

TEACHING EDITORIAL

A Brief Survey of Methods for Preparing Protein Conjugates with Dyes, Haptens, and Cross-Linking Reagents

Michael Brinkley

Molecular Probes, Inc., 4849 Pitchford Avenue, Eugene, Oregon 97402. Received July 24, 1991

I. INTRODUCTION

Modification of proteins, DNA, and other biopolymers by labeling them with reporter molecules has become a very powerful research tool in immunology, histochemistry, and cell biology. A number of excellent reviews of this subject have been published (1-6). In addition, there are a growing number of commercial applications of these modified biomolecules, including clinical immunoassays, DNA hybridization tests, and gene fusion detection systems. In these techniques, a small molecule with special properties, such as fluorescence or binding specificity, is covalently bound to a protein, a DNA strand, or other biomolecule. Specific examples include fluorescent-labeled antibodies for detection and localization of cell-surface antigens, biotin-labeled single-stranded DNA probes for detection of DNA hybridization, and hapten-labeled proteins that, when introduced into a suitable host animal, generate hapten-specific antibodies.

This review will focus on the experimental design and procedures for preparing protein conjugates with dyes, biotin, and haptens such as drugs and hormones. Methods for covalently linking two unlike biopolymers through the judicious choice of cross-linking reagents will also be discussed. The following specific topics will be addressed: (a) reactive groups of proteins that are available for modification, including their naturally occurring amino acids, and reactive groups introduced by chemical modification, (b) reagents that can be used to couple molecules to these reactive sites, (c) experimental procedures for preparing conjugates, (d) purification and isolation of conjugates, and (e) techniques for determining the degree of labeling.

II. GENERAL DISCUSSION OF METHODS

A. Reactive Groups of Proteins. Proteins and peptides are amino acid polymers containing a number of reactive side chains. In addition to, or as an alternative to, these intrinsic reactive groups, specific reactive moieties can be introduced into the polymer chain by chemical modification. These groups, whether or not they are naturally a part of the protein or are artificially introduced, serve as "handles" for attaching a wide variety of molecules, including other proteins. The intrinsic reactive groups of proteins are described in the following section.

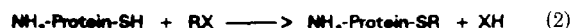
(1) *Amines (Lysines, α -Amino Groups).* One of the most common reactive groups of proteins is the aliphatic ϵ -amine of the amino acid lysine. Lysines are usually present to some extent and are often quite abundant. For example, the protein bovine insulin contains only a single lysine amine, while avidin, a protein found in egg whites, contains 36 lysines (7). Lysine amines are reasonably good nucleophiles above pH 8.0 ($pK_a = 9.18$) (8) and therefore react easily and cleanly with a variety of reagents to form

stable bonds (eq 1). Other reactive amines that are found



in proteins are the α -amino groups of the N-terminal amino acids. The α -amino groups are less basic than lysines and are reactive at around pH 7.0. Sometimes they can be selectively modified in the presence of lysines. There is usually at least one α -amino acid in a protein, and in the case of proteins that have multiple peptide chains or several subunits, there can be more (one for each peptide chain or subunit). Bovine insulin has one N-terminal glycine residue and one N-terminal phenylalanine (9). There are proteins that do not possess free α -amino groups, such as cytochrome C and ovalbumin. In these molecules, the N-terminal amino group is N-acylated, and therefore not reactive toward the usual modification reagents. Since either N-terminal amines or lysines are almost always present in any given protein or peptide, and since they are easily reacted, the most commonly used method of protein modification is through these aliphatic amine groups.

(2) *Thiols (Cystine, Cysteine, Methionine).* Another common reactive group in proteins is the thiol residue from the sulfur-containing amino acid cystine and its reduction product cysteine (or half-cystine), which are counted together as one of the 20 amino acids. Cysteine contains a free thiol group, which is more nucleophilic than amines and is generally the most reactive functional group in a protein. It reacts with some of the same modification reagents as do the amines discussed in the previous section and in addition can react with reagents that are not very reactive toward amines. Thiols, unlike most amines, are reactive at neutral pH, and therefore they can be coupled to other molecules selectively in the presence of amines (eq 2). This selectivity makes the thiol

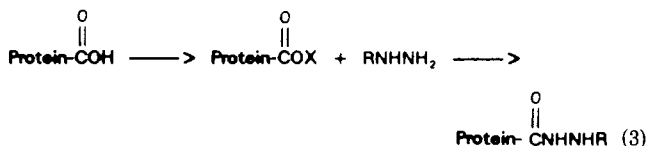


group the linker of choice for coupling two proteins together, since methods which only couple amines (e.g., glutaraldehyde, dimethyl adipimidate coupling) can result in formation of homodimers, oligomers, and other unwanted products (10). Since free sulfhydryl groups are relatively reactive, proteins with these groups often exist in their oxidized form as disulfide-linked oligomers or have internally bridged disulfide groups. Immunoglobulin M is an example of a disulfide-linked pentamer, while immunoglobulin G is an example of a protein with internal disulfide bridges bonding the subunits together. In proteins such as this, reduction of the disulfide bonds with a reagent such as dithiothreitol (DTT) is required to generate the reactive free thiol (11). In addition to cystine and cysteine, some proteins also have the amino acid methionine, which contains sulfur in a thioether linkage. When cysteine is absent, methionine can sometimes react

with thiol-reactive reagents such as iodoacetamides (12). However, selective modification of methionine is difficult to achieve and therefore is seldom used as a method of attaching small molecules to proteins.

(3) *Phenols (Tyrosine)*. The phenolic substituent of the amino acid tyrosine can react in two ways. The phenolic hydroxyl group can form esters and ether bonds, and the aromatic ring can undergo nitration or coupling reactions with reagents such as diazonium salts at the position adjacent to the hydroxyl group. There is considerable literature describing the reaction of tyrosyl residues with diazonium compounds (13). For example, a *p*-aminobenzoyl biocytin derivative has been diazotized and reacted with protein tyrosine groups (14). Modification of tyrosines has primarily been used in structural studies, rather than as a means for attaching specific labels, since acetylation and nitration can give useful information concerning the participation of tyrosine in the binding properties of proteins. Often, the reactivity of tyrosines with amine-selective modification reagents to form unstable carboxylic acid esters or sulfate esters is an unwanted side reaction resulting in conjugates that slowly hydrolyze during storage. Methods for preventing this problem are discussed in a later part of this teaching editorial (section V.B.1).

(4) *Carboxylic Acids (Aspartic Acid, Glutamic Acid)*. Proteins contain carboxylic acid groups at the carboxy-terminal position and within the side chains of the dicarboxylic amino acids aspartic acid and glutamic acid. The low reactivity of carboxylic acids in water usually makes it difficult to use these groups to selectively modify proteins and other biopolymers. In the cases where this is done, the carboxylic acid group is usually converted to a reactive ester by use of a water-soluble carbodiimide



and then reacted with a nucleophilic reagent such as an amine or a hydrazide (15, 16). The amine reagent should be weakly basic in order to react specifically with the activated carboxylic acid in the presence of the other amines on the protein. This is because protein cross-linking can occur when the pH is raised to above 8.0, the range where the protein amines are partially unprotonated and reactive. For this reason, hydrazides, which are weakly basic, are useful in coupling reactions with a carboxylic acid (17). This reaction can also be used effectively to modify the carboxy terminal group of small peptides.

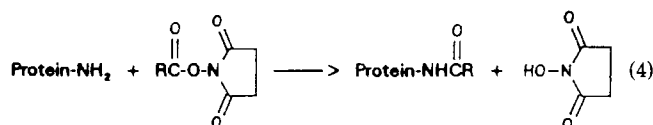
(5) *Other Amino Acid Side Chains (Arginine, Histidine, Tryptophan)*. Chemical modification of other amino acid side chains in proteins has not been extensive, compared to the groups discussed above. The high pK_a of the guanidine functional group of arginine ($pK_a = 12-13$) necessitates more drastic reaction conditions than most proteins can survive. Arginine modification has been accomplished primarily with glyoxals and α -diketone reagents (18). Tryptophan modification requires harsh conditions and is seldom carried out except as a method of analysis in structural or activity studies. Histidines have been subjected to photooxidation (19) and reaction with iodoacetates (20).

B. Protein Modification Reagents. This section will survey the extensive selection of reagents that are available

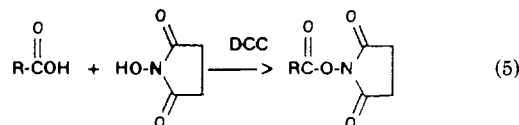
for the purpose of protein modification. The fundamental principles for understanding how to use these reagents are (1) recognition of the reactive group(s) on the protein or peptide that can be modified and (2) knowledge of the type of chemical reactions these reactive groups will participate in and the nature of the chemical bonds that will result from these reactions.

(1) *Amine-Reactive Reagents*. These reagents are those which will react primarily with lysines and the α -amino groups of proteins and peptides under both aqueous and nonaqueous conditions. Some amine-reactive reagents are more reactive, and therefore less selective, than others, and it will be necessary to understand this property in order to choose the best reagent for modification of a specific protein. The following amine-reactive reagents are available.

(a) *Reactive Esters (Formation of an Amide Bond)*. Reactive esters, especially *N*-hydroxysuccinimide (NHS) esters, are among the most commonly used reagents for modification of amine groups (21). These reagents have intermediate reactivity toward amines, with high selectivity toward aliphatic amines. Their reaction rate with aromatic amines, alcohols, phenols (tyrosine), and histidine is relatively low. Reaction of NHS esters with amines under nonaqueous conditions is facile, so they are useful for derivatization of small peptides and other low molecular weight biomolecules. The optimum pH for reaction in aqueous systems is 8.0–9.0. The aliphatic amide products which are formed are very stable (eq 4). The

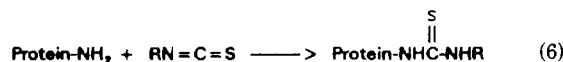


NHS esters are slowly hydrolyzed by water (22), but are stable to storage if kept well desiccated. Virtually any molecule that contains a carboxylic acid or that can be chemically modified to contain a carboxylic acid can be converted into its NHS ester (eq 5), making these reagents



among the most powerful protein-modification reagents available. Newly developed NHS esters are available with sulfonate groups that have improved water solubility (23). A short list of reactive NHS ester derivatives of fluorescent probes, biotin, and other molecules is given in Table I.

(b) *Isothiocyanates (Formation of a Thiourea Bond)*. Isothiocyanates, like NHS esters, are amine-modification reagents of intermediate reactivity and form thiourea bonds with proteins and peptides (eq 6). They are



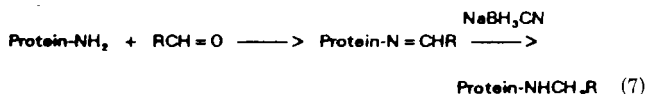
somewhat more stable in water than the NHS esters and react with protein amines in aqueous solution optimally at pH 9.0–9.5. Since this is a higher pH than the optimal pH for NHS esters (which undergo competing hydrolysis at pH 9.0–9.5), isothiocyanates may not be as suitable as NHS esters when modifying proteins that are sensitive to alkaline pH conditions. One of the most commonly used fluorescent derivatization reagents for proteins is fluorescein isothiocyanate (FITC). A number of other fluo-

Table I. Succinimidyl Ester Probes

probes	structure	function	ref
succinimidyl fluorescein-5-(and -6-)carboxylate		fluorescent label	75, 76
succinimidyl <i>N,N,N',N'</i> -tetramethylrhodamine-5-(and -6-)carboxylate		fluorescent label	76
succinimidyl 7-amino-4-methylcoumarin-3-acetate		fluorescent label	77
succinimidyl X-rhodamine-5-(and -6-)carboxylate		fluorescent label	75, 78
succinimidyl D-biotin		ligand, affinity label	79
succinimidyl 3-(4-hydroxyphenyl)propionate		radioiodination label	80

rescent dyes (coumarins and rhodamines) have been coupled to proteins via their reactive isothiocyanates (24).

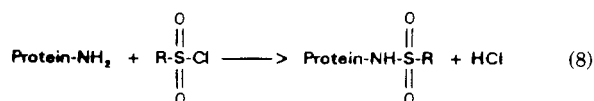
(c) *Aldehydes (Formation of Imine, Reduction to Alkylamine Bond)*. Aldehyde groups react under mild aqueous conditions with aliphatic and aromatic amines to form an intermediate known as a Schiff base (an imine), which can be selectively reduced by the mild reducing agent sodium cyanoborohydride to give a stable alkylamine bond (eq 7) (44, 53). This method of amine modification is not used



in protein conjugations as frequently as the activated ester method, but when the molecule to be attached has an aldehyde group, or can be easily converted to an alde-

hyde, the method is mild, simple, and very effective. Aldehydes (glyoxals) can also react with protein arginine groups (25, 26) and the nucleic acid base guanosine, making them of some use in nucleic acid modification (27).

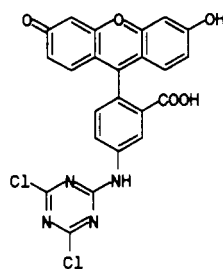
(d) *Sulfonyl Halides (Formation of a Sulfonamide Bond)*. Sulfonyl halides are highly reactive amine-modifying reagents. They are unstable in water, especially at the pH required for reaction with aliphatic amines, but they form extremely stable sulfonamide bonds which can survive even amino acid hydrolysis (eq 8). It is for this



reason that sulfonamide conjugates are useful for amine-terminus derivatization (Dansyl-Edman degradation) and

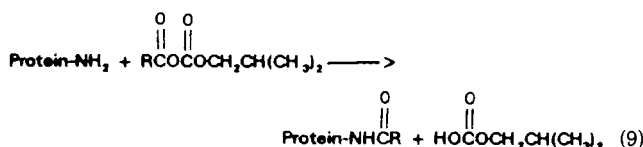
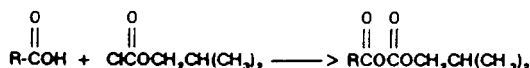
as tracers (28). In addition to amines, sulfonyl halides also react with phenols (tyrosine), thiols (cysteine), and imidazoles (histidine) on proteins (29); therefore, they are less selective than either NHS esters or isothiocyanates. The conjugates formed with thiols, imidazoles, and phenols are all unstable and, if not removed during purification, can lead to loss of the label from the protein during long-term storage (see section V.B.1). One of the most widely used long-wavelength fluorescent probes, Texas Red, is a sulfonyl chloride. It has the longest wavelength spectral properties of any of the common amine-reactive fluorescent labeling reagents (30).

(e) *Miscellaneous Amine Reactive Reagents (Dichlorotriazines, Alkyl Halides, Anhydrides)*. The dichlorotriazine derivative of fluorescein, known as DTAF (I), has



I

high reactivity with protein amines and has been used to prepare fluorescein tubulin with minimal loss of activity (31). In addition to amines, dichlorotriazines will react with alcohols at elevated temperatures (60–90 °C) and are used to prepare polysaccharide conjugates (32). Some alkyl halides, including iodoacetamides commonly used to modify thiols, will react with amines of proteins if the pH is in the range 9.0–9.5 (33). Other reagents that have been used to modify amines of proteins are acid anhydrides. Succinic anhydride is commonly used to succinylate amine groups of basic proteins for the purpose of changing their isoelectric point and other charge-related properties (34). Mixed anhydrides derived from reaction of a carboxylic acid with carbitol or 2-methylpropanol chloroformates (eq 9) are excellent reagents for modification of amines under



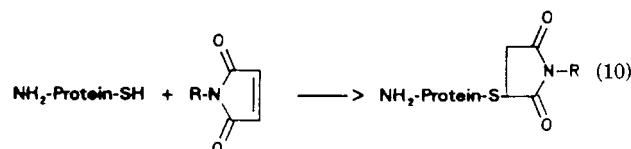
mild conditions (35). Of these, the carbitol mixed anhydride is relatively water soluble and is the preferred reagent for modification of amines in aqueous solution.

(2) *Thiol-Reactive Reagents*. Thiol-reactive reagents are those that will couple to thiol groups on proteins to give thioether-coupled products. These reagents react rapidly at neutral (physiological) pH and therefore can be reacted with thiols selectively in the presence of amine groups.

(a) *Haloacetyl Derivatives (Formation of a Thioether Bond)*. These reagents (usually iodoacetamides) are among the most frequently used reagents for thiol modification. In most proteins, the site of reaction is at cysteine groups that are either intrinsically present or that

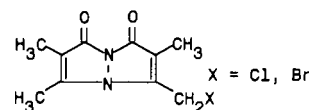
result from reduction of cystines. The reaction of iodoacetate with cysteine is approximately twice as fast as that with bromoacetate and 20–100 times as rapid as that with chloroacetate (36). As mentioned previously, in the absence of cysteines, methionines can sometimes react with haloacetamides (12). Reaction of haloacetamides with thiols occurs rapidly at neutral pH at room temperature or below, and under these conditions, most aliphatic amines are unreactive. In addition to proteins, haloacetamides have been reacted with thiolated peptides and thiolated primers for DNA sequencing (37), and also with RNA (on thiouridine) (38). The thioether linkages formed from reaction of haloacetamides are very stable. A potential problem in using iodoacetamides as modification reagents is their instability to light, especially in solution; therefore, they must be protected from light in storage and during reaction. The fluorescein and rhodamine iodoacetamides are among the most intensely fluorescent sulfhydryl reagents available for protein and peptide modification.

(b) *Maleimides (Formation of a Thioether Bond)*. Maleimides (eq 10) are similar to iodoacetamides in their



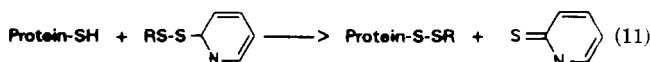
application as reagents for thiol modification; however, they are more selective than iodoacetamides, since they do not react with histidine, methionine, or thionucleotides (39, 40). The optimum pH for the reaction of maleimides is near 7.0. Above pH 8.0, hydrolysis of maleimides to nonreactive maleamic acids can occur (41).

(c) *Miscellaneous Thiol-Reactive Reagents*. These reagents include bromomethyl derivatives and pyridyl disulfides. The bromomethyl derivatives are similar in reactivity to iodoacetamides. The haloalkyl derivatives monobromobimane and monochlorobimane (II) react with

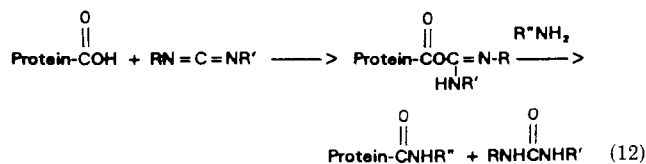


II

glutathione and other thiols in cells to give fluorescent adducts, thus providing a method of quantitation of thiols (42). Pyridyl disulfides react in an exchange reaction with protein thiols to give mixed disulfides (eq 11) (43).



(3) *Carboxylic Acid- and Aldehyde-Reactive Reagents*. (a) *Amines and Hydrazides (Formation of Amide or Alkylamine Bonds)*. Amines and hydrazides can be coupled to carboxylic acids of proteins via activation of the carboxyl group by a water-soluble carbodiimide followed by reaction with the amine or hydrazide. As mentioned previously (section II.A.4), the amine or hydrazide reagent must be weakly basic so that it will react selectively with the carbodiimide-activated protein in the presence of the more highly basic protein ϵ -amines (lysines). The reaction of these probes with carbodiimide-activated carboxyl groups leads to the formation of stable amide bonds (eq 12).



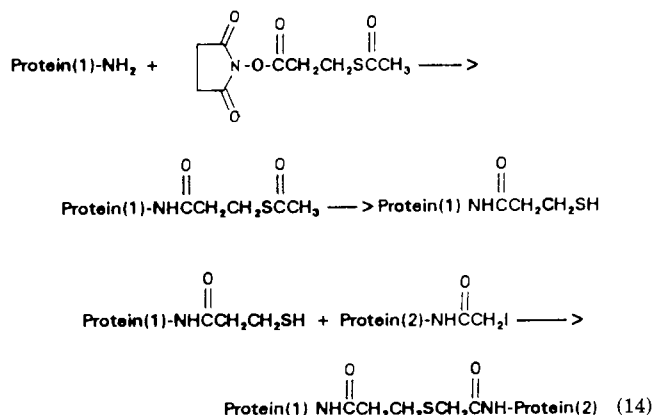
Amines and hydrazides are also able to react with aldehyde groups, which can be generated on proteins by periodate oxidation of carbohydrate residues on the protein. In this case, a Schiff base intermediate is formed (eq 13), which can be reduced to an alkylamine with sodium



cyanoborohydride, a mild and selective water-soluble reducing agent (44) (see also section II.B.1.c). Since the Schiff base formation is reversible, it is possible to minimize formation of protein-protein products by adding a large excess of amine or hydrazide reagent.

(4) *Bifunctional Reagents*. Bifunctional, or cross-linking, reagents are specialized reagents having reactive groups that will form a bond between two different groups, either on the same molecule or two different molecules. Bifunctional reagents can be divided into two types: those with the same reactive group at each end of the molecule (homobifunctional) and those with different reactive groups at each end of the molecule (heterobifunctional). Recent trends are heavily in favor of the use of heterobifunctional cross-linkers where the bifunctional reagent has two reactive sites, each with selectivity toward different functional groups (amine reactive and thiol reactive, for example). These reagents, some of which are available in a range of chain lengths, are well-suited to the task of controlled coupling of unlike biomolecules, such as two different proteins. Table II lists some frequently used heterobifunctional cross-linkers along with their reactivities and references describing their use.

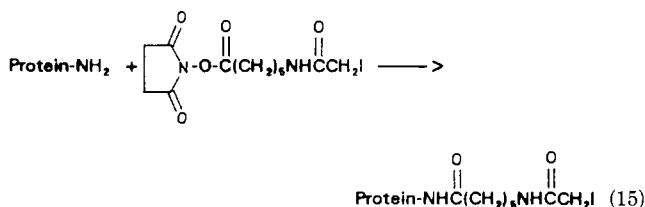
(a) *Amine Reactive—Thiol or Protected Thiol*. Because thiols will react selectively in the presence of amines with a variety of reagents, these functional groups are very useful for attaching two different proteins together. Thiol-coupling methods are frequently employed to prepare protein-enzyme conjugates. If the proteins to be coupled do not contain intrinsic thiols, the procedure is typically carried out by introducing a single thiol group to an amine of one of the proteins by means of a heterobifunctional reagent (eq 14). Traut's reagent (iminothiolane) has been



extensively used for the purpose of introducing thiol groups selectively to proteins (45, 46). Many other bifunctional

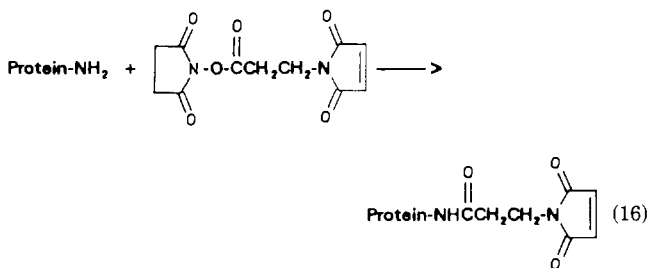
reagents contain both an amine-reactive and a protected thiol group, such as succinimidyl (acetylthio)acetate (SATA) (47, 48) or succinimidyl 3-(2-pyridyldithio)propionate (SPDP) (43, 49). After deprotection, the thiol-containing protein is then reacted with a thiol-reactive group on the other protein, which has been introduced by a similar technique. Alternatively, proteins with synthetic thiol groups that have been introduced by modification can be used to couple to a number of thiol-reactive derivatives of dyes, biotin, haptens, or other molecules.

(b) *Amine Reactive—Iodoacetamide*. Iodoacetamides are primarily thiol-reactive groups with the reaction occurring rapidly at physiological pH, but they can react with amines under more alkaline conditions (greater than pH 9.0) and long reaction times (section II.B.2.a). Iodoacetamides can be introduced into a protein or peptide that does not have intrinsic thiols via amine-reactive derivatives (eq 15) (50). The resulting modified protein



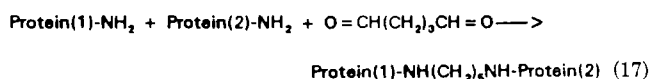
can then be coupled to any thiol-containing molecule. The second molecule is usually a thiol-containing protein.

(c) *Amine Reactive—Maleimide*. The introduction of maleimides into a protein or peptide can be carried out with heterobifunctional reagents that have an amine-reactive group at one end and the thiol-specific maleimide at the other end (eq 16). The applications are very



similar to those for the iodoacetamides discussed in the preceding section. Specific applications include coupling of ricin to monoclonal antibodies (51) and linking of oligonucleotides to enzymes (52).

(d) *Amine Reactive—Aldehyde*. Aldehydes do not occur naturally in proteins, but can be introduced in two ways. In the first method, carbohydrate groups on proteins are treated with an oxidizing reagent, such as sodium periodate, or are converted via a galactose oxidase/catalase enzyme method, both of which split the sugar to form aldehyde groups (53). Not all proteins contain carbohydrate groups, and therefore a second method of introducing aldehydes via the reagent glutaraldehyde has been employed (10). Glutaraldehyde has been used extensively to couple two proteins together via their amine groups (eq 17); however, like other homobifunctional reagents, glu-



taraldehyde is being replaced with more selective heterobifunctional reagents such as those discussed above.

Table II. Heterobifunctional Cross-Linking Reagents

reagent	structure	reactivity	ref
succinimidyl 3-(2-pyridyldithio)propionate (SPDP)		primary amine, thiol	49
succinimidyl <i>trans</i> -4-(<i>N</i> -maleimidymethyl)cyclohexane-1-carboxylate (SMCC)		primary amine, thiol	54, 48
succinimidyl (acetylthio)acetate (SATA)		primary amine, thiol	47, 48
4-[(succinimidyl)oxy]carboxyl- α -methyl- α -(2-pyridyldithio)toluene (SMPT)		primary amine, thiol	55, 48
succinimidyl 4-[[[iodoacetyl]amino]methyl]-cyclohexane-1-carboxylate (SIAC)		primary amine, thiol	50
succinimidyl <i>p</i> -azido benzoate (SAB)		primary amine, nonselective	56

(5) *Photoactivatable Reagents*. Reagents are available that can be activated by light (photons) to produce a reactive intermediate that can couple to various functional groups on biomolecules. Two of the most frequently used photoactivatable reagents for this purpose are aromatic azides and benzophenones.

(a) *Aromatic Azides*. Aromatic azides are efficiently photolyzed by illumination with an ultraviolet light at 300–350 nm. The reactive molecule produced by this photolysis is a nitrene, which reacts rapidly and nonspecifically with either solvent molecules or with functional groups on biomolecules. Almost any functional group or amino acid can be modified, since the nitrene is very reactive. Recent improvements in azide-based protein modification reagents have resulted in perfluorinated azides that generate nitrene intermediates with greater stability, thus giving reagents with higher efficiency (up to 40%) of reaction with the protein (57, 58). One of the primary uses of these highly reactive reagents is to carry out photoaffinity labeling experiments. In these experiments, the aromatic azide is attached to a drug or other molecule which binds specifically to a protein binding site (an example is an enzyme inhibitor or a nucleotide analogue) and then photolyzed. The location and type of bond formed in this process provides information about the environment near the binding site (59). In addition to their role as photoaffinity labels, aryl azides are useful as heterobifunctional cross-linkers. Succinimidyl azido benzoate (SAB), *p*-azidophenacyl bromide, and 4-maleimidobenzophenone have been employed to couple proteins through dark reaction with amines or thiols followed by light activation (56, 58, 60, 61).

(b) *Benzophenones*. Benzophenones are like azides in that they are photoactivatable by ultraviolet light, but once they have been activated, they can either react with functional groups or return to the ground state. Thus, these molecules can sometimes be reactivated if they do not react on the first activation. These reagents are also used as photoaffinity labels in a manner similar to that of the aromatic azides (62).

III. PRACTICAL CONSIDERATIONS

Along with a thorough knowledge of protein reactivity and the available reagents for the desired type of protein modification, it is of crucial importance that the researcher understand the practical aspects of carrying out reactions between highly reactive small organic molecules and large, complex, conformationally sensitive, water-soluble biopolymers. The following discussion will address some of the general rules, problems, and pitfalls of protein-modification chemistry.

A. Choosing the Right Buffer. Conjugations should be carried out in a well-buffered system at a pH that is optimal for the reaction. The ionic strength should, in most cases, be in the range of 25–100 mM. For modification of thiol groups and α -amino groups, which occurs selectively at physiological pH (7.0–7.5), phosphate buffers are ideally suited. The more strongly basic lysine amines require more alkaline pH, in the range of 8.0–9.5, where phosphate solutions do not buffer well. For these reactions, carbonate/bicarbonate (pH of 100 mM bicarbonate is 9.2) or borate buffers are quite satisfactory. As an example, conjugations with NHS esters are best carried out in pH 8.2 bicarbonate buffer, while isothiocyanates require the

higher pH (9.0–9.5) provided by carbonate or borate buffers. The choice of buffer will in some cases be directed by compatibility of the protein.

B. Cosolvents. If the reagent that is to be attached to the biomolecule is readily soluble at millimolar concentrations in water or buffer, no cosolvent is needed, and the reagent can be added as a concentrated aqueous solution to the buffered reaction solution. Unfortunately, aqueous systems are very often incompatible with the reagent, as a result of poor solubility or high reactivity with water. In these cases, a water-miscible cosolvent must be employed that will dissolve the reagent without causing its decomposition. At the same time, the cosolvent must not cause irreversible denaturation or precipitation of the biomolecule. Some cosolvents that have been successfully utilized in protein modifications are methanol, ethanol, 2-propanol, 2-methoxyethanol, dioxane, dimethylformamide (DMF), and dimethyl sulfoxide (DMSO).

The most versatile of these cosolvents are DMF and DMSO. They are recommended because of the following desirable properties: (a) they are inert to many of the reactive reagents used in preparing conjugates, (b) they are miscible with water in all proportions, and (c) they are compatible with most aqueous protein solutions even at up to 30% v/v ratios. DMF is the solvent of choice for reactions of sulfonyl chlorides, since these reagents will react with DMSO. It is usually important that cosolvents be carefully dried and stored over a drying agent to prevent competing hydrolysis of the reactive modification reagent.

C. Reaction Conditions. As a general rule, conjugation reactions should be done at below room temperature, since the rate of reaction of most conjugation reagents is rapid at low temperature. Low temperatures tend to increase the selectivity of the reaction, resulting in fewer side reactions and more consistent and reproducible results. A convenient procedure is to add the reagent to a gently stirred buffered solution of the protein in an ice-bath and then allow the bath to warm to room temperature over a period of about 2 h. Very reactive reagents such as sulfonyl chlorides should be reacted under more carefully controlled conditions, such as 4 °C for 1 h. Stirring can be done with a magnetic stir-bar and should not be excessively fast, since proteins can be denatured by violent mixing. Addition of the reagent should be carried out dropwise and as slowly as possible, since gradual addition increases the selectivity of the reaction.

(1) *Protein Concentration.* Because the kinetics of conjugation of these reagents is bimolecular, but the hydrolysis rates are pseudo-first-order, dilution results in competition between conjugation and loss of reagent by hydrolysis. Protein concentrations above 10 μ M are strongly recommended, with an optimum in the range of 50–100 μ M.

(2) *pH.* In modification of amines, only the unprotonated form is reactive, and therefore it is necessary to maintain a pH at which a significant number of amines are unprotonated. An average pK_a above 9 for lysines indicates that the higher the pH, the better. Offsetting this are the factors that the rate of reagent hydrolysis increases rapidly above pH 9 and that proteins tend to be unstable at a higher pH. A free amine terminus has a pK_a near 7 and is sometimes preferentially modified when the reaction is run at neutral pH. An effective compromise in most cases is to use a pH close to 9.0–9.2 if the protein is stable, but a lower pH combined with more reagent and longer reaction times if the protein is unstable. The succinimidyl esters and DTAF appear to react more efficiently at a lower pH than the isothiocyanates and sulfonyl

chlorides. Our experience with succinimidyl esters indicates that a reaction pH of around 8.2 gives excellent results for most proteins.

(3) *Reaction Time.* Usually, 1–2 h is sufficient time for conjugation reactions to go to completion. Longer reaction times, if convenient, are acceptable, since the degree of labeling is generally limited by the ratio of the reagent to protein, rather than the reaction time. Many published procedures specify overnight reaction times. Obviously, the more reactive the reagent, the shorter the reaction time; sulfonyl chloride reactions are faster than NHS ester reactions.

IV. FACTORS INFLUENCING CHOICE OF MOLAR RATIO OF REACTANTS

A. End Use of Reagents. (1) *Immunogen—High Degree of Labeling.* Protein conjugates are frequently prepared for use in producing specific antibodies to a drug or other hapten in a host animal. The drug or hapten is conjugated to a high molecular weight protein carrier molecule and injected into the animal to elicit an immune response, and over a period of time, specific antibodies to the drug or hapten are produced. For these purposes, a high degree of labeling of the protein carrier is desirable, since more labels generally increase the strength and specificity of the immune response.

(2) *Labeled Antibody or Enzyme—Low to Moderate Degree of Labeling.* Antibodies and enzymes are relatively sensitive to substitution, since there are usually reactive amino acid side chains (amines, thiols, histidines) in or near the binding sites. For this reason, a low to moderate degree of labeling is preferred in order to preserve binding specificity or enzyme activity. Excessive labeling can also result in decreased solubility of the conjugates, which also reduces the overall activity. In the case of many fluorescent labels, a high dye to protein ratio causes a dramatic decrease in the fluorescence efficiency of the conjugates (63,64). In our experience with antibodies, a substitution ratio in the range of 4–6 is usually optimal for good retention of binding activity.

(3) *Fluorescent Labeled Proteins/Peptides—Low to Moderate Degree of Labeling.* Fluorescent labels are often very sensitive to their molecular environment and therefore their fluorescence intensity is almost always decreased when they are bound to proteins and other biomolecules. Fluorescence also decreases when the fluorescent labels are located in close proximity to one another, probably as a result of transfer of excited-state energy (quenching) from one molecule to another (65). When proteins are labeled with fluorescent dyes, the fluorescence increases as more dyes are added; at the same time, however, the fluorescence efficiency decreases as a result of the quenching described above. Some dyes are more sensitive to quenching than others. FITC is about 50–70% quenched on IgG at a dye/protein ratio of 5 (66), while Cascade Blue, a newly developed blue fluorescent dye (67), retains nearly 100% of its fluorescence efficiency under the same conditions. The number of dyes that can be conjugated to a protein without substantial loss of fluorescence will depend on the size of the protein and the distance between the functional groups to which the label is attached. Usually, more dyes can be attached to a large protein than a small protein or peptide. A general rule for conjugates of fluorescein is 4–6 dyes/protein and for rhodamines, 2–3 dyes/protein. The degree of labeling depends on the relative reactivity of the labeling reagent to the protein and to water, the molecular weight and number of reactive amines on the protein, the reactant concentrations (es-

pecially of the protein), and other factors. The exact amount of label to use must be determined by experiment; however, as a guideline, 10 mol of a typical isothiocyanate or NHS ester is needed to label 1 mol of a protein. Because of the faster competitive hydrolysis rate, 20 mol of a sulfonyl chloride, such as Texas Red, is required to label 1 mol of a protein.

B. Number of Reactive Groups on the Protein. Proteins vary greatly in the number of reactive amino acid groups. For example, some proteins have 40 or more reactive amine groups, while others may have only one or two amines or thiol groups. The reactivity of these groups with the labeling reagent and their effective concentration in solution will then have an effect on the amount of labeling reagent required to achieve the desired degree of substitution. This means that small molecular weight proteins or peptides with few reactive groups will require more labeling reagent per gram than large molecular weight proteins with many reactive groups.

C. Solubility of Modification Reagent in Reaction Solution. (1) *Cosolvent Sometimes Required.* The use of cosolvents was explained in section III.B. In some cases the labeling reagent is very hydrophobic and, even though it is readily soluble in DMF or DMSO, it precipitates when added to the buffered protein solution. It is often possible to circumvent this problem by adding some cosolvent gradually, with stirring, to the buffered protein solution until the protein solution contains 20–25% cosolvent. The ionic strength of the buffer should be no more than 50 mM so that the buffer does not salt out upon addition of the cosolvent. Then the solution of labeling reagent in cosolvent is added so that the final volume percent cosolvent in the reaction mixture is around 30%. This modification often is successful in preventing precipitation of the labeling reagent. Many proteins are stable in 30% DMSO or DMF; however the stability of the protein to these conditions should be determined before carrying out this technique.

(2) *Two-Stage Labeling as a Last Resort.* If the technique described in section IV.C.1 is used and the labeling reagent still precipitates when added to the protein solution, it may be possible to purify the conjugate and then repeat the labeling procedure to increase the degree of substitution.

D. Solubility of Conjugate. (1) *Conjugate Is Often Less Soluble Than Native Protein.* Problems with solubility of the conjugate can occur, most often when the labeling reagent is hydrophobic or contains multiple ionic groups. These physical properties of the label can upset the natural folding of the protein and cause the conjugate to be significantly less soluble than the native protein (30).

(2) *Overlabeling Can Cause Precipitation of Conjugate.* Overlabeling can produce the same undesirable results noted above. The best solution to these problems is to use a lower ratio of labeling reagent to protein, resulting in a conjugate with a lower degree of substitution.

V. PURIFICATION OF CONJUGATES

A. Removal of Excess Noncovalently Bound Labeling Reagent. (1) *Dialysis—Simple, Inexpensive Purification Method—Inefficient for Hydrophobic Molecules.* Dialysis is the simplest, but most time-consuming, method of purifying protein conjugates. Not all molecules dialyze efficiently; the rate of dialysis depends on their relative affinity for the protein versus the dialysis solution. Molecules that are sparingly soluble in water or strongly adsorbed to the protein surface will take a long time to dialyze. Dialysis works best when the labeling reagent

and its unreacted byproducts are hydrophilic. When purifying conjugates by dialysis, a dialysis buffer volume of at least 100 times the volume of the conjugate solution should be used and the dialysis buffer should be changed at least five times. Allow at least 4 h for dialysis between buffer changes.

(2) *Gel Filtration—Faster Than Dialysis—Effectively Removes Most Hydrophilic and Hydrophobic Labeling Reagents.* Gel exclusion chromatography separates conjugates from excess noncovalently bound labeling reagent and other small molecular weight impurities by selectively adsorbing the small molecules, while allowing the larger protein conjugate molecules to pass through the void space in the gel. This method is very fast and effective for purifying conjugates from both hydrophobic and hydrophilic labeling reagents. A common technique employs a Sephadex G-25 or similar column containing about a 2-mL bed volume/mg of protein that can be packed in any suitable buffer (30). Upon elution in the case of dyes, the conjugate and free dye bands are usually clearly visible; many other types of labels can be visualized by holding a hand-held UV lamp close to the column during chromatography. Automatic fraction-collecting devices with UV monitors are also frequently used. If partial precipitation has occurred during the reaction, the samples should be centrifuged before running the column. The solution of labeled protein will contain a mixture of species with variable degrees of substitution. If required, separation of the lightly and heavily labeled fractions can be done by ion-exchange chromatography. Usually one passage through a gel filtration column is sufficient to remove most of the unreacted label; however, some proteins bind small molecules with high avidity. To completely purify these conjugates it may be necessary to carry out additional purification steps.

(3) *Hydrophobic Interaction Adsorbents—Removes Strongly Bound Hydrophobic Labeling Reagents.* Some labeling reagents have a very strong affinity for certain proteins and cannot be completely removed by gel filtration. These conjugates can be further purified (after gel filtration to remove most of the unreacted label) by treatment with microporous, hydrophobic polystyrene beads (68). In this procedure, the conjugate is simply mixed with the beads, and the small hydrophobic molecules are selectively adsorbed into the micropores while the larger conjugate molecules are excluded.

B. Removal of Labeling Reagent Attached by Unstable Covalent Bonds. (1) *Hydroxylamine Treatment—Hydrolysis of Tyrosine Ester Bonds under Mild Conditions.* Section II.A.3 describes the formation of tyrosine esters. Several of the reagents commonly used for protein modification, including NHS esters, isothiocyanates, and sulfonyl chlorides, can react with tyrosines to form these esters. These adducts are unstable and can hydrolyze even at physiological pH, resulting in loss of label over a period of time. Since any measurable loss of label can interfere with the intended use of many conjugates, it is advisable to pretreat all conjugates prepared with these types of reagents to remove any esters that may have formed in the conjugation reaction. This can be effectively done in most cases by treating the conjugate before purification with hydroxylamine (69, 70). In this method, a 1.5 M solution of hydroxylamine at pH 8.0 is added to the conjugate solution to a final concentration of 0.1 M and the solution is stirred at room temperature for 1 h. The conjugate is then purified by gel filtration or dialysis.

VI. EXPERIMENTAL METHODS FOR PREPARING PROTEIN CONJUGATES

The general experimental procedures that follow describe methods for conjugating amine-reactive and thiol-reactive probes to proteins. They should be useful as a guide for the experimentalist; however, it is strongly suggested that the numerous literature references given in this review and others be consulted for additional specific information. Because of the very wide variety of experimental conditions required for coupling proteins with bifunctional reagents, it is difficult to generate a simple general procedure and the reader is advised to consult the literature for specific procedures.

A. Amine-Reactive Probes. The following general procedure is recommended for the first trial and is adaptable to amine-reactive dye, biotin, hapten, and bifunctional linker conjugations. The procedure may be modified after the degree of substitution has been determined (see below) after purification.

Step 1. Dissolve the protein at 50–100 μ M in 50–100 mM sodium bicarbonate buffer at pH 9.2 at room temperature. Borate buffer is also suitable. Amine-based buffers, such as TRIS are not recommended. Conjugations with succinimide esters and reagents such as DTAF [5-[(4,6-dichlorotriazin-2-yl)amino]fluorescein] should be done at a lower pH. In these cases, a suitable buffer is 50–100 mM pH 8.2 sodium bicarbonate.

Step 2. Add sufficient protein-modification reagent from a stock solution to contain about 10 mol of isothiocyanate or succinimide ester for each mole of protein or about 20 mol of sulfonyl chloride for each mole of protein. Although most protein modification reagents have some solubility in water, it is recommended that a stock solution be prepared immediately before use in a water-miscible nonhydroxylic solvent such as dimethyl formamide (DMF), dimethyl sulfoxide (DMSO), or dioxane. The stock solution should be prepared fresh each time, since it is very difficult to store these solutions for any length of time without decomposition of the reagent taking place. As a guideline, it is recommended to prepare a stock solution at about 10–20 mM of the protein-modification reagent in dry DMF. The fluorescent dyes Texas Red, Lissamine rhodamine B, and other sulfonyl chlorides must *never* be used in DMSO, with which they react. These stock solutions (prepared in dry DMF) are usually diluted about 10-fold into the protein, while being agitated to avoid high local concentrations of reagent. Some reagents are quite hydrophobic, having little solubility in the aqueous protein solution. This is particularly true of some of the rhodamine and biotin succinimidyl esters. A technique that helps in these cases is to add a 20% volume of DMF or DMSO slowly to the protein/buffer solution before adding the stock solution of the reagent in DMF or DMSO (see section IV.C.1).

Isothiocyanates and Succinimidyl Esters. Add the solution of the modification reagent dropwise using a microliter syringe during a period of about 1 min to the stirred protein solution while in an ice-water bath. Allow the reaction mixture to warm to room temperature and continue to stir for at least 2 h.

Sulfonyl Chlorides. Add the solution of the reagent quickly using a micropipet to the stirred protein solution in an ice bath or in a cold room. Allow to react at 4 $^{\circ}$ C for 1 h.

Step 3. Separate the conjugate from unreacted dye on a gel filtration column using the appropriate buffer as described in section V. Texas Red and certain other rhodamine-based conjugates will still retain varying

amounts of noncovalently adsorbed dye even after purification by gel chromatography. This protein-adsorbed dye can be removed by treating the conjugate with a hydrophobic adsorbent as described in section V.A.3.

B. Thiol-Reactive Probes. A general procedure suitable for conjugation of thiol-reactive probes, including maleimides, iodoacetates, and alkyl halides, is outlined below. As a rule, thiol-reactive reagents are more stable to water than the reactive esters; however, they should be handled carefully and stored in a freezer with protection from light and moisture. As with the reactive esters and isothiocyanates discussed above, only freshly prepared reagent solutions should be used. Protection from light is particularly important for iodoacetamides.

Step 1. Dissolve the protein at 50–100 μ M in a suitable buffer at pH 7.0–7.5 (10–100 mM phosphate, TRIS, HEPES) at room temperature. At this pH range, the protein thiol groups are sufficiently nucleophilic so that they react almost exclusively with the reagent in the presence of the more numerous protein amines, which are protonated and relatively unreactive. As a general rule, it is advisable to carry out thiol modifications in an oxygen-free environment, since some thiols can be oxidized to disulfides. This is particularly important if the modification reagent is to be reacted with a cystine group that has been previously reduced with a reagent such as dithiothreitol. In this case, all buffers should be deoxygenated and the reactions carried out under an inert atmosphere to prevent re-formation of disulfide.

Step 2. Add sufficient protein modification reagent from a stock solution of the reagent to contain 10–20 mol of reagent for each mole of protein. If the reagent is water-soluble, an aqueous solution can be used; otherwise, the reagent can be dissolved in one of the water-miscible nonhydroxylic solvents recommended for use with amine-reactive reagents. The reagent concentration should be about 10–20 mM. Upon completion of the reaction with the protein, an excess of glutathione, mercaptoethanol, or other soluble low molecular weight thiol can be added to consume excess modification reagent, thus ensuring that no reactive species are present during the purification step.

Iodoacetamides. Reactions with iodoacetamides should be carried out in the dark, since light can cause reagent decomposition. Add the stock reagent solution dropwise and slowly to the gently stirred solution of the protein at room temperature over a period of about 1 min. Continue stirring for 2 h.

Maleimides. Reaction conditions are essentially the same as with iodoacetamides; however, the selectivity of maleimides toward thiol groups is greater, allowing somewhat more latitude in the buffer pH. Decomposition to maleamic acids above pH 8.0 is a competing reaction. Add the stock reagent solution dropwise and slowly to the gently stirred protein solution at room temperature over a period of about 1 min and allow the mixture to react for 2 h.

Step 3. Separate the conjugate from unreacted modification reagent as described in section V.

C. Storage of Conjugates. Conjugates should be stored as one normally stores the parent protein. If the protein is stable to freezing, then lyophilization is recommended for long term storage. Sodium azide at 2 mM or thimerosal may be added to inhibit bacterial growth. **CAUTION:** These preservatives may be toxic in live-cell use of conjugates. In addition, sodium azide is an inhibitor of the enzyme horseradish peroxidase (HRP). Therefore, thimerosal should be substituted as a preservative in situations where the conjugate is derived from HRP or it is anticipated that the conjugate will be used in the

presence of HRP. Fluorescent dye conjugates should be protected from light.

VII. DETERMINATION OF THE DEGREE OF SUBSTITUTION OF PROTEIN CONJUGATES

Several methods are available for determining the degree of substitution of modified proteins. If the modification results in the creation of thiol residues, as is often the case with bifunctional reagents, it is relatively straightforward to determine the degree of substitution by quantitation of thiols. Several colorimetric methods for thiol determination are available (43, 45, 47). Maleimides introduced into proteins can be determined by back-titration with 2-mercaptoethanol (81). Dyes and many other types of molecules introduced into proteins are usually determined by spectroscopic techniques, as described below.

This general procedure should be applicable to dyes and other molecules that have significant absorption above 280 nm.

The determination of dye/protein (D/P) levels by spectroscopy is accomplished by determining the apparent concentration of dye in the conjugate by measuring its absorption at its characteristic λ_{\max} and then measuring the protein concentration of the conjugate by its absorption at 280 nm. Because most dyes have some absorption at 280 nm, the absorption of the conjugate at 280 nm must be corrected for the contribution of the dye to obtain the correct protein concentration. The ratio of these two concentrations, calculated by use of Beer's law ($A = \epsilon Cl$, where ϵ = extinction coefficient, A = molar absorbance, C = molar concentration, and l = path length), is then equal to the D/P ratio.

This method is inexact, because there is no way to know precisely how the spectral characteristics of the dye change when it is conjugated to the protein. The following assumptions and approximations are made.

(1) The extinction coefficient of the protein-bound dye at its absorption maximum is about the same as the extinction coefficient of the free dye in solution at its absorption maximum. Although there are undoubtedly some differences, experiments have shown that this assumption is at least approximately correct (64).

(2) The absorption of the protein-bound dye at 280 nm is about the same as the absorption of the free dye in solution. This assumption may be less reliable than the previous assumption, since there is probably more contribution from the linking group to this portion of the spectrum, and this group can be substantially changed when attached to the protein. The following question arises: what is the "free dye"? There is no unambiguous answer to this question, since the dye, when attached to the protein, is different than the free dye, and the spectral properties will be somewhat different. The best choice of free dye if the NHS ester was used as the reagent is probably the free acid or lysine amide derivative. These may be available or can be synthesized. *Do not use the NHS ester as the free dye, since the N-succinimidyl group absorbs strongly at 280 nm.* In other cases, sulfonic acids can be used when the protein modification reagent was a sulfonyl chloride.

(3) The extinction coefficient of the conjugate at 280 nm is about the same as the extinction coefficient of the native protein. However, extensive modification of the protein may change the spectral absorption at 280 nm in an unknown manner.

Although there are obvious questionable assumptions, spectroscopy remains the easiest and most convenient method of determining D/P ratios. One alternative is to

determine the protein concentration by weighing the conjugate, which eliminates problems in assumption 3, but this is tedious and includes the danger that the conjugate will denature when dried without buffer, or the lyophilized conjugate may contain entrapped buffer salts. This method does not eliminate errors from assumptions 1 and 2. Another alternative is to digest a known amount of the conjugate chemically or with a proteolytic enzyme to degrade the molecule to small fragments containing the dye and then determine the concentration of the dye by spectroscopy. This is even more tedious and still does not usually give a pure dye product which can be compared spectrally with a known derivative. Because of the lack of convenient and suitable alternatives, direct spectroscopic determination is the most frequently used method of estimating D/P ratios (64, 71-74).

Procedure. *Step 1.* Obtain absorption spectra of the free dye and the dye-protein conjugate (note 1).

Step 2. Obtain extinction coefficients of the free dye and protein from a handbook of dyes and protein tables (8, 50).

Step 3. Perform these calculations:

$$C_d = A_{\lambda_{\max}}/\epsilon_d$$

$$F = A_{d(280)}/A_d$$

$$C_p = [A_{280} - (A_{\lambda_{\max}}F)]/\epsilon_p$$

$$D/P = C_d/C_p$$

where ϵ_d is the extinction coefficient of free dye at λ_{\max} , A_d is the absorbance of free dye at λ_{\max} , $A_{d(280)}$ is the absorbance of free dye at 280 nm, $A_{\lambda_{\max}}$ is the absorbance of dye in conjugate at λ_{\max} , ϵ_p is the extinction coefficient of protein at 280 nm, A_{280} is the absorbance of protein in conjugate at 280 nm, C_d is the concentration of dye in conjugate (mol/L), and C_p is the concentration of protein in conjugate (mol/L).

ACKNOWLEDGMENT

I thank Dr. Rosaria Haugland and Danuta Szalecki for helpful discussions and advice concerning experimental details. I also thank Nan Minchow for preparing the structures and tables.

LITERATURE CITED

- (1) (a) Means, G. E., and Feeney, R. E. (1971) *Chemical Modification of Proteins*. Holden-Day, San Francisco, CA.
(b) Means, G. E., and Feeney, R. E. (1990) *Chemical Modification of Proteins: History and Applications*. *Bioconjugate Chem.* 1, 2.
- (2) Glazer, A. N., Delange, R. J., and Sigman, D. S. (1975) *Chemical Modification of Proteins. Laboratory Techniques in Biochemistry and Molecular Biology* (T. S. Work, and E. Work, Eds.) American Elsevier Publishing Co., New York.
- (3) Lundblad, R. L., and Noyes, C. M. (1984) *Chemical Reagents for Protein Modification*, Vols. I and II, CRC Press, New York.
- (4) Pfeleiderer, G. (1985) *Chemical Modification of Proteins*. In *Modern Methods in Protein Chemistry* (H. Tschesche, Ed.) Walter DeGruyter, Berlin and New York.
- (5) Eyzaguirro, J. (1987) *Chemical Modification of Enzymes. Active Site Studies*. John Wiley & Sons, New York.
- (6) Wong, S. H. (1991) *Chemistry of Protein Conjugation and Cross-linking*, CRC Press, Boca Raton, FL.
- (7) De Lange, R. J., and Huang, T. S. (1971) Egg white avidin. III. sequence of the 78-residue middle cyanogen bromide peptide. Complete amino acid sequences of the protein subunit. *J. Biol. Chem.* 246, 698.

- (8) Fasman, G. D., Ed. (1989) *Practical Handbook of Biochemistry and Molecular Biology*, p 13, CRC Press, Boca Raton, FL.
- (9) White, A., Handler, P., and Smith, E. L. (1982) *Principles of Biochemistry*, p 142, McGraw-Hill, New York.
- (10) (a) Korn, A. H., Fearheller, S. H., and Filachione, E. M. (1972) Glutaraldehyde: nature of the reagent. *J. Mol. Biol.* 66, 525. (b) Hardy, P. M., Nicholls, A. C., and Rydon, N. H. (1976) The nature of the crosslinking of proteins by glutaraldehyde. Part 1. Interaction of glutaraldehyde with the amino group of β -aminohexanoic acid and of α -N-acetyl-lysine. *J. Chem. Soc. Perkin Trans. 1*, 958.
- (11) Cleland, W. W. (1964) Dithiothreitol, a new protective reagent for SH groups. *Biochemistry* 3, 480.
- (12) Gundlach, H. G., Moore, S., and Stein, W. H. (1959) The reaction of iodoacetate with methionine. *J. Biol. Chem.* 234, 1761.
- (13) Riordan, J. F., and Vallee, B. L. (1972) Diazonium salts as specific reagents and probes of protein configuration. *Methods Enzymol.* 25, 251.
- (14) Wilchak, M., Ben-Hur, H., and Bayer, E. A. (1966) p-Diazobenzoyl biocytin—A new biotinylating reagent for the labelling of tyrosines and histidines in proteins. *Biochem. Biophys. Res. Commun.* 136, 872.
- (15) Hoare, D. G., and Koshland, D. E., Jr. (1966) A procedure for the selective modification of carboxyl groups in proteins. *J. Am. Chem. Soc.* 88, 2087.
- (16) Yamada, H., Imoto, T., Fujita, K., Ozaki, K., and Motomura, M. (1981) Selective modification of aspartic acid 101 in lysozyme by carbodiimide reaction. *Biochemistry* 20, 4836.
- (17) Renthal, R., Cothran, M., Dawson, N., and Harris, G. J. (1987) Fluorescent labeling of bacteriorhodopsin: implications for helix connections. *Biochim. Biophys. Acta* 897, 384.
- (18) Yankeelov, J. A., Jr., Mitchell, C. D., and Crawford, T. H. (1968) A simple trimerization of 2,3-butanediones yielding a selective reagent for the modification of arginine in proteins. *J. Am. Chem. Soc.* 90, 1664.
- (19) Bond, J. S., Francis, S. H., and Park, J. H. (1970) An essential histidine in the catalytic activities of 3-phosphoglycerate dehydrogenase. *J. Biol. Chem.* 245, 1041.
- (20) Stark, G. R., Stein, W. H., and Moore, S. (1961) Relationships between the conformation of ribonuclease and its reactivity toward iodoacetate. *J. Biol. Chem.* 236, 436.
- (21) Bragg, P. D., and Hou, C. (1975) Subunit composition, function and spatial arrangement in the Ca^{2+} and Mg^{2+} -activated adenosine triphosphatases of *Escherichia coli* and *Salmonella typhimurium*. *Arch. Biochem. Biophys.* 167, 311.
- (22) Lomants, A. J., and Fairbanks, G. (1976) Chemical probes of extended biological structures: synthesis and properties of the cleavable protein cross-linking reagent [^{35}S]dithiobis(succinimidyl propionate). *J. Mol. Biol.* 104, 243.
- (23) Staros, J. V. (1982) *N*-hydroxysulfosuccinimide active esters: Bis(*N*-hydroxysulfosuccinimide) esters of two dicarboxylic acids are hydrophilic, membrane-impermeant protein cross-linkers. *Biochemistry* 21, 3950.
- (24) Brantzaag, P. (1975) Rhodamine conjugates: specific and non-specific binding properties in immunohistochemistry. *Ann. N.Y. Acad. Sci.* 254, 35.
- (25) Takihashi, K. (1968) The reaction of phenylglyoxal with arginine residues. *J. Biol. Chem.* 243, 6171.
- (26) Konishi, K., and Fujioka, M. (1987) Chemical modification of a functional arginine residue of rat liver glycine methyltransferase. *Biochemistry* 26, 8496.
- (27) Wagner, R., and Gassen, H. G. (1975) On the covalent binding of mRNA models to the part of the 16S RNA which is located in the mRNA binding site of the 30S ribosome. *Biochem. Biophys. Res. Commun.* 65, 519.
- (28) Gray, W. R. (1967) Sequential degradation plus dansylation. *Methods Enzymol.* 11, 469.
- (29) Hartley, B., and Massey, V. (1956) The active center of chymotrypsin I. Labelling with a fluorescent dye. *Biochim. Biophys. Acta* 21, 58.
- (30) Titus, J., Haugland, R., Sharrow, S. O., and Segal, D. M. (1982) Texas Red, a hydrophilic, red-emitting fluorophore for use with fluorescein in dual parameter flow microfluorometric and fluorescence microscopic studies. *J. Immunol. Methods* 50, 193.
- (31) Wadsworth, P., and Salmon, E. (1986) Preparation and characterization of fluorescent analogs of tubulin. *Methods Enzymol.* 134, 519.
- (32) De Belder, A. N., and Granath, K. (1973) Preparation and properties of fluorescein labeled dextrans. *Carbohydr. Res.* 30, 375.
- (33) Gurd, F. R. N. (1967) Carboxymethylation. *Methods Enzymol.* 11, 532.
- (34) Shiao, D. D. F., Lumry, R., and Rajender, S. (1972) Modification of protein properties by change in charge. *Eur. J. Biochem.* 29, 377.
- (35) Singh, P. (1977) Carbamazepine antigens and antibodies. U.S. Patent 4,058,511.
- (36) Lundblad, R. L., and Noyes, C. M. (1984) *Chemical Reagents for Protein Modification*, Vol. I, p 55, CRC Press, New York.
- (37) Ansorge, W. (1988) Non-radioactive automated sequencing of oligonucleotides by chemical degradation. *Nucleic Acids Res.* 16, 2203.
- (38) Johnson, A. E., Adkins, H. J., Matthews, E. A., and Cantor, C. R. (1962) Distance moved by transfer RNA during translocation from the A site to the P site on the ribosome. *J. Mol. Biol.* 156, 113.
- (39) Smyth, D. G., Blumenfeld, O. O., and Konigsberg, W. (1964) Reaction of *N*-ethylmaleimide with peptides and amino acids. *Biochem. J.* 91, 589.
- (40) Brown, R. D., and Matthews, K. S. (1979) Chemical modification of lactose repressor proteins using *N*-substituted maleimides. *J. Biol. Chem.* 254, 5128.
- (41) Ishi, S. S., and Lehrer, J. (1966) Effects of the state of the succinimido-ring on the fluorescence and structural properties of pyrene maleimide labeled α -tropomyosin. *Biophys. J.* 50, 75.
- (42) Kosower, N. S. (1979) Bimane fluorescent labels: labeling of normal human red cells under physiological conditions. *Proc. Natl. Acad. Sci. U.S.A.* 76, 3382.
- (43) Carlsson, J., Drevin, H., and Axen, R. (1978) Protein thiolation and reversible protein-protein conjugation. *N*-succinimidyl 3-(2-pyridyldithio)propionate, a new heterobifunctional reagent. *Biochem. J.* 173, 723.
- (44) Jentoft, J. E., and Dearborn, P. G. (1979) Labeling of proteins by reductive methylation using sodium cyanoborohydride. *J. Biol. Chem.* 254, 4359.
- (45) Jue, R., Lambert, J. M., Pierce, L. R., and Traut, R. R. (1978) Addition of sulfhydryl groups to *Escherichia coli* ribosomes by protein modification with 2-iminothiolane (methyl 4-mercaptobutyrimidate). *Biochemistry* 17, 5399.
- (46) McCall, M. J., Diril, H., and Meares, C. F. (1990) Simplified method for conjugating macrocyclic bifunctional chelating agents to antibodies via 2-iminothiolane. *Bioconjugate Chem.* 1, 222.
- (47) Julian, R. (1983) A new reagent which may be used to introduce sulfhydryl groups into proteins, and its use in the preparation of conjugates for immunoassay. *Anal. Biochem.* 132, 68.
- (48) Ghetie, V., Till, M. A., Ghetie, M., Tucker, T., Porter, J., Patzer, E. J., Richardson, J. A., Uhr, J. W., and Vitetta, A. (1990) Preparation and characterization of conjugates of recombinant CD4 and deglycosylated ricin A chain using different cross-linkers. *Bioconjugate Chem.* 1, 24.
- (49) Cumber, J. A., Forrester, J. A., Foxwell, B. M. J., Ross, W. C. J., and Thorpe, P. E. (1985) Preparation of antibody-toxin conjugates. *Methods Enzymol.* 112, 207.
- (50) Haugland, R. P. (1989) *Handbook of Fluorescent Probes and Research Chemicals*, p 54, Molecular Probes, Inc., Eugene, OR.
- (51) Youle, R. J., and Neville, D. M. (1980) Anti-Thy 1.2 monoclonal antibody linked to ricin is a potent cell-type specific toxin. *Proc. Natl. Acad. Sci. U.S.A.* 77, 5483.
- (52) Ghosh, S. S., Kao, P. N., McCue, A. W., and Chappelle, H. L. (1990) Use of maleimide-thiol coupling chemistry for efficient synthesis of oligonucleotide-enzyme conjugate hybridization probes. *Bioconjugate Chem.* 1, 71.

- (53) (a) Komatsu, S. K., Devries, A. L., and Feeney, R. E. (1970) Studies of the structure of freezing point-depressing glycoproteins from an Antarctic fish. *J. Biol. Chem.* 245, 2909. (b) Vanderheede, J., Ahmed, A. I., and Feeney, R. E. (1972) Structure and role of carbohydrate in freezing point-depressing glycoproteins from an Antarctic fish. *J. Biol. Chem.* 247, 7885.
- (54) Freytag, J. W. (1984) Affinity column-mediated immunoassays: influence of affinity column ligand and valency of antibody-enzyme conjugates. *Clin. Chem.* 30, 1494.
- (55) Thorpe, P. E. (1987) New coupling reagents for the synthesis of immunotoxins containing a hindered disulfide bond with improved stability *in vivo*. *Cancer Res.* 47, 5924.
- (56) Ji, I., and Ji, T. H. (1981) Both α and β subunits of human chorionic gonadotropin photoaffinity label the hormone receptor. *Proc. Natl. Acad. Sci. U.S.A.* 78, 5465.
- (57) Keana, J. F. W., and Cai, S. X. (1989) functionalized perfluorophenyl azides: New reagents for photoaffinity labeling. *J. Fluorine Chem.* 43, 151.
- (58) Crocker, P. J., Imai, N., Rajagopalan, K., Boggess, M. A., Kwiatkowski, S., Dwyer, L. D., Vanaman, T. C., and Watt, D. S. (1990) Heterobifunctional cross-linking reagents incorporating perfluorinated aryl azides. *Bioconjugate Chem.* 1, 419.
- (59) Batra, S. P., and Nicholson, B. H. (1982) 9-Azidoacridine, a new photoaffinity label for nucleotide and aromatic binding sites in proteins. *Biochem. J.* 207, 101.
- (60) Hixson, S. H., and Hixson, S. S. (1975) *p*-Azidophenacyl bromide, a versatile photolabile bifunctional reagent. Reaction with glyceraldehyde-3-phosphate dehydrogenase. *Biochemistry* 14, 4251.
- (61) Bayley, H. (1983) *Photogenerated Reagents in Biochemistry and Molecular Biology*. Elsevier, New York.
- (62) Tao, T., Lamkin, M., and Scheiner, C. (1984) Studies on the proximity relationships between thin filament proteins using benzophenone-4-maleimide as a site-specific photoreactive crosslinker. *Biophys. J.* 45, 261.
- (63) Valdes-Aguilera, O., and Neckers, D. C. (1989) Aggregation phenomena in xanthene dyes. *Acc. Chem. Res.* 22, 171.
- (64) Midoux, P., Roche, A. C., and Monsigny, M. (1987) Quantitation of the binding, uptake, and degradation of fluoresceinylated neoglycoproteins by flow cytometry. *Cytometry* 8, 327.
- (65) Stryer, L., and Haugland, R. P. (1967) Energy transfer: A spectroscopic ruler. *Proc. Natl. Acad. Sci. U.S.A.* 58, 719.
- (66) Zuk, R. F., Rowley, G. L., and Uliman, E. F. (1979) Fluorescence protection immunoassay: A new homogeneous assay technique. *Clinical Chem.* 25, 1554.
- (67) Whitaker, J. E., Haugland, R. P., Moore, P. L., Hewitt, P. C., Reese, M., and Haugland, R. P. Cascade Blue derivatives: water soluble, reactive, blue emission dyes evaluated as fluorescent labels and tracers. *Anal. Biochem.* In press.
- (68) Spack, E. G., Jr., Packare, B., Wier, M. L., and Edidin, M. (1986) Hydrophobic adsorption chromatography to reduce nonspecific staining by rhodamine-labeled antibodies. *Anal. Biochem.* 158, 233.
- (69) Carraway, K. L., and Koshland, D. E., Jr. (1968) Reaction of tyrosine residues in proteins with carbodiimide reagents. *Biochem. Biophys. Acta* 160, 272.
- (70) Smyth, D. G. (1967) Acetylation of amine and tyrosine hydroxyl groups. *J. Biol. Chem.* 242, 1592.
- (71) Van Dalen, J. P. R., and Haajlman, J. J. (1974) Determination of the molar absorption coefficient of bound tetramethylrhodamine isothiocyanate relative to fluorescein isothiocyanate. *J. Immunol. Methods* 5, 103.
- (72) Wessendorf, M. W., Tallaksen-Greene, S. J., and Wohlueter, R. M. (1990) A spectrophotometric method for determination of fluorophore-to-protein ratios in conjugates of the blue fluorophore 7-amino-4-methylcoumarin-3-acetic acid (AMCA). *J. Histochem. Cytochem.* 38, 87.
- (73) Guar, R. K., and Gupta, K. C. (1989) A spectrophotometric method for the estimation of amino groups on polymer supports. *Anal. Biochem.* 180, 253.
- (74) Srivastava, P. C., Buchsbaum, D. J., Allred, J. F., Brubaker, P. G., Hanna, D. E., and Spiker, J. K. (1990) A new conjugating agent for radioiodination of proteins: Low *in vivo* deiodination of a radiolabeled antibody in a tumor model. *Biotechniques* 8, 536.
- (75) Vlgers, G. P. A., Cove, M., and McIntosh, J. R. (1988) Fluorescent microtubules break up under illumination. *J. Cell. Biol.* 107, 1011.
- (76) Kellogg, D. R., Michison, T. J., and Alberts, B. M. (1988) Behavior of microtubules and actin filaments in living *Drosophila* embryos. *Development* 103, 675.
- (77) Khalfan, H. (1986) Aminomethylcoumarin acetic acid: a new fluorescent labelling reagent for proteins. *Histochem. J.* 18, 497.
- (78) Gorbsky, G. J., Sammak, P. J., and Borisy, G. G. (1988) Microtubule dynamics and chromosome motion visualized in living anaphase cells. *J. Cell. Biol.* 106, 1185.
- (79) Hoffman, K., Finn, F., and Kiso, Y. (1978) Avidin-biotin affinity columns. General methods for attaching biotin to peptides and proteins. *J. Am. Chem. Soc.* 100, 3585.
- (80) Bolton, A. E., and Hunter, W. M. (1973) The labelling of proteins to high specific radioactivities by conjugation to a ^{125}I -containing acylating agent. Application to the radioimmunoassay. *Biochem. J.* 133, 529.
- (81) Duncan, J. S., Weston, P. D., and Wigglesworth, R. (1982) A new reagent which may be useful to introduce sulfhydryl groups into proteins, and its use in the preparation of conjugates for immunoassay. *Anal. Biochem.* 132, 68.

ARTICLES

New Synthesis of Immunogenic N^6 -Isopent-2-enyladenosine-Protein Conjugate. Preparation, Purification, and Specificity of Related Antibodies

Marie-Pierre Papet,[†] Didier Delay, Patrick Dumas,[‡] and Francis Delmotte*

Centre de Biophysique Moléculaire, Département de Biochimie des Glycoconjugués et Lectines Endogènes C.N.R.S. et Université d'Orléans, 1 rue Haute, 45071 Orléans Cedex 2, France. Received April 24, 1991

An original procedure which preserves the structure of the sugar ring is described to link a plant hormone as N^6 -isopent-2-enyladenosine ([9R]iP) onto a protein carrier to prepare a more specific immunogen. This cytokinin is bound to bovine serum albumin (BSA) and ovalbumin by a five-step procedure. These [9R]iP-protein conjugates have a maximal absorption at 269 nm and show molar ratios of hormone bound to proteins in the range of 12:1 and 18:1 for BSA and ovalbumin, respectively. Polyclonal antibodies were raised in rabbits against [9R]iP-BSA and were purified by affinity chromatography. Titers and specificity of the antisera and purified antibodies were determined by ELISA and RIA. These antibodies are highly specific for [9R]iP and do not cross-react with zeatin and ribosylzeatin. An immunoaffinity matrix was prepared with a capacity of 1 μ g of [9R]iP/mL of gel.

INTRODUCTION

The quantitative analysis of plant hormones by immunoassays has gained considerable importance in the last years (1, 2). One crucial factor for the successful development of such assays is the preparation of an immunogen which preserves the structure of the antigen or the hapten. Immunogenic cytokinin ribosyl-protein conjugates are always prepared according to an original procedure (3, 4) with minor modification (5, 6). The procedure used for cytokinin immunogens is based on the reaction of periodate-oxidized riboside with amino groups of the protein carrier. According to this method, the sugar moiety is destroyed and yields a morpholino derivative after reduction by borohydride.

In order to protect the ribofuranosyl ring of the N^6 -isopent-2-enyladenosine ([9R]iP)¹ during its linkage to BSA, we decided to use the primary hydroxyl group for this coupling. The present work describes the synthesis of an original N^6 -isopent-2-enyladenosine-BSA conjugate, which was used to generate specific related antibodies, which were purified by affinity chromatography. The preparation of a corresponding immunoaffinity matrix is also presented.

EXPERIMENTAL PROCEDURES

Chemical Syntheses. General Methods. 1-Ethyl-3-[3-(dimethylamino)propyl]carbodiimide, iP, [9R]iP, Z,

[9R]Z, BSA, bovine hemoglobin, ovalbumin, Freund adjuvants, gelatin, anti-rabbit IgG (whole molecule), goat anti-rabbit alkaline phosphatase conjugate, and *p*-nitrophenyl phosphate were purchased from Sigma (La Verpillière, France). 6-Aminohexanoic acid, benzyltrimethylammonium hydroxide (Triton B), 1,1'-carbonyldiimidazole, cyclohexane, cyanogen bromide, 2,2-dimethoxypropane, triethylamine, and *p*-toluenesulfonic acid were obtained from Aldrich-Chimie (Strasbourg, France); *N,N'*-dicyclohexylcarbodiimide was purchased from Fluka (Buchs, Switzerland) and agarose from Difco/Osibio (Paris, France). Trisacryl GF 05, Trisacryl GF 2000, and agarose A4 were provided by IBF-Biotechnics (Villeneuve-la-Garenne, France) and Affi-Gel 10 by Bio-Rad (Paris, France). Thin-layer plates and chemicals (if not otherwise stated) were purchased from Merck (Nogent-sur-Marne, France). [³H][9R]iP dialcohol was prepared according to the method of MacDonald and Morris (7). All the solvents were freshly distilled.

Nuclear magnetic resonance spectra were measured on an AM 300 WB Brüker spectrometer. UV and visible spectra were recorded with an Uvikon 860 spectrophotometer.

Preparation of N^6 -Isopent-2-enyladenosine-Protein Conjugates. [9R]iP (1) was bound to BSA and ovalbumin by a five-step procedure (Scheme I). Firstly, 2'- and 3'-hydroxyl groups of the ribofuranosyl ring from 1 were protected by an isopropylidene group to give compound 2. Then, 6-aminohexanoic acid was coupled by its amino group to the 5'-hydroxyl of the ribofuranosyl moiety by a carbamate linkage (4) using 1,1'-carbonyldiimidazole in order to activate the 5'-hydroxyl of the ribosyl derivative. After elimination of the isopropylidene group (5), the carboxylic group of the aliphatic arm was activated with *N*-hydroxysuccinimide (6) to react further with the free amino groups from the proteins.

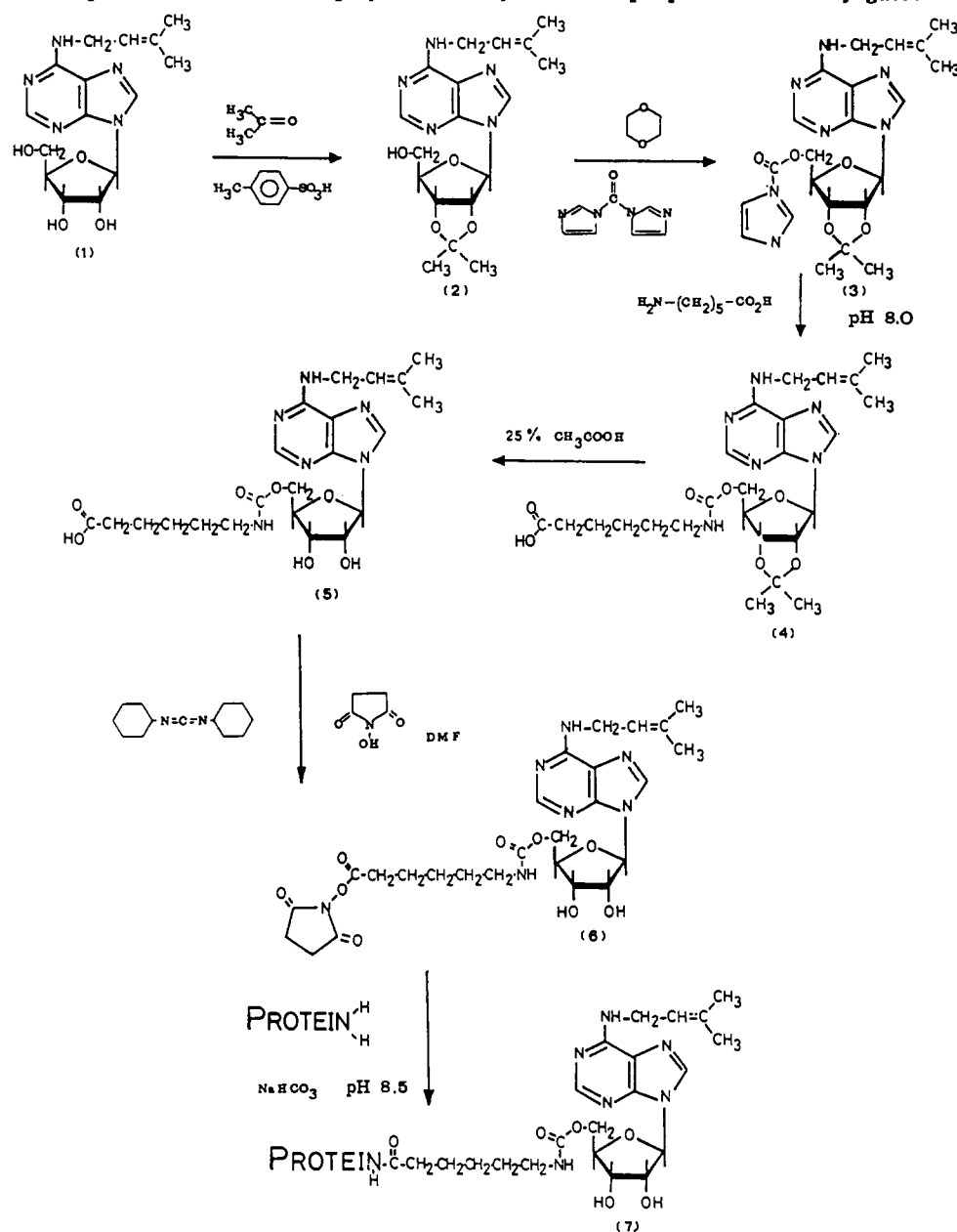
Synthesis of 2',3'-*O*-Isopropylidene- N^6 -isopent-2-enyladenosine (2) According to a General Procedure (8). *p*-Toluenesulfonic acid (285 mg, 1.5 mmol) was added, with exclusion of moisture, to a magnetically stirred

[†] Present address: Centre Essais des Tabacs, 4 rue André Des-saux, 45400 Fleury-les-Aubrais, France.

[‡] Station d'Amélioration des Arbres Forestiers, I.N.R.A., Ardon, 45160 Olivet, France.

¹ Abbreviations used: BSA, bovine serum albumin; ELISA, enzyme linked immunosorbent assay; DMF, *N,N*-dimethylformamide; DMSO, dimethyl sulfoxide; iP, N^6 -isopent-2-enyladenosine or 6-[(3-methyl-2-butenyl)amino]purine; [9R]iP, N^6 -isopent-2-enyladenosine or 6-[(3-methyl-2-butenyl)amino]-9- β -D-ribofuranosylpurine; PBS, phosphate-buffered saline; RIA, radioimmunoassay; Z, zeatin or 6-[(4-hydroxy-3-methyl-*trans*-2-butenyl)amino]purine; [9R]Z, ribosylzeatin or 6-[(4-hydroxy-3-methyl-*trans*-2-butenyl)amino]-9- β -D-ribofuranosylpurine.

Scheme I. Reaction Sequence Which Was Employed in the Synthesis of [9R]iP-Protein Conjugates



suspension of [9R]iP (1, 500 mg, 1.5 mmol; dried over P_2O_5 at 40 °C under reduced pressure) in anhydrous acetone (100 mL, dried over Drierite and distilled from P_2O_5). Then 2,2-dimethoxypropane (1 mL, 7.5 mmol) was added and the mixture stirred for 20 h at room temperature. After neutralization by adding sodium hydrogen carbonate, the mixture was filtered off and the filtrate was evaporated under reduced pressure. Purification was achieved by chromatography on a silica gel column (85 × 2 cm) using chloroform/methanol/triethylamine (90:10:1) as solvent. The pure fractions corresponding to R_f 0.70 with the same solvent were combined, evaporated to dryness, and then precipitated from a chloroform/cyclohexane mixture (1:3). The white solid compound 2 (450 mg, 80%) was identified by its ^1H NMR spectra (in $\text{DMSO}-d_6$) (primed locants correspond to protons on the D-ribose portion): δ 1.32 and 1.54 (2 s, 2 × 3 H, methyl from isopropylidenyl group), 1.66 and 1.69 (2 s, 2 × 3 H, methyl from isopentenyl group), 3.53 (m, 2 H, methylene from isopentenyl group), 4.07 (m, 2 H, H-5'), 4.21 (dt, 1 H, H-4'), 4.96 (dd, 1 H, H-3'), 5.28 (m, 1 H, ethylenyl H from isopentenyl group), 5.33 (dd, 1 H, H-2'), 6.12 (d, 1 H, J =

3 Hz, H-1'), 7.89 (m, br, 1 H, NH), 8.21 and 8.32 (2 s, 2 H, H-2 and H-8).

Coupling of 6-Aminohexanoic Acid to 2',3'-*O*-Isopropylidene-*N*⁶-isopent-2-enyladenosine by Using a Carbonylating Reagent. Compound 2 (30 mg, 91 μmol), dried over P_2O_5 at 25 °C under reduced pressure overnight, was dissolved in anhydrous dioxane (1 mL), and 1,1'-carbonyldiimidazole (30 mg, 178 μmol) was added in two equal portions within 90 min. This mixture was stirred for 18 h at room temperature. Under these conditions, we got quantitatively an imidazolyl carbonate derivative (3) which moved on TLC with R_f 0.65 and 0.59 in chloroform/methanol (9:1 and 8:2 as developers, respectively). This active compound 3 was not isolated and was reacted further with the 6-aminohexanoate salt of benzyltrimethylammonium (Triton B) (127.5 mg, 455 μmol). After stirring for 24 h, TLC on silica gel in the solvent system chloroform/methanol (4:1) revealed the presence of compound 4 as the major component (R_f 0.66) and some 2',3'-*O*-isopropylidene-*N*⁶-isopent-2-enyladenosine (2; R_f 0.75). Compound 4 was isolated by chromatography on a silica gel column (85 × 2 cm) using chloroform/methanol/triethyl-

amine (80:20:1) as solvent. The pure fractions corresponding to R_f 0.66 were combined and evaporated to dryness. In order to obtain a derivative (4) with a free carboxylic group, the above residue was dissolved in chloroform (2 mL) and the organic solution was washed successively with aqueous potassium hydrogen sulfate and water (1 mL) and dried over anhydrous sodium sulfate. Evaporation of the solvent gave a white solid residue identical to 4 by ^1H NMR (CDCl_3): δ 1.31 and 1.56 (2 s, 2×3 H, methyl from isopropylidene group), 1.25–1.62 (m, 3×2 H, methylene from aminohexanoic acid), 1.68 (s, 2×3 H, methyl from isopentenyl group), 2.29 (t, 2 H, $J = 7$ Hz, methylene in α from carboxylic group), 3.10 and 3.18 (2 m, 2 H, methylene from isopentenyl group), 4.16 (m, 2 H, methylene in α from carbamate), 4.23 (t, 2 H, $J = 4$ Hz, H-5'), 4.90 (dd, 1 H, H-3'), 5.13 (m, 1 H, ethylenyl H from isopentenyl group), 5.18 (dd, 1 H, H-2'), 5.32 (dt, 1 H, H-4'), 6.17 (d, 1 H, H-1'), 6.42 (m, br, 1 H, NH), 8.08 and 8.35 (2 s, 2 H, H-2 and H-8).

Synthesis of ϵ -Aminohexanoic Acid-[9R]iP Conjugate 5. Removal of isopropylidene substituent from compound 4 has been accomplished by acid hydrolysis. A solution of 4 (10 mg/mL) in acetic acid (25%) was kept for 3 h at 100 °C. After cooling, the solution was evaporated to dryness and the residual syrup was purified by chromatography on a silica gel column (85 \times 2 cm) using chloroform/methanol (55:45) as solvent. The ϵ -aminohexanoic acid-[9R]iP derivative 5 had R_f 0.75 on TLC (silica gel) in the above solvent system. Compound 5 was identified by ^1H NMR ($\text{DMSO}-d_6$): δ 1.22 (m, 2 H, methylene from aminohexanoic acid), 1.41 (m, 2×2 H, methylene from aminohexanoic acid), 1.65 and 1.68 (2 s, 2×3 H, methyl from isopentenyl group), 2.07 (t, 2 H, methylene in α from carboxylic group), 2.94 (m, 2 H, methylene in α from carbamate), 4.00–4.27 (m, 6 H, methylene from isopentenyl group, H-3', H-4', H-5'), 4.66 (t, 1 H, $J = 5$ Hz, H-2'), 5.30 (m, 1 H, ethylenyl H from isopentenyl group), 5.92 (d, 1 H, $J = 6$ Hz, H-1'), 7.28 (t, 1 H, NH), 7.84 (m, br, 1 H, NH), 8.22 and 8.33 (2 s, 2 H, H-2 and H-8).

Synthesis of N -Hydroxysuccinimide Ester 6 from ϵ -Aminohexanoic Acid-[9R]iP Conjugate 5. To a solution of compound 5 (25 mg, 51 μmol) in N,N -dimethylformamide (0.5 mL) were successively added N -hydroxysuccinimide (6.8 mg, 75 μmol) and N,N' -dicyclohexylcarbodiimide (11.7 mg, 75 μmol) at -10 °C. Then this mixture was stirred for 4 h at 4 °C and finally 16 h at room temperature. Dicyclohexylurea was filtered off and the filtrate was further reacted with a protein (BSA or ovalbumin). TLC analysis of this solution showed a major compound with R_f 0.70 on silica gel in chloroform/methanol (4:1).

Preparation of Immunogenic Protein-[9R]iP Conjugates 7. Compound 6 (25 mg, 42 μmol) in N,N -dimethylformamide (0.5 mL) was added to a solution of BSA (170 mg, 2.5 μmol) in 0.02 M sodium borate at pH 8.7 (21 mL). After stirring for 24 h at 4 °C, this mixture was dialyzed against water and freeze-dried. This residue was resuspended in distilled water containing 5% 1-butanol (v/v). The insoluble material was discarded after spinning the suspension at 12000g for 30 min. The supernatant was loaded on a Trisacryl GF 05 column (15 \times 3 cm) equilibrated with 1-butanol/water (5:95). The protein fraction recovered in the void volume of this column was freeze-dried. The average number of [9R]iP residues bound to the BSA was calculated from the measurement of the absorbance at 280 and 240 nm, respectively; and the free amino groups were determined by a colorimetric method using 2,4,6-trinitrobenzenesulfonate (TNBS) (9).

According to the same procedure, compound 6 was bound to ovalbumin.

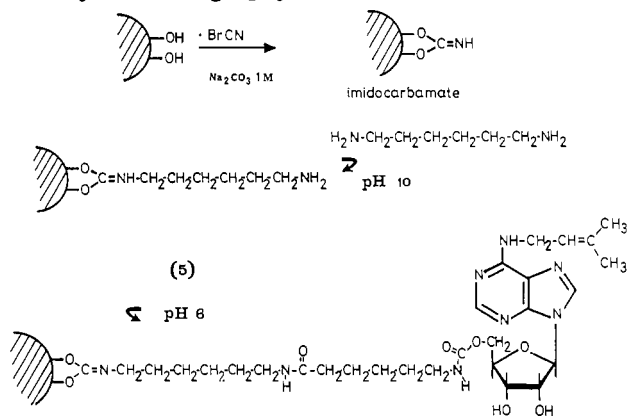
Immunization Schedule. Antisera against [9R]iP-BSA were raised in three rabbits (A, B, C) by multiple sc injections of the antigen suspension in complete Freund's adjuvant, on days 0, 7, and 14. Each rabbit received 1 mL of an emulsion of 0.5 mL antigen fraction (1 mg) in saline and of 0.5 mL complete Freund's adjuvant. Booster doses of this antigen in incomplete Freund's adjuvant were given after 3 weeks and rabbits were bled (50 mL) 7 days later, from the marginal ear vein. Crude sera were stored at -20 °C.

Immunodiffusion. Double-diffusion analyses (10) were performed with 2% agar in barbital buffer (pH 8.2) on glass microscope slides. IgG was identified by using goat anti-rabbit IgG.

Enzyme Linked Immunosorbent Assays. Wells in polystyrene immunoplates (type Nunc I, Denmark) were coated with 100 μL of [9R]iP-ovalbumin conjugate (50 $\mu\text{g}/\text{mL}$ in 0.05 M carbonate/hydrogen carbonate buffer, pH 9.6). Standards and samples were processed in triplicate. The plates were incubated for 2 h at 37 °C, after washing with phosphate-buffered saline (PBS), the plate was shaken dry, and 200 μL of PBS containing 0.5% (w/v) gelatin was added to each well to block unbound solid-phase sites and to minimize nonspecific binding in further steps. The plates were then incubated for 2 h at 37 °C, and washed as described above. Antiserum against [9R]iP-BSA conjugate was diluted 1:100 to 1:10000 in PBS; 50 μL of diluted antisera was added to microtiter wells and incubated for 45 min at 22 °C. After washing with PBS, 100 μL of goat anti-rabbit alkaline phosphatase conjugate [diluted 1:400 (v/v) in PBS] was added to each well and incubated for 45 min at room temperature. After four washings to eliminate the excess conjugate, 200 μL of p -nitrophenyl phosphate (1 mg/mL in 0.5 M sodium carbonate pH 10.6 supplemented with 1 mM MgCl_2) was added to wells, and the wells were incubated for 1 h at 37 °C. After adding 20 μL of 5 N sodium hydroxide, the phosphatase activity bound to the plate was measured spectrophotometrically at 405 nm on a Dinattech Micro-Elisa autoreader (Artek System Corp., Farmingdale, NY).

Radioimmunoassays. RIA were performed according to the procedure of Weiler (4) modified by MacDonald et al. (5). Briefly, assays for serum titration were performed in Eppendorf tube as follows: standards and samples were processed in triplicate. The incubation mixture contained 50 μL of dilute tracer solution (^3H)[9R]iP dialcohol, 9000 cpm), 300 μL of buffer (0.02 M phosphate, 0.17 M sodium chloride, pH 7.2, supplemented with 0.1% gelatin and 1% ovalbumin), and 50 μL of dilute antiserum (1:10 to 1:1000 range). After mixing, the tubes were incubated for 20 min at room temperature, and 600 μL of 90% saturated ammonium sulfate solution was added to precipitate the proteins. After 10 min at room temperature, the tubes were centrifuged for 1 min in a microcentrifuge. The supernatants were carefully removed using a Pasteur pipet and discarded. The pellets were resuspended in 100 μL of methanol, and after 30 min, 1 mL of scintillation cocktail (Readymicro, Beckman, France) was added. After thorough mixing, the Eppendorf tubes as vial inserts were counted for radioactivity (^3H assay) on a Beckman LS1801 counter for 4 min. The results were computed in a programmed calculator.

Cross-reactivities of various purines with anti-[9R]iP serum were assessed under the following conditions: iP, [9R]iP, Z, and [9R]Z in methanol solution (50–10000 pg ranges) were added in 1.5-mL Eppendorf centrifuge tube

Scheme II.^a Schematic Protocol for Synthesis of Affinity Chromatography Matrix

^a Cyanogen bromide activated agarose A4 was substituted by a eight-atom spacer arm as hexane-1,6-diamine. The carboxylated compound 5 was attached to this [(6-aminoethyl)imino]methylene gel using 1-ethyl-3-[3-(dimethylamino)propyl]carbodiimide.

to 350 μ L of the above described pH buffer containing 9000 cpm of [³H][9R]iP dialcohol, and then the assays were performed as above described.

Preparation of Substituted Agaroses A4. [9R]iP was bound to agarose A4 via a [[6-[(ϵ -aminohexanoyl)-amino]hexyl]imino]methylene spacer arm (Scheme II). In a first step, agarose A4 activated with cyanogen bromide was reacted with hexane-1,6-diamine to afford [(6-aminoethyl)imino]methylene-agarose A4. Then, this substituted agarose was coupled to ϵ -aminohexanoic acid-[9R]iP derivative 5 to give the affinity chromatography gel expected.

[(6-Aminoethyl)imino]methylene-Agarose A4. Ultragel A4 (100 mL) activated with cyanogen bromide in acetonitrile (10 mL) (11, 12) was reacted overnight at 4 °C with hexane-1,6-diamine (20 g in 100 mL of distilled water adjusted to pH 10 with 12 N HCl) and then washed with distilled water.

[9R]iP-[[6-[(ϵ -Aminoheptanoyl)amino]hexyl]imino]methylene-Agarose A4. [(6-Aminoethyl)imino]methylene-agarose A4 (20 mL) was suspended in a solution of compound 5 (40 mg in 10 mL water). The slurry was adjusted to pH 6.0, 1-ethyl-3-[3-(dimethylamino)propyl]carbodiimide hydrochloride (80 mg, 420 μ mol) was added, and the gel stirred for 16 h at 4 °C. After washing with distilled water, the slurry was resuspended in 20 mL of 0.2 M sodium hydrogen carbonate, and the remaining free amino groups were blocked at 0 °C by adding a few drops of acetic anhydride (~100 μ L). The gel was stirred for 4 h at 4 °C and then washed extensively with distilled water and stabilized in 0.05 M Tris-HCl buffer, pH 7.2.

Preparation of BSA-Trisacryl GF 2000 Matrix. BSA was coupled directly to the Trisacryl GF 2000 gel according to the usual procedure (13). The Trisacryl gel was activated by using *p*-nitrophenyl chloroformate in anhydrous acetone in the presence of *N*-methylmorpholine that serves both as a scavenger for the hydrochloric acid released and as a catalyst. BSA was coupled to the activated Trisacryl gel in 0.1 M sodium hydrogen carbonate, pH 8.5.

Preparation of Immunoaffinity Column. The affinity-purified antibodies from the Trisacryl GF 05 column (15 mL) were coupled to Affi-Gel 10 (13 mL) in 0.1 M sodium hydrogen carbonate (pH 8.3) at 4 °C during 4 h. The slurry was filtered, and the unbound protein was spectrophotometrically determined at 280 nm after acidifi-

Table I. Immunological Response Raised in Rabbit (B) by Subcutaneous Injections of [9R]iP-BSA Conjugate and Determined by ELISA Titration

delay after the first injection in weeks	dilution of sera ^a	delay after the first injection in weeks	dilution of sera ^a
7	1:100	15	1:1000
8	1:250	19	1:3500
9	1:250	20	1:5000
13	1:750	21	1:2500
14	1:2600		

^a Dilutions of sera required to give $A_{405\text{nm}} = 0.5$.

cation of the filtrate at pH 2.0 by hydrochloric acid. Coupling efficiency was 80% with 0.5 mg of antibody/mL of gel. The immunoaffinity matrix was stored in 0.13 M ammonium acetate (pH 7.0) at 4 °C and supplemented with 0.02% sodium azide.

RESULTS AND DISCUSSION

Immunogen Synthesis and Immunological Response. In order to preserve the structure of the ribofuranosyl cycle, [9R]iP was bound to a protein, BSA or ovalbumin, by the five-step procedure summarized in Scheme I. An efficient conversion (80% yield) of [9R]iP to its 2',3'-*O*-isopropylidene derivative (2) was obtained using *p*-toluenesulfonic acid as catalyst in acetone and 2,2-dimethoxypropane for maintaining the anhydrous conditions necessary for such conversion. 1,1'-Carbonyldiimidazole, widely used as a carbonylating reagent for the activation of agarose affinity matrix (14), was allowed to quantitatively activate the 5'-hydroxyl group of compound 2. The nucleophilic attack of 6-aminoheptanoate salt on the imidazolyl carbonate derivative 3 led to the major compound 4. The acidic hydrolysis of the isopropylidene derivative 4 gave quantitatively ϵ -aminoheptanoic acid-[9R]iP conjugate 5. The ϵ -amino groups of proteins were substituted with [9R]iP derivative upon activation of the carboxyl group of compound 5. The molar ratios of hormone bound to proteins in our conditions were in the range of 12:1 and 18:1 for BSA and ovalbumin, respectively. These conjugates showed a maximal absorption at 269 nm. In the literature, ratios in the range of 6:1 to 17:1 were described for binding [9R]iP on BSA after periodate oxidization (6, 7, 15-19).

These molar ratios had given satisfactory results for the immunological response in two rabbits as shown by ELISA titer determination. As an example, the titers of the sera from rabbit B are reported in Table I. The highest titer (1:5000) was reached after eight injections.

For ELISA optimization, we checked the polystyrene immunoplates from various brands (Nunc I, Nunc II, and Greiner) and the nature of the protein used to block unbound solid-phase sites. For this purpose bovine hemoglobin (2%), gelatin (0.1, 0.5, and 1.0%), and proteins of milk (Régilait from a local grocery) (1.5 and 10%) were tested. In our hands, the nonspecific binding was minimized by using type Nunc I immunoplate substituted with [9R]iP-ovalbumin (0.05 mg/mL) and saturation with 0.5% gelatin.

Specificity of Crude Antisera by Radioassays. In a preliminary experiment the optimal antiserum dilution to be used for the competition studies was determined from typical standard curves (Figure 1). The crude antiserum bound 50% of [³H][9R]iP radiotracer at a dilution of 1:2400. The standard curves (Figure 2) and Table II show that the polyclonal anti-[9R]iP antisera have a good specificity for [9R]iP, no binding occurs with [9R]Z and Z, but the antisera partially cross-reacts with iP. This

Table II. Cross-Reactivities^a of Polyclonal Anti-[9R]iP-BSA Antisera with Cytokinins and Related Purines ([9R]iP, iP, [9R]Z, and Z) Compared to Published Works on Antisera

competitor	this study	ref 5	ref 15	ref 16	ref 17	ref 18	ref 19	INRA ^b
[9R]iP	100	100	100	100	100	100	100	100
iP	55	100	64	60	56	49	51	85
[9R]Z	<0.5	nd ^c	<0.1	1.0	1.8	3	0.3	0.5
Z	<0.5	nd	<0.1	0.3	0.9	1	0.1	0.5

^a Based on 50% inhibition values in the RIA. ^b Antiserum prepared at INRA according to the procedure of Sotta et al. (16). ^c nd, not determined.

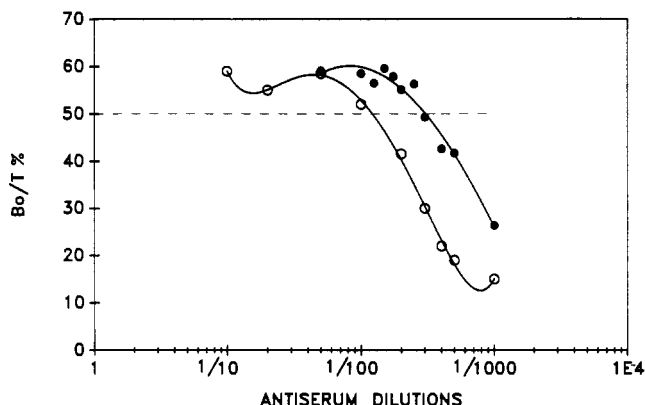


Figure 1. Standard dilution curves for [9R]iP radioimmunoassays. Assays were performed using either crude rabbit antiserum (●) or purified antibodies (○). [³H][9R]iP dialcohol was used as tracer (9000 cpm). Each point is the mean value from triplicate assays. Each curve resulted from a curvilinear regression of magnitude 4: Bo, amount of radiolabel bound with antibodies; T, total amount of radiolabel.

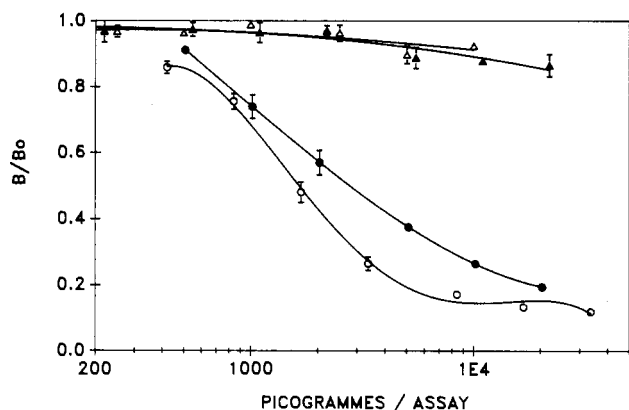


Figure 2. Standard curves for the [³H][9R]iP dialcohol radioimmunoassay. The assays were performed using a 1:2400 final dilution of antiserum. [9R]iP (●), iP (○), [9R]Z (▲), and Z (Δ) were used as competitor as described in the Experimental Procedures. Each point is the mean value from triplicate assays and curves resulted from curvilinear regressions: B, amount of radiolabel bound in the presence of different amounts of unlabelled derivatives; Bo, amount of radiolabel bound in the absence of competitor.

cross-reaction (55%) was lower than that previously observed (100%) by MacDonald et al. (5), (64%) by Cahill et al. (15) and (60%) by Sotta et al. (16) and that which we obtained (85%) with the antiserum from INRA prepared according to the method of Sotta et al. (16). Weiler and Spanier (17), Barthe and Stewart (18), and Hansen et al. (19) obtained approximately the same cross-reaction as we did in our work. The antibodies raised against [9R]iP linked to BSA via the 5'-hydroxyl from ribosyl residue can recognize the isopentenyl adenosyl group associated with the unbroken sugar cycle, in contrast to [9R]iP linked after periodate oxidization. However, Badenoch-Jones et al. (20) found that antibodies raised in rabbit against [9R]Z-BSA prepared from periodate-oxidized derivative showed 100% cross-reactivity with [9R-

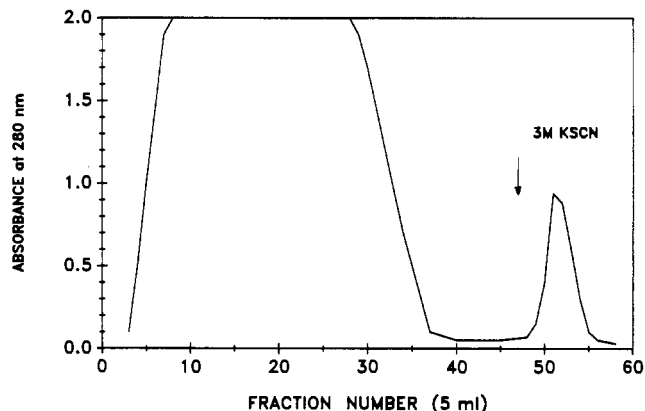


Figure 3. Affinity chromatography on [9R]iP-[6-[(ε-amino-hexanoyl)amino]hexyl]imino]methylene-agarose A4 of anti-[9R]iP immunoglobulins. This affinity column (9 × 1 cm) was equilibrated in 0.05 M Tris-HCl buffer (pH 7.2) (flow rate 15 mL/h). A pool of anti-[9R]iP antisera (90 mL) was precipitated in the 30–50% ammonium sulfate saturation range at 4 °C. The precipitate P_{30–50} was dialyzed overnight at 4 °C against 0.05 M Tris-HCl buffer (pH 7.2). This material was then passed through a DEAE-Trisacryl column (10 × 4.5 cm) and a BSA-Trisacryl affinity column (5 × 1 cm) equilibrated in the above buffer in order to remove the anti-BSA antibodies; the unbound material (50 mL) which contained the anti-[9R]iP antibodies was run directly onto the [9R]iP-[6-[(ε-amino-hexanoyl)amino]hexyl]imino]methylene-agarose A4 column equilibrated with the same buffer. The column was washed with 0.05 M Tris-HCl buffer (pH 7.2), and the specific anti-[9R]iP IgG were eluted with 3 M KSCN. Proteins were monitored by absorbance at 280 nm; fractions of 5 mL were collected and made free of the chaotropic agent by desalting on a Trisacryl GF05 column (34 × 2 cm).

(5'P)]Z and 50% cross-reactivity with Z. The cross-reaction may be due to the presence of the morpholino group.

Purification of Antibodies. A pool of rabbit (B) antiserum (90 mL) was precipitated at 4 °C in the 30–50% ammonium sulfate saturation range. The precipitate (P_{30–50}) was left to settle overnight and collected by centrifugation at 4000g for 20 min. The pellet was suspended in 0.05 M Tris-HCl buffer at pH 7.2 (10 mL) and dialyzed against the same buffer with two changes for 24 h at 4 °C. The protein solution from the previous step was applied directly to a DEAE-Trisacryl column (10 × 4.5 cm) equilibrated with 0.05 M Tris-HCl (pH 7.2) and washed with the same buffer at 4 °C. The IgG immunoglobulins passed through the column (21). In order to eliminate the antibodies against BSA, the unbound material was loaded on a BSA-Trisacryl affinity column (5 × 1 cm) stabilized in 0.05 M Tris-HCl (pH 7.2) (flow rate 15 mL/h) and washed with the same buffer. Unbound material (150 mL) was then loaded onto [9R]iP-[6-[(ε-amino-hexanoyl)amino]hexyl]imino]methylene-agarose A4 (9 × 1 cm) and eluted at a flow rate of 12 mL/h at room temperature. The column was washed with 0.05 M Tris-HCl buffer (pH 7.2), and the specific antibodies were eluted with 0.05 M Tris-HCl buffer at pH 7.2 containing 3 M KSCN as chaotropic agent. IgG antibodies eluted as a sharp peak (Figure 3) and were desalted by gel filtration on a Trisacryl GF 05 (34 × 2 cm) column stabilized in 0.1

M sodium hydrogen carbonate (pH 8.3) at 4 °C. The protein fraction from the void volume was sterilized by filtration through a 0.22- μ m Millipore filter and stored at 4 °C. From 90 mL of crude antiserum we obtained 9 mg of antibodies. The protein content was photometrically estimated assuming a specific absorbance of $A_{280\text{nm}} = 12$ (1 cm, 1%).

Characterization and Specificity of the Purified Antibodies. Crude rabbit antiserum against [9R]iP-BSA gave a precipitation band with BSA, [9R]iP-BSA, and [9R]iP-ovalbumin in double immunodiffusion on agar plate. After DEAE-Trisacryl and BSA-Trisacryl GF 2000 affinity chromatography, the unbound material gave a single precipitation band against [9R]iP-ovalbumin and did not react with BSA. At this step, the protein fraction was devoid of any anti-BSA antibodies. The same result was obtained with the material eluted from [9R]iP-substituted agarose by 3 M KSCN and desalted on Trisacryl GF 05. The purified antibodies were identified as IgG by immunoprecipitation with goat antiserum anti-rabbit IgG.

The purification of the anti-[9R]iP IgG from the crude antiserum did not modify the specificity of these antibodies, as determined by ELISA or RIA tests (data not shown).

Capacity of the Immunoaffinity Matrix. Antibodies raised against a number of cytokinins have been coupled to a variety of supports including cellulose (6, 7, 22). For this study, we used Affi-Gel 10, which allowed rapid and high efficiency coupling of proteins with the ϵ -amino group of lysine residues, forming a stable amide bond. This cross-linked agarose is supplied with a spacer arm which prevents steric hindrance and is activated by *N*-hydroxysuccinimide ester. According to the described conditions, we have bound 0.5 mg of antibody/mL of gel. A solution of [9R]iP (10 μ g, 30 nmol) in 0.13 M ammonium acetate (10 mL) was loaded on the immunoaffinity matrix (3 mL) with a flow rate of 0.2 mL/min. The column was washed with the same buffer. Low pH (0.1 M acetic acid, pH 3.0) or high ionic strength (1 M ammonium acetate) were inefficient to elute bound [9R]iP from the immunoaffinity matrix. A 50% methanol solution was needed to elute [9R]iP as previously described (6). The binding capacity of this column was 1 μ g of [9R]iP/mL of gel, 15-fold higher than a similar immunoaffinity matrix (70 ng/mL) prepared by Bollmark et al. (23).

ACKNOWLEDGMENT

Research was supported in part by grants from M.E.N. Biologie 1985 and Arbocentre to F.D.; M.-P.P. was a recipient of a fellowship from Conseil Régional, Région Centre. We thank Professor L. Johnson (University of South Carolina) and Miss R. MacKay, for their kind help in improving the English of this paper, and P. Label for preparing antiserum [INRA]. We are grateful for Professor M. Monsigny's encouragement. Acknowledgment is also due to Mrs. A.-M. Camus for typing the manuscript.

LITERATURE CITED

- Weiler, E. W. (1984) Immunoassay of Plant Growth Regulators. *Ann. Rev. Plant Physiol.* 35, 85-95.
- Weiler, E. W., Eberle, J., Mertens, R., Atzorn, R., Feyereabend, M., Jourdan, P. S., Arnscheidt, A., and Wiczorek, U. (1986) Antisera and Monoclonal Antibody Based Immunoassay of Plant Hormones. *Immunology in Plant Science* (T. L. Wang, Ed.) pp 27-58, Cambridge University Press, New York.
- Erlanger, B. F., and Beiser, S. M. (1964) Antibodies Specific for Ribonucleosides and Ribonucleotides and their Reaction with DNA. *Proc. Natl. Acad. Sci. U.S.A.* 52, 68-74.
- Weiler, E. W. (1980) Radioimmunoassays for *trans*-Zeatin and Related Cytokinins. *Planta* 149, 155-162.
- MacDonald, E. M. S., Akiyoshi, D. E., and Morris, R. O. (1982) Combined High Performance Liquid Chromatography-Radioimmunoassay for Cytokinins. *J. Chromatogr.* 214, 101-109.
- Wang, T. L., Cook, S. K., and Knox, J. P. (1987) Monoclonal Antibodies for the Analysis and Purification of Isopentenyl Adenine Cytokinins. *Phytochemistry* 26, 2447-2452.
- MacDonald, E. M. S., and Morris, R. O. (1985) Isolation of Cytokinins by Immunoaffinity Chromatography and Analysis by High-Performance Liquid Chromatography Radioimmunoassay. *Methods Enzymol.* 110, 347-358.
- Hampton, A. (1961) Nucleotides. II. A New Procedure for the Conversion of Ribonucleosides to 2',3'-O-Isopropylidene Derivatives. *J. Am. Chem. Soc.* 83, 3640-3645.
- Fields, R. (1972) The Rapid Determination of Amino Groups with TNBS. *Methods Enzymol.* 25, 464-468.
- Ouchterlony, O. (1962) Diffusion in Gel Methods for Immunological Analysis. *Prog. Allergy* 6, 375-381.
- March, S., Parikh, I., and Cuatrecasas, P. (1974) A Simplified Method for Cyanogen Bromide Activation of Agarose for Affinity Chromatography. *Anal. Biochem.* 60, 149-152.
- Delmotte, F., and Goldstein, I. (1980) Improved Procedures for Purification of the *Bandeiraea simplicifolia* I Isolectins and *Bandeiraea simplicifolia* II Lectin by Affinity Chromatography. *Eur. J. Biochem.* 112, 219-223.
- Miron, T., and Wilchek, M. (1985) Activation of Trisacryl Gels with Chloroformates and Their Use for Affinity Chromatography and Protein Immobilization. *Appl. Biochem. Biotech.* 11, 445-456.
- Bethell, G. S., Ayers, J. S., Hancock, W. S., and Hearn, M. T. (1979) A Novel Method of Activation of Cross-Linked Agaroses with 1,1'-Carbonyldiimidazole which Gives a Matrix for Affinity Chromatography Devoid of Additional Charged Groups. *J. Biol. Chem.* 254, 2572-2574.
- Cahill, D. M., Weste, G. M., and Grant, B. R. (1986) Changes in Cytokinin Concentrations in Xylem Exudate following Infection of *Eucalyptus marginata* Donn ex Sm with *Phytophthora cinnamomi* Rands. *Plant Physiol.* 81, 1103-1109.
- Sotta, B., Pilate, G., Pelese, F., Sabbagh, I., Bonnet, M., and Maldiney, R. (1987) An Avidin-Biotin Solid Phase ELISA for Femtomole Isopentenyladenine and Isopentenyladenosine Measurements in HPLC Purified Plant Extracts. *Plant Physiol.* 84, 571-573.
- Weiler, E. W., and Spanier, K. (1981) Phytohormones in the Formation of Crown Gall Tumors. *Planta* 153, 326-337.
- Barthe, G. A., and Stewart, I. (1985) Enzyme Immunoassay (EIA) of Endogenous Cytokinins in Citrus. *J. Agric. Food Chem.* 33, 293-297.
- Hansen, C. E., Meins, F., Jr., and Milani, A. (1985) Clonal and Physiological Variation in the Cytokinin Content of Tobacco-Cell Lines Differing in Cytokinin Requirement and Capacity for Neoplastic Growth. *Differentiation (Berlin)* 29, 1-6.
- Badenoch-Jones, J., Letham, D. S., Parker, C. W., and Rolfe, B. G. (1984) Quantitation of Cytokinins in Biological Samples Using Antibodies against Zeatin Riboside. *Plant Physiol.* 75, 1117-1125.
- Kieda, C. M. T., Delmotte, F. M., and Monsigny, M. L. P. (1977) Protein-sugar Interactions: Preparation, Purification, and Properties of Rabbit Antibodies against di-*N*-Acetylchitobiose. *Proc. Natl. Acad. Sci. U.S.A.* 74, 168-172.
- Knox, J. P., and Galfre, G. (1986) Use of Monoclonal Antibodies to Separate the Enantiomers of Abscissic Acid. *Anal. Biochem.* 155, 92-94.
- Bollmark, M., Kubat, B., and Eliasson, L. (1988) Variation in Endogenous Cytokinin Content During Adventitious Root Formation in Pea Cuttings. *J. Plant Physiol.* 132, 262-265.

Registry No. 2, 20268-92-2; 3, 137823-55-3; 4, 137823-56-4; 5, 137823-57-5; 6, 137823-58-6; $\text{H}_2\text{N}(\text{CH}_2)_5\text{CO}_2\text{H}$, 60-32-2; $\text{H}_2\text{N}(\text{CH}_2)_6\text{NH}_2$, 124-09-4; Ultragel A4, 62168-82-5; [(6-aminohexyl)-imino]methylene-agarose A4, 58856-73-8; [4R]iP-[[[6-(ϵ -aminohexanoyl)amino]hexyl]imino]methylene-agarose A4, 137868-26-9.

Gadolinium Complexes of [(Myristoyloxy)propyl]diethylenetriaminetetraacetate: New Lipophilic, Fatty Acyl Conjugated NMR Contrast Agents[†]

Sung K. Kim, Gerald M. Pohost, and Gabriel A. Elgavish*

Division of Cardiovascular Disease, Department of Medicine, University of Alabama at Birmingham, Birmingham, Alabama 35294. Received May 30, 1991

New lipophilic contrast agents, 1-[3'-(myristoyloxy)propyl]diethylenetriamine-1,4,7,7-tetraacetic acid (1MP-DTTA), 4-[3'-(myristoyloxy)propyl]diethylenetriamine-1,1,7,7-tetraacetic acid (4MP-DTTA), and 4-[3'-(myristoyloxy)propyl]-2,6-dioxodiethylenetriamine-1,1,7,7-tetraacetic acid (4MPD-DTTA), were prepared from either diethylenetriamine or 3-amino-1-propanol (overall yield 16-23%). Liposome-incorporated Gd complexes of ligands 1MP-DTTA, 4MP-DTTA, and 4MPD-DTTA were prepared by mixing GdCl₃ and the prepared vesicles consisting of ligand, egg lecithin, and cholesterol (molar ratio 1:1.5:1) followed by further sonication, and their in vitro relaxivities were determined. The relaxivities of these agents were higher than those of the Gd³⁺ aquoion, Gd(EDTA), or Gd(DTPA) at both 0.23 and 0.47 T. Gd(4MPD-DTTA) displayed the highest relaxivities (24.0 ± 0.4 and 34.7 ± 0.4, at 0.23 and 0.47 T, respectively) among these new Gd complexes. The relaxivities of these three agents increased from the lower to the higher magnetic field, indicating a positive field dependence. Stability constants (log K) of Gd(1MP-DTTA), Gd(4MP-DTTA), and Gd(4MPD-DTTA) were found to be 18.2 ± 0.2, 18.4 ± 0.2, and 15.7 ± 0.8, respectively. A lower limit of 0.3 mmol/kg was found for LD₅₀ for these three agents.

INTRODUCTION

Although the gadolinium (Gd) complex of diethylenetriaminepentaacetate (DTPA) has been widely used to enhance contrast in NMR imaging (1-3), attempts to overcome disadvantages of the DTPA complex such as low relaxivity, low tissue specificity, and rapid clearance have been made recently (4-9). These mainly concentrated on the conjugation of the DTPA ligand with various molecules such as proteins, polymers, and either fatty acids or phospholipids using the reaction of these molecules with the anhydride of DTPA (4-9). In these reactions one of the five carboxylates of the DTPA ligand was used for monoconjugation, leaving four free carboxylates as the metal-binding moiety. Another approach included the encapsulation of paramagnetic agents, such as manganese chloride and Gd(DTPA), into liposomes (10, 11).

Previously, we demonstrated that the introduction of a carbonyl group into the metal-binding moiety increased in vitro relaxivities, compared with those of Gd(DTPA), at 0.23 and 0.47 T (12). To further explore the structure and relaxivity relationship, we prepared new imino polycarboxylates conjugated with myristic acid. The newly designed metal-binding moiety mimics the DTPA portion monoconjugated with macromolecules. Thus, a hydroxypropyl group for the conjugation of fatty acids was attached at different positions in the diethylenetriamine backbone to evaluate the effects on relaxivity of the position of the hydroxypropyl group. Furthermore, we introduced a carbonyl group into the metal-binding moiety to also assess the effect of the carbonyl group on relaxivity. Subsequently, the prepared Gd complexes of these ligands were incorporated into liposomes and relaxivities were measured. The effect on relaxivity of the structural

changes provides information about the structure and relaxivity relationship in these systems and may assist in the design of optimal contrast agents. Also, the results may suggest an optimal position of the covalent attachments of the chelate to macromolecules, thus improving relaxivity.

EXPERIMENTAL PROCEDURES

Melting points were determined in open capillaries with a Gallenkamp melting point apparatus and are uncorrected. High-resolution proton NMR spectra to confirm intermediates and identify products were recorded on a Bruker AM-360 instrument. Either Me₄Si (CDCl₃, DMSO-*d*₆) or 3-(trimethylsilyl)propionic-2,2,3,3-*d*₄ acid sodium salt (TSP) (D₂O) were used as internal standard. Chemical shifts (in ppm, downfield from the internal standard) are reported along with peak multiplicities: br, broad; m, multiplet; t, triplet; d, doublet; s, singlet. Elemental analyses were performed by Atlantic Microlab Inc. (Norcross, GA).

1-(3'-Hydroxypropyl)diethylenetriamine (2). Following a published procedure (13), 3-chloro-1-propanol (9.45 g, 0.1 mol) was added to a refluxing solution of diethylenetriamine (30.95 g, 0.3 mol) and NaOH (4 g, 0.1 mol) in 30 mL of H₂O, and reflux was continued for 2 h. H₂O was removed under reduced pressure and the residue was distilled at 134-138 °C (0.7 mmHg), affording 9.74 g (60%) of compound 2 used for the next reaction without further purification. NMR (D₂O): 1.6-1.8 (m, 2 H), 2.5-2.8 (m, 10 H), 3.65 (t, 2 H).

Tetrabenzyl 1-(3'-Hydroxypropyl)diethylenetriamine-1,4,7,7-tetraacetate (3). A solution of amino alcohol 2 (4.03 g, 0.025 mol) and triethylamine (12.65 g, 0.125 mol) in 35 mL of DMF was added dropwise to a cold (0 °C) solution of benzyl bromoacetate (28.64 g, 0.125 mol) in 25 mL of DMF during a period of 1 h, and the resulting mixture was stirred overnight at room temperature. After partition of the mixture between ethyl acetate (EtOAc) and water, the organic layer was washed with saturated brine, dried with MgSO₄, filtered, and concentrated under reduced pressure. The residue was purified through a

* Address all correspondence to Gabriel A. Elgavish, Ph.D., University of Alabama at Birmingham, Division of Cardiovascular Disease, Department of Medicine, Room 336, Tinsley Harrison Tower, Birmingham, AL 35294.

[†] Results from this work were presented at the 201st American Chemical Society Meeting, Division of Medicinal Chemistry, Atlanta, Georgia, April 14-19, 1991.

silica gel column using EtOAc/hexane (3:1) as eluent, affording 8.86 g (47%) of compound 3. NMR (CDCl₃): 1.5–1.7 (m, 2 H), 2.6–2.8 (m, 8 H), 2.85 (t, 2 H), 3.38 (s, 2 H), 3.46 (s, 2 H), 3.59 (s, 4 H), 3.70 (t, 2 H), 5.09 (s, 2 H), 5.10 (s, 4 H), 5.11 (s, 2 H), 7.2–7.4 (m, 20 H). Anal. Calcd for C₄₃H₅₁N₃O₉: C, 68.51; H, 6.82; N, 5.57. Found: C, 68.39; H, 6.84; N, 5.61.

Tetrabenzyl 1-[3'-(Myristoyloxy)propyl]diethylenetriamine-1,4,7,7-tetraacetate (4). To a solution of hydroxy ester 3 (3.02 g, 4 mmol) and triethylamine (0.61 g, 6 mmol) in 20 mL of carbon tetrachloride was added a solution of myristoyl chloride (1.48 g, 6 mmol) in 15 mL of carbon tetrachloride at 0 °C, and the resulting solution was stirred overnight at room temperature. The CCl₄ layer was washed with saturated brine and concentrated. The residue was purified by silica gel column chromatography [hexane/EtOAc (2:1)], affording 2.97 g (77%) of compound 4. NMR (CDCl₃): 0.88 (t, 3 H), 1.25 (br s, 20 H), 1.5–1.8 (m, 4 H), 2.25 (t, 2 H), 2.64 (t, 2 H), 2.70 (s, 4 H), 2.76 (t, 2 H), 2.84 (t, 2 H), 3.39 (s, 2 H), 3.46 (s, 2 H), 3.61 (s, 4 H), 4.04 (t, 2 H), 5.09 (s, 2 H), 5.10 (s, 6 H), 7.2–7.4 (m, 20 H). Anal. Calcd for C₅₇H₇₇N₃O₁₀: C, 71.00; H, 8.05; N, 4.36. Found: C, 70.89; H, 8.08; N, 4.38.

1-[3'-(Myristoyloxy)propyl]diethylenetriamine-1,4,7,7-tetraacetic Acid (5). A mixture of benzyl ester 4 (2.12 g, 2.2 mmol) and 10% Pd/C (0.5 g) in 30 mL of ethanol and 15 mL of cyclohexene was heated at reflux for 2 h and the catalyst was removed through a Celite pad. After the solvent had been removed under reduced pressure, the residue was recrystallized from ethanol, affording 1.06 g (80%) of compound 5. Mp: 152–155 °C. NMR (DMSO-*d*₆): 0.85 (t, 3 H), 1.24 (br s, 20 H), 1.4–1.6 (m, 2 H), 1.6–1.8 (m, 2 H), 2.27 (t, 2 H), 2.75 (t, 2 H), 2.8–3.1 (m, 8 H), 3.35 (s, 2 H), 3.45 (s, 4 H), 3.49 (s, 2 H), 4.02 (t, 2 H). Anal. Calcd for C₂₉H₅₃N₃O₁₀·H₂O: C, 56.02; H, 8.92; N, 6.76. Found: C, 56.42; H, 8.72; N, 6.87.

N-(3-Hydroxypropyl)-2,2'-iminodiacetamide (7). A solution of 3-amino-1-propanol (1.88 g, 0.025 mol) and triethylamine (6.33 g, 0.063 mol) in 20 mL of dry acetonitrile was added to a suspension of iodoacetamide (9.71 g, 0.053 mol) in 35 mL of dry acetonitrile at 0 °C and the resulting solution was stirred for 1 h at 0 °C followed by stirring overnight at room temperature. The solid in the reaction mixture was collected, washed with hot chloroform, and recrystallized from a mixture of methanol and acetone, affording 2.69 g (57%) of compound 7. Mp: 114–116 °C. NMR (D₂O): 1.7–1.8 (m, 2 H), 2.67 (t, 2 H), 3.29 (s, 4 H), 3.65 (t, 2 H). Anal. Calcd for C₇H₁₅N₃O₃: C, 44.43; H, 7.99; N, 22.21. Found: C, 44.57; H, 8.05; N, 22.22.

Tetrabenzyl 4-(3'-Hydroxypropyl)diethylenetriamine-1,1,7,7-tetraacetate (8). Amide 7 (2.52 g, 13.3 mmol) was added portionwise to 130 mL of BH₃·THF at 0 °C, and the resulting mixture was refluxed overnight. Subsequently, methanol (30 mL) was added to the reaction mixture at 0 °C and stirring was continued for 16 h at room temperature. HCl gas was introduced to the reaction mixture (pH 1) and the solvent was removed under reduced pressure. The residue in 25 mL of DMF was treated with Et₃N (15 mL), and the solid was removed by filtration. The filtrate was added to a solution of benzyl bromoacetate (15.23 g, 66.5 mmol) in 15 mL of DMF at 0 °C during a period of 1 h, and stirring was continued overnight. The reaction mixture was diluted with EtOAc, and the organic solution was washed with saturated brine, dried with MgSO₄, filtered, and concentrated under reduced pressure. Purification through a silica gel column using CHCl₃/EtOAc/methanol (7:2:1) as eluent afforded 4.98 g (50%) of compound 8. NMR (CDCl₃): 1.5–1.8 (m, 2 H), 2.4–2.6

(m, 6 H), 2.85 (t, 4 H), 3.60 (s, 8 H), 3.67 (t, 2 H), 5.11 (s, 8 H), 7.2–7.5 (m, 20 H). Anal. Calcd for C₄₃H₅₁N₃O₉: C, 68.51; H, 6.82; N, 5.57. Found: C, 68.43; H, 6.83; N, 5.63.

Tetrabenzyl 4-[3'-(Myristoyloxy)propyl]diethylenetriamine-1,1,7,7-tetraacetate (9). Compound 9 was prepared in the same way as described for the preparation of compound 4. Thus, compound 8 (1.51 g, 2 mmol) gave 1.39 g (72%) of compound 9. NMR (CDCl₃): 0.88 (t, 3 H), 1.25 (br s, 20 H), 1.6–1.8 (m, 4 H), 2.26 (t, 2 H), 2.44 (t, 2 H), 2.54 (t, 4 H), 2.79 (t, 4 H), 3.61 (s, 8 H), 4.01 (t, 2 H), 5.11 (s, 8 H), 7.2–7.4 (m, 20 H). Anal. Calcd for C₅₇H₇₇N₃O₁₀: C, 71.00; H, 8.05; N, 4.36. Found: C, 70.89; H, 8.00; N, 4.43.

4-[3'-(Myristoyloxy)propyl]diethylenetriamine-1,1,7,7-tetraacetic Acid (10). Compound 10 was prepared from 9 (0.85 g, 0.88 mmol) according to procedures identical to those described for the preparation of 5 from 4, affording 0.41 g (77%) as a white solid. An EtOAc/ethanol solvent mixture was used for recrystallization. Mp: 195–197 °C. NMR (DMSO-*d*₆): 0.85 (t, 3 H), 1.24 (br s, 20 H), 1.4–1.6 (m, 2 H), 1.8–2.0 (m, 2 H), 2.29 (t, 2 H), 2.8–3.2 (m, 10 H), 3.38 (s, 8 H), 4.06 (t, 2 H). Anal. Calcd for C₂₉H₅₃N₃O₁₀·H₂O: C, 56.02; H, 8.92; N, 6.76. Found: C, 56.15; H, 8.72; N, 6.94.

Tetrabenzyl 4-(3'-Hydroxypropyl)-2,6-dioxodiethylenetriamine-1,1,7,7-tetraacetate (12). A solution of 3-amino-1-propanol (0.804 g, 10.7 mmol) and triethylamine (3.25 g, 32.1 mmol) in 10 mL of DMF was added to a solution of compound 11 (see ref 12 for the synthesis of this intermediate) (10.22 g, 23.54 mmol) in 10 mL of DMF, and the resulting solution was stirred for 5 h at room temperature. The reaction mixture was partitioned between EtOAc and H₂O and the organic layer was washed with saturated brine, dried with MgSO₄, filtered, and concentrated under reduced pressure. The residue was purified through a silica gel column using hexane/EtOAc (1:3) as eluent, yielding 3.68 g (44%) of compound 12. NMR (CDCl₃): 1.4–1.6 (m, 2 H), 2.66 (t, 2 H), 3.40 (s, 4 H), 3.64 (t, 2 H), 4.17 (s, 4 H), 4.36 (s, 4 H), 5.12 (s, 4 H), 5.16 (s, 4 H), 7.2–7.5 (m, 20 H). Anal. Calcd for C₄₃H₄₇N₃O₁₁: C, 66.06; H, 6.06; N, 5.37. Found: C, 65.95; H, 6.05; N, 5.34.

Tetrabenzyl 4-[3'-(Myristoyloxy)propyl]-2,6-dioxodiethylenetriamine-1,1,7,7-tetraacetate (13). Compound 13 was prepared in the same way as described for the preparation of compound 4. Thus, compound 12 (1.72 g, 2.2 mmol) gave 1.62 g (74%) of compound 13. NMR (CDCl₃): 0.88 (t, 3 H), 1.25 (br s, 20 H), 1.5–1.7 (m, 4 H), 2.25 (t, 2 H), 2.60 (t, 2 H), 3.35 (s, 4 H), 3.98 (t, 2 H), 4.17 (s, 4 H), 4.41 (s, 4 H), 5.12 (s, 4 H), 5.15 (s, 4 H), 7.2–7.5 (m, 20 H). Anal. Calcd for C₅₇H₇₃N₃O₁₂: C, 69.00; H, 4.23; N, 7.42. Found: C, 68.72; H, 4.30; N, 7.38.

4-[3'-(Myristoyloxy)propyl]-2,6-dioxodiethylenetriamine-1,1,7,7-tetraacetic Acid (14). Compound 14 was prepared from 13 (1.4 g, 1.41 mmol) according to procedures identical to those described for the preparation of 5 from 4, affording 0.62 g (71%) of compound 14. Ethanol was used for recrystallization. Mp: 185–188 °C. NMR (DMSO-*d*₆): 0.85 (t, 3 H), 1.24 (br s, 20 H), 1.4–1.6 (m, 2 H), 1.6–1.8 (m, 2 H), 2.25 (t, 2 H), 2.60 (t, 2 H), 3.37 (s, 4 H), 3.94 (s, 4 H), 3.98 (t, 2 H), 4.31 (s, 4 H). Anal. Calcd for C₂₉H₄₉N₃O₁₂·H₂O: C, 53.61; H, 7.91; N, 6.48. Found: C, 53.71; H, 7.76; N, 6.49.

Preparation of the Gd Complexes of Compounds 5, 10, and 14. Gd complexes of target compounds 5, 10, and 14 were prepared according to published procedure (8). Thus, a solution of GdCl₃·6H₂O (0.87 g, 2.34 mmol) in 2 mL of distilled water was added dropwise to a solution of compound 5 (0.942 g, 1.56 mmol) in 25 mL of pyridine,

and stirring was continued for 30 min at room temperature. The solvent was completely removed under reduced pressure and the residue was suspended in distilled water to remove excess GdCl_3 . The solid in water was collected by filtration and dried under vacuum, affording 1.1 g (81.4%) of Gd-complexed compound 5. Anal. Calcd for $\text{C}_{29}\text{H}_{50}\text{N}_3\text{O}_{10}\text{Gd}\cdot 6\text{H}_2\text{O}$: C, 40.72; H, 7.22; N, 4.85. Found: C, 40.36; H, 6.82; N, 4.80.

Similarly, compound 10 (0.326 g, 0.54 mmol) yielded 0.34 g (76%) of Gd-complexed compound 10. Anal. Calcd for $\text{C}_{29}\text{H}_{50}\text{N}_3\text{O}_{10}\text{Gd}\cdot 4\text{H}_2\text{O}$: C, 41.96; H, 7.04; N, 5.06. Found: C, 41.63; H, 6.89; N, 4.93.

Compound 14 (0.442 g, 0.7 mmol) yielded 0.489 g (83.2%) of Gd-complexed compound 14. Anal. Calcd for $\text{C}_{29}\text{H}_{46}\text{N}_3\text{O}_{12}\text{Gd}\cdot 3\text{H}_2\text{O}$: C, 41.46; H, 6.24; N, 5.00. Found: C, 41.82; H, 6.53; N, 5.00.

Incorporation of Gd Complexes 5, 10, and 14 into Liposomes. According to modification of a published procedure (9), the dry lipids of ligand (5.5 μmol), egg lecithin (20 mg, Avanti Co., 20 mg/mL in chloroform), and cholesterol (2 mg) (molar ratio 1.1:5:1) were suspended in 4 mL of buffer solution containing 0.9% saline and 20 mM HEPES (pH 7.4), and the resulting suspension was sonicated using a Bransonic ultrasonic device (Model B-5200R-4) for 3 h at 4 $^\circ\text{C}$. A 5 μmol amount of GdCl_3 solution [concentration of the stock solution was determined by published procedures (22)] was added with fast vortexing to the prepared vesicles and sonication was continued further for 4 h. The pH was adjusted to 7.4 and the final volume was brought to 5 mL, affording a 1 mM solution of Gd complexes used for the measurement of relaxivities.

NMR Relaxivity Measurements. The liposome-incorporated complexes of Gd^{3+} with compounds 5, 10, and 14 as ligands were used for water proton NMR relaxation rate ($1/T_1$) measurements at pH 7.4 and probe temperature 40 $^\circ\text{C}$ as a function of the concentration of each complex (0.2–1.0 mM) on IBM PC-10 (10 MHz, 0.23 T) and IBM PC-20 (20 MHz, 0.47 T) Multispec NMR instruments. For each sample, $1/T_1$ was calculated from three consecutive $1/T_1$ measurements. From the slope of $1/T_1$ versus varying concentrations of the Gd complex, the relaxivity of each complex was determined.

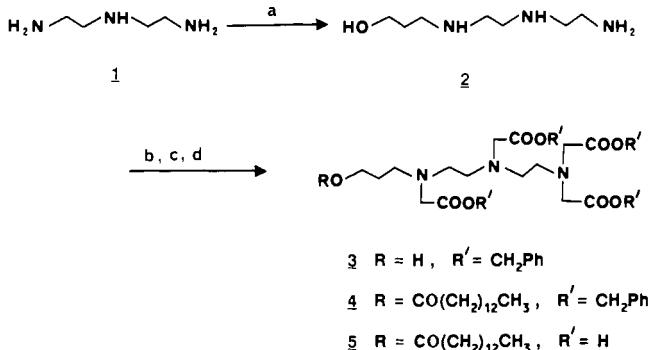
Determination of Stability Constants. Based on the approach (15) of a competitive-equilibrium relaxivity experiment between a Gd complex of unknown stability and $\text{Gd}(\text{EDTA})$, we have developed a method of simultaneous determination of the stability constant and of the relaxivity of such a Gd complex (20). Using this method, we obtained log K values as well as relaxivities for the Gd complexes of 1MP-DTTA, 4MP-DTTA, and 4MPD-DTTA from the measurement of $1/T_1$ versus the concentration of added EDTA using an IBM PC-20 Multispec NMR instrument. In the calculations we made use of the known stability constant (log $K = 17.3$) of $\text{Gd}(\text{EDTA})$ (21) and its separately measured relaxivity.

Toxicity. Liposome-incorporated Gd complexes for toxicity experiments were prepared as described above. Seven Sprague–Dawley rats (270–330 g body weight) were used for each compound and the administered volume for rat was 2.5 mL/330 g of body weight corresponding to a dosage of 0.3 mmol/kg of body weight. The animals were anesthetized with ether and the liposome-incorporated Gd complex was administered by bolus injection (1 mL/min) via the tail vein. The animals were observed for 10 days (see Table II).

RESULTS AND DISCUSSION

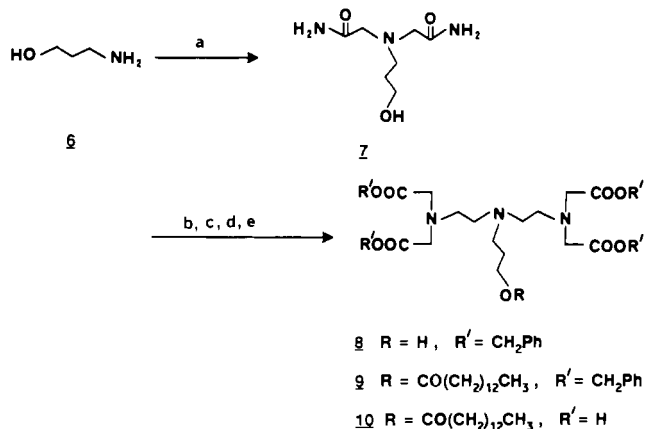
Synthetic Aspects. Scheme I describes synthetic

Scheme I.^a Synthesis of 1MP-DTTA



^a (a) $\text{HOCH}_2\text{CH}_2\text{CH}_2\text{Cl}$, NaOH ; (b) $\text{BrCH}_2\text{COOCH}_2\text{Ph}$, Et_3N , DMF; (c) $\text{CH}_3(\text{CH}_2)_{12}\text{COCl}$, Et_3N ; (d) 10% Pd/C, cyclohexene, EtOH.

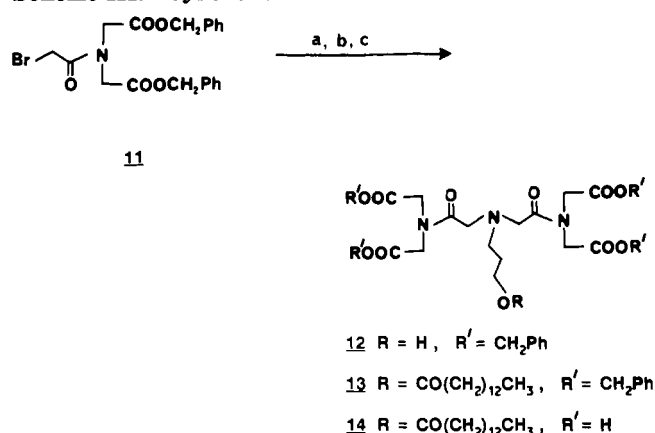
Scheme II.^a Synthesis of 4MP-DTTA



^a (a) $\text{ICH}_2\text{CONH}_2$, Et_3N , CH_3CN ; (b) $\text{BH}_3\cdot\text{THF}$, HCl ; (c) $\text{BrCH}_2\text{COOCH}_2\text{Ph}$, Et_3N ; (d) $\text{CH}_3(\text{CH}_2)_{12}\text{COCl}$, CCl_4 ; (e) 10% Pd/C, cyclohexene, EtOH.

sequences for the preparation of 1MP-DTTA (5). Following hydroxypropylation of triethylenediamine (13), alkylation of the resulting intermediate 2 using benzyl bromoacetate and triethylamine in DMF afforded compound 3 with 47% yield. In this alkylation step, amino alcohol 2 and triethylamine should be added slowly to an excess of benzyl bromoacetate to avoid cyclic-amide formation. An attempt to use reverse addition resulted in poor yield of compound 3. Only trace amounts of product were detected. Subsequent treatment of intermediate 3 with myristoyl chloride in carbon tetrachloride produced compound 4 with 77% yield. Although catalytic hydrogenation for removal of benzyl group in compound 4 was satisfactory, we used transfer hydrogenation (14) for the cleavage of the benzyl ester in intermediate 4, affording an 80% yield of 1MP-DTTA.

The synthetic sequences for the preparation of 4MP-DTTA (10) and 4MPD-DTTA (14) are depicted in Schemes II and III, respectively. 3-Amino-1-propanol was treated with iodoacetamide, affording intermediate 7 with 57% yield. Subsequently, reduction of the carbonyl groups in compound 7 using a $\text{BH}_3\cdot\text{THF}$ complex, followed by alkylation with benzyl bromoacetate, gave compound 8. Similarly, compound 12 was prepared by reaction of bromo compound 11 with 3-amino-1-propanol with 44% yield. Target ligands 10 and 14 were obtained from 8 and 12, respectively, using the methods described for the preparation of 5 from 3. Thus, following monomyristoylation of 8 and 12, transfer hydrogenation of 9 and 13 provided target ligands 10 and 14 with 77% and 71% yield, respectively.

Scheme III.^a Synthesis of 4MPD-DTTA

^a (a) $HOCH_2CH_2CH_2NH_2$, DMF; (b) $CH_3(CH_2)_{12}COCl$, CCl_4 ; (c) 10% Pd/C, cyclohexene, EtOH.

Following a published procedure (8), the 1:1 complexes of Gd^{3+} with ligands 5, 10, and 14 were prepared with good yields (76–83%). Thus, a solution of $GdCl_3$ in water was treated with ligands in pyridine for 30 min at room temperature, and the solvent was subsequently removed. The residue was washed with water to remove excess $GdCl_3$. Purity of the Gd complexes of 5, 10, and 14 was confirmed by elemental analysis. Gd complexes of these ligands were incorporated into liposomes by mixing $GdCl_3$ with sonicated vesicles consisting of ligand, cholesterol, and egg lecithin, followed by further sonication using a Bransonic ultrasonic device (B-5200R-4).

Relaxivity. Water proton NMR relaxation rate ($1/T_1$) was measured at varying agent concentrations at pH 7.4 and 40 °C, using an inversion recovery sequence with eight delay times, on IBM PC-10 (0.23 T) and IBM PC-20 (0.47 T) Multispec NMR instruments to determine relaxivities of the liposome-incorporated Gd complexes of the ligands 1MP-DTTA, 4MP-DTTA, and 4MPD-DTTA. For each sample, $1/T_1$ was obtained from the average of three consecutive $1/T_1$ measurements. The $1/T_1$ values versus the concentration of each of the three Gd complexes at both fields are shown in Figures 1, 2, and 3, respectively. Straight lines were fitted to the data points by least-squares analysis, obtaining $R^2 > 0.99$. From the slope of these lines the relaxivity of each complex was determined. The resulting relaxivities were compiled in Table I.

The relaxivities of the liposome-incorporated Gd complexes of target ligands 5, 10, and 14 increased between 19% and 44% from 0.23 to 0.47 T, indicating a positive field dependence. Furthermore, relaxivities of these agents were much larger than those of the Gd^{3+} aquoion, Gd(EDTA), or Gd(DTPA) at 0.23 and 0.47 T. It is likely that both the enhanced relaxivity and the positive field dependence of complexes 5, 10, and 14 are the result of a long enough rotational reorientation time, τ_R , due to larger molecular weights of these complexes compared with those of EDTA and DTPA. Similarly, previous studies have shown that increased relaxivities of Gd(DTPA) conjugated with macromolecules such as bovine immunoglobulin and albumin compared with unconjugated Gd(DTPA) were due to prolonged rotational correlation times (15, 16).

The relaxivities of the Gd complexes of the DTTA-type ligands presented here were found to be about 1.4- and 2.4-fold higher than those of the free Gd^{3+} aquoion. Furthermore, the relaxivities of these Gd complexes were 2.4- and 3.9-fold larger than those of Gd(EDTA). Compared with Gd(DTPA), 2.8- and 4.5-fold increases in relaxivities of Gd(1MP-DTTA) at 0.23 and 0.47 T, respec-

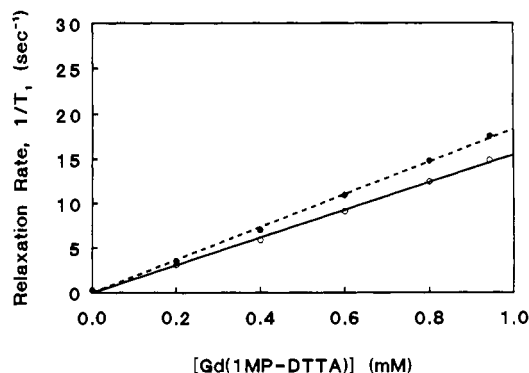


Figure 1. 1H NMR relaxation rate ($1/T_1$) versus concentration of the liposome-incorporated Gd complex of 1-[3'-(myristoyloxy)propyl]diethylenetriamine-1,4,7,7-tetraacetic acid (1MP-DTTA, 5). The liposome-incorporated 1:1 complex of Gd^{3+} with compound 5 as a ligand was used for water proton NMR relaxation rate ($1/T_1$) measurements at pH 7.4 as a function of the concentration of the complex (0.2–1.0 mM) on IBM PC-10 (10 MHz, 0.23 T, open circles) and IBM PC-20 (20 MHz, 0.47 T, filled circles) Multispec NMR instruments. $1/T_1$ measurements were taken at a probe temperature of 40 °C, and $1/T_1$ values were corrected with subtraction of the diamagnetic contribution from the observed $1/T_1$ values. For each sample, $1/T_1 \pm SEM$ was calculated from three consecutive $1/T_1$ measurements. The typical SEM is 0.11. No error bars are shown since they are smaller than the dimension of the data symbols. The straight lines (continuous line, 0.47 T; broken line, 0.23 T) were obtained by a linear least-squares method for fitting lines to data points ($R^2 > 0.99$). From the slope of $1/T_1$ versus concentration of the Gd complex, the relaxivity of the complex was determined with an accuracy of ± 0.08 (SEM).

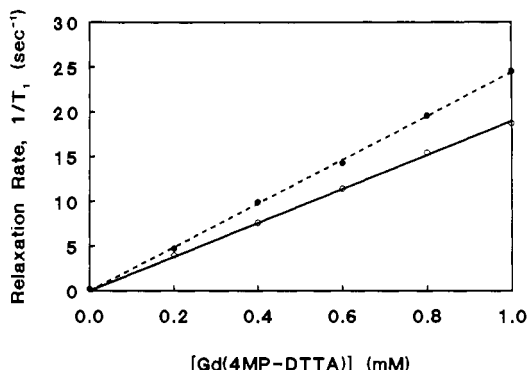


Figure 2. 1H NMR relaxation rate ($1/T_1$) versus concentration of the liposome-incorporated Gd complex of 4-[3'-(myristoyloxy)propyl]diethylenetriamine-1,1,7,7-tetraacetic acid (4MP-DTTA, 10). The liposome-incorporated 1:1 complex of Gd^{3+} with compound 10 as a ligand was used for water proton NMR relaxation rate ($1/T_1$) measurements at pH 7.4 as a function of the concentration of the complex (0.2–1.0 mM) on IBM PC-10 (10 MHz, 0.23 T, open circles) and IBM PC-20 (20 MHz, 0.47 T, filled circles) Multispec NMR instruments. $1/T_1$ measurements were taken at a probe temperature of 40 °C, and $1/T_1$ values were corrected with subtraction of the diamagnetic contribution from the observed $1/T_1$ values. For each sample, $1/T_1 \pm SEM$ was calculated from three consecutive $1/T_1$ measurements. The typical SEM is 0.21. No error bars are shown since they are smaller than the dimension of the data symbols. The straight lines (continuous line, 0.47 T; broken line, 0.23 T) were obtained by a linear least-squares method for fitting lines to data points ($R^2 > 0.99$). From the slope of $1/T_1$ versus concentration of the Gd complex, the relaxivity of the complex was determined with an accuracy of ± 0.08 (SEM).

tively, were observed. On the other hand, Gd(4MP-DTTA) revealed a 3.5- and 6.0-fold increase at both fields. Interestingly, Gd(4MPD-DTTA) showed the largest increase in relaxivities at both fields. Thus 4.4- and 8.5-fold increases in relaxivities of Gd(4MPD-DTTA) were ob-

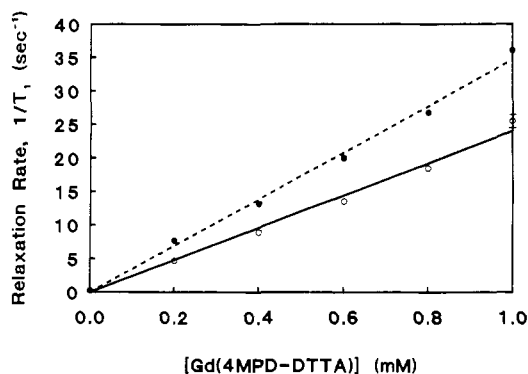


Figure 3. ^1H NMR relaxation rate ($1/T_1$) versus concentration of the liposome-incorporated Gd complex of 4-[3'-(myristoyloxy)propyl]-2,6-dioxodiethylenetriamine-1,1,7,7-tetraacetic acid (4MPD-DTTA, 14). The liposome-incorporated 1:1 complex of Gd^{3+} with compound 14 as a ligand was used for water proton NMR relaxation rate ($1/T_1$) measurements at pH 7.4 as a function of the concentration of the complex (0.2–1.0 mM) on IBM PC-10 (10 MHz, 0.23 T, open circles) and IBM PC-20 (20 MHz, 0.47 T, filled circles) Multispec NMR instruments. $1/T_1$ measurements were taken at a probe temperature of 40 °C, and $1/T_1$ values were corrected with subtraction of the diamagnetic contribution from the observed $1/T_1$ values. For each sample, $1/T_1 \pm \text{SEM}$ was calculated from three consecutive $1/T_1$ measurements. The typical SEM is 0.55. No error bars are shown since they are smaller than the dimension of the data symbols. The straight lines (continuous line, 0.47 T; broken line, 0.23 T) were obtained by a linear least-squares method for fitting lines to data points ($R^2 > 0.99$). From the slope of $1/T_1$ versus concentration of the Gd complex, the relaxivity of the complex was determined with an accuracy of ± 0.37 (SEM).

Table I. Longitudinal Relaxivity (ρ_1) of Several Gadolinium Complexes at Two Magnetic Fields^a and Molecular Weight of Ligands

complex	MW ^b	ρ_1 (s ⁻¹ mM ⁻¹)		ref
		0.23 T	0.47 T	
Gd(1MP-DTTA)	603.76	15.5 \pm 0.1	18.4 \pm 0.1	c
Gd(4MP-DTTA)	603.76	19.0 \pm 0.1	24.4 \pm 0.1	c
Gd(4MPD-DTTA)	631.72	24.0 \pm 0.4	34.7 \pm 0.4	c
Gd(MHE-DTTA)	704.82	22.4 \pm 0.1	31.9 \pm 0.7	12
Gd(BME-DTTA)	915.18	18.8 \pm 0.2	27.1 \pm 0.3	12
Gd ³⁺ aquoion		14.0	11.0	23
Gd(EDTA)	292.24	8.0	6.6	23
Gd(DTPA)	393.35	5.5	4.1	24

^a Mean \pm SEM. ^b Molecular weight of ligand. ^c This work.

served, compared with those of Gd(DTPA), at 0.23 and 0.47 T, respectively.

Gd(4MPD-DTTA) produced the largest relaxivities among these Gd complexes at both fields, suggesting an effect on relaxivities of the carbonyl groups in the 4MPD ligand. Such effects may be due to the prevention of Gd^{3+} coordination by the nitrogen atom positioned next to the carbonyl group. Such reduction in ligand coordination could result in an increased number of water molecules in the hydration sphere of the Gd^{3+} ion, affording an increased relaxivity.

Although the structures of 1MP-DTTA and 4MP-DTTA were similar and the only structural difference between these two ligands was the location of one of the carboxylate groups, the relaxivities of Gd(4MP-DTTA) were slightly higher (1.2–1.3-fold) than those of Gd(1MP-DTTA) at both fields. The slight difference in relaxivities between Gd(4MP-DTTA) and Gd(1MP-DTTA) may be related to the differences in the distance between lipophilic and metal-binding moieties in both complexes. Thus, in Gd(4MP-DTTA) the water molecules may have easier access to the hydration sphere of the Gd^{3+} ion, yielding slightly higher relaxivities. This easier access may

be due to a longer distance between the lipophilic and the metal-binding moieties compared with the distance in Gd(1MP-DTTA). Alternatively, the higher relaxivity of the 4MP-DTTA complex versus that of 1MP-DTTA may be the result of the possibility that moving the covalent attachment between the chelating group and the fatty acyl group from the terminal carboxyl group of DTTA to the central carboxyl improves relaxivity. If this were the case generally, DTPA-type, macromolecule-conjugated contrast agents could also gain improved relaxivity if the central, rather than a terminal, carboxyl of the chelating group were used for conjugation.

The relaxivities of the Gd complexes of ligands such as 4MPD-DTTA, MHE-DTTA (12), and BME-DTTA (12) increased by about 43% from 0.23 to 0.47 T. However, the relaxivities of Gd(1MP-DTTA) and (4MP-DTTA) showed only about 23% increase from the lower to the higher field. This observation suggests that the relaxivities of the gadolinium complexes of carbonyl-bearing ligands may be more τ_c -dependent at high field, owing to the larger molecular weight (see Table I) of these ligands, compared with those of 1MP-DTTA and 4MP-DTTA, resulting in a slower molecular tumbling of the Gd complexes of 4MPD-DTTA, MHE-DTTA, and BME-DTTA.

The relaxivity depends on the number of water molecules in the first coordination sphere of the metal ion and the weighted average of the intrinsic relaxation rates ($1/T_{1M}$) of the protons of these water molecules. The dependence of $1/T_{1M}$ on molecular and NMR parameters is governed by the Solomon-Bloembergen equation (17, 18) as shown in eq 1, where C is a constant composed of nuclear

$$\frac{1}{T_{1M}} = \frac{C}{r^6} \left(\frac{3\tau_c}{1 + \omega_i^2 \tau_c^2} + \frac{7\tau_c}{1 + \omega_s^2 \tau_c^2} \right) \quad (1)$$

parameters pertaining to protons and the gadolinium ion; ω_i and ω_s are the proton and electron Larmor frequency, respectively. The effective correlation time of the complex, τ_c , is given in eq 2, where τ_R , τ_s , and τ_M are the rotational

$$\frac{1}{\tau_c} = \frac{1}{\tau_R} + \frac{1}{\tau_s} + \frac{1}{\tau_M} \quad (2)$$

reorientation time, the longitudinal electron-spin relaxation time (T_{1e}), and the lifetime of a water molecule in the hydration sphere of the gadolinium ion, respectively. The lifetime, τ_M , of water of hydration on lanthanide ions has been determined (25), and for Gd^{3+} it is 0.94 ns, somewhat longer than either τ_R (0.05–0.1 ns for small molecular weight complexes) or τ_s (0.04–0.1 ns at low magnetic fields). Therefore, the third term in eq 2 is small in comparison to the other two, and usually is neglected. In most small molecular size gadolinium complexes $\tau_R < \tau_s$, and thus τ_R largely determines the overall τ_c . As a result, the gadolinium aquoion, Gd(DTPA), Gd(EDTA), and most other small molecular weight contrast agents possess a negative field dependence displaying a sharp decrease of relaxivity from a higher to a significantly lower plateau with an inflection point around 0.2 T. This inflection results from the dispersive effect (19) of the second Lorentzian term in eq 1, and it occurs at the magnetic field that corresponds to the electron Larmor frequency given by $\omega_s = 1/\tau_c$. In practice, this means a reduced efficacy of such agents when used in conjunction with most NMR imagers of higher magnetic fields (1–4 T) that are expected to be in current and future use. Obviously, for such fields, contrast agents that possess a positive field dependence would be desirable. A positive field dependence would

Table II. Stability Constants,^a Relaxivities,^a and Toxicity^b of Gd Complexes in a Buffer of 20 mM HEPES in 0.9% Saline^c

	log <i>k</i>	ρ_1 (0.47 T)	dosage ^d	animals ^e	LD ₅₀ ^d
Gd(1MP-DTTA)	18.2 ± 0.2	18.4 ± 0.6	0.3	2/7	>0.3
Gd(4MP-DTTA)	18.4 ± 0.2	24.4 ± 0.7	0.3	1/7	>0.3
Gd(4MPD-DTTA)	15.7 ± 0.8	36.4 ± 3.6	0.3	1/7	>0.3

^a The stability constants and relaxivities presented in this table were simultaneously obtained in competition experiments between ligand and EDTA (mean ± 95% confidence intervals). ^b Due to limited solubility, only a lower limit is given. ^c pH 7.4. ^d Dosage, in mmol/kg of body weight, in toxicity experiments. ^e Mortality/total no.

consist of an increase in relaxivity, to a higher plateau as the magnetic field strength is increased above the inflection point. The relaxivity values at the two magnetic fields of the agents reported here seem to indicate such a desirable positive field dependence for these agents.

On the basis of the above theory, the observed positive field dependence of the relaxivities of the Gd complexes of all DTTA-type compounds (see Table I) may be ascribed to the increased size of the complexes resulting in increased τ_R values. This would make the relaxivity of these complexes more τ_s -dependent. The electron relaxation rate, $1/T_{1e}$, itself displays a negative field dependence because of considerations similar to those described above for proton relaxivities. Since τ_s is T_{1e} , a strong dependence of the overall correlation time on τ_s would result in an inverted, positive profile for the proton relaxivity in the 0.1–4 T range. It is worth noting that because of the dispersion of τ_s itself, a sharp decrease of relaxivity is expected above 4 T. Thus, also the somewhat more pronounced positive field dependence of the complexes of the three carbonyl-bearing ligands, 4MPD-DTTA, MHE-DTTA, and BME-DTTA, compared with those of 1MP-DTTA and 4MP-DTTA, may be the result of the larger molecular weights of the former complexes.

Comparing the relaxivities among the three Gd complexes of carbonyl-bearing ligands at 0.23 and 0.47 T showed the largest relaxivities for Gd(4MPD-DTTA) at both fields. This may be explained by the differences among the three complexes in the extent of metal coordination by nitrogen atoms. Thus, 4MPD-DTTA has one less nitrogen than either MHE-DTTA or BME-DTTA, possibly resulting in an increased number of water molecules in the hydration sphere of the Gd³⁺ ion, leading to increased relaxivities.

Stability Constants and Toxicity. The stability constants of Gd(1MP-DTTA), Gd(4MP-DTTA), and Gd(4MPD-DTTA) were determined by competitive equilibrium between Gd(ligand) and Gd(EDTA), measuring water proton relaxivity as a function of [ligand]/[EDTA] (20). On the basis of the known stability constant (log *K* = 17.3) of Gd(EDTA) (21), the log *K* values of Gd(1MP-DTTA), Gd(4MP-DTTA), and Gd(4MPD-DTTA) were calculated to be 18.2 ± 0.2, 18.4 ± 0.2, and 15.7 ± 0.8, respectively (see Table II). The Gd complexes of 1MP-DTTA and 4MP-DTTA display 1 log unit higher stabilities than that of Gd(EDTA). However, the Gd complex of the ligand 4MPD-DTTA was less stable than that of EDTA. These results are probably due to higher coordination numbers in 1MP-DTTA and 4MP-DTTA, and a lower coordination number in 4MPD-DTTA, compared with that of EDTA.

The relaxivities at 0.47 T of these three complexes were redetermined by the competitive equilibrium method, simultaneously with the determination of the stability constants. The resulting relaxivities are also compiled in Table II and are similar, within experimental error, to those determined separately and shown in Table I. Consistent with the effect of the carbonyl groups in

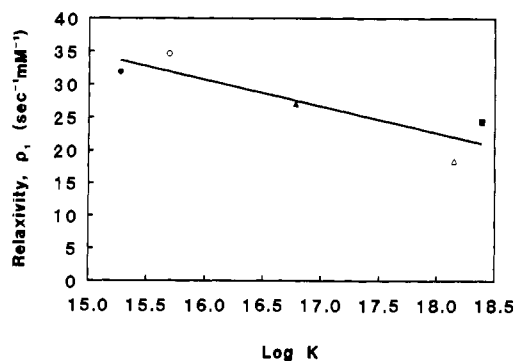


Figure 4. Relaxivities (ρ_1) at 0.47 T versus stability constants (log *K*) of the Gd complex of 1MP-DTTA (opened triangle), 4MP-DTTA (filled square), 4MPD-DTTA (opened circle), MHE-DTTA (filled circle), and BME-DTTA (filled triangle). The straight line was obtained by a linear least-squares method for fitting a line to data points ($R^2 > 0.77$).

Gd(4MPD-DTTA) on the relaxivity due to the reduction of the ligand coordination, the larger relaxivity of Gd(4MPD-DTTA), compared with those of Gd(1MP-DTTA) and Gd(4MP-DTTA), correlates well with the somewhat lower stability constant of Gd(4MPD-DTTA) compared with those of Gd(1MP-DTTA) and Gd(4MP-DTTA) (see Figure 4). Thus, stability constants and relaxivities seem to be inversely related among the gadolinium complexes of this family of DTTA-type ligands.

The LD₅₀ of these three Gd complexes in rat was >0.3 mmol/kg (iv). Specific LD₅₀ could not be determined due to an upper concentration limit for liposome-incorporated Gd complexes 5, 10, and 14 and due to limitations in total volume of bolus to be administered. Nevertheless, a lower limit for LD₅₀ of these three agents was obtained (see Table II). As we expected, based on the relative similarity of their stability constants, the toxicities of Gd(1MP-DTTA), Gd(4MP-DTTA), and Gd(4MPD-DTTA) displayed similar lower limits of LD₅₀ values.

CONCLUSIONS

The new lipophilic bifunctional contrast agents, Gd(1MP-DTTA), Gd(4MP-DTTA), and Gd(4MPD-DTTA), showed relatively low toxicity, good stability, high relaxivity, and a positive field profile. These characteristics suggest potential usefulness for NMR imaging at high magnetic fields. Also, we have shown that certain structural properties of ligands, such as functional groups that modify the coordination number and molecular weight, may have effects on relaxivity, on the field profile of relaxivity, and on the stability constant, in a correlated manner that can be utilized in the design of future contrast agents.

ACKNOWLEDGMENT

We gratefully acknowledge the help of Dr. Katharine A. Kirk with the statistical analyses in the determination of the stability constants.

LITERATURE CITED

- Weinmann, H. J., Brasch, R. C., Press, W. R., and Wesbey, G. E. (1984) Characteristics of gadolinium-DTPA complex: A potential NMR contrast agent. *Am. J. Roentgenol.* 142, 619–624.
- McNamara, M. T., Higgins, C. B., Ehman, R. L., Revel, D., Sievers, R., and Brasch, R. C. (1984) Acute myocardial ischemia: Magnetic resonance contrast enhancement with gadolinium-DTPA. *Radiology* 153, 157–163.

- (3) Johnston, D. L., Liu, P., Lauffer, R. B., Newell, J. B., Wedeen, V. J., Rosen, B. R., Brady, T. J., and Okada, R. D. (1987) Use of gadolinium-DTPA as a myocardial perfusion agent: Potential applications and limitations for magnetic resonance imaging. *J. Nucl. Med.* 28, 871-877.
- (4) Lauffer, R. B., and Brady, T. J. (1985) Preparation and water relaxation properties of proteins labelled with paramagnetic metal chelates. *Magn. Reson. Imaging* 3, 11-16.
- (5) Schmiedl, U., Ogan, M. D., Moseley, M. E., and Brasch, R. C. (1986) Comparison of the contrast-enhancing properties of albumin-(Gd-DTPA) and Gd-DTPA at 2.0T: An experimental study in rats. *Am. J. Roentgenol.* 147, 1263-1270.
- (6) Shreve, P., and Aisen, A. M. (1986) Monoclonal antibodies labeled with polymeric paramagnetic ion chelates. *Magn. Reson. Med.* 3, 336-340.
- (7) Gibby, W. A., Bogdam, A., and Ovitt, T. W. (1989) Cross-linked DTPA polysaccharides for magnetic resonance imaging: synthesis and relaxation properties. *Invest. Radiol.* 24, 302-309.
- (8) Kabalka, G. W., Buonocore, E., Hubner, K., Davis, M., and Huang, L. (1988) Gadolinium-labeled liposomes containing paramagnetic amphipathic agents: Targeted MRI contrast agents for the liver. *Magn. Reson. Med.* 8, 89-95.
- (9) Grant, C. W. M., Karlik, S., and Florio, E. (1989) A liposomal MRI contrast agent: Phosphatidylethanolamine-DTPA. *Magn. Reson. Med.* 11, 236-243.
- (10) Magin, R. L., Wright, S. M., Niesman, M. R., Chan, H. C., and Swartz, H. M. (1986) Liposome delivery of NMR contrast agents for improved tissue imaging. *Magn. Reson. Med.* 3, 440-447.
- (11) Vion-Dury, J., Masson, S., Devoisselle, J. M., Sciaky, M., Desmoulin, F., Confort-Gouny, S., Coustaut, D., and Cozzzone, P. J. (1989) Liposome-mediated delivery of gadolinium-diethylenetriaminopentaacetic acid to hepatic cells: A P-31 NMR study. *J. Pharmacol. Exp. Ther.* 250, 1113-1118.
- (12) Kim, S. K., Pohost, G. M., and Elgavish, G. A. (1991) Fatty-acyl iminopolycarboxylates: Lipophilic bifunctional contrast agents for NMR imaging. *Magn. Reson. Med.* 22, 57-67.
- (13) Timakova, L. M., Rusina, M. N., Yaroshenko, G. F., and Temkina, V. Y. (1977) Synthesis and complex-forming properties of *N*-(2-hydroxyethyl)-diethylenetriamine-*N,N',N'',N'''*-tetraacetic Acid. *Zh. Obsh. Khim.* 47, 691-694.
- (14) Anantharamaiah, G. M., and Sivamandaiah, K. M. (1977) Transfer hydrogenation: a convenient method for removal of some commonly used protecting groups in peptide synthesis. *J. Chem. Soc. Perkin Trans. 1* 490-491.
- (15) Lauffer, R. B., Brady, T. J., Brown, R. D., Baglin, C., and Koenig, S. H. (1986) $1/T_1$ NMRD profiles of solution of Mn^{2+} and Gd^{3+} protein-chelate conjugates. *Magn. Reson. Med.* 3, 541-548.
- (16) Ogan, M. D., Schmiedl, U., Moseley, M. E., Grodd, W., Paa-janen, H., and Brasch, R. C. (1987) Albumin labeled with Gd-DTPA an intravascular contrast-enhancing agent for magnetic resonance blood pool imaging: preparation and characterization. *Invest. Radiol.* 22, 665-671.
- (17) Solomon, I. (1955) Relaxation processes in a system of two spins. *Phys. Rev.* 99, 559-565.
- (18) Bloembergen, N. (1957) Proton relaxation times in paramagnetic solutions. *J. Chem. Phys.* 27, 572-573.
- (19) Koenig, S. H., Baglin, C., and Brown, R. D. (1984) Magnetic field dependence of solvent proton relaxation induced by Gd^{3+} and Mn^{2+} complexes. *Magn. Reson. Med.* 1, 496-501.
- (20) Kim, S. K., Pohost, G. M., and Elgavish, G. A. *Magn. Reson. Med.* Submitted.
- (21) Martell, A. E., and Smith, R. M. (1974) *Critical Stability Constants*, Vol. 1, Plenum, New York.
- (22) Korbl, J., and Pribil, R. (1956) New indicator for the EDTA titration. *Chemist-Analyst* 45, 102-103.
- (23) Brown, M. A., and Johnson, G. A. (1984) Transition metal-chelate complexes as relaxation modifiers in nuclear magnetic resonance. *Med. Phys.* 11, 67-72.
- (24) Weinman, H. J., and Gries, H. (1984) Paramagnetic contrast media in NMR tomography: Basic properties and experimental studies in animals. *Magn. Reson. Med.* 1, 271-272.
- (25) Cossy, C., Helm, L., and Merbach, A. E. (1988) Oxygen-17 nuclear magnetic resonance kinetic study of water exchange on the lanthanide(III) aqua ions. *Inorg. Chem.* 27, 1973-1979.

Registry No. 1, 111-40-0; 2, 118633-37-7; 3, 137203-69-1; 4, 137203-70-4; 5, 137203-71-5; 6, 156-87-6; 7, 137203-72-6; 8, 137203-73-7; 9, 137259-43-9; 10, 137203-74-8; 11, 137259-44-0; 12, 137203-75-9; 13, 137259-45-1; 14, 137203-76-0; $HOCH_2CH_2CH_2Cl$, 627-30-5; $CH_3(CH_2)_{12}COCl$, 112-64-1; ICH_2CONH_2 , 144-48-9; $BrCH_2COOCH_2Ph$, 5437-45-6.

Nuclear Magnetic Spin-Lattice Relaxation of Water Protons Caused by Metal Cage Compounds

Lidia S. Szczepaniak,[†] Alan Sargeson,[‡] I. I. Creasey,[‡] R. J. Geue,[‡] Michael Tweedle,[§] and Robert G. Bryant^{*,†,||}

Department of Biophysics, University of Rochester Medical Center, Rochester, New York 14642, Department of Chemistry, University of Rochester, Rochester, New York 14523, Research School of Chemistry, Australian National University, P.O. Box 4, Canberra, A.C.T. 2600, Australia, and Bristol-Meyers Squibb Pharmaceutical Research Institute, P.O. Box 191, New Brunswick, New Jersey 08903-0191. Received May 3, 1991

The nuclear magnetic spin-lattice relaxation rates of water protons are reported for solutions of manganese(II), copper(II), and chromium(III) cage complexes of the sarcophagine type. As simple aqueous solutions, the complexes are only modest magnetic relaxation agents, presumably because they lack protons on atoms in the first-coordination-sphere protons that are sufficiently labile to mix the large relaxation rate at the metal complex with that of the bulk solvent. The relaxation is approximately modeled using spectral density functions derived for translational diffusion of the interacting dipole moments with the modification that the electron spin relaxation rate is directly included as a contribution to the correlation time. In all cases studied, the electron spin relaxation rate is sufficiently large that it contributes directly to the water-proton spin relaxation process. The poor relaxation efficiency of the cage compound may, however, be improved dramatically by binding the complex to a protein. The efficiency is improved even further if the rotational motion of the protein is reduced drastically by an intermolecular cross-linking reaction. The relaxation efficiency of the cross-linked protein-cage complexes rivals that of the best first-coordination-sphere relaxation agents like $[\text{Gd}(\text{DTPA})(\text{H}_2\text{O})]^{2-}$ and $[\text{Gd}(\text{DOTA})(\text{H}_2\text{O})]^-$.

The development of magnetic resonance imaging as a routine clinical diagnostic procedure drives the exploration of methods for controlling water-proton nuclear magnetic relaxation rates because they determine, in very large measure, the contrast in a magnetic resonance image (1). We focus here on methods for controlling spin-lattice relaxation rates using transition metal complexes that are paramagnetic. The approaches used to date have emphasized metal complexes with high metal-ligand affinity, but which leave one or more metal coordination positions open for the rapid exchange of water molecules (2, 3). The rapid nuclear spin relaxation of the protons when water is coordinated in the complex is carried to the bulk solvent by the chemical exchange of the coordinated water with the bulk solvent. Thus, nonlabile first-coordination-sphere protons make little contribution to the net observed relaxation (4). We have shown previously that amine ligand systems are generally not sufficiently labile, except for the more labile ammonia and ethylenediamine complexes of copper(II), to provide significant first-coordination-sphere relaxation in water protons. The observed water-proton relaxation in complexes like (triethylenetetramine)copper(II) solutions is caused by through-space electron-nuclear dipole-dipole coupling often referred to as outer-sphere relaxation (5). Although the relaxation efficiency of such complexes is modest, the kinetic and thermodynamic benefits of minimizing toxic effects by completely encapsulating the metal ion appear to be significant. We report here an examination of such molecules and find, in some cases, surprising potential for effective relaxation.

The cage molecule of interest is shown in Figure 1. All six secondary N atoms bind to the metal ions to give complexes with average D_3 symmetry. The transition

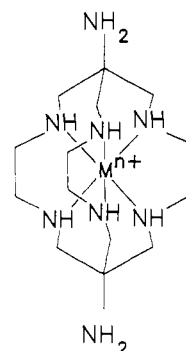


Figure 1. The structure of the metal complexes studied.

metal ion complexes are particularly stable thermodynamically and are kinetically inert with respect to dissociation of the metal ion. Tracer studies have shown that Co^{3+} , Co^{2+} , Cu^{2+} , and Mn^{2+} do not escape the cage in 24 h in vitro. To date, these molecules as ligands or even as tripositively charged ions are not toxic other than at high concentrations (>100 mg/kg), where they show a mild cholinesterase inhibition (6). In situations where $\text{Co}(\text{III})$ complexes have been administered orally or intraperitoneally to rats, the animals did not appear stressed and the ^{57}Co was eliminated essentially quantitatively in the feces and urine, respectively (7). So far it does not appear that the animal systems or bacteria, fungi, or molds have the capability of removing the metal ion from the cage, and therefore, the usual metal ion toxicology in liver and kidneys is not evident. These complexes simply filter readily through the kidney tubules and are eliminated in the urine unaltered. All six coordination positions are taken by the nitrogen atoms of the macrobicyclic ligand. There is no evidence yet that water can also bind the metal ion in the cage. In fact, the ligand fits around the metal ion so tightly that the prospect of increasing the coordination number to seven seems extremely unlikely. The strain thereby induced would be prohibitive. In situations

[†] University of Rochester Medical Center.

[‡] Australian National University.

[§] Bristol-Meyers Squibb Pharmaceutical Research Institute.

^{||} Department of Chemistry, University of Rochester.

where there is evidence of another ligand bound to the metal ion, one strand of the ligand has dissociated and the metal ion has moved into a square planar macrocyclic configuration (14). These processes, along with nitrogen-proton exchange rates, all appear too slow ($<10^5 \text{ s}^{-1}$) to make a significant contribution to the water-proton relaxation rate, a conclusion supported by earlier reports (5, 8).

EXPERIMENTAL PROCEDURES

The nuclear magnetic relaxation rates were measured over a range of magnetic field strengths corresponding to proton Larmor frequencies between 0.01 and 30 MHz using a field-cycling spectrometer described elsewhere (9, 10). This instrument switches the current in a copper solenoidal magnet to vary the field according to a program that initially polarizes the spins at a high field and then switches to the magnetic field of interest (measure field) for a variable delay time, after which it switches to a resonance field corresponding to a proton Larmor frequency of 7.25 MHz, where the remaining magnetization is measured by numerically integrating a spin echo or a free induction decay. Samples are contained in Pyrex test tubes sealed with both a rubber stopper and a Teflon screw cap. The sample chamber of the magnet system is bathed in recirculating perchloroethylene that is thermostated using a Neslab RTE-8 temperature controller. Typically 32 points are taken on the magnetization decay curve and fitted to a single exponential using software developed in this laboratory by Dr. Cathy C. Lester (11). The magnetic relaxation dispersion plots are generated by changing the measure field over the range of interest.

The synthesis of the cage molecules has been described in detail (12–14). Bovine serum albumin (Sigma Chemical Co.) was dialyzed and lyophilized to eliminate preparative salts. Aqueous solutions of the metal complexes were made by weight, and optical absorbance was measured on an Hewlett-Packard Model 8451A diode-array spectrophotometer. Protein solutions were cross-linked using a glutaraldehyde reaction with the cross-linking agent in approximately 100-fold excess over the molar concentration of protein. The excess cross-linking reagent was not removed from the sample. Since the agent cross-links amines, the capping groups of the metal complex will be conjugated to the protein by cross-linking reagent because the protein-cage complex was treated with cross-linking agent. The affinity of the metal complex for binding to the protein is very high (27) and involves a number of binding sites. Equilibrium dialysis experiments demonstrate that there are in excess of 30 binding sites with individual binding constants of approximately 2200 M^{-1} , assuming equivalent sites. Therefore, under the conditions of the magnetic relaxation experiment, there is an insignificant concentration of unbound metal complex.

RESULTS AND DISCUSSION

The water-proton nuclear spin-lattice relaxation rate is shown as a function of magnetic field strength plotted as proton Larmor frequency in Figure 2 for manganese, chromium(III), and copper(II) complexes at 298 and 279 K. In all cases the paramagnetic contributions to the relaxation rates are small, which is expected for complexes without labile first-coordination-sphere protons close to the metal. The inefficiency of the proton relaxation permits an estimate of a lower bound for the proton lifetime in ligand nitrogen atom bonds of about 10^{-5} s . This slow exchange rate is consistent with amines in general as well as with other metal complexes (6). The protons on the capping nitrogen atoms are more labile; however, these

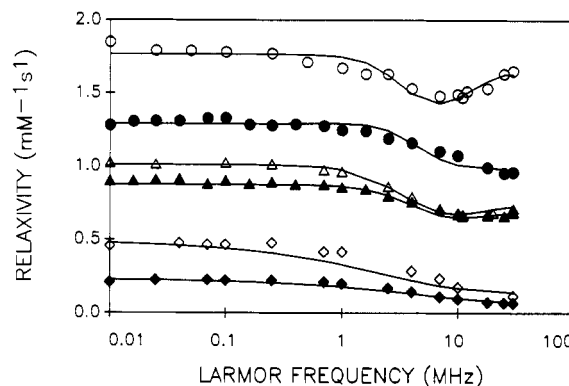


Figure 2. The water-proton nuclear magnetic spin-lattice relaxation rates as a function of the magnetic field strength plotted as the proton Larmor frequency for manganese (O, ●), chromium(III) (Δ, ▲), and copper(II) (◇, ◆) cage complexes. The filled symbols are for 298 K and the open symbols are for 279 K. The pH of all solutions was between 7.0 and 7.2. The ordinate is the relaxation rate for a 1.00 mM solution of the complex also called the relaxivity. The solid lines were computed using the outer-sphere relaxation equation presented by Freed (19) and the parameters summarized in Table I.

protons are much further away from the metal center. Therefore, based on the increased distance, relaxation at these sites should be less efficient by a factor of approximately 40. Thus, we conclude that the water-proton relaxation is dominated by the metal-water-proton dipole-dipole coupling modulated by the translational motion of the water and the complex. That is, relaxation derives from outer-sphere effects.

Outer-sphere relaxation has been treated by Pfeifer (15, 16), Hubbard (17), and Freed (18, 19) and discussed in the context of metal ion outer-sphere relaxation elsewhere (4). We use the development of Freed

$$1/T_1 = (32\pi/405)\gamma_I^2\gamma_S^2\hbar^2 S(S+1)(N_a/1000)([S]/bD) \times \{j_2(\omega_S - \omega_I) + 3j_1(\omega_I) + 6j_2(\omega_S + \omega_I)\} \quad (1)$$

with the spectral density function $j_k(\omega)$:

$$j_k(\omega) = \text{Re}\{(1 + s/4)/(1 + s + 4s^2/9 + s^3/9)\} \quad (2)$$

$$s = b\{i\omega + (T_k^S)^{-1}/D\}^{1/2} \quad (3)$$

where

$$1/T_{1S} = B[\tau_v/(1 + \omega^2\tau_v^2) + 4\tau_v/(1 + 4\tau_v^2\omega^2)] \quad (4)$$

$$1/T_{2S} = B/2[3\tau_v + 5\tau_v/(1 + \tau_v^2\omega^2) + 2\tau_v/(1 + 4\tau_v^2\omega^2)] \quad (5)$$

where γ_I and γ_S are the proton and electron magnetogyric ratios respectively, ω_I and ω_S are the nuclear and the electron Larmor frequencies, \hbar is Planck's constant divided by 2π , S is the electron spin, the square brackets indicate molar concentration, N_a is Avogadro's number, b is the distance of closest approach between the centers of the interacting magnetic moments, and D is the relative translational diffusion constant, i.e., the sum of the water and cage complex diffusion constants. If the magnetic field dependence of electron spin relaxation is neglected, poor fits to the data are achieved; however, when the effects of the electron spin relaxation are included approximately by assuming an elementary relaxation equation for the field dependence of the electron relaxation rate (19, 20), the solid curves through the data are obtained with the parameters listed in Table I.

Table I. Relaxation Parameters

metal ion	temp, K	$b \times 10^8$, cm	$D \times 10^5$, cm ² s ⁻¹	$\tau_v \times 10^{11}$, s	$B \times 10^{-19}$, s ⁻²	$\tau_d \times 10^{10}$, s	$\tau_e \times 10^{10}$, s
Mn	279	6	0.83	5.2	3.5	4.4	1.14
Mn	298	6	1.5	5.3	3.4	2.4	1.10
Cr	279	5.3	0.91	3.4	4.4	3.1	1.36
Cr	298	5.3	1	4	4.5	2.8	1.10
Cu	279	5.1	1.2			1.3	
Cu	298	5.1	2.6			0.9	
MnBSA	279	6.25	0.5	27.4	0.1	7.8	7.3
MnBSA	298	6.25	1.0	22.8	0.11	3.9	8.0

Copper(II) complexes are among the simplest magnetically because of the single unpaired electron and the generally long electron spin relaxation times. Thus, copper serves as a reasonable standard against which the other complexes may be compared. The relaxation rates of both chromium and manganese complexes are higher as expected because of their larger magnetic moments. However, the metal magnetic moment is proportional to $S(S + 1)$. If other contributions are equal, the ratio of the relaxation rates should be 3:15:35 for Cu:Cr:Mn. It is clear from the magnitudes of the low field relaxation rates shown in Figure 2 that the relaxation rates are not simply proportional to the size of the electron magnetic moment. Limitations in the effective correlation time for the electron-nuclear coupling provided by a short electron relaxation rate are consistent with this observation.

The increase in the proton relaxation rate for the manganese complex at high field provides a clear signal that the electron relaxation time, which is field dependent and increases with increasing magnetic field, makes a contribution to the correlation time for the electron-nuclear coupling. This is a common observation for chromium complexes, but is less common for manganese(II) complexes of high symmetry. This observation derives from some oxidation of the manganese(II) to the manganese(III) complex, as will be demonstrated later. The near temperature independence of the chromium-induced water-proton relaxation rate is interesting in that the solution dynamical properties such as viscosity change by approximately a factor of 2 over this range. This behavior may be caused by compensating changes in the contributions to the correlation time, i.e., the translational correlation time and the electron spin relaxation time. This situation could also result if the electron spin relaxation time was independent of temperature and dominated the correlation time.

The manganese data require further comment. The complex prepared is the manganese(II) complex; however, it oxidizes in air readily to a yellow manganese(III) complex. Similar changes are found with manganese porphyrins, where the manganese(III) complex also has a dominant contribution to the relaxation efficiency from the limiting behavior of the electron relaxation time (21, 22). The oxidation problem may be avoided by two strategies: preparation and handling in oxygen-free solutions and reduction by dithionite. The magnetic relaxation profile for the uncontaminated manganese(II) complex is different from that of Figure 2, as shown in Figure 3. The relaxation rates for the manganese(II) complex are higher than those for the manganese(III) or perhaps a mixture of the two, and the relaxation rates at high field do not increase, but provide a relaxation profile that is more classically diffusional in shape. To avoid difficulties, we have worked in either a nitrogen atmosphere or in the presence of a 5-fold excess of dithionite to reduce any manganese(III) formed. We note that use of a 100-fold excess of dithionite leads to a dependence of the solution relaxation rate at long times that we do not understand.

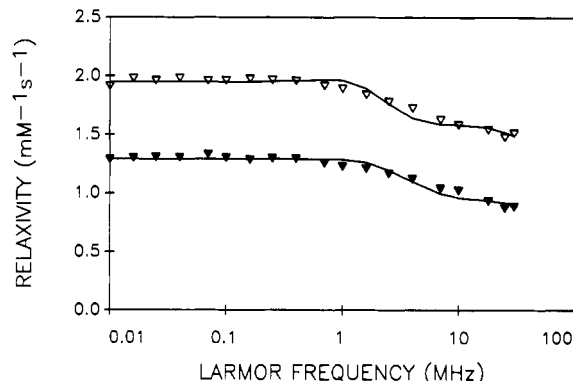


Figure 3. The water-proton nuclear magnetic spin-lattice relaxation rate as a function of the magnetic field strength plotted as the proton Larmor frequency for manganese(II) cage at pH 6.9 and (▽) 279 K and (▼) 298 K.

In summary, the relaxation induced by all three metal complexes may be described by an outer-sphere mechanism. The electron relaxation parameters are estimated from the fits of the data to the theory; however, we point out that these parameters are just that, and while it is clear that electron relaxation times make a crucial contribution to the nuclear relaxation rates, the model used for the electron relaxation rate is the most elementary. Modeling the electron relaxation problem more accurately is difficult; however, successful attempts have been made in some cases (20). The result is to add significantly to the parameter set needed to characterize the data, which in the present case is already accommodated reasonably well by the assumptions of the crude model. Therefore, we have stopped with the present model, but underscore the caution that the entries to Table I are approximations to the electron relaxation rates at best.

The distance of closest approach deduced from the data for the different complexes is on the order of 5–6 Å, which appears to be consistent with the structural chemistry of the encapsulated metals (13). The relative translational diffusion constant, which is the sum of the diffusional motion of the water and the complex, is also not far from that of the bulk water, which is consistent with other work on outer-sphere relaxation induced by metal complexes that provide no first-coordination-sphere positions.

The relaxation efficiency of metal complexes generally changes with change in the size of the complex because the relaxation rate is proportional, within certain limits, to the correlation times for rotation and translation. In the present cases, the translational correlation time for the complex may be changed by binding the macrocyclic system to a protein. We expect that the relaxation rate should change little because the correlation time for the electron-nuclear coupling should be dominated by the highly mobile water translational motion. The data in Figure 4 demonstrate that more than a 2-fold increase in paramagnetic relaxation rate is obtained if the manganese cage complex is measured in an equimolar solution of serum albumin. This increase may arise from the slower diffu-

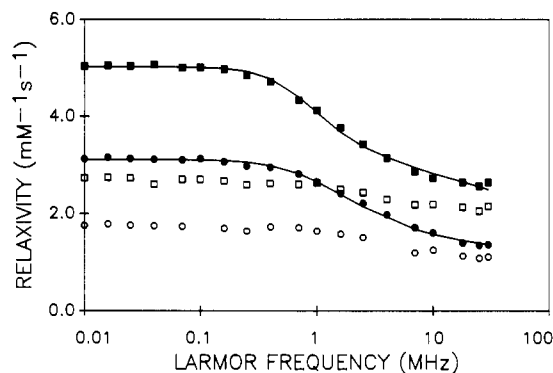


Figure 4. The water-proton nuclear magnetic spin-lattice relaxation rates as a function of the magnetic field strength plotted as the proton Larmor frequency for aqueous solutions of bovine serum albumin and the manganese(II) cage complex each at 1.0 mM and pH 7: (●) the full relaxation rate at 298 K and (○) the paramagnetic contribution at 298 K, (■) the full relaxation rate at 279 K and (□) the paramagnetic contribution at 279 K. The solid lines were computed using the outer-sphere model of Freed (19) and the parameters summarized in Table I.

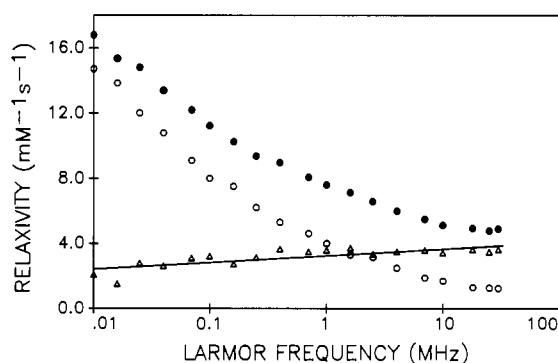


Figure 5. The water-proton nuclear magnetic spin-lattice relaxation rates as a function of the magnetic field strength plotted as the proton Larmor frequency at pH 7 and 281 K: (○) 1.0 mM aqueous cross-linked serum albumin, (●) 1.0 mM serum albumin and 1.0 mM manganese(II) cage complex cross-linked with glutaraldehyde, (Δ) the paramagnetic contribution obtained by subtracting the diamagnetic rate from the full relaxation rate. The solid line is a linear least squares fit through the paramagnetic contribution.

sional motion of water at the protein surface to which the complex is bound (23).

An important change in the character of the system dynamics occurs when the protein rotational motion is stopped. In the present experiments we accomplish this with a glutaraldehyde cross-linking reaction (24). As previously reported (25, 26), the proton relaxation in the protein system changes profoundly as a consequence of this dynamical change because the proton-proton dipole-dipole couplings are no longer averaged by the bulk rotational motion of the molecule. The consequence is efficient spin-spin coupling within the protein matrix and rapid equilibration of the protein spin system with itself. This situation provides several crucial consequences discussed elsewhere (25, 26) that include complex water-proton relaxation behavior, and amplification of paramagnetic effects by the protein proton matrix and its interactions with water.

Figure 5 shows data obtained on cross-linked bovine serum albumin samples at 281 K in the presence and absence of the manganese cage complex. The metal-free relaxation dispersion curve has been discussed elsewhere (11). The addition of the manganese complex causes an enhanced relaxation rate at all magnetic fields studied. Further, the paramagnetic contribution increases with

increasing magnetic field strength. If the metal complex did not bind to the protein matrix, the metal-induced relaxation would add a relaxation contribution similar to that shown in Figure 3 and the relaxation efficiency at high magnetic fields would be lower relative to the diamagnetic sample rather than higher. We therefore conclude that the complex binds to the protein matrix. That the paramagnetic contribution is greater at higher magnetic fields than at lower magnetic fields is strong evidence that the electron relaxation time makes a significant contribution to the correlation time for the electron-nuclear coupling as in the solution data of Figure 2. As in the protein solution case, the relaxation efficiency of the metal complex will be compromised if it is not all bound to the protein matrix. If there is rapid equilibrium between bound and free environments for the manganese complex, the observed relaxation properties should represent a superposition of the proton relaxation induced by each environment because the chemical exchange is unlikely to be fast enough to provide an exchange-averaged electron relaxation spin relaxation rate. Nevertheless, the data of Figure 5 imply a lower limit for the relaxation efficiency of the manganese complex in association with a rotationally immobilized protein matrix which places such complexes in a competitive range with other soluble first-coordination-sphere agents.

LITERATURE CITED

- (1) Morris, P. G. (1986) *Nuclear Magnetic Resonance Imaging in Medicine and Biology*, Clarendon Press, Oxford.
- (2) Lauffer, R. B. (1987) Paramagnetic metal complexes as water proton relaxation agents for NMR imaging. *Chem. Rev.* 87, 901.
- (3) Koenig, S. H., and Brown, R. D., III, (1984) Relaxation of solvent protons by paramagnetic ions and its dependence on magnetic field and chemical environment: Implications for NMR imaging. *Magn. Reson. Med.* 1, 478.
- (4) Lester, C. C., and Bryant, R. G. (1990) Outer coordination sphere: Characterization by nuclear magnetic resonance dispersion. *J. Phys. Chem.* 94, 2843.
- (5) Szczepaniak, L. S., and Bryant, R. G. (1991) Proton nuclear magnetic relaxation in aqueous copper(II) amine chelate solutions. *Inorg. Chim. Acta*, 184, 7.
- (6) Koch, J. H., Gyrfas, E. C., and Dwyer, F. P. (1956) Biological activity of complex ions. Mechanism of inhibition of acetylcholinesterase. *Aust. J. Biol. Sci.* 9, 371.
- (7) Behm, C. A., Creaser, I. I., Maddalera, D. Snowden, G., and Sargeson, A. M., unpublished results.
- (8) Basolo, F., and Pearson, R. G. (1967) *Mechanisms of Inorganic Reactions, A Study of Metal Complexes in Solution*, p 185, J. Wiley & Sons, New York.
- (9) Hernandez, G. H., Brittain, H. G., Tweedle, M. F., and Bryant, R. G. (1990) Nuclear magnetic relaxation in aqueous solutions of Gd(HEDTA) complex. *Inorg. Chem.* 29, 985.
- (10) Lester, C. C., and Bryant, R. G. Magnetically coupled paramagnetic relaxation agents. *Magn. Reson. Med.* In press.
- (11) Lester, C. C. (1990) Nuclear magnetic relaxation studies of water in paramagnetic and heterogeneous systems. Ph.D. Thesis, University of Rochester, Rochester, NY.
- (12) Comba, P., Sargeson, A. M., Engelhardt, L. M., Harrowfield, J. M., White, A. H., Horn, E., and Snow, M. R. (1985) Analysis of trigonal-prismatic and octahedral and preferences in hexamine cage complexes. *Inorg. Chem.* 24, 2325.
- (13) Comba, P., Creaser, I. I., Gahan, L. R., Harrowfield, J. M., Lawrence, G. A., Martin, L. L., Mau, A. W. H., Sargeson, A. M., Sasse, W. H. F., and Snow, M. R. (1986) Macrobicyclic chromium(III) hexamine complexes. *Inorg. Chem.* 25, 384.
- (14) Sargeson, A. M. (1986) Developments in the synthesis and reactivity of encapsulated metal ions. *Pure Appl. Chem.* 58, 1511 and references therein.
- (15) Pfeifer, H. (1961) *Ann. Phys. Leipzig* 8, 1.
- (16) Pfeifer, H. (1962) *Z. Naturforsch.* 17a, 279.

- (17) Hubbard, P. S. (1966) Theory of electron-nuclear-Overhauser effects in liquids containing free radicals. *Proc. R. Soc. London, Ser. A* 291, 537.
- (18) Hwang, L. P., and Freed, J. H. (1975) Dynamic effects of pair correlation functions on spin relaxation by translational diffusion in liquids. *J. Chem. Phys.* 63, 4017.
- (19) Freed, J. H. (1978) Dynamic effects of pair correlation functions on spin relaxation by translational diffusion in liquids: II. Finite jumps and independent T_1 processes. *J. Chem. Phys.* 68, 4034.
- (20) Bertini, I., and Luchinat, C. (1986) NMR of Paramagnetic Molecules in Biological Systems, p 71, Benjamin/Cummings, Menlo Park, CA.
- (21) Koenig, S. H., Brown, R. D., III, and Spiller, M. (1987) The anomalous relaxivity of Mn^{3+} (TPPS₄). *Magn. Reson. Med.* 4, 252.
- (22) Hernandez, G., and Bryant, R. G. (1991) Proton magnetic relaxation of Manganese(II) tetrakis(4-sulfophenyl)porphine ion in water. *Bioconjugate Chem.* 2, 394-397.
- (23) Polnaszek, C. F., and Bryant, R. G. (1984) Nitroxide radical induced solvent proton relaxation: Measurement of localized translational diffusion. *J. Chem. Phys.* 81, 4038.
- (24) Quioco, F. A., and Richards, F. M. (1966) The enzymic behavior of carboxypeptidase-A in the solid state. *Biochemistry* 5, 4062.
- (25) Lester, C. C., and Bryant, R. G. (1991) Water proton nuclear magnetic relaxation in heterogeneous systems: Hydrated lysozyme results. *Magn. Reson. Med.* 22, 143.
- (26) Lester, C. C., Mendelson, D., and Bryant, R. G. (1991) The magnetic field dependence of proton spin relaxation in tissues. *Magn. Reson. Med.* 21, 117.
- (27) Friedberg, F. (1975) Albumin as the major metal transport agent in blood. *FEBS Lett.* 59, 140.
- Registry No.** Manganese(2+), (3,6,10,13,16,19-hexaazabicyclo[6.6.6]eicosane-1,8-diamine- $N^3, N^6, N^{10}, N^{13}, N^{16}, N^{19}$)-, (OC-6-11)-, 96164-40-8; copper(2+), (3,6,10,13,16,19-hexaazabicyclo[6.6.6]eicosane-1,8-diamine- $N^3, N^6, N^{10}, N^{13}, N^{16}, N^{19}$)-, (OC-6-11)-, 96164-52-2; chromium(3+), (3,6,10,13,16,19-hexaazabicyclo[6.6.6]eicosane-1,8-diamine- $N^3, N^6, N^{10}, N^{13}, N^{16}, N^{19}$)-, (OC-6-11)-, 94090-55-8.

Preparation of Novel Cyclosporin A Derivatives

P. A. Paprica,[†] A. Margaritis,[‡] and N. O. Petersen^{*,†}

Department of Chemistry and Department of Chemical and Biochemical Engineering, University of Western Ontario, London, Ontario, Canada N6A 5B7. Received June 24, 1991

The hydroxyl group on the 2-*N*-methyl-*R*-((*E*)-2-butenyl)-4-methyl-L-threonine residue of cyclosporin A was protected by acetylation, then the double bond on the same amino acid residue was oxidatively cleaved using a periodate/permanganate reagent. The resultant derivative of cyclosporin A contained a carboxylic acid group which was subsequently reacted with the nucleophiles 5-(aminoacetamido)fluorescein and poly(L-lysine), in the presence of 1-ethyl-3-[3-(dimethylamino)propyl]carbodiimide, to furnish novel cyclosporin A conjugates.

INTRODUCTION

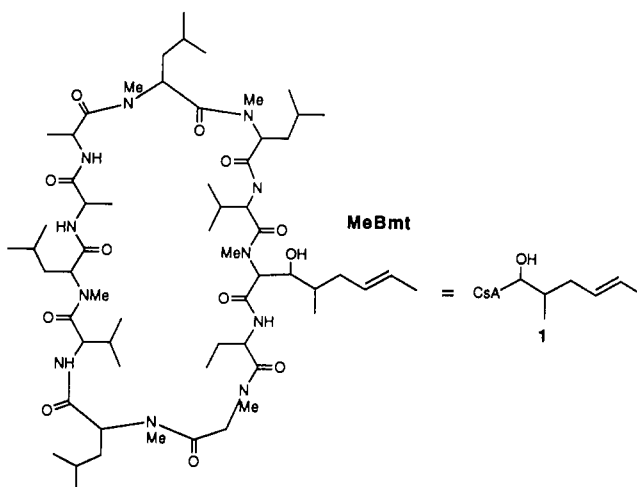
Cyclosporin A (CsA, 1) is a secondary metabolite produced by the fungus *Beauveria nivea* (1). CsA is an undecapeptide (Chart I, Schemes I and II) which is prescribed as an immunosuppressant to prevent rejection of transplanted organs in human patients (2, 3). Because of its wide prescription throughout North America and Europe, cyclosporin A research is widespread; however, few synthetic schemes for modification of cyclosporin A are known (4-8). Previously published schemes for modification of cyclosporin A involve in vivo amino acid substitution (4), total synthesis of CsA starting from tartaric acid (5-7), or a low-yield oxidation of CsA to a derivative which contains a reactive aldehyde moiety (8). In our laboratory we have prepared a novel cyclosporin A derivative in good yield and used this derivative to prepare conjugates for fluorescence and immunological studies. This report presents the syntheses of four new molecules synthesized from cyclosporin A (3, 8, 11b, 11c, Schemes II-IV).

EXPERIMENTAL PROCEDURES

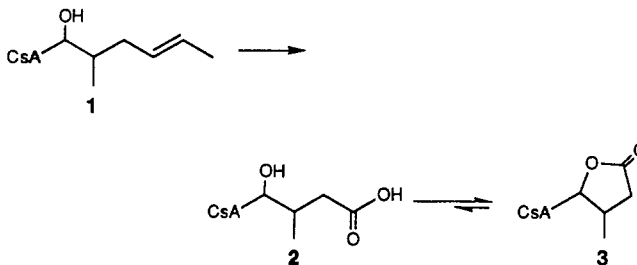
Cyclosporin A (1) was obtained as a generous gift from Dr. J. Borel of Sandoz. 2-[*N*-Methyl-*N*-(7-nitrobenz-2-oxa-1,3-diazo-4-yl)amino]ethanoic acid (10) was prepared by methods described elsewhere (9). 5-(Aminoacetamido)-fluorescein (7) was purchased from Molecular Probes Inc. (Eugene, OR). Poly-(L-lysine)hydrobromide (average MW = 26 500) (9) was purchased from Sigma Chemical Co. (St. Louis, MO). All other reagents were purchased from Aldrich Chemical Co. (Milwaukee, WI) or British Drug House (BDH) (Toronto, ON, Canada); KMnO₄, NaIO₄, and K₂CO₃ were recrystallized prior to use as described elsewhere (10).

¹H NMR spectra and ¹³C NMR APT spectra were recorded on a Varian Gemini 200-MHz spectrometer. Chemical shifts are reported in ppm relative to TMS as an internal standard unless otherwise stated. Mass spectroscopy analyses were performed on a Finnigan MAT 8320 by the chemical ionization (CI) or fast atom bombardment (FAB) technique. Fourier transform infrared spectra were recorded using a Bruker IRS 32 source and an IBM system 9000 processing system. FTIR samples were prepared as thin films from CHCl₃ solutions on NaCl disks. Reactions and purification procedures were monitored by thin-layer chromatography (TLC) using plastic-backed silica gel 60 UV/254 plates (Merck) as the stationary

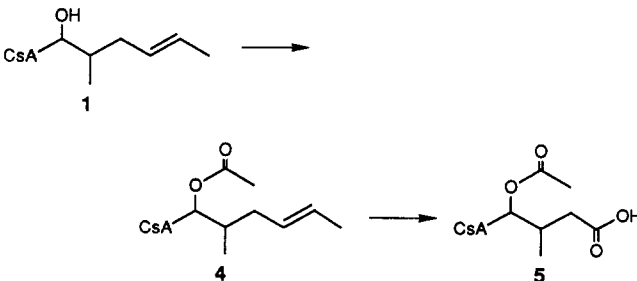
Chart I



Scheme I



Scheme II



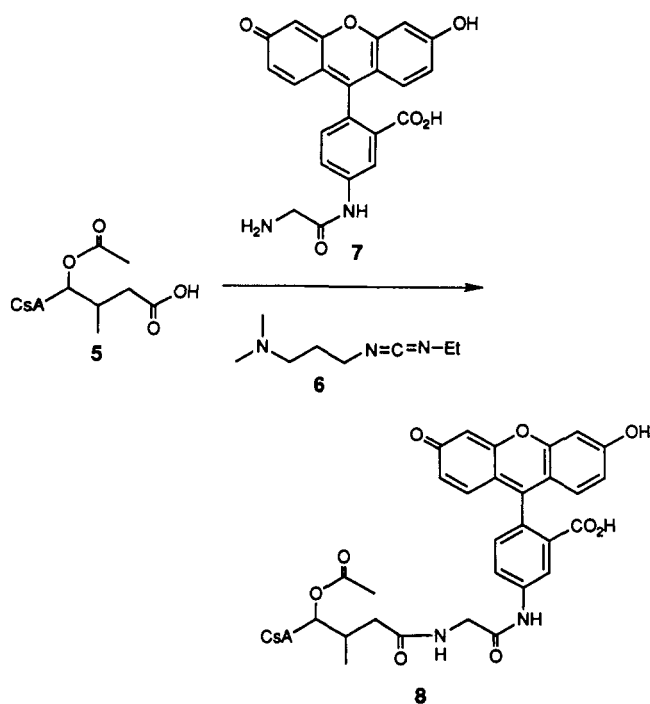
phase and 60/40 (v/v) ethyl acetate/acetone with 1% tri-fluoroacetic acid as the mobile phase. UV spectra were obtained using a Shimadzu UV-160 UV-visible recording spectrophotometer.

Automatic pH-stat work was performed with a radiometer system (Copenhagen) consisting of a PHM82

[†] Department of Chemistry.

[‡] Department of Chemical and Biochemical Engineering.

Scheme III



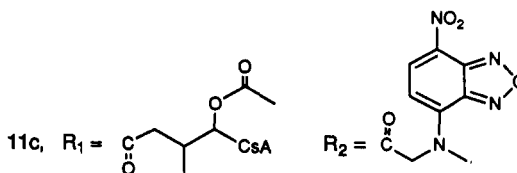
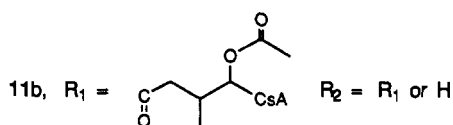
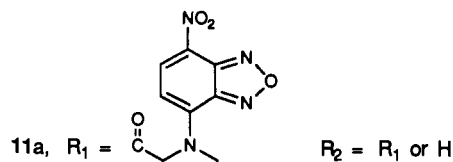
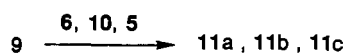
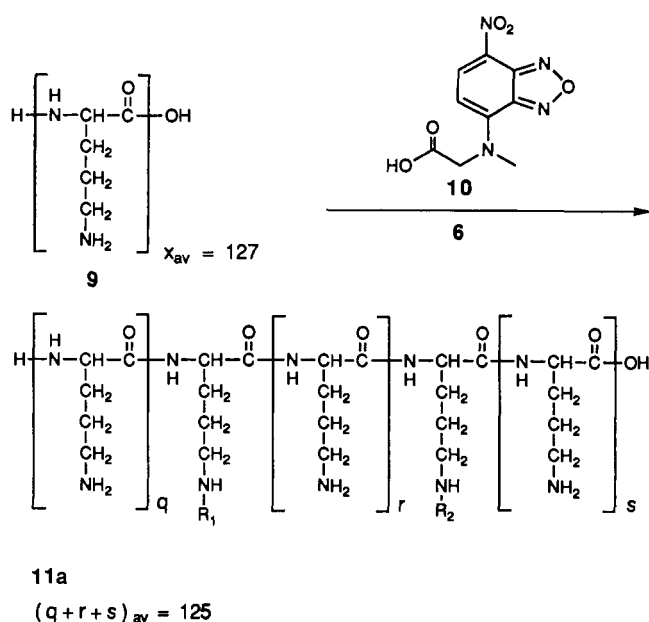
standard pH meter, a TTT80 titrator, and an ABU80 autoburette.

CsA Lactone 3. The title compound was prepared by a modification of the periodate/permanegase oxidation used to cleave unsaturated fatty acids (10). In a typical preparation, 490 μL of 0.15 M aqueous K_2CO_3 (73.5 μmol) and 490 μL of 0.20 M aqueous NaIO_3 (98.0 μmol) were added to a solution of 14.7 mg of CsA (1) (12.2 μmol) in 1.48 mL of *tert*-butyl alcohol. Deionized distilled water was added dropwise until all NaIO_4 had dissolved, then 98.0 μL of 0.025 M aqueous KMnO_4 (2.45 μmol) was added. The solution was stirred at room temperature under $\text{N}_2(\text{g})$ for 14 h, and then an additional 98 μL of 0.025 M aqueous KMnO_4 (2.45 μmol) was added to the reaction mixture. Stirring at room temperature under $\text{N}_2(\text{g})$ was continued for an additional 6 h (total reaction time 20 h), at which point the solution was pale brownish pink. The reaction was stopped by the addition of 0.147 mL of freshly prepared 40% (w/v) aqueous $\text{Na}_2\text{S}_2\text{O}_5$ solution (309 μmol), 0.250 mL of 1.0 M H_2SO_4 (250 μmol), and 2.5 mL of deionized distilled water. The mixture was stirred for 10 min, and then the aqueous solution was extracted with 3×40 mL of diethyl ether.

The solvent was removed from the ether extracts under reduced pressure, and then the dry product was dissolved in 2 mL of methanol and loaded on 20 g of Sephadex LH-20 gel filtration media (Pharmacia) which had been previously swollen in methanol. The fractions were analyzed by TLC and the fractions containing the first compound to elute from the gel filtration column were collected. Removal of solvent under reduced pressure furnished 12.2 mg (84%) of white solid product 3. ^1H NMR (CDCl_3): NH groups, δ 8.42, 7.92, 7.50, 7.46 (all d, each 1 H); NCH_3 groups, 3.46, 3.39, 3.17, 3.05, 2.66, 2.64 (all s, each 3 H). ^{13}C NMR (CDCl_3): CH_2 carbons, δ 49.92, 40.57, 36.51, 39.05, 36.51, 35.90, 35.20, 25.14, CHOR, 82.77; $\text{CH}=\text{CH}$ carbons, 126.72, 130.14. IR: carbonyl stretch (lactone), 1787 cm^{-1} . MS: m/e expected 1188, found 1188 (M^+).

O-Acetyl-CsA 4. O-Acetyl-CsA was prepared according to the method of Traber et al. (11). ^1H NMR (CDCl_3): NH groups, δ 8.48, 7.97, 7.43, 7.38 (all d, each 2 H); NCH_3

Scheme IV



groups, 3.38, 3.18, 3.16, 3.13, 3.01, 2.60, 2.58 (all s, each 3 H), $\text{OC}(\text{O})\text{CH}_3$ 1.93 (s, 3 H) (the complete ^1H NMR spectrum is available as supplementary material). ^{13}C NMR (CDCl_3): CH_2 carbons, δ 49.82, 40.79, 37.95, 36.79, 35.61, 33.48, 24.74; $\text{HCOC}(\text{O})\text{CH}_3$, 72.31; $\text{HCOC}(\text{O})\text{CH}_3$, 168.21; $\text{CH}=\text{CH}$ carbons 129.21, 126.35. All NMR assignments are in accord with those expected on the basis of previous assignments of the ^1H and ^{13}C NMR spectra of CsA (12). IR: carbonyl stretch, 1746 cm^{-1} (in addition to a strong amide stretch at 1628 cm^{-1}). MS: m/e (FAB) expected 1245, found 1245 (M^+).

O-Acetyl-CsA 5. The title compound was prepared from O-acetyl-CsA 4 by the same method used to prepare CsA lactone 3. Yield: 100%. ^1H NMR (CDCl_3) (dominant conformer): NH groups, δ 8.38, 8.02, 7.72, 7.45 (d, each 1 H); NCH_3 groups, 3.49, 3.24, 3.09, 2.69, 2.67, (all s, each 3 H), 3.25 (s, 6 H); $\text{OC}(\text{O})\text{CH}_3$, 2.01 (s 3 H) (the complete ^1H NMR spectrum is available as supplementary material). ^{13}C NMR (CDCl_3): CH_2 carbons, δ 40.50, 38.79, 34.40, 24.92 (multiple conformations of the peptide in solution complicated the ^{13}C spectrum and precluded the assignment of all expected methylene ^{13}C signals); HCOC -

(O)CH₃, 72.31; HCOC(O)CH₃, 167.34. IR: carbonyl stretch, 1745 cm⁻¹. MS: *m/e* (FAB) expected 1249, found 1249 (M)⁺.

5-(Aminoacetamido)fluorescein-*O*-Acetyl-CsA Amide 8. Compound 8 was prepared using a modification of the procedure routinely used to react carboxylic acid groups on proteins (13). In a typical preparation, 33.1 mg (173 μmol) of 1-ethyl-3-[3-(dimethylamino)propyl]carbodiimide (EDC, 6) and 2.5 mg (5.24 μmol) of 5-(aminoacetamido)fluorescein (7) were dissolved in 12 mL of deionized distilled water which had been made basic by the addition of 2 drops of 10% NaOH solution. A solution of 10 mg (8 μmol) of *O*-acetyl-CsA acid 5 in 200 μL of *tert*-butyl alcohol was added to the aqueous solution and the solution was transferred to an autotitrator set on pH-stat, where the pH of the solution was adjusted to 5.50 by titration with 1.0 M HCl. The reaction was allowed to proceed in the dark for 5 h, during which time the pH of the solution was maintained at 5.50 by automatic titration with 1.0 M HCl. After 5 h the reaction was stopped by the addition of 1 mL of pH 4.75 acetate buffer and the solvent was removed by freeze-drying.

The methanol-soluble dried products were dissolved in 2 mL of methanol and loaded on 20 g of Sephadex LH-20 gel filtration media (Pharmacia) which had been previously swollen in methanol. The fastest running colored compound was collected and the methanol was removed under reduced pressure. CHCl₃ (25 mL) was added to the flask containing the dried products, and then the solution of the colored product in CHCl₃ was washed with 3 × 20 mL of pH 7.40 phosphate buffer to remove side products. Removal of the CHCl₃ under vacuum furnished 12.0 mg (87%) of orange solid product 8. ¹H NMR (CDCl₃): NCH₃ groups (major conformer in solution) δ 3.48, 3.11, 3.06, 2.74, 2.71, (all s, each 3 H), 3.25 (s, 6 H); aromatic region multiplets, 8.62, 8.34, 7.77, 7.66, 6.78.

Compound 11a. The title compound was prepared by the same method used to prepare compound 8. In a typical reaction 80 mg of 2-[*N*-methyl-*N*-(7-nitrobenz-2-oxa-1,3-diazo-4-yl)amino]ethanoic acid (10) (317 μmol) was allowed to react with 18.3 mg of poly(L-lysine) (9) [0.691 μmol of poly(L-lysine), 87.7 μmol lysine residues] in the presence of 161.1 mg of EDC (6) (840 μmol) in 13 mL of deionized distilled water at pH 5.50. After 5 h the reaction was stopped by the addition of 2 mL of pH 4.75 acetate buffer and the total volume of the solution was reduced to 2 mL by freeze-drying. Purification of products was performed on a column of 20 g of Bio-Gel P-2 gel filtration media (Bio-Rad) which had been previously swollen in pH 7.4 phosphate buffer solution. The desired product was easily identified as the first colored compound to elute from the column. ¹H NMR (D₂O) indicated the presence of poly(L-lysine) but was not sensitive enough to detect peaks corresponding to protons on the fluorescent moiety. ¹H NMR (D₂O): C(O)NHCH, δ 4.11 (t, 1 H); CH₂NH₂, 2.80 (t, 2 H); CH₂CH₂NH₂, 1.49 (quint, 2 H); CHCH₂CH₂CH₂NH₂, 1.24 (m, 2 H). UV: λ = 480 nm.

Compound 11b. The title compound was prepared by the same method used to prepare compound 8. In a typical reaction 6.23 mg of poly(L-lysine) [0.235 μmol of poly(L-lysine), 29.9 μmol of lysine residues] was combined with 1.5 mg of 2-[*N*-methyl-*N*-(7-nitrobenz-2-oxa-1,3-diazo-4-yl)amino]ethanoic acid (10) (5.95 μmol) and 80 mg of EDC (6) (417 μmol) in 12 mL of deionized distilled water which had been made basic by the addition of 2 drops of 10% NaOH solution. A solution of 10 mg of *O*-acetyl-CsA acid 5 (8.01 μmol) in 1 mL of *tert*-butyl alcohol was added and the solution was stirred for 5 h while the pH was maintained

at 5.50. Products were purified as per 11a. The first band to elute from the column presumably contained compounds 11a-c and unreacted poly(L-lysine). Unreacted *O*-acetyl-CsA acid 5 and low molecular weight products from side reactions of 10 were collected in later fractions and identified by ¹H NMR. The ¹H NMR of the products 11a-c and 9 contained signals corresponding to both poly(L-lysine) and *O*-acetyl-CsA acid, but ¹H NMR was not a sensitive enough technique to detect peaks corresponding to protons on the fluorescent moiety. ¹H NMR (D₂O): poly(L-lysine) peaks, δ 4.05, 2.74, 1.50, 1.22; cyclosporin A related peaks, 2.92, 2.62, 2.60, 1.90, 0.73.

RESULTS AND DISCUSSION

Cyclosporin A (CsA, 1) is an undecapeptide which contains only two chemically reactive sites that can be modified without destruction of the amide bonds within the peptide (see Chart I). Both of these functional groups, the hydroxyl group and the double bond, are located on the 2-*N*-methyl-*(R)*-(*E*)-2-butenyl-4-methyl-L-threonine (MeBmt) residue of cyclosporin A, and the chemical reactivity of both groups is diminished by steric factors arising from the three-dimensional conformation of CsA in solution (13).

It has been shown elsewhere (11) that the alcohol moiety of CsA is sufficiently reactive to produce *O*-acetyl-CsA when combined with acetic anhydride. Consequently, in our initial experiments we aimed to exploit the reactivity of the alcohol group and incorporate a new reactive fundamental group on CsA by allowing the alcohol moiety to undergo esterification with small carboxylic acid chlorides containing terminal primary bromide groups (i.e. 4-bromobutyric acid chloride, 3-bromopropionic acid chloride).

When 2-octanol is allowed to react with 4-bromobutyric acid chloride in deuteriochloroform in an NMR tube, it is possible to follow the reaction by monitoring the ¹H NMR spectrum, since the ¹H signal corresponding to the methylene group adjacent to the carbonyl in 4-bromobutyric acid chloride is 0.58 ppm downfield from the analogous signal of 4-bromobutyric acid 2'-octyl ester (3.02 vs 2.43 ppm). Using this information we hoped to follow the reaction of the alcohol group on CsA with 4-bromobutyric acid chloride; however the ¹H NMR spectra indicated that no new signal at ~2.43 ppm was evident after 5 h, i.e. no reaction had occurred. Additional experiments where cyclosporin A was combined with 4-bromobutyric acid chloride and 3-bromopropionic acid chloride in the presence of a pyridine catalyst also showed that no ester product was formed, even after 24 h. The lack of success with the above strategy is perplexing in view of the reactivity of CsA with acetic anhydride (10), and can most likely be attributed to the fact that the alcohol moiety of CsA does not readily react intermolecularly with acid chlorides because of steric hindrance of the alcohol moiety due to the three-dimensional conformation of the peptide (13).

Since attempts to react the alcohol group of CsA were unsuccessful, a new synthetic strategy was developed based on oxidative cleavage of the double bond of the MeBmt residue, by analogy with a previous preparation of a CsA derivative containing an aldehyde function (4). Using a modification of a mild oxidation procedure used to cleave the double bonds of unsaturated fatty acids, cyclosporin A was converted to compound 2 (Scheme I). As expected (15), ¹H and ¹³C NMR indicated that the equilibrium between 2 and the lactone 3 strongly favored lactone formation to the exclusion of 2. Additional evidence for

lactone formation was obtained from the FTIR spectrum, which exhibited a characteristic strong stretch at 1787 cm^{-1} .

From the spectral data of 3 it was clear that the reaction had proceeded cleanly and without any oxidation of amide bonds in the peptide. However, the fact that lactone 3 was the dominant species of the equilibrium with carboxylic acid 2 suggested that secondary reactions involving intramolecular nucleophilic attack of the alcohol on a modified terminal carboxylic acid group might occur at a later stage in any synthetic scheme. Accordingly, *O*-acetyl-CsA acid 5 which is incapable of lactonization, was prepared by oxidation of *O*-acetyl-CsA (4) (Scheme II).

O-Acetyl-CsA acid 5 was found to be reactive with primary amines in aqueous solution when combined with 1-ethyl-3-[3-(dimethylamino)propyl] carbodiimide (EDC, 6), a well-known reagent for modification of carboxylic acid groups in aqueous media (10). By reacting *O*-acetyl-CsA acid 5 with 5-(aminoacetamido)fluorescein (7), a commercially available fluorescent compound, in the presence of EDC (6), the fluorescent derivative of cyclosporin A (8) was obtained (Scheme III). Fluorescent product 8 was easily identified and isolated as the first colored compound to elute from a gel filtration column which fractionates compounds over the molecular weight range 100–1800 g/mol.

One of the main purposes of the cyclosporin A manipulations undertaken in this laboratory was to generate an immunogen with CsA as a hapten which could be used to obtain monoclonal antibodies directed against CsA. It was necessary to prepare an immunogen because cyclosporin A is an immunosuppressant and is also liable to be too small to illicit an immune response in a live animal. The initial synthetic strategy for preparation of an immunogen derived from CsA involved the reaction of *O*-acetyl-CsA acid 5 with bovine serum albumin (BSA) in the presence of EDC (6); however, verification of the coupling of 5 to BSA by amino acid analysis proved difficult for several reasons. Amino acid analysis is based on the hydrolysis of amide bonds, therefore the amide bond linking *O*-acetyl-CsA acid 5 and BSA is necessarily cleaved by this technique. Consequently, using amino acid analysis, one cannot verify whether 5 is chemically linked to BSA, or whether the two species are simply present in the same solution. Moreover, the coupling efficiency of the reaction of 5 with BSA in the presence of EDC (6) is very low, and evidence of CsA was not detectable in the hydrolysis mixture.

To address these general problems involved with detection of the immunogen, we decided to increase the coupling probability of the reaction by using poly(L-lysine) rather than BSA and to verify the coupling by introducing a small amount of fluorescent acid as a tracer. The assumption made was that if we can identify a fluorescent adduct of poly(L-lysine), there is a high probability that the poly(L-lysine)-*O*-acetyl-CsA acid conjugate will also be present.

The compound 2-[*N*-methyl-*N*-(7-nitrobenz-2-oxa-1,3-diazo-4-yl)amino]ethanoic acid (10) was prepared because it is a fluorescent water-soluble compound containing a carboxylic acid group, which should couple to poly(L-lysine) competitively with *O*-acetyl-CsA acid. In our first experiment, poly(L-lysine) (9) was allowed to react with 10 in the presence of EDC (6) (Scheme IV). Fluorescent product 11a was isolated as the first colored compound to elute from a gel filtration column and ^1H NMR confirmed the presence of poly(L-lysine), but was not sensitive enough to detect peaks corresponding to protons on the fluorescent

moiety. The UV spectrum of adduct 11a confirmed that the fluorophore was present, and that the overall coupling efficiency for the reaction was low [10% of the poly(L-lysine) in solution reacted to produce conjugate 11a].

Once the reaction of poly(L-lysine) (9) with fluorescent carboxylic acid 10 had been ascertained, poly(L-lysine) (9) and *O*-acetyl-CsA acid 5 were allowed to react in the presence of EDC (6) and a small amount of 10 (Scheme IV). The colored high molecular weight products 11a, and presumably 11c, eluted from a Bio-Gel P-2 column with unreacted poly(L-lysine) (9), and presumably poly(L-lysine)-*O*-acetyl-CsA acid conjugate, 11b. The presence of colored products 11a and 11c allowed for facile isolation of the mixture of poly(L-lysine) adducts by gel filtration chromatography, and served to indicate that reaction between poly(L-lysine) and carboxylic acids in solution had occurred. Fractions containing unreacted *O*-acetyl-CsA acid 5 and products from side reactions of 10 eluted after the fractions containing products 11a–c and were characterized by ^1H NMR.

We felt it was necessary to include the tracer compound 10 in our reaction scheme to ensure that conjugation was occurring; however, the presence of 10 inevitably gave rise to the mixture of products 11a–c which could not be separated. Consequently, it was necessary to inject the mixture of products 11a–c into the live animal, in the expectation that antibodies will be raised against all antigens. Though it is always preferable to inject a single antigen (in our case 11b would be the desired antigen) when generating antibodies, fortunately it is possible to select only those antibodies directed against *O*-acetyl-CsA acid by competitive ELISA screening techniques, or by a competitive binding assay using fluorescent derivative 8. Thus we anticipate that screening techniques will furnish antibodies directed against the *O*-acetyl-CsA acid moiety of 11b, though compound 11b could not be isolated itself.

CONCLUSIONS

The synthesis of compound 5 is an important step toward the synthesis of novel cyclosporin A derivatives. The novel compounds 8, 11b, and 11c represent a few examples of the numerous cyclosporin A derivatives which can be prepared by reacting 5 with primary amines or other nucleophiles.

ACKNOWLEDGMENT

Funding for the work described in this paper was provided by an NSERC postgraduate fellowship (P.A.P.), by NSERC operating grant #3272 (N.O.P.), and by an NSERC Biotechnology Strategic Grant #STR0040839 (A.M., principal investigator). We thank Dr. J. Borel of Sandoz for providing a cyclosporin A sample.

Supplementary Material Available: ^1H NMR spectra of 1, 4, and 5 (6 pages). Ordering information is given on any current masthead page.

LITERATURE CITED

- (1) Margaritis, A., and Chahal, P. S. (1989) Development of a Fructose Medium for Biosynthesis of Cyclosporin A by *Beauveria nivea*. *Biotechnology Lett.* 11, 765–768.
- (2) Borel, J. F. (1983) Cyclosporine: Historical Perspectives. *Transplant Proc.* 15, Suppl. 1, 2230–2241.
- (3) Stiller, C. R., and Keown, P. A. (1984) Cyclosporin Therapy in Perspective. *Progress in Transplantation* (P. J. Morris, and N. L. Tilney, Eds.) pp 11–45, Churchill Livingstone Publishers, London.

- (4) Wenger, R., Traber, R. P., Kobel, H., and Hofmann, H. (1985) Cyclosporin Derivatives and Their Use. French Patent # 561 651 A1.
- (5) Wenger, R. M. (1986) Synthesis of Cyclosporin and Analogs: Structural and Conformational Requirements for Immunosuppressive Activity. *Prog. Allergy* 38 (Cyclosporin), 46-64.
- (6) Wenger, R. (1983) Synthesis of Cyclosporine and Analogues: Structure Activity Relationships of New Cyclosporine Derivatives. *Transplant. Proc.* 15, Suppl. 1, 2230-2241.
- (7) Wenger, R. (1982) Chemistry of Cyclosporin. *Cyclosporin A, Proceedings of the International Conference* (D. White, Ed.) pp 19-34, Elsevier Biomedical Press, Amsterdam, Netherlands.
- (8) Abbot Laboratories (1988) Fluorescence Polarization Assay for Cyclosporin A and Metabolites and Related Immunogens and Antibodies. European Patent # EP 0283 801 A2.
- (9) Petersen, N. O. (1985) Intramolecular Fluorescence Energy Transfer in Nitrobenzoxadiazole Derivatives of Polyene Antibiotics. *Can. J. Chem.* 63, 1, 77-85.
- (10) Longmair, K. J., Rossi, M. E., and Resele-Tiden, C. (1987) Determination of Monoenoic Fatty Acid Double Bond Position by Permanganate-Periodate Oxidation Followed by High Performance Liquid Chromatography of Carboxylic Phenacyl Esters. *Anal. Biochem.* 167, 213-221.
- (11) Traber, R., Loosli, H., Hoffman, H., Kuhn, M., and Von Wartburg, A. (1982) Isolation and Structure Determination of New Cyclosporins E, F, G, H and I. *Helv. Chim. Acta* 65, Fasc 5, 1655-1677.
- (12) Kessler, H., Loosli, H., and Oschkinat, H. (1985) Assignment of the ^1H -, ^{13}C -, and ^{14}N -NMR Spectra of Cyclosporin A in CDCl_3 and C_6D_6 by a Combination of Homo- and Heteronuclear Two-Dimensional Techniques. *Helv. Chim. Acta* 68, 661-681.
- (13) Carraway, K. L., and Koshland, D. E. (1972) Carbodiimide Modification of Proteins. *Methods Enzymol.* 25B, 616-623.
- (14) Loosli, H.; Kessler, Oschkinat, Weber, H., Petcher, T. J., and Windmer, A. (1985) The Conformation of Cyclosporin A in the Crystal and in Solution. *Helv. Chim. Acta* 68, 682-704.
- (15) Streitwieser, A., Jr., and Heathcock, C. H. (1985) Chapter 27 Hydroxy Acids. *Introduction to Organic Chemistry*, 3rd ed., pp 859-861, Macmillan Publishing Co., New York.
- Registry No.** 1, 59865-13-3; 3, 137718-40-2; 4, 83602-41-9; 5, 137718-41-3; 7, 137718-42-4; 8, 137718-43-5; 9 (homopolymer), 25104-18-1; 9 (SRU), 38000-06-5.

Biotinylated Peptides Containing a Factor XIIIa or a Tissue Transglutaminase-Reactive Glutaminyl Residue That Block Protein Cross-Linking Phenomena by Becoming Incorporated into Amine Donor Sites

L. Lorand,* K. N. Parameswaran, P. T. Velasco, and S. N. P. Murthy

Department of Biochemistry, Molecular Biology, and Cell Biology, Northwestern University, Evanston, Illinois 60208. Received July 10, 1991

Biotinylated peptides Biot-Gln-Gln-Ile-Val and Biot- ϵ -Aca-Gln-Gln-Ile-Val were shown to act as acceptor substrates for amines in reactions catalyzed by both tissue transglutaminase and coagulation factor XIIIa. Moreover, the peptides could be employed for specifically blocking the potential amine donor sites of protein substrates participating in biological cross-linking with these enzymes. The presence of the biotin label allowed for ready detectability of the marked donor substrates during the cross-linking of crystallins in lens homogenate by the intrinsic transglutaminase and that of the α chains of human fibrin by factor XIIIa.

Recent reports from this laboratory (1, 2) demonstrated that protein-to-protein cross-linking reactions catalyzed by transglutaminase (protein-glutamine:amine γ -glutamyl-transferase, EC 2.3.2.13) and activated fibrin-stabilizing factor (coagulation factor XIIIa) could be inhibited by the addition of glutamine-containing short peptide analogues patterned on the N-terminal portion of the fibronectin molecule. Among the compounds thus far examined, Boc-Gln-Gln-Ile-Val,¹ Boc-Ala-Gln-Gln-Ile-Val, pGlu-Ala-Gln*-Gln-Ile-Val, Dns-Ala-Gln-Gln-Ile-Val, and Dns-Pro-Gly-Gly-Gln-Gln-Ile-Val were found to be effective in this regard. The first glutaminyl residue marked in the pGlu-Ala-Gln*-Gln-Ile-Val sequence was shown to act as the amine acceptor in the enzymatic transamidations, and it was also concluded that inhibition by these compounds resulted from the enzyme-directed blocking of select ϵ -lysine donor sites which would have participated in the cross-linking of the protein substrates if no peptides were present. In order to widen the scope of utility of compounds designed for the probing of transglutaminase and factor XIIIa-mediated bioconjugating processes in various settings, we have now also prepared the biotinylated derivatives Biot-Gln-Gln-Ile-Val and Biot- ϵ -Aca-Gln-Gln-Ile-Val. The present paper shows that such biotinylated peptides will, indeed, be useful for the specific labeling, rapid identification, and exploration of the enzyme-reactive amine donor sites in proteins.

EXPERIMENTAL PROCEDURES

Peptide Synthesis. Reagents and solvents were purchased from Aldrich Chemical Co. (Milwaukee, WI) and Sigma (St. Louis, MO). Biotin *N*-hydroxysuccinimide ester (NHS Biotin) was prepared according to published procedures (3). TLC was performed on Whatman (Hill-

boro, OR) K₆F silica gel glass plates (0.25 mm) using the following solvent systems (v/v): (A) ethyl acetate/heptane 2:1; (B) chloroform/methanol/glacial acetic acid 10:3:1; (C) 1-butanol/glacial acetic acid/water 15:6:5; (D) chloroform/methanol/2-propanol 10:4:4; (E) 1-propanol/water/concentrated ammonium hydroxide/ethanol 7:4:2:3; (F) 1-propanol/water 7:3. The plates were viewed under UV light or were developed with ninhydrin (0.25% in 1-butanol for N-deblocked peptides) or with hypochlorite (10%) followed by starch/KI spray for N-blocked peptides (4) and a reagent [0.2% solution of *p*-(dimethylamino)cinnamaldehyde in ethanol containing 2% sulfuric acid] specific for the biotin ring system (5). Melting points were determined with a Büchi apparatus and are uncorrected. NMR spectra were recorded on a Varian XLA-400 spectrometer. Chemical shifts are reported as parts per million (ppm, δ) relative to tetramethylsilane in DMSO-*d*₆. Elemental analyses were performed by Searle Laboratories (Skokie, IL).

General Procedures for Peptide Synthesis. *Peptide Coupling.* To a stirred and cooled (0 °C) 0.5–0.8 M solution of the pertinent Boc-amino acid in dry DMF were added equimolar amounts of 1-hydroxybenzotriazole and 1-ethyl-3-[3-(dimethylamino)propyl]carbodiimide hydrochloride. The mixture was stirred at 0 °C for 40 min and then added to a solution of the trifluoroacetate salt of the peptide benzyl ester (obtained by acidolytic deblocking of the Boc-peptide benzyl ester) in dry DMF which was pre-neutralized with *N*-methylmorpholine. The reaction mixture was stirred at 0 °C for 1 h and then at room temperature for 18–36 h. The mixture was evaporated under reduced pressure to remove DMF and the residue was stirred with 3% sodium bicarbonate for 15 min. The precipitate was filtered off, washed with 5% NaHCO₃, water, cold 0.5 N HCl, and water, and dried in vacuo in a P₂O₅ desiccator for 12–18 h. When necessary, the product was reprecipitated from DMF–water.

Deblocking of the Boc Group. To 1.0 mmol of the Boc-peptide benzyl ester was added 2 mL of 50% trifluoroacetic acid in anhydrous dichloromethane. The solution was allowed to stand at room temperature for 1 h, and excess trifluoroacetic acid was removed by adding fresh dichloromethane to the mixture followed by evaporation under reduced pressure. Upon addition of anhydrous ether to the residue, the precipitated TFA salt of the peptide

* To whom correspondence should be addressed: Department of Biochemistry, Molecular Biology and Cell Biology, Northwestern University, 2153 Sheridan Rd, Evanston, IL 60208-3500.

¹ Abbreviations: Boc, *tert*-butoxycarbonyl; pGlu, pyroglutamate; Dns or dansyl, [5-(dimethylamino)-1-naphthalenyl]sulfonyl; Biot, biotinyl; ϵ -Aca, ϵ -aminocaproyl; dansylcadaverine, *N*-(5-aminopentyl)-5-(dimethylamino)-1-naphthalenesulfonamide; DMSO, dimethyl sulfoxide; DMF, dimethylformamide; TFA, trifluoroacetic acid; OBzl, benzyl ester; SDS, sodium dodecyl sulfate; PAGE, polyacrylamide gel electrophoresis.

benzyl ester was filtered off, washed with anhydrous ether, and dried under vacuum in a desiccator for 2 h before proceeding with the coupling reaction.

Boc-Ile-Val-OBzl: yield 90%; mp 93–95 °C; TLC homogeneous, R_f 0.8 (A), 0.95 (B), 0.94 (C), 0.9 (D); ^1H NMR δ 0.77 (6 H, appt, γ' , δCH_3 Ile), 0.85 (6 H, overlapping d, γCH_3 Val), 1.05 (1 H, m, γCH_2 Ile), 1.35 (10 H, s, t -Bu of Boc superimposed on one of the multiples of γCH_2 Ile), 1.63 (1 H, m, βCH Ile), 2.05 (1 H, m, βCH Val), 3.88 (1 H, appt, αCH Ile), 4.22 (1 H, appt, αCH Val), 5.1 (2 H, s, $\text{OCH}_2\text{C}_6\text{H}_5$), 6.75 (1 H, d, NH Ile), 7.35 (5 H, s, C_6H_5), 8.05 (1 H, d, NH , Val).

Boc-Gln-Ile-Val-OBzl: yield 92%; mp 192–194 °C; TLC homogeneous, R_f 0.93 (B), 0.91 (C), 0.85 (D); ^1H NMR δ 0.78 (6 H, appt, γ' , δCH_3 Ile), 0.85 (6 H, overlapping d, γCH_3 Val), 1.05 (1 H, m, γCH_2 Ile), 1.37 (10 H, s, t -Bu of Boc superimposed on one of the multiples of γCH_2 Ile), 1.65 (2 H, m, βCH Ile + βCH_2 Gln), 1.8 (1 H, m, βCH_2 Gln), 2.07 (3 H, m, βCH Val + γCH_2 Gln), 3.87 (1 H, m, αCH Ile), 4.18 (1 H, appt, αCH Val), 4.32 (1 H, appt, αCH Gln), 5.11 (2 H, s, $\text{OCH}_2\text{C}_6\text{H}_5$), 6.77 (1 H, s, CONH_2 Gln), 7.03 (1 H, d, CONH Ile), 7.24 (1 H, s, CONH_2 Gln), 7.36 (5 H, s, C_6H_5), 7.6 (1 H, d, CONH Gln), 8.28 (1 H, d, CONH Val). Anal. Calcd for $\text{C}_{28}\text{H}_{44}\text{N}_4\text{O}_7$: C, 61.29; H, 8.08; N, 10.21. Found: C, 61.17; H, 8.05; N, 10.13.

Boc-Gln-Gln-Ile-Val-OBzl: yield 88%; mp 239–241 °C dec; TLC homogeneous, R_f 0.1 (A), 0.82 (C), 0.73 (D); ^1H NMR δ 0.78 (6 H, appt, γ' , δCH_3 Ile), 0.86 (6 H, overlapping d, γCH_3 Val), 1.05 (1 H, m, one of the γCH_2 Ile), 1.37 (10 H, s of t -Boc superimposed on one of the m due to γCH_2 Ile), 1.68 (3 H, m, βCH Ile + βCH_2 Gln), 1.82 (2 H, m, βCH_2 Gln), 2.08 (5 H, m, γCH_2 Gln + βCH Val), 3.87 (1 H, m, αCH Ile), 4.2 (1 H, appt, αCH Val), 4.3 (2 H, appt, αCH Gln), 5.11 (2 H, s, $\text{OCH}_2\text{C}_6\text{H}_5$), 6.78 (2 H, s, CONH_2 Gln), 7.0 (1 H, d, CONH Ile), 7.25 (2 H, s, CONH_2 Gln), 7.36 (5 H, s, C_6H_5), 7.9 (2 H, d, CONH Gln), 8.26 (1 H, d, CONH Val). Anal. Calcd for $\text{C}_{33}\text{H}_{52}\text{N}_6\text{O}_9$: C, 58.56; H, 7.75; N, 12.42. Found: C, 58.00; H, 7.72; N, 12.18.

Boc-Ala-Gln-Gln-Ile-Val-OBzl: yield 90%; mp 275–277 °C dec; TLC homogeneous R_f 0.8 (C), 0.75 (D), 0.86 (E); ^1H NMR δ 0.8 (6 H, overlapping t + d, γ' , δCH_3 Ile), 0.9 (6 H, overlapping d, γCH_3 Val), 1.05 (1 H, m, one of the γCH_2 Ile), 1.19 (3 H, d, βCH_3 Ala), 1.4 (10 H, s of t -Boc superimposed on one of the m γCH_2 Ile), 1.7 (3 H, m, βCH Ile + βCH_2 Gln), 1.85 (2 H, m, βCH_2 Gln), 2.1 (5 H, m, γCH_2 Gln + βCH Val), 3.98 (1 H, m, αCH Ala), 4.2–4.38 (4 H, overlapping m, αCH of Val, Ile, and Gln), 5.14 (2 H, s, $\text{OCH}_2\text{C}_6\text{H}_5$), 6.79 (2 H, s, CONH_2 Gln), 7.0 (1 H, d, CONH Ile), 7.23 (2 H, s, CONH_2 Gln), 7.39 (5 H, s, C_6H_5), 7.82 (1 H, d, CONH Ala), 7.9 (1 H, d, CONH Gln), 8.05 (1 H, d, CONH Gln), 8.28 (1 H, d, CONH Val). Anal. Calcd for $\text{C}_{36}\text{H}_{57}\text{N}_7\text{O}_{10}$: C, 57.81; H, 7.68; N, 13.11. Found: C, 57.85; H, 7.72; N, 13.03.

Biot-Gln-Gln-Ile-Val. The trifluoroacetate salt of Gln-Gln-Ile-Val benzyl ester, obtained by deblocking of Boc-Gln-Gln-Ile-Val benzyl ester (1) with 50% trifluoroacetic acid in anhydrous dichloromethane for 1 h at room temperature, was allowed to react with 20% molar excess of biotin N -hydroxysuccinimide ester in the presence of 2 equiv of N -methylmorpholine in dimethylformamide at room temperature overnight. Water and 3% NaHCO_3 were added, and the reaction mixture was stirred for an additional 15 min. The precipitate was separated by centrifugation, washed successively with 3% NaHCO_3 , water, 0.3 N HCl, and water, and dried under vacuo to give a 91% yield of a white, crystalline, blocked intermediate, Biot-Gln-Gln-Ile-Val benzyl ester: mp 280–282 °C dec; TLC homogeneous, R_f 0.75 (B), 0.74 (C), 0.8 (E),

0.62 (F). Anal. Calcd for $\text{C}_{38}\text{H}_{58}\text{N}_8\text{O}_9\text{S}\cdot\text{H}_2\text{O}$: C, 55.59; H, 7.36; N, 13.65. Found: C, 55.92; H, 7.18; N, 13.53. The above benzyl ester was dissolved in dimethyl sulfoxide at 60 °C and cooled to 40 °C, and a 3-fold molar excess of NaOH was added to give a final concentration of 0.2 N NaOH. After stirring for 1 h, the mixture was diluted with water and filtered. The filtrate was acidified to pH 3.0 with 1 N HCl. The precipitate was collected by centrifugation, washed with water and dried in vacuo to yield 76% of Biot-Gln-Gln-Ile-Val as white crystals: mp 270–272 °C dec; TLC homogeneous, R_f 0.15 (B), 0.58 (C), 0.66 (E), 0.46 (F). Anal. Calcd for $\text{C}_{31}\text{H}_{52}\text{N}_8\text{O}_9\text{S}\cdot\text{H}_2\text{O}$: C, 50.94; H, 7.45; N, 15.32. Found: C, 50.97; H, 7.55; N, 14.87.

Biot- ϵ -Aca-Gln-Gln-Ile-Val. This was synthesized by a procedure essentially similar to the one above. Reaction of the trifluoroacetic acid salt of Gln-Gln-Ile-Val benzyl ester with biotinyl- ϵ -aminocaproic acid N -hydroxysuccinimide ester followed by saponification of the benzyl ester gave the desired Biot- ϵ -Aca-Gln-Gln-Ile-Val in 60% yield: mp 255–257 °C dec; TLC homogeneous, R_f 0.06 (B), 0.49 (C), 0.68 (E), 0.57 (F). Anal. Calcd for $\text{C}_{37}\text{H}_{63}\text{N}_9\text{O}_{10}\text{S}\cdot 0.5\text{H}_2\text{O}$: C, 53.22; H, 7.72; N, 15.10. Found: C, 53.27; H, 7.45; N, 14.93.

Enzyme-Mediated Coupling of Dansylcadaverine to Peptides. Analysis by TLC (Polyamide-6; aqueous 1% pyridine, pH 5.4; Macherey & Nagel, Alltech Associates, Deerfield, IL), designed to demonstrate that the biotinylated peptides could serve as amine acceptors in transamidating reactions, were performed as previously described with guinea pig liver transglutaminase or human factor XIIIa as catalysts (1, 6).

Inhibition of Crystallin Cross-Linking by the Endogenous Transglutaminase in Lens Homogenate with Simultaneous Labeling of Select Subunits. Incubations of rabbit lens homogenate with the biotinylated peptides, SDS-PAGE, and electroblotting were carried out according to methods previously described (1). Following electroblotting, unbound sites on the nitrocellulose were blocked with 10 mM sodium phosphate (pH 7.5), 0.9% NaCl, 0.05% Tween 20 (TPBS) for 30 min. Biotin labeling was visualized using an avidin-biotinylated peroxidase conjugate. Avidin and biotinylated peroxidase from a Vectastain ABC kit (Vector Laboratories, Burlingame, CA) were diluted 1:5000 into TPBS and a complex was allowed to form for 30 min before incubating with the nitrocellulose sheet for 90 min. Following washing with 10 mM sodium phosphate (pH 7.5) and 0.9% NaCl (PBS; 3 \times 5 min), the peroxidase label was developed for 5 min with a freshly prepared mixture of 50 mL of PBS, 10 mL of 4-chloro-1-naphthol (3 mg/mL in ice-cold methanol) and 30 μL of 30% H_2O_2 ; the reaction was stopped by extensive washing with water.

Factor XIIIa-Directed Labeling of the α Chains of Fibrin. The effects of biotinylated peptides on the cross-linking of human fibrin by human factor XIIIa were evaluated by published methods (1). Detection of biotin labeling on nitrocellulose transblots was as described above.

RESULTS

In order to widen the scope of utility of compounds designed for the probing of transglutaminase and factor XIIIa-mediated cross-linking processes in various biological settings (1, 2), we have prepared the following biotinylated derivatives: Biot-Gln-Gln-Ile-Val and Biot- ϵ -Aca-Gln-Gln-Ile-Val. It was first shown that the two new compounds could, indeed, serve as acceptors in the enzyme-catalyzed reactions with the synthetic amine dansylca-

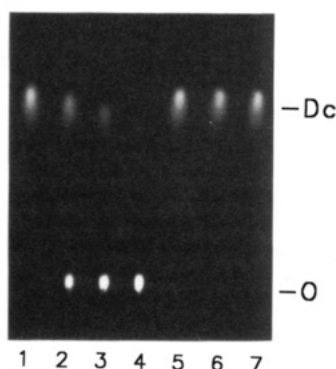


Figure 1. Coupling of dansylcadaverine to Biot-Gln-Gln-Ile-Val as catalyzed by guinea pig liver transglutaminase. Incubations were carried out at 37 °C for 60 min and analyzed by TLC as previously described (1, 6). Reactions comprised 50 mM Tris-HCl (pH 7.5), 0.2 mM dansylcadaverine, 10 mM dithiothreitol, and 12 μ g/mL transglutaminase and contained either no peptide (lanes 5 and 6) or 0.25 mM (lane 2), 0.5 mM (lane 3), or 1.0 mM Biot-Gln-Gln-Ile-Val (lanes 1 and 4) and either 2 mM EDTA (lanes 1 and 5) or 10 mM CaCl_2 (lanes 2–4 and 6). Lane 7 was spotted with dansylcadaverine (Dc) as reference; the origin is marked as O.

daverine as donor. As analyzed by TLC on Polyamide (1, 6), the fluorescent coupling products remained close to the origin, whereas unreacted dansylcadaverine moved with an approximate R_f of 0.45. The experiment presented in Figure 1 with tissue transglutaminase pertains to Biot-Gln-Gln-Ile-Val as the acceptor; results with the other biotinylated substrate, Biot- ϵ -Aca-Gln-Gln-Ile-Val (not shown), were quite similar. The apparent affinities of the biotinylated peptides compared favorably with those of the previously published compound: Boc-Gln-Gln-Ile-Val (1). The biotinylated peptide, similarly to the *tert*-butoxycarbonyl derivative, was a considerably better substrate for tissue transglutaminase than for human factor XIIIa. No unreacted dansylcadaverine was left with tissue transglutaminase and 1 mM Biot-Gln-Gln-Ile-Val after 60 min of reaction (Figure 1, lane 4), whereas in the same time frame significant amounts of the free amine remained in the reaction using similar concentrations of factor XIIIa and 8 mM of the acceptor peptide (not shown).

Two biological cross-linking systems were employed to examine the effects of the newly synthesized biotinylated peptide derivatives. The results presented in Figure 2 relate to Biot-Gln-Gln-Ile-Val and those in Figure 3 to Biot- ϵ -Aca-Gln-Gln-Ile-Val. The key observations with regard to the Ca^{2+} -promoted cross-linking of crystallin subunits occurring in the rabbit lens homogenate under catalysis by the intrinsic transglutaminase can be summarized as follows. Increasing concentrations of Biot-Gln-Gln-Ile-Val (0.125, 0.25, and 0.5 mM; lanes 4–6, panel A, Figure 2) caused marked reduction in the amount of the cross-linked dimeric β crystallin products, marked $\text{X}\beta_2$. Simultaneously (as best recorded in lanes 4'–6' of panel B, Figure 2), a number of parent crystallin subunits incorporated the biotinylated peptide marker, which could be readily identified with the avidin-based blotting procedure. Consistent with taking on such sizeable branched peptide decorations, several (if not all) of the modified crystallin subunits were displaced to apparently higher M_r values on SDS-PAGE. This is easily recognized in the ~ 31 –35K region of M_r values in lanes 4–6, Figure 2.

The human factor XIIIa-mediated selective modification of α chains of human fibrin was examined in the presence of 20 mM Biot- ϵ -Aca-Gln-Gln-Ile-Val (Figure 3). The biotinylated peptide clearly inhibited production of the α_n chain type of polymers (compare lanes 2 and 3 in panel

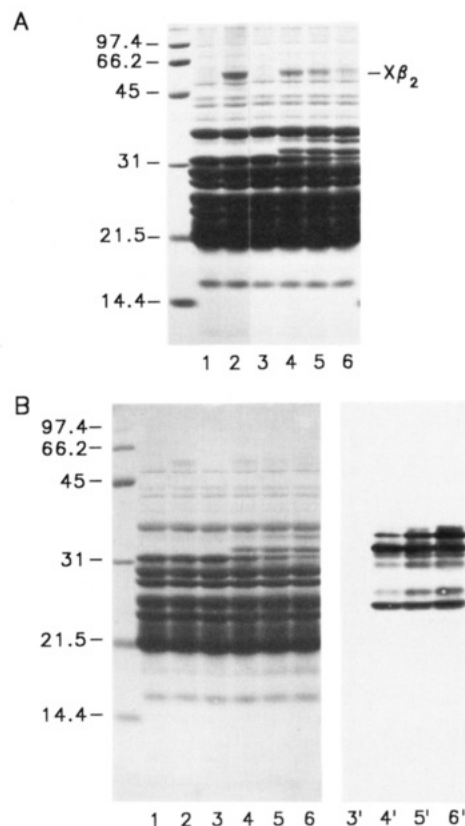


Figure 2. Inhibition of crystallin cross-linking in lens homogenates by Biot-Gln-Gln-Ile-Val with simultaneous labeling of certain subunits. Incubations were carried out at 37 °C for 90 min as previously described (1, 2). Reactions comprised lens homogenate (~ 50 mg of protein per mL), 20% (v/v) glycerol, 2 mM leupeptin, either no peptide (lanes 1 and 2) or 0.125 mM (lane 4), 0.25 mM (lane 5) or 0.5 mM Biot-Gln-Gln-Ile-Val (lanes 3 and 6), and either 2 mM EDTA (lanes 1 and 3) or 8 mM CaCl_2 (lanes 2 and 4–6). Samples were analyzed by SDS-PAGE and stained with Coomassie Brilliant Blue R (panel A). Alternatively (panel B), the gel was electroblotted onto nitrocellulose which was either stained with AmidoBlack (lanes 1–6) or probed for biotin (lanes 3'–6'). Cross-linked dimeric β crystallins ($M_r \sim 55,000$) are marked $\text{X}\beta_2$.

A) and incorporation of the biotin-containing label could be readily visualized by the avidin-based blotting procedure (lane 3 in panel C). Though most of the tracer was found to be associated with monomeric α chains, a low degree of labeling of γ - γ' dimers was also evident.

DISCUSSION

Of the two biological transamidating examples presented in this study, that involving human factor XIIIa represents an extracellular cross-linking event, whereas that in the rabbit lens is characteristic of the action of tissue transglutaminases in an intracellular environment. The functioning of factor XIIIa or activated fibrin-stabilizing factor is essential for normal hemostasis. As the last enzyme generated on the blood coagulation cascade, factor XIIIa—which similarly to tissue transglutaminases operates through a cysteine active center (7) and requires Ca^{2+} —brings about the fusion of fibrin molecules by promoting the formation of a few intermolecular *N*-(γ -glutamyl)lysine bonds between two γ chains and several α chains (8). These side-chain bridges augment the mechanical rigidity of the clot network (9–11) and greatly increase its resistance to lysis by thrombolytic agents (12–15). The intracellular phenomenon of transglutaminase-mediated protein cross-linking in lens is thought to be involved in the remodeling of fiber cells and also in the

Scheme I

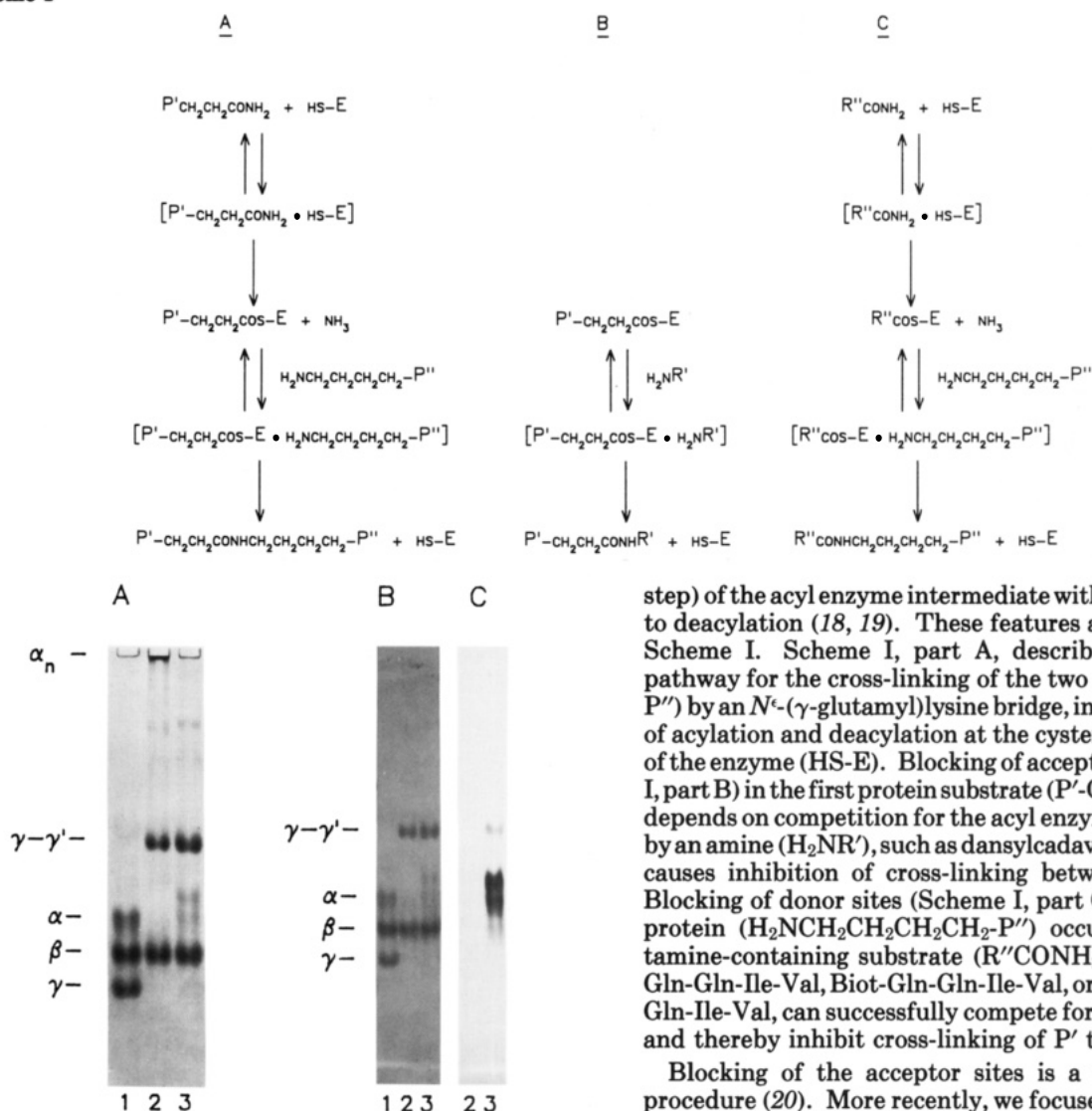


Figure 3. Incorporation of Biot- ϵ -Aca-Gln-Gln-Ile-Val into the parent α chains of human fibrin during reaction with human factor XIIIa. Incubations were carried out at 37 °C for 2 h as previously reported (1). Reactions comprised 50 mM Tris-HCl (pH 7.5), 100 mM NaCl, 2.5 mg/mL human fibrinogen, 20 μ g/mL factor XIII, 0.7 unit/mL human α -thrombin, either no peptide (lanes 1 and 2) or 20 mM Biot- ϵ -Aca-Gln-Gln-Ile-Val (lanes 3), and either 5 mM EDTA (lanes 1) or 5 mM CaCl_2 (lanes 2 and 3). Samples were analyzed by SDS-PAGE and stained with Coomassie Brilliant Blue R (panel A). Alternatively (panel B), the gel was electroblotted onto nitrocellulose and either stained with Amidoblack (panel B) or probed for biotin (panel C).

development of cataract. Certain subunits of β crystallin are specific targets for the endogenous transglutaminase which can be activated merely by the immersion of lens in a Ca^{2+} -containing medium. The earliest cross-linked products are the ca. 55 000 weight ($\text{X}\beta_2$) cross-linked β crystallin dimers (16, 17).

The kinetic pathway of catalysis by these transamidating enzymes is essentially the same as that of papain, for example, where a Michaelis-type of complexation is followed by the chemical steps of acylation and deacylation. What sets them apart from papain, however, is their remarkable affinity (over water) for the electron-donating second substrate comprising a primary amine so that aminolytic deacylation prevails over hydrolysis. Unlike with proteases, in general, there is a readily discernible additional complexation (a second Michaelis

step) of the acyl enzyme intermediate with the amine prior to deacylation (18, 19). These features are illustrated in Scheme I. Scheme I, part A, describes the catalytic pathway for the cross-linking of the two proteins (P' and P'') by an N^ϵ -(γ -glutamyl)lysine bridge, involving the steps of acylation and deacylation at the cysteine active center of the enzyme (HS-E). Blocking of acceptor sites (Scheme I, part B) in the first protein substrate ($\text{P}'\text{-CH}_2\text{CH}_2\text{CONH}_2$) depends on competition for the acyl enzyme intermediate by an amine ($\text{H}_2\text{NR}'$), such as dansylcadaverine (20), which causes inhibition of cross-linking between P' and P'' . Blocking of donor sites (Scheme I, part C) in the second protein ($\text{H}_2\text{NCH}_2\text{CH}_2\text{CH}_2\text{CH}_2\text{-P}''$) occurs when a glutamine-containing substrate ($\text{R}''\text{CONH}_2$), such as Dns-Gln-Gln-Ile-Val, Biot-Gln-Gln-Ile-Val, or Biot- ϵ -Aca-Gln-Gln-Ile-Val, can successfully compete for the free enzyme and thereby inhibit cross-linking of P' to P'' .

Blocking of the acceptor sites is a well-established procedure (20). More recently, we focused on developing reagents for the enzyme-directed labeling of donor functionalities. Short synthetic peptides containing *endo*-glutamyl residues, as found in the N-terminal sequence of fibronectin, could be shown to effectively interfere with protein-to-protein cross-linking reactions catalyzed either by tissue transglutaminases or by coagulation factor XIIIa (1). Moreover, concurrent with inhibition of cross-linking, labeling of select protein substrates was obtained. Since these enzymes are known to catalyze the formation of N^ϵ -(γ -glutamyl)lysine cross-links and since the synthetic peptides contained only enzyme-reactive glutamyl residues, it was concluded that interference with protein cross-linking was due to the specific blocking of ϵ -lysine functionalities of the donor protein substrate. In order to further capitalize on the advantages of the enzyme-directed and site-specific labeling of donor groups in biological systems, first Dns-Ala-Gln-Gln-Ile-Val and Dns-Pro-Gly-Gly-Gln-Gln-Ile-Val (2) and then Biot-Gln-Gln-Ile-Val and Biot- ϵ -Aca-Gln-Gln-Ile-Val were synthesized, as described in the present paper, and were shown to be effective in inhibiting protein cross-linking. While the dansylated derivatives allowed for the visualization of the blocked proteins by fluorescence as well as by immune detection with antibody to the incorporated dansyl hapten, fluorescence alone may not be universally applicable to all biological systems (21). We also found that only a few available anti-dansyl antibodies are useful for immunoblotting the dansyl peptides which become attached to

proteins. Thus, it is important to know that biotinylated peptide probes are now available for carrying out transglutaminase- and factor XIIIa-directed bioconjugation experiments to explore the amine donor sites in the protein substrates of these enzymes.

ACKNOWLEDGMENT

This work was aided by a U.S. Public Health Service Research Career Award (HL-03512) and by grants from the National Institutes of Health (EY-03942 and HL-02212).

LITERATURE CITED

- (1) Parameswaran, K. N., Velasco, P. T., Wilson, J., and Lorand, L. (1990) Labeling of ϵ -lysine crosslinking sites in proteins with peptide substrates of factor XIIIa and transglutaminase. *Proc. Natl. Acad. Sci. U.S.A.* 87, 8472-8475.
- (2) Lorand, L., Parameswaran, K. N., and Velasco, P. T. (1991) Sorting-out of acceptor-donor relationships in the transglutaminase-catalyzed cross-linking of crystallins by the enzyme-directed labeling of potential sites. *Proc. Natl. Acad. Sci. U.S.A.* 88, 82-83.
- (3) Parameswaran, K. N. (1990) A facile synthesis of biotin N-hydroxysuccinimide ester. *Org. Prep. Proc. Int.* 22, 119-121.
- (4) Stewart, J. M., and Young, J. D. (1969) Laboratory techniques in solid phase peptide synthesis. *Solid Phase Peptide Synthesis*, pp 62-63, Freeman, San Francisco, CA.
- (5) McCormick, D. B., and Roth, J. A. (1970) Specificity, stereochemistry, and mechanism of the color reaction between *p*-dimethylaminocinnamaldehyde and biotin analogs. *Anal. Biochem.* 34, 226-236.
- (6) Lorand, L., and Campbell, L. K. (1971) Transamidating enzymes I. Rapid chromatographic assays. *Anal. Biochem.* 44, 207-220.
- (7) Curtis, C. G., Brown, K. L., Credo, R. B., Domanik, R. A., Gray, A., Stenberg, P., and Lorand, L. (1974) Calcium-dependent unmasking of active center cysteine during activation of fibrin stabilizing factor. *Biochemistry* 13, 3774-3780.
- (8) Schwartz, M. L., Pizzo, S. V., Hill, R. L., and McKee, P. A. (1971) The effect of fibrin-stabilizing factor on the subunit structure of human fibrin. *J. Clin. Invest.* 50, 1506-1513.
- (9) Roberts, W. W., Lorand, L., and Mockros, L. F. (1973) Viscoelastic properties of fibrin clots. *Biorheology* 10, 29-42.
- (10) Mockros, L. F., Roberts, W. W., and Lorand, L. (1974) Viscoelastic properties of ligation-inhibited fibrin clots. *Biophys. Chem.* 2, 164-169.
- (11) Shen, L., and Lorand, L. (1983) Contribution of fibrin stabilization to clot strength. Supplementation of factor XIII-deficient plasma with the purified zymogen. *J. Clin. Invest.* 71, 1336-1341.
- (12) Lorand, L., and Jacobsen, A. (1962) Accelerated lysis of blood clots. *Nature* 195, 911-912.
- (13) Bruner-Lorand, J., Pilkington, T. R. E., and Lorand, L. (1966) Inhibitors of fibrin cross-linking: relevance for thrombolysis. *Nature* 210, 1273-1274.
- (14) Nilsson, J. L. G., Stenberg, P., Ljunggren, C., Hoffman, K. J., Lunden, R., Eriksson, O., and Lorand, L. (1972) Fibrin-stabilizing factor inhibitors. *Ann. N.Y. Acad. Sci.* 202, 286-296.
- (15) Lorand, L., and Nilsson, J. L. G. (1972) Molecular approach for designing inhibitors to enzymes involved in blood clotting. *Drug Design* (E. J. Ariens, Ed.) Vol. 3, pp 415-447, Academic Press, New York.
- (16) Lorand, L., Conrad, S. M., and Velasco, P. T. (1985) Formation of a 55 000-weight cross-linked β crystallin dimer in the Ca^{2+} -treated lens. A model for cataract. *Biochemistry* 24, 1525-1531.
- (17) Lorand, L., Conrad, S. M., and Velasco, P. T. (1987) Inhibition of β crystallin cross-linking in the Ca^{2+} -treated lens. *Invest. Ophthalmol. Vis. Sci.* 28, 1218-1222.
- (18) Curtis, C. G., Stenberg, P., Brown, K. L., Baron, A., Chen, K., Gray, A., Simpson, I., and Lorand, L. (1974) Kinetics of transamidating enzymes. Production of thiol in the reactions of thiol esters with fibrinolytic enzymes. *Biochemistry* 13, 3257-3262.
- (19) Stenberg, P., Curtis, C. G., Wing, D., Tong, Y. S., Credo, R. B., Gray, A., and Lorand, L. (1975) Transamidase kinetics. Amide formation in the enzymic reactions of thiol esters with amines. *Biochem. J.* 147, 155-163.
- (20) Lorand, L., Rule, N. G., Ong, H. H., Furlanetto, R., Jacobsen, A., Downey, J., Oner, N., and Bruner-Lorand, J. (1968) Amine specificity in transpeptidation. Inhibition of fibrin cross-linking. *Biochemistry* 7, 1214-1223.
- (21) Kvedar, J. C., Bilodeau, E. A., Daryanani, H. A., Pion, I. A., and Baden, H. P. (1990) The in-vivo localization of transglutaminase mediated cross-linking in murine epidermis. *J. Cell. Biol.* 111, 442a, abstract 2468.

Preparation and Characterization of a β -Lactamase-Fab' Conjugate for the Site-Specific Activation of Oncolytic Agents

Damon L. Meyer,^{*,†} Louis N. Jungheim,[‡] Stephen D. Mikolajczyk,[†] Timothy A. Shepherd,[‡] James J. Starling,[‡] and Clarence N. Ahlem[†]

Hybritech Incorporated, P.O. Box 269006, San Diego, California 92196-9006, and Lilly Research Laboratories, Eli Lilly and Company, Indianapolis, Indiana 46285. Received July 24, 1991

Antibody-directed catalysis (ADC) is a two-step method for the targeted delivery of chemotherapeutic agents in which enzyme-antibody conjugates, prelocalized to antigen-bearing cells, activate prodrugs designed to be substrates for the enzyme. An enzyme-Fab' conjugate exhibiting both native β -lactamase activity and immunoreactivity toward carcinoembryonic antigen (CEA) was constructed. Treatment of CEA-expressing LS174T cells with this conjugate imparted β -lactamase activity to the cells; β -lactamase activity was not imparted by treatment with unconjugated β -lactamase and not to CEA negative cells treated with conjugate. Cephalosporin-based prodrugs, and other substrates synthesized as model compounds, were found to have wide variations in their kinetic parameters toward the conjugate, with k_{cat} values ranging from 16 to 3300 s⁻¹ and K_M values ranging from 5 to 160 μ M. The prodrug derived from desacetylvinblastine-3-carboxylic acid hydrazide (DAVLBHYD) was studied in vitro and found to be 5-fold less cytotoxic to LS174T cells than the parent DAVLBHYD. For antigen-positive cells preincubated with conjugate, however, the prodrug showed the same potency as the parent drug. Thus, the combination of conjugate and prodrug appears to provide antigen-dependent toxicity to tumor cells.

INTRODUCTION

Antibody-directed catalysis (ADC¹) is a form of non-covalent drug delivery in which an enzyme-antibody conjugate is localized to a tumor target, where it converts subsequently administered prodrug to active drug. The ADC approach has been adopted as one way of overcoming potential difficulties with the delivery of therapeutic levels of free drugs to tumor targets using covalent protein-based delivery systems.

Demonstration of accumulation and retention of radiolabeled haptens by prelocalized bifunctional antibodies showed that the latter act as artificial receptors and proved that targeting of small molecules in vivo does not require covalent linkage to the targeting molecule. Furthermore, these studies showed that two-step noncovalent delivery has advantages for certain applications over covalent delivery. For instance, bifunctional antibody-based non-covalent delivery of isotopically labeled haptens results in decreased radiation exposure of normal tissues relative to covalent delivery (1). ADC represents an extension of this system in which the synthetic receptor not only binds the ligand but also activates and releases it. A number of enzyme-prodrug systems have been described for the antibody targeted activation of prodrugs (2-9).

[†] Hybritech Inc.

[‡] Eli Lilly and Co.

¹ Abbreviations: ADC, antibody-directed catalysis; CEA, carcinoembryonic antigen; DAVLBHYD, desacetylvinblastine-3-carboxylic acid hydrazide; β -l, β -lactamase; β -ICEM, β -lactamase-CEM231 Fab' 1:1 conjugate; sulfo-SMCC, sulfosuccinimido 4-(*N*-malimidomethyl)cyclohexane-1-carboxylate; BBS, 50 mM sodium borate, 100 mM sodium chloride (pH 8.2), containing 0.01% NP40 (Pierce); NP40, Nonidet P40; NHS, *N*-hydroxysuccinimide; DTPA, diethylenetriaminepentaacetic acid; DTNB, 5,5'-dithiobis(2-nitrobenzoic acid); PMSF, phenylmethanesulfonyl fluoride; PAGE, polyacrylamide gel electrophoresis; SDS, sodium dodecyl sulfate; RIA, radioimmunoassay; PADAC 2-[(*N,N*-dimethylanilin-4-yl)azo]pyridinium 3'-cephalosporin; PBS, 15 mM sodium phosphate, 100 mM NaCl (pH 7.4), containing 0.01% NP40; EBSS-MEM, Eagle basic salt solution-minimal essential media.

Of the multitude of enzymatic reactions which could potentially be used to activate prodrugs, the most directly and generally applicable appeared to be the type in which a molecule is cleaved into two pieces, especially that subset in which the enzyme recognizes only a portion of the substrate and is relatively insensitive to the identity of the remainder. Reactions catalyzed by β -galactosidase, exopeptidases, and various phosphatases are among those for which substrate recognition depends predominantly on one portion of the molecule and is independent of the remainder. However, a disadvantage of these enzymes is that they each cleave only a small number of linkage types, e.g. acetal, peptide, phosphate ester, which limits the variety of drugs that can be used. Ideally, the enzyme of choice should be capable of cleaving substrates connected through a wide range of functional groups, providing the ability to deliver several drugs with a single enzyme-antibody conjugate.

In addition, enzymatic activity that does not occur in eucaryotic organisms is advantageous for clinical use because it avoids interference from endogenous enzymes in nontarget tissues (activity which may be induced by the prodrug), or from endogenous substrates, inhibitors, etc. Other factors affecting enzyme selection included requirements for diffusible cofactors, molecular weight, and stability. β -Lactamase meets all of these criteria and, in addition, is relatively easy to obtain and purify. The β -lactamase produced by the P99 strain of *Enterobacter cloacae*, is particularly attractive since it can be produced as a substantial fraction of the cell's total protein (10, 11), has good cephalosporinase activity (12), and is relatively insensitive to substrate side-chain modification. The amino acid sequence for this enzyme has been determined, both by amino acid analysis and by gene sequencing (13), and the enzyme has been crystallized (14), though a high-resolution crystal structure has not yet been published.

β -Lactamase can cause the release of many different substituents from the 3' position of cephalosporins (15), depending on their leaving group propensity. This is because the release occurs in a reaction that is secondary

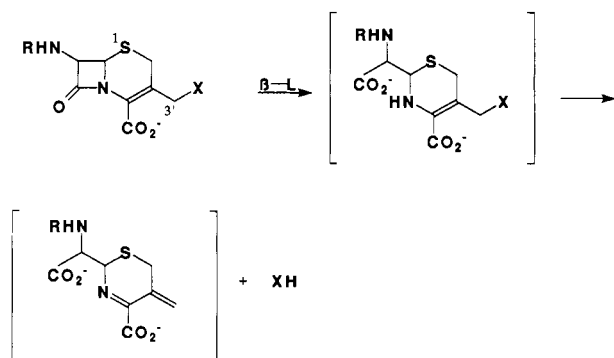


Figure 1. β -Lactamase catalyzes the hydrolysis of the cephalosporin β -lactam ring. Expulsion occurs subsequent to ring opening depending on the leaving group propensity of the 3' substituent.

to β -lactam ring hydrolysis (16, 17), the reaction actually catalyzed by the enzyme (Figure 1). Consequently, the linkage between cephem and drug is not directly acted upon by the enzyme and the 3' substituent generally does not impede catalysis. Advantage has been taken of the 3' substituent release upon ring opening to design dual-action antibiotics which act primarily as cephalosporins but release a secondary antibiotic when cleaved by a β -lactamase in the target bacteria (18, 19).

One of the goals of the ADC system was to make use of the carcinoembryonic antigen CEA. Potential barriers preventing the effective use of CEA for immunochemotherapy, such as low or heterogeneous antigen expression and shedding of the antigen into interstitial space, could be circumvented by the amplifying properties of enzyme targeting and the ultimate release of a readily diffusable drug. CEA has been the target in many preclinical antibody-drug conjugate studies (20–24), including a few in which bifunctional-antibody-mediated noncovalent localization of vinca alkaloids to tumors provided an enhanced therapeutic effect (25–27).

The conjugation methodology is derived from procedures described by Yoshitake et al. (28). The heterobifunctional cross-linker sulfo-SMCC (Pierce) covalently connects lysine ϵ -amino groups on the β -lactamase to naturally occurring sulfhydryls in the hinge region of the antibody Fab' fragment. This provides a heterogeneous conjugate that is regiospecific with respect to Fab', is comparable in immunoreactivity and enzymatic activity to the proteins from which it is derived, and has a known molecular weight as small or smaller than Fab'₂ fragments.

This paper describes the conjugation procedure, properties of the conjugates, and kinetic parameters obtained with selected substrates. A detailed description of prodrug syntheses is in preparation. Behavior of the system in nude mouse models is under investigation.

EXPERIMENTAL PROCEDURES

Syntheses of LY262319, LY262594, and LY266070 will be reported elsewhere. The synthesis of LY191026 has been described (9). All were shown to be analytically pure by HPLC, and structures were identified by NMR and MS before being tested as substrates. LY223425 (29) and DAVLBHYD (30) were generous gifts from G. Cullinan of Lilly Research Laboratories. Their preparation has been described. Keflin (cephalothin) was the gift of B. Jackson of Lilly Research Laboratories and is commercially available (Sigma).

Derivatization of β -Lactamase with Sulfo-SMCC. β -Lactamase was purified according to the method of Cartwright (31) after isolation from cell paste by a combination

of freeze-thaw and sonication. The purified enzyme was dialyzed into BBS and concentrated to 10 mg/mL. Its concentration was determined by A_{280} , assuming $A_{280}^{1\%} = 14$ (32). To 2 mL of the protein solution was added an aqueous solution containing 2.0 molar equiv of sulfo-SMCC (Pierce).

The concentration of this reagent was determined by measuring the release of NHS in a basic aqueous solution (70 mM Na_2CO_3). The molarity of the active ester was calculated by measuring the rise in OD_{260} using $\Delta\epsilon_{260} = 8 \times 10^3$.

The β -lactamase-SMCC reaction mixture was allowed to incubate at room temperature for 1 h, unstirred. The reaction mixture was then applied to a $1.5 \times \sim 23$ cm P6DG (Bio-Rad) column and eluted with 50 mM ammonium citrate, 100 mM sodium chloride, 1 mM DTPA (pH 6.3). The peak was collected manually in a single fraction. The concentration of protein in the peak fraction was measured by A_{280} again and was typically between 2.5 and 4.0 mg/mL. The average number of maleimide residues per enzyme molecule was determined by cysteine titration and quantitation of unreacted cysteine with DTNB (Aldrich).

A typical maleimide determination used 10 nmol of β -lactamase and 20 nmol of cysteine in a 500- μL reaction volume. Cysteine oxidation in the absence of maleimide was also determined as a control. The maleimide to β -lactamase ratio was typically 0.8–1.0 under the conditions described.

Preparation of Fab'. CEM-231 (murine IgG1) Fab'₂ fragments were prepared from intact antibody, which has been shown to react with CEA (33), by digestion with 3% pepsin (pepsin:Ab) (Boehringer Mannheim) at pH 4.1 in 0.1 M NaOAc, 0.1 M NaCl, at 37 °C for 4–6 h. The digestion was terminated by neutralization, followed by dialysis in 0.1 M sodium borate, 0.1 M NaCl (pH 8.2).

The Fab'₂ fragments were reduced to Fab' with 20 mM cysteine, in the presence of 1 mM DTPA, at 37 °C for 10 min. SDS PAGE was used to confirm that these conditions give complete hinge-region reduction with minimal heavy-light chain reduction. Cysteine was removed by P6DG (Bio-Rad) gel filtration in 50 mM ammonium citrate, 0.1 M NaCl, 0.5 mM DTPA (pH 6.3). DTNB assay showed between 2 and 3 reactive sulfhydryls per fragment.

Parent antibody and antibody fragment concentrations were determined by A_{280} assuming $A_{280}^{1\%} = 14$.

Conjugation of β -Lactamase to Fab'. To the maleimide- β -lactamase solution was added Fab' at a concentration of either 1.0 or 1.5 molar equiv of Fab' per maleimide (see results). After a 1-h incubation at room temperature, the reaction was stopped by addition of a 10-fold excess of *N*-ethylmaleimide as a 1 M ethanolic solution. The mixture was then applied to a 2×100 cm Sephadex G-150 superfine gel filtration column and eluted with BBS. Critical fractions were analyzed by PAGE and then pooled according to purity of the desired molecular weight component. The conjugate was then concentrated by ultrafiltration to 2–4 mg/mL for storage and diluted to the desired concentration for use. Purity of the conjugate was determined by SDS PAGE and by gel permeation HPLC, using two 0.9×30 cm Zorbax 250 columns (Du Pont) in series, eluted with 100 mM sodium phosphate (pH 7.0), at a flow rate of 1 mL/min.

Immunoreactivity of the β -Lactamase-Fab' Conjugate. Immunoreactivity of the conjugates, with reactant antibody and Fab' as control, was measured in a solid-phase assay as described by Phelps et al. (34). Conjugate binding was also checked in a competitive binding assay. Serial 2-fold dilutions of antibody from a starting con-

centration of 3.3 μM were prepared in DMEM + 10% fetal calf serum. To 10^6 LS174T cells were added 50 μL of the above dilution and 50 μL of 100 $\mu\text{g}/\text{mL}$ CEM 231-FITC. Cells were incubated with antibody for 1 h at 4 $^\circ\text{C}$ and then washed three times and fixed in 1% paraformaldehyde. Fluorescence was determined by flow cytometry and is reported as linear equivalent relative fluorescent intensity.

Enzymatic Activity of the β -Lactamase-Fab' Conjugate. β -Lactamase activity was measured by monitoring the change in absorbance of the chromogenic substrate PADAC (Calbiochem) at 570 nm in a stirred cuvette at 37 $^\circ\text{C}$ in PBS. Absorbance was measured every 5 s for 120 s using a Hewlett-Packard 8451A spectrophotometer, and linear portions of the rate plots were used to obtain reaction velocities. K_M and k_{cat} were determined from the slope and intercept of Lineweaver-Burk plots of the velocity data. PADAC's ϵ_{570} was taken to be 4.8×10^4 (product label).

Because of PADAC's low solubility and high extinction coefficient, the assay was run under conditions in which the rate is dependent on the substrate concentration. Consequently, the runs comparing activity between different preparations were all performed with a starting $A_{570} \approx 0.5$.

Substrate Kinetic Parameters. Kinetic parameters for conjugate acting on Keflin, LY262319, and LY262594 were measured as for PADAC, except that the change in absorbance was monitored at around 260 nm. LY262319 and LY262594 have a residual absorbance after hydrolysis, so $\Delta\epsilon$'s were obtained by completely hydrolyzing a known concentration of the substrate and calculating $\Delta\epsilon$ from the change in absorbance: $\Delta\epsilon_{258}$ for LY262319 = 6.60×10^3 (cm M^{-1}); $\Delta\epsilon_{260}$ for LY262594 = 8.4×10^3 (cm M^{-1}).

The spectral change on β -lactamase-catalyzed hydrolysis of prodrug substrates LY191026 and LY266070 was too small to be useful for quantitative determination of the rates. Consequently, HPLC methods were developed to monitor these reactions. Vials containing 1.5-mL solutions of varying concentrations of substrate at 37 $^\circ\text{C}$ in PBS (pH 7.4) were treated with 0.11 nM β -lactamase. Samples were quenched after 90 s by adding 0.5 mL of reaction solution to 0.5 mL of 34% acetonitrile in 200 mM potassium phosphate (pH 3.0). Control experiments were performed to determine appropriate concentrations so that less than 10% of the substrate would be consumed during the 90-s reaction, to assure a linear reaction rate. Duplicate samples of the quenched reaction mixtures were injected onto a 0.46×15 cm C-18 reverse-phase HPLC column eluted isocratically at 1 mL/min with the buffer containing 34% acetonitrile in 200 mM potassium phosphate. The starting prodrug and/or product concentration was monitored by absorbance at 266 nm.

Determination of Antigen-Mediated β -Lactamase Activity. Antigen-positive (LS174T) and -negative (MOLT4) tumors were harvested from nude mice. Single cell suspensions were prepared at 2×10^7 cells/mL: LS174T 23% viable, MOLT4 75% viable.² To 1 mL of cells was added sufficient conjugate or β -lactamase to bring the assay concentration to the desired level. Cells were incubated either 1 or 10 min and washed with PBS. The activity was measured by the difference in absorbance at 570 nm before and after a 10-min incubation with PADAC. Results were recorded as the percent change in 570-nm absorbance over the incubation period.

² Cell viability was not considered crucial to the successful performance of the assay.

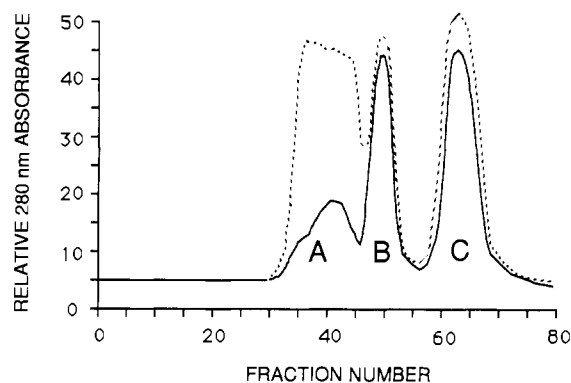


Figure 2. Purification by gel permeation chromatography of the Fab'-maleimido- β -lactamase reaction mixture. Comparison of elution patterns for 1:1 (dashed line) and 1.5:1 (solid line) Fab':maleimido- β -lactamase reaction mixtures. Ten milliliters of 15 mg/mL protein was loaded on a 2×100 cm column of Sephadex G-150 superfine equilibrated with BBS and eluted with BBS at 0.1–0.2 mL/min. Fractions were approximately 4.5 mL. Peak A contains high molecular weight byproducts, B contains the 1:1 conjugate with which studies were performed, and C contains unreacted β -lactamase and Fab'.

In Vitro Conjugate-Mediated Prodrug Activation. Target cells resuspended in 75% leucine-deficient EBSS-MEM + 10% dialyzed fetal bovine serum + gentamicin were seeded into 96-well plates (2×10^4 cells/well) and incubated overnight. All incubations were performed at 37 $^\circ\text{C}$, 5% CO_2 . The supernatants were removed, and appropriate wells treated with CEM or β -lactamase at 25 $\mu\text{g}/\text{mL}$ (280 nM) for 1 h. The wells were washed and 0.2 mL of the drug or prodrug at 10, 1, 0.1, 0.01, or 0.001 $\mu\text{g}/\text{mL}$ vinca content were added to the cells. The plates were incubated for the desired length of time (1–48 h). At the end of the treatment period the cells were washed and incubated in fresh media for the remainder of the 48-h period. Supernatants were then removed, 4 μCi of tritiated leucine in 0.2 mL of leucine-deficient media was added to each well, and the plates were incubated overnight. The cells were harvested, and the uptake of tritiated leucine was determined by liquid scintillation counting. All samples were run in quadruplicate.

RESULTS

The G-150 elution profile of conjugation reactions performed under two different sets of conditions (Figure 2) shows that products are formed in three molecular weight ranges. The components consist of 1:1 β -1 to Fab' conjugate (peak B), along with unreacted Fab' and β -1 (peak C), and higher molecular weight adducts (peak A). The higher molecular weight adducts are the result of either the reaction of more than one sulfhydryl in the Fab' hinge region with a sulfo-SMCC-modified β -1 or the reaction of Fab's with more than one maleimide on a single β -1 molecule. Increasing the ratio in the reaction mixture of Fab' to maleimido- β -lactamase from 1:1 to 1.5:1 caused an overall improvement in the yield of 1:1 conjugate. The purification also improved due to decreased peak overlap with a smaller amount of high molecular weight product.

Analytical gel filtration of the purified product (peak B, Figure 2) on Zorbax G-250 columns (broken line, Figure 3) showed that the conjugate has a molecular weight in the desired range. Molecular weights were also confirmed by polyacrylamide gel electrophoresis (not shown) comparing purified product to Fab', β -lactamase, Fab'₂, and whole antibody. Immunoreactivity of the conjugate was evaluated in a whole-cell assay (Figure 4) in which binding of fluorescent-labeled whole CEM231 to LS174T cells was

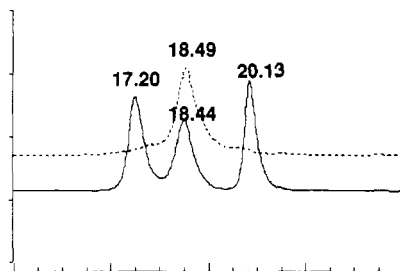


Figure 3. Analytical gel sizing HPLC profile of purified conjugate (dashed line) monitored by absorbance at 280 nm. Elution positions of known proteins (solid line): whole antibody (17.20 min) and β -1 (20.13 min) mixed with 1:1 β -1-Fab' conjugate. Analyses were performed using two 0.9 \times 30 cm Zorbax 250 columns in series eluted with 100 mM sodium phosphate (pH 7.0) at 1 mL/min. Molecular weight identification was confirmed by SDS PAGE.

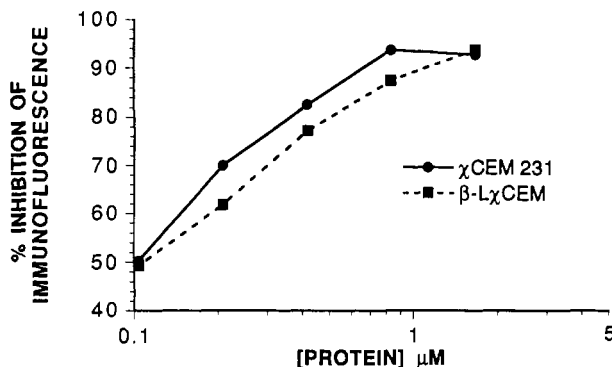


Figure 4. Competitive binding immunoreactivity comparison of parent antibody and conjugate. The ability of conjugate (dashed line) and parent antibody (solid line) to competitively inhibit the binding of FITC-labeled parent antibody to antigen-positive LS174T cells was determined as described in the Experimental Procedures.

Table I. Comparison of PADAC Kinetic Parameters for Conjugate and Enzyme

enzyme	K_M , μ M	k_{cat} , s^{-1}
β -lactamase	53 ± 18^a	106 ± 33
β -lCEM	55 ± 12	135 ± 31

^a Standard deviations of the parameters are calculated from the standard deviations of the slope and intercept (data analyzed using the linear regression module of the RS/1 computer program, BBN Software Products Corp.) of a single Lineweaver-Burk plot. Velocities were measured at four different concentrations in either duplicate or triplicate at each, and at least 11 points were used to calculate each velocity.

competitively inhibited by conjugate, and by direct binding of iodinated conjugate to an antigen-bearing solid phase. In the whole-cell assay, conjugate immunoreactivity was comparable to that of parent antibody. In the solid-phase assay, the conjugate showed immunoreactivity of 79%, while a single binding arm bifunctional antibody was 96% immunoreactive.

Enzymatic activity of the conjugate was determined by comparing Lineweaver-Burk plots for conjugate and native enzyme using PADAC as substrate (Table I). Both K_M and k_{cat} are experimentally indistinguishable. The marginal difference in k_{cat} could be due to inexact values for the protein extinction coefficients. Modification of β -lactamase by sulfo-SMCC was found to have no effect on β -lactamase activity.

Catalytic parameters were measured for a set of available substrates in an attempt to predict the impact of drug structure on catalytic activity. K_M , k_{cat} , and their ratio were found to vary substantially (Table II) among the

compounds tested. The finding that the cephem β -sulfoxides tested exhibited better hydrolytic stability than the native cephem's (see Conclusions) led us to test their activity as β -lactamase substrates. The results (Table II: LY262594 vs LY262319) show that the cephem sulfoxides can be better substrates, in terms of k_{cat}/K_M ratio, than their native cephem analogues.

Large relative errors (on the order of 50%) are associated with the k_{cat} and K_M values for PADAC, LY191026, and LY266070. In the case of PADAC and LY266070, this is because insolubility prevented velocity determinations at concentrations above about 20% of the K_M . Consequently, there are no points close to the intercept of the Lineweaver-Burk plot. Obtaining more points in the low substrate concentration range does not improve the confidence limit. This actually amounts to an inability to measure k_{cat} and K_M independently, since the slope of the plot, which represents the ratio, can be determined relatively precisely.

In the case of LY191026, the uncertainty is due to the fact that measurements of the very rapid velocity require very low substrate concentrations to remain in the linear range, and consequently, the ability to accurately integrate the HPLC peaks becomes limiting.

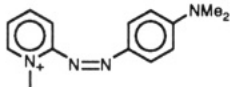

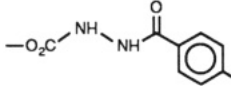
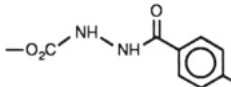
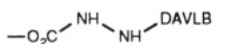
The bifunctional nature of the conjugate, i.e. its ability to simultaneously bind antigen and catalyze cephem ring opening, was tested by allowing it to bind with antigen-bearing cells, rinsing the cells to remove unbound conjugate, and then measuring the ability of cells resuspended in buffer to hydrolyze PADAC. The results (Table III) show that the conjugate has the ability to bind to cells in vitro and thereby impart β -lactamase activity. The quantity of the enzymatic activity associated with the cells depended on the time and concentration of conjugate in the incubation mixture. Treatment of antigen-positive cells with β -lactamase showed that the activity could not be attributed to nonantigen-mediated adherence of β -1 to the cells. Treatment of antigen-negative cells with conjugate confirmed that interaction of conjugate with cells is mediated strictly through the antibody binding site. A background level of "activity" (5–7% Δ OD) was observed in the negative controls, attributable to dilution in the assay. The slightly higher activity observed at the high β -1 level may have resulted from insufficient washing.

The in vitro cytotoxicity of LY266070 or DAVLBHYD incubated for various times in the presence of CEM or β -lCEM is shown in Figure 5. The cytotoxicity of DAVLBHYD is not affected significantly by incubation in the presence of CEM or β -lCEM, whereas LY266070 toxicity is greatly enhanced (lower ID_{50} values) by incubation for 1, 3, or 5 h in the presence of the conjugate. LY266070 toxicity cannot be distinguished from DAVLBHYD at the 24-h time point. In one experiment irrelevant (nonantigen binding) β -lactamase conjugate control was evaluated for LY266070 activation, at drug exposure times of 1 and 3 h. At the 3-h point the ID_{50} values of LY266070 and DAVLBHYD were 0.83 and 0.024 μ g/mL, respectively, indicating no enhanced cytotoxicity attributable to the irrelevant conjugate and, therefore, that the activation demonstrated in Figure 5 is an antigen-mediated event.

CONCLUSIONS

A conjugation procedure has been developed that produces a conjugate with the essential properties required for an ADC system. The conjugate has a single binding arm and a molecular weight of about 90 000. Pharmacokinetic studies of antibody fragments in mouse models have shown that mono- and bifunctional Fab'2 exhibit rapid serum clearance relative to tumor residence in comparison

Table II. Kinetic Parameters for Substrates

	X	Y	k_{cat} , s ⁻¹	K_M , μ M	k_{cat}/K_M , (s μ M) ⁻¹
KEFLIN	OAc	.. ^a	50	5	10
PADAC		..	135	55	2.5
LY191026		..	3300	9	400
LY262319		..	16	2	9
LY262594		O	1000	38	26
LY266070		O	1700	160	11

^a Electron lone pair.Table III. Antigen-Dependent β -Lactamase Activity

enzyme	concn, nM	antigen expression	time, min	% Δ ^a
β -1	50	+ ^b	10	13 ^c
	10	+	10	5
β -ICEM	50	+	10	77
	10	+	10	54
	50	+	1	64
	10	+	1	38
β -ICEM	50	- ^d	10	7
	10	-	10	6

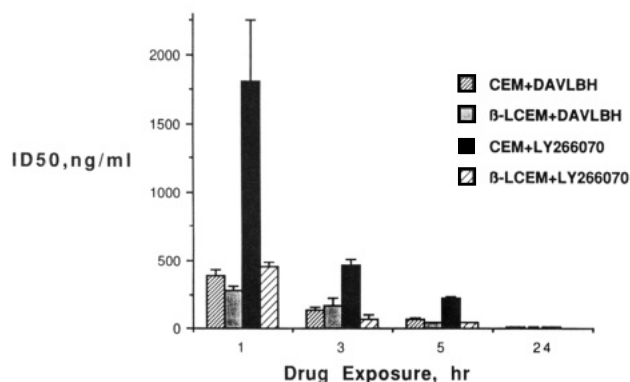
^a Percent decrease in 570-nm absorbance by PADAC under conditions described in the paper. A large number indicates catalytic degradation of PADAC due to β -lactamase on the cell surface.^b LS174T cells. ^c A small decrease in absorbance may result from dilution in the assay, uncatalyzed hydrolysis of PADAC, or insufficient washing of the cells. ^d MOLT4 cells.

Figure 5. In vitro cytotoxicity was determined as described in the Experimental Procedures. The dose of drug required to inhibit the incorporation of tritiated leucine to 50% of the control value (ID_{50}) is given on the ordinate, while the time of drug exposure is indicated on the abscissa. The data shown in the figure is from a representative experiment. Similar data were obtained in four separate experiments which included drug exposure times of 1, 3, 5, 24, and 48 h. All samples were run in quadruplicate, and the mean \pm SD values are indicated in the figure.

to whole antibodies (35). Hence, a single binding arm conjugate of less than 100 000 molecular weight shows relatively high tumor to blood concentration ratios at times longer than about 48 h after injection. Furthermore,

studies with synthetic bifunctional Fab'₂ have provided evidence that two-step delivery systems can cause localization of small molecules administered independently to antigen-bearing target cells (1).

The heterobifunctional cross-linker used for the conjugation, sulfo-SMCC, reacts nonregiospecifically with ϵ -amino groups of lysine residues on proteins. Since β -1 activity was not significantly impaired under the conditions described, it is probable that neither of the lysine residues in the vicinity of the active site of this enzyme are particularly reactive with this reagent. The lack of impact of conjugation on immunoreactivity of the antibody fragment results from the fact that the sulfhydryls available for reaction occur naturally in the hinge region, away from the binding site.

The finding that all of the substrates developed for the ADC delivery system are readily cleaved by the *E. cloacae* β -lactamase (Table II) is in accord with findings of studies on the mechanism of catalyzed and uncatalyzed breakdown of cephalosporins (15–17, 36–42) and with the known tolerance of this particular enzyme for substitution of the cephalosporin nucleus. Despite large relative errors associated with these measurements, it is clear that there is a very wide variation in k_{cat} and K_M and their ratio and that simple substrates, such as Keflin, are not necessarily the most rapidly hydrolyzed. Although this observation is consistent with previous reports (43–46), the phenomenon is only poorly understood. Of particular interest is the finding that cephem β -sulfoxides are excellent substrates. Cursory data suggest that they are also more stable to hydrolysis than their native cephem analogues and therefore may be preferred candidates for use in an ADC system.

The conjugate is conveniently assayed using the chromogenic substrate PADAC (47, 48). Alternatively, nitrocefin could be used (49), but nitrocefin undergoes a spectral change on binding to albumin (50) which interferes with its ability to act as a chromogenic substrate. PADAC was chosen so that its use could be applied to samples containing serum.

That the conjugate combined enzymatic activity and antigen binding activity simultaneously was demonstrated

by treating antigen positive cells sequentially with conjugate and PADAC. Cells expressing the antigen clearly exhibited β -lactamase activity, indicating that conjugate was able to perform both the binding and the catalytic function. Negative results in the case of antigen-positive cells treated with native β -lactamase showed that non-specific interaction of enzyme with cell or antigen was not responsible for the interaction, and negative results in the case of antigen negative cells treated with conjugate illustrated the antibody binding site dependence of the phenomenon.

A reproducible difference in potency between prodrug and drug was observed in leucine incorporation assays on antigen-positive cells in culture. Pretreatment of the cells with conjugate eliminated the differential, thus demonstrating activation of the prodrug, in an antigen-dependent manner. The diminished potency of the prodrug with respect to the drug, and the ability of cell-bound conjugate to activate the prodrug, demonstrated that both prodrug and conjugate had the requisite properties for antibody-directed catalysis. The combination of potency differential and activation was also the primary criterion for selecting candidate prodrugs for further study.

ACKNOWLEDGMENT

We acknowledge extensive contributions to this work made by Thomas R. Parr, Jr., who provided us with β -lactamase; George Cullinan, who supplied starting materials for preparation of the vinca prodrugs; Daniel G. Mackensen and Pamela Resch, who provided cells and other support; and Kevin L. Law and Jeanette Fegan, who performed immunoreactivity and cytotoxicity determinations. In addition, we are indebted to the Hybritech Therapeutics and Lilly Research organizations, which provided an environment in which this investigation could flourish.

LITERATURE CITED

- (1) Stickney, D. R., Slater, J. B., Kirk, G. A., Ahlem, C. N., Chang, C. H., and Frincke, J. M. (1989) Bifunctional Antibody: ZCE/CHA¹¹¹ Indium BLEDTA-IV Clinical Imaging in Colorectal Carcinoma. *Antibody Immunoconjugates Radiopharm.* 2, 1-13.
- (2) Senter, P. D., Saulnier, M. G., Schreiber, G. J., Hirschberg, D. L., Brown, J. P., Hellström, I., and Hellström, K. E. (1988) Anti-tumor Effects of Antibody-Alkaline Phosphatase Conjugates in Combination with Etoposide Phosphate. *Proc. Natl. Acad. Sci., U.S.A.* 85, 4842-6.
- (3) Senter, P. D., Schreiber, G. J., Hirschberg, D. L., Ashe, S. A., Hellström, K. E., and Hellström, I. (1989) Enhancement of the In Vitro and In Vivo Antitumor Activities of Phosphorylated Mitomycin C and Etoposide Derivatives by Monoclonal Antibody-Alkaline Phosphatase Conjugates. *Cancer Res.* 49, 5789-92.
- (4) Senter, P. D. (1990) Activation of Prodrugs by Antibody-Enzyme Conjugates: A New Approach to Cancer Therapy. *FASEB J.* 4, 188-93.
- (5) Kerr, D. E., Senter, P. D., Burnett, W. V., Hirschberg, D. L., Hellström, I., and Hellström, K. E. (1990) Antibody-Penicillin-V-Amidase Conjugates Kill Antigen Positive Tumor Cells When Combined with Doxorubicin phenoxyacetamide. *Cancer Immunol. Immunother.* 31, 202-6.
- (6) Sahin, U., Hartmann, F., Senter, P., Pohl, C., Engert, A., Diehl, V., and Pfreundschuh, M. (1990) Specific Activation of the Prodrug Mitomycin Phosphate by a Bispecific Anti-CD30/Anti-Alkaline Phosphatase Monoclonal Antibody. *Cancer Res.* 50, 6944-8.
- (7) Springer, C. J., Antoniwi, P., Bagshawe, K. D., Searle, F., Bisset, G. M. F., and Jarman, M. (1990) Novel Prodrugs Which Are Activated to Cytotoxic Alkylating Agents by Carboxypeptidase G2. *J. Med. Chem.* 33, 677-81.
- (8) Bagshawe, K. D., Springer, C. J., Searle, F., Antoniwi, P., Sharma, S. K., Melton, R. G., and Sherwood, R. F. (1988) A Cytotoxic Agent Can Be Generated Selectively at Cancer Sites. *Br. J. Cancer* 58, 700-3.
- (9) Shepherd, T. A., Jungheim, L. N., Meyer, D. L., and Starling, J. J. (1991) A Novel Targeted Delivery System Utilizing a Cephalosporin-Oncolytic Prodrug Activated by an Antibody β -Lactamase Conjugate for the Treatment of Cancer. *BioMed. Chem. Lett.* 1, 21-6.
- (10) Lindberg, F., and Normark, S. (1987) Common Mechanism of *ampC* β -Lactamase Induction in Enterobacteria: Regulation of the Cloned *Enterobacter cloacae* P99 β -Lactamase Gene. *J. Bacteriol.* 169, 758-63.
- (11) Gootz, T. D., Sanders, C. C., and Goering, R. V. (1982) Resistance to cefamandole: Depression of β -lactamases by cefoxitin and mutation in *Enterobacter cloacae*. *J. Infect. Dis.* 146, 34-42.
- (12) Fleming, P. C., Goldner, M., and Glass, D. G. (1963) Observations on the Nature, Distribution, and Significance of Cephalosporinase. *Lancet* 1399-401.
- (13) Galleni, M., Lindberg, F., Normark, S., Cole, S., Honore, N., Joris, B., and Frère, J.-M. (1988) Sequence and Comparative Analysis of Three *Enterobacter cloacae ampC* β -Lactamase Genes and their Products. *Biochem. J.* 250, 753-60.
- (14) Charlier, P., Dideberg, O., Frère, J.-M., Moews, P. C., and Knox, J. R. (1983) Crystallographic Data for the β -Lactamase from *Enterobacter cloacae* P99. *J. Mol. Biol.* 171, 237-8.
- (15) Boyd, D. B., and Lunn, W. H. W. (1979) Electronic Structures of Cephalosporins and Penicillins. 9. Departure of a Leaving Group in Cephalosporins. *J. Med. Chem.* 22, 778-84.
- (16) Pratt, R. F., and Faraci, W. S. (1986) Direct observation by ¹H NMR of Cephalosporate Intermediates in Aqueous Solution during the Hydrazinolysis and β -Lactamase-Catalyzed Hydrolysis of Cephalosporins with 3'-Leaving Groups: Kinetics and Equilibria of the 3'-Elimination Reaction. *J. Am. Chem. Soc.* 108, 5328-33.
- (17) Faraci, S. W., and Pratt, R. F. (1984) Elimination of a Good Leaving Group from the 3'-Position of a Cephalosporin Need Not Be Concerted with β -Lactam Ring Opening: TEM-2 β -Lactamase-Catalyzed Hydrolysis of Pyridine-2-azo-4'-(N',N'-dimethyl)aniline Cephalosporin (PADAC) and of Cephaloridine. *J. Am. Chem. Soc.* 106, 1489-90.
- (18) Mobashery, S., Lerner, S. A., and Johnston, M. (1986) Conscripting β -Lactamase for Use in Drug Delivery. Synthesis and Biological Activity of a Cephalosporin C10-Ester of an Antibiotic Dipeptide. *J. Am. Chem. Soc.* 108, 1685-6.
- (19) Albrecht, H. A., Beskid, G., Christenson, J. G., Durkin, J. W., Fallat, V., Georgopapadakou, N. H., Keith, D. D., Konzelmann, F. M., Lipschitz, E. R., McGarry, D. H., Siebelist, J., Wei, C. C., Weigle, M., and Yang, R. (1991) Dual-Action Cephalosporins: Cephalosporin 3'-Quaternary Ammonium Quinolones. *J. Med. Chem.* 34, 669-75.
- (20) Bernier, L. G., Page, M., Gaudreault, R. C., and Joly, L. P. (1984) A Chlorambucil-anti-CEA Conjugate Cytotoxic for Human Colon Adenocarcinoma Cells In Vitro. *Br. J. Cancer* 49, 245-6.
- (21) Rowland, G. F., Simmonds, R. G., Gore, V. A., Marsden, C. H., and Smith, W. (1986) Drug Localization and Growth Inhibition Studies of Vindesine-Monoclonal anti-CEA Conjugates in a Human Tumor Xenograft. *Cancer Immunol. Immunother.* 21, 183-7.
- (22) Shih, L. B., and Goldenberg, D. M. (1990) Effects of Methotrexate-Carcinoembryonic-Antigen-Antibody Immunoconjugates on GW-39 Human Tumors in Nude Mice. *Cancer Immunol. Immunother.* 31, 197-201.
- (23) Page, M., Delorme, F., Lafontaine, F., and Dumas, L. (1984) Chemotherapy with Daunorubicin-anti-CEA Conjugates in Human Colon Adenocarcinoma Grafted in Nude Mice. *Semin. Oncol.* 11, 56-8.
- (24) Iwahashi, T., Tone, Y., Usui, J., Watanabe, H., Sugawara, I., Mori, S., and Okazaki, H. (1989) Selective Killing of Carcinoembryonic-Antigen (CEA)-Producing Cells In Vitro by the Immunoconjugate Cytorhodin-S and CEA-Reactive Cytorhodin-S Antibody CA208. *Cancer Immunol. Immunother.* 30, 239-46.

- (25) Corvalan, J. R. F., Smith, W., Gore, V. A., and Brandon, D. R. (1987) Specific In Vitro and In Vivo Drug Localization to Tumor Cells Using a Hybrid-Hybrid Monoclonal Antibody Recognizing Both Carcinoembryonic Antigen (CEA) and Vinca Alkaloids. *Cancer Immunol. Immunother.* 24, 133-7.
- (26) Corvalan, J. R. F., and Smith, W. (1987) Construction and Characterization of a Hybrid-Hybrid Monoclonal Antibody Recognizing Both Carcinoembryonic Antigen (CEA) and Vinca Alkaloids. *Cancer Immunol. Immunother.* 24, 127-32.
- (27) Corvalan, J. R. F. (1988) Tumor Therapy with Vinca Alkaloids Targeted by a Hybrid-Hybrid Monoclonal Antibody Recognizing both CEA and Vinca Alkaloids. *Int. J. Cancer*, Suppl. 2, 22-5.
- (28) Yoshitake, S., Yamada, Y., Ishikawa, E., and Masseyeff, R. (1979) Conjugation of Glucose Oxidase from *Aspergillus niger* and Rabbit Antibodies Using N-Hydroxysuccinimide Ester of N-(4-Carboxycyclohexylmethyl)-Maleimide. *Eur. J. Biochem.* 101, 395-9.
- (29) Conrad, R. A., Cullinan, G. J., Gerzon, K., and Poore, G. A. (1979) Structure-Activity Relationships of Dimeric Catharanthus Alkaloids. 2. Experimental Antitumor Activities of N-Substituted Deacetylvinblastine Amide (Vindesine) Sulfates. *J. Med. Chem.* 22, 391-400.
- (30) Barnett, C. J., Cullinan, G. J., Gerzon, K., Hoying, R., Jones, W. E., Newlon, W. M., Poore, G. A., Robison, R. L., Sweeney, M. J., and Todd, G. C. (1978) Structure-Activity Relationships of Dimeric Catharanthus Alkaloids. 1. Deacetylvinblastine Amide (Vindesine) Sulfate. *J. Med. Chem.* 21, 88-96.
- (31) Cartwright, S. J., and Waley, S. G. (1984) Purification of β -Lactamases by Affinity Chromatography on Phenylboronic Acid-Agarose. *Biochem. J.* 221, 505-12.
- (32) Cartwright, S. J., and Waley, S. G. (1987) Cryoenzymology of β -Lactamases. *Biochem. J.* 26, 5329-37.
- (33) Beidler, C. B., Ludwig, J. R., Cardenas, J., Phelps, J., Papworth, C. G., Melcher, E., Sierzega, M., Myers, L. J., Unger, B. W., Fisher, M., David, G. S., and Johnson, M. J. (1988) Cloning and High Level Expression of a Chimeric Antibody with Specificity for Human Carcinoembryonic Antigen. *J. Immunol.* 141, 4053-60.
- (34) Phelps, J. E., Beidler, D. E., Jue, R. A., Unger, B. W., and Johnson, M. W. (1990) Expression and Characterization of a Chimeric Antibody with Therapeutic Applications. *J. Immunol.* 145, 1200-4.
- (35) Mackensen, D. G., Courtney, L. P., Desmond, W. J., Hansen, N., Resch, P. A., Sanders, V. L., Lowe, S. R., Ahlem, C. N., Anderson, L. D., and Frincke, J. M. (1989) Enhanced Antitumor Effect of Multiple Course Radioimmunotherapy Using a Bifunctional Antibody. *J. Nucl. Med.* 31 (5th Supplement), 911.
- (36) Faraci, W. S., and Pratt, R. F. (1986) Interactions of Cephalosporins with the *Streptomyces* R61 DD-Transpeptidase/Carboxypeptidase. Influence of the 3'-Substituent. *Biochem. J.* 238, 309-12.
- (37) Boyd, D. B. (1985) Leaving Group Ability and pK_a in Elimination Reactions. *J. Org. Chem.* 50, 885-6.
- (38) Boyd, D. B. (1985) Elucidating the Leaving Group Effect in the β -Lactam Ring Opening Mechanism of Cephalosporins. *J. Org. Chem.* 50, 886-8.
- (39) Boyd, D. B. (1984) Electronic Structures of Cephalosporins and Penicillins. 15. Inductive Effect of the 3-Position Side Chain in Cephalosporins. *J. Med. Chem.* 27, 63-6.
- (40) Boyd, D. B., Hermann, R. B., Presti, D. E., and Marsh, M. M. (1975) Electronic Structures of Cephalosporins and Penicillins. 4. Modeling Acylation by the β -Lactam Ring. *J. Med. Chem.* 18, 408-17.
- (41) Page, M. I., and Proctor, P. (1984) Mechanism of β -Lactam Ring Opening in Cephalosporins. *J. Am. Chem. Soc.* 106, 3820-5.
- (42) Rao, S. N., and O'Ferrall, R. A. M. (1990) A Structure-Reactivity Relationship for Base-Promoted Hydrolysis and Methanolysis of Monocyclic β -Lactams. *J. Am. Chem. Soc.* 112, 2729-35.
- (43) James, R. (1983) Relative Substrate Affinity Index Values: a Method for Identification of Beta-Lactamase Enzymes and Prediction of Successful Beta-Lactam Therapy. *J. Clin. Microbiol.* 17, 791-8.
- (44) Labia, R., Morand, A., Tiwari, K., Sirot, J., Sirot, D., and Petit, A. (1988) Interactions of New Plasmid-Mediated β -Lactamases with Third-Generation Cephalosporins. *Rev. Infect. Dis.* 10, 885-91.
- (45) Galleni, M., Amicosante, G., and Frere, J.-M. (1988) A Survey of the Kinetic Parameters of Class C β -Lactamases. Cephalosporins and Other β -Lactam Compounds. *Biochem. J.* 255, 123-9.
- (46) Mazzella, J., and Pratt, R. F. (1989) Effect of the 3'-Leaving Group on Turnover of Cephem Antibiotics by a Class C β -Lactamase. *Biochem. J.* 259, 255-60.
- (47) Schindler, P., and Huber, G. (1980) Use of PADAC, A Novel Chromogenic β -Lactamase Substrate, for the Detection of β -Lactamase Producing Organisms and Assay of β -Lactamase Inhibitors/Inactivators. *Enzyme Inhibitors* (U. Brodbeck, Ed.) pp 169-76, Verlag Chemie, Weinheim.
- (48) Thornsberry, C., W. J. Novick, J., and Jones, R. N. (1982) PADAC. Its Use as an Indicator of Relevant Beta-Lactamase Production In Clinical Bacterial Isolates. Calbiochem-Behring product brochure, 10933 N. Torrey Pines R., La Jolla, CA, 92037.
- (49) O'Callaghan, C. H., Morris, A., Kirby, S. M., and Shingler, A. H. (1972) Novel Method for Detection of β -Lactamase by Using a Chromogenic Cephalosporin Substrate. *Antimicrob. Ag. Chemother.* 1 (4), 283-8.
- (50) Jones, R. N., Wilson, H. W., and W. J. Novick, J. (1982) In Vitro Evaluation of Pyridine-2-azo-p-dimethylaniline Cephalosporin (PADAC), a New Diagnostic Chromogenic Reagent Compared to Nitrocefin, Cephacetrile, and Other Beta-Lactam Compounds. *J. Clin. Microb.* 15, 954-8.

Registry No. PADAC, 77449-91-3; LY191026, 134762-02-0; LY262319, 137848-34-1; LY262594, 137848-35-2; LY266070, 137848-36-3; keflin, 58-71-9; desacetylvinblastine-3-carboxylic acid hydrazide, 55383-37-4.

Synthesis, Conformation, Biodistribution, and in Vitro Cytotoxicity of Daunomycin–Branched Polypeptide Conjugates†

F. Hudecz,*‡ J. A. Clegg,§ J. Kajtár,|| M. J. Embleton,§ M. Szekerke,† and R. W. Baldwin§

Research Group for Peptide Chemistry, Hungarian Academy of Science, and Institute of Organic Chemistry, Eötvös L. University, Budapest 112 POB 32, H-1518 Hungary, and Cancer Research Campaign Laboratories, University of Nottingham, University Park, Nottingham NG7 2RD, United Kingdom. Received August 2, 1991

Daunomycin has been attached to various structurally related synthetic branched polypeptides with a polylysine backbone, using its acid-labile *cis*-aconityl derivative (cAD). Due to the importance of the side-chain structure in α -helix formation and immunological and pharmacological properties of branched polypeptides, we have investigated the conformation, biodistribution, and in vitro cytotoxicity of cAD-carrier conjugates with polypeptides containing amino acid residues of different identity and/or configuration at the side-chain end (XAK type) or at the position next to the polylysine backbone (AXK type), where X = Leu, D-Leu, Pro, Glu, or D-Glu. According to CD studies, polycationic conjugates with hydrophobic Leu in the side chains could assume a highly ordered conformation, while amphoteric conjugates containing Glu proved to be unordered in PBS. The reduction of in vitro cytotoxic activity of cAD by conjugation to carriers and the biodistribution profile of the conjugates were found to be dependent predominantly on the charge properties and on the side-chain sequence of the carrier polypeptide. It was demonstrated that by proper combination of structural elements of the carrier molecule, it is feasible to construct a cAD-branched polypeptide conjugate with significantly prolonged blood survival and with no reduction in in vitro cytotoxicity of the drug.

INTRODUCTION

Daunomycin (Dau)¹ is one of the clinically important anthracycline antitumor antibiotics. However, its efficacy is restricted by a range of undesirable side effects such as cumulative myocardial toxicity. Considerable efforts have been made to improve the therapeutic index, including attempts at site-specific targeting or providing controlled release of Dau by using natural macromolecules [e.g., hormones (1), enzymes (2), poly- and monoclonal antibodies (3, 4), or DNA (5)].

Daunomycin has also been linked to various synthetic polymers such as poly(Lys) (6–8), poly(Asp) (9), SPDP-modified poly(Glu) (10), poly[Glu(N₂H₃)] (11), poly(divinyl ether-*co*-maleic anhydride) (12), *N*-(2-hydroxypropyl)-methacrylamide (HPMA) (13), poly[acryloyl-2-amido-2-(hydroxymethyl)-1,3-propanediol] (14), and dextran (15). Some of these daunomycin conjugates, prepared with dex-

tran (16), HPMA (17), or derivatives of poly(Glu) (10, 11), have been used for coupling to cell-specific poly- or monoclonal antibodies.

The methods for conjugation of daunomycin to synthetic carriers have involved (a) the α -amino group of daunomycin using a cross-linking agent [e.g., carbodiimide (10)], anhydride (12), or active ester (13) of the polymer's carboxylic groups, (b) cleavage of the bond between C-3 and C-4 of the amino sugar (15), (c) the methyl ketone side chain of the aglycon by nucleophilic substitution of its 14-bromo derivative (8, 9, 11). Conjugates have been synthesized by the incorporation of leucyl or aspartyl (14), maleyl or *cis*-aconityl (6), and succinyl or several other diacidic (7) spacers.

Although considerable work has been performed with preparation and analysis of daunomycin–polymer conjugates (6–15), few empirical studies have been reported to establish the structure–activity relationships of carrier molecules in terms of their biological properties required for optimized daunomycin delivery and/or targeting.

In the past decade new groups of branched polypeptides with the general formula poly[Lys-(X_i-DL-Ala_m)] (XAK) or poly[Lys-(DL-Ala_m-X_i)] (AXK), where $i < 1$ and $m \sim 3$, have been developed (18–21) and characterized (20–24) by our laboratories. Potential advantages provided by this water-soluble, biodegradable group of polymeric polypeptides include (a) beneficial chemical characteristics, like a large number of α -amino groups available for simple and efficient coupling of daunomycin derivative without polymer cross-linking, (b) reliable determination of conjugate composition and conformation, and (c) comparative analysis of the functional properties (e.g. cytotoxicity, immunogenicity, biodistribution) of carriers with respect to their size, primary structure, charge (polycationic vs amphoteric compounds), and secondary structure (ordered vs unordered). The aim of present work is to provide a logical basis for selection of synthetic macromolecular carrier for constructing conjugates with daunomycin. In order to achieve this, Dau has been attached to various structurally related polymeric polypeptides with

* To whom all correspondence and reprint requests should be addressed.

† Presented in part at the 31st Annual Meeting of the British Association of Cancer Research, Brighton, UK, March 19–22, 1990, and at the 21st European Peptide Symposium, Barcelona, Spain, September 2–7, 1990.

‡ Hungarian Academy of Science, Eötvös L. University.

§ Cancer Research Campaign Laboratories, University of Nottingham.

|| Institute of Organic Chemistry, Eötvös L. University.

¹ Abbreviations used (in order of appearance in the text): Dau, daunomycin; SPDP, *N*-succinimidyl 3-(2-pyridyldithio)propionate; HPMA, *N*-(2-hydroxypropyl) methacrylamide; XAK, poly[Lys-(X_i-DL-Ala_m)] where X = Glu, D-Glu, Leu, D-Leu, or Pro; AXK, poly[Lys-(DL-Ala_m-X_i)] where X = Glu or Leu; cAD, *cis*-aconityldaunomycin; CD, circular dichroism; HSA, human serum albumin; CMC, *N*-cyclohexyl-*N'*-(2-morpholinoethyl)carbodiimide methyl *p*-toluenesulfonate; DS, average degree of substitution; XAK-cAD, poly[Lys-(cAD_i-X_i-DL-Ala_m)] where X = Glu, D-Glu, Leu, D-Leu, or Pro; AXK-cAD, poly[Lys-(cAD_i-DL-Ala_m-X_i)] where X = Glu or Leu; DP_n, number average of the degree of polymerization; AK, poly[Lys-(DL-Ala_m)] ; MEM, minimum essential medium; NBCS, newborn calf serum.

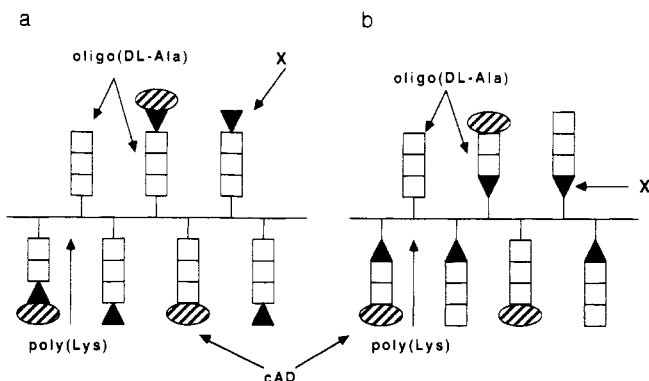


Figure 1. Schematic representation of branched polypeptide-cis-aconityldaunomycin (cAD) conjugates: (a) poly[Lys-(cAD)_X-DL-Ala_m] (XAK-cAD), (b) poly[Lys-(cAD)_X-DL-Ala_m-X_i] (AXK-cAD).

different chemical (20, 21), immunological (25–28), and pharmacokinetic (29) properties.

In this paper we describe the synthesis of daunomycin-branched polypeptide conjugates (Figure 1), in which an acid-labile, *cis*-aconityl derivative of daunomycin (cAD) was applied (6). To understand the possible role of the secondary structure, the solution conformation of these conjugates has been analyzed by circular dichroism (CD) spectroscopy. Comparative studies have been performed on cAD conjugates to determine predominant structural features of the carrier polypeptide influencing the conjugate's biodistribution (blood-clearance profile, whole-body survival, tissue distribution) and cytotoxicity. Conjugates have been tested and their *in vitro* cytotoxicity compared with that of free drug and of other conjugates like cAD-HSA or cAD-monoclonal antibody (791T/36) on osteogenic sarcoma cell line 791T.

EXPERIMENTAL PROCEDURES

Abbreviations used in this paper follow the rules of the IUPAC-IUB Commission of Biochemical Nomenclature (30) in accord with the recommended nomenclature of graft polymers (31).

Materials. Daunomycin hydrochloride was obtained from Wyeth; *cis*-aconitic anhydride and *N*-cyclohexyl-*N'*-(2-morpholinoethyl)carbodiimide methyl *p*-toluenesulfonate (CMC) were from BDH (UK). *cis*-Aconityldaunomycin (cAD) was prepared as reported elsewhere (4). Branched polypeptides used in these studies were synthesized in our laboratory as described previously (20, 21). Briefly, poly(Lys) was prepared by the polymerization of *N*^α-carboxy-*N*^ε-(benzyloxycarbonyl)lysine anhydride under conditions that allowed an average degree of polymerization (DP_n) of approximately either 80–120 or 400–500. After cleavage of protecting groups from poly[Lys(Z)], either poly[Lys-(DL-Ala_m)] (AK) was prepared by grafting of short oligomeric DL-Ala side chains onto the ε-amino groups of poly(Lys) or protected amino acid was coupled by the active ester method. Poly[Lys-(X_i-DL-Ala_m)] (XAK) was synthesized by reacting a suitably protected amino acid pentachlorophenyl ester to the α-amino groups of AK. Blocking groups were removed completely with HBr in glacial acetic acid, as confirmed by UV spectroscopy at 254 nm. Poly[Lys-(DL-Ala_m-X_i)] (AXK) was prepared by the introduction of DL-Ala oligomers to the previously deprotected α- and ε-amino groups of poly[Lys-(X_i)] by the aid of *N*-carboxy-DL-Ala anhydride. The primary structure of polypeptides was studied by amino acid analysis, by the identification of the branch-terminating amino acid residue (32), and by the determination of the enantiomer

composition of the side chains (33). The size of these compounds was analyzed by sedimentation analysis and gel chromatography (18).

Methods. Synthesis of Branched Polypeptide-cAD Conjugates. Coupling of *cis*-aconityldaunomycin to the branched polypeptides was performed using the method previously described for the conjugation of cAD to monoclonal antibodies (4), with some modifications. Briefly, 5.0–9.5 μmol (3.4–6.5 mg) of cAD in 144–210 μL of PBS was diluted with PBS (pH 5) to a final concentration of 4 mg/mL. The solution was stirred and treated with 7.5–14.25 μmol (3.1–6.0 mg) of CMC dissolved in 400–600 μL of distilled water (i.e., a 1.5 times molar excess of carbodiimide reagent) for 30 min at room temperature. This mixture was added dropwise to 20 mg (0.1–0.5 μmol) of polypeptide in 10 mL of 0.05 M carbonate buffer (pH 9.0). After stirring for 2 h, the reaction was allowed to proceed for 16 h at room temperature. The final concentration of polypeptide was 1.6 mg/mL. The input molar ratio of cAD to polypeptide was between 20:1 and 90:1. After conjugation, the reaction mixture was applied to a Sephadex G-25 (medium grade) column equilibrated with PBS. The appropriate macromolecular peak as defined by UV detection at 275 nm was collected. The cAD was determined spectrophotometrically as described previously (4). It was assumed that the cAD coupled to the α-amino group of terminal amino acid has the same molar extinction coefficient at λ = 476 nm as cAD itself (ε = 8000). Analytical data on the conjugates are presented in Table I.

HPLC Analysis of Branched Polypeptide-cAD Conjugates. Instrumentation. The HPLC system consisted of one Model 302 and one Model 303 liquid-delivery module, a Model HM/HPLC Holochrome UV-visible detector, a Model 811 dynamic mixer, a Model 802 manometric module, a Model N1 recorder (all from Gilson France S.A.), a Model 7125 injector valve, and 100-μL and 200-μL sample loops (Rheodyne, Inc., Cotati, CA). A 25 cm × 4.6 mm column and a 3 cm × 4.6 mm Aquapore RP-300 guard column (Brownlee Labs., Inc., Santa Clara, CA) were used. Both columns contained spherical 7-μm silica (300-Å pore size) with a hydrophobic bonded phase.

Conditions. The mobile phase consisted of 0.2 M ammonium carbonate/methanol (50:50, v/v). Ammonium carbonate solution was prepared daily using high-purity (Analar) salt and distilled, deionized water and was mixed with methanol 20 min before use. The injection volume was 100 μL containing 0.3 μg (0.53 nmol) of daunomycin and/or 0.3 μg (0.44 nmol) of cAD dissolved in eluent or 200 μL containing 1.1–5.7 μg (1.5–10.1 nmol) of cAD coupled to branched polypeptide in PBS. Daunomycin hydrochloride and cAD were used separately as standards and their retention times were determined. UV absorbance was monitored at a wavelength of 280 nm. All analyses were carried out at room temperature with a flow rate of 1.0 mL/min.

Spectroscopic Measurements. Absorption spectra were recorded on an ultraviolet-visible spectrophotometer (Unicam-Pye) in a cell of optical path 1.0 cm at room temperature. cAD and conjugates were dissolved in PBS at pH 7.3. Conformations of the conjugates were studied by CD spectroscopy. CD spectra were recorded using a Roussel-Jouan (Jobin-Yvon) Model III dichrograph in quartz cells of optical paths 1.0, 0.2, and 0.1 cm at room temperature under constant nitrogen flush. The dichrograph was calibrated with epiandrosterone at 304 nm and D-(–)-pantoyl lactone at 220 nm (34). The samples were dissolved in PBS at pH 7.3. The concentration of

Table I. Characteristics of Branched Polypeptide-*cis*-Aconityldaunomycin Conjugates

conjugate	abbreviation ^a	molar ratio		% \overline{DS}^b	$\overline{M}_w^c \pm 5\%$	% free of ^d cAD/Dau
		polypeptide	cAD			
poly[Lys-(cAD) ₁ -DL-Ala _{2,94}]	ak-cAD	1	5.5	5.5	37700	0.7
poly[Lys-(cAD) ₁ -DL-Ala _{3,1}]	AK-cAD	1	24.3	5.4	172300	0.8
poly[Lys-(cAD) ₁ -DL-Ala _{2,9} -Leu _{0,79}]	alk-cAD	1	4.8	4.8	42100	0.7
poly[Lys-(cAD) ₁ -Leu _{0,81} -DL-Ala _{2,94}]	lak-cAD	1	4.5	4.5	37000	0.9
poly[Lys-(cAD) ₁ -Leu _{0,98} -DL-Ala _{3,1}]	LAK-cAD	1	24.8	5.5	223100	0.8
poly[Lys-(cAD) ₁ -D-Leu _{0,9} -DL-Ala _{2,94}]	D-lak-cAD	1	4.8	4.8	37200	<0.5
poly[Lys-(cAD) ₁ -D-Leu _{0,98} -DL-Ala _{3,1}]	D-LAK-cAD	1	20.8	4.6	219900	<0.5
poly[Lys-(cAD) ₁ -Pro _{0,94} -DL-Ala _{2,94}]	pak-cAD	1	16.0	16.0	56100	<0.5
poly[Lys-(cAD) ₁ -Pro _{0,96} -DL-Ala _{3,1}]	PAK-cAD	1	70.0	15.5	245300	<0.5
poly[Lys-(cAD) ₁ -DL-Ala _{2,67} -Glu _{1,0}]	aek-cAD	1	5.3	5.3	48140	<0.5
poly[Lys-(cAD) ₁ -Glu _{0,93} -DL-Ala _{2,94}]	eak-cAD	1	12.5	12.5	53800	<0.5
poly[Lys-(cAD) ₁ -Glu _{0,96} -DL-Ala _{3,1}]	EAK-cAD	1	61.9	13.8	253200	<0.5
poly[Lys-(cAD) ₁ -D-Glu _{0,95} -DL-Ala _{3,1}]	D-EAK-cAD	1	63.1	14.0	254000	<0.5

^a Based on one-letter symbols of amino acids and abbreviation of *cis*-aconityldaunomycin (cAD). Capital or small letters denote the size of the conjugates. ^b Average degree of substitution, expressed as percentage of side chains modified with cAD. ^c Calculated from the average degree of polymerization of poly(L-Lys) and of the side chain composition as described in the Experimental Procedures. ^d Determined by reversed-phase HPLC as described in the Experimental Procedures.

solutions was approximately 0.5 mg/mL. CD band intensities are expressed as $\Delta\epsilon$ values, representing the difference of molar absorptivity of the left and right circularly polarized components. $\Delta\epsilon$ values were related either to one lysine residue in the main chain including a whole side chain (in the range of the spectrum between 190 and 250 nm) or to the cAD content of the conjugate (in the 250–600-nm absorption range). Interpretation of CD spectra was based on the secondary structure analysis of the well characterized poly(Lys) (20, 22, 23).

Cytotoxicity Assay. Osteogenic sarcoma cell line 791T was grown in monolayer culture in Eagle's minimum essential medium supplemented with 10% newborn calf serum (MEM + NBCS). It was harvested for routine passage and for cytotoxicity assays with a mixture of 0.25% trypsin and 0.1% ethylenediaminetetraacetic acid in phosphate-buffered saline, adjusted to pH 7.2. Cells suspended in MEM + NBCS were adjusted to a concentration of 5×10^4 per mL and plated at 100 μ L (5×10^3 cells) per well in 96-well flat-bottom tissue culture grade microtiter plates (Falcon 3072). They were incubated at 37 °C for 4 h until fully adherent. Drugs (Dau and cAD) and conjugates in PBS were diluted in MEM + NBCS to twice the desired final concentration and a range of 10-fold dilutions prepared. Each dilution was added in 100 μ L to quadruplicate wells, the concentrations stated in the Results being the final concentrations in the wells at this point. Control wells were treated with 100 μ L of MEM + NBCS alone. The cells were incubated for 48 h and then labeled with [⁷⁵Se]selenomethionine (Amersham International plc, Amersham, UK) (0.1 μ Ci in 50 μ L per well) for 16 h. They were gently washed three times with 0.9% NaCl solution and dried down, and the dry contents of the wells were sealed in with Nobecutane spray (Astra Pharmaceuticals Ltd). The wells were separated with a band saw and their radioactivity was measured as counts per minute (cpm) in a γ -spectrometer. Percent cytotoxicity was calculated by the formula

$$\frac{\text{mean cpm in controls} - \text{mean cpm in treated wells}}{\text{mean cpm in controls}} \times 100$$

Radioiodination of Branched Polypeptides-cAD Conjugates. Branched polypeptides-cAD conjugates were labeled with *N*-succinimidyl 3-(4-hydroxy-5-[¹²⁵I]-iodophenyl)propionate (Amersham International plc, Amersham, UK) using the Bolton and Hunter procedure (35). Reagent solution (10–20 μ L) was added to plastic microfuge tubes and evaporated to dryness under a stream of

nitrogen. Then 500 μ L of conjugate solution at 1 mg/mL in 0.1 M borate buffer (pH 8.6) was reacted with iodinated ester (2.0 mol of ester/mol of conjugate). The reaction was allowed to proceed for 20 min at 0 °C and terminated by adding 500 μ L of 0.2 M glycine in the same buffer for 5 min at 0 °C. The [¹²⁵I]-labeled conjugate was purified on a G-25 Sephadex gel column using 0.066 M phosphate buffer (pH 7.6) containing 0.25% gelatin as eluent. Electrophoresis on native polyacrylamide gel with a continuous 8–25% gradient (PhastGel gradient 8-25 Pharmacia-LKB, Uppsala, Sweden) was applied to assess the low molecular weight labeled product content of the preparation.

Blood-Clearance and Tissue-Distribution Studies. Balb/c mice (Bantin and Kingman, Hull, UK) were used throughout these studies. Drinking water was supplemented with 0.1% w/v sodium iodide. Groups of mice ($n = 3$) received a single injection (0.2 mL) of [¹²⁵I]-labeled conjugate via a tail vein. Serial blood samples (10 μ L) were taken from the tail tip up to 24 h after injection. At this time the mice were killed and dissected. The blood samples, visceral organs, and residual carcasses were weighed and assayed for radioactivity. Results of the blood-clearance study were expressed as a percentage of the zero-time count rate assuming the blood volume of the mouse (mL) to be 11.2% of the body weight (g) (36). Area under the blood concentration–time curve up to 6 h following injection was calculated by the trapezoidal rule (37). Results of the tissue-distribution analyses were expressed as (i) a percentage of the injected dose of radioactivity per gram of tissue or blood and as (ii) ratios of radioactivity per gram of tissue to radioactivity per gram of blood (tissue to blood). Levels of statistical difference between groups of animals were assessed by Student's *t*-test.

RESULTS

Synthesis and Chemical Characterization of Branched Polypeptide-cAD Conjugates. The coupling of cAD to branched polypeptides was achieved by a carbodiimide method in which one carboxyl group of the molecule was linked to the α -amino group of the side-chain terminal amino acid to provide covalent α -amide bonding. First, the carboxyl groups of cAD were activated by water-soluble carbodiimide under conditions (i.e., 1.5 times molar excess of carbodiimide, at pH 5.0) described in detail elsewhere (4). In the second step, the carboxyl-activated derivative was added to the amino component (polypeptide) and the coupling reaction allowed to proceed

in alkaline solution (pH 9.0). It should be noted that no precipitate was detected during the synthesis of conjugates under these conditions. The conjugates composed of cAD and XAK or AXK type polypeptide were purified by gel filtration and characterized by reversed-phase HPLC, cAD content, and \overline{M}_w determination. These data are summarized in Table I. The results presented in this table indicate that the amount of cAD incorporated into the polypeptide conjugate depends on the size of the polymer and on the identity of the terminal amino acid residue of the side chain.

The average molar substitution ratio was in the range of 4.5–16.0 *cis*-aconityldaunomycin per carrier molecule in the case of small relative molar mass polypeptides ($\overline{DP}_n = 100$) or in the range of 20.8–70.0 in the case of large relative molar mass polymers ($\overline{DP}_n = 450$). Thus the total number of cAD molecules in conjugates was found to correlate with the size of the carrier polypeptide (e.g., the number of cAD per polypeptide molecule is 24.3 for poly[Lys-(cAD)₇-DL-Ala_{3,1}] (AK-cAD) and 5.5 for poly[Lys-(cAD)₇-DL-Ala_{2,94}] (ak-cAD) or 61.9 for poly[Lys-(cAD)₇-Glu_{0,96}-DL-Ala_{3,1}] (EAK-cAD) and 12.5 for poly[Lys-(cAD)₇-Glu_{0,93}-DL-Ala_{2,94}] (eak-cAD). In order to compare the coupling efficacy in conjugate groups of different size, the average degree of cAD substitution (\overline{DS}) has been also calculated and expressed as percent of modified side chains in the conjugates. No significant differences have been observed between the respective \overline{DS} values of high ($\overline{DP}_n = 450$) and low ($\overline{DP}_n = 100$) relative molar mass polypeptides [\overline{DS} for poly[Lys-(cAD)₇-Leu_{0,81}-DL-Ala_{2,94}] (lak-cAD) = 4.5% and for poly[Lys-(cAD)₇-Leu_{0,98}-DL-Ala_{3,1}] (LAK-cAD) = 5.5%, or for poly[Lys-(cAD)₇-Pro_{0,94}-DL-Ala_{2,94}] (pak-cAD) = 16.0% and for poly[Lys-(cAD)₇-Pro_{0,96}-DL-Ala_{3,1}] (PAK-cAD) = 15.5%].

The choice of carrier polypeptide could also influence the composition of the conjugates. The highest coupling efficacy was obtained with polypeptides containing Pro or Glu/D-Glu at the terminal positions of the side chains ($\overline{DS}_{PAK} = 15.5\%$, $\overline{DS}_{EAK} = 13.8\%$, $\overline{DS}_{D-EAK} = 14.0\%$). Under identical conditions CMC-mediated synthesis of conjugates made of branched polypeptides with N-terminal DL-Ala or Leu/D-Leu led to much lower \overline{DS} values (e.g., $\overline{DS}_{LAK} = 5.5\%$, $\overline{DS}_{eak} = 5.3\%$, or $\overline{DS}_{AK} = 5.4\%$). The absolute configuration of the side chain terminal amino residue had no significant influence on cAD incorporation into the conjugates studied ($\overline{DS}_{LAK} = 5.5\%$, $\overline{DS}_{D-LAK} = 4.6\%$ or $\overline{DS}_{EAK} = 13.8\%$, $\overline{DS}_{D-EAK} = 14.0\%$).

Following purification by gel filtration, HPLC was used to detect free anthracycline derivatives in the samples of polypeptide-cAD conjugates. Quantitative analysis, performed on a reversed-phase column (pore size of 300 Å, isocratic elution), indicated no detectable amount of free daunomycin and the presence of less than 1% of cAD could be demonstrated in the conjugates using peak-area measurement calibrated with appropriate standards.

Conformation of Branched Polypeptide-cAD Conjugates. The chiroptical properties of branched polypeptide-cAD conjugates in water solution was studied by CD spectroscopy in the wavelength region 190–360 nm. The CD curves of ak-cAD, lak-cAD, and eak-cAD conjugates in PBS at pH 7.3 are shown in Figure 2.

In the 190–250-nm wavelength region, the circular dichroic spectra indicate the formation of a helical secondary structure for lak-cAD, but only marginally ordered conformation for ak-cAD and eak-cAD conjugates (Figure 2A). Highly ordered conformation was also observed with

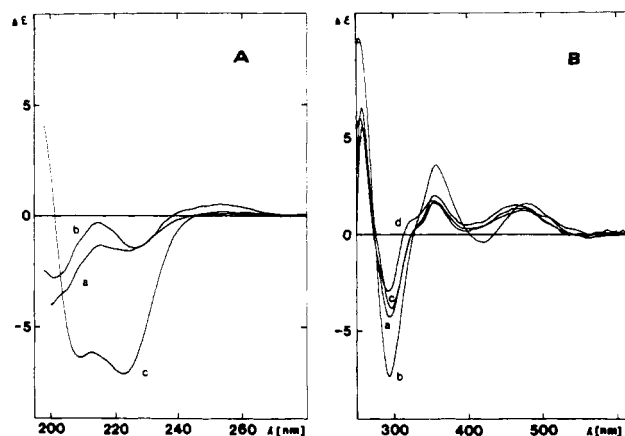


Figure 2. CD spectra of branched polypeptide-cAD conjugates and cAD in PBS of pH 7.3: (a) ak-cAD, (b) eak-cAD, (c) lak-cAD, (d) cAD.

poly[Lys-(cAD)₇-DL-Ala_{2,9}-Leu_{0,79}] (alk-cAD) (data not shown). The CD signals in this range originated from the optical activity of amide bonds and from the contribution of the cAD moiety. In order to consider this, the ellipticity values ($\Delta\epsilon$) are related to one lysine residue in the main chain including a whole cAD substituted side chain. Due to the relative low cAD content of the conjugates (4.5–14.0%), the CD contribution of cAD was found to be negligible and therefore the pattern of the curves reflects predominantly the secondary structure of conjugates. It should be noted that the CD spectra of the unconjugated polypeptides lak and alk correspond to a highly ordered helical conformation (23), while ak (22) and eak (23) proved to be completely unordered under identical circumstances. These conjugates also have optical activity in the 250–360-nm absorption range, which is distinct from the amide chromophores and corresponds only to the structure of cAD. Consequently, this region of the CD spectra could be used to monitor the presence of the drug and local chromophore interaction in the conjugates. CD spectra in the range of 250–360 nm demonstrated the presence of daunomycin moieties in conjugates (Figure 2B). In the case of ak-cAD and lak-cAD, the shape and the characteristic values of the CD curves were similar to that of free cAD, indicating no interaction between coupled *cis*-aconityldaunomycin groups. In contrast, a significant red-shift could be demonstrated in the CD spectrum of eak-cAD conjugate as compared to free cAD. The minimum at 380 nm and the maximum at 450 nm in the cAD spectrum shifted to 420 nm and to 480 nm, respectively. These observations are in agreement with changes detected in the UV spectra of cAD and eak-cAD conjugate (data not shown).

Cytotoxicity against Tumor Cells in Vitro. Modification of daunomycin by substitution of a *cis*-aconityl group significantly reduced its cytotoxicity against 791T osteogenic sarcoma cells ($P < 0.001$) compared with that of the free drug, as shown in Figure 3. Comparison of the cytotoxicity curves around the 50% inhibitory concentrations showed that this reduction was about 8-fold. Conjugation of *cis*-aconityldaunomycin to a branched polypeptide carrier caused a further reduction in cytotoxicity. This reduction was not significantly influenced by differences in the size of the branched polypeptide-cAD molecule. Thus, the example in Figure 3 shows a reduction of cAD cytotoxicity by approximately 1 order of magnitude following conjugation to ak (conjugate \overline{M}_w 37700) and a similar reduction in the case of AK-cAD (\overline{M}_w 172300) ($P < 0.001$). This pattern was consistent using other polypeptides where only the molecular size was changed,

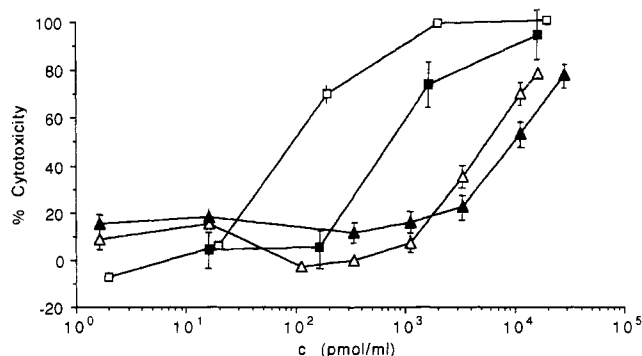


Figure 3. Molecular size of the polypeptide carrier molecule in relation to daunomycin cytotoxicity and comparison with free drug: (□) free daunomycin, (■) *cis*-aconityldaunomycin (cAD), (Δ) ak-cAD, (▲) AK-cAD.

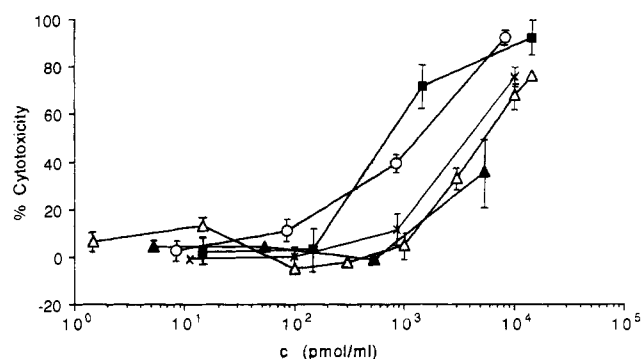


Figure 4. Influence of different side-chain terminal amino acids on cytotoxicity of polypeptide-*cis*-aconityldaunomycin conjugates and comparison with a protein carrier: (■) cAD, (○) eak-cAD, (Δ) ak-cAD, (▲) lak-cAD, (×) HSA-cAD.

Table II. Cytotoxicity of Daunomycin (Dau), *cis*-Aconityldaunomycin (cAD), and Branched Polypeptide-cAD Conjugates against 791T Osteogenic Sarcoma Cells

compound	IC ₅₀ ^a pmol/mL	compound	IC ₅₀ ^a pmol/mL
daunomycin	9.3×10^1	pak-cAD	3.3×10^3
cAD	7.1×10^2	PAK-cAD	3.0×10^3
ak-cAD	5.3×10^3	aek-cAD	7.2×10^3
AK-cAD	9.6×10^3	eak-cAD	1.2×10^3
alk-cAD	1.0×10^4	EAK-cAD	1.2×10^3
lak-cAD	$>6.0 \times 10^3$	D-EAK-cAD	8.1×10^3
LAK-cAD	4.3×10^3	HSA-cAD	4.0×10^3
D-lak-cAD	$>5.0 \times 10^3$	791T/36-cAD	9.6×10^3
D-LAK-cAD	3.8×10^3		

^aConcentration is expressed in terms of molar daunomycin or cAD content of conjugates.

although the extent of the reduction differed according to the amino acid residue in the side chain (Table II).

The identity of the terminal amino acid in the side chains had a marked influence on cAD cytotoxicity (Figure 4). The addition of leucine to produce lak-cAD resulted in a similar reduction to that seen with ak-cAD, but the addition of glutamic acid to make the conjugate amphoteric (eak-cAD) resulted in a more cytotoxic conjugate. The cytotoxicity of eak-cAD was not significantly different from that of cAD alone, while both ak-cAD and lak-cAD were significantly less cytotoxic ($P < 0.001$). A control conjugate of cAD prepared with human serum albumin (HSA) as a carrier showed activity similar to that of ak-cAD and lak-cAD (Figure 4).

The configuration of the terminal amino acid residue had different effects on cytotoxicity, depending on the amino acid involved. Replacement of L-leucine with D-

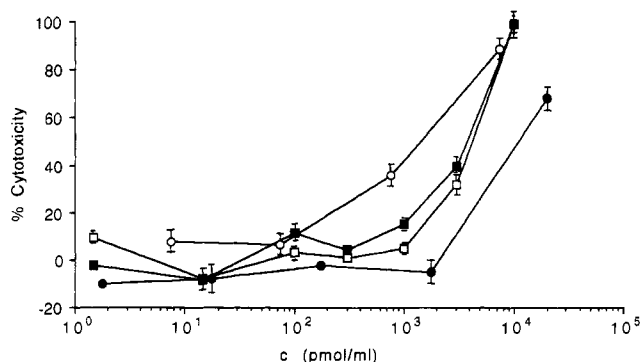


Figure 5. Influence of amino acid configuration of the terminal side chain on cytotoxicity of polypeptide-*cis*-aconityldaunomycin conjugates: (■) D-LAK-cAD, (□) LAK-cAD, (●) D-EAK-cAD, (○) EAK-cAD.

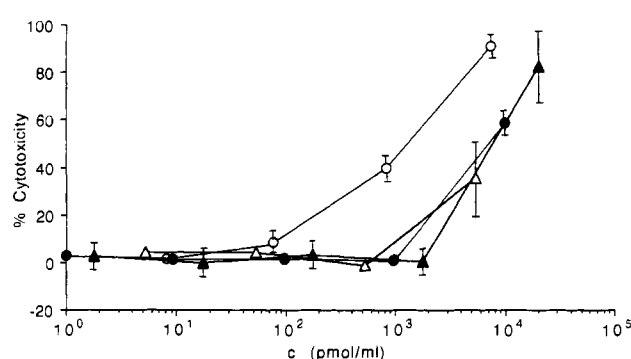


Figure 6. Influence of amino acid sequence of the side chain on cytotoxicity of polypeptide-*cis*-aconityldaunomycin conjugates: (Δ) lak-cAD, (▲) alk-cAD, (○) eak-cAD, (●) aek-cAD.

leucine to make poly[Lys-(cAD)₇-D-Leu_{0.95}-DL-Ala_{3.1}] (D-LAK-cAD) had no effect on cytotoxicity compared with that of LAK-cAD (Figure 5), but in the case of EAK-cAD a similar replacement had a profound effect. EAK-cAD was significantly more cytotoxic than LAK-cAD ($P < 0.05$ around 10^3 pmol/mL), as also observed with the smaller relative molar mass variants in Figure 4, but poly[Lys-(cAD)₇-D-Glu_{0.95}-DL-Ala_{3.1}] (D-EAK-cAD) was much less active (Figure 5). Cytotoxicity of D-EAK-cAD was about 7 times less than that observed with D-LAK-cAD ($P < 0.01$ at concentrations above 10^3 pmol/mL).

The importance of the sequence of the amino acids in the side chain was also tested (Figure 6). In the case of conjugates containing a polycationic polypeptide, lak-cAD was compared with alk-cAD. Both compounds had similar cytotoxic activity. In contrast, cytotoxic activity of the amphoteric cAD-polypeptide conjugates eak or aek was found to be significantly different. Eak-cAD was about 6 times more active than poly[Lys-(cAD)₇-DL-Ala_{2.67}-Glu_{1.0}] (aek-cAD) (Figure 6). It was concluded that the side-chain sequence could have little (in polycationic conjugates) or marked (in amphoteric conjugates) influence on cytotoxicity of cAD, depending on the identity of the amino acid X involved (Table II).

Biodistribution of Branched Polypeptide-cAD Conjugates. The blood survival of iodinated alanylated polylysine-cAD conjugates following iv administration is shown in Figure 7. There was no significant difference in the area under the blood-clearance curve (AUC_{0-6h}) for conjugates prepared with either the higher (AK-cAD) or lower (ak-cAD) relative molecular mass branched polypeptide. Twenty-four hours following iv injection the whole-body survivals for AK-cAD and ak-cAD were $7.5 \pm 1.6\%$ injected dose and $7.6 \pm 0.7\%$ injected dose, respectively. The tissue-distribution profiles of these two

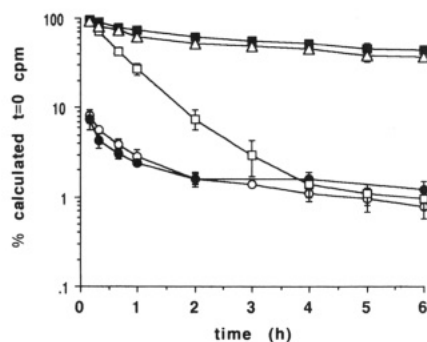


Figure 7. Blood-clearance profiles of ^{125}I -branched polypeptide-cAD and HSA-cAD conjugates following iv administration to Balb/c mice. $\text{AUC}_{0-6\text{h}}$ calculated from these data are given in Table III. Results are expressed as mean \pm standard deviation for groups of three animals: (O) ak-cAD, (●) AK-cAD, (□) lak-cAD, (■) eak-cAD, (Δ) HSA-cAD.

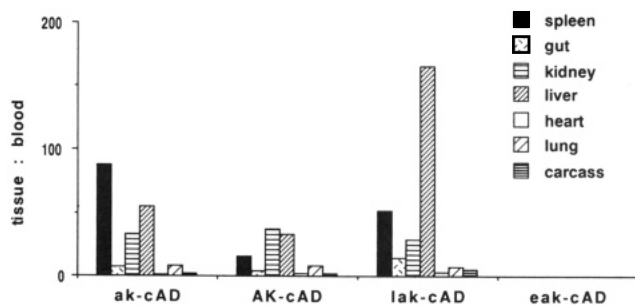


Figure 8. Tissue distribution of ^{125}I -branched polypeptide-cAD conjugates in Balb/c mice 24 h after iv administration. Results are expressed as mean for groups of three animals.

Table III. Biodistribution Parameters of Branched Polypeptide-cAD Conjugate

conjugate	$\text{AUC}_{0-6\text{h}}$, % of cpm-h at $t = 0$ (mean \pm SD)	WBS at $t = 24$ h, % injected dose (mean \pm SD)	% dose/g blood at $t = 24$ h (mean \pm SD)
ak-cAD	21.5 ± 3.9	7.6 ± 0.7	0.07 ± 0.01
AK-cAD	20.3 ± 2.3	7.5 ± 1.6	0.10 ± 0.04
alk-cAD	277.4 ± 37.2	31.4 ± 2.2	7.4 ± 1.4
lak-cAD	77.8 ± 8.1	14.2 ± 2.6	0.07 ± 0.02
D-lak-cAD	50.4 ± 4.2	11.4 ± 0.7	0.08 ± 0.02
aek-cAD	145.2 ± 11.6	8.6 ± 0.4	4.1 ± 0.3
eak-cAD	360.9 ± 22.6	22.6 ± 1.0	11.5 ± 1.8
EAK-cAD	279.8 ± 7.5	15.3 ± 1.2	6.8 ± 0.3
D-EAK-cAD	275.4 ± 6.0	16.8 ± 1.9	9.2 ± 1.9
HSA-cAD	311.7 ± 9.4	22.6 ± 0.7	6.5 ± 0.2
791T/36-cAD	482.7 ± 18.9	58.0 ± 0.8	18.2 ± 1.8

conjugates were also very similar (Figure 8), both compounds being taken up by spleen, kidney, and liver.

In contrast, changes in the identity in the terminal side chain amino acid of the conjugates resulted in dramatic changes in their biodistribution profiles. Substitution of both leucine and glutamic acid at the terminal side chain position of the peptide significantly prolonged blood survival (Figure 7). The $\text{AUC}_{0-6\text{h}}$ for lak-cAD was increased 4-fold compared to that of ak-cAD and for eak-cAD it was 16-fold compared to that of ak-cAD. The 24-h tissue distributions of these three conjugates are compared in Figure 8. Although lak-cAD had a significantly higher WBS compared to that of ak-cAD (Table III), the tissue distribution of conjugate 24 h after iv administration was very similar. Tissue to blood ratios for spleen, liver, and kidney were greater than 25 for both conjugates. However, tissue to blood ratios for eak-cAD were less than 0.3 in all tissues with the percent dose/gram of blood at $t = 24$ h being 100 times greater than for lak-cAD or ak-cAD.

Substitution of the D isomer into the terminal side chain position of the polypeptide had no significant effect on

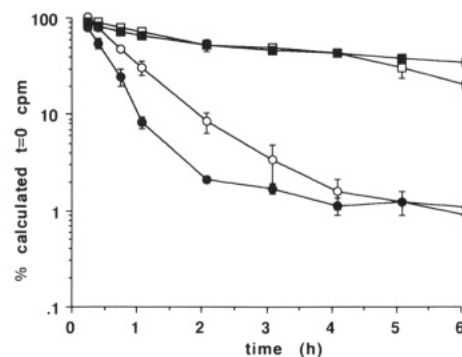


Figure 9. A comparison of the blood clearance of ^{125}I -labeled EAK-cAD and D-EAK-cAD and of ^{125}I -labeled lak-cAD and D-lak-cAD in Balb/c mice following iv administration. $\text{AUC}_{0-6\text{h}}$ calculated from these data are given in Table III. Results are expressed as mean \pm standard deviation for groups of three mice: (□) EAK-cAD, (■) D-EAK-cAD, (O) lak-cAD, (●) D-lak-cAD.

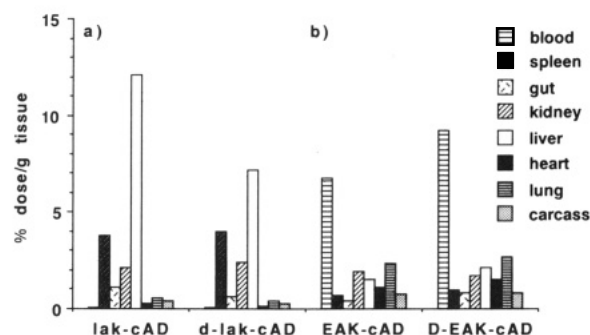


Figure 10. Effect of absolute configuration of the terminal side chain amino acid on tissue distribution of ^{125}I -labeled branched polypeptide-cAD conjugates in Balb/c mice: (a) lak-cAD and D-lak-cAD and (b) EAK-cAD and D-EAK-cAD. Results are the mean of three animals.

the biodistribution of the conjugates studied. There was little change in blood clearance (Figure 9) for the polycationic leucine-containing pair (lak-cAD, D-lak-cAD) or the amphoteric glutamic acid containing pair of conjugates (EAK-cAD, D-EAK-cAD). Twenty-four hours following iv administration the tissue-distribution profiles of each pair were very similar (Figure 10). Both lak-cAD and D-lak-cAD were taken up predominantly into spleen, liver, and kidney. In contrast EAK-cAD and D-EAK-cAD had tissue to blood ratios of less than 0.4 for all tissues. There was no significant difference in percent dose/gram of blood at 24 h between the L and D amino acid containing conjugates for both pairs studied.

The effect of changing the side chain amino acid sequence of the branched polypeptides on the biodistribution of the polypeptide-cAD conjugates is illustrated in Figures 11 and 12 and was different for polycationic and amphoteric conjugates. In the case of polycationic conjugates, when leucine was substituted for a side-chain alanine adjacent to the polylysine backbone, the blood survival of its cAD conjugate (alk-cAD) was considerably prolonged compared to a conjugate containing leucine in the terminal side chain position (lak-cAD). The $\text{AUC}_{0-6\text{h}}$ for alk-cAD was 3.5 times greater than for lak-cAD (Table III). Twenty-four hours after iv administration the WBS for alk-cAD was $31.4 \pm 2.2\%$ injected dose compared to $17.2 \pm 2.6\%$ injected dose for lak-cAD. Figure 12 illustrates that at 24 h postinjection there was 100 times more alk-cAD in the blood and 8 times more alk-cAD in the spleen compared to lak-cAD. In contrast, for the amphoteric conjugates investigated, when glutamic acid was substituted for a side chain alanine adjacent to the polylysine backbone, the blood survival of the conjugate (aek-cAD)

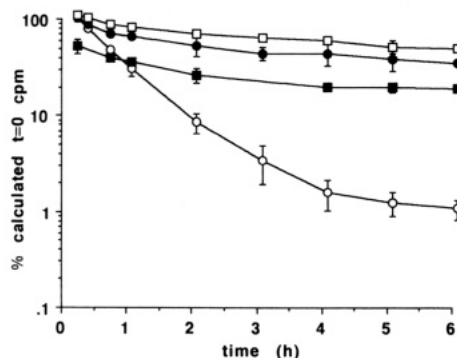


Figure 11. Effect of side-chain sequence on blood survival of ^{125}I -labeled branched polypeptide-cAD conjugates following iv administration of Balb/c mice. AUC_{0-6h} calculated from these data are given in Table III: (□) eak-cAD, (■) aek-cAD, (○) lak-cAD, (●) alk-cAD.

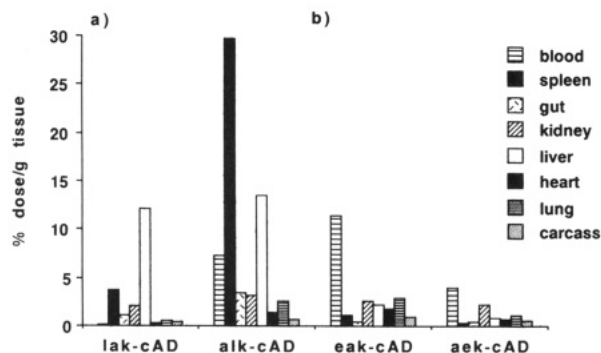


Figure 12. Effect of side-chain sequence on the tissue distribution of ^{125}I -labeled branched polypeptide-cAD conjugates in Balb/c mice: (a) lak-cAD and alk-cAD and (b) eak-cAD and aek-cAD. Data shown are the mean of three mice.

was reduced, with a 2-fold reduction in AUC_{0-6h} (Table III) compared to a conjugate containing glutamic acid at the terminal side chain position. Figure 12 shows that although the WBS of aek-cAD was much lower than for eak-cAD, the tissue distribution profiles of these two conjugates were very similar with tissue to blood ratio all less than 1.0.

DISCUSSION

In the design of polymer-drug conjugates, selection of polymeric compounds is an important factor to be considered. In order to provide a rational basis for identification of structural elements essential for drug-carrier function, daunomycin has been coupled to chemically related branched polymeric polypeptides. These conjugates have been synthesized using a *cis*-aconityl derivative of Dau (cAD), ensuring the same type of drug-polymer linkage in all compounds prepared. Two groups of polypeptides with basically identical side chain composition, but of different size (29), were used for syntheses. As a result of standardized coupling procedure, cAD conjugates of both groups had a similar average degree of molar substitution (Table I), allowing the effect of size to be studied. In view of the importance of charge and side-chain structure of branched polypeptides in α -helix formation (20, 21) and immunological (39, 40) and pharmacological (29, 40) properties, we have investigated the conformation, the biodistribution, and in vitro cytotoxicity of cAD-carrier conjugates with polypeptides containing amino acid residues of different identity and/or configuration (e.g., Leu, D-Leu, Glu, D-Glu) at the side-chain end (XAK type) or at the position next to the polylysine backbone (AXK type).

CD spectra of conjugates showed significant differences correlating with the identity of the side chain terminating amino acid residue, but not with the sequential order of amino acid residues in the side chains of the carrier. Polycationic conjugates could assume a highly ordered conformation (lak-cAD and alk-cAD) or a random steric arrangement (ak-cAD), depending on the presence of a hydrophobic amino acid (Leu) in the side chain. The CD spectrum of the amphoteric conjugate (eak-cAD) corresponded to an unordered structure. These results demonstrate that conformational properties of cAD-polypeptide conjugates are very similar to those of unconjugated polypeptides (20, 21). Consequently, the introduction of daunomycin molecules with an average degree of substitution of up to 12.5% has no significant influence on the conformation of the free carrier molecule under comparable conditions. Additional information regarding the secondary structure of the conjugate could be derived from the differences observed in the 250–360-nm absorption range. The shape of the CD curve of cAD-eak might be attributed to the interaction of eak-coupled cAD chromophores. Similar changes in the CD spectrum of daunomycin have been interpreted as "self-association" of free drug molecules in solution (38).

The data presented in this study indicate that the covalent binding of daunomycin to branched polypeptides could result in reduction of drug cytotoxicity. This observation is not unique for polymeric derivatives of toxic agents (17), but has also been described for protein conjugates of antitumor drugs (e.g., ref 3). In our case, this decrease is partly due to the derivatization of daunomycin by *cis*-aconitic anhydride and partly caused by its coupling to branched polypeptides. The reduction of cytotoxic activity was found to be independent of size, but influenced by the side-chain structure of the carrier polypeptide. Conjugation to polycationic polymers, regardless of the identity, configuration, and position of amino acid X (where X = Leu, D-Leu, or Pro) in the carrier side chain resulted in a reduction of cAD cytotoxicity. In contrast, amphoteric conjugates bearing L-Glu at the side chain terminal position produced an agent with cytotoxicity similar to that of free cAD. However, the replacement of L-Glu by its enantiomer or a change in sequential position of the negative charge (eak \rightarrow aek) lowered the cytotoxic potential of the conjugate. This observation might be explained by the unordered conformation of eak-cAD, which could provide (a) preferential orientation of cAD (L-Glu vs D-Glu) or (b) proper surface charge density (eak vs aek) for cell to conjugate interactions.

The fate of these conjugates after introduction into the organism was studied in detail. The elimination of polypeptide conjugates from the blood and their tissue-distribution profiles after iv injection showed no correlation to the average molecular mass or to the absolute configuration of amino acid X in the carrier side chains. In contrast, blood clearance of these compounds could be significantly prolonged by using either amphoteric polypeptides (EAK or aek) or a carefully selected polycationic one (alk). It should be noted that the retarded blood survival of amphoteric and polycationic conjugates was not accompanied by similar tissue distribution. Conjugates with a polycationic polypeptide, regardless of their blood clearance, were directed predominantly to spleen, liver, and kidney, while conjugates with glutamic acid at the end of the side chains were taken up by the lung, kidney, and liver.

In summary, these studies have indicated that changes in the primary/secondary structure of the branched poly-

peptide carrier molecule can alter the biodistribution profile of the conjugate and the in vitro cytotoxic activity of daunomycin. In this report we showed that a daunomycin-branched polypeptide conjugate constructed from an amphoteric carrier (e.g., eak) (a) can sustain the cytotoxic activity of cAD and (b) can be present in the circulation for an extended period of time. These findings suggest that amphoteric branched polypeptide-daunomycin conjugates are good candidates for further conjugation to site-specific targeting agents such as monoclonal antibodies. In contrast, a conjugate based on a polycationic polypeptide (e.g., lak) leaves the circulation in a short period of time and accumulates in the liver. Therefore, in spite of its reduced in vitro cytotoxicity as compared to free cAD, this conjugate could be useful also for direct liver-specific targeting without further coupling to recognition unit. In conclusion, this investigation suggests that it is feasible to modulate beneficially the body distribution, retention time, and in vitro cytotoxicity of daunomycin by proper combination of structural elements (side chain sequence, configuration, and identity of amino acid X in the side chain) of the carrier molecule. We are currently studying the therapeutic efficacy of the conjugates reported and also immunoconjugates prepared with monoclonal antibodies.

ACKNOWLEDGMENT

This work was partly supported by the Cancer Research Campaign, London, U.K., and partly by a grant (T-405/1990) from the Ministry of Health, Budapest, Hungary.

LITERATURE CITED

- (1) Varga, J. M., Asato, N., Lande, S., and Lerner, A. B. (1977) Melanotropin-daunomycin conjugate shows receptor-mediated cytotoxicity in cultured murine melanoma cells. *Nature* 267, 56-58.
- (2) Zunino, F., Gambetta, R., Vigevari, A., Penco, S., Geroni, C., and DiMarco, A. (1981) Biological activity of daunorubicin linked to proteins via the methylketone side chain. *Tumori* 67, 521-524.
- (3) Upešlaciš, J., and Hinman, L. (1988) Chemical modification of antibodies for cancer chemotherapy. *Annual Reports in Medicinal Chemistry* (N. Saltzman, Ed.) pp 151-160, Academic Press, New York.
- (4) Hudecz, F., Ross, H., Price, M. R., and Baldwin, R. W. (1990) Immunoconjugate design: a predictive approach for coupling of daunomycin to monoclonal antibodies. *Bioconjugate Chem.* 1, 197-204.
- (5) Trouet, A., and Jolles, G. (1984) Targeting of daunorubicin by association with DNA or proteins: A review. *Semin. Oncol.* 11, 64-72.
- (6) Shen, W. C., and Ryser, H. J. P. (1981) *cis*-Aconityl spacer between daunomycin and macromolecular carriers: a model of pH-sensitive linkage releasing drug from lysosomotropic conjugate. *Biochem. Biophys. Res. Commun.* 102, 1048-1054.
- (7) Arnold, L. J., Jr. (1985) Polylysine-drug conjugates. *Methods Enzymol.* 112, 270-285.
- (8) Zunino, F., Savi, G., Giuliani, F., Gambetta, R., Supino, R., Tinelli, S., and Pezzoni, G. (1984) Comparison of antitumor effects of daunorubicin covalently linked to poly-L-amino acid carriers. *Eur. J. Cancer Clin. Oncol.* 20, 421-425.
- (9) Zunino, F., Giuliani, F., Sovi, G., Dasdia, T., and Gambetta, R. (1982) Anti-tumour activity of daunorubicin linked to poly-L-aspartic acid. *Int. J. Cancer* 30, 465-470.
- (10) Tsukada, Y., Kato, Y., Umemoto, N., Takeda, Y., Hara, T., and Hirai, H. (1984) An anti- α -fetoprotein antibody-daunorubicin conjugate with a novel poly-L-glutamic acid derivative as intermediate drug carrier. *J. Natl. Cancer Inst.* 73, 721-729.
- (11) Hurwitz, E., Wilchek, M., and Pitha, J. (1980) Soluble macromolecules as carriers for daunorubicin. *J. Appl. Biochem.* 2, 25-35.
- (12) Hirano, T., Ohashi, S., Morimoto, S., Tsukada, K., Kobayashi, T., and Tsukagoshi, S. (1986) Synthesis of antitumor-active conjugates of adriamycin or daunomycin with the copolymer of divinyl ether and maleic anhydride. *Macromol. Chem.* 187, 2815-2824.
- (13) Duncan, R., Kopečková-Rejmanová, P., Strohalm, J., Hume, I., Cable, H. C., Pohl, J., Lloyd, J. B., and Kopeček, J. (1987) Anticancer agents coupled to *N*-(2-hydroxypropyl) methacrylamide copolymers. I. Evaluation of daunomycin and puromycin conjugates in vitro. *Br. J. Cancer* 55, 165-174.
- (14) Daussin, F., Boschetti, E., Delmotte, F., and Monsigny, M. (1988) *p*-Benzylthiocarbamoyl-aspartyl-daunorubicin-substituted poly-trisacryl. A new drug acid-labile arm-carrier conjugate. *Eur. J. Biochem.* 176, 625-628.
- (15) Bernstein, A., Hurwitz, E., Maron, R., Arnon, R., Sela, M., and Wilchek, M. (1978) Higher antitumor efficacy of daunomycin when linked to dextran. In vivo and in vitro studies. *J. Natl. Cancer Inst.* 60, 379-384.
- (16) Hurwitz, E., Maron, R., Bernstein, A., Wilchek, M., Sela, M., and Arnon, R. (1978) The effect in vivo of chemotherapeutic drug-antibody conjugates in two murine experimental tumor systems. *Int. J. Cancer* 21, 747-755.
- (17) Rihova, B., Kopečková, P., Strohalm, J., Rossmann, P., Vetrivka, V., and Kopeček, J. (1988) Antibody-directed affinity therapy applied to the immune system: in vivo effectiveness and limited toxicity of daunomycin conjugated to HPMAC copolymers and targeting antibody. *Clin. Immunol. Immunopathol.* 46, 100-114.
- (18) Hudecz, F., and Szekerke, M. (1980) Investigation of drug-protein interactions and the drug-carrier concept by the use of branched polypeptides as model systems. Synthesis and characterization of the model peptides. *Collect. Czech. Chem. Commun.* 45, 933-940.
- (19) Hudecz, F., and Szekerke, M. (1985) Synthesis of new branched polypeptides with poly-lysine backbone. *Collect. Czech. Chem. Commun.* 50, 103-113.
- (20) Hudecz, F., Votavova, H., Gaál, D., Šponar, J., Kajtár, J., Blaha, K., and Szekerke, M. (1985) Branched polypeptides with poly(L-lysine) backbone: synthesis, conformation and immunomodulation. In *Polymeric Materials in Medicine* (Ch. G. Gebelein, and Ch. E. Carraher, Eds.) pp 265-289, Plenum Press, New York.
- (21) Mezö, G., Hudecz, F., Kajtár, J., Szókan, Gy., and Szekerke, M. (1989) The influence of the side chain sequence on the structure-activity correlations of immunomodulatory branched polypeptides. *Biopolymers* 28, 1801-1826.
- (22) Votavova, H., Hudecz, F., Šponar, J., Szekerke, M., and Blaha, K. (1982) Conformation of branched polypeptides based on poly(L-lysine). Effect of the ionic strength and of the presence of alcohols. *Collect. Czech. Chem. Commun.* 47, 3437-3446.
- (23) Votavova, H., Hudecz, F., Kajtár, J., Šponar, J., Blaha, K., and Szekerke, M. (1985) Conformation of branched polypeptides based on poly(L-lysine): the effect of terminal amino acids in the branches. *Collect. Czech. Chem. Commun.* 50, 228-244.
- (24) Hudecz, F., Kutassi-Kovács, S., Mezö, G., and Szekerke, M. (1989) Biodegradability of synthetic branched polypeptide with poly(L-lysine)/backbone. *Biol. Chem. Hoppe-Seyler* 370, 1019-1026.
- (25) Rajnavölgyi, É., Hudecz, F., Mezö, G., Szekerke, M., and Gergely, J. (1986) Isotype distribution and fine specificity of the antibody response on inbred mouse strains to four compounds belonging to a new group of synthetic branched polypeptides. *Mol. Immunol.* 23, 27-37.
- (26) Rajnavölgyi, É., Lányi, Á., Hudecz, F., Kurucz, I., Kiss, K., László, G., Szekerke, M., and Gergely, J. (1989) Structural characteristics influencing the carrier function of synthetic branched polypeptides based on poly[Lys-(DL-Ala)₃] backbone. *Mol. Immunol.* 26, 949-958.
- (27) Gaál, D., Hudecz, F., and Szekerke, M. (1984) Immunomodulatory effect of synthetic branched polypeptides. *J. Biol. Response Modif.* 3, 174-184.

- (28) Gaál, D., Hudecz, F., Kovács, A. L., and Szekerke, M. (1986) Immunomodulatory effect of synthetic branched polypeptides II. *J. Biol. Response Modif.* 5, 148-159.
- (29) Clegg, J. A., Hudecz, F., Pimm, M. V., and Baldwin, R. W. (1990) Drug-carrier design: Biodistribution of branched polypeptides with poly-L-lysine backbone. *Bioconjugate Chem.* 2, 425-430.
- (30) IUPAC-IUB Commission on Biochemical Nomenclature (1972) *Biochem. J.* 127, 753-756.
- (31) IUPAC-IUB Commission on Biochemical Nomenclature (1984) *Eur. J. Biochem.* 138, 9-37.
- (32) Hudecz, F., and Szókán, Gy. (1985) Structure analysis of branched chain poly- and isopeptides based on HPLC of their dansyl derivatives. In *Chromatography, the State of the Art* (H. Kalász, and L. S. Ettre, Eds.) pp 273-286, Akadémiai Kiadó, Budapest.
- (33) Szókán, Gy., Mezö, G., and Hudecz, F. (1988) Application of Marfey's reagent in racemization studies of amino acids and peptides. *J. Chromatogr.* 444, 115-122.
- (34) Schippers, P. H., and Dekkers, H. P. J. (1981) Direct determination of absolute circular dichroism data and calibration of commercial instruments. *Anal. Chem.* 53, 778-782.
- (35) Bolton, A. E., and Hunter, W. M. (1973) The labelling of proteins to high specific radioactivities by conjugation to a ^{125}I -containing acylating agent. *Biochem. J.* 133, 529-539.
- (36) Pimm, M. V., Clegg, J. A., and Baldwin, R. W. (1987) *Eur. J. Cancer Chem. Oncol.* 23, 521.
- (37) Rowland, M., and Tozer, T. N. (1989) *Clinical Pharmacokinetics, Concepts and Application*, 2nd ed., pp 459-463, Lea and Fibiger, Philadelphia.
- (38) Martin, S. R. (1980) Absorption and circular dichroic spectral studies on the self-association of daunorubicin. *Biopolymers* 19, 713-721.
- (39) Rajnavölgyi, É., Hudecz, F., Mezö, G., Watari, E., Heber-Katz, E., Gaál, D., Kurucz, I., Szekerke, M., and Gergely, J. (1990) Synthetic branched polypeptides as carriers for low-molecular weight antigens: correlation between chemical structure and biological functions. *Chimica Oggi* 8, 21-28.
- (40) Hudecz, F., Gaál, D., Lányi, Á., Kurucz, I., Kovács, A. L., Mezö, G., Rajnavölgyi, É., and Szekerke, M. (1991) Carrier design: cytotoxicity and immunogenicity of branched polypeptides with polylysine backbone. *J. Controlled Release*. In press.

Rational Design of a Chimeric Toxin: An Intramolecular Location for the Insertion of Transforming Growth Factor α within *Pseudomonas* Exotoxin as a Targeting Ligand

Robert J. Kreitman, Vijay K. Chaudhary,[†] Clay B. Siegall,[‡] David J. FitzGerald, and Ira Pastan*

Laboratory of Molecular Biology, Division of Cancer Biology, Diagnosis and Centers, National Cancer Institute, National Institutes of Health, 9000 Rockville Pike, 37/4E16, Bethesda, Maryland 20892. Received August 6, 1991

To investigate the potential utility of *Pseudomonas* exotoxin (PE) in forming rationally designed chemotherapeutic agents, we inserted a cDNA encoding transforming growth factor α (TGF α) at several locations in a gene encoding a mutant full-length PE (PE^{4E}) which does not bind to the PE receptor. After expression in *Escherichia coli*, we purified the chimeric toxins to near homogeneity and showed that they were specifically cytotoxic to human epidermoid, ovarian, colon, and hepatocellular carcinoma lines. Like the previously reported TGF α -PE40 (11), one of the new molecules (TGF α -PE^{4E}) contains the ligand at the amino terminus. Two additional chimeras (PE^{4E}-TGF α and PE^{4E}-TGF α -598-613) each contain TGF α inserted near the carboxyl terminus of PE. We show that preservation of the correct PE carboxyl-terminal amino acid sequence, REDLK, allows the toxins containing TGF α carboxyl inserts to retain significant cytotoxicity against target cells, since another molecule (PE^{4E}-TGF α -ILK) containing a nonfunctional carboxyl-terminal sequence was over 100-fold less active. The chimeric toxins with TGF α had the same binding affinity for the EGF receptor whether the ligand occupied the amino or carboxyl position. Molecules with TGF α near the carboxyl position were consistently less active against target cells but also less toxic to mice than those with TGF α at the amino terminus, indicating both types of molecules might be therapeutically effective. Our results establish that a ligand can be placed near the carboxyl terminus of PE, within the portion of the toxin that translocates to the cytosol. The amino-terminal position in such molecules is then available for the placement of other targeting ligands.

INTRODUCTION

Pseudomonas exotoxin A (PE) is produced by *Pseudomonas aeruginosa* and kills mammalian cells which express the PE receptor (1). PE is composed of three structural domains (2). A combination of structural and functional studies (2, 3) has established that domain Ia of PE is responsible for cell recognition, domain II for translocation across cell membranes into the cytosol, and domain III for catalyzing the ADP ribosylation of elongation factor 2, the step that leads to cell death. When domain Ia is removed from PE, a 40-kDa protein is produced (PE40) that still has translocating and ADP ribosylation activity, but lacks the ability to bind and to enter cells. However, when cDNAs encoding TGF α , IL2, IL4, IL6, CD4, or anti-Tac(Fv) are fused to the 5' end of the gene segment encoding PE40, chimeric toxic proteins can be produced which are specifically cytotoxic to malignant cells expressing appropriate receptors (4-11). Because these recombinant molecules kill target cells at extremely low concentrations, they make attractive potential chemotherapeutic agents.

Transforming growth factor α (TGF α), which is similar structurally and functionally to the epidermal growth factor, appears to be involved in the growth and maintenance of many human solid tumors, including those of lung, breast, head and neck, prostate, brain, liver, and bladder, and of endometrial, renal, and gastrointestinal origin (12-18). The use of chemotherapy in eradicating or even partially reducing metastatic disease from these

sites has been disappointing at best. TGF α -PE40 in vitro is extremely cytotoxic to many of these human solid tumors (11, 19). Moreover, in nude mouse xenographs of human prostate and epidermoid carcinomas (19) and hepatocellular cancer (Siegall, C. B., FitzGerald, D. J., and Pastan, I., unpublished results), a therapeutic window exists between the dose required to kill tumor cells and the dose-limiting toxicity due to the EGF receptors on normal tissues.

From the standpoint of rational drug design, it would be useful to place one (or more) ligand(s) in different locations within the toxin, especially within the region that translocates into the cytosol. However, when TGF α was placed at the carboxyl end of PE40, a molecule was produced (PE40-TGF α) that was much less active than TGF α -PE40 and could not be purified by anion exchange and sizing chromatography (4, 11). Furthermore, PE40-IL2, PE40-IL4, and PE40-IL6 were all produced and found to have no detectable cytotoxic activity on receptor-bearing target cells (unpublished data). The explanation for the difference in activity between the amino- and carboxyl-terminal chimeric toxins emerged recently when we established that the last five amino acids of PE, REDLK, while unnecessary for ADP ribosylation activity, are needed for cytotoxicity (20). These results suggested that the reason for the reduced cytotoxic activity of molecules such as PE40-TGF α was that the TGF α molecule blocked REDLK and prevented as essential step in translocation of the toxin's active fragment into the cytosol.

To determine if a cell-targeting ligand could be placed at a location other than the amino terminus where it would still bind to EGF receptors and also be translocated into the cytosol, we decided to insert TGF α near the carboxyl terminus of PE^{4E}. We used PE^{4E}, in which Lys⁶⁷, His²⁴⁶, Arg²⁴⁷, and His²⁴⁹ are all replaced by glutamates (21), rather than PE40, in which domain Ia is deleted, because its

* To whom correspondence should be sent.

[†] Current address: Department of Biochemistry, University of Delhi, South Campus, Benito Juarez Rd, New Delhi 110021, India.

[‡] Current address: Pharmaceutical Research and Development Division, Bristol-Myers Squibb Co., 5 Research Parkway, Dept. 207, Wallingford, CT 06492.

expression level is better and it is more readily purified. Additionally, we have found that the chimeric toxins IL2-PE^{4E} and IL6-PE^{4E} are several-fold more active than IL2-PE40 and IL6-PE40, respectively (22, 23). Accordingly, two carboxyl-terminal TGF α recombinant constructions were prepared and expressed in *E. coli*; both contain the necessary REDLK terminal sequence. The first, PE^{4E}-TGF α , contains amino acids 1–607 of PE followed by TGF α , then amino acids 604–613 of PE. The second, PE^{4E}-TGF α -598–613, differs from the first in that TGF α is followed by amino acids 598–613 of PE so that more of the natural carboxyl terminus of PE remains undisturbed. A third molecule, PE^{4E}-TGF α -ILK, contains an improper carboxyl end following the TGF α insert and hence should be less cytotoxic. Using cell lines with varying numbers of EGF receptors, the cytotoxic and cell-binding activities of these three PE^{4E} molecules with carboxyl-inserted TGF α were compared to those of PE derivatives with an amino-attached TGF α (TGF α -PE^{4E} and TGF α -PE40). The chimeric toxins were also tested in vivo to determine their lethality to mice.

EXPERIMENTAL PROCEDURES

Materials. Restriction endonucleases and DNA ligase were obtained from New England Biolabs (Beverly, MA) or Bethesda Research Laboratories (Gaithersburg, MD) and used as recommended. Alkaline phosphatase was obtained from Boehringer Mannheim (Indianapolis, IN). [³H]Leucine and [¹²⁵I]EGF were purchased from Amersham Corporation (Arlington Heights, IL) or from New England Nuclear (Boston, MA). EGF was purchased from Bioproducts for Science (Indianapolis, IN). FPLC columns and media were purchased from Pharmacia (Piscataway, NJ).

Cell Lines. OVCAR3 cells were a gift from T. Hamilton (NCI). HUT102 cells were a gift from T. Waldmann (NCI). Other cell lines were from the American Type Culture Collection (Rockville, MD).

Plasmids. All the plasmids utilize a lactose-inducible T7 promoter expression system (24). All the constructions were carried out using standard cloning techniques involving restriction enzyme digestions and separation of fragments on low melting point agarose gels, followed by in-gel ligations.

Plasmid pVC 47195 f+T, reported previously (20), encodes the *OmpA* signal sequence, followed by PE amino acids 1–607, RPMPGD, and finally PE amino acids 598–613. The DNA sequence of the heptapeptide linker (5'-AGGCCTCATATGCCCGGGGAT-3') provides unique *StuI* and *NdeI* sites, in addition to *BamHI* and *SmaI* sites. Following the linker, mutation of PE codon 604 to 5'-CCC-3' inserts a second *SmaI* site in the plasmid for cloning purposes. A cDNA encoding TGF α with *NdeI* restriction sites at the 5' and 3' ends was inserted into *NdeI*-digested pVC 47195 f+T, resulting in pVC 47395 f+T. pVC 47355 f+T was prepared from pVC 47395 f+T by digesting with *SmaI* and selfligating the 5.3-kb fragment.

Plasmid pVC 4715 f+T is similar to pVC 47195 f+T, except that it contains sequences which encode ILK at the carboxyl terminus of the gene-fusion product, instead of PE amino acids 598–613 (20). The TGF α cDNA was ligated into the *NdeI*-digested plasmid to produce pVC 47315 f+T.

Plasmids pVC 4731/4E f+T, 4735/4E f+T, and 4739/4E f+T encode PE^{4E}-TGF α -ILK, PE^{4E}-TGF α , and PE^{4E}-TGF α -598–613, respectively, which do not carry the *OmpA* signal sequence. They were prepared from plasmids pVC 47315 f+T, pVC 47355 f+T, and pVC 47395 f+T, respec-

tively, by ligating the 4.0-kb *XbaI*-*SstII* fragment of each plasmid with a 1.3-kb *XbaI*-*SstII* fragment of pVC4/4E f+T, which encodes PE^{4E} (5, 21, 25).

pVC 34/4E f+T encoding TGF α -PE^{4E} was prepared by inserting the *NdeI* insert containing TGF α into *NdeI*-digested pVC 4/4E f+T.

Protein Expression and Purification. *E. coli* BL21 (λ DE3) cells, which carry a T7 RNA polymerase gene in a lysogenic and inducible form, were used as a host for transformation and expression of the above plasmids. The fusion proteins were isolated from the insoluble fraction (inclusion bodies) as described previously (6). The inclusion bodies were denatured in 7 M guanidine hydrochloride and renatured in phosphate-buffered saline (PBS). The crude dialyzed mixture was purified by sequential Q-Sepharose, Mono-Q (Pharmacia), and gel filtration chromatography as has been reported previously (26). Using a step NaCl gradient for Q-Sepharose and linear gradient for Mono-Q, the desired chimeric toxin eluted at a salt concentration of 0.2–0.24 M with chromatograms appearing similar to those obtained for the purification of DT388-antiTac(Fv) (26). Protein concentration of the purified chimeric toxins was determined by the Bradford assay (Pierce, Rockford, IL) using BSA as a standard. This method has agreed well with results from amino acid analysis of similar molecules.

In Vitro Assay. Cytotoxicity assays were generally performed as described previously (7). Adherent cells were plated at a density of 1×10^5 cells/mL on the day prior to addition of recombinant toxins. HUT102 and U266 cells, which grew in suspension, were washed and plated immediately at a density of 4×10^5 cells/mL prior to toxin addition. Assays were performed in 24-well plates containing 1 mL of cells per well. After a 16–20-h incubation with toxins, [³H]leucine (2 μ Ci per well) was added for 60–90 min and incorporation into cellular protein was measured. Data was obtained from the average of duplicates, which generally varied from the mean by 5–10%. Total counts per minute (cpm) in the absence of toxin was 12–14 000. The assay reported was representative of several confirmatory assays.

Binding Studies To Determine Receptor Number. PLC/PRF/5, HEPG2, OVCAR3, and HT29 cells were each plated at 5×10^4 /mL, 1 mL/well, in 24-well plates. Twenty-four hours later, cells were washed twice with binding buffer (DMEM containing 50 mM BES (pH 6.8) and BSA 1 mg/mL). The 24-well plates were placed on ice, and 200 μ L of binding buffer containing either 0.037, 0.11, 0.33, 1, 2, or 6 ng of [¹²⁵I]EGF (0.1 μ Ci/ng), each with or without 1.2 μ g of cold EGF, was added. Each of the 12 combinations were performed in duplicate. After 1–2 h of equilibration at 4 °C with rocking, cells were washed three times with binding buffer and lysed with 0.01 M Tris-HCl (pH 7.4) containing 0.5% SDS and 1 mM EDTA, and bound ligand was quantitated with a γ detector. Receptor number was determined from Scatchard plots as described previously (27). K_d 's for each cell line were similar and varied between 0.8 and 2×10^{-9} M. Receptor numbers shown for other cell lines in Table I were determined previously (28, 29).

[¹²⁵I]EGF Displacement Studies. A431 cells were plated at 8×10^3 cells/well, 1 mL/well, in 24-well plates. After 24 h, the cells were washed twice with binding buffer, fixed with formaldehyde, washed again with binding buffer, and treated with 200 μ L of binding buffer containing 0.5 ng (0.05 μ Ci) of [¹²⁵I]EGF, combined with either 0, 0.16, 0.8, 4, 20, or 100 pmol of chimeric toxin. After equilibration for 1–2 h on a rocker, the cells were washed, lysed, and

Table I. Cytotoxicity of TGF α -Toxins against Human Malignant Cells

cell line, type	EGF receptors sites/cell $\times 10^3$	ID ₅₀ , ^a ng/mL				
		TGF α -PE40	TGF α -PE ^{4E}	PE ^{4E} -TGF α	PE ^{4E} -TGF α -598-613	PE ^{4E} -TGF α -ILK
A431, epidermoid	3000	0.05	0.02	0.3	0.3	130
KB, epidermoid	200	0.5	0.3	5	7	>1000
HT29, colon	100	0.5	1.7	2.5	3	>1000
OVCAR3, ovarian	70	0.75	0.45	1.7	2.4	>1000
PLC/PRF/5, hepatoma	20	0.16	0.05	0.4	0.3	>1000
HEPG2, hepatoma	9	3	4	33	65	>1000
U266, myeloma	<1	>1000	>1000	>1000	>1000	>1000
HUT102, T leukemia	—	>1000	>1000	>1000	>1000	>1000

^a ID₅₀'s constituted the concentrations needed for half-maximal protein synthesis inhibition. Values were calculated using the two concentration points on either side of the 50% of control (represented by dashed lines in Figure 3).

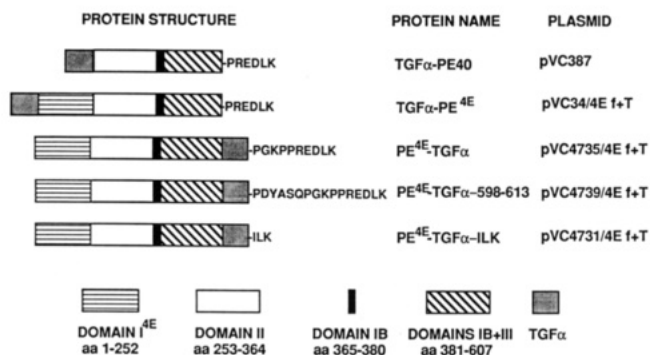


Figure 1. Schematic of expressed proteins. The amino acids listed in the one-letter code are the C-terminal residues.

counted as above. Data was obtained from the medians of triplicate values, and reported values were taken from one of several independent confirmatory assays.

In Vivo Studies. Athymic female (nude) mice, strain BALB/c, were supplied by the Frederick Cancer Research Center, National Cancer Institute. LD₅₀ studies were performed by intraperitoneal injection of the various chimeric toxins in phosphate-buffered saline supplemented with 0.2% human serum albumin (0.5 mL).

RESULTS

Construction of Recombinant Toxins. Our goal is to construct chimeric toxins which can bind to cells using ligands placed at locations other than the amino terminus of the PE molecule. A second goal is to have a ligand in the 37-kDa carboxy terminal position of PE, where it could be translocated into the cytosol. Recent experiments demonstrating the importance of the last several amino acids of PE (20) suggested to us that toxin activity could be better preserved if the ligand were placed near rather than at the carboxyl terminus. The location we chose for TGF α was after amino acid 607 of PE, since residues after 602 are not required for ADP ribosylation activity (20). To retain two different lengths of the native carboxyl terminus of PE, we inserted TGF α prior to either PE amino acids 604-613 or 598-613 (Figure 1). The recombinant proteins, expressed in *E. coli* and recovered from inclusion bodies by denaturation and renaturation, were purified to near homogeneity (Figure 2) and purified chimeric toxins were used for further studies.

Activity on Cell Lines. To determine if TGF α could be inserted into the carboxyl terminus of PE and still target PE to cells expressing EGF receptors, we determined the cytotoxic activities of PE^{4E}-TGF α and PE^{4E}-TGF α -598-613 against cell lines expressing different numbers of EGF receptors (Table I). The cell lines A431, KB, HT29, OVCAR3, and PLC/PRF/5 were all very sensitive to TGF α -PE40 and were quite sensitive to both PE^{4E}-TGF α and PE^{4E}-TGF α -598-613, with ID₅₀'s ranging from 0.3 to

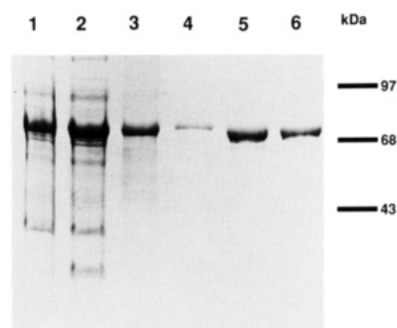


Figure 2. SDS-PAGE (10% reducing) of PE^{4E}-TGF α : lane 1, total cell; lane 2, spheroplast; lane 3, inclusion bodies; lane 4, pooled fractions after Q-Sepharose chromatography; lane 5, pooled fractions after mono-Q chromatography; and lane 6, pooled fractions after TSK sizing column. For lanes 1-3, 30 μ L based on the original culture volume (90 min after induction at an OD₆₅₀ of 1.0) was loaded in each lane. Less than 1 μ g was loaded in lane 4, and 2-4 μ g was loaded in lanes 5 and 6. Gels were stained by coomassie blue.

7 ng/mL. The cell line A431, with 3×10^6 receptors/cell, was more sensitive to the chimeric toxins than KB cells, which have 2×10^5 receptors/cell. The cell line HEPG2, which has only 9000 receptors/cell, showed less sensitivity to the two carboxyl inserts. Interestingly, PLC/PRF/5 cells, which express EGF receptors in numbers similar to HEPG2 cells, were 20-200-fold more sensitive to the TGF α -toxins than were HEPG2 cells. The cell lines U266 and HUT102, which are resistant to TGF α -PE40, were resistant to the new molecules, even at toxin concentrations of 1000 ng/mL. Specificity for target cells was demonstrated by competition with excess EGF. Figure 3 shows that inhibition of protein synthesis by both toxins in A431 cells could be reversed by 2 μ g/mL EGF. Reversal by excess EGF was also demonstrated for KB, OVCAR3, HEPG2, PLC/PRF/5, and HT29 cells (data not shown).

To demonstrate the importance of retaining a proper carboxyl end, we also made and tested PE^{4E}-TGF α -ILK (Figure 1). In the sensitive cell lines, this change in the last several amino acids of PE resulted at least in a 150-3000-fold loss of activity against A431, KB, HT29, OVCAR3, and PLC/PRF/5 cells (Table I).

To evaluate the effect of moving the ligand from the amino to the carboxyl position, we made TGF α -PE^{4E}, which has TGF α at the amino terminus of PE^{4E}. TGF α -PE^{4E} is several-fold more active than TGF α -PE40, a chimeric toxin that is missing all of domain I and is cytotoxic to a variety of cell lines expressing EGF receptors (11). Comparison of ID₅₀'s for each sensitive cell line shows greater cytotoxicity when TGF α occupies the amino terminal position (Table I).

EGF displacement studies were performed to determine whether the decreased cytotoxicity of PE^{4E}-TGF α and PE^{4E}-TGF α -598-613 relative to that of TGF α -PE^{4E} was

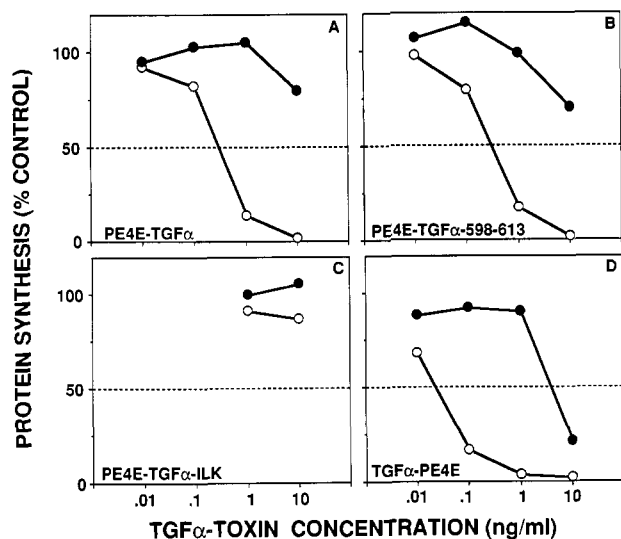


Figure 3. Protein synthesis inhibition of A431 cells by PE^{4E}-TGF α , PE^{4E}-TGF α -598-613, PE^{4E}-TGF α -ILK, and TGF α -PE^{4E}: (O) toxin alone, (●) toxin + EGF, 2 μ g/mL. Total cpm in the absence of toxin was 12–14 000.

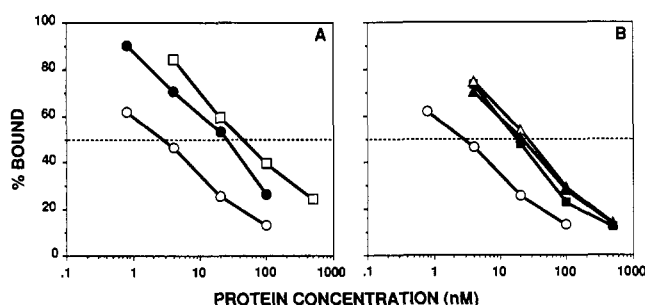


Figure 4. Displacement of [¹²⁵I]EGF from A431 cells by (O) TGF α and (A) the amino-terminal constructs (●) TGF α -PE40 and (□) TGF α -PE^{4E} and (B) the carboxyl-insert constructs (■) PE^{4E}-TGF α -ILK, (Δ) PE^{4E}-TGF α , and (▲) PE^{4E}-TGF α -598-613. nM values were calculated from ng/mL assuming approximate molecular weights of 6 kDa for TGF α , 46 kDa for the TGF α -PE₄₀, and 72 kDa for PE^{4E}-TGF α -ILK, PE^{4E}-TGF α , PE^{4E}-TGF α -598-613, and TGF α -PE^{4E}.

Table II. LD₅₀ Analysis

molecule	amount injected, μ g (μ g/kg)	no. deaths/no. mice	molecule	amount injected, μ g (μ g/kg)	no. deaths/no. mice
TGF α -PE40	0.75 (38)	0/4	PE ^{4E} -TGF α	5.0 (250)	0/3
	1 (50)	0/4		6.0 (300)	2/4
	2 (100)	2/3		8.0 (400)	2/3
	2.5 (125)	2/2	PE ^{4E} -TGF α -598-613	1.0 (50)	0/2
TGF α -PE ^{4E}	0.2 (10)	0/2		4.0 (200)	0/2
	0.8 (40)	0/4		6.0 (300)	1/4
	1.5 (75)	1/2		8.0 (400)	1/2
	3.0 (150)	2/2		10.0 (500)	2/2

due to a reduction in binding affinity of the inserted TGF α ligand to the EGF receptor. Figure 4 shows that PE^{4E}-TGF α -ILK, PE^{4E}-TGF α , and PE^{4E}-TGF α -598-613, which contain TGF α near the carboxyl terminus, and TGF α -PE40 and TGF α -PE^{4E}, which contain TGF α at the amino terminus, all displace [¹²⁵I]EGF from A431 cells in a similar manner and 6–15-fold less well than free TGF α .

Animal Toxicity Studies. To determine the animal toxicity of these new chimeric toxins, we injected several different doses into the intraperitoneal cavity of nude mice. Table II shows that the approximate single dose LD₅₀ of PE^{4E}-TGF α was 6 μ g (300 μ g/kg), which was similar to the 8 μ g (400 μ g/kg) value obtained for PE^{4E}-TGF α -598-613. We were able to give several-fold more of the carboxyl inserts than TGF α -PE^{4E}, which had an LD₅₀ of 1.5 μ g/

mouse (75 μ g/kg). The LD₅₀ of TGF α -PE40 in nude mice is the same as that of TGF α -PE^{4E}, despite the difference in activity on several cell lines (Table I).

DISCUSSION

Until now, obtaining chimeric toxins of high cytotoxic activity against human cancer cells has required placing the binding ligand at the amino terminus of PE or PE derivatives in which domain Ia is deleted or mutated. Placement of ligands at the carboxyl terminus produced molecules with greatly reduced or no activity. The current study shows that the ligand TGF α can be inserted near the carboxyl terminus of PE, and this insertion results in molecules with specific cytotoxicity for EGF receptor-bearing cells.

The function of the PE carboxyl terminal sequence appears to be to allow a fragment of the toxin containing all of domain III and part of domain II to translocate to the cytosol (20,30). The two chimeric toxins with a correct carboxyl terminus following the TGF α insert were several orders of magnitude more cytotoxic to target cells than a similar molecule with ILK at the carboxyl terminus, despite having the same binding affinity to the EGF receptor (Table I and Figure 4). The reason why PE^{4E}-TGF α -ILK (Table I) or the impure PE40-TGF α (4) have any activity against A431 cells remains unclear, but it is possible that the carboxyl-terminal sequences of these molecules may allow for a very low level of translocation into the A431 cytosol. TGF α alone had less than 50% protein synthesis inhibition of A431 cells at 1000 ng/mL (data not shown).

PE^{4E}-TGF α and PE^{4E}-TGF α -598-613 are 2–15-fold less cytotoxic to target cells than comparable molecules with TGF α at their amino terminus (Table I). Displacement analysis has determined that they all bind equally well to the EGF receptor. Therefore, there must be another basis for the decreased cytotoxic activity. The insertion of TGF α plus 9 or 15 extra amino acids could lead to a decreased rate of proteolytic processing in domain II (30). Alternatively, there may be a reduction in the rate or extent of translocation into the cytosol of the ADP ribosylating activity contained in domain III.

The new molecule TGF α -PE^{4E}, as expected, was generally more cytotoxic to target cells than TGF α -PE40. It was surprising that it was not several-fold more toxic to mice in view of the *in vivo* data comparing the toxicity of IL2-PE^{4E} and IL6-PE^{4E} to that of IL2-PE40 and IL6-PE40, respectively (22, 31). These results make TGF α -PE^{4E} an attractive molecule for further study.

From a therapeutic standpoint, inserting TGF α near the carboxyl terminus may be just as useful as placing it at the amino terminus in spite of the decrease in cytotoxicity of PE^{4E}-TGF α relative to that of TGF α -PE^{4E}, since specificity for EGF receptors is apparently preserved, and several-fold more toxin can be given to mice. Furthermore, using this approach, it should now be possible to utilize this carboxyl insertion position for other ligands. Some ligands, which require a relatively unhindered carboxyl terminus, may be more effective near the carboxyl terminus than at the amino terminus of PE. Molecules such as IL2, which bind to the α and β subunits of their receptors, might show selective binding to one or the other subunit when placed at the N- or C-terminus. By placing the same or different ligands at both locations, one may be able to improve binding of the chimeric toxin to a target cell, or to enhance binding to dimeric receptors.

Another possible use of the carboxyl insert position could take advantage of the fact that this region is within the 37-kDa carboxyl fragment of PE which translocates to the

cytosol (30). One may be able to target functional proteins to the cytoplasm of mammalian cells by inserting a biologically active polypeptide into the PE carboxyl terminus. The polypeptide may be an additional toxin active in the cytosol of an unwanted cell (such as the ADP ribosylating portion of diphtheria toxin or the ribosome-inactivating portion of ricin and Shiga toxins) or a protein required in the cytoplasm of a metabolically defective non-malignant cell.

LITERATURE CITED

- (1) Pastan, I., and FitzGerald, D. (1989) *Pseudomonas* exotoxin: Chimeric toxins. *J. Biol. Chem.* 264, 15157-15160.
- (2) Allured, V. S., Collier, R. J., Carroll, S. F., and McKay, D. B. (1986) Structure of exotoxin A of *Pseudomonas aeruginosa* at 3.0-Å resolution. *Proc. Natl. Acad. Sci. U.S.A.* 83, 1320-1324.
- (3) Hwang, J., FitzGerald, D. J., Adhya, S., and Pastan, I. (1987) Functional domains of *Pseudomonas* exotoxin identified by deletion analysis of the gene expressed in *E. coli*. *Cell* 48, 129-136.
- (4) Chaudhary, V. K., FitzGerald, D. J., Adhya, S., and Pastan, I. (1987) Activity of a recombinant fusion protein between transforming growth factor type α and *Pseudomonas* toxin. *Proc. Natl. Acad. Sci. U.S.A.* 84, 4538-4542.
- (5) Chaudhary, V. K., Xu, Y., FitzGerald, D., Adhya, S., and Pastan, I. (1988) Role of domain II of *Pseudomonas* exotoxin in the secretion of proteins into the periplasm and medium by *Escherichia coli*. *Proc. Natl. Acad. Sci. U.S.A.* 85, 2939-2943.
- (6) Chaudhary, V. K., Mizukami, T., Fuerst, T. R., FitzGerald, D. J., Moss, B., Pastan, I., and Berger, E. A. (1988) Selective killing of HIV-infected cells by recombinant human CD4-*Pseudomonas* exotoxin hybrid protein. *Nature* 335, 369-372.
- (7) Chaudhary, V. K., Queen, C., Junghans, R. P., Waldmann, T. A., FitzGerald, D. J., and Pastan, I. (1989) A recombinant immunotoxin consisting of two antibody variable domains fused to *Pseudomonas* exotoxin. *Nature* 339, 394-397.
- (8) Lorberboum-Galski, H., FitzGerald, D., Chaudhary, V., Adhya, S., and Pastan, I. (1988) Cytotoxic activity of an interleukin 2-*Pseudomonas* exotoxin chimeric protein produced in *Escherichia coli*. *Proc. Natl. Acad. Sci. U.S.A.* 85, 1922-1926.
- (9) Ogata, M., Chaudhary, V. K., FitzGerald, D. J., and Pastan, I. (1989) Cytotoxic activity of a recombinant fusion protein between interleukin 4 and *Pseudomonas* exotoxin. *Proc. Natl. Acad. Sci. U.S.A.* 86, 4215-4219.
- (10) Siegall, C. B., Chaudhary, V. K., FitzGerald, D. J., and Pastan, I. (1988) Cytotoxic activity of an interleukin 6-*Pseudomonas* exotoxin fusion protein on human myeloma cells. *Proc. Natl. Acad. Sci. U.S.A.* 85, 9738-9742.
- (11) Siegall, C. B., Xu, Y., Chaudhary, V. K., Adhya, S., FitzGerald, D., and Pastan, I. (1989) Cytotoxic activities of a fusion protein comprised of TGF α and *Pseudomonas* exotoxin. *FASEB J.* 3, 2647-2652.
- (12) Lau, J. L. T., Fowler, J. E., Jr., and Ghosh, L. (1988) Epidermal growth factor in the normal and neoplastic kidney and bladder. *J. Urol.* 139, 170-175.
- (13) Real, F. X., Rettig, W. J., Chesa, P. G., Melamed, M. R., Old, L. J., and Mendelsohn, J. (1986) Expression of epidermal growth factor receptor in human cultured cells and tissues: Relationship to cell lineage and stage of differentiation. *Cancer Res.* 46, 4726-4731.
- (14) Hendler, F. J., and Ozanne, B. W. (1984) Human squamous cell lung cancers express increased epidermal growth factor receptors. *J. Clin. Invest.* 74, 647-651.
- (15) Jones, N. R., Rossi, M. L., Gregoriou, M., and Hughes, J. T. (1990) Epidermal growth factor receptor expression in 72 meningiomas. *Cancer* 66, 152-155.
- (16) Reynolds, R. K., Talavera, F., Roberts, J. A., Hopkins, M. P., and Menon, K. M. J. (1990) Characterization of epidermal growth factor receptor in normal and neoplastic human endometrium. *Cancer* 66, 1967-1974.
- (17) Wilding, G., Valverius, E., Knabbe, C., and Gelmann, E. P. (1989) Role of transforming growth factor- α in human prostate cancer cell growth. *Prostate* 15, 1-12.
- (18) Scambia, G., Panici, P. B., Battaglia, F., Ferrandina, G., Almadori, G., Paludetti, G., Maurizi, M., and Mancuso, S. (1991) Receptors for epidermal growth factor and steroid hormones in primary laryngeal tumors. *Cancer* 67, 1347-1351.
- (19) Pai, L. H., Gallo, M. G., FitzGerald, D. J., and Pastan, I. (1991) Anti-tumor activity of a transforming growth factor α -*Pseudomonas* exotoxin fusion protein (TGF- α -PE40). *Cancer Res.* 51, 2808-2812.
- (20) Chaudhary, V. K., Jinno, Y., FitzGerald, D., and Pastan, I. (1990) *Pseudomonas* exotoxin contains a specific sequence at the carboxyl terminus that is required for cytotoxicity. *Proc. Natl. Acad. Sci. U.S.A.* 87, 308-312.
- (21) Chaudhary, V. K., Jinno, Y., Gallo, M. G., FitzGerald, D., and Pastan, I. (1990) Mutagenesis of *Pseudomonas* exotoxin in identification of sequences responsible for the animal toxicity. *J. Biol. Chem.* 265, 16306-16310.
- (22) Lorberboum-Galski, H., Garsia, R. J., Gately, M., Brown, P. S., Clark, R. E., Waldmann, T. A., Chaudhary, V. K., FitzGerald, D. J. P., and Pastan, I. (1990) IL2-PE66^{Glu}, a new chimeric protein cytotoxic to human-activated T lymphocytes. *J. Biol. Chem.* 265, 16311-16317.
- (23) Siegall, C. B., FitzGerald, D. J., and Pastan, I. (1990) Cytotoxicity of IL6-PE40 and derivatives on tumor cells expressing a range of IL6 receptor levels. *J. Biol. Chem.* 265, 16318-16323.
- (24) Studier, F. W., and Moffatt, B. A. (1986) Use of bacteriophage T7 RNA polymerase to direct selective high-level expression of cloned genes. *J. Mol. Biol.* 189, 113-130.
- (25) Jinno, Y., Ogata, M., Chaudhary, V. K., Willingham, M. C., Adhya, S., FitzGerald, D., and Pastan, I. (1989) Domain II mutants of *Pseudomonas* exotoxin deficient in translocation. *J. Biol. Chem.* 264, 15953-15959.
- (26) Chaudhary, V. K., Gallo, M. G., FitzGerald, D. J., and Pastan, I. (1990) A recombinant single-chain immunotoxin composed of anti-Tac variable regions and a truncated diphtheria toxin. *Proc. Natl. Acad. Sci. U.S.A.* 87, 9491-9494.
- (27) Siegall, C. B., Nordan, R. P., FitzGerald, D. J., and Pastan, I. (1990) Cell-specific toxicity of a chimeric protein composed of interleukin-6 and *Pseudomonas* exotoxin (IL6-PE40) on tumor cells. *Mol. Cell. Biol.* 10, 2443-2447.
- (28) De Larco, J. E., Reynolds, R., Carlberg, K., Engle, C., and Todaro, G. J. (1980) Sarcoma growth factor from mouse sarcoma virus-transformed cells. *J. Biol. Chem.* 255, 3685-3690.
- (29) Lyall, R. M., Hwang, J., Cardarelli, C., FitzGerald, D., Akiyama, S., Gottesman, M. M., and Pastan, I. (1987) Isolation of human KB cell lines resistant to epidermal growth factor-*Pseudomonas* exotoxin conjugates. *Cancer Res.* 47, 2961-2966.
- (30) Ogata, M., Chaudhary, V. K., Pastan, I., and FitzGerald, D. J. (1990) Processing of *Pseudomonas* exotoxin by a cellular protease results in the generation of a 37,000-Da toxin fragment that is translocated to the cytosol. *J. Biol. Chem.* 265, 20678-20685.
- (31) Siegall, C. B., Kreitman, R. J., FitzGerald, D. J., and Pastan, I. (1991) Antitumor effects of interleukin 6-*Pseudomonas* exotoxin chimeric molecules against the human hepatocellular carcinoma PLC/PRF/5 in mice. *Cancer Res.* 51, 2831-2836.

Properties of Chimeric Toxins with Two Recognition Domains: Interleukin 6 and Transforming Growth Factor α at Different Locations in *Pseudomonas* Exotoxin

Robert J. Kreitman, Clay B. Siegall,[†] Vijay K. Chaudhary,[‡] David J. FitzGerald, and Ira Pastan*

Laboratory of Molecular Biology, DCBDC, National Cancer Institute, National Institutes of Health, Bethesda, Maryland 20892. Received August 6, 1991

Pseudomonas exotoxin (PE) is a potent cytotoxic agent that is composed of 613 amino acids arranged into three major domains. We have previously identified two positions where ligands can successfully be placed in PE to direct it to cells with specific surface receptors. One site is at the amino terminus and the other is close to but not at the C-terminus. To examine the possibility of constructing onco-toxins with two different recognition elements that will bind to two different receptors, we have placed cDNAs encoding either transforming growth factor α (TGF α) or interleukin 6 (IL6) at the 5' end of a PE gene and also inserted a cDNA encoding TGF α near the 3' end of the PE gene. The plasmids encoding these chimeric toxins were expressed in *Escherichia coli* and the chimeric proteins purified to near homogeneity. In all the new toxins, the TGF α near the C-terminus was inserted after amino acid 607 of PE and followed by amino acids 604-613 so that the correct PE C-terminus (REDLK) was preserved. For each chimera, the toxin portion was either PE^{4E}, in which the cell binding domain (domain Ia) is mutated, PE40, in which domain Ia is deleted, or PE38, in which domain Ia and part of domain Ib are deleted. These derivatives of PE do not bind to the PE receptor and allow 607, 355, or 339 amino acids, respectively, between the two ligands. Chimeric toxins containing two TGF α ligands were all cytotoxic to human cancer cells expressing EGF receptors, while those containing one IL6 and one TGF α ligand were cytotoxic toward cells expressing either IL6 or EGF receptors, or both. The effect of distance separating the two ligands was evaluated using cytotoxicity assays and [¹²⁵I]EGF displacement assays. The animal toxicity of two of the bifunctional chimeric toxins was investigated in mice. Our results establish that two ligands can be placed in different locations within PE simultaneously and that adding IL6 to the amino terminus of PE which already contains TGF α near the carboxyl terminus decreases animal toxicity in vivo and yet increases cytotoxicity against some cell lines in vitro.

INTRODUCTION

Receptor-targeted therapy of cancer or autoimmune disease is gaining interest as many of these diseases remain incurable despite chemotherapeutic and steroidal therapy. Not only do many tumors express higher levels of certain growth factor receptors or antigens than normal cells, but they often express receptors for more than one ligand. For example, human melanoma cells have been found to express both nerve growth factor and epidermal growth factor (EGF) receptors (1, 2). Renal, breast, and esophageal carcinomas have been found to express both insulin-like growth factor I (IGF-I) and EGF receptors (3-5). Interleukin 6 and EGF receptors have also been found on epidermoid, prostate, and hepatocellular carcinoma cells (6-8). Recently, our laboratory has described chimeric toxins containing either IL6 or TGF α fused to derivatives of *Pseudomonas* exotoxin (PE) (9, 10) which have shown efficacy against epidermoid, prostate, and hepatocellular carcinoma cells both in vitro and in nude mice (11, 12).

PE is a 66-kDa 613 amino acid protein consisting of a domain which binds to the PE receptor of normal cells (domain Ia, amino acids 1-252), a domain which undergoes proteolytic cleavage and mediates translocation of the 37-kDa carboxyl terminal segment of PE into the cytoplasm (domain II, amino acids 253-364), and a domain which

ADP-ribosylates elongation factor II (domain III, amino acids 400-613) (13-15). The function of domain Ib (amino acids 365-399), which is between domains II and III, is unclear, but much of it (amino acids 365-380) can be removed without adversely affecting cytotoxicity (16).

In order to generate chimeric toxins which have minimal binding to normal cells, we have modified PE in several ways so that it does not bind to the PE receptor. One method is to remove domain Ia, which results in PE40. Recently, we have shortened PE40 to PE38 by removing amino acids 365-380 of domain Ib (16). A third method is to mutate four amino acids within domain Ia (Lys⁵⁷, His²⁴⁶, Arg²⁴⁷, and His²⁴⁹) to glutamates (17), resulting in PE^{4E}. We have then fused these modified PE molecules to ligands that will direct PE to target cells. In IL6 chimeric toxins (IL6-PE40 and IL6-PE^{4E}), we have genetically fused IL6 to the amino terminus of either PE40 or PE^{4E}, respectively (6, 9). With TGF α , we have not only made TGF α -PE40 and TGF α -PE^{4E}, in which TGF α is located at the amino terminus of the modified toxin, but also PE^{4E}-TGF α , which contains TGF α inserted near the carboxyl terminus of PE^{4E} (10, 18). By inserting the TGF α ligand after PE amino acid 607 and before PE amino acids 604-613, we preserved the correct PE carboxyl terminus REDLK, which is necessary for cytotoxicity (18, 19).

In the current study, we wished to determine if we could target a chimeric toxin to either EGF- or IL6-receptor-bearing cells, or to both EGF and IL6 receptors on the same cell. Therefore, we made chimeric toxins which contain TGF α in the carboxyl insert position of PE, and IL6 at the amino terminus. We also made chimeric toxins

* To whom correspondence should be sent.

[†] Current address: Pharmaceutical Research Institute, Bristol-Myers Squibb Co., 5 Research Parkway, Wallingford, CT 06492.

[‡] Current address: Department of Biochemistry, University of Delhi, South Campus, Benito Juarez Road, New Delhi 110021, India.

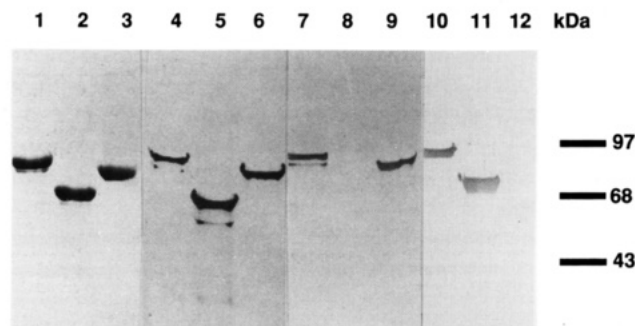


Figure 2. SDS-PAGE analysis of chimeric proteins. Ten percent reducing gel (stained by coomassie blue) showing 4 μ g of purified IL6-PE^{4E}-TGF α in lane 1, PE^{4E}-TGF α in lane 2, and IL6-PE^{4E} in lane 3. The three proteins IL6-PE^{4E}-TGF α , PE^{4E}-TGF α , and IL6-PE^{4E} were respectively visualized in immunoblots by anti-PE antibodies in lanes 4–6; anti-IL6 antibodies in lanes 7–9, and anti-TGF α antibodies in lanes 10–12. One hundred nanograms of each chimera was added to lanes 4–9, and 1 μ g to lanes 10–12.

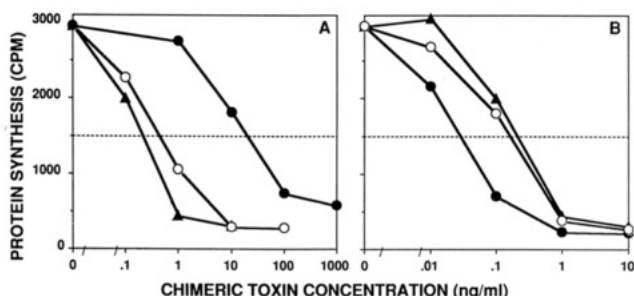


Figure 3. Cytotoxicity of various chimeric toxins on A431 cells. In A, the cytotoxic activity against A431 cells of IL6-PE^{4E}-TGF α (○) was compared to IL6-PE^{4E} (●) and PE^{4E}-TGF α (▲). Similarly, in B, TGF α -PE^{4E}-TGF α (○) was compared to its two components TGF α -PE^{4E} (●) and PE^{4E}-TGF α (▲).

To study the cytotoxic effect of adding a second ligand to a chimeric toxin, we first examined the cell line A431, which expresses a high number of EGF receptors. In Figure 3A, we compare the cytotoxicity of IL6-PE^{4E}-TGF α to that of its component toxins IL6-PE^{4E} and PE^{4E}-TGF α . Toward A431 cells, IL6-PE^{4E}-TGF α was 40-fold more cytotoxic than IL6-PE^{4E} ($ID_{50} = 0.5$ vs 20 ng/mL), but was 2–3-fold less active than PE^{4E}-TGF α . Using A431 cells in Figure 3B, we compare the cytotoxicity of TGF α -PE^{4E}-TGF α with that of its component toxins PE^{4E}-TGF α and TGF α -PE^{4E}. As noted previously (18), PE^{4E}-TGF α is 1 order of magnitude less cytotoxic than TGF α -PE^{4E}, probably from partially impaired cytosolic translocation due to the TGF α ligand contained in the translocated portion of PE (15). Figure 3B shows that the cytotoxicity of TGF α -PE^{4E}-TGF α is more similar to that of PE^{4E}-TGF α than that of TGF α -PE^{4E}.

To evaluate the relationship of the distance between two ligands on cytotoxicity, we compared the molecules which had ligands in PE^{4E}, PE40, and PE38 (Figure 4). PE^{4E}, PE40, and PE38 would separate ligands by 607, 355, and 339 amino acids, respectively. In Figure 4A, we show that IL6-PE^{4E}-TGF α is nearly 1 order of magnitude more cytotoxic than either IL6-PE40-TGF α or IL6-PE38-TGF α . We then compared the cytotoxicity of TGF α -PE^{4E}-TGF α with that of TGF α -PE40-TGF α and TGF α -PE38-TGF α . Figure 4B shows that the separation of the two TGF α ligands had only a marginal effect on the cytotoxicity toward A431 cells. The ID_{50} 's of TGF α -PE^{4E}-TGF α , TGF α -PE40-TGF α , and TGF α -PE38-TGF α were 0.15, 0.25, and 0.4 ng/mL, respectively.

Because our goal was to improve targeting by improving binding affinity through addition of a second binding

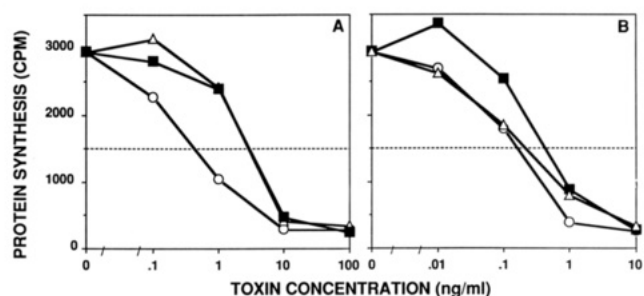


Figure 4. Cytotoxicity of various chimeric toxins on A431 cells. In A, A431 cytotoxicity was observed when the IL6 and TGF α were separated by 607 amino acids in IL6-PE^{4E}-TGF α (○), 355 amino acids in IL6-PE40-TGF α (Δ), and 339 amino acids in IL6-PE38-TGF α (■). In B, TGF α -PE^{4E}-TGF α (○) was compared to TGF α -PE40-TGF α (Δ) and TGF α -PE38-TGF α (■).

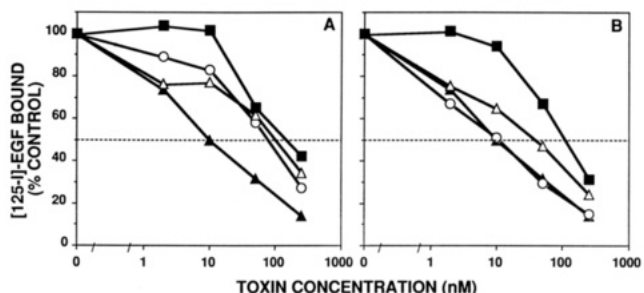


Figure 5. Displacement of EGF binding by TGF α -containing chimeric toxins. [¹²⁵I]EGF displacement from A431 cells by IL6-PE^{4E}-TGF α (○), IL6-PE40-TGF α (Δ), IL6-PE38-TGF α (■), and PE^{4E}-TGF α (▲) in A, and TGF α -PE^{4E}-TGF α (○), TGF α -PE40-TGF α (Δ), TGF α -PE38-TGF α (■), and PE^{4E}-TGF α (▲) in B. Nanomolar values were calculated from nanograms/milliliter assuming molecular weights of 93 kDa for IL6-PE^{4E}-TGF α , 67 kDa for IL6-PE40-TGF α , 65 kDa for IL6-PE38-TGF α , 73 kDa for PE^{4E}-TGF α , 79 kDa for TGF α -PE^{4E}-TGF α , 53 kDa for TGF α -PE40-TGF α , and 51 kDa for TGF α -PE38-TGF α .

domain, we decided to directly test the new toxins in [¹²⁵I]-EGF displacement assays. In Figure 5A, we examine toxins where IL6 and TGF α are separated by 607, 355, or 339 amino acids, by comparing EGF displacement to that seen with PE^{4E}-TGF α . In previous studies, we found that PE^{4E}-TGF α bound to the EGF receptor with an affinity similar to that of TGF α -PE40 or TGF α -PE^{4E} (18). We found that IL6-PE^{4E}-TGF α , IL6-PE40-TGF α , and IL6-PE38-TGF α each had significantly less binding affinity than PE^{4E}-TGF α (Figure 5A). Adding IL6 to the amino terminus of PE containing TGF α near the carboxyl terminus interfered with EGF-receptor binding on A431 cells (which have relatively few IL6 receptors), regardless the distance separating the IL6 and TGF α ligands. This was in contrast to the situation when TGF α was added to the amino terminus of PE^{4E}-TGF α (Figure 5B). Here, the addition of a second TGF α ligand to the amino terminus of PE^{4E}-TGF α did not interfere with binding. However, as the distance separating the two TGF α ligands progressively decreased, binding affinity decreased as well. The ability to displace EGF from A431 cells is approximately 10-fold less for TGF α -PE38-TGF α compared to TGF α -PE^{4E}-TGF α (Figure 5B), while TGF α -PE^{4E}-TGF α was only a few-fold more cytotoxic than TGF α -PE38-TGF α (Figure 4B).

To confirm that the IL6 moiety of IL6-PE^{4E}-TGF was binding to the IL6 receptor, we showed that it was cytotoxic toward U266 myeloma cells, which have few if any EGF receptors (Table I). We also found that cytotoxicity was prevented by an excess of enzymatically inactive IL6-containing protein (data not shown). The protein synthesis inhibition of IL6-PE^{4E}-TGF α like that of IL6-PE^{4E} could

Table I. Activity of PE^{4E} with Ligands at the N-Terminus and/or near the C-Terminus on Malignant Cells

cell line ^a	type	receptors, sites/cell × 10 ³		ID ₅₀ , ng/mL				
		EGF	IL6	IL6-PE ^{4E}	IL6-PE ^{4E} -TGF α	PE ^{4E} -TGF α	TGF α -PE ^{4E} -TGF α	TGF α -PE ^{4E}
A431	epidermoid	3000	2.3	20	0.5	0.2	0.15	0.03
KB	epidermoid	200		>1000	3.5	4.5	1.8	0.3
LNCAP	prostate	30	1.3	1.5	0.2	0.4	0.17	0.025
DU145	prostate	100	2.6	25	14	2.5	2	0.3
PLC/PRF/5	hepatoma	20	2.3	1.5	0.3	0.1	0.15	0.025
HEPG2	hepatoma	9	0.4	20	4	15	5	4
HEP3B	hepatoma	200	1.2	40	15	5	1.5	0.2
OVCAR-3	ovarian	70		>1000	9	2	2	0.7
HT29	colon	100		>1000	7	5	2	0.7
U266	myeloma	<1	16	0.6	3	>1000	>1000	>1000

^a TGF α alone at 1000 ng/mL did not significantly inhibit any of the cell lines.

be reversed by 20 μ g/mL of IL6-PE^{4E}D553, which lacks ADP-ribosylation activity (12), but not by the same concentration of IL2-PE^{4E}.

To determine if the bifunctional toxin IL6-PE^{4E}-TGF α would be more cytotoxic than its component toxins IL6-PE^{4E} and PE^{4E}-TGF α if the IL6 and EGF receptor numbers were different, we tested the toxins against cell lines other than A431 (Table I). EGF and IL6 receptor numbers were either taken from previous references or determined using the same methods as previously reported (7, 18, 20). We noted that in all of the cell lines with more EGF than IL6 receptors, IL6-PE^{4E}-TGF α is more cytotoxic than IL6-PE^{4E}. Only in U266 cells, which have few if any EGF receptors, is IL6-PE^{4E}-TGF α less cytotoxic than IL6-PE^{4E}. In considering the effect of IL6 ligand addition to PE^{4E}-TGF α , we noted that IL6-PE^{4E}-TGF α is more cytotoxic than PE^{4E}-TGF α in both LNCaP and HEPG2 cells. In the prostate carcinoma line LNCaP, IL6-PE^{4E}-TGF α is 2-fold more cytotoxic than PE^{4E}-TGF α (ID₅₀ improves from 0.4 to 0.2 ng/mL). This small difference was reproducible in multiple confirmatory assays. In the hepatocellular carcinoma line HEPG2, the bifunctional toxin is nearly 4-fold more cytotoxic (ID₅₀ improves from 15 to 4 ng/mL). Both LNCaP and HEPG2 cells have lower numbers of EGF receptors than A431 cells, but also lower numbers of IL6 receptors. In KB and HT29 cells, which are resistant to IL6-toxins, the difference between IL6-PE^{4E}-TGF α and PE^{4E}-TGF α was not more than 1.5-fold, and an improvement of IL6-PE^{4E}-TGF α over PE^{4E}-TGF α was not seen in repeat assays of these cell lines. On A431, DU145, PLC/PRF/5, HEP3B, and OVCAR3 cells, which have varying numbers of IL6 and EGF receptors, IL6-PE^{4E}-TGF α was 3–5-fold less cytotoxic than PE^{4E}-TGF α .

To further evaluate the effect of a toxin containing two of the same kind of binding ligand instead of one, we compared the cytotoxicities of TGF α -PE^{4E}-TGF α , PE^{4E}-TGF α , and TGF α -PE^{4E} against cell lines with varying numbers of EGF receptors (Table I). In view of our observation that insertion of TGF α near the carboxyl terminus of PE^{4E} decreases the toxin's cytotoxicity, we expected to find that TGF α -PE^{4E} was more cytotoxic than TGF α -PE^{4E}-TGF α toward all of the EGF-receptor-bearing cell lines. We were more interested in comparing the cytotoxicity of TGF α -PE^{4E}-TGF α to PE^{4E}-TGF α , since both have the carboxy insertion. In many cell lines, there is a slight to several-fold improvement in ID₅₀ when TGF α is added to the amino terminus of PE^{4E}-TGF α . At least several-fold improvements occurred against KB, LNCaP, HEPG2, HEP3B, and HT29, whereas A431, DU145, PLC/PRF/5, and OVCAR3 cells each differed less in their sensitivities to TGF α -PE^{4E}-TGF α and PE^{4E}-TGF α .

To judge whether by adding a second ligand we had made a chimeric toxin more or less potentially useful from a therapeutic standpoint, we administered some of the

Table II. Toxicity of PE^{4E} Containing TGF α and/or IL6 in Mice

	ip dose, μ g/kg	deaths
PE ^{4E} -TGF α	150	0/2
	300	2/3
TGF α -PE ^{4E} -TGF α	75	0/2
	150	3/3
	600	3/3
IL6-PE ^{4E} -TGF α	300	0/3
	600	0/3
	1200	3/3

new toxins to mice. We chose IL6-PE^{4E}-TGF α and TGF α -PE^{4E}-TGF α for this purpose, so that we could compare the LD₅₀ of these with the known LD₅₀ of the carboxyl terminal component toxin PE^{4E}-TGF α . We previously found in nude mice that the LD₅₀ of PE^{4E}-TGF α was 300 μ g/kg, compared to 75 μ g/kg for TGF α -PE^{4E} (18). Table II, reporting data using white Balb/C mice (used because of lower cost), confirms the LD₅₀ of approximately 300 μ g/kg for PE^{4E}-TGF α . The LD₅₀ for IL6-PE^{4E}-TGF α appears to be 2–4-fold higher, 600–1200 μ g/kg, which indicates that adding IL6 to the amino terminus of PE^{4E}-TGF α decreased its toxicity to mice. In contrast, adding TGF α to the amino terminus of PE^{4E}-TGF α increased its toxicity to mice, since the LD₅₀ of TGF α -PE^{4E}-TGF α was between 75 and 150 μ g/kg, or 2–4-fold more toxic than PE^{4E}-TGF α . With the cell lines LNCaP and HEPG2, the ratio between the LD₅₀ in vivo and the ID₅₀ in vitro improves when one adds IL6 to the amino terminus of PE^{4E}-TGF α , but changes little if one adds TGF α to the amino terminus of PE^{4E}-TGF α .

DISCUSSION

Our goal was to construct recombinant chimeric toxins containing two ligands, determine if such molecules could be expressed and purified as monomers, and to investigate the cytotoxicity of these agents as a function of ligand separation distance and number of receptors on the target cells. Unlike TGF α -anti-Tac(Fv)-PE40, which has both TGF α and anti-Tac(Fv) at the amino terminus of PE40 and targets the toxin to either of two different types of cells (21), we wished to target PE to a given cell using both ligands. We have previously found that an immunotoxin such as OVB3-PE binds to target cells via the anti-ovarian cancer monoclonal antibody OVB3 as well as domain Ia of PE (22), but for this study we preferred two ligands that would both bind selectively to tumor cells. We found we could construct recombinant toxins containing TGF α near the carboxyl terminus and either TGF α or IL6 at the amino terminus of three different derivatives of PE (PE^{4E}, PE40, and PE38) and that all six new toxins could be adequately purified. Further, we found that adding IL6 to the amino terminus of PE^{4E}-TGF α not only decreased

Table III. IL6-PE^{4E}-TGF α and Component Toxins against Cells with Both EGF and IL6 Receptors

cell line	receptor ratio EGF/IL6	ID ₅₀ ratio IL6-PE ^{4E} /PE ^{4E} -TGF α	cell line	receptor ratio EGF/IL6	ID ₅₀ ratio IL6-PE ^{4E} /PE ^{4E} -TGF α
A431	1300	100	PLC/PRF/5	9	15
LNCaP	25	4	HEPG2	25	1.3
DU145	40	10	HEP3B	170	8

the toxicity to mice but also improved the cytotoxicity toward two cell lines containing both IL6 and EGF receptors.

Purification of IL6-TGF α Toxins. By isolating recombinant chimeric toxins from inclusion bodies, we were able to achieve over 90% purity. Figure 2 shows a minor band several kilodaltons less than the major band for PE^{4E}-TGF α and IL6-PE^{4E}-TGF α . When we attempted to purify PE^{4E}-TGF α from periplasm, this minor band was >50% of the total protein. Because the band stained with anti-PE but not anti-TGF α and because the lower band nearly disappears when PE^{4E}-TGF α devoid of amino acids 596–607 is expressed in periplasm (unpublished data), we believe it represents the toxin after proteolytic cleavage proximal to the TGF α insert. Similarly, the minor band for IL6-PE^{4E}-TGF α in Figure 2 stains with anti-PE and anti-IL6 but not anti-TGF α , indicating it is probably IL6-PE^{4E}-TGF α after proteolytic cleavage proximal to the TGF α insert. Because it should have no cytotoxicity and is a minor contaminant, it should have little influence on our results.

Cytotoxicity of IL6-TGF α Toxins against Malignant Cells. When we compared IL6-PE^{4E}-TGF α , IL6-PE40-TGF α , and IL6-PE38-TGF α to their amino terminal component toxins IL6-PE^{4E}, IL6-PE40, and IL6-PE38, respectively, we found that the new chimeric toxins containing TGF α were more cytotoxic toward IL6-receptor-bearing cell lines that also expressed EGF receptors (Table I, other data not shown). Since EGF receptors outnumber IL6 receptors by 1–3 orders of magnitude on such cells, it is likely that the presence or absence of TGF α is more important than IL6 for binding and cytotoxicity toward the cells.

Of the cell lines with both IL6 and EGF receptors, two cell lines (LNCaP and HEPG2) were more sensitive to IL6-PE^{4E}-TGF α than to either of its component toxins PE^{4E}-TGF α or IL6-PE^{4E}. This suggests that on those cell lines both IL6 and TGF α ligands bind to receptors simultaneously, or that binding occurs more frequently because either ligand can bind. The LNCaP and HEPG2 data also suggest that the decrease in binding affinity of IL6-PE^{4E}-TGF α compared to PE^{4E}-TGF α against A431 cells (Figure 5A) is not due to improper folding of IL6-PE^{4E}-TGF α , but is due to cell related factors.

It is unclear why IL6-PE^{4E}-TGF α was more cytotoxic than its component toxins toward HEPG2 and LNCaP cells, but not toward the other cell lines. Table III was constructed to help identify factors which might make a cell line more sensitive to IL6-PE^{4E}-TGF α than to PE^{4E}-TGF α . One possibility is that in order for a cell line to be more sensitive to a toxin containing both IL6 and TGF α ligands than a toxin containing only a TGF α ligand, it must have a relatively low ratio of EGF to IL6 receptors. Indeed, HEPG2 and LNCaP cells each have an EGF/IL6 receptor number ratio of 25, which is lower than most of the other cell lines in Table III. However, the PLC/PRF/5 cell line, which is less sensitive to IL6-PE^{4E}-TGF α than PE^{4E}-TGF α , has the lowest EGF/IL6 receptor number ratio. Perhaps more relevant than receptor number is how easily a receptor on a target cell internalizes its ligand

and how readily the toxin containing that ligand translocates to the cytosol. We found that the ratio of the cytotoxic activities of the component toxins IL6-PE^{4E} and PE^{4E}-TGF α on each cell line was predictive of that cell line's sensitivity to IL6-PE^{4E}-TGF α . Table III shows that as this ratio approached unity, the cell line was more likely to be sensitive to the bifunctional chimeric toxin IL6-PE^{4E}-TGF α than either of its component toxins IL6-PE^{4E} or PE^{4E}-TGF α . It is possible that IL6-PE^{4E}-TGF α is less toxic to mice than PE^{4E}-TGF α because the normal murine cells affected are much more sensitive to PE^{4E}-TGF α than to IL6-PE^{4E}.

PE Containing Two TGF α Ligands. Part of the goal of the present study was to see whether two of the same ligand would be better than one in directing a toxin to a target cell. Our data from most of the EGF receptor-bearing cell lines tested indicate that the cytotoxicity of PE^{4E}-TGF α improves 2–3-fold when a second TGF α ligand is added to the amino terminus. The modest improvement in cytotoxicity is probably related to improved receptor binding which could not be detected by the [¹²⁵I]EGF displacement study on A431 cells (Figure 5B). Improved binding to murine EGF receptors on normal tissues was probably why TGF α -PE^{4E}-TGF α was several-fold more toxic to mice than PE^{4E}-TGF α (Table II). TGF α -PE^{4E} was more cytotoxic than TGF α -PE^{4E}-TGF α or PE^{4E}-TGF α , indicating that the position of the TGF α ligand had a greater effect on cytotoxicity than the number of ligands.

Distance between Two Ligands Affects Cytotoxicity and Affinity. For both IL6-TGF α and TGF α -TGF α toxins, cytotoxicity worsened when the two ligands were separated by 339 amino acids as in the PE38 toxins compared to the PE^{4E} toxins, which allowed a separation distance of 607 amino acids. We were able to show that the ability of a toxin which contains two TGF α ligands to displace EGF from A431 cells improves more than 10-fold when the distance separating the two TGF α ligands increases from 339 to 607 amino acids. Perhaps this indicates either that the shorter distance prevents the toxin from binding to two receptors simultaneously or that the shorter distance interferes with folding of the toxin and decreases binding affinity from either ligand. Because of the large number of EGF receptors on A431 cells, 10-fold differences in binding affinity may result in less differences in cytotoxicity between TGF α -PE^{4E}-TGF α and TGF α -PE₃₈-TGF α .

We have shown that by using recombinant technology, it is possible to combine two chimeric toxins into one by placing two ligands into different locations in PE. IL6-PE^{4E}-TGF α , which has less toxicity to mice than PE^{4E}-TGF α but has improved *in vitro* cytotoxicity against a prostate and a hepatocellular cancer cell line, deserves further study. In addition, we would like to use different ligands at the amino terminus such as IGF-I or fibroblast growth factor. Of particular interest as an occupant for the amino terminus of PE^{4E}-TGF α is single-chain Fv fragments of antibodies. Such bifunctional immunotoxins may be particularly useful against EGF-receptor-bearing cancer cells which express high levels of noninternalizing antigen.

ACKNOWLEDGMENT

We appreciate the assistance of B. Lovelace and A. Harris in cell culture. We thank A. Gaddis and P. Andryszak for help in manuscript preparation.

LITERATURE CITED

- (1) Real, F. X., Rettig, W. J., Chesa, P. G., Melamed, M. R., Old, L. J., and Mendelsohn, J. (1986) Expression of epidermal growth factor receptor in human cultured cells and tissues: Relationship to cell lineage and stage of differentiation. *Cancer Res.* 46, 4726-4731.
- (2) Fabricant, R. N., DeLarco, J. E., and Todaro, G. J. (1977) Nerve growth factor receptors on human melanoma cells in culture. *Proc. Natl. Acad. Sci. U.S.A.* 74, 565-569.
- (3) Chen, S., Chou, C., Wong, F., Chang, C., and Hu, C. (1991) Overexpression of epidermal growth factor and insulin-like growth factor-I receptors and autocrine stimulation in human esophageal carcinoma cells. *Cancer Res.* 51, 1898-1903.
- (4) Pekonen, F., Partanen, S., Makinen, T., and Rutanen, E. (1988) Receptors for epidermal growth factor and insulin-like growth factor I and their relation to steroid receptors in human breast cancer. *Cancer Res.* 48, 1343-1347.
- (5) Pekonen, F., Partanen, S., and Rutanen, E. (1989) Binding of epidermal growth factor and insulin-like growth factor I in renal carcinoma and adjacent normal kidney tissue. *Int. J. Cancer* 43, 1029-1033.
- (6) Siegall, C. B., FitzGerald, D. J., and Pastan, I. (1990) Cytotoxicity of IL6-PE40 and derivatives on tumor cells expressing a range of IL6 receptor levels. *J. Biol. Chem.* 265, 16318-16323.
- (7) Siegall, C. B., Schwab, G., Nordan, R. P., FitzGerald, D. J., and Pastan, I. (1990) Expression of the interleukin 6 receptor and interleukin 6 in prostate carcinoma cells. *Cancer Res.* 50, 7786-7788.
- (8) Wilding, G., Valverius, E., Knabbe, C., and Gelmann, E. P. (1989) Role of transforming growth factor- α in human prostate cancer cell growth. *Prostate* 15, 1-12.
- (9) Siegall, C. B., Chaudhary, V. K., FitzGerald, D. J., and Pastan, I. (1988) Cytotoxic activity of an interleukin 6-*Pseudomonas* exotoxin fusion protein on human myeloma cells. *Proc. Natl. Acad. Sci. U.S.A.* 85, 9738-9742.
- (10) Siegall, C. B., Xu, Y., Chaudhary, V. K., Adhya, S., FitzGerald, D., and Pastan, I. (1989) Cytotoxic activities of a fusion protein comprised of TGF α and *Pseudomonas* exotoxin. *FASEB J.* 3, 2647-2652.
- (11) Pai, L. H., Gallo, M. G., FitzGerald, D. J., and Pastan, I. (1991) Anti-tumor activity of a transforming growth factor α -*Pseudomonas* exotoxin fusion protein (TGF- α -PE40). *Cancer Res.* 51, 2808-2812.
- (12) Siegall, C. B., Kreitzman, R. J., FitzGerald, D. J., and Pastan, I. (1991) Antitumor effects of interleukin 6-*Pseudomonas* exotoxin chimeric molecules against the human hepatocellular carcinoma PLC/PRF/5 in mice. *Cancer Res.* 51, 2831-2836.
- (13) Allured, V. S., Collier, R. J., Carroll, S. F., and McKay, D. B. (1986) Structure of exotoxin A of *Pseudomonas aeruginosa* at 3.0-Å resolution. *Proc. Natl. Acad. Sci. U.S.A.* 83, 1320-1324.
- (14) Hwang, J., FitzGerald, D. J., Adhya, S., and Pastan, I. (1987) Functional domains of *Pseudomonas* exotoxin identified by deletion analysis of the gene expressed in *E. coli*. *Cell* 48, 129-136.
- (15) Ogata, M., Chaudhary, V. K., Pastan, I., and FitzGerald, D. J. (1990) Processing of *Pseudomonas* exotoxin by a cellular protease results in the generation of a 37,000-Da toxin fragment that is translocated to the cytosol. *J. Biol. Chem.* 265, 20678-20685.
- (16) Siegall, C. B., Chaudhary, V. K., FitzGerald, D. J., and Pastan, I. (1989) Functional analysis of domains II, Ib, and III of *Pseudomonas* exotoxin. *J. Biol. Chem.* 264, 14256-14261.
- (17) Chaudhary, V. K., Jinno, Y., Gallo, M. G., FitzGerald, D., and Pastan, I. (1990) Mutagenesis of *Pseudomonas* exotoxin in identification of sequences responsible for the animal toxicity. *J. Biol. Chem.* 265, 16306-16310.
- (18) Kreitzman, R. J., Chaudhary, V. K., Siegall, C. B., FitzGerald, D. J., and Pastan, I. (1992) Rational design of a chimeric toxin: An intramolecular location for the insertion of transforming growth factor alpha within *Pseudomonas* exotoxin as a targeting ligand. *Bioconjugate Chem.*, preceding paper in this issue.
- (19) Chaudhary, V. K., Jinno, Y., FitzGerald, D., and Pastan, I. (1990) *Pseudomonas* exotoxin contains a specific sequence at the carboxyl terminus that is required for cytotoxicity. *Proc. Natl. Acad. Sci. U.S.A.* 87, 308-312.
- (20) Siegall, C. B., Nordan, R. P., FitzGerald, D. J., and Pastan, I. (1990) Cell-specific toxicity of a chimeric protein composed of interleukin-6 and *Pseudomonas* exotoxin (IL6-PE40) on tumor cells. *Mol. Cell. Biol.* 10, 2443-2447.
- (21) Batra, J. K., Chaudhary, V. K., FitzGerald, D., and Pastan, I. (1990) TGF α -anti-Tac(Fv)-PE40: A bifunctional toxin cytotoxic for cells with EGF or IL2 receptors. *Biochem. Biophys. Res. Commun.* 171, 1-6.
- (22) Willingham, M. C., FitzGerald, D. J., and Pastan, I. (1987) *Pseudomonas* exotoxin coupled to a monoclonal antibody against ovarian cancer inhibits the growth of human ovarian cancer cells in a mouse model. *Proc. Natl. Acad. Sci. U.S.A.* 84, 2474-2478.

Registry No. EGF, 62229-50-9.

Application of an *N*-(4-Azido-2,3,5,6-tetrafluorobenzoyl)tyrosine-Substituted Peptide as a Heterobifunctional Cross-Linking Agent in a Study of Protein O-Glycosylation in Yeast

Richard R. Drake,*† James T. Slama,‡ Katherine A. Wall,‡ Margaret Abramova,† Crislyn D'Souza,† Alan D. Elbein,† Peter J. Crocker,§ and David S. Watt§

Department of Chemistry, University of Kentucky, Lexington, Kentucky 40506, Department of Biochemistry, University of Texas Health Science Center, San Antonio, Texas 78284, and Department of Medicinal and Biological Chemistry, College of Pharmacy, University of Toledo, Toledo, Ohio 43606. Received September 6, 1991

In order to investigate the *O*-mannosyltransferase involved in the initial *O*-mannosylation of glycoproteins in *Saccharomyces cerevisiae*, a photoactive hexapeptide, [¹²⁵I]-*N*-(4-azido-2,3,5,6-tetrafluorobenzoyl)-3-iodo-Tyr-Asn-Pro-Thr-Ser-Val ([¹²⁵I]azidoTyr-peptide), was synthesized by solid-phase techniques using a new photoactive cross-linking reagent, *N*-(4-azido-2,3,5,6-tetrafluorobenzoyl)tyrosine, and resin-bound Asn-Pro-Thr(tBu)-Ser(tBu)-Val. When this modified hexapeptide substrate was incubated with *O*-mannosyltransferase preparations, the hexapeptide was an acceptor of [¹⁴C]-mannose from dolichol phosphate-[¹⁴C]mannose. After partially purifying the *O*-mannosyltransferase and photolabeling these enzyme preparations with [¹²⁵I]azidoTyr-peptide, a ca. 82-kDa protein was shown to be the only apparent photolabeled protein that was protected by unmodified hexapeptide. This ca. 82-kDa protein may be the catalytic subunit of the *O*-mannosyltransferase. The susceptibility of the *N*-(4-azido-2,3,5,6-tetrafluorobenzoyl) moiety to reducing agents in aqueous buffers was also examined.

INTRODUCTION

In *Saccharomyces cerevisiae* and other fungal cells, the majority of glycoproteins contain high-mannose *N*- and *O*-linked oligosaccharides. In *O*-glycosylation, the initial mannose residue is transferred from dolichol phosphate-mannose (Man-P-Dol) to a serine or threonine residue on the protein (1). This Man-P-Dol:protein *O*-mannosyltransferase has also been shown to transfer a mannose from Man-P-Dol to an artificial hexapeptide substrate, Tyr-Asn-Pro-Ser-Thr-Val (2). Using this peptide, the enzyme from *Saccharomyces cerevisiae* was partially purified 150-fold (3) and to apparent homogeneity (4). The recent availability of a perfluorinated aryl azide derivative of tyrosine (5), the ability to incorporate a radioiodinated version of this derivative into peptides, the anticipated high cross-linking efficiency of the perfluorinated aryl azides (6-12) in photoaffinity labeling experiments, and the difficulty in purifying the *O*-mannosyltransferase suggested the development of a radiolabeled, photoactive version of the hexapeptide substrate as a logical way to identify the *O*-mannosyltransferase. This report describes the preparation of [¹²⁵I]-*N*-(4-azido-2,3,5,6-tetrafluorobenzoyl)-3-iodo-Tyr-Asn-Pro-Thr-Ser-Val ([¹²⁵I]azidoTyr-peptide) (4), outlined in Scheme I, the photolabeling of *O*-mannosyltransferase partially purified from *Saccharomyces cerevisiae* with this photoactive hexapeptide, and the behavior of the photoactive component of this photoactive hexapeptide in aqueous medium in the presence of reducing agents.

EXPERIMENTAL PROCEDURES

Peptide Synthesis. The pentapeptide Asn-Pro-Thr-Ser-Val was synthesized on an Applied Biosystems 430A peptide synthesizer at the University of Texas Health Science Center at San Antonio Biopolymer Sequencing and Synthesis Facility. Fluorenylmethoxycarbonyl (Fmoc) amino acid derivatives were coupled to 0.25 mmol of a preloaded *N*-α-Fmoc-L-valine-(Wang) resin (#RFMC260, Bachem, Torrance, CA) using standard procedures. The side-chain-protected peptide-resin was dried and removed after addition of the Asn and removal of the *N*-terminal Fmoc protecting group. The composition of the pentapeptide was verified by acid hydrolysis followed by amino acid analysis on a Beckman 7300 analyzer.

Preparation of *N*-Succinimidyl *N*-(4-Azido-2,3,5,6-tetrafluorobenzoyl)tyrosinate (2). To 1 mL of THF¹ that had been dried by passage through an activated alumina column were added 15 mg (36 μmol) of *N*-(4-azido-2,3,5,6-tetrafluorobenzoyl)tyrosine (1 in Scheme I) (5), 12 mg (99 μmol) of *N*-hydroxysuccinimide, and 13 μL (83 μmol) of *N,N'*-diisopropylcarbodiimide in a sealed 2-mL Wheaton vial with stirring. The reaction progress was monitored by TLC on silica gel using 1:99 HOAc-EtOAc or 1:99 HOAc-MeOH. NHS-activated ester 2 had *R*_f = 0.9 compared to an *R*_f = 0.8 for *N*-(4-azido-2,3,5,6-tetrafluorobenzoyl)tyrosine (1). Conversion to activated ester 2 appeared to be quantitative after 22 h at 25 °C. After activation, the THF was removed under reduced pressure, and NHS ester 2 was resuspended in 0.5 mL of DMF prior to use in the peptide coupling procedure.

Preparation of *N*-(4-Azido-2,3,5,6-tetrafluorobenzoyl)-Tyr-Asn-Pro-Thr-Ser-Val (AzidoTyr-peptide)

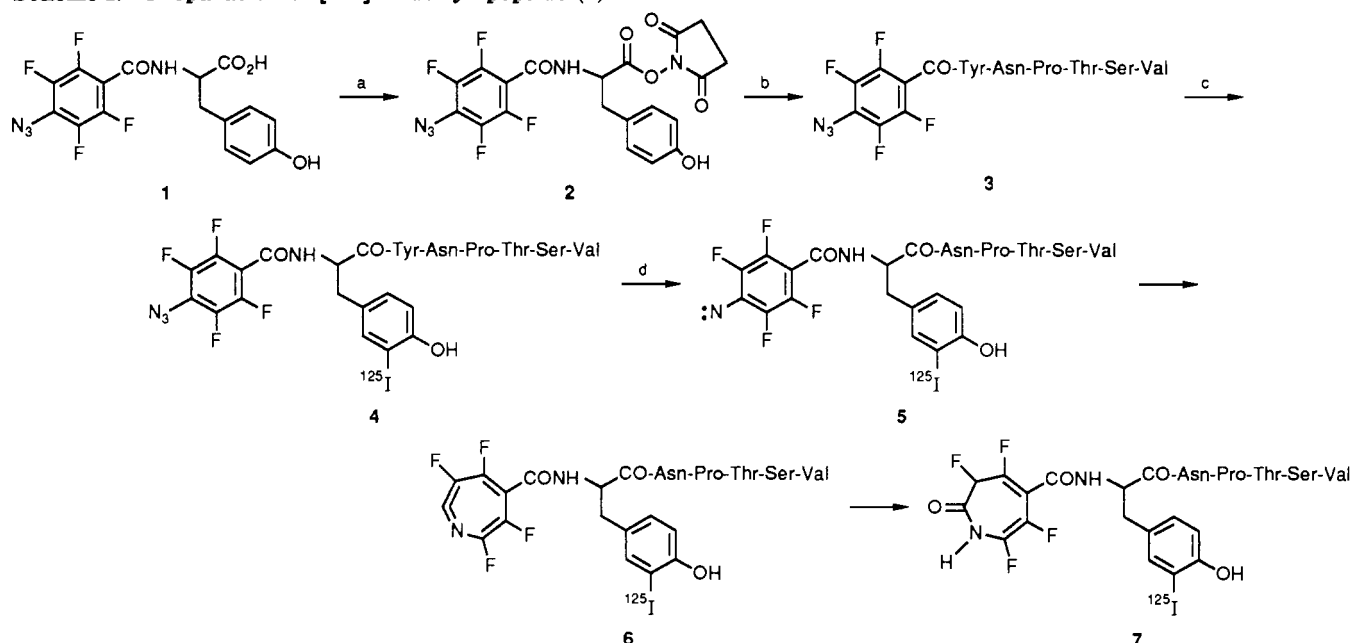
¹ Abbreviations used: azidoTyr-peptide, *N*-(4-azido-2,3,5,6-tetrafluorobenzoyl)Tyr-Asn-Pro-Thr-Ser-Val; DEAE, 2-(diethylamino)ethyl; DMF, *N,N*-dimethylformamide; HEPES, 4-(2-hydroxyethyl)-1-piperazineethanesulfonic acid; NHS, *N*-hydroxysuccinimide; TCA, trichloroacetic acid; TFA, trifluoroacetic acid; THF, tetrahydrofuran.

* Author to whom correspondence should be addressed: Richard R. Drake, Department of Biochemistry and Molecular Biology, University of Arkansas for Medical Sciences, Little Rock, AR 72205.

† University of Texas Health Science Center.

‡ University of Toledo.

§ University of Kentucky.

Scheme I.^a Preparation of [¹²⁵I]AzidoTyr-peptide (4)

^a Legend: (a) *N*-hydroxysuccinimide, *N,N'*-diisopropylcarbodiimide, THF; (b) Asn-Pro-Thr(tBu)-Ser(tBu)-Val-resin, DMF and then released from resin with 95% TFA; (c) [¹²⁵I]NaI, oxidant (14); (d) photolysis.

(3). A 0.5-mL DMF solution of NHS ester 2 was added to an excess of the dry Asn-Pro-Thr(tBu)-Ser(tBu)-Val-resin (150 mg of pentapeptide). This mixture was slowly agitated on a rocker arm for 3 h, and the solution above the resin was monitored for loss of UV absorbance at 256 nm, characteristic of the perfluorinated aryl azide group. No apparent NHS ester 2 or acid 1 was detected after 3 h. The mixture was filtered on a Whatman 1 filter, and the resin was washed three times with 2-mL portions of DMF and three times with 4-mL portions of CH₂Cl₂. The filter and resin were dried for ca. 12 h in a vacuum desiccator. The dried peptide was cleaved from the resin and deprotected using 10 mL of 95% TFA at 25 °C for 2 h (13). AzidoTyr-peptide (3) was separated from unreacted pentapeptide by preparative, reversed-phase (C₁₈) HPLC (Vydac, 2.2 × 25 cm). The azidoTyr-peptide (3) was dissolved in 0.1:20:79.9 TFA-CH₃CN-H₂O and washed isocratically for 20 min at a flow rate of 4 mL/min. Fractions were monitored at 210 or 256 nm. The unmodified pentapeptide eluted after ca. 15 min. AzidoTyr-peptide (3) was eluted with acetonitrile.

AzidoTyr-peptide (3) Characterization. The composition of azidoTyr-peptide (3) was established by amino acid analysis and fast-atom bombardment mass spectrometry that displayed an MH⁺ ion at the expected *m/z* 897. AzidoTyr-peptide (3) was also identified by its characteristic absorbance maximum at 256 nm and the loss of this absorbance after UV irradiation.

Preparation of [¹²⁵I]AzidoTyr-peptide (4). AzidoTyr-peptide (3) was radioiodinated (1 mCi) using a vapor-phase iodination procedure (14). [¹²⁵I]AzidoTyr-peptide (4) was separated from free ¹²⁵I by gel filtration on a Sephadex G-10 column (1 cm × 6 cm) equilibrated in 50 mM HEPES (pH 7.5). The specific activity of [¹²⁵I]azidoTyr-peptide (4) was 0.1 mCi/μmol.

Preparation of Yeast *O*-Mannosyltransferase Extracts. *Saccharomyces cerevisiae* (MEC 428 B) cells were grown and harvested as previously described (3) except that the cells were disrupted by rapid vortexing of 3 mL of cell suspension with 0.5-cm glass beads (1:1, v/v) five times for 1 min. Mannosyltransferase assays, prep-

aration of microsomal fractions, solubilization in 0.5% Triton X-100, and purification by ion-exchange chromatography on DEAE-cellulose were done as previously described (3) except for the use of 0.01% and 0.1% 2-mercaptoethanol in the lysis and assay buffers, respectively.

Photolabeling of *O*-Mannosyltransferase with [¹²⁵I]AzidoTyr-peptide (4). In 1.5-mL Eppendorf tubes, 100–200 μg of *O*-mannosyltransferase extract and 5 mM MgCl₂ were added to 50–150 μM [¹²⁵I]azidoTyr-peptide (4) to obtain a final volume of 0.1 mL. This mixture was irradiated with a hand-held UV lamp (254 nm) at a distance of 3 cm for 2 min at 25 °C. The reactions were terminated by the addition of 0.2 mL of 10% TCA and centrifuged for 2 min at 13 500 rpm. The precipitated proteins were resuspended in a protein-solubilizing mix and separated on 10% SDS-polyacrylamide gels as previously described (15). Any deviation from this photolabeling protocol is described in the appropriate figure legends. Prephotolysis experiments contained the same reaction components except that the photoactive peptide was UV irradiated for 1–2 min prior to addition of the enzyme.

RESULTS

NHS azidotyrosine reagent 2, shown in Scheme I, was coupled to a side-chain-protected Asn-Pro-Thr(tBu)-Ser(tBu)-Val peptide still linked to the resin following automated synthesis using Fmoc chemistry. The use of the perfluorinated aryl azide moiety had two advantages with respect to the characterization of the peptide product. The increased hydrophobicity of azidoTyr-peptide (3) relative to the unmodified pentapeptide allowed the modified hexapeptide to be easily separated from non-reacted pentapeptide using reversed-phase HPLC. Secondly, each step of the synthesis and purification could be readily monitored by following the UV absorbance at 256 nm characteristic of azidoTyr-peptide (3) as shown in Figure 1 and consistent with the λ_{max} at 256 nm (ε 19 000) of *N*-(4-azido-2,3,5,6-tetrafluorobenzoyl)tyrosine (5). The corresponding, nonphotoactive hexapeptide had a λ_{max} at

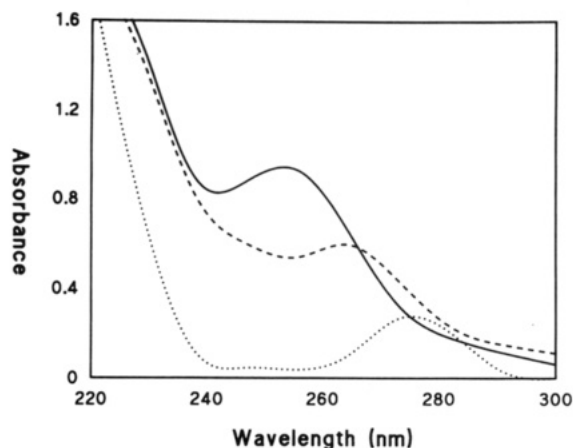


Figure 1. Ultraviolet spectra of the unmodified hexapeptide (dotted line), azidoTyr-peptide (3) before photolysis (solid line), and azidoTyr-peptide (3) after photolysis (dashed line).

276 nm consistent with the λ_{max} of 275 nm (ϵ 1000) for Tyr (16). UV irradiation of the photoactive peptide shifted the absorbance from 256 to 270 nm, indicating that a photochemical reaction had occurred. The UV spectrum of [^{125}I]azidoTyr-peptide (4) was the same as that of the noniodinated azidoTyr-peptide (data not shown).

The photoactive peptide was tested as an acceptor of mannose transferred from [^{14}C]Man-P-Dol by the *O*-mannosyltransferase according to published procedures (3). At the concentrations of hexapeptide (0.5–1 mM) routinely used in these enzyme assays, the photoactive peptide accepted the mannose with the same or slightly better efficiency than the unmodified hexapeptide (data not shown). The added hydrophobicity of the perfluorinated aryl azide may even enhance mannose transfer since this enzyme activity is membrane-associated. Photoinactivation of the enzyme by cross-linking of the photoactive peptide to the enzyme was observed but could not be reproducibly accomplished; the effect varied from 50% inhibition to no effect (data not shown). Several factors may account for this including a very high K_m of 10 mM for the hexapeptide (3), the impurity of the *O*-mannosyltransferase preparations, and the susceptibility of the photoprobe to thiol reducing agents (17–19) necessary to maintain enzyme activity (Figure 3).

The tyrosine residue in the photoactive azidoTyr-peptide was iodinated with [^{125}I] (14). Radiolabeled photoactive peptide 4 was used to photolabel enzyme fractions enriched in *O*-mannosyltransferase activity, and as shown in the autoradiograph in Figure 2, several proteins were radiolabeled after UV irradiation. No proteins were labeled if the reaction mixture was not UV irradiated (Figure 2, lane 1). Yeast microsomal preparations containing *O*-mannosyltransferase activity were solubilized and further purified by DEAE-cellulose ion-exchange chromatography as previously described (3). The solubilized microsomes and the DEAE-cellulose fractions were then photolabeled with [^{125}I]azidoTyr-peptide (4) in the presence and absence of nonradiolabeled, unmodified hexapeptide. As shown in Figure 2, only the photolabeling of a ca. 82-kDa protein in both the solubilized microsomes and the DEAE-cellulose fractions was protected with competing peptide. Photolabeling of this ca. 82-kDa protein was protected by nonradioiodinated azidoTyr-peptide (3) (data not shown). Since this ca. 82-kDa protein was present in each enzyme preparation of increasing purity for the *O*-mannosyltransferase activity and its photolabeling was competitively inhibited by the unmodified hexapeptide

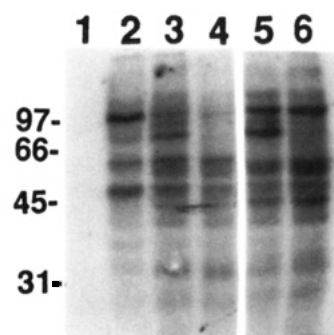


Figure 2. Photolabeling of yeast *O*-mannosyltransferase fractions of increasing purity. Microsomal *O*-mannosyltransferase fractions that were solubilized using Triton-X100 and partially purified on DEAE-cellulose were photolabeled with 200 μM [^{125}I]azidoTyr-peptide (4) as described in the Results section. Lanes 1 and 2: microsomal preparations (180 μg) minus UV irradiation and plus UV irradiation, respectively. Lanes 3 and 4: Triton X-100 solubilized preparation (60 μg) photolabeled in the absence (lane 3) and the presence (lane 4) of 0.9 mM unmodified hexapeptide. Lanes 5 and 6: DEAE-cellulose-purified enzyme (55 μg) photolabeled in the absence (lane 5) and the presence (lane 6) of 0.9 mM unmodified hexapeptide. The final concentration of 2-mercaptoethanol was 1 mM in each lane.

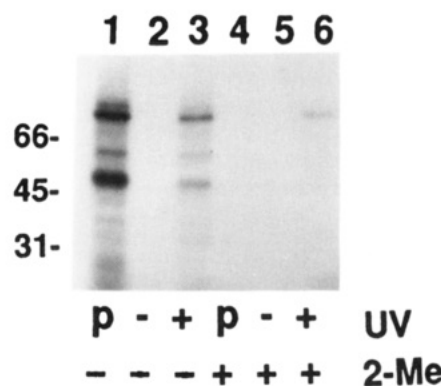


Figure 3. Effects of 2-mercaptoethanol and "prephotolysis" on the photolabeling of *O*-mannosyltransferase with [^{125}I]azidoTyr-peptide (4). Microsomes were prepared according to a literature procedure (3) except that no 2-mercaptoethanol was included in the buffers. Lanes 1–3: labeling of microsomes (100 μg) in the absence of 2-mercaptoethanol with 165 μM [^{125}I]azidoTyr-peptide (4). Lanes 4–6: labeling of microsomes (100 μg) in the presence of 14 mM 2-mercaptoethanol. Legend: p = "prephotolysis" experiment in which the photoprobe was photolyzed before the addition of the enzyme; – = enzyme plus photoprobe but no UV irradiation; + = enzyme plus photoprobe UV irradiated for 2 min; 2-Me = 14 mM 2-mercaptoethanol.

substrate, this protein could be the catalytic subunit of *O*-mannosyltransferase.

The photolysis of perfluorinated aryl azides in nonaqueous media generates a singlet nitrene intermediate (9) that is thought to be the putative cross-linking species. To examine the nature of the intermediate generated upon photolysis in aqueous solvents, a "prephotolysis" labeling experiment was conducted in which a solution of [^{125}I]azidoTyr-peptide (4) was irradiated prior to the addition of *O*-mannosyltransferase. As shown in Figure 3, the same bands photolabeled in the normal photolysis experiment (lane 3) are also labeled in the "prephotolysis" sample (lane 1). No labeling was observed in an experiment conducted without irradiation (lane 2). These results suggest that some type of long-lived photogenerated intermediate was responsible for the labeling. When yeast microsomal preparations were added, in separate experiments at varying time points after "prephotolysis" of identical [^{125}I]azidoTyr-peptide samples, a 50% decrease in the labeling of the yeast microsomal proteins was

observed after 8 min (data not shown). Since a singlet nitrene generated from a related perfluoroaryl azide has a half-life of 10 ns (9), these results suggest that the photogenerated intermediate derived from [125 I]azidoTyr-peptide (4) is unlikely to be a singlet nitrene. As additional controls, either 1 mM sodium iodide or 1 mM tyramine was included in the photolabeling reaction mixture to determine whether the iodine or tyrosine moieties in [125 I]-azidoTyr-peptide were affecting the photolabelings. Inclusion of these compounds during photolabeling had no effect on the labeling patterns of the yeast proteins described in Figure 2 (data not shown).

A potential source for generating or stabilizing the long-lived intermediate was the presence of 2-mercaptoethanol in the enzyme preparation. The addition of 14 mM (0.1%) 2-mercaptoethanol completely abolishes the UV absorbance of the azidoTyr-peptide (3) at 256 nm after 1 min (data not shown). To determine the effect of 2-mercaptoethanol on photolabeling of the yeast enzymes, a microsomal preparation was made without the reducing agent. In Figure 3, lanes 1–3, there was no reducing agent present. In lanes 4–6, 0.1% 2-mercaptoethanol was included. These results indicate that the long-lived intermediate generated upon photolysis was not due to 2-mercaptoethanol but that this intermediate was sensitive to its presence, as demonstrated by the decreased labeling in both the normal and "prephotolyzed" labeling experiments (compare lanes 1 and 4, 3 and 6). When dithiothreitol was added to the yeast membranes at similar concentrations, there was little effect on the normal and "prephotolyzed" labeling experiments (data not shown).

DISCUSSION

A photoactive, radioiodinated hexapeptide analogue, [125 I]azidoTyr-peptide (4), of a known hexapeptide substrate for yeast *O*-mannosyltransferase was synthesized (Scheme I) and shown to be an acceptor of [14 C]mannose from [14 C]Man-P-Dol. After partially purifying the *O*-mannosyltransferase and photolabeling these fractions with [125 I]azidoTyr-peptide (4), a ca. 82-kDa protein appeared to be the only protein whose photolabeling was competitively inhibited by the hexapeptide substrate. Since azidoTyr-peptide (3) serves as a mannose acceptor in enzyme assays and photolabeling of the ca. 82-kDa protein by the [125 I]azidoTyr-peptide (4) was competitively inhibited by the hexapeptide substrate, this ca. 82-kDa protein may be the catalytic subunit of *O*-mannosyltransferase. However, this *O*-mannosyltransferase has recently been purified to apparent homogeneity and reported to be of ca. 92-kDa molecular weight (4). Additionally, an antibody raised against this 92-kDa protein was used to immunoprecipitate *O*-mannosyltransferase activity (4). It is possible that the 82-kDa protein, identified by [125 I]-azidoTyr-peptide photoaffinity labeling, may represent a protease- or glycosidase-generated product of the 92-kDa protein since no inhibitors were included in the disruption and purification buffers. Treatment of a partially purified *O*-mannosyltransferase with endoglycosidase F, a known deglycosylating enzyme of glycopeptides, changed the gel migration of the 92-kDa protein to 84 kDa (4). It is also possible that the photoincorporated 82-kDa protein is not the Man-P-Dol:protein *O*-mannosyltransferase, but a similar glycosyl transferase with a higher affinity for the peptide substrate.

Two limiting factors in the use of this type of photoaffinity peptide analogue are its susceptibility to reducing agents (17–19) and the generation of a long-lived intermediate upon photolysis (20). 2-Mercaptoethanol, present

at 1–14 mM concentrations (see legends to Figures 2 and 3), quickly inactivated the photoactive properties of the compound, consistent with the known ability of thiols to promote the reduction of azides. This was also observed as a loss of absorbance at 256 nm when the same concentrations of 2-mercaptoethanol were added to the photoprobe and analyzed by UV spectrophotometry (data not shown). Photolabeling using [125 I]azidoTyr-peptide (4) in the presence of 2-mercaptoethanol was detected if UV irradiation was initiated immediately following addition of the photoprobe to the enzyme (Figures 2 and 3). Less severe inactivation of the reagent was observed with 1 mM dithiothreitol in photolabeling reactions and UV spectral analysis (data not shown). This suggests that if a reducing must be present to maintain enzyme activity, as was necessary for the *O*-mannosyltransferase, dithiothreitol would be the optimal choice.

The nature of the long-lived intermediate generated upon UV irradiation is unknown. This photogenerated intermediate was sensitive to reducing agents, especially 2-mercaptoethanol, as demonstrated by the reduced labeling in Figure 3. It is possible, as shown in Scheme I, that the singlet nitrene 5 undergoes ring expansion to the dehydroazepine 6 that subsequently traps water to afford the azepinone 7, a possible long-lived intermediate that would be sufficiently reactive to intercept nucleophilic residues on the target protein unless other more reactive nucleophiles, like 2-mercaptoethanol, were present. The uncertain nature of the intermediate does not detract from the effectiveness of using this type of photoaffinity analogue as demonstrated by the specific labeling and protection of the ca. 82-kDa protein. Another long-lived intermediate generated in the photolysis of an α -diazo ketone was reported to result in specific labeling (20). The importance of doing appropriate control experiments, as described in this report, must be stressed for any photoaffinity labeling experiments but particularly for experiments using the perfluorinated aryl azide reagent *N*-(4-azido-2,3,5,6-tetrafluorobenzoyl)tyrosine (1), in order to ensure that the results represent meaningful, specific labeling. As demonstrated with similar perfluorinated aryl azide derivatives linked to calmodulin (5), these peptide derivatives may be more useful when used to label pure polypeptides than when used in less pure systems as reported here. In addition, the *O*-mannosyltransferase in yeast was not an optimal experimental system for this type of photo-cross-linking experiment due to the high K_m (10 mM) of the hexapeptide substrate (3). The identification of the ca. 82-kDa protein suggests that additional studies involving the electroelution and production of antisera may further define the role of this enzyme in the *O*-mannosylation of yeast glycoproteins.

ACKNOWLEDGMENT

We thank the National Science Foundation (CHE-8607441 to D.S.W.), the National Institutes of Health (DK 21800 to A.D.E.), and the University of Kentucky Research Committee for the purchase of GC and HPLC instrumentation (for D.S.W.).

LITERATURE CITED

- (1) Tanner, W., and Lehle, L. (1987) Protein glycosylation in yeast. *Biochim. Biophys. Acta* 906, 81–99.
- (2) Lehle, L., and Bause, E. (1984) Primary structural requirements for N- and O-glycosylation of yeast mannoproteins. *Biochim. Biophys. Acta* 799, 246–251.
- (3) Sharma, C. B., D'Souza, C., and Elbein, A. D. Purification and characterization of a mannosyltransferase involved in the

- O-mannosylation of glycoproteins from *Saccharomyces cerevisiae*. *Glycobiology*. In press.
- (4) Strahl-Bolsinger, S., and Tanner, W. (1991) Protein O-glycosylation in *Saccharomyces cerevisiae*: purification and characterization of the dolichyl-phosphate-D-mannose-protein O-D-mannosyltransferase. *Eur. J. Biochem.* 196, 185-190.
- (5) Crocker, P. J., Imai, N., Rajagopalan, K., Boggess, M. A., Kwiatkowski, S., Dwyer, L. D., Vanaman, T. C., and Watt, D. S. (1991) Heterobifunctional cross-linking agents incorporating perfluorinated azides. *Bioconjugate Chem.* 2, 419-424.
- (6) Levy, E., Munoz, D., and Platz, M. S. (1989) Photochemistry of fluorinated aryl azides in toluene solution and in frozen polycrystals. *J. Org. Chem.* 54, 5938-5945.
- (7) Young, M. J. T., and Platz, M. S. (1989) Polyfluorinated aryl azides as photoaffinity labelling reagents: The room temperature CH insertion reactions of singlet pentafluorophenyl nitrene with alkanes. *Tetrahedron Lett.* 30, 2199-2202.
- (8) Soundararajan, N., and Platz, M. (1990) Descriptive photochemistry of polyfluorinated azide derivatives of methyl benzoate. *J. Org. Chem.* 55, 2034-2039.
- (9) Schuster, G. B., and Platz, M. S. Photochemistry of Phenyl Azide. *Chem. Rev.* In press.
- (10) Keana, J. F. W., and Cai, S. X. (1990) New reagents for photoaffinity labeling: Synthesis and photolysis of functionalized perfluorophenyl azides. *J. Org. Chem.* 55, 3640-3647.
- (11) Keana, J. F. W., and Cai, S. X. (1989) Functionalized perfluorophenyl azides: New reagents for photoaffinity labeling. *J. Fluorine Chem.* 43, 151-154.
- (12) Cai, S. X. and Keana, J. F. W. (1989) 4-Azido-2-iodo-3,5,6-trifluorophenylcarbonyl derivatives. A new class of functionalized and iodinated perfluorophenyl azide photolabels. *Tetrahedron Lett.* 30, 5409-5412.
- (13) Lundt, B. F., Johansen, N. L., Volund, A., and Markussen, J. (1978) Removal of t-butyl and t-butoxycarbonyl protecting groups with trifluoroacetic acid. *Int. J. Pept. Protein Res.* 12, 258-268.
- (14) Siekierka, J. J., and DeGudicibus, S. (1988) Radioiodination of Interleukin 2 to high specific activities by the vapor-phase chloramine T method. *Anal. Biochem.* 172, 514-517.
- (15) Drake, R. R., Evans, R. K., Wolf, M. J., and Haley, B. E. (1989) Synthesis and properties of 5-azido-UDP-glucose: Development of photoaffinity probes for nucleotide diphosphate sugar binding sites. *J. Biol. Chem.* 264, 11928-11933.
- (16) Kamlet, M. J., Ed. (1960) *Organic Electronic Spectral Data*, Vol. 1, p 268, Interscience, New York.
- (17) Staros, J. V., Bayley, H., Standring, D. N., and Knowles, J. R. (1978) Reduction of aryl azides by thiols: Implications for the use of photoaffinity reagents. *Biochem. Biophys. Res. Commun.* 80, 568-572.
- (18) Bayley, H., Standring, D. N., and Knowles, J. R. (1978) Propane-1,3-dithiol: A selective reagent for the efficient reduction of alkyl and aryl azides to amines. *Tetrahedron Lett.* 39, 3633-3634.
- (19) Czarnecki, J., Geahlen, R., and Haley, B. (1979) Synthesis and use of azido photoaffinity analogs of adenine and guanine nucleotides. *Methods. Enzymol.* 56, 642-653.
- (20) Payne, D. W., Katzenellenbogen, J. A., and Carlson, K. E. (1980) Photoaffinity labeling of rat α -fetoprotein. *J. Biol. Chem.* 255, 10359-10367.

Selective Modification of Cytosines in Oligodeoxyribonucleotides

Paul S. Miller* and Cynthia D. Cushman

Department of Biochemistry, School of Hygiene and Public Health, The Johns Hopkins University, 615 North Wolfe Street, Baltimore, Maryland 21205. Received October 17, 1991

A single deoxycytidine residing in an oligodeoxyribonucleotide which also contains 5-methyldeoxycytidines can be selectively derivatized with various alkylamines by sodium bisulfite-catalyzed transamination. Selective transamination results because 5-methylcytosine, unlike cytosine, does not form a bisulfite adduct. When the reaction is carried out at pH 7.1, transamination in the oligomer appears to occur to greater than 95% with little or no deamination. This procedure has been used to introduce aminoalkyl or carboxyalkyl side chains at the N⁴-position of a deoxycytidine in oligonucleotides. These side chains contain potentially reactive amine or carboxy groups which could serve as a sites for further conjugation of the oligomer with a variety functional groups. Oligonucleotides which carry these side chain form duplexes and triplexes with appropriate complementary single-stranded or double-stranded oligodeoxyribonucleotide target molecules. The stabilities of the duplexes are similar to those formed by unmodified oligomers, whereas the stability of the triplexes is approximately 18 °C lower than that formed by unmodified oligomers.

INTRODUCTION

Oligonucleotides and oligonucleotide analogues conjugated with functional groups have unusual properties which make them useful as hybridization probes and antisense reagents (1-3). These functional groups can include intercalators such as acridine, reporter groups such as fluorescent or spin labels, immunoreactive groups such as biotin, or chemically reactive groups such as alkylating groups, psoralen, or metal chelators. In many cases the functional groups are conjugated with the oligomer via a linker arm of variable chain length. The linker arm in turn may be attached to the 3'- or 5'-end of the oligomer, to the internucleotide linkage of the oligomer, or to a modified base located at a specific site within the oligomer.

A variety of methods are available for introducing the linker into the oligomer. Solid-phase supports, some of which are commercially available, have been developed which incorporate a linker as part of the support (4-9). These allow synthesis of oligomers having linkers at the 3'-end of the molecule. Linkers may be introduced at the 3'- or 5'-position by derivatization of terminal phosphate groups with diaminoalkanes or amino acids (10-14). H-phosphonate chemistry has been used to introduce linkers at specific internucleotide bonds within the oligomer (15-18). Protected phosphoramidite reagents and nucleoside phosphoramidite synthons have been developed which allow incorporation of linkers or linker-modified nucleosides during the course of oligonucleotide synthesis (19-23).

The N⁴-position of cytosine can be modified by means of a bisulfite-catalyzed transamination reaction (24). We have found that it is possible to use this reaction to selectively introduce aminoalkyl or carboxyalkyl linker arms at a specific deoxycytidine site within oligonucleotides which also contain 5-methyldeoxycytidine residues. The resulting oligonucleotides contain a single amine or carboxylic acid functionality which can serve as site for selective attachment of a variety of functional groups. The linker-arm-conjugated oligomers are capable of forming stable duplexes with complementary single-stranded oligodeoxyribonucleotides as well as stable triplexes with target oligodeoxyribonucleotide duplexes.

EXPERIMENTAL PROCEDURES

Base-protected 5'-O-(4,4'-dimethoxytrityl)deoxyribonucleoside 3'-O-[(diisopropylamino)- β -cyanoethyl phosphoramidites] were purchased from Curachem. Nucleoside-derivatized controlled pore glass supports were purchased from American Bionetics. All chemicals used were reagent grade or better. Proton NMR spectra were recorded on a Bruker 300-MHz spectrometer.

Oligonucleotide Synthesis. Oligodeoxyribonucleotides were synthesized on a 1- μ mol scale on a Biosearch 8700 DNA synthesizer using controlled pore glass supports and base-protected 5'-O-dimethoxytrityldeoxyribonucleoside 3'-O-[(diisopropylamino)- β -cyanoethyl phosphoramidite] synthons. The oligomers were deprotected and removed from the support by treatment with a solution containing pyridine/concentrated ammonium hydroxide (1:1 v/v) for 5 h at 60 °C. The support was removed by filtration, and the solvents were evaporated. The residue was dissolved in water and the solution was loaded onto a BioGel TSK-DEAE-5-PW HPLC ion-exchange column (7.5 \times 75 mm). The column, which was monitored at 254 nm, was eluted with a 50-mL linear gradient of 0.1-0.5 M sodium chloride in 10 mM Tris-HCl at pH 7.0 at flow rate of 0.8 mL/min. The solution containing the oligomer was loaded onto a SEP-PAK cartridge which had been previously equilibrated with the following solutions: 10 mL of acetonitrile, 10 mL of acetonitrile/water (1:1 v/v), and 10 mL of 0.1 M sodium phosphate buffered at pH 5.8. The SEP-PAK cartridge was washed with 10 mL of water and the oligomer was eluted with 3 mL of acetonitrile/water (1:1 v/v). The purity of the oligomer was checked by gel electrophoresis on a 15% denaturing gel after the oligomer had been phosphorylated using [γ -³²P]ATP and polynucleotide kinase (25). Each oligomer migrated as a single band on the gel.

Transamination Reactions—General Procedure. Transamination solutions were freshly prepared by mixing the appropriate components as described in Table I. The final pH of each solution was 7.1. The nucleoside (24 A₂₅₄ units, \sim 3.5 μ mol) or oligonucleotide (10 A₂₅₄ units, \sim 96 nmol) was dissolved in 96 μ L of transamination solution containing 4 μ L of 0.1 M hydroquinone in 95% ethanol. The solution was incubated for 48 h at 50 °C. The reaction mixture was diluted with 0.5 mL of 0.1 M sodium hydroxide

Table I. Transamination Solutions

amine (mmol)	sodium bisulfite, mg	water, mL	8 N sodium hydroxide, mL	12 N hydrochloric acid, mL
4-aminobutyric acid (3.0)	104	0.90	0.10	
1,4-diaminobutane (3.0)	104	0.30		0.47
1-aminobutane (3.0)	104	0.80		0.20

and the solution was incubated for 1 h at room temperature. The solution was then further diluted with 1 mL of 0.1 M sodium phosphate buffered at pH 5.8. The oligonucleotide was purified by preparative reversed-phase HPLC on a Whatman Partisil 5 RAC ODS-3 10-cm column. The column was eluted with a 50-mL linear gradient of 2%–20% acetonitrile in 0.1 M sodium phosphate (pH 5.8) at a flow rate of 2.5 mL/min. The fraction containing the pure oligomer was diluted with 0.1 M sodium phosphate to give a final acetonitrile concentration of 5% and the solution was desalted on a SEP-PAK cartridge as described above.

Transamination of Deoxycytidine with 4-Aminobutyric Acid. A solution of deoxycytidine (48 A_{254} units, 7.7 μ mol) in 12 μ L of water was added to 180 μ L of transamination buffer prepared as described in Table I and 8 μ L of 0.1 M hydroquinone in 95% ethanol. The solution was incubated at 50 °C for 48 h and then treated with 1 mL of 0.1 M sodium hydroxide at room temperature for 2 h. The solution was passed through a Dowex 50X column which contained 1 mL of resin in the pyridinium form. The column was washed with 3 mL of water, and the combined eluant and washings were evaporated to dryness. The residue was dissolved in 0.6 mL of water and the product purified by reversed-phase HPLC on a Partisil 5 RAC ODS-3 10-cm column. The column was eluted with 30 mL of a linear gradient of 0%–3% acetonitrile in 0.1 M sodium phosphate at a flow rate of 2.5 mL/min. A total of 28 A_{254} units was obtained. The UV spectrum showed λ_{max} at 239 and 271 nm and λ_{min} at 230 and 250 nm in 0.1 M sodium phosphate (pH 5.8). ^1H NMR ($^2\text{H}_2\text{O}$): δ 1.83 (m, $\text{NHCH}_2\text{CH}_2\text{CH}_2\text{COOH}$), 2.23 (m, H-2'), 2.96 (t, $\text{NHCH}_2\text{CH}_2\text{CH}_2\text{COOH}$), 3.30 (t, $\text{NHCH}_2\text{CH}_2\text{CH}_2\text{COOH}$), 3.74 (m, H-5'), 4.00 (m, H-4'), 4.39 (m, H-3'), 5.94 (d, H-5), 6.24 (t, H-1'), 7.63 (d, H-6).

Proton NMR Spectra of Nucleosides in 1 M Sodium Bisulfite. Two milligrams of deoxycytidine or 2 mg of 5-methyldeoxycytidine was dissolved in 0.5 mL of $^2\text{H}_2\text{O}$ containing 52 mg of sodium bisulfite. The solutions were incubated overnight at room temperature and the proton NMR spectra were then recorded.

Base Ratio Determination. The oligonucleotide (0.2 A_{254} units) was dissolved in 48 μ L of digestion buffer which contained 2 mM magnesium chloride and 10 mM Tris-HCl (pH 8.2). Snake venom phosphodiesterase, 5 ng in 2 μ L, and bacterial alkaline phosphatase, 0.4 units in 2 μ L, were added, and the reaction mixture was incubated for 16 h at 37 °C. The solution was diluted with 200 μ L of 0.1 M sodium phosphate (pH 5.8). Aliquots were analyzed by reversed-phase HPLC on a Whatmann ODS-3 RACII column using an 18-mL linear gradient of 0%–3% acetonitrile in 0.1 M sodium phosphate followed by a 12-mL linear gradient of 3%–20% acetonitrile in 0.1 M sodium phosphate (pH 5.8) at a flow rate of 1.5 mL/min. The column was monitored at 254 nm. The peak areas, which were determined by weighing or by integration, were normalized by dividing the extinction coefficient of the nucleoside. The following extinction coefficients at 254

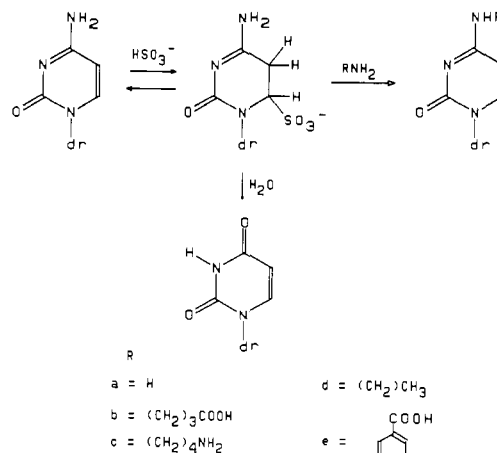


Figure 1. Bisulfite-catalyzed transamination and deamination of deoxycytosine.

nm were used: 5-methyldeoxycytidine, 3700; deoxycytidine or N⁴-modified deoxycytidine, 6260; and thymidine, 7250.

Determination of Oligomer Extinction Coefficients. Four samples of the oligomer (0.2–0.5 A_{254} unit) were dissolved in 48 μ L of digestion buffer. Duplicate samples of the oligomer were treated with 2 μ L (5 ng) of snake venom phosphodiesterase or with 2 μ L of water. The solutions were incubated for 16 h at 37 °C and then diluted with 1.0 mL of water. The A_{254} values of the enzyme-treated solutions were used to determine the amount of oligomer hydrolyzed and this amount was then used to calculate the oligomer extinction coefficient based upon the A_{260} of the water-treated, nonhydrolyzed samples.

Determination of Melting Temperatures of Duplexes and Triplexes. The melting temperatures of the duplexes and triplexes were determined using a Varian 219 spectrophotometer fitted with a thermostated cell compartment connected to a Neslab RTE 100 circulating, programmable temperature bath. The temperature of the cell holder was monitored by a Varian temperature readout unit and the sample compartment was continuously purged with dry nitrogen throughout the experiment. All experiments were carried out in melt buffer which consisted of 0.1 M sodium chloride, 20 mM magnesium chloride, and 50 mM Tris-HCl buffered at pH 7.0. Duplexes were formed by mixing 0.5 mL of a 1.0 μ M solution of each oligomer. Triplexes were formed by mixing 0.5 mL of a 1.0 μ M solution of the oligomer with 0.5 mL of a 1.0 μ M solution of the preformed target duplex. The A_{260} of the duplexes or triplexes were recorded as a function of temperature as the solutions were heated from 0 to 60 °C at a rate of 1 °C/min.

RESULTS

Transamination of Deoxycytidine and 5-Methyldeoxycytidine. In order to optimize the conditions for the transamination reaction, which is shown schematically in Figure 1, the reaction of deoxycytidine with 4-aminobutyric acid was performed at various pHs. Reactions were carried out at pH 6.4, 7.1, or 8.2 in the presence of 1 M sodium bisulfite and 3 M 4-aminobutyric acid at 50 °C. Hydroquinone was added to inhibit radical-generated modification of the nucleoside (26). The products of the reaction were analyzed by reversed-phase HPLC. As shown in Figure 2, reactions carried out at pH 7.1 gave the highest yield of N⁴-(3-carboxypropyl)deoxycytidine, whose structure was confirmed by UV and proton NMR spectroscopy. These conditions produced minimum amounts

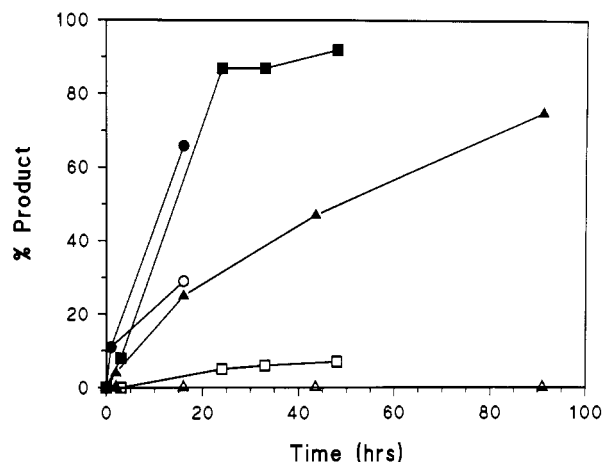


Figure 2. Rate of formation of N^4 -(3-carboxypropyl)deoxycytidine (filled symbols) and deoxyuridine (open symbols) upon incubation of 2'-deoxycytidine with 1 M sodium bisulfite and 3 M 4-aminobutyric acid at 50 °C at pH 6.4 (O), pH 7.1 (□), or pH 8.2 (Δ).

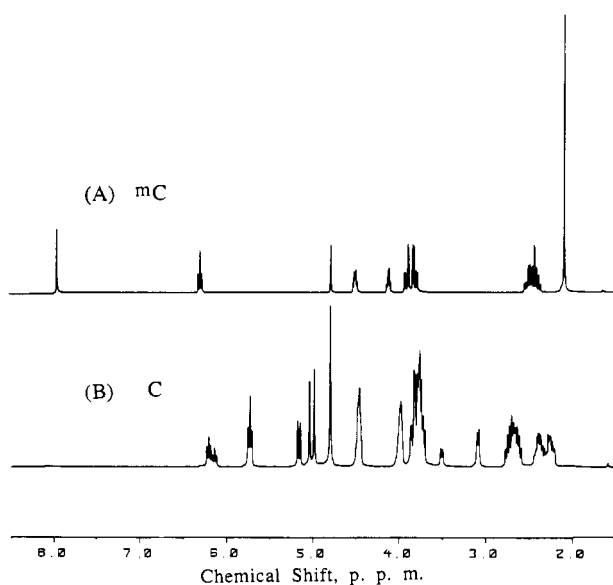


Figure 3. Proton NMR spectra of (A) 5-methyl-2'-deoxycytidine or (B) 2'-deoxycytidine in 1 M sodium bisulfite.

of deoxyuridine, a side product generated by deamination of deoxycytidine. The rate of deamination increased at pH 6.4, whereas at pH 8.2, no deamination was observed. However, at the higher pH, the rate of transamination was reduced to approximately one-fifth that at pH 7.1. The rate of transamination was also reduced when the concentrations of either sodium bisulfite or 4-aminobutyric acid were reduced or when the temperature of the reaction was reduced (data not shown).

Similar results were obtained when transamination was carried out in the presence of 1,4-diaminobutane, aminobutane, or 3-aminobenzoic acid. The limited solubility of the latter allowed only a 1 M solution to be prepared. In this case the extent of transamination was approximately 30% after 48 h.

In contrast to the behavior of deoxycytidine, 5-methyldeoxycytidine was found to be completely unreactive when incubated at 50 °C in transamination buffer containing 4-aminobutyric acid at either pH 6.4, 7.1, or 8.2. The reaction of 5-methyldeoxycytidine with 1 M sodium bisulfite was examined by proton NMR. As shown in Figure 3, incubation of deoxycytidine with 1 M sodium bisulfite resulted in the disappearance of the H-5 and H-6

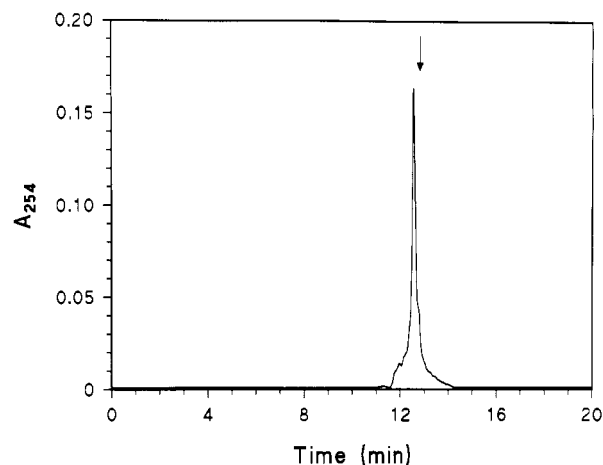


Figure 4. Reversed-phase HPLC of the products of reaction of d-CTT·CTT·TTT·TCT·TTT (IIa) with 1 M sodium bisulfite and 3 M 4-aminobutyric acid. The elution conditions are described in the text and the arrow indicates the retention time of oligomer IIa.

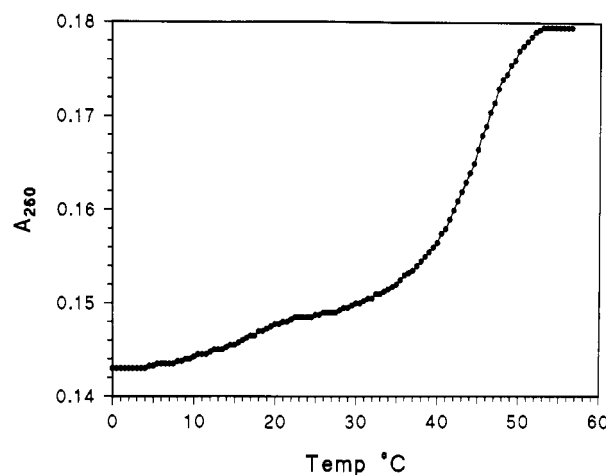


Figure 5. Absorbance versus temperature profile of a solution containing 0.5 μ M IIb and 0.5 μ M double-stranded DNA target IV in 0.1 M sodium chloride, 20 mM magnesium chloride, and 50 mM Tris, at pH 7.0.

resonances at 6.0 and 7.7 ppm, respectively, and the appearance of new resonances at 5.0, 5.2, and 5.8 ppm, which correspond to the formation of the bisulfite adduct. The appearance of two sets of sugar proton resonances, for example the two sets of H-1' resonances at 6.1 and 6.2 ppm, suggests that the bisulfite adducts of both deoxycytidine and its deamination product, deoxyuridine, are present in the reaction mixture. No change in the proton NMR spectrum of 5-methyldeoxycytidine was observed under these conditions.

Transamination of Oligodeoxyribonucleotides. Two oligodeoxyribonucleotides, d-CTT·CTT·TTT·TC (Ia) and d-CTT·CTT·TTT·TCT·TTT (IIa), where C represents 5-methyldeoxycytidine, were synthesized. Transamination of Ia or IIa was carried out under the same conditions used to transaminate deoxycytidine. Under these conditions, little or no degradation of the oligomer was observed. As shown in Figure 4, transamination of IIa with 4-aminobutyric acid resulted in the formation of a single major product, IIb, whose retention time on a reversed-phase HPLC column was distinct from that of IIa. Transamination of Ia or IIa with 1,4-diaminobutane or 1-aminobutane also gave single products, Ic, IIc, and IId, respectively, as assayed by reversed-phase HPLC.

Digestion of IIb with a combination of snake venom phosphodiesterase and bacterial alkaline phosphatase

Table II. Enzymatic Digestion of Modified Oligodeoxyribonucleotides

oligomer	X	base ratio			ε at 260 nm
		d-C	d-X	d-T	
d-C <u>T</u> T-T <u>T</u> T-T <u>T</u> T-TX					
Ia	C	1.0	0.5	4.1	84 800
Ic	N ⁴ -(4-aminobutyl)C	1.0	0.5 ^a	3.6	68 900
d-C <u>T</u> T-T <u>T</u> T-T <u>T</u> T-TXT-T <u>T</u> T					
IIa	C	1.0	0.5	6.1	104 400
IIb	N ⁴ -(3-carboxypropyl)C	1.0	0.6	6.1	102 200
IIc	N ⁴ -(4-aminobutyl)C	1.0	0.6 ^a	5.5	93 600
IId	N ⁴ -butyl-C	1.0	0.6	5.8	90 800

^a d-TpX, X = N⁴-(4-aminobutyl)C.

Table III. Melting Temperatures of Duplexes Containing Modified Oligodeoxyribonucleotides

duplex	X	T_m , °C
d-CTT-CTT-TTT-TX GAA-GAA-AAA-AGA-AAA-d		
Ia	C	40
Ib	N ⁴ -(4-aminobutyl)C	37
d-CTT-CTT-TTT-TXT-TTT GAA-GAA-AAA-AGA-AAA-d		
IIa	C	47
IIb	N ⁴ -(3-carboxypropyl)C	43
IIc	N ⁴ -(4-aminobutyl)C	45
IId	N ⁴ -butyl-C	44

^a The melting temperatures were determined at an oligomer strand concentration of 0.5 μ M in 0.1 M sodium chloride, 20 mM magnesium chloride, and 50 mM Tris (pH 7.0).

yielded three nucleosides, thymidine, deoxycytidine, and N⁴-(3-carboxypropyl)deoxycytidine in the expected molar ratios as shown in Table II. The reversed-phase HPLC mobility of the latter nucleoside was identical to that of authentic N⁴-(3-carboxypropyl)deoxycytidine produced by transamination of deoxycytidine by 4-aminobutyric acid. No deoxyuridine was detected in the digest of the oligomer. In a similar manner, oligomer IId gave the expected products thymidine, deoxycytidine, and N⁴-butyldeoxycytidine following enzymatic digestion. However digestion of oligomers Ic or IId gave thymidine, deoxycytidine, and a new product whose reversed-phase HPLC mobility was consistent with that of a dinucleoside monophosphate. Analysis of the base ratios suggested that the dimer was d-TpX, where X is N⁴-(4-aminobutyl)deoxycytidine. This was confirmed by preparing d-TpX by transamination of d-TpC with 1,4-diaminobutane. The reversed-phase HPLC mobility of this modified dimer was identical to that of the dimer observed in the digests of the oligomers.

Interaction of Transaminated Oligodeoxyribonucleotides with Complementary DNA Targets. The ability of oligodeoxyribonucleotides Ia or IIa and their transaminated derivatives to form duplexes with the complementary single-stranded DNA target, d-AAA-AGA-AAA-AAG-AAG (III), was studied. The experiments were carried out in a buffer consisting of 0.1 M sodium chloride 20 mM magnesium chloride and 50 mM Tris at pH 7.0. Stoichiometric mixtures of the oligomers and the target gave melting curves with a single transition. The melting temperatures of the duplexes formed by the transaminated oligomers were between 2 and 4 °C lower than the comparable duplex formed by the parent oligomer as shown in Table III.

The transaminated 15-mers also form triple-stranded complexes with the double-stranded DNA target d-GAA-GAA-AAA-AGA-AAA/d-TTT-TCT-TTT-TTC-TTC (IV). As shown in Figure 4, a one to one mixture of IIb and IV gives two cooperative transitions in a plot of A_{260}

Table IV. Melting Temperatures of Triplexes Containing Modified Oligodeoxyribonucleotides

d-CTT-CTT-TTT-TXT-TTT d-GAA-GAA-AAA-AGA-AAA CTT-CTT-TTT-TCT-TTT-d } IV		T_m , °C	
triplex	X	b	c
IIa	C	34	45
IIb	N ⁴ -(3-carboxypropyl)C	16	44
IIc	N ⁴ -(4-aminobutyl)C	16	45
IId	N ⁴ -butyl-C	16	44

^a The melting temperatures were determined at an oligomer strand concentration of 0.5 μ M in 0.1 M sodium chloride, 20 mM magnesium chloride, and 50 mM Tris (pH 7.0). ^b Transition from triplex to third strand + duplex. ^c Transition from duplex to single strands.

versus temperature with midpoints at 16 and 45 °C. The first transition corresponds to melting the third-strand oligomer IIb and the second transition corresponds to melting of the target duplex IV. Similar results were obtained for the other derivatized oligomers as shown by the data in Table IV. The third-strand melting temperatures of the triplexes formed by the derivatized oligomers were 18 °C lower than that of the triplex formed by oligomer IIa.

DISCUSSION

Bisulfite-catalyzed transamination of cytosine is a well-known reaction which has been used to modify and probe the structure of nucleic acids (24, 26–30). In this context, the reaction shows selectivity for C residues which occur in single-stranded regions of nucleic acids. The reaction, however, would ordinarily not be expected to be sequence selective for C residues which occur in single-stranded oligonucleotides. Our results demonstrate that site-selective transamination in oligonucleotides can be achieved by substituting 5-methylcytosine for cytosine at positions where transamination is not desired. The single remaining cytosine residue then becomes a target for transamination. Oligomers which are modified in this manner are still capable of hybridizing to complementary nucleic acids because 5-methylcytosine can readily participate in normal Watson-Crick or Hoogsteen base pairing interactions which lead to the formation of double- and triple-stranded complexes, respectively.

Reaction of cytosine with bisulfite can lead to both deamination as well as transamination as is shown in Figure 1 (24). Our results are essentially in agreement with those of Draper (26), who showed that the rates of deamination and transamination are sensitive to the pH of the reaction solution. The rate of deamination appears to be accelerated at lower pH whereas deamination is suppressed above pH 7. Both deamination and transamination proceed via the bisulfite adduct which can be detected by proton NMR as shown in Figure 3. In contrast to cytosine, 5-methylcytosine shows no evidence of forming the bisulfite adduct. Consequently, no reaction is observed when 5-methylcytidine is subjected to conditions under which deoxycytidine undergoes either deamination or transamination.

Efficient transamination of deoxycytidine occurred when the reaction was carried out in the presence of 1 M sodium bisulfite and 3 M amine at pH 7.2 at a temperature of 50 °C. Under these conditions, the nucleoside was converted to 90% or greater of the transaminated product as determined by HPLC analysis. For example, transamination by 4-aminobutyric acid gave 93% of N⁴-(3-carboxypropyl)deoxycytidine, 6% deoxyuridine, and

1% deoxycytidine. Similar results were obtained when transamination was carried out with 1,4-diaminobutane or 1-aminobutane. Less efficient transamination was observed with 3-aminobenzoic acid, which gave *N*⁴-(3-carboxyphenyl)deoxycytidine in approximately 30% yield. In this case the lower extent of reaction could be attributed to the bulky nature of the amine and to the lower solubility of the amine.

Conditions which led to efficient transamination of the nucleoside also resulted in efficient transamination of deoxycytosine residues in oligodeoxyribonucleotides. Little or no hydrolysis of the oligomer was observed and the reaction appeared to be selective for deoxycytidine residues. Thus treatment of d-GAA-GAA-AAA-AGA-AAA, an oligomer which contains only purine nucleosides, with 1,4-diaminobutane transamination solution for 2 days at 50 °C resulted in no change in the oligomer as judged by HPLC. This result, coupled with the observation that 5-methylcytosine is inert to transamination, suggests that it should be possible to specifically modify C residues in an oligonucleotide which contains A, G, T, C and 5-Me-C.

Oligomers Ia, IIa, IIb, and IIc were completely hydrolyzed to their component nucleosides when treated with a mixture of snake venom phosphodiesterase and bacterial alkaline phosphatase. The resulting nucleosides were obtained in the expected molar ratios. Essentially no deoxycytidine or deoxyuridine was observed in the digests of the transaminated oligomers IIb or IIc. This result indicates that transaminated oligomers were successfully purified from nontransaminated oligomer and that the extent of deamination, if any, was below the limits of detection by HPLC.

In contrast to the behavior of the oligomers containing *N*⁴-(3-carboxypropyl)cytosine or *N*⁴-butylcytosine, oligomers Ib and IIb, which contain an *N*⁴-(4-aminobutyl)cytosine, were hydrolyzed to a mixture of thymidine, 5-methyldeoxycytidine, and the dimer d-Tp-[*N*⁴-(4-aminobutyl)]C. It appears that the presence of the aminobutyl side chain protects the internucleotide linkage on the 5'-side of the modified base from hydrolysis by the exonucleolytic activity of the snake venom phosphodiesterase. This inhibitory effect could be due to the size of the aminobutyl side chain, although the 3-carboxypropyl side chain, which is also five atoms long, does not cause inhibition. Alternatively, the primary amino group of the side chain, which should be protonated under these conditions, may directly interact with the enzyme. On the basis of examination of molecular models, it appears less likely that protection arises for interaction of the protonated amino group of the aminobutyl side chain with the negatively charged phosphodiester internucleotide bond.

Oligomers which carry a single linker arm at the *N*⁴-position of cytosine are able to form stable duplexes with complementary single-stranded DNA targets. The melting temperatures of these duplexes are only slightly less than that of the duplex formed by unmodified oligomers Ia or IIa. The position of the modification within the oligomer chain does not appear to effect the stability of the duplex. Thus the duplex formed by oligomer Ib, which contains an aminobutyl group at the 3'-end of the oligomer, shows the same reduction in melting temperature as the duplex formed by oligomer IIc, which contains an internal aminobutyl group. These results suggest that the *N*⁴-modified cytosines of the transaminated oligomers most likely are able to form normal Watson-Crick base pairs with the complementary G in the target strand.

The transaminated oligomers are also capable of forming

triplexes with a double-stranded DNA target. In this case the melting temperature of the derivatized third-strand oligomer from the triplex is considerably lower than that of the unmodified third-strand oligomer. This decrease in stability could be due to steric interactions between the side chain and components in the major groove of the triplex, although examination of molecular models suggests that the side chains should be accommodated in this environment. Alternatively, the p*K* of the modified cytosines may be higher than that of cytosine as a result of modification of the *N*⁴-position. In this case protonation of the modified base would be less likely to occur at pH 7.0 and the modified base would then be capable of forming only a single hydrogen bond to the O-6 carbonyl of guanine in the G-C base pair of the target.

Oligomers carrying the 3-carboxypropyl or the 4-aminobutyl side chain contain a reactive amino or carboxyl group which would allow conjugation with a variety of molecules. For example, the carboxyl group should serve as a site for carbodiimide-mediated esterification or amidation, whereas the amino group would be expected to be reactive toward isothiocyanates or *N*-hydroxysuccinimide esters of carboxylic acids. Thus it should be possible to conjugate the oligomers with, for example, fluorescent groups such as fluorescein or tetramethylrhodamine. Based on the melting studies described above, these derivatized molecules could be expected to form stable duplexes with complementary single-stranded nucleic acids and under the appropriate conditions, triplexes with double-stranded nucleic acids.

ACKNOWLEDGMENT

The research described in this report was supported by a grant from the National Institutes of Health (GM 45012). We thank Dr. Lou-Sing Kan for the NMR spectra and Dr. Purshotam Bhan for helpful discussions.

LITERATURE CITED

- (1) Goodchild, J. (1990) Conjugates of Oligonucleotides and Modified Oligonucleotides: A Review of Their Synthesis and Properties. *Bioconjugate Chem.* 1, 165-187.
- (2) Uhlmann, E., and Peyman, A. (1990) Antisense Oligonucleotides: A New Therapeutic Principle. *Chem. Rev.* 90, 544-584.
- (3) Englisch, U., and Gauss, D. H. (1991) Chemically Modified Oligonucleotides as Probes and Inhibitors. *Angew. Chem., Int. Ed. Engl.* 30, 613-629.
- (4) Zuckermann, R., Corey, D., and Schultz, P. (1987) Efficient Methods for Attachment of Thiol Specific Probes to the 3' Ends of Synthetic Oligodeoxyribonucleotides. *Nucleic Acids Res.* 15, 5305-5321.
- (5) Nelson, P. S., Frye, R. A., and Liu, E. (1989) Bifunctional Oligonucleotide Probes Synthesized Using a Novel CPG Support are able to Detect Single Base Pair Mutations. *Nucleic Acids Res.* 17, 7187-7194.
- (6) Haralambidis, J., Duncan, L., Angus, K., and Tregear, G. W. (1990) The Synthesis of Polyamide-Oligonucleotide Conjugate Molecules. *Nucleic Acids Res.* 18, 493-498.
- (7) Asseline, U., and Thuong, N. T. (1990) New Solid-Phase for Automated Synthesis of Oligonucleotides Containing an Amino-Alkyl Linker at Their 3'-End. *Tetrahedron Lett.* 31, 81-84.
- (8) Gupta, K. C., Sharma, P., Kumar, P., and Sathyanarayana, S. (1991) A General Method for the Synthesis of 3'-Sulphydryl and Phosphate Group Containing Oligonucleotides. *Nucleic Acids Res.* 19, 3019-3025.
- (9) Bonfils, E., and Thuong, N. T. (1991) Solid Phase Synthesis of 5',3'-Bifunctional Oligodeoxyribonucleotides Bearing a Masked Thiol Group at the 3'-End. *Tetrahedron Lett.* 32, 3053-3056.

- (10) Chu, B. C. F., Wahl, G. M., and Orgel, L. E. (1983) Derivatization of Unprotected Polynucleotides. *Nucleic Acids Res.* 11, 6513-6529.
- (11) Chollet, A., and Kawashima, E. H. (1985) Biotin Labeled Synthetic Oligodeoxyribonucleotides: Chemical Synthesis and Uses as Hybridization Probes. *Nucleic Acids Res.* 13, 1529-1541.
- (12) Teare, J., and Wollenzien, P. (1989) Specificity of the Site Directed Psoralen Addition to RNA. *Nucleic Acids Res.* 17, 3359-3372.
- (13) Bhan, P., and Miller, P. S. (1990) Photochemical Cross-Linking of Psoralen-Derivatized Oligonucleoside Methylphosphonates with Synthetic DNA Containing a Promoter for T7 RNA Polymerase. *Bioconjugate Chem.* 1, 82-88.
- (14) Gottikh, M., Asseline, U., and Thuong, N. T. (1990) Synthesis of Oligonucleotides Containing a Carboxyl Group at Either Their 5'-End or 3'-End and Their Subsequent Derivatization by an Intercalating Agent. *Tetrahedron Lett.* 31, 6657-6660.
- (15) Agrawal, S., and Tang, J.-Y. (1990) Site-Specific Functionalization of Oligodeoxynucleotides for Non-Radioactive Labeling. *Tetrahedron Lett.* 31, 1543-1546.
- (16) Agrawal, S., and Zamecnik, P. C. (1990) Site Specific Functionalization of Oligonucleotides for Attaching Two Different Reporter Groups. *Nucleic Acids Res.* 18, 5419-5423.
- (17) Gryaznov, S. M., and Potapov, V. K. (1991) A New Approach to the Synthesis of Oligodeoxyribonucleotides with Alkylamino Groups Linked to Internucleotide Phosphate Groups. *Tetrahedron Lett.* 30, 3715-3718.
- (18) Murakami, A., Nakaura, M., Nakatsuji, Y., Nagahara, S., Tran-Cong, Q., Makino, K. (1991) Fluorescent-labeled Oligonucleotide Probes: Detection of Hybrid Formation in Solution by Fluorescence Polarization Spectroscopy. *Nucleic Acids Res.* 19, 4097-4102.
- (19) Agrawal, S., Christodoulou, C., and Gait, M. J. (1986) Efficient Methods for Attaching Non-Radioactive Labels to the 5' Ends of Synthetic Oligodeoxyribonucleotides. *Nucleic Acids Res.* 14, 6227-6245.
- (20) Roduit, J.-P., Shaw, J., Chollet, A., and Chollet, A. (1987) Synthesis of Oligodeoxyribonucleotides Containing an Aliphatic Amino Linker Arm at Selected Adenine Bases and Derivatization with Biotin. *Nucleosides Nucleotides* 6, 349-352.
- (21) Sproat, B. S., Lamond, A. I., Beijer, B., Neuner, P., and Ryder, U. (1989) Highly Efficient Chemical Synthesis of 2-O-Methyloligoribonucleotides and Tetrabiotinylated Derivatives; Novel Probes that are Resistant to Degradation by RNA or DNA Specific Nucleases. *Nucleic Acids Res.* 17, 3373-3386.
- (22) Nelson, P., Sherman-Gold, R., and Leon, R. (1989) A New and Versatile Reagent for Incorporating Multiple Primary Aliphatic Amines into Synthetic Oligonucleotides. *Nucleic Acids Res.* 17, 7179-7186.
- (23) Pei, D., Ulrich, H. D., and Schultz, P. G. (1991) A Combinatorial Approach Toward DNA Recognition. *Science* 253, 1408-1411.
- (24) Shapiro, R., and Weigras, J. M. (1970) Bisulfite-Catalyzed Transamination of Cytosine and Cytidine. *Biochem. Biophys. Res. Commun.* 40, 839-843.
- (25) Maniatis, T., Fritsch, E. F., and Sambrook, J. (1982) *Molecular Cloning, A Laboratory Manual*, p 396, Cold Spring Harbor Laboratory, Cold Spring Harbor, NY.
- (26) Draper, D. E. (1984) Attachment of Reporter Groups to Specific, Selected Cytidine Residues in RNA Using a Bisulfite-Catalyzed Transamination Reaction. *Nucleic Acids Res.* 12, 989-1002.
- (27) Hayatsu, H. (1976) Reaction of Cytidine with Semicarbazide in the Presence of Bisulfite. A Rapid Modification Specific for Single-Stranded Polynucleotides. *Biochemistry* 15, 2677-2682.
- (28) Negishi, K., Harada, F., Nishimura, S., and Hayatsu, H. (1977) A Rapid Cytosine-Specific Modification of *E. coli* tRNA^{leu} by Semicarbazide-Bisulfite, A Probe for Polynucleotide Conformations. *Nucleic Acids Res.* 4, 2283-2292.
- (29) Draper, D. E., and Gold, L. M. (1980) A Method for Linking Fluorescent Labels to Polynucleotides: Application to Studies of Ribosome-Ribonucleic Acid Interactions. *Biochemistry* 19, 1774-1781.
- (30) Schulman, L. H., Pleka, H., and Reines, S. A. (1981) Attachment of Protein Affinity-Labeling Reagents of Variable Length and Amino Acid Specificity to *E. coli* tRNA^{Met}. *Nucleic Acids Res.* 9, 1203-1217.

Studies of the Influence of Different Cross-Linking Reagents on the Immune Response against a B-Epitope

A. Delmas,* A. Brack, and Y. Trudelle

Centre de Biophysique Moléculaire, 1A, Avenue de la Recherche Scientifique, 45071 Orléans Cedex 2, France.
Received July 22, 1991

We have previously shown that the carrier polytuftsin obtained by polycondensation of tuftsin, a naturally occurring macrophage activator, increases significantly the antibody response against a linked B-epitope. In the present work, we have studied the influence of different cross-linking reagents on the quality of the conjugation and on the immune response, at both B-cell and T-cell levels. We observed that the cross-linking method used for coupling the B-epitope to the carrier influences the immune response. A hypothesis is put forward to explain the differences observed.

INTRODUCTION

Chemically synthesized peptide immunogens have been shown to be able to elicit a strong immune response only when attached to a carrier protein (8) or coadministered with an immunopotentiating agent or adjuvant (21). The further use of synthetic peptide immunogens as vaccines depends on the finding of suitable adjuvants and carriers for widespread use in humans and animals. Different strategies have been explored with the aim of increasing their potency in eliciting an effective and long-lasting immune response (18, 21). A promising immunostimulant is tuftsin, Thr-Lys-Pro-Arg, a naturally occurring macrophage activator (6). It is derived from the CH₂ domain of human IgG. Tuftsin was shown to exert a strong immunopotentiating activity (3) and seems to be nonimmunogenic by itself (14). In order to develop new carriers for synthetic vaccines devoid of any side effects, such as cross-reactions with host proteins (19) or epitopic suppression (7), we have previously synthesized the polypeptide polytuftsin (PTF in abbreviated form). First results showed that PTF increased significantly the antibody response against a linked B-epitope, the 10-26 sequence of the Pre-S₂ region of the hepatitis B surface antigen, hereafter referred to as 10-26PreS₂, when glutaraldehyde was used as cross-linking reagent (20). But, when using glutaraldehyde as coupling reagent, a random cross-linking occurs, thus generating a number of different products (15 and references herein cited). So as to prepare better-characterized conjugates and to investigate more accurately the immune response, heterobifunctional cross-linkers should be used so that the peptide will be coupled specifically and in a predictable manner to the carrier. As bifunctional cross-linkers for immunological purposes, maleimide derivatives are preferred to *N*-succinimidyl 3-(2-pyridyldithio)propionate (SPDP), which generates a disulfide bond not completely stable to reductive cleavage by ubiquitously occurring thiol compounds. The spacer between the carrier and the antigen obtained by use of aliphatic maleimide reagents elicits less antibodies against itself than when cyclic or aromatic reagents are used (17). Moreover the linkage thus obtained is more flexible and stable in aqueous solutions (17). For these reasons, we chose succinimidyl 3-*N*-maleimidopropionate (MPS) (9, 13) possessing two CH₂ only, to get a spacer resembling as closely as possible the SPPS spacer, the weakest immunogenic one.

In the present work, we synthesized the conjugate 10-26PreS₂-PTF by use of MPS, a heterobifunctional reagent. The conjugate thus obtained was compared to the pre-

viously described glutaraldehyde conjugate (20) with respect to the antibody response. Contrary to expected results, the chemically well-defined conjugate does not elicit any antibody response. We have also investigated the influence of the conjugation method at the T-cell level of the immune response. A hypothesis is put forward to explain the differences observed in antibody production.

EXPERIMENTAL PROCEDURE

Peptides. The polypeptide PTF and the 10-26PreS₂ peptide were synthesized as already described by Trudelle et al. (20). An extra ¹⁴C-labeled alanine was added to 10-26PreS₂ in the N-terminal position to facilitate the monitoring of the conjugation.

Bifunctional Reagents. Succinimidyl 3-*N*-maleimidopropionate (MPS) was purchased from Fluka (Switzerland). Succinimidyl *S*-acetylthioacetate (SATA) was synthesized according to the method of Duncan et al. (4).

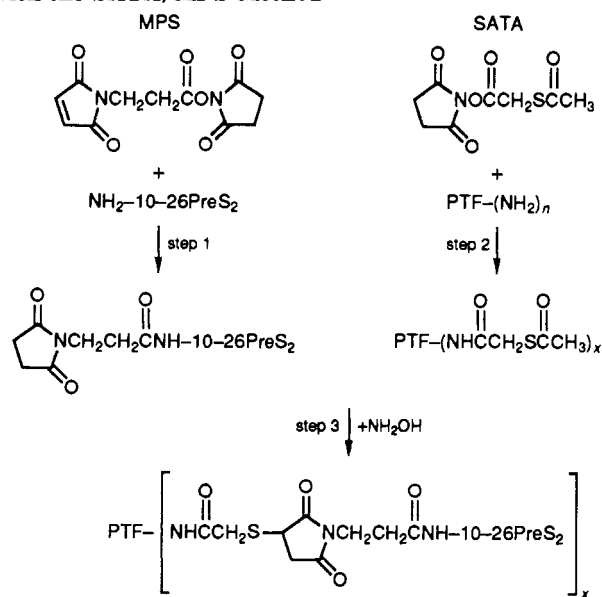
Preparation of Conjugates. The preparation of conjugates via the glutaraldehyde cross-linking method is described in ref 20.

Coupling of the 10-26PreS₂ to PTF with a heterobifunctional reagent was performed according to the method of Duncan et al. (4), with the following modifications.

(a) *SATA Attachment to PTF.* SATA (0.6075 μmol) dissolved in 10 μL of DMF was added with stirring to PTF, corresponding to 2.43 μequiv of ε-NH₂, dissolved in 1 mL of phosphate buffer (50 mM, pH 7.5). The stirring was continued for a further 30 min at room temperature. The solution was then exhaustively dialyzed against bidistilled water using dialysis tubing with a molecular weight cutoff of 6000-8000 and lyophilized. The coupling yield was determined by the Ellman's sulfhydryl titration method (5) after deacetylation of SATA by hydroxylamine as described in ref 4.

(b) *MPS Attachment to 10-26PreS₂.* To 7 μmol of 10-26PreS₂, dissolved in 4 mL phosphate buffer (50 mM, pH 7.5), was added a 10-fold molar excess of MPS (dissolved in 20 μL of DMF). The reaction mixture was stirred for 30 min at room temperature. HPLC on a semipreparative RP-C18 (Merck) column was used to purify the derivatized peptide with a linear gradient of water/acetonitrile/trifluoroacetic acid, 85/15/0.1 to 60/40/0.1 in 35 min and a flow rate of 3 mL/min. For the determination of the amount of attached maleimide groups, these were first reacted with an excess of 2-mercaptoethanol, which was then back-titrated by the Ellman's method.

(c) *Conjugation.* The MPS-treated 10-26PreS₂, dissolved in 1 mL of phosphate buffer (50 mM, pH 7.5), was

Scheme I. Preparation of 10-26PreS₂-PTF Conjugate with the SATA/MPS Method^a

^a *n*: NH₂ number per PTF macromolecule. *x*: degree of substitution.

added to the SATA-treated PTF, dissolved in 3 mL of phosphate buffer (50 mM, pH 7.5). A 400- μ L portion of a 50 mM solution of hydroxylamine hydrochloride, adjusted to pH 7.5 by addition of solid disodium hydrogen phosphate, was added for deacetylating SATA-treated PTF. The concentrations used corresponded to a maleimide/S_H ratio of 2. After stirring for 1 h at room temperature, the reaction was stopped by adding a 2-fold molar excess of 2-mercaptoethanol (referring to initial maleimide) and then, 15 min later, a 2-fold molar excess of *N*-ethylmaleimide (referring to total S_H). The solution was then dialyzed extensively against water, lyophilized, and stored at -20 °C until used. The ratio of 10-26PreS₂ to tuftsin unit in PTF was estimated by amino acid analysis after acid hydrolysis by HCl 5.6 N at 110 °C for 72 h, and by counting the radiolabeled 10-26PreS₂.

Immunization. Balb/c mice were purchased from Iffa Credo (France). Groups of seven mice, about 8 weeks old, were immunized intraperitoneally on days 1, 27, 57 with either free or coupled 10-26PreS₂ corresponding to 3 nmol of 10-26PreS₂ dissolved in 100 μ L of 0.9% NaCl/complete Freund adjuvant (CFA) 1/1 v/v for priming and in 100 μ L 0.9% NaCl/incomplete Freund adjuvant (IFA) 1/1 v/v for boosters. The animals were bled in the retroorbital sinus 14 days after priming and 14 days after the second booster. The sera of each group were pooled and frozen at -20 °C until used. Anti-10-26PreS₂ antibody titration was performed by ELISA 14 days after priming and 14 days after the second booster.

Enzyme-Linked Immunosorbent Assay (ELISA). Mouse antisera were assayed according to the general procedure for ELISA. Briefly, immunoplate wells (Nunc, Denmark) were coated with 1 μ g of 10-26PreS₂ peptide and then saturated with BSA (2% in PBS). Rabbit anti-mouse total immunoglobulin serum coupled to horseradish peroxidase (Nordic, Netherlands) was used as immunoconjugate (1/4000) and *o*-phenylenediamine as substrate. The reaction was stopped by addition of 1 N H₂SO₄. The absorbance (*A*) was measured at 492 nm. Each pool of sera was tested in duplicate and the test was repeated two times.

Assay for Proliferative Responses of Antigen-Specific T-Cells. Balb/c mice were injected in the hind

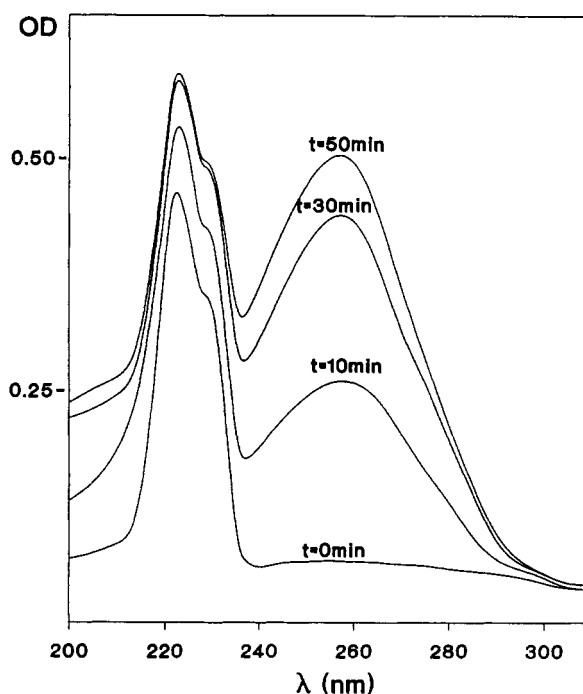


Figure 1. Hydrolysis of MPS. To 10 mL of phosphate buffer (pH 7.5, 50 mM) was added 100 μ g of MPS dissolved in 12.6 μ L of DMSO. The spectrum was recorded at times 0, 10, 30, and 50 min in a 1-cm cell.

footpads with 25 μ g of either glutaraldehyde- or SATA-treated PTF, dissolved in 25 μ L of 0.9% NaCl, both emulsified in 25 μ L of CFA. Ten days later, draining popliteal and inguinal lymph nodes were removed, and a single cell suspension of T-cells was prepared in RPMI 1640 (Gibco laboratories) supplemented with 2 mM L-glutamine, antibiotics, 5×10^{-5} M 2-mercaptoethanol, and 10% fetal calf serum. T-cells were cultured in 0.2 mL at a final concentration of 2.5×10^6 cells in 96-well plates with or without antigen. After 4 days of culture (37 °C, 7.5% CO₂) the cells were pulsed for 18 h with [³H]thymidine and then collected on glass-fiber filters with a Mash cell harvester. Incorporated radioactivity was determined by liquid scintillation counting. Results were expressed as the difference between cpm with and without antigen (Δ cpm) as means of quadruplicate cultures.

Viscosity Measurements. PTF was reacted with either glutaraldehyde or SATA according to a procedure mimicking a cross-linking reaction except that no antigen was added.

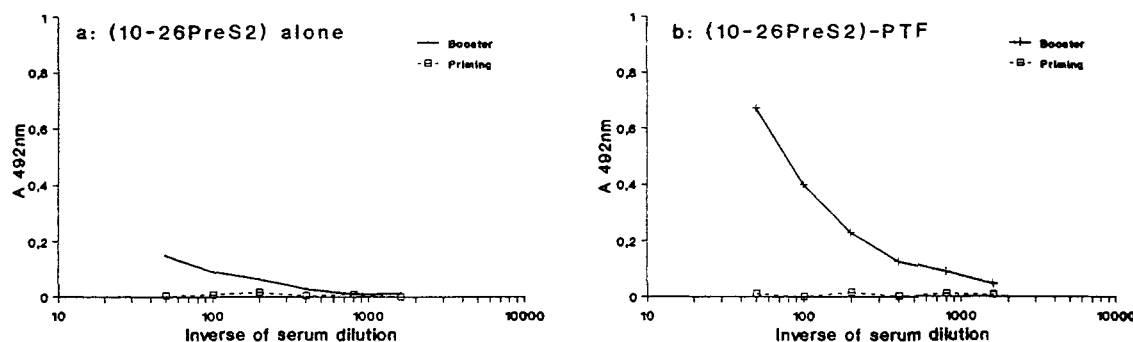
(a) *Treatment with Glutaraldehyde.* A 5.9-mL portion of PTF solution corresponding to 15 μ equiv of ϵ -NH₂ of lysine in 0.1 M sodium bicarbonate was transferred after thorough filtration into a water-jacketed Ubbelohde viscometer thermostated at 25 ± 0.01 °C. A 7.1- μ L portion of 25% glutaraldehyde water solution (from Fluka) corresponding to 17.75 μ mol was then added, and flow times were measured repeatedly by means of an automatic Viscomatic Fica instrument over a 10-h period.

(b) *Treatment with SATA.* A 5-mL sample of PTF solution, corresponding to 11.96 μ equiv of ϵ -NH₂ of lysine in 0.05 M phosphate buffer (pH 7.5), was handled as described above. SATA (3.03 μ mol) dissolved in 50 μ L of DMF was then added, and flow times were measured over a 2-h period.

RESULTS AND DISCUSSION

Scheme I describes the preparation of the 10-26PreS₂-PTF conjugate via SATA/MPS method. MPS was reacted

A: Coupling reagent: glutaraldehyde



B: Coupling reagent: SATA / MPS

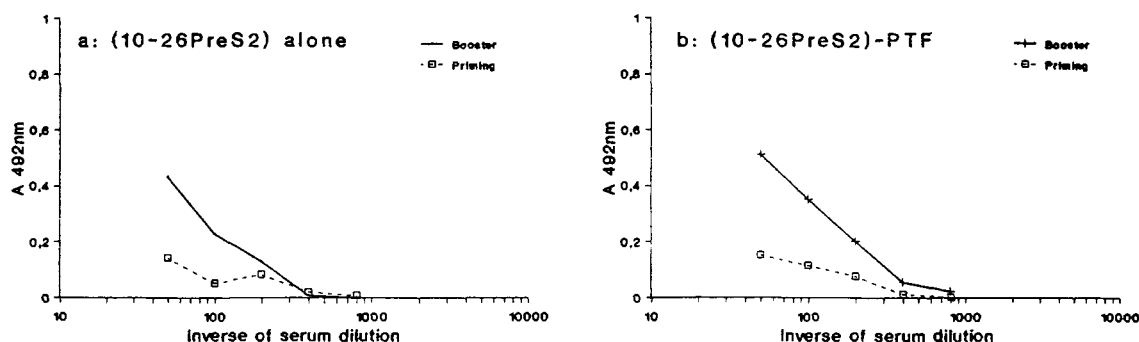


Figure 2. Antibody production after immunization with either free or coupled 10-26PreS₂ using glutaraldehyde (upper panel) or SATA/MPS (lower panel) coupling reagent.

Table I. Substitution Level of PTF Conjugates by 10-26PreS₂ Obtained by Glutaraldehyde or MPS Reagent

	10-26PreS ₂	tuftsin unit ^a
glutaraldehyde	1	20
MPS	1	24

^a The average molecular weight of PTF estimated by viscometry (1) was found to be 16.8 kDa.

with the α -NH₂ of 10-26PreS₂ (step 1) rather than with ϵ -NH₂ groups of PTF. Indeed, we found that, even when using a 10-fold excess, no MPS group could be coupled to ϵ -NH₂ of lysine of PTF (unpublished data) because, at pH values required for deprotonating ϵ -NH₂ of lysine, hydrolysis of MPS is so fast (Figure 1) that no aminolysis occurred. The MPS-10-26PreS₂ was purified by HPLC. MPS loading was determined by Ellman's back-titration. PTF was derivatized by reacting some lysine side-chains with SATA (step 2) to obtain the thiol groups required for the addition reaction to maleimide, so avoiding the addition of an extra cysteinyl residue. SH functions are generated by a deacetylation reaction with hydroxylamine at neutral pH (step 3). This step can be achieved in the presence of maleimide groups, thus minimizing the oxidation of thiols groups to disulfide. The derivatized PTF was purified by dialysis rather than by chromatographic methods because of the strong adsorption of PTF on reverse-phase or permeation chromatographic supports. The conjugate was purified by dialysis for the same reasons. The degree of substitution of PTF by 10-26PreS₂ was determined by measuring the radioactivity of ¹⁴C (incorporated at the end of the 10-26PreS₂ synthesis) and by amino acid analysis. The different conjugates used in this work are collected in Table I.

For each conjugate, two groups of mice were immunized with either 10-26PreS₂ alone as control or 10-26PreS₂ coupled to PTF. It is clear from Figure 2A that only the glutaraldehyde-treated 10-26PreS₂-PTF conjugate elicits

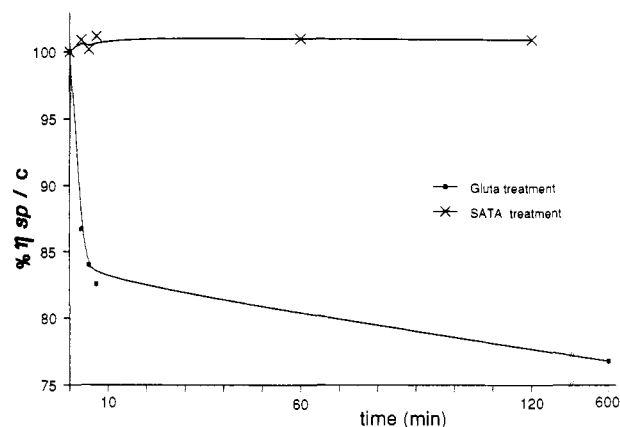


Figure 3. Percentage of variation of the viscosity versus time during the reaction between PTF and either glutaraldehyde or SATA. Viscosity (η_{sp}/c) is calculated by the expression $(t - t_0)/(t_0 \times c)$ where t and t_0 are the flow times at 25 °C of solution and solvent, respectively, and c is the polymer concentration in g/mL.

a significant enhancement of anti-10-26PreS₂ antibody production as compared to that elicited by 10-26PreS₂ alone. On the contrary, the conjugate obtained via SATA/MPS method has no noticeable activity on the antibody production (Figure 2B).

The use of heterobifunctional reagents such as SATA and MPS gives well-characterized conjugates, because all intermediates formed can be checked up by titration of introduced reactive groups. Furthermore, no significant variation of the viscosity could be detected when PTF was treated with SATA in the same operating conditions as used for the preparation of conjugates (Figure 3). These data demonstrate that the conformation of PTF remains essentially unaffected by the conjugation procedure. On the contrary, the chemical reactions between glutaraldehyde and amino groups, especially ϵ -NH₂ of lysine, are not

Table II. Amino Acid Analysis after Acidolytic Hydrolysis^a

	theory	PTF	glutaraldehyde-treated PTF
Thr	1	0.93	1.05
Lys	1	1.14	0.73
Pro	1	ND ^b	ND
Arg	1	1.00	1.00

^a Acidolytic hydrolysis: 5.6 N HCl, 72 h at 120 °C. ^b Not determined.

yet fully understood. When PTF is submitted to a glutaraldehyde treatment in the absence of antigen, in the same concentration and pH conditions as in the conjugation procedure (20), we observed a decrease of the lysine content estimated by amino acid analysis after acidolytic degradation (Table II). Therefore, the linkage formed by the reaction of glutaraldehyde with ϵ -NH₂ of lysine is stable to acid hydrolysis (12). Furthermore, Figure 3 shows a lowering of PTF viscosity during glutaraldehyde treatment. This lowering of viscosity probably results from an intramolecular cross-linking between lysine side chains of PTF, consistent with the decrease of the lysine content. It is clear that such a modification occurs in the presence of antigen also, because of the large excess of glutaraldehyde used.

To elicit an antibody response, an antigen must include both a B- and a T-epitope. Indeed, previous studies have demonstrated that the induction of antibody responses against a haptenic determinant is mediated through cognate interaction between hapten-specific B-cells and carrier-specific helper T-cells (11). To enlist T-cell help, most short synthetic peptides have therefore to be conjugated to larger protein carrier providing the necessary T-cell epitopes. The 10-26PreS₂ peptide has been chosen because it was known to be a B-epitope only (15). Indeed, Milich et al. (10) found that 9-19Pre-S₂ and 14-26Pre-S₂ peptides of HBsAg were respectively nonstimulatory and minimally reactive in the T-cell proliferative assay. Their experiments used C3Hq mice. We found that 10-26PreS₂ peptide is also minimally reactive whether C3Hq or Balb/c mice were used (data not shown). Therefore, the difference in antibody production elicited by glutaraldehyde and SATA/MPS conjugates was thought to be due to a dissimilar reactivity at the T-cell level. In other words, the chemical modification of PTF by glutaraldehyde is likely to influence the immune response at the T-cell level.

To test this hypothesis, we undertook a T-epitope determination in the carrier moiety of the conjugates by the lymph node T-cell proliferative assay. Figure 4 shows that glutaraldehyde-treated PTF is capable of eliciting a significant T-cell proliferative response at antigen concentration up to 75 μ g/mL. Beyond this concentration, glutaraldehyde-treated PTF exhibits an inhibitory activity. In the case of SATA-treated PTF, the stimulation of the proliferative activity is clearly less pronounced and its inhibitory activity on T-cell proliferative response is on the same order of value. The inhibitory activity seems to be nonspecific and due to a toxic effect, since 58% living cells were counted after 4 days incubation with 40 μ g/mL PTF. Thus the absence of antibody production elicited by the SATA/MPS conjugate in which the PTF carrier part has not been damaged by any unnecessary chemical modification arises probably from the poor activity of SATA-treated PTF for stimulating the proliferative response of T-cells. On the other hand, the significant antibody production induced by the glutaraldehyde conjugate results from the T-epitope activity of glutaraldehyde-treated PTF. Furthermore the nonnatural modi-

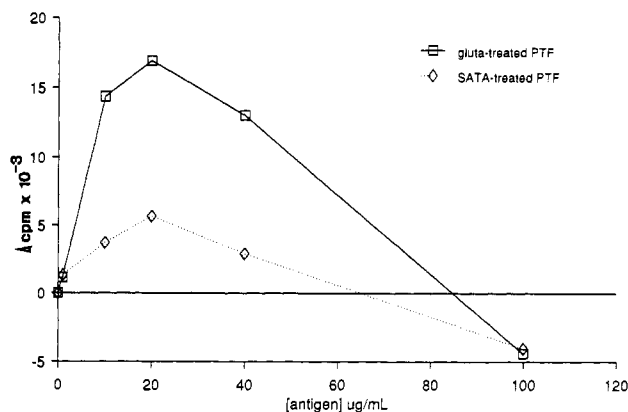


Figure 4. Proliferative response of T-cells from Balb/c mice with either glutaraldehyde- or SATA-treated PTF. Balb/c mice were immunized in the hind footpads with 50 μ g of PTF, glutaraldehyde-treated PTF, or SATA-treated PTF and in vitro stimulated with the same antigen. T-cell proliferation was determined by incorporation of [³H]thymidine and expressed as the difference between cpm with and without antigen (Δ cpm). Standard deviation of quadruplicate culture were about 10% of the mean.

fication of lysine side chains, almost irreversible (16), should remain stable in vivo and should confer on glutaraldehyde-treated PTF a longer in vivo lifetime (2).

In conclusion, it must be emphasized that the type of linkage of the peptide to PTF is of considerable importance for successful immunizations. As PTF appears to be an interesting carrier because of its poor immunogenicity (20), other tuftsin derivatives are currently being evaluated to diminish the in vitro toxicity on T-cells and to understand at the molecular level why the treatment with either glutaraldehyde or SATA modifies differently the T-epitope activity of this carrier.

ACKNOWLEDGMENT

We gratefully acknowledge Dr. C. Spach and Ms. N. Bureaud for their help with the T-cell proliferative assay and Dr. P. Rivaille for his gift of 10-26PreS₂ peptide. We thank Dr. A. Chabin for amino acid analysis.

LITERATURE CITED

- (1) Brack, A., and Trudelle, Y. (1985) Molecular weight determination of polypeptides from viscosity measurements. *Polym. Commun.* 26, 369-370.
- (2) Cheung, D. T., Tong, D., Perlman, N., Ertl, D., and Nimni, M. E. (1990) Mechanism of crosslinking of proteins by glutaraldehyde IV: in vitro and in vivo stability of a cross-linked collagen matrix. *Connect. Tissue Res.* 25, 27-34.
- (3) Dagan, S., Tzehoval, E., Fridkin, M., and Feldman, M. (1987) Tuftsin and tuftsin conjugates potentiate immunogenic processes: effects and possible mechanisms. *J. Biol. Response Modif.* 6, 625-636.
- (4) Duncan, R. J. S., Weston, P. D., and Wrigglesworth, R. (1983) A new reagent which may be used to introduce sulfhydryl groups into proteins, and its use in the preparation of conjugates for immunoassays. *Anal. Biochem.* 132, 68-73.
- (5) Ellman, G. L. (1959) Tissue sulfhydryl groups. *Arch. Biochem. Biophys.* 82, 70-77.
- (6) Fridkin, M., and Najjar, V. A. (1989) Tuftsin: its chemistry, biology and clinical potential. *Critical Reviews in Biochemistry and Molecular Biology* (G. D. Fasman, Ed.) Vol. 24, pp 1-40, CRC Press, Boca Rota, FL.
- (7) Herzenberg, L. A., Tokuhisa, T., and Herzenberg, L. A. (1980) Carrier-priming leads to hapten-specific suppression. *Nature* 285, 664-667.

- (8) Katz, D. H. (1980) Adaptive differentiation of lymphocytes. Theoretical implications for cell-cell recognition and regulation of immune response. *Adv. Immunol.* 29, 137-207.
- (9) Keller, O., and Rudinger, J. (1975) Preparation and some properties of maleimido acids and maleoyl derivatives of peptides. *Helv. Chim. Acta* 58, 531-541.
- (10) Milich, D. R., McLachlan, A., Chisari, F. V., and Thornton, G. B. (1986) Nonoverlapping T and B cell determinants on an hepatitis B surface antigen PreS₂ region synthetic peptide. *J. Exp. Med.* 164, 532-547.
- (11) Mitchison, N. A. (1971) The carrier effect in the secondary response to hapten-protein conjugates. I: Measurement of the effect with transferred cells and objections to the local environment hypothesis. *Eur. J. Immunol.* 1, 10-18.
- (12) Monsan, P., Puzo, G., and Mazarguil, H. (1975) *Biochimie* 57, 1281-1292.
- (13) Moroder, L., Nyfeler, R., Gemeiner, M., Kalbacher, H., and Wünsch, E. (1983) Immunoassays of peptide hormones and their chemical aspects. *Biopolymers* 22, 481-486.
- (14) Naim, J. O., Hinshaw, J. R., and Van Oss, C. J. (1989) The lack of antigenicity of tuftsin: a naturally occurring phagocytosis stimulating tetrapeptide. *Immunol. Invest.* 18, 817-824.
- (15) Neurath, A. R., Kent, S. B. H., Strick, N., and Parker, K. (1988) Delineation of contiguous determinants essential for biological functions of the Pre-S sequence of the hepatitis B virus envelope protein: its antigenicity, immunogenicity and cell-receptor recognition. *Ann. Inst. Pasteur/Virol.* 139, 13-38.
- (16) Okuda, K., Urabe, I., Yamada, Y., and Okada, H. (1991) Reaction of glutaraldehyde with amino and thiol compounds. *J. Ferment. Bioeng.* 71, 100-105.
- (17) Peeters, J. M., Hazendonk, T. G., Beuvery, E. C., and Tesser, G. I. (1989) Comparison of four bifunctional reagents for coupling peptides to proteins and the effect of the three moieties on the immunogenicity of the conjugates. *J. Immunol. Methods* 120, 133-143.
- (18) Plaue, S., Muller, S., Briand, J. P., and Van Regenmortel, M. H. V. (1990) Recent advances in solid-phase peptide synthesis and preparation of antibodies to synthetic peptides. *Biologicals* 18, 147-157.
- (19) Sakata, S., and Atassi, M. Z. (1981) Immune recognition of serum albumin. XIII: Autoreactivity with rabbit serum albumin of rabbit antibodies against bovine and human serum albumins and autoimmune recognition of rabbit serum albumin. *Mol. Immunol.* 18 (12), 961-967.
- (20) Trudelle, Y., Brack, A., Delmas, A., Pedoussaut, S., and Rivaille, P. (1987) Synthesis of a new carrier for immunization: polytuftsin. *Int. J. Pept. Protein Res.* 30, 54-60.
- (21) Warren, H. S., and Chedid, L. A. (1988) Future prospects for vaccine adjuvants. *CRC Crit. Rev. Immunol.* 88, 83-101.

TECHNICAL NOTES

An Improved CPG Support for the Synthesis of 3'-Amine-Tailed Oligonucleotides

Charles R. Petrie,* Michael W. Reed, A. David Adams, and Rich B. Meyer, Jr.

MicroProbe Corporation, 1725 220th Street SE #104, Bothell, Washington 98021. Received August 27, 1991

A new controlled-pore glass (CPG) support is described that allows for the direct synthesis of oligonucleotides bearing a 3'-aminoethyl tail. This solid support (AH-CPG) exhibits superior performance as compared to a commercially available 3'-amine CPG. The AH-CPG is prepared from 6-aminoethanol-1-ol with a unique protecting group for the amine that also functions as the site of attachment to the CPG. A 3'-amine-tailed oligodeoxynucleotide (ODN) was prepared from this support using standard phosphoramidite coupling and deprotection conditions. The 3'-amine-tailed ODN was subsequently modified with an acridinylpropionic acid tetrafluorophenyl ester. Facile synthesis of the AH-CPG and the stability of the deprotected product makes this functionalized solid support especially useful for preparation of oligonucleotides bearing 3'-amine tails and other modifications.

Oligodeoxynucleotide (ODN) hybridization has become a powerful tool in genetic research, biomedical research, and clinical diagnostics (1). Typically, radiolabeled ODN probes are hybridized to a DNA or RNA sample that has been directly or indirectly immobilized on a solid support. Because of the inconveniences associated with radioisotopes (e.g. potential health hazards, disposal problems, and the inherent instability of many radioisotopes), efforts are being made to develop analogous nonisotopic labeled ODNs.

Modified ODNs are also finding widespread application in "antisense" and "antigene" therapeutics (2, 3). The modification of ODNs is useful for many reasons in this new field, such as inhibition of nuclease degradation, enhancement of cellular transport, and the incorporation of intercalators and other functional groups.

Methods for modification of ODNs have been reviewed (3, 4). Many of these methods utilize special phosphoramidite reagents during automated DNA synthesis. Phosphoramidites that incorporate primary amines into ODNs are now commercially available. ODNs modified with these reagents can be subsequently derivatized with enzymes, biotin, fluorophores, or other reporting groups. In addition, reagents have been described that can incorporate thiol (5), aldehyde (6), or carboxyl (6), groups on the 5'-terminus of an ODN. Recently, two novel controlled-pore glass (CPG) supports (7, 8) have been described that directly introduce an amine onto the 3'-terminus of an ODN.

In our ongoing programs on DNA probe diagnostics and antisense therapeutics we have required the selective introduction of a primary amine onto the 3'-termini of ODNs. We have previously reported (9) that the commercially available 3'-amine CPG (Amine-ON CPG, Clontech) described by Nelson et al. (7) gives unpredictable results. Recently, a seven-step synthesis of a solid support that introduces an aminoethyl tail on the 3'-terminus of an ODN was described (8). However, the report gives little experimental detail and only a brief description of its performance as a solid support for ODN synthesis.

We have now prepared a 3'-aminoethyl CPG (AH-CPG) that exhibits superior performance in comparison to the commercially available 3'-amine CPG and is more con-

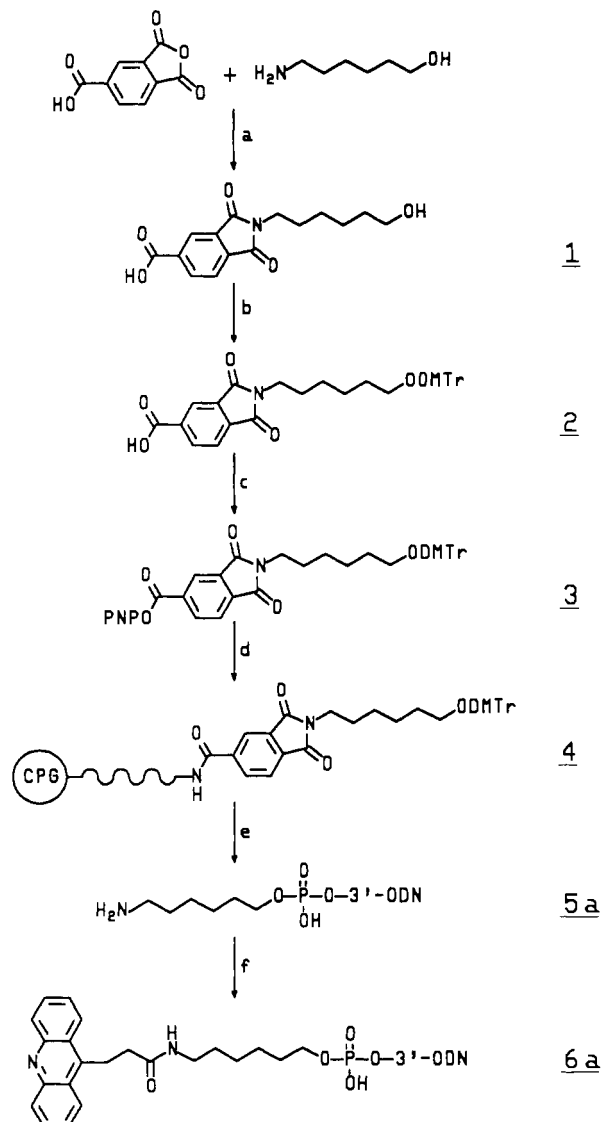
venient to synthesize (four steps, good yield) than the reported 3'-aminoethyl CPG (8).

The AH-CPG is prepared from 6-aminoethanol-1-ol with a unique protecting group for the amine that also functions as the site of attachment to the CPG. The AH-CPG is compatible with all protocols used on commercially available DNA synthesizers; however, removal of the 3'-amine-tailed ODN from the CPG is best accomplished off the instrument.

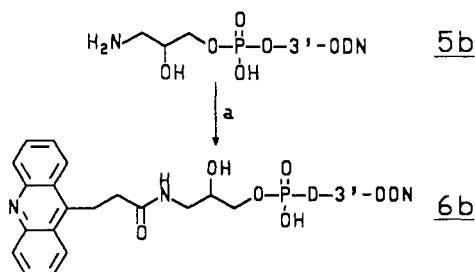
The synthesis of the AH-CPG is shown in Scheme I. Excess 6-amino-1-hexanol was treated with 1,2,4-benzenetricarboxylic anhydride to give phthalimide 1 in good yield. Following protection of the primary hydroxyl with a dimethoxytrityl group, the crude carboxylic acid (2) was converted to the p-nitrophenyl ester 3. Long chain alkylamine CPG (LCAA-CPG) was treated with 3 to give 3'-aminoethyl CPG 4. After capping with acetic anhydride, the dimethoxytrityl loading of the AH-CPG was determined to be 20 $\mu\text{mol/g}$.

An 11-mer ODN (5a) was synthesized using the AH-CPG and was compared to the same ODN (5b, Scheme II) prepared using the Clontech Amine-ON CPG. The functional performance of these 3'-amine tails was evaluated by derivatizing each with 2,3,5,6-tetrafluorophenyl (TFP) 3-(9-acridinyl)propionate (9). The 3'-amine-tailed ODN prepared from the AH-CPG appeared as a single distinct product by both polyacrylamide gel electrophoresis (PAGE) and reversed-phase HPLC (Figure 1, panel A). In addition, derivatization of this amine-tailed ODN proceeded rapidly to completion, giving a quantitative yield of the acridine-modified ODN (6a) without the need for HPLC purification (Figure 1, panel B). Chromatographically pure 6a was obtained by gel filtration of the crude extraction mixture (Figure 1, panel C).

In contrast, the 3'-amine-tailed ODN (5b, Scheme II) prepared from the Clontech Amine-ON CPG was not homogeneous and exhibited unusual behavior (9). Although, the ODN 5b appeared as a single peak by reversed-phase HPLC, PAGE indicated the presence of more than one compound. HPLC analysis of the reaction of 5b with TFP 3-(9-acridinyl)propionate indicated that conversion of 5b to 6b was incomplete even after 22 h. Reversed-phase HPLC purification was required for purification of

Scheme I.^a Synthesis of AH-CPG and 3'-Amine-Tailed ODN and Reaction of the 3'-Amine-Tailed ODN with TFP Acridinylpropionate

^a (a) fusion, 175–225 °C; (b) pyridine, Et₃N, DMTrCl; (c) (1) p-nitrophenyl chloroformate, Et₃N, CH₂Cl₂, (2) DMAP; (d) (1) LCAA-CPG, pyridine, Et₃N, (2) Ac₂O, pyridine; (e) automated DNA synthesis, NH₄OH deprotection; (f) TFP 3-(9-acridinyl)propionate, 0.1 M sodium borate (pH 8.3), 1-methyl-2-pyrrolidinone.

Scheme II.^a Synthesis of an Acridine-Modified ODN Using a 3'-Amine-Tailed ODN Prepared from Amine-ON CPG

^a (a) TFP 3-(9-acridinyl)propionate, 0.1 M sodium borate (pH 8.3), 1-methyl-2-pyrrolidinone.

6b in order to separate the mixture of ODN products and the isolated yield was only 14%. PAGE analysis suggested that the major product of ODN synthesis using the Amine-ON CPG does not possess a cationic tail, rendering this product unreactive with the active ester.

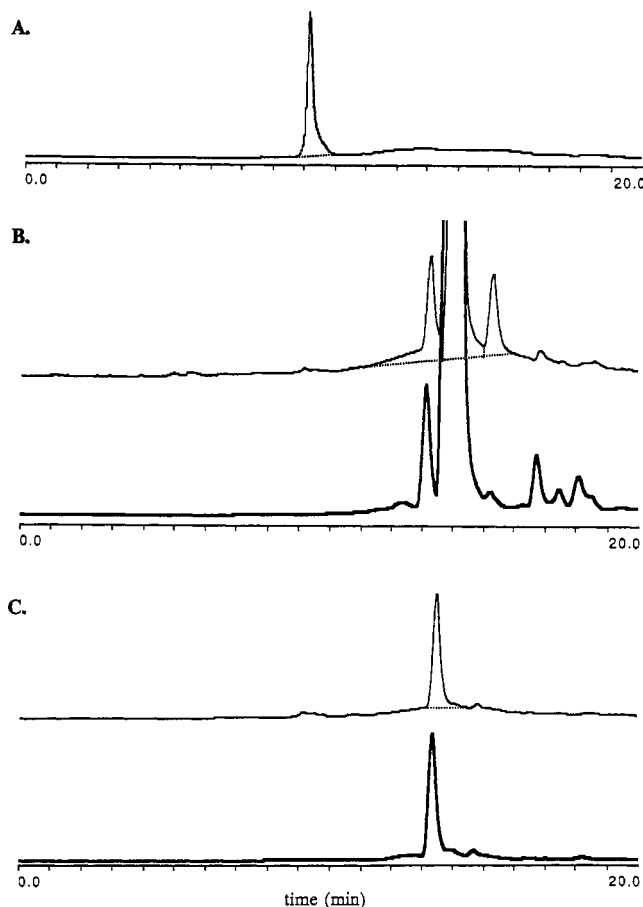


Figure 1. Reversed-phase HPLC chromatograms describing the reaction of ODN 5a with TFP acridinylpropionate. The HPLC system used a 300-Å, C-18 column (7.5 mm i.d. × 250 mm) and a 20 min gradient of 5–45% acetonitrile in 0.1 M triethylammonium acetate (pH 7.5) with a 2 mL/min flow rate. Detection was by UV absorbance at 260 nm; the lower trace (bold) is fluorescence detection. Panel A: 3'-hexylamine-tailed 11-mer ODN 5a. Panel B: reaction with acridine TFP ester after 1 h shows complete reaction of 5a (9-min peak) to the desired 3'-acridine ODN 6a (13-min peak). The peak at 14 min is acridinylpropionic acid. Panel C: 3'-acridine-tailed ODN 6a after purification by gel filtration.

EXPERIMENTAL PROCEDURES

Oligonucleotide synthesis was performed on either an ABI 380B or a Milligen-Bioscience 7500 DNA synthesizer. Amine-ON CPG columns were purchased from Clontech (Palo Alto, CA). Long chain alkylamine CPG (LCAA-CPG) was from Sigma Chem. Co. (St. Louis, MO). All reagents were purchased from Aldrich Chemical Co., unless otherwise indicated. Removal of solvents at 15–30 Torr was accomplished on a rotary evaporator at <30 °C. Melting points were determined in an open glass capillary tube using a Mel-Temp melting point apparatus and are uncorrected. UV spectra were obtained with a Beckman DU-40 spectrophotometer using 0.1-mL quartz cuvettes. Proton magnetic resonance spectra were recorded using a Varian Gemini FT-200 (200 MHz) spectrometer. Appropriate solvent resonances were consistently used as internal references. All chemical shifts are reported in ppm downfield from tetramethylsilane. Elemental analyses were performed by Quantitative Technologies, Inc. (Bound Brook, NJ). Flash chromatography was performed with EM Science silica gel 60 (230–400 mesh). Analytical thin-layer chromatography was carried out on EM Science F₂₅₄ aluminum-backed, fluorescence-indicator plates. Detection of components on TLC was by UV light and 10% H₂SO₄ in MeOH with heating. Unless otherwise stated,

yields refer to isolated compounds of greater than 95% purity, as determined by ^1H NMR spectroscopy.

1,3-Dihydro-1,3-dioxo-2-(6-hydroxyhex-1-yl)isoin-dole-5-carboxylic Acid (1). A mixture of 6-aminohe-xan-1-ol (11.7 g, 10 mmol) and 1,2,4-benzenetricarboxylic anhydride (7.68 g, 4 mmol) was heated to 175–225 °C until evolution of H_2O vapor stopped (~15 min). The melt was poured into water to give a white crystalline solid. The solid was collected by vacuum filtration and dried overnight in vacuo to give 9.1 g (78%) of analytically pure 1: mp 127–135 °C; ^1H NMR ($\text{DMSO}-d_6$) δ 8.34 (1 H, d, H-7[6]), 8.21 (1 H, s, H-4), 7.97 (1 H, d, H-6[7]), 3.58 (2 H, t, H-1'[6']), 3.36 (2 H, t, H-6'[1']), 1.7–1.2 (8 H, m, H-2',3',4',5'). Anal. Calcd for $\text{C}_{15}\text{H}_{17}\text{N}_1\text{O}_5$: C, 61.85; H, 5.88; N, 4.81. Found: C, 61.56; H, 6.12; N, 4.98.

1,3-Dihydro-1,3-dioxo-2-[6-[bis(4-methoxyphenyl)-phenylmethoxy]hex-1-yl]isoin-dole-5-carboxylic Acid (2). To a solution of 1 (2.91 g, 10 mmol) in pyridine (50 mL) and triethylamine (1.9 mL) was added dimethoxy-trityl chloride (7.11 g, 20 mmol) and 4-(dimethylamino)-pyridine (63 mg). The solution was stirred overnight and then evaporated to dryness. The residue was dissolved in CH_2Cl_2 (100 mL). The resulting solution was washed with ice-cold 1 M citric acid (100 mL) and with H_2O (100 mL), dried over Na_2SO_4 , and then evaporated to a stiff syrup. The yellow syrup was used in the next step without further purification: TLC, $\text{CH}_2\text{Cl}_2/\text{MeOH}$ (9:1), $R_f = 0.5$, develops orange color when sprayed with 10% H_2SO_4 in MeOH and then chars when heated.

p-Nitrophenyl 1,3-Dihydro-1,3-dioxo-2-[6-[bis(4-methoxyphenyl)phenylmethoxy]hex-1-yl]isoin-dole-5-carboxylate (3). To a mixture of 2 (2.4 g, 4 mmol) in CH_2Cl_2 was added triethylamine (405 mg, 4 mmol). After cooling of the solution in an ice/water bath, freshly sublimed p-nitrophenyl chloroformate (806 mg, 4 mmol) was added and the solution stirred for 5 h at 4 °C. 4-(Dimethylamino)pyridine (50 mg) was added and then the solution was allowed to warm to ambient temperature. After stirring overnight at ambient temperature, the solution was repeatedly extracted with saturated NaHCO_3 (5 \times 100 mL) and then once with ice-cold 1 M citric acid. The organic phase was dried over Na_2SO_4 and evaporated to dryness. The residue was flash chromatographed on a silica gel column (29 \times 150 mm) using toluene/EtOAc (5:1) as the eluent. Fractions containing pure material were pooled and evaporated to dryness to give 1.7 g (60%) of analytically pure 3 as a pale yellow foam: TLC, toluene/ethyl acetate (5:1), $R_f = 0.75$, develops yellow color when sprayed with 0.1 N NaOH, orange color when sprayed with 10% H_2SO_4 in MeOH, and then chars when heated; ^1H NMR (CDCl_3) δ 8.7–6.8 (20 H, m, aromatic H), 3.80 (6 H, s, 2 OCH_3), 3.79–3.61 (4 H, 2 t, H-6',1'), 1.8–1.2 (8 H, m, H-2',3',4',5'). Anal. Calcd for $\text{C}_{42}\text{H}_{38}\text{N}_2\text{O}_9$: C, 70.58; H, 5.36; N, 3.92. Found: C, 70.57; H, 5.22; N, 3.84.

Preparation of the 3'-Amine CPG Support (4). Long chain alkylamine CPG (1 g) was treated with a solution of 3 (143 mg, 0.2 mmol) in pyridine (10 mL) and Et_3N (1 mL). The reaction mixture was gently agitated for 24 h. The CPG was filtered and washed with pyridine (50 mL) and then with acetonitrile (50 mL). The remaining amines were capped by treating with acetic anhydride (0.5 mL) in pyridine (10 mL) and gently agitating for 24 h. The AH-CPG was filtered, washed with pyridine (1 \times 5 mL), washed with acetonitrile (3 \times 5 mL), and air-dried. The AH-CPG was then dried in vacuo for 2 days at ambient temperature. Analysis of the AH-CPG by treatment with perchloric acid indicated a dimethoxytrityl loading of 20 $\mu\text{mol/g}$ (10). The AH-CPG (50 mg, 1 μmol) was packed into standard 1- μmol synthesizer columns.

Preparation of ODNs Using the 3'-Amine CPG Supports. 3'-Amine-tailed ODNs 5a and 5b (9) with the base sequence 5'-TCCATGTTTCGTA were synthesized and purified as previously described (9) using 1- μmol columns of either the AH-CPG (4) or the Clontech Amine-ON CPG. Isolated yields were 1.39 and 1.45 mg, respectively, for an 11-mer as determined by UV absorbance at 260 nm (11). ODN purity was determined by reversed-phase HPLC and PAGE.

Preparation of Acridine-Modified ODNs. The acridine-derivatized ODN 6a was prepared from HPLC-purified 5a (100 μg , 29 nmol) by the method previously described for the preparation of 6b from 5b (9). Purification of the acridine-modified ODN 6a was accomplished by gel filtration through a prepacked column containing Sephadex G-25 (NAP-25 column, Pharmacia). After equilibration of the column with 25 mL of water, the crude reaction mixture was applied to the top of the column and the product was eluted with water (0.5-mL fractions). The fractions containing pure product (as evidenced by reversed-phase HPLC) were combined and concentrated on a Speed-Vac. The pale yellow solid residue was reconstituted with 200 μL of water and analyzed by UV at 260 nm. The concentration was determined to be 108 $\mu\text{g}/200 \mu\text{L}$ (100% yield).

ACKNOWLEDGMENT

The competent technical assistance of Dina Furin is greatly appreciated. We also thank John Tabone and Debra Leith for helpful discussions. We thank NeoRx Corp. for use of the NMR spectrometer. This research was supported by grants from the National Institutes of Health (R43 GM46143-01 and R44 CA45905) and the Department of Defense (DAMD 17-88-C-8201).

LITERATURE CITED

- (1) *Nucleic Acid Probes*. (R. H. Symons, Ed.) CRC Press, Inc., Boca Raton, FL.
- (2) Cohen, J. (1989) *Oligodeoxynucleotides, Antisense Inhibitors of Gene Expression*, Macmillan Press, London.
- (3) Uhlmann, E., and Peyman, A. (1990) Antisense oligonucleotides: a new therapeutic principle. *Chem. Rev.* 90, 543.
- (4) Goodchild, J. (1990) Conjugates of oligonucleotides and modified oligonucleotides: a review of their synthesis and properties. *Bioconjugate Chem.* 1, 165.
- (5) Connolly, B. A., and Rider, P. (1985) Chemical synthesis of oligonucleotides containing a free sulphhydryl group and subsequent attachment of thiol specific probes. *Nucleic Acid Res.* 13, 4485–4502.
- (6) Kremsky, J. N., Wooters, J. L., Dougherty, J. P., Meyers, R. E., Collins, M., and Brown, E. L. (1987) Immobilization of DNA via oligonucleotides containing an aldehyde or carboxylic acid group at the 5' terminus. *Nucleic Acids Res.* 15, 2891–2909.
- (7) Nelson, P. S., Frye, R. A., and Liu, E. (1989) Bifunctional oligonucleotide probes synthesized using a novel CPG support are able to detect single base pair mutations. *Nucleic Acids Res.* 17, 7187.
- (8) Asseline, U., and Thuong, N. T. (1990) New solid-phase for automated synthesis of oligonucleotides containing an amino-alkyl linker at their 3' end. *Tetrahedron Lett.* 31, 81–84.
- (9) Reed, M. W., Adams, A. D., Nelson, J. S., and Meyer, R. B. (1991) Acridine- and Cholesterol-Derivatized Solid Supports for Improved Synthesis of 3'-Modified Oligonucleotides. *Bioconjugate Chem.* 2, 217–225.
- (10) Atkinson, T., and Smith, M. (1984) Solid-phase synthesis of oligodeoxyribonucleotides by the phosphite-triester method. In *Oligonucleotide Synthesis, A Practical Approach* (M. Gait, Ed.) pp 35–81, IRL Press, Washington, DC.
- (11) Cantor, C. R., Warshaw, M. M., and Shapiro, H. (1970) Oligonucleotide interactions. III. Circular dichroism studies of the conformation of deoxyoligonucleotides. *Biopolymers* 9, 1059.

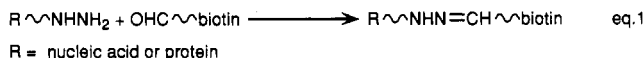
Synthesis of *N*-[6-(Ethylenedioxy)hexyl]biotinamide: A Biotinyl Aldehyde Precursor for Labeling Hydrazine-Modified Biomolecules

Gary F. Musso,[†] Gerard R. Scarlato,[‡] and Soumitra S. Ghosh^{*,§}

SISKA Diagnostics, Inc., and The Salk Institute Biotechnology/Industrial Associates, Inc., P.O. Box 85200, San Diego, California 92138. Received September 10, 1991

Synthetic approaches for obtaining biotinyl aldehydes are described. While such aldehydes have limited shelf life, the acetal derivative, *N*-[6-(ethylenedioxy)hexyl]biotinamide, IX, was found to be indefinitely stable upon storage at -20 °C. Mild acid hydrolysis conveniently unmasks the aldehyde, which can then be used to label hydrazine-tagged biomolecules.

The high affinity (10^{-15} M⁻¹) between the glycoprotein avidin and biotin has been exploited for a wide variety of bioanalytical applications such as affinity chromatography, localization, immunodiagnosics, and detection of nucleic acids (1). A key feature of the avidin-biotin technology requires the prior covalent modification of the biological probe or matrix with biotinylated derivatives. Thus, a number of biotinylating reagents have been reported, which include biotinyl-*p*-nitrophenyl and biotin *N*-hydroxysuccinimide esters (2), biotin and biocytin hydrazides (3, 4), photobiotin (5), and 3-(*N*-maleimidopropionyl)biocytin (6). We were interested in diagnostic approaches which entailed functionalizing biomolecules, such as proteins (7) and nucleic acids (8), with hydrazine groups. In order to take advantage of the facile hydrazone-forming ability of hydrazines with aldehydes and ketones (eq 1) and the high yields of hydrazone formation (7), we



have developed synthetic pathways to biotin analogues which contain aldehyde groups linked to the hapten via appropriate alkyl spacers.

Our initial approach, as depicted in Scheme I, focused on the condensation of 6-amino-1-hexanol, I, with biotin *N*-hydroxysuccinimide ester, followed by selective oxidation of the primary alcohol to the aldehyde. While the acylation reaction in dimethylformamide (DMF)¹ proceeded in 93% yield, conversion to the aldehyde using the "activated" dimethyl sulfoxide method (9) or pyridinium chlorochromate (PCC) (10) was unsuccessful. However, treatment of alcohol derivative II with pyridinium dichromate (PDC) (11) in methylene chloride or DMF provided aldehyde III in 15% yield. A promising alternate method for synthesizing biotinyl aldehydes was the reaction of biotin hydrazide, IV (3), with an excess of dialdehyde such as glutaraldehyde or 1,10-decanedialdehyde,² wherein the desired aldehydes, V, were isolated in 65% and 70% yields, respectively (Scheme I). Unfortunately, the aldehyde derivatives prepared by either route

decomposed with time, even when stored at -20 °C under an inert atmosphere.

Since the aldehyde derivatives were unstable, a biotinyl acetal derivative was considered to be a more practical target molecule. The acetal was expected to have an extended shelf life and be readily converted to the aldehyde upon exposure to mild acidic conditions. Scheme II depicts the reaction scheme for the synthesis of this biotin aldehyde precursor. Selective trifluoroacetylation of 6-amino-1-hexanol, I, with *S*-ethyl trifluorothioacetate (12) provided the amide (13) in 79% yield. Oxidation of this intermediate with PDC furnished 6-(trifluoroacetamido)-1-hexanol, VI (14), in 70% yield. Protection of the aldehyde was achieved using the Noyori procedure (15) to afford acetal VII, in 77% yield. The trifluoroacetyl protecting group of VII was then removed either by treatment with 10% piperidine in water or by potassium carbonate in aqueous methanol. The resulting amine, VIII, was treated with biotin *N*-hydroxysuccinimide ester in the presence of an equimolar amount of 4-(*N,N*-dimethylamino)pyridine to afford the desired biotinyl acetal derivative, IX, in 50% yield.

As anticipated, biotinyl acetal derivative IX is indefinitely stable when stored at -20 °C. When required, the acetal can be quantitatively hydrolyzed to biotinyl aldehyde III upon treatment with 80% aqueous acetic acid for 3 h at 37 °C. The lyophilized aldehyde reacts rapidly to form stable hydrazones with (2,4-dinitrophenyl)hydrazine, 5'-oligonucleotide hydrazide derivatives (16), and long nucleic acids transaminated with hydrazine/bisulfite treatment (17). In view of the specificity of its reactions, this biotinylating reagent should find utility for attaching the hapten to a variety of hydrazine-functionalized biomolecules and polymeric supports.

EXPERIMENTAL PROCEDURES

All solvents were freshly distilled over argon. ¹H NMR and IR spectra were recorded on a 360-MHz Nicolet NMR spectrometer and a Mattson Cygnus 25 FTIR spectrometer, respectively. Chemical shifts are given in ppm relative to tetramethylsilane. High-resolution mass spectra were obtained using a VG analytical 70-250 EHF-GC/MS/DS spectrometer. Elemental analyses were performed by Galbraith Laboratories, Knoxville, TN. Melting points were determined on a Thomas Hoover capillary melting point apparatus and are uncorrected. Thin-layer chromatography was performed on silica gel precoated (0.25-mm thickness) glass plates (Merck).

6-(Trifluoroacetamido)-1-hexanol. To 4.0 g (34.2 mmol) of 6-amino-1-hexanol in 20 mL of 0.05 M sodium bicarbonate, pH 10, was added 5.8 mL (45.3 mmol) of

* To whom correspondence should be addressed.

[†] Alkermes, Inc., Cambridge, MA 02139.

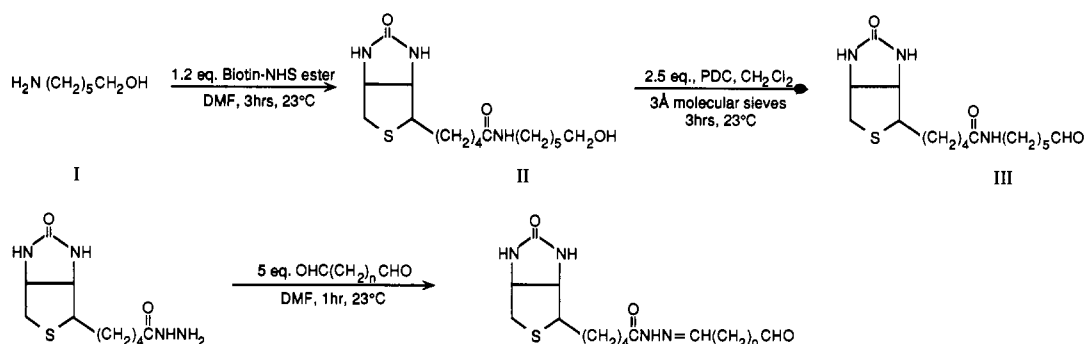
[‡] Gensia Pharmaceuticals, Inc., San Diego, CA 92121.

[§] Baxter Diagnostics, Inc., Life Sciences Research Laboratory, P.O. Box 910492, San Diego, CA 92191-0492.

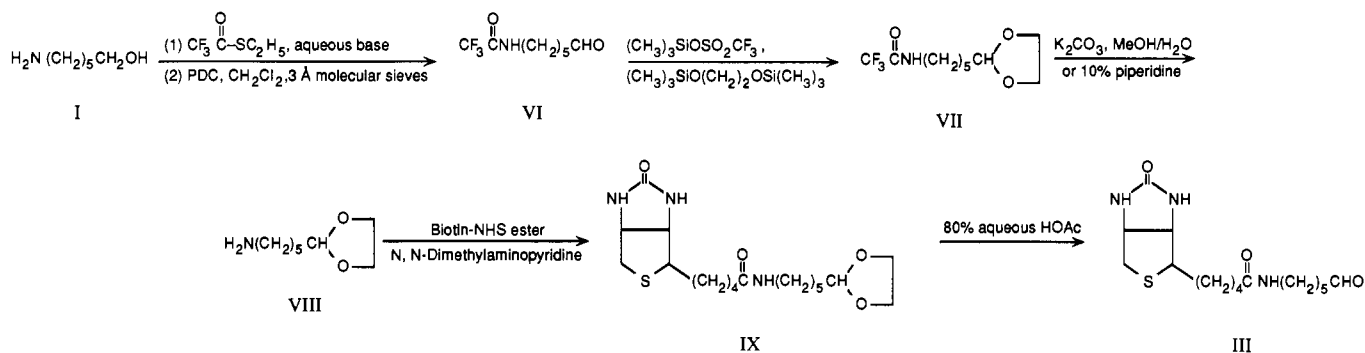
¹Abbreviations: dimethylformamide, DMF; pyridinium chlorochromate, PCC; pyridinium dichromate, PDC.

²1,10-Decanedialdehyde was prepared by oxidation of 1,10-decanediol with PDC in methylene chloride in 58% yield.

Scheme I



Scheme II



S-ethyl trifluorothioacetate with stirring at 23 °C. The pH was maintained between 9.5 and 10.0 with 1 N NaOH, and after 3 h, the aqueous solution was extracted with five 50-mL volumes of chloroform. The chloroform solution was dried over anhydrous MgSO₄ and concentrated under reduced pressure. Recrystallization from chloroform afforded 5.6 g (77 %) of 6-(trifluoroacetamido)-1-hexanol. Mp: 51–52 °C (lit. (13) mp: 52–53 °C). ¹H NMR (CDCl₃): δ 9.39 (s, 1 H), 4.34 (t, 1 H), 3.34 (m, 3 H), 3.17 (br s, 1 H), 1.55–1.2 (m, 8 H). IR: 1706 cm⁻¹.

6-(Trifluoroacetamido)-1-hexanol (VI). To 2.1 g (9.9 mmol) of 6-(trifluoroacetamido)-1-hexanol in 40 mL of methylene chloride was added 4.0 g (10.6 mmol) of PDC and 4.4 g of 3-Å molecular sieves, and the reaction mixture was stirred for 3 h at 23 °C. After addition of 250 mL of ethyl acetate, the reaction mixture was filtered through a small bed of silica gel 60 and concentrated in vacuo. Flash chromatography using 50% ethyl acetate in hexane afforded 1.5 g (71 %) of **VI** as an oil [TLC, ethyl acetate–hexane (1:1), *R_f* 0.5]. ¹H NMR (CDCl₃): δ 9.8 (s, 1 H), 7.5 (br s, 1 H), 3.32 (m, 2 H), 2.54 (t, 2 H), 1.7 (m, 4 H), 1.4 (m, 2 H). IR: 1729, 1709 cm⁻¹.

N-[6-(Ethylenedioxy)-1-hexyl]trifluoroacetamide (VII). To 1.4 g (6.6 mmol) of **VI** in 21 mL of methylene chloride under nitrogen at –78 °C was added 1.8 mL (7.5 mmol) of 1,2-bis(trimethylsiloxy)ethane and 140 μL (0.7 mmol) of trimethylsilyl trifluoromethanesulfonate. The solution was stirred for 3 h at –78 °C, followed by another 0.5 h at 23 °C. The reaction mixture was taken up in 100 mL of methylene chloride and washed with 30 mL of saturated NaHCO₃. The aqueous layer was extracted with 50 mL of methylene chloride, and the organic layers were combined, dried over MgSO₄, and concentrated. The crude product was purified by flash chromatography using 50% ethyl acetate in hexane to afford 1.3 g (77 %) of **VII** as an oil [TLC, ethyl acetate–hexane (2:8), *R_f* 0.2]. ¹H NMR (CDCl₃): δ 9.39 (s, 1 H), 4.75 (t, 1 H), 3.79 (m, 4 H), 3.16 (m, 2 H), 1.51 (m, 4 H), 1.31 (m, 4 H). Anal. Calcd for C₁₀H₁₆O₃NF₃: C, 47.06; H, 6.27; N, 5.49. Found: C, 46.6; H, 6.14; N, 6.01.

6-(Ethylenedioxy)-1-hexylamine (VIII). To 380 mg (1.5 mmol) of **VII** in 7.5 mL of 20% water in methanol was added 0.3 g (2.2 mmol) of potassium carbonate, and the mixture was stirred for 14 h at 23 °C. After concentration of the reaction mixture, the residue was taken up in 15 mL of brine and extracted with four 50-mL volumes of diethyl ether, followed by another four 50-mL volumes of chloroform. The organic layers were dried over anhydrous MgSO₄, combined, and concentrated to give 190 mg (80 %) of the product as an oil. Alternately, the same conversion can be carried out in quantitative yield by treating **VII** with 10% piperidine in water for 45 min at 23 °C, followed by lyophilization. ¹H NMR (CDCl₃): δ 4.74 (t, 1 H), 3.83 (m, 4 H), 3.16 (br s, 2 H), 1.50–1.21 (m, 8 H).

N-[6-(Ethylenedioxy)hexyl]biotinamide (IX). A mixture of 90 mg (264 μmol) of biotin *N*-hydroxysuccinimide ester, 32 mg (262 μmol) of 4-(*N,N*-dimethylamino)pyridine, and 50 mg (315 μmol) of **VIII** in 4 mL of dry dimethylformamide was stirred for 14 h at 23 °C. Concentration of the solution under vacuo, followed by medium-pressure liquid chromatography on a Lobar Si 60 column (Merck, Darmstadt, West Germany), provided 50 mg of **IX** as an oil in 50% yield [TLC, methanol–chloroform (1:9), *R_f* 0.4]. ¹H NMR (DMSO-*d*₆): δ 7.73 (t, 1 H), 6.42 (s, 1 H), 6.35 (s, 1 H), 4.74 (t, 1 H), 4.3 (m, 1 H), 4.13 (m, 1 H), 3.71–3.89 (m, 4 H), 2.79 (dd, 1 H), 2.04 (t, 2 H), 1.49 (m, 6 H), 1.29 (m, 8 H). High-resolution mass spectrum calcd for C₁₈H₃₁O₄N₃S 385.2035, found 385.2039. Anal. Calcd for C₁₈H₃₁O₄N₃S: C, 56.08; H, 8.10; N, 10.90. Found: C, 55.78; H, 8.09; N, 10.72.

ACKNOWLEDGMENT

We wish to thank Dr. J. Vaughn of Rockefeller University for NMR spectra and Mr. B. Williams of the University of Chicago for high-resolution mass spectra.

LITERATURE CITED

- (1) Wilchek, M., and Bayer, E. A. (1988) The avidin-biotin complex in bioanalytical applications. *Anal. Biochem.* 171, 1–32.

- (2) Becker, J. M., Wilchek, M., and Katchalski, E. (1971) Irreversible inhibition of biotin transport in yeast by biotinyl-*p*-nitrophenyl ester. *Proc. Natl. Acad. Sci., U.S.A.* 68, 2604–2607.
- (3) Bayer, E. A., and Wilchek, M. (1980) The use of avidin-biotin complex as a tool in molecular biology. *Methods Biochem. Anal.* 26, 1–45.
- (4) Bayer, E. A., Ben-Hur, H., and Wilchek, M. (1988) Biotin hydrazide—a selective label for sialic acids, galactose and sugars in glycoconjugates using avidin-biotin technology. *Anal. Biochem.* 170, 271–281.
- (5) Forster, A. C., McInnes, J. L., Skingle, D. C., and Symons, R. H. (1985) Non-radioactive hybridization probes prepared by the chemical labelling of DNA and RNA with a novel reagent, photobiotin. *Nucleic Acids Res.* 13, 745–761.
- (6) Bayer, E. A., Zalis, M. G., and Wilchek, M. (1985) 3-(*N*-Maleimidopropionyl)biotin: a versatile thiol-specific biotinylating reagent. *Anal. Biochem.* 149, 529–536.
- (7) King, T. P., Zhao, S. W., and Lam, T. (1986) Preparation of protein conjugates via intermolecular hydrazone linkage. *Biochemistry* 25, 5774–5779.
- (8) Hayatsu, H. (1986) Reaction of cytidine with semicarbazide in the presence of bisulfite. A rapid modification specific for single-stranded polynucleotide. *Biochemistry* 15, 2677–2682.
- (9) Omura, K., and Swern, D. (1978) Oxidation of alcohols by “activated” dimethyl sulfoxide. A preparative, steric and mechanistic study. *Tetrahedron* 34, 1651–1660.
- (10) Corey, E. J., and Suggs, W. (1975) Pyridinium chloroformate. An efficient reagent for oxidation of primary and secondary alcohols to carbonyl compounds. *Tetrahedron Lett.* 2647–2650.
- (11) Corey, E. J., and Schmidt, G. (1979) Useful procedures for the oxidation of alcohols involving pyridinium dichromate in aprotic media. *Tetrahedron Lett.* 2647–2650.
- (12) Goldberger, R. F. (1967) Trifluoroacetylation of ϵ -amino groups. *Methods Enzymol.* 11, 317–323.
- (13) Connolly, D. T., Roseman, S., and Lee, Y. C. (1980) Preparation of anomeric pairs of 1-thioglycosides: Use of anomericization catalyzed by boron trifluoride. *Carbohydr. Res.* 87, 227–239.
- (14) Bartlett, D. L., King, C-H. R., and Poulter, C. D. (1985) Purification of farnesyl pyrophosphate synthetase by affinity chromatography. *Methods Enzymology* 110 (Pt. A), 171–184.
- (15) Tsunoda, T., Suzuki, M., and Noyori, R. (1980) A facile procedure for acetalization under aprotic conditions. *Tetrahedron Lett.* 1357–1358.
- (16) Ghosh, S. S., Kao, P. M., and Kwok, D. Y. (1989) Synthesis of 5'-oligonucleotide hydrazide derivatives and their use in preparation of enzyme-nucleic acid hybridization probes. *Anal. Biochem.* 178, 43–51.
- (17) Musso, G. F., Ghosh, S. S., Orgel, L. E., Wahl, G. M., and Kaiser, E. T. (1989) Compounds for tagging nucleic acid probes. United States Patent 4,833,251.

Registry No. I, 4048-33-3; II, 106451-92-7; III, 124884-09-9; IV, 66640-86-6; V ($n = 3$), 138008-88-5; V ($n = 8$), 124884-11-3; VI, 97228-89-2; VII, 124884-02-2; VIII, 124883-96-1; IX, 124884-03-3; S-ethyl trifluorothioacetate, 383-64-2; 6-(trifluoroacetamido)-1-hexanol, 40248-34-8; biotin *N*-hydroxysuccinimide ester, 35013-72-0; glutaraldehyde, 111-30-8; 1,10-decanedialdehyde, 45037-67-0.

Bioconjugate Chemistry

MARCH/APRIL 1992
Volume 3, Number 2

© Copyright 1992 by the American Chemical Society

REVIEW

Radiolabeling of Monoclonal Antibodies and Fragments with Technetium and Rhenium

Gary L. Griffiths,*† David M. Goldenberg,‡ Anastasia L. Jones,† and Hans J. Hansen†

Immunomedics, Inc., Warren, New Jersey 07059, and Center for Molecular Medicine and Immunology and Garden State Cancer Center, Newark, New Jersey 07103. Received October 23, 1991

INTRODUCTION

The use of radiolabeled monoclonal antibodies (mAbs)¹ and mAb fragments in the radioimmunodetection (RAID) of cancer with ¹³¹I, ¹¹¹In, and ¹²³I has been described (1–9). More recently, however, increased effort has been made to label these reagents with ^{99m}Tc. Indeed, successful clinical application of commercial monoclonal antibody imaging products will probably be dependent on the development of simple, inexpensive methods to label antibody and/or antibody fragments with this radionuclide. When compared with other radionuclides used to label mAbs, ^{99m}Tc has the following advantages: low cost, ready availability, ideal nuclear properties for γ cameras, and reduced patient radiation exposures per millicurie of radionuclide administered. Strategies employed by different investigators to label antibodies and antibody fragments with ^{99m}Tc fall into two major categories. In one approach, efforts have been made to use a ligand to attach ^{99m}Tc indirectly to the antibody. The second approach has been to bind the radionuclide directly to reduced disulfide on the protein backbone of the antibody molecule. Both approaches are theoretically capable of extension to isotopes of rhenium.

In this review we discuss the following topics: (1) a brief overview of the chemistry of technetium and rhenium, (2) the chemistry involved in the ^{99m}Tc labeling of ligands, (3)

the progress made in the development of ^{99m}Tc-labeled antibody and antibody fragments using direct labeling methods, and (4) the extension of the direct labeling approach to rhenium isotopes for use in radioimmunotherapy (RAIT).

CHEMISTRY OF TECHNETIUM AND RHENIUM

^{99m}Tc has a 6-h half-life and upon decay emits a single photon with a γ energy of 140 keV. It is produced from the parent radionuclide, ⁹⁹Mo, a fission product with a half-life of 2.78 days. The availability of ^{99m}Tc to most hospitals and research scientists was made possible by the development of a simple ⁹⁹Mo–^{99m}Tc generator (10). In this generator, molybdate is adsorbed to a column of alumina and ^{99m}Tc is formed by decay of ⁹⁹Mo. The ^{99m}Tc, in the form of ^{99m}TcO₄, is eluted from the column with saline. The column is enclosed in a lead shield that contains ports for introduction of saline onto the top of the column and collection of the ^{99m}Tc-containing eluent from the bottom of the alumina column. In practice, a vial of sterile saline can be attached onto a syringe needle at the top of the generator and when an evacuated vial is attached to the outlet port the saline is drawn through the generator, eluting the ^{99m}Tc. These generators have an effective life of 2 weeks before the ⁹⁹Mo in the column has decayed too far to be useful.

^{99m}Tc produced by the generator is never carrier-free. Fifteen percent of ⁹⁹Mo decays directly to the extremely long-lived isotope ⁹⁹Tc ($t_{1/2} = 2.13 \times 10^5$ y), which is also the single decay product of ^{99m}Tc. The two isotopes have identical chemical properties (11). The specific activity of eluted ^{99m}Tc is dependent upon the time between generator elutions, because the longer the time between elutions the more ^{99m}Tc decays to ⁹⁹Tc. The mole fraction of the metastable isomer (^{99m}Tc) present in the eluted Tc varies from 0.836, at 0.5 h postelution, to 0.277, at 24 h postelution, and to 0.077, at 72 h postelution (11).

* To whom correspondence should be addressed at Immunomedics, Inc., 5 Bruce Street, Newark, NJ 07103.

† Immunomedics, Inc.

‡ Center for Molecular Medicine and Immunology and Garden State Cancer Center.

¹ Abbreviations used: CSAP, colon-specific antigen p; DTPA, diethylenetriaminepentaacetic acid; Fc, crystallizable fragment; HPLC, high-performance liquid chromatography; IgG, immunoglobulin G; ITLC, instant thin-layer chromatography; mAb, monoclonal antibody.

As discussed above, the products eluted from the generator are the pertechnetate anions, $^{99m}\text{TcO}_4^-$ and $^{99}\text{TcO}_4^-$, which have a negative charge of one. No effective chemistry exists that can be used to attach the negatively charged pertechnetate ions to small molecules (ligands) or proteins. Reduction of pertechnetate to a lower oxidation state results in the formation of highly reactive forms that complex to many compounds, such as DTPA and albumin. Because of its nearly optimal redox properties, stannous chloride has proven to be the most effective reducing agent, and with few exceptions, most commercial kits employ stannous chloride to reduce pertechnetate (12). Preparation and use of stannous chloride is not a trivial task. Because conversion of stannous chloride to stannic chloride occurs rapidly, it must be prepared just prior to use, which involves dissolving tin in hydrochloric acid under nonoxidizing conditions. This acid solution can be stored for a period of several hours in an inert atmosphere. Upon adjustment of this solution to physiologic pH, the formation of insoluble tin oxide occurs. This is minimized by use of a chelating ligand, such as citrate or tartrate. Despite the formidable problems of preparing and stabilizing stannous ions, Eckelman and co-workers succeeded in developing stannous ion-containing kits and stabilizing them by lyophilization (13). This has resulted in the formulation of "instant-use" pharmaceutical imaging agents that require only the addition of pertechnetate and mixing, prior to injection.

Most of the ^{99m}Tc kits now used in nuclear medicine can be classified into one of two types: those in which reduced pertechnetate is complexed to a small ligand and those in which reduced pertechnetate is directly complexed into a macromolecule (protein or colloid). An example of the latter is ^{99m}Tc -human serum albumin, directly labeled by adding the protein to a vial containing stannous chloride and [^{99m}Tc]pertechnetate (14). Examples of small ligands employed in kits are DTPA and 2,3-mercaptosuccinic acid (used for imaging of kidneys), gluceptate (used for imaging brain and kidneys), methylenediphosphonate (used for bone imaging), and iminodiacetic acid (used to image the hepatobiliary tree) (12).

As mentioned above, for the past decade attempts have been made to label antibodies with ^{99m}Tc , first by direct labeling of the antibody by the addition of reduced [^{99m}Tc]pertechnetate to the antibody (15) and, secondly, through the use of a bifunctional chelate of DTPA (16). More recently, sulfur-containing chelates have been used to bind reduced [^{99m}Tc]pertechnetate to antibody and antibody fragments; dimercaptide analogue tetradentate chelating agents, developed by Fritzberg et al., and bis-thiosemicarbazone analogues, developed by Hosotani et al., are examples of these new chelates (17, 18). Each will be discussed later in this review.

Rhenium chemistry is very similar to technetium chemistry due to the periodic relationship of the two elements (19, 20). It, too, forms a stable anionic species, the perrhenate ion, ReO_4^- , and will not bind to organic ligands without reduction to a lower oxidation state. Fortunately, there are two isotopes of rhenium which may be considered as candidates for RAIT. Rhenium-186 decays with a half-life of 3.68 days with an E_{max} of 1.07 MeV and has a γ component at 137 keV (9% abundance) which should allow imaging during therapy. Rhenium-188 also has an imagable γ -ray at 155 keV (15% abundance) and an intense β emission, E_{max} 2.12 MeV. It has a 16.98 h half-life. Rhenium-186 is produced by neutron irradiation of rhenium-185 targets and can be prepared with specific activities ranging up to 5 mCi/mg of rhenium when

using natural rhenium (37.4% ^{185}Re) targets. The specific activity achievable is dependent upon the flux of the neutron beam used for the irradiation. Rhenium-188 is produced by double neutron capture on a tungsten-186 target to produce tungsten-188. Tungsten-188 decays with a 69-day half-life to rhenium-188, which in turn decays to stable osmium-188. Taking advantage of the chemical differences between tungsten and rhenium has led to the development of generator systems along similar lines to the molybdenum/technetium system mentioned above.

Interest in rhenium-188 for both diagnostic and therapeutic purposes is not new (21–25). Renewed interest in the past few years has led to the development of at least two different types of tungsten-188/rhenium-188 generator systems. A system based on the use of a zirconium tungstate gel has been described (26). The second system (27) uses an alumina column to adsorb tungsten as sodium tungstate and selectively elutes the daughter perrhenate ion with physiological saline.

For clinical use, a reasonably concentrated solution (5–20 mCi/ml) of the radioisotope in sterile physiological saline would be ideal. However, too concentrated a solution and, more especially, too concentrated an amount of rhenium-188 on the generator itself may be expected to lead to radiolysis problems. Under certain conditions, the decay of rhenium-188 can lead to the production of hydroxyl radicals and, subsequently, to the reduction of perrhenate to lower oxidation states which may then be unavailable for antibody binding.

Rhenium radiolabeling of mAbs has been approached from the same viewpoint as technetium radiolabeling, and most usually by the initial reduction of rhenium onto a low molecular weight bifunctional chelating agent, followed by the conjugation of the rhenium-chelate complex to mAb. This chemistry has been diligently pursued in the $\text{N}_2\text{S}_2/\text{N}_3\text{S}$ chelate systems to where the biodistribution, pharmacokinetic, and radioimmunotherapy experiments using the carrier-added ^{186}Re isotope has been described recently (28, 29). We have pursued the alternative direct labeling approach to both technetium and rhenium radiolabeling of monoclonal antibodies. This approach is perceived by some investigators (30), incorrectly we believe, to result in a metal-mAb bond too unstable to be of use with RAID and RAIT. The rapidity and efficiency of mAb and fragment direct labeling with ^{99m}Tc prompted us to try to extend the method to rhenium, particularly to generator-produced ^{188}Re . The rhenium isotopes might offer some significant advantages over other potential RAIT isotopes. Firstly, in comparison to yttrium-90, rhenium should not have the same bone accretion problem because of its different aqueous chemistry. Secondly, both rhenium-186 and rhenium-188 have γ emissions of an energy which allows for imaging during therapy. Thirdly, rhenium-188, as a carrier-free isotope, allows for preparation of radiolabeled conjugates in high-specific activity. Fourthly, the availability of ^{188}Re from a generator system permits the on-site "elution" of the radioisotope in essentially the same fashion as ^{99m}Tc is currently obtained. Concerns about shipping the isotope are therefore eliminated. Since the generator can be eluted with sterile saline, the perrhenate is ready for use. Fifthly, the direct radiolabeling approach will allow very high yields of rhenium-labeled antibody to be produced with minimum manipulation and ideally with no post-radiolabeling purification of conjugate required. The development of a single-vial kit formulation would enable a radioimmun-conjugate to be made merely by reconstituting a vial with perrhenate, and then after a short labeling time, to have

an injectable agent. For any widespread adoption of RAID for cancer therapy to occur, we felt that simplicity and minimal manipulation in the interests of safety and convenience for the nuclear medicine personnel, who would be required to handle multimillicurie doses of these powerful β emitters, to be of prime practical importance.

Tungsten-rhenium generators have currently been fabricated with up to 200 mCi of tungsten loaded onto an alumina column. Generators have proven to be very predictable on a day-to-day elution basis, with 70–80% of the available rhenium-188 elutable in a 20-mL elution volume. The eluate consistently assays for one species by HPLC analysis as sodium perrhenate, which has a retention time of approximately 13 min on a Zorbax GF-250 size-exclusion column. By the use of γ -ray spectroscopy, we have never detected any parent tungsten-188 breakthrough in the eluates and are able to confidently estimate any possible breakthrough at below $2 \times 10^{-4}\%$. A fuller discussion of generator performance as it relates to radionuclide purity has been published (31).

^{99m}Tc LIGAND RADIOLABELING

The use of bifunctional chelates to complex reduced ^{99m}Tc to antibody would appear preferable to direct methods of incorporation of the radionuclide into antibodies/fragments. In theory, the radionuclide should be bound more effectively by a well-defined chemical structure, in contrast with the binding of ^{99m}Tc to heterogeneous receptor groups native to the protein backbone of the antibody molecule. However, the application in practice of the use of chelates to bind reduced ^{99m}Tc to antibodies/fragments has proven to be difficult. Successful labeling of antibodies with ^{111}In , using bifunctional chelates of DTPA, encouraged several investigators to attempt to specifically incorporate reduced ^{99m}Tc into DTPA-antibody chelates. As early as 1982, Khaw et al. claimed specific incorporation of ^{99m}Tc into a DTPA-Fab prepared from an antibody to human cardiac myosin (32). However, in a study published in 1985, Childs and Hnatowich performed a more critical evaluation of the incorporation of ^{99m}Tc into a DTPA-antibody conjugate. They concluded that "it was not possible to reduce to negligible levels nonspecific binding of ^{99m}Tc to the antibody" (33).

With the development of a better understanding of the chemistry of technetium, chelates were designed to complex reduced pertechnetate specifically to antibodies. The chelates that have been evaluated most extensively are the dithio, diamido derivatives developed by Fritzberg et al. (34); this class of chelates is commonly referred to as N_2S_2 ligands. These superior chelates did not resolve the problems that prevented the specific incorporation of ^{99m}Tc into DTPA-antibody conjugates, i.e., nonspecific binding of the reduced radionuclide to the antibody.

In an attempt to circumvent these problems, Fritzberg's group developed elaborate technology to load the ligand with ^{99m}Tc , purify the ^{99m}Tc -ligand complex from free ^{99m}Tc and impurities, and then covalently couple the ^{99m}Tc -activated ligand to antibodies and fragments. NeoRx Corp. has developed a kit based on this technology and has conducted clinical trials to evaluate a ^{99m}Tc - N_2S_2 -Fab' prepared with this kit for melanoma imaging (35, 36). Because of the complexity of the labeling kit, two of the advantages of using ^{99m}Tc have been compromised, i.e., low cost of the final product and its ease of preparation. Indeed, it is unlikely that this kit can be adapted for use by the hospital nuclear medicine laboratory, and thus its use will be limited to regional radiopharmacies. Clinical performance of this RAID product to detect tumor in the abdomen and pelvis was compromised by liver uptake and

hepatobiliary excretion of the radionuclide (35, 36). For reasons that remain to be defined, localization of tumor required preadministration of 40 mg of irrelevant IgG and 7.5 mg of unlabeled specific anti-melanoma IgG. This resulted in induction of high levels of human anti-murine antibody (HAMA) in most of the patients, certainly an undesirable property of a RAID product (36).

We encountered many similar problems in an attempt to develop another second-generation ^{99m}Tc chelate, bis-thiosemicarbazone (unpublished information). When we used antibody coupled with the chelate it was not possible to obtain quantitative incorporation into the chelate. Experiments to preload the chelate with ^{99m}Tc and attach it to the antibody were successful. However, experiments in mice bearing human tumor xenografts demonstrated high uptake of the labeled antibody by normal organs. This approach has been described by another group (37), with a 60% incorporation of ^{99m}Tc into chelate-IgG at 30 min, rising to an 87–90% incorporation of ^{99m}Tc at 3 h. However, unconjugated IgG showed 45% of ^{99m}Tc bound to protein at 30 min and 40% at 3 h postlabeling. The possibility of incorporation of ^{99m}Tc into protein sulfhydryl groups rather than into the bifunctional chelate, due to the reducing conditions employed in the radiolabeling, cannot be ruled out.

Other bifunctional chelates for technetium-99m labeling of antibodies have been described (38–40), with prelabeling of chelate prior to antibody conjugation being a requirement. One type of chelating agent which has been demonstrated to be capable of postconjugation, site-specific labeling with technetium-99m is that based on hydrazino nicotinamides (41, 42). Using this type of chelate, greater than 90% of ^{99m}Tc -glucoheptonate could be incorporated into a protein conjugate in 1 h at room temperature, while a control nonconjugated protein incorporated only 6% of the radioactivity.

In a different approach, Brown and co-workers used a cross-linking agent to conjugate antibodies with metallothionein (43, 44). Radiolabeling with ^{99m}Tc , by exchange labeling, gave a 70–95% radiolabeling efficiency in 1–2 h at room temperature. Of note is the faster blood clearance of ^{99m}Tc -labeled IgG compared to the corresponding ^{131}I -IgG.

DIRECT ANTIBODY RADIOLABELING WITH ^{99m}Tc

One of the first reports of successful direct labeling of IgG with ^{99m}Tc was described by Wong et al. in 1978 (45). They labeled human polyclonal IgG, using trisodium citrate as a chelator, and obtained 95–100% incorporation of reduced ^{99m}Tc into the protein within 30 min. They claimed localization of human tumors as determined by scintigraphic scans, putatively due to the presence of tumor-specific antibody in the preparation. The existence of "tumor-specific antibodies" in normal human polyclonal IgG, in the light of current knowledge, appears highly doubtful. Tumor imaging obtained with this reagent was probably due to nonspecific localization of the labeled macromolecule in the tumor.

Using this method, Mishkin et al. successfully labeled IgG prepared using antisera from rabbits hyperimmunized with bacterial antigens (46). They raised high-titer antibody in rabbits to *Staphylococcus aureus*, isolated the IgG, and labeled the IgG with ^{99m}Tc previously reduced by the addition of stannous chloride in 0.05 N HCl. Reduction was performed under acidic conditions to prevent formation of insoluble oxides of both tin and technetium. The pH of the solution was then adjusted to neutral pH using sodium citrate (the citrate ion acts as a

weak chelating ligand, stabilizing both the stannous ion and the reduced pertechnetate). These investigators demonstrated that 98% of the radionuclide was incorporated into the IgG. The labeled antibody was administered to rabbits that had aortic valves infected with either staphylococcus or enterococcal bacteria. Impressive localization ratios of aortic valve/normal tissue were demonstrated in animals with staphylococcal infection; the labeled antibody did not localize in enterococcal-infected control aortic valves. Despite highly significant localization of the antibody in the bacterial vegetations of the experimental animals, *in vivo* imaging failed to detect the infection. Indeed, these investigators rediscovered the "blood-pool background" problem of using intact IgG for *in vivo* imaging identified by Goldenberg and co-workers several years previously (1).

In the work described above, receptor groups intrinsic to the native polyclonal IgG, probably free thiol groups, were effectively labeled without prior activation of the IgG. The conditions used to reduce pertechnetate, usually a stabilized stannous ion, can lead to incorporation of technetium into IgG, as described as long ago as 1980 (47). This type of method was developed into a procedure where antibodies were "pretinned" with a relatively large amount of stannous ion for extended periods prior to lyophilization or radiolabeling. Incorporations of around 80% of technetium-99m into proteins were achieved (48). The slow reduction of protein disulfide groups with tin(II) has been advantageously replaced with a fast reduction reaction prior to radiolabeling. Thiol groups are not present in many murine monoclonal antibodies of the IgG subclass and the effective incorporation of reduced [^{99m}Tc]pertechnetate into the intact IgG requires exposure of the IgG to reducing agents such as mercaptoethanol. In order to generate thiol groups for incorporation of reduced ^{99m}Tc into murine mAb-IgG, Schwarz and Steinsträsser have pretreated murine monoclonal antibodies with mercaptan-reducing agents and have stabilized the partially reduced IgG by lyophilization and storage of the vial under nitrogen (49). They have then used stannous chloride complexed with phosphonates or pyrophosphate to reduce [^{99m}Tc]pertechnetate prior to incorporation of the radionuclide into the reduced antibody.

Utilizing the labeling method of Schwarz and Steinsträsser, Baum et al. have labeled an anti-CEA-mAb (intact IgG) and imaged 40 patients with colorectal carcinoma (50). Tumor detection was observed 6–24 h postinjection, with a sensitivity of 92% reported in detecting known lesions. Sensitivity of detecting occult, CEA-producing tumors was 73%. Despite these impressive results, these investigators report several problems that need to be solved. Nonspecific liver uptake was relatively high, varying from patient to patient, and the high blood-pool activity caused problems in early images, especially in patients with questionable lung metastases. Finally, nonspecific accumulation of the isotope in the large bowel presented difficulties in interpretation. Apparently this problem was minimized by the administration of a laxative.

In 1986, Rhodes et al. reported localization of a tumor in a nude mouse with an antitumor antibody fragment labeled with ^{99m}Tc (48). F(ab')₂ fragments, prepared from a anti-HCG monoclonal antibody, were incubated with stannous chloride and then lyophilized. ^{99m}Tc was added to the lyophilized vial and incubated for 30 min. A molecular sieve column, containing Sephadex-G25 pretreated with stannous phthalate and gentisate, was used to remove free pertechnetate and isotope bound to low-affinity sites. The purified product was a mixture of labeled F(ab')₂ and

Fab', with Fab' being the dominant labeled fragment. Although the preclinical animal studies reported by Rhodes et al. were disappointing, Summa Medical Corp. (Albuquerque, NM) continued to pursue development of the Rhodes technology. In a recent publication, Zimmer et al. described results obtained in an athymic mouse-human/colonic tumor xenograft with a ^{99m}Tc-labeled anti-CEA-F(ab')₂, formulated by Summa (51). Results of this study were markedly better than those reported by Rhodes et al. using the anti-HCG-labeled mAb fragment. Positive localization ratios were obtained when tumor was compared with several normal organs, and specificity was demonstrated using a control labeled fragment, the one important exception being the liver. The percent injected dose/gram (%ID/g) observed in the liver exceeded the %ID/g in the tumor at 24 h postinjection of the labeled fragment. In agreement with the findings of Rhodes et al., these investigators observed that the primary labeled product was Fab'; however, the predominant protein in the preparation, prior to addition of the isotope, was F(ab')₂. They speculated that the pretinning process caused some reduction in disulfide bonds, with subsequent generation of monomeric fragments, and that this Fab' minor component was preferentially labeled with reduced [^{99m}Tc]pertechnetate.

Buraggi et al. (52) have employed a modified "Rhodes" procedure to label F(ab')₂ fragments prepared from anti-melanoma mAbs; the primary modification of the original method was the substitution of an ion-exchange column to remove free ^{99m}Tc, in place of the special gel-filtration-tin column used by Rhodes. Siccardi et al., in a large multicenter study, compared a ^{99m}Tc-labeled fragment to an ¹¹¹In-labeled fragment (53). Overall, 74% of antigen-positive lesions were detected with the ^{99m}Tc-labeled fragment and 59% with the ¹¹¹In-labeled fragment. The optimal imaging time was between 6 and 12 h for the ^{99m}Tc-labeled fragment. Although the size of the ^{99m}Tc fragment was not reported, the optimal imaging time of 6–12 h could indicate that the predominant labeled fragment was Fab'.

We have also developed a direct method to label Fab' fragments with ^{99m}Tc. One of our goals was to obtain a labeled fragment that would give positive tumor/normal liver ratios within 24 h after injection into athymic mice bearing a xenograft of colonic carcinoma. We considered this prerequisite to performing phase I RAID studies in patients with colorectal carcinoma, because the liver is the primary organ to which these tumors metastasize. This goal has been achieved. The Fab' fragment prepared from Immu-4, a mAb that is specific for high molecular weight CEA, has been formulated in a single vial and labeled by simply adding [^{99m}Tc]pertechnetate eluted from a generator. Essentially quantitative incorporation of the isotope into the fragment is complete within 5 min after its addition to the vial containing the lyophilized fragment (54). Clinical studies have demonstrated the effectiveness of the labeled fragment to image colorectal and other carcinomas (55).

Although we expected that it would be possible to incorporate ^{99m}Tc into Fab'-SH, the quantitative incorporation achieved within 5 min of adding pertechnetate to the preparation was unexpected. To date, we have labeled Fab' prepared from anti-CEA, anti-AFP, and other mAbs of the IgG₁ subclass and have routinely incorporated >99% of 20 mCi of ^{99m}Tc into 1 mg of Fab'. It is apparent that the hinge region sulfhydryl groups of the Fab' fragment have an extremely high affinity for reduced ^{99m}Tc. In generating the free sulfhydryl groups by pepsin

digestion of $F(ab')_2$, minimal damage to the fragment due to exposure to reducing agents is achieved. Furthermore, the quantity of sulfhydryl groups in each preparation is controlled, assuring that enough are present to bind ^{99m}Tc of low specific activity, i.e., eluate from a generator that has not been eluted for 3 days.

With intact IgG, from one to nine SH groups per IgG molecule, as analyzed for by the Ellman reaction (56), may be generated by the reduction of IgG with mercaptoethanol (57). No change in elution times on Zorbax-GF 250 size-exclusion HPLC was noted even with nine SH groups per mAb. In the interest of minimal disruption of antibody, normally one or two SH groups were generated. Mixing of the prereduced antibody with as little as 0.5 μg of stannous ion followed immediately by addition of pertechnetate resulted, at the 5-min analysis period, in the quantitative incorporation of ^{99m}Tc into the mAb. The intact IgG could be lyophilized in the same manner as the Fab' to give "instant" one-vial kits for clinical technetium radiolabeling. With no thiol reduction prior to mixing of the mAb with $Sn(II)$ and pertechnetate, only 5–15% of the radioactivity eluted with the mAb on HPLC. With IgG, as with Fab' - and $F(ab')_2$ -labeled fragments, over 95% of activity applied to the HPLC could be recovered. The avidity of reduced mAb for reduced technetium species was also demonstrated by subsequent stability tests. Incubation of ^{99m}Tc -mAb in human serum for 24 h at 37 °C showed no evidence of reoxidation of technetium or of the transfer of technetium to serum proteins. These results were remarkable to us, in the light of then current thinking, which suggested that technetium chemistry was plagued by problems of reoxidation, colloid formation during labeling (estimated in our procedure at below 2% by ITLC), and instability and variability in some final radiolabeled products. Reduced IgG seemed to surpass, in ease of labeling, purity of product, resistance to reoxidation, and stability to challenge, a number of low molecular weight chelates being developed for various purposes. Essentially the same results have been described by Mather and Ellison (58). In their report, by the addition of pertechnetate to a mixture of stannous ion and antibody, greater than 97% incorporation of technetium to antibody was obtained in a few minutes. The resultant ^{99m}Tc -IgG was stable to DTPA challenge.

mAb $F(ab')_2$ fragments might offer an alternative to Fab' and IgG when labeled with technetium-99m for RAID because of potentially lower kidney uptake than the ^{99m}Tc - $F(ab')_2$ and quicker blood clearance than the ^{99m}Tc -IgG. However, our attempts to thiol-reduce $F(ab')_2$, in an analogous manner to IgG, prior to technetium radiolabeling always resulted in a small amount of Fab' in the product. Upon addition of stannous ion and technetium, a quantitative incorporation of radioactivity was seen but as an approximately 50:50 mixture of ^{99m}Tc - $F(ab')_2$ and ^{99m}Tc - Fab' , as analyzed by size-exclusion HPLC. Earlier workers had noted the same problem with $F(ab')_2$ (48). We recently solved the problem of production of pure ^{99m}Tc - $F(ab')_2$ by a simple modification of our procedures. Originally, we had thiol-reduced $F(ab')_2$ to generate free sulfhydryl groups, in order to obtain a mixture of ^{99m}Tc - Fab' and ^{99m}Tc - $F(ab')_2$ upon radiolabeling. Instead, we thiol-reduced intact IgG to generate one or two SH groups per mAb and then pepsin-digested the reduced IgG. We theorized that a controlled reduction of IgG would target less critical disulfide bonds away from the hinge region, such that upon digestion we would obtain a thiol-reduced pure $F(ab')_2$ after purification. Because of the lack of any Fab' contaminant in this preparation, subsequent stan-

Table I. Biodistribution of ^{99m}Tc -Mu-9-IgG, $-F(ab')_2$, and $-Fab'$ in Nude Mice Bearing LS174T Tumors, 24 h Postinjection^a

tissue	mean % injected dose/g in tissue \pm SD		
	^{99m}Tc -IgG	^{99m}Tc - $F(ab')_2$	^{99m}Tc - Fab'
LS174T	30.08 \pm 3.85	8.71 \pm 1.54	1.21 \pm 0.08
liver	4.31 \pm 0.91	2.17 \pm 0.23	0.52 \pm 0.09
kidney	8.21 \pm 0.67	30.67 \pm 5.67	40.29 \pm 5.74
blood	8.17 \pm 1.76	0.75 \pm 0.10	0.19 \pm 0.08
stomach	0.87 \pm 0.10	1.36 \pm 0.32	0.23 \pm 0.06
small int	1.14 \pm 0.13	0.94 \pm 0.74	0.20 \pm 0.03
large int	1.14 \pm 0.24	1.33 \pm 0.39	0.57 \pm 0.22

^a Five animals per group.

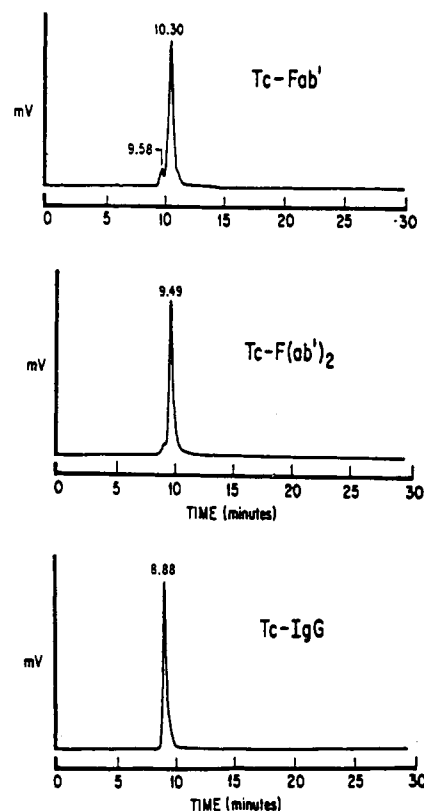


Figure 1. Size-exclusion HPLC analysis of radiolabeled ^{99m}Tc - Fab' , ^{99m}Tc - $F(ab')_2$, and ^{99m}Tc -IgG showing each at 5 min postlabeling. No pertechnetate (retention time, 13 min) or reduced low molecular weight technetium species (retention time, 11.2 min) is present in any of the preparations.

nous ion/pertechnetate addition resulted in ^{99m}Tc - $F(ab')_2$ uncontaminated with ^{99m}Tc - Fab' . The in vivo biodistribution of a Fab' , $F(ab')_2$, and intact mAb, when radiolabeled with technetium, is shown in Table I, and the HPLC analyses of the three radiolabeled agents, prior to injection, are shown in Figure 1.

DIRECT ANTIBODY RADIOLABELING WITH RHENIUM ISOTOPES

Initial attempts to radiolabel mAb with rhenium were performed with low specific activity rhenium-186 and various lyophilized kit preparations used for radiolabeling with technetium-99m. Some incorporations were seen, although the reactions were slow and labeling volumes had to be kept to a minimum. Vials containing 1.25 mg of antibody, reconstituted with a 0.5-mL volume of $Na^{186}ReO_4$, showed high incorporation of Re to protein at 18 h and good incorporation at 3–4 h postreconstitution (57). The same vials, of course, labeled with Tc -99m within 5 min in a quantitative manner. This is in agreement

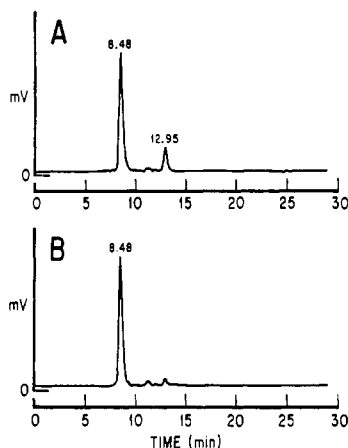


Figure 2. Optimized conditions for the ¹⁸⁸Re labeling of Mu-9: (A) ¹⁸⁸Re-Mu-9 at 15 mCi/1 mg at 30 min and (B) at 60 min (from Griffiths et al. (58), with permission of the publisher).

with the different redox properties of technetium and rhenium discussed by other workers (20, 59). Of interest to us, at this point, was the control vial which contained no mAb, but was otherwise labeled under the same conditions. Rhenium reduction was poor, and at the 3-h time point had reached a maximum. By 6 h the reduced rhenium had reoxidized to perrhenate (data not shown). This result, and the technetium results discussed above, reinforced the notion that proteins labeled with these elements were more stable than one might expect. Continual refinement of labeling conditions, using mainly the ¹⁸⁸Re isotope, has enabled us to develop labeling sufficiently to reconstitute 1-mg vials with 10 mL (15 mCi) of ¹⁸⁸ReO₄ and, later, 10-mg vials with up to 20 mL of generator eluate. Representative HPLC traces of one such conjugate, ¹⁸⁸Re-labeled Mu-9 IgG (an anti-CSAp antibody), are shown in Figure 2.

In terms of in vitro stability, the ¹⁸⁸Re-IgG conjugates show only moderate stability in saline solution, but enhanced stability to serum challenge with from 0–15% loss of label to perrhenate over the initial 48-h challenge, with no transfer of rhenium to serum proteins being observed. The dissociation in serum, being considerably slower than that in saline, suggests a protective effect of serum proteins against the processes of reoxidation (57).

In Balb/c mice the ¹⁸⁸Re-Mu-9 conjugate compared to sodium perrhenate (Table II) shows enhanced retention in the circulation with the perrhenate localizing in the stomach and thyroid at early time points (1–4 h) and essentially fully cleared at 24 h. ¹⁸⁸Re-Mu-9 showed 29% and 10% of the percent injected dose/gram in the circulation at 4 and 24 h, respectively. Low stomach, thyroid, and intestinal activity was noted, with most activity passing and clearing through the liver and kidney.

Comparison of the ¹⁸⁸Re-Mu-9, the corresponding ¹³¹I-Mu-9, and a nonspecific control mAb, ¹⁸⁸Re-AFP (α -fetoprotein), illustrates the specific tumor uptake of the first two agents relative to the ¹⁸⁸Re-AFP, and demonstrates that both rhenium-labeled antibodies show little nontarget organ accretion in liver, gut, or bone (Table III). Furthermore, the rhenium-labeled antibodies cleared the bloodstream faster than the iodinated antibody, which enabled the ¹⁸⁸Re-Mu-9 to achieve a higher tumor/blood ratio than ¹³¹I-Mu-9 at 24–48 h postinjection. In previous work with colorectal carcinoma xenograft models, the importance of the tumor localization index, defined as the tumor/blood ratio of radiolabeled antibody divided by the tumor/blood ratio of radiolabeled nonspecific antibody, has been described (60). In the comparison of ¹⁸⁸Re-Mu-

Table II. Biodistribution of ¹⁸⁸Re-Mu-9-IgG and Na¹⁸⁸ReO₄ in Balb/c Mice at 1, 4, and 24 h Postinjection^a

tissue	time post-injection (h)	mean % injected dose/g tissue \pm SD	
		¹⁸⁸ Re-Mu-9	Na ¹⁸⁸ ReO ₄
blood	1	28.02 \pm 1.86	5.56 \pm 0.53
	4	29.66 \pm 3.83	4.68 \pm 0.85
	24	10.20 \pm 1.10	0.02 \pm 0.00
liver	1	13.55 \pm 0.77	3.91 \pm 0.38
	4	11.61 \pm 0.74	3.46 \pm 0.71
	24	4.46 \pm 0.23	0.01 \pm 0.00
stomach	1	1.78 \pm 0.41	85.80 \pm 23.70
	4	2.98 \pm 0.42	53.60 \pm 3.87
	24	0.81 \pm 0.05	0.12 \pm 0.01
small int	1	1.92 \pm 0.04	1.53 \pm 0.15
	4	3.00 \pm 0.33	1.40 \pm 0.24
	24	1.01 \pm 0.11	0.01 \pm 0.00
large int	1	0.95 \pm 0.05	1.38 \pm 0.19
	4	2.69 \pm 0.65	1.17 \pm 0.26
	24	1.13 \pm 0.23	0.01 \pm 0.00
thyroid	1	3.87 \pm 0.71	45.02 \pm 7.61
	4	6.04 \pm 0.87	40.47 \pm 12.31
	24	2.97 \pm 0.31	0.13 \pm 0.05
kidney	1	11.76 \pm 1.11	2.84 \pm 0.13
	4	13.76 \pm 1.99	2.69 \pm 0.59
	24	5.10 \pm 0.47	0.08 \pm 0.00

^a Five animals per group (from Griffiths et al. (58), with permission of the publisher).

9 to ¹⁸⁸Re-AFP, localization indices of 2.07, 3.60, and 2.84 were seen at 24, 48, and 72 h, respectively.

Work with ¹⁸⁶Re-mAb by the group at NeoRx, using the bifunctional chelate approach, described the extended lifetime of ¹⁸⁶Re-IgG in the bloodstream with the best tumor/blood ratios seen between 3 and 6 days postinjection, and low tumor/blood ratios up to 48 h postinjection (28). The faster blood clearance of ¹⁸⁸Re-Mu-9 described above, compared to that of the ¹⁸⁶Re-IgG prepared by the bifunctional chelate approach, is an essential prerequisite to the use of the 17-h half-life ¹⁸⁸Re in RAIT. ¹⁸⁸Re-mAbs are currently being examined in animal therapy experiments by us.

The current clinical shortcomings of using ¹³¹I-labeled mAbs for RAIT must include the hazardous prospect of radiolabeling with 50–200 mCi doses of potentially volatile iodine, and the undesirability of using a nuclide with such a high-energy, high-abundance (364 keV, 81%) γ component. The use of yttrium-90 was attractive, before the bone accretion problem was identified. Stronger yttrium chelates have somewhat ameliorated the bone accretion rate (61), and even stronger chelates may further improve this isotope's usefulness (62). However, great care will always be needed in ensuring that the yttrium is not non-specifically bound to antibody, and postlabeling purification of ⁹⁰Y-IgG is always a requirement. With regard to the bone accretion problem with the use of other metal(III) cation radioimmunoconjugates, the approach of Schlom et al. in using a less penetrating β emitter is worthy of note (63). Also, RAIT with phosphorus-32, although as the PO₄³⁻ anion it is a potent bone-seeking agent (64), is another potentially interesting approach (65). However, the most immediate replacement for ¹³¹I-labeled mAbs for RAIT may be Re-labeled mAbs. The ¹⁸⁶Re-mAb conjugates prepared using bifunctional chelates have been evaluated in the clinic (66), and our own direct-labeled ¹⁸⁸Re-mAbs will be tested shortly. Because of the advantages of availability, chemistry, nonaccretion in normal tissue, ease of labeling, and enhanced conjugate clearance outlined in this section, we believe that ¹⁸⁸Re-labeled mAbs may have a promising future in RAIT.

Table III. Biodistribution at 2, 24, 48, and 72 h of ^{188}Re -Mu-9-IgG, ^{188}Re -AFP-IgG, and ^{131}I -Mu-9 in Nude Mice Bearing LS174T Xenografts^a

tissue	time post-injection (h)	mean % injected dose/g in tissue \pm SD		
		^{188}Re -Mu-9 % of ID/g	^{188}Re -AFP % of ID/g	^{131}I -Mu-9 % of ID/g
LS174T tumor	2	9.98 \pm 1.23	7.09 \pm 1.89	8.59 \pm 1.99
	24	16.30 \pm 1.74	5.54 \pm 1.02	14.96 \pm 1.97
	48	14.94 \pm 1.36	2.39 \pm 0.54	18.86 \pm 1.19
	72	9.86 \pm 1.18	1.62 \pm 0.20	23.75 \pm 2.03
blood	2	28.27 \pm 1.41	22.44 \pm 2.21	23.69 \pm 3.30
	24	9.16 \pm 1.47	9.57 \pm 1.91	15.39 \pm 1.31
	48	5.59 \pm 1.21	3.22 \pm 0.53	13.55 \pm 0.88
	72	3.46 \pm 0.80	2.38 \pm 0.23	13.13 \pm 2.90
liver	2	10.44 \pm 1.67	10.32 \pm 1.57	7.84 \pm 1.90
	24	3.69 \pm 0.51	5.27 \pm 1.34	4.68 \pm 0.44
	48	2.60 \pm 0.39	1.82 \pm 0.29	3.75 \pm 0.47
	72	1.58 \pm 0.28	1.48 \pm 0.42	3.67 \pm 1.12
spleen	2	8.68 \pm 2.21	11.07 \pm 2.38	6.82 \pm 2.58
	24	2.74 \pm 0.49	5.19 \pm 1.44	3.45 \pm 0.90
	48	2.08 \pm 0.37	ND ^b	3.46 \pm 0.95
	72	1.47 \pm 0.43	ND	3.17 \pm 1.18
stomach	2	3.35 \pm 0.56	4.91 \pm 2.27	2.06 \pm 0.59
	24	1.63 \pm 0.27	1.95 \pm 0.52	1.17 \pm 0.44
	48	1.39 \pm 0.68	1.24 \pm 0.55	1.27 \pm 0.24
	72	0.59 \pm 0.06	1.85 \pm 0.47	1.31 \pm 0.40
small int	2	2.58 \pm 0.20	2.20 \pm 0.51	2.03 \pm 0.25
	24	1.07 \pm 0.09	1.18 \pm 0.36	1.30 \pm 0.09
	48	0.82 \pm 0.11	0.57 \pm 0.11	1.24 \pm 0.19
	72	0.58 \pm 0.08	0.64 \pm 0.12	1.10 \pm 0.26
large int	2	1.65 \pm 0.58	2.09 \pm 0.34	1.29 \pm 0.27
	24	1.16 \pm 0.11	1.33 \pm 0.30	0.83 \pm 0.18
	48	0.82 \pm 0.11	0.57 \pm 0.11	0.71 \pm 0.09
	72	0.49 \pm 0.06	0.93 \pm 0.16	0.65 \pm 0.10
thyroid	2	ND	5.48 \pm 1.71	3.96 \pm 0.86
	24	ND	3.07 \pm 0.86	3.52 \pm 0.35
	48	ND	2.71 \pm 0.59	3.03 \pm 0.22
	72	ND	0.93 \pm 0.16	2.80 \pm 0.55
kidney	2	10.19 \pm 1.98	10.38 \pm 1.17	7.78 \pm 1.04
	24	4.44 \pm 0.54	3.6 \pm 1.56	4.80 \pm 0.57
	48	3.54 \pm 0.41	3.51 \pm 0.94	4.00 \pm 0.20
	72	2.47 \pm 0.16	4.87 \pm 1.36	4.03 \pm 0.74
bone	2	4.74 \pm 0.82	3.57 \pm 2.50	3.82 \pm 1.41
	24	1.97 \pm 0.21	3.01 \pm 0.56	2.30 \pm 0.33
	48	2.00 \pm 0.33	3.68 \pm 0.92	2.05 \pm 0.29
	72	1.67 \pm 0.41	6.66 \pm 13.20	1.72 \pm 0.40

^a From Griffiths et al. (58), with permission of the publisher. ^b ND, not done.

CONCLUSIONS

From the above discussion it is apparent that significant progress has been made toward the strong binding of reduced ^{99m}Tc and Re to antitumor monoclonal antibodies and antibody fragments, while the immunoreactivity of the antibody is maintained. Many of these reagents are now being evaluated in clinical trials. One significant difference that has been reported using ^{99m}Tc -labeled mAb, instead of ^{131}I -labeled mAb, is the ability to obtain early tumor imaging. Preclinical studies using animal models predict that superior imaging results should be obtained with labeled ^{99m}Tc -Fab' or ^{99m}Tc -F(ab')₂ versus labeled ^{99m}Tc -IgG at time points up to 24 h postinjection. However, in light of the excellent results reported by Baum et al. (50), carefully controlled clinical studies are needed to compare the effectiveness of imaging with intact IgG versus labeled fragments, with each reagent being prepared from the same monoclonal antibody. Resolution of this issue is of paramount importance. The decision to use intact IgG or fragments is not a trivial matter if therapy with a monoclonal antibody is to be attempted. Intact IgG is much more immunogenic than are similar doses of antibody fragments (67). Further, it has been documented that preexisting human anti-murine antibodies present

in human sera are primarily reactive with determinants on the Fc of mAbs, and it appears that primary sensitization with intact mAb not only results in an increase of Fc-reactive HAMA but also in sensitization to Fab' epitopes (68, 69). Obviously, use of fragments for imaging is preferred, assuming at least equal performance of Fab' and/or F(ab')₂ to intact IgG reagents. For therapy, the rhenium isotopes' physical and chemical advantages discussed above would be further enhanced if the direct-labeling approach, so successfully applied to technetium by a number of groups, were extendable to rhenium. To this end, we have developed the direct radiolabeling of mAbs with rhenium-188 taken from an in-house generator. Tumor targeting in animals with ^{188}Re -Mu-9 mAb is better, at early time points, than with ^{131}I -Mu-9. Enhanced clearance of ^{188}Re -Mu-9 from the circulation is an important observation, as is the lack of accretion of metabolic products in nontarget tissues. We are currently evaluating ^{188}Re -mAbs in radioimmunotherapy studies.

ACKNOWLEDGMENT

This work was supported in part by NIH contract SBIR CM 87778 from the National Cancer Institute and USPHS grant CA 39841 from the NIH.

LITERATURE CITED

- Goldenberg, D. M., DeLand, F. H., Kim, E. E., Bennett, S., Primus, F. J., Van Nagell, J. R., Estes, N., DeSimone, P., and Rayburn, P. (1978) Use of radiolabeled antibodies to carcinoembryonic antigen for the detection and localization of diverse cancers by external photoscanning. *N. Engl. J. Med.* 298, 1384-1388.
- Goldenberg, D. M., Kim, E. E., DeLand, F. H., Bennett, S., and Primus, F. J. (1980) Radioimmunodetection of cancer with radioactive antibodies to carcinoembryonic antigen. *Cancer Res.* 40, 2984-2992.
- Mach, J. P., Buchegger, F., Forni, M., Ritschard, J., Berche, C., Lambroso, J. D., Schreyer, M., Girardet, C., Accalla, R. S., and Carrel, S. (1981) Use of radiolabeled monoclonal anti-CEA antibodies for the detection of human carcinomas by external photoscanning and tomoscintigraphy. *Immunol. Today* 2, 239-249.
- Epenetos, A., Britton, K. E., Mather, S., Shepherd, J., Granowska, M., Taylor-Papadimitriou, J., Nimmon, C. C., Durbin, H., Hawkins, L. R., Malpas, J. S., and Bodmer, W. F. (1982) Targeting of iodine-I-123 tumor-associated antibodies to ovarian, breast and gastrointestinal tumors. *Lancet* 2, 999-1005.
- Goldenberg, D. M., Kim, E. E., Bennett, S. J., Nelson, M. D., and DeLand, F. H. (1983) CEA radioimmunodetection in the evaluation of colorectal cancer and in the detection of occult neoplasms. *Gastroenterology* 84, 524-532.
- Beatty, J. D., Duda, R. B., Williams, L. E., Sheibani, K., Paxton, R. J., Beatty, B. G., Philben, B. J., Werner, J. L., Shively, J. E., Vlahos, W. G., Kokal, W. A., Riihimaki, D. U., Terz, J. J., and Wagman, L. D. (1986) Preoperative imaging of colorectal carcinoma with ^{111}In -labeled anticarcinoembryonic antigen monoclonal antibody. *Cancer Res.* 46, 6494-6502.
- Granowska, M., Britton, K. E., Shepherd, J. H., Nimmon, C. C., Mather, S., Ward, B., Osborne, R. J., and Slevin, M. L. (1986) A prospective study of ^{125}I -labeled monoclonal antibody imaging in ovarian cancer. *J. Clin. Oncol.* 4, 730-736.
- Epenetos, A. A., Carr, D., Johnson, P. M., Bodmer, W. F., and Lavender, J. P. (1986) Antibody-guided radiolocalization of tumors in patients with testicular or ovarian cancer using two radioiodinated monoclonal antibodies to placental alkaline phosphatase. *Br. J. Radiol.* 59, 117-125.
- Colcher, D., Esteban, J. M., Carrasquillo, J. A., Sugarbaker, P., Reynolds, J. C., Bryant, G., Larson, S. M., and Schlom, J. (1987) Quantitative analysis of selective radiolabeled monoclonal antibody localization in metastatic lesions of colorectal cancer patients. *Cancer Res.* 47, 1185-1189.

- (10) Tucker, W. D., Green, M. W., and Weiss, A. J. (1958) Methods of preparation of some carrier-free radioisotopes involving adsorption on alumina, BNL 3746. Annual Meeting, American Nuclear Society, Los Angeles, CA, June 1958. *Trans. Am. Nucl. Soc.* 1, 160.
- (11) Lamson, M., III, Hotte, C. E., and Ice, R. D. (1976) Practical generator kinetics. *J. Nucl. Med. Technol.* 4, 21–27.
- (12) Kowalsky, R. J., and Perry, J. R. (1987) Chemistry of radiopharmaceuticals. *Radiopharmaceuticals in Nuclear Medicine Practice* (S. Baum, Ed.) pp 75–95, Appleton & Lange, Norwalk, CT.
- (13) Eckelman, W. C., and Richards, P. (1970) Instant ^{99m}Tc -DTPA. *J. Nucl. Med.* 11, 761.
- (14) Kowalsky, R. J., and Perry, J. R. (1987) Heart. In *Radiopharmaceuticals in Nuclear Medicine Practice* (S. Baum, Ed.) pp 217–218, Appleton & Lange, Norwalk, CT.
- (15) Pettit, W. A., DeLand, F. H., Bennett, S. J., and Goldenberg, D. M. (1980) Radiolabeling of affinity-purified goat anti-carcinoembryonic antigen immunoglobulin G with technetium-99m. *Cancer Res.* 40, 3043–3045.
- (16) Eckelman, W. C., and Paik, C. H. (1986) Comparison of ^{99m}Tc and ^{111}In -labeling of conjugated antibodies. *Nucl. Med. Biol.* 13, 335–343.
- (17) Fritzberg, A. R., Kasina, S., Reno, J. M., Srinivasan, A., Wilbur, D. S., Vanderheyden, J.-L., Schroff, R. W., and Morgan, A. C., Jr. (1986) Radiolabeling of antibodies with Tc-99m using N_2S_2 ligands. *J. Nucl. Med.* 27, 957–958.
- (18) Hosotani, T., Yokoyama, A., Arano, Y., Horiuchi, K., Wasaki, H., Saji, H., and Torizuka, K. (1986) In the procurement of a neutral and compact monomeric complex of dithiosemicarbazone (DTS) derivative: ^{99m}Tc -KTS. *Int. J. Nucl. Med. Biol.* 12, 431–437.
- (19) Cotton, F. A., and Wilkinson, G. (1980) Technetium and rhenium. *Advanced Inorganic Chemistry*, 4th ed., pp 883–901, Wiley Interscience, New York.
- (20) Deutsch, E., Libson, K., Vanderheyden, J.-L., Ketrang, A. R., and Maxon, H. R. (1986) The chemistry of rhenium and technetium as related to the use of isotopes of these elements in therapeutic and diagnostic nuclear medicine. *Nucl. Med. Biol.* 13, 465–477.
- (21) Hayes, R. L., and Rafter, J. J. (1966) Rhenium-188 as a possible diagnostic agent. *J. Nucl. Med.* 7, 797 (abstract).
- (22) Lewis, R. E., and Eldridge, J. S. (1966) Production of 70-d tungsten-188 and development of a 17h rhenium-188 generator. *J. Nucl. Med.* 7, 804–805.
- (23) Hayes, R. L., and Rafter, J. J. (1966) Rhenium-188 as a possible diagnostic agent. In Research Report, pp 7, 74–77, Medical Division, Oak Ridge Associated Universities.
- (24) Mikheev, N. B., Popovich, V. B., Rumer, I. A., Savelev, G. I., and Volkova, N. C. (1972) Rhenium-188 generator. *Iso-topenpraxis* 8, 248–251.
- (25) Kodina, G., Tulsakaya, T., Gureev, E., Brodskaya, G., Gapurova, O., and Drosdovsky, B. (1990) Production and investigation of rhenium-188 generator. In *Technetium and Rhenium in Chemistry and Nuclear Medicine*, 3rd ed. (M. Nicolini, G. Bandoli, and U. Mazzi, Eds.) pp 635–641, Raven Press, New York.
- (26) Earhardt, G. J., Ketrang, A. R., Turpin, T. A., Razavi, M. S., Vanderheyden, J.-L., and Fritzberg, A. R. (1987) An improved tungsten-188/rhenium-188 generator for radiotherapeutic applications. *J. Nucl. Med.* 28, 656–657.
- (27) Callahan, A. P., Rice, D. E., and Knapp, F. F. Jr. (1989) Rhenium-188 for therapeutic applications from an alumina-based tungsten-188/rhenium-188 radionuclide generator. *Nucl. Med. Eur./Am. Commun. Nucl. Med.* 20, 3–6.
- (28) Goldrosen, M. H., Biddle, W. C., Pancook, J., Bakshi, S., Vanderheyden, J.-L., Fritzberg, A. R., Morgan, A. C., Jr., and Foon, K. A. (1990) Biodistribution, pharmacokinetic and imaging studies with ^{186}Re -labeled NR-Lu-10 whole antibody in LS174T colonic tumor-bearing mice. *Cancer Res.* 50, 7973–7978.
- (29) Beaumier, P. L., Venkatesan, P., Vanderheyden, J.-L., Burqua, W. D., Kunz, L. L., Fritzberg, A. R., Abrams, P. G., and Morgan, A. C., Jr. (1991) ^{186}Re radioimmunotherapy of small cell lung carcinoma xenografts in nude mice. *Cancer Res.* 57, 676–681.
- (30) Eckelman, W. C., Paik, C. H., and Steigman, J. (1989) Three approaches to radiolabeling antibodies with ^{99m}Tc . *Nucl. Med. Biol.* 16, 171–176.
- (31) Coursey, B. M., Calhoun, J. M., Cessna, J., Hoppes, D. D., Schima, F. J., Unterweger, M. P., Golas, D. G., Callahan, A. P., Mirzadeh, S., and Knapp, F. F., Jr. (1990) Assay of the eluent from the alumina-based tungsten-188-rhenium-88 generator. *Radioact. Radiochem.* 3, 38–49.
- (32) Khaw, B. A., Strauss, H. W., Carvalho, A., Locke, E., Gold, H. K., and Haber, E. (1982) Technetium-99m labeling of antibodies to cardiac myosin Fab and to human fibrinogen. *J. Nucl. Med.* 23, 1011–1019.
- (33) Childs, R. L., and Hnatowich, D. J. (1985) Optimum conditions for labeling of DTPA-coupled antibodies with technetium-99m. *J. Nucl. Med.* 26, 293–299.
- (34) Fritzberg, A. R., Abrams, P. G., Beaumier, P. L., Kasina, S., Morgan, A. C., Jr., Rao, T. N., Reno, J. M., Sanderson, J. A., Srinivasan, A., Wilbur, D. S., and Vanderheyden, J.-L. (1988) Specific and stable labeling of antibodies with technetium-99m with a diamide dithiolate chelating agent. *Proc. Natl. Acad. Sci. U.S.A.* 85, 4025–4029.
- (35) Eary, J. F., Schroff, R. W., Abrams, P. G., Fritzberg, A. R., Morgan, A. C., Kasina, S., Reno, J. M., Srinivasan, A., Woodhouse, C. S., Wilbur, D. S., Natale, R. B., Collins, C., Stehlin, J. S., Mitchell, M., and Nelp, W. B. (1989) Successful imaging of malignant melanoma with technetium-99m-labeled monoclonal antibodies. *J. Nucl. Med.* 30, 25–32.
- (36) Salk, D. and the Multicenter Study Group (1988) Technetium-labeled monoclonal antibodies for imaging metastatic melanoma: Results of a multicenter clinical study. *Semin. Oncol.* 15, 609–618.
- (37) Arano, Y., Yokoyama, A., Furukana, T., Horiuchi, K., Yahata, T., Saji, H., Sakahara, H., Nakashima, T., Koizumi, M., Endo, K., and Torizuka, K. (1987) Technetium-99m-labeled monoclonal antibody with preserved immunoreactivity and high in vivo stability. *J. Nucl. Med.* 28, 1027–1033.
- (38) Franz, J., Wolkert, W. A., Barefield, E. K., and Holmes, R. A. (1987) The production of Tc-99m labeled conjugated antibodies using a cyclam based bifunctional chelating agent. *Nucl. Med. Biol.* 26, 293–299.
- (39) Misra, H. K., Virzi, F., Hnatowich, D. J., and Wright, G. (1989) Synthesis of a novel diaminedithiol ligand for labeling proteins and small molecules with technetium-99m. *Tetrahedron Lett.* 30, 1885–1888.
- (40) Linder, K. E., Wen, M. D., Nowotnik, D. P., Malley, M. F., Gougoutas, J.-L., Nunn, A. D., and Eckelman, W. C. (1991) Technetium labeling of monoclonal antibodies with functionalized BATOs. 1. $\text{TcCl}(\text{DMG})_3\text{PITC}$. *Bioconjugate Chem.* 2, 160–170.
- (41) Abrams, M. J., Juweid, M., Tarkate, C. I., Schwartz, D. A., Hauser, M. M., Gaul, F. E., Fuccello, A. J., Rubin, R. H., Strauss, H. W., and Fischman, A. J. (1990) Technetium-99m-human polyclonal IgG radiolabeled via the hydrazino nicotinamide derivative for imaging focal sites of infection in rats. *J. Nucl. Med.* 31, 2022–2028.
- (42) Schwartz, D. A., Abrams, M. J., Hauser, M. M., Gaul, F. E., Larsen, S. K., Rauh, D., and Zubleta, J. A. (1991) Preparation of hydrazino-modified proteins and their use for the synthesis of ^{99m}Tc -protein conjugates. *Bioconjugate Chem.* 2, 333–336.
- (43) Brown, B. A., Drozynski, C. A., Dearborn, C. B., Hadjian, R. A., Liberatore, F. A., Tulip, T. H., Tolman, G. L., and Haber, S. B. (1988) Conjugation of metallothionein to a murine monoclonal antibody. *Anal. Biochem.* 177, 22–28.
- (44) Brown, B. A., Dearborn, C. B., Drozynski, C. A., and Sands, H. (1990) Pharmacokinetics of ^{99m}Tc -metallothionein-B72.3 and its $\text{F}(\text{ab}')_2$ fragment. *Cancer Res.* 50, 835–839.
- (45) Wong, D. W., Mishkin, F. S., and Lee, T. (1978) A rapid chemical method of labeling human plasma proteins with ^{99m}Tc -pertechnetate at pH 7.4. *Int. J. Appl. Radiat. Isot.* 29, 251–253.
- (46) Mishkin, F. S., Wong, D. W., and Dhawan, V. K. (1983) Radiolabeled antibody in the detection of infection using endocarditis as a model. *Radioimmunoimaging and Radioimmunotherapy* (S.W. Burchiel, and B.A. Rhodes, Eds.) pp 299–369, Elsevier Science, New York.

- (47) Pettit, W. A., DeLand, F. H., Bennett, S. J., and Goldenberg, D. M. (1980) Improved protein labeling by stannous tartrate reduction of pertechnetate. *J. Nucl. Med.* 21, 59-62.
- (48) Rhodes, B. A., Zamora, P. O., Newell, K. D., and Valdez, E. F. (1986) Technetium-99m labeling of murine monoclonal antibody fragments. *J. Nucl. Med.* 27, 685-693.
- (49) Schwarz, A., and Steinsträsser, A. (1987) A novel approach to Tc-99m-labeled monoclonal antibodies. *J. Nucl. Med.* 28, 721 (abstract).
- (50) Baum, R. P., Hertel, A., Lorenz, M., Schwarz, A., Encke, A., and Hör, G. (1989) Tc-99m labeled anti-CEA monoclonal antibody for tumor immunoscintigraphy: First clinical results. *Nucl. Med. Commun.* 10, 345-352.
- (51) Zimmer, A. M., Kazikiewicz, J. M., Rosen, S. T., and Spies, S. A. (1987) Pharmacokinetics of $^{99m}\text{Tc}(\text{Sn})$ - and ^{131}I -labeled anti-carcinoembryonic antigen monoclonal antibody fragments in nude mice. *Cancer Res.* 47, 1691-1694.
- (52) Buraggi, G. L., Callegaro, L., Turrin, A., Cascinelli, N., Attili, A., Emanuelli, H., Gasparini, M., Deleide, D., Plassio, G., Dovis, M., Marini, G., Natali, P. G., Scassellati, G. A., Rosa, U., and Ferrone, S. (1984) Immunoscintigraphy with ^{123}I , ^{99m}Tc , and ^{111}In -labeled $\text{F}(\text{ab}')_2$ fragments of monoclonal antibodies to human high molecular weight-melanoma associated antigen. *J. Nucl. Med. Allied Sci.* 28, 283-295.
- (53) Siccardi, A. G., Buraggi, G. L., Callegaro, L., Mariani, G., Natali, P. G., Abbati, A., Betagno, M., Caputo, V., Mansi, L., Masi, R., Paganelli, G., Riva, P., Salvatore, M., Sanguineti, M., Troncone, L., Turco, G. L., Scasselatti, G. A., and Ferrone, S. (1986) Multicenter study of immunoscintigraphy with radiolabeled monoclonal antibodies in patients with melanoma. *Cancer Res.* 46, 4817-4822.
- (54) Hansen, H. J., Jones, A. L., Sharkey, R. M., Grebenau, R., Blazejewski, N., Kunz, A., Buckley, M. J., Newman, E. S., Ostella, F., and Goldenberg, D. M. (1990) Preclinical evaluation of an "instant" ^{99m}Tc -labeling kit for antibody imaging. *Cancer Res.* 50, 794-798.
- (55) Goldenberg, D. M., Goldenberg, H., Sharkey, R. M., Higginbotham-Ford, E., Lee, R. E., Swayne, L. C., Burger, K. A., Tsai, D., Horowitz, J. A., Hall, T. C., Pinsky, C. M., and Hansen, H. J. (1990) Clinical studies of cancer radioimmunodetection with carcinoembryonic antigen monoclonal antibody fragments labeled with ^{123}I or ^{99m}Tc . *Cancer Res.* 50, 909-921.
- (56) Ellman, G. L. (1959) Tissue sulfhydryl groups. *Arch. Biochem. Biophys.* 82, 70-77.
- (57) Griffiths, G. L., Goldenberg, D. M., Knapp, F. F., Jr., Callahan, A. P., Chang, C.-H., and Hansen, H. J. (1991) Direct radiolabeling of monoclonal antibodies with generator-produced rhenium-188 for radioimmunotherapy: Labeling and animal biodistribution studies. *Cancer Res.* 51, 4594-4602.
- (58) Mather, S. J., and Ellison, D. (1990) Reduction-mediated technetium-99m labeling of monoclonal antibodies. *J. Nucl. Med.* 31, 692-697.
- (59) Quadri, S. M., and Wessels, B. W. (1986) Radiolabeled biomolecules with ^{186}Re : Potential for radioimmunotherapy. *Nucl. Med. Biol.* 13, 447-451.
- (60) Pimm, M. V., Armitage, N. C., Perkins, A. C., Smith, W., and Baldwin, R. W. (1985) Localization of an anti-CEA monoclonal antibody in colorectal carcinoma xenografts. *Cancer Immunol. Immunother.* 19, 8-17.
- (61) Kozak, R. W., Raubitschek, A., Mirzadeh, S., Brechbiel, M. W., Junghaus, R., Gansow, O. A., and Waldmann, T. A. (1989) Nature of the bifunctional chelating agent used for radioimmunotherapy with yttrium-90 monoclonal antibodies: Critical factors in determining in vivo survival and organ toxicity. *Cancer Res.* 49, 2639-2644.
- (62) Moi, M. K., Meares, C. F., and DeNardo, S. J. (1988) The peptide way to macrocyclic bifunctional chelating agents: Synthesis of 2-(p-Nitrobenzyl)-1,4,7,10-tetraazacyclododecane- $\text{N},\text{N}',\text{N}'',\text{N}'''$ -tetraacetic acid and study of its yttrium(III) Complex. *J. Am. Chem. Soc.* 110, 6266-6267.
- (63) Schlom, J., Siler, K., Milenic, D. E., Eggensperger, D., Colcher, D., Miller, L. S., Houchens, D., Cheng, R., Kaplan, D., and Goeckeler, W. (1991) Monoclonal antibody-based therapy of a human tumor xenograft with a ^{177}Lu -labeled immunoconjugate. *Cancer Res.* 51, 2889-2896.
- (64) Recommendations of the International Commission on Radiological Protection (1968) ICRP Publication 10, Pergamon Press, London.
- (65) Foxwell, B. M. J., Band, H. A., Long, J., Jeffrey, W. A., Snook, D., Thorpe, P. E., Watson, G., Parker, P. J., Epenetos, A. A., and Creighton, A. M. (1988) Conjugation of monoclonal antibodies to a synthetic peptide substrate for protein kinase: A method for labeling antibodies with ^{32}P . *Br. J. Cancer* 57, 489-493.
- (66) Schroff, R. W., Weiden, P. L., Appelbaum, J., Fer, M. F., Breitz, H., Vanderheyden, J.-L., Ratliff, B. A., Fisher, D., Foisie, D., Hanelin, L. G., Morgan, A. C., Jr., Fritzberg, A. R., and Abrams, P. G. (1990) Rhenium-186 labeled antibody in patients with cancer: Report of a pilot phase I study. *Antibody Immunoconjugate Radiopharm.* 3, 99-111.
- (67) Covell, D. G., Barbet, J., Holton, O. D., Black, C. D. V., Parker, R. J., and Weinstein, J. N. (1986) Pharmacokinetics of Immunoglobulin G, $\text{F}(\text{ab}')_2$, and Fab' in mice. *Cancer Res.* 46, 3969-3978.
- (68) Courtenay-Luck, N. S., Epenetos, A. A., Winearls, C. G., and Ritter, M. A. (1987) Preexisting human anti-murine immunoglobulin reactivity due to polyclonal rheumatoid factors. *Cancer Res.* 47, 4520-4525.
- (69) Courtenay-Luck, N. S., Epenetos, A. A., Moore, R., Larche, M., Pectasides, D., Dhokia, B., and Ritter, M. A. (1986) Development of primary and secondary immune responses to mouse monoclonal antibodies used in the diagnosis and therapy of malignant neoplasms. *Cancer Res.* 46, 6489-6493.

Registry No. ^{99}Tc , 14133-76-7.

LETTER

Design of a Sequence-Specific DNA-Cleaving Molecule Which Conjugates a Copper-Chelating Peptide, a Netropsin Residue, and an Acridine Chromophore

Christian Bailly,[†] Jian-Sheng Sun,[‡] Pierre Colson,[§] Claude Houssier,[§] Claude Hélène,[‡] Michael J. Waring,^{||} and Jean-Pierre Hénichart^{*†}

INSERM U16, Place de Verdun, 59045 Lille, France, Muséum National d'Histoire Naturelle, rue Cuvier, 75231 Paris, France, Laboratoire de Chimie Macromoléculaire et Chimie Physique, Université de Liège au Sart-Tilman, 4000 Liège, Belgium, and Department of Pharmacology, University of Cambridge, Tennis Court Road, CB2 1QJ Cambridge, England. Received October 7, 1991

Artificial control of gene expression could be achieved if one could design sequence-specific ligands for duplex DNA. Small ligands such as netropsin have been shown to bind specifically to the minor groove of DNA (1), and irreversible reactions can be induced at specific DNA sequences if the ligand is equipped with a reactive group (2). We previously reported the DNA-binding properties of a hybrid (minor-groove binder–intercalator) ligand endowed with sequence specificity and high affinity (3). This molecule consists of the oligopyrrolecarboxamide part of netropsin (Net) covalently linked to an intercalating 9-(4-glycylanilino)acridine derivative (GA). Here we show that a tripeptide glycylhistidyllysine (GHK), which has growth-factor-like properties (5), can be hooked to NetGA.¹ A remarkable feature is that the GHK–Cu complex binds to the minor groove of DNA (6), just like netropsin. Therefore, the DNA-binding configurations of these two moieties are perfectly compatible and synergistic effects may be expected. In the presence of copper ions and a reducing agent, this conjugate GHK~NetGA (Figure 1) induces site-specific cleavage of duplex DNA.

To investigate the interaction between GHK~NetGA and DNA, electric linear dichroism (ELD) spectroscopy was employed because this method can independently reveal the orientations of both netropsin and acridine parts of the molecule relative to the DNA bases (Figure 2). The drug–DNA complex oriented by the electric field displays two ELD bands of opposite sign. The positive signal between 295 and 335 nm is due to outside binding of the netropsin part, presumably in the minor groove (3). At 440 nm the signal is negative and its magnitude varies with the GHK~NetGA/DNA ratio. The minimum occurs

at binding ratios between 0.05 and 0.1. The intensity of the ELD signal is also a function of the degree of alignment of the DNA molecules in the electric field. The reduced dichroism depends upon field strength similarly at 260 and 440 nm (Figure 2 inset). This demonstrates that the acridine ring is tilted close to the plane of the DNA bases, consistent with an intercalative mode of binding.

Comparing this behavior with that of a netropsin–acridine hybrid (NetGA) unsubstituted by GHK, we observed that the tripeptide does not inhibit but rather facilitates the groove-binding process and allows complete intercalation of the acridine ring. The affinity constant² of GHK~NetGA for calf thymus DNA is $2.2 \times 10^7 \text{ M}^{-1}$, more than 20-fold greater than that of NetGA ($K_a = 9.1 \times 10^5 \text{ M}^{-1}$), reinforcing the conclusion that GHK contributes positively to the DNA binding. The binding constant diminishes with increasing ionic strength, pointing to additional ionic contacts between the drug (most likely the side chain of lysine) and DNA. Spectroscopic analysis (7) has revealed that GHK binds copper in a square planar configuration, as observed with the analogous tripeptide GGH (8), also used as a cutting agent for DNA-cleaving metalloproteins (9). ESR spectra of GHK~NetGA–Cu(II) confirm that the copper is tetracoordinated³ and produces radical species in the presence of hydrogen peroxide.⁴

* Address correspondence to Jean-Pierre Hénichart, INSERM Unit 16, Place de Verdun, 59045 Lille, France.

[†] INSERM U16.

[‡] Muséum National d'Histoire Naturelle.

[§] Université de Liège.

^{||} University of Cambridge.

¹ To attach GHK to the N-terminus of the netropsin–acridine hybrid, *N*~[(*tert*-butoxycarbonyl)-glycyl-L-histidyl]-*N*~(benzoyloxycarbonyl)-L-lysine (4a) was coupled with methyl 4-[(4-amino-1-methyl-1-pyrrol-2-yl)carbonyl]amino-1-methylpyrrole-2-carboxylate (4b) in the presence of dicyclohexylcarbodiimide (DCC) and hydroxybenzotriazole (HOBt) at 0 °C. After saponification of the methyl ester GHK~Net with sodium hydroxide, the corresponding free acid was subjected to a coupling reaction with 4-(9-acridinylamino)-*N*-glycylaniline (4a) in the presence of DCC/HOBt. After terminal protecting group removal by hydrobromic acid in acetic acid medium, the drug was purified by flash chromatography and fully characterized by conventional spectroscopic methods.

² Binding parameters were determined using spectrophotometric readings from absorbance titration experiments. The apparent association constant K (M^{-1}) was estimated from Scatchard plots using a two-site model which assumes the existence of two independent noncooperative types of binding sites. The program Enzfitter (Elsevier Biosoft) was used to secure the best fit of the data to this model.

³ The Cu(II) atom is tetracoordinated from the imidazole nitrogen, a peptide nitrogen, the terminal glycyl amino group, and an oxygen atom from a water molecule (5–7). The ESR spectrum of the Cu–GHK~NetGA complex was obtained from a frozen, aqueous solution (0.5 mM) in the presence of CuClO_4 (0.25 mM) at 77 K and 9.32 GHz. The magnetic parameters are $A_{\parallel} = 190 \text{ G}$, $g_{\parallel} = 2.22$, and $g_{\perp} = 2.06$.

⁴ Spin-trapping techniques have shown that the drug can serve as a source of oxygen-based free radicals, with hydroxy radicals OH^{\bullet} probably the ultimate reactive species. In the presence of 5,5-dimethyl-1-pyrroline *N*-oxide (DMPO), solutions of GHK~NetGA–Cu complex containing hydrogen peroxide generate an ESR spectrum characteristic of the DMPO-OH radical adduct ($a_N = a_H = 15.2 \text{ G}$). However, direct evidence that these radicals are involved in DNA strand scission is not yet available. The deoxyribose cleavage positions are closely clustered, which may not be consistent with a diffusible radical-mediated DNA cleavage process.

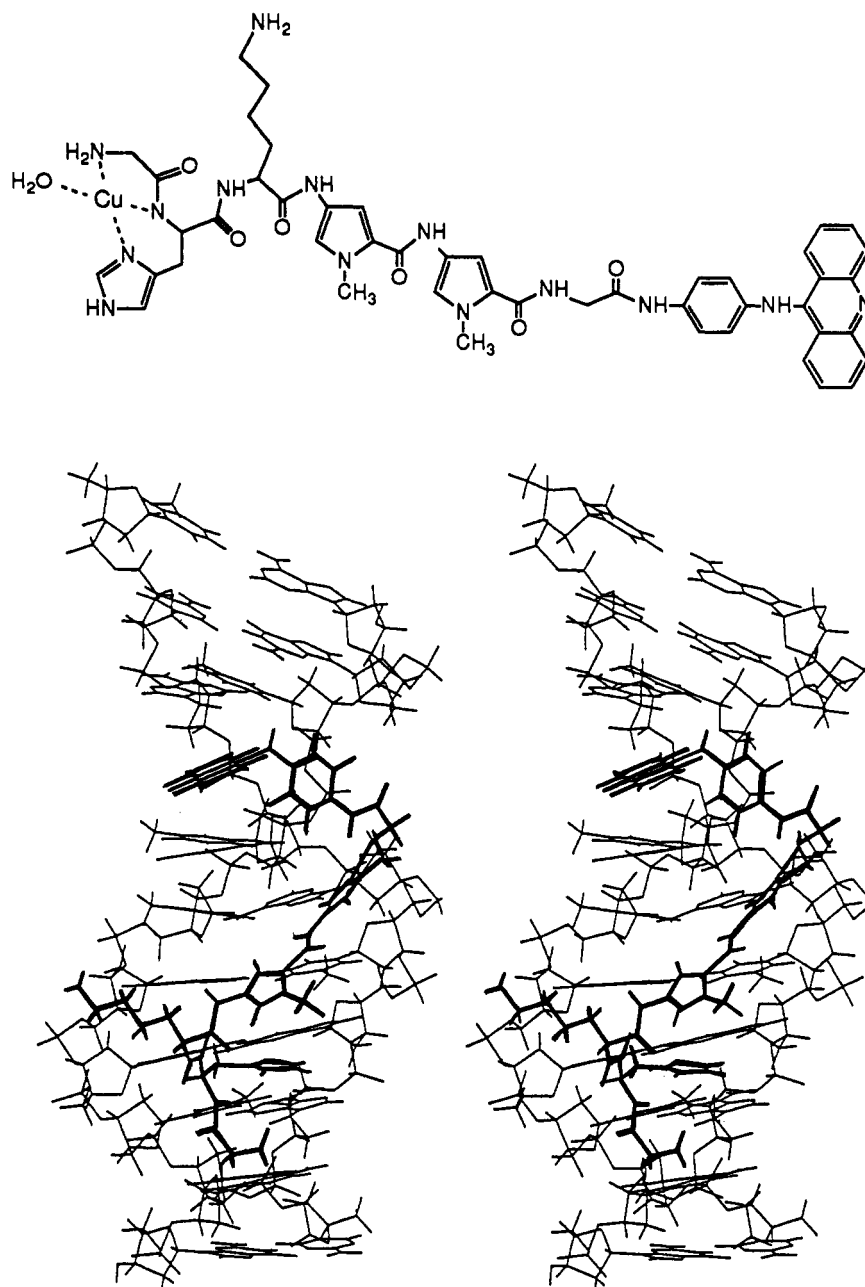


Figure 1. Structure of the GHK~NetGA-Cu(II) complex and stereopair drawing of the complex of GHK~NetGA (dark bonds) with the DNA duplex d(CATTTGATATG):d(GTAAACTATAC).⁷

DNAase I footprinting was used to map GHK~NetGA binding sites on the *Escherichia coli* *tyr* T DNA fragment⁵ (10) (Figure 3a). The major protected duplex region extends from positions 82 to 92 and represents the juxtaposition of two AT-containing tetranucleotides (previously identified with the same DNA fragment as netropsin binding sites (11) flanked by GC base pairs (known as preferential binding steps for numerous intercalators). Surrounding the protected sequence we

⁵ The 160 base pair *tyr* T DNA fragment containing the tyrosine tRNA promoter was isolated from the plasmid pKMA-98 and labeled according to published procedures (10, 11). Incubation with reverse transcriptase and [α -³²P]dCTP led to selective labeling of the 3' end of the top strand (Watson strand) whereas incubation with [α -³²P]dATP led to selective labeling of the 3' end of the bottom strand (Crick strand). DNAase I digestions were performed at 37 °C in buffer with aliquots removed from the digestion mixture 1 and 5 min after the addition of DNAase I (0.03 unit/mL). Reactions were stopped by adding 3 μ L of gel loading solution containing formamide. Samples were heated to 90 °C for 4 min prior to electrophoresis at 1700 V for 2 h.

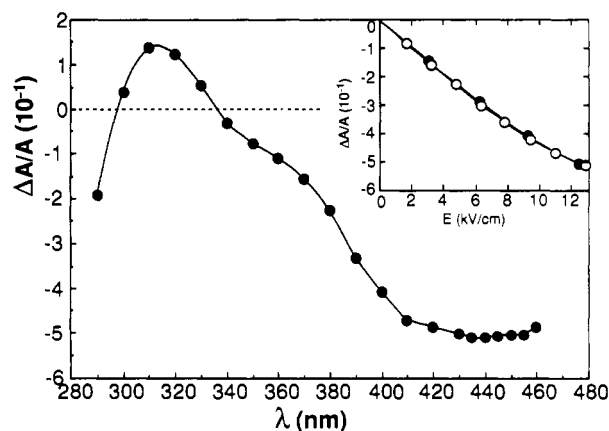


Figure 2. Electric linear dichroism spectra of GHK~NetGA-DNA complex at a drug-DNA ratio of 0.1 and 12.5 kV/cm, in 1 mM Tris HCl buffer, pH 7.0. Inset shows the electric field dependence of the ELD of calf thymus DNA alone at 260 nm (○) compared to that of the GHK~NetGA-DNA complex at 440 nm (●).

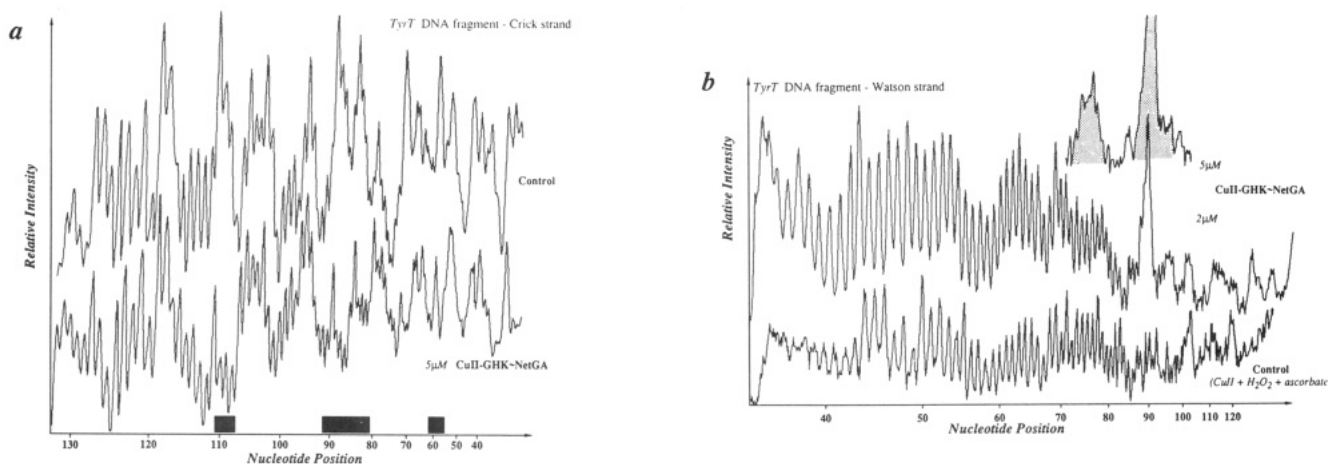


Figure 3. Densitometric traces of the results of (a) DNAase I reaction⁵ with the bottom (Crick) strand of the *tyr* T DNA in the absence (top tracing) and the presence (bottom tracing) of 5 μM GHK~NetGA. (b) DNA cleavages⁶ in the absence (bottom tracing) and presence (top tracing) of GHK~NetGA under reducing conditions. In b both control and drug samples contain hydrogen peroxide (100 μM), ascorbate (100 μM), and Cu(II) (5 μM). Bands were assigned by reference to a dimethyl sulfate-piperidine marker track for guanines. The relative intensity (in arbitrary units) of individual maxima in the control and the drug-treated samples can be compared. The sequence of the DNA is shown in Figure 4.

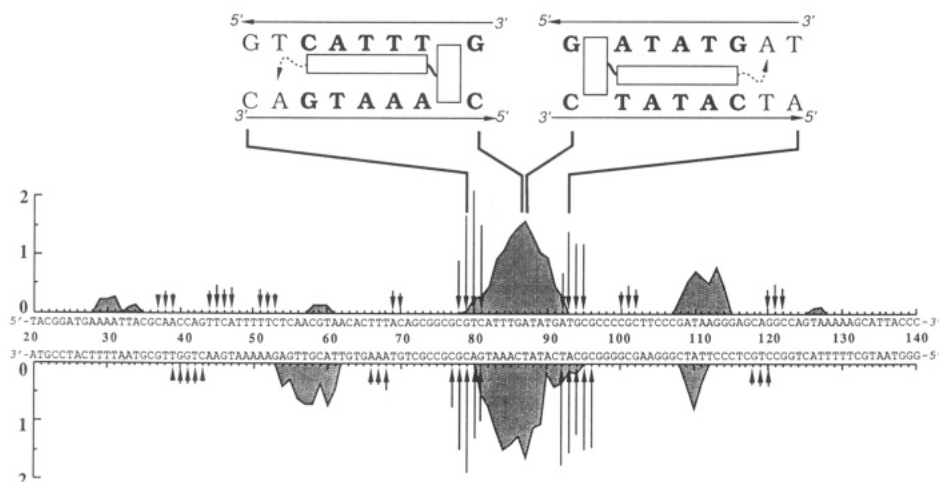


Figure 4. Map of GHK~NetGA binding and cutting of the 160-bp *tyr* T DNA restriction fragment. Areas represent extent of protection from DNAase I cleavage by bound GHK~NetGA. Arrows indicate positions of cleavage by activated drug; lengths of arrows are proportional to the frequency of cleavage. Extent of protection and cleavage were determined by densitometry followed by quantitative analysis. Schematic representation of the two proposed types of binding of GHK~NetGA to DNA.

observed regions of enhanced DNAase I cutting, most notably on the 5' side of the drug-protected sequence. Two other loci of inhibited DNAase I cutting are revealed, one located at positions 108–113 of the top strand, the other at positions 54–62 of the bottom strand. Both these sites are more evident on one strand of the DNA duplex than the other, and both lie some 17–19 base pairs from the 3' end of the principal recognized sequence. The asymmetrical, equidistant appearance of these partial footprints suggests some altered structure detectable by DNAase I since cutting by this enzyme is known to be affected by steric disturbances to the helix. Linkage of the tripeptide GHK increases the strength of binding (and probably the half-life of the drug–DNA complex) so that the specific recognition process can be more readily detected by footprinting.

Addition of sodium ascorbate and hydrogen peroxide initiated cleavage of DNA.⁶ On both strands of the DNA duplex two major cleavage loci at nucleotide positions 80 and 93 (Figure 3b), on each side of the protected sequence revealed, were detected. However, several other minor cleavage loci were also detected along the DNA fragment (Figure 4).

The size of the binding site revealed by footprinting is twice that expected from computer-modeling analysis

(Figure 1). Moreover cleavage occurs on both sides of the recognized duplex sequence although the ligand bears only one cleaving functionality. These observations leave little room for doubt that the target sequence corresponds in fact to two juxtaposed drug binding sites, to which GHK~NetGA binds in opposite orientations: firstly, with the netropsin moiety at the sequence ATTT and the acridine ring intercalated on the 5' side of the central GC base pair and, secondly, with the netropsin bound to the TATA box and with acridine ring intercalated on the 3' side of the central GC. Molecular modeling⁷ (12) of

⁶ 5 μM GHK~NetGA–Cu(II) was allowed to react with the end-labeled *tyr* T DNA for 2 h at room temperature (in 10 mM NaCl, 10 mM Tris-HCl, pH 7.2) in the presence of excess hydrogen peroxide–ascorbate (100 μM of each). Controls established that neither the drug–Cu complex in the absence of H₂O₂–ascorbate nor the drug in the absence of copper gave any detectable cleavage. Under reducing conditions, Cu(II) at micromolar concentrations was found to cleave the DNA randomly with more or less equal intensity at all four nucleotides. At a 1:1 drug–copper(II) ratio, the observed cleavage pattern was a superimposition of specific (GHK~NetGA induced) and nonspecific (copper induced) cutting. Quantitative analysis was performed by subtracting control intensities from those obtained from cleavage of DNA by GHK~NetGA–Cu.

GHK~NetGA bound to the target oligonucleotide reveals that intercalation of the acridine chromophore and simultaneous minor-groove binding of the netropsin part, together with interactive anchorage of the tripeptide, are energetically feasible and supports the two drug orientations shown in Figure 4.

These results establish that attachment of GHK converts a bifunctional DNA-binding ligand composed of two well-characterized antitumor moieties into an artificial endonuclease-like molecule capable, under activation, of attacking a short DNA sequence at a specifically recognized position in the minor groove. This type of small synthetic molecule—a "designer drug" in the true sense—had its origins in a consideration of the molecular mechanism of action of a nuclease acting in the major groove. On this basis there is a brighter prospect of using chemical knowledge to design sequence-specific artificial endonucleases.

ACKNOWLEDGMENT

This work was supported by grants from the INSERM, the CNRS (France), the FNRS (Belgium), the MRC, and the Cancer Research Campaign (U.K.).

LITERATURE CITED

- (1) Kopka, M. L., Yoon, C., Goodsell, D., Pjura, P., and Dickerson, R. E. (1985) The molecular origin of DNA-drug specificity in netropsin and distamycin. *Proc. Natl. Acad. Sci. U.S.A.* 82, 1376–1380.
- (2) (a) Dervan, P. B. (1986) Design of sequence-specific DNA-binding molecules. *Science* 232, 464–471. (b) Lown, J. W., Sondhi, S. M., Ong, C. W., Skorobogaty, A., Kishikawa, H., and Dabrowiak, J. C. (1986) Deoxyribonucleic acid cleavage specificity of a series of acridine- and acodazole-iron porphyrins as functional bleomycin models. *Biochemistry* 25, 5111–5117. (c) Ward, B., Skorobogaty, A., Kishikawa, H., and Dabrowiak, J. C. (1986) DNA cleavage specificity of a group of cationic metalloporphyrins. *Biochemistry* 25, 6875–6883. (d) Barton, J. K. (1986) Metals and DNA: molecular left-handed complements. *Science* 233, 727–734. (e) Sluka, J. P., Horvath, S. J., Bruist, M. F., Simon, M. I., and Dervan, P. B. (1987) Synthesis of a sequence-specific DNA-cleaving peptide. *Science* 238, 1129–1132. (f) Perrouault, L., Asseline, U., Rivalle, C., Thuong, N. T., Bisagni, E., Giovannangeli, C., Le Doan, T., and Hélène, C. (1990) Sequence specific artificial photo-induced endonucleases based on triple helix-forming oligonucleotides. *Nature* 344, 358–360. (g) Sigman, D. S. (1990) Chemical nucleases. *Biochemistry* 29, 9097–9105.
- (3) Bailly, C., Helbecque, N., Hénichart, J. P., Colson, P., Houssier, C., Rao, K. E., Shea, R. G., and Lown, J. W. (1990) Molecular recognition between oligopeptides and nucleic acids. DNA sequence specificity and binding properties of an acridine-linked netropsin hybrid ligand. *J. Mol. Recognit.* 3, 26–35.
- (4) (a) Morier-Teissier, E., Bailly, C., Bernier, J. L., Houssin, R., Helbecque, N., Catteau, J. P., Colson, P., Houssier, C., and Hénichart, J. P. (1989) Synthesis, biological activity and DNA interaction of anilinoacridine and bithiazole peptide derivatives related to the anti-tumor drugs m-AMSA and bleomycin. *Anti-Cancer Drug Des.* 4, 37–52. (b) Bailly, C., Pommery, N., Houssin, R., and Hénichart, J. P. (1989) Design, synthesis, DNA-binding, and biological activity of a series of DNA minor-groove-binding intercalating drugs. *J. Pharm. Sci.* 78, 910–917.
- (5) Pickart, L., Freedman, J. H., Loker, W. J., Peisach, J., Perkins, C. M., Stenkamp, R. E., and Weinstein, B. (1980) Growth-modulating plasma tripeptide may function by facilitating copper uptake into cells. *Nature* 288, 715–717.
- (6) Chikira, M., Sato, T., Antholine, W. E., and Petering, D. H. (1991) Orientation of non-blue cupric complexes on DNA fibers. *J. Biol. Chem.* 266, 2859–2863.
- (7) (a) Freedman, J. H., Pickart, L., Weinstein, B., Mims, W. B., and Peisach, J. (1982) Structure of the glycyl-L-histidyl-L-lysine-copper(II) complex in solution. *Biochemistry* 21, 4540–4544. (b) Laussac, J. P., Haran, R., and Sarkar, B. (1983) N.m.r. and e.p.r. investigation of the interaction of copper(II) and glycyl-L-histidyl-L-lysine, a growth-modulating tripeptide from plasma. *Biochem. J.* 209, 533–539.
- (8) Camerman, N., Camerman, A., and Sarkar, B. (1976) Molecular design to mimic the copper(II) transport site of human albumin. The crystal and molecular structure of the copper(II)-glycyl-glycyl-L-histidine-N-methyl amide monoaquo complex. *Can. J. Chem.* 54, 1309–1316.
- (9) (a) Mack, D. P., Iverson, B. L., and Dervan, P. B. (1988) Design and chemical synthesis of a sequence-specific DNA-cleaving protein. *J. Am. Chem. Soc.* 110, 7572–7574. (b) Mack, D. P., and Dervan, P. B. (1990) Nickel-mediated sequence-specific oxidative cleavage of DNA by a designed metalloprotein. *J. Am. Chem. Soc.* 112, 4604–4606.
- (10) Drew, H. R., and Travers, A. A. (1984) DNA structural variations in the *E. coli* *tyrT* promoter. *Cell* 37, 491–502.
- (11) Portugal, J., and Waring, M. J. (1987) Comparison of binding sites in DNA for berenil, netropsin and distamycin. *Eur. J. Biochem.* 167, 281–289.
- (12) Lavery, R. (1988) *Structure and Expression, Vol. 3, DNA Bending and Curvature* (W. K. Olson, M. H. Sarma, R. H. Sarma, and M. Sundaralingam, Eds.) pp 191–211, Adenine Press, Guilderland, NY.

⁷ The GHK~NetGA/DNA complex was modeled by conformational energy minimization using the JUMNA program package (12). The ligand was docked into the minor groove of B-DNA to avoid steric clashes using the Insight program (Biosym Inc.). Minimization was effected by successively decreasing the number of constraints. Calculations were performed on a Silicon Graphics 4D/120GTXB workstation.

ARTICLES

Photoactivation of Toxin Conjugates[†]

Victor S. Goldmacher,* Peter D. Senter,[†] John M. Lambert, and Walter A. Blättler

ImmunoGen, Inc., 148 Sidney Street, Cambridge, Massachusetts 02139. Received July 1, 1991

A novel photocleavable protein cross-linking reagent has been used for conjugation of the ribosome-inactivating protein pokeweed antiviral protein from seeds of *Phytolacca americana* (PAP-S), with either the monoclonal antibody 5E9 directed against the human transferrin-receptor or the B-chain of ricin that binds to cell-surface oligosaccharides bearing terminal D-galactose residues. When irradiated with near-UV light (350 nm), the linker of these conjugates undergoes photolytic degradation, resulting in the release of native toxin that is fully functional. The cytotoxicities of these 5E9-PAP-S and ricin B-chain-PAP-S conjugates for HeLa cells could be enhanced by irradiating the cells with light after they had internalized the conjugates.

INTRODUCTION

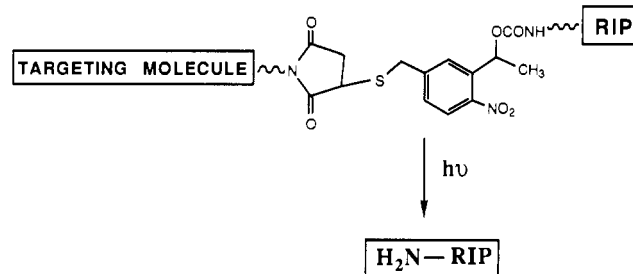
We have previously described the synthesis of novel photocleavable cross-linking reagents which can be used for constructing conjugates between ribosome-inactivating proteins and targeting molecules such as monoclonal antibodies or lectins (1). UV irradiation (350 nm) of such conjugates results in the photolytic fragmentation of the linker and release of nonmodified toxin that is fully active in a cell-free translation system (Scheme I). Here we report the cytotoxic effects on cultured human cells of conjugates of the ribosome-inactivating protein PAP-S¹ to two different targeting molecules made with photocleavable cross-linking reagents. One targeting molecule, the monoclonal antibody 5E9, binds to the human transferrin receptor, but does not compete with transferrin for binding, and is not cytotoxic (2). The other targeting molecule, ricin B-chain, binds to terminal D-galactose residues of oligosaccharide components of cell-surface molecules (3).

EXPERIMENTAL PROCEDURES

Synthesis of Photocleavable Cross-Linking Reagents. The chloroformate derivative of S-[4-nitro-3-(1-hydroxyethyl)phenyl]methyl thioacetate (see Scheme II, top of left column) was synthesized as described previously (1).

The chloroformate of 1-[5-(N-maleimidomethyl)-2-nitrophenyl]ethanol (see Scheme II, top of right column) was synthesized as follows. 1-[5-(Bromomethyl)-2-nitrophenyl]ethanol (see ref 1) was converted with aqueous ammonia in methanol to the corresponding 1-[5-(aminomethyl)-2-nitrophenyl]ethanol. The amine was reacted with 1 equiv of maleic anhydride in methanol, thus forming the corresponding amido carboxylic acid. Ring closure to form a maleimido group was effected with anhydrous sodium acetate in acetic anhydride. The resulting O-acetyl derivative of 1-[5-(N-maleimidomethyl)-2-nitrophenyl]ethanol was then hydrolyzed to the final hydroxy com-

Scheme I. Release of the Ribosome-Inactivating-Protein (RIP) Moiety from Its Conjugate with a Targeting Molecule upon Irradiation with Light



pound by refluxing in a mixture of tetrahydrofuran and 3% aqueous perchloric acid (2:1, v/v) under an atmosphere of nitrogen for 20 h. After chromatography on silica, 1-[5-(N-maleimidomethyl)-2-nitrophenyl]ethanol was obtained as a light yellowish solid, which was converted to the corresponding chloroformate as described in ref 1.

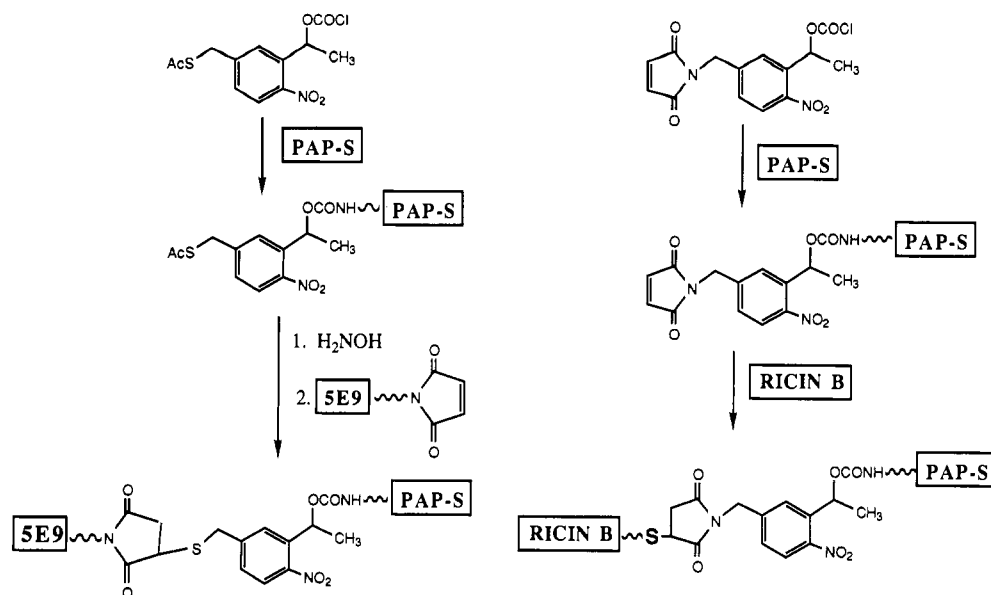
Preparation of Conjugates. The conjugate between the monoclonal antibody 5E9 [IgG₁, anti-human transferrin receptor (2), purified as described previously (4)] and PAP-S² was prepared as illustrated in Scheme II (left column) using procedures described previously (1). Briefly, PAP-S was reacted with the chloroformate of S-[4-nitro-3-(1-hydroxyethyl)phenyl]methyl thioacetate using conditions described previously (1), and free sulfhydryl groups were generated by treating the modified PAP-S with 50 mM hydroxylamine at pH 7.3 for 30 min at 25 °C followed by gel filtration through Sephadex G 25 equilibrated with 100 mM potassium phosphate buffer (pH 7.0). An average of 0.7 sulfhydryl groups per molecule of PAP-S were introduced in this way, as measured by Ellman's reagent (5). The modified PAP-S was mixed at pH 7.0 with 5E9 antibody which had been functionalized with succinimidyl 4-(N-maleimidomethyl)cyclohexane-1-carboxylate so as to introduce an average of 1.5 maleimido groups per antibody molecule using procedures for antibody modification described previously (1, 5). The incorporation of maleimido groups was assayed with [¹⁴C]cysteine using the method described previously (5). The conjugation

[†] This work was done during the authors' appointment in the Division of Tumor Immunology of the Dana-Farber Cancer Institute and Harvard Medical School.

* Present address: Oncogen, Inc., Seattle, WA 98121.

¹ PAP-S, pokeweed antiviral protein from seeds of *Phytolacca americana*.

² The source and purification of PAP-S has been reported elsewhere (5).

Scheme II. Construction of Light-Sensitive Conjugates of PAP-S with either 5E9 Antibody (left) or Ricin B-Chain (right)

reaction mixture was kept at 4 °C for 4 h and the conjugate was then purified by ion-exchange chromatography followed by gel filtration as described previously (1), yielding conjugates of similar purity to those described previously as shown by polyacrylamide/sodium dodecyl sulfate gel electrophoresis (1).

PAP-S was conjugated to ricin B-chain (Scheme II, right column) by first reacting PAP-S (1 mg/mL) with the chloroformate derivative of 1-[5-(*N*-maleimidomethyl)-2-nitrophenyl]ethanol (20-fold molar excess) in 100 mM NaHCO₃ at 0 °C for 30 min followed by gel filtration through a column of Sephadex G-25 equilibrated in 100 mM sodium phosphate buffer (pH 7.0). The modified PAP-S was then reacted with 1 mol equiv of ricin B-chain (Worthington, Freehold, NJ). After a 3-h incubation, the reaction mixture was applied to a column (2 × 90 cm) of Sephadex G-100 equilibrated in 5 mM bistris/acetate (pH 5.8) containing lactose (50 mM), NaCl (50 mM), EDTA (1 mM), and dithioerythritol (1 mM). Fractions were analyzed by polyacrylamide/sodium dodecyl sulfate gel electrophoresis, and those fractions containing the conjugate (1:1 ratio of ricin B-chain and PAP-S) were dialyzed against 10 mM potassium phosphate buffer (pH 7.2) containing NaCl (145 mM) and stored in aliquots (90 μL) at -80 °C.

Irradiation of Cells. Samples were irradiated with near-UV light for 7 min at room temperature. A Rayonet fluorescence UV lamp (Southern New England Ultraviolet Co., Middletown, CT) with an emission peak at 350 nm was used as a source of UV light. The lamp was placed at a 15-cm distance from the Petri dishes with samples. SDS gel electrophoresis showed that ≥85% of the conjugate was cleaved under these conditions.

Cells and Cell Culture Maintenance. HeLa cells (ATCC CCL 2) were grown as monolayer cultures in a growth medium composed of RPMI-1640 medium supplemented with 10% heat-treated (30 min at 56 °C) fetal calf serum and 2 mM L-glutamine (all three from GIBCO). Cells were passaged twice a week, using the standard trypsin-Versen mixture (Whittaker M.A. Bioproducts, Walkersville, MD) to suspend the cells.

Cytotoxicity Studies. Cytotoxicities of toxin conjugates were determined by a clonogenic assay. Cells were plated onto 20 cm² polystyrene tissue culture grade Petri

dishes in 10 mL of growth medium at a density of 5–1000 cells/cm² and left for 24 h at 37 °C in a humidified atmosphere containing 5% CO₂. Within this interval of time, the cells adhered to the substratum and resumed exponential growth, and the expression of cell-surface transferrin receptors and binding sites for ricin returned to normal after being decreased during the trypsinization procedure (data not shown). Medium was then replaced with 10 mL of fresh growth medium containing a toxin conjugate. After a desired time period of exposure to the toxin at 37 °C, Petri dishes (with the lid on) were irradiated for 7 min with near-UV light at room temperature. Following the irradiation, the cells were rinsed with warm growth medium and incubated in 10 mL of fresh medium for 8 days. Colonies of 20 or more cells were enumerated as described previously (6).

RESULTS

We have previously established that irradiation of photocleavable conjugates with UV light under conditions used in experiments with cells induced dissociation of more than 85% of the toxin molecules, as determined by polyacrylamide/SDS gel electrophoresis (1). The 5E9-PAP-S and the ricin B-chain-PAP-S conjugates were cleaved using identical conditions (results not shown). As described previously (1), we also further confirmed the release of fully active PAP-S from the photocleavable conjugates by measuring its ability to inhibit protein synthesis in a cell-free translation system (1, 7). PAP-S released from these conjugates was as efficient at inactivating protein synthesis as native PAP-S.

The cytotoxicity of the toxin conjugates was examined by measuring the colony-forming ability of HeLa cells which had been exposed to the reagents for a desired period of time under normal growth conditions. Plating efficiency of control HeLa cells in these experiments was 0.4–0.5. UV irradiation of cells in the absence of toxins under conditions described in Experimental Procedures was non-toxic (surviving fractions ≥ 0.9).

Photocleavable conjugates had a significant cytotoxicity even in the dark (Figure 1), which was consistent with our observation (1) that PAP-S conjugated with an antibody via a photocleavable linker could inactivate ribosomes in a cell-free translation system. Irradiation of

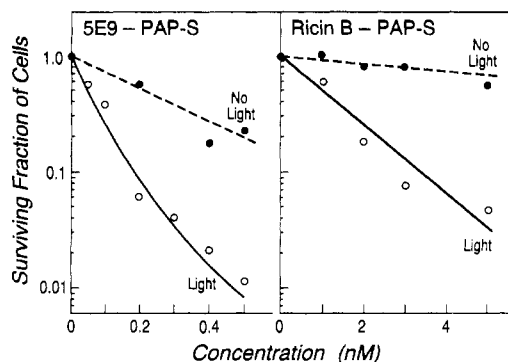


Figure 1. Cytotoxicity of photocleavable conjugates 5E9-PAP-S and ricin B-chain-PAP-S. Cells were incubated with a conjugate for 24 h under normal growth conditions, and then the cells were either light irradiated (empty symbols) or not (filled symbols). The dishes with the cells were then rinsed and placed into fresh medium, and the surviving fractions of cells were determined by their ability to form colonies.

cells that had been exposed for 24 h to ricin B-PAP-S or 5E9-PAP-S with UV light caused a further profound decrease in the surviving fraction (Figure 1).

The following controls have been done in order to confirm the specificity of the cytotoxic effects. Photocleavable conjugates 5E9-PAP-S (0.4 nM) mixed with 1 μ M 5E9 antibody or ricin B-chain-PAP-S (2 nM) mixed with 30 mM α -lactose were essentially not cytotoxic (surviving fractions ≥ 0.9) whether followed or not by UV irradiation of the cells. PAP-S, 5E9, or ricin B-chain alone, with or without the UV-irradiation step, were not toxic to the cells at concentrations up to 50 nM.

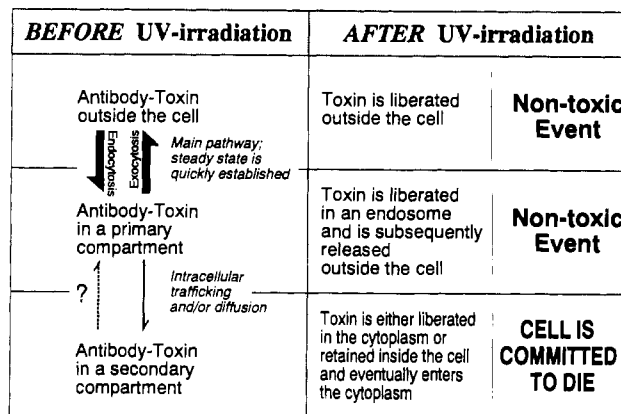
A short (1 h) exposure of cells to photocleavable ricin B-PAP-S (20 nM), or to 5E9-PAP-S (1 nM) with or without subsequent UV irradiation, was not toxic for HeLa cells (surviving fractions ≥ 0.95).

DISCUSSION

It has been reported previously that immunotoxins in which antibody and single-chain ribosome-inactivating protein moieties are linked via a disulfide bond are more cytotoxic than similar immunotoxins linked in a noncleavable manner, presumably because the disulfide bond is reductively cleaved in the cells (5,9–12). The data reported here indicate that the disulfide linkage is not unique in this respect and suggest that other linkers which allow release of the single-chain ribosome-inactivating protein inside cells will permit the formation of a cytotoxic immunotoxin. In this respect photocleavable conjugates of PAP-S were similar to conjugates of antibodies or ricin B-chain with PAP-S or with gelonin linked via a disulfide bond (5). Gelonin is a single-chain ribosome-inactivating protein that is similar to PAP-S in its enzymatic activity and specificity and its cytotoxicity properties (5,8). Cytotoxicities of ricin B-gelonin and of 5E9-gelonin conjugates linked via a disulfide bond for HeLa cells after a 24-h exposure [with the IC_{37} being 0.12 nM for the both conjugates (13)] are very similar to those of the photolabile conjugates described in this report ($IC_{37} = 0.05$ and 1.3 nM for photocleavable conjugates of 5E9-PAP-S and ricin B-chain-PAP-S after a 24-h exposure followed by UV irradiation, respectively).

It is well-established (14–16) that endocytosis is an obligatory step in the process of intoxication of cells by antibody conjugated to single-chain ribosome-inactivating proteins or ricin A-chain. In particular, experiments with a large number of disulfide-linked conjugates of gelonin with antibodies showed that, invariably, those conjugates

Scheme III. Internalization of a PAP-S Conjugate and Release of PAP-S Moiety from Its Conjugate



that were not endocytosed exhibited low cytotoxicity similar to that of free gelonin, while those conjugates that were endocytosed demonstrated enhanced cytotoxicity (14). Similar results were obtained in experiments with disulfide-linked PAP-S conjugates (Goldmacher, V. S., Lambert, J. M., and Blättler, W. A., unpublished results). The observation that free PAP-S at 50 nM did not have a cytotoxic effect on HeLa cells also suggested that the PAP-S moieties of the conjugates which were located outside the cell at the time of the irradiation were not toxic to the cells. These results imply that only the internalized PAP-S molecules were involved in killing cells.

Endocytosis delivers proteins into endosomes and lysosomes that are acidified to pH 4.5–5.5 (17). The photolysis of *o*-nitrobenzyl alcohol derivatives is thought to involve an *aci*-nitro intermediate that decomposes to the final product (18). This decomposition is catalyzed by protons. Therefore, the acidified compartments create a favorable environment for the reaction. Thus, photolytic cleavage of the photocleavable conjugates is possible in any intracellular compartments, including the acidified ones.

The fact that a short (1 h) incubation of cells with photocleavable PAP-S conjugates followed by UV irradiation of the cells does not induce any noticeable cytotoxic effect is of interest. It suggests that a single round of endocytosis is not sufficient for achieving an intracellular concentration of PAP-S conjugate that is high enough to kill the cell upon the release of free toxin by UV irradiation. Endocytosis for a 24-h period appears to be necessary to accumulate sufficient amounts of the conjugates to kill the cells once the PAP-S can be released.

The compartment where this accumulation of the conjugate takes place is probably a compartment that is distinct from the primary endosome. Previously we have shown that most molecules of ricin B-chain and 5E9 antibody that had been internalized by cells via endocytosis are quickly transported back to the cell surface via exocytosis (14). PAP-S molecules liberated from the conjugate in endosomes might therefore be quickly excreted into the external medium and thus would not cause any cytotoxic effect. The tentative pathway of intoxication of cells by photocleavable conjugates is depicted in Scheme III. The intracellular site of cleavage of disulfide-linked conjugates is also unknown. It seems likely that such conjugates would be cleaved under reducing conditions in the cell. Such conditions are not found in endosomes or lysosomes (19), but rather in the cytoplasm that contains 1–10 mM glutathione (20), or in the endoplasmic reticulum or the Golgi complex that contain protein disulfide isomerase (19).

We have demonstrated that the cytotoxicity of conjugates prepared with photocleavable linkers can be induced by photolysis. Such conjugates may be of interest as a research tool because their cytotoxicity can be increased by an external signal at the desired site and/or at the desired moment in time.

LITERATURE CITED

- (1) Senter, P. D., Tansey, M. J., Lambert, J. M., and Blättler, W. A. (1985) Novel photocleavable protein crosslinking reagents and their use in the preparation of antibody-toxin conjugates. *Photochem. Photobiol.* **42**, 231-237.
- (2) Haynes, B. F., Hemler, M., Cotner, T., Mann, D. L., Eisenbarth, G. S., Strominger, J. L., and Fauci, A. S. (1981) Characterization of a monoclonal antibody (5E9) that defines a human cell surface antigen of cell activation. *J. Immunol.* **127**, 347-351.
- (3) Olsnes, S., and Pihl, A. (1982) Toxic lectins and related proteins. In *Molecular Action of Toxins and Viruses* (P. Cohen, and S. van Heyningen, Eds.) pp 195-234, Elsevier, Amsterdam.
- (4) Scott, C. F., Goldmacher, V. S., Lambert, J. M., Jackson, J. V., and McIntyre, G. D. (1987) An immunotoxin composed of a monoclonal anti-transferrin receptor antibody linked by a disulfide bond to the ribosome-inactivating protein gelonin: potent in vitro and in vivo effects against human tumors. *J. Natl. Cancer Inst.* **79**, 1163-1172.
- (5) Lambert, J. M., Senter, P. D., Yau-Young, A., Blättler, W. A., Goldmacher, V. S. (1985) Purified immunotoxins that are reactive with human lymphoid cells. Monoclonal antibodies conjugated to the ribosome-inactivating proteins gelonin and the pokeweed antiviral proteins. *J. Biol. Chem.* **160**, 12035-12041.
- (6) Goldmacher, V. S., Tinnel, N. L., and Nelson, B. C. (1986) Evidence that pinocytosis in lymphoid cells has a low capacity. *J. Cell Biol.* **102**, 1312-1319.
- (7) Pelham, H. R., and Jackson, R. J. (1976) An efficient mRNA-dependent translation system from reticulocyte lysates. *Eur. J. Biochem.* **67**, 247-256.
- (8) Endo, Y., Tsurugi, K., and Lambert, J. M. (1988) The site of action of six different ribosome-inactivating proteins from plants on eukaryotic ribosomes: The RNA *N*-glycosidase activity of the proteins. *Biochem. Biophys. Res. Commun.* **150**, 1032-1036.
- (9) Oeltman, T. N., and Forbes, J. T. (1981) Inhibition of mouse spleen cell function by diphtheria toxin fragment A coupled to anti-mouse Thy-1.2 and by ricin A chain coupled to anti-mouse IgM. *Arch. Biochem. Biophys.* **209**, 362-370.
- (10) Masuho, Y., Kishida, K., Saito, M., Umemoto, N., and Hara, T. (1982) Importance of the antigen-binding valency and the nature of the crosslinking bond in ricin A-chain conjugates with antibody. *J. Biochem.* **91**, 1583-1591.
- (11) Blythman, H. E., Bord, A., Buisson, I., Jansen, F. K., Richer, G., and Thurneyssen, O. (1984) Antitumor effect of immunotoxin in mouse and human tumor models. *Protides* **32**, 421-424.
- (12) Ramakrishnan, S., and Houston, L. L. (1984) Comparison of the selective cytotoxic effects of immunotoxins containing ricin A chain or pokeweed antiviral protein and anti-Thy 1.1 monoclonal antibodies. *Cancer Res.* **44**, 201-208.
- (13) Goldmacher, V. S., Blättler, W. A., Lambert, J. M., McIntyre, G., and Stewart, J. (1990) Cytotoxicity of gelonin conjugated to targeting molecules: effects of weak amines, monensin, adenovirus, and adenoviral capsid proteins penton, hexon, and fiber. *Mol. Pharmacol.* **36**, 818-822.
- (14) Goldmacher, V. S., Scott, C. F., Lambert, J. M., McIntyre, G. D., Blättler, W. A., Collinson, A. R., Stewart, J. K., Chong, L. D., Cook, S., Slayter, H. S., Beaumont, E., and Watkins, S. (1989) Cytotoxicity of gelonin and its conjugates with antibodies is determined by the extent of their endocytosis. *J. Cell. Physiol.* **141**, 222-234.
- (15) Preijers, F. W. M. B., Tax, W. J. M., De Witte, T., Janssen, A., Heijden, H. V. D., Vidal, H., Wessels, J. M. C., and Capel, P. J. A. (1988) Relationship between internalization and cytotoxicity of ricin A-chain immunotoxins. *Br. J. Haematol.* **70**, 289-294.
- (16) Wargalla, U. C., and Reisfeld, R. A. (1989) Rate of internalization of an immunotoxin correlates with cytotoxic activity against human tumor cells. *Proc. Natl. Acad. Sci. U.S.A.* **86**, 5146-5150.
- (17) Yamashiro, D. J., and Maxfield, F. R. (1984) Acidification of endocytic compartments and the intracellular pathways of ligands and receptors. *J. Cell. Biochem.* **26**, 231-246.
- (18) Walker, J. W., Reid, G. P., McGray, J. A., and Trentham, D. R. (1988) Photolabile 1-(2-nitrophenyl)ethyl phosphate esters of adenine nucleotide analogues. Synthesis and mechanism of photolysis. *J. Am. Chem. Soc.* **110**, 7170-7177.
- (19) Feener, E. P., Shen, W.-C., and Ryser, H. J.-P. (1990) Cleavage of disulfide bonds in endocytosed macromolecules. A processing not associated with lysosomes or endosomes. *J. Biol. Chem.* **265**, 18780-18785.
- (20) Meister, A. (1988) Glutathione metabolism and its selective modification. *J. Biol. Chem.* **263**, 17205-17208.

Registry No. S-[4-Nitro-3-(1-hydroxyethyl)phenyl]methyl thioacetate chloroformate derivative, 99821-62-2; 1-[5-(*N*-maleimidomethyl)-2-nitrophenyl]ethanol chloroformate derivative, 114317-16-7; 1-[5-(bromomethyl)-2-nitrophenyl]ethanol, 99821-60-0; 1-[5-(aminomethyl)-2-nitrophenyl]ethanol, 138957-91-2; 1-[5-(aminomethyl)-2-nitrophenyl]ethanol maleic acid derivative, 138957-92-3; 1-[5-(*N*-maleimidomethyl)-2-nitrophenyl]ethanol *O*-acetyl derivative, 138957-93-4; 1-[5-(*N*-maleimidomethyl)-2-nitrophenyl]ethanol, 138957-94-5.

Convenient Synthesis of Bifunctional Tetraaza Macrocycles

Thomas J. McMurry,* Martin Brechbiel, Krishan Kumar, and Otto A. Gansow

Radiation Oncology Branch, National Cancer Institute, National Institutes of Health, Building 10, Room B3-B69, Bethesda, Maryland 20892. Received August 5, 1991

A convenient synthesis of 4-nitrobenzyl-substituted macrocyclic tetraamines and their conversion to bifunctional poly(amino carboxylate) chelating agents is described. Cyclization of (4-nitrobenzyl)-ethylenediamine with appropriate BOC-protected amino disuccinimido esters in dioxane at 90 °C resulted in the formation of 12- and 14-membered ring diamides in 40% and 44% yield, respectively. A 12-membered macrocyclic triamide was also prepared in 44% yield by cyclization of *N*-(2-aminoethyl)-4-nitrophenylalaninamide with disuccinimidyl *N*-(*tert*-butoxycarbonyl)iminodiacetate. Deprotection (HCl/dioxane) and reduction with borane gave the substituted macrocyclic amines which were then alkylated with either bromoacetic acid or *tert*-butyl bromoacetate. Preparation of the isothiocyanate derivatives and ¹⁴C labeled chelating agents are described. Attempts to prepare a 9-membered macrocyclic diamide using this cyclization technique resulted instead in a 20% yield of a 10:1 mixture of isomeric fused 5,6 ring acylamidines. Deprotection (HCl/dioxane) and reduction with borane gave a substituted piperazine derivative in 55% yield.

INTRODUCTION

The notion that a tumor-seeking monoclonal antibody (mAb) can act as a biological "magic bullet" has prompted extensive investigations to determine the utility of radiolabeled antibody in cancer diagnosis and therapy (1). Radioiodination was first employed to label antibodies (2) and has been used to prepare [¹³¹I]mAb conjugates for clinical studies (3). However, neither ¹³¹I nor ¹²⁵I has proved to be ideal for scintigraphy or therapy (4). Fortunately, exploitation of the broad array of decay properties available within the metallic radionuclides is possible provided the antibody can be altered to incorporate a strong metal-binding site. Methodology required to introduce a exogenous metal-binding site into protein was demonstrated in 1974 by Meares and co-workers, who reported the synthesis of a bifunctional EDTA (5) molecule bearing a *p*-diazophenyl moiety capable of functionalizing serum albumin and fibrinogen (6-8). Linkage of a metal complex to mAb and the subsequent tumor localization of ¹¹¹In in mice was first achieved (9) using the mixed anhydride DTPA-isobutylcarboxylic carbonic anhydride (10), which reacts with proteins to form a modified tetraacetic acid ligand.

Tetraacetic acid chelates of the type noted above did not have sufficient thermodynamic and kinetic stability to prevent in vivo loss of radionuclides such as ⁹⁰Y, an energetic β emitter proposed for use in cancer therapy (11-13). Because dissociated yttrium accumulates in the bone (14) and would provide an undesirable dose to the radiosensitive marrow, the need to efficiently sequester the ion is apparent. Efforts to improve the thermodynamic and kinetic stability of the radionuclide complexes has led to the development of DTPA chelating agents which satisfy the requirements of the typically 8-9 coordinate (15, 16) yttrium ion (17, 18). Biological experiments have clearly demonstrated the advantages of these DTPA chelates for in vivo sequestration of ⁹⁰Y (19) and ¹¹¹In (17, 18). We have recently reported the synthesis of a series of modified DTPA ligands in which backbone alkyl substituents have been added to increase the kinetic inertness of the chelates (20). Concurrent with that work, we have been exploring the chemistry of macrocyclic poly(amino

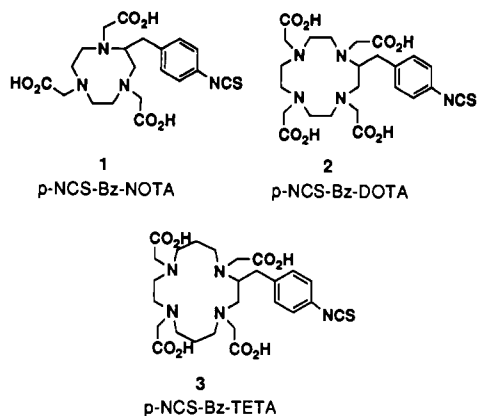
carboxylates) known to form unusually stable metal complexes (21-23).

Complexes of macrocyclic ligands typically show enhanced thermodynamic and kinetic stability relative to an open-chain analogue. The thermodynamic "macrocyclic effect" is attributed to the enthalpic and entropic contributions resulting from the "preorganization" (24) enjoyed by the macrocycle (25). The 9-, 12-, and 14-membered ring poly(amino carboxylates) 1,4,7-triazacyclononane-*N,N',N''*-triacetic acid (NOTA), 1,4,7,10-tetraazacyclododecane-*N,N',N'',N'''*-tetraacetic acid (DOTA), and 1,4,8,11-tetraazacyclotetradecane-*N,N',N'',N'''*-tetraacetic acid (TETA) form an attractive series of ligands in which the variation in cavity size and the number of donor atoms confer unique properties on the metal complexes (21, 26-28). For example, DOTA has been shown to form remarkably stable complexes of both divalent and trivalent metals, including yttrium and the lanthanides (29, 30), prompting the synthesis of several C- and N-functionalized derivatives of DOTA (33-36) and TETA (37, 38) suitable for linkage to mAb. Biological experiments with ⁸⁸Y-labeled DOTA/Lym-1 conjugates have confirmed that the Y[DOTA]⁻ complex exhibits high stability in vivo (39). Our interest in synthesizing a bifunctional DOTA ligand was stimulated by the observation that the complexes [Pb(DOTA)]²⁻ and [Bi(DOTA)]⁻ were kinetically inert within the pH ranges of 4-10 (40), suggesting the utility of DOTA as a chelating agent for the α emitter ²¹²Bi and its parent ²¹²Pb (41). We report here the synthesis of the macrocyclic bifunctional poly(amino carboxylates) 2 and 3 by a synthetic route employing a diamide cyclization reaction. Our attempts to prepare 1 were thwarted by the propensity of the 9-membered macrocyclic diamide precursor to undergo a transannular reaction, resulting in the formation of a fused 5,6 ring acyl amidine.

EXPERIMENTAL PROCEDURES

Materials and Methods. Anhydrous solvents (THF, dioxane, and DMF) were obtained from Aldrich. Triethylamine was distilled from CaH₂. Diborane was used as received (Aldrich). Ethylenediamine-*N,N'*-dipropionic acid dihydrochloride was obtained from American Tokyo Kasei. (*p*-Nitrobenzyl)ethylenediamine dihydrochloride

* Author to whom correspondence should be addressed.



(4) and *N*-(2-aminoethyl)-4-nitrophenylalaninamide (5) were prepared as described previously (17). Ion-exchange resins were purchased from Bio-Rad; the AG50W-X8 resin was further purified by literature methods (42). Silica used for flash chromatography was purchased from Fluka (silica gel 60, 230–400 mesh).

Proton and ^{13}C NMR spectra were obtained using a Varian 300XL instrument unless otherwise noted. Chemical shifts are reported in ppm on the δ scale relative to TMS, TSP, or the following internal references (noted in text): *t*-BuOD (^1H , 1.25; ^{13}C , 31.1), CD_3CN (^1H , 1.93; ^{13}C , 1.30), CD_3CN (^{13}C , 118.2), $\text{dmsO}-d_6$ solvent (^1H , 2.49; ^{13}C , 39.5), CDCl_3 solvent (^{13}C , 77.0). Proton chemical shifts are annotated as follows: ppm (multiplicity, integral, coupling constant (Hz)). Chemical ionization mass spectra (CI-MS) were obtained on a Finnegan 3000 instrument. Electron impact (EI-MS) mass spectra were recorded on an LKB9000 instrument. Fast atom bombardment (FAB-MS) mass spectra were taken by the Mass Spectroscopy Laboratory, College of Chemistry, University of California, Berkeley, CA. Elemental analyses were performed by Galbraith Laboratories (Knoxville, TN) or Atlantic Microlabs (Atlanta, GA). Carbon-14-labeled compounds prepared in this work were not submitted for elemental analysis, exact mass measurement, or NMR due to the possibility of radioactive contamination. However, chromatographic behavior of the carbon-14-labeled compounds was identical to that observed for the unlabeled analogues.

Analytical HPLC was performed using a Beckman gradient system equipped with Model 114M pumps controlled by System Gold software and a Model 165 dual-wavelength detector operating at 254 and 280 nm. A Waters C-18 reverse-phase column (15- μm particles, 100-Å pore size, 3.9×300 mm) and a binary gradient of 0–100% B/25 min (solvent A = 0.05 M AcOH/ Et_3N , pH 5.5, solvent B = MeOH) at 1.0 mL/min were used for all analyses.

***N,N'*-Bis(*tert*-butoxycarbonyl)ethylenediamine-*N,N'*-diacetic Acid (6).** Triethylamine (22.3 mL, 0.16 mol) was added to a suspension of ethylenediamine-*N,N'*-diacetic acid (Aldrich, 7.0 g, 39.7 mmol) in 50% aqueous dioxane (200 mL). To the clear solution, 2-[(*tert*-butoxycarbonyl)oxy]imino]-2-phenylacetonitrile (Aldrich BOC-ON, 20.1 g, 81.5 mmol) was added. The reaction was stirred for 5 days at room temperature and then extracted with EtOAc (200 mL). The layers were separated, and the aqueous solution was extracted with EtOAc (2 \times 200 mL). The aqueous solution was cooled in an ice bath and acidified with 3 N HCl to pH 2.0. The cloudy solution was extracted with EtOAc (3 \times 200 mL), and the combined organic fractions were dried with MgSO_4 , filtered, and concentrated to approximately 50 mL. The product was isolated by adding petroleum ether to effect a cloudy solution, refrigerating (4 $^\circ\text{C}$) for 18 h, and

collecting the white powdery solid by filtration (12.82 g, 86%): IR (Nujol) 3548, 3420, 1746, 1730, 1686; ^1H NMR ($\text{dmsO}-d_6$) δ 3.841 (d, 2 H, J = 6.5), 3.806 (s, 2 H), 3.27 (m, 4 H), 1.384, 1.368, 1.322 (3 s, total 18 H, ratio 1:1:1.67); ^{13}C NMR ($\text{dmsO}-d_6$, ref = solvent) δ 171.25, 171.11, 154.71, 154.50, 79.00, 78.87, 49.10, 48.29, 45.93, 45.71, 45.64, 45.32, 27.86, 27.78; MS (CI/ NH_3) m/e 221 (M - BOC- $\text{CH}_2\text{C}(\text{CH}_3)_2$ + 1), 177 (M - 2BOC + 1). Anal. Calcd for $\text{C}_{16}\text{H}_{28}\text{N}_2\text{O}_8$: C, 51.06; H, 7.45; N, 7.45. Found: C, 51.31; H, 7.37; N, 7.38.

Disuccinimidyl *N,N'*-Bis(*tert*-butoxycarbonyl)ethylenediamine-*N,N'*-diacetate (7). *N*-Hydroxysuccinimide (7.34 g, 63.8 mmol), compound 6 (11.71 g, 31.1 mmol), and EDC [1-[3-(dimethylamino)propyl]-3-ethylcarbodiimide hydrochloride] (12.24 g, 63.8 mmol) were dissolved in a 4:1 mixture of EtOAc and DMF (300 mL). The reaction was stirred at room temperature for 18 h. The resulting white precipitate was filtered, washed with hexanes, and vacuum dried to give 14.80 g (83%) of the disuccinimido ester: mp 212–214 $^\circ\text{C}$ dec; IR (Nujol) 1840, 1803, 1759 (sh), 1708 cm^{-1} ; ^1H NMR ($\text{dmsO}-d_6$) δ 4.372 (m, 4 H), 3.360 (m, 4 H), 2.798 (s, 8 H), 1.407, 1.395, 1.363 (3 s, total 18 H, ratio 1:0.71:2); ^{13}C NMR ($\text{dmsO}-d_6$, ref = solvent) δ 169.76, 166.45, 166.20, 154.41, 154.03, 80.05, 47.03, 46.38, 45.98, 45.75, 45.50, 45.26, 27.50, 25.37; MS (CI/ NH_3) m/e 588 (M + NH_4), 571 (M + 1). Anal. Calcd for $\text{C}_{24}\text{H}_{34}\text{N}_4\text{O}_{12}$: C, 50.52; H, 6.01; N, 9.82. Found: C, 50.45; H, 6.01; N, 9.67.

***N,N'*-Bis(*tert*-butoxycarbonyl)ethylenediamine-*N,N'*-dipropionic Acid (8).** Ethylenediamine-*N,N'*-dipropionic acid dihydrochloride (15.5 g, 56.0 mmol) was reacted with Et_3N (32 mL, 0.23 mol) and BOC-ON (28.8 g, 0.117 mol) in 50% aqueous dioxane (250 mL) as described for 6. After extractive workup and acidification, a precipitate was collected and dried (20.2 g, 89%): ^1H NMR (D_2O , pH = 9.5) δ 3.424 (m, 8 H), 2.404 (m, 4 H), 1.454 (s, 18 H); ^{13}C NMR (D_2O , pH 9.5, ref = CD_3CN) δ 179.26, 155.87, 80.17, 43.53, 43.04, 34.97, 26.79; MS (CI/ NH_3) m/e 405 (M + 1). Anal. Calcd for $\text{C}_{18}\text{H}_{32}\text{N}_2\text{O}_8$: C, 53.45; H, 7.97; N, 6.93. Found: C, 53.33; H, 7.97; N, 6.97.

Disuccinimidyl *N,N'*-Bis(*tert*-butoxycarbonyl)ethylenediamine-*N,N'*-dipropionate (9). Dicarbamate 8 (9.0 g, 22.3 mmol) and *N*-hydroxysuccinimide (5.25 g, 45.7 mmol) were suspended in 50% DMF/EtOAc (300 mL) and stirred until a clear solution formed. EDC (8.75 g, 45.6 mmol) was added and the reaction was stirred for 18 h under argon. The white precipitate was collected and vacuum dried (11.35 g, 85%): ^1H NMR ($\text{dmsO}-d_6$) δ 3.438 (m, 4 H), 3.310 (m, 4 H, partially obscured by D_2O in solvent), 2.917 (t, 4 H, J = 7.5), 2.813 (s, 8 H), 1.393 (s, 18 H); ^{13}C NMR ($\text{dmsO}-d_6$) δ 169.95, 167.31, 154.31, 79.13, 54.78, 27.87, 25.37; MS (CI/ NH_3) m/e 599 (M + 1). Anal. Calcd for $\text{C}_{26}\text{H}_{38}\text{N}_4\text{O}_{12}$: C, 52.17; H, 6.36; N, 9.37. Found: C, 51.92; H, 6.46; N, 9.27.

***N*-(*tert*-Butoxycarbonyl)iminodiacetic Acid (10).** Iminodiacetic acid (15.0 g, 0.113 mol) was treated with Et_3N (39.2 mL, 0.282 mol) and BOC-ON (Aldrich, 27.8 g, 0.113 mol) as described for 6. After aqueous workup, the combined EtOAc fractions were dried over MgSO_4 , filtered, and rotary evaporated to dryness (23.5 g, 89%): ^1H NMR (220 MHz, $\text{dmsO}-d_6$) δ 3.90 (s, 2 H), 3.86 (s, 2 H), 1.35 (s, 9 H); MS (CI/ NH_3) m/e 234 (M + 1). Anal. Calcd for $\text{C}_9\text{H}_{15}\text{NO}_6$: C, 46.35; H, 6.44; N, 6.00. Found: C, 46.62; H, 6.52; N, 5.87.

Disuccinimidyl *N*-(*tert*-Butoxycarbonyl)iminodiacetate (11). Compound 10 (19.14 g, 82 mmol), *N*-hydroxysuccinimide (18.98 g, 165 mmol), and EDC (32.51 g, 169.6 mmol) were combined in EtOAc (300 mL) and stirred for 18 h. The solution was transferred to a separatory funnel and extracted sequentially with saturated NaCl

solution (2×200 mL), 5% NaHCO_3 (3×200 mL), and salt solution again (200 mL). The organic solution was dried over MgSO_4 , filtered, and concentrated to about 50 mL with some precipitation of product. Hexanes (50 mL) were added to the suspension, and the flask was cooled at -20°C for 3 h. The precipitate was collected, washed with hexanes, and dried in vacuo (30.9 g, 88%). ^1H NMR ($\text{dms}\text{-}d_6$) δ 4.546 (s, 2 H), 4.528 (s, 2 H), 2.812 (s, 8 H), 1.396 (s, 9 H); MS (CI/NH_3) m/e 428 ($M + 1$). Anal. Calcd for $\text{C}_{17}\text{H}_{21}\text{N}_3\text{O}_{10}$: C, 47.78; H, 4.95; N, 9.83. Found: C, 47.49; H, 5.03; N, 9.68.

1,4-Bis(*tert*-butoxycarbonyl)-8-(4-nitrobenzyl)-6,11-dioxo-1,4,7,10-tetraazacyclododecane (12). A 5-L three-neck flask was equipped with a stirbar, two 500-mL Normag water-jacketed addition funnels, and a Claisen adapter fitted with a thermometer and reflux condenser. After purging with argon, anhydrous dioxane was introduced and the temperature was increased to 90°C . (*p*-Nitrobenzyl)ethylenediamine dihydrochloride (4, 2.68 g, 10 mmol) and Et_3N (4.2 mL, 30 mmol) were added to a 250-mL round-bottom flask containing anhydrous DMF (200 mL). The solution was stirred 5 min, filtered, and then transferred to addition funnel "A". DMF was added to increase the total volume to 250 mL. Diester 7 (5.88 g, 10 mmol) was dissolved in DMF (250 mL) by heating to 60°C and then transferred to funnel "B" (preheated to 60°C). The contents of the addition funnels were added simultaneously to the stirring dioxane solution over an 8-h period. The temperature of the solution was maintained at 90°C for 12 h, after which time the reaction was cooled to room temperature and the solvent was removed by rotary evaporation. The residual brown oil was redissolved in EtOAc (200 mL) and extracted with H_2O (2×200 mL), 5% NaHCO_3 (2×200 mL), and saturated NaCl (2×100 mL). The EtOAc was dried (Na_2SO_4) and evaporated to a brown solid. Recrystallization from hot MeOH gave a tan precipitate which was further purified by flash chromatography (Fluka, 230–400 mesh silica, 41×250 mm, 2% $\text{MeOH}/\text{CH}_2\text{Cl}_2$) to give 2.19 g (4.0 mmol, 40%): IR (Nujol) 3290, 3080 (w), 1710 (s), 1693 (sh), 1655 (s) cm^{-1} ; ^1H NMR ($\text{dms}\text{-}d_6$) δ 8.29 (d, 1 H, $J = 6.7$), 8.20 (d, 1 H, $J = 10.3$), 8.16 (d, 2 H, $J = 8.64$), 7.49 (d, 2 H, $J = 8.64$), 4.18 (m, 3 H), 3.803 (m, 3 H), 3.2 (m, 2 H), 2.944 (m, 2 H), 2.744 (m, 3 H), 1.405 (s, 9 H), 1.379 (s, 9 H); MS (CI/NH_3) m/e 536 ($M + 1$), 480, 436, 424, 406, 380, 336, 306. Anal. Calcd for $\text{C}_{25}\text{H}_{37}\text{N}_5\text{O}_8 \cdot 0.5\text{H}_2\text{O}$: C, 55.14; H, 7.03; N, 12.86. Found: C, 55.08; H, 7.01; N, 12.82.

1-(*tert*-Butoxycarbonyl)-5-(4-nitrobenzyl)-3,6,11-trioxo-1,4,7,10-tetraazacyclododecane (13). Diester 11 (12.81 g, 30 mmol) and *N*-(2-aminoethyl)-4-nitrophenylalaninamide (5, 7.56 g, 30 mmol) were each dissolved in DMF (100 mL) and one-half of each solution was loaded into a 50-mL gas-tight syringe. The two syringes were locked onto a syringe pump and the two reactants were added to ca. 4 L of efficiently stirred anhydrous dioxane under argon at 95°C such that the addition was complete after 24 h. The syringe-pump addition was then repeated using the second half of the two solutions. After the second addition had finished, the reaction was heated for an additional 18 h and then cooled to room temperature. The solution was concentrated to about 300 mL during which a large amount of precipitate formed. The flask was cooled at 4°C for 18 h, after which the gelatinous crude product was collected on a Buchner funnel with constant trituration with petroleum ether (300 mL). The resulting light tan solid was dried under high vacuum (8.50 g). The crude product was suspended in CHCl_3 (300 mL) and heated to boiling. MeOH was slowly added until the solution was clear. The flask was lightly stoppered and the solution was cooled to

room temperature and then to -20°C for 48 h. The off-white precipitate was collected and dried in vacuo. The filtrate was concentrated and a second crop was collected (5.97 g, 44%): ^1H NMR ($\text{dms}\text{-}d_6$) δ 8.583 (br t, 1 H), 8.145 (d, 2 H, $J = 8.5$), 7.699 (m, 1 H), 7.519 (d, 2 H, $J = 8.5$), 7.137 (m, 1 H), 4.371 (q, 1 H, $J = 15.0, 9.0$), 3.986 (dt, 2 H, $J = 15.5, 3.6$), 3.885 (br t, 2 H, $J = 16.0$), 3.580 (m, 1 H), 3.365 (m, 1 H), 3.160 (dd, 1 H, $J = 14.0, 6.0$), 2.950 (m, 3 H), 1.384 (s, 9 H); ^{13}C NMR ($\text{dms}\text{-}d_6$) δ 170.71, 169.34, 154.72, 146.37, 146.16, 130.32, 123.14, 79.63, 54.62, 54.38, 50.65, 50.32, 49.98, 49.79, 37.99, 37.91, 36.55, 36.43, 34.83, 27.80; MS (CI/NH_3) m/e 450 ($M + 1$). Anal. Calcd for $\text{C}_{20}\text{H}_{27}\text{N}_5\text{O}_7$: C, 53.45; H, 6.06; N, 15.58. Found: C, 53.35; H, 6.13; N, 15.52.

2-(4-Nitrobenzyl)-1,4,7,10-tetraazacyclododecane Trihydrochloride (14). Route A (via Diamide 12). In a 200-mL Schlenk flask, compound 12 (2.06 g, 3.79 mmol) was suspended in anhydrous dioxane (20 mL) and cooled to ca. 10°C . HCl -saturated dioxane (10 mL) was added and the reaction was stirred at room temperature for 14 h protected from atmospheric water by a Drierite-filled drying tube. The HCl /dioxane was then evaporated in vacuo by transferring to a liquid nitrogen trap. After vacuum drying at 0.1 mmHg for 48 h, the diamide dihydrochloride was obtained as a tan solid (1.6 g). This solid (1.6 g) was suspended in anhydrous THF (150 mL) and cooled to 0°C before adding $\text{BH}_3\cdot\text{THF}$ (1.0 M, 19.4 mL, 19.4 mmol). The reaction was stirred at 0°C for 1 h and 45°C for 48 h. The solution was cooled in an ice bath, quenched with MeOH (150 mL), and then evaporated to dryness. The residue was redissolved in MeOH (60 mL), heated to boiling, and evaporated. This procedure was repeated once with MeOH and once with absolute EtOH . The residue was then taken up in absolute EtOH (90 mL), cooled in an ice bath, and saturated with HCl(g) . The flask was equipped with a reflux condenser and drying tube, and the reaction refluxed for 24 h. The EtOH solution was concentrated to ca. 30 mL and cooled to 4°C . The resulting white precipitate was filtered on a medium frit under argon, washed with Et_2O , and vacuum dried. Recrystallization was achieved by dissolving in boiling MeOH and allowing the solution to stand at room temperature for 24 h. The white solid (0.91 g, 55%) was isolated as a trihydrochloride salt: ^1H NMR (D_2O , pH = 1.0) δ 8.230 (d, 2 H, $J = 8.5$), 7.530 (d, 2 H, $J = 8.5$), 3.443 (m, 1 H), 3.25–2.90 (m, 16 H); ^{13}C NMR (D_2O , pH = 1.0, ref = *tert* butyl alcohol) δ 148.14, 146.17, 131.74, 125.47, 55.59, 49.05, 45.98, 45.58, 45.29, 44.42, 43.89, 42.19, 38.16; MS (CI/NH_3) m/e 308 ($M + 1$). Anal. Calcd for $\text{C}_{15}\text{H}_{25}\text{N}_5\text{O}_2 \cdot 3\text{HCl} \cdot \text{H}_2\text{O}$: C, 41.44; H, 6.91; N, 16.12; Cl, 24.48. Found: C, 41.42; H, 6.94; N, 15.92; Cl, 24.09.

Route B (via Triamide 13). Triamide 13 (5.62 g, 12.5 mmol) was added to a solution of anhydrous dioxane (300 mL) previously saturated with HCl(g) and then stirred for 18 h under argon. Diethyl ether (100 mL) was added and the suspension was cooled at 4°C for 6 h. The solid was collected and dried under vacuum for 18 h.

The deprotected material was washed into a three-necked round-bottom flask with THF (50 mL) and the solution was cooled in an ice bath. Diborane/THF (1 M, 75 mL) was added via syringe and the reaction was heated at 50°C for 48 h. The solution was cooled to 0°C and MeOH (50 mL) was added. After stirring at room temperature for 1 h, the solution was evaporated to dryness. The residue was taken up in 100% EtOH and saturated with HCl . The saturated solution was then refluxed for 6 h under argon. After stirring at room temperature for 12 h, the reaction was left at 4°C for 24 h. The white precipitate was collected and vacuum dried. The trihydrochloride salt was recrystallized by dissolving in hot

100% MeOH (65 mL) and being allowed to cool slowly to 4 °C (2.03 g, 37%). Analytical data was indistinguishable from that described above for the product obtained via route A.

2-(4-Nitrobenzyl)-1,4,7,10-tetraazacyclododecane-*N,N,N',N''*-tetraacetic Acid Hydrochloride (15). Tetraazacyclododecane 14 (1.25 g, 2.87 mmol) was dissolved in H₂O (15 mL) at 47 °C. The solution was neutralized with 5 M NaOH (0.625 mL) prior to adding BrCH₂CO₂H (3.25 g, 23.7 mmol). The solution was then neutralized with 5 M NaOH, the pH stat endpoint set to pH = 8.5, and the reaction stirred for 14 h. The pH was lowered to 1.0 by the addition of concentrated HCl and the solution applied to a AG50W-X8 cation-exchange resin (H⁺ form, 200–400 mesh, 16 × 200 mm). The column was washed with water (ca. 500 mL) prior to elution of the amino carboxylate with 2 M NH₄OH. The fractions containing product were evaporated to near dryness and then applied to an AG1-X2 resin (200–400 mesh, acetate form, 20 × 200 mm). The column was washed with water (500 mL), and the product eluted with an acetic acid gradient (0–1.5 M over 2 L). Twenty-milliliter fractions were collected, with the product 2 eluted in tubes 25–38. The fractions were combined, concentrated to ca. 20 mL by rotary evaporation, and then lyophilized to give a pale yellow, fluffy solid. Residual acetic acid was removed by re-lyophilizing twice from 30 mL of water to give 0.8 g (1.39 mmol, 48%): MS (EI, exhaustively silylated with *N,O*-Bis(trimethylsilyl)-trifluoroacetamide/CH₃CN) *m/e* 827 (M⁺), 812 (M – 15). Anal. Calcd for C₂₃H₃₃N₅O₁₀·2H₂O: C, 48.00; H, 6.48; N, 12.17. Found: C, 47.70; H, 6.18; N, 12.57.

A portion of 15 was purified by recrystallization from aqueous HCl. Pale yellow 15 (0.7 g) was suspended in ca. 1 mL of water. Approximately 6 mL of concentrated HCl was added. The solution was heated to reflux briefly and then allowed to stand for 14 h. The resulting pale yellow crystals were collected on a fine frit and washed with concentrated HCl and then 2-propanol before drying at 75 °C (0.1 mmHg) for 48 h (0.7 g, 95%, 46% conversion from 14): ¹H NMR (D₂O, pH = 11.2, ND₄OD, ref = *t*-BuOD) δ 8.20 (d, 2 H, *J* = 8.57), 7.49 (d, 2 H, *J* = 8.57), 3.652 (s, 2 H), 3.561 (s, 2 H), 3.48–3.06 (m, 11 H), 3.04–2.80 (m, 6 H), 2.74–2.58 (m, 2 H); ¹³C NMR (D₂O, pH = 11.2, ND₄OD, ref = CD₃CN) δ 179.36, 178.71, 175.88, 175.62, 148.66, 147.15, 131.19, 124.81, 59.93, 58.65, 57.66, 57.12, 55.42, 53.61, 53.00, 52.45, 49.99, 47.45; MS (FAB, *m*-nitrobenzyl alcohol) *m/e* 540 (M + 1). Anal. Calcd for C₂₃H₃₃N₅O₁₀·1.6HCl·0.5H₂O: C, 45.52; H, 5.91; N, 11.54; Cl, 9.35. Found: C, 45.39; H, 5.94; N, 11.52; Cl, 9.41.

2-(4-Aminobenzyl)-1,4,7,10-tetraazacyclododecane-*N,N,N',N''*-tetraacetic Acid (16). In a 25-mL three-neck flask, recrystallized compound 15 (130 mg, 0.21 mmol) was dissolved in H₂O (6 mL). Following the addition of 130 mg of 10% Pd/C catalyst, the flask was attached to an atmospheric hydrogenation apparatus. After hydrogen uptake ceased (ca. 5 h), the suspension was filtered (Whatman glass-fiber filter) and lyophilized to give a pure white solid (110 mg, 85%): ¹H NMR (D₂O, pH = 11.2, ND₄OD) δ 7.084 (d, 2 H, *J* = 7.82), 6.806 (d, 2 H, *J* = 7.81), 3.60–2.5 (m, 23 H), 2.30 (br m, 2 H); ¹H NMR (D₂O, pH = 2.0) δ 7.429 (m, 4 H), 4.13–3.87 (m, 4 H), 3.79–3.33 (m, 12 H), 3.27–2.83 (m, 8 H), 2.710 (dd, 1 H, *J* = 12.6, 9.9); ¹³C NMR (D₂O, pH = 2, ref = TSP) δ 176.43, 173.06, 140.80, 133.75, 131.78, 126.46, 58.70, 58.42, 58.15, 57.24, 56.42, 54.68, 54.28, 53.55, 52.92, 52.37, 50.05, 49.36; MS (FAB, thioglycerol/glycerol) *m/e* 510 (M + H), 532 (M + Na), 554 (M + 2Na – H); analytical HPLC *t*_R = 8.42 min. Anal. Calcd for C₂₃H₃₆N₅O₈·2HCl·2H₂O: C, 44.66; H, 6.68; N, 11.32. Found: C, 44.75; H, 6.74; N, 11.37.

2-(4-Isothiocyanatobenzyl)-1,4,7,10-tetraaza-

cyclododecane-*N,N,N',N''*-tetraacetic Acid (2). In a 2.5-mL polypropylene vial, compound 16 (35 mg, 0.57 μmol) was dissolved in H₂O (250 μL). A 1 M solution of thiophosgene in CHCl₃ (77 μL) was added and the two-phase reaction shaken vigorously for 30 s and then stirred for 2 h. The aqueous phase was removed via pipet and the CHCl₃ washed with H₂O (3 × 200 μL). The combined aqueous washings were lyophilized to give a pale yellow solid (34 mg, 86%): IR (Nujol) 2080 cm⁻¹; ¹H NMR (D₂O, pH = 1.3) δ 7.416 (s, 4 H), 4.46–3.34 (m, 17 H), 3.32–2.70 (m, 8 H); MS (FAB, thioglycerol/glycerol) *m/e* 552 (M + H), 574 (M + Na); analytical HPLC *t*_R = 17.79 min. Anal. Calcd for C₂₄H₃₃N₅O₈S·2HCl·4H₂O: C, 41.38; H, 6.22; N, 10.05. Found: C, 41.59; H, 6.04; N, 10.28.

2-(4-Nitrobenzyl)-1,4,7,10-tetraazacyclododecane-*N,N,N',N''*-tetra(1-¹⁴C)acetic Acid Hydrochloride (15-¹⁴C). The synthesis of ¹⁴C-labeled 2 was performed as described above for 15 by alkylating 14 (0.63 g, 1.44 mmol) with (1-¹⁴C) bromoacetic acid (2.0 mCi) prior to adding nonradioactive bromoacetic acid (1.36 g, 9.92 mmol). Compound 15-¹⁴C was purified by ion-exchange chromatography and recrystallized from HCl as described above.

The specific activity of the chelate was determined by dissolving a known weight of chelate in a volumetric flask, calculating the exact concentration by spectrophotometry (ϵ = 8260 L mol⁻¹ cm⁻¹, pH = 6.2 MesCl, determined for analytically pure 15), and averaging the counts of three 50-μL aliquots: 3.51 × 10⁶ dpm/μmol.

2-(4-Aminobenzyl)-1,4,7,10-tetraazacyclododecane-*N,N,N',N''*-tetra(1-¹⁴C)acetic Acid (16-¹⁴C). Compound 15-¹⁴C (115 mg) was dissolved in H₂O (5 mL) and hydrogenated as described above for the preparation of 16: analytical HPLC *t*_R = 8.23 min (purity > 95%).

2-(4-Isothiocyanatobenzyl)-1,4,7,10-tetraazacyclododecane-*N,N,N',N''*-tetra(1-¹⁴C)acetic Acid (2-¹⁴C). In a 2-mL polypropylene vial, compound 16-¹⁴C (37 mg) was dissolved in H₂O (0.5 mL). Thiophosgene (109 μL of a 1 M CHCl₃ solution) was added and the reaction shaken vigorously for 30 s and then stirred at room temperature for 2 h. The product was isolated as described above for the preparation of 2: analytical HPLC *t*_R = 17.76 min (purity > 96%).

1,4-Bis(*tert*-butoxycarbonyl)-9-(4-nitrobenzyl)-7,12-dioxo-1,4,8,11-tetraazacyclotetradecane (17). A 5-L three-necked round bottom flask was fitted with a condenser, two 0.5-L water-jacketed Normag addition funnels, one of which was heated to 60 °C, and an argon inlet. The flask was charged with anhydrous 1,4-dioxane (ca. 3.5 L) and heated to 90 °C. Diester 9 (8.97 g, 15 mmol) was dissolved in hot anhydrous DMSO (120 mL) and transferred into the heated addition funnel. In anhydrous DMSO (100 mL), 4 (4.02 g, 15 mmol) was dissolved and treated with triethylamine (4.17 mL, 30 mmol). The volume of the solution was adjusted to 120 mL with dry DMSO and transferred into the second addition funnel. The two reactants were added dropwise over ca. 8 h and the reaction was stirred for 18 h. An identical set of additions was made to the heated solution on each of the following two days, 45 mmol total in each reactant.

After cooling, the reaction solution was concentrated to about 0.5 L and transferred to a separatory funnel. Water (200 mL) and CHCl₃ (400 mL) were added and the layers were separated. The organic layer was then extracted with 1 N HCl (3 × 300 mL), saturated NaCl solution (3 × 300 mL), 5% NaHCO₃ (3 × 300 mL), and saturated NaCl solution again (3 × 300 mL). After drying over MgSO₄ and filtering, the solution was concentrated to about 150 mL. One-third of the solution was loaded onto a 3.7 × 50 cm silica column in CHCl₃. The product was eluted with

1% MeOH in CHCl_3 . The remaining two-thirds of the crude product solution was similarly chromatographed. The purified product solutions were combined and concentrated to a light yellow solid (11.14 g, 44%): TLC on silica (5% MeOH/ CHCl_3) R_f = 0.20; ^1H NMR (CDCl_3) δ 8.072 (d, 2 H, J = 8.5), 7.324 (d, 2 H, J = 8.5), 7.05 (br m, 2 H), 4.101 (m, 1 H), 3.70–3.20 (m, 8 H), 2.98 (m, 4 H), 2.751 (dd, 1 H, J = 14.0, 7.0), 2.35 (m, 4 H), 1.387 (s, 9 H), 1.367 (s, 9 H); ^{13}C NMR (CDCl_3) δ 172.89, 171.27, 154.99, 154.65, 145.96, 144.39, 129.09, 122.77, 79.31, 79.15, 52.06, 48.06, 47.36, 44.85, 44.15, 42.19, 37.90, 36.16, 35.88, 27.45; MS (CI/NH_3) m/e 564 (M + 1). Anal. Calcd for $\text{C}_{27}\text{H}_{41}\text{N}_5\text{O}_8$: C, 57.53; H, 7.33; N, 12.42. Found: C, 57.60; H, 7.32; N, 12.33.

2-(4-Nitrobenzyl)-1,4,8,11-tetraazacyclotetradecane Tetrahydrochloride (18). Diamide 17 (5.0 g, 8.88 mmol) was added to anhydrous 1,4-dioxane (200 mL) previously saturated with $\text{HCl}(\text{g})$ and stirred under argon for 18 h. Diethyl ether (100 mL) was added and the flask was held at 4 °C for 4 h. The solid was filtered off and vacuum dried for 18 h. The dried solid was washed into a three-necked round bottom flask with THF (150 mL). The flask was cooled in an ice bath and $\text{BH}_3\cdot\text{THF}$ (1 M, 62 mL) was injected. The reaction was heated at 50 °C for 48 h after which additional borane (10 mL) was added. After 48 h, the solution was cooled, MeOH (100 mL) was added, and the solution was rotary evaporated to dryness. The solid was taken up in 100% EtOH (110 mL) and saturated with $\text{HCl}(\text{g})$ while cooling in an ice bath. The solution was then refluxed for 4 h under argon and left stirring at room temperature for 18 h. The flask, now containing a fine white precipitate, was stoppered and held at 4 °C for 18 h. The solid was collected, washed with ether, and vacuum dried (2.88 g, 66%): ^1H NMR (D_2O , pH = 1.0) δ 8.251 (d, 2 H, J = 8.5), 7.569 (d, 2 H, J = 8.5), 3.77 (m, 1 H), 3.55–2.96 (m, 17 H), 2.20–1.92 (m, 4 H); ^{13}C NMR (D_2O , pH = 1.0, ref = CD_3CN) δ 146.43, 139.84, 129.70, 123.31, 52.22, 42.61, 42.36, 41.04, 40.79, 40.15, 38.34, 37.95, 34.34, 18.82, 18.48; MS (CI/NH_3) m/e 336 (M + 1). Anal. Calcd for $\text{C}_{17}\text{H}_{29}\text{N}_5\text{O}_2\cdot 4\text{HCl}\cdot 0.5\text{H}_2\text{O}$: C, 41.65; H, 6.99; N, 14.28; Cl, 28.95. Found: C, 41.50; H, 6.96; N, 14.02; Cl, 28.79.

2-(4-Nitrobenzyl)-1,4,8,11-tetraazacyclotetradecane- N,N,N',N'' -tetraacetic Acid (19). Tetraamine 18 (0.5 g, 1.02 mmol) and Na_2CO_3 (0.492 g, 4.64 mmol) were added to a 50-mL flask with DMF (20 mL) and heated to about 80 °C after which *tert*-butyl bromoacetate (1.04 g, 5.3 mmol) was added. The reaction was heated for 18 h and after cooling, the solution was poured into a separatory funnel with CH_2Cl_2 (60 mL). The solution was extracted with water (3 \times 100 mL), separated, dried over MgSO_4 , filtered, and concentrated under high vacuum to a thick dark oil. The oil was stirred with trifluoroacetic acid (20 mL) for 18 h under argon. The solution was rotary evaporated and the residue dissolved in water (25 mL). The solution was loaded onto a column of AG50W-X8 cation-exchange resin (H^+ form, 200–400 mesh, 2.6 \times 15 cm) and washed with water until the eluant was neutral. The crude product was then eluted from the column with 2 M NH_4OH (1 L). The solution was taken to dryness and the solid was redissolved in water (5 mL) and then loaded onto an AG1-X8 anion-exchange column (acetate form, 200–400 mesh, 1.2 \times 30 cm). The column was washed with water to collect 11 fractions (18 \times 150 mm tubes). The column was then eluted with a 2-L gradient of acetic acid, 0.0–2.0 M. Fractions 60–82 were combined and upon concentration a white precipitate formed. After the total volume was reduced to about 10 mL, the flask was left at 4 °C for 1 week. The resulting fine white power was collected on a small Hirsh funnel and then dried at 90 °C

(0.01 mmHg) for 18 h (178 mg, 29%): ^1H NMR (D_2O , pH = 11.5) δ 8.195 (d, 2 H, J = 8.5), 7.499 (d, 2 H, J = 8.5), 3.38–3.04 (m, 8 H), 2.94–2.28 (m, 17 H), 1.84–1.56 (m, 4 H); ^{13}C NMR (D_2O , pH = 11.5, ref = TSP) δ 183.03, 181.82, 152.54, 148.72, 133.05, 126.51, 62.39, 62.15, 61.97, 58.55, 56.54, 54.44, 54.32, 54.05, 52.28, 52.13, 51.49, 35.79, 27.13, 26.42; MS (FAB, glycerol/thioglycerol) m/e 568 (M + 1). Anal. Calcd for $\text{C}_{25}\text{H}_{37}\text{N}_5\text{O}_{10}\cdot 2\text{H}_2\text{O}$: C, 49.75; H, 6.85; N, 11.60. Found: C, 49.46; H, 6.59; N, 11.09.

2-(4-Aminobenzyl)-1,4,8,11-tetraazacyclotetradecane- N,N,N',N'' -tetraacetic Acid (20). Tetraacid 19 (73 mg, 0.121 mmol) was suspended in H_2O (2 mL) and 1 drop of concentrated NH_4OH was added to affect a clear pale yellow solution. The solution was added to a suspension of 10% Pd/C in H_2O (3 mL) presaturated with H_2 attached to an atmospheric hydrogenation apparatus. After H_2 uptake had ceased, the catalyst was filtered off with a fine frit and Celite 577. The filtrate was lyophilized to a fine white powder (68 mg, 98%): ^1H NMR (D_2O , pH = 1.0) δ 7.460 (d, 2 H, J = 8.5), 7.395 (d, 2 H, J = 8.5), 4.20–2.90 (m, 24 H), 2.735 (dd, 1 H, J = 13.5, 8.5), 2.15 (m, 2 H), 1.95 (m, 2 H); (D_2O , pH = 13.0) δ 7.103 (d, 2 H, J = 9.0), 6.817 (d, 2 H, J = 9.0), 3.40–2.40 (m, 22 H), 2.24 (m, 3 H), 1.70 (m, 4 H); ^{13}C NMR (D_2O , pH = 13.0, ref = CD_3CN) δ 181.01, 180.14, 179.79, 132.16, 144.89, 130.88, 117.39, 60.58, 60.39, 60.17, 56.32, 55.32, 52.77, 52.55, 50.85, 49.35, 31.68, 25.70, 24.85; MS (FAB, thioglycerol/glycerol) m/e 538 (M + 1); analytical HPLC t_R = 9.35 min (purity > 98%).

2-(4-Isothiocyantobenzyl)-1,4,8,11-tetraazacyclotetradecane- N,N,N',N'' -tetraacetic Acid (3). Aniline 20 from above was dissolved in H_2O (2 mL), and thiophosgene (20 μL , 0.26 mM) in CHCl_3 (10 mL) was added in one portion with maximum stirring. After 2 h, the organic phase was removed by rotary evaporation without heating. The aqueous residue was lyophilized to leave an off-white powder (57.5 mg, 78%): IR (Nujol) 2110 cm^{-1} ; ^1H NMR (D_2O , pH = 3.5) δ 7.297 (s, 4 H), 3.8–2.5 (m, H), 1.70 (m, 4 H); MS (FAB, thioglycerol/glycerol) m/e 580 (M + 1), 602 (M + Na); analytical HPLC t_R = 17.99 min (purity > 98%).

2-(4-Nitrobenzyl)-1,4,7,10-tetraazacyclotetradecane- N,N,N',N'' -tetra(1- ^{14}C)acetic Acid (19- ^{14}C). A modified procedure for the preparation of 19 was followed. Tetraamine 18 (0.86 g, 1.79 mmol) and Na_2CO_3 (1.7 g, 16 mmol) were combined in DMF (20 mL) and heated to ca. 80 °C. Tertiary butyl bromo(1- ^{14}C)acetate (Amersham, 2 mCi, 12 mCi/mmol) was added with two 1-mL rinses of DMF for each ampoule. After 2 h, *tert*-butyl bromoacetate (1.56 g, 8 mmol) was added and the reaction was continued for 18 h. After cooling to room temperature, the solution was extracted into CH_2Cl_2 (30 mL) and washed with water (2 \times 100 mL). The organic phase was dried over MgSO_4 and filtered into a Schlenk flask. The contents were then frozen in liquid nitrogen. The flask was then attached to two liquid nitrogen traps in line and the system was evacuated. After disconnecting the vacuum system, the frozen material was allowed to reach room temperature and eventually was heated gently to transfer any volatile radioactive residue to the traps. With the transfer completed, trifluoroacetic acid (25 mL) was added to the contents of the Schlenk flask and the solution was stirred for 18 h. The solution was concentrated to a thick oil, dissolved in H_2O , and loaded onto an AG50W-X8 cation-exchange column (H^+ form, 200–400 mesh, 26 \times 300 mm). The column was washed with water until the eluant was neutral. The crude product was then eluted from the column with 1 L of 4 M NH_4OH and the solution was rotary evaporated to leave a solid. The solid was taken up in water and loaded onto an AG1-X8 anion-

exchange column (acetate form, 200–400 mesh, 1.6×30 cm). The column was washed with water and twenty fractions (ca. 20 mL) were taken, after which the column was eluted with a 0.0–2.0 M HOAc gradient (2 L). Fractions 60–82 were combined and concentrated to 50 mL, during which a fine white precipitate formed. The flask was stoppered and left at 4 °C for 48 h. The product was collected on a small Hirsh funnel, transferred to a vial, and dried for 18 h (0.02 mmHg, 90 °C).

The specific activity was determined by counting three aliquots (100, 200, and 300 μ L) of a solution of the ligand (pH = 7.4, 0.1 M PO_4^{3-} buffer, 0.05% NaN_3) with the ^{14}C standards and correcting for quenching. The concentration of the solution was determined via UV ($\epsilon = 7730 \text{ L mol}^{-1} \text{ cm}^{-1}$). The averaged result was $2.72 \times 10^6 \text{ dpm/mol}$. Analytical HPLC $t_R = 11.95 \text{ min}$ (purity = 95%).

2-(4-Isothiocyantobenzyl)-1,4,8,11-tetraazacyclotetradecane- N,N,N',N'' -tetra(1- ^{14}C)acetic Acid (3- ^{14}C). Compound 19- ^{14}C (52 mg) was dissolved in H_2O (3 mL) and hydrogenated as described for the preparation of 20. Compound 20- ^{14}C (45 mg) was taken up in H_2O (3 mL) and thiophosgene (15 mL in 10 mL of CHCl_3) was added with vigorous stirring. The stirring was continued for 2 h at room temperature and the product was isolated as described for 3.

1,4,7-Triaza-3(2)-(4-nitrobenzyl)-7-(*tert*-butoxycarbonyl)-9-oxobicyclo[4.3.0]-4-nonene (21a and 21b). In a 50-mL volumetric flask, 4 (1.5 g, 5.6 mmol) was dissolved in anhydrous DMF (30 mL). Et_3N (3.9 mL, 28 mmol) was added, and the volume adjusted to 50 mL with DMF. The resulting suspension was sonicated for 5 min, cooled to 4 °C, and then filtered to remove insoluble triethylamine hydrochloride. The filtrate was taken up in a 50-mL gas-tight syringe. Diester 11 (2.39 g, 5.6 mmol) was dissolved in anhydrous DMF (50 mL) and taken up with a 50 mL gas-tight syringe. A 5-L three-neck flask was placed under an argon atmosphere, charged with dioxane (4 L), and heated to 90 °C. The contents of the two syringes were added via an Orion Model 355 syringe pump to the efficiently stirred dioxane over an 8-h period. This addition procedure was repeated three more times over the next 48 h (22.4 mmol total).

The dioxane was evaporated to an oil, which was concentrated to a thick slurry on a vacuum rotary evaporator and vacuum dried for 14 h. The residue was taken up in EtOAc (300 mL) and extracted with 5% NaHCO_3 (4 \times 150 mL). A final extraction was performed with H_2O (150 mL), using saturated NaCl to break up the resulting emulsion. The EtOAc was dried (Na_2SO_4) and evaporated to give a brownish-orange solid. Purification was achieved using flash chromatography (230–400 mesh silica, $40 \times 300 \text{ mm}$) and a gradient of 0–1% $\text{MeOH}/\text{CH}_2\text{Cl}_2$ (1 L of CH_2Cl_2 , 2 L of 0.25% $\text{MeOH}/\text{CH}_2\text{Cl}_2$, 2 L of 0.5% $\text{MeOH}/\text{CH}_2\text{Cl}_2$, 2 L of 0.75% $\text{MeOH}/\text{CH}_2\text{Cl}_2$, 1 L of 1% $\text{MeOH}/\text{CH}_2\text{Cl}_2$). The fractions containing product were evaporated to give a 10:1 mixture of 21a and 21b (pale yellow foam, 17.6 g, 4.7 mmol, 21%): MS (CI/ NH_3) m/e 375 (M + H), 319 (M – $\text{CH}_2\text{C}(\text{CH}_3)_2$ + H), 275 (M – BOC + H). Anal. Calcd for $\text{C}_{18}\text{H}_{22}\text{N}_4\text{O}_5$: C, 57.75; H, 5.92; N, 14.96. Found: C, 57.30; H, 5.92; N, 14.79.

Separation of 21a from 21b was achieved using HPLC (Waters 10 μm , 125 Å, $19 \times 300 \text{ mm}$ silica, flow = 17 mL/min) and a 25-min linear gradient of 25% $\text{CH}_2\text{Cl}_2/\text{hexane}$ to 100% IPA. Fraction 21a eluted at 15.7 min and was evaporated to give 1.4 g of pure 1,4,7-triaza-3-(4-nitrobenzyl)-7-(*tert*-butoxycarbonyl)-9-oxobicyclo[4.3.0]-4-nonene (21a): ^1H NMR ($\text{dms}-d_6$) δ 8.235 (d, 2 H, $J = 8.57$), 7.633 (d, 2 H, $J = 8.57$), 4.507 (m, 1 H), 4.401 (d, 2 H, $J = 9.94$), 4.145 (d, 2 H, $J = 18.6$), 3.816 (dd, 1 H, $J = 10.4$, 11), 3.450 (dd, 1 H, $J = 6.7$, 11.2), 3.050 (d, 2 H, $J = 6.9$),

1.472 (s, 9 H); ^{13}C NMR (CDCl_3) δ 164.34, 154.16, 153.36, 147.09, 145.03, 130.20, 123.80, 82.09, 65.91, 47.27, 47.03, 41.71, 41.61, 28.25; MS (CI/ NH_3) m/e 375 (M + H), FAB ($\text{CHCl}_3/m\text{-NO}_2\text{BzOH}$) m/e 375 (M + H), 319 (M – $\text{CH}_2\text{C}(\text{CH}_3)_2$ + H), (EI) m/e 375 (M + H), 374 (M^+), 301 (M – $\text{O}(\text{CH}_3)_3$), 238 (M – CH_2PhNO_2), 182 (M – CH_2PhNO_2 – $\text{CH}_2\text{C}(\text{CH}_3)_2$). Anal. Calcd for $\text{C}_{18}\text{H}_{22}\text{N}_4\text{O}_5$: C, 57.75; H, 5.92; N, 14.96. Found: C, 57.13; H, 6.04; N, 14.61.

Fraction 21b eluted at 17.5 min and was evaporated to give 0.16 g of 1,4,7-triaza-2-(4-nitrobenzyl)-7-(*tert*-butoxycarbonyl)-9-oxobicyclo[4.3.0]-4-nonene (21b): ^1H NMR ($\text{dms}-d_6$) δ 8.105 (d, 2 H, $J = 8.67$), 7.289 (d, 2 H, $J = 8.67$), 4.545 (m, 1 H), 4.38–4.00 (m, 4 H), 3.858 (dd, 1 H, $J = 9.59$, 15.66), 3.646 (dd, 1 H, $J = 4.85$, 15.66), 3.330 (dd, 1 H, $J = 3.12$, 13.4), 2.901 (dd, 1 H, $J = 8.83$, 13.4), 1.472 (s, 9 H); ^{13}C NMR (CDCl_3) δ 164.75, 153.95, 153.34, 147.25, 143.74, 130.29, 123.78, 82.09, 58.89, 56.63, 47.26, 41.80, 41.69, 38.23, 28.25; MS (CI/ NH_3) m/e 375 (M + H), 319 (M – $\text{CH}_2\text{C}(\text{CH}_3)_2$ + H), 275 (M – BOC + H). Anal. Calcd for $\text{C}_{18}\text{H}_{22}\text{N}_4\text{O}_5 \cdot 0.5\text{H}_2\text{O}$: C, 56.39; H, 6.05; N, 14.29. Found: C, 56.39, H, 6.05, N, 14.61.

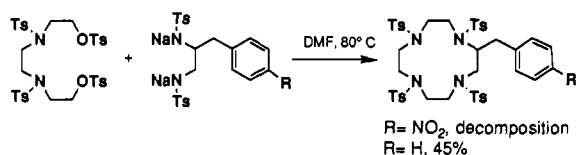
1,4,7-Triaza-3-(4-nitrobenzyl)-9-oxobicyclo[4.3.0]-4-nonene Hydrochloride (22). In a 250-mL Schlenk flask, the mixture of 21a + 21b (1.1 g, 2.94 mmol) was dissolved in 30 mL of anhydrous dioxane under argon. Dioxane saturated with HCl gas (30 mL) was added and the reaction vessel sealed under positive argon pressure. The reaction was stirred for 14 h at room temperature, at which time a white precipitate was evident. HCl gas and dioxane were removed by trap-to-trap distillation under vacuum. The solid residue was dried for 24 h at 0.1 mmHg (0.95 g): IR (Nujol) 3400 (w, br), 1760 (w), 1707 (s) cm^{-1} ; ^1H NMR ($\text{dms}-d_6$) δ 9.67 (br s, 3 H), 8.199 (d, 2 H, $J = 8.77$), 7.592 (d, 2 H, $J = 8.77$), 4.574 (mult, 1 H), 4.216 (s, 2 H), 3.935 (s, 2 H), 3.870 (dd, 1 H, $J = 11.1$, 10.5), 3.570 (s, dioxane impurity, 0.14 equiv), 3.497 (dd, 1 H, $J = 11.4$, 6.4); ^{13}C NMR ($\text{dms}-d_6$) δ 161.20, 160.91, 152.63, 146.22, 146.03, 144.56, 130.75, 130.49, 123.46, 123.28, 66.28, 64.39, 55.60, 47.29, 44.57, 40.39, 37.20; MS (CI/ NH_3): 275 (M + H).

N -[2-Amino-3-(4-nitrophenyl)propyl]piperazine (23). In a 200-mL Schlenk flask, 22 (0.87 g, 2.8 mmol) was suspended in anhydrous THF (50 mL) under argon. After cooling to 0 °C, 1 M $\text{BH}_3 \cdot \text{THF}$ (14 mL) was added. The reaction was warmed to room temperature for 1 h and then 45 °C for 2 h. The reaction was quenched by the addition of MeOH (20 mL) and evaporated to a brown oil. The oil was redissolved in MeOH (20 mL), heated to boiling, and evaporated to an oil. This procedure was repeated two more times with MeOH and once with anhydrous EtOH. The oil was dissolved in anhydrous EtOH (50 mL) and saturated with HCl gas at 0 °C. The suspension was warmed to 40 °C for 6 h and then cooled to 4 °C. The resulting precipitate was collected on a medium frit under a blanket of argon, washed with Et_2O , and vacuum-dried. This procedure yielded 0.6 g of product which was converted to the free base using 40% NaOH, extracted into CHCl_3 , and then flash chromatographed ($\text{CH}_2\text{Cl}_2/\text{CH}_3\text{OH}/\text{NH}_4\text{OH}$ 24/8/1, 230–400 mesh silica, $20 \times 200 \text{ mm}$) to give a brown oil. The oil was dissolved in absolute EtOH and precipitated with anhydrous HCl(g) to give 0.5 g of the hydrochloride salt. An additional 0.1 g of this pure material was obtained by evaporation of the original HCl/EtOH filtrate, giving a total of 0.6 g (1.53 mmol, 55%): ^1H NMR (D_2O , pH = 1.6, ref = *t*-BuOD) δ 8.272 (d, 2 H, $J = 8.67$), 7.580 (d, 2 H, $J = 8.67$), 3.897 (m, 1 H), 3.363 (t, 4 H, $J = 5.3$), 3.225–3.160 (m, 2 H), 3.12–3.01 (m, 2 H), 2.94–2.84 (m, 4 H); ^{13}C NMR (D_2O , pH = 1.6, CD_3CN) 148.04, 144.02, 131.37, 125.06, 58.98, 50.19, 50.04, 43.81, 37.11; MS (CI/ NH_3) m/e 265 (M + 1). Anal. Calcd

for $C_{13}H_{20}N_4O_2 \cdot 3HCl \cdot H_2O$: C, 39.86; H, 6.43; N, 14.30; Cl, 27.15. Found: C, 40.14; H, 6.61; N, 14.05; Cl, 26.95.

RESULTS AND DISCUSSION

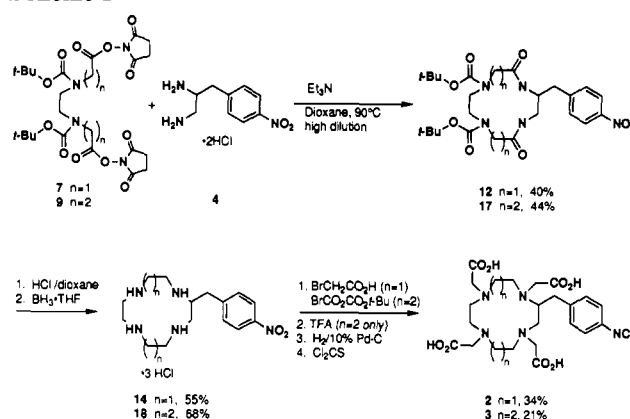
Because poly(amino carboxylates) are readily prepared from the corresponding polyamine by alkylation with haloacetic acids or their esters, the preparation of pure macrocyclic polyamines constitutes the most crucial aspect of synthesizing these bifunctional macrocyclic poly(amino carboxylates). Representative examples of important cyclization procedures which have been used to form macrocyclic polyamines include the aminolysis of malonates with polyamines (43), high dilution acylation of diamines by acid chlorides and their derivatives (44–48), intramolecular reaction of amines with active esters (49,50), metal-mediated cyclization reactions (51), the "crablike" cyclization of a bis(α -chloroamide) with amines (52), and the cyclization of deprotonated tosylamides with tosylates or mesylates in aprotic solvents (53). The last reaction, known as the Richman–Atkins cyclization, provides an efficient and convenient means of preparing unsubstituted macrocyclic polyamines. Yields of 40–50% are commonly obtained for bimolecular cyclizations without resorting to high dilution. While several groups have synthesized functionalized macrocyclic polyamines employing a bimolecular Richman–Atkins cyclization step, none have incorporated the versatile aryl nitro group (54–58). However, Moi et al. have described a unique *intramolecular* variant of this technique to prepare *p*-NO₂-Bz-DOTA, 15 (33). Our initial efforts to prepare the substituted DOTA precursor 2-(4-nitrobenzyl)-*N,N',N'',N'''*-tetrakis(*p*-tolylsulfonyl)-1,4,7,10-tetraazacyclododecane by a bimolecular Richman–Atkins reaction of 3,6-bis(*p*-tolylsulfonyl)-1,8-bis[(*p*-tolylsulfonyl)oxy]-3,6-diazaoctane with *N,N'*-disodio-*N,N'*-bis(*p*-tolylsulfonyl)-1-(4-nitrobenzyl)ethylenediamine in dry DMF at 80 °C was not synthetically useful, and produced only trace amounts of product. In contrast, cyclization of *N,N'*-disodio-*N,N'*-(*p*-tolylsulfonyl)-1-benzylethylenediamine with



the same ditosylate was facile, forming 2-benzyl-*N,N',N'',N'''*-tetrakis(*p*-tolylsulfonyl)-1,4,7,10-tetraazacyclododecane in 45% yield, thus implicating the nitro group and not adverse steric interactions as the culprit in the failed cyclization attempt (59). These preliminary results prompted the search for another cyclization procedure which would allow convenient entry into nitroaryl-functionalized macrocyclic polyamines of varying ring size.

The reaction of (4-nitrobenzyl)ethylenediamine with carbamate-protected amino disuccinimido esters 7 and 9 under high-dilution conditions (90 °C, dioxane, Et₃N) afforded the macrocyclic diamides 12 and 17 in 41% and 44% yield, respectively, after purification by flash chromatography or recrystallization (Scheme I). No higher molecular weight cyclic oligomers were isolated. The ready availability of carbamate-protected amino diesters from the corresponding aminoacetic acids as well as the substituted diamine (17) makes this an efficient route for constructing C-functionalized polyaza macrocyclic rings. In contrast to some other cyclizations employing disuccinimido esters and diamines which work efficiently at 0 °C (60), reaction temperatures lower than 90 °C were found to adversely affect the yield of the macrocycles. Sheh and

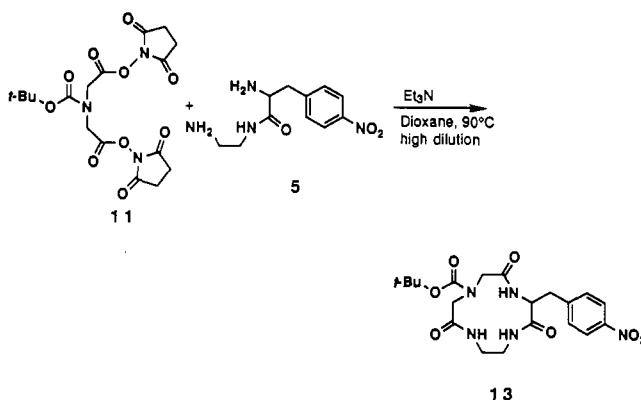
Scheme I



Mokotoff have reported the preference for monomeric cyclotetrapeptide formation in an intramolecular pentafluorophenyl ester cyclization was enhanced at 80–90 °C (61).

Deprotection of the BOC protecting groups was effected by stirring the macrocycles in anhydrous HCl(g)/dioxane for 14 h. Following removal of the solvent and drying, the resulting diamide amine hydrochloride was reduced to the corresponding amine with borane/THF. Purification of the amine was accomplished by crystallization of the hydrochloride salt.

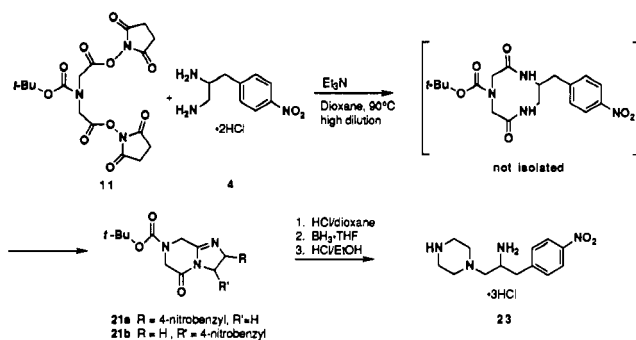
The 12-membered ring polyamine 14 was also prepared by an independent route employing the same cyclization chemistry but with a different diamine starting material.



Thus, ester 11 was reacted with 5 in dioxane at 90 °C to form the macrocyclic triamide 13 in 44% yield. While the cyclization yield is similar to the above reaction employing diamine 4, this approach had two practical advantages for preparing the 12-membered ring tetraamine. First, ester 11 was much more soluble in a variety of solvents than ester 7, thus allowing use of a syringe pump instead of a thermostated addition funnel for the preparation of diamide 12. Secondly, the product triamide conveniently precipitated upon concentration of the reaction solution, which facilitated purification. Conversion to the tetraamine was effected uneventfully by procedures described above for the macrocyclic diamides.

With the pure cyclic carbon substituted amines in hand, alkylation of the macrocyclic amines to form the poly(amino carboxylates) (62) was accomplished in one step by using BrCH₂CO₂H (pH = 8.5) or in two steps by using BrCH₂COO-*t*-Bu (Na₂CO₃/DMF) followed by deprotection with TFA. Preparation of an internally labeled ¹⁴C ligand was most conveniently performed at this step using either bromo(1-¹⁴C)acetic acid or *tert*-butyl bromo(1-¹⁴C)-acetate, thus permitting an accurate and sensitive determination of the number of ligands ultimately attached to the mAb. Following the alkylation, the crude ligand was

Scheme II



then subjected to cation-exchange chromatography to remove acid and salt (AG50W-X8 column). The organic components were then further purified by anion-exchange chromatography on an AG1-X8(2) resin. We, and others (28), have noted that these macrocyclic poly(amino carboxylates), particularly *p*-NO₂-Bz-DOTA (15), need to be handled carefully to avoid adventitious sequestering of divalent metals, especially calcium. For that reason, the alkylation step and subsequent steps were performed in acid-washed glassware or metal-free plasticware. In addition, 15 was recrystallized from aqueous HCl to insure metal-free purity.

Catalytic reduction of the 4-nitrobenzyl-substituted macrocycles in the presence of 10% Pd/C (H₂O) proceeded to give the aniline derivatives in nearly quantitative yield. Conversion to the isothiocyanate was accomplished by vigorously stirring an aqueous solution of the aniline with thiophosgene in CHCl₃. Conversion typically was complete in 1–2 h and was readily verified by HPLC (see Experimental Procedures). The product isothiocyanate was characterized by a strong stretch at 2100 cm⁻¹ in the infrared spectrum and a singlet for the aromatic protons in the 300-MHz proton NMR spectrum. MAb/bismuth-(III) complex conjugates using 2 have been shown to be stable *in vivo*, as evidenced by indistinguishable biodistribution data for both ^{205/206}Bi-DOTA/103A and biosynthetically labeled ³⁵S-103A (63).

Attempts to prepare a 9-membered ring triaza diamide by the reaction of 11 with 4 followed an unexpected course deserving of additional comment (Scheme II). Following aqueous workup, a product with chromatographic behavior similar to the 12- and 14-membered ring BOC-protected macrocycles was isolated and purified by flash chromatography. Proton NMR revealed the presence of a minor component 21b (ca. 10%), which was ultimately separated from the major fraction 21a by HPLC. Both fractions exhibited the following mass spectral features, indicating that fractions 21a and 21b were isomeric. Electron impact mass spectroscopy revealed a parent ion at *m/e* 374, 18 mass units less than the molecular weight calculated for the expected macrocyclic diamide product, as well as a significant ion at *m/e* 375 attributed to self chemical ionization. Fragments consistent with loss of carbamate (M – OC(CH₃)₃, M – BOC) and nitrobenzyl group (M – 136) were observed. In addition, both CI/NH₃ and FAB mass spectra gave molecular ions at 375 (M + H)⁺, consistent with a molecular weight of 374 and supported by elemental analysis.

Although an amide stretch was apparent in the IR (1680 cm⁻¹), examination of the ¹H NMR of 21a and 21b revealed no D₂O exchangeable amide protons, suggesting a lack of secondary amides. In the carbonyl region of the carbon-13 NMR, each isomer was characterized by one amide resonance (164.338 (21a)/164.749 (21b)), one carbamate resonance (154.160/153.945), and a resonance (153.355/153.343) not characteristic of the larger BOC-protected

macrocycles. Upon reaction with 1.55 equiv of NaCNBH₃ at pH = 6, the unique resonance disappeared, suggesting the presence of an imine bond. Consistent with this interpretation, the CI/NH₃ mass spectrum of the reduced material exhibited a parent ion at *m/e* 377. Taken together, these results provide convincing evidence for the structure of the cyclization products as being the isomeric acyl amidines 21a and 21b. Presumably the products are derived from the initial macrocyclic diamide cyclization product by transannular acylation of an amide nitrogen, followed by dehydration of an intermediate azacyclol. Although unanticipated, literature precedence exists for the transannular reaction of lactam nitrogens with ketones (64) and amides (65, 66) in medium-ring compounds. Interestingly, the distribution of products was identical when the cyclization was performed at 45 °C, although the yield dropped to less than 1%. Our observations may offer an explanation why the "crablike" cyclization of *N,N'*-bis(α-chloroacetamide)ethylenediamine with benzylamine failed to give an identifiable 9-membered ring diamide, while the corresponding *N*-methyl tertiary amide derivative gave the anticipated triazacyclononane in 44% yield (52).

Following deprotection with HCl/dioxane, two attempts were made to reductively expand the fused ring system to the macrocyclic triamine. First, reduction of the mixture of the deprotected 21a and 21b with borane/THF converted the fused 6,5-membered ring acylamidines into *N*-[2-amino-3-(4-nitrophenyl)propyl]piperazine, which was purified by chromatography (silica, CH₂Cl₂/CH₃OH/NH₄OH 24/8/1) and isolated in 55% yield as a trihydrochloride salt. The structure of the triamine was confirmed by acylation with 3.3 equiv of acetyl chloride in CH₂Cl₂ and characterization of the product diamide. The efficient production of piperazine 23 at the expense of a macrocyclic triazacyclononane suggests that reductive cleavage of the neighboring C–N bond is preferred over that of the central C–N bond for this system. Such a result would be predicted on the basis of the results obtained by Takeuchi et al. for the preparation of benzoannelated cyclic 1,5 diamines from fused ring quinazolinones (67). In that work, the moderate yield of a medium-ring cyclic diamine was explained by the high strain energy of the resulting 11-membered ring. A second attempt to reductively cleave the central C–N bond using DIBALH (68) in refluxing toluene resulted in the formation of many products and was therefore deemed not useful for synthetic purposes.

Thus, a noteworthy limitation of the synthetic route described herein is the inability to prepare medium-ring diamides due to the formation of fused-ring acylamidines under the reaction conditions employed. However, larger ring macrocyclic diamides are prepared in good yield from readily accessible starting materials and are easily purified, thus providing an efficient means of preparing the bifunctional macrocyclic poly(amino carboxylates) *p*-NCS-Bz-DOTA (2) and *p*-NCS-Bz-TETA (3). The macrocyclic chelating agents described here have been synthesized in sufficient quantity and high purity to permit the study of the thermodynamic and kinetic properties of the metal complexes of interest, as well as biological evaluation of the mAb conjugates.

ACKNOWLEDGMENT

We thank Dr. Henry Fales for insightful discussions concerning the structure and mass spectrum of compound 21.

LITERATURE CITED

- (1) Parker, D. (1990) Tumor targeting with radiolabeled macrocycle-antibody conjugates. *Chem. Soc. Rev.* 19, 271–291.

- (2) Pressman, D., and Kieghtley, G. J. (1948) The zone of activity of antibodies as determined by the use of radioactive tracers; the zone of activity of nephritoxenic antiserum. *J. Immunol.* 59, 141-146.
- (3) Goldenberg, D. (1990) *Cancer Imaging and Radiolabeled Antibodies*, Kluwer Academic Press, Boston.
- (4) Fritzberg, A. R., Berninger, R. W., Hadley, S. W., and Wester, D. W. (1988) Approaches to Radiolabeling of antibodies for diagnosis and therapy of cancer. *Pharm. Res.* 6, 325-334.
- (5) Abbreviations used in the text: EDTA, ethylenediamine-tetraacetic acid, DTPA, diethylenetriaminepentaacetic acid, NOTA, 1,4,7-triazacyclononane-*N,N',N''*-triacetic acid, DOTA, 1,4,7,10-tetraazacyclododecane-*N,N',N'',N'''*-tetraacetic acid, TETA, 1,4,8,11-tetraazacyclotetradecane-*N,N',N'',N'''*-tetraacetic acid. BOC-ON, 2-[[*tert*-butoxycarbonyl]oxy]imino]-2-phenylacetoneitrile.
- (6) Sundberg, M. W., Meares, C. F., Goodwin, D. A., and Diamanti, C. I. (1974) Chelating agents for the binding of metal ions to macromolecules. *Nature* 250, 587-588.
- (7) Sundberg, M. W., Meares, C. F., Goodwin, D. A., and Diamanti, C. I. (1974) Selective binding of metal ions to macromolecules using bifunctional analogs of EDTA. *J. Med. Chem.* 17, 1304-1307.
- (8) Meares, C. F., Goodwin, D. A., Leung, C. S.-H., Girgis, A. Y., Silvester, D. J., Nunn, A. D., and Lavender, P. J. (1976) Covalent attachment of metal chelates to proteins: The stability in vivo and in vitro of the conjugate of albumin with a chelate of indium-111. *Proc. Natl. Acad. Sci. U.S.A.* 73, 3803-3806.
- (9) Scheinberg, D. A., Strand, M., and Gansow, O. A. (1982) Tumor imaging with radioactive metal chelates conjugated to monoclonal antibodies. *Science* 215, 1511-1513.
- (10) Krejcarek, G. E., and Tucker, K. L. (1977) Covalent attachment of chelating groups to macromolecules. *Biochem. Biophys. Res. Commun.* 77, 581-585.
- (11) Vaughn, A. T. M., Keeling, A., and Ynakuba, S. C. S. (1985) The production and biodistribution of yttrium-90 labelled antibodies. *Int. J. Appl. Radiat. Isot.* 36, 803-806.
- (12) Hnatowich, D. J., Vrzi, F., and Doherty, P. W. (1985) ⁹⁰Y labeled monoclonal antibody for cancer therapy. *J. Nucl. Med.* 26, 503-509.
- (13) Washburn, L. C., Hwa Sun, T. T., Crook, J. E., Byrd, B. L., Carlton, J. E., Hung, Y. W., and Steplewski, Z. S. (1986) ⁹⁰Y-labeled monoclonal antibodies for cancer therapy. *Nucl. Med. Biol.* 13, 453-458.
- (14) Durbin, P. W. (1960) Metabolic characteristics within a chemical family. *Health Phys.* 2, 225-238.
- (15) Hart, F. A. (1987) Scandium, Yttrium, and the Lanthanides. In *Comprehensive Coordination Chemistry* (G. Wilkinson, Ed.) pp 1059-1127, Pergamon Press, Oxford, UK.
- (16) Cossy, C., Barnes, A. C., Enderby, J. E., and Merbach, A. E. (1989) The hydration of Dy³⁺ and Yb³⁺ in aqueous solution: A neutron scattering first order difference study. *J. Chem. Phys.* 90, 3254-3260.
- (17) Brechbiel, M. W., Gansow, O. A., Atcher, R. W., Schlom, J., Esteban, J., Simpson, D. E., and Colcher, D. (1986) Synthesis of 1-(*p*-isothiocyanatobenzyl) derivatives of DTPA and EDTA. Antibody labeling and tumor-imaging studies. *Inorg. Chem.* 25, 2772-2781.
- (18) Westerberg, D. A., Carney, P. L., Rodgers, P. E., Kline, S. J., and Johnson, D. K. (1989) Synthesis of novel bifunctional chelators and their use in preparing monoclonal antibody conjugates for tumor targeting. *J. Med. Chem.* 32, 236-243.
- (19) Kozak, R. W., Raubitchek, A., Mirzadeh, S., Brechbiel, M. W., Jungmans, R., Gansow, O. A., and Waldmann, T. (1989) Nature of the bifunctional chelating agent used for radioimmunotherapy with yttrium-90 monoclonal antibodies: Critical factors in determining in vivo survival and organ toxicity. *Cancer Res.* 49, 2639-2644.
- (20) Brechbiel, M. W., and Gansow, O. A. (1991) Backbone-substituted DTPA ligands for ⁹⁰Y radioimmunotherapy. *Bioconjugate Chem.* 2, 187-194.
- (21) Delgado, R., and Frausto da Silva, J. J. R. (1982) Metal complexes of cyclic tetraazatetra-acetic acids. *Talanta* 29, 815-822.
- (22) Stetter, H., and Frank, W. (1976) Complex formation with tetraazacycloalkane-*N,N',N'',N'''*-tetraacetic acids as a function of ring size. *Angew. Chem. Int. Ed. Engl.* 15, 686.
- (23) Stetter, H., Frank, W., and Mertens, R. (1981) *Tetrahedron* 37, 767-772.
- (24) Cram, D. J., Kaneda, T., Helgeson, R. C., Brown, S. B., Knobler, C. B., Maverick, E., and Trueblood, K. N. (1985) Host-guest complexation. 35. Spherands, the first completely preorganized ligand systems. *J. Am. Chem. Soc.* 107, 3645.
- (25) Hancock, R. D., and Martell, A. E. (1988) The chelate, cryptate, and macrocyclic effects. *Comments Inorg. Chem.* 6, 237.
- (26) Weighardt, K., Bossek, U., Chaudhuri, P., Herrmann, W., Menke, B. C., and Weiss, J. (1982) 1,4,7-triazacyclononane-*N,N',N''*-triacetate (TCTA), a hexadentate ligand for divalent and trivalent metal ions. Crystal structures of [Cr^{III}(TCTA)], [Fe^{III}(TCTA)], and Na[Cu^{II}(TCTA)]·2NaBr·8H₂O. *Inorg. Chem.* 21, 4308-4314.
- (27) van der Merwe, M. J., Boeyens, J. C. A., and Hancock, R. D. (1983) Optimum ligand hole sizes for stabilizing nickel(II). Structure of the nickel(II) complex of 1,4,7-triazacyclononane-*N,N',N''*-triacetate. *Inorg. Chem.* 22, 3489-3490.
- (28) Broan, C. J., Cox, J. P. L., Craig, A. S., Katak, R., Parker, D., Harrison, A., Randall, A. M., and Ferguson, G. (1991) Structure and solution stability of indium and gallium complexes of 1,4,7-triazacyclononane-*N,N',N''*-triacetate and of yttrium complexes of 1,4,7,10-tetraazacyclododecane-*N,N',N'',N'''*-tetraacetate and related ligands: kinetically stable complexes for use in imaging and radioimmunotherapy. X-ray molecular structure of the indium and gallium complexes of 1,4,7-triazacyclononane-1,4,7-triacetic acid. *J. Chem. Soc. Perkin Trans. 2*, 87-99.
- (29) Loncin, M. F., Desreux, J. F., and Merciny, E. (1986) Coordination of lanthanides by two polyamino polycarboxylic macrocycles: Formation of highly stable lanthanide complexes. *Inorg. Chem.* 25, 2646-2648.
- (30) Cacheris, W. P., Nickle, S. K., and Sherry, A. D. (1987) Thermodynamic study of lanthanide complexes of 1,4,7-triazacyclononane-*N,N',N''*-triacetic acid and 1,4,7,10-tetraazacyclododecane-*N,N',N'',N'''*-tetraacetic acid. *Inorg. Chem.* 26, 958-960.
- (31) Riesen, A., Zehnder, M., and Kaden, T. A. (1986) 219. Metal complexes of macrocyclic ligands. Part XXIV. Binuclear complexes with tetraazamacrocyclic-*N,N',N'',N'''*-tetraacetic acids. *Helv. Chim. Acta* 69, 2074-2080.
- (32) Moi, M. K., Yanuck, M., Deshpande, S. V., Hpo, H., DeNardo, S. J., and Meares, C. F. (1987) X-ray crystal structure of a macrocyclic copper chelate stable enough for use in living systems. Copper(II) dihydrogen 6-(*p*-nitrobenzyl)-1,4,8,11-tetraazacyclotetradecane-1,4,8,11-tetraacetate. *Inorg. Chem.* 26, 3458-3463.
- (33) Moi, M. K., Meares, C. F., and DeNardo, S. J. (1988) The peptide way to macrocyclic bifunctional chelating agents: Synthesis of 2-(*p*-nitrobenzyl)-1,4,7,10-tetraazacyclododecane-*N,N',N'',N'''*-tetraacetic acid and study of its yttrium(III) complex. *J. Am. Chem. Soc.* 110, 6266-6267.
- (34) Cox, J. P. L., Craig, A. S., Helps, I. M., Jankowski, K. J., Parker, D., Eaton, M. A. W., Millican, A. T., Millar, K., Beeley, N. R. A., and Boyce, B. A. (1990) Synthesis of C- and N-functionalized derivatives of 1,4,7-triazacyclononane-1,4,7-triyltriacetic acid (NOTA), 1,4,7,10-tetraazacyclododecane-1,4,7,10-tetrayltetra-acetic acid (DOTA), and diethylenetriaminepenta-acetic acid (DTPA): Bifunctional complexing agents for the derivatization of antibodies. *J. Chem. Soc. Perkin Trans. 1* 2567-2576.
- (35) Kline, S. J., Betebenner, D. A., and Johnson, D. K. (1991) Carboxymethyl-substituted bifunctional chelators: Preparation of aryl isothiocyanate derivatives of 3-(carboxymethyl)-3-azapentanedioic acid, 3,12-bis(carboxymethyl)-6,9-dioxo-3,12-diazatetradecanedioic acid, and 1,4,7,10-tetraazacyclododecane-*N,N',N'',N'''*-tetraacetic acid for use as protein labels. *Bioconjugate Chem.* 2, 26-31.
- (36) McCall, M. J., Diril, H., and Meares, C. F. (1991) Simplified method for conjugating macrocyclic bifunctional chelating agents to antibodies via 2-iminothiolane. *Bioconjugate Chem.* 1, 222-226.
- (37) Moi, M. K., Meares, C. F., McCall, M. J., Cole, W. C., and DeNardo, S. J. (1985) Copper chelates as probes of biological

- systems: stable copper complexes with a macrocyclic bifunctional chelating agent. *Anal. Biochem.* 148, 249–253.
- (38) Morphy, J. R., Parker, D., Alexander, R., Bains, A., Carne, A. F., Eaton, M. A. W., Harrison, A., Millican, A., Rhind, S. K., Titmas, R., and Weatherby, D. (1988) Antibody labelling with functionalized cyclam macrocycles. *J. Chem. Soc. Chem. Commun.* 156–158.
- (39) Deshpande, S. V., DeNardo, S. J., Kukis, D. L., Moi, M. K., McCall, M. J., DeNardo, G. L., and Meares, C. F. (1990) Yttrium-90-labeled monoclonal antibody for therapy: Labeling by a new macrocyclic bifunctional chelating agent. *J. Nucl. Med.* 31, 473–479.
- (40) Kumar, K., Magerstadt, M., and Gansow, O. (1989) Lead(II) and bismuth(III) complexes of the polyazacycloalkane-*N*-acetic acids nota, dota, and teta. *J. Chem. Soc., Chem. Commun.* 3, 145.
- (41) Gansow, O. A., Atcher, R. W., Link, D. C., Friedman, A. M., Seever, R. H., Anderson, W., Scheinberg, D. A., and Strand, M. Radionuclide Generators: New Systems for Nuclear Medicine Applications. In *ACS Symposium Series* #241 (F. F. Knapp, Jr., and T. A. Butler, Eds.) pp 215–227, American Chemical Society, Washington, DC.
- (42) Buhr, J. D. (1978) Ph.D. Dissertation, Stanford University.
- (43) Tabushi, I. (1977) Preparation of C-alkylated macrocyclic amines. *Tetrahedron Lett.* 12, 1049–1052.
- (44) Stetter, H., and Marx, J. (1957). *Liebigs Ann. Chem.* 59, 607.
- (45) Stetter, H., and Mayer, K.-H. (1961). *Chem. Ber.* 94, 1410–1416.
- (46) Vellaccio, F., Jr., Penzar, R. V., and Kemp, D. S. (1977) The reaction of dialkylmalonyl dichlorides with 1,3-diaminopropanes: a new route to macrocyclic polyamides and polyamines. *Tetrahedron Lett.* 6, 547–550.
- (47) Nagao, Y., Seno, K., Miyasaka, T., and Fujita, E. (1980) Monitored aminolysis of 3-acylthiazolidine-2-thione: a new synthesis of macrocyclic amides. *Chem. Lett.* 159–162.
- (48) Uoto, K., Tomohiro, T., and Okuno, H. (1990) Preparation of large macrocyclic tetraamines consisting of a methylene backbone and a cyclophane type skeleton. *J. Heterocycl. Chem.* 27, 893.
- (49) Schmidt, U., Griesser, H., Lieberknecht, A., and Talbiersky, J. (1981) A novel method for preparation of ansapeptides, synthesis of model peptide alkaloids. *Angew. Chem. Int. Ed. Engl.* 3, 280–281.
- (50) Schmidt, U., Lieberknecht, A., Griesser, H., Utz, R., Beuttler, T., and Bartkowiak, B. (1986) Amino acids and peptides, 55. Synthesis of biologically active cyclopeptides, 7. Total synthesis of chlamydocin. *Synthesis* 361–366.
- (51) For example, see: Barefield, K. E., Wagner, F., and Hodges, K. D. (1976) Synthesis of macrocyclic tetraamines by metal ion assisted cyclization reactions. *Inorg. Chem.* 15, 1370–1377.
- (52) Krakowiak, K. E., Bradshaw, J. S., and Izatt, R. M. (1990) Preparation of a variety of macrocyclic di- and tetraamides and their peraza-crown analogs using the crab-like cyclization reaction. *J. Heterocycl. Chem.* 27, 1585.
- (53) Richman, J. E., and Atkins, T. J. (1974) Nitrogen analogs of crown ethers. *J. Am. Chem. Soc.* 96, 2268–2270.
- (54) Craig, A. S., Helps, I. M., Jankowski, K. J., Parker, D., Beeley, N. R. A., Boyce, B. A., Eaton, M. A. W., Millican, A. T., Millar, K., Phipps, A., Rhind, S. K., Harrison, A., and Walker, C. (1989) Towards tumor imaging with indium-111 labeled macrocycle-antibody conjugates. *J. Chem. Soc. Chem. Commun.* 794–796.
- (55) Cox, J. P. L., Jankowski, K. J., Katak, R., Parker, D., Beeley, N. R. A., Boyce, B. A., Eaton, M. A. W., Millar, K., Millican, A. T., Harrison, A., and Walker, C. (1989) Synthesis of a kinetically stable yttrium-90 labelled macrocycle-antibody conjugate. *J. Chem. Soc. Chem. Commun.* 797–798.
- (56) Deutsch, J., Gries, H., Conrad, J., and Weinmann, H.-J. (1988) International Patent Application, WO 88/08422, 1988.
- (57) Marecek, J. F., and Burrows, C. J. (1986) Synthesis of an optically active spermine macrocycle, (S)-6-(hydroxymethyl)-1,5,10,14-tetraazacyclooctadecane, and its complexation at ATP. *Tetrahedron Lett.* 27, 5943–5946.
- (58) Wagler, T. R., and Burrows, C. J. (1987) Synthesis of an optically active C-functionalized cyclam: (S)-5-(hydroxymethyl)-1,4,8,11-tetra-azacyclotetradecane and its nickel(II) complex. *J. Chem. Soc. Chem. Commun.* 277–278.
- (59) Nitro groups are known to activate aryl groups to nucleophilic attack; see: Strauss, M. J. (1970) Anionic sigma complexes. *Chem. Rev.* 70, 667–712.
- (60) Diederich, F., Dick, K., and Griebel, D. (1986) Complexation of arenes by macrocyclic hosts in aqueous and organic solution. *J. Am. Chem. Soc.* 108, 2273–2286.
- (61) Sheh, L., and Mokotoff, M. (1985) Cyclization studies of tetrapeptide homologs. *Tetrahedron Lett.* 26, 5755–5758.
- (62) Desreux, J. F. (1980) NMR spectroscopy of lanthanide complexes of a tetraacetate tetraaza macrocycle. Unusual conformational properties. *Inorg. Chem.* 19, 1319–1324.
- (63) Reugg, C. L., Anderson-Berg, W. T., Brechbiel, M. W., Mirzadeh, S. M., Gansow, O. A., and Strand, M. (1990) Improved in vivo stability and tumor targeting of bismuth-labeled antibody. *Cancer Res.* 50, 4221–4226.
- (64) Cohen, L. A., and Witkop, B. (1955) Transannular reactions of peptides. The peptide nitrogen in a 10-membered ring. *J. Am. Chem. Soc.* 6595–6600.
- (65) Shemyakin, M. M., Antonov, V. K., Shkrob, A. M., Shchelokov, V. I., and Agadzhanian, Z. E. (1965) Activation of the amide group by acylation. *Tetrahedron* 21, 3537–3572.
- (66) Antonov, V. K., and Shemyakin, M. M. (1965) Further data on aminoacyl incorporation in peptides. *Acta. Chim. Hung. Tomus* 44, 93–98.
- (67) Takeuchi, H., Matsushita, Y., and Eguchi, S. (1991) Novel ring enlargement of lactams via quinazolinone annelation. A facile route to benzoannelated large-membered cyclic 1,5-diamines. *J. Org. Chem.* 56, 1535–1537.
- (68) Yamamoto, H., and Maruoka, K. (1981) Regioselective carbonyl amination using diisobutylaluminum hydride. *J. Am. Chem. Soc.* 103, 4186–4186.
- Registry No.** 2, 127985-74-4; 2-¹⁴C isomer, 138878-33-8; 3, 138878-17-8; 3-¹⁴C isomer, 138878-35-0; 4, 105359-57-7; 6, 53049-03-9; 7, 53049-04-0; 8, 138878-18-9; 9, 138878-19-0; 10, 56074-20-5; 11, 123317-48-6; 12, 138878-20-3; 13, 138878-21-4; 14, 138878-22-5; 14 base, 135825-00-2; 15, 138878-23-6; 15-¹⁴C isomer, 138878-32-7; 16, 123317-52-2; 16-¹⁴C isomer, 138898-85-8; 17, 138878-24-7; 18, 138878-25-8; 19, 138878-26-9; 19-¹⁴C isomer, 138878-34-9; 20, 138878-27-0; 21a, 138878-28-1; 21b, 138878-31-6; 22, 138878-29-2; 23, 138878-30-5; *N,N'*-ethylenediaminediacetic acid, 5657-17-0; bromoacetic acid, 79-08-3; 2-[[*tert*-butoxycarbonyl]oxylimino]-2-phenylacetone nitrile, 80994-44-1; 1-[3-(dimethylamino)propyl]-3-ethylcarbodiimide hydrochloride, 25952-53-8; ethylenediamine-*N,N'*-dipropionic acid dihydrochloride, 32705-91-2; iminodiacetic acid, 142-73-4; *N*-hydroxysuccinimide, 6066-82-6.

Structure-Function Relationships in Indium-111 Radioimmunoconjugates

Kimberly D. Brandt and David K. Johnson*

Abbott Laboratories, Department 90M, Abbott Park, Illinois 60064. Received September 19, 1991

Conjugates formed by reaction of monoclonal antibody B72.3 with benzyl isothiocyanate derivatives of four amino polycarboxylate chelators (NTA, EGTA, EDTA, DTPA) were labeled with indium-111 and administered iv to athymic mice bearing antigen-positive (LS174T) and antigen-negative (A375) human tumor xenografts. Conjugate immunoreactivities, antibody dose, and xenograft size were controlled, so that the effects of varying chelate structure could be evaluated under conditions where immunological and physiological factors were effectively held constant. Tissue distribution and excretion of the radiometal at 24 and 48 h postinjection were shown to correlate directly with chelate thermodynamic stability (NTA < EGTA < EDTA < DTPA). Radioactivity levels in the blood and the LS174T xenograft increased, while kidney levels and excretion levels decreased, with increasing chelate stability. The kidney was the only normal organ that accumulated non-antibody-bound ¹¹¹In, uptake of radioactivity into all other tissues, and in particular the liver, being unaffected by changes in chelate structure. Mean transferrin saturation in the tumor-bearing athymic mice was found to be 65%. It is proposed that uptake of free ¹¹¹In by serum transferrin is precluded in this model, leading to the observed renal localization of unbound label. Kidney: blood and kidney: LS174T activity ratios at 48 h postinjection provided the most sensitive indices of conjugate instability in vivo, spanning 50- and 20-fold ranges, respectively, between the least stable and the most stable conjugate. It is concluded that this antigen/antibody system and mouse model are well-suited to structure-function studies of immunoglobulin labels.

Antibody-chelator conjugates labeled with the radio-metal indium-111 have been widely used in tumor radio-immunoscintigraphy (1-8). The results of these trials have been mixed, with high background activity in normal tissues, particularly the liver, often being a major factor that limits tumor detection. Although these findings may reflect inherent limitations on the tissue discrimination achievable in man with such immunoproteins, it is also likely that the true potential of these agents has been obscured by artifacts related to the radiolabeling process. The majority of human trials to date have employed antibody-DTPA¹ conjugates prepared by procedures (9-11) that have the potential to produce both antibody denaturation and unstable indium binding sites, and these effects would be expected to increase normal tissue background (12). Recognition of these shortcomings has prompted the development of alternative bifunctional chelators intended for use in indium-111 radioimmuno-scintigraphy (13-18).

An important objective is to obtain chelates that remain completely stable throughout the period required to conduct a radioimmunosintigraphy study (typically several days when whole immunoglobulin is used). Nevertheless, there are few well-established and generally applicable methods for evaluating the in vivo stability of indium-111 radioimmunoconjugates. Incubation in human serum at 37 °C, with periodic size-exclusion HPLC analysis to determine the percentage of the radiolabel

present in antibody-bound form, has been used to assess the likely stability of a chelate conjugate in the circulation (19). However, because such in vitro serum incubations do not mimic all of the conditions to which a conjugate may be exposed in vivo (e.g. the low pH environment within lysosomes), animal model studies have also generally been undertaken. The most sophisticated of these have used anti-chelate monoclonal antibodies to probe for the presence of intact chelate (20, 21), while many investigators have also attempted to interpret biodistribution data from nude mouse/human tumor xenograft models in terms of the stability of the indium-111 chelate label (13, 14, 22-24). In the latter situation, as in man, it has often been difficult to distinguish nontarget tissue uptakes that are due to chelate instability from those caused by intrinsic factors (e.g. immune complex formation, physiological processing of immunoglobulin by liver and kidney) or other label-related phenomena (e.g. reticuloendothelial scavenging of denatured protein). A case in point is the high liver background often seen when indium-111-labeled antibodies have been administered to athymic mice implanted with a variety of tumor xenografts. This has been ascribed to immune mechanisms in some studies (25), to chelate instability in others (14, 22), and, most recently, to an artifact in the labeling process (26). Such disparities point to the need for experimental designs that allow independent investigation of each of the various factors, intrinsic and label-related, that can potentially impact tissue distribution.

The present study was designed to isolate the relationship between chelate stability and indium-111 biodistribution in a widely used nude mouse model of human colon cancer, employing the IgG₁ murine monoclonal antibody B72.3 (13, 14, 22-24, 27). The intention was to use a single antibody and derivatization chemistry to prepare a series of different chelator conjugates of equivalent immuno-reactivity and to study these at a fixed dose in athymic mice bearing antigen-positive and antigen-negative xe-

¹ Abbreviations used: BSA, bovine serum albumin; BSM, bovine submaxillary mucin; CEA, carcinoembryonic antigen; DTPA, diethylenetriaminepentaacetic acid; DTTA, diethylenetriaminetetraacetic acid; EDTA, ethylenediaminetetraacetic acid; EGTA, ethylene glycol tetraacetic acid; ELISA, enzyme-linked immunosorbent assay; HRPO, horseradish peroxidase; ID, injected dose; ND, not determined; NTA, nitrilotriacetic acid; OPD, o-phenylenediamine; PBS, phosphate-buffered normal saline (pH 7.4); RD, recovered dose; TAG, tumor-associated glycoprotein; TIBC, total iron binding capacity.

Chart I

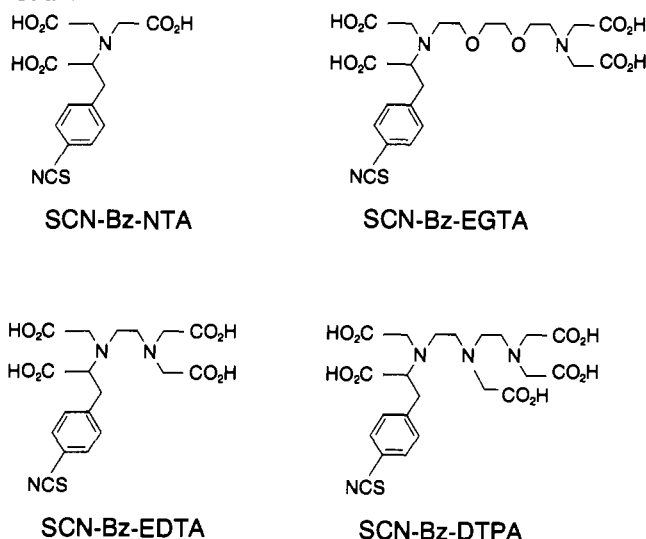


Table I. Characteristics of Chelate Labels

chelator	maximum denticity	log β for In(III) chelate
NTA	4	15.9 \pm 0.19 ^{a,b}
EGTA	8	15–20 ^{b,c}
EDTA	6	25.8 \pm 0.21 ^{a,b}
DTPA	8	28.5 \pm 0.08 ^{a,b}

^a Data taken from ref 28. ^b Studies with model chelates of SCN-Bz-EDTA (29) suggest that formation constants for complexes formed by the carboxymethyl-substituted bifunctional ligands are ca. 20% lower than those for the corresponding undervatized chelates. ^c Data unavailable. The range shown is an estimate based on corresponding values for other trivalent metals.

nografts of fixed size. Under these conditions, physiologic and immunological factors were expected to remain uniform across all groups of animals studied. Conjugates were constructed using benzyl isothiocyanate derivatives of a series of structurally related chelators (Chart I) that span a range of indium chelate thermodynamic stabilities (Table I), with the expectation that the least stable system (NTA) would be likely to dissociate extensively in vivo while the most stable (DTPA) should show minimal dissociation. Complete metabolic balance studies were performed, in order to define the impact of chelate instability on both tissue distribution and excretion of the radiometal.

EXPERIMENTAL PROCEDURES

Preparation of Antibody-Chelator Conjugates. The hybridoma producing B72.3 (American Type Culture Collection, Rockville, MD) was grown in tissue culture using a hollow-fiber bioreactor (Amicon Corp., Danvers, MA), the antibody being purified from the culture medium by affinity chromatography on protein A Sepharose 4B (12, 13). Bifunctional chelating agents were synthesized as described elsewhere (13, 30) and were coupled to the antibody following the same procedure previously developed for the preparation of B72.3-chelator conjugates (12, 13). All conjugations were carried out at pH 8.5 and 37 °C for 3 h, using an input stoichiometry of chelator: antibody of 3:1 and an antibody concentration of 10 mg/mL.

Immunoassay of Antibody-Chelator Conjugates. Microtiter plate ELISA assays that employed BSM as the antigen were used to evaluate the chelator conjugates for differences in retained immunological activity. A detailed description of the assay procedure may be found elsewhere

(12, 13). Briefly, 96-well microtiter plates (Dynatech Laboratories, Arlington, VA) were coated with BSM (Cooper Biomedical, Malvern, PA), overcoated with BSA, and stored at 2–8 °C until needed. Each plate was then washed with PBS and serial 2-fold dilutions of the B72.3-chelator conjugates were applied, using conjugate stock solutions adjusted to an initial concentration of 4 μ g/mL. After incubation at 37 °C for 1 h, the plate was emptied and washed with PBS and a goat anti-mouse antibody-HRPO conjugate (Kirkegaard & Perry Laboratories, Gaithersburg, MD) was applied. After a further 1-h incubation at 37 °C, the plate was again emptied and washed with PBS and then the color was developed by addition of OPD and, after quenching with H₂SO₄, was read at 490 nm using a microtiter plate reader (Dynatech). The chelator conjugates (B72.3-NTA, B72.3-EGTA, B72.3-EDTA, and B72.3-DTPA) were assayed, in duplicate, on the same plate.

Indium-111 Labeling of Antibody-Chelator Conjugates. B72.3-chelator conjugates, at concentrations of 5–10 mg/mL in 0.05 M citrate buffer (pH 6.0), were incubated at 37 °C with sufficient ¹¹¹InCl₃ (Nordion International, Inc., Kanata, Ontario, Canada) to give a specific activity of 1 mCi/mg if completely incorporated. Radiochemical yields were determined by ITLC following a brief challenge with excess DTPA (12, 13). The EGTA, EDTA, and DTPA conjugates incorporated >90% of the radiolabel after overnight incubation and were used in subsequent animal studies without further purification. The radiochemical yield of ¹¹¹In-B72.3-NTA achieved after overnight incubation was only 60% and this conjugate was therefore purified further by TSK-250 size-exclusion HPLC to give a preparation in which >90% of the radiolabel was bound to the antibody. For biodistribution studies, conjugates were diluted into normal saline to a final concentration of 10–50 μ g/mL. The solution of indium-111 citrate that was used as a control in the biodistribution studies was prepared following the same procedure employed in labeling the conjugates; i.e. ¹¹¹InCl₃ was incubated in 0.05 M citrate buffer (pH 6.0) for 30 min at 37 °C and then diluted into normal saline.

Biodistribution Studies. Female athymic mice (nu/nu, BALB/c background, Charles River Biotechnology Services, Wilmington, MA) were injected subcutaneously with 7.5 \times 10⁶ A375 human melanoma cells (American Type Culture Collection) in one flank. Two weeks later, 2.5 \times 10⁶ LS174T human colon carcinoma cells (American Type Culture Collection) were injected subcutaneously into the opposing flank. When the solid tumors that developed at the injection sites reached sizes of ca. 50–500 mg, the mice were divided into groups of five and 1–5 μ g of ¹¹¹In-labeled B72.3-chelator conjugate in 100 μ L of normal saline was administered to each mouse via a tail vein. Each group of animals was then housed in a separate metabolic cage (Bio-Serv., Inc., Frenchtown, NJ) and provided with food and drinking water. Control groups received iv indium-111 citrate (ca. 1 μ Ci) in 100 μ L of normal saline and were similarly housed in metabolic cages.

At either 24 or 48 h after administration of the conjugate, the mice were killed by cervical dislocation and the tumors and all internal organs were removed, weighed, and counted in a γ -counter (LKB 1272 Clinigamma, Pharmacia LKB Biotechnology Inc., Gaithersburg, MD). Weighed aliquots of blood, muscle, and skin were also counted and the tail was counted separately to check for extravasation at the injection site. The residual carcass was counted and an estimate of whole body retention of radioactivity obtained, by totaling the carcass counts and all individual tissue

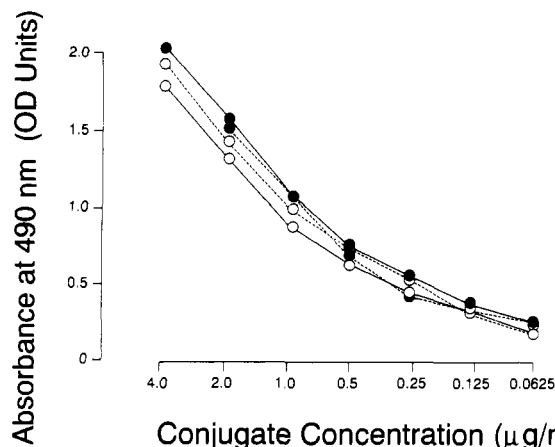


Figure 1. ELISA titration curves for binding of B72.3-NTA (○—○), B72.3-EGTA (□—□), B72.3-EDTA (●—●), and B72.3-DTPA (■—■) to a BSM-coated microtiter plate. Each data point represents the mean of two duplicate determinations.

counts. A 100-μL aliquot of each injectate was counted at the same time as the corresponding tissues and the radioactivity in each tissue was expressed as a percentage of this injected dose per gram of tissue.

Stool and urine samples that had accumulated over the study period were removed and each cage was then rinsed with deionized H₂O and wiped down with gauze. The stool and urine samples plus the rinse H₂O and gauze (hereafter "washings") from each group were counted together with the corresponding injectate standard, the counts for each group being divided by 5 to arrive at the average output per animal.

Differences in radioactivity distribution were evaluated for statistical significance by the two-tailed Student *t*-test.

Transferrin Saturation Measurements. Four athymic mice bearing LS174T and A375 xenografts (prepared as for, but not used in, biodistribution studies) were bled via a retroorbital sinus and the serum was separated. The iron concentration and TIBC of each serum sample were determined using a commercially available colorimetric assay (A-GENT, Abbott Laboratories). Values for percent transferrin saturation were then calculated from the measured serum iron and TIBC levels.

RESULTS

For the purposes of this study, it was important to exclude the possibility that differences in label biodistribution might be caused by differences in retained immunological activity between the various B72.3-chelator conjugates. All preparations were therefore tested and shown to differ by less than 20% in the midpoint absorbance of their ELISA titration curves (Figure 1), indicating no significant differences in immunoreactivity between the different chelator conjugates (12). Other potential variables that were controlled included the size of tumor xenografts (31). Mean tumor weights were kept above 50 mg, to avoid unusually high uptakes due to facile vascular access in very small tumors, and below 500 mg, to avoid artifactually low uptakes reflecting necrosis and poor vascularization. The dose of antibody given to each mouse was also held in a narrow range (1–5 μg), so as to minimize any dependence of biodistribution on protein dose (20).

To mimic the extreme case of a conjugate undergoing complete dissociation of the radiometal immediately on entering the circulation, control groups were given iv indium-111 citrate. As anticipated, these animals had only

low levels of radioactivity remaining in the blood by 24 h postinjection, with low (and equivalent) uptakes in both xenografts (Table II). Indium-111 activity was concentrated in the kidneys, but not in the liver or spleen. Radioactivity levels at 48 h postinjection were unchanged from those at 24 h for all tissues, indicating that the observed distribution was achieved rapidly, as would be expected for a low molecular weight species.

Tissue distributions of indium-111 administered in the form of the NTA conjugate were indistinguishable from those produced by indium-111 citrate, except for minor differences in activity levels in the blood and both tumors. Although low, blood levels at 24 h postinjection in animals given the NTA conjugate were significantly higher than those in both the 48-h ¹¹¹In B72.3-NTA group (*p* < 0.01) and the 24-h citrate controls (*p* < 0.01), while uptake into both tumors was some 1.5–2-fold higher for the NTA conjugate than for free indium-111. In some instances, the latter differences were statistically significant (e.g. 24-h LS174T levels: citrate vs NTA conjugate, *p* < 0.001), although in others the large standard deviations characteristic of xenograft tissue in this model obscured the effect. This uptake most likely represented nonspecific trapping within xenografts of indium-111 reaching the tumor in macromolecular form, as levels in the antigen-negative xenograft were elevated (relative to indium-111 citrate) in all groups that received conjugated indium-111. These observations suggest that the ¹¹¹In-B72.3-NTA conjugate underwent complete loss of the indium-111 label by 48 h postinjection, but that some fraction of the radiometal remained bound to the antibody long enough to produce a nonspecific elevation of tumor levels and a low, but detectable, concentration of conjugated indium-111 still present in the circulation after 24 h.

In contrast to animals given the NTA conjugate, those receiving the EGTA analogue showed clear evidence for specific tumor targeting of the radiolabel. The ratio of LS174T:A375 activity was ca. 2:1 at both 24 and 48 h after administration of the antibody, and the absolute amounts of radioactivity in the LS174T xenograft were 3-fold higher than those seen with indium-111 citrate and 2-fold higher than those for the corresponding NTA groups. There was a 2-fold reduction in kidney uptake of the radiolabel and clearance from the circulation was markedly prolonged, with blood levels at 48 h being 8-fold higher than those seen with either indium-111 citrate or ¹¹¹In-B72.3-NTA. Viewed in isolation, these characteristics of the ¹¹¹In-B72.3-EGTA conjugate (specific tumor targeting, prolonged blood clearance, limited normal tissue uptake) could be taken as evidence for retention of conjugate integrity in vivo. However, when biodistribution data for the EGTA conjugate were compared to those for the EDTA analogue, it was immediately apparent that the former underwent significant dissociation.

Blood levels of indium-111 activity in animals given ¹¹¹In-B72.3-EDTA were significantly higher by 48 h postinjection than those in the corresponding EGTA group (*p* < 0.01), while LS174T levels were 2-fold higher and renal activity 2-fold lower in the EDTA animals than in those given the EGTA conjugate. Tissue levels of indium-111 following administration of the DTPA conjugate were not significantly different from those produced by ¹¹¹In-B72.3-EDTA, except that kidney uptake was lower in the DTPA group (*p* < 0.01).

It is noteworthy that liver uptake of indium-111 was unaffected by chelate instability in this model. There was no statistically significant difference between liver activity in the citrate controls and that in any group

Table II. Tissue Distribution of Indium-111 Activity at 24 and 48 h after Intravenous Administration of Indium-111 Citrate and Indium-111-Labeled B72.3-Chelator Conjugates to Athymic Mice Bearing Subcutaneous Antigen-Positive (LS174T) and Antigen-Negative (A375) Xenografts

tissue	% injected dose of In-111 activity per gram of tissue [mean (\pm SD) for $n = 5$]									
	indium-111 citrate		¹¹¹ In-B72.3-NTA		¹¹¹ In-B72.3-EGTA		¹¹¹ In-B72.3-EDTA		¹¹¹ In-B72.3-DTPA	
	24 h	48 h	24 h	48 h	24 h	48 h	24 h	48 h	24 h	48 h
blood	1.9 (0.4)	1.1 (0.3)	3.4 (0.6)	1.1 (0.3)	13.5 (2.3)	8.5 (2.0)	13.6 (1.9)	13.9 (0.8)	ND	12.9 (2.6)
LS174T ^a	4.0 (0.4)	4.2 (0.5)	7.5 (0.7)	6.0 (0.7)	13.7 (4.7)	14.4 (2.9)	17.6 (3.6)	30.5 (8.6)	ND	25.3 (5.0)
A375 ^b	4.6 (0.6)	4.3 (1.1)	7.6 (3.8)	8.4 (3.8)	7.3 (1.4)	8.0 (1.2)	6.1 (1.9)	8.2 (1.2)	ND	8.7 (1.7)
kidney	18.7 (3.8)	18.0 (1.7)	23.6 (3.2)	21.9 (2.5)	10.8 (3.6)	13.6 (2.9)	4.7 (0.7)	6.5 (0.6)	ND	4.7 (0.8)
liver	4.2 (0.3)	5.3 (0.8)	5.2 (0.4)	5.2 (0.7)	5.4 (1.5)	6.1 (0.8)	4.6 (0.9)	6.6 (1.3)	ND	7.5 (2.7)
spleen	4.6 (0.5)	5.4 (0.4)	4.7 (0.6)	5.0 (0.7)	5.0 (1.6)	5.9 (1.3)	5.0 (0.7)	5.2 (0.8)	ND	6.5 (1.6)
lungs	3.2 (0.3)	4.0 (1.3)	3.8 (0.5)	3.3 (0.4)	6.7 (1.0)	5.3 (1.1)	5.8 (0.7)	6.2 (0.6)	ND	6.1 (1.2)
heart	2.8 (0.1)	2.8 (0.3)	3.5 (0.3)	2.8 (0.3)	6.1 (1.1)	4.2 (0.7)	5.4 (0.9)	4.9 (0.6)	ND	5.4 (1.8)
GI tract	2.8 (0.1)	2.3 (0.6)	4.1 (0.4)	2.7 (0.2)	2.2 (0.4)	2.3 (0.5)	1.4 (0.4)	1.4 (0.4)	ND	1.6 (0.2)
muscle	1.6 (0.3)	1.9 (0.4)	1.8 (0.3)	1.9 (0.5)	2.1 (0.5)	2.3 (0.6)	1.9 (0.4)	2.2 (0.4)	ND	2.0 (0.3)
skin	3.3 (0.6)	4.1 (0.7)	3.8 (0.6)	3.4 (0.4)	4.0 (0.9)	3.6 (1.2)	3.4 (0.7)	4.3 (0.7)	ND	3.4 (0.8)

^a Mean tumor weights in grams (\pm SD): 24-h groups—indium-111 citrate, 0.32 (0.14); ¹¹¹In-B72.3-NTA, 0.10 (0.04); ¹¹¹In-B72.3-EGTA, 0.23 (0.04); ¹¹¹In-B72.3-EDTA, 0.27 (0.09); 48-h groups—indium-111 citrate, 0.28 (0.11); ¹¹¹In-B72.3-NTA, 0.12 (0.07); ¹¹¹In-B72.3-EGTA, 0.36 (0.13); ¹¹¹In-B72.3-EDTA, 0.28 (0.06); ¹¹¹In-B72.3-DTPA, 0.36 (0.15). ^b Mean tumor weights in grams (\pm SD): 24-h groups—indium-111 citrate, 0.28 (0.08); ¹¹¹In-B72.3-NTA, 0.05 (0.02); ¹¹¹In-B72.3-EGTA, 0.10 (0.06); ¹¹¹In-B72.3-EDTA, 0.20 (0.15); 48-h groups—indium-111 citrate, 0.22 (0.10); ¹¹¹In-B72.3-NTA, 0.05 (0.03); ¹¹¹In-B72.3-EGTA, 0.11 (0.06); ¹¹¹In-B72.3-EDTA, 0.33 (0.16); ¹¹¹In-B72.3-DTPA, 0.12 (0.04).

Table III. Distribution of Injected Indium-111 Activity between Tissues and Excreta at 24 and 48 h after Intravenous Administration of Indium-111 Citrate and Indium-111-Labeled B72.3-Chelator Conjugates to Athymic Mice Bearing Subcutaneous Antigen-Positive (LS174T) and Antigen-Negative (A375) Xenografts

	indium-111 citrate		¹¹¹ In-B72.3-NTA		¹¹¹ In-B72.3-EGTA		¹¹¹ In-B72.3-EDTA		¹¹¹ In-B72.3-DTPA	
	24 h	48 h	24 h	48 h	24 d	48 h	24 h	48 h	24 h	48 h
% ID in mouse [mean (\pm SD) for $n = 5$]	60.4 (3.9)	61.9 (6.6)	80.3 (3.5)	67.1 (2.7)	81.0 (14.8)	75.6 (14.0)	67.1 (9.0)	70.6 (6.2)	ND	80.0 (12.0)
% ID in urine (mean for $n = 5$)	12.0	11.2	3.6	5.2	3.0	3.0	4.5	5.7	ND	4.0
% ID in stool (mean for $n = 5$)	7.1	8.7	5.6	10.4	3.8	8.2	4.5	4.7	ND	3.8
% ID in washings (mean for $n = 5$)	6.0	6.2	3.0	3.1	1.6	2.4	3.8	3.0	ND	2.4
total % ID recovered (mean for $n = 5$)	85.5	88.0	92.5	85.8	89.4	89.2	79.9	84.0	ND	90.2

Table IV. Tissue and Excreta Data from Table III Restated in the Form of Whole-Body Retention and Overall Excretion Values Expressed as a Percentage of the Radioactivity Recovered from Each Group

	indium-111 citrate		¹¹¹ In-B72.3-NTA		¹¹¹ In-B72.3-EGTA		¹¹¹ In-B72.3-EDTA		¹¹¹ In-B72.3-DTPA	
	24 h	48 h	24 h	48 h	24 h	48 h	24 h	48 h	24 h	48 h
mean % RD in mouse ($n = 5$)	70.6	70.3	86.8	78.2	90.6	84.8	84.0	84.0	ND	88.7
mean % RD excreted (stool + urine + washings, $n = 5$)	29.4	29.7	13.2	21.8	9.4	15.2	16.0	16.0	ND	11.3

receiving indium-111 in conjugated form ($p > 0.1$). The liver, heart, and lungs did show a trend toward slightly increased activity with increasing chelate stability, but this probably reflected the increasing radioactivity levels in blood trapped within these highly perfused organs. The only tissues that were responsive to changes in chelate structure were the kidney, the LS174T xenograft, and the blood. Blood levels of unsaturated transferrin, which is assumed to mediate distribution of indium-111 once lost from the immunoglobulin, were found to be lower in tumor-bearing nude mice than in normal man. The mean serum iron concentration in athymic mice bearing LS174T and A375 xenografts was 250 μ g/dL (range, 189–301 μ g/dL) with a TIBC of 388 μ g/dL (range, 312–435 μ g/dL), giving a mean saturation of 65% (range, 51–81%).

Patterns of excretion of the indium-111 label (Table III) were consistent with the overall trends found in the tissue-distribution data, although metabolic studies proved to be of limited utility due to the relatively low levels of label excretion that were seen. There were no clear cut trends in the distribution of excreted activity among stool, urine, and washings, and given the inherent imprecision

of these measurements, the data are best combined and expressed as values for total label excretion in each group. While whole-body retention of radioactivity could be shown to be significantly higher for some conjugates than for indium-111 citrate (e.g. 24 h ¹¹¹In-B72.3-NTA vs indium-111 citrate, $p < 0.001$), this was not true in other cases where the standard deviations were large (e.g. 24 h ¹¹¹In-B72.3-EDTA vs indium-111 citrate, $p > 0.1$). The mean recovery of radioactivity over nine groups of animals was 87.2%, and as mechanical losses were minimal, this shortfall (relative to a 100 μ L counting standard) probably represents the actual mean volume of injectate received by the animals. It is therefore useful to restate the metabolic data in the form of whole-body retention and overall excretion values, expressed as a percentage of the counts recovered from each group rather than a percentage of the estimated counts injected (Table IV). Viewed in this way, a trend toward increased whole-body retention and decreased overall excretion of the radiometal with increasing chelate stability is more readily apparent.

Comparison of the 24-h data with the corresponding 48-h values in Table IV also confirms other inferences

drawn from the tissue-distribution measurements. Those groups where the label was either so unstable that distribution appeared complete by 24 h postinjection (indium-111 citrate) or so stable that nontarget distribution changed little during 24 h (^{111}In -B72.3-EDTA) showed no incremental excretion of the radiometal between 24 and 48 h after administration. In contrast, those groups in which tissue data suggested a progressive loss of indium-111 from the conjugate throughout the study period (^{111}In -B72.3-NTA, ^{111}In -B72.3-EGTA) showed a decrease in whole-body activity and a corresponding increase in overall excretion between the 24- and 48-h time points. Although excretion data therefore reinforced the conclusions drawn from tissue-distribution studies, the narrow range between the least stable and the most stable conjugate (10% RD at 48 h, Table IV) made excretion a relatively insensitive index of conjugate instability *in vivo*. This is well-illustrated by the EDTA and EGTA conjugates, which were indistinguishable on the basis of 48-h excretion values yet showed readily observable differences in tissue distribution of the radiometal at that time point. It is thus unlikely that excretion patterns alone could be used to differentiate conjugates of varying stability in this model.

DISCUSSION

When a unique biological entity (e.g. a protein or polynucleotide having a particular specificity) is coupled to a unique reporter or effector molecule (e.g. an enzyme or fluorophore) and evaluated in a biological assay system that is also often unique, the singular nature of the results obtained makes comparison with those for any other conjugate, particularly between different laboratories, difficult if not impossible. Nevertheless, systematic intercomparisons of related conjugates in common assay systems are likely to be needed if the rules that govern construction of optimum reagents of this type are to become fully understood. In particular, research in which the reporter/effector molecule is a low molecular weight organic moiety (e.g. a drug or chelate) should lend itself to the structure-function approach often taken in medicinal chemistry when developing such molecules in non-conjugated form, provided that potential variables associated with the biological moiety and the bioassay can be held constant. This study was undertaken to test the feasibility of applying such an approach to antibody-chelator conjugates for radiosciintigraphic use, where the function of the reporter/effector molecule is to bind a metal in stable fashion *in vivo*.

Control of all variables arising from the antibody and mouse model appears to have been adequate in this study, as the patterns of indium-111 distribution and excretion that were seen can be rationalized entirely on the basis of differences in the structure, and hence thermodynamic stability, of the various chelates employed. In order to retain indium-111 *in vivo*, a chelator must be able to compete effectively with endogenous metal-binding molecules and, in particular, with the iron transport protein transferrin, which has a high affinity for indium(III) [$\log K$ for the 1:1 In-transferrin complex was recently estimated to be 18.8 (32)]. Complete saturation of the coordination sphere of a metal, which has recently been shown to require an octadentate ligand in the case of indium (33), may also be needed for maximum chelate stability. It is therefore unsurprising that NTA, a tetradentate chelator with a relatively modest affinity for indium, gave a conjugate that appeared to completely lose the radiometal after 48 h *in vivo*. It is perhaps more surprising that this

dissociation process was relatively slow, the tissue data and metabolic studies together providing substantial evidence that breakdown of the ^{111}In -B72.3-NTA conjugate was still incomplete at 24 h postinjection. This finding is in keeping with previous observations (21) that transchelation reactions, even when favored thermodynamically, can be slow when substituted amino polycarboxylate ligands are used. It was therefore uncertain at the outset whether the EGTA ligand would give conjugates that were stable *in vivo*. The formation constant for the EGTA complex of indium is unavailable, but it is known that this chelator can function as an octadentate ligand (34) and it seemed possible that kinetic barriers to the dissociation of a coordinatively saturated indium chelate might be sufficient to produce acceptable inertness *in vivo*. That this proved not to be the case is evident from the data in Tables II and IV. In contrast, the EDTA and DTPA chelates gave conjugates that appeared to be highly stable *in vivo*, although a question remains as to whether meaningful performance differences exist between the latter two preparations.

While the ^{111}In -B72.3-EDTA and ^{111}In -B72.3-DTPA conjugates were indistinguishable on the basis of blood levels and LS174T uptake, the DTPA conjugate did produce a significantly lower level of activity in the kidney, which was the only normal organ to accumulate unbound indium. In addition, whole-body retention of indium-111 activity was higher, and excretion lower, in animals given ^{111}In -B72.3-DTPA than in those receiving the EDTA analogue, although this difference was not statistically significant. A previous study in which the B72.3-EDTA and B72.3-DTPA conjugates were compared in nude mice bearing LS174T tumors (13) gave similar results (equivalent LS174T and blood levels, significantly lower kidney uptake and higher, but not statistically significant whole-body retention with the DTPA conjugate). Taken together, these findings suggest that the DTPA conjugate is probably slightly more stable than the EDTA analogue, but this difference in performance is small and could not be demonstrated unequivocally within the present study design.

That chelate structure can be shown to correlate with function in this context is perhaps of less significance than is a clear definition of the physiological consequences when that function (stable binding of indium to antibody) is not adequately fulfilled. Identification of the kidney as the sole normal organ responsive to changes in the stability of these chelates is advantageous, inasmuch as it simplifies the animal model, but also disadvantageous, as it indicates that the animal model does not mimic the way that unbound indium is handled in man. Trace amounts of indium in "ionic" form are rapidly taken up by the iron-binding sites of serum transferrin when the radiometal is administered *iv* in normal man (35). As most of the iron in transit in the bloodstream at any given time is destined to be stored as ferritin until needed for erythropoiesis, the primary organ of deposition of the ^{111}In tracer becomes the primary organ responsible for iron storage, namely the liver. That this is not the case in the nude mouse suggests that distribution of free indium-111 in the latter may occur through alternative mechanisms.

The rapid blood clearance and renal localization of radioactivity in animals given indium-111 citrate have been previously described in similar models (24, 36) and are certainly consistent with glomerular trapping of indium-111 being filtered from the bloodstream in low molecular weight form. This, in turn, infers that there exists some type of barrier to binding of free indium-111 by serum

transferrin in the nude mouse. When such a barrier was intentionally created (36), by administering a saturating dose of iron 1 h before giving indium-111 citrate, kidney activity at 48 h postinjection in MF1-nu/01a mice bearing HX99 breast carcinoma xenografts was reported to increase 4-fold (from $10 \pm 3.1\%$ ID/g to $40.0 \pm 14.4\%$ ID/g) while liver activity was unaffected ($4.1 \pm 1.2\%$ ID/g without presaturation vs $4.8 \pm 1.9\%$ ID/g with presaturation). Although such intentional presaturation had not been performed in the present study, we speculated that ambient levels of transferrin saturation in the nude mouse might be significantly higher than in man. Serum iron and TIBC measurements confirmed that this was indeed the case. In normal man, ca. 35% of serum transferrin binding sites are occupied by iron (37), whereas the analogous value measured in the mice used in this study was 65%. This disparity may reflect intrinsic differences in iron metabolism between man and the athymic mouse, or it may be that the presence of the rapidly growing xenograft tissue produces an elevated demand for iron [a growth factor essential for tumor proliferation (38)] that translates into elevated serum levels as dietary and storage iron is transported to the xenograft to satisfy this demand. Whatever its origin, the elevation is transferrin saturation that was documented in the tumor-bearing athymic mice used in this study should not have been sufficient to prevent binding of the injected dose of indium-111 on strictly stoichiometric grounds. However, the two iron-binding sites of transferrin are known to differ in their metal-chelating properties (39). If indium were to be able to bind with high affinity to only one of these sites in the nude mouse and if, at 65% saturation, that site were to be preferentially occupied by iron, uptake of indium by the transport protein would be preempted. Such a hypothesis offers the best explanation for the observed behavior of nonantibody-bound indium-111 in this paradigm.

Recognition that the liver is not a site of accumulation of unbound indium-111 in this model narrows the range of possible explanations for the elevated liver activities that have certainly been produced by some preparations (22, 23). Reticuloendothelial uptake of antibody that has become denatured during conjugation remains a likely source of high liver backgrounds when coupling is achieved using cross-linking agents such as the bicyclic dianhydride of DTPA (23). However, elevated liver activities have also been reported even when non-cross-linking conjugation methods were used [e.g. 14% ID/g for B72.3 labeled via an SCN-Bz-EDTA chelator (22)]. In such cases, the most likely source is first-pass hepatic clearance of immune complexes formed as a result of antigen being shed from the xenograft into the circulation. Such a mechanism has been proposed in the case of CEA (25) but not, to our knowledge, in the case of the TAG-72 antigen system. As leakage of antigen into the bloodstream is likely to depend both on the level of its expression and on physiological factors, such as the size and vascular integrity of the xenograft, elevations in liver background due to this source would be expected to be sporadic and difficult to control.

Although the model is clearly imperfect in duplicating the fate of indium once released from a radioimmunoconjugate, the fact that this fate is fixation in a single organ system (as opposed to translocation to a serum protein and subsequent redistribution to a variety of possible tissues) simplifies the selection of biological endpoints. Kidney:blood (K:B) and kidney:LS174T (K:T) activity ratios at 48 h postinjection provide the most

sensitive indices of in vivo instability, spanning 50- and 20-fold ranges, respectively, between the least stable (K:B = 20; K:T = 3.7) and most stable (K:B = 0.4; K:T = 0.2) conjugate. It is unclear how low these ratios would become if a conjugate were to remain absolutely stable in vivo. Kidney activity produced by ^{111}In -B72.3-DTPA in this model has previously been shown to be the same as that produced by ^{125}I -labeled B72.3 (12), inferring that the residual renal activity seen with the DTPA conjugate represents immunoglobulin and not free label. In clinical radioimmunoscinigraphy trials that have employed the SCN-Bz-DTPA chelator (Chart I), translocation of the indium-111 label to serum transferrin has not been detectable by SDS-PAGE, immunoprecipitation, and size-exclusion HPLC analyses of patient sera (40), and hepatic metastases have been readily visualized in a high proportion of cases (40-43). These observations suggest that the apparent stability that the DTPA label shows in nude mice is also evident in man and, consequently, that the K:B and K:T values produced by ^{111}In -B72.3-DTPA in the mouse model probably approach the theoretical minima. Nevertheless, low levels of ^{111}In -transferrin have been detected in patient sera when anti-transferrin affinity chromatography was used (44), indicating that the SCN-Bz-DTPA chelator certainly does not meet the criterion of absolute stability in vivo under all circumstances. It is possible that alternative chelators that more closely approach this ideal would produce significantly lower K:B and K:T values, although, as with the EDTA and DTPA conjugates of this study, modified experimental designs are likely to be required if a small difference in performance between two high-affinity chelates is to be demonstrated with any degree of statistical confidence.

Although access to many antibody/antigen systems is limited, the B72.3 hybridoma, the LS174T and A375 tumor cell lines, and the BSM antigen used in the immunoreactivity assay are all freely available to any investigator. This model is thus well-suited to serve as a generic test-bed for evaluating different labeling chemistries in circumstances where the results can be readily compared with an existing body of data and where duplication of results between different laboratories could be undertaken. Without such studies, it is likely that attempts to understand the in vivo behavior of synthetic moieties used to label immunoglobulins will continue to be confounded by variables that, in reality, are unrelated to the label but rather arise from often unrecognized idiosyncracies of a particular antibody/antigen system and its host.

LITERATURE CITED

- (1) Fairweather, D. S., Bradwell, A. R., Dykes, P. W., Vaughan, A. T., Watson-James, S. F., and Chandler, S. (1983) Improved tumor localization using indium-111 labeled antibodies. *Br. Med. J.* 287, 167-170.
- (2) Murray, J. L., Rosenblum, M. G., Sobol, R. L., Bartholomew, R. M., Plager, C. E., Haynie, T. P., Jahns, M. F., Glenn, H. J., Lamki, L. M., Benjamin, R. S., Papadopoulos, N., Boddie, A. W., Frincke, J. M., David, G. S., Carlo, D. J., and Hersh, E. M. (1985) Radioimmunoimaging in malignant melanoma with ^{111}In -labeled monoclonal antibody 96.5. *Cancer Res.* 45, 2376-2381.
- (3) Patt, Y. Z., Lamki, L. M., Haynie, T. P., Unger, M. W., Rosenblum, M. G., Shirkhoda, A., and Murray, J. L. (1988) Improved tumor localization with increasing dose of indium-111 labeled anti-carcinoembryonic antigen monoclonal antibody ZCE-025 in metastatic colorectal cancer. *J. Clin. Oncol.* 6, 1220-1230.
- (4) Maguire, R. T., Schmelter, R. F., Pascucci, V. L., and Conklin, J. L. (1989) Immunoscintigraphy of colorectal adenocarcinoma: results with site-specifically radiolabeled

- B72.3 (¹¹¹In-CYT-103). *Antibody Immunoconjugates Radiopharm.* 2, 257-269.
- (5) Beatty, J. D., Hyams, D. M., Morton, B. A., Beatty, B. G., Williams, L. E., Yamauchi, D., Merchant, B., Paxton, R. J., and Shively, J. E. (1989) Impact of radiolabeled antibody imaging on management of colon cancer. *Am. J. Surg.* 157, 13-19.
- (6) Siccardi, A. G., Buraggi, G. L., Callegaro, L., Colella, A. C., De Filippi, P. G., Galli, G., Mariani, G., Masi, R., Palumbo, R., Riva, P., Salvatore, M., Scassellati, G. A., Scheidhauer, K., Turco, G. L., Zaniol, P., Benini, S., Deleide, G., Gasparini, M., Lastoria, S., Mansi, L., Paganelli, G., Salvischiani, E., Seregini, E., Viale, G., and Natali, P. G. (1989) Immunoscintigraphy of adenocarcinomas by means of radiolabeled F(ab')₂ fragments of an anti-carcinoembryonic antigen monoclonal antibody: A multicenter study. *Cancer Res.* 49, 3095-3103.
- (7) Chatal, J.-F., Saccavini, J.-C., Gestin, J.-F., Thédrez, P., Curtet, C., Kremer, M., Guereau, D., Nolibé, D., Fumoleau, P., and Guillard, Y. (1989) Biodistribution of indium-111 labeled OC 125 monoclonal antibody intraperitoneally injected into patients operated on for ovarian carcinomas. *Cancer Res.* 49, 3087-3094.
- (8) Patt, Y. Z., Lamki, L. M., Shanken, J., Jessup, J. M., Charnsangavej, C., Ajani, J. A., Levin, B., Merchant, B., Halverson, C., and Murray, J. L. (1990) Imaging with indium-111-labeled anticarcinoembryonic antigen monoclonal antibody ZCE-025 of recurrent colorectal or carcinoembryonic antigen-producing cancer in patients with rising serum carcinoembryonic antigen levels and occult metastases. *J. Clin. Oncol.* 8, 1246-1254.
- (9) Krejcarek, G. E., and Tucker, K. L. (1977) Covalent attachment of chelating groups to macromolecules. *Biochem. Biophys. Res. Commun.* 77, 581-585.
- (10) Hnatowich, D. J., Layne, W. W., Childs, R. L., Lanteigne, D., Davis, M. A., Griffin, T. W., and Doherty, P. W. (1983) Radioactive labeling of antibody: A simple and efficient method. *Science* 220, 613-615.
- (11) Paxton, R. J., Jakowatz, J. G., Beatty, J. D., Beatty, B. J., Vlahos, W. G., Williams, L. E., Clark, B. R., and Shively, J. E. (1985) High specific activity ¹¹¹In-labeled anticarcinoembryonic antigen antibody: Improved method for the synthesis of diethylenetriaminepentaacetic acid conjugates. *Cancer Res.* 45, 5694-5699.
- (12) Carney, P. L., Rogers, P. E., and Johnson, D. K. (1989) Dual isotope study of iodine-125 and indium-111-labeled antibody in athymic mice. *J. Nucl. Med.* 30, 374-384.
- (13) Westerberg, D. A., Carney, P. L., Rogers, P. E., Kline, S. J., and Johnson, D. K. (1988) Synthesis of novel bifunctional chelators and their use in preparing monoclonal antibody conjugates for tumor targeting. *J. Med. Chem.* 32, 236-243.
- (14) Brechbiel, M. W., Gansow, O. A., Atcher, R. W., Schlom, J., Esteban, J., Simpson, D. E., and Colcher, D. (1986) Synthesis of 1-(p-isothiocyanatobenzyl) derivatives of DTPA and EDTA. Antibody labeling and tumor-imaging studies. *Inorg. Chem.* 25, 2772-2781.
- (15) Craig, A. S., Helps, I. M., Jankowski, K. J., Parker, D., Bealey, N. R. A., Boyce, B. A., Eaton, M. A. W., Millican, A. T., Millar, K., Phipps, A., Rhind, S. K., Harrison, A., and Walker, C. (1989) Towards tumor imaging with indium-111 labelled macrocycle-antibody conjugates. *J. Chem. Soc. Chem. Commun.* 794-796.
- (16) Mathias, C. J., Sun, Y., Connett, J. M., Philpott, G. W., Welch, M. J., and Martell, A. E. (1990) A new bifunctional chelate, BrMe₂HBED: An effective conjugate for radiometals and antibodies. *Inorg. Chem.* 29, 1475-1480.
- (17) Mathias, C. J., Sun, Y., Welch, M. J., Connett, J. M., Philpott, G. W., and Martell, A. E. (1990) N,N'-Bis(2-hydroxybenzyl)-1-(4-bromoacetamidobenzyl)-1,2-ethylenediamine-N,N'-diacetic acid: A new bifunctional chelate for radiolabeling antibodies. *Bioconjugate Chem.* 1, 204-211.
- (18) Ruser, G., Ritter, W., and Maecke, H. R. (1990) Synthesis and evaluation of two new bifunctional carboxymethylated tetraazamacrocyclic chelating agents for protein labeling with indium-111. *Bioconjugate Chem.* 1, 345-349.
- (19) Cole, W. C., DeNardo, S. J., Meares, C. F., McCall, M. J., DeNardo, G. L., Epstein, A. L., O'Brian, H. A., and Moi, M. K. (1987) Comparative serum stability of radiochelates for antibody radiopharmaceuticals. *J. Nucl. Med.* 28, 83-90.
- (20) Adams, G. P., DeNardo, S. J., Deshpande, S. V., DeNardo, G. L., Meares, C. F., McCall, M. J., and Epstein, A. L. (1989) Effect of mass of ¹¹¹In-benzyl-EDTA monoclonal antibody on hepatic uptake and processing in mice. *Cancer Res.* 49, 1707-1711.
- (21) Deshpande, S. V., Subramanian, R., McCall, M. J., DeNardo, S. J., DeNardo, G. L., and Meares, C. F. (1990) Metabolism of indium chelates attached to monoclonal antibody: Minimal transchelation of indium from benzyl-EDTA chelate in vivo. *J. Nucl. Med.* 31, 218-224.
- (22) Esteban, J. M., Schlom, J., Gansow, O. A., Atcher, R. W., Brechbiel, M. W., Simpson, D. E., and Colcher, D. (1987) New method for the chelation of indium-111 to monoclonal antibodies: Biodistribution and imaging of athymic mice bearing human colon carcinoma xenografts. *J. Nucl. Med.* 28, 861-870.
- (23) Brown, B. A., Comeau, R. D., Jones, P. L., Liberatore, F. A., Neacy, W. P., Sands, H., and Gallagher, B. M. (1987) Pharmacokinetics of the monoclonal antibody B72.3 and its fragments labeled with either ¹²⁵I or ¹¹¹In. *Cancer Res.* 47, 1149-1154.
- (24) Roselli, M., Schlom, J., Gansow, O. A., Raubitschek, A., Mirzadeh, S., Brechbiel, M. W., and Colcher, D. (1989) Comparative biodistributions of yttrium- and indium-labeled monoclonal antibody B72.3 in athymic mice bearing human colon carcinoma xenografts. *J. Nucl. Med.* 30, 672-682.
- (25) Beatty, B. G., Beatty, J. D., Williams, L. E., Paxton, R. J., Shively, J. E., and O'Connor-Tressel, M. (1989) Effect of specific antibody pretreatment on liver uptake of ¹¹¹In labeled anticarcinoembryonic antigen monoclonal antibody in nude mice bearing human colon cancer xenografts. *Cancer Res.* 49, 1587-1594.
- (26) Schuhmacher, J., Klivényi, G., Matys, R., Kirchgebner, H., Hauser, H., Maier-Borst, W., and Matzku, S. (1990) Uptake of indium-111 in the liver of mice following administration of indium-111-DTPA-labeled monoclonal antibodies: Influence of labeling parameters, physiologic parameters, and antibody dose. *J. Nucl. Med.* 31, 1084-1093.
- (27) Keenan, A. M., Colcher, D., Larson, S. M., and Schlom, J. (1984) Radioimmunoscintigraphy of human colon cancer xenografts in mice with radioiodinated monoclonal antibody B72.3. *J. Nucl. Med.* 25, 1197-1203.
- (28) Subramanian, K. M., and Wolf, W. (1990) A new radiochemical method to determine the stability constants of metal chelates attached to a protein. *J. Nucl. Med.* 31, 480-488.
- (29) Betebenner, D. A., Carney, P. L., Zimmer, A. M., Kazikiewicz, J. M., Brucher, E., Sherry, A. D., and Johnson, D. K. (1991) Hepatobiliary delivery of polyaminopolycarboxylate chelates: Synthesis and characterization of a cholic acid conjugate of EDTA and biodistribution and imaging studies with its indium-111 chelate. *Bioconjugate Chem.* 2, 117-123.
- (30) Kline, S. J., Betebenner, D. A., and Johnson, D. K. (1991) Carboxymethyl-substituted bifunctional chelators: Preparation of aryl isothiocyanate derivatives of 3-(carboxymethyl)-3-azapentanedioic acid, 3,12-bis(carboxymethyl)-6,9-dioxo-3,12-diazatetradecanedioic acid, and 1,4,7,10-tetraazacyclododecane-N,N',N'',N'''-tetraacetic acid for use as protein labels. *Bioconjugate Chem.* 2, 26-31.
- (31) Williams, L. E., Duda, R. B., Proffitt, R. T., Beatty, B. G., Beatty, J. D., Wong, J. Y. C., Shively, J. E., and Paxton, R. J. (1988) Tumor uptake as a function of tumor mass: A mathematical model. *J. Nucl. Med.* 29, 103-109.
- (32) Bannochie, C. J., and Martell, A. E. (1989) Affinities of racemic and meso forms of N,N'-ethylenebis(2-(o-hydroxyphenyl)glycine) for divalent and trivalent metal ions. *J. Am. Chem. Soc.* 111, 4735-4742.
- (33) Maecke, H. R., Riesen, A., and Ritter, W. (1989) The molecular structure of indium-DTPA. *J. Nucl. Med.* 30, 1235-1239.
- (34) Schauer, C. K., and Anderson, O. P. (1987) Calcium-selective ligands. 2. Structural and spectroscopic studies on calcium and cadmium complexes of EGTA⁴⁻. *J. Am. Chem. Soc.* 109, 3646-3656.

- (35) Hosain, F., McIntyre, P. A., Poulose, K., Stern, H. S., and Wagner, H. N. (1969) Binding of trace amounts of ionic indium-113m to plasma transferrin. *Clin. Chim. Acta* 24, 69-75.
- (36) Ward, M. C., Roberts, K. R., Westwood, J. H., Coombes, R. C. C., and McCready, V. R. (1986) The effect of chelating agents on the distribution of monoclonal antibodies in mice. *J. Nucl. Med.* 27, 1746-1750.
- (37) Ramsay, W. N. M. (1957) The determination of the total iron-binding capacity of serum. *Clin. Chim. Acta* 2, 221-226.
- (38) Weinberg, E. D. (1984) Iron withholding: A defense against infection and neoplasia. *Physiol. Rev.* 64, 65-102.
- (39) See, for example: Luk, C. K. (1971) Study of the nature of the metal-binding sites and estimate of the distance between the metal-binding sites in transferrin using trivalent lanthanide ions as fluorescent probes. *Biochemistry* 10, 2838-2843. Donovan, J. W., and Ross, K. D. (1975) Non-equivalence of the metal-binding sites of conalbumin (ovotransferrin). Calorimetric and spectrophotometric studies of binding and displacement of aluminum. *Fed. Proc.* 34, 593. Princiotto, J. V., and Zapolski, E. J. (1975) Difference between the two iron-binding sites of transferrin. *Nature* 255, 87-88. Cannon, J. C., and Chasteen, N. D. (1975) Nonequivalence of the metal binding sites in vanadyl labeled human serum transferrins. *Biochemistry* 14, 4573-4577.
- (40) Griffin, T. W., Brill, A. B., Stevens, S., Collins, J. A., Bokhari, F., Bushe, H., Stochl, M. C., Gionet, M., Rusckowski, M., Stroupe, S. D., Kiefer, H. C., Sumerdon, G. A., Johnson, D. K., and Hnatowich, D. J. (1991) Initial clinical study of indium-111-labeled clone 110 anti-carcinoembryonic antigen antibody in patients with colorectal cancer. *J. Clin. Oncol.* 9, 631-640.
- (41) Divgi, C. R., McDermott, K., Johnson, D. K., Schnobrich, K. E., Finn, R. D., Cohen, A. M., and Larson, S. M. (1991) Detection of hepatic metastases from colorectal carcinoma using indium-111 labeled monoclonal antibody: MSKCC experience with mAb ¹¹¹In-C110. *Nucl. Med. Biol.* 18, 705-710.
- (42) Johnson, D. K., SeEVERS, R. H., Schnobrich, K. E., Golick, J. A., Carney, P. L., Vijayakumar, V., and Blend, M. J. (1991) Detection of hepatic metastases from colorectal carcinoma using indium-111 labeled antibody: Initial clinical results with B72.3. *Antibody Immunoconjugates Radiopharm.* 4, 223.
- (43) Vijayakumar, V., Blend, M. J., Johnson, D. K., Schnobrich, K. E., and Golick, J. (1992) Detection of recurrent colon cancer with In-111-labeled MoAb B72.3 in a patient who had normal CEA and TAG-72 levels. *Clin. Nucl. Med.* In press.
- (44) Hnatowich, D. J., Rusckowski, M., Brill, A. B., Siebecker, D. A., Misra, H., Mardirossian, G., Bushe, H., Rescigno, A., Stevens, S., Johnson, D. K., and Griffin, T. W. (1990) Pharmacokinetics in patients of an anti-CEA antibody labeled with indium-111 using a novel diethylenetriaminepentaacetic acid chelator. *Cancer Res.* 50, 7272-7278.
- Registry No.** SCN-Bz-EDTA, 117499-22-6; SCN-Bz-DTPA, 117499-23-7.

Conjugation and Evaluation of 7E3 \times P4B6, a Chemically Cross-Linked Bispecific F(ab')₂ Antibody Which Inhibits Platelet Aggregation and Localizes Tissue Plasminogen Activator to the Platelet Surface

Donald S. Neblock,* Chien-Hsing Chang, Mary Ann Mascelli, Melanie Fleek, Lisa Stumpo, Mary Margaret Cullen, and Peter E. Daddona

Department of Immunobiology, Centocor Inc., 200 Great Valley Parkway, Malvern Pennsylvania 19355.
Received October 7, 1991

A bispecific F(ab')₂ monoclonal antibody which recognizes both the platelet GPIIb/IIIa receptor and human tissue plasminogen activator was produced to target tPA to platelets for enhancement of thrombolysis. A stable, thioether-cross-linked bispecific F(ab')₂ (7E3 \times P4B6) combining the GPIIb/IIIa-specific monoclonal antibody 7E3, which inhibits platelet aggregation, and a nonneutralizing anti-tPA monoclonal antibody (P4B6) was produced. This was performed by coupling each of the parental Fab' moieties with the homobifunctional cross-linker bis(maleimido methyl) ether (BMME). 7E3 \times P4B6 was sequentially purified using gel-filtration chromatography and hydrophobic interaction (HIC) HPLC. HIC was shown to completely resolve each of the parental F(ab')₂ species from the bispecific one. 7E3 \times P4B6 was shown to retain completely each of the parental immunoreactivities in GPIIb/IIIa and tPA binding EIA's. The bispecific antibody inhibited platelet aggregation in vitro at levels comparable to those for 7E3 Fab. Recruitment of tPA activity to washed human platelets was demonstrated using the S-2251 chromogenic substrate assay. 7E3 \times P4B6 recruited 12-fold more tPA to the washed platelets than a mixture of the parental F(ab')₂ molecules used as controls.

INTRODUCTION

Thrombolytic therapy with recombinant tissue plasminogen activator (rtPA¹) has received widespread clinical use in the treatment of acute myocardial infarction, significantly reducing associated mortality and morbidity (Collen, 1990). Despite the successful use of this thrombolytic agent in the clinic, there are still problems associated with its use. Short serum half-life (requiring high doses and prolonged infusions), serious nonspecific hemorrhagic complications, and risk of reocclusion are among these unresolved problems (Verstaete, 1990). These issues have promoted interest in the development of third-generation plasminogen activators, including forms of tPA modified via recombinant DNA technology to have longer circulating half-lives, and the production of novel antibody-plasminogen activator hybrid molecules and immunoconjugates aimed at increasing the thrombus specificity of tPA and other plasminogen activators (Haber et al., 1989; Dewerchin & Coller, 1991; Hayzer et al., 1991). In addition, the combined use of thrombolytics with potent inhibitors of platelet aggregation is seen as an approach to the reduction of the time to reperfusion and frequency of coronary vessel reocclusion currently accompanying thrombolytic therapy (Coller, 1990).

* Author to whom all correspondence should be addressed.

¹ Abbreviations used: 7E3, murine IgG₁ anti-GPIIb/IIIa monoclonal antibody; P4B6, murine IgG₁ anti-tPA monoclonal antibody; 7E3 \times P4B6, chemically cross-linked bispecific anti-GPIIb/IIIa anti-tPA (F(ab')₂); S-2251, H-D-valyl-L-leucyl-L-lysine-p-nitroanilide dihydrochloride; BMME, bis(maleimidomethyl) ether; rtPA, recombinant human tissue-type plasminogen activator; SDS-PAGE, sodium dodecyl sulfate polyacrylamide gel electrophoresis; Tris, tris(hydroxymethyl)aminomethane; TBS, Tris-buffered saline; PBS, phosphate-buffered saline; DTT, dithiothreitol; DTNB, 5,5'-dithio-bis(2-nitrobenzoic acid); EDTA, ethylenediaminetetraacetic acid; HPLC, high-performance liquid chromatography; EIA, enzyme immunoassay; OPD, o-phenylenediamine; NEM, N-ethylmaleimide; PRP, platelet-rich plasma.

Antibody targeting of tPA and other plasminogen activators to thrombi via a high-affinity monoclonal antibody directed against the amino terminus of the β -chain of fibrin has been the topic of recent research which demonstrated an increase rate of fibrinolysis in vitro and in vivo for a number of plasminogen activator-antifibrin antibody conjugates (Bode et al., 1985; Runge et al., 1987) and bispecific antibodies (Runge et al., 1990; Bode et al., 1989; Runge et al., 1987; Runge et al., 1988a,b). As a major component of arterial thrombi, platelets provide an additional target for the antibody recruitment of tPA. This may be especially useful in the case of thrombolysis-resistant platelet-rich arterial thrombi occurring in acute myocardial infarction or during acute reocclusion subsequent to thrombolytic therapy (Yasuda et al., 1990; Gold & Leinbach, 1987). As one approach, targeting to activation-specific platelet antigens would direct a platelet-specific thrombolytic agent only to platelet-rich thrombi, circumventing binding to circulating platelets. This approach has been described recently for immunoconjugates of recombinant single-chain urokinase-type plasminogen activator (Dewerchin et al., 1991). However, the use of a potent inhibitor of platelet aggregation which does bind to circulating resting platelets as the fibrinolysis targeting antibody, such as the anti-GPIIb/IIIa monoclonal antibody 7E3, might yield additional benefits in terms of preventing reocclusion as well as hastening reperfusion. Experimentally, this concept was demonstrated recently by acceleration of in vitro platelet-rich clot lysis and inhibition of platelet aggregation with a 7E3-urokinase immunoconjugate (Bode et al., 1991). Toward this end, targeting of tPA to platelets via a bispecific antibody comprised of 7E3 and an anti-tPA monoclonal antibody would combine potent inhibition of platelet aggregation in vivo via the 7E3 half of the molecule (Coller et al., 1988; Gold et al., 1987; Gold et al., 1990) with the recruitment of the plasminogen activator to both the platelet-rich thrombus and circulating platelets. The potential advantages of this approach over currently available or next-

generation thrombolytics may include increased specificity for platelet-rich thrombi, recruitment of endogenous and pharmacological tissue plasminogen activator, increase of avidity by combining platelet and fibrin binding specificities in one molecule, and combination of anti-platelet and thrombolytic functions in one agent. In the present study, a bispecific F(ab')₂, 7E3 × P4B6, recognizing both human tissue plasminogen activator as well as GPIIb/IIIa, was prepared by chemical conjugation of the parental Fab' antibodies via a nonreducible thioether cross-link and was biochemically and functionally characterized. A bispecific antibody with these dual specificities might allow the targeting of both pharmacologically administered tPA and endogenously released tPA to circulating platelets and the platelet-rich thrombus in vivo.

EXPERIMENTAL PROCEDURES

Recombinant tPA (Activase) was obtained from Genentech (San Francisco, CA). BMME was purchased from Calbiochem. S-2251, plasminogen, and fibrin fragments were purchased from Helena Laboratories (Beaumont, TX). All other chemicals were purchased from Sigma (St. Louis, MO).

Electrophoresis. Phastsystem gels and supplies (Pharmacia, Piscataway, NJ) were used for all SDS-PAGE analyses. Samples of the BMME cross-linking steps were prepared for electrophoresis by incubating 1 volume of sample for 10 min on ice in the presence of 2 volumes of 200 mM *N*-ethylmaleimide, followed by dilution 1:2 in 2× sample buffer (4% SDS, 20% glycerol, 0.250 M Tris-HCl (pH 6.8), and 0.002% bromophenol blue) and heating for 3 min at 100 °C. Other samples were processed for SDS-PAGE by dilution into 2× sample buffer and heating for 3 min at 100 °C in the presence or absence of 100 mM DTT. A mixture of prestained molecular weight standards consisting of myosin (200 kDa), phosphorylase B (97.4 kDa), bovine serum albumin (68 kDa), ovalbumin (43 kDa), carbonic anhydrase (29 kDa), β -lactoglobulin (18.4 kDa), and lysozyme (14.3 kDa) was purchased from Bethesda Research Laboratories (Gaithersburg, MD).

Monoclonal Antibodies. An IgG₁ mouse monoclonal antibody (7E3) specific for the glycoprotein GPIIb/IIIa fibrinogen receptor on platelets was produced by methods previously described (Coller, 1985). The P4B6 hybridoma was provided for research purposes by Dr. Desire Collen (Leuven, Belgium). The hybridoma secretes an IgG1 which is specific for tPA.

Purification and Characterization of Parental F(ab')₂ Antibodies. 7E3 F(ab')₂ fragment was obtained from the pepsin digestion of 7E3 IgG as previously described (Yasuda et al., 1988). P4B6 IgG was purified from tissue culture supernatant fluid using protein A chromatography equilibrated in 1.5 M glycine and 3 M NaCl (pH 8.9). The IgG was eluted from the column by using a pH gradient in 100 mM sodium citrate buffer starting at pH 6.5 and ending at pH 3.5. The purified IgG was diafiltered into 100 mM sodium citrate at pH 3.9 and digested in the presence of 2% (w/w) pepsin for 16 h at 37 °C. The F(ab')₂ fragment of P4B6 was purified by cation-exchange FPLC using a Mono S HR 10/10 column equilibrated in 50 mM sodium acetate at pH 4.2. The bound F(ab')₂ was eluted with a 0–1 M NaCl gradient under conditions which resolved undigested IgG and low molecular weight fragments from the F(ab')₂.

Cross-Linking of Bispecific Antibodies. Immediately before cross-linking, 10 mg of each of the parental F(ab')₂ fragments was reduced to Fab' fragments using a modification of previously described methods (Chang et al., 1986; Glennie et al., 1987). The fragments were buffer exchanged into 50 mM sodium borate, 100 mM NaCl, and

1 mM EDTA (pH 8.0) and reduced with 20 mM L-cysteine (free base form) at 37 °C for 1 h, yielding Fab' fragments. Both Fab' fragments were desalted on a separate 1.0 × 18 cm column of P6DG equilibrated with 50 mM ammonium citrate, 100 mM NaCl, and 1 mM EDTA (pH 6.3) (conjugation buffer). The P4B6 Fab' was maintained as the free sulfhydryl form (Fab'-SH) while the 7E3 Fab' was derivatized with BMME. The 7E3 Fab' was added dropwise to an approximately 30-fold molar excess of 50 mM BMME in dimethylformamide with constant mixing and allowed to react at room temperature for 10 min. The 7E3-BMME derivative was desalted on a 1.8 × 10 cm P6DG column equilibrated in conjugation buffer. The BMME-derivatized 7E3 Fab' was reacted with P4B6 Fab'-SH at a 1:1 molar ratio for 60 min at room temperature. Each of the reaction steps was analyzed after reaction with excess NEM by PhastSDS-PAGE under nonreducing conditions to determine the efficiency of reduction and cross-linking. The reaction products were treated with 1 mM DTNB to cap remaining sulfhydryl groups and stored at 4 °C until purification.

Purification of Bispecific Antibodies. The reaction mixture containing the bispecific F(ab')₂ was concentrated by ultrafiltration using a 30 kDa cutoff membrane in a stirred cell and was applied to a column of Sephacryl S-200 (1.6 × 90 cm) equilibrated in 10 mM sodium phosphate and 150 mM NaCl (pH 7.2). The F(ab')₂ pool of the S-200 step was applied to a 7.5 × 75 mm Biogel TSK phenyl-5-PW HPLC column for hydrophobic interaction chromatography (HIC). The HIC column was equilibrated with 100 mM sodium phosphate at pH 6.3 containing 1 M (NH₄)₂SO₄. The bispecific F(ab')₂ fragment was eluted with a 1–0 M ammonium sulfate gradient in the same phosphate buffer over a period of 55 min, followed by isocratic elution with 100 mM sodium phosphate for 15 min using a flow rate of 1 mL/min. The purified bispecific F(ab')₂ was biochemically characterized by gel filtration HPLC using a 9.6 × 250 mm Zorbax GF-250 column equilibrated in 200 mM sodium phosphate at pH 6.8, SDS-PAGE under reducing and nonreducing conditions using a Phastsystem, and analytical HIC as described above.

Native Reduction Analysis. The presence of the nonreducible cross-link between the parental heavy chains in the bispecific F(ab')₂ was demonstrated by reduction of the bispecific or the parental F(ab')₂ species followed by gel-filtration HPLC. All samples were reduced at 37 °C for 1 h after the addition of 1/10 final volume of 1 M Tris-HCl (pH 8.0) and DTT to 1 mM final concentration. After reduction, the samples were reacted with 1/10 final volume of 50 mM NEM and analyzed by GF-HPLC for the presence of Fab' or F(ab')₂ as described previously.

Immunoassays. The immunoreactivity of the parental antibodies and the 7E3 × P4B6 specific and control antibodies was quantified using EIA's specific for GPIIb/IIIa and tPA, respectively. Polystyrene 96-well plates were coated with 100 μ L per well containing 5 μ g/mL of affinity-purified human platelet GPIIb/IIIa (Blum et al., 1989) in 100 mM Tris-HCl (pH 9.5), 1 mM CaCl₂, and 0.02% sodium azide buffer for 1 h at room temperature. The plates were washed in TBS containing 1 mM CaCl₂ and 0.05% Tween-80 and blocked in the same buffer containing 1% bovine serum albumin (BSA) for 1 h at room temperature. After washing, the plates were incubated in the presence of dilutions of the test antibodies for 1 h at room temperature, washed, and incubated with a 1:5000 dilution of affinity-purified goat anti-murine F(ab')₂ conjugated to horseradish peroxidase (HRP). After the final washing, the plates were developed with 50 μ L/well of 1.2 mg/mL OPD and 0.16% H₂O₂ in 20 mM sodium citrate and 50 mM sodium phosphate buffer at pH 5. The color was

read at 490 nm. The format for the tPA EIA was identical to that for the GPIIb/IIIa EIA with the exception of coating the rtPA in 50 mM in sodium carbonate (pH 8.9) and performing all incubations in PBS containing 1% (w/v) bovine serum albumin diluent instead of the TBS/CaCl₂ used in the GPIIb/IIIa assay. The tPA was coated at 5 µg/mL. In both EIA's, the color development in the bispecific F(ab')₂ was compared to the respective parental antibody as the Fab' fragment and to nonrelevant control antibodies for the determination of a binding constant defined as the inverse of the concentration corresponding to half of the maximum signal.

Platelet Aggregation. The inhibition of platelet aggregation by 7E3 and the 7E3 × P4B6 bispecific antibody was assayed using a two-channel aggregometer (Chronolog). Platelet-rich plasma (PRP) anticoagulated with 15% acidified citrate dextrose (ACD) solution was prepared according to standard centrifugal technique (Collier, 1979). Platelet counts were adjusted to 250 000–300 000 per microliter with autologous platelet-poor plasma. Platelet aggregation studies were performed at 37 °C in siliconized glass cuvettes with continuous stirring. A stable baseline was established for each sample, followed by stimulation of the PRP with 10 µM ADP to initiate aggregation. The aggregation response in the presence or absence of test antibodies was measured as the rate of change in light transmittance in the platelet aggregometer for sample volumes of 0.5 mL. Test antibodies were preincubated with PRP at room temperature for 5 min prior to initiation of aggregation.

tPA Activity Assay. The recruitment of rtPA to human platelets *in vitro* was assayed by incubation of citrated platelet-rich plasma in the presence of test antibodies and controls at 10 µg/mL for 1 h at room temperature. A total of 1×10^6 platelets per well were then added to 96-well plates. The platelets were washed by centrifugation at 3000g for 10 min at room temperature and washed with TBS/CaCl₂. A 5 units/mL portion of recombinant human tPA (Activase) in TBS/CaCl₂ was added to each well and allowed to incubate for 1 h at room temperature. The wells were washed with TBS and incubated for up to 2 h at 37 °C in the presence of S-2251, plasminogen, and fibrin fragments. The color resulting from the plasmin-mediated release of *p*-nitroaniline was quantified every 15 min in a plate reader set to 405-nm absorbance. The activity recruited to the platelets was compared to a standard curve of tPA in solution containing 10–0.125 units/mL incubated simultaneously in wells containing no platelets.

RESULTS

Production of the Bispecific F(ab')₂. The bispecific F(ab')₂ cross-linking was monitored by nonreducing SDS-PAGE as shown in Figure 1. The selective, complete reduction of the parental F(ab')₂ hinge-region disulfides by L-cysteine was indicated by the presence of the approximately 40 kDa Fab' band for either parent in these nonreducing gels (lanes 2 and 3), with no detectable 100 kDa F(ab')₂ bands. The presence of low molecular weight bands in the Fab's analyzed in overloaded nonreducing gels (not shown) indicated a low level of reduction of the H-L disulfides did occur. NEM capping of the Fab' fragments prevented any possible reoxidation to larger fragments in these analyses. Spontaneous reoxidation of either parental Fab' to F(ab')₂ after desalting into conjugation buffer was prevented by the maintenance of low pH and the presence of 1 mM EDTA. Lane 4 depicts the BMME-derivatized 7E3 Fab', demonstrating that the conjugation of BMME to 7E3 Fab' had no effect on the molecular weight of the Fab' and that no formation of

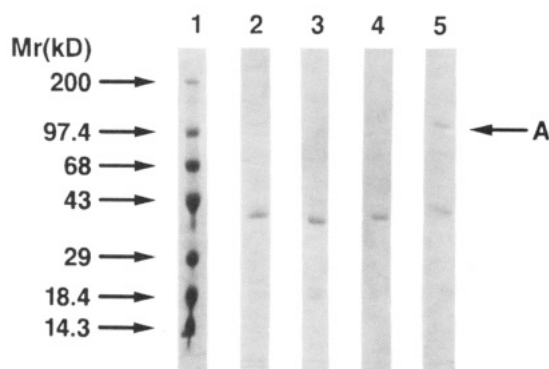


Figure 1. Nonreducing SDS-PAGE of the BMME cross-linking of 7E3 and P4B6. 10–15% gradient Phastsystem SDS-PAGE (Pharmacia) was electrophoresed under nonreducing conditions according to the manufacturer's instructions and manually stained with Coomassie Brilliant Blue R. Samples were prepared for electrophoresis by incubation on ice for 10 min in the presence of excess *N*-ethylmaleimide and then heated to 100 °C for 3 min in 2× sample buffer without DTT. The prestained molecular weight calibrators are shown in lane 1, with respective molecular weights as indicated by the arrows; lane 2, P4B6 Fab', 0.09 µg; lane 3, 7E3 Fab', 0.07 µg; lane 4, 7E3 Fab'-BMME, 0.04 µg; lane 5, products of cross-linking P4B6 Fab' and 7E3 Fab'-BMME for 60 min at room temperature; A, F(ab')₂ sized band produced by P4B6 Fab'-7E3 Fab'-BMME conjugation.

BMME-mediated 7E3 homodimers or F(ab')₂ reoxidation occurred. No F(ab')₂ formation was evident for either parent until the addition of the P4B6 Fab' to the BMME-modified 7E3. After mixing, the F(ab')₂ formed via the coupling of 7E3-BMME to P4B6 at the end of 60 min is shown in lane 5 by the appearance of a 100 kDa band. A significant level of unreacted Fab' was present in the final mixture, as well as lower levels of non-F(ab')₂ byproducts of molecular weight intermediate between those of the F(ab')₂ and Fab'. These immunoglobulin-derived fragments likely result from the recombination of intact Fab' with completely reduced light or heavy chains.

S-200 Sephacryl was used to separate the bispecific F(ab')₂ from residual Fab' in the first purification step after capping the mixture with DTNB (not shown). The reaction mixture chromatographed into two partially resolved peaks of approximately 100 and 50 kDa. The fractions enriched in F(ab')₂ were pooled for further purification by HIC HPLC.

The preparative and analytical hydrophobic interaction chromatography HPLC is shown in Figure 2. This step was employed to remove residual parental F(ab')₂ species or parental F(ab')₂ which may have formed via sulfhydryl oxidation, since resolution of the parental F(ab')₂ species was obtained under the conditions used in this separation (panels A and B). The technique was also employed to remove low amounts of BMME-coupled 7E3 homodimer which might have formed during the cross-linking reaction or other non-F(ab')₂ byproducts of the reaction. The preparative HIC of the S-200 F(ab')₂-sized pool containing the bispecific (panel C) species yielded a major peak of UV absorbance with a retention time of 45–53 min, as well as two prominent peaks with retention times of 32 min (compare to 30.2 min for P4B6 F(ab')₂ standard in panel A) and 68 min (compare to 66.4 min for the 7E3 F(ab')₂ in panel B). The 45–53-min peak was pooled, concentrated, and rechromatographed under the same conditions, resulting in a single peak of approximately 47.5 min (panel D). An overall yield of approximately 16% was obtained for the production of the bispecific F(ab')₂ through the two chromatographic steps. The purified bispecific antibody was shown to be predominantly F(ab')₂ by nonreducing SDS-PAGE (not shown), containing low levels of low molecular weight, copurifying byproducts. The pu-

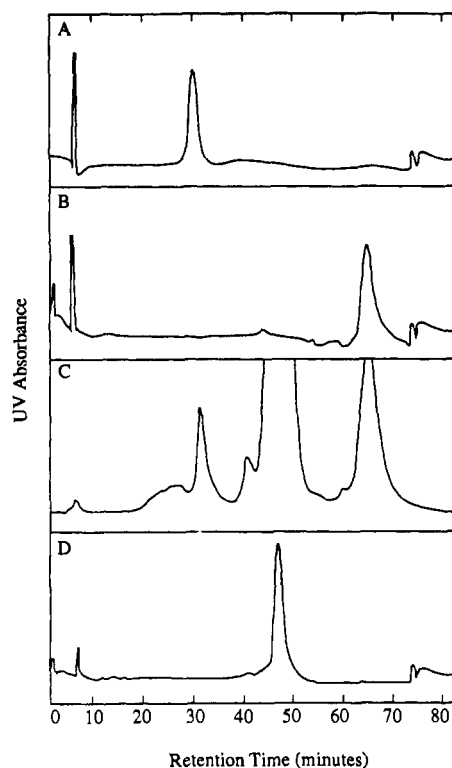


Figure 2. Hydrophobic interaction HPLC of 7E3 \times P4B6 and parental F(ab')₂ fragments. All samples were diluted with an equal volume of 2 M ammonium sulfate and injected onto a 75 \times 7.5 mm Biogel TSK phenyl-5-PW HIC column which had been equilibrated in 1 M ammonium sulfate and 100 mM sodium phosphate (pH 6.3) at a 1 mL/min flow rate. Column elution was performed as described in the text. Protein detection was by UV absorbance at 214 nm (panel C) or 280 nm (panels A, B, and D): panel A, 33 μ g of P4B6 F(ab')₂; panel B, 33 μ g of 7E3 F(ab')₂; panel C, 1 mL of the S-200 F(ab')₂ pool containing the bispecific F(ab')₂; panel D, 27 μ g of purified bispecific F(ab')₂ rechromatographed on HIC.

rified bispecific F(ab')₂ was shown to be approximately 93% pure as determined by gel-filtration HPLC (Figure 3, panel A).

Biochemical Characterization. Support for the formation of the nonreducible cross-link in the bispecific F(ab')₂ was obtained by performing native reduction analysis by HPLC as shown in Figure 3. The bispecific and parental F(ab')₂ species were subjected to native reduction in the presence of 1 mM DTT under conditions shown to result in complete conversion of F(ab')₂ to Fab' (Pak et al., 1991). After reduction, the antibodies were capped with NEM to prevent in situ reoxidation to F(ab')₂ and analyzed by gel-filtration HPLC. Panel A shows a retention time of 8.3 min for the reduced and capped bispecific F(ab')₂ (dotted line) and 8.3 min for the nonreduced bispecific F(ab')₂ (solid line), consistent with approximately 100 kDa molecular weight. In contrast, the retention times for reduced and capped P4B6 (panel B, dotted line) increased to 9.1 min from 8.2 min for the nonreduced sample (solid line). Similarly the reduced and capped 7E3 (panel C, dotted line) shifted to 9.2 min from 8.3 min (solid line). This shift indicates the conversion to Fab' by the predicted molecular weight of approximately 40–50 kDa as compared to molecular weight calibrators. These data indicate that the bispecific F(ab')₂ was not reducible to Fab', consistent with the presence of the thioether cross-linking the heavy chains of the two parental Fab' fragments.

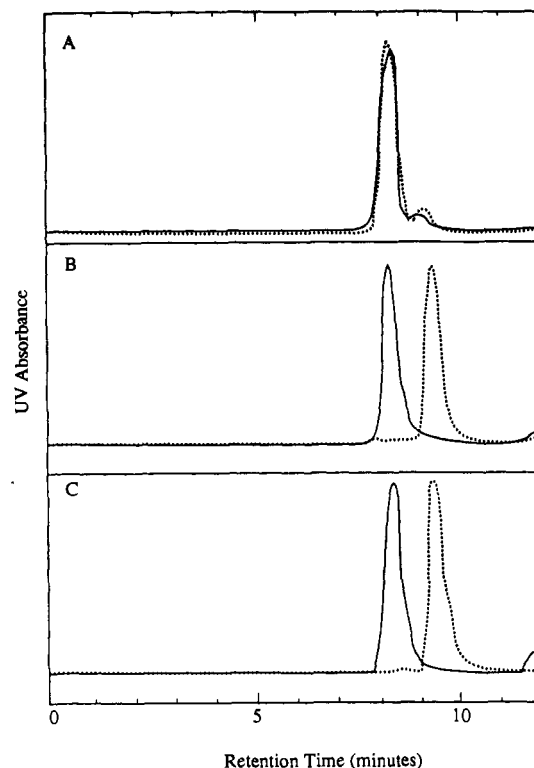


Figure 3. Native reduction analysis of the bispecific F(ab')₂ by gel-filtration HPLC. 7E3 \times P4B6 (panel A), P4B6 (panel B), and 7E3 (panel C) F(ab')₂ were reduced and capped with NEM as described in the text. The samples (16–20 μ g) were analyzed by GF-HPLC (dotted lines) as described in the text and compared to molecular weight standards and to chromatograms of nonreduced samples (solid lines). The reduced bispecific antibody was retained 8.3 min (panel A, dotted line) and the nonreduced sample was retained 8.3 min. The reduced P4B6 (panel B, dotted line) was retained 9.1 min while the nonreduced form was retained 8.2 min. The reduced 7E3 (panel C, dotted line) was retained 9.2 min while the nonreduced (panel C, solid line) form was retained 8.3 min.

Table I. Binding Constants for 7E3 \times P4B6 and Parental Antibodies in Antigen Binding EIA's

test antibody	GPIIb/IIIa ^a binding constant, M ⁻¹	tPA ^b binding constant, M ⁻¹
7E3	5 \times 10 ⁸	ND
P4B6	ND	2 \times 10 ⁹
7E3 \times P4B6	1 \times 10 ⁹	1 \times 10 ¹⁰

^a Relative binding constant for human GPIIb/IIIa determined in purified GPIIb/IIIa EIA as described in Experimental Procedures. Inverse molar concentrations yielding half of the maximal signal were compared between 7E3 Fab' fragment and the monovalent 7E3 \times P4B6 F(ab')₂. ^b Relative binding constant for tPA determined in purified tPA EIA as described in Experimental Procedure. Inverse molar concentrations yielding half of the maximal signal were compared between P4B6 Fab' and 7E3 \times P4B6 F(ab')₂.

Immunoreactivity. The relative association constants of 7E3 \times P4B6 relative to each parental immunoreactivity were quantified in antigen binding EIA's as described in Experimental Procedures. In these EIA's, the association constant was defined as the inverse of the concentration corresponding to half of the maximum signal. These data are summarized in Table I and show that the bispecific F(ab')₂ fully retained both its anti-tPA (relative binding constant approximately 1 \times 10¹⁰ M⁻¹) and anti-GPIIb/IIIa (relative binding constant approximately 1 \times 10⁹ M⁻¹) immunoreactivities.

Inhibition of Platelet Aggregation. The ability of the 7E3 \times P4B6 bispecific F(ab')₂ to inhibit platelet aggregation in vitro was compared to that of the Fab' fragment of 7E3. Figure 4 shows the percent inhibition

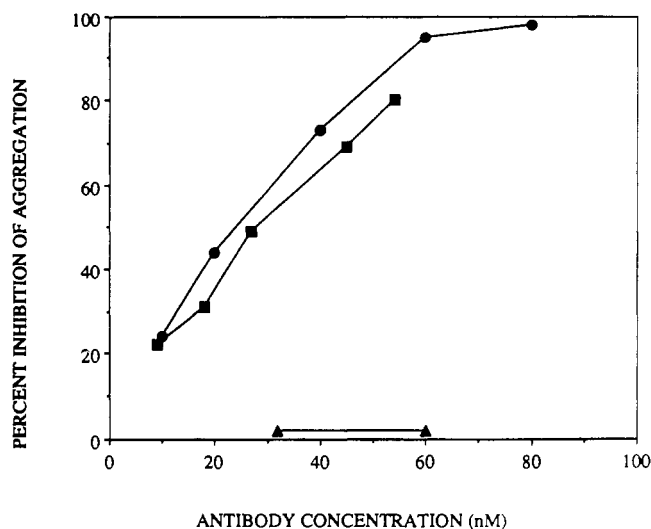


Figure 4. Inhibition of platelet aggregation by 7E3 \times P4B6. Human platelet-rich plasma was preincubated in the presence of test samples and then aggregated at 37 °C by stimulation with 10 μ M ADP. Aggregation was quantified in a two-channel platelet aggregometer as described in the text, and the percent inhibition of aggregation in the presence of antibody was calculated: \bullet , 7E3 Fab; \blacksquare , 7E3 \times P4B6 F(ab')₂; \blacktriangle , P4B6 F(ab')₂.

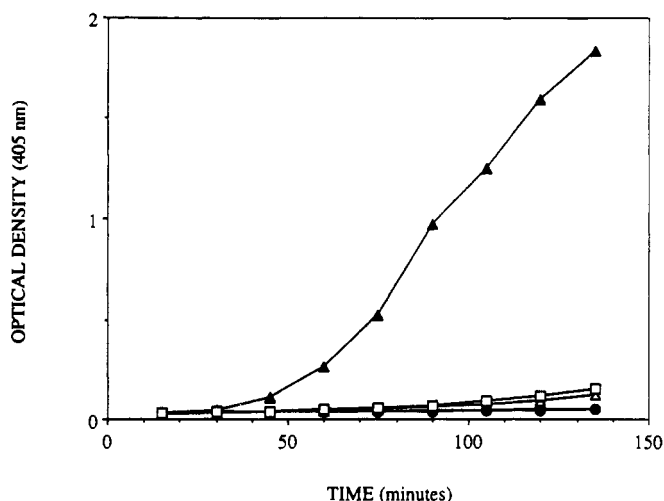


Figure 5. Measurement of tPA activity in the S-2251 assay. The amount of tPA activity recruited to 1×10^6 platelets per well by 7E3 \times P4B6 or controls was quantified by incubation of the washed platelets in the presence of the plasmin substrate S-2251 as described in the text. The activation of plasmin from plasminogen was detected by the release of *p*-nitroaniline with absorbance at 405 nm. \blacktriangle , 7E3 \times P4B6 plus 5 units/mL rtPA; \bullet , no antibody or rtPA; \triangle , rtPA with no antibody; \square , mixture of 7E3 F(ab')₂ and P4B6 F(ab')₂ plus rtPA; overlap of data points has occluded certain symbols. The experiment shown was representative of three separate experiments.

of ADP-induced platelet aggregation associated with varying concentrations of 7E3 \times P4B6, 7E3 Fab, or P4B6 F(ab')₂. The inhibition curves for both 7E3 Fab and 7E3 \times P4B6 were comparable, showing equivalent levels of inhibition at all concentrations tested. The P4B6 parent showed no inhibition of platelet aggregation at comparable concentrations.

Plasminogen Activation Assay. The recruitment of tPA to the surface of platelets via 7E3 \times P4B6 with concomitant activation of plasminogen to plasmin was demonstrated in the S-2251 assay as indicated in Figure 5. Human platelets which had previously been incubated in the presence of saturating levels of the bispecific or control antibodies (10 μ g/mL) were washed and then incubated in the presence of 5 units/mL of rtPA. The specific recruitment of rtPA to platelets was demonstrated

by washing the platelets to remove free rtPA and then incubating the wells in the presence of S-2251, plasminogen, and fibrin fragments. As indicated in Figure 5, plasmin activity was associated only with the platelets which had been incubated in the presence of the bispecific F(ab')₂. When compared to a standard curve of soluble rtPA incubated simultaneously in the absence of platelets, it was calculated that approximately 1.5 units/mL of rtPA activity had been recruited to the platelets (1×10^6 /well), a difference of approximately 12-fold over the background binding of tPA in the presence of the mixture of the parental F(ab')₂ antibodies.

DISCUSSION

The anti-GPIIb/IIIa monoclonal antibody 7E3 and the anti-tPA monoclonal P4B6 have been chemically cross-linked as Fab' fragments to produce a bispecific F(ab')₂ molecule containing both parental specificities. 7E3 was chosen for its ability to target platelets and inhibit fibrinogen-mediated platelet aggregation, and P4B6 was selected for its ability to bind tPA with high affinity and preservation of plasminogen activation. The combination of these two immunoreactivities in one F(ab')₂ species in postulated to have clinical utility via the targeting of endogenous or pharmacologically administered tPA to platelet-rich thrombi.

The cross-linking of Fab' fragments via bis-maleimides has been widely used for its speed, simplicity, yields (Glennie et al., 1987), and predicted resistance of the resulting thioether linkage to reduction in vivo (Stickney et al., 1989). BMME conjugates of this type have been used in human clinical trials successfully in a cancer imaging application (Stickney et al., 1989) and have been used to target cytotoxic T-cells to ovarian carcinoma cells in vitro and in vivo (Mezzananza et al., 1991). In the case of the present report, the BMME-cross-linked bispecific species was produced and purified to an overall yield of approximately 16% using a combination of gel filtration and hydrophobic interaction chromatography. The conjugation step was shown to result in the formation of an F(ab')₂ containing a nonreducible cross-link. This immunoconjugate was shown to retain both parental immunoreactivities, inhibit the aggregation of platelets in vitro, and recruit 12-fold more active tPA to platelets in vitro than mixtures of the parental antibodies, resulting in the activation of soluble plasminogen to plasmin in the S-2251 assay. While double immunoaffinity chromatography of bispecific antibodies has been used (Runge et al., 1990), this purification strategy would be difficult to perform in large-scale production. In contrast, hydrophobic interaction chromatography is scalable and nondenaturing. In this study, HIC was capable of resolving F(ab')₂ fragments (Figure 2) derived from the two parental murine IgG1 antibodies based on their relative hydrophobicities. The retention times observed for the bispecific and parental F(ab')₂ species in Figure 2 were consistent with the intermediate hydrophobicity expected for the heterodimer containing both of the parental Fab' fragments. This chromatographic technique is thus capable of extremely powerful resolution based on the hydrophobicity differences attributable to the variable region of murine antibodies or primary sequence and posttranslational modification differences in nonvariable regions within an isotype. This separation technique may lend itself to similar applications such as in the resolution of complex product mixtures secreted by hybrid-hybridomas (quadromas). Purification of distinct parental antibodies must nevertheless be evaluated on a case-by-case basis for this application.

It is believed that a potential benefit of platelet targeting of tPA through this bispecific antibody may reside in com-

binning targeting to lysis-resistant, platelet-rich thrombus and to circulating platelets, potentially hastening the rate of lysis and subsequent reperfusion of the occluded vessel as well as decreasing reocclusion. The recruitment of tPA to circulating platelets via 7E3 × P4B6 may be advantageous in coronary thrombolysis by preventing aggregation through the 7E3 function of the bispecific antibody, as shown in this study, and promoting disaggregation by generation of a fibrinolytic surface at the platelet membrane (Loscalzo and Vaughan, 1987). This second mechanism may be responsible for the observed potentiation of platelet aggregation inhibiting capacity of 7E3-urokinase compared to 7E3 alone (Bode et al., 1991). Future evaluation of the effects of this bispecific antibody on the rates of reperfusion and reocclusion in vivo in animal models of thrombolysis will provide valuable insight into these mechanisms.

ACKNOWLEDGMENT

We thank Dr. Desire Collen for the generous gift of the anti-tPA hybridoma P4B6 and other anti-tPA murine hybridoma lines and Ms. Joani Wendel and Ms. Camille Thompson for preparation of the manuscript.

LITERATURE CITED

- Blum, M., Jordan, R., Wagner, C., and Mattis, J. (1989) Immunopurification and Functional Characterization of Platelet GPIIb/IIIa Complexes. *Blood* 74 (Suppl. I), 398a.
- Bode, C., Matsueda, G. R., Hui, K. Y., and Haber, E. (1985) Antibody-Directed Urokinase: A Specific Fibrinolytic Agent. *Science* 229, 765-767.
- Bode, C., Runge, M. S., Branscomb, E. E., Newell, J. B., Matsueda, G. R., and Haber, E. (1989) Antibody-Directed Fibrinolysis: An Antibody Specific for Both Fibrin and Tissue Plasminogen Activation. *J. Biol. Chem.* 264, 944-948.
- Bode, C., Meinhardt, G., Runge, M. S., Freitag, M., Nordt, T., Arens, M., Newell, J. B., Kubler, W., and Haber, E. (1991) Platelet-Targeted Fibrinolysis Enhances Clot Lysis and Inhibits Platelet Aggregation. *Circulation* 84, 805-813.
- Chang, C.-H., Ahlem, C. N., Wolfert, B., Hochswender, S. M., Jue, R., Frincke, J. M., and Carlo, D. J. (1986) Preparation and Characterization of Bifunctional Antibodies with Reactivity to Carcinoembryonic Antigen and Indium Benzyl EDTA. *J. Nucl. Med.* 27, 1041.
- Collen, D. (1990) Coronary Thrombolysis: Streptokinase or Recombinant Tissue-Type Plasminogen Activator. *Ann. Int. Med.* 112, 529-538.
- Coller, B. S. (1979) Platelet Aggregation by ADP, Collagen and Ristocetin: A Critical Review of Methodology and Analysis in *CRC Handbook Series in Clinical Laboratory Science* (R. M. Schmidt, Ed.) Vol. 1, p 301, CRC, Boca Raton, FL.
- Coller, B. S. (1985) A New Murine Monoclonal Antibody Reports an Activation-Dependent Change in the Conformation and/or Microenvironment of the Platelet Glycoprotein IIb/IIIa Complex. *J. Clin. Invest.* 97, 101-108.
- Coller, B. S. (1990) Platelets and Thrombolytic Therapy. *N. Engl. J. Med.* 322, 33-42.
- Coller, B. S., Scudder, L. E., Berger, H. J., and Iulucci, J. D. (1988) Inhibition of Human Platelet Function In Vivo with a Monoclonal Antibody with Observations on the Newly Dead as Experimental Subjects. *Ann. Int. Med.* 109, 635-638.
- Dewerchin, M., and Collen, D. (1991) Enhancement of the Thrombolytic Potency of Plasminogen Activators by Conjugation with Clot Specific Antibodies. *Bioconjugate Chem.* 2, 293-300.
- Dewerchin, M., Lijnen, H. R., Stassen, J. M., DeCook, F., Quartermous, T., Ginsberg, M. H., Plow, E. F., and Collen, D. (1991) Effect of Chemical Conjugation of Recombinant Single-Chain Urokinase-Type Plasminogen Activator with Monoclonal Antiplatelet Antibodies on Platelet Aggregation and Plasma Clot Lysis in Vivo. *Blood* 78, 1005-1018.
- Glennie, M. J., McBride, H. M., Worth, A. T., and Stevenson, G. T. (1987) Preparation and Performance of Bispecific F(ab')₂ Antibody Containing Thioether-Linked Fab' Fragments. *J. Immunol.* 139, 2367.
- Gold, H. K., and Leinbach, R. C. (1987) Prevention of Acute Reocclusion after Thrombolysis with Intravenous Recombinant Tissue Plasminogen Activator. In *Tissue Plasminogen Activator in Thrombolytic Therapy* (B. E. Sobel, D. Collen, and E. B. Grossbard, Eds.) p 115, Marcel Dekker, New York.
- Gold, H. K., Coller, B. S., Yasuda, T., Saito, R., Fallon, J. T., Guerrero, J. L., Leinbach, R. C., Ziskind, A. A., and Collen, D. (1987) Rapid and Sustained Coronary Artery Recanalization with Combined Bolus Injection of Recombinant Tissue-Type Plasminogen Activator and Monoclonal Antiplatelet GPIIb/IIIa Antibody in a Canine Preparation. *Circulation* 77, 670.
- Gold, H. K., Gimple, L. W., Yasuda, T., Leinbach, R. C., Werner, W., Holt, R., Jordan, R., Berger, H., Collen, D., and Coller, B. S. (1990) Pharmacodynamic Study of F(ab')₂ Fragments of Murine Monoclonal Antibody 7E3 Directed Against Human Platelet Glycoprotein IIb/IIIa in Patients with Unstable Angina Pectoris. *J. Clin. Invest.* 86, 651-659.
- Haber, E., Quartermous, T., Matsueda, G. R., and Runge, M. S. (1989) Innovative Approaches to Plasminogen Activator Therapy. *Science* 243, 51-56.
- Hayzer, D. J., Lubin, I. M., and Runge, M. S. (1991) Conjugation of Plasminogen Activators and Fibrin-Specific Antibodies To Improve Thrombolytic Therapeutic Agents. *Bioconjugate Chem.* 2, 301-308.
- Loscalzo, J., and Vaughan, D. E. (1987) Tissue Plasminogen Activation Promotes Platelet Disaggregation in Plasma. *J. Clin. Invest.* 79, 1749-1755.
- Mezzanzanica, D., Garrido, M. A., Neblock, D. S., Daddona, P. E., Andrew, S. M., Zurawski, V. R., Jr., Segal, D. M., and Wunderlich, J. R. (1991) Human T-Lymphocytes Targeted Against an Established Human Ovarian Carcinoma with a Bispecific F(ab')₂ Antibody Prolong Host Survival in a Murine Xenograft Model. *Cancer Res.* 51, 5716-5721.
- Pak, K. Y., Nedelman, M. A., Fogler, W. E., Tam, S. H., Wilson, E., van Haarlem, L. J. M., Colognola, R., Warnaar, S. O., and Daddona, P. E. (1991) Evaluation of the 323/A3 Monoclonal Antibody and the Use of Technetium-99m Labeled 323/A3 Fab' for the Detection of Pan Adenocarcinoma. *Nucl. Med. Biol.* 18, 483-497.
- Runge, M. S., Bode, C., Matsueda, G. R., and Haber, E. (1987) Antibody-enhanced thrombolysis: Capture of Tissue Plasminogen Activator by a Bispecific Antibody and Direct Targeting by an Antifibrin-Tissue Plasminogen Activator Conjugate In Vivo. *Trans. Assoc. Am. Phys.* 100, 250-255.
- Runge, M. S., Quartermous, T., Matsueda, G. R., and Haber, E. (1988a) Increasing Selectivity of Plasminogen Activators with Antibodies. *Clin. Res.* 56, 501-506.
- Runge, M. S., Bode, C., Matsueda, G. R., and Haber, E. (1988b) Conjugation to an Antifibrin Monoclonal Antibody Enhances the Fibrinolytic Potency of Tissue Plasminogen Activator in Vitro. *Biochemistry* 27, 1153.
- Runge, M. S., Bode, C., Savard, C. E., Matsueda, G. R., and Haber, E. (1990) Antibody-Directed Fibrinolysis: A Bispecific F(ab')₂ that Binds to Fibrin and Tissue Plasminogen Activator. *Bioconjugate Chem.* 1, 274-277.
- Stickney, D. R., Slater, J. B., Kirk, G. A., Ahlem, C., Chang, C.-H., and Frincke, J. M. (1989) Bifunctional Antibody: ZCH/CHA¹¹¹ Indium BLEDTA-IV Clinical Imaging in Colorectal Carcinoma. *Immunoconjugates Radiopharm.* 2, 1-13.
- Verstraete, M. (1990) Thrombolytic Treatment in Acute Myocardial. *Circulation* 82 (Suppl. II), II-96-II-109.
- Yasuda, T., Gold, H. K., Fallon, J. T., Leinbach, R. C., Guerrero, J. L., Scudder, L. E., Kanke, M., Shealy, D., Ross, M. J., Collen, D., and Collen, B. S. (1988) Monoclonal Antibody Against the Platelet Glycoprotein (GP) IIb/IIIa Receptor Prevents Coronary Artery Reocclusion after Reperfusion with Recombinant Tissue-Type Plasminogen Activation in Dogs. *J. Clin. Invest.* 81, 1284-1291.
- Yasuda, T., Gold, H. K., Yaolta, H., Leinbach, R. C., Guerrero, J. L., Jang, I. K., Holt, R., Fallon, J. T., and Collen, D. (1990) Comparative Efforts of Aspirin, A Synthetic Thrombin Inhibitor and a Monoclonal Antiplatelet Glycoprotein IIb/IIIa Antibody on Coronary Artery Reperfusion and Bleeding with Recombinant Tissue-Type Plasminogen Activator in a Canine Preparation. *J. Am. Coll. Cardiol.* 16, 1728-1735.

Preparation and Properties of the Immunoconjugate Composed of Anti-Human Colon Cancer Monoclonal Antibody and Mitomycin C-Dextran Conjugate¹

Akinori Noguchi,* Toshio Takahashi, Toshiharu Yamaguchi, Kazuya Kitamura, Yoshinobu Takakura,† Mitsuru Hashida,† and Hitoshi Sezaki†

Department of Surgery, Kyoto Prefectural University of Medicine, Kawaramachi, Hirokoji, Kamikyo-ku, Kyoto, 602, Japan, and Department of Basic Pharmaceutics, Faculty of Pharmaceutical Sciences, Kyoto University. Received October 7, 1991

Monoclonal antibody (mAb) A7, produced against human colon cancer, was conjugated with a polymeric prodrug of mitomycin C (MMC), the MMC-dextran conjugate with an anionic charge (MMCD_{an}) and a molecular weight of 70 000. The amino groups were introduced into the MMCD_{an} by reacting ethylenediamine with the carboxyl group in the spacer arm of the dextran bridge by a carbodiimide-catalyzed reaction. The coupling to mAb A7 was performed using SPDP. A 15 M excess of ethylenediamine produced an optimal MMCD_{an} with amino groups, which resulted in a homogenous conjugate (A7-MMCD) with minimal formation of high-molecular-weight aggregates in about a 30% yield of both IgG and MMC. The molar binding ratio of IgG:dextran:MMC in A7-MMCD was estimated to be 1:1.2:40. A7-MMCD, having MMC prodrug properties, released active MMC with a half-life of 29.1 h and had an almost neutral electric charge under physiological conditions. A competitive binding assay using ¹²⁵I-labeled A7 revealed that the A7-MMCD almost fully retained its antibody-binding activity. The cytotoxicity of A7-MMCD was assayed by determining the degree of inhibition of [³H]-thymidine incorporation in two different ways using the human colon cancer cell line SW1116. A 48-h continuous exposure test revealed that the pharmacological activity of MMC in A7-MMCD was completely preserved. In addition, A7-MMCD exhibited about a 14-fold greater cytotoxicity than MMCD_{an} when the IC₅₀ values determined using a 2-h pretreatment exposure system were compared. These results suggest that A7-MMCD could be useful in immunotargeting chemotherapy for colorectal cancer.

INTRODUCTION

One of the major limitations of cancer chemotherapy is the indiscriminate toxicity of anticancer drugs toward both cancer cells and proliferating normal cells. To overcome such adverse effects, targeting chemotherapy using various drug-carrier systems, involving tumor-specific and non-specific carriers (1-3), has been widely developed. Of these approaches, the production of monoclonal antibodies (4) has focused a great deal of attention on the antibody-mediated delivery of cytotoxic agents to targeted cancer cells (5-8).

We have prepared mAb A7 against human colon cancer (9) and its conjugate with a protein antitumor antibiotic, neocarzinostatin (A7-NCS) (10). We obtained a favorable response to the application of A7-NCS in patients with colorectal carcinoma without serious side effects (11). In addition, we have developed a polymeric prodrug of MMC, MMC-dextran conjugate (MMCD), for passive targeting chemotherapy (3). MMC is a well-known antitumor antibiotic widely used for a number of cancers, especially gastrointestinal adenocarcinomas (12).

The physicochemical, pharmacokinetic, and pharmacodynamic characteristics of MMCD have also been extensively investigated (13-18). These studies revealed

that MMCD acts as a reservoir of MMC, supplying active MMC to the body, and has altered pharmacokinetic behavior according to the size and electric charge of the carrier dextran. Regarding systemic administration, it was concluded that MMCD_{an}, which has a molecular weight of 70 000, is most suitable in that it has a long circulating life and is taken up less by the reticuloendothelial system due to its polyanionic nature (19).

Therefore, we attempted to conjugate mAb A7 with MMCD, to enhance the delivery of MMC to the target cancer tissue. This paper focuses on the coupling method and the characteristics of the novel immunoconjugate, designated as A7-MMCD, including its physicochemical properties and in vitro antitumor activities.

EXPERIMENTAL PROCEDURES

Chemicals. MMC was kindly supplied by Kyowa Hakkō Kogyo Co. (Tokyo, Japan). Dextran with an average molecular weight of about 70 000 (T-70) was purchased from Pharmacia (Uppsala, Sweden). Heterobifunctional reagent *N*-succinimidyl 3-(2-pyridyldithio)propionate (SPDP) was purchased from Pharmacia Fine Chemicals (Sweden), and dithiothreitol (DTT) was obtained from Wako Pure Chemicals Industries Co. Ltd. (Osaka). All other chemicals were reagent-grade products obtained commercially.

Monoclonal Antibody. mAb A7 was produced by a hybridoma generated by the fusion of splenocytes from a mouse immunized against human colon carcinoma cells and murine myeloma P3.X63.Ag8.653 cells as described previously (9). mAb A7 was class IgG1 and the antigenic determinant recognized by mAb A7 was a glycoprotein with a molecular weight of 40 000 (20). mAb A7 was

¹ Abbreviations used: mAb, monoclonal antibody; MMC, mitomycin C; MMCD, MMC-dextran conjugate; MMCD_{an}, MMCD with an anionic charge; MMCD_{cat}, MMCD with a cationic charge; SPDP, *N*-succinimidyl 3-(2-pyridyldithio)propionate; DTT, dithiothreitol; EDC, 1-ethyl-3-(3-dimethylamino)propyl carbodiimide; PDP, 3-(2-pyridyldithio)propionated.

* To whom correspondence should be addressed.

† Kyoto University.

revealed to react specifically with human colon cancer tissues and with some cultured human colon cancer cell lines. In the present study, the mAb A7 was purified from ascites fluid in BALB/C mice by affinity chromatography on immobilized protein A (Affi-Gel Protein A Monoclonal Antibody Purification System, MAPS, Bio-Rad). The eluted antibody was dialyzed against phosphate-buffered saline (PBS), pH 7.2, and stocked in a deep freezer (-70 °C).

Cell Line. Cells of the human colon cancer cell line SW1116 were used as target cells in this study. The cells were grown as monolayer cultures in RPMI 1640 supplemented with 10% heat-inactivated fetal bovine serum.

Synthesis of MMCD_{an}. MMCD_{an}, a polymeric pro-drug of mitomycin C, was synthesized by the following two steps.

(1) 6-Bromohexanoic acid was introduced into the hydroxyl group in dextran through an ether linkage. Namely, 1 g of dextran (MW 70 000) was dissolved in a 4 M NaOH solution (10 mL), and 6-bromohexanoic acid (2.8 g) was added. The mixture was kept at about 80 °C for 3 h with occasional stirring. The product, spacer-introduced dextran, was dialyzed against water.

(2) MMC was conjugated to the spacer-introduced dextran by a carbodiimide-catalyzed reaction. One gram of 1-ethyl-3-[3-(dimethylamino)propyl]carbodiimide was added to the solution of spacer-introduced dextran, and the pH of the solution was maintained between 5.0 and 5.5 with 1 N HCl. MMC was stepwise dissolved in this solution, and the reaction was allowed to proceed for 12 h at room temperature in the dark. The product was washed with water and concentrated by ultrafiltration. (UK-20, TOYO, Tokyo, Japan).

The anionic charge was given to the MMCD_{an} by the remaining free carboxyl group since all of the spacer arms were not used for coupling. The MMCD_{an} was estimated to contain 8% (w/w) MMC and to release active MMC with a half-life of 24 h by chemical hydrolysis. The conversion was not accelerated by the tissue homogenate (17).

Synthesis of the Immunoconjugate Composed of mAb A7 and MMCD_{an} (A7-MMCD). The amino groups were introduced to the MMCD_{an} and the coupling to mAb A7 was performed using the heterobifunctional reagent SPDP. The coupling procedure consisted of the following three steps.

(1) MMCD_{an} with amino groups was synthesized by reacting ethylenediamine with the carboxyl group of the spacer arm of the dextran backbone soon after conjugating MMC by the carbodiimide-catalyzed reaction. That is, 50 mg of EDC was added to the solution of spacer-introduced dextran (50 mg), and 7.5 mg of MMC was dropwise dissolved in this solution. Thirty minutes later, a 15 M excess of ethylenediamine (300 μ L, 0.35 M) was added stepwise, and the reaction was allowed to proceed for 12 h at room temperature in the dark. The pH of the solution was maintained between 5.0 and 5.5 with 0.1 N HCl throughout the procedure. The product was washed with water and concentrated by ultrafiltration.

(2) The MMCD_{an} with amino groups (50 mg) was incubated first with a 10-fold molar excess of SPDP in 5 mL of 0.1 M phosphate buffer (pH 7.5) at room temperature for 30 min. The reaction was terminated by the addition of 0.5 mL of 0.1 M Tris HCl buffer (pH 8.0) and the product was washed with PBS, and concentrated by ultrafiltration. The 3-(2-pyridyldithio)propionated (PDP) MMCD_{an} was reduced with 10 mM DDT in a 0.1 M acetate buffer (pH 4.5) at room temperature for 20 min. The resulting MMCD_{an} with thiol groups introduced (HS-MMCD_{an}) was washed with acetate buffer and concen-

trated by ultrafiltration. In another process, mAb A7 (45 mg) was also incubated with a 10-fold molar excess of SPDP in 5 mL of 0.1 mol/L phosphate buffer (pH 7.5) at room temperature for 30 min. The PDP-A7 was passed immediately through a Sephadex G-25 (Pharmacia, Uppsala, Sweden) column equilibrated with phosphate buffer (pH 7.5).

(3) Finally, the PDP-A7 was mixed with an equal mole amount of HS-MMCD_{an}, the pH was adjusted to 7.5, and the mixture was allowed to stand at room temperature overnight in the dark. Then, the mixture was applied to a Toyopearl HW-60S (Toyo Soda Kogyo, Co., Tokyo, Japan) column (2.4 \times 65 cm) equilibrated with phosphate buffer (pH 7.0) and eluted with the same buffer. The peak fractions were pooled, concentrated, frozen, and stored at -20 °C in the dark.

Estimation of the Degree of Substitution with 2-Pyridyl Disulfide Residues. The number of SPDP groups introduced into MMCD_{an} with amino groups or mAb A7 was quantified by measuring the release of pyridine-2-thione (absorbance at 343 nm).

Determination of the Binding Molar Ratio of the Conjugate. The concentration of each component of the conjugate was determined and the binding molar ratio was calculated. The concentration of the antibody was measured by the method of Lowry et al. (21) using normal mouse IgG as a reference standard. Dextran was quantified by the anthrone-sulfuric acid method (22). MMC was quantified by determining the absorbance at 363 nm.

In Vitro Release Experiment. The release rate of MMC from the conjugates was determined with a dialysis system. A Visking dialysis tube containing 2 mL of a pH 7.4 isotonic phosphate buffer solution of the conjugate was immersed in 50 mL of the same buffer maintained at 37 °C and shaken continuously. At fixed intervals, 1 mL of sample was taken from the outer medium and the amount of MMC was measured spectrophotometrically at 364 nm. The release rate and half-life were calculated by the least-squares method.

Molecular Charge Estimation. The molecular charge of the conjugates was estimated by a batch method using a DEAE-Sephadex A-50 anion exchanger and a CM-Sephadex C-50 cation exchanger (Pharmacia Fine Chemicals, Uppsala, Sweden). The anion exchanger (25 mg) was suspended in 5 mL of 20 mM *N*-(2-hydroxyethyl)piperadine-*N*-2-ethanesulfonic acid (Hepes)-buffered saline (pH 7.2) and shaken with 0.5 mL of the conjugate solution (160- μ g equivalent of MMC/mL). After 30 min, the samples were centrifuged. The amount of conjugate in the supernatant was determined spectrophotometrically at 364 nm and the percent adsorption on the ion exchanger was calculated.

mAb A7 Radiolabeling Procedure. mAb A7 was labeled with ¹²⁵I (New England Nuclear, Boston, MA) by a chloramine T method. Briefly, 50 μ L of antibody (1 μ g/mL) was mixed first with Na¹²⁵I (500 μ Ci) for 15 s and then with 50 μ L of chloramine T (400 μ g/mL). The radiolabeled reaction was terminated with the addition of 200 μ L of Na₂S₂O₃ (400 μ L/mL). The reaction mixture was applied onto an anion exchange resin column (AG1-X4, 100–200 mesh, chloride form, Bio-Rad) to remove free iodine from the mixture. The specific activity of ¹²⁵I was 5 μ Ci/ μ g.

Determination of the Antibody Activity of the Conjugate. The ability of the conjugate to retain its antibody activity was determined by a competitive binding assay using radiolabeled A7. A standard curve of antibody activity was constructed by measuring the radioactivity of tumor cells incubated with a saturating amount of radiolabeled antibody for 1 h at 4 °C in competition with

known amounts of unlabeled antibody in the range of 0.05–10 μg . The relative antibody-binding activity of the conjugate competing against radiolabeled antibody can be determined using this standard curve. Namely, SW1116 cells (4×10^5) were suspended in 100 μL of growth medium (0.5-mL Eppendorf tube) containing various concentrations of the conjugate or mAb A7, and 100 μL of ^{125}I -labeled mAb A7 (10^5 cpm) in PBS containing BSA was added to each tube. After incubation for 1 h at 4 $^{\circ}\text{C}$, the cells were washed three times with ice-cold PBS and centrifuged for 5 min at 1000 rpm. Then, the cell pellets were transferred to tubes for γ counting.

In Vitro Antitumor Activity. The conjugate was assayed for cytotoxicity by determining the degree of inhibition of [³H]thymidine incorporation in the following two different ways using SW1116.

(1) *The 48-h Continuous Drug Exposure System.* One hundred microliter of growth medium suspending 1×10^4 cells per well was plated out in 96 flat-bottom plates (Becton-Dickinson Co.) and incubated for 2 h to allow the cells to become adherent. Then, various dilutions of the drug or conjugates were added to each well and the plates were incubated for 48 h at 37 °C.

(2) *The 2-h Pretreatment System.* In a sample tube (Bio Plastics Co.) 1×10^4 cells were exposed to various concentrations of the drug or conjugates for 2 h at 37 °C, and then washed twice with the fresh growth medium by centrifugation. Drug-treated cells were plated in 96-well microplates and incubated for 48 h at 37 °C.

After the 48-h incubation, 1 μ Ci of [3 H]thymidine (specific activity, 20 Ci/mmol; Amersham) was added to each well and the cells were cultured for a further 12 h. After three washings, the cells were treated with 0.25% trypsin-containing EDTA and harvested on a Whatman glass-fiber filter. Radioactivity incorporated into the cells was counted in a liquid scintillation counter (Packard 460). In another experiment, the cells were incubated with various concentrations of A7-MMCD containing an excess of neat mAb A7 (10 μ g/well) and then subjected to the [3 H]thymidine incorporation assay of the 2-h pretreatment system.

The growth inhibition curve was calculated as follows:

$$\% \text{ growth inhibition} = (1 - T/C) \times 100$$

where T and C represented the number of surviving cells in the treated group and in the untreated group, respectively. Experiments were carried out in triplicate. The IC_{50} values, concentrations exhibiting 50% growth inhibition, were calculated from the growth-inhibition curve.

RESULTS

Synthesis of A7-MMCD. Measuring the degree of 2-pyridyl disulfide residue substitution revealed that four to five sulfhydryl residues were introduced into each IgG using a 10-fold molar excess of SPDP. The number of sulfhydryl residues introduced into each MMCD_{an} with amino groups using a 10-fold molar excess of SPDP ranged from 0.76 to 2.55. The number varied with the molar excess (5–20) of ethylenediamine used. Ethylenediamine reacts with spacer-introduced dextran and its concentration determines the number of amino groups introduced into MMCD_{an} (Table I). A 15-fold molar excess of ethylenediamine was chosen in this experiment to react with spacer-introduced dextran. With this concentration 1.62 sulfhydryl residues were introduced into each MMCD_{an}. In preliminary conjugation experiments using nonspecific IgG as a counterpart, it was clarified that these conditions produced the most homogenous conjugate in satisfactory yields of IgG (41.9%) with minimal formation of high-

Table I. Effect of the Molar Excess of Ethylenediamine Reacting with Spacer-Introduced Dextran on the Degree of 2-Pyridyl Disulfide Residue Substitution of MMCD_{an} with Amino Groups and the Yield of IgG from the Resulting Conjugate

molar excess of ethylenediamine reacting against spacer-introduced dextran	number of 2-pyridyl disulfide residues introduced into a MMCD _{an} with amino groups	% yield of IgG
5	0.76	28.7
10	1.33	34.3
15	1.62	41.9
20	2.55	39.2

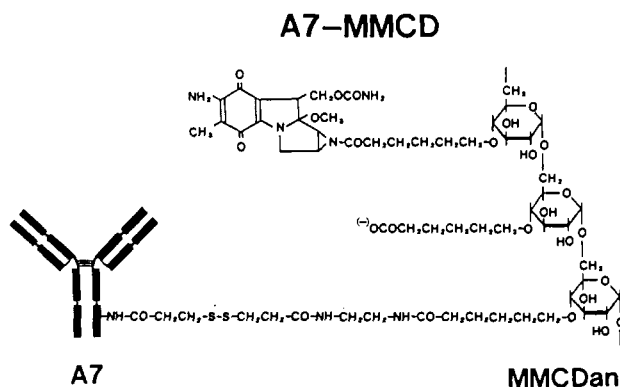


Figure 1. Chemical structure of A7-MMCD.

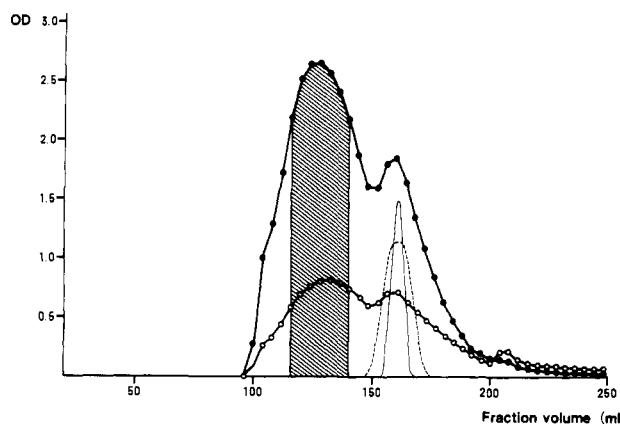


Figure 2. Elution profile of a reaction mixture of PDP-A7 and HS-MMCD_{an} with amino groups using Toyopearl HW-60S column chromatography (2.4 × 65 cm; each fraction 4.0 mL). The protein and the MMC concentrations were monitored by measuring absorbance at 280 and 363 nm, respectively; MMC (●), IgG (○). Control profiles of MMCD_{an} (---) and mAb A7 (—) were also shown for reference. Fractions indicated by the shaded region were pooled and used as A7-MMCD conjugate.

molecular-weight aggregates, compared to other MMCD_{an} conjugates having a different number of 2-pyridyl disulfide residues (Table I). Toyopearl HW-60S column chromatography was performed on the reaction mixture of HS-MMCD_{an} and PDP-A7, and two peaks at 280 and 364 nm were found by absorption (Figure 2). When unconjugated MMCD_{an} and A7 were applied to the column, although their molecular sizes are approximately 70 000 and 150 000, respectively, a single peak appeared almost in the same position (fraction volume 165–170 mL) because the Stokes' radius of dextran (T-70) is similar to that of the globular protein IgG. From the elution position, the materials corresponding to the second peak appeared to be free A7 and MMCD_{an}, and the first peak (fraction volume 110–130 mL) appeared to correspond to the desired conjugate, which was concentrated, frozen, and stored at -20 °C. Thus, MMCD_{an} was conjugated with mAb A7 through a disulfide bond, and was designated A7-MMCD.

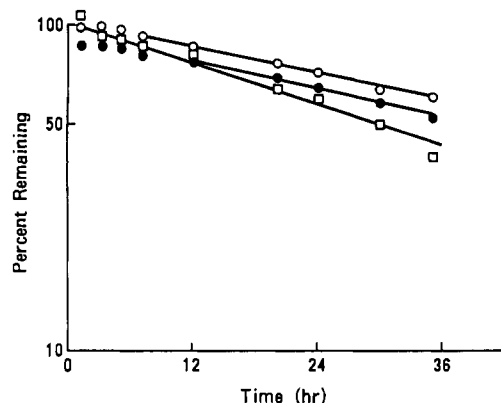


Figure 3. In vitro release of MMC from MMCD_{an} (●), MMCD_{an} with amino groups (○), and A7-MMCD (□), in a pH 7.4 isotonic phosphate buffer at 37 °C.

Table II. Molecular Charge of MMCD_{an}, MMCD_{an} with Amino Groups, and A7-MMCD

	% adsorption at pH 7.2	
	CM-Sephadex	DEAE-Sephadex
MMCD _{an}	0	9.3
MMCD _{an} with amino groups	3.9	0
A7-MMCD	0.5	0

The proposed molecular structure of A7-MMCD is shown in Figure 1.

Molar Binding Ratio. By quantitative analysis, the molar binding ratio of IgG:dextran:MMC in the conjugate was estimated to be 1:1.2:40. The yields were calculated to be 26.7% for IgG, 27.7% for dextran, and 29.1% for MMC.

In Vitro Release of MMC. Figure 3 shows the in vitro release of MMC from MMCD_{an} (T-70), MMCD_{an} with amino groups, and A7-MMCD. A7-MMCD, and similarly MMCD_{an} and MMCD_{an} with amino groups, showed a monoexponential liberation of MMC under the present conditions (pH 7.4, 37 °C). The release rates were not affected by the addition of rat plasma (data not shown). The release half-lives observed were 42.3 h for MMCD_{an}, 45.4 h for MMCD_{an} with amino groups, and 29.1 h for A7-MMCD.

Molecular Charge Estimation. As shown in Table II, MMCD_{an} with amino groups introduced was adsorbed on a cation exchanger (CM-Sephadex) to some extent, while MMCD_{an} was adsorbed on an anion exchanger (DEAE-Sephadex). Ethylenediamine might give the cationic charge to the MMCD_{an} by reacting with the remaining free carboxyl group which itself provides an anionic charge. On the other hand, the net electric charge of A7-MMCD was almost neutral due to the anionic charge of mAb A7.

Determination of Antibody Activity. The antibody-binding activity of A7-MMCD was measured by a competitive binding assay using radiolabeled mAb A7, and a comparison was made with unconjugated mAb A7 (Figure 4). The antibody activity of A7-MMCD was roughly equivalent to that of unconjugated mAb A7, indicating that the reactivity was almost preserved through the coupling procedure.

Cytotoxicity. The cytotoxic activity of A7-MMCD against the human colon cancer cell line SW1116 was compared with that of MMCD_{an} and free MMC by determining the degree of inhibition of [³H]thymidine uptake by the cells. A cytotoxicity test in which target cells were continuously exposed to the test compounds for 48 h was designed to assess the conjugate's ability to retain its pharmacological activity (Figure 5). In this experiment, A7-MMCD, although having less in vitro cytotoxic effect

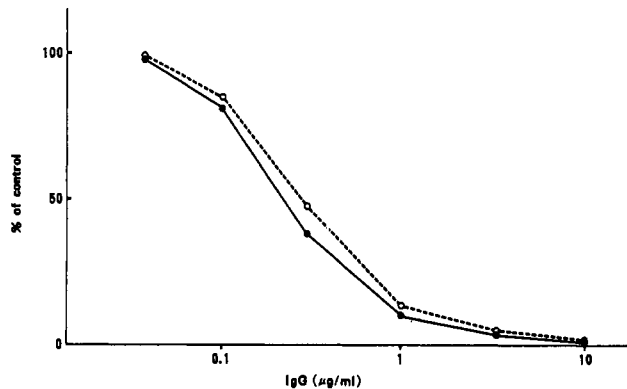


Figure 4. Antibody binding activity of A7-MMCD. The antibody binding activities of A7-MMCD (○) and intact A7 (●) were measured by competitive binding radioimmunoassay. SW1116 cells were suspended with various concentrations of A7-MMCD or intact A7, and a saturating amount of [¹²⁵I]-labeled A7 was added to each tube. After incubation for 1 h at 4 °C, the cells were washed and counted in a γ counter.

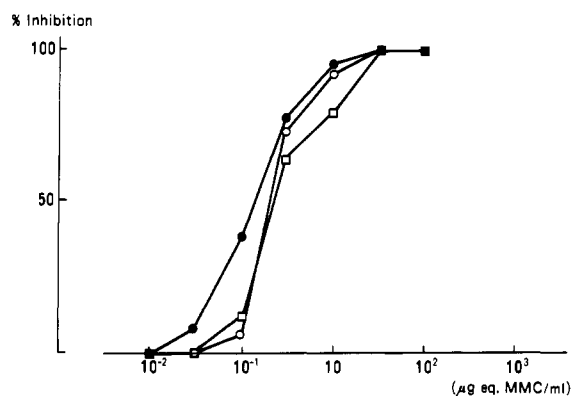


Figure 5. In vitro cytotoxic activity of A7-MMCD assayed using a 48-h continuous exposure system. The cytotoxic effects of free MMC (●), MMCD_{an} (○), and A7-MMCD (□) on SW1116 cells were assayed by a 48-h continuous exposure cytotoxic test in terms of the percent inhibition of [³H]thymidine incorporation. For details, see Experimental Procedures. The points represent mean values of experiments performed in triplicate.

than MMC, had almost the same cytotoxicity as MMCD_{an}, which indicates that the pharmacological activity of MMC bound to MMCD_{an} was almost completely preserved after the conjugation procedure. To assess the specific cytotoxicity of the conjugate under conditions somewhat comparable to the in vivo situation, the cytotoxic activity was measured using a 2-h pretreatment system (Figure 6). The system was designed on the basis of our observation that the binding of mAb A7 to SW1116 cells reached maximal level within 2 h at 37 °C (data not shown). Under these conditions, A7-MMCD was as cytotoxic as free MMC, and had about a 14-fold greater cytotoxicity than MMCD_{an} (IC₅₀ values: 28.7 μ g for A7-MMCD, 395 μ g for MMCD_{an}). Furthermore, the cytotoxicity of A7-MMCD was reduced by the addition of excessive A7, which indicated that it was mediated through the specific antigen-antibody binding. Previous work has shown that mAb A7 alone has no cytotoxicity against SW1116 cells (9).

DISCUSSION

In this study, we have developed a novel immunoconjugate composed of mAb A7 and MMCD_{an} using SPDP as a coupling reagent without losing activity in either the antibody or MMC. In our previous study, we directly conjugated MMC with mAb A7 using the cyanogen bromide method (A7-MMC) (23, 24). Though exhibiting

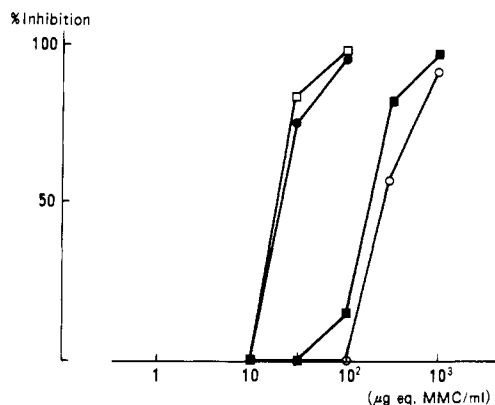


Figure 6. In vitro cytotoxic activity of A7-MMCD assayed using a 2-h pretreatment system. The cytotoxic effects of free MMC (●), MMCD_{an} (○), A7-MMCD (□), and A7-MMCD containing an excess of neat mAb A7 (■) on SW1116 cells were assayed by a 2-h pretreatment cytotoxic test in terms of the percent inhibition of [³H]thymidine incorporation. For details, see Experimental Procedures. The points represent mean values of experiments performed in triplicate.

strong antitumor effects on colon carcinoma in vitro and in vivo, the amount of MMC was not large enough for clinical use because the extent of substitution was only 2 mol of MMC/mol of IgG since the direct linkage method was used.

Recently, there have been many reports on immunoconjugates which were synthesized by employing intermediate carriers such as dextran, serum albumin, and synthetic polymers to increase the amount of drug attached to the antibody without significantly impairing its antigen-binding activity (25–28). MMC has also been linked to the antibody using periodate-oxidized dextran and serum albumin (29–31). However, in these cases, the physicochemical properties of the intermediate macromolecules must be considered because they, as well as the specificity of the antibody, might affect the in vivo behavior of the immunoconjugates. From this point of view, MMCD appears to be most suitable for conjugating with the antibody since its physicochemical properties and in vivo disposition characteristics have been extensively examined (13–19).

MMCD, which is a polymeric prodrug of MMC containing approximately 10% of MMC (w/w) covalently bound to the spacer-introduced dextran bridge, releases active MMC with a half-life of 22–40 h by chemical hydrolysis in the body (14). The total molecular size of MMCD can be altered freely by changing the size of the carrier dextran. The charge of MMCD, cationic or anionic, can be manipulated by different chemical structures of the spacer arm (13, 17). Pharmacokinetic studies have revealed that MMCD with a cationic charge (MMCD_{cat}), particularly if it also has a high molecular weight of around 500 000, is suitable for local administration because of its sustained retention at the injected site (15). In fact, a remarkable reduction in tumor size was observed in a clinical trial involving its intratumoral administration (32). On the other hand, with regard to its intravenous administration, MMCD with an anionic charge (MMCD_{an}) and having a molecular weight of 70 000 showed a long circulating life due to less cellular interaction with the reticuloendothelial system including the liver and spleen. This resulted in a higher level of tumor accumulation. MMCD_{cat}, on the other hand, was rapidly removed from circulation due to its polycationic nature (19). For this reason, we chose MMCD_{an} with a molecular weight of 70 000 as a candidate for conjugation with mAb A7, expecting a superior in vivo tumor localization and therapeutic efficacy.

The synthesis of A7-MMCD was performed using a heterobifunctional reagent, SPDP, which reacts with amino groups of the lysyl residues in the antibody molecule and also with amino groups introduced to the spacer arms of the dextran backbone by ethylenediamine. Whether the conjugation provided a sufficient yield with minimal formation of high-molecular-weight aggregates depended mainly on the number of amino groups introduced into the MMCD_{an}. Through repeated conjugation experiments, we found that the optimal molar excess of ethylenediamine against MMCD_{an} was 15, which resulted in 1.62 mol of 2-pyridyl disulfide groups being introduced into each mole of MMCD_{an}. Before mixing with SPDP-treated mAb A7, the SPDP-treated MMCD_{an} was reduced by DTT to produce free sulfhydryl groups. Generally, MMC is inactivated by reducing agents because it exhibits its cytotoxicity through bioreductive alkylation (33). However, incubation with DTT under these reaction conditions (20 mM, 20 min) did not impair the biological activity of MMC, as confirmed in an in vitro cytotoxicity test using the 48-h continuous exposure system.

A7-MMCD, thus synthesized, had an appropriate binding molar ratio (IgG:dextran:MMC = 1:1.2:40), which appeared to contribute to the full retention of antigen-binding activity, as evidenced by the competitive binding assay using radiolabeled A7. The properties of a latent form or prodrug of MMC which will continuously release active MMC under physiological conditions was also confirmed by an in vitro release experiment using A7-MMCD. The release rate of MMC was accelerated by conjugation with the antibody, probably due to some steric effect or altered electric charge. Concerning the molecular charge, since the in vivo behavior of neutrally charged dextran is comparable to that of MMCD_{an} (19), the neutral charge of A7-MMCD is considered to pose no problem for intravenous administration.

In the cytotoxicity test using a 48-h continuous exposure system, which was designed to assess the pharmacological activity of MMC, A7-MMCD was found to be less cytotoxic than free MMC. This appears to be ascribed to the properties of A7-MMCD as a prodrug; that is, MMC bound to the spacer arm of dextran through an aziridylamide bond shows little activity by itself and A7-MMCD exhibits its major cytotoxicity only after liberating active MMC by chemical hydrolysis. In this cytotoxicity test, the cytotoxicity of A7-MMCD was comparable to that of unconjugated MMCD_{an}. This result suggests that during the A7-MMCD conjugation procedure the biological activities of MMC are almost completely preserved.

Using a 2-h pretreatment system, which was designed to assess cytotoxicity under conditions closer to the in vivo situation, the cytotoxicity of A7-MMCD was found to be greater than that of MMCD_{an}. We supposed that A7-MMCD bound to the tumor cell surface by antigen-antibody interaction after the 2-h exposure remained there even after washing and liberated intact MMC in the growth medium during the successive culture period. On the other hand, MMCD_{an} was removed from the growth medium by washing. Furthermore, A7-MMCD was found to be as cytotoxic as free MMC in this 2-h pretreatment test. As the plasma clearance of MMC is considered to be very rapid in the body after intravenous administration (34), the antitumor activity of A7-MMCD is probably stronger than that of free MMC in vivo.

Although the internalization of A7-MMCD remains to be investigated, A7-MMCD bound to the antigen determinant on the tumor cell surface is considered to liberate active MMC at a constant rate by chemical hydrolysis and to show cytotoxicity against not only the targeted cells but also surrounding cells which might not

have the antigen recognized by mAb A7. Therefore, A7-MMCD, like antibody-radioisotope conjugates, may have an advantage in that the heterogeneity of tumor cells in the expression of tumor-associated antigens might not reduce its therapeutic effect. Thus, A7-MMCD could be a useful tool in immunotargeting chemotherapy for colorectal cancer.

LITERATURE CITED

- (1) Takahashi, T., Ueda, S., Kohno, K., and Majima, S. (1976) Attempt at local administration of anticancer agents in the form of fat emulsion. *Cancer* 38, 1504-1514.
- (2) Hagiwara, A., Takahashi, T., Lee, R., Ueda, T., Takeda, M., and Itoh, T. (1987) Chemotherapy for carcinomatous peritonitis and pleuritis with MMC-CH, mitomycin C adsorbed on activated carbon particles. *Cancer* 59, 245-251.
- (3) Sezaki, H., and Hashida, M. (1984) Macromolecular-drug conjugates in targeted cancer chemotherapy. *CRC Crit. Rev. Ther. Drug Carrier Syst.* 1, 1-38.
- (4) Kohler, G., and Milstein, C. (1975) Continuous culture of fused cells secreting antibody of predefined specificity. *Nature* 256, 495-497.
- (5) Pietersz, G. A., Kanellos, J., Smyth, M. J., Zalberg, J., and McKenzie, I. F. C. (1987) The use of monoclonal antibody conjugates for the diagnosis and treatment of cancer. *Immunol. Cell Biol.* 65, 111-125.
- (6) Baldwin, R. W., Embleton, M. J., Gallego, J., Garnett, M., Pimm, M. V., and Price, M. R. (1986) Monoclonal Antibody Drug Conjugates for Cancer Therapy. In *Monoclonal Antibodies in Cancer: Advances in Diagnosis and Treatment* (J. A. Roth, Ed.) pp 215-257, Futura Publishing Co. Inc., New York.
- (7) Sela, M., and Hurwitz, E. (1987) Conjugates of Antibodies with Cytotoxic Drugs. In *Immunoconjugates: Antibody Conjugates in Radioimaging and Therapy of Cancer* (C.-W. Vogel, Ed.) pp 3-7, Oxford University Press, New York.
- (8) Ghose, T. (1987) The design of cytotoxic-agent-antibody conjugates. *CRC Crit. Rev. Ther. Drug Carrier Syst.* 3, 263-359.
- (9) Kotanagi, H., Takahashi, T., Masuko, T., Hashimoto, Y., and Koyama, K. (1986) A monoclonal antibody against human colon cancers. *Tohoku J. Exp. Med.* 148, 353-360.
- (10) Fukuda, K. (1985) Study of targeting chemotherapy against gastrointestinal cancer: Preparation of anticancer drug-monoclonal antibody conjugates and investigation about its biological activities (in Japanese). *Akita J. Med.* 12, 415-468.
- (11) Takahashi, T., Yamaguchi, T., Kitamura, K., Suzuyama, H., Honda, M., Yokota, T., Kotanagi, H., Takahashi, M., and Hashimoto, Y. (1988) Clinical application of monoclonal antibody drug conjugates for immunotargeting chemotherapy of colorectal carcinoma. *Cancer* 61, 25-33.
- (12) Crooke, S. T. (1979) Mitomycin C: An Overview. In *Mitomycin C: Current Status and New Developments* (S. K. Carter, and S. T. Crooke, Eds.) pp 1-4, Academic Press, New York.
- (13) Kojima, T., Hashida, M., Muranishi, S., and Sezaki, H. (1980) Mitomycin C-dextran conjugate: A novel high molecular weight pro-drug of mitomycin C. *J. Pharm. Pharmacol.* 32, 30-34.
- (14) Hashida, M., Takakura, Y., Matsumoto, S., Sasaki, H., Kato, A., Kojima, T., Muranishi, S., and Sezaki, H. (1983) Regeneration characteristics of mitomycin C-dextran conjugate in relation to its activity. *Chem. Pharm. Bull.* 31, 2055-2063.
- (15) Takakura, Y., Matsumoto, S., Hashida, M., and Sezaki, H. (1984) Enhanced lymphatic delivery of mitomycin C conjugated with dextran. *Cancer Res.* 44, 2505-2510.
- (16) Matsumoto, S., Yamamoto, A., Takakura, Y., Hashida, M., Tanigawa, N., and Sezaki, H. (1986) Cellular interaction and in vitro antitumor activity of mitomycin C-dextran conjugate. *Cancer Res.* 46, 4463-4468.
- (17) Takakura, Y., Kitajima, M., Matsumoto, S., Hashida, M., and Sezaki, H. (1987) Development of a novel polymeric pro-drug of mitomycin C, mitomycin C-dextran conjugate with anionic charge. I. Physicochemical characteristics and in vivo antitumor activities. *Int. J. Pharm.* 37, 135-143.
- (18) Takakura, Y., Atsumi, R., Hashida, M., and Sezaki, H. (1987) Development of a novel polymeric prodrug of mitomycin C, mitomycin C-dextran conjugate with anionic charge. II. Disposition and pharmacokinetics following intravenous and intramuscular administration. *Int. J. Pharm.* 37, 145-154.
- (19) Takakura, Y., Takagi, A., Hashida, M., and Sezaki, H. (1987) Disposition and tumor localization of mitomycin C-dextran conjugates in mice. *Pharm. Res.* 4, 293-300.
- (20) Kitamura, K., Takahashi, T., Yamaguchi, T., Yokota, T., Noguchi, A., Amagai, T., and Imanishi, J. (1989) Immunotargeting characterization of the antigen recognized by the murine monoclonal antibody A7 against colorectal cancer. *Tohoku J. Exp. Med.* 157, 83-93.
- (21) Lowry, O. H., Rosebrough, N. J., Farr, A. L., and Randall, R. J. (1951) Protein measurement with the folin phenol reagent. *Biol. Chem.* 28, 265-275.
- (22) Scott, T. A., and Melvin, E. H. (1953) Determination of dextran with anthrone. *Anal. Chem.* 25, 1656-1661.
- (23) Suzuki, T., Sato, E., Goto, K., Katurada, Y., Unno, K., and Takahashi, T. (1981) The preparation of mitomycin C, adriamycin and daunomycin covalently bound to antibodies as improved cancer chemotherapeutic agents. *Chem. Pharm. Bull.* 29, 844-848.
- (24) Kotanagi, H., Fukuda, K., and Ogata, N. (1987) Potent effect of the monoclonal antibody-mitomycin C conjugate on human colon cancers. *Jpn. J. Surg.* 17, 47-50.
- (25) Hurwitz, E., Marson, R., Arnon, R., Wilchek, M., and Sela, M. (1978) Daunomycin-immunoglobulin conjugates, uptake and activity in vitro. *Eur. J. Cancer* 14, 1213-1220.
- (26) Schechter, B., Pauzner, R., Arnon, R., Haimovich, J., and Wilchek, M. (1987) Selective cytotoxicity against tumor cells by cisplatin complexed to antitumor antibodies via carboxymethyl dextran. *Cancer Immunol. Immunother.* 25, 225-230.
- (27) Garnett, M. C., and Baldwin, R. W. (1986) An improved synthesis of a methotrexate-albumin-791T/36 monoclonal antibody conjugate cytotoxic to human osteogenic sarcoma cell line. *Cancer Res.* 46, 2407-2412.
- (28) Kato, Y., Umemoto, N., Kayama, Y., Fukushima, H., Takeda, Y., Hara, T., and Tsukada, Y. (1984) A novel method of conjugation of daunomycin with antibody with a poly-L-glutamic acid derivative as intermediate drug carrier. An anti- α -fetoprotein antibody-daunomycin conjugate. *J. Med. Chem.* 27, 1602-1607.
- (29) Manabe, Y., Tsubota, T., Haruta, T., Kataoka, K., Okazaki, M., Haisa, S., Nakamura, K., and Kimura, I. (1985) Production of a monoclonal antibody-mitomycin C conjugate, utilizing dextran T-40, and its biological activity. *Biochem. Pharmacol.* 34, 289-291.
- (30) Umemoto, N., Kato, Y., Takeda, Y., Saito, M., Hara, T., Seto, M., and Takahashi, T. (1984) Conjugates of mitomycin C with the immunoglobulin M monomer fragment of a monoclonal anti-MM46 immunoglobulin M antibody with or without serum albumin as intermediary. *J. Appl. Biochem.* 6, 297-307.
- (31) Ohkawa, K., Tsukada, Y., Hibi, N., Umemoto, N., and Hara, T. (1986) Selective in vitro growth inhibition against human yolk sac tumor cell lines by purified antibody against human α -fetoprotein conjugated with mitomycin C via human serum albumin. *Cancer Immunol. Immunother.* 23, 81-86.
- (32) Honda, K., Satomura, K., Hashida, M., and Sezaki, H. (1985) Topical application of mitomycin C conjugated with dextran (MMC-D): A high molecular weight derivative of mitomycin C. *Jpn. J. Cancer Chemother.* 12, 311-317.
- (33) Lin, A. J., Cosby, L. A., and Sartorelli, A. C. (1974) Quinones as anticancer agents: Potential bioreductive agents. *Cancer Chemother. Rep.* 4, 23-25.
- (34) Schwartz, H. S., and Philips, F. S. (1961) Pharmacology of mitomycin C 2. Renal excretion and metabolism by tissue homogenates. *J. Pharmacol. Exp. Ther.* 133, 335-342.

Site-Directed Conjugation of Nonpeptide Groups to Peptides and Proteins via Periodate Oxidation of a 2-Amino Alcohol. Application to Modification at N-Terminal Serine

Kieran F. Geoghegan* and Justin G. Stroh

Central Research Division, Pfizer Inc., Groton, Connecticut 06340. Received October 15, 1991

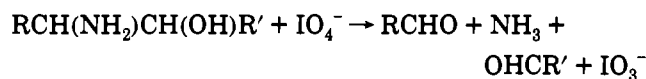
The 2-amino alcohol structure $\text{-CH(NH}_2\text{)CH(OH)-}$ exists in proteins and peptides in N-terminal Ser or Thr and in hydroxylysine. Its very rapid oxidation by periodate at pH 7 generates an aldehyde in the peptide and is the first step in a method for site-directed labeling with biotin or a fluorescent reporter. The modifying group is a hydrazide, RCONHNH_2 , which reacts with the new aldehyde to form a hydrazone-peptide conjugate, RCONHN=CH-peptide . Experiments with two synthetic peptides, Ser-Ile-Gly-Ser-Leu-Ala-Lys and Ser-Tyr-Ser-Met-Glu-His-Phe-Arg-Trp-Gly, and with recombinant murine interleukin-1 α (an 18-kDa cytokine with N-terminal Ser) demonstrated this method of peptide tagging. The use of a low molar ratio of periodate to peptide minimized the potential for side reactions during the oxidation, and the desired oxidation was rapid and highly specific. The hydrazones formed were stable at pH 6-8 for at least 12 h at 22 °C, but were labile at more acidic pH values. Potential uses of this method include the attachment of biotin, reporter groups, metal chelating groups, imaging agents, and cytotoxic drugs to peptides.

INTRODUCTION

Covalent conjugates of polypeptides with nonpeptide "labels" or "tags" form a useful class of reagents in protein and peptide research. A conjugate is usually intended to retain the native properties of the peptide while gaining a new, non-native property due to the label. Biotinylation, for example, permits proteins to be separated, quantitated, or immobilized by mechanisms based on the strong interaction of biotin with avidin or streptavidin (1). Fluorescent or metal-chelating groups can also be introduced in order to generate newly bifunctional modified peptides.

It would be convenient to be able to introduce a non-peptide label as the peptide is produced, but this is only sometimes feasible in chemical synthesis (2, 3) and is impractical when the peptide is produced biologically. Generally, the conjugate must be formed by treating the peptide with a group-specific reagent that contains the label. Unless the peptide contains only one group attacked by the reagent, this procedure yields a mixture of products. This random form of labeling is sometimes adequate, but it is often preferable to modify a peptide at a single specified site and to employ the modified product in purified form. For such cases, it would be valuable to have a method of directing the modifying group into a single, preselected location. This precisely targeted chemical modification could be termed site-directed peptide tagging. Several schemes for N-terminal (4, 5) or C-terminal (6-8) site-directed tagging have already been described.

This paper describes and illustrates a method which can potentially lead to site-directed modification at any locus within a synthetic peptide and at the N-terminus of proteins with N-terminal Ser or Thr. The method is based on the very fast oxidation by periodate of the 2-amino alcohol grouping



to create a single aldehyde function at a known site in the peptide (9-13). The aldehyde is then reacted with the tagging group in the form of a hydrazide, R''CONHNH_2 , to form a hydrazone, $\text{R''CONHN=CH-peptide}$. R'' can be any of a variety of useful groups, and the hydrazones are adequately stable for many biochemical applications in the range pH 6-8. Site-selectivity is possible because the target site for the periodate reaction exists in peptides only when the N-terminus is Ser or Thr, or when hydroxylysine is present; hence the location at which an aldehyde is generated is known or can be selected in advance. (Hydroxylysine is only known to occur naturally in collagen, but in principle can be placed anywhere in a synthetic peptide.) Results presented here introduce the method by demonstrating site-directed modification at N-terminal Ser.

EXPERIMENTAL PROCEDURES

Reagents. Biotin-X-hydrazide,¹ Lucifer Yellow, and Cascade Blue hydrazide were purchased from Molecular Probes (P.O. Box 22010, 4849 Pitchford Ave., Eugene, OR 97402). The peptides SIGSLAK and SYSMEHFRWG were from Sigma (P.O. Box 14508, St. Louis, MO 63178). Recombinant mIL-1 α was produced as described (14). Avidin-HRP conjugate and biotinylated M_r markers were from Pierce (P.O. Box 117, Rockford, IL 61105). Sodium *m*-periodate was from Aldrich (1001 West Saint Paul Ave., Milwaukee, WI 53233). Periodate solutions were prepared on the day of use and kept in a foil-wrapped tube.

¹ Abbreviations used: PDMS, plasma desorption mass spectrometry; ESMS, electrospray mass spectrometry; biotin-X-hydrazide, 6-(biotinoylamino)caproic acid hydrazide; Lucifer Yellow, Lucifer Yellow CH; mIL-1 α , murine interleukin-1 α ; IEF, isoelectric focusing; SDS-PAGE, SDS-polyacrylamide gel electrophoresis; PVDF, polyvinylidene difluoride; Tris, tris(hydroxymethyl)aminomethane; Mes, 2-morpholinoethanesulfonic acid; CAPS, 3-(cyclohexylamino)-1-propanesulfonic acid; the one-letter code for representing amino acid residues in peptide sequences may be found in most textbooks of biochemistry.

* Correspondence: Dr. K. F. Geoghegan, Pfizer Central Research, Eastern Point Road, Groton, CT 06340.

Chromatography. For the experiments with SIGSLAK and SYSMEHFRWG, HPLC was performed using a gradient system from LDC Analytical or a Hewlett-Packard 1090 Series II system. A Vydac C4 column (4.6 × 150 mm; type 214TP10415) (Separations Group, Hesperia, CA 92345) was used with linear gradients of CH₃CN in 0.1% TFA (1 mL/min flow rate). Peaks selected for PDMS were dried in a SpeedVac (Savant Instruments, 110-103 Bi-County Blvd., Farmingdale, NY 11735) to 1–5 μ L.

Peptide mapping was performed on the Hewlett-Packard system using a C18 Aquapore cartridge (2.1 × 100 mm) (Applied Biosystems, 850 Lincoln Centre Dr., Foster City, CA 94404) with a flow rate of 0.2 mL/min. The solvents were A, 0.1% TFA in 5% (v/v) CH₃CN; and B, 0.085% TFA in 70% (v/v) CH₃CN. A linear gradient from 0% to 80% solvent B was run from 2 to 66 min after injection. Peaks were collected by hand.

Reversed-phase HPLC of mIL-1 α and its oxidized and biotinylated forms was performed on the Hewlett-Packard system, which was equipped with a diode-array detector to allow measurement of the UV-visible absorption spectrum of each component. A Vydac C4 column (2.1 × 50 mm; type 214TP5205) was used with solvents as follows: A, 0.1% TFA; and B, 0.085% TFA in 80% (v/v) CH₃CN. The flow rate was 0.2 mL/min. A linear gradient from 10% to 82% solvent B was run from 2 to 16 min after injection.

Protein/Peptide Sequencing. Sequence analysis was performed using an Applied Biosystems Model 470A gas-phase sequencer equipped with a Model 120A PTH analyzer.

Electrophoresis. IEF, SDS-PAGE, and electroblotting to PVDF membrane (ProBlott; Applied Biosystems) were performed using a PhastSystem (Pharmacia LKB, 800 Centennial Ave., Piscataway, NJ 08854) and gels were developed using a PhastGel silver kit (Pharmacia LKB). Western blots were tested for biotinylated proteins using avidin-HRP conjugate.

Mass Spectrometry. PDMS was performed using a Bio-Ion 20 spectrometer (Applied Biosystems). Samples were dissolved in 15 μ L of 20% CH₃CN and applied to nitrocellulose targets (Applied Biosystems). The instrument was run in the positive ion mode with an acceleration potential of 15 kV. Masses were estimated by placing the twin cursors on each side of the peak at the bottom of the Gaussian-shaped area and calculating a centroid. This procedure generally produced a value of mass accuracy within 0.2%.

ESMS data were obtained on a Finnigan TSQ-700 mass spectrometer operating in the positive-ion mode. The instrument was scanned over the m/z range 450–2200. Thirty-two spectra were averaged and the averaged data were smoothed using a seven-point smoothing routine. Spectra of mIL-1 α and its derivatives were collected on the HPLC column fractions with no further concentration. Samples were infused into the ES ion source at 2 μ L/min with a sheath liquid flow of 2 μ L/min of 2-methoxyethanol.

Periodate Oxidations and Coupling Reactions. (1) **Ser-Ile-Gly-Ser-Leu-Ala-Lys (SIGSLAK).** SIGSLAK (2 × 10⁻⁴ M) in 0.01 M sodium phosphate, pH 7.0, was treated with a 2-fold molar excess of NaIO₄ for 4 min at 22 °C. The reaction mixture (200 μ L) was then injected into the HPLC and fractionated using a linear gradient from 0% to 42% CH₃CN between 5 and 20 min after injection. A small portion of the product peak was used for PDMS, and the remainder was dried.

The oxidation product α -N-glyoxylyl-IGSLAK (1.5 mM)

was reacted with biotin-X-hydrazide (10 mM) in 0.03 M sodium acetate (pH 4.5)/16% CH₃CN for 70 min at 22 °C, after which the 30- μ L reaction mixture was diluted to 220 μ L with water and injected into the HPLC (see Results). Separately, α -N-glyoxylyl-IGSLAK (1.5 mM) was allowed to react with Lucifer Yellow (16 mM) in 0.03 M sodium acetate (pH 4.5) for 120 min at 22 °C, after which this reaction mixture was fractionated by HPLC (see Results). Products were characterized by PDMS.

(2) **Ser-Tyr-Ser-Met-Glu-His-Phe-Arg-Trp-Gly (SYSMEHFRWG).** In a series of reactions at different pH values, SYSMEHFRWG (28 μ M) was treated with NaIO₄ (44 μ M) in a mixed buffer containing 7 mM each of sodium acetate, Mes, and sodium phosphate. The experiment was performed with the buffer set to pH 4.0, 5.0, 6.0, 7.0, and 8.0. After 2 min at 22 °C, the reactions were terminated by HPLC injection. (In preliminary experiments, the major oxidation products were mass analyzed; mass data interpreted in terms of Met oxidation were confirmed by showing that components suspected of containing Met sulfoxide failed to undergo cleavage by CNBr).

N-Terminally oxidized peptide α -N-glyoxylyl-SYSMEHFRWG was coupled to biotin-X-hydrazide as described. The conjugate was then used in a study of the stability of peptide-hydrazone conjugates. Biotin-X-SYSMEHFRWG was separately incubated at 22 °C in a series of buffers with pH in the range pH 2–10, and the samples were analyzed by automated injection into the HPLC. Buffers used were 0.05 M sodium phosphate (pH 2.0), 0.05 M sodium acetate (pH 4.0), 0.05 M Mes (pH 6.0), 0.05 M Tris-HCl (pH 8.0), 0.05 M CAPS (pH 10.0).

(3) **Murine Interleukin-1 α (mIL-1 α).** In a 2.2-mL reaction, mIL-1 α (13 μ M) was incubated at 0 °C for 30 min with NaIO₄ (40 μ M) in 0.02 M sodium phosphate (pH 7.0). Periodate was removed by gel filtration using Sephadex G-25 equilibrated with 0.05 M sodium acetate (pH 4.5). Quantitative oxidation of the N-terminus was confirmed by IEF, and the N-terminally oxidized protein was concentrated using a Centricon 10 (Amicon, 24 Cherry Hill Dr., Danvers, MA 01923) before reaction with biotin-X-hydrazide. The coupling reaction contained 57 μ M oxidized mIL-1 α with 8 mM biotin-X-hydrazide in 25% acetonitrile/0.038 M sodium acetate (pH 4.5). After 16 h at 22 °C, the protein was gel filtered into 0.02 M Tris (pH 7.0) to remove biotin-X-hydrazide and subjected to anion-exchange chromatography (MonoQ HR 5/5, Pharmacia LKB) using a flow rate of 1 mL/min and a NaCl gradient of 0.0–0.1 M NaCl in 20 min in 0.02 M Tris (pH 7.0). The modified product was characterized by SDS-PAGE and by Western blotting followed by detection of the biotin label with avidin-HRP. Control samples were treated as described above with the omission of periodate from the oxidation stage or of biotin-X-hydrazide from the coupling stage.

Tryptic Digestion of mIL-1 α . Unmodified and oxidized samples of mIL-1 α were treated in parallel with trypsin to prepare digests. In a first attempt, 0.2 mL of each protein sample at 0.14 mg/mL (28 μ g of mIL-1 α) was incubated with 1 μ g of sequencing-grade trypsin (Boehringer Mannheim, P.O. Box 50414, Indianapolis, IN 46250) for 18 h at 37 °C in 0.1 M Tris (pH 8.0). When it was found that this accomplished no digestion, the samples were made 1 M in guanidinium chloride, a further 2 μ g of trypsin was added, and the tubes were again incubated at 37 °C for 18 h. These conditions led to a substantial, though incomplete, digestion of the mIL-1 α samples which sufficed to permit isolation and characterization of the

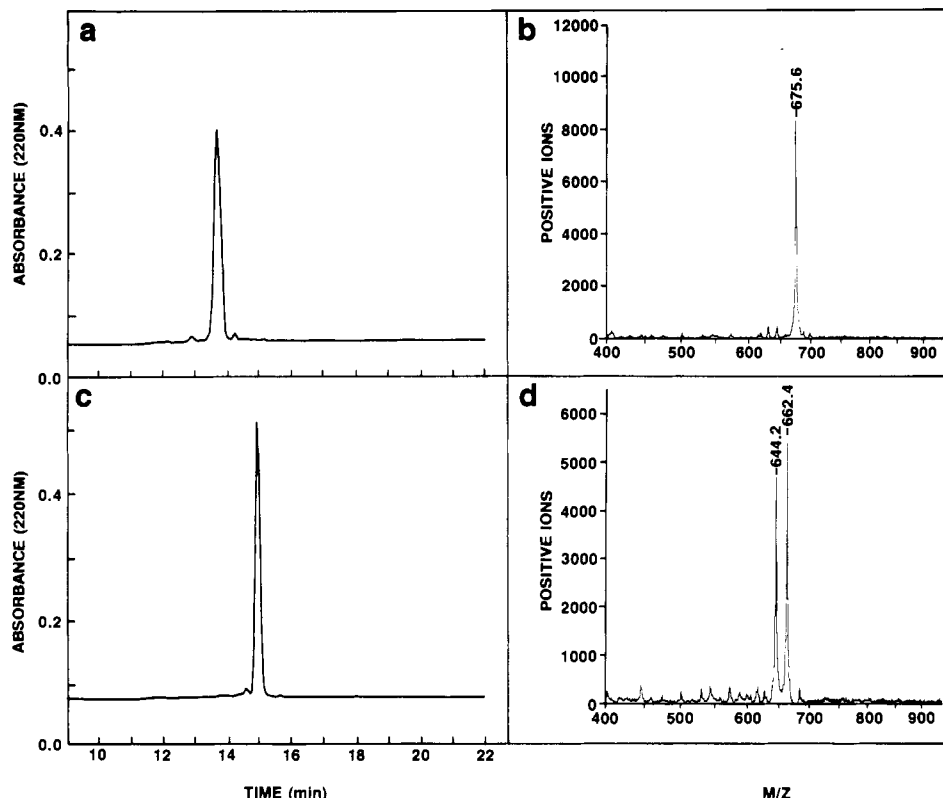
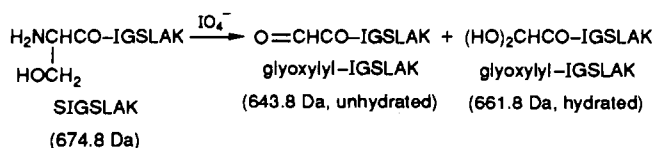


Figure 1. HPLC and PDMS analyses of periodate oxidation of SIGSLAK. See the methods for experimental details. (a) HPLC analysis of SIGSLAK before oxidation; the 13.7-min peak was collected for PDMS. (b) PDMS analysis of SIGSLAK peak; the calculated MH^+ for SIGSLAK is 675.8. (c) HPLC fractionation of periodate oxidation of SIGSLAK; the 14.9-min peak was collected for PDMS. (d) PDMS analysis of peak from SIGSLAK oxidation reaction; the calculated MH^+ for α -N-glyoxylyl-IGSLAK is 644.8 (unhydrated form of aldehyde) and 662.8 (hydrated form).

unmodified and oxidized forms of the anticipated N-terminal undecapeptide (see Results).

RESULTS

Initial Test of Oxidation and Coupling. Oxidation and coupling experiments were first performed using SIGSLAK, a peptide in which the only periodate-sensitive residue was the N-terminal Ser. SIGSLAK gave a single major peak in HPLC (Figure 1a), and in PDMS (Figure 1b) gave an MH^+ of 675.6 (calculated MH^+ 675.8). The reaction of SIGSLAK with a 2-fold molar excess of periodate (see Methods) gave a single product (Figure 1c). PDMS of this material gave two species with MH^+ values of 644.2 and 662.4, respectively (Figure 1d), assigned to the unhydrated (calculated MH^+ 644.8) and hydrated (calculated MH^+ 662.8) forms of the expected product, α -N-glyoxylyl-IGSLAK.



Prewetting the nitrocellulose target for PDMS with ethanol resulted in a third peak in addition to the two seen in Figure 1d (spectrum not shown). The new peak, corresponding to an MH^+ of 690.8, was assigned to a hemiacetal formed by ethanol with α -N-glyoxylyl-IGSLAK (calculated MH^+ 690.8 Da).

α -N-Glyoxylyl-IGSLAK was dried and then allowed to react with 10 mM biotin-X-hydrazide for 70 min or 16 mM Lucifer Yellow for 120 min (see the methods) in 0.03 M sodium acetate (pH 4.5) at 22 °C. Reactions were

terminated by injection into the HPLC, and the products were collected, concentrated, and characterized by PDMS. The reaction of α -N-glyoxylyl-IGSLAK with biotin-X-hydrazide gave a single major product which was the 18.9-min peak in Figure 2a; the broad peak at 12–13 min (Figure 2a) was due to biotin-X-hydrazide. The calculated MH^+ for the hydrazone conjugate of biotin-X-hydrazide with α -N-glyoxylyl-IGSLAK was 998.3; in agreement with this, the product gave an MH^+ of 997.9 (Figure 2b).

Reaction with Lucifer Yellow also converted α -N-glyoxylyl-IGSLAK to a single product (Figure 2c). PDMS (Figure 2d) showed that the product had an MH^+ of 1072.3, in agreement with the calculated MH^+ of 1072.1 for the hydrazone formed by Lucifer Yellow and α -N-glyoxylyl-IGSLAK. The Lucifer Yellow adduct gave a weak mass spectrum lacking any dominant component unless the nitrocellulose target was first washed with 0.1% TFA.

Very similar oxidation and coupling experiments were successfully performed using the peptide TIGSLAK, in which the N-terminus is Thr rather than Ser. These results confirmed the expectation that N-terminal Ser and Thr are equally viable targets for site-directed modification.

Selectivity of Periodate Oxidation. As periodate can oxidize several amino acid side chains in proteins (15), it was important to define optimum conditions for selective oxidation of the 2-amino alcohol. This was done by studying periodate oxidation of another synthetic peptide, SYSMEHFRWG, which in addition to N-terminal Ser contained one residue each of Tyr, Met, His, and Trp. Apart from Cys, which was excluded from consideration because of its presumed sensitivity to oxidation (10), these were the residues most likely to undergo side reactions with periodate (15). The effect of treating SYSMEHFRWG with low molar ratios of periodate was examined

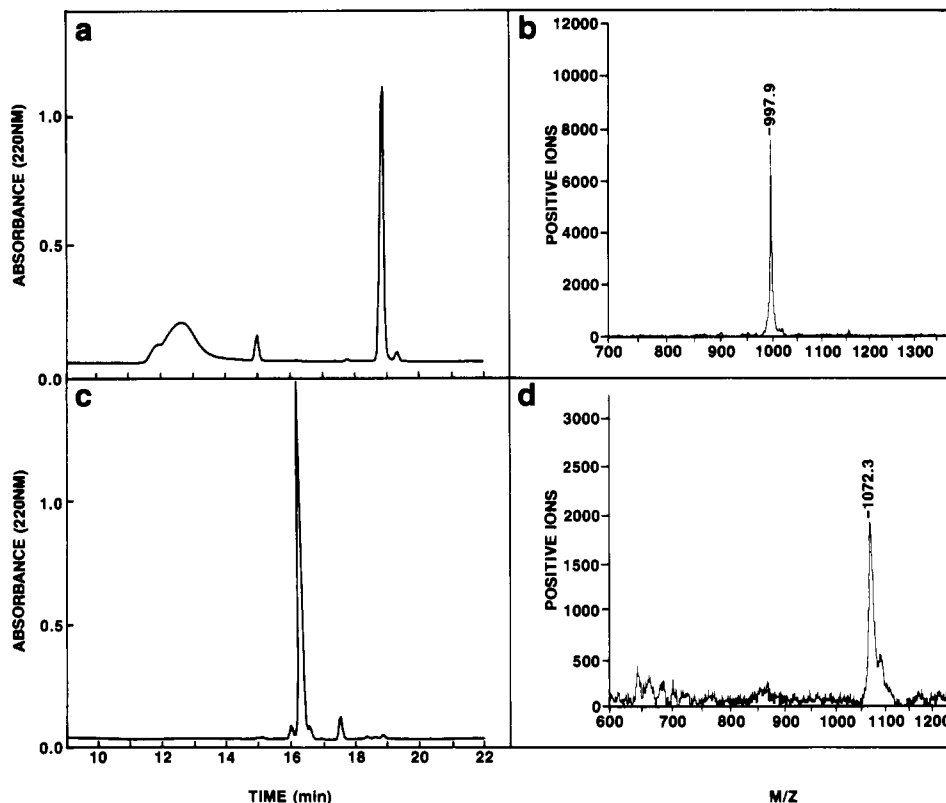


Figure 2. HPLC and PDMS analyses of coupling reactions between α -N-glyoxylyl-IGSLAK and hydrazide reagents. See the methods for experimental details. (a) HPLC analysis of coupling reaction with biotin-X-hydrazide; the 18.9-min peak was collected for PDMS. (b) PDMS analysis of hydrazone adduct between biotin-X-hydrazide and α -N-glyoxylyl-IGSLAK; the calculated MH^+ for the desired adduct is 998.3. (c) HPLC analysis of coupling reaction with Lucifer Yellow; the 16.2-min peak was collected for PDMS. (d) PDMS analysis of hydrazone adduct between Lucifer Yellow and α -N-glyoxylyl-IGSLAK; the calculated MH^+ for the desired adduct is 1072.1.

in the pH range 4–8, and reaction products were separated by HPLC and characterized by PDMS. Only three significant products were detected in addition to unreacted peptide. In order of increasing HPLC retention time (Figure 3a), the products were (I) the methionine sulfoxide form of the peptide, characterized by mass spectrometry and its inability to be cleaved by CNBr; (II) the methionine sulfoxide form, also N-terminally oxidized; (III) unmodified peptide; and (IV) the peptide modified only by the desired N-terminal oxidation.

The effect of pH on the distribution of reaction products was then examined using an IO_4^- :SYSMEHFRWG ratio of 1.6:1.0 (Figure 3b). At pH 4.0, the principal reaction was oxidation of Met to its sulfoxide. The yield of this product diminished with increasing pH, and at pH 7.0 the amount of the desired N-terminal oxidation product, α -N-glyoxylyl-SYSMEHFRWG, was 40-fold higher and accounted for >90% of the total peptide (Figure 3a,b). Thus, at neutral pH, the desired oxidation of N-terminal Ser was rapid and highly favored. This was not true at pH 4–6 (Figure 3b), where oxidation of Met was favored. His, Tyr, and Trp were much less reactive to oxidative attack by periodate than either the N-terminus or the thioether group of Met. Very similar results were reported from an earlier study of periodate oxidation of corticotropin (16), of which SYSMEHFRWG is the N-terminal decapeptide.

Stability of the Hydrazone Adduct. α -N-Glyoxylyl-SYSMEHFRWG, the product of N-terminal oxidation of SYSMEHFRWG, was coupled to biotin-X-hydrazide as described above for α -N-glyoxylyl-IGSLAK. The product was isolated by HPLC (not shown) and gave a mass spectrum consistent with the expected hydrazone (calculated MH^+ 1622.9, MH^+ observed 1623.6).

The stability of biotin-X-SYSMEHFRWG at pH 2–10 at 22 °C was then analyzed by HPLC sampling over 12 h

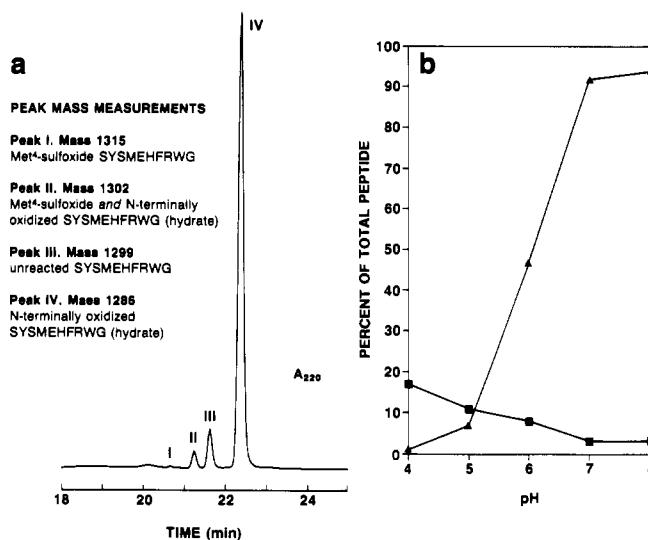


Figure 3. Effect of pH on periodate oxidation of SYSMEHFRWG. See the methods for experimental details. (a) HPLC analysis of oxidation of SYSMEHFRWG with a 1.6-fold molar excess of sodium periodate at pH 7. Peak identifications (inset text) were based on preliminary experiments from which peaks were collected and mass analyzed. (b) Percent of total SYSMEHFRWG undergoing (■) conversion to Met sulfoxide at the Met residue, and (▲) N-terminal oxidation in experiments which were identical to that in panel a except for variation of the pH.

(Figure 4). The hydrazone broke down rapidly at pH 2, was less labile at pH 4, and remained intact through the course of the experiment at pH 6 and 8. Slow breakdown occurred at pH 10, but the hydrazone was still >95% intact after 12 h.

Modification of mIL-1 α with Biotin-X-hydrazide.

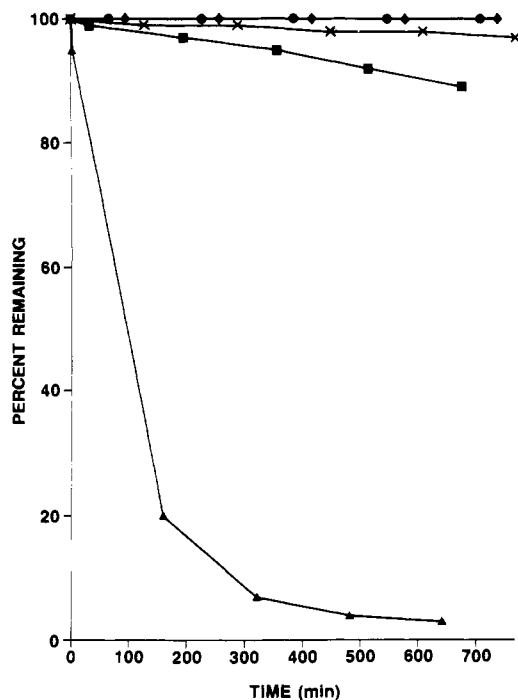


Figure 4. Stability of Biotin-X-YSMEHFRWG in the pH range 2–10. See the methods for experimental details. The hydrazone was incubated at 22 °C at (▲) pH 2.0, (■) pH 4.0, (●) pH 6.0, (◆) pH 8.0, and (×) pH 10.0.

mIL-1 α , a 156-residue single-chain cytokine, was produced by expression of a synthetic gene in *Escherichia coli* (14). As it contained no thiol groups but had an N-terminal Ser, it was a good candidate for site-directed modification by the present method.

mIL-1 α (1.4×10^{-5} M) in 0.02 M sodium phosphate (pH 7.0) was treated with a 3-fold molar excess of sodium periodate at 0 °C for 30 min. Periodate was then removed by gel filtration, at the same time buffer-exchanging the protein into 0.05 M sodium acetate (pH 4.5) in preparation for the coupling reaction.

Oxidation of N-terminal Ser would convert a positively charged site into a neutral one, lowering the isoelectric point of the protein and allowing the reaction to be monitored by IEF (Figure 5A). As anticipated, IEF showed that mIL-1 α was quantitatively converted to a modified form with a more acidic pI, consistent with oxidation of the N-terminus. A minor band in the preparation, originally with a more acidic pI than the major component, also shifted upon oxidation. This minor component has not been identified, but may be a deamidated form of mIL-1 α .

A 500-pmol sample of periodate-oxidized mIL-1 α gave no sequence result in the gas-phase sequencer, with the quantity of protein submitted being verified by amino acid analysis. This loss of capacity to undergo automated Edman degradation confirmed that mIL-1 α had undergone modification of its N-terminus.

To characterize the modification further, unmodified and oxidized mIL-1 α were digested with trypsin in the presence of 1 M guanidinium chloride and the digests were compared by reversed-phase HPLC peptide mapping (Figure 6a,c). Selective modification of N-terminal Ser would result in the maps differing only by a shift in the position of the predicted N-terminal undecapeptide, SAPYTYQSDLR, due to its oxidation. With one additional discrepancy (see below), this was the result obtained. The peak near 19 min in the map of unmodified mIL-1 α was missing from the oxidized map, but the oxidized map

contained a new component at about 20.1 min. In PDMS, the peak eliminated by periodate oxidation had an MH⁺ of 1302.5 (calculated MH⁺ for SAPYTYQSDLR, 1301.4) (Figure 6B). The 20.1-min fragment from oxidized MH⁺ gave components with MH⁺ values of 1271.4 and 1289.7 [calculated MH⁺ for α -N-glyoxylyl-APYTYQSDLR, 1270.4 (unhydrated) and 1288.4 (hydrated)] (Figure 6d). Sequence analysis of the putative SAPYTYQSDLR derived from unmodified mIL-1 α confirmed its identity, also showing that the discrepancy between observed and calculated MH⁺ values was not due to deamidation of the Gln residue, but was due to normal error in the PDMS.

The maps also differed by the presence of a minor peak at about 15 min in the map of unmodified mIL-1 α (Figure 6a) which was absent from the digest of oxidized protein (Figure 6c). Sequence and mass analyses showed that this was due to a mixture of three fragments of mIL-1 α . It was apparent from analysis of other peaks (not shown) that digestion of mIL-1 α in the presence of 1 M guanidinium chloride was incomplete and that several peaks in the maps were due to fragments containing a potentially trypsin-labile bond. Thus, the presence of this small extra peak in the unmodified map was attributed to inconsistency between two incomplete digestions.

Following overnight coupling with biotin-X-hydrazide (see the methods), the samples were gel filtered into 0.02 M Tris (pH 7.0) to remove the hydrazide and prepare them for anion-exchange chromatography using a Pharmacia MonoQ column. All three protein samples gave sharp single peaks; as an example, Figure 7 shows chromatography of the product from the biotinylation reaction. The oxidized/nonbiotinylated and oxidized/biotinylated forms of the protein were eluted slightly later in the NaCl gradient (~ 0.07 M NaCl) than unmodified mIL-1 α (~ 0.06 M NaCl) (Figure 7).

The samples were next examined by SDS-PAGE (Figure 5B). The unmodified and oxidized/nonbiotinylated forms of mIL-1 α ran together in a position consistent with their respective masses of ~ 18 kDa. The oxidized/biotinylated form of mIL-1 α , however, gave a single band of slightly reduced mobility, consistent with covalent attachment of biotin-X-hydrazide (M_r of 371.5). To confirm that this was due to modification with biotin-X-hydrazide, a similar gel was electroblotted to a PVDF membrane and the blot was developed using avidin-HRP conjugate (Figure 5C). A single positive band at ~ 18 kDa was found in the lane loaded with oxidized/biotinylated mIL-1 α ; no bands were present in the lanes loaded with control mIL-1 α samples. Thus, the small mass increase in the oxidized/biotinylated protein could be attributed to attachment of biotin-X-hydrazide. Conversion of the oxidized mIL-1 α to the biotinylated form appeared quantitative (Figure 5B), and the adduct was stable to SDS-PAGE.

For definitive mass analysis of the modified cytokine, unmodified and modified forms of mIL-1 α were desalted by reversed-phase HPLC and subjected to ESMS. In the HPLC step (Figure 8A), the unmodified, oxidized, and biotinylated forms of the protein were eluted in the same relative order as similar series prepared from much smaller peptides (e.g. Figures 1 and 2). The absorption spectra of the unmodified and oxidized forms of the protein were essentially equivalent, but the biotinylated protein had a strong new absorption band centered at about 264 nm (Figure 8B). This was assigned to the hydrazone formed by biotin-X-hydrazide at the oxidized N-terminus. In support of this assignment, the hydrazone adduct of the aromatic-free peptide oxidation product α -N-glyoxylyl-IGSLAK with biotin-X-hydrazide possessed a very similar

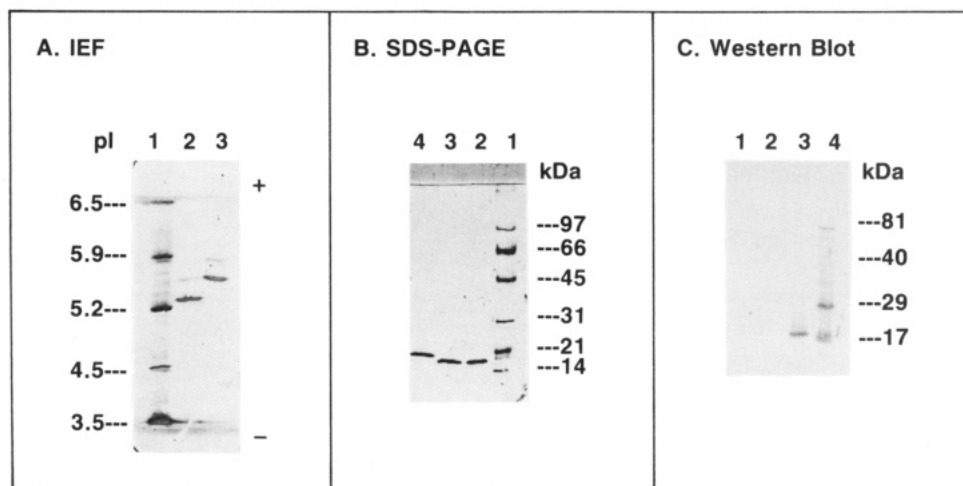


Figure 5. Electrophoretic analysis of N-terminal oxidation and biotinylation of mIL-1 α . (A) IEF of periodate oxidation showing, lane 1, pI standards; lane 2, mIL-1 α before periodate oxidation; lane 3, mIL-1 α after periodate oxidation. The gel was a Phast IEF pH 4–6.5 premade gel, silver stained. (B) SDS-PAGE of biotinylation reaction, lane 1, M_r markers; lane 2, mIL-1 α which was not periodate oxidized or treated with biotin-X-hydrazide; lane 3, mIL-1 α which was periodate oxidized but not treated with biotin-X-hydrazide; lane 4, mIL-1 α which was periodate oxidized and allowed to react with biotin-X-hydrazide. The gel (PhastGel 12% homogeneous) was silver stained. (C) Western blot analysis of biotinylation of mIL-1 α . A gel similar to that in the preceding panel was used, except that biotinylated M_r markers were used. Lane 1, mIL-1 α which was not periodate oxidized or treated with biotin-X-hydrazide; lane 2, mIL-1 α which was periodate oxidized but not treated with biotin-X-hydrazide; lane 3, mIL-1 α periodate oxidized and reacted with biotin-X-hydrazide; lane 4, biotinylated M_r markers.

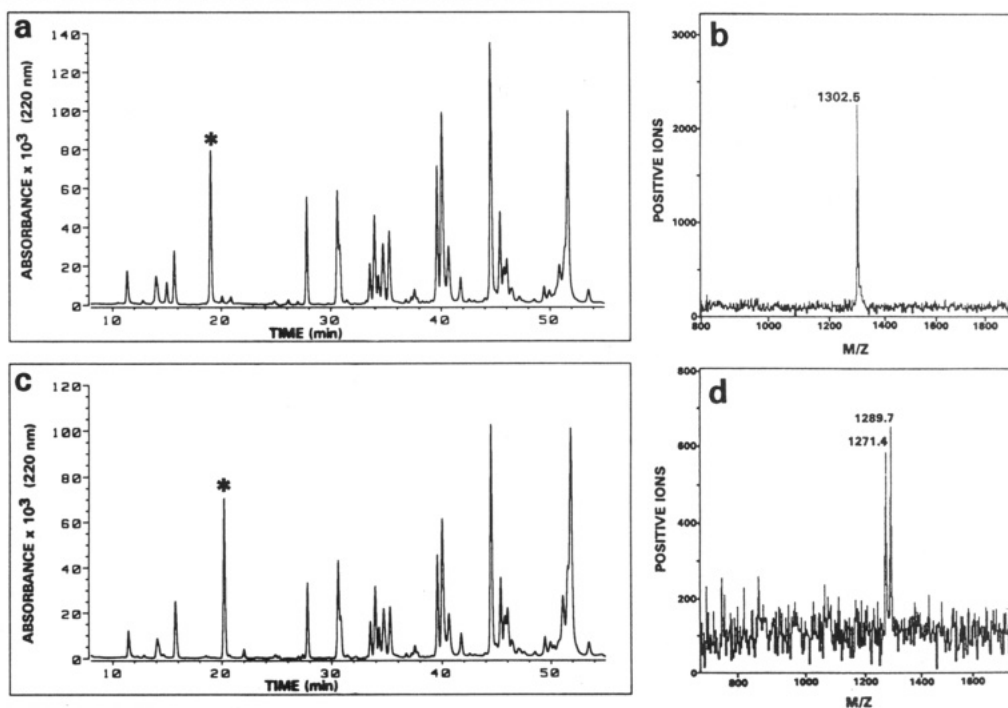


Figure 6. Comparative reversed-phase HPLC peptide mapping of unmodified and periodate-oxidized mIL-1 α . (a) HPLC peptide map of unmodified mIL-1 α digested with trypsin in the presence of 1 M guanidinium chloride (see Experimental Procedures). The peak marked with an asterisk was selected for PDMS. (b) PDMS analysis of selected peak from digest of unmodified mIL-1 α . The calculated MH^+ for SAPYTYQSDLR, the predicted N-terminal tryptic peptide of mIL-1 α , was 1301.4. (c) HPLC peptide map of periodate-oxidized mIL-1 α digested with trypsin in the presence of 1 M guanidinium chloride. The peak marked with an asterisk was selected for PDMS. (d) PDMS analysis of selected peak from digest of oxidized mIL-1 α . The calculated MH^+ for α -N-glyoxylyl-APYTYQSDLR was 1270.4 (unhydrated) and 1288.4 (hydrated).

absorption band (not shown); hence, the new band was not due to chemical modification or changes in the environment of aromatic residues in mIL-1 α .

ESMS gave a result of $17\,989.6 \pm 7.2$ for unmodified mIL-1 α (theoretical mass, 17 990.3 Da) (Figure 9a; see inset text for deconvolution of the m/z peak series to a mass result). The biotinylated product gave a result of $18\,314.8 \pm 1.2$ (theoretical mass, 18 312.8) (Figure 9b). As the standard deviation provided information about the precision of the estimate rather than its accuracy, these

observed and theoretical values were not significantly discrepant; in fact, the error of about 0.01 % was consistent with standard estimates of the accuracy of ESMS. Thus, the result confirmed other indications that mIL-1 α had been monobiotinylated by the specific site-directed chemistry.

Mass analysis of the oxidized intermediate form of mIL-1 α gave no clear result, probably due to the difficulty of separating contributions from the hydrated and unhydrated forms of the α -N-glyoxylyl N-terminus.

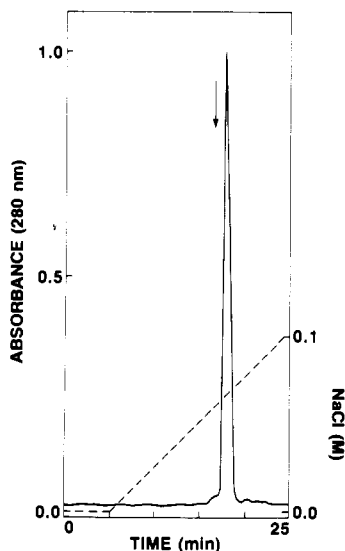


Figure 7. Anion-exchange chromatography of product from reaction of periodate-oxidized mIL-1 α with biotin-X-hydrazide. See the text for conditions. The arrow shows the position at which unmodified mIL-1 α was eluted in a similar run.

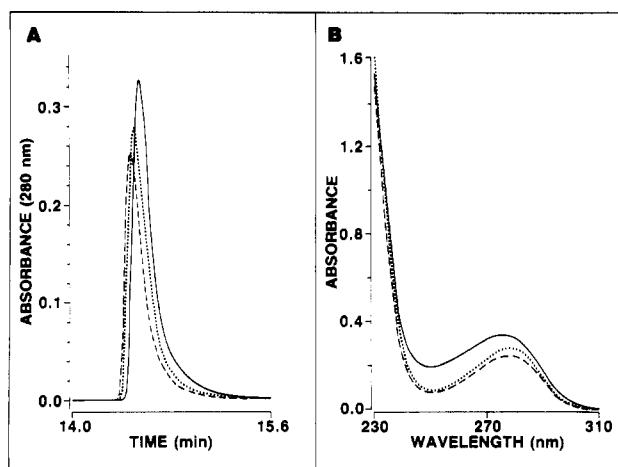


Figure 8. Reversed-phase HPLC of unmodified, periodate-oxidized and biotinylated mIL-1 α . See the text for conditions. (A) Portion of chromatograms showing peaks due to (---) unmodified, (···) periodate-oxidized, and (—) biotinylated mIL-1 α . (B) Absorption spectra corresponding to 280-nm peaks observed in panel A recorded by diode-array detector in HPLC (linestyles as in panel A).

The receptor binding and other biologically relevant activities of periodate-oxidized and biotinylated mIL-1 α were indistinguishable from those of control unmodified samples. A detailed account of the biological activities of biotinylated mIL-1 α will be presented elsewhere (Otterness, I. G., Geoghegan, K. F., et al., in preparation).

Numerous hydrazide tagging reagents are available. Those tested successfully in the present work have been biotin hydrazide (in three forms differing by the length of spacer group), Lucifer Yellow, and Cascade Blue hydrazide (not shown). One practical problem was the presence of hydrazine in the Cascade Blue hydrazide as supplied (probably a residue from synthesis); as hydrazine competed avidly for aldehyde, it had to be removed by passing the reagent through Dowex resin in the sulfonic acid form before use. As a further practical note, it was important to avoid introducing periodate-quenching substances such as glycerol into the protein sample before oxidation. Glycerol is present in some commercial membrane devices, such as the Centricon concentrator; use of these units was avoided until after the periodate reaction.

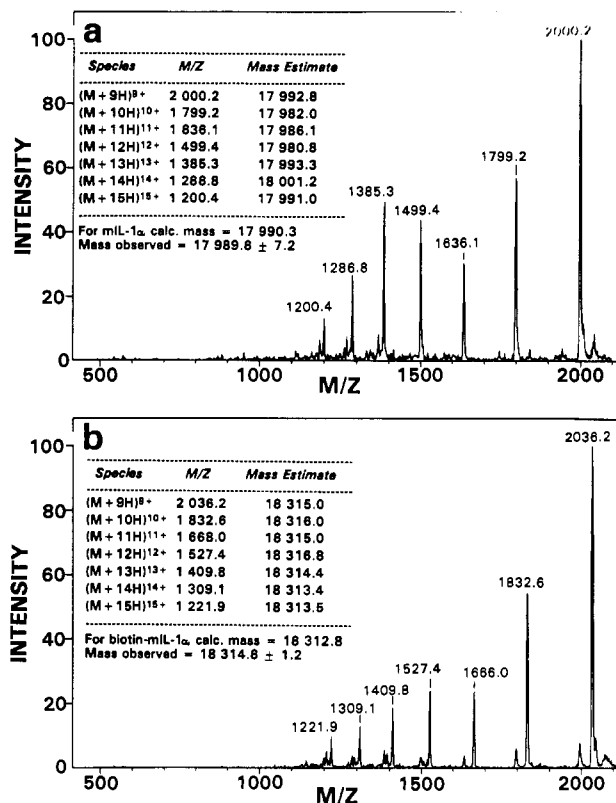


Figure 9. Electrospray mass spectrometry of unmodified and biotinylated mIL-1 α . See the text for conditions; text inset to each panel of the figure shows the basis for the mass estimate in each experiment, in which the mean of estimates provided by a series of multiply-charged ions is computed as the final result. (a) ESMS analysis of unmodified mIL-1 α (theoretical mass 17 990.3). (b) ESMS analysis of mIL-1 α monobiotinylated by hydrazone linkage at the N-terminus (theoretical mass 18 312.8).

DISCUSSION

Broadly applicable methods for site-directed tagging—the ability to deliver a label or reporter group to a single locus in a polypeptide—would reduce the tedium and complexity associated with the preparation of peptide conjugates. They would also promote the ability to apply knowledge of structure–function relationships in peptides to the selection of target sites for chemical modification. Modification of regions relevant to the biological function of a peptide could be avoided, maximizing the chances of producing conjugates with full biological activity.

The need for such technology is widely appreciated (4–8, 13), and three main approaches to the problem have been proposed: (i) to alter the peptide sequence so that only one group of the type to be tagged is present; examples are introduction of a single surface-accessible thiol into interleukin-1 β by site-directed mutagenesis (17, 18) and elimination of all but one Lys from calcitonin to leave a single ϵ -amino group for modification (19); (ii) to use an enzyme to confer specificity, as in C-terminal biotinylation of proteins (6) or C-terminal incorporation of a hydrazide or other group as the locus for secondary modification (7, 8); and (iii) to synthesize peptides with site-directed modification in mind, so that a uniquely reactive group is present or can be generated. An example is incorporation of a protected thiol group at the N-terminus of synthetic products which may be exposed to provide a locus for site-directed coupling (4).

The present strategy most closely resembles the third of these approaches. This paper has implemented a

scheme for N-terminal modification of peptides equipped with an N-terminal Ser or Thr (13), but the approach has wider potential for site-directed modification at N-terminal, internal, or C-terminal locations in synthetic peptides. For proteins produced biosynthetically, it will remain a means of N-terminal modification alone for the foreseeable future. Site-directed mutagenesis can be used to introduce N-terminal Ser or Thr when needed.

In this procedure, a 2-amino alcohol group in a protein or peptide (N-terminal Ser or Thr, or any hydroxylysine side chain) is first oxidized with periodate to generate an aldehyde, and this is derivatized with a hydrazide reagent to form a hydrazone adduct. Both chemical steps are classical, direct, and reliable; thus, it was readily possible to demonstrate selective N-terminal modification both of small peptides (Figures 1–3) and a larger protein (Figures 5, 6, and 9). The major issues requiring study have been the selectivity with which the desired oxidation can be achieved, and the stability of the hydrazone adducts once formed. The method could not be effective if periodate invariably caused widespread oxidation at different amino acid residues, nor would it be satisfactory if it generated conjugates that lacked the requisite stability for biochemical experiments such as receptor binding assays and cell sorting.

Considerations relating to the oxidative step should also apply to the method described by Rose et al. (8). To effect C-terminal site-directed tagging, they proposed the use of carboxypeptidase-catalyzed coupling of 1,3-diamino-2-propanol to peptides followed by periodate oxidation of the resulting 2-amino alcohol as a means to generate an aldehyde for subsequent modification.

Periodate oxidation of 2-amino alcohols $\text{—CH(NH}_2\text{)CH(OH)—}$ is a very fast reaction, reportedly 1000-fold faster than the periodate oxidation of 1,2-diols (9–13, 20, 21). As a result, selective oxidation of a 2-amino alcohol structure in a protein is possible even though other side chains are potentially susceptible to oxidation. This was used to convert N-terminal Ser to Gly in corticotropin (16) and to reverse reductive hydroxyisopropylation (22) or reductive dihydroxypropylation (23) of amino groups. Periodate effects quantitative oxidation of N-terminal Ser when present in only a low molar excess over peptide, as demonstrated by the oxidations of SYSMEHFRWG (Figure 3a) and mIL-1 α (Figure 5A). The use of mass spectrometry has recently simplified the analysis of oxidative reactions in peptides, so that anomalous instances of a competing reaction that matches or exceeds the rate of the desired process can readily be detected.

Periodate oxidation of SYSMEHFRWG in the pH range 4–8 occurred at the N-terminus and at Met. The Tyr, Trp, and His residues were not appreciably oxidized under the conditions of the experiment (see the methods). The conversion of Met to its sulfoxide was favored by acidification, while the desired N-terminal reaction was strongly favored at pH 7–8 (Figure 3) (12). Met residues in peptides vary in their susceptibility to oxidation (24, 25), and there may be cases where oxidation of a particular Met will be accelerated to a rate closer to that of the reaction with N-terminal Ser; in synthetic peptides, a possible countermove will be to replace the sensitive Met with norleucine. Peptides containing a free thiol probably should not be used because of their extreme susceptibility to oxidation (10), but the possibility of protecting thiols by reversible blocking remains to be explored.

We have not studied the periodate susceptibility of either disulfide bonds or protein-linked carbohydrates in relation to the rapid oxidation of 2-amino alcohols. It seems quite

possible, given the reported preferential oxidation of 2-amino alcohols relative to 1,2-diols at pH 7–8, that the present method can be applied successfully to glycoproteins. Conversely, however, O'Shannessy and Wilchek (26) noted that periodate oxidation of glycoproteins with N-terminal Ser or Thr probably cannot be directed selectively to the carbohydrates without also generating an aldehyde at the N-terminus.

The conjugation of α -N-glyoxylyl peptides with hydrazides proceeds under mild conditions, generally going to near completion in 2–16 h at room temperature. Aqueous buffers of pH 4.5 have been used, sometimes with the addition of 8%–25% acetonitrile to maintain solubility of a hydrophobic reagent such as biotin-X-hydrazide. Progress of the reactions can be monitored by reversed-phase HPLC, although when hydrazides containing a highly electronegative substituent (such as Cascade Blue hydrazide) are used, the solvent pH should be pH 4–7; the hydrazone formed between glyoxylyl-YS-MEHFRWG and Cascade Blue hydrazide decomposed with increasing time of residence when adsorbed on a column in the presence of solvents containing 0.1% TFA (not shown).

While hydrazones are acid-labile, they are relatively stable at pH 6–8 (Figure 4) and form the basis of several schemes for conjugating biomolecules (26, 27). The ability of N-terminally biotinylated mIL-1 α to remain stable through SDS-PAGE (including sample preparation with heating in the presence of β -mercaptoethanol and SDS) (Figure 5B) is a good indication of the stability of such conjugates. In addition, our many successful recoveries of hydrazone conjugates from HPLC experiments performed using solvents containing 0.1% TFA (pH \sim 2.1) show that at least a selection of them, although perhaps not all (see Results), can endure this valuable procedure. In all such cases, however, samples have been kept cold when possible and the acidic solvent has been removed at the first opportunity. Labile hydrazones require chromatography at pH 4–7.

Application of the method described here to site-directed modification at internal and C-terminal loci will require peptides synthesized with a strategically located residue of hydroxylysine. A barrier has been the commercial unavailability of L-hydroxylysine, which (in suitably protected form) is required for the synthesis of peptides that contain hydroxylysine and have an all-L peptide backbone. Using such peptides, it will be possible to produce peptide conjugates which are tagged at the site of the hydroxylysine. Hydroxylysine in peptides has been shown to undergo rapid periodate oxidation to create an aldehyde (28).

The experiments presented here document the feasibility of an approach to site-directed chemical modification of peptides and certain proteins. The use of periodate does create a need for careful analysis of products for potential side reactions. On the other hand, the desired reaction of periodate with 2-amino alcohols is very fast and selective, and the potential for side reactions can be limited by using very low periodate:protein molar ratios. Also, the routine application of mass spectrometry to peptide and protein chemistry has greatly increased the precision with which peptide modifications can be monitored. This simple and direct procedure may prove to be a useful option among strategies for site-directed protein and peptide tagging.

ACKNOWLEDGMENT

We thank many colleagues for helpful advice and support, including G. C. Andrews, L. J. Contillo, G. O.

Daumy, D. E. Danley, H. B. F. Dixon, M. E. Kelly, A. J. Lanzetti, I. G. Otterness, A. R. Proctor, K. J. Rosnack, N. A. Saccomano, A. D. Vodenlich, R. A. Volkmann, and P. T. Wingfield.

LITERATURE CITED

- (1) Bayer, E. A., and Wilchek, M. (1990) Protein Biotinylation. *Methods Enzymol.* 184, 138-160.
- (2) Laveille, S., Chassaing, G., Beaujouan, J. C., Torrens, Y., and Marquet, A. (1984) Binding affinities to rat brain synaptosomes—synthesis of biotinylated analogues of Substance P. *Int. J. Pept. Protein Res.* 24, 480-487.
- (3) Arya, R., and Gariépy, J. (1991) Rapid Synthesis and Introduction of a Protected EDTA-like Group during the Solid-Phase Assembly of Peptides. *Bioconjugate Chem.* 2, 323-326.
- (4) Drijfhout, J. W., Bloemhoff, W., Poolman, J. T., and Hoogerhout, P. (1990) Solid-Phase Synthesis and Applications of N-(S-Acetylmercaptoacetyl) Peptides. *Anal. Biochem.* 187, 349-354.
- (5) Wetzel, R., Halualani, R., Stults, J. T., and Quan, C. (1990) A General Method for Highly Selective Cross-linking of Unprotected Polypeptides via pH-controlled Modification of N-terminal α -Amino Groups. *Bioconjugate Chem.* 1, 114-122.
- (6) Schwarz, A., Wandrey, C., Bayer, E. A., and Wilchek, M. (1990) Enzymatic C-Terminal Biotinylation of Proteins. *Methods Enzymol.* 184, 160-162.
- (7) Rose, K., Vilaseca, L. A., Werlen, R., Meunier, A., Fisch, I., Jones, R. M. L., and Offord, R. E. (1991) Preparation of Well-Defined Protein Conjugates Using Enzyme-Assisted Reverse Proteolysis. *Bioconjugate Chem.* 2, 154-159.
- (8) Rose, K., Jones, R. M. L., Sundaram, G., and Offord, R. E. (1989) Attachment of Linker Groups to Carboxyl Termini Using Enzyme-assisted Reverse Proteolysis. *Peptides 1988* (G. Jung, and E. Bayer, Eds.) pp 274-276, Walter de Gruyter & Co., New York.
- (9) Nicolet, B. H., and Shinn, L. A. (1939) The Action of Periodic Acid on α -Amino Alcohols. *J. Am. Chem. Soc.* 61, 1615.
- (10) Dixon, H. B. F., and Fields, R. (1972) Specific Modification of NH_2 -Terminal Residues by Transamination. *Methods Enzymol.* 25, 409-419.
- (11) Dixon, H. B. F. (1984) N-Terminal Modification of Proteins—A Review. *J. Protein Chem.* 3, 99-108.
- (12) Sklarz, B. (1967) Organic Chemistry of Periodates. *Q. Rev., Chem. Soc.* 21, 3-28.
- (13) Offord, R. E. (1990) Chemical Approaches to Protein Engineering. *Protein Design and the Development of New Therapeutics and Vaccines* (J. B. Hook and G. Poste, Eds.) pp 253-282, Plenum Publishing Corporation, New York.
- (14) Daumy, G. O., Merenda, J. M., McColl, A. S., Andrews, G. C., Franke, A. E., Geoghegan, K. F., and Otterness, I. G. (1989) Isolation and Characterization of Biologically Active Murine Interleukin-1 α Derived from Expression of a Synthetic Gene in *Escherichia coli*. *Biochim. Biophys. Acta* 998, 32-42.
- (15) Clamp, J. R., and Hough, L. (1965) The Periodate Oxidation of Amino Acids with Reference to Studies on Glycoproteins. *Biochem. J.* 94, 17-24.
- (16) Dixon, H. B. F., and Weitkamp, L. R. (1962) Conversion of the N-Terminal Serine Residue of Corticotrophin into Glycine. *Biochem. J.* 84, 462-468.
- (17) Wingfield, P., Graber, P., Shaw, A. R., Gronenborn, A. M., Clore, G. M., and MacDonald, H. R. (1989) Preparation, characterization, and application of interleukin-1 β mutant proteins with surface-accessible cysteine residues. *Eur. J. Biochem.* 179, 565-571.
- (18) Chollet, A., Bonnefoy, J.-Y., and Odermatt, N. (1990) Preparation, application and biological characterization of interleukin-1 β mutant protein biotinylated at a single site. *J. Immunol. Methods* 127, 179-185.
- (19) D'Santos, C. S., Nicholson, G. C., Mosely, J. M., Evans, T., Martin, T. J., and Kemp, B. E. (1988) Biologically Active, Derivatizable Salmon Calcitonin Analog: Design, Synthesis and Applications. *Endocrinology* 123, 1483-1488.
- (20) Barlow, C. B., Guthrie, R. D., and Prior, A. M. (1966) Periodate Oxidation of Amino Sugars. *Chem. Commun.* pp 268-269.
- (21) Geoghegan, K. F., and Dixon, H. B. F. (1989) Synthesis of 2-Aminoethylarsonic acid. A new synthesis of primary amines. *Biochem. J.* 260, 295-297.
- (22) Geoghegan, K. F., Ybarra, D. M., and Feeney, R. E. (1979) Reversible Reductive Alkylation of Amino Groups in Proteins. *Biochemistry* 18, 5392-5399.
- (23) Acharya, A. S., and Manjula, B. N. (1987) Dihydroxypropylation of Amino Groups of Proteins: Use of Glyceraldehyde as a Reversible Reagent for Reductive Alkylation. *Biochemistry* 26, 3524-3530.
- (24) Knowles, J. R. (1965) The Role of Methionine in α -Chymotrypsin-Catalyzed Reactions. *Biochem. J.* 95, 180-190.
- (25) Penner, M. H., Yamasaki, R. B., Osuga, D. T., Babin, D. R., Meares, C. F., and Feeney, R. E. (1983) Comparative Oxidations of Tyrosines and Methionines in Transferrins: Human Serum Transferrin, Human Lactotransferrin, and Chicken Ovotransferrin. *Arch. Biochem. Biophys.* 225, 740-747.
- (26) O'Shannessy, D. J., and Wilchek, M. (1990) Immobilization of Glycoconjugates by Their Oligosaccharides: Use of Hydrazido-Derivatized Matrices. *Anal. Biochem.* 191, 1-8.
- (27) Kaneko, T., Willner, D., Monkovic, I., Knipe, J. O., Braslawsky, G. R., Greenfield, R. S., and Vyas, D. M. (1991) New Hydrazone Derivatives of Adriamycin and Their Immunoconjugates—A Correlation between Acid Stability and Cytotoxicity. *Bioconjugate Chem.* 2, 133-141.
- (28) Van Slyke, D. D., Hiller, A., and MacFadyen, D. A. (1941) The Determination of Hydroxylysine in Proteins. *J. Biol. Chem.* 141, 681-705.

Registry No. SIGSLAK, 115918-58-6; SYSMEHFRWG, 2791-05-1; TIGSLAK, 138354-10-6; α -N-glyoxylyl-(IGSLAK), 138354-05-9; α -N-glyoxylyl-(YSMEHFRWG), 138354-06-0; biotin-X-(YSMEHFRWG), 138354-09-3; biotin-X-hydrazide/ α -N-glyoxylyl-(IGSLAK) hydrazone conjugate, 138354-07-1; lucifer yellow/ α -N-glyoxylyl-(IGSLAK) hydrazone, 138354-08-2; biotin-X-hydrazide lucifer yellow CH, 67769-47-5.

Site-Specific Modification of a Fragment of a Chimeric Monoclonal Antibody Using Reverse Proteolysis¹

Igor Fisch,* Gabriel Künzi, Keith Rose, and Robin E. Offord

Département de Biochimie Médicale, Centre Médical Universitaire, 1 rue Michel-Servet, 1211 Geneva 4, Switzerland. Received November 7, 1991

We propose a novel method for the site-specific labeling of antibodies under mild conditions and give as an example the modification of an F(ab')₂-like fragment of the chimeric monoclonal antibody B72.3. The F(ab')₂-like fragment was produced by the action of the protease lysyl endopeptidase. Reverse proteolysis, catalyzed by the same enzyme, was then used to attach carbohydrazide specifically to the carboxyl termini of the heavy chains of the fragment. Finally, a radiolabeled chelator possessing an aldehyde group was conjugated to the modified fragment through a hydrazone linkage. The resulting site-specifically labeled F(ab')₂-like fragment was characterized by gel electrophoresis and by enzymic digestion. It was found to possess immunoreactivity equivalent to that of the unmodified F(ab')₂-like fragment as determined by immunofluorescence and ELISA (enzyme-linked immunosorbent assay) techniques. The advantages and disadvantages of this labeling method, which appear to be of quite general applicability, are discussed.

INTRODUCTION

Monoclonal antibodies usually require modification if they are to be used successfully for in vivo diagnosis (immunoscintigraphy) or for therapy. For immunoscintigraphy, monoclonal antibodies are labeled with γ -emitting isotopes by coupling, for example, iodine-131 or iodine-123 to tyrosine residues (Goldenberg et al., 1978; Moldofsky et al., 1984), or by coupling to lysine residues a chelator which binds a radiometal such as indium-111 (Rainsbury et al., 1983; Khaw et al., 1980; Scheinberg et al., 1982; Hnatowitch et al., 1983; Murray et al., 1985), or by the passive adsorption of species such as technetium-99m (Morrison et al., 1984). For therapeutic applications, antibodies are coupled to radioactive isotopes (e.g. Epenetos et al., 1982; Order et al., 1980; Carrasquillo et al., 1984), cytotoxic drugs (e.g. Baldwin et al., 1982; Ghose & Blair, 1978; Hurwitz et al., 1979; Gallego et al., 1984), or toxins (e.g. Youle & Neville, 1980) in an attempt to target such cytotoxic substances to pathological sites. These modifications of an antibody generally involve covalent attachment of an agent either to the side chain of residues such as tyrosine, lysine, aspartic, and glutamic acid or to sulfhydryl groups, the latter being generated either by reduction of cystine residues or by reaction of the antibody with reagents such as 2-iminothiolane or *N*-succinimidyl 3-(pyridyldithiol)propionate (SPDP). All of the methods mentioned above for labeling antibodies have a major disadvantage: a heterogeneous product is generated with regard to the site of labeling. This disadvantage may be avoided by directing the modification to a specific site, ideally far from the antigen-binding site. Site-specific labeling of oxidized carbohydrate present on immunoglobulins of the IgG class has already been reported (Murrayama et al., 1978) and exploited (e.g. Rodwell et al., 1986; Pochon et al., 1989). However, this latter labeling technique is clearly not applicable to polypeptides or proteins that do not carry a sugar moiety, as is often the

case for F(ab')₂ or Fab fragments of an antibody. In addition, for those IgG molecules that possess more than one glycosylated site, oxidation of carbohydrate will not be restricted to a single site.

More recently, the specificity of proteases working in reverse has been used to attach, to the carboxyl terminus of a polypeptide chain, a chemical group which is not present in proteins and the reactivity of which can be used to conjugate other materials, for example chelated radiometals, cytotoxic drugs, or toxins. Thus, lysyl endopeptidase has been used to couple carbohydrazide to the carboxyl terminus of des-Ala^{B30}-insulin (Rose et al., 1991). The modified insulin was then conjugated to the chelator HCO-*m*-C₆H₄CH=NOCH₂CO-ferrioxamine through a hydrazone bond. The conditions for both the coupling and conjugation reactions are very mild indeed, which prompted us to use this potentially general site-specific method to label the carboxyl terminus of the heavy chains of a monoclonal antibody fragment. A preliminary account of some of our work in this field has already appeared (Fisch et al., 1991).

The F(ab')₂ fragment of an antibody is often a better carrier of radionuclides for immunoscintigraphy than is the intact antibody (Kurkela et al., 1988). Loss of the Fc region of the antibody frequently leads to decreased nonspecific binding (Lamoyi, 1986), and the more rapid kinetics of clearance of F(ab')₂ fragments from healthy organs may increase the tumor to background ratio (Buehger et al., 1983; Herlyn et al., 1983; Mach et al., 1985; Mather et al., 1987), both of which factors should improve the quality of images obtained during immunoscintigraphy.

We chose to work with the F(ab')₂-like fragment derived from a chimeric form of the monoclonal antibody B72.3 (Whittle et al., 1984). The chimeric form, cB72.3, has a human IgG₄ constant region (γ 4) and binds to a glycoprotein complex with a molecular weight of about 220-440 kDa named TAG-72 and present in many carcinomas. cB72.3 reacts with approximately 50% of human mammary carcinomas and with 80% of the colon carcinomas tested, but does not react appreciably with normal mammary tissue, with normal colon tissue, or with a variety of normal adult human tissues tested using immunohistochemical techniques (Nutti et al., 1982; Colcher et al.,

¹ Abbreviations used: ELISA, enzyme-linked immunosorbent assay; SDS-PAGE, sodium dodecyl sulfate polyacrylamide gel electrophoresis; KTI, kallikrein trypsin inhibitor; FITC, fluorescein isothiocyanate; BSA, bovine serum albumin; DMSO, dimethyl sulfoxide; PBS, phosphate-buffered saline.

* Author to whom correspondence should be addressed.

1984). In the present study, we describe conditions for attaching a carbonylhydrazide group to the carboxyl terminus of the shortened heavy chains of the F(ab')₂-like fragment generated by lysyl endopeptidase digestion of the antibody. We also give conditions for the conjugation of a chelator to the carbonylhydrazide group of the modified F(ab')₂-like fragment. Preliminary work with a series of other antibodies (not described) shows that our two-step site-specific modification procedure is of fairly general applicability.

EXPERIMENTAL PROCEDURES

Preparation of the Conjugate—Time-Course Studies. *Proteolysis of cB72.3.* To 0.86 mL of cB72.3 (19 mg/mL in 0.1 M ammonium bicarbonate) was added 16.3 μ L of lysyl endopeptidase (freshly prepared as a solution 10 mg/mL in water; from *Achromobacter lyticus*, WAKO Pure Chemical Co., Japan; final enzyme:substrate ratio of 1:100, w/w). After incubation at 37 °C for 8 h, the digest was cooled to 0 °C, at which temperature it may be stored for up to 96 h. Aliquots were removed for analysis by SDS-PAGE (sodium dodecyl sulfate polyacrylamide gel electrophoresis), under both reducing and nonreducing conditions (see below).

Coupling of Carbonylhydrazide by Reverse Proteolysis. A 420- μ L portion of the digest, now at a concentration of 18.6 mg/mL in 0.1 M ammonium bicarbonate, was added to 132.7 mg of solid carbonylhydrazide (Fluka, Buchs, Switzerland), giving a final concentration of 2.5 M carbonylhydrazide. The pH was lowered to 5.5 (uncorrected glass electrode) by addition of 12.5 μ L of glacial acetic acid. Lysyl endopeptidase (80 μ L of a freshly prepared solution 10 mg/mL in water) was added in order to obtain a final enzyme:substrate ratio of 1:10 (w/w). The sample was incubated at room temperature (23 °C). At various times (1, 2, 4, 8, and 24 h), an aliquot of 112 μ L of the coupling reaction solution was removed and the reaction stopped by addition of 20.5 μ L of kallikrein trypsin inhibitor (KTI or Trasylol, BAYER), freshly prepared as a 78 mg/mL solution in water (final enzyme:inhibitor ratio of 1:10, w/w). In a control series of experiments, the enzyme used for the coupling step was replaced by 80 μ L of KTI at 10 mg/mL in water. At each time point, for experimental samples and for controls, carbonylhydrazide and enzyme were separated from the F(ab')₂-like fragment by gel filtration on a Superose-12 column (30 cm \times 1 cm i.d. FPLC system, Pharmacia, Uppsala, Sweden) equilibrated and eluted with 0.1 M acetate buffer (counterion, Na⁺) at pH 4.6, at a flow rate of 0.4 mL/min. Effluent was monitored at 280 nm. The peak containing the protein fragment was collected in the presence of 20.5 μ L of KTI (78 mg/mL in water), to avoid possible residual action on the coupled F(ab')₂-like fragment of any unseparated enzyme. The samples (experimental and controls) were then concentrated at 4 °C in a centrifugal membrane concentrator having a molecular weight cutoff of 10 kDa (Centricon-10, AMICON). The concentrations of the experimental and control samples were estimated by UV absorption at 280 nm using an extinction coefficient of $\epsilon^{1\%}_{280} = 14.75$. This value is that of the intact cB72.3, the amino acid sequence of which is known (Whittle et al., 1984). The F(ab')₂-like fragment, which contains a similar proportion of Tyr and Trp residues to the intact antibody, will have a similar weight-based extinction coefficient. The concentration of the antibody fragment was thus overestimated due to the presence of any residual KTI (relative molecular mass, 6.5 kDa) which was not removed by the centrifugal membrane concentrator (cutoff 10 kDa), but this overestimation is of no consequence (see Results and

Discussion). The gel filtration step which followed the conjugation reaction with HCO-*m*-C₆H₄CH=NOCH₂CO-ferrioxamine (see below) permitted the proportion of remaining KTI to be established.

Preparation of HCO-*m*-C₆H₄CH=NOCH₂CO-ferrioxamine. Desferrioxamine was loaded with iron-55 according to a published procedure (Prelog & Walser, 1962) but on a much smaller scale. The isotope was supplied by Amersham, England, as iron(III) chloride in 0.1 M HCl and was of low (1–50 mCi/mg) specific activity. The resulting ferrioxamine was converted to [(aminooxy)-acetyl]ferrioxamine as previously described (Pochon et al., 1989). Conversion of the labeled compound to HCO-*m*-C₆H₄CH=NOCH₂CO-ferrioxamine followed techniques already described for unlabeled material (Rose et al., 1991). The specific activity of the chelator was determined by optical absorption at 430 nm, using an extinction coefficient of $\epsilon^{1M}_{430} = 2650$, and by the radioactivity, which was measured with a scintillant liquid (Pico-fluor 40, Packard, Canberra, Australia) in a liquid scintillation counter (Beckman, Model LS6800). The specific activity of the chelator was thus determined to be 8.2×10^4 dpm/nmol of HCO-*m*-C₆H₄CH=NOCH₂CO-ferrioxamine for both the time-course studies and the characterization studies.

Hydrazone Formation. For each time point, the carbonylhydrazide-coupled F(ab')₂-like fragment (at the nominal concentration estimated by UV absorption at 280 nm) was incubated in 0.1 M acetate buffer at pH 4.6, counterion Na⁺, with a nominal excess of 5 equiv (mol/mol) of the chelator HCO-*m*-C₆H₄CH=NOCH₂CO-ferrioxamine labeled with iron-55. The chelator was added as a portion of a 3.1 mM stock solution in the acetate buffer. The control series was treated similarly. After 20 h at room temperature, the conjugated fragment was separated from residual KTI and free labeled chelator on the Superose-12 gel filtration column equilibrated and eluted with 0.1 M ammonium bicarbonate buffer, at 0.8 mL/min. The effluent was monitored at 280 nm. Fractions containing the conjugated fragment were pooled; the final solution was analyzed by UV spectroscopy, and portions were counted for radioactivity. The optical density at 280 nm due to the conjugated HCO-*m*-C₆H₄CH=NOCH₂CO-ferrioxamine was then calculated from the UV spectrum of the model hydrazone (CH₃)₃COCONHNHCONHN=HC-*m*-C₆H₄CH=NOCH₂CO-ferrioxamine ($\epsilon^{1M}_{280} = 26\,500$). Subtraction of this contribution to the absorbance at 280 nm, from the observed absorbance of the protein conjugate at this wavelength, permitted calculation of the protein concentration, and thus the conjugation ratio was expressed as moles of iron-55 per mole of F(ab')₂-like fragment.

Characterization of the Conjugate. Cleavage of the Chelator from the Protein. An 80- μ L portion of the labeled F(ab')₂-like fragment prepared as described above, at a nominal concentration of 0.47 mg/mL (measured by UV absorption at 280 nm as before, in 0.1 M ammonium bicarbonate buffer) and a specific activity of 1.4×10^5 dpm/nmol, was incubated with 0.75 μ L of lysyl endopeptidase (freshly prepared as a 1 mg/mL solution in water). After 6 h at 37 °C, 1 μ L of KTI (7.8 mg/mL in water) was added to stop the reaction. In a control experiment, the enzyme was replaced by addition of 0.75 μ L of KTI (1 mg/mL in water). The F(ab')₂-like fragment was then separated from enzyme, inhibitor, and released chelator by gel filtration on the Superose-12 column equilibrated and eluted with 0.1 M ammonium bicarbonate buffer, at 0.8 mL/min. The effluent was monitored at 280 nm. Fractions containing the fragment were pooled; the final

solution was analyzed by UV spectroscopy and SDS-PAGE (see below), and portions were counted for radioactivity.

In vitro Immunoreactivity Tests. (1) Cell Binding. LS174T cells (ATCC, Rockville, Maryland) were used for the immunofluorescence test as described (Nairn, 1976). Briefly, cells were removed from flasks with 0.1% trypsin containing 5 mM EDTA and washed twice in 1× PBS (Gibco, Brl) containing 0.2% BSA and 0.05% NaN₃. A 1-mL portion of the suspension containing 1 million cells was centrifuged at 1000 rpm for 5 min (Megafuge, Heraeus S.A., Zurich, Switzerland) and the supernatant was removed. A 50-μL sample of iron-55-labeled F(ab')₂-like fragment (coupled 4 h with carbonylhydrazide and having a specific activity of 1.4×10^5 dpm/nmol; 5 μg in PBS containing 0.2% BSA and 0.05% NaN₃) was applied to the pellet and gently mixed, and the suspension was incubated for 1 h at room temperature (23 °C). Cells were centrifuged as described above and washed twice with 1 mL of PBS containing 0.2% BSA and 0.05% NaN₃. A 50-μL sample of FITC-coupled anti-human IgG (Sigma cat. no. F 0132, 20-fold diluted in PBS containing 0.2% BSA and 0.05% NaN₃) was added to the pellet, gently mixed, and incubated for 1 h at room temperature (23 °C). Cells were centrifuged as described above, washed twice with 1 mL of PBS containing 0.2% BSA and 0.05% NaN₃, and observed with a fluorescence microscope (Dialux 20 ED, Leitz, Wetzlar GMBH, Germany).

(2) Antigen Binding. Quantitation of the immunoreactivity using an enzyme-linked immunosorbent assay (ELISA) test was performed as already described (Engvall, 1980).

SDS-PAGE. Sodium dodecyl sulfate polyacrylamide gel electrophoresis (SDS-PAGE) was performed according to Laemmli (1970). The acrylamide:bisacrylamide ratio was 30:0.8, w/w. For nonreducing conditions, the concentration of this mixture was 8% (w/w), and for reducing conditions it was 12% (w/w).

RESULTS AND DISCUSSION

Lysyl Endopeptidase Digestion of cB72.3. Lysyl endopeptidase is a protease which cleaves a polypeptide chain specifically at the carboxyl side of lysine residues (Masaki et al., 1981). A time-course of the digestion of cB72.3 with lysyl endopeptidase was followed by SDS-PAGE analysis, but only the 8-h digestion is shown. Under nonreducing conditions (Figure 1A), the intact cB72.3 (lane 3) shows a major band whose mobility corresponds to a relative molecular mass of 150 kDa and also some contaminants at about 130 and 70 kDa. The band whose mobility corresponds to a relative molecular mass of 150 kDa (intact antibody, lane 3) disappeared after 8 h of digestion and a new band was formed (lane 4), whose relative molecular mass (110 kDa) is similar to that of a peptic F(ab')₂ fragment. The intensity of the band at 110 kDa in lane 4 (the digest) is lower than observed in lanes 5–8 (fractions from gel filtration). This is due to the residual activity of the protease, which was still present when the digest was loaded onto the gel.

Under reducing conditions (Figure 1B), the band with a relative molecular mass of 50 kDa (heavy chain) in the undigested cB72.3 (Figure 1B, lane 2) was absent after 8 h of digestion and a new band whose mobility corresponds to 28 kDa appeared (lane 3). In contrast, the band with a relative molecular mass of 26 kDa (light chain) in the undigested cB72.3 (lane 2) remained intact after 8 h of digestion (lane 3). As discussed above, the relative intensities of the bands in lane 3 (the digest) are lower than those in lanes 4–7 (fractions from gel filtration) due

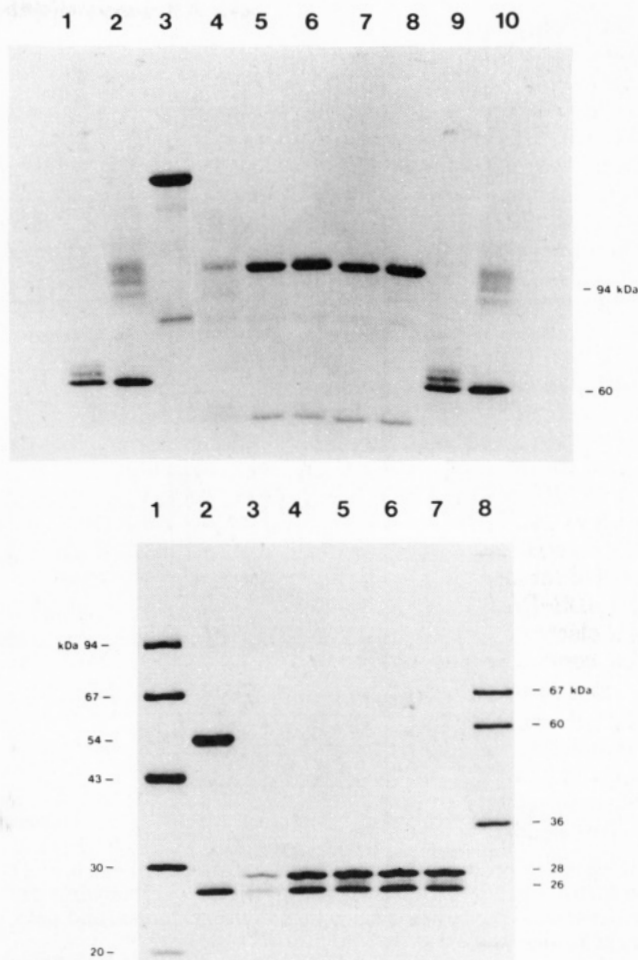


Figure 1. (A) SDS-PAGE under nonreducing conditions of the coupling reaction, stained with Coomassie Blue R250: lanes 1, 2, 9, and 10, molecular weight markers; lane 3, intact antibody cB72.3; lane 4, cB72.3 digested with 1% (w/w) lysyl endopeptidase for 8 h at 37 °C; lanes 5 and 7, F(ab')₂-like fragment coupled with carbonylhydrazide for 4 and 24 h, respectively; lanes 6 and 8, control samples of F(ab')₂-like fragment after 4 and 24 h, respectively, in coupling conditions but without lysyl endopeptidase. (B) SDS-PAGE under reducing conditions [5% (v/v) β-mercaptoethanol] of the coupling reaction, stained with Coomassie Blue R250: lanes 1 and 8, the molecular weight markers; lane 2, intact antibody cB72.3; lane 3, cB72.3 digested with 1% (w/w) lysyl endopeptidase for 8 h at 37 °C; lanes 4 and 6, F(ab')₂-like fragment coupled with carbonylhydrazide for 4 and 24 h, respectively; lanes 5 and 7, control samples of the F(ab')₂-like fragment after 4 and 24 h, respectively, in coupling conditions but without lysyl endopeptidase.

to the presence of protease. When protease is removed by gel filtration, no bands with lower relative molecular mass appeared (lanes 4–7), indicating the absence of nicks on the light chains of the digested cB72.3. Thus, SDS-PAGE data show that lysyl endopeptidase produces, very efficiently, a F(ab')₂-sized fragments from cB72.3. Examination of the sequence of the heavy chain (Whittle et al., 1984) in the CH2 domain provides only two possible sites of cleavage. These are Lys²⁴⁰ and Lys²⁴².

Reverse Proteolytic Coupling of Carbonylhydrazide to the F(ab')₂-like Fragment of cB72.3. The coupling of carbonylhydrazide by reverse proteolysis to the carboxyl terminus of a polypeptide chain (insulin) has already been described (Rose et al., 1991), and it was shown that the coupling yield was increased in the presence of an organic cosolvent. In 50% DMSO (dimethyl sulfoxide), yields up to 95% were obtained, whereas in the absence of DMSO, the coupling yields approached only 84%. In the present

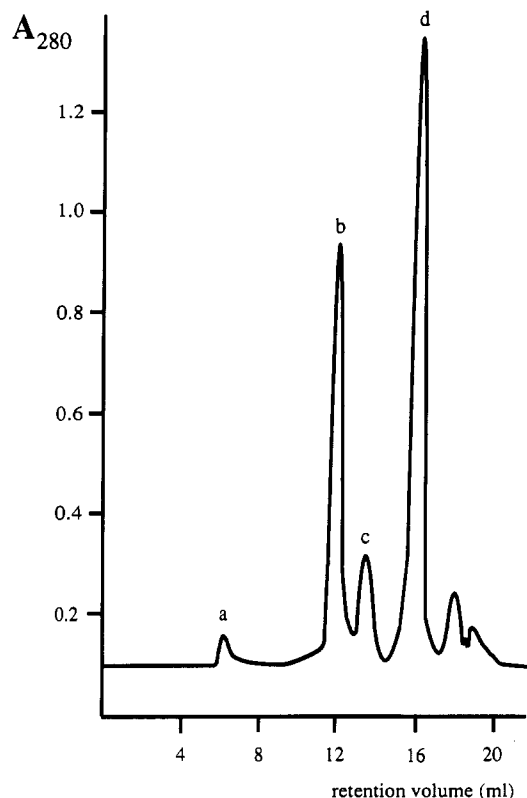


Figure 2. Gel filtration profile of the coupling reaction between a $F(ab')_2$ -like fragment and carbohydrazide, after 4 h. Peak a, at 6.8 mL, is probably due to aggregated material. Peak b, at 12 mL, is the $F(ab')_2$ -like fragment coupled with carbohydrazide. Peak c, at 13.5 mL, is the enzyme-inhibitor complex, and peak d, at 16 mL, the excess of inhibitor (KTI).

study, preliminary attempts to couple carbohydrazide in 50% DMSO led to precipitation of the $F(ab')_2$ -like fragment, and so all subsequent work was performed in fully aqueous solution, which in any case would be preferable from the point of view of immunoreactivity preservation. Given that no organic cosolvent, which tends to suppress further proteolytic cleavage, was used, and given the large quantity of enzyme added for the coupling step, SDS-PAGE analysis was performed to test for any degradation of the $F(ab')_2$ -like fragment during the coupling reaction. Under nonreducing (Figure 1A) and reducing conditions (Figure 1B), no evidence for the production of lower molecular weight material was found, even after 24 h (Figure 1A, lane 7, and Figure 1B, lane 6). Figure 2 shows the gel filtration profile of the coupling reaction after 4 h of incubation with carbohydrazide. The coupled $F(ab')_2$ -like fragment is seen to elute separate from enzyme-inhibitor complex, inhibitor, and carbohydrazide.

Hydrazone Formation. The degree of incorporation of carbohydrazide into the $F(ab')_2$ -like fragment cannot be directly measured, but is obtained by conjugation with iron-55-labeled $HCO-m-C_6H_4CH=NOCH_2CO$ -ferrioxamine through a hydrazone linkage. The stability of hydrazone linkages has been discussed by King et al. (1986), who showed that 98% of a model hydrazone (*N*-acetylhydrazone of *p*-carboxybenzaldehyde) remained intact at pH 8.0, even after 72 h of incubation at 25 °C. The specificity of such conjugation reactions for a hydrazone (rather than side-chain amino) group has already been demonstrated in previous work (Rose et al., 1991; King et al., 1986). Figure 3 shows the gel filtration profile of the conjugation reaction between the $F(ab')_2$ -like fragment (coupled with carbohydrazide for 4 h) and iron-55-labeled $HCO-m-C_6H_4CH=NOCH_2CO$ -ferrioxamine. An excel-

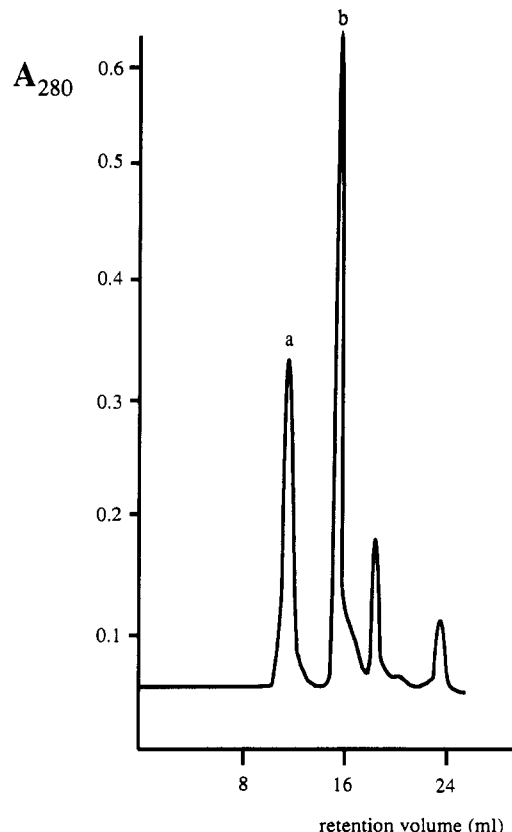


Figure 3. Gel filtration profile of the conjugation reaction between carbohydrazide-coupled $F(ab')_2$ -like fragment and $HCO-m-C_6H_4CH=NOCH_2CO$ -ferrioxamine after 20 h. Peak a, at 12 mL, represents the conjugated $F(ab')_2$ -like fragment, and peak b, at 16 mL, the inhibitor (KTI).

Table I. Hydrazone Formation

sample ^a	nominal concentration, ^b mg/mL	nmol coupled ^c	specific activity of the fragment, dpm/nmol of conjugate $\times 10^{-4}$
E ₁	4.4	5	5.5
E ₂	3.0	3.3	12
E ₄	4.0	4	14
E ₈	4.0	5	9.5
E ₂₄	2.9	4.4	16
C ₁	3.3	5	0.3
C ₂	3.2	5	0.9
C ₄	2.5	5	0.8
C ₈	3.7	5	2.7
C ₂₄	3.7	5	4.8

^a E_n and C_n represent the experimental and control samples, respectively, after *n* hours of coupling with carbohydrazide. ^b Nominal concentration after the coupling step with carbohydrazide, overestimated due to the presence of residual KTI. ^c Represents the quantity, based on the nominal concentrations, of $F(ab')_2$ -like fragment (which had been incubated with carbohydrazide) which was conjugated with iron-55-labeled $HCO-m-C_6H_4CH=NOCH_2CO$ -ferrioxamine.

lent separation of protein and small molecules is achieved. The KTI which was not removed during the membrane concentration step is clearly visible (Figure 3) and may be quantitated. Correction of the nominal fragment concentration (see Table I) for the contribution due to residual KTI permitted calculation of the actual ratios of reagent to fragment used for the conjugation reaction. This ratio, found to be between 8.3 and 16.1, was always in excess of the nominal 5-fold excess of reagent, thus the initial overestimation of fragment concentration is without consequence because reaction is essentially quantitative when using this reagent (Rose et al., 1991). Using the specific activity of the reagent (8.2×10^4 dpm/nmol) and

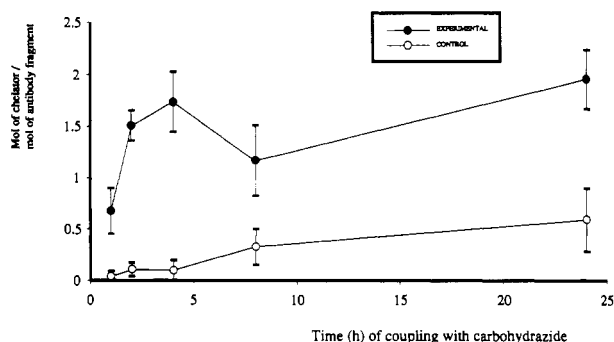


Figure 4. Time-course of the enzymatic coupling reaction: the incorporation (expressed in moles of iron-55-labeled $\text{HCO}-m\text{-C}_6\text{H}_4\text{CH}=\text{NOCH}_2\text{CO}$ -ferrioxamine/mole of $\text{F}(\text{ab}')_2$ -like fragment of the cB72.3) is shown as a function of the time of coupling with carbohydrazide. Filled circles represent the experimental samples, and open circles the control samples.

radioactivity counting of a portion of the protein peak, the concentration of the conjugated label was calculated. The results of the conjugation reaction (hydrazone formation) are given in Table I as measured specific activities and are shown graphically in Figure 4 as calculated conjugation ratios. After 4 h of coupling with carbohydrazide, the resulting coupled $\text{F}(\text{ab}')_2$ -like fragment incorporates about 1.7 mol of iron-55-labeled $\text{HCO}-m\text{-C}_6\text{H}_4\text{CH}=\text{NOCH}_2\text{CO}$ -ferrioxamine/mol of $\text{F}(\text{ab}')_2$ -like fragment. The control experiment, where during the reverse proteolysis coupling steps lysyl endopeptidase was replaced by a protease inhibitor (KTI or Trasylol), showed after 4 h of incubation with carbohydrazide an incorporation of 0.1 mol of labeled $\text{HCO}-m\text{-C}_6\text{H}_4\text{CH}=\text{NOCH}_2\text{CO}$ -ferrioxamine/mol of $\text{F}(\text{ab}')_2$ -like fragment.

Figure 4 shows, for the experimental sample, a rapid increase of the incorporation of labeled $\text{HCO}-m\text{-C}_6\text{H}_4\text{CH}=\text{NOCH}_2\text{CO}$ -ferrioxamine with the duration of the coupling step. The value of about 1.7 mol of $\text{HCO}-m\text{-C}_6\text{H}_4\text{CH}=\text{NOCH}_2\text{CO}$ -ferrioxamine per mol of $\text{F}(\text{ab}')_2$ -like fragment, attained after 4 h, is close to that expected from model experiments with insulin under similar conditions (Rose et al., 1991), where, in the absence of DMSO, about 0.7 mol of carbohydrazide was incorporated per mole of carboxyl terminal Lys. As hydrazone formation is almost quantitative when $\text{HCO}-m\text{-C}_6\text{H}_4\text{CH}=\text{NOCH}_2\text{CO}$ -ferrioxamine is used as the reagent (Rose et al., 1991; Fisch et al., 1991), and as the $\text{F}(\text{ab}')_2$ -like fragment possesses two heavy chains to which carbohydrazide may be coupled by the protease, an incorporation of 1.7 mol of $\text{HCO}-m\text{-C}_6\text{H}_4\text{CH}=\text{NOCH}_2\text{CO}$ -ferrioxamine/mol of $\text{F}(\text{ab}')_2$ -like fragments corresponds to about 0.85 mol of carbohydrazide at the C-terminus of each heavy chain. If coupling to each heavy chain is an independent event, then the value of 1.7 mol/mol corresponds (binomial distribution) to 72% of the $\text{F}(\text{ab}')_2$ -like fragment with carbohydrazide coupled to the C-terminus of both heavy chains, 26% with carbohydrazide coupled to the C-terminus of a single chain, and 2% with no carbohydrazide at all.

The control experiment (Figure 4) was performed in order to estimate any nonspecific incorporation of carbohydrazide. Values of apparent incorporation found at coupling times of 4 h or less show that, for the $\text{F}(\text{ab}')_2$ -like fragment of cB72.3, such nonspecific incorporation is a minor process. One mechanism by which carbohydrazide might be incorporated, other than enzymatically to the $\text{F}(\text{ab}')_2$ -like fragment, is through deamidation of Asn or Gln accompanied by nucleophilic attack by carbohydrazide (which is present at very high concentrations, see Experimental Procedures) rather than by a water molecule. An

alternative interpretation of the control curve of Figure 4 would be the presence of residual active enzyme from the digest, which was not totally inhibited by addition of KTI. Given the relatively low values found for the control at coupling times of 4 h and less, we did not investigate this effect further. The apparent fall in conjugation ratio at 8 h (Figure 4) was consistently observed, and we have no explanation. The optimum coupling time is about 4 h and the overall yield (moles of labeled $\text{F}(\text{ab}')_2$ -like fragment compared to moles of intact antibody taken) of the preparation of the conjugated fragment was between 30 and 45%.

Cleavage of the Labeled Fragment. To determine whether the label is in the expected position, i.e. at the carboxyl terminus of the heavy chains, the iron-55-conjugated $\text{F}(\text{ab}')_2$ -like fragment was digested with the same enzyme used in the coupling step (lysyl endopeptidase). It was expected that the enzyme, used at pH 8.0 and in the absence of carbohydrazide, would cleave the bond which had been formed at pH 5.5 in the presence of 2.5 M carbohydrazide. Such cleavage would release the label from the carboxyl terminus of antibody fragment, without degrading the latter. After 6 h of digestion at 37 °C, analysis by gel filtration showed that the specific radioactivity of the antibody fragment had been reduced from 1.4×10^5 to 8.6×10^3 dpm/nmol, i.e. to 6% of its original value. The mobility of the protein fragment on reducing and nonreducing SDS-PAGE gels remained unaffected (data not shown). In a control redigestion experiment, the enzyme was replaced by the inhibitor KTI. Under these conditions, no diminution of specific radioactivity of the conjugated $\text{F}(\text{ab}')_2$ -like fragment was observed (1.4×10^5 dpm/nmol recovered). These results indicate that the lysyl endopeptidase had coupled carbohydrazide specifically at the carboxyl termini and was then able to cleave the Lys-carbohydrazide bond of the conjugated fragment. Since lysyl endopeptidase was shown to act on the heavy chains (Figure 1) and since a degree of incorporation was found which is similar to that obtained with the insulin model (Rose et al., 1991), it is most likely that the modification is mainly restricted to the truncated heavy chains in the case of cB72.3. Indeed, autoradiography of a reducing SDS-PAGE gel to which the fragment conjugated to chelator labeled with ^{67}Ga had been applied showed labeling of the heavy chain alone (data not shown). Taking into account the uniform background of the exposed film, we were able to estimate that labeling of the light chains, if it occurs at all, represents less than 10% of that of the heavy chains. Furthermore, examination of the amino acid sequence (Whittle et al., 1984) shows the C-terminus residue of the light chain to be Cys, which is not recognized by lysyl endopeptidase. In the case of a fragment possessing Lys at the carboxyl-terminal residue of the light chain, incorporation of carbohydrazide would be expected to occur there also. This would lead to an even higher conjugation ratio, yet the modification, by being restricted to the carboxyl termini, would be remote from the antigen-binding region and would not be expected to interfere with it.

In Vitro Immunoreactivity Tests. ELISA and immunofluorescence tests were performed to investigate the effect, on the immunoreactivity of the $\text{F}(\text{ab}')_2$ -like fragment, of coupling to carbohydrazide and then conjugating a labeled aldehyde chelator to the carboxyl terminus. Results show (Figure 5) that the affinity for the antigen of the conjugated fragment remained essentially unchanged. Immunofluorescence tests showed that both the coupled and the conjugated fragment were able to bind

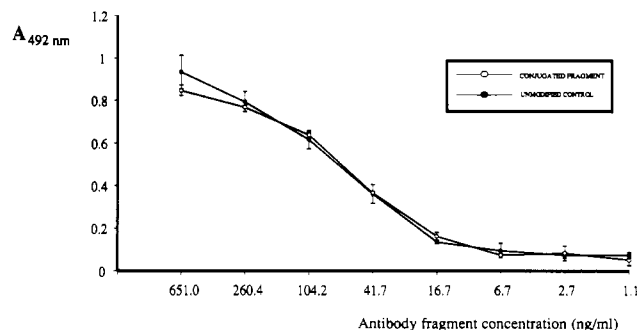


Figure 5. ELISA of unmodified F(ab')₂-like fragment (filled circles) and the fragment conjugated with iron-55-labeled HCO-m-C₆H₄CH=NOCH₂CO-ferrioxamine (open circles).

to the cell-surface antigen expressed by the cell line. Similar results (not shown) were obtained with the gallium-containing chelator derivative (prepared according to Rose et al., 1991). Gallium-67 is a γ -emitting isotope useful in radioimmunoscintigraphy which is tightly held by the desferrioxamine chelator in vivo (e.g. Pochon et al., 1989).

As the binding of the conjugated F(ab')₂-like fragment for its antigen remained essentially unchanged, it will be interesting to test such a specifically modified antibody fragment in in vivo systems. Experiments with the conjugate labeled with gallium-67 show that targeting to tumor tissue occurs in a mouse xenograft model (data not shown). Results of these experiments, including full details of the procedures used to label the chelator with small quantities of gallium-67 of high specific activity, will be published elsewhere.

CONCLUSION

Lysyl endopeptidase may be used to obtain an F(ab')₂-like fragment of the chimeric monoclonal antibody cB72.3. Reverse proteolysis may be used to attach carbohydrazide to the carboxyl terminus of the heavy chains of the F(ab')₂-like fragment. Conjugation of HCO-m-C₆H₄CH=NOCH₂CO-ferrioxamine labeled with iron-55 (and with gallium-67) to the carbohydrazide-modified F(ab')₂-like fragment did not decrease its capacity to bind antigen.

The two-step approach to protein modification described here offers the following advantages: (1) site-specific modification, giving a relatively homogeneous product, (2) carboxyl-terminal modification, far from the antigen-binding region of the antibody, (3) very mild conditions, (4) production of an intermediate of general application (coupled fragment) to which a wide variety of molecules may be attached, provided that they carry or can be made to carry an aldehyde or a keto function (Rose et al., 1991).

Our own preliminary experiments with a series of monoclonal antibodies show that the two-step approach is of fairly general applicability. Different enzymes (trypsin for example) have been employed and conjugated Fab fragments have also been produced (data not shown).

Further experiments with other monoclonal antibodies and tumor cell lines will be necessary to determine whether the site-specific labeling of an antibody fragment has more than just a theoretical advantage over the techniques currently used for labeling antibodies.

ACKNOWLEDGMENT

We thank Brigitte Dufour for expert technical assistance and Gwynfor Davies for helpful advice during the preparation of the manuscript. This work was supported by the Fonds National Suisse de la Recherche Scientifique and the Schmidheiny Foundation. We thank Celltech,

Ltd., Slough, U.K., for the gift of antibodies and for financial support. Igor Fisch thanks the Ligue Suisse contre le Cancer for a bursary.

LITERATURE CITED

- Baldwin, R. W., Embleton, M. J., and Pimm, M. W. (1982) Monoclonal antibodies for radioimmunoassay of tumors and for targeting. *Bull. Cancer* 70, 132-136.
- Buchegger, F., Haskell, C. M., Schreyer, M., Scazziga, B. R., Randin, S., Carrel, S., and Mach, J. P. (1983) Radiolabeled fragments of monoclonal antibodies against carcinoembryonic antigen for localisation of human colon carcinoma grafted into nude mice. *J. Exp. Med.* 158, 413-427.
- Carrasquillo, J. A., Krohn, K. A., Beaumier, P., McGuffin, R. W., Brown, J. P., Hellstrom, K. E., and Larson, S. M. (1984) Diagnosis of and therapy for solid tumors with radiolabeled antibodies and immune fragments. *Cancer Treat. Rep.* 68, 317-328.
- Colcher, D., Keenan, A. M., Larson, S. M., and Schlom, J. (1984) Prolonged binding of a radiolabeled monoclonal antibody (B72.3) and for the in situ radioimmunoassay of human colon carcinoma xenografts. *Cancer Res.* 44, 5744-5751.
- Engvall, E. (1980) Enzyme immunoassay ELISA and EMIT. *Methods Enzymol.* 70, 419-439.
- Epenetos, A. A., Britton, K. E., Mather, S., Shepherd, J., Granowska, M., Taylor-Papadimitriou, J., Nimmon, C. C., Durbin, H., Hawkins, L. R., Malpas, J. S., and Bodmer, W. F. (1982) Targeting of iodine-123-labelled tumor associated monoclonal antibodies to ovarian, breast, and gastrointestinal tumours. *Lancet* 2, 999-1005.
- Fisch, I., Pochon, S., Werlen, R., Jones, R. M. L., Rose, K., and Offord, R. E. (1991) Site-specific modification of antibodies by enzyme-assisted reverse proteolysis. *Peptides 1990* (E. Giralt, and D. Andreu, Eds.) pp 819-821, ESCOM, Leiden, The Netherlands.
- Gallego, J., Price, M. R., and Baldwin, R. W. (1984) Preparation of four daunomycin-monoclonal antibody 791T/36 conjugated with antitumor activity. *Int. J. Cancer* 33, 737-744.
- Ghose, T., and Blair, A. H. (1978) Antibody-linked cytotoxic agents in the treatment of cancer: current status and future prospects. *J. Natl. Cancer Inst.* 61, 657-676.
- Goldenberg, D. M., DeLand, F., Kim, E. E., Benett, S. S., Primus, F. J., VanNagell, J. R., Jr., Ester, N., DeSimone, P., and Rayburn, P. (1978) Use of radiolabeled antibodies to carcinoembryonic antigen for the detection and localization of diverse cancers by external photoscanning. *N. Engl. J. Med.* 297, 1384-1386.
- Halpern, S. E., Hagan, P. L., Garver, P. R., Koziol, J. A., Chen, A. W. N., Frincke, J. N., Bartholomew, R. M., Davies, J. S., and Adams T. H. (1983) Stability, characterization, and kinetics of ¹¹¹In-labeled monoclonal antibodies in normal animals and nude mouse-human tumor models. *Cancer Res.* 43, 5347-5355.
- Herlyn, D., Powe, J., Alair, A., Mattis, J. A., Herlyn, M., Ernst, C., Vaum, R., and Koprowski, H. (1983) Radioimmunoassay of human tumor xenografts by monoclonal antibodies. *Cancer Res.* 43, 2731-2735.
- Hnatowich, D. J., Layne, W. W., Childs, R. L., Lantaigne, D., Davies, M. A., Griffin, T. W., and Doherty, P. W. (1983) Radioactive labeling of antibody: a simple and efficient method. *Science* 220, 613-615.
- Hurwitz, E., Schecter, B., Arnon, R., and Sela, M. (1979) Binding of antitumor-immunoglobulins and their daunomycin conjugates to the tumor and its metastases. In vitro and in vivo studies with Lewis lung carcinoma. *Int. J. Cancer* 24, 461-470.
- Khaw, B. A., Fallon, J. T., Strauss, H. W., and Haber, E. (1980) Myocardial infarct imaging of antibodies to canine cardiac myosine with indium-111-diethylenetriamine pentaacetic acid. *Science* 209, 295-297.
- King, T. P., Zhao, S. W., and Lam, T. (1986) Preparation of a protein conjugates via intermolecular hydrazone linkage. *Biochemistry* 25, 5774-5779.

- Kurkela, R., Vuolas, L., and Vihko, P. (1988) Preparation of $F(ab')_2$ fragments from monoclonal mouse IgG1 suitable for use in radioimaging. *J. Immunol. Methods* 110, 229-236.
- Laemmli, U. K. (1970) Cleavage of structural proteins during the assembly of the head of bacteriophage T4. *Nature* 227, 680-685.
- Lamoyi, E. (1986) Preparation of $F(ab')_2$ fragments from mouse IgG of various subclasses. *Methods Enzymol.* 121, 652-657.
- Mach, J. P., Buchegger, F., Grob, J. Ph., Van Fliduer, V., Carrel, S., Barreth, L., Bishop-Delaloye, A., and Delaloye, B. (1985) In *Monoclonal Antibodies for Cancer Detection and Therapy* (R.W. Baldwin, and V. S. Bryers, Eds.), pp 53-65, Academic Press, London.
- Masaki, T., Fujihashi, T., Nakamura, K., and Soejima, M. (1981) Studies on a new proteolytic enzyme from *Achromobacter lyticus* M497-1. II. Specificity and inhibition studies of *Achromobacter* protease I. *Biochim. Biophys. Acta* 660 (1), 51-55.
- Mather, S. J., Durbin H., and Taylor-Papadinitriou, J. (1987) Identification of immunoreactive monoclonal antibody fragment for improved immunoscintigraphy. *J. Immunol. Methods* 96, 255-264.
- Moldofsky, P. J., Sears, H. F., Mulhearn, C. B., Jr., and Hammond, N. D. (1984) Detection of metastatic tumor in normal-sized retroperitoneal lymph nodes by monoclonal-antibody imaging. *N. Engl. J. Med.* 311, 106-107.
- Morrison, R. T., Lyster, D. M., Alcorn, L., Rhodes, B. A., Breslow, K., and Burchiel, S. W. (1984) Radioimmunoimaging with ^{99m}Tc monoclonal antibodies: Clinical Studies. *Int. J. Nucl. Med. Biol.* 11, 184-188.
- Murayama, A., Shimada, K., and Yamamoto, T. (1978) Modification of immunoglobulin G using specific reactivity of sugar moiety. *Immunochemistry* 15, 523-528.
- Murray, J. L., Rosenblum, M. G., Sobol, R. E., Bartholomew, R. M., Plager, C. E., Haynie, T. P., Jahns, M. F., Glenn, H. J., Lamki, L., Benjamin, R. S., Papadopoulos, N., Boddie, A. W., Frincke, J. M., David, G. S., Carlo, D. J., and Hersch, E. M. (1985) Radioimmunoimaging in malignant melanoma with ^{111}In -labeled monoclonal antibody 96.5. *Cancer Res.* 45, 2376-2381.
- Nairn, R. C. (1976) in *Fluorescent Protein Tracing*, 4th ed., Churchill Livingstone, Edinburgh.
- Nuti, M., Teramoto, Y. A., Mariani-Costantini, R., Horan-Hand, P., Colcher, D., and Schlom, J. A. (1982) A monoclonal antibody (B72.3) defines pattern of distribution of a novel tumor-associated antigen in human mammary carcinoma cell population. *Int. J. Cancer* 29, 539-545.
- Order, S. E., Klein, J. L., Ettinger, D., Alderson, P., Siegelman, S., and Leichner, P. (1980) Use of isotopic immunoglobulin in therapy. *Cancer Res.* 40, 703-710.
- Pochon, S., Buchegger, F., Pélegrin, A., Mach, J. P., Offord, R. E., Ryser, J. E., and Rose, K. (1989) A novel derivative of the chelon desferrioxamine for site-specific conjugation to antibodies. *Int. J. Cancer* 43, 1188-1194.
- Prelog, V., and Walser, A. (1962) *Helv. Chim. Acta* 45, 631-637.
- Rainsbury, R. M., Westwood, J. H., Coombes, R. C., Neville, A. M., Oh, R. J., Kalirai, T. S., McCready, V. R., and Gazet, J. C. (1983) Location of metastatic breast carcinoma by a monoclonal antibody chelate labelled with indium-111. *Lancet* 2, 934-938.
- Rodwell, J. D., Alvarez, V. L., Lee, C., Lopez, A. D., Goers, J. W. F., King, H. D., Powsner, H. J., and McKearn, T. J. (1986) Site-specific modification of monoclonal antibodies: in vitro and in vivo evaluations. *Proc. Natl. Acad. Sci. U.S.A.* 83, 2632-2636.
- Rose, K., Vilaseca, L. A., Werlen, R., Meunier, A., Fisch, I., Jones, R. M. L., and Offord, R. E. (1991) Preparation of a well-defined protein conjugates using enzyme-assisted reverse proteolysis. *Bioconjugate Chem.* 2, 154-159.
- Scheinberg, D. A., Strand, M., and Gansow, O. A. (1982) Tumor imaging with radioactive metal chelates conjugated to monoclonal antibodies. *Science* 215, 1511-1513.
- Whittle, N., Adair, J., Lloyd, C., Jenkins, L., Schlom, J., Raubitschek, A., Colcher, D., and Bodmer, M. (1984) Expression in COS cells of a mouse-human chimaeric B72.3 antibody. *Protein Eng.* 1 (6), 499-505.
- Youle, R. J., and Neville, D. M. (1980) Anti-thy 1.2 monoclonal antibody linked to ricin is a potent cell-type-specific toxin. *Proc. Natl. Acad. Sci. U.S.A.* 77, 5483-5486.
- Registry No.** Lysyl endopeptidase, 78642-25-8; carbonyldrazide, 497-18-7; $HCO-m-C_6H_4-CH=N-O-CH_2-CO$ -ferrioxamine, 138984-27-7.

Molecular Amplifiers: Synthesis and Functionalization of a Poly(aminopropyl)dextran Bearing a Uniquely Reactive Terminus for Univalent Attachment to Biomolecules

Jeffrey S. Mann,[†] Jin Cheng Huang, and John F. W. Keana*

Department of Chemistry, University of Oregon, Eugene, Oregon 97403. Received November 18, 1991

The synthesis and characterization of the versatile dextran-based molecular amplifier **6** is described. Dextran ($M_r = 40\,000$) was selectively monofunctionalized in high yield at its reducing terminus via reductive amination with 2-(4-nitrophenyl)ethylamine to give **1**. The nitro group in **1** serves as a masked amino group which is eventually converted into a reactive isothiocyanato group used for monovalent attachment of the completed assembly to a target molecule. Cyanoethylation of **1** gave the terminally nitrophenylated poly(cyanoethyl)dextran **5** which was selectively reduced to the corresponding poly(aminopropyl) derivative **6** with $\text{BH}_3\cdot\text{THF}$, a reagent which preserved the end nitro group. Conjugation of amplifier **6** with the isothiocyanate-derivatized Gd(III) chelate **7** gave conjugate **9** containing about 22 mol of chelate/mol of amplifier. The T_1 relaxivity per Gd(III) ion of **9** in H_2O was $15.0\text{ mM}^{-1}\text{ s}^{-1}$, about 3-fold higher than that of free Gd(III)DTPA in H_2O . The nitro group of **9** was then selectively reduced to the corresponding amine **10**, which was converted into isothiocyanate **11**. The reactivity of the single isothiocyanate group in **11** was demonstrated by coupling to 5-aminoeosin, giving conjugate **12**. Amplifier **6** was also conjugated with the acid-labile *N*-cis-aconityl derivative **8** of the potent anticancer agent daunomycin. The nitro group of the resulting conjugate **13** was then reduced and the resulting amine **14** was converted into mono isothiocyanate **15**. Compound **15** reacted with a water-insoluble amine-containing solid support to give **16**. Free daunomycin was released from **16** by exposure to citrate-phosphate buffer at pH 4.0.

The conjugation of therapeutically or diagnostically relevant small molecules (agents) to biomolecules with intrinsic tissue specificity provides a means of targeting the agent to a desired tissue. Due to their exquisite selectivity, monoclonal antibodies (mAbs) have been actively studied as carriers for drug molecules (1). Diverse agents such as anthracyclines (2, 3), methotrexate (4), ricin A (5), and metal chelates (6) have been attached to mAbs.

In general, the methods used to achieve agent-antibody conjugation involve the random modification of mAb amino acid side chain amines with drug derivatives and frequently result in an unacceptable reduction in the mAb immunoreactivity at useful levels of drug incorporation (7). Recent approaches have involved the modification of specific sites on the antibody such as the mAb carbohydrate moiety (8) or interchain disulfide bridge (9, 10). While use of site-specific labeling techniques avoids many of the pitfalls of random labeling, site-specific labeling methods have the disadvantage of providing immunoconjugates with low levels of agent incorporation.

In order to maximize the amount of the agent borne by the mAb, macromolecular carrier molecules such as poly(L-amino acids) (11), human serum albumin (12), and polyaldehyde dextran (13) have been used. In principle, the macromolecule is capable of carrying a large number of drug molecules, amplifying the amount of drug that the antibody is able to carry to its target while causing minimal loss of the mAb immunoreactivity. Polyaldehyde dextran, produced by periodate oxidation of dextran, has been conjugated with mitomycin C (14), methotrexate (15), daunomycin (16), and the hydrazides of the antineoplastic drugs ellipticine and CI-921 (17). The resulting drug-carrier assemblies have been coupled with a mAb. Drug-

dextran-mAb conjugates have been shown to offer therapeutic advantages in several instances (16, 18, 19). The drug-dextran conjugation is conducted in a manner which leaves several of the dextran aldehyde functions unmodified. The carrier-drug assembly is attached to the mAb through the remaining aldehydes by reductive amination of amino acid side chains of the mAb. A limitation of the polyaldehyde carrier-drug assembly is its ability to act as a mAb cross-linking agent, causing antibody aggregation. A dextran-based carrier which, after labeling with drug molecules, bears one mAb-reactive group would represent a significant improvement over the polyaldehyde dextran carrier.

The following account details the synthesis of a poly(aminopropyl)dextran derivative which is monofunctionalized at its reducing terminus with a masked amine-reactive functional group. The aminopropyl groups were conjugated to a derivative of the magnetic resonance imaging (MRI) contrast agent Gd-DTPA, which is functionalized to allow its attachment to other molecules at a site distinct from its chelating moieties (20). Previously studied dextran-DTPA-Gd(III) conjugates were constructed through ester or amide linkages using a DTPA carboxylate and result in a substantial loss of chelate stability (10^{18} vs 10^{22}) (21, 22). A conjugate was also prepared by functionalizing the amines with daunomycin via the acid-labile *N*-cis-aconityldaunomycin derivative (23, 24). The release of daunomycin from the resulting conjugate at pH 4 and 8 was studied.

EXPERIMENTAL PROCEDURES

Materials. Dextran ($M_r = 40\,000$, Lot No. 15779), *cis*-aconitic anhydride, daunomycin, and 1-ethyl-3-[3-(dimethylamino)propyl]carbodiimide (EDCI) were purchased from Sigma. Dextran was dried at 80°C and 0.05 mmHg over P_2O_5 for 24 h prior to use. EAH Sepharose

[†] Current Address: Contrast Media Laboratory, Department of Radiology, University of California, San Francisco, CA 94143.

(7–11 μmol amine/mL) was purchased from Pharmacia. Acrylonitrile, tetramethylammonium chloride (TMAC), 2-(4-nitrophenyl)ethylamine hydrochloride, $\text{BH}_3\cdot\text{THF}$ (1.0 M in THF), and anhydrous DMSO (Gold Label) were purchased from Aldrich. 5-Amino eosin was purchased from Molecular Probes. *N*-cis-Aconityldaunomycin was prepared by the method of Shen (24). The isothiocyanatobenzyl-DTPA–Gd chelate 7 was prepared as described earlier (20).

NMR Spectroscopy. Proton NMR spectra were obtained using a G.E. QE 300 spectrometer. The samples were dissolved in DMSO (2.49 ppm) or D_2O (4.80 ppm) and the chemical shifts reported in ppm on the δ scale using the residual proton absorptions of these solvents as references. Proton NMR relaxation measurements were carried out at 10 MHz using a Praxis 2 spectrometer. T_1 values were measured using the inversion-recovery method, 180° – τ – 90° –fid–delay, where the delay was $5 \times T_1$.

Infrared Spectroscopy. Infrared spectra of dextran derivatives as KBr pellets were obtained on a Nicolet 5DXB FTIR spectrometer.

Ultraviolet Spectroscopy. UV absorbance spectra of aqueous solutions were measured using a Beckman DU-7 instrument. The concentrations of free and bound daunomycin were estimated from the height of the absorbance maximum at 475 nm ($\epsilon = 9860$) in the UV spectra of aqueous solutions (24). The concentration of 2-(4-nitrophenyl)ethylamine was estimated from the absorbance maximum at 275 nm ($\epsilon = 9.7 \times 10^3$). Concentrations of the thiourea derivative of 5-amino eosin were estimated in a similar manner from an absorbance maximum at 525 nm ($\epsilon = 9.0 \times 10^4$).

Analyses. Elemental analyses (C, H, N) were performed by Desert Analytics (Tucson, AZ). Metal ion analysis (Gd^{3+}) was performed by Galbraith Laboratories, Inc. (Knoxville, TN), using atomic absorption spectroscopy. Molecular weight analyses were performed by Arco Laboratories, Inc. (Joliet, IL), using gel permeation chromatography.

Thin-Layer Chromatography. TLC of daunomycin and *N*-cis-aconityldaunomycin was performed on silica gel (60 F₂₅₄, 0.2-mm thickness) from EM Science using a 17:3:1 acetone– HCCl_3 –AcOH system as eluent.

Gel Permeation Chromatography. Before use the Sephadex G-25 gel was swelled with the aqueous eluting buffer at 25 °C for 16 h or 80 °C for 1 h. The poured columns were equilibrated with the eluting buffer by passing five column volumes of the buffer through the column. Column void volumes were determined using a solution of blue dextran (5 mg/mL). During chromatography the column effluent was monitored continuously at 254 nm with an ISCO UA-4 detector. The chromatograms displayed complete baseline separation of the macromolecular and small molecule components in all cases.

1-[(4-Nitrophenethyl)amino]dihydrodextran (1). The free base of 2-(4-nitrophenyl)ethylamine hydrochloride was obtained by chloroform extraction (4×25 mL) of an emulsion produced by basifying a solution of the amine hydrochloride (1.01 g, 5.0 mmol) to pH 12–13 with 2 N NaOH (3 mL). The extracts were pooled, dried (K_2CO_3), and evaporated to dryness. The resulting dark orange oil (800 mg) was purified by chromatography over silica gel (30 g) and elution with HCCl_3 –MeOH–concentrated NH_4OH (4:1:0.1) afforded the free base (750 mg, 90%) as a yellow oil. NMR (CDCl_3): δ 1.261 (s, 2), 2.286 (t, 2), 3.023 (t, 2), 7.349–8.175 (AA'BB', 4). UV (0.5% EtOH): $\lambda_{\text{max}} = 278$ nm ($\epsilon = 8.6 \times 10^3$).

Dextran (1.10 g, 2.75×10^{-2} mmol) was dissolved in anhydrous DMSO (5.5 mL) with gentle heating (45 °C) and allowed to return to 25 °C. 2-(4-Nitrophenyl)eth-

ylamine (680 mg, 4.1 mmol) and crushed 4-Å molecular sieves (130 mg) were added. The flask was flushed with Ar for 3 min and then sealed with a serum cap. The reaction mixture was stirred for 24 h at 37 °C. NaBH_4 (17 mg, 0.44 mmol) was added, the flask was flushed with Ar, and the suspension was stirred for 24 h at 37 °C. The viscous brown mixture was cooled in an ice bath as water (10 mL) was slowly added. The pH was adjusted to 5.5 by the addition of glacial acetic acid (about 0.4 mL). The orange suspension was centrifuged and the supernatant was loaded onto a column of Sephadex G-25 (2.5 cm \times 65 cm) and eluted with 0.1 M NH_4OAc . The modified polysaccharide eluted off in the void volume (150 mL). It was collected as one fraction (80 mL), evaporated to approximately 15 mL, dialyzed against flowing distilled water for 18 h, and lyophilized to afford 984 mg (90% recovery based on starting dextran) of a cream-colored solid. NMR (D_2O): δ 3.477–3.989 (m, 7), 4.970 (s, 1); at increased gain δ 8.205 (d), 7.495 (d). UV (H_2O): $\lambda_{\text{max}} = 278.0$ nm ($\epsilon = 8.5 \times 10^3$). The yield of functionalization (97–98%) was calculated from the above absorbance (see discussion in the text). A commercial molecular weight analysis by gpc gave an M_r value of ~ 40 200.

1-[(4-Aminophenethyl)amino]dihydrodextran (2). End-group modified dextran 1 (10.2 mg, 2.52×10^{-4} mmol) was dissolved in H_2O (5 mL) and 30% Pd/C (5 mg) was added. The suspension was shaken under 40 psi of H_2 for 6 h and then filtered through Celite and lyophilized. The resulting powder was dried at 1 mmHg over P_2O_5 at 80 °C for 18 h, giving 8.8 mg (86%) of 2 as a white powder. NMR (D_2O): δ 3.480–3.968 (m, 7), 4.966 (s, 1); at increased gain δ 7.130 (d), 6.815 (d).

1-[(4-Isothiocyanatophenethyl)amino]dihydrodextran (3). Dextran 2 (8.8 mg, 2.2×10^{-4} mmol) was dissolved in H_2O (1 mL) and 0.1 M NaHCO_3 (1 mL) was added. The stirred solution was cooled in an ice bath and thiophosgene (100 μL , 1.4×10^{-3} mmol) was added. The mixture was stirred at 0 °C for 2 h then at 25 °C for 30 min. The mixture was extracted with Et_2O (3×5 mL), transferred to dialysis tubing, and dialyzed against 1 L of distilled H_2O (pH = 6.5) at 4 °C for 16 h and then lyophilized. The resulting solid was dried at 1 mmHg over P_2O_5 at 35 °C for 18 h, giving 5.5 mg (62%) of a cream-colored powder.

5-Amino eosin Derivative 4 of Dextran. Isothiocyanate-derivatized dextran 3 (5.5 mg, 1.4×10^{-4} mmol) was dissolved in H_2O (1 mL), and MeOH (200 μL) was added. To this stirred solution were added 0.1 M NaHCO_3 (1 mL) and 5-amino eosin (10 mg, 1.4×10^{-2} mmol). The bright red solution was stirred for 16 h at 25 °C and then loaded onto a Sephadex G-25 column (1.5 \times 26 cm) and eluted with 0.1 M NH_4OAc . The modified polysaccharide eluted in the void volume (5 mL) as a bright red band and was collected in one fraction (2 mL), dialyzed against 4 L of distilled water at 4 °C for 18 h, and then lyophilized, giving 5.0 mg of a bright red solid.

UV Determination of 5-Amino eosin Incorporation into 4. The extent of 5-amino eosin incorporation into 4 was estimated from the UV spectrum of solutions of varying concentrations in 4. A blank prepared using unmodified dextran (11.0 mg, 2.7×10^{-4} mmol) showed that the extent of noncovalent binding of 5-amino eosin, estimated from the UV spectrum of the blank, was 2.4%. The extent of covalent binding of 5-amino eosin in 4 was 90%. This agreed closely with the extent of incorporation of the 2-(4-aminophenyl)ethylamine group estimated from the intensity of the absorbance of the aromatic nitro chromophore at 278.0 nm ($\epsilon = 8.6 \times 10^3$) in the UV spectrum of 1.

1-[(4-Nitrophenethyl)amino]dihydropoly(2-cyanoethyl)dextran (5). (Nitrophenyl)dextran 1 (744 mg, 1.85×10^{-2} mmol) was slurried in H₂O (1 mL) containing tetramethylammonium chloride (30 mg, 0.3 mmol) with stirring. The slurry was stirred to produce a clear solution (~20 min) and then freshly distilled acrylonitrile (15 mL) was added. NaOH (12%, 750 μ L, 2.2 mmol) was added and the resulting mixture was stirred for 1 h. At the end of this time 2-propanol (40 mL) was added to the reaction mixture and the resulting viscous mixture was triturated with fresh portions of 2-propanol (3×40 mL) until a free-flowing suspension was produced. The white solid was isolated by filtration, washed with EtOH (2×25 mL) and Et₂O (2×25), and dried at 40 °C over P₂O₅ for 16 h at 1 mmHg, giving 825 mg (85% based on degree of substitution = 0.5) of a white powder. IR: 2254 cm⁻¹. NMR (D₂O): δ 2.811 (s, 2), 3.497–4.020 (m, 7), 4.956 (s, 1). Anal. Calcd for (C₆H₉O₅)_n(C₃H₄N)_{0.5n}(H₂O)_{0.5n}: C, 47.87; H, 5.85; N, 3.72. Found: C, 47.68; H, 5.85; N, 3.72.

1-[(4-Nitrophenethyl)amino]dihydropoly(3-aminopropyl)dextran (6). Dextran derivative 5 (668 mg, 1.4×10^{-2} mmol) was suspended with stirring in anhydrous THF (20 mL) and cooled to 0 °C. BH₃·THF (20 mL, 20 mmol) was added via syringe and the suspension was refluxed for 18 h. At the end of this time the suspension was cooled to 0 °C and MeOH (25 mL) was added slowly via syringe. The volatiles were removed by rotary evaporation and the resulting white solid was treated again with MeOH (15 mL). The suspension was evaporated to dryness and the solid was slurried in dioxane (10 mL) with stirring. A mixture of Et₃N (1 mL) and H₂O (9 mL) was added slowly to the stirring suspension. The reaction mixture was stirred for 2 h at 25 °C, during which time the solid dissolved completely. The resulting solution was evaporated to near dryness, redissolved in water (5 mL), loaded onto a Sephadex G-25 column (2.5 cm \times 50 cm), and eluted with 0.1 M NH₄OAc. The modified polysaccharide eluted in the void volume (23 mL), was collected as one fraction (10 mL), dialyzed against distilled water (4 L) at 4 °C for 18 h, and lyophilized. The resulting white solid was dried at 0.05 mmHg over P₂O₅ at 60 °C for 24 h, giving 570 mg (85%) of 6 as a white powder. An aqueous solution (2 mg/mL) of 6 gave a positive reaction when treated with a 5% solution of ninhydrin in EtOH and heated to 40 °C for 1 min. NMR (D₂O): δ 4.980 (s, 1), 3.291–4.223 (m, 10), 2.730–2.950 (m, 1). Anal. Calcd for (C₆H₉O₅)_n-(C₃H₈N)_{0.5n}(H₂O)_{0.5n}: C, 45.22; H, 7.03; N, 3.52. Found: C, 45.31; H, 6.87; N, 3.38.

Coupling of Isothiocyanatobenzyl-DTPA-Gd 7 and Poly(aminopropyl)dextran 6 To Give Conjugate 9. End-modified poly(aminopropyl)dextran 6 (202 mg, 4.21×10^{-3} mmol, 0.826 mequiv of amine) was dissolved in 0.1 M NaHCO₃ (5 mL) with stirring. A solution of isothiocyanatobenzyl-DTPA-Gd chelate 7 (820 mg, 1.11 mmol) in H₂O (8 mL) was added and the resulting solution was stirred for 16 h at 25 °C. At the end of this time the mixture was centrifuged to remove a small amount of a white solid and the supernatant was drawn off. The supernatant did not give a positive reaction to 5% ninhydrin in EtOH. To ensure that all of the available amines were "capped", the supernatant was cooled to 0 °C and taken to pH 9 with saturated NaHCO₃, and acetic anhydride (500 μ L, 5.23 mmol) was added. The resulting solution was stirred for 2 h, dialyzed against 4 L of distilled H₂O at 4 °C for 16 h, lyophilized, and dried at 0.05 mmHg over P₂O₅ at 60 °C for 16 h, giving 233 mg (75% recovery, see below) of 9 as a white powder. A commercial Gd(III) analysis by atomic absorption spectroscopy showed that 9 contained 7.45% Gd. The Gd(III) analysis corresponds to a conjugate with 22 mol of 7/mol of 6. The relaxivity

of a solution of 9 in water at 10 MHz and 37 °C was 330.3 mM⁻¹ s⁻¹, corresponding to a relaxivity per Gd(III) ion of 15.0 mM⁻¹ s⁻¹.

Conjugate 10. End group modified dextran conjugate 9 (100.6 mg, 6.37×10^{-4} mmol) was dissolved in H₂O (10 mL) and 30% Pd/C (30 mg) was added. The suspension was shaken under 30 psi of H₂ for 8 h and then filtered through Celite; the filtrate was lyophilized, giving 90 mg (90%) of conjugate 10 as a white powder.

Isothiocyanate-Derivatized Conjugate 11. Conjugate 10 (90.0 mg, 6.2×10^{-4} mmol) was dissolved in H₂O (8 mL) and 0.1 M NaHCO₃ (2 mL) was added. The solution was cooled in an ice bath and a 0.2 M solution of thiophosgene (500 μ L, 0.1 mmol) in HCCl₃ was added. The mixture was stirred at 0 °C for 3 h and then evaporated to dryness. The residual solid was dissolved in H₂O (2 mL) and dialyzed against flowing distilled water for 16 h. The contents of the dialysis tubing were concentrated to about 1 mL and the product was precipitated with acetone. The precipitate was isolated by centrifugation, washed with acetone (3×5 mL), and dried at 0.05 mmHg at 25 °C for 24 h, giving 88 mg (90%) of a slightly yellow powder.

5-Amineoosin Derivative 12 of Conjugate 11. Isothiocyanate-derivatized dextran conjugate 11 (10 mg, 6.33×10^{-5} mmol) was dissolved in H₂O (1 mL) and MeOH (200 μ L) was added. To this stirred solution were added 0.1 M NaHCO₃ (500 μ L) and 5-amineoosin (2.8 mg, 4×10^{-3} mmol). The bright red solution was stirred for 16 h at 25 °C then loaded onto a Sephadex G-25 column (1.5 cm \times 26 cm) and eluted with 0.1 M NH₄OAc. The modified polysaccharide eluted in the void volume (5 mL) as a bright red band and was collected in one fraction (2.5 mL), dialyzed against 4 L of distilled water at 4 °C for 18 h, and then lyophilized to provide 9.6 mg (96%) of conjugate 12 as a bright red powder. UV (H₂O): λ_{\max} = 525 nm (ϵ = 9.0×10^4).

UV Determination of 5-Amineoosin Incorporation into 12. The extent of 5-amineoosin incorporation into 12 was estimated from the UV spectra of solutions varying in concentrations of 12. A blank was prepared as a control by submitting a sample (3.1 mg, 5.5×10^{-5} mmol) of the Gd(III)-derivatized (nitrophenyl)dextran conjugate 9 to the conditions of the 5-amineoosin incorporation reaction used to produce 12. The extent of noncovalent binding of 5-amineoosin was estimated at 4.0% from the blank. The extent of covalent binding of 5-amineoosin in 11 was determined to be 88%.

Conjugation of *N*-cis-Aconityldaunomycin (8) with Poly(aminopropyl)dextran 6 Giving Conjugate 13. *N*-cis-Aconityldaunomycin (8) was conjugated to dextran 6 using the procedure of Shen (24). The resulting red solution was stirred in the dark for 17 h. The solution gave a positive ninhydrin test. To "cap" the remaining amines the solution was taken to pH 8 with 0.1 M NaHCO₃ (2 mL) and treated at 0 °C with Ac₂O (500 μ L, 5.0×10^{-3} mmol). The resulting mixture was stirred until it gave a negative ninhydrin test (2 h). The reaction mixture was loaded onto a Sephadex G-25 column eluted with 0.1 M NH₄OAc (pH 8). The modified polysaccharide eluted in the void volume (7.5 mL) and was collected in one fraction (2.5 mL). An aliquot (50 μ L) of this solution was diluted to 3.0 mL with H₂O and the extent of coupling was estimated from the UV spectrum to be 48 mol of 8/mol of 6. The two solutions were recombined, dialyzed against distilled H₂O (4 L) at 4 °C for 24 h, and lyophilized, giving 2.3 mg of 13 as a pink solid. IR (KBr): cm⁻¹ 1554.7 (carboxylate, *cis*-aconityl group).

A control was prepared by submitting 6 (1.6 mg, 3.5×10^{-5} mmol) and 8 to the above reaction conditions without the addition of EDCI. The control was purified as above,

lyophilized, and redissolved in H₂O (2.00 mL). The extent of coupling was estimated from the A_{475} of this solution to be 1.0×10^{-2} mol of 8/mol of 6.

N-cis-Aconityldaunomycin-Dextran Conjugate 14. The nitro group of 13 was reduced to amine 14 by a modification of the procedure of Avery et al. (25). To a 5-mL round-bottomed flask equipped with a magnetic stirrer were added PtO₂ (5 mg) and water (3 mL). H₂ gas was bubbled through the suspension for 3 min, and then an aliquot (1.0 mL, 1.5×10^{-5} mmol) of a solution of conjugate 13 in water was added. The flask was flushed with H₂ for 3 min and sealed. The suspension was stirred at 1 atm of H₂ at 25 °C for 4 h and then filtered through Celite. The filtrate containing 14 was used for the next experiment without further purification.

Isothiocyanate-Derivatized Conjugate 15. The filtrate containing 14 was taken to pH 8.5 with 0.1 M NaHCO₃. The solution was cooled in an ice bath and thiophosgene (50 μ L, 7.0×10^{-4} mmol) was added. The reaction mixture was stirred at 0 °C for 2 h and at 25 °C for 30 min and then dialyzed against 1 L of distilled H₂O (pH = 6.8) at 4 °C for 16 h. The resulting solution was diluted to 5.00 mL with distilled H₂O. An aliquot of this solution was used in the next experiment.

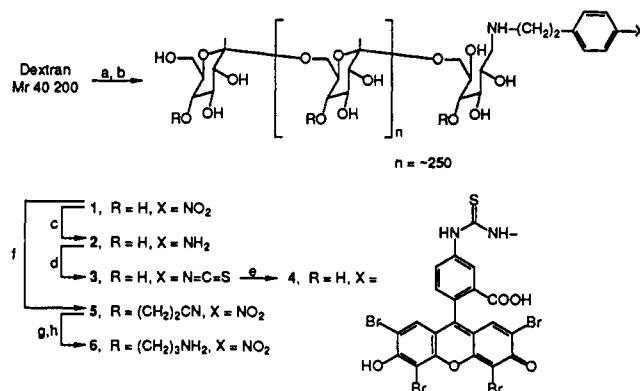
Reaction of Conjugate 15 with EAH Sepharose To Give Water-Insoluble Conjugate 16. A 1.7-mL aliquot of EAH Sepharose (7–11 μ mol of amino groups/mL) was centrifuged and the pellet was washed with water (3×2 mL). A 250- μ L aliquot of the solution containing 15 from the above experiment was diluted to 1.00 mL with 0.1 M NaHCO₃ and the UV spectrum was recorded (A_{475} = 0.2337). This solution of compound 15 was added to the gel pellet and the suspension was stirred for 4 h. The mixture was centrifuged and the supernatant was removed. The amount of 15 bound to the EAH Sepharose, estimated from the UV spectrum (A_{475} = 0.0684) of the supernatant, was 71 % of the amount originally in the supernatant. The pellet of 16 was washed with water (3×3 mL) to remove any unbound 15 and then suspended in citrate-phosphate buffer (pH 4.0) with stirring for 8 h. The suspension was centrifuged every 2 h during the course of the reaction and the extent of daunomycin release was estimated from the UV spectrum of the supernatant. A plateau was reached at 8 h (A_{475} = 0.1107) that corresponded to release of 65 % of the total bound daunomycin. TLC (17:3:1 acetone-CHCl₃-AcOH) of the supernatant against a known sample of daunomycin gave identical R_f values (0.16) for the two solutions. The supernatant was adjusted to pH 7.5 with 1 N NaOH (1 drop) and then extracted with HCCl₃ (3×10 mL). The organic layers were pooled and evaporated to dryness, affording 0.6 mg of a pale pink solid. The IR spectrum (KBr) of this material was identical to that of daunomycin.

A second sample of conjugate 16 was prepared in an identical manner and suspended at 25 °C in citrate-phosphate buffer (pH 7.0) with stirring. After 48 h there was no significant release of daunomycin in the supernatant detected by UV spectroscopy.

RESULTS AND DISCUSSION

Synthesis of the Dextran Amplifier. The synthesis of amplifier 6 is detailed in Scheme I. The reducing terminus of dextran (40 200) was derivatized with a masked reactive group by reductive amination with 2-(4-nitrophenyl)ethylamine in DMSO under anhydrous conditions. The macromolecular component was separated from excess 2-(4-nitrophenyl)ethylamine by chromatography over Sephadex G-25. A molecular weight analysis by gel permeation chromatography (gpc) revealed that the degree

Scheme I^{a,b}

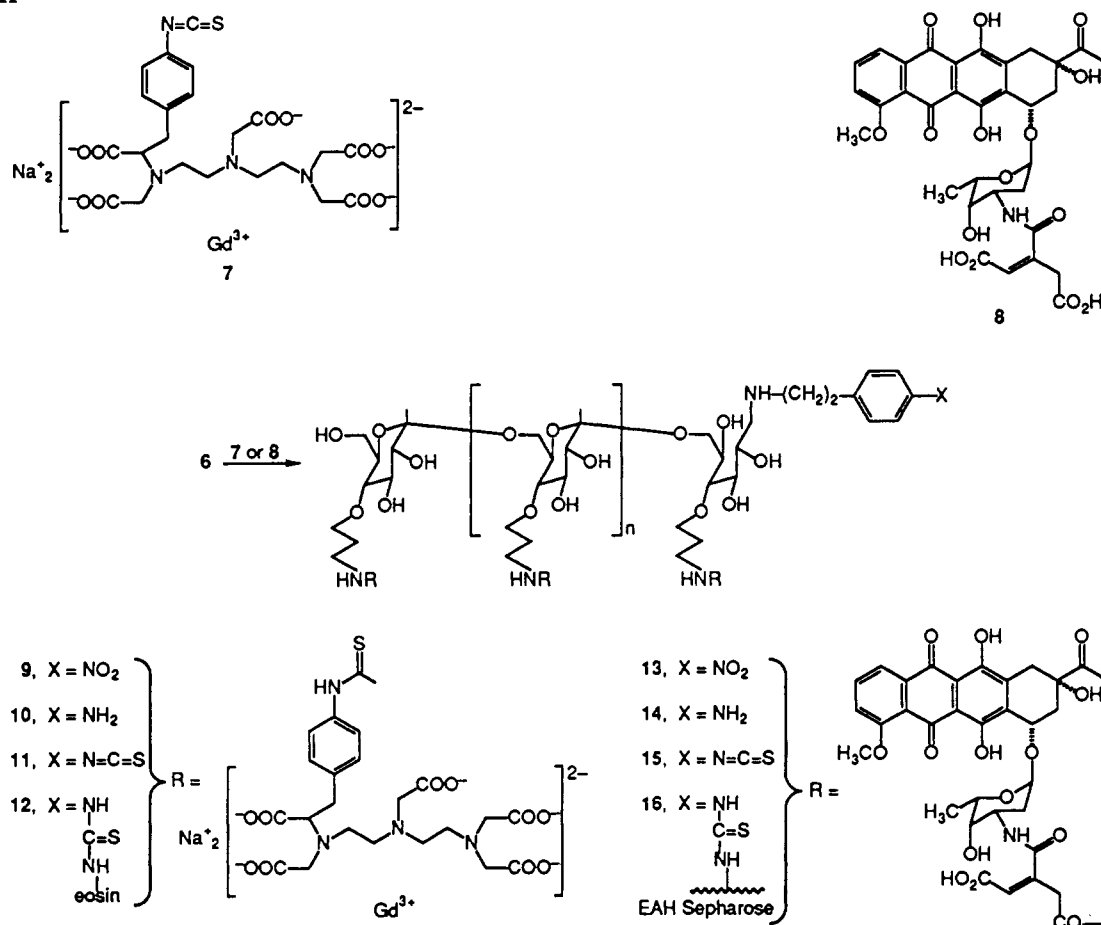


^a (a) 2-(4-Nitrophenyl)ethylamine/DMSO/molecular sieves; (b) NaBH₄; (c) Pd/C, H₂; (d) C(S)Cl₂/NaHCO₃(aq); (e) 5-aminoeosin/NaHCO₃(aq); (f) 12 % aqueous NaOH/Me₄N⁺Cl⁻/acrylonitrile; (g) BH₃-THF; (h) 9:1 H₂O:Et₃N/dioxane. ^b For convenience the R group is shown attached to O-4 although the actual point of attachment likely varies along the dextran backbone. R = H for many of the glucose residues.

of polymerization of the product, dextran 1, was identical to that of the starting dextran. The extent of derivatization was estimated at 98–99 % from the absorbance of the 2-(4-nitrophenyl)ethylamine chromophore at 278 nm (ϵ = 8.6×10^3). The protons of the *p*-nitrophenyl group were readily observed in the high-gain ¹H NMR spectrum of 1. The extent of end-group derivatization in 1 was confirmed by the conversion of 1 into 5-aminoeosin derivative 4 via amine 2 and isothiocyanate 3. The observed absorbance at 525 nm (ϵ = 9.0×10^4) of an aqueous solution of 4, adjusted for a 2.4 % background binding of 5-aminoeosin to unmodified dextran, corresponded to a 90 % yield of covalent incorporation. This reaction sequence also served as a model for the introduction of an isothiocyanate group into the new derivatized dextrans described below.

End-modified dextran 1 was next cyanoethylated to give 5 by adapting the procedure of Daly (26). The appearance of a broad singlet at 2.811 ppm in the ¹H NMR (D₂O) spectrum of 5 was indicative of cyanoethylation. The extent of cyanoethylation could be estimated by comparing the integrals of the dextran anomeric protons (4.956 ppm) and the peak at 2.811 ppm in the ¹H spectrum of 5 in D₂O. Further confirmation of the presence of the cyanoethyl groups came from the IR spectrum (KBr) which showed a sharp peak at 2254 cm⁻¹. A series of dextrans differing in their degree of cyanoethylation was synthesized by varying the amount of 12 % NaOH(aq) added to the reaction mixture. Poly(cyanoethyl)dextrans of degree of substitution (DS) > 1.0 cyanoethyl groups per subunit formed hazy gels with water. A poly(cyanoethyl)dextran which was soluble in water to at least 50 mg/mL was produced by lowering the DS to 0.5 cyanoethyl groups per glucose subunit as determined by elemental (C, H, N) and NMR analysis. Cyanoethylation by the above procedure was reproducible to within ± 0.1 cyanoethyl group/subunit.

Selective reduction of poly(cyanoethyl)dextran 5 to the corresponding poly(aminopropyl)dextran 6 was effected by refluxing a suspension of the cyanoethylated dextran in THF containing excess BH₃-THF for 18 h followed by hydrolysis of the intermediate borotriazine (27) using dilute aqueous triethylamine. Reduction was confirmed by the disappearance of the nitrile absorbance at 2254 cm⁻¹. A solution of 6 in water (5 mg/mL) had a pH of 8.8 and gave a positive reaction with 5 % ninhydrin in EtOH, indicating the presence of primary amines. A molecular weight analysis of 6 by gpc indicated that the product had approximately the same average molecular weight as the

Scheme II^a^a See footnote b, Scheme I.

starting material. The chromatogram generated by this analysis displayed a tailing peak for the analyte which was most likely indicative of nonideal interactions between the polyamino analyte and the column (28). The increased retention of the analyte caused by these nonideal interactions gave the appearance of a decrease in average molecular weight to approximately 37 000. Although the possibility of degradation cannot be ruled out, it is unlikely that this would occur under the mild conditions used. An elemental analysis of this compound gave results consistent with a DS = 0.5 aminopropyl groups/subunit.

The UV and ¹H NMR spectra of 6 confirmed that the nitrophenyl group survived the reductive conditions necessary to convert the cyanoethyl groups to propylamines. As a control a sample dextran 1 was treated with BH₃·THF in a manner identical to that used to convert 5 to 6. The starting nitro compound was recovered in nearly quantitative yield.

Attachment of Agents to Dextran Amplifier 6. The thiourea-linked conjugate 9 between amplifier 6 and Gd-DTPA derivative 7 was produced by mixing the two components under basic conditions (Scheme II). The remaining amines were "capped" by acetylation with acetic anhydride to ensure that they would not interfere with the subsequent conversion of the nitro group to an isothiocyanate or react with this group once it was in place (see below). The success of the conjugation reaction was confirmed by the appearance of a strong phenylthiourea absorbance at 246 nm in the UV spectrum of 9. A Gd(III) analysis by atomic absorption spectroscopy was consistent with a derivative containing 22 mol of chelate 7/mol of amplifier 6. The moderate degree of chelate incorporation is likely due to the steric requirements of the bulky che-

late or repulsions due to the buildup of negative charge on the dextran with the binding of the chelate.

As conjugate 9 contains multiple Gd(III) chelates and is of interest as a new agent for MRI contrast enhancement, its ability to affect the *T*₁ relaxation of water is of considerable interest. The *T*₁ of an aqueous solution of this conjugate was measured at a field strength of 0.25 T by the inversion-recovery method (180°-τ-90°). The *T*₁ relaxivity of 9 in H₂O was 15.0 mM⁻¹ s⁻¹ per Gd(III). For comparison the *T*₁ relaxivity of Gd(DTPA) in H₂O is 4.9 mM⁻¹ s⁻¹ (29).

The aromatic nitro group of 9 was reduced with H₂ and 30% Pd/C to give the corresponding amine 10 which was subsequently converted to isothiocyanate 11 by the action of C(S)Cl₂. In order to determine the extent of the ability of 11 to react with amino groups on other target molecules, the isothiocyanate was allowed to react with 5-aminoeosin to form 12 in a manner identical to that used in the preparation of 4. Calculations based on the UV absorbance maxima of 12 (λ_{max} = 525 nm, ε = 9.0 × 10⁴) gave a value of 95% for the incorporation of 5-aminoeosin. As a control, 5-aminoeosin was stirred with nitro dextran 1 under conditions identical to those used to produce 4. Calculations based on the UV spectrum of the control gave a value of 4.0% for the extent of noncovalent incorporation of the 5-aminoeosin. The corrected yield of covalent binding involving the isothiocyanate group of 11 was therefore 91%.

The next series of experiments demonstrates the attachment and release of the anthracycline daunomycin, a potent cytotoxin widely used in cancer chemotherapy (30). The previously reported *N*-cis-aconityl derivative 8 of daunomycin was synthesized in 80% yield following

the procedure of Shen (24). The acid-labile derivative was attached to poly(aminopropyl)dextran 6 in aqueous solution at pH 6.0 using EDCI. Conjugate 13 was purified by chromatography over a column of Sephadex G-25 eluted with citrate-phosphate buffer (pH 8) (31).

The solution of 13 which eluted off the column gave a positive test toward the ninhydrin reagent, indicating the presence of unreacted amine groups. To ensure that the remaining amines would not interfere with the formation of the isothiocyanate group the unreacted amino groups were "capped" by acetylation with acetic anhydride at pH 8 and 0 °C. The resulting solution was purified on a column of Sephadex G-25 eluted with citrate-phosphate buffer (pH 8). Recovery of a dextran from the Sephadex G-25 column was shown to be quantitative using underivatized 6. Quantitative recovery of the applied capped dextran 13 is assumed in the following calculations.

The extent of the attachment of 8 to 6 was estimated at 48 mol of daunomycin/mol of dextran from the UV absorbance of the *cis*-aconityldaunomycin chromophore at 475 nm (λ_{max} , ϵ = 9860) (24) of an aqueous solution of 13. To confirm that the binding in 13 was covalent, a control was performed by mixing an excess of 8 with dextran 6 without the addition of EDCI. After a workup identical to that used in the preparation of 13 the UV spectrum of an aqueous solution of the control was measured. No significant amount of binding of 8 to 6 was observed.

The procedure of Avery (25) allowed the selective reduction of the nitro group of 13 to the corresponding amine 14 with H₂ (1 atm) and PtO₂. Amine 14 was converted to its isothiocyanate derivative 15 by the action of C(S)Cl₂ at pH 8.5. The presence of the isothiocyanate moiety of 15 was confirmed and quantified by reaction of 15 at pH 8.5 with EAH Sepharose (EAH), a water-insoluble amine-containing solid support, to form 16. The extent of the binding of 15 to EAH was estimated to be 71% by measuring the decrease in the absorbance at 475 nm of the supernatant of the reaction suspension.

Free daunomycin could be released from the insoluble conjugate 16 by suspending a sample of 16 in citrate-phosphate buffer at pH 4.0. The extent of daunomycin released at pH 4.0 was estimated from the absorbance of the supernatant at 475 nm to be 65% of the total amount of daunomycin bound to the EAH Sepharose. The TLC and IR behavior of an HCCl₃ extract of the supernatant corresponded to that of authentic daunomycin. A suspension of conjugate 16 in citrate-phosphate buffer at pH 7.0 was stable toward release of daunomycin for 48 h at 25 °C.

The preceding has detailed the synthesis and characterization of a versatile dextran-based homopolyfunctionalized "amplifier" molecule 6 derivatized selectively at its reducing terminus for attachment to biomolecules. Poly(aminopropyl)dextran 6 is stable and can be prepared in high yield from inexpensive precursors. The utility and versatility of this compound was demonstrated by its conjugation to a modifier Gd-DTPA chelate, a useful contrast-enhancing agent for MRI and to an acid-labile prodrug of the potent cytotoxin daunomycin. An efficient two-step conversion of the aromatic nitro group to an isothiocyanate allows for the monovalent attachment of the assembly to other amine-containing molecules.

ACKNOWLEDGMENT

This work was supported by NIH Grant GM-27137. We thank Drs. Johannes Volwerk, Bruce Birrell, and Olivier Clement for helpful discussions.

LITERATURE CITED

- (1) Pietersz, G. A. (1990) *Bioconjugate Chem.* 1, 89-95.
- (2) Pietersz, G. A., Smyth, M. J., and McKenzie, I. F. C. (1988) In *Targeted Diagnosis and Therapy*, (J. D. Rockwell, Ed.) Vol. 1, pp 25-32, Marcel Dekker, New York.
- (3) Ghose, T., and Blair, T. H. (1986) *Crit. Rev. Ther. Drug Carrier Syst* 3, 263-359.
- (4) Garnett, M. C., and Baldwin, R. W. (1986) *Cancer Res.* 46, 2407-2412.
- (5) Senter, P. D., Saulnier, M. G., Schreiber, G. J., Hirschberg, D. L., Brown, J. P., Hellstrom, I., and Hellstrom, K. E. (1988) *Proc. Natl. Acad. Sci. U.S.A.* 85, 4842-4846.
- (6) McCall, M. J., Diril, H., and Meares, C. F. (1990) *Bioconjugate Chemistry* 1, 222-226.
- (7) Arnon, R. (1982) In *Targeting of Drugs*, (G. Gregoriadis, Ed.) pp 31-54, Plenum Press, New York.
- (8) Barton, R., Starling, J., Hinson, A., Maciak, R., and Koppel, G. (1988) *Abstracts of Papers, Third International Conference on Monoclonal Antibody Immunoconjugates for Cancer*, p 78.
- (9) del Rosario, R. B., Wahl, R. L., Brocchini, S. J., Lawton, R. G., and Smith, R. H. (1990) *Bioconjugate Chem.* 1, 51-59.
- (10) del Rosario, R. B., and Wahl, R. L. (1989) *J. Nucl. Med. Biol.* 16, 525-529.
- (11) Zunino, F., Savi, G., Guilian, F., Gambetta, R., Supino, R., Tinelli, S., and Pezzoni, G. (1981) *Eur. J. Cancer Clin. Oncol.* 20, 421-425.
- (12) Pietersz, G. A., Cunningham, Z., and McKenzie, I. F. C. (1988) *Immunol. Cell Biol.* 66, 43-49.
- (13) Shih, L., Sharkey, R. M., Primus, F. J., and Goldenberg, D. M. (1988) *Int. J. Cancer* 4, 832-839.
- (14) Manabe, Y., Tsubota, T., Haruta, Y., Kataoka, K., Okazaki, M., Haisa, S., Nakamura, K., and Kimura, I. (1985) *Biochem. Pharm.* 34, 289-291.
- (15) Manabe, Y., Tsubota, T., Haruta, Y., Kataoka, K., Okazaki, M., Haisa, S., Nakamura, K., and Kimura, I. (1984) *J. Lab. Clin. Med.* 104, 445-453.
- (16) Tsukada, Y., Hurwitz, E., Kahi, R., Sela, M., Hibi, N., Hara, A., and Hirai, H. (1982) *Proc. Natl. Acad. Sci. U.S.A.* 79, 7896-7899.
- (17) Heindel, N. D., Zhao, H., Leiby, J., VanDongen, J. M., Lacey, C. J., Lima, D. A., Shabsoug, B., and Buzby, J. H. (1990) *Bioconjugate Chem.* 1, 77-82.
- (18) Takakura, Y., Takagi, A., Hashida, M., and Sezaki, H. (1987) *Pharm. Res.* 4, 293-300.
- (19) Kato, Y., Tsukada, Y., Hara, T., and Hirai, H. (1983) *J. Appl. Biochem.* 5, 313-319.
- (20) Keana, J. F. W., and Mann, J. S. (1990) *J. Org. Chem.* 55, 2868-2871.
- (21) Armitage, F. E., Richardson, D. E., and Li, K. C. P. (1990) *Bioconjugate Chem.* 1, 365-374.
- (22) Blich, S. W. A., Harding, C. T., Sadler, P. J., Bulman, R. A., Bydder, G. M., Pennock, J. M., Kelly, J. D., Latham, I. A., and Marriott, J. A. (1991) *Magn. Reson. Med.* 17, 516-532.
- (23) Diener, E., Diner, U. E., Sinha, A., Xie, S., and Vergidis, R. (1986) *Science* 231, 148-150.
- (24) Shen, W. C., and Ryser, J. P. (1981) *Biochem. Biophys. Res. Commun.* 102, 1048-1054.
- (25) Avery, M. A., Verlander, M. S., and Goodman, M. (1980) *J. Org. Chem.* 45, 2750.
- (26) Daly, W. H., and Munir, A. J. (1984) *J. Polym. Sci. Chem. Ed.* 22, 975-984.
- (27) Yoshizaki, T., Watanabe, H., and Nakagawa, T. (1968) *Inorg. Chem.* 7, 422-29.
- (28) Joan Rohl, Arro Laboratory, P.O. Box 686, Caton Farm Road, Joliet, IL 60434. Personal communication.
- (29) Weinmann, H.-J., Brasch, R. C., Press, W. R., and Wesbey, G. E. (1984) *Am. J. Roentgenol.* 142, 619-624.
- (30) Carter, S. K., Bakowski, M. T., and Hellman, K. (1977) *Chemotherapy Cancer*, John Wiley, New York.
- (31) Gomori, G. (1955) *Methods in Enzymology*, Vol. I, p 141, Academic Press, New York.

Registry No. 2-(4-Nitrophenyl)ethylamine, 24954-67-4; 5-aminoeosin, 75900-75-3; acrylonitrile, 107-13-1.

Photochemical Cross-Linking of Guanosine 5'-Triphosphate to Phosphoenolpyruvate Carboxykinase (GTP)

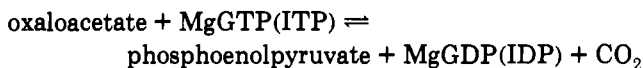
Cristina T. Lewis,[†] Jerome M. Seyer,[‡] and Gerald M. Carlson*

Department of Biochemistry, The University of Tennessee, Memphis, College of Medicine, Memphis, Tennessee 38163. Received November 19, 1991

Mammalian phosphoenolpyruvate carboxykinase (PEPCK) specifically requires a guanosine or inosine nucleotide as a substrate; however, the structural basis for this nucleotide specificity is not yet known. Because affinity labels derived from guanosine have not yielded a stable, modified peptide in quantities sufficient for sequence analysis, we have investigated the utility of direct photochemical cross-linking of GTP to PEPCK in order to identify the nucleotide binding site. UV irradiation at a distance of 2 cm by a Mineralight lamp (330 $\mu\text{W}/\text{cm}^2$) results in the attachment of [α - ^{32}P]GTP to PEPCK via a stable, covalent linkage in a reaction that is dependent upon GTP concentration and duration of irradiation. After 10 min of irradiation, more than 0.2 mol of [α - ^{32}P]GTP is incorporated per mole of PEPCK; under these conditions the GTP concentration required for half-maximal labeling is 69 μM . The substrates phosphoenolpyruvate, ITP, and GDP provide protection against photolabeling, as do Mn^{2+} and Mg^{2+} . One major and one minor radioactive peptide derived from proteolytic digests of photolabeled PEPCK have been isolated and identified. The major modified peptide has been provisionally assigned to an acidic region near the C-terminus, and the minor peptide has been identified as Ser₄₆₂-Ly₈₄₇.

INTRODUCTION

Mammalian phosphoenolpyruvate carboxykinase (EC 4.1.1.32), referred to hereafter as PEPCK,¹ catalyzes the conversion of oxaloacetate to phosphoenolpyruvate in the first committed step of gluconeogenesis. The enzyme



displays a specific substrate requirement for guanosine or inosine nucleotides; adenosine nucleotides are neither substrates nor inhibitors and do not bind to the enzyme in a detectable manner (Miller et al., 1968). Although the gene coding for the cytosolic carboxykinase has been cloned and the amino acid sequence of the enzyme has been determined (Beale et al., 1985), the nucleotide binding site of PEPCK has not been directly identified, and very little is known about the structure of the enzyme's active site. Furthermore, even though PEPCK does contain three consensus sequences that may represent the guanine nucleotide binding region (Cook et al., 1986), the enzyme does not share extensive regions of homology with other GTP-binding proteins.

Chemical modification and affinity labeling are traditional techniques that have made significant contributions to the identification of functionally important enzyme residues, and such procedures have been exploited in several efforts to elucidate the mechanism of PEPCK's binding specificity. To date, however, modification of

PEPCK with a variety of nucleotide affinity labels (including 8-azidoGTP, 5'-[*p*-(fluorosulfonyl)benzoyl]guanosine, and the 2',3'-dialdehyde derivative of GTP) has not resulted in the identification of a modified peptide (Lewis et al., 1989a; Jadus et al., 1981; Anthony et al., 1990). For example, previous results from our laboratory established that the photoaffinity label 8-N₃GTP specifically modifies PEPCK, ultimately causing formation of a cystine disulfide, but does not yield sufficient quantities of a stable, derivatized peptide for sequence analysis (Lewis et al., 1989a). These results reflect a significant concern regarding attempts to modify PEPCK with nucleotide affinity labels, namely, potential complications caused by the enzyme's unusual sulfhydryl chemistry. Recently, we reported the identity of a very reactive cysteine residue (Cys₂₈₈) that is critical for catalytic activity and that lies between two of the consensus sequences for a GTP binding site (Lewis et al., 1989b; Carlson et al., 1978). In addition, chemical modification and photoaffinity labeling studies provide substantial evidence for the existence of at least two cysteine residues within or near the enzyme's nucleotide-binding site (Lewis et al., 1989a,b). As part of a continuing effort to characterize the active site of PEPCK, we now report the development of a protocol for directly photolabeling the enzyme with its nucleotide substrate.

The technique of direct photolabeling offers several potential advantages over the use of photoaffinity or chemically reactive GTP analogues. Several GTP analogues have a chemically reactive moiety that can react with thiols [e.g., 5'-[*p*-(fluorosulfonyl)benzoyl]guanosine (Jadus et al., 1981) or 5'-(bromoacetamido)-5'-deoxyguanosine (Samant and Sweet, 1983)]. Consequently, one might predict that a sulfhydryl-directed probe could readily modify the hyperreactive Cys₂₈₈; if that were the case, it would be difficult to eliminate the possibility that the thiol was modified simply because of its hyperreactivity rather than because of its location within the enzyme's active site. Because direct photolabeling can lead to the modification of a variety of residues, this potential difficulty may be avoided. In addition, because it is the C-8 position of GTP that typically participates

[†] Recipient of the Doggett Predoctoral Fellowship from the College of Graduate Health Sciences, The University of Tennessee, Memphis. Present address: Departments of Chemistry and Molecular Biology, The Scripps Research Institute, 10666 North Torrey Pines Road, La Jolla, CA 92037.

[‡] Primary address: Veterans Administration Medical Center, 1030 Jefferson Avenue, Memphis, TN 38104.

* To whom correspondence should be addressed.

¹ Abbreviations used: PEPCK, phosphoenolpyruvate carboxykinase (GTP); HPLC, high-performance liquid chromatography; PTC, phenylthiocarbonyl; PTH, phenylthiohydantoin.

in covalent bond formation during photolabeling (Steinmaus et al., 1971), this technique may target different amino acids than affinity labels derivatized at the phosphoryl portion of the nucleotide, such as GMP-pyridoxal phosphate (Ohmi et al., 1988). Finally, direct photolabeling results in the cross-linking of the natural ligand to the enzyme by "freezing" existing contact points, thus increasing the probability that the modification is specific and occurs within the active site.

EXPERIMENTAL PROCEDURES

Materials. Radioactive [α - 32 P]GTP (10–25 Ci/mmol) and *Staphylococcus aureus* V8 protease were from ICN Biomedicals, TPCK-treated trypsin was from Sigma Chemical Co., HPLC-grade acetone was from Mallinckrodt, ultrapure urea was from Research Organics, and amino acid standards were from Pierce Chemical Co. All other reagents were of the highest quality commercially available. All glassware used for amino acid analyses was rinsed with constant-boiling HCl. PEPCK was purified to homogeneity and assayed as previously described (Lewis et al., 1989b).

Standard Conditions for Direct Photolabeling. As previously observed (Sperling, 1976; Sperling and Havron, 1976), the addition of acetone as a photosensitizer increased the extent of covalent incorporation of the radioactive nucleotide (Figure 1A). However, with increasing time and concentrations of acetone, the extent of apparent changes in protein structure was also increased (Figure 1B); after extended irradiation in the presence of higher concentrations of acetone, PEPCK migrated as a more broad, diffuse band during polyacrylamide gel electrophoresis in the presence of sodium dodecyl sulfate. We observed that inclusion of dithiothreitol in the photolabeling reaction mixture decreased the amount of apparent changes in protein structure and also caused a significant increase in the extent of nucleotide incorporation (data not shown). Inasmuch as sulfhydryls are vulnerable to oxidation by ultraviolet radiation (Zaremba et al., 1984; Nath et al., 1985), increased photolabeling in the presence of dithiothreitol may simply be due to prevention of cysteine oxidation. On the basis of these results, standard conditions were established to maximize photoincorporation of [α - 32 P]GTP while photochemical damage to the enzyme was minimized. PEPCK (2–10 μ M) was incubated in the presence of 6 mM TES, 3% (v/v) glycerol, 0.5 mM EDTA, 100 μ M dithiothreitol, 1.1% (v/v) acetone, and 200 μ M [α - 32 P]GTP (30–200 Ci/mol) in a glass well in a total volume of 100 μ L at 0 °C. The sample was irradiated at a distance of 2 cm by a UVG-11 Mineralight lamp (330 μ W/cm²) for 10 min. After irradiation, the covalent incorporation of [α - 32 P]GTP into PEPCK was routinely measured by precipitation of the labeled enzyme onto filter paper in the presence of 10% trichloroacetic acid (Reimann et al., 1971; King et al., 1982). The filter paper was washed and the radioactivity was determined by liquid scintillation counting. Alternatively, quantification of [α - 32 P]GTP incorporation was performed by liquid scintillation counting and protein assays after gel filtration of the modified enzyme over a column (1.25 \times 37 cm) of Sephadex G-50 in the presence of 100 mM ammonium bicarbonate (pH 8.0), 1 mM EDTA, and 2 M urea; unmodified PEPCK in the presence of an equivalent concentration of urea was used as the protein standard.

Preparation and Isolation of Labeled Peptides. PEPCK was labeled under standard conditions, solid urea was added to 6 M, and the modified enzyme was separated from free [α - 32 P]GTP by gel filtration over Sephadex G-

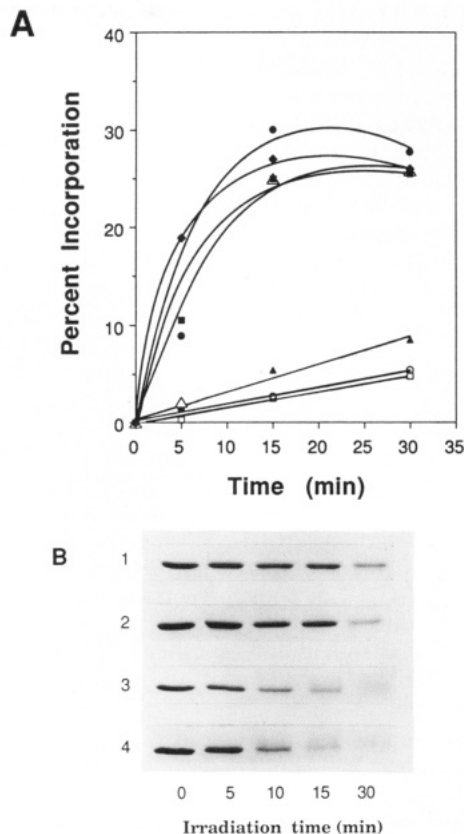


Figure 1. Panel A: time-dependence of photoincorporation. PEPCK was labeled under standard conditions for the indicated times in the presence of 200 μ M GTP and increasing concentrations of acetone: 0% (v/v), □; 0.2%, ○; 0.4%, ▲; 0.7%, △; 1.1%, ■; 1.5%, ●; 2.2%, ◆. Panel B: assessment of changes in protein structure. PEPCK was photolabeled under standard conditions for the indicated times and in the presence of increasing concentrations of acetone: 0% (v/v), row 1; 0.4%, row 2; 1.1%, row 3; 2.2%, row 4. After irradiation, an aliquot of each reaction mixture was subjected to polyacrylamide gel electrophoresis in the presence of sodium dodecyl sulfate. Only the region of interest of the polyacrylamide gel is shown; no other bands were apparent in any other area of the gel.

50 in the presence of 100 mM ammonium bicarbonate (pH 8.0), 1 mM EDTA, and 2 M urea. Tryptic digests were performed in this buffer in the presence of 2% (w/w) trypsin for 36 h at 37 °C, with an additional 2% (w/w) trypsin added after the first 12 h.

Proteolytic (*S. aureus* V8 protease) and CNBr digests were also prepared from enzyme labeled under standard conditions. Solid guanidine hydrochloride was added to 4 M, and the modified enzyme was separated from free [α - 32 P]GTP by gel filtration over a column (1.25 \times 37 cm) of Sephadex G-50 in the presence of 10 mM ammonium bicarbonate (pH 8.0) and 2 M guanidine hydrochloride. The sample was then digested with 2% V8 protease for 30 h at 37 °C, with an additional 2% V8 protease added after the first 12 h (Drapeau, 1976). Alternatively, the gel-filtered enzyme was lyophilized, solubilized in 70% formic acid, and digested with CNBr (60-fold molar excess over total methionine residues) under nitrogen for 24 h at 25 °C.

Initial attempts to purify the radiolabeled tryptic peptide(s) were performed by reversed-phase HPLC over a C₁₈ column (Delta-Pak, 300 Å, 3.9 \times 300 mm, 15 μ m; Waters Associates). Tryptic peptides were eluted with 20 mM ammonium acetate (pH 6.0) and acetonitrile, using a triphasic linear gradient of acetonitrile: 0–25% from 10 to 100 min, 25–35% from 100 to 200 min, 35–80% from 200 to 230 min. All subsequent proteolytic digests were

fractionated by anion-exchange HPLC after first desalting the lyophilized digests over a column of Bio-Gel P-2 (1.25 × 37 cm) equilibrated in water or in 10 mM ammonium bicarbonate (pH 7.5). Under these conditions the proteolytic peptides (detected by their absorbance at 210 nm) and the radioactivity eluted within the void volume of the P-2 column. The pooled fractions were lyophilized and then relyophilized after solubilization in water. The samples were then dissolved in 10 mM acetic acid (pH 3.5) and were purified by HPLC over an anion-exchange column (PL-SAX, 1000 Å, 8 µm, 50 × 4.6 mm, Polymer Laboratories). Peptides were eluted with solvent A (10 mM acetic acid, pH 3.5) and solvent B (500 mM acetic acid, pH 3.5) using a linear gradient of 0–60% B (tryptic digest) or 0–100% B (V8 proteolytic digest) from 20 to 110 min. Fractions (2 min) were collected, and the major peak of radioactivity was lyophilized. The radioactive tryptic fragment was further purified by desalting over a column of Sephadex G-10 equilibrated in 10 mM ammonium bicarbonate (pH 7.5), whereas the radioactive V8 proteolytic fragment was rechromatographed over Bio-Gel P-2 in H₂O. The pooled fractions were lyophilized prior to amino acid analysis. At each step of the purifications, the yield and quantity of the labeled peptide was estimated on the specific radioactivity of the [α -³²P]GTP.

Sequencing and Amino Acid Analysis of the Labeled Peptides. Independent samples of the purified proteolytic peptides (obtained from different enzyme preparations) were subjected to amino acid sequencing as previously described (Lewis et al., 1989b). Amino acid analyses were performed using standard protocols and according to published procedures (Jarrett et al., 1986). Additional samples of the labeled proteolytic peptides were also submitted to the Harvard Microchem Facility for amino acid analysis or sequencing. Portions of these samples were hydrolyzed in 6 N HCl for 24 h and derivatized with phenyl isothiocyanate using a 420A derivatizer from Applied Biosystems. The resulting PTC amino acids were analyzed via reversed-phase HPLC using an Applied Biosystems 130A HPLC. Aliquots of the samples were also subjected to sequencing using an Applied Biosystems 477A protein sequencer equipped with a 120A online PTH-amino acid analyzer.

RESULTS

Photoincorporation of [α -³²P]GTP. A primary objective of this study was to establish conditions by which radioactive GTP could covalently label PEPCK in yields sufficient for isolation of a modified peptide. Under the established standard conditions described in Experimental Procedures, the extent of photoincorporation is approximately 0.2 mol of [α -³²P]GTP/mol of PEPCK (Figure 1A), and changes in protein structure, as evidenced by polyacrylamide gel electrophoresis, are minimal (Figure 1B, lane 3). The enzyme retains approximately 20% of native activity after irradiation under these standard conditions. Considering the low power of the ultraviolet lamp and the minimal duration of irradiation, the extent of covalent incorporation of the nucleotide is high, and is sufficient for isolation of a labeled peptide.

Because it is possible for indiscriminate photochemical reactions to occur during these experiments, it is important to ascertain the specificity of the covalent modification. The data in Table I illustrate that photoincorporation of GTP requires native PEPCK. Enzyme that had been previously denatured by boiling was not labeled, and significant labeling did not occur in the presence of

Table I. Specificity of Photolabeling by [α -³²P]GTP^a

condition	% incorporation
2 µM PEPCK	17.8
2 µM PEPCK + 0.2% sodium dodecyl sulfate	1.1
2 µM PEPCK (boiled)	0.9
2 µM albumin	1.2

^a Photolabeling was carried out under standard conditions. The data represent the mean for duplicate analyses.

Table II. Substrate Protection against Photolabeling by [α -³²P]GTP^a

addition	% of control	addition	% of control
none	100	1 mM phosphoenolpyruvate	35.5 ± 0.6
200 µM ITP	35.0 ± 0.1	1 mM oxaloacetate	89.7 ± 0.3
200 µM GDP	33.7 ± 0.3	1.5 mM Mg(CH ₃ COO) ₂	61.4 ± 3.7
200 µM AMP	64.1 ± 3.3	1.5 mM MnCl ₂	54.4 ± 1.2

^a Photolabeling was carried out under standard conditions in the presence of 2 µM PEPCK, 200 µM [α -³²P]GTP, and the indicated concentrations of substrates. Incorporation of [α -³²P]GTP into PEPCK was measured by precipitation of the modified enzyme onto filter paper as described in Experimental Procedures. The results are expressed as a percentage of the incorporation observed in the absence of substrates (control, set to 100%), and the data represent an average of triplicate experiments (mean ± SD).

denaturant. The inability of [α -³²P]GTP to covalently label albumin, a protein of similar size but which does not bind the nucleotide, provides further evidence that the photolabeling of PEPCK is not merely due to nonspecific photochemical cross-linking.

If the covalent incorporation of [α -³²P]GTP does occur through a specific reaction at the nucleotide-binding site of PEPCK, then the addition of other substrates should affect the extent of labeling. Table II shows that this is indeed the case; alternative substrates such as ITP and GDP provide substantial protection against photoincorporation of [α -³²P]GTP. AMP, which is not a substrate for the enzyme, is much less effective than ITP or GDP. The protection that is afforded by AMP may be due to the ability of the nucleotide to absorb ultraviolet light at 254 nm and to thus decrease the efficiency of photolabeling. Divalent cations also decrease the extent of photolabeling. Phosphoenolpyruvate affords nearly as much protection against photolabeling as ITP, whereas oxaloacetate has no significant effect.

The specificity of the photolabeling reaction was also assessed by measuring the dependence of photoincorporation on [α -³²P]GTP concentration. As shown in Figure 2, the extent of labeling displayed saturation at higher nucleotide concentrations, indicating that the covalent modification step is preceded by reversible binding of [α -³²P]GTP to PEPCK. As determined from the double-reciprocal replot (inset), the concentration of [α -³²P]GTP required for half-maximal labeling was 69 ± 6 µM.

Isolation and Characterization of the Modified Tryptic Peptides. Fractionation of a tryptic digest of modified PEPCK by reversed-phase HPLC in 20 mM ammonium acetate (pH 6.0) revealed two peaks of radioactivity (Figure 3). The first peak (designated as peak I) was not retained by the C₁₈ column and accounted for 95% of the total eluted radioactivity. The second peak (peak II) was only slightly retarded by the C₁₈ column and accounted for 5% of the total eluted radioactivity. Peak II was isolated and lyophilized; sequence analysis of the purified peptide yielded exclusively the following sequence:

Ser-Glu-Ala-Thr-Ala-Ala-Ala-Glu-X-Lys

No PTH-amino acid could be identified for the ninth cycle of sequencing and no significant PTH-derivatives were

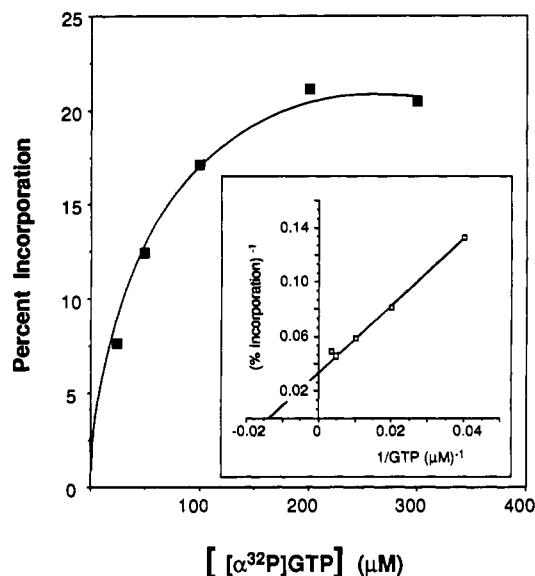


Figure 2. Concentration dependence of photolabeling. PEPCK was labeled under standard conditions in the presence of the indicated concentrations of [α - 32 P]GTP.

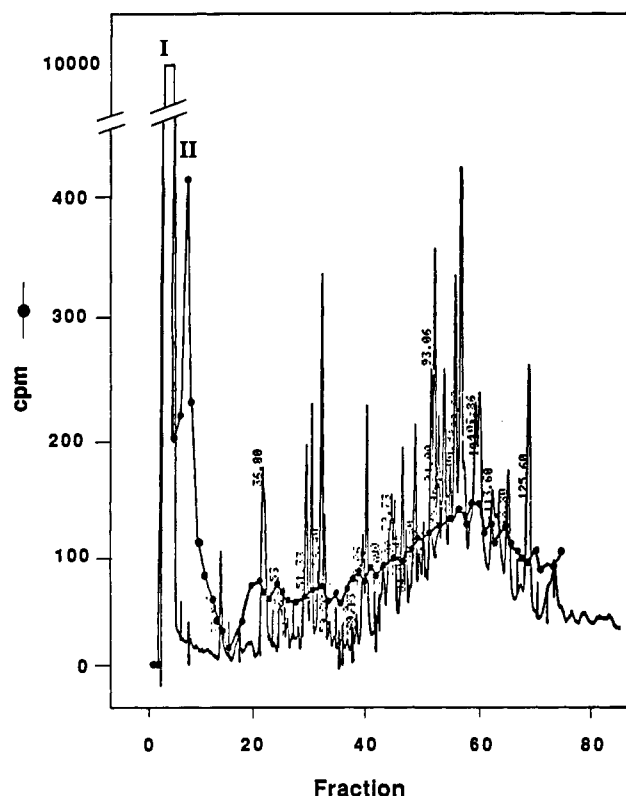


Figure 3. Reversed-phase HPLC of a tryptic digest of modified PEPCK. The tryptic digest of PEPCK was prepared and subjected to reversed-phase HPLC in 20 mM ammonium acetate (pH 6.0) as described in Experimental Procedures. Peptides were detected by their absorbance at 210 nm, and aliquots of each fraction were assayed for radioactivity (●) using liquid scintillation counting.

detected after cycle 10. This sequence matches that of the tryptic peptide Ser₄₆₂-Lys₄₇₁ of PEPCK, which contains a histidine residue at position 470 (Beale et al., 1985).

It should be emphasized that the modified enzyme had been purified from free [α - 32 P]GTP prior to tryptic digestion, suggesting that peak I, bearing the majority of the radioactive label, must represent a hydrophilic labeled peptide that was simply not retained by the reversed-phase column. Two-dimensional peptide maps of tryptic

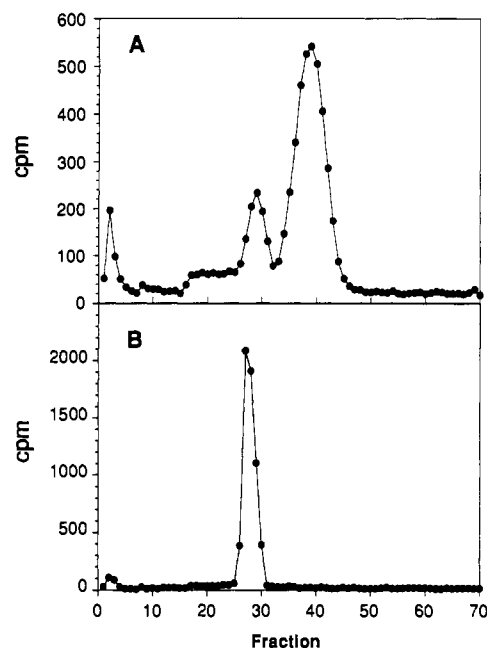


Figure 4. Ion-exchange HPLC of the proteolytic digests of modified PEPCK. The tryptic (A) or *S. aureus* V8 proteolytic (B) digest of PEPCK was prepared and subjected to anion-exchange HPLC in 10 mM acetic acid (pH 3.6) as described in Experimental Procedures. Detection of a significant corresponding peak in absorbance at 220 nm was difficult due to a large background subtraction from the acetic acid gradient.

digests of the modified enzyme indicated that the radioactivity was associated with a peptide and did not represent either undigested enzyme, [α - 32 P]GTP, or a fragment of [α - 32 P]GTP. The major radioactive spot derived from the tryptic digest migrated closer to the anode than did [α - 32 P]GTP, suggesting the presence of one or more acidic residues (data not shown). Therefore, a purification strategy was devised to take advantage of the highly anionic nature of a tryptic peptide labeled with guanosine triphosphate. After gel filtration, a tryptic digest of modified PEPCK was passed over a strong anion-exchange HPLC column at pH 3.6. Under these conditions, most of the tryptic peptides were not retained. The column was then eluted with acetic acid (Figure 4A). The peak eluting between fractions 35 and 45 contained at least 75% of the total eluted radioactivity; this peak was pooled and subjected to sequencing and amino acid analysis. Under these conditions, this major peak did not have the same retention time as free [α - 32 P]GTP. The two smaller radioactive peaks were not analyzed.

Three independently derived samples of the major peak shown in Figure 4A were submitted for sequence analysis; in each case a sequence could not be determined. The yield of PTH derivatives that could be detected at each cycle was very low and accounted for less than 5% of the applied sample. These results suggested that the amino terminus of this labeled tryptic peptide was blocked; the remaining samples were therefore characterized by amino acid analysis. The amino acid compositions of each of the three independent samples were very similar, and each contained relatively high amounts of Asx and Glx (data not shown), which is consistent with this tryptic peptide being highly acidic. However, the composition could not be unambiguously assigned to any single modified tryptic peptide predicted from the known sequence of PEPCK (Beale et al., 1985). The quantity of the peptides subjected to amino acid analyses was estimated from the specific radioactivity, assuming one molecule of [α - 32 P]GTP was incorporated per peptide. It should be emphasized that

the quantity of amino acids detected was within 10% of this estimate.

Characterization of the Labeled CNBr Fragment. It was anticipated that a cyanogen bromide fragment of the labeled enzyme might permit the unequivocal identification of a modified peptide. Following lyophilization, a CNBr digest was solubilized in aqueous 0.1% trifluoroacetic acid and was applied to a C_{18} reversed-phase HPLC column equilibrated in the same buffer. Under these conditions, >75% of the applied radioactivity was not retained by the column. Because the radioactive CNBr fragment(s) eluted from a Bio-Gel P-2 column as a broad peak with a greater retention time than [α - 32 P]-GTP, we reasoned that the CNBr fragment might be smaller than the nucleotide itself. This supposition was supported by two-dimensional peptide maps of the CNBr digest, which showed that the radioactive CNBr fragment(s) coelectrophoresed with [α - 32 P]GTP but migrated somewhat faster than GTP in the second chromatography dimension (data not shown). These data suggest that the derivatized peptide was not stable under the highly acidic conditions used for CNBr cleavage, a result that has been reported by several other laboratories (Abraham et al., 1983; Peter et al., 1988; Hoppe et al., 1983). Fractionation of a peptic digest by reversed-phase HPLC also indicated that most of the radioactivity was not retained by the C_{18} column. We therefore sought yet another cleavage method for isolation of the modified peptide.

Isolation and Characterization of the Modified *S. aureus* V8 Proteolytic Peptide. The radiolabeled fragment derived from a V8 proteolytic digestion of modified PEPCK eluted as a single radioactive peak during anion-exchange HPLC (Figure 4B). Sequence analysis of the purified peptide yielded exclusively the following sequence:

Asp-Gln-Val-Asn-Ala-Asp-Leu-Pro

Although serine and glycine appeared as contaminating PTH derivatives in the first cycle (<30%), no contaminating PTH derivatives appeared in any subsequent cycles. Scintillation counting of the eluent from each cycle of sequencing revealed that all of the radioactivity remained associated with the filter and the seal on which the sample was applied. Because of diminishing yields, no PTH derivatives were detected beyond the eighth cycle of sequencing. This sequence overlaps with the *S. aureus* V8 proteolytic peptide that would be produced from PEPCK under our experimental conditions (cleavage at glutamate only): Asp₅₉₈-Gln-Val-Asn-Ala-Asp-Leu-Pro-Tyr-Glu₆₀₇ (Beale et al., 1985).

DISCUSSION

In spite of the advantages afforded by modifying with the natural ligand, it is nevertheless important to characterize the specificity of the photochemical reaction. Our results indicate that the standard conditions chosen for photolabeling yield substantial amounts of covalently modified PEPCK without sacrificing specificity. Although the addition of acetone as a photosensitizer substantially increased incorporation of the nucleotide, at higher concentrations it also caused greater changes in the enzyme's structure as detected by polyacrylamide gel electrophoresis in the presence of sodium dodecyl sulfate. However, as was discussed previously, inclusion of dithiothreitol in the photolabeling reaction mixture diminished apparent alterations in protein structure. In summary, by including dithiothreitol and by minimizing the con-

centration of acetone and the duration of irradiation, we established standard conditions for photolabeling that cause minimal damage to the enzyme. Under these conditions, the incorporation of the nucleotide is approximately 0.2 mol/mol of enzyme, as measured by precipitation of the labeled enzyme onto filter paper or by gel filtration in the presence of a denaturant.

Several lines of evidence indicate that [α - 32 P]GTP is specifically incorporated into the active site of native PEPCK. First, there was no significant photolabeling of denatured enzyme or albumin under conditions in which incorporation into native PEPCK was approximately 20%. Second, the pattern of substrate protection was consistent with specific modification of the nucleotide binding site. Substrates that would be expected to compete with [α - 32 P]GTP for the active site (ITP, GDP, and phosphoenolpyruvate) provided substantial protection against photolabeling, whereas AMP and oxaloacetate had little effect. It is not clear from these studies whether the divalent metal ions decreased the extent of photolabeling by chelation of the nucleotide or through a general charge effect. Third, the extent of labeling displayed saturation with increasing nucleotide concentration, indicating that covalent modification was preceded by reversible binding. These data indicate that direct photolabeling by [α - 32 P]-GTP under standard conditions results in the specific modification of the enzyme's active site; thus, the peptide that bears the majority of the radioactive label should define a portion of the GTP binding site that interacts with the purine ring.

Isolation of the major radioactive fragment generated from a V8 proteolytic digest of the modified enzyme yielded exclusively the peptide Asp₅₉₈-Pro₆₀₅, which lies near the carboxyl terminus of this 621 amino acid protein (Beale et al., 1985). Although the sequence of the modified tryptic peptide derived from peak II of Figure 3 (Ser₄₆₂-Lys₄₇₁) revealed a distinct blank in one sequencing cycle (usually indicative of a modified residue), the sequence analysis of the V8 peptide did not display such a pattern. We therefore analyzed the radioactivity recovered from the filter, seal, and from aliquots of each sequencing cycle by liquid scintillation counting; the results showed that all of the radioactivity remained associated with the filter and the seal onto which the sample had been applied. However, our inability to detect radioactivity at any of the sequencing cycles of the modified peptide is not without precedent. Independent sequence analyses of several radioactive carboxymethylated peptides (modified by [3 H]- or [14 C]iodoacetate) derived from PEPCK also showed that the majority of radioactivity remained associated with the filter and seal (unpublished data). Similarly, although Hesse et al. (1987) isolated and sequenced a radioactive peptide from a preparation of β -tubulin photolabeled with GTP, the labeled residue was not identified because all of the radioactivity remained on the sequencing filter. On the basis of their results, the authors concluded that the GTP-peptide bond was apparently sensitive to the degrading chemicals, but that the phenylthiohydantoins were nevertheless extracted and identified. We considered the possibility that Asp₅₉₈-Pro₆₀₅ represented a highly acidic, contaminating, unlabeled peptide that copurified on the anion-exchange HPLC column with the radiolabeled triphosphate-containing peptide; however, a number of facts argue against this possibility. Sequence analyses of the V8 proteolytic peptide revealed no substantial quantities of contaminating PTH derivatives; therefore, if contaminating peptides were present then they would have to be blocked at the N-terminus.

The fact that the moles of amino acids detected within the tryptic peptide agreed with the amounts that were predicted from the specific radioactivity of [α - 32 P]GTP argues against the comigration of significant amounts of contaminating peptides during anion-exchange HPLC. Finally, the high percentage of acidic residues in the labeled peptide is consistent with the negligible retention of radioactivity on a C₁₈ reversed-phase HPLC column and with the observation by two-dimensional peptide mapping that the major radiolabeled tryptic peptide was more negatively charged than GTP. Despite these arguments, the use of a purification protocol that selects for negatively charged peptides imposes a caveat on our identification of an acidic peptide as the site of labeling. We cannot definitely exclude the possibility that contamination by the C-terminal peptide, caused by UV-mediated covalent cross-linking or comigration of acidic peptides during anion-exchange HPLC chromatography, obscured the identification of a small [α - 32 P]GTP-labeled peptide.

Fractionation by reversed-phase HPLC of a tryptic digest of modified PEPCK revealed two radioactive peaks, one bearing a major portion and the other a minor portion of the total eluted radioactivity. Although conditions were established for purification of the major radioactive tryptic peptide by anion-exchange HPLC, this particular peptide, unlike the V8 proteolytic peptide, could not be identified by sequencing or by amino acid analysis. It is possible that a residue(s) was covalently modified during photolabeling or peptide isolation such that the resultant tryptic peptide was resistant to Edman degradation. For example, an O-acyl group of a serine or threonine can undergo O \rightarrow N migration under alkaline conditions to form the N-acylserine/threonine, thus rendering the peptide resistant to degradation (Allen, 1981; Jornvall, 1970). Considering the methodology and the current lack of information concerning the photochemistry of amino acid side chains, our inability to identify this tryptic peptide by amino acid analysis is not necessarily surprising. One report of direct photolabeling described tryptic peptides that were apparently cross-linked and that could not be interpreted in terms of a single peptide chain (Sperling and Havron, 1976). Amino acids that become modified subsequent to, or independent of, labeling by the nucleotide could also obstruct peptide identification. For example, tyrosine residues can become cross-linked to each other (Andersen, 1964), and Carroll et al. found that UV-mediated covalent labeling can be accompanied by cleavage of bonds in the modified amino acid side chains as well as in the label (Carroll & Collier, 1984; Carroll et al., 1985).

Sequence analysis of the tryptic peptide bearing the smaller portion of the radioactivity revealed that the modified peptide was Ser₄₆₂-Lys₄₇₁. The absence of the predicted histidine residue at cycle 9 suggests that His₄₇₀ was modified by [α - 32 P]GTP. This peptide is quite hydrophilic and resides within a putative α -helical domain of the enzyme (Beale et al., 1985); all of the residues within this peptide are conserved among the cytosolic and mitochondrial isoenzymes from rat, chicken, and *Drosophila melanogaster* (Beale et al., 1985; Weldon et al., 1990; Gundelfinger et al., 1987). However, because this minor peptide represents only 5% of the total eluted radioactivity, we are hesitant to assign it unequivocally as a portion of the GTP binding site.

In summary, our results demonstrate that specific modification of the active site of PEPCK, in yields sufficient for peptide isolation, can be performed by direct photolabeling under relatively mild conditions. Two peptides representing the major and the minor portion of the

radioactive label were isolated and identified. Although the previously discussed limitations prevent us from concluding with certainty that these two peptides represent portions of the GTP binding site, our results are nevertheless most consistent with that conclusion. In general, the convenience of using the natural substrate as a probe, rather than an expensive or synthetically difficult affinity label, may continue to be of practical utility in the identification of nucleotide-binding proteins and the characterization of their active sites.

ACKNOWLEDGMENT

This work was supported in part by Research Grants from the National Science Foundation (DMB 85-20311 to G.M.C.) and by research funds from the Veterans Administration (J.M.S.). We thank Dr. Bob Cassell of the Veterans Administration Medical Center of Memphis and Dr. Bill Lane and colleagues of the Harvard Microchemistry Facility for excellent technical assistance in peptide sequencing and amino acid analysis. We are also grateful to Dr. Harry Jarrett of the University of Tennessee, Memphis, for assistance with amino acid analyses.

LITERATURE CITED

- Abraham, K. I., Haley, B., and Modak, M. J. (1983) Biochemistry of Terminal Deoxynucleotidyltransferase: Characterization and Properties of Photoaffinity Labeling with 8-Azidoadenosine 5'-Triphosphate. *Biochemistry* 22, 4197-4203.
- Allen, G. (1981) *Laboratory Techniques in Biochemistry and Molecular Biology: Sequencing of Proteins and Peptides*, Elsevier/North Holland Biomedical Press, Amsterdam, The Netherlands.
- Andersen, S. O. (1964) The Cross-links in Resilin Identified as Dityrosine and Trityrosine. *Biochim. Biophys. Acta* 93, 213-215.
- Anthony, D. D., Kinzy, T. G., and Merrick, W. C. (1990) Affinity Labeling of Eukaryotic Initiation Factor 2 and Elongation Factor 1- α β γ with GTP Analogs. *Arch. Biochem. Biophys.* 281, 157-162.
- Beale, E. G., Chrapkiewicz, N. B., Scoble, H. A., Metz, R. J., Quick, D. P., Noble, R. L., Donelson, J. E., Biemann, K., and Granner, D. K. (1985) Rat Hepatic Cytosolic Phosphoenolpyruvate Carboxykinase (GTP): Structures of the Protein, Messenger RNA, and Gene. *J. Biol. Chem.* 260, 10748-10760.
- Carlson, G. M., Colombo, G., and Lardy, H. A. (1978) A Vicinal Dithiol Containing an Essential Cysteine in Phosphoenolpyruvate Carboxykinase (Guanosine Triphosphate) from Cytosol of Rat Liver. *Biochemistry* 17, 5329-5338.
- Carroll, S. F., and Collier, R. J. (1984) NAD Binding Site of Diphtheria Toxin: Identification of a Residue within the Nicotinamide Subsite by Photochemical Modification with NAD. *Proc. Natl. Acad. Sci. U.S.A.* 81, 3307-3311.
- Carroll, S. F., McCloskey, J. A., Crain, P. F., Oppenheimer, N. J., Marschner, T. M., and Collier, R. J. (1985) Photoaffinity Labeling of Diphtheria Toxin Fragment A with NAD: Structure of the Photoproduct at Position 148. *Proc. Natl. Acad. Sci. U.S.A.* 82, 7237-7241.
- Cook, J. S., Weldon, S. L., Garcia-Ruiz, J. P., Hod, Y., and Hanson, R. W. (1986) Nucleotide Sequence of the mRNA Encoding the Cytosolic Form of Phosphoenolpyruvate Carboxykinase (GTP) from the Chicken. *Proc. Natl. Acad. Sci. U.S.A.* 83, 7583-7587.
- Drapeau, G. R. (1976) Protease from *Staphylococcus aureus*. *Methods Enzymol.* 45, 469-475.
- Gundelfinger, E. D., Hermans-Borgmeyer, I., Grennengloh, G., and Zopf, D. (1987) Nucleotide and Deduced Amino Acid Sequence of the Phosphoenolpyruvate Carboxykinase (GTP) from *Drosophila melanogaster*. *Nucleic Acids Res.* 15, 9745.
- Hesse, J., Thierauf, M., and Ponstingl, H. (1987) Tubulin Sequence Region 8155-174 Is Involved in Binding Exchangeable Guanosine Triphosphate. *J. Biol. Chem.* 262, 15472-15475.

- Hoppe, J., Montecucco, C., and Friedl, P. (1983) Labeling of Subunit *b* of the ATP Synthase from *Escherichia coli* with a Photoreactive Phospholipid Analogue. *J. Biol. Chem.* 258, 2882-2885.
- Jadus, M., Hanson, R. W., and Colman, R. F. (1981) Inactivation of Phosphoenolpyruvate Carboxykinase by the Guanosine Nucleotide Analogue 5'-*p*-Fluorosulfonyl-benzoylguanosine. *Biochem. Biophys. Res. Commun.* 101, 884-892.
- Jarrett, H. W., Cooksy, K. D., Ellis, B., and Anderson, J. M. (1986) The Separation of *o*-Phthalaldehyde Derivatives of Amino Acids by Reversed-Phase Chromatography on Octyl-silica Columns. *Anal. Biochem.* 153, 189-198.
- Jornvall, H. (1970) Horse Liver Alcohol Dehydrogenase: The Primary Structure of the Protein Chain of the Ethanol-Active Isoenzyme. *Eur. J. Biochem.* 16, 25-40.
- King, M. M., Carlson, G. M., and Haley, B. E. (1982) Photoaffinity Labeling of the β Subunit of Phosphorylase *b* Kinase by 8-Azidoadenosine 5'-Triphosphate and Its 2',3'-Dialdehyde Derivative. *J. Biol. Chem.* 257, 14058-14065.
- Lewis, C. T., Haley, B. E., and Carlson, G. M. (1989a) Formation of an Intramolecular Cystine Disulfide during the Reaction of 8-Azidoguanosine 5'-Triphosphate with Cytosolic Phosphoenolpyruvate Carboxykinase (GTP) Causes Inactivation without Photolabeling. *Biochemistry* 28, 9248-9255.
- Lewis, C. T., Seyer, J. M., and Carlson, G. M. (1989b) Cysteine 288: An Essential Hyperreactive Thiol of Cytosolic Phosphoenolpyruvate Carboxykinase (GTP). *J. Biol. Chem.* 264, 27-33.
- Miller, R. S., Mildvan, A. S., Chang, H.-C., Easterday, R. L., Maruyama, H., and Lane, M. D. (1968) Purification and Properties of Rabbit Skeletal Muscle Adenosine 3',5'-Monophosphate-dependent Protein Kinases. *J. Biol. Chem.* 243, 6030-6040.
- Nath, J. P., Eagle, G. R., and Himes, R. H. (1985) Direct Photoaffinity Labeling of Tubulin with Guanosine 5'-Triphosphate. *Biochemistry* 24, 1555-1560.
- Ohmi, N., Hoshiro, M., Tagaya, M., Fukui, T., Kauakita, M., and Hattori, S. (1988) Affinity Labeling of *ras* Oncogene Product p21 with Guanosine Diphospho- and Triphosphopyridoxals. *J. Biol. Chem.* 263, 14261-14266.
- Peter, M. E., Wittmann-Liebold, B., and Sprinzl, M. (1988) Affinity Labeling of the GDP/GTP Binding Site in *Thermus thermophilus* Elongation Factor Tu. *Biochemistry* 27, 9132-9139.
- Reimann, E. M., Walsh, D. A., and Krebs, E. G. (1971) Purification and Properties of Rabbit Skeletal Muscle Adenosine 3',5'-Monophosphate-dependent Protein Kinases. *J. Biol. Chem.* 246, 1986-1995.
- Samant, B. R., and Sweet, F. (1983) 5'-Bromoacetamido-5'-deoxyadenosine. *J. Biol. Chem.* 258, 12779-12782.
- Sperling, J. (1976) Photochemical Crosslinking of ATP to Histone H4. *Photochem. Photobiol.* 23, 323-326.
- Sperling, J., and Havron, A. (1976) Photochemical Crosslinking of Neighboring Residues in Protein-Nucleic Acid Complexes: RNase and Pyrimidine Nucleotide Inhibitors. *Biochemistry* 15, 1489-1495.
- Steinmaus, H., Rosenthal, I., and Elad, D. (1971) Light- and γ -Ray-Induced Reactions of Purines and Purine Nucleosides with Alcohols. *J. Org. Chem.* 36, 3594-3598.
- Weldon, S. L., Rando, A., Matathias, A. S., Hod, Y., Kalonick, A., Savon, S., Cook, J. S., and Hanson, R. W. (1990) Mitochondrial Phosphoenolpyruvate Carboxykinase from the Chicken: Comparison of the cDNA and Protein Sequences with the Cytosolic Isozyme. *J. Biol. Chem.* 265, 7308-7317.
- Zaremba, T. G., LeBon, T. R., Millar, D. B., Smejkal, R. M., and Hawley, R. J. (1984) Effects of Ultraviolet Light on the in vitro Assembly of Microtubules. *Biochemistry* 23, 1073-1080.
- Registry No.** PEPCK(GTP), 9013-08-5; GTP, 86-01-1; Mg^{2+} , 7439-95-4; Mn^{2+} , 7439-96-5.

Vinylstannylated Alkylating Agents as Prosthetic Groups for Radioiodination of Small Molecules: Design, Synthesis, and Application to Iodoallyl Analogues of Spiperone and Diprenorphine

John L. Musachio and John R. Lever*

Division of Radiation Health Sciences, Department of Environmental Health Sciences, The Johns Hopkins University School of Hygiene and Public Health, Baltimore, Maryland 21205-2179. Received December 2, 1991

The preparation and synthetic utility of *p*-toluenesulfonate esters of (*E*)- and (*Z*)-3-(tri-*n*-butylstannyl)-prop-2-en-1-ol as bifunctional reagents for radioiodination are described. These vinylstannylated alkylating agents are prepared in two steps from propargyl alcohol, and readily couple with nucleophilic functionality (amide nitrogen, secondary amine, tertiary alcohol) in good yields (48–95%) to provide derivatives of the neuroreceptor ligands spiperone and diprenorphine. Regio- and stereospecific radioiododestannylation with retention of configuration occurs under mild, no-carrier-added conditions to give the corresponding radiolabeled *N*- or *O*-iodoallyl analogues in good radiochemical yields (55–95%) with high specific radioactivities. The methodology is versatile and well-suited to selective labeling of small molecules with radioisotopes of iodine such as ^{125}I or ^{123}I .

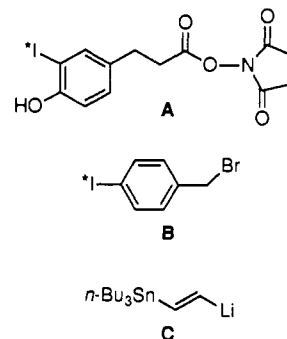
INTRODUCTION

Radioiodinated tracers have diverse applications in biomedical research, and there are a number of methods for incorporation of radioiodine into organic substrates (Seever & Counsell, 1982; Coenen et al., 1983; Baldwin, 1986). Direct electrophilic radioiodination is most commonly employed, but many compounds are not suited to this procedure because they lack activating functionality, are not stable upon iodination, or lose biological activity when iodinated at the chemically favored site. In such circumstances, the use of a prosthetic group is advisable in order to enhance reactivity, promote stability, control regiospecificity, and avoid harsh reaction conditions.

A variety of radioiodinated aromatics, exemplified by the Bolton–Hunter reagent (Chart I, A), have been tailored for conjugation to proteins, antibodies, and glycosides (Bolton & Hunter, 1973; Lowndes et al., 1988; Wilbur et al., 1989; Lin et al., 1989; Vaidyanathan & Zalutsky, 1990). However, these techniques are of limited applicability to small molecules due to the relatively large size of the reagents. Notwithstanding, the Bolton–Hunter method is quite useful in some instances, including the preparation of certain neuroreceptor ligands (Korner et al., 1986; Ponchant et al., 1988). *p*-Iodobenzyl bromide (Chart I, B), one of the few prosthetic groups chiefly intended for radiolabeling small molecules with either ^{125}I or ^{123}I (Wilson et al., 1986), has been applied to radioiodinated glucose analogues (Saji et al., 1987). This reagent is particularly appropriate when the benzyl moiety is an integral feature of the target, as in the case of the muscarinic cholinergic receptor antagonist 4-iododexetimide (Wilson et al., 1989).

Prosthetic groups which impart less steric bulk and lipophilicity are especially desirable for radioiodination of small molecules, since minimal perturbation of structural and physicochemical parameters increases the likelihood of preserving favorable properties of the parent compound. The smallest prosthetic group for radioiodination is a lithiated vinylstannane (Chart I, C), which, after nucleophilic

Chart I.* Prosthetic Groups for Radioiodination



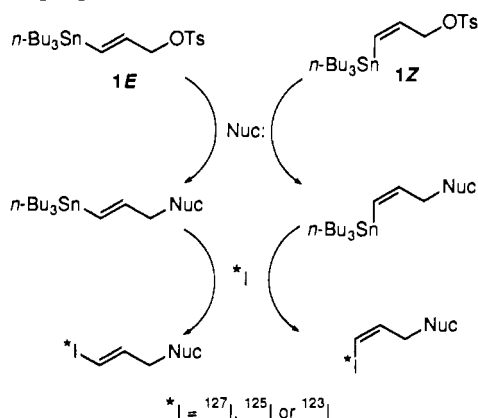
*I = radioisotopes of iodine.

addition to carbonyl groups and halodemetalation, gives iodovinyl derivatives (Hanson & Seitz, 1982; Hanson et al., 1982). Since radioiododestannylation is fast and reliable (Kabalka & Varma, 1989), complementary electrophilic reagents for the introduction of vinylstannylated prosthetic groups would be of considerable synthetic value.

In a recent communication, we described bifunctional alkylating agents 1*E* and 1*Z*, which render vinylstannanes for radioiodination as depicted in Scheme I (Musachio & Lever, 1989). Several factors provided the rationale for selection of 1*E* and 1*Z* as prosthetic groups. The allylic framework, in conjunction with the leaving-group ability of tosylate, allows ready coupling to nucleophilic functionality. The intermediacy of vinylstannanes permits radioiodination in high yield under mild, no-carrier-added conditions. Radiolabeling at the end of the synthetic procedure mitigates exposure to and handling of radioactive materials. Finally, the sequence gives a vinyl carbon–iodine bond which is stronger than the often used aryl carbon–iodine bond (Coenen et al., 1983). Of note, the allylic linkage is the smallest unit which accommodates sites which facilitate conjugation as well as stable incorporation of radioiodine.

In our initial studies, 1*E* and 1*Z* were employed for syntheses of *N*-iodoallyl analogues of spiperone radiolabeled with ^{125}I ($t_{1/2}$ = 60 d) or the diagnostic imaging radioisotope ^{123}I ($t_{1/2}$ = 13.3 h). These ligands display high affinities for serotonin 5-HT₂ and dopamine D₂ receptors in vitro, and are suited for in vivo studies of D₂

* Address correspondence and offprint requests to John R. Lever, Ph.D., Department of Environmental Health Sciences, The Johns Hopkins University School of Hygiene and Public Health, 2001 Hume, 615 N. Wolfe St., Baltimore, Maryland 21205-2179.

Scheme I. Radioiodination via Vinylstannylated Alkylating Agents

sites including single photon emission computed tomography (Lever et al., 1989; Lever et al., 1990a). Here we provide full details for the preparation of **1E** and **1Z**, as well as for (*E*)- and (*Z*)-3-*N*-(iodoallyl)sipiperone. Further, we illustrate the general utility of the approach through syntheses of *N*- and *O*-iodoallyl analogues of diprenorphine, a potent opioid receptor ligand.

EXPERIMENTAL PROCEDURES

Chemicals and solvents were reagent grade and used as received from commercial sources unless otherwise stated. Dry DMF was prepared by sequential distillations under reduced pressure from CaH_2 and then BaO. No-carrier-added [^{125}I]NaI was obtained from Amersham Corp. (1 mCi/10 μL of dilute NaOH, pH 7–11). [^{123}I]NaI, produced by the (p, 5n) reaction and dispensed in 0.1 N NaOH (50–200 μL), was purchased from Nordion Intl. Uncorrected melting points were determined with a Thomas-Hoover capillary apparatus. ^1H NMR spectra were obtained with a Bruker WM-300 (300.13 MHz) unless otherwise stated. Chemical shifts are reported in ppm (δ) relative to internal Me_4Si in CDCl_3 . Proton assignments for sipiperone derivatives (4–7) were made by analogy to previous reports (Burns et al., 1984; Chi et al., 1987) while assignments for morphinans (8–16) were based upon a 2D NMR study of diprenorphine (Mazza et al., 1990). HRMS via EI, CI, or FAB was performed at the University of Minnesota Mass Spectrometry Facility. Elemental analyses were determined by Atlantic Microlab, Inc. Analytical TLC was conducted on Macherey Nagel silica gel 60 F-254 plates (250 μm). Short-path column chromatography was performed using E. Merck 7729 (<230 mesh) silica gel under N_2 pressure. HPLC equipment consisted of a Rheodyne 7125 injector, Waters 510EF pumps, Waters 490 UV absorbance detector (254 nm unless otherwise noted), a flow-through NaI(Tl) crystal scintillation detector comprised of EE&G Ortec components, and Shimadzu CR-3A integrating recorders. Waters C-18 Nova-Pak columns were used for semipreparative (7.8 mm \times 30 cm, 6 μm) and analytical (radial compression module, 8 mm \times 10 cm, 4 μm) reverse-phase HPLC unless otherwise noted. Analytical Alltech silica columns (Econosil, 4.6 mm \times 25 cm, 10 μm) were used for normal-phase HPLC. Radioactivity was measured with a radioisotope dose calibrator (Capintec CRC-7), assuring similar counting geometries and vessel types for each reading. Specific radioactivities were determined for aliquots of known radioactivity using analytical HPLC for determination of the mass associated with the UV absorbance peak area for the carrier. The HPLC response curve was established using nonradioactive standards.

(*E,Z*)-3-(Tri-*n*-butylstannyl)prop-2-en-1-ol (**2E** and **2Z**) and 2-(Tri-*n*-butylstannyl)prop-2-en-1-ol (**3**). Vinylstannylated alcohols (**2E**, **2Z**, and **3**) were prepared by minor modifications of the procedure of Jung and Light (1982). Propargyl alcohol (5.61 g, 100 mmol) was treated with tri-*n*-butyltin hydride (14.5 g, 50 mmol) and AIBN (0.10 g, 0.73 mmol). After heating at 60 $^\circ\text{C}$ for 2 h, excess propargyl alcohol was removed under reduced pressure. The crude mixture was applied to a short-path column and eluted with hexane/EtOAc (96:4). Fractions were monitored by TLC (hexane/EtOAc, 8:1) with visualization by ethanolic phosphomolybdic acid. As previously reported, **2Z/3** (8.10 g, 23.3 mmol; 47%) were obtained as an inseparable mixture (R_f = 0.51), while **2E** (3.20 g, 9.22 mmol; 18%) was readily isolated (R_f = 0.43). Appropriate ^1H NMR spectral characteristics were observed for **2E** and the **2Z/3** (1.1:1) mixture.

(*E*)- and (*Z*)-3-(Tri-*n*-butylstannyl)prop-2-en-1-ol, *p*-Toluenesulfonate (**1E** and **1Z**). **1E**. To a solution of **2E** (5.50 g, 15.8 mmol) in diethyl ether (30 mL) under N_2 and cooled to -25°C was added TsCl (3.24 g, 17.0 mmol) in diethyl ether (20 mL). Potassium trimethylsilanolate (10.16 g, 79.1 mmol) was added in portions over 30 min. The mixture was stirred vigorously at -25°C for 2 h, poured into ice water (75 mL), and extracted with diethyl ether (2 \times 75 mL). The combined organic extracts were washed with ice cold water (50 mL) and dried (Na_2SO_4). Filtration, concentration under reduced pressure at ambient temperature, and short-path chromatography (hexane/EtOAc, 98:2) gave **1E** (5.17 g, 10.3 mmol) as a colorless oil in 65% yield. ^1H NMR: (CDCl_3 , δ) 0.83–0.94 (m, 15 H, *n*-Bu), 1.24–1.56 (m, 12 H, *n*-Bu), 2.45 (s, 3 H, PhCH_3), 4.53 (dd, 2 H, J = 5.3, 1.2 Hz, CH_2O), 5.90 (dt, 1 H, J = 19.0, 5.3 Hz, CHCH_2), 6.29 (dt, 1 H, J = 19.0, 1.2 Hz, SnCH), 7.33 (d, 2 H, J = 8.3 Hz), 7.80 (d, 2 H, J = 8.3 Hz). HRMS-EI: m/z calcd, 502.1563; found, 445.0838 ($\text{M}^+ - n\text{-Bu}$, 40). Anal. Calcd for $\text{C}_{22}\text{H}_{38}\text{O}_3\text{SSn}$: C, 52.71; H, 7.64; S, 6.40. Found: C, 52.49; H, 7.66; S, 6.29.

1Z. As described for **1E**, a mixture of **2Z/3** (1.1:1, 1.38 g, 3.98 mmol) in diethyl ether (6 mL) at -25°C was treated with TsCl (0.84 g, 4.40 mmol) in diethyl ether (10 mL) and potassium trimethylsilanolate (2.56 g, 19.9 mmol) to give, after workup and short-path chromatography, **1Z** (0.460 g; 0.92 mmol) in 42% yield. ^1H NMR: (400 MHz, CDCl_3 , δ) 0.80–0.94 (m, 15 H, *n*-Bu), 1.22–1.47 (m, 12 H, *n*-Bu), 2.45 (s, 3 H, PhCH_3), 4.44 (dd, 2 H, J = 6.5, 1.0 Hz, CH_2O), 6.24 (dt, 1 H, J = 13.0, 1.0 Hz, SnCH), 6.49 (dt, 1 H, J = 13.0, 6.5 Hz, CHCH_2), 7.35 (d, 2 H, J = 8.4 Hz), 7.80 (d, 2 H, J = 8.4 Hz). HRMS-EI: m/z calcd, 502.1563; found, 445.0832 ($\text{M}^+ - n\text{-Bu}$, 58). Anal. Calcd for $\text{C}_{22}\text{H}_{38}\text{O}_3\text{SSn}$: C, 52.71; H, 7.64; S, 6.40. Found: C, 52.86; H, 7.68; S, 6.33.

(*E*)- and (*Z*)-3-*N*-[3-(Tri-*n*-butylstannyl)prop-2-enyl]sipiperone (**4E** and **4Z**). **4E**. NaH (0.036 g, 1.5 mmol) was added to a stirred solution of sipiperone (0.100 g, 0.25 mmol) in DMF (1.0 mL) under N_2 at ambient temperature. After 3 min, a solution of **1E** (0.150 g, 0.30 mmol) in DMF (1 mL) was added. After 2 min, the reaction was quenched by slow addition of saturated NH_4Cl (2 mL). The solution was made basic (1.0 N NaOH) and extracted with CH_2Cl_2 (3 \times 15 mL). The extracts were washed with saturated NaHCO_3 (15 mL) and concentrated under reduced pressure. Residual DMF was removed by bulb-to-bulb distillation (3 mm; 55 $^\circ\text{C}$). Short-path column chromatography (hexane/EtOAc/ Et_3N , 70:30:1) gave **4E** (0.086 g, 0.12 mmol) as a colorless oil in 48% yield. ^1H NMR: (CDCl_3 , δ) 0.85–0.98 (m, 15 H, *n*-Bu), 1.23–1.53 (m, 12 H, *n*-Bu), 1.67 (bd, 2 H, J = 13.8 Hz), 1.97 (quin, 2 H, J = 7.1 Hz, COCH_2CH_2), 2.51 (t, 2 H, J = 7.1 Hz, COCH_2),

2.60–2.68 (m, 2 H), 2.82–2.85 (m, 4 H), 3.02 (t, 2 H, $J = 7.1$ Hz, $\text{COCH}_2\text{CH}_2\text{CH}_2$), 4.06 (d, 2 H, $J = 5.4$ Hz, CONCH_2CH), 4.61 (s, 2 H, NCH_2N), 5.88 (dt, 1 H, $J = 18.7, 5.4$ Hz, CONCH_2CH), 6.21 (d, 1 H, $J = 18.7$ Hz, SnCH), 6.82–6.88 (m, 3 H), 7.13 (t, 2 H, $J = 8.7$ Hz), 7.24 (t, 2 H, $J = 7.3$ Hz), 8.02 (m, 2 H). HRMS-EI: m/z calcd, 725.3378; found 725.3356 (M^+ , 2), 707.3248 ($\text{M}^+ - \text{H}_2\text{O}$, 40). Anal. Calcd for $\text{C}_{38}\text{H}_{56}\text{N}_3\text{O}_2\text{FSn}$: C, 62.99; H, 7.79; N, 5.80. Found: C, 63.07; H, 7.83; N, 5.79.

4E. As described for **4E**, treatment of spiperone (0.888 g, 2.25 mmol) in DMF (8.8 mL) with NaH (0.324 g, 13.5 mmol) followed by addition of **1Z** (1.350 g, 2.69 mmol) in DMF (8.0 mL) gave, after workup and chromatography, **4Z** (0.814 g, 1.12 mmol) in 49% yield. Characteristic ^1H NMR (CDCl_3 , δ) for **4Z**: 4.06 (d, 2 H, $J = 5.7$ Hz, CONCH_2CH), 6.19 (d, 1 H, $J = 12.5$ Hz, SnCH), 6.44 (dt, 1 H, $J = 12.5$ Hz, 5.7 Hz, CONCH_2CH). HRMS-EI: m/z calcd, 725.3378; found, 707.3210 ($\text{M}^+ - \text{H}_2\text{O}$, 3). Anal. Calcd for $\text{C}_{38}\text{H}_{56}\text{N}_3\text{O}_2\text{FSn}$: C, 62.99; H, 7.79; N, 5.80. Found: C, 62.87; H, 7.80; N, 5.75.

(E)- and (Z)-3-N-(3-Iodoprop-2-enyl)spiperone (5E and 5Z). **5E.** To a solution of **4E** (0.403 g, 0.556 mmol) in CH_2Cl_2 (1 mL) was added I_2 (0.148 g, 0.583 mmol) in CH_2Cl_2 (9.4 mL). The reaction was stirred for 1.5 h at ambient temperature and quenched with an aqueous solution (25 mL) of $\text{Na}_2\text{S}_2\text{O}_5$ (0.211 g, 1.11 mmol). The aqueous phase was made basic (1.0 N NaOH), the layers were separated, and the aqueous phase was extracted with CH_2Cl_2 (25 mL). The combined organic extracts were dried (K_2CO_3) and concentrated under reduced pressure. Short-path column chromatography (hexane/EtOAc/ Et_3N , 54:46:1) gave **5E** (0.124 g, 0.221 mmol) as a white powder (mp 120 °C, sharp) in 40% yield. Characteristic ^1H NMR (CDCl_3 , δ) for **5E**: 3.99 (d, 2 H, $J = 5.9$ Hz, CONCH_2CH), 6.42 (d, 1 H, $J = 14.6$ Hz, ICH), 6.53 (dt, 1 H, $J = 14.6, 5.9$ Hz, CONCH_2CH). HRMS-EI: m/z calcd, 561.1288; found, 561.1268 (M^+ , 1), 543.1189 ($\text{M}^+ - \text{H}_2\text{O}$, 32). Anal. Calcd for $\text{C}_{26}\text{H}_{29}\text{N}_3\text{O}_2\text{FI} \cdot 0.5\text{H}_2\text{O}$: C, 54.74; H, 5.30; N, 7.37; I, 22.25. Found: C, 54.77; H, 5.28; N, 7.32; I, 22.37.

5Z. As described for **5E**, treatment of **4Z** (0.436 g, 0.602 mmol) with 1.05 equiv of I_2 in CH_2Cl_2 gave, after workup and chromatography, **5Z** (0.282 g, 0.504 mmol) as a white powder (mp 122–124 °C) in 84% yield. Characteristic ^1H NMR (CDCl_3 , δ) for **5Z**: 4.16 (d, 2 H, $J = 6.6$ Hz, CONCH_2CH), 6.29 (overlapping dt, 1 H, $J = 7.3, 6.6$ Hz, CONCH_2CH), 6.61 (d, 1 H, $J = 7.3$ Hz, ICH). HRMS-FAB: m/z calcd, 561.1288; found, 562.1389 ($\text{M}^+ + 1$). Anal. Calcd for $\text{C}_{26}\text{H}_{29}\text{N}_3\text{O}_2\text{FI}$: C, 55.62; H, 5.21; N, 7.48; I, 22.60. Found: C, 55.68; H, 5.22; N, 7.39; I, 22.50.

Stereochemistry of Iodostannylation. By reverse-phase HPLC, **5E** and **5Z** were inseparable. However, normal-phase HPLC (hexane/EtOAc/ Et_3N , 50:49:1; 3 mL/min; 280-nm detection) provided baseline resolution of **5E** ($t_R = 7.4$ min, $k' = 5.4$) from **5Z** ($t_R = 6.2$ min, $k' = 4.4$). With solutions of **5E** and **5Z** mixed in known ratios, <0.5% of one isomer is detectable in the presence of the other. Based upon this method, the iodostannylation reactions were stereospecific.

(E)- and (Z)-3-N-(3-Chloroprop-2-enyl)spiperone (6E and 6Z). To a stirred solution of spiperone (0.144 g, 0.364 mmol) in DMF (5 mL) under N_2 was added NaH (52 mg, 2.16 mmol). After 2 min at ambient temperature, freshly distilled (*E,Z*)-1,3-dichloroprop-2-ene (0.403 g, 3.63 mmol; *E:Z*, 1:4) and a catalytic amount of KI (6.0 mg, 0.036 mmol) were added. The reaction was heated at 90 °C for 10 min and quenched by slow addition of saturated NH_4Cl (3 mL). The mixture was diluted with H_2O (10

mL), made basic, and extracted with CH_2Cl_2 (3 \times 15 mL). The combined extracts were concentrated under reduced pressure, and residual DMF was removed by bulb-to-bulb distillation (3 mm; 90 °C) to give a brown oil. Short-path chromatography (hexane/EtOAc/ Et_3N ; 55:45:1) gave **6** (53.0 mg, 0.113 mmol) as a colorless oil in 31% yield with an *E:Z* ratio of 1:4 by ^1H NMR. Characteristic ^1H NMR (CDCl_3 , δ) for **6E** and **6Z**: 4.04 (d, 0.2 H, $J = 6.9$ Hz, (*E*) CONCH_2CH), 4.25 (d, 0.8 H, $J = 6.7$ Hz, (*Z*) CONCH_2CH), 5.81–5.88 (m, 0.8 H, (*Z*) CONCH_2CH), 5.89–5.97 (m, 0.2 H, (*E*) CONCH_2CH), 6.28 (d, 0.2 H, $J = 13.7$ Hz, (*E*) ClCH), 6.33 (d, 0.8 H, $J = 7.0$ Hz, (*Z*) ClCH). Anal. Calcd for $\text{C}_{26}\text{H}_{29}\text{N}_3\text{O}_2\text{FCl}$: C, 66.44; H, 6.22; N, 8.94; Cl, 7.54. Found: C, 66.69; H, 6.29; N, 8.85; Cl, 7.63. By reverse-phase HPLC, **6E** and **6Z** were inseparable. Normal-phase HPLC provided partial resolution ($R_s = 0.63$) with hexane/EtOAc/ Et_3N (50:49:1) at 3 mL/min (**6Z**, $t_R = 5.8$ min, $k' = 3.7$; **6E**, $t_R = 7.1$ min, $k' = 4.8$) to give samples of **6E** and **6Z** for HRMS-FAB: m/z calcd, 469.1932; found, (**6E**) 470.1995 ($\text{M}^+ + 1$), (**6Z**) 470.2031 ($\text{M}^+ + 1$).

3-N-Prop-2-enylspiperone (7). To a solution of spiperone (158 mg, 0.40 mmol) in DMF (4 mL) under N_2 was added NaH (58 mg, 2.4 mmol). The mixture was stirred for 3 min at ambient temperature before addition of allyl bromide (58 mg, 0.48 mmol). After 2.5 min, the reaction was quenched with saturated NH_4Cl (5 mL). The mixture was made basic (1.0 N NaOH) and extracted with CH_2Cl_2 (3 \times 15 mL). The combined organic extracts were concentrated, and residual DMF removed by bulb-to-bulb distillation (3 mm; 60 °C). Short-path chromatography (hexane/EtOAc/ Et_3N ; 70:30:1) gave **7** (54.0 mg, 0.124 mmol) as a colorless oil in 31% yield. Characteristic ^1H NMR (80 MHz, CDCl_3 , δ) for **7**: 4.03 (d, 2 H, $J = 5.6$ Hz, CONCH_2CH), 5.12–5.40 (m, 2 H, $\text{NCH}_2\text{CHCH}_2$), 5.55–6.05 (m, 1 H, $\text{NCH}_2\text{CHCH}_2$). HRMS-EI: m/z calcd, 435.2322; found, 435.2317 (M^+ , 1), 417.2182 ($\text{M}^+ - \text{H}_2\text{O}$, 39). Anal. Calcd for $\text{C}_{26}\text{H}_{30}\text{N}_3\text{O}_2\text{F}$: C, 71.70; H, 6.94; N, 9.65. Found: C, 71.50; H, 6.98; N, 9.58.

[^{125}I]-5E and [^{125}I]-5Z. Method A: [^{125}I]-5E. To **4E** (0.87 mg, 1.2 μmol) in a glass vial sealed with a Teflon-faced septum was added [^{125}I]NaI (15 μL , ca. 0.75 nmol; 1.0 mCi) followed by CH_3CN containing 10% aqueous H_2SO_4 (100 μL ; 65:35 v/v). Aqueous chloramine-T trihydrate (25 μL , 3.5 mM) was added, and the mixture incubated at ambient temperature for 1 min. The reaction was quenched with $\text{Na}_2\text{S}_2\text{O}_5$ (100 μL , 6.3 mM). Semipreparative reverse-phase HPLC (Whatman C-18 Partisil M-9, 9.4 mm \times 50 cm) using 52:48 MeOH/0.05 N NH_4HCO_2 containing 1% v/v glacial HOAc (5 mL/min) afforded [^{125}I]-**5E** ($t_R = 26.6$ min, $k' = 11.1$) which was well-separated from **7** ($t_R = 13.7$ min, $k' = 5.2$) and potential chlorinated products **6E** or **6Z** ($t_R = 18.4$ min, $k' = 7.4$). Concentration under reduced pressure gave [^{125}I]-**5E** (0.93 mCi) in 95% radiochemical yield. Nearly quantitative radioiodide incorporation was observed for a range of **4E** concentrations (0.25–1.5 mg/145 μL).

[^{125}I]-5Z. Similar treatment of **4Z** (0.25 mg, 0.36 μmol) with [^{125}I]NaI (0.61 mCi) and chloramine-T (25 μL , 3.5 mM) gave [^{125}I]-**5Z** (0.41 mCi) in 66% radiochemical yield.

Method B: [^{125}I]-5E. To **4E** (0.26 mg, 0.36 μmol) in a glass vial sealed with a Teflon-faced septum was added [^{125}I]NaI (20 μL , ca. 1.0 nmol; 1.77 mCi) followed by MeOH containing glacial HOAc (100 μL ; 99:1 v/v). Aqueous chloramine-T trihydrate (25 μL , 3.5 mM) was added, and the mixture incubated at ambient temperature for 1 min. The reaction was quenched with $\text{Na}_2\text{S}_2\text{O}_5$ (100 μL , 6.3 mM). Semipreparative reverse-phase HPLC using 55:45 MeOH/0.05 N NH_4HCO_2 containing 1% v/v glacial HOAc (6 mL/

min) gave [^{125}I]-5E ($t_R = 18.9$ min, $k' = 12.9$) in a 25-mL volume. After dilution with water (25 mL), the solution was passed through an activated solid-phase extraction minicolumn (Waters Sep-Pak, 150 mg of C-18 adsorbent). The column was flushed with water (10 mL), to remove salts, and then with air. Elution with ethanol (3 mL) gave [^{125}I]-5E (1.38 mCi) in 78% radiochemical yield.

Purity, Specific Radioactivity, and Stereochemistry. Aliquots of [^{125}I]-5E or [^{125}I]-5Z were examined by analytical reverse-phase HPLC using 60:40 MeOH/0.05 N NH_4HCO_2 containing 1% v/v glacial HOAc at 3 mL/min. Under these conditions, both radioligands have the same retention time ($t_R = 7.5$ min, $k' = 5.9$). Radiochemical purities of [^{125}I]-5E and [^{125}I]-5Z were consistently >97% while specific radioactivities were 1329–2000 mCi/ μmol . Normal-phase HPLC as described for 5E and 5Z indicated that radioiododestannylation proceeds stereospecifically with retention of configuration.

[^{123}I]-5E. To a sealed vial containing [^{123}I]NaI [19.7 mCi; dispensed in 0.1 N NaOH (76 μL) and taken to dryness] were added the following in sequence: 1.0 N H_2SO_4 (8 μL), 95:5 MeOH/glacial HOAc (150 μL) containing 4E (0.31 mg, 0.43 μmol), and chloramine-T trihydrate (25 μL , 3.5 mM). After 5 min at ambient temperature, the reaction was quenched with $\text{Na}_2\text{S}_2\text{O}_5$ (100 μL , 50 mM). Semipreparative reverse-phase HPLC (50:50 MeOH/0.05 N NH_4HCO_2 containing 1% v/v glacial HOAc; 6 mL/min) gave [^{123}I]-5E ($t_R = 33.0$ min, $k' = 23.3$) in a 50-mL volume. After dilution with water (100 mL) and solid-phase extraction, [^{123}I]-5E was isolated in ethanol. The ethanol was removed under reduced pressure, and the radioligand formulated in 0.9% saline to give [^{123}I]-5E (10.8 mCi) in 55% radiochemical yield (not corrected for decay). By analytical HPLC, radiochemical purity was >92% while the specific radioactivity was >5050 mCi/ μmol based upon the UV absorbance detection limit.

(E)-17-[3-(Tri-*n*-butylstannyl)prop-2-enyl]-4,5 α -epoxy-18,19-dihydro-3,6-dimethoxy-7 α -(1-hydroxy-1-methylethyl)-6,14-endo-ethenomorphinan (11). A mixture of 10 (301 mg, 0.78 mmol), prepared as previously described (Bentley & Hardy, 1967a,b; Bentley et al., 1967), and 1E (600 mg, 1.20 mmol) was treated with Na_2CO_3 (176 mg, 1.66 mmol) in absolute ethanol (14 mL) at reflux for 13 h, cooled to room temperature, and filtered. The filtrate was concentrated under reduced pressure, and the residue purified by short-path chromatography (hexane/EtOAc/ Et_3N , 9:1:0.01) to give 11 (528 mg; 0.74 mmol) as a colorless oil in 95% yield. ^1H NMR: (CDCl_3 , δ) 0.75–1.10 (m, 18 H, *n*-Bu 15 H, H-18 2 H, H-8 α 1 H), 1.17 (s, 3 H, CH_3), 1.22–1.32 (m, 6 H, *n*-Bu), 1.35 (s, 3 H, CH_3), 1.43–1.56 (m, 6 H, *n*-Bu), 1.63–1.70 (m, 1 H, H-15 $_{\text{eq}}$), 1.73–1.79 (m, 2 H, H-19), 1.90 (t, 1 H, $J = 10.0$ Hz, H-7 β), 2.01 (m, 1 H, H-15 $_{\text{ax}}$), 2.19 (dd, 1 H, $J = 18.4, 6.4$ Hz, H-10 α), 2.25–2.35 (m, 1 H, H-16 $_{\text{ax}}$), 2.49 (dd, 1 H, $J = 11.6, 4.9$ Hz, H-16 $_{\text{eq}}$), 2.78 (d, 1 H, $J = 6.4$ Hz, H-9 α), 2.87 (m, 1 H, H-8 β), 3.03 (d, 1 H, $J = 18.4$ Hz, H-10 β), 3.10 (d, 2 H, $J = 5.2$ Hz, $\text{NCH}_2\text{-CHCHSn}$), 3.52 (s, 3 H, 6-OCH $_3$), 3.86 (s, 3 H, 3-OCH $_3$), 4.39 (s, 1 H, H-5 β), 5.06 (s, 1 H, OH), 5.89 (dt, 1 H, $J = 19.0$ Hz, 5.2 Hz, $\text{NCH}_2\text{CHCHSn}$), 6.08 (d, 1 H, $J = 19.0$ Hz, $\text{NCH}_2\text{CHCHSn}$), 6.54 (d, 1 H, $J = 8.1$ Hz, H-1), 6.69 (d, 1 H, $J = 8.1$ Hz, H-2). HRMS-Cl: m/z calcd, 715.3622; found, 716.3664 ($M^+ + 1$, 15). Anal. Calcd for $\text{C}_{38}\text{H}_{61}\text{NO}_4\text{Sn}$: C, 63.87; H, 8.60; N, 1.96. Found: C, 63.78; H, 8.64; N, 1.93.

(E)-17-[3-(Tri-*n*-butylstannyl)prop-2-enyl]-4,5 α -epoxy-18,19-dihydro-3-hydroxy-6-methoxy-7 α -(1-hydroxy-1-methylethyl)-6,14-endo-ethenomorphinan (12). To a solution of 11 (65 mg, 0.091 mmol) in DMF (5

mL) under argon was added sodium propanethiolate (89 mg, 0.91 mmol). The reaction was heated at reflux for 30 min, cooled to ambient temperature, and quenched with saturated NaHCO_3 (2 mL). The mixture was diluted with water (10 mL) and the pH adjusted to 9.5 with 1.0 N NaOH. The aqueous phase was extracted with CH_2Cl_2 (3 \times 15 mL), the extracts were combined, and the solvent was evaporated. Residual DMF was removed by bulb-to-bulb distillation under vacuum (3 mm; 60 $^\circ\text{C}$). Short-path column chromatography (hexane/EtOAc/ Et_3N , 3:1:0.01) gave 12 (45 mg, 0.064 mmol) in 70% yield as a colorless oil. Characteristic ^1H NMR (CDCl_3 , δ) for 12: 3.13 (d, 2 H, $J = 5.3$ Hz, NCH_2CHCH), 3.53 (s, 3 H, 6-OCH $_3$), 5.90 (dt, 1 H, $J = 19.0$ Hz, 5.3 Hz, $\text{NCH}_2\text{CHCHSn}$), 6.11 (d, 1 H, $J = 19.0$ Hz, $\text{NCH}_2\text{CHCHSn}$). HRMS-Cl: m/z calcd for $\text{C}_{37}\text{H}_{59}\text{NO}_4\text{Sn}$, 701.3466; found, 702.3507 ($M^+ + 1$, 49).

(E)-17-(3-Iodoprop-2-enyl)-4,5 α -epoxy-18,19-dihydro-3-hydroxy-6-methoxy-7 α -(1-hydroxy-1-methylethyl)-6,14-endo-ethenomorphinan (8). A mixture of 12 (35 mg, 0.050 mmol) and I_2 (13 mg, 0.051 mmol) in CH_2Cl_2 (4.6 mL) was stirred for 2 h at ambient temperature before addition of Celite (250 mg). The solvent was removed by evaporation under reduced pressure, and the Celite was applied to a short-path silica gel column. Elution with hexane/EtOAc/ Et_3N (65:35:0.35) gave 8 (21.7 mg, 0.040 mmol) as a foam in 80% yield. Characteristic ^1H NMR (CDCl_3 , δ) for 8: 2.94–3.04 (m, 3 H, H-10 β , $\text{NCH}_2\text{-CHCH}$), 6.24 (d, 1 H, $J = 14.6$ Hz, NCH_2CHCH), 6.48–6.57 (m, 2 H, H-1, NCH_2CHCH). HRMS-EI ($\text{C}_{25}\text{H}_{32}\text{INO}_4$): m/z calcd, 537.1376; found, 537.1378 (M^+ , 63).

[^{125}I]-8. To 12 (0.45 mg, 0.84 μmol) in a glass vial sealed with a Teflon-faced septum was added [^{125}I]NaI (10 μL , ca. 0.5 nmol; 0.98 mCi) followed by MeOH containing glacial HOAc (100 μL ; 95:5 v/v) and aqueous chloramine-T trihydrate (25 μL , 3.5 mM). After 1.5 min at ambient temperature, the reaction was quenched with $\text{Na}_2\text{S}_2\text{O}_5$ (100 μL , 6.3 mM). Semipreparative reverse-phase HPLC (70:30 MeOH/0.05 N NH_4HCO_2 containing 1% v/v glacial HOAc; 6 mL/min) gave [^{125}I]-8 ($t_R = 24.2$ min, $k' = 16.9$) in a 20-mL volume. Dilution with water (20 mL) and solid-phase extraction provided an ethanolic solution of [^{125}I]-8 (0.71 mCi) in 72% radiochemical yield. An aliquot (130 μCi) was reconstituted in HPLC mobile phase (75:25 MeOH/0.05 N NH_4HCO_2) for examination by analytical reverse-phase HPLC (2 mL/min). The radioproduct ($t_R = 6.9$ min, $k' = 5.0$) was of >99% radiochemical purity with a specific radioactivity of 1647 mCi/ μmol .

(E)-17-(Cyclopropylmethyl)-4,5 α -epoxy-18,19-dihydro-3-methoxy-6-[[3-(tri-*n*-butylstannyl)prop-2-enyl]-oxy]-7 α -(1-hydroxy-1-methylethyl)-6,14-endo-ethenomorphinan (14). To a 5-mL conical vial containing 30 mg (0.070 mmol) of 13 (Lever et al., 1987) in DMF (2 mL) was added NaH (17 mg, 0.71 mmol). The mixture was stirred for 1 min before addition of 1E (177 mg, 0.35 mmol) in DMF (1 mL). After stirring for 90 min at ambient temperature, saturated NH_4Cl (0.8 mL) was added. Extractive workup followed by semipreparative reverse-phase HPLC (Alltech Econosil C-18, 10 mm \times 25 cm, 10 μm) using MeOH/0.05 N NH_4HCO_2 (95:5 v/v) at 8 mL/min provided 27 mg (0.036 mmol) of 14 ($t_R = 51.6$ min, $k' = 41.0$) in 51% yield. ^1H NMR: (CDCl_3 , δ) 0.10 (m, 2 H, *c*- C_3H_5), 0.50 (m, 2 H, *c*- C_3H_5), 0.78–0.81 (m, 2 H, H-18, *c*- C_3H_5), 0.84–0.90 (m, 15 H, *n*-Bu), 1.04–1.12 (m, 2 H, H-8 α , H-18), 1.21 (s, 3 H, CH_3), 1.23–1.35 (m, 6 H, *n*-Bu), 1.41 (s, 3 H, CH_3), 1.42–1.53 (m, 6 H, *n*-Bu), 1.64–1.70 (m, 1 H, H-15 $_{\text{eq}}$), 1.80 (m, 2 H, H-19), 1.98 (m, 1 H, H-7 β), 2.04 (m, 1 H, H-15 $_{\text{ax}}$), 2.18–2.41 (m, 4 H, $\text{CH}_2\text{-c-C}_3\text{H}_5$; 2 H, H-10 α , H-16 $_{\text{ax}}$), 2.63 (dd, 1 H, $J = 11.8$ Hz, 4.9 Hz, H-16 $_{\text{ax}}$), 2.87 (m, 1 H, H-8 β),

2.97–3.02 (m, 2 H, H-10 β , H-9 α), 3.89 (s, 3 H, C-3 OCH₃), 4.23 (dd, 1 H, J = 12.9, 4.8 Hz, CH₂O), 4.43 (s, 1 H, H-5 β), 4.48 (dd, 1 H, J = 12.9, 4.8 Hz, CH₂O), 5.2 (s, 1 H, OH), 6.03 (dt, 1 H, J = 19.1, 4.8 Hz, SnCHCH), 6.20 (d, 1 H, J = 19.1 Hz, SnCHCH), 6.52 (d, 1 H, J = 8.0 Hz, H-1), 6.70 (d, 1 H, J = 8.0 Hz, H-2). HRMS-Cl (C₄₁H₆₅NO₄Sn): m/z calcd, 755.3935; found, 756.4025 (M^+ + 1, 10), 698.3208 (M^+ - n -Bu, 100).

(E)-17-(Cyclopropylmethyl)-4,5 α -epoxy-18,19-dihydro-3-hydroxy-6-[[3-(tri- n -butylstannyl)prop-2-enyl]oxy]-7 α -(1-hydroxy-1-methylethyl)-6,14-*endo*-ethenomorphinan (15). To a solution of 14 (52 mg, 0.069 mmol) in DMF (5 mL) under argon was added sodium propanethiolate (339 mg, 3.45 mmol). The mixture was heated at reflux for 8 min, cooled to ambient temperature, and quenched by addition of saturated NH₄Cl (2 mL). Extractive workup followed by semipreparative reverse-phase HPLC (Alltech Econosil C-18, 10 mm \times 25 cm, 10 μ m) using 95:5 MeOH/0.05 N NH₄HCO₂ at 8 mL/min provided 20.0 mg (0.027 mmol, 39%) of 15 (t_R = 13.16 min, k' = 9.36) and 13.5 mg (0.030 mmol, 43%) of 16 (t_R = 2.70 min, k' = 1.12). Characteristic ¹H NMR (CDCl₃, δ) for 15: 4.19 (ddd, 1 H, J = 12.1, 4.9, 1.2 Hz, CH₂O), 4.41–4.46 (overlapping s and ddd, 2 H, H-5 β , CH₂O), 4.80 (br s, 1 H, 3-OH), 6.04 (dt, 1 H, J = 19.1, 4.9 Hz, SnCHCH), 6.21 (d, 1 H, J = 19.1 Hz, SnCHCH). HRMS-Cl (15, C₄₀H₆₃NO₄Sn): m/z calcd, 741.3779; found 742.3818 (M^+ + 1). Characteristic ¹H NMR (CDCl₃, δ) for 16: 5.93 (m, 1 H, H₂CCHCH₂O), 5.28 (dd, 1 H, J = 17.2, 1.5 Hz, H₂CCHCH₂O), 5.15 (dd, 1 H, J = 10.5, 1.5 Hz, H₂CCHCH₂O), 4.43–4.46 (overlapping s and dd, 2 H, H-5 β , H₂CCHCH₂O), 4.19 (dd, 1 H, J = 12.2, 5.4 Hz, H₂CCHCH₂O). HRMS-Cl (16, C₂₈H₃₇NO₄): m/z calcd, 451.2722; found, 452.2802 (M^+ + 1).

(E)-17-(Cyclopropylmethyl)-4,5 α -epoxy-18,19-dihydro-3-hydroxy-6-[[3-iodoprop-2-enyl]oxy]-7 α -(1-hydroxy-1-methylethyl)-6,14-*endo*-ethenomorphinan (9). To 15 (16 mg, 0.022 mmol) in CH₂Cl₂ (1.0 mL) was added I₂ (0.024 mmol) in CH₂Cl₂ (0.55 mL, 0.043 M). The mixture was stirred at room temperature for 10 min and then applied to a preparative TLC silica plate (Analtech, 20 cm \times 20 cm, 1000 μ m) which was developed in hexane/EtOAc/Et₃N (2:1:0.01). The major component (R_f = 0.54) was desorbed using EtOAc containing 1% Et₃N. Filtration followed by concentration gave 7.0 mg (0.012 mmol, 55%) of 9 as an oil. Characteristic ¹H NMR (CDCl₃, δ) for 9: 4.14 (ddd, 1 H, J = 12.7, 5.8, 1.4 Hz, CH₂O), 4.37–4.44 (overlapping s and ddd, 2 H, H-5 β , CH₂O), 6.41 (dt, 1 H, J = 14.6, 1.4 Hz, ICHCH), 6.65 (dt, 1 H, J = 14.6, 5.8 Hz, ICHCH). HRMS-Cl (C₂₈H₃₆INO₄): m/z calcd, 577.1688; found, 578.1767 (M^+ + 1).

[¹²⁵I]-9. To a solution of 15 (0.30 mg, 0.40 μ mol) in MeOH (50 μ L) in a glass vial sealed with a Teflon-faced septum was added [¹²⁵I]NaI (5 μ L, ca. 0.25 nmol; 0.54 mCi) followed by MeOH containing glacial HOAc (50 μ L; 95:5 v/v) and aqueous chloramine-T trihydrate (25 μ L, 4.3 mM). After 1 min at ambient temperature, the reaction was quenched with Na₂S₂O₅ (100 μ L, 50 mM). Semipreparative reverse-phase HPLC using MeOH/0.05 N NH₄HCO₂ (60:40 v/v) at 6 mL/min gave [¹²⁵I]-9 (t_R = 30.7 min, k' = 21.0) in a 20-mL volume. Dilution with water (35 mL) and solid-phase extraction provided an ethanolic solution of [¹²⁵I]-9 (0.38 mCi) in 71% radiochemical yield. An aliquot was reconstituted in mobile phase (MeOH/0.05 N NH₄HCO₂, 75:25 v/v) for examination by analytical reverse-phase HPLC at 3 mL/min. The radioproduct (t_R = 6.1 min, k' = 4.4) was of >99% radiochemical purity with specific radioactivity of 1405 mCi/ μ mol.

Scheme II. Synthesis of Bifunctional Reagents 1E and 1Z

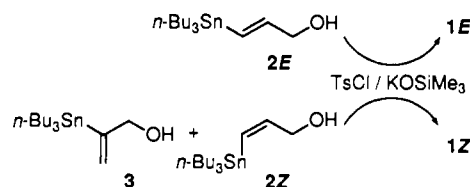
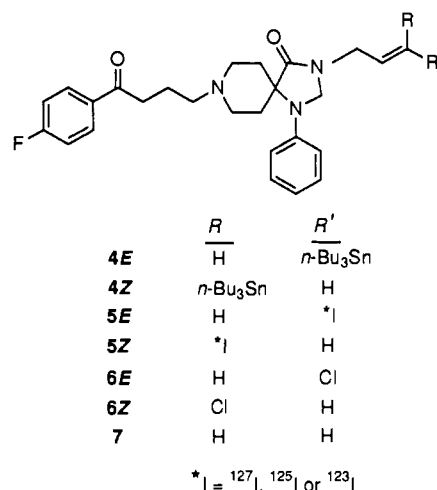


Chart II. Alkyl Derivatives of Spiperone at the N-3 Position



RESULTS AND DISCUSSION

Allylic alcohols 2E and 2Z, the precursors to 1E and 1Z, were prepared by treatment of propargyl alcohol with tri- n -butyltin hydride and AIBN as described by Jung and Light (1982). This route allows convenient access in one step to both 2E and 2Z along with structural isomer 3 (Scheme II). Chromatographic isolation afforded pure 2E, while 2Z and 3 were obtained as an inseparable mixture. Alternatively, 2E and 2Z can be individually obtained from propargyl alcohol in stereospecific fashion by palladium-catalyzed syn hydrostannylation (2E, Miyake & Yamamura, 1989) or by hydroalumination followed by stannylation (2Z; Corey & Eckrich, 1984).

Standard conditions for esterification with TsCl in pyridine (Tipson, 1944) proved unsuccessful for 2E even when using aqueous copper sulfate for removal of pyridine. A procedure for tosylation of allylic alcohols (Johnson & Dutra, 1973) was then modified by substitution of the organic-soluble potassium trimethylsilanolate (Laganis & Chenard, 1984) for freshly ground sodium hydroxide. Treatment of 2E with the silanolate and TsCl in diethyl ether at -25 °C gave 1E in 65% yield (Scheme II). In similar fashion, the mixture of 2Z and 3 gave 1Z (42%) without concomitant esterification of 3. Once purified, 1E and 1Z suffer negligible decomposition upon storage for at least 6 months at -20 °C.

To ascertain the utility of vinylstannylated alkylating agents 1E and 1Z for selective radioiodination of drugs having multiple functionality, we investigated the preparation of (*E*)- and (*Z*)-3-*N*-(iodoallyl)spiperone (Chart II). These targets were selected because spiperone derivatives with bulky substituents at the amide nitrogen maintain high affinity for dopamine D₂ receptors (Agui et al., 1988; Welch et al., 1988). Accordingly, vinylstannanes 4E and 4Z were prepared as precursors for iodination in approximately 50% yield by NaH-promoted alkylation with either 1E or 1Z in DMF. By contrast to fluoroalkylations of spiperone (Chi et al., 1987), imino ester formation

by O-alkylation was not detected in the reaction mixture by ^1H NMR. In fact, no evidence was observed for competitive pathways, such as C-alkylation adjacent to the carbonyl group (Burns et al., 1984) or 3-N-alkylation in $\text{S}_{\text{N}}2'$ fashion.

Routes to allylic vinylstannanes frequently involve reaction of organotin hydrides with alkynes. For instance, **4E** has been prepared by hydrostannylation of 3-*N*-propargylpiperone (Hanson & Ranade, 1989; Lisic et al., 1989). Hydrostannylation is not always well-defined stereochemically, and a benefit of the present method is controlled availability of both *E*- and *Z*-isomers. In addition, some multifunctional substrates which are not compatible with hydrostannylation reaction conditions would be suited to alkylation with **1E** or **1Z**. A structural congener of **1E**, (*E*)-1-chloro-3-(tri-*n*-butylstannyl)prop-2-ene, has also been reported by Hanson (1989). The better leaving-group ability of tosylate with respect to chloride should make **1E** or **1Z** preferred for alkylation of weak nucleophiles.

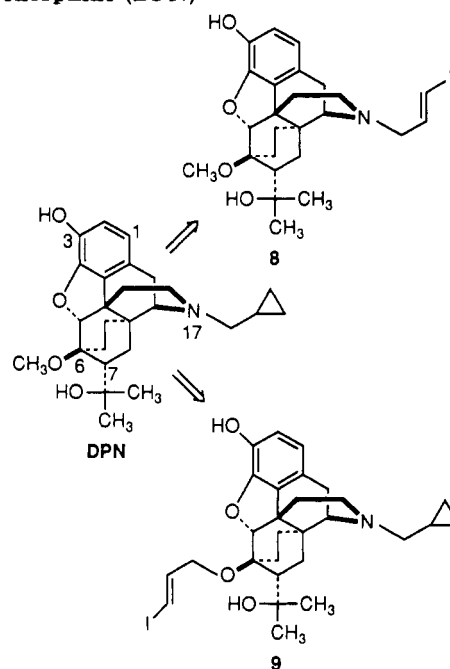
Vinylstannanes **4E** and **4Z** were converted to the corresponding vinyl iodides **5E** and **5Z** (Chart II) with iodine in CH_2Cl_2 in 40% and 84% yields, respectively. Even though the anilino rings are activated toward electrophiles, only ipso-substitution of the vinylstannane was observed. Retention of configuration was confirmed by appropriate ^1H NMR vicinal couplings for the ABX_2 spin systems of **5E** ($^3J_{\text{AB}} = 14.6$ Hz) and **5Z** ($^3J_{\text{AB}} = 7.3$ Hz). On the basis of normal-phase HPLC, which allows detection of <0.5% of one isomer mixed with the other, the iododestannylation is stereospecific. Cleavage of the vinyl carbon-tin bond was expected to take place with retention since electrophilic destannylations typically occur in this fashion (Baekelmans et al., 1968). While retention of configuration is the rule, non-ipso electrophilic substitution of vinylstannanes by carbon electrophiles has recently been reported (Reetz & Hois, 1989).

As a prelude to radioiodination of **4E** and **4Z**, additional piperone derivatives which might be expected as byproducts of radiolabeling were prepared by 3-*N*-alkylation with appropriate alkyl halides and NaH in DMF (Chart II). These include chloroalkyl compounds **6E** and **6Z**, which might result from the use of chlorinated oxidants, and allyl analogue **7**, which would be formed by simple protodemetalation. In previous studies of aromatic radioiododestannylation, both chloro- and protodestannylation were significant (Moerlein & Coenen, 1985; Moerlein et al., 1988). The alkylation with (*E,Z*)-1,3-dichloroprop-2-ene was catalyzed by inclusion of KI, and gave **6** in 31% yield with an *E:Z* ratio of 1:4. Alkylation with allyl bromide was uneventful, and gave **7** in 31% yield.

Armed with appropriate standards, radioiodination of the vinylstannanes at the no-carrier-added level was explored. Treatment of **4E** or **4Z** with ^{125}I NaI and chloramine-T in CH_3CN containing 10% aqueous H_2SO_4 at ambient temperature afforded ^{125}I -**5E** or ^{125}I -**5Z**, respectively. The radioiododestannylation proceeds stereospecifically with retention of configuration as established by normal-phase HPLC. Radioiodide incorporation was not dependent upon precursor concentration over the 6-fold range studied, and was nearly quantitative within 1 min. For multiple preparations, ^{125}I -**5E** and ^{125}I -**5Z** were obtained in good radiochemical yields (66–95%) with radiochemical purities >97%. Specific radioactivities ranged from 1329 to 2000 mCi/ μmol , and were comparable to that of the batches of ^{125}I NaI employed.

During reverse-phase HPLC isolation of the ^{125}I -labeled products, *N*-allyl derivative **7** was observed as the

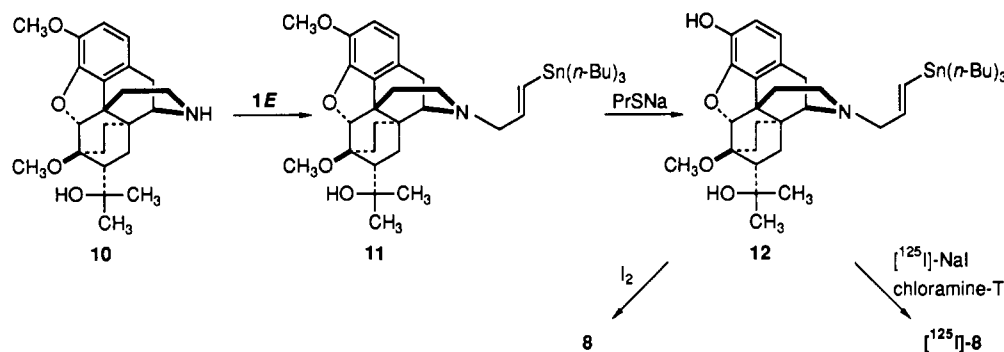
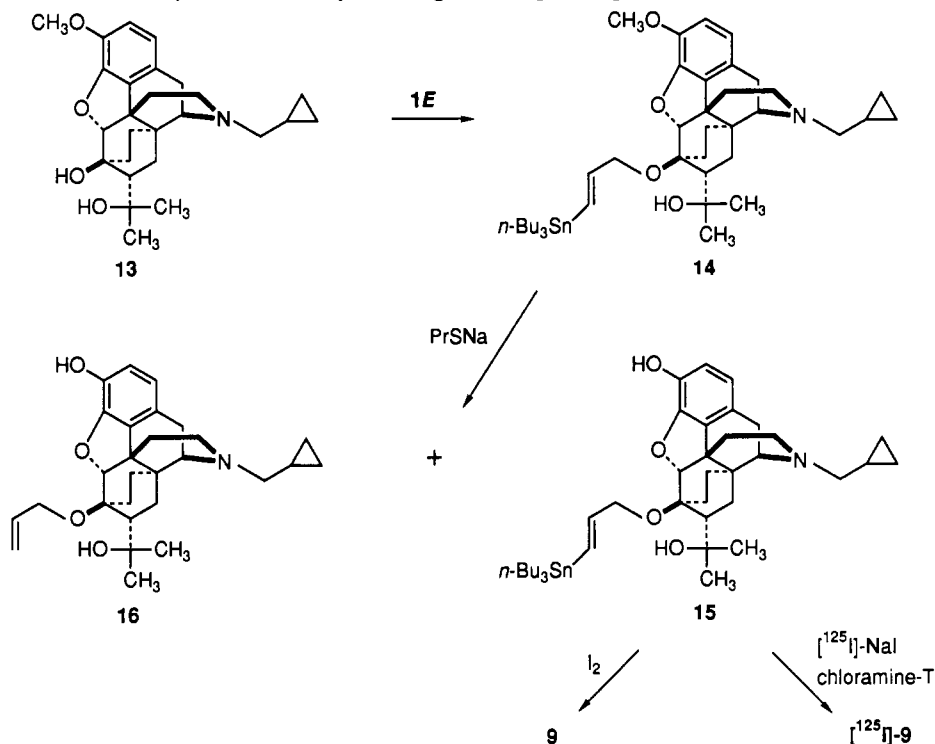
Chart III. Structures of *N*- and *O*-Iodoalkyl Analogues of Diprenorphine (DPN)



major nonradioactive product, while chloroalkyl analogues (**6E**, **6Z**) were not detected. Side reactions can complicate radiotracer purification, and it is noteworthy that chlorination is averted with these vinylstannanes. Extensive protodestannylation does not adversely effect radioiododestannylation, and **7** is readily separated from ^{125}I -**5E** or ^{125}I -**5Z**. Nevertheless, conditions were sought which would minimize protodemetalation and thereby expedite radiotracer purification in general. With a less acidic solvent system, methanol containing 1% glacial acetic acid, **4E** suffers no protodemetalation (0.2% HPLC detection limit) while incorporation of radioiodide is >95%.

The procedures were easily adapted to radiolabeling with ^{123}I by neutralizing the variable amounts of base contained in dispensing solutions of ^{123}I NaI with aqueous acid (1 equiv). For a typical preparation on a 20 mCi scale, ^{123}I -**5E** was synthesized, purified, and formulated within 2 h in 55% yield (not corrected for decay). The radiochemical purity of ^{123}I -**5E** was >92% while the specific radioactivity was >5050 mCi/ μmol . Normal-phase HPLC confirmed retention of configuration.

To further explore the scope and limitations of radioiodination via vinylstannylated alkylating agents, we selected *N*- and *O*-iodoalkyl analogues **8** and **9** of diprenorphine as targets (Chart III). Coupling to secondary amine and tertiary alcohol residues would serve as a measure of the alkylating ability of **1E** and **1Z**. Further, the highly activated aromatic ring provides a stringent test of the ability of the stannyl group to direct iodination. In addition to testing synthetic constraints, the preparation of **8** and **9** might lead to radioligands for opioid receptor studies. A prosthetic group is necessary since direct substitution of the aromatic ring with heavy halogens leads to a substantial reduction in potency of 4,5-epoxymorphinans such as diprenorphine (Casy & Parfitt, 1986). The *N*- ^{18}F fluoroalkyl analogues of diprenorphine similar to **8** retain affinity for opioid receptors, and show promise for positron emission tomography (Bai et al., 1990; Chesis et al., 1990). Moreover, **9** was of interest because structurally related oxymorphones with bulky substituents at C-6 display good biological activity at opioid receptors (Hazum et al., 1982).

Scheme III. Synthetic Route to 8, the *N*-Iodoallyl Analogue of Diprenorphine**Scheme IV. Synthetic Route to 9, the *O*-Iodoallyl Analogue of Diprenorphine**

The route employed for the preparation of 8 is shown in Scheme III. Alkylation of secondary amine 10, obtained from thebaine in five steps (Bentley & Hardy, 1967a,b; Bentley et al., 1967), with 1E in ethanol containing Na_2CO_3 smoothly provided 11 in 95% yield. Phenol 12 was obtained in 70% yield by cleavage of the aromatic methyl ether with sodium propanethiolate (10 equiv) in DMF at reflux. Even in the presence of the highly activated aromatic ring, treatment of 12 with iodine (1 equiv) in CH_2Cl_2 gave exclusively ipso-substitution product 8 in 82% yield. Retention of configuration was confirmed by ^1H NMR of the ABX_2 spin system ($^3J_{\text{AB}} = 14.6$ Hz). Radioiodination of 12 using $[^{125}\text{I}]\text{NaI}$ and chloramine-T at ambient temperature in methanolic acetic acid for 1.5 min gave $[^{125}\text{I}]\text{-8}$ (1647 mCi/ μmol) in 72% radiochemical yield with >99% radiochemical purity. Although standards for proto- and chlorodestannylation were not prepared in this case, no significant nonradioactive side products were observed during HPLC purification of $[^{125}\text{I}]\text{-8}$.

For the synthesis of 9 (Scheme IV), diol 13 was prepared from 10 as previously reported (Lever et al., 1987). Selective *O*-alkylation of the C-6 hydroxyl with 1E and NaH in DMF gave 14 in 51% yield. As a consequence of steric hindrance (Bentley et al., 1967; Lever et al., 1987; Lever et al., 1990b), *O*-alkylation of the tertiary hydroxyl moiety attached to C-7 α was not observed. Submission

of 14 to sodium propanethiolate (50 equiv) in DMF at reflux for 8 min rendered the desired phenol 15 in an unoptimized 39% yield accompanied by demetalated phenol 16 (43%). The unexpected formation of 16 is presumably due to nucleophilic attack of thiolate on tin; however, no attempt was made to isolate an organotin sulfide. Some precedent for this type of reaction exists in the alkali-induced cleavage of aryltrimethylstannanes (Eaborn et al., 1967). Treatment of 15 with iodine in CH_2Cl_2 gave 9 in 55% yield with retention of configuration based upon ^1H NMR of the ABXX' spin system ($^3J_{\text{AB}} = 14.6$ Hz). Radioiododestannylation of 15 with $[^{125}\text{I}]\text{NaI}$ and chloramine-T at ambient temperature in methanolic acetic acid for 1.0 min provided $[^{125}\text{I}]\text{-9}$ (1405 mCi/ μmol) in 71% radiochemical yield with >99% radiochemical purity. With the fortuitous availability of 16 as a reference standard, protodestannylation of 15 to give 16 was not observed (ca. 1% HPLC detection limit) during purification of the reaction mixture. Using the same reaction conditions except for the omission of radioiodide, no indication of side-product formation (e.g., chlorination) was found by HPLC.

In summary, 1E and 1Z are versatile bifunctional alkylating agents which couple readily with nucleophilic residues, including amide nitrogen, secondary amine, and tertiary alcohol, to provide vinylstannylated intermediates

in good yields (48–95%). Subsequent regio- and stereospecific radioiododestannylation with retention of configuration occurs under mild, no-carrier-added conditions to give products with high specific radioactivities in good isolated radiochemical yields (55–95%). The radioiodination is rapid, efficient, and dependable, and is suited to preparation of [125 I]- or [123 I]-labeled tracers without requiring extensive optimization of reaction conditions. Oxidant-promoted chlorination is not a significant side reaction, and conditions have been established which minimize protodemetalation. Thus, 1E and 1Z allow access to iodoallyl analogues from highly functionalized structural classes. The stability of such adducts has yet to be determined, and is likely to depend upon overall structure. For example, iodovinyl estradiols (Hanson et al., 1982) and iodovinyl fatty acids (Knapp et al., 1984) are quite stable in vivo, while certain iodovinyl antibody conjugates suffer metabolic degradation (Hadley & Wilbur, 1990). The novel reagents 1E and 1Z complement the arsenal of existing prosthetic groups and should prove useful for radioiodination of a variety of biologically active small molecules.

ACKNOWLEDGMENT

This research was supported by DHHS NCI CA-32845 and by predoctoral fellowships (JLM) from DHHS NIDA NRSA 1F31DA05428, DHHS NCI CA-09199, the Education and Research Foundation of the Society of Nuclear Medicine, and the Metropolitan Washington DC Chapter of the ARCS Foundation. NMR spectra (300 MHz) were obtained through the Biophysics NMR Facility of Johns Hopkins University established by NIH Grant GM 27512.

LITERATURE CITED

- Agui, T., Amlaiky, N., Caron, M. G., and Keabian, J. W. (1988) Binding of [125 I]-N-(p-aminophenethyl)spiroperidol to the D-2 dopamine receptor in the neurointermediate lobe of the rat pituitary gland: A thermodynamic study. *Mol. Pharmacol.* 32, 163–169.
- Baekelmans, P., Gielen, M., Malfroid, P., and Nasielski, J. (1968) Mechanism for the cleavage of carbon-tin bonds. *Bull. Soc. Chim. Belges* 77, 85–97.
- Bai, L. Q., Teng, R. R., Shiue, C. Y., Wolf, A. P., Dewey, S. L., Holland, M. J., Simon, E. J. (1990) No-carrier-added (NCA) N-(3-[18 F]fluoropropyl)-N-norbuprenorphine and N-(3-[18 F]fluoropropyl)-N-nordiprenorphine—Synthesis, anatomical distribution in mice and rats, and tomographic studies in baboon. *Nucl. Med. Biol.* 17, 217–227.
- Baldwin, R. M. (1986) Chemistry of radioiodine. *Appl. Radiat. Isot.* 37, 817–821.
- Bentley, K. W., and Hardy, D. G. (1967a) Novel analgesics and molecular rearrangements in the morphine-thebaine group. I. Ketones derived from 6,14-endo-ethenotetrahydrothebaine. *J. Am. Chem. Soc.* 89, 3267–3273.
- Bentley, K. W., and Hardy, D. G. (1967b) Novel analgesics and molecular rearrangements in the morphine-thebaine group. III. Alcohols of the 6,14-endo-ethenotetrahydrothebaine series and derived analogs of N-allylnormorphine and -nocodeine. *J. Am. Chem. Soc.* 89, 3281–3292.
- Bentley, K. W., Hardy, D. G., and Meek, B. (1967) Novel analgesics and molecular rearrangements in the morphine-thebaine group. II. Alcohols derived from 6,14-endo-etheno- and 6,14-endo-ethanotetrahydrothebaine. *J. Am. Chem. Soc.* 89, 3273–3280.
- Bolton, A. E., and Hunter, W. M. (1973) The labelling of proteins to high specific radioactivities by conjugation to a I-125-containing acylating agent. *Biochem. J.* 133, 529–539.
- Burns, H. D., Dannals, R. F., Langström, B., Ravert, H. T., Zemyan, S. E., Duelfer, T., Wong, D. F., Frost, J. J., Kuhar, M. J., and Wagner, H. N., Jr. (1984) (3-N-[14 C]methyl)piperone, a ligand binding to dopamine receptors: Radiochemical synthesis and biodistribution studies in mice. *J. Nucl. Med.* 25, 1222–1227.
- Casy, A. F., and Parfitt, R. T. (1986) *Opioid Analgesics Chemistry and Receptors*, Plenum Publishing Corp., New York.
- Chesis, P. L., Hwang, D.-R., and Welch, M. J. (1990) N-(3-[18 F]fluoropropyl)-N-nordiprenorphine: Synthesis and characterization of a new agent for imaging opioid receptors with positron emission tomography. *J. Med. Chem.* 33, 1482–1490.
- Chi, D. Y., Kilbourn, M. R., Katzenellenbogen, J. A., and Welch, M. J. (1987) A rapid and efficient method for the fluoroalkylation of amines and amides. Development of a method suitable for incorporation of the short-lived positron-emitting radionuclide F-18. *J. Org. Chem.* 52, 658–664.
- Coenen, H. H., Moerlein, S. M., and Stöcklin, G. (1983) No-carrier-added radiohalogenation methods with heavy halogens. *Radiochim. Acta* 34, 47–68.
- Corey, E. J., and Eckrich, T. M. (1984) A new route to Z-disubstituted olefins. A simple synthesis of polyunsaturated fatty acids by reiterative coupling. *Tetrahedron Lett.* 25, 2419–2422.
- Eaborn, C., Hornfeld, H. L., and Walton, D. R. (1967) Aromatic reactivity. Part XXXV. Alkali cleavage of aryltrimethylstannanes: An unusual electrophilic aromatic substitution. *J. Chem. Soc. B*, 1036–1040.
- Hadley, S. W., and Wilbur, D. S. (1990) Evaluation of iodovinyl antibody conjugates: Comparison with a p-iodobenzoate conjugate and direct radioiodination. *Bioconjugate Chem.* 1, 154–161.
- Hanson, R. N. (1989) Application of organotin chemistry to radiopharmaceutical design: Preparation of N-(tri-butylstannyl)allyl derivatives. *J. Labelled Compds. Radiopharm.* 26, 3 [Abstract].
- Hanson, R. N., and Seitz, D. E. (1982) Radioiododestannylation: A method for specifically labeled radiopharmaceuticals. *J. Labelled Compds. Radiopharm.* 19, 1585–1586.
- Hanson, R. N., and Ranade, M. (1989) Haloallyl derivatives of spiperone and cleopride: potential radioligands for the dopamine D-2 receptor. *Abstracts of the 197th American Chemical Society National Meeting*, Dallas, Texas, American Chemical Society, Washington, DC.
- Hanson, R. N., Seitz, D. E., and Botarro, J. C. (1982) E-17(α)-[I-125]iodovinylestradiol: an estrogen-receptor-seeking radiopharmaceutical. *J. Nucl. Med.* 23, 431–436.
- Hazum, E., Chang, K.-J., Leighton, H. J., Lever, O. W. Jr., and Cuatrecasas, P. (1982) Increased biological activity of dimers of oxymorphone and enkephalin: Possible role of receptor cross-linking. *Biochem. Biophys. Res. Commun.* 104, 347–353.
- Johnson, C. R., and Dutra, G. A. (1973) Reactions of lithium diorganocuprates(I) with tosylates. I. Synthetic aspects. *J. Am. Chem. Soc.* 95, 7777–7788.
- Jung, M. E., and Light, L. A. (1982) Preparation of iodoallylic alcohols via hydrostannylation: Spectroscopic proof of structures. *Tetrahedron Lett.* 23, 3851–3854.
- Kabalka, G. W., and Varma, R. S. (1989) The synthesis of radiolabeled compounds via organometallic intermediates. *Tetrahedron* 45, 6601–6621.
- Knapp, F. F., Jr., Goodman, M. M., Kabalka, G. W., and Sastry, K. A. R. (1984) Synthesis and evaluation of radioiodinated (E)-18-iodo-17-octadecenoic acid as a model iodoalkenyl fatty acid for myocardial imaging. *J. Med. Chem.* 27, 94–97.
- Korner, M., Bouthenet, M.-L., Ganellin, C. R., Garbarg, M., Gros, C., Ife, R. J., Sales, N., and Schwartz, J.-C. (1986) [125 I]iodobolpyramine, a highly sensitive probe for histamine H₁-receptors in guinea-pig brain. *Eur. J. Pharmacol.* 120, 151–160.
- Laganis, E. D., and Chenard, B. L. (1984) Metal silanates: Organic soluble equivalents for O². *Tetrahedron Lett.* 25, 5831–5834.
- Lever, J. R., Dannals, R. F., Wilson, A. A., Ravert, H. T., and Wagner, H. N., Jr. (1987) Synthesis of carbon-11 diprenorphine: A radioligand for positron emission tomographic studies of opiate receptors. *Tetrahedron Lett.* 28, 4015–4018.
- Lever, J. R., Musachio, J. L., Scheffel, U. A., Stathis, M., and Wagner, H. N., Jr. (1989) Synthesis of [I-125/123]-N-iodoal-

- lylsipiperone for in vivo studies of dopamine D₂ receptors. *J. Nucl. Med.* 30, 803 [Abstract].
- Lever, J. R., Scheffel, U. A., Stathis, M. S., Musachio, J. L., and Wagner, H. N., Jr. (1990a) In vitro and in vivo binding of (*E*) and (*Z*)-N-(iodoallyl)sipiperone to dopamine D₂ and serotonin 5-HT₂ neuroreceptors. *Life Sci.* 46, 1967-1976.
- Lever, J. R., Mazza, S. M., Dannals, R. F., Ravert, H. T., Wilson, A. A., and Wagner, H. N., Jr. (1990b) Facile synthesis of [¹¹C]-buprenorphine for positron emission tomographic studies of opioid receptors. *Appl. Radiat. Isot.* 41, 745-752.
- Lin, C. M., Mihal, K. A., and Krueger, R. J. (1989) N-Iodoacetyltyramine: Preparation and use in ¹²⁵I labeling by alkylation of sulfhydryl groups. *Anal. Biochem.* 179, 389-395.
- Lisic, E. C., McPherson, D. W., Strivastava, P. C., and Knapp, F. F., Jr. (1989) Radioiodinated N-(ω-iodoalkenyl)sipiperone analogs for potential dopamine receptor imaging by SPECT. *J. Nucl. Med.* 30, 925 [Abstract].
- Lowndes, J. M., Hokin-Neaverson, M., and Ruoho, A. E. (1988) N-(3-(*p*-azido-*m*-[¹²⁵I]iodophenyl)propionyl)-succinimide, a heterobifunctional reagent for the synthesis of radioactive photoaffinity ligands: Synthesis of a carrier-free ¹²⁵I-labeled cardiac glycoside photoaffinity label. *Anal. Biochem.* 168, 39-47.
- Mazza, S. M., Erickson, R. H., Blake, P. R., and Lever, J. R. (1990) Two-dimensional homonuclear and heteronuclear correlation NMR studies of diprenorphine: A prototypic 6α,14α-endo-ethanotetrahydrothebaine. *Magn. Reson. Chem.* 28, 675-681.
- Miyake, H., and Yamamura, K. (1989) Palladium(0) catalyzed hydrostannylation of alkynes. Stereospecific syn addition of tributyltin hydride. *Chem. Lett.* 981-984.
- Moerlein, S. M., and Coenen, H. H. (1985) Regiospecific no-carrier-added radiobromination and radioiodination of aryl-trimethyl group IVb organometallics. *J. Chem. Soc. Perkin Trans. 1* 1941-1947.
- Moerlein, S. M., Beyer, W., and Stöcklin, G. (1988) No-carrier-added radiobromination and radioiodination of aromatic rings using in situ generated peracetic acid. *J. Chem. Soc. Perkin Trans. 1* 779-786.
- Musachio, J. L., and Lever, J. R. (1989) Radioiodination via vinylstannylated alkylating agents. *Tetrahedron Lett.* 30, 3613-3616.
- Ponchant, M., Beaucourt, J.-P., Vanhove, A., Daval, G., Verge, D., Hamon, M., and Gozlan, H. (1988) ¹²⁵I-BH-8-MeO-N-PAT, a new ligand for studying 5-HT_{1A} receptors in the central nervous system. *C. R. Acad. Sci. Paris* 306, 147-152.
- Reetz, M. T., and Hois, P. (1989) Non-*ipso* electrophilic substitution of vinylstannanes and silanes. *J. Chem. Soc. Chem. Commun.* 1081-1082.
- Saji, H., Magata, Y., Arano, Y., Horiuchi, K., Torizuka, K., and Yokoyama, A. (1987) 2-O-(*p*-Iodobenzyl)-D-glucose: a new radiopharmaceutical for SPECT studies of cerebral glucose transport. *J. Nucl. Med.* 28, 571 [Abstract].
- Seever, R. H., and Counsell, R. E. (1982) Radioiodination techniques for small molecules. *Chem. Rev.* 82, 575-590.
- Tipson, R. S. (1944) On esters of *p*-toluenesulfonic acid. *J. Org. Chem.* 9, 235-241.
- Vaidyanathan, G., and Zalutsky, M. R. (1990) Radioiodination of antibodies via N-succinimidyl 2,4-dimethoxy-3-(trialkylstannyl)benzoates. *Bioconjugate Chem.* 1, 387-393.
- Welch, M. J., Katzenellenbogen, J. A., Mathias, C. J., Brodack, J. W., Carlson, K. E., Chi, D. Y., Dence, C. S., Kilbourn, M. R., Perlmutter, J. S., Raichle, M. E., and Ter-Pogossian, M. M. (1988) N-(3-[¹⁸F]fluoropropyl)-spiperone: The preferred ¹⁸F labeled spiperone analog for positron emission tomographic studies of the dopamine receptor. *Nucl. Med. Biol.* 15, 83-97.
- Wilbur, D. S., Hadley, S. W., Hylarides, M. D., Abrams, P. G., Beaumier, P. A., Morgan, C., Reno, J. M., and Fritzberg, A. R. (1989) Development of a stable radioiodinating reagent to label monoclonal antibodies for radiotherapy of cancer. *J. Nucl. Med.* 30, 216-226.
- Wilson, A. A., Dannals, R. F., Ravert, H. T., Burns, H. D., and Wagner, H. N., Jr. (1986) I-125 and I-123 labelled iodobenzyl bromide, a useful alkylating agent for radiolabelling biologically important molecules. *J. Labelled Compd. Radiopharm.* 23, 83-93.
- Wilson, A. A., Dannals, R. F., Ravert, H. T., Frost, J. J., and Wagner, H. N., Jr. (1989) Synthesis and biological evaluation of [¹²⁵I]- and [¹²³I]-4-Iododexetimide, a potent muscarinic cholinergic receptor antagonist. *J. Med. Chem.* 32, 1057-1062.

Monoclonal Antibody- β -Lactamase Conjugates for the Activation of a Cephalosporin Mustard Prodrug

Håkan P. Svensson,[†] John F. Kadow,[‡] Vivekananda M. Vrudhula,[†] Philip M. Wallace,[†] and Peter D. Senter^{*†}

Bristol-Myers Squibb Pharmaceutical Research Institute, 3005 First Avenue, Seattle, Washington 98121, and 5 Research Parkway, Wallingford, Connecticut 06492. Received December 20, 1991

Cephalosporin mustard (CM) was designed as an anticancer prodrug that could be activated in a site-specific manner by monoclonal antibody- β -lactamase conjugates targeted to antigens present on tumor cell surfaces. Purified β -lactamases from *Bacillus cereus* (BC β L) and *Escherichia coli* (EC β L) catalyzed the release of phenylenediamine mustard (PDM) from CM through a fragmentation reaction which occurs after the β -lactam ring of CM is hydrolyzed. The K_m and V_{max} values were 5.7 μ M and 201 μ mol/min per mg for BC β L and 43 μ M and 29 μ mol/min per mg for EC β L, respectively. Conjugates of BC β L were prepared by combining the F(ab')₂ fragments of the maleimide-substituted monoclonal antibodies L6 and 1F5 with thiolated BC β L. The conjugates showed little loss in enzymatic activity and bound nearly as well as the unmodified F(ab')₂ monoclonal antibodies to antigens expressed on the H2981 human lung adenocarcinoma cell line (L6 positive, 1F5 negative). PDM was approximately 50-fold more cytotoxic than CM to H2981 cells. Treatment of the cells with L6-BC β L followed by CM resulted in a level of cytotoxic activity that was comparable to that of PDM. This was most likely due to activation of CM by conjugate that bound to cell-surface antigens, since pretreatment of H2981 cells with BC β L or 1F5-BC β L enhanced the activity of CM to a lesser extent. Thus, we have shown that CM is a prodrug, and that it can be activated with immunological specificity by a monoclonal antibody- β -lactamase conjugate.

INTRODUCTION

The treatment of cancer with conventional chemotherapy is often hampered by low drug specificity, dose-limiting side effects, and poor antitumor activities (1). To address these issues, we have explored a two-step approach in which relatively nontoxic drug precursors (prodrugs) are activated by targeted enzymes (for a review, see ref 2). In the first step, monoclonal antibodies (mAbs)¹ are used to deliver enzymes to antigens present on tumor cell surfaces. After the unbound conjugate has undergone a sufficient degree of clearance from nontarget tissues, a prodrug is administered that can be converted by the enzyme into an active anticancer drug.

We initially tested the feasibility of this approach using mAb-alkaline phosphatase conjugates for the hydrolysis of phosphorylated anticancer drug derivatives (2-5). While significant in vivo antitumor activities were observed, in only one case was the prodrug substantially less toxic than the corresponding drug (5). A larger differential in toxicity will most likely require the use of enzymes that carry out reactions not readily occurring in the body, or are confined to areas inaccessible to the prodrug. Many such enzymes for prodrug activation have been described. They include carboxypeptidase G2 (6, 7), carboxypeptidase A (8), penicillin amidase (9), β -lactamase (10-12), cytosine deaminase (13), and nitroreductase (14).

Several factors must be taken into account in selecting an enzyme for prodrug activation. These include the molecular weight and physical properties of the enzyme, its activity and stability under physiological conditions, the presence of the enzyme or related enzymes within the body, and the nature of the drug that the enzyme generates. Ideally, the enzyme should be able to activate a panel of anticancer drugs that differ mechanistically and have synergistic activities. In these respects, many β -lactamases hold a great deal of potential because of their favorable kinetics (15) and broad substrate specificities (16), as well as their abilities to effect the elimination of substituents appended to the 3'-position of cephalosporin substrates (10-12, 17, 18). This report describes the activation of CM, a cephalosporin derivative of phenylenediamine mustard (PDM), by β -lactamases from *Escherichia coli*, *Bacillus cereus*, and mAb- β -lactamase conjugates.

EXPERIMENTAL PROCEDURES

Materials. Crude *B. cereus* penicillinase (catalog number P0389) and pepsinogen were obtained from Sigma Chemical Co. The *E. coli* strain expressing the TEM-2 plasmid-mediated β -lactamase was a gift from Dr. Karen Bush (Bristol-Myers Squibb, Princeton, NJ). L6 (19) and IF5 (20) are IgG_{2a} mAbs that bind to antigens on human carcinomas and to the CD20 antigen on normal and neoplastic B-cells, respectively. The human lung adenocarcinoma cell line H2981 has been described previously (19, 21). L6 binds strongly to these cells, while IF5 shows very weak binding.

The F(ab')₂ fragments of L6 and IF5 were obtained by digestion of the mAbs with 2.2% pepsinogen (w/w) in 0.2 M sodium acetate at pH 4.2 for 7-9 h at 37 °C. The reaction mixture was brought to pH 7-8 with 1.0 M Tris base, and the F(ab')₂ fragments were purified on a Sephacryl S-200 (Pharmacia) column equilibrated in PBS. The purified product was concentrated by ultrafiltration to 5-10 mg/mL.

[†] Seattle, WA.

[‡] Wallingford, CT.

¹ Abbreviations used: BC β L, *Bacillus cereus* β -lactamase (II); CM, cephalosporin mustard; DMF, dimethylformamide; EC β L, *Escherichia coli* β -lactamase; EDTA, ethylenediaminetetraacetic acid; FITC, fluorescein isothiocyanate; LFE, linear fluorescence equivalence; mAb, monoclonal antibody; PBS, phosphate-buffered saline; PDM, phenylenediamine mustard; SDS-PAGE, sodium dodecyl sulfate polyacrylamide gel electrophoresis; SMCC, N-succinimidyl 4-(maleimidomethyl)cyclohexane-1-carboxylate; 2-IT, 2-iminothiolane hydrochloride.

Preparation of CM. To a solution of 4 g (9.7 mmol) of 3-acetoxy-7-(phenylacetamido)cephalosporanic acid sodium salt (22) in 50 mL of 0.1 M bicarbonate buffer at pH 9 was added 11.7 g of immobilized esterase (Bristol-Myers Squibb Industrial Division, Syracuse, NY). After 48 h at room temperature, TLC analysis of the supernatant (SiO₂ plate, ethyl acetate/methanol/acetic acid, 8:1:1) indicated that the reaction was complete. The product was filtered, partially concentrated, and purified by chromatography on C-18 silica gel (3 × 24 cm column) equilibrated with H₂O. The column was first washed with H₂O (280 mL) and then with 20% methanol in H₂O. Fractions 4–22 (10 mL each) contained the sodium salt of 3-(hydroxymethyl)-7-(phenylacetamido)cephalosporanic acid. Lyophilization gave 3.55 g of a pale yellow powder which was used without further purification. The ¹H NMR (DMSO-*d*₆) showed loss of the acetate methyl group and a new signal at δ 4.0 for the C-7 CH₂ group.

To a magnetically stirred green suspension of PDM hydrochloride (23) (650 mg, 2.4 mmol) in absolute THF (24 mL) under N₂ at 0 °C was added diisopropylethylamine (0.42 mL, 2.4 mmol). After 10 min at 0 °C, a solution of phosgene in toluene (1.9 M, 1.3 mL) was added dropwise. Analysis by TLC (SiO₂ plate, ethyl acetate/hexane, 1:4) indicated that the reaction was complete after 1 h and that a less polar product was formed.

A suspension of the sodium salt of 3-(hydroxymethyl)-7-(phenylacetamido)cephalosporanic acid (750 mg) in anhydrous toluene (100 mL) was evaporated to dryness under reduced pressure. The residue was dissolved in DMF (40 mL) and cooled to 0 °C under N₂, and 1.1 mL of diisopropylethylamine was added. After 5 min, the ice-cold solution of PDM isocyanate was introduced via a cannula into the DMF solution. The orange solution was allowed to warm to room temperature. After 2 h, the reaction mixture was treated with 1 N HCl (1.5 mL), and volatiles were removed under reduced pressure. To the residue was added ethyl acetate (100 mL) and H₂O (50 mL), and the pH was adjusted to 3.0 with 1 N HCl with vigorous stirring. The layers were separated, and the aqueous portion was extracted with ethyl acetate (50 mL). The combined organic layers solution was concentrated to about 25 mL, 10 g of C-18 silica gel was added, and volatiles were removed under reduced pressure. The residual brown powder was applied to a C-18 column (2 × 12 cm) and eluted with 50% and 70% acetonitrile in 1% aqueous acetic acid (250 mL each). A total of 448 mg (38% yield) of CM was obtained. A portion (300 mg) was triturated with dichloromethane (5 mL) and filtered to give CM (280 mg) as a white fluffy solid. High-resolution mass spectrometry: *M*⁺ 606.1116 (obsd), 606.1107 (calcd). ¹H NMR (DMSO-*d*₆, 300 MHz): δ 9.42 (s, 1 H), 9.10 (d, 1 H, NH, *J* = 6 Hz), 7.24 (m, 7 H, Ar-H), 6.68 (d, 2 H, Ar-H, *J* = 9 Hz), 5.66 (dd, 2 H, H-7, *J* = 6 Hz and *J* = 9 Hz), 5.09 (d, 1 H, H-6, *J* = 6 Hz), 4.88 (dd, 2 H, C3-CH₂O, *J* = 12 Hz), 3.67 (s, 8 H, (NCH₂CH₂Cl)₂), 3.53 (dd, 2 H, H-2, *J* = 15 Hz).

Enzymatic Activity. Enzymatic activities of BC β L and mAb conjugates of BC β L were determined using nitrocefin as a substrate (24). Solutions containing BC β L (50 ng/mL) were incubated with nitrocefin (40 μ M) in PBS containing 75 μ g/mL bovine serum albumin in 96-well polystyrene microtiter plates. The absorbance at 490 nm was determined every 2.0 min for 10 min starting 2.0 min after the reaction was initiated. Under these conditions, the increase of absorbance at 490 nm was linear and was directly proportional to the specific activities of the BC β L-containing solutions.

Enzyme Purification. (A) From *B. cereus*. BC β L was purified using a modification of the method of Davies et

al. (25). Crude β -lactamase from Sigma was taken up in H₂O, dialyzed into 10 mM sodium phosphate at pH 7.5 containing 50 mM NaCl, and incubated for 30 min at 60 °C. Precipitated material was removed by centrifugation (2 × 900*g* for 30 min) and the supernatant was applied to a Mono S column (Pharmacia) which was equilibrated with the above phosphate buffer. Purified enzyme was eluted off the column with 10 mM sodium phosphate at pH 7.5 containing 0.3 M NaCl. The protein was concentrated to 2–4 mg/mL by ultrafiltration, filtered through a 0.2- μ m filter, and stored at 4 °C. The purity of the BC β L thus obtained was assessed by SDS-PAGE and by specific activity measurements. β -Lactamase concentration was determined spectrophotometrically at 280 nm using *E*_{1%} of 10.5.

(B) From *E. coli*. Tryptic soybean broth was inoculated with pure colonies of β -lactamase expressing *E. coli*. The cultures were incubated for 18 h at 37 °C and centrifuged (6400*g* for 15 min at 4 °C). The pellet was washed with PBS, resuspended in PBS, frozen, and then quickly thawed. The debris was centrifuged off (21500*g* for 20 min at 4 °C) and resuspended in 0.2 M sodium acetate at pH 5.0. Supernatants from four such freeze-thaw cycles were pooled and dialyzed extensively against 20 mM triethanolamine hydrochloride containing 0.5 M NaCl at pH 7.0. After centrifugation (900*g* for 30 min at 4 °C), the supernatant was applied to a boronic acid affinity column (26) which was equilibrated in 20 mM triethanolamine hydrochloride containing 0.5 M NaCl at pH 7.0. The column was washed with this buffer until *A*_{280 nm} was zero, and the enzyme was then eluted with 0.5 M sodium borate containing 0.5 M NaCl at pH 7.0. EC β L was concentrated by ultrafiltration and the protein concentration was determined using the BCA assay (Pierce Chemical Co.).

HPLC Analysis of Drug Release. The release of PDM from CM (50 μ M in PBS at 37 °C) by crude BC β L (0.3 μ g/mL total protein) was investigated by HPLC using a C-18 column (4.6 × 250 mm). The gradient conditions were 45–90% acetonitrile in 0.08% diethylamine and 0.08% phosphoric acid (pH 2.3) over 15 min at 1 mL/min. The eluant was monitored at 254 nm. Under these conditions, the retention times of PDM and CM were 6.4 and 8.8 min, respectively.

Enzyme Kinetics with CM. Kinetic parameters for the β -lactamases (25 ng/mL for BC β L and 1 μ g/mL for EC β L) using CM (in PBS containing 12.5 μ g/mL bovine serum albumin) as a substrate (4–65 μ M with BC β L, 5–50 μ M with EC β L) were obtained by determination of the initial velocity of the reaction as a function of substrate concentration. This was estimated from the loss of absorbance at 266 nm ($\Delta\epsilon_{266\text{nm}} = 1.8 \times 10^4 \text{ M}^{-1} \text{ cm}^{-1}$) that occurs upon β -lactam hydrolysis. The reaction was monitored in a cuvette at room temperature by reading *A*_{266nm} every 0.1 min for 1.05 min starting at 0.15 min after the addition of enzyme. Lineweaver-Burk plots of the data were used to estimate the *K*_m and *V*_{max} values.

The rate of hydrolysis of CM by BC β L in the presence of EDTA was investigated by incubating the enzyme (1.0 μ g/mL in PBS) with 0 (control), 1.0, and 2.5 mM EDTA for 1 h at room temperature. Upon addition of CM (40 μ M in PBS), the reaction rate was determined as previously described.

Conjugate Preparation. SMCC (Pierce Chemical Co.) was dissolved in DMF at 5.0 mM and added to solutions of the F(ab')₂ mAbs at 5–10 mg/mL in PBS to give a final SMCC concentration of 0.25 mM. The solution was incubated for 30 min at 30 °C. Unreacted SMCC was removed by gel filtration through Sephadex G-25 (PD-10, Pharmacia) equilibrated in 40 mM sodium phosphate at pH 7.5 containing 0.6 M NaCl. The number of maleim-

ides (1.1–1.4) incorporated into the mAbs was estimated by adding an excess amount of mercaptoethanol to an aliquot of the solution, followed by titration of free thiols with 5,5'-dithiobis(2-nitrobenzoic acid).

2-IT (Pierce Chemical Co.) was dissolved in 0.5 M sodium borate at pH 8.5 (final concentration 18.7 mM) and added to BC β L at 2–4 mg/mL in 10 mM sodium phosphate containing 0.3 M NaCl at pH 7.5 to give a final 2-IT concentration of 1.7 mM. After incubation for 90 min at 4 °C, unreacted 2-IT was removed by gel filtration through Sephadex G-25 (PD-10) equilibrated in 40 mM sodium phosphate at pH 7.5 containing 0.6 M NaCl. The number of thiol groups (1.1–1.4) was determined using 5,5'-dithiobis(2-nitrobenzoic acid).

Maleimide-substituted F(ab')₂ and thiolated BC β L were mixed at a 1:1 molar ratio and incubated for 1 h at room temperature. The solution was cooled to 4 °C, and subsequent manipulations were carried out at this temperature. The reaction was terminated by the addition of 2-aminoethanethiol hydrochloride (100 μ M final concentration) and *N*-ethylmaleimide (200 μ M final concentration) in rapid succession. The mixture was concentrated by ultrafiltration and purified on a Sephacryl S-300 column equilibrated with 10 mM Tris HCl at pH 7.5 containing 150 mM NaCl. Fractions containing monomeric mAb-BC β L adducts (determined by SDS-PAGE and relative activity) were pooled, dialyzed into 10 mM Tris HCl at pH 7.5 containing 50 mM NaCl, and applied to a CM-Sephadex column (Pharmacia) equilibrated in the above Tris HCl buffer. The conjugate was eluted with a linear gradient of 50–300 mM NaCl (10 \times column volume) in 10 mM Tris HCl at pH 7.5. Alternatively, a stepwise gradient (10 mM Tris HCl at pH 7.5 containing first 0.1 M NaCl and then 0.3 M NaCl) was used to elute the bound material from the column. The conjugate eluted in the high-salt fractions. Fractions were analyzed by SDS-PAGE and relative enzyme activity. Those fractions containing primarily 1:1 conjugated proteins were pooled, dialyzed into saline, concentrated by ultrafiltration to 1.5–3.0 mg/mL, filtered through a 0.2- μ m filter, and stored at –70 °C. Concentrations of conjugated mAb and BC β L were determined spectrophotometrically at 280 nm using an $E^{1\%}$ of 16.6 and 66, respectively. The purity of conjugates was assessed by SDS-PAGE.

Cell Binding. L6-F(ab')₂-BC β L was tested for its ability to bind to H2981 cells relative to L6-F(ab')₂. Cells (7.5 \times 10⁵) in 0.2 mL of incomplete modified Dulbecco's medium with 10% fetal bovine serum (v/v) were incubated at 4 °C for 30 min with different proportions of FITC-labeled whole L6 and either unlabeled L6-F(ab')₂ or L6-F(ab')₂-BC β L. The total concentration of L6 for the solution was kept constant at 400 nM. After the incubation, the cells were washed twice with medium and analyzed on a fluorescence activated cell sorter for fluorescence intensity. The mean channel number of fluorescence was converted into linear fluorescence equivalence (LFE) and percent of binding was calculated using the following formula:

$$\% \text{ binding} = 100 - 100[(\text{LFE}_{100\% \text{ L6-FITC}} - \text{LFE}_{\text{sample}}) / (\text{LFE}_{100\% \text{ L6-FITC}} - \text{LFE}_{\text{no mAb}})]$$

In Vitro Cytotoxicity. H2981 cells in incomplete modified Dulbecco's medium with 10% fetal bovine serum (v/v) were plated into 96-well microtiter plates at 8000 cells/well and allowed to adhere overnight at 37 °C. The cells were exposed to analytically pure CM or PDM for 1 h at 37 °C, washed three times, and incubated an additional 18 h at 37 °C. This was followed by a 6-h pulse with [³H]-thymidine (1 μ Ci/well). The cells were detached by

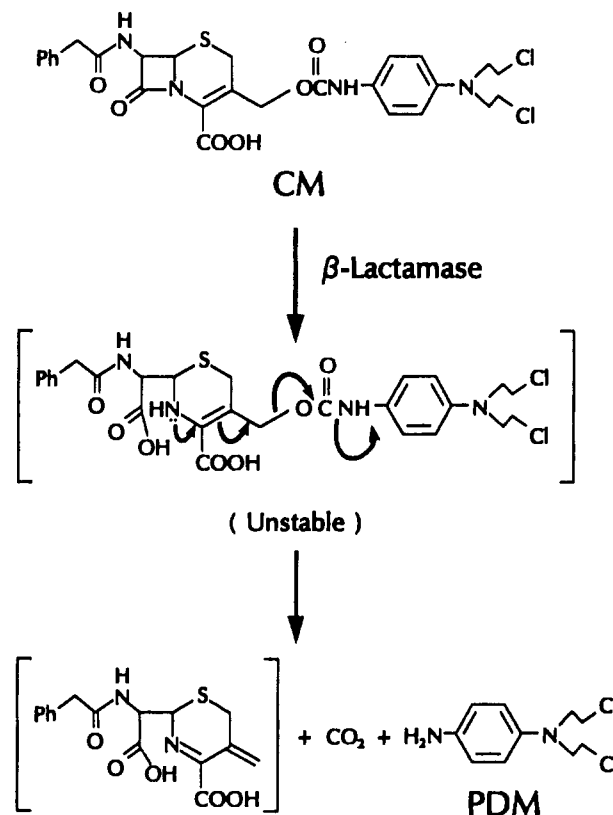


Figure 1. Structures of CM and PDM and the mechanism of drug release catalyzed by β -lactamase.

freezing at –20 °C and then harvested onto filter mats using an LKB WALLAC 1295-001 cell harvester. The filter mats were counted on an LKB WALLAC 1205 liquid scintillation counter. Cells that were pretreated with mAb- β -lactamase conjugates were exposed to the conjugates at 10 μ g/mL (mAb concentration) for 30–40 min at 4 °C, washed five times with cold medium, and then treated with CM. The cells were then washed, incubated, and pulsed as described above. A control experiment included cells that were pretreated with BC β L (2.5 μ g/mL), washed five times, and then exposed to CM.

RESULTS

Preparation and Reactivity of CM. CM (Figure 1) was prepared in two steps from 3-acetoxy-7-(phenylacetamido)cephalosporanic acid (22) by enzymatic removal of the acetoxy group followed by condensation of the resulting 3-(hydroxymethyl)-containing product with the isocyanate derivative of PDM (23). The structure of CM was confirmed using high-field NMR and high-resolution mass spectrometry.

Preliminary studies were undertaken in order to identify enzymes that were capable of effecting the transformation depicted in Figure 1. Commercially available crude β -lactamase preparations from *E. coli*, *B. cereus*, and *Enterobacter cloacae* were incubated with CM, and the formation of PDM was monitored by analytical methods such as HPLC and UV spectroscopy. It was found that all three enzyme preparations catalyzed the hydrolysis of CM and that PDM was released. With crude *B. cereus* β -lactamase (0.3 μ g/mL), the half-life for the conversion of CM (50 μ M in PBS) to PDM was 10 min. Identity of the product formed was determined by HPLC comparison with an authentic sample of PDM.

Purification and Characterization of β -Lactamases. Crude β -lactamase from *B. cereus* was obtained commercially as a mixture of proteins having penicilli-

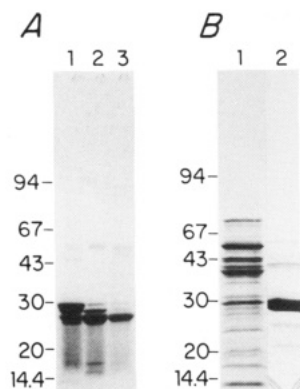


Figure 2. SDS-PAGE analyses (4–20%, nonreducing) of fractions obtained in the purification of β -lactamases. (A) From *B. cereus*: lane 1, unpurified protein from Sigma; lane 2, after heat precipitation; lane 3, BC β L after cation-exchange chromatography. (B) From *E. coli*: lane 1, supernatant from the first freeze-thaw cycle; lane 2, EC β L after purification on a boronic acid affinity column.

nase and cephalosporinase activities. Analysis of the mixture by SDS-PAGE (Figure 2A, lane 1) revealed the presence of a major component at 30 kDa and a minor component at 25 kDa. These proteins could be separated using a modification of the method of Davies et al. (25). The 30-kDa protein underwent precipitation when the protein mixture was heated at 60 °C. After centrifugation (Figure 2A, lane 2), purified *B. cereus* β -lactamase (II) (BC β L) was obtained by cation-exchange chromatography (Figure 2A, lane 3).

E. coli β -lactamase (EC β L), from a strain that produced a TEM-2 plasmid-mediated enzyme (16), was isolated according to a previously described procedure (26). Briefly, several freeze-thaw cycles of the cells, followed by centrifugation, provided a crude enzyme preparation (Figure 2B, lane 1). Purification was achieved by passing the material through a boronic acid affinity column. SDS-PAGE indicated that the enzyme purified in this manner had an apparent molecular weight of 30 kDa (Figure 2B, lane 2).

It was possible to spectrophotometrically follow the β -lactam hydrolysis by measuring the decrease in absorbance at 266 nm. With CM as the substrate, the K_m and V_{max} values for both enzymes were obtained from Lineweaver-Burk plots (Figure 3). BC β L had a K_m of 5.7 μ M and a V_{max} of 201 μ mol/min per mg (Figure 3A). The K_m and V_{max} values obtained for EC β L were 43 μ M and 29 μ mol/min per mg, respectively (Figure 3B).

The two enzymes were compared with each other using an in vitro cytotoxicity assay. H2981 human lung adenocarcinoma cells were incubated with CM and varying concentrations of either BC β L or EC β L. The concentration required to achieve 50% cell death was significantly lower for BC β L (4 ng/mL) compared to EC β L (30 ng/mL) (Figure 4). These results are in agreement with the kinetic analyses which show that CM is more rapidly hydrolyzed by BC β L than by EC β L.

At this stage, it became necessary to more fully characterize BC β L and to compare its properties with those of the previously reported *B. cereus* β -lactamase (25). Incubation of the purified enzyme with 2.5 mM EDTA prior to addition of CM resulted in complete inhibition of enzyme activity, indicating the presence of an essential metal cofactor. This is consistent with a previous report indicating that BC β L is a zinc metalloenzyme (25). Further confirmation of the identity of the enzyme was obtained by N-terminal amino acid sequence analysis (10 residues, data not shown), which correlated to the published amino acid sequence for the *B. cereus* enzyme (27).

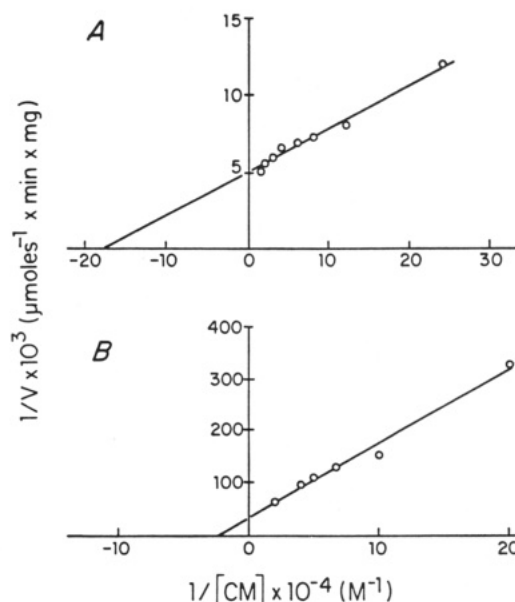


Figure 3. Kinetics of CM hydrolysis catalyzed by (A) BC β L (25 ng/mL), and (B) EC β L (1 μ g/mL). K_m and V_{max} values were obtained from the intercepts of the x and y axes, respectively. The R values were 0.993 for both plots.

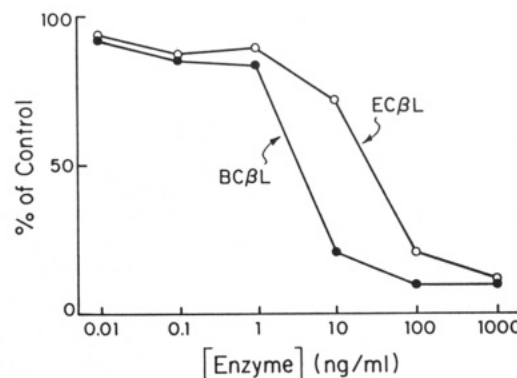


Figure 4. Cytotoxic effects of β -lactamases combined with CM (10 μ M, 1 h exposure) on H2981 cells.

Conjugate Preparation, Purification, and Characterization. The F(ab')₂ fragments of the mAbs L6 (anticarcinoma, 19) and 1F5 (anti B-lymphoma, 20) were covalently linked to BC β L through stable thioether bonds. This was achieved by combining maleimide-substituted mAbs with thiolated BC β L. The formation of high molecular weight aggregates could be minimized by carefully controlling the extent to which each of the proteins was modified. Optimal results were obtained when 1.1–1.4 modifying groups per protein molecule were introduced.

The composition of the crude conjugation mixture is shown in Figure 5 (lane 2). Purification of the conjugate was achieved using a two-step procedure. Gel filtration was used to separate high molecular weight aggregates and unreacted enzyme from the conjugate-containing fractions (Figure 5, lane 3). Unconjugated mAbs could be removed by cation-exchange chromatography. The resulting conjugate consisted almost exclusively of a 1:1 mAb:BC β L adduct which had a molecular weight of approximately 125 kDa (Figure 5, lane 4).

A competitive binding assay was used to establish how effectively the conjugates could bind to cell-surface antigens. In this assay, H2981 cells (L6 positive) were exposed to different proportions of L6-BC β L and FITC-modified L6. It was found that L6-BC β L and unmodified L6 were nearly equal in their abilities to compete

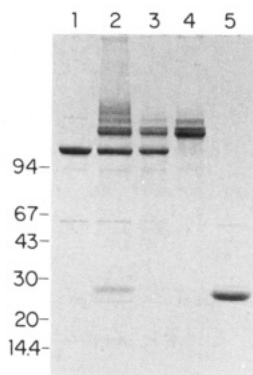


Figure 5. SDS-PAGE analyses (4–20%, nonreducing) of fractions obtained in the purification of L6-BC β L: Lane 1, L6-F(ab')₂; lane 2, conjugation product before purification; lane 3, after gel filtration; lane 4, L6-BC β L after cation-exchange chromatography; lane 5, BC β L.

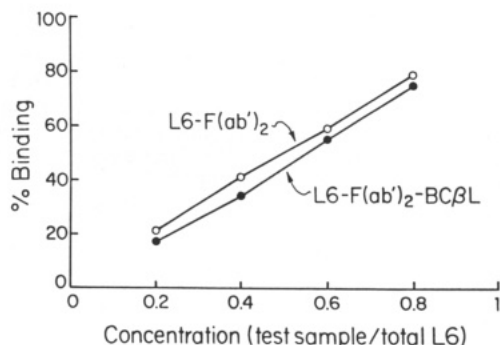


Figure 6. Competition binding assay: H2981 cells were incubated with various combinations of the test samples (L6-F(ab')₂, or L6-F(ab')₂-BC β L) and FITC-modified whole L6, keeping the total mAb concentration (tested L6 + L6-FITC) constant at 400 nM. Fluorescence intensity was determined by fluorescence activated cell sorter analysis.

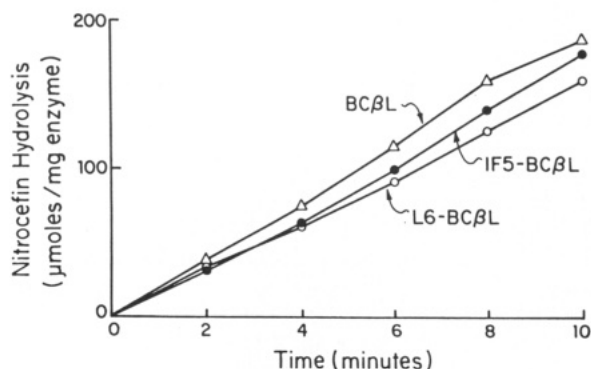


Figure 7. Enzymatic activities of BC β L (50 ng/mL) and mAb-BC β L conjugates (50 ng BC β L component/mL) using nitrocefin (40 μ M) as a substrate.

with FITC-modified L6 for cell-surface binding (Figure 6), indicating that the conjugation chemistry used did not significantly alter the capability of the L6 moiety to bind to cell surface antigens. 1F5 binds very weakly to H2981 cells (3–5).

Enzymatic activity measurements with the purified conjugates were done using nitrocefin as a substrate (24). Typically, the conjugates retained 70–85% of the enzyme's specific activity compared to unmodified BC β L (Figure 7). This small loss was probably not directly due to the addition of thiol groups to BC β L with 2-IT, since the thiolated enzyme retained 90–100% of its original activity (data not shown).

Conjugate-Mediated Cytotoxicity. In vitro cytotoxicity experiments were performed using the H2981 human lung adenocarcinoma cell line (L6 positive, 1F5 negative).

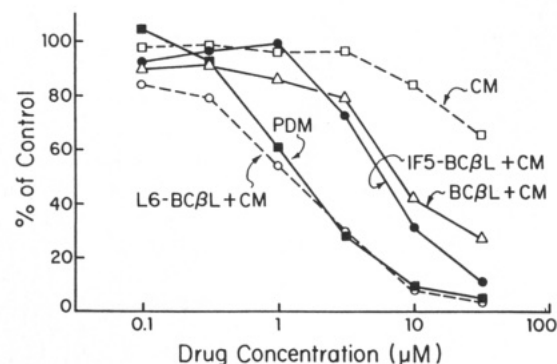


Figure 8. In vitro cytotoxicity of CM and PDM, on previously untreated H2981 cells (L6 positive, 1F5 negative), and of CM on cells that were pretreated with either L6-BC β L, 1F5-BC β L, or BC β L (2.5 μ g of BC β L component/mL).

Cells were treated with CM or PDM for 1 h, washed, and incubated for a total of 24 h. The incorporation of [³H]-thymidine into DNA was used as a measure of cell viability. It was found that CM (IC₅₀ > 30 μ M) was significantly less cytotoxic than PDM (IC₅₀ = 1.5 μ M, Figure 8). The cytotoxic activity of CM on cells that were pretreated with L6-BC β L was equal to that of PDM. This activation showed signs of immunological specificity based on the finding that the control conjugate, 1F5-BC β L, caused a smaller degree of enhancement. The cytotoxic effect of CM on 1F5-BC β L-treated cells might be due to insufficient washing or to interactions between the enzyme and the cell surface, since a similar degree of activation was observed when cells were treated with BC β L before exposure to CM.

DISCUSSION

The reaction of β -lactamases with appropriately substituted cephalosporins can result in the fragmentation of the 3'-substituent through the mechanism shown in Figure 1. This has led to the development of "dual-action cephalosporins" for the treatment of bacterial strains that are antibiotic resistant due to their levels of β -lactamases. Antibacterial activity was obtained when such strains were treated with 3'-substituted cephalosporins that released antibiotics when the β -lactam ring was hydrolyzed (17, 18). Application of this strategy for the release of anticancer drugs such as PDM (12), other nitrogen mustards (12), and vinca alkaloids (10, 11) from corresponding 3'-substituted cephalosporins have recently been reported. The β -lactamases used to catalyze the release of these drugs were obtained from *E. cloacae*.

We have demonstrated that the mechanistically different (25, 26) β -lactamases from *B. cereus* and *E. coli* catalyze the conversion of the prodrug CM into PDM. These enzymes have pronounced structural differences. They share no significant amino acid sequence homology (27, 28), and would not be expected to have immunological cross-reactivity. In therapeutic applications, it may therefore be possible to switch enzymes if an immune response against the β -lactamase used initially precludes further treatment.

One of the greatest advantages of using β -lactamases for prodrug activation is that a variety of drugs can be released upon hydrolysis of the β -lactam ring (10–12, 17, 18). Many anticancer agents with amino groups that are essential for activity would be rendered inactive when attached to cephalosporins through carbamate linkages as shown in this paper. Our finding that CM was at least 50 times less cytotoxic than PDM is consistent with what others have reported concerning the effect that electron-

withdrawing groups have on the activities of *N,N*-bis(2-chloroethyl)anilines (29, 30).

The activation of CM by L6-BC β L is a further example of a targeted enzyme capable of activating a relatively noncytotoxic prodrug (2-14). We are currently investigating the in vivo activities of CM combined with monoclonal antibody-BC β L conjugates. In addition, we are developing a variety of other prodrugs that can be activated by β -lactamases.

ACKNOWLEDGMENT

We wish to thank Karl Erik and Ingegerd Hellström for their support throughout the course of this work, Hans Marquardt and Steven Klohr for analyses, and Karen Bush and David Lowe for discussions and useful reagents.

LITERATURE CITED

- (1) Zubrod, C. G. (1982) Principles of Chemotherapy. *Cancer Medicine* (J. F. Holland and E. Frei, Eds.) pp 627-632, Lea and Febiger, Philadelphia.
- (2) Senter, P. D. (1990) Activation of prodrugs by antibody-enzyme conjugates: A new approach to cancer therapy. *FASEB J.* 4, 199-193.
- (3) Senter, P. D., Saulnier, M. G., Schreiber, G. J., Hirschberg, D. L., Brown, J. P., Hellström, I., and Hellström, K. E. (1988) Antitumor effects of antibody-alkaline phosphatase conjugates in combination with etoposide phosphate. *Proc. Natl. Acad. Sci. U.S.A.* 85, 4842-4846.
- (4) Senter, P. D., Schreiber, G. J., Hirschberg, D. L., Ashe, S. A., Hellström, K. E., and Hellström, I. (1988) Enhancement of the in vitro and in vivo antitumor activities of phosphorylated mitomycin C and etoposide derivatives by monoclonal antibody-alkaline phosphatase conjugates. *Cancer Res.* 49, 5789-5792.
- (5) Wallace, P. M., and Senter P. D. (1991) In vitro and in vivo activities of monoclonal antibody-alkaline phosphatase conjugates in combination with phenol mustard phosphate. *Bioconjugate Chem.* 2, 349-352.
- (6) Bagshawe, K. D., Springer, C. J., Searle, F., Antoniow, P., Sharma, S. K., Melton, R. F. (1988) A cytotoxic agent can be generated selectively at cancer sites. *Br. J. Cancer* 58, 700-703.
- (7) Springer, C. J., Bagshawe, K. D., Sharma, S. K., Searle, F., Boden, J. A., Antoniow, P., Burke, P. J., Rogers, G. T., Sherwood, R. F., and Melton, R. G. (1991) Ablation of human choriocarcinoma xenografts in nude mice by antibody-directed enzyme prodrug therapy (ADEPT) with three novel compounds. *Eur. J. Cancer* 27, 1361-1366.
- (8) Esswein, A., Hanseler, E., Montejano, Y., and Huennekens, F. M. (1991) Construction and chemotherapeutic potential of carboxypeptidase-A/monoclonal antibody conjugate. *Adv. Enzyme Regul.* 31, 3-12.
- (9) Kerr, D. E., Senter, P. D., Burnett, W. V., Hirschberg, D. L., Hellstrom, I., and Hellstrom, K. E. (1990) Antibody-penicillin-V amidase conjugates kill antigen-positive tumor cells when combined with doxorubicin phenoxylacetamide. *Cancer Immunol. Immunother.* 31, 202-206.
- (10) Shepherd, T. A., Jungheim, L. N., Meyer, D. L., and Starling, J. J. (1991) A novel targeted delivery system utilizing a cephalosporin-oncolytic prodrug activated by an antibody β -lactamase conjugate for the treatment of cancer. *Bioorg. Med. Chem. Lett.* 1, 21-26.
- (11) Meyer, D. L., Jungheim, L. N., Mikolajczyk, S. D., Shepherd, T. A., Starling, J. J., and Ahlem, C. N. (1992) Preparation and characterization of β -lactamase-Fab' conjugates for the site-specific activation of oncolytic agents. *Bioconjugate Chem.* 3, 42-48.
- (12) Alexander, R. P., Beeley, N. R. A., O'Driscoll, M., O'Neill, F. P., Millican, T. A., Pratt, A. J., and Willenbrock, F. W. (1991) Cephalosporin nitrogen mustard carbamate prodrugs for "ADEPT". *Tetrahedron Lett.* 32, 3269-3272.
- (13) Senter, P. D., Su, P. C. D., Katsuragi, T., Sakai, T., Cosand, W. L., Hellström, I., and Hellström, K. E. (1991) Generation of 5-fluorouracil from 5-fluorocytosine by monoclonal antibody-cytosine deaminase conjugates. *Bioconjugate Chem.* 2, 447-451.
- (14) Sunters, A., Baer, J., and Bagshawe, K. D. (1991) Cytotoxicity and activation of CB1954 in a human tumour cell line. *Biochem. Pharmacol.* 9, 1293-1298.
- (15) Waley, S. G. (1988) β -Lactamases: A major cause of antibiotic resistance. *Sci. Prog. (Oxford)* 72, 579-597.
- (16) Bush, K. (1989) Characterization of β -lactamases. *Antimicrob. Agents Chemother.* 33, 259-263.
- (17) Mobashery, S., Lerner, S. A., and Johnston, M. (1986) Conscripting β -lactamase for use in drug delivery. Synthesis and biological activity of a cephalosporin C10-ester of an antibiotic dipeptide. *J. Am. Chem. Soc.* 108, 1685-1686.
- (18) Albrecht, H. A., Beskid, G., Christenson, J. G., Durkin, J. W., Fallet, V., Georgopapadakou, N. H., Keith, D. D., Konzelmann, F. M., Lipschitz, E. R., McGarry, D. H., Siebelist, J., Wei, C. C., Weigle, M., and Yang, R. (1991) Dual-action cephalosporins: Cephalosporin 3'-quaternary ammonium quinolones. *J. Med. Chem.* 34, 669-675.
- (19) Hellström, I., Horn, D., Linsley, P. S., Brown, J. P., Brankovan, V., and Hellström, K. E. (1986) Monoclonal antibodies raised against human lung carcinoma. *Cancer Res.* 46, 3917-3923.
- (20) Clark, E. A., Shu, G., and Ledbetter, J. A. (1985) Role of the Bp35 cell surface polypeptide in human B cell activation. *Proc. Natl. Acad. Sci. U.S.A.* 82, 1766-1770.
- (21) Hellström, I., Beaumier, P. L., and Hellström, K. E. (1986) Antitumor effects of L6, an IgG_{2a} antibody that reacts with most human carcinomas. *Proc. Natl. Acad. Sci. U.S.A.* 83, 7059-7063.
- (22) Cocker, J. D., Cowley, B. R., Cox, J. S. G., Eardley, S., Gregory, G. I., Lazenby, J. K., Long, A. G., Sly, J. C. P., and Somerfield, G. A. (1965) Cephalosporanic acids. Part II. Displacement of the acetoxy-group by nucleophiles. *J. Chem. Soc.* 1965, 5015-5031.
- (23) Everett, J. L., and Ross, W. C. J. (1949) Aryl-2-halogenoalkylamines. Part II. *J. Chem. Soc.* 1949, 1972-1983.
- (24) Madgwick, P. J., and Waley, S. G. (1987) β -Lactamase I from *Bacillus cereus*. *Biochem. J.* 248, 657-662.
- (25) Davies, R. B., and Abraham, E. P. (1974) Separation, purification and properties of β -lactamase I and β -lactamase II from *Bacillus cereus* 569/H/9. *Biochem. J.* 143, 115-127.
- (26) Cartwright, S. J., and Waley, S. G. (1984) Purification of β -lactamases by affinity chromatography on phenylboronic acid-agarose. *Biochem. J.* 221, 505-512.
- (27) Ambler, R. P., Daniel, M., Fleming, J., Hermoso, J. M., Pang, C., and Waley, S. G. (1985) The amino acid sequence of the zinc-requiring β -lactamase from the bacterium *Bacillus cereus* 569. *FEBS Lett.* 189, 207-211.
- (28) Ambler, R. P., and Scott, G. K. (1978) Partial amino acid sequence of penicillinase coded by *Escherichia coli* plasmid R6K. *Proc. Natl. Acad. Sci. U.S.A.* 75, 3732-3736.
- (29) Palmer, B. D., Wilson, W. R., Pullen, S. M., and Denny, W. (1990) Hypoxia-selective antitumor agents. 3. Relationships between structure and cytotoxicity against cultured tumor cells for substituted *N,N*-bis(2-chloroethyl)anilines. *J. Med. Chem.* 33, 112-121.
- (30) Chakravarty, P. K., Carl, P. L., Weber, M. J., and Katzenellenbogen, J. A. (1983) Plasmin-activated prodrugs for cancer therapy. 1. Synthesis and biological activity of peptidylcivicin and peptidylphenylenediamine mustard. *J. Med. Chem.* 26, 633-638.

Introduction of Aliphatic Amino and Hydroxy Groups to Keto Steroids Using O-Substituted Hydroxylamines[†]

Heikki Mikola* and Elina Hänninen[‡]

Wallac Chemical Laboratories, P.O. Box 10, SF-20101 Turku, Finland. Received January 7, 1992

(Aminoxy)butyl- and -hexylamines and alcohols were synthesized by the Ing-Manske modification of the Gabriel synthesis. The aminoxy group of these heterobifunctional spacer reagents is a far more powerful nucleophile than the amino or hydroxy group because of the oxygen atom adjacent to the amino group (α -effect). The aminoxy group reacts readily with keto groups while the amino or hydroxy (or other) group remains free for further reactions. These excellent heterobifunctional spacer reagents were used here to derivatize keto steroids in an alkaline alcoholic solution. Using the described, general, and easy one-step synthesis, aliphatic amino or hydroxy groups with a spacer arm have been introduced to testosterone, 6-ketoestradiol, and cortisol.

INTRODUCTION

In many biochemical applications, haptens coupled covalently to other molecules are needed (1). For example in affinity chromatography and in immunoassays haptens immobilized on solid matrix are used. In antibody production the hapten needs to be coupled covalently to a carrier before immunization, and in competitive immunoassays the hapten is traditionally coupled to a label molecule to be used as a tracer. Usually before coupling, a spacer arm and a suitable reactive group have to be introduced to the hapten molecule, for example by using bifunctional spacer reagents. The coupling site, the chemical structure of the linkage, and the length of the spacer arm between the hapten and the label or the carrier have important roles in the recognition of the hapten by the antibody (1-5).

O-(Carboxymethyl)oximes, hemisuccinates, carboxyethyl ethers, and thioethers are frequently used as derivatives in steroid immunoassays (1). The spacer arm in all of these derivatives is quite short. α,ω -Diamino-hydrocarbons have been coupled to testosterone 3-[O-(carboxymethyl)oxime] (6) to get longer spacer arms containing an aliphatic amino group. The yield of this reaction is quite low because of the large excess of diamino compound needed, which has to be removed from the reaction mixture. Amino sterols have also been used as starting materials for some bridged steroid derivatives (3, 7) instead of keto or hydroxy steroids.

In the present study aliphatic (aminoxy)alkylamines and alcohols were synthesized. In a one-step synthesis these were used to incorporate a spacer arm with primary aliphatic amino or hydroxy group to the keto group of testosterone, 6-ketoestradiol, and cortisol. Similar (aminoxy)butyl compounds have so far been utilized as enzyme inhibitors or bacteriostatics (8-13) and to introduce aliphatic amino (14) or hydroxyl groups (15) to nucleotides.

The use of these synthesized steroid derivatives in immunoassays will be described later.

EXPERIMENTAL PROCEDURES

Materials. The reagents for syntheses were purchased either from Aldrich-Chemie, E. Merck, or Fluka and used without further purification. The solvents were p.a. grade either from E. Merck or Baker. TLC plates and silica for short-column chromatography were obtained from E. Merck.

¹H NMR spectra were recorded on either JEOL GX 400 or Hitachi Perkin-Elmer R-600 spectrometers using tetramethylsilane (TMS) or 3-(trimethylsilyl)propanesulfonic acid (DSS) as internal standard. UV spectra were obtained on a Shimadzu UV-2100 spectrophotometer. Mass spectra were recorded on a VG7070E mass spectrometer by using an electronic ionization energy of 70 or 15 eV (EI 70 eV and EI 15 eV) and chemical ionization with ammonia as reagent gas (CI). Melting points are uncorrected and were measured on a Gallenkamp capillary melting point apparatus.

Syntheses of Aminoxy-Group-Containing Heterobifunctional Spacer Reagents. *N*-(4-Bromobutyl)phthalimide (I). A mixture of 55.6 g of potassium phthalimide, 95.5 mL of 1,4-dibromobutane, and 3.5 mL of dimethylformamide was stirred at 160 °C for about 17 h. The warm reaction mixture was filtered and the precipitate was washed with ethanol. The solvents were evaporated under reduced pressure, and the remainder was recrystallized twice from ethanol to produce *N*-(4-bromobutyl)phthalimide (I). Yield: 59.7 g (71%). Mp: 77-80 °C.

N-(6-Bromohexyl)phthalimide (II). The title compound was synthesized by the method employed for *N*-(4-bromobutyl)phthalimide (I) starting from 55.6 g of potassium phthalimide and 114.5 mL of 1,6-dibromohexane. Yield: 66.9 g (72%). Mp: 52-55 °C.

N-[4-(Phthalimidooxy)butyl]phthalimide (III). A mixture of 17.6 g of *N*-(4-bromobutyl)phthalimide (I), 11.0 g of *N*-hydroxyphthalimide, and 63 mL of dry dimethylformamide was heated to 60 °C. Triethylamine (9.5 mL) was added and the mixture was stirred at room temperature for 30 h. Water (250 mL) was added and the precipitate was collected and washed with water. The crude product (III) was dried at room temperature. Yield: 18.4 g (81%). Mp: 159-161 °C.

N-[6-(Phthalimidooxy)hexyl]phthalimide (IV). The title compound was synthesized as *N*-[4-(phthalimidooxy)butyl]phthalimide (III) from 17.6 g of *N*-(6-bromohexyl)-

* Author to whom correspondence should be addressed.

[†] Presented in part as a poster at the 8th International IUPAC Conference on Organic Synthesis, Helsinki, Finland, July 23-27, 1990.

[‡] Present address: Orion Corp., Farmos, P.O. Box 425, SF-20101 Turku, Finland.

phthalimide (II) and 11.0 g of *N*-hydroxyphthalimide. Yield: 21.5 g (97%). Mp: 114–118 °C.

4-(Aminoxy)butylamine Dihydrochloride (V). A mixture of 18.0 g of *N*-[4-(phthalimidooxy)butyl]phthalimide (III), 9.5 mL of hydrazine hydrate, and 50 mL of ethanol was stirred for 2 h at 80 °C and then 2 days at room temperature. Concentrated hydrochloric acid (100 mL) was added and refluxed for 1 h. Water (125 mL) was added and the ethanol was evaporated under reduced pressure. The precipitated phthalhydrazide was separated by filtration; the solution was concentrated, made alkaline, and evaporated to dryness. Ethanol (50 mL) was added to solubilize the product and the remaining solid was filtered. The ethanol solution was acidified using 6 M HCl, filtered, and evaporated to dryness. The solid product was crystallized from methanol/ethyl acetate to give 6.8 g (97%) of 4-(aminoxy)butylamine dihydrochloride (V). ¹H NMR: δ (D₂O) 1.70 (4 H, m, -CH₂CH₂-), 3.03 (2 H, t, NH₂CH₂), 3.77 ppm (2 H, t, NH₂OCH₂). MS: free base, *m/z* (relative intensity) (CI) 105 (37), 90 (31), 88 (30), 72 (100); [M + H]⁺ calcd for C₄H₁₂N₂O + H, 105.1028, found 105.069; (EI 15 eV) 105 (5), 88 (11), 72 (100), 55 (36); [M + H]⁺ found 105.10; (EI 70 eV) 88, 72, 55.

6-(Aminoxy)hexylamine Dihydrochloride (VI). The title compound was synthesized by the method employed for 4-(aminoxy)butylamine dihydrochloride (V). ¹H NMR: δ (D₂O) 1.40 (4 H, m, -CH₂-), 1.68 (4 H, m, -CH₂-), 3.00 (2 H, t, NH₂CH₂), 3.93 ppm (2 H, t, NH₂OCH₂).

4-Bromobutyl Acetate (VII). Acetyl bromide (10.0 g) was dropped into refluxing tetrahydrofuran (200 mL) and the product, 4-bromobutyl acetate (VII), was distilled at reduced pressure. Yield: 14 g (88%). Bp: 92 °C (12 mmHg).

***N*-[(4-Acetylbutyl)oxy]phthalimide (VIII).** A mixture of 80 g of *N*-hydroxyphthalimide and 100 g of 4-bromobutyl acetate (VII) was added into 200 mL of dry dimethylformamide and 70 mL of dry triethylamine and stirred at room temperature for 16 h and at 100 °C for 30 min. The mixture was cooled to room temperature and poured into 2 L of water. The precipitate was collected, washed with water, dried in a vacuum desiccator, and used without further purification.

4-(Aminoxy)butanol (IX). Crude *N*-[(4-acetylbutyl)oxy]phthalimide (VIII) from the previous step was refluxed in a mixture of acetic acid (135 mL) and concentrated hydrochloric acid (75 mL) for 45 min. After cooling, the precipitated phthalic acid was filtered off and the filtrate concentrated and coevaporated five times with 50 mL of water to dryness to remove the traces of acids. Water (100 mL) was added and the pH was adjusted to 13–14 using 30% sodium hydroxide. The product was extracted from water with ethyl acetate in a continuous extraction system for 8 h. Distillation at reduced pressure yielded 28 g (50%) of 4-(aminoxy)butanol (IX). Bp: 98 °C (1 mmHg). ¹H NMR: δ (D₂O) 1.62 (4 H, m, -CH₂-), 3.63 (2 H, t, OHCH₂), 3.76 ppm (2 H, t, NH₂OCH₂). MS: free base, *m/z* (relative intensity) (CI) 106 (85), 88 (38), 73 (30), 55 (100); [M + H]⁺ calcd for C₄H₁₁NO₂ + H 106.0868, found 106.096; (EI 15 eV) 106 (3), 88 (4), 73 (72), 55 (100); [M + H]⁺ found 106.03; (EI 70 eV) 73, 55.

***N*-[(6-Bromohexyl)oxy]phthalimide (X).** A mixture of 8.16 g of *N*-hydroxyphthalimide and 30.5 g of 1,6-dibromohexane in 125 mL of dry dimethylformamide and 6.9 mL of triethylamine was stirred at 60 °C for 2 h and then at room temperature for 24 h. After filtration the reaction mixture was distilled at reduced pressure and the re-

mainder was crystallized from ethanol to produce *N*-[(6-bromohexyl)oxy]phthalimide (X). Yield: 11 g (68%). Mp: 57–62 °C.

***N*-[(6-Acetylhexyl)oxy]phthalimide (XI).** A mixture of 0.98 g of *N*-[(6-bromohexyl)oxy]phthalimide (X) and 2.46 g of sodium acetate in 50 mL of acetic acid was refluxed for 36 h and evaporated to dryness. The product, *N*-[(6-acetylhexyl)oxy]phthalimide (XI), was used without further purification.

6-(Aminoxy)hexanol Hydrochloride (XII). A mixture of 1.83 g of crude *N*-[(6-acetylhexyl)oxy]phthalimide (XI) and 1.17 mL of hydrazine hydrate in 5 mL of ethanol was stirred overnight at 62 °C. Concentrated hydrochloric acid (10 mL) was added and refluxed for 2.5 h. Water (20 mL) was added and the ethanol was evaporated. The precipitated phthalhydrazide was separated by filtration and the solution was concentrated. The concentrate was purified with a short silica column using first 30% methanol in chloroform and then 50% methanol in chloroform, which eluted the product, 6-(aminoxy)hexanol hydrochloride (XII). ¹H NMR: δ (D₂O) 1.68 (4 H, m, -CH₂-), 1.42 (4 H, m, -CH₂-), 3.60 (2 H, t, OHCH₂), 3.73 ppm (2 H, t, NH₂OCH₂).

General Procedures for the Synthesis of Steroid O-Alkylloximes. **Testosterone 3-[O-(6-Aminoethyl)oxime].** A solution of 100 mg of testosterone and 360 mg of 6-(aminoxy)hexylamine dihydrochloride (VI) in 3 mL of 90% ethanol and 150 mg of sodium acetate was stirred at room temperature for 1 h and then refluxed for 4 h. The reaction mixture was filtered and evaporated to dryness. The product, testosterone 3-[O-(6-aminoethyl)oxime], was purified with a short silica column using gradient elution from 0 to 20% of methanol in chloroform. Yield: 120 mg (85%). ¹H NMR: δ (CDCl₃ + CD₃OD) 0.77 (3 H, s, 18-CH₃), 1.07 (3 H, s, 19-CH₃), 1.42 (4 H, m, -CH₂CH₂-), 1.74 (4 H, m, -CH₂CH₂-), 2.93 (2 H, d, CH₂NH₂), 3.61 (1 H, d, *J* = 8.5 Hz, 17 α -H), 4.02 (2 H, t, NOCH₂), 5.74 and 6.36 ppm (1 H, 2 s, 4-H anti- and syn-isomer, respectively). MS: (EI 70 eV) *m/z* (relative intensity) 402 (8), 372 (5), 314 (3), 286 (38), 116 (100); M⁺ calcd for C₂₅H₄₂N₂O₂ 402.3236, found 402.288.

6-Ketoestradiol 6-[O-(6-Hydroxyhexyl)oxime]. A solution of 290 mg of 6-ketoestradiol and 400 mg of 6-(aminoxy)hexanol hydrochloride (XII) in 20 mL of 90% ethanol and 650 mg of sodium acetate was treated as above. The product, estradiol 6-[O-(6-hydroxyhexyl)oxime] was purified by thin-layer chromatography using 20% methanol in chloroform to develop the plates. Yield: ~130 mg (30%). ¹H NMR: δ (CDCl₃ + CD₃OD) 0.78 (3 H, s, 18-CH₃), 1.48 (m, -CH₂CH₂-), 1.78 (m, -CH₂CH₂-), 3.00 (m, CH₂OH), 3.73 (1 H, m, 17 α -H), 4.18 (2 H, t, NOCH₂), 6.89 (1 H, dd, *J* = 2.8 and 8.5, 2-H), 7.20 (1 H, d, *J* = 8.5, 1-H), 7.43 ppm (1 H, d, *J* = 2.8, 4-H). MS: (EI 70 eV) *m/z* (relative intensity) 401 (13), 371 (5), 313 (3), 284 (100), 226 (5), 172 (19), 117 (50); M⁺ calcd for C₂₄H₃₅NO₄ 401.2557, found 401.225.

Cortisol 3-[O-(6-Aminoethyl)oxime]. A solution of 1 g of cortisol and 0.7 mL of pyrrolidine in 15 mL of methanol was stirred for 15 min. Pyrrolidine (0.7 mL) and 566 mg of 6-(aminoxy)hexylamine dihydrochloride (VI) were added, and the reaction mixture was heated to 60 °C for 5 min and then stirred at room temperature for 2 h. The mixture was evaporated to dryness and purified with a short silica column using 20% methanol in chloroform as eluent. Yield: 300 mg (26%). ¹H NMR: δ (CDCl₃ + CD₃OD) 0.87 (3 H, s, 18-CH₃), 1.32–1.47 (7 H, m, -CH₂CH₂- and 19-CH₃), 1.78 (4 H, m, -CH₂CH₂-), 2.96 (2 H, d, CH₂-NH₂), 4.02 (2 H, t, NOCH₂), 4.39 (1 H, m, 11 α -H), 5.66 and

6.25 ppm (1 H, 2 s, 4-H anti- and syn-isomer, respectively). MS: (EI 15 eV) m/z (relative intensity) 446 (5), 368 (8), 301 (37), 256 (18), 207 (40), 135 (100); (CI) (relative intensity) 477 (4), 447 (8), 433 (11), 419 (57), 391 (100), 363 (28), 279 (47), 173 (64); $[M + H]^+$ calcd for $C_{27}H_{44}N_2O_5 + H$ 477.3328, found 477.25.

RESULTS AND DISCUSSION

O-(Carboxymethyl)oximes have been used extensively while conjugating steroids to other molecules. During the synthesis of such steroid derivatives (aminooxy)acetic acid has been used as a heterobifunctional spacer reagent. In spite of this the same method of incorporating other spacer arms and aliphatic functional groups to steroids has remained almost unnoticed. Here the method is used to couple some aminooxy-group-containing bifunctional reagents to keto steroids. Methods of synthesizing (aminooxy)alkylamines and alcohols are described as examples of how to synthesize these bifunctional spacer reagents, which are quite stable and useful, as hydrochlorides. While using other aminooxy compounds, like (aminooxy)alkyl carboxylic acids or thiols, other reactive groups can easily be introduced to keto compounds by the same method.

There are quite a number of methods of synthesizing aminooxy compounds (O-substituted hydroxylamines) (13, 16). Here the Ing-Manske modification of the Gabriel synthesis (the phthalimido method) (17) was used because of our experience with phthalimido derivatives of dibromoalkanes during the synthesis of chemiluminescent derivatives of steroids (18). Other suitable methods for synthesizing these aminooxy compounds are, for example, the use of benzohydroxamic acid (12) or ethyl *N*-hydroxyacetimidate (19). In both cases the conditions during the reaction and hydrolysis of the protecting groups are relatively mild.

The mass spectrometric characterization of the synthesized aminooxy compounds seems to indicate that these molecules can act as ionization reactants. Under normal electronic ionization conditions (70 eV), no molecular ions were detectable, and with a very high concentration of the aminooxy compound and a lower ionization energy (15 eV), the molecular ions could be detected as $[M + H]^+$. When normal chemical ionization with ammonia was applied, the molecular ions were clearly obtainable as $[M + H]^+$. In all the spectra, characteristic fragmentation was observed and the major ions detected originated from loss of ONH_2 , and NH_2 or OH , or both.

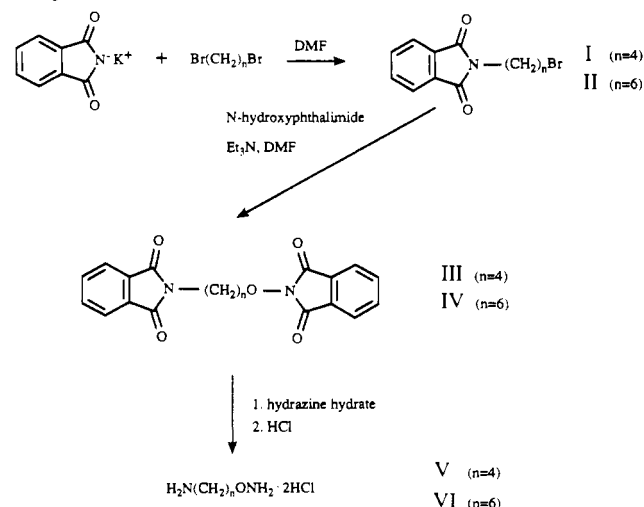
Synthesis of (Aminooxy)alkylamine Dihydrochlorides. (Aminooxy)alkylamine dihydrochlorides (V, VI) have been synthesized according to the method of Adarichev and co-workers (14) as shown in the Scheme I.

Synthesis of Aminooxy Alcohols. 4-(Aminooxy)butanol (IX) was synthesized using the method of Petrenko and co-workers (15) as presented in the Scheme II. 4-(Aminooxy)butanol (IX) was easily extracted from an alkaline water solution by a continuous extraction system and purified by distillation.

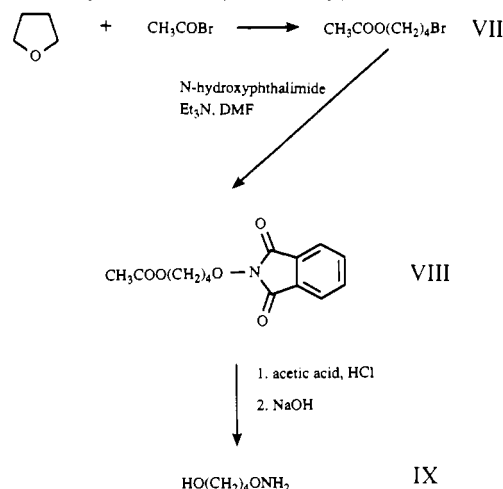
6-(Aminooxy)hexanol hydrochloride (XII) was synthesized as presented in the Scheme III. The protecting phthalimido and acetyl groups were then cleaved by hydrazine hydrate and concentrated hydrochloric acid treatment, although the same method as with 4-(aminooxy)butanol could be also used. 6-(Aminooxy)hexanol hydrochloride was purified by using short-column chromatography.

Introduction of the Spacer Arm and Reactive Group to Keto Steroids (Scheme IV). The aminooxy group reacts in refluxing alkaline (NaOH or CH_3OONa)

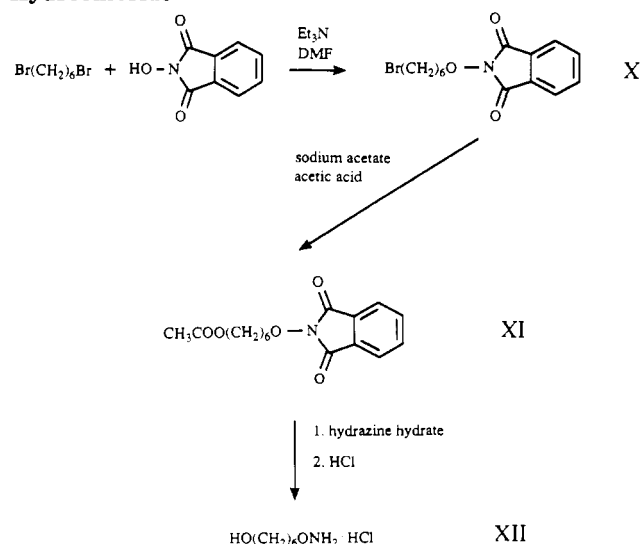
Scheme I. Synthesis of (Aminooxy)alkylamine Dihydrochlorides



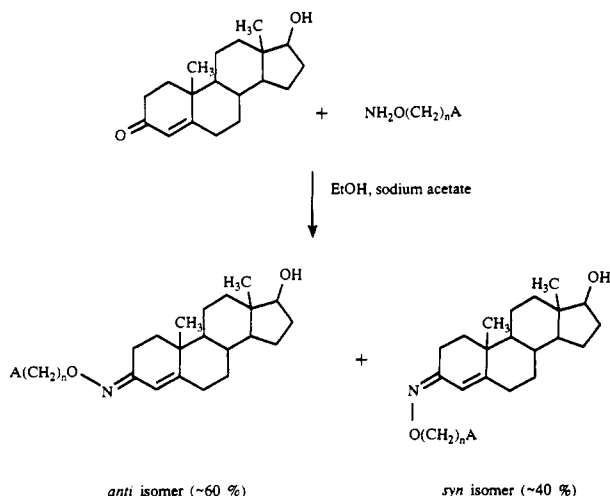
Scheme II. Synthesis of (Aminooxy)butanol



Scheme III. Synthesis of (Aminooxy)hexanol Hydrochloride



alcoholic solution readily with keto groups of steroids to produce alkyl oximes (20). The aminooxy group is far more reactive than the amino or hydroxy group because of the oxygen atom adjacent to the amino group (the α -effect), which greatly increases the nucleophilicity of the amino group (21, 22). For an example of the use of these

Scheme IV. Synthesis of Testosterone *O*-Alkyloximes

bifunctional aminoxy compounds, testosterone 3-, 6-ketoestradiol 6-, and cortisol 3-(*O*-alkyloximes) were synthesized. Testosterone and estradiol alkyloximes were synthesized from aminoxy compound and testosterone and 6-ketoestradiol, respectively, in refluxing alcoholic solution. When preparing cortisol 3-derivatives, the 3-keto group has to be activated, for example, by using pyridine (23) because of the other reactive keto group at 21-position. The same method can be used while derivatizing other 3-keto steroids and has to be used while derivatizing 3-keto steroids which have several keto groups, e.g. progesterone. The chemical structure linking the bridge to the steroid is the same as in the *O*-(carboxymethyl)oximes, but the bridge itself is three or five carbon atoms longer.

The mass spectra of the synthesized steroid derivatives clearly showed the cleavage of the introduced side chain. With electronic ionization of 15 eV, no molecular ion could be detected in the spectrum of the cortisol derivative because of the obvious fragmentation of the parent cortisol structure. While using chemical ionization the $[M + H]^+$ of the cortisol derivative was detectable.

In the UV spectra of the synthesized cortisol and testosterone derivatives a characteristic shift of the absorption maximum from about 240 nm for 3-keto steroids to 250 nm for the corresponding oxime derivatives has been detected. In estradiol derivatives a similar shift of the maxima from 256 and 327 nm for 6-ketoestradiol to 260 and 311 nm for the oxime derivative has also been observed.

Since the formed C=N double bond restricts free rotation, the oximes of steroids exist as syn- and anti-isomers. In estradiol oximes these isomers could not be detected from the ^1H NMR spectra, where the chemical shift of the aromatic proton at the C-4 carbon of 6-alkyloximes and underivatized estradiol were 7.43 and 6.56 ppm, respectively. In oxime derivatives of 4-en-3-one steroids, such as cortisol and testosterone, these isomers can be detected from the ^1H NMR spectra. The most striking difference between the ^1H NMR spectra of these two isomers is the chemical shift of the olefinic proton at the C-4 carbon. The chemical shifts were 5.66 and 5.74 ppm for the anti-isomer and 6.25 and 6.36 ppm for the syn-isomer of cortisol and testosterone 3-(alkyloximes), respectively, while these shifts for underivatized cortisol and testosterone were 5.65 and 5.73 ppm, respectively. The ratio (syn/anti) of these two isomers in these reaction conditions varied from 1/1.2 for cortisol to 1/1.5 for testosterone. The ratio is influenced by the reaction conditions and solvent used (24). The isomers can be

separated for example on sulfoethyl Sephadex LH-20 (22) or to some extent on silica TLC plates using 20% methanol in chloroform to develop the plates. The yield, which varied from 26 to 85%, is greatly influenced by the molar ratio of the reagents (steroid/aminoxy compound), which varied in this study from 1/1.6 to 1/7.8 during the synthesis of testosterone and cortisol, respectively.

The amino, hydroxy, or other similarly prepared derivatives of bridged steroids can be coupled to other molecules and used, for example, in steroid immunoassays (25).

LITERATURE CITED

- (1) Pratt, J. J. (1978) Steroid immunoassay in clinical chemistry. *Clin. Chem.* 24, 1869-1890.
- (2) Lavastre, I., Besancon, J., Brossier, P., and Moise, C. (1990) The synthesis of metallocene-labelled drugs for biological assays. *Appl. Organomet. Chem.* 4, 9-17.
- (3) Tiefenauer, L. X., and Andres, R. Y. (1990) Biotinyl-estradiol derivatives in enzyme immunoassays: Structural requirements for optimal antibody binding. *J. Steroid Biochem.* 35, 633-639.
- (4) Bermudez, J. A., Coronado, V., Mijares, A., Leon, C., Velazquez, A., Noble, P., and Mateos, J. L. (1975) Stereochemical approach to increase the specificity of steroid antibodies. *J. Steroid Biochem.* 6, 283-290.
- (5) Mikola, H., and Miettinen, P. (1991) Preparation of europium labeled derivatives of cortisol for time-resolved fluoroimmunoassays. *Steroids* 56, 17-21.
- (6) Evrain, Ch., Rajkowski, K. M., Cittanova, N., and Jayle, M. F. (1980) The preparation of three fluorescence-labelled derivatives of testosterone. *Steroids* 35, 611-619.
- (7) Cuilleron, C. Y., Mappus, E., Forest, M. G., and Bertrand, J. (1981) Synthesis and stereochemistry of 7 β - and 7 α -amino-, acetamido-, hemisuccinamido- and terephthalamido derivatives of testosterone. *Steroids* 38, 607-632.
- (8) McHale, D., Green, J., and Mamalis, P. (1960) Amino-oxy-derivatives. Part I. Some α -amino-oxy-acids and α -amino-oxy-hydrazides. *J. Chem. Soc.* 225-229.
- (9) Mamalis, P., Green, J., and McHale, D. (1960) Amino-oxy-derivatives. Part II. Some derivatives of N-hydroxydiguanide. *J. Chem. Soc.* 229-238.
- (10) Schulmann, E. L., Paquette, L. A., Heinzelman, R. V., Wallach, D. P., DeVanzo, J. P., and Greig, M. E. (1962) The synthesis and γ -aminobutyric acid transaminase inhibition of aminoxy acids and related compounds. *J. Med. Chem.* 5, 464-477.
- (11) Satshenko, L. P., Severin, E. S., and Khomutov, R. M. (1968) On the inhibition of decarboxylase of L-glutamic acid by derivatives of hydroxylamine and relative compounds. *Biokhimiya (Moscow)* 33, 142-147.
- (12) Pankaskie, M. C., and Scholtz, S. A. (1989) An improved synthetic route to aminoxypropylamine (APA) and related homologs. *Synth. Commun.* 19, 339-344.
- (13) McKay, A. F., Garmaise, D. L., Paris, G. Y., and Gelblum, S. (1960) Bacteriostats. III. Oxyamines and their derivatives. *Can. J. Chem.* 38, 343-358.
- (14) Adarichev, V. A., Dymshits, G. M., Kalachikov, S. M., Pozdnyakov, P. I., and Salganik, R. I. (1987) Introduction of aliphatic amino groups into DNA and their labelling with fluorochromes in preparation of molecular hybridisation probes. *Bioorg. Chem.* 13, 1066-1069.
- (15) Petrenko, V. A., and Pozdnyakov, P. I. (1983) Synthesis of triester analogs of di(deoxynucleoside)phosphates containing hydroxylamine residue. *Bioorg. Chem.* 9, 832-837.
- (16) Ilvespää, A. O., and Marxer, A. (1964) O-Substituted hydroxylamines and their derivatives. *Chimia* 18, 1-36.
- (17) Rougny, A., and Daudon, M. (1976) Use of N-hydroxylamines for the synthesis of primary alkoxyamines. *Bull. Soc. Chim. Fr.* 5-6, 833-838.
- (18) Lindström, L., Meurling, L., and Lövgren, T. (1982) The measurement of serum cortisol by a solid-phase chemiluminescence immunoassay. *J. Steroid Biochem.* 16, 577-580.

- (19) Khomutov, R. M. (1961) Hydroxylamine derivatives I. Synthesis of O-substituted hydroxylamines. *Zh. Obshch. Khim. SSSR* 31, 1992-1995.
- (20) Erlanger, B. F., Borek, F., Beiser, S. M., and Lieberman, S. (1957) Steroid-protein conjugates I. Preparation and characterization of conjugates of bovine serum albumin with testosterone and with cortisone. *J. Biol. Chem.* 228, 713-727.
- (21) Klopman, G., Tsuda, K., Louis, J. B., and Davis, R. E. (1970) Supernucleophiles I. The α effect. *Tetrahedron* 26, 4549-4554.
- (22) Grekov, A. P., and Vasselov, V. Y. (1978) α -effect in the chemistry of organic compounds. *Usp. Khim.* 47, 1200-1230.
- (23) Janoski, A. H., Shulman, F. C., and Wright, G. E. (1974) Selective 3-(O-carboxymethyl)oxime formation in steroidal 3,20-diones for hapten immunospecificity. *Steroids* 23, 49-64.
- (24) Axelson, M., Sjövall, J., Drakenberg, T., and Forsen, S. (1978) Separation and configuration of syn and anti isomers of testosterone oxime. *Anal. Lett. B11*, 229-237.
- (25) Mikola, H., Hänninen, E., and Höglund, A.-C. (1990) Preparation of europium labeled steroid derivatives for time-resolved fluoroimmunoassays (Abstract). *J. Steroid Biochem.* 36 Suppl. 115S.

Microparticle-Enhanced Nephelometric Immunoassay with Microsphere-Antigen Conjugates

Paul Montagne,* Pierre Varcin, Marie Louise Cuillière, and Jean Duheille

Immunology Laboratory, Faculty of Medicine, BP 184, F-54505 Vandoeuvre les Nancy, France.

Received September 17, 1991

γ -Irradiation of acrolein and other acrylic monomers allowed the synthesis of spherical polyfunctional hydrophilic microparticles in the size range of 50 to 300 nm, on which antigens (immunoglobulins G, chorionic gonadotropin hormone, prealbumin) could be covalently bound. Microsphere-antigen conjugates clustered together in the presence of specific antiserum or monoclonal antibodies and their agglutination was quantified by light-scattering measurement performed with a specially designed nephelometer. Essential factors concerning the conjugate agglutination and its quantitation (size of microsphere, amount of antigen bound on microsphere, concentration of conjugate, concentration of agglutinating reagent, angle of light-scattering observation) were successively studied. A microparticle-enhanced nephelometric immunoassay for prealbumin was finally developed as an example of application. It was based on the inhibition of the immunoagglutination of microspheres-prealbumin conjugate by free prealbumin. This prealbumin immunoassay was easy to perform (one-step assay without washing or phase separation), fast (30 min), reliable (variation coefficients ranged from 3.6% to 7.5% for within- and between-assay determination), and sensitive (1 $\mu\text{g/L}$ detected). It was correlated with conventional immunonephelometry and radial immunodiffusion (correlation coefficients, 0.98). Microparticle-enhanced nephelometric immunoassay offered many advantages over the last two methods. Its better sensitivity allowed a lower reagent consumption and a larger sample dilution (contrary to the conventional immunonephelometry, sample pretreatment and sample blank measurement were unnecessary). Its inhibition mode induced a total accuracy for sample with high analyte concentration (a risk of underevaluation in antigen excess conditions existed in all method based on a noncompetitive antigen-antibody reaction) and provided the possibility to quantify haptens. Fully automated and fast, it was better adapted to large series of measurement and produced results more rapidly than radial immunodiffusion.

INTRODUCTION

For several years, conventional immunonephelometry (CIN)¹ has been used to quantify various proteins in biological fluids: serum, plasma, urine, and cerebrospinal fluid (Sieber & Gross, 1976; Schliep & Felgenhauer, 1978; Schmitz-Huebner et al., 1980). CIN is based on the nephelometric measurement of antigen-antibody complexes. This method is easy to perform, but its detection limit (about 1 mg/L) remains poor, compared with other immunoassays such as radioimmunoassay or immunochemistry. Several authors have attempted to improve the sensibility of the CIN by using agglutination of latexes coated with antigens or antibodies (Grange et al., 1977; Von Schulthess et al., 1976, 1980; Ripoll et al., 1980). Cell counting (Cambiaso et al., 1977; Cambiaso & Limet, 1989), turbidimetry (Kimura, 1980), and laser Doppler spectrometry (Uzgiris, 1976) have also been used to quantify latex agglutination. These latexes, usually made of polystyrene, were hydrophobic and often unstable.

Stable hydrophilic immunolatexes have been synthesized as markers for scanning electron microscopy (Molloy et al., 1975; Rembaum et al., 1979; Bene et al., 1982) and later on as the solid phase in radioimmunoassay (Pines & Margel, 1986). They were also used for the nephelometric detection of Clq-binding immune complexes (Montagne et al., 1980) and as immunization carrier (Jambon et al., 1981), but they were unsuitable for general use as

a reagent in nephelometric immunoassay (extra steps of activation for protein binding, inadequate size, overly-long reaction time).

This study describes the synthesis of stable hydrophilic microspheres (Ms) that are physicochemically well-defined and optimally devised for immunological reaction support. It reports the preparation of Ms-antigen conjugates and assesses conditions of their use as reagent in an improved microparticle-enhanced nephelometric immunoassay. The performance of this assay is demonstrated by an example of application to the prealbumin (PA) quantitation in human serum.

EXPERIMENTAL PROCEDURES

Chemical Reagents. Acrolein, 2-hydroxyethyl methacrylate, and methacrylic acid were obtained from Merck (Darmstadt, Germany); *N,N'*-methylenebisacrylamide was from Eastman Kodak Co. (Rochester, NY); Sodium dodecyl sulfate, hydroquinone, 2-aminoethanol, sucrose, sodium chloride, sodium dihydrogenophosphate, disodium hydrogenophosphate, and sodium azide, of analytical-reagent grade, were purchased from Prolabo-Rhône Poulenc (Paris, France). Most immunonephelometric assays were carried out with the buffer for nephelometry supplied by Diagnostics Pasteur (Marnes, France).

Biochemical Reagents. Human immunoglobulins G (IgG) were isolated from a pool of normal human sera by DEAE-Trisacryl (IBF, Paris, France) chromatography using an elution gradient of increasing ionic strength (Cuillière et al., 1991). The purity of the IgG preparation (about 98%) was checked by immunoelectrophoresis and polyacrylamide gel electrophoresis. Human chorionic gonadotropin (hCG) from urine was a Sigma (St. Louis, MO)

* Author to whom correspondence should be addressed.

¹ Abbreviations used: CIN, conventional immunonephelometry; Ms, microsphere; PA, prealbumin; IgG, immunoglobulins G; hCG, chorionic gonadotropin hormone; PB, phosphate buffer; HSA, human serum albumin; RID, radial immunodiffusion.

product (3326 IU/mg according to the second international standard). Eight anti-hCG monoclonal antibodies (mAb) were kindly supplied by Sanofi (Paris, France): six of them were hCG- β specific with affinity about 10^8 M $^{-1}$, the other two reacted against the whole hCG molecule ($\alpha + \beta$) with higher affinity (10^9 and 10^{10} M $^{-1}$). Purified PA (95% electrophoretically pure), anti-PA goat antiserum, PA standard (0.35 ± 0.03 g/L), and anti-IgG (γ) goat antiserum were Diagnostics Pasteur products. Behring (Marburg, Germany) protein standards were used as control sera in the PA immunoassay; their PA concentrations, determined by radial immunodiffusion and compared with international WHO standard preparations, were 0.12 ± 0.02 g/L and 0.40 ± 0.05 g/L. Human sera were randomly chosen from the patients of the University Hospital of Nancy (France).

Preparation and Characterization of Ms. Acrolein, 2-hydroxyethyl methacrylate, and methacrylic acid were freshly distilled under Ar and mixed with *N,N'*-methylenebisacrylamide in respective percentages: 47%, 49.7%, 2%, and 1.3% (v/v) of total monomers. Various concentrations of total monomers (50, 80, 100, and 120 g/L) were used. Sodium dodecyl sulfate was added as a surfactant at concentrations of 0.6, 0.8, 0.9, and 1 g/L. Deaerated and Ar-saturated monomer mixtures were γ -irradiated using a ^{60}Co source (ORIS, Nucleart, CENG, Grenoble, France) for 3 h under vacuum at a flux of 23 krad $\cdot\text{cm}^{-2}\cdot\text{h}^{-1}$. After irradiation, the polymerized Ms were stored in amine-free suspension, at 4 °C under Ar, with hydroquinone (1 g/L) (Duheille et al., 1982).

Ms suspension concentration was calculated by dry weight determination at 110 °C. Ms size measurement was carried out by transmission electron microscopy (JEOL 200 CX; Tokyo, Japan) after drying on a formvar filmed grid (200 mesh) and with a granulometer (Autosizer II; Malvern Instruments, Worcs, England) in aqueous suspension. Shape and dispersion were evaluated by scanning electron microscopy (Cambridge S250) after gold shadowing.

Binding of Antigens to Ms. Antigen (IgG, PA, and hCG) solution and Ms suspension were mixed in 0.1 M phosphate buffer (PB) (pH 7.2) and 0.3 M NaCl for IgG, 0.01 M PB (pH 7.2) and 0.14 M NaCl for PA, or 0.005 M PB (pH 7.2) for hCG. The final concentrations in the binding mixtures were 10 g/L for Ms and 1.3 g/L for IgG, 1.6 g/L for PA, and 0.2, 0.4, 0.8, 1.6, and 3.2 g/L for hCG. After gentle stirring for 18 h at 4 °C, unreacted aldehyde groups of the Ms were blocked by 2-aminoethanol, 0.12 M in pH 8 buffered solution, for 4 h at room temperature. The uncoupled proteins were then eliminated by centrifugation on a discontinuous sucrose gradient (200/800 g/L) buffered at pH 7.2 (Ultracentrifuge Spinco L, Rotor Beckmann SW50, 3000–12000g according to the Ms size, 1 h, 4 °C). The Ms-antigen conjugates were finally collected at the interface of sucrose solutions and stored at 4 °C in 0.1 M PB (pH 7.2) containing 2 g/L of sodium azide.

The yields of antigen binding were calculated by measuring the uncoupled protein by CIN for IgG and PA and by determining the amount of labeled hCG in Ms-hCG conjugates, using a ^{125}I -hCG probe prepared by the chloramine-T method (Greenwood & Hunter, 1963). Amounts of immunoreactive hCG on the Ms-hCG conjugates were evaluated with anti-hCG mAb by a radioimmunoassay using ^{125}I -hCG as competitor and free hCG as calibrator.

Nephelometric and Immunonephelometric Assays. The influence of several factors (Ms size, amount of antigen

bound on Ms, stability of Ms-antigen conjugate, concentration of Ms-antigen conjugate in reaction mixture, concentration of agglutinating reagent, angle of observation of the light scattering) were defined by nephelometric assays of native Ms and immunonephelometric assays of Ms-antigen conjugates. These studies were performed by measurement of the light scattered by dispersed native Ms, Ms-antigen conjugates, and clusters of Ms-antigen conjugate, performed with the Diagnostics Pasteur nephelometer (Nephelia N600), perfected during this work. Its light source was an He-Ne laser (power, 2 mW; wavelength, 632.8 nm). The reagents were dispensed in disposable microcuvettes (light path, 1 cm) and scattered light was collimated at an angle of 10° on a light-sensitive silicon diode. To measure the light scattered at various angles, an experimental prototype (laboratory made) photogoniometer was used. Its physical characteristics are the same as those of the Diagnostics Pasteur nephelometer, but the light scattering can be measured between 7.4° and 40.2° every 0.8° with a scan period of 4 s.

Microparticle-Enhanced Nephelometric Immunoassay of PA. The microparticle-enhanced nephelometric immunoassay of serum PA was a one-step immunoassay: 0.03 mL of 200-fold diluted unknown human serum was mixed with anti-PA antiserum, Ms-PA conjugate (125 nm in diameter), and buffer for nephelometry in a total volume of 0.3 mL, to obtain a sample dilution in the reaction mixture of $1/2000$ with 2100-fold diluted antiserum and 100 mg/L of Ms-PA conjugate. All predilutions and dispensations were performed with an automated dilutor (Hamilton, Bonaduz, Switzerland). Light scattering was measured with the Diagnostics Pasteur nephelometer after 30-min incubation at room temperature. For the standard curves, six serial dilutions of the PA standard were used in the place of unknown serum. The precision of the assay was assessed by measuring high, middle, and low PA concentration in 20 assays repeated within 1 day (within-assay precision) and assays repeated on each of 10 days (between-assay precision) with fresh reagents taken each time from the same batches.

Other Methods. For interference and comparison studies, rheumatoid factor was determined with a latex slide-agglutination test (Latex-RF reagent, Behring), PA concentrations were measured in human sera by CIN (Behring laser nephelometer and Behring reagents) and radial immunodiffusion (RID) (Behring M-Partigen) following the manufacturer's recommendations.

RESULTS

Ms-Antigen Conjugates. Above-described copolymerizations produced spherical, monodispersed, polyfunctional, and hydrophilic microparticles. Effects of polymerization time, irradiation flux, agitation, and relative concentration of monomers and surfactant on yield, size, and chemical characteristics of Ms were previously reported (Duheille et al., 1982). Sizes of the Ms synthesized in this study are given in Table I. Mean dry diameters were between 50 and 295 nm with an acceptable dispersion (2% to 17%) for each sample.

IgG, PA, and hCG were covalently bound to the native Ms in physiological conditions by a one-step reaction with formation of imine bonds between aldehyde functions on the Ms (acrolein residues) and primary amino groups of the ligand. Previous reaction of the Ms with concentrated HSA solution (higher than 12 g/L) inhibited the ligand binding. Ms-antigen conjugates were stable several months at 4 °C with sodium azide as preservative and could be frozen and lyophilized. On account of this good

Table I. Influence of Relative Concentrations of Total Monomers (TM) and Sodium Dodecyl Sulfate (SDS) on the Size of Microspheres (Ms)

concentration of reagents, g/L		dry diameter of Ms		
TM	SDS	mean, nm	SD, ^a nm	n ^b
50	1.0	50	5	39
50	0.8	100	17	30
80	0.8	125	16	43
100	0.6	200	6	27
120	0.9	295	4	7

^a SD, standard deviation. ^b n, number of data.**Table II.** Influence of the Ms Size on the Light Scattered at an Angle of 10° by Dispersed Ms and Ms Clusters

Ms diameter, nm	Ms concentration, mg/L		amplification of light scattered during Ms agglutination ^c
	range with linearity between concentration and light scattered ^a	significantly detected ^b	
50	300–4800	20	32
100	40–1700	3	21
125	10–300	2	17
200	6–230	0.2	12
295	2.5–150	0.01	4

^a $P < 0.001$. ^b Expressed as the Ms concentration giving an intensity of light scattering 3 SD higher than the intensity of light scattered by the empty nephelometer microcuvettes. ^c Expressed as the ratio of the maximum light scattered by Ms clusters (pH 4) to the light scattered by the same dispersed Ms (pH 7).

stability, imine bonds of the Ms–antigen conjugates were not reduced by treatment with a metallic hydride.

Binding yield varied with binding conditions, particularly with relative concentrations of antigen and Ms in the binding mixture. Binding yield of hCG ranged from 19% to 94% when hCG concentration decreased from 3.2 to 0.2 g/L. The best immunoreactivity of bound hCG molecules (76%) was obtained when 1.6 g (4×10^{-5} mol) of hCG was present in the binding mixture (1 L) with 10 g of Ms (200 nm in diameter). Under these conditions, each Ms was coated by about 1000 hCG molecules, but only a fraction of these bound hCG molecules was thus recognized by anti-hCG mAb. The ratio of immunoreactive versus total hCG molecules bound to Ms changed (18% to 76%) according to the mAb used, and there was probably a close connection between the large disparity of the immunoreactivity and a poor accessibility of some epitopes on the hCG molecules bound on the Ms surface.

Nephelometric Assays of Native and Aggregated Ms. According to the physical laws (Rayleigh, 1899; Mie, 1908; Debye, 1944), the intensity of light scattered by a suspension of Ms depended on the Ms size and the concentration of the suspension. Light scattering increased with increasing Ms concentration, but reached a maximum and decreased by absorption for the highest concentrations (above 300 mg/L) of the largest Ms (295 nm in diameter). As can be seen in Table II, the intensity of light scattered by dispersed Ms and the concentration of the suspension were in linear relation ($P < 0.001$) for large ranges of concentration, variable with the Ms size. When the Ms diameter increased from 50 to 295 nm, the Ms concentration significantly detected by the nephelometer, as giving an intensity of light scattering 3 SD higher than the intensity of light scattered by the empty nephelometer microcuvettes, decreased from 20 to 0.01 mg/L (Table II).

In solutions of neutral pH and physiological ionic strength, Ms were stabilized by their hydrophilic and charged surface (hydroxyl and carboxyl groups of 2-hy-

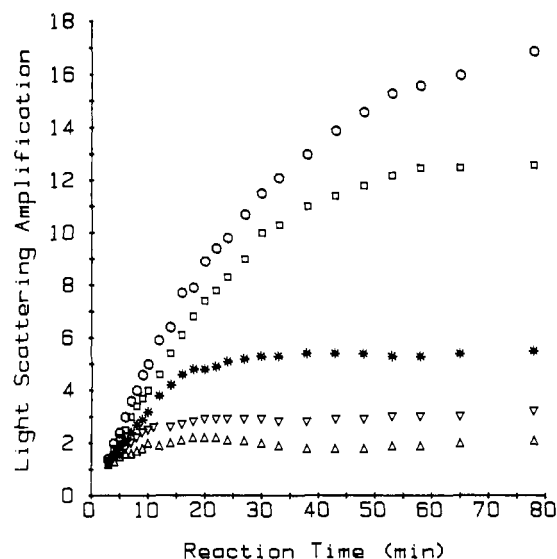


Figure 1. Agglutination kinetics of Ms–IgG conjugate (100 nm in diameter, 200 mg/L) with anti-IgG antiserum (120-fold diluted) for various angles of measure of the light-scattering intensity: 9.8° (○), 12.2° (□), 20.2° (*), 31.4° (▽), and 40.2° (Δ). Light-scattering amplification is the ratio of the light scattered by Ms–IgG conjugate clusters to the light scattered by dispersed Ms–IgG conjugates (0.01 M PB, pH 7.2, 0.14 M NaCl; experimental photogoniometer).

droxyethyl methacrylate and methacrylic acid residues). They were not spontaneously autoagglutinated and their sedimentation was slow: intensity of light scattered by the largest Ms (295 nm) slightly decreased (1% to 6% according to their concentration) when Ms remained at rest for 24 h. But the intensity of light scattered increased (Table II) when Ms were aggregated by increasing ionic strength or decreasing pH. Amplification of the light scattering during the Ms agglutination was a maximum for the smallest Ms (32-fold for 50 nm diameter Ms) and decreased when their size increased (4-fold for the 295 nm diameter Ms only).

Immunonephelometric Assays of Ms–Antigen Conjugates. Figure 1 shows the importance of the angle of light-scattering observation. At the beginning of the immunological agglutination of Ms–IgG conjugate (100-nm diameter) by anti-IgG antiserum, the intensity of light scattered by small clusters of Ms–IgG conjugate was slight and not very different, whatever the angle of measurement between 9.8° and 40.2° (Rayleigh's diffusion). Then, with the formation of big aggregates of Ms–IgG conjugate (Mie's diffusion), light-scattering amplification increased and was higher (up to 17-fold the light scattered by the suspended conjugate alone) at small angles (9.8° and 12.2°) than at the largest angles (between 2- and 5-fold the light scattered by unagglutinated conjugate only). In addition to the detection of a limited amplification of the light, the measure at a large angle was more disturbed by the light scattered by small scattering centers (Rayleigh's diffusion) present in the reaction mixture (components of antiserum, sample, buffer).

Level of light-scattering amplification during agglutination of Ms–antigen conjugate and kinetics of this agglutination were functions of the Ms–antigen conjugate concentration and antiserum dilution. The curves of Figure 2 were obtained by variation of anti-IgG antibody concentration while Ms–IgG conjugate concentration was kept constant. Increasing dilution of antiserum reduced the light scattering amplification and lengthening of the reaction time was required to obtain the same light-scattering levels. However, Figure 2 shows that under

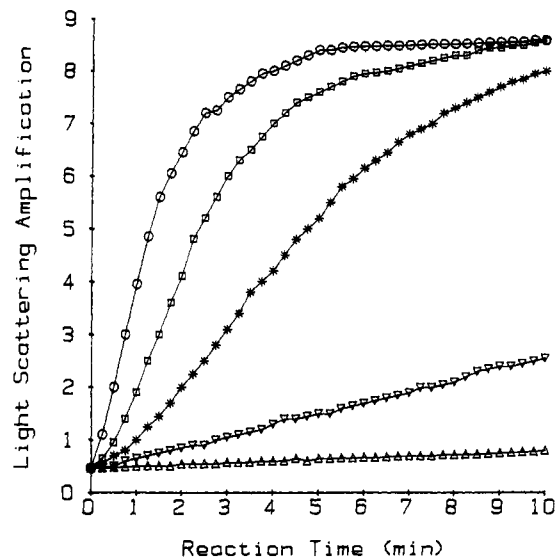


Figure 2. Agglutination kinetics of Ms-IgG conjugate (100 nm in diameter, 350 mg/L) for five dilutions of anti-IgG antiserum: $1/800$ (Δ), $1/400$ (∇), $1/240$ (*), $1/120$ (\square), and $1/60$ (\circ). Light scattering amplification is the ratio of the light scattered by Ms-IgG conjugate clusters to the light scattered by dispersed Ms-IgG conjugates (0.01 M PB, pH 7.2, 0.14 M NaCl; experimental photogoniometer at 9.8°).

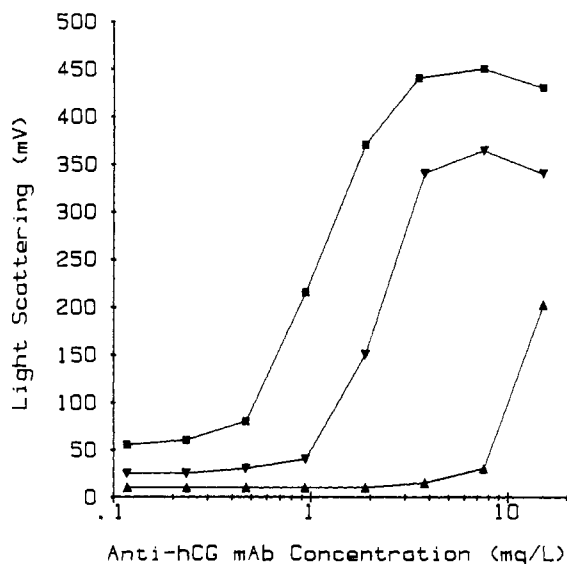


Figure 3. Light scattered by Ms-hCG conjugate (40 mg/L) agglutinated by anti-hCG mAb for three diameters of Ms: 50 (Δ), 100 (∇), and 200 nm (\blacksquare); reaction time, 2 h; buffer for nephelometry and nephelometer from Diagnostics Pasteur.

appropriate conditions the nephelometric quantification of immunoagglutination can be fast (10 min).

Figure 3 presents agglutination of three Ms-hCG conjugates (50, 100, and 200 nm in diameter) as a function of anti-hCG mAb concentration. For the two largest Ms diameters (200 and 100 nm), the scattered light reached a maximum (450 and 350 mV) in the same range of anti-hCG mAb concentration. Then, the light scattered decreased with the mAb concentration but always remained higher for 200 nm diameter Ms than for 100 nm diameter Ms. For the 50 nm diameter Ms-hCG conjugate, the agglutination curve was observed only at high mAb concentration and the intensity was much less.

The number of hCG molecules present on each Ms was very important for the immunoagglutination of Ms-hCG conjugate. An optimal hCG concentration in the binding mixture of Ms could be experimentally defined: for the

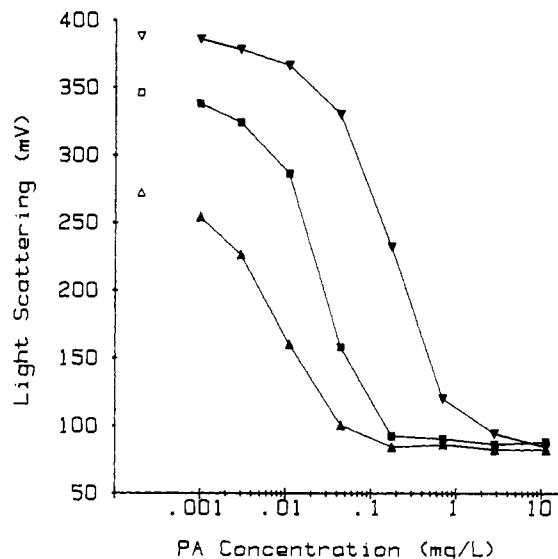


Figure 4. Inhibition of the agglutination of Ms-PA conjugate (295 nm in diameter, 50 mg/L) by free PA, in the presence of three different dilutions of anti-PA antiserum: $1/8000$ (∇), $1/32000$ (\blacksquare), and $1/128000$ (Δ). Controls without PA (∇ , \square , Δ); reaction time, 30 min; buffer for nephelometry and nephelometer from Diagnostics Pasteur.

200 nm diameter Ms, this hCG concentration was 1.6 g/L (4.10^{-5} mol/L) for 10 g/L of Ms. This corresponded to the concentration previously observed as necessary to coat each Ms by about 1000 hCG molecules with the best immunoreactivity (76%).

Ms-PA Conjugate as Reagent for Microparticle-Enhanced Nephelometric Immunoassay of PA in Human Serum. Inhibition of agglutination, like agglutination, can be studied with the nephelometer: Figure 4 shows the quantification of inhibition by free PA of Ms-PA conjugate (295 nm in diameter) agglutination observed for three dilutions of the anti-PA antiserum. The total inhibition observed assessed the specificity of the agglutination. Sensitivity of the assay increased with the dilution of antiserum: 50% of inhibition was obtained for about 200 $\mu\text{g/L}$ of free PA when the anti-PA antiserum was 8000-fold diluted, 35 $\mu\text{g/L}$ for $1/32000$, and about 7 $\mu\text{g/L}$ for $1/128000$. For this last antiserum dilution, the smallest concentration of PA detectable was 1 $\mu\text{g/L}$, when it was defined as that giving an intensity of light scattered 3 SD lower ($n = 30$, mean = 254.8 mV, SD = 5.8 mV) than the mean of the intensity of light scattered without PA ($n = 30$, mean 272.2 mV, SD = 5.7 mV).

Ms-PA conjugates could be used for a sensitive PA measurement in human serum by microparticle-enhanced nephelometric immunoassay. In the described assay conditions (serum 2000-fold diluted in the reaction mixture), the intensity of light scattered by serum samples ($n = 60$, mean = 3.4 mV, SD = 0.7 mV) was not different from that of the empty nephelometer microcuvettes ($n = 60$, mean = 3.1 mV, SD = 0.3 mV) and slight compared with the intensity of light scattered by the Ms-PA conjugate alone ($n = 60$, mean = 39.3 mV, SD = 1.1 mV). This last intensity was not different from that of the Ms-PA conjugate in the presence of serum samples ($n = 60$, mean = 38.9 mV, SD = 1.9 mV). These results showed that a clarifying pretreatment and a blank measurement were unnecessary for serum samples and they confirmed results previously observed for bovine whole milk samples which were used without skimming (Marchal et al., 1991). Furthermore, they gave proof of the stability of the Ms-PA conjugate under the conditions of the assay.

Table III. Precision of Prealbumin Assay

	within-assay precision			between-assay precision			
<i>n</i> ^a	30	30	30	10	10	10	10
\bar{C} ^b	0.0553	0.1137	0.2231	0.0596	0.1163	0.2318	0.4754
SD ^c	0.0037	0.0050	0.0157	0.0045	0.0042	0.0089	0.0219
CV ^d	6.6	4.4	7.0	7.5	3.6	3.8	4.6

^a *n*, number of determinations. ^b \bar{C} , mean of measured concentrations, g/L. ^c SD, standard deviation, g/L. ^d CV, coefficient of variation, %.

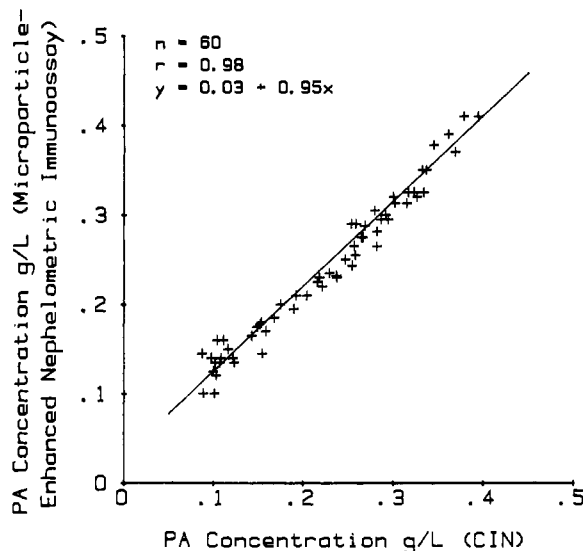


Figure 5. Comparison by linear-regression analysis between results of serum PA assay obtained by microparticle-enhanced nephelometric immunoassay and by conventional immunonephelometry; number of data, *n*; correlation coefficient, *r*.

The calibration range for PA assay using 2000-fold diluted serum extended from 0.038 to 1.200 g/L, and largely encompassed reference seric concentrations of PA (0.10 g/L to 0.40 g/L; mean = 0.25 g/L) as well as the lower pathological values seen with protein malnutrition (Ingenbleek et al., 1972), liver diseases (Hutchinson et al., 1981), burn injury (Moody, 1982), and cancers (Mollinshead et al., 1977).

A reproducibility study, performed at high, middle, and low PA concentrations, gave coefficients of variation for within-assay ranging from 4.4% to 7.0%, and from 3.6% to 7.5% for between-assay (Table III). The target concentrations of control sera (0.12 ± 0.02 and 0.40 ± 0.05 g/L) were well-attained (*n* = 19, mean = 0.12 g/L, SD = 0.01 g/L and *n* = 19, mean = 0.36 g/L, SD = 0.01 g/L). The concentration of PA was simultaneously determined by microparticle-enhanced nephelometric immunoassay, CIN, and RID in 60 human sera and results were submitted to linear-regression analysis. Figures 5 and 6 show the correlations (correlation coefficients, 0.98) obtained with CIN and RID, respectively. Rheumatoid factors were detected in 18 of the 60 sera, but no interference, such as a under- or overevaluation of results, was observed in the three compared methods.

DISCUSSION

Inadaptation of microparticles previously used in agglutination-based immunoassays was largely due to their hydrophobicity. Previous synthesis of polyacrylic Ms in our laboratory (Montagne et al., 1980) and their use in nephelometric assay had shown there was still the necessity of further increasing their hydrophilic character, optimizing their charge, and introducing chemical functions facilitating the covalent binding of biological molecules.

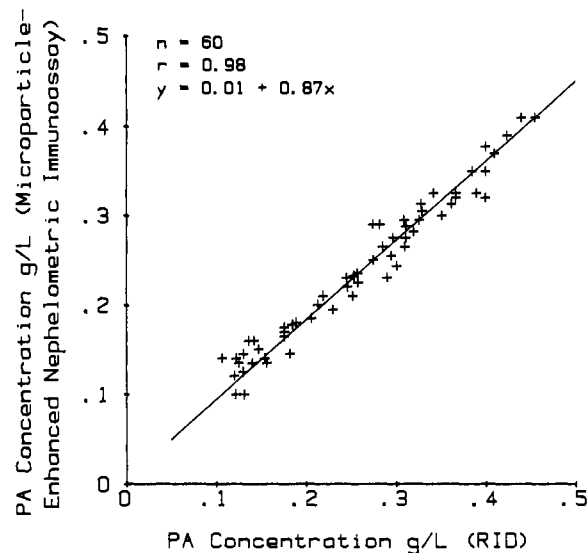


Figure 6. Comparison by linear regression analysis between results of serum PA assay obtained by microparticle-enhanced nephelometric immunoassay and by radial immunodiffusion; number of data, *n*; correlation coefficient, *r*.

The Ms synthesis described herein allowed compliance with these necessities. Ms obtained were hydrophilic (hydroxyl and carboxyl functions), stable (charges brought by carboxyl groups), and covalently coated (aldehyde groups) with ligands containing primary amino groups such as proteic antigens. Ms-antigen conjugates were not spontaneously autoagglutinated, their sedimentation was very slow, and they remained immunoreactive for several months. These three qualities are judged essential for their use as a nephelometric reagent. Latexes usually made of plain or modified polystyrene were used for immunoassay: compared with our Ms, these particles were more hydrophobic and often unstable, with autoagglutination, nonspecific protein adsorption, and protein releasing being pitfalls. Their investigators have pointed out the necessity of hydrophilic coating of these hydrophobic particles (Litchfield et al., 1984), of sonication prior to use, to ensure dispersion of the latex aggregates (Passelecq et al., 1988), or of sample pretreatment to warrant latex stability (Wilkins et al., 1988).

Nephelometric and immunonephelometric studies of Ms-antigen conjugates permitted determination of their optimum usage conditions as reagents in microparticle-enhanced nephelometric immunoassay. Ms size, amount of antigen bound on Ms, concentration of Ms-antigen conjugate in the reaction mixture, concentration of agglutinating reagent, and angle of observation of the light scattering were thus systematically studied. Influence of these factors on the stability of Ms-antigen conjugates, on their ability to be specifically agglutinated, and on their capacity as nephelometric marker of this agglutination was determined. The results observed for Ms size and concentration adhered to Rayleigh's (diluted small size Ms) and Mie's (big Ms and clusters) theories. Concentration of Ms-antigen conjugate usable in assay was chosen from a range where intensity of light scattered was proportional to the Ms concentration and, at the same time, where the highest amplification of light scattered during agglutination was obtained (e.g., between 100 and 300 mg/L for 125 nm diameter Ms). Size of Ms in Ms-protein conjugates, amount of antigen bound on each Ms, and optimum agglutinating concentration of antibody were in close connection on account of the variation of Ms-antigen conjugate total surface with Ms diameter. A low

angle (10° to the incident beam) was chosen for the measure of light scattering in the nephelometer specially designed for microparticle-enhanced nephelometric immunoassay. It allowed a good discrimination between the background (light scattered by small scattering centers present in the reaction mixture) and the conjugate agglutination specific for the immunological reaction (high amplification of the light).

Microparticle-enhanced nephelometric immunoassay was particularly easy to perform (one-step assay without washing or phase separation) and fully automatable. For PA assay, chosen herein as an example of application, the incubation time has been fixed at 30 min, but it could be decreased (10 min) and measurement time itself was short (10–15 s per sample), allowing numerous measurements (240 samples/h at least). The great dilution of antiserum or mAb used as agglutinating reagent decreased their consumption. The sensitivity of the PA assay was good (1 µg/L significantly detected) and an adequate concentration range was easily covered with a satisfactory reproducibility (CV from 3.6% to 7.5%). This sensitivity allowed the great dilution of human serum samples ($1/2000$ in the reaction mixture) and gave the possibility of use of a very small volume of serum in malnourished children (Ingenbleek et al., 1972) and premature infants (Moskowitz et al., 1983). This large dilution also eliminated interference by sample turbidity, sample blank measurement, and clarifying pretreatment. Finally, results observed by microparticle-enhanced nephelometric immunoassay for serum PA correlated well with those obtained by CIN and RID.

The sensitivity, accuracy, and practicality of these three methods can be compared. Only 1.5 and 22 mg/L of PA was detected, with CV ranging from 3.5% to 9.0% and from 7.0% to 12.9% by CIN and RID, respectively, and only CIN was reliable for low PA concentrations (Romette et al., 1984). Others authors (Virella & Fudenberg, 1977; Patricot & Cadot, 1982; Guiguet et al., 1983) had given similar results for comparison between CIN and RID performed with other proteins besides PA. A time of diffusion between 24 and 48 h was necessary to obtain reliable results by RID (linearity and slope of the standard curve). This wait was too protracted to assay protein with short biological half-life (about 45 h for PA); thus, RID did not allow a fast enough determination of the variations of PA concentration in protein-energy depletion and parenteral nutrition (Shetty, 1979; Zazzo et al., 1984), and it was less adapted to a large series of measurements. Human serum was used only 20-fold diluted in the PA assay performed by CIN. Such a dilution required sample pretreatment (Voigt, 1977) with a clarifying reagent, then centrifugation. Furthermore, according to the manufacturers' recommendations, a blank measurement was often still necessary after pretreatment. These constraints increased cost, duration, and complexity of the assay. Microparticle-enhanced nephelometric immunoassay preserved the advantages of CIN (specially as a one-step assay) but overcame drawbacks (poor sensitivity, risk of under-evaluation in antigen excess conditions) and provided the opportunity to assay haptens (Duheille et al., 1984; Gartner et al., 1991).

Microparticle-enhanced nephelometric immunoassay using specifically conceived Ms appeared as a choice method for routine quantitation of a large variety of biological molecules. Applications to serum components (Cuillère et al., 1991; Montagne et al., 1991a, 1992) and to milk proteins (Montagne et al., 1991b; El Bari et al., 1991; Collard-Bovy et al., 1991; Marchal et al., 1991; Hum-

bert et al., 1991) had been already developed. This report described the study of factors essential for the use of Ms-antigen conjugates in nephelometry and their optimization so that other molecules occurring at lower concentration and currently measured by more sophisticated methods could be determined.

ACKNOWLEDGMENT

This work was supported by grants from the Ministère Français de la Recherche et de la Technologie (Contracts 81 MO835 and 84 M1121). Paul Montagne is research engineer, Institut National de la Santé et de la Recherche Médicale. Marie Louise Cuillère is study engineer, Centre National de la Recherche Scientifique.

LITERATURE CITED

- Bene, M. C., Faure, G., Montagne, P., Jambon, B., Rembaum, A., and Duheille, J. (1982) SEM visualization of human lymphocytes membranes receptors for "Facteur Thymique sérique" (FTS). SEM congress, Anaheim.
- Cambiaso, C. L., and Limet, J. N. (1989) Latex agglutination assay for human anti-Brucella IgM antibodies. *J. Immunol. Methods* 122, 169–175.
- Cambiaso, C. L., Leek, A. E., De Steenwinkel, F., Billen, J., and Masson, P. L. (1977) Particle counting immunoassay (PA-CIA). I. A general method for the determination of antibodies, antigens and haptens. *J. Immunol. Methods* 18, 33–44.
- Collard-Bovy, C., Marchal, E., Humbert, G., Linden, G., Montagne, P., El Bari, N., Duheille, J., and Varcin, P. (1991) Microparticle-enhanced nephelometric immunoassay: I. Measurement of alpha- and kappa casein. *J. Dairy Sci.* 74, 3695–3701.
- Cuillère, M. L., Montagne, P., Bessou, Th., El Omari, R., Riochet, D., Varcin, P., Laroche, P., Prud'homme, Ph., Marchand, J., Flecheux, O., Pau, B., and Duheille, J. (1991) Microparticle-Enhanced Nephelometric Immunoassay (Nephelia[®]) for Immunoglobulins G, A, and M. *Clin. Chem.* 37, 20–25.
- Debye, P. (1944) Light scattering in solutions. *J. Appl. Phys.* 15, 338–374.
- Duheille, J., Pau B., and Gros, P. (1982) European Patent 0104101B1.
- Duheille, J., Montagne, P., Riochet, D., Bessou, Th., Varcin, P., Cuillère, M. L., Marchand, J., and Pau, B. (1984) XII International Congress of Clinical Chemistry, Rio De Janeiro, Abstract 1410.
- El Bari, N., Montagne, P., Humbert, G., Cuillère, M. L., Varcin, P., Linden, G., and Duheille, J. (1991) Development of a microparticle-enhanced nephelometric immunoassay for the quantification of beta-casein in milk. *Food Agric. Immunol.* 3, 63–71.
- Gartner, A., Carles, C., Montagne, P., Cuillère, M. L., and Duheille, J. (1991) A microparticle-enhanced nephelometric immunoassay (Nephelia[®]) applied to thymulin measurement. *J. Immunoassay* 12, 521–542.
- Grange, J., Roch, A. M., and Quash, G. A. (1977) Nephelometric assay of antigens and antibodies with latex particles. *J. Immunol. Methods* 18, 365–375.
- Greenwood, F. C., and Hunter, W. M. (1963). The preparation of ¹³¹I-labelled growth hormone of high specific activity. *Biochem. J.* 89, 114–121.
- Guiguet, M., Padieu, P., and Mack, G. (1983) Laser nephelometric measurement of seven serum proteins compared with radial immunodiffusion. *J. Clin. Chem. Clin. Biochem.* 21, 217–221.
- Humbert, G., Collard-Bovy, C., Marchal, E., Linden, G., Montagne, P., Duheille, J., and Varcin, P. (1991) Microparticle-enhanced nephelometric immunoassay: III. Applications to milk and dairy products. *J. Dairy Sci.* 74, 3709–3715.
- Hutchinson, D. R., Halliwell, R. P., Smith, M. G., and Parke, D. V. (1981) Serum prealbumin as an index of liver function in human hepatobiliary diseases. *Clin. Chim. Acta* 114, 69–73.

- Ingenbleeck, Y., De Visscher, M., and De Nayer, Ph. (1972) Measurement of prealbumin as index of protein-calorie malnutrition. *Lancet II*, 106-109.
- Jambon, B., Montagne, P., Bene, M. C., Brayer, M. P., Faure, G., and Duheille, J. (1981) Immunohistologic localisation of "Facteur Thymique Sérique" (FTS) in human thymic epithelium. *J. Immunol.* 127, 2055-2059.
- Kimura, H. (1980) Immunoassay with stable polystyrene latex particles. *J. Immunol. Methods* 38, 353-360.
- Litchfield, W. J., Craig, A. R., Frey, W. A., Leflar, C. C., Looney, C. E., and Luddy, M. A. (1984) Novel shell/core particles for automated turbidimetric immunoassays. *Clin. Chem.* 30, 1489-1493.
- Marchal, E., Collard-Bovy, C., Humbert, G., Linden, G., Montagne, P., Duheille, J., and Varcin, P. (1991) Microparticle-enhanced nephelometric immunoassay: II. Measurement of alpha-lactalbumin and beta-lactoglobulin. *J. Dairy Sci.* 74, 3702-3708.
- Mie, G. (1908) *Ann. Phys.* 25, 377-455.
- Molday, R. S., Dreyer, W. J., Rembaum, A., and Yen, S. P. S. (1975) New immunolabelled spheres: visual markers of antigens on lymphocytes for scanning electron microscopy. *J. Cell. Biol.* 64, 75-88.
- Mollinshead, A. C., Chuang, C. Y., Cooper, E. H., and Catalona, W. J. (1977) Interrelationship of prealbumin and alpha-1 acid glycoprotein in cancer patient sera. *Cancer* 40, 2993-2999.
- Montagne, P., Cuillière, M. L., and Duheille, J. (1980) Highly sensitive immunonephelometric assay detecting Clq-binding immune complexes. 4th International Congress of Immunology, Paris, France, Abstract 15-7-15.
- Montagne, P., Laroche, P., Cuillière, M. L., Riochet, D., Flecheux, O., Varcin, P., Marchand, J., Pau, B., and Duheille, J. (1991a) Polyacrylic microspheres as a solid phase for microparticle-enhanced nephelometric immunoassay (Nephelia[®]) of transferrin. *J. Immunoassay*, 12, 165-183.
- Montagne, P., Gavriloff, C., Humbert, G., Cuillière, M. L., Duheille, J., and Linden, G. (1991b) Microparticle-enhanced nephelometric immunoassay for immunoglobulins G in cow's milk. *Lait* 71, 493-499.
- Montagne, P., Laroche, P., Cuillière, M. L., Varcin, P., Pau, B., and Duheille, J. (1992) Microparticle-enhanced nephelometric immunoassay for human C-reactive protein. *J. Clin. Lab. Anal.* In press.
- Moody, B. J. (1982) Changes in the serum concentrations of thyroxine-binding prealbumin and retinol-binding protein following burn injury. *Clin. Chim. Acta* 118, 87-92.
- Moskowitz, S. R., Pereira, G., Spitzer, A., Heaf, L., Amsel, J., and Watkins, J. B. (1983) Prealbumin as a biochemical marker of nutritional adequacy in premature infants. *J. Pediatr.* 102, 749-753.
- Passelecq, B., De Bo, M., Huber, C., Gennart, J. P., Bernard, A., and Lauwerys, R. (1988) Latex immunoassays of serum alpha-fetoprotein using polyethylene glycol pretreatment. *J. Immunol. Methods* 109, 69-74.
- Patricot, M. C., and Cadot, R. (1982) *Pathol. Biol.* 30, 188-192.
- Pines, M., and Margel, S. (1986) Polyacrolein microspheres as a new solid phase for radioimmunoassay. *J. Immunoassay* 7, 97-111.
- Rayleigh, L. (1899) On the transmission of light through an atmosphere containing small particles in suspension and on the origin of the blue of the sky. *Philos. Mag.* 47, 375-384.
- Rembaum, A., Yen, S. P. S., and Molday, R. S. (1979) Synthesis and reactions of hydrophilic functional microspheres for immunological studies. *J. Macromol. Sci. Chem.* 13, 603-632.
- Ripoll, J. P., Roch, A. M., Quash, G. A., and Grange, J. (1980) An automatic continuous flow method for the determination of antipolyamine antibodies in human sera. *J. Immunol. Methods* 33, 159-173.
- Romette, J., Mallet, B., and Di Constanzo, J. (1984) *Ann. Biol. Clin.* 42, 227-229.
- Saint Blancard, J., and Kinzin, J. M. (1981) Preparation of albumin and IgGs on CM-Trisacryl[®] M. Fourth international symposium affinity chromatography, Valldhoven.
- Schliep, G., and Felgenhauer, K. (1978) Rapid determination of proteins in serum and cerebrospinal fluid by laser nephelometry. *J. Clin. Chem. Clin. Biochem.* 16, 631-635.
- Schmitz-Huebner, U., Nachbar, J., and Asbeck, F. (1980) The determination of antithrombin III, alpha 2-macroglobulin and alpha 2-antiplasmin in plasma by laser nephelometry. *J. Clin. Chem. Clin. Biochem.* 18, 221-225.
- Shetty, P. S. (1979) Rapid turnover transport protein: an index of subclinical protein-energy malnutrition. *Lancet I*, 230-234.
- Sieber, A., and Gross, J. (1976) Determination of proteins by laser nephelometry. *Laborblätter* 26, 117-123.
- Uzgiris, E. E. (1976) A laser Doppler assay for the Antigen-Antibody Reaction. *J. Immunol. Methods* 10, 85-96.
- Virella, G., and Fudenberg, H. (1977) Comparison of immunoglobulin determination in pathological sera by radial immunodiffusion and laser nephelometry. *Clin. Chem.* 23, 1925-1928.
- Voigt, H. W. (1977) *Laborblätter* 27, 168-172.
- Von Schulthess, G. V., Cohen, R. J., Sakato, N., and Benedek, G. B. (1976) Laser light scattering spectroscopic immunoassay for mouse IgA. *Immunochemistry* 13, 955-962.
- Von Schulthess, G. V., Giglio, M., Cannell, D. S., and Benedek, G. B. (1980) Detection of agglutination reactions using anisotropic light scattering: An immunoassay of high sensitivity. *Mol. Immunol.* 17, 81-92.
- Wilkins, T. A., Brouwers, G., Mareschal, J. C., and Cambiaso, C. L. (1988) High sensitivity, homogeneous particle-based immunoassay for thyrotropin (Multipact[™]) *Clin. Chem.* 34, 1749-1752.
- Zazzo, J. F., Millat, B., Vauzelle, D., and Abella, A. (1984) Effects of nutrition on the post-operative serum levels of Prealbumine (PA), Transferrin (T) and fibronectin (Fn). Retrospective study in 30 peritonitis. *Marker proteins in inflammation 2* (P. Arnaud, J. Bienvenu, and P. Laurent, Eds.) pp 493-495, Walter de Gruyter, Berlin.

Registry No. SDS, 151-21-3; 2-propenoic acid, 2-methyl-, polymer with 2-hydroxyethyl 2-methyl-2-propenoate, *N,N'*-methylenebis[2-propenamide] and 2-propenal, 90119-91-8.

Activation of Mouse Macrophages by Muramyl Dipeptide Coupled with an Anti-Macrophage Monoclonal Antibody

Patrick Midoux,[†] Anne Martin, Brigitte Collet, Michel Monsigny,[†] Annie-Claude Roche,[†] and Louis Toujas*

Service d'Immunologie-Immunothérapie, Centre Régional de Lutte contre le Cancer, Pontchaillou, 35033 Rennes Cedex, France, and Département de Biochimie des Glycoconjugués et Lectines Endogènes, Centre de Biophysique Moléculaire, CNRS, INSERM et Université, 1, rue Haute, 45071 Orléans Cedex 2, France. Received December 9, 1991

A rat IgG_{2a} monoclonal antibody (mAb3A33) directed against the mouse Mac-1 antigen was conjugated with muramyl dipeptide (MDP) by using an intermediate polymer; under such conditions 75 MDP molecules were bound to one antibody molecule. A poly(L-lysine) polymer substituted with muramyl dipeptide and 3-(2-pyridyldithio)propionyl residues was prepared, the remaining lysine ϵ -amino groups were acylated with D-gluconolactone, leading to a neutral polymer; then a few polymer conjugates were coupled to mAb3A33 via a disulfide bridge. The binding capacity of the monoclonal antibody was preserved after conjugation with MDP-polymer molecules. Mouse peritoneal macrophages, incubated for 24 h with MDP-mAb3A33 conjugate became cytostatic against P815 mastocytoma cells, whereas unconjugated mAb3A33 and MDP-bound to a nonspecific rat IgG_{2a} were ineffective. An enhancement of the cytostatic activity induced by MDP-mAb3A33 conjugate was obtained in the presence of γ -IFN. These results show that several tens of MDP molecules can be linked to a macrophage-specific monoclonal antibody by using a neutral intermediate polymer without impairing the binding antibody capacity and that this type of MDP conjugate can efficiently activate macrophages and therefore could be the basis of the development of new antitumor therapy.

INTRODUCTION

Mouse macrophages have been shown to acquire cytotoxic properties against tumor cells after incubation with either γ -IFN, bacterial lipopolysaccharides, or muramyl dipeptide (MDP) (1). MDP, the smallest active component isolated from mycobacterial cell wall (2) or obtained by synthesis (3), exhibits adjuvant properties comparable to those of mycobacteria and activates *in vitro* various macrophage functions such as the release of collagenase and prostaglandins (4), interleukin-1 (5), and oxygen metabolites (6). MDP, which is able to stimulate *in vitro* macrophage cytostasis against tumor cells, is inefficient *in vivo* because of its rapid blood clearance (7) and the lack of a specific cell surface receptor (8). Increased MDP efficiency was obtained by binding MDP to macromolecular carriers designed to be recognized and internalized by macrophages. The killing of tumor cells (tumoricidal activity) by alveolar macrophages was enhanced *in vitro* and *in vivo* by using liposome-encapsulated MDP (9, 10). MDP bound to mannosylated bovine serum albumin or mannosylated polymers which are recognized and internalized by macrophages via mannose-specific membrane lectins was shown to activate *in vitro* macrophages more efficiently than free MDP (11, 12) and to reduce *in vivo* lung metastases in a lung carcinoma mouse model (13). MDP bound to monoclonal antibodies which recognized tumor cells rendered the macrophages cytostatic (14). MDP-anti-MDP antibody complexes which are recognized

by the macrophage Fc receptors were more efficient than free MDP in activating macrophages *in vitro* (15).

Recently, we obtained a monoclonal antibody (mAb3A33) which binds selectively to the cell surface of mouse macrophages (16). This antibody is a rat IgG_{2a} which was shown to react with Mac-1 antigen, to immunoprecipitate its 95 and 170 kDa components, to compete for cellular binding with the anti-Mac-1 M1/70 antibody (17), and to block rosette formation. Radiolabeled mAb3A33 injected intravenously in mice was found to be localized on cells of the peritoneal cavity more efficiently than nonspecific antibody. This monoclonal antibody was also shown to be efficient in the visualization of inflammatory lesions and tumors by γ scintigraphy (18). Therefore, this monoclonal antibody seems a good candidate as a carrier for modifiers of the biological response.

In the present work, MDP was conjugated to mAb3A33 antibody in an original manner such that a high number of MDP residues were bound to the carrier molecule while preserving its antibody specificity and affinity. A synthetic, biodegradable, water-soluble, and neutral polymer carrying 15 MDP residues was prepared and several polymer molecules were coupled to mAb3A33 via disulfide bridges. The immunostimulant properties of the MDP-mAb3A33 conjugate were tested *in vitro* on mouse peritoneal macrophages.

EXPERIMENTAL PROCEDURES

The mAb3A33 antibody was generated by cell fusion between the mouse plasmacytoma SP2/0 and B lymphocytes from rats immunized against mouse macrophages as previously described (16). The hybridoma was grown intraperitoneally in nude mice and the antibody was purified from ascitic fluid by ion-exchange chromatography (19). A rat IgG_{2a} polyclonal antibody provided by H. Bazin (20), which did not recognize mouse peritoneal macrophages, was used as control. Murine recombinant γ -IFN was

* Author to whom reprint requests and correspondence should be addressed.

[†] CNRS, INSERM et Université.

¹ Abbreviations used: DMF, dimethylformamide; DMSO, dimethylsulfoxide; DTT, dithiothreitol; FCS, fetal calf serum; GlcA, gluconoyl; γ -IFN, γ interferon; LPS, lipopolysaccharides; MDP, *N*-acetylmuramyl dipeptide; PBS, phosphate-buffered saline; PDP, 3-(2-pyridyldithio)propionyl; PEC, peritoneal exudate cells; PLK, poly(L-lysine); SPDP, *N*-succinimidyl 3-(2-pyridyldithio)propionate; TEA, triethylamine.

kindly provided by J. Wietzerbin (Institut Curie, Paris, France). MDP was synthesized as described by Merse et al. (3).

Preparation of a Polymer Substituted with 3-(2-Pyridyldithio)propionyl (PDP) and *N*-Acetylmuramyl Dipeptide (MDP). Half the lysine residues of poly(L-lysine) hydrobromide (30 000–50 000) containing about 190 lysine residues (Bachem, Feinchemikalien, Bendorff, Switzerland) was gluconoylated as described by Derrien et al. (11). The polymer (300 mg; 10 μ mol) was reacted with SPDP (Pierce, Rockford, IL) (60 mg; 200 μ mol) (21) for 10 h in a 3-mL mixture of DMF/DMSO (1:1; v/v) in the presence of TEA (1 mmol). The substituted polymer was precipitated by adding 10 volumes of a mixture of dichloromethane/ethyl acetate/*n*-butanol (1:1:1; v/v/v). After centrifugation, the polymer was washed with the same solvent, dissolved in distilled water, and freeze-dried. The number of PDP groups bound per polymer molecule, determined from the absorbance at 343 nm upon treatment with dithiothreitol (DTT) (Serva, Heidelberg, FRG) (21), was found to be 7. The PDP-bound polymer (100 mg; 1.67 μ mol), dissolved in 10 mL of DMF/DMSO (1:1, v/v) in the presence of TEA (60 μ mol), was reacted for 10 h at 20 °C with MDP *N*-hydroxysuccinimide ester (30 mg; 52 μ mol) prepared as previously described (12). The remaining lysine ϵ -amino groups were acylated by reaction with *D*-gluconolactone in order to remove any cationic charge on the polymer (11). The polymer (60 000 average molecular mass) was purified by precipitation, washed, dissolved in distilled water, and freeze-dried as described above. The number of MDP residues bound per polymer molecule, determined by the *p*-(dimethylamino)benzaldehyde assay (22) was found to be 15.

Introduction of 2-Pyridyl Disulfide Groups onto Antibodies. mAb3A33 antibody (5.5 mg) in 6 mL of 0.1 M NaCl, 0.1 M phosphate buffer (pH 8.5) (pH adjusted with 0.2 M sodium carbonate) was reacted for 5 h at 4 °C with SPDP (0.57 mg; 1.82 μ mol) dissolved in 100 μ L of ethanol. Rat IgG_{2a} antibody (25 mg) in 3 mL of 0.1 M NaCl, 0.1 M borate buffer (pH 8.5) was reacted for 5 h at 4 °C with SPDP (2 mg; 6.4 μ mol) dissolved in 100 μ L of ethanol. The PDP-antibody conjugates were precipitated by adding ammonium sulfate up to 40% saturation at 4 °C and purified by gel filtration (20 \times 1 cm column) on trisacryl GF 05 (Sepracor, Villeneuve-la-Garenne, France) in 0.1 M NaCl and 0.1 M phosphate buffer (pH 7.0). The numbers of PDP groups bound to mAb3A33 and rat IgG_{2a}, determined as described above from the absorbances at 343 nm in the presence of DTT, were 24 and 14, respectively.

Thiolation of the Polymer. Gluconoylated poly(L-lysine) bearing 15 MDP and 7 PDP residues was dissolved in 0.1 M sodium acetate buffer (pH 4.5) (outgassed by bubbling oxygen-free nitrogen). DTT was added to a final concentration of 25 mM and the mixture reacted for 30 min at 20 °C. Then, DTT, its oxidized derivative, and pyridine-2-thione were extracted five times with 5 volumes of an ethyl acetate/degassed water (40:1; v/v) mixture in which the polymer is not soluble. After the last extraction, no trace of these compounds is detectable.

Coupling of mAb3A33 and Rat IgG_{2a} Antibodies with MDP-Bound Polymer. The polymer bearing 15 MDP and 7 thiol residues (16 mg in 0.5 mL of sodium acetate buffer) was added to the mAb3A33 antibody coupled to 24 PDP residues (4 mg in 3.3 mL of 0.1 M NaCl, 0.1 M phosphate buffer, pH 7.0). The same polymer (33 mg in 0.5 mL of sodium acetate buffer) was added to

rat IgG_{2a} antibody coupled to 14 PDP residues (7 mg in 2 mL of 0.1 M NaCl, 0.1 M phosphate buffer, pH 7.0). The pH of the solutions was adjusted to 7.0 with 0.2 M sodium carbonate and the mixture was stirred for 20 h at 4 °C. Then, iodoacetamide (1% final concentration) (Pierce) was added and the solution kept for 30 min at 4 °C. After addition of ammonium sulfate up to 40% saturation, the conjugates were precipitated overnight at 4 °C, spun down (3500g; 15 min), and dissolved in PBS. Antibody-polymer conjugates were purified by gel filtration on Sephacryl S200 (Pharmacia, Uppsala, Sweden) eluted with PBS. The number of MDP and polymer molecules per immunoglobulin molecule was determined by the *p*-(dimethylamino)benzaldehyde assay. The antibody concentration was determined using $E^{1\%}_{280\text{nm}} = 14$, the absorbance of MDP substituted polymer at 280 nm being insignificant.

Macrophage Activation and Cytostatic Assays. Peritoneal exudate cells (PEC) were collected from (C57BL/6 \times DBA/2) F1 hybrid female mice 2 days after ip injection of 1 mL of fetal calf serum (FCS) (Anval, 35830 Betton, France). The exudate cells contained 40% neutral red positive phagocytic cells and reacted strongly with the mAb3A33 antibody. PEC were suspended at 5×10^6 per mL in RPMI 1640 culture medium (Aqual, AES Laboratoires, 35370 Combourg, France) supplemented with Hepes buffer (Eurobio, Paris, France), 4 mM L-glutamine (Biomérieux, 69269 Charbonnière-les-bains, France), 5×10^{-5} mercaptoethanol, 160 μ g/mL gentamycin, 10% FCS, and 10 ng/mL *Escherichia coli* O55B5 LPS (Difco, Paris, France). In preliminary experiments, it was found that the addition of a low concentration of LPS (10 ng/mL) to the culture medium was necessary to prime macrophages and to improve their cytostaticity, in agreement with the data published by Barratt et al. (23). MDP-mAb3A33 conjugate or control preparations were mixed with PEC in suspensions that were subsequently distributed in 96-well microplates. After overnight incubation at 37 °C, the wells were washed three times and nonadherent cells were discarded. Then, 100 μ L of P815 cells (10^5 cells/mL) and 100 μ L of tritiated [³H]thymidine (1.85 MBq/mL) (Amersham, UK) were added per well and the microplates were further incubated for 24 h at 37 °C. All cultures were done in at least five replicates. The activation step was always 24 h, after which 20 μ L of 1 M NaOH was added to each well. The cells were harvested on a glass-fiber filter (Beckman, Irvine, CA) with a multiple automated sample harvester, and the radioactivity was counted in a Beckman LS7500 liquid scintillation counter. Cytostatic activity was expressed by the equation $100 \times (C - A)/C$, where *C* and *A* are the number of cpm recorded in control and activated PEC cultures, respectively.

Flow Cytometry Analysis. Peritoneal exudate macrophages (2×10^5 in 1 mL of complete medium) (RPMI 1640 medium containing 2 mM L-glutamine and antibiotics) were plated into 24-well tissue culture plates. After 4 h of incubation at 37 °C, nonadherent cells were removed by washing with complete medium and the plates were further incubated for 20 h at 37 °C in the same medium. Cells were washed and incubated for 45 min at 4 °C in complete PBS (PBS supplemented with 1 mM CaCl₂, 0.5 mM MgCl₂, and 0.5% BSA) in the presence of either mAb3A33 or MDP-mAb3A33 conjugate. The cells were then washed with cold complete PBS and further incubated for 45 min at 4 °C with fluoresceinylated goat anti-rat IgG F(ab)₂ fragment (Cappel, West Chester, U.K.) diluted 50-fold. Cells were washed in cold complete PBS and resuspended in PBS. The cell fluorescence intensity was measured using a FACS analyzer (Becton Dickinson,

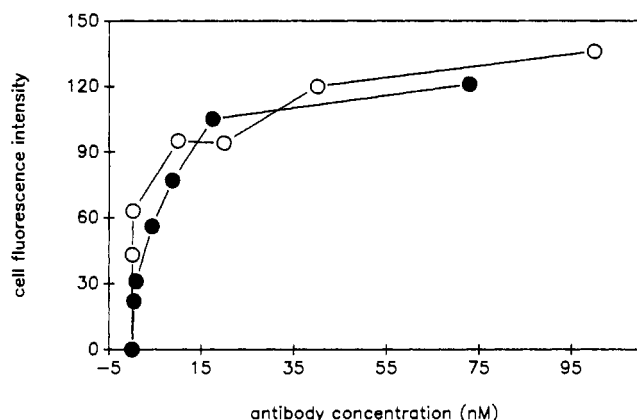


Figure 1. Flow cytometry analysis of the binding of MDP-bound to mAb3A33. Mouse peritoneal macrophages were incubated first with either mAb3A33 (○) or mAb3A33 conjugated with MDP-polymer molecules (●) and then with fluoresceinylated goat anti-rat IgG F(ab')₂ fragments.

Sunnyvale, CA, USA) equipped with the FACSLite unit (Becton Dickinson). A 488-nm excitation wavelength was produced by a 25-mW cold air argon laser. A 540-nm short-pass filter as splitter and a 520 ± 10-nm interference filter were installed to collect the emitted green fluorescence. The three parameters (90° light scatter, volume, and green fluorescence) were simultaneously recorded in list mode on 5000 cells at 300 events per second and the data were analyzed in biparameter cytograms using the Consort 30 device (Hewlett-Packard). The fluorescence intensity value of identical cells was expressed as the mean value of the fluorescence intensity of cells contained in the gated cell population. The fluorescence intensity was corrected with calibrated fluoresceinylated beads (24) so that experiments done at different times were comparable.

RESULTS

Preparation of MDP-Antibody Conjugates. In order to bind a large number of *N*-acetylmuramyl dipeptide (MDP) molecules onto mAb3A33 without losing the antibody binding activity, a neutral, water-soluble, and biodegradable polymer bearing MDP molecules was prepared and coupled to the monoclonal antibody via a disulfide bridge. Fifteen MDP molecules were bound onto a polymer made of poly(L-lysine) containing about 190 lysine residues substituted with seven 3-(2-pyridyldithio)propionyl (PDP) groups and with gluconoyl residues. The residual lysine ε-amino groups of the polymer were acylated by reaction with *D*-gluconolactone in order to remove any cationic charges and to prevent nonspecific binding on the cell surfaces. The MDP substituted polymer, with an average molecular mass of 60 000, was treated with dithiothreitol in order to generate thiol groups and then coupled to antibodies bearing PDP groups. The thiol groups of the polymer which have not reacted with antibodies were irreversibly blocked by alkylation with iodoacetamide. With this procedure, an average of five polymer molecules each bearing 15 MDP residues were linked to one mAb3A33 molecule (MDP to antibody molar ratio was 75:1; 246 μg of MDP/mg of mAb3A33). By the same procedure, an average of two molecules of the polymer were bound to a rat IgG_{2a} polyclonal antibody molecule (MDP to antibody molar ratio was 30:1; 89 μg of MDP/mg of IgG_{2a}). The capacity of mAb3A33 substituted with MDP to bind to macrophages was compared to that of native mAb3A33 (Figure 1). Macrophages were incubated first with either MDP-mAb3A33 conjugate or native mAb3A33, then with fluoresceinylated goat anti-rat IgG

Table I. Cytostatic Activity of Mouse Peritoneal Macrophages on P815 Tumor Cells after Incubation with Free MDP, MDP-mAb3A33, or MDP-IgG_{2a} Conjugates

MDP, μg/mL	cpm uptake × 10 ⁻³ (% cytostasis) ^a		
	MDP-mAb3A33	MDP-IgG _{2a}	MDP
0	80.3 ± 6.9	63.7 ± 4.8	58.2 ± 5.1
(control)			
0.3	81.0 ± 6.9	72.6 ± 5.9	ND
	(neg)	(neg)	
1	62.3 ± 13.3	63.4 ± 3.0	ND
	(22)*	(0)	
3	49.9 ± 2.25	60.4 ± 3.9	62.0 ± 1.5
	(38)*	(5)	(neg)
10	38.6 ± 2.1	58.1 ± 2.2	57.9 ± 4.0
	(52)*	(9)*	(0)
30	23.8 ± 0.9	63.3 ± 1.4	54.7 ± 1.0
	(70)*	(0)	(6)

^a Radioactivity uptake is expressed as cpm ± SD and the percentage of cytostasis is shown in parentheses. The radioactivity uptake by macrophages in the absence of P815 cells was 15 800 ± 600 cpm. The radioactivity uptake by P815 cells in the absence of macrophages was 162 000 ± 11 800 cpm. ND: not done. neg: negative value for percentage cytostasis (radioactivity uptake in treated cells higher than in controls). *: significantly different from control (macrophages incubated in the absence of MDP conjugates) as shown by Student's *t* test for *p* < 0.05.

(Fab')₂ fragments, and the cell fluorescence intensity was measured by flow cytometry. Peritoneal macrophages were homogeneously labeled by mAb3A33 substituted with MDP-polymer conjugates as well as by mAb3A33, and the binding of mAb3A33 coupled with MDP-polymer conjugates was not significantly reduced compared to that of mAb3A33 (Figure 1). These results indicate that the binding capacity of the monoclonal antibody was preserved after conjugation with several MDP-polymer molecules.

Cytostatic Activity of Mouse Peritoneal Macrophages Induced by MDP-mAb3A33 Conjugate. Mouse peritoneal exudate cells (PEC) were cultured in the presence of various concentrations of free MDP, MDP conjugated to mAb3A33 (246 μg/mg of mAb3A33), or MDP conjugated to rat IgG_{2a} (89 μg/IgG_{2a} mg). After a 24-h incubation at 37 °C, PEC were cocultivated with P815 cells for 24 h in the presence of tritiated thymidine. All experiments were performed by using macrophages primed with a low concentration of LPS (10 ng/mL). Under these conditions, macrophages were slightly cytostatic in the absence of either free or conjugated MDP, but were highly responsive to the presence of free or conjugated MDP. MDP-mAb3A33 conjugate was found to induce a dose-related cytostatic activity with a maximum effect (70%) obtained with 30 μg/mL of MDP conjugated to mAb3A33 (121 μg of antibody/mL) (Table I). At the same MDP concentration, free MDP and MDP conjugated to non-specific rat IgG_{2a} did not induce significant macrophage activation (Table I). Ten micrograms/milliliter of MDP bound to mAb3A33 antibody (40 μg/mL) was able to induce 50% cytostatic activity. At higher concentrations (100 and 300 μg/mL) of MDP conjugated to mAb3A33 antibody or to the unspecific IgG_{2a}, cells no longer adhered and the cytostatic activity was no longer assessable. mAb3A33 substituted by PDP groups alone was also used as control (Table II). PDP-mAb3A33 conjugate (50 μg/mL) did not induce any significant cytostatic effect whereas the same concentration of MDP-mAb3A33 conjugate (12.5 μg of MDP/mL) induced 59% cytostaticity.

Cytostatic Activity of MDP in the Presence of Murine γ-IFN. γ-IFN, a lymphokine secreted by T lymphocytes upon antigen or mitogen stimulation, is known to render macrophages primed or elicited and suitable to be easily triggered by bacterial LPS (25). The cytostatic

Table II. Cytostatic Activity of Mouse Peritoneal Macrophages on P815 Tumor Cells after Incubation with MDP-mAb3A33 or PDP-mAb3A33 Conjugates

mAb3A33, $\mu\text{g/mL}$	cpm uptake $\times 10^{-3}$ (% cytostasis) ^a	
	MDP-mAb3A33	PDP-mAb3A33
0 (control)	72.2 \pm 5.4	
0.5	74.0 \pm 4.6	94.7 \pm 3.3 (neg)*
1.5	68.4 \pm 2.2 (5)	86.1 \pm 4.5 (neg)*
5	62.2 \pm 2.2 (14)*	72.6 \pm 2.5
15	47.7 \pm 1.7 (34)*	72.7 \pm 4.5
50	29.6 \pm 4.7 (59)*	81.2 \pm 2.1 (neg)*

^a Radioactivity uptake is expressed as cpm \pm SD and the percentage of cytostasis is shown in parentheses. The radioactivity uptake by macrophages in the absence of P815 cells was 12 000 \pm 900 cpm. The radioactivity uptake by P815 cells in the absence of macrophages was 206 900 \pm 5500 cpm. neg: negative value for percentage cytotoxicity (radioactivity uptake in treated cells higher than in controls). *: significantly different from control as shown by Student's *t* test for *p* < 0.05.

Table III. Cytostatic Activity of Macrophages Incubated with Both MDP-mAb3A33 Conjugate and γ -IFN

γ -IFN, units/ mL	cpm uptake $\times 10^{-3}$ (% cytostasis) ^a			
	O ^b	0.25 ^b	0.75 ^b	2.5 ^b
0	172.2 \pm 3.6 (0)	148.3* \pm 7.0 (14)	142.1* \pm 6.5 (17)	138.0* \pm 17.1 (20)
3	155.4* \pm 9.7 (10)	165.0 \pm 16.0 (4)	152.7* \pm 9.0 (11)	150.0* \pm 11.7 (13)
10	109.6* \pm 5.8 (36)	108.5** \pm 6.5 (37)	74.7*** \pm 3.9 (57)	51.2*** \pm 3.3 (70)

^a Radioactivity uptake is expressed as cpm \pm SD and the percentage of cytostasis is shown in parentheses. The radioactivity uptake by P815 cells in the absence of macrophages was 283 000 \pm 10 100 cpm.

^b Conjugated MDP in $\mu\text{g/mL}$. *: significantly different from control (macrophages incubated without MDP bound to mAb3A33 and without γ -IFN) as shown by Student's *t* test for *p* < 0.05. **: significantly different from control (macrophages incubated with MDP bound to mAb3A33 alone) as shown by Student's *t* test for *p* < 0.05. ***: significantly different from control (macrophages incubated with 10 units/mL γ -IFN alone) as shown by Student's *t* test for *p* < 0.05.

activity of macrophages incubated in the presence of MDP-mAb3A33 conjugate was significantly enhanced in the presence of 10 units/mL γ -IFN (Table III). When used independently, 10 units/mL γ -IFN gave 36% cytostasis while 2.5 $\mu\text{g/mL}$ MDP-mAb3A33 conjugate gave 20% cytostasis. The cytostatic activity reached 70% when both immunomodulators were present. There were no additive effect of these immunomodulators when γ -IFN was used at 3 units/mL and MDP-mAb3A33 conjugate at 0.25, 0.75, or 2.5 $\mu\text{g/mL}$. These data show that γ -IFN and MDP used together, under optimal concentrations, can have additive effect on the cytostatic activity of mouse peritoneal macrophages.

DISCUSSION

MDP conjugated to an anti-macrophage (Mac-1 antigen) IgG_{2a} monoclonal antibody (mAb3A33) was found to stimulate the cytostatic activity of mouse peritoneal macrophages against tumor cells under conditions where free MDP, unsubstituted mAb3A33, and MDP bound to an unspecific immunoglobulin had no activity. The cytostatic effect was dose dependent, and macrophage activation induced by MDP-mAb3A33 conjugate was specifi-

cally dependent on the recognition of Mac-1 macrophage antigen by mAb3A33 antibody. Despite certain variations in cytostatic assays due to a variability in macrophage response, it appears that free MDP failed to activate macrophages. Even if mAb3A33 substituted with PDP groups and MDP bound to a nonspecific rat IgG_{2a} antibody incidentally induced significant macrophage cytostasis, they were much less effective than MDP-mAb3A33 conjugate. Macrophage activation was already obtained by using MDP bound to monoclonal antibodies directed against tumor cells (14): 45 MDP residues were covalently bound per IgM molecule (i.e. 6 MDP/100,000 molecular weight fraction), which led to conjugates with a significant reduced antigen affinity. In order to increase the number of MDP molecules which can be linked to a monoclonal antibody and to avoid decrease of the antibody affinity, MDP was first bound to an intermediate, synthetic, biodegradable, water-soluble, and neutral polymer, and then, a few polymer molecules were linked to mAb3A33 antibody via a disulfide bridge. This type of synthetic, biodegradable, water-soluble, and neutral polymer, substituted both with mannose or mannose 6-phosphate residues, which are ligands of membrane lectins, and with a biological response modifier (MDP) (11) or an antiviral drug (26), was able to render macrophages cytostatic or to inhibit the multiplication of herpes simplex virus in human macrophages, respectively. An average of five polymer molecules bearing 15 MDP residues each were linked to mAb3A33 antibody, leading to an antibody substituted with 75 MDP; an average of two polymer molecules and 30 MDP residues were linked to the polyclonal unspecific IgG_{2a}. The coupling reactions were performed using a polymer substituted with MDP and the antibody in a molar ratio of 10:1, which reduced the probability of getting conjugates containing more than one antibody molecule per polymer molecule. By flow cytometry, we showed that mAb3A33 antibody substituted with several MDP-polymer molecules were able to bind target cells as well as native mAb3A33 antibody and that the substitution of the monoclonal antibody with MDP-polymer molecules did not significantly impair the binding capacity of the antibody. Indirect conjugation of drugs to monoclonal antibodies via intermediate carriers have been reported to increase the amount of drug attached to antibody without impairing its antigen-binding activity: human serum albumin (27-33), dextran (34-39), poly(L-glutamate acid) (40), a copolymer of N-(2-hydroxypropyl)methacrylamide containing an oligopeptide sequence (41), and succinylated polylysine (42) were used as intermediate carriers. In this paper, we used gluconoylated poly(L-lysine), a nonimmunogenic (43) and neutral polymer; the gluconoylation prevents a nonspecific binding to cells and increases the water solubility of poly(L-lysine) (11).

Mac-1 antigen is also expressed on monocytes, granulocytes, and NK cells (44). Since both granulocyte oxidative burst (45) and NK cytotoxic activity (46) are induced by MDP, MDP-mAb3A33 conjugate might be effective to stimulate these cells. Using radiolabeled mAb3A33, it has been shown that this monoclonal antibody localized in tumors (18), suggesting that it might be used as a vector for MDP to activate macrophages surrounding tumor cells. An anti-macrophage monoclonal antibody might have some advantages over other MDP vectors in view of an in vivo use (47): targeting would be more specific than when using neoglycoproteins and liposomes, and diffusion into tissues would be more efficient.

MDP encapsulated in liposomes has been reported to act synergistically with interferon (48). We observed an

additive effect when macrophages were incubated with both γ -IFN and MDP-mAb3A33 conjugate. It is of interest to note that MDP activates macrophages more efficiently in the presence of minute amounts of LPS (23) and that γ -IFN and MDP have additive effects. Ex vivo activation of human monocytes or macrophages for antitumor immunotherapy is currently under investigation, and protocols using γ -IFN as stimulating agent have been proposed (49, 50). Mac-1 antigen has a known human counterpart, CD11b, against which several monoclonal antibodies are available. A molecular conjugate consisting of a monoclonal antibody, directed against the human CD11b antigen and substituted with MDP, might be helpful to increase the γ -IFN antitumor activity in man.

ACKNOWLEDGMENT

This work was supported by a grant from the ARC (Association de la Recherche contre le cancer); A.C.R. is "Directeur de recherche INSERM", A.M. and P.M. are "Chargé de recherche INSERM", L.T. is "Chef de Service".

LITERATURE CITED

- (1) Adam, A., Petit, J. F., Lefrancier, P., and Lederer, E. (1981) Muramyl peptides: Chemical structure, biological activity and mechanism of action. *Mol. Cell Biochem.* 41, 27-47.
- (2) Adam, A., Ciorbaru, R., Ellouz, F., Petit, J. F., and Lederer, E. (1974) Adjuvant activity of monomeric bacterial cell wall peptidoglycans. *Biochem. Biophys. Res. Commun.* 56, 561-567.
- (3) Merse, C., Sinay, P., and Adam, A. (1975) Total synthesis and adjuvant activity of bacterial peptidoglycan derivatives. *Biochem. Biophys. Res. Commun.* 66, 1316-1322.
- (4) Wahl, S. M., Wahl, L. M., McCarthy, J. B., Chedid, L., and Mergenhagen, S. E. (1979) Macrophage activation by mycobacterial water soluble compounds and synthetic muramyl dipeptide. *J. Immunol.* 122, 2226-2231.
- (5) Tenu, J. P., Lederer, E., and Petit, J. F. (1980) Stimulation of thymocyte mitogenic protein and cytostatic activity of mouse peritoneal macrophages by trehalose dimycolate and muramyl dipeptide. *Eur. J. Immunol.* 10, 647-653.
- (6) Pabst, M. J., and Johnson, R. B. (1980) Increased production of superoxide anion by macrophages exposed in vitro to muramyl dipeptide or lipopolysaccharide. *J. Exp. Med.* 151, 101-108.
- (7) Parant, M., Parant, F., Chedid, L., Yapo, A., Petit, J. F., and Lederer, E. (1979) Fate of the synthetic immunoadjuvant, muramyl dipeptide (14 C-labeled) in the mouse. *Int. J. Immunopharmacol.* 1, 35-41.
- (8) Tenu, J. P., Roche, A. C., Yapo, A., Kieda, C., Monsigny, M., and Petit, J. F. (1982) Absence of cell surface receptors for muramyl peptides in mouse peritoneal macrophages. *Biol. Cell* 44, 157-164.
- (9) Fidler, I. J., Sone, S., Fogler, W. E., and Barnes, Z. L. (1981) Eradication of spontaneous metastases and activation of alveolar macrophages by intravenous injection of liposomes containing muramyl dipeptide. *Proc. Natl. Acad. Sci. U.S.A.* 78, 1680-1684.
- (10) Fidler, I. J., Barnes, Z., Fogler, W. E., Kirsh, R., Bugelski, P., and Poste, G. (1982) Involvement of macrophages in the eradication of established metastasis following intravenous injection of liposome containing macrophage activators. *Cancer Res.* 42, 496-501.
- (11) Derrien, D., Midoux, P., Petit, C., Nègre, E., Mayer, L., Monsigny, M., and Roche, A. C. (1989) Muramyl dipeptide bound to poly-L-lysine substituted with mannose and glucosyl residues as macrophage activators. *Glycoconjugate J.* 6, 241-255.
- (12) Monsigny, M., Roche, A. C., and Bailly, P. (1984) Tumor-icidal activation of murine alveolar macrophages by muramyl dipeptide substituted mannoseylated serum albumin. *Biochem. Biophys. Res. Commun.* 121, 579-584.
- (13) Roche, A. C., Bailly, P., and Monsigny, M. (1985) Macrophage activation by MDP bound to neoglycoproteins: Metastasis eradication in mice. *Invasion Metastasis* 5, 218-232.
- (14) Roche, A. C., Bailly, P., Midoux, P., and Monsigny, M. (1984) Selective macrophage activation by muramyl dipeptide bound to monoclonal antibodies specific for mouse tumor cells. *Cancer Immunol. Immunother.* 18, 155-159.
- (15) Leclerc, C., Bahr, G. L., and Chedid, L. (1984) Marked enhancement of macrophage activation induced by synthetic muramyl dipeptide (MDP) conjugate using monoclonal anti-MDP antibodies. *Cell. Immunol.* 86, 269-277.
- (16) Martin, A., Le Corre, R., Pellen, P., Bourel, D., Merdignac, G., Genetet, B., and Toujas, L. (1986) A monoclonal antibody reacting with a mouse-specific epitope of Mac-1 antigen. *Tissue Antigens* 28, 14-23.
- (17) Springer, T. A., Galfre, G., Secher, D. S., and Milstein, C. (1979) Mac-1: A macrophage differentiation antigen identified by monoclonal antibody. *Eur. J. Immunol.* 9, 301-306.
- (18) Collet, B., Pellen, P., Martin, A., Moisan, A., Bourel, D., and Toujas, L. (1988) Scintigraphic detection in mice of inflammatory lesions and tumours by an indium-labelled monoclonal antibody directed against Mac-1 antigen. *Cancer Immunol. Immunother.* 26, 237-242.
- (19) Dazord, L., Bourel, D., Martin, A., Bourguet, P., Bohy, J., Saccavini, J. C., Delaval, P., Louvet, M., and Toujas, L. (1987) A monoclonal antibody (Po66) directed against human lung squamous cell carcinoma. Immunolocalization of tumor xenografts in nude mice. *Cancer Immunol. Immunother.* 24, 263-268.
- (20) Bazin, H., Beckers, A., and Querinjean, P. (1974) Three classes and four (sub)classes of rat immunoglobulins: IgM, IgA, IgE and IgG1, gG2a, IgG2b, IgG2c. *Eur. J. Immunol.* 4, 44-48.
- (21) Carlsson, J., Drevin, H., and Axen, R. (1978) Protein thiolation and reversible protein-conjugation. N-succinimidyl 3-(2-pyridyldithio) propionate, a new heterobifunctional reagent. *Biochem. J.* 173, 723-737.
- (22) Levy, G. A., and McAllan, A. (1959) The N-acetylation and estimation of hexosamines. *Biochem. J.* 73, 127-132.
- (23) Barratt, G., Tenu, J. P., Petit, J. F., and Nolibé, D. (1986) Sub-optimal concentrations of LPS are necessary for in vitro activation of rat alveolar macrophages by muramyl peptides. In *Biological Properties of Peptidoglycans* (Seidl P. H., and Schleifer, K. H., Eds.) p 249, Walter De Gruyten and Co., Berlin.
- (24) Monsigny, M., Roche, A. C., and Midoux, P. (1984) Uptake of neoglycoproteins via membrane lectin(s) of L1210 cells evidenced by quantitative flow cytofluorometry and drug targeting. *Biol. Cell* 51, 187-196.
- (25) Adams, D. O., and Hamilton, T. A. (1984) The cell biology of macrophage activation. *Annu. Rev. Immunol.* 2, 283-318.
- (26) Midoux, P., Nègre, E., Roche, A. C., Mayer, R., Monsigny, M., Balzarini, J., De Clercq, E., Mayer, E., Ghaffar, A., and Gangemi, J. D. (1990) Drug targeting: Anti-HSV-1 activity of mannosylated polymer-bound 9-(2-phosphonylmethoxyethyl) adenine. *Biochem. Biophys. Res. Commun.* 167, 1044-1049.
- (27) Embleton, M. J., Garnett, M. C., Jacobs, E., and Baldwin, R. W. (1984) Antigenicity and drug susceptibility of human osteogenic sarcoma cells "escaping" a cytotoxic methotrexate-albumin-monoclonal antibody conjugate. *Br. J. Cancer.* 49, 559-565.
- (28) Endo, N., Kato, Y., Takeda, Y., Saito, M., Umemoto, N., and Kishida, K. (1987) In vitro cytotoxic of a human serum albumin-monoclonal antibody conjugate of methotrexate with anti-MM46 monoclonal antibody. *Cancer Res.* 47, 1076-1080.
- (29) Garnett, M. C., and Baldwin, R. W. (1986) An improved synthesis of a methotrexate-albumin-971T/36 monoclonal antibody conjugate cytotoxic to human osteogenic sarcoma cell lines. *Cancer Res.* 46, 2407-2412.
- (30) Garnett, M. C., Embleton, M. J., Jacobs, E., and Baldwin, R. W. (1983) Preparation and properties of a drug-carrier-antibody conjugate showing selective antibody-directed cytotoxicity in vitro. *Int. J. Cancer* 31, 661-670.
- (31) Ohkawa, K., Tsukada, Y., Hibi, N., Umemoto, N., and Hara, T. (1986) Selective in vitro and in vivo growth inhibition against human yolk sac tumor cell lines by purified antibody against

- human alpha-fetoprotein conjugated with mitomycin C via human serum albumin. *Cancer Immunol. Immunother.* 23, 81-86.
- (32) Pimm, M. V., Clegg, J. A., Caten, J. E., Ballantyne, K. D., Perkins, A. C., Garnett, M. C., and Baldwin, R. W. (1987) Biodistribution of methotrexate-monoconal antibody conjugates and complexes: Experimental and clinical studies. *Cancer Treat. Rev.* 14, 411-420.
- (33) Umemoto, N., Kato, Y., Takeda, Y., Saito, M., Hara, T., Seto, M., and Takahashi, T. (1984) Conjugates of mitomycin C with the immunoglobulin M monomer fragment of a monoclonal anti-MM46 immunoglobulin M antibody with or without serum albumin as intermediary. *J. Appl. Biochem.* 6, 297-307.
- (34) Hurwitz, E., Kashi, R., Burowsky, D., Arnon, R., and Haimovich, J. (1983) Site-directed chemotherapy with a drug bound to anti-idiotypic antibody to a lymphoma cell-surface IgM. *Int. J. Cancer.* 31, 745-748.
- (35) Hurwitz, E., Maron, R., Arnon, R., Wilchek, M., and Sela, M. (1978) Daunomycin-immunoglobulin conjugates, uptake and activity in vitro. *Eur. J. Cancer* 14, 1213-1220.
- (36) Manabe, Y., Tsubota, T., Haruta, Y., Kataoka, K., Okazaki, M., Haisa, S., Nakamura, K., and Kimura, I. (1984) Production of a monoclonal antibody-methotrexate conjugate utilizing dextran T-40 and its biological activity. *J. Lab. Clin. Med.* 104, 445-454.
- (37) Tsukada, Y., Bishof, W. F.-D., Hibi, N., Hirai, H., Hurwitz, E., and Sela, M. (1982) Effect of a conjugate of daunomycin and antibodies to rat alpha-fetoprotein on the growth of alpha-fetoprotein-producing tumor cells. *Proc. Natl. Acad. Sci. U.S.A.* 79, 621-625.
- (38) Tsukada, Y., Hurwitz, E., Kashi, R., Sela, M., Hibi, N., Hara, A., and Hirai, H. (1982) Chemotherapy by intravenous administration of conjugates of daunomycin with monoclonal and conventional anti-rat-fetoprotein antibodies. *Proc. Natl. Acad. Sci. U.S.A.* 79, 7896-7899.
- (39) Tsukada, Y., Ohkawa, K., and Hibi, N. (1987) Therapeutic effect of treatment with polyclonal or monoclonal antibodies to fetoprotein that have been conjugated to daunomycin via a dextran bridge: Studies with an alpha-fetoprotein-producing rat hepatoma tumor model. *Cancer Res.* 47, 4293-4295.
- (40) Tsukada, Y., Kato, Y., Umemoto, N., Takeda, Y., Hara, T., and Hirai, H. A. (1984) Anti α -fetoprotein antibody-daunorubicin conjugate with a novel poly-L-glutamic acid derivative as intermediate drug carrier. *J. Natl. Cancer. Inst.* 73, 721-729.
- (41) Rihova, B., Kopecek, J., Kopeckova-Rejmanova, P., Strohalm, J., and Plocova, D. (1986) Bioaffinity therapy with antibodies and drugs bound to soluble synthetic polymers. *J. Chromatogr.* 376, 221-233.
- (42) Hurwitz, E., Stancovski, I., Wilchek, M., Shouval, D., Takahashi, H., Wands, J. R., and Sela, M. (1990) A conjugate of 5-fluorouridine-poly(L-lysine) and an antibody reactive with human colon carcinoma. *Bioconjugate Chem.* 1, 285-290.
- (43) Derrien, D. (1988) Thesis, Orléans, France.
- (44) Springer, T. A. (1985) Murine macrophage differentiation antigens defined by monoclonal antibodies. In *Monoclonal Hybridoma Antibodies: Techniques and Applications* (J. G. R., Hurrell, Ed.) p 169, CRC Press, Boca Raton, FL.
- (45) Jupin, C., Parant, M., Chedid, L., and Damais, C. (1987) Enhanced oxidative burst without IL1 production by normal human PMN primed with muramyl dipeptide. *Inflammation* 11, 153-161.
- (46) Le Garrec, Y., and Morin, P. (1987) Modulation of natural killer activity by muramyl peptides: Relationship with adjuvant and anti-infectious properties. *Nat. Immun. Cell Growth* 6, 65-76.
- (47) Tabata, Y., and Ikada, Y. (1990) Drug delivery systems for antitumor activation of macrophages. *Crit. Rev. Ther. Drug Carrier Sys.* 7, 121-148.
- (48) Sone, S., and Fidler, I. J. (1980) Synergistic activation by lymphokines and muramyl dipeptide of tumoricidal properties in rat alveolar macrophages. *J. Immunol.* 125, 2454-2460.
- (49) Dumont, S., Hartman, D., Poindron, P., Oberling, F., Faradji, A., and Bartholeyns, J. (1988) Control of the antitumoral activity of human macrophages produced in large amounts in view of adoptive transfer. *Eur. J. Clin. Oncol.* 24, 1691-1698.
- (50) Andreesen, R., Scheibenbogen, C., Brugger, W., Krause, S., Meerpohl, H.-G., Leser, H.-G., Engler, H., and Löhr, G. W. (1990) Adoptive transfert of tumor cytotoxic macrophages generated in vitro from circulating blood monocytes: A new approach to cancer immunotherapy. *Cancer Res.* 50, 7450-7456.

TECHNICAL NOTE

Activating Hydroxyl Groups of Polymeric Carriers Using 4-Fluorobenzenesulfonyl Chloride¹

Yu-An Chang,* Adrian Gee, Alan Smith, and William Lake

Baxter Healthcare Corporation, Fenwal Division, 3015 South Daimler Street, Santa Ana, California 92705.
Received November 15, 1991

4-Fluorobenzenesulfonyl chloride (fosyl chloride), due to the strong electron-withdrawing property of its fluoride atom, is found to be an excellent activating agent for the covalent attachment of biologicals to a variety of solid supports (e.g. functionalized polystyrene microspheres, Sepharose beads, or cellulose rods and hollow fibers). This reagent reacts rapidly with primary or secondary hydroxyl groups, at ambient temperature and pressure, to form 4-fluorobenzenesulfonate leaving groups. The activated solid support can be used immediately or preserved for several months without loss of activity by freeze-drying or by storage at 4 °C in aqueous solution at pH 5. Enzymes, antibodies, avidin, and other biologicals can be covalently attached to the activated solid phase with excellent retention of biological function. Potential therapeutic applications of the fosyl chloride chemistry for bioselective separation of human lymphocyte subsets from whole blood and tumor cells from bone marrow are presented.

INTRODUCTION

Bioselective-separation technology can be used to perform separations of a specific target population of cells, proteins, or antibodies from a heterogeneous solution without the need of tedious and extensive chemical or physical separation techniques. This technology uses affinity supports which are typically formed from hydroxyl-bearing polymeric carriers, in the form of columns, gels, or polymeric beads. A biologically active ligand is chemically bound to the carrier to provide a selective affinity for binding to the desired target population, i.e. cells, proteins, enzymes, antibodies, and antigens from solutions.

Various methods have been used for chemically coupling biologically active ligands to hydroxyl-bearing polymeric carriers (1). Cyanogen bromide (CNBr) (2) is one of the earliest and most widely used methods. Present methods using CNBr and similar reagents (3, 4) have several limitations. The activated solid supports are unstable, side reactions occur during activation and coupling, and the linkages formed between supports and ligands are labile (4). In addition, CNBr is a noxious, lachrymatory, and poisonous chemical which requires special handling.

Mukaiyama et al. (6) first reported the use of 1-methyl-2-fluoropyridinium *p*-toluenesulfonate (FMP) for the preparation of various sulfides and amines from alcohols. Ngo (7) used this reagent to activate hydroxyl groups on polysaccharides such as agarose and Sepharose. A positively charged amine group on the FMP-activated polymeric carrier makes displacement of this group by similarly charged ligands difficult and inefficient.

Mosbach and Nilsson (8a,b) have activated hydroxyl groups using *p*-toluenesulfonyl chloride (tosyl chloride) and 2,2,2-trifluoroethanesulfonyl chloride (tresyl chloride). Due to the electron-donating character of the methyl group on the *p*-toluenesulfonate, reaction with the nucleophilic groups on the biological often requires 16-24 h under

conditions of pH 8.0 or higher. Such harsh conditions can denature biologicals and may decrease the usefulness of the ligand-coupled carrier. Tresyl chloride is toxic, highly reactive, and volatile. The volatility and high reactivity of tresyl chloride requires that activation with this chemical be performed under strictly anhydrous conditions, making use difficult.

In this study we describe a coupling chemistry which overcomes many of these disadvantages. 4-Fluorobenzenesulfonyl chloride (fosyl chloride) has a fluorine atom at the para position, providing a strong electron-withdrawing group to increase the reactivity of the sulfonate. Fosyl chloride is a solid of low volatility and requires no special handling conditions. Use of this reagent to activate hydroxyl carriers yields stable activated supports with minimal side reactions. In this study, we investigated fosyl chloride activation of different solid supports and the resultant biological activity of bound ligands.

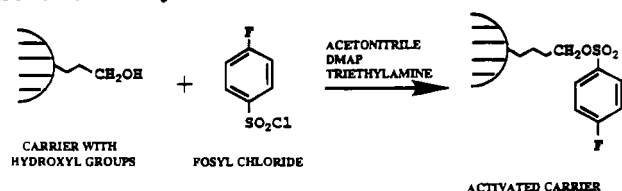
EXPERIMENTAL PROCEDURES

4-Fluorobenzenesulfonyl chloride, *p*-toluenesulfonyl chloride, cyanogen bromide (CNBr), pyridine, triethylamine, and acetonitrile were purchased from Aldrich Chemical Co. (Milwaukee, WI). 4-(Dimethylamino)pyridine (DMAP) was purchased from Fluka (Ronkonkoma, NY). Tween-20 and bovine serum albumin (BSA) were purchased from Sigma, St. Louis, MO. BCA micro protein assay reagents were purchased from Pierce (Rockford, IL). Bolton-Hunter reagent was purchased from Du Pont Co. NEN Research Products (Boston, MA). Dynal M-450 beads were purchased from Dynal Inc. (Great Neck, NY). Goat anti-mouse IgG was purchased from Jackson Immunoresearch Lab. (West Grove, PA). Anti-Leu 1 (CD 3), anti-Leu 3a (CD 4), and anti-Leu 4 (CD 5) antibodies were purchased from Becton Dickinson (Mountain View, CA).

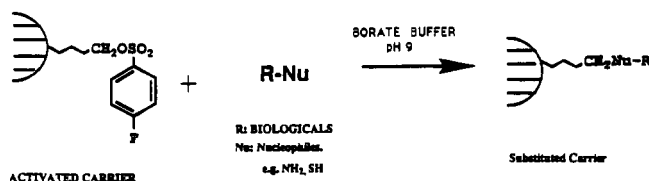
General Reaction for Fosyl Chloride Activation of Hydroxyl Groups. The activation of hydroxylated carriers was performed in the presence of a base such as triethylamine or pyridine. DMAP was used as a catalyst in a dry polar aprotic organic solvent such as acetonitrile.

¹A preliminary poster presentation has been given at the 200th American Chemical Society national meeting (Division of Medicinal Chemistry), Washington, DC, August 26-31, 1990.

Scheme I. Fosyl Chloride Activation



Scheme II. Coupling of Fosyl Chloride Activated Carrier



The fosyl chloride reacted rapidly with the hydroxyl groups under ambient temperature and pressure to form 4-fluorobenzenesulfonate groups. This reactive derivative can be used immediately, preserved by freeze-drying, or stored at 4 °C and pH 5 in aqueous solution for future use. The unreacted reagents can be removed by washing with organic solvents (e.g. acetonitrile and acetone) followed by deionized water. The carrier can be made of polystyrene with copolymers which contain hydroxyl groups or polysaccharides such as cellulose or Sepharose. The carriers can be in the form of microspheres, beads, fibers, or rods. The activation of carriers and coupling of ligands are illustrated in Scheme I.

General Coupling Procedure of Biologicals to Activated Solid Supports. Biologicals containing amino or sulfhydryl groups are suitable for use as ligands to displace the 4-fluorobenzenesulfonate groups. The coupling reaction can be carried out under various conditions, e.g. temperature, pH, and solvents. The unreacted 4-fluorobenzenesulfonate groups can be easily removed by incubation with 0.05 M Tris buffer (pH 8). Scheme II illustrates the coupling of various biologicals to activated solid supports and the following examples illustrate specific coupling procedures.

(1) *Activation of Polystyrene Paramagnetic Beads and Coupling of Goat Anti-Mouse (GAM) IgG to Activated Magnetic Polystyrene Beads.* Dynal M 450 polystyrene paramagnetic beads (5 mL) were washed with deionized water (3 mL) three times followed by acetonitrile (3 mL) three times. The beads were then resuspended in 6 mL of acetonitrile, and pyridine (0.08 mL), DMAP (160 mg), and fosyl chloride (600 mg) were added to the solution. The sample was rotated at ambient temperature for 6 h and then the beads were washed four times with acetonitrile (3 mL) and then washed four times with deionized water (3 mL). Part of the sample was freeze-dried and stored at 4 °C; the remaining sample was used directly for coupling to biologicals. Borate buffer (20 mL, 0.05 M, pH 9) was added to fosyl chloride activated beads (1.24×10^9 beads) and 18.6 mg of a goat anti-mouse IgG preparation was added to the beads. The beads were rotated at ambient temperature overnight and then washed with Dulbecco's phosphate-buffered saline (DPBS) and stored at 4 °C. These GAM Ab coated beads were used for cell separation experiments (see below).

(2) *Activation of Sepharose Beads.* Sepharose beads (2.04 g, Sigma, CL-4B-200) were filtered under reduced pressure and washed once with 15 mL of deionized water and then with 15 mL of acetonitrile three times to remove water. A solution of acetonitrile/DMAP/triethylamine (9

mL/100 mg/1 mL; 7 mL) and fosyl chloride (2.03 g) was added to the beads. The mixture was rotated at ambient temperature for 1 h.

The reagents were removed by filtration under reduced pressure, and then the beads were washed with acetonitrile (7 mL) and deionized water (7 mL). Deionized water (10 mL) and 3 drops of 1 N HCl were added to the beads to decrease the solution pH to 5 and the activated beads were sealed in the test tube with Parafilm and stored at 4 °C for future coupling of biologicals.

(3) *Activation of Cellulose Rods and Coupling of ^{125}I -Labeled GAM.* Cellulose rods (3 mg; 1 cm long) were added to each of two glass test tubes. To the tubes was added 4 mL of dry acetonitrile along with the quantity of reagents as follows:

sample no.	reagents	quantity
1	DMAP	300 mg
	pyridine	150 μL
	fosyl chloride	500 mg
2	DMAP	300 mg
	pyridine	150 μL
	tresyl chloride	450 mg

The samples were incubated at ambient temperature for 6 h and then washed with 0.05 M borate buffer (pH 9.5, 2 mL) two times, acetonitrile (2 mL) three times, and borate buffer (2 mL) three times. The samples were resuspended in the borate buffer (3 mL). ^{125}I -Labeled GAM (1 mg/mL, specific activity = 1998 cpm/mg) was prepared using Bolton-Hunter reagent as per the manufacturer's procedure. A 90- μL sample of ^{125}I -labeled GAM was added to each sample and incubated at room temperature overnight.

Samples were then counted in the γ counter for total counts to determine the quantity of antibody bound in each sample. Each sample was washed three times with 0.05% Tween/PBS and then resuspended in 1.0 mL of 0.05% Tween/PBS solution and transferred to new tubes. Tubes used for the original incubation were washed with 0.5 mL of buffer, and the wash was added to the new tubes. The tubes were then counted for the radioactivity of each sample by a γ counter.

RESULTS AND DISCUSSION

(1) *Comparison of Fosyl Chloride to Other Activation Agents.* (A) *Comparison of Fosyl Chloride and Tresyl Chloride Activation of Cellulose Rods and Their Binding of ^{125}I -Labeled GAM Antibody.* Cellulose rods activated by fosyl chloride and tresyl chloride under the same conditions were incubated with ^{125}I -labeled GAM Ab, and then samples were washed and transferred to new tubes. The tubes were counted for radioactivity and the quantity of the ^{125}I -labeled GAM bound to the cellulose rod samples was thus determined (See Figure 1).

(B) *Cell Depletion by Fosyl Chloride vs Tosyl Chloride Activated Polystyrene Beads.* Goat anti-mouse Ab coupled polystyrene beads activated by fosyl chloride and tosyl chloride under the same conditions were used for separation of lymphocyte subsets, such as CD 3, CD 4, and CD 5 positive cells,² following the reported procedure (9). Comparable results were obtained (Table I).

²Lymphocyte subsets used in these experiments are human T-lymphocytes which express different surface antigens such as CD 3, CD 4, and CD 5. Consequently, these cells can be identified and separated using specific antibodies against these surface antigens.

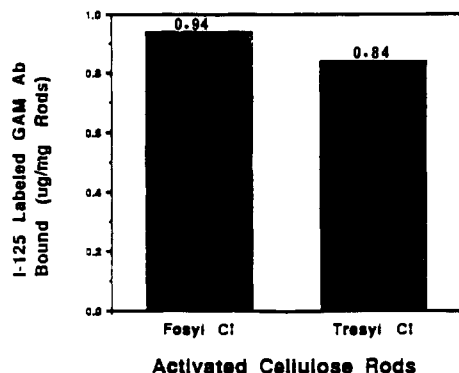


Figure 1. ^{125}I -Labeled GAM Ab bound to fosyl or tresyl chloride activated cellulose rods.

Table I. Comparison of Percent Cell Depletion by Fosyl Chloride and Tosyl Chloride Activated GAM Ab Coupled Beads

lymphocyte subset	% cell depletion	
	fosyl chloride	tosyl chloride
CD 3	90.1	82.2
CD 4	99.9	99.9
CD 5	93.5	88.0

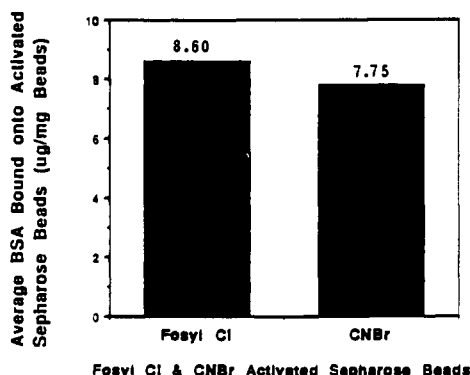


Figure 2. Fosyl chloride vs CNBr activation.

(C) *Binding of BSA to Fosyl Chloride and CNBr Activated Sepharose Beads.* Sepharose beads (Sigma, CL-4B-200) were activated by CNBr (2) and fosyl chloride, respectively, and the activated samples were incubated with BSA under the same conditions. The quantities of the BSA bound to the samples were determined by BCA micro protein assay (Figure 2). The amount of BSA coupled was similar with both activation chemistries.

The *p*-fluoro substitution imparts a strong electron-withdrawing effect, making the 4-fluorobenzenesulfonate an excellent leaving group. Consequently, substitution of ligand for the 4-fluorobenzenesulfonate on the solid supports can be completed faster than that with *p*-toluenesulfonate. The reaction time is thus reduced while biological activity is conserved.

4-Fluorobenzenesulfonyl chloride can be used to activate a broad spectrum of solid supports, e.g. cross-linked agarose beads, cellulose fiber, cellulose rod, maleated cellulose rod, and polystyrene paramagnetic beads. The activation

time can be as short as 30 min and the activated solid support can be stored at 4 °C for several weeks without loss of binding activity.

In summary, fosyl chloride was found to be a versatile reagent for the activation of a variety of solid supports which have a wide range of applications. Examples of other biologicals which have been successfully coupled to fosyl chloride activated solid supports include (1) avidin (a protein which has high affinity for biotinylated biologicals), (2) the enzyme catalase, and (3) human factor VIII, an anticoagulant protein (unpublished results available upon request).

Potential therapeutic applications of the 4-fluorobenzenesulfonyl chloride chemistry for bioselective separation of human lymphocyte subsets from whole blood, tumor cells from bone marrow, and allergenic antibodies from whole blood are currently under investigation.

LITERATURE CITED

- (1) Scouten, W. (1987) A Survey of Enzyme Coupling Techniques. In *Methods in Enzymology* (K. Mosbach, Ed.) Vol. 135, pp 30-64, Academic Press, New York.
- (2) Porath, J., and Axen, R. (1976) Immobilization of Enzymes to Agar, Agarose, and Sephadex Supports. In *Methods in Enzymology* (K. Mosbach, Ed.) Vol. 44, pp 19-45, Academic Press, New York.
- (3) Kohn, J., and Wilcheck, M. (1982) A new approach (cyanotransfer) for cyanogen bromide activation of Sepharose at neutral pH, which yields activated resins free of interfering nitrogen derivatives. *Biochem. Biophys. Res. Commun.* 107, 878-884.
- (4) Kohn, J., and Wilcheck, M. (1983) New approaches for the use of cyanogen bromide and related cyanylating agents for the preparation of activated polysaccharide resins. In *Affinity Chromatography and Biological Recognition* (I. M. Chaiken, M. Wilcheck, and I. Parikh, Eds.) pp 197-207, Academic Press, New York.
- (5) (a) Tesser, G. I., Fisch, H. U., and Schwyzler, R. (1974) Limitations of affinity chromatography: Solvolytic detachment of ligands from polymeric supports. *Helv. Chim. Acta* 57, 1718-1730. (b) Kohn, J., and Wilcheck, M. (1983) Activation of polysaccharide resins by CNBr. In *Solid Phase Biochemistry* (W. H. Scouten, Ed.) pp 599-630, Wiley, New York.
- (6) Mukaiyama, T., Ikeda, S., and Kobayashi, S. (1975) A novel method for the preparation of various 2-pyridyl sulfides from alcohols. *Chem. Lett.* 1159-1162.
- (7) Ngo, T. T. (1986) Method of Activating Hydroxyl Groups of a Polymeric Carrier Using 2-Fluoro-1-methylpyridinium Toluene-4-sulfonate. U.S. Patent # 4,582,875.
- (8) (a) Mosbach, K. H., and Nilsson, K. G. I. (1983) Method of Covalently Binding Biologically Active Organic Substances to Polymeric Substances. U.S. Patent # 4,415,665. (b) Nilsson, K., and Mosbach, K. (1984) Immobilization of Ligands with Organic Sulfonyl Chlorides. In *Methods in Enzymology* (W. B. Jakoby, Ed.) Vol. 104, pp 56-69, Academic Press, New York.
- (9) Gee, A. P., Mansour, V., and Weiler, M. (1989) T-Cell Depletion of Human Bone Marrow *J. Immunogenet.* 16, 103-115.

Registry No. DMAP, 1122-58-3; CNBr, 506-68-3; fosyl chloride, 349-88-2; catalase, 9001-05-2; human factor VIII, 9001-27-8; Dynal M 450 polystyrene paramagnetic beads, 114451-54-6; Sepharose beads CL-4B-200, 61970-08-9; cellulose, 9004-34-6; pyridine, 110-86-1; tresyl chloride, 1648-99-3.

Bioconjugate Chemistry

MAY/JUNE 1992
Volume 3, Number 3

© Copyright 1992 by the American Chemical Society

Modification of Dry 1,2-Dipalmitoylphosphatidylcholine Phase Behavior with Synthetic Membrane-Bound Stabilizing Carbohydrates¹

Mary A. Testoff and Alan S. Rudolph*

The Center for Biomolecular Science and Engineering, Code 6090, Naval Research Laboratory, Washington, D.C. 20375-5000. Received October 23, 1991

Carbohydrates, particularly disaccharides, have been shown to accumulate in organisms as protective solutes during periods of stress such as freezing and desiccation. Cholesterol and lipid derivatives containing the protective carbohydrates galactose or maltose, *O*-[11-(1- β -D-galactosyloxy)-3,6,9-trioxaundecanyl]ol (TEC-GAL), *O*-[11-(1- β -D-maltosyloxy)-3,6,9-trioxaundecanyl]ol (TEC-MAL), and 14-(galactosyloxy)-*N,N*-dimethyl-*O*-(dipalmitoylphosphatidyl)-6,9,12-trioxa-3-azoniatetradecanol (DP-GAL), have been synthesized to investigate the interaction of a protective carbohydrate moiety tethered to the 1,2-dipalmitoylphosphatidylcholine (DPPC) bilayer surface. Toward this goal, we have investigated the calorimetric and infrared spectroscopic behavior of mixtures of DPPC codried with these glycolipids. The synthetic glycolipids are shown to decrease significantly the main transition temperature ($\max C_p$) of dry DPPC with a concomitant reduction in the cooperativity of the transition, as evidenced by a decrease in the enthalpy with increasing glycolipid. The decrease in transition temperature is shown to be related to chain melting monitored by the CH₂ symmetric stretch frequency through the transition using FTIR. We also present evidence that the glycolipids interact with the interfacial region of DPPC, as shown by the decrease in the phosphate symmetric stretch intensity with increasing concentration of glycolipid. These observed effects are similar to the action of bulk protective sugars with DPPC; however, the concentration of glycolipid and the associated carbohydrate concentration needed to effect the observed changes are reduced compared to the quantity of bulk carbohydrate previously shown to give similar results with DPPC.

INTRODUCTION

The presence of water is essential for proper assembly of the constituents of biomembranes (i.e. phospholipids, sterols, membrane proteins) and the proper maintenance of critical membrane metabolic and physiological cellular processes such as energy transduction and molecular recognition. The interplay between water and biological membranes still remains an active area of research, as the nature and physiological role of membrane associated water has not been fully elucidated (1-5). Hydrogen bonding of water to the polar regions of membrane components is thought to provide the necessary structural and functional maintenance critical to biomembranes (1, 2). Water removal during freezing and desiccation results

in functional and structural defects of biomembranes by inducing a number of changes in membrane structure.

¹ Abbreviations used: DPPC, 1,2-dipalmitoylphosphatidylcholine; DPPC-*d*₆₂, 1,2-dipalmitoyl-*d*₆₂-*sn*-glycerol-3-phosphocholine; DOPE, dioleoylphosphatidylethanolamine; DP-GAL, 14-(galactosyloxy)-*N,N*-dimethyl-*O*-(dipalmitoylphosphatidyl)-6,9,12-trioxa-3-azoniatetradecanol; TEC, triethoxycholesterol or *O*-(11-hydroxy-3,6,9-trioxaundecyl)cholesterol; TEC-GAL, triethoxycholesterol galactose or *O*-[11-(1- β -D-galactosyloxy)-3,6,9-trioxaundecanyl]cholesterol; TEC-MAL, triethoxycholesterol maltose or *O*-[11-(1- β -D-maltosyloxy)-3,6,9-trioxaundecanyl]cholesterol; EDTA, ethylenediaminetetraacetic acid; TLC, thin-layer chromatography; DSC, differential scanning calorimetry; FT-IR, Fourier transform infrared spectroscopy; FAB, fast atom bombardment; CI, chemical ionization.

Dehydration- and freezing-induced phase separation of membrane components has been shown to result in damage to embedded membrane proteins as well as provide structural defects which may lead to membrane fusion and leakage of intracellular contents (1-3, 5).

In the search for mechanisms by which biomembranes are protected from damage by water removal, recent focus has been placed on the interaction of water replacement solutes found in organisms that survive freezing or desiccation with biomembranes (1, 3-5). One class of such solutes are the polyhydroxy compounds of which the carbohydrates are found to commonly accumulate in large quantities during the induction of hydration stress. A variety of disaccharides (e.g. trehalose, sucrose) have been found to accumulate at high concentrations in biological systems during dehydration or freezing (1, 3, 4). Infrared spectroscopic studies on the interaction of disaccharides and dry DPPC suggest that these solutes hydrogen bond to hydration sites of phospholipids, of which the phosphate group may be a potential site of interaction (1, 2). This action results in the reduction in the observed transition temperature of dry DPPC dihydrate and in anhydrous DPPC (1). The maximal effect resulted in the reduction of the transition temperature of the dry system to around 24 °C, significantly below the transition temperature of DPPC in excess water (6). It has been found that the effect of trehalose on dry DPPC depends on the phase from which the lipid is dried, with the most significant reduction observed when DPPC is dried from the liquid-crystalline phase (6, 7). The phase which arises due to the association of trehalose and dry DPPC has been designated L_k and has been characterized by phospholipids with restricted rotational motion of the acyl chains with increased intermolecular volume of the acyl chains compared to dry DPPC in the absence of trehalose (8, 9).

One approach to the further study of the action of protective carbohydrates with lipid systems is to construct glycolipids that have protective carbohydrates covalently linked to the phospholipid head group. The strategy employed in the synthesis of cryoprotective glycolipids is to use an amphiphilic membrane anchor that will incorporate into a phospholipid bilayer. The covalent attachment of the carbohydrate to the amphiphile is extended through the hydrophobic region of the bilayers by a linker group (oxyethylene). The oxyethylene linkage is designed to give the carbohydrate mobility to localize at the interfacial region of the membrane surface and hydrogen bond to hydration sites on the bilayer. This model also allows maximal interaction of the hydrophilic carbohydrates with the membrane and does not require efforts to ensure homogeneous mixing of carbohydrate and lipid assemblies in bulk solution before the induction of freezing or desiccation. Incorporation of lipid molecules with inherent protective carbohydrates into such membrane systems (or cellular biomembranes) could induce stability to hydration stress which may be required for other technologies relying on lipid amphiphiles.

Two glycolipids that have been synthesized previously (8) focused on cholesterol derivatives covalently attached to a protective sugar via a similar oxyethylene linkage, namely triethoxycholesterol galactose (TEC-GAL) and triethoxycholesterol maltose (TEC-MAL) (Figure 1) (10). Goodrich et al. have studied the changes in the lipid phase behavior of *hydrated* DPPC and DOPE influenced by the addition of the linker triethoxycholesterol (TEC) and TEC-GAL, which were characterized by fluorescence polarization, ^{31}P NMR, DSC, and freeze-fracture electron microscopy (10). The addition of TEC and TEC-GAL

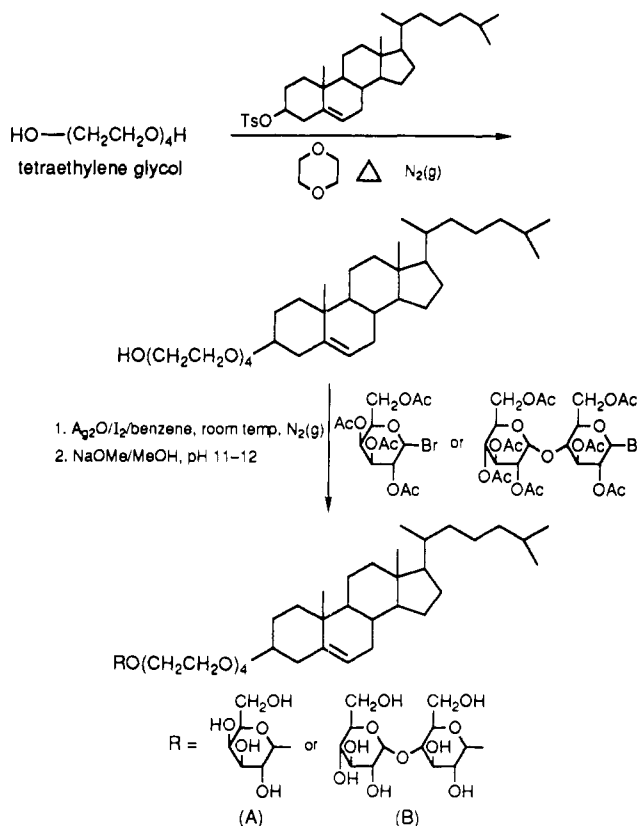


Figure 1. Synthetic scheme and structure of sterol-based glycolipids: (A) TEC-GAL, *O*-[11-(1- β -D-galactosyloxy)-3,6,9-trioxaundecanyl]cholesterol; (B) TEC-MAL, *O*-[11-(1- β -D-maltosyloxy)-3,6,9-trioxaundecanyl]cholesterol. TsO = *p*-toluenesulfonate and OAc = acetate.

resulted in a reduction in the measured anisotropy of the gel state and an increase in the liquid-crystalline phase similar to the order-disorder effect observed with cholesterol (10). The difference between the glycolipid sterol derivatives and cholesterol is the ability of the derivatives to decrease the gel to liquid-crystalline phase-transition temperature of DPPC and to increase the lamellar to hexagonal phase-transition temperature of DOPE in a concentration-dependent manner (10). Infrared and Raman spectroscopic investigations of the interaction of TEC-GAL and TEC-MAL with DPPC also reveal that the phosphate symmetric stretch frequency of DPPC is shifted in a similar fashion as that observed with bulk protective sugars (11). The cryoprotectant action of these compounds has also been recently demonstrated by examining the ability of TEC-GAL and TEC-MAL to inhibit freeze-thaw-induced fusion and leakage (12). As a further extension of this work, we have studied the calorimetric and spectroscopic phase behavior of dry films of DPPC codried with different mole percentages of TEC-GAL and TEC-MAL to observe the concentration-dependent capability of these molecules to alter the phase properties of dry DPPC.

In addition, we have synthesized a new modified phospholipid membrane component composed of a carbohydrate (galactose) attached to DPPC by an oxyethylene linkage. This glycolipid, 14-(galactosyloxy)-*N,N*-dimethyl-*O*-(dipalmitoylphosphatidyl)-6,9,12-trioxa-3-azoniatetradecanol (DP-GAL) (Figure 2), and its effects on the lipid phase behavior of dry DPPC films have been investigated by DSC and FT-IR. Dry DPPC films were codried with various mole percentages of DP-GAL to study the importance of the concentration effects of the sugar moiety of DP-GAL on the acyl chain interactions of DPPC.

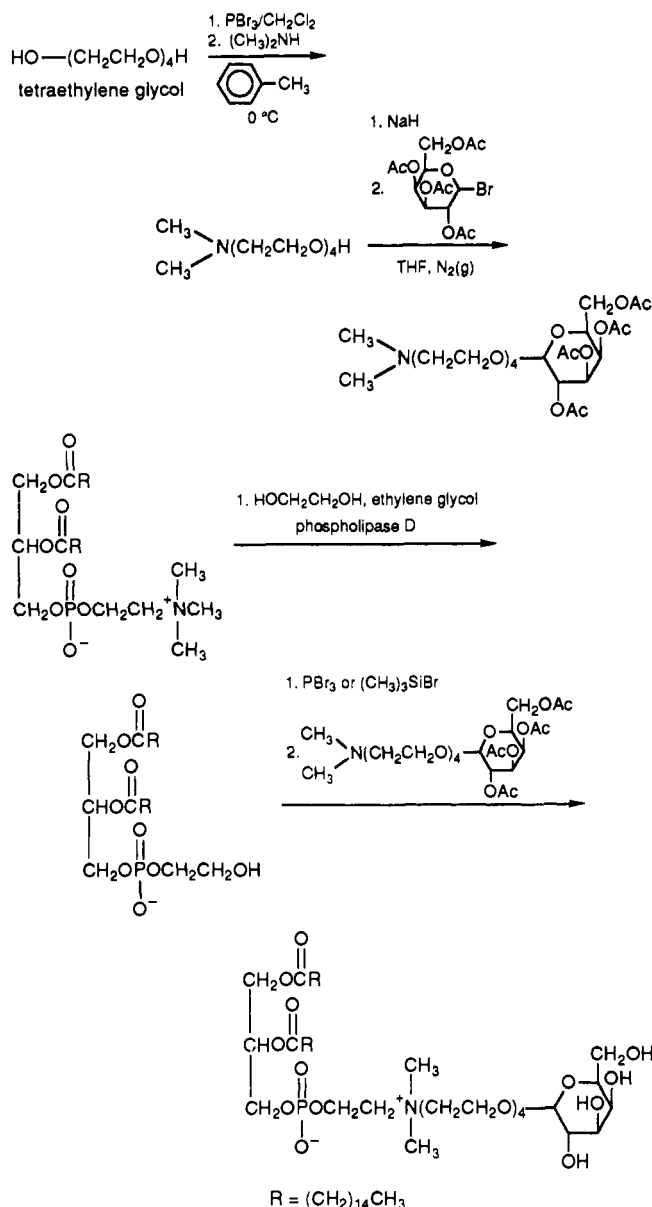


Figure 2. Synthetic scheme and structure of DP-GAL, 14-(galactosyloxy)-*N,N*-dimethyl-*O*-(dipalmitoylphosphatidyl)-6,9,12-trioxa-3-azoniatetradecanol. OAc = acetate.

EXPERIMENTAL PROCEDURES

All reagent-grade chemicals and solvents were purchased from Aldrich Chemical Co. (Milwaukee, WI). Tetrahydrofuran, chloroform, methanol, and dimethylformamide were further purified by distillation and dried over molecular sieves. DPPC and deuterated $\text{L-}\alpha$ -DPPC- d_{62} , obtained through Avanti Polar Lipids, Inc. (Alabaster, AL), were stored at -70°C in dry powder form or in chloroform. Tetra-*O*-acetyl- α -D-glucopyranosyl bromide (acetobromo- α -D-galactose) was purchased from Fluka Chemical Co. (Ronkonkoma, NY). Hepta-*O*-acetyl- α -maltosyl bromide (acetobromo- α -maltose) was supplied by Sigma Chemical Co. (St. Louis, MO). Silica gel 60 (EM 70–230 mesh) was used for all column chromatography purification, and thin-layer chromatography (TLC) was performed on EM silica gel 60 plates, both supplied by Merck (Germany). The plates were visualized by non-destructive iodine vapors. Some plates were further treated and characterized by orcinol ferric chloride (Bial's reagent), ninhydrin, Dragendorff's reagent, and/or molybdenum blue stain supplied by the Sigma Chemical Co. Amberlite IR-120 (16–45 mesh) was obtained from

Fluka Chemical Co. and 200–400 mesh AG 1-X2 hydroxide-form cation-exchange resin was supplied by Bio-Rad (Richmond, CA).

Analysis. FT-IR spectra were obtained on a Model 1800 Perkin-Elmer Fourier transform spectrophotometer and data analyzed by a Model 7700 Perkin-Elmer data station (Perkin Elmer Corp., Norwalk, CT). Differential scanning calorimetry was performed using a Perkin-Elmer DSC7 (Perkin-Elmer Corp., Norwalk, CT). The transition temperatures, onsets, and enthalpies were calculated using the Perkin-Elmer thermal analysis software. The mass spectrometry was performed on a Finnigan triple quadrupole mass spectrometer (MAT, Inc., San Jose, CA). Residual moisture of samples was determined by the Karl Fischer titration utilizing the Brinkmann 684 KF coulometer (Metrohm Inc., Switzerland). Melting points were determined by an Electrothermal melting point apparatus and are uncorrected.

Synthesis of TEC-Gal and TEC-MAL. TEC-GAL and TEC-MAL were synthesized according to the experimental procedure described by Goodrich et al. and Patel et al. (10, 13). Cholesteryl *p*-toluenesulfonate was refluxed with tetraethylene glycol in the presence of anhydrous dioxane. Acetobromo- α -D-galactose or acetobromo- α -maltose in benzene was added to the sterol derivative in the presence of silver oxide, iodine, and 4-Å powdered molecular sieves. The acetate groups of each carbohydrate moiety were removed with treatment of sodium methoxide. The suspension was neutralized when passed over an Amberlite IR-120 exchange resin. TEC-GAL and TEC-MAL were characterized by FT-IR, TLC, and mass spectra and agreed with previous results obtained by Goodrich et al. and Patel et al. (10, 13).

Synthesis of DP-GAL. *Synthesis of 11-Bromo-3,6,9-trioxaundecanol.* Phosphorous tribromide (8.928 g, 33 mmol) in 10 mL of anhydrous dichloromethane was slowly added dropwise to a tetraethylene glycol (19.4 g, 100 mmol)/anhydrous dichloromethane (50 mL) suspension at 0°C to ensure a low probability of synthesizing the dibromo product. The resultant light brown oil was purified over a silica gel column to give a pale yellow oil (20% yield, 5.14 g); R_f (chloroform/methanol, 90:10, v/v) 0.82; IR (neat, cm^{-1}) 3460, 2880, 1150, 670.

Synthesis of 11-(Dimethylamino)-3,6,9-trioxaundecanol. A 60% solution of dimethylamine in water was slowly added to potassium hydroxide pellets with constant stirring at room temperature. The resultant dimethylamine was obtained by condensing the gaseous vapors in a side flask that was placed in a -10°C dry ice/ethanol bath. Dimethylamine (2.3 g, 51 mmol) was added to 11-bromo-3,6,9-trioxaundecanol (4.0 g, 16 mmol) and 1 mL of anhydrous toluene. The reaction mixture was sealed under nitrogen and placed in a 4–8 $^\circ\text{C}$ refrigerator overnight, during which time crystallization of white spindles in a yellow suspension occurred (82% yield, 2.9 g); R_f (chloroform/methanol, 90:10, v/v) 0.27; IR (neat, cm^{-1}) 3400, 2980–2750, 2450, 1475, 1350, 1250–1050; mp $205\text{--}208^\circ\text{C}$; mass spectrum (FAB, glycerol) $m/e = 222$.

Attachment of Acetobromo- α -D-galactose to 11-(Dimethylamino)-3,6,9-trioxaundecanol. Sodium hydride (40% by weight in oil, 55.2 mg, 2.3 mmol) was rinsed three times with 25 mL of anhydrous tetrahydrofuran (THF) and weighed. 11-(Dimethylamino)-3,6,9-trioxaundecanol (0.50 g, 2.3 mmol) in 5 mL of anhydrous THF was slowly added to the sodium hydride suspension. Acetobromo- α -D-galactose (0.945 g, 2.3 mmol) was dissolved in 50 mL of anhydrous THF and slowly added to the alcohol reaction mixture under nitrogen at room temperature. This

mixture was stirred constantly for 7 days at room temperature. The crude product was purified over a silica gel column to give a pale yellow oil (39% yield, 0.495 g): R_f (chloroform/methanol, 90:10, v/v) 0.76; IR (neat, cm^{-1}) 3480, 3000–2850, 1750, 1650, 1450, 1375, 1250, 1150–1050, 760; mp 92–95 °C; mass spectrum (FAB, glycerol) m/e = 109, 127, 169, 264, 331, 543, 552, 594; (CI, isobutane) m/e = 169, 222, 331, 552.

Synthesis of the Hydroxyl Phospholipid Derivative. Preparation of the enzyme extract phospholipase D from white cabbage was performed as previously described (14). The protein content of the cabbage extract (2.6–3.0 mg/mL) was determined by Lowry's assay (15). The reaction parameters used to obtain the hydroxyl derivative of the phospholipid DPPC was described by Yang et al. (16). DPPC (1.0 g, 1.4 mmol) was dissolved in 50 mL of diethyl ether. In successive order, 3.4 mL of ethylene glycol, 20 mL of enzymatic buffer (0.2 M sodium acetate, 0.08 M calcium chloride, pH 5.6), and 34 mL of phospholipase D extract (3 mg/mL) were added to the lipid suspension. After 7 days, the reaction was quenched by removing the solvent under reduced pressure and EDTA (0.05 M, pH 8.5) was added to bind calcium, prohibiting further enzymatic activity (14). After solvent removal, the crude product was recrystallized by acetone precipitation to give a white solid (85% yield, 0.823 g): R_f (chloroform/methanol/water, 65:25:4, v/v) 0.84; IR (film and KBR, cm^{-1}) 3300–3200, 2960–2850, 1730, 1650, 1470, 1250, 1150–1050, 960.

Synthesis of the Brominated Phospholipid Derivative. Two methods were employed to brominate the hydroxyl lipid derivative. One method of bromination used reacted phosphorus tribromide with the hydroxyl derivative and the second method was to treat the hydroxyl derivative with trimethylsilyl bromide (13, 14). Phosphorus tribromide (51.0 mg, 0.19 mmol) in 2 mL of anhydrous dichloromethane was slowly added to the hydroxyl lipid derivative of DPPC (0.40 g, 0.578 mmol)/anhydrous dichloromethane (5 mL) suspension under the experimental conditions described by Singh and Marchywka (17). After column purification, the crude material was recrystallized by acetone precipitation to produce pale white crystals (10% yield, 44.0 mg).

Trimethylsilyl bromide was used as an alternative method to brominate the hydroxyl lipid derivative. Trimethylsilyl bromide (1.32 g, 8.62 mmol) was added directly to the hydroxyl lipid derivative of DPPC (3.0 g, 4.34 mmol) in 20 mL of anhydrous chloroform. The reaction was allowed to proceed at 55 °C under nitrogen, as described by Jung et al. (18). After column purification, the crude crystals were recrystallized by acetone precipitation to give pale white crystals (20% yield, 0.655 g): R_f (chloroform/methanol/water, 65:25:4, v/v) 0.60; IR (film, cm^{-1}) 3000–2850, 1740, 1470, 1250, 1150–1050, 720; mass spectrum (CI, isobutane) m/e = 335, 409, 471, 647, 753.

Attachment of the Galactose Linker to the Brominated Phospholipid Derivative. The brominated lipid derivative of DPPC (3.0 g, 3.97 mmol) was dissolved in 30 mL of anhydrous dimethylformamide with gentle heating. The sugar-11-(dimethylamino)-3,6,9-trioxaundecanol complex (2.19 g, 3.97 mmol) was dissolved in anhydrous dimethylformamide and added directly to the lipid mixture. The material was sealed and placed in a 60 °C oven for 7 days. Reactions were performed without anhydrous solvents but were unsuccessful in producing the quaternary compound. The mixture was purified over a silica gel column and the solvent was removed under reduced pressure, which caused crystallization of a light brown solid. The solid was re-

crystallized by acetone precipitation to give beige crystals (84% yield, 4.08 g): R_f (chloroform/methanol/water, 65:25:4, v/v) 0.64; IR (film, cm^{-1}) 3500–3200, 3000–2850, 1735, 1650, 1475, 1375, 1250, 1150–1050.

The acetylated glycolipid (4.112 g, 3.35 mmol) was dissolved in ethanol/tetrahydrofuran (1:1, v/v) (33 mL of solvent mixture/g of glycolipid) with gentle heating. The warm suspension of glycolipid was subjected to an Ag1-X2 exchange resin in ethanol (16 mL/glycolipid), the method described by Chabala and Shen (19). After the solvent was removed under reduced pressure, the crude deacetylated glycolipid was recrystallized by acetone precipitation to give light beige crystals (10% yield, 0.345 g): R_f (chloroform/methanol/water, 65:25:4, v/v) 0.14; IR (film, cm^{-1}) 3400–3200, 3000–2850, 1740, 1560, 1475, 1440, 1150–1050.

Differential Scanning Calorimetry. DPPC was dissolved in chloroform at the concentration of 25 mg/mL. The glycolipid containing the sterol derivatives TEC-GAL and TEC-MAL was taken up in chloroform at a concentration of 25 mg/mL. The glycolipid containing the lipid derivative DP-GAL was dissolved in methanol/water (2:1, v/v) at a concentration of 25 mg/mL. Samples were prepared by codrying the individual solutes with DPPC at specific molar percentages as thin films into previously weighed stainless steel pans under nitrogen on a hot plate. Before deposition, methanol and water were added to ensure complete solubility of all material of the desired samples. Approximately 3 mg of each suspension containing the varying mole percentages of solute were dispensed into the stainless steel pans. To ensure complete evaporation of solvents, the pans were then placed in a vacuum oven at room temperature under nitrogen overnight or until use. Each pan was sealed and weighed prior to scanning. The calorimetric scans were run at 2 °C/min. Duplicate scans were run for the samples. Enthalpies and transition temperatures were calculated, normalized (to the mass of DPPC present), and calibrated using multilamellar vesicles of DPPC. Determination of the percentage of water was performed by the Karl Fischer titration on DPPC samples containing TEC-GAL and TEC-MAL. Aliquots of stock solutions of DPPC, TEC-GAL, and TEC-MAL (as described above) were mixed at specific molar concentrations. These samples were codried as thin films under nitrogen and desiccated until use. The DPPC/TEC-GAL and DPPC/TEC-MAL mixtures were taken up in 100 μL of chloroform and chloroform/methanol (1:2, v/v), respectively, at the total concentration of 75 mg/mL. The DPPC samples were taken up in 100 μL of both solvent mixtures at the identical concentration for background comparison. Titrations were performed in triplicate using 10 μL for each run. A solvent background was subtracted from the samples containing the appropriate solvent.

Fourier Transform Infrared Spectroscopy. DPPC, DPPC- d_{62} , TEC-GAL, and TEC-MAL were each suspended in chloroform in a concentration of 25 mg/mL, as described in the calorimetry section. The DP-GAL was also suspended in methanol/water (2:1, v/v) at a concentration of 25 mg/mL. The glycolipids were individually aliquoted at specific mole percentages with DPPC or DPPC- d_{62} . Methanol and water were added to desired samples to ensure complete solubility of all material. The mixtures were codried and deposited as thin films on silver chloride, KRS-5, or calcium fluoride windows under nitrogen. Approximately 1–2 mg of each sample was deposited. For complete evaporation of solvents, the samples were placed in a vacuum oven at room temper-

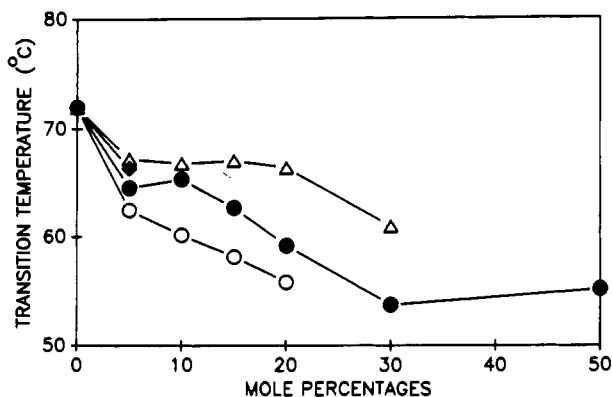


Figure 3. Calorimetric effects of increasing mole percents of glycolipid on the phase transition of dry DPPC; scan rate, 2 °C/min: ○, TEC-GAL; ●, TEC-MAL; △, DP-GAL; ◆, cholesterol.

Table I. Enthalpic Changes in the Calorimetric Transition of Dry Mixtures of Cryoprotectant Glycolipids with DPPC

mol % glycolipid	ΔH , J/g		
	TEC-GAL	TEC-MAL	DP-GAL
0	43.71	43.71	43.71
5	24.31	34.58	27.62
10	26.86	19.72	25.07
15	26.28	13.43	23.77
20	19.73	16.10	21.82
30		12.09	15.33
50		7.49	

ature overnight or until use. The windows were placed in a thermostated, water-jacketed cell mount controlled by a RTE-110 programmable water bath (Neslab Instruments, Inc., Newington, NH). The temperature was monitored by a thermocouple attached to the windows. The spectra (4000–450 cm^{-1}) were collected through the temperature range of 25–80 °C at 2 °C intervals (scan rate of 1 °C/min) over the transition temperature region. The data were analyzed after baseline corrections of specific regions, with frequencies and bandwidths (at half-absorbance) determined using a center of gravity algorithm (20, 21).

Mass Spectroscopy. Mass spectra were determined by two techniques, fast atom bombardment (FAB) and desorption chemical ionization (CI) mass spectrometry. FAB mass spectrometry involved mixing the sample with a viscous matrix such as sodium iodide in the presence of glycerol and applying the sample directly to the tip of a copper probe.

In the desorption chemical ionization process, the sample was coated on a copper wire and subjected to a chemical ionization reagent gas such as isobutane or ammonia. An electrical current was applied to the tip of the copper wire containing the sample, rapidly increasing the temperature, favoring desorption over decomposition. The desorbed molecules were protonated by the selected reagent gases.

RESULTS

The phase behavior of most biological lipids is dramatically influenced by the degree of hydration, due to their amphiphilic nature (22–26). The DSC scans of dry DPPC films in the present study resulted in a transition temperature of 71.2 °C, which suggests that this lipid is in a dihydrate form (24, 27, 28). Melting scans of dry DPPC films codried with TEC-GAL, TEC-MAL, and DP-GAL revealed a decrease in the main chain melting transition temperature (max C_p) with increasing mole percent of glycolipid (Figure 3). The largest decrease is observed with TEC-MAL at 30 mol % or greater where

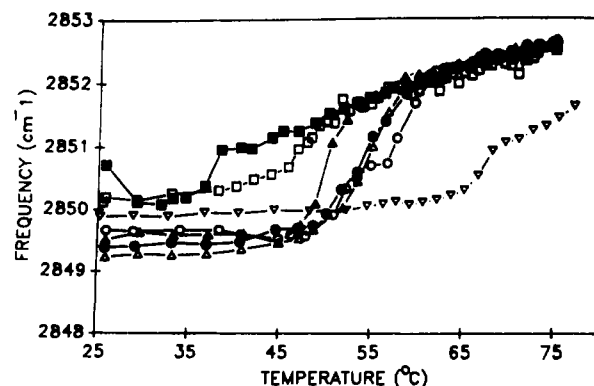


Figure 4. The effect of the temperature-dependent frequency of the CH_2 symmetric stretching vibration of DPPC containing increasing mole percents of TEC-GAL: ○, 5%; ●, 10%; △, 15%; ▲, 20%; □, 30%; ■, 50%; ▽, dry DPPC.

the transition temperature is reduced almost 20 °C from the transition temperature of the pure DPPC dihydrate. TEC-GAL showed nearly the same decrease in transition temperature (an approximate 18 °C reduction in transition temperature at 20 mol %), while DP-GAL at 30 mol % showed a 10 °C reduction in transition temperature. The phase transition of the glycolipid/DPPC systems also showed a decrease in enthalpy (ΔH) with increasing mole percentage of glycolipid (Table I). The observed reduction in the enthalpy of these films correlates with an increase in the transition width and thus reflects reduced cooperativity of the transition. The enthalpy of the dry DPPC film transition, 43.71 J/g, agrees with previous measurements for the melting of the dihydrate form (24, 25, 27, 28). TEC-GAL showed the greatest reduction in enthalpy at 5 mol %, with almost a 20 J/g reduction in the enthalpy of the transition. At higher mole percentages of glycolipid, the enthalpy was further reduced (19.73 J/g at 20 mol % for TEC-GAL, 7.49 J/g at 50 mol % for TEC-MAL, and 15.33 J/g at 30 mol % DP-GAL). Calorimetric scans of the pure glycolipids TEC-GAL, TEC-MAL, and DP-GAL did not show a cooperative phase transition at the sensitivity of the calorimeter in either the dry or hydrated state when tested through the same calorimetric temperature range.

We have contrasted the affects of TEC-GAL, TEC-MAL, and DP-GAL with the calorimetric effect of increasing cholesterol in films codried with DPPC. A cooperative phase transition in the films was not observed after 5 mol % (Figure 3). This concentration of cholesterol is far below the concentration required to inhibit the gel to liquid-crystalline phase transition of DPPC in excess water.

Infrared spectroscopy has been used to monitor vibrational modes which are sensitive to the changes in the phase behavior of the two-component dry films. The frequency in the CH_2 symmetric stretch of dry cast films of DPPC dihydrate shows a 1.4- cm^{-1} increase in frequency over the temperature range in which the calorimetric transition is observed (approximately 63 to 77 °C) (Figure 4). The change in frequency observed in cast films of dry DPPC with increasing TEC-GAL begins at lower temperatures and occurs over a broader temperature range. For example, increasing the mole percentage of TEC-GAL to 30 mol % results in an observed change in the CH_2 symmetric stretch frequency, which begins at 45 °C, compared to that of DPPC alone, which occurs at 65 °C. At lower TEC-GAL concentrations (5 and 10 mol %), the DPPC CH_2 symmetric stretch of the dry films occurs over a narrower temperature range (47 to 57 °C). Above the phase transition temperature, at all concentrations of TEC-

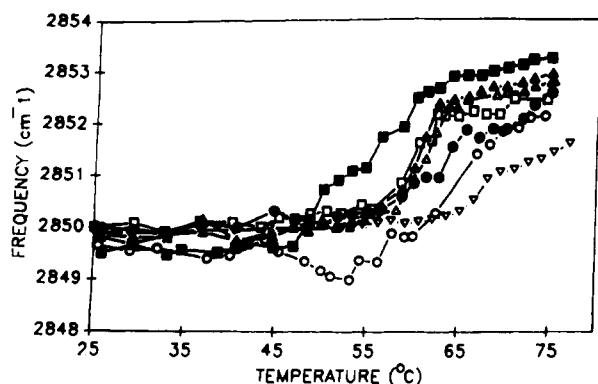


Figure 5. The effect on the temperature-dependent frequency of the CH_2 symmetric stretching vibration of DPPC containing increasing mole percents of TEC-MAL: \circ , 5%; \bullet , 10%; \blacktriangle , 15%; \triangle , 20%; \square , 30%; \blacksquare , 50%; ∇ , dry DPPC.

GAL examined the CH_2 symmetric stretch is observed to be greater than the frequency observed in the pure DPPC films. In addition, above the phase transition, there is a slight increase (2 cm^{-1}) in frequency with increasing temperature in the DPPC and TEC-GAL/DPPC mixtures. The infrared spectra of dry DPPC containing increasing mole percent of TEC-MAL also show a decrease in the temperature over which the change in CH_2 symmetric is observed (Figure 5). The observed reduction is not as marked as is observed with TEC-GAL, which correlates with the calorimetric observation. Similar to TEC-GAL/DPPC films, the TEC-MAL/DPPC films also show an increase in frequency above the phase transition, although in the TEC-MAL films this increase appears to be linearly related to the TEC-MAL concentration, with the maximal effect observed at 50 mol % TEC-MAL.

To study spectroscopically the effect of DP-GAL on the phase behavior of DPPC, we have used $\text{DPPC-}d_{62}$ in the two-component system of DP-GAL/DPPC to monitor the acyl chain regions of the two individual components of the dry film. The CD_2 symmetric stretch of the $\text{DPPC-}d_{62}$ cast films increased 4.5 cm^{-1} (from 2089 to 2093.5 cm^{-1}) over the temperature range of $54\text{--}63.5\text{ }^\circ\text{C}$ (Figure 6A). This temperature range is much reduced compared to that of the perhydro-DPPC film. The CD_2 symmetric stretch frequency above the transition temperature is increased compared to that of the pure $\text{DPPC-}d_{62}$ films, similar to the effect observed with the TEC-GAL/DPPC and TEC-MAL/DPPC films. However, unlike TEC-GAL and TEC-MAL, the temperature over which the change in CD_2 symmetric stretch frequency is observed in the DP-GAL/DPPC- d_{62} films is not significantly altered (Figure 6B).

Changes in the CH_2 symmetric stretch of the acyl chains of DP-GAL in the DP-GAL/DPPC films show that the temperature range over which the frequency increases is reduced by $13\text{ }^\circ\text{C}$ compared to the range for DPPC alone (Figure 6B). The CH_2 symmetric stretch for the DP-GAL acyl chains is also 1.8 cm^{-1} higher (2851.8 cm^{-1}) than the CH_2 symmetric stretch for dry DPPC alone. This increase is observed throughout the entire temperature range examined. The change in frequency over the transition temperature range for the CH_2 stretch of DP-GAL through the transition is 1.8 cm^{-1} compared to 1.4 cm^{-1} for the dry DPPC film. Notably, the acyl chains of DP-GAL in the deuterated DP-GAL/DPPC show a cooperative change in the CH_2 symmetric stretch frequency despite the lack of an observable cooperative transition of DP-GAL in the DSC (Table I).

A more direct measure of the interaction of TEC-MAL, TEC-GAL, and DP-GAL with the interfacial region of

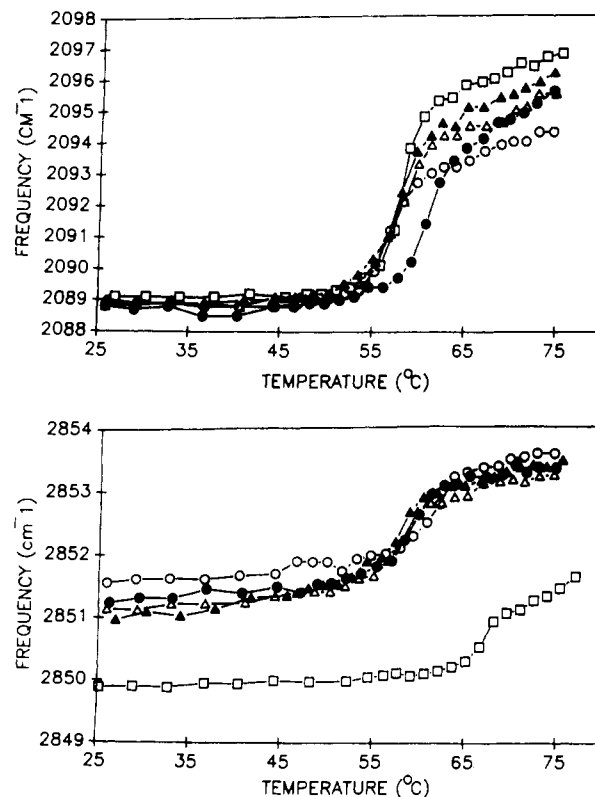


Figure 6. (A) The effect on the temperature-dependent frequency of the CD_2 symmetric stretching vibration of perdeuterated DPPC ($\text{DPPC-}d_{62}$, 1,2-dipalmitoyl- d_{62} -sn-glycerol-3-phosphocholine) containing increasing mole percents of DP-GAL: \circ , $\text{DPPC-}d_{62}$; \bullet , 10%; \blacktriangle , 20%; \triangle , 30%; \square , 50%. (B) The effect on the temperature-dependent frequency of the CH_2 symmetric stretching vibration of dry DPPC and increasing mole percents of DP-GAL in a perdeuterated DPPC system: \circ , 10%; \bullet , 20%; \blacktriangle , 30%; \triangle , 50%; \square , dry DPPC.

DPPC is seen by examining potential sites of hydrogen bonding on the DPPC surface. One such site is the phosphate moiety, which has been previously suggested as the site of action of the bulk carbohydrates in dry lipid/carbohydrate mixtures (2). Figure 7A–C shows a decrease in intensity of the asymmetric PO_2 stretch (1250 cm^{-1}) of dry DPPC with increasing mole percents of TEC-GAL, TEC-MAL, and DP-GAL. The reduction in intensity is accomplished by band broadening. In the case of DP-GAL/DPPC (Figure 7C) there is a shift in frequency of the band to 1225 cm^{-1} with smaller shifts observed for TEC-GAL and TEC-MAL. The C–O–C stretch ($1150\text{--}1000\text{ cm}^{-1}$) also shows a decrease in intensity as the mole percent of glycolipids is increased. Examination of this vibration in TEC-MAL shows an 8-cm^{-1} shift in frequency at 50 and 75 mol %, indicating significant perturbation of the glycerol backbone by the sterol group.

DISCUSSION

The mixtures of dry DPPC with TEC-GAL, TEC-MAL, and DP-GAL have been examined to elucidate the effect of these glycolipids on the phase behavior of dry DPPC. The results from the DSC data indicate miscibility of the glycolipids with DPPC in the two-component system. It has been suggested that a decrease in enthalpy associated with a decreased transition temperature is indicative of reduced cooperative interactions of the acyl chains of the lipid system (29, 30). The cooperativity of the transition in the DPPC mixtures of TEC-GAL, TEC-MAL, and DP-GAL is markedly reduced with increasing concentration of the glycolipids. Increasing mole percents of DP-GAL

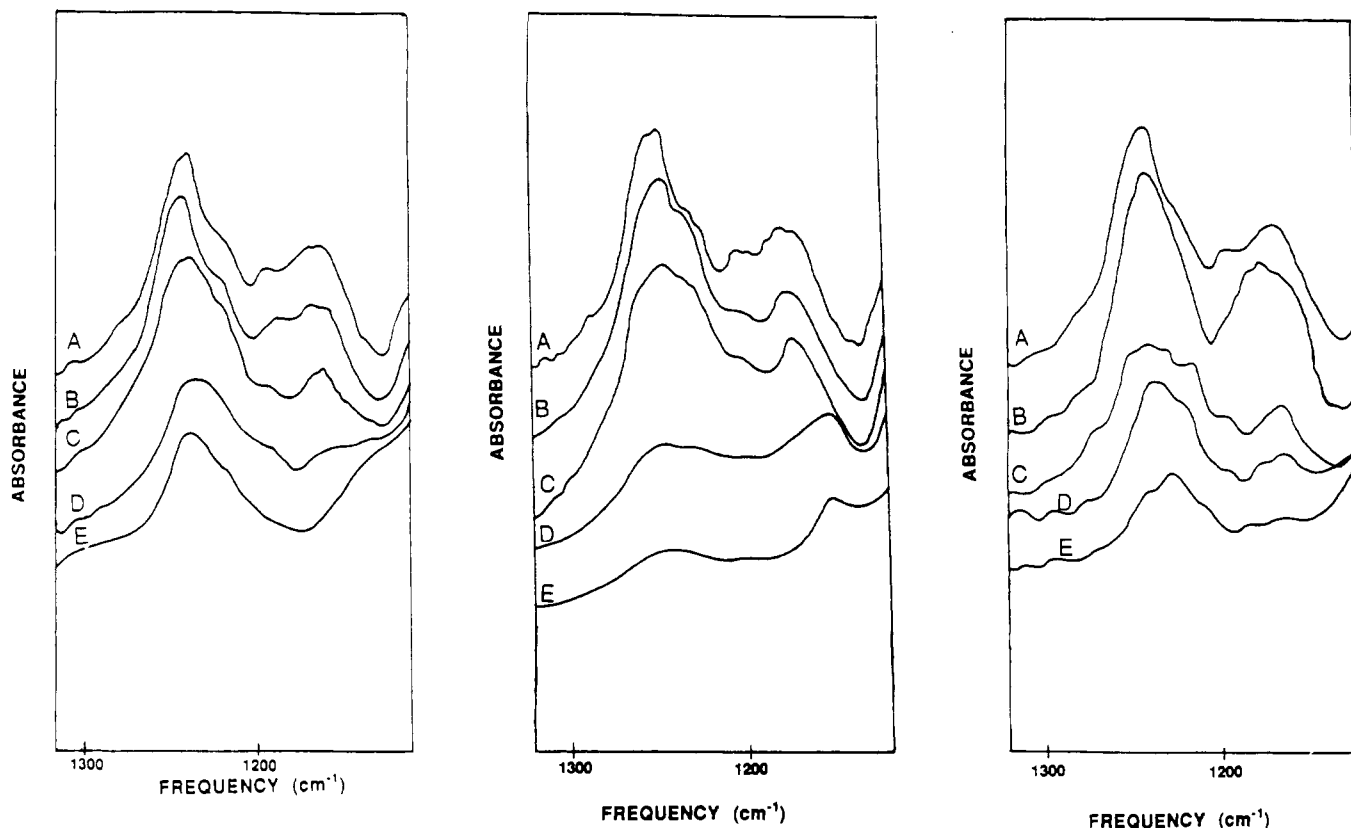


Figure 7. (A) FT-IR spectra of the asymmetric phosphate, P=O, stretch region (1250 cm^{-1}) of dry DPPC containing increasing mole percents of TEC-GAL: A, dry DPPC; B, 10 mol %; C, 20 mol %; D, 50 mol %; and E, 75 mol %. (B) FT-IR spectra of the asymmetric phosphate, P=O, stretch region (1250 cm^{-1}) of dry DPPC containing increasing mole percents of TEC-MAL: A, dry DPPC; B, 10 mol %; C, 20 mol %; D, 50 mol %; and E, 75 mol %. (C) FT-IR spectra of the asymmetric phosphate, P=O, stretch region (1250 cm^{-1}) of dry DPPC containing increasing mole percents of DP-GAL: A, dry DPPC; B, 10 mol %; C, 20 mol %; D, 50 mol %; and E, 75 mol %.

decreased the enthalpy and transition temperature (max C_p) of DPPC to a lesser degree than TEC-GAL and TEC-MAL. The observed calorimetric differences in the reduction of enthalpy and transition temperature of DP-GAL/DPPC mixtures as compared to the TEC-GAL/DPPC and TEC-MAL/DPPC mixtures suggest that acyl chains of DP-GAL may cooperatively mix with the dry DPPC film. In the case of TEC-GAL/DPPC and TEC-MAL/DPPC, the sterol moiety intercalates into the bilayers of DPPC, reducing cooperativity of the melting of the acyl chains. The further reduction of the transition temperature of TEC-GAL/DPPC and TEC-MAL/DPPC mixtures compared to that of cholesterol/DPPC may indicate that the carbohydrate moiety of TEC-GAL and TEC-MAL may interact directly with the interfacial region of DPPC, enhancing the effect observed with the sterol alone.

At low water concentration, some lipids exhibit highly ordered phases (23–25). For DPPC, the acyl chains become rigid, with a specific angle of tilt, and appear to be packed with some degree of rotational disorder (24). The addition of bulk water results in an increase in the surface area between phosphate head groups, decreasing the packing density of the hydrocarbon chains and decreasing the van der Waals attractions. Consequently, the transition temperature from the gel to liquid-crystalline phase decreases. Bulk carbohydrates have also been shown with calorimetry and FTIR to reduce the phase transition of dry DPPC (1, 2). Studies with X-ray diffraction and solid-state NMR (8, 9) reveal that the acyl chains of DPPC/carbohydrate mixtures are disordered in the dry state, although there may be some restriction of acyl chain rotational motion. This has led to the designation of a new liquid-crystalline

phase, L_k (8, 9). For example, previous studies have shown that at 0.45 g of trehalose/g of DPPC, a 1:1 molar ratio, the phase temperature of dry DPPC resembles the transition temperature of fully hydrated DPPC (1, 31). Further reduction in T_m was observed when DPPC was lyophilized from a liquid-crystalline phase at 2.5:1 mole ratio of trehalose:DPPC (6). The depression of the phase transition has been attributed to the hydrogen bonding of the disaccharide hydroxyl groups to the interfacial region of DPPC membranes, increasing the molecular area between phosphate head groups (1, 4). At the highest concentrations of TEC-MAL and TEC-GAL, a significant reduction in the transition temperature (approaching the hydrated transition temperature) was also observed.

Changes in the CH_2 stretch of the acyl chains of DPPC are indicative of changes in the *trans*/*gauche* conformers of the acyl chains. The increased frequency of the CH_2 symmetric stretch as the temperature increases through the main chain melting temperature is indicative of increased *gauche* conformers. The partitioning of cholesterol in hydrated DPPC has been shown to increase the average number of *gauche* conformers (with an increase in the CH_2 stretch frequency) in hydrocarbon chains in the gel phase and to decrease them in the liquid-crystalline phase (29, 32–35). For mixtures of TEC-GAL/DPPC and TEC-MAL/DPPC, the temperature range over which additional *gauche* conformers are observed is increased, in agreement with the calorimetric observation of reduced cooperativity and transition temperature. The CH_2 symmetric stretch frequency in the low-temperature phase of the dry mixtures of both TEC-GAL and TEC-MAL was not significantly different from that of DPPC alone. Above the phase transition, however, there was a concentration-

dependent increase in the frequency, indicating a larger number of gauche conformers and thus disorder in the high-temperature phase. We currently do not know how this effect is mediated, although future experiments will be aimed at determining the effect of different linker lengths and their mobility in the high temperature phase. These results agree with previous measurements of 30% TEC-MAL incorporated into dry DPPC bilayers which showed a similar increase in the CH₂ asymmetric stretch at a reduced T_m compared to DPPC alone (11).

The FT-IR spectra of the asymmetric phosphate stretch shows band broadening and a decrease in intensity as the mole percentage of the glycolipids in dry DPPC is increased (Figure 7A-C). In addition, the frequency of this band shifts slightly to lower frequency. This effect is suggestive that the dielectric environment around the phosphate moiety is changed and could result from the hydrogen bonding of carbohydrate moieties of the glycolipids to the interfacial region of the bilayer. Alternatively, the tetraethoxy linkage could significantly change the dielectric environment of the phosphate. The changes observed in the phosphate infrared spectra of mixtures of TEC-GAL, TEC-MAL, and DP-GAL are consistent with previous measurements of 30% TEC-MAL/DPPC, which showed a shift to lower frequency when compared to measurements of dry DPPC alone (11). Raman spectra of the C-N asymmetric stretch were also consistent with an expanded interfacial region (11).

One advantage to constructing lipids with cryoprotectant moieties may be the localization of the cryoprotectant moiety at the surface of the lipid surface. Thus, one might suppose that the concentration of carbohydrate required to mediate these effects may be less than that required for bulk carbohydrate action. For example, the optimal concentration of TEC-MAL found to reduce the phase-transition temperature of dry DPPC was approximately 50 mol %. The mole percentage of maltose per mole of lipid is 44.4 mol %. The mole percent of trehalose which lowered the phase-transition temperature of dry DPPC dihydrate to that of the hydrated DPPC was 87.3 mol % (1). Further reduction in the transition temperature was reached with anhydrous DPPC at somewhat lower mole ratios of trehalose (6). The additional bulk carbohydrates required to preserve membranes may be related to the need to form a glass. This may also be why the glycolipids do not show a reduction of the transition temperature down to the hydrated transition as do the bulk carbohydrates. Future experiments will be aimed at determining whether these glycolipids can form two-dimensional glasses at the membrane surface.

In addition, as the carbohydrates are known to be hygroscopic, we have measured residual moisture of the dry mixtures to examine whether the observed effects were based on differential water retention. The results indicate that the mixtures do not significantly differ in percent water to percent lipid (approximately 3%) as compared to DPPC alone (data not shown). This is supported by previous measurements of the residual water content of dry liposomes preserved with bulk trehalose which demonstrate that the productive effect of the bulk sugar does not require retention of residual water (36).

In summary, we have demonstrated the synthesis of three glycolipids that have cryoprotective carbohydrate moieties attached by a tetraethoxy linkage to either cholesterol or DPPC. Dry mixtures of DPPC and the glycolipids show some of the same effects as bulk carbohydrates in their calorimetric and spectroscopic effects. The utility of synthesizing new cryoprotectant groups may be

the controlled localization of the cryoprotectant at a fixed distance from the interfacial region of the lipid surface. Amphiphilic cryoprotectants such as these may also be easier to incorporate into membrane systems, imparting protection from freezing or desiccation.

ACKNOWLEDGMENT

We gratefully acknowledge the support of the Office of Naval Research through its CORE funds in conjunction with the Naval Research Laboratory. We thank Dr. Barry Spargo, Dr. Alok Singh, and Dr. Beth Goins for their technical advice and helpful discussions and John Callahan for acquisition and analysis of the mass spectra.

LITERATURE CITED

- (1) Crowe, L. M., Crowe, J. H., and Chapman, D. (1985) Interaction of Carbohydrates with Dry Dipalmitoylphosphatidylcholine. *Arch. Biochem. Biophys.* 236, 289-296.
- (2) Crowe, J. H., Crowe, L. M., and Chapman, D. (1984) Infrared spectroscopic Studies on Interactions of Water and Carbohydrates with a Biological Membrane. *Arch. Biochem. Biophys.* 232, 400-407.
- (3) Rudolph, A. S., and Crowe, J. H. (1985) Membrane Stabilization during Freezing: The Role of Two Natural Cryoprotectants, Trehalose and Proline. *Cryobiology* 22, 367-377.
- (4) Crowe, J. H., Crowe, L. M., Carpenter, J. F., Rudolph, A. S., Wistrom, C. A., Spargo, B. J., and Anchordoguy, T. J. (1988) Interactions of Sugars with Membranes. *Biochem. Biophys. Acta* 947, 367-384.
- (5) Crowe, L. M., Crowe, J. H., Rudolph, A. S., Womersley, C., and Appel, L. (1985) Preservation of Freeze-Dried Liposomes by Trehalose. *Arch. Biochem. Biophys.* 242, 240-247.
- (6) Crowe, L. M., and Crowe, J. H. (1988) Trehalose and dry dipalmitoylphosphatidylcholine revisited. *Biochem. Biophys. Acta* 946, 193-201.
- (7) Tsvetkova, N., Tenchov, B., Tsonev, L., and Tsvetkov, T. (1988) The Effect of Trehalose on Membrane Phospholipids Depends on the Initial Phase from Which Drying Occurs. *Cryobiology* 25, 256-263.
- (8) Lee, C. W. B., Waugh, J. S., and Griffin, R. G. (1986) Solid-State NMR Study of Trehalose/1,2-Dipalmitoyl-sn-phosphatidylcholine Interactions. *Biochemistry* 25, 3737-3742.
- (9) Lee, C. W. B., Das Gupta, S. K., Mittai, J., Shipley, G. G., Abdel-Mageed, O. H., Makriyannis, A., and Griffin, R. G. (1989) Characterization of the L Phase in Trehalose-Stabilized Dry Membranes by Solid-State NMR and X-ray Diffraction. *Biochemistry* 28, 5000-5009.
- (10) Goodrich, R. P., Handel, T. M., and Baldeschwieler, J. D. (1988) Modification of Lipid Phase Behavior with Membrane-Bound Cryoprotectants. *Biochim. Biophys. Acta* 938, 143-154.
- (11) Goodrich, R. P., Crowe, J. H., Crowe, L. M., and Baldeschwieler, J. D. (1991) Alterations in Membrane Surfaces Induced by Attachment of Carbohydrates. *Biochemistry* 30, 5313-5318.
- (12) Goodrich, R. P., and Baldeschwieler, J. D. (1991) The Cryoprotective Action of Synthetic Glycolipids. *Cryobiology* 28, 327-334.
- (13) Patel, K. R., Li, M. P., Schuh, J. R., and Baldeschwieler, J. D. (1984) The Pharmacological Efficacy of a Rigid Non-Phospholipid Liposome Drug Delivery System. *Biochim. Biophys. Acta* 797, 20-26.
- (14) Eibl, H., and Kovatchen, S. (1981) Preparation of Phospholipids and Their Analogs by Phospholipase D. *Methods Enzymol.* 72, 632-639.
- (15) Lowery, O. H., Rosebrough, N. J., Farr, A. L., and Randall, R. J. (1951) Protein Measurement with the Folin Phenol Reagent. *J. Bio. Chem.* 193, 265-275.
- (16) Yang, S. F., Freer, S., and Benson, A. A. (1967) Transphosphatidylolation by Phospholipase D. *J. Bio. Chem.* 242, 477-484.

- (17) Singh, A., and Marchywka, S. (1989) Synthesis and Characterization of Headgroup Modified 1,3 Diacetylenic Phospholipids. *Polym. Mater. Sci. Eng.* 61, 675-678.
- (18) Jung, M. E., and Hatfield, G. L. (1978) Preparation of Bromides from Alcohols via Treatment with Trimethylsilyl Bromide. *Tetrahedron Lett.* 46, 4483-4486.
- (19) Chabala, J., and Shen, T. Y. (1978) The Preparation of 3-Cholesteryl 6-(Glycosylthio)hexyl Ethers and Their Incorporation into Liposomes. *Carbohydr. Res.* 67, 55-63.
- (20) Kauppinen, J. K., Moffatt, D. J., Cameron, D. G., and Mantsch, H. H. (1981) Noise in Fourier Self-Deconvolution. *Appl. Opt.* 20, No. 10, 1866-1879.
- (21) Kauppinen, J. K., Moffatt, D. J., Mantsch, H. H., and Cameron, D. G. (1981) Fourier Self-Deconvolution: A Method for Resolving Intrinsically Overlapped Bands. *Appl. Spectrosc.* 65, No. 3, 271-276.
- (22) Small, D. M. (1986) *Handbook of Lipid Research: The Physical Chemistry of Lipids* (D. J. Hanahan, Ed.) Chapter 12, pp 475-485, Plenum Press Corp., New York.
- (23) Luzzati, V., and Tardieu, A. (1974) Lipid Phases: Structure and Structural Transitions. *Annu. Rev. Phys. Chem.* 25, 79-94.
- (24) Tardieu, A., Luzzati, V., and Reman, F. C. (1973) Structure and Polymorphism of the Hydrocarbon Chains of Lipids: A Study of Lecithin-Water Phases. *J. Mol. Biol.* 75, 711-733.
- (25) Chapman, D. (1983) Physicochemical Properties of Phospholipids and Lipid-Water Systems. *Liposome Technology* (G. Gregoriadis, Ed.) Chapter 1, Vol. 1, pp 1-18, CRC, Boca Raton, FL.
- (26) Hauser, H., Pascher, I., Pearson, R. H., and Sundell, S. (1981) Preferred Conformation and Molecular Packing of Phosphatidylethanolamine and Phosphatidylcholine. *Biochim. Biophys. Acta* 650, 21-51.
- (27) Fringeli, U. P. (1981) A New Crystalline Phase of L- α -Dipalmitoylphosphatidylcholine Monohydrate. *Biophys. J.* 34, 173-187.
- (28) Phillips, M. C., Williams, R. M., and Chapman, D. (1969) On the Nature of Hydrocarbon Chain Motions in Lipid Liquid Crystals. *Chem. Phys. Lipids* 3, 234-244.
- (29) Brauner, J. N., and Mendelsohn, R. (1986) A Comparison of Differential Scanning Calorimetric and Fourier Transform Infrared Spectroscopic Determination of Mixing Behavior in Binary Phospholipid Systems. *Biochim. Biophys. Acta* 861, 16-24.
- (30) Mabrey, S., Mateo, P. L., and Sturtevant, J. M. (1978) High-Sensitivity Scanning Calorimetric Study of Mixtures of Cholesterol with Dimyristoyl- and Dipalmitoylphosphatidylcholines. *Biochemistry* 17, 2464-2468.
- (31) Tsvetkov, T. D., Tsonev, L. I., Tsvetkova, N. M., Koynova, R. D., and Tenchov, B. G. (1989) Effect of Trehalose on the Phase Properties of Hydrated and Lyophilized Dipalmitoylphosphatidylcholine Multilayers. *Cryobiology* 26, 162-169.
- (32) Umemura, J., Cameron, D. G., and Mantsch, H. M. (1980) A Fourier Transform Infrared Spectroscopic Study of the Molecular Interaction of Cholesterol with 1,2-Dipalmitoyl-sn-glycerol-3-phosphocholine. *Biochim. Biophys. Acta* 602, 32-44.
- (33) Gennis, R. B. (1989) *Biomembranes: Molecular Structure and Function* (C. R. Cantor, Ed.) Chapters 2 and 5, pp 36-84 and 166-198, Springer-Verlag New York, Inc., New York.
- (34) Casal, H. L., and Mantsch, H. H. (1984) Polymorphic Phase Behaviour of Phospholipid Membranes Studied by Infrared Spectroscopy. *Biochim. Biophys. Acta* 779, 381-401.
- (35) Davies, M. A., Schuster, H. F., Brauner, J. W., and Mendelsohn, R. (1990) Effects of Cholesterol on Conformational Disorder in Dipalmitoylphosphatidylcholine Bilayers. A Quantitative IR Study of the Depth Dependence. *Biochemistry* 29, 4368-4373.
- (36) Crowe, J. H., Spargo, B. J., and Crowe, L. M. (1987) Preservation of Dry Liposomes Does Not Require Retention of Residual Water. *Proc. Natl. Acad. Sci. U.S.A.* 84, 1537-1540.

Coupling of DTPA to Proteins: A Critical Analysis of the Cyclic Dianhydride Method in the Case of Insulin Modification¹

Federico Maisano, Luigia Gozzini,* and Christoph de Haën

Research and Development Division, Bracco S.p.A, Via E. Folli, 50, 20134 Milan, Italy. Received November 19, 1991

The reaction between the cyclic dianhydride of diethylenetriaminepentaacetic acid (DTPA), a bifunctional reagent, and proteins under various conditions was studied using porcine insulin as a model protein. The reaction was compared with that between citraconic anhydride, a monofunctional reagent, and insulin. Products were characterized chromatographically and electrophoretically before and after deesterification by hydroxylamine. A DTPA-conjugated product was further characterized by proteolytic fragmentation. The reaction with citraconic anhydride yielded the expected number of products exclusively acylated on amino groups. In contrast, the reaction with the cyclic dianhydride of DTPA under all conditions examined yielded a much higher number of products than expected. Among the products formed were O-acylated ones and products of intermolecular cross-linking. It is concluded that the use of the cyclic dianhydride of DTPA does not allow the reliable preparation of proteins or other macromolecules conjugated with a high number of DTPA molecules in which each molecule of DTPA is linked to one amino group of the macromolecule through a single amide bond.

INTRODUCTION

The chemical modification of proteins with chelating agents has been studied mainly in the context of the preparation of antibody-based radiopharmaceuticals (Meares & Wensel, 1984). A low stoichiometric ratio of chelator to protein is usually satisfactory for this purpose. Recently, chelators were attached to proteins (Lauffer & Brady, 1985; Ogan et al., 1987) and to other polymers such as polylysine (Deutsch et al., 1989) and polysaccharides (Jacobsen, 1986) in order to obtain macromolecular paramagnetic metal ion complexes as contrast agents for magnetic resonance imaging. For this, a high stoichiometric ratio of chelator to macromolecule is required.

The reagent most commonly used for the covalent modification of proteins with a chelating agent is the cyclic dianhydride of DTPA² (*N,N*-bis[2-(2,6-dioxo-4-morpholinyl)ethyl]glycine) (Hnatowich et al., 1983b; Lauffer & Brady, 1985; Ogan et al., 1987). Although the reagent contains two reactive sites, which create the potential for undesirable cross-linking reactions (Hnatowich et al., 1983a; Paik et al., 1989), products sufficiently defined for nuclear medicine applications have been obtained. However, when the DTPA dianhydride was employed in the extensive modification of serum albumin for magnetic resonance imaging (Lauffer & Brady, 1985; Ogan et al., 1987), the complexity of the products precluded a detailed characterization of the chemistry that had taken place.

In order to gain more insight into the complexity of the reaction and detect possible unwanted reaction products, the extensive modification of insulin with DTPA dianhydride was studied. In particular, we intended to investigate whether hydrolysis of the anhydride function competed with aminolysis to such an extent that cross-linking reactions would become negligible. Moreover, we

wanted to clarify whether the reaction enabled the selective modification of amino groups without the concomitant modification of tyrosine hydroxyl groups.

Insulin was chosen as a model protein first because it has only three amino groups (one lysine side chain and two α amino groups), so that the number of distinct reaction products is limited, and second because it contains four tyrosine residues that potentially compete with amino groups for the reagent. Moreover, insulin lends itself to convenient enzymatic fragmentation, which, in turn, facilitates the characterization of the chemical modification sites. Finally, a vast experience in the chemical modification of this molecule is available.

The reaction between insulin and DTPA dianhydride was compared with the reaction between insulin and citraconic anhydride both under moderate and high anhydride concentrations. Citraconic anhydride, a monofunctional anhydride, was chosen in place of DTPA monoanhydride, since a convincing preparation of the latter is not yet available.³ Moreover, the products of partial citraconylation of insulin were studied in detail and no unpredicted side reactions were reported (Naithani & Gattner, 1982).

EXPERIMENTAL PROCEDURES

Insulin Modification. The reaction between insulin (porcine insulin, sodium salt, Calbiochem) and DTPA dianhydride (Aldrich) was performed as follows: about 20 mg of insulin was dissolved in 2 mL of 1 M $H_3BO_3/NaOH$ at pH 8.5. The exact insulin concentration was determined by reading the absorbance at 277.5 nm ($\epsilon = 5530 \text{ M}^{-1} \text{ cm}^{-1}$; Harrison & Garrat, 1969). Dry DTPA dianhydride corresponding to the desired molar ratio was dissolved at a concentration of 9% (w/v) at 40 °C in dimethyl sulfoxide that had been dried over 4-Å molecular sieves (E. Merck). At intervals of 3 min, the dianhydride solution was added in five portions to the stirred insulin solution while an automatic titroprocessor maintained the pH at the value of 8.5 with 2 M NaOH. The temperature was held constant

* To whom correspondence should be addressed at Biochemistry Dept., Research and Development Division, Bracco S.p.A., Via E. Folli, 50, 20134 Milan, Italy.

¹ Part of this work has been presented at the Jerker Porath 70 Symposium, June 16-19, 1991, Uppsala, Sweden.

² Abbreviations used: DTPA, diethylenetriaminepentaacetic acid; SDS, sodium dodecylsulfate; PAGE, polyacrylamide gel electrophoresis; Na_2EDTA , ethylenediaminetetraacetic acid disodium salt; HPLC, high performance liquid chromatography.

³ In our hands, the synthesis of DTPA anhydride outlined by Halpern et al. (1983) did not yield appreciable amounts of monoanhydride, as judged from NMR analysis.

by keeping the reaction vessel immersed in a water bath that was maintained at room temperature ($22 \pm 0.5^\circ\text{C}$).

The reaction with citraconic anhydride was performed according to published procedures (Naithani & Gattner, 1982), which are similar to those described above for DTPA dianhydride. The only differences were that the buffer was 0.1 M sodium tetraborate-HCl (pH 8.5) and that the anhydride was dissolved at 5% (v/v) in dry dioxane. These conditions were adopted to conform to the published procedure, while the 1 M borate buffer used in the case of DTPA dianhydride was necessary to avoid large pH fluctuations.

When indicated, the reaction mixture was subjected to a deesterification treatment with 1 M $\text{NH}_2\text{OH}\cdot\text{HCl}/\text{NaOH}$ (pH 8) for 1 h at room temperature ($22 \pm 0.5^\circ\text{C}$).

Product Purification. The crude reaction mixture was desalted on a Sephadex G-25 column ($2.2 \times 40\text{ cm}$) which was equilibrated in water and was run at 2 mL/min, at 4°C . The protein pool was lyophilized, dissolved in 1 mL of 20 mM $\text{H}_3\text{BO}_3/\text{NaOH}$ (pH 7.3) and 7 M urea (Buffer A), and loaded on a (trimethylamino)ethyl-based anion-exchange column (Fractogel EMD TMAE-650, $10 \times 150\text{ mm}$; E. Merck) that was equilibrated with buffer A. Buffer B was 50 mM $\text{H}_3\text{BO}_3/\text{NaOH}$ (pH 7.3), 7 M urea, and 0.5 M NaCl. Both buffers were made up from an 8 M urea stock solution which had been freshly deionized by passage through a mixed ion-exchange resin bed. The anion-exchange column was developed with different gradients, depending on the type and the concentration of the anhydride (see legends to the figures). The chromatography was carried out in a cold room (4°C) at a flow rate of 0.7 mL/min. The eluant absorbance was monitored at 280 nm, and 1.4-mL fractions were collected.

To further purify some protein pools obtained by anion-exchange chromatography, size-exclusion chromatography was performed on a column ($1 \times 95\text{ cm}$) of Fractogel TSK-HW 50 Superfine (E. Merck). Elution was accomplished at a 0.4 mL/min flow rate in 0.1 M triethylammonium acetate (pH 7.3), which contained 35% acetonitrile to suppress dimerization of insulin (McLeod & Wood, 1984). The fractions of interest were pooled and lyophilized.

SDS-Polyacrylamide Gel Electrophoresis. SDS-PAGE was performed on a PhastSystem (Pharmacia), using either 20% Homogeneous PhastGels or High Density PhastGels, according to the instructions of the manufacturer. The protein bands were stained with Coomassie Blue using a slight modification of the method of Schagger & von Jagow (1987) that avoids the elution of small proteins. In brief, after a fixing step (5 min in 5:4:1 methanol/water/acetic acid at 20°C), the gel was stained for 15 min at 40°C in a solution of 0.025% (w/v) Coomassie Blue G (Serva Blue G, Serva) in 10% (v/v) acetic acid. Then two destaining steps were carried out at 40°C in 10% acetic acid, for 5 and 10 min, respectively. Molecular weight markers for the 20% Homogeneous PhastGel were obtained from Bio-Rad; their molecular weights are as reported in the manufacturer's catalogue, except for bovine serum albumin, the molecular weight of which has been recently corrected (Feng et al., 1991). For the High Density PhastGel, the molecular weight markers were the CNBr fragments of horse heart myoglobin (E. Merck); their molecular weights were assigned on the basis of a recent revision (Kratzin et al., 1989).

Protein Fragmentation. Two procedures were adopted. The first procedure was a *Staphylococcus aureus* V8 protease (Pierce) digestion. It was carried out for 3 h at 37°C , using 13 μg (8 units according to the titer on the

label) of V8 protease and 25 μg of insulin or a derivative thereof, in 50 μL 0.2 M Tris-HCl (pH 7.3). The digestion was stopped by addition of HCl up to 0.1 M and incubation for 5 min at 95°C . The second procedure was a mixed enzymatic/chemical cleavage, which consisted of digestion with clostripain followed by reduction/alkylation of disulfides. Clostripain (Sigma) was activated according to the supplier's instructions and incubated with 50 μg of insulin or a derivative thereof (ratio: 2 milliunits/ μg of protein to be digested) for 135 min at 25°C in 25 μL of 50 mM phosphate buffer (pH 7.6), 7.5 mM dithiothreitol, and 0.5 mM CaCl_2 . After enzyme inactivation (5 min at 95°C), 75 μL of 0.2 M phosphate buffer pH 9, 7 M guanidinium hydrochloride, 2 mM Na_2EDTA , and 10 μL of 55 mM dithiothreitol were added. Reduction was carried out for 30 min at 37°C . Alkylation was performed by addition of 10 μL of 0.36 M iodoacetamide and incubation for 20 min at 37°C . Excess iodoacetamide was destroyed by addition of 8 μL of 0.6 M dithiothreitol and incubation for 5 min at 37°C .

Reversed-Phase HPLC. The peptide mixtures obtained by the above fragmentation procedures were cleared by centrifugation (14926g, 5 min) and directly injected (about 5 μg) into the HPLC system (Merck-Hitachi). The reversed-phase column ($4 \times 250\text{ mm}$ LiChrospher 300 RP-18, 10 μm) was eluted at 40°C with a gradient between water (A) and acetonitrile (B), both containing 0.1% (v/v) trifluoroacetic acid. The gradient was programmed as follows: from 17 to 19% B in 5 min, from 19 to 30% B in 11 min, from 30 to 45% B in 8 min, and from 45 to 55% B in 4 min. Detection was at 214 nm; the flow rate was 1 mL/min.

RESULTS AND DISCUSSION

Despite the fact that the reactions with the two anhydrides were performed under comparable conditions (pH 8.5 and anhydride to insulin molar ratio 4:1, without considering the double functionality of DTPA dianhydride), quite different chromatograms were obtained from the anion-exchange column. At least 10 major peaks were observed for the reaction with DTPA dianhydride, and these peaks indicated further heterogeneity (Figure 1a). Only five peaks were resolved in the citraconic anhydride reaction mixture (Figure 1b). In both chromatograms of Figure 1, the first peak had the same retention time as unmodified insulin. Insulin has three amino groups, yielding theoretically a maximum of eight products (including unreacted insulin), which are separable on the basis of their electrical charge. Since more species were formed with DTPA dianhydride, additional reactions must have taken place. Most likely, these were products of inter- and intramolecular cross-linking, since the two reagents used mainly differed in their functionality, one being monofunctional, the other bifunctional. The protein pools obtained by anion-exchange chromatography were analyzed using SDS-PAGE under nonreducing conditions (Figure 2). Although with this technique it is not possible to obtain molecular weight estimates of proteins with intact disulfide bridges, molecular weight markers were included for general reference and for quality control. Lane 0 shows untreated insulin. Lanes 1–10 correspond to peaks 1–10 of Figure 1a. Lanes 2 and 3 refer to two components, which were well-separated from insulin by anion-exchange chromatography and therefore represent insulin substituted by DTPA. It must be concluded that such a modification does not alter mobility under the adopted electrophoretic conditions (20% Homogeneous PhastGel). Lanes 4–10 show several protein species that have lower electrophoretic mobility than insulin. Since substitution

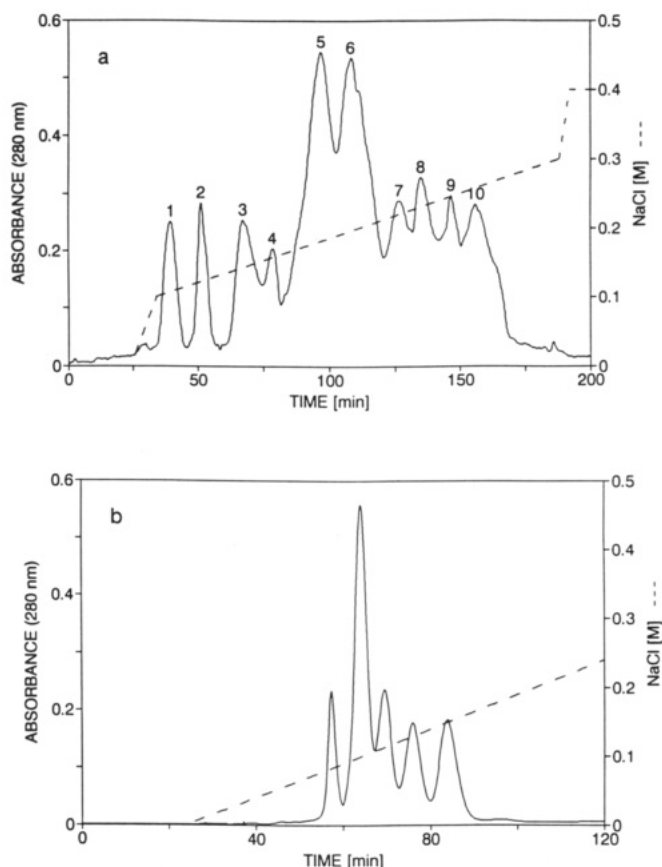


Figure 1. Anion-exchange chromatograms of insulin reacted with anhydrides. The reaction was carried out at an anhydride-to-insulin molar ratio of 4:1, at pH 8.5. The chromatographic conditions are described under Experimental Procedures: (a) reaction with DTPA dianhydride (salt gradient: from 0 to 20% B in 10 mL, then from 20 to 60% B in 100 mL, and last from 60 to 80% B in 5 mL), (b) reaction with citraconic anhydride (salt gradient from 0 to 50% B in 70 mL).

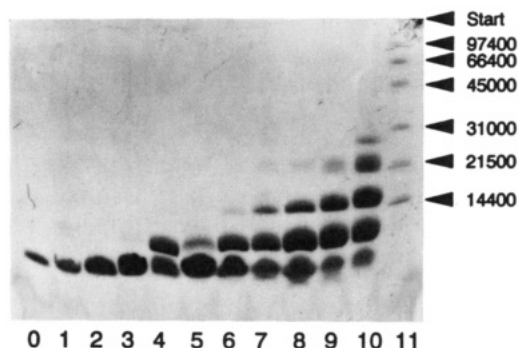


Figure 2. SDS-PAGE of unreduced protein pools obtained by anion-exchange chromatography. Electrophoresis was run on a 20% Homogeneous PhastGel. No disulfide reduction was performed except in the marker sample. Lane 0, untreated insulin, lanes 1–10 correspond to the peaks 1–10 of the chromatogram in Figure 1a; lane 11, low molecular weight markers (Bio-Rad).

by DTPA does not explain the altered mobility, these protein species must be products of intermolecular cross-linking.

The reaction with DTPA dianhydride was repeated at pH 7, a pH that should favor anhydride hydrolysis rather than coupling to amino groups and cross-linking. Even under these conditions (pH 7, molar ratio 4:1) some cross-linked species were formed as judged by SDS-PAGE (data not shown) and, due to the increased anhydride hydrolysis, about 80% of the insulin was unmodified. The reaction was repeated at the same pH using a large excess

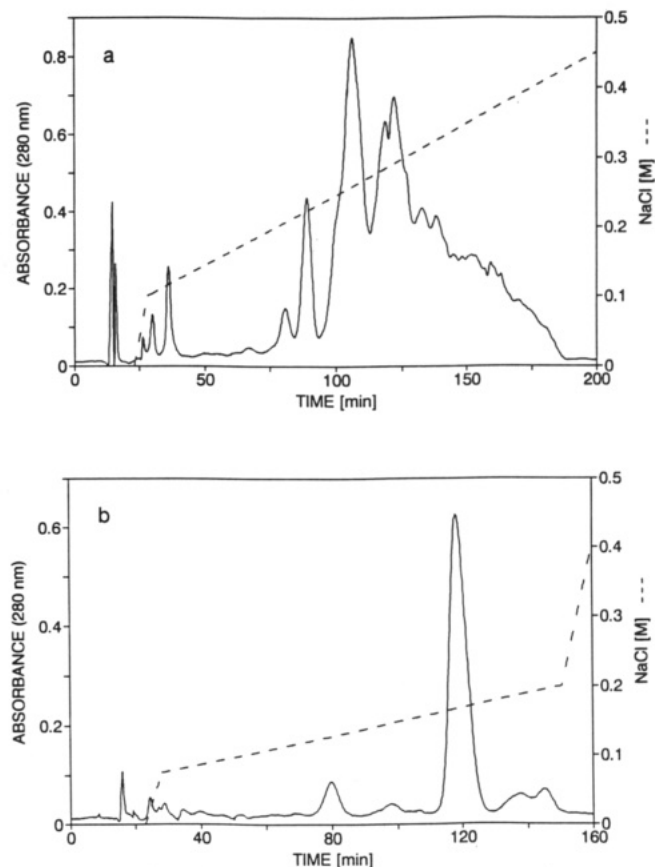


Figure 3. Anion-exchange chromatograms of insulin reacted with anhydrides. The reaction was carried out at an anhydride to insulin molar ratio of 200:1, at pH 7. The chromatographic conditions are described under Experimental Procedures: (a) reaction with DTPA dianhydride (salt gradient: from 0 to 20% B in 5 mL, then from 20 to 100% B in 160 mL), (b) reaction with citraconic anhydride (salt gradient, from 0 to 15% B in 5 mL, then from 15 to 40% B in 85 mL, and last from 40 to 100% B in 10 mL).

of the anhydride over insulin (molar ratio 200:1). In the absence of side reactions, the use of a large excess of acylating reagent should result in the formation of a main product, i.e., the trisubstituted monomeric insulin. Since negative charges are introduced with the modification, this product should be in the last eluting peak in the anion-exchange chromatography.

Under these conditions (pH 7, molar ratio 200:1), a main product was formed in the case of citraconic anhydride (Figure 3b). It was identified as tricitraconylinsulin on the basis of similarities with the product described by Naithani and Gattner (1982). Some minor peaks with higher negative charge were also observed. They were probably due to some deamidated species that are known to exist in insulin preparations (Berson and Yalow, 1966) and that might have also formed during the reaction with the large excess of the anhydride.

In contrast, the reaction with DTPA dianhydride resulted in a complex mixture of products with high negative charge (Figure 3a). This complexity can only be explained by the modification of other side-chain functional groups and/or with the occurrence of intra- and intermolecular cross-linking. Similar results were obtained at pH 8.5.

In order to assess whether tyrosine residues had been acylated even at pH 7, the reaction mixture, after desalting and lyophilization, was subjected to deesterification by hydroxylamine. This treatment reduced the number of ionic species resolved by anion-exchange chromatog-

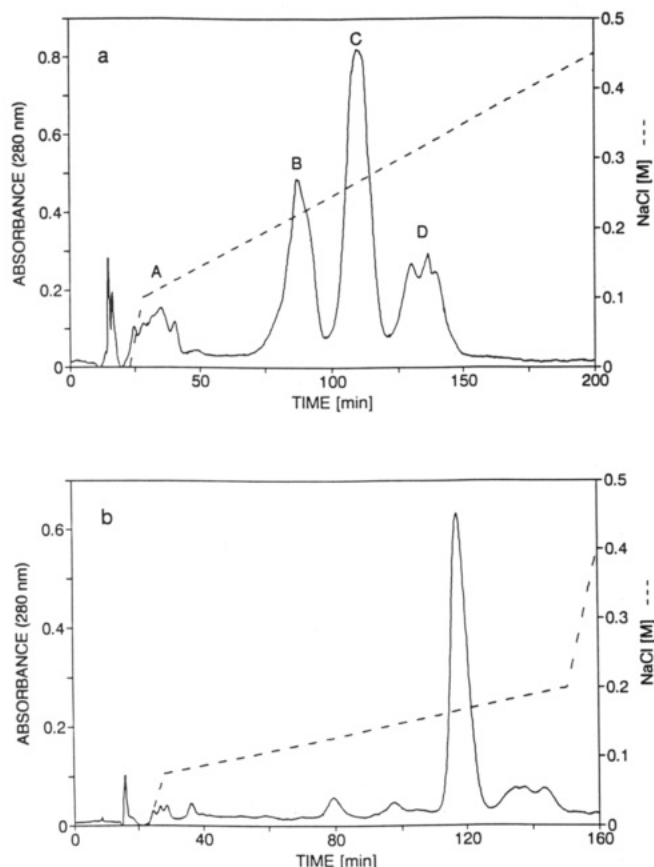


Figure 4. Anion-exchange chromatograms of insulin conjugates treated with hydroxylamine. The reaction of insulin with anhydrides was performed as described in the legend to Figure 3 and was followed by deesterification. The chromatographic conditions are described under Experimental Procedures (salt gradients are as described in the legend to Figure 3): (a) reaction with DTPA dianhydride, (b) reaction with citraconic anhydride.

raphy (compare Figure 4a with Figure 3a). Thus, despite the fact that at pH 7 only 0.25% of the tyrosine residues are expected to be protonated ($pK_a = 9.6$; Tanford & Epstein, 1954), some of them were modified by DTPA dianhydride. In contrast, tyrosine residues were not acylated by citraconic anhydride as shown by the chromatographic profiles before and after treatment with hydroxylamine (Figure 3b and Figure 4b).

Potential tyrosine modification is a problem since the resulting esters would be susceptible to hydrolysis and aminolysis, the latter yielding products of intra- and intermolecular cross-linking. Serine and threonine residues are likely to be much less modified than tyrosine residues. Still, product stability will be impaired, if these residues are modified. The possible modification of histidine residues was not examined since acylimidazoles are quite unstable in aqueous solution and hydrolyze spontaneously (Riordan & Vallee, 1972). Moreover, aminolysis of acylimidazole intermediates would have yielded the desired products. Thus, neither the modification of serine and threonine residues nor that of histidine residues was investigated here.

In the course of our study, one of the insulin-DTPA conjugates was isolated and characterized. The fractions from a chromatogram similar to Figure 4a were collected into four pools (pool A, 20–40 min; pool B, 70–90 min; pool C, 100–120 min; pool D, 125–150 min). The pools were purified using size-exclusion chromatography on Fractogel TSK-HW 50 Superfine. Each pool yielded reasonably sharp peaks; only pool A and pool D showed some front tailing and back tailing, respectively. Pool C was identified

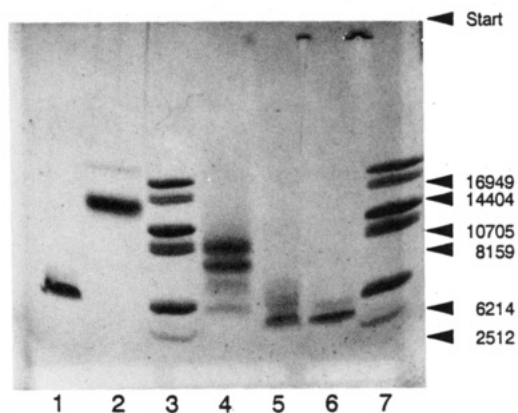


Figure 5. SDS-PAGE of the purified pool C. Electrophoresis was run on a High Density PhastGel. Lanes: (1) unreduced insulin, (2) unreduced pool C, (3 and 7) myoglobin CNBr fragments as molecular weight markers (E. Merck), (4) disulfide-reduced pool C, (5) disulfide-reduced insulin, (6) performic acid oxidized insulin B-chain. Molecular weight estimates were obtained from the straight line linking $\log(M_r)$ to the migration distance in lane 3 ($r = 0.960$).

as the most homogeneous pool and was subjected to further characterization.

By SDS-PAGE under nonreducing conditions pool C gave a single band (Figure 5, lane 2) with a much lower mobility than that of insulin (lane 1). After disulfide reduction, two major bands with apparent molecular weights of 7300 and 8700 were observed for pool C (lane 4). Under these conditions, only the insulin B-chain ($M_r = 3398$) was visible in the reduced insulin lane (lane 5), the A-chain being too small to be detected. This high density polyacrylamide gel allows good resolution in the molecular weight range below 10000 so that the difference in mobility due to three DTPA substituents can potentially be detected. However, the marked differences in the migration distance that were observed between insulin and pool C (both under reducing and nonreducing conditions) could only be explained by cross-linking between insulin molecules. It is very unlikely that a single DTPA molecule ($M_r = 393$) could account for the large increase in the molecule weight of the insulin A-chain from 2380 (not visible on the gel) to 7300 (lane 4). The same observation holds for the insulin B-chain and for the entire insulin molecule.

Further evidence that cross-linking had occurred was obtained after enzymatic treatment of pool C. Complete cleavage of pool C with *S. aureus* V8 protease resulted in the formation of six fragments as analyzed by reversed-phase HPLC (Figure 6a). Insulin has four glutamic acid residues and no aspartic acid residues. Consequently, four fragments should be obtained by V8 protease cleavage, one of which is a disulfide-bridged two-chain molecule. As reported by Grau (1985) and shown in Figure 6b, only three of them were retained by the reversed-phase HPLC column, the insulin A-chain-(1–4)-tetrapeptide eluting with the solvent front. A similar chromatographic profile is to be expected for the V8 protease digest of a monomeric DTPA-modified insulin and was, indeed, observed after digestion of a trisubstituted DTPA-insulin obtained by a selective procedure.⁴ Moreover, it was noted that the DTPA moiety has little, if any, influence on the fragment retention times under the adopted HPLC conditions. Thus, in the case of pool C, the number of fragments and the high retention times observed for some of them demonstrated that cross-linking had occurred between insulin molecules.

⁴ Unpublished results.

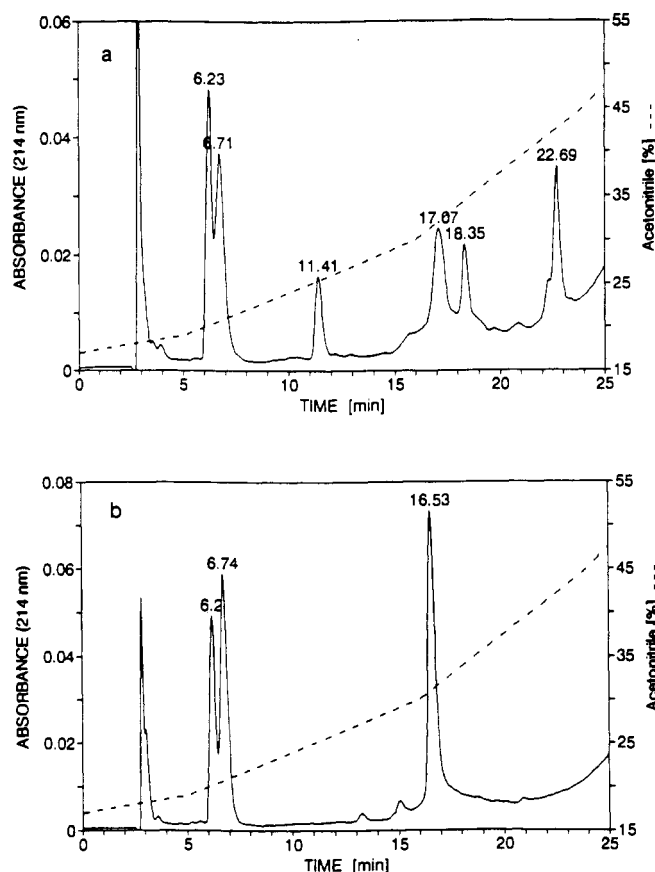


Figure 6. Reversed-phase HPLC analysis of peptides after V8 protease digestion. The chromatographic conditions are described under Experimental Procedures: (a) pool C, (b) insulin.

Treatment of pool C with clostripain followed by reduction of disulfides and alkylation with iodoacetamide yielded six fragments that were retained by the reversed-phase HPLC column (Figure 7a). As expected, cleavage of insulin gave three fragments (Figure 7b) since clostripain selectively cleaves at the only arginine residue (B22). On comparison with the alkylated A- and B-chain, they were identified as insulin B-chain-(23–30)-octapeptide (6.9 min), [S-(carbamoylmethyl)-Cys^{6,7,11,20}]insulin A-chain (13.71 min), and [S-(carbamoylmethyl)-Cys^{7,19}]insulin B-chain-(1–22)-peptide (20.97 min). Again, the extra peaks observed in the pool C fragmentation pattern could only be explained by the presence of cross-linked insulin fragments.

In conclusion, full citraconylation of the three amino insulin groups can be readily achieved using excess anhydride, whereas the coupling of DTPA to proteins via its dianhydride is accompanied by side reactions, namely cross-linking and tyrosine residue acylation. Tyrosine modification was detected using a rather high anhydride to insulin molar ratio (200:1), at a pH value as low as 7.0. Cross-linking occurred to a considerable extent even at a low anhydride to protein molar ratio (i.e. 4:1, that is an anhydride to amino group ratio of 1.3:1). Therefore, monomeric protein species carrying a high number of DTPA substituents attached through a single amide bond are not practically accessible via the dianhydride reaction. The use of low protein concentrations might reduce the intermolecular cross-linking but it has no effect on intramolecular cross-linking, which represents a major risk in the case of highly flexible macromolecules such as polylysine. Products from such side reaction cannot be detected and separated by conventional purification techniques based on charge and size discrimination.

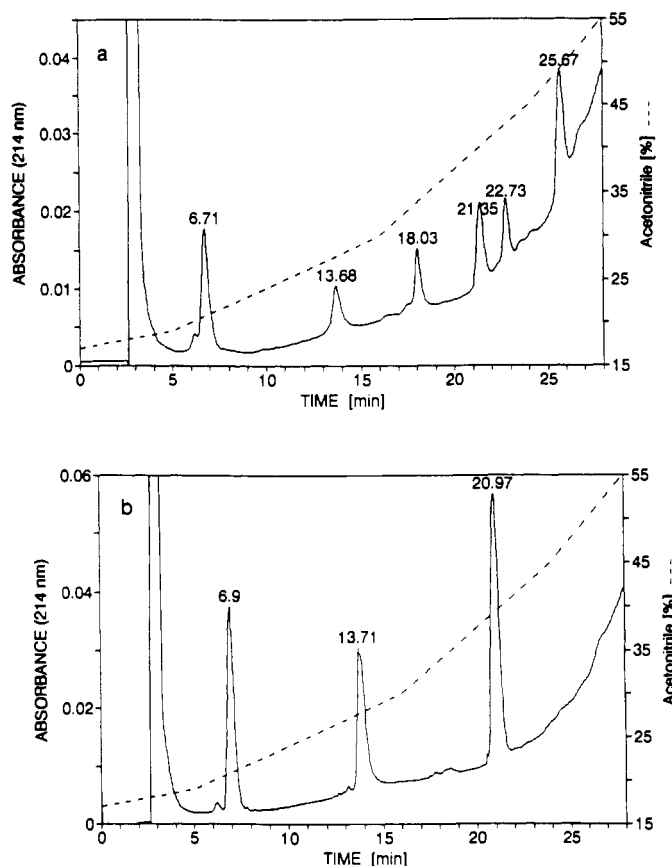


Figure 7. Reversed-phase HPLC analysis of peptides after clostripain digestion followed by reduction of disulfides and alkylation with iodoacetamide. The chromatographic conditions are described under Experimental Procedures: (a) pool C, (b) insulin.

Moreover, intramolecular cross-linking creates weak chelation sites, which impair efficacy and safety of the macromolecular chelate used as contrast agent.

On these grounds, the need for a monoreactive DTPA compound which would enable extensive and specific acylation of amino groups in macromolecules is still vivid.

ACKNOWLEDGMENT

We thank Laura Alessandroni and Fabio Castellini for their excellent technical assistance and Assunta Picciocchi for her help in preparing the manuscript.

LITERATURE CITED

- Berson, S. A., and Yalow, R. S. (1966) Deamidation of Insulin during Storage in Frozen State. *Diabetes* 15, 875–879.
- Deutsch, J., Schmitt-Willich, H., Gries, H., Conrad, J., and Neumeier, R. (Schering AG) (1989) Polymer-bonded Complexing Agents and Their Complexes for Use in Pharmaceuticals. Ger. Offen. DE 3,806,795 (Cl. CO8G73/04), 07 Sept 1989 (Appl. 29 Feb. 1988).
- Feng, R., Konishi, Y., and Bell, A. W. (1991) High Accuracy Molecular Weight Determination and Variation Characterization of Proteins Up to 80 ku by Ionspray Mass Spectrometry. *J. Am. Soc. Mass Spectrom.* 2, 387–401.
- Grau, U. (1985) Fingerprint Analysis of Insulin and Proinsulins. *Diabetes* 34, 1174–1180.
- Halpern, S., Stern, P., Hagan, P., Chen, A., Frincke, J., Bartholomew, R., David, G., and Adams, T. (1983) Labeling of Monoclonal Antibodies with Indium-111: Technique and Advantages Compared to Radioiodine Labeling. *Radioimmunoimaging and Radioimmunotherapy* (Burchiel, S. W., and Rhodes B. A., Eds.) pp. 197–205, Elsevier Science Publishing Co., Inc., New York.

- Harrison, D. M., and Garrat, C. J. (1969) The Accurate Measurement of Insulin Molarity. *Biochem. J.* 113, 733-734.
- Hnatowich, D. J., Childs, R. L., Lanteigne, D., and Najafi, A. (1983a) The Preparation of DTPA-Coupled Antibodies Radiolabeled with Metallic Radionuclides: An Improved Method. *J. Immunol. Methods* 65, 147-157.
- Hnatowich, D. J., Layne, W. W., Childs, R. L., Lanteigne, D., Davis, M. A., Griffin, T. W., and Doherty, P. W. (1983b) Radioactive Labeling of Antibody: A Simple and Efficient Method. *Science* 220, 613-615.
- Jacobsen, T. (Nyegaard & Co. A/S) (1986) Paramagnetic Contrast Agents for Use in "In Vivo" Diagnostic Methods Using NMR, and Their Preparation. Eur. Pat. Appl. EP 186,947 (Cl. A61K49/00), 09 Jul 1986 (SE Appl. 84/5,499,01 Nov 1984).
- Kratzin, H. D., Wiltfang, J., Karas, M., Neuhoﬀ, V., and Hilschmann, N. (1989) Gas-Phase Sequencing after Electrophoretic Separation on Polyvinylidene Difluoride Membranes Assigns Correct Molecular Weights to Myoglobin Molecular Weight Markers. *Anal. Biochem.* 183, 1-8.
- Lauffer, R. B., and Brady, T. J. (1985) Preparation and Water Relaxation Properties of Proteins Labeled with Paramagnetic Metal Chelates. *Magn. Reson. Imag.* 3, 11-16.
- McLeod, A., and Wood, S. P. (1984) High-Performance Liquid Chromatography of Insulin. *J. Chromatogr.* 285, 319-331.
- Meares, C. F., and Wensel, T. G. (1984) Metal Chelates as Probes of Biological Systems. *Acc. Chem. Res.* 17, 202-209.
- Naithani, V. K., and Gattner, H. G. (1982) Preparation and Properties of Citraconylinsulins. *Hoppe-Seyler's Z. Physiol. Chem.* 363, 1443-1448.
- Ogan, M. D., Schmiedl, U., Moseley, M. E., Grodd, W., Paajanen, H., and Brasch, R. C. (1987) Albumin Labeled with Gd-DTPA. An Intravascular Contrast-Enhancing Agent for Magnetic Resonance Blood Pool Imaging: Preparation and Characterization. *Invest. Radiol.* 22, 665-671.
- Paik, C. H., Yokoyama, K., Reynolds, J. C., Quadri, S. M., Min, C. Y., Shin, S. Y., Maloney, P. J., Larson, S. M., and Reba, R. C. (1989) Reduction of Background Activities by Introduction of a Diester Linkage Between Antibody and a Chelate in Radioimmunoassay of Tumor. *J. Nucl. Med.* 30, 1693-1701.
- Riordan, J. F., and Vallee, B. L. (1972) Acetylation. *Methods Enzymol.* 25, 494-499.
- Schägger, H., and von Jagow, G. (1987) Tricine-Sodium Dodecyl Sulfate-Polyacrylamide Gel Electrophoresis for the Separation of Proteins in the Range from 1 to 100 kDa. *Anal. Biochem.* 166, 368-379.
- Tanford, C., and Epstein, J. (1954) Physical Chemistry of Insulin I. Hydrogen Ion Titration Curves of Zinc-Free Insulin. *J. Am. Chem. Soc.* 76, 2163-2165.
- Registry No.** DTPA cyclic anhydride, 23911-26-4; procine insulin, 12584-58-6; citraconic anhydride, 616-02-4.

Characterization of Mercapturic Acid and Glutathionyl Conjugates of Benzo[a]pyrene-7,8-dione by Two-Dimensional NMR[†]

Varanasi S. Murty[‡] and Trevor M. Penning*

Department of Pharmacology, University of Pennsylvania School of Medicine, Philadelphia, Pennsylvania 19104-6084. Received December 3, 1991

Non-K-region polycyclic aromatic hydrocarbon (PAH) *o*-quinones represent alternative metabolites of PAH *trans*-dihydro diol proximate carcinogens. These PAH *o*-quinones react readily with glutathione and *N*-acetyl-L-cysteine, and these adducts may be responsible for their detoxication. Reactions between benzo[a]pyrene-7,8-dione and either *N*-acetyl-L-cysteine or glutathione gave three predominant products which were purified by semipreparative reverse-phase high-pressure liquid chromatography and characterized by homonuclear two-dimensional correlation spectroscopy (COSY). The first product corresponded to a Michael type, 1,4-addition product isolated at the level of quinone oxidation. The second product converted to the first and is a presumptive 1,4-addition product isolated at the level of hydroquinone oxidation. The third product was 7,8-dihydroxybenzo[a]pyrene (a hydroquinone) and was formed as a result of the reductive potential of the thiol. Additional proof for the catechol structure was obtained by its conversion to its diacetate and its identity with authentic 7,8-diacetoxybenzo[a]pyrene. The structures of these adducts and intermediates confirm that thiol addition involves formation of the ketol and rearrangement to give a catechol followed by oxidation to yield the quinone adduct. No evidence was obtained for the formation of either bisphenol or bisglutathionyl adducts. The COSY spectra provide the first complete structure of a benzo[a]pyrenyl-peptide conjugate.

INTRODUCTION

Polycyclic aromatic hydrocarbons (PAH)¹ are widespread environmental pollutants that cause cancer (1, 2). PAH which contain a terminal benzo ring are activated by metabolism to form non-K-region *trans*-dihydro diols which act as immediate precursors of the *anti*-diol epoxides (3), which are ultimate carcinogens. For benzo[a]pyrene this pathway of activation involves conversion of (\pm)-*trans*-7,8-dihydroxy-7,8-dihydrobenzo[a]pyrene (B[a]P-diol) to (\pm)-*trans*-7,8-dihydroxy-*anti*-9,10-epoxy-7,8,9,10-tetrahydrobenzo[a]pyrene (*anti*-BPDE), which then reacts with the 2-amino group of guanine within DNA (4-7).

One of several enzymes that can suppress the formation of the *anti*-diol epoxides is dihydrodiol dehydrogenase [DD; EC 1.3.1.20 (8)]. Previous studies from this laboratory have shown that homogeneous dihydrodiol dehydrogenase catalyzes the oxidation of non-K-region *trans*-dihydro diols to yield intermediate catechols which then air oxidize to form the corresponding non-K-region *o*-quinones (9, 10). These PAH *o*-quinones react with buffer nucleophiles but can be trapped from the reaction mixture as thiol ether adducts with 2-mercaptoethanol (10). Thus, B[a]P-diol is oxidized by DD to yield benzo[a]pyrene-7,8-dione, which then reacts with the thiol scavenger. ¹H

NMR and mass spectrometry have established the structure of the 2-mercaptoethanol adduct of benzo[a]pyrene-7,8-dione as a 1,4-Michael addition product, leading to the proposal that a ketol and catechol are also intermediates in adduct formation, but these were never isolated.

To assess the contribution of DD to B[a]P-diol metabolism, subcellular fractions of rat liver have been fortified with appropriate cofactors to optimize the activities of enzymes that would compete for this proximate carcinogen. In these studies, rat liver S₁₀₀ fortified with NAD(P)⁺ produced significant amounts of benzo[a]pyrene-7,8-dione. Indeed the amount of dione formed was only superseded by the formation of tetrols of benzo[a]pyrene (7,8,9,10-tetrahydroxy-7,8,9,10-tetrahydrobenzo[a]pyrenes) by microsomes fortified with an NADPH generating system, (Penning and Shou, in preparation). These tetrols arise from the hydrolysis of the *anti*-BPDE which is a product of the microsomal oxygenation of B[a]P-diol. Together, these data imply that benzo[a]pyrene-7,8-dione may be an important cellular metabolite of B[a]P-diol.

Once formed PAH *o*-quinones have the potential to be cytotoxic species, thus by entering redox cycles they could generate semiquinone and superoxide anion radicals. An examination of the cytotoxicity of several PAH *o*-quinones (naphthalene-1,2-dione, 7,12-dimethylbenzo[a]anthracene-3,4-dione, and benzo[a]pyrene-7,8-dione) indicated that benzo[a]pyrene-7,8-dione was the least cytotoxic to rat H-4IIe hepatoma cells (11), suggesting that elimination pathways exist for this quinone. These findings indicate that further examination of benzo[a]pyrene-7,8-dione conjugate chemistry is warranted if the elimination and/or toxicity of this PAH *o*-quinone is to be understood.

In the present study we report the synthesis and characterization by homonuclear two-dimensional correlation (COSY) spectroscopy of the mercapturic acid and glutathionyl conjugates of benzo[a]pyrene-7,8-dione. The studies show that although 1,4-addition products can be isolated the reactions are complicated by the formation of hydroquinone conjugates. The elucidation of the struc-

* Address all correspondence to Dr. Trevor M. Penning, Dept. of Pharmacology, University of Pennsylvania School of Medicine, 37th & Hamilton Walk, Philadelphia, PA 19104-6084.

[†] A preliminary account of this work was presented at the American Association for Cancer Research Annual Meeting in Houston, Texas, and was published in abstract form: *Proc. Am. Assoc. Cancer Res.* (1991) 32, Abst.# 735.

[‡] Present address: Uniroyal Chemical Co., Middlebury, CT.

¹ Abbreviations: PAH, polycyclic aromatic hydrocarbons; DD, dihydrodiol dehydrogenase, *trans*-1,2-dihydrobenzene-1,2-diol: dehydrogenase (EC 1.3.1.20); B[a]P-diol, (\pm)-*trans*-7,8-dihydroxy-7,8-dihydrobenzo[a]pyrene; *anti*-BPDE, (\pm)-*trans*-7,8-dihydroxy-*anti*-9,10-epoxy-7,8,9,10-tetrahydrobenzo[a]pyrene COSY, correlation spectroscopy; TFA, trifluoroacetic acid; and RP-HPLC, reverse-phase high-pressure liquid chromatography.

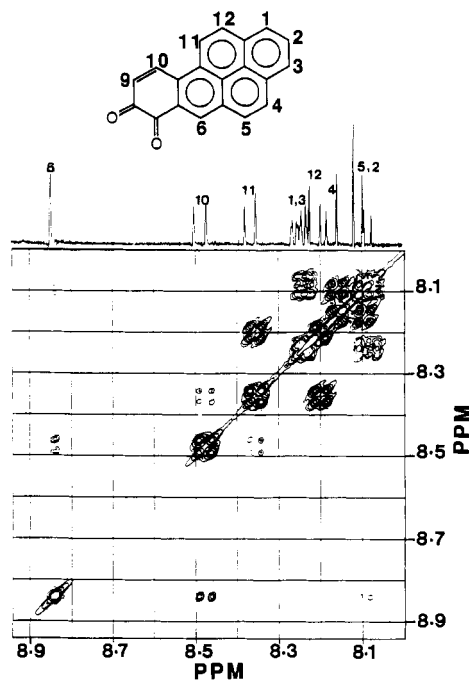


Figure 1. The 500 MHz ^1H -COSY spectrum of benzo[a]pyrene-7,8-dione (with solvent suppression). The sample is 1 mg/0.5 mL in $\text{DMSO}-d_6$. The pulse sequence applied is described in Experimental Procedures, and spectra were collected into 16K data points and 64 scans were taken.

tures of the *N*-acetyl-L-cysteine and glutathionyl conjugates of benzo[a]pyrene-7,8-dione now permit their use as synthetic standards for studies on the further metabolism of benzo[a]pyrene-7,8-dione. The correlation spectra reported here provide unequivocal proton assignments of a benzo[a]pyrenyl-glutathione conjugate which may be useful in assigning structure to other PAH-peptidyl conjugates. To date a complete structure of the *S*-glutathionyl adduct of *anti*-BPDE has not been described.

EXPERIMENTAL PROCEDURES

General. The work described involves the synthesis and handling of hazardous or potentially hazardous agents. Work was therefore conducted in accordance with "NIH Guidelines for the Laboratory Use of Chemical Carcinogens".

Materials. Benzo[a]pyrene-7,8-dione was synthesized according to published procedures (12). *N*-Acetyl-L-cysteine and reduced glutathione were purchased from Sigma (St. Louis, MO) and were used without further purification. HPLC-grade trifluoroacetic acid (TFA) was obtained from Pierce (Rockford, IL). Deuterated solvents and trimethylsilane (TMS) were purchased from Aldrich (Milwaukee, WI).

NMR Spectroscopy. Spectra were obtained on a Bruker AM-500 spectrometer equipped with an ASPECT 3000 computer operating at 500.13 MHz. Samples were dissolved in $\text{DMSO}-d_6$ or dioxane- d_8 /D $_2$ O mixtures. Chemical shifts are expressed relative to TMS. To acquire the COSY spectra the two-pulse experiment described by Aue et al. (13) was used. In this experiment the preparatory phase ends with a nonselective rf pulse at time $t = 0$ (preparatory pulse). A flip angle of 90° was employed to generate the off-diagonal elements, and at the end of the evolution period a second rf field (mixing pulse) was applied at a time $t = t_1$ (13, 14).

Synthesis of Mercapturic Acid and Glutathionyl Conjugates of Benzo[a]pyrene-7,8-dione. The synthesis of *N*-acetyl-*S*-(7,8-dihydro-7,8-dioxobenzo[a]pyren-

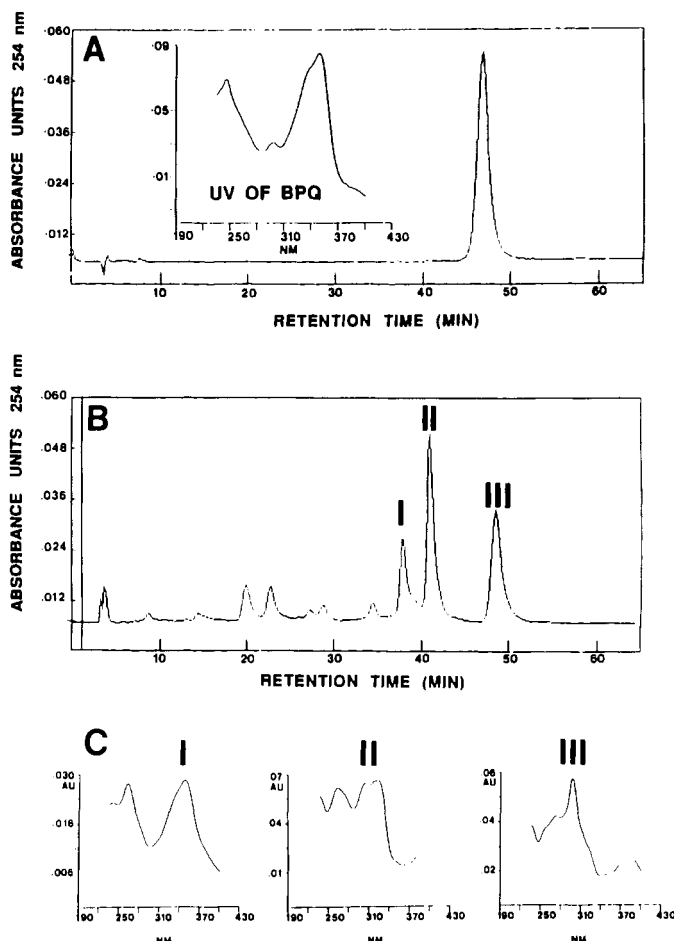


Figure 2. RP-HPLC chromatography of reaction mixtures resulting from *N*-acetyl-L-cysteine addition to benzo[a]pyrene-7,8-dione: Elution profile for benzo[a]pyrene-7,8-dione (A), elution profile for *N*-acetyl-L-cysteine-benzo[a]pyrene-7,8-dione adducts obtained at 24 h (B), and UV spectra of *N*-acetyl-L-cysteine-benzo[a]pyrene-7,8-dione adducts (C). Similar data were obtained for the addition of glutathione to benzo[a]pyrene-7,8-dione (not shown).

10-yl)cysteine and *S*-(7,8-dihydro-7,8-dioxobenzo[a]pyren-10-yl)glutathione were conducted in a similar manner. Benzo[a]pyrene-7,8-dione (1 equiv) was reacted with glutathione (2 equiv) in dioxane/water (2:1, v/v) for 24 h under N_2 at 25°C . The dioxane was removed under vacuum, excess quinone was removed with ethyl acetate, and the aqueous layer was lyophilized. The residue was reconstituted in a small volume of aqueous dioxane and purified by semipreparative ion-pair RP-HPLC using an acetonitrile/water gradient containing 0.1% TFA, in which the acetonitrile concentration was increased from 40 to 60% over 50 min at a flow rate of 1.0 mL/min. Peak fractions were collected, concentrated, and analyzed by ion-pair RP-HPLC using a Perkin-Elmer LC-480 with diode-array detection.

RESULTS

NMR Chemical Shift Assignments and Coupling Constants for Benzo[a]pyrene-7,8-dione. A 2D-COSY spectrum of benzo[a]pyrene-7,8-dione was acquired (Figure 1) from which it was possible to assign all the protons unequivocally. The appropriate connectivities obtained from the cross-peaks are listed in Table I. All of the assignments obtained in this 2D experiment confirmed the chemical shifts reported for ^1H NMR (270 MHz) of the quinone (12) with one exception. In our experiments H-12 has a chemical shift of 8.21 ppm instead of 7.62 ppm;

Table I. Proton Assignments for Benzo[a]pyrene-7,8-dione

proton	chemical shift (ppm), multiplicity	coupling constants, J (Hz)	connectivities
H-1 or H-3	8.25, dd; 8.24, dd	8, 1.2	
H-2	8.09, t	8	H-1/H-3 (8.25/8.24) with H-2 (8.09)
H-4	8.16, d	9	H-4 (8.16) with H-5 (8.11)
H-5	8.11, d	9	H-5 (8.11) with H-4 (8.16)
H-6	8.84, s		
H-9	6.59, d	10.5	H-9 (6.59) with H-10 (8.48)
H-10	8.48, d	10.5	H-10 (8.48) with H-9 (6.59)
H-11	8.36, d	9.5	H-11 (8.36) with H-12 (8.21)
H-12	8.21, d	9.5	H-12 (8.21) with H-11 (8.36)

however, the coupling constant with H-11 is unchanged, $J_{11,12} = 9.5$ Hz. It seems likely that the original assignment was in error since others have reported the difficulty in assigning PAH aromatic protons based on ^1H NMR data (15).

Formation of *N*-Acetyl-L-cysteinyl and Glutathionyl Conjugates of Benzo[a]pyrene-7,8-dione. Reactions between benzo[a]pyrene-7,8-dione and either *N*-acetyl-L-cysteine or glutathione were monitored by RP-HPLC using a diode-array detector. After 24 h three products had formed (I, II, and III). Peak I gave a UV spectrum identical to benzo[a]pyrene-7,8-dione and is a presumptive thiol ether adduct obtained at the level of quinone oxidation (Figure 2a,b). The 2D-COSY spectra of peak I obtained from both reactions are presented later. Attempts to isolate peak II showed that upon further purification and chromatography, peak II was converted to peak I. Inspection of the UV spectra for peak II indicates that it contains a mixture of two chromophores, that observed with the quinone (peak I) and that observed with the hydroquinone (peak III; presented later). Thus the UV spectra support the view that, in each reaction, peak II is a hydroquinone conjugate which autooxidizes to yield the quinone conjugate. Peak III was isolated from each reaction and the 2D-COSY spectrum indicates that this is 7,8-dihydroxybenzo[a]pyrene (also presented later).

2D-COSY Spectra of *N*-Acetyl-L-cysteine Adducts of Benzo[a]pyrene-7,8-dione. The 2D-COSY spectrum of product I obtained from the reaction of *N*-acetyl-L-cysteine and benzo[a]pyrene-7,8-dione is shown in Figure 3 and corresponds to *N*-acetyl-S-(7,8-dihydro-7,8-dioxobenzo[a]pyren-10-yl)cysteine. The aliphatic region shows the presence of Cys α (4.83 ppm) and Cys β 1 (3.70 ppm) and Cys β 2 (3.50 ppm). A complete list of the connectivities obtained from the cross peaks is given in Table II. In the aromatic region key chemical shifts show the presence of a vinylic proton at 6.7 ppm which corresponds to H-9, and confirms that the conjugate is a quinone rather than a hydroquinone. The vinylic proton corresponding to H-10 (8.49 ppm) is also absent, indicating that this is the position of thiol substitution.

Rapid anaerobic handling of product III isolated from the reaction of *N*-acetyl-L-cysteine with benzo[a]pyrene-7,8-dione led to the recovery of 7,8-dihydroxybenzo[a]pyrene. A 2D-COSY spectrum of this product permitted the assignment of all the protons (Figure 4). The spectrum indicates that all the protons are aromatic (see Table III for a complete list of the connectivities). Absent from the spectrum are vinylic protons that correspond to H-9 and H-10. Careful inspection of the spectrum indicates that a number of smaller cross-peaks exist that can be assigned to a structure that would coincide with benzo[a]pyrene-7,8-dione. It is estimated that the isolated 7,8-dihydroxybenzo[a]pyrene exists as a mixture of (6:1) hydroquinone/

o-quinone. Further, proof of the structure of the hydroquinone came from trapping the unstable compound as its diacetate (acetic anhydride/pyridine). The product of this reaction gave an identical retention time and UV spectra by diode-array RP-HPLC to a synthetically prepared standard obtained via reductive acetylation of benzo[a]pyrene-7,8-dione (16). ^1H NMR of the trapped diacetate gave chemical shifts that corresponded to the methyl groups of the two acetates observed in the authentic standard at 2.55 and 2.35 ppm.

2D-COSY Spectra of Glutathionyl Adducts of Benzo[a]pyrene-7,8-dione. S-Glutathionyl conjugates of benzo[a]pyrene-7,8-dione were prepared as previously described in the Experimental Procedures. From the product profile it was anticipated that, of the three products, one would correspond to a glutathionyl conjugate obtained at the level of quinone oxidation, one would correspond to a glutathionyl conjugate obtained at the level of hydroquinone oxidation, and one would correspond to 7,8-dihydroxybenzo[a]pyrene. Isolation of the putative quinone-glutathionyl conjugate gave pure material as judged by RP-HPLC and this was subjected to 2D-COSY spectroscopy. Examination of the spectrum indicates that although a large solvent peak exists in the aliphatic region it is possible by examination of the cross peaks to assign all the aliphatic protons in glutathione (Table IV). It is also possible to assign all the aromatic protons present in benzo[a]pyrene-7,8-dione, and together these support a simple 1,4-Michael addition product with thiol conjugation occurring at C-10. Thus, there is an isolated vinyl proton that corresponds to H-9, while the benzylic vinyl proton at H-10 is absent from the spectrum. Since all the aromatic protons can be accounted for, the product does not correspond to a bisphenol adduct; similarly, since all the aliphatic protons can be accounted for, the product does not correspond to a bisglutathionyl adduct. The compound thus corresponds to S-(7,8-dihydro-7,8-dioxobenzo[a]pyren-10-yl)glutathione.

Recently, the confirmations of free and lanthanide-complexed glutathione have been determined in solution by ^1H and ^{13}C NMR (17). Comparison of the chemical shifts for the protons of the tripeptide with those obtained in this study are in close agreement, with the exception of Cys β 1 and Cys β 2, which have been shifted downfield by 0.50 and 0.65 ppm, respectively. This shift is consistent with the formation of a benzylic thiol. In the earlier study the confirmation of glutathione was predicted by using the coupling constants to predict torsion angles. Of the pertinent coupling constants, the constants for Glu α coupling with Glu β should be 2.8 and 13.5 Hz, if standard proton-proton vicinal trans and gauche couplings are observed. In the structure of the benzo[a]pyrenyl-glutathionyl conjugate these constants are 7.5 and 15.0 Hz, respectively, indicating that within the adduct the confirmation of glutathione has been distorted. It should be emphasized that it is not possible to predict the complete confirmation of glutathione within the benzo[a]pyrenyl adduct since the spectra were taken in a dioxane-*d*/D₂O mixture which will promote the exchange of the amide and carboxyl group protons. Chemical shifts for these protons along with the coupling constants observed with adjacent methylene and methine protons are required for the complete confirmational analysis of the tripeptide. In the earlier work (17) the spectrum of glutathione was taken in H₂O containing 10% D₂O, a solvent incompatible with the solubility of a benzo[a]pyrene adduct.

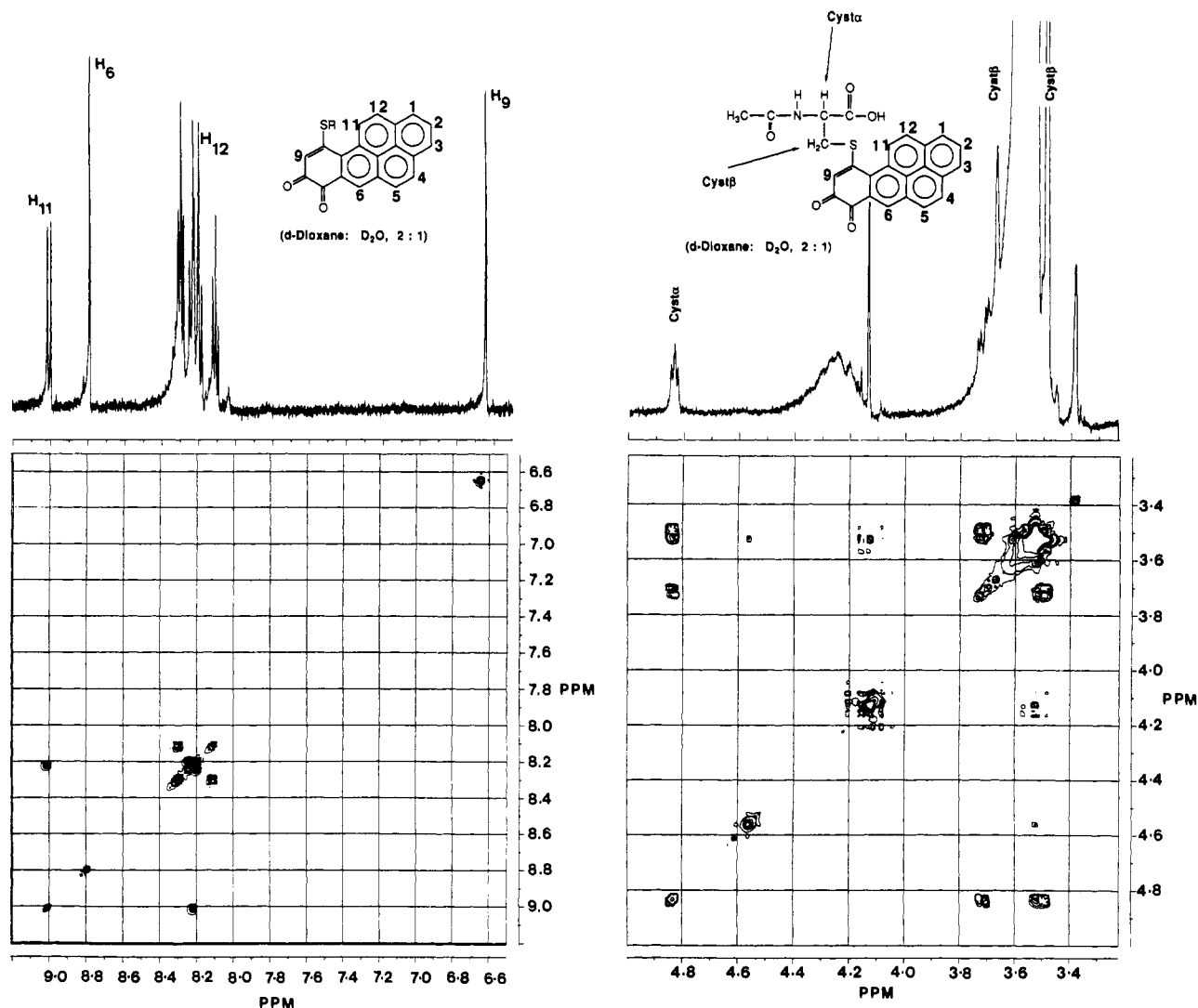


Figure 3. The 500-MHz ^1H -COSY spectrum of the *N*-acetyl-L-cysteine adduct of benzo[a]pyrene-7,8-dione (with solvent suppression). Panel A shows the aromatic region and panel B shows the aliphatic region. The sample is 1 mg/0.5 mL in dioxane-*d*/ D_2O . The pulse sequence applied is described in the Experimental Procedures and spectra were collected into 16K data points and 80 scans were taken.

DISCUSSION

Benzo[a]pyrene-7,8-dione represents a novel metabolite of B[a]P-diol which is a potent proximate carcinogen. It can form *in vitro* as a result of the reaction catalyzed by dihydrodiol dehydrogenase, in which B[a]P-diol undergoes a formal dehydrogenation to yield a ketol which then rearranges to a catechol and undergoes air oxidation to form benzo[a]pyrene-7,8-dione. Benzo[a]pyrene-7,8-dione *in turn* is reactive and can be trapped as a thiol ether adduct (10).

Benzo[a]pyrene-7,8-dione has also been detected as a major metabolite of B[a]P-diol in rat liver S_{100} supplemented with NAD(P) $^+$ (Penning and Shou, unpublished observations), suggesting that the conversion of B[a]P-diol to benzo[a]pyrene-7,8-dione may represent a significant route of B[a]P-diol metabolism. This paper describes the synthesis and complete characterization of *N*-acetyl-L-cysteine (mercapturic acid) and glutathionyl conjugates of benzo[a]pyrene-7,8-dione that could represent the ultimate water-soluble forms of this *o*-quinone. The availability of these conjugates will permit their use as synthetic standards to identify their formation *in vivo*.

2D-COSY has permitted the assignment of each proton resonance in the thiol conjugates. In each case the predominant stable product is the simple 1,4-Michael addition product obtained at the level of quinone oxidation.

This is supported by the presence of an isolated vinyl proton corresponding to H-9, and the lack of a benzylic vinyl proton at H-10. It has been proposed that a ketol and catechol are intermediates in thiol ether formation (10). The studies described here support this mechanism since in the presence of excess thiol, adducts were detected as hydroquinones which autooxidize to quinone conjugates upon sample handling.

In the pathway proposed (Scheme I), *N*-acetyl-L-cysteine or glutathione attacks benzo[a]pyrene-7,8-dione to yield a ketol. Enolization then occurs to yield the corresponding hydroquinone conjugate, which could either autooxidize or cross-oxidize to yield the *o*-quinone conjugate. Although, these reactions were conducted under a nitrogen atmosphere, it is difficult to exclude all the oxygen, and therefore autooxidation with molecular oxygen acting as the oxidant is favored. For example, when the reductive addition of glutathione to 2-(hydroxymethyl)-1,4-naphthoquinone is followed, molecular oxygen is consumed and H_2O_2 is formed (18). Interestingly, the rates of oxygen consumption and H_2O_2 production were unaffected by superoxide dismutase. This suggests that superoxide anion is rapidly depleted by redox transitions with the hydroquinone and/or the anion of reduced glutathione to yield H_2O_2 . In contrast, cross-oxidation, which requires one molecule of unconjugated *o*-quinone to oxidize

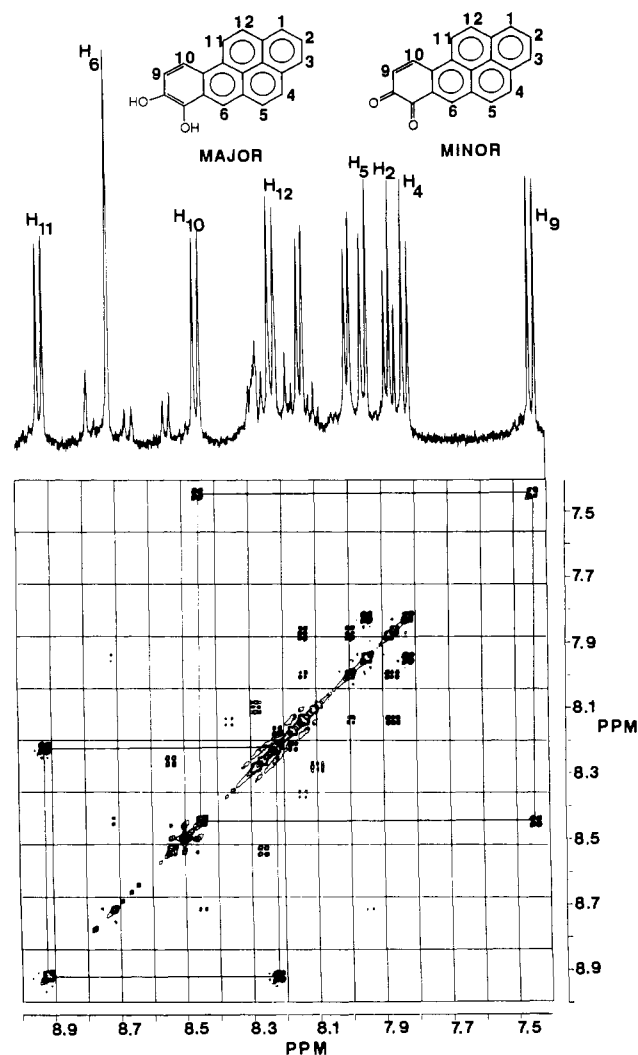


Figure 4. The 500-MHz ^1H -COSY spectrum of a 6:1 mixture of 7,8-dihydroxybenzo[a]pyrene and benzo[a]pyrene-7,8-dione obtained from thiol addition reactions. The sample is 1 mg/0.5 mL in dioxane- d_6 /D $_2$ O. The pulse sequence applied is described in the Experimental Procedures and spectra were collected into 16K data points and 112 scans were taken.

Table II. Proton Assignments for *N*-Acetyl-*S*-(7,8-dihydro-7,8-dioxobenzo[a]pyren-10-yl)cysteine

proton	chemical shift (ppm), multiplicity	coupling constant, J (Hz)	connectivities
H-1 or H-3	8.29, dd; 8.30, dd	7.5	
H-2	8.11, t	7.6	H-1/H-3 (8.29/8.30) with H-2 (8.11)
H-4	8.24, d		H-4 (8.24) with H-5 (8.19)
H-5	8.19, d		H-5 (8.19) with H-4 (8.24)
H-6	8.79, s		
H-9	6.70, s		
H-10	absent		
H-11	9.00, d	9.5	H-11 (9.00) with H-12 (8.21)
H-12	8.21, d	9.5	H-12 (8.21) with H-11 (9.00)
Cysβ1	3.70, dd	11.75	Cysβ1 (3.7) with Cysβ2 (3.50)
Cysβ2	3.50, dd	13.20	Cysβ2 (3.5) with Cysβ1 (3.7)
Cysα	4.83, t		Cysα (4.8) with Cysβ1 (3.70) Cysα (4.8) with Cysβ2 (3.50)
CH ₃ (acetyl)	1.88, s		

a molecule of hydroquinone conjugate is not favored. Thus, in the reductive addition of glutathione to 2-(hydroxymethyl)-1,4-naphthoquinone, cross-oxidation only occurred when the [GSH]:[quinone] ratio was 0.35. In the reactions described here the [RSH]:[benzo[a]pyrene-7,8-dione] ratio was 2.0. On this basis, it is predicted that the autooxidation of thiol conjugates of 7,8-dihydroxybenzo-

Table III. Proton Assignments for 7,8-Dihydroxybenzo[a]pyrene^a

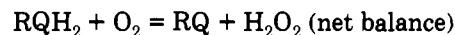
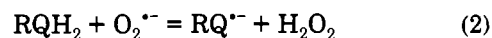
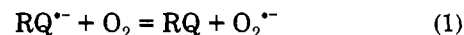
proton	chemical shift (ppm), multiplicity	coupling constants (Hz), J	connectivities
H-1 or H-3	8.00, dd; 8.15, dd	7.5, 7.9	
H-2	7.88, t	7.5	H-1/H-3 (8.00/8.15) with H-2 (7.88)
H-4	7.83, d	9.1	H-4 (7.83) with H-5 (7.95)
H-5	7.95, d	9.1	H-5 (7.95) with H-4 (7.83)
H-6	8.72, s		
H-9	7.45, d	9.2	H-9 (7.45) with H-10 (8.45)
H-10	8.45, d	9.3	H-10 (8.45) with H-9 (7.45)
H-11	8.92, d	9.1	H-11 (8.92) with H-12 (8.22)
H-12	8.22, d	9.1	H-12 (8.22) with H-11 (8.92)

^a Ratio of catechol/quinone observed in this experiment is 6:1 (based on peak ratios).

Table IV. Proton Assignments for *S*-(7,8-Dihydro-7,8-dioxobenzo[a]pyren-10-yl)glutathione

proton	chemical shift (ppm), multiplicity	coupling constants (Hz), J	connectivities
H-1 or H-3	8.21, dd; 8.19, dd	10.0	
H-2	8.04, t	9.0	H-1/H-3 (8.21/8.19) with H-2 (8.04)
H-4 or H-5	8.08, dd; 8.10, dd	10.0	H-4 with H-5
H-6	8.53, s		
H-9	6.62, s		
H-10	absent		
H-11	8.82, d	10.0	H-11 (8.82) with H-12 (7.96)
H-12	8.10, d	10.0	H-12 (8.10) with H-11 (8.82)
Cysβ1 or β2	3.43, dd; 3.60, dd		Cysβ1 (3.43) with Cysβ2 (3.60)
Cysα	4.78, t	15.0	Cysα (4.71) with Cysβ1/β2 (3.43/3.60)
Gluγ	2.40, t	7.5	Gluγ (2.4) with Gluβ (2.0)
Gluβ	2.0, t	15.0	Gluβ (2.0) with Gluγ (2.5)
Gluα	3.7, t	5.0	Gluα (3.7) with Gluβ (2.0)
Glyα	3.86, s		

[a]pyrene would be initiated by the reaction of the semiquinone radical with molecular oxygen to yield the *o*-quinone conjugate and superoxide anion. The superoxide anion would then propagate formation of the *o*-quinone conjugate by oxidizing the hydroquinone and forming hydrogen peroxide (see eqs 1 and 2, where $\text{RQ}^{\cdot-}$



= semiquinone radical of a thiol ether conjugate of benzo[a]pyrene-7,8-dione; RQ = thiol ether conjugate of benzo[a]pyrene-7,8-dione; RQH₂ = thiol ether conjugate of 7,8-dihydroxybenzo[a]pyrene).

Because the reactions described here were conducted in the presence of a molar ratio of [RSH]:[quinone] = 2.0, the thiol is consumed by at least two processes. First, reductive addition of the thiol to the quinone will deplete RSH (Scheme I). Second, RSH oxidation may be coupled to redox transitions that involve the thiyl radical. This radical may be produced by interaction of RSH with superoxide anion, hydroxyl radical, or semiquinone radical. Reaction of RSH with the semiquinone radical would produce the hydroquinone, while dimerization of resultant thiyl radicals would yield RSSR. These reactions have

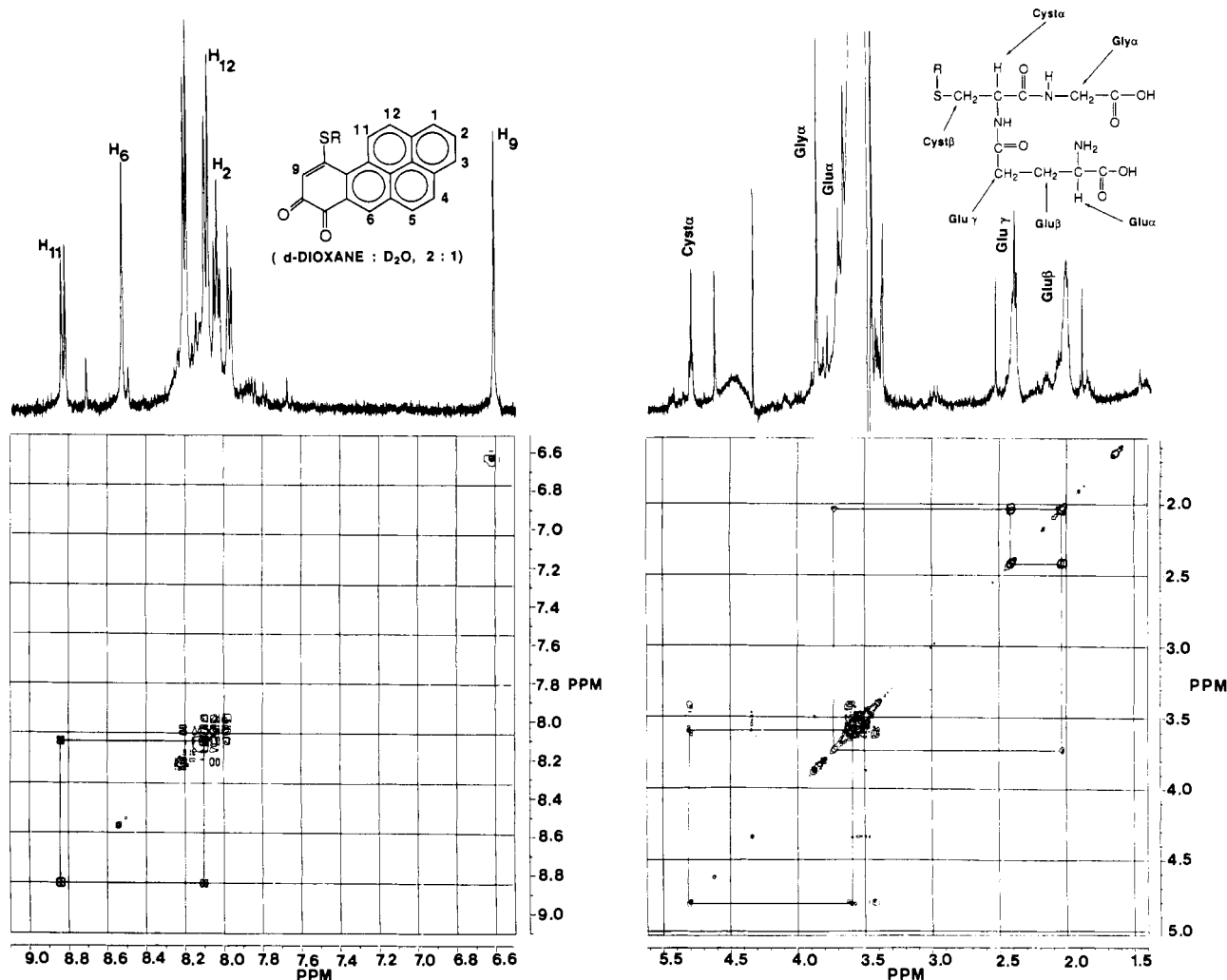
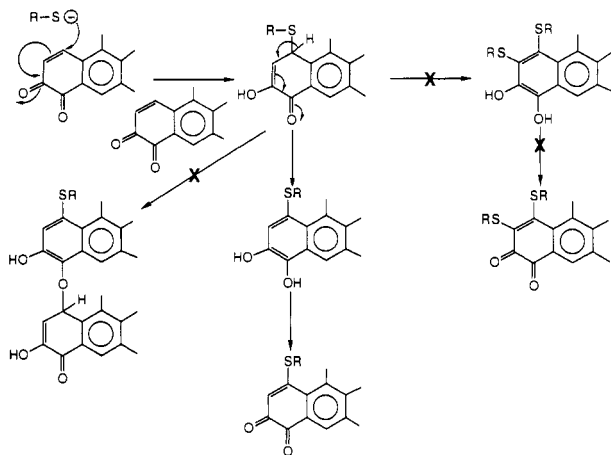


Figure 5. The 500-MHz ^1H -COSY spectrum of the glutathionyl conjugate of benzo[a]pyrene-7,8-dione (with solvent suppression). Panel A shows the aromatic region and panel B shows the aliphatic region. The sample is 1 mg/0.5 mL in dioxane- d_6 /D $_2$ O. The pulse sequence applied is described in the Experimental Procedures and spectra were collected into 16K data points and 80 scans were taken.

Scheme I. Mechanism of Formation of Thiol Ether Conjugates of Benzo[a]pyrene-7,8-dione (R-SH = glutathione or N -acetyl-L-cysteine)



been well-documented for the addition of GSH to 2-(hydroxymethyl)-1,4-naphthoquinone (18) and would provide an explanation for the chromatographic profiles shown in Figure 2. It is clear that the intermediates that form and their redox transitions are critically dependent on the $[\text{RSH}]:[\text{quinone}]$ ratio. However, once these reactions are handled aerobically, fully oxidized thiol conjugates of benzo[a]pyrene-7,8-dione are obtained.

Although it is conceivable that N -acetyl-L-cysteine and glutathione might add directly to the hydroquinone (7,8-dihydroxybenzo[a]pyrene) this possibility is ruled out on mechanistic grounds (18-21).

Since all the aliphatic and aromatic protons in the 2D-NMR spectra can be assigned to mono adducts, the formation of bisphenol and bisglutathionyl adducts are ruled out. Our results are in contrast to other studies which have examined the formation of thiol ether adducts of p -quinones (22, 23). Thus, bisglutathionyl conjugates have been described for 2-bromobenzoquinone (22). In addition, reactions between p -quinone and L-cysteine may not be simple 1,4-Michael additions. Studies on the L-cysteinyl adducts of 2-bromobenzoquinone indicate that intramolecular Schiff's base formation occurs, leading to cyclization reactions that result in the formation of 1,4-benzothiazines (23). The studies described here may have avoided the formation of these complex products since N -acetyl-L-cysteine rather than cysteine was used as a reactant.

We have recently described the cytotoxicity of a variety of PAH o -quinones in H-4IIE (rat hepatoma) cells. Benzo[a]pyrene-7,8-dione (20 μM) was the least cytotoxic of the PAH o -quinones examined. It reduced cell viability without having an adverse effect on cell survival. This effect was accompanied by a concomitant depletion of glutathione which was not accompanied by a change in GSH/GSSG ratios (11). This implies that benzo[a]pyrene-

7,8-dione does not cause a change in redox state and generate superoxide anion as observed in vitro but rather depletes glutathione by forming glutathionyl conjugates. The glutathionyl conjugate characterized in this study may represent the metabolite that is responsible for the elimination of this quinone from hepatoma cells and its limited cytotoxicity.

It is clear from our work that B[a]P-diol can act as a branch point in benzo[a]pyrene metabolism giving rise to either *anti*-BPDE or benzo[a]pyrene-7,8-dione. Both metabolites can react with glutathione and can be eliminated as glutathione conjugates. This paper describes the first complete structure of a benzo[a]pyrenyl-glutathionyl conjugate. The structure of the glutathionyl conjugate of *anti*-BPDE has not been fully characterized.

ACKNOWLEDGMENT

This work was supported by U.S. Public Health Service Grant CA35904 (to T.M.P.) from the National Cancer Institute and NIH Research Career Development Award CA01335 (to T.M.P.). Portions of this work were supported by the High-Resolution NMR facility in the Department of Biochemistry and Biophysics at the University of Pennsylvania. Dr. Kurt Loening of Topterm, North American Division was responsible for the nomenclature of the compounds.

LITERATURE CITED

- (1) Gelboin, H. V. (1980) Benzo[a]pyrene metabolism, activation and carcinogenesis: Role and regulation of mixed function oxidases and related enzymes. *Physiol Rev.* 60, 1107-1166.
- (2) Conney, A. H. (1982) Induction of microsomal enzymes by foreign chemicals and carcinogens by polycyclic aromatic hydrocarbons: GHA Clowes Memorial Lecture. *Cancer Res.* 42, 4875-4917.
- (3) Lehr, R. E., Kumar, S., Levin, W., Wood, A. W., Chang, R. L., Conney, A. H., Yagi, H., Sayer, J. M., and Jerina, D. M. (1985) The bay region theory of polycyclic aromatic hydrocarbon carcinogenesis. In *Polycyclic Hydrocarbons and Carcinogenesis* (R. G. Harvey, Ed.) pp 63-84, American Chemical Society, Washington, DC.
- (4) Yang, S. K., McCourt, D. W., Roller, P. P., and Gelboin, H. V. (1976) Enzymatic conversion of benzo[a]pyrene leading predominantly to the diol-epoxide *r*-7,8-dihydroxy-*t*-9,10-oxo-7,8,9,10-tetrahydrobenzo[a]pyrene through a single enantiomer of *r*-7,8-dihydroxy-7,8-dihydroxybenzo[a]pyrene. *Proc. Natl. Acad. Sci. U.S.A.* 73, 2594-2598.
- (5) Jeffrey, A. M., Jennette, K. W., Blobstein, S. H., Weinstein, I. B., Beland, F. A., Harvey, R. G., Kasai, H., Miura, I., and Nakanishi, H. (1976) Benzo[a]pyrene-nucleic acid derivative found *in vivo*. Structure of a benzo[a]pyrenetetrahydrodiol epoxide-guanosine adduct. *J. Am. Chem. Soc.* 98, 5714-5715.
- (6) Koreeda, M., Moore, P. D., Wislocki, P. G., Levin, W., Conney, A. H., Yagi, H., and Jerina, D. M. (1978) Binding of benzo[a]pyrene-7,8-diol-9,10-epoxides to DNA, RNA and protein of mouse skin occurs with high stereoselectivity. *Science* 199, 778-780.
- (7) Buening, M. K., Wislocki, P. G., Levin, W., Yagi, H., Thakker, D. R., Akagi, H., Koreeda, M., Jerina, D. M., and Conney, A. H. (1978) Tumorigenicity of the optical enantiomers of the diastereomeric benzo[a]pyrene-7,8-diol-9,10-epoxides in newborn mice: Exceptional activity of (+)-7 β ,8 α -dihydroxy-9 α ,10 α -epoxy-7,8,9,10-tetrahydrobenzo[a]pyrene. *Proc. Natl. Acad. Sci. U.S.A.* 75, 5358-5361.
- (8) Glatt, H. R., Vogel, K., Bentley, P., and Oesch, F. (1979) Reduction of benzo[a]pyrene mutagenicity by dihydrodiol dehydrogenase. *Nature* 277, 319-320.
- (9) Smithgall, T. E., Harvey, R. G., and Penning, T. M. (1986) Regio- and stereospecificity of homogeneous 3 α -hydroxysteroid/dihydrodiol dehydrogenase for *trans*-dihydrodiol metabolites of polycyclic aromatic hydrocarbons. *J. Biol. Chem.* 261, 6184-6191.
- (10) Smithgall, T. E., Harvey, R. G., and Penning, T. M. (1988) Spectroscopic identification of *o*-quinones as the products of polycyclic aromatic *trans*-dihydrodiol oxidation catalyzed by dihydrodiol dehydrogenase. *J. Biol. Chem.* 263, 1814-1820.
- (11) Flowers, L., Harvey, R. G., and Penning, T. M. (1991) Cytotoxicity of polycyclic aromatic hydrocarbon *o*-quinones in H-4IIE cells. *Proc. Am. Assoc. Cancer Res.* 32, Abstract 696.
- (12) Sukumaran, K. B., and Harvey, R. G. (1980) Synthesis of the *o*-quinones and dihydro diols of polycyclic aromatic hydrocarbons from the corresponding phenols. *J. Org. Chem.* 45, 4407-4413.
- (13) Aue, W. P., Bartholdi, E., and Ernst, R. R. (1976) Two-dimensional spectroscopy. Application to nuclear magnetic resonance. *J. Chem. Phys.* 64, 2229-2246.
- (14) Nagayama, K., Kumar, A., Wuethrich, K., and Ernst, R. R. (1980) Experimental techniques of two dimensional correlated spectroscopy. *J. Magn. Reson.* 40, 321-324.
- (15) Williamson, D. S., Cremonesi, P., Cavalieri, E., Nagel, D. L., Markin, R. S., and Cohen, S. M. (1986) Assignment of ¹H-NMR spectra of polycyclic aromatic hydrocarbons by multiple quantum filtration. *J. Org. Chem.* 51, 5210-5213.
- (16) Cho, H., and Harvey, R. G. (1976) Synthesis of hydroquinone diacetates from polycyclic aromatic quinones. *J. Chem. Soc. Perkin Trans. 1* 836-839.
- (17) Podanyi, B., and Reid, R. S. (1988) NMR Study of the conformations of free and lanthanide-complexed glutathione in aqueous solution. *J. Am. Chem. Soc.* 110, 3805-3810.
- (18) Goin, J., Gibson, D. D., McCay, P. B., and Cadenas, E. (1991) Glutathionyl- and hydroxyl radical formation coupled to the redox transitions of 1,4-naphthoquinone bioreductive alkylation agents during glutathione two-electron reductive addition. *Arch. Biochem. Biophys.* 288, 386-396.
- (19) Finley, K. T., (1974) The addition and substitution chemistry of quinones. In *The Chemistry of Quinoid Compounds* (K. Patai, Ed.) pp 877-1144, John Wiley & Sons., New York.
- (20) Gant, T. W., Doherty, d'A.M., Odowole, D., Sales, K. D., and Cohen, G. M. (1988) Semiquinone anion radicals formed by the reaction of quinones with glutathione or amino acids. *FEBS Lett.* 201, 296-300.
- (21) Takahashi, N., Schreiber, J., Fischer, V. and Mason, R. P. (1987) Formation of glutathione-conjugated semiquinones by the reaction of quinones with glutathione. An ESR study. *Arch. Biochem. Biophys.* 252, 41-48.
- (22) Monks, T. J., Highet, P. J., and Lau, S. S. (1988) 2-Bromo-(diglutathion-S-yl)hydroquinone nephrotoxicity: Physiological, biochemical and electrochemical determinants. *Mol. Pharmacol.* 34, 492-500.
- (23) Monks, T. J., Highet, P. J., and Lau, S. S. (1990) Oxidative cyclization, 1,4-benzothiazine formation and dimerization of 2-bromo-3-(glutathionyl)hydroquinone. *Mol. Pharmacol.* 38, 121-127.

Effect of Different Binding Proteins on the Detection Limits and Sensitivity of Assays Based on Biotinylated Adenosine Deaminase

Minas S. Barbarakis, Sylvia Daunert, and Leonidas G. Bachas*

Department of Chemistry, University of Kentucky, Lexington, Kentucky 40506-0055. Received December 9, 1991

The properties of binding proteins that control the nature and magnitude of inhibition of the enzyme-ligand conjugates in homogeneous enzyme-linked competitive binding assays were investigated. An assay for biotin that employed adenosine deaminase as the enzyme-label was used as a model system because of the availability of several biotin-specific binders with different characteristics. It was found that the association constant between the ligand and the binding protein, as well as the depth of the binding pocket, affect the response characteristics of the assay. In addition, the reported data suggest that steric-hindrance effects also contribute toward the sensitivity and detection-limit capabilities of the assay.

INTRODUCTION

Homogeneous enzyme-linked competitive binding assays have found numerous applications in bioanalysis. Usually, in these assays, the activity of an enzyme-labeled ligand (conjugate) is inhibited upon binding to a ligand-specific binder (e.g., antibody, binding protein, lectin, etc.). The inhibition of the enzymatic activity can be modulated by a competition between the unlabeled ligand (analyte) and the enzyme conjugate for the binding sites of the binder (1, 2). The sensitivity and detection limits of these assays are controlled by (a) the ability to measure low levels of enzymatic activity, (b) the extent of the change in the activity of the enzyme-ligand conjugate upon binding to the ligand-specific binder, (c) the binding constant between the ligand and its specific binder, and (d) the assay susceptibility to interference (3). Consequently, a variety of factors (e.g., assay conditions, enzyme-label employed (4), affinity of the binding system involved (5), amplification of the detection scheme (6), use of better transducers capable of discriminating small signal changes from background noise) have been considered in order to improve the sensitivity and detection limits of these assays (7-9).

Studies performed to elucidate the parameters that control the activity of the enzyme-ligand conjugates demonstrated that the inhibition is a result of either steric exclusion of the substrate from the active site of the enzyme or a conformational change of the enzyme molecule (3, 10, 11). Therefore, the response characteristics of these assays may be affected by the ability of a particular binder to induce such conformational changes. In that respect, it is important to know how different properties of the binder affect the inhibition of the enzyme-ligand conjugates.

In this report, several properties of the binder that may control the nature and magnitude of the inhibition have been investigated. The studies were performed by using an assay for biotin based on the enzyme adenosine deaminase (ADA). This assay was chosen as a model system because of the commercial availability of several well characterized biotin-specific binders (e.g., avidin, streptavidin, anti-biotin antibody). These binders differ in size, isoelectric point, depth of the binding pocket, and association constant with biotin. This investigation revealed that both the depth of the binding pocket of the ligand-specific binder and the modification of the side chains of its amino acids affect the response characteristics of homogeneous enzyme-linked competitive binding assays.

EXPERIMENTAL PROCEDURES

Reagents. The reagents and procedure for the isoelectric focusing experiments have been described previously (12). Avidin (egg white, lyophilized) was obtained from Calbiochem (La Jolla, CA) and streptavidin from InFerGene (Benicia, CA). 4'-Hydroxyazobenzene-2-carboxylate (HABA) and 1,2,4,5-benzenetetracarboxylic dianhydride (PMDA), a reactive form of pyromellitic acid (PML), were obtained from Aldrich (Milwaukee, WI). Sulfo-succinimidyl 6-(biotinamido)hexanoate (biotin-LC-NHS) was from Pierce (Rockford, IL). Tris(hydroxymethyl)aminomethane (Tris) (ultra pure) was obtained from Research Organics (Cleveland, OH). *N*-Hydroxysuccinimide biotin (biotin-NHS), adenosine deaminase (ADA) from calf intestinal mucosa (type VI), bovine serum albumin (BSA), *N*-hydroxysuccinimide (NHS), 1-ethyl-3-[3'-(dimethylamino)propyl]carbodiimide hydrochloride (EDAC), and folic acid were purchased from Sigma (St. Louis, MO). The assay buffer was 0.0100 M Tris-sulfate containing 6.5×10^{-5} M ethylenediaminetetraacetic acid (EDTA), pH 7.40. The biotin and avidin standards were prepared in assay buffer containing 0.10% (w/v) BSA. Deionized (Milli-Q Water Purification System; Millipore, Bedford, MA) distilled water was used for all solutions.

Apparatus. A Perkin-Elmer (Lambda 6) UV/vis spectrophotometer (Norwalk, CT) was employed for all spectrophotometric experiments. An isoelectric focusing apparatus (Model 111 Mini IEF Cell; Bio-Rad, Richmond, CA), along with a standard power supply (Gelman Instrument, Ann Arbor, MI), was used to determine the isoelectric points of the avidin conjugates. The electrophoresis was performed in a nonsieving medium (polyacrylamide gel) in the presence of a carrier ampholyte (Bio-Lyte 3/10 or Bio-Lyte 4/6 from Bio-Rad).

Preparation of the ADA Conjugates. The ADA-biotin conjugate was prepared as described by Kjellström and Bachas (4) using an initial enzyme/biotin mole ratio of 1/500. The ADA-LC-biotin conjugate was prepared in a similar way. The solutions of the enzyme conjugates were stored at 4 °C. The enzymatic activity of the conjugates was monitored potentiometrically (4).

Preparation of the Avidin-PML Conjugates. Avidin was dissolved in a 0.100 M NaHCO₃ (pH 8.50) solution. A 30-fold excess of HABA was added to protect the binding sites of avidin from modification. Aliquots of 2.00 mL of the above solution were used for conjugation. To each aliquot containing 1.0 mg/mL of avidin were added various amounts of a freshly prepared aqueous solution of PMDA.

The mixture was incubated with magnetic stirring at room temperature for 4 h. The pH was maintained between 8.0 and 8.5 throughout the reaction by adjusting with 1.0 M NaOH. The reaction mixture was dialyzed against four changes of 1.0 L of 0.0100 M Tris-sulfate (pH 7.40). The avidin-PML conjugates were characterized by determining their isoelectric point (*pI*). The higher the amount of PML attached to avidin, the lower the *pI* of the conjugate.

Preparation of the Avidin-Folate Conjugates. The avidin-folate conjugates were synthesized by the *N*-hydroxysuccinimide ester method. The activated folate ester was prepared as described by Bachas et al. (13). To prepare the avidin-folate conjugates, the activated folate ester solution was added in aliquots at 5-min intervals into a solution of 3.0 mg mL⁻¹ of avidin in 0.100 M NaHCO₃ (pH 8.50). The conjugation reaction was run under magnetic stirring in an ice bath for 4 h as described for the avidin-PML conjugates. Three avidin-folate conjugates were prepared using initial mole ratios of 1/20, 1/30 and 1/40 of avidin/folate.

Inhibition Studies for the ADA-Biotin System. One hundred microliters of variable concentrations of a biotin-specific binder, 100 μ L of 2.4×10^{-8} M ADA-biotin conjugate (or ADA-LC-biotin), 100 μ L of assay buffer, and 200 μ L of a 0.10% (w/v) BSA solution in assay buffer (to prevent nonspecific binding) were incubated together for 15 min. Then, 1.20 mL of 2.7×10^{-4} M adenosine was added to the assay cup, followed by 15 min of incubation. The enzymatic reaction was stopped by adding 100 μ L of 0.100 M AgNO₃, and then the amount of NH₄⁺ produced was determined. An inhibition graph was generated by plotting the percent inhibition observed vs the moles of binding sites in the assay mixture. The moles of binding sites were determined by titrating each binder with biotin and using HABA as an indicator (14).

Dose-Response Curves. The dose-response characteristics of the assay were studied by incubating biotin standards with the enzyme-biotin conjugate and a biotin-specific binder (4). One hundred microliters each of the enzyme conjugate, binder, and biotin standard were incubated for 20 min prior to the addition of 1.20 mL of 2.7×10^{-5} M adenosine. Dose-response curves were prepared by plotting the percent inhibition observed vs the logarithm of the concentration of the biotin in the standards.

RESULTS AND DISCUSSION

In conventional homogeneous enzyme-linked competitive binding assays the activity of an enzyme-ligand conjugate is inhibited by a ligand-specific binder. The ideal enzyme conjugate for these assays should have high enzymatic activity and should be inhibited at or near 100% by an excess of binder. In this study, native and modified biotin-specific binders were employed in a homogeneous enzyme-linked competitive binding assay for biotin in an attempt to understand how the properties of the binder affect the inhibition of enzyme-ligand conjugates.

Adenosine deaminase was reacted with biotin-NHS to form the respective ADA-biotin conjugate. This enzyme conjugate could be fully inhibited by either avidin or streptavidin. However, for the same concentration of conjugate the inhibition curve obtained by using streptavidin as the binder was shifted toward lower concentrations compared to the one obtained using avidin (Figure 1). As shown in Figure 1, a lower concentration of streptavidin compared to avidin is needed to achieve the same level of inhibition. Consequently, the dose-response curve obtained for streptavidin allows for the determination of

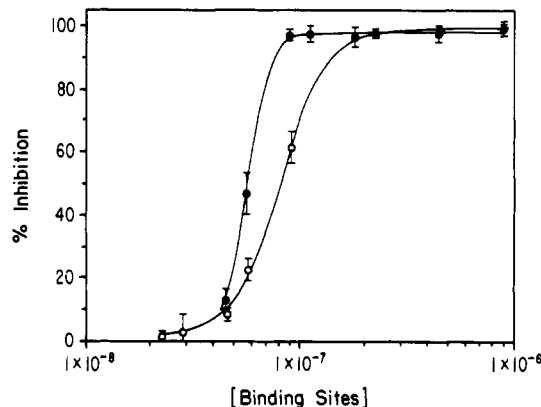


Figure 1. Inhibition curves of the ADA-biotin conjugate obtained by using streptavidin (●) and avidin (○). Error bars indicate \pm one standard deviation ($n = 3$).

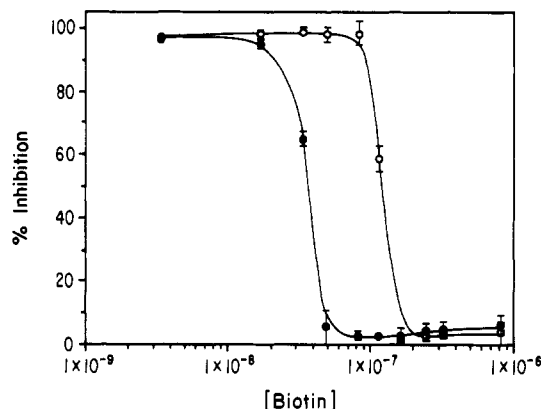


Figure 2. Dose-response curves for biotin obtained by using the ADA-biotin conjugate and streptavidin (●) or avidin (○). Error bars indicate \pm one standard deviation ($n = 3$).

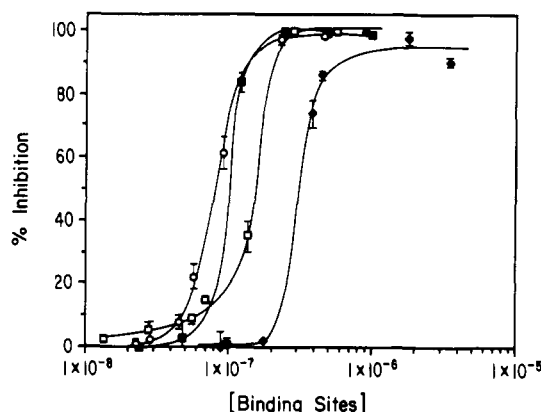
lower concentrations of biotin than the one for avidin (Figure 2). Specifically, the detection limit was found to be 1×10^{-7} M and 2×10^{-8} M biotin when using avidin and streptavidin, respectively. This observation provided the motivation for the present study, since a better understanding of the factors responsible for the lower detection limit obtained by using streptavidin may reveal ways to improve the detection limits of other homogeneous enzyme-linked competitive binding assays.

Avidin and streptavidin are naturally occurring biotin-specific binders that, although they have very different origins, share the same high affinity for biotin. The dissociation constants of both proteins with biotin are on the order of 1×10^{-15} M (15). With respect to physical properties, both molecules are approximately of the same size and both are tetramers comprised of identical subunits (15, 16). The primary structures of the two proteins are almost homologous with respect to the amino acid residues involved in the construction of the biotin binding site (17–19). However, streptavidin is not a glycoprotein whereas avidin is. In addition, streptavidin has a *pI* of ca. 5 and therefore is negatively charged at pH 7.40; in contrast the *pI* of avidin is ca. 10, which causes avidin to be positively charged at pH 7.40 (20).

Because of the large difference in the surface charge between streptavidin and avidin, it was thought that charge interactions may influence the ability of the binder to inhibit ADA-biotin. This led to the hypothesis that a modified avidin with reduced surface charge may improve the detection limits of the assay. In order to test this hypothesis, avidin was modified with PML by formation of an amide bond between the ϵ -amino group of the lysine

Table I. Isoelectric Points (pI) of Conjugates of Avidin with Pyromellitic Acid and Folate

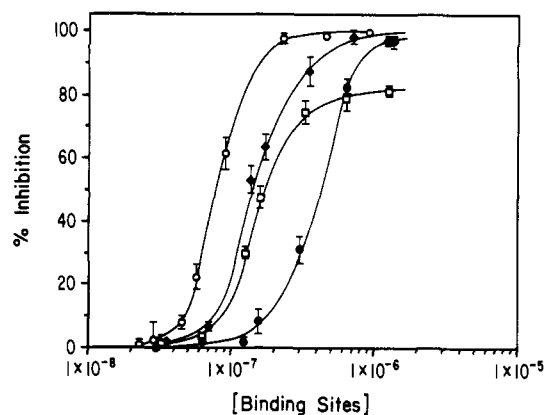
conjugate	initial molar ratio		pI
	PMDA/avidin	folate/avidin	
avidin-PML-1	2/1		9.3
avidin-PML-2	20/1		8.3
avidin-PML-3	60/1		5.7
avidin-folate-1		20/1	8.8
avidin-folate-2		30/1	8.0
avidin-folate-3		40/1	6.0

**Figure 3.** Effect of the modification of the binder on the inhibition of ADA-biotin: avidin (○), avidin-PML-1 (■), avidin-PML-2 (□), and avidin-PML-3 (◆). Error bars indicate \pm one standard deviation ($n = 3$).

residues on the avidin and PML. Three avidin-PML conjugates were prepared, which presented reduced pI values compared to that of avidin (Table I). The inhibition curves obtained with these modified binders demonstrate that a reduction of the positive surface charge of avidin by increasing the amount of conjugated PML (a fact indicated by the decrease in the pI value of the modified avidin) worsens the detection limit attainable by the system (Figure 3). This is also true for the modified avidin that had a pI less than the assay buffer (i.e., overall negatively charged under the conditions of the assay). Therefore, the observed differences in the inhibition caused by avidin and streptavidin cannot be attributed to differences in charge. The above data may be explained by considering that the PML molecules bound on avidin sterically hinder the binding between the enzyme-labeled biotin and avidin leading to assays with worse detection limits.

These observations were further confirmed by modifying avidin with folic acid. Three avidin-folate conjugates were prepared that had a lower surface charge than avidin (Table I). In accordance to the results obtained with the avidin-PML conjugates, it was found that by decreasing the charge of avidin, the detection limits obtained with this system worsen as well (Figure 4). In addition and because of the bulkiness of the structure of folic acid (in comparison to PML), the induced steric hindrance in the interaction between the ADA-biotin and the modified avidin molecules was more pronounced when folate was used as the modifier. Indeed, a comparison of Figures 3 and 4 reveals that avidin-folate conjugates shift the inhibition curve to worse detection limits than avidin-PML conjugates with similar pI values.

It should be noted that the affinity of avidin for biotin may decrease upon modification with PML and folic acid. In such an instance, the inhibition curve should also shift to worse detection limits, since it is known that the association constant between the binder and its specific ligand affects the detectability in binding assays (5). However, no significant difference in the inhibition curves

**Figure 4.** Effect of the modification of the binder on the inhibition of ADA-biotin: avidin (○), avidin-folate-1 (◆), avidin-folate-2 (□), and avidin-folate-3 (●). Error bars indicate \pm one standard deviation ($n = 3$).

of ADA-LC-biotin obtained with avidin and avidin-folate-3 was observed. ADA-LC-biotin was prepared from a derivative of biotin that contains one aminopentanoic acid residue attached to the carboxylic group of biotin by an amide bond. This provides an additional spacer of seven atoms between the attached biotin and the enzyme. The fact that the long-chain conjugate (ADA-LC-biotin) was not as affected by the modifications of avidin as was the short-chain conjugate (ADA-biotin) further supports the steric hindrance argument. Finally, control experiments indicated that an excess of either PML or folic acid does not affect the inhibition of ADA-biotin conjugate by avidin in solution.

On the basis of the above results, it may be concluded that the increased inhibition of biotinylated ADA by streptavidin in comparison to avidin does not arise from its lower surface charge. Further, it should be mentioned that nonglycosylated avidin has been reported to have the same biotin-binding properties as native (glycosylated) avidin (21). Therefore, the difference in the carbohydrate content between the two proteins may not account for the displacement of the inhibition curves depicted in Figure 1. Rather, a possible explanation could involve the consideration that streptavidin binds with biotin in a stronger manner than avidin. The dissociation constants between biotin and avidin or streptavidin are considered to be ca. 1×10^{-15} M (15). Because of the lack of accuracy in the value of the reported dissociation constants, there is no direct support for the hypothesis that streptavidin may bind with biotin more strongly than avidin. However, there is some evidence in the literature that suggests the existence of a higher association constant between biotin and streptavidin than between biotin and avidin. Specifically, streptavidin and avidin were found to have different dissociation rate constants with biotin (22). In addition, Finn et al. found that a greater inhibition of the hormonal activity of biotinylated insulin is observed in the presence of streptavidin than in the presence of avidin (23). These authors proposed that streptavidin is capable of forming a more stable complex with biotinylinsulin than avidin.

Besides the higher association constant with biotin, streptavidin appears to have a deeper binding pocket than avidin as indicated by differences observed in photochemically induced dynamic nuclear polarization experiments (24) and in the shielding of the disulfide bond of Bio-12-SS-dUTP (a biotinylated nucleotide that contains a S-S bond in the linker arm joining biotin to the pyrimidine base) (25).

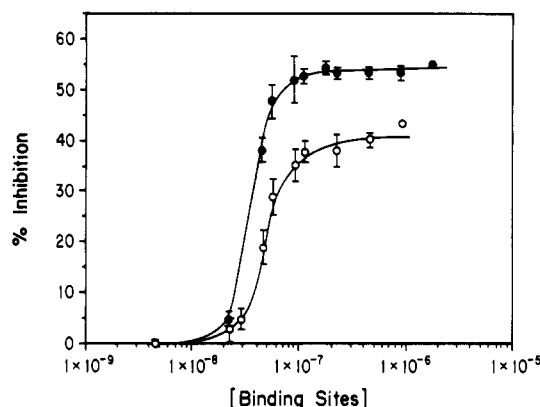


Figure 5. Inhibition curves of the ADA-LC-biotin conjugate obtained by using streptavidin (●) and avidin (○). Error bars indicate \pm one standard deviation ($n = 3$).

It is well-established that in the avidin-biotin complex the carboxylic group of biotin is at least 9 Å beneath the van der Waals surface of the binding protein (15, 26). However, the link provided by the lysine residue in the biotinylated ADA allows only for 7.1 Å between the carboxylic group of biotin and the polypeptide chain of the enzyme. Therefore, formation of the avidin-biotin complex may bring the avidin right to the polypeptide backbone of the ADA-biotin conjugate and either cause a conformational change of the enzyme or physically block its active site (4, 27). In that respect, the depth of the binding pocket of the binder should affect the inhibition of biotinylated ADA. To investigate this, biotin was coupled to the enzyme through a spacer arm of seven atoms to yield the ADA-LC-biotin conjugate. It was found that this conjugate was inhibited to a significantly different extent by streptavidin than by avidin (Figure 5). Indeed, ADA-LC-biotin was inhibited by streptavidin up to 54%, whereas avidin inhibits this enzyme conjugate up to 43%. This observation is consistent with streptavidin having a deeper binding pocket than avidin. Thus, formation of the streptavidin-biotin complex may bring the streptavidin closer (compared to avidin) to the polypeptide backbone of the enzyme conjugate and either cause a conformational change of the enzyme or physically block its active site.

Finally, incubation of the ADA-biotin conjugate with an excess of an anti-biotin antibody did not inhibit the enzymatic activity. Although the lower binding constant between the antibody and the conjugate (28) may play a role in the inhibition of the enzymatic activity, this observation may also be explained by the depth of the binding pocket of the binder, which is lower in the case of antibodies (26).

In conclusion, it was found that the characteristics of the binder significantly affect the detection capabilities of a homogeneous enzyme-linked competitive binding assay for biotin. Such characteristics include the affinity of the binder for its specific ligand and the depth of its binding pocket. It was also found that chemical modification of the binder can lead to undesirable steric hindrance effects. Finally, the information gained through these studies may be useful in the design of optimization strategies for homogeneous enzyme-linked binding assays. In particular, when developing this type of assays one should not only be concerned about the type of ligand derivative chosen for conjugation to the enzyme-label but also about the binding properties of the binder, especially in cases where many ligand-specific binders are available. Moreover, when the assay protocol involves chemical

modification of the various assay reagent components (29), the possible impact of these modifications on the sensitivity and detection limit of the assay should be taken into consideration.

ACKNOWLEDGMENT

This research was supported by a grant from the National Institutes of Health (GM 40510).

LITERATURE CITED

- (1) Ngo, T. T., and Lenhoff, H. M. (1981) Recent advances in homogeneous and separation-free enzyme immunoassays. *Appl. Biochem. Biotechnol.* 6, 53-64.
- (2) Monroe, D. (1984) Enzyme immunoassay. *Anal. Chem.* 56, 920A-931A.
- (3) Ullman, E. F., and Maggio, E. T. (1980) Principles of homogeneous enzyme-immunoassay. *Enzyme-Immunoassay* (E. T. Maggio, Ed.) pp 105-134, CRC Press, Boca Raton, FL.
- (4) Kjellström, T. L., and Bachas, L. G. (1989) Potentiometric homogeneous enzyme-linked competitive binding assays using adenosine deaminase as the label. *Anal. Chem.* 61, 1728-1732.
- (5) Bachas, L. G., and Meyerhoff, M. E. (1986) Theoretical models for predicting the effect of bridging group recognition and conjugate substitution on hapten enzyme-immunoassay dose-response curves. *Anal. Biochem.* 156, 223-238.
- (6) Gleria, K., Hill, H. A. O., and Chambers, J. A. (1989) Homogeneous amperometric ligand-binding assay amplified by a proteolytic enzyme cascade. *J. Electroanal. Chem.* 267, 83-91.
- (7) Mattiasson, B., and Borrebaeck, C. (1980) Novel approaches to enzyme-immunoassay. *Enzyme-Immunoassay* (E. T. Maggio, Ed.) pp 213-248, CRC Press, Boca Raton, FL.
- (8) Chan, W. D. (1987) General principle of immunoassay. *Immunoassay* (W. D. Chan, and T. M. Perlstein, Eds.) pp 1-23, Academic Press, San Diego, CA.
- (9) Feldkamp, S. C., and Stuart, W. S. (1987) Practical guide to immunoassay method evaluation. *Immunoassay* (W. D. Chan, and T. M. Perlstein, Eds.) pp 49-95, Academic Press, San Diego, CA.
- (10) Rubenstein, K. E., Schneider, R. S., and Ullman, E. F. (1972) Homogeneous enzyme immunoassay. A new immunochemical technique. *Biochem. Biophys. Res. Commun.* 47, 846-851.
- (11) Rowley, G. L., Rubenstein, K. E., Huisjen, J., and Ullman, E. F. (1975) Mechanism by which antibodies inhibit hapten-malate dehydrogenase conjugates. An enzyme immunoassay for morphine. *J. Biol. Chem.* 250, 3759-3766.
- (12) Barbarakis, M. S., and Bachas, L. G. (1991) Isoelectric focusing electrophoresis of protein-ligand conjugates; Effect of the degree of substitution. *Clin. Chem.* 37, 87-90.
- (13) Bachas, L. G., Lewis, P. F., and Meyerhoff, M. E. (1984) Cooperative interaction of immobilized folate binding protein with enzyme-folate conjugate: An enzyme-linked assay for folate. *Anal. Chem.* 56, 1723-1726.
- (14) Green, N. M. (1965) A spectrophotometric assay for avidin and biotin based on binding of dyes by avidin. *Biochem. J.* 94, 23c-24c.
- (15) Green, N. M. (1975) Avidin. *Adv. Protein Chem.* 29, 85-133.
- (16) Chaiet, L., and Wolf, F. J. (1964) The properties of streptavidin, a biotin-binding protein produced by streptomycetes. *Arch. Biochem. Biophys.* 106, 1-5.
- (17) Argaraja, C. E., Kuntz, I. D., Birken, S., Axel, R., and Cantor, C. R. (1986) Molecular cloning and nucleotide sequence of the streptavidin gene. *Nucleic Acids Res.* 14, 1871-1882.
- (18) DeLange, R. J., and Huang, T. S. (1971) Egg white avidin. III. Sequence of the 78-residue middle cyanogen bromide peptide. Complete amino acid sequence of the protein subunit. *J. Biol. Chem.* 246, 698-709.
- (19) Bayer, E. A., and Wilchek, M. (1990) Application of avidin-biotin technology to affinity-based separations. *J. Chromatogr.* 510, 3-11.
- (20) Buckland, R. M. (1986) Strong signals from streptavidin-biotin. *Nature* 320, 557-558.

- (21) Hiller, Y., Bayer, E. A., and Wilchek, M. (1990) Nonglycosylated avidin. *Methods Enzymol.* 184, 68-70.
- (22) Piran, U., and Riordan, W. J. (1990) Dissociation rate constant of the biotin-streptavidin complex. *J. Immunol. Methods* 133, 141-143.
- (23) Finn, F. S., Gail, T., and Hofmann, K. (1984) Ligands for insulin receptor isolation. *Biochemistry* 23, 2554-2558.
- (24) Gitlin, G., Khait, I., Bayer, E. A., Wilchek, M., and Muszkat, K. A. (1989) Studies on the biotin-binding sites of avidin and streptavidin. A chemically induced dynamic nuclear polarization investigation of the status of tyrosine residues. *Biochem. J.* 259, 493-498.
- (25) Herman, T. M., Lefever, E., and Shimkus, M. (1986) Affinity chromatography of DNA labeled with chemically cleavable biotinylated nucleotide analogs. *Anal. Biochem.* 156, 48-55.
- (26) Green, N. M., Konieczny, L., Toms, E. J., and Valentine, R. C. (1971) The use of bifunctional biotinyl compounds to determine the arrangement of subunits in avidin. *Biochem. J.* 125, 781-791.
- (27) Daunert, S., Bachas, L. G., and Meyerhoff, M. E. (1988) Homogeneous enzyme-linked competitive binding assay for biotin based on the avidin-biotin interaction. *Anal. Chim. Acta* 208, 43-52.
- (28) Bayer, E. A., and Wilchek, M. (1990) Application of avidin-biotin technology to affinity-based separations. *J. Chromatogr.* 510, 3-11.
- (29) Bacquet, C. A., and Twumasi, D. Y. (1984) A homogeneous enzyme immunoassay with avidin-ligand conjugate as the enzyme-modulator. *Anal. Biochem.* 136, 487-490.
- Registry No.** PMDA, 89-32-7; streptavidin, 9013-20-1.

Efficient Photoaffinity Labeling of Human β -Hexosaminidase A. Synthesis and Application of 3-Azi-1-[(2-acetamido-2-deoxy-1- β -D-glucopyranosyl)thio]- and -galactopyranosyl)thio]butane

Cai-Steffen Kuhn,[†] Jochen Lehmann,^{*,†} and Konrad Sandhoff[‡]

Institut für Organische Chemie und Biochemie der Universität Freiburg, Albertstrasse 21, D-7800 Freiburg i. Br., Germany, and Institut für Organische Chemie und Biochemie der Universität Bonn, Gerhard-Domagk-Strasse, D-5300 Bonn, Germany. Received December 11, 1991

Two photolabile thioglycosides (8 and 9) were synthesized by Koenigs-Knorr type glycosylation. These compounds, being enzyme-resistant analogues of *N*-acetylhexosaminides, were shown to be good competitive inhibitors of lysosomal β -hexosaminidase (2-acetamido-2-deoxy- β -D-hexoside acetamidodeoxyhexohydrolase, EC 3.2.1.52) action. For photoaffinity labeling ³H-labeled 8a was prepared by enzymatic oxidation with galactose oxidase followed by reduction with sodium [³H]borohydride. Compound 8a, when photolyzed in the presence of hexosaminidase, specifically labeled both subunits of the enzyme.

INTRODUCTION

Photoaffinity labeling with suitable ligands has been successfully applied to probe receptor binding sites (1). For probing binding sites of glycoside hydrolases, which usually have a high glycon specificity, the photolabile group must be introduced into the aglycon of an enzyme-resistant glycoside in order to gain sufficient affinity as well as stability against enzyme-catalyzed hydrolysis (2). We recently published the synthesis of the "C-glycoside" 4-acetamido-3,7-anhydro-2-azi-1,2,4-trideoxy-D-glycero-D-gulo-octitol as a potential photoaffinity reagent for human hexosaminidase (3). Although the K_i value (10 mM) of this compound with human hexosaminidase A was acceptable, the efficiency of photoaffinity labeling was unsatisfactory (4). We now describe facile syntheses of two photolabile thiohexosaminides and their successful application as photoaffinity reagents.

EXPERIMENTAL PROCEDURES

General Methods. All reactions were monitored by TLC on silica gel 60 F₂₅₄ (Merck), using the solvents indicated. Flash column chromatography (5) was performed on ICN silica gel (32-63, 60A). Melting points are uncorrected, and the optical rotations were measured with a Polartronic I spectrometer (Schmidt and Haensch). ¹H NMR spectra were recorded with a Bruker WM 250 spectrometer on CDCl₃ solutions (internal Me₄Si). Kinetic data were determined with a fluorimeter (Perkin-Elmer 165/10S). Radioactive material was detected either radioautographically (Agfa-Gevaert Curix X-ray film) or with a Berthold Automatic TLC linear analyzer. Radioactive samples in solution were assayed in a Berthold BF-815 liquid scintillation counter, using the scintillator indicated. Photolabile compounds were irradiated with a Rayonet RPR 100 reactor equipped with 16 lamps (RPR 3500 A, emitting at λ_{\max} = 350 nm) and a ventilator for cooling. NaB³H₄ was purchased from Amersham-Buchler.

Enzymes. Human β -hexosaminidase A (2-acetamido-2-deoxy- β -D-hexoside acetamidodeoxyhexohydrolase, EC

3.2.1.52) from lysosomes was purified by chromatography on concanavalin-A sepharose, ion-exchange chromatography, and gel filtration (the specific activity was 40.5 units/mg) (6). Galactose oxidase (D-galactose:oxygen 6-oxidoreductase, EC 1.1.3.9) from *Dactylium dendroides* (87 units/mg lyophilisate) was purchased from Sigma. Catalase (hydrogen-peroxide:hydrogen-peroxide oxidoreductase, EC 1.11.1.6) from bovine pancreas was purchased from Boehringer Mannheim.

Benzoyl 2-Acetamido-3,4,6-tri-O-acetyl-2-deoxy-1-thio- β -D-galactopyranoside (3). A solution of acetochlorogalactosamine 1 (0.5 g, 1.4 mmol) and potassium thiobenzoate (0.35 g, 2.0 mmol) in dry acetone (10 mL) was heated under reflux. After 1 h the mixture was filtrated and concentrated to dryness; the residue was subjected to flash chromatography (cyclohexane/ethyl acetate 3:1) and recrystallized from ethanol to give 3 (0.46 g, 70%): mp 141 °C; TLC (cyclohexane/ethyl acetate 3:1) R_f 0.21; [α]_D +6.1° (c 1, chloroform); ¹H NMR (CDCl₃) δ 1.89, 2.03, 2.05, 2.18 (4 \times s, 12 H, OAc), 4.10 (t, 1 H, H-5), 4.12 (d, 2 H, H-6a,b), 4.67 (dd, 1 H, $J_{2,3}$ = 10.5 Hz, H-2), 5.21 (dd, 1 H, $J_{3,4}$ = 3.75 Hz, H-3), 5.49 (d, 1 H, $J_{1,2}$ = 10.35 Hz, H-1), 6.16 (d, 1 H, J_{NH_2} = 9.5 Hz, NH), 7.47-7.97 (m, 7 H, Bz). Anal. Calcd for C₂₁H₂₅NO₉S: C, 53.95; H, 5.39; N, 2.99; S, 6.86. Found: C, 54.00; H, 5.38; N, 2.84; S, 6.65.

Benzoyl 2-Acetamido-3,4,6-tri-O-acetyl-2-deoxy-1-thio- β -D-glucopyranoside (4). Acetochloroglucosamine 2 (4 g, 14 mmol) in dry acetone (20 mL) was treated with potassium thiobenzoate (2.5 g, 14 mmol) and chromatographed (cyclohexane/ethyl acetate 3:1), as described for 3. Compound 4 crystallized from ethanol to give white crystals (3.75 g, 73.6%): mp 160 °C; TLC (cyclohexane/ethyl acetate 3:1) R_f 0.25; [α]_D -10.5° (c 1, chloroform); ¹H NMR (CDCl₃) δ 1.91, 2.05, 2.07, 2.08 (4 \times s, 12 H, OAc), 3.89 (ddd, 1 H, $J_{5,6a}$ = 4.65 Hz, $J_{5,6b}$ = 2.35 Hz, H-5), 4.14 (dd, 1 H, H-6a), 4.29 (dd, 1 H, H-6b), 4.53 (m, 1 H, H-2), 5.21 (m, 2 H, H-3,4), 5.43 (d, 1 H, $J_{1,2}$ = 10.5 Hz, H-1), 6.01 (d, 1 H, J_{NH_2} = 9.5 Hz, NH), 7.49-7.94 (m, 7 H, Bz). Anal. Calcd for C₂₁H₂₅NO₉S: C, 53.95; H, 5.39; N, 2.99; S, 6.86. Found: C, 53.74; H, 5.36; N, 3.21; S, 6.89.

3-Azi-1-[(2-acetamido-3,4,6-tri-O-acetyl-2-deoxy- β -D-galactopyranosyl)thio]butane (6). A solution of 3 (0.4 g, 0.85 mmol) and 3-azi-1-[(*p*-tolylsulfonyl)oxy]bu-

* Author to whom correspondence should be addressed.

[†] Universität Freiburg.

[‡] Universität Bonn.

tane 5 (0.26 g, 1 mmol) in dry methanol (5 mL) was treated with 1 M methanolic sodium methylate (200 μ L). The mixture was stirred 2 h at room temperature, deionized with Amberlite IR 120 H⁺ resin, evaporated to dryness, and reacylated in pyridine/acetic acid (5 mL, 2:1). The usual workup and flash chromatography (cyclohexane/ethyl acetate 1:1) gave 6 as white solid (350 mg, 61%); TLC (cyclohexane/ethyl acetate 1:1) R_f 0.25; $[\alpha]_D +2.6^\circ$ (c 1, chloroform); ¹H NMR (CDCl₃) δ 1.06 (s, 3 H, H-4'), 1.65 (m, 2 H, H-2'a,b), 1.97, 2.00, 2.07, 2.17 (4 \times s, 12 H, OAc), 2.61 (m, 2 H, H-1'a,b), 3.93 (t, 1 H, H-5), 4.11 (d, 2 H, H-6a,b), 4.21 (dd, 1 H, $J_{2,3} = 10.65$ Hz, H-2), 4.62 (d, 1 H, $J_{1,2} = 10.35$ Hz, H-1), 5.39 (d, 1 H, $J_{3,4} = 3.7$ Hz, H-4), 5.77 (d, 1 H, $J_{NH,2} = 9.5$ Hz, NH).

3-Azi-1-[(2-acetamido-3,4,6-tri-*O*-acetyl-2-deoxy- β -D-glucopyranosyl)thio]butane (7). A solution of 4 (1 g, 2.12 mmol) and 5 (0.65 g, 2.5 mmol) in anhydrous methanol (10 mL) was treated with methanolic sodium methoxide (0.5 mL) as described for compound 6. After evaporation and reacylation the crude product was purified by flash chromatography (cyclohexane/ethyl acetate 2:1). Crystallization from ethyl acetate/ethanol gave white crystals of 7 (578 mg, 61%); mp 153 $^\circ$ C; TLC (cyclohexane/ethyl acetate 2:1) R_f 0.19; $[\alpha]_D -41.5^\circ$ (c 1, chloroform); ¹H NMR (CDCl₃) δ 1.04 (s, 3 H, H-4'), 1.65 (m, 2 H, H-2'a,b), 1.97, 2.03, 2.05, 2.11 (4 \times s, 12 H, OAc), 2.58 (m, 2 H, H-1'a,b), 3.68 (ddd, 1 H, $J_{5,6a} = 2.4$ Hz, $J_{5,6b} = 2.5$ Hz, H-5), 4.07 (t, 1 H, $J_{2,3} = 9.35$ Hz, H-2), 4.15 (d, 1 H, $J_{6a,6b} = 2.5$ Hz, H-6a), 4.22 (dd, 1 H, H-6b), 4.56 (d, 1 H, $J_{1,2} = 10.5$ Hz, H-1), 5.25 (d, 1 H, $J_{3,4} = 3.75$ Hz, H-4), 5.67 (d, 1 H, $J_{NH,2} = 9.5$ Hz, NH).

3-Azi-1-[(2-acetamido-2-deoxy- β -D-galactopyranosyl)thio]butane (8). A solution of compound 6 (0.2 g, 0.45 mmol) in dry methanol (5 mL) was stirred with 1 M methanolic sodium methoxide (100 μ L) for 0.5 h, when TLC (ethyl acetate/methanol 5:1) indicated the absence of 6. Filtration through a short column of silica gel, evaporation of the solvent, and lyophilization yielded 8 (138 mg, 96%); $[\alpha]_D +5.6^\circ$ (c 1.0, water); TLC (ethyl acetate/methanol/water 7:2:1) R_f 0.46. Anal. Calcd for C₁₂H₂₁N₃O₅S: C, 45.13; H, 6.63; N, 13.15; S, 10.04. Found: C, 44.04; H, 6.43; N, 12.77; S, 10.14.

3-Azi-1-[(2-acetamido-2-deoxy- β -D-glucopyranosyl)thio]butane (9). Peracetate 7 (0.5 g, 1.12 mmol) was deacetylated as described for compound 6. Crystallization from ethanol/ethyl acetate gave 9 (325 mg, 91%; colorless crystals); mp 168–171 $^\circ$ C; TLC (ethyl acetate/methanol 5:1) R_f 0.25; $[\alpha]_D -38^\circ$ (c 1.0, water). Anal. Calcd for C₁₂H₂₁N₃O₅S: C, 45.13; H, 6.63; N, 13.15; S, 10.04. Found: C, 43.87; H, 6.38; N, 12.78; S, 9.88.

3-Azi-1-[(6-³H]-2-acetamido-2-deoxy- β -D-galactopyranosyl)thio]butane (8a). Compound 8 (30 mg, 94 μ mol) was dissolved in sodium phosphate buffer (1 mL, pH 7.2, 10 mM). D-Galactose oxidase (0.4 mg, 87 units/mg) and catalase (30 μ L, 1300 units/mL) were added at 37 $^\circ$ C. Formation of the 6-aldehyde compound was indicated by TLC (ethyl acetate/methanol/water 17:2:1, R_f 0.24). After 11 h, when no educt was detected by TLC, the reaction mixture was passed through a column (silica gel, 0.5 \times 3 cm) with water as eluent. The eluate was concentrated under diminished pressure to 200 μ L, made alkaline with aqueous sodium hydroxide (1 M, pH 9), and added to an ampule containing NaB³H₄ (100 mCi, specific activity 5 Ci/mmol). After 12 h, the mixture was neutralized (acetic acid) and concentrated to dryness. The residue was subjected to column chromatography (ethyl acetate/methanol/water 17:2:1) to give 33 mCi of the 6-³H-labeled 8a (specific activity, 1.25 Ci/mmol). The

radioactivity cochromatographed with unlabeled 8 on two-dimensional TLC (ethyl acetate/methanol/water 7:2:1).

Determination of the Inhibition Constants (K_i). Fluorescent substrate umbelliferyl 4-methyl-2-acetamido-2-deoxy- β -D-glucopyranoside (Fluka) was used as substrate (1–2.5 mM) in sodium citrate buffer (pH 4.5, 50 mM) at 37 $^\circ$ C (7). Inhibitors were used in the following concentrations: 8, 0–6 mM; 9, 0–10 mM. Each assay involved 0.25 mUnit/mL β -hexosaminidase A.

Irreversible Deactivation of β -Hexosaminidase with Compounds 8 and 9. Solutions of enzyme (0.1 mL, 3 units/mL) with compounds 8 (18 mM) or 9 (49 mM) were each irradiated for 20 min with UV light ($\lambda_{max} = 350$ nm). This experiment was repeated with solutions of the same compositions each containing additional compound 10 (155 mM). For reference a solution of the enzyme without photolabile reagent was treated in the same manner. After diluting with citrate buffer (1:100), enzyme activity was assayed in each mixture as described above.

Reaction of 3-Azi-1-[(6-³H]-2-acetamido-2-deoxy- β -D-galactopyranosyl)thio]butane with β -Hexosaminidase A. Compound 8a (3.6 μ mol) was dissolved in a solution of β -hexosaminidase A (100 μ g) in 200 μ L sodium citrate buffer (solution A). Part (100 μ L) of solution A was incubated with an excess (155 mM) of compound 10 (solution B). Solutions A and B were deoxygenated by bubbling with nitrogen gas for 2 min, then irradiated at 350 nm for 20 min, and dialyzed against buffer and water, until no more radioactivity was released into the dialysate. The radioactivity of the protein solutions was determined by liquid scintillation counting of an aliquot with Quickszint 1 (Zinsser). For solution A 0.19 nmol and for B 0.02 nmol of incorporated radioactive ligand was found per 0.416 nmol of β -hexosaminidase A.

Reduction and Carboxymethylation of ³H-Labeled β -Hexosaminidase. The samples (A and B) were freeze-dried, reduced (50 mM dithiothreitol at 60 $^\circ$ C for 10 min), and then alkylated (100 mM sodium iodoacetate at room temperature for 1 h) in 7 M guanidinium hydrochloride/0.5 M Tris-HCl, pH 8.5 (0.2 μ L). The reaction was stopped by adding an excess of 2-mercaptoethanol (10 μ L). After deionization with Sephadex-G25 (PD 10 column, Pharmacia), the samples were dried in a Speed Vac concentrator.

Gel Electrophoresis. Sodium dodecyl sulfate polyacrylamide gel electrophoresis (SDS-PAGE) was performed according to the method of Laemmli (8). A separation gel (12 cm long) containing 10% acrylamide was used in combination with a stacking gel (2 cm long, 4.5% acrylamide). The reduced and alkylated samples (50 μ g) were dissolved in 0.1 mL of Tris-HCl buffer (62.5 mM, pH 6.8) containing 2% SDS, 10% glycerol, 5% 2-mercaptoethanol, and 0.001% bromphenol blue. Electrophoresis was carried out until the bromphenol blue marker reached the bottom of the gel. After electrophoresis the protein bands were localized by staining with Serva Blue. The molecular weight was estimated by the standard calibration kit from Pharmacia Fine Chemicals (Uppsala, Sweden). For determination of the incorporated radioactivity the gel was cut into 2-mm slices, each of which was submerged in Biolute-S (Zinsser, 0.5 mL) and left overnight. Quickszint-501 (4 mL) was then added, the mixture was kept for 1 h in the cold, and the radioactivity was then counted.

RESULTS

Lysosomal β -hexosaminidase (2-acetamido-2-deoxy- β -D-hexoside acetamidodeoxyhydrolase, EC 3.2.1.52) exists

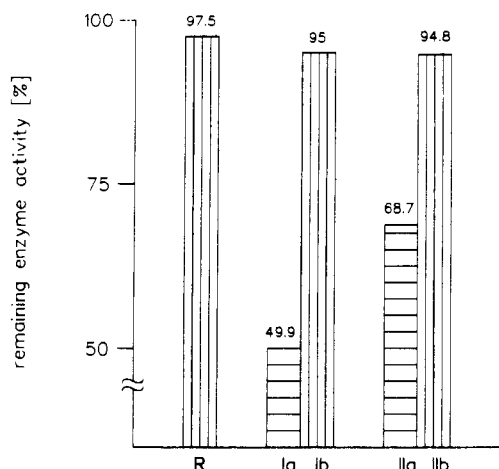


Figure 1. Deactivation of β -hexosaminidase A by 3-azi-1-[(2-acetamido-2-deoxy-1- β -D-glucopyranosyl)thio]- and -galactopyranosyl)thio]butane (8 and 9). Each sample contained enzyme and had been irradiated for 20 min at $\lambda_{\max} \approx 350$ nm under cooling by ventilation: R, reference without additive; Ia, with compound 8; Ib, with compounds 8 and 10; IIa, with compound 9; IIb, with compounds 9 and 10.

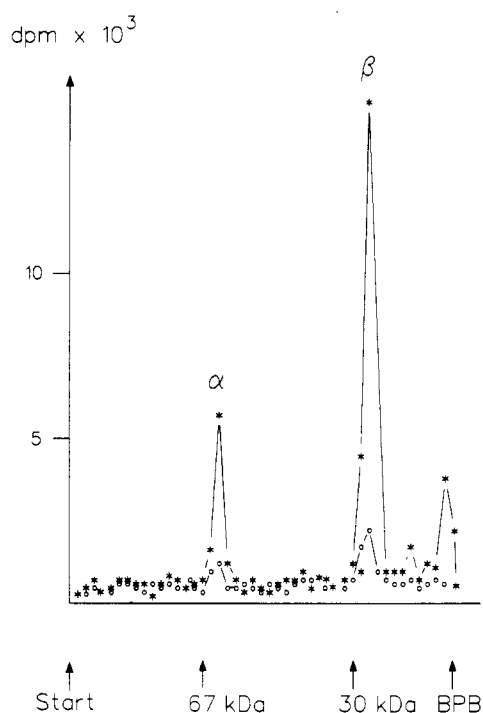
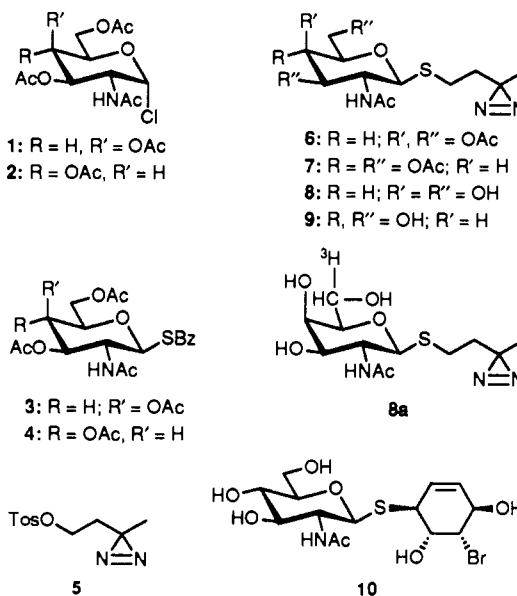


Figure 2. SDS-PAGE of radioactively labeled β -hexosaminidase A. Radioactivity is associated with both α - and β -subunits, the β -subunit being labeled more efficiently. The arrows indicate the position of calibration proteins and the marker bromophenol blue (BPB). Radioactivity was determined using a liquid scintillation counter: (*) protein, photoaffinity labeled by 3-azi-1-[(6- 3 H)-2-acetamido-2-deoxy-1- β -D-galactopyranosyl)thio]butane (8a), (O) protein, photoaffinity labeled by compound 8a in the presence of the competitive inhibitor compound 10 (155 mM).

as two main oligomeric proteins, hexosaminidase A ($M = 120\,000$) and hexosaminidase B ($M = 130\,000$) composed of the subunits α (54 kDa) (9) and β (56 kDa), where A is $\alpha\beta$ and B is 2β . The β -subunit consists of two peptide chains of approximately 30 000 Da each, which are linked by disulfide bridges (10). Under denaturing conditions (reduction with dithiothreitol and carboxymethylation with sodium iodoacetate) the peptides come apart and show as a single band in SDS-PAGE (compare Figure 2). Hexosaminidase A has two active sites, one on each

subunit, with significant differences in specificity for N -acetylhexosaminides (11). Elucidation of the structure and function of the enzyme is of general clinical interest, because genetic defects in the α - (Tay Sachs' disease) or β -subunit (Sandhoff's disease) cause fatal accumulation of the ganglioside G_M2 (12). Thioglycosides are resistant against enzyme-catalyzed hydrolytic cleavage and therefore useful and generally potent competitive inhibitors. Especially the β -thioglycosides are easily prepared by Koenigs-Knorr type glycosylation of a thionucleophile (13).

2-Acetamido-3,4,6-tri- O -acetyl-2-deoxy- α -D-galactopyranosyl chloride (1) (14) and 2-acetamido-3,4,6-tri- O -acetyl-2-deoxy- α -D-glucopyranosyl chloride (2) (15) were



both converted into the corresponding benzoyl 2-acetamido-3,4,6-tri- O -acetyl-2-deoxy-1-thio- β -D-hexosaminides (3 and 4) using potassium thiobenzoate as nucleophile. 3-Azi-1-(tosyloxy)butane (5) (16) is a versatile alkylating agent for the facile introduction of the photolabile 3-azibutyl group into thio derivatives of carbohydrates (17). Compounds 3 and 4 were deacylated in situ by dilute sodium methoxide, alkylated with compound 5 and acetylated to yield 3-azi-1-[(2-acetamido-3,4,6-tri- O -acetyl-2-deoxy- β -D-galactopyranosyl)thio]butane (6) and - β -D-glucopyranosyl)thio]butane (7). For the de- O -acetylated thioglycosides 8 and 9, the inhibition constants K_i were determined by Dixon plot to be 1.8 (8) and 4.9 mM (9). When a solution of β -hexosaminidase A in buffer was irradiated for 20 min in the presence of either 8 or 9, using 350-nm UV light, the enzyme became irreversibly deactivated to 50.1% and 31.3%, respectively. In the absence of 8 or 9, irradiation had hardly any effect on enzyme activity. In the presence of the competitive nonreactive inhibitor 10 the enzyme could be protected against photodeactivation by compounds 8 or 9 (Figure 1). Because of its higher affinity, the N -acetylgalactosaminide was chosen for radioactive labeling with tritium. Compound 8 was oxidized by galactose oxidase and the resulting aldehyde reduced with sodium borohydride to give 3-azi-1-[(6- 3 H)-2-acetamido-2-deoxy- β -D-galactopyranosyl)thio]butane (8a). This material having a specific radioactivity of 1.25 Ci/mmol, was used for radiolabeling hexosaminidase A. Irradiation of an incubation mixture in the presence of 8a gave radioactively labeled protein. Radiolabeling could almost totally be suppressed when the competitive inhibitor 10 (18) had been added before

irradiation. Incorporation of covalently bound ligand was 45%/mol of protein as calculated from the measured radioactivity in the thoroughly dialyzed solution. Electrophoresis in polyacrylamide under denaturing conditions separates labeled hexosaminidase A into the unequally labeled subunits (Figure 2). The α -subunit carries 30%, the β -subunit 70%, of the total radioactivity.

ACKNOWLEDGMENT

J.L. thanks the Deutschen Forschungsgemeinschaft (DFG) for financial support.

LITERATURE CITED

- (1) Knowles, J. R., and Bayley, H. (1977) *Methods Enzymol.* 46, 69–114.
- (2) Kuhn, C.-S., and Lehmann, J. (1987) *Carbohydr. Res.* 160, C6–C8.
- (3) Ats, S. C., Lausberg, E., Lehmann, J., and Sandhoff, K. (1990) *Liebigs Ann. Chem.* 1261–1264.
- (4) Ats, S. C., Lausberg, E., Lehmann, J., and Sandhoff, K. Unpublished results.
- (5) Still, M. C., Kahn, M., and Mitra, A. (1978) *J. Org. Chem.* 43, 2923–2925.
- (6) Sandhoff, K., Conzelmann, E., and Nehrhorn, H. (1977) *Hoppe-Seyler's Z. Physiol. Chem.* 358, 779–787.
- (7) Leaback, D. H., and Walker, P. G. (1961) *Biochem. J.* 78, 151–156.
- (8) Laemmli, U. K. (1970) *Nature* 227, 680–685.
- (9) Mahuran, D. L., and Lowden, J. A. (1980) *Can. J. Biochem.* 58, 287–294.
- (10) Mahuran, D. J., Tsui, F., Gravel, R. A., and Lowden, J. A. (1982) *Proc. Natl. Acad. Sci. U.S.A.* 79, 1602–1605.
- (11) Kytzia, H.-J., and Sandhoff, K. (1985) *J. Biol. Chem.* 260, 7568–7572.
- (12) Sandhoff, K., Conzelmann, E., Neufeld, E. F., Kaback, M. M., and Susuki, K. (1989) *The Metabolic Basis of Inherited Disease*, 6th ed., (C. R. Scriver, A. L. Beaudet, W. S. Sly, D. Valle, Eds.) pp 1807–1842, McGraw-Hill, New York.
- (13) Horton, D. (1963) *Methods Carbohydr. Chem.* 2, 435–436.
- (14) Tarasiejska, Z., and Jeanloz, R. W. (1958) *J. Am. Chem. Soc.* 80, 6325–6327.
- (15) Horton, D. (1972) *Methods Carbohydr. Chem.* 6, 282–285.
- (16) Church, R. F., and Weiss, M. J. (1970) *J. Org. Chem.* 35, 2465–2471.
- (17) Kuhn, C.-S., Lehmann, J., and Steck, J. (1990) *Tetrahedron Lett.* 46, 3129–3134.
- (18) Kuhn, C.-S., Lehmann, J., and Sandhoff, K. (1992) *Liebigs Ann. Chem.* In press.

Molecular Probes for Muscarinic Receptors: Derivatives of the M₁-Antagonist Telenzepine

Yishai Karton,^{§,†,‡} Jesse Baumgold,[§] Jeffrey S. Handen,[§] and Kenneth A. Jacobson^{*†}

Israel Institute for Biological Research, Nes Ziona, Israel, Department of Radiology, George Washington University Medical Center, Washington, D.C. 20037, and Laboratory of Bioorganic Chemistry, NIDDK, National Institutes of Health, Bethesda, Maryland 20892. Received January 6, 1992

Functionalized congeners of the M₁-selective muscarinic antagonist telenzepine (4,9-dihydro-3-methyl-4-[(4-methyl-1-piperazinyl)acetyl]-10H-thieno[3,4-b][1,5]benzodiazepin-10-one) were developed and found to bind to the receptor with affinities (K_i values) in approximately the nanomolar range. The derivatives contain a 10-aminodecyl group, which provides a nucleophilic functionality for further derivatization. The attachment of a spacer chain to the distal piperazinyl nitrogen was based on previous findings of enhanced affinity at muscarinic receptors in an analogous series of alkylamino derivatives of pirenzepine [*J. Med. Chem.* (1991) 34, 2133-2145]. The telenzepine derivatives contain prosthetic groups for radioiodination, protein cross-linking, photoaffinity labeling, and fluorescent labeling and biotin for avidin complexation. The affinity for muscarinic receptors in rat forebrain (mainly m₁ subtype) was determined in competitive binding assays vs [³H]-N-methylscopolamine. A (*p*-aminophenyl)-acetyl derivative for photoaffinity labeling had a K_i value of 0.29 nM at forebrain muscarinic receptors (16-fold higher affinity than telenzepine). A biotin conjugate displayed a K_i value of 0.60 nM at m₂-receptors and a 5-fold selectivity versus forebrain. The high affinity of these derivatives makes them suitable for the characterization of muscarinic receptors in pharmacological and spectroscopic studies, for peptide mapping, and for histochemical studies.

INTRODUCTION

Acetylcholine acts as a neurotransmitter through both muscarinic (1) and nicotinic receptors (2), in the central nervous system and at peripheral sites, such as heart and ileum. Five subtypes of muscarinic acetylcholine receptors (m₁-m₅) have been cloned (3). The receptors belong to the functional and structural class of G-protein-coupled receptors, which contain seven transmembrane helices (4). The binding sites for agonists and antagonists are thought to be nonequivalent, although there is little direct evidence (5) for which amino acid residues are involved in the binding of ligands. The details of the conformational changes in the receptor protein produced by ligand binding are unknown.

In general, structural knowledge of the G-protein-linked receptors has been obtained through site-directed mutagenesis (6) and by using specialized ligands as molecular probes (5, 7-12). Such molecular probes include irreversible affinity labels containing chemically- and photochemically-reactive groups (5, 7-9), fluorescent labels and other spectroscopic reporter groups (10-11), biotinylated probes (10, 12). We have developed a functionalized congener approach to the design of muscarinic ligands (13, 14), which in this study is extended to sites for the attachment of reporter groups to high-affinity antagonists. We have derivatized the M₁-selective antagonist telenzepine (20) in a manner analogous to our previous work with the structurally similar pirenzepine (14). These functionalized ligands are also potentially suited for affinity chromatography and histochemical characterization of the receptors.

EXPERIMENTAL PROCEDURES

¹H NMR spectra were recorded using a Varian XL-300 FT-NMR spectrometer and all values are reported in parts per million (ppm, δ) downfield from tetramethylsilane (TMS). Chemical ionization MS using ionized NH₃ gas were recorded using a Finnigan 1015D mass spectrometer modified with EXTREL electronics. Fast atom bombardment MS was carried out on a JEOL JMS-SX102 mass spectrometer, and parent ion peaks measured at high resolution are listed in Table II. Thin-layer chromatography (TLC)¹ analyses were carried out using EM Kieselgel 60 F254, DC-Alufolien 200- μ m plates and were visualized in an iodine chamber and/or with 1% ninhydrin in ethanol. R_f values in two solvent systems are given in Table II. Silica gel columns used MN-Kieselgel 60 (230-400 mesh) silica gel. Elemental analyses were performed by Atlantic Microlabs, Inc. (Atlanta, GA). The term in vacuo refers to a water aspirator (15-30 mmHg) rotary evaporator. Percent yields are rounded to the nearest whole number.

4,9-Dihydro-3-methyl-4-(1-piperazinylacetyl)-10H-thieno[3,4-b][1,5]benzodiazepin-10-one (2). Telenzepine dihydrochloride (0.527 g, 1.20 mmol; Research Biochemicals Inc., Natick MA) was dried in vacuo over P₂O₅. Chloroform (7 mL) and *N,N*-diisopropylethylamine (1.66 mL) were added, and the mixture was cooled in an ice bath and stirred until a solution formed. α -Chloroethyl chloroformate (1.4 g, 9.8 mmol) was added dropwise, and the solution was warmed for 0.5 h at 40 °C. The CHCl₃ was removed in vacuo, and the solid [consisting mainly of the *N*-(α -chloroethoxycarbonyl) intermediate which was not isolated] was dissolved in methanol and sufficient 1 M HCl in ether to lower the pH to 0-1. The solution was refluxed for another 0.5 h and after cooling

* Address for correspondence: Dr. Kenneth A. Jacobson, Bldg 8A, Rm B1A-17, NIH, Bethesda, MD.

[†] Israel Institute for Biological Research.

[‡] NIH.

[§] George Washington University Medical Center.

¹ Abbreviations used: ASA, 4-azidosalicylic acid; Boc, *tert*-butoxycarbonyl; DITC, 1,3-phenylene diisocyanate; DMF, dimethylformamide; NMS, *N*-methylscopolamine; TFA, trifluoroacetic acid; TLC, thin-layer chromatography.

immediately basified with aqueous sodium carbonate and washed with ether. The aqueous layer was saturated with sodium chloride and extracted into CHCl_3 . The organic extracts were evaporated in vacuo, and the residue was purified by silica gel column chromatography (chloroform/methanol/ammonia, 90:10:1, by vol) to provide 159 mg (37% yield) of **2**: The ^1H NMR (CDCl_3) spectrum showed a characteristic singlet for the thiophene CH_3 (3 H) at δ 2.43 ppm; MS (CI/NH_3) m/e 357 (MH^+ , base).

4,9-Dihydro-3-methyl-4-[[4-(10-aminodecyl)-1-piperazinyl]acetyl]-10H-thieno[3,4-*b*][1,5]benzodiazepin-10-one (4). A solution of **2** (158 mg, 0.43 mmol), 1,10-dibromodecane (1.1 g, 3.6 mmol) and *N,N*-diisopropylethylamine (0.2 g) was stirred in chloroform (3 mL) at 55 °C for 6 h. The reaction was judged complete by TLC, and all volatile materials were removed in vacuo. The resulting clear mixture was evaporated under N_2 , and the residue was washed several times with petroleum ether to give **4,9-dihydro-3-methyl-4-[[4-(10-bromodecyl)-1-piperazinyl]acetyl]-10H-thieno[3,4-*b*][1,5]benzodiazepin-10-one (3)**, which was used without further purification.

The powder, **3**, was dissolved in 2 mL of methanol, treated with 1 mL of concentrated NH_4OH , and heated for 6 h at 50 °C. The reaction mixture was cooled and extracted with ether (6 \times 10 mL). The ether extracts were evaporated in vacuo, leaving 0.27 g of the crude product, **4**, which was purified on a silica gel column (chloroform/methanol/ammonia, 90:10:1, by vol). An analytical sample of the trihydrochloride salt of **4** was prepared. Anal. Calcd ($\text{C}_{28}\text{H}_{44}\text{N}_5\text{Cl}_3\text{O}_2\cdot 2\text{H}_2\text{O}$): 51.18, C; 7.36, H; 10.66, N. Found: 51.10, C; 7.22, H; 10.48, N.

The purity of **4** was demonstrated using HPLC. With a gradient of 20 to 80% acetonitrile in water (both solvents containing 0.1% TFA, LKB Ultrapak C-18 Column, 25 \times 0.4 cm, flow rate 1 mL/min, detection at 254 nm, pressure <2K psi), a single peak emerged at 9.9 min. Telenzepine under the same conditions had a retention time of 8.3 min.

4,9-Dihydro-3-methyl-4-[[4-[10-[[3-(4-hydroxyphenyl)propionyl]amino]decyl]-1-piperazinyl]acetyl]-10H-thieno[3,4-*b*][1,5]benzodiazepin-10-one (5). Compound **4** (5.0 mg, 7.6 μmol) was dissolved in chloroform (0.7 mL). *N*-Succinimidyl 3-(4-hydroxyphenyl)propionate (5.5 mg, 21 μmol) was added. The reaction was judged complete by TLC after 6 h at 25 °C. Methanolic HCl was added (pH 1), and the solution was kept in a refrigerator overnight. The precipitate was washed successively with chloroform and dried to give **5**. The product, visualized using UV and iodine vapors, was pure by TLC. The product had a retention time of 14 min using HPLC (same conditions as given above for **4**).

4,9-Dihydro-3-methyl-4-[[4-[10-[[4-(4-aminophenyl)acetyl]amino]decyl]-1-piperazinyl]acetyl]-10H-thieno[3,4-*b*][1,5]benzodiazepin-10-one (6) and 4,9-Dihydro-3-methyl-4-[[4-[10-[[4-((*tert*-butoxycarbonyl)amino]phenyl)acetyl]amino]decyl]-1-piperazinyl]acetyl]-10H-thieno[3,4-*b*][1,5]benzodiazepin-10-one (7). Compound **4** (5.0 mg, 7.6 μmol) was dissolved in benzene/chloroform (0.25 mL, 3:2, by vol). *N*-Succinimidyl *p*-[(*tert*-butoxycarbonyl)amino]phenylacetate was prepared as described in ref 7, dissolved (5.0 mg, 14 μmol) in chloroform (0.5 mL), and added to the solution of **4** with stirring. The reaction was complete after 1 h. Methanolic HCl was added carefully in the cold to acidify the mixture to pH 1–2. Following the addition of 0.2 mL of ether the product precipitated slowly, overnight at 0 °C. A total of two crops of the product was collected, combined, and washed with chloroform. The product, visualized

using UV or iodine vapors, was pure by thin-layer chromatography and was used as such for the preparation of **6**.

TFA was added slowly to the solid Boc-protected amine derivative **7**, and the reaction was stirred for 10 min. The excess TFA was removed under a stream of N_2 , and the resulting oily residue was washed with ether and dried for 24 h at 50 °C under high vacuum (0.1 mmHg) to yield the free arylamine **6**.

4,9-Dihydro-3-methyl-4-[[4-[10-[(4-azido-2-hydroxybenzoyl)amino]decyl]-1-piperazinyl]acetyl]-10H-thieno[3,4-*b*][1,5]benzodiazepin-10-one (8). Compound **4** (5.0 mg, 7.6 μmol) was dissolved in benzene/chloroform (0.25 mL, 3:2, by vol). The *N*-succinimidyl ester of 4-azidosalicylic acid (NHS-ASA, Pierce Chemical Co., Rockford, IL; 6.0 mg, 21.7 μmol) was added. The reaction was kept in the dark and was complete after 0.5 h. Following the addition of 0.2 mL of ether the product precipitated slowly, during 2 days at 0 °C. The product was collected and washed with chloroform and was shown to be pure by reversed-phase HPLC. With a gradient of 20 to 80% acetonitrile in water, both containing 0.1% trifluoroacetic acid (same conditions as given for compound **4**), the retention time of **8** was 18 min. An isocratic run at 50% acetonitrile showed a single peak at 5.8 min. A DMSO solution stored at –20 °C in the dark for 2 months remained pure: ^1H NMR (CDCl_3) δ 1.2–1.5 (m, 16 H), 2.4 (s, 3 H), 3.2–3.8 (m, 14 H), 6.5 (m, br d, 1 H), 6.6 (s, 1 H), 7.2–7.5 (m, 4 H), 7.8 (br s, 1 H) ppm.

4,9-Dihydro-3-methyl-4-[[4-[10-[[5-(hexahydro-2-oxo-1H-thieno[3,4-*d*]imidazol-4-yl)-1-oxopentyl]amino]decyl]-1-piperazinyl]acetyl]-10H-thieno[3,4-*b*][1,5]benzodiazepin-10-one (9). Compound **4** (5.0 mg, 7.6 μmol) was dissolved in benzene/chloroform (0.25 mL, 3:2, by vol). (+)-Biotin *N*-hydroxysuccinimide ester (Fluka, Ronkonoma, NY; 6.5 mg, 19 μmol , dissolved in 0.4 mL of dimethylformamide) was added. The reaction was stirred for 1 h. Methanolic HCl was added causing the product to precipitate slowly, overnight. The precipitate was washed successively with chloroform and ether to yield **9** (1 mg, 20% yield). The product, which was visualized using UV or iodine vapors, was pure by thin-layer chromatography (alumina 5550, Merck, chloroform/methanol/ammonia, 90:10:1): ^1H NMR (CDCl_3) δ 1.2–1.5 (m, 24 H), 2.4 (s, 3 H), 7.1–7.5 (m, 4 H), 7.8 (s, 1 H) ppm.

4,9-Dihydro-3-methyl-4-[[4-[10-[[[(3-isothiocy-anatophenyl)amino]thiocarbonyl]amino]decyl]-1-piperazinyl]acetyl]-10H-thieno[3,4-*b*][1,5]benzodiazepin-10-one (10). Compound **4** (2.8 mg, 5.7 μmol , prepared as described in ref 14) was dissolved in DMF (0.2 mL) and treated with 1,3-phenylene diisothiocyanate (6 mg, 31 μmol). After 0.5 h, ethyl acetate (1 mL) and petroleum ether (3 mL) were added, and the cloudy mixture was stored at 4 °C overnight. The supernatant was decanted from the oily residue. The residue solidified upon trituration with dry ether to give 2.0 mg (51% yield) of pure product: ^1H NMR (CDCl_3) δ 1.2–1.5 (m, 16 H), 2.4 (s, 3 H), 7.1–7.4 (m, 4 H), 7.8 (s, 1 H) ppm.

4,9-Dihydro-3-methyl-4-[[4-[10-[[[(3,5-diisothiocy-anatophenyl)amino]thiocarbonyl]amino]decyl]-1-piperazinyl]acetyl]-10H-thieno[3,4-*b*][1,5]benzodiazepin-10-one (12). Compound **12** was prepared by a method similar to compound **10**, except that 1,3,5-benzenetriyl triisothiocyanate (**8**) was used.

4,9-Dihydro-3-methyl-4-[[4-[10-[[[(4-isothiocy-anatophenyl)amino]thiocarbonyl]amino]decyl]-1-piperazinyl]acetyl]-10H-thieno[3,4-*b*][1,5]benzodiazepin-10-one (13). Compound **4** (5.0 mg, 7.6 μmol) was dissolved

in a mixture of benzene and chloroform (0.25 mL, 3:2, by vol). 1,4-Phenylene diisothiocyanate (13 mg, 67 μ mol, dissolved in 0.5 mL of chloroform) was added dropwise and with agitation. The mixture was left for 1 h at 25 °C. The volume was reduced under a stream of nitrogen, and the residue was washed with petroleum ether. The product was pure by thin-layer chromatography: ^1H NMR (CDCl_3) δ 1.2–1.5 (m, 16 H), 2.4 (s, 3 H), 7.1–7.4 (m, 4 H), 7.8 (s, 1 H) ppm.

4,9-Dihydro-3-methyl-4-[[4-[10-[[[4-carboxy-3-(6-hydroxy-3-oxo-3H-xanth-9-yl)phenyl]amino]decyl]-1-piperazinyl]acetyl]-10H-thieno[3,4-b]-[1,5]benzodiazepin-10-one Oxalate (14). Compound 4 (2.0 mg, 3.0 μ mol) was dissolved in benzene/chloroform (0.2 mL, 3:2, by vol). *N*-Succinimidyl 6-carboxyfluorescein (Research Organics, Inc., Cleveland, OH; 3.0 mg, 6.3 μ mol, dissolved in 0.3 mL of dimethylformamide) was added. The reaction was followed by TLC (2 h), and the product, precipitated as an oxalate salt, was pure (silica, chloroform/methanol/acetic acid, 75:25:5, by vol): ^1H NMR (CDCl_3) δ 1.1–1.3 (m, 16 H), 2.3 (s, 3 H), 6.4 (m, 2 H), 6.5 (s, 1 H), 7.0–7.3 (m, 6 H), 7.6 (s, 1 H), 7.9 (bd, 1 H), 8.1 (bs, 1 H) ppm.

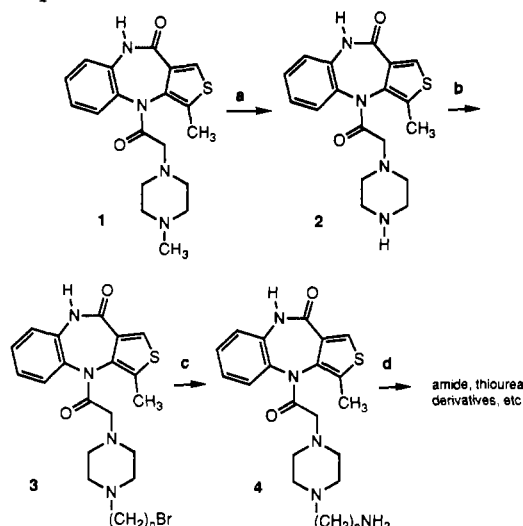
4,9-Dihydro-3-methyl-4-[[4-[10-[[[4-carboxy-3-(2,4,5,7-tetrabromo-6-hydroxy-3-oxo-3H-xanth-9-yl)phenyl]amino]thiocarbonyl]amino]decyl]-1-piperazinyl]acetyl]-10H-thieno[3,4-b]-[1,5]benzodiazepin-10-one (15). Compound 4 (5.0 mg, 7.6 μ mol) was dissolved in benzene/chloroform (0.25 mL, 3:2, by vol). Eosin 5-isothiocyanate (Molecular Probes, Eugene OR; 3.0 mg, 6.3 μ mol) dissolved in dimethylformamide (0.25 mL) was added, and the mixture was left at 25 °C for 48 h. The product was precipitated as a hydrochloric acid salt, and purified by chromatography on a thin-layer plate (250 μ) using chloroform/methanol/acetic acid, 85:10:5 as an eluant.

Binding Assays. Crude membrane fractions from rat forebrain (mostly m_1 -receptors) and from rat heart (m_2 -receptors) were obtained by homogenizing (Polytron, 3 \times 15 s, 75% max) tissue in phosphate-buffered saline at pH 7.2 and centrifuging at 28000g for 20 min. The resulting pellet was washed several more times by resuspension in fresh buffer followed by centrifugation. The final pellet was resuspended at 3 mg/mL and stored at -70 °C until needed.

Inhibition of [^3H]NMS binding to membranes from either tissue was determined by incubating (37 °C for 60 min) varying concentrations of the analog with 0.5 nM [^3H]NMS in phosphate-buffered saline, pH 7.2, and a quantity of membranes containing 100–300 μ g of protein. The total volume in each tube was 1 mL. The mixture was then rapidly filtered over GF/B filters using a Brandel cell harvester, and the filters were equilibrated in scintillation cocktail and counted in a liquid scintillation counter. Nonspecific binding was determined by incubation with 1 μ M atropine, and amounted to less than 15% of the total counts. It was routinely subtracted from the total counts. Competition binding experiments using membranes from transfected A9L cells (m_1 - and m_3 -receptors) and from NG108-15 cells (m_4 -receptors) were carried out as previously described (14).

All competition binding data were analyzed by nonlinear regression using the GraphPAD computer program (GraphPAD, San Diego, CA), and IC_{50} values were converted to K_i values using the Cheng-Prusoff equation (15). The K_d values, used in these calculations, for [^3H]NMS binding to forebrain muscarinic receptors and to

Scheme I.^a Synthesis of Functionalized Congeners of Telenzepine



^a Reagents: (a) *N,N*-diisopropylethylamine, α -chloroethyl chloroformate; (b) 1,10-dibromodecane, *N,N*-diisopropylethylamine; (c) NH_3 ; (d) isothiocyanates or activated carboxylic esters.

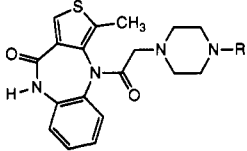
cardiac muscarinic receptors were 0.350 and 0.425 nM, respectively.

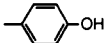
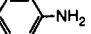
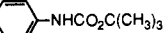
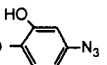
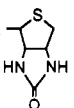
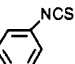
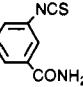
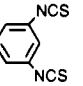
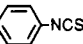
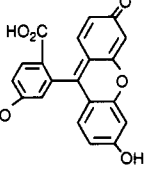
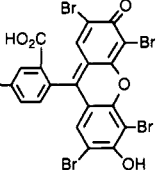
To assay for irreversible inhibition, saturation by [^3H]NMS before and after treatment of the membranes with a potential affinity label was measured. Aliquots of brain membranes were incubated with the indicated concentration (typically 100 nM) of an isothiocyanate derivative, freshly diluted from a DMSO stock solution (stored at -20 °C) into phosphate-buffered saline (pH 8.0, 10 mM phosphate, 0.15 M sodium chloride) for 60 min at room temperature, and then centrifuged at 15 000 rpm for 10 min. The resulting pellet was resuspended in 25 mL of fresh phosphate-buffered saline (pH 7.2) and centrifuged as above. The pellet was again resuspended in fresh buffer and centrifuged, and aliquots were taken for [^3H]NMS binding experiments as above.

RESULTS

Telenzepine (20) was derivatized with functionalized chains by a scheme analogous to that developed for pirenzepine (14). The *N*-methyl group was removed from the piperazine ring (Scheme I) and replaced with a terminally functionalized alkyl chain, with the expectation that this modification would not interfere with receptor binding. The demethylation was accomplished using α -chloroethyl chloroformate under basic conditions (14). The secondary amine 2 was purified chromatographically and alkylated with 1,10-dibromodecane, present in excess, to provide the ω -bromoalkyl intermediate 3. The chain length of $n = 10$ was selected on the basis of previously explored structure-activity relationships (SAR) for pirenzepine (14). An aminodecyl derivative of pirenzepine and acylated derivatives were more potent in muscarinic receptor binding assays than shorter homologs. Compound 3 was treated with ammonia in situ, to give a telenzepine amine congener (TAC), 4. This amine derivative was purified and could be readily acylated using active esters or isothiocyanate derivatives, to give amide and thiourea derivatives, respectively, that were subsequently tested for affinity at muscarinic receptors (Table I). These derivatives were characterized using fast atom bombardment mass spectrometry in the high resolution mode for accurate mass determination (Table II).

Table I. Structures of Telenzepine Derivatives Synthesized and Their Affinity at Muscarinic Receptors



no.	R	receptor subtype and K_i values ^a (nM)		
		forebrain	heart	other
1	—CH ₃ (telenzepine)	4.67 ± 0.53	66.9 ± 32	m ₁ (A9L), 1.8; m ₃ , 6.9; m ₄ , 17.4
2	—H	<i>b</i>	<i>b</i>	
4	—(CH ₂) ₁₀ NH ₂	<i>b</i>	3.7	m ₁ (A9L), 2.39; m ₃ , 7.5; m ₄ , 1.3
5	—(CH ₂) ₁₀ NHCO(CH ₂) ₂ — 	2.22 ± 0.48	1.75 ± 0.52	
6	—(CH ₂) ₁₀ NHCOCH ₂ — 	0.29 ± 0.03	0.31 ± 0.07	
7	—(CH ₂) ₁₀ NHCOCH ₂ — 	<i>b</i>	<i>b</i>	
8	—(CH ₂) ₁₀ NHCO— 	1.25 ± 0.12	3.7 ± 0.5	
9	—(CH ₂) ₁₀ NHCO(CH ₂) ₄ — 	3.20 ± 1.33	0.60 ± 0.22	
10	—(CH ₂) ₁₀ NHCSNH— 	42.5 ± 10.0	43.7 ± 12.2	
11	—(CH ₂) ₁₀ NHCSNH— 	10.5 ± 0.7	<i>b</i>	
12	—(CH ₂) ₁₀ NHCSNH— 	116 ± 17.5	82.1 ± 11	
13	—(CH ₂) ₁₀ NHCSNH— 	1.21 ± 0.12	1.38 ± 0.15	
14	—(CH ₂) ₁₀ NHCO— 	20.1 ± 6.2	<i>b</i>	
15	—(CH ₂) ₁₀ NHCSNH— 	11.8 ± 3.4	<i>b</i>	

^a K_i values for inhibition of binding of [³H]NMS are given. Values are expressed as average for a single experiment run in triplicate or as mean ± SEM for three experiments. Membranes from rat brain (mostly m₁-receptors) or rat heart (m₂-receptors) were isolated as described in Experimental Procedures. Varying concentrations of compound were incubated with 0.5 nM [³H]NMS and a quantity of membranes containing 100–300 µg of protein for 60 min at 37 °C and then rapidly filtered over GF/B filters. Competition binding experiments using membranes from transfected A9L cells (m₁- and m₃-receptors) and from NG108-15 cells (m₄-receptors) were carried out as previously described (14). The resulting data were analyzed by nonlinear regression, and IC₅₀ values were converted to K_i values using the Cheng–Prusoff equation (15) with the following K_d values for [³H]NMS binding: 0.350 nM with brain membranes and 0.425 nM with cardiac membranes. ^b Not determined.

N-Hydroxysuccinimide esters were used in the synthesis of compounds 5 [TAC conjugate with Bolton–Hunter reagent (16) for radioiodination], 8 [ASA-TAC (17) for radioiodination and/or photoaffinity labeling of the receptor], 9 [biotinyl-TAC (12)], and 14 [a fluorescein isothiocyanate conjugate of TAC (11)]. Compound 6 [PAPA-TAC, the (*p*-aminophenyl)acetyl conjugate (18)], for radioiodination and conversion to the azide for pho-

toaffinity labeling, was prepared via the corresponding (*tert*-butoxycarbonyl)amino derivative (17), 7, which was deprotected in neat trifluoroacetic acid. Compound 7 was synthesized from the amine congener 4 and the appropriate *N*-hydroxysuccinimide ester (7).

In addition to amide conjugates, thiourea conjugates of TAC were prepared. Compounds 10–13, which contain the isothiocyanate group for chemical affinity labeling,

Table II. Characterization of Compounds Synthesized

compd ^e	formula	R_f		low resolution ^a	high resolution ^a	
		A ^d	B ^d		calcd	found
3	C ₂₈ H ₃₉ BrN ₄ O ₂ S	0.66		577, ^b 575, ^b 497, 317, 185	575.2055 577.2038	575.2027 577.2029
4	C ₂₈ H ₄₁ N ₅ O ₂ S	0.15	0	512, ^b M ⁺ (511), ^c 368, ^c 327, ^c 314, ^c 254 ^c	512.3059	512.3073
5	C ₃₇ H ₄₉ N ₅ O ₄ S	0.51	0.53	660, ^b 402, 277, 185	660.3584	660.3607
6	C ₃₆ H ₄₈ N ₆ O ₃ S	0.41	0.32	645, ^b 387, 318, 229	645.3584	645.3608
8	C ₃₅ H ₄₄ N ₈ O ₄ S	0.69	0.75	674, ^b 647, 553, 461, 369, 277	673.3284	673.3344
9	C ₃₈ H ₅₅ N ₇ O ₄ S ₂	0.39	0.26	738, ^b 468, 342, 227	738.3835	738.3848
10	C ₃₆ H ₄₅ N ₇ O ₂ S ₃	0.83	0.93	704, ^b 688, 307, 242	704.2875	704.2894
11	C ₃₇ H ₄₈ N ₈ O ₃ S ₃		0.58	747, ^b 461, 369, 277	747.2933	747.2964
12	C ₃₇ H ₄₄ N ₈ O ₂ S ₄	0.85	0.9	761, ^b 729, 553, 461, 369	761.2548	761.2570
13	C ₃₆ H ₄₅ N ₇ O ₂ S ₃	0.89	0.94	704, 553, 461, 369, 277	704.2875	704.2891
14	C ₄₉ H ₅₁ N ₅ O ₈ S	0	0.31	870, ^b 613, 461, 309	870.3534	870.3535
15	C ₄₉ H ₄₈ Br ₄ N ₆ O ₇ S ₂		0.30	1217 ^b	1212.9838	1212.984

^a Unless noted, by fast atom bombardment mass spectroscopy, using glycerol matrix, in the positive ion mode. ^b M + 1. ^c EI mass spectroscopy. ^d Solvent A = chloroform/methanol/ammonia, 90:10:1; solvent B = chloroform/methanol/acetic acid, 85:10:5. ^e Refer to Table I for structures. Yields for conjugates of TAC (compounds 5 and 7–13) were generally in the range of 50–80%.

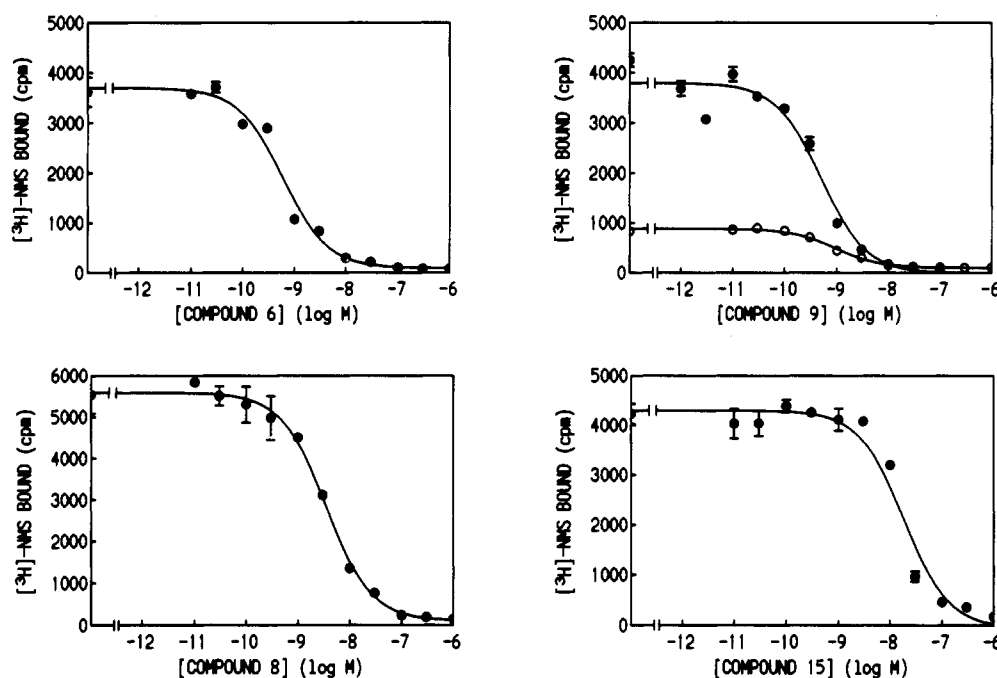


Figure 1. Inhibition curves for the displacement of [³H]-N-methylscopolamine by PAPA-TAC (6), ASA-TAC (8), biotinyl-TAC (9), and the eosine isothiocyanate conjugate of TAC (15). Specific counts are shown versus concentration of the inhibitor for rat forebrain membranes (●) and rat heart membranes (○). Inhibition of [³H]NMS binding was determined by incubating the analog and membranes with 0.5 nM [³H]NMS in phosphate-buffered saline at pH 7.2 at 37 °C for 60 min. Nonspecific binding was determined by coinubation with 1 μM atropine.

were prepared from the corresponding phenylenediisothiocyanate (DITC) derivatives (7, 8), present in large stoichiometric excess to avoid formation of bis-adducts. Compound 15, which is a fluorescent eosin derivative intended for the technique of photosensitized labeling of proteins in proximity to the receptor (19), was also prepared from the amine congener 4 and the appropriate isothiocyanate.

The affinity of the analogs for muscarinic receptors was determined in competitive binding assays vs [³H]-N-methylscopolamine (summarized in Table I, selected curves in Figure 1). The selectivities of chosen derivatives were determined by comparison of K_i values in rat forebrain membranes (mainly m_1 receptors) and in rat heart membranes (mainly m_2 receptors). The affinities generally appeared in the 10^{-10} – 10^{-8} M range, and many of the derivatives were more potent than telenzepine. The compound of highest affinity was an aniline derivative PAPA-TAC, 6, which had a K_i value of 0.29 nM at rat forebrain muscarinic receptors (16-fold higher affinity than telenzepine for these receptors). The 4-azido-2-hydrox-

ybenzoyl derivative (ASA-TAC) 8, also for photoaffinity labeling, displayed nanomolar affinity at forebrain muscarinic receptors. The high affinity of these derivatives make them suitable for the characterization of muscarinic receptors in pharmacological and spectroscopic studies, for peptide mapping, and for histochemical studies. Compounds 4–6 were nonselective for forebrain versus heart receptors. Curiously, compound 9, which displayed a K_i value of 0.60 nM at cardiac muscarinic receptors, was 5-fold selective for m_2 -muscarinic receptors.

Compounds 10–13 contain an aryl isothiocyanate for labeling of the receptors through the formation of a covalent bond with a nucleophilic residue of the receptor protein (most reactive would be amino or thiol groups). These compounds were first examined under "reversible binding" conditions, and the apparent K_i values are reported in Table I. The para-substituted analog 13, with K_i values of approximately 1 nM at both forebrain and cardiac muscarinic receptors, was clearly more potent than the mono- and di-meta-substituted derivatives.

The ability of compounds 10–13 to irreversibly inhibit

Table III. Irreversible Inhibition of Rat Muscarinic Receptors Resulting from Incubation of Membranes with an Isothiocyanate Derivative at a Concentration of 100 nM

compd	% decrease in binding ^a	
	brain	heart
10	43	11
12	12	15
13	62	32

^a Decrease in specific binding of a single concentration (0.50 nM) of [³H]N-methylscopolamine from rat forebrain or rat heart membranes. Membranes were incubated with the indicated isothiocyanate derivative, freshly diluted from a DMSO stock solution (stored at -20 °C) into phosphate-buffered saline (pH 8.0, 10 mM phosphate, 0.15 M sodium chloride) for 60 min at room temperature followed by radioligand binding.

muscarinic receptors was examined (Table III). Membranes were incubated with a fixed concentration of each isothiocyanate derivative, then washed exhaustively to remove excess, noncovalently bound ligand, and finally subjected to either radioligand saturation experiments or binding with single concentrations of radioligand. It was found that a 1 h preincubation of rat brain receptors with 10 at a concentration of 1.0 μ M resulted in a nearly total loss of the specific receptor binding sites. The detailed pharmacological characterization of the isothiocyanate derivatives will be reported elsewhere.

Variations in activity dependent on structure were observed for the isothiocyanate derivatives (Table III). The most effective in irreversible inhibition appeared to be the *p*-DITC conjugate 13, which at a concentration of 100 nM blocked with more than half of the [³H]NMS (0.5 nM) binding sites. Compounds 10 and 12 blocked less than half of these sites.

DISCUSSION

We have shown that telenzepine may be derivatized as a long chain alkylamino derivative (TAC, compound 4), which retains high affinity for muscarinic receptors, albeit with diminished selectivity. Compound 4 has been subsequently coupled to a variety of reporter groups resulting in high-affinity probes for detection and characterization of muscarinic receptors. The new conjugates, in spite of having much higher molecular weights than telenzepine, were potent inhibitors of [³H]NMS binding in rat brain membranes. These probes include analogs for radiolabeling (5, 6, and 8), a biotin conjugate (9), ligands for chemical affinity labeling (bearing electrophilic groups, 10–13) and photoaffinity cross-linking (an aryl amine, 6), and fluorescent derivatives (14 and 15) for nonradioactive receptor assays. Compound 5, the conjugate with Bolton-Hunter reagent, is intended for use as an iodinated radioligand, due to the phenolic prosthetic group. Compound 6, the (*p*-aminophenyl)acetyl (PAPA) conjugate, is also intended for use as an iodinated radioligand, with the added feature of potentially being cross-linked to the receptor protein by conversion of the aryl amine to an azide or by use of a photoaffinity cross-linking reagent such as SANPAH. A similar scheme has been developed using ligands bearing the PAPA prosthetic group to affinity label adenosine receptors (18). Compound 8, the ASA conjugate of TAC, is intended for use as an iodinated photoaffinity ligand radioligand, which is already photoactivated due to the azido group.

The iodination of TAC conjugates bearing phenols or aryl amines could be carried out by first iodinating a precursor of prosthetic group, such as *N*-succinimidyl 3-(*p*-hydroxyphenyl)propionate, used to prepare compound 5. Alternately, the final compound may be iodinated

through a standard iodination procedure, such as the chloramine T/sodium iodide method (18). Telenzepine itself is unaffected upon brief exposure to a mixture of chloramine T/sodium iodide (data not shown), thus it is expected that the iodination of compounds such as 5 or 6 would occur on phenolic or aniline ring, respectively.

The isothiocyanate derivatives 10–13 have been shown to irreversibly inhibit the binding site of muscarinic receptors. The apparent K_i values under "reversible" conditions (Table I) in most cases indicate the intrinsic affinity of the compound for the antagonist binding site. However, for compound 10 at forebrain muscarinic receptors, this value does not reflect solely "equilibrium" conditions, since the K_i value is similar to the IC_{50} value in irreversible binding (see Table III). The degree of irreversible binding (Table III) likely reflects a combination of factors, including the intrinsic receptor binding affinity of the compound and the proximity of a nucleophilic group to the NCS of the ligand in the bound state (relating to the intrinsic labeling efficacy).

The para-substituted isothiocyanate 13 was consistently the most potent antimuscarinic compound among the isothiocyanates under apparent "equilibrium" conditions. Under irreversible conditions, at a concentration 83 times its K_i value, 13 resulted in a 62% loss of forebrain [³H]NMS binding. Compound 10 inhibited nearly half of the forebrain [³H]NMS binding at only 2.4 times its K_i value. Compound 12, a diisothiocyanate, was relatively weak in both assays. At roughly half receptor occupancy, it inhibited only a small fraction of [³H]NMS binding. Thus, there is no SAR advantage of the additional NCS group present in 12. Compounds 10 and 13 showed some selectivity for the forebrain versus cardiac receptors in irreversible binding. There is considerable potential for using these affinity labels and related derivatives as pharmacological probes (7, 8, 22), particularly if selectivity is demonstrated in further testing and structural modification.

This series of telenzepine derivatives includes chemically reactive chains, such as amines (4 and 6), phenols (5 and 8), and isothiocyanates (10–13), potentially of use in anchoring these high-affinity ligands to a solid matrices for isolation of muscarinic receptors by affinity chromatography. In previous studies only the nonselective ligand aminobenzotropine (23) has served this purpose.

Fluorescent analogs 14 and 15 retain sufficient affinity for muscarinic receptors to be explored for use in non-radioactive receptor assays (11). These compounds and other fluorescent conjugates of TAC may also be useful for fluorescent histochemical studies to microscopically locate muscarinic receptors in tissue slices.

We have shown that the selectivity in this series of muscarinic antagonists may be modulated to some extent by distal structural changes. The analogues have been shown to be either nonselective or moderately m_2 -selective, depending on the group with which TAC is acylated. Although this series is based on the m_1 -selective antagonist telenzepine (here 14-fold selective for forebrain versus cardiac muscarinic receptors), compound 9 displayed a reversal of this selectivity. This may be due to an interaction of the biotin group with a distal site on the receptors that is more energetically favorable in the case of m_2 -receptors. The isothiocyanate-bearing derivatives were highly variable in measured affinity at rat forebrain receptors, depending on the positions of substitution and substituents of the distal phenyl ring. It appears that a *p*-isothiocyanate group (compound 13) is favored in that series in competitive binding (Table I), and the *m*-isothiocyanate group (compound 10) is highly efficient in

irreversible inhibition relative to the degree of receptor occupancy (Tables I and III).

Telenzepine is known to consist of two relatively stable enantiomers, which have very divergent affinities at muscarinic receptors, differing by as much as several orders of magnitude (21). The principle potent and selective muscarinic antagonist is the (+)-form, and the (–)-form is of much lower affinity. Nevertheless, in future studies with these compounds it would be desirable to resolve enantiomers in order to maximize potency and to avoid concerns about heterogeneity of biologically active species.

ACKNOWLEDGMENT

We thank Dr. Lewis Pannell and Dr. H. Lee of NIDDK for carrying out mass spectral determinations. We thank Dr. Yossef Raviv of NIDDK for helpful discussions.

LITERATURE CITED

- (1) Brown, J. H., Ed. (1989) *The Muscarinic Receptors*, Humana Press, Clifton, NJ.
- (2) Connolly, J. G. (1989) Structure–function relationships in nicotinic acetylcholine receptors. *Comp. Biochem. Biophys.* 93A, 221–231.
- (3) (a) Bonner, T. I., Buckley, N. J., Young, A. C., and Brann, M. R. (1987) Identification of a family of muscarinic acetylcholine receptor genes. *Science* 237, 527–532. (b) Bonner, T. I., Young, A. C., Brann, M. R., and Buckley, N. J. (1988) Cloning and expression of human and rat m5 muscarinic acetylcholine receptor genes. *Neuron* 1, 403–410. (c) Peralta, E. G., Ashkenazi, A., Winslow, J. W., Ramachandran, J., and Capon, D. J. (1988) Differential regulation of PI hydrolysis and adenylyl cyclase by muscarinic receptor subtypes. *Nature* 334, 434–437.
- (4) Dohlman, H. G., Thorner, J., Caron, M. G., and Lefkowitz, R. J. (1991) Model systems for the study of seven-transmembrane-segment receptors. *Ann. Rev. Biochem.* 60, 653–688.
- (5) Curtis, C. A., Wheatley, M., Bansal, S., Birdsall, N. J., Eveleigh, P., Pedder, E. K., Poyner, D., and Hulme, E. C. (1989) Propylbenzylcholine mustard labels an acidic residue in transmembrane helix 3 of the muscarinic receptor. *J. Biol. Chem.* 264, 489–495.
- (6) Fraser, C. M., Wang, C. D., Robinson, D. A., Gocayne, J. D., and Venter, J. C. (1989) Site-directed mutagenesis of m1 muscarinic receptors: Conserved aspartic acids play important roles in receptor function. *Mol. Pharmacol.* 36, 840–847.
- (7) Jacobson, K. A., Barone, S., Kammula, U., and Stiles, G. L. (1989) Electrophilic derivatives of purines as irreversible inhibitors of A₁-adenosine receptors. *J. Med. Chem.* 32, 1043–1051.
- (8) Boring, D. L., Ji, X.-D., Zimmet, J., Taylor, K. E., Stiles, G. L., and Jacobson, K. A. (1991) Trifunctional agents as a design strategy for tailoring ligand properties: Irreversible inhibitors of A₁ adenosine receptors. *Bioconjugate Chem.* 2, 77–88.
- (9) Avissar, S., Amitai, G., and Sokolovsky, M. (1983) Oligomeric structure of muscarinic receptors is shown by photoaffinity labeling: Subunit assembly may explain high- and low-affinity agonist states. *Proc. Natl. Acad. Sci. U.S.A.* 80, 156–159.
- (10) Jacobson, K. A., Ukena, D., Padgett, W., Kirk, K. L., and Daly, J. W. (1987) Molecular probes for extracellular adenosine receptors. *Biochem. Pharmacol.* 36, 1697–1707.
- (11) McCabe, R. T., de Costa, B. R., Miller, R. L., Havunjan, R. H., Rice, K. C., and Skolnick, P. (1990) Characterization of benzodiazepine receptors with fluorescent ligands. *FASEB J.* 4, 2934–2940.
- (12) Wilchek, M., and Bayer, E., Eds. (1990) Avidin-Biotin Technology. *Methods in Enzymology*, Vol. 184, Academic Press, New York.
- (13) Jacobson, K. A., Bradbury, B. J., and Baumgold, J. (1990) A functionalized congener approach to muscarinic ligands. In *Novel Treatments and Models for Alzheimer's Disease* (E. Meyer, J. Simpkins, and J. Yamamoto, Eds.) Plenum Press, New York, pp 1–10.
- (14) Karton, Y., Bradbury, B. J., Baumgold, J., Paek, R., and Jacobson, K. A. (1991) Functionalized congener approach to muscarinic antagonists: Analogues of pirenzepine. *J. Med. Chem.* 34, 2133–2145.
- (15) Cheng, Y.-C. and Prusoff, W. H. (1973) Relationship between the inhibition constant (K_i) and the concentration of inhibitor which causes 50 percent inhibition (IC₅₀) of an enzyme reaction. *Biochem. Pharmacol.* 22, 3099–3108.
- (16) Bolton, A. E. and Hunter, W. M. (1973) The labelling of proteins to high specific radioactivities by conjugation to a ¹²⁵I-containing acylating agent. *Biochem. J.* 133, 529–539.
- (17) Shanahan, M. F., Wadzinski, B. E., Lowndes, J. M., and Ruoho, A. E. (1985) Photoaffinity labeling of the human erythrocyte monosaccharide transporter with an aryl azide derivative of D-glucose. *J. Biol. Chem.* 260, 10897–10900.
- (18) Barrington, W. W., Jacobson, K. A., and Stiles, G. L. (1989) Demonstration of distinct agonist and antagonist conformations of the A₁ adenosine receptor. *J. Biol. Chem.* 264, 13157–13164.
- (19) Raviv, Y., Pollard, H. B., Bruggemann, E. P., Pastan, I., and Gottesman, M. M. (1990) Photosensitized labeling of a functional multidrug transporter in living drug-resistant tumor cells. *J. Biol. Chem.* 265, 3975–3980.
- (20) Eltze, M., Gönne, S., Riedel, R., Schlotke, B., Schudt, C., Simon, W. A. (1985) Pharmacological evidence for selective inhibition of gastric acid secretion by telenzepine, a new antimuscarinic drug. *Eur. J. Pharmacol.* 112, 211–224.
- (21) Schudt, C., Boer, R., Eltze, M., Riedel, R., Grundler, G., and Birdsall, N. J. M. (1989) The affinity, selectivity, and biological activity of telenzepine enantiomers. *Eur. J. Pharmacol.* 165, 87–96.
- (22) Newman, A. H. (1990) Irreversible ligands for drug characterization. In *Annual Reports in Medicinal Chemistry*, Vol. 25, pp 271–280.
- (23) Haga, K., and Haga, T. (1983) Affinity chromatography of the muscarinic acetylcholine receptor. *J. Biol. Chem.* 258, 13575–13579.

Carboranyl Peptide-Antibody Conjugates for Neutron-Capture Therapy: Preparation, Characterization, and in Vivo Evaluation

Raymond J. Paxton,[†] Barbara G. Beatty,[‡] Aravamuthan Varadarajan,[§] and M. Frederick Hawthorne^{*§}

Division of Immunology, Beckman Research Institute of the City of Hope, Duarte, California 91010, Department of General Oncologic Surgery, City of Hope National Medical Center, Duarte, California 91010, and Department of Chemistry and Biochemistry, University of California at Los Angeles, Los Angeles, California 90024.

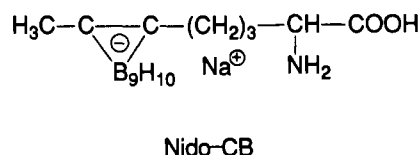
Received January 13, 1992

Two model peptides rich in boron and prepared by Merrifield syntheses, dansyl-(*nido*-CB)₂ (1) and dansyl-(*nido*-CB)₁₀-Lys-Ac (2), where *nido*-CB represents the α -amino acid [*nido*-7-CH₃-8-(CH₂)₃CH-(NH₂)COOH-7,8-C₂B₉H₁₀]⁻, were conjugated with the anti-CEA mAb T84.66 using peptide active ester reagents. The dansyl groups provided a means of fluorimetric analysis of mAb conjugates which was augmented by conventional amino acid analyses for *nido*-CB. The conjugate of 1 contained an average of 63 B atoms per mAb molecule. The mAb conjugate of 2 was chromatographically separated into a strongly fluorescent high molecular weight aggregated fraction (HMW) and a less intensely fluorescent monomeric fraction. Both fractions retained immunoreactivity. The HMW species contained an average of ca. 490 B atoms/mAb molecule, as determined by amino acid analysis. Biodistribution data were collected using nude mice bearing LS174T xenografts and ¹²⁵I-labeled mAb conjugates. While the lightly B-loaded dipeptide conjugate gave biodistribution results which resembled those of native T84.66 mAb, the undecapeptide conjugate displayed greatly enhanced liver uptake and decreased tumor accretion. These results suggest that as the boron-containing burden on the supporting immunoprotein is greatly increased, as in the case of the T84.66-2 conjugate, loss of circulating conjugate to liver effectively competes with the desired tumor localization. Means which might be taken to circumvent this difficulty have been described elsewhere (ref 15).

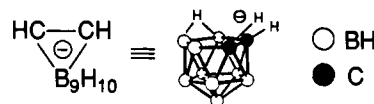
INTRODUCTION

Of the many possible methods of ¹⁰B delivery to tumor cells for the purpose of boron-neutron-capture therapy (BNCT) (1) the immunological approach remains as a potentially viable method, providing that about 10³ ¹⁰B atoms can be attached to each tumor-associated immunoprotein molecule while its immunoreactivity is retained as well as any inherent ability to enter the cell by endocytosis. A number of previous studies have demonstrated the limitations associated with attaching large numbers of small B-containing molecules to mAb (2-4). Attention was then focused upon the linkage of inhomogeneous boron-rich polymers to mAb (5-14). The latter studies demonstrated that although >10³ B atoms could be attached to each mAb molecule, the resulting conjugates suffered from either a serious loss of immunoreactivity or a reduced tumor uptake. In two recent publications (15, 16) we have described an approach to this synthesis and conjugation problem which utilizes oligomeric peptides of defined structure containing a large predetermined number (100-500) of boron atoms randomly conjugated to an immunoprotein such as anti-CEA mAb T84.66. The boron-containing peptide reagents have been given the trivial name "boron trailer" and conceived as being derived from synthetic hydrophilic α -amino acids assembled using the Merrifield peptide synthesis methodology (15, 16). The carborane-containing α -amino acid employed in this study (*nido*-CB) was previously described (15, 16) and its structure is reproduced in Scheme I. The anionic [*nido*-7,8-C₂B₉H₁₁]⁻ cage incorporated in the amino acid structure was a device employed to enhance peptide hydrophilicity as the sodium salt of the α -amino acid repeating unit. The chirality of the *nido*- α -amino acid

Scheme I



Note: Throughout this text



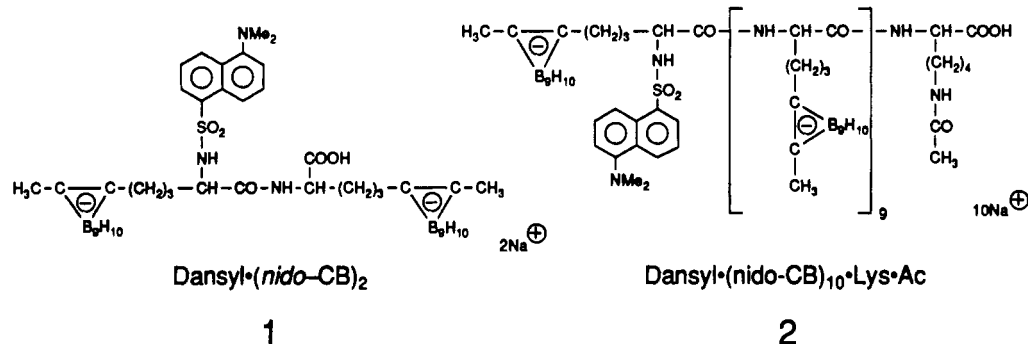
originating at the α -carbon atom and the unsymmetrically substituted *nido*-carborane cage was ignored in order to simplify peptide synthesis procedures although it is recognized that the oligomeric peptides derived in this fashion from two sets of racemic diastereomeric repeating units were complex mixtures of diastereomers. Nonetheless, the physical and chemical properties of these isomer mixtures probably introduced only minor differences in biological response over the whole population of diastereomers examined. The much more important requirement of uniformity of oligomer size was achieved through synthesis methodology. In accordance with the trivial nomenclature employed elsewhere (15, 16) the dansylated dipeptide and undecapeptide are denoted as dansyl-(*nido*-CB)₂ (1) and dansyl-(*nido*-CB)₁₀-Lys-Ac (2), respectively. Their structures are presented in Scheme II and their syntheses are reported elsewhere (16). Results obtained by conjugation of these two peptide trailers with T84.66 anti-CEA mAb and the biodistributions of the resulting conjugates in nude mice bearing CEA-producing LS174T tumor xenografts are presented here.

[†] Beckman Research Institute of the City of Hope.

[‡] City of Hope National Medical Center.

[§] University of California at Los Angeles.

Scheme II



EXPERIMENTAL PROCEDURES

Materials. Carboranyl peptides (Scheme II) were synthesized as previously described (15, 16). Anti-carcinoembryonic antigen (CEA) mAb T84.66 (17, 18) was purified from ascites by 40% ammonium sulfate precipitation and protein A affinity chromatography. T84.66 is a murine IgG₁, is specific for CEA, and has an affinity constant for CEA of $>2 \times 10^{10} \text{ M}^{-1}$. LS174T, a CEA-producing human colon cancer derived cell line, was grown in continuous culture in supplemented RPMI medium (19).

Activation of Dansyl-(nido-CB)₂ (1) and Conjugation to T84.66. A solution of 1 was converted to its *N*-succinimidyl active ester and reacted with T84.66 in phosphate buffer as previously described (16). A control reaction was also performed in which the unactivated 1 was added to T84.66. The conjugate and the control reaction were initially purified by ultrafiltration using Centricon-30 (Amicon, Danvers, MA) membrane concentrators. The concentrates were repeatedly washed with phosphate buffer until the filtrates exhibited no detectable fluorescence. Subsequent purification was performed by gel filtration chromatography on a $1 \times 30 \text{ cm}$ Superose 12 column (Pharmacia) equilibrated with phosphate-buffered saline (PBS, 0.01 M Na₂HPO₄, 0.15 M NaCl, pH 7.5) and eluted at 1 mL/min. Chromatography was performed with a Pharmacia FPLC system monitored at 280 nm, and protein peaks were collected manually. Fluorescence was monitored with a Gilson SpectroGlo fluorescence detector positioned after the UV detector. Excitation and emission wavelengths were 313 and 515 nm, respectively.

Activation of Dansyl-(nido-CB)₁₀-Lys-Ac (2) and Conjugation to T84.66. (i) *Conjugation 1.* A solution of 2 (6.40 mM, 34 μL) in phosphate buffer (0.1 M Na₂HPO₄, pH 4.35) was treated with solutions of *N*-hydroxysulfosuccinimide (92.1 mM, 4.8 μL) in water and *N,N*-diisopropylcarbodiimide (64 mM, 6.9 μL) in dimethylformamide, and the mixture was vortexed continuously at ambient temperature for 55 min. An aliquot of the active ester solution (20.9 μL) was added to a solution of T84.66 (26.7 μM , 250 μL) in bicarbonate buffer [0.1 M NaHCO₃, pH 8.5, 0.01% (v/v) Tween-20], and the mixture was vortexed continuously at ambient temperature for 30 min. Assuming complete conversion of 2 to its active ester, the molar ratio of active ester to antibody was 15:1. Control reactions of T84.66 with an equivalent amount of unactivated 2 and T84.66 alone were also performed. Conjugate and control reactions were purified by gel filtration chromatography using a $0.7 \times 28 \text{ cm}$ column of Sephacryl S200 (Pharmacia) equilibrated with PBS, pH 8.0 containing 0.01% (v/v) Tween-20. Chromatography was performed at 0.3 mL/min with a Pharmacia FPLC system as described above.

(ii) *Conjugation 2.* A solution of 2 (6.70 mM, 30 μL) in phosphate buffer (0.1 M Na₂HPO₄, pH 4.35) was treated

with solutions of *N*-hydroxysulfosuccinimide (92.1 mM, 4.4 μL) in water and *N,N*-diisopropylcarbodiimide (64 mM, 6.3 μL) in dimethylformamide, and the mixture was vortexed continuously at ambient temperature for 55 min. An aliquot of the active ester solution (13.5 μL) was added to a solution of T84.66 (26.7 μM , 250 μL) in bicarbonate buffer (0.1 M NaHCO₃, pH 8.6), and the mixture was vortexed continuously at ambient temperature for 60 min. Assuming complete conversion of 2 to its active ester, the molar ratio of active ester to antibody was 10:1. Control reactions of T84.66 with an equivalent amount of unactivated 2 and T84.66 alone were also performed. Conjugate and control reactions were adjusted to 0.05% Tween-20, vortexed continuously at ambient temperature for 60 min, and purified by gel filtration chromatography using a $1 \times 30 \text{ cm}$ Superose 12 column equilibrated with PBS (pH 8.0) containing 0.05% (v/v) Tween-20. Chromatography was performed at 0.5 mL/min with a Pharmacia FPLC system as described above.

Radioiodination of T84.66-Carboranyl Peptide Conjugates. T84.66 conjugates prepared with dansyl-(nido-CB)₂ and dansyl-(nido-CB)₁₀-Lys-Ac peptides were radiolabeled with ¹²⁵I using the chloramine-T method. Gel-filtration-purified conjugates containing 10–35 μg of protein in 50–100 μL of chromatography buffer were treated with 1 mCi Na¹²⁵I (New England Nuclear, $\sim 17 \text{ mCi/mg}$) and chloramine-T (3.5 mM, 10 μL) in phosphate buffer (0.1 M NaH₂PO₄, pH 7.5) for 1 min with gentle mixing. Reactions were stopped by adding sodium bisulfite (0.6 mg/mL, 10 μL) in phosphate buffer and mixing gently for 1 min. Human serum albumin (250 mg/mL, 4 μL) was then added to each reaction and each radiolabeled conjugate was purified by gel filtration chromatography on a freshly packed $0.7 \times 13 \text{ cm}$ Sephadex G50 Fine column equilibrated with PBS (pH 8.0). Tween-20 (0.01%) was included for the T84.66-dansyl-(nido-CB)₁₀-Lys-Ac conjugates. T84.66 was similarly radioiodinated for control purposes. All operations were performed at ambient temperature, and ¹²⁵I incorporation ranged from 30 to 69%.

Immunoreactivity of T84.66-Carboranyl Peptide Conjugates. Microtiter plates coated with CEA (5 $\mu\text{g/mL}$) were incubated with serial dilutions starting at 10 $\mu\text{g/mL}$ of T84.66-dansyl-(nido-CB)₂ and T84.66-dansyl-(nido-CB)₁₀-Lys-Ac conjugates. A double sandwich enzyme immunoassay was then performed, and the resulting binding curves were compared to those for nonconjugated T84.66 (20).

In Vivo Evaluation of T84.66-Carboranyl Peptide Conjugates. Groups of 6–8-week-old athymic (nude) female mice (Simonsen) were injected subcutaneously in the left flank with 10^6 LS174T cells in 0.2 mL of phosphate-buffered saline. Ten to fourteen days later the animals were injected intravenously with either ¹²⁵I-labeled T84.66-dansyl-(nido-CB)₂, ¹²⁵I-labeled T84.66-dansyl-(nido-CB)₁₀-Lys-Ac, or ¹²⁵I-labeled T84.66 as a control.

Animals were sacrificed 48, 72, or 120 h after antibody injection, and tissues were removed, weighed, and counted for radioactivity using a γ well counter. An aliquot of the injected dose (ID) was counted with the tissues to correct for radionuclide decay. Uptake of radiolabel was expressed as a percent of the injected dose per gram (%ID/g) of tissue (mean \pm SE).

Analytical Procedures. Protein concentrations were determined by absorbance measurement at 280 nm based on an absorbance of 1.42 for a 1 mg/mL solution. Quantitative fluorescence measurements were performed on a Spex fluorimeter using 313 and 515 nm for the excitation and emission wavelengths, respectively. Standard solutions of 1 in water were prepared and the fluorescence intensity measured for each of these solutions was plotted against the respective concentration to obtain a linear correlation. Aliquots of T84.66–dansyl-(*nido*-CB)₂ conjugate or T84.66 control were diluted in water, and the fluorescence intensity was measured. From the standard calibration curve, the concentration of the peptide in the conjugate or control was obtained.

Quantitative amino acid analysis was also used to determine the amount of carboranyl peptide incorporation in antibody conjugates. Hydrolyses were performed in the vapor phase using 6 N HCl with 0.1% (v/v) 2-mercaptoethanol at 115 °C for 24 h. Hydrolysates were dried under vacuum, dissolved in loading buffer, and analyzed on a Beckman 6300 amino acid analyzer according to the manufacturer's instructions.

RESULTS AND DISCUSSION

Preparation and Characterization of T84.66–Dansyl-(*nido*-CB)₂ Conjugates. The synthesis of the dipeptide dansyl-(*nido*-CB)₂ (1, Scheme II) and conditions for its conjugation to anti-CEA mAb T84.66 were previously described by Varadarajan and Hawthorne (16). The resulting conjugate, designated T84.66–(CB)₂, for simplicity, and the control antibody (T84.66 treated with unactivated dipeptide) were initially purified by ultrafiltration and then by Superose 12 gel filtration chromatography. The control antibody (Figure 1A) showed a sharp protein peak corresponding to monomeric T84.66 with a small amount (~2% by peak height) of high molecular weight species preceding the main antibody peak.

Very little fluorescence was associated with either protein species, indicating that 1 did not bind nonspecifically to the antibody. T84.66–(CB)₂ (Figure 1B) showed a similar protein elution profile; however, the significant fluorescence eluted with the antibody was indicative of the covalent attachment of 1 to the antibody. The high molecular weight species contained a disproportionate amount of the fluorescent label. This suggests that the high molecular weight species is more reactive toward activated 1 or that a small percentage of the monomeric antibody reacts at a disproportionately rapid rate with activated 1 (cascade conjugation, vide infra) generating a highly conjugated, high molecular weight species.

Monomeric T84.66–(CB)₂ and control T84.66 were collected and used for fluorescence, electrophoretic, immunoreactivity, and in vivo tumor-targeting studies. On the basis of the measured fluorescence intensity and protein concentration T84.66–(CB)₂ contained an average of 3.5 molecules of 1 (63 boron atoms) per antibody molecule, whereas control T84.66 contained <0.1 molecules per antibody. Sodium dodecyl sulfate–polyacrylamide gel electrophoresis (SDS–PAGE) of monomeric T84.66–(CB)₂ and control T84.66 exhibited identical electrophoretic migrations (data not shown), indicating that there was no

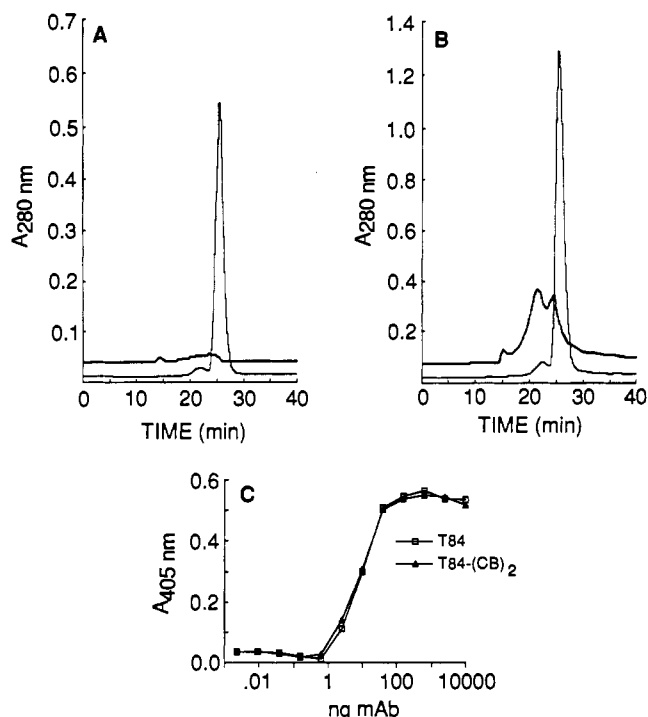


Figure 1. Characterization of T84.66–(CB)₂ conjugate. T84.66 was treated with unactivated or activated 1, partially purified by Centricon-30 ultrafiltration, and chromatographed on a Superose 12 column FPLC system as described in Experimental Procedures. Panels A and B show the chromatograms for T84.66 treated with unactivated and activated 1, respectively. The fluorescence signal (upper line) precedes the absorbance signal (lower line) by ~1 min on the chromatograms. The sharp monomeric antibody peaks (~25.5 min) were collected separately from the high molecular weight peaks (~22.5 min) and used for fluorescence, electrophoretic immunoreactivity, and tumor-targeting analyses. Panel C shows the enzyme immunoassay of monomeric T84.66–(CB)₂ conjugate and untreated T84.66. Beginning with 10 μ g/mL of each sample, 1:4 serial dilutions were prepared in microtiter plates previously coated with 5 μ g/mL CEA. Bound antibody was detected with goat anti-mouse IgG conjugated alkaline phosphatase.

gross alteration of protein structure. Enzyme immunoassay (Figure 1C) of monomeric T84.66–(CB)₂ and control T84.66 showed identical immunoreactivities. These results are consistent with other studies which have shown that the conjugation of T84.66 with bifunctional chelating ligands such as diethylenetriaminepentaacetic acid (21) and bisdicarbollide Venus flytrap cluster reagent (22) do not affect the immunoreactivity of the antibody.

For tumor-targeting analyses, aliquots of monomeric T84.66–(CB)₂ and control T84.66 were radioiodinated using Na¹²⁵I and chloramine-T. In the case of T84.66–(CB)₂ conjugate, this procedure potentially labeled not only the protein but also conjugated 1 due to the similar reactivity of the *nido*-carborane moiety and tyrosine residues toward iodination (4). Nude mice bearing CEA-producing LS174T tumor xenografts were administered 92 μ g of unlabeled T84.66–(CB)₂ together with 0.4 μ g of ¹²⁵I–T84.66–(CB)₂ as a marker. Similar amounts of ¹²⁵I–T84.66 were used as a control.

The biodistribution studies are summarized in the Table I. At the three time points studied (24, 48, and 120 h) tumor was the principal site of mAb uptake. The tumor-to-blood (T/B) ratio increased from 1.94 at 48 h to 22.63 at 120 h while the tumor-to-liver (T/L) ratio remained nearly constant at 4.10–4.93. ¹²⁵I–T84.66, which was studied only at 120 h, showed a T/L ratio of 11.57, although the T/B ratio was 9.26, somewhat less than for T84.66–

Table I. Biodistribution of ^{125}I -Labeled T84.66-(CB) $_2$ in Nude Mice Bearing LS174T Xenografts^a

	% injected dose/gram of tissue ^b			
	48 h	72 h	120 h	
	T84.66-(CB) $_2$	T84.66-(CB) $_2$	T84.66-(CB) $_2$	T84.66 (control)
tissue				
blood (B)	7.35 \pm 0.49	6.26 \pm 0.75	0.43 \pm 0.13	1.28 \pm 0.38
liver (L)	3.48 \pm 0.15	2.99 \pm 0.32	1.67 \pm 0.17	0.87 \pm 0.05
spleen	1.77 \pm 0.07	1.56 \pm 0.16	0.69 \pm 0.11	0.45 \pm 0.02
kidney	1.69 \pm 0.05	1.58 \pm 0.15	0.33 \pm 0.07	0.41 \pm 0.08
lung	2.91 \pm 0.22	2.40 \pm 0.21	0.41 \pm 0.11	0.64 \pm 0.10
tumor (T)	14.21 \pm 0.81	14.50 \pm 0.91	6.96 \pm 0.57	9.87 \pm 0.58
T/L	4.10 \pm 0.30	4.93 \pm 0.27	4.19 \pm 0.07	11.57 \pm 1.21
T/B	1.94 \pm 0.08	2.40 \pm 0.19	22.63 \pm 5.47	9.26 \pm 1.76
tumor wt (g)	1.52 \pm 0.06	1.74 \pm 0.13	2.56 \pm 0.20	2.15 \pm 0.19

^a $3\ \mu\text{Ci}$ ($\sim 0.4\ \mu\text{g}$) of ^{125}I -labeled T84.66-(CB) $_2$ together with $92\ \mu\text{g}$ of unlabeled T84.66-(CB) $_2$ was injected iv in nude mice bearing 14-day-old subcutaneous LS174T tumors. Equivalent amounts of ^{125}I -labeled and unlabeled T84.66 were used as a control. Groups of four or five mice were sacrificed at the indicated times after antibody injection, and the tumor and tissues were weighed and counted to determine the percent injected dose per gram of tissue. ^b Values quoted are mean \pm standard error.

(CB) $_2$. On a per organ basis, the tumor accumulation was 20.66, 24.66, and 17.25% ID/organ at the three time points for T84.66-(CB) $_2$ conjugate and 20.84% ID/organ for control T84.66.

Preparation and Characterization of T84.66-Dansyl-(nido-CB) $_{10}$ -Lys-Ac Conjugates. The undeca-peptide dansyl-(nido-CB) $_{10}$ -Lys-Ac (2, Scheme II) was synthesized as previously described (16) and conjugated to T84.66 as described in Experimental Procedures (Conjugation 1). Two control samples were also prepared: T84.66 treated with unactivated undeca-peptide and T84.66 alone. Preliminary studies with the resulting conjugate, designated T84.66-(CB) $_{10}$ for simplicity, and the control reactions suggested that the hydrophobic nature of 2 resulted in nonspecific (noncovalent) binding of 2 to T84.66, as well as incomplete recovery of T84.66-(CB) $_{10}$, T84.66, and unconjugated 2 during chromatographic procedures. A number of gel filtration media and buffers, which included organic solvents and nonionic detergents, were tested in order to alleviate these problems. Chromatography on Sephadex type media (i.e. G50, G100, and G150) equilibrated with PBS containing 0.01–0.05% (v/v) Tween-20 appeared to prevent the nonspecific binding of 2 to T84.66 and also provided a good recovery of unconjugated 2. However, these media were unable to resolve unconjugated 2 and T84.66, presumably due to the large micelle that formed between 2 and Tween-20. Resolution of 2 and T84.66, however, was obtained on Sephacryl S200 with PBS containing 0.01% Tween-20. Single, symmetrical protein peaks were obtained for untreated T84.66 (Figure 2A) and T84.66 treated with unactivated 2 (Figure 2B). As expected, little if any fluorescence was associated with untreated T84.66. For T84.66 treated with unactivated 2, <5% of the fluorescence eluted with the antibody, with >95% of the fluorescence eluting later than and well-resolved from the antibody peak. For T84.66-(CB) $_{10}$ a nonsymmetrical UV-absorbing peak was obtained (Figure 2C), apparently due to the formation of a high molecular weight species (~ 14 min) which did not resolve from monomeric antibody (~ 15 min). A sharp fluorescent peak corresponding to 15–20% of the total fluorescence was associated with the high molecular weight species, with a lesser amount associated with the monomeric component. Because the high molecular weight and monomeric species

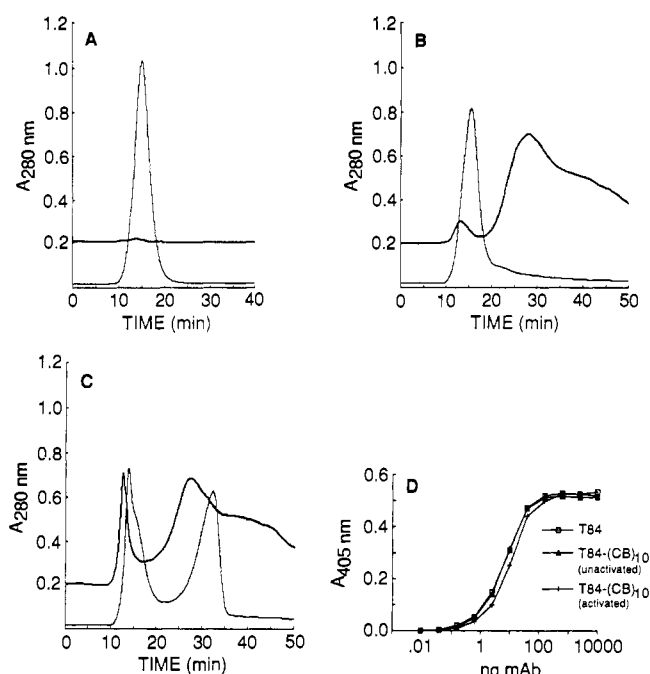


Figure 2. Characterization of T84.66-(CB) $_{10}$ conjugate and unconjugated T84.66 controls (Conjugation 1). T84.66 was treated with unactivated or activated 2. Samples were chromatographed on a Sephacryl S200 column as described in Experimental Procedures. Panel A shows a chromatogram for untreated T84.66. Panels B and C show the chromatograms for T84.66 treated with unactivated and activated 2, respectively. The fluorescence signal (upper line) precedes the absorbance signal (lower line) by ~ 2 min on the chromatograms. The antibody peaks were collected and used for fluorescence, electrophoretic, immunoreactivity, and tumor-targeting analyses. In the case of the T84.66-(CB) $_{10}$ conjugate (panel C), the high molecular weight (~ 14 min) and monomeric species were collected together. The UV-absorbing peak eluting at ~ 32 min is due to *N*-hydroxysulfosuccinimide from the activation of 2. Panel D shows the enzyme immunoassay of T84.66-(CB) $_{10}$ conjugate and unconjugated T84.66 controls. The assay was performed as previously described.

were not well-resolved, they were collected together for further analyses.

Quantitative fluorescence measurements showed that two molecules of 2 (180 boron atoms) were incorporated per antibody molecule. The heavy and light chains of the three purified antibody peaks appeared to be identical by SDS-PAGE (data not shown), although the heavy chain of T84.66-(CB) $_{10}$ may have been slightly retarded. Immunoreactivities for the two controls were equivalent, while the immunoreactivity of T84.66-(CB) $_{10}$ was slightly decreased (Figure 2D). For tumor-targeting analyses, aliquots of T84.66-(CB) $_{10}$ and untreated T84.66 were radioiodinated as described above. Nude mice bearing CEA-producing LS174T tumor xenografts were administered $56\ \mu\text{g}$ of unlabeled T84.66-(CB) $_{10}$ together with $0.25\ \mu\text{g}$ of ^{125}I -T84.66-(CB) $_{10}$ as a marker. Similar amounts of untreated T84.66 were used as a control. Biodistribution studies were performed at a single time point of 48 h and are summarized in Table II.

Although tumor showed an appreciable uptake of T84.66-(CB) $_{10}$, liver and spleen were the organs of greatest accretion. These results suggest that the conjugation of 2 to T84.66 and/or the formation of high molecular species accelerate the deposition of antibody in liver and spleen. Despite the high uptake of antibody by these organs, a reasonable tumor-to-blood ratio of 2.63 was obtained. The T84.66 control behaved as expected and gave a biodistribution similar to that observed at 48 h for T84.66-(CB) $_2$.

These results suggested that the formation of high mo-

Table II. Biodistribution of ^{125}I -Labeled T84.66–(CB) $_{10}$ in Nude Mice Bearing LS174T Xenografts^a

tissue	% injected dose/gram of tissue ^b	
	T84.66–(CB) $_{10}$	T84.66 (control)
blood (B)	1.35 \pm 0.06	11.20 \pm 1.99
liver (L)	36.84 \pm 2.08	3.22 \pm 0.70
spleen	12.80 \pm 1.26	2.08 \pm 0.51
kidney	3.77 \pm 2.10	2.62 \pm 0.47
lung	2.10 \pm 0.13	4.14 \pm 0.98
tumor (T)	3.54 \pm 0.17	16.41 \pm 0.94
T/L	0.097 \pm 0.004	6.01 \pm 1.45
T/B	2.63 \pm 0.12	1.61 \pm 0.26
tumor wt (g)	0.83 \pm 0.14	0.53 \pm 0.15

^a 7 μCi ($\sim 0.25 \mu\text{g}$) of ^{125}I -labeled T84.66–(CB) $_{10}$ together with 56 μg of unlabeled T84.66–(CB) $_{10}$ was injected iv in nude mice bearing 10-day-old subcutaneous LS174T tumors. Equivalent amounts of ^{125}I -labeled and unlabeled T84.66 was used as a control. Groups of six mice were sacrificed 2 days after antibody injection, and the tumor and tissues were weighed and counted to determine the percent injected dose per gram of tissue. ^b Values quoted are mean \pm standard error.

lecular weight T84.66–(CB) $_{10}$ conjugates was responsible for their accelerated deposition in liver and spleen. To test this hypothesis, an alternative purification procedure capable of separating monomeric and high molecular weight antibody species was employed. The conjugation of 2 to T84.66 was carried out as described in Experimental Procedures (Conjugation 2). Control reactions of T84.66 treated with unactivated undecapeptide and T84.66 alone were also performed. The conjugate and the two controls were brought to a final concentration of 0.05% Tween-20 and purified by Superose 12 chromatography. A sharp, monomeric antibody peak was obtained for untreated T84.66 with a minor high molecular weight species (Figure 3A).

As expected, little if any fluorescence was associated with these peaks. T84.66 treated with unactivated 2 also showed a sharp, monomeric antibody peak (Figure 3B); however, the high molecular weight species was slightly larger than seen with T84.66 alone. A small amount of fluorescence was associated with each of these peaks, with the free peptide eluting as a symmetrical peak after the monomeric antibody peak. The amount of unconjugated 2 was less than that observed when chromatography was performed on a Sephacryl S200 column (Figure 2B), suggesting that Superose 12 may have a greater affinity for unconjugated 2 despite the higher concentration of Tween-20, i.e. 0.05% for Superose 12 versus 0.01% for Sephacryl S200. For T84.66–(CB) $_{10}$ (Figure 3C), a sharp, monomeric antibody peak was obtained with a sizeable peak due to a high molecular weight species. A significant amount of fluorescence was associated with the antibody peak relative to the unactivated 2 control (Figure 3B). As was seen in the previously described experiments with T84.66–(CB) $_2$, the fluorescence was disproportionately associated with the higher molecular weight species and attributed to cascade conjugation. However, a significant amount of fluorescence was associated with monomeric T84.66. The high molecular weight (HMW) and monomeric antibody species were collected and analyzed separately.

Background fluorescence due to the presence of 0.05% Tween-20 prevented quantitative fluorescence measurements. To circumvent this problem, the conjugates were subjected to amino acid analysis to determine the level of 2 in the conjugates. Model studies with 1 and 2 showed a ninhydrin-reactive species eluting just before aspartic

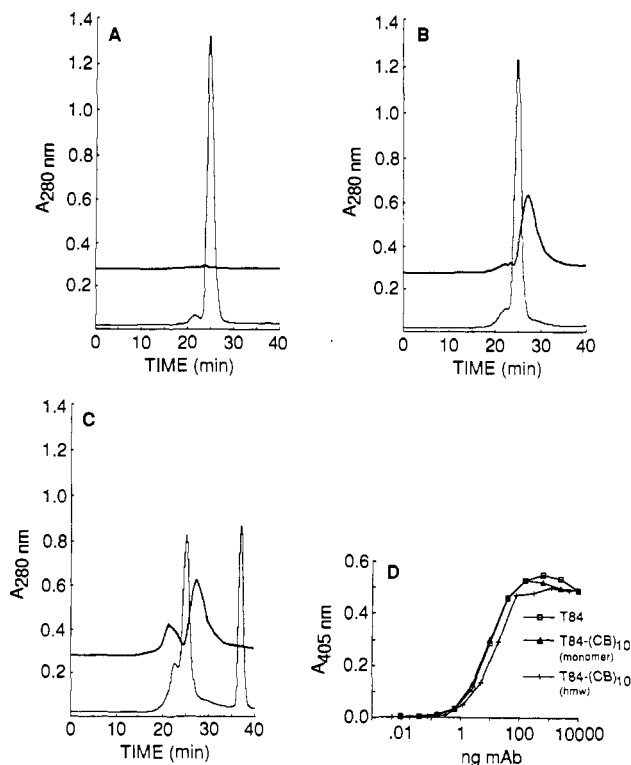


Figure 3. Characterization of T84.66–(CB) $_{10}$ conjugate and unconjugated T84.66 controls (Conjugation 2). T84.66 was treated with unactivated or activated 2. Samples were chromatographed on a Superose 12 column FPLC system as described in Experimental Procedures. Panel A shows a chromatogram for untreated T84.66. Panels B and C show the chromatograms for T84.66 treated with unactivated and activated 2, respectively. The fluorescence signal (upper line) precedes the absorbance signal (lower line) by ~ 1 min on the chromatogram. The antibody peaks were collected and used for fluorescence, immunoreactivity, and tumor-targeting analyses. For the controls (Panels A and B) only the monomeric species (~ 25.5 min) was collected and analyzed. In the case of the T84.66–(CB) $_{10}$ conjugate (panel C), the high molecular weight (~ 22.5 min) and monomeric (~ 25.5 min) species were collected and analyzed separately. Panel D shows the enzyme immunoassay of the high molecular weight and monomeric T84.66–(CB) $_{10}$ conjugates (panel C) and the untreated antibody (panel A). The assay was performed as previously described.

acid when the peptides were hydrolyzed and analyzed using standard conditions. This elution position is consistent with the anionic nature of the *nido*- α -amino acid. The yield of this peak was linear with concentration although its color yield was $\sim 10\%$ of that for common amino acids, perhaps due to partial destruction during hydrolysis. This peak was present in hydrolysates of T84.66–(CB) $_{10}$ but not in control T84.66. Analysis of HMW T84.66–(CB) $_{10}$ showed an average of 5.4 molecules (486 boron atoms) of 2 per antibody molecule. Monomeric T84.66–(CB) $_{10}$ was not analyzed due to the low level of 2 fluorescence detected during chromatography.

Immunoreactivities for the HMW and monomeric antibody species were compared to untreated T84.66 as shown Figure 3D. Monomeric T84.66–(CB) $_{10}$ retained its native immunoreactivity while there was a slight decrease in the immunoreactivity of the HMW species. For tumor-targeting analyses, aliquots of both the HMW and monomeric T84.66–(CB) $_{10}$ and untreated T84.66 were radioiodinated as described above. Nude mice bearing CEA-producing LS174T tumor xenografts were administered 27 μg of either HMW or monomeric T84.66–(CB) $_{10}$ together with 0.3 μg of the corresponding ^{125}I -T84.66–(CB) $_{10}$ conjugate as a marker. Similar amounts of untreated T84.66 were used as a control. Biodistribution studies

Table III. Biodistribution of ^{125}I -Labeled T84.66-(CB) $_{10}$ in Nude Mice Bearing LS174T Xenografts^a

tissue	% injected dose/gram of tissue ^b		
	T84.66-(CB) $_{10}$ (HMW)	T84.66-(CB) $_{10}$ (monomer)	T84.66 (control)
blood (B)	1.20 \pm 0.24	1.90 \pm 0.15	7.93 \pm 1.42
liver (L)	43.84 \pm 4.23	37.48 \pm 2.12	2.89 \pm 0.16
spleen	13.98 \pm 1.36	8.07 \pm 0.80	1.65 \pm 0.07
kidney	2.30 \pm 0.33	3.08 \pm 0.21	1.86 \pm 0.18
lung	1.61 \pm 0.17	2.36 \pm 0.10	3.26 \pm 0.26
tumor (T)	4.35 \pm 0.57	5.14 \pm 0.41	23.19 \pm 5.12
T/L	0.099 \pm 0.009	0.139 \pm 0.014	7.85 \pm 1.23
T/B	3.79 \pm 0.31	2.74 \pm 0.23	2.91 \pm 0.28
tumor wt (g)	0.64 \pm 0.20	0.57 \pm 0.19	0.86 \pm 0.21

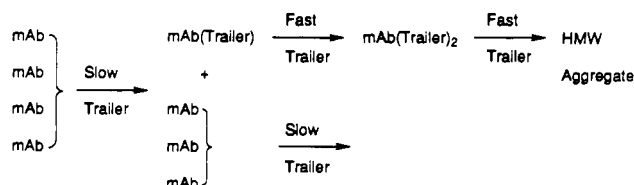
^a 7 μCi ($\sim 0.30 \mu\text{g}$) of ^{125}I -labeled T84.66-(CB) $_{10}$ samples together with 27 μg of the respective unlabeled T84.66-(CB) $_{10}$ samples were injected iv in nude mice bearing 10-day-old subcutaneous LS174T tumors. Equivalent amounts of ^{125}I -labeled and unlabeled T84.66 was used as a control. Groups of five or six mice were sacrificed 2 days after antibody injection, and the tumor and tissues were weighed and counted to determine the percent injected dose per gram of tissue. ^b Values quoted are mean \pm standard error.

were performed at a single time point of 48 h and are summarized in Table III.

As with the previous T84.66-(CB) $_{10}$ conjugate (Table II), tumor showed an appreciable uptake of both HMW and monomeric T84.66-(CB) $_{10}$, although liver and spleen were again the organs of greatest localization. In comparing HMW and monomeric T84.66-(CB) $_{10}$, slightly better tumor uptake and decreased liver and spleen uptake were seen with the monomeric species. This suggests that the conjugation of 2 to T84.66 alone accelerates the deposition of T84.66 in liver and spleen and that aggregate formation can further accelerate the deposition. T84.66 control behaved as expected and gave a biodistribution similar to that observed at 48 h for the other controls (Tables I and II).

CONCLUSIONS

In progressing from trailer 1 to trailer 2 the problems associated with nonspecific binding of peptide trailer to mAb, the increase in the proportion of HMW species formed during conjugation, and the appearance of cascade conjugation in greater amounts were exacerbated. Paralleling these changes is the enhancement of liver uptake of the conjugated mAbs relative to that of tumor. The nonspecific binding of activated and unactivated 2 with T84.66 mAb probably arises from the interaction of ambiphilic 2 with hydrophobic regions of T84.66. Cascade conjugation of 1 and 2 with mAb led to the disproportionate quantity of fluorescent label attached to the HMW species (or aggregate) accompanied by the creation of additional aggregate. In terms of reaction mechanisms, the initial lysine conjugation reaction with ambiphilic 2 in a hydrophobic mAb region appears to open the mAb structure, thus exposing additional reactive sites in the hydrophobic region which are attacked ever more rapidly as conjugation proceeds and the mAb structure becomes increasingly perturbed. Eventually, this cascade effect allows the growth of exposed hydrophobic or ambiphilic regions of the conjugate to proceed to the point that inter-mAb hydrophobic bonding results in the formation of aggregate (HMW) species. The HMW aggregate formed by this process would be strongly fluorescent relative to monomeric conjugate. The equations below demonstrate this competitive conjugation complication. Both HMW and monomeric T84.66-(CB) $_{10}$ conjugates have good immu-



noassay responses. The reduction in tumor uptake is the apparent result of competitive loss of mAb and HMW conjugates to liver.

The observations recorded in this contribution emphatically support the conclusion that random conjugation of complete IgG molecules with very large boron trailer reagents will become excessively cumbersome as the boron burden is increased. Consequently, if immunoproteins are to mediate the delivery of ^{10}B to tumor antigens, the antibody must be simplified with respect to size and its chemical functionality made specific at only one or two points of attachment. In short, increased simplicity and greater structural certainty will be required to secure a successful (and reproducible) conjugate. Two new approaches of this type were recently suggested and are now being evaluated (15).

ACKNOWLEDGMENT

This research was supported by Grant RO1-CA31753 from the National Institutes of Health.

LITERATURE CITED

- (1) Barth, R. F., Soloway, A. H., and Fairchild, R. A. (1990) Boron Neutron Capture Therapy of Cancer. *Cancer Res.* 50, 1061-1070.
- (2) Mizusawa, E., Dahlman, H. L., Bennett, S. J., Goldenberg, D. M., and Hawthorne, M. F. (1982) Neutron-Capture Therapy of Human Cancer: In Vitro Results on the Preparation of Boron-Labeled Antibodies to Carcinoembryonic Antigen. *Proc. Natl. Acad. Sci. U.S.A.* 79, 3011-3014.
- (3) Goldenberg, D. M., Sharkey, R. M., Primus, F. J., Mizusawa, E., and Hawthorne, M. F. (1984) Neutron-Capture Therapy of Human Cancer: In Vivo Results on Tumor Localization of Boron-10-Labeled Antibodies to Carcinoembryonic Antigen in the GW-39 Tumor Model System. *Proc. Natl. Acad. Sci. U.S.A.* 81, 560-563.
- (4) Mizusawa, E. A., Thompson, M. R., and Hawthorne, M. F. (1985) Synthesis and Antibody-Labeling Studies with the *p*-Isothiocyanatobenzene Derivatives of 1,2-Dicarba-closo-dodecaborane(12) and the Dodecahydro-7,8-dicarba-nido-undecaborate(1-) Ion for Neutron Capture Therapy of Human Cancer. Crystal and Molecular Structure of $\text{Cs}^+[\text{nido-7-(p-C}_6\text{H}_4\text{NCS)-9-I-7,8-C}_2\text{B}_9\text{H}_{11}]^-$. *Inorg. Chem.* 24, 1911-1916.
- (5) Alam, F., Soloway, A. H., Barth, R. F., Johnson, C. W., Carey, W. E., and Knoth, W. E. (1983) Boronation of Polyclonal and Monoclonal Antibodies for Neutron Capture. *First International Symposium on Neutron Capture Therapy. Brookhaven National Laboratory Report No. BNL-51730* (R. G. Fairchild, and G. L. Brownwell, Eds.) pp 229-236, Cambridge, MA, Oct 12-14.
- (6) Alam, F., Soloway, A. H., Barth, R. F., Mafune, N., Adams, D. M., and Knoth, W. H. (1989) Boron Neutron Capture Therapy: Linkage of a Boronated Macromolecule to Monoclonal Antibodies Directed against Tumor Associated Antigens. *J. Med. Chem.* 32, 2326-2330.
- (7) Barth, R. F., Fazlul, A., Soloway, A. H., and Adams, D. M. (1985) Delivery of Boron-10 for Neutron Capture Therapy by Means of Polyclonal and Monoclonal Antibodies: Progress and Problems. *Proceedings of the Second International Symposium on neutron Capture Therapy*, Oct 18-20, Tokyo, Japan, pp 346-352.
- (8) Barth, R. F., Fazlul, A., Soloway, A. H., Adams, D. M., and Steplewski, Z. (1986) Boronated Monoclonal Antibody 17-1A

- for Potential Neutron Capture Therapy of Colorectal Cancer. *Hybridoma* 5, Suppl. 1, s43-s50.
- (9) Alam, F., Soloway, A. H., McGillire, J. E., Barth, R. F., Carey, W. E., and Adams, D. (1985) Dicesium *N*-Succinimidyl 3-(undecahydro-*closo*-dodecaboranyldithio)propionate, a Novel Heterobifunctional Boronating Agent. *J. Med. Chem.* 28, 522-525.
- (10) Barth, R. F., Mafune, N., Adams, D. M., Soloway, A. H., Makroglou, G. E., Oredipe, O. A., Bule, T. E., and Stepkowski, Z. (1989) Conjugation, Purification and Characterization of Boronated Monoclonal Antibodies for Use in Neutron Capture Therapy. *Strahlenther. Onkol.* 165, 142-145.
- (11) Elmore, J. J., Jr., Borg, D. C., Gabel, D., Fairchild, R. G., Temponi, M., and Ferrone, S. (1985) Boronated Dextran-Monoclonal Antibody Conjugates for NCT. *Proceedings of the Second International Symposium on Neutron Capture Therapy*, Oct 18-20, Tokyo, Japan, pp 367-381.
- (12) Abraham, R., Muller, R., and Gabel, D. (1989) Boronated Antibodies for Neutron Capture Therapy. *Strahlenther. Onkol.* 165, 148-151.
- (13) Pettersson, M. L., Courel, M. N., Girard, N., Gabel, D., and Delpech, B. (1989) In Vitro Immunological Activity of a Dextran-Boronated Monoclonal Antibody. *Strahlenther. Onkol.* 165, 151-152.
- (14) Tamat, S. R., Patwardhan, A., Moore, D. E., Kabral, A., Bradstock, K., Hersey, P., and Allen, B. J. (1989) Boronated Monoclonal Antibodies for Potential Neutron Capture Therapy of Malignant Melanoma and Leukaemia. *Strahlenther. Onkol.* 165, 145-147.
- (15) Hawthorne, M. F. (1991) Biochemical Applications of Boron Cluster Chemistry. *Pure and Appl. Chem.* 24, 327-334.
- (16) Varadarajan, A., and Hawthorne, M. F. (1991) Novel Carboranyl Amino Acids and Peptides: Reagents for Antibody Modification and Subsequent Neutron-Capture Studies. *Bioconjugate Chem.* 2, 242-253.
- (17) Wagener, C., Clark, B. R., Rickard, K. J., and Shively, J. E. (1983) Monoclonal Antibodies for Carcinoembryonic Antigen and Related Antigens as a Model System: Determination of Affinities and Specificities of Monoclonal Antibodies by Using Biotin-Labeled Antibodies and Avidin as Precipitating Agent in Solution Phase Immunoassay. *J. Immunol.* 130, 2302-2307.
- (18) Wagener, C., Yang, Y. H. J., Crawford, F. G., and Shively, J. E. (1983) Monoclonal Antibodies for Carcinoembryonic Antigen and Related Antigens as a Model System: A Systematic Approach for the Determination of Epitope Specificities of Monoclonal Antibodies. *J. Immunol.* 130, 2308-2315.
- (19) Baldwin, H. T., Rutzky, L. P., Jakstys, M. M., Oyasu, R., Kaye, C. I., and Kahan, B. D. (1976) Human Colonic Adenocarcinoma Cells, I. Establishment and Description of a New Line. *In Vitro (Rockville)* 12, 180-191.
- (20) Beatty, J. D., Beatty, B. G., and Viahos, W. G. (1987) Methods of Analysis of Noncompetitive Enzyme-Immunoassays for Antibody Quantification. *J. Immunol. Methods* 100, 161-172.
- (21) Paxton, R. J., Jakowatz, J. G., Beatty, J. D., Beatty, B. G., Viahos, W. G., Williams, L. E., Clark, B. R., and Shively, J. E. (1985) High-Specific-Activity ¹¹¹In-Labeled Anticarcinoembryonic Antigen Monoclonal Antibody: Improved Method for the Synthesis of Diethylenetriaminepentaacetic Acid Conjugates. *Cancer Res.* 45, 5694-5699.
- (22) Paxton, R. J., Beatty, B. G., Hawthorne, M. F., Varadarajan, A., Williams, L. E., Curtis, F. L., Knobler, C. B., Beatty, J. D., and Shively, J. E. (1991) A Transition Metal Complex (Venus Flytrap Cluster) for Radioimmunodetection and Radioimmunotherapy. *Proc. Natl. Acad. Sci. U.S.A.* 88, 3387-3391.

New Chelating Agent for Attaching Indium-111 to Monoclonal Antibodies: In Vitro and in Vivo Evaluation

R. Subramanian,* J. Colony, S. Shaban, H. Sidrak, M. V. Haspel, N. Pomato, M. G. Hanna, Jr., and R. P. McCabe

Organon Teknika, Biotechnology Research Institute, 1330A Piccard Drive, Rockville, Maryland 20850.
Received January 13, 1992

¹¹¹In possesses excellent radiophysical properties suitable for use in immunoscintigraphy of cancerous tissues when attached to an antitumor antibody. However, ¹¹¹In has a tendency to accumulate in normal tissues such as liver. Instability of the linkage between ¹¹¹In and antibody may contribute to this problem. To avoid this, we developed a new bifunctional chelating agent, 1,3-bis[*N*-(2-aminoethyl)-2-aminoethyl]-2-aminoacetamido]-2-(4-isothiocyanatobenzyl)propane-*N,N,N',N'',N''',N''''*,-*N''''',N''''''*-octaacetic acid (LiLo), that forms a kinetically stable chelate with metal ions such as indium. Using LiLo, indium-111 was conjugated to a human monoclonal antibody, 16.88. Competitive binding analysis revealed that the 16.88-LiLo conjugate is as immunoreactive as the unconjugated native antibody. This conjugate was compared with ¹¹¹In-16.88, where diethylenetriaminepentaacetic acid dianhydride (DTPAa) was used as the chelating agent. In vitro stability studies showed that ¹¹¹In was more stably bound to 16.88-LiLo than to 16.88-DTPA. Biodistribution studies in athymic mice bearing colorectal tumor xenografts indicated less liver retention with 16.88-LiLo than with 16.88-DTPA. These results demonstrate that LiLo is superior to DTPAa for attachment of ¹¹¹In to the monoclonal antibodies.

A recently completed imaging study in colon cancer patients using ¹³¹I-labeled human monoclonal antibody (16.88) indicated a sensitivity in tumor detection of 79% for lesions >2 cm that express the relevant antigen (1). Encouraged by this result, we are developing improved methods of tumor imaging with human monoclonal antibodies to increase the sensitivity of detection of lesions <2 cm in diameter. ¹¹¹In possesses radiophysical properties superior to ¹³¹I for detection of small tumors and has been used by several investigators in clinical imaging studies with murine monoclonal antibodies (2). However, in these investigations retention of ¹¹¹In in normal tissues has been a limitation in the application of the radionuclide (3). Improved clearance of ¹¹¹In from liver tissue has been investigated with a labile linkage between the antibody and the chelator (4, 5) and alteration of the structure of the chelator to provide for higher stability under in vivo conditions (6, 7). Both approaches have been successful in experimental studies.

Our aim was to develop a new chelation structure that could be coupled to human monoclonal antibodies without compromising antibody activity or altering antibody pharmacokinetics and that would bind ¹¹¹In to antibody under in vivo conditions with greater kinetic stability than is achieved with the commonly used chelators such as diethylenetriaminepentaacetic acid dianhydride (DTPAa).

When choosing a chelator several factors must be considered. The chelator must readily bind the radiometal through simple chemical reactions. The chelator must not be toxic to humans. The chelator must bind the metal strongly such that under physiological conditions the rate of loss is very slow—preferably negligible. Often the indium-111-labeled radiopharmaceutical is administered intravenously, where it encounters metal-binding proteins such as transferrin and albumin in concentrations 100–1000-fold greater than that of the radiopharmaceutical. Loss of radiometal to serum proteins leads to accumulation of radioactivity in normal tissues, especially liver, spleen, and kidney, reducing the radioactivity available for tumor uptake. Kinetic stability of the ra-

dioimmunoconjugate is a critically important factor in determining its usefulness for in vivo applications (8).

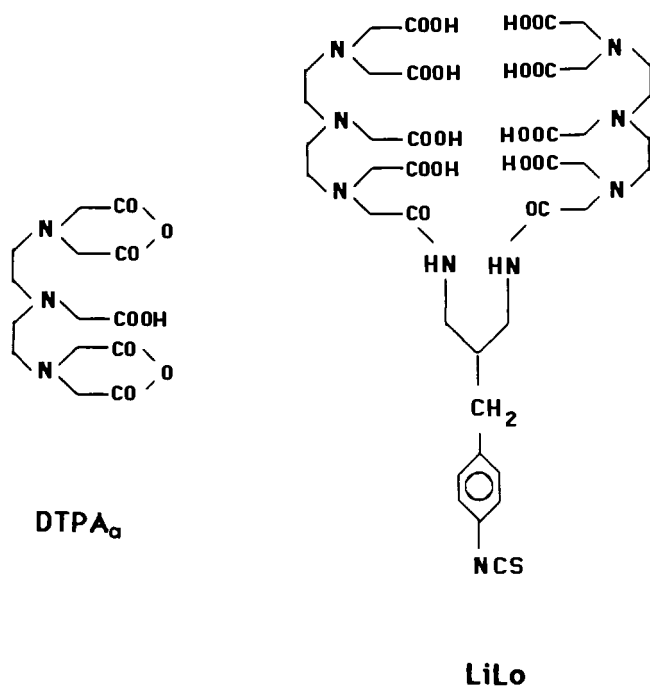
Many chelating agents used to attach radiometals to antibodies are poly(amino carboxylates), such as ethylenediaminetetraacetic acid (EDTA), DTPA, and their derivatives, which are capable of binding a variety of metal ions (3). This paper describes the synthesis, characterization, and in vivo behavior of 1,3-bis[*N*-(2-aminoethyl)-2-aminoethyl]-2-aminoacetamido]-2-(4-isothiocyanatobenzyl)propane-*N,N,N',N'',N''',N''''*,-*N''''',N''''''*-octaacetic acid (LiLo, Chart I), a polycarboxylate molecule suitable for attaching radiometals to antibodies. LiLo forms a stable radioimmunoconjugate with indium. High specific activity without loss of immunoactivity was achieved using this chelating agent. Biodistribution studies in mice indicated reduced liver retention of ¹¹¹In with the new chelator.

EXPERIMENTAL PROCEDURES

Materials and Methods. All the chemicals used in this investigation were obtained from Aldrich Chemical Co. and/or Sigma Chemical Co. Indium-111 chloride was purchased from Du Pont-New England Nuclear. Chelex 100 and Sephadex resins (G25 and G50) were obtained from Pharmacia Fine Chemicals and/or Sigma Chemical Co. The TLC plates were obtained from E. Merck (silica gel 60 F₂₅₄ precoated plastic sheets, Cat. No. 5725).

Absorption measurements were carried out using a Perkin-Elmer Lambda 4B spectrophotometer. Infrared spectral analyses were performed on a Perkin-Elmer 1600 series FTIR spectrophotometer. Melting points were determined using an apparatus obtained from Electrothermal (Model 1A 8101). NMR studies were carried out using a Varian 60-MHz spectrometer (Model EM360L) or Bruker 200-MHz NMR spectrometer. Fast atom bombardment mass spectral analyses were carried out with a Finnigan Model VG 7070E spectrometer. For mass spectral measurements, water, chloroform, and/or *p*-nitrobenzyl alcohol were used as the solvent. Radioactivity

Chart I. Structures of LiLo and DTPAa



was measured using a Capintec CR7 dose calibrator and/or a Pharmacia-LKB CompuGamma radiation spectrometer.

HPLC measurements were performed with a TSK 4000 column (Beckman Instruments) and a Waters chromatography system consisting of two pumps (Model 501), an absorption detector (Model 481), a recorder (Model 745B), an injector (U6K), and an automated gradient controller unit.

Stability studies were carried out at 37 °C, 7% CO₂, in a carbon dioxide incubator (Forma Scientific Model 3158). The experimental details are described elsewhere (8). Radiochromatographic analyses were performed using a Radiomatic (Model A100) radioisotope detector attached to the HPLC system.

Antibody. Human monoclonal antibody 16.88 (IgM isotype) is produced by an Epstein-Barr virus transformed human lymphoblastoid cell line derived from the peripheral blood lymphocytes of a colon carcinoma patient specifically immunized with autologous tumor cells (9, 10). Antibody 16.88 recognizes a cytoplasmic antigen with an apparent avidity in the range of 5×10^8 l/M. Immunochemical analyses indicated specificity for epitopes on a unique molecular structure as well as shared epitopes with cytokeratins 8, 18, and 19 (11).

Synthesis of LiLo. The synthesis of LiLo is outlined in Scheme I.

I. Diethyl 2-(4-Nitrobenzyl)malonate (12). Sodium metal (10.9 g, 0.47 mol) was added in portions to a stirring solution of 473 mL of absolute ethanol under a nitrogen atmosphere. After all the metal had dissolved, 151 g (0.943 mol) of diethyl malonate was slowly added dropwise to the solution followed by the addition of 102 g (0.47 mol) of 4-nitrobenzyl bromide. The solution was heated to reflux for 24 h and the precipitated byproduct was filtered off. The solution was cooled in an ice bath, and the crystallized product was filtered and rinsed with cold ethanol (62.5 g, 45%). Mp: 60 °C. IR (KBr pellet): 1736, 1524, 1346, 1151, 852 cm⁻¹. ¹H NMR (CDCl₃) δ: 8.14 (d, 2 H), 7.37 (d, 2 H), 4.15 (q, 4 H), 3.64 (t, 1 H), 3.30 (d, 2 H), 1.22 (t, 6 H). Anal. Found (Calcd): C, 56.85 (56.93); H, 5.79 (5.81); N, 4.72 (4.74).

II. 2-(4-Nitrobenzyl)malondiamide. I (42.8 g, 0.145 mol) was dissolved in 300 mL of methanol and cooled to 4 °C, and ammonia was bubbled through the solution to the point of saturation. The solution was kept at 4 °C for 36 h. The precipitated product was filtered and rinsed with methanol. The product was washed with boiling acetonitrile, filtered, and dried (28.4 g, 83 %). Mp: 238–240 °C. IR (KBr pellet): 3441, 3392, 1678, 1657 cm⁻¹. ¹H NMR (DMSO-*d*₆) δ: 8.13 (d, 2 H), 7.47 (d, 2 H), 7.17 (d, 4 H), 3.33 (m, 3 H). Anal. Found (Calcd): C, 50.68 (50.62); H, 4.64 (4.68); N, 17.74 (17.72).

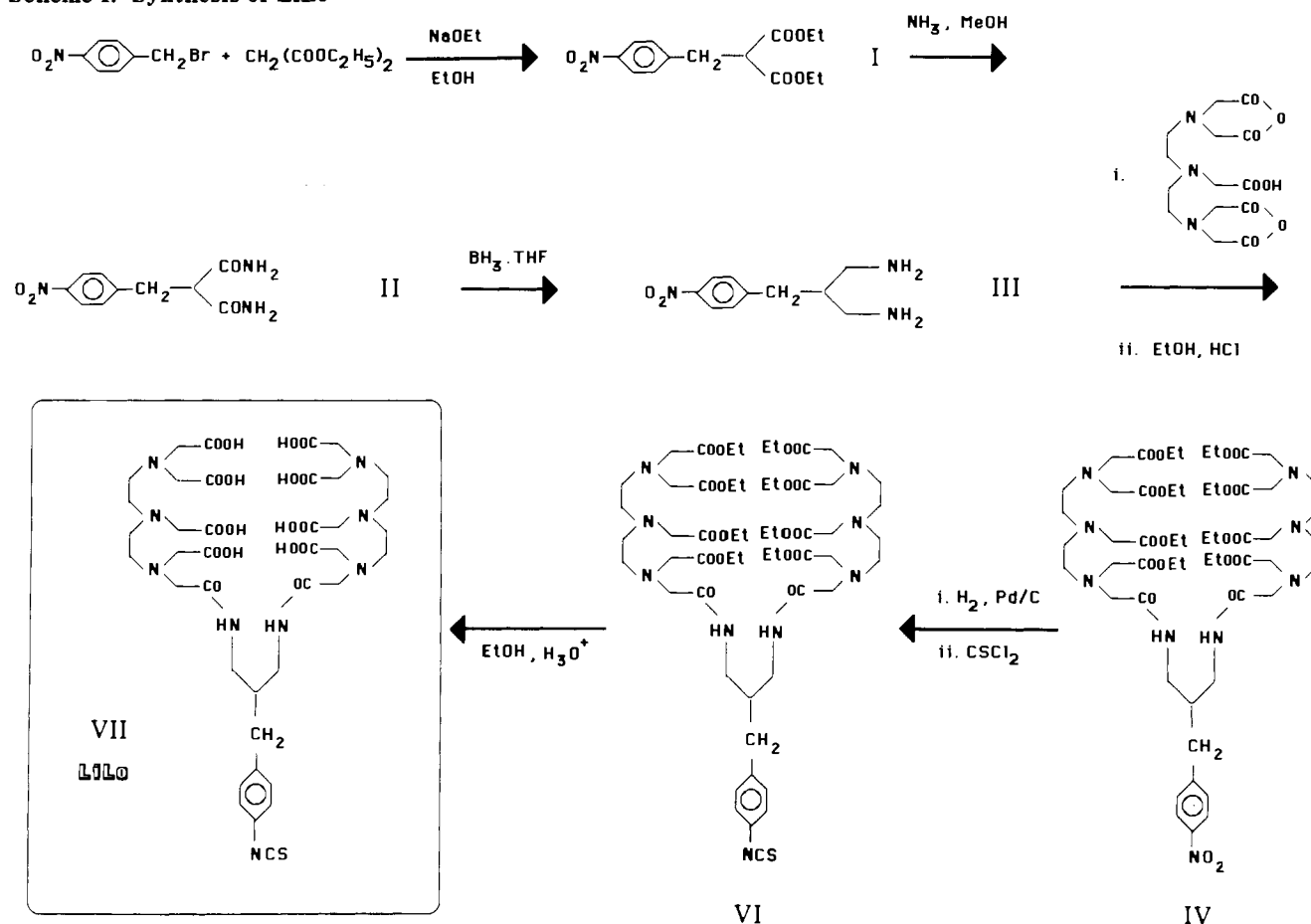
III. 1,3-Diamino-2-(4-nitrobenzyl)propane Dihydrochloride. II (24.6 g, 0.104 mol) was added to 500 mL (0.5 mol) of 1 M borane-THF solution under a nitrogen atmosphere. The solution was refluxed for 20 h. Concentrated HCl was added dropwise cautiously until no more evolution of gas occurred. The solvent was evaporated off and the white solid dissolved in 200 mL of concentrated HCl (37%) and refluxed for 1 h. The solution was then evaporated to dryness and the remaining solid dissolved in 100 mL of 40% NaOH solution. The organic layer was extracted with methylene chloride, dried with magnesium sulfate, and filtered. HCl gas was bubbled through 100 mL of absolute ethanol to the point of saturation. This was added to the extracted product (ca. 500 mL) and the solution cooled in an ice bath. The precipitated product was filtered, rinsed with methylene chloride, and dried (17.55 g, 60%). The product was recrystallized in 5 M HCl. TLC: R_f 0.20 (75:24:1 methylene chloride/methanol/ammonium hydroxide), fluorescamine positive; FTIR (KBr pellet): 2910, 1603, 1509, 1353, 854 cm^{-1} . ^1H NMR (D_2O) δ : 7.97 (d, 2 H); 7.29 (d, 2 H); 2.90 (m, 7 H). Anal. Found (Calcd): C, 42.65 (42.56); H, 6.08 (6.08); N, 14.89 (14.89). FABMS m/e : (M + 1) 210.

IV. 1,3-Bis[N-[N-(2-aminoethyl)-2-aminoethyl]-2-aminoacetamido]-2-(4-nitrobenzyl)propane-*N,N,N',N'',N''',N''''N''''''N''''''N''''''*-octaacetic Acid Octakis(ethyl ester). DTPA anhydride was prepared as described by Hnatowich et al. (14). DTPA anhydride (24 g, 64.0 mmol) was dissolved in 45 mL of acetonitrile, 30 mL of dimethylformamide, and 10 mL of triethylamine under a nitrogen atmosphere. Three grams (10.6 mmol) of III was added in portions to the solution with strong stirring every 2 h over a period of 3 days. The solution was stirred at room temperature for 3 more days. The solvent was then evaporated under vacuum. Absolute ethanol (300 mL) was added to the reaction mixture and then it was saturated with HCl gas. The reaction was then refluxed for 15 h. The solvent was evaporated and the resulting product dissolved in 200 mL of saturated sodium carbonate solution and extracted with methylene chloride. The organic layer was dried with anhydrous magnesium sulfate, filtered, and evaporated. The resulting oil was run down a silica gel column (2–7% methanol in methylene chloride)¹ (4.56 g, 36%). IR (KBr pellet): 1738, 1667, 1520, 1346, 1193 cm⁻¹. UV (methanol): 275 nm. TLC: *R_f* 0.430 (93:7 methylene chloride/methanol). ¹H NMR (CDCl₃) δ: 8.18 (d, 2 H); 7.50 (d, 2 H); 4.15 (q, 16 H); 3.40 (m, 25 H); 2.78 (s, 20 H); 1.25 (t, 24 H). FABMS *m/e*: (M + 1) 1185. Anal. Found (Calcd): C, 54.58 (54.75); H, 7.61 (7.59); N, 10.59 (10.64).

V. 1,3-Bis[N-[N-(2-aminoethyl)-2-aminoethyl]-2-aminoacetamido]-2-(4-aminobenzyl)propane-N,N,N',N'',N''',-

¹ Using silica gel column chromatography, a small amount of (~5%) the cyclic product, 3-(4-nitrobenzyl)-6,16-dioxo-1,5,8-, 11,14-pentaazacyclohexadecane-N,N',N''-triacetic acid tris(ethyl ester) (HETA) was also isolated (TLC: *R_f* 0.613, 93:7 methylene chloride/methanol). The details of this product will be reported separately.

Scheme I. Synthesis of LiLo



N''''',N''''',N'''''-octaacetic Acid Octakis(ethyl ester). IV (1.5 g, 1.27 mmol) was dissolved in absolute ethanol and added to a stirring solution of a catalytic amount of 10% palladium on carbon in absolute ethanol under hydrogen atmosphere. Hydrogen was bubbled through the solution for 8 h with occasional addition of catalyst. The reaction was followed by change in UV spectra (13). The catalyst was then filtered off and the solvent evaporated (934 mg, 64%). TLC: R_f 0.332 (93:7 methylene chloride/methanol) fluorescamine positive. IR (KBr pellet): 3351, 2981, 1738, 1660, 1524, 1195 cm^{-1} (loss of peak at 1347 cm^{-1}). UV (ethanol): 240 nm.

VI. 1,3-Bis[N-[N-(2-aminoethyl)-2-aminoethyl]-2-aminoacetamido]-2-(4-isothiocyanatobenzyl)propane-N,N,N',N'',N''',N'''',N'''''-octaacetic Acid Octakis(ethyl ester). V (100 mg, 86.7 μmol) was dissolved in 20 mL of methylene chloride and 0.5 mL of thiophosgene was added with stirring under a nitrogen atmosphere. The solution was stirred for 4 h. The solvent was evaporated, and the oil dissolved in 30 mL of saturated sodium carbonate solution, extracted with methylene chloride, dried with anhydrous magnesium sulfate, filtered, and evaporated. The product was purified by a silica gel column chromatography (2–7% methanol in methylene chloride) (70 mg, 68%). TLC: R_f 0.353 (93:7 methylene chloride/methanol), fluorescamine negative. IR (KBr pellet): 2981, 2116, 1736, 1671, 1194 cm⁻¹. UV (ethanol): 272 nm. FABMS m/e: (M + 1) 1197. Anal. Found (Calcd): C, 53.99 (55.20); H, 7.51 (7.44); N, 10.43 (10.54); S, 2.63 (2.68).

VII. 1,3-Bis[N-[N-(2-aminoethyl)-2-aminoethyl]-2-aminoacetamido]-2-(4-isothiocyanatobenzyl)propane-N,N,N',N'',N''',N'''',N'''''-octaacetic Acid (LiLo). The octakis(ethyl ester) derivatives of LiLo isothiocyanate

(VI) was hydrolyzed by adding 1 mL of 1 M HCl to 70 mg of VI and allowing the acid hydrolysis to proceed at room temperature for 7 days. The product was lyophilized, and IR spectral analysis, NMR, and TLC analysis confirmed the hydrolysis of the product. Alternately, LiLo was prepared from amino LiLo ester (V) by first hydrolyzing to amino LiLo ester using 1 M NaOH, followed by conversion of the amino LiLo acid to LiLo isothiocyanate, using thiophosgene as described earlier, and lyophilization. Product characterization was identical. IR (KBr pellet): 3414, 2119, 1750, 1677, 1566, 1381, 1225 cm^{-1} . UV (H_2O): 270 nm. TLC: R_f 0.702 (4:1 methanol/ammonium hydroxide), fluorescamine negative. ^1H NMR ($\text{DMSO}-d_6$) δ : 7.38 (s, 4 H), 4.10 (m, 23 H), 3.50 (m, 20 H) FABMS m/e ($M + 1$) 973.

Conjugation of LiLo/DTPAA to Proteins. DTPAA conjugations to human serum albumin and the IgM monoclonal antibody 16.88 were carried out as described previously (4, 14). A small amount of DTPA dianhydride in chloroform solution was dried with dry nitrogen gas as a film on the walls of an acid-washed microcentrifuge test tube. The protein solution (10 mg/mL; phosphate buffered saline solution, PBS, pH 7.2, 0.05 M) was added. The reaction mixture was allowed to sit at room temperature for about 15 min with occasional stirring. The contents of the tube were poured onto a G-50 Sephadex gel filtration column and eluted with PBS buffer (pH 7.2, 0.05 M) using a Gilson fraction collector. The absorbance at 280 nm of the eluant fractions was measured. The fractions of the first peak were pooled and concentrated using Amicon Centricon/Centriprep membrane filters.

Antibody LiLo conjugates were prepared by incubating 16.88 and LiLo (1:10 molar ratio) at 37 °C, pH 8.5, in phosphate buffer for 2 h (3). The conjugate was purified

by Sephadex G50 gel filtration chromatography as in the case of 16.88-DTPA. Conjugates were analyzed by SDS/PAGE gel electrophoresis, HPLC, and a competitive binding analysis. The number of chelate molecules per antibody was determined as described previously (4). The number of chelates per protein molecule ranged from three to five for both conjugates (16.88-DTPA and 16.88-LiLo).

¹¹¹In Labeling of Immunoconjugate. ¹¹¹InCl₃ (3–4 mCi, 0.1 mL) in a mixture of acetate (0.6 M, pH 5.5) and citrate (0.06 M, pH 5.5) buffers (0.2 mL) was added to the immunoconjugate (3 mg, 0.3 mL) and incubated at room temperature for 30–60 min. Excess DTPA was added to bind the unreacted indium. The radiolabeled immunoconjugate was further purified by gel filtration chromatography. The elution profile for 16.88-LiLo-¹¹¹In is shown in Figure 2. When a Sephadex G-50 was used for purification, 16.88-LiLo-¹¹¹In eluted in the void volume using phosphate buffered saline solution (0.05 M, pH 7.2). Radiochemical purity was determined by thin-layer chromatography using 10% ammonium acetate/methanol (50:50 v/v) solvent system. Radiochemical purity in all cases was greater than 95%. The TLC sheets were cut into several small strips and the strips were counted in a γ well counter (4). Radiolabeling yield was $70 \pm 10\%$, with respect to ¹¹¹In. Depending on the amount of ¹¹¹In taken, specific activity ranged from 1 to 3 mCi/mg.

TLC Studies of ¹¹¹In-Labeled Chelates. ¹¹¹In-labeled chelates (In-EDTA, In-DTPA, In-LiLo) were prepared by incubating ¹¹¹InCl₃ and the chelate solution in acetate buffer (0.5 M, pH 5.5). The solution was passed through a Chelex 100 column to remove the unbound ¹¹¹In. The chromatographic behavior of the chelates was studied using 10 cm long silica gel plates with 10% ammonium acetate and methanol (1:1) as the solvent system (15).

In-LiLo Complexation. 1,3-Bis[*N*-(2-aminoethyl)-2-aminoethyl]-2-aminoacetamido]-2-(4-nitrobenzyl)propane-*N,N,N',N'',N''',N''''*-octaacetic acid octakis-(ethyl ester) (IV) was hydrolyzed in the presence of HCl as described earlier (see Experimental Procedures, synthesis of LiLo, VII). FABMS *m/e*: (*M* + 1) 691. Nitro-LiLo (hydrolyzed IV) (52.2 mg) was added to 14.3 mg of indium sulfate in 1 mL of deionized water. The solution was stirred for 10–15 min until the solution turned yellow. Concentrated NaOH solution was added in drops to this solution to adjust the pH to approximately 5. A small amount of ethanol was added to this solution and the solution was left at room temperature undisturbed until crystals were formed (21). FABMS *m/e*: (*M* + 1) 1386, (Na₄In-LiLo·12H₂O).

Immunoreactivity. Competitive Binding Assays. The immunoreactivity of the antibody conjugates was determined by competitive binding comparing the reactivity of 16.88-LiLo with native 16.88 in its ability to compete with ¹²⁵I-16.88 for binding to the 16.88 antibody cognate antigen (CTA-1). Immulon I Remov-a-wells (Dynatech Laboratories) were coated with a solution of CTA-1 (2 μ g/mL in PBS, pH 7.2) at 4 °C. CTA-1 was purified as described (12). Fish gelatin from Norland Chemical Co. (3% in PBS) was used to block nonspecific sites of attachment (2 h at 4 °C), and the wells were washed with a solution of 1% glycerol and 0.5% Tween 20. Native 16.88 or 16.88-LiLo (0.156 μ g/mL to 40 μ g/mL) was then added followed by an equal volume (0.05 mL) of ¹²⁵I-16.88. The quantity of ¹²⁵I-16.88 was in the range of 10–30 ng/mL as determined by previous titration to yield a high level of binding below the plateau level. After overnight incubation at 4 °C, the wells were washed and counted for bound ¹²⁵I-16.88. Values were determined in triplicate, and the binding fraction

(bound/total, B/T) was plotted against the quantity of native 16.88 or conjugate added.

Cell Binding Assay. The immunoreactivity of ¹¹¹In-labeled 16.88-DTPA and 16.88-LiLo conjugates was determined by direct cell binding using the WiDr colon carcinoma cell lines as described by Lindmo et al. (16). Approximately 20 ng of ¹¹¹In-16.88 was incubated with 1.25×10^6 to 5×10^6 glutaraldehyde-fixed WiDr cells in 1 mL of PBS solution containing 1% BSA for 18–24 h with constant mixing at room temperature. The suspension was centrifuged, and the radioactivity in the pellet and supernatant was determined. Measurements were done in triplicate. The inverse of the binding fraction (T/B) was determined and plotted against the inverse of the cell number (mL/10⁶ cells). The inverse of the y-intercept (1/Y) is expressed as the maximal binding fraction at infinite antigen concentration. As per this assay, the immunoreactivity of 16.88-LiLo-¹¹¹In was $90 \pm 5\%$.

Stability Studies. The kinetic stabilities of the radiolabeled immunoconjugates were determined in PBS buffer, pH 7.2, at 37 °C, 7% CO₂) by competition in presence of an excess of DTPA (LiLo:DTPA, 1:>5000). At intervals an aliquot of the solution was removed and analyzed by thin-layer chromatography. ¹¹¹In not bound to 16.88 migrated as In-DTPA (*R_f* 0.7; See Table I), whereas indium bound to 16.88 remained at the origin. Measurements were performed in triplicate. TLC plates were cut into equal portions and counted in a γ counter as described by Meares et al. (15). Serum stability measurements were done as described by Deshpande et al. (9).

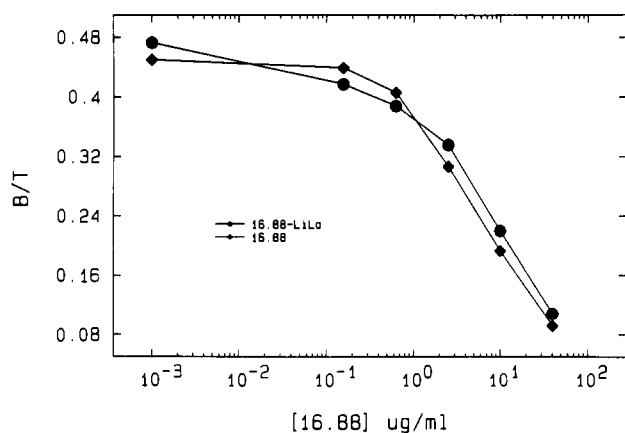
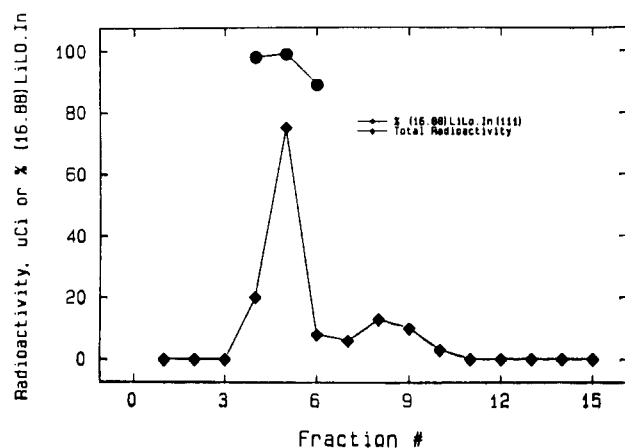
Tissue Distribution Studies. Tumor retention studies were conducted in athymic mice bearing 0.8–1.5 cm diameter xenografts of the THO colon carcinoma prepared from enzymatically dissociated cells as described elsewhere (10, 17). Six-to-eight-week old athymic male mice (Balb/c, nu/nu) were injected in the tail vein with 50 μ g (50 μ Ci) quantities of 16.88-DTPA-¹¹¹In or 16.88-LiLo-¹¹¹In. Animals were sacrificed at intervals from 1 h to 8 days after administration. Blood was collected and sera counted for ¹¹¹In at periodic intervals. Liver, kidney, spleen, intestine, thigh muscle, and femur were excised, weighed, and counted for ¹¹¹In. Results were expressed as a percentage of the injected dose per organ for dosimetry measurements and as a percentage of the injected dose per gram of tissue or per milliliter of serum for distribution studies. The counts were decay corrected. Whole-body clearance was monitored with a dose calibrator. Absorbed dose estimates were calculated using the MIRD formalism of the Society of Nuclear Medicine (18). Pharmacokinetic data were calculated using least squares regression analysis and a microcomputer program (RStrip, Micro-math Scientific Software, Salt Lake City, UT).

RESULTS

Synthesis. A diagram of the LiLo synthesis procedure is provided in Scheme I. The intermediates diester (I), diamide (II), diamine (III), and LiLo esters (IV–VI) were identified by spectral means. The structure of LiLo (VII) was confirmed by spectral methods such as FABMS, IR, and UV/vis. The chromatographic behavior of radiolabeled LiLo in methanol/ammonium acetate solvent system resembled the behavior of ethyl ester of LiLo in methanol/ammonia solvent system. Silica gel TLC analysis showed that the greater the number of carboxyl groups per chelate, the less the chromatographic mobility of the chelate on silica gel (Table I). DTPA chelates with five carboxyl

Table I. Chromatographic Behavior of Radiometal Chelates

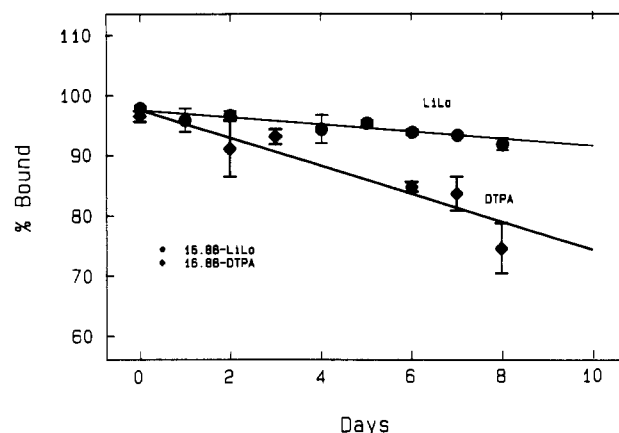
chelate	R_f
^{111}In -EDTA	0.9
^{111}In -DTPA	0.7
^{111}In -LiLo	0.6
^{111}In -16.88	0.0

**Figure 1.** Competitive binding assay: the immunoactivity of the antibody (16.88-LiLo, ●) was estimated by comparison with native antibody (16.88, ◆), in its ability to compete with ^{125}I -16.88 for binding to the cognate antigen for 16.88 (CTA-1).**Figure 2.** Radiochromatography: the radiolabeled immunoconjugate (●) was purified by gel filtration chromatography. The labeled antibody came off the column in the first peak. (Radiochemical purity as determined by TLC analysis is >95%.)

groups moved slower (R_f 0.7) than EDTA chelates with four carboxyl groups (R_f 0.9). LiLo with eight carboxyl groups had an R_f value of 0.6 in this system. The radiolabeled antibody chelate conjugate (16.88-LiLo- ^{111}In) under our experimental conditions stayed at the origin (R_f 0–0.2).

Conjugation and Labeling. The bifunctional chelating agent LiLo was easily coupled to HSA and monoclonal antibody 16.88. The immunoreactivity of the antibody was not affected by the presence of LiLo or the conjugation procedures used. Competitive binding studies demonstrated that 16.88-LiLo behaves similarly to 16.88 in its ability to bind to antigen CTA-1 (Figure 1). The immunoconjugate was labeled by incubating with ^{111}In in a buffer solution containing acetate and citrate. The radioimmunoconjugate was purified by gel filtration chromatography (Figure 2).

Stability Studies. The stability of DTPA and LiLo conjugates was determined in a challenge experiment with a 5000 molar excess of DTPA to conjugate. Under identical experimental conditions, 16.88-LiLo retained ^{111}In much

**Figure 3.** Stability studies—16.88-LiLo- ^{111}In (●) vs 16.88-DTPA- ^{111}In (◆): stability studies were carried out in PBS buffer (pH 7.2, 37 °C) with excess DTPA. Error bars represent the SD values.

better than 16.88-DTPA (Figure 3). After 8 days of incubation 95 % of ^{111}In was bound to 16.88-LiLo, whereas only 80 % of ^{111}In was bound to 16.88-DTPA.

Biodistribution Studies. In vivo stability of the 16.88-LiLo- ^{111}In and 16.88-DTPA- ^{111}In conjugates was studied in athymic mice bearing human colon tumor xenografts. Retention of ^{111}In in various normal tissues as well as in the tumor xenograft was determined as a percentage of the injected dose per gram of tissue (Table II). Stability of 16.88-LiLo- ^{111}In compared with the DTPA conjugate was most apparent in the liver, where significant differences between the two conjugates were seen from 4 h ($p < 0.005$) to 24 h after administration ($p < 0.020$). During the distribution phase up to 4 h following administration apparent differences were not significant (Figure 4A).

A typical biphasic serum clearance curve was obtained with both 16.88-LiLo- ^{111}In and 16.88-DTPA- ^{111}In . Least squares regression analysis gave an initial distribution phase half-life of 39 min with an elimination phase half-life of 10.5 h for 16.88-LiLo- ^{111}In . The values for 16.88-DTPA- ^{111}In (2.2 and 16.3 h, respectively) suggested longer retention of 16.88-DTPA- ^{111}In in the circulation, but these differences were not significant and area under the curve determinations actually indicated longer retention of 16.88-LiLo- ^{111}In (Figure 4B). Maximum blood concentration with a 50- μg dose of the LiLo-chelate conjugate was 13.3 $\mu\text{g}/\text{mL}$ and was 12.3 $\mu\text{g}/\text{mL}$ for the DTPA conjugate. At 4 and 24 h following administration, when the liver values showed the greatest difference, no significant differences in ^{111}In retention in other normal tissues was apparent. Similarly, whole-body clearance of ^{111}In occurred at the same rate with both chelates (Figure 4C). These results were similar to those obtained with ^{125}I -16.88 (17).

Somewhat more activity was seen in tumor xenografts of animals receiving 16.88-LiLo- ^{111}In (max = 3.4 %) than in those from the 16.88-DTPA- ^{111}In group (max 2.9 %) (Table II), but the differences between the two groups were not significant. For both groups tumor-to-blood ratios were greater than unity from 2 days after administration, ranging from 2.4:1 to 29:1 for the LiLo group and 2.6:1 to 16:1 for the DTPA group. Tumor-to-liver ratios over the 8-day evaluating period averaged 0.30 ± 0.06 for 16.88-LiLo- ^{111}In and 0.14 ± 0.05 for 16.88-DTPA- ^{111}In .

Dosimetry calculations based on the murine data indicated that patients receiving 16.88-LiLo- ^{111}In would receive less radiation exposure to normal tissues than

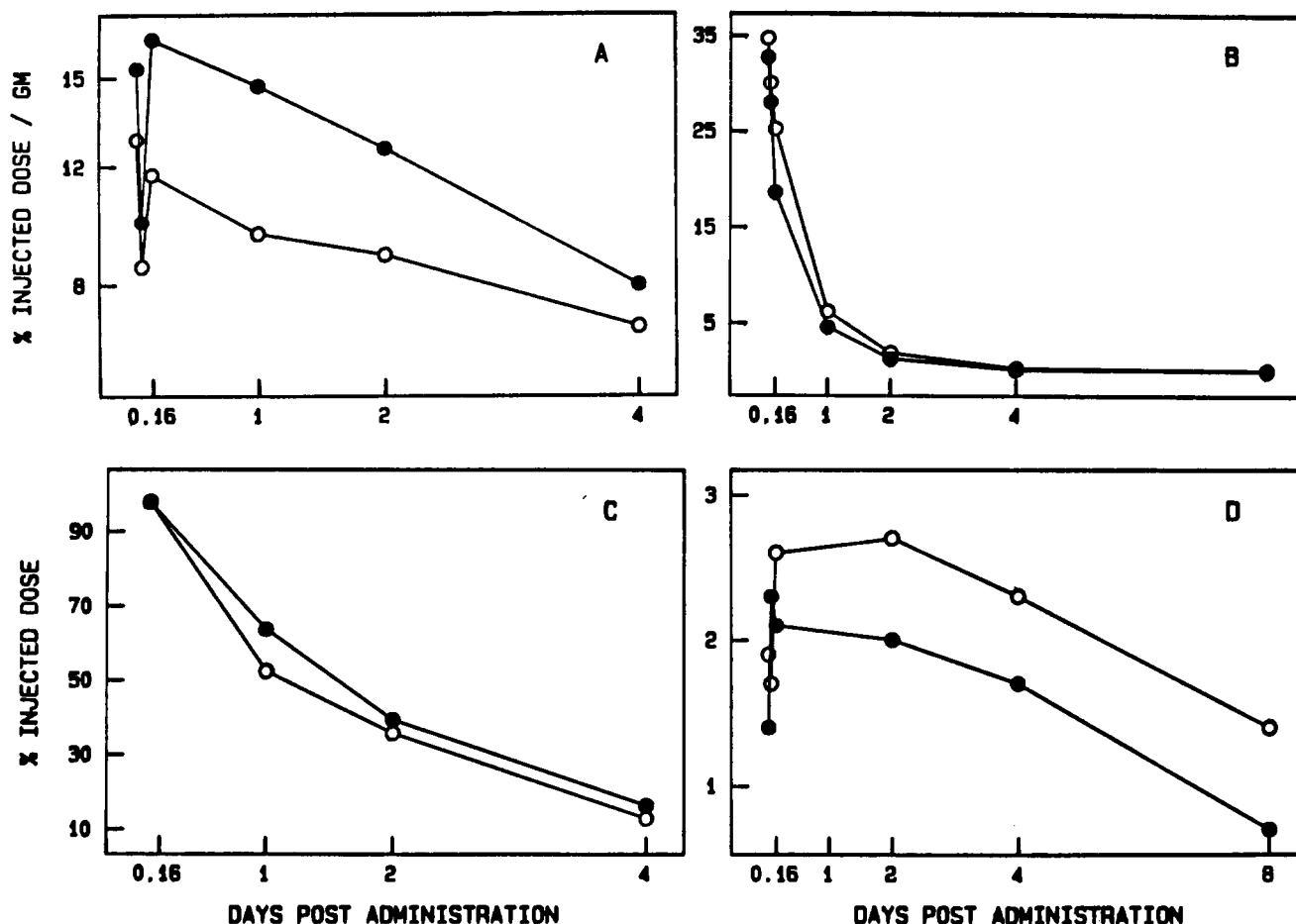


Figure 4. Tissue uptakes of 16.88-DTPA- ^{111}In and 16.88-LiLo- ^{111}In in nude mice: (A) liver, (B) serum, (C) whole body, (D) tumor. Human colon xenografts were developed in 6–8-week-old athymic Balb/c mice from enzymatically dissociated human tumor cells. Fifty micrograms of the labeled antibodies was injected into tail veins of the mice for biodistribution studies ($n = 6$ –12). ●, DTPA; ○, LiLo.

Table II. Tissue Distribution of ^{111}In from 16.88-LiLo- ^{111}In or 16.88-DTPA- ^{111}In in Nude Mice Bearing Human Colon Tumor Xenograft ($n = 6$ –12)

tissue	% injected dose per gram of tissue (\pm SD)													
	16.88-LiLo- ^{111}In							16.88-DTPA- ^{111}In						
	1 h	2 h	4 h	1 d	2 d	4 d	8 d	1 h	2 h	4 h	1 d	2 d	4 d	8 d
serum	34.7 (8.1)	30.0 (9.2)	25.2 (11.5)	6.2 (1.6)	1.9 (0.4)	0.3 (0.1)	0.08 (0.02)	32.7 (2.1)	28.0 (8.6)	18.6 (1.9)	4.6 (0.7)	1.3 (0.2)	0.2 (0.06)	0.07 (0.02)
liver	12.9 (7.6)	8.6 (3.6)	11.7 (3.1)	9.7 (4.5)	9.0 (3.6)	6.6 (2.7)	5.1 (2.8)	15.3 (0.8)	10.1 (3.9)	16.3 (4.9)	14.7 (5.3)	12.6 (5.5)	8.0 (2.5)	5.4 (3.0)
spleen	3.5 (0.9)	3.7 (0.9)	5.9 (3.7)	6.6 (2.4)	8.7 (2.1)	8.3 (3.9)	6.6 (2.4)	4.6 (1.9)	4.2 (2.2)	4.6 (0.7)	5.7 (0.9)	6.1 (1.5)	4.2 (0.8)	3.1 (0.7)
kidney	7.4 (2.3)	7.3 (3.6)	8.9 (3.3)	7.0 (2.6)	5.6 (1.7)	3.5 (1.0)	2.0 (0.6)	5.8 (0.56)	4.9 (0.57)	6.2 (0.67)	7.4 (1.89)	6.8 (2.04)	4.1 (1.04)	2.6 (0.78)
sm. intestine	4.1 (2.6)	2.0 (0.83)	1.6 (0.51)	1.3 (0.56)	1.1 (0.41)	0.5 (0.15)	0.2 (0.0)	3.5 (0.42)	2.7 (0.35)	1.9 (0.85)	1.3 (0.3)	1.0 (0.35)	0.4 (0.10)	0.2 (0.06)
bone (femur)	2.7 (1.0)	3.2 (1.21)	3.4 (1.10)	4.4 (1.73)	4.3 (1.71)	2.1 (1.02)	1.2 (0.57)	2.1 (0.21)	2.1 (0.42)	2.3 (0.10)	2.8 (0.5)	2.5 (0.70)	1.1 (0.31)	1.0 (0.15)
skeletal muscle	0.8 (0.67)	0.6 (0.36)	0.5 (0.17)	0.4 (0.23)	0.3 (0.21)	0.2 (0.13)	0.1 (0.0)	6.5 (0.14)	0.4 (0.0)	1.4 (0.06)	0.2 (0.06)	0.2 (0.06)	0.1 (0.06)	0.1 (0.06)
tumor	1.9 (0.5)	1.7 (0.27)	2.6 (0.29)	3.4 (1.14)	2.7 (0.43)	2.3 (0.46)	1.4 (0.5)	1.4 (0.28)	2.3 (1.07)	2.1 (0.2)	2.9 (0.2)	2.0 (0.3)	1.7 (0.44)	0.7 (0.22)

patients receiving an equal dose of 16.88-DTPA- ^{111}In (Table III). The difference was most apparent in the estimate of the liver dose, where the LiLo patients would receive slightly more than half the dose of the patients receiving 16.88-DTPA- ^{111}In .

DISCUSSION

DTPA dianhydride has been widely used to link radiometals such as ^{111}In to proteins such as human serum albumin and monoclonal antibodies. However, these coupling reactions are difficult to control because hydroly-

sis of cyclic anhydride competes with the protein coupling reaction. In addition, because of the presence of two anhydride moieties, aggregate formation frequently occurs. Although DTPA dianhydride can be coupled to human IgM class antibodies, preparation and purification by gel filtration chromatography can result in considerable loss of radioimmunoconjugate. Halpern et al. reported that only 30% of ^{111}In -labeled human IgM was recovered when DTPA was used as the chelating agent (19).

To avoid these losses and to obtain kinetically inert radioimmunoconjugates with a variety of radiometals, we

Table III. Estimated Radiation Dose to Patients per Millicurie of Administered 16.88-LiLo-¹¹¹In or 16.88-DTPA-¹¹¹In

tissue	rads/mCi	
	16.88-LiLo- ¹¹¹ In preclinical	16.88-DTPA- ¹¹¹ In preclinical
whole body	0.22	0.38
blood	0.40	0.56
spleen	0.93	0.96
kidneys	1.02	1.46
liver	1.28	2.27
bone	0.24	0.32
bone marrow	0.15	0.21

have prepared a new poly(amino carboxylate) chelator suitable for attachment to human monoclonal antibodies and other proteins. The synthesis of the bifunctional chelate involves the condensation between *p*-nitrobenzyl bromide and diethyl malonate. The diethyl (*p*-nitrobenzyl)malonate obtained is converted to a diamine by reacting the ester with ammonia to give a diamide and then by reducing the diamide to a diamine. The diamine was coupled to DTPA and esterified to obtain LiLo ethyl ester. This compound was purified by silica gel column chromatography, reduced to an aminobenzyl derivative, and converted to a isothiocyanate derivative. This was further hydrolyzed in the presence of hydrochloric acid to obtain LiLo.

The final step in the synthesis of LiLo involves the reaction between the diamine and DTPA anhydride. This reaction leads to the formation of LiLo ester and DTPA ester. Upon silica gel column chromatography using chloroform/methanol as the eluant, DTPA ester elutes first followed by LiLo ester. NMR, infrared, and mass spectral analyses of the product confirmed the structure of LiLo.

As seen from the structure, LiLo has six nitrogen atoms and eight carboxyl groups suitable for binding radiometals (Chart I). Each arm can bind a metal ion, or alternately, both arms together can bind one or more metal ions. The nature of such binding may depend on the reaction conditions and the type of metal ions involved. Metal ions with very high coordination numbers (e.g., actinides, lanthanides, etc.) may bind easily to this molecule. We focused our efforts on binding of indium, a radiometal used in cancer imaging with radiolabeled antibodies.

The results of the in vitro stability measurements demonstrated that 16.88-LiLo-¹¹¹In was more stable than 16.88-DTPA-¹¹¹In. The stability of ¹¹¹In chelator was determined using G-50 gel filtration chromatography in normal human serum at 37 °C. It was found that over a period of 7 days, less than 1% of the ¹¹¹In was released from the chelate. In vitro stability studies have shown that LiLo may be suitable for attaching yttrium to 16.88 (data not shown). Current experiments evaluating the pharmacokinetic behavior of 16.88-LiLo-⁹⁰Y in animal model systems will be reported separately.

Although the thermodynamic stability of a metal chelate is an important factor in determining the ease with which the chelation occurs, kinetic stability data are critical for in vivo applications of radiometal chelates. Kinetic stability of a radioimmunoconjugate will be influenced by several factors including the nature of the metal ion, the nature of the chelating agent, and the nature of the linkage between the chelator and the antibody, and, to some extent, the characteristics of the antibody. Earlier stability measurements demonstrated that chelators such as isothiocyanatobenzyl-EDTA or isothiocyanatobenzyl-DTPA attached to proteins are kinetically more stable than DTPA

cyclic anhydride linked proteins. Recent experiments have shown that benzyl-EDTA chelates attached to proteins are more stable in human serum than benzyl-DTPA chelate linked proteins (9). Similar results were also obtained by Carney et al. (20). There are several reasons for the instability of DTPA conjugates prepared from cyclic dianhydride. During conjugation of DTPA anhydride to protein one of the five carboxyl groups of DTPA is involved in coupling to an amine group of the protein, leaving four carboxyl groups available for binding to radiometals. Recent crystal structure studies have shown that In-DTPA complexation involves coordination between indium and five oxygens and three nitrogens of DTPA (21), necessitating the presence of at least five carboxyl groups for optimal chelation with indium. The *p*-nitrobenzyl group in the backbone carbon chain may further contribute to kinetic stability of LiLo-antibody conjugates. Meares and co-workers have shown that bulky substituents in the chelator molecule will reduce loss of ¹¹¹In from the conjugate to other metal-binding proteins in vivo (3, 9). To reduce the uptake of radioactivity in normal organs, several approaches have been taken. A recent report suggested that the liver uptake of ¹¹¹In-labeled antibodies may depend on the method of purification (22).

Another method to reduce the normal organ uptake is the use of cleavable linkers between the antibody and chelator. In an attempt to reduce the background activity, we conjugated a DTPA analogue to 16.88 through a diester linkage. Biodistribution studies in nude mice bearing THO human colon tumor xenografts indicated that diester-linked conjugate was retained to a lesser extent in tumor and normal organs such as liver and kidney as compared to the peptide conjugate (23). LiLo contains an isothiocyanato group for coupling to antibody, ensuring that aggregation through antibody cross-linking is prevented. HPLC analysis using a molecular-sieve chromatography showed that, under similar experimental conditions, aggregate formation with LiLo was almost negligible (<1%). The conjugates prepared using DTPA dianhydride normally contained 10% aggregates (data not shown).

In vivo stability of 16.88-LiLo-¹¹¹In was demonstrated in animal studies. It can be clearly seen that liver uptake of 16.88-LiLo-¹¹¹In was lower than that of 16.88-DTPA-¹¹¹In (Tables II and III). This observation is in agreement with in vitro stability measurements. The tumor uptakes of radiolabeled human IgM class monoclonal antibodies are lower than reported for murine IgG monoclonal antibodies in mouse models. This may be related to differences in Ig class and species of origin of the antibody. Recent experiments with radiolabeled human IgGs resulted in higher tumor uptakes (24).

The encouraging in vitro and in vivo results obtained using the bifunctional chelating agent LiLo demonstrate that this molecule is suitable for attaching radiometals such as indium to the human monoclonal antibodies.

ACKNOWLEDGMENT

We are thankful to Drs. Carolyn Preyor of University of Maryland and Frans Kaspersen of Organon, for the spectral analyses of the compounds, and to Debra Balachalk and Ping Jiang-Baucom, for the technical assistance.

LITERATURE CITED

- Steis, R. G., Carrasquillo, J. A., McCabe, R. P., Bookman, M. A., Reynolds, J. C., Larson, S., Smith, J. W., II, Clark, J. W., Dailey, V., Velvetchio, S., Shuke, N., Pinsky, C. M., Urba, W.

- J., Haspel, M. V., Parentesis, P., Paris, B., Longo, D. L., and Hanna, M. G., Jr. (1990) Toxicity, immunogenicity, and tumor radioimmunodetecting ability of two human monoclonal antibodies in patients with metastatic colorectal carcinoma. *J. Clin. Oncol.* 8, (3), 476-490.
- (2) Lamki, L. M., Patt, Y. Z., and Murray, J. L. (1990) In-111 monoclonal antibody immunoscintigraphy of colorectal cancer. *Cancer Imaging with Radiolabeled Antibodies* (D.M. Goldenberg, Ed.) pp 293-312, Kluwer Academic, Boston.
- (3) Subramanian, R., and Meares, C. F. (1990) Bifunctional chelating agents for radiometal labeled monoclonal antibodies. *Cancer Imaging with Radiolabeled Antibodies* (D.M. Goldenberg, Ed.) pp 183-199, Kluwer Academic Publishers, Boston.
- (4) Subramanian, R., Paik, C. H., McCabe, R. P., Quadri, S. M., Kim, H. J., Pomato, N., Haspel, M. V., Reba, R., and Hanna, M. G., Jr. (1990) Tissue distribution of ¹¹¹In labeled human monoclonal antibody 16.88 in nude mice bearing tumor xenografts: Effect of diester linkage. *Antibody, Immunoconjugates, Radiopharm.* 3, 127-136.
- (5) Haseman, M. K., Goodwin, D. A., Meares, C. F., Kaminski, M. S., Wensel, T. G., McCall, M. J., and Levy, R. (1986) Metabolizable ¹¹¹In chelate conjugated antiidiotypic monoclonal antibody for radioimmunodetection of lymphoma in mice. *Eur. J. Nuc. Med.* 12, 455-60.
- (6) Moi, M. K., Meares, C. F., and DeNardo, S. J. (1988) The peptide ways to macrocyclic bifunctional chelating agents: Synthesis of 2-(p-nitrobenzyl)-1,4,7,10-tetraazacyclodecane-N,N',N'',N'''-tetraacetic acid and study of its yttrium(111) complex. *J. Am. Chem. Soc.* 110, 6266-6267.
- (7) Esteban, J. E., Schlom, J., Gansow, O. A., Atcher, R. W., Brechbiel, M. W., Simpson, D. E., and Colcher, E. J. (1987) New methods for the chelation of indium-111 to monoclonal antibodies: Biodistribution and imaging of athymic mice bearing human colon carcinoma xenografts. *Nucl. Med.* 28, 861-870.
- (8) Deshpande, S. V., Subramanian, R., McCall, M. J., DeNardo, S. J., DeNardo, G. J., and Meares, C. F. (1990) Metabolism of indium chelates attached to monoclonal antibody: Minimal transchelation of indium from benzyl-EDTA chelate in vivo. *J. Nucl. Med.* 31, 218-224.
- (9) Peters, L. C., Brandhorst, J. S., and Hanna, M. G., Jr. (1979) Preparation of immunotherapeutic autologous tumor cell vaccines from solid tumors. *Cancer Res.* 39, 1353-1360.
- (10) Haspel, M. V., McCabe, R. P., Pomato, N., Janesch, N. J., Knowlton, J. V., Peters, L. C., Hoover, H. C., Jr., and Hanna, M. G., Jr. (1985) Generation of tumor cell-reactive human monoclonal antibodies using peripheral blood lymphocytes from actively immunized colorectal carcinoma patients. *Cancer Res.* 45, 3951-61.
- (11) Pomato, N., Murray, J. H., Bos, E., Haspel, M. V., McCabe, R. P., and Hanna, M. G., Jr. (1989) Identification and characterization of a human colon tumor-associated antigen, CTAA-16.88, recognized by a human monoclonal antibody. *Human Tumor Antigens and Specific Tumor Therapy* (R.S. Metzgar, and M.S. Mitchell, Eds.) pp 127-136, Alan R. Liss, New York.
- (12) Moi, M. K., Meares, C. F., McCall, M. J., Cole, W. C., and DeNardo, S. J. (1985) Copper chelates as probes of biological systems: Stable copper complexes with a macrocyclic bifunctional chelating agent. *Anal. Biochem.* 148, 249-253.
- (13) Mikkala, V. M., Mikola, H., and Hemmila, I. (1989) The synthesis and use of activated N-benzyl derivatives of diethylenetriaminetetraacetic acids: Alternative reagents for labeling of antibodies with metal ions. *Anal. Biochem.* 176, 319-325.
- (14) Hnatowich, D. J., Layne, W. W., and Childs, R. L. (1983) Radioactive labeling of antibody. *Science* 220, 613-15.
- (15) Meares, C. F., McCall, M. J., Reardan, D. J., Goodwin, D. A., Diamanti, C. I., and McTigue, M. (1985) Conjugation of antibodies with bifunctional chelating agents: Isothiocyanate and bromoacetamide reagents, methods of analysis and subsequent addition of metal ions. *Anal. Biochem.* 142, 68-78.
- (16) Lindmo, T., Boven, E., Cuttitta, F., Fedorko, J., and Bunn, P. A., Jr. (1984) Determination of the immunoreactive fraction of radiolabeled monoclonal antibodies by linear extrapolation to binding at infinite antigen excess. *J. Immunol. Methods* 72, 77-89.
- (17) McCabe, R. P., Peters, L. C., Haspel, M. V., Pomato, N., Carrasquillo, J. C., and Hanna, M. G., Jr. (1988) Preclinical studies on the pharmacokinetic properties of human monoclonal antibodies to colorectal cancer and their use for detection of tumors. *Cancer Res.* 48, 4348-4353.
- (18) Lovinger, R., Budinger, T., Watson, E. (1988) *MIRD primer for absorbed dose calculations*, The Society of Nuclear Medicine, New York, NY 10016.
- (19) Halpern, S. E., Hagen, P. L., Chen, A., Birdwell, C. R., Bartholomew, R. M., Bunnett, K. G., David, G. S., Poggenburg, K., Merchant, B., and Carlo, D. J. (1988) Distribution of radiolabeled human and mouse monoclonal IgM antibodies in murine models. *J. Nucl. Med.* 29, 1688-1696.
- (20) Carney, P. L., Rogers, P. E., and Johnson, D. K. (1989) Dual isotope study of iodine-125 and indium-111 labeled antibody in athymic mice. *J. Nucl. Med.* 30, 374-384.
- (21) Maecke, H. R., Riesen, A., and Ritter, W. (1989) The molecular structure of indium-DTPA. *J. Nucl. Med.* 30, 1235-1239.
- (22) Schuhmacher, J., Klivenyi, G., Matys, R., Kirchgebnner, H., Nauser, N., Mäyser-Bovst, W., and Matzku, S. (1990) Uptake of indium-111 in the liver of mice following administration of indium-111-DTPA-labeled monoclonal antibodies: Influence of labeling parameters, physiologic parameters, and antibody dose. *J. Nucl. Med.* 31, 1084-1093.
- (23) Paik, C. H., McCabe, R. P., Quadri, S. M., Subramanian, R., Lynn, F., Kim, J. J., and Reba, R. C. (1988) Tumor targeting of radiolabeled human monoclonal antibody 16.88 after modification of chemical bonds. *J. Nucl. Med.* 29, 889.
- (24) Subramanian, R., Haspel, M. V., De Jager, R., Pomato, N., Hanna, Jr., M. G., and McCabe, R. P. (1991) Technetium-99m labeled human monoclonal antibody 88BV59-1: Pharmacokinetic evaluation. *Antibody, Immunoconjugate, Radiopharm.* 4, 221.

Registry No. I, 7598-70-1; II, 119822-20-7; III, 140437-93-0; IV, 140175-48-0; V, aminobenzyl derivative, 140175-50-4; VI, 140175-49-1; VII, 134439-56-8; DTPAa, 23911-26-4; diethyl Malonate, 105-53-3; 4-nitrobenzyl bromide, 100-11-8; thiophosgene, 463-71-8.

New Strategy in Glycopolymer Syntheses. Preparation of Antigenic Water-Soluble Poly(acrylamide-*co-p*-acrylamidophenyl β -lactoside)

René Roy,* François D. Tropper, and Anna Romanowska

Department of Chemistry, University of Ottawa, Ottawa, Ontario, Canada K1N 6N5. Received February 19, 1992

Stereospecific phase-transfer-catalyzed glycosidation of acetobromolactose 3 with *p*-nitrophenoxide gave the peracetylated 1,2-*trans*- β -D-4-nitrophenyl lactoside 4. Functionalization of 4 into an *N*-acryloyl monomer was achieved by catalytic transfer hydrogenation of the nitro group, followed by *N*-acryloylation of the resulting amino group, on both *O*-acetyl-protected and unprotected disaccharides. Copolymerization of 4-acrylamidophenyl β -lactoside (9) with acrylamide, initiated by ammonium persulfate, afforded a water-soluble carbohydrate copolymer (glycopolymer). The antigenicity of the new polymer was demonstrated by agar gel diffusion with *Arachis hypogaea* (peanut) and *Ricinus communis* (castor bean) lectins. Quantitative precipitation and enzyme linked lectin assays (ELLA) were also performed with peanut lectin.

INTRODUCTION

Carbohydrates are ubiquitous components of cell wall membranes and occur as glycolipids, glycoproteins, proteoglycans, and capsular polysaccharides (1). As such, they can participate in forefront intramolecular and intracellular events. Apart from their recognized roles in the physicochemical properties of glycolipids and glycoproteins, the carbohydrate residues can also serve as cell surface receptors for toxins, hormones, enzymes, antibodies, viruses, and bacteria (2). It is therefore not surprising that tremendous efforts have been directed at the syntheses of artificial carbohydrate-protein conjugates (neoglycoproteins) used as antigens (3-5) and immunogens¹ (6) in order to mimic some of the above interactions.

However, much less attention has been directed at the syntheses of water-soluble carbohydrate copolymers (7-10) (we propose the term glycopolymer²) which share some of the antigenic properties of their neoglycoprotein counterparts. A number of the previous glycopolymer syntheses relied on the copolymerization of allyl glycosides (7-9) and acrylamides. Most recently, we (10-13) and others (14, 15) have modified the method using *N*-acryloylated carbohydrate monomers having lengthened spacer arms. They also have an improved reactivity when compared to that of alkenyl monomers. In our approaches, intermediates were designed with dual functional properties. Thus, the *N*-acryloyl moieties could also be used as Michael acceptors for amine groups of proteins (13, 16), thus providing access to both neoglycoproteins and glycopolymers from single precursors.

¹ The terms antigens and immunogens are used throughout in their contemporary sense as defined in refs 26 and 27. Antigens can react with antibodies and can thus produce immune complexes without necessarily inducing antibody formations as opposed to immunogens. Therefore, in this context, antigens would be equivalent to multivalent haptens, because haptens cannot, on their own, form insoluble (cross-linked) immune complexes as determined by double immunodiffusion or quantitative precipitation assays.

² Glycopolymer is introduced here for the first time. It is suggested as a replacement for "pseudopolysaccharide" previously used. The term has been chosen in analogy to glycoproteins and glycolipids. In the present context, it is used to mean water-soluble polymers bearing covalently bound carbohydrates. However, the term should be equally well applicable to insoluble polymers such as those used in affinity chromatography.

The present work describes the application of the above strategy by combining the ease and usefulness of phase-transfer catalysis to the stereospecific synthesis of 4-nitrophenyl β -lactoside, which serves as a precursor to the 4-acrylamidophenyl β -lactoside comonomer. The advantages of using glycopolymers instead of protein conjugates are obvious: lower costs, improved thermal and biological stabilities (17), and controlled determinants (18). It was also shown that they are suitable coating antigens in solid-phase enzyme linked lectin assays (ELLA), in agar gel diffusion, and in quantitative precipitation assays.

EXPERIMENTAL PROCEDURES

General Methods. Melting points were determined on a Gallenkamp apparatus and are uncorrected. The ¹H- and ¹³C-NMR spectra were recorded on a Varian XL-300 at 300 and 75.4 MHz, respectively. The proton chemical shifts (δ) are given relative to internal chloroform (7.24 ppm) for CDCl₃ solutions, and to internal acetone (2.216 ppm) for D₂O solutions. The carbon chemical shifts are given relative to deuteriochloroform (77.0 ppm) and to acetone (31.1 ppm) for D₂O solutions. The analyses were done as a first-order approximation and assignments were based on COSY and HETCOR experiments. Optical rotations were measured on a Perkin-Elmer 241 polarimeter and were run at 23 °C for 1% solutions. Mass spectra were recorded on a VG 7070-E spectrometer (CI, ether) and Kratos Concept IIH (FAB, glycerol). Thin-layer chromatography (TLC) was performed using silica gel 60 F-254 and column chromatography on silica gel 60 (230-400 mesh, E. Merck No. 9385).

4-Nitrophenyl 2,3,6,2',3',4',6'-Hepta-*O*-acetyl- β -lactoside (4). To a solution of acetobromolactose 3 (5.20 g, 7.43 mmol), tetrabutylammonium hydrogen sulfate (2.50 g, 1 equiv), and *p*-nitrophenol (2.01 g, 14.5 mmol) in methylene chloride (50 mL) was added 1.0 M NaOH (50 mL). The reaction mixture was gently warmed until no solid precipitate appeared. The two-liquid-phase mixture was then vigorously stirred at room temperature for 2.5 h. TLC in hexane/ethyl acetate (1/1) containing 0.5% 2-propanol indicated complete consumption of bromide 3 into lactoside 4. The resulting organic phase was successively washed with 1 M NaOH and water and dried over sodium sulfate. The residue obtained after filtration and evaporation of the solvent was purified by silica gel column chromatography using the above solvent as eluent. Crystallization of the pooled fractions from ethanol gave 3.19

g (57%) of 4: mp 183.2–185.2 °C; $[\alpha]_D -15^\circ$ ($c = 1.16$, CHCl_3) [lit. (19) mp 132–133 °C; $[\alpha]_D -35.4^\circ$ (CHCl_3)]; ^1H NMR (CDCl_3) δ 8.19 (d, 2 H, $J = 9.3$ Hz, H-meta), 7.03 (d, 2 H, H-ortho), 5.35 (dd, 1 H, $J_{3,4} = 3.4$, $J_{4,5} = 1.0$ Hz, H-4'), 5.29 (ABM pattern, 1 H, H-3), 5.18 (AB pattern, 2 H, H-1, H-2), 5.12 (dd, 1 H, $J_{1,2} = 7.9$, $J_{2,3} = 10.4$ Hz, H-2'), 4.95 (dd, 1 H, H-3'), 4.50 (d, 1 H, $J_{1,2} = 7.9$ Hz, H-1'), 4.50 (dd, 1 H, $J_{5,6} = 1.8$, $J_{6,6'} = 12.1$ Hz, H-6), 4.01–4.15 (m, 3 H, H-6, 2 \times H-6'), 3.80–3.92 (m, 3 H, H-4, H-5, H-5'), 1.96, 2.04, 2.05, 2.06 (2 \times), 2.07, 2.15 (7 s, OAc); ^{13}C NMR (CDCl_3) δ 169.2, 169.6, 169.7, 170.1, 170.2 (2 C), 170.4 (C=O), 161.2 (C-*ipso*), 143.2 (C-*para*), 125.7 (C-*meta*), 116.5 (C-*ortho*), 101.1 (C-1'), 97.6 (C-1), 75.8 (C-4), 73.0 (C-3), 72.4 (C-5), 71.0 (C-3'), 70.7 (C-2), 70.6 (C-5'), 68.9 (C-2'), 66.5 (C-4'), 61.7 (C-6), 60.7 (C-6'), 20.2, 20.4 (4 C), 20.5 (2 C) (Ac); mass spectrum (pos FAB) (rel intensity) m/e 727 (M – NO, 1.4), 711 (M – NO₂, 1.3), 619 (M – OPhNO₂, 5.3). Anal. Calcd for $\text{C}_{32}\text{H}_{39}\text{NO}_{20}$: C, 50.73; H, 5.19; N, 1.85. Found: C, 50.87, H, 5.25, N, 1.85.

4-Nitrophenyl β -Lactoside (5). Peracetylated lactoside 4 (1.21 g, 1.60 mmol) was dissolved in warm methanol (30 mL) containing 1 M NaOMe (40 μL). After a few hours at room temperature, 5 had partially crystallized. To ensure complete de-O-acetylation, more methanol was added (20 mL) and the solution was warmed again. The solution was stirred overnight at room temperature and ether (25 mL) was added to the cooled solution to ensure complete crystallization. Pure 5 (733 mg) was thus obtained after filtration and drying in 99% yield: mp 249.0–250.2 °C; $[\alpha]_D -39.1^\circ$ ($c = 1.25$, DMSO) [lit. (19) mp 258–260 °C dec; $[\alpha]_D -74.2^\circ$ (H_2O)]; ^1H NMR (D_2O) δ 8.27 (d, 2 H, $J = 9.3$ Hz, H-meta), 7.25 (d, 2 H, H-ortho), 5.30 (d, 1 H, $J_{1,2} = 7.7$ Hz, H-1), 4.48 (d, 1 H, $J_{1,2} = 7.7$ Hz, H-1'), 3.55–3.99 (m, 12 H, ring H); ^{13}C NMR ($\text{DMSO}-d_6$) 162.6 (C-*ipso*), 142.0 (C-*para*), 126.0 (C-*meta*), 116.7 (C-*ortho*), 104.0 (C-1'), 99.4 (C-1), 80.0 (C-4), 75.7 (C-3), 75.2 (C-5), 74.8 (C-2), 73.0 (C-3'), 72.9 (C-5'), 70.6 (C-2'), 68.2 (C-4'), 60.5 (C-6), 60.0 (C-6'); mass spectrum (pos FAB) (rel intensity) m/e 556 (M + 1 + glycerol, 1), 464 (M + 1, 1.4). Anal. Calcd for $\text{C}_{18}\text{H}_{25}\text{NO}_{13}$: C, 46.66; H, 5.44; N, 3.02. Found: C, 46.67; H, 5.43; N, 2.99.

4-Aminophenyl 2,3,6,2',3',4',6'-Hepta-O-acetyl- β -lactoside (6). A solution of 4-nitrophenyl β -lactoside 4 (483 mg, 0.638 mmol) and ammonium formate (800 mg) in MeOH (80 mL) containing 10% Pd/C (100 mg) was gently warmed for 5–10 min in a stoppered round-bottom flask. After cooling, the reaction mixture was filtered through Celite which was rinsed with methylene chloride. The solvents were evaporated, and the residue was dissolved in CH_2Cl_2 . The organic phase was washed with water and dried (Na_2SO_4). The residue obtained from the solvent gave pure 6 (456 mg) in 98% yield, which was crystallized from ethanol/methanol: mp 183.2–185.2 °C; $[\alpha]_D -15.0^\circ$ ($c = 1.16$, CHCl_3); ^1H NMR (CDCl_3) δ 6.79 (d, 2 H, $J = 8.8$ Hz, H-meta), 6.57 (d, 2 H, H-ortho), 5.33 (dd, 1 H, $J_{3,4} = 3.4$, $J_{4,5} = 1.0$ Hz, H-4'), 5.23 (dd, 1 H, $J_{2,3} = 9.4$, $J_{3,4} = 9.1$ Hz, H-3), 5.10 (dd, 1 H, $J_{1,2} = 7.8$, $J_{2,3} = 9.4$ Hz, H-2), 5.10 (dd, 1 H, $J_{1,2} = 7.8$, $J_{2,3} = 10.4$ Hz, H-2'), 4.93 (dd, 1 H, $J_{2,3} = 10.4$, $J_{2,3} = 3.4$ Hz, H-3'), 4.85 (d, 1 H, $J_{1,2} = 7.8$ Hz, H-1), 4.48 (d, 1 H, $J_{1,2} = 7.8$ Hz, H-1'), 4.47 (dd, 1 H, $J_{6,6'} = 11.9$, $J_{5,6} = 2.0$ Hz, H-6), 4.01–4.14 (m, 3 H, H-6, 2 \times H-6'), 3.84 (m, 2 H, H-4, H-5'), 3.68 (ddd, 1 H, $J_{4,5} = 9.9$, $J_{5,6} = 2.0$, $J_{5,6'} = 5.4$ Hz, H-5), 3.51 (b s, 2 H, NH₂), 1.95–2.14 (7 s, OAc); ^{13}C NMR (CDCl_3) δ 168.9–170.2 (7 s, C=O), 149.6 (C-*ipso*), 142.4 (C-*para*), 118.8 (C-*meta*), 115.7 (C-*ortho*), 101.0 (C-1'), 100.2 (C-1), 76.2 (C-4), 72.8 (C-3), 72.7 (C-5), 71.6 (C-2), 70.9 (C-3'), 70.7 (C-5'), 69.1 (C-2'), 66.6 (C-4'), 62.0 (C-6), 60.8 (C-6'), 20.6–20.9 (7 s,

Ac); mass spectrum (CI) (rel intensity) m/e 727 (M, 18), 619 (M – OPhNH₂, 23.8). Anal. Calcd for $\text{C}_{32}\text{H}_{41}\text{NO}_{18}$: C, 52.82; H, 5.68; N, 1.92. Found: C, 52.73; H, 5.50; N, 1.75.

4-Aminophenyl β -Lactoside (7). The catalytic transfer hydrogenation method described above for 6 was applied to de-O-acetylated lactoside 5. Compound 5 (178 mg, 0.384 mmol), ammonium formate (120 mg, 5 equiv) and 10% Pd/C (25 mg) were warmed in MeOH (25 mL) in a stoppered round-bottom flask. When TLC in $\text{CHCl}_3/\text{MeOH}/\text{H}_2\text{O}$ (30:10:1) indicated complete conversion (15 min), the reaction mixture was cooled to room temperature. The solids were filtered through Celite and rinsed with MeOH. The filtrate was evaporated to dryness to give 7 still containing ammonium formate. The salt was removed by repeated freeze-drying from water. The homogeneous product (quantitative) was crystallized from warm (not hot) ethanol (mp 237.0–238.5 °C) or water (mp 270.2–271.5 °C); $[\alpha]_D -24.2^\circ$ ($c = 1.26$, DMSO) [lit. (19) mp 233 °C dec; $[\alpha]_D -36.4^\circ$ (H_2O)]; ^1H NMR (D_2O) δ 7.00 (d, 2 H, $J = 9.0$ Hz, H-meta), 6.81 (d, 2 H, H-ortho), 4.99 (d, 1 H, $J_{1,2} = 7.9$ Hz, H-1), 4.47 (d, 1 H, $J_{1,2} = 7.7$ Hz, H-1'), 3.53–4.00 (m, 12 H, ring-H); ^{13}C NMR ($\text{DMSO}-d_6$) δ 148.6 (C-*ipso*), 142.5 (C-*para*), 117.7 (C-*meta*), 114.5 (C-*ortho*), 103.8 (C-1'), 101.6 (C-1), 80.3 (C-4), 75.6 (C-3), 74.9 (C-5), 74.8 (C-2), 73.3 (C-3), 73.1 (C-5), 70.6 (C-2), 68.2 (C-4), 60.5 (C-6'), 60.3 (C-6); mass spectrum (pos FAB) (rel intensity) m/e 548 (M + Na + glycerol, 1.2), 456 (M + Na, 10.2), 434 (M + 1, 5.3).

4-Acrylamidophenyl 2,3,6,2',3',4',6'-Hepta-O-acetyl- β -lactoside (8). A solution of compound 6 (419 mg, 0.576 mmol) and triethylamine (350 μL) in CH_2Cl_2 (40 mL) was cooled to 0 °C. Acryloyl chloride (60 μL , 1.25 equiv) in CH_2Cl_2 (15 mL) was added dropwise while the temperature was allowed to reach room temperature. The reaction mixture was stirred for 30 min. MeOH (2 mL) was then added and the reaction mixture was stirred at room temperature for a further hour. Water (60 mL) was then added and the organic phase was successively washed with 0.5 M HCl (2 \times 60 mL), saturated NaHCO₃, and water. The dried (Na_2SO_4) organic phase was filtered and evaporated to dryness (<30 °C). The residue was purified by silica gel column chromatography with $\text{CHCl}_3/\text{EtOAc}$ (1/1). Pure 8 (426 mg) was obtained as a white solid in 95% yield and failed crystallization: mp 117.8–118.7 °C (slow evaporation from CH_2Cl_2) $[\alpha]_D -18.8^\circ$ ($c = 1.0$, CHCl_3); ^1H NMR (CDCl_3) δ 7.21 (d, 2 H, $J = 9.1$ Hz, H-meta), 6.93 (d, 2 H, H-ortho), 6.41 (dd, 1 H, $J_{\text{gem}} = 1.3$, $J_{\text{trans}} = 10.2$ Hz, H-trans), 6.20 (dd, 1 H, $J_{\text{cis}} = 6.8$, $J_{\text{trans}} = 10.2$ Hz, CHCO), 5.75 (dd, 1 H, H-cis), 5.34 (dd, 1 H, $J_{3,4} = 3.4$, $J_{4,5} = 1.0$ Hz, H-4'), 5.25 (dd, 1 H, $J_{2,3} = 9.1$, $J_{3,4} = 8.7$ Hz, H-3), 5.14 (dd, 1 H, $J_{1,2} = 9.7$, $J_{2,3} = 9.1$ Hz, H-2), 5.11 (dd, 1 H, $J_{1,2} = 7.8$, $J_{2,3} = 10.4$ Hz, H-2'), 4.98 (d, 1 H, $J_{1,2} = 7.7$ Hz, H-1), 4.94 (dd, 1 H, H-3'), 4.47 (dd, 1 H, $J_{5,6} = 2.1$, $J_{6,6'} = 12.0$ Hz, H-6), 4.48 (d, 1 H, $J_{1,2} = 7.8$ Hz, H-1'), 4.01–4.14 (m, 3 H, H-6, 2 \times H-6'), 3.86 (m, 2 H, H-4, H-5'), 3.75 (ddd, 1 H, $J_{4,5} = 9.8$, $J_{5,6} = 2.1$, $J_{5,6'} = 5.9$ Hz, H-5); ^{13}C NMR (CDCl_3) δ 169.2–170.2 (7 s, COCH₃), 163.2 (COCH=CH₂), 153.4 (C-*ipso*), 133.2 (C-*para*), 130.9 (CH=), 127.8 (=CH₂), 121.3 (C-*meta*), 117.5 (C-*ortho*), 101.0 (C-1'), 99.1 (C-1), 76.2 (C-4), 72.8 (C-3), 72.7 (C-5), 71.4 (C-2), 70.9 (C-3'), 70.7 (C-5'), 69.1 (C-2'), 67.0 (C-4'), 62.0 (C-6), 60.8 (C-6'), 20.6–20.9 (7 s, Ac); mass spectrum (pos FAB) (rel intensity) m/e 874 (M + 1 + glycerol, 1.7), 619 (M – aglycon, 3.9). Anal. Calcd for $\text{C}_{35}\text{H}_{43}\text{NO}_{19}$: C, 53.78, H, 5.54; N, 1.79. Found, C, 53.64; H, 5.58; N, 1.68.

4-Acrylamidophenyl β -Lactoside (9). Method A. Per-O-acetylated N-acryloyl derivative 8 (350 mg, 0.448

mmol) was treated with methanolic sodium methoxide as above for 5. Analytically pure **9** (441 mg) was obtained in 98% yield after crystallization from the reaction mixture as above: mp 252.6–254.8 °C (MeOH); $[\alpha]_D^{25} -26.7^\circ$ ($c = 0.81$, DMSO); ^1H NMR (D_2O) δ 7.45 (d, $J = 9.1$ Hz, H-meta), 7.15 (d, H-ortho), 6.52 (dd, 1 H, $J_{\text{trans}} = 17.0$, $J_{\text{cis}} = 9.8$ Hz, $\text{CH}=\text{CH}_2$), 6.31 (dd, 1 H, $J_{\text{gem}} = 1.7$ Hz, H-trans), 5.86 (dd, 1 H, H-cis), 5.14 (d, 1 H, $J_{1,2} = 7.8$ Hz, H-1), 4.48 (d, 1 H, $J_{1,2} = 7.8$ Hz, H-1'), 3.52–4.01 (m, 12 H, ring-H); ^{13}C NMR ($\text{DMSO}-d_6$) δ 162.6 (C=O), 153.2 (C-ipso), 133.2 (C-para), 131.8 (CH=), 126.3 ($\text{CH}_2=$), 120.4 (C-meta), 116.4 (C-ortho), 103.7 (C-1'), 100.2 (C-1), 80.1 (C-4), 75.5 (C-3), 74.8 (C-2, C-5), 73.2 (C-3'), 72.9 (C-5'), 70.5 (C-2'), 68.1 (C-4'), 60.4 (C-6'), 60.1 (C-6). Anal. Calcd for $\text{C}_{21}\text{H}_{29}\text{NO}_{12}$: C, 51.74; H, 6.00; N, 2.87. Found: C, 51.97; H, 5.99; N, 2.76.

Method B. *N*-Acryloylation of the Unprotected Lactoside **7.** Compound **7** (141 mg, 0.326 mmol) was treated with triethylamine (200 μL) in cold MeOH (20 mL, 0 °C) by dropwise addition of acryloyl chloride (35 μL) in CHCl_3 (4 mL). After complete addition, the reaction mixture was stirred at room temperature for an additional hour. The ions were removed by successive treatment with anionic resin (OH^-) and then cationic resin (H^+) until the solution reached neutrality. Compound **9** was obtained in 94% yield after freeze-drying of the methanolic residue. It was homogeneous by TLC in $\text{CHCl}_3/\text{MeOH}/\text{H}_2\text{O}$ (30:10:1) and had the physical properties described above.

Poly(acrylamide-co-*p*-acrylamidophenyl β -lactoside) (10**).** Compound **9** (29 mg, 60 μmol) and acrylamide (42.3 mg, 600 μmol) were dissolved in deoxygenated water (750 μL) obtained by multiple cool-thaw cycles and bubbling with nitrogen. Ammonium persulfate (12 μL of a stock solution, 50 mg/mL) and TMEDA (4 μL) were then added. The reaction mixture was stirred under nitrogen at 90 °C for 12 min. TLC indicated remaining monomers. The same amount of the initiators was added and the mixture reacted for a further 12 min at 90 °C. The cooled reaction mixture was diluted with water (25 mL) and dialyzed (10 000 MW cutoff) exhaustively against distilled water (6 \times 5 L). The aqueous solution of the polymer was lyophilized to afford lactosyl copolymer **10** (46 mg) in 65% yield: $[\alpha]_D^{25} +3.6^\circ$ ($c = 1.02$, H_2O); ^1H NMR (300 MHz, D_2O) δ 7.40 (d, 2 H, $J = 8$ Hz, H-meta), 7.15 (d, 2 H, $J = 8$ Hz, H-ortho), 4.88 (b s, 1 H, H-1), 4.48 (d, 1 H, $J = 8.4$ Hz, H-1'), 3.57–3.98 (m, 12 H, ring H), 3.31 (app s, 1 H, CHCONHPh), 2.77 (app s, 2 H, $\text{CH}_2\text{-CHCONHPh}$), 2.3 and 2.2 (2 b s, 12 H), 1.7 and 1.6 (2 b s, 20 H); ^{13}C NMR (75.4 MHz, D_2O): δ (ppm), 180.3 (C=O), 155.0 (C-ipso), 132.4 (C-para), 124.8, (C-meta), 118.0 (C-ortho), 103.8 (C-1'), 101.0 (C-1), 78.9 (C-4), 76.2 (C-5), 75.8 (C-3), 75.0 (C-2), 73.5 (C-3'), 73.4 (C-5'), 71.8 (C-2'), 69.4 (C-4'), 61.9 (C-6'), 60.8 (C-6), 52.1 ($\text{CH}_2\text{CHCONHPh}$), 44.2 (CHCONHPh), 43.0 (b), 42.9 (b), 42.6 (b), (CH backbone), 36.9, 36.7, 35.7, 35.5 (b, CH_2 backbone). Anal. Found for $(\text{C}_3\text{H}_5\text{NO})_{10.1}(\text{C}_{21}\text{H}_{29}\text{NO}_{12})_{1.0}(\text{H}_2\text{O})_{6.4}$: C, 46.71; H, 6.19, N, 11.78 (20).

Molecular Weight Determination. Molecular weight determination was effected on a Waters Model 991/625LC HPLC system equipped with a diode-array detector. The calibration was done with proteins (Boehringer Mannheim, cat. no. 1213-776) and polyacrylamide standards (Polysciences, Inc.) in 0.1 M phosphate buffer (pH 7.0) on a TSK G4000 SWXL column (7.5 \times 30 cm) at a flow rate of 1 mL/min. Absorbances were measured at 205 (polyacrylamides) or 280 nm (proteins and **10**).

Agar Gel Diffusion. Agar gel diffusion experiments were performed on 1% agarose (BDH) containing 2% poly-

(ethylene glycol) (PEG, MW 8000, Sigma) in phosphate-buffered saline (PBS) according to Ouchterlony and Nilsson (21). The polymer conjugate **10** and the lectins (Sigma) were used at a concentration of 1 mg mL $^{-1}$ in PBS. The precipitin bands were allowed to form overnight at 4 °C.

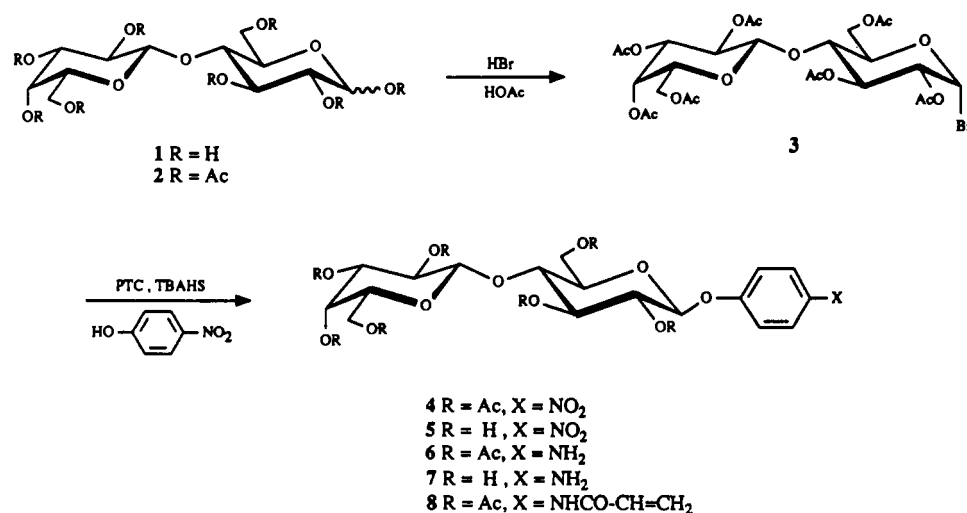
Quantitative Precipitation Assays with Lectin. The lectin from *Arachis hypogaea* (peanut, Sigma No. L-0811) was diluted to 200 μg mL $^{-1}$ in PBS, and 100- μL solutions were added to 1.5-mL Eppendorf microfuge tubes (Brinkmann Instruments Co., Westbury, NY). Aliquots of 1.0–200 μL of a stock solution of the polymer **10** (1.0 mg mL $^{-1}$) in PBS were added to the tubes. The final volume of all the tubes was then adjusted to 300 μL . The reactions were run in triplicate. The solutions were gently agitated and allowed to incubate for 2 h at 37 °C and then for 4 days at 4 °C. The tubes were centrifuged for 15 min at 14000g in a Fisher Microcentrifuge Model 235 B. The precipitin pellets were washed three times with 300 μL of cold PBS with centrifugation between washes. The protein content of the pellets was determined using the bicinchoninic acid (22) (BCA) protein assay reagents of Pierce following the enhanced protocol described in the instruction manual. The absorbances were measured at 562 nm.

Enzyme Linked Lectin Assays (ELLA). The wells of Linbro EIA microtiter plates (Flow Laboratories, Mississauga, ON, Canada) were coated at room temperature overnight by using 100 μL of 2-fold dilutions of polymer **10** (16 μg mL $^{-1}$) in PBS. The plates were blocked with 300 μL of 0.2% BSA in PBS for 1 h at room temperature. After washing (four times), the wells were filled with 100 μL of 300 \times diluted (PBS) horseradish peroxidase-labeled peanut lectin (1 mg/mL, Sigma No. L7759). The plates were incubated at room temperature for 3 h and then washed five times with PBS. The enzyme substrate 2,2'-azino bis(3-ethylbenzothiazoline-6-sulfonic acid) (ABTS, 250 μg mL $^{-1}$, (50 μL /well) in citrate-phosphate buffer (0.2 M, pH 4.0 with 0.01% H_2O_2) was added. After 15 min the optical density was measured at 410 nm on a Dynatech MR 600 spectrophotometer.

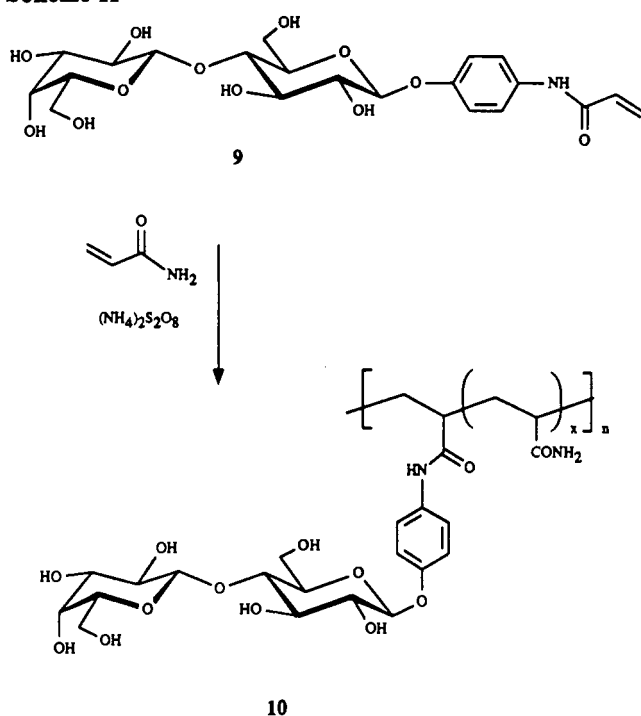
RESULTS AND DISCUSSION

Synthesis. Lactose (**1**) was chosen as a good ligand model because it is an important hepatocyte receptor (23, 24). Thus, transformation of disaccharide **1** into a suitable glycosyl donor **3** through the intermediary of octa-*O*-acetyl derivative **2** was effected using standard procedures (HBr, HOAc). Lactosyl bromide **3** was then glycosidated with complete anomeric stereocontrol using phase transfer catalyzed (PTC) conditions in the presence of *p*-nitrophenol and tetrabutylammonium hydrogen sulfate to afford **4** in 57% overall yield from **2** (Scheme I). There was no α -glycoside detected, as judged by the ^1H -NMR spectrum of the crude reaction mixture. Dehydrobromination and hydrolysis were the major side reactions to occur (5). To the best of our knowledge, this report, together with ongoing research (25), represents the first example of high stereoselective disaccharide syntheses under PTC conditions. It is also worthy to mention that 4-nitrophenyl glycosides are useful glycohydrolase substrates and many of them are commercially available. Thus, the strategy described here should be of general interest. Transformation of the nitro group to the *N*-acryloyl function was then effected on both the per-*O*-acetylated precursor **4** and the unprotected derivative **5** obtained in quantitative yield by Zemplén de-*O*-acetylation of **4** with the aim of demonstrating the generality of the approach.

Scheme I



Scheme II



Catalytic transfer hydrogenation with 10% Pd/C in the presence of ammonium formate was found to be most efficient for the reduction of 4 and 5 to 4-aminophenyl β -lactosides 6 and 7, obtained in almost quantitative yields. Compound 7 was also produced from 6 following Zemplén de-O-acetylation in methanol containing a catalytic amount of sodium methoxide. The syntheses of the monomer precursors 8 and 9 were also straightforward using *N*-acryloyl chloride in a mixture of methylene chloride (for 6) or methanol (for 7) and triethylamine at (0 °C) (>94% yield). Zemplén de-O-acetylation of 8 afforded 9 in quantitative yield. Care should be taken in the manipulation of 8 and 9 since they were prone to homopolymerization, especially if small quantities of acrylic acid were present. The scheme employing per-O-acetylated intermediates 4, 6, and 8 offers the most convenient and easiest route in terms of purification and isolation of the desired products.

Finally, 4-acrylamidophenyl β -lactoside monomer 9 was copolymerized with acrylamide (1:10 molar ratio) using ammonium persulfate and heat or *N,N,N',N'*-tetrame-

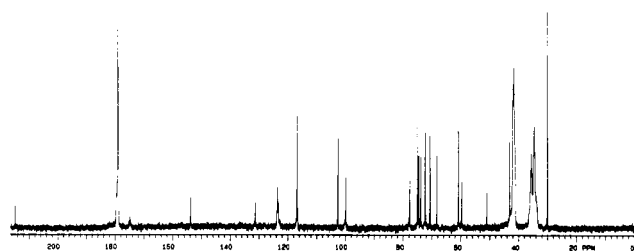


Figure 1. ¹³C-NMR spectrum (75.4 MHz) of the poly-lactose-co-acrylamide polymer 10 in D₂O at 37 °C.

thylethylenediamine (TMEDA) in aqueous solutions as previously described for nonaromatic *N*-acryloylated glycosides (8–13). Thin-layer chromatography of the reaction mixture was used to monitor the transformation of the carbohydrate monomer 9 into 10, which was obtained as a white fluffy material after exhaustive dialysis in water and freeze-drying (65% yield). The ¹H NMR spectrum of 10 in D₂O and elemental analyses were used to establish the molar ratio of the reactants incorporated into the glycopolymer (20). There was no remaining unreacted monomer 9 in the polymer, thus illustrating the efficiency of the dialysis in removing all low molecular weight components. Both results gave an incorporation identical to the stoichiometry used in the reaction mixture, thus proving the advantage of *N*-acryloylated comonomers over allyl glycosides. Hence, the water-soluble glycopolymer 10 contained disaccharide and acrylamide residues in a 1:10 ratio, as calculated from the intensities of the bulk signals attributed to the carbohydrate units (intensities verified with the anomeric, aromatic, and ring protons) relative to those of the methine and methylene groups of the polyacrylamide backbone in the 300-MHz ¹H-NMR spectra. The ¹³C-NMR spectrum of 10 is shown (Figure 1). HPLC chromatograms of 10 (Figure 2) showed a rather narrow molecular weight distribution centered at around 120 kDa.

Binding Assays. The usefulness of co-polyacrylamide lactoside 10 to act as antigen was first demonstrated by radial diffusion in agar gel (21) with two different lectins. Sharp precipitin bands were observed (Figure 3) with *A. hypogaea* (peanut) lectin and *Ricinus communis* (castor bean agglutinin) (2). The relative mobilities of 10 and the lectins in the agarose gel indicated a relative molecular weight of approximately 50–150 kDa, similar to those previously observed (8–13), thus confirming the HPLC results (Figure 2). The capacity of multivalent haptens to form insoluble cross-linked complexes with lectins can

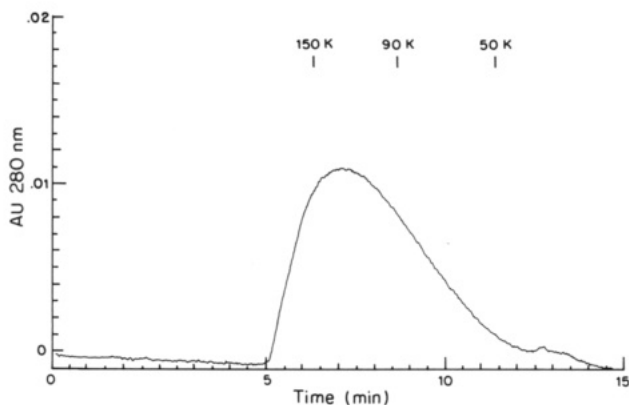


Figure 2. HPLC profile of glycopolymer 10 on a TSK G4000 SWXL column in 0.1 M phosphate buffer, pH 7.0. Bars indicate the molecular weight of polyacrylamide standards.

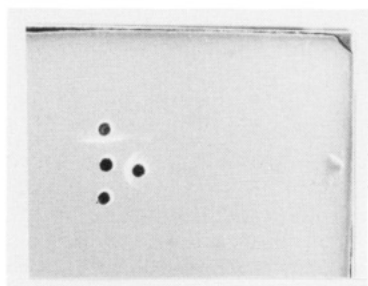


Figure 3. Agar gel diffusion of polymer 10 (middle well) with peanut lectin (top well), castor bean lectin (right well), and wheat germ agglutinin (bottom well, as negative control).

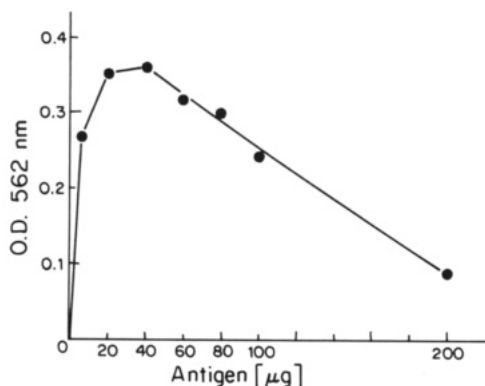


Figure 4. Quantitative precipitin curve of poly(acrylamide-*co*-*p*-acrylamidophenyl β -lactoside) 10 with *A. hypogaea* lectin.

be demonstrated by quantitative precipitation experiments. Thus, as shown in Figure 4, when using a fixed amount of peanut lectin, the usual quantitative precipitin curve can be obtained with increasing concentration of the glycopolymer 10. The added advantage of the glycopolymers in such experiments is that the amount of protein in the precipitates is directly related to the lectin used since the polymer is nonreactive in the colorimetric protein assays (22). Control experiments using an unrelated lectin (wheat germ agglutinin), specific for *N*-acetylglucosamine and sialic acid, showed no binding, thus demonstrating the specificity of the interactions.

Moreover, we also demonstrated the ability of such carbohydrate *co*-acrylamide polymer to serve as coating antigen in solid-phase enzyme binding assays. Two-fold serial dilutions in 10 in PBS were used to coat the wells of enzyme immunoassays (EIA) microtiter plates. The plates were washed and blocked in the usual manner. Direct binding with horseradish peroxidase-labeled peanut lectin was demonstrated using ABTS/ H_2O_2 as enzyme substrates (Figure 5). With a preestablished lectin con-

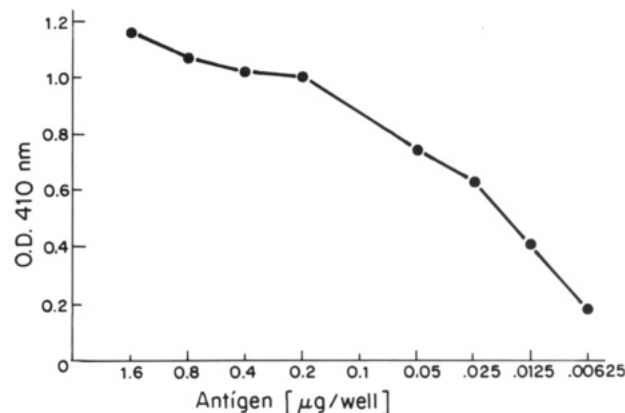


Figure 5. Enzyme linked lectin assay (ELLA) of the conjugate 10 as coating antigen with horseradish peroxidase-labeled *A. hypogaea* lectin using ABTS as enzyme substrate.

centration, the absorbance at 410 nm could be directly correlated with the antigen-polymer concentrations. Thus, glycopolymer 10 at 1 μ g/well in the above lectin assay is as sensitive as a protein could be in similar assays.

In conclusion, stereospecific glycosidation of glycobiosyl bromide with *p*-nitrophenol under PTC conditions afforded the monomer precursor. Following catalytic transfer hydrogenation, *N*-acryloylation, and copolymerization with acrylamide, water-soluble antigenic glycopolymers were obtained. The method is general and application to other biologically relevant carbohydrates is in progress (18).

ACKNOWLEDGMENT

This work was supported by NSERC. F.D.T. is grateful to NSERC for a graduate fellowship.

LITERATURE CITED

- (1) Sharon, N. (1975) In *Complex Carbohydrates. Their Chemistry, Biosynthesis, and Functions*, Addison-Wesley, Reading, MA.
- (2) Goldstein, L. J., and Poretz, R. D. (1986) in *The Lectins. Properties, Functions, and Applications in Biology and Medicine* (I. E. Liener, N. Sharon, and I. J. Goldstein, Eds.) Academic Press, Orlando, FL.
- (3) Stowell, C. P., and Lee, Y. C. (1980) Neoglycoproteins. The Preparation and Application of Synthetic Glycoproteins. *Adv. Carbohydr. Chem. Biochem.* 37, 225-281.
- (4) Roy, R., and Laferrière, C. A. (1990) Synthesis of protein conjugates and analogues of *N*-acetylneuraminic acid. *Can. J. Chem.* 68, 2045-2054.
- (5) Roy, R., Tropper, R. D., Romanowska, A., Letellier, M., Cousineau, L., Meunier, S., and Boratynski, J. (1991) Expedient syntheses of neoglycoproteins using phase transfer catalysis and reductive amination as key reactions. *Glycoconjugate J.* 8, 75-81.
- (6) Dick, W. E., and Beureet, M. (1989) Glycoconjugates of bacterial carbohydrate antigens. In *Contributions to Microbiology and Immunology. Conjugate Vaccines* (J. L. Cruse, and R. E. Lewis, Jr., Eds.) Vol. 10, pp 48-114, Karger, Switzerland.
- (7) Hořekš, V., Smolek, P., and Kocourek, J. (1978) Water-soluble O-glycosyl polyacrylamide derivatives for specific precipitation of lectins. *Biochim. Biophys. Acta* 538, 293-298.
- (8) Roy, R., Laferrière, C. A., Gamian, A., and Jennings, H. J. (1987) *N*-acetylneuraminic acid: Neoglycoproteins and pseudopolysaccharides *J. Carbohydr. Chem.* 6, 161-165.
- (9) Kosma, P., Waldstätten, P., Daoud, L., Schulz, G., and Unger, F. M. (1989). Synthesis of poly(acrylamide) copolymers containing 3,5-dideoxy-D-arabino-2-octulopyranosylonic (5-deoxy-KDO) residues. *Carbohydr. Res.* 194, 145-154.

- (10) Roy, R., and Tropper, F. D. (1988) Synthesis of copolymer antigens containing 2-acetamido-2-deoxy- α - or β -D-glucopyranosides. *Glycoconjugate J.* 5, 203-206.
- (11) Roy, R., and Laferrière, C. A. (1988) Synthesis of antigenic copolymers of N-acetylneuraminic acid binding to wheat germ agglutinin and antibodies. *Carbohydr. Res.* 88, C1-C4.
- (12) Roy, R., and Tropper, F. D. (1988) Synthesis of antigenic carbohydrate polymers recognized by lectins and antibodies. *J. Chem. Soc. Chem. Commun.* 1058-1060.
- (13) Roy, R., and Laferrière, C. A. (1990) Michael Addition as the key step in the synthesis of sialyloligosaccharide-protein conjugates from N-acryloylated glycopyranosyl-amines. *J. Chem. Soc. Chem. Commun.* 1709-1711.
- (14) Kallin, E., Lönn, H., Norberg, T., and Elofsson, M. (1989) Derivatization procedures for reducing oligosaccharides, Part 3: preparation of oligosaccharide glycosylamines, and their conversion into oligosaccharide-acrylamide copolymers. *Glycoconjugate J.* 8, 597-611.
- (15) Chernyak, A. Y., Sharma, G. V. M., Kononov, L. O., Krishna, P. R., Rao, A. V. R., and Kochetkov, N. K. (1991) Synthesis of glycuronamides of amino acids, constituents of microbial polysaccharides and their conversion into neoglycoconjugates of copolymer type. *Glycoconjugate J.* 8, 82-89.
- (16) Roy, R., Tropper, F. D., Morrison, T., and Boratynski, J. (1991) Syntheses and transformations of glycohydrolase substrates into protein conjugates based on Michael additions. *J. Chem. Soc. Chem. Commun.* 536-538.
- (17) Similar copolymers were kept for 4 years at room temperature, without loss of antigenic properties as shown by agar gel diffusion and quantitative precipitation assays.
- (18) Other sialic acid and N-acetylglucosamine homo and copolymers with acrylic acid, methacrylamide, hydroxyethyl methacrylate of various molar ratios (1:0 to 1:40) were similarly prepared. Their binding properties to the influenza A virus hemagglutinin and wheat germ agglutinin will be described elsewhere.
- (19) Babers, F. H., and Goebel, W. F. (1934) The synthesis of p-aminophenol β -glycosides of maltose, lactose, cellobiose, and gentiobiose. *J. Biol. Chem.* 105, 473-480.
- (20) The monomer incorporations calculated by elemental analysis should be established using $(C_3H_5NO)_x(C_{21}H_{29}NO_{12})_y(H_2O)_n$ as the general structure of the copolymer obtained after freeze-drying since polyacrylamides are known to strongly retain some water of hydration. By setting up three equations for percent C, H, and N in addition to $x + y$

+ $n = 1$, four simultaneous equations with three unknowns can be solved and verified algebraically:

$$\% \text{ element} = \frac{\text{am}_{\text{element}} \sum_{x,y,n} E_{\text{mu}} M_{\text{mu}}}{\text{MW of the average repeating unit}}$$

- where $\text{am}_{\text{element}}$ = atomic mass of the element, E_{mu} = number of elements per monomer unit, and M_{mu} = molar fraction of each monomer unit (x, y, n). (Example for %C: %C = $12.0115(3x + 21y)/(71.0786x + 487.4596y + 18.0152n)$.) Note that this method has the distinct advantage that the water content (variable from batch to batch) in the polymers can be calculated and taken into consideration during serological studies. Thus, for the elemental analysis obtained, $x:y:n = 10.1:1:6.3$ or a copolymer of 1:10.1 ratio with 8.6% (w/w) water content.
- (21) Ouchterlony, Ö., and Nilsson, L. A. (1978) Immunodiffusion and immunoelectrophoresis. In *Handbook of Experimental Immunology* (D. M. Weir, Ed.) Chapter 19, Blackwell Scientific Publications, Oxford.
 - (22) Smith, P. K., Krohn, R. I., Hermanson, G. T., Mallia, A. K., Gartner, F. H., Prorenzano, M. D., Fukimoto, E. K., Goeke, N. M., Olson, B. J., and Klenck, D. C. (1985) Measurements of Protein using Bicinchoninic Acid. *Anal. Biochem.* 150, 76-85.
 - (23) Hudgin, R. L., Pricer, Jr., W. E., and Ashwell, G. (1974) The isolation and properties of a rabbit liver binding protein specific for asialoglycoproteins. *J. Biol. Chem.* 249, 5536-5543.
 - (24) Lee, R. T., and Lee, Y. C. (1987) Preparation of cluster glycosides of N-acetylgalactosamine that have subnanomolar binding constants towards the mammalian hepatic Gal/GalNAc-specific receptor. *Glycoconjugate J.* 4, 317-328.
 - (25) Tropper, F. D., Andersson, F. O., Grand-Maitre, C., and Roy, R. (1991) Stereospecific synthesis of 1,2-trans-1-phenylthio- β -D-disaccharides under phase transfer catalysis. *Synthesis* 734-736.
 - (26) Catty, D. (1988) In *Antibodies: A Practical Approach*. Chapter 1, p 7, IRL Press Ed., Oxford, England.
 - (27) Roitt, I. (1991) In *Essential Immunology*, 7th Edition, Chapter 4, p 65 Blackwell Scientific Publications, Oxford, England.
- Registry No.** 3, 5160-10-1; 4, 84034-75-3; 5, 4419-94-7; 6, 135253-84-8; 7, 17691-02-0; 8, 135253-86-0; 9, 135253-89-3; 10, 140440-47-7; p-nitrophenol, 100-02-7; acryloyl chloride, 814-68-6.

Construction of Protein Analogues by Site-Specific Condensation of Unprotected Fragments

Hubert F. Gaertner,^{*,†} Keith Rose,[†] Ron Cotton,[†] David Timms,[†] Roger Camble,[†] and Robin E. Offord[†]

Département de Biochimie Médicale, Centre Médical Universitaire, 1 rue Michel Servet, 1211 Geneva 4, Switzerland, and ICI Pharmaceuticals, Mereside, Alderley Park, Macclesfield, Cheshire SK 10 4TG, U.K.

Received January 23, 1992

The extreme sensitivity to periodate of 1-amino, 2-hydroxy compounds permits the selective conversion of N-terminal serine and threonine to an aldehydic group. We have used this reaction to construct analogues of human granulocyte colony stimulating factor (G-CSF) by allowing such oxidized peptides to react with others that have had a hydrazide derivative attached to the C-terminus by reversed proteolysis. Two recombinant analogues of G-CSF were used as starting materials. Both had only a single lysine residue (at position 62 and 75, respectively) followed immediately by a serine. Digestion of each analogue by the lysine-specific protease from *Achromobacter lyticus* gave two fragments, one of which could be N-terminally oxidized and the other converted to the C-terminal hydrazide derivative by reversed proteolysis using the same enzyme. After preliminary studies with model peptides, we first reacted the corresponding peptide pairs together and then, in order to eliminate the 64-74 disulfide loop, fragment 1-62 from the first analogue with fragment 76-174 from the second. Reactions are efficient (up to 80% product based on the oxidized fragment) and take place under very mild conditions. The hydrazone bond can easily be stabilized by reduction with NaBH₃CN. This method represents a new, reasonably general route for the construction of large protein chimeras of precisely controlled structure.

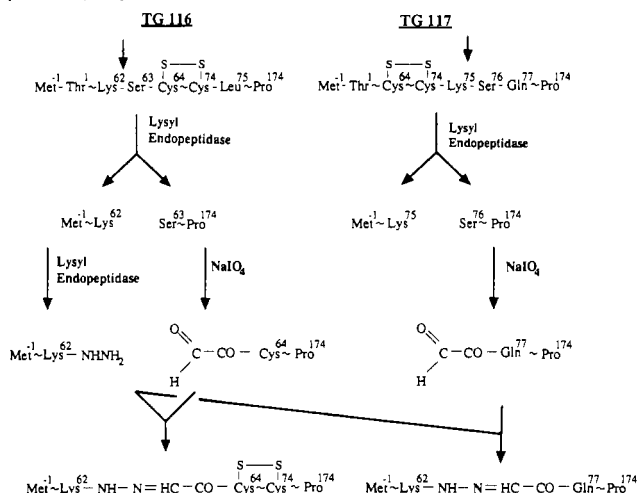
The rebuilding of proteins from two or more fragments has been used for many years to investigate structure-function relationships of proteins (for reviews, Chaiken, 1981; Offord, 1990). Though mutation of recombinant proteins is now a more generally suitable approach for these studies, the coupling of protein fragments remains important in three areas: firstly, for the introduction of noncoded structures (e.g. D-amino acids and peptide mimics; Offord, 1990); secondly, to overcome the length limitations of solid-phase peptide synthesis (Kent, 1992); and thirdly, to conjugate site-specifically various structures, as for example introducing a "reporter" group for structural studies of a protein or arming antibodies with peptidic toxins (Waldman, 1991). For such purposes, the ability of proteolytic enzymes to catalyse peptide-bond synthesis has been widely investigated with the aim of developing new methods of fragment coupling which can be achieved with great specificity and minimum use of protecting groups (Laskowski, 1978; Jakubke et al., 1985). Conversion of porcine insulin to human insulin (Moriyama et al., 1979) as well as amidation of a peptide hormone (Breddam et al., 1991) have been successfully achieved enzymically under the thermodynamic influence of a high concentration of the amino component, and (usually) the presence of an organic cosolvent, thus shifting the equilibrium toward synthesis. However, proteases have been applied to the fragment condensation of long-chain peptides only in a limited number of cases, usually those where there is some assistance either by specific interaction between acyl and amine components or by the presence of a molecular trap (Homandberg et al., 1982; Sahni et al., 1989). The principal factors limiting more general applications are the low solubility of long-chain peptides in terms of molar concentration and the more likely presence, within longer peptides, of several sites of unwanted cleavage by the proteases used for the condensation.

Protein semisynthesis, which utilizes polypeptide fragments of natural origin for the construction of larger molecules, may be facilitated by using mutagenesis techniques to produce protein analogues tailored to eliminate unwanted cleavage sites and introduce new ones at specified sites along the peptide chain (Camble et al., 1985; Wallace et al., 1991). Reverse proteolysis catalyzed by the same enzyme that was used for protein fragmentation is an efficient means for introducing C-terminal groups that are not normally found in proteins, and such an approach has already been exploited for attachment of amino acid dichlorophenyl esters with subsequent conjugation by aminolysis (Rose et al., 1988a) or attachment of hydrazine as a prelude to azide coupling (Jones & Offord, 1982). But in both cases, if there is no conformational assistance, coupling to the desired amino group involves protection and deprotection of any other amino groups present. On the other hand, protection and deprotection is not required if one forms a link between two groups that have a unique and complementary chemical reactivity and that do not normally exist in proteins. One such approach to site-specific condensation is reaction between a specifically introduced C-terminal hydrazide nucleophile and a component carrying an aldehyde or keto group (Offord & Rose, 1986; Rose et al., 1991). Such a latter function can be generated at a unique site in the protein by very mild oxidation of an N-terminal serine or threonine residue (Fields & Dixon, 1968; Geoghegan & Stroh, 1992). An enzymically introduced C-terminal hydrazide function will be the only nucleophile present that, under acidic conditions, is able to form a stable product with the terminal glyoxal function produced by oxidation of N-terminal serine or threonine.

In this paper we report such an approach using two recombinant G-CSF analogues, each engineered to contain a single lysine residue which is immediately followed by a serine. It was first established that all four lysine residues present in natural human G-CSF can be replaced by arginine residues with retention of biological activity (Cam-

[†] Centre Médical Universitaire.

^{*} ICI Pharmaceuticals.

Scheme I. Construction of Protein Analogues (1-62)-(63-174) Hydrazone and (1-62)-(76-174) Hydrazone


ble et al., unpublished results). A single novel lysine residue was then substituted into the lysine-free analogue at specified positions along the polypeptide chain. In one analogue the lysine-serine bond is between residues 62 and 63, i.e. just before the disulfide-loop region between Cys⁶⁴ and Cys⁷⁴ (Wingfield et al., 1988), and in the other analogue the lysine-serine bond is between residues 75 and 76, i.e. just after the loop region. Both proteins give, upon enzymatic cleavage with the lysine specific protease from *Achromobacter lyticus* (Masaki et al., 1981), two fragments, one fragment having a C-terminal lysine, the other an N-terminal serine. After preliminary studies with model peptides, we first reacted the corresponding peptide pairs together (Scheme I), and then, in order to eliminate the 64-74 disulfide loop, we reacted fragment 1-62 from the first analogue with fragment 76-174 from the second.

EXPERIMENTAL PROCEDURES

Except where otherwise specified, solvents and reagents of analytical grade or better, were obtained from commercial sources, and were used without further purification. Room temperature was approximately 23 °C.

A. lyticus protease (lysyl endopeptidase) was from Wako Pure Chemical Co., Osaka, Japan. Hydrazine was from Pierce, Boc-hydrazide was from Aldrich, carbonyldiimidazole, and adipohydrazide were from Fluka (Buchs, Switzerland). Ser-Leu-Leu was purchased from Bachem (Bubendorf, Switzerland), and Ac-Pro-Gln-Ser-Phe-Leu-Lys(Boc)-OH was provided by ICI Pharmaceuticals.

This latter peptide was Boc deprotected by incubation in trifluoroacetic acid (TFA) for 1 h at room temperature and the hydrazide derivative was obtained by esterification of the deprotected peptide (8 mg in 2 mL of 0.1 M HCl in methanol 4 h at room temperature), followed by hydrazinolysis in methanol (10 mg/mL) with a 200-fold excess of hydrazine over the peptide, for 5 h at room temperature. The hydrazide derivative was recovered by dilution with 2 volumes of 0.1% TFA, followed by adsorption to a Sep-Pak C18 (Waters Associates) cartridge, previously washed with methanol and equilibrated with 0.1% TFA. After washing the Sep-Pak thoroughly with 0.1% TFA, the sample was eluted with 5 mL of 0.1% TFA containing 80% acetonitrile and dried under vacuum (weight, 7.8 mg; yield, 95%). The product was characterized by fast atom bombardment mass spectrometry (calcd M + H, *m/z* 888.5; found, *m/z* 888.6).

HPLC was performed on a Waters 625 LC system equipped with a Wisp 712 sample processor and a Model 441 UV detector. For analytical work, a column 250 × 4 mm i.d. (Nucleosil C8, 300 Å, 5 μm, Macherey Nagel, Oensingen, Switzerland) was used at a flow rate of 0.6 mL/min, and effluent monitored at 214 nm. For preparative work, a column 250 × 10 mm i.d. of Nucleosil C4 or C8 (300 Å, 5 μm, Macherey Nagel) was used at a flow rate of 3 mL/min. Solvent A was 1 g of trifluoroacetic acid (Pierce) added to 1 L of water (MilliQ system). Solvent B was prepared by adding 1 g of trifluoroacetic acid to 100 mL of water and bringing the solution up to 1 L with acetonitrile (Lichrosolv, Merck).

Recombinant Analogues of G-CSF. Two recombinant analogues of G-CSF were produced in *Escherichia coli* at ICI Pharmaceuticals. These analogues, TG116 (Cys 17 → Ser; Lys 16, 23, 34, 40 → Arg; Ser 62 → Lys) and TG117 (Cys 17 → Ser; Lys 16, 23, 34, 40 → Arg; Leu 75 → Lys), each contained a single lysine-serine linkage for proteolytic cleavage by *A. lyticus* protease.

Fragment Preparation. The protein concentration was spectrophotometrically determined using an extinction coefficient of 0.86 at 280 nm and a 1-cm path for a 0.1% protein solution. G-CSF analogues, in phosphate-buffered saline (PBS), were concentrated to 2 mg/mL in the presence of 0.5% sodium lauroyl sarcosinate (Sarcosyl) in Centricon 10 (Amicon) concentrators. Digestion with *Achromobacter* protease (enzyme/substrate ratio of 1/200, w/w) at 37 °C was followed by electrophoresis on polyacrylamide gels in the presence of sodium dodecyl sulfate (SDS-PAGE) over 8 h. In a preparative experiment the enzyme was inactivated by incubation for 5 h with diisopropyl phosphorofluoridate (DFP) at a 2 mM final concentration. Protein samples were then dialyzed at 4 °C versus PBS to remove detergent and then against water and freeze-dried. Fragments were purified by reversed-phase HPLC on a 250 × 10 mm i.d. column packed with Nucleosil C4 using a flow rate of 3 mL/min and a linear gradient of 30-70% (by vol) B over 40 min. The N-terminal fragments (1-62 or 1-75) eluted at about 40% B and the C-terminal fragments (63-174 or 76-174) at about 55% B. Acetonitrile was removed by rotary evaporation, and the protein fragments were lyophilized. Since the C-terminal fragment could not be separated from undigested protein under preparative conditions, traces of intact protein that remained after digestion were removed by gel filtration on Sephacryl S-100 in Tris-HCl 50 mM, Sarcosyl 0.3% (v/v), pH 8.0, using a 90.0 × 1.6 cm i.d. column with a 4.0 mL/h flow rate.

The homogeneity of the fragments was checked by SDS-PAGE, by analytical reversed-phase HPLC using a 250 × 4 mm diameter column packed with Nucleosil C8, and by electrospray ionization mass spectrometry.

Hydrazide Formation by Reverse Proteolysis. The C-terminal lysine residue of 1-62 was converted to a hydrazide derivative by the reverse reaction of *Achromobacter* protease. Solutions (1 M) of Boc-hydrazide and carbonyldiimidazole were prepared in dimethyl sulfoxide/0.1 M sodium acetate pH 5.5 buffer (1:1 v/v), and the apparent pH was adjusted to 5.5 with pure acetic acid using an uncorrected glass electrode calibrated with aqueous standards. Adipohydrazide was used as a 0.4 M solution in acetonitrile/0.1 M sodium acetate pH 5.5 buffer (1:1 v/v), and the pH adjusted to 5.5 with pure acetic acid. The fragment was dissolved in the hydrazide solutions at 20 mg/mL. *Achromobacter* protease was added as a freshly prepared solution in water (10 mg/mL) at an enzyme/substrate ratio of 1:50 (w/w) and the sample incubated at

room temperature for 15 h (Rose et al., 1991). The extent of modification was followed by analytical HPLC, on a C8 column, using a linear gradient from 35 to 60% B over 50 min. The Boc-hydrazide derivative eluted later than the unmodified fragment, while the carbohydrazide and adipohydrazide derivatives eluted earlier. Boc-hydrazide and carbohydrazide derivatives were recovered by acidification with 5 volumes of pure acetic acid and dilution with 20 volumes of 0.1% TFA followed by adsorption to a Sep-Pak C₁₈ cartridge, previously washed with methanol and equilibrated with 0.1% TFA. After washing with 5 mL of 0.1% TFA containing 30% CH₃CN, the sample was eluted with 5 mL of 0.1% TFA containing 90% CH₃CN. Solvent was removed in the vacuum centrifuge and the hydrazide derivative lyophilized. The amino protection of the Boc-hydrazide derivative was removed by dissolving 20 mg of product in 250 μ L of TFA for 45 min at room temperature. TFA was removed by rotary evaporation, the material was taken up in water, lyophilized, and characterized by electrospray ionization mass spectrometry.

Oxidation of the N-Terminal Serine. A 1-mL portion of a solution of Ser-Leu-Leu (10 mM in water) was added to 8 mL of 50 mM imidazole hydrochloride buffer (pH 6.9) and reacted with 1 mL of 20 mM NaIO₄. The oxidation was stopped after 10 min by the addition of ethylene glycol (2 equiv over periodate). The reaction mixture was applied to a C18 Sep-Pak cartridge previously washed with methanol and equilibrated with 0.1% TFA. The Sep-Pak was washed with 5 mL of 0.1% TFA containing 10% CH₃CN to remove the reagents and the product was then eluted with 5 mL of 0.1% TFA containing 80% CH₃CN. Solvent was removed in the vacuum centrifuge and the peptide lyophilized. The product was eluted as a single peak from an analytical HPLC C4 column with a linear gradient from 0 to 100% B over 50 min (t_R = 33.7 min, while unoxidized Ser-Leu-Leu standard eluted at t_R = 32.7 min) and gave the expected molecular weight as determined by FAB-MS (calcd M + H, m/z 301.2; found, m/z 301.2).

The protein fragment 63–174 or 76–174 was dissolved in the imidazole buffer at 2 mg/mL in the presence of 1% Sarcosyl and oxidation performed with a 5-fold molar excess of periodate over the polypeptide. After 10 min of incubation at room temperature, unreacted periodate was destroyed with 2 equiv (over periodate) of ethylene glycol, and reagents were removed by dialysis against 0.1 M NaOAc buffer (pH 5.3) containing 0.1% Sarcosyl, which was also the buffer for the coupling reaction.

Hydrazone Formation. Equal volumes of Ac-Pro-Gln-Ser-Phe-Leu-Leu-Lys-NHNH₂ (10 mM in water) and oxidized Ser-Leu-Leu (5 mM in 0.2 M NaOAc, pH 4.6) were mixed in order to obtain a 2-fold molar excess of hydrazide over aldehyde. The coupling reaction, which proceeded at room temperature, was followed by analytical HPLC, and the hydrazone was finally isolated by preparative HPLC, with collection over dry ice to minimize hydrolysis. Solvents were removed in the vacuum centrifuge without heating.

As in the case of the model peptides, a 2-fold molar excess of fragment (1–62)-NHNH₂ (2.5 mM in water initially) over the oxidized C-terminal fragment (2 mg/mL in 0.1 M NaOAc pH 5.3 buffer in the presence of 0.1% Sarcosyl, initially) was used. The coupling reaction was followed by analytical HPLC, using a linear gradient of 50–80% (by vol) B over 30 min. Coupled product was separated from unreacted fragments by reversed-phase HPLC on a 250 \times 10 mm i.d. Nucleosil C8 column with

a flow rate of 3 mL/min and a linear gradient from 50 to 80% B over 30 min, and 5 mL fractions were collected in tubes already containing 1 mL of 0.1 M sodium phosphate buffer (pH 8.0) to minimize hydrolysis. Acetonitrile was removed by rotary evaporation and the product dialyzed against 50 mM sodium phosphate buffer (pH 7.0) in the presence of 0.3% Sarcosyl. For electrospray analysis, a portion was collected without sodium phosphate buffer, the solvent was removed in a vacuum centrifuge, and the residue freeze-dried.

Reduction of Hydrazone Linkage. In the case of the model peptide, the reaction mixture consisted of 0.1 mM hydrazone and 0.2 M NaBH₃CN in 0.1 M sodium acetate buffer (pH 4.6). During incubation at room temperature, portions were removed and analyzed by reversed-phase HPLC on a C8 column, using a linear gradient from 0% to 100% B over 50 min.

In the case of coupled protein fragments, 1 volume of protein solution (0.5–1.0 mg/mL in 50 mM sodium phosphate buffer containing 0.3% Sarcosyl) was diluted with 1 volume of acetonitrile, followed by 2 volumes of a 0.4 M solution of NaBH₃CN in 0.1 M sodium acetate (pH 4.6). The pH was then adjusted to 4.6 with glacial acetic acid.

SDS-PAGE. SDS-PAGE was performed on a Phast-System electrophoresis apparatus (Pharmacia) using 20% polyacrylamide gels. Protein samples were applied to the gel for 90 V h at 15 $^{\circ}$ C and visualized by silver staining. Protein standards were from Sigma: ovalbumin (45 kDa), carbonic anhydrase, (29 kDa), soybean trypsin inhibitor (20.1 kDa), and α -lactalbumin (14.2 kDa).

Mass Spectrometry. Mass spectra of model peptides were obtained using fast-atom bombardment equipment and operating conditions as previously described (Rose et al., 1988b). Protein fragments were analyzed by electrospray ionization mass spectrometry using a VG Trio 2 machine equipped with a 3000 amu rf generator and operated under Lab-Base software. For electrospray, protein samples previously desalted by HPLC and dried were taken up in a mixture (50/50/1, by vol) of methanol, water, and acetic acid at concentrations between 20 and 50 pmol/ μ L. The flow rate of the sample solution into the ion source was 2–3 μ L/min.

RESULTS AND DISCUSSION

Hydrazone Bond Formation with Model Peptides and Reduction with Sodium Cyanoborohydride. The hydrazone formed between Ac-Pro-Gln-Ser-Phe-Leu-Leu-Lys-NHNH₂ and oxidized Ser-Leu-Leu was obtained under optimal conditions developed by King et al. (1986), with a yield of about 70% after 20-h incubation at room temperature. The coupled peptide had the expected molecular weight, as determined by FAB-MS (calcd M + H, m/z 1170.7; found, m/z 1171.0).

The hydrazone linkage can be stabilized by reduction with sodium cyanoborohydride (King et al., 1986). Reduction of the conjugate with 0.2 M NaBH₃CN at pH 4.6 was followed by HPLC as shown in Figure 1, the reduced peptide eluted a little earlier than the hydrazone derivative. In this way, the yield of reduced product was estimated to be about 60 and 95% at 24 and 48 h, respectively. It is noteworthy that the amount of hydrolyzed conjugate visible in Figure 1 did not increase with time during incubation under slightly acidic conditions (pH 4.6), and was thus probably formed during isolation and drying of the hydrazone prior to reduction. The reduced conjugate was purified by HPLC and the molecular weight confirmed by FAB-MS (calcd M + H, m/z 1172.7; found, m/z 1172.8).

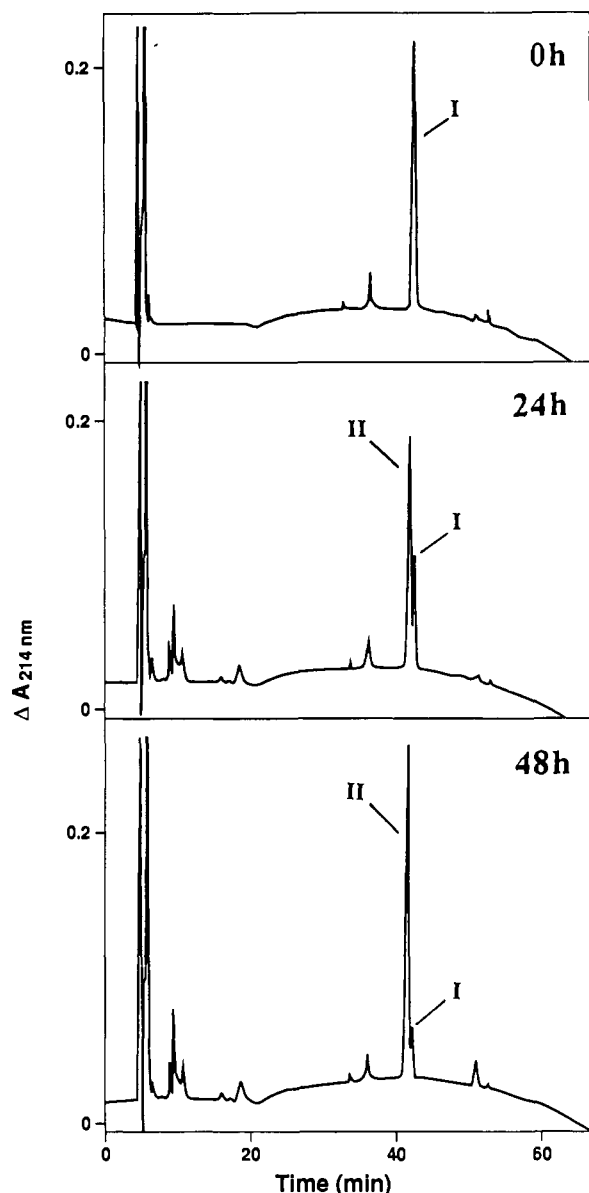


Figure 1. Analytical reversed-phase HPLC analysis of reduction of hydrazone linkage in the case of Ac-Pro-Gln-Ser-Phe-Leu-Leu-Lys-NHN=CHCO-Leu-Leu-OH. Reaction conditions: hydrazone and NaBH_3CN concentrations were initially 0.1 mM and 0.2 M, respectively, in 0.1 M NaOAc (pH 4.6). Hydrazone (I) and reduced hydrazone (II) elute at $t_R = 40.5$ and 39.5 min, respectively. Small peaks eluting at $t_R = 32.0$ and 35.5 min correspond to the hydrolyzed products, i.e. oxidized Ser-Leu-Leu and Ac-Pro-Gln-Ser-Phe-Leu-Leu-Lys-NHNH₂, respectively.

Pyridine-borane, which has been reported to be a more efficient reducing agent for proteins (Wong et al., 1984), was also investigated and the extent of reduction using 60 mM reagent at pH 4.6 was approximately 30% after 20-h incubation at room temperature.

Fragment Preparation. Digestion of G-CSF analogues with *Achromobacter* protease to give the two expected fragments was found to be almost quantitative within 8 h (data not shown). Purified fragments were characterized by electrospray ionization mass spectrometry. All fragments had the expected molecular weight (Table I).

Enzymatic Synthesis of Protein Fragment Hydrazides. Reverse proteolysis permitted the conjugation of a hydrazide group to the C-terminus of isolated fragment 1-62, under conditions already developed with des-AlaB³⁰ insulin (Rose et al., 1991). Coupling of Boc-hydrazide and

Table I. Characterization of Fragments and Protein Analogues by Electrospray Ionization Mass Spectrometry

sample	mass, Da	
	calcd ^a	measured ^b
TG 16	18 935.9	18 935.9 ± 1.2
fragment 1-62	6 934.1	6 934.0 ± 0.4
fragment 63-174	12 019.8	12 020.0 ± 3.3
(1-62)-NHNH ₂	6 948.1	6 948.1 ± 1.4
(1-62)-NHNHCONHNH ₂	7 006.2	7 005.7 ± 0.4
(1-62)-NHNHCO(CH ₂) ₄ CONHNH ₂	7 090.3	7 090.1 ± 0.2
TG 117	18 909.8	18 910.9 ± 14.5
fragment 1-75	8 178.5	8 178.3 ± 0.4
fragment 76-174	10 749.3	10 748.8 ± 11.3
(1-62)-(63-174) hydrazone	18 918.9	18 930.4 ± 3.4
(1-62)-(76-174) hydrazone	17 648.4	17 656.3 ± 2.0
(1-62)-(76-174) carbohydrazone	17 706.5	17 714.2 ± 1.8
(1-62)-(76-174) adipohydrazone	17 790.6	17 796.8 ± 1.2

^a Values represent the average mass of the uncharged species.

^b Standard deviation refers to the precision of the measured mass rather than its accuracy. Calibration was determined to be accurate to 0.005%.

carbohydrazide in 50% DMSO was almost quantitative after 15-h incubation, as determined by HPLC, so that adsorption on to a C18 Sep-Pak, which separated the excess of hydrazide from the protein fragment, was sufficient to isolate the wanted product. The modified peptides had the expected molecular weight (Table I). Adipohydrazone is poorly soluble in 50% DMSO and when the coupling reaction was performed in a fully aqueous medium (0.5 M in 0.1 M NaOAc, pH 5.5), a yield of about 30% at equilibrium was obtained. However, the yield could be increased to 55% by using 0.4 M adipohydrazide in 50% acetonitrile. Preparative HPLC was used to isolate the fragment (1-62)-adipohydrazone.

Fragment Coupling by Hydrazone Formation. The amino-terminal serine residue of proteolytic fragments 63-174 and 76-174 was oxidized under mild conditions. In contrast with the reaction with the model peptide Ser-Leu-Leu, the protein fragments were very sensitive to overreaction during periodate oxidation, as shown by the production of a cluster of peaks on analytical reversed-phase HPLC. Reaction time had to be carefully controlled to get a single peak, but oxidized fragments could not be characterized by electrospray ionization mass spectrometry.

Upon addition of the fragment (1-62)-NHNH₂ to the oxidized fragment, itself previously purified by dialysis to remove the excess of ethylene glycol and the formaldehyde byproduct, a new component was generated, eluting earlier from the HPLC column (Figure 2), with a retention time comparable to that of initial G-CSF analogue (data not shown). By using a 2-fold molar excess of hydrazide over the aldehydic fragment, after 20-h incubation at pH 5.3, the yield of hydrazone (ratio of product to remaining aldehydic fragment) was as high as 80%. The same profile was obtained after 48-h incubation, suggesting that equilibrium was achieved under these conditions in less than 20 h. Though the yield of hydrazone at equilibrium depends on reagent concentration and chemical structure (King et al., 1986), it appears that 2 equiv of fragment (1-62)-hydrazide over aldehyde with concentrations of protein fragments on the order of 200 μM were sufficient to obtain a high coupling efficiency. Furthermore, the presence of 0.1% Sarcosyl to solubilize one of the components did not prevent coupling. As shown in Figure 3, the coupling reaction proceeded cleanly and no trace of reaction occurred with nonoxidized fragment (lane 4) which is evidence that fragments 1-62 and 63-174 are linked by a hydrazone bond. This was confirmed by electrospray

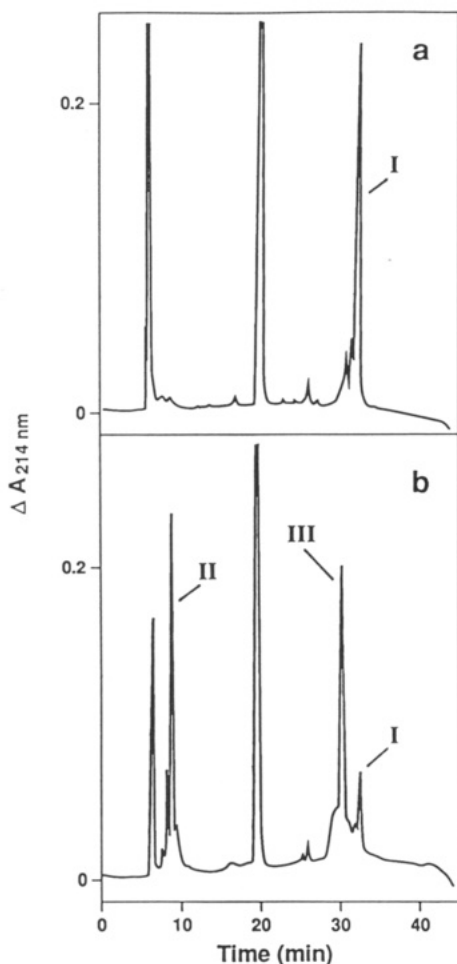


Figure 2. HPLC chromatograms of oxidized fragment 63–174, and coupling reaction with fragment (1–62)–NHNH₂. Panel a: oxidized fragment 63–174 (I) alone. Panel b: incubation of oxidized fragment 63–174 with fragment (1–62)–NHNH₂ after a reaction time of 20 h. Fragment (1–62)–NHNH₂ (II), oxidized fragment 63–174 (I), and the hydrazone reaction product (III) elute at t_R = 7.0, 31.5, and 29.5 min, respectively. The peak eluted at 18 min corresponds to Sarcosyl.

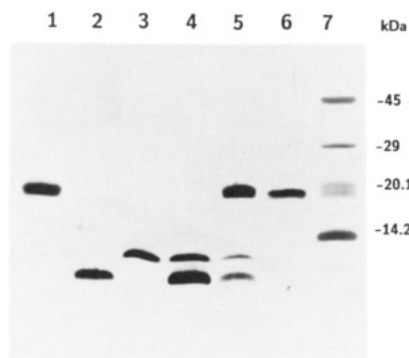


Figure 3. Conjugation of oxidized fragment 63–174 with fragment (1–62)–NHNH₂ by hydrazone bond formation: lane 1, G-CSF analogue TG-116; lane 2, fragment (1–62)–NHNH₂; lane 3, fragment 63–174; lane 4, control incubation of unoxidized fragment 63–174 with fragment (1–62)–NHNH₂ after 20 h; lane 5, incubation of oxidized fragment 63–174 with fragment (1–62)–NHNH₂ after 20 h; lane 6, (1–62)–(63–174) hydrazone after HPLC purification; lane 7, protein markers α -lactalbumin, trypsin inhibitor, carbonic anhydrase, and ovalbumin.

ionization mass spectrometry (Table I). The measured masses of this and other coupled products are consistently higher than the calculated values. This is in contrast with the values obtained for the starting proteins and their fragments. The fact that the measured masses are slightly

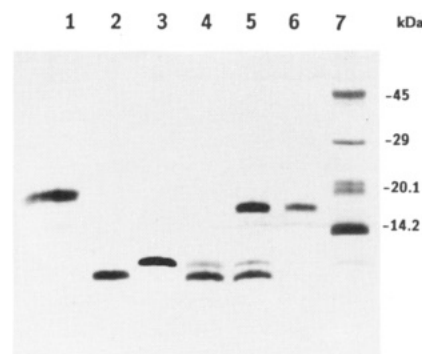


Figure 4. SDS–polyacrylamide gel electrophoresis of coupling between fragment (1–62)–NHNH₂ and oxidized fragment 76–174: lane 1, G-CSF analogue TG-117; lane 2, fragment (1–62)–NHNH₂; lane 3, fragment 76–174; lane 4, control incubation of unoxidized fragment 76–174 with fragment (1–62)–NHNH₂ after 20 h; lane 5, incubation of oxidized fragment 76–174 with fragment (1–62)–NHNH₂ after 20 h; lane 6, (1–62)–(76–174) hydrazone after HPLC purification; lane 7, protein markers as in Figure 3.

in excess of the calculated values may be due to adduct formation with alkali metals (especially sodium) or to oxidation of the thioether side chain of Met residues of which the C-terminal fragment contains three. Oxidation of Met to the sulfoxide may occur during exposure to periodate, but it has been recently shown that under the conditions of neutral pH and limited quantities of reagent as used here, sulfoxide formation is about 40 times slower than oxidation of N-terminal Ser (Geoghegan & Stroh, 1992). The peak profiles obtained during analysis by electrospray ionization mass spectrometry were asymmetric (tailing toward higher mass) but showed no shoulders, so it was not possible to decide whether the displacement of the centroid toward higher mass was due to sodium (increment 22 amu) or to oxygen (16 amu). Operation at higher mass resolution was not successful since sensitivity was then inadequate. The possibility that oxidation of Met occurs to a small degree cannot therefore be excluded. While oxidation of Met can occasionally adversely affect biological activity, much harsher oxidation conditions are regularly used without affecting the antigen binding properties of antibodies (e.g. Rodwell et al., 1986). In other cases, reduction of the sulfoxide to the thioether may be undertaken (Houghton & Li, 1983) after reduction of the hydrazone with cyanoborohydride.

The same procedure was used in the coupling of oxidized fragment 76–174 with fragment (1–62)–NHNH₂, fragment (1–62)–carbohydrazide or fragment (1–62)–adipohydrazide (Figure 4). In all cases, 2 equiv of hydrazide derivative over the oxidized proteolytic fragment led to a hydrazone yield of about 80% after 20-h incubation. All the resulting coupled products were characterized by electrospray ionization mass spectrometry (Table I) and correspond to protein analogues lacking the 64–174 disulfide loop, but relinked by nonpeptide bridging compounds of increasing size. These are the first protein analogues to be constructed by conjugation of two fragments resulting from enzymatic digestion of two different recombinant proteins. The way is now open for reassembly of the protein around a chemically synthesized segment that mimics the excised disulfide loop Cys64–Cys74 more effectively than the compounds used here.

It appears that substituted hydrazides are excellent linkers for the two-step coupling reaction. In the first step, the specific coupling to C-terminal lysine of a protein fragment, hydrazine derivatives have pK values close to the pK of the carboxyl group, which is the necessary

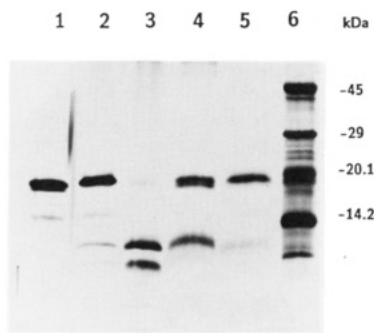


Figure 5. Reduction of the hydrazone bond in the presence of NaBH_3CN as determined by the resistance to hydrolysis under acidic conditions: lane 1, G-CSF analogue TG-116; lane 2, (1-62)-(63-174) hydrazone; lane 3, (1-62)-(63-174) hydrazone reacted for 48 h at room temperature with 1 mM $\text{H}_2\text{N}-\text{OCH}_3$ in 0.1% TFA/ CH_3CN , 1:1 v/v brought to pH 2.0 with formic acid; lane 4, as in lane 3 but with prior treatment of the hydrazone with 0.2 M NaBH_3CN for 60 h at room temperature; lane 5, as in lane 4 but with prior NaBH_3CN treatment for 110 h; lane 6, protein markers as in Figure 3.

condition for shifting equilibria in enzyme-catalyzed reactions toward synthesis (Homandberg et al., 1978). Such groups are thus more appropriate for reversed proteolysis than the usual amino groups, which have pK values of approximately 7–9. If the protein is easily denatured by the presence of a cosolvent, the enzymatic coupling step can be performed in fully aqueous media, with yields of over 70% (Rose et al., 1991). On the other hand, if cosolvents can be tolerated, nearly quantitative introduction of Boc-hydrazine and carbohydrazide was observed in 50% DMSO. In the second step, a C-terminal hydrazide group with a pK of 3–4 provides, under acidic conditions, a unique nucleophilic group in the protein fragment able to react with the aldehyde group to form a relatively stable product, so that blocking of the α -amino group and other side chain groups is not required.

Reduction of Hydrazone Linkage of Protein Analogues. Hydrazones are known to be stable at neutral pH, but are susceptible to hydrolysis at pH values less than 7. This provides another means to characterize a hydrazone bond in a recoupled protein. Though previous observations with model compounds (King et al., 1986) showed that susceptibility to hydrolysis of the hydrazone linkage was influenced by the presence of electron-donating or -withdrawing groups near the aldehyde function, it is interesting to point out the rather high stability of the linkage in protein analogues described here, which may be related to the presence of a carboxamide adjacent to the aldehyde group. Incubation of the analogue in 0.1% TFA, pH 2.0, at room temperature led to slow hydrolysis which reached about 60% after 48 h. However, as shown in Figure 5, at pH 2.0 (0.1% TFA containing 50% CH_3CN) in the presence of 1 mM methoxamine, the (1-62)-(63-174) hydrazone was almost completely dissociated by an exchange reaction into fragment (1-62)- NHNH_2 and the (presumed) methoxime derivative of 63-174 (lane 3). Such a reaction was used to follow reduction of the hydrazone linkage during incubation of the recoupled protein in 0.2 M NaBH_3CN at pH 4.6, the protein being previously ultrafiltered on a Centricon 10 microconcentrator to remove the large excess of NaBH_3CN . After 60-h reduction, it was still possible to demonstrate the presence of hydrolyzable material, while after 110-h reduction, the single initial band was observed after methoxamine treatment, thus confirming that reduction of the hydrazone was essentially complete.

CONCLUSION

The presence of N-terminal serine in a peptide or a protein offers a means for its site-specific activation as a prelude to fragment coupling by hydrazone bond formation, since such a residue can be converted, under mild conditions, to an aldehyde group by periodate oxidation (Fields & Dixon, 1968). Moreover this procedure is equally applicable to amino-terminal threonine (Geoghegan & Stroh, 1992). The very considerable reactivity toward periodate of 1-amino, 2-hydroxy compounds relative to diols suggests that the oxidation could be carried out even if a carbohydrate moiety was present. Indeed, Rose et al. (1989) were able to oxidize such a compound in the presence of 300 equiv of ethylene glycol. However, such selectivity may be difficult to achieve in the presence of sialic acid, which is very susceptible to periodate (Zara et al., 1991). The new approach to fragment condensation described here, which does not require side-chain protection, extends the importance of a previously described technique, that of enzyme-catalyzed reverse proteolysis for the specific attachment of the reactive hydrazide compound to peptide or protein C-termini. Although in our case we used an engineered protein fragment not containing any other susceptible bond, it is possible to apply reverse proteolysis to large fragments of antibodies (Fisch et al., 1992). In the present work, conversion of the protein fragment to the hydrazide was facilitated by the presence of a single C-terminal lysine, a high-affinity substrate of *Achromobacter* protease. The same approach, cleavage followed by reversed proteolysis, can be used with other specific endoproteases.

The high yields in the enzymatic coupling step reported in this paper, as in previous studies (Yagisawa, 1981; Rose et al., 1991), show that the enzymatic approach is a general tool for the site-specific modification of proteins. The condensation between the two specifically modified fragments (which constitutes the second step of the procedure) was achieved under mild conditions and low concentrations of reagents. This approach is an improvement over chemical methods developed for the preparation of protein conjugates and involving heterobifunctional reagents such as *N*-succinimidyl 3-(2-pyridyldithio)propionate (Carlsson et al., 1978) or 2,2-bis(2-maleimidoethoxy)propane (Srinivasachar & Neville, 1989). These latter methods lack site specificity and give rise to conjugated proteins that are heterogenous, since the number and location of reacting sites are not easily controlled. The recombinant DNA approach is an alternative way to produce fusion proteins and is often preferred where fragments must be joined by a peptide linkage (Dewerchin & Collen, 1991; Hayzer et al., 1991). In other cases, the same goal can be achieved with greater flexibility by the semisynthetic approach described in this paper: a peptide bond is not always absolutely essential as the means of joining two domains, and it may even be precluded if subsequent slow release of a fragment (by hydrazone hydrolysis for example) is desired or if some types of noncoded elements are to be incorporated into the new structure.

ACKNOWLEDGMENT

This work was supported by the Strategic Research Fund of ICI Pharmaceuticals (Macclesfield, U.K.) and the Fonds National de la Recherche Scientifique for mass spectrometry. We thank the Biotechnology Department of ICI Pharmaceuticals for the production of recombinant G-CSF analogues TG116 and TG117. We also thank P. O. Regamey for mass spectrometric analyses.

LITERATURE CITED

- Breddam, K., Widmer, F., and Meldal, M. (1991) Amidation of growth hormone releasing factor(1-29) by serine carboxypeptidase catalyzed transpeptidation. *Int. J. Pept. Protein Res.* 37, 153-160.
- Camble, R., Edge, M. D., and Moore, V. E. (1985) Properties of Interferon α_2 analogues produced from synthetic genes. *Proc. 9th Am. Pep. Symp.* 375-384.
- Carlsson, J., Drevin, H., and Axen, R. (1978) Protein thiolation and reversible protein-protein conjugation. *Biochem. J.* 173, 723-737.
- Chaiken, I. M. (1981) Semisynthetic peptides and proteins. *Crit. Rev. Biochem.* 11, 255-301.
- Dewerchin, M., and Collen, D. (1991) Enhancement of the thrombolytic potency of plasminogen activators by conjugation with clot-specific monoclonal antibodies. *Bioconjugate Chem.* 2, 293-300.
- Fields, R., and Dixon, H. B. F. (1968) A spectrophotometric method for the microdetermination of periodate. *Biochem. J.* 108, 883-887.
- Fisch, I., Künzi, G., Rose, K., and Offord, R. E. (1992) Site specific modification of a fragment of a chimeric monoclonal antibody using reverse proteolysis. *Bioconjugate Chem.* 3, 147-153.
- Geoghegan, K. F., and Stroh, J. G. (1992) Site-directed conjugation of nonpeptide groups to peptides and proteins via periodate oxidation of a 2-amino alcohol. Application to modification at N-terminal Serine. *Bioconjugate Chem.* 3, 138-146.
- Hayzer, D. J., Lubin, I. M., Runge, M. S. (1991) Conjugation of plasminogen activators and fibrin-specific antibodies to improve thrombolytic therapeutic agents. *Bioconjugate Chem.* 2, 301-308.
- Homandberg, G. A., Mattis, J. A., and Laskowski, M., Jr. (1978) Synthesis of peptide bonds by proteinases. Addition of solvents shifts peptide bond equilibria towards synthesis. *Biochemistry* 17, 5220-5227.
- Homandberg, G. A., Komoriya, A. and Chaiken, I. M. (1982) Enzymatic condensation of nonassociated peptide fragments using a molecular trap. *Biochemistry* 21, 3385-3389.
- Houghton, R. A., and Li, C. H. (1983) Reduction of sulfoxides in peptides and proteins. *Methods Enzymol.* 91, 549-559.
- Jakubke, H. D., Kuhl, R., and Kónnecke, A. (1985) Enzymatic peptide synthesis. *Angew. Chem., Int. Ed. Engl.* 24, 85-93.
- Jones, R. M. L., and Offord, R. E. (1982) The proteinase-catalyzed synthesis of peptide hydrazides. *Biochem. J.* 203, 125-129.
- Kent, S. P. H. (1992) Total chemical synthesis, crystal structures and engineering of the HIV protease: nature and beyond. In *Innovation and Perspectives in Solid Phase Synthesis and Related Technologies* (R. Epton, Ed.) SPCC, Birmingham (in press).
- King, T. E., Zhao, S. W., and Lam, T. (1986) Preparation of protein conjugates via intermolecular hydrazone linkage. *Biochemistry* 25, 5774-5779.
- Kuga, T., Komatsu, Y., Yamasaki, M., Sekine, S., Miyaji, H., Nishi, T., Sato, M., Yokoo, Y., Asano, M., Okabe, M., Morimoto, M., and Itoh, S. (1989) Mutagenesis of human granulocyte colony stimulating factor. *Biochem. Biophys. Res. Commun.* 159, 103-111.
- Laskowski, M., Jr. (1978) The use of proteolytic enzymes for the synthesis of specific peptide bonds in globular proteins. In *Semisynthetic Peptides and Proteins* (R. E. Offord and C. Di Bello, Eds.) pp 255-262, Academic Press, London.
- Masaki, T., Fujihashi, T., Nakamura, K., and Soejima, M. (1981) Studies on a new proteolytic enzyme from *Achromobacter lyticus* M497.1 II. Specificity and inhibition studies of *Achromobacter* protease I. *Biochem. Biophys. Acta* 660, 51-55.
- Moriyama, K., Oka, T., and Tsuzuki, H. (1979) Semi-synthesis of human insulin by trypsin catalyzed replacement of Ala-B30 by Thr in porcine insulin. *Nature* 280, 412-413.
- Offord, R. E. (1990) Chemical approaches to protein engineering. In *Protein Design and the Development of New Therapeutics and Vaccines* (J. B. Hook, and G. Poste, Eds.) pp 253-282, Plenum, New York.
- Offord, R. E., and Rose, K. (1986) Press-stud protein conjugates. In *Protides of the Biological Fluids* (H. Peeters, Ed.) pp 35-38, Pergamon, Oxford.
- Rodwell, J. D., Alvarez, V. L., Lee, C., Lopes, A. D., Goers, J. W. F., King, H. D., Powsner, H. J., and McKearn, T. J. (1986) Site-specific covalent modification of monoclonal antibodies: In vitro and in vivo evaluations. *Proc. Natl. Acad. Sci. U.S.A.* 83, 2632-2636.
- Rose, K., Herrero, C., Proudfoot, A. E. I., Offord, R. E., and Wallace, C. J. A. (1988a) Enzyme-assisted semisynthesis of polypeptide active esters and their use. *Biochem. J.* 249, 83-89.
- Rose, K., Savoy, L. A., Simona, M. G., Offord, R. E., and Wingfield, P. (1988b) C-terminal peptide identification by fast atom bombardment mass spectrometry. *Biochem. J.* 250, 253-259.
- Rose, K., Jones, R. M. L., Sundaram, G., and Offord, R. E. (1989) Attachment of linker groups to carboxyl termini using enzyme-assisted reverse proteolysis. In *Peptides 1988* (G. Jung, and E. Bayer, Eds.) pp 274-276, W. de Gruyter, Berlin.
- Rose, K., Vilaseca, A., Werlen, R., Meunier, A., Fisch, I., Jones, R. M. L., and Offord, R. E. (1991) Preparation of well-defined protein conjugates using enzyme-assisted reverse proteolysis. *Bioconjugate Chem.* 2, 154-159.
- Sahni, G., Cho, Y. J., Iyer, K. S., Kahn, S. A., Seetharam, R., and Acharya, A. S. (1989) Semisynthetic hemoglobin A: Reconstitution of functional tetramer from semisynthetic α -globin. *Biochemistry* 28, 5456-5461.
- Srinivasachar, K., and Neville, D. M. (1991) New protein cross-linking reagents that are cleaved by mild acid. *Biochemistry* 28, 2501-2508.
- Waldmann, T. A. (1991) Monoclonal antibodies in diagnosis and therapy. *Science* 252, 1657-1662.
- Wallace, C. J. A., Guillemette, J. G., Hibiya, Y., and Smith, M. (1991) Enhancing protein engineering capabilities by combining mutagenesis and semisynthesis. *J. Biol. Chem.* 266, 21355-21357.
- Wingfield, P., Benedict, R., Turcatti, G., Allet, B., Mermod, J. J., Delamarter, I., Simona, M. G., and Rose, K. (1988) Characterization of recombinant-derived granulocyte-colony stimulating factor (G-CSF). *Biochem. J.* 256, 213-218.
- Wong, W. S. D., Osuga, D. T., and Feeney, R. E. (1984) Pyridine borane as a reducing agent for proteins. *Anal. Biochem.* 139, 58-67.
- Yagisawa, S. (1981) Studies on protein semisynthesis. I. Formation of esters, hydrazides and substituted hydrazides of peptides by the reverse reaction of trypsin. *J. Biochem. (Tokyo)* 89, 491-501.
- Zara, J. J., Wood, R. D., Boon, P., Kim, C. H., Pomato, N., Bredehorst, R., and Vogel, C. W. (1991) A carbohydrate-directed heterobifunctional cross-linking reagent for the synthesis of immunoconjugates. *Anal. Biochem.* 194, 156-162.

Bioconjugate Chemistry

JULY/AUGUST 1992
Volume 3, Number 4

© Copyright 1992 by the American Chemical Society

REVIEWS

Purifying Antibody-Plasminogen Activator Conjugates[†]

Christoph Bode,* Marschall S. Runge,[‡] and Edgar Haber[§]

Medical Clinic III (Cardiology), University of Heidelberg, 6900 Heidelberg, Germany, Division of Cardiology, Emory University School of Medicine, Atlanta, Georgia 30322, and Harvard School of Public Health, Boston, Massachusetts 02115. Received December 2, 1991

INTRODUCTION

Conjugates of monoclonal antibodies and plasminogen activators have been constructed in an effort to target these therapeutically useful enzymes to thrombi. Because thrombi may contain fibrin-rich and platelet-rich material, antifibrin as well as antiplatelet antibodies have been investigated as targeting devices. To reduce the antigenicity and alter the pharmacokinetic properties of these potential therapeutic agents, efforts were made to reduce the molecular size of the conjugate's antibody portion by using the antigen-binding fragment (Fab) rather than the whole antibody. To obtain a homogeneous preparation of conjugate and to facilitate production, recombinant antibody-plasminogen activator constructs have been produced.

Bispecific monoclonal antibodies containing one binding site that recognizes a thrombus and one binding site that recognizes a plasminogen activator have been shown to concentrate plasminogen activator at the surface of a thrombus. Theoretically, such bispecific antibodies could be used to enhance the potency of endogenous plasminogen activators. Alternatively, bispecific antibodies or bispecific (Fab')₂ could be combined with a plasminogen activator and used as immunoconjugates.

The potential therapeutic use of these constructs has been reviewed previously (1, 2). The present review focuses on the purification of antibody-plasminogen activator conjugates and bispecific antibodies.

PURIFICATION OF CHEMICAL AND RECOMBINANT ANTIBODY-PLASMINOGEN ACTIVATOR CONJUGATES

Purification by Gel Filtration. The chemistry used to synthesize the antibody-plasminogen activator molecule can be controlled to the extent that predominantly 1:1 conjugates of whole antibody or Fab' and plasminogen activator are formed. In addition to the desired conjugate the reaction mixture always contains uncoupled antibody and uncoupled plasminogen activator. For example, with a conjugation mixture of antifibrin IgG (150 kDa) and the B-chain of urokinase (30 kDa), the uncoupled B-chain of urokinase could be effectively separated from the antifibrin antibody-urokinase conjugate (180 kDa) by gel filtration on Sephacryl 2-200 (3). However, the conjugate could not be completely separated by uncoupled antibody. Resolution on Sephacryl 2-300 did produce better results, but the S-300 column was still unsuitable for the evaluation of conjugates with antibodies that exhibit functional properties of their own (e.g. platelet inhibition). These antibodies had to be separated quantitatively from the conjugate so that they would not interfere with assays comparing the functional properties of conjugated versus unconjugated enzyme.

Although it is possible to separate 104 kDa conjugates of antifibrin Fab' (50 kDa) and urokinase (54 kDa) by gel filtration, this method has not been extensively applied because other purification procedures are superior (see below).

Affinity Purification Based on Functional Properties. The use of two sequential affinity procedures, one selecting for active enzyme and the other for functionally intact antibody, has proved to be the method of choice for purifying active conjugate. This method is schematically presented in Figure 1.

For the plasminogen activators urokinase (4, 5) and tissue-type plasminogen activator (t-PA) (6, 7), which are

* Address for correspondence: Dr. Christoph Bode, Medizinische Klinik III (Kardiologie), Universität Heidelberg, Bergheimerstrasse 58, 6900 Heidelberg, Germany.

[†] This research was supported in part by a grant from the Deutsche Forschungsgemeinschaft (Bo 726/3-2).

[‡] Emory University School of Medicine.

[§] Harvard School of Public Health.

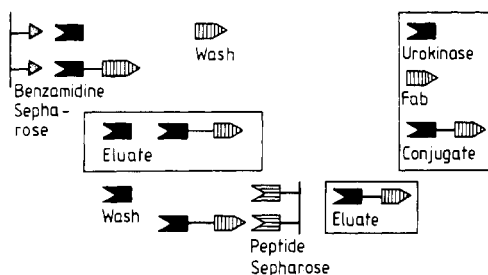


Figure 1. The principle of sequential affinity chromatography based on functional properties. This is the method of choice for purifying highly active conjugates of plasminogen activators and antifibrin antibodies or antifibrin Fab.

both serine proteases, the specific inhibitor benzamidine was used as an immobilized ligand (8). Only enzyme-antibody conjugates in which the enzymatic center remained intact during the coupling procedure (and uncoupled intact enzyme from the reaction mixture) could bind and be retained by the benzamidine-Sepharose affinity column. Uncoupled whole antibody or uncoupled antibody fragments such as Fab have no affinity for benzamidine and were thus not retained on the column. To reduce nonspecific binding on the affinity column to a minimum, a high-salt washing step was performed prior to elution (Figure 2). Free antibody in the nonbinding fraction from the column could then be collected and reused for conjugation in order to enhance yield. The desired conjugate (and uncoupled enzyme) was eluted by a mild change in pH. Application of an elution buffer containing 0.1 M sodium acetate and 0.1 M sodium chloride, pH 4.0, regularly resulted in complete elution without measurable loss of enzyme activity. The pH of the eluate was adjusted to 7.4 with a 3.0 M Tris-HCl solution, pH 8.6.

In the case of antifibrin antibody-plasminogen activator conjugates, the eluate was then applied to a (Gly-His-Arg-Pro-Leu-Asp-Lys-Cys)-MB-lysine-Sepharose column (peptide-Sepharose). The peptide, which was used as an antigen to raise monoclonal antifibrin antibodies, represents the seven amino-terminal residues of the fibrin B-chain (B β 15-22) (9). The cysteine residue was added to allow for predefined coupling to lysine immobilized on cyanogen bromide-activated Sepharose C1-4B using the heterobifunctional cross-linking reagent *p*-maleimidobenzoic acid succinimido ester (MBS). Peptide-Sepharose has been used as an efficient purification matrix for antifibrin antibody, antifibrin Fab', and their respective conjugates. Because this matrix was used for the eluate of the benzamidine-Sepharose purification step, which contained only uncoupled enzyme and conjugate and no free antibody, only the conjugate was retained. Elution was effected again through pH change (0.2 M glycine, pH 2.8). As the capacity of the peptide-Sepharose matrix was very high (usually in excess of 20 mg of antibody/mL of affinity gel) the column could be used to concentrate conjugate, making concentration by filtration in pressure cells (Amicon) unnecessary. Figure 2 shows a representative elution profile. Purification results were confirmed by SDS-PAGE (10, 11) and Western blotting (11).

Sequential affinity chromatography as described above has yielded conjugates with an active enzyme portion and an antibody portion capable of binding to the intended target. Because the conjugation chemistry was controlled so that predominantly 1:1 conjugates were synthesized, further purification by gel filtration to eliminate active aggregates has usually been unnecessary.

The purification of chemical conjugates by sequential affinity chromatography yields active, predominantly 1:1

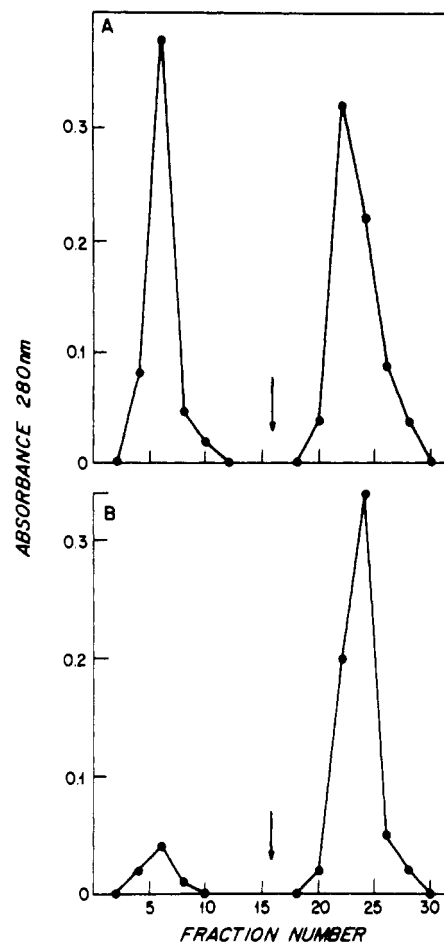


Figure 2. Purification of antibody-urokinase conjugates by affinity chromatography based on functional properties. Antibody-urokinase conjugates were first purified by passage over a benzamidine-Sepharose column. (A) the reaction mixture (6 mL at 2 mg/mL) was loaded onto a 4-mL benzamidine-Sepharose column pre-equilibrated with PBSA (0.1 M NaH₂PO₄, 0.1 M NaCl, 0.2% sodium azide, pH 6.6). After a washing step with PBSA and then 0.1 M sodium phosphate, 0.5 M NaCl, 0.02% sodium azide, pH 7.4, the bound material was eluted with 0.1 M sodium acetate, 0.1 M NaCl, pH 4.0. The arrow marks the beginning of the elution. The eluted material was neutralized with 3 M Tris-HCl, pH 8.6. (B) the material eluted from the benzamidine-Sepharose column was loaded onto a peptide-Sepharose column pre-equilibrated with PBSA. This column was also washed with 0.1 M sodium phosphate, 0.5 M NaCl, 0.02% sodium azide, and the bound material was eluted with 0.2 M glycine, pH 2.8. The arrow marks the beginning of the elution (from ref 4).

conjugates that are, however, not completely homogeneous because the heterobifunctional cross-linking reagent *N*-succinimidyl 3-(2-pyridylthio)propionate (SPDP) can react with different amino groups on the plasminogen activator. Using this purification procedure for recombinant conjugates yields a uniform, homogeneous preparation (12).

Purification by Immunoaffinity. In most cases affinity purification can be performed by immobilizing an antibody to one of the conjugate components on a cyanogen bromide-activated Sepharose matrix. For example, a goat antibody directed against mouse Fab (goat anti-mouse Fab) has been used to select for antiplatelet Fab', antiplatelet IgG, and their respective conjugates (13). Using benzamidine-Sepharose first and then goat anti-mouse Fab-Sepharose we were able to efficiently purify antiplatelet-urokinase conjugates. However, this procedure does not select for antibody (or Fab) in the conjugate that has retained its capacity to bind to the antigen. Therefore,

we suggest that affinity chromatography based on functional criteria be used whenever such an approach is feasible.

Immunoaffinity chromatography (on an anti-plasminogen activator column) has also been combined with affinity chromatography based on functional properties (on a fibrin fragment D-dimer column) to purify antibody-plasminogen activator conjugates (14, 15). Because binding with the immunoaffinity column is based on antigen recognition rather than functional activity, this approach may in theory result in conjugates with diminished specific activity because the final preparation may contain a mixture of active and inactive components. The reported conjugates (14, 15), however, showed specific activities on fibrin plate assays or toward chromogenic substrate that were comparable to those of uncoupled activator. Thus the theoretical limitation of this approach may not always be of practical importance. Another method for selecting intact IgG that might be contained within a conjugate is the use of protein A immobilized on Sepharose. Protein A is a streptococcal protein that binds to the constant domains of immunoglobulins with high affinity. As our goal has been to develop strategies that eliminate the constant domains from conjugates by using Fab fragments, this approach has not been widely practiced in our laboratories.

PURIFICATION OF BISPECIFIC ANTIBODIES AND IMMUNOCONJUGATES

Purification by Gel Filtration. Bispecific antibodies have been constructed by chemically coupling IgG (or Fab') molecules (16, 17) of the same isotype but different specificity. The example discussed below was synthesized from a monoclonal antifibrin antibody and a monoclonal anti-tPA antibody.

Bispecific IgG molecules (300 kDa) have been purified by gel filtration from reaction mixtures containing the two antibodies (each 150 kDa). Usually 9 mL of reaction mixture was applied to a Sephacryl S-300 column (2.5 × 85 cm). Fractions from the first peak contained the desired bispecific antibody. Fractions from the second peak (at about 150 kDa) presumably contained both antibody monomers.

An immunochemical complex (immunoconjugate) made up of tPA and bispecific antibody was formed by mixing a 3:1 molar excess (tPA:bispecific antibody) of tPA (3.5 mg) with bispecific antibody (5 mg). This mixture was again applied in a 9-mL volume to the Sephacryl S-300 column. Chromatography revealed a peak at approximately 400 kDa, which was interpreted as tPA bound to the bispecific antibody, and a second peak of approximately 70 kDa, representing unbound tPA. On the basis of enzymatic activity in a chromogenic substrate assay (S-2288), approximately 1.5 mol of tPA appeared to bind per mole of bispecific antibody.

Purification by gel filtration is an effective way to obtain bispecific antibodies in high yield. Harsh elution conditions can be avoided. However, antibodies that have lost function during the coupling procedure are not removed. In addition, the resolving power of most gel filtration resins is insufficient to discriminate effectively between bispecific antibody-tPA complexes (370 kDa) and bispecific antibody alone (300 kDa). Therefore, the preparation may contain functionally inactive molecules.

Affinity Purification Based on Functional Groups. The method of choice for purifying bispecific antibodies is affinity purification based on functional criteria. Bispecific (Fab')₂ molecules made from the Fab' of an an-

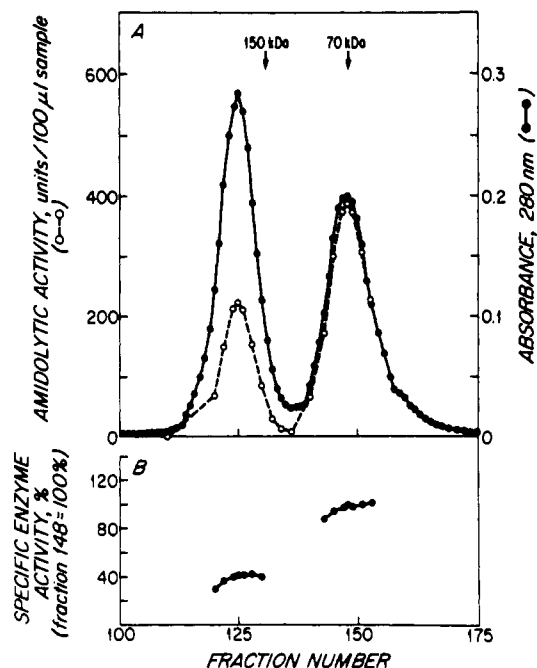


Figure 3. Gel filtration on a calibrated Sephacryl S-300 column of the tPA-bispecific (Fab')₂ complex. (A) The gel filtration resulted in two protein peaks, both of which contained enzymatic activity. Profiles of absorbance at 280 nm (filled circles) and amidolytic activity (open circles) are shown. On the basis of molecular weights and the relative specific enzymatic activities of the two peaks (B), peak 1 (170 kDa) was judged to contain a 1:1 molar conjugate of bispecific (Fab')₂ and tPA and peak 2 was judged to contain unbound tPA (from ref 17).

tifibrin antibody and the Fab' of an anti-tPA antibody have been synthesized using a procedure that yields 1:1 conjugates imitating the natural structure of an (Fab')₂ fragment. No cross-linking reagent was required (17). Alternatively, identical molecules could be produced by the hybrid-hybridoma technique (18) and subsequent pepsin digestion to generate (Fab')₂. In both cases, recovery from the reaction mixture or from the digest was best effected by sequential affinity chromatography.

First, the reaction mixture was applied to peptide-Sepharose (see above). This column retained antifibrin Fab' and bispecific (Fab')₂ but not uncoupled anti-Fab'. The eluate from this column was then applied to Sepharose on which tPA had been immobilized. Here, only the bispecific (Fab')₂ was retained while antifibrin-Fab' was washed out. Elution from this column with 0.2 M glycine, pH 2.8, yielded a homogeneous 100 kDa band on sodium dodecyl sulfate polyacrylamide gel electrophoresis.

An immunoconjugate consisting of tPA and bispecific (Fab')₂ was formed by mixing 3.5 mg of tPA with 5 mg of bispecific (Fab')₂. The immunoconjugate was purified by gel filtration on a calibrated Sephacryl S-300 column equilibrated with PBSA (Figure 3). A first peak was detected at 170 kDa, corresponding to tPA bound to the bispecific (Fab')₂, and a second peak at 70 kDa, corresponding to unbound tPA. On the basis of enzymatic activity, exactly 1 mol of tPA appeared to bind per mole of bispecific (Fab')₂. This finding underscores the fact that only functionally intact bispecific (Fab')₂ molecules were selected by affinity chromatography.

CONCLUSION

This review has focused on strategies used to purify bispecific antibodies and conjugates of antibodies and plasminogen activators. In our view, the best results were obtainable by using sequential affinity chromatography

based on functional criteria. Whenever this approach was not possible, an immunoaffinity procedure could be used as a substitute. In cases where the coupling chemistry could not be well controlled, it was possible to combine the two strategies with a final gel filtration step to eliminate aggregates.

The use of these methods has resulted in the purification of chemical conjugates and recombinant constructs that are many times more potent and more specific than their parent enzymes, in vitro as well as in vivo. Whether these superior enzymes translate into improved therapy remains to be proved.

LITERATURE CITED

- (1) Bode, C., Runge, M. S., and Haber, E. (1990) Future directions in plasminogen activator therapy. *Clin. Cardiol.* 13, 375-381.
- (2) Bode, C., Runge, M. S., and Haber, E. (1990) Improving on nature: Antibody-targeted enzymes. In *The Year in Immunology 1989-1990. Molecules and Cells of Immunity*, (J. M. Cruse, and R. E. Lewis, Eds.) Vol. 6, pp 186-196, Karger Publishing, Basel.
- (3) Bode, C., Matsueda, G. R., Hui, K. Y., and Haber, E. (1985) Antibody-directed urokinase: A specific fibrinolytic agent. *Science* 229, 765-767.
- (4) Bode, C., Runge, M. S., Newell, J. B., Matsueda, G. R., and Haber, E. (1987) Characterization of a urokinase-antibody conjugate: A plasminogen activator targeted to fibrin. *J. Biol. Chem.* 262, 10819-10823.
- (5) Bode, C., Runge, M. S., Newell, J. B., Matsueda, G. R., and Haber, E. (1987) Thrombolysis by a fibrin-specific antibody Fab'-urokinase conjugate. *J. Mol. Cell. Cardiol.* 19, 335-341.
- (6) Runge, M. S., Bode, C., Matsueda, G. R., and Haber, E. (1988) Conjugation to an antifibrin monoclonal antibody enhances the fibrinolytic potency of tissue plasminogen activator in vitro. *Biochemistry* 27, 1153-1157.
- (7) Runge, M. S., Bode, C., Matsueda, G. R., and Haber, E. (1987) Antibody-enhanced thrombolysis: Targeting of tissue plasminogen activator in vivo. *Proc. Natl. Acad. Sci. U.S.A.* 84, 7659-7662.
- (8) Holmberg, L., Bladh, B., and Astedt, B. (1976) Purification of urokinase by affinity chromatography. *Biochim. Biophys. Acta* 445, 215-222.
- (9) Hui, K. Y., Haber, E., and Matsueda, G. R. (1983) Monoclonal antibodies to a synthetic fibrin-like peptide bind to human fibrin but not fibrinogen. *Science* 222, 1129-1131.
- (10) Bode, E., Runge, M. S., Schönermark, S., Eberle, T., Newell, J. B., Kübler, J. B., and Haber, E. (1990) Conjugation to antifibrin Fab' enhances fibrinolytic potency of single-chain urokinase plasminogen activator. *Circulation* 81, 1974-1980.
- (11) Runge, M. S., Quertermous, T., Zavodny, P. J., Love, T. W., Bode, C., Freitag, M., Shaw, S.-Y., Huang, P. L., Chou, C.-C., Mullins, D., Schnee, J. M., Savard, C. E., Rothenberg, M. E., Newell, J. B., Matsueda, G. R., and Haber, E. (1990) A recombinant chimeric plasminogen activator with high affinity for fibrin has increased thrombolytic potency in vitro and in vivo. *Proc. Natl. Acad. U.S.A.* 88, 10337-10341.
- (12) Schnee, J. M., Runge, M. S., Matsueda, G. R., Hudson, N. W., Seidman, J. G., Haber, E., and Quertermous, T. (1987) Construction and expression of a recombinant antibody-targeted plasminogen activator. *Proc. Natl. Acad. Sci. U.S.A.* 84, 6904-6908.
- (13) Bode, C., Meinhardt, G., Runge, M. S., Freitag, M., Nordt, T., Arens, M., Newell, J. B., Kübler, W., and Haber, E. (1991) Platelet-targeted fibrinolysis enhances clot lysis and inhibits platelet aggregation. *Circulation* 84, 805-813.
- (14) Dewerchin, M., Lijnen, H. R., Van Hoef, B., De Cock, F., and Collen, D. (1989) Biochemical properties of conjugates of urokinase-type plasminogen activator with a monoclonal antibody specific for cross-linked fibrin. *Eur. J. Biochem.* 185, 141-149.
- (15) Collen, D., Dewerchin, M., Rapold, H., Lijnen, H. R., and Stassen, J. M. (1990) Thrombolytic and pharmacokinetic properties of a conjugate of recombinant single-chain urokinase-type plasminogen activator with a monoclonal antibody specific for cross-linked fibrin in a baboon venous thrombosis model. *Circulation* 82, 1744-1753.
- (16) Bode, C., Runge, M. S., Branscomb, E. E., Newell, J. B., Matsueda, G. R., and Haber, E. (1989) Antibody-directed fibrinolysis. An antibody specific for both fibrin and tissue plasminogen activator. *J. Biol. Chem.* 264, 944-948.
- (17) Runge, M. S., Bode, C., Savard, C. E., Matsueda, G. R., and Haber, E. (1990) Antibody-directed fibrinolysis: A specific (Fab')₂ that binds to fibrin and tissue plasminogen activator. *Bioconjugate Chem.* 1, 274-277.
- (18) Branscomb, E. E., Runge, M. S., Savard, C. E., Adams, K. M., Matsueda, G. R., and Haber, E. (1990) Bispecific monoclonal antibodies produced by somatic cell fusion increase the potency of tissue plasminogen activator. *Thromb. Haemostasis* 64, 260-266.

LETTERS

Protein Radiolabeling with Bolton-Hunter Reagent in Surfactant Reversed Micelles in Organic Solvent[†]

Vladimir I. Slepnev, Nikolai S. Melik-Nubarov, and Alexander V. Kabanov*

Laboratory of Biopolymer Chemistry, Russian Research Center of Molecular Diagnostics and Therapy, Simferopolskii Boulevard 8, Moscow 113149, Russia. Received February 3, 1992

Surfactant reversed micelle (RM) systems are widely used in fundamental and applied biochemistry (1-6). In particular, they are regarded as a very promising reaction media for enzymology, biochemical analysis, protein extraction, and purification. We have demonstrated before that RM systems can be used as microreactors for protein and oligonucleotide modification with water-insoluble reagents (7-10) and for introduction of fluorescent dyes into proteins (11). These reactions are characterized by high yields resulting from good solubility of a modifying reagent in the RM system, low rate of its hydrolysis (observed, for example, in the cases of chloranhydrides or activated esters), and its concentration in the micelle interface in the vicinity of the modified biopolymer group. The simplicity of preparation of the RM reaction system and of recovering biopolymer from it makes the methods suggested (7-11) very convenient. In this paper we describe the rapid and effective procedure for protein radiolabeling in the Aerosol OT RM system using [¹²⁵I]Bolton-Hunter reagent.

In a typical experiment from 7.0 to 10 MBq of the [¹²⁵I]-Bolton-Hunter reagent (1.4-10¹¹ MBq/mol) in toluene was placed in a 1.5-mL Eppendorf tube and the solvent was evaporated by the stream of dried nitrogen. In order to avoid radioactivity contamination, the tube was isolated from the atmosphere by an outlet equipped with a granulated charcoal filter. The reagent was solubilized in 50 μ L of 0.3 M Aerosol OT solution in octane. In another tube, 10 μ L of from 0.2 to 1.0 mg/mL protein solution in 0.1 M H₃BO₃ buffer (pH 8.5-9.3) was mixed with 100 μ L of 0.3 M Aerosol OT in octane. This mixture was shaken in order to obtain an optically transparent RM solution, which after 5-min incubation was added to the [¹²⁵I]Bolton-Hunter solution. After 2-h incubation of the system at room temperature, the reaction was stopped by addition of 2 μ L of 1 M Tris-HCl (pH 9.3). The protein was precipitated from the micellar system by addition of from 600 to 750 μ L of cold (-20 °C) acetone, and centrifuged at 8000 rpm in an Eppendorf centrifuge for 5 min. The precipitate was washed three times (resuspended and then centrifuged again) with cold acetone, dried, dissolved in 100 μ L of PBS (pH 7.4), and dialyzed against 1 L of the same buffer. For determination of ¹²⁵I incorporation, the labeled protein was precipitated by 10% trichloroacetic acid. The concentration of protein was measured using the Bradford procedure (12) and its radioactivity was determined using a Minigamma-II γ -counter.

This method was used for radiolabeling the various proteins presented in Table I. Using the tests described

Table I. ¹²⁵I Labeling of Proteins in the RM System^a

protein	specific ¹²⁵ I radioactivity (Ci/mmol)	% yield ^b
mouse IgG (antibodies to human μ -chain)	130 \pm 13	6.4 \pm 0.6
human transferrin	105 \pm 10	5.0 \pm 0.5
protein A	110 \pm 15	11.0 \pm 1.5
α_2 -interferon	66 \pm 18	7.3 \pm 1.6

^a The values are mean \pm SEM for three to five independent experiments. ^b The part of the radioactive label incorporated in the protein related to the total amount of the label introduced in the system during protein modification.

Table II. Determination of Protein Biological Activity after Radiolabeling

protein	biological activity after radiolabeling	method used
antibodies to human μ -chain	The titer after radiolabeling is 80-90% of the initial value	indirect enzyme immunoassay (13)
human transferrin	The specific binding with human fibroblasts is not affected	radioligand assay (14)
α_2 -interferon	The antiviral titer is 80-90% of the initial value	inhibition of VSV cytopathogenic effect on pig kidney cells (15)

Table III. Specific Radioactivity of Mouse IgG (Antibodies to Human μ -Chain) Labeled in the RM System and in Homogeneous Aqueous Solution^a

conditions ^b	specific ¹²⁵ I radioactivity (Ci/mmol)	% yield ^c
aqueous solution	52 \pm 6	2.6 \pm 0.3
RM system	130 \pm 13	6.4 \pm 0.4

^a The values are mean \pm SEM for three to five independent experiments. ^b Protein radiolabeling in the RM system was performed as described in the text. Briefly, 30 μ L of IgG solution (0.5 mg/mL) in 1 M H₃BO₃ (pH 8.5) was solubilized in 300 μ L of Aerosol OT solution and then mixed with 50 mL of Aerosol OT solution containing 7 MBq Bolton-Hunter. The system was then incubated and the protein was recovered from it as described for the typical experiment. In order to modify the protein in aqueous solution 30 μ L of IgG solution (0.5 mg/mL) in 1 M H₃BO₃ (pH 8.5) was placed in an Eppendorf tube containing 7 MBq Bolton-Hunter. The reaction system was incubated for 2 h at 4 °C and then the protein was purified by the gel filtration on Sephadex G-50. In both cases the protein: Bolton Hunter molar ratio is equal to 2:1. ^c The part of the radioactive label incorporated in the protein related to the total amount of the label introduced in the system during protein modification.

in Table II, we demonstrated that the proteins retained their biological activity after iodination in the RM system. This result is in good agreement with previous data (11) demonstrating that proteins of various origin are modified in the RM system and extracted from it without significant loss of their specific biological activity.

* Author to whom correspondence should be addressed.

[†] Abbreviations used: Aerosol OT, sodium 1,4-bis(2-ethylhexyl) sulfosuccinate; [¹²⁵I]Bolton-Hunter reagent, *N*-hydroxysuccinimide ester of 3-[*p*-hydroxy([¹²⁵I]diiodophenyl)]propionic acid; PBS, phosphate-buffered saline; RM, reversed micelle.

The modification procedure was easy and fast. In particular, in this case, the protein purification step is significantly simplified compared with the conventional method described by Bolton and Hunter (16). The major part (>90%) of nonbound [125 I]Bolton-Hunter reagent is separated from the radiolabeled protein in the course of protein precipitation from the RM system. The remaining 10% separates after dialysis.

The efficiency of protein radiolabeling in the RM system was compared with that achieved using the conventional Bolton and Hunter method. The data presented in Table III show that the yield of protein coupling with Bolton-Hunter in RM is higher than that achieved in homogeneous aqueous solution.

We believe that the method suggested may become useful for radiolabeling of proteins solubilized in non-aqueous media, for example hydrophobic proteins which are extracted from the cell in an organic solvent using RM systems (17).

LITERATURE CITED

- (1) Martinek, K., Levashov, A. V., Klyachko, N. L., Khmel'nitskii, Yu. L. and Berezin, I. V. (1986) Micellar enzymology. *Eur. J. Biochem.* 155, 453-468.
- (2) Waks, M. (1986) Proteins and peptides in water-restricted environments. *Proteins* 1, 4-15.
- (3) Luisi, P. L., Giomini, M., Pileni, M. P., and Robinson, B. H. (1988) Reverse micelles as hosts for proteins and small molecules. *Biochim. Biophys. Acta* 947, 209-246.
- (4) Dekker, M., Hilhorst, R., and Laane, C. (1989) Isolating enzymes by reversed micelles. *Anal. Biochem.* 178, 217-226.
- (5) Martinek, K., Klyachko, N. L., Kabanov, A. V., Khmel'nitskii, Yu. L., and Levashov, A. V. (1989) Micellar enzymology: its relation to membranology. *Biochim. Biophys. Acta* 981, 161-172.
- (6) Pileni, M. P., Ed. (1989) *Structure and reactivity in reverse micelles*. Elsevier, Amsterdam, Oxford, New York, Tokyo.
- (7) Levashov, A. V., Kabanov, A. V., Khmel'nitskii, Yu. L., Berezin, I. V., and Martinek, K. (1984) Chemical modification of proteins (enzymes) with water-insoluble reagents. (in Russian) *Dokl. Acad. Nauk SSSR, Ser. Biokhim.* 278, 246-248 (Engl. Ed. (1985) 295-297).
- (8) Kabanov, A. V., Levashov, A. V., and Martinek, K. (1987) Transformation of water-soluble enzymes into membrane active form by chemical modification. *Ann. N.Y. Acad. Sci.* 501, 63-66.
- (9) Kabanov, A. V., Klibanov, A. L., Torchilin, V. P., Martinek, K., and Levashov, A. V. (1987) Efficiency of protein amino group acylation with fatty acid chlorides in reversed micelles of Aerosol OT in octane. (in Russian) *Bioorg. Khim.* 13, 1321-1324.
- (10) Kabanov, A. V., Vinogradov, S. V., Ovcharenko, A. V., Krivosos, A. V., Melik-Nubarov, N. S., Kiselev, V. I., and Severin, E. S. (1990) A new class of antivirals: antisense oligonucleotides combined with a hydrophobic substituent effectively inhibit influenza virus reproduction and synthesis of virus-specific proteins in MDCK cells. *FEBS Lett.* 259, 327-330.
- (11) Kabanov, A. V., Alakhov, V. Yu., and Chekhonin, V. P. (1992) Enhancement of biopolymer penetration into the cell and nontraditional drug delivery systems. *Soviet Scientific Reviews D. Physicochemical Biology* (V.P. Skulachev, Ed.) Gordon and Breach, in press.
- (12) Bradford, M. M. (1976) A rapid and sensitive method for the quantitation of microgram quantities of protein utilizing the principle of protein-dye binding. *Anal. Biochem.* 72, 248-254.
- (13) Voller, A., Bidwell, D. E., and Bertlett, A. (1976) Enzyme immunoassay in diagnostic medicine. Theory and practice. *Bull. WHO* 53, 55-65.
- (14) Dautry-Varsat, A., Ciechanove, A., and Lodish, H. F. (1983) pH and recycling of transferrin during receptor-mediated endocytosis. *Proc. Natl. Acad. U.S.A.* 80, 2258-2262.
- (15) Fimter, N. B. (1969) Dye uptake methods for assessing viral cytopathogeny and their application to interferon assays. *J. Gen. Virol.* 5, 419-429.
- (16) Bolton, A. M., and Hunter, R. M. (1973) The labelling of proteins to high specific radioactivities by conjugation to a I^{125} -containing alkylating agent. *Biochem. J.* 133, 529-539.
- (17) Nicot, C., and Waks, M. (1989) Reverse micelles as a model for the study of membrane proteins at myelin interlamellar aqueous phase. *Structure and Reactivity in Reverse Micelles* (M. P. Pileni, Ed.) pp 342-360.

Registry No. Bolton-Hunter reagent, 60285-92-9; aerosol OT, 577-11-7.

Synthesis of Poly(ethylene oxide) with Heterobifunctional Reactive Groups at Its Terminals by an Anionic Initiator

Masayuki Yokoyama,* Teruo Okano, and Yasuhisa Sakurai

Institute of Biomedical Engineering, Tokyo Women's Medical College, Kawada-cho, 8-1, Shinjuku-ku, Tokyo 162, Japan

Akira Kikuchi, Nobuyuki Ohsako, Yukio Nagasaki, and Kazunori Kataoka*

Department of Materials Science and Technology, Faculty of Industrial Science and Technology, Science University of Tokyo, Yamazaki 2641, Noda-shi, Chiba 278, Japan. Received March 10, 1992

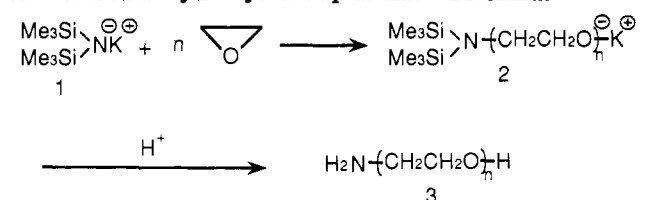
Much attention has been focused on utilization of poly(ethylene oxide) (PEO) for biological and biomedical fields. These applications include cell fusion for hybridoma production (1), protein modification for decreased antigenicity (2) or for suppression of reagenic antibody response (3), drug targeting (4, 5), and controlled drug release (6). In these applications, PEO was mixed with or bound to other components. Since ethylene oxide (EO) units possess no reactive functional groups, PEO is bound to the other components with its end groups. Several kinds of terminal-derivatized PEOs (7) have been synthesized for the binding of PEO to the other components. Most of these PEOs, however, are limited to homobifunctional polymers (e.g. PEO with primary amines at the both terminals) and polymers with one reactive terminal and one unreactive terminal (e.g. PEO with amine and methoxy groups at its terminals, respectively). For more functionalized conjugates containing PEO chains, PEOs with heterogeneous reactive groups at its two terminals are warranted. Sépúlchre et al. (8) reported a polymerization of EO by an anionic initiator which contained a masked primary amino group binding to a bulky aliphatic group (3,5,5-trimethylcyclohexyl group). Huang et al. (9) reported a preparation of the PEO with a primary amine and a hydroxyl groups at each terminal up to polymerization degree of 33 (molecular weight = 1500). They used $C_6H_5CH=NCH_2CH_2ONa$ for an initiator of polymerization of EO.

This paper reports a facile synthetic method of PEO with a primary amino group and a hydroxyl group at each terminal using a commercially available reagent, potassium bis(trimethylsilyl)amide ($[(CH_3)_3Si]_2NK$, 1), as an initiator of EO polymerization. Characterization of the high molecular weights of the polymers obtained under these conditions suggests this method will be useful for the biological applications.

As shown in Scheme I, EO was polymerized by 1 to obtain PEO with bis(trimethylsilyl)amine and potassium oxide terminals (2). These terminals are changed into a primary amine and a hydroxyl group, respectively, by subsequent acid treatment.

EO was dissolved in tetrahydrofuran (THF) at $-79^\circ C$. A solution of 1 at a concentration of 0.50 M in toluene (Aldrich Chemicals, Inc.) was added, and the mixture was stirred in a degassed sealed glass tube at $20^\circ C$. Quantities of the reagents are summarized in Table I. For run 1, the mixture was divided into five samples of almost equal quantity to follow the polymerization. After a defined period, the mixture was treated with acid (1 mL of 1 N HCl for 4 and 16 h, or 1 mL of 11% (v/v) acetic acid solution in THF for 28, 48, and 96 h) to prepare samples for gel permeation chromatography (GPC). For run 2, the mixture was poured into a 15-fold volume of diethyl ether.

Scheme I. Synthesis of Poly(ethylene oxide) with an Amino and a Hydroxyl Group at Each Terminal



The precipitate was washed with diethyl ether and dried in vacuo. For run 3, 10 mL of the reaction mixture was poured into 120 mL of diethyl ether to obtain the precipitated polymer. The residual mixture (20 mL) was transferred to a pear-shape flask, and solvent was evaporated. Both polymers obtained in run 3 were dissolved in 30 mL of THF, followed by an addition of a few drops of 0.1 N hydrochloric acid. This solution was stirred for 3 min at room temperature and poured into 300 mL of diethyl ether to obtain the precipitated polymer.

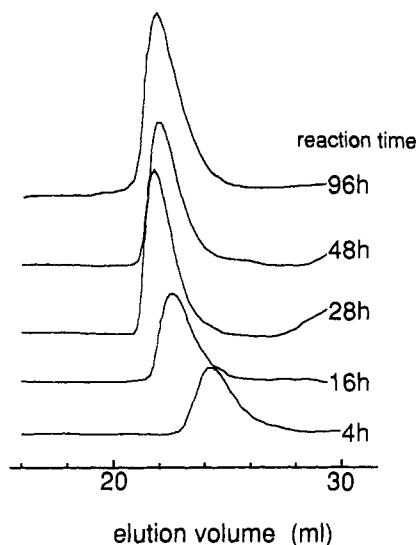
The polymerization of EO by the initiator (1) was found to have progressed successfully by GPC analysis. As shown in Figure 1, the elution volume of the sample decreased as the reaction time increased from 4 to 28 h for run 1. No change in elution volume was observed between 28 and 48 h. This indicated that polymerization of run 1 was completed within 28 h. Therefore, the polymerizations of runs 2 and 3 with smaller monomer/initiator ratios and longer reaction times than run 1 were also considered complete. The elution volume of run 1 (for 48 and 96 h) was found to correspond to molecular weights of 5.2×10^3 and 6.0×10^3 , respectively, using PEO standards. These values were almost identical with the molecular weight (4.8×10^3) calculated from the monomer/initiator ratio. Run 2 also resulted in a polymer whose molecular weight was almost the same as the calculated value. Therefore, the polymerization of EO initiated by 1 proceeded with theoretical efficiency. The molecular weight distributions of these polymers, characterized by GPC, were very narrow with ratios of weight-average molecular weight and number-average molecular weight (\bar{M}_w/\bar{M}_n) of approximately 1.1. This indicated that the initiator (1) produced polymerization without side reactions.

Run 3 brought about two samples before the acid treatment; one by precipitation and the other by evaporation. These two samples were found to have the same molecular weight (2.7×10^3) by GPC. This indicates that precipitation did not affect the molecular weight of the obtained sample. After the acid treatment, the two polymers were mixed, followed by purification on an ion-exchange resin. The mixed polymer was dissolved in 40 mL of distilled water and applied to 200 mL of Diaion PK216 (SO_3H type). After washing the column with 400 mL of distilled water, 1000 mL of 5% ammonia aqueous solution was added and the eluent was collected. The

* Author to whom correspondence should be addressed.

Table I. Polymerization of Ethylene Oxide (EO) by $[(CH_3)_3Si]_2NK$

run	quantity		EO/initiator (mol ratio)	reaction time, h	M^a (calculated)	$\overline{M}_w/\overline{M}_n^a$
	EO, g	THF, mL				
1	15.31	40	105	96	6.0×10^3 (4.8×10^3)	1.15
2	3.18	10	58	149	2.5×10^3 (2.8×10^3)	1.08
3	6.64	20	52	50	2.7×10^3 (2.5×10^3)	1.07

^a Determined by GPC using PEO standard.**Figure 1.** Gel permeation chromatogram of run 1. Gel permeation chromatography was carried out using a Toyosoda Model HLC-8020 equipped with TSK gel G2000Hxl, TSK gel G3000Hxl, and TSK gel G4000Hxl columns (gel-exclusion molecular weight is 1×10^4 , 6×10^4 , and 4×10^5 , respectively) at 40 °C in THF at a flow rate of 1.0 mL/min. Detection was performed by refractive index.

eluent was freeze-dried, the polymer was redissolved in benzene, and the solution again was freeze-dried. The yield of this purification was 94.1%. This high yield suggested successful incorporation of amino terminals, and this was confirmed by acid-base titration in chloroform with $HClO_4$ in acetic acid using methyl violet as an indicator. The purified sample was found to contain 4.0×10^{-4} mol equiv of base/g, approximately the same as 3.7×10^{-4} , calculated from the molecular weight determined by GPC on the assumption that every polymer chain carries the amino group at one terminal.

In summary, this letter reports a facile method to obtain

poly(ethylene oxide)s possessing a primary amino and a hydroxyl group at each terminal with the molecular weight well controlled by the monomer/initiator ratio as well as with narrow molecular weight distributions. In conventional methods which substitute hydroxyl terminals of PEO with other functional groups, substitution yields are dependent on a molecular weight of PEO; therefore, the more difficult it is to obtain high yields for the higher molecular weight of PEO. Furthermore, for preparation of the heterobifunctional (both reactive) PEO, yields must be low due to separation procedures from unsubstituted PEO and substituted PEO at both the terminals. On the other hand, this more convenient method introduces a primary amine to the polymer by an anionic initiator. Indeed, this method can provide 100% incorporation of an amino group even for high molecular weight polymers. Thus obtained heterobifunctional PEO is considered very useful for biological applications. For one example, this PEO may be utilized to design the directional drug-carrier systems which bind drugs and targeting moieties at each terminal of the PEO, respectively.

LITERATURE CITED

- (1) Köhler, G., and Milstein, C. (1975) *Nature* 256, 495.
- (2) Abuchowski, A., van Es, T., Palczuk, N. C., and Davis, F. F. (1977) *J. Biol. Chem.* 252, 3582.
- (3) Lee, W. Y., and Sehon, A. H. (1977) *Nature* 267, 618.
- (4) Yokoyama, M., Okano, T., Sakurai, Y., Ekimoto, H., Shibazaki, C., and Kataoka, K. (1991) *Cancer Res.* 51, 3229.
- (5) Yokoyama, M., Miyauchi, M., Yamada, N., Okano, T., Sakurai, Y., Kataoka, K., and Inoue, S. (1990) *Cancer Res.* 50, 1693.
- (6) Graham, N. B., and McNeil, M. E. (1984) *Biomaterials* 5, 27.
- (7) Harris, J. M., Struck, E. C., Case, M. G., Paley, S., Yalpani, M., van Alstine, J. M., and Brooks, D. (1984) *J. Polym. Sci., Polym. Chem. Ed.* 22, 341.
- (8) Sépulchre, M., Paulus, G., and Jérôme, R. (1983) *Makromol. Chem.* 184, 1849.
- (9) Huang, Y.-H., Li, Z.-M., Morawetz, H. (1985) *J. Polym. Sci., Polym. Chem. Ed.* 23, 795.

Registry No. 3, 32130-27-1; $[(CH_3)_3Si]_2NK$, 40949-94-8.

ARTICLES

Uptake by Macrophages of a Biotinylated Oligo- α -deoxythymidylate by Using Mannosylated Streptavidin[†]

Edwige Bonfils, Christina Mendes, Annie-Claude Roche, Michel Monsigny, and Patrick Midoux*

Laboratoire de Biochimie des Glycoconjugués et Lectines endogènes, Centre de Biophysique Moléculaire, CNRS et Université d'Orléans, 1, rue Haute 45071, Orléans Cedex 02, France. Received December 23, 1991

Streptavidin substituted with mannose residues increased by 20-fold the intracellular concentration of a biotinylated dodecakis(α -deoxythymidylate) in macrophages by comparison with the uptake of free oligodeoxynucleotide. Streptavidin, the bacterial homologue of the very basic avidin, which does not contain any carbohydrate moieties and is a neutral protein, was substituted with 12 mannose residues in order to be recognized and internalized by mannose-specific lectins on the surface of macrophages. A 3'-biotinylated and 5'-fluoresceinylated dodecakis(α -deoxythymidylate) was synthesized and bound onto mannosylated streptavidin. The conjugate was isolated, and by using flow cytometry, it was shown that the uptake of fluoresceinylated oligodeoxynucleotides bound to mannosylated streptavidin by macrophages is 20-fold higher than that of free oligodeoxynucleotides and that the uptake was competitively inhibited by mannosylated serum albumin. Glycosylated streptavidin conjugates recognizing specific membrane lectins on different cells provide the possibility to target biotinylated antisense oligodeoxynucleotides and to increase the biological effect of these chemotherapeutic agents.

INTRODUCTION

Synthetic oligodeoxynucleotides and particularly antisense oligodeoxynucleotides have been found to control the gene expression in various systems and could be used as antiviral drugs (for reviews see refs 1 and 2). However, their use in therapy is impaired by their absence of cell specificity and their limited cell uptake. In order to increase oligodeoxynucleotide uptake by cells, derivatives with cholesterol (3), phospholipid (4) and poly(L-lysine) (5, 6) have been described. Although these derivatives increase the oligodeoxynucleotide cellular uptake, they do not allow specific targeting. The attachment of an antisense oligodeoxynucleotide to a specific macromolecule recognized and internalized by cells via a receptor-mediated endocytosis will offer both a specific targeting and an increase of the intracellular uptake. Since (i) macrophages are potential targets for viruses, (ii) macrophages possess several membrane lectins (sugar binding receptors), one of them induces endocytosis of mannose-terminated glycoproteins (7), (iii) mannosylated neoglycoproteins and mannosylated neutral polymers have been used to target an immunomodulator (8-11) and an antiviral drug (12), (iv) the linking of biotin to oligodeoxynucleotides has been reported to be either onto the 5'- or 3'-ends or onto the purine or pyrimidine bases (13-15), and (v) the interaction between biotin and streptavidin is very strong ($K_d = 10^{-15}$ M) with a very low dissociation rate

constant (9×10^{-8} s⁻¹) (16, 17), we planned to use mannosylated streptavidin to target biotinylated oligodeoxynucleotides to macrophages and to increase their intracellular concentration.

In this report, we describe the synthesis of a 3'-biotinylated 5'-fluoresceinylated dodecakis(α -deoxythymidylate) and the preparation of mannosylated streptavidin and demonstrate by flow cytometry that mannosylated streptavidin increases 20-fold the internalization of this oligodeoxynucleotide into a macrophage cell line.

EXPERIMENTAL PROCEDURES

Streptavidin, bovine serum albumin fraction V (BSA), α -deoxythymidine, and 1,4-diazobicyclo[2.2.2]octane (DABCO) were purchased from Sigma (St. Louis, MO); 1,1'-carbonyldiimidazole, hexamethylenediamine, iodoacetamide, and L-glutamine were from Merck (Darmstadt, Germany); dithiothreitol (DTT) was from Serva (Heidelberg, Germany); fluorescein isothiocyanate (FITC isomer I) was from Molecular Probes (La Jolla, CA); N-(6-biotinamidoethyl)-3-(2'-pyridyldithio)propionamide (biotin-HPDP) was from Pierce (Rockford, IL); monensin was from Calbiochem (La Jolla, CA); Trisacryl GF05 and Ultrogel ACA54 were from Sepracor (Villeneuve la Garenne, France); sodium dodecyl sulfate (SDS) and Biogel P2 were from Bio-Rad (Richmond, CA); fetal bovine serum was from Gibco (Reufrewshire); penicillin (100 units/mL) and streptomycin (0.1 mg/mL) were from Eurobio (Paris, France). 4- α -D-mannopyranosylphenylisothiocyanate and mannosylated BSA (Man-BSA) containing 20 mannose residues were prepared as described (18, 19).

Preparation of Mannosylated Streptavidin. Streptavidin (6.5 mg, 0.1 μ mol) in 1 mL of 0.3 M NaCl, 0.1 M sodium carbonate buffer (pH 9) was reacted for 20 h at 4 °C with 4- α -D-mannopyranosylphenyl isothiocyanate (2 mg, 6 μ mol in 70 μ L of DMSO). The conjugate was purified by gel filtration on Trisacryl GF05 (column size 20 \times 2 cm) in PBS. The number of mannose residues bound per

* To whom reprint request should be addressed.

[†] Abbreviations used: biotin-HPDP, N-(6-biotinamidoethyl)-3-(2'-pyridyldithio)propionamide; BSA, bovine serum albumin; DABCO, 1,4-diazobicyclo[2.2.2]octane; EDTA, ethylenediaminetetraacetic acid; DMF, dimethylformamide; DMSO, dimethyl sulfoxide; DTT, dithiothreitol; FI, fluoresceinyl; FI-(α -dT)₁₂-RSS-HPbiotin, 5'-fluoresceinylated 3'-biotinylated dodecakis(α -deoxythymidylate); FI-(α -dT)₁₂-RSCH₂CONH₂, 5'-fluoresceinyl 3'-thioacetamide dodecakis(α -deoxythymidylate); Man-BSA, mannosylated BSA; PBS, phosphate-buffered saline; α -dT, α -deoxythymidine; SDS, sodium dodecyl sulfate.

streptavidin molecule was determined by the resorcinol sulfuric micromethod (20). The streptavidin concentration was determined spectrophotometrically by using $E_{282\text{nm}}^{1\%} = 34$ (17). The concentration of mannosylated streptavidin was determined spectrophotometrically at 300 nm (where mannose residues did not absorb) by using $E_{280\text{nm}}^{1\%}/E_{300\text{nm}}^{1\%} = 5.2$.

Oligonucleotide Synthesis. Preparation of 5'-Fluoresceinylated Dodecakis(α -deoxythymidylate) [Fl-(α -dT)₁₂-RSSROH] Where R = -(CH₂)₂O(CH₂)₂O-(CH₂)₂-. A dodecakis(α -deoxythymidylate) was obtained by solid-phase synthesis on a Milligen DNA synthesizer 7500 (Milligen, Saint Quentin en Yvelines, France) using 5'-O-(4,4'-dimethoxytrityl)-2'-deoxy-1'- α -thymidine 3'-(2-cyanoethyl *N,N*-diisopropylphosphoramidite) prepared from α -thymidine and the phosphoramidite method (21, 22). The chain elongation was performed on a modified solid support (10- μ mol scale) allowing the synthesis of an oligomer bearing a 3'-thiol function as previously described (23). After detritylation, the free 5'-hydroxyl group of the oligodeoxynucleotide 5'-end was activated on the solid support at 20 °C for 5 h in 5 mL of 0.3 M 1,1'-carbonyldiimidazole in dioxane. After washing with dioxane and then with dry pyridine, the activated 5'-hydroxyl was reacted for 12 h at 20 °C with 5 mL of 0.45 M hexamethylenediamine in dry pyridine (24). The cleavage and the deprotection of the oligodeoxynucleotide from the support was conducted for 4 h at 20 °C in concentrated ammonia. The oligodeoxynucleotide was purified by HPLC ion exchange chromatography on a Mono Q 5/10 column (Pharmacia, Uppsala, Sweden) with a FPLC GP 250/500 apparatus (Pharmacia) using a linear NaCl gradient from 0 to 0.9 M in 20 min in 0.01 M phosphate buffer (pH 6.8) containing 20% acetonitrile. The oligodeoxynucleotide was eluted with a retention time of 10.1 min (flow rate, 4 mL/min). Acetonitrile was removed under reduced pressure. The oligodeoxynucleotide solution was desalted by gel filtration on Biogel P2 equilibrated with water and then freeze-dried.

Fluorescein isothiocyanate (20 mg, 52 μ mol in 1.5 mL of DMF) was reacted at 20 °C for 5 h with the 5'-end amine function of the above oligodeoxynucleotide (5 mg, 0.13 μ mol) in 3 mL of 0.1 M carbonate/bicarbonate buffer (pH 9.6). Excess of unbound fluorescein was removed by gel filtration on Biogel P2 equilibrated with water. Then, the fluoresceinylated oligodeoxynucleotide was further purified by reverse-phase chromatography on C18 column (Lichrocart 250 mm \times 10 mm packed with 7- μ m Lichrospher 100 RP-18 from Merck) using a Waters G 25 LC system apparatus and a Waters 600 E (system controller) equipped with a photodiode-array detector Waters 990. The fluoresceinylated oligodeoxynucleotide was purified using a linear gradient of acetonitrile from 5% to 27.5% in 30 min in 0.1 M triethylammonium acetate (pH 7) and eluted with a retention time of 22.3 min (flow rate, 4 mL/min). Acetonitrile was removed under reduced pressure and finally the oligodeoxynucleotide solution was freeze-dried.

Preparation of 5'-Fluoresceinyl 3'-Thiol Dodecakis(α -deoxythymidylate) [Fl-(α -dT)₁₂-RSH]. The fluoresceinylated oligodeoxynucleotide (1 mg, 0.026 μ mol) was reduced by treatment for 6 h at 20 °C with 0.1 M DTT in 0.4 mL of 0.1 M NaCl, 0.1 M sodium acetate buffer (pH 4.5) in the presence of 1.7 M EDTA. Then, DTT was removed by gel filtration on Biogel P2 equilibrated with the acetate buffer.

Preparation of 5'-Fluoresceinyl 3'-Thioacetamide Dodecakis(α -deoxythymidylate) [Fl-(α -dT)₁₂-RSCH₂-

CONH₂]. The Fl-(α -dT)₁₂-RSH oligodeoxynucleotide in acetate buffer was reacted with iodoacetamide in order to block the 3'-thiol function. The pH of the solution was adjusted to 7 with 0.2 M sodium carbonate, and solid iodoacetamide (1% final concentration) was added. Fl-(α -dT)₁₂-RSCH₂CONH₂ was purified by gel filtration on Biogel P2 equilibrated with water and used as "free oligodeoxynucleotide" in uptake experiments.

Biotinylation of the Oligodeoxynucleotide [Fl-(α -dT)₁₂-RSS-HPbiotin]. Biotin-HPDP (1.4 mg, 2.6 μ mol in 300 μ L of DMF) was added to Fl-(α -dT)₁₂-RSH (0.5 mg, 0.11 μ mol) in 0.6 mL of 0.1 M acetate buffer (pH 4.5) with stirring. The solution pH was adjusted to 7.4 with a 0.2 M sodium carbonate and the solution stirred for 20 h at 20 °C. Fl-(α -dT)₁₂-RSSHPbiotin was purified by gel filtration on Biogel P2 equilibrated with PBS.

Fluoresceinylated Oligodeoxynucleotide and Mannosylated Streptavidin Conjugate. Mannosylated streptavidin (1.2 mg, 0.02 μ mol) in 1 mL of PBS was mixed with Fl-(α -dT)₁₂-RSSHPbiotin (0.4 mg, 0.09 μ mol) in 1.3 mL of PBS and stirred for 3 h at 20 °C. Then, the conjugate was purified by gel filtration on Ultrogel ACA54 (column size 1 \times 40 cm) equilibrated with complete PBS (PBS containing 1 mM CaCl₂ and 0.5 mM MgCl₂). The number of molecules bound per mannosylated streptavidin molecule was spectrophotometrically determined by using $E_{495\text{nm}}^{1\%} = 12.6$ for the fluoresceinylated oligodeoxynucleotide.

Gel Electrophoresis. Polyacrylamide gel electrophoresis was performed in the presence of sodium dodecyl sulfate (SDS/PAGE). Electrophoresis was carried out for 6 h at 70 mA with 5% stacking gel and either 15% or 20% separating gels. The running buffer was 0.1% SDS (w/v) in 25 mM Tris-glycine buffer (pH 8.9). For electrophoresis performed under reducing conditions, samples contained 1% SDS, 0.1 M DTT, and 0.8% bromophenol blue in PBS. Samples were reduced to their monomer form(s) upon boiling for 3 min. Then 50% (w/v) saccharose was added. For electrophoresis performed under nonreducing conditions, samples contained 0.1% SDS, 0.8% bromophenol blue, and 50% (w/v) saccharose in PBS and were not boiled. After electrophoresis, gels were stained with 0.1% Coomassie Brilliant Blue R 250 in a mixture of methanol, acetic acid, and water (5:2:5, v/v/v), destained in the same solvent, and dried under vacuum.

Cells. The J774 clone E cell line (J774E), kindly given by Dr. P. Stahl (Washington University Medical School, St. Louis, MO) is a variant of murine macrophage-like J774 cell line, selected, upon treatment with 5-azacytidine, because it expressed mannose membrane lectin (25). Cells were grown at 37 °C in RPMI medium (RPMI supplemented with 10% heat-inactivated fetal bovine serum, 2 mM L-glutamine, and antibiotics). Cells were passaged by harvesting in PBS for 3 min at 37 °C in the presence of 2.5 μ g/mL trypsin and 0.02% EDTA. Cells were mycoplasma free as evidenced by the BVC-Kanamycin A staining method (26). The cells were plated and incubated with fluoresceinylated compounds in either complete PBS containing 1% BSA, RPMI containing 1% BSA, or RPMI medium for a long incubation period.

Flow Cytometry Analysis. Cells were washed and suspended in sheath fluid (134 mM NaCl, 3.75 mM KCl, 1.9 mM KH₂PO₄, 16.53 mM Na₂HPO₄, 15.24 mM NaF, 0.2% 2-phenoxyethanol) (27). The cell fluorescence intensity was measured using a FACS analyzer (Becton Dickinson, Sunnyvale, CA) equipped with the FACSlite unit (Becton Dickinson). A 488-nm excitation wavelength was produced by a 25-mW cold-air argon laser. A 520 \pm

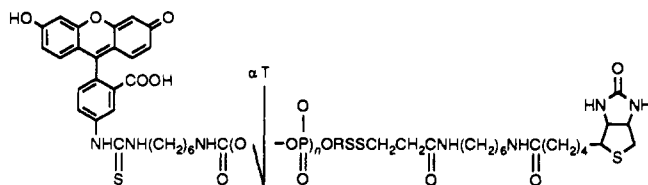


Figure 1. Structure of the 5'-fluoresceinylated 3'-biotinylated dodecakis(α -deoxythymidylate); $R = -(CH_2)_2O(CH_2)_2O(CH_2)_2-$. 10 nm interference filter was set to collect the emitted green fluorescence. Three parameters (90° light scatter, electric volume, and green fluorescence) were simultaneously recorded in the list mode. The data from 5000 cells collected at 300 events/s were analyzed using the Consort 30 device (Hewlett-Packard). The cell fluorescence intensity was measured before and after a postincubation at 4°C with $50\ \mu\text{M}$ monensin in order to estimate the uptake efficacy as previously described (19, 27, 28). Cell fluorescence intensity values were expressed as the mean value statistically calculated from the data of cells contained in the gated cell population. Fluoresceinylated beads (19) were used both to compare experiments done at different times and to quantitate the amount of fluoresceinylated oligodeoxynucleotide associated to the cells.

Microscopy Analysis. Cell-associated fluorescence was localized with a confocal fluorescence microscope (Lasersharp MRC-600, Bio-Rad, Oxfordshire, U.K.) operating with a 488-nm argon laser excitation wavelength.

RESULTS

A dodecakis(α -deoxythymidylate) [$\text{Fl}-(\alpha\text{-dT})_{12}\text{-RSS-ROH}$] bearing a fluoresceinyl group at the 5'-end and a disulfide group at the 3'-end was synthesized using the solid support previously described (23). Then, the 3'-thiol function, liberated upon reduction with DTT, was reacted with the dithiopyridinyl group of biotin-HPDP, leading to a 5'-fluoresceinylated oligodeoxynucleotide bearing a biotinyl group at the 3'-end (Figure 1). Streptavidin was mannosylated in order to prepare a specific macromolecular ligand for macrophages. Streptavidin was substituted with an activated mannose derivative (*p*-isothiocyanatophenyl α -D-mannopyranoside) which reacted with the ϵ -amino groups of the lysine residues of streptavidin. The absorbance spectrum of purified streptavidin substituted with mannose residues was modified between 240 and 290 nm compared to native streptavidin, because *N*-(*p*- α -D-mannopyranosylphenyl)thioamidyl residues bound to streptavidin also absorb in this wavelength region (Figure 2). The number of mannose residues bound per streptavidin molecule was determined by resorcinol sulfuric micromethod (20) and according to the method of ref 28 by using 14 000 Da as the streptavidin subunit molecular mass (16, 17). Mannosylated streptavidin was found to contain three mannose residues per subunit molecule (12 mannose residues per tetramer and $35\ \mu\text{g}$ of mannose per mg of protein). The purity and the molecular size of mannosylated streptavidin was checked and estimated by SDS/PAGE analysis (Figure 3). Under nonreducing conditions, the apparent molecular masses of mannosylated and native streptavidin were 62 000 and 68 100 Da, respectively. Mannosylated streptavidin migrated faster, corresponding to an apparent smaller molecular mass than native streptavidin. Under reducing conditions, the apparent molecular mass of the subunit of both mannosylated and native streptavidin was 14 000 Da. Substitution of a large number of lysine residues with sugar residues may have altered the streptavidin structure and led to an increase in its migration in polyacrylamide gel in the presence of SDS.

A fluorescent oligonucleotide-mannosylated streptavidin conjugate was prepared by mixing in PBS the 3'-biotinylated 5'-fluoresceinylated dodecakis(α -deoxythymidylate) and the mannosylated streptavidin (oligonucleotide to protein molar ratio was 4:1), and the conjugate was purified by gel filtration on a Ultrogel ACA 54 column. On the basis of the absorbance at 495 nm, the main peak was found to contain the mannosylated streptavidin with three biotinylated and fluoresceinylated dodecakis(α -deoxythymidylate) molecules per mannosylated streptavidin molecule.

Oligonucleotide Endocytosis. J774E cells were incubated at 37°C in the presence of various concentrations of fluoresceinylated oligodeoxynucleotides either free [$\text{Fl}-(\alpha\text{-dT})_{12}\text{-RSSCH}_2\text{CONH}_2$] or bound to mannosylated streptavidin. After 2 h, the cell fluorescence intensity was analyzed by flow cytometry before and after a monensin posttreatment (Figure 4). Monensin, a proton/sodium ionophore, was used to neutralize (29) acidic compartments (endosomes and/or lysosomes) of the cells, in order to recover the total fluorescence intensity of fluoresceinylated oligodeoxynucleotides inside the cells. The fluorescence intensity of cells incubated with the fluoresceinylated oligodeoxynucleotide was very low, even after a monensin posttreatment, indicating that the oligodeoxynucleotide was poorly internalized by J774E cells. The fluorescence intensity of cells incubated in the presence of the fluoresceinylated oligodeoxynucleotide bound to mannosylated streptavidin was much higher than that of cells incubated with free oligodeoxynucleotide. The enhancement of the cell fluorescence intensity upon monensin treatment demonstrates that the oligodeoxynucleotide linked to mannosylated streptavidin was mainly internalized into acidic compartments. The binding and the uptake of mannosylated streptavidin carrying fluoresceinylated oligodeoxynucleotides were saturable at $2\ \mu\text{M}$ oligodeoxynucleotide, in agreement with an endocytosis mediated by receptors (Figure 4). The uptake of fluoresceinylated oligodeoxynucleotides-mannosylated streptavidin conjugate was inhibited (up to 75%) in the presence of an excess of mannosylated BSA, showing that mannosylated streptavidin was recognized by receptors specific for mannose (Figure 5). Upon incubation of cells with nonbiotinylated oligonucleotide, either in the absence or in the presence of mannosylated streptavidin, the cell fluorescence intensities were identically low (Figure 6). This result indicates that nonbiotinylated oligonucleotide does not interact with mannosylated streptavidin to form a nonspecific conjugate. Therefore, biotinylated oligonucleotides were conjugated with mannosylated streptavidin by a specific binding to biotin sites of streptavidin, and the endocytosis of the conjugate was mediated by the mannose membrane lectins of J774E cells.

The cells were also analyzed by fluorescence microscopy using a confocal microscope (Figure 7). The fluorescence microscopy patterns of cells incubated with the fluoresceinylated oligodeoxynucleotides-mannosylated streptavidin conjugate showed that the conjugate entered the cells more efficiently than the unconjugated oligonucleotide. Furthermore, the fluorescence was mainly localized inside intracellular vesicles, a very mild fluorescence in the cytosol and almost nothing in nucleus. These results are in agreement with data obtained by using flow cytometry and specially with the enhancement of the cell fluorescence intensity measured after a postincubation with monensin, indicating that the fluorescent material was mainly in an acidic environment.

Time Course of the Oligonucleotide Uptake. Flu-

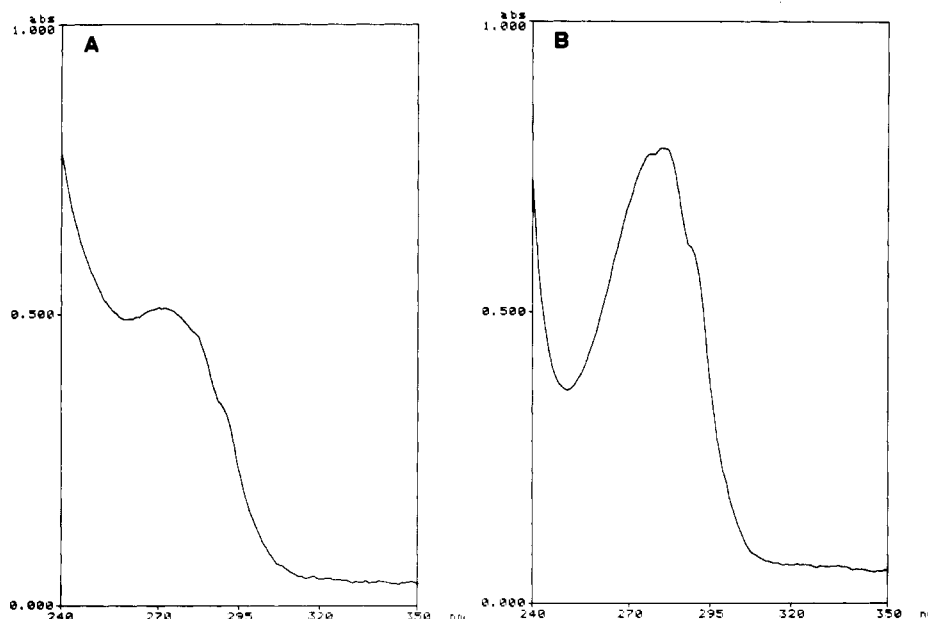


Figure 2. Absorbance spectra of (A) mannosylated streptavidin (2.0 μ M) and (B) streptavidin (3.5 μ M) in PBS.

oresceinylated oligodeoxynucleotide (2 μ M) either free or bound to mannosylated streptavidin was incubated at 37 $^{\circ}$ C for 24 h with J774 clone E cells and the cell fluorescence intensity was measured at different times before and after a postincubation with monensin (Figure 8). The uptake of oligodeoxynucleotide bound to mannosylated streptavidin increased significantly during 6 h whereas the uptake of the free oligodeoxynucleotide remained very low even after 24 h of incubation. After 24-h incubation, the fluorescence intensity of cells incubated with the oligodeoxynucleotides-streptavidin conjugate was close to that obtained after 6-h incubation. The amount of fluoresceinylated oligodeoxynucleotide associated with a single cell was calculated from the enhancement of the cell fluorescence intensity measured after monensin treatment and using calibrated fluoresceinylated beads as previously described (28). The intracellular concentrations of oligodeoxynucleotide bound to mannosylated streptavidin were found to be 3 and 12.2 μ M after 1 and 6 h, respectively (assuming a cell volume of 1.76×10^{-6} μ L). Under similar conditions, cells incubated with free oligodeoxynucleotide contained 0.14 and 0.60 μ M oligodeoxynucleotide, respectively.

DISCUSSION

In this report, we describe the use of streptavidin bearing mannose residues to allow an efficient and specific uptake of a synthetic oligodeoxynucleotide by a macrophage-like cell line. Streptavidin, a protein which does not contain any carbohydrate moieties, binds four biotin molecules with a dissociation constant of about 10^{-15} M (16). SDS/PAGE analysis of streptavidin from Sigma used in our experiments showed an apparent molecular mass of 68 100 and 14 000 for streptavidin and its subunits, respectively. These values are close to those published by Green (17) and are in agreement with data reported by Bayer et al. (30) showing that commercial streptavidin is a truncated form of streptavidin related to a proteolytic digestion occurring during the isolation process. Streptavidin containing 16 lysine residues (17) which are not directly involved in the binding of biotin (31) was substituted with 12 mannose residues by allowing 4- α -D-mannopyranosylphenyl isothiocyanate to react with the lysine amino group of the protein. A mannosylated streptavidin

substituted with 12 mannose residues is supposed to be recognized by mannose-specific lectins of the macrophage surface as glycoproteins exposing terminal mannose residues do. J774E cells, a macrophage cell line bind and internalize mannosylated protein via their mannose-specific membrane lectin (25). A dodecakis(α -deoxythymidylate) [$(\alpha$ -dT) $_{12}$] resistant to nuclease degradation was synthesized and modified at the 5'-end by coupling a fluoresceinyl group and at the 3'-end by coupling a biotinyl group via a disulfide bridge. The fluoresceinylated and biotinylated oligodeoxynucleotide strongly interacted with mannosylated streptavidin, which was easily substituted by three 3'-biotinylated 5'-fluoresceinylated dodecakis(α -deoxythymidylate) molecules. This indicated that the glycosylation of streptavidin by 12 mannose residues did not impair the accessibility of the biotin binding sites. The dissociation rate constant ($k_{\text{off}} = 9 \times 10^{-8}$ s $^{-1}$) (17) between biotin and streptavidin is so low that the biotinylated oligodeoxynucleotide-mannosylated streptavidin conjugate is as stable as a conjugate in which oligodeoxynucleotides would have been bound by a covalent linkage. This type of conjugate can be isolated by chromatographic methods. The 3'-thiol and 5'-fluoresceinyl dodecakis(α -deoxythymidylate) is linked to biotin by a disulfide bond. It was shown previously that this type of linkage is stable in culture medium: a 5'-radioiodinated oligodeoxyribonucleotide conjugated to 6-phosphomannosylated bovine serum albumin (neoglycoprotein) via a disulfide bridge was not released from the carrier after 4 h at 37 $^{\circ}$ C in the culture medium supplemented with heat-inactivated fetal calf serum. Conversely, when J774E cells were incubated for 2 h in the presence of the oligonucleotide-neoglycoprotein conjugate, it was found by cell fractionation that the cell-associated radiolabeled oligonucleotide was no longer linked with the carrier (32, and unpublished results). The release of the oligonucleotide may come from the reduction of the disulfide bond, reduction that may occur somewhere from the plasma membrane (33, 34) to any of the internal compartments where the conjugate may reach.

The endocytosis of both fluoresceinylated oligodeoxynucleotide free or bound to mannosylated streptavidin was measured by a flow cytometry method as previously described (19, 27, 28). The uptake of macromolecules by

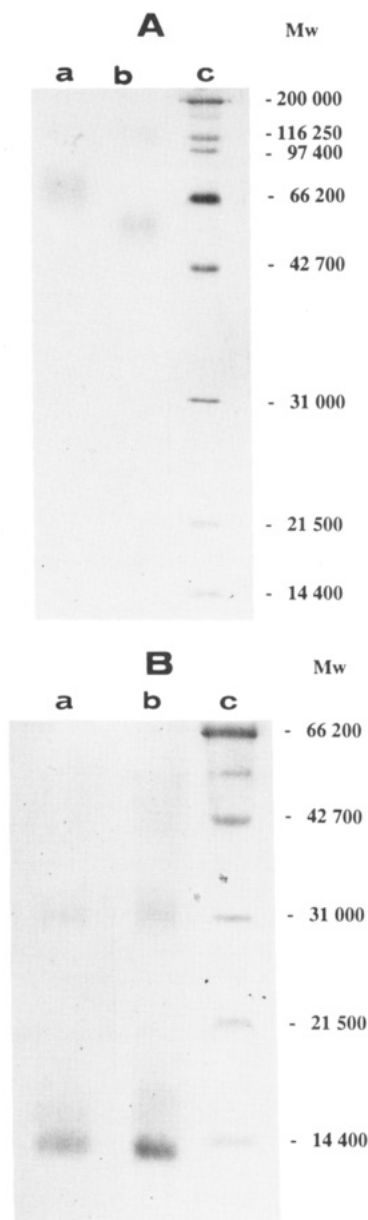


Figure 3. SDS/PAGE pattern of mannosylated and native streptavidin. Mannosylated and native streptavidin were subjected to SDS/PAGE: (A) 15% gel and unboiled samples and (B) 20% under reducing conditions; proteins were stained by Coomassie Brilliant Blue; lanes a, 25 μ g of streptavidin; lanes b, 40 μ g of mannosylated streptavidin; lanes c, the standard protein markers from Bio-Rad [myosin (MW 200 000), β -galactosidase (MW 116 250), phosphorylase B (MW 97 400), bovine serum albumin (MW 66 200), ovalbumin (MW 42 700), bovine carbonic anhydrase (MW 31 000), soybean trypsin inhibitor (MW 21 500), and hen egg white lysozyme (MW 14 400)].

receptor-mediated endocytosis generally occurs via acidic vesicles—such as endosomes and ultimately lysosomes—in which the fluorescein fluorescence is partially quenched (35–37). The internalization of fluoresceinylated macromolecules can be evidenced by cell fluorescence intensity measurements before and after a postincubation in the presence of monensin, which allows neutralization of the acidic compartments. The enhancement of the cell fluorescence intensity after monensin treatment proves that the fluoresceinylated macromolecules were contained in acidic vesicles upon endocytosis. We showed by using flow cytometry that the fluoresceinylated dodecakis(α -deoxythymidylate) conjugated with mannosylated streptavidin was intensely internalized by J774E cells by a receptor-mediated endocytosis process using the mannose

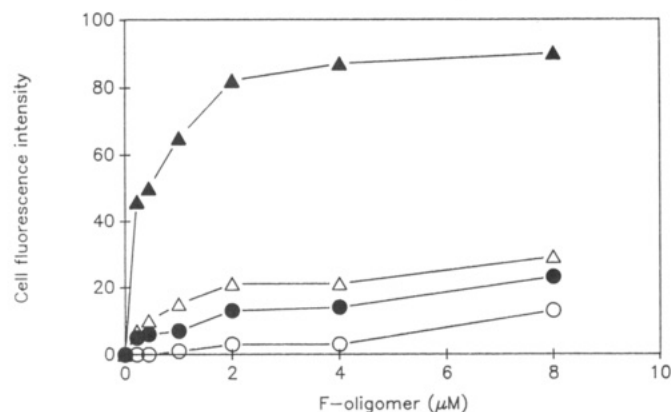


Figure 4. Flow cytometry analysis of the uptake by J774E cells of 5'-fluoresceinylated dodecakis(α -deoxythymidylate) free and bound to mannosylated streptavidin. Cells were incubated at 37 $^{\circ}$ C for 2 h in RPMI containing 1% BSA in the presence of Fl-(α -dT)₁₂-RSCH₂CONH₂ (O, ●) or 5'-fluoresceinylated dodecakis(α -deoxythymidylate) bound to mannosylated streptavidin (Δ , ▲). Cell fluorescence intensities were measured by flow cytometry before (O, Δ) and after (●, ▲) a postincubation for 30 min at 4 $^{\circ}$ C with 50 μ M monensin.

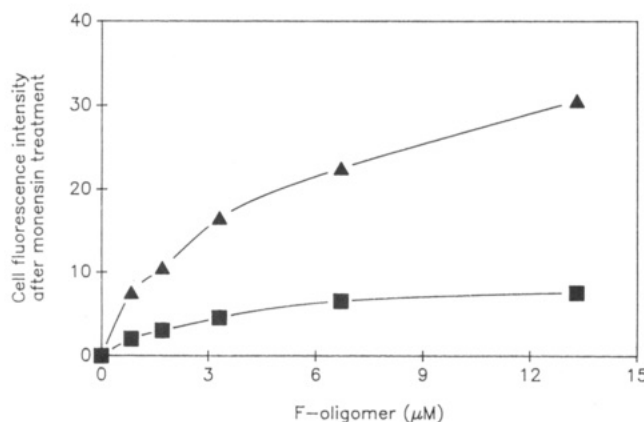


Figure 5. Specificity of the binding and uptake of 5'-fluoresceinylated dodecakis(α -deoxythymidylate) bound to mannosylated streptavidin. J774E cells were first incubated at 37 $^{\circ}$ C for 30 min in complete PBS containing 1% BSA in the absence (Δ) or presence (\blacksquare) of mannosylated bovine serum albumin (1 mg/mL; 13 μ M), and then 1 h at 37 $^{\circ}$ C with 5'-fluoresceinylated dodecakis(α -deoxythymidylate) bound to mannosylated streptavidin. Cell fluorescence intensities were measured by flow cytometry after a postincubation for 30 min at 4 $^{\circ}$ C with 50 μ M monensin.

membrane lectin of these cells. Conversely, the carrier-free fluoresceinylated oligonucleotide entered the cells poorly. The endocytosed oligonucleotide targeted by mannosylated streptavidin as well as the carrier-free fluoresceinylated oligonucleotide are mainly located in vesicles, as suggested by flow cytometry analysis and confirmed by fluorescence confocal microscopy analysis. Intracellular oligodeoxynucleotide concentration was only 30% of the extracellular concentration when cells were incubated with free oligodeoxynucleotide. Zamecnik et al. reported that 1.5 μ M of an eicosakis(β -deoxythymidylate) was found in Hela cells after 15-min incubation in the presence of 20 μ M oligodeoxynucleotide (38). Incubating cells with 2 μ M oligodeoxynucleotide bound to mannosylated streptavidin gave an intracellular oligodeoxynucleotide concentration 1.5 and 6 times higher than the extracellular concentration after 1 and 6 h, respectively. Therefore, mannosylated streptavidin concentrated the dodecakis(α -deoxythymidylate) inside J774E cells. Moreover, the cellular uptake of oligodeoxynucleotide bound to mannosylated streptavidin was 20-fold higher than that of free

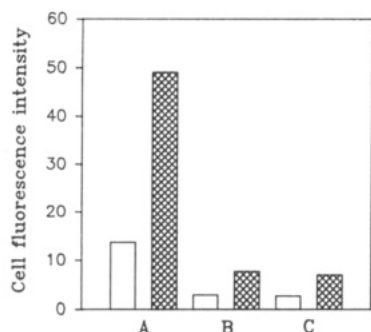


Figure 6. Flow cytometry analysis of the uptake by J774E cells of 5'-fluoresceinylated dodecakis(α -deoxythymidylate) conjugated with mannosylated streptavidin. Cells were incubated at 37 °C for 2 h in RPMI containing 1% BSA in the presence of (A) 5 μ M 5'-fluoresceinylated dodecakis(α -deoxythymidylate) bound to mannosylated streptavidin (40 μ g/mL), (B) 5 μ M Fl-(α -dT)₁₂-RSCH₂CONH₂, and (C) 5 μ M Fl-(α -dT)₁₂-RSCH₂CONH₂ mixed with 40 μ g/mL mannosylated streptavidin. Cell fluorescence intensities were measured by flow cytometry before (open) and after (hatched) a postincubation for 30 min at 4 °C with 50 μ M monensin.

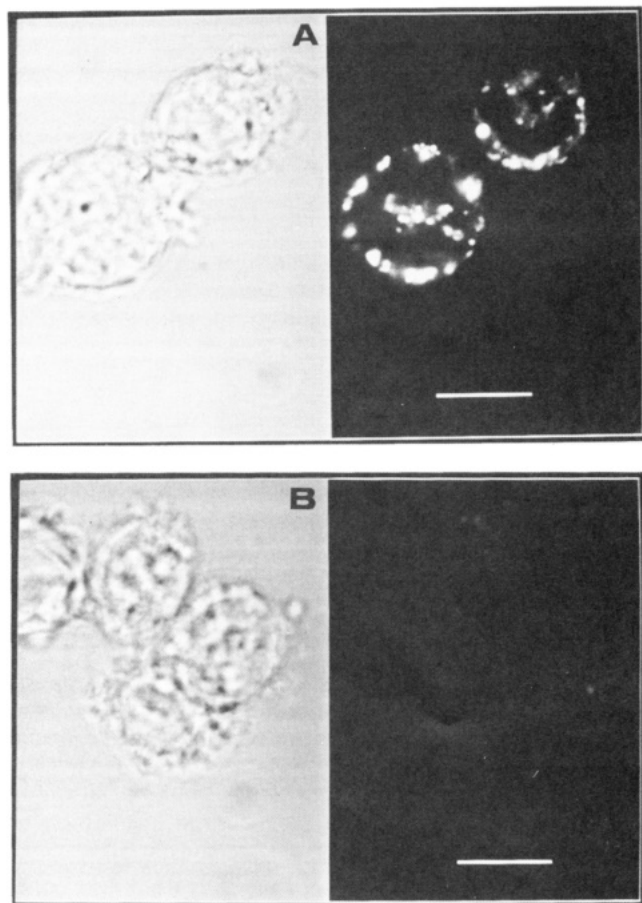


Figure 7. Intracellular localization of 5'-fluoresceinylated dodecakis(α -deoxythymidylate) either free or bound to mannosylated streptavidin. J774E cells were incubated at 37 °C for 2 h in RPMI containing 1% BSA in the presence of either (A) 5 μ M 5'-fluoresceinylated dodecakis(α -deoxythymidylate) conjugated with 40 μ g/mL mannosylated streptavidin or (B) 5 μ M Fl-(α -dT)₁₂-RSCH₂CONH₂. Cells were washed, incubated for 30 min at 4 °C with 50 μ M monensin, and fixed at 4 °C in 1% paraformaldehyde in PBS. Cells were mounted in PBS/glycerol (v/v) containing 1% DABCO as antifade agent (scale bar, 10 μ m).

oligodeoxynucleotide. These values are close to those obtained using cholesterol, phospholipid, or poly(L-lysine) oligodeoxynucleotide derivatives. Attachment of a cholesterol residue at the 3'-end of a decakis(β -deoxythymidylate) increased 6- and 8-fold its intracellular concentration

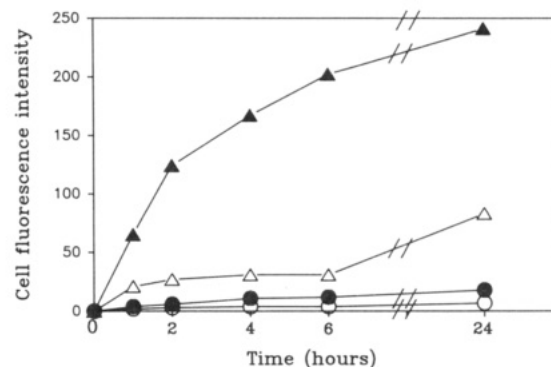


Figure 8. Time course of the J774E cell uptake of 5'-fluoresceinylated dodecakis(α -deoxythymidylate) either free or bound to mannosylated streptavidin. Cells were incubated at 37 °C in RPMI medium in the presence of 2 μ M Fl-(α -dT)₁₂-RSCH₂CONH₂ (O; ●) or 2 μ M 5'-fluoresceinylated dodecakis(α -deoxythymidylate) bound to mannosylated streptavidin (15 μ g/mL) (Δ; ▲). Cell fluorescence intensities were measured by flow cytometry before (O; Δ) and after (●; ▲) a postincubation for 30 min at 4 °C with 50 μ M monensin.

and 15- and 20-fold its internalization by comparison with those of underivatized oligodeoxynucleotide when 2.5 and 0.5 μ M cholesterol-derivatized oligodeoxynucleotide conjugates were incubated for 2 h with L929 and Krebs-2 cells, respectively (3). Attachment of a phospholipid tail to the 5'-end of a pentadecakis(β -oligodeoxynucleotide) increased 10-fold its cellular uptake after 4-h incubation by comparison with the uptake of phosphorothioate and phosphodiester derivatives and concentrated 4-fold the oligodeoxynucleotide inside L929 cells (4). Attachment of a fluoresceinylated pentadecakis(β -oligodeoxynucleotide) to the polycationic poly(L-lysine) increased its internalization 12-fold by comparison with that of free oligodeoxynucleotide when L929 cells were incubated for 4 h with 1 μ M fluoresceinylated oligodeoxynucleotide-polylysine conjugate (6). Recently, a 4-fold increase of the uptake by brain capillaries of a biotinylated antisense uneicosakis(β -oligodeoxynucleotide) was obtained after conjugation with avidin (39). In this case, it is the cationic properties of avidin that mediated the uptake of the conjugate. Indeed, when streptavidin, which is a neutral protein, was used, there was no increase in the uptake of the uneicosakis(β -oligodeoxynucleotide) (39). The use of poly(L-lysine) and avidin cannot be considered as true targeting since polycationic molecules will interact with any cells. Biotinylated oligodeoxyribonucleotides can be easily synthesized and conjugated to streptavidin substituted with mannose to allow targeting to macrophages. A conjugate containing three oligodeoxynucleotide molecules was easily obtained and isolated from free oligodeoxynucleotides with a greater yield than conjugates prepared using covalent linkages between oligodeoxynucleotides and protein.

Membrane lectins have been evidenced at the surface of many normal cells (including hepatocytes, monocytes, macrophages, endothelial cells, and lymphocytes) and tumor cells and specific glycoconjugates have been used to target drugs (for reviews see refs 40–42). Streptavidin could be substituted by various monosaccharides or complex oligosaccharides, provided that the biotin binding site accessibility be preserved and so could be used to target membrane lectins on different cell types. Various glycosylated streptavidins may be obtained and therefore open the possibility (i) to target antisense oligodeoxynucleotides to different cells; (ii) to increase their cellular uptake, and (iii) to study their intracellular traffic, in a chemotherapeutic strategy. Streptavidin could also be

used as an intermediate carrier to bind biotinylated antisense oligonucleotides to specific biotinylated vectors such as monoclonal antibodies, glycoproteins, cytokines, or growth factors.

Antisense oligonucleotides, which have been found to control the gene expression in cultured cells, enter the cells mainly by pinocytotic vesicles (43); few molecules may reach, by a still unknown process, the cytosol and/or the nucleus, and, there, interact with their targets (mRNA translation initiation sites, pre-mRNA splicing sites, or genes). The use of macromolecular carriers such as mannosylated streptavidin allows an increased uptake of fluoresceinylated dodecakis(α -deoxythymidylate) into macrophages by a receptor-mediated endocytotic process. The increased intracellular concentration of the oligonucleotide is clearly observed inside endocytotic vesicles. According to the fact that the internalized oligonucleotide is carrier free, it may be expected that the cytosolic and/or the nuclear oligonucleotide concentration will also increase. The mechanism of the uptake of free oligonucleotides is not yet understood; it has been proposed that specific receptors are involved (43), but even in this case, the free oligonucleotides are taken up by an endocytotic process. Therefore, oligonucleotides targeted by mannosylated streptavidin have the opportunity to enter the cells and to reach a higher intracellular concentration, which may in turn significantly increase the cytosolic and nuclear concentrations.

ACKNOWLEDGMENT

We thank Dr. C. Hélène for helpful discussions and his interest in this work, and Dr. N. T. Thuong for his valuable help in oligonucleotide synthesis. This work was supported by grants from "Agence Nationale de Recherche sur le Sida" (ANRS). E.B. and C.M. received a fellowship from ANRS and MRT, respectively. A.C.R. is "Directeur de recherche INSERM" and P.M. is "Chargé de recherche INSERM".

LITERATURE CITED

- Hélène, C., and Toulmé, J. J. (1990) Specific regulation of gene expression by antisense, sense and antigene nucleic acid. *Biochim. Biophys. Acta* 1049, 99–125.
- Uhlmann, E., and Peyman, A. (1990) Antisense oligonucleotides: A new therapeutic principle. *Chem. Rev.* 90, 543–584.
- Boutorin, A. S., Gus'kova, L. V., Ivanova, E. M., Kobetz, N. D., Zarytova, V. F., Rytte, A. S., Yurchenko, L. V., and Vlassov, V. V. (1989) Synthesis of alkylating oligonucleotide derivatives containing cholesterol or phenazinium residues at their 3'-terminus and their interaction with DNA within mammalian cells. *FEBS Lett.* 254, 129–132.
- Shea, R. G., Marsters, J. C., and Bischoffberger, N. (1990) Synthesis, hybridization properties and antiviral activity of lipid-oligodeoxynucleotide conjugates. *Nucleic Acids Res.* 18, 3777–3783.
- Lemaitre, M., Bayard, B., and Lebleu, B. (1987) Specific antiviral activity of a poly(L-lysine)-conjugate oligodeoxyribonucleotide sequence complementary to vesicular stomatitis virus N protein mRNA initiation site. *Proc. Natl. Acad. Sci. U.S.A.* 84, 648–652.
- Leonetti, J. P., Degols, G., and Lebleu, B. (1990) Biological activity of oligonucleotide-Poly(L-lysine) conjugates: Mechanism of cell uptake. *Bioconjugate Chem.* 1, 149–153.
- Wileman, T., Harding, C., and Stahl, P. (1985) Receptor-mediated endocytosis. *Biochem. J.* 232, 1–14.
- Monsigny, M., Roche, A. C., and Bailly, P. (1984) Tumoricidal activation of murine alveolar macrophages by muramyl dipeptide substituted mannosylated serum albumin. *Biochem. Biophys. Res. Commun.* 121, 579–584.
- Roche, A. C., Bailly, P., and Monsigny, M. (1985) Macrophage activation by MDP bound to neoglycoproteins: Metastasis eradication in mice. *Invasion Metastasis* 5, 218–232.
- Derrien, D., Midoux, P., Petit, C., Nègre, E., Mayer, R., Monsigny, M., and Roche, A. C. (1989) Muramyl Dipeptide Bound to Poly-L-Lysine Substituted with Mannose and Glucosyl Residues as Macrophage Activators. *Glycoconjugate J.* 6, 241–255.
- Petit, C., Monsigny, M., and Roche, A. C. (1990) Macrophages activation by muramyl dipeptide bound to neoglycoproteins and glycosylated polymers: Cytotoxic factor production. *J. Biol. Response Modif.* 9, 33–43.
- Midoux, P., Nègre, E., Roche, A. C., Mayer, R., Monsigny, M., Balzarini, J., De Clercq, J., Mayer, E., Ghaffar, A., and Gangemi, J. D. (1990) Drug targeting: Anti-HSV-1 activity of mannosylated polymer-bound 9-(2-phosphonylmethoxyethyl)-adenine. *Biochem. Biophys. Res. Commun.* 167, 1044–1049.
- Goodchild, J. (1990) Conjugates of oligonucleotides and modified oligonucleotides: A review of their synthesis and properties. *Bioconjugate Chem.* 1, 165–187.
- Temsamani, J., Agrawal, S., and Pederson, T. (1991) Biotinylated antisense methylphosphonate oligodeoxynucleotides. *J. Biol. Chem.* 266, 468–472.
- Sproat, B., Lamond, A. I., Beijer, B., Neuner, P., and Ryder, U. (1989) Highly efficient chemical synthesis of 2'-O-methyloligoribonucleotides and tetrabiotinylated derivatives; novel probes that are resistant to degradation by RNA or DNA specific nucleases. *Nucleic Acids Res.* 17, 3373–3386.
- Chaiet, L., and Wolf, K. J. (1964) The properties of streptavidin, a biotin-binding protein produced by streptomyces. *Arch. Biochem. Biophys.* 106, 1–5.
- Green, N. M. (1975) Avidin. *Adv. Protein Chem.* 29, 85–133.
- Roche, A. C., Barzilay, M., Midoux, P., Junqua, S., Sharon, N., and Monsigny, M. (1983) Sugar-specific endocytosis of glycoproteins by Lewis lung carcinoma cells. *J. Cell. Biochem.* 22, 131–140.
- Monsigny, M., Roche, A. C., and Midoux, P. (1984) Uptake of neoglycoproteins via membrane lectin(s) of L 1210 cells evidenced by quantitative flow cytofluorometry and drug targeting. *Biol. Cell* 251, 187–196.
- Monsigny, M., Petit, C., and Roche, A. C. (1988) Colorimetric determination of neutral sugars by a resorcinol sulfuric acid micromethod. *Anal. Biochem.* 175, 525–530.
- Beaucage, S. L., and Caruthers, M. H. (1981) Deoxynucleoside phosphoramidites—A new class of key intermediates for deoxypolynucleotide synthesis. *Tetrahedron Lett.* 22, 1859–1862.
- Matteucci, M. D., and Caruthers, M. H. (1981) Synthesis of deoxyoligonucleotides on a polymer support. *J. Am. Chem. Soc.* 103, 3185–3191.
- Bonfils, E., and Thuong, N. T. (1991) Solid phase synthesis of 5',3'-bifunctional oligodeoxyribonucleotides bearing a masked thiol group at the 3'-end. *Tetrahedron Lett.* 32, 3053–3056.
- Wachter, L., Jablonski, J., and Ramachandran, K. L. (1986) A simple and efficient procedure for the synthesis of 5'-aminoalkyl oligonucleotides. *Nucleic Acids Res.* 14, 7985–7994.
- Diment, S., Leech, M. S., and Stahl, P. D. (1987) Generation of macrophage variants with 5-azacytidine: Selection for mannose receptor expression. *J. Leukocyte Biol.* 42, 485–490.
- Monsigny, M., Midoux, P., Depierreux, C., Bebear, C., Le Bris, M.-T., and Valeur, B. (1990) Benzoxazinone kanamycin A conjugate. A new fluorescent probe suitable to detect mycoplasmas in cell culture. *Biol. Cell* 70, 101–105.
- Midoux, P., Roche, A. C., and Monsigny, M. (1987) Quantitation of the binding, uptake and degradation of fluoresceinylated neoglycoproteins by flow cytometry. *Cytometry* 8, 327–334.
- Midoux, P., Roche, A. C., and Monsigny, M. (1986) Degradation of endocytosed materials estimated by flow cytofluorometry using two neoglycoproteins containing different numbers of fluorescein molecules. *Biol. Cell* 58, 221–226.
- Maxfield, F. R. (1982) Weak bases and ionophores rapidly and reversibly raise the pH of endocytic vesicles in cultured mouse fibroblasts. *J. Cell Biol.* 95, 676–681.

- (30) Bayer, E. A., Ben-Hur, H., Hiller, Y., and Wilchek, M. (1989) Postsecretory modifications of streptavidin. *Biochem. J.* 259, 369–376.
- (31) Wilchek, M., and Bayer, E. A. (1989) Avidin-biotin technology ten years on: Has it lived up to its expectations? *Trends Biochem. Sci.* 14, 408–412.
- (32) Bonfils, E. (1991) Thesis, Orléans, France.
- (33) Feener, E. P., Shen, W.-C., and Ryser, H. J. P. (1990) Cleavage of disulfide bonds in endocytosed macromolecules. *J. Biol. Chem.* 265, 18780–18785.
- (34) Ryser, H. J. P., Mandel, R., and Ghani, F. (1991) Cell surface sulfhydryls are required for the cytotoxicity of diphtheria toxin but not of ricin in Chinese hamster ovary cells. *J. Biol. Chem.* 266, 18439–18442.
- (35) Mellman, I., Fuchs, R., and Helenius, A. (1986) Acidification of the endocytic and exocytic pathways. *Annu. Rev. Biochem.* 55, 663–700.
- (36) Ohkuma, S., and Poole, B. (1978) Fluorescence probe measurement of the intralysosomal pH in living cells and the perturbation of pH by various agents. *Proc. Natl. Acad. Sci. U.S.A.* 75, 3327–3331.
- (37) Yamashiro, D. J., and Maxfield, F. R. (1984) Acidification of endocytic compartments and the intracellular pathways of ligands and receptors. *J. Cell. Biochem.* 26, 231–246.
- (38) Zamecnik, P. C., Goodchild, J., Taguchi, Y., and Sarin, P. S. (1986) Inhibition of replication and expression of human T-cell lymphotropic virus type III in cultured cells by exogenous synthetic oligonucleotides complementary to viral RNA. *Proc. Natl. Acad. Sci. U.S.A.* 83, 4143–4146.
- (39) Pardridge, W. M., and Boado, R. J. (1991) Enhanced cellular uptake of biotinylated antisense oligonucleotide or peptide mediated by avidin, a cationic protein. *FEBS Lett.* 288, 30–32.
- (40) Monsigny, M., Kieda, C., and Roche, A. C. (1983) Membrane glycoproteins, glycolipids and membrane lectins as recognition signals in normal and malignant cells. *Biol. Cell* 47, 95–110.
- (41) Monsigny, M., Roche, A. C., Kieda, C., Midoux, P., and Obrenovitch, A. (1988) Characterization and biological implications of membrane lectins in tumor, lymphoid, and myeloid cells. *Biochimie* 70, 1633–1649.
- (42) Monsigny, M., Roche, A. C., Mayer, R., Midoux, P., Nègre, E., and Bonfils, E. (1991) NATO workshop on endocytosis. In press.
- (43) Loke, S. L., Stein, C. A., Zhang, X. H., Mori, K., Nakanishi, M., Subasinghe, C., Cohen, J. S., and Neckers, L. M. (1989) Characterization of oligonucleotide transport into living cells. *Proc. Natl. Acad. Sci. U.S.A.* 86, 3474–3478.

Registry No. F-(α -dT)₁₂-R-SS-ROH, 141436-86-4; F-(α -dT)₁₂-RSH, 141436-84-2; F-(α -dT)₁₂-RS-CH₂-CONH₂, 141436-85-3; F-(α -dT)₁₂-RSS-HPbiotin, 141436-87-5; streptavidin, 9013-20-1; 4- α -D-mannopyranosylphenyl isothiocyanate, 96345-79-8; mannose, 31103-86-3.

Covalent Linkage of Ruthenium Polypyridyl Compounds to Poly(L-lysine), Albumins, and Immunoglobulin G

Eleanor M. Ryan,[†] Richard O'Kennedy,[‡] Martin M. Feeney,[§] John M. Kelly,[§] and Johannes G. Vos^{*†}

Schools of Chemical Sciences and Biological Sciences, Dublin City University, Dublin 9, Ireland, and Department of Chemistry, University of Dublin, Dublin 2, Ireland. Received January 27, 1992

A series of ruthenium polypyridyl complexes has been covalently bound to poly(L-lysine), bovine serum albumin, human serum albumin, ovalbumin, and immunoglobulin G using different binding methods. The conjugation ratios and the luminescence properties of the bioconjugates are reported. All conjugates show nonsingle-exponential decay curves. Quenching of the emission by oxygen has been studied.

INTRODUCTION

At present much research is in progress to find substitutes for radioisotopic labels for biomolecules. Radio-labeling methods have been used, and although they are extremely sensitive, they have environmental disadvantages (1, 2). Nonisotopic systems developed include the use of enzymic, chemiluminescent, and fluorescent labels (3). Recently ruthenium compounds have been receiving attention as nonradioactive probes and labels for biomolecules.

Ruthenium polypyridyl complexes have been used in DNA probe technology and their use as labels for proteins has also been reported (4-10).

Ruthenium compounds offer certain advantages over conventional fluorescent labels such as fluorescein isothiocyanate (FITC) because the ruthenium compounds have a larger Stokes' shift (160-170 nm) than FITC (30 nm). This will decrease problems with light-scattering effects. The longer emission lifetime of the ruthenium compounds is a clear advantage, as the lifetime can be used as a probe for the local environment of the emitting species. It is hoped that by studying the emission lifetime of the ruthenium labels detailed information about the binding site can be obtained. By using different binding methods the binding location of the labels can be controlled; furthermore, covalent bonding will also enable one to control very carefully the loading of the emitting label.

In this paper the use of ruthenium complexes as new types of reporter molecules for proteins is described. The conjugation of bovine serum albumin (BSA), human serum albumin (HSA), ovalbumin (OVA), goat anti-mouse immunoglobulin G (IgG), and poly(L-lysine) (PLL) to the complexes $[\text{Ru}(\text{L-L})_2(\text{NCSphen})]^{2+}$ and $[\text{Ru}(\text{L-L})_2(\text{NH}_2\text{phen})]^{2+}$, where L-L = 2,2'-bipyridyl (bpy) or 1,10-phenanthroline (phen), NH_2phen is 5-amino-1,10-phenanthroline, and NCSphen is 5-isothiocyanato-1,10-phenanthroline is described. Poly(L-lysine) conjugates are used as polar tracers for cell lineage tracing in embryonic cells (11) and have also been reported as having antiviral activity (12) and anticancer activity (13). Fluorescent conjugates of bovine serum albumin and ovalbumin find application as polar tracers with applications in cell microinjection for the study of dynamic activities of living cells and as probes of phagocytosis (11). Antibody conjugates are used extensively in immunoassay and immunofluorescence procedures.

Usually, labeling of proteins involves the modification of amino acid side chains. These include tyrosines, the ϵ -amino groups of lysines, carboxyl groups of glutamic and aspartic acids, and sulfhydryl groups generated by mild reduction of cysteines (14). The site at which modification takes place has special significance when labeling of immunoglobulins is involved. The polypeptide moieties of immunoglobulins impart their specific antigen binding ability, and modification of the amino acid side chains may result in partial or complete loss of immunological activity. In contrast, the carbohydrate moieties of immunoglobulins are not involved in the antigen binding properties of these molecules, and modification should not directly affect antigen binding (15). The albumins and IgG have therefore been conjugated to the reporter molecule through both the ϵ -amino group of the lysine residues and also through modification of the carbohydrate moieties on these proteins.

EXPERIMENTAL PROCEDURES

Reagents and Materials. Mouse IgG (I-5381), goat anti-mouse IgG (M8642), anti-goat IgG peroxidase conjugate (A3540), dialysis tubing (D-0405), *o*-phenylenediamine (P-9029), poly(L-lysine) (P-1274), lysine (L-5501), ovalbumin (A-3154), human serum albumin (A-8763), and PBS tablets (P-4417) were purchased from Sigma Chemical Co. Bovine serum albumin was purchased from BDH Chemicals Ltd. Nunc-Immuno Plate Maxi-Sorp 96-well plates were purchased from Intermed Nunc. RuCl_3 was a gift from Johnson-Matthey. The ligands 2,2'-bipyridine, 4,4'-dimethyl-2,2'-bipyridine, 1,10-phenanthroline, and 5-amino-1,10-phenanthroline (NH_2phen) were obtained from Aldrich Chemical Co., Riedel de Haen Chemical Co., and Polysciences Inc. The ligand 4,4'-dicarboxy-2,2'-bipyridine (dcbpy) was prepared from 4,4'-dimethyl-2,2'-bipyridine according to literature methods (16). Synthesis of the complex $[\text{Ru}(\text{bpy})_2(\text{dcbpy})](\text{PF}_6)_2$ and its conversion to the active ester were carried out according to the method of Bard (7). All other reagents or solvents used were reagent grade unless otherwise specified.

Equipment and Physical Measurements. Infrared spectra were recorded on a Perkin-Elmer 983G infrared spectrometer using pressed KBr disks. Emission spectra were recorded on either a Perkin-Elmer LS-5 luminescence spectrometer or a Perkin-Elmer LS-50 luminescence spectrometer controlled from a personal computer using the Perkin-Elmer Fluorescence Data Manager software. Both spectrometers were equipped with a red-sensitive Hamamatsu R928 detector, and an emission slit width of 10 nm was used at room temperature. The results were

[†] School of Chemical Sciences, Dublin City University.

[‡] School of Biological Sciences, Dublin City University.

[§] University of Dublin.

not corrected for photomultiplier response. UV/vis spectra were recorded on a Shimadzu UV-240 spectrometer with matched quartz cells. All spectroscopic measurements were carried out in 0.1 M carbonate buffer (pH 9.6). High-performance liquid chromatography (HPLC) was carried out using methods described in an earlier paper (17). Lifetime measurements were carried out using an Edinburgh Instruments FL900 time-correlated single photon counting apparatus. The nF900 lamp was N₂-filled and was operated at 25 kHz. The intensity was increased by shorting the resistor across the electrodes, this also increased the pulse width (FWHM = 5.0 ns). Excitation and emission wavelengths were 337 and 600 nm, respectively. Signals were detected on a cooled R955-type photomultiplier and processed by conventional CFD and TAC units. Data were analyzed by nonlinear least squares deconvolution methods using the Marquardt algorithm provided by Edinburgh Instruments.

Samples were thermostated at 25 °C and measured in aerated 0.1 M carbonate buffer (pH 9.60). Solutions were degassed with nitrogen or oxygenated for 30 min, then about 0.2 mL of the bioconjugate was added and the mixture further degassed for 15 min. Upon prolonged degassing of the bioconjugate solutions by bubbling through nitrogen, denaturation of the proteins was observed.

Synthesis of Labels. Compounds of the type $[Ru(L-L)_2(5-NH_2phen)](PF_6)_2$ were synthesized according to general literature procedures (18, 19). Anal. Calcd for $[Ru(bpy)_2(NH_2phen)](PF_6)_2 \cdot \frac{1}{2}(CH_3)_2CO$: C, 43.36; H, 3.02; N, 10.57. Found: C, 43.40; H, 3.04; N, 10.37. Anal. Calcd for $[Ru(phen)_2(NH_2phen)](PF_6)_2$: C, 45.66; H, 2.63; N, 10.36. Found: C, 45.16; H, 2.67; N, 10.28.

$[Ru(L-L)_2(NCSphen)]^{2+}$. $[Ru(L-L)_2(NH_2phen)](PF_6)_2$ (2.2×10^{-4} M) in 10 mL of distilled water was stirred in the presence of Amberlite anion exchange resin (Cl⁻) to exchange the PF₆⁻ anion for Cl⁻ ions to produce a compound more soluble in aqueous solution. The solution obtained was filtered to remove the resin. The amine compound was then reacted with thiophosgene (0.01 M) in acetone which was added dropwise to the aqueous solution over 30 min. During this time the reaction vessels were kept in an ice bath to inhibit the evaporation of the thiophosgene. After addition was complete the reaction was allowed to proceed at room temperature overnight in a covered vessel. The complex $[Ru(phen)_2(NCSphen)]Cl_2$ was isolated by filtration and dried under vacuum. The complex $[Ru(bpy)_2(NCSphen)]^{2+}$ remained in solution and was isolated by evaporation of excess thiophosgene under reduced pressure, followed by precipitation using a saturated aqueous solution of NH₄PF₆. The compounds were dried under vacuum. All procedures were carried out with care due to the toxicity of thiophosgene. Gloves were worn, and due to the volatility of the thiophosgene, each stage was carried out in a fume hood.

The purity of the amino and isothiocyanate compounds was checked by HPLC.

Conjugation Procedures. *Conjugation of $[Ru(L-L)_2(NH_2phen)]^{2+}$ to Albumins.* The direct conjugation of the amino complexes involves firstly the periodate oxidation of the albumin, which is followed by conjugation to the amino complex. The appropriate albumin (BSA, HSA, or OVA) (10–25 mg) was dissolved in 0.1 M NaHCO₃ (1–2 mL) and treated with 2.5 mL of 16 mM NaIO₄ for 2 h at 4 °C in the dark (20). The label solution was then added (50 molar excess) dropwise to the protein solution. The ruthenium compound was dissolved in a minimum volume of dimethylformamide (DMF) and 0.1 M carbonate

buffer (pH 9.6). The total reaction volume was kept to a minimum. The conjugation reaction was allowed to proceed overnight at 4 °C, in the dark with minimal agitation. The conjugate was extensively dialyzed against 0.1 M carbonate buffer (pH 9.6) to remove unbound label for not less than 72 h. In order to reduce excess oxidized sites on the protein, 4 vol of NaBH₄ (5 mg/mL) was added and reacted for 1 h at 4 °C in the dark. Finally, the conjugate was again dialyzed (two changes of buffer) to remove all small molecules.

Conjugation of $[Ru(bpy)_2(NH_2phen)]^{2+}$ to Goat Anti-Mouse IgG. The above described conjugation procedure was used; 1–2 mg of pure goat anti-mouse IgG was used per conjugation and the material was dissolved in 0.1 M acetate buffer (pH 5.5). The IgG was oxidized using 1 mL of 10 mM NaIO₄ (21).

Conjugation of $[Ru(L-L)_2(NCSphen)]^{2+}$ to Albumins, Goat Anti-Mouse IgG and Poly(L-lysine). Albumin, poly(L-lysine) (10–25 mg), or goat anti-mouse IgG (1–2 mg) was dissolved in 1–2 mL 0.1 M carbonate buffer (pH 9.6). The ruthenium compound (50 molar excess) was dissolved in the minimum volume of DMF/0.1 M carbonate buffer (pH 9.6) and added dropwise to the protein or poly(L-lysine) solution. The conjugation reaction was allowed to proceed overnight at 4 °C, in the dark, with minimal agitation. The conjugate was then extensively dialyzed against 0.1 M carbonate buffer to remove unbound label.

Conjugation of the Active Ester of $[Ru(bpy)_2(dcbpy)](PF_6)_2$ to Albumins and PLL. The active ester was prepared according to literature methods (7). Twenty milligrams of albumin/PLL was dissolved in 1–2 mL of 0.1 M carbonate buffer (pH 9.6). The active ester solution was added dropwise in amounts which were equivalent to a 50 molar excess of the ester to the albumin or PLL. The conjugation reaction was allowed to proceed overnight at 4 °C, in the dark, with minimal agitation. The complex was extensively dialyzed against 0.1 M carbonate buffer (pH 9.6).

Estimate of Conjugation Ratio. The amount of ruthenium compound present was determined by its absorption maximum at 450 nm. The extinction coefficients of the unbound labels were measured in 0.1 M carbonate buffer (pH 9.6). No allowance was made for a change in the extinction coefficient on binding to protein. The protein concentration was determined using the Folin-Lowry method (22). The conjugation ratio was calculated according to Nairn's method (23) using molecular weights of 160 000 (anti IgG), 68 000 (BSA), 67 000 (HSA), 43 000 (OVA), and 109 000 (PLL).

Enzyme Linked Immunosorbent Assay (ELISA). The wells of a 96-well Nunc maxisorb microtiter plate were coated overnight at 4 °C with 100 µL of mouse IgG (10 µg/mL in phosphate-buffered saline (PBS), pH 7.4). The plate was emptied by inversion and washed (3×) with Tween 20-PBS (0.05% v/v) for 3 min at room temperature. Blocking of free adsorption sites was achieved by the addition of 100 µL of lysine (1 mg/mL in Tween-20/PBS 0.05% v/v) and incubation for 2 h at 37 °C. The plate was emptied and washed as before. Dilutions of samples and standards (positive controls) were prepared in PBS (the samples used were the ruthenium-labeled anti IgG conjugates, and standards were unconjugated anti IgG), and 100 µL of blank (PBS), sample, or standard was added and incubated at 37 °C for 1 h. The plates were emptied and washed as before. A 100-µL sample of a 1/750 dilution of rabbit anti-goat IgG conjugated to horse radish peroxidase (HRP) was added to the wells and incubated for 2 h at room temperature. The plates were

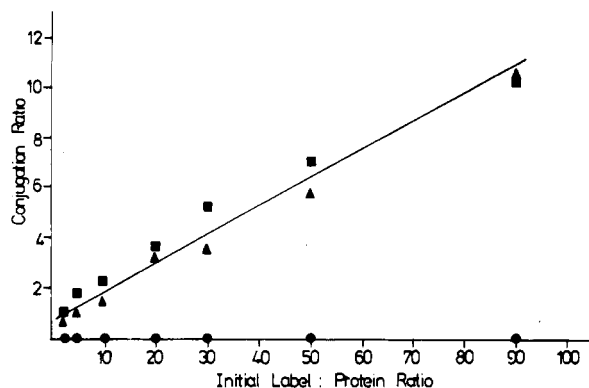


Figure 1. Conjugation profile obtained for the reaction of $[\text{Ru}(\text{bpy})_2(\text{NCSphen})]^{2+}$ with BSA. Conjugation carried out at (○) pH 4.3 (0.1 citrate buffer), (▲) pH 7.4 (0.1 M phosphate buffer), and (■) pH 9.6 (0.1 M carbonate buffer).

Table I. Electronic Data for the Complexes $[\text{Ru}(\text{L-L})_2(\text{NH}_2\text{phen})]^{2+}$ and $[\text{Ru}(\text{L-L})_2(\text{NCSphen})]^{2+}$

compound	maxima, nm	
	absorption ^a (log)	emission
$[\text{Ru}(\text{bpy})_2(\text{NH}_2\text{phen})]^{2+}$	454 (4.14)	609
$[\text{Ru}(\text{bpy})_2(\text{NCSphen})]^{2+}$	452 (4.17)	610
$[\text{Ru}(\text{phen})_2(\text{NH}_2\text{phen})]^{2+}$	452 (4.24)	604
$[\text{Ru}(\text{phen})_2(\text{NCSphen})]^{2+}$	447 (4.16)	608
$[\text{Ru}(\text{bpy})_2(\text{dc bpy})]^{2+}$	460	639
active ester of $[\text{Ru}(\text{bpy})_2(\text{dc bpy})]^{2+}$	458	642

^a Solvent, 0.1 M carbonate buffer (pH 9.6); extinction coefficient in $\text{L mol}^{-1} \text{cm}^{-1}$.

emptied and washed. The substrate was freshly prepared, 10 mg of *o*-phenylenediamine (OPD) in 0.5 M Na_2HPO_4 and 0.1 M citric acid (pH 5.0) and 5 μL of H_2O_2 were added to the substrate solution just prior to addition to the microtiter plate. The plate was incubated for 30 min at room temperature. A 50- μL portion of H_2SO_4 (20% v/v) was added to each well to stop the reaction. The absorbance of 414 nm was measured using a Titertek Twin-reader Plus ELISA reader.

RESULTS

Conjugation. The purity of the potential labels was checked by HPLC. The amino and carboxyl compounds were found to be pure while the isothiocyanate compounds were found to contain a small amount (<5%) of an impurity, probably the amino compound. However, for the purpose of conjugation, the small impurity in these compounds is not particularly important, since after conjugation the unbound reporter molecule is removed by extensive dialysis. In initial experiments the conjugation of the NCS labels was carried out at three different pH's, 4.3, 7.4, and 9.6. The conjugation ratios obtained are shown in Figure 1. While the conjugation ratios obtained at pH 7.4 and 9.6 were the same within experimental error, at pH 4.3 no conjugation was obtained. In further experiments a pH of 9.6 was used.

The absorption and emission data for the complexes are presented in Table I. Infrared spectra taken using pressed KBr disks confirmed the presence of the isothiocyanate moiety (24) with a band at 2056 cm^{-1} and 2051 cm^{-1} for $[\text{Ru}(\text{bpy})_2(\text{NCSphen})]^{2+}$ and $[\text{Ru}(\text{phen})_2(\text{NCSphen})]^{2+}$, respectively.

BSA, HSA, and OVA were conjugated to $[\text{Ru}(\text{L-L})_2(\text{NH}_2\text{phen})]^{2+}$ and $[\text{Ru}(\text{L-L})_2(\text{NCSphen})]^{2+}$. PLL was conjugated to $[\text{Ru}(\text{L-L})_2(\text{NCSphen})]^{2+}$. Goat anti-mouse IgG was conjugated to $[\text{Ru}(\text{bpy})_2(\text{NH}_2\text{phen})]^{2+}$ and to $[\text{Ru}(\text{bpy})_2(\text{NCSphen})]^{2+}$. In all cases the proteins or PLL

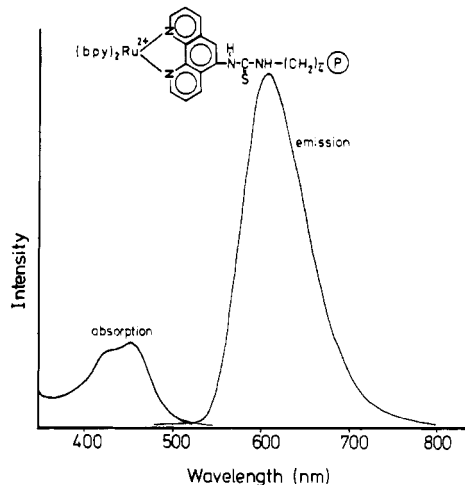


Figure 2. The absorption and emission spectra of (a) $[\text{Ru}(\text{bpy})_2(\text{NH}_2\text{phen})]^{2+}$ and (b) $[\text{Ru}(\text{bpy})_2(\text{NCSphen})]^{2+}$ bound to BSA in 0.1 M carbonate buffer (pH 9.6).

Table II. Assessment of the Extent of Conjugation of $[\text{Ru}(\text{L-L})_2(\text{NCSphen})]^{2+}$ to BSA, HSA, OVA, PLL, and Goat Anti-Mouse IgG

conjugate	F:P ^a	% label eff ^b	maxima, ^c nm	
			abs	em
$[\text{Ru}(\text{bpy})_2(\text{NCSphen})]^{2+}/\text{BSA}$	20–21	35	455	606
$[\text{Ru}(\text{bpy})_2(\text{NCSphen})]^{2+}/\text{HSA}$	19–22	35	454	608
$[\text{Ru}(\text{bpy})_2(\text{NCSphen})]^{2+}/\text{OVA}$	9–10	44	454	607
$[\text{Ru}(\text{bpy})_2(\text{NCSphen})]^{2+}/\text{PLL}$	20–24	3.0	454	608
$[\text{Ru}(\text{bpy})_2(\text{NCSphen})]^{2+}/\text{anti IgG}$	2–4		452	614
$[\text{Ru}(\text{phen})_2(\text{NCSphen})]^{2+}/\text{BSA}$	15–18	29	450	600
$[\text{Ru}(\text{phen})_2(\text{NCSphen})]^{2+}/\text{HSA}$	12–14	22	450	600
$[\text{Ru}(\text{phen})_2(\text{NCSphen})]^{2+}/\text{OVA}$	5–7	33	449	601
$[\text{Ru}(\text{phen})_2(\text{NCSphen})]^{2+}/\text{PLL}$	29–33	4.5	451	604
$[\text{Ru}(\text{bpy})_2(\text{dc bpy})]^{2+}/\text{BSA}$	12–16	24	467	657
$[\text{Ru}(\text{bpy})_2(\text{dc bpy})]^{2+}/\text{HSA}$	14–16	26	467	657
$[\text{Ru}(\text{bpy})_2(\text{dc bpy})]^{2+}/\text{OVA}$	5–6	30	465	655
$[\text{Ru}(\text{bpy})_2(\text{dc bpy})]^{2+}/\text{PLL}$	30–33	4.3	465	660

^a F:P = label to protein ratio after conjugation. ^b Ratio of bound to total amount of active groups on protein. ^c Absorption and emission maximum obtained in 0.1 M carbonate buffer (pH 9.6).

Table III. Assessment of the Extent of Conjugation of $[\text{Ru}(\text{L-L})_2(\text{NH}_2\text{phen})]^{2+}$ to BSA, HSA, OVA, and Goat Anti-Mouse IgG

conjugate	F:P ^a	maxima, ^b nm	
		abs	em
$[\text{Ru}(\text{bpy})_2(\text{NH}_2\text{phen})]^{2+}/\text{BSA}$	3–4	454	609
$[\text{Ru}(\text{bpy})_2(\text{NH}_2\text{phen})]^{2+}/\text{HSA}$	2–3	454	610
$[\text{Ru}(\text{bpy})_2(\text{NH}_2\text{phen})]^{2+}/\text{OVA}$	1–3	454	608
$[\text{Ru}(\text{bpy})_2(\text{NH}_2\text{phen})]^{2+}/\text{anti IgG}$	<1	450	610
$[\text{Ru}(\text{phen})_2(\text{NH}_2\text{phen})]^{2+}/\text{BSA}$	4–5	450	606
$[\text{Ru}(\text{phen})_2(\text{NH}_2\text{phen})]^{2+}/\text{HSA}$	3–4	448	610
$[\text{Ru}(\text{phen})_2(\text{NH}_2\text{phen})]^{2+}/\text{OVA}$	1–2	449	609

^a F:P = label to protein ratio after conjugation. ^b Absorption and emission maxima in 0.1 M carbonate buffer (pH 9.6).

was treated with a 50 molar excess of label. Some typical absorption and emission spectra are shown in Figure 2.

Protein concentration was measured using the Folin-Lowry method and absorbance of the protein solutions was determined at 750 nm (22). A standard curve for each protein/PLL was prepared simultaneously with the conjugate samples. The conjugation ratios were determined and are tabulated in Tables II and III.

Luminescence Lifetimes. The lifetimes of the excited states of the protein-bound ruthenium complexes and those of the free labels using the time-correlated single

Table IV. Emission Decay Lifetimes for the Free Labels and Bioconjugates

compound/conjugate	lifetime, ns		
	oxygenated	aerated	degassed
[Ru(bpy) ₂ (NH ₂ phen)] ²⁺	195	353	639
when bound to BSA	314 (73)	308 (55)	373 (55)
	807 (27)	915 (45)	1103 (45)
[Ru(bpy) ₂ (NCSphen)] ²⁺	191		856
when bound to BSA	350 (70)	487 (62)	587 (57)
	699 (30)	930 (38)	1130 (43)
when bound to PLL	197 (81)	251 (48)	209 (50)
	513 (19)	613 (52)	614 (50)
Ru(phen) ₂ (NH ₂ phen)] ²⁺	171	496	733
when bound to BSA	300 (70)	326 (69)	413 (51)
	827 (30)	1037 (31)	1341 (49)
[Ru(phen) ₂ (NCSphen)] ²⁺	188	664	1055
when bound to BSA	329 (67)	455 (49)	454 (49)
	793 (33)	1190 (51)	1286 (51)
when bound to PLL	163 (72)	237 (41)	250 (47) ^b
	486 (28)	736 (59)	866 (53)

^a Measured in 0.1 M carbonate buffer (pH 9.6); decay curves were analyzed using the function $I(t) = A + B_1e^{-t/\tau_1} + B_2e^{-t/\tau_2}$; values in parentheses are B_1 and B_2 given as percent. ^b This sample gave a poor correlation ($\chi^2 = 1.52$), triple-exponential analysis gives 71 (29), 479 (44), and 1014 (27).

photon counting technique are listed in Table IV. Examples of some fitted decay curves are given in Figure 3.

The excited state decay of both [Ru(phen)₂(NH₂phen)]²⁺ and [Ru(bpy)₂(NH₂phen)]²⁺ can be fitted well by single-exponential kinetics. The lifetime of the phen derivative is longer than that of its bipyridyl analogue, as has been reported for other phen and bpy complexes (25). The excited states of both are efficiently quenched by oxygen. Lifetimes of the [Ru(phen)₂(NCSphen)]²⁺ and [Ru(bpy)₂(NCSphen)]²⁺ intermediates were found to be significantly longer than for the NH₂ derivatives, possibly indicating a role for the NH₂ group in the deactivation of the excited-state complex. The lifetime of the NCS compounds is possibly affected by the presence of the earlier mentioned small impurity. This impurity is most likely the corresponding amino compound. As the lifetimes of the amino and the NCS compounds are similar, especially in oxygen-flushed and aerated solutions, this effect is not thought to be very important. In degassed solutions the values obtained for the NCS compound are possibly shortened somewhat, but this is not thought to be a major problem. The decay of the excited states has been measured in argon-flushed, aerated, and oxygen-flushed solutions.

None of the lifetimes of the excited states of the conjugates could be fitted to a single exponential (either in the presence or absence of oxygen). This is consistent with the metal complex center occupying a number of different sites. A satisfactory fit ($\chi^2 \leq 1.36$) is found for double-exponential analysis. However fitting to two exponentials is almost certainly an approximation, as it is likely that there are more than two sites.

DISCUSSION

The most likely site for the conjugation of isothiocyanate groups is the ϵ -amino group of lysine residues on the protein (23, 30–32). The pH behavior of the NCS conjugation is in agreement with binding through the protein amino groups, as a high pH will prohibit protonation of the amino groups (26). Quite a noticeable difference in conjugation ratio for the NCS labels is observed between the HSA or BSA and the OVA conjugates. This is as expected since both BSA and HSA contain about 13% lysine with 57 and 58 lysine residues, respec-

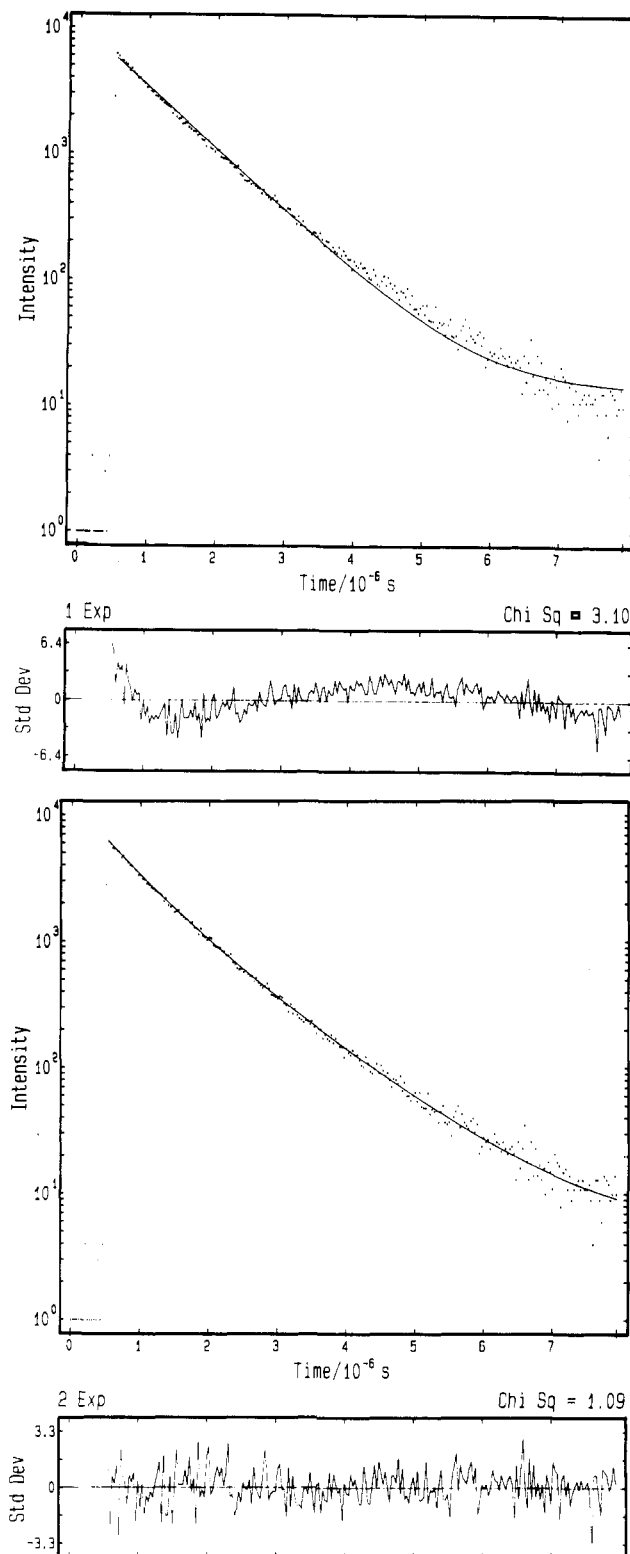


Figure 3. Emission decay profile for [Ru(bpy)₂(NCSphen)]²⁺ bound to BSA (a) fitted to a single-exponential fit and (b) fitted to a double-exponential fit.

tively (27), while OVA contains 6.3% lysine (28) or about 18 lysine residues. The conjugation ratios for the OVA conjugates are approximately half those obtained for the BSA/HSA conjugates. The same difference has been reported by Samuel et al. (29) for OVA-FITC and BSA-FITC conjugates. Their final conjugation ratios are lower but the initial reaction conditions had FITC: protein ratios of 5:1.

Assuming conjugation only occurs at the lysine residues and taking an average of the conjugation ratio in Tables

II or III gives labeling efficiencies of about 40% for $[\text{Ru}(\text{bpy})_2(\text{NCSphen})]^{2+}$ and of about 30% for $[\text{Ru}(\text{phen})_2(\text{NCSphen})]^{2+}$. For both labels higher labeling efficiencies for the OVA conjugates compared to the BSA/HSA conjugates were achieved. This may reflect differing degrees of accessibility of the label compounds for the different albumins. For OVA-FITC conjugates, a labeling efficiency of 44% has been reported where the initial fluorochrome:protein ratio was 5:1 (29). In this paper all conjugates were prepared using initial fluorochrome:protein ratios of 50:1. The similar efficiencies observed for the labels reported here may indicate that there is only limited accessibility of the label to the lysine moieties due to the structural conformation of the albumin. The results obtained also suggest that access may indeed differ between albumins and other proteins. Steric hindrance due to the size and structure of the label molecule as well as the proximity of lysine residues to each other probably also plays a role in determining how much label may be attached to the protein. Table II also includes conjugation ratios obtained with the active ester of $[\text{Ru}(\text{bpy})_2(\text{dcbpy})]^{2+}$, a compound described by Bard (7). This label also binds to the ϵ -amino group of the lysine residues on the albumin.

The conjugation ratios and labeling efficiencies calculated for these conjugates are quite similar to those for the isothiocyanate compounds.

Assuming there are about 750 lysine residues per molecule in the PLL used (molecular weight is 109 000), and averaging the conjugation ratios as before, labeling efficiencies of between 3 and 5% were achieved. With the label to polymer ratio of 50:1 used in the conjugation, the highest efficiency possible is 6.7%. The efficiency observed is therefore very good. The fact that a lower than maximum loading is obtained might suggest that steric hindrance may play a role in the number of label molecules which can bind to the polymer, or that side reactions occur.

The much lower proportion of carbohydrate moieties compared to lysine residues on the protein molecules is clearly reflected in the conjugation ratios obtained for the albumins which were bound to the $[\text{Ru}(\text{L-L})_2(\text{NH}_2\text{phen})]^{2+}$ compounds, with slightly higher ratios obtained for the higher molecular weight albumins. About 1–5 label molecules per albumin molecule were determined.

Goat anti-mouse IgG was conjugated through its lysine residues to $[\text{Ru}(\text{bpy})_2(\text{NCSphen})]^{2+}$ and through its carbohydrate moiety to $[\text{Ru}(\text{bpy})_2(\text{NH}_2\text{phen})]^{2+}$. Conjugation ratios for the isothiocyanate conjugate were determined to be about 2–4 label molecules per anti IgG molecule. Generally for immunoglobulin conjugation 1–4 molecules of FITC per IgG is recommended for tissue-staining procedures and higher ratios lead to nonspecific staining (33, 34). Higher ratios could also lead to loss of immunological activity (23). For conjugation ratios of 4–7 FITC molecules per IgG molecule, initial ratios are usually between 5:1 and 25:1 (33). Up to 8.5 molecules of rhodium isothiocyanate complex were incorporated into human IgG (35). On the basis of these results the ratios reported in this paper are somewhat lower than what may be expected, especially since quite a large initial molar excess of the ruthenium isothiocyanate complex was used (50:1). This again may reflect the limited accessibility of the binding sites on the proteins. Anti IgG conjugates were also prepared using initial ratios of 100:1 and 200:1 and gave the same conjugation ratio as the 50:1 reaction.

Periodate oxidation of the goat anti-mouse IgG and conjugation to $[\text{Ru}(\text{bpy})_2(\text{NH}_2\text{phen})]^{2+}$ yielded a conjugation ratio of about 1. The average carbohydrate content

of IgGs is about 3% (21), so the low conjugation ratio is not surprising. Emission from the label can however be detected; see Table III.

Periodate oxidation of the carbohydrate moiety is of use where there is a possibility of loss of immunological activity due to conjugation through the amino groups which are located close to the antigen binding site (14).

The retention of immunological activity of the goat anti-mouse IgG after conjugation to the isothiocyanate and amino ruthenium compounds was investigated using ELISA. For all conjugates the immunological activity was found to be retained. Thus these ruthenium labels may have potential applications in immunoassay techniques. The use of the active ester of $[\text{Ru}(\text{bpy})_2(\text{dcbpy})]^{2+}$ in immunofluorescent techniques (7) and in time-resolved immunoassay techniques (8) has been reported. However, preliminary investigations into the use of the isothiocyanate complexes reported here in fluorescence microscopy techniques have not proved successful. Bright red emission was observed for the albumin conjugates where the conjugation ratio was quite high but not for the anti IgG conjugates. An attempt was made to prepare stained mouse spleen cells with the anti-mouse IgG isothiocyanate complex but no emission was observed under the microscope.

The extent of conjugation has been calculated assuming the molar extinction coefficient of protein bound ruthenium to be the same as that of the unbound ruthenium complexes. This is assumed generally for FITC conjugates, but it has been shown that the extinction coefficients are higher after binding to protein. If so, the extent of conjugation may be somewhat smaller than indicated (29).

The luminescence decay of the ruthenium complexes when conjugated could not be fitted to a single-exponential function, indicating that there must be more than one emitting site. This behavior was found for both BSA and PLL conjugates and for samples prepared via $[\text{Ru}(\text{L-L})_2(\text{NH}_2\text{phen})]^{2+}$ or $[\text{Ru}(\text{L-L})_2(\text{NCSphen})]^{2+}$. The decay data in most cases can be fitted well to a double-exponential function, although it is probable that the situation is more complex with a spectrum of sites being present, especially for the BSA samples.

In degassed solution, analysis of the data from the BSA conjugates reveals one decay which is substantially longer than that of the free label and another which is significantly shorter. A lengthening of the lifetime would be expected for molecules in a more hydrophobic environment, as deactivation due to interaction with water would be reduced. Such behavior is also found for ruthenium complexes bound to DNA (4, 5). The shortened lifetime of the other site is more difficult to explain. Deactivation due to interaction of two excited complexes can be discounted because of the low excitation intensity. Similarly quenching of the excited state by ground-state ruthenium complexes should not be efficient given the low Ru:amino acid ratio in each sample. It would therefore appear that quenching is due to interaction with the protein, possibly because of electron transfer between the excited state and certain amino acid moieties. In the case of PLL the lifetimes of the excited states are significantly shorter than for the BSA conjugates. This may be attributed to the tertiary structure of PLL providing fewer hydrophobic pockets for the complex, and a more open structure which allows easier access for water molecules. A more open structure for PLL, compared to BSA, is consistent with the oxygen-quenching data which reveal that the emitting sites are much better protected against deactivation by oxygen in BSA.

CONCLUDING REMARKS

We have shown that ruthenium compounds may be covalently linked through both the lysine and carbohydrate moieties on protein molecules. The absorption and emission maxima of the labels are not substantially altered; upon conjugation the emission lifetime is however markedly affected. In the case of immunoglobulin conjugation, immunological activity was preserved. Thus these compounds may have application in fluoroimmunoassay techniques.

ACKNOWLEDGMENT

Support from EOLAS, the Irish Board for Science and Technology, the Research and Postgraduate Studies Committee, Dublin City University, and the Childrens Leukemia Research Project are gratefully acknowledged. Johnson Matthey are thanked for a generous loan of ruthenium trichloride.

LITERATURE CITED

- (1) Soini, E., and Hemmila, I. (1979) Fluoroimmunoassay: Present status and key problems. *Clin. Chem.* 25, 353-361.
- (2) Smith, D. S., Al-Hakim, M. M. H., Landon, J. (1981) A review of fluoroimmunoassay and immunofluorimetric assay. *Annu. Clin. Biochem.* 18, 253-274.
- (3) O'Sullivan, M. J., Bridges, J. W., and Marks, V. (1979) Enzyme immunoassay: A review. *Annu. Clin. Biochem.* 6, 221-239.
- (4) Pyle, A. M., Rehmann, J. P., Meshoyrer, R., Kumar, C. V., Turro, N. J. and Barton, J. K. (1989) Mixed-ligand complexes of ruthenium(II): Factors governing binding of DNA. *J. Am. Chem. Soc.* 111, 3051-3058.
- (5) Tossi, A. B. and Kelly, J. M. (1989) A study of some polypyridylruthenium(II) complexes as DNA binders and photocleavage reagents. *Photochem. Photobiol.* 49, 545-556.
- (6) Bannwarth, W. and Schmidt, D. (1989) A simple specific labelling for oligonucleotides by bathophenanthroline Ru(II) complexes as non-radioactive label molecules. *Tetrahedron Lett.* 30, 1513-1516.
- (7) Bard, A. J. (1986) Luminescent metal chelate labels and means for detection. US Patent Application PCT/US85/02153.
- (8) Davidson, R. S. (1987) Transition metal complexes and method for time-resolved luminescence binding assay. Patent Application PCT Int. Appl. WO 87 04,523.
- (9) Chang, I.-Y., Gray, H. B. and Winkler, J. R. High-driving-force electron transfer in metalloproteins: Intramolecular oxidation of ferrocyclochrome c by Ru(2,2'-bpy)₂(im)(His-33)³⁺. *J. Am. Chem. Soc.* 113, 7056-7057.
- (10) Grover, N. and Thorp, H. H. (1991) Efficient Electrocatalytic and stoichiometric oxidative cleavage of DNA by oxoruthenium(IV). *J. Am. Chem. Soc.* 113, 7030-7031.
- (11) Haughland, R. P. (1989) *Molecular Probes. Handbook of fluorescent probes and research chemicals.* Molecular Probes, Inc., Eugene, OR.
- (12) Degols, G., Leonetti, J.-P., Gaynor, C., Lemaitre, M. and Lebleu, B. (1989) Antiviral activity and possible mechanisms of action of oligonucleotides-poly-L-lysine conjugates targeted to vesicular stomatitis virus mRNA and genomic RNA. *Nucleic Acids Res.* 17, 9341-9350.
- (13) Hurwitz, E., Stancovski, I., Wilchek, M., Shouval, D., Takahashi, H., Wands, J. R. and Sela, M. (1990) A conjugate of 5-fluorouridine-poly(L-lysine) and an antibody reactive with human colon carcinoma. *Bioconjugate Chem.* 1, 285-290.
- (14) O'Shannessy, D. J. and Quarles, R. H. (1987) Labeling of the oligosaccharide moieties of immunoglobulins. *J. Immunol. Methods* 99, 153-161.
- (15) O'Shannessy, D. J., Dobersen, M. J. and Quarles, R. H. (1984) A novel procedure for labeling immunoglobulins by conjugation to oligosaccharide moieties. *Immunology Lett.* 8, 273-277.
- (16) Sprintschnik, G., Sprintschnik, H. W., Kirsch, P. P. and Whitten, D. G. (1977) Preparation and Photochemical Reactivity of Surfactant Ruthenium(II) Complexes in Monolayer Assemblies and at Water-Solid Interfaces. *J. Am. Chem. Soc.* 99, 4947-4953.
- (17) Buchanan, B. E., Wang, R., Vos, J. G., Hage, R., Haasnoot, J. G., Reedijk, J. and Vos, J. G. (1990) Chromatographic separation and characterization of linkage isomers of the 3-(pyridin-2-yl)-1H-1,2,4-triazole complex of ruthenium(II) bis-(2,2'-bipyridyl). *Inorg. Chem.* 29, 3263-3265.
- (18) Ellis, C. D., Margerum, L. D., Murray, R. W. and Meyer, T. J. (1983) Oxidative and electropolymerization of polypyridyl complexes of ruthenium. *Inorg. Chem.* 22, 1283-1291.
- (19) Hage, R., Haasnoot, J. G., Nieuwenhuis, H. A., Reedijk, J., de Ridder, D. J. A. and Vos, J. G. (1990) Synthesis, X-ray structure and spectroscopic and electrochemical properties of novel heteronuclear ruthenium-osmium complexes with an asymmetric triazolate bridge. *J. Am. Chem. Soc.* 112, 9245-9251.
- (20) Tijssen, P. (1985) *Practice and Theory of Enzyme Immunoassays*, Elsevier, New York.
- (21) O'Shannessy, D. J. and Quarles, R. H. (1985) Specific conjugation reactions of the oligosaccharide moieties of immunoglobulins. *J. Appl. Biochem.* 7, 347-355.
- (22) Holme, D. J., and Peck, H. Eds., (1983) *Analytical Biochemistry*, Chapter 11, Longman, New York.
- (23) Ward, H. A., Fothergill, J. E. (1976) In *Fluorescent Protein Tracing* (R. C. Nairn, Ed.) Chapter 3, Churchill Livingstone, New York.
- (24) McKinney, R. M., Spillane, J. T. and Pearce, G. W. (1964) Determination of purity of fluorescein isothiocyanates. *Anal. Biochem.* 7, 74-86.
- (25) Juris, A., Balzani, V., Barigelletti, F., Campagna, S., Belser, P. and von Zelewsky, A. (1988) Ru(II) Polypyridine Complexes: Photophysics, Photochemistry, Electrochemistry and Chemiluminescence. *Coord. Chem. Rev.* 84, 85-277.
- (26) Mirzadeh, S., Brechbiel, M. W., Atcher, R. W. and Ganson, O. A. (1990) Radiometal labeling of immunoproteins: Covalent linkage of 2-(4-isothiocyanatobenzyl)diethylene triaminepentacetic acid. *Bioconjugate Chem.* 1, 59-65.
- (27) Fasman, G. D. Ed. (1976) *Handbook of Biochemistry and Molecular Biology. Proteins*, 3rd ed., Vol. 3, CRC Press, Cleveland, OH.
- (28) Long, C., Ed. (1961) *Biochemist's Handbook*. E. and F. N. Spon Ltd., London.
- (29) Samuel, D., Patt, R. J. and Abuknesha, R. A. (1988) A sensitive method of detecting proteins on dot and Western blots using a monoclonal antibody to FITC. *J. Immunol. Methods* 107, 217-224.
- (30) Smith, D. S., Hassan, H. and Nargessi, R. D. (1981) In *Modern Fluorescence Spectroscopy 3* (E. L. Wehry, Ed.) Chapter 4, Plenum Press, New York.
- (31) Bromer, W. W., Sheehan, S. K., Berns, A. W. and Arquilla, E. R. (1967) Preparation and properties of fluorescein-thiocarbamyl insulins. *Biochemistry* 6, 2378-2388.
- (32) Tietze, F., Mortimore, G. E. and Lomax, N. R. (1962) Preparation and properties of fluorescent insulin derivatives. *Biochim. Biophys. Acta (Amst.)* 59, 336-346.
- (33) The, T. H. and Feltkamp, T. E. W. (1970) Conjugation of fluorescein isothiocyanate to antibodies. I. Experiments on the conditions of conjugation. *Immunology* 18, 865-873.
- (34) Der-Balian, G. P., Kameda, N. and Rowley, G. L. (1988) Fluorescein labeling of Fab' while preserving single thiol. *Anal. Biochem.* 173, 59-63.
- (35) Pillai, M. R. A., John, C. S. and Troutner, D. E. (1990) Labeling of human-IgG with rhodium-105 using a new pentadentate bifunctional ligand. *Bioconjugate Chem.* 1, 191-197.

Registry No. [Ru(bpy)₂(NH₂phen)]²⁺, 84537-85-9; [Ru(bpy)₂(NCSphen)]²⁺, 141292-49-1; [Ru(phen)₂(NH₂phen)]²⁺, 141292-50-4; [Ru(phen)₂(NCSphen)]²⁺, 141292-51-5; [Ru(bpy)₂(dcbbpy)]²⁺, 65354-20-3; poly(L-lysine) homopolymer, 25104-18-1; poly(L-lysine) SRU, 38000-06-5.

Synthesis and Characterization of Singly Modified (Carboxyferrocenyl)cytochrome *c* Derivatives

Antonius C. F. Gorren,[†] Man Ling Chan, Brian R. Crouse, and Robert A. Scott*

Departments of Chemistry and Biochemistry and the Center for Metalloenzyme Studies, University of Georgia, Athens, Georgia 30602. Received February 5, 1992

Carbodiimide-activated coupling chemistry has been used to covalently attach 1,1'-dicarboxyferrocene (dcFc) to the ϵ -amine of surface lysine residues of horse heart cytochrome *c*. Conditions have been found that optimize the production of singly modified (dcFc)cytochrome *c* derivatives and the presence of one free carboxylate per modification site allows separation and purification of about 10 of these derivatives by cation-exchange chromatography. Reversed-phase HPLC tryptic peptide mapping techniques have been used to identify the attachment sites of eight pure (dcFc)cytochrome *c* derivatives (at lysines 7, 8, 13, 25, 60, 72, 73, and 100). Through-space distances from these lysines to the nearest heme edge span the 6–16 Å range and these derivatives should prove useful in exploring the distance dependence of long-range intramolecular electron transfer in cytochrome *c*.

INTRODUCTION

In recent years much research has been devoted to the fundamental mechanism of long-range biological electron transfer and to the dependence of the electron transfer rate on parameters like driving force or distance of separation of acceptor and donor sites (1–5). One method for varying the donor-acceptor distance in proteins is to attach a second redox center to amino acid side chains at different locations on the surface of a single-site redox protein. This approach was originally taken by Gray and Isied and their co-workers, who coupled $\text{Ru}(\text{NH}_3)_5$ to His-33 of horse heart cytochrome *c* (6–8). Similar derivatives have since been obtained for a number of other proteins as well (9–18). Alternatively, other metal complexes can be attached to different surface groups of cytochrome *c*. For example, recent efforts in this laboratory have generated cytochrome *c* derivatives with the cobalt cage complex $\text{Co}(\text{diAMsar})^1$ coupled to the carboxylates of several aspartic and glutamic acid residues (19, 20).

The presence of 19 lysine residues on horse heart cytochrome *c* suggests that covalent attachment strategies directed at lysine ϵ -amines may result in numerous derivatives with a range of probe-heme distances. Millett and co-workers generated a number of such derivatives with $[\text{Ru}(\text{bpy})_2(\text{dcbpy})]$ (bpy = 2,2'-bipyridine; H_2dcbpy = 4,4'-dicarboxy-2,2'-bipyridine) as the lysine-attached moiety (21, 22). We have recently attached $[\text{Ru}(\text{NH}_3)_5\text{-in}]^{2+}$ (inH = 4-carboxypyridine, isonicotinic acid) to cytochrome *c* lysines (20).

As part of our continuing effort to generate series of probe-labeled cytochrome *c* derivatives with which to study distance effects of biological electron transfer, we have

used a ferrocene derivative as a lysine-modifying reagent. Heller and co-workers have demonstrated that 1-ethyl-3-[3-(dimethylamino)propyl]carbodiimide (EDC) will activate the carboxyl group of carboxyferrocene toward nucleophilic attack by surface lysine ϵ -amines of glucose oxidase, generating derivatives with about 12 ferrocenes per protein molecule (23). We have chosen to use 1,1'-dicarboxyferrocene (dcFc) in a similar reaction to generate singly labeled cytochrome *c* derivatives. The presence of the negative charge from the second carboxylate allows the separation of a number of these (dcFc)cytochrome *c* derivatives from native cytochrome *c* and from one another.

EXPERIMENTAL PROCEDURES

Cytochrome *c* (Sigma type VI) was purified according to a literature method (24) and 1,1'-dicarboxyferrocene was synthesized according to literature methods (25–27). Anal. Calcd for $\text{C}_{12}\text{H}_{10}\text{O}_4\text{Fe}$: C, 52.59; H, 3.68. Found: C, 52.58; H, 3.71.

Coupling Reaction. 1,1'-Dicarboxyferrocene (dcFc) (3 mmol) was suspended in 9 mL water and the pH increased with concentrated NaOH to a value between 7.5 and 8.0, at which stage the dcFc dissolved. A cytochrome *c* solution (15 μmol in 6 mL of 100 mM potassium phosphate (KP_i) buffer, pH 7.0) was then added and the pH adjusted to 7.5. All subsequent steps were carried out in the dark. The reaction was started by the addition of solid EDC (0.3 mmol) and the mixture was stirred for 1 h at room temperature, followed by exhaustive ultrafiltration (Amicon YM 5 membrane).

Separation and Purification of (dcFc)cytochromes *c*. A crude separation was achieved on a $2.5 \times 70\text{-cm}$ column of S-Sepharose Fast Flow resin (Pharmacia/LKB), using a pH 8.0 elution buffer containing 4 mM NaP_i and 1 mM ascorbic acid and a linear gradient running from 0 to 200 mM NaCl in 1 L. Further purification of the derivatives was accomplished by FPLC on a HR 5/5 Mono S column with the same elution buffer and gradients in the range between 0 and 100 mM NaCl.

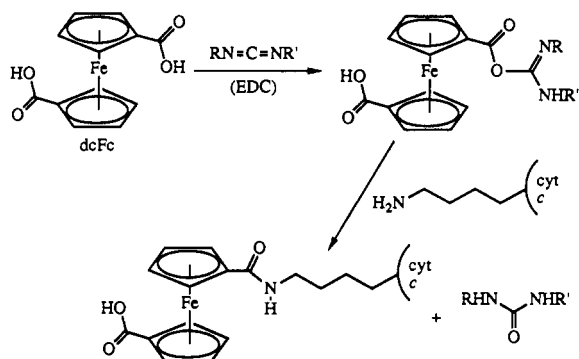
Methods. Absorbance spectra were measured on a Cary 219 UV/visiblespectrophotometer. Heme *c* concentrations of cytochrome *c* solutions were measured using $\epsilon_{410} = 1.05 \times 10^5 \text{ M}^{-1} \text{ cm}^{-1}$ (28). Electrochemical measurements were performed by differential pulse voltammetry (DPV) using an EG&G Princeton Applied Research Model 264A polarographic analyzer/stripping voltammeter (connected to

* Address all correspondence to Robert A. Scott, Department of Chemistry, University of Georgia, Cedar Drive, Athens, GA 30602-2556.

[†] Present address: Department of Microbiology and Enzymology, Delft University of Technology, Julianalaan 67, 2628 BC Delft, the Netherlands.

¹ Abbreviations used: bpy, 2,2'-bipyridine; $\text{Co}(\text{diAMsar})$, [1,8-diamino-3,6,10,13,16,19-hexaazabicyclo[6.6.6]icosanyl]cobalt dcbpy²⁻, 4,4'-dicarboxy-2,2'-bipyridine; dcFc, 1,1'-dicarboxyferrocene; DPV, differential pulse voltammetry; EDC, 1-ethyl-3-[3-(dimethylamino)propyl]carbodiimide; ICP/AES, inductively coupled plasma/atomic emission spectrometry; in-, isonicotinate (4-carboxylatopyridine); NHE, normal hydrogen electrode.

Scheme I



a MFE 815 M Plotmatic XY-recorder) with a Au working electrode, a Ag/AgCl reference electrode (both from Bio-Analytical Systems), and a Pt wire as the counter electrode. All electrochemical measurements were carried out in the presence of 100 mM NaCl, 50 mM NaP_i (pH 8.0), and 10 mM 4,4'-bipyridine. ICP/AES metal analyses were performed by the Institute of Ecology, University of Georgia. Tryptic digests and reversed-phase HPLC peptide maps were obtained as previously described (29) using a Waters 600E HPLC with a Delta-Pak C₁₈ column (300 Å, 5 µm; 3.9 mm × 15.0 cm). Tryptic peptide sequencing was performed by the Molecular Genetics Instrumentation Facility, University of Georgia.

Through-space distances from modification sites (lysine ε-amine nitrogens) to the nearest porphyrin ring carbon of the heme (and their standard deviations) were estimated by time-averaging such distances from structures calculated at each ps of a 100-ps molecular dynamics simulation of solvated horse heart cytochrome *c* (30) using the Amber 3 software package (31). These computations will be described in detail elsewhere (Conrad, D. W., Zhang, H., Stewart, D., Scott, R. A., manuscript in preparation).

RESULTS

Coupling Reaction and Product Separation. Reaction of cytochrome *c* with dcFc in the presence of EDC (Scheme I) resulted in a highly reproducible mixture of protein products that are separable by cation-exchange chromatography. Figure 1a shows the FPLC Mono-S elution pattern for a typical product mixture. Rechromatography on FPLC Mono-S (Figure 1b–g) allowed separation of a number of subfractions, suggesting the formation of at least 13 distinct (dcFc)cytochrome *c* derivatives. ICP/AES determination of total iron and spectrophotometric determination of heme *c* concentration demonstrated that fractions 2–6 each had a total iron to heme ratio of about 2, indicative of the presence of one dcFc moiety per cytochrome *c* molecule. Fraction 7 (Fe:heme, 1:1) was the unmodified protein, whereas fraction 1 (not shown; Fe:heme, 12:1) eluted before the start of the gradient and consisted of a mixture of free dcFc and cytochrome *c* that had incorporated two or more ferrocenes.

The ratio of modified to unmodified cytochrome *c* varied with reactant concentrations. When EDC or dcFc was omitted from the reaction mixture, no modification was observed. The reaction conditions employed in Figure 1 (cyt *c*:EDC:dcFc, 1:20:200; 1 mM cyt *c*) were chosen to minimize the formation of multiply modified derivatives. Increasing the EDC and dcFc concentrations (cyt *c*:EDC:dcFc, 1:30:300) resulted in formation of more singly modified protein but also produced significant amounts of doubly modified protein. The reaction pH (7.5) was chosen at about the higher of the pK_a values of the dcFc

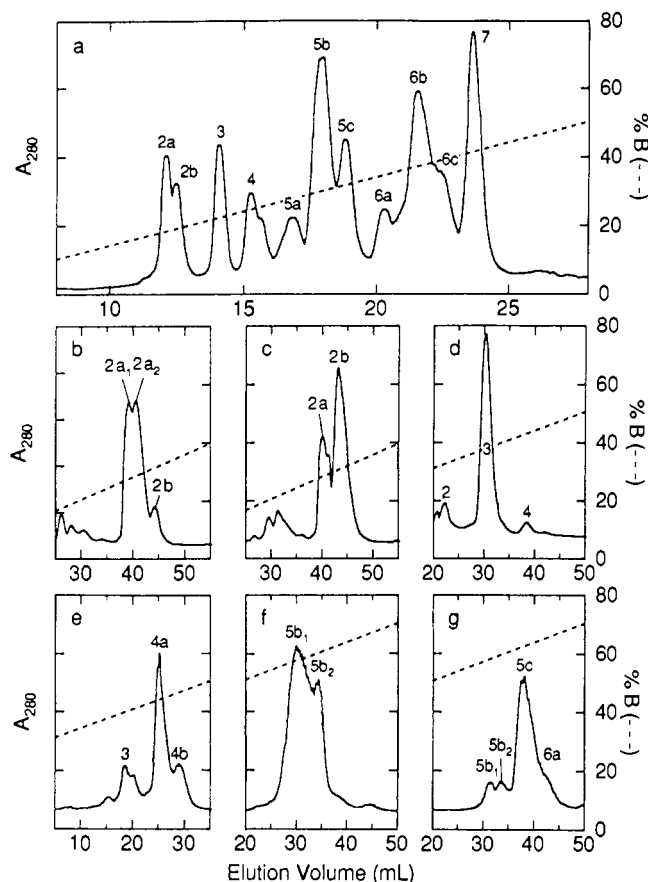


Figure 1. Cation-exchange separation of the (dcFc)cytochrome *c* derivatives. (a) Separation of the crude reaction mixture on a Pharmacia LKB FPLC HR 5/5 Mono-S column. In all cases, buffer A is 4 mM NaP_i, pH 8.0, with 1 mM ascorbic acid, and buffer B is buffer A plus 100 mM NaCl. All flow rates were 1.0 mL min⁻¹. Rechromatographic purifications of subfractions under the same conditions are shown for fractions 2a (b), 2b (c), 3 (d), 4 (e), 5b (f), and 5c (g).

carboxylate groups (6.5 and 7.6 (32)). Variation of the reaction pH between 7.3 (at lower values the solubility of dcFc in water decreases rapidly) and 8.0 did not appreciably change the overall yield but did change the relative proportions of fractions 2–6.

Chromatographic separation was performed at pH 8.0 to ensure that the free carboxylate group of the bound dcFc was deprotonated. This improved the separation of the modified derivatives, presumably owing to the larger change in charge distribution. During the incubation with dcFc, the cytochrome *c* heme became *partly* reduced, significantly complicating the separation and identification of modified derivatives. For this reason, ascorbic acid was added to the elution buffer to keep the derivatives fully reduced. It is remarkable that, although the extent to which cytochrome *c* was reduced during the coupling reaction varied from one experiment to another, the *relative* degree of reduction of the different fractions followed a regular pattern, always systematically decreasing with increasing fraction number.

It is essential that the (dcFc)cytochrome *c* derivatives be kept in the dark. When two samples of product mixture were stored overnight at 4 °C, one in the dark and one in room light, FPLC of the former resulted in the usual elution pattern, whereas the elution profile of the latter was completely different, indicating that exposure to light caused the derivatives to decompose.

Differential pulse voltammetry of the (dcFc)cytochrome *c* derivatives showed oxidation waves for both the cy-

Table I. Assignment of Attachment Site for Purified (dcFc)cytochrome *c* Fractions of Figure 1

FPLC elution fraction	estimated % purity	fragments missing from tryptic map ^a	sequence of modified tryptic fragment	modification site	corresponding fraction no. from refs 21, 22	estimated heme-Lys N ₁ distance (Å) ^b
2a ₁	≥90	T3, T4	IFVQX: T3	Lys 13	2B	6.2 ± 0.6
3	100	T11, T11', T12', T10/11, T10/11'		Lys 72	3A	10.2 ± 0.9
4a	100	T3		Lys 8	3B	14.8 ± 0.7
4b	80	T12, T12', T11', T10/11'		Lys 73	—	14.7 ± 0.6
5b ₁	85		GXX: T2'	Lys 7	4'	12.9 ± 0.5
5c	100		GGXHL: T5/6	Lys 25	4A	14.0 ± 0.7
6a	100		XATNE: T18'	Lys 100	6AB	14.8 ± 0.6
6b ₁	100	T10, T11, T11', T10/11, T10/11'		Lys 60	5B	15.5 ± 0.5

^a Horse heart cytochrome *c* tryptic fragments are named as follows: T1, (1–5); T2, (6–7); T2', (6–8); T3, (9–13); T4, (14–22); T5, (23–25); T6, (26–27); T7, (28–38); T7', (28–39); T8, (40–53); T9, (54–55); T10, (56–60); T11, (61–72); T11', (61–73); T12, (74–79); T12', (73–79); T13, (80–86); T14, (87–88); T15, (89–91); T16, (92–97); T17, (98–99); T18, (101–104); T18', (100–104). ^b Estimated by molecular dynamics simulations as described in Experimental Procedures.

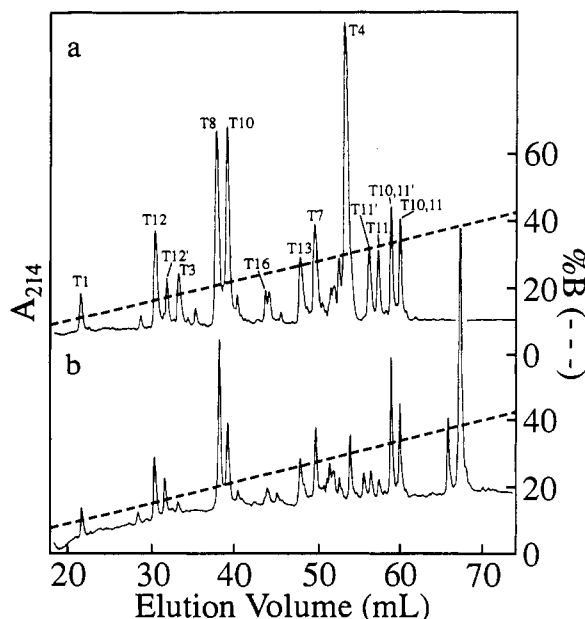


Figure 2. Reversed-phase HPLC tryptic maps of (a) native cytochrome *c* and (b) subfraction 2a₁ (Figure 1b). Note the absence of tryptic fragments T3 and T4 in b and the appearance of the major new peak at an elution volume of about 68 mL, which was identified by sequencing as the double-modified fragment T3-(dcFc)T4. (See footnote a of Table I for tryptic fragment assignments.)

tochrome *c* heme at 265 mV (vs NHE) and of the dcFc moiety at 760 mV. The latter value, which is 100 mV higher than that observed for free dcFc, was found at both pH 6.4 and 8.0. The optical absorbance spectra of the modified fractions were very similar to that of native cytochrome *c*, as might be expected considering the relatively low absorbance of free dcFc [λ_{\max} (ϵ): 446 nm ($238 \text{ M}^{-1} \text{ cm}^{-1}$), 306 nm ($1.04 \times 10^3 \text{ M}^{-1} \text{ cm}^{-1}$)].

Identification of Attachment Sites. To determine the attachment site of dcFc the purified derivatives were subjected to trypsin digestion followed by reversed-phase HPLC. Since dcFc-modified lysines are no longer recognized as cleavage sites by trypsin, modification generally results in the disappearance from the peptide map of the two fragments that are connected by the modified lysine, with the concomitant appearance of a new peak representing the modified double fragment. Since the HPLC elution positions of the tryptic fragments of native cytochrome *c* are known (20) (Figure 2a), the modification site could in most cases be determined from the tryptic map alone. An example is shown in Figure 2b, in which the reduction in intensity of peaks assigned to T3 and T4 and sequencing of the major new peak eluting after all native fragments allows the assignment of the modification

site as Lys-13. In derivatives for which modified lysines connected two fragments neither of which appeared in the native map, identification was accomplished by collecting and sequencing the new double fragment. The results for eight of the purest fractions are summarized in Table I.

DISCUSSION

Millett and co-workers recently obtained a number of singly modified cytochrome *c* derivatives that have [Ru(bpy)₂(dcbpy)] attached to single lysine residues (21, 22). Perhaps not surprisingly, the lysines that were modified (by dcbpy initially) in those experiments and the order of cation-exchange chromatographic elution of the resulting derivatives closely parallel the results of this study. The elution order seems to reflect the positions of the modified lysines projected along an axis that coincides with the calculated molecular dipole axis of cytochrome *c* (33). Since the positive end of the dipole is located near the exposed heme edge, modification nearest the heme causes the largest change in the molecular dipole, altering the cation-exchange mobility the most, predicting that the dcFc-heme distances should increase with increasing fraction number. As shown in Table I, this trend is approximately observed.

The incorporation of a second redox-active center at different positions in a single-site-redox protein is the most straightforward method to investigate the way in which distance affects long-range electron transfer in proteins. A complete understanding of the effects of donor-acceptor distance and intervening medium on electron transfer rates will require a large body of rate data on different proteins with different donor/acceptor combinations. The necessity of this is evident from the fact that thus far a clear but unexplained discrepancy exists between the rates found with cytochrome *c* and myoglobin on one hand (12), and the blue copper proteins on the other (14, 16, 17). Results obtained recently in this laboratory with cytochrome *c*, modified at carboxylate groups with Co(di-AMsar), showed an insignificant distance dependence (20). Determination of the intramolecular electron transfer rates from the heme to the carboxyferrocenyl group in the derivatives reported here, which have estimated dcFc-heme distances that range from about 6 to 16 Å (Table I), may shed more light on the relationship between electron-transfer rate and distance.

ACKNOWLEDGMENT

Dr. Greg Frauenhoff is acknowledged for the synthesis of 1,1'-dicarboxyferrocene. Hui Zhang and Dr. David Stewart are gratefully acknowledged for help with the molecular dynamics simulations. The University of Georgia

Computing and Networking Services provided Cyber 205 time for these computations. Gary Brayer is acknowledged for providing the atomic coordinates for horse heart cytochrome *c*. B.R.C. acknowledges summer support from the NSF Research Training Group Award to the Center for Metalloenzyme Studies (DIR 90-14281).

LITERATURE CITED

- (1) Marcus, R. A., and Sutin, N. (1985) Electron Transfers in Chemistry and Biology. *Biochim. Biophys. Acta* 811, 265-322.
- (2) Scott, R. A., Mauk, A. G., and Gray, H. B. (1985) Experimental Approaches to Studying Biological Electron Transfer. *J. Chem. Educ.* 62, 932-938.
- (3) McLendon, G. (1988) Long-Distance Electron Transfer in Proteins and Model Systems. *Acc. Chem. Res.* 21, 160-167.
- (4) Williams, R. J. P. (1989) Electron Transfer in Biology. *Biochem. Int.* 18, 475-499.
- (5) Gray, H. B., and Malmström, B. G. (1989) Long-Range Electron Transfer in Multisite Metalloproteins. *Biochemistry* 28, 7499-7505.
- (6) Yocom, K. M., Shelton, J. B., Shelton, J. R., Schroeder, W. A., Worosila, G., Isied, S. S., Bordignon, E., and Gray, H. B. (1982) Preparation and Characterization of a Pentaammineruthenium(III) Derivative of Horse Heart Ferricytochrome *c*. *Proc. Natl. Acad. Sci. U.S.A.* 79, 7052-7055.
- (7) Winkler, J. R., Nocera, D. G., Yocom, K. M., Bordignon, E., and Gray, H. B. (1982) Electron-Transfer Kinetics of Pentaammineruthenium(III)(histidine-33)-Ferricytochrome *c*. Measurement of the Rate of Intramolecular Electron Transfer between Redox Centers Separated by 15 Å in a Protein. *J. Am. Chem. Soc.* 104, 5798-5800.
- (8) Isied, S. S., Kuehn, C., and Worosila, G. (1984) Ruthenium-Modified Cytochrome *c*: Temperature Dependence of the Rate of Intramolecular Electron Transfer. *J. Am. Chem. Soc.* 106, 1722-1726.
- (9) Therien, M. J., Selman, M., Gray, H. B., Chang, I. J., and Winkler, J. R. (1990) Long-Range Electron Transfer in Ruthenium-Modified Cytochrome *c*: Evaluation of Porphyrin-Ruthenium Electronic Couplings in the *Candida krusei* and Horse Heart Proteins. *J. Am. Chem. Soc.* 112, 2420-2422.
- (10) Osvath, P., Salmon, G. A., and Sykes, A. G. (1988) Preparation, Characterization, and Intramolecular Rate Constant for Ru(II) → Fe(III) Electron Transfer in the Pentaammineruthenium Histidine Modified Cytochrome *c*₅₅₁ from *Pseudomonas stutzeri*. *J. Am. Chem. Soc.* 110, 7114-7118.
- (11) Crutchley, R. J., Ellis, W. R., and Gray, H. B. (1986) Long Range Electron Transfer in Pentaammineruthenium(His-48)-Myoglobin. *Frontiers in Bioinorganic Chemistry* (A. V. Xavier, Ed.) pp 679-693, VCH, Weinheim, Germany.
- (12) Axup, A. W., Albin, M., Mayo, S. L., Crutchley, R. J., and Gray, H. B. (1988) Distance Dependence of Photoinduced Long-Range Electron Transfer in Zinc/Ruthenium-Modified Myoglobins. *J. Am. Chem. Soc.* 110, 435-439.
- (13) Margalit, R., Kostic, N. M., Che, C.-M.; Blair, D. F., Chiang, H.-J., Pecht, I., Shelton, J. B., Shelton, J. R., Schroeder, W. A., and Gray, H. B. (1984) Preparation and Characterization of Pentaammineruthenium(histidine-83)azurin: Thermodynamics of Intramolecular Electron Transfer from Ruthenium to Copper. *Proc. Natl. Acad. Sci. U.S.A.* 81, 6554-6558.
- (14) Kostic, N. M., Margalit, R., Che, C.-M., and Gray, H. B. (1983) Kinetics of Long-Distance Ruthenium-to-Copper Electron Transfer in [Pentaammineruthenium histidine-83]azurin. *J. Am. Chem. Soc.* 105, 7765-7767.
- (15) Farver, O., and Pecht, I. (1989) Preparation and Characterization of a Ruthenium Labeled *Rhus* Stellacyanin. *FEBS Lett.* 244, 376-378.
- (16) Farver, O., and Pecht, I. (1989) Long-Range Intramolecular Electron Transfer in *Rhus vernicifera* Stellacyanin: A Pulse Radiolysis Study. *FEBS Lett.* 244, 379-382.
- (17) Jackman, M. P., McGinnis, J., Powls, R., Salmon, G. A., and Sykes, A. G. (1988) Preparation and Characterization of Two His-59 Ruthenium-Modified Algal Plastocyanins and an Unusually Small Rate Constant for Ruthenium(II) → Copper(II) Intramolecular Electron Transfer over ~12 Å. *J. Am. Chem. Soc.* 110, 5880-5887.
- (18) Jackman, M. P., Lim, M.-C., Salmon, G. A., and Sykes, A. G. (1988) Preparation of a Penta-ammineruthenium(III) Derivative of *Chromatium vinosum* HiPIP and the Kinetics of Intramolecular Electron Transfer. *J. Chem. Soc., Chem. Commun.* 179-180.
- (19) Conrad, D. W., and Scott, R. A. (1989) Long-Range Electron Transfer in a Cytochrome *c* Derivative Containing a Covalently Attached Cobalt-Cage Complex. *J. Am. Chem. Soc.* 111, 3461-3463.
- (20) Scott, R. A., Conrad, D. W., Eidsness, M. K., Gorren, A. C., and Wallin, S. A. (1990) Long-Range Electron Transfer in Cytochrome *c* Derivatives with Covalently Attached Probe Complexes. *Metal Ions in Biological Systems* (H. Sigel, and A. Sigel, Eds.) Vol. 27, pp 199-222, Marcel Dekker, New York.
- (21) Pan, L. P., Durham, B., Wolinska, J., and Millett, F. (1988) Preparation and Characterization of Singly Labeled Ruthenium Polypyridine Cytochrome *c* Derivatives. *Biochemistry* 27, 7180-7184.
- (22) Durham, B., Pan, L. P., Long, J. E., and Millett, F. (1989) Photoinduced Electron-Transfer Kinetics of Singly Labeled Ruthenium Bis(bipyridine) Dicarboxybipyridine Cytochrome *c* Derivatives. *Biochemistry* 28, 8659-8665.
- (23) Degani, Y., and Heller, A. (1987) Direct Electrical Communication between Chemically Modified Enzymes and Metal Electrodes. 1. Electron Transfer from Glucose Oxidase to Metal Electrodes via Electron Relays, Bound Covalently to the Enzyme. *J. Phys. Chem.* 91, 1285-1289.
- (24) Brautigan, D. L., Ferguson-Miller, S., and Margolias, E. (1978) Mitochondrial Cytochrome *c*: Preparation and Activity of Native and Chemically Modified Cytochromes *c*. *Methods Enzymol.* 53, 128-164.
- (25) Benkeser, R. A., Goggin, D., and Schroll, G. (1954) A Route to Monosubstituted Ferrocene Compounds. *J. Am. Chem. Soc.* 76, 4025-4026.
- (26) Mayo, D. W., Shaw, P. D., and Rausch, M. (1957) Effect of Tetrahydrofuran on the Lithiation of Ferrocene. *Chem. Ind.* 1388-1389.
- (27) Rausch, M., Vogel, M., and Rosenberg, H. (1957) Derivatives of Ferrocene. I. The Metalation of Ferrocene. *J. Org. Chem.* 22, 900-903.
- (28) Margolias, E., and Frohwirt, N. (1959) Spectrum of Horse-Heart Cytochrome *c*. *Biochem. J.* 71, 570-572.
- (29) Conrad, D. W. (1990) Long-Range Intramolecular Electron Transfer in Cobalt-Labeled Cytochrome *c*. Ph.D. Thesis, University of Illinois at Urbana-Champaign.
- (30) Bushnell, G. W., Louie, G. V., and Brayer, G. D. (1990) High-Resolution Three-Dimensional Structure of Horse Heart Cytochrome *c*. *J. Mol. Biol.* 214, 585-595.
- (31) Weiner, S. J., Kollman, P. A., Nguyen, D. T., and Case, D. A. (1986) An All Atom Force Field for Simulations of Proteins and Nucleic Acids. *J. Comput. Chem.* 7, 230-252.
- (32) Woodward, R. B., Rosenblum, M., and Whiting, M. C. (1952) A New Aromatic System. *J. Am. Chem. Soc.* 74, 3458-3459.
- (33) Koppenol, W. H., and Margolias, E. (1982) The Asymmetric Distribution of Charges on the Surface of Horse Cytochrome *c*. Functional Implications. *J. Biol. Chem.* 257, 4426-4437.

Registry No. dcFc, 1293-87-4; cytochrome *c*, 9007-43-6; lysine, 56-87-1.

Preparation of Micelle-Forming Polymer-Drug Conjugates

Masayuki Yokoyama,* Glenn S. Kwon, Teruo Okano, Yasuhisa Sakurai, Takashi Seto,† and Kazunori Kataoka*‡

Institute of Biomedical Engineering, Tokyo Women's Medical College, Kawada-cho, 8-1, Shinjuku-ku, Tokyo 162, Japan, Nippon Kayaku Company, Ltd., Iwahana 269, Takasaki-shi, Gunma 370-12, Japan, and Department of Materials Science and Technology, Faculty of Industrial Science and Technology, Science University of Tokyo, Yamazaki 2641, Noda-shi, Chiba 278, Japan. Received February 13, 1992

Adriamycin, a hydrophobic anticancer drug, was conjugated with poly(ethylene oxide)-poly(aspartic acid) block copolymers composed of various lengths of each block copolymer segment ranging from 1000 to 12 000 in molecular weight and from 10 to 80 units, respectively. Conjugation was achieved without precipitation by adjusting the ratio of adriamycin to aspartic acid residues of the block copolymer and the quantity of DMF used for the reaction. Thus obtained conjugates showed high water solubility irrespective of a large amount of the conjugated adriamycin. Furthermore, these conjugates were found to form micellar structures with a hydrophobic inner core and a hydrophilic outer shell. This micellar architecture may be utilized for effective drug targeting.

INTRODUCTION

Drug targeting using drug carriers is a very attractive "target" both for basic sciences and medical applications. The ideal drug is expected to act only at the designated target site of the drug and not at the other sites and, consequently, to express specificity and high activity without toxic side effects. To realize this ideal drug-targeting system, several types of drug carriers (e.g., microspheres, liposomes, and polymeric carriers) have been investigated especially for anticancer drugs. However, successful practical applications have not yet been obtained mainly due to the nonselective scavenging by normal cells even in the case of monoclonal antibodies (1-4). It is expected that drug targeting by carriers cannot succeed without maintenance of their stable circulation in blood. For microspheres (5) and liposomes (6), nonspecific scavenging by the reticuloendothelial system is the main obstacle to effective drug targeting unless these microspheres and liposomes were appropriately modified (5, 7, 8). For polymeric carriers, low water solubility of drug-polymer conjugates often causes problems in their synthesis (9-11) and in their injection into the blood stream (12). Since most drugs have a hydrophobic character, conjugation of the drugs with a polymer easily leads to precipitation because of the high, localized concentration of hydrophobic drug molecules bound along the polymer chain.

The authors have been investigating polymeric micelles as an alternative drug-carrier system (13-15). An AB-type block copolymer composed of hydrophilic and hydrophobic components can form a micellar structure as a result of its amphiphilic character as illustrated in Figure 1. The hydrophobic drug-binding segment forms the hydrophobic core of the micelle, while the hydrophilic segment surrounds this core as a hydrated outer shell. With a core-shell structure, polymeric micelles may maintain their water solubility by inhibiting intermicellar aggregation of the hydrophobic cores irrespective of high hydrophobicity of the inner cores. That is, polymeric micelles can utilize the hydrophobicity of the drug-binding segment, which causes precipitation in conventional

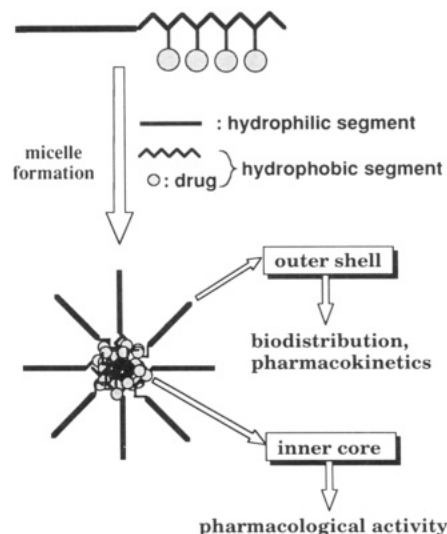


Figure 1. Concept of a micelle-forming polymeric drug.

polymeric drugs, to achieve a suitable structure for drug targeting. Furthermore, the functions which are required for drug carriers can be shared by the structurally separated segments of the block copolymer. The outer shell is responsible for interactions with the biocomponents such as proteins and cells. These interactions may determine pharmacokinetic behavior and biodistribution of drugs, therefore, in vivo delivery of drugs may be controlled by the outer shell independently of the inner core of the micelle which expresses pharmacological activities. This heterogeneous structure is more favorable to construct highly functionalized carrier systems than the conventional polymeric carrier systems.

Until now, few studies were done to focus on the application of polymeric micelles to drug carriers. Ringsdorf et al. reported an idea of application of polymeric micelles to sustained release of drugs (16, 17). Although Ringsdorf's group suggested micelle formation of their polymer-drug conjugate on the basis of the data from dye-solubilization and retardation in release rate of the bound drug, they did not confirm micelle formation by more direct methods. Kavanov et al. (18) reported an increase in in vivo activity of a drug associated with a polymeric amphiphile. Kavanov, however, did not distinguish the effect of formation of a polymer-drug conjugate on efficient

* Author to whom correspondence should be addressed.

† Nippon Kayaku Co., Ltd.

‡ Science University of Tokyo.

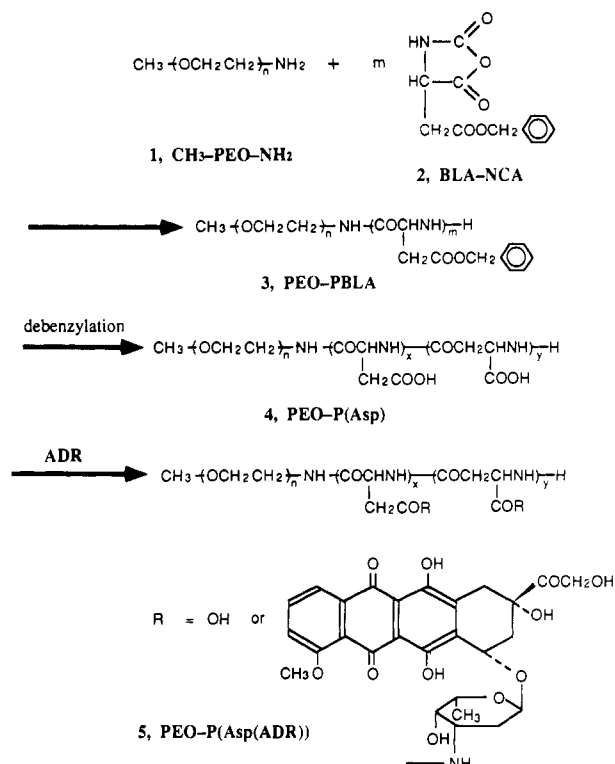


Figure 2. Synthesis of PEO-P(Asp(ADR)).

delivery to the target from that on an increase in permeability of biological membranes given by the polymeric amphiphile, and that study did not present evidence for micelle formation in a physiological condition. We have been studying polymeric micelles to realize a drug-carrier system stably existing under in vivo conditions for a long time period, and we directly confirmed micelle formation in vitro (13, 14) and in vivo (19) with adriamycin-conjugated poly(ethylene oxide)-poly(aspartic acid) block copolymer [PEO-P(Asp(ADR))¹] by dynamic laser light scattering and gel-filtration chromatography. Furthermore, this micelle-forming polymeric drug was shown to express significantly higher in vivo anticancer activity than free adriamycin (ADR) against P388 murine leukemia (14) and several solid tumors such as murine adenocarcinoma C 26 (19). The chemical structure of the micelle-forming polymeric drug synthesized by the authors previously (13, 20) is shown in Figure 2. One segment of the block copolymer is poly(ethylene oxide), which becomes the outer shell of the micelle, and the other segment is poly(aspartic acid), which becomes the inner core after binding a hydrophobic anticancer drug, ADR.

This paper describes preparations of various compositions of this micelle-forming polymeric anticancer drug [PEO-P(Asp(ADR))] by changing chain lengths of both the polymer segments. Evidence for micelle formation of these PEO-P(Asp(ADR))s is presented.

EXPERIMENTAL PROCEDURES

Chemicals. Adriamycin hydrochloride (ADR·HCl) was purchased from Sanraku Inc., Yatsushiro, Japan. 1-Ethyl-

3-[3-(dimethylamino)propyl]carbodiimide (EDC) was purchased from Peptide Institute, Inc., Osaka, Japan. α -Methyl- ω -aminopoly(oxyethylene) (CH₃-PEO-NH₂, 1 in Figure 2) was purchased from Nippon Oil & Fats Co., Ltd., Kawasaki, Japan. β -Benzyl *N*-carboxy-L-aspartate anhydride (2) was purchased from Kokusan Chemical Works, Ltd., Tokyo, Japan. Other chemicals were of reagent grade and were used as purchased unless otherwise stated.

General Procedures. ¹H-NMR spectra were obtained in CDCl₃ (PEO-PBLA) or D₂O (PEO-P(Asp)) with a Varian Gemini-500 NMR instrument. HPLC was carried out using a JASCO HyPer LC-800 system (Tokyo, Japan) at a flow rate of 1.0 mL/min at 40 °C with a Shodex OHPak KB-802.5 column and a KB-803 column in 0.1 M phosphate-buffered solution (pH 7.4) for PEO-P(Asp) and with an Asahipak GS-520 H column in 0.1 M phosphate-buffered solution (pH 7.4, containing 0.3 M NaCl) for PEO-P(Asp(ADR)). One hundred microliter samples were injected into the columns at a concentration of 0.2 wt % in distilled water for PEO-P(Asp) and 20 μ g ADR·HCl equiv/mL in phosphate-buffered saline (Na/Na, pH 7.4, 0.155 M) for PEO-P(Asp(ADR)). The detection of the polymers was performed by refractive index (with a JASCO 830-RI detector) for PEO-P(Asp) or absorption at 485 nm (with a JASCO 870-UV detector) for PEO-P(Asp(ADR)). Laser scattering measurements on the conjugate solutions were carried out using a Photol dynamic laser scattering spectrometer DLS-700 (Otsuka Electronics Co. Ltd., Tokyo, Japan) with an argon laser beam at a concentration of 20 μ g ADR·HCl equiv/mL in phosphate-buffered saline (Na/Na, pH 7.4, 0.155 M) at 25 °C, and the values are expressed in weight fraction and weight average.

The synthetic route of PEO-P(Asp(ADR)) is shown in Figure 2. The procedure was based on the previously reported one (14) with slight modifications.

Abbreviations used for block copolymers were based on molecular weight of poly(ethylene oxide) (PEO) chain and polymerization degree of BLA (or Asp) units; for example, 1-10 means a block copolymer composed of a PEO chain of MW = 1000 and a PLBA or P(Asp) chain which has 10 units of BLA (or Asp).

Synthesis of Poly(ethylene oxide)-Poly(β -benzyl L-aspartate) Block Copolymer (PEO-PBLA). β -Benzyl *N*-carboxy-L-aspartate anhydride (BLA-NCA, 2) was dissolved in doubly distilled *N,N*-dimethylformamide (DMF), followed by an addition of distilled chloroform. α -Methyl- ω -aminopoly(oxyethylene) (CH₃-PEG-NH₂, 1) was dissolved in distilled chloroform and added to the solution of 2. Quantities of the solvents in the reaction mixture were adjusted to 1.5 mL of DMF and 15 mL of chloroform per 1 g of BLA-NCA. The reaction mixture was stirred at 35 °C in a stream of dry nitrogen until BLA-NCA disappeared by the detection of characteristic peaks (1850 and 1790 cm⁻¹) in an IR spectrum. Then, the reaction mixture was poured into a 10-fold volume of diethyl ether at 0 °C, and a precipitate was collected by filtration and washed with diethyl ether, followed by drying in vacuo.

Synthesis of Poly(ethylene oxide)-Poly(aspartic acid) Block Copolymer (PEO-P(Asp)). Three-fold equivalents of sodium hydroxide to benzyl groups of the block copolymer was added to PEO-PBLA with 0.5 N NaOH aqueous solution. The reaction mixture was vigorously stirred at room temperature. When the reaction mixture clarified, the solution was neutralized with acetic acid, followed by dialysis against distilled water using a Spectrapor 6 dialysis membrane (molecular weight cutoff = 1000) until low molecular weight contaminants such as acetic acid could not be detected by ¹H-NMR measure-

¹ Abbreviations used: EDC, 1-ethyl-3-[3-(dimethylamino)propyl]carbodiimide; ADR, adriamycin; ADR·HCl, adriamycin hydrochloride; Asp, aspartic acid; BLA-NCA, β -benzyl *N*-carboxy-L-aspartate anhydride; PEO, poly(ethylene oxide); PBLA, poly(β -benzyl L-aspartate); P(Asp), poly(aspartic acid); PEO-PBLA, poly(ethylene oxide)-poly(β -benzyl L-aspartate) block copolymer; PEO-P(Asp), poly(ethylene oxide)-poly(aspartic acid) block copolymer; PEO-P(Asp(ADR)), adriamycin-conjugated poly(ethylene oxide)-poly(aspartic acid) block copolymer.

Table I. Synthesis of PEO-PBLA

run	feed composition		reaction time (h)	yield (g) [%] ^b	BLA units ^c
	MW of PEO chain	MeO-PEO-NH ₂ (g)			
1-10 ^a	1000	2.01	14.0	5.31 [86.5]	10.4
1-20	1000	1.51	17.5	6.52 [84.6]	22.6
1-40	1000	0.50	26.0	4.18 [90.9]	40.0
1-80	1000	0.25	27.5	3.95 [90.8]	73.3
2-10	2000	2.50	13.5	4.33 [85.4]	9.6
2-20	2000	2.50	14.5	7.01 [91.9]	19.4
2-40	2000	1.00	38.0	4.65 [91.2]	38.3
2-80	2000	0.50	38.5	4.15 [90.2]	72.0
5-10	5000	4.00	26.0	5.13 [91.0]	9.0
5-20	5000	7.01	21.5	11.73 [91.9]	19.3
5-40	5000	2.00	24.0	4.82 [91.2]	38.6
5-80	5000	1.21	26.0	4.74 [91.4]	75.3
12-20	12000	4.00	17.0	4.82 [89.8]	19.5
12-40	12000	4.00	20.5	6.08 [90.3]	38.0
12-80	12000	2.50	22.5	5.18 [87.6]	73.5

^a Abbreviation was used based on molecular weight of the PEO chain and polymerization degree of BLA units; for example, 1-10 means a block copolymer composed of the PEO chain of MW 1000 and the PBLA chain which has 10 units of BLA. ^b Percent yield was calculated with the weight of (CH₃-PEO-NH₂ + BLA-NCA × 0.823) as 100%. ^c Determined by ¹H NMR using methylene proton (OCH₂CH₂, 3.7 ppm) of the PEO chain and benzyl proton (CH₂C₆H₅, 5.1 ppm) of the PBLA chain.

ment. Then, poly(ethylene oxide)-poly(aspartic acid) block copolymer [PEO-P(Asp), 4] was obtained by freeze-drying.

Binding of ADR to PEO-P(Asp). ADR-HCl was mixed with DMF, followed by an addition of 1.3 equiv of triethylamine (with 10 v/v % solution in DMF) with vigorous stirring at 0 °C. PEO-P(Asp) (4), dissolved in distilled water, and 1-ethyl-3-[3-(dimethylamino)propyl]-carbodiimide (EDC) were successively added to the solution of ADR. The reaction mixture was stirred at 0 °C for 4 h, followed by the second addition of EDC. Then, the reaction mixture was stirred for 15 h at room temperature. The resulting solution was dialyzed overnight against 0.1 M sodium acetate buffered solution (pH 4.5, using approximately 100-fold volume dialysate) using a Spectrapor 6 membrane (MW cutoff = 1000). It seems that this transfer from an environment in an organic solvent to aqueous medium induces micelle formation of the drug-block copolymer conjugates with a hydrophobic drug-binding inner core and hydrophilic PEO outer shell. For several samples listed in Table IV, the resulting solution was further purified by ultrafiltration using a Minitan ultrafiltration system (Japan Millipore Ltd.) and Amicon ultrafiltration cells Model 8050 and 8200 (Grace). The content of ADR in the conjugate [PEO-P(Asp(ADR)), 5] was determined by measuring absorbance at 485 nm in DMF on the assumption that ϵ_{485} of the ADR residue bound to the polymer was the same as that of free ADR.

RESULTS

Synthesis of PEO-PBLA. Fifteen compositions of PEO-PBLA were synthesized with combinations of four lengths of the PEO chains and four lengths of the BLA units as summarized in Table I. Polymerizations of BLA-NCA in all the runs had progressed homogeneously in the mixed solvent of DMF and chloroform (1:10), and they were found to complete within 38.5 h by confirming the disappearance of the characteristic peaks of BLA-NCA in IR spectra. All samples were obtained in high yields over 85%. The number of the BLA units in PEO-PBLA was determined by the peak ratio of methylene protons (OCH₂CH₂, 3.7 ppm) of the PEO chain and benzyl protons (CH₂C₆H₅, 5.1 ppm) of the PBLA chain in a ¹H-NMR spectrum measured in CDCl₃. These numbers agreed well with the theoretical values.

Synthesis of PEO-P(Asp). The reaction mixtures became homogeneous within 2 h after an addition of the NaOH solution for all the runs except 2-80. Successful

debenzylation was confirmed by ¹H-NMR spectroscopy in D₂O. No residual benzyl groups were detected in the obtained polymer samples, and the numbers of the Asp units in the PEO-P(Asp) chain determined by the peak ratio of methylene protons (3.7 ppm) of the PEO chain and methylene protons (2.8 ppm) of the P(Asp) chain were identical to the numbers of BLA units of the corresponding PEO-PBLA within experimental error of the NMR measurement. PEO-P(Asp) were obtained in high yields over 90% for most runs. Yields were found to exceed 100% for some runs. That was likely due to incorporated sodium as sodium salts in carboxyl groups of the P(Asp) chain, and due to some water that could not be removed even after lyophilization. It is known that α -amide bonds of the BLA units were transformed into β -amide bonds by alkaline hydrolysis to a considerable degree (21). The content of the β -amide bond was found to be 75 mol % among all the amide bonds in the P(Asp) chain of PEO-P(Asp) 5-20 by measuring a peak ratio of methine protons of α -amide (4.66 ppm) and β -amide (4.47 ppm) of a ¹H-NMR spectrum in D₂O at pD 9.2. For other samples, contents of the β -amide bond were not measured; however, these contents seem to be around 75 mol % independent of their compositions, since it was reported (23) that 75 mol % of the β -amide bond was also found in P(Asp) homopolymer obtained from PBLA homopolymer (degree of polymerization = 110) by an alkaline hydrolysis procedure.

The molecular weight distribution of PEO-P(Asp) was evaluated by gel-filtration chromatography as summarized in Table II. Two peaks were observed for block copolymers 1-10 and 2-10, while the other block copolymers possessed one peak in their chromatograms, as typified by PEO-P(Asp) 2-10, 2-20, and 2-40 in Figure 3. This heterogeneity is considered to result from an acceleration effect of NCA polymerization above a degree of polymerization of eight (22). It was reported (23) that elongation of γ -benzyl L-glutamate units in poly(γ -benzyl L-glutamate) chains composed of over about 8 units progressed more rapidly in dioxane than the polymer chains not reaching this polymerization degree. It is expected that such bimodal molecular weight distribution was obtained with a valley which corresponds to PEO-P(Asp) with about eight Asp units. For the block copolymers with 20, 40, and 80 Asp units, unimodal molecular weight distribution was obtained possibly because this acceleration effect could be negligible in high ratios of NCA/initiator. For block copolymer 5-10, the difference in the Asp unit number

Table II. Synthesis of PEO-P(Asp)

run	feed composition		reaction time (min)	yield (g) [%] ^b	Asp units ^c	elution volume ^d (mL)
	PEO-PBLA (g)	0.5 N NaOH solution (mL)				
1-10 ^a	1.76	35.0	53	1.21 [98.0]	9.5	14.6, 15.9
1-20	1.46	35.0	26	nd ^e [nd]	20.5	14.6
1-40	1.35	35.0	54	0.93 [113]	41.6	14.1
1-80	1.27	35.0	120	0.79 [105]	83.8	13.4
2-10	2.42	35.0	50	1.75 [92.4]	8.8	14.2, 15.6
2-20	1.80	35.0	20	1.34 [105]	18.8	14.1
2-40	1.51	35.0	70	1.11 [113]	39.5	13.5
2-80	1.36	35.0	180	f		
5-10	4.44	35.0	40	3.10 [79.1]	8.1	15.1
5-20	2.72	35.0	22	2.16 [98.7]	17.6	14.7
5-40	1.96	35.0	80	1.53 [107]	36.0	13.9
5-80	1.59	35.0	25	1.22 [115]	75.2	13.3
12-20	2.40	17.5	12	2.02 [94.5]	17.9	14.1
12-40	2.54	29.2	12	2.10 [101]	35.8	13.7
12-80	2.15	35.1	20	1.63 [100]	70.8	13.2

^a Abbreviation used was based on molecular weight of the PEO chain and polymerization degree of BLA units, in the same way as in Table I. ^b Percent yield was calculated with the theoretical weight of PEO-P(Asp) transformed from PEO-PBLA as 100%. ^c Determined by ¹H NMR using methylene proton (3.7 ppm) of the PEO chain and methylene proton (2.8 ppm) of the P(Asp) chain. ^d Gel-filtration chromatography with a Shodex OHpak KB-802.5 column and a KB-803 column in 0.1 M phosphate-buffered solution (pH 7.4). ^e nd: not determined. ^f The reaction mixture remained heterogeneous after 3 h of stirring.

Table III. Introduction of ADR to PEO-P(Asp)

PEO-P(Asp)	reaction ^a condition		status ^b after dialysis	PEO-P(Asp)	reaction ^a condition		status after dialysis
	ADR (mg)	DMF (mL)			ADR (mg)	DMF (mL)	
1-10	25.0	2.0	precipitation	2-20	25.0	2.0	precipitation
	12.5	8.0	precipitation	2-40	25.0	2.0	precipitation
1-20	25.0	2.0	precipitation		25.0	4.0	precipitation
	25.0	8.0	precipitation		25.0	8.0	opaque
	12.5	4.0	precipitation		12.5	4.0	homogenous
	12.5	8.0	opaque		12.5	8.0	homogenous
	6.3	16.0	homogenous	5-10	25.0	2.0	homogenous
1-40	25.0	2.0	precipitation	5-20	25.0	2.0	homogenous
	25.0	8.0	precipitation	5-40	25.0	2.0	opaque
	12.5	16.0	precipitation	5-80	25.0	2.0	precipitation
	6.3	16.0	homogenous		25.0	4.0	opaque
1-80	25.0	2.0	precipitation		12.5	2.0	homogenous
	25.0	16.0	precipitation		12.5	4.0	homogenous
	12.5	16.0	precipitation	12-20	25.0	2.0	homogenous
2-10	25.0	2.0	precipitation	12-40	25.0	2.0	homogenous
	25.0	4.0	opaque	12-80	25.0	2.0	homogenous
	25.0	8.0	homogenous		12.5	4.0	homogenous
	12.5	4.0	homogenous				
	12.5	8.0	homogenous				

^a Reaction conditions: triethylamine, 1.3 equiv to ADR; EDC, 13 μ L + 13 μ L; PEO-P(Asp), quantity containing 9.1×10^{-4} mol of Asp unit; distilled water, 200 μ L; reaction time, 4 h (0 °C) + 15 h (room temperature). 25.0 mg of ADR·HCl corresponds to a mol equiv (9.1×10^{-4} mol) of Asp units to PEO-P(Asp). ^b Status is shown with three words: precipitation, opaque, and homogenous.

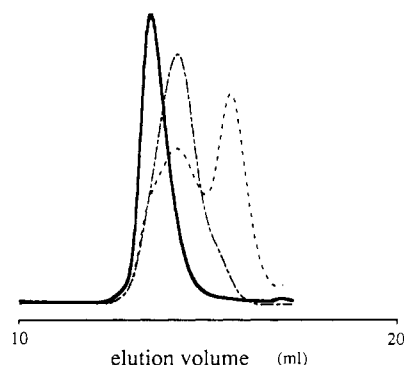


Figure 3. Gel-filtration chromatograms of PEO-P(Asp) 2-10 (---), 2-20 (····), and 2-40 (—): Column, Shodex OHpak KB-802.5 + KB-803; eluent, 0.1 M phosphate-buffered solution (pH 7.4); flow rate, 1.0 mL/min; temperature, 40 °C; detection, refractive index.

was expected to become negligible in its molecular weight distribution due to its relatively long PEO chain.

Binding of ADR to PEO-P(Asp). To obtain a water-soluble conjugate PEO-P(Asp(ADR)), several reaction conditions were investigated in the covalent attachment

of ADR to PEO-P(Asp) by changing quantities of ADR and DMF as summarized in Table III. The faculty of obtaining a water-soluble conjugate was revealed to be primarily dependent on the composition of PEO-P(Asp) as compared in the reaction conditions as follows: 25.0 mg of ADR·HCl, 7.8 μ L of triethylamine, PEO-P(Asp) containing 1 molequiv of aspartic acid (Asp) units to ADR, 200 μ L of distilled water, and 13 μ L + 13 μ L of EDC. Experiments carried out with high PEO content (e.g., 12-20) brought about homogeneous solutions after overnight dialysis against 0.1 M sodium acetate buffer solution (pH 4.5), while runs with low PEO content such as 1-20 resulted in precipitation. The precipitation behavior, however, was not only dependent on the composition but also on lengths of the polymer chains. Run 12-80, which brought about a homogeneous conjugate, contains smaller weight fraction (59.6%) of the PEO chain than run 2-10 (66.5%) having resulted in precipitation in these conditions. This fact suggests that longer PEO chains were able to inhibit precipitate formation more efficiently than shorter PEO chains. For runs that resulted in precipitation under these conditions, homogeneous solutions were obtained by decreasing the ADR molar ratio and increasing the

Table IV. Synthesis of PEO-P(Asp(ADR))

run ^a	ADR-HCl (mg)/ DMF (mL)	PEO-P(Asp) (mg)/ H ₂ O (mL)	ultrafiltration ^b	conjugated ADR ^c (mg) [% yield]	substitution ^d ratio (%)	diameter ^e (nm)
1-40	500/1280	480/16.0	A	110.9 [22.2]	12	nd/ ^f
2-10	700/224	829/11.2	B	509.6 [72.8]	44	nd/ ^f
2-40	700/224	400/11.2	B	404.0 [57.7]	30	21, 123
5-10	600/48	763/4.8	B	428.7 [71.5]	73	24, 131
5-80	600/96	375/9.6	A	398.4 [66.4]	46	36, 118
12-20	600/48	810/4.8	A	369.2 [61.5]	104	40
12-40	600/48	465/4.8	C	454.6 [77.4]	78	58
12-80	600/48	295/4.8	A	252.9 [42.2]	84	14, 91

^a Abbreviation used based on molecular weight of PEO chain and polymerization degree of Asp units, in the same way as with Table I.

^b Ultrafiltration procedure is abbreviated as follows: (A) with a Minitan system (Millipore) equipped with a membrane of molecular weight cutoff 100 000, followed by Amicon stirring cells equipped with a PM-30 membrane (Amicon; molecular weight cutoff 30 000), (B) with a Minitan system equipped with a membrane of molecular weight cutoff 10 000, followed by Amicon stirred cells equipped with a UK-10 membrane (Advantec, Tokyo, Japan; molecular weight cutoff 10 000), (C) with Amicon stirred cells equipped with a PM-30 membrane.

^c Measured by absorbance at 485 nm in DMF. ^d Percent molar substitution of ADR with respect to Asp residues of PEO-P(Asp). Calculation method is described in the text. ^e Weight average diameter of each peak is shown. ^f nd: not detected; diameter was not detected above 10 nm.

quantity of DMF. For 2-10 with ADR ratio of 1, solution status after the dialysis was changed from precipitation to homogeneity by increasing the quantity of DMF from 2.0 to 8.0 mL. Decreasing the molar ratio of ADR was also effective to prevent precipitation from occurring in the introduction reaction as shown by several examples such as 5-80.

According to the study of the reaction conditions in Table III, ADR was introduced to eight kinds of compositions of PEO-P(Asp) as summarized in Table IV. For all the eight runs, the reaction had proceeded homogeneously, and the reaction mixtures were homogeneous after the dialysis against 0.1 M sodium acetate buffer (pH 4.5) for 6 h. Then, the reaction mixtures were purified by repeated ultrafiltration with distilled water until the ADR concentration of the filtrate was reduced to less than $1/1000$ of the ADR concentration of the residual solution on ultrafiltration membranes. The amounts of the conjugated ADR in the polymeric drugs were determined by measuring the absorbance at 485 nm in DMF. The substitution ratios of the Asp units with ADR were calculated after lyophilization. The weight of the PEO-P(Asp) fraction in a dried PEO-P(Asp(ADR)) sample was obtained by subtracting the conjugated ADR weight from the total weight of the lyophilized sample. The substitution ratios were calculated on the assumption that the compositions of PEO-P(Asp) did not change during the conjugation reaction and the following purification procedures. These ratios are expressed as mole percents with respect to the aspartic acid (Asp) residues of the PEG-P(Asp) chain as summarized in Table IV. For all the runs except 1-40 and 2-40, higher ADR contents were obtained than the previously reported value (30 mol %) for 5-20 (14). A decrease in DMF quantity was found to contribute to obtaining conjugates with high ADR contents, since DMF quantity in the previous paper corresponded to 9.4 times that for 5-20 in Table III. For 12-20, a substitution ratio resulted in a value over 100%. It is considered that this value was reflected by an error in the ¹H-NMR measurement of PEO-P(Asp).

Micelle formation was confirmed by gel-filtration chromatography for all eight samples of PEO-P(Asp(ADR)) as typified by charts of 1-40, 2-10, 5-10, and 12-20 in Figure 4. A peak at the gel-exclusion volume (4.2 mL), which corresponds to a molecular weight of over 300 000 on the pullulan standard, was observed for all runs. This peak indicated the elution of the conjugates as polymeric micelles because the molecular weights of these conjugates were much smaller than 300 000. The elution profile was, however, dependent on the composition. For PEO-P(Asp(ADR)) 1-40, a small fraction appeared at the gel-exclusion volume, followed by a larger peak at 6.9 mL, which was

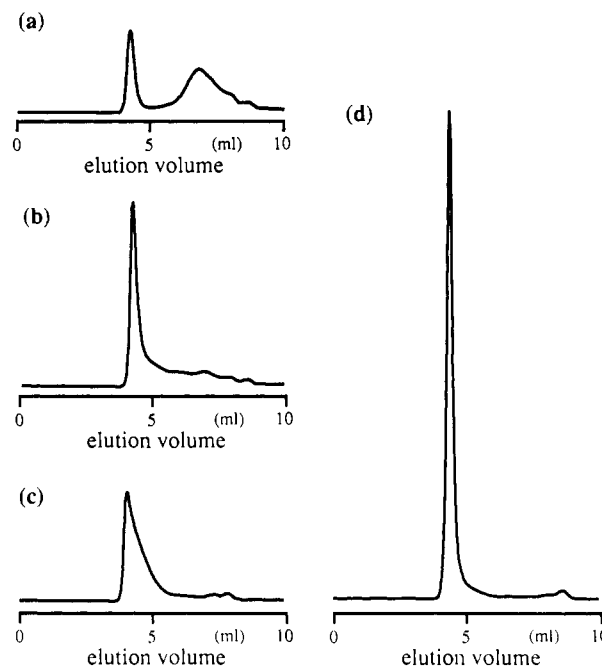


Figure 4. Gel-filtration chromatograms of PEO-P(Asp(ADR)) (a) 1-40, (b) 2-10, (c) 5-10, (d) 12-20: Column, Asahipak GS-520 H; eluent, 0.1 M phosphate-buffered solution (pH 7.4, containing 0.3 M NaCl); flow rate, 1.0 mL/min; temperature, 40 °C; detection, absorption at 485 nm.

considered a polymer fraction not forming a micellar structure. For PEO-P(Asp(ADR)) 2-10, a sharp peak at the gel-exclusion volume was accompanied by a small shoulder around 7 mL. PEO-P(Asp(ADR)) 5-10 gave a broader peak than the others. The other compositions were observed to show distinct micelle formation by a sharp peak at the gel-exclusion volume as typified by a chart of 12-20. From these facts, it is considered that longer chains are favorable in both the segments to form distinct micellar structures.

Micelle size was measured by dynamic laser light scattering. For 1-40 and 2-10, micelles of over 10 nm in diameter were not observed, possibly due to short chain lengths of the PEO segment. Unimodal diameter distribution was obtained only for 12-20 and 12-40, while the other composition brought about bimodal distribution as summarized in Table IV and shown in Figure 5. These micelles were revealed to be formed by noncovalent hydrophobic interaction since all the micelle peaks in the laser scattering measurements disappeared by an addition of 1 wt % of sodium dodecyl sulfate. Although diameters of the micelles were not determined only by the chain lengths of the conjugates, possibly because of variety in

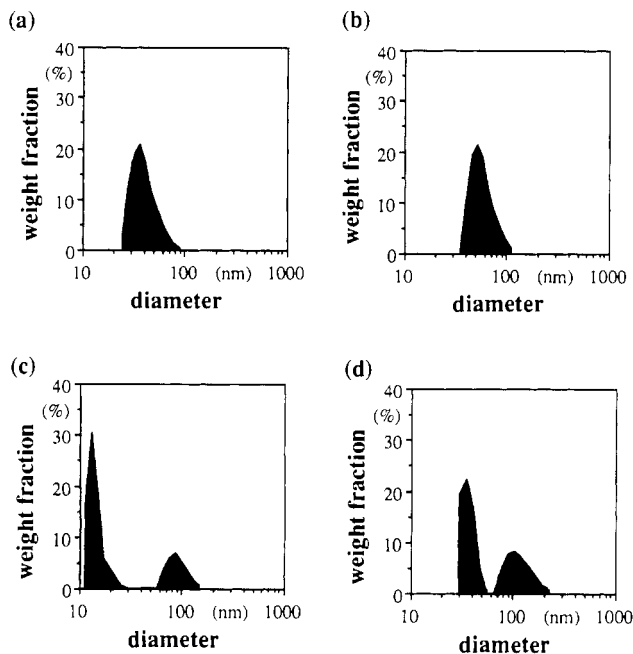


Figure 5. Diameter distribution of PEO-P(Asp(ADR)): (a) 12-20, (b) 12-40, (c) 12-80, (d) 5-80, measured with a dynamic laser light scattering spectrometer equipped with an argon laser beam at a concentration of 20 μ g ADR-HCl equiv/mL in phosphate-buffered saline (Na/Na, pH 7.4, 0.155 M) at 25 $^{\circ}$ C.

the aggregation numbers of the micelles, it was found that micelle-forming polymeric drugs with a range from approximately 10 to 100 nm in diameter were obtained with various compositions in the block copolymer.

It was found that all the runs in Table IV maintained water solubility irrespective of high loading of hydrophobic ADR residues to the block copolymer even after being concentrated to 20 mg ADR equiv/mL, and that they were able to be injected into tail vein of mice without sudden deaths caused by precipitation in the blood vessels. The results of *in vivo* anticancer activity of these conjugates will be reported elsewhere.

DISCUSSION

The conjugates of ADR and PEO-P(Asp) were successfully synthesized without precipitation for the four lengths in both the segments by changing the ratio of ADR to the Asp residues and the quantity of DMF. Although water-soluble conjugates were not obtained for four copolymers, 1-10, 1-80, 2-20, and 5-40, it is considered that ADR could be bound to PEO-P(Asp) block copolymer without precipitation for all the samples except 1-80 because ADR could be successfully bound to the block copolymer with a shorter P(Asp) chain by the reaction conditions which brought about a homogeneous conjugate for the block copolymer with a longer P(Asp) chain. For example, the conjugate 1-10 may be synthesized by the reaction conditions (6.3 mg of ADR and 16.0 mL of DMF) which brought about the water-soluble conjugate for 1-20. As a result, micelle-forming conjugates were obtained from PEO-P(Asp) containing from 17 wt % (1-40) to 85 wt % (12-20) of the PEO chain. Generally, the range of composition for block copolymers to form micellar structures is not so large. For one example, PEO-poly(styrene) block copolymer was reported to form micellar structures in distilled water of PEO weight content only from 61% to 80% (24). The wider range of PEO weight content for PEO-P(Asp(ADR)) than that for the PEO-poly(styrene) block copolymer is considered to result from the binding method of ADR to PEO-P(Asp) because the hydrophobic-hydrophilic balance of the conjugate can be adjusted to

form micellar structures by changing the ADR ratio to the Asp residues. Efficient targeting of the micelles can be optimized with this wide range of chain lengths of both segments.

As shown in Table IV, micelles with diameter of from approximately 10 to 100 nm were obtained with PEO-P(Asp(ADR)). This diameter range is very interesting for drug targeting because it was reported that some specially designed liposomes (7, 8) with diameter of about 100 nm circulated stably in blood for long time periods and that nanospheres (25) (microspheres below 1 μ m in diameter) could be utilized for drug targeting by intravenous injection. Furthermore, the architecture of polymeric micelles is very unique among all the drug-delivery systems because of their hydrated soft shells, and this architecture cannot be obtained in the other types of carrier systems. Therefore, polymeric micelles are expected to express their targeting behavior (e.g. biodistribution, interaction with cells, and permeation into tissues) differently from the conventional systems. The diameter of the polymeric micelles could be primarily controlled by the chain lengths mainly of PEO. Fine control of the micelle size, however, was not achieved, possibly because of various aggregation numbers of the micelles. Detailed physicochemical studies to describe the relationship between the composition of PEO-P(Asp(ADR)) and micelle size and stability are needed to design the polymeric micelle carrier for more efficient drug targeting.

High water solubility of the conjugates in Table IV proved an outstanding property of a micellar form for carrying hydrophobic drugs while maintaining high water solubility. For conventional polymeric carriers, several groups reported maximum mole percent substitution of side carboxyl groups of polymer chains by ADR or daunomycin (an ADR analogue): 5 mol % (10) and 10 mol % (26) for poly(glutamic acid), 8 mol % (27) for pyran copolymer, and 3 mol % (9) for poly[N-(2-hydroxypropyl)methacrylamide]. For PEO-P(Asp(ADR)), ADR was bound to the side carboxyl groups almost quantitatively as shown by 12-20. As compared in ADR weight percent in the conjugates, PEO-P(Asp(ADR)) also afforded much larger values (60% for 12-80) than those of the conventional polymer drugs: 17 wt % (10) and 26 wt % (26) for poly(glutamic acid), 35 wt % (27) for pyran copolymer, and 10 wt % (9) for poly[N-(2-hydroxypropyl)methacrylamide]. Furthermore, PEO-P(Asp(ADR)) containing many ADR residues did not cause a precipitate by the concentrating procedure or temperature change from 0 $^{\circ}$ C to room temperature, while a conventional polymer drug was reported to precipitate by temperature change at around room temperature (9). Such stable water solubility is expected to contribute to safe injection of the conjugate into the blood stream by inhibiting precipitation in the blood vessels. This excellent water solubility is considered to result from the core-shell structure of the micelle in which the outer shell can inhibit aggregation of the hydrophobic cores very efficiently. All these results pointed out that micellar forms are very suitable to design a hydrophobic drug-carrying system.

Although detailed physicochemical characterization of the micelles is indispensable to establish this new carrier system, a unique delivery system may be constructed with polymeric micelles. For polymeric micelles, factors to determine their pharmacokinetic behavior and biodistribution are the chemical characters of the outer shell and the size and stability of the micelles. These three factors are independent of drugs bound to the inner core. Therefore, drug delivery with polymeric micelles can be controlled drug-independently, while delivery of the conventional polymeric drug was affected by bound drug

because the bound drug faces outside to interact with bio-components. If a polymeric micelle is analyzed pharmacokinetically, many kinds of drugs can be applied to this polymeric micelle system by only adjusting the quantity of bound drug to correct the hydrophobic-hydrophilic balance of the conjugate for micelle formation. Therefore, this polymeric micelle drug-carrying system can be applied to many kinds of hydrophobic drugs.

This paper presented successful preparations of the block copolymer-drug conjugates PEO-P(Asp(ADR)) of various chain lengths in both the segments, and showed excellent water solubility of these conjugate irrespective of the large amount of bound ADR. This paper also showed micelle formation of these conjugates with diameters ranging from approximately 10 to 100 nm. These micelles can pass through filters with submicron pores, and therefore can be easily sterilized by a simple filtration procedure. This is another preferable pharmaceutical property of the polymeric micelles.

LITERATURE CITED

- (1) Uadia, P., Blair, A. H., and Ghose, T. (1984) Tumor and tissue distribution of a methotrexate-anti-EL4 immunoglobulin conjugate in EL4 lymphoma-bearing mice. *Cancer Res.* 44, 4263-4266.
- (2) Koizumi, M., Endo, K., Kunitatsu, M., Sakahara, H., Nakashima, T., Watanabe, Y., Saga, T., Konishi, J., Yamamuro, T., Hosoi, S., Toyama, S., Arano, Y., and Yokoyama, A. (1988) ⁶⁷Ga-labeled antibodies for immunoscintigraphy and evaluation of tumor targeting of drug-antibody conjugates in mice. *Cancer Res.* 48, 1189-1194.
- (3) Yang, H. M., and Reisfeld, R. (1988) Doxorubicin conjugated with a monoclonal antibody directed to a human melanoma-associated proteoglycan suppresses the growth of established tumor xenografts in nude mice. *Proc. Natl. Acad. Sci. U.S.A.* 85, 1189-1193.
- (4) Thédrez, P., Saccavini, J.-C., Nolibé, D., Simoen, J.-P., Guereau, D., Gustin, J. F., Kremer, M., and Chatal, J. F. (1989) Biodistribution of indium-111-labeled OC125 monoclonal antibody after intraperitoneal injection in nude mice intraperitoneal grafted with ovarian carcinoma. *Cancer Res.* 49, 3081-3086.
- (5) Davis, S. S., and Illum, L. (1986) Colloidal delivery systems—Opportunities and challenges. *Site-Specific Drug Delivery* (E. Tomlinson, and S. S. Davis, Ed.) pp 93-110, John Wiley & Sons Ltd., Lancing, Sussex, UK.
- (6) Gregoriadis, G., Senior, J., Wolff, B., and Kirby, C. (1984) Fate of liposomes in vivo: control leading to targeting. *Receptor-Mediated Targeting of Drugs* (G. Gregoriadis, G. Poste, J. Senior, and A. Trouet, Ed.) pp 243-266, Plenum Press, New York.
- (7) Allen, T. M., and Chonn, A. (1987) Large unilamellar liposomes with low uptake into the reticuloendothelial system. *FEBS Lett.* 223, 42-86.
- (8) Gabizon, A., and Papahadjopoulos, D. (1988) Liposome formulations with prolonged circulation time in blood and enhanced uptake by tumors. *Proc. Natl. Acad. Sci. U.S.A.* 85, 6949-6953.
- (9) Duncan, R., Kopeckova-Rejmanova, P., Strohm, J., Hume, I., Cable, H. C., Pohl, J., Lloyd, J. B., and Kopecek, J. (1987) Anticancer agents coupled to N-(2-hydroxypropyl)methacrylamide copolymers I. Evaluation of daunomycin and piro-mycin conjugates in vitro. *Br. J. Cancer* 55, 165-174.
- (10) Hoes, C. J. T., Potman, W., van Heeswijk, W. A. R., Mud, J., de Grooth, B. G., Grave, J., and Feijen, J. (1985) Optimization of macromolecular prodrugs of the antitumor antibiotic adriamycin. *J. Controlled Release* 2, 205-213.
- (11) Endo, N., Umemoto, N., Kato, Y., Takeda, Y., and Hara, T. (1987) A novel covalent modification of antibodies at their amino groups with retention of antigen-binding activity. *J. Immunol. Methods* 104, 253-258.
- (12) Zunino, F., Pratesi, G., and Micheloni, A. (1989) Poly(carboxylic acid) polymers as carriers for anthracyclines. *J. Controlled Release* 10, 65-73; Description was made in Table II.
- (13) Yokoyama, M., Inoue, S., Kataoka, K., Yui, N., Okano, T. (1989) Molecular design for missile drug: Synthesis of adriamycin conjugated with IgG using poly(ethylene glycol)-poly(aspartic acid) block copolymer as intermediate carrier. *Makromol. Chem.* 190, 2041-2054.
- (14) Yokoyama, M., Miyauchi, M., Yamada, N., Okano, T., Sakurai, Y., Kataoka, K., and Inoue, S. (1990) Characterization and anticancer activity of the micelle-forming polymeric anticancer drug adriamycin-conjugated poly(ethylene glycol)-poly(aspartic acid) block copolymer. *Cancer Res.* 50, 1693-1700.
- (15) Yokoyama, M., Miyauchi, M., Yamada, N., Okano, T., Sakurai, Y., Kataoka, K., and Inoue, S. (1990) Polymer micelles as novel carrier: Adriamycin-conjugated poly(ethylene glycol)-poly(aspartic acid) block copolymer. *J. Controlled Release* 11, 269-278.
- (16) Bader, H., Ringsdorf, H., and Schmidt, B. (1984) Water-soluble polymers in medicine. *Angew. Chem.* 123/124, 457-485.
- (17) Pratten, M. K., Lloyd, J. B., Hörpel, G., and Ringsdorf, H. (1985) Micelle-forming block copolymers: Pinocytosis by macrophages and interaction with model membranes. *Makromol. Chem.* 186, 725-733.
- (18) Kabanov, A. V., Chekhonin, V. P., Alakhov, V. Yu., Batrakova, E. V., Lebedev, A. S., Melik-Nubarov, N. S., Arzhakov, S. A., Levashov, A. V., Morozov, G. V., Severin, E. S., and Kabanov, V. A. (1989) The neuroleptic activity of haloperidol increases after its solubilization in surfactant micelles; Micelles as microcontainers for drug targeting. *FEBS Lett.* 258, 343-345.
- (19) Yokoyama, M., Okano, T., Sakurai, Y., Ekimoto, H., Shibazaki, C., and Kataoka, K. (1991) Toxicity and antitumor activity against solid tumors of micelle-forming polymeric anticancer drug and its extremely long circulation in blood. *Cancer Res.* 51, 3229-3236.
- (20) Yokoyama, M., Inoue, S., Kataoka, K., Yui, N., and Sakurai, Y. (1987) Preparation of adriamycin-conjugated poly(ethylene glycol)-poly(aspartic acid) block copolymer. *Makromol. Chem. Rapid Commun.* 8, 431-435.
- (21) Saudek, V., Picova, H., and Drobnik, J. (1981) NMR study of poly(aspartic acid). II. α - and β -peptide bonds in poly(aspartic acid) prepared by common methods. *Biopolymers* 20, 1615-1623.
- (22) Sekiguchi, H. (1981) Mechanism of N-carboxy- α -amino acid anhydride (NCA) polymerization. *Pure Appl. Chem.* 53, 1689-1714.
- (23) Lundberg, R. D., and Doty, P. (1957) Polypeptides. XVII. A study of the kinetics of the primary amine-initiated polymerization of N-carboxy-anhydrides with special reference to configurational and stereochemical effects. *J. Am. Chem. Soc.* 79, 3961-3972.
- (24) Wilhelm, M., Zhao, C.-L., Wang, Y., Xu, R., Winnik, M. A., Mura, J.-L., Riess, G., and Croucher, M. D. (1991) Poly(styrene-ethylene oxide) block copolymer micelle formation in water: a fluorescence probe study. *Macromolecules* 24, 1033-1040.
- (25) Douglas, S. J., Illum, E., and Davis, S. S. (1986) Poly(butyl 2-cyanoacrylate) nanoparticles with differing surface charges. *J. Controlled Release* 3, 15-23.
- (26) Tsukada, Y., Kato, Y., Umemoto, N., Takeda, Y., Hara, T., and Hirai, H. (1984) An anti- α -fetoprotein antibody-daunorubicin conjugate with a novel poly-L-glutamic acid derivative as intermediate drug carrier. *J. Natl. Cancer Inst.* 73, 721-729.
- (27) Hirano, T., Ohashi, S., Morimoto, S., Tsukada, K., Kobayashi, T., and Tsukagoshi, S. (1986) Synthesis of antitumor-active conjugates of adriamycin or daunomycin with the copolymer of divinyl ether maleic anhydride. *Makromol. Chem.* 187, 2815-2824.

CORRECTIONS

Volume 3, Number 4, July/August 1992

PREPARATION OF MICELLE-FORMING POLYMER-DRUG CONJUGATES

Masayuki Yokoyama,* Glenn S. Kwon, Teruo Okano, Yasuhisa Sakurai, Takashi Seto, and Kazunori Kataoka*

Page 298. In footnote *a* of Table III, each value 9.1×10^{-4} mol should read 4.31×10^{-5} mol.

Cytotoxicity of Chimeric (Human-Murine) Monoclonal Antibody BR96 IgG, F(ab')₂, and Fab' Conjugated to *Pseudomonas* Exotoxin

Clay B. Siegall,* Susan L. Gawlak, Jeffrey J. Chin, Mary E. Zoeckler,† Kathleen F. Kadow,† Joseph P. Brown, and Gary R. Braslawsky†

Cellular and Molecular Biology Department and Immunology Department, Bristol-Myers Squibb Pharmaceutical Research Institute, 5 Research Parkway, Wallingford, Connecticut 06492. Received February 6, 1992

We have made antigen-specific cytotoxic reagents by conjugating the chimeric antibody BR96 (chiBR96) to *Pseudomonas* exotoxin A (PE), as either native PE or a truncated form (LysPE40) devoid of the cell-recognition region (domain I). PE kills cells by ADP-ribosylation of elongation factor 2, thereby inhibiting protein synthesis. Chimeric BR96 immunotoxins were constructed by chemical conjugation of the toxin to Fab', F(ab')₂, and intact IgG and purified by anion-exchange and gel-filtration chromatography. Chimeric BR96 [IgG and F(ab')₂] immunotoxins were cytotoxic against tumor cell lines displaying the BR96 antigen, with EC₅₀ values ranging from 0.1 to 110 pM. Immunotoxins constructed with chiBR96 Fab' were 50-100-fold less cytotoxic. Competition analysis showed that the immunotoxins were specifically active through their BR96 antigen-binding ability. The binding of chiBR96-PE and chiBR96-LysPE40 to antigen was equivalent to that of BR96 itself and these immunotoxins were found to internalize very rapidly, displaying 90% of their cytotoxicity within 1 h. Binding assays determined that chiBR96 F(ab')₂-LysPE40 bound as well as chiBR96-LysPE40; however, chiBR96 Fab'-LysPE40 bound 20-fold less efficiently. The chiBR96 Fab'-LysPE40 internalized similarly to the F(ab')₂ or the IgG immunotoxins. Therefore, the chiBR96 Fab'-LysPE40 immunotoxin is less cytotoxic toward target cells because of reduced antigen binding. This is may be due to the monovalent nature of chiBR96 Fab'-LysPE40. This study shows that the monoclonal antibody chiBR96-*Pseudomonas* exotoxin A immunotoxins can be effective at inhibiting protein synthesis in target cells.

INTRODUCTION

Immunotoxins have been investigated as a new approach for treating tumors and disease in man (1-3). By coupling a potent but nonselective bacterial or plant protein toxin with an antibody directed against tumor-associated membrane antigens, cytotoxicity of the toxin can be preferentially directed toward neoplastic cells.

Immunotoxins have shown promise in preclinical models using human tumor xenografts in nude mice (4-6). The studies outlined here focus on immunotoxins prepared by conjugating *Pseudomonas* exotoxin A (PE) and a 40-kDa (LysPE40) form of the toxin conjugated to the chimeric (human-murine) antibody BR96. BR96 binds to Lewis Y antigen present on a large number of breast, colon, lung, and ovarian carcinomas (7). The antibody has low cross-reactivity to normal tissue, limited to the upper gastrointestinal tract. More importantly, the unconjugated antibody is rapidly internalized after binding antigen, a requirement that has been demonstrated for antibody-directed cytotoxicity in several studies of antibody-toxin conjugates (8) and antibody-drug conjugates (9, 10).

Chimeric BR96 was constructed by a two-step homologous recombination method, in which DNA encoding human IgG1 heavy chain and human κ light chain were attached to the murine BR96 variable region (11). In this study, we have tested immunotoxins using the whole antibody molecule as well as antibody fragments [F(ab')₂ and Fab'] as a first step toward designing optimal recombinant molecules. PE, produced by *Pseudomonas aeruginosa*, is a polypeptide comprising three domains (12). Domain I encodes the cell-binding ability, domain II encodes the proteolytic sensitivity site and the membrane translocation ability, and domain III encodes the

ADP-ribosylation activity of the toxin (13, 14). PE kills cells by ADP-ribosylating elongation factor 2 and catalytically inhibiting protein synthesis. By removing domain I from PE, a truncated 40-kDa toxin is formed (PE40) (15). PE40 is weakly toxic to cells, since it lacks the binding domain for the PE receptor (15). In order to conjugate this molecule to an antibody, the amino terminus of PE40 has been modified to include a lysine residue, hence LysPE40 (6).

In this report, PE and LysPE40 were coupled to the various antibody forms either by thiolation with 2-iminothiolane or by direct attachment to intact antibody by reduction with DTT. Monovalent Fab' conjugates showed antibody-directed cytotoxicity, although at much higher protein concentrations than those obtained using bivalent IgG and F(ab')₂ toxins. Differences in cytotoxic potential were attributed to binding differences between the various forms of the antibody, and not to internalization differences.

EXPERIMENTAL PROCEDURES

Reagents. *N*-succinimidyl 4-(*N*-maleimidomethyl) cyclohexane-1-carboxylate (SMCC) and 2-iminothiolane were purchased from the Pierce Chemical Corp. (Rockford, IL). Soluble pepsin was purchased from Sigma Chemical Co. (St. Louis, MO). Na¹²⁵I and [³H]leucine were purchased from New England Nuclear (Boston, MA). Native PE was purchased from Berna Products (Coral Gables, FL). Mono Q columns were purchased from Pharmacia (Uppsala, Sweden). TSK-3000 columns were purchased from TosoHaas, Inc. (Philadelphia, PA). Immunoblots were performed using mouse (anti-idiotypic BR96) and rabbit (anti-PE) ABC kits (Vector Laboratories, Burlingame, CA). Rabbit polyclonal anti-PE antibody and mouse anti-PE monoclonal antibody (M40/1) were kindly supplied by Drs. Ira Pastan and David FitzGerald, National Institutes of Health (Bethesda, MD). Anti-idiotypic BR96

* To whom correspondence should be addressed.

† Immunology Department.

antibody (757-4-1) was provided by Dr. Bruce Mixan, Bristol-Myers Squibb (Seattle, WA).

Cell Culture and Plasmids. All cells were cultured in RPMI 1640 supplemented with 10% fetal bovine serum except L929, which was cultured in DMEM supplemented with 10% fetal bovine serum. Plasmid pMS8, which encodes the gene for LysPE40 under control of the T7 promoter, was previously described (6).

Expression and Purification of LysPE40. The plasmid pMS8 encoding LysPE40 (6) was transformed into *Escherichia coli* BL21(λ DE3) cells and cultured in Super Broth (Digene, Inc., Silver Spring, MD) containing 75 μ g of ampicillin/mL at 37 °C. When absorbance at 650 nm was 2.0 or greater, isopropyl 1-thio- β -D-galactopyranoside was added (1 mM), and cells were harvested 90 min later. The bacteria were washed in sucrose buffer (20% sucrose, 30 mM Tris-HCl (pH 7.4), 1 mM EDTA) and osmotically shocked in ice-cold H₂O to isolate the periplasm. LysPE40 protein was purified from the periplasm by successive anion-exchange and gel-filtration chromatography with a Pharmacia fast protein liquid chromatography (FPLC) system, as described previously (6).

Generation of BR96 F(ab')₂ and Fab' Fragments. F(ab')₂ fragments were generated from chiBR96 (4 mg/mL) by pepsin digestion (25 μ g/mL in 0.1 M citrate buffer, pH 4.0). After 6 h at 37 °C, digestion was stopped by adjusting the pH to 7.2 with phosphate-buffered saline (PBS). Purity of the digest preparation was 90–95% F(ab')₂, determined by SDS-PAGE and Coomassie Blue staining.

Fab' was prepared from chiBR96 F(ab')₂ by reduction with cysteine to break the remaining interchain disulfide bonds (16). Briefly, F(ab')₂ molecules (2–4 mg/mL) in 0.1 M Tris-HCl (pH 7.5) were incubated at 37 °C for 2 h with cysteine (0.01 M final concentration). Free sulfhydryl groups on the Fab' molecule were alkylated with 0.02 M iodoacetamide (CalBiochem, San Diego, CA) for 30 min at room temperature to prevent recombination of the Fab' to F(ab')₂. The reaction mixture was dialyzed against PBS. Purity was greater than 85% as assessed by SDS-PAGE.

Immunotoxin Construction and Purification. Chimeric BR96 (6–10 mg/mL) was thiolated by addition of a 3-fold molar excess of 2-iminothiolane (2-IT) in 0.2 M sodium phosphate buffer (pH 8.0), 1 mM EDTA for 1 h at 37 °C (4). Unreacted 2-iminothiolane was removed by PD-10 column chromatography (Pharmacia). Alternatively, free thiol groups were generated by reduction with dithiothreitol (DTT). Chimeric BR96 was incubated with a 20-fold molar excess of DTT for 2.5 h at 42 °C. Excess DTT was removed by overnight dialysis against PBS under nitrogen. The number of thiol groups on the antibody was determined by DTNB reduction (Ellman's reagent, Sigma Chemical Co., St. Louis, MO) (17). This procedure routinely gave four thiol groups per BR96 antibody, with no reduction in antibody binding reactivity or protein concentration. The procedure was not used with F(ab')₂ or Fab' fragments.

Thiolated BR96 antibody was condensed with maleimide-modified PE or LysPE40. A maleimide group was attached to lysine residues on the toxin (PE or LysPE40; 6–8 mg/mL) by mixing with a 3-fold molar excess of SMCC in 0.2 M sodium phosphate (pH 7.0), 1 mM EDTA at room temperature for 30 min and purified on a PD-10 column. Modified toxin and thiolated antibody were mixed in a 4:1 molar ratio and incubated at room temperature for 14–16 h to allow a thioether linkage to form. Immunotoxins were purified by anion exchange (Mono Q) to remove unreacted antibody and gel-filtration chro-

matography (TSK-3000) to remove unconjugated toxin as previously described (4, 6, 15).

Inhibition of Protein Synthesis Assay. Tumor cells (10⁵ cells/mL) in growth media were added to 96-well flat bottom tissue culture plates (0.1 mL/well) and incubated at 37 °C for 16 h. Dilutions of toxin or toxin-conjugates were made in growth media, and 0.1 mL was added to each well (three wells/dilution) for 1 h or 20 h at 37 °C. After the appropriate incubation time unreacted material was removed by washing the monolayer with growth media. Cells were incubated in 0.2 mL of growth media for a total of 20 h and pulse labelled with [³H]leucine (1 μ Ci/well) for an additional 4 h at 37 °C. The cells were lysed by freezing and thawing at 37 °C and were harvested using a Tomtec cell harvester (Orange, CT). Cellular protein labeled with [³H]leucine was determined by counting the incorporated radioisotope using a LKB Beta Plate liquid scintillation counter.

Competition for Cytotoxicity Analysis. Tumor cells were plated and incubated at 37 °C as described above. Chimeric BR96 diluted to 50 μ g/mL in growth media was added to the cell monolayer (0.5 mL/well). After incubation at 37 °C for 1 h, dilutions of chiBR96 immunconjugates (50 μ L) were added and incubated an additional 1 h and cell supernatants were removed and washed with RPMI. Growth media (0.2 mL) was added to each well, and cells were incubated at 37 °C (20 h) and labeled with [³H]leucine as described above.

Binding Activity. Competition Binding. L2987 cells were removed from monolayer culture with 0.2% trypsin and washed with RPMI 1640 containing 2% FCS (wash buffer). Cell suspensions (1.0 \times 10⁶ cells/0.1 mL) were incubated with 0.1 mL of fluorescein isothiocyanate (FITC) labeled chiBR96 (13.3 μ g/mL final concentration) and 0.1 mL of diluted antibody or immunotoxin 4 °C for 1 h and washed, and the amount of cell-bound FITC-labeled chiBR96 was quantified on an EPICS V Model 753 flow cytometer (Coulter Corp., Hialeah, FL).

Direct Binding. Two-fold serially diluted immunotoxins or antibody was incubated for 1 h at 4 °C in 0.2 mL of wash buffer containing 1 \times 10⁶ L2987 cells. Cells were washed and then incubated in wash buffer containing 1:40 diluted FITC-labeled goat anti-human K antibody (Bethyl Labs, Montgomery, TX) for an additional 30 min at 4 °C. Cells were washed and analyzed for cell-surface fluorescence on a flow cytometer.

Antigenic Modulation and Internalization. The level of membrane-associated immunotoxin bound to target cell populations during antigenic modulation was quantified using an [¹²⁵I]anti-PE monoclonal antibody M40/1. Previously, the M40/1 epitope was mapped to a 44 amino acid region in PE domain II (18). The M40/1 antibody was radioiodinated using Na¹²⁵I (New England Nuclear, MA) and chloramine T (Kodak Chemical Co., Rochester, NY) according to ref 19). Radioiodinated M40/1 was separated from unbound iodine by PD10 column chromatography (Pharmacia). Specific activities ranged from 2 to 5 \times 10⁵ cpm/ μ g.

Modulation of intact chiBR96, F(ab')₂, or Fab' immunotoxins was assayed on L2987 cells propagated as 90–95% confluent monolayer cultures in 96 well microtiter plates prepared as described above. Target cells were pulsed for 1 h at 4 °C with 0.1 mL of 2-fold serially diluted immunotoxin ranging from 1.6 to 3.2 \times 10⁻⁷ M antibody protein in binding buffer. Subsequently, cultures were washed using growth medium and individual plates were incubated in complete medium at either 4 or 37 °C.

At specific time points during incubation at 37 or 4 °C,

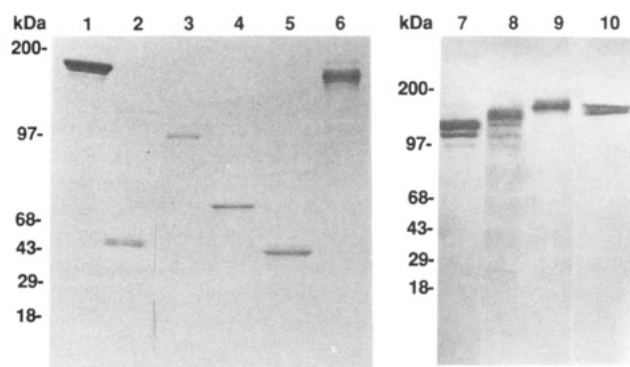


Figure 1. Nonreducing SDS-PAGE analysis of conjugated and unconjugated chiBR96 IgG, Fab', F(ab')₂. 4–20% gels were stained with Coomassie Blue. Lanes: 1, chiBR96 IgG; 2, chiBR96 Fab'; 3, chiBR96 Fab'-LysPE40; 4, native PE; 5, LysPE40; 6, chiBR96 IgG-LysPE40; 7, chiBR96 (Fab')₂; 8, chiBR96 F(ab')₂-LysPE40; 9, chiBR96 IgG-LysPE40; 10, chiBR96 IgG.

triplicate sets of wells were washed twice with wash buffer and pulse-labeled with 0.1 mL ¹²⁵I-labeled M40/1 antibody (0.5 µg/mL in wash buffer containing 0.2% sodium azide). After 15 min, unbound label was removed from the monolayers, and cell-bound cpm determined by solubilization of the cell monolayer with 0.5 N NaOH. Cell-bound radioactivity was determined using a LKB Model 1272 γ counter. Nonspecific binding was determined by incubation of target cells with a similar concentration of unconjugated chiBR96. In certain experiments, unconjugated PE was used to determine background binding levels. ¹²⁵I-labeled M40/1 antibody did not react with membrane bound antibody or PE.

RESULTS

Construction and Purification of chiBR96-Toxin Conjugates. Reduced chiBR96-drug conjugates have been successfully used as (in vivo) antitumor agents. In this study, we have used a similar approach in constructing chiBR96-toxin conjugates. Chimeric BR96, thiolated by condensation with 2-iminothiolane or after mild reduction using DTT, was chemically conjugated to both PE (66 kDa) and LysPE40 (40 kDa). LysPE40 was additionally conjugated to chiBR96 Fab' and F(ab')₂ antibody forms. The immunotoxins were purified as described in Experimental Procedures. Chimeric BR96 IgG-LysPE40 (190 kDa), Fab'-LysPE40 (96 kDa), and F(ab')₂-LysPE40 (145 kDa) conjugates were analyzed by nonreducing SDS-polyacrylamide gel electrophoresis to determine the size of the native conjugate (Figure 1). From the Coomassie Blue stained gels, we determined that there was less than 5% unconjugated antibody after purification.

Binding Activity of chiBR96-Immunotoxins. Two methods were used to determine whether there was an alteration in antibody binding activity after conjugation to PE or LysPE40. Competition binding analysis showed that both immunotoxins competed with FITC-labeled chiBR96 as efficiently as unconjugated chiBR96 antibody (Figure 2), indicating that binding affinity for the BR96 antigen was not perturbed after chemical conjugation. Similar results were obtained using the direct binding assay for both PE and LysPE40 conjugates (results not shown). Binding activities of LysPE40-conjugated and unconjugated IgG, F(ab')₂, and Fab' were also compared by direct binding to L2987 tumor cells. Cell-bound antibody protein was quantitated using FITC-labeled goat anti-human K light chain antibody. Binding of the LysPE40 immunotoxin was similar to that obtained using unconjugated chiBR96 antibody (Figure 3A) and agrees with results

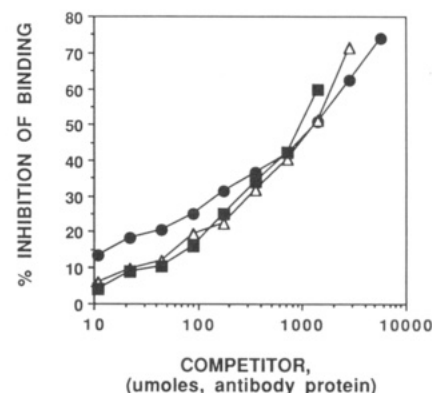


Figure 2. Competition of chiBR96-PE and chiBR96-LysPE40 binding. Inhibition of FITC labeled chiBR96 (40 µg/mL) by chiBR96 (●); chiBR96-PE (■), and chiBR96-LysPE40 (Δ) using L2987 target cells.

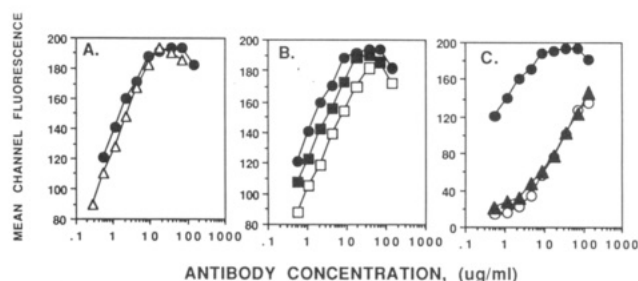


Figure 3. Direct binding of intact chiBR96-LysPE40, F(ab')₂-LysPE40, and Fab'-LysPE40 to L2987 cells. Cells were incubated (4 °C, 1 h) with immunotoxin or antibody as described in Experimental Procedures. Cell-bound antibody was quantitated with FITC labeled anti-human κ antibody. The amount of immunotoxin or antibody remaining on the cell surface was determined by measuring cell-surface fluorescence. Legend: ChiBR96 (●), chiBR96-LysPE40 (Δ), chiBR96 F(ab')₂ (□), chiBR96 F(ab')₂-LysPE40 (■), chiBR96 Fab' (○), chiBR96 Fab'-LysPE40 (▲).

obtained using the competition binding assay (Figure 2). Figure 3B compares the binding activity of intact IgG to that of F(ab')₂ and F(ab')₂-LysPE40. There was no loss in immunoreactivity with the F(ab')₂ and F(ab')₂-immunotoxin as compared to chiBR96 IgG. Conjugation of PE40 to Fab' did not affect immunoreactivity (Figure 3C); however, binding of the Fab' was significantly decreased as compared to intact IgG (Figure 3C), most likely due to the monovalency of the Fab' molecule.

Modulation and Internalization of chiBR96-Immunotoxins. BR96 has been shown to be a rapidly internalizing antibody (7). The ability of chiBR96-PE and chiBR96-LysPE40 to induce antigenic modulation was initially measured by determining the loss of immunotoxin from the cell surface membrane (Figure 4). There was no difference in modulation kinetics between PE or LysPE40 immunotoxins with approximately 50% of the original cell-bound immunotoxin modulated from the surface membrane 30 min after warming to 37 °C. Cells incubated under conditions which do not allow antigenic modulation (4 °C) showed essentially no loss of cell surface toxin within 6 h (Figure 4a). In order to confirm that the loss of cell-surface immunotoxin was due to endocytosis, cells were incubated with a ¹²⁵I-labeled immunotoxin complex for 1 h at 4 °C to permit binding, washed, and subsequently modulated at 37 °C. As demonstrated in Figure 4B, essentially all the radiolabeled immunotoxin remained cell-associated, despite the concomitant loss of immunotoxin from the cell-surface membrane (Figure 4A). These findings confirm that most if not all of the membrane-associated BR96 immunotoxins were rapidly

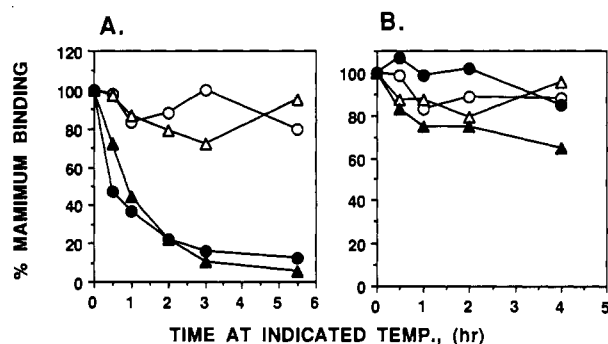


Figure 4. Endocytosis of cell-surface immunotoxin after modulation with chiBR96-PE or chiBR96-LysPE40 immunotoxins. (A) Loss of cell surface immunotoxin was measured by incubating the cell populations under modulating (37 °C) or nonmodulating (4 °C) conditions. The amount of immunotoxin remaining on the cell surface at each individual time point was quantitated with [¹²⁵I]M-40/1 (anti-PE) antibody. (B) Internalization of cell-bound immunotoxin was measured by incubating the immunotoxin plus [¹²⁵I]M-40/1 complex at 37 or 4 °C. Cell-bound radioactivity was determined as described in Experimental Procedures. Chimeric BR96/PE coated cells incubated at 4 °C (○) or at 37 °C (●); chiBR96-LysPE40 coated cells incubated at 4 °C (△) or at 37 °C (▲).

Table I. Internalization of Chimeric BR96-Immunotoxins from the Cell Surface Membrane of L2987 Cells

	% internalization	
	2.5 h	4.5 h
chiBR96-LysPE40	74.0	85.0
chiBR96 F(ab') ₂ -LysPE40	72.0	91.6
chiBR96 Fab'-PE40	12.0	89.6

internalized, and that internalization rates were similar for PE and LysPE40 immunotoxins.

The capacity of chiBR96 F(ab')₂-LysPE40 and Fab'-LysPE40 immunotoxins to internalize was also determined by measuring the loss of cell surface toxin using radiolabeled anti-PE antibody. Essentially all of the chiBR96 immunotoxins were completely internalized after 4.5 h including Fab'-immunotoxin (Table I). However, rate differences were observed. At 2.5 h, when 76% of the intact IgG toxin and 72% of the F(ab')₂ were internalized, only 12% of the Fab'-immunotoxin was internalized. Therefore, IgG-, F(ab')₂-, and Fab'-LysPE40 immunotoxins were modulated from the cell surface membrane, but at different rates.

In Vitro Cytotoxicity of Intact IgG-PE Immunotoxins. Having established the binding and internalizing activities of these chimeric molecules, we assayed their cytotoxicity against cancer cells by comparing inhibition of protein synthesis on antigen-positive and antigen-negative cell lines (Table II). BR96 antigen-positive cell lines MCF-7, L2987, and RCA were the most sensitive to chiBR96-PE with EC₅₀ values of 0.14, 0.28, and 1.4 pM, respectively. The immunotoxin was also more inhibitory than native PE, which had EC₅₀ values of 200, 140, and 380 pM. When tested on antigen-negative cell lines, little difference in EC₅₀ values between PE and the immunotoxin was observed. Specificity (antibody directed cell-killing) must also take into consideration the different sensitivities of the various cell lines to native PE. Thus, the chiBR96 immunotoxins were 100–500-fold more potent than native PE against the antigen positive cell lines.

Cytotoxicity of chiBR96 Antibody and Enzymatic Fragments Linked to LysPE40 against MCF-7 Cells. We also compared the cytotoxic activity of chiBR96 in Fab', F(ab')₂, and IgG form linked by LysPE40 (Table III). As with the chiBR96-PE immunotoxin (Table II), MCF-7

and L2987 cells are the most sensitive cell lines tested. The IgG- and F(ab')₂-LysPE40 molecules showed similar cytotoxic activity against MCF-7 cells (EC₅₀ = 8–14 pM) while the Fab'-LysPE40 conjugate was much less active (EC₅₀ = 780 pM) (Figure 5). Specificity of protein synthesis inhibition activity of Fab' and F(ab')₂ conjugates was also preserved, with little or no inhibitory activity observed against the antigen negative cell lines A2780.

Specificity of Growth Inhibition by chiBR96-LysPE40. Specificity was confirmed by abrogating the protein synthesis inhibition by chiBR96-LysPE40 with unconjugated chiBR96. Addition of excess chiBR96 antibody (50 µg) with chiBR96-LysPE40 immunotoxin, resulted in a decrease of in vitro potency (Figure 6). At 20 pM of chiBR96-LysPE40, approximately 50% of its cytotoxic effect was blocked by the addition of excess unconjugated antibody, while at 4 pM, the excess chiBR96 completely blocked the cytotoxic activity of chiBR96-LysPE40.

Kinetics of Cytotoxicity of chiBR96 Immunotoxins and Native PE. In part, the effectiveness of immunotoxins may depend upon the rate of internalization after binding to antigen positive cells. To determine the cytotoxic activity of chiBR96-PE, chiBR96-LysPE40, and PE, we performed a time-course analysis where cells were incubated with toxin for up to 20 h as described in Experimental Procedures.

After a 1-h incubation, MCF-7 cells were sensitive to chiBR96-PE and chiBR96-LysPE40, with EC₅₀ values of 1 and 60 pM, respectively, but not to the native toxin (EC₅₀ > 10 000 pM). After 20 h MCF-7 cells were slightly more sensitive to chiBR96-PE and chiBR96-LysPE40, but much more sensitive to PE; EC₅₀ = 200 pM (Figure 7). We also repeated this assay at 2, 4, and 6 h time points (data not shown). At each time point, PE was considerably less cytotoxic against MCF-7 cells than chiBR96-immunotoxins. This may be due in part to the mechanism by which the toxin molecule is delivered to target cells.

DISCUSSION

We have produced immunotoxins containing the carcinoma-reactive monoclonal antibody chiBR96 and *Pseudomonas* exotoxin A. The antibody was used in forms including intact IgG, F(ab')₂, and Fab'. The toxin component of the immunotoxin was either native PE or NLysPE40 (referred to as LysPE40 in this paper), a truncated form containing a genetically modified amino terminus that includes a lysine residue for conjugation purposes (4). Chimeric BR96-toxin conjugates were found to be cytotoxic to cells which display Lewis Y, the epitope recognized by BR96. The most cytotoxic of the conjugates produced was chiBR96-PE, which was 1000-fold more potent than PE itself against MCF-7 breast carcinoma cells. Chimeric BR96-LysPE40 was also extremely cytotoxic toward BR96 antigen-positive cells (1000-fold more potent than LysPE40). Both chiBR96-PE and chiBR96-LysPE40 were produced using two procedures to generate sulfhydryl groups on the antibody, mild reduction or treatment with 2-iminothiolane. The former procedure gave a greater yield of conjugate, but conjugates produced by both procedures resulted in chimeric molecules of identical activities.

Chimeric BR96-PE and chiBR96-LysPE40 were almost fully active with 1-h incubation, while PE was relatively inactive (Figure 7). With continued incubation, chiBR96-immunotoxins increase cytotoxic activity only slightly while PE becomes cytotoxic to the MCF-7 cells at later time points. This rapid efficacy of chiBR96-immunotoxins is evidence of the utility of chiBR96 in targeting cell populations for elimination.

Table II. Cytotoxicity of Chimeric BR96-PE on Human Tumor Cells

cell line	type	BR96 antigen	EC ₅₀ , ^a pM		
			DTT-reduced chiBR96-PE	2-iminothiolane-treated chiBR96-PE	native PE
MCF-7	breast cancer	+	0.10	0.14	200.0
L2987	lung cancer	+	0.25	0.28	140.0
RCA	colon cancer	+	1.2	1.4	380.0
A2780	ovarian cancer	+	23.0	23.0	60.0
L929	mouse fb1st	-	13.5	14.0	3.0
KB	epidermoid cancer	-	220.0	231.0	227.0

^a EC₅₀ represents the amount of immunotoxin or toxin required to inhibit 50% of the protein synthesis as determined by [³H]leucine incorporation in cellular protein.

Table III. Cytotoxicity of 2-Iminothiolane-Substituted Chimeric BR96-LysPE40 on Human Tumor Cells

cell line	type	BR96 antigen	EC ₅₀ , ^a pM			
			IgG-PE40	F(ab') ₂ -PE40	Fab'-PE40	LysPE40
MCF-7	breast cancer	+	8	14	780	15000
L2987	lung cancer	+	37	70	2700	17500
RCA	colon cancer	+	84	110	5000	15000
A2780	ovarian cancer	+	650	2500	11000	15000
KB	epidermoid cancer	-	>5000	ND	ND	>25000

^a EC₅₀ is described in the Table I footnote. ND = not determined.

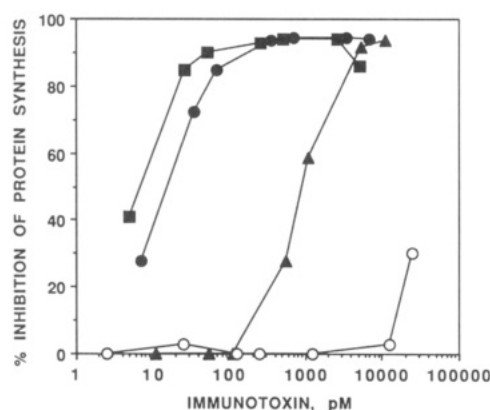


Figure 5. Cytotoxicity of various chiBR96 forms conjugated to LysPE40 against MCF-7 cells. Immunotoxins were incubated for 20 h, and protein synthesis was determined as described in Experimental Procedures. Legend: chiBR96-PE40 (■), chiBR96 F(ab')₂-PE40 (●), chiBR96 Fab'-PE40 (▲), PE40 (○).

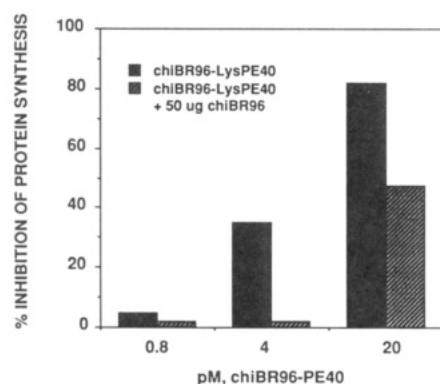


Figure 6. Competition of chiBR96-PE40 cytotoxic activity against MCF-7 cells. Chimeric BR96-PE40 was added at 0.8, 4, and 20 pM concentrations to MCF-7 cells in presence or absence of 50 µg (333 pM) chiBR96 antibody. Cytotoxicity was determined as described in Experimental Procedures.

We also examined the binding and internalization activities of chiBR96-immunotoxins. Immunconjugates prepared with intact IgG or its F(ab')₂ or Fab' enzymatic digest products were not affected in terms of binding by chemical conjugation to LysPE40 (Figure 3) or PE (data not shown). Differences in binding activity between Fab' and F(ab')₂ or IgG conjugates may be attributed to

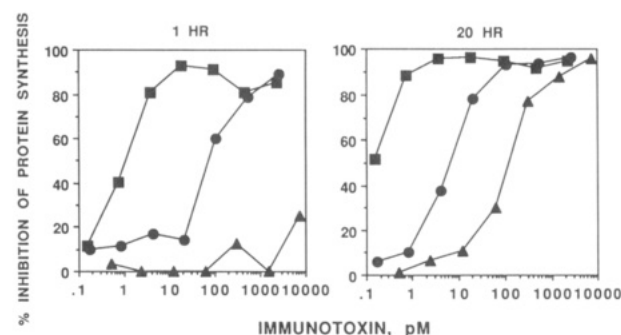


Figure 7. Protein synthesis inhibition analysis of chiBR96-PE/LysPE40 vs PE against MCF-7 cells. Immunotoxins were added to the cells at various concentrations and either removed and replaced with fresh media at 1 h or not disturbed. After 20 h, the cells were pulsed with [³H]leucine and harvested as described. Legend: chiBR96-PE (■), chiBR96-PE40 (●), PE (▲).

differences in avidity due to the monovalence of the Fab' molecule. We also cannot exclude the possibility that the enzymatic method used to generate Fab' did not contribute to the decreased avidity. Of most interest was the comparison between chiBR96-LysPE40 and the enzymatic fragment immunotoxins chiBR96 F(ab')₂-LysPE40 and chiBR96 Fab'-LysPE40. This finding is also reflected in the cytotoxicity data (Table III).

The decreased potency of the Fab'-immunoconjugate could not be attributable to the inability to internalize, although minor rate differences were observed between the Fab' and F(ab')₂ or IgG toxin conjugates. Other groups have used fragments of antibodies to direct toxins toward certain cell populations (20, 21). F(ab')₂ and Fab' fragments are smaller than IgG molecules, and can perhaps penetrate the inside of tumors more readily (22). Our own results (manuscript in preparation) have shown that antibody Fab' fragments have a shorter serum lifetime and penetrate into the tumor at a faster rate than IgG or F(ab')₂ fragments. It will be important to determine the serum lifetime and the maximum tolerated dose for these immunotoxin forms. A bivalent BR96 immunotoxin molecule may be necessary to achieve maximal binding efficacy, but a Fab'-immunotoxin molecule may achieve faster penetration into the tumor mass and allow for a greater input of material despite a shorter serum half-life of the molecule.

Chimeric toxins similar to chiBR96-PE have been shown to be effective as antitumor agents in vivo (5). In this report, we have shown that both intact PE and LysPE40 immunotoxins as well as F(ab')₂ and Fab' immunotoxins demonstrate cytotoxic activity in vitro. Potency differences between the various immunotoxins were most likely attributable to avidity differences and could not be due to the ability of the immunotoxins to deliver the toxin to the appropriate intracellular target. The critical question is whether the pharmacokinetic differences between a monovalent Fab' and a bivalent IgG or F(ab')₂ immunotoxin will translate into a better therapeutic response. Experiments which will determine the in vivo potency of chiBR96-PE conjugates have been initiated in models of human tumors.

ACKNOWLEDGMENT

We thank Drs. I. Pastan, D. FitzGerald, B. Mixan, P. Fell, K. E. Hellstrom, S. McAndrew, and P. Friedman, for reagents and helpful comments, and L. Howe, for expert secretarial assistance.

LITERATURE CITED

- (1) Pastan, I., and FitzGerald, D. (1991) Recombinant toxins for cancer treatment. *Science* 254, 1173-1177.
- (2) FitzGerald, D., and Pastan, I. (1991) Redirecting *Pseudomonas* exotoxin. *Semin. Cell Biol.* 2, 31-37.
- (3) Vitetta, E. S., Krolick, K. A., Miyama-Inaba, M., Cushley, W., and Uhr, J. W. (1987) Immunotoxins: A new approach to cancer therapy. *Science* 235, 644, 650.
- (4) Batra, J. K., Jinno, Y., Chaudhary, V. K., Kondo, T., Willingham, M. C., FitzGerald, D. J., and Pastan, I. (1989) Antitumor activity in mice of an immunotoxin made with anti-transferrin receptor and a recombinant form of *Pseudomonas* exotoxin. *Proc. Natl. Acad. Sci. U.S.A.* 86, 8545-8549.
- (5) Pai, L. H., Batra, J. K., FitzGerald, D. J., Willingham, M. C., and Pastan, I. (1991) Anti-tumor activities of immunotoxins made of monoclonal antibody B3 and various forms of *Pseudomonas* exotoxin. *Proc. Natl. Acad. Sci. U.S.A.* 88, 3358-3362.
- (6) Debinski, W., Karlsson, B., Lindholm, L., Siegall, C. B., Willingham, M., FitzGerald, D., and Pastan, I. (1991) Monoclonal antibody C242-*Pseudomonas* exotoxin A: A specific and potent immunotoxin with antitumor activity. *J. Clin. Invest.* in press.
- (7) Hellstrom, I., Garrigues, H. J., Garrigues, U., and Hellstrom, K. E. (1990) Highly tumor-reactive, internalizing, mouse monoclonal antibodies to Le^x-related cell-surface antigens. *Cancer Res.* 50, 2183-2190.
- (8) Carriere, D., Casella, P., Richer, G., Gros, P., and Jansen, F. (1985) Endocytosis of an antibody-ricin A chain conjugate (immuno-A toxin) adsorbed on colloidal gold. *Exp. Cell. Res.* 156, 327-340.
- (9) Nio, Y., Shiraishi, T., Imai, S., Ohgaki, K., and Tobe, T. (1989) Binding and internalization of human immunoglobulin G conjugated with melphalan (K18) to human tumor cell lines. *Anticancer Res.* 9, 59-64.
- (10) Braslawsky, G. R., Kadow, K., Knipe, J., McGoff, K., Edson, M., Kaneko, T., and Greenfield, R. S. (1991) Adriamycin (Hydrazine) antibody conjugates require internalization and intracellular acid hydrolysis for antitumor activity. *Cancer Immunol. Immunother.* 33, 367-374.
- (11) Fell, H. P., Yarnold, S., Hellstrom, I., and Hellstrom, K. E. (1989) Homologous recombination in hybridoma cells: Heavy chain chimeric antibody produced by gene targeting. *Proc. Natl. Acad. Sci. U.S.A.* 86, 8507-8511.
- (12) Allured, V., Collier, R. J., and McKay, D. B. (1986) Structure of exotoxin A of *Pseudomonas aeruginosa* at 3.0-angstrom resolution. *Proc. Natl. Acad. Sci. U.S.A.* 83, 1320-1324.
- (13) Hwang, J., FitzGerald, D. J. P., Adhya, S., and Pastan, I. (1987) Functional domains of *Pseudomonas* exotoxin identified by deletion analysis of the gene expressed in *E. coli*. *Cell* 48, 129-136.
- (14) Siegall, C. B., Chaudhary, V. K., FitzGerald, D. J., and Pastan, I. (1989) Functional analysis of domains II, Ib and III of *Pseudomonas* exotoxin. *J. Biol. Chem.* 264, 14256-14261.
- (15) Kondo, T., FitzGerald, D., Chaudhary, V. K., Adhya, A., and Pastan, I. (1988) Activity of immunotoxins constructed with modified *Pseudomonas* exotoxin A lacking the cell recognition. *J. Biol. Chem.* 263, 9470-9475.
- (16) Parham, P. (1986) Preparation and purification of active fragments from mouse monoclonal antibodies. In *Handbook of Experimental Immunology*, (Weir, D. M., Ed.) pp 1-23, Blackwell Scientific Publishers, New York.
- (17) Deakin, H., Ord, M. G., and Stocken, L. A. (1963) "Glucose 6-phosphate-dehydrogenase" activity and thiol content of thymus nuclei from control and x-irradiated rats. *Biochem. J.* 89, 296-304.
- (18) Ogata, M., Pastan, I. and FitzGerald, D. (1991) Analysis of *Pseudomonas* exotoxin activation and conformational changes by using monoclonal antibodies as probes. *Infect. Immun.* 59, 407-414.
- (19) McConahey, P. J., and Dixon, F. J. (1966) A method for trace iodination of proteins for immunological studies. *Arch. Allergy Appl.* 29, 185-188.
- (20) Roffler, S. R., Yu, M.-H., Chen, B. M., Tung, E., and Yeh, M.-Y. (1991) Therapy of human cervical carcinoma with monoclonal antibody-*Pseudomonas* exotoxin conjugates. *Cancer Res.* 51, 4001-4007.
- (21) Wawrzynczak, E. J., and Thorpe, P. E. (1988) Effect of chemical linkage upon the stability and cytotoxic activity of A chain immunotoxins. In *Immunotoxins* (A. E. Frankel, Ed.) Kluwer Academic Publishers, New York.
- (22) Jain, R. K. (1989) Delivery of novel therapeutic agents in tumors: Physiological barriers and strategies. *J. Natl. Cancer Inst.* 81, 570-576.

Light-Induced Coupling of Aqueous-Soluble Proteins to Liposomes Formed from Carbene-Generating Phospholipids

Michael Sanger,* Franois Borle, Manfred Heller, and Hans Sigrist

Institute of Biochemistry, University of Berne, Freiestrasse 3, CH-3012 Berne, Switzerland.

Received March 18, 1992

A novel bilayer-forming phospholipid analogue with a photoactivatable carbene-generating head group was synthesized and characterized with respect to molecular structure and light-induced reactivity. *N'*-(1,2-Dimyristoyl-*sn*-glycero-3-phosphoethyl)-*N*-[*m*-[3-(trifluoromethyl)diazirin-3-yl]phenyl]thiourea (PED) was prepared by thiocarbamylation of synthetic dimyristoylphosphatidylethanolamine with 3-(trifluoromethyl)-3-(*m*-isothiocyanophenyl)diazirine. PED formed liposomes in aqueous media. Gel to liquid-crystalline transitions occurred at 10.5 C. Neither PED- nor PED/dimyristoylphosphatidylcholine mixed liposomes underwent major structural changes when photoactivated. Liposome sizes, determined by electron microscopy, were not altered upon light exposure. PED combines the advantages of facile synthesis and timed carbene reactivity by photoactivation at wavelengths ≥ 320 nm. Conditions used for PED photoactivation did not inactivate catalytically active or complex-forming proteins. Light-induced binding of aqueous-soluble proteins to PED containing liposomes was attained through photoactivation in the presence of myoglobin, streptavidin, or trypsin. The proteins mentioned were utilized to characterize carbene-initiated ligand coupling. Procedures described establish a new and versatile method for the formation of proteoliposomes.

There is an increasing interest in analytical, diagnostic, and medical applications of liposomes: Liposomes coated with antibodies, cell-specific ligands, or peptides are utilized as carriers for the delivery of therapeutic or diagnostic agents to target tissues (review in ref 1) or for the design of vaccines (reviews in refs 2 and 3). Moreover, proteoliposomes are applied in immunoassays which are based on the lysis of liposomes (4). Recently, targeted liposomes were employed for biomolecule isolation (5) and purification (6). A decisive step in either of the applications mentioned is the process of ligand immobilization under mild and nonlytic conditions. Proteoliposome surface engineering by accustomed methods requires specific reaction conditions or invasive coupling reagents (7). Ligand immobilization procedures described so far are based on the availability of reactive functional groups on the ligand surface. If functional groups are missing or inappropriate with respect to reactivity or topology, they need to be introduced by chemical means or by protein engineering. Both procedures are time-consuming and inherently restrictive. Treatments mentioned may cause protein denaturation or incorrect folding and, as a consequence, hamper biological activities. Light-induced immobilization of proteinaceous ligands is therefore proposed as an alternative procedure for surface ligand coupling. Photocoupling approaches have been employed in former studies, which were designed to delineate lipid/protein interactions in biological membranes (8, 9).

This study introduces a new carbene-generating lipid and describes its application in liposomal surface engineering. Central to this investigation is the usage of PED,¹

a bilayer-forming phospholipid analogue carrying a photoactivatable head group (Figure 1). In contrast to the above-mentioned molecular probe studies, the objective of this investigation is the demonstration of light-induced covalent bond formation between few abundant reactants. Immobilization of protein ligands onto lipid layers by carbene-initiated mechanisms is attractive in that specific, ligand-born functional groups are not required for coupling. Photoactivation of diazirines at wavelengths ≥ 320 nm leads to the formation of highly reactive carbene intermediates (10). Covalent binding of aqueous-soluble proteins to liposomes occurs by insertion of photogenerated carbenes into chemical bonds of target proteins. Furthermore, photoactivation is independent of invasive coupling agents. Specific reaction conditions are not required except light. The diazirine-phospholipid used in this study has previously been shown to form stable planar bilayers (11).

EXPERIMENTAL PROCEDURES

Materials. Trypsin (from bovine pancreas), cholic acid sodium salt, and dimyristoylphosphatidylcholine (DMPC) were purchased from Fluka. Dimyristoyl- and dipalmitoylphosphatidylethanolamine (DMPE and DPPE), myoglobin (from horse skeletal muscle), and trypsin inhibitor (from soybean) were from Sigma. [¹⁴C]biotin was from Amersham and streptavidin from Boehringer. The trypsin substrate S-2251 was supplied by KabiVitrum (Stockholm, Sweden). Silica gel 60 (particle size 0.040–0.063 mm) was purchased from Merck. Thin-layer chromatography was performed on Alugram Sil G/UV₂₅₄-plates from Machery-Nagel. All other chemicals were reagent grade.

Synthesis of 3-(Trifluoromethyl)-3-(*m*-isothiocyanophenyl)diazirine (TRIMID). The synthesis of TRIMID was accomplished as described by Dolder et al. (12) with the following modifications: The product of the reaction of 3-(trifluoromethyl)-3-(*m*-aminophenyl)diazirine with thiophosgene was purified by flash chromatography (13) on silica gel 60 with hexane/ethyl acetate (6:1 v/v) as eluent.

Synthesis of *N'*-(1,2-Dimyristoyl-*sn*-glycero-3-phosphoethyl)-*N*-[*m*-[3-(trifluoromethyl)diazirin-3-yl]phenyl]thiourea (PED). DMPE (0.26 mmol) and triethyl-

¹ Abbreviations used: PED, *N'*-(1,2-dimyristoyl-*sn*-glycero-3-phosphoethyl)-*N*-[*m*-[3-(trifluoromethyl)diazirin-3-yl]phenyl]thiourea; C₁₆-PED, *N'*-(1,2-dipalmitoyl-*sn*-glycero-3-phosphoethyl)-*N*-[*m*-[3-(trifluoromethyl)diazirin-3-yl]phenyl]thiourea; TRIMID, 3-(trifluoromethyl)-3-(*m*-isothiocyanophenyl)diazirine; DMPC, dimyristoylphosphatidylcholine; DPPC, dipalmitoylphosphatidylcholine; DMPE, dimyristoylphosphatidylethanolamine; DPPE, dipalmitoylphosphatidylethanolamine; SDS, sodium dodecyl sulfate; Tris, tris(hydroxymethyl)aminomethane; HEPES, 4-(2-hydroxyethyl)-1-piperazineethanesulfonic acid; DSC, differential scanning calorimetry; SUV, small unilamellar vesicles.

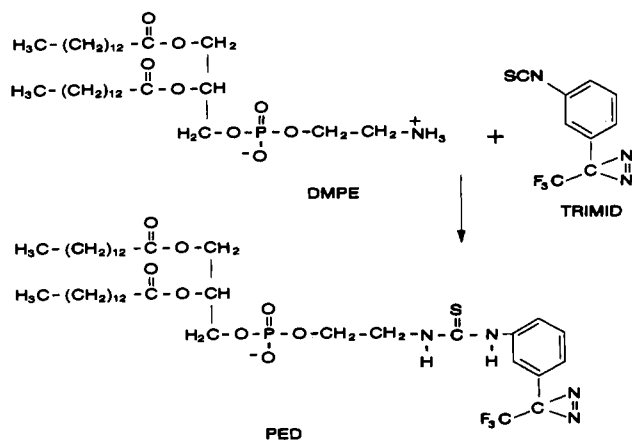


Figure 1. PED synthesis scheme.

amine (0.35 mmol) were dissolved in 6 mL of chloroform/methanol (6:1 v/v). TRIMID (0.33 mmol), dissolved in 1.5 mL of chloroform, was added to the DMPE/triethylamine mixture. The solution was stirred at room temperature in the dark. After 1 h triethylamine (0.18 mmol) was added, the reaction continued for an additional hour, and the solvent removed under reduced pressure. Reactants in excess and the reaction product were redissolved in a small amount of chloroform and purified by flash chromatography on silica gel 60 with chloroform/methanol (4:1 v/v) as the eluent. Solvent evaporation of pooled UV- and phosphate-positive (14), ninhydrin-negative fractions yielded 173 mg (75%) of PED with a R_f value of 0.62 on TLC with chloroform/methanol/water (65:25:4 v/v) as the solvent system.

$^1\text{H NMR}$: (Bruker, 360 MHz, δ = chemical shift in ppm, CD_3OD) δ 0.9 (t, 6 H), 1.3 (m, 40 H), 1.55 (m, 4 H), 2.3 (q, 4 H), 3.83 (t, 2 H), 4.05 (m, 4 H), 4.2 (q, 1 H), 4.45 (q, 1 H), 5.25 (m, 1 H), 7.0 (d, 1 H), 7.4 (t, 1 H), 7.59 (m, 2 H). UV/vis: ϵ_{355} (methanol): $560 \text{ M}^{-1} \text{ cm}^{-1}$.

PED was stored in chloroform/methanol (4:1 v/v) in the dark at -20°C .

Synthesis of *N*-(1,2-Dipalmitoyl-*sn*-glycero-3-phosphoethyl)-*N*-[*m*-[3-(trifluoromethyl)diazirin-3-yl]phenyl]thiourea (C_{16} -PED). C_{16} -PED was synthesized in an identical manner as PED. Chloroform/methanol (4:1 v/v) was used as the solvent for the reaction of TRIMID with DPPE in the presence of triethylamine.

Preparation of Liposomes. PED Liposomes. Single-component PED liposomes were prepared by the ethanol-injection method introduced by Batzri and Korn (15). Liposomes utilized for photocoupling of myoglobin or streptavidin were prepared by the following procedure: PED (4.4 mg, 5 μmol) dissolved in 2.5 mL of chloroform/methanol (4:1 v/v) was dried in a stream of nitrogen. Dried lipid was redissolved in 200 μL of ethanol at 37°C and rapidly injected through a syringe (Hamilton, 100 μL) into 1.2 mL of buffer at 37°C (5 mM Tris-HCl, pH 7.0, for photocoupling experiments with myoglobin; 5 mM Tris-HCl, pH 7.5, for streptavidin).

PED/DMPC Liposomes. Mixed liposomes consisting of PED and DMPC were prepared by the detergent dialysis method (16). PED (7–9.9 μmol), DMPC (7 μmol), and sodium cholate (23.9 μmol) were dissolved in 2.5 mL chloroform/methanol (4:1 v/v). After evaporation of the solvent in a stream of nitrogen, micelles were prepared by the addition of 7 mL of buffer A (0.1 M NaCl, 5 mM HEPES, pH 7.5) followed by sonication for 30 s in a bath-type sonicator (Laboratory Supplies Co., Hicksville, NY). Dialysis was carried out with a Dianorm-4 system (Dianorm-Geraete, Munich, Germany). Aliquots of the micellar suspension were distributed among three Macro-2

Teflon cells covered with dialysis membranes (molecular weight cutoff 10 000 Da, Diachema, Dianorm). Liposomes were formed by dialysis in buffer A (22 h at 35°C in the dark).

Electron Microscopy. Liposomes were adsorbed to carbon-coated parlodion films that were mounted on electron microscope grids and rendered hydrophilic by glow discharge at low pressure in air. After washing in Tris-HCl buffer (5 mM, pH 7.0) the liposomes were negatively stained with 0.75% uranyl formate (pH 4.2). Images were recorded on Kodak SO-163 film at a nominal magnification of 50 000 under low-dose conditions using a Hitachi H-7000 transmission electron microscope operated at 100 kV.

Differential Scanning Calorimetry. DSC was carried out on a Perkin-Elmer DSC-2. Dried PED (5–6 mg) or C_{16} -PED was dissolved at 37°C in 100 μL of ethanol and rapidly injected into 200 μL of water at 37°C in a plastic tube. A pellet was formed by centrifugation for 90 s on a table-top centrifuge (Eppendorf). The supernatant was discarded. A concentrated lipid dispersion was formed by resuspending the pellet in 10 μL of water. Aliquot samples (15 μL) were sealed in aluminum pans. DSC scans were recorded with a heating rate of $2.5^\circ\text{C}/\text{min}$.

Photoactivation of PED Liposomes. PED liposomes suspended in water (1 mg of lipid/mL) were prepared by the ethanol injection method and irradiated in quartz cuvettes. Samples of 1 mL were percolated with argon for 5 min before and during irradiation. The quartz cuvettes were positioned 40 cm from the light source (HBO 350 mercury lamp, Osram). Liposome suspensions were irradiated with light (200 W) filtered by a Schott WG 320 filter and a saturated solution of CuSO_4 in water (path-length, 1 cm). This filter combination efficiently screens short UV radiation.

Photocoupling of Aqueous-Soluble Proteins to PED-Containing Liposomes. Photocoupling of Myoglobin to PED Liposomes. PED liposome suspensions (1.4 mL) in 5 mM Tris-HCl, pH 7.0, were mixed with 900 μL of 0.27 mM myoglobin in 5 mM Tris-HCl, pH 7.0, in a molar lipid to protein ratio of 20:1. The liposome/protein mixture (1 mL) was percolated with argon for 5 min in the dark before and during irradiation which was performed for 20 s as described for PED liposomes. Photoactivation of PED was monitored by TLC, monitoring R_f changes of lipid products with chloroform/methanol/water (65:25:4 v/v/v) as the solvent system. Irradiated liposome/protein solutions (800 μL) were mixed with 400 μL of 5 mM Tris-HCl, pH 7.0, containing 0.2 M NaCl. Liposome-bound myoglobin was separated from free myoglobin by gel filtration. Aliquot samples (500 μL) were applied to a Sephacryl S-300 HR 10/30 column (Pharmacia) and eluted with 0.1 M NaCl, 5 mM Tris-HCl, 0.02% NaN_3 , pH 7.0, by FPLC procedures at a flow rate of 1 mL/min. Absorbance at 280 nm was recorded, and 1-mL fractions were collected. Nonirradiated samples served as a control. The liposome/protein mixture was treated identically, but photoactivation was omitted. Heme absorption was recorded on a Uvikon 810 spectrophotometer with photoactivated and control liposomes after separation of free myoglobin. Phospholipid contents were assayed by the method of Chen et al. (17).

Photocoupling of Streptavidin to PED Liposomes. Mixtures of PED liposomes and streptavidin (400 μL ; 5 mM Tris-HCl, pH 7.5) were prepared at a molar lipid to protein ratio of 125:1. Samples were percolated with argon for 5 min before and during irradiation (3 min). After photocoupling liposome/streptavidin mixtures were diluted with 350 μL of 5 mM Tris-HCl buffer (pH 7.5) containing 0.2 M NaCl. Liposome-bound streptavidin was

separated from free streptavidin by chromatography on Superose 12 (Pharmacia 10/30 column, sample volume of 500 μ L). Elution was carried out with 0.1 M NaCl, 5 mM Tris-HCl, 0.02% NaN₃, pH 7.5, at a flow rate of 1 mL/min. Control samples were treated identically, but photoactivation was omitted. The extent of streptavidin photocoupling to PED liposomes was assayed by monitoring [¹⁴C]biotin binding. Briefly 25 μ L of [¹⁴C]biotin (18.7 μ M, 53 μ Ci/ μ mol) in water was added to Superose 12 fractionated liposomes (300 μ L of fraction 4) of photoactivated or nonphotoactivated samples. Following incubation (4 h) at room temperature, unbound [¹⁴C]biotin was removed from the liposomes by gel chromatography on Sephadex G 25 (10/10, Pharmacia, flow 1 mL/min) equilibrated with 0.1 M NaCl, 5 mM Tris-HCl, 0.02% NaN₃, pH 7.5. Fractions (1 mL) were collected and analyzed for [¹⁴C]radioactivity by scintillation counting (K 3000, Kontron).

Photocoupling of Trypsin to PED/DMPC Liposomes. Suspensions of PED/DMPC liposomes at a molar ratio of 1.4:1 in 0.1 M NaCl, 5 mM HEPES, pH 7.5 (buffer B), were prepared by the detergent dialysis method. Aliquot samples (650 μ L) were mixed with 350 μ L of 0.36 mM trypsin in 0.1 M NaCl, 5 mM HEPES, 2 mM CaCl₂, pH 7.5, at a molar lipid to protein ratio of 16:1. The mixture was percolated with argon for 5 min in the dark and during 5-min irradiation. Irradiated liposome/protein mixtures (800 μ L) were diluted with 400 μ L of 0.1 M NaCl, 5 mM HEPES, 2 mM CaCl₂, 0.02% NaN₃, pH 7.8 (buffer C). Separation of liposome-bound trypsin and free trypsin was achieved by fractionation of 500- μ L samples on Superose 12 equilibrated with buffer C at a flow rate of 1 mL/min. Fractions of 1 mL were collected. Nonphotoactivated samples served as a control. The hydrolytic activity of liposome-associated trypsin was assayed with the chromogenic substrate S-2251 (H-D-valyl-L-leucyl-L-lysine *p*-nitroanilide dihydrochloride). After separation of free trypsin, liposomes (500 μ L) of either photoactivated or nonphotoactivated preparations were mixed with 110 μ g of S-2251 dissolved in 50 μ L of water. Release of *p*-nitroaniline was recorded at 405 nm on a Uvikon 810 at 25 $^{\circ}$ C immediately after substrate addition. In inhibition experiments 20 μ g of soybean trypsin inhibitor was included in the assay medium prior to substrate addition.

RESULTS

Synthesis of PED. The photoactivatable phospholipid was produced by coupling the heterobifunctional photoactivatable reagent TRIMID to synthetic dimyristoylphosphatidylethanolamine (Figure 1). The structure of PED was confirmed by ¹H NMR. The photoactivatable lipids remained structurally intact over months when stored in the dark at -20 $^{\circ}$ C in chloroform/methanol (4:1 v/v). PED was handled under normal laboratory conditions; exposure to intense sunlight and artificial light was avoided.

Differential Scanning Calorimetry. To set the optimum thermal conditions for liposome formation (18), the thermotropic transition T_c of PED was determined by DSC. PED suspensions were prepared by injecting lipids into water. C₁₆-PED served as a reference. Within the temperature range of the analysis, a major PED phase transition occurred at 10.5 $^{\circ}$ C. In comparison, C₁₆-PED showed a phase transition at 28.5 $^{\circ}$ C. DSC data were collected at the second heating cycle; they thus represent reversible phase transitions. Major effects of residual ethanol on T_c were ruled out on the basis of the following control experiments: DSC of DMPC lipid suspensions prepared by hydration of a lipid film or by ethanol

injection yielded a T_c of 23.5 $^{\circ}$ C, which is in agreement with published data (19). A ΔT_c of 18 $^{\circ}$ C between PED and C₁₆-PED is consistent for phospholipids with the same head group but differing in the saturated hydrocarbon chain by two carbon atoms (DMPC, T_c = 23 $^{\circ}$ C; DPPC, T_c = 41 $^{\circ}$ C (19)). Arylthiocarbamoylation of the primary amine of DMPE shifts the phase transition from 50 (18) to 10.5 $^{\circ}$ C. The bulky headgroup of PED and its interrelation with neighboring molecules may prevent close lipid packing in the gel phase (20, 21).

Formation and Characterization of Liposomes. Single component PED liposomes were formed by ethanol injection. The procedure is mild, does not degrade phospholipids, and gives reasonably homogeneous SUVs (15). For photocoupling of proteins, PED was dissolved in ethanol and injected into buffered media at 37 $^{\circ}$ C, a temperature well above the phase transition of PED. The liposome suspension contained 14% ethanol and 3.1 mg (3.5 μ mol) of PED/mL of buffer. It has been noted for this lipid that 14% ethanol had no effect on the formation of PED liposomes, but influenced their size and size distribution. SUVs composed of PED and DMPC in a molar ratio of 1:1 to 1.4:1 were prepared by detergent dialysis. Mixed micelles (PED/DMPC/sodium cholate 1-1.4:1:3.4) were dialyzed against HEPES buffer in the dark for 22 h. Extended preparation times and elevated temperatures (35 $^{\circ}$ C) did not affect the photoreactivity of PED. Electron microscopy of negatively stained PED/DMPC liposomes (1:1) revealed SUVs with a mean radius of 20 nm (Figure 2A). Liposome size changes were not observed upon photoactivation for 5 min (Figure 2B). Ethanol injected, nonphotoactivated, negatively stained single component PED liposomes with radii varying from 48 to 20 nm are depicted in Figure 3A. As observed for the above mentioned PED/DMPC liposomes, single component PED liposomes did neither decompose nor change their radii upon irradiation. Both statements are based on electron microscopic evidence. Concentrated PED liposome suspensions were prepared for protein immobilization purposes by injecting 3.5 μ mol of PED, dissolved in 200 μ L of ethanol, into 1.2 mL of buffer. This protocol yields less homogeneous liposomes with radii ranging from 16 to 84 nm (Figure 3B).

Photoactivation of PED. Upon irradiation with UV light (≥ 320 nm) the PED diazirine head group decays to a highly reactive carbene intermediate and nitrogen (10). The diazirine of the parent compound TRIMID showed an absorption maximum at 347 nm (12). Photolabel coupling to the primary amine of DMPE by arylthiocarbamoylation induced a shift to 355 nm. Photoactivation was spectroscopically monitored by recording the disappearance of the diazirine absorption band (Figure 4). For kinetic studies the concentration C_t of the diazirine at a defined irradiation time (t) was quantitated by the absorption difference $A_t - A_{\infty}$ at 355 nm, where A_{∞} is the absorption under saturating light (30 s for PED liposomes; 240 s for PED in methanol). $\log [(A_t - A_{\infty})/(A_0 - A_{\infty})]$ expressed as a function of the irradiation time yielded straight lines (Figure 5), which concurs with first-order kinetic processes (22). In order to compare the diazirine decay kinetics in PED-liposomes and monomeric PED in methanol, identical PED concentrations (0.57 mM) and light intensities were used for sample activation. With reference to the liposomal system a 7.7-fold slower decay of PED was observed when photolyzed in methanol. The half-life time was 4.7 s for PED in liposomes and 36.2 s for PED in methanol.

Photocoupling of Water-Soluble Proteins to PED-Containing Liposomes. *Photocoupling of Myoglobin to PED Liposomes.* Myoglobin has been chosen as a

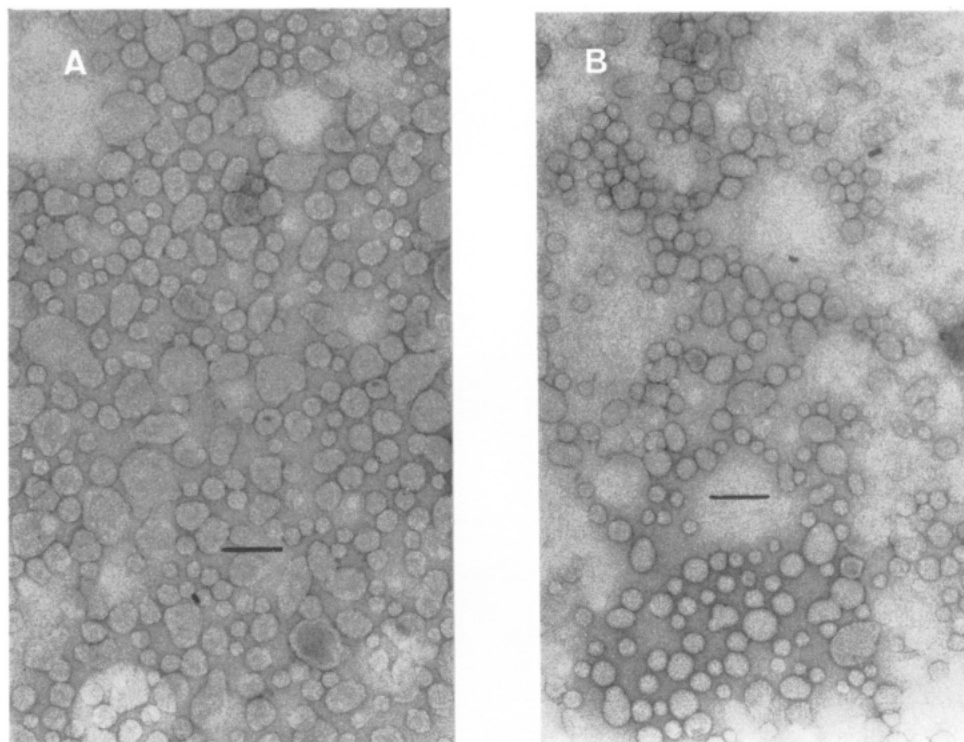


Figure 2. (A) Negatively stained, nonphotoactivated PED/DMPC (1:1 molar ratio) small unilamellar vesicles in 0.1 M NaCl, 5 mM HEPES, pH 7.5 (prepared by cholate dialysis); scale bar, 100 nm. (B) Same liposome preparation after 5 min irradiation.

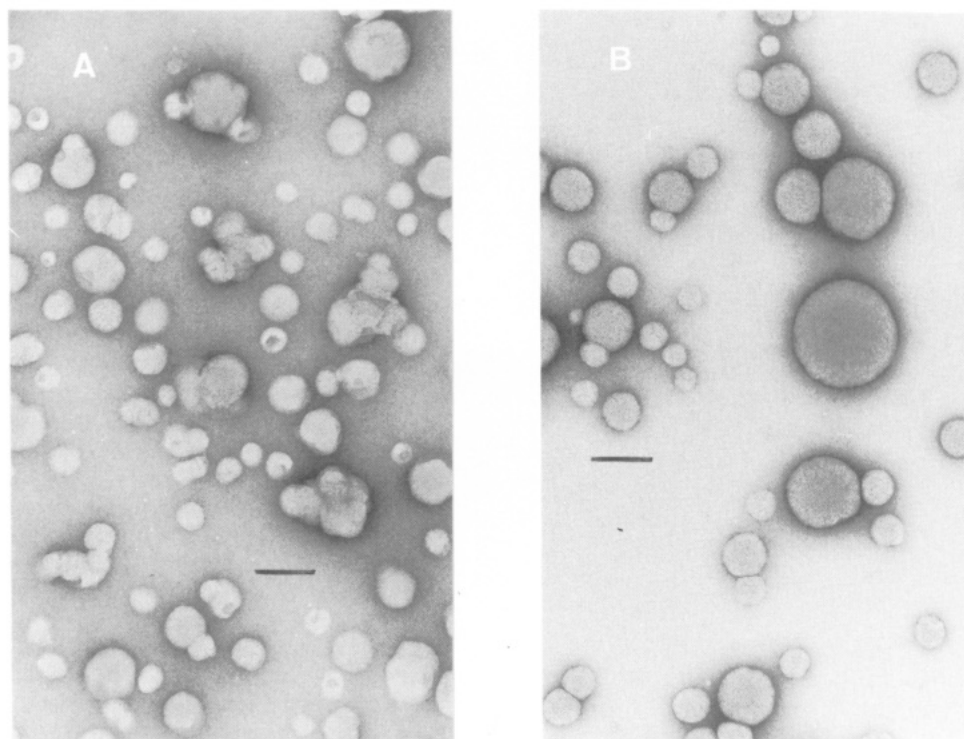


Figure 3. (A) Negatively stained, nonphotoactivated PED liposomes prepared by injecting 3.5 μ mol PED into 3 mL of 0.1 M NaCl, 5 mM Tris-HCl, pH 7.5, at 37 $^{\circ}$ C; scale bar, 100 nm. (B) Negatively stained PED liposomes prepared by injecting 3.5 μ mol PED into 1.2 mL of 0.1 M NaCl, 5 mM Tris-HCl, pH 7.5, at 37 $^{\circ}$ C. The liposome preparation was irradiated for 5 min before staining and electron microscopic analysis.

reference protein: Its molecular weight (18.8 kDa) is in the range of ligands to be utilized for the fabrication of targetable liposomes. Myoglobin coupling to single-component PED liposomes was assayed and quantitated spectroscopically by its heme absorption band at 410 nm. PED liposomes were mixed with myoglobin in a buffer of low ionic strength (5 mM Tris-HCl, pH 7.0). The liposome/protein mixture was photoactivated under argon for 20 s. Nonirradiated control samples containing PED liposomes and myoglobin were processed analogously. After dilution

with a high ionic strength buffer (0.2 M NaCl, 5 mM Tris-HCl, pH 7.0) liposome-bound myoglobin was separated from free myoglobin by gel chromatography on Sephacryl S-300. A UV/vis spectrum of chromatographically separated PED liposomes photoactivated in the presence of myoglobin is shown in Figure 6 together with the absorbance of a nonirradiated control sample. The extent of net ligand binding was 120 μ g/ μ mol PED. Light-independent myoglobin adsorption to PED liposomes was below 15 μ g/ μ mol PED.

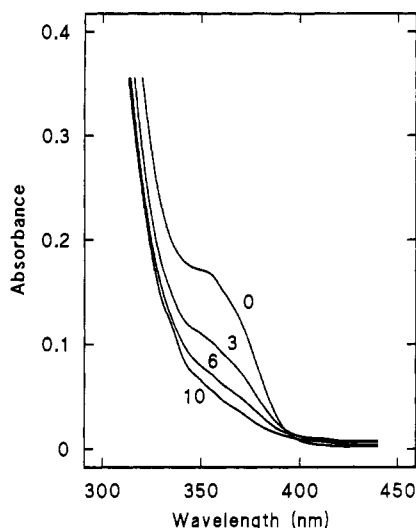


Figure 4. PED photolysis. PED liposomes in water (0.57 mM PED) were irradiated for the indicated time lengths (0, 3, 6, 10 s) and ultraviolet spectra were recorded.

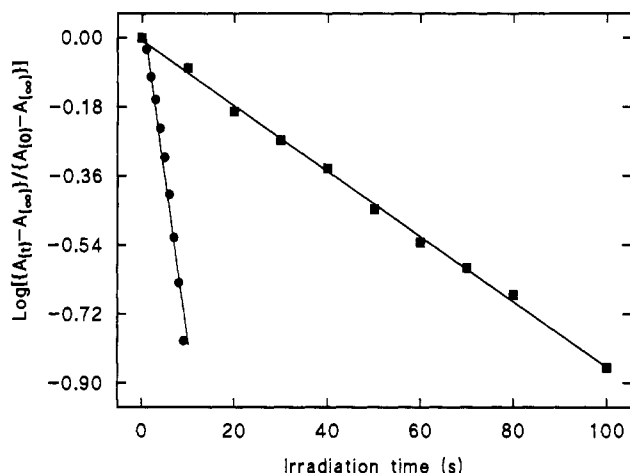


Figure 5. Kinetics of PED photolysis. Kinetics of diazine decay of PED liposomes (0.57 mM PED) suspended in water (●); monomeric PED (0.57 mM) in methanol (■).

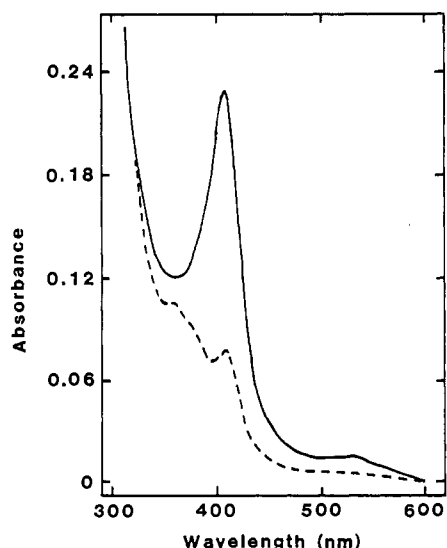


Figure 6. Photocoupling of myoglobin to PED liposomes. UV/vis spectra of PED liposome fractions after separation of free myoglobin: (—) PED liposomes photoactivated in the presence of myoglobin, (---) nonphotoactivated control sample.

Exposure of myoglobin to light (wavelengths ≥ 320 nm) did not cause chromophore absorption changes, indicating photostability of the chromoprotein. SDS gel electro-

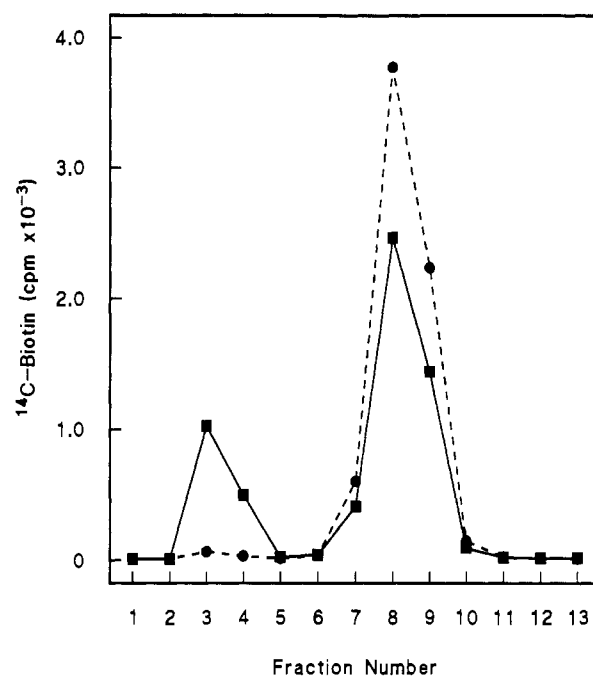


Figure 7. [^{14}C]Biotin binding to streptavidin photoimmobilized on PED liposomes. PED liposomes were photoactivated (control without light exposure) in the presence of streptavidin and—after separation of free streptavidin—incubated with [^{14}C]biotin. Streptavidin-[^{14}C]biotin proteoliposomes were subsequently separated from free [^{14}C]biotin by gel chromatography on Sephadex G-25: (■) Sephadex G-25 elution diagram showing that [^{14}C]biotin coelution with PED liposomes photoactivated in the presence of streptavidin. (Streptavidin-biotin conjugates on PED liposomes elute in fraction 3 and 4.) (●) Elution diagram as above recording [^{14}C]biotin binding to nonphotoactivated control samples.

phoretic analysis of myoglobin-proteoliposomes and non-irradiated myoglobin revealed identical mobilities for both protein samples (15% SDS-polyacrylamide gel according to ref 23). Occurrence of photopolymerized myoglobin is therefore excluded. It has further been shown that the amount of myoglobin adsorbed to preirradiated liposomes was equal to the extent of protein adsorbed to nonphotoactivated PED liposomes.

Photocoupling of Streptavidin to PED Liposomes. Streptavidin has been photocoupled to PED liposomes in order to investigate photoeffects on biotin binding. Single component PED liposomes were photoactivated under argon in the presence of streptavidin. Free streptavidin was separated from liposome coupled streptavidin by gel chromatography on Superose 12 equilibrated with Tris-HCl buffer (pH 7.5). The extent of streptavidin photocoupling to PED liposomes was assayed by [^{14}C]biotin binding. Superose 12 fractionated liposomes (photoactivated or nonphotoactivated) were incubated with [^{14}C]biotin. [^{14}C]Biotin-streptavidin proteoliposomes were separated by gel chromatography on Sephadex G-25 (Figure 7). [^{14}C]Biotin binding to PED liposomes photoactivated in the presence of streptavidin exceeded the label incorporation in control samples by a factor of 10. Photocoupling of $12.2\ \mu\text{g}$ streptavidin/ μmol PED is inferred, with four biotin binding sites accessible.

Photocoupling of Trypsin to PED/DMPC Liposomes. Trypsin, chosen as a reference enzyme, reports on the fate of its catalytic activity when exposed to light under photocoupling conditions. Mixed liposomes of PED and DMPC were used in order to study the coupling efficiency of the photoactivatable lipid in the presence of lipids other than PED. Mixed liposomes were prepared by detergent dialysis and combined with trypsin in HEPES buffer (pH

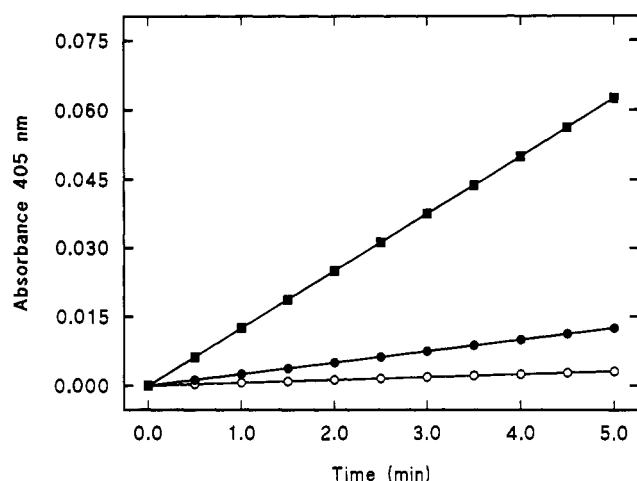


Figure 8. Photoimmobilization of trypsin on PED/DMPC liposomes. Time-dependent release of *p*-nitroaniline from the substrate S-2251 effected by photoimmobilized trypsin on PED/DMPC liposomes (1.4:1 molar ratio) at 25 °C: (■) Protease activity on PED/DMPC liposomes photoactivated in the presence of trypsin, (●) nonphotoactivated samples, (○) remaining protease activity on PED/DMPC liposomes photoactivated in the presence of trypsin after addition of soybean trypsin inhibitor.

7.5). Liposome/protein mixtures were photoactivated under argon. Liposome-bound trypsin was separated from free trypsin by gel chromatography at a slightly higher pH (HEPES buffer, pH 7.8). Proteoliposomes eluted in the void volume. They were assayed for protease activity with the chromogenic substrate S-2251 (Figure 8). Results obtained showed significantly higher (5-fold) protease activities in the trypsin-proteoliposome fraction than in the corresponding control samples. Moreover, inhibition of protease activity by the soybean trypsin inhibitor further documents the photostability of the enzyme.

DISCUSSION

Synthesis and (Photo)Chemical Properties of PED.

The product of the one-step reaction between the primary amine of DMPE and TRIMID is a negatively charged phospholipid (Figure 1). The synthesis is facile and large-scale production is envisaged. It has been shown earlier that PED forms planar bilayers upon apposition of surface spread monolayers. Irradiated and nonirradiated planar membranes remain stable for hours (11). Results reported in this study further document the phospholipid's ability to form bilayer membrane structures. The carbene-generating lipid spontaneously forms liposomes, prepared by either ethanol injection or detergent dialysis, but not by hydrating dried lipid films and subsequent sonication. When organized as a bilayer, PED was recognized and catalytically processed by the enzyme phospholipase A₂ (data not shown). Therefore, replacement of the fatty acid at the sn-2 position can be achieved by semisynthetic procedures (24).

To date, numerous phospholipids with photoactivatable groups incorporated in the fatty acyl chain (8) and two phospholipid analogues with diazirine head groups (9) were applied as molecular probes in native and reconstituted membrane systems. The synthesis of the latter lipids are considerably more complex than PED. Their application was restricted to the structural investigation of a multicomponent biomembrane system where coupling yields with individual components were discouragingly low.

Photoactivation of PED is most effective in liposomes where diazirine activation is completed within seconds. In addition to PED photolysis (interaction of the photo-

generated carbene with water) intraliposomal cross-links occur (data not shown). However, on the basis of circumstantial evidence extensive interlipid cross-linking is excluded: Photoactivation of PED bilayers did not impair diffusion of valinomycin within photoactivated planar membranes (11).

PED Liposomes. DSC revealed gel to liquid-crystalline phase transitions for PED at 10.5 °C. This allows preparation of liposomes and formation of proteoliposomes at ambient temperatures. The ethanol-injection method has been chosen as the preferred preparation procedure. With reference to proteoliposome fabrication this method allows fast processing under mild conditions. In accordance with observations reported by Kremer et al. (25), the size and size distribution of injected liposomes varied with varying lipid and organic solvent concentrations. Larger PED liposomes were obtained when concentrated lipid solutions were injected. Electron microscopic analysis revealed disperse liposomes. Their size and size distribution did not alter upon photoactivation.

Proteoliposomes from Photoactivatable Lipids and Aqueous-Soluble Proteins. Current methods of proteoliposome formation follow the general route of cross-linking ligands to functionalized lipids by thermochemical reactions. This study employs for the first time photochemical reactions for covalent ligand (protein) coupling to preformed liposomes. Myoglobin, streptavidin, and trypsin were chosen as reference proteins (enzymes) to elaborate the basic procedures for light-induced liposome coating. Photoactivation is carried out at wavelengths ≥ 320 nm, which limits UV-induced damage of proteins (biomolecules), and radiation effects on the photosensitive amino acids tyrosine and tryptophan are negligible (11, 26). Photocoupling of myoglobin to PED liposomes yields proteoliposomes with 7 myoglobin molecules per 1000 phospholipid molecules. This corresponds to a 15% liposome surface coverage, assuming a lipid surface area of 74 Å² (27) and an area of 1575 Å² per myoglobin molecule (28). Presuming that similar coupling yields are attained with any protein selected for targeting, the photocoupling procedure proves as efficient as current approaches. Large-scale preparation of homogeneously sized PED liposomes and biocompatible lipid composition (29) is in progress. With respect to future in vivo applications, it has been noted that photoactivated PED liposomes are not immunogenic (Sigrist, H., and Lerch, P., unpublished). Coupling of streptavidin to liposomes yields a polyvalent system, which allows conjugation of any biotinylated ligand. Covalent streptavidin-liposome conjugates have been generated by thermochemical coupling of thiolated streptavidin to *N*-[4-(*p*-maleimidophenyl)butyryl]phosphatidylethanolamine-containing liposomes (30). Coupling yields attained by thermochemical procedures are 15–50 μg streptavidin/μmol lipid. Photochemical ligand immobilization yields 12 μg streptavidin/μmol PED. Besides the ease of liposome preparation and the fact that the protein is utilized in its native, unmodified form, the successful photocoupling of streptavidin entails an additional important feature: Binding of biotin to photoimmobilized streptavidin is not affected by irradiation at wavelengths ≥ 320 nm, although the biotin binding pocket is a complex arrangement of several aromatic amino acid residues including tryptophan (Trp 79, 92, 108, 120 (31)). Retention of biotin binding capacity thus documents the biocompatibility of the irradiation process. Moreover, preservation of catalytic activity is documented with trypsin immobilized on PED/DMP liposomes. Recovery of liposome-bound enzyme activity and inhibition of the enzymatic activity by an externally added inhibitor implies that the photocoupled enzyme is structurally stable.

Photochemical versus Thermochemical Ligand Coupling. There are fundamental differences concerning the mechanisms of ligand binding by photochemical and thermochemical procedures. Thermochemical coupling of ligands requires either functionalized lipids and correspondingly reactive functional groups at the ligand's surface or vice versa. Ligand binding occurs only when two reactive groups—in some protocols even additional activating agents—are close and appropriately oriented. These requirements limit the versatility of the thermochemical approach. Photogenerated carbenes, however, are highly reactive and insert in all amino acid side-chain structures with a distinct pattern of preference (32). The only requirement for successful surface linking is molecular proximity of the ligand at the time of carbene generation. By judicious selection of liposome-forming lipids the noncovalent interaction of ligands with the liposomal surface prior to photoactivation may be enforced. As a consequence the probability of successful covalent ligand coupling increases. Photogenerated carbenes which do not encounter a ligand will photolyze, react with buffer components or neighboring lipids. In general terms, this new technology of ligand coupling is considered exceptionally advantageous for versatile surface engineering, including photoimmobilization of peptides, nucleic acids, and carbohydrates to coated or "inert" supports. Procedures presented may prove useful in liposome targeting and the liposome-based design of vaccines.

ACKNOWLEDGMENT

We are grateful to Prof. Dr. A. Engel and Mr. A. Hefti for the preparation of electron micrographs. This work was supported by the Swiss National Science Foundation (Grant No. 31-26234.89) and the "Studienstiftung der Basler Chemischen Industrie".

LITERATURE CITED

- (1) Leserman, L., and Machy, P. (1988) Ligand Targeting of Liposomes. In *Liposomes: From Biophysics to Therapeutics* (M. Ostro, Ed.) pp 157–194, Marcel Dekker, New York.
- (2) Alving, C. R. (1987) Liposomes as carriers for vaccines. In *Liposomes: From Biophysics to Therapeutics* (M. Ostro, Ed.) pp 195–218, Marcel Dekker, New York.
- (3) Gregoriadis, G. (1990) Immunological adjuvants: A role for liposomes. *Immunol. Today* 11, 89–97.
- (4) Ho, R. J. Y., and Huang, L. (1988) Immunoliposome assays: Perspectives, progress and potential. In *Liposomes as Drug Carriers* (G. Gregoriadis, Ed.) pp 527–547, John Wiley & Sons, Chichester.
- (5) Golubev, A., and Sidorova, E. (1989) The use of targeted liposomes to isolate cells bearing immunoglobulin receptors. *J. Immunol. Methods* 125, 29–34.
- (6) Powers, J. D., Kilpatrick, P. K., and Carbonell, R. G. (1990) Trypsin purification by affinity binding to small unilamellar liposomes. *Biotechnol. Bioeng.* 36, 506–519.
- (7) Martin, F. J., Heath, T. D., and New, R. R. C. (1990) Covalent attachment of proteins to liposomes. In *Liposomes: A practical approach* (R. R. C. New, Ed.) pp 163–182, Oxford University Press, Oxford.
- (8) Brunner, J., and Richards, F. M. (1980) Analysis of membranes photolabeled with lipid analogues. *J. Biol. Chem.* 255, 3319–3329.
- (9) Burnett, B. K., Robson, R. J., Takagaki, Y., Radhakrishnan, R., and Khorana, H. G. (1985) Synthesis of phospholipids containing photoactivatable carbene precursors in the head-groups and their crosslinking with membrane proteins. *Biochim. Biophys. Acta* 815, 57–67.
- (10) Bayley, H. (1983) *Photogenerated Reagents in Biochemistry and Molecular Biology*, Elsevier Science Publishers, Amsterdam.
- (11) Borle, F., Sänger, M., and Sigrist, H. (1991) Planar bilayer membranes from photoactivable phospholipids. *Biochim. Biophys. Acta* 1066, 144–150.
- (12) Dolder, M., Michel, H., and Sigrist, H. (1990) 3-(Trifluoromethyl)-3-(m-Isothiocyano-phenyl)Diazirine: Synthesis and chemical characterization of a heterobifunctional carbene-generating crosslinking reagent. *J. Protein Chem.* 9, 407–415.
- (13) Still, W. C., Kahn, M., and Mitra, A. (1978) Rapid chromatographic technique for preparative separations with moderate resolution. *J. Org. Chem.* 43, 2923–2925.
- (14) Dittmer, J. C., and Lester, R. L. (1964) A simple, specific spray for the detection of phospholipids on thin-layer chromatograms. *J. Lipid. Res.* 5, 126–127.
- (15) Batzri, S., and Korn, E. (1973) Single bilayer liposomes prepared without sonication. *Biochim. Biophys. Acta* 298, 1015–1019.
- (16) Zumbuehl, O., and Weder, H. G. (1981) Liposomes of controllable size in the range of 40 to 180 nm by defined dialysis of lipid/detergent mixed micelles. *Biochim. Biophys. Acta* 640, 252–262.
- (17) Chen, P. S., Toribara, T. Y., and Warner, H. (1956) Microdetermination of phosphorus. *Anal. Chem.* 28, 1756–1758.
- (18) Szoka, F., and Papahadjopoulos, D. (1980) Comparative properties and methods of preparation of lipid vesicles (liposomes). *Annu. Rev. Biophys. Bioeng.* 9, 467–508.
- (19) Chapman, D. (1984) Physicochemical properties of phospholipids and lipid-water systems. In *Liposome Technology* (G. Gregoriadis, Ed.) Vol. I, pp 1–18, CRC Press, Boca Raton, FL.
- (20) Traeuble, H., Teubner, M., Wooley, P., and Eibl, H. (1976) Electrostatic interactions at charged lipid membranes. I. Effects of pH and univalent cation on membrane structure. *Biophys. Chem.* 4, 319–326.
- (21) Casal, H. L., and Mantach, H. H. (1983) The thermotropic phase behavior of N-methylated dipalmitoylphosphatidylethanolamines. *Biochim. Biophys. Acta* 735, 387–396.
- (22) Nassal, M. (1983) 4-(1-Azi-2,2,2-trifluoroethyl)benzoic acid, a highly photolabile carbene generating label readily fixable to biochemical agents. *Liebigs Ann. Chem.* 1510–1523.
- (23) Laemmli, U. K. (1970) Cleavage of structural proteins during the assembly of the head of bacteriophage T4. *Nature* 227, 680–685.
- (24) Eibl, H. (1980) Synthesis of glycerophospholipids. *Chem. Phys. Lipids* 26, 405–429.
- (25) Kremer, J. M. H., v. d. Esker, M. W. J., Pathmamanoharan, C., and Wiersma, P. H. (1977) Vesicles of variable diameter prepared by a modified injection method. *Biochemistry* 16, 3932–3935.
- (26) Busath, D., and Waldbillig, R. C. (1983) Photolysis of gramicidin A channels in lipid bilayers. *Biochim. Biophys. Acta* 736, 28–38.
- (27) Huang, C., and Mason, J. T. (1978) Geometric packing constraints on egg phosphatidylcholine vesicles. *Proc. Natl. Acad. Sci. U.S.A.* 75, 308–310.
- (28) Stryer, L. (1988) *Biochemistry*, 3rd ed., p 145, W. H. Freeman, New York.
- (29) Gregoriadis, G. (1988) Fate of injected liposomes: observation of entrapped solute retention, vesicle clearance and tissue distribution in vivo. In *Liposomes as Drug Carriers* (G. Gregoriadis, Ed.) pp 527–547, John Wiley & Sons, Chichester.
- (30) Loughrey, H. C., Wong, K. F., Choi, L. S., Cullis, P. R., and Bally, M. B. (1990) Protein-liposome conjugates with defined size distributions. *Biochim. Biophys. Acta* 1028, 73–81.
- (31) Weber, P. C., Ohlendorf, D. H., Wendoloski, J. J., and Salemme, F. R. (1989) Structural origins of high-affinity biotin binding to streptavidin. *Science* 243, 85–88.
- (32) Sigrist, H., Muehleemann, M., and Dolder, M. (1990) Philicity of amino acid side-chains for photogenerated carbenes. *J. Photochem. Photobiol. B:7*, 277–287.

In Vivo Antitumor Activity of a Panel of Four Monoclonal Antibody-Vinca Alkaloid Immunoconjugates Which Bind to Three Distinct Epitopes of Carcinoembryonic Antigen

James J. Starling,*† Ronald S. Maciak,† N. Ann Hinson,† Cynthia L. Nichols,† Stephen L. Briggs,† Bennett C. Laguzza,† William Smith,† and Jose R. F. Corvalan†

Lilly Research Laboratories, Department MC7R1, Eli Lilly and Company, Lilly Corporate Center, Indianapolis, Indiana 46285, and Lilly Research Centre Ltd., Eli Lilly and Company, Erl Wood Manor, Windlesham, Surrey GU20 6PH, UK. Received March 31, 1992

A panel of four murine monoclonal antibodies apparently directed against three distinct epitopes of carcinoembryonic antigen (CEA) was conjugated via oxidized carbohydrate groups to 4-desacetylvinblastine-3-carboxhydrazide. The resulting antibody-vinca conjugates were evaluated for antitumor activity against 2-9-day-established LS174T human colorectal carcinoma xenografts. The antibodies (immunoglobulin G, IgG) employed in this study were 11.285.14 (IgG₁), 14.95.55 (IgG_{2a}), CEM231 (IgG₁), ZCE025 (IgG₁). Additive immunofluorescence studies indicated that CEM231 and ZCE025 recognized the same or a closely related epitope(s) on CEA which was distinct from the two epitopes bound by 11.285.14 and 14.95.55. The in vivo antitumor efficacy studies demonstrated that chemoimmunoconjugates prepared from 14.95.55 and ZCE025 were more active than the conjugates constructed from the 11.285.14 and CEM231 antibodies. The 14.95.55 and ZCE025 immunoconjugates were also more efficacious than free drug or drug conjugated to irrelevant murine IgG. The presence of increased carbohydrate content on the light chain of ZCE025 may have been responsible for the ability to construct ZCE025-vinca conjugates with about twice the drug content (~10 mol of vinca/mol of IgG) than was achieved with the other antibodies. The highly conjugated form of ZCE025 demonstrated similar efficacy but was much less toxic than a ZCE025 conjugate containing 5 mol of vinca/mol of IgG. These data indicated that significant differences existed in the ability of monoclonal antibodies to target a cytotoxic agent for effective antitumor activity even when the immunoconjugates recognized the same antigen or even the same or closely related antigenic epitope(s). Furthermore, these differences could not have been identified without extensive in vivo evaluation for antitumor efficacy.

INTRODUCTION

CEA¹ is perhaps the most widely studied and utilized human tumor marker (1, 2). The normal physiologic role of CEA is still unclear, but recent studies have identified it as an adhesion-related protein and a member of the immunoglobulin supergene family (3). mAbs directed against numerous epitopes of CEA have been characterized (4-11) and many papers have described the diagnostic and therapeutic potential of radio-, toxin-, and chemoimmunoconjugates constructed using anti-CEA mAbs (12-31). A number of recent publications have elucidated the potent in vivo antitumor activity of mAb-DAVLBHYD conjugates directed against various human solid tumor membrane antigens. These antigen systems included KS1/4 (32-34), squamous cell carcinoma membrane antigens (35, 36), TAG72 (37), and epidermal growth factor receptor (38). The studies enumerated in this report will extend this list to include a panel of mAb-DAVLBHYD conjugates directed against at least three distinct epitopes of CEA.

EXPERIMENTAL PROCEDURES

Monoclonal Antibodies and Immunoconjugates. The hybridoma cell lines secreting the CEM231 (39) and

ZCE025 (same clone as Mab 35 described by Haskell et al., ref 40) anti-CEA mAbs were obtained from Dr. Richard Bartholomew, Hybritech, Inc., San Diego, CA. These hybridoma cultures as well as the cell lines secreting the 11.285.14 and 14.95.55 (11) anti-CEA mAbs were grown as ascites and each antibody was purified from the corresponding ascites fluid by Protein A chromatography. Non-antigen-binding mAbs of the IgG₁ and IgG_{2b} subtypes were also purified from ascites fluid in the same manner. Additive immunofluorescence was performed by incubating 50 µg/mL mAb-FITC conjugates (containing 1.5-1.7 mol of fluorescein/mol of antibody, kindly supplied by Dr. Maurice Scheetz, Lilly Research Laboratories, Indianapolis, IN) alone or in combination with another mAb-FITC conjugate in the presence of antigen-positive tumor cells and quantifying the amount of antibody bound by flow cytometry. Purified CEM231, 11.285.14, 14.95.55, and irrelevant IgG were conjugated to DAVLBHYD as previously described (41). Briefly, mAbs were concentrated to about 10 mg/mL by vacuum dialysis in phosphate-buffered saline and subsequently dialyzed against 0.1 M sodium acetate, pH 5.6. The antibodies were oxidized by treatment for 21 min with 160 mM sodium metaperiodate and purified by Sephadex G-25 chromatography in acetate buffer. Conjugation to DAVLBHYD was performed by incubating the mAb for 24 h at 4 °C in the presence of 5 mM vinca. ZCE025 was conjugated to DAVLBHYD using similar methodology, but the periodate oxidation reaction was done for either 10 or 21 min to generate conjugates with different amounts of DAVLBHYD attached per mole of mAb. This procedure routinely resulted in the conjugation of 3-6 mol of DAVLBHYD/mol of 11.285.14,

* Author to whom correspondence should be addressed.

† Lilly Research Laboratories.

† Lilly Research Centre Ltd.

¹ Abbreviations used: CEA, carcinoembryonic antigen; mAb, monoclonal antibody; FITC, fluorescein isothiocyanate; IgG, immunoglobulin G; DAVLBHYD, 4-desacetylvinblastine-3-carboxhydrazide; SDS-PAGE, sodium dodecyl sulfate polyacrylamide gel electrophoresis; endo F, endo-β-N-acetylglucosaminidase; DMEM, Dulbecco's modified Eagle's medium; LD, lethal dose; RIA, radioimmunoassay.

14.95.55, CEM231, or irrelevant IgG₁ mAb as determined by dual-wavelength UV spectroscopy (41). The 10- or 21-min periodate oxidation reactions resulted in the conjugation of approximately 5 or 10 mol of DAVLBHYD/per mol of ZCE025, respectively. Immunoreactivity of mAbs and mAb-drug conjugates was evaluated against antigen-positive or antigen-negative human tumor cells using solid-phase radioimmunoassay and flow cytometry of live cells (32). The presence of aggregates was assessed by reduced and nonreduced SDS-PAGE and Superose 12 column chromatography (32). The glycosylation of the ZCE025 light chain was characterized by treating the antibody with the enzyme endo F (42) and analyzing the resultant products on SDS-PAGE.

Human Tumor Cell Lines and Nude Mouse Xenograft. LS174T human colon carcinoma cells were purchased from the American Type Culture Collection and propagated in vitro in DMEM containing 10% fetal calf serum, L-glutamine, and 50 μ g/mL gentamicin. M14 human melanoma cells (43) were kindly provided by Dr. Thomas Bumol, Lilly Research Laboratories, Indianapolis, IN, and grown in the same tissue culture medium used for LS174T. Human colon carcinoma cell lines SW948, Colo 205, SW403, HCT116, LoVo, DLD-1, and HCT-15 were also purchased from the American Type Culture Collection and propagated in vitro using the recommended culture conditions. For in vivo studies, LS174T cells were grown in vitro, removed from the substratum, and washed three times in phosphate-buffered saline. Cells (1×10^7) were injected sc in the hindquarters of 25-27-g female outbred nude mice (Charles River Breeding Laboratories, Boston, MA). The tumors were allowed to establish for various times, and treatments of phosphate-buffered saline, mAb-DAVLBHYD conjugates, free mAb, and free DAVLBHYD were given iv at defined intervals. Tumor size was determined by caliper measurements and tumor mass in milligrams was estimated from the formula $l \times w^2/2$, where l is the larger and w is the smaller of perpendicular diameters. Control groups contained 10-14 animals, whereas treatment groups comprised 5-7 mice each.

RESULTS

Live cell immunofluorescence (Figure 1) indicated that all four anti-CEA mAbs had similar cell surface binding to LS174T tumor cells. These data also demonstrated that additive binding was observed for various antibody combinations with the exception of CEM231 and ZCE025. These results suggested that CEM231 and ZCE025 are reactive with the same or closely related antigenic epitope(s) which is different than the two epitopes recognized by 11.285.14 and 14.95.55. Our data are in agreement with a previous report which stated that 11.285.14 and 14.95.55 bound different epitopes on the CEA molecule (11).

The mAb-DAVLBHYD conjugates used for the in vivo experiments described below exhibited good immunoreactivity as determined by solid-phase RIA against LS174T tumor cells which display the CEA target antigen (Figure 2). Immunofluorescence studies with M14 melanoma cells demonstrated that the conjugates did not bind to CEA antigen-negative human tumor cells (data not shown). Size-exclusion chromatography and SDS-PAGE analyses indicated that the anti-CEA immunoconjugates possessed low levels of aggregates (usually <10% and not exceeding 15%) similar to the mAb-DAVLBHYD conjugates described previously (32, 41; data not shown). 11.285.14, 14.95.55, and CEM231 gave conjugates with 3-6 mol of drug bound/mol of IgG, which is quite typical for this conjugation procedure (41).

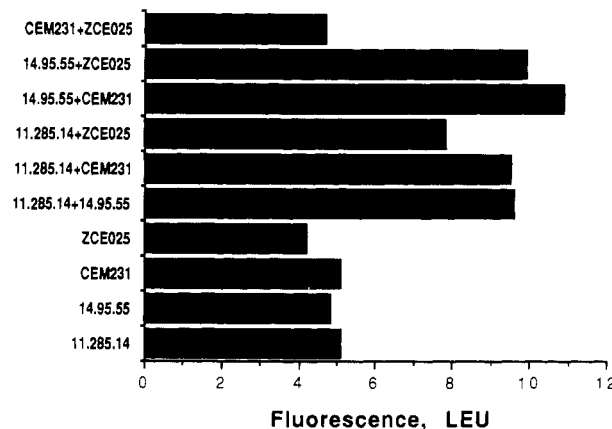


Figure 1. Additive membrane fluorescence analysis of anti-CEA mAbs. LS174T tumor cells were grown in vitro and removed from the substratum with trypsin-EDTA. The cells were washed and resuspended at a concentration of 1×10^7 cells/mL in 0.1 mL of cold tissue culture medium containing 50 μ g/mL mAb-FITC conjugate. The cells were incubated for 1 h at 4 °C and washed. The cell pellets were resuspended in 1% paraformaldehyde in phosphate-buffered saline and mean fluorescence intensities were determined with an Epics V flow cytometer. Linear equivalent units (LEU) were calculated by multiplying the mean fluorescence intensity by 0.0118 and taking the antilog as suggested by the manufacturer.

During the construction of the anti-CEA-DAVLBHYD immunoconjugates, however, it was noticed that ZCE025 routinely yielded conjugates with relatively high amounts of drug per mole of antibody. Analysis by reduced SDS-PAGE indicated that the light chain of ZCE025 had an apparent M_r of 28 kDa (Figure 3, lane A), which was considerably higher than the light chain of the other anti-CEA mAbs (illustrated with CEM231) used in these studies (Figure 3, lane E). One possible explanation, therefore, for the increased vinca incorporation into ZCE025 via oxidized carbohydrate groups was that the ZCE025 light chain was highly glycosylated relative to the other mAbs which resulted in a higher degree of drug attachment to ZCE025. To test this possibility ZCE025 was incubated with endo F, which is an enzyme capable of cleaving glycans of both the high-mannose and complex type linked through asparagine to the protein backbone (42). The data shown in Figure 3, lane C, demonstrated that treatment with endo F caused a significant amount of the ZCE025 light chain to migrate with a M_r that was indistinguishable from the CEM231 light chain (Figure 3, lane G). This result strongly suggested that the light chain of ZCE025 was indeed highly glycosylated and that this could be the site of increased vinca incorporation during the conjugation reaction. No significant change was observed in the apparent M_r for the CEM231 light chain (Figure 3, lane G) or the heavy chains of either mAb (Figure 3, lanes C and G) as a result of endo F treatment. The change induced in the ZCE025 light chain M_r was enzyme specific since no effects were observed in antibody samples handled identically to the endo F treated samples but incubated without the enzyme (Figure 3, lanes B and F). The failure of endo F to cause all of the ZCE025 light chain to migrate with a lower apparent M_r may indicate incomplete digestion of the susceptible carbohydrate groups and/or the presence of light chain carbohydrate that is resistant to endo F treatment. Advantage was taken of the ability of ZCE025 to incorporate relatively large amounts of vinca to construct immunoconjugates with "high" (~ 10 mol of vinca/mol of mAb) and "low" (~ 5 mol of vinca/mol of mAb) amounts of drug attached for direct comparison in the human tumor xenograft studies.

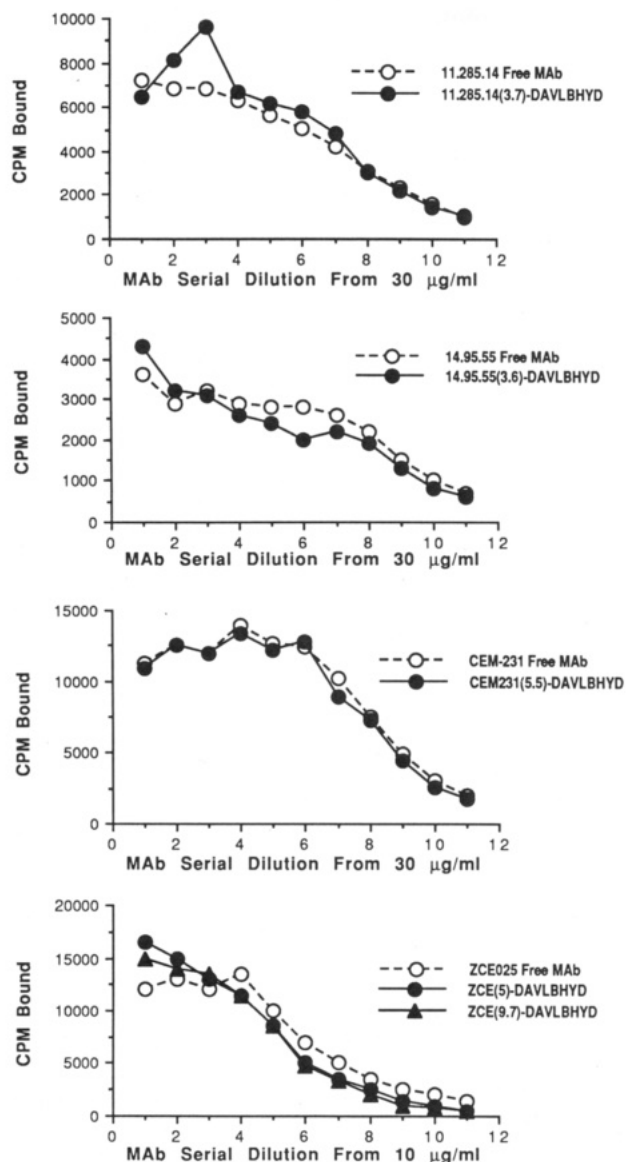


Figure 2. Immunoreactivity of anti-CEA-DAVLBHYD immunoconjugates. mAbs or immunoconjugates were diluted to 10 or 30 $\mu\text{g/mL}$ as indicated. Serial 2-fold dilutions were prepared and the binding activity was determined in a solid-phase RIA (32) against air-dried LS174T human colon carcinoma cells (150 000 cells per well in a 96-well microtiter plate). Numbers in parentheses are the mole of DAVLBHYD conjugated per mole of IgG.

The *in vivo* antitumor activity of the anti-CEA-DAVLBHYD conjugates was determined against LS174T human tumor xenografts using various dosing schedules. The LS174T cell line was chosen for these studies because immunofluorescence analyses of a number of human colon carcinoma cell lines including LS174T, SW948, Colo 205, SW403, HCT116, LoVo, DLD-1, and HCT-15 indicated that LS174T exhibited the highest level of surface CEA expression for the mAbs described in this paper (data not shown).

The first *in vivo* study was performed with immunoconjugates constructed from the 11.285.14 and 14.95.55 anti-CEA mAbs (Figure 4). The dose-response effect of the anti-CEA-DAVLBHYD conjugates was compared to irrelevant IgG_{2b}-DAVLBHYD and free DAVLBHYD in 9-day-established LS174T tumor xenografts. Significant antitumor activity was observed for all drug treatment groups at the 3 mg/kg dose (vinca content) although free DAVLBHYD was considerably more toxic than the mAb-DAVLBHYD conjugates (Figure 4, panel A). No toxic

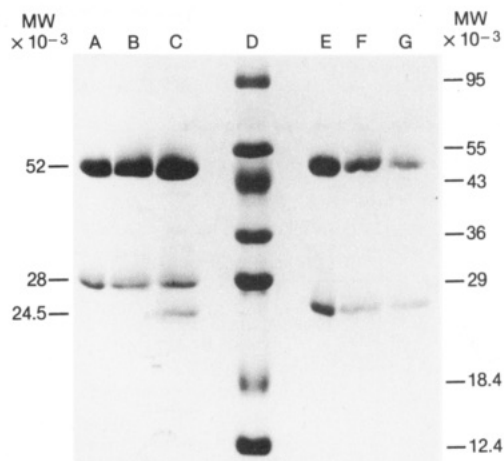


Figure 3. Analysis of ZCE025 light chain glycosylation. ZCE025 and CEM231 mAbs were diluted to 0.5 mg/mL and dialyzed against a buffer containing 0.017 M $\text{Na}_2\text{H}_2\text{PO}_4$, 0.083 M NaH_2PO_4 , 0.05 M disodium EDTA, pH 6.1. Nonidet P-40 was added to the samples after dialysis to a final concentration of 1% (assay buffer). Pretreatment buffer was made by adding 50 μL of 10% SDS, 50 μL of nonidet P-40, and 50 μL of 2-mercaptoethanol to 350 μL of assay buffer. Ten microliters of mAb was mixed with 1 μL of pretreatment buffer and boiled at 100 °C for 1 min. Twenty microliters of endo F (42) and 20 μL of assay buffer were added and the samples were incubated overnight at 37 °C (incubation control samples received 40 μL of assay buffer and 0 μL of enzyme). Fifty-two microliters double strength Laemmli dialysis buffer (47) and 5 μL of 0.05% bromophenol blue were added, and each sample was boiled for 5 min. The above samples were subjected to SDS-PAGE on a discontinuous Laemmli gel (47) composed of a 5.5% stacking and 12.5% separating gel. After electrophoresis the gels were stained with Coomassie Brilliant Blue and destained. Molecular weight standards were also run on the gel and the molecular weights of the various bands are indicated in the figure. A, untreated ZCE025; B, ZCE025 incubated overnight at 37 °C without endo F; C, ZCE025 treated with endo F; D, molecular weight standards; E, untreated CEM231; F, CEM231 incubated overnight at 37 °C without endo F; G, CEM231 treated with endo F.

deaths were observed in the 1.5 mg/kg treated animals (Figure 4, panel B) and 14.95.55-DAVLBHYD appeared to be more efficacious than either free DAVLBHYD or 11.285.14-DAVLBHYD. The antitumor activity of 14.95.55-DAVLBHYD, however, was not significantly different than irrelevant IgG_{2b}-DAVLBHYD. 14.95.55-DAVLBHYD was clearly the most efficacious therapy at the 0.75 mg/kg dose (Figure 4, panel C) while 11.285.14-DAVLBHYD exhibited antitumor activity similar to free DAVLBHYD. None of the drug treatments were significantly different than the saline control group at the 0.38 mg/kg dose (Figure 4, panel D). Since 11.285.14-DAVLBHYD did not demonstrate superior antitumor activity to both irrelevant IgG₁-DAVLBHYD and free DAVLBHYD at any dose tested in this experiment, this anti-CEA mAb was not used for further study.

Immunoconjugates constructed from 14.95.55 and CEM231 were compared for *in vivo* activity against the low tumor burden LS174T xenograft model shown in Figure 5. All drug treatments exhibited good antitumor activity at the 3 mg/kg (vinca content) dose although free DAVLBHYD and 14.95.55-DAVLBHYD demonstrated considerable toxicity relative to the other treatments at this dose. The lack of 14.95.55-DAVLBHYD toxicity at the 3 mg/kg dose in the previous experiment (Figure 4) may have been due to the longer time interval between dosing (three doses in 6 days) compared to the study shown in Figure 5 (three doses in 5 days). Both anti-CEA-DAVLBHYD conjugates appeared to be more efficacious than

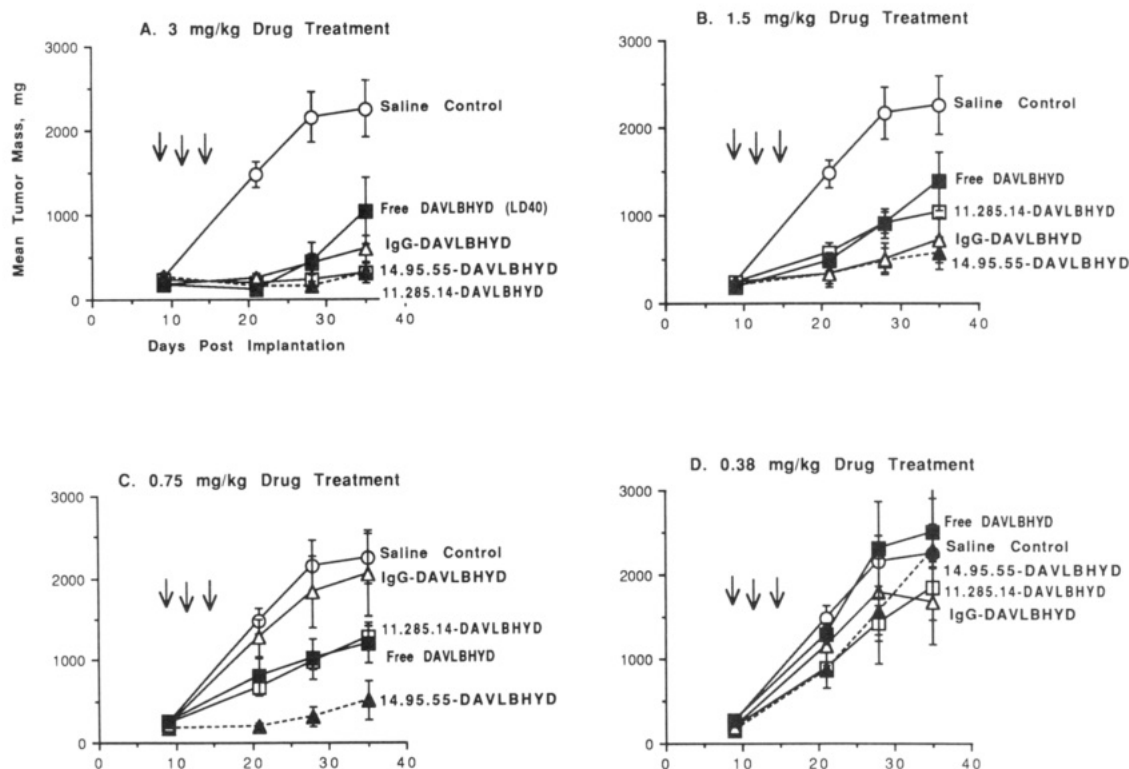


Figure 4. In vivo efficacy of 11.285.14- and 14.95.55-DAVLBHYD against 9-day-established LS174T xenografts. Nude mice were given injections sc of 1×10^7 LS174T tumor cells. Animals were treated iv on days 9, 12, and 15 with 11.285.14-DAVLBHYD, 14.95.55-DAVLBHYD, irrelevant IgG_{2b}-DAVLBHYD, free DAVLBHYD, or saline. The quantity of antibody injected (mg/kg) at the 3 mg/kg vinca dose was 160, 214, and 308 for 11.285.14-, 14.95.55-, and irrelevant IgG_{2b}-DAVLBHYD, respectively. The ordinate is the mean tumor mass in milligrams; abscissa, days after implantation; points, means; bars, SE: A, 3 mg/kg vinca dose; B, 1.5 mg/kg vinca dose; C, 0.75 mg/kg vinca dose; D, 0.38 mg/kg vinca dose.

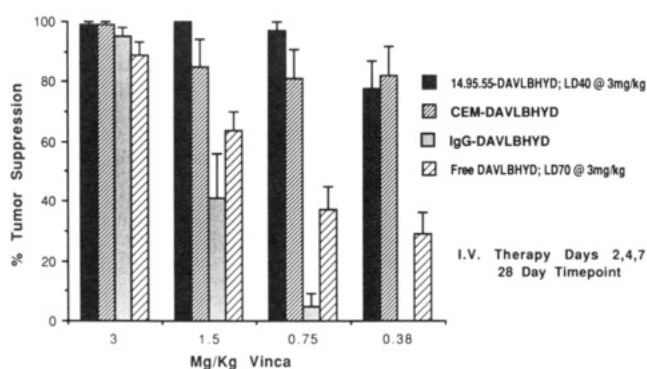


Figure 5. In vivo efficacy of 14.95.55- and CEM231-DAVLBHYD against a low tumor burden (2-day-established) LS174T tumor model. 14.95.55-DAVLBHYD, CEM231-DAVLBHYD, irrelevant IgG₁-DAVLBHYD, or free DAVLBHYD was given iv at days 2, 4, and 7 after implantation. The quantity of antibody (mg/kg) injected at the 3 mg/kg vinca dose was 194, 146, and 126 for 14.95.55-, CEM231-, and irrelevant IgG₁-DAVLBHYD, respectively. The abscissa is the treatment dose given in mg/kg vinca equivalent, while the ordinate is tumor suppression (given as a percentage). Tumor suppression is defined as $[1 - (a/b)] \times 100$, where a is the mean tumor mass of treated animals, and b is the mean tumor mass of the saline-injected control group. Columns are mean values, and bars are the SE.

irrelevant IgG₁-DAVLBHYD or free DAVLBHYD at the 1.5, 0.75, and 0.38 mg/kg doses (Figure 5). Since an earlier report had indicated that unconjugated 14.95.55 could suppress human tumor nude mouse xenograft growth (27), we tested this antibody at 100 mg/kg (antibody content) against the low tumor burden (iv treatment performed on days 2, 5, 7 after tumor implantation) and the established (iv treatment on days 13, 17, 20, and 24 after tumor implantation; mean tumor size at initiation of therapy was approximately 300 mg) LS174T tumor models. No

significant antitumor activity was observed for 14.95.55 against LS174T in either experiment (data not shown).

In order to further evaluate the relative potencies of 14.95.55- and CEM231-DAVLBHYD we examined these conjugates against 7-day-established LS174T tumors as shown in Figure 6. These data indicated that the 14.95.55 conjugate and free DAVLBHYD were toxic at the 3 mg/kg (vinca content) dose whereas no deaths were observed in the CEM231- or irrelevant IgG₁-DAVLBHYD treated groups (Figure 6, panel A). CEM231-DAVLBHYD exhibited significant antitumor activity at the 3 mg/kg dose (Figure 6, panel A) but was no more active than the non-antigen-binding control immunoconjugate. 14.95.55-DAVLBHYD was more efficacious than free drug or irrelevant IgG₁-DAVLBHYD at the 1.5 and 0.75 mg/kg doses (Figure 6, panels B and C). CEM231-DAVLBHYD, in contrast, was not significantly more active than the control conjugate at any dose tested (Figure 6).

As stated above, the presence of light chain carbohydrate allowed ZCE025-DAVLBHYD conjugates to be constructed with widely varying amounts of drug attached. We therefore prepared immunoconjugates with 5 or 9.7 mol of vinca/mol of mAb and tested their therapeutic efficacy in the same in vivo experiment (Figure 7). The data in Figure 7 (panel A) demonstrated that at the 3 mg/kg (vinca content) dose, free DAVLBHYD and ZCE025 with 5 mol of vinca bound were quite toxic compared to the irrelevant conjugate and ZCE025 with 9.7 mol of vinca attached. At the 2 mg/kg dose (Figure 7, panel B), both ZCE025 conjugates displayed similar antitumor activity, which was significantly better than irrelevant conjugate but only marginally more active than free DAVLBHYD. No deaths were observed for the highly conjugated ZCE025 construct at the 2 mg/kg dose while treatment with the less conjugated ZCE025-DAVLBHYD (5 mol of vinca/

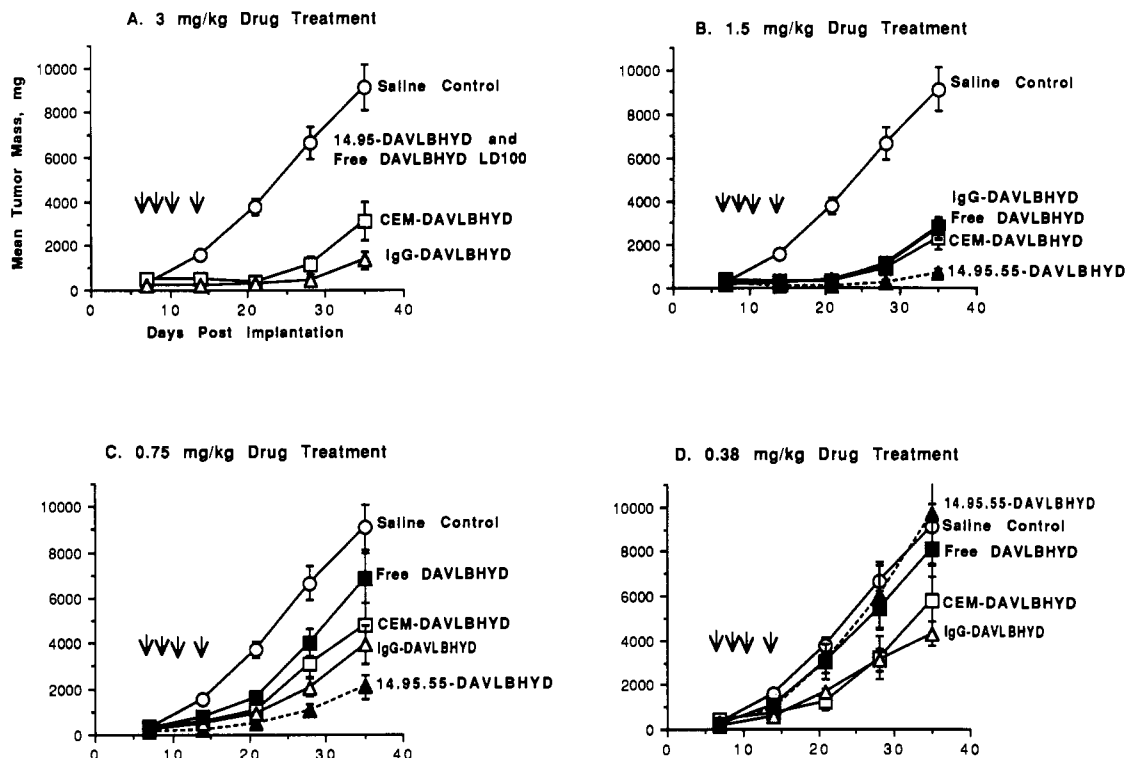


Figure 6. In vivo efficacy of 14.95.55- and CEM231-DAVLBHYD against 7-day-established LS174T xenografts. Animals were treated iv on days 7, 9, 11, and 14 with 14.95.55-DAVLBHYD, CEM231-DAVLBHYD, irrelevant IgG₁-DAVLBHYD, free DAVLBHYD, or saline. The quantity of antibody (mg/kg) injected at the 3 mg/kg vinca dose was 194, 146, and 126 for 14.95.55-, CEM231-, and irrelevant IgG₁-DAVLBHYD, respectively. The ordinate is the mean tumor mass in mg; the abscissa, days after implantation; points, means; bars, SE: A, 3 mg/kg vinca dose; B, 1.5 mg/kg vinca dose; C, 0.75 mg/kg vinca dose; D, 0.38 mg/kg vinca dose.

mol of mAb) resulted in the death of one out of five mice (Figure 7, panel B). All drug treatment groups demonstrated similar activity at the 1 mg/kg dose (Figure 7, panel C). These data suggested that the more highly conjugated ZCE025 had an improved therapeutic index relative to ZCE025 with 5 mol of vinca/mol of mAb. This experiment was repeated for the 3 mg/kg dose (animals injected on days 7, 10, 14, 17 after implantation) with similar results (ZCE025(9.7)-DAVLBHYD 0/5 deaths, ZCE025(5)-DAVLBHYD 4/5 deaths; data not shown).

The final in vivo experiment compared the therapeutic activity of CEM231-DAVLBHYD, 14.95.55-DAVLBHYD, and a highly conjugated form (9.1 mol of vinca/mol of mAb) of ZCE025-DAVLBHYD against LS174T xenografts (Figure 8). At the drug dose (2 mg/kg vinca) and schedule (treatment on days 7, 9, 11, 14) utilized in this experiment, immunoconjugates constructed from the 14.95.55 and ZCE025 mAbs were clearly superior to all other drug treatment groups. Irrelevant IgG₁-DAVLBHYD and CEM231-DAVLBHYD displayed comparable activity to each other in this experiment, which was in agreement with the data shown in Figure 6 while free DAVLBHYD was toxic under these conditions.

DISCUSSION

A panel of four murine anti-CEA mAbs was conjugated to DAVLBHYD and evaluated for preclinical antitumor activity. A wide range of preclinical efficacy was observed for the mAb-drug conjugates even though all of the mAbs displayed similar membrane binding activity against the LS174T target cell line utilized in the xenograft experiments (Figure 1). The affinity constants of the mAbs, however, varied significantly. CEM231 and ZCE025 bind to the same apparent CEA epitope (Figure 1) with K_a 's of 5×10^9 and 6×10^9 M⁻¹, respectively (39, 44), while the K_a 's for the distinct epitopes recognized by 11.285.14 and

14.95.55 were both estimated to be 5×10^8 M⁻¹ (J. R. F. Corvalan and W. Smith, unpublished observations). In spite of the similarities between CEM231 and ZCE025, the chemoimmunoconjugates constructed from these mAbs displayed disparate characteristics in the preclinical studies.

CEM231-DAVLBHYD was no more active than irrelevant IgG₁-DAVLBHYD against established LS174T tumors when examined at a number of different drug doses (Figures 6 and 8) while ZCE025-DAVLBHYD was significantly more efficacious than irrelevant conjugate and CEM231-DAVLBHYD in the same tumor model at the 2 mg/kg (vinca content) dose (Figure 8). The reason(s) for this disparity is not clear although it was observed that the light chain of ZCE025 was glycosylated to a significantly greater extent than the light chain of CEM231 (Figure 3). Immunoglobulin carbohydrate side chains can affect antibody biodistribution (for review see ref 45) but it is not known if this was a factor in the ability of ZCE025-DAVLBHYD to outperform CEM231-DAVLBHYD in the LS174T tumor xenograft experiment (Figure 8). The glycosylated light chain of ZCE025 may have been responsible for the construction of highly substituted vinca conjugates which appeared to have an improved therapeutic index relative to a less conjugated form of the mAb (Figure 7). The improved therapeutic index may have been related to the reduced antibody content required for the highly conjugated ZCE025-DAVLBHYD to deliver an equivalent drug dose relative to the less conjugated form of ZCE025 (at the 3 mg/kg vinca dose, 64 mg/kg antibody was required for the 9.7 mol of vinca/mol of IgG conjugate versus 125 mg/kg antibody for the 5 mol of vinca/mol of IgG construct; Figure 7). Previous studies (46) have shown that nude mouse liver uptake of ¹¹¹In-labeled ZCE025 was significantly enhanced by the presence of LS174T tumors. The explanation for this finding was that CEA was released

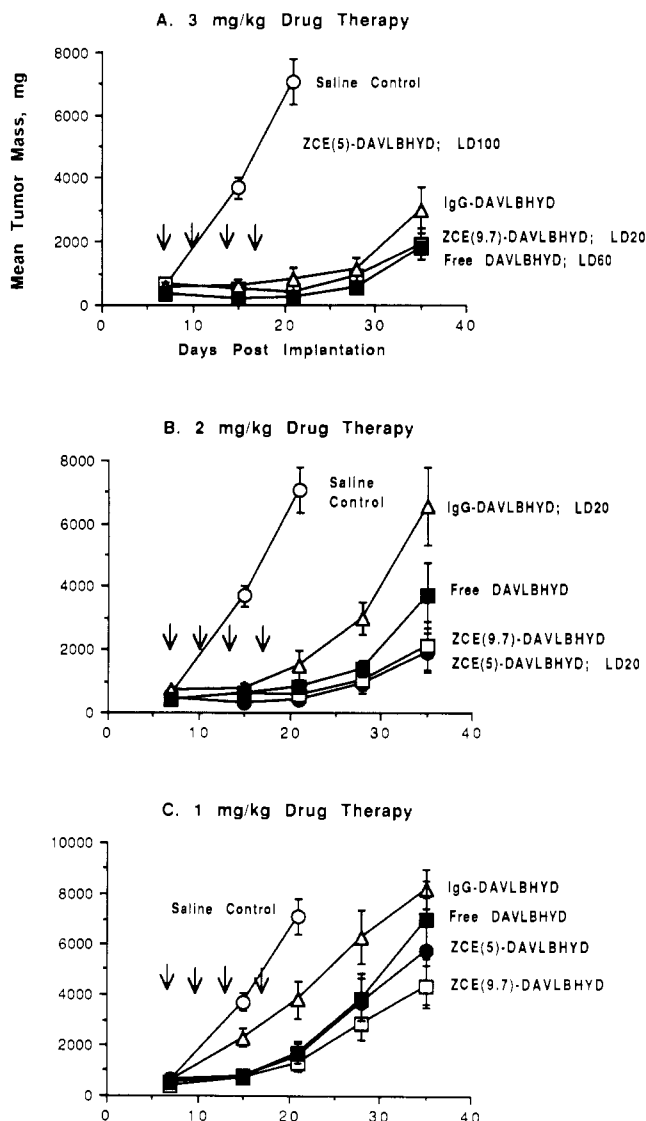


Figure 7. In vivo efficacy of "high"- and "low"-conjugated ZCE025-DAVLBHYD against 7-day-established LS174T xenografts. Animals were treated iv on days 7, 10, 14, and 17 with ZCE025-DAVLBHYD conjugated to 5 mol of vinca, ZCE025-DAVLBHYD conjugated to 9.7 mol of vinca, irrelevant IgG₁-DAVLBHYD, free DAVLBHYD, or saline. The quantity of antibody (mg/kg) injected at the 3 mg/kg vinca dose was 125, 64, and 112 for ZCE(5)-, ZCE(9.7)-, or irrelevant IgG₁-DAVLBHYD, respectively. The ordinate is the mean tumor mass in mg; the abscissa, days after implantation; points, means; bars, SE: A, 3 mg/kg vinca dose; B, 2 mg/kg vinca dose; C, 1 mg/kg vinca dose.

into the circulation by the human tumor xenograft and that the resulting ¹¹¹In-ZCE025-CEA complexes were removed from circulation by the liver (46). The amount of labeled antibody found in the liver was substantially reduced if animals were pretreated with an appropriate amount of unlabeled ZCE025 (46). The mechanism of mAb-drug-induced toxicity observed in Figure 7 is unknown, but it is conceivable that the lower mass of the highly conjugated ZCE025-DAVLBHYD conjugate required to deliver 3 mg/kg vinca equivalent may have resulted in a more favorable (less toxic) biodistribution. It is also quite possible that the toxicity associated with the less conjugated form of ZCE025 is independent of liver biodistribution. A previous report (49) indicated that an anti-KS1/4-DAVLBHYD conjugate exhibited significant leucopenia in rats and primates. It is not known if leucopenia and/or hepatotoxicity were responsible for the animal deaths observed after treatment with the anti-

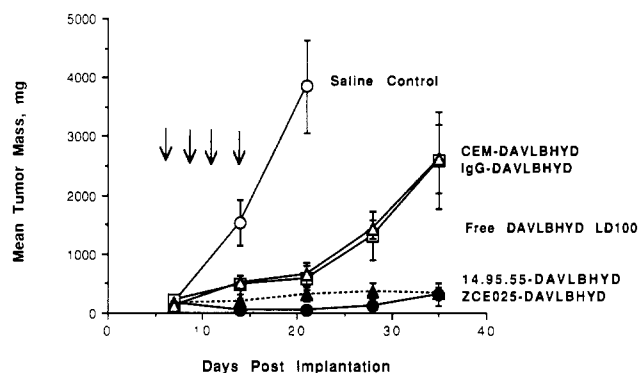


Figure 8. In vivo efficacy of 14.95.55-, ZCE025-, and CEM231-DAVLBHYD against 7-day-established LS174T xenografts. Animals were treated iv on days 7, 9, 11, and 14 with 2 mg/kg vinca equivalent of 14.95.55-DAVLBHYD, ZCE025-DAVLBHYD conjugated to 9.1 mol of vinca, CEM231-DAVLBHYD, irrelevant IgG₁-DAVLBHYD, free DAVLBHYD, or saline. The amount of antibody injected (mg/kg) was 86, 46, 115, or 89 for 14.95.55-, ZCE025-, CEM231, or irrelevant IgG₁, respectively. The ordinate is the mean tumor mass in mg; the abscissa, days after implantation; points, means; bars, SE.

CEA-DAVLBHYD immunoconjugates (Figures 5–7). Possible differences in the biodistribution of the "high"- and "low"-conjugated form of ZCE025 and any relationship to toxicity will of course have to be experimentally determined.

14.95.55-DAVLBHYD exhibited similar antitumor activity as ZCE025-DAVLBHYD (Figure 8) and was more efficacious than conjugates constructed from 11.285.14 (Figure 4) and CEM231 (Figure 6 and 8). Interestingly, CEM231-DAVLBHYD efficacy was comparable to that of 14.95.55-DAVLBHYD in the low tumor burden LS174T tumor model (Figure 5) but the former conjugate was not significantly more active than irrelevant mAb-vinca in established tumors (Figures 6 and 8).

It is apparent from the above data that the preclinical in vivo efficacy of chemoimmunoconjugates constructed from this panel of anti-CEA mAbs could not be predicted on the basis of the level of membrane reactivity with the target tumor cell line (Figure 1), CEA epitope specificity (Figure 1), or the affinity of antigen binding (see above). Other reports have also shown that in vivo targeting of anti-CEA mAbs could not be predicted on the basis of antigen binding affinity (17). It should also be noted that no significant differences were observed among the anti-CEA-DAVLBHYD conjugates with regard to in vitro cytotoxicity against LS174T tumor cells (data not shown).

Differences in biological processing of antigen-antibody complexes at the target cell membrane could explain the variation in antitumor efficacy of the anti-CEA conjugates although preliminary investigations have revealed that none of these mAbs were rapidly internalized to a major extent after binding to LS174T cells in vitro (J. J. Starling, unpublished observations). Previous reports from our laboratory (37, 48) have demonstrated that mAb-DAVLBHYD conjugates constructed as described by Laguzza et al. (41) do not require rapid internalization for antitumor activity. The cytotoxicity of these immunoconjugates may be due to the release of free drug from the conjugate at the periphery of the tumor cell followed by intracellular transport (37, 48).

Previous studies have utilized 11.285.14 and 14.95.55 to deliver vinca alkaloids to CEA expressing tumors in vivo (27–30). Corvalan et al. (28–30) described the use of a hybrid-hybrid mAb constructed from 11.285.14 and an anti-vinca mAb to enhance the therapeutic efficacy of vin-

blastine against the MAWI human tumor xenograft. 11.285.14 and 14.95.55 were also utilized to prepare mAb-vindesine immunoconjugates which were evaluated for in vivo antitumor activity against the MAWI xenograft (27). Significant growth suppression was observed for both immunoconjugates although unmodified 14.95.55 demonstrated similar efficacy as its vinca-conjugated form (27). Unconjugated 14.95.55 (100 mg/kg) did not exhibit significant antitumor activity against the low tumor burden LS174T tumor model depicted in Figure 5 (data not shown) even though substantial efficacy was observed for 14.95.55-DAVLBHYD at an antibody equivalent dose of only 25 mg/kg (0.38 mg/kg vinca dose in Figure 5). Unconjugated 14.95.55 was also inactive against LS174T tumors which had grown to an average size of 300 mg prior to four treatments (twice weekly) of 100 mg/kg of this anti-CEA mAb. These observations strongly suggested that the antitumor effects demonstrated for 14.95.55-DAVLBHYD in Figures 4-6 and 8 were not due to unmodified antibody.

The antitumor activity of the anti-CEA-DAVLBHYD conjugates was not simply due to diminished tumor growth in sick animals. This statement is supported by the observation that significant efficacy was observed for 14.95.55-DAVLBHYD at the 0.75 (Figures 4-6) and 0.38 mg/kg (Figure 5) doses, where no significant weight loss was observed in the mice undergoing therapy (data not shown). This was also true for the 0.75 and 0.38 mg/kg dose groups of CEM231-DAVLBHYD shown in Figure 5 (data not shown). It should also be noted that the 1.5 mg/kg treatment group of 14.95.55-DAVLBHYD shown in Figure 6 experienced a maximum loss of 1.2% of starting body weight while the free-drug-treated group exhibited a 21% loss of weight and had more rapid tumor growth than the conjugate-treated animals (weight data not shown). Similar observations were noted for the other anti-CEA-DAVLBHYD conjugates (data not shown).

A number of other drugs including 5-fluorouridine (25), methotrexate (26), and doxorubicin (31) have been conjugated to anti-CEA mAbs via an aminodextran linker and evaluated for in vivo antitumor activity. These conjugates also demonstrated greater efficacy than free drug or irrelevant conjugates and caused less systemic toxicity than free drug.

In conclusion, extensive in vivo preclinical evaluation was required to identify the two most active immunoconjugates that could be constructed from a panel of four anti-CEA mAbs. These two anti-CEA mAb-DAVLBHYD immunoconjugates were shown to be more efficacious than free drug or an irrelevant conjugate against established LS174T tumor xenografts. The ultimate designation of antitumor activity will of course depend on the clinical evaluation of these immunoconjugates. The preclinical studies presented in this paper, however, have provided a rational basis to select ZCE025 and/or 14.95.55 for the construction of the anti-CEA-DAVLBHYD chemoimmunoconjugates to be utilized in clinical trials.

LITERATURE CITED

- (1) Shively, J. E. (1985) CEA-related antigens: Molecular biology and clinical significance. *Crit. Rev. Oncol. Hematol.* 2, 355-399.
- (2) Begent, R., and Rustin, G. J. S. (1989) Tumour markers: From carcinoembryonic antigen to products of hybridoma technology. *Cancer Surv.* 8, 107-121.
- (3) Johnson, J. P. (1991) Cell adhesion molecules of the immunoglobulin supergene family and their role in malignant transformation and progression to metastatic disease. *Cancer Metastasis Rev.* 10, 11-22.
- (4) Muraro, R., Wunderlich, D., Thor, A., Lundy, J., Noguchi, P., Cunningham, R., and Schlom, J. (1985) Definition by monoclonal antibodies of a repertoire of epitopes on carcinoembryonic antigen differentially expressed in human colon carcinomas versus normal adult tissues. *Cancer Res.* 45, 5769-5780.
- (5) Savoie, S. C., and Sikorska, H. M. (1991) Immunohistochemical characterization of a new anticarcinoembryonic antigen monoclonal antibody. *Anticancer Res.* 11, 1-12.
- (6) Tsujisaki, M., Imai, K., Hishikawa, N., Tokuchi, S., Hinoda, Y., Matsukawa, H., Oikawa, S., Nakazato, H., and Yachi, A. (1991) Preparation and characterization of monoclonal antibodies specific to synthetic peptide of carcinoembryonic antigen. *Int. J. Cancer* 47, 267-273.
- (7) Teh, J.-G., and McKenzie, I. F. C. (1990) Monoclonal antibodies to carcinoembryonic antigen. *Immunol. Cell Biol.* 68, 263-268.
- (8) Price, M. R. (1988) Epitopes of carcinoembryonic antigen (CEA) defined by monoclonal antibodies. *Br. J. Cancer* 57, 165-169.
- (9) Hedin, A., Zoubir, F., Lundgren, T., and Hammarstrom, S. (1986) Epitope specificity and cross-reactivity pattern of a large series of monoclonal antibodies to carcinoembryonic antigen. *Mol. Immunol.* 23, 1053-1061.
- (10) Matsunaga, A., Kuroki, M., Higuchi, H., Arakawa, F., Takakura, K., Okamoto, N., and Matsuoka, Y. (1987) Antigenic heterogeneity of carcinoembryonic antigen in the circulation defined by monoclonal antibodies against the carbohydrate moiety of carcinoembryonic antigen and closely related antigens. *Cancer Res.* 47, 56-61.
- (11) Corvalan, J. R. F., Axton, C. A., Brandon, D. R., Smith, W., and Woodhouse, C. (1983) Classification of anti-CEA monoclonal antibodies. *Protides Biol. Fluids* 31, 921-924.
- (12) Duda, R. B., Beatty, J. D., Sheibani, K., Williams, L. E., Paxton, R. J., Beatty, B. G., Shively, J. E., Vlahos, W. G., Werner, J. L., Kemeny, M. M., Kokal, W. A., Riihimaki, D. U., Wagman, L. D., and Terz, J. J. (1986) Imaging of human colorectal adenocarcinoma with indium-labeled anticarcinoembryonic antigen monoclonal antibody. *Arch. Surg.* 121, 1315-1319.
- (13) Abdel-Nabi, H. H., Schwartz, A. N., Higano, C. S., Wechter, D. G., and Unger, M. W. (1987) Colorectal carcinoma: Detection with indium-111 anticarcinoembryonic-antigen monoclonal antibody ZCE-025. *Radiology* 164, 617-621.
- (14) Abdel-Nabi, H. H., Schwartz, A. N., Goldfogel, G., Ortman-Nabi, J. A., Matsuoka, D. M., Unger, M. W., and Wechter, D. G. (1988) Colorectal tumors: Scintigraphy with In-111 anti-CEA monoclonal antibody and correlation with surgical, histopathologic and immunohistochemical findings. *Radiology* 166, 747-752.
- (15) Lind, P., Smola, M. G., Lechner, P., Ratschek, M., Klima, G., Koltringer, P., Steindorfer, P., and Eber, O. (1991) The immunoscintigraphic use of Tc-99m-labelled monoclonal anti-CEA antibodies (BW431/26) in patients with suspected primary, recurrent and metastatic breast cancer. *Int. J. Cancer*, 47, 865-869.
- (16) Pimm, M. V., and Baldwin, R. W. (1987) Comparative biodistributions and rates of catabolism of radiolabelled anti-CEA monoclonal antibody and control immunoglobulin in nude mice with human tumour xenografts showing specific antibody localization. *Eur. J. Nucl. Med.* 13, 258-263.
- (17) Hedin, A., Wahren, B., and Hammarstrom, S. (1982) Tumor localization of CEA - containing human tumors in nude mice by means of monoclonal anti-CEA antibodies. *Int. J. Cancer* 30, 547-552.
- (18) Patt, Y. Z., Lamki, L. M., Shanken, J., Jessup, J. M., Charnsangavej, C., Ajani, J. A., Levin, B., Merchant, B., Halverson, C., and Murray, J. L. (1990) Imaging with indium-111-labeled anticarcinoembryonic antigen monoclonal antibody ZCE-025 of recurrent colorectal or carcinoembryonic antigen-producing cancer in patients with rising serum carcinoembryonic antigen levels and occult metastases. *J. Clin. Oncol.* 8, 1246-1254.
- (19) Buchegger, F., Vacca, A., Carrel, S., Schreyer, M., and Mach, J.-P. (1988) Radioimmunotherapy of human colon carcinoma by ¹³¹I-labelled monoclonal anti-CEA antibodies in a nude mouse model. *Int. J. Cancer* 41, 127-134.

- (20) Sharkey, R. M., Pykett, M. J., Siegel, J. A., Alger, E. A., Primus, F. J., and Goldenberg, D. M. (1987) Radioimmunotherapy of the GW-39 human colonic tumor xenograft with ¹³¹I-labeled murine monoclonal antibody to carcinoembryonic antigen. *Cancer Res.* 47, 5672-5677.
- (21) Sharkey, R. M., Kaltovich, F. A., Shih, L. B., Fand, I., Gov-elitz, G., and Goldenberg, D. M. (1988) Radioimmunotherapy of human colonic cancer xenografts with ⁹⁰Y-labeled monoclonal antibodies to carcinoembryonic antigen. *Cancer Res.* 48, 3270-3275.
- (22) Esteban, J. M., Hyams, D. M., Beatty, B. G., Wanek, P., and Beatty, J. D. (1989) Effect of yttrium-90-labeled anti-carcinoembryonic antigen monoclonal antibody on the morphology and phenotype of human tumors grown as peritoneal carcinomatosis in athymic mice. *Cancer* 63, 1343-1352.
- (23) Levin, L. V., Griffin, T. W., Childs, L. R., Davis, S., and Haagen, D. E. (1987) Comparison of multiple anti-CEA immunotoxins active against human adenocarcinoma cells. *Cancer Immunol. Immunother.* 24, 202-206.
- (24) Byers, V. S., Pawluczyk, I., Berry, N., Durrant, L., Robins, R. A., Garnett, M. C., Price, M. R., and Baldwin, R. W. (1988) Potentiation of anti-carcinoembryonic antigen immunotoxin cytotoxicity by monoclonal antibodies reacting with co-expressed carcinoembryonic antigen epitopes. *J. Immunol.* 140, 4050-4055.
- (25) Shih, L. B., Xuan, H., Sharkey, R. M., and Goldenberg, D. M. (1990) A Fluorouridine-anti-CEA immunoconjugate is therapeutically effective in a human colonic cancer xenograft model. *Int. J. Cancer* 46, 1101-1106.
- (26) Shih, L. B., and Goldenberg, D. M. (1990) Effects of methotrexate-carcinoembryonic-antigen-antibody immunoconjugates on GW-39 human tumors in nude mice. *Cancer Immunol. Immunother.* 31, 197-201.
- (27) Rowland, G. F., Axton, C. A., Baldwin, R. W., Brown, J. P., Corvalan, J. R. F., Embleton, M. J., Gore, V. A., Hellstrom, I., Hellstrom, K. E., Jacobs, E., Marsden, C. H., Pimm, M. V., Simmonds, R. G., and Smith, W. (1985) Antitumor properties of vindesine-monoclonal antibody conjugates. *Cancer Immunol. Immunother.* 19, 1-7.
- (28) Corvalan, J. R. F., Smith, W., Gore, V. A., Brandon, D. R., and Ryde, P. J. (1987) Increased therapeutic effect of vinca alkaloids targeted to tumour by a hybrid-hybrid monoclonal antibody. *Cancer Immunol. Immunother.* 24, 138-143.
- (29) Corvalan, J. R. F., Smith, W., and Gore, V. A. (1988) Tumour therapy with vinca alkaloids targeted by a hybrid-hybrid monoclonal antibody recognising both CEA and vinca alkaloids. *Int. J. Cancer Supplement* 2, 22-25.
- (30) Smith, W., Gore, V. A., Brandon, D. R., Lynch, D. N., Cranstone, S. A., and Corvalan, J. R. F. (1990) Suppression of well-established tumour xenografts by a hybrid-hybrid monoclonal antibody and vinblastine. *Cancer Immunol. Immunother.* 31, 157-163.
- (31) Shih, L. B., Goldenberg, D. M., Xuan, H., Lu, H., Sharkey, R. M., and Hall, T. C. (1991) Anthracycline immunoconjugates prepared by a site-specific linkage via an amino-dextran intermediate carrier. *Cancer Res.* 51, 4192-4198.
- (32) Starling, J. J., Maciak, R. S., Hinson, N. A., Nichols, C. L., Briggs, S. L., and Laguzza, B. C. (1989) In vivo efficacy of monoclonal antibody-drug conjugates of three different subtypes which bind the human tumor-associated antigen defined by the KS1/4 monoclonal antibody. *Cancer Immunol. Immunother.* 28, 171-178.
- (33) Starling, J. J., Maciak, R. S., Hinson, N. A., Hoskins, J., Laguzza, B. C., Gadske, R. A., Strnad, J., Rittmann-Grauer, L., DeHerdt, S. V., Bumol, T. F., and Moore, R. E. (1990) In vivo selection of human tumor cells resistant to monoclonal antibody-vinca alkaloid immunoconjugates. *Cancer Res.* 50, 7634-7640.
- (34) Apelgren, L. D., Zimmerman, D. L., Briggs, S. L., and Bumol, T. F. (1990) Antitumor activity of the monoclonal antibody-vinca alkaloid immunoconjugate LY203725 (KS1/4-4-desacetylvinblastine-3-carboxhydrazide) in a nude mouse model of human ovarian cancer. *Cancer Res.* 50, 3540-3544.
- (35) Johnson, D. A., and Laguzza, B. C. (1987) Antitumor xenograft activity with a conjugate of a Vinca derivative and the squamous carcinoma-reactive monoclonal antibody PF1/D. *Cancer Res.* 47, 3118-3122.
- (36) Johnson, D. A., Baker, A. L., Laguzza, B. C., Fix, D. V., and Gutowski, M. C. (1990) Antitumor activity of L/1C2-4-desacetylvinblastine-3-carboxhydrazide immunoconjugates in xenografts. *Cancer Res.* 50, 1790-1794.
- (37) Starling, J. J., Maciak, R. S., Law, K. L., Hinson, N. A., Briggs, S. L., Laguzza, B. C., and Johnson, D. A. (1991) In vivo antitumor activity of a monoclonal antibody-vinca alkaloid immunoconjugate directed against a solid tumor membrane antigen characterized by heterogeneous expression and non-internalization of antibody-antigen complexes. *Cancer Res.* 51, 2965-2972.
- (38) Gutowski, M. C., Briggs, S. L., and Johnson, D. A. (1991) Epidermal growth factor receptor-reactive monoclonal antibodies: xenograft antitumor activity alone and as drug immunoconjugates. *Cancer Res.* 51, 5471-5475.
- (39) Beidler, C. B., Ludwig, J. R., Cardenas, J., Phelps, J., Papworth, C. G., Melcher, E., Sierzega, M., Myers, L. J., Unger, B. W., Fisher, M., David, G. S., and Johnson, M. J. (1988) Cloning and high level expression of a chimeric antibody with specificity for human carcinoembryonic antigen. *J. Immunol.* 141, 4053-4060.
- (40) Haskell, C. M., Buchegger, G., Schreyer, M., Carrel, S., and Mach, J.-P. (1983) Monoclonal antibodies to carcinoembryonic antigen: ionic strength as a factor in the selection of antibodies for immunoscintigraphy. *Cancer Res.* 43, 3857-3864.
- (41) Laguzza, B. C., Nichols, C. L., Briggs, S. L., Cullinan, G. J., Johnson, D. A., Starling, J. J., Baker, A. L., Bumol, T. F., and Corvalan, J. R. F. (1989) New antitumor monoclonal antibody-vinca conjugates LY203725 and related compounds: design, preparation, and representative in vivo activity. *J. Med. Chem.* 32, 548-555.
- (42) Elder, J. H., and Alexander, S. (1982) *Endo-β-N*-acetylglucosaminidase F: Endoglycosidase from *Flavobacterium meningosepticum* that cleaves both high-mannose and complex glycoproteins. *Proc. Natl. Acad. Sci. U.S.A.* 79, 4540-4544.
- (43) Chee, D. O., Boddie, A. L., Jr., Roth, J. A., Holmes, E. C., and Morton, D. L. (1976) Production of melanoma-associated antigen(s) by a defined malignant melanoma cell strain grown in chemically defined medium. *Cancer Res.* 36, 1503-1509.
- (44) Buchegger, F., Schreyer, M., Carrel, and Mach, J.-P. (1984) Monoclonal antibodies identify a CEA crossreacting antigen of 95 kD (NCA-95) distinct in antigenicity and tissue distribution from the previously described NCA of 55 kD. *Int. J. Cancer* 33, 643-649.
- (45) Zuckier, L. S., Rodriguez, L. D., and Scharff, M. D. (1989) Immunologic and pharmacologic concepts of monoclonal antibodies. *Semin. Nucl. Med.* 19, 166-186.
- (46) Beatty, B. G., Beatty, J. D., Williams, L. E., Paxton, R. J., Shively, J. E., and O'Connor-Tressel, M. (1989) Effect of specific antibody pretreatment on liver uptake of ¹¹¹In-labeled anticarcinoembryonic antigen monoclonal antibody in nude mice bearing human colon cancer xenografts. *Cancer Res.* 49, 1587-1594.
- (47) Laemmli, U. K. (1970) Cleavage of structural proteins during the assembly of the head of the bacteriophage T4. *Nature (London)* 227, 680-685.
- (48) Starling, J. J., Hinson, N. A., Marder, P., Maciak, R. S., and Laguzza, B. C. (1988) Rapid internalization of antigen-immunoconjugate complexes is not required for anti-tumor activity of monoclonal antibody-drug conjugates. *Antibody Immunoconjugate Radiopharm.* 1, 311-324.
- (49) Johnson, I. S., Spearman, M. E., Todd, G. C., Zimmermann, J. L., and Bumol, T. F. (1987) Monoclonal antibody drug conjugates for site-directed cancer chemotherapy: Preclinical pharmacology and toxicology studies. *Cancer Treat. Rev.* 14, 193-196.

Use of N-Terminal Modified Poly(L-lysine)-Antibody Conjugate as a Carrier for Targeted Gene Delivery in Mouse Lung Endothelial Cells

Vladimir S. Trubetskoy,^{*,†‡} Vladimir P. Torchilin,^{†‡} Stephen J. Kennel,[§] and Leaf Huang^{†,||}

Department of Biochemistry, University of Tennessee, Knoxville, Tennessee 37996, and Biology Division, Oak Ridge National Laboratory, Oak Ridge, Tennessee 37831. Received January 21, 1992

A DNA targeted delivery and expression system has been designed based on an N-terminal modified poly(L-lysine) (NPLL)-antibody conjugate, which readily forms a complex with plasmid DNA. Monoclonal antibodies against the cell-surface thrombomodulin conjugated with NPLL were used for targeted delivery of foreign plasmid DNA to an antigen-expressing mouse lung endothelial cell line in vitro and to mouse lungs in vivo. In both cases significant amounts of DNA can be specifically bound to the target cells or tissues. Specific gene expression was observed in the treated mouse lung endothelial cells.

INTRODUCTION

Since the mainstream of DNA-delivery research has shifted to in vivo elaboration of practically useful gene-therapy strategies, the need for a tissue-specific and stable transfection agent has become a matter of primary importance. Among the preparations which have been employed for DNA-mediated transfection of mammalian cells, special attention has been paid to the cationic liposomes (1,2) and protien-PLL¹ conjugates (3-5). However, cationic liposomes, despite of their transfection efficiency, demonstrate a complete lack of specificity toward different tissues or cell types. The use of protein-PLL conjugates seems to represent a sound alternative to the cationic liposomes. Wu and Wu have used an asialoorosomucoid-PLL conjugate for DNA delivery into the asialoglycoprotein receptor-positive HepG2 hepatoma cells (3) as well as into mammalian liver hepatocytes in vivo (4). Wagner et al. have used a similar approach for designing the DNA-delivery system based on a transferrin-PLL conjugate (5). Unfortunately, in the former example only the liver can serve as the target organ, while in the latter case the organ specificity is absent and the method in general may only be applied for in vitro experiments. It seems that antibody molecules could be used as targeting ligands to achieve a broader range of organ or tissue specificity. Antibodies have already been widely used as a targeting molecules for the deliver of liposomes (6-8) and drug conjugates (9,10) to different cells and tissues both in vitro and in vivo. Another advantage of antibody-based systems is the well-developed coupling chemistry (11,12). In this paper we describe the first successful attempt to synthesize an Ab-PLL conjugate suitable for the targeted delivery and expression of foreign DNA in mammalian cells.

EXPERIMENTAL PROCEDURES

Synthesis of N-Terminal Modified PDP-NPLL. Poly(ϵ -CBZ-L-lysine) (30 mg, M_w = 3000, Sigma), SPDP

(7 mg, Pharmacia), and 5 μ L of triethanolamine (Pierce) were mixed in 0.5 mL of dry dimethylformamide (Fluka). The reaction mixture was allowed to incubate overnight at room temperature. N-terminal modified poly(ϵ -CBZ-L-lysine) was precipitated with 10 mL of distilled water. The precipitate was washed with water and freeze-dried. The product (21 mg) was dissolved in a solution of HBr in glacial acetic acid (2 mL). After 0.5-h incubation the precipitate of deprotected PDP-NPLL was formed. The final product was washed several times with dry ether (30 mL) and dried in vacuo. The final product recovery was 15 mg.

Up to 90% of the PDP groups in the polymer were found to be active toward mercaptoethanol using the 2-thiopyridone release assay (13). PDP-NPLL was labeled with a trace amount of fluorescamine (14) in order to monitor the coupling reaction with antibody.

Modification of Monoclonal Antibodies. Rat monoclonal IgG_{2a} antibodies 34A and 14 (15,16) were dialyzed against degassed and N₂-purged HBS containing 5 mM EDTA, pH 7.3, at 4 °C following dilution with the same buffer to 5 mg/mL. Iminothiolane (250 μ g, Pierce) was added to the solution of antibody and the reaction was allowed to proceed for 1 h at room temperature. Antibodies were dialyzed against HBS containing 5 mM EDTA at 4 °C for 10 h with several changes of buffer. In order to remove large aggregates the preparation was centrifuged at 14000g for 10 min after the dialysis. Using the 5,5'-dithiobis(2-nitrobenzoic acid) assay (17), the antibodies were found to contain five to six SH groups per IgG molecule.

The thiolated antibodies and fluorescamine-labeled PDP-NPLL were mixed in HBS at an antibody/PDP-NPLL weight ratio of 20:1 and reaction was allowed to proceed overnight at 4 °C. The reaction mixture was then incubated with 2 mM N-ethylmaleimide for 1 h and subjected to gel chromatography (Bio-Gel A 0.5-m column, 40 \times 1.5 cm). Fluorescamine fluorescence ($\lambda_{ex}/\lambda_{em}$ = 380nm/480nm) was determined in each fraction and the first peak containing IgG was pooled. Two to three PDP-NPLL molecules were conjugated with one IgG. This parameter was calculated using fluorescamine fluorescence readings of known amount of the labeled polymer and the protein content of the conjugate determined with the Bio-Rad Protein Assay reagent under the assumption that polymer fluorescence is not changed upon coupling to antibody.

Cells and Cell Culture. Thrombomodulin-expressing mouse lung endothelial cells established as a continuous

[†] University of Tennessee.

[‡] Present address: Center for Imaging and Pharmaceutical Research, MGH-East, Charlestown, MA 02129.

[§] Oak Ridge National Laboratory.

^{||} Present address: Department of Pharmacology, University of Pittsburgh School of Medicine, Pittsburgh, PA 15261.

¹ Abbreviations used: NPLL, N-terminal modified poly-L-lysine; PLL, poly(L-lysine); SPDP, N-succinimidyl 3-(2-pyridyldithio)propionate; PDP, 3-(2-pyridyldithio)propionyl; CBZ, benzyloxycarbonyl; HBS, HEPES-buffered saline; Ab, antibody; CAT, chloramphenicolacetyl transferase.

culture (15) were used. Cells were cultured in 10-cm plastic dishes containing DMEM medium (Gibco-BRL) supplemented with 10% fetal calf serum (Hy-Clone) and a penicillin/streptomycin mixture at 37 °C in 5% CO₂.

All binding experiments were performed in serum-free DMEM medium. ³²P-DNA/Ab-PLL complexes diluted with the medium were applied to the cells and incubated for 4 h at 37 °C. The cells were washed three times with medium and harvested with trypsin/EDTA for radioactivity counting. ³²P-counting was performed using a standard toluene/Triton X-100 scintillation cocktail.

Plasmid Preparation. pUCSV2CAT plasmid was grown and purified as described earlier (18). DNA preparations were labeled with ³²P using a nick-translation kit (Gibco-BRL). Labeling DNA with ¹²⁵I for biodistribution studies was performed according to ref 19. Agarose gel electrophoresis of DNA and DNA/Ab-NPLL complexes was performed as in (18).

Preparation of Targeted DNA Complexes and Transfection. Targeted complexes were obtained by direct mixing of Ab-NPLL and DNA solutions which had been previously diluted to the desired concentrations with HBS, pH 7.3. For transfection experiments both specific DNA/34A-NPLL and nonspecific DNA/14-NPLL complexes were diluted with the serum-free medium and incubated with cells in the same way as for the binding experiments. After the incubation period serum-free medium was replaced with the complete medium and cells were allowed to grow for 48 h. Cells were scraped using a cell scraper and processed for CAT activity assay using fluorescent BODIPY-chloroamphenicol (Molecular Probes) as a substrate (20).

Targeting of ¹²⁵I-Labeled DNA Preparation in Vivo. One microgram of ¹²⁵I-labeled DNA (either alone or complexed with 20 µg of 34A-NPLL or 14-NPLL) was injected intravenously into 6-week-old female BALB/c mice. Each group contained three animals. After 0.5 h the mice were sacrificed and the major organs were counted for ¹²⁵I radioactivity. Organ dose uptake was calculated as a percent of the injected dose per gram of tissue.

RESULTS

Ab-NPLL Conjugate Synthesis. For the synthesis of N-terminal single-point reactive derivatives of PLL we took advantage of the fact that fully protected poly(ϵ -CBZ-L-lysine) possesses only one reactive NH₂ group—i.e., the N-terminal one. This group can be easily modified with conventional bifunctional reagents such as SPDP in organic solvent to produce an N-terminal SH-reactive moiety. Finally, all protective CBZ groups can be removed to give free PDP-NPLL without damaging the 3-(2-pyridyldithio)propionyl group (Figure 1). A similar procedure was described recently for the synthesis of antibody-polylysine-DTPA conjugates (21).

We have used the monoclonal antibody 34A against thrombomodulin of the mouse lung endothelial cells. Intravenously injected free antibody 34A accumulates efficiently in the mouse lung (15). This antibody has already been employed for the successful immunoliposome targeting both in vitro and in vivo (22, 26). Isotype-matched rat monoclonal antibody 14 of unknown specificity was used as the negative control. The antibodies were thiolated using the conventional iminothiolane method and further conjugated with N-terminal modified PDP-PLL. The resulting reaction mixture was separated using a Bio-Gel A 0.5-m column and the major fraction of fluorescent-labeled PDP-NPLL was coeluted with the antibody fraction (Figure 2). In order to demonstrate the

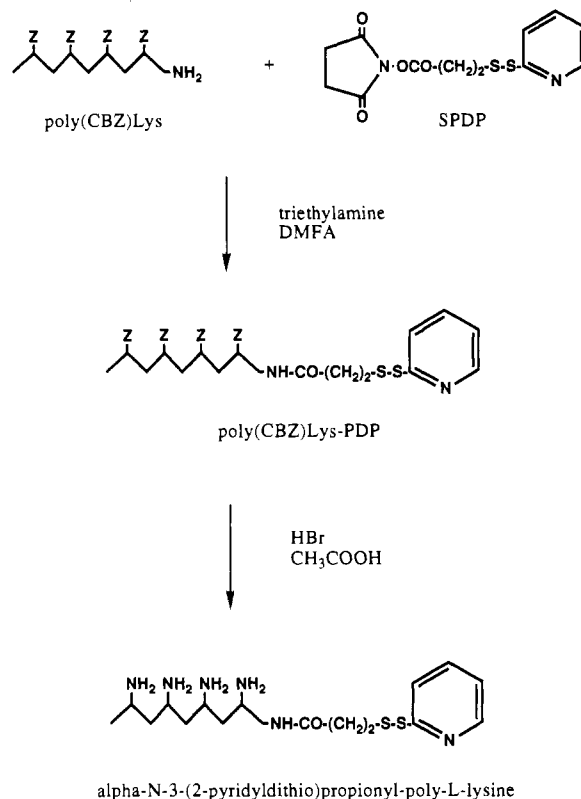


Figure 1. Synthesis of N-terminal modified 3-(2-pyridyldithio)propionyl-poly(L-lysine).

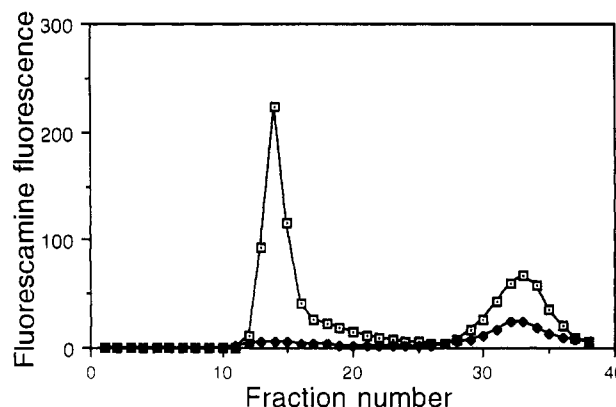


Figure 2. Bio-Gel A 0.5-m gel-chromatography of 34A-NPLL (□) and reduced conjugate (◆). 0.5-mL aliquot of the Ab-NPLL peak (250 µg of protein) was incubated with 50 mM mercaptoethanol and then rechromatographed on the same column.

reducibility of the linkage between NPLL and antibody, an aliquot of the first peak was incubated with 50 mM mercaptoethanol and then rechromatographed on the same column. In this case almost all label was eluted as free PLL, indicating that PLL moiety had been detached from IgG (Figure 2).

Properties of Ab-NPLL Conjugate. We have routinely obtained the conjugate preparations containing two to three PLL "tails" per single molecule of 34A or 14 antibody (see Experimental Procedures). Using partially purified mouse thrombomodulin (23) as an antigen in the ELISA binding assay, we have shown that the introduction of that amount of NPLL into 34A antibody resulted in a decreased binding affinity of the conjugate in comparison with nonmodified 34A antibody. However, the remaining binding activity of the 34A-NPLL conjugate was still substantially higher than the nonspecific binding activity of the 14-NPLL conjugates (Figure 3).

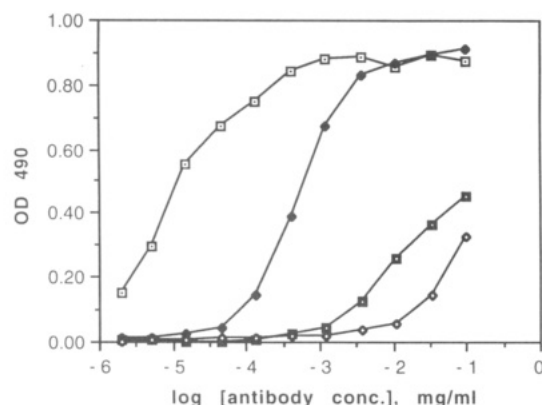


Figure 3. ELISA for native 34A (□) and 14 (■) antibodies and 34A-NPLL (◇) and 14-NPLL (◇) conjugates. Mouse lung thrombomodulin was used as antigen for plate coating. Peroxidase-labeled goat anti-mouse IgG were used as the second antibody.



Figure 4. Electrophoretic migration of pUCSV2CAT DNA complexed with increasing amount of 34A-NPLL conjugate. Lanes 1-7, 100 ng of DNA complexed with 34A-NPLL in weight ratios 1:30, 1:20, 1:15, 1:10, 1:7, 1:5, 1:3, respectively; lane 8, the same amount of DNA alone.

DNA Complexing. Ab-PLL conjugates were found to form avid complexes with plasmid DNA upon mixing of their dilute solutions. Figure 4 shows that plasmid DNA complexed with an increasing amount of Ab-NPLL was prevented from entering the agarose gel under standard electrophoresis conditions. This phenomenon, known as DNA migration retardation, occurs reputedly due to the neutralization of DNA negative charges with the positive charges of PLL moiety and has been observed in previous work with protein-PLL/DNA-delivery systems (3, 5). Using this assay we have also found that mixing 34A-PLL with DNA at a 20:1 weight ratio resulted in the complete binding of DNA by Ab-NPLL as judged from the disappearance of free DNA bands in the gel. The final DNA/Ab-NPLL complex formed no precipitate and remained in solution when the components were mixed at optimum ratio. The complex can also be filtered through the 0.22- μ m filter without removal of the DNA from solution.

Targeted DNA Delivery in Vitro and in Vivo. Using 34A-NPLL, plasmid DNA can be specifically delivered to the cultured target cells in vitro. Figure 5 shows considerable difference in target-cell DNA delivery mediated by specific and nonspecific conjugates. 34A-NPLL conjugate could also deliver the plasmid DNA to the target in vivo. Figure 6 shows the biodistribution patterns of 125 I-DNA/Ab-NPLL preparations 0.5 h after intravenous injection into mice. The specific accumulation of labeled DNA in the lung was clearly demonstrated.

Having shown that 34A-PLL conjugate can effectively

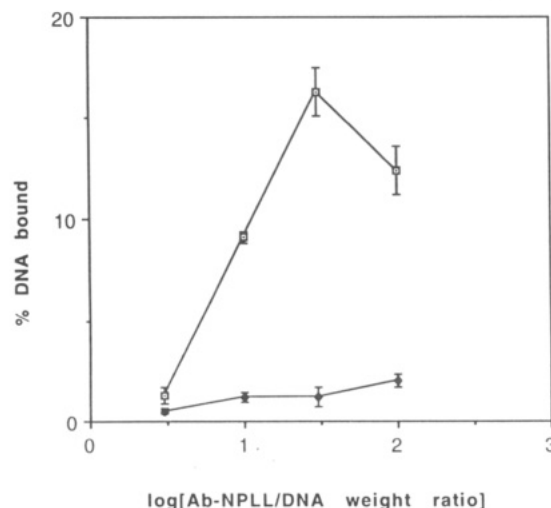


Figure 5. Binding of 32 P-labeled pUCSV2CAT DNA complexed with 34A-NPLL (□) and 14-NPLL (●) at different weight ratios to the cultured mouse lung endothelial cells.

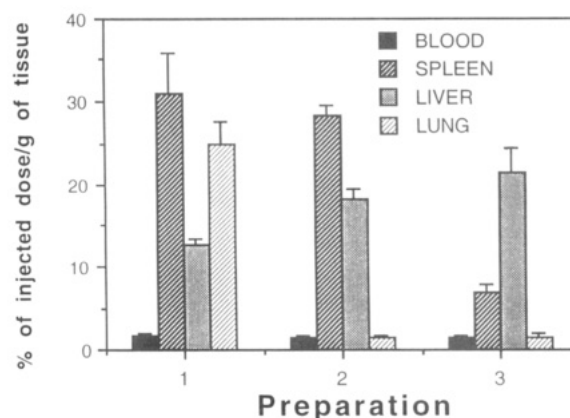


Figure 6. Biodistribution of 125 I-labeled DNA alone (3) and complexed with 34A-NPLL (1) and 14-NPLL (2) in BALB/c mice.

and specifically deliver genetic material to the antigen-positive target cells both in vitro and in vivo, we tried to evaluate whether this DNA can be expressed in the mouse lung endothelial cells. We have found that 2 days after the standard transfection procedure using 5 μ g of pUCSV2CAT complexed with different amounts of 34A-PLL one could observe specific CAT gene expression although the level of expression was rather modest (Figure 7).

DISCUSSION

In the present paper we describe the design of a targeted DNA-delivery system based on the use of antibody-NPLL conjugates. In principle the system described resembles ligand-PLL conjugates described earlier (3-5) but definitely represents a more general approach because the antibody is used as the targeting ligand. Theoretically, conjugates with a broad range of specificity can be designed with appropriate monoclonal antibodies. The advantages of the particular targeting system based on 34A monoclonal Ab are as follows: the availability of the cell culture and partially purified antigen and the possibility to carry out the in vivo targeting.

An additional advantage of our conjugate design is the use of an N-terminal PLL-antibody linkage which helps to avoid inter-IgG cross-linking and makes available the whole bulk of PLL amino groups for DNA binding. One can speculate that the decrease in 34A-NPLL binding to

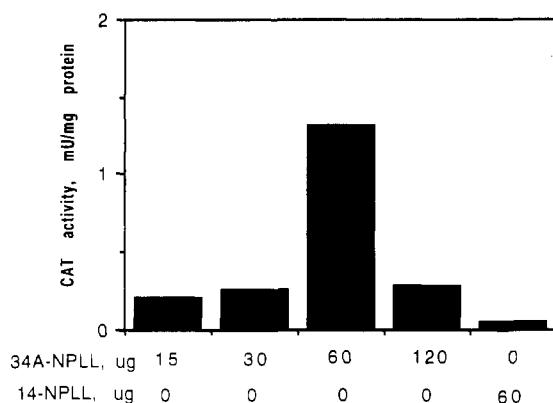


Figure 7. Transfection efficiency of different DNA/Ab-NPLL preparations. For each transfection 3 μ g of pUCSV2CAT was complexed with (1) 15 μ g of 34A-NPLL, (2) 30 μ g of 34A-NPLL, (3) 60 μ g of 34A-NPLL, (4) 120 μ g of 34A-NPLL, (5) 60 μ g of 14-NPLL.

the antigen as compared with the native 34A binding is probably caused by steric hindrance created by PLL chains (Figure 4). This circumstance results in a lower lung accumulation of the labeled DNA/34A-NPLL in vivo (Figure 6) as compared with the free 34A (up to 300% of injected dose/g tissue for 34A (15) vs 25%/g tissue for 125 I-DNA/34A-NPLL).

As emphasized in the previous studies with ligand/receptor based systems of DNA delivery, the endocytosis of DNA/cationized ligand is required for the successful transfection. In human umbilical vein endothelial cells thrombomodulin has been shown to undergo active endocytosis when exposed to either thrombin or specific antibody or both (24, 25). Figure 5 shows that a substantial amount of DNA can be specifically delivered to the thrombomodulin-positive target cells in vitro when complexed with 34A-NPLL (up to 15% of total DNA added). Despite of this, the level of specific CAT gene in vitro expression in transfected cells was rather modest (Figure 7). Thus, the level of CAT gene expression in the cells transfected with DNA/cationic liposome complex was found to be at least 1 order of magnitude higher (2, 18), depending on the cell line. Low expression levels can be explained by two possibilities: (1) unlike the free antibody, the complex is not internalized into the cell; and (2) DNA is subjected to intralysosomal degradation. The former case is not likely as the DNA/34A-NPLL complex is quite small in size. Furthermore, immunoliposomes containing covalently bound 34A are rapidly endocytosed by mouse artery endothelial cells (26). The endocytosed plasmid would have to be released into the cytoplasm before it can be delivered to the lysosome for degradation. Little is known about the mechanism by which the PLL-bound DNA escapes the endosomal compartment. This process is probably dependent on the nature of the specific ligand/receptor system and its endocytic pathway. Inefficient release of DNA from the endosomes would result in the lysosomal degradation of DNA and a low level of gene expression in the transfected cells. Excess of the Ab-NPLL component may alter the structure of final transfection complex, which may result in decreasing transfection activity. This hypothesis can explain why CAT gene expression level at elevated 34A-NPLL/DNA ratio is lower (120 μ g vs 60 μ g of 34A-NPLL in Figure 7). The phenomenon was also observed and discussed by other authors for other transfection agents (5, 18).

As proposed earlier by us (18), an efficient DNA-targeting vehicle should consist of three major components: a target-specific ligand for target binding, a polycation for

complexing the negatively charged DNA, and a lipophilic part which reputedly helps DNA to enter the cell cytoplasm (27). The present conjugate system contains the first two components, but not the third component. It is conceivable that the low level of the foreign DNA expression might be improved by adding to the system a lipophilic moiety as its constituent. This hypothesis will be tested in future experiments.

Thus, we have succeeded in demonstrating the principal possibility of targeted transfection using an Ab-based conjugate system. If successful, these experiments may result in the appearance of new agents for genetic modification of selected cells which can leave normal tissues untouched.

ACKNOWLEDGMENT

This work was supported by NIH Grant AI 29893. We thank X. Gao for the generous gift of purified thrombomodulin.

LITERATURE CITED

- (1) Felgner, P. L., Gadek, T. R., Holm, M., Roman, R., Chan, H. W., Wenz, M., Northrop, J. P., Ringold, G. M., and Danielsen, M. (1987) Lipofection: A highly efficient, lipid-mediated DNA-transfection procedure. *Proc. Natl. Acad. Sci. U.S.A.* 84, 7413-7417.
- (2) Gao, X., and Huang, L. (1991) A novel cationic liposome reagent for efficient transfection of mammalian cells. *Biochem. Biophys. Res. Commun.* 179, 280-285.
- (3) Wu, G. Y., and Wu, C. H. (1988) Evidence for targeted gene delivery to HepG2 hepatoma cells in vitro. *Biochemistry* 27, 887-892.
- (4) Wu, C. H., Wilson, J. M., and Wu, G. Y. (1989) Targeted genes: Delivery and persistent expression of a foreign gene driven by mammalian regulatory elements in vivo. *J. Biol. Chem.* 264, 16985-16978.
- (5) Wagner, E., Zenke, M., Cotten, M., Beug, H., and Birnstiel, M. L. (1990) Transferrin-polycation conjugates as carriers for DNA uptake into cells. *Proc. Natl. Acad. Sci. U.S.A.* 87, 3410-3414.
- (6) Martin, F. J., and Papahadjopoulos, D. (1982) Irreversible coupling of immunoglobulin fragments to preformed vesicles. An improved method for liposome targeting. *J. Biol. Chem.* 257, 286-292.
- (7) Wang, C.-Y., and Huang, L. (1987) pH-sensitive immunoliposomes mediate target cell specific delivery and controlled expression of a foreign gene in mouse. *Proc. Natl. Acad. Sci. U.S.A.* 84, 7851-7855.
- (8) Wright, S., and Huang, L. (1989) Antibody directed liposomes as drug delivery vehicles. *Adv. Drug Delivery Rev.* 3, 343-389.
- (9) Gallego, J., Price, M. R., and Baldwin, R. W. (1984) Preparation of four daunomycin-monooclonal antibody 791T/36 conjugates with antitumor activity. *Int. J. Cancer* 33, 737-744.
- (10) Hurvitz, E., Kashi, R., Arnon, R., Wilchek, M., and Sela, M. (1985) The covalent linking of two nucleotide analogues to antibodies. *J. Med. Chem.* 28, 137-140.
- (11) Torchilin, V. P., and Klibanov, A. L. (1991) The antibody-linked chelating polymers for nuclear therapy and diagnostics. *Ther. Drug Carrier Syst.* 7, 275-308.
- (12) Peeters, J. M., Hazendonk, T. G., Beuvery, E. C., and Tesser, G. I. (1989) Comparison of four bifunctional reagents for coupling peptides to proteins and the effect of the three moieties on the immunogenicity of the conjugates. *J. Immunol. Methods* 120, 133-143.
- (13) Carlsson, J., Drevin, H., and Axen, R. (1978) Protein thiolation and reversible protein-protein conjugation. N-succinimidyl 3-(2-pyridyldithio)propionate, a new heterobifunctional reagent. *Biochem. J.* 173, 723-737.
- (14) Chen, R. F., Smith, P. D., and Maly, M. (1978) The fluorescence of fluorescamine-amino acids. *Arch. Biochem. Biophys.* 189, 241-250.

- (15) Kennel, S. J., Lankford, T., Huges, B., and Hotchkiss, J. A. (1988) Quantitation of a murine lung endothelial cell protein, P112, with a double monoclonal antibody assay. *Lab. Invest.* 59, 692-701.
- (16) Ford, V. A., Stringer, C. and Kennel, S. J. (1992) Thrombomodulin is preferentially expressed in Balb/c lung microvessels. *J. Biol. Chem.* 267, 5446-5450.
- (17) Deakin, H., Ord, M. G., and Stocken, L. A. (1963) Glucose-6-phosphate dehydrogenase activity and thiol content of thymus nuclei from control and X-irradiated rats. *Biochem. J.* 89, 296-302.
- (18) Zhou, X., Klivanov, A. L., and Huang, L. (1991) Lipophilic polylysines mediate efficient DNA transfection in mammalian cells. *Biochim. Biophys. Acta* 1065, 8-14.
- (19) Prenskey, W. (1976) The radiiodination of RNA and DNA to high specific activities. *Methods Cell Biol.* 13, 121-152.
- (20) Hruby, D. E., Brinkley, J. M., Kang, H. C., Haugland, R. P., Young, S. L., and Melner, M. H. (1990) Use of fluorescent chloramphenicol derivative as a substrate for CAT assays. *Bio-techniques* 8, 65-71.
- (21) Slinkin, M. A., Klivanov, A. L., and Torchilin, V. P. (1991) Terminal-modified polylysine based chelating polymers; highly efficient coupling to antibody with minimal loss in immunoreactivity. *Bioconjugate Chem.* 2, 342-348.
- (22) Maruyama, K., Kennel, S. J., and Huang, L. (1990) Lipid composition is important for highly efficient target binding and retention of immunoliposomes. *Proc. Natl. Acad. Sci. U.S.A.* 87, 5744-5748.
- (23) Salem, H. H., Maruyama, I., Ishii, H., and Majerus, P. W. (1984) Isolation and characterization of thrombomodulin from human placenta. *J. Biol. Chem.* 260, 12246-12251.
- (24) Maruyama, I., and Majerus, P. W. (1985) The turnover of thrombin-thrombomodulin complex in cultured human umbilical vein endothelial cells and A549 lung cancer cells. *J. Biol. Chem.* 260, 15432-15438.
- (25) Maruyama, I., and Majerus, P. W. (1987) Protein C inhibits endocytosis of thrombin-thrombomodulin complex in A549 lung cancer cells and human umbilical vein endothelial cells. *Blood* 69, 1481-1484.
- (26) Holmberg, E., Maruyama, K., Kennel, S. J., Klivanov, A. L., Torchilin, V. P., Ryan, U., and Huang, L. (1990) Target specific binding of immunoliposomes in vivo. *J. Liposome Res.* 1, 393-406.
- (27) Hug, P., and Sleight, R. G. (1991) Liposomes for the transformation of eukaryotic cells. *Biochim. Biophys. Acta* 1097, 1-17.

Photoaffinity Labeling of Scallop Myosin with 2-[(4-Azido-2-nitrophenyl)amino]ethyl Diphosphate: Identification of an Active Site Arginine Analogous to Tryptophan-130 in Skeletal Muscle Myosin[†]

Bruce A. Kerwin and Ralph G. Yount*

Department of Biochemistry and Biophysics and Department of Chemistry, Washington State University, Pullman, Washington 99164-4660. Received April 6, 1992

The ADP photoaffinity analogue 2-[(4-azido-2-nitrophenyl)amino]ethyl diphosphate (NANDP) was used to photolabel the ATP binding site of scallop myosin. Approximately 1 mol of NANDP per mol of myosin was trapped at the active site by complexation with vanadate and manganese. ADP, but not AMP, inhibited trapping of NANDP. The trapped NANDP photolabeled up to 37% of the myosin upon UV irradiation. Papain subfragment-1 prepared from the photolabeled myosin was digested with trypsin, and the major photolabeled tryptic peptides were isolated by reversed-phase HPLC. The amino acid sequence of the major labeled peptide was X-Leu-Pro-Ile-Tyr-Thr-Asp-Ser-Val-Ile-Ala-Lys, where X represents the photolabeled amino acid Arg¹²⁸. Previously, Trp¹³⁰ of rabbit skeletal muscle myosin has been shown to be photolabeled by NANDP [Okamoto, Y., and Yount, R. G. (1985) *Proc. Natl. Acad. Sci. U.S.A.* 82, 1575-1580]. Scallop and rabbit skeletal muscle myosin display a high degree of sequence similarity in this region with Arg¹²⁸ in an equivalent position as Trp¹³⁰. These results suggest that the composition of the purine binding site is analogous in both myosins and that Arg and Trp play a similar role in binding ATP, despite the marked differences of their side chains.

INTRODUCTION

Myosin II (or conventional myosin) from skeletal muscle is the most extensively studied of the many actin-based molecular motors. It is a multidomain protein composed of six subunits: two heavy chains and four light chains of two types. The C-terminal halves of two heavy chains form an α -helical coiled-coil rod which make up the backbone of the thick filament while the N-terminus of each heavy chain folds into a globular head responsible for binding actin and hydrolyzing ATP. Each head contains a pair of light chains (one regulatory and one essential) which appear to modify or regulate contraction (for a review see Adelstein & Eisenberg, 1980). In smooth muscle this occurs via specific phosphorylation of the regulatory light chains (Sobieszek & Small, 1977; Sherry et al., 1978; for a review see Trybus, 1991). A similar myosin-based regulation occurs in the striated muscle of scallops (Kenrick-Jones et al., 1970; Szent-Györgyi & Szentkiralyi, 1973). Here, Ca²⁺ binding to a regulatory complex composed of the two light chains and a portion of the heavy chain (Kwon et al., 1990) regulates ATPase activity and tension development. In both of these systems, although the basic components of the regulatory mechanisms have been identified, little is known concerning the regions of the active site which may be involved with regulation.

In the absence of X-ray crystallographic data, amino acids within the active site of myosin can be identified using photoaffinity labeling with analogues of ATP or ADP (Yount et al., 1992). This technique has been used to map the amino acids near the ribose ring binding site of skeletal (Mahmood et al., 1989; Kennedy et al., 1991) and smooth muscle myosin (Cole & Yount, 1990) and portions of the

purine binding site of *Acanthamoeba* myosin II (Atkinson et al., 1986) and smooth muscle myosin (Garabedian & Yount, 1990, 1991). The region of the active site of skeletal muscle myosin which binds near C-2 of the adenine ring of ATP has been mapped using 2-azido-ATP (Yount et al., 1987; H. Kuwayama, unpublished results) and the photoreactive ADP analogue NANDP (Okamoto and Yount, 1985). NANDP¹ (Figure 1) has proven to be exceptionally useful in studying skeletal myosin due to its high photoincorporation and the stability of its photoadducts (Nakamaye et al., 1985). Trp¹³⁰ of skeletal MHC was identified as the major photolabeled amino acid when either 2-azido-ATP or NANDP was used. Analysis of the amino acid sequence of scallop MHC (Nyitray et al., 1991) shows that Arg¹²⁸ replaces Trp¹³⁰ (skeletal). The introduction of a positively charged residue at the adenine binding site is surprising and may reflect a structural change that is important in myosin-based regulation.

As a first step toward identifying amino acids in the purine binding region which may be involved in myosin-based regulation, we have used NANDP to photolabel the active site of scallop myosin. Here we demonstrate that NANDP is an excellent substrate for scallop myosin and that NANDP is stably trapped at the active site with Mn²⁺ and V_i. This step allowed the unbound NANDP to be separated from the myosin complex before irradiation. Approximately 35% of the trapped NANDP photoincorporated into the heavy chain with less than 2% photoincorporation into the light chains. Arg¹²⁸ was identified as the major photolabeled amino acid, suggesting that Arg¹²⁸ (scallop) and Trp¹³⁰ (skeletal) are in analogous

* Author to whom correspondence should be addressed.

[†] Supported by grants from NIH (DK05195) and MDA. B.A.K. is an MDA postdoctoral fellow.

¹ Abbreviations used: high-performance liquid chromatography, HPLC; myosin heavy chain, MHC; myosin regulatory light chain, RLC; myosin subfragment 1, S1; 2-[(4-azido-2-nitrophenyl)amino]ethyl diphosphate, NANDP; phenylthiohydantoin, PTH; polyacrylamide gel electrophoresis, PAGE; sodium dodecyl sulfate, SDS; trifluoroacetic acid, TFA; vanadate, V_i.

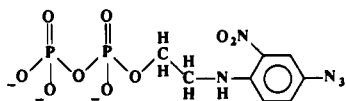


Figure 1. Schematic diagram of 2-[(4-azido-2-nitrophenyl)amino]ethyl diphosphate, NANDP.

positions within the purine binding site. Thus, it is highly likely that this region of the ATP binding site is similar for the two myosins even though they contain amino acids with quite different properties.

EXPERIMENTAL PROCEDURES

Purification of Scallop Myosin. Bay scallops (*Aequipecten irradians*), preserved in 50% polyethylene glycol, were a generous gift from Dr. Andrew G. Szent-Györgyi. Myosin was purified from the striated adductor muscle according to the method of Chantler and Szent-Györgyi (1978) as modified by Szent-Györgyi (personal communication). Briefly, 10–50 g of scallops was homogenized in ice cold buffer in a Waring blender by pulsing three times for 10 s and three times for 15 s. The homogenate was placed on ice for 2–3 min between each pulse. The myofibrils were spun down at 7000g and resuspended with a Dounce homogenizer (A. H. Thomas) in 40 mM NaCl, 5 mM NaP_i, pH 7.0, 3 mM MgCl₂, 0.1 mM EGTA, and 0.1 mM DTT. The pH of the myofibril solution was adjusted to 7.5 with 0.5 M Na₂HPO₄ and fresh DTT was added to 1.0 mM. MgCl₂ and ATP were then added to 5 mM and NaCl was added to 0.6 M while the pH was kept constant at 7.5 using 0.5 M Na₂HPO₄. The solution was centrifuged at 16000g for 20 min at 4 °C. MgCl₂ and ATP were then added to the supernatant to 10 mM, and either solid or saturated solution of ammonium sulfate was added to 45% saturation while the pH was kept constant at 7.0 using 0.5 M Na₂HPO₄. The suspension was centrifuged at 16000g for 20 min at 4 °C to remove precipitated actin and tropomyosin. The decanted supernatant was brought to 65% saturation by addition of solid ammonium sulfate. The myosin precipitate was centrifuged at 16000g for 20 min; the pellet was resuspended in a minimal volume of 20 mM NaCl, 10 mM NaP_i, pH 6.5, 0.1 mM EGTA, 3 mM MgCl₂, 0.1 mM DTT, and 0.1 mM NaN₃ and dialyzed overnight against 6 L of the same buffer. The resulting myosin filaments were either washed extensively with 30 mM KCl and 20 mM Tris, pH 7.5 after centrifugation or were dialyzed into 30 mM KCl, 20 mM Tris, pH 7.5, and 0.1 mM DTT, and then washed extensively as above. This is referred to as filamentous myosin. Protein concentrations were determined using $\epsilon_{280}^{1\%} = 5.3$, after dissolving the myosin filaments in 0.5 M KCl and 20 mM Tris, pH 8.0, at 4 °C. The myosin was used immediately for trapping of [β -³²P]NANDP.

ATPase and NANTPase Assays. CaATPase assays were done as described by Wells et al. (1979) except that the release of P_i was measured after 2 and 8 min.

Synthesis of NANTP and [β -³²P]NANDP. NANTP and [β -³²P]NANDP were prepared as described by Nakamaye et al. (1985) and Okamoto and Yount (1985), respectively. Carrier-free ³²P (10 mCi in 1 mL) was purchased from New England Nuclear (Du Pont). Purity of each compound was determined by chromatography on silica gel TLC (60 F₂₅₄, Merck) using isobutyric acid/concentrated NH₄OH/water 66:1:33 as a solvent. [β -³²P]NANDP with an initial specific activity of 144 000 cpm/nmol was stored at -20 °C in methanol.

Trapping of [β -³²P]NANDP on Scallop Myosin. NANDP was trapped on scallop myosin based on the

method of Goodno (1979). Filamentous scallop myosin was dissolved in 0.5 M KCl and 20 mM Tris, pH 8.0, at a concentration of 4–5 mg/mL (300–600 mg of myosin was normally used in a photolabeling experiment). MnCl₂ was added to a final concentration of 2 mM, [β -³²P]NANDP was added to a concentration of 2–4 times the number of ATP binding sites and V_i was added to a final concentration of 1 mM. The solution was incubated for 25 min at 25 °C followed by a 3–4-h incubation on ice. Solid ammonium sulfate was added to 65% saturation and the precipitated myosin was collected by centrifugation at 16000g for 20 min at 4 °C. The pellet was resuspended in a minimal volume of 30 mM KCl, 20 mM Tris, pH 6.5, and 0.1 mM DTT, then dialyzed overnight against 6 L of the same buffer. The following day the dialyzate containing filamentous myosin was centrifuged at 7000g for 10 min at 4 °C and the resulting myosin-MnNANDP-V_i pellet washed twice with low-salt buffer (30 mM KCl and 20 mM Tris, pH 7.5). The final pellet was resuspended to a final concentration of approximately 5 mg/mL in the low-salt buffer (this was the final myosin-Mn-nucleotide-V_i complex used for photolysis).

Photolysis of the Myosin-Mn[β -³²P]NANDP-V_i Complex. Photolysis was based on the procedure of Cremona et al. (1991). Briefly, filamentous myosin (10–12 mL of ~5 mg/mL solution) containing trapped [β -³²P]NANDP was irradiated for 3 min on ice in a 9-cm Petri dish with a Pyrex cover using a 450-W medium-pressure Hg lamp (Hanovia, Ace Glass) at a distance of approximately 9 cm. To determine the extent of photolabeling, aliquots of irradiated myosin (100–200 μ L) were precipitated with 1 mL of ice-cold 5% trichloroacetic acid and incubated for 2–3 h on ice. The precipitates were collected in a microcentrifuge tube, resuspended in 0.5 mL of 4% SDS/50 mM Tris-base, and incubated overnight at room temperature prior to scintillation counting.

SDS-PAGE Analysis. Myosin samples were analyzed by SDS-PAGE on 18 × 20 cm 7–20% gels according to the procedure of Laemmli (1970). Protein bands were visualized by staining with a solution of 0.05% Coomassie Blue in 45% methanol, 45% water, and 10% glacial acetic acid. Gel strips containing the bands of interest were excised, placed in 20-mL glass vials, and solubilized by heating for 2–4 h at 70 °C in 0.75 mL of 30% H₂O₂. After cooling, 18 mL of BCS scintillant (Amersham) was added and the radioactivity was determined in a scintillation counter.

Scintillation Counting. Aliquots of samples (0.01–1.0 mL) were diluted to 4.5 mL with BCS scintillant and radioactively determined.

Proteolytic Digestion of Photolabeled Myosin. Photolabeled myosin in low salt buffer was brought to 10 mM EDTA, pH 7.5, and incubated for 25 min on ice, then 5 min at 25 °C. Activated papain (Sigma, St. Louis, MO) (0.1 units/mg of myosin) was added (Lowey et al., 1969) and the mixture incubated for 15 min at 25 °C. Papain was inactivated by addition of iodoacetic acid (0.1 M in 0.25 M Na₂HPO₄) to 5 mM and the solution incubated an additional 5 min. MgCl₂ (1 M) was added to 20 mM, and the reactions were incubated on ice for 20 min and then centrifuged at 16000g for 10 min at 4 °C to remove aggregated rods and undigested myosin. Solid ammonium sulfate was added to the supernatant to 70% saturation and the precipitated S1 collected by centrifugation as above. The S1 pellet was dissolved in 30 mM KCl and 20 mM Tris, pH 7.5, and the concentration adjusted to 1–2 mg/mL based on $\epsilon_{280}^{1\%} = 8.0$. CaCl₂ (1 M) was added to 1 mM, and urea (Ultrapure, ICN Biomedicals Inc., Cleveland, OH) added to 1 M. The S1 (1–2 mg/mL) was digested

Table I. ATPase and NANTPase Activities of Scallop Myosin^a

assay system	$\mu\text{mol P}_i$ / min per mg		NANTPase/ ATPase
	NANTPase	ATPase	
Ca ²⁺ /Mg ²⁺ (high salt)	0.074 \pm 0.002	0.078 \pm 0.009	0.95
Ca ²⁺ (high salt)	0.19 \pm 0.03	1.9 \pm 0.1	0.1
Ca ²⁺ /Mg ²⁺ (low salt)	0.18 \pm 0.03	0.12 \pm 0.01	1.5
Ca ²⁺ /Mg ²⁺ /F-actin			
pCa 4 (low salt)	0.39 \pm 0.03	0.29 \pm 0.03	1.4
pCa 9 (low salt)	0.058 \pm 0.011	0.044 \pm 0.007	1.3
pCa 4/pCa 9	6.6	6.8	

^a A freshly prepared myosin stock solution of 4.3 mg/mL was assayed at 25 °C with substrate concentrations of 2 mM. The high-salt Ca²⁺ assay used 0.46 μM myosin, 0.5 M KCl, 20 mM Tris, pH 7.5, and 5 mM CaCl₂. The high-salt Ca²⁺/Mg²⁺ assay used 0.92 μM myosin, 0.5 M KCl, 20 mM Tris, pH 7.6, 0.11 mM CaCl₂, and 3 mM MgCl₂. The low-salt Ca²⁺/Mg²⁺ assay was similar but with 30 mM KCl replacing 0.5 M KCl. The Ca²⁺/Mg²⁺/F-actin pCa 4 assay contained 0.46 μM myosin, 4.6 μM F-actin, 30 mM KCl, 20 mM Tris, pH 7.6, 0.11 mM CaCl₂, and 3 mM MgCl₂. The comparable pCa 9 assay contained in addition 3.41 mM EGTA. Each activity value is expressed as the average and standard deviation calculated from the data from six experiments.

at room temperature with TPCK-treated trypsin (in 1 mM HCl) (Sigma, St. Louis, MO) at a 1:50–1:100 ratio of trypsin:S1. Three additions of trypsin were made at 0, 30, and 60 min, and the solution was allowed to digest overnight.

Purification of Peptides by HPLC. HPLC separations were performed at room temperature using a microprocessor-controlled Altex/Beckman dual-pump set-up connected to a Beckman 165 dual-wavelength detector. Initial separations were carried out on a semipreparative (7.0 \times 250 mm) 300-Å pore C8 reversed-phase column (Aquapore RP-300, Brownlee Labs) equilibrated in 0.11% trifluoroacetic acid (TFA), pH 2, at a flow rate of 2.0 mL/min. All subsequent separations were carried out on an analytical (4.6 \times 220 mm) 300-Å pore C8 reversed-phase column (Aquapore RP-300, Brownlee Labs) at a flow rate of 1.0 mL/min. Prior to separation on the analytical column, samples were acidified with TFA to approximately pH 2 (by litmus), and β -mercaptoethanol was added to 10 mM. The samples were then passed through a 0.45-mm Nylon-66 filter syringe (Rainin) before loading via a 7.5-mL sample loop. Volumes greater than 6.0 mL were loaded on the column by multiple loadings. Following each separation samples which were radioactive and absorbed at 320 nm were concentrated to one-half their volume on a SpeedVac (Savant, Farmingdale, NY) to remove acetonitrile and then diluted with the appropriate equilibrating buffer and brought to 1.0 mM with β -mercaptoethanol before further HPLC chromatographic separations.

RESULTS

NANTP as a Substrate for Scallop Myosin. The ability of scallop myosin to utilize NANTP as a substrate was investigated using a variety of assay conditions. As shown in Table I the ATPase and NANTPase activities of scallop myosin differ by less than a factor of 2 for a number of assay conditions. Comparison of the degree of calcium activation for the actin activated NANTPase and ATPase activities at pCa 4 and 9 in the presence of Mg²⁺ demonstrated no significant difference between the two activities, suggesting that the rate-limiting steps for hydrolysis of these two substrates is the same with or without Ca²⁺. The only activity which differed significantly were those measured in 5 mM Ca²⁺ and high salt. Here the

ATPase activity was a factor of 10 greater than the NANTPase for unknown reasons.

Trapping of [β -³²P]NANDP at the Active Site of Scallop Myosin. Previous studies have shown that Co²⁺ can be used in conjunction with V_i to trap nucleoside diphosphates at the ATP binding site of both skeletal and smooth muscle myosin (Grammer et al., 1988; Cole & Yount, 1990; Garabedian & Yount, 1990, 1991). However, when 2 mM Co²⁺ was added to scallop myosin under normal trapping conditions the myosin formed a white flocculent precipitate (B. Kerwin, unpublished observations). Previous studies have shown that Mn²⁺ and Ni²⁺ can also be used to trap nucleoside diphosphate and quench the photoreaction of V_i with myosin (Grammer et al., 1988). Both of these metals effectively trapped nucleoside diphosphates on scallop myosin without precipitating the myosin, although the time course of trapping with the Mn²⁺ was much faster than that with Ni²⁺ (data not shown). Trapping of [β -³²P]NANDP and [¹⁴C]ADP with V_i and Mn²⁺ on scallop myosin in high salt was complete within 5 min (data not shown). Approximately 62% of the ATP binding sites were complexed with [β -³²P]NANDP using Mn²⁺ and V_i with a parallel decrease in the CaATPase activity to a value approximately 30% of that for untrapped myosin. Trapping was done in high salt because these conditions produced the highest percent trapping. Trapping with [¹⁴C]ADP under identical conditions blocked approximately 73% of the ATP binding sites. We were unable to increase the percentage trapping of the myosin-Mn[β -³²P]NANDP-V_i complex through either subsequent additions of [β -³²P]NANDP after 10 min of incubation or readdition of Mn²⁺, V_i, and [β -³²P]NANDP after purification of the trapped myosin (data not shown). Control experiments with skeletal muscle myosin S1 and [β -³²P]NANDP under identical conditions also resulted in only 60% trapping. Following trapping in high salt the myosin-Mn[β -³²P]NANDP-V_i complex was dialyzed into a low-salt buffer to produce myosin filaments. The final percent trapping under these conditions was approximately 52% and 54% for the myosin-Mn[β -³²P]NANDP-V_i complex and the myosin-Mn[¹⁴C]ADP-V_i complex, respectively, with concomitant increases in the CaATPase activities.

Further evidence that [β -³²P]NANDP was trapped at the ATP binding site of scallop myosin came from trapping inhibition studies. Figure 2 shows that ADP, but not AMP, inhibited the trapping of [β -³²P]NANDP on scallop myosin. Inhibition occurred in a 1:1 manner (Figure 2, inset) such that 50% inhibition of trapping occurred when the concentration of ADP equaled that of [β -³²P]NANDP. These results demonstrate that NANDP and ADP compete for the same binding site with nearly identical binding constants.

Photoincorporation of [β -³²P]NANDP into Scallop Myosin. As seen in Figure 3 maximum photoincorporation of [β -³²P]NANDP into myosin filaments occurred within 2–3 min of irradiation. Approximately 37% of the total trapped [β -³²P]NANDP was covalently incorporated as determined by trichloroacetic acid precipitation of the protein. In order to determine if the photoincorporated adducts were stable in the low-salt buffer and to determine if nonspecific dark reactions were occurring (Staros & Bayley, 1984), a photolyzed sample of [β -³²P]NANDP-trapped scallop myosin was stored on ice in the dark and aliquots were precipitated with trichloroacetic acid to determine the extent of covalent modification. Figure 4 shows that the covalently incorporated [β -³²P]NANDP was stable over a period of 5 h. In addition, precipitable counts did

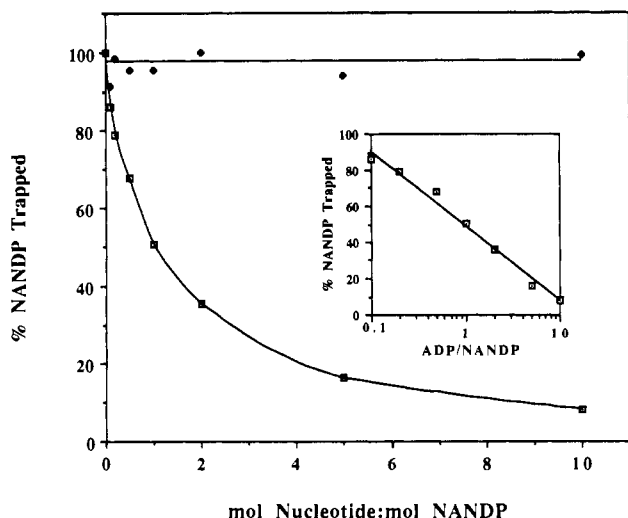


Figure 2. ADP-dependent inhibition of $[\beta\text{-}^{32}\text{P}]\text{NANDP}$ trapping. Aliquots (1 mL) of freshly prepared scallop myosin in 0.5 M KCl, 20 mM Tris, pH 8.0, $[\beta\text{-}^{32}\text{P}]\text{NANDP}$ at a 2 times excess over active sites and either ADP or AMP were added to 2 mM MnCl_2 and 1 mM V_i and incubated for 20 min at 25 °C. The reactions were quenched by the addition of ATP to 25 times excess over the $[\beta\text{-}^{32}\text{P}]\text{NANDP}$ and excess nucleotides were removed by centrifugation through columns of Sephadex G-50 (Penefsky, 1977). Radioactivity was determined by counting duplicate 200- μL aliquots as described under Experimental Procedures. Protein concentrations were measured by the absorbance at 280 nm. Increasing concentrations of ADP (\square) or AMP (\blacklozenge) were added to each reaction mixture. The percent NANDP trapped ($\sim 62\%$) was normalized to 100%.

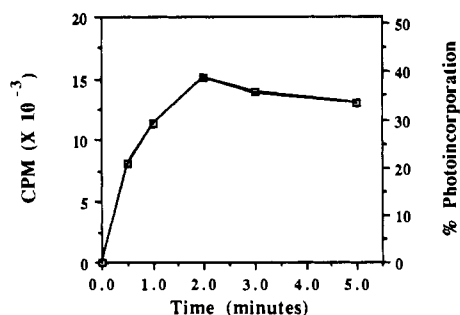


Figure 3. Photoincorporation of $[\beta\text{-}^{32}\text{P}]\text{NANDP}$. Scallop myosin was trapped with $[\beta\text{-}^{32}\text{P}]\text{NANDP}$ and transferred into the low-salt buffer as described under Experimental Procedures. Trapped myosin (10 mL, 54% trapped) was irradiated as described under Experimental Procedures. Three 100- μL aliquots were removed at each of the indicated times and precipitated with trichloroacetic acid (Experimental Procedures). The Y-axis is defined as the percent of the originally trapped myosin that became covalently labeled with $[\beta\text{-}^{32}\text{P}]\text{NANDP}$.

not increase over time, indicating that dark reactions were not occurring. Furthermore, if the active site of unmodified scallop myosin was blocked with the $\text{MnADP}\cdot\text{V}_i$ complex followed by addition of free $[\beta\text{-}^{32}\text{P}]\text{NANDP}$ (equal to one-half of the total number of ATP binding sites) immediately prior to irradiation, photoincorporation appeared to be nonspecific. As seen in Figure 5A no distinct radiolabeled peptides were evident following photolysis in the presence of uncomplexed $[\beta\text{-}^{32}\text{P}]\text{NANDP}$. When the $[\beta\text{-}^{32}\text{P}]\text{NANDP}$ was trapped at the active site with V_i and Mn^{2+} , though, only a discrete number of peptides were labeled (Figure 5B). Taken together these results indicate that $[\beta\text{-}^{32}\text{P}]\text{NANDP}$ must be trapped at the ATP binding site for specific photoincorporation to occur and that long-lived reactive intermediates were not labeling the scallop myosin following irradiation.

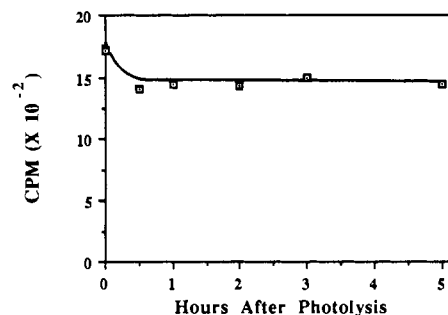


Figure 4. Stability of photoincorporated $[\beta\text{-}^{32}\text{P}]\text{NANDP}$. Scallop myosin was trapped with $[\beta\text{-}^{32}\text{P}]\text{NANDP}$, transferred into low-salt buffer, and 10 mL was photolyzed as described under Experimental Procedures. Following photolysis three 150- μL aliquots were removed at each of the indicated times and precipitated with trichloroacetic acid, and the amount of radioactivity present was determined as described under Experimental Procedures.

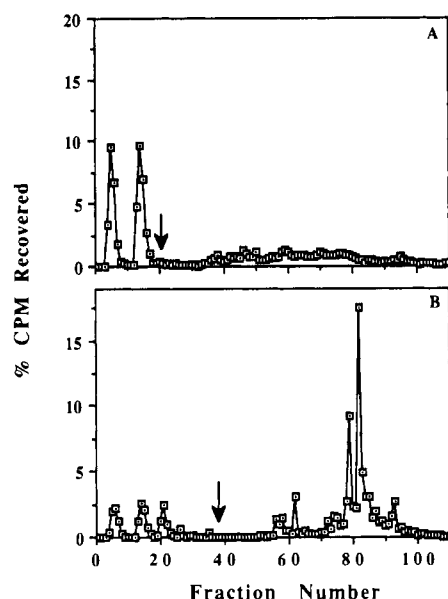


Figure 5. Photolabeling of ADP-blocked scallop myosin with free $[\beta\text{-}^{32}\text{P}]\text{NANDP}$. Scallop myosin (120 mg) was inactivated by complexation with ADP, Mn^{2+} , and V_i and transferred into low-salt buffer as described for trapping of $[\beta\text{-}^{32}\text{P}]\text{NANDP}$ under Experimental Procedures. To 10 mL of $\text{MnADP}\cdot\text{V}_i$ trapped myosin (5.1 mg/mL), $[\beta\text{-}^{32}\text{P}]\text{NANDP}$ was added equal to one-half the total number of ATP binding sites. The sample was photolyzed for 3 min, then S1 was prepared and digested with trypsin (1:100, trypsin:myosin) as described under Experimental Procedures. The tryptic digest was filtered, chromatographed, and analyzed on a RP-300 semipreparative HPLC column as described in the legend for Figure 7. Aliquots (1.0 mL) were analyzed for ^{32}P as described under Experimental Procedures. Panel A, radioactive profile of HPLC separation of tryptic peptides from ADP-blocked scallop myosin photolabeled with free $[\beta\text{-}^{32}\text{P}]\text{NANDP}$. Panel B, radioactive profile of HPLC separation of tryptic peptides from scallop myosin photolabeled with trapped $[\beta\text{-}^{32}\text{P}]\text{NANDP}$ (see Figure 7). Arrows indicate the beginning of the elution gradient as described in the legend to Figure 7. The two initial peaks in "A" and three early peaks in "B" resulted from loading the tryptic digestion mixture of S1 in two steps and three steps, respectively, and presumably is free photolyzed ^{32}P -NANDP.

The photoincorporation was limited to the S1 heavy chain. As seen in Figure 6, less than 2% of the total photoincorporated counts were in the light chains or the rod. SDS-PAGE analysis of a limited tryptic digestion of photolabeled S1 indicated that the photolabel was present in the NH_2 -terminal 75 and 63 kDa tryptic fragments (data not shown). These results indicate that $[\beta\text{-}^{32}\text{P}]\text{NANDP}$

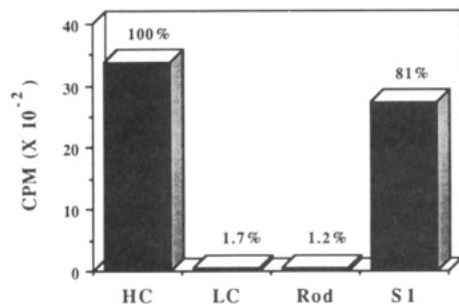


Figure 6. Subunit location of photoincorporated [β - 32 P]NANDP. Scallop myosin was trapped with [β - 32 P]NANDP, transferred into low-salt buffer and 10-mL aliquots were photolyzed as described under Experimental Procedures. Following photoincorporation the myosin was digested with papain and the resulting S1 was purified as described under Experimental Procedures. Equivalent radioactivity for photolyzed whole myosin, whole myosin and rod, and S1 were loaded on a 7–20% SDS-PAGE gel. After electrophoresis, the appropriate bands were excised and solubilized with H_2O_2 , and the amount of radioactivity was determined as described under Experimental Procedures. Less than 2% of the photoincorporated [β - 32 P]NANDP was present in either the myosin light chains or the rod subfragment.

forms a stable photoadduct with an amino acid residue(s) only in the NH_2 -terminus of the heavy chain, which is believed to contain the ATP binding site (Nyitrai et al., 1991).

Isolation of the Photolabeled Peptides. Papain S1 isolated from photolabeled scallop myosin was digested with trypsin as described under Experimental Procedures. The tryptic digest was chromatographed on a C8 reversed-phase semipreparative column (Figure 7). Two radioactive peaks containing a total of 28 nmol of labeled peptide (49% of the recovered radioactivity) were eluted at approximately 45 and 48 min. The fractions eluting between 44 and 51 min were pooled and further purified on a C8 reversed-phase analytical column (Figure 7, inset). Two radioactive peaks were clearly resolved with peak I (52 min) containing 6.6 nmol of labeled peptide and peak II (63 min) containing 9.5 nmol of labeled peptide. Because peaks I and II were treated in an identical manner, only the purification of peak II will be described. Peak II was further purified at pH 6.9 on the analytical HPLC column (Figure 8). By the fourth HPLC column peak II had become well-resolved into a single peak with few apparent contaminating peptides (Figure 8, inset). Following purification at pH 6.9, peak II was desalted at pH 2 with trifluoroacetic acid/acetonitrile (Figure 9). Since other peptides were still present and peak II appeared to be resolving into two or more radioactive peptides, the fractions containing the radioactive peptides were further purified by a shallower acetonitrile gradient. We were unable to obtain further separation of the peaks though, and the fractions from the final HPLC purification corresponding to 74 (peak IIA, Figure 9) and 78 (peak IIB, Figure 9) were used for amino acid sequence analysis.

Amino Acid Sequence and Composition Analysis of Photolabeled Peptides. The results of pulsed liquid-phase sequencing of photolabeled tryptic peptide IIA (Table II) indicated it corresponded to the tryptic peptide X-Leu-Pro-Ile-Tyr-Thr-Asp-Ser-Val-Ile-Ala-Lys of scallop myosin. No amino acids were detected in the first cycle of sequence analysis. The first amino acid (X) corresponded to Arg¹²⁸ of the scallop myosin heavy chain sequence (Nyitrai et al., 1991) and is believed to be the photolabeled amino acid. Essentially no radioactivity was detected from any of the sequencing cycles. All the radioactivity remained on the filter.

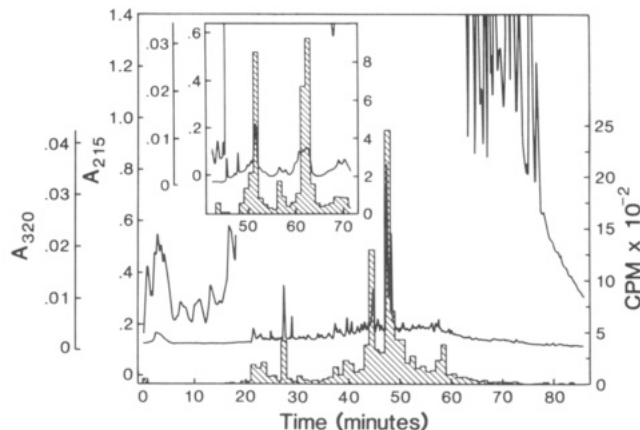


Figure 7. HPLC separation of tryptic peptides from photolabeled scallop myosin. Scallop myosin (570 mg) was complexed with [β - 32 P]NANDP, Mn, and V_i in low-salt buffer and photolabeled as described in Experimental Procedures. Papain S1 was prepared and digested with trypsin, and the tryptic peptides were loaded in three steps onto a Brownlee RP-300 semipreparative column as described under Experimental Procedures. The column was developed with a 1%/min linear gradient of 0.11% TFA/60% CH_3CN/H_2O at a flow rate of 2 mL/min. One-minute fractions were collected. Aliquots (25 μ L) of each fraction were analyzed for their radioactive content (shaded bar graphs). The top solid line is the A_{215nm} while the bottom line is the A_{320nm} . Inset, HPLC column fractions 44–51 from the semipreparative column loaded on an analytical column equilibrated in 0.11% TFA/ H_2O . The column was developed with a 1%/min linear gradient of 0.11% TFA/60% CH_3CN/H_2O for 30 min followed by a 0.1%/min linear gradient. One-minute fractions were collected at a flow rate of 1 mL/min and 10- μ L aliquots were analyzed for their radioactive content. Two major radioactive peaks (bar graph) eluted from the column. The first peak (~52 min) contained 6.6 nmol (29% of the total) of radiolabeled peptides, and the second peak (~63 min) contained 9.5 nmol (41% of the total) of radiolabeled peptide.

The amino acid composition of peak IIA was also determined to confirm the amino acid sequence data (Table II). The amino acids expected from the sequence analysis were all present in ratios approximating their theoretical yields. Surprisingly, arginine was also present, indicating that the [β - 32 P]NANDP–arginine adduct was not stable to the strong acid hydrolysis. Partial mole fractions of glutamate, glycine, phenylalanine, and histidine were also detected in this preparation, but they were not detected by amino acid sequence analysis. They may represent a small amount of a contaminating NH_2 -blocked peptide which would not sequence.

Two other isolated tryptic peptides, I (Figure 7, inset) and IIB (Figure 9), were sequenced (data not shown). As with tryptic peptide IIA, no amino acid was detected in the first cycle of sequence analysis. Peptide I gave the partial sequence X-Leu-Pro-Ile-Tyr- with the first amino acid corresponding to Arg¹²⁸. Tryptic peptide IIB (isolated from a different batch of photolabeled myosin than for peptide I) was fully sequenced and shown to stop at Thr¹³³ (X-Leu-Pro-Ile-Tyr-Thr¹³³). The unusual cut site of trypsin may be due to the presence of 1 M urea during the digestion or may reflect the presence of small amounts of chymotrypsin not inactivated by TPCK.

To further establish the site of photolabeling, we digested photolabeled S1 with chymotrypsin in the presence of 1 M urea. The chymotryptic peptides were separated by reversed-phase HPLC as described for the tryptic peptides (data not shown). The major chymotryptic peptide gave a sequence of Arg¹²⁷-X-Leu-Pro-Ile-Tyr, where X corresponded to Arg¹²⁸. The residue preceding Arg¹²⁷ is Tyr, indicating that chymotrypsin followed its normal specificity. These data show that

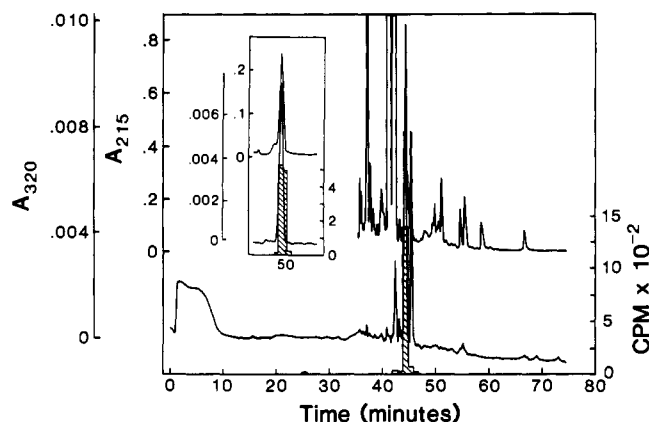


Figure 8. HPLC purification peak II (pH 6.9). Fractions 61–64 from the second HPLC column (peak II, Figure 7, inset) were prepared as described under Experimental Procedures. The pH of the peptide solution was adjusted to 6–7 (by litmus paper) with 0.5 M Na_2HPO_4 and loaded onto an analytical column equilibrated with 5 mM NaP_i , pH 6.9. The column was washed for 10 min with the equilibrating buffer (not shown on chromatogram) then developed with a 1%/min linear gradient 65% $\text{CH}_3\text{CN}/\text{H}_2\text{O}$. One-minute fractions were collected at a flow rate of 1 mL/min and 10 μL aliquots were analyzed for their radioactive content. A total of 7.4 nmol of radiolabeled peptide, 99% of the recovered radioactivity, was present in the 44-min fraction. Inset, fraction 44 from the third HPLC column was prepared and loaded onto an analytical column equilibrated in NaP_i , pH 6.9. The gradient was changed to 0.1%/min after 25 min. A total of 6.4 nmol of radiolabeled peptide was collected in fractions 49 and 50 and accounted for 100% of the radioactivity loaded on the column. The lines and bar graph are the same as in Figure 7.

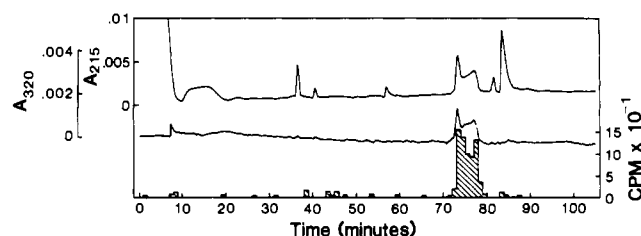


Figure 9. HPLC purification of peak II at pH 2. Fractions 49 and 50 from the fourth HPLC column (Figure 8, inset) were combined and prepared for HPLC analysis as described in Figure 7. The peptide solution was loaded onto an analytical column equilibrated with 0.11% TFA/ H_2O and washed for 10 min with the equilibrating buffer (data not shown). The column was developed with a 1%/min gradient of 0.11% TFA/60% $\text{CH}_3\text{CN}/\text{H}_2\text{O}$ for 25 min followed by a 0.25%/min gradient. One-minute fractions were collected at a flow rate of 1 mL/min and 10- μL aliquots were analyzed for their radioactive content. A total of 4.3 nmol of radiolabeled peptide was collected in fractions 74–78, accounting for 88% of the radioactivity loaded onto the column.

Arg¹²⁸ is the major labeled amino acid under these photolabeling conditions.

DISCUSSION

The purpose of this study was to probe the active site of scallop myosin with the ADP photoaffinity analog NANDP. Our purpose was 2-fold. First, NANDP was shown to specifically photolabel Trp¹³⁰ in the heavy chain of rabbit skeletal muscle myosin (Okamoto & Yount, 1985). In scallop myosin this tryptophan is replaced with an arginine (Nyitray et al., 1991) in an otherwise highly conserved region of the amino acid sequence (see below). We wished to address the question as to whether arginine could occupy a similar position as tryptophan in the purine binding site despite its quite different chemical properties. Second, Peyser et al. (1990) recently reported that Trp¹³⁰ of skeletal

Table II. Amino Acid Sequence and Composition Analysis of the Photolabeled Peptide IIA

cycle no.	residue found	amino acid sequence analysis ^a		amino acid composition ^c		
		amino acid (pmol)	cpm	amino acid	relative yield	theoretical yield
1	X ^b	Nil	0	Arg	1.37	{0}
2	Leu	129	14	Leu	1.11	1.0
3	Pro	28	2	Pro	0.91	1.0
4	Ile	114	12	Ile	1.72	2.0
5	Tyr	67	0	Tyr	0.71	1.0
6	Thr	41	0	Thr	0.75	1.0
7	Asp	55	0	Asp	1.05	1.0
8	Ser	14	0	Ser	0.80	1.0
9	Val	31	0	Val	1.02	1.0
10	Ile	20	0			
11	Ala	20	0	Ala	1.03	1.0
12	Lys	7	0	Lys	1.00	1.0
filter			1304			

^a A 185-pmol (1164 cpm) sample of the [β -³²P]NANDP-labeled peptide IIA was sequenced using an ABI 475A pulse liquid sequencer (Applied Biosystems Inc.). Data acquisition and analyses were performed with standard program Run 470-I (ABI). One-half of each >PhNCS amino acid extract was assayed for its amino acid concentration and its ³²P content respectively. The average yield of >PTH-amino acid determined at each cycle was $82 \pm 1\%$. ^b There were no >PTH-amino acids detected at this step. ^c A 1.02-nmol sample of the [β -³²P]NANDP-labeled peptide (isolated separately from that used for the amino acid sequence analysis shown) was used for amino acid composition analyses. Amino acids were determined with a Beckman Model 121 MB amino acid analyzer after hydrolysis in 6 N HCl for 22 h at 110 °C. Yields were determined by comparison with standard amino acids and normalized to that obtained for lysine. The theoretical composition is based on the sequence Arg¹²⁸-Leu-Pro-Ile-Tyr-Thr-Asp-Ser-Val-Ile-Ala-Lys (Nyitray et al., 1991). Other amino acids, Glu (0.56 nmol), Gly (0.80 nmol), Phe (0.15 nmol), and His (0.15 nmol) were also detected in these analyses but were not seen during amino acid sequence analyses of the peptide.

myosin can be chemically modified with little effect on the actin-activated MgATPase activity. These results suggest that Trp¹³⁰ may not be part of the active site or at least not a critical residue. If this were true then we would not expect Arg¹²⁸ of scallop myosin to be photolabeled by NANDP.

As a first step, it was important to show that NANDP bound to the active site of scallop myosin in a manner analogous to ATP. As we had observed previously with skeletal myosin (Nakamaye et al., 1985), NANDP and ATP were hydrolyzed by scallop myosin with almost identical kinetic properties (Table I). Importantly, the physiologically relevant Ca^{2+} activation of the F-actin stimulated NANDPase and ATPase activities were nearly identical (6.6 vs 6.8, Table I). The only exception occurred in high salt (0.5 M KCl) and high Ca^{2+} (5 mM), where the NANDPase activity was 1/10 that of the ATPase (Table I). Here the high Ca^{2+} may be binding to low-affinity sites normally occupied by Mg^{2+} (Goodwin et al., 1990), a condition which may accentuate small differences in the hydrolysis rates of the two substrates.

Further evidence that NANDP specifically occupied the ATP binding site came from experiments in which ADP, but not AMP, was able to inhibit formation of the MnNANDP-Vi complex (Figure 2). The trapped NANDP specifically photolabeled only the heavy chain of the S1 subfragment (Figure 6). This photolabeling appeared to be specific for the active site because photolysis of NANDP in the presence of scallop myosin whose active site was previously blocked with MnADP-Vi failed to demonstrate significant photolabeling of any particular peptide (Figure 5). Furthermore, no additional labeling was observed if the trapped photolyzed NANDP complex was allowed to stand in the dark for up to 5 h (Figure 4). Such electro-

Table III. Comparison of the Partial Amino Acid Sequence of Scallop Myosin Heavy Chain with Other Myosin Heavy Chains^c

scallop (<i>A. quipecten</i>)	I	A	V	N	P	Y	R	R ¹²⁸	L	P	I	Y	(Nyitray et al., 1991)
acanthamoeba (myosin II)	V	V	V	N	P	Y	R	R	L	P	V	Y	(Hammer et al., 1987)
nematode (<i>C. elegans</i>)	V	V	I	N	P	Y	K	R	L	P	I	Y	(Karn et al., 1983)
<i>Dictyostelium discoideum</i>	V	A	V	N	P	F	K	R	I	P	I	Y	(Warrick et al., 1986)
yeast	V	A	I	N	P	Y	H	N	L	N	L	Y	(Watts et al., 1987)
chicken gizzard	V	V	I	N	P	Y	K	Q	L	P	I	Y	(Yanagisawa et al., 1987)
rabbit skeletal	V	T	V	N	P	Y	K*	W ¹³⁰	L	P	V	Y	(Tong & Elzinga, 1983)
chicken skeletal	V	T	V	N	P	Y	K*	W	L	P	V	Y	(Maita et al., 1987)
rat skeletal	V	T	V	N	P	Y	K	W	L	P	V	Y	(Strehler et al., 1986)
human skeletal	V	T	V	N	P	Y	K	W	L	P	V	Y	(Stedman et al., 1990)

^c An asterisk denotes lysine residues that are trimethylated.

philic labeling in the dark by rearranged products of nitroaryl nitrenes has been observed previously with compounds similar to NANDP (Mas et al., 1980; see discussion in Staros & Bayley, 1984). Taken together the above observations point to the specificity of the photolabeling reaction for the active site.

Sequence analysis of a series of purified radiolabeled peptides demonstrated that Arg¹²⁸ was the major photolabeled amino acid. Three distinct tryptic radiolabeled peptides all lacked an identifiable PTH-amino acid in the first sequencing cycle but gave a subsequent sequence identical to that known to follow Arg¹²⁸ (Nyitray et al., 1991). The absence of a NANDP-PTH-arginine adduct in the HPLC analysis following the Edman cycle cleavage was expected because the negatively charged diphosphate moiety binds strongly to the positively charged polybrene-coated filter used for sequencing. Thus it would not be extracted by the butyl chloride used to remove the PTH amino acids from the filter. Further evidence for the specific photolabeling of Arg¹²⁸ came from the sequence analysis of the major radiolabeled peptide isolated from a chymotryptic digest of [β -³²P]NANDP-labeled myosin (data not shown). Here again only Arg¹²⁸ was missing from the sequence cycle. The first amino acid, Arg¹²⁷, was clearly identified, indicating that only Arg¹²⁸ reacted with the putative nitrene from photolyzed NANDP. Interestingly, the bulky photomodification did not inhibit trypsin cleavage of the Arg¹²⁷-Arg¹²⁸ bond or the chymotryptic cleavage of the Tyr¹²⁶-Arg¹²⁷ bond. A computer search of the literature has not revealed any other reports detailing photolabeling of an arginine with a reactive azide. Because the NANDP-arginine adduct was sensitive to the acid conditions used for hydrolysis of peptide bonds, we speculate that a N-N bond was formed between the aryl nitrene from NANDP and a nitrogen of the arginine guanido group. Acid treatment may have cleaved the postulated N-N bond to regenerate unmodified arginine. The characterization of the photoadduct is planned in order to determine the chemical structure of the postulated unusual arginine-nitrene adduct.

The amino acid sequence surrounding Arg¹²⁸ of scallop myosin appears to be highly conserved among a wide variety of species (Table III). This region is most highly conserved among the skeletal muscle myosins with some conservative substitutions among the invertebrate myosins. Interestingly, Arg¹²⁸ of scallop myosin has been maintained at the analogous position in a number of other invertebrate and nonmuscle myosins but has been replaced by Trp in skeletal and cardiac muscle myosin. Both amino acids, though, are apparently in similar positions of the myosin structure since, as mentioned above, Trp¹³⁰ of rabbit skeletal myosin is also photolabeled with NANDP (Okamoto & Yount, 1985). The role of Arg¹²⁸ or Trp¹³⁰ in the function of the active site is unclear because they can be replaced by either an asparagine (yeast) or a glutamine (gizzard). Regardless of the role, there are constraints on

the nature of the amino acid at this position because no myosins have yet been found which have an acidic residue at this position.

Molecular modeling shows that the azido group of NANDP is in essentially the same position as the azido group of 2-azido-ADP when the analogues are in their most extended conformation, i.e., when 2-azido-ADP is anti (S. Johns & R. Yount, unpublished observations). NMR and X-ray crystallographic data have shown that ATP is in the anti conformation when it is bound to a number of ATP binding proteins (Brunie et al., 1990; Brick et al., 1988; Watson et al., 1982; Rould et al., 1989; Kabsch et al., 1990; Yan et al., 1990; Rosevear et al., 1987; Brito et al., 1991; Williams & Rosevear, 1991; Garin et al., 1988). The fact that 2-azido-ADP (H. Kuwayama & R. Yount, unpublished results; Yount et al., 1987) and NANDP (Okamoto & Yount, 1985) both photolabel Trp¹³⁰ of rabbit skeletal myosin support the idea that both molecules are in equivalent positions within the purine binding site. In scallop myosin Arg¹²⁸ may in fact lay across the purine ring with the guanido group hydrogen bonding with N1 or N3 of ADP and the hydrophobic alkyl side chain interacting with the purine ring in a manner similar to the interaction of Lys¹¹⁷ of H-ras p21 with GTP (Pai et al., 1990). Likewise the tryptophan residue of skeletal myosin may form aromatic-aromatic interactions with the purine ring of ATP. The observation that in the absence of ATP Trp¹³⁰ is the most readily modified of five tryptophans in the head region of the myosin (Peyser et al., 1990; Werber et al., 1987) suggests it is on the surface of the protein, where an arginine residue would also be expected to reside. Therefore, it is possible that Trp¹³⁰ and Arg¹²⁸, although chemically different, may play similar roles in binding the purine ring.

ACKNOWLEDGMENT

We are deeply indebted to A. G. Szent-Györgyi for his generous gift of scallops and for his continuing advice on the preparation and properties of scallop myosin. We thank Dr. Gerhard Munske of the WSU Laboratory for Bioanalysis and Biotechnology for amino acid sequence analysis and Dr. Gurusidiah for amino acid composition analysis. The advice of Jean Grammer and Christine Cremo was invaluable in all aspects of this work.

LITERATURE CITED

- Adelstein, R. S., and Eisenberg, E. (1980) Regulation and Kinetics of the actin-myosin-ATP Interaction. *Ann. Rev. Biochem.* 49, 921-956.
- Atkinson, M. A. L., Robinson, E. A., Appella, E., and Korn, E. D. (1986) Amino Acid Sequence of Acanthamoeba Myosin II. *J. Biol. Chem.* 261, 1844-1848.
- Brick, P., Bhat, T. N., and Blow, D. M. (1988) Structure of Tyrosyl-tRNA Synthetase Refined at 2.3 Å Resolution. *J. Mol. Biol.* 208, 83-98.

- Brito, R. M. M., Rudolph, F. B., and Rosevear, P. R. (1991) Conformation of NADP⁺ Bound to a Type II Dihydrofolate Reductase. *Biochemistry* 30, 1461-1469.
- Brunie, S., Zelwer, C., and Risler, J.-L. (1990) Crystallographic Study at 2.5 Å Resolution of the Interaction of Methionyl-tRNA Synthetase from *Escherichia coli* with ATP. *J. Mol. Biol.* 216, 411-424.
- Chantler, P. D., and Szent-Györgyi, A. G. (1978) Spectroscopic Studies on Invertebrate Myosins and Light Chains. *Biochemistry* 17, 5440-5448.
- Cole, D. G., and Yount, R. G. (1990) Photolabeling of 6 and 10 S Conformations of Gizzard Myosin with 3'-(2')-O-(4-Benzoyl)-benzoyl-ATP. *J. Biol. Chem.* 265, 22537-22546.
- Cremo, C. R., Grammer, J. C., and Yount, R. G. (1991) Vanadate-Mediated Photocleavage of Myosin. *Methods Enzymol.* 196, 442-449.
- Garabedian, T. E., and Yount, R. G. (1990) Direct Photoaffinity Labeling of Gizzard Myosin with [³H]Uridine Diphosphate Places Glu¹⁸⁵ of the Heavy Chain at the Active Site. *J. Biol. Chem.* 265, 22547-22553.
- Garabedian, T. E., and Yount, R. G. (1991) Direct Photoaffinity Labeling of Gizzard Myosin with Vanadate-Trapped Adenosine Diphosphate. *Biochemistry* 30, 10126-10132.
- Garin, J., Vignais, P. F., Gronenborn, A. M., Clore, G. M., Gao, Z., and Baeuerlein, E. (1988) 1H-NMR Studies on Nucleotide Binding to the Catalytic Sites of Bovine Mitochondrial F1-ATPase. *FEBS Lett.* 242, 178-182.
- Goodno, C. (1979) Inhibition of Myosin ATPase by Vanadate Ion. *Proc. Natl. Acad. Sci. U.S.A.* 76, 2620-2624.
- Goodwin, E. B., Leinwand, L. A., and Szent-Györgyi, A. G. (1990) Regulation of Scallop Myosin by Mutant Regulatory Light Chains. *J. Mol. Biol.* 216, 85-93.
- Grammer, J. C., Cremo, C. R., and Yount, R. G. (1988) UV-Induced Vanadate-Dependent Modification and Cleavage of Skeletal Myosin Subfragment 1 Heavy Chain. 1. Evidence for Active Site Modification. *Biochemistry* 27, 8408-8414.
- Hammer, J. A., III, Bowers, B., Paterson, B. M., and Korn, E. D. (1987) Complete Nucleotide Sequence and Deduced Polypeptide Sequence of a Nonmuscle Myosin Heavy Chain Gene from *Acanthamoeba*: Evidence of a Hinge in the Rodlike Tail. *J. Cell Biol.* 105, 913-925.
- Kabsch, W., Mannherz, H. G., Suck, D., Pai, E. F., and Holmes, K. C. (1990) Atomic Structure of the Actin:DNase I Complex. *Nature* 347, 37-44.
- Karn, J., Brenner, S., and Barnett, L. (1983) Protein Structural Domains in the *Caenorhabditis elegans unc-54* Myosin Heavy Chain Gene are not Separated by Introns. *Proc. Natl. Acad. Sci. U.S.A.* 80, 4253-4257.
- Kendrick-Jones, J., Lehman, W., and Szent-Györgyi, A. G. (1970) Regulation in Molluscan Muscles. *J. Mol. Biol.* 54, 313-326.
- Kennedy, D. L., Cole, D. C., and Yount, R. G. (1991) Photoaffinity Labeling of Skeletal and Smooth Muscle Myosin S1 with Vanadate Trapped [3H]2',3'-O-[3-[N-(4-Azido-2-nitrophenyl)amino]propionyl] ADP (NANPAP-ADP). *Biophys. J.* 59, 226a.
- Kwon, H., Goodwin, E. B., Nyitray, L., Berliner, E., O'Neal-Hennessey, E., Melandri, F. D., and Szent-Györgyi, A. G. (1990) Isolation of the Regulatory Domain of Scallop Myosin: Role of the Essential Light Chain in Calcium Binding. *Proc. Natl. Acad. Sci. U.S.A.* 87, 4771-4775.
- Laemmli, U. K. (1970) Cleavage of Structural Proteins During the Assembly of the Head of Bacteriophage T4. *Nature* 227, 680-685.
- Lowey, S., Slayter, H. S., Weeds, A. G., and Baker, H. (1969) Substructure of the Myosin Molecule. I. Subfragments of Myosin by Enzyme Degradation. *J. Mol. Biol.* 42, 1-29.
- Mahmood, R., Elzinga, M., and Yount, R. G. (1989) Serine-324 of Myosin's Heavy Chain is Photoaffinity-Labeled by 3'-(2')-O-(4-Benzoylbenzoyl)adenosine Triphosphate. *Biochemistry* 28, 3989-3995.
- Maita, T., Hayashida, M., Tanioka, Y., Komine, Y., and Matsuda, G. (1987) The Primary Structure of the Myosin Head. *Proc. Natl. Acad. Sci. U.S.A.* 84, 416-420.
- Mas, M. T., Wang, J. K., and Hargrave, P. A. (1980) Topography of Rhodopsin in Rod Outer Segment Disk Membranes. Photochemical Labeling with N-(4-Azido-2-nitrophenyl)-2-aminoethanesulfonate. *Biochemistry* 19, 684-691.
- Nakamaye, K. L., Wells, J. A., Bridenbaugh, R. L., Okamoto, Y., and Yount, R. G. (1985) 2-[(4-Azido-2-nitrophenyl)amino]ethyl Triphosphate, a Novel Chromophoric and Photoaffinity Analogue of ATP. Synthesis, Characterization, and Interaction with Myosin Subfragment 1. *Biochemistry* 24, 5276-5285.
- Nyitray, L., Goodwin, E. B., and Szent-Györgyi, A. G. (1991) Complete Primary Structure of a Scallop Striated Muscle Myosin Heavy Chain. *J. Biol. Chem.* 266, 18469-18476.
- Okamoto, Y., and Yount, R. G. (1985) Identification of an Active Site Peptide of Skeletal Myosin after Photoaffinity Labeling with N-(4-azido-2-nitrophenyl)-2-aminoethyl Diphosphate. *Proc. Natl. Acad. Sci. U.S.A.* 82, 1575-1579.
- Pai, E. F., Krenkel, U., Petsko, G. A., Goody, R. S., Kabsch, W., and Wittinghofer, A. (1990) Refined Crystal Structure of the Triphosphate Conformation of H-ras p21 at 1.35 Å Resolution: Implications for the Mechanism of GTP Hydrolysis. *EMBO J.* 9, 2351-2359.
- Penefsky, H. S. (1977) Reversible Binding of P_i by Beef Heart Mitochondrial Adenosine Triphosphatase. *J. Biol. Chem.* 252, 2891-2899.
- Peyser, M. Y., Muhrad, A., and Werber, M. M. (1990) Tryptophan-130 is the most reactive tryptophan residue in rabbit skeletal myosin subfragment-1. *FEBS Lett.* 259, 346-348.
- Rosevear, P. R., Fox, T. L., and Mildvan, A. S. (1987) Nuclear Overhauser Effect Studies of the Conformation of MgATP Bound to the Active and Secondary Sites of Muscle Pyruvate Kinase. *Biochemistry* 26, 3487-3493.
- Rould, M. A., Perona, J. J., Soll, D., and Steitz, T. A. (1989) Structure of *E. coli* Glutamyl-tRNA Synthetase complexed with tRNA(Gln) and ATP at 2.8 Å Resolution. *Science* 246, 1135-1142.
- Sherry, J. M. F., Gorecka, A., Aksoy, M. O., Dabrowska, R., and Hartshorne, D. J. (1978) Roles of Calcium and Phosphorylation in the Regulation of the Activity of Gizzard Myosin. *Biochemistry* 17, 4411-4418.
- Sobieszek, A., and Small, J. V. (1977) Regulation of the Actin-myosin Interaction in a Vertebrate Smooth Muscle: Activation via a Myosin Light Chain Kinase and the Effect of Tropomyosin. *J. Mol. Biol.* 112, 559-576.
- Staros, J. V., and Bayley, H. (1984) In *Azides and Nitrenes; Reactivity and Utility* (E. F. Scriven, Ed.) Academic Press Inc., Orlando, FL.
- Stedman, H. H., Eller, M., Jullian, E. H., Fertels, S. H., Sarkar, S., Sylvester, J. A., Kelly, A. M., and Rubinstein, N. A. (1990) The Human Embryonic Myosin Heavy Chain. *J. Biol. Chem.* 265, 3568-3576.
- Strehler, E. E., Strehler-Page, M.-A., Perriard, J.-C., Periasamy, M., and Nadal-Ginard, B. (1986) Complete Nucleotide and Encoded Amino Acid Sequence of a Mammalian Myosin Heavy Chain Gene: Evidence Against Intron-Dependent Evolution of the Rod. *J. Mol. Biol.* 190, 291-317.
- Szent-Györgyi, A. G., and Szentkiralyi, E. M. (1973) The Light Chains of Scallop Myosin as Regulatory Subunits. *J. Mol. Biol.* 74, 179-203.
- Tong, S. W., and Elzainaga, M. (1983) The Sequence of the NH₂-terminal 204-residue Fragment of the Heavy Chain of Rabbit Skeletal Muscle Myosin. *J. Biol. Chem.* 258, 13100-13110.
- Trybus, K. M. (1991) Regulation of Smooth Muscle Myosin. *Cell. Mobil. Cytoskeleton* 18, 81-85.
- Warrick, H. M., De Lozanne, A., Leinwand, L., and Spudich, J. A. (1986) Conserved Protein Domains in a Myosin Heavy Chain Gene from *Dictyostelium discoideum*. *Proc. Natl. Acad. Sci. U.S.A.* 83, 9433-9437.
- Watson, H. C., Walker, N. P. C., Shaw, P. J., Bryant, T. N., Wendell, P. L., Fothergill, L. A., Perkins, R. E., Conroy, S. C., Dobson, M. J., Tuite, M. F., Kingsman, A. J., and Kingsman, S. M. (1982) Sequence and Structure of Yeast Phosphoglycerate Kinase. *EMBO J.* 1, 1635-1640.
- Watts, F. Z., Shiels, G., and Orr, E. (1987) The Yeast MYO1 Gene Encoding a Myosin-like Protein Required for Cell Division. *EMBO J.* 6, 3499-3505.
- Wells, J. A., Werber, M. M., and Yount, R. G. (1979) Inactivation of Myosin Subfragment One by Cobalt(II)/Cobalt(III) Phenanthroline.

- thioline Complexes. 2. Cobalt Chelation of Two Critical SH Groups. *Biochemistry* 18, 4800-4805.
- Werber, M. M., Peyser, Y. M., and Muhlrud, A. (1987) Modification of Myosin Subfragment 1 Tryptophan by Dimethyl(2-hydroxy-5-nitrobenzyl)sulfonium Bromide. *Biochemistry* 26, 2903-2909.
- Williams, J. S., and Rosevear, P. R. (1991) Nuclear Overhauser Effect Studies on the Conformation of Mg(α,β -methylene)ATP Bound to *Escherichia coli* Methionyl-tRNA Synthetase. *J. Biol. Chem.* 266, 2089-2098.
- Yan, H., Dahnke, T., Zhou, B., Nakazawa, A., and Tsai, M.-D. (1990) Mechanism of Adenylate Kinase. Critical Evaluation of the X-ray Model and Assignment of the AMP Site. *Biochemistry* 29, 10956-10964.
- Yanagisawa, M., Hamada, Y., Katsuraguwa, Y., Imamura, M., Mikawa, T., and Masaki, T. (1987) Complete Primary Structure of Vertebrate Smooth Muscle Myosin Heavy Chain Deduced from its Complementary DNA Sequence. *J. Mol. Biol.* 198, 143-157.
- Yount, R. G., Okamoto, Y., Mahmood, R., Nakamaye, K., Grammer, J., Huston, E., and Kuwayama, H. (1987) In *Perspectives of Biological Energy Transduction* (Y. Mukohata, M. F. Morales, and S. Fleischer, Eds.) pp 67-72, Academic Press, Orlando, FL.
- Yount, R. G., Cremo, C. R., Grammer, J. C., and Kerwin, B. A. (1992) Photochemical Mapping of the Active Site of Myosin. *Philos. Trans. R. Soc. London B* 336, 55-61.

TECHNICAL NOTES

Synthesis of Novel 1,4,7-Triazacyclononane-*N,N',N''*-triacetic Acid Derivatives Suitable for Protein Labeling

Martin Studer and Claude F. Meares*

Department of Chemistry, University of California, Davis, California 95616. Received December 23, 1991

C-Functionalized derivatives of the macrocycle 1,4,7-triazacyclononanetriacetic acid that are suitable for labeling proteins have been synthesized starting from the peptide *p*-NO₂Phe-Gly-Gly.

INTRODUCTION

There is a growing interest in polyazamacrocycles with N-bonded acetate groups (1-8). Besides the formation of thermodynamically stable metal complexes (9) and some selectivity in complexation (10, 11), they also offer the big advantage of forming kinetically stable complexes. In vivo applications like magnetic resonance imaging (2), radiotherapy, and radiodiagnostics require the metal ions of interest to be bound very tightly to the complexing agent, because the validity of the procedure depends on it and also because the metal ions involved may be toxic when not complexed.

Until now, most of the work in this area has been done with the 14-membered macrocycle TETA¹ (1), the 12-membered DOTA (5), and the 9-membered NOTA. Of these compounds, not only have the plain macrocycles been described, but also C-substituted derivatives (5-8). The side chains were designed to allow the covalent attachment of the chelator to a biomolecule like a monoclonal antibody.

The best known side chain for this purpose is the nitrobenzyl group. Such derivatives of the open chain EDTA (12, 13) and DTPA (14, 15) as well as of the macrocyclic TETA (1) and DOTA (5) have been prepared and attached to biomolecules (16). They have already found a wide range of applications, including new areas like protein structure probing (14, 17). What makes the nitrobenzyl group such a favorable candidate is the fact that it can be carried through a wide variety of chemical reactions without being altered or destroyed. Furthermore, it is an easily detectable chromophore which facilitates experimental procedures.

NOTA is known to form very stable complexes with a wide variety of metal ions (8). Since the net charge of these metal complexes with di- and trivalent metal ions is lower than that of the DOTA and TETA complexes, NOTA complexes are more lipophilic. This is considered advantageous for imaging organs like the brain and the heart. It might also result in a faster liver clearance than seen for more highly charged metal complexes (18). On the other hand, the complex formation reactions of NOTA

are much faster than for other triazamacrocycles (7), or for DOTA and TETA (4). Since a reasonably fast binding of the metal ions is imperative for work with radioactive metals in low concentrations, this is a valuable feature.

Moi et al. described a new approach for C-substituted macrocycles that they called "the peptide way to macrocycle bifunctional chelating agents" (5). They used a tetrapeptide that had the carbon and nitrogen frame of the desired macrocycle. After reduction of the amides and the carboxylic acid, they cyclized the previously tosylated amino alcohol and obtained the macrocyclic nitrobenzyl-DOTA precursor. This new way to obtain macrocycles should allow preparation of a wide variety of different ring sizes and substituents, provided the cyclization is practical and the side chains are not destroyed by the procedure. Since the starting materials *N*-*t*-BOC-*p*-NO₂-Phe and Gly-Gly are relatively cheap and the synthesis described for a butylamino-substituted NOTA with 10 steps is rather complicated (7), we sought an alternative NOTA preparation. Here we describe the synthesis of the new macrocycle nitrobenzyl-NOTA and its tri-*tert*-butyl derivative.

EXPERIMENTAL PROCEDURES

General. Proton NMR spectra were recorded on a GE 300 spectrometer at 300 MHz. Chemical shifts are relative to either HDO (4.70 ppm) or residual CHCl₃ (7.21 ppm). Mass spectra and exact mass measurements were obtained on a ZAB-HS-2F mass spectrometer (VG analytical instruments). IR spectra were recorded on an IBM IR/32 spectrometer. γ -Radiation counting was done with a Beckman Model 310. For UV/vis measurements, a Hewlett-Packard Model 8450 spectrophotometer was used.

Reagents. Pure water (18 M Ω) was employed throughout. Tetrahydrofuran (THF) was dried by distillation from benzophenone-sodium ketyl. Triethylamine was dried by standing over KOH pellets and distilling from BaO. BrCH₂COOC(CH₃)₃, 10% Pd/C, Cs₂CO₃, toluenesulfonyl chloride, BrCH₂COOH, BH₃·THF, and BrCH₂COBr were purchased from Aldrich Chemical Co. 1-Hydroxybenzotriazole (HOBt), 1,3-dicyclohexylcarbodiimide (DCC), *N*-(*tert*-butoxycarbonyl)-*L*-*p*-nitrophenylalanine (*N*-*t*-BOC-*p*-NO₂-Phe), and Gly-Gly were from Sigma Chemical Co. Citric acid, phenol, triethylamine, and CF₃COOH were from Fischer Scientific. Silica gel for column chromatography (60-200 mesh) was from J. T. Baker. All other reagents were at least reagent grade.

Chromatography. Thin-layer chromatography (TLC) was run on plastic-backed silica gel plates (Kieselgel 60

* Author to whom correspondence should be addressed.

¹Abbreviations used: TETA, 1,4,8,11-tetraazacyclotetradecane-*N,N',N'',N'''*-tetraacetate; DOTA, 1,4,7,10-tetraazacyclododecane-*N,N',N'',N'''*-tetraacetate; NOTA, 1,4,7-triazacyclononane-*N,N',N''*-triacetate; EDTA, ethylenediaminetetraacetic acid; DTPA, diethylenetriaminepentaacetic acid; Ts, *p*-CH₃C₆H₄SO₂ moiety.

F₂₅₄, EM Science). For syntheses, various systems were used as described with the experiments. For the metal binding assays (19), a 10% (w/v) aqueous ammonium acetate/methanol (1:1 v/v) solution was used as the eluent. High-performance liquid chromatography was performed on a Rainin Rabbit HP system. For UV detection, an ISCO UA-5 was used (254 nm). Dynamax C₁₈ and silica gel columns (21.4 × 250 mm for preparative, 4.6 × 250 mm for analytical runs) were purchased from Rainin Instruments. Solvent gradients were controlled by MacRabbit software on a Macintosh computer and were as follows. System 1: CH₂Cl₂ and CH₃CN, 12.5 mL/min; 0–25 min, linear 2–15% CH₃CN; 25–30 min, linear 15–100% CH₃CN. System 2: 0.1% CF₃COOH in water and 0.1% CF₃COOH in CH₃CN, 12.5 mL/min; 0–5 min, linear 15–20% 0.1% CF₃COOH in CH₃CN; 5–20 min, linear 20–31.5% 0.1% CF₃COOH in CH₃CN. System 3: 0.1 M ammonium acetate, pH 4, and CH₃OH, 12.5 mL/min; 15% CH₃OH, isocratic. System 4: 0.1 M sodium acetate, pH 6.2, containing 1 mmol EDTA, and CH₃OH, 1 mL/min; 0–20 min, linear 0–100% CH₃OH. System 5: CH₂Cl₂ and CH₃OH, 12.5 mL/min; 0–20 min, linear 30–50% CH₃OH; 20–21 min, linear 50–100% CH₃OH.

Preparation of *N*-*t*-BOC-*p*-NO₂-Phe-Gly-Gly (2). *N*-*t*-BOC-*p*-NO₂-Phe (3.00 g, 9.7 mmol) and HOBT·H₂O (1.48 g, 9.7 mmol) were dissolved in 100 mL of dry *N,N*-dimethylformamide (DMF). After cooling to 0 °C, DCC (2.00 g, 9.7 mmol) was added, the mixture was held at 0 °C for 2.5 h and then at 25 °C for 1 h. Gly-Gly (1.28 g, 9.7 mmol) was added, the mixture was kept at 25 °C for 16 h. After evaporation to dryness, the semisolid was taken up in 150 mL of ethyl acetate and 50 mL of aqueous citric acid (10% by weight) and transferred into a separatory funnel. The organic layer was extracted with aqueous citric acid (3 × 50 mL) and saturated NaCl solution (50 mL). The ethyl acetate was dried over anhydrous Na₂SO₄ and evaporated to dryness to yield 2.73 g of 2 (6.41 mmol, 66%). ¹H NMR (CDCl₃/D₂O): δ 1.30 (s, 9 H), 2.90–3.40 (m, 2 H), 3.80–4.20 (m, 4 H), 4.55 (m, 1 H), 7.30 (d, 2 H), 8.00 (d, 2 H). MS *m/e* for C₁₈H₂₅N₄O₈ (M + H⁺): 425.

Preparation of *p*-NO₂-Phe-Gly-Gly CF₃COOH Salt 3. Compound 2 (2.73 g, 6.41 mmol) was dissolved in 60 mL of neat CF₃COOH. After stirring for 2 h at 25 °C, the solution was evaporated to dryness in vacuo to yield 3.50 g of 3·2CF₃COOH (6.34 mmol, 99%). ¹H NMR (D₂O): δ 3.35 (d, 2 H), 4.00 (br, 4 H), 4.30 (t, 1 H), 7.45 (d, 2 H), 8.15 (d, 2 H). MS *m/e* for C₁₃H₁₇N₄O₆ (M + H⁺): 325.

Preparation of 8-(*p*-Nitrobenzyl)-3,6,9-triazanolanol (4). BH₃·THF (77 mL, 1 M) in THF was added dropwise to a stirring solution of 3 (3.50 g, 6.34 mmol) in 100 mL of dry THF at 0 °C under N₂. After the addition, the mixture was refluxed for 20 h. At 0 °C, 50 mL of dry methanol was slowly added, and then the mixture was saturated with gaseous HCl. After refluxing for 2 h, the solution was evaporated to dryness. The semisolid was taken up in H₂O and the pH was adjusted to 10.5 with 50% NaOH. The aqueous solution was continually extracted with CHCl₃ for 16 h. After drying of the organic layer over anhydrous Na₂SO₄, the CHCl₃ was evaporated to dryness. Purification was carried out on an open silica gel column (35 × 400 mm) step eluted with 500 mL of CHCl₃, 500 mL of (CHCl₃/CH₃OH (1:1 v/v), 400 mL of CHCl₃/CH₃OH/NH₄OH (28–30%, aqueous) 10:10:1 v/v/v, and 500 mL of CHCl₃/CH₃OH/NH₄OH (28–30%, aqueous) (2:2:1 v/v/v). The fractions from the last elution were combined and dried under high vacuum to give 0.90 g of 4 (3.19 mmol, 51%). ¹H NMR (CDCl₃/D₂O): δ

2.50–3.00 (m, 10 H), 3.15 (m, 1 H), 3.65 (t, 2 H), 7.40 (d, 2 H), 8.25 (d, 2 H). IR (KBr) no amide or carboxylate carbonyl stretch. MS *m/e* for C₁₃H₂₃N₄O₃ (M + H⁺): 283.

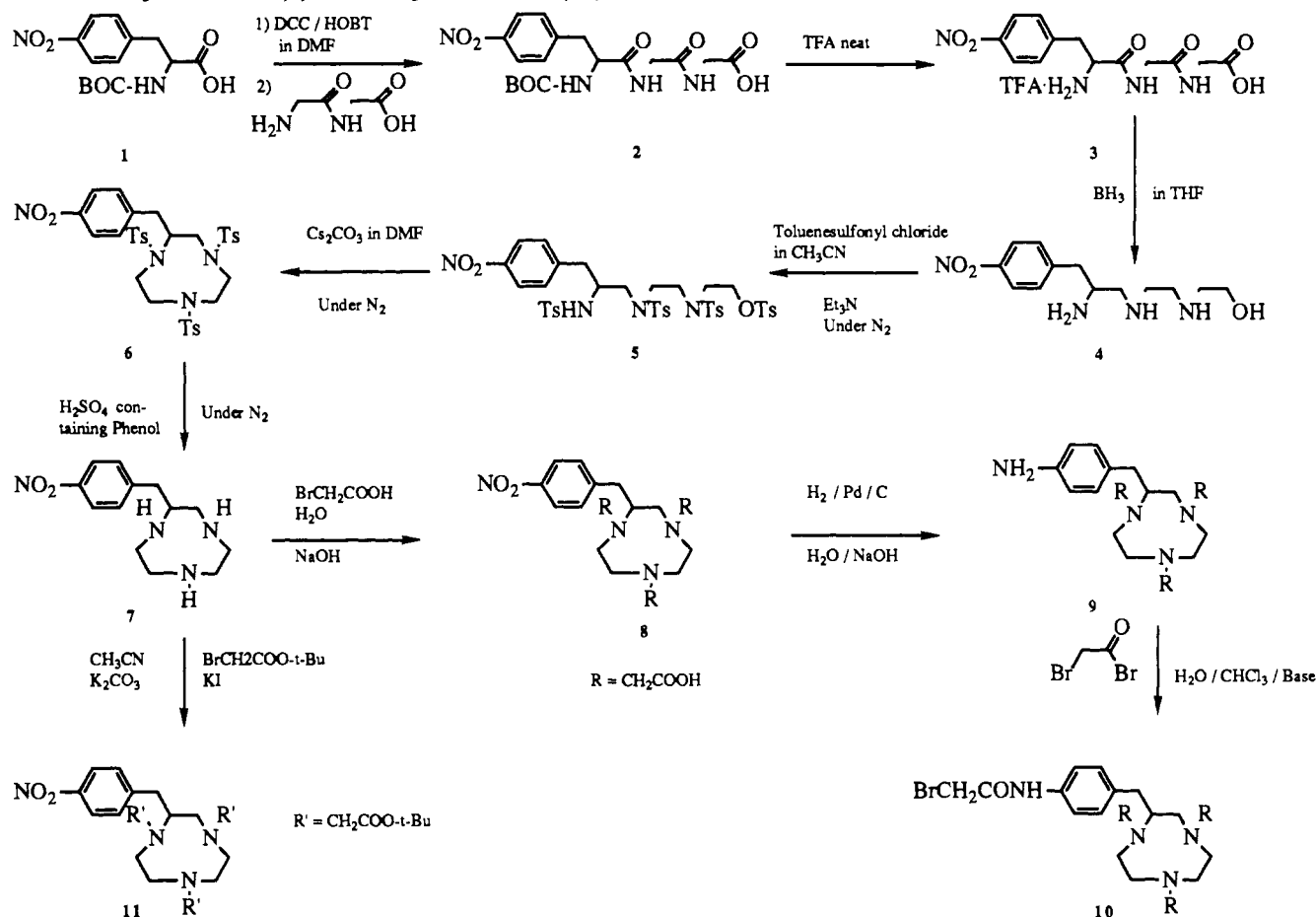
Preparation of 8-(*p*-Nitrobenzyl)-*N,N,N'*,*O*-tetraakis(tolylsulfonyl)-3,6,9-triazanolanol (5). Toluene sulfonyl chloride (2.94 g, 15.4 mmol) was added in small portions to a stirring suspension of 4 (0.90 g, 3.19 mmol) in 20 mL of dry CH₃CN and 14 mL of triethylamine at 25 °C under N₂. After 16 h, the mixture was evaporated to dryness. The residue was taken up in 80 mL of ethyl acetate and 50 mL of 1 M HCl. The organic layer was extracted with 1 M HCl (3 × 35 mL) and saturated aqueous NaCl (50 mL). The ethyl acetate layer was dried over Na₂SO₄ and evaporated to dryness. Purification was carried out by normal-phase HPLC (preparative silica gel column, system 1). The peak that eluted with 12% CH₃CN was collected and dried to give 1.00 g of 5 (1.11 mmol, 33%). ¹H NMR (CDCl₃): δ 2.35 (s, 3 H), 2.50 (br s, 9 H), 2.75 (m, 2 H), 3.10–3.50 (m, 8 H), 3.80 (m, 1 H), 4.15 (m, 2 H), 5.20 (d, 1 H), 7.00–8.00 (m, 20 H). MS *m/e* for C₄₁H₄₇N₄O₁₁S₄ (M + H⁺): 899.

Preparation of 2-(*p*-Nitrobenzyl)-*N,N,N'*-tris-(tolylsulfonyl)-1,4,7-triazacyclononane (6). Cs₂CO₃ (339 mg, 1.04 mmol) was added to a stirring solution of 5 (1.00 g, 1.11 mmol) in 50 mL of dry DMF at 25 °C under N₂. After 12 h, the brown mixture was evaporated to dryness. The residue was taken up in 80 mL of ethyl acetate and 50 mL of 1 M NaCl. The organic layer was extracted with 1 M NaCl (3 × 50 mL), dried over Na₂SO₄, and evaporated to dryness. Purification was carried out by normal-phase HPLC (preparative silica gel column, system 1). The peak that eluted with 10% CH₃CN was collected and dried to give 340 mg of 6 (0.468 mmol, 42%). ¹H NMR (CDCl₃): δ 2.4 (s, 9 H), 2.50–3.90 (m, 12 H), 4.70 (m, 1 H), 7.10–8.20 (m, 16 H). MS *m/e* for C₃₄H₃₉N₄O₈S₃ (M + H⁺): 727.

Preparation of 2-(*p*-Nitrobenzyl)-1,4,7-triazacyclononane (7). A 10-mL quantity of 96% H₂SO₄ was added to a mixture of 6 (340 mg, 0.468 mmol) and phenol (620 mg, 6.59 mmol). The mixture was heated to 115 °C under N₂. After 37 h, the solution was poured over 200 mL of ice. The stirred solution was heated to 80 °C and treated slowly with Ba(OH)₂·8H₂O (56.8 g, 0.180 mol). The hot mixture was filtered; the filtrate was concentrated to 10 mL. Purification was carried out by reversed-phase HPLC (preparative C₁₈ column, system 2). The peak that eluted with 25% 0.1% CF₃COOH in CH₃CN was collected and dried to give 250 mg of 7·3CF₃COOH (0.412 mmol, 88%). ¹H NMR (D₂O): δ 2.70–3.70 (m, 13 H), 7.55 (d, 2 H), 8.20 (d, 2 H). MS *m/e* for C₁₃H₂₁N₄O₂ (M + H⁺): 265.

Preparation of 2-(*p*-Nitrobenzyl)-1,4,7-triazacyclononane-*N,N,N'*-triacetic Acid (8). Bromoacetic acid (286 mg, 2.06 mmol) was added to a solution of 7·3CF₃COOH (250 mg, 0.412 mmol) in 5 mL of H₂O. The mixture was heated to 80 °C. A pH of 10 was maintained with 3 M NaOH during 3 h. After neutralization, the purification was carried out by reversed-phase HPLC (preparative C₁₈ column, system 3). The peak that eluted at 30 min was collected and dried to give 60 mg of 8 (0.14 mmol, 33%). ¹H NMR (D₂O): δ 2.70–4.20 (m, 19 H), 7.50 (d, 2 H), 8.20 (d, 2 H). MS *m/e* calcd for C₁₉H₂₇N₄O₈ (M + H⁺): 439.18289. Found: 439.18209. The visible spectral data of an aqueous solution of 8 and CuSO₄·5H₂O (molar ratio 1:0.9) are given in Table I.

Preparation of 2-(*p*-Aminobenzyl)-1,4,7-triazacyclononane-*N,N,N'*-triacetic Acid (9). Compound 8 (20 mg, 0.046 mmol) was dissolved in 10 mL of H₂O. After the addition of 10% Pd/C (5 mg), the pH was adjusted to

Scheme I. Synthesis of 1,4,7-Triazacyclononane-*N,N',N''*-triacetic Acid Derivatives

11.3 with 3 M NaOH and the reaction vessel was attached to an atmospheric-pressure hydrogenation apparatus. The mixture was cooled with ice, purged with N_2 , and filled with H_2 . After 16 h, the pH was adjusted to 5.8 with 3 M HCl and the catalyst was removed by filtration. The filtrate, now positive to a test for primary amines using fluorescamine (20), was evaporated to dryness to yield 64%, assuming 9 has the same UV absorption properties as *p*-toluidine (21). The purity of 9 was checked by HPLC (analytical C_{18} column, system 4, elution of 9 with 58% CH_3OH). ^1H NMR (D_2O): δ 2.60–4.00 (m, 19 H), 6.80 (d, 2 H), 7.20 (d, 2 H). MS m/e calcd for $\text{C}_{19}\text{H}_{28}\text{N}_4\text{O}_6$ ($M + \text{H}^+$): 409.

Preparation of 2-[*p*-(Bromoacetamido)benzyl]-1,4,7-triazacyclononane-*N,N',N''*-triacetic Acid (10, BAN). Compound 9 (0.031 mmol) was added to a solution of *N,N*-diisopropylethylamine (30 mg, 0.23 mmol) in 2 mL of H_2O . BrCH_2COBr (28 μL , 0.32 mmol) dissolved in 2 mL of CHCl_3 was added to this mixture. The reaction was stirred vigorously for 30 min and then transferred into a separation funnel. After extraction with CHCl_3 (2 \times 8 mL), the pH was adjusted to 1 with 1 M HCl. The solution was extracted with CHCl_3 until the organic extracts were negative to a test of alkylating agents using 4-(*p*-nitrobenzyl)pyridine (22). The pH was adjusted to 8 and the solution was frozen with liquid N_2 and stored at -80°C . The yield was 48%, assuming 10 has the same UV absorption properties as *p*-acetotoluidide (18). The purity of 10 was checked by HPLC (analytical C_{18} column, system 4, elution of 10 with 76% CH_3OH). MS m/e calcd for $\text{C}_{21}\text{H}_{30}\text{BrN}_4\text{O}_7$ ($M + \text{H}^+$): 529.

Preparation of 2-(*p*-Nitrobenzyl)-*N,N',N''*-tris-[(*tert*-butoxycarbonyl)methyl]-1,4,7-triazacy-

clononane (11). To 7- $3\text{CF}_3\text{COOH}$ (100 mg, 0.165 mmol), dissolved in 10 mL of dry CH_3CN , were added K_2CO_3 (179 mg, 1.19 mmol) and KI (34 mg, 0.21 mmol). With stirring, $\text{BrCH}_2\text{COOC}(\text{CH}_3)_3$ (0.098 mL, 0.629 mmol) was added; the reaction mixture was kept at room temperature for 20 h. After evaporation to dryness, the yellow oil was dissolved in CH_3OH and filtered through a frit containing 2 cm of silica gel. The filtrate was dried under vacuum and the residue was dissolved in a $\text{CH}_3\text{OH}/\text{CH}_2\text{Cl}_2$ (1:1 v/v) mixture. The purification was carried out by normal phase HPLC (preparative silica gel column, system 5). The peak that eluted with 38% CH_3OH was collected and dried to give 50 mg of 11 (0.082 mmol, 50%). ^1H NMR (CDCl_3): δ 1.25–1.50 (m, 27 H), 2.60–4.05 (m, 19 H), 7.50 (d, 2 H), 8.15 (d, 2 H). MS m/e for $\text{C}_{31}\text{H}_{50}\text{N}_4\text{O}_8$ ($M + \text{H}^+$): 607.

RESULTS AND DISCUSSION

Derivatives of DOTA (5, 8), TETA (1), and NOTA (7) that can be attached to biomolecules are currently being evaluated for their use in cancer diagnosis and therapy with ^{67}Cu (23, 24), ^{90}Y (25), and ^{111}In (7). The interest in more lipophilic metal complexes and the relatively high liver concentration of the radiometal observed when using these ligands make the synthesis of different NOTA derivatives desirable.

Moi et al. (4) described the synthesis of the 12-membered macrocycle nitrobenzyl-DOTA starting from the tetrapeptide *p*- NO_2 -Phe-Gly-Gly-Gly. With the use of *p*- NO_2 -Phe-Gly-Gly we hoped to obtain the 9-membered ring with the same side chain.

The synthesis could be carried out through steps analogous to those described for DOTA (See Scheme I).

Table I. Spectrophotometric Data for 8 + Cu²⁺

pH	λ_{\max} , nm	ϵ , M ⁻¹ cm ⁻¹	pH	λ_{\max} , nm	ϵ , M ⁻¹ cm ⁻¹
2.3	710	140	8.1	742	146
4.7	742	131	11.2	746	140
6.0	742	136			

The HOBt ester of *N*-*t*-BOC-*p*-NO₂Phe (1) was reacted with Gly-Gly to give 2 (66% yield). Subsequently, the *t*-BOC group was cleaved off in neat CF₃COOH to give 3 (99%). The resulting tripeptide *p*-NO₂-Phe-Gly-Gly was reduced with BH₃-THF to the corresponding amino alcohol 4 (51%). The OH group and the amines were tosylated with toluenesulfonyl chloride and triethylamine as a base to form the tosyl ester and tosylamides (33%). 5 was cyclized in an intramolecular reaction to give the tosylated 9-membered macrocycle 6 (42%). The deprotection was carried out in 96% H₂SO₄ under N₂ to give 7 (88%). The ligand nitrobenzyl-NOTA 8 could be obtained by carboxymethylation with BrCH₂COO⁻ at pH 10 (33%).

In order to obtain a product that can be attached to a biomolecule, the nitro group of 8 was reduced to the corresponding amine 9 (64%) according to Meares et al. (19). The last step, the reaction of the aromatic amino group with BrCH₂COBr, was performed according to the method of Mukkala et al. (26) and McCall et al. (16) to give 10 (48%). The bromoacetamido compound BAN could subsequently be used to label the monoclonal antibody Lym-1. The results of this labeling, the serum stability of the metal complexes, and the animal studies will be reported elsewhere.

The visible spectra of an aqueous solution of 8 and CuSO₄·5H₂O (molar ratio 1:0.9) showed only small changes between pH 2.3 and 11.2. As shown in Table I, λ_{\max} was in the range of 710–746 nm, with $136 \leq \epsilon \leq 146$ M⁻¹ cm⁻¹. This suggests that the new ligand 8 forms Cu(II) complexes of similar geometry and high stability like the unsubstituted NOTA described by Wieghardt et al. (27). They found for a crystal containing Cu(II)NOTA complexes $\lambda_{\max} = 750$ nm and $\epsilon = 72$ M⁻¹ cm⁻¹. Besides nitrobenzyl-NOTA, we were also able to synthesize the esterified derivative of this compound. Using the *tert*-butyl ester of BrCH₂COOH for the alkylation, we obtained the analogous triester 11 (50%). The lipophilic *tert*-butyl groups eliminated the need for carefully avoiding every metal contamination, since this compound could be handled and purified in organic solvents. As we have shown for the tetra-*tert*-butyl ester of nitrobenzyl-EDTA (18, 28), such derivatives are versatile starting materials for a variety of reactions.

Our synthesis presents a new application of the peptide route to macrocyclic bifunctional chelating agents. It allows the synthesis of nitrobenzyl-NOTA, a new and promising ligand for many applications, in a relatively easy seven-step synthesis.

ACKNOWLEDGMENT

We thank Michael McCall, Habibe Diril, and Tariq Rana for helpful discussions. The research was supported by NIH Research Grant CA16861 from the National Cancer Institute.

LITERATURE CITED

- Moi, M. K., Meares, C. F., McCall, M. J., Cole, W. C., and DeNardo, S. J. (1985) Copper Chelates as Probes of Biological Systems: Stable Copper Complexes with a Macrocyclic Bifunctional Chelating Agent. *Anal. Biochem.* 148, 249–253.
- Lauffer, R. B. (1987) Paramagnetic Metal Complexes as Water Proton Relaxation Agents for NMR Imaging: Theory and Design. *Chem. Rev.* 87, 901–927.
- Parker, D. (1990) Tumor Targeting with Radiolabelled Macrocyclic-Antibody Conjugates. *Chem. Soc. Rev.* 19, 271–291.
- Brucher, E., and Sherry, A. D. (1990) Kinetics of Formation and Dissociation of the 1,4,7-Triazacyclononane-N,N',N''-triacetate Complexes of Cerium(III), Gadolinium(III), and Erbium(III) Ions. *Inorg. Chem.* 29, 1555–1559.
- Moi, M. K., and Meares, C. F. (1988) The Peptide Way to Macrocyclic Bifunctional Chelating Agents: Synthesis of 2-(*p*-Nitrobenzyl)-1,4,7,10-tetraazacyclododecane-N,N',N''-tetraacetic Acid and Study of Its Yttrium(III) Complex. *J. Am. Chem. Soc.* 110, 6266–6267.
- Moi, M. K., Yanuck, M., Deshpande, S. V., Hope, H., DeNardo, S. J., and Meares, C. F. (1987) X-ray Crystal Structure of a Macrocyclic Copper Chelate Stable Enough for Use in Living Systems: Copper(II) Dihydrogen 6-(*p*-Nitrophenyl)-1,4,8,11-tetraazacyclotetradecane-1,4,8,11-tetraacetate. *Inorg. Chem.* 26, 3458–3463.
- Cox, J. P. L., Jankowski, K. J., Katakly, R., Parker, D., Beeley, N. R. A., Boyce, B. A., Eaton, M. A. W., Millar, K., Millican, A. T., Harrison, A., and Walker, C. (1989) Synthesis of a Kinetically Stable Yttrium-90 Labelled Macrocyclic-Antibody Conjugate. *J. Chem. Soc., Chem. Commun.* 797–798.
- Craig, A. S., Helps, I. M., Jankowski, K. J.; Parker, D., Beeley, N. R. A., Boyce, B. A., Eaton, M. A. W., Millican, A. T., Millar, K., Phipps, A., Rhind, S. K., Harrison, A., and Walker, C. (1989) Towards Tumor Imaging with Indium-111-Labelled Macrocyclic-Antibody Conjugates. *J. Chem. Soc., Chem. Commun.* 794–796.
- Smith, R. M., and Martell, A. E. (1975, 1977, 1982, and 1989) Critical Stability Constants, Vol. 2, 3, 5, and 6, Plenum Press, New York.
- Van der Merwe, M. J., Boeyens, J. C. A., and Hancock, R. D. (1985) Crystallographic and Thermodynamic Study of Metal Ion Size Selectivity in the Ligand 1,4,7-Triazacyclononane-N,N',N''-triacetate. *Inorg. Chem.* 24, 1208–1213.
- Bevilaqua, A., Gelb, R. I., Hebard, W. B., and Zompa, L. J. (1987) Equilibrium and Thermodynamic Study of the Aqueous Complexation of 1,4,7-Triazacyclononane-N,N',N''-triacetic Acid with Protons, Alkaline-Earth-Metal Cations, and Copper(II). *Inorg. Chem.* 26, 2699–2706.
- Yeh, S. M., Sherman, D. A., and Meares, C. F. (1979) A New Route to "Bifunctional" Chelating Agents: Conversion of Amino Acids to Analogs of Ethylenedinitrilotetraacetic Acid. *Anal. Biochem.* 100, 152–159.
- DeRiemer, L. H., Meares, C. F., Goodwin, D. A., and Diamanti, C. I. (1981) BLEDTA II: Synthesis of a new tumor-visualizing derivative of cobalt(III)-bleomycin. *J. Labelled Compds. Radiopharm.* 18, 1517–1534.
- Meares, C. F., and Wensel, T. G. (1984) Metal Chelates as Probes of Biological Systems. *Acc. Chem. Res.* 17, 202–209.
- Brechbiel, M. W., Gansow, O. A., Atcher, R. W., Schlom, J., Esteban, J., Simpson, D. E., and Colcher, D. (1986) Synthesis of 1-(*p*-Isothiocyanatobenzyl) derivatives of DTPA and EDTA. Antibody Labeling and Tumor-Imaging Studies. *Inorg. Chem.* 25, 2772–2781.
- McCall, M. J., Diril, H., and Meares, C. F. (1990) Simplified Method for Conjugating Macrocyclic Bifunctional Chelating Agents to Antibodies via 2-Iminothiolane. *Bioconjugate Chem.* 1, 222–226.
- Rana, T. M., and Meares, C. F. (1990) Specific Cleavage of a Protein by an Attached Iron Chelate. *J. Am. Chem. Soc.* 112, 2457–2458.
- Studer, M., Meares, C. F., DeNardo, S. J., Kukis, D. L., and Kroger, L. A. (1991) Influence of a Peptide Linker on Biodistribution and Metabolism of Antibody Conjugated Benzyl-EDTAs. Comparison of Enzymatic Digestion in Vitro and in Vivo. *Bioconjugate Chem.* Submitted for publication.
- Meares, C. F., McCall, M. J., Reardan, D. T., Goodwin, D. A., Diamanti, C. I., and McTigue, M. (1984) Conjugation of Antibodies with Bifunctional Chelating Agents: Isothiocyanate and Bromoacetamide Reagents, Methods of Analysis, and Subsequent Addition of Metal Ions. *Anal. Biochem.* 142, 68–78.
- Udenfriend, S., Stein, S., Bohlen, P., Wallace, D., Leimgruber, W., and Weigle, M. (1972) Fluorescamine: A reagent

- for assay of amino acids, peptides, proteins and primary amino acids in the picomolar range. *Science (Washington, DC)* 178, 871-872.
- (21) The Sadtler Standard Spectra, Published by Sadtler Research Laboratories, Subsidiary of Block Engineering, 3316 Spring Garden St, Philadelphia, PA 19104. *p*-Toluidine: spectrum UV 1745, recorded 1966. *p*-Acetotoluidide: spectrum UV 832, recorded 1960.
- (22) Kramer, S. P., Goodman, L. E., Dorfman, H., Soloman, R., Gutenberg, A. M., Pineda, E., Nason, L. L., Ulfohn, A., Gaby, S. D., Bakal, D., Williamson, C. E., Miller, J. I., Sass, S., Witten, B., and Seligman, A. M. (1963) Enzyme alterable alkylating agents VI. Synthesis, chemical properties, toxicities and clinical trial of haloacetates and haloacetamides containing enzyme susceptible bonds. *J. Natl. Cancer Inst.* 31, 297-326.
- (23) Deshpande, S. V., DeNardo, S. J., Meares, C. F., McCall, M. J., Adams, G. P., and DeNardo, G. L. (1988) Copper-67-Labeled Monoclonal Antibody Lym-1, A Potential Radiopharmaceutical for Cancer Therapy: Labeling and Biodistribution in RAJI Tumored Mice. *J. Nucl. Med.* 29, 217-225.
- (24) Moi, M. K., DeNardo, S. J., and Meares, C. F. (1990) Stable Bifunctional Chelates of Metals Used in Radiotherapy. *Cancer Res. (Suppl.)* 50, 789s-793s.
- (25) Deshpande, S. V., DeNardo, S. J., Kukis, D. L., Moi, M. K., McCall, M. J., DeNardo, G. L., and Meares, C. F. (1990) Yttrium-90-Labeled Monoclonal Antibody for Therapy: Labeling by a New Macrocyclic Bifunctional Chelating agent. *J. Nucl. Med.* 30, 473-479.
- (26) Mikkala, V. M., Mikola, H., and Hemmila, I. (1989) The Synthesis and Use of Activated *N*-Benzyl Derivatives of Diethylenetriaminetetraacetic Acids: Alternative Reagents for Labeling of Antibodies with Metal Ions. *Anal. Biochem.* 176, 319-325.
- (27) Wieghardt, K., Bossek, U., Chaudhuri, P., Herrmann, W., Menke, B. C., and Weiss, J. (1982) 1,4,7-Triazacyclononane-*N,N,N'*-triacetate (TCTA), a Hexadentate Ligand for Divalent and Trivalent Metal Ions. Crystal Structures of [Cr^{III}(TCTA)], [Fe^{III}(TCTA)], and Na[Cu^{II}(TCTA)]·NaBr·8H₂O. *Inorg. Chem.* 21, 4308-4314.
- (28) Studer, M., and Meares, C. F. (1991) An Improved and Flexible Approach for Introducing Linkers on Benzyl-EDTAs. *Bioconjugate Chem.* Submitted for publication.
- Registry No.** 1, 33305-77-0; 2, 64936-29-4; 3, 142131-31-5; 4, 142131-32-6; 5, 142131-33-7; 6, 142131-34-8; 7, 142131-35-9; 8, 142131-36-0; 9, 142131-37-1; 10, 142131-38-2; 11, 142131-39-3; H-Gly-Gly-OH, 556-50-3; BrCH₂COOH, 79-08-3; BrCH₂COOBu_t, 5292-43-3; BrCH₂COBr, 598-21-0.

Spectrophotometric Method for the Determination of a Bifunctional DTPA Ligand in DTPA-Monoclonal Antibody Conjugates

C. Greg Pippin,* Tammy A. Parker,[†] Thomas J. McMurry, and Martin W. Brechbiel

Chemistry Section, Radiation Oncology Branch, National Cancer Institute, National Institutes of Health, Building 10, Room B3-B69, Bethesda, Maryland 20892. Received January 13, 1992

A simple spectrophotometric method was developed to quantitate micromolar concentrations of a bifunctional DTPA ligand in DTPA monoclonal antibody (mAb) conjugates. Titration of a brightly colored 1:2 yttrium(III) complex of arsenazo III with the ligand 1B4M-DTPA obeyed Beer's law over the concentration range 0–2.0 μ M 1B4M-DTPA at 652 nm. From a calibration plot of absorbance versus 1B4M molarity, concentrations of 1B4M-DTPA conjugated to mAb were determined. Mole ratios of 1B4M-DTPA to mAb agreed satisfactorily with the ratios obtained by a radioanalytical technique using carbon-14-labeled 1B4M-DTPA and a binding assay using ¹¹¹In. The spectrophotometric method was applied successfully to the preparation of 1B4M-DTPA mAb anti-TAC, a mAb conjugate used in clinical trials of ⁹⁰Y radioimmunotherapy.

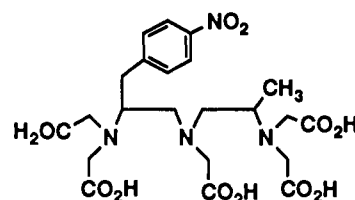
INTRODUCTION

Radiolabeled monoclonal antibodies (mAbs) are being developed and evaluated for the diagnosis and treatment of cancer in many clinical laboratories (1–4). Efforts to develop practical radiolabeled mAbs usually involve the conjugation of a bifunctional ligand to the mAb, followed by labeling the ligand–mAb conjugate with a radioactive metal ion (5). In order to maintain optimal and reproducible behaviors of radiolabeled mAbs in clinical investigations, it is necessary to establish the relationship between targeting efficacy of the mAb and the number of ligands per mAb molecule. It has been amply documented that the targeting efficacy and catabolism of mAbs should not be altered by conjugation or radiolabeling procedures (for review see refs 1 and 2).

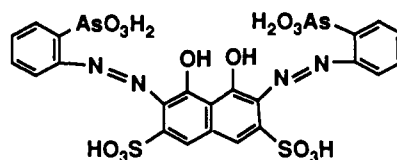
Several analytical methods can quantitate the number of strong metal binding sites in ligand–mAb conjugates. For the amino polycarboxylate class of ligands (e.g. bifunctional EDTA,¹ DTPA, etc.), these methods include ¹¹¹In (6, 7) and ⁵⁷Co (8) binding assays, Tb fluorescence titrations (9), and use of ¹⁴C-labeled ligands (10). In this laboratory, mAb conjugates with ¹⁴C labeled ligands were prepared for preclinical studies, but these conjugates have been restricted from use in patients because of the ¹⁴C label. This restriction and our desire to use rapid, simple procedures to quantitate bifunctional ligands led us to develop a spectrophotometric method to quantitate a bifunctional DTPA ligand currently used in clinical trials of ⁹⁰Y radioimmunotherapy. The spectrophotometric method is based on the reaction between a 1B4M-DTPA ligand (11) mAb conjugate and a yttrium(III) complex of arsenazo III (see Chart I). Arsenazo III is a highly sensitive colorimetric reagent for yttrium, the lanthanides, and other metal ions (12, 13). Because of its sensitivity, several authors (14–16) have studied coordination complexes with arsenazo III even at micromolar concentrations.

In this study our prime objectives were (a) to determine whether the spectrophotometric method used in this laboratory would be quantitative for the 1B4M-DTPA ligand and, if so, (b) to compare the results of the method with previously documented analytical techniques for ligand quantitation, especially the ¹⁴C radioanalytical

Chart I



1B4M-DTPA



Arsenazo III

technique (10). Because the ¹⁴C radioanalytical technique measures the *total* binding sites and metal ion titrations measure the *available* binding sites, a secondary objective was to measure these two distinct physical properties of 1B4M-DTPA–mAb conjugates.

EXPERIMENTAL PROCEDURES

Reagents. A stock solution of 0.100 M Y(III) in 10^{−3} M HCl was prepared from YCl₃·6H₂O (Aldrich, 99.9%) and standardized by titration with EDTA using xylenol orange as indicator. Arsenazo III (ca. 98%, < 0.01 μ mol Ca²⁺/mg) was purchased from Sigma Chemical Co. **Caution:** Arsenazo III is a possible carcinogen! Avoid skin contact and inhalation of the solid material. All mAb conjugate stocks were prepared as described earlier (17) in concentrations that ranged from 9.6 to 45.4 mg/

* Author to whom correspondence should be addressed.

[†] Student Intern at NIH during Summer 1991 from San Jose State University.

¹ Abbreviations used: DTPA, diethylenetriaminepentaacetate; 1B4M-DTPA, 2-methyl-6-(p-nitrobenzyl)diethylenetriamine-N,N,N',N'',N''-pentaacetate; EDTA, ethylenediaminetetraacetate; arsenazo III, 3,6-bis[(2-arsenophenyl)azo]-4,5-dihydroxy-2,7-naphthalenedisulfonic acid.

mL. Each conjugate was stored at 4 °C in solutions of 0.020 mM MES buffer (CALBIOCHEM, passed through a column of Chelex-100 resin, Na⁺ form), 0.15 M NaCl, 0.05% NaN₃, pH 6.2. Weighed quantities of the ligand 1B4M-DTPA, available from previous studies (11), were dissolved in deionized water with 3 equiv of NaOH. Indium(III) nitrate (Specpure, Johnson Matthey) was obtained as a 1000 µg/mL atomic absorption standard. The radionuclide ¹¹¹In chloride was obtained from New England Nuclear. All solutions were prepared with high-purity deionized water (Hydroservices Picosystem, >18 Ω cm).

Procedures. A 500-mL stock solution of the Y(III)-arsenazo III complex (hereafter designated as Y(AAIII)₂) was prepared with the following composition: 5.0 µM AAIII, 1.6 µM Y(III), 0.15 M sodium acetate buffer, pH 4.00. Among the factors which led to the selection of this composition, the three prime factors were as follows: (1) the maximum absorbance of Y(AAIII)₂ at 652 nm, 0.111, was sufficient for quantitative measurements, (2) Beer's law was obeyed when Y(III) was equal to or less than 1.6 µM in this medium, and (3) the 0.15 M acetate buffer adequately maintained pH 4.00 when mAb conjugates in 0.02 M MES buffer were added to Y(AAIII)₂.

To determine the mole ratio of 1B4M to mAb, 3.00 mL of Y(AAIII)₂ was added to a cuvette and the absorbance measured at 652 nm in a diode-array spectrophotometer (Hewlett-Packard 8450A). The 0.15 M acetate buffer, pH 4.00, served as the reference solution for all measurements. From four to six 10 µL additions of 0.123 mM 1B4M-DTPA ligand were added serially to the cuvette. Absorbance values were recorded after each addition of ligand and corrected for volumetric dilution, e.g. corrected back to the initial volume of 3.00 mL. Data from three independently prepared stock solutions of 1B4M-DTPA and Y(AAIII)₂ were used to construct a calibration plot of A₆₅₂ versus [1B4M-DTPA].

A similar procedure was followed for a ¹⁴C-labeled 1B4M-DTPA mAb anti-TAC conjugate, i.e. four 20-µL aliquots were added to 3.00 mL of Y(AAIII)₂. However, in this experiment, a minimum of 10 min elapsed between addition of the mAb conjugate and measurement of the absorbance of Y(AAIII)₂ in order to ensure equilibrium. From the previously constructed calibration plot, the 1B4M-DTPA molarity was calculated for each of the four 20-µL additions of mAb conjugate. After correction for mAb dilution, the mole ratios of 1B4M-DTPA to mAb were calculated as the quotient [1B4M-DTPA]/[mAb]. These experiments were done in triplicate.

One mAb anti-TAC conjugate served as a secondary standard for subsequent determinations of the mole ratios of 1B4M-DTPA to mAb. Specifically, determination of [1B4M]/[mAb anti-TAC] before a new measurement ensured reproducibility² and also obviated additional calibrations with the 1B4M-DTPA ligand. Beer's law was observed for each mAb conjugate determination (see sample data in Figure 2 inset). In addition, few metal ion contaminants or strong metal binding sites were found in the mAb anti-TAC or IgG stocks. For example, when ≤2.0 µM concentrations of mAb anti-TAC or IgG were maintained in Y(AAIII)₂ for 10 min, the absorbance of Y(AAIII)₂

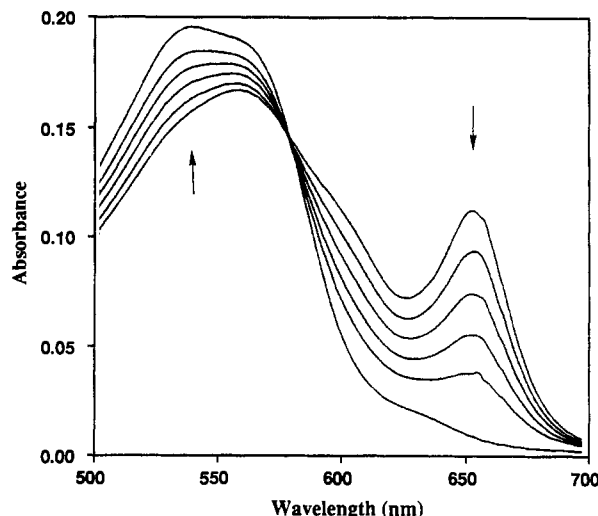


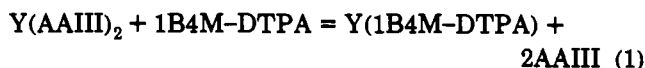
Figure 1. Visible spectra recorded during the titration of a yttrium complex of arsenazo III with bifunctional 1B4M-DTPA: Y(AAIII)₂ + 1B4M-DTPA = Y(1B4M-DTPA) + 2AAIII. For the absorption band centered at 652 nm, the spectra in decreasing order correspond to 0, 0.409, 0.815, 1.22, 1.62, and 2.02 µM 1B4M-DTPA: [Y]_T = 1.6 µM, [arsenazo III]_T = 5.0 µM, pH 4.00, I = 0.15 M (NaAc). The lowest spectrum is that of the arsenazo III reagent: [arsenazo III]_T = 5.0 µM, pH 4.00, I = 0.15 M (NaAc).

decreased at 652 nm by 6–8%. This decrease was within the precision of the method (vide infra).

For experiments using ¹⁴C-labeled 1B4M-DTPA (specific activity = 1.145 × 10⁶ dpm/µmol), the β radioactivity of ¹⁴C was measured by standard liquid scintillation techniques. Similarly, ¹¹¹In was assayed by γ-ray spectroscopy using a NaI detector which had been interfaced to a multichannel analyzer (Canberra Series 40 MCA). Concentrations of mAbs were estimated from their absorbance values at 280 nm [ε = 1.35 (mg/mL)⁻¹].

RESULTS

The predominant equilibrium reaction which occurred in the spectrophotometric titration of Y(AAIII)₂ with 1B4M-DTPA can be written as



based on measurements of reaction stoichiometry. Figure 1 shows the absorbance of Y(AAIII)₂ (λ_{max} = 662 nm) decreases upon the addition of 1B4M-DTPA while the corresponding absorbance of AAIII (λ_{max} = 538 nm) increases. The Y(AAIII)₂ and arsenazo III are the only absorbing species in solution; neither 1B4M-DTPA nor its Y(III) complex have any absorbance in this wavelength region.³ The isosbestic point observed at 585 nm is consistent with only two absorbing species for reaction (1).

Figure 2 shows the dependence of the absorbance at 652 nm on 1B4M-DTPA molarity. The linearity of the data demonstrates that Beer's law is obeyed over the concentration range 0–2.0 µM 1B4M-DTPA. These data were adequately adjusted by the equation, $y = 0.1106 - (4.599 \times 10^{-4})x$ ($R^2 = 0.997$). Identifying $y = A_{652}$ and $x = [1\text{B4M}]$, unknown concentrations of 1B4M-DTPA were readily calculated.

²The stock solutions of Y(AAIII)₂ and arsenazo III showed reproducible behavior over a 5 month period when their containers were kept in the dark. By contrast, very dilute concentrations (<0.1 mM) of the ligand 1B4M had to be prepared just prior to each calibration experiment. When these conditions were met, the mole ratios of 1B4M to mAb could be reproduced for mAb conjugates kept stored at 4 °C over the same 5 month period.

³Several absorption bands of Y(AAIII)₂ and arsenazo III appeared at wavelengths below 500 nm; however, these bands were of little analytical utility because of extensive spectral overlap. For a more detailed description of the absorption and complexation properties of these species, see refs 12 and 13.

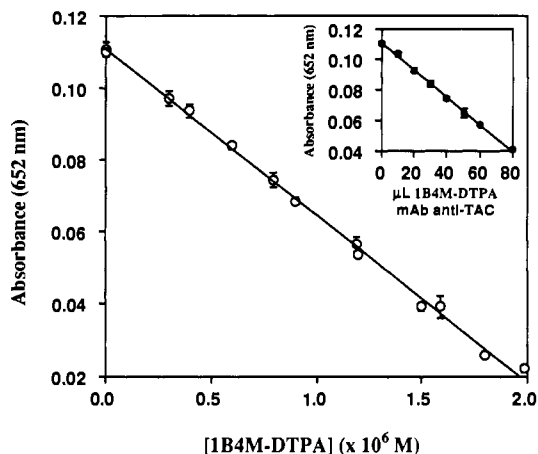


Figure 2. Relationship between the absorbance of the yttrium complex of arsenazo III at 652 nm and the molarity of 1B4M-DTPA. The solid line represents the linear regression fit ($R^2 = 0.997$) and the data points are mean values $\pm \sigma$. The inset shows the linear relationship between the absorbance, $A_{652 \text{ nm}}$, and the volume of added titrant during a sample titration of the yttrium complex of arsenazo III with a 1B4M-DTPA mAb anti-TAC conjugate.

Table I. Comparison between Spectrophotometric and ^{14}C Radioanalytical Methods for the Determination of the Mole Ratios of 1B4M-DTPA to mAb^{a,b}

mAb	[1B4M-DTPA]/[mAb]	
	spectrophotometric method	^{14}C radioanalytical method
anti-Tac	1.08 ± 0.16	1.04 ± 0.12
UPC10	2.01 ± 0.32	1.99 ± 0.08
IgG	2.42 ± 0.54	2.44 ± 0.10
clinical anti-Tac	0.90 ± 0.13	^c

^a Standard deviations are listed at the 2σ level for 4–12 titrations of a single stock solution. ^b The mole ratios were previously referred to as $(\text{C/P})_t$ in ref 17. ^c Quantity was not determined.

In order to assess whether the spectrophotometric method would provide results comparable to the ^{14}C radioanalytical technique, experiments were performed with 1B4M-DTPA ligands in which the nitro moiety had been converted to the isothiocyanate (10) and thereafter with the ligand conjugated to mAbs (17). When 120 μL of stock [^{14}C]-p-SCN-1B4M-DTPA were added to 3.00 mL of $\text{Y}(\text{AAIII})_2$, the absorbance at 652 nm was 0.0500. From the above linear equation and after correction for dilution, the concentration of the stock solution was calculated to be 0.0343 mM, a value which was in good agreement with the molarity of the stock solution, 0.0358 mM, determined by the ^{14}C technique. The results of subsequent experiments with 1B4M ligands conjugated to mAbs are listed in Table I. This table shows that, for the three mAb conjugates tested, the results of spectrophotometric and ^{14}C methods agree satisfactorily with each other.

The ^{111}In binding assay provides an independent test of the validity of the results listed in Table I. In experiments following the procedures of ref 6, the use of 0.010 mM ($^{111}\text{In} + \text{In}$) Cl_3 , 0.0709 mM anti-TAC, and 0.40 M acetate buffer, pH 5.0, allowed determination of the mole ratio of ^{14}C -labeled 1B4M to anti-TAC to be 0.85 ± 0.14 . By comparison, the respective mole ratios determined by the spectrophotometric and ^{14}C methods were 1.08 ± 0.16 and 1.04 ± 0.12 . Because of agreement among the three independent techniques for this anti-TAC mAb conjugate, the mole ratio of the 1B4M to mAb anti-TAC used in clinical trials was determined by the spectrophotometric method (see Table I).

DISCUSSION

The titration of $\text{Y}(\text{AAIII})_2$ with the ligand 1B4M and its mAb conjugates provided quantitative results at micromolar concentrations. The agreement between the ^{14}C and spectrophotometric methods not only validates the spectrophotometric method but also indicates, importantly, that few, if any, of the mAb DTPA sites were occupied by strongly bound metal ions at pH 4.00. This observation is not surprising, however, as trace metal ion impurities which may interfere with radiolabeling efficiency are usually removed by mAb purification procedures.

The precision of the method was found to be 8–12% for identical samples. Major factors which affected precision were fluctuation of the lamp intensity, positioning of the sample cuvette, and trace metal contamination of both the stock solutions and glassware. The precision could be improved if more concentrated $\text{Y}(\text{AAIII})_2$ stock solutions were utilized, such that the absorbance values at 652 nm are larger. However, this condition would decrease the sensitivity of the method and consume greater amounts of 1B4M-DTPA-mAb conjugate stock. For this reason, we feel the precision is satisfactory for most 1B4M-DTPA ligand determinations.

We conclude that the spectrophotometric method reported here provides a useful method for 1B4M ligand quantitation. The method is rapid, simple, and does not require chromatographic separations of radioactive material. It can be utilized with minimal reagents and common lab equipment. Furthermore, it is reasonable to assume that this method could be adapted to other mAb conjugate systems (including systems with other metal ions), providing the specific system obeys Beer's law. The spectrophotometric method may not be considered useful, however, when the equilibrium displacement of the metal ion from AAIII exhibits slow reaction kinetics or is thermodynamically unfavorable, and this restricts the method's applicability.

ACKNOWLEDGMENT

We thank Dr. O. A. Gansow for his support of this work and Dr. T. Waldmann for the supply of mAb anti-TAC. T. Parker acknowledges the support of a Minority Access to Research Careers (MARC) Internship at NCI during Summer 1991 through NIH Grant No. 5T34-GM-08253.

LITERATURE CITED

- (1) Waldmann, T. A. (1991) Monoclonal Antibodies in Diagnosis and Therapy. *Science* 252, 1661.
- (2) Kozak, R. W., Raubitschek, A., Mirzadeh, S., Brechbiel, M. W., Junghans, R., Gansow, O. A., and Waldmann, T. A. (1989) Nature of the Bifunctional Chelating Agent Used for Radioimmunotherapy with Yttrium-90 Monoclonal Antibodies: Critical Factors in Determining In Vivo Survival and Organ Toxicity. *Cancer Res.* 49, 2639–2644.
- (3) Goldenberg, D. M., Ed. (1990) *Cancer Imaging with Radiolabeled Monoclonal Antibodies*, Kluwer Academic Press, Boston.
- (4) Fritzberg, A. R., Berminger, R. W., Hadley, S. W., and Wester, D. W. (1988) Approaches to Radiolabeling of Antibodies for Diagnosis and Therapy of Cancer. *Pharm. Res.* 5, 325–334.
- (5) Meares, C. F. (1984) Metal Chelates as Probes of Biological Systems. *Acc. Chem. Res.* 17, 202–209.
- (6) Mathias, C. J., Sun, Y., Connett, J. M., Philpott, G. W., Welch, M. J., and Martell, A. E. (1990), A New Bifunctional Chelate, BrMe_2HBED : An Effective Conjugate for Radiometals and Antibodies. *Inorg. Chem.* 29, 1475–1480 and references therein.
- (7) Paik, C. H., Murphy, P. R., Eckelman, W. A., Volkert, W. A., and Reba, R. C. (1983) Optimization of the DTPA Mixed-

- Anhydride Reaction with Antibodies at Low Concentration. *J. Nucl. Med.* 24, 932-936.
- (8) Meares, C. F., Mcall, M. J., Reardon, D. T., Goodwin, D. A., Diamanti, C. I., and McTigue, M. (1984) Conjugation of Antibodies with Bifunctional Chelating Agents: Isothiocyanate and Bromoacetamide Reagents, Methods of Analysis and Subsequent Addition of Metal Ions. *Anal. Biochem.* 142, 68-78.
- (9) Brandt, K. D., Schnobrich, K. E., and Johnson, D. K. Characterization of Antibody-Chelator Conjugates: Determination of Chelator Content by Terbium Fluorescence Titration. *Bioconjugate Chem.* 1, 59-65.
- (10) Brechbiel, M. W., Gansow, O. A., Atcher, R. W., Schlom, J., Esteban, J., Simpson, D. E., and Colcher, D. (1986) Synthesis of 1-(p-isothiocyanatobenzyl) derivatives of DTPA and EDTA. Antibody labeling and tumor imaging studies. *Inorg. Chem.* 25, 2772-2781.
- (11) Brechbiel, M. W., and Gansow, O. A. (1991) Backbone-Substituted DTPA Ligands for ^{90}Y Radioimmunotherapy. *Bioconjugate Chem.* 2, 187-194.
- (12) Savin, S. B. (1961) Analytical Use of Arsenazo III. *Talanta* 8, 673-685.
- (13) Budesinsky, B. (1969) Monoaryldazo and Bis(Aryldazo) Derivatives of Chromotropic Acid as Photometric Reagents. *Chelates in Analytical Chemistry* (H. A. Flaschka, and A. J. Barnard, Eds.) pp 1-91, Marcel Dekker, New York.
- (14) Pippin, C. G., Sullivan, J. C., and Wester, D. W. (1984) A Kinetic Study of the Reactions Between Tetravalent Actinide Ions and Arsenazo III. *Radiochim. Acta* 37, 99-100.
- (15) Sherry, A. D., Cacheris, W. P., and Kuan, K. T. (1988) Stability Constants for Gd Binding to Model DTPA-Conjugates and DTPA-Proteins: Implications for Their Use as Magnetic Resonance Contrast Agents. *Magnetic Resonance in Medicine* 8, 180-190.
- (16) Cacheris, W. P., Nickle, S. K., and Sherry, A. D. (1987) Thermodynamic Study of Lanthanide Complexes of 1,4,7-Triazacyclononane- $\text{N},\text{N}',\text{N}''$ -triacetic Acid and 1,4,10-Tetraazacyclododecane- $\text{N},\text{N}',\text{N}'',\text{N}'''$ -tetraacetic Acid. *Inorg. Chem.* 26, 958-960.
- (17) Mirzadeh, S., Brechbiel, M. W., Atcher, R. W., and Gansow, O. A. (1990) Radiometal Labeling of Immunoproteins: Covalent Linkage of 2-(4-Isothiocyanatobenzyl)diethylenetriaminepentaacetic Acid Ligands to Immunoglobulin. *Bioconjugate Chem.* 1, 59-65.
- Registry No.** 1B4M-DTPA, 108415-02-7; arsenazo III, 1668-00-4.

An Improved Method for Labeling Monoclonal Antibodies with Samarium-153: Use of the Bifunctional Chelate 2-(*p*-Isothiocyanatobenzyl)-6-methyldiethylenetriaminepentaacetic Acid

M. E. Izard,[†] G. R. Boniface,^{*†} K. L. Hardiman,[†] M. W. Brechbiel,[‡] O. A. Gansow,[‡] and K. Z. Walkers[§]

Biomedicine and Health Program, ANSTO, Lucas Heights, New South Wales, Australia, Chemistry Section, National Cancer Institute, NIH, Bethesda, Maryland, and Centenary Institute for Cancer Medicine and Cell Biology, Sydney, New South Wales, Australia. Received April 10, 1992

Samarium-153 (^{153}Sm) radioimmunoconjugates of the monoclonal antibody K-1-21 were produced using the bifunctional chelate 2-(*p*-isothiocyanatobenzyl)-6-methyldiethylenetriaminepentaacetic acid (Mx-DTPA). The specific activity (up to 150 MBq mg^{-1}) and percent retained immunoreactivity (>75%) were similar to that of ^{153}Sm -K-1-21 conjugates formed with cyclic DTPA anhydride (cDTPAa). In vivo biodistribution studies showed specific localization of ^{153}Sm -Mx-DTPA-K-1-21 to target antigen implants and higher blood pool and lower uptake in liver, spleen, kidney, and bone when compared to ^{153}Sm -cDTPAa-K-1-21. The improved in vivo distribution of ^{153}Sm -Mx-DTPA-K-1-21 should result in lower radiotoxicity to nontarget tissues when used for radioimmunotherapy purposes.

INTRODUCTION

Samarium-153 (^{153}Sm) is a β -/ α -emitting radionuclide of intermediate half-life and β energy which may be appropriate for the production of radioimmunoconjugates with various antitumor monoclonal antibodies (mAb) for radioimmunotherapy. We have previously reported the successful labeling of the monoclonal antibody K-1-21 with ^{153}Sm using the bifunctional chelate cyclic DTPA dianhydride (cDTPAa) at specific activities up to 150 MBq mg^{-1} (1).

The mAb K-1-21 binds to free monomers and dimers of human κ light chains (LC) but not heavy-chain-associated light chains. It also recognizes a tumor-associated antigen on some κ myeloma and κ lymphoma cells (2, 3). Biodistribution studies of ^{153}Sm conjugates of the mAb K-1-21 indicated specific localization to subcutaneous implants of the κ antigen covalently linked to Sepharose 6MB CNBr-activated beads (Pharmacia) in a rat tumor model system to a similar degree to ^{131}I - or ^{111}In -labeled K-1-21. However, significant radioactivity was also noted in liver, kidneys, and osteous bone. In addition, serum levels of radioactivity were significantly lower than ^{131}I - or ^{111}In -labeled K-1-21 indicating some in vivo dissociation of the radiolabel (1). A similar biodistribution pattern was also observed when ^{153}Sm conjugates of the anti-bladder cancer mAb BLCA-38 were injected systemically into nude mice bearing tumor xenografts of the human bladder cancer cell line BL17 (4). Although the ^{153}Sm -BLCA-38 conjugates showed significant tumoricidal activity, a dose-limiting radiotoxicity to liver and bone marrow was calculated from dosimetric estimations (5).

The synthesis of a number of diethylenetriaminepentaacetic acid based bifunctional chelating agents containing an isothiocyanato benzyl group as protein linker have been described (6). The synthesis of the chelating agent used here was described by Brechbiel (7) and Brechbiel

and Gansow (8) as Mx-DTPA [2-(*p*-isothiocyanatobenzyl)-6-methyldiethylenetriaminepentaacetic acid] and its structure has been confirmed by Cummins et al. (9). This bifunctional chelator has recently been shown to improve the in vivo stability of both ^{111}In and ^{90}Y mAb conjugates (10, 11). In this study we have investigated the suitability of Mx-DTPA as a bifunctional chelator for preparing ^{153}Sm -mAb conjugates. In addition the biodistribution of ^{153}Sm -Mx-DTPA-K-1-21 was compared with that of ^{153}Sm -cDTPAa-K-1-21 in the κ antigen implant rat tumor model system (12). The number of chelator molecules per antibody molecule was determined with ^{14}C intrinsically labeled Mx-DTPA (7).

EXPERIMENTAL PROCEDURES

Monoclonal Antibody Production and Purification.

The IgG₁ mAb K-1-21 was purified from ascites by ammonium sulfate fractionation and affinity chromatography on ROW κ LC conjugated to Sepharose CL-4B beads (Pharmacia, Uppsala, Sweden). Purified antibody was suspended in phosphate-buffered saline, pH 7.2 (PBS), at 14.8 mg mL^{-1} and stored at -20°C .

Preparation of ^{153}Sm . Samarium oxide ($^{152}\text{Sm}_2\text{O}_3$) enriched to 98.7% purity was activated (n, γ) in a neutron flux of $5 \times 10^{13} \text{ n cm}^{-2} \text{ s}^{-1}$ in the ANSTO HIFAR reactor to a specific activity of 31 GBq mg^{-1} . The activated oxide was dissolved in 6 N HCl and evaporated to dryness. The $^{153}\text{SmCl}_3$ was dissolved in ultrapure water to a radioactive concentration of 18.5 GBq mL^{-1} at pH 5.3. ^{153}Sm was used as the citrate salt at pH 7 following dilution with 0.2 M sodium citrate, pH 7, to a specific activity of 10 GBq mL^{-1} .

Cyclic DTPA Anhydride Conjugation to mAb.

Cyclic DTPA anhydride (cDTPAa) (Sigma Chemical Co., St. Louis, MO) was conjugated to K-1-21 (14.8 mg mL^{-1}) at a reactive molar ratio of 20:1 cDTPAa:K-1-21 as previously described (1). The cDTPAa-K-1-21 was separated from unconjugated DTPA by centrifugal size-exclusion chromatography (13) and buffer exchanged into 0.2 M, pH 7 citrate buffer on Bio-Gel P-6DG (Bio-Rad, Richmond, CA).

Mx-DTPA Conjugation to mAb. Mx-DTPA or ^{14}C -Mx-DTPA was freshly dissolved in ultrapure water and reacted with K-1-21 at Mx-DTPA:K-1-21 molar ratios

* Corresponding author: Graeme R. Boniface, BIOMIRA INC, Research Centre One, Edmonton Research & Development Park, 9411-20 Ave, Edmonton, Alberta, Canada T6N 1E5.

[†] ANSTO.

[‡] NIH.

[§] Centenary Institute for Cancer Medicine and Cell Biology.

between 2.5:1 and 25:1 in 0.14 M phosphate buffer, pH 9 (6, 13, 14). Concentration of the antibody in the conjugation reaction was 7 mg mL⁻¹. The reaction was maintained at pH 9 and incubated at 37 °C for 2.5 h, prior to purification and buffer exchange into 0.2 M, pH 7 citrate buffer. The number of chelator molecules per antibody molecule was determined by liquid scintillation counting of the purified ¹⁴C-Mx-DTPA-K-1-21 conjugate and ¹⁴C-Mx-DTPA standards suspended in scintillation fluor (Instagel, Packard).

Labeling of cDTPAa-K-1-21 and Mx-DTPA-K-1-21 with ¹⁵³Sm. Fifty megabecquerel of ¹⁵³Sm (10 GBq mL⁻¹ in 0.2 M, pH 7 citrate buffer) was added to the purified cDTPAa- or Mx-DTPA-conjugated K-1-21 (200 µg) and incubated at room temperature for 30 min. The labeled antibody was then purified by either centrifugal size-exclusion chromatography or by elution from a 20 mm × 150 mm P-6DG (Bio-Rad) size-exclusion column. The purified conjugates were adjusted to a volume of about 300 µL with citrate buffer (0.01 M, pH 7) in a Centricon-30 microconcentrator (Amicon). Citrate buffer (500 µL, 0.01 M, pH 7) was added to the microconcentrator and the volume reduced to about 300 µL by centrifuging at 1600g for 8 min. This washing procedure was repeated four times. The conjugates were finally washed in sterile physiological saline before injection into animals. Total activity retained on the antibody was determined after each wash with an isotope dose calibrator.

Nonspecific Binding of ¹⁵³Sm to K-1-21. Stock K-1-21 (200 µg) in PBS was buffer exchanged via a centrifugal P-6DG column into 0.2 M, pH 7 citrate buffer. The column eluent was incubated with samarium-153 citrate (50 MBq, 10 GBq mL⁻¹) for 30 min and then purified through either a 20 mm × 150 mm or a centrifugal P-6DG gel column. Activity in the second column eluent was measured with an isotope dose calibrator.

Immunoreactivity of ¹⁵³Sm-K-1-21. The immunoreactivity of the ¹⁵³Sm-K-1-21 conjugates was assessed by a solid phase binding assay to immobilized κ LC Sepharose beads as previously described (1, 12).

HPLC Analysis of ¹⁵³Sm-K-1-21. Size-exclusion HPLC (Biosil TSK 250 (Bio-Rad), 0.2 M Tris, pH 7.2) was performed on representative samples of the labeled conjugates as previously described (1).

Biodistribution Studies. Male Fisher 334 rats aged between 10 and 15 weeks were used for biodistribution studies. κ (test) and λ (control) LC-conjugated Sepharose beads (ca. 0.5 mL) were implanted into opposite flanks of the animals as previously described (12). Twenty four hours after the placement of implants, groups of five animals were injected ip with 10–20 µg (0.3–1 MBq) of ¹⁵³Sm-cDTPAa-K-1-21 or ¹⁵³Sm-Mx-DTPA-K-1-21. Six days after injection each animal was exsanguinated, dissected, and selected organs counted in a γ counter (Riagamma, LKB/Wallac, Sweden).

After 6 days each gel implant was covered by a thin vascularized membrane which facilitated its removal as an intact capsule. These gel capsules were cleared of fat and connective tissue before weighing and counting. Tissue distribution profiles of percent injected dose per gram (% ID g⁻¹), percent injected dose per organ (% ID), tissue:blood (T:B) ratio, implant:blood ratio, and κ:λ specificity index were calculated using a computer biodistribution program. Data were compared by Student's *t*-test.

RESULTS

Conjugation of Mx-DTPA to K-1-21. The conjugation of the bifunctional chelate Mx-DTPA to the K-1-21 mAb

Table I. Conjugation of ¹⁴C-Mx-DTPA to K-1-21

mole ratio of Mx-DTPA:K-1-21	Mx-DTPA:K-1-21 incorporation ^a (mol:mol)	specific activity of ¹⁵³ Sm-K-1-21 (MBq mg ⁻¹) ^b	% retained immuno- reactivity
25:1	6.3	130	87
10:1	2.4	56	85
5:1	1.9	44	88
2.5:1	0.2	24	86

^a Reacted for 2.5 h at 37 °C. ^b Using samarium-153 citrate at 31 GBq mg⁻¹.

Table II. Effect of ¹⁵³Sm Concentration on Specific Activity of ¹⁵³Sm-Mx-DTPA-K-1-21

mole ratio of ¹⁵³ Sm: Mx-DTPA-K-1-21	specific activity of ¹⁵³ Sm-Mx-DTPA-K-1-21	
	before wash	after wash
12:1	133	117
0.6:1	37	30

was studied using ¹⁴C labeled Mx-DTPA and liquid scintillation counting. A near linear relationship was observed between the amount of ¹⁴C incorporated onto the mAb and the Mx-DTPA:K-1-21 molar ratio employed (Table I). At a starting Mx-DTPA:K-1-21 molar ratio of 2.5:1, an average of 0.2 mol of Mx-DTPA were added to the mAb within 2.5 h. At a Mx-DTPA:K-1-21 molar ratio of 25:1, an average of 6.3 mol of Mx-DTPA was added. These were the reaction conditions selected for subsequent conjugation preparations for biodistribution studies using unlabeled Mx-DTPA bifunctional chelate.

Conjugation of cDTPAa to mAb. The conjugation of cDTPAa to mAb at various ratios of cDTPAa:K-1-21 and HPLC analyses of the labeled conjugates have been previously described (1). The number of cDTPAa molecules attached to the mAb was not quantified, but at the cDTPAa:K-1-21 ratio of 20:1, chosen for the biodistribution studies, there was minimal cross-linking of the conjugate and immunoreactivity remained at about 90% after preparation.

Preparation of ¹⁵³Sm-Mx-DTPA-K-1-21. Successful labeling of K-1-21 occurred with the use of Mx-DTPA as bifunctional chelate. The specific activity of the labeled conjugate depended on both the mole ratio of Mx-DTPA:K-1-21 in the conjugation reaction and the total activity of the ¹⁵³Sm in the chelation reaction. Using excess samarium-153 citrate with specific activity of 31 GBq mg⁻¹ and Mx-DTPA:K-1-21 ratios of between 2.5:1 and 25:1 produced ¹⁵³Sm-Mx-DTPA-K-1-21 conjugates with specific activities between 24 and 130 MBq mg⁻¹ (Table I).

Size exclusion purified Mx-DTPA-K-1-21 conjugate (Mx-DTPA:K-1-21, 25:1) labeled at ¹⁵³Sm:K-1-21 mole ratios of 12:1 and 0.6:1 produced labeled conjugates with specific activities of 133 and 37 MBq mg⁻¹ before citrate wash and 117 and 30 MBq mg⁻¹ after three washes (Table II). Retained immunoreactivity, determined by solid phase binding assay, remained above 80% for these preparations. When the mole ratio of Mx-DTPA:K-1-21 in the conjugation reaction was raised to 50:1 the specific activity of the labeled conjugate produced was increased to 230 MBq mg⁻¹; however, immunoreactivity decreased to 64%.

Nonspecific Binding of ¹⁵³Sm to K-1-21. No ¹⁵³Sm was detected in the column eluent containing the antibody when unconjugated K-1-21 incubated with ¹⁵³Sm was purified through the 20 mm × 150 mm size-exclusion chromatography column. Less than 0.5% of total activity added to the unconjugated K-1-21 was recovered following purification by the centrifugal column technique.

Citrate Wash of Labeled Conjugates. Following purification of the labeled antibody through size-exclusion

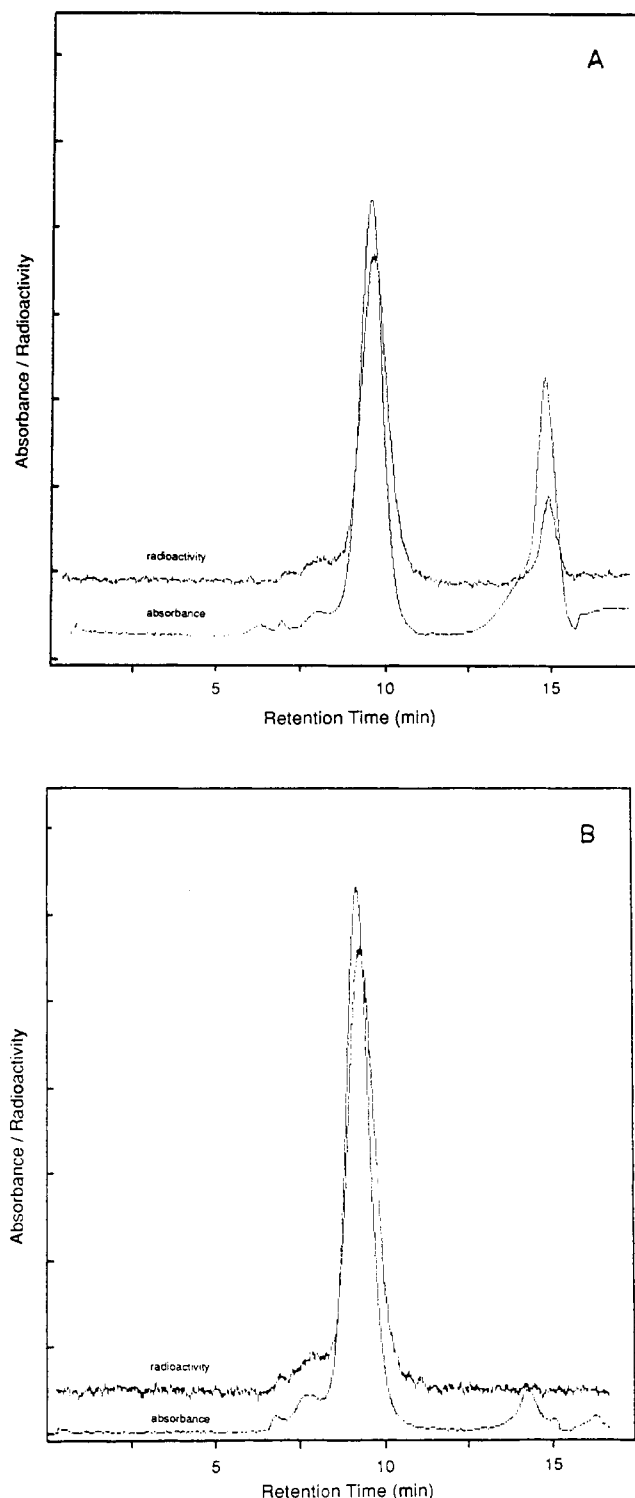


Figure 1. Size-exclusion HPLC chromatograms of gel column purified ^{153}Sm -Mx-DTPA-K-1-21 (A) before and (B) after citrate wash. Retention time of ^{153}Sm -Mx-DTPA-K-1-21 at 9.68 min, non-antibody-bound ^{153}Sm at 13.8 min (Biosil TSK-250, Tris buffer 0.2 M, pH 7.2, 1 mL/min).

columns, HPLC analysis revealed the antibody to be clearly labeled with minimal cross-linking (Figure 1). It also showed the presence of some ^{153}Sm activity not associated with the antibody. This activity was completely removed by the citrate washing.

Biodistribution Studies. Biodistribution studies confirmed that both ^{153}Sm -cDTPAa-K-1-21 and ^{153}Sm -Mx-DTPA-K-1-21 exhibited specific localization to the κ antigen implants at 6 days postinjection.

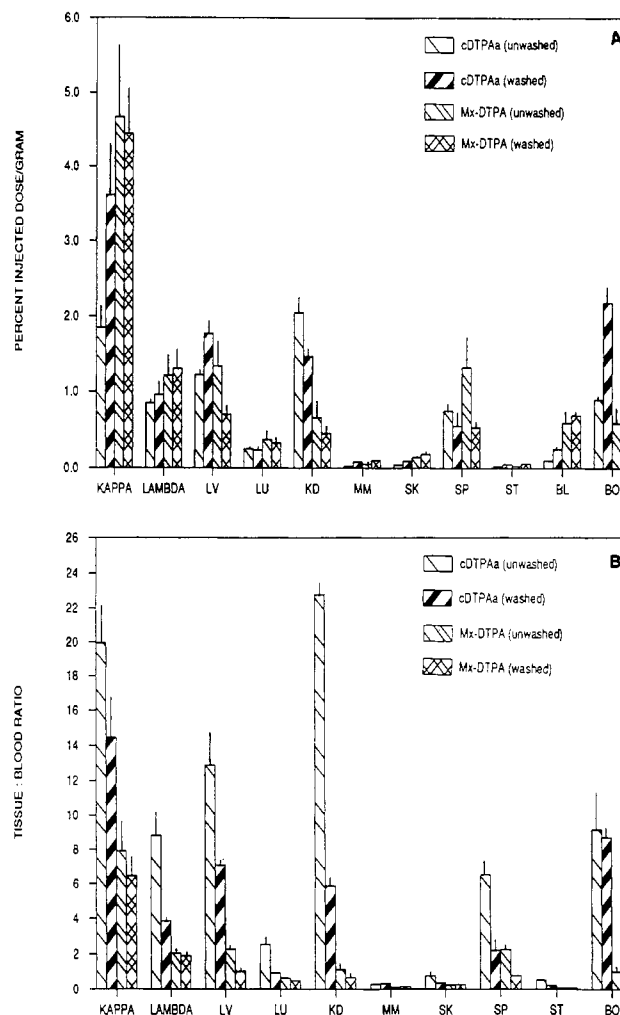


Figure 2. Biodistribution of ^{153}Sm -K-1-21 in Fisher rats 6 days postinjection (mean \pm SEM, $n = 5$); (A) percent injected dose per gram, (B) tissue:blood ratio. Abbreviations: KAPPA = κ antigen implant, LAMBDA = λ antigen implant, LV = liver, LU = lung, KD = kidney, MM = muscle, SK = skin, SP = spleen, ST = stomach, BL = blood, BO = bone.

The resultant κ implant uptakes were 1.9 ± 0.2 and $3.6 \pm 0.1\%$ ID g^{-1} for unwashed and washed ^{153}Sm -cDTPAa-K-1-21 and 4.67 ± 1.0 and $4.45 \pm 0.9\%$ ID g^{-1} for ^{153}Sm -Mx-DTPA (Figure 2). The $\kappa:\lambda$ (control implant) specificity index was 2.0 and 3.76 for unwashed and washed ^{153}Sm -cDTPAa-K-1-21 and 3.85 and 3.42 for unwashed and washed ^{153}Sm -Mx-DTPA-K-1-21.

Blood retention for the unwashed ^{153}Sm -cDTPAa-K-1-21 was $4.2 \pm 0.6\%$ ID and $5.09 \pm 0.7\%$ ID for the washed preparation. Both ^{153}Sm -Mx-DTPA-K-1-21 preparations showed increased blood retention with $9.38 \pm 1.8\%$ ID for the unwashed and $10.46 \pm 2.0\%$ ID for the washed. This increased blood retention resulted in reduced tissue:blood ratios in all organs in comparison to the ^{153}Sm -cDTPAa-K-1-21 preparations (Figure 2). More importantly however, the implant:liver, implant:kidney, and implant:bone ratios for both unwashed (3.5, 7.1, 7.9) and washed (6.3, 9.9, 18.5) ^{153}Sm -Mx-DTPA-K-1-21 were significantly higher than those seen with the ^{153}Sm -cDTPAa-K-1-21 conjugate both unwashed (1.5, 0.9, 2.3) and washed (2.0, 2.4, 1.7).

DISCUSSION

The potential of radioimmunotherapy of tumors by the use of systemically administered β -emitting radionuclide-mAb conjugates has been limited to date due to a number

of factors associated with the nonspecific accumulation of radioimmunoconjugate in nontarget tissues, particularly the liver and bone (1, 13, 15). This uptake has been particularly prevalent when radiolanthanides, such as yttrium or samarium, have been conjugated to mAbs via cyclic DTPA anhydride. The natural predilection of intact mAbs to be metabolized in the liver (16), combined with significant transchelation of radionuclide to subcellular components within the hepatocyte, has resulted in unacceptably high liver dose predictions at therapeutic dose levels. In addition, the natural bone-seeking properties of yttrium, and to a lesser extent samarium, ions have resulted in significant transchelation of these radionuclides from the mAb to osteous bone matrix, with resultant high radiation doses to neighboring marrow. This is of particular concern with ^{90}Y due to the higher penetration of the more energetic β emissions of this radionuclide.

In order to reduce the nontarget uptake of radiolabeled mAbs for radioimmunotherapeutic purposes, several alternative regimens have been proposed including the use of metabolizable linkers, antibody fragments, or heterobifunction antibodies, with radiochelate chase (13, 15). Other workers have proposed the use of macrocycle bifunctional chelates to enhance binding of metal ions to mAbs (17, 18).

While it is still conjecture whether enhancing the stability of the radionuclide-mAb attachment will alone diminish the hepatic transchelation of some metal ions, there is clear evidence that bone transchelation can be minimized. The use of bifunctional chelates which elicit improved chemical stability of the radionuclide to the mAb by retaining the denticity of the DTPA moiety have recently been shown to reduce the "off rate" of radiolabel from the mAb in vivo. Using a series of backbone-substituted DTPA analogues (Mx-DTPA, 1M3B-DTPA, 1B3M-DTPA) Kozak and colleagues have shown significant increases in the in vivo stability of ^{111}In and ^{90}Y labeled anti-Tac mAb in comparison to cDTPAa conjugates (10). A reduction in bone uptake, together with a reduced plasma clearance of ^{90}Y labeled anti-Tac, was seen using these derivatives in comparison to cDTPAa. However, liver uptake remained unaffected.

Our studies extend these findings by demonstrating that the biodistribution of ^{153}Sm labeled mAb in animals bearing model tumor implants is improved by using the DTPA derivative 2-(p-isothiocyanatobenzyl)-6-methyldiethylenetriaminepentaacetic acid rather than the cyclic DTPA anhydride. A reduction in bone uptake and increased retention in the blood was observed with ^{153}Sm -Mx-DTPA-K-1-21. Despite these improvements the liver uptake of ^{153}Sm was not significantly reduced for Mx-DTPA conjugates of K-1-21 purified by conventional gel chromatography methods only. HPLC analyses of these size-exclusion-purified conjugates revealed, along with the labeled antibody, some activity unassociated with the antibody. The activity was not nonspecifically bound ^{153}Sm but may have been due to postpurification release of ^{153}Sm weakly chelated to conjugated Mx-DTPA. Dissociation in vivo from the conjugate of any weakly chelated ^{153}Sm not removed by the purification regime would contribute to liver uptake seen in the biodistributions of those conjugates without the citrate wash. The purification regime with citrate buffer of ^{153}Sm -Mx-DTPA-K-1-21 produced a conjugate whose liver uptake diminished to the level of the blood pool.

The Mx-DTPA bifunctional chelate appears to be an attractive alternative to cDTPAa for producing ^{153}Sm -

mAb radioimmunoconjugates yielding reduced osteous deposition and improved blood retention.

Further studies are continuing with ^{153}Sm -Mx-DTPA conjugates of the anti-bladder mAbs BLCA-38 and BLCA-8 for the intravesical and systemic radioimmunotherapy of bladder cancer in cancer xenograft animal models (2, 3).

ACKNOWLEDGMENT

We thank Mr. P. Sorby and D. Henderson of ANSTO for the production of ^{153}Sm . The expert technical assistance of Ms. Sharon Parkes of ANSTO with HPLC and immunoreactivity estimations is also gratefully acknowledged.

LITERATURE CITED

- (1) Boniface, G. R., Izard, M. E., Walker, K. Z., McKay, D. R., Sorby, P. J., Turner, J. H., and Morris, J. G. (1989) Labeling of monoclonal antibodies with samarium-153 for combined radioimmunoscinigraphy and radioimmunotherapy. *J. Nucl. Med.* 30, 683-691.
- (2) Boux, H. A., Raison, R. L., Walker, K. Z., Hayden, G. E., and Basten, A. (1983) A tumour-associated antigen specific for human kappa myeloma cells. *J. Exp. Med.* 158, 1769-1794.
- (3) Goodnow, C. C., and Raison, R. L. (1985) Structural analysis of the myeloma-associated membrane antigen KMA. *J. Immunol.* 135, 1276-1280.
- (4) Walker, K. Z., Boniface, G. R., Lightfoot, D. V., Ormsby, S., Izard, M. E., Parkes, S. L., Weedon, A., and Russell, P. J. (1990) Samarium-153-labeled monoclonal antibody BLCA-38. I. Biodistribution studies in a nude mouse xenograft model. *Antibodies, Immunoconjugates Radiopharm.* (submitted).
- (5) Lightfoot, D. V., Walker, K. Z., Boniface, G. R., Hetherington, E. L., Izard, M. E., and Russell, P. J. (1991) Dosimetric and therapeutic studies in nude mice xenograft models with samarium-153 labelled monoclonal antibody. *Antibodies, Immunoconjugates Radiopharm.* 4 (3), 319-330.
- (6) Brechbiel, M. W., Gansow, O. A., Atcher, R. W., Schlom, J., Esteban, J., Simpson, D. E., and Colcher, D. (1986) Synthesis of 1-(p-isothiocyanatobenzyl) derivatives of DTPA and EDTA. Antibody labeling and tumor-imaging studies. *Inorg. Chem.* 25, 2772-2781.
- (7) Brechbiel, M. W. (1988) New bifunctional ligands for radioimmunimaging and radioimmunotherapy. Ph.D Thesis, The American University, Washington, D.C.
- (8) Brechbiel, M. W., and Gansow, O. A. (1991) Backbone-substituted DTPA ligands for Y-90 radioimmunotherapy. *Bioconjugate Chem.* 2, 187-194.
- (9) Cummins, C. H., Rutter, E. W., and Fordyce, W. A. (1991) A convenient synthesis of bifunctional chelating agents based on diethylenetriaminepentaacetic acid and their co-ordination chemistry with yttrium (III). *Bioconjugate Chem.* 2, 180-186.
- (10) Kozak, R. W., Raubitschek, A., Mirzadeh, S., Brechbiel, M. W., Junghaus, R., Gansow, O. A., and Waldmann, T. A. (1989) Nature of the bifunctional chelating agent used for radioimmunotherapy with yttrium-90 monoclonal antibodies: Critical factors in determining in vivo survival and organ toxicity. *Cancer Res.* 49, 2639-2644.
- (11) Roselli, M., Schlom, J., Gansow, O. A., Raubitschek, A., Mirzadeh, S., Brechbiel, M. W., and Colcher, D. (1989) Comparative biodistributions of yttrium- and indium-labeled monoclonal antibody B72.3 in athymic mice bearing human colon carcinoma xenografts. *J. Nucl. Med.* 30, 672-682.
- (12) Walker, K. Z., Seymour-Munn, K., Keech, F. K., Axiak, S. M., Bautovich, G. J., Morris, J. G., and Basten, A. (1986) A rat model system for radioimmunodetection of kappa myeloma antigen on malignant B cells. *Eur. J. Nucl. Med.* 12, 461-467.
- (13) Meares, C. F., McCall, M. J., Reardan, D. T., Goodwin, D. A., Diamanti, C. I., and McTigue, M. (1984) Conjugation of antibodies with bifunctional chelating agents: Isothiocyanate and bromoacetamide reagents, methods of analysis and subsequent addition of metal ions. *Anal. Biochem.* 142, 68-78.

- (14) Meares, C. F., and Goodwin, D. A. (1984) Linking radio-metals to proteins with bifunctional chelating agents. *J. Prot. Chem.* 3 (2), 215-228.
- (15) Deshpande, S. V., DeNardo, S. J., Meares, C. F., McCall, M. J., Adams, G. P., and DeNardo, G. L. (1989) Effect of different linkages between chelates and monoclonal antibodies on levels of radioactivity in the liver. *J. Nucl. Med. Biol.* 16, 587-597.
- (16) Sands, H., and Jones, P. L. (1987) Methods for the study of the metabolism of radiolabelled monoclonal antibodies by liver and tumor. *J. Nucl. Med.* 28, 390-398.
- (17) Craig, A. S., Helps, I. M., Jankowski, K. J., Parker, D., Beeley, N. R. A., Boyce, B. A., Eaton, M. A. W., Millican, A. T., Millar, K., Phipps, A., Rhind, S. K., Harrison, A., and Walker, C. (1989) Towards tumour imaging with indium-111 labelled macrocycle-antibody conjugates. *J. Chem. Soc. Chem. Commun.* 12, 794-798.
- (18) Moi, M. K., Meares, C. F., and DeNardo, S. J. (1988) The peptide way to macrocyclic bifunctional chelating agents: Synthesis of 2-(p-Nitrobenzyl)-1,4,7,10-tetraazacyclododecane-N,N',N'',N'''-tetracetic acid and study of its yttrium (III) complex. *J. Am. Chem. Soc.* 110, 6266-6267.

Bioconjugate Chemistry

SEPTEMBER/OCTOBER 1992
Volume 3, Number 5

© Copyright 1992 by the American Chemical Society

REVIEWS

Conjugates of Anticancer Agents and Polymers: Advantages of Macromolecular Therapeutics in Vivo

Hiroshi Maeda,*† Len W. Seymour,‡§ and Yoichi Miyamoto†

Department of Microbiology, Kumamoto University School of Medicine, 2-2-1 Honjo, Kumamoto 860, Japan, and Cancer Research Campaign's Polymer-Controlled Drug Delivery Group, Department of Biological Sciences, Keele University, Keele, Staffordshire ST5 5BG, U.K. Received June 11, 1992

1. INTRODUCTION

There is a pressing need for the development of more effective and yet less toxic drugs for the treatment of diseases such as cancer and AIDS. The use of sophisticated macromolecular drugs offers many new therapeutic strategies (1–5), although so far investigation and development of such materials has been surprisingly limited. Synthetic macromolecular therapeutic agents have never previously been used in clinical practice, although naturally-occurring macromolecules have been used routinely. Immunoglobulins, growth hormones, insulin, interferons, plasma albumin, fibrinogen, plasminogen activator, heparins, chondroitin sulfate, etc., are all widely used, and their basic therapeutic principle is for the supplementation of deficient patients. Hence molecular size alone should not be a factor prohibiting the development of synthetic macromolecular drugs. One reason for the slow development is probably a lack of perception of the potential advantages and therapeutic benefits, although another may be connected with the perceived complexity and diverse chemical structures of the materials involved.

Interest in synthetic polymer–drug conjugates can be traced back before the 1950s, but the understanding of pharmacology, polymer chemistry, subcellular/cellular biology, and purification technology was then so poorly developed that the precise requirements for a macromolecular drug could be neither identified nor met at that

time. One exception may be polyvinylpyrrolidone iodine complex (Isodine) (6), which was developed as a topical antiseptic agent and even now remains one of the best antiseptics available.

In recent years great advances have been made in pharmacology, purification technology, and allied sciences, and the development of sophisticated macromolecular drugs is now a real possibility. As the clinical benefits of this new approach become gradually established, the field is likely to achieve an increasing momentum of growth.

Macromolecular anticancer drugs are usually either conjugates of proteins with polymers (e.g. SMANCS¹) or immunoglobulins (e.g. antibody–ricin conjugates), or conjugates of low molecular weight drugs with synthetic polymers (e.g. HPMA) or proteins (e.g. IgG or albumin). The common aspects of the polymer conjugates are that the polymers function as carriers or stabilizers, frequently resulting in decreased drug toxicity, altered biodistribution, and mostly increased therapeutic efficacy.

Firstly we shall review mechanistic principles of tumor targeting of polymer–drug conjugates in relation to the pathophysiology of tumor tissue, followed by brief comments on representative polymer-conjugated anticancer drugs.

¹ Abbreviations used: SMA, styrene–maleic acid/anhydride copolymer; SMANCS, poly(styrene-co-maleic acid *n*-butyl ester)-conjugated neocarzinostatin; HPMA, *N*-(2-hydroxypropyl)-methacrylamide copolymer; $t_{1/2}$, plasma half-life in vivo; NCS, neocarzinostatin; EPR effect, enhanced permeability and retention effect; HMKG, high molecular weight kininogen; Hyp³-BK, [hydroxypropyl³]bradykinin; PEG, polyethylene glycol; SOD, superoxide dismutase; DIVEMA–NCS, divinyl ether–maleic acid copolymer- or pyran copolymer-conjugated NCS; LD₅₀, dose giving 50% lethality; A7–NCS, an anti-human colorectal carci-

* Author to whom correspondence should be addressed.

† Kumamoto University School of Medicine.

‡ Keele University.

§ Current address: Department of Clinical Oncology, Queen Elizabeth Hospital, University of Birmingham, Edgbaston, Birmingham B15 2TH, U.K.

Table I. Plasma Clearance Time of Various Proteins, Polymer-Conjugated or Modified Proteins, and Synthetic Polymers

protein or polymer	type of polymer or modification	daltons $\times 10^{-3}$	$t_{1/2}$	$t_{1/10}$	test animal	refs
neocarzinostatin (NCS)	none	12	1.8 min	15 min	mouse	8, 70
SMANCS	SMA ^a -conjugated NCS	16	19 min	5 h	mouse	8, 70
ribonuclease	none	13.7	5 min	30 min	mouse	109
ribonuclease dimer	cross-linked	27	18 min	5 h	mouse	109
soybean trypsin inhibitor (SBTI ^b)	none	20	<2.0 min	3 min	rabbit	47
dextran-SBTI	dextran	127	~20 min	>80 min	rabbit	47, 48
ovomucoid	DTPA ^c / ⁵¹ Cr	29	5 min	34 min	mouse	8
Cu ²⁺ , Zn ²⁺ superoxide dismutase (SOD)	none	32	5 min	30 min	rat	8
SOD-SMA ^a	SMA conjugate	40	>5 h	>10 h	rat	9
SOD-DIVEMA ^d	divinyl ether-maleic acid conjugate	43	30 min	>10 h	mouse	71
SOD-PVA _L ^e	polyvinyl alcohol (low mol wt)	67	3 h	>10 h	mouse	UD
SOD-PVA _H ^f	polyvinyl alcohol (high mol wt)	118	7.8 h	>15 h	mouse	UD
SOD-suc-gelatin ^g	succinyl gelatin	92	25 min	66 min	mouse	UD
bilirubin oxidase	none	50	15 min	74 min	rat	49
PEG ^h -bilirubin oxidase	PEG	70	5 h	48 h	rat	49
serum albumin	none	68	3-4 days ⁱ		mouse	8
serum albumin	Evans blue dye		2 h	30 h	mouse	8, 11
formaldehyde-modified serum albumin	formaldehyde/ ¹²⁵ I		25 min	4 h	rat	110
L-asparaginase	none	65 \times (2-8)	1.5-3.4 h		rat	42
L-asparaginase-PEG	PEG ₂ -linked	>500	56 h	11 days	mouse	42
HPMA ^j	iodination/ ¹²⁵ I	22	<6 min	1 h	mouse	UD
HPMA	iodination/ ¹²⁵ I	40	6 h	20 h	mouse	UD
HPMA	iodination/ ¹²⁵ I	78	20 h	70 h	mouse	UD
HPMA	iodination/ ¹²⁵ I	148	20 h	>72 h	mouse	UD
HPMA	iodination/ ¹²⁵ I	556	25 h	>72	mouse	UD
immunoglobulin G	DTPA/ ⁵¹ Cr	150	60 h		rat	8
α_2 -macroglobulin	iodination/ ¹²⁵ I	180 \times 4	140 h	22 days	mouse	111
α_2 -macroglobulin-plasmin complex	iodination/ ¹²⁵ I	180 \times 2	2.5 min	20 min	mouse	111

^a SMA, styrene-maleic acid/anhydride copolymer butyl ester, Mr 1600. It confers albumin binding capacity. ^b SBTI, Kunitz type. ^c DIVEMA, divinyl ether-maleic acid (pyran) copolymer, Mr 5600. ^d PVA_L, polyvinyl alcohol, Mr 4500. ^e PVA_H, polyvinyl alcohol, Mr 11200. ^f Suc-gelatin, succinylated gelatin, Mr 10 000. ^g PEG, polyethylene glycol, Mr 6000. ^h DTPA, diethylenetriaminepentaacetic acid. ⁱ Human albumin in humans: 19 days. ^j HPMA, *N*-(2-hydroxypropyl)methacrylamide copolymer. ^k UD, unpublished data.

2. PLASMA HALF-LIFE OF MACROMOLECULAR DRUGS

The profile of plasma concentration of drugs is generally of great pharmacological and therapeutic significance. To attain a high concentration in any peripheral target tissue or organ following systemic administration, a high plasma concentration (generally measured as the area under the clearance curve) is essential (1-3). Consequently it is important that the material demonstrates good blood and tissue compatibility. For this purpose a neutral or slightly negative electric charge appears to be optimal since polycationic polymers are rapidly captured by the first pass effect and also during circulation (7). The reason for this is that the endothelial surfaces of the blood vessels are covered with negatively charged components such as chondroitin sulfate, heparan sulfate, and glycocalyx. The bioadhesiveness of polycationic drugs may make them more suitable for topical or local application than for intravenous injection.

Molecular size is another important parameter. Small proteins less than 40 000 Da are cleared rapidly into the urine, with a plasma half-life in vivo ($t_{1/2}$) of usually less than 5 min in mice (e.g. superoxide dismutase, 30 kDa) (1-4, 8, 9) (Table I). On the other hand, low molecular weight drugs which bind to albumin or other large plasma proteins exhibit relatively high plasma concentrations for prolonged periods. Conjugation of the small anticancer protein neocarzinostatin (NCS, 12 kDa) with two copolymers of styrene-maleic acid/anhydride (SMA, 1.6 kDa), a conjugate designated SMANCS, has a molecular mass

of only 15.5 kDa. However, conjugation results in a prolongation of plasma $t_{1/2}$ in mice from 1.9 min for NCS to 20 min for the conjugate (8, 9), as a result of binding of SMANCS to albumin (10). Systematic studies using plasma proteins or synthetic polymers with various molecular weights have shown clearly that noncationic materials larger in size than the renal threshold frequently display extended plasma circulation times (11, 12, and unpublished data, Seymour et al.).

3. INCREASED PERMEABILITY OF TUMOR VASCULATURE

In inflammatory conditions the permeability of the blood vessels is greatly increased by factors acting on endothelial cells and opening the tight intercellular junctions. These factors include agents such as bradykinin, histamine, prostaglandins, and tumor necrosis factor. This has also been shown to be the case with certain microbial infections, where the bradykinin-generating cascade is activated and hence edema is formed (13).

In tumor tissue there are at least two substances known to be involved in modulation of vascular permeability. Vascular permeability factor (VPF), initially described by Dvorak et al. (14, 15), is a protein of about 38 kDa with sequence homology to platelet derived growth factor (PDGF) (16, 17). VPF is produced by a range of cancer cells and also by pituitary follicular cells (18, 19). This factor possesses endothelial growth (angiogenic) activity and mitogenic activity in vivo, and is thought to be involved in a range of physiological processes such as inflammation and wound healing (20, 21).

Bradykinin (or kinin) is generated from high molecular weight kininogen (HMKG) by limited proteolysis of kallikrein (22-24). Kallikrein is generated from prekallikrein, a proenzyme, by the action of activated Hageman factor (also called clotting factor XII). The cascade of the proteolytic reactions to generate bradykinin is shown in

noma monoclonal antibody A7-conjugated NCS; *T/C*, a ratio of the value obtained in the treatment group to that in the control group; DOX, doxorubicin; OXD-DOX, oxidized dextran-DOX conjugate; DIVEMA-DOX, divinyl ether-maleic acid copolymer-DOX conjugate; MMC-D, mitomycin C-dextran conjugate; MMC-D_{cat}, cationic MMC-D; MMC-D_{an}, anionic MMC-D.

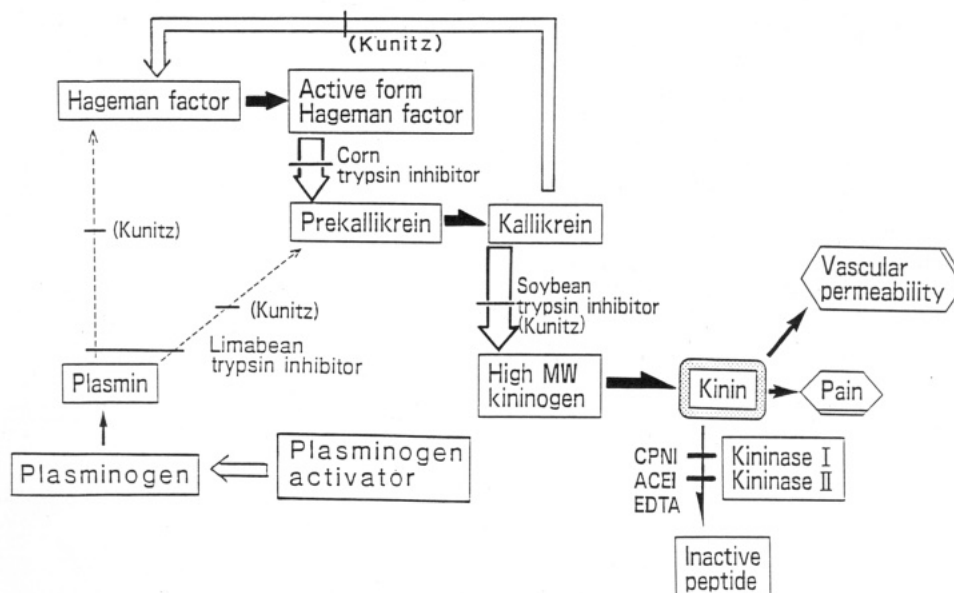


Figure 1. Kinin-generating and -degrading cascade and points of inhibition by various inhibitors: CPNI, carboxypeptidase N inhibitor; ACEI, angiotensin converting enzyme inhibitor (from ref 23 with permission).

Bradykinin H-Arg-Pro-Pro-Gly-Phe-Ser-Pro-Phe-Arg-OH

[Hyp³]-Bradykinin H-Arg-Pro-Hyp-Gly-Phe-Ser-Pro-Phe-Arg-OH

Figure 2. Amino acid sequences of bradykinin and Hyp³-bradykinin. (See ref 22.)

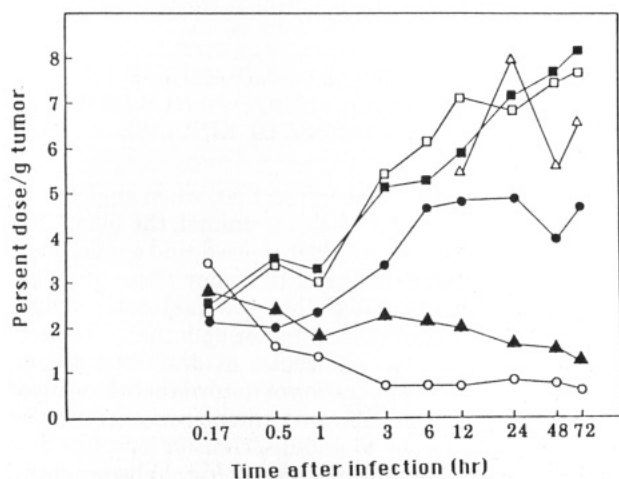


Figure 3. Intratumor accumulation of proteins with different sizes injected intravenously. All proteins were labeled with ⁵¹Cr via the chelating agent DTPA (diethylenetriaminepentaacetic acid): □, bovine serum albumin; ■, mouse serum albumin; △, mouse IgG; ●, SMANCS; ▲, ovomucoid (29 kDa), and ○, neocarcinostatin (12 kDa) (from ref 11 with permission).

Figure 1. Bradykinin is an endogenous vasoactive peptide and it acts on smooth muscle cells, particularly in post capillary venules, inducing an enlarged gap between endothelial cells. Many tumor cells are known to produce plasminogen activator, which activates one or more steps in the kinin-generating cascade. Tumor cells also frequently produce plasminogen activator inhibitors, which controls expression of plasminogen activator activity (24). We have tested this kinin-generating cascade in vivo as well as in vitro, analyzing human blood plasma, and found that in cancer patients the levels of prekallikrein and HMKG are lower than those in healthy subjects as a result of increased conversion of precursors to their active form (24). Additionally, we could quantify elevated bradykinin levels in pleural or ascitic fluid of carcinomatoses (22, 23).

Table II. Accumulation of ¹⁴C-Labeled Iodinated Fatty Acid*

organs, tissues	radioactivity dpm/g (×10 ³)		organs, tissues	radioactivity dpm/g (×10 ³)	
	15 min	3 days		15 min	3 days
tumor	1252.58	130.94	muscle	<0.1	0.46
liver (adjacent)	566.25	17.02	skin	<0.1	1.42
liver (remote)	28.95	6.89	mes lymph node	0.15	2.21
sm intestine	1.06	4.44	cer lymph nodes	0.22	1.61
lung	2.66	2.02	thymus	0.22	0.93
kidney	1.61	2.57	serum	0.58	1.03
stomach	10.97	—	plasma cells	0.86	1.57
heart	2.65	1.72	bone marrow	<0.1	2.97
lg intestine	0.35	1.06	urine (exc)	—	1.14
spleen	2.39	3.28	urine (vesical)	<0.1	1.06
bladder	0.28	1.31	bile	70.91	1.78
brain	<0.1	0.46			

* Intrahepatic arterial dose, 0.3 mL. (From ref 29 with permission.)

In cancerous exudate fluid a large amount of a new (previously unreported) form of bradykinin was identified, [hydroxyprolyl³]bradykinin (Hyp³-BK), in which proline in the third position is replaced with Hyp (Figure 2) (22).

It has been shown that fluid accumulation in tumors and the leakage of plasma proteins out of the blood vessels is indeed a result of kinin action (23), since inhibition of the kinin-generating cascade by specific inhibitors, such as soybean trypsin inhibitor, resulted in the suppression of formation and accumulation of ascitic fluid in ascitic tumors (23, 25). This effect may contribute toward the hypoalbuminemia of cachexic cancer patients (26). Similarly, high concentrations of kinin at the site of generation (tumor) can be maintained by inhibiting its degradation using kininase inhibitor (also known as angiotensin converting enzyme inhibitor) (23, 25). In addition to VPF and bradykinin, interleukin-2 (27), prostaglandins, tumor necrosis factor, and other agents are also known to influence the vascular permeability of tumors, although currently many questions into their regulation and mechanisms of action remain unanswered.

It is now well-established that macromolecules greater than 50 kDa circulating for extended periods in the bloodstream show substantial tumor accumulation (2-4, 11) (Table I and Figure 3). Although smaller molecules would also be subjects of increased permeability in tumor

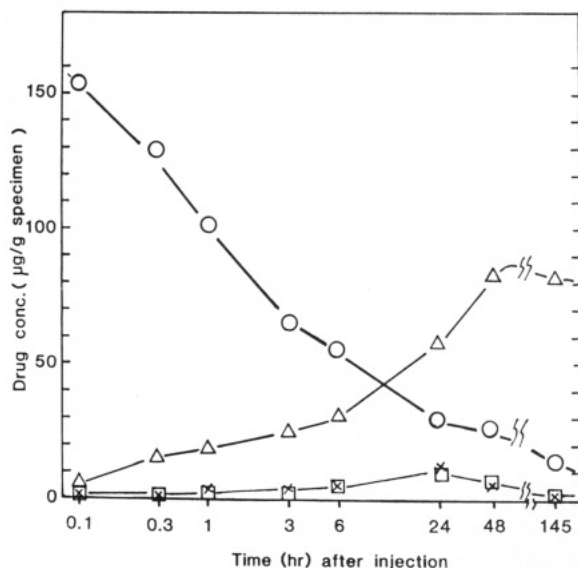


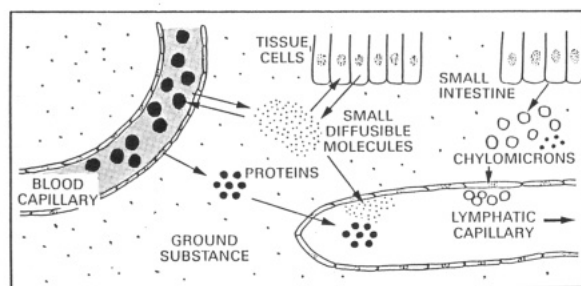
Figure 4. Clearance of Evans blue-albumin complex (a model for macromolecular drug) from blood plasma and its accumulation in the tumor tissue and the normal skin in tumor-bearing mice. Tumor S-180 (5×10^6 cells) was injected into the skin of mice, and after 7 days Evans blue was injected intravenously. The tumor became progressively blue due to the accumulation of Evans blue-albumin complex. The amount of Evans blue-albumin complex in tissues were quantified after removal and extraction: O, plasma; □, normal skin; ×, normal muscle; Δ, tumor (from ref 11 with permission).

tissue, they are more diffusible out of tumor tissue into blood circulation again, and no significant tumor accumulation would be expected in the long run, which is a clear contrast to large molecules as described below.

4. PROLONGED RETENTION OF MACROMOLECULES IN TUMOR TISSUE: THE ENHANCED PERMEABILITY AND RETENTION (EPR) EFFECT

Another factor operates in influencing the passive tumor accumulation of circulating macromolecules. In addition to the enhanced tumor vascular permeability, patterns of the lymphatic drainage are substantially modified in neoplastic tissue (28–32). Indeed, there is now overwhelming evidence that the lymphatic drainage system does not operate effectively in tumor tissue (1–3, 11, 28–32). As a consequence, macromolecular drugs and drug vehicles such as Lipiodol or medium-chain triglycerides are retained for a prolonged period of time in the tumor interstitium (Table II). Lipids and albumin are known to be cleared from the normal interstitium only via drainage through the lymphatics or by action of the reticuloendothelial system (33). However they remain in tumor tissue for a much longer period than in normal tissue, following both direct injection into the tumor and indirect accumulation from the bloodstream (1–3, 11, 23, 28–32) (Figure 4). The combination of poor tissue drainage with increased tumor vascular permeability (described in the preceding section) results in a phenomenon termed the EPR (enhanced permeability and retention) effect. The effect appears to apply to all tumors so far examined, suggesting that passive accumulation of macromolecular drugs may be a universal phenomenon. Hence the rationale justifying the development of macromolecular anticancer drugs is clear. A schematic representation of architectural differences of normal and tumor tissues is shown in Figure 5, in which the high density of tumor blood capillaries, as a result of tumor angiogenesis, and lack of lymphatic capillaries should be noted.

A Normal Tissues



B Tumor Tissues

(Hypervascularity, no lymphatic capillary)

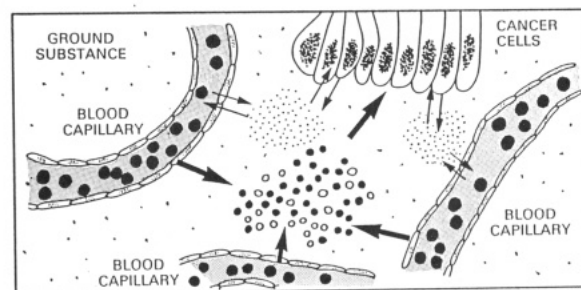


Figure 5. Diagrammatic representation of normal and tumorous vascular structures and transport of various substances into or out of capillaries. Note the much enhanced leakage of macromolecules in tumorous tissue but no lymphatic recovery. Furthermore, there is no backward flow of macromolecules into the blood capillary (from ref 3 with permission).

5. ENHANCEMENT OF MACROMOLECULAR DRUG ACCUMULATION UNDER ANGIOTENSIN II-INDUCED HYPERTENSION AND/OR USE OF KININASE INHIBITOR

Suzuki et al. initially observed that, when angiotensin II was applied to a tumor-bearing animal, the blood flow in tumor tissue was selectively increased, and applied drug could be selectively delivered to tumor tissue (34, 35). However, it is anticipated that low molecular weight compounds may traverse the tumor endothelial barriers more freely than macromolecules as described earlier, resulting in a rapid equilibration of the drug between tumor and blood. Thus, the elevated tumor concentration of drug achieved may be maintained only briefly before a rapid decline for low molecular drugs (unpublished data).

With macromolecular drugs, on the contrary, we found the tumor concentration of the drug was increased about 2-fold even 6 h following administration of angiotensin II. In addition, the drug accumulation by the bone marrow and the small intestine, two representative drug-sensitive normal tissues, decreased under hypertensive therapy to 60–80% of the value of normotensive controls (unpublished data). The enhanced drug deposition in tissue coupled with decreased delivery to normal tissues means that hypertensive chemotherapy could become a very useful chemotherapeutic technique.

A second tactic to improve tumor drug delivery involves manipulation of the local kinin concentration described above. By inhibiting kinin degradation using oral administration of kininase II inhibitor (enalapril), we were able to increase drug delivery to the tumor significantly (23, 25). The usefulness of this method was further confirmed using ^{131}I -labeled monoclonal antibody (A-7) in nude mice bearing SW116 tumor. In these studies, hypertension alone produced about 27% increased drug delivery to the tumor compared with normotensive con-

trols, and the combination of enalapril plus angiotensin II gave about 100% increase (36). In addition, the plasma concentration of the ^{131}I -A-7 remained 50–70% higher in the enalapril-treated group compared with untreated controls, and 86% higher in the combination group (36). These results give a clear indication of the potential therapeutic advantage of these tactics.

6. MODULATION OF IMMUNOGENICITY

Two different types of immune response are expressed in antigen-injected hosts, namely humoral/antibody production and the cellular immune response which involves a number of different types of leukocytes and interleukins.

In earlier studies of the antigenicity of proteins it became evident that some protein modifications resulted in a loss of antigenic potential (37–39). For example, succinylation of proteins or conjugation of poly(D-Glu-D-Ala-D-Lys) or poly(D-Glu-D-Lys) were all found to decrease substantially the immunogenicity of albumin, lactoglobulin, myoglobin, γ -globulin, and lysozyme. Other synthetic polymers and peptides were also found to be effective in modifying immunogenicity (40, 41). Detailed accounts are described in the references. Here we will consider some pharmacologically important proteins, with particular regard to their conversion to nonantigenic states by tailoring with synthetic polymers.

L-Asparaginase is an enzyme produced by *Escherichia coli*, which hydrolyzes L-asparagine to yield L-aspartic acid and ammonia. The depletion of L-asparagine from blood plasma can be used to inhibit tumor growth since L-asparagine is a nutrient essential for the growth of some tumor cells. Asparaginase was first introduced for the treatment of lymphocytic leukemia and lymphoma in the 1960s. However, it was soon found that an anti-L-asparaginase antibody was produced in patients which nullified the pharmacological activity. Another limitation documented was the relatively short plasma half-life ($t_{1/2} = 1.5$ h). These problems were solved simultaneously by conjugating the enzyme with polyethylene glycol (PEG). The immunogenic potential of the conjugate was reduced to about 1% of its native counterpart and plasma circulation was greatly extended (42). Polymer-tailored L-asparaginase is now being developed for clinical applications in the U.S.A. as a second generation drug of L-asparaginase.

Abuchowski et al. initially developed a number of PEG-conjugated proteins including PEG-albumin, -superoxide dismutase, and -catalase. In every case they found the immunogenicity of the protein was greatly reduced following conjugation (43, 44).

The antitumor protein NCS (Mw 12 000) is produced by *Streptomyces carzinostaticus* variant F-41. It is a very potent antitumor agent expressing inhibition of DNA synthesis and cell growth in the nanomolar range (about $0.05 \mu\text{g/mL}$) (45). Although it was anticipated to demonstrate significant antigenicity, it was actually found that very few patients developed antibodies against it (46). Among the bladder cancer patients who did not respond to the drug, it was found that their plasma contained a protease activity that was capable of degrading NCS (46). The very weak immunogenicity found for NCS may be attributed to its very rapid clearance rate ($t_{1/2} = 1.9$ min in mice). Subsequently we developed a polymer conjugate SMANCS, which is described in the following section. In retrospect it crystallized a number of properties important for many macromolecular therapeutic agents: low antigenicity, good stability in vitro and in vivo, a prolonged plasma half-life, lymphotropicity, the ability to cross the

tumor endothelial layer in certain situations, and the possibility for formulation in lipid carriers (1–3).

Immunological properties studied in depth included the capacity of the conjugate to induce antibody, its reactivity to the antibody and also to antibody prepared against the parent protein NCS, and its induction of passive cutaneous anaphylaxis. Each of these tests showed that the antigenicity of NCS was decreased 8–16 times as the conjugate SMANCS (1). It should be noted that these biological responses vary among the strains of the same species and depend on the conditions they are kept under. Recent clinical results suggest that SMANCS could actually be very weakly antigenic, like penicillin (unpublished data), which does not detract from its clinical benefit.

Recently we prepared a conjugate of soybean trypsin inhibitor (Kunitz type, Mw 20 000) with dextran (Mw 6000) (47, 48), testing its immunogenicity before and after conjugation. We found that induction of antibody formation in rabbits was greatly decreased following dextran conjugation, and the passive cutaneous anaphylaxis reaction was decreased in parallel.

Bilirubin oxidase is a fungal extracellular protein of *Myrotherium verrucaria* which was derivatized with PEG (49). When injected subcutaneously with Freund's complete adjuvant, native bilirubin oxidase induced a potent immune response, whereas the corresponding PEG conjugate produced only a minor response (decreased approximately 20-fold). Intravenous injection of PEG-bilirubin oxidase did not induce detectable formation of any antibody (49).

Hershiel et al. prepared a conjugate of bovine adenosine deaminase with PEG and applied it clinically for the treatment of patients with congenital adenosine deaminase deficiency (50). The extended plasma $t_{1/2}$ of the enzyme and the decreased antigenicity made the treatment effective over a period of several months without any adverse immunological effects (50). Similar pharmacokinetic improvements were obtained also for interleukin 2 (51) and interferon-gelatin conjugates (52).

In short, it is now clear that the immunogenicity of proteins can be decreased by conjugation with various polymers. The main challenge now is to maintain the activity of the protein, and this is easier to achieve when the substrate is a small molecule (e.g. asparagine) which can penetrate through the shielding polymer coils, rather than macromolecules or cell surface (53).

7. POLYMER-CONJUGATED ANTICANCER AGENTS

(1) **SMANCS.** SMANCS is a derivative of NCS in which two amino groups, one at the amino-terminal alanine and the other at lysine 20, were used for conjugation with the acid anhydride of maleyl residues in the SMA (Figures 6 and 7). NCS consists of a single-chained polypeptide with 112 amino acids plus two disulfide bridges (54, 55) and a prosthetic chromophore with a highly unstable bicyclododecadienediyne structure (56). In early studies the SMA units used had a mean molecular mass of 5000 Da (57). Subsequently, more refined SMA was prepared with a mean molecular weight of 1500 and a Mw/Mn ratio of 1.2 or less (58). As with NCS, SMANCS' molecular mechanism of action is by induction of DNA damage and inhibition of DNA synthesis (59). In addition, the induction of interferon (mainly γ -type) (60) and the activation of macrophages and killer T-cells have been described (61–63) following SMANCS administration. These effects are typical of the features induced by many materials after polymer conjugation, particularly with polyanions (64, 92). It should be also noted that SMANCS

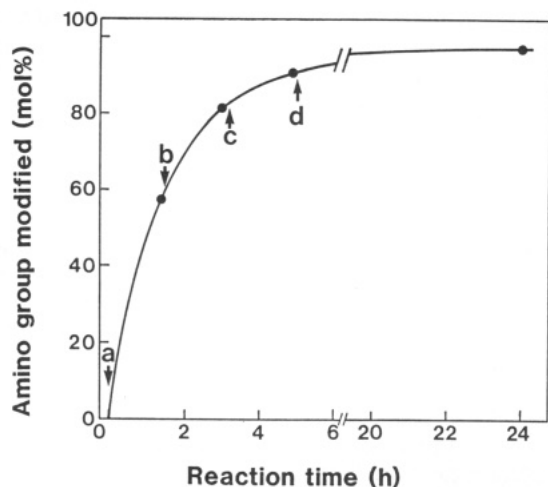


Figure 6. Reaction of NCS with partially hydrolyzed SMA. To a solution of NCS (0.2 g) in 0.8 M NaHCO_3 (5 mL) at 4 °C in the dark was added powdered SMA at the times indicated by the arrows (a, 0.3 g; b, 0.3 g; c, 0.2 g; d, 0.1 g). The reaction mixture was stored in a refrigerator after the complete dissolution of the last addition (d). Twenty-four hours after the start of the reaction, the amino group modified was 97.3 mol % (from ref 58 with permission).

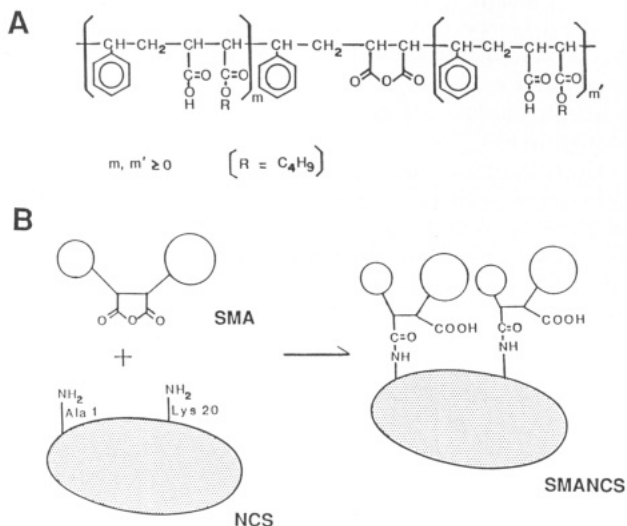


Figure 7. (A) Structure of SMA, poly(styrene-co-maleic acid/anhydride) half butyl ester and (B) diagrammatic representation of the reaction with NCS to produce the conjugate SMANCS.

with molecular weight of 15 000 can bind to albumin; hence, the effective molecular mass of SMANCS in plasma is probably about 83 000 Da as described (10). The non-protein chromophore of NCS appears to be stable during preparation or handling since equivalent molar activity is found to between NCS and SMANCS (58, 59).

The greatly improved stability of NCS as SMANCS in aqueous as well as in lipid medium has been described (65). This seems to be a common feature among many polymer conjugates.

In a pilot clinical study SMANCS demonstrated a remarkable antitumor effect when administered arterially as an oily formulation with the lipid contrast medium Lipiodol (2, 30, 32, 66). All patients entered into this trial had advanced disease and were inoperable. A control group, administered conventional chemotherapy with or without surgery, achieved a median life expectancy of only 6 months (mean about 4 months). As shown in Figure 8, survival rates at years 3 and 4 ranged from 30 to 90%, depending upon the stage and grade of the tumor in patients with hepatocellular carcinoma. It is clear that

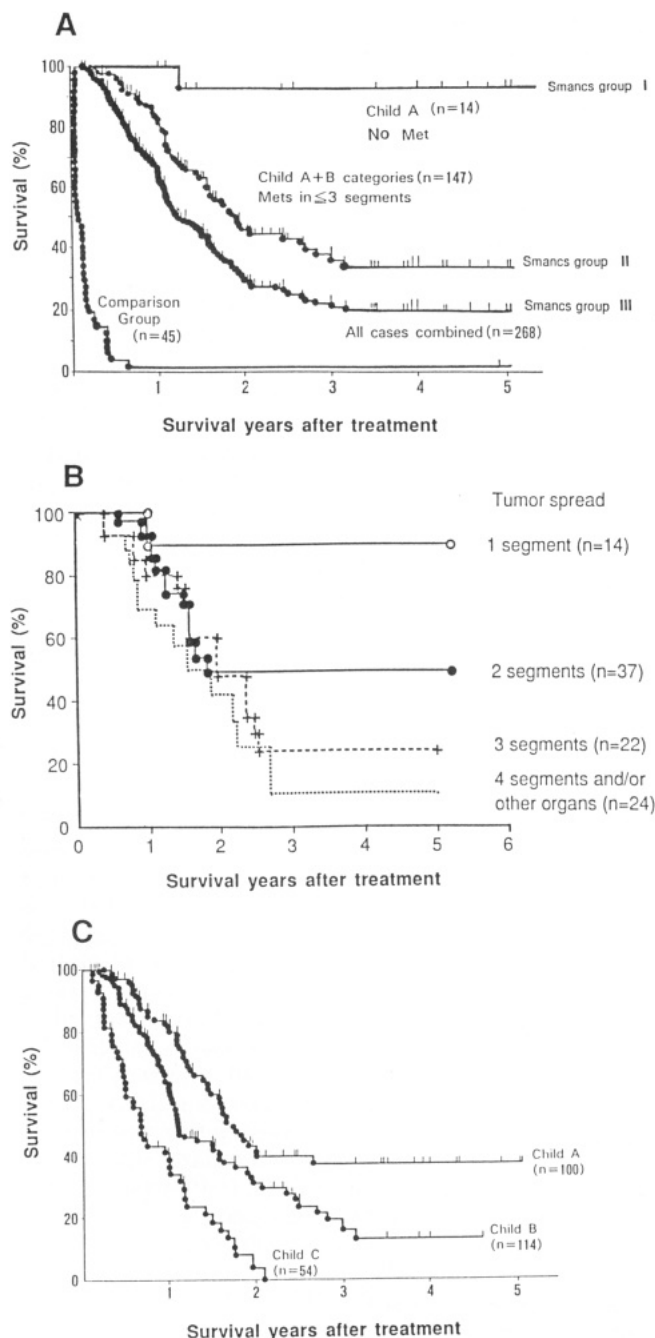


Figure 8. Survival of patients with unresectable hepatocellular carcinoma (HCC) treated with intra-arterial administration of SMANCS/Lipiodol. (A) Comparison of survival of patients after conventional therapy and after SMANCS/Lipiodol. (B) Survival of HCC patients classified according to metastatic spread of tumor in the liver. (C) Survival of HCC patients classified according to the extent of liver cirrhosis (Child class A, B, and C). All SMANCS-treated patients are inoperable and/or in advanced stage (Met, metastasis) (data courtesy of Dr. T. Konno and SMANCS Pilot Study Group, Kumamoto University).

for this tumor, SMANCS treatment represents the only successful procedure. Efficacy in other tumors using intraarterial SMANCS administration is currently undergoing intensive evaluation. Tumors showing an effective response to date include the following: lung cancer (adenocarcinoma and squamous cell carcinoma) (30), renal carcinoma (67), pleural or ascitic carcinomatosis, some pancreatic, bile duct, and ovarian tumors, and leiomyosarcoma (30 and unpublished data).

Intravenous administration of SMANCS in aqueous formulation is also effective. Recently, a significant

regression in tumor size was observed in 95% of chemically-induced mammary tumors in rats, after intravenous administration of aqueous SMANCS, without severe side effects (68). A preliminary clinical study in our group has shown some effect on tumors of the brain, lung (69), esophagus, stomach, kidney, urinary bladder, adrenal gland, colon, and ovary. SMANCS clearly has profound potential and its activity seems broad against a range of tumors; whether it is particularly suited to the treatment of one individual tumor type remains to be established.

(2) Divinyl Ether-co-maleic Anhydride Copolymer-NCS (DIVEMA-NCS or Pyran-NCS). We have prepared this polymer conjugate in an attempt to achieve more selective tumor targeting and longer $t_{1/2}$, while simultaneously decreasing the bone marrow toxicity (70). The polymer (pyran copolymer) has a molecular weight of about 5600 and two chains were conjugated to each NCS molecule in a manner analogous to that of SMANCS. The final conjugate has a molecular weight of about 25 000. It was found that this size was too small to achieve the desired prolonged half-life although a slightly higher tumor concentration was detected, compared with parent NCS, and decreased toxicity (LD_{50} increased 50–70%) was seen. The most interesting aspect was that the bone marrow toxicity was reduced to one-third that of NCS at the same dose, measured using a precise stem cell colony formation assay (70). An important lesson is that this size of drug conjugate is not necessarily large enough to exploit the EPR effect of macromolecular therapeutics. When the same pyran copolymer was conjugated with SOD, resulting in an approximate molecular weight of 40 000, the $t_{1/2}$ (about 10–20 min) was somewhat longer than that of the above NCS derivative of 25 000 Da (71).

(3) Monoclonal Antibody A7-Neocarzinostatin Conjugate (A7-NCS). Takahashi et al. prepared a conjugate of NCS and an anti-human colorectal carcinoma monoclonal antibody A7 (A7-NCS) using *N*-succinimidyl 3-(2-pyridyldithio)propionate (SPDP) as a linker (72). A7 is also known to react with some gastric and mammary tumors. The conjugation ratio was 2–3 mol of NCS/mol of A7 (72). A7-NCS was 4 times more cytotoxic to the cultured human colon cancer cells in vitro than free NCS at the same concentration. Antitumor activity of A7-NCS in vivo was studied in the human tumor xenografted into nude mice. A7-NCS displayed an inhibitory effect on tumor growth with a T/C of 1.22, whereas NCS or A7 alone had no effect. This conjugate was also applied clinically in the treatment of colorectal cancer including patients with postoperative metastasis. Three of the eight patients with liver metastases showed evidence of tumor reduction. In addition a chimeric antibody containing the Fab fragment of A7 and Fc of human immunoglobulin was prepared for conjugation with NCS in order to reduce the production of antibodies against the conjugate (73). Indeed, in an attempt to circumvent the intrinsic problem of anti-A7 antibody generation in vivo, polyethylene glycol-conjugated A7-NCS was also prepared (74). A7 has also been developed as a carrier of mitomycin C (75).

(4) HPMA Copolymer-Doxorubicin Conjugates. Copolymers based on *N*-(2-hydroxypropyl)methacrylamide have been developed extensively as soluble drug carriers, particularly for targeted delivery of drugs (76). The homopolymer is biologically well-tolerated, being essentially nonimmunogenic (77) and without observable toxicity both in in vitro cell systems and in vivo (78). The versatile chemistry of HPMA means that a range of side chains and pendant drugs or targeting moieties can be introduced into the structure, and the resulting conjugates

are usually well-tolerated by biological systems (53, 79, 80). Indeed, HPMA copolymers are capable of decreasing the immunogenicity of proteins conjugated to them (81).

Many different drugs have been linked covalently to the HPMA copolymer backbone, including various anti-cancer agents. Doxorubicin (DOX) has been incorporated using peptide sequences, linking through the amino function of the daunosamine sugar residue. Peptide spacers used here such as Gly-Phe-Leu-Gly were designed to be stable extracellularly but cleaved (and the drug activated) rapidly following pinocytic internalization into cells. The above tetrapeptide spacers proved particularly useful for this purpose since the cleavage of the conjugate by lysosomal enzymes released free DOX in a quantitative fashion (82). In addition targeting groups such as antibodies (53), hormones (83), or simple sugars (84) have been incorporated into the conjugate. The incorporation of galactose is particularly interesting since it affords the possibility of targeting therapeutic doses of DOX into the liver, for organ-specific delivery and treatment of primary hepatoma (85).

Of particular interest has been the mechanism of action and antitumor efficacy of untargeted HPMA copolymer-DOX conjugate. Free DOX has a very short plasma half-life (ca. 2 min in mice) and it diffuses rapidly through membranes, achieving high cardiac concentrations which correlate with a cumulative cardiotoxicity. DOX shows relatively little tumor-selective accumulation (86). HPMA-DOX conjugate, on the other hand, has an extended plasma half-life (ca. 60 min) (87) and shows substantial accumulation in peripheral tumors. Following intravenous administration to mice bearing solid subcutaneous B16F10 melanomas, free DOX (5 mg of DOX/kg of body wt) produced tumor levels of only 0.55 μ g of DOX/g of tumor, while the same dose of DOX administered as polymer conjugate achieved levels of up to 7.5 μ g/g. The decreased cardiotoxicity of polymer-conjugated DOX permits the use of greater doses, and administration of doses of 18 mg DOX/kg results in tumor levels of drug up to 22 μ g/g (Seymour, unpublished observations).

This passive targeting of HPMA copolymer-DOX conjugates to solid tumors is thought to result from their prolonged circulation in the plasma and nonspecific capture by tumors as a result of the EPR effect described earlier. In studies of anticancer efficacy, this tumor accumulation of drugs is mirrored by an impressive therapeutic effect in mice (88, 89). Large numbers of long-term survivors are obtained when the conjugates are used to treat model systems such as intraperitoneal L1210 leukemia, and they also demonstrate remarkable anti-cancer activity when applied to a range of solid rodent and human xenografted tumor systems (82). These conjugates are currently undergoing clinical evaluation in the United Kingdom.

(5) Oxidized Dextran-Anthracycline Conjugates. Bernstein et al. originally showed that dextran oxidized to a polyaldehyde could be coupled to daunomycin, producing a conjugate which actually had greater therapeutic activity than the free drug, as well as decreased toxicity at equivalent doses (90). Subsequently DOX has been coupled to oxidized dextran 70 (OXD-DOX) and the efficacy, toxicity, and pharmacokinetics of the conjugate have been compared with those of free DOX (91). DOX is linked to the polymer via a Schiff's base which is stable at neutral pH, but the conjugate rapidly liberates free DOX in the acidic milieu of the secondary lysosome intracellularly. The conjugate contains about 30% (wt/wt) DOX. While the LD_{50} of OXD-DOX for animals is

about 3–4-fold higher than that for free DOX, the therapeutic efficacy is simultaneously higher than that of the free drug. The plasma level of OXD–DOX was higher and persisted for a longer period compared with that of free DOX, and there was very effective passive tumor targeting. The tumor level of DOX after iv injection of OXD–DOX to S-180 sc tumor-bearing mice was 4 times as much as that after injection of the same dose of free DOX. High concentration of the drug in tumor tissue was also confirmed in the other animal-tumor systems. In addition to the possible enhanced endocytic uptake activity of tumor cells, the EPR effect may account for the tumor accumulation of this conjugate.

(6) DIVEMA–Doxorubicin Conjugate (DIVEMA–DOX). The hydrolyzed copolymer of divinyl ether and maleic anhydride (DIVEMA) demonstrates inherent antitumor activity via stimulation of the immune system (92). The use of macromolecules with their own anticancer action as carriers for cytotoxic agents is a particularly interesting possibility for macromolecular therapeutics. Hirano et al. synthesized conjugates of DOX and DIVEMA (Mw 7000) (DIVEMA–DOX) by reacting the amino group of the drug with the anhydride group of the copolymer, followed by hydrolysis of the remaining anhydride groups (93). The conjugate contained up to 36% (wt/wt) drug and the resulting decreased toxicity made it possible to increase the amount of drug administered (93). When DIVEMA–DOX was injected intraperitoneally into mice bearing an intraperitoneal tumor, the survival rate of the animals was improved. Sixty days following inoculation of tumor, 50% of the DIVEMA–DOX (287 mg/kg as DOX) injected mice were still surviving, while all of the free DOX (10 mg/kg) group survived for less than 3 weeks (93). Prolonged retention of the conjugate in the peritoneal cavity may contribute to the antitumor effect of the drug, although it is also reported that this conjugate is more effective than free DOX for treatment of animals bearing solid tumors (94).

(7) Mitomycin C–Dextran Conjugate (MMC–D). The pharmacokinetics of mitomycin C–dextran conjugates (MMC–D) with various molecular weights (10, 70, and 500 kDa) and electrical charges were studied by Hashida et al. (95, 96). Cationic MMC–D (MMC–D_{cat}), prepared using ϵ -aminocaproic acid as a spacer, exhibited a high affinity for the cell surface *in vitro* and hence showed stronger cytotoxicity compared with free mitomycin C or anionic MMC–D (MMC–D_{an}), prepared using 6-bromohexanoic acid as a spacer (96). When the conjugates were injected intravenously into mice, the plasma $t_{1/2}$ of MMC–D_{an} was much longer than that of MMC–D_{cat}; the latter tended to be trapped by the liver and the blood vessels and cleared from the blood circulation rapidly. MMC–D_{an} (T-70, 70 kDa) showed a persistent high plasma level and gradually accumulated in peripheral solid tumors (95, 96). MMC–D_{an} (T-70) was shown to exhibit a stronger antitumor effect on the subcutaneous S-180 tumor in mice than an equitoxic dose of free mitomycin C (95). This tumoritropic behavior of MMC–D_{an} (T-70) is almost certainly a result of the EPR effect.

(8) Human Immunoglobulin G–Melphalan Conjugate (K-18). K-18 (Mw 15 kDa) is a conjugate of human immunoglobulin G (IgG) with the alkylating agent melphalan (97) containing about five melphalan molecules in each conjugate. It shows similar antitumor activity as melphalan following intravenous or oral administration, but with a reduction of peripheral toxicities such as bone marrow suppression (97). When administered orally, K-18 was absorbed from the small intestine via both the portal

and lymphatic routes and showed a selective distribution into tumor tissue. K-18 showed efficient accumulation by tumor cells but not by bone marrow cells (97). Since the IgG used for preparation of K-18 is not an antitumor antibody, time-dependent intratumoral accumulation of K-18 may also be explained by the EPR effect, possibly followed by pinocytotic internalization into tumor cells.

(9) Other Polymer Conjugates. In addition to the above there are many other studies of macromolecular cytotoxic drug conjugates, including pyran–DOX (98), albumin–daunorubicin (99), gelatin–interferon α (52), transferrin–neocarzinostatin (100), transferrin–rich (100), and polyaspartic acid–DOX (101). The many advantages of macromolecular drug conjugates are clear in each case. However, only a few are currently scheduled for thorough clinical evaluation, including SMANCS, A7–NCS, and K-18 (in Japan) and HPMA–DOX (in the U.K.). In the recent reviews by Duncan (5) and Seymour (4), some other polymer conjugate drugs were discussed. Conjugations with plasma proteins and various enzymes were reviewed by Poznansky and Juliano (102).

8. CONCLUSION

Macromolecular drugs have shown superiority in a number of therapeutic applications, most notably in oncology. The use of antibodies for targeted cancer therapy has shown considerable preclinical promises (103, 104) and many different systems are currently undergoing thorough clinical evaluation (105, 106). As discussed earlier, synthetic macromolecules have achieved particular success in abrogating the immunogenicity of a variety of therapeutic molecules, including many different allogenic enzymes, and adding biological response modifying effects as described briefly. This approach can be particularly powerful when the substrate for recognition is a low molecular weight material such as asparagine, superoxide radical, or bilirubin, capable of penetrating the shielding layer of polymers. However, when the substrate for recognition is another macromolecule or a cell surface it becomes extremely difficult to maintain activity of the protein while simultaneously decreasing its immunogenicity. Currently sophisticated conjugation techniques appear to be the best way to overcome this limitation, but so far success has been limited (4, 5, 107).

Probably the single most important advance resulting from the application of macromolecules in cancer therapy has been the possibility to stabilize low molecular weight drugs in the bloodstream. Not only are the rates of renal excretion of drugs often diminished and their circulation time increased by this process, particularly when the carrier is an inert polymer, but their distribution kinetics, especially tumor accumulation, are also enhanced. Hence such constructs show substantial passive accumulation in peripheral tumors even following intravenous administration. Although use of polymeric carriers is a relatively new innovation, it may make a contribution to the cancer chemotherapy of a number of other established anticancer agents. For example, the widely-used agent methotrexate binds to plasma proteins and presumably shows decreased rates of renal excretion and increased passive accumulation in tumors as a result.

The ingenuity of the pharmaceutical scientist, in combination with angiographic expertise, could take advantage of the EPR effect. Careful choice of administration route, appropriate formulation of the drug, and coapplication of vasoactive agents can sometimes achieve extremely high tumor-to-blood ratios of cytotoxic drugs (28–32, 108). The clinical benefits of some of these approaches have already

been demonstrated against certain diseases, but widespread realization of the potential usefulness of macromolecular drugs is eagerly awaited.

ACKNOWLEDGMENT

L.W.S is grateful for the support of the Cancer Research Campaign. The international interaction has been sponsored by the Japan Society for the Promotion of Science and by the Royal Society. H.M. is grateful for Monbusho (Ministry of Education, Science and Culture) of Japan for supporting the research work described herein.

LITERATURE CITED

- (1) Maeda, H., Matsumoto, T., Konno, T., Iwai, K., and Ueda, M. (1984) Tailor-making of protein drugs by polymer conjugation for tumor targeting. A brief review on smancs. *J. Protein Chem.* 3, 181-193.
- (2) Maeda, H. (1991) SMANCS and polymer-conjugated macromolecular drugs: advantages in cancer chemotherapy. *Adv. Drug Delivery Rev.* 6, 181-202.
- (3) Maeda, H., and Matsumura, Y. (1989) Tumorotropic and lymphotropic principles of macromolecular drugs. *Crit. Rev. Ther. Drug Carrier Syst.* 6, 193-210.
- (4) Seymour, L. (1992) Passive tumour-targeting of soluble macromolecules and drug conjugates. *Crit. Rev. Ther. Drug Carrier Syst.* 9, 135-187.
- (5) Duncan, R. (1992) Drug-polymer conjugates: potential for improved chemotherapy. *Anti-Cancer Drugs* (in press).
- (6) Shelanski, H. A., and Shelanski, M. V. (1956) PVP-iodine: history, toxicity and therapeutic uses. *J. Intern. Coll. Surgeons* 25, 727-734.
- (7) Takakura, Y., Takagi, A., Hashida, M., and Sezaki, H. (1987) Disposition and tumor localization of mitomycin C-Dextran conjugates in mice. *Pharm. Res.* 4, 293-300.
- (8) Maeda, H., Matsumura, Y., Oda, T., and Sasamoto, K. (1986) Cancer selective macromolecular therapeutics: tailoring of an antitumor protein drug. *Protein Tailoring for Food and Medical Uses* (R. E. Feeny and J. R. Whitaker, Eds.) pp 353-382, Marcel Dekker Inc., New York.
- (9) Ogino, T., Inoue, M., Ando, Y., Arai, M., Maeda, H., and Morino, Y. (1988) Chemical modification of superoxide dismutase. Extension of plasma half-life of the enzyme through its reversible binding to the circulating albumin. *Int. J. Pept. Protein Res.* 32, 153-159.
- (10) Kobayashi, A., Oda, T., and Maeda, H. (1988) Protein binding of macromolecular anticancer agent SMANCS: Characterization of poly(styrene-comaleic acid) derivatives as an albumin binding ligand. *J. Bioact. Compat. Polym.* 3, 319-328.
- (11) Matsumura, Y., and Maeda, H. (1986) A new concept for macromolecular therapeutics in cancer chemotherapy: Mechanism of tumorotropic accumulation of proteins and antitumor agent smancs. *Cancer Res.* 46, 6387-6392.
- (12) Seymour, L. W., Duncan, R., Strohalm, J., and Kopecek, J. (1987) Effect of molecular weight (Mw) of N-(2-hydroxypropyl)methacrylamide copolymers on body distribution and rate of excretion after subcutaneous, intraperitoneal and intravenous administration to rats. *J. Biomed. Mater. Res.* 21, 1341-1358.
- (13) Matsumoto, K., Yamamoto, T., Kamata, R., and Maeda, H. (1986) Enhancement of vascular permeability upon serratia infection: Activation of Hageman factor-kallikrein-kinin cascade. *Kinin IV, part B* (L. B. Greenbaum and H. S. Margolis, Ed.) pp 71-78 (AEMB 198B), Plenum Press, New York.
- (14) Senger, D. R., Galli, S. J., Dvorak, A. M., Perruzzi, C. A., Harvey, V. S., and Dvorak, H. F. (1983) Tumor cells secrete a vascular permeability factor that promotes accumulation of ascitic fluid. *Science* 219, 983-985.
- (15) Dvorak, H. F., Nagy, J. A., Dvorak, J. T., and Dvorak, A. M. (1988) Identification and characterization of the blood vessels of solid tumors that are leaky to circulating macromolecules. *Am. J. Pathol.* 133, 95-109.
- (16) Leung, D. W., Cachianes, G., Kuang, W.-J., Goeddel, D. V., and Ferrara, N. (1989) Vascular endothelial growth factor is a secreted angiogenic mitogen. *Science* 246, 1306-1309.
- (17) Keck, P. J., Hauser, S. D., Krivi, G., Sanzo, K., Warren, T., Feder, J., and Connolly, D. T. (1989) Vascular permeability factor and endothelial cell mitogen related to PDGF. *Science* 246, 1309-1312.
- (18) Senger, D. R., Perruzzi, C. A., Feder, J., and Dvorak, H. F. (1986) A highly conserved vascular permeability factor secreted by a variety of human and rodent tumor cells. *Cancer Res.* 46, 5629-5632.
- (19) Senger, D. R., Connolly, D. T., Van de Water, L., Feder, J., and Dvorak, H. F. (1990) Purification and NH₂-terminal amino acid sequences of guinea pig tumor-secreted vascular permeability factor. *Cancer Res.* 50, 1774-1778.
- (20) Brock, T. A., Dvorak, H. F., and Senger, D. (1991) Tumor-secreted vascular permeability factor increases cytosolic calcium and von Willebrand factor release in human endothelial cells. *Am. J. Pathol.* 138, 213-221.
- (21) Olander, J. V., Connolly, D. T., and DeLarco, J. E. (1991) Specific binding of vascular permeability factor to endothelial cells. *Biochem. Biophys. Res. Commun.* 175, 68-76.
- (22) Maeda, H., Matsumura, Y., and Kato, H. (1988) Purification and identification of [hydroxypropyl³]-bradykinin in ascitic fluid from a patient with gastric cancer. *J. Biol. Chem.* 263, 16051-16056.
- (23) Matsumura, Y., Kimura, M., Yamamoto, T., and Maeda, H. (1988) Involvement of kinin-generating cascade in enhanced vascular permeability in tumor tissue. *Jpn. J. Cancer Res.* 79, 1327-1334.
- (24) Matsumura, Y., Maruo, K., Kimura, M., Yamamoto, T., Konno, T., and Maeda, H. (1991) Kinin-generating cascade in advanced cancer patients and in vitro study. *Jpn. J. Cancer Res.* 82, 732-741.
- (25) Matsumura, Y., Maeda, H., and Kato, H. (1990) Degradation pathway of kinins in tumor ascites and inhibition by kininase inhibitors: Analysis by HPLC. *Agents Actions* 29, 172-180.
- (26) Fleck, A., Hawker, F., Wallace, P. I., Raines, G., Trotter, J., Ledingham, I. McA., and Calman, K. C. (1985) Increased vascular permeability: A major cause of hypoalbuminemia in disease and injury. *Lancet* Apr 6, 781-784.
- (27) Ettinghausen, S. E., Puri, R. J., and Rosenberg, S. A. (1988) Increased vascular permeability in organs mediated by the systemic administration of lymphokine-activated killer cells and recombinant interleukin-2 in mice. *J. Natl. Cancer Inst.* 80, 177-187.
- (28) Iwai, K., Maeda, H., and Konno, T. (1984) Use of oily contrast medium for selective drug targeting to tumor: Enhanced therapeutic effect and X-ray image. *Cancer Res.* 44, 2114-2121.
- (29) Iwai, K., Maeda, H., Konno, T., Matsumura, Y., Yamashita, R., Yamasaki, K., Hirayama, S., and Miyauchi, Y. (1987) Tumor targeting by arterial administration of lipids: Rabbit model with VX-2 carcinoma in the liver. *Anticancer Res.* 7, 321-328.
- (30) Konno, T., Maeda, H., Iwai, K., Maki, S., Tashiro, S., Uchida, M., and Miyauchi, Y. (1984) Selective targeting of anticancer drug and simultaneous image enhancement in solid tumors by arterially administered lipid contrast medium. *Cancer* 54, 2367-2374.
- (31) Maki, S., Konno, T., and Maeda, H. (1985) Image enhancement in computerized tomography for sensitive diagnosis of liver cancer and semiquantitation of tumor selective drug targeting with oily contrast medium. *Cancer* 56, 751-757.
- (32) Konno, T., Maeda, H., Iwai, K., Tashiro, S., Maki, S., Morinaga, T., Mochinaga, M., Hiraoka, T., and Yokoyama, I. (1983) Effect of arterial administration of high-molecular-weight anticancer agent SMANCS with lipid lymphographic agent on hepatoma: A preliminary report. *Eur. J. Cancer Clin. Oncol.* 19, 1053-1065.
- (33) Coutice, F. C. (1963) The origin of lipoprotein in lymph. *Lymph and the Lymphatic System*. (Meyersen, H. S., Chairman) pp 89-126, C. C. Thomas, Springfield, IL.
- (34) Suzuki, M., Hori, K., Abe, I., Saito, S., and Sato, H. (1981) A new approach to cancer chemotherapy: Selective enhance-

- ment of tumor blood flow with angiotensin II. *J. Natl. Cancer Inst.* 67, 663-669.
- (35) Hori, K., Suzuki, M., Abe, I., Saito, S., and Sato, H. (1985) Increase in tumor vascular area due to increased blood flow by angiotensin II in rats. *J. Natl. Cancer Inst.* 74, 453-459.
 - (36) Noguchi, A., Takahashi, T., Yamaguchi, T., Kitamura, K., Noguchi, A., Tsurumi, H., Takashima, K., and Maeda, H. (1992) Enhanced tumor localization of monoclonal antibody by treatment with kininase II inhibitor and angiotensin II. *Jpn. J. Cancer Res.* 83, 240-243.
 - (37) Sela, M. (1969) Antigenicity: Some molecular aspects. *Science* 166, 1365-1374.
 - (38) Habeeb, A. F. S. A., Cassidy, H. G., and Singer, S. F. (1958) Molecular structural effects produced in proteins by reaction with succinic anhydride. *Biochim. Biophys. Acta* 29, 587-593.
 - (39) Jones, V. E., and Leskowitz, S. (1965) Role of the carrier in development of delayed sensitivity to the azophenyl-azonate group. *Nature* 207, 596-597.
 - (40) Rajnavolgyi, E., Hudecz, F., Mezo, G., Szekerke, M., and Gergely, J. (1986) Isotope distribution and fine specificity of the antibody response of inbred mouse strain to four compounds belonging to a new group of synthetic branched polypeptide. *Mol. Immunol.* 23, 27-37.
 - (41) Hunter, R. L., and Bennet, B. (1984) The adjuvant activity of nonionic block polymer surfactants. Antibody formation and inflammation related to the structure of triblock and octablock copolymer. *J. Immunol.* 133, 3167-3175.
 - (42) Kamisaki, Y., Wada, H., Yagura, H., Matsushima, A., and Inada, Y. (1981) Reduction in immunogenicity and clearance rate of *Escherichia coli* L-asparaginase by modification with monomethoxypoly(ethylene glycol). *J. Pharmacol. Exp. Ther.* 216, 410-414.
 - (43) Abuchowski, A., Es, T. V., Palczuk, N. C., and Davis, F. F. (1977) Alteration of immunological properties of bovine serum albumin by covalent attachment of polyethylene glycol. *J. Biol. Chem.* 252, 3578-3581.
 - (44) Abuchowski, A., McCoy, J. R., Palczuk, N. C., Es, T. V., and Davis, F. F. (1977) Effect of covalent attachment of polyethylene glycol on immunogenicity and circulating life of bovine liver catalase. *J. Biol. Chem.* 252, 3582-3586.
 - (45) Maeda, H. (1981) Neocarzinostatin in cancer chemotherapy—A review. *Anticancer Res.* 1, 175-186.
 - (46) Sakamoto, S., Maeda, H., Matsumoto, T., and Ogata, J. (1978) Experimental and clinical studies on the formation of antibody to neocarzinostatin, a new protein antibiotic. *Cancer Treat. Rep.* 62, 2063-2070.
 - (47) Takakura, T., Kaneko, Y., Fujita, T., Hashida, M., Maeda, H., and Sezaki, H. (1989) Control of pharmaceutical properties of soybean trypsin inhibitor by conjugation with dextran. I. Synthesis and characterization. *J. Pharm. Sci.* 78, 117-121.
 - (48) Takakura, Y., Fujita, T., Hashida, M., Maeda, H., and Sezaki, H. (1989) Control of pharmaceutical properties of soybean trypsin inhibitor by conjugation with dextran. II. Biopharmaceutical and pharmacological properties. *J. Pharm. Sci.* 78, 219-222.
 - (49) Kimura, M., Matsumura, Y., Miyauchi, Y., and Maeda, H. (1988) A new tactic for the treatment of jaundice: An injectable polymer-conjugated bilirubin oxidase. *Proc. Soc. Exp. Biol. Med.* 188, 364-369.
 - (50) Hershfield, M. S., Buckley, R. H., Greenberg, M. L., Melton, A. L., Schiff, R., Hatem, C., Kurtzberg, J., Martert, M. L., Kobayashi, R. H., Kobayashi, A. L., and Abuchowski, A. (1987) Treatment of adenosine deaminase deficiency with polyethylene glycol-modified adenosine deaminase. *New Engl. J. Med.* 316, 589-596.
 - (51) Katre, N. V., Knauf, M. J., and Laird, W. J. (1987) Chemical modification of recombinant interleukin 2 by polyethylene glycol increases its potency in murine Meth A sarcoma model. *Proc. Natl. Acad. Sci.* 84, 1487-1491.
 - (52) Tabata, Y., Uno, K., Yamaoka, T., Ikada, Y., and Muramatsu, S. (1991) Effect of recombinant α -interferon-gelatin conjugate on in vivo murine tumor cell growth. *Cancer Res.* 51, 5532-5538.
 - (53) Seymour, L. W., Flanagan, P. A., Al-Shamkhani, A., Subr, V., Ulbrich, K., Cassidy, J. A., and Duncan, R. (1991) Synthetic polymers conjugated to monoclonal antibodies: Vehicles for tumour-targeted drug delivery. *Sel. Cancer Ther.* 7, 59-73.
 - (54) Kuromizu, K., Tsunawasa, S., Maeda, H., Abe, O., and Sakiyama, F. (1986) Reexamination of the primary structure of an antitumor protein, neocarzinostatin. *Arch. Biochem. Biophys.* 246, 199-205.
 - (55) Kuromizu, K., Abe, O., and Maeda, H. (1991) Location of the disulfide bonds in the antitumor protein, neocarzinostatin. *Arch. Biochem. Biophys.* 286, 569-573.
 - (56) Edo, K., Mizugaki, M., Koide, Y., Seto, H., Furihata, K., Otake, N., and Ishida, N. (1985) The structure of neocarzinostatin chromophore possessing a novel bicyclo-(7,3,0)-dodecadiene system. *Tetrahedron Lett.* 26, 331-334.
 - (57) Maeda, H., Takeshita, J., and Kanamura, R. (1979) A lipophilic derivative of neocarzinostatin. *Int. J. Pept. Protein Res.* 14, 81-87.
 - (58) Maeda, H., Ueda, M., Morinaga, T., and Matsumoto, T. (1985) Conjugation of poly(styrene-co-maleic acid) derivative to the antitumor protein neocarzinostatin: Pronounced improvements in pharmacological properties. *J. Med. Chem.* 29, 455-461.
 - (59) Oda, T., Sato, F., Yamamoto, H., Akagi, M., and Maeda, H. (1987) Cytotoxicity of smancs in comparison with other anticancer agents against various cells in culture. *Anticancer Res.* 9, 261-266.
 - (60) Suzuki, F., Munakata, T., and Maeda, H. (1988) Interferon induction by SMANCS. *Anticancer Res.* 8, 97-104.
 - (61) Oda, T., Morinaga, T., and Maeda, H. (1986) Stimulation of macrophage by polyanions and its conjugated proteins and effect on cell membrane. *Proc. Soc. Exp. Biol. Med.* 181, 9-17.
 - (62) Suzuki, F., Pollard, R. B., and Maeda, H. (1989) Stimulation of non-specific resistance to tumor in the mouse using a poly-(maleic acid-styrene) conjugated neocarzinostatin. *Cancer Immunol. Immunother.* 30, 97-104.
 - (63) Suzuki, F., Pollard, R. B., Uchimura, S., Munakata, T., and Maeda, H. (1990) Role of natural killer cells and macrophages in the non-specific resistance to tumors in mice stimulated with SMANCS. A polymer-conjugated derivative of neocarzinostatin. *Cancer Res.* 50, 3897-3904.
 - (64) Seymour, L. (1991) Synthetic polymers with intrinsic anticancer activity. *J. Bioact. Compat. Polym.* 6, 178-216.
 - (65) Hirayama, S., Sato, F., Oda, T., and Maeda, H. (1986) Stability of high molecular weight anticancer agent SMANCS and its transfer from oil-phase to water-phase. *Jpn. J. Antibiot.* 39, 815-822.
 - (66) Konno, T., and Maeda, H. (1987) Targeting chemotherapy of hepatocellular carcinoma: arterial administration of smancs/lipiodol. *Neoplasm of the Liver* (K. Okuda and K. G. Ishak, Ed.) Chapter 27, pp 343-352, Springer-Verlag, New York.
 - (67) Kobayashi, M., Imai, K., Sugihara, S., Maeda, H., Konno, T., and Yamanaka, H. (1991) Tumor targeted chemotherapy with lipid contrast medium and macromolecular anticancer drug (SMANCS) for renal cell carcinoma. *Urology* 37, 288-294.
 - (68) Kimoto, A., Konno, T., Kawaguchi, T., Miyauchi, Y., and Maeda, H. (1992) Antitumor effects of SMANCS on rat mammary tumor induced by 7, 12 dimethylbenz[a]anthracene. *Cancer Res.* 52, 1013-1017.
 - (69) Maeda, H. (1992) The tumor blood vessel as an ideal target for macromolecular anticancer agents. *J. Controlled Release* 19, 315-324.
 - (70) Yamamoto, H., Miki, T., Oda, T., Hirano, T., Sera, Y., Akagi, M., and Maeda, H. (1990) Reduced bone marrow toxicity of neocarzinostatin by conjugation with divinylether-maleic acid copolymer. *Eur. J. Cancer* 26, 253-260.
 - (71) Maeda, H., Oda, T., Matsumura, Y., and Kimura, M. (1988) Improvement of pharmacological properties of protein drug by tailoring with synthetic polymers. *J. Bioact. Compat. Polym.* 3, 27-43.
 - (72) Takahashi, T., Yamaguchi, T., Kitamura, K., Suzuyama, H., Honda, M., Yokota, Y., Kotanagi, Y., Takahashi, M., and Hashimoto, Y. (1988) Clinical application of monoclonal antibody drug conjugates for immunotargeting chemotherapy of colorectal carcinoma. *Cancer* 61, 25-33.
 - (73) Takahashi, T., Yamaguchi, T., Kitamura, K., and Noguchi, A. Targeting chemotherapy using monoclonal antibody-drug

- conjugate for patients with digestive cancers. *Proceeding of the Second Joint Meeting of the American Association for Cancer Research and the Japanese Cancer Association. "Molecular Oncology as a Basis for New Strategies in Cancer Therapy"*; February 10-14, 1992, Hawaii.
- (74) Kitamura, K., Takahashi, T., Yamaguchi, T., Noguchi, A., Noguchi, A., Takashima, K., Tsurumi, H., Inagake, M., Toyokuni, T., and Hakomori, S. (1991) Chemical engineering of the monoclonal antibody A7 by polyethylene glycol for targeting cancer chemotherapy. *Cancer Res.* 51, 4310-4315.
- (75) Suzuki, T., Sato, E., Goto, K., Katsurada, Y., Unno, K., and Takahashi, T. (1981) The preparation of mitomycin C, adriamycin and daunomycin covalently bound to antibodies as improved cancer chemotherapeutic agents. *Chem. Pharm. Bull.* 29, 844-848.
- (76) Kopecek, J., Rejmanova, P., Duncan, R., and Lloyd, J. B. (1985) Controlled release of drug model from N-(2-hydroxypropyl)methacrylamide copolymers. *Ann. N.Y. Acad. Sci.* 446, 93-104.
- (77) Rihova, B., Kopecek, J., Ulbrich, K., and Chytrý, V. (1985) Immunogenicity of N-(2-hydroxypropyl)methacrylamide copolymers. *Makromol. Chem., Suppl.* 9, 13-24.
- (78) Duncan, R. (1985) Biological effects of soluble synthetic polymers as drug carriers. *CRC Crit. Rev. Ther. Drug Carrier Syst.* 4, 281-310.
- (79) Rihova, B., Ulbrich, K., Strohalm, J., Vetricka, V., Bilej, M., Duncan, R., and Kopecek, J. (1989) Biocompatibility of N-(2-hydroxypropyl)methacrylamide copolymers containing adriamycin. Immunogenicity, effect on haematopoietic stem cells in bone marrow in vivo and effect on mouse splenocytes and human peripheral blood lymphocytes in vitro. *Biomaterials* 10, 335-342.
- (80) Flanagan, P. A., Kopeckova, P., Kopecek, J., and Duncan, R. (1989) Evaluation of antibody-N-(2-hydroxypropyl)methacrylamide copolymer conjugates as targetable drug carriers. 1. Binding, pinocytic uptake and intracellular distribution of anti-transferrin receptor antibody-conjugates. *Biochim. Biophys. Acta* 993, 83-91.
- (81) Flanagan, P. A., Rihova, B., Subr, V., Kopecek, J., and Duncan, R. (1990) Immunogenicity of protein-N-(2-hydroxypropyl)methacrylamide copolymer conjugates measured in A/J and B10 mice. *J. Bioact. Compat. Polym.* 5, 151-166.
- (82) Duncan, R., Seymour, L. W., O'Hare, K. B., Flanagan, P. A., Wedge, S., Ulbrich, K., Strohalm, J., Subr, V., Spreafico, F., Grandi, M., Ripamonti, M., Farao, M., Suarato, A. (1992) Preclinical evaluation of polymer-bound doxorubicin. *J. Controlled Release* 18, 123-132.
- (83) O'Hare, K. B., Duncan, R., Strohalm, J., Kopeckova, P., Kopecek, J., and Ulbrich, K. Macromolecular prodrugs containing doxorubicin and melanocyte stimulating hormone in vitro and in vivo evaluation against murine melanoma. *Br. J. Cancer* (in press).
- (84) Duncan, R., Seymour, L. C. W., Scarlett, L., Lloyd, J. B., Rejmanova, P., and Kopecek, J. (1986) N-(2-hydroxypropyl)methacrylamide copolymers with pendant galactosamine residues. Fate after intravenous administration to rats. *Biochim. Biophys. Acta* 880, 62-71.
- (85) Seymour, L. W., Ulbrich, K., Strohalm, J., and Duncan, R. (1991) Pharmacokinetics of a polymeric drug carrier targeted to the hepatocyte galactose receptor. *Br. J. Cancer* 63, 859-866.
- (86) Stallard, S., Morrison, J. G., George, W. D., and Kaye, S. B. (1990) Distribution of doxorubicin to normal breast and tumor tissue in patients undergoing mastectomy. *Cancer Chemother. Pharmacol.* 25, 286-290.
- (87) Seymour, L. W., Ulbrich, K., Strohalm, J., Kopecek, J., and Duncan, R. (1990) Pharmacokinetics of polymer-bound adriamycin. *Biochem. Pharmacol.* 39, 1125-1131.
- (88) Duncan, R., Kopeckova-Rejmanova, P., Strohalm, J., Hume, I., Lloyd, J. B., and Kopecek, J. (1988) Anticancer agents coupled to N-(2-hydroxypropyl)methacrylamide copolymers. 2. Evaluation of daunomycin conjugates in vivo against L1210 leukaemia. *Br. J. Cancer* 57, 147-156.
- (89) Duncan, R., Hume, I. C., Kopeckova, P., Ulbrich, K., Strohalm, J., and Kopecek, J. (1989) Anticancer agents coupled to N-(2-hydroxypropyl)methacrylamide copolymers. 3. Evaluation of adriamycin conjugates against mouse leukaemia L1210 in vivo. *J. Controlled Release* 10, 51-63.
- (90) Bernstein, A., Hurwitz, E., Maron, R., Arnon, R., Sela, M., and Wilchek, M. (1978) Higher antitumor efficacy of daunomycin when linked to dextran: In vivo and in vitro studies. *J. Natl. Cancer Inst.* 60, 379-384.
- (91) Fujita, H., Okamoto, M., and Takao, A. (1991) Pharmacokinetics of adriamycin-oxidized dextran conjugate (ADM-OXD) in experimental animals (in Japanese). *Drug Delivery Syst.* 6, 133-138.
- (92) Merigan, T. C., and Regelson, W. (1967) Interferon induction in man by a synthetic polyanion of defined composition. *N. Engl. J. Med.* 277, 1283-1287.
- (93) Hirano, T., Ohashi, S., Morimoto, S., Tsuda, K., Kobayashi, T., and Tsukagoshi, S. (1986) Synthesis of antitumor-active conjugates of adriamycin or daunomycin with the copolymer of divinyl ether and maleic anhydride. *Makromol. Chem.* 187, 2815-2824.
- (94) Ohashi, S., Hirano, T., Morimoto, S., Kobayashi, T., Inaba, M., and Tsukagoshi, S. (1987) Antitumor activity of the conjugate of adriamycin with the copolymer of divinyl ether and maleic anhydride against M5076 fibrosarcoma. *Proceedings of 46th annual meeting of the Japanese Cancer Association*. No. 1624. September, 1987, Tokyo (in Japanese).
- (95) Sezaki, H., and Hashida, M. (1984) Macromolecule-drug conjugates in targeted cancer chemotherapy. *CRC Crit. Rev. Ther. Drug Carrier Syst.* 1, 1-38.
- (96) Takakura, Y., Kitajima, M., Matsumoto, S., Hashida, M., and Sezaki, H. (1987) Development of a novel polymeric prodrug of mitomycin C, mitomycin C-dextran conjugate with anionic charge. I. Physicochemical characteristics and in vivo and in vitro antitumor activities. *Int. J. Pharm.* 37, 135-143.
- (97) Nio, Y., Imai, S., Ohgaki, K., and Tobe, T. (1988) Selective accumulation of a new antineoplastic agent, K-18 (human immunoglobulin conjugated melphalan), in Ehrlich carcinoma transplanted in mice. *In Vivo* 2, 177-188.
- (98) Zunino, F., Pratesi, G., and Pezzoni, G. (1987) Increased therapeutic efficacy and reduced toxicity of doxorubicin linked to pyran copolymer via the side chain of the drug. *Cancer Treat. Rep.* 71, 367-373.
- (99) Trouet, A., Masquelier, M., Baurain, R., and Campeneere, D. D.-D. (1982) A covalent linkage between daunorubicin and proteins that is stable in serum and reversible by lysosomal hydrolases, as required for a lysosomotropic drug-carrier conjugate: in vitro and in vivo studies. *Proc. Natl. Acad. Sci. U.S.A.* 79, 626-629.
- (100) Kohgo, Y., Nittsu, Y., Nishisato, T., Urushizaki, Y., Kondo, H., Fukushima, M., Tsushima, N., and Urushizaki, I. (1985) Transferrin receptors of tumor cells-potential tools for diagnosis and treatment of malignancies. In *Proteins of iron storage and transport*. (J. Spik, J. Montreuil, R. R. Crichton, and J. Mazurier, Eds.) pp 155-169, Elsevier Science Publishers B. V., Amsterdam.
- (101) Bogliolo, G., Muzzulini, C., Lerza, R., and Pannacchiulli, I. (1986) Activity of doxorubicin linked to poly-L-aspartic acid on normal murine hematopoietic progenitor cells. *Cancer Treat. Rep.* 70, 1275-1281.
- (102) Poznansky, M. J., and Juliano, R. L. (1984) Biological approaches to the controlled delivery of drugs: A critical review. *Pharmacol. Rev.* 36, 277-336.
- (103) Wallace, P. M., and Senter, P. D. (1991) In vitro and in vivo activities of monoclonal antibody-alkaline phosphatase conjugates in combination with phenol mustard phosphate. *Bioconjugate Chem.* 2, 349-352.
- (104) Melton, R. G., Searle, F., Sherwood, R. F., Bagshawe, K. D., and Bden, J. A. (1990) The potential of carboxypeptidase G2: Antibody conjugates as anti-tumour agents. II. In vivo localising and clearance properties in a choriocarcinoma model. *Br. J. Cancer* 61, 420-424.
- (105) Bagshawe, K. D., Sharma, S. K., Springer, C. J., Antoniwi, P., Boden, J. A., Rogers, G. T., Burke, P. J., Melton, R. G., and Sherwood, R. F. (1991) Antibody directed enzyme prodrug therapy (ADEPT): A clinical report. *Dis. Markers* 9, 233-238.
- (106) Vitetta, E. S., Stone, M., Amlot, P., Fay, J., May, R., Till, M., Newman, J., Clark, P., Collins, R., Cunningham, D., Ghetie,

- V., Uhr, J. W., and Thorpe, P. E. (1991) Phase I immunotoxin trial in patients with B-cell lymphoma. *Cancer Res.* 51, 4052-4058.
- (107) Goldberg, J. A., Thomson, J. A. K., Brodnam, M. S., Fenner, J., Bessent, R. G., McKillop, J. H., Kerr, D. J. and McArdle, C. S. (1991) Angiotensin II as a potential method of targeting cytotoxic-loaded microspheres in patients with colorectal liver metastases. *Br. J. Cancer* 64, 114-119.
- (108) Seymour, L. W., Flanagan, P. A., Al Shamkhani, A., Subr, V., Ulbrich, K., Cassidy, J., and Duncan, R. (1991) Synthetic polymers conjugated to monoclonal antibodies: Vehicles for tumour-targeted drug delivery. *Select. Cancer Ther.* 7, 59-73.
- (109) Bartholeyns, J., and Moore, S. (1974) Pancreatic ribonuclease: enzymatic and physiological properties of a cross-linked dimer. *Science* 186, 444-445.
- (110) Buys, C. H. C. M., Dejong, A. S. H., Bouma, J. D. W., and Gruber, M. (1975) Rapid uptake by liver sinusoidal cells of serum albumin modified with retention of its compact conformation. *Biochim. Biophys. Acta* 392, 95-100.
- (111) Ney, K. A., Gidwitz, S., and Pizzo, S. V. (1985) Binding and endocytosis of α_2 -macroglobulin-plasmin complex. *Biochemistry* 24, 4586-4592.

LETTERS

Immobilization of Human Thrombomodulin on Glass Beads and Its Anticoagulant Activity

Mitsuru Akashi,^{*†} Ikuro Maruyama,^{*‡} Norihiro Fukudome,[§] and Eiji Yashima[†]

Department of Applied Chemistry and Chemical Engineering, Faculty of Engineering, Kagoshima University, 1-21-40 Korimoto, Kagoshima 890, Japan, The Third Department of Internal Medicine, Faculty of Medicine, Kagoshima University, Usuki-cho 1208, Kagoshima 890, Japan, and Department of Industrial Chemistry, Miyakonojo National College of Technology, 473-1 Yoshio, Miyakonojo, Miyazaki 885, Japan.
Received May 27, 1992

Human thrombomodulin (TM) was for the first time immobilized on glass beads by the reaction between the carboxyl group of TM and the amino group of glass beads using water-soluble carbodiimide. Immobilized human TM exhibited both anticoagulant activity and inhibition of platelet aggregation of human blood.

Thrombomodulin (TM) is a newly described endothelial cell associated protein that functions as a potent natural anticoagulant by converting thrombin from a procoagulant protease to an anticoagulant (1, 2). Very recently, the preparation of human TM was achieved by using gene technology (3, 4), and since then biomaterials containing human TM have been of interest. The antithrombogenicity of immobilized TM has previously been demonstrated by Miura et al. using bovine lung TM that had been bound to agarose (5). In this study we were able to use recombinant human TM.

In a previous paper (6), we showed that poly(vinyl chloride) (PVC) containing heparin-immobilized hydrogels provides high antithrombogenicity and PVC containing prostaglandin I₂-immobilized hydrogels inhibits platelet aggregation sufficiently. The results show that the combination of pharmaceutically active compounds and polymer materials is important for development of antithrombogenic biomaterials.

In this article, we report the immobilization of human TM on glass beads as a first part of our study on human TM conjugated biomaterials.

As shown in Scheme I, TM is an integral membrane protein and the active site of it has been thought to be located on the surface of blood vessel endothelia. Because only the amino terminal part of TM is involved in the interaction with thrombin, TM was immobilized on the surface of the glass by means of its carboxyl terminal part. The condensation between the amino group of *N*-(2-aminoethyl)-3-aminopropyl-substituted glass and the carboxyl group of TM using water-soluble carbodiimide gave glass-immobilized TM in a 0.2 M phosphate buffer

Scheme I. Antithrombogenicity of the Endothelial Cell Surface

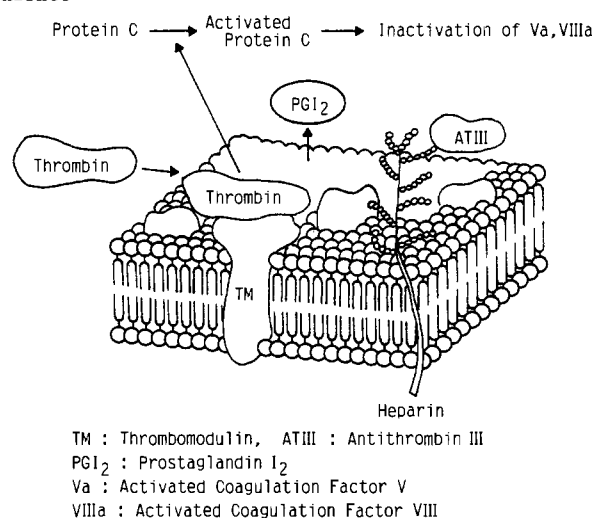


Table I. Activated Partial Thromboplastin Time (aPTT) of Glass-TM

sample	aPTT (s)	
	$3.3 \times 10^{-3} \mu\text{g}/\mu\text{L}^a$	$6.6 \times 10^{-3} \mu\text{g}/\mu\text{L}^a$
glass-TM	32	35
glass	28	31

^a Final concentration of glass-TM or glass.

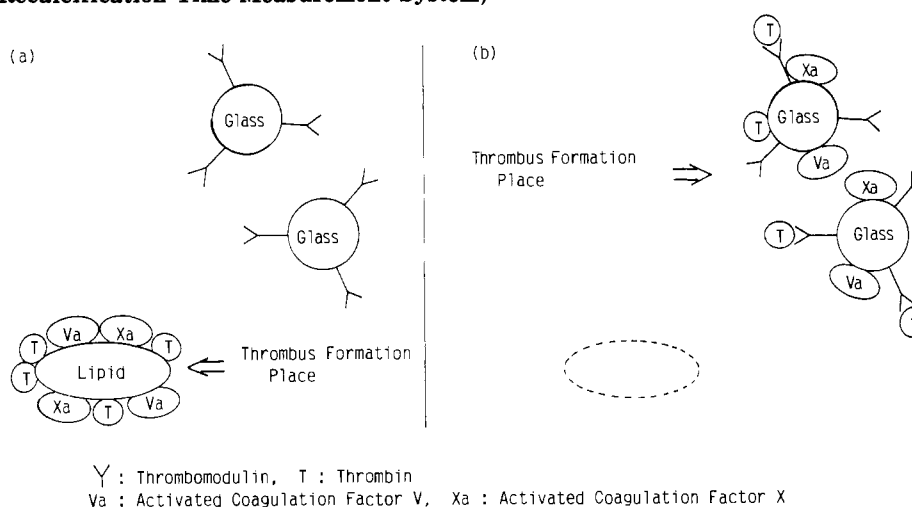
solution. After washing with phosphate buffer solution and drying in vacuo, the antithrombogenic activity of the resulting glass-immobilized human TM was first evaluated by the method previously reported (6). As shown in Table I, no significant difference between glass and glass-TM was observed. When lipid was added first, the lipid prevented the complex formation between thrombin and TM on the glass. Therefore, thrombus formation started in the vicinity of lipid and it was difficult for thrombin occurring with activation of coagulative factor to make a complex with TM on the glass bead as shown in Scheme

* To whom correspondence should be addressed.

[†] Department of Applied Chemistry and Chemical Engineering, Kagoshima University.

[‡] The Third Department of Internal Medicine, Kagoshima University.

[§] Department of Industrial Chemistry, Miyakonojo National College of Technology.

Scheme II. Mechanism of Measurement for the Data Outlined in Tables I (a, aPTT Measurement System) and II (b, Modified Plasma Recalcification Time Measurement System)**Table II. Modified Plasma Recalcification Time of Glass-TM**

material	modified plasma recalcification time ^a (s)
glass-TM ^b	225.0 ± 4.8 (n = 4)
glass	172.6 ± 1.5 (n = 4)

^a Mean ± SE. ^b Final concentration was 6.7 mg/mL.

II (part a). In order to clarify the role of TM on the glass, modified plasma recalcification time was evaluated without lipid, and the results are summarized in Table II. Glass-immobilized TM was found to exhibit excellent prolongation of modified plasma recalcification time compared with control glass. This result shows that the coagulation factor was activated on the glass surface to produce thrombin and then TM immobilized on the glass surface formed a complex with it (Scheme II, part b).

In blood-compatible materials, it is also required that platelet adhesion to endothelial cells be inhibited. It is known that biomaterials with immobilized prostaglandins show excellent antithrombotic effect by inhibiting platelet aggregation, regardless of either chemical (7-10) or physical immobilization (6). TM on glass is also expected to play a role in inhibiting platelet aggregation induced by thrombin. Typical platelet aggregation curves for platelet plasma from human blood exposed to glass-immobilized TM are shown in Figure 1. As seen in the figure, it was found that immobilized TM had an effect on inhibition of platelet aggregation in a dose-dependent manner. The turbidity observed in the control experiments traced platelet aggregation and coagulation induced by thrombin. It is thought that fibrin clotting took place. In the system containing enough glass-immobilized TM, however, fibrin clotting was not observed. This fact suggests that immobilized TM could combine with thrombin as seen in blood vessels.

It is concluded that glass-immobilized human TM is a very active inhibitor of both coagulation and platelet aggregation of human blood. Since chemically immobilized TM is active enough as seen on the surface of blood vessel endothelia, TM-immobilized biomaterials are expected to inhibit platelet adhesion to their surface. They are also important as a model system of endothelia. Further study on TM-immobilized biopolymers is now in progress.

Experimental Procedures. Human TM was supplied by Asahi-Kasei Ltd. Aminopropyl glass beads were

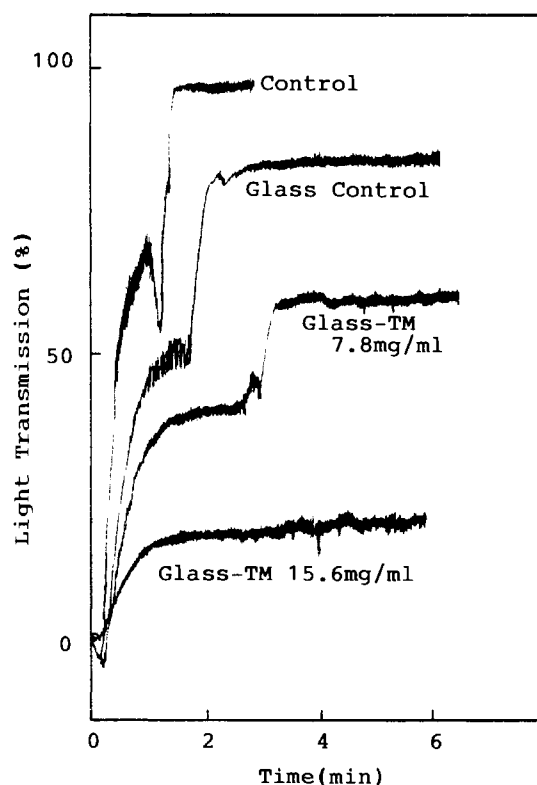


Figure 1. Inhibition of thrombin-induced platelet aggregation by glass-immobilized TM: control, only platelet plasma poured into a test tube; glass control, glass beads suspended in platelet-rich plasma and poured into a test tube.

purchased from Sigma Chemical Co. Turbidimetry was performed with an aggregometer (Syenco).

Glass-Immobilized Human TM. Phosphate buffer solution (3.18 mL, pH 5.0) including 3 mg of human TM and 0.72 mg of 1-ethyl-3-[3-(dimethylamino)propyl]carbodiimide hydrochloride was added to 1 g of *N*-(2-aminoethyl)-3-aminopropyl-glass suspended in 8.0 mL of phosphate buffer solution. The immobilization reaction was performed at 0 °C for 48 h, and the obtained glass-immobilized TM was repeatedly washed with phosphate buffer solution (pH 7.4) and dried in vacuo over night.

Measurement of Activated Partial Thromboplastin Time (aPTT). aPTT was measured similarly to the method described in the literature (6).

Measurement of Modified Plasma Recalcification Time. Glass-TM suspension (100 μL) was added to 100

μ L of platelet-rich plasma and the mixture was incubated for 2 min at 37 °C. Then the clotting was started by 0.025 M CaCl_2 addition.

Measurement of Platelet Aggregation. Platelet aggregation was measured by the turbidimetric assay (11) using thrombin (0.50 unit/mL) as an inducer in glass-immobilized TM suspended in platelet-rich plasma.

ACKNOWLEDGMENT

We thank Miss M. Uchikado for her experimental support. We are also grateful to Professor N. Miyauchi of Kagoshima University for helpful discussions.

LITERATURE CITED

- (1) Maruyama, I., and Majerus, P. W. (1985) The turnover of thrombin-thrombomodulin complex in cultured human umbilical vein endothelial cells and A549 lung cancer cells. Endocytosis and degradation of thrombin. *J. Biol. Chem.* **260**, 15432-15438.
- (2) Maruyama, I., and Majerus, P. W. (1987) Protein C inhibits endocytosis of thrombin-thrombomodulin complexes in A549 lung cancer cells and human umbilical vein endothelial cells. *Blood* **69**, 1481-1484.
- (3) Suzuki, K., Kusumoto, H., Deyashiki, Y., Nishioka, J., Maruyama, I., Zushi, M., Kawahara, S., Honda, G., Yamamoto, S., and Horiguchi, S. (1987) Structure and expression of human thrombomodulin, a thrombin receptor on endothelium acting as a cofactor for protein C activation. *EMBO J.* **6**, 1891-1897.
- (4) Sirai, T., Shiojiri, S., Ito, H., Yamamoto, S., Kusumoto, H., Deyashiki, Y., Maruyama, I., and Suzuki, K. (1988) Gene structure of human thrombomodulin, a cofactor for thrombin-catalyzed activation of protein C. *J. Biochem.* **103**, 281-285.
- (5) Yagi, K., Hirota, K., Yamasaki, S., Uwai, A., and Miura, Y. (1989) Anticoagulant Activity of Immobilized Thrombomodulin. *Chem. Pharm. Bull.* **37**, 732-734.
- (6) Akashi, M., Takeda, S., Miyazaki, T., Yashima, E., Miyauchi, N., Maruyama, I., Okadome, T., and Murata, Y. (1989) Antithrombogenic Poly(vinyl chloride) with Heparin- and/or Prostaglandin I_2 -Immobilized in Hydrogels. *J. Bioact. Compat. Polym.* **4**, 4-16.
- (7) Grode, G. A., Pitman, J., Crowley, J. P., Leininger, R. I., and Falb, R. D. (1974) Surface-Immobilized Prostaglandin as a Platelet Protective Agent. *Trans. Am. Soc. Artif. Intern. Organs* **20**, 38-41.
- (8) Ebert, C. D., Lee, E. S., and Kim, S. W. (1982) The Antiplatelet Activity of Immobilized Prostacyclin. *J. Biomed. Mater. Res.* **16**, 629-638.
- (9) Jacobs, H. A., Okano, T., and Kim, S. W. (1989) Antithrombogenic Surfaces: Characterization and Bioactivity of Surface Immobilized PGE_1 -heparin Conjugate. *J. Biomed. Mater. Res.* **23**, 611-630.
- (10) Chandy, T., and Sharma, C. P. (1984) The antithrombotic effect of prostaglandin E_1 immobilized on albuminated polymer matrix. *J. Biomed. Mater. Res.* **18**, 1115-1124.
- (11) O'Brien, J. R. (1962) Platelet aggregation I. Some effects of the adenosine phosphates, thrombin, and cocaine upon platelet adhesiveness. *J. Clin. Pathol.* **15**, 446-452.

ARTICLES

A Non-Nucleotide-Based Linking Method for the Preparation of Psoralen-Derivatized Methylphosphonate Oligonucleotides

Mark A. Reynolds,* Terry A. Beck, Richard I. Hogrefe, Anton McCaffrey, Lyle J. Arnold, Jr., and Morteza M. Vaghefi

Genta Inc., 3550 General Atomics Court, San Diego, California 92121. Received January 30, 1992

A method is reported for conjugating an analog of 4'-(aminomethyl)-4,5',8-trimethylpsoralen to methylphosphonate oligonucleotides. This method enables the psoralen moiety to be coupled to the phosphonate backbone between any two desired bases in a sequence. When hybridized to a target mRNA, the psoralen moiety can be directed toward a uridine base and, in turn, can undergo a photo-addition reaction with the target under UV irradiation at 365 nm. Several different non-nucleotide-based amino-linker reagents have been prepared for incorporation into methylphosphonate oligonucleotides by standard phosphoramidite chemistry. In addition, an *N*-hydroxysuccinimide activated ester analog of 4'-[(3-carboxypropionamido)methyl]-4,5',8-trimethylpsoralen has been synthesized for conjugation to the amino-linker moieties. Using this approach, we have prepared a number of psoralen-methylphosphonate-oligonucleotide conjugates which are complementary to the chimeric *bcr/abl* mRNA associated with chronic myelogenous leukemia. Solution hybridization studies with a 440-base subfragment of the *bcr/abl* RNA have shown that the psoralen moiety does not adversely affect duplex stability. Polyacrylamide gel electrophoresis analyses have demonstrated that the psoralen-oligonucleotide conjugates undergo photo-addition to the RNA in a sequence-specific manner. Optimal photo-addition occurs when the psoralen moiety is inserted adjacent to one or more adenine residues in the oligonucleotide sequence, particularly between adenine and thymine (5'-3'). This internal labeling approach greatly increases the number of potential target sites available for photo-cross-linking experiments.

INTRODUCTION

Methylphosphonate oligonucleotides (MP-oligomers) are known to inhibit protein synthesis in a sequence-specific manner (1-3). These compounds are not substrates for ribonuclease H (4, 5) and, to date, have not been found to interact with proteins or enzymes that normally bind to or modify DNA or RNA. Thus, their primary mode of action appears to be through the formation of short duplexes with mRNA resulting in blockage of translation. Based on this assumption, the potency of MP-oligomers should correlate, at least in part, with the stability of these duplexes. One method for enhancing potency is to increase the length of the MP-oligomer. This has practical limitations, however, due to reduced specificity (6, 7). Another method is to form a cross-link between the MP-oligomer and mRNA, thereby driving the equilibrium between the two strands to an irreversible duplex form.

Psoralen-derivatized methylphosphonate oligonucleotides have been described for photochemical cross-linking to single-stranded DNA and RNA (8-11). The two types reported to date possess either 3-[(2-aminoethyl)carbamoyl]psoralen or 4'-[[*N*-(aminoethyl)amino]methyl]-4,5',8-trimethylpsoralen coupled at the 5'-terminus via a phosphoramidate bond. Following duplex formation, the psoralen moiety is directed toward a neighboring pyrimidine base on the target nucleic acid, preferably a thymidine or uridine. Irradiation at 365 nm produces a 2 + 2 cycloaddition reaction between the psoralen and the 5,6-double bond of the pyrimidine base, resulting in a covalent

cross-link between the two strands. Such cross-linking has been demonstrated, for example, by denaturing polyacrylamide gel electrophoresis. Furthermore, these derivatives have been shown to be 30-50-fold more potent than their unmodified counterparts as inhibitors of protein synthesis in both cell-free systems and intact mammalian cells (3, 10).

Psoralen conjugates of normal phosphodiester oligonucleotides have also been described. For example, a cleavable psoralen moiety ("site-specific psoralen") has been reported with a side chain containing an internal disulfide bond and terminating in a reactive primary amine (12). This compound can be coupled to oligonucleotides containing a 5'-terminal phosphate group using carbodiimide. Psoralen has also been derivatized with a 6'-iodohexyl side chain for coupling to oligonucleotides containing a 5'-terminal thiophosphate group (13). Oligonucleotides derivatized at internal locations have been prepared by irradiating preformed duplexes in the presence of free psoralen and then purifying the furan-side thymidine monoadducts (14, 15). Automated phosphoramidite coupling procedures have also been reported for attaching psoralen at the 5'-terminus (16, 17) or at internal positions via an adenine analog derivatized with psoralen at the C-8 position (18).

Here we present the synthesis of several non-nucleotide-based linking reagents for the incorporation of reactive primary amines into oligonucleoside methylphosphonates. These primary amines permit the subsequent conjugation of a wide variety of chemical moieties by simple aqueous chemistries. We also report the synthesis of an activated analog of 4'-(aminomethyl)-4,5',8-trimethylpsoralen for

* Author to whom correspondence should be addressed.

addition to primary amines. These two reagents provide a simple and quantitative means of attaching one or more psoralen moieties to any desired location within a methylphosphonate oligonucleotide sequence.

We shall also describe the effect of linker length and position within a sequence on the efficiency of photo-cross-linking to an RNA target. The target sequence chosen for this study is the junction region of the chimeric *bcr/abl* mRNA associated with chronic myelogenous leukemia (19). Various sites of linker insertion and different linker lengths have been evaluated to optimize the photo-cross-linking reaction.

EXPERIMENTAL PROCEDURES

L-Threonine methyl ester was purchased from Sigma. (9-Fluorenylmethoxy)carbonyl (Fmoc), *N*-hydroxysuccinimide, *N*-Fmoc-6-aminocaproic acid, *N*-Fmoc-glycine, and *N*-Fmoc-succinimidyl carbonate were from Bachem. 4,4'-Dimethoxytrityl chloride (DMT-Cl), lithium aluminum hydride (1 M solution in THF), *N,N*-diisopropylethylamine, 4,5',8-trimethylpsoralen, trimethylacetyl chloride, anhydrous ammonia, succinic anhydride, 4-(dimethylamino)pyridine, *N*-hydroxysuccinimide, *N,N'*-dicyclohexylcarbodiimide, acetic anhydride, iodine crystals (99.99%), and trichloroacetic acid were purchased from Aldrich. Solvents were reagent grade and, unless specified otherwise, were dried by refluxing and distillation over calcium hydride in a dry argon atmosphere. Unless stated otherwise, all synthetic reactions were run under a dry argon atmosphere. Reactions were monitored by TLC on precoated silica gel 60 F-254 plates purchased from EM Reagents. Preparative flash chromatography was performed using silica gel 60 (230–400 mesh), also from EM Reagents. ¹H-NMR spectra were run on a JW 360 NMR spectrometer using either trimethylsilyl propionate (DMSO-*d*₆) or tetramethylsilane (CDCl₃) as internal standards. Elemental analyses were done by Robertson Laboratory (Madison, NJ). Melting points were determined by standard procedures and are uncorrected. Monomers for the synthesis of oligonucleotides methylphosphonates were provided by JBL Scientific, Inc. (a subsidiary of Genta, Inc.). Other reagents for oligonucleotide synthesis were obtained from Milligen-Bioscience, Inc. SEP-PAK C-18 reversed-phase cartridges were obtained from Milligen-Waters. High-performance liquid chromatography (HPLC) was conducted on a Beckman System Gold instrument with Hamilton PRP-1 10-μm reversed-phase columns: analytical (250 × 4.1 mm); semipreparative (305 × 7.0 mm). The analytical column was eluted at a flow rate of 1.5 mL/min with a linear gradient of 0%–50% acetonitrile in 50 mM triethylammonium acetate buffer (pH 7.0) over 30 min. For the semipreparative column, the gradient time was extended to 45 min and the flow rate was increased to 2.5–3 mL/min. Peak detection was determined by UV absorbance at 260 nm (analytical) and 297 nm (semipreparative). [γ-³²P]ATP and Nensorb-20 oligonucleotide purification columns were purchased from New England Nuclear/Du Pont. T4-polynucleotide kinase was from Stratagene, Inc. Gel electrophoresis was carried out with 6% polyacrylamide/bisacrylamide (19:1) containing 0.089 M Tris, 0.089 M boric acid, 0.2 mM EDTA, and 7 M urea. The gels were dried onto 3MM blotting paper and exposed to XAR-5 film overnight. The resulting autoradiographs were used to locate the bands on the gels, which were then cut out and counted in scintillation fluid (Cytoscint, ICN) using a scintillation counter.

Synthesis of (2*S*,3*R*)-2-Amino-1,3-butanediol. This compound was prepared by reduction of L-threonine

methyl ester with lithium aluminum hydride as described elsewhere (20). The crude product was purified by silica gel flash chromatography with methanol/dichloromethane (1:1) as the eluent.

Synthesis of (2*S*,3*R*)-2-*N*[(Fluoren-9-ylmethoxy)carbonyl]-2-amino-1,3-butanediol (1). (2*S*,3*R*)-2-Amino-1,3-butanediol (1.5 g, 14 mmol) was treated with *N*[(9-fluorenylmethoxy)carbonyl]oxy)succinimide (Fmoc-NHS, 5 g, 15 mmol) in a solution of acetone/water (1:1, 35 mL) containing sodium hydrogen carbonate (5 g). The reaction was monitored by spotting aliquots onto silica gel TLC plates and developing with ninhydrin reagent. Following complete protection of the amine, the mixture was evaporated under reduced pressure. The residue was taken up in dichloromethane (40 mL), extracted twice with water (50 mL), dried over anhydrous MgSO₄, and concentrated to an oil under reduced pressure. The product was purified by silica gel flash chromatography using 2% methanol in dichloromethane as the eluent (3.46 g, 69% yield). ¹H NMR (DMSO-*d*₆): δ 1.20 (CH₃), 2.85 (NH), 3.26 (CH), 3.48 (CH), 3.72 (OH), 7.3–7.8 (8 aromatic protons). Anal. Calcd for C₁₉H₂₁NO₄: C, 69.71; H, 6.47; N, 4.28. Found: C, 69.66; H, 6.22; N, 4.39.

Synthesis of (2*S*,3*R*)-2-[2'-*N*[(Fluoren-9-ylmethoxy)carbonyl]-2-aminoethanamido]-1,3-butanediol (2). *N*-Fmoc-glycine (5.0 g, 17 mmol) was dried by coevaporation with dry pyridine (3 × 30 mL). The residue was dissolved in dry dimethylformamide (30 mL) and dry tetrahydrofuran (30 mL) was added. The solution was cooled to 0 °C and *N,N*-diisopropylethylamine (17 mmol, 1 equiv) was added. Trimethylacetyl chloride (18.7 mmol, 1.1 equiv) was then added dropwise with stirring over a period of 45 min. Next, a solution of (2*S*,3*R*)-2-amino-1,3-butanediol (25.5 mmol, 1.5 equiv) in dry dimethylformamide (30 mL) was added and the reaction mixture was allowed to return to room temperature. The reaction was monitored by TLC using dichloromethane/methanol/acetic acid (10:1:0.1) as the solvent system. After completion of the reaction (typically 1 h), the solvent was removed under reduced pressure and the residue was mixed with ethyl acetate (50 mL). The water-soluble materials were removed by extraction first with saturated aqueous sodium bicarbonate (40 mL) and then with water (20 mL). The organic layer was then dried over anhydrous MgSO₄. The product (2) was purified by crystallization from ethyl acetate (5.2 g, 80% yield, mp 143–144 °C). ¹H NMR (DMSO-*d*₆): δ 1.03 (CH₃ of reduced L-threonine), 3.35 (OH), 3.3–3.45 (2 CH), 3.91 (NH), 4.27 (NH), 4.31 (OH), 4.34 (CH₂), 4.63 (CH and CH₂ of Fmoc), 7.3–7.9 (8 aromatic protons). Anal. Calcd for C₂₁H₂₄N₂O₅: C, 65.61; H, 6.29; N, 7.29. Found: C, 65.39; H, 6.07; N, 7.10.

Synthesis of (2*S*,3*R*)-2-[4'-*N*[(Fluoren-9-ylmethoxy)carbonyl]-4-aminobutanamido]-1,3-butanediol (3). Fmoc-NHS (5 g, 15 mmol) and 4-aminobutyric acid (1.8 g, 17.5 mmol) were reacted in a solution of acetone/water (1:1, 35 mL) containing sodium hydrogen carbonate (1.24 g) with stirring overnight. The reaction mixture was then acidified to pH 2 with 1 N HCl, and the solvents were evaporated under reduced pressure. Next, the residue was taken up into ethanol (20 mL) and filtered. The resulting solution was evaporated under reduced pressure to give the product, 4-*N*-Fmoc-4-aminobutyric acid (4, 4.5 g, 14 mmol). ¹H NMR (DMSO-*d*₆): δ 1.61 (CH₂), 2.2 (CH₂), 3.01 (CH₂N), 4.32 (CH₂C=O), 4.22 (NH), 7.25–7.95 (8 aromatic protons). Next, compound 4 (3.0 g) was coupled with (2*S*,3*R*)-2-amino-1,3-butanediol (3.0 g) using trimethylacetyl chloride according to the procedure described above for compound 2. Product 3 was crystallized from

ethyl acetate (3.1 g, 89% yield, mp 141–142 °C). ^1H NMR (DMSO- d_6): δ 1.03 (CH_3 of reduced L-threonine), 1.62 (CH_2), 2.14 (CH_2), 2.91 (CH), 2.97 (CH_2), 3.3–3.5 (2 CH), 3.63 (OH), 3.84 (OH), 4.23 (CH), 4.33 (CH and CH_2 of Fmoc), 7.3–7.9 (8 aromatic protons). Anal. Calcd for $\text{C}_{23}\text{H}_{28}\text{N}_2\text{O}_5$: C, 66.97; H, 6.84; N, 6.79. Found: C, 66.56; H, 6.81; N, 6.51.

Synthesis of (2*S*,3*R*)-2-[6'-*N*-(Fluoren-9-ylmethoxy)carbonyl]-6'-aminohexanamido]-1,3-butanediol (5). *N*-Fmoc-6-aminocaproic acid (3.5 g, 11 mmol) was coupled with (2*S*,3*R*)-2-amino-1,3-butanediol (1.2 equiv) using trimethylacetyl chloride according to the procedure described above for compound 2. The material was crystallized from ethyl acetate to give 5 (2.5 g, 58% yield). ^1H NMR (DMSO- d_6): δ 1.03 (CH_3 of reduced L-threonine), 1.3–1.7 (3 CH_2), 2.52 (CH_2N), 3.12 ($\text{CHC}=\text{O}$), 3.8–3.9 (2 OH), 4.1–4.2 (2 CH), 4.41 (CH_2 of Fmoc), 5.22 (NH), 6.48 (NH), 7.3–7.9 (8 aromatic protons). Anal. Calcd for $\text{C}_{25}\text{H}_{32}\text{N}_2\text{O}_5$: C, 68.16; H, 7.32; N, 6.36. Found: C, 68.07; H, 7.21; N, 6.09.

Synthesis of (2*S*,3*R*)-2-[6'-*N*-[2''-*N*-(Fluoren-9-ylmethoxy)carbonyl]-2''-aminoethanamido]-6'-amino-hexanamido]-1,3-butanediol (6). *N*-Fmoc-glycine (5 g, 17 mmol) was dried by repeated coevaporation with dry pyridine (3 \times 30 mL). The dried material was then dissolved in dry dimethylformamide (30 mL) and dry tetrahydrofuran (30 mL) was added. The solution was cooled to 0 °C and *N,N*-diisopropylethylamine (3 mL, 17 mmol) was added. While stirring, trimethylacetyl chloride (2.08 mL, 17 mmol) was added dropwise and stirring was continued at 0 °C for 45 min. Next, 6-aminohexanoic acid (2.5 g, 20.4 mmol) was added and the reaction mixture was warmed to room temperature and stirred overnight. The solvents were then evaporated under reduced pressure, and the residue was reconstituted with water (50 mL) and the pH was adjusted to 2 with 1 *N* HCl. This mixture was extracted with ethyl acetate (100 mL) and the organic phase was separated, washed with water (20 mL), and dried over anhydrous MgSO_4 . Following filtration, the solvent was concentrated under reduced pressure. Hexane was added dropwise to the resulting solution until a cloudy suspension resulted which could be clarified by gentle heating with a heat gun. This solution was then allowed to stand overnight at room temperature. A crystalline product resulted (7, 4.9 g, 70% yield, mp 126–128 °C) which could be recovered by filtration. ^1H NMR (DMSO- d_6): δ 1.30 (CH_2), 1.39 (CH_2), 1.48 (CH_2), 2.20 (CH_2N), 3.06 (CH_2 of Fmoc), 3.58 (CH_2COOH), 4.24 (2 NH), 4.34 (CH of Fmoc and CH_2 of glycine), 7.3–7.9 (8 aromatic protons). Anal. Calcd for $\text{C}_{23}\text{H}_{26}\text{N}_2\text{O}_5$: C, 67.30; H, 6.38; N, 6.82. Found: C, 66.98; H, 6.33; N, 6.57. Next, compound 7 (4.5 g, 11 mmol) was coupled with (2*S*,3*R*)-2-amino-1,3-butanediol using trimethylacetyl chloride according to the procedure described above for compound 2. The material was crystallized from ethyl acetate to give 6 (4.33 g, 79% yield). ^1H NMR (DMSO- d_6): δ 1.01 (CH_3 of reduced L-threonine), 1.22–1.52 (3 CH_2 protons from 6-aminohexanoyl group), 3.62 and 3.84 (2 OH), 5.35 (NH), 6.18 (NH), 7.3–7.9 (8 aromatic protons). Anal. Calcd for $\text{C}_{27}\text{H}_{35}\text{N}_3\text{O}_6$: C, 65.17; H, 7.09; N, 8.44. Found: C, 64.95; H, 7.02; N, 8.32.

Dimethoxytritylation of Primary Hydroxyl Groups on Compounds 1–3, 5, and 6. The primary hydroxyls of these compounds were protected using 4,4'-dimethoxytrityl chloride (DMT-Cl) to give compounds 8–12, respectively, according to the following general procedure. Either compound 1–3, 5, or 6 (6 mmol) was dried by repeated coevaporations in dry pyridine (3 \times 30 mL) and

then dissolved in dry pyridine (15 mL). A solution of DMT-Cl (2.2 g) in dry dichloromethane/pyridine (1:1, 20 mL) was added dropwise with stirring and the reaction was allowed to proceed at room temperature for 45 min. The progress of the reaction was monitored by TLC. Then, the reaction was quenched by addition of methanol (2 mL) and stirring was continued for 10 min. The solvents were removed under reduced pressure, and the residue was dissolved in dichloromethane (50 mL) and extracted with saturated sodium hydrogen carbonate (2 \times 50 mL) followed by water (30 mL). The organic phase was dried over anhydrous MgSO_4 and filtered. After filtration and removal of the solvent, the product was purified by silica gel flash chromatography eluting with 2% methanol in dichloromethane containing 0.5% triethylamine. Compound 8. ^1H NMR (CDCl_3): δ 1.18 (CH_3 of reduced L-threonine), 1.63 (CH), 2.83 (NH), 3.77 (2 CH_3 of DMT), 3.82 (CH_2 of Fmoc), 5.48 (CH_2ODMT), 6.82–7.90 (21 aromatic protons). Anal. Calcd for $\text{C}_{40}\text{H}_{39}\text{NO}_6$: C, 76.29; H, 6.24; N, 2.22. Found: C, 76.56; H, 6.26; N, 1.93. Data for compound 9 follows. ^1H NMR (CDCl_3): δ 1.18 (CH_3 of reduced L-threonine), 3.78 (2 CH_3 from DMT), 4.35 (CH_2ODMT), 5.98 (NH), 6.8–7.78 (21 aromatic protons). Anal. Calcd for $\text{C}_{42}\text{H}_{42}\text{N}_2\text{O}_7$: C, 73.49; H, 6.16; N, 4.08. Found: C, 73.22; H, 5.45; N, 3.78. Data for compound 10 follows. ^1H NMR (CDCl_3): δ 1.18 (CH_3 of reduced L-threonine), 1.83 (CH_2), 2.28 (CH_2), 3.74 (2 CH_3 of DMT), 4.21 (OH), 4.38 (CH_2 of Fmoc), 5.22 and 6.42 (2 NH), 6.80–7.65 (21 aromatic protons). Anal. Calcd for $\text{C}_{44}\text{H}_{46}\text{N}_2\text{O}_7$: C, 73.93; H, 6.49; N, 3.92. Found: C, 73.63; H, 6.73; N, 3.96. Data for compound 11 follows. ^1H NMR (CDCl_3): δ 1.12 (CH_3 of reduced L-threonine), 1.3–1.6 (3 CH_2), 3.75 (2 CH_3 of DMT), 4.38 (CH_2 of Fmoc), 6.80–7.90 (21 aromatic protons). Anal. Calcd for $\text{C}_{46}\text{H}_{46}\text{N}_2\text{O}_7$: C, 74.37; H, 6.78; N, 3.77. Found: C, 74.02; H, 6.77; N, 3.78. Data for compound 12 follows. ^1H NMR (CDCl_3): δ 1.12 (CH_3 of reduced L-threonine), 3.80 (2 CH_3 of DMT), 5.42 (CH_2 of Fmoc), 6.18 and 6.32 (2 NH), 6.82–7.80 (21 aromatic protons). Anal. Calcd for $\text{C}_{48}\text{H}_{53}\text{N}_3\text{O}_8$: C, 72.07; H, 6.68; N, 5.25. Found: C, 71.86; H, 6.57; N, 5.63.

Methoxyphosphinylation of the Secondary Hydroxyl Moieties on Compounds 8–12. Compounds 8–12 were converted to the corresponding activated methylphosphonamidite monomers 13–17, respectively, according to the following procedure. *N,N*-diisopropylmethylphosphonamidic chloride was prepared as previously described (21). Any of the compounds 8–12 (4 mmol) was dried by several coevaporations with dry pyridine (3 \times 30 mL) and then dissolved in dry dichloromethane (20 mL). *N,N*-diisopropylethylamine (1.5 equiv) and *N,N*-diisopropylmethylphosphinamidic chloride (1.2 equiv) were added dropwise with stirring and the reaction was continued for 45 min. The solvent was removed under reduced pressure and the residue was purified by silica gel flash chromatography. The columns were packed with ethyl acetate/hexane (1:1) containing 5% triethylamine and the products were then eluted with ethyl acetate/hexane (1:1) containing 1% triethylamine. The purity of these compounds was estimated to be greater than 95% on the basis of ^{31}P NMR analysis.

Synthesis of 4'-(Aminomethyl)-4,5',8-trimethylpsoralen. 4'-(Chloromethyl)-4,5',8-trimethylpsoralen was synthesized as previously described (22). This compound (330 mg) was then dissolved in dry acetonitrile (100 mL) and cooled to 10 °C. The resulting solution was then saturated with anhydrous ammonia at –10 °C and the reaction was allowed to warm to room temperature with stirring. Stirring was continued overnight. The solvent

and unreacted ammonia were removed under reduced pressure, and the residue was taken up into tetrahydrofuran/acetone (3:1, 80 mL) and filtered to remove ammonium chloride. Removal of the solvent gave nearly a quantitative yield of the desired product. The purity was estimated to be greater than 95% on the basis of ^1H NMR analysis with comparison to published values (22). This material was used in the next reaction without further purification.

Synthesis of 4'-[(3-Carboxypropionamido)methyl]-4,5',8-trimethylpsoralen (18). 4'-(Aminomethyl)-4,5',8-trimethylpsoralen (300 mg) was dried by coevaporation with dry pyridine (3×30 mL) and then dissolved in dry pyridine (30 mL). To this solution were added succinic anhydride (550 mg) and 4-(dimethylamino)pyridine (50 mg). The mixture was stirred at room temperature for 3 h. The solvent was removed under reduced pressure and the residue was dissolved in dichloromethane (30 mL). The material was precipitated by addition of methanol (5 mL), and the crystals were collected after 2 h to give 18 (370 mg, 67% yield, mp 252–260 °C dec). ^1H NMR: δ 2.31 (CH_2), 2.48–2.51 (3 CH_3), 2.53 (CH_2), 4.38 (CH_2N), 6.27 (Ar), 7.81 (Ar), 8.40 (NH), 12.02 (COOH). Anal. Calcd for $\text{C}_{19}\text{H}_{19}\text{NO}_6$: C, 63.86; H, 5.36; N, 3.92. Found: C, 64.02; H, 5.44; N, 3.88.

Synthesis of 4'-[(3-Carboxypropionamido)methyl]-4,5',8-trimethylpsoralen, *N*-Hydroxysuccinimide Ester (Psoralen-NHS Reagent, 19). The product from the previous step, 18 (100 mg), was dried by coevaporation with dry pyridine (3×30 mL) and then dissolved in a 1:1 mixture of dry dimethylformamide/dioxane (40 mL). To this solution was added, with stirring, dry *N*-hydroxysuccinimide (700 mg) and an aliquot (2 mL) from a 20% solution of *N,N'*-dicyclohexylcarbodiimide in dry dioxane. The resulting reaction mixture was stirred at room temperature overnight. The precipitate was then removed by filtration and washed with dioxane (30 mL). The combined filtrate and washings were evaporated to dryness under reduced pressure, and the resulting solid was triturated with ethyl acetate (40 mL), by sonication for 5 min. The product was then recovered by filtration to give 19 (110 mg, 87% yield, mp 150–160 °C dec.).

Synthesis of Oligonucleoside Methylphosphonates and Oligonucleoside Methylphosphonates Modified with Non-Nucleotide-Based Amino Linkers. Oligomers were synthesized using 5'-(Dimethoxytrityl)nucleoside 3'-[(*N,N*-diisopropylamino)methyl]phosphonamidite monomers as previously described (6, 23). Solid-phase synthesis was performed on CPG supports with a Biosearch Model 8750 DNA synthesizer according to the manufacturer's recommendations, except for the following modifications: monomers were dissolved in either 1:1 acetonitrile/dichloromethane ("G") or acetonitrile ("A", "C", and "T") at concentrations of 100 mM. Deblocking reagent = 2.5% dichloroacetic acid in dichloromethane. Oxidizing reagent = 25 g/L iodine in 2.5% water, 25% 2,6-lutidine, 72.5% tetrahydrofuran. CAP A = 10% acetic anhydride in acetonitrile. CAP B = 0.625% 4-(*N,N*-dimethylamino)pyridine in pyridine. Where desired, non-nucleotide linkers were inserted into the sequence using 100 mM solutions of compounds 13–17 in acetonitrile using the same coupling routine. A 5'-phosphodiester linkage was added by introducing a standard β -cyanoethyl phosphoramidite monomer at the last coupling cycle. (This enables the oligomer to be labeled with polynucleotide kinase, as described below.) The 5'-DMT protecting group was left on at the end of each synthesis to facilitate purification. Oligomers were cleaved from the support

and deprotected as described elsewhere (6). The crude oligomers were then freed from failure sequences using SEP-PAK C18 cartridges. The crude deprotected oligomers were dissolved in 1:1 acetonitrile/water, diluted with 25 mM triethylammonium bicarbonate (TEAB, pH 7.5) to a final acetonitrile concentration of 5%, and applied to the SEP-PAK cartridge. The cartridge was washed with 20% acetonitrile in 25 mM TEAB and then treated with 2% trifluoroacetic acid followed immediately by 25 mM TEAB. The detritylated product oligomers were then recovered from the cartridge by washing with water and eluting with 1:1 acetonitrile/water. The products were further purified by preparative reversed-phase HPLC on a Hamilton PRP-1 10- μm column (7.0 \times 3.5 mm) and obtained in isolated yields ranging from 20 to 48%.

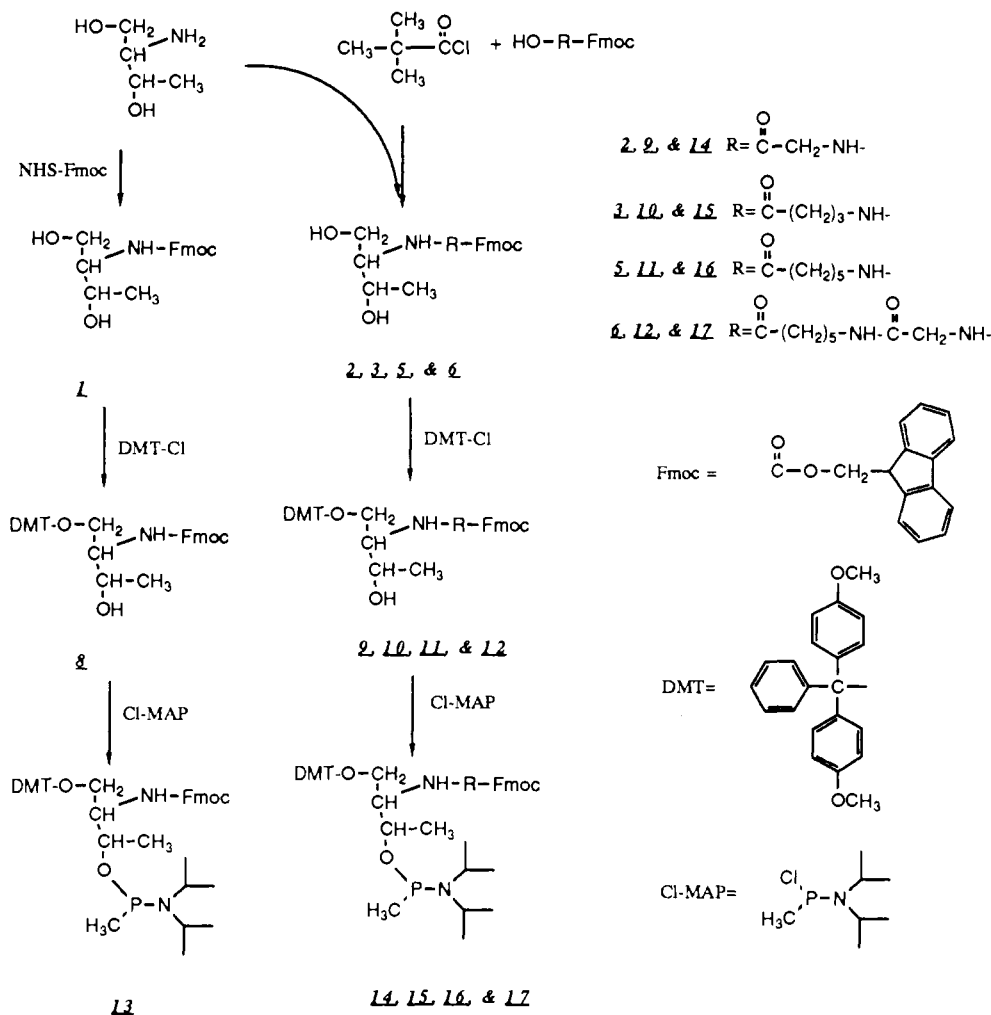
Derivatization of Linker-Modified Oligonucleoside Methylphosphonates with 4,5',8-Trimethylpsoralen. Linker-modified methylphosphonate oligomers (3–5 mg, 99–150 OD₂₆₀ units) were dissolved in 100 μL of 1:1 acetonitrile/water and transferred to 1.5 mL polypropylene microcentrifuge tubes. Reagents were added with brief vortexing after each addition in the following order: dimethyl sulfoxide (170 μL), water (100 μL), 1 M HEPES buffer, pH 8.0 (50 μL), and 50 mM psoralen-NHS reagent in dimethyl sulfoxide (80 μL). Total volume = 500 μL . The mixtures were reacted at room temperature in the dark for 2–4 h. Ethanol (1 mL) was added, and the mixtures were chilled at –20 °C overnight. The tubes were then spun in a microcentrifuge for 5 min and the supernatants were aspirated and discarded. The resulting pellets were resuspended in 1:1 acetonitrile/water and purified by preparative HPLC on a Hamilton PRP-1 10- μm column (7.0 \times 305 mm). Isolated yields of psoralen-modified oligomers ranged from 45 to 85%.

Photo-Cross-Linking Reactions between Psoralen-Modified Oligonucleoside Methylphosphonates and an RNA Target. A 440-base RNA transcript was prepared from a pGEM vector clone. This represents a portion of a biological chimeric *bcr/abl* mRNA which contains a *bcr/abl* junction at approximately the middle of the sequence. Psoralen-modified oligonucleoside methylphosphonates were labeled with ^{32}P using [γ - ^{32}P]ATP (3000 Ci/mmol) and T4 polynucleotide kinase as described elsewhere (24). The resulting ^{32}P -labeled psoralen-oligomer conjugates were purified on Nensorb-20 cartridges according to the manufacturer's instructions, except that the ^{32}P -kinased oligomer was eluted with 1:1 acetonitrile/water. Hybridizations and photo-cross-linking reactions were conducted in borosilicate glass autosampler vials (2 mL) with Teflon-lined caps. ^{32}P -labeled psoralen-oligomer (0.03 pmol, ca. 20 000 cpm) and unlabeled tandem methylphosphonate oligomers (5 pmol) were prehybridized with RNA target (0.3 pmol) in 10 μL of 20 mM potassium phosphate buffer (pH 7.4) containing 0.1 mM EDTA and 0.03% sarkosylate. The resulting solutions were then irradiated with a Model B-100A long-wavelength ultraviolet lamp (UVP, Inc.) either on crushed ice or in a thermostat-controlled water bath at a distance of 15 cm. For most reactions, the irradiations were carried out for 30 min. Following irradiation, the solutions were diluted with 5 μL of 90% formamide containing 1 \times Tris-borate buffer and 0.1% bromophenol blue dye. The final solutions were analyzed by polyacrylamide gel electrophoresis as described above.

RESULTS

Non-Nucleotide-Based Linking Reagents. Five different non-nucleotide-based linking reagents were syn-

Scheme I



thesized for incorporation into MP-oligonucleotides using an automated DNA synthesizer (Scheme I). Each of these reagents contains a three-carbon chain which, once coupled into the oligomer, closely mimics the spacing of a traditional ribose moiety. The starting material for these syntheses, L-threonine, was reduced with lithium aluminum hydride to form (2*S*,3*R*)-2-amino-1,3-dihydroxybutane. (Although L-threonine was used exclusively in these syntheses, other chiral forms of threonine are commercially available and could also be used.) Next, the 2-amino group of reduced L-threonine was either protected with a (fluoren-9-ylmethoxy)carbonyl group (Fmoc) or condensed with a series of carboxylic side chains terminating in an Fmoc-protected primary amine. The primary hydroxyl groups were then selectively protected with dimethoxytrityl chloride (DMT-Cl) in essentially quantitative yields. Finally, the secondary hydroxyl groups were activated with *N,N*-diisopropylmethylphosphonamidic chloride. The products (14–17) were purified by silica gel glass chromatography with estimated purities of greater than 95% based on ^1H NMR, ^{31}P NMR, and thin-layer chromatography.

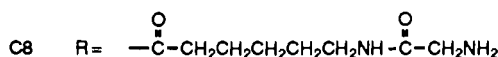
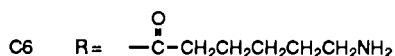
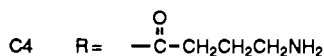
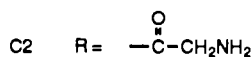
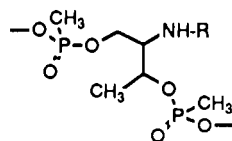
Methylphosphonate Oligonucleotides Containing Non-Nucleotide-Based Linking Moieties. Reagents 14–17 were used along with standard methylphosphonamidite monomers on an automated DNA synthesizer essentially as described elsewhere (6). In order to improve coupling efficiencies, the oxidation reagent was reformulated with a lower water content (2.5%) and oxidation was performed immediately following the coupling step. With these modifications, coupling efficiencies were

typically greater than 95% based on A_{502} measurements of released DMT protecting groups. As reported elsewhere (25), the Fmoc protecting groups were stable in the presence of the DNA synthesis reagents. A traditional B-cyanoethyl phosphoramidite base was used in the final coupling cycle for radiolabeling purposes (see below). Once the synthesis was completed, the oligonucleotides were deprotected as previously described (6). The resulting amino-linker-modified MP-oligonucleotides contained non-nucleotide-based moieties with side chains of different lengths inserted into the backbone as illustrated in Scheme II. (These side chains are designated C_0 – C_8 according to the number of carbon atoms.)

The 5'-trityl groups were left attached to the oligomers to assist in purification. Cleavage from the solid support and removal of the protecting groups was performed as described elsewhere (6). The 5'-tritylated oligomers were separated from shorter (trityl-off) failure sequences using a short column of SEP-PAK C-18 adsorbent. The bound, tritylated oligomers were detritylated on the column by treatment with 2.5% trifluoroacetic acid, neutralized with triethylammonium bicarbonate buffer, and then eluted. Further purification was achieved by reversed-phase HPLC.

Psoralen-Derivatized Methylphosphonate Oligonucleotides. A series of psoralen-derivatized methylphosphonate oligomers was prepared in order to evaluate the effects of different linker-arm lengths and insertion sites on photo-cross-linking efficiency. These oligomers are 18 or 19 bases on length and are complementary to the

Scheme II



bcr/abl junction region of a chimeric mRNA associated with the Philadelphia [9:22] chromosomal translocation (19).

Coupling sites in the methylphosphonate oligomer sequence were chosen to direct the psoralen moiety toward one or more uridine residues in the RNA strand following duplex formation (Scheme III). A C₄ linker arm moiety was inserted at positions b, c, and d opposite the 3'-U-U-5' diad, located approximately in the middle of the duplex. Also, a C₄ linker moiety was inserted in place of a guanine base at position a with the intention of looping out the cytosine base of the target strand and forming a 5'-T-A-3' stacked base pair. (5'-T-A-3' diads are known to be preferred sites for cross-linking in DNA with free psoralen reagents (26).) Another 5'-T-A-3' site was created by attaching an additional adenine base at the 3'-end and inserting a C₄ linker moiety at position e. In order to examine the effects of different linker lengths on cross-linking efficiency, C₀–C₈ linker moieties were inserted at position c.

The primary-amino-modified methylphosphonate oligomers were derivatized with an *N*-hydroxysuccinimide activated ester form of 4'-*N*-modified-4'-(aminomethyl)-4,5,8-trimethylpsoralen (19, Scheme IV). The resulting psoralen-derivatized oligomers were separated from underivatized oligomers by reversed-phase HPLC. Product peaks were identified by their absorbance at 340 nm (due to the psoralen moiety). Typical isolated yields from small scale (5 mg) syntheses ranged from 45 to 85%. A nearly quantitative yield was obtained for oligomer 9 when prepared on a 100-mg scale.

Photo-Cross-Linking Experiments. The RNA target strand used in these studies was a 440-base cloned transcript containing the *bcr/abl* junction region at approximately the middle of the sequence. Site-specificity of the photo-cross-linking reaction was demonstrated with one of the psoralen-oligomers (oligomer 5). This oligomer was labeled with [³²P]phosphate at the 5'-terminus using T4 polynucleotide kinase and [γ-³²P]ATP. (The presence of a phosphate diester linkage at the 5'-end of this oligomer permitted it to be used as a substrate for this enzyme (24).) Annealing reactions were conducted in borosilicate glass vials with the ³²P-labeled psoralen oligomer and a 10-fold excess of the RNA target strand. To minimize competing secondary structures from the RNA strand, two tandem 18-mer methylphosphonate oligomers were also included (complementary to regions immediately adjacent to the 3'- and 5'-ends of the psoralen-oligomer), each in 5-fold excess over the RNA target strand. Omitting

the tandem oligomers from the annealing reactions resulted in insignificant reductions in the levels of photo-cross-linking that were measured (data not shown). Some of these annealing reactions also included either a 10-fold excess of nonradioactive phosphodiester oligomer, having the same sequence as the psoralen-oligomer, or a 1- or 2-fold excess of the nonradioactive psoralen oligomer. Following the annealing step, the vials were placed on crushed ice and irradiated with a long-wavelength ultraviolet lamp (Model B-100A, UVP, Inc.) at a distance of 15 cm for 30 min. The products from photo-irradiation were then analyzed by polyacrylamide gel electrophoresis. The nonradioactive oligomers specifically competed with the ³²P-labeled psoralen-oligomer for cross-linking to the RNA target (Figure 1). To further demonstrate specificity, a ³²P-labeled nonsense psoralen-oligomer was included in the annealing reaction in place of the ³²P-labeled antisense oligomer. In this case, no photo-cross-linking was observed. Therefore, photo-cross-linking of oligomer 5 to the RNA target proceeded in a sequence-specific manner.

Extents of photo-cross-linking were examined over time and at various temperatures with two of the psoralen-oligomer conjugates (oligomers 5 and 9, Figure 2). As reported elsewhere (11), the photo-cross-linking reaction was essentially complete after 30 min at 4 °C. The extents of photo-cross-linking decreased dramatically as the temperature was raised above 35 °C, suggesting that duplexes formed between these psoralen-oligomer conjugates and the biological RNA target are mostly denatured above this temperature.

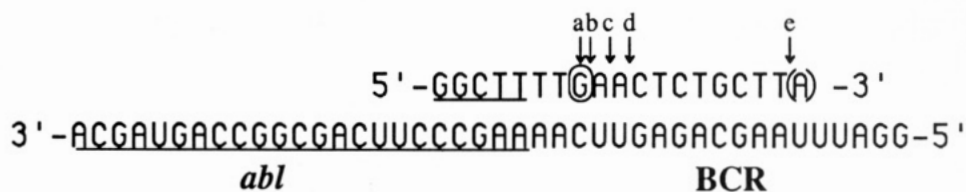
A thermal denaturation experiment was conducted to measure the effect of our psoralen conjugation chemistry on the hybridization characteristics of one of the psoralen-oligonucleotide conjugates (Figure 3). In this experiment, a psoralen-oligonucleotide conjugate (oligomer 5), its C₄-amino-linker-modified precursor, and an unmodified oligonucleotide having the same base sequence were each individually annealed to a complementary oligoribonucleotide target. Insertion of the C₄-amino linker into the oligonucleotide had a negligible effect on its thermal denaturation profile. On the other hand, the psoralen-oligonucleotide conjugate had a slightly higher thermal transition temperature (Δ*T*_m ≈ +3 °C), consistent with the psoralen moiety acting as a weak intercalator.

Finally, photo-cross-linking efficiencies were compared for the entire series of psoralen-derivatized oligomers 1–9 (Figure 4). Averages from a number of photo-cross-linking experiments are summarized in Table I. The shortest linker-arm length yielded the highest level of photo-cross-linking, presumably due to entropic effects. As expected, directing the psoralen moiety toward the middle of the 3'-U-U-5' site gave a high level of photo-cross-linking (site c), whereas positioning it to the 3'- or 5'-side of this site gave less photo-cross-linking (sites b and d). Locating the psoralen moiety in place of a guanine base (site a) also yielded a high level of cross-linking. Presumably, this leads to the formation of a 5'-T-A-3' intercalation site for the psoralen moiety with the opposing cytosine base "looped out" of the duplex. Another 5'-T-A-3' intercalation site was created by adding an adenine base to the 3'-terminus and locating the psoralen moiety at site e. This psoralen-oligomer conjugate (oligomer 9) exhibited the highest level of photo-cross-linking in the series.

DISCUSSION

This report describes a method for conjugating various chemical moieties to methylphosphonate oligonucleotides at internal positions within the sequence. Since conju-

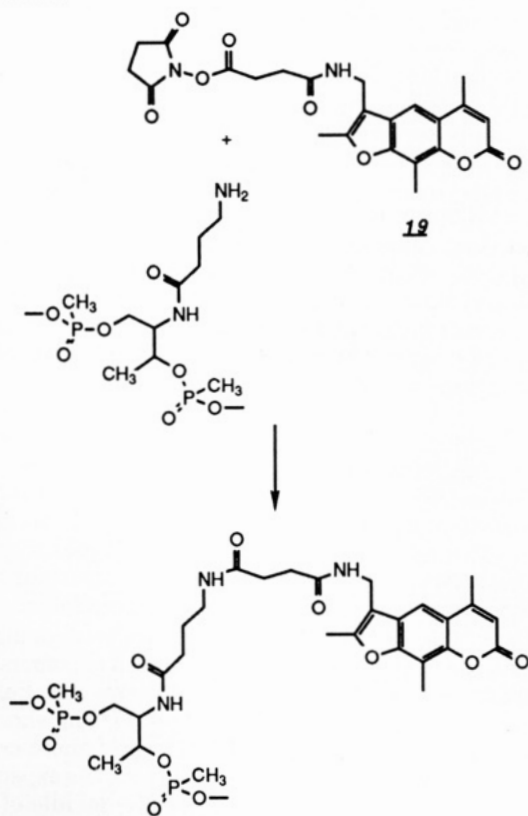
Scheme III



The underline indicates *abl* sequences.

Oligo Number	Conjugation Site	Linker Length
1	a	C4
2	b	C4
3	c	C0
4	c	C2
5	c	C4
6	c	C6
7	c	C8
8	d	C4
9	e	C4

Scheme IV



gation is not limited to the 3'- or 5'-termini, the method permits the chemical moiety to be directed toward any desired base (or bases) on a complementary target strand.

Such an approach is ideally suited for conjugation with 4'-(aminomethyl)-4,5',8-trimethylpsoralen, where the optimal target sites are opposite a thymidine or uridine base. Our non-nucleotide-based linking approach was intended to provide attachment sites which neither participate in nor interfere with the normal hybridization characteristics of the oligonucleotide. Indeed, our results show that the non-nucleotide linker has a negligible effect on the base-stacking interactions occurring around its site of insertion. This property undoubtedly enhances the ability of the tethered psoralen moiety to intercalate and engage in photo-cross-linking interactions with the RNA target strand.

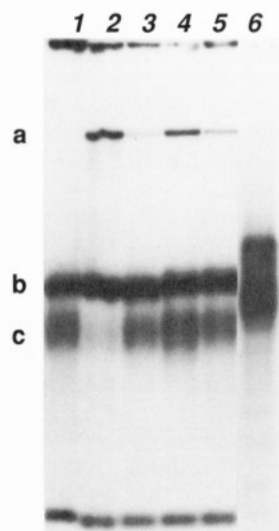


Figure 1. PAGE analysis demonstrating site-specific cross-linking of psoralen-methylphosphonate-oligonucleotide 5 to the 440-base *bcr/abl* RNA target: 0.1 pmol of ^{32}P labeled psoralen-oligonucleotide was annealed in the presence or absence of 1 pmol of the RNA target in 10 μL of 10 mM Tris-HCl (pH 7.2), 0.03% sarkosyl, 0.1 mM EDTA; 5 pmol each of two tandem methylphosphonate oligomers (18 bases in length) were also included in these annealing reactions. Annealing reactions were irradiated at 365 nm for 30 min on ice prior to analysis. Three bands are observed on the gel: (a) ^{32}P -psoralen-oligonucleotide that has been photo-cross-linked to the RNA target, (b) free ^{32}P -psoralen-oligonucleotide (not photo-cross-linked), and (c) free ^{32}P -psoralen-oligonucleotide which has had its psoralen moiety photodegraded during UV irradiation. Lane 1, control (no RNA); lane 2, plus RNA; lane 3, RNA plus 10 pmol of a normal diester oligonucleotide having the same sequence as the ^{32}P -psoralen-oligonucleotide; lanes 4 and 5, RNA plus 1 or 2 pmol of nonradioactive psoralen-oligonucleotide; lane 6, control, RNA plus ^{32}P -labeled nonsense psoralen-methylphosphonate oligonucleotide 5'-ApCTAAAATT-TAATATGAA-(C₄-psoralen)-T-3'.

Improvements in photo-cross-linking efficiency were observed with psoralen-oligonucleotide conjugates containing shorter linker arms (C₀ and C₂). This indicates that a shorter tether length is more efficient for directing the psoralen moiety toward its intercalation site(s). Absorption of a photon can lead to degradation of the psoralen moiety when it is outside of the duplex, whereas the expected 2 + 2 cycloaddition reaction occurs when it is intercalated into the duplex. Such a result is clearly evident on our polyacrylamide gels, where photodegraded

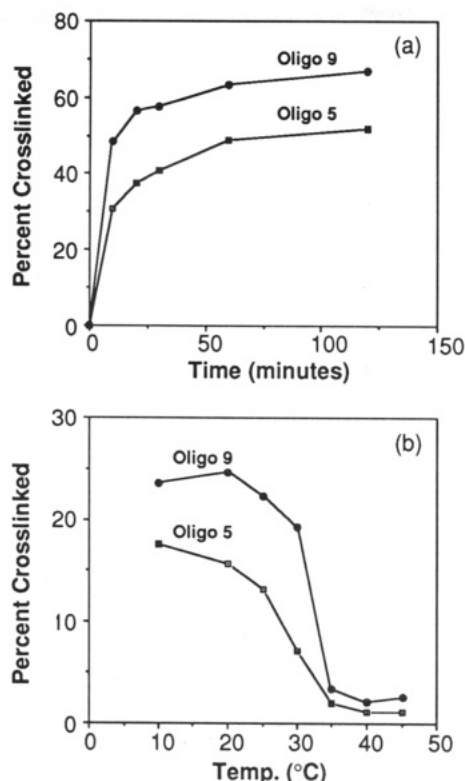


Figure 2. Photo-cross-linking of ^{32}P -labeled psoralen-methylphosphonate-oligonucleotides **5** and **9** to a 440-base *bcr/abl* RNA target: (a) irradiation on ice as a function of time, (b) vials immersed 1 cm below the surface of a circulating water bath at various temperatures with 30-min irradiations at a distance of 10 cm above the surface.

psoralen oligonucleotides are detected as faster running bands than those of the parent compounds (see Figure 1).

The method of photo-cross-linking analysis reported here differs from previous studies (9, 11) in that the ^{32}P -labeled psoralen-oligomer conjugates were monitored in the presence of excess RNA target strands. (In previous reports, ^{32}P -labeled target strands were monitored in the presence of excess psoralen-oligomers.) This method permitted the entire population of psoralen-methylphosphonate-oligomers to be detected by gel electrophoresis, i.e., those which were cross-linked to the RNA target (upper bands), unmodified (middle bands), or photodegraded (lower bands). The data generated permits an analysis of the degree to which the hybridization characteristics of methylphosphonate oligomers are compromised due to chirality at phosphorus. Each oligomer actually exists in 2^n different chiral forms, where n is the number of methylphosphonate linkages existing in either the R_p or S_p conformation. Up to 70% of psoralen-oligomer **9** was cross-linked to the RNA target under our assay conditions (see Figure 2). Furthermore, the RNA target strand clearly protected each psoralen-oligomer from photodegradation (see Figure 1). These observations suggest that chirality does not significantly limit the population of methylphosphonate oligomers available for duplex formation with an RNA target.

Our non-nucleotide-based linking approach is not limited to conjugations with psoralen since a wide variety of other chemical moieties can be attached by the same general approach. Furthermore, the method is not restricted to methylphosphonate oligonucleotides since a variety of other oligonucleotide analogs (e.g., phosphoramidites, phosphorothioates, etc.) can be modified with non-nucleotide linker arms through simple modifications of the chemistry presented above.

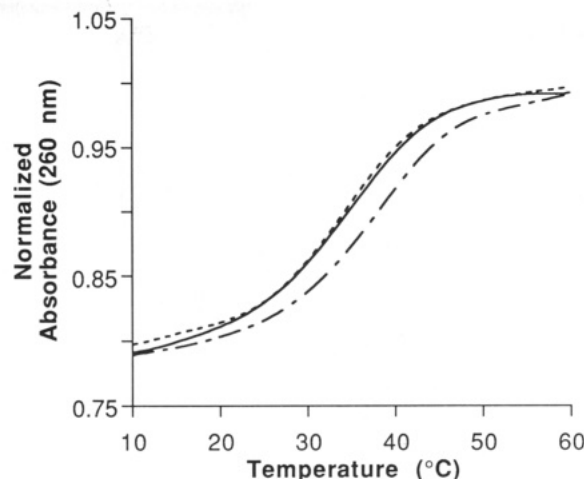


Figure 3. Thermal denaturation profiles for a completely unmodified oligomer 5'-GpGCTTTTGAAGCTCTGCTTA-3' (---), an oligomer containing an internal non-nucleotide C_4 -linker 5'-GpGCTTTTGA-(C_4)-ACTCTGCTTA-3' (—), and an oligomer containing an internal non-nucleotide C_4 -linker that has been conjugated with psoralen 5'-GpGCTTTTGA-(C_4)-psoralen-ACTCTGCTTA-3' (- - -). Each oligomer was hybridized with a synthetic RNA target strand 5'-UAAGCAGAGUCAAAGCC-3' in 20 mM potassium phosphate (pH 7.2), 0.03% potassium sarkosylate, 0.01 mM EDTA (1:1 molar ratios, total strand concentration 2.4×10^{-6} M). The solutions were incubated from 80 °C to room temperature over about 4 h and then stored at 4 °C overnight. Optical measurements were performed on a Perkin-Elmer Lambda 3 spectrophotometer interfaced with an IBM PC-compatible computer. Temperature control was provided by a programmable interface (Softways, Inc.) connected to a refrigerated ethylene glycol-water bath (Neslab RTE-100). Digitized absorbance and temperature values were stored on the computer for subsequent plotting and analysis. The temperature variation was 0.5 °C/min.

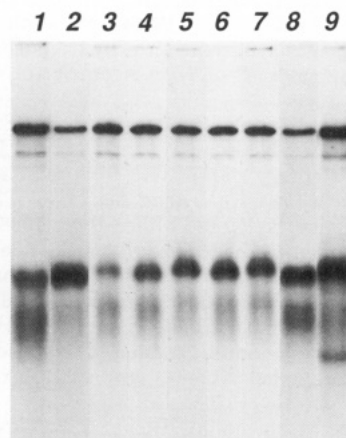


Figure 4. PAGE analysis of ^{32}P -labeled psoralen-methylphosphonate-oligonucleotides **1-9** after annealing to a 440-base *bcr/abl* RNA target and irradiation at 365 nm for 30 min on ice. Annealing conditions and analysis were similar to those described for Figure 1, except that the annealing reaction buffer was 10 mM potassium phosphate, pH 7.2, 0.03% potassium sarkosylate, 0.01 mM EDTA. Lane 1, oligomer **1**; lane 2, oligomer **2**; lane 3, oligomer **3**; lane 4, oligomer **4**; lane 5, oligomer **5**; lane 6, oligomer **6**; lane 7, oligomer **7**; lane 8, oligomer **8**; lane 9, oligomer **9**.

ACKNOWLEDGMENT

We thank Melissa Almazan for preparing the 440-base *bcr/abl* RNA transcript used in these studies. We are also grateful to Ben Tseng and Tom Adams for helpful discussions.

Table I. Average Photo-Cross-Linking Values for Psoralen-MP-Oligomer Conjugates

oligomer no.	site	linker	% photo-cross-linked, 4 °C (n)
(a) Varying Linker-Arm Length			
3	c	C ₀	59.6 ± 9.6 (9)
4	c	C ₂	44.5 ± 7.2 (9)
5	c	C ₄	43.8 ± 7.7 (9)
6	c	C ₆	36.9 ± 4.5 (5)
7	c	C ₈	39.2 ± 5.2 (9)
(b) Varying Sites of Insertion			
1	a	C ₄	34.8 ± 5.4 (5)
2	b	C ₄	22.7 ± 5.9 (5)
5	c	C ₄	43.8 ± 7.7 (9)
8	d	C ₄	16.0 ± 1.6 (5)
9	e	C ₄	44.7 ± 3.2 (5)

LITERATURE CITED

- (1) Ts'o, P. O. P., Miller, P. S., Aurelian, L., Murakami, A., Agris, C., Blake, K. R., Lin, S.-B., and Smith, C. (1987) An approach to chemotherapy based on base sequence information and nucleic acid chemistry: Matagen (Masking Tape for Gene Expression). *Ann. N.Y. Acad. Sci.* 507, 220-241.
- (2) Miller, P. S. (1989) Non-ionic antisense oligonucleotides. In *Oligonucleotides: Antisense Inhibitors of Gene Expression* (J. S. Cohen, Ed.) pp 79-95, CRC Press, Boca Raton, FL.
- (3) Chang, E. H., Miller, P. S., Cushman, C., Devadas, C., Pirolo, K. F., Ts'o, P. O. P., and Yu, Z. P. (1991) Antisense inhibition of *ras* p21 expression that is sensitive to a point mutation. *Biochemistry* 30, 8283-8286.
- (4) Furdon, P. J., Dominski, Z., and Kole, R. (1989) RNase H cleavage of RNA hybridized to oligonucleotides containing methylphosphonate, phosphorothioate and phosphodiester bonds. *Nucleic Acids Res.* 17, 9193-9204.
- (5) Quartin, R. S., Brakel, C. L., and Wetmur, J. G. (1989) Number and distribution of methylphosphonate linkages in oligodeoxynucleotides affect exo- and endonuclease activity and ability to form RNase H substrates. *Nucleic Acids Res.* 17, 7253-7262.
- (6) Sarin, P. S., Agrawal, S., Civeira, M. P., Goodchild, J., Ikeuchi, T., and Zamechnik, P. C. (1988) Inhibition of acquired immunodeficiency syndrome virus by oligodeoxynucleoside methylphosphonates. *Proc. Natl. Acad. Sci. U.S.A.* 85, 7448-7451.
- (7) Freier, S. M., Kierzek, R., Jaeger, J. A., Sugimoto, N., Caruthers, M. H., Neilson, T., and Turner, D. H. (1986) Improved free-energy parameters for predictions of RNA duplex stability. *Proc. Natl. Acad. Sci. U.S.A.* 83, 9373-9377.
- (8) Lee, B. L., Blake, K. R., and Miller, P. S. (1988) Interaction of psoralen-derivatized oligodeoxyribonucleoside methylphosphonates with synthetic DNA containing a promoter for T7 RNA polymerase. *Nucleic Acids Res.* 16, 10681-10697.
- (9) Lee, B. L., Murakami, A., Blake, K. R., Lin, S.-B., and Miller, P. S. (1988) Interaction of psoralen-derivatized oligodeoxynucleoside methylphosphonates with single-stranded DNA. *Biochemistry* 27, 3197-3203.
- (10) Kean, J. M., Murakami, A., Blake, K. R., Cushman, C. D., and Miller, P. S. (1988) Photochemical cross-linking of psoralen-derivatized oligonucleoside methylphosphonates to rabbit globin messenger RNA. *Biochemistry* 27, 9113-9121.
- (11) Bhan, P., and Miller, P. S. (1990) Photo-cross-linking of psoralen-derivatized oligonucleoside methylphosphonates to single-stranded DNA. *Bioconjugate Chem.* 1, 82-88.
- (12) Teare, J., and Wollenzein, P. (1989) Specificity of site directed psoralen addition to RNA. *Nucleic Acids Res.* 17, 3359-3372.
- (13) Takasugi, M., Guendouz, A., Chassignol, M., Decout, J. L., Lhomme, J., Thuong, N. T., and Helene, C. (1991) Sequence-specific photo-induced cross-linking of the two strands of double-helical DNA by a psoralen covalently linked to a triple helix-forming oligonucleotide. *Proc. Natl. Acad. Sci. U.S.A.* 88, 5602-5606.
- (14) Van Houten, B., Gamper, H., Hearst, J. E., and Sancar, A. (1986) Construction of DNA substrates modified with psoralen at a unique site and study of the action mechanism of ABC exonuclease on these uniformly modified substrates. *J. Biol. Chem.* 261, 14135-14141.
- (15) Gasparro, F. P., Edelson, R. L., O'Malley, M. E., Ugent, S. J., and Wong, H. H. (1991) Photoactivatable antisense DNA: suppression of ampicillin resistance in normally resistant *Escheria coli*. *Antisense Res. Dev.* 1, 117-140.
- (16) Pieleles, U., and English, U. (1989) Psoralen covalently linked to oligodeoxyribonucleotides: synthesis, sequence specific recognition of DNA and photo-cross-linking to pyrimidine residues of DNA. *Nucleic Acids Res.* 17, 285-299.
- (17) Duval-Valentin, G., Thuong, N. T., and Helene, C. (1992) Specific inhibition of transcription by triple helix-forming oligonucleotides. *Proc. Natl. Acad. Sci. U.S.A.* 89, 504-508.
- (18) Pieleles, U., Sproat, B. S., and Cramer, R. (1989) Preparation of a novel psoralen containing deoxyadenosine building block for the facile solid phase synthesis of psoralen-modified oligonucleotides for a sequence specific crosslink to a given target sequence. *Nucleic Acids Res.* 17, 8967-8978.
- (19) Adams, J. M. (1985) Oncogene activation by fusion of chromosomes in leukaemia. *Nature* 315, 542-543.
- (20) Stanfield, C. F., Parker, J. E., and Kanellis, P. (1981) Synthesis of protected amino acid alcohols: a comparative study. *J. Org. Chem.* 46, 4799-4800.
- (21) Jaeger, A. and Engels, J. (1984) Synthesis of methylphosphonates via a phosphoramidite approach. *Tetrahedron Lett.* 25, 1437-1440.
- (22) Isaacs, S. T., Shen, C. J., Hearst, J. E., and Rapoport, H. (1977) Synthesis and characterization of new psoralen derivatives with superior photoreactivity with DNA and RNA. *Biochemistry* 16, 1058-1064.
- (23) Miller, P. S., Reddy, M. P., Murakami, A., Blake, K. R., Lin, S.-B., and Agris, C. H. (1986) Solid phase syntheses of oligodeoxynucleoside methylphosphonate. *Biochemistry* 25, 5092-5097.
- (24) Murakami, A., Blake, K. R., and Miller, P. S. (1985) Characterization of sequence-specific oligodeoxyribonucleoside methylphosphonates and their interaction with rabbit globin mRNA. *Biochemistry* 24, 4041-4046.
- (25) Nelson, P. S., Sherman-Gold, R., and Leon, R. (1989) A new and versatile reagent for incorporating multiple primary aliphatic amines into synthetic oligonucleotides. *Nucleic Acids Res.* 17, 7179-7186.
- (26) Esposito, F., Brankamp, R. G., and Sinden, R. R. (1988) DNA sequence specificity of 4',5,8-trimethylpsoralen cross-linking. *J. Biol. Chem.* 263, 11466-11472.

Preparation and Characterization of Recombinant Proricin Containing an Alternative Protease-Sensitive Linker Sequence

Michael Westby, Richard H. Argent, Carol Pitcher, J. Michael Lord, and Lynne M. Roberts*

Department of Biological Sciences, University of Warwick, Coventry CV4 7AL, U.K. Received February 26, 1992

The aim of this study was to determine the feasibility of utilizing a factor Xa-specific cleavage site within a recombinant protein containing the ricin A chain (RTA) sequence. Release of RTA is believed to be an essential step during the intracellular phase of ricin intoxication. Failure to incorporate such cleavage sites in fusions containing RTA results in a loss of toxin action (O'Hare, M., et al. (1990) *FEBS Lett.* 273, 200. Kim, J., and Weaver, R. F. (1988) *Gene* 68, 315). In this report we describe the introduction of a factor Xa-specific site in the linker of proricin, which we use here as a model substrate. Upon purification of the recombinant mutant proricin after expression in *Xenopus* oocytes, we demonstrate that the protease does have access to the engineered recognition sequence (albeit at low efficiency) and that the presence of the latter does not interfere with disulfide bond formation or the lectin activity of the ricin B chain moiety. Upon cleavage and reduction, the RTA polypeptide displays ribosome-inactivating ability, indicating that the presence of the modified linker at its C-terminus does not interfere with its catalytic activity. The general applicability of using such a cleavage site in recombinant fusions with RTA is discussed.

INTRODUCTION

Ricin is a heterodimeric cytotoxin produced in the seeds of the castor oil plant, *Ricinus communis*. The mature toxin consists of a 32-kDa A chain (RTA) linked by a disulfide bond to a 34-kDa galactose-binding B chain (RTB) (1). Ricin intoxication of eukaryotic cells is initiated when the holotoxin interacts with cell surface glycoproteins and glycolipids containing galactose. This binding is mediated entirely by RTB, which is also believed to play a role in correctly transporting RTA during the ensuing endocytosis (2, 3). Membrane translocation of RTA, possibly from a Golgi compartment (4, 5), is then followed by catalytic inactivation of ribosomes in a step mediated entirely by reduced RTA. RTA is an RNA-specific N-glycosidase which acts on 28S or 26S rRNA leading to a specific depurination within a highly conserved region thought to be crucial in the interaction with elongation factors (6).

Ricin is synthesized in *Ricinus* seeds as a preproprotein which is converted to its mature form by a number of co- and post-translational modifications (7, 8). These begin as the protein is being segregated into the ER lumen and terminate after vesicular transport when the protein is finally deposited in protein body organelles where ricin accumulates. The initial preproricin molecule contains a 35 residue presequence (including a signal peptide), followed by RTA, a 12 amino acid residue linker, and the RTB sequence (9). The final processing steps include proteolytic removal of the linking peptide by enzymes contained within protein bodies (8). A study of the activities of the proricin precursor has shown that although it possesses sugar binding activity, it is unable to depurinate 28S rRNA (10). Catalytic activity is present only when peptide continuity between RTA and RTB is disrupted. Thus synthesis of RTA as an inactive proenzyme contributes to the safeguards which ensure that RTA does not inactivate endogenous plant ribosomes.

Ricin and RTA have been used extensively in a variety of conjugates designed for selective cell destruction (reviewed in ref 11). Conventionally, the toxin is linked

to an antibody, lymphokine, or other protein entity by chemical means, which also introduces a reducible disulfide bond. Many such conjugates exert a potent cytotoxic effect upon their target cells. Increasingly, however, recombinant cytotoxic conjugates are being produced directly by expression of the relevant gene fusions. This has been a particularly successful approach with the bacterial toxins diphtheria toxin (DT) and *Pseudomonas* exotoxin A (PE). By fusing fragments of these toxins with alternative cell binding proteins such as α -melanocyte stimulating hormone (12), soluble CD4 (13), or a single chain Fv antibody fragment (14), cell-specific, single-chain cytotoxins have been generated. Similar single-chain fusions containing RTA are not cytotoxic (15, 16). It is believed that during intoxication, RTA must be released from its cell binding ligand to be competent for membrane translocation. Unlike DT and PE, RTA lacks a specific proteolytic cleavage site recognized by target cell proteases encountered upon cellular uptake. Introduction of a trypsin-sensitive sequence into an RTA-protein A (PA) fusion protein demonstrated for the first time that a noncytotoxic fusion protein containing RTA could be converted into a cytotoxic conjugate (16).

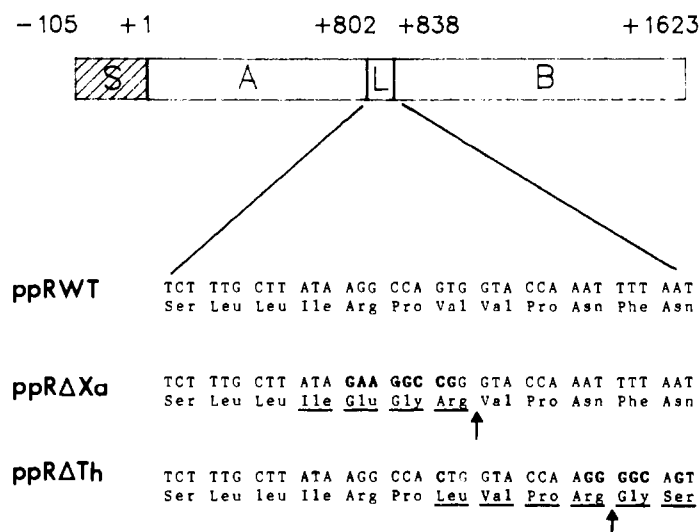
In the present report we describe the production and characterization of a recombinant variant possessing an alternative protease-sensitive linker separating RTA from RTB. Using proricin as a model recombinant fusion, we reveal that, as in native proricin, the mutant precursor possesses lectin activity but has no RTA activity until treated with the appropriate protease and reduced. Specific cleavage generates disulfide-bonded subunits with the biological properties of native holotoxin. This particular arrangement of modified linker and flanking cysteines, which does not significantly perturb the structure of the component polypeptides, may have general applicability in creating disulfide-linked conjugates from single-chain recombinant polypeptides containing RTA.

EXPERIMENTAL PROCEDURES

Construction of Plasmids. Preproricin cDNA (9) was subjected to site-directed mutagenesis to create a mutant clone with a linker encoding a factor Xa recognition

* Author to whom correspondence should be addressed.

A



B

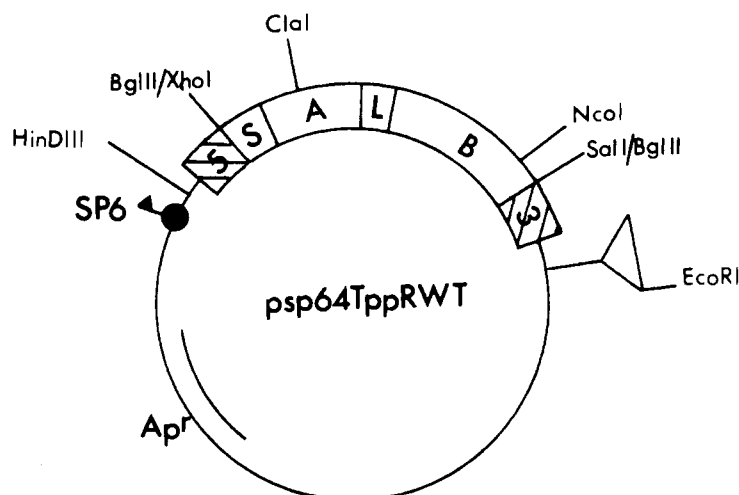


Figure 1. Mutagenesis of the proricin linker. (A) DNA and predicted amino acid sequences of the linker regions in wild-type preproricin cDNA (ppRWT) and factor X-site containing preproricin (ppRΔXa). Mutated bases are shown in bold type and the amino acids comprising the protease recognition site are underlined. The arrow indicates the predicted site of cleavage. Nucleotide numbers refer to the preproricin cDNA (9). S refers to signal sequence, A, L, and B to RTA, linker, and RTB, respectively. (B) The wild-type and mutant preproricin sequences were ligated into pSP64T as described in the methods and shown here for the wild-type sequence. 5 and 3 refer to the 5' and 3' untranslated regions of *Xenopus* β globin cDNA which, upon transcription, provide stability to the RNA when injected into *Xenopus* oocytes (18). HindIII refers to a *HindIII* site between the SP6 promoter and the *BglII* expression site. Other sites characteristic of the vector or preproricin sequence are also indicated.

sequence (IEGR). The template for mutagenesis was derived from a 552 base pair *BglII* fragment which spans the preproricin linker region. This fragment was cloned into the *BglII* site of pIC20-H (17), and an *EcoRI* and a *HindIII* fragment were subsequently ligated into M13-mp19. Mutagenesis was performed by standard techniques using an oligonucleotide-directed mutagenesis kit (Amersham Corp.) as directed by the manufacturer. Mutations were confirmed by dideoxy sequencing. Oligonucleotides for mutagenesis were synthesized on an Applied Biosystems Model 380 B DNA synthesizer. The eight base pair mismatch to create the factor Xa site was achieved in a single round of mutagenesis using the oligonucleotide 5'-TTTGCTTATAGAAGGCCGGGTACCAAAT-3'. The mismatches are indicated by underlining. The *BglII* fragment was then substituted into the wild-type preproricin clone and sequenced. The nucleotide and predicted amino acid sequences corresponding to the

new linker is shown in Figure 1A. Wild-type and mutant proricins were subsequently recloned into the *BglII* expression site of pSP64T, a vector which has been successfully used for the production of stable transcripts suitable for expression in *Xenopus laevis* oocytes (18).

Expression of Preproricin Transcripts. Transcripts were synthesized *in vitro* in the presence of the capping dinucleotide 7-Me(5')GpppG(5')OH and SP6 RNA polymerase as described previously (19). Purified RNA was dissolved in water at a concentration of 1 mg/mL. Oocytes were injected with approximately 50 ng of RNA, pulse labeled with [³⁵S]methionine, and homogenized as described previously (19), except that the protease inhibitor phenylmethanesulfonylfluoride was omitted. Proricin was either affinity purified (below) or, standardly, batches of 10 oocytes were homogenized for immunoprecipitation (20).

Affinity Purification of Proricin Mutants. Recombinant proricens were purified by affinity chromatography using a 1.0 mL column of SeLectin-2 beads (10) (lactose coupled to acrylamide; Pierce, Rockford, IL) equilibrated in oocyte homogenization buffer (19). Soluble protein from 10 homogenized oocytes was typically passed through the column a total of three times. The column was washed with three 1.0-mL aliquots of oocyte homogenization buffer prior to the elution of bound material in either homogenization buffer or protease digestion buffer (10 mM Tris-HCl, 1 mM EDTA, 140 mM NaCl, pH 7.6) containing 50 mM galactose.

Proteolytic Digestion. Affinity selected proricin was eluted from the SeLectin-2 matrix in protease digestion buffer containing 50 mM galactose. Proricin substrate was then incubated for 60 min at 26 °C with 1/10 volume of human factor Xa (kindly provided by P. Esnouf, The Radcliffe Hospital, Oxford, UK). Factor Xa, at a concentration of 240 µg/mL was stored frozen at -20 °C.

Depurination of 28S rRNA. Affinity-selected and protease-treated proricin was incubated for 30 min at 30 °C with 30 µg of salt-washed rabbit ribosomes prepared from a non-nuclease-treated rabbit reticulocyte lysate (Promega) (21) in 1X Endo buffer (25 mM Tris-HCl, 25 mM KCl, 5 mM MgCl₂, pH 7.6) before or after reduction of the interchain disulfide bond using 5% (v/v) β-mercaptoethanol for 30 min at room temperature. RNA was then extracted and analyzed for the RTA-specific modification of ribosomal RNA using the acetic-aniline reagent, exactly as described previously (22). This assay is based on the observation that RTA-modified ribosomes which carry a 28S rRNA depurinated at a position close to the 3' end, are extremely sensitive to hydrolysis using acetic-aniline. Thus brief aniline treatment of RNA extracted from ribosomes will release a 390 base RNA fragment only if the ribosomes were inactivated with a catalytically active RTA. Non-aniline-treated samples should not release a visible RNA fragment. Purified recombinant RTA on ribosomes was used to give a positive control signal.

Other Methods. Published procedures were followed for translation of in vitro transcripts in wheat germ cell-free lysates (23), sodium dodecyl sulfate-polyacrylamide gel electrophoresis, fluorography, immunoprecipitation (20), and enzymic deglycosylation using endo-*N*-acetyl glucosaminidase H (8). Antibodies for immunoprecipitation were raised in rabbits against glycosylated RTB and crossreact with RTA, RTB, and proricin.

RESULTS

Mutagenesis and Cloning. Oligonucleotide site-directed mutagenesis of the preproricin cDNA was performed to create a factor Xa recognition sequence within the naturally occurring linker which separates the RTA and RTB coding regions. The nucleotide and amino acid sequences of the wild type (pp RWT) and mutant (ppRΔXa) are shown in Figure 1A. Preproricin encoding sequences were then cloned into the transcription vector pSP64T as to generate an expression plasmid as illustrated in Figure 1B.

Expression and Purification of Proricin. Transcripts were prepared for wild-type preproricin and the variant using SP6 RNA polymerase. Transcripts were microinjected into *Xenopus* oocytes and the [³⁵S]-methionine-labeled products were subsequently analyzed after homogenization and purification by selection on columns of immobilized lactose (Figure 2). In both cases a good proportion of the proricin synthesized possessed

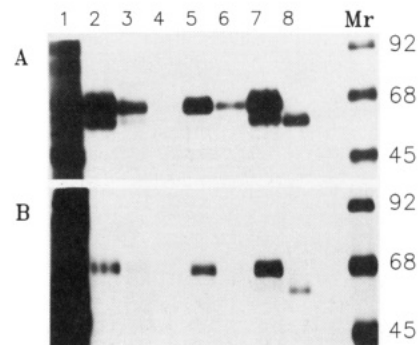


Figure 2. Wild-type and mutant proricens synthesized in *Xenopus* oocytes are glycosylated and bind lactose. [³⁵S]-methionine-labeled homogenates from 10 oocytes were applied to a 1.0-mL SeLectin-2 (Pierce) column as described in the methods. A and B refer to wild-type and mutant proricens, respectively. Lane 1, unbound protein; lane 2, immunoprecipitate of proricin from the unbound fraction; lanes 3 and 4, immunoprecipitated proricin in the first two 0.5-mL column washes with homogenization buffer; lanes 5 and 6, nonimmunoprecipitated material eluted in buffer containing 50 mM galactose; lanes 7 and 8, immunoprecipitates from crude homogenates not treated and treated with endo-*N*-acetylglucosaminidase H, respectively. M refers to molecular weight markers. Immunoprecipitations (where appropriate) were performed using rabbit anti-B chain antisera which cross react with both subunits separately and with the proricin precursors. All samples were run by SDS-PAGE in reducing buffer.

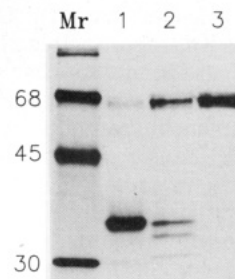


Figure 3. Protease susceptibility of mutant proricin: lane 1, oocyte produced RTB control; lanes 2 and 3, affinity purified proricin eluted in reaction buffer containing 50 mM galactose was incubated with and without factor Xa as described in the methods. Samples are electrophoresed on SDS-PAGE in a reducing sample buffer.

lactose binding ability, as judged by the amount of radioactive proricin released from the SeLectin-2 matrix in buffer containing 50 mM galactose (Figure 2, lanes 2 and 5). As observed previously (10), the only labeled protein to be retained by the column was the *Ricinus* lectin molecule (Figure 2, lane 5). In this track the sample represents a nonimmunoprecipitated sample. When immunoprecipitated samples of total homogenate (lane 7) were treated with endo-*N*-acetyl glucosaminidase H (lane 8), the multiple proricin species were converted to single polypeptides of greater electrophoretic mobility (i.e. deglycosylated), confirming that they had become *N*-glycosylated within *Xenopus* oocytes. The faster migrating species in the proricin immunoprecipitate from total homogenates (lanes 2 and 7) is most likely a nonglycosylated form of proricin which runs with the same mobility as the endo H treated sample (lane 8). The nonglycosylated form is not always seen (e.g. Figure 2B) and appears to be dependent upon the oocyte batch.

Protease Susceptibility of the Modified Linker. Affinity purified mutant proricin was treated with protease to confirm specific susceptibility (Figure 3). Recombinant RTB produced in *Xenopus* oocytes and affinity purified was used to indicate the electrophoretic mobility of this

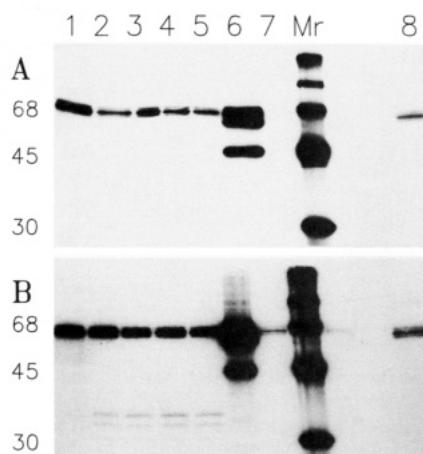


Figure 4. Cleavage and disulfide bonding of mutant proricin: affinity purified proricin from 10 oocytes were digested for up to 1 h with factor Xa as described in the methods and subsequently immunoprecipitated. A and B refer to wild-type and mutant proricins, respectively. All tracks but lane 8 on the SDS-PAGE were run in the presence of reducing agent. Lanes 1–5, material eluted from the column incubated in the first galactose-containing wash with factor Xa for 0, 15, 30, 45, and 60 min, respectively; lane 6, immunoprecipitate of the unbound material; lane 7, protein eluted in the second galactose wash; lane 8, a duplicate samples of the 60-min protease sample (lane 5) electrophoresed in the absence of reducing agent. M refers to molecular weight markers.

particular subunit (Figure 3, lane 1). Using the mutant proricin and factor Xa, reproducible cleavage products were visualized (Figure 3, lane 2) that were absent in a duplicate incubation minus protease (Figure 3, lane 3). Cleavage was incomplete but reproducible, using the batch of enzyme provided. The production of three fragments is discussed later.

Cleavage and Disulfide-Bond Formation. Affinity-purified wild-type or mutant proricins were digested for up to 60 min with factor Xa (Figure 4). Aliquots of each reaction were immunoprecipitated under nonreducing conditions and then subjected to SDS-PAGE in the presence of reducing agent. Wild-type proricin was not cleaved by factor Xa (Figure 4A) whereas the mutant polypeptide was, albeit at low efficiency using the conditions described here (Figure 4B). It would appear that after 15 min there was little further digestion. When an equivalent aliquot of the 60-min mutant digestion was electrophoresed in the absence of reducing agent, the cleavage fragments had apparently disappeared, indicating they were covalently coupled by a disulfide bond in the native protein. (Figure 4B, lane 8).

Ribosome Inactivation. Figure 5 shows the activities of the various forms of proricin toward mammalian ribosomes. As shown, the RNA fragment diagnostic of RTA activity (see the methods for explanation) was absent in samples containing cleaved but unreduced proricin (Figure 5A, lanes 1–4), but present if the connecting disulfide bond had been reduced by pretreatment with 5% (v/v) β -mercaptoethanol (Figure 5A, lanes 5–7). The decreasing intensity of fragment in these lanes correlates with the amounts of cleaved substrate added to the ribosomes. Noncleaved proricin was not catalytically active (Figure 5, lane 9, and ref 10). Controls include ribosomes treated with 0.1 ng of recombinant RTA or 10 ng of nonreduced or reduced recombinant RTB (Figure 5A, lanes 10–12, respectively), plus non-aniline-treated samples (Figure 5A, lanes 13–18). To check that the high concentration (5% (v/v)) of β -mercaptoethanol did not itself interfere with the assay, ribosomes were incubated in the presence or absence of recombinant RTA in the

presence or absence of reducing agent. Figure 5B shows that ribosomes were only modified in the presence of RTA, irrespective of the presence or absence of 5% (v/v) β -mercaptoethanol.

DISCUSSION

We show here that it is possible to make proricin containing a novel protease-sensitive cleavage site within the naturally occurring linker region without significantly perturbing the structures and therefore the biological properties of the component A and B chains. The factor X site was recognized by its protease although cleavage was generally poor under the conditions used here. Nevertheless, in the proportion of proricin which was cleavable it is clear that the new linker had not become buried in the fusion protein but remained accessible and presumably surface-exposed. Furthermore, presence of a modified linker did not affect disulfide bond formation between Cys 259 of RTA and Cys 4 of RTB.

The natural linker in wild-type proricin (Figure 1A) is cleaved by endoproteases contained within plant cell vacuoles. The cleavage specificity of at least one of these enzymes is known. The unique asparagine-specific endoprotease activity (responsible for cleavage after the terminal Asn 279 in the proricin linker) has been widely implicated in the processing of many plant vacuolar proteins (25). Its activity was recognized some years ago (26), but the enzyme has been purified only recently (27). It is an extremely unstable protease after purification, but nevertheless has been shown to convert several plant proprotein precursors into their mature forms. However a second endoprotease, presumably responsible for generating the mature C-terminus of the RTA subunit in proricin, has not yet been identified.

To exert a cytotoxic effect, RTA must be released from RTB intracellularly (16). In native ricin the linker has already been removed during protein maturation, thus the holotoxin requires no further treatment other than intracellular reduction to render it cytotoxic (28). In contrast, the bacterial toxins DT and PE and Shiga toxin are not proteolytically processed during their biosynthesis (29). However, their enzymatic ADP ribosylating or ribosome inactivating fragments are released from the holotoxins as a result of trypsin-like cleavages within a disulfide-bonded loop sequence (29). Such nicking can be revealed experimentally and appears to occur upon endocytosis when the toxins encounter an appropriate serine protease (30). Clearly, this requirement for a releasable toxic fragment has implications for the design of selective cell-killing reagents.

In the development of these reagents, immunotoxins (ITs) (antibody-toxin conjugates), have emerged as a major group with potentially enormous clinical value (reviewed in refs 31–34). In the so-called third and subsequent generations of conjugates, tailor-made recombinant proteins with the desired activities are anticipated. Although not yet routine, this approach also extends to the manufacturer of entire single chain antibody-toxin or other recombinant cell-toxin fusion proteins (12–14).

We have shown previously that RTA, as part of a recombinant fusion protein containing protein A in place of RTB, was biologically active in vitro but was not cytotoxic unless a cleavable sequence was inserted between the two protein moieties (16). On this previous occasion we used the DT disulfide loop as our protease-sensitive region. However, it was difficult to analyze cleavage and disulfide bonding in vitro due to the presence of multiple trypsin-sensitive sites within the RTA molecule and the

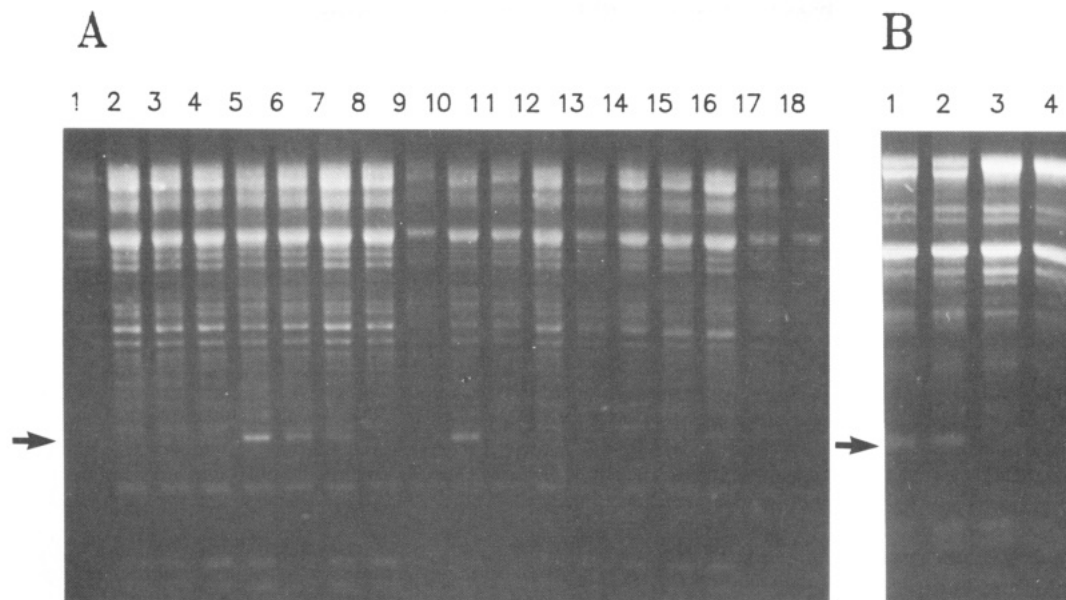


Figure 5. Cleaved proricin exhibits ribosome inactivating ability only after reduction of the interchain disulfide bond. (A) After incubation with ribosomes total RNA was analyzed as described previously (22). Lanes 1–12 represent extracted RNAs treated with aniline: lanes 1–4, serial dilutions of cleaved but nonreduced proricin; lanes 5–8, serial dilutions of cleaved and reduced proricin; lane 9, reduced but noncleaved proricin; lane 10, 0.1 ng of recombinant RTA; lanes 11 and 12, 10 ng of recombinant RTB, reduced and nonreduced, respectively; lanes 13–18 represent non-aniline-treated aliquots of RNA samples shown in lanes 1, 2, 5, 6, 10, and 11, respectively. (B) Lanes 1 and 2, aniline-treated RNA after incubation of ribosomes with 1 ng of recombinant RTA, reduced or nonreduced, respectively; lanes 3 and 4, equivalent incubations in which the extracted RNA was not treated with aniline. The arrow indicates the position of the small RNA fragment released after aniline-treatment of RNA extracted from RTA-modified ribosomes.

cleavage procedure required judicious use of protease. Furthermore, a different construct containing RTA linked to IL2 by the DT loop did not generate a disulfide-bonded heterodimer upon trypsin cleavage (L.M.R., unpublished). It appears that the DT loop may have limited application depending upon its context in a particular fusion. It is therefore timely to search for other possible joining sequences susceptible to specific cleavage and disulfide bonding.

In this report we have used native preproricin as our model to test the potential of an alternative, highly specific cleavage site within the linker. The human factor Xa recognition sequence (IEGR) has been used successfully to create cleavable recombinant proteins on previous occasions (35, 36). The minimal change of three amino acid residues to create such a site in the proricin linker was shown here not to prevent accessibility to the active protease nor to detrimentally affect disulfide bonding between cysteines which flank the linker, nor to disrupt the normal biological properties of the precursor substrate. A potentially spurious site (IVGR↓) occurs 16 residues within the RTB sequence. At first it was suspected that the smallest of the three cleavage products (e.g., Figure 3, lane 2, Figure 4B, lanes 2–5) might represent a fragment of RTB anomalously cleaved at just such a site, the larger two fragments representing RTA and RTB released after cleavage at the defined linker site. However, wild-type proricin when treated with factor Xa did not produce such a fragment (Figure 4A). Furthermore, if the smallest fragment were derived from a cleavage site lying outside the cysteines connecting RTA and RTB, it should still be observed when the cleaved proricin is run under non-reducing conditions (Figure 4B, lane 8). The fragment was not observed under these conditions. Its exact nature is therefore unclear but we believe it most likely represents an underglycosylated subunit. RTA and RTB have two potential N-glycosylation sites each (9), but frequently RTA carries just one N-linked oligosaccharide (37). This heterogeneity is visualized as a smear using SDS-PAGE

(Figure 2, lane 2). Endo-N-acetyl-glucosaminidase H treatment converts the multiple forms of proricin into a single, faster migrating species (Figure 2, lanes 7 and 8). In addition to the partly and fully glycosylated forms of proricin, a nonglycosylated version is also produced in oocytes (compare Figure 2, lanes 2 and 8). This form does not possess lectin activity as judged by its inability to bind to the affinity matrix. Since N-glycosylation, like disulfide bond formation, is an ER-catalyzed event, we assume that the affinity purified material tested in this report is from that proportion contained within the oocyte endomembrane system.

Xenopus oocytes were used in this study because we have previously found it to be an excellent system for the expression and analysis of soluble and stable forms of ricin containing the RTB region (10, 19, 24). This contrasts with the RTB made in *Escherichia coli* which was unstable and had a propensity to aggregate (38). Although a good system in which to purify substrate for in vitro analyses, the oocyte clearly has one major drawback. With yields of 1–13 ng of proricin/oocyte, insufficient material can be purified to perform microsequence analysis on the cleavage products or to perform a cytotoxicity assessment. We therefore base our assumption that cleavage occurs at the correct site on comparison of the size of the released fragments with control recombinant RTB using SDS-PAGE (Figure 3, lanes 1 and 2). Cleavage also generates a disulfide-bonded conjugate possessing the activities previously ascribed to processed proricin (10) (viz., ribosome-inactivating ability associated with correctly processed and reduced holotoxin). This, and previous findings with the RTA-protein A fusions (16), leads us to assume the cleaved molecule would possess cytotoxic ability.

To take the analysis further, an alternative eukaryotic expression system would clearly be desired for the production of useful amounts of proricin. N-glycosylation appears to be important in conferring solubility and stability to the molecule, or more specifically to the RTB component of the precursor (24). This requirement

precludes development of a bacterial expression system. However, fusions of RTA-linker sequences with alternative cell binding ligands having less stringent requirements could well be prepared on large scale using a bacterial host.

Recombinant mutant RTB molecules deficient in galactose (cell) binding (24), or in some other property, may be produced in association with RTA carrying a factor Xa site at its C-terminus as described in this report. This strategy would ensure correct folding of the mutant RTB moiety and production of stoichiometric amounts of both subunits. The cleaved proricins made this way could then be coupled by more conventional means to a cell-targeting antibody to produce versions of the highly potent holotoxin-containing ITs (11). However, the usefulness of the factor Xa cleavage site in conjunction with RTA goes further. Since the presence of eight additional residues at the C-terminus of RTA does not negate its ribosome inactivating- or RTB-reassociation abilities, one might conceive the design of recombinant fusions containing RTA, the modified linker, and the first few residues of RTB (to provide a connecting cysteine) with a whole range of alternative cell-binding ligands.

Other cleavage sites for use in recombinant fusions containing RTA or other plant ribosome inactivating proteins may also be considered. Mutation of proricin to generate an α -thrombin-specific site (IVPRGS) (Figure 1A) has also been accomplished (data not shown). Upon expression in *Xenopus* oocytes the precursor is soluble and sensitive to thrombin and the disulfide bond is correctly formed. Thus lack of an asparagine-specific protease within the endocytic compartments of target eukaryotic cells need no longer preclude construction of cytotoxic recombinant fusions containing RTA.

ACKNOWLEDGMENT

We thank Dr. P. Esnouf of The Radcliffe Hospital, Oxford, for the gift of factor Xa and ICI plc for recombinant RTA. This work was supported by the UK Science and Engineering Research Council via Grant GR/G 00877.

LITERATURE CITED

- (1) Olsnes, S., and Phil, A. (1982) In *Molecular Action of Toxins and Viruses* (P. Cohen, and S. Van Heyningen, Eds.) pp 51-105, Elsevier, Amsterdam.
- (2) Youle, R. J., Murray, G. J., and Neville, D. M. (1979) Ricin linked to monophosphopentamannose binds to fibroblast lysosomal hydrolase receptors, resulting in a cell-type specific toxin. *Proc. Natl. Acad. Sci. U.S.A.* 76, 5559-5562.
- (3) McIntosh, D. P., Edwards, D. C., Cumber, A. J., Parnell, G. D., Dean, C. J., Ross, W. C. J., and Forrester, J. A. (1983) Ricin B chain converts nontoxic antibody-ricin A chain conjugate into a potent and specific cytotoxic agent. *FEBS Lett.* 164, 17-20.
- (4) van Deurs, B., Sandvig, K., Petersen, O. W., Olsnes, S., Simons, K., and Griffiths, G. (1988) Estimation of the amount of internalized ricin that reaches the trans-Golgi network. *J. Cell. Biol.* 106, 253-267.
- (5) Sandvig, K., Prydz, K., Hansen, S. H., and van Deurs, B. (1991) Ricin transport in Brefeldin A-treated cells: Correlation between Golgi structure and toxic effect. *J. Cell. Biol.* 115, 971-981.
- (6) Endo, Y., Mitsui, K., Motizuki, M., and Tsurugi, K. (1987) The mechanism of action of ricin and related toxic lectins on eukaryotic ribosomes. *J. Biol. Chem.* 262, 551-559.
- (7) Lord, J. M. (1985) Synthesis and intracellular transport of lectin and storage protein precursors in endosperm from castor bean. *Eur. J. Biochem.* 146, 403-409.
- (8) Lord, J. M. (1985) Precursors of ricin and *Ricinus communis* agglutinin: glycosylation and processing during synthesis and intracellular transport. *Eur. J. Biochem.* 146, 411-416.
- (9) Lamb, F. I., Roberts, L. M., and Lord, J. M. (1985) Nucleotide sequence of cloned cDNA coding for preproricin. *Eur. J. Biochem.* 148, 265-270.
- (10) Richardson, P. T., Westby, M., Roberts, L. M., Gould, J. H., Colman, A., and Lord, J. M. (1989) Recombinant proricin binds galactose but does not depurinate 28S rRNA. *FEBS Lett.* 255, 15-20.
- (11) Vitetta, E. S., and Thorpe, P. E. (1991) Immunotoxins containing ricin or its A chain. *Semin. Cell Biol.* 2, 47-58.
- (12) Murphy, J. R., Bishai, W., Borowski, M., Miyahara, A., Boyd, J., and Nagle, S. (1986) Genetic construction, expression and melanoma-selective cytotoxicity of a diphtheria toxin-related α -melanocyte-stimulating hormone fusion protein. *Proc. Natl. Acad. Sci. U.S.A.* 83, 8258-8262.
- (13) Chaudhary, V. K., Mizukani, T., Fuerst, T. R., FitzGerald, D. J., Moss, B., Pastan, I., and Berger, E. A. (1988) Selective killing of HIV-infected cells by recombinant human CD4-PE hybrid protein. *Nature* 335, 369-372.
- (14) Chaudhary, V. K., Gallo, M. G., FitzGerald, D. J., and Pastan, I. (1990) A recombinant single-chain immunotoxin of anti-Tac variable region and a truncated diphtheria toxin. *Proc. Natl. Acad. Sci. U.S.A.* 87, 9491-9494.
- (15) Kim, J., and Weaver, R. F. (1988) Construction of a recombinant expression plasmid encoding a staphylococcal protein A-ricin A fusion protein. *Gene* 68, 315-321.
- (16) O'Hare, M., Brown, A. N., Hussain, K., Gebhardt, A., Watson, G., Roberts, L. M., Vitetta, E. S., Thorpe, P. E., and Lord, J. M. (1990) Cytotoxicity of a recombinant ricin A-chain fusion protein containing a proteolytically cleavable spacer sequence. *FEBS Lett.* 273, 200-204.
- (17) Marsh, J. L., Erfle, M., and Wykes, E. J. (1984) The pIC plasmid and phage vectors with versatile cloning sites for recombinant selection by insertional inactivation. *Gene* 32, 481-485.
- (18) Krieg, P. A., and Melton, D. A. (1984) Functional mRNAs are produced by SP6 *in vitro* transcription of cloned cDNAs. *Nucleic Acids Res.* 12, 7057-7071.
- (19) Richardson, P. T., Gilmartin, P., Colman, A., Roberts, L. M., and Lord, J. M. (1988) Expression of functional ricin B chain in *Xenopus* oocytes. *Biotechnology* 6, 565-570.
- (20) Roberts, L. M., and Lord, J. M. (1981) The synthesis of *Ricinus communis* agglutinin. *Eur. J. Biochem.* 119, 31-41.
- (21) Blobel, G. (1971) Release, identification and isolation of mRNA from mammalian ribosomes. *Proc. Natl. Acad. Sci. U.S.A.* 68, 832-835.
- (22) May, M. J., Hartley, M. R., Roberts, L. M., Krieg, P. A., Osborn, R. W., and Lord, J. M. (1989) Ribosome inactivation by ricin A chain: a sensitive method to assess the activity of wild-type and mutant polypeptides. *EMBO J.* 8, 301-308.
- (23) Anderson, C. W., Straws, J. W., and Dudock, B. S. (1983) Preparation of a cell-free protein-synthesizing system from wheat germ. *Methods Enzymol.* 101, 635-644.
- (24) Wales, R., Richardson, P. T., Roberts, L. M., Woodland, H. R., and Lord, J. M. (1991) Mutational analysis of the galactose binding ability of recombinant ricin B chain. *J. Biol. Chem.* 266, 19172-19179.
- (25) Lord, J. M., and Robinson, C. (1986) Role of Proteolytic Enzymes in the post-translational modification of proteins. In *Plant Proteolytic Enzymes*. (M. J. Dalling, Ed.) Vol. II, CRC Press, Inc., Boca Raton, FL.
- (26) Harley, S. M., and Lord, J. M. (1985) *In vitro* endoproteolytic cleavage of castor bean lectin precursors. *Plant Sci.* 41, 111-116.
- (27) Hara-Nishimura, I., Inoue, K., and Nishimura, M. (1991) A unique vacuolar processing enzyme responsible for the conversion of several proprotein precursors into the mature forms. *FEBS Lett.* 294, 89-93.
- (28) Wright, H. T., and Robertus, J. D. (1987) The intersubunit disulfide bridge of ricin is essential for cytotoxicity. *Arch. Biochem. Biophys.* 256, 280-284.
- (29) Olsnes, S., Kozlov, J. V., van Deurs, B., and Sandvig, K. (1991) Bacterial protein toxins acting on intracellular targets. *Semin. Cell Biol.* 2, 7-14.

- (30) Ogata, M., Chaudhary, V. K., Pastan, I., and FitzGerald, D. J. (1990) Processing of *Pseudomonas* exotoxin by a cellular protease results in the generation of a 37,000-Da toxin fragment that is translocated to the cytosol. *J. Biol. Chem.* 265, 20678–20685.
- (31) Frankel, A. E., Ed. (1988) *Immunotoxins*, Kluwer, Boston.
- (32) FitzGerland, D. J., and Pastan, I. (1989) Targeted toxin therapy for the treatment of cancer. *J. Natl. Cancer Inst.* 81, 1455–1462.
- (33) Byers, V. S., and Baldwin, R. W. (1991) Rationale for clinical use of immunotoxins in cancer and autoimmune disease. *Semin. Cell. Biol.* 2, 59–70.
- (34) Wawrzynczak, E. (1991) Systemic immunotoxin therapy of cancer: Advances and prospects. *Br. J. Cancer* 64, 624–630.
- (35) Nagai, K., and Thorgersen, H. C. (1984) Generation of β -globin by sequence specific proteolysis of a hybrid protein produced in *Escherichia coli*. *Nature* 309, 810–812.
- (36) Smith, D. B., and Johnson, K. S. (1988) Single-step purification of polypeptides expressed in *Escherichia coli* as fusions with glutathione S-transferase. *Gene* 67, 31–40.
- (37) Foxwell, B. M. J., Donovan, T. A., Thorpe, P. E., and Wilson, G. (1985) The removal of carbohydrates from ricin with endoglycosidases H, F and D and α -mannosidase. *Biochim. Biophys. Acta* 840, 193–203.
- (38) Hussain, K., Bowler, C., Roberts, L. M., and Lord, J. M. (1989) Expression of ricin B chain in *Escherichia coli*. *FEBS Lett.* 244, 383–387.

Metalloprotein Complexes for the Study of Electron-Transfer Reactions. Characterization of Diprotein Complexes Obtained by Covalent Cross-Linking of Cytochrome *c* and Plastocyanin with a Carbodiimide[†]

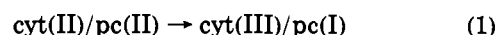
Jian S. Zhou, Herb M. Brothers II, John P. Neddersen, Linda M. Peerey, Therese M. Cotton, and Nenad M. Kostić*

Department of Chemistry, Iowa State University, Ames, Iowa 50011. Received March 23, 1992

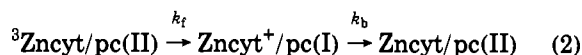
Cytochrome *c* (cyt) and zinc cytochrome *c* (Zncyt) are separately cross-linked to plastocyanin (pc) by the carbodiimide EDC according to a published method. The changes in the protein reduction potentials indicate the presence of approximately two amide cross-links. Chromatography of the diprotein complexes cyt/pc and Zncyt/pc on CM-52 resin yields multiple fractions, whose numbers depend on the eluent. UV-vis, EPR, CD, MCD, resonance Raman, and surface-enhanced resonance Raman spectra show that cross-linking does not significantly perturb the heme and blue copper active sites. Degrees of heme exposure show that plastocyanin covers most of the accessible heme edge in cytochrome *c*. Impossibility of cross-linking cytochrome *c* to a plastocyanin derivative whose acidic patch had been blocked by chemical modification shows that it is the acidic patch that abuts the heme edge in the covalent complex. The chromatographic fractions of the covalent diprotein complex are structurally similar to one another and to the electrostatic diprotein complex. Isoelectric points show that the fractions differ from one another in the number and distribution of *N*-acylurea groups, byproducts of the reaction with the carbodiimide. Cytochrome *c* and plastocyanin are also tethered to each other via lysine residues by *N*-hydroxysuccinimide diesters. Tethers, unlike direct amide bonds, allow mobility of the cross-linked molecules. Laser-flash-photolysis experiments show that, nonetheless, the intracomplex electron-transfer reaction $\text{cyt(II)/pc(II)} \rightarrow \text{cyt(III)/pc(I)}$ is undetectable in complexes of either type. Only the electrostatic diprotein complex, in which protein rearrangement from the docking configuration to the reactive configuration is unrestricted, undergoes this intracomplex reaction at a measurable rate.

Metalloproteins are involved in various biological oxidoreduction processes, and it is important to understand the kinetics and mechanisms of their electron-transfer reactions (1). The heme protein cytochrome *c* (designated cyt) and the blue copper protein plastocyanin (designated pc) are well-suited to kinetic and mechanistic studies because their structures and properties are known in detail. Cytochrome *c* has a positively charged (basic) patch near the exposed heme edge (2, 3), whereas plastocyanin has a negatively charged (acidic) patch remote from the copper atom and an electroneutral (hydrophobic) patch proximate to this atom (4). According to quantum-chemical calculations, electron-transfer paths connecting the copper atom to the hydrophobic patch are more efficient than paths connecting this atom to the acidic patch (5). The presence in plastocyanin of two putative sites for interaction with redox partners makes this protein especially interesting.

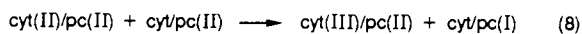
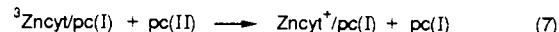
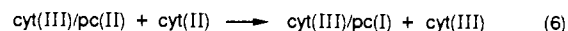
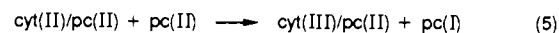
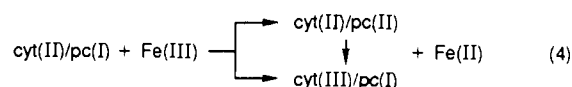
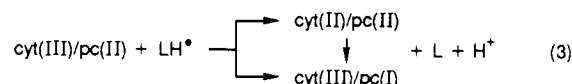
Reaction of plastocyanin with cytochrome *c*, and a reaction between two redox proteins in general, involves three general steps: association of the proteins, electron transfer, and dissociation of the diprotein complex (6). The second step (eq 1) can be experimentally separated



from the other two by varying ionic strengths and by cross-linking the proteins. The photoinduced "forward" reaction k_f is followed by the thermal "back" reaction k_b (eq 2).



Besides these unimolecular reactions within diprotein complexes, there are also bimolecular reactions between diprotein complexes on the one side and various external redox agents on the other (eqs 3-9). The Roman numerals



show oxidation states of iron and copper; the one oxidation state omitted in eq 8 is irrelevant.

Kinetic and mechanistic studies in this laboratory of the reactions in eqs 1-9 have yielded unexpected results (7-12). The electron-transfer reaction in eq 1 within the electrostatic complex (1200 s^{-1}) is abolished (less than 0.2 s^{-1}) when this complex is reinforced by noninvasive cross-links, promoted by the carbodiimide EDC, which prevent

[†] Abbreviations used: CD, circular dichroism; cyt, cytochrome *c*; cyt(II), ferrocyanochrome *c*; cyt(III), ferricytochrome *c*; DST, disuccinimidyl tartarate; EDC, 1-ethyl-3-[3-(dimethylamino)propyl]carbodiimide hydrochloride; EGS, ethylene glycol bis(succinimidyl succinate); L, flavin; LH*, flavin semiquinone; MCD, magnetic circular dichroism; MOPS, 3-(*N*-morpholino)propanesulfonate; NHE, normal hydrogen electrode; pc, plastocyanin; pc(I), cuproplastocyanin; pc(II), cupriplastocyanin; RF, riboflavin; RFH*, riboflavin semiquinone; RRS, resonance Raman spectroscopy; SDS, sodium dodecyl sulfate; SERRS, surface-enhanced resonance Raman spectroscopy; Zncyt, zinc cytochrome *c*.

protein rearrangement. But the reactions k_f and k_b in eq 2 within the two covalent complexes still occur ($k_f = 2.2 \times 10^4$ and $k_b = 7 \times 10^4 \text{ s}^{-1}$, respectively) despite identical cross-linking. This remarkable contrast can be explained on assumption that the amide cross-links connect residues near the heme edge to those in the acidic patch. Native cytochrome *c*, a weak reductant ($E^\circ = 0.26 \text{ V vs NHE}$), apparently cannot reduce cupriplastocyanin ($E^\circ = 0.36 \text{ V vs NHE}$) from the acidic patch, which is remote from the copper atom. The triplet state of zinc cytochrome *c*, a strong reductant ($E^\circ = -0.88 \text{ V vs NHE}$) (13), apparently can reduce cupriplastocyanin from the acidic patch. Since the native and zinc-substituted cytochrome *c* have similar conformations, topographies, and charge distributions, protein-protein orientation for electron transfer apparently depends on the driving force for this reaction.

Reactivity of the cross-linked proteins toward flavin semiquinones, designated LH^\bullet (eq 3), and toward ferric complexes, designated Fe(III) (eq 4), cannot be predicted simply on the basis of the reactivity of separate proteins. The surprisingly small steric shielding of the iron and copper sites in the covalent complex may indicate that the proteins have multiple reaction domains on their surfaces, or that the complex is dynamical, or both. This shielding is greater in the reactions between diprotein complexes and single proteins (eqs 5–7), and even greater in the reactions between diprotein complexes (eqs 8 and 9). The reactions in eqs 1, 2, and 5–9 perhaps are relevant to processes involving oligomeric redox enzymes.

Our analyses of the kinetic results and the aforementioned conclusions rested on suppositions and indirect evidence about the configuration of cytochrome *c* and plastocyanin in the covalent complex *cyt/pc* and about the causes of heterogeneity of this complex when it is subjected to cation-exchange chromatography. Direct evidence, presented here, confirms previous hypotheses and validates previous conclusions. Carbodiimides are routinely used for cross-linking of proteins, but the resulting complexes and aggregates are often studied *in situ*, without isolation. In this study, however, purification and characterization of diprotein complexes may show the pitfalls of cross-linking.

Besides this analytical part, this report has a kinetic part. Cytochrome *c* and plastocyanin are cross-linked by bifunctional *N*-hydroxysuccinimide diesters. These flexible diprotein complexes, which contain tethers, are compared with rigid complexes, which contain direct amide bonds, in their (un)reactivity with respect to intracomplex electron transfer (eq 1).

EXPERIMENTAL PROCEDURES

Chemicals. Chromatographic supplies, riboflavin, protein standards for determination of molecular mass, EDC, and MOPS were obtained from Sigma Chemical Co., the laser dye LD-425 was from Exciton Co., and DST and EGS were from Pierce Chemical Co. Other chemicals were of the reagent grade, and water was demineralized to a resistivity greater than $10 \text{ M}\Omega \text{ cm}$. All the phosphate buffers had a pH of 7.0, and their concentrations or ionic strengths are specified.

Protein Purification, Reconstitution, and Modification. Horse heart ferricytochrome *c* (type III from Sigma Chemical Co.) was purified by cation-exchange chromatography (14). The free-base form of this protein was prepared, purified, and reconstituted with zinc by standard procedures, in the dark (15,16). Zinc cytochrome *c* was always handled in the dark. French bean plastocyanin was isolated by standard methods (17) and purified

repeatedly by gel-filtration chromatography on Sephadex G-25 and G-75 columns with 50 mM acetate buffer at pH 6.0 and by anion-exchange chromatography on a Sephadex DEAE A-25 column with the same buffer, which was made 0.200 M in NaCl. The purifications continued until the absorbance quotient A_{278}/A_{597} became less than 1.20. The acidic patch was chemically modified by ethylenediamine by a published method (18); the chromatographic fraction containing four to six blocked carboxylic groups (19,20) was used in further experiments. Ultrafiltration was done in Amicon cells, with YM-5 membranes, at 4°C , under pressure of pure nitrogen.

Protein Cross-Linking with EDC. The covalent complex *cyt/pc* was prepared by an extension (7) of the published method (21). The product was purified on a column of Sephadex G-75 (50 mesh) sized $1.0 \times 75 \text{ cm}$, with an 85 mM phosphate buffer at pH 7.0 as an eluent. The major band (70–90%), containing the covalent complex *cyt/pc*, was followed by two minor bands, containing the separate proteins.

The complex (37 mg or $1.6 \mu\text{mol}$) was dialyzed by ultrafiltration into a 5 or 10 mM phosphate buffer at pH 7.0, treated with a small excess of $\text{K}_3[\text{Fe}(\text{CN})_6]$ dissolved in this buffer, concentrated, and chromatographed on a CM-52 column sized 2.5×8.5 or $1.5 \times 20 \text{ cm}$ that had previously been equilibrated first with a concentrated and then with a 5 or 10 mM phosphate buffer at pH 7.0. Elution with a 5 mM phosphate buffer at pH 7.0 yielded 12 bands, but only the first, second, fourth, and seventh were major. Elution with a 10 mM phosphate buffer at pH 7.0 yielded four bands, and the fourth one required a shallow gradient from a 10 to a 30 mM buffer. The four major bands in the former procedure correspond in their mobility to the four bands in the latter procedure. Subsequent experiments were done with the latter. The average chromatographic yields of these bands from several syntheses were 19, 26, 29, and 26% in the order of elution.

In another cross-linking procedure, native plastocyanin was replaced by a derivative whose acidic patch had been blocked by ethylenediamine (see the preceding subsection). The mixture after incubation was chromatographed on a CM-52 column sized $2.5 \times 15 \text{ cm}$. Two plastocyanin bands were eluted with a 20 mM phosphate buffer at pH 7.0; two cytochrome *c* bands and two more plastocyanin bands were eluted with an 85 mM phosphate buffer at pH 7.0. Each fraction was oxidized with a small excess of dissolved $\text{K}_3[\text{Fe}(\text{CN})_6]$ and examined by UV–vis spectrophotometry.

In yet another cross-linking procedure native cytochrome *c* was replaced by zinc cytochrome *c*, and larger quantities of the proteins were used: 132 mg ($10.6 \mu\text{mol}$) of zinc cytochrome *c* and 110 mg ($10.6 \mu\text{mol}$) of plastocyanin. Experiments were done in the dark as often as possible. Photodegradation of zinc cytochrome *c* was not detected. The *Zncyt/pc(II)* complex eluted from Sephadex G-75 was dialyzed into a 5 mM phosphate buffer at pH 7.0, concentrated, and chromatographed on a CM-52 column sized $2.5 \times 30 \text{ cm}$. The first two bands were eluted with a 5 mM phosphate buffer at pH 7.0, and the following six required a shallow gradient from an 8.5 to a 40 mM phosphate buffer at pH 7.0.

Chromatographic separations of the covalent complexes *cyt/pc* and *Zncyt/pc* are reproducible and in reasonable agreement with each other: four bands for the former and four major bands for the latter, with correspondingly similar retention times. Since the latter procedure involved larger amounts of proteins, four additional minor bands became evident. Since the presence of cytochrome *c* makes the complex strongly colored, separation was

Table I. Cross-Linking of Ferricytochrome *c* and Cupriplastocyanin by Homobifunctional *N*-Hydroxysuccinimide Diesters

diester	diester concn (mM)	protein concn (mM)	pH ^a	time (h)	NaCl concn (M)	diprotein complex(es)	
						cyt (%)	pc (%)
DST ^b	0.40	0.050	7.0	6	0	5	5
EGS ^c	0.40	0.050	7.0	6	0	14	12
	15	0.50	7.0	39	0	31	16
	15	0.50	7.0	39	0.20	24	18
	1.0	0.030	6.5	39	0	5	5
	1.0	0.030	6.5	39	0.20	0	0

^a A 5 mM MOPS buffer. ^b Disuccinimidyl tartarate. ^c Ethylene glycol bis(succinimidyl succinate).

followed visually. Fraction collectors were unnecessary, and chromatograms were not recorded.

Protein Modification with EDC. Cytochrome *c* and plastocyanin were separately incubated with EDC and chromatographed as described above for the covalent complex cyt/pc. Only the monomeric fractions from Sephadex G-75 were investigated further. The cytochrome *c* fraction was dialyzed into an 85 mM phosphate buffer at pH 7.0 and chromatographed with it on a CM-52 column sized 2.5 × 25 cm. Three bands, with relative yields of 5, 85, and 10%, were eluted in this order. These three fractions were separately oxidized and compared with native cytochrome *c* for their mobility on CM-52 columns; the first fraction proved to contain the native protein. The plastocyanin derivatives were dialyzed into a 5 mM phosphate buffer at pH 7.0 and chromatographed with it on a Sephadex DEAE A-25 column sized 1.5 × 15 cm. The first two bands were eluted with this buffer, and the third one required a 40 mM phosphate buffer at pH 7.0. Again, these three fractions were separately oxidized and compared with native plastocyanin in their mobility on DEAE A-25 columns; the third fraction proved to contain the native protein.

Protein Cross-Linking with DST and EGS. Experimental details are summarized in Table I. Gel-filtration chromatography in all cases was done as in the EDC procedures described above. Further separations of the EGS products were tested with DEAE A-25 and CM-52 columns, with various phosphate and cacodylate buffers, isocratically and with gradients. The diprotein complexes were retained by the DEAE A-25 resin. The CM-52 resin and a 1.0 mM phosphate buffer at pH 7.0 proved most effective; this chromatography gave three bands.

Molecular Mass. Size-exclusion chromatography was done as in previous studies (7, 22). Electrophoresis was done with a Mini Protean II Dual Slab Cell and supplies from Bio-Rad, Inc. Samples were denatured by the addition of SDS. A Laemmli Tris-glycine buffer and an 18% polyacrylamide gel were used. The markers had molecular mass of 6.5, 14.5, 21.5, 31.0, 45.0, 66.0, and 97.4 kDa. Protein bands were stained with Coomassie Blue.

Spectroscopy. Absorption spectra at 25 ± 1 °C were recorded and protein concentrations determined as in previous studies (7, 10). Each compartment of the tandem mixing cell had a pathway of 4.00 mm.

The EPR spectra were recorded at 4–6 K with a Bruker ER200D X-band instrument. The CD and MCD spectra were recorded at ambient temperature, with a JASCO ORD/UV-5 spectropolarimeter equipped with a CD accessory and a permanent magnet. Its field strength, 600 G, was determined with K₃[Fe(CN)₆] as a standard (23). Molar ellipticity, [θ]_m, in MCD experiments was corrected by making the measurements with and without the

magnetic field. Each CD and MCD spectrum was scanned at least twice, between 600 and 230 nm, at a rate of 100 nm h⁻¹. The path lengths were 1.00 mm in MCD experiments and 1.00 mm or 1.00 cm in CD experiments. Concentrations of the samples were adjusted so that the absorbance at 410 nm was 1.06 for MCD experiments and 1.60 in a 1.00-cm cell for CD experiments.

Heme exposure in native ferricytochrome *c* and in the covalent and electrostatic complexes cyt(III)/pc(II) was determined from the effect of ethylene glycol on the UV-vis spectra (24, 25), recorded in a tandem mixing cell. From the composite spectrum of the protein and of ethylene glycol, both dissolved in phosphate buffer at pH 7.0, was subtracted the spectrum of their mixture, whose final concentrations were 3.0–10.0 mM in each protein and 20% by weight in ethylene glycol. The buffer concentration was 85 mM in the case of the covalent complex and only 0.3 mM in the case of the electrostatic complex. The electrostatic complex was prepared by mixing the two proteins in the ratio 0.67:1.00 in order to maximize the fraction of bound cytochrome *c*.

Both RR and SERR spectra were obtained by irradiating the samples with the 413.1 nm line of a Kr⁺ laser (Coherent, Innova 100). The scattered light was collected in a back-scattering configuration and focused onto the entrance slit of a monochromator/spectrograph (Spex, Triplemate 1877) by a pair of lenses. The spectrograph stage, containing a grating with 1800 grooves/mm, provided dispersion of 0.93 nm/mm and a bandpass of 10 cm⁻¹. The spectra were accumulated and processed with an intensified diode-array detector (PARC 1420) coupled with a multichannel analyzer (PARC OMA II). Integration time was 2 s. The spectrometer was calibrated with indene.

Protein samples for RR and SERR experiments were oxidized with a small excess of dissolved K₃[Fe(CN)₆], dialyzed into a 5 mM phosphate buffer at pH 7.0, and concentrated; the last two operations were done by centrifugation in Amicon Centricon 3 cells. Silver sol reduced by citrate was prepared by a standard method (26), with vigorous stirring. The absorption spectrum of the sol had a maximum at 410 nm.

Redox Potentials and Isoelectric Points. Differential-pulse voltammograms were obtained as in previous studies (7, 22).

Spectrophotometric titrations of cytochrome *c* were done with the K₃[Fe(CN)₆]/K₄[Fe(CN)₆] couple, whose redox potential is 420 mV vs NHE; such titrations of plastocyanin were done with the [Co(trpy)₂](ClO₄)₃/[Co(trpy)₂](ClO₄)₂ couple, whose redox potential is assumed to be 280 mV vs NHE. The two cobalt complexes were prepared by a published method (27). Oxidized and reduced forms of cytochrome *c* and of plastocyanin were quantitated by their absorbances at 550 and 557 nm, respectively.

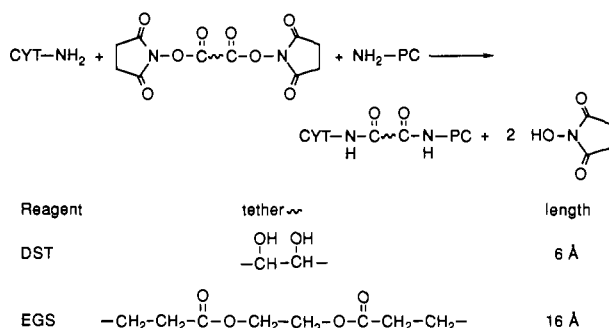
Isoelectric points were determined in focusing experiments with a PhastSystem from Pharmacia and with a Bio-Phoresis horizontal electrophoresis cell from Bio-Rad.

Kinetics. Experiments with laser-flash photolysis were done as before (10, 28, 29). A phosphate buffer at pH 7.0 had ionic strength of 10 mM. Since the complex cyt(II)/pc(II) was in large excess over riboflavin semiquinone, simultaneous reduction of both proteins was improbable.

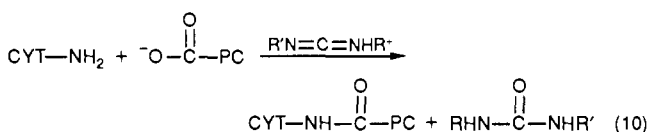
RESULTS AND DISCUSSION

Heterogeneity of the Covalent Complexes cyt/pc. Carbodiimides soluble in water are routinely used for direct cross-linking of amino groups (i.e., lysine residues) and carboxylate groups (i.e., aspartate or glutamate residues)

Scheme I



according to eq 10. Application of this method to redox proteins has been critically reviewed (30). Homobifunctional *N*-hydroxysuccinimide diesters are used for tethering of amino groups (i.e., lysine residues) according to Scheme I. This method has also been reviewed (31). Direct cross-linking of cytochrome *c* and plastocyanin is one, and their cross-linking via tethers the other, aspect of the present study.



Cytochrome *c* and plastocyanin are typical proteins for they contain multiple side chains for cross-linking. Because the complex cyt/pc was likely to be heterogeneous, in this study size-exclusion chromatography was followed by ion-exchange chromatography. Indeed, multiple bands were separated. Although heterogeneity was noted before in the case of direct cross-linking of cytochrome *c* and cytochrome *c* peroxidase (32, 33), to our knowledge the complex cyt/pc is the first one for which both chromatographic heterogeneity and protein configuration were examined.

Electrostatic Complex cyt/pc. Because of their opposite charges, +7 and -8 at pH 7.0, ferricytochrome *c* and cupriplastocyanin form an electrostatic complex in solution at low ionic strength. Chemical modification (18–20, 34, 35), electrochemical response (36), competitive inhibition (37), dependence of the cross-linking yield on ionic strength (21), NMR spectroscopy (38, 39), and computer graphics combined with electrostatic calculations (40) all clearly showed that the association involves the positively charged patch around the exposed heme edge in cytochrome *c* and the negatively charged patch near Tyr 83 in plastocyanin. These interaction domains are approximately defined by the lysine residues 13, 25, 27, 86, and 87 in the horse cytochrome *c* and aspartate residues 43 and 45 and glutamate residues 44, 46, 60, 61, and 62 in the bean plastocyanin, as shown in Figure 1. Since substitution of zinc for iron does not noticeably alter the conformation of cytochrome *c* (41) and its association with other proteins (15, 16), electrostatic complexes cyt/pc and Zncyt/pc most likely have similar configurations. But the configuration that is optimal for binding and recognition need not be optimal for reaction, as recent studies from this (7–10) and other (42) laboratories have shown.

Composition of the Covalent Complexes cyt/pc. Amide cross-links probably involve the same (but not necessarily all) amino and carboxylic groups that are responsible for the electrostatic attraction. Peptide mapping proved inadequate for complete and unambiguous location of amide bonds induced by carbodiimide (30, 43,

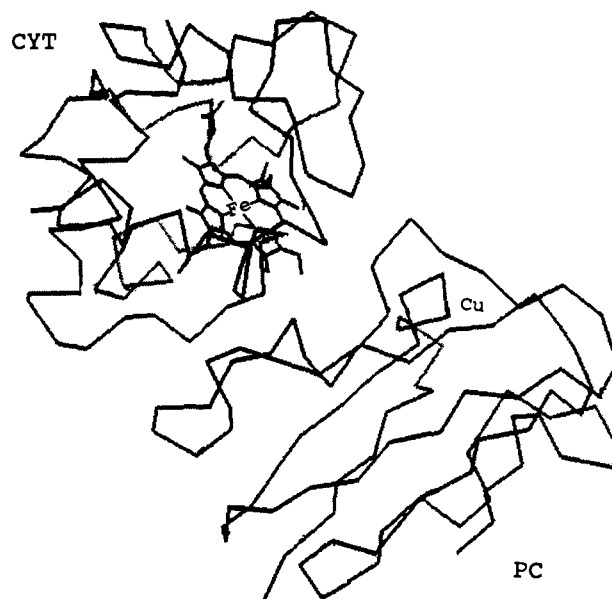


Figure 1. The α -carbon chains of cytochrome *c* and plastocyanin in the electrostatic complex. The atomic coordinates correspond to the theoretical maximum-overlap model described in ref 40.

Table II.^a Properties of Ferricytochrome *c*, Cupriplastocyanin, and Their Covalent Complex Formed in the Presence of the Carbodiimide EDC^b

property ^c	cyt(III)	pc(II)	cyt(III)/pc(II)
molecular mass (kDa) ^d	12.5	10.5	27.0 ± 1.2
EPR <i>g</i> values			
<i>g_x</i>	1.26		1.3
<i>g_y</i> ^e	2.25		2.3
<i>g_z</i>	3.02		3.09
<i>g</i>		2.2	2.3
<i>g_⊥</i>		2.053	2.056
reduction potential at 25 °C (mV vs NHE)			
Fe	256 ± 2/ ^f		245 ± 5/ ^g
Cu		360 ± 4/ ^{h,i}	385 ± 5/ ^h

^a Adapted from ref 7. ^b 1-Ethyl-3-[3-(dimethylamino)propyl]carbodiimide hydrochloride. ^c In 85 mM phosphate buffer at pH 7.0. ^d Determined by size-exclusion chromatography and SDS-PAGE. ^e Measured at peak maximum. ^f Determined by differential-pulse voltammetry with 4,4'-bipyridine as mediator. ^g Reference 2. ^h Determined by spectrophotometric titration with [Fe(CN)₆]⁴⁻. ⁱ Reference 4.

44), and radiolabeling is inapplicable to this task because carbodiimide atoms are not incorporated into the cross-links. Exact locations of the cross-links, and the static structure that it implies, are relatively unimportant because the complex cyt/pc seems to be dynamical. Both the reactivity of the covalent complex, discussed in the introduction (7, 10), and the absence of nuclear Overhauser effects between the protein molecules in the electrostatic complex (45) point to dynamical flexibility. Fortunately, protein configuration in the covalent complex cyt/pc can be defined without pinpointing the cross-links, and other methods proved applicable.

Others (21) purified the complex cyt/pc by size-exclusion chromatography and determined its composition and some properties. We corroborated their findings and added those in Tables II (7) and III.

The apparent molecular mass of both covalent complexes cyt/pc and Zncyt/pc is 27.0 ± 1.2 kDa, an average of several determinations by size-exclusion chromatography and SDS polyacrylamide gel electrophoresis. This value is by ca. 17% greater than the sum of the molecular masses of the individual proteins because molecular mass

Table III. Magnetic Circular Dichroism Properties of Free Ferricytochrome *c* and of Its Covalent Complex with Cupriplastocyanin, Formed in the Presence of the Carbodiimide EDC^a

protein	λ_{max} (nm) ^b	$\Delta\epsilon_m/H$ (M ⁻¹ cm ⁻¹ T ⁻¹) ^c
cyt(III)	400	71
	414	-77
cyt(III)/pc(II) derivative		
1	401	75
	414	-87
2	403	75
	417	-81
3	399	61
	414	-77
4	400	73
	414	-81

^a 1-Ethyl-3-[3-(dimethylamino)propyl]carbodiimide hydrochloride. ^b ± 2 . ^c ± 10 .

is only an approximate measure of the biopolymer size and because $\log M_r$ is strictly proportional to elution time only for protein molecules of similar shapes. This phenomenon was semiquantitatively studied in our laboratory with diprotein complexes whose elongation varied with the size of the metal complex used for cross-linking (22, 46, 47). The visible absorption spectra confirmed the protein ratio of 1.00 ± 0.08 in each of the four fractions of cyt/pc obtained by cation-exchange chromatography on CM-52 resin.

Since the cross-linking reactions with the reagents DST and EGS require that the cationic lysine side chains in the two proteins face each other, and since both of these diesters hydrolyze in water, the yields of the complexes cyt/pc are at most 15%, as Table I shows. This electrostatic repulsion is more detrimental to the shorter DST than to the longer EGS. Lower protein concentration and shorter incubation times favor the formation of the desired heterodiprotein complexes, cyt/pc. Higher concentrations and longer times were avoided because they yielded the undesired homodiprotein complexes, especially cyt/cyt, which cannot be fully separated from cyt/pc by size-exclusion chromatography. The low yields of the DST complex and of the three fractions of the EGS complex obtained by cation-exchange chromatography precluded their detailed study.

Raman Spectroscopy of the Covalent Complex cyt/pc. Resonance Raman spectra (RRS) are obtained with proteins in aqueous solution. Surface-enhanced resonance Raman spectra (SERRS) are obtained with proteins adsorbed onto a roughened silver surface, but cytochrome *c* retains its native structure under these conditions (48, 49). Since both of these methods are noninvasive (50, 51), they are well-suited to examination of possible structural perturbations of the heme and of its protein environment owing to electrostatic association and covalent cross-linking of proteins.

The spectra of ferricytochrome *c* in Figure 2 are consistent with those reported previously (49). Peaks ν_{10} , ν_2 , and ν_3 at 1634, 1585, and 1501 cm⁻¹, respectively, are characteristic of the low-spin state. Peak ν_4 at 1369 cm⁻¹ is characteristic of the ferric form. The spectra of the electrostatic complex cyt(III)/pc(II) in Figure 3 differ only slightly from those of the free ferricytochrome *c*. The peak at 749 cm⁻¹ is absent from Figure 3A, and the relative intensities of the peaks at 397 and 410 cm⁻¹ are altered. The peak at 353 cm⁻¹ in Figure 3B has a greater relative intensity than the peak at 347 cm⁻¹ in Figure 3A. Figure 4 typifies the spectra of all four derivatives (chromatographic fractions) of the covalent complex cyt(III)/pc(II). The only apparent difference between native cytochrome

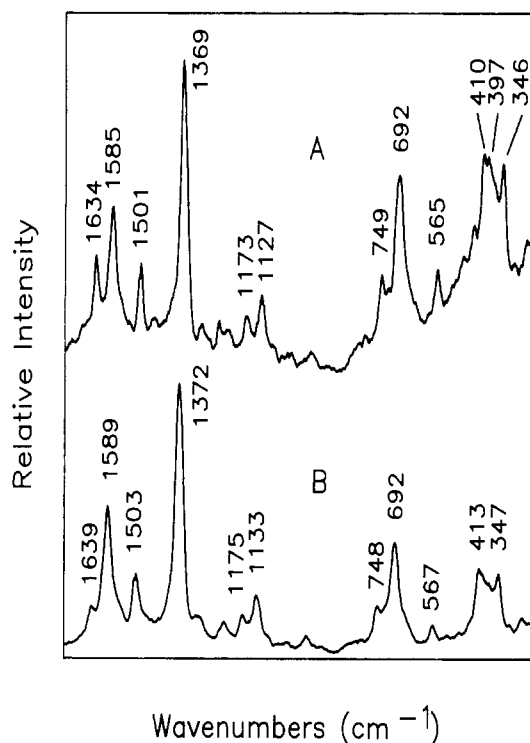


Figure 2. Vibrational spectra of ferricytochrome *c* in a 5 mM phosphate buffer at pH 7.0, at room temperature. The protein concentrations are 3.3×10^{-4} M for the resonance Raman spectrum (A) and 1.6×10^{-5} M for the surface-enhanced resonance Raman spectrum (B).

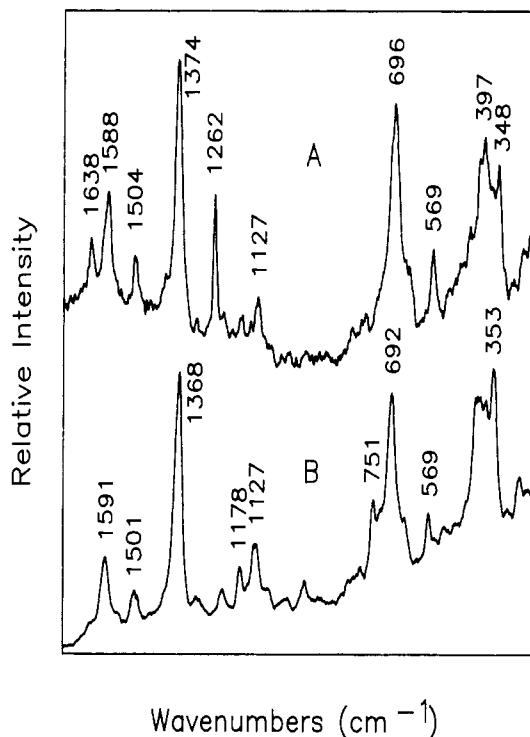


Figure 3. Vibrational spectra of the electrostatic complex between ferricytochrome *c* and cupriplastocyanin in a 5 mM phosphate buffer at pH 7.0, at room temperature. The concentrations of each protein are 1.9×10^{-4} M for the resonance Raman spectrum (A) and 9.2×10^{-6} M for the surface-enhanced resonance Raman spectrum (B).

c and the complex is the slight decrease in the intensity of the peak at 397 cm⁻¹ in Figure 2A, which becomes a shoulder in Figure 4A. Although the protein solutions for surface-enhanced Raman spectra are 21 times more dilute

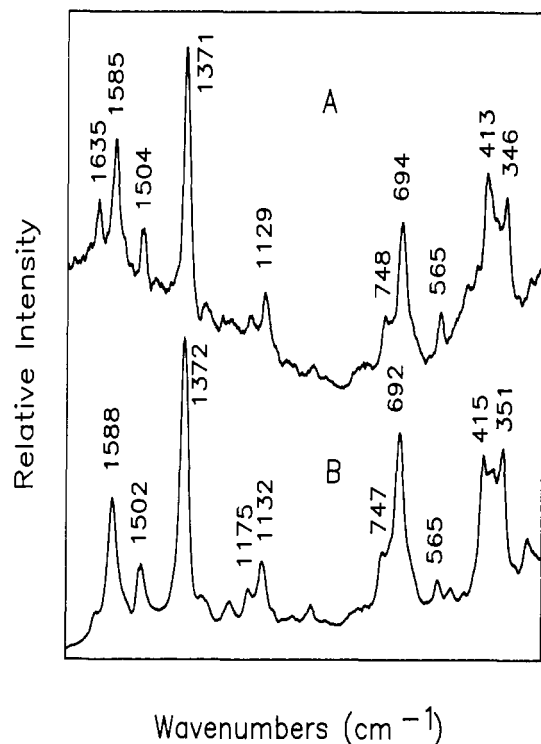


Figure 4. Vibrational spectra of the first chromatographic fraction of the covalent complex between ferricytochrome *c* and cupriplastocyanin in a 5 mM phosphate buffer at pH 7.0, at room temperature. The complex concentrations are 4.7×10^{-4} M for the resonance Raman spectrum (A) and 2.2×10^{-5} M for the surface-enhanced resonance Raman spectrum (B).

than the solutions for resonance Raman spectra, band intensities are comparable. This is an evidence of the surface effect.

These Raman spectra show that ferriheme retains its six-coordinate structure and low-spin state and remains virtually unperturbed upon electrostatic association and covalent cross-linking between cytochrome *c* and plastocyanin. A previous resonance Raman spectroscopic study showed the same for native cytochrome *f* and its covalent complex with plastocyanin, formed with the reagent EDC (44). The four derivatives of the covalent complex are indistinguishable from one another and from the electrostatic complex.

Number of Direct Amide Cross-Links in the Complex cyt/pc. The number of cross-links induced by EDC can perhaps be estimated from the reduction potentials. As Table II shows, cross-linking lowers the reduction potential of cytochrome *c* by ca. 10 mV and raises that of plastocyanin by ca. 25 mV (7). The following interpretation is based on the assumption that this small divergence is due mainly to neutralization of the cationic side chain(s) in the former and of the anionic side chain(s) in the latter. Formation of single amide bonds between one amino group of $\text{H}_2\text{NCH}_2\text{CH}_2\text{NH}_2$ and different carboxylate groups in the anionic domain (residues 42–45 and 59–61) raises the reduction potential of spinach plastocyanin by 15–20 mV (19). Somewhat smaller increases were reported in an earlier study (52). Because the remaining amino group in ethylenediamine is protonated, this modification converts an anionic residue into a cationic one. The cross-linking with cytochrome *c*, however, converts an anionic residue in plastocyanin into a neutral one, so the reduction potential of plastocyanin probably increases by less than 15–20 mV per amide bond. If this protein is treated as a low-dielectric cavity with charges smeared on the surface, the expected increase is 12 mV per lost charge (53). The

observed increase of ca. 25 mV corresponds to approximately two cross-links, on the average, in the four chromatographic fractions of the covalent complex cyt/pc. Although the change in reduction potentials upon cross-linking may be caused by various factors in addition to charge neutralization, the preceding simple analysis should be useful. To our knowledge, no other method for estimating the number of direct amide cross-links has been proposed; this may be the first time that this difficult problem has been addressed.

Other Spectroscopy of the Covalent Complex cyt/pc. The EPR spectra are summarized in Table II. The overlapping g_y component for ferricytochrome *c* and the g_1 component for cupriplastocyanin were identified nonetheless (7). The MCD spectra, summarized in Table III, are characteristic of low-spin ferriheme; indeed, the absorption band at 695 nm, diagnostic of axial ligation of Met 80 in cytochrome *c*, is evident in the spectra of all four chromatographic fractions. The electrostatic complex cyt(III)/pc(II) (a solution in a 3.0 mM phosphate buffer that is 160 μM in each protein) and all four fractions of the covalent complex cyt(III)/pc(II) gave superimposable UV-vis, CD, and MCD spectra. Although EPR, UV-vis, CD, and MCD spectra are not very sensitive to small structural changes, it is fair to conclude that electrostatic association and direct cross-linking do not significantly perturb the electronic structure of the iron and copper sites and the gross conformations of the proteins.

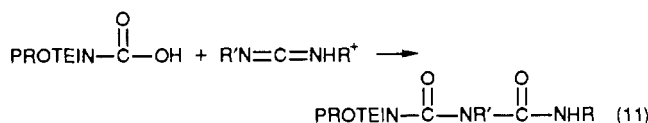
Protein Docking in the Complex cyt/pc. The heme exposures in native ferricytochrome *c*, in the electrostatic complex cyt(III)/pc(II), and in the covalent complex cyt(III)/pc(II) are 24.2 ± 1.3 , 5.6 ± 0.3 , and $4.5 \pm 0.2\%$, respectively. In the first two cases, the margins of error reflect the reproducibility of the experiments; in the third case, the margin reflects the comparison among the four chromatographic fractions of the covalent complex. These findings confirm the previous findings by others (see above) that plastocyanin covers most of the exposed heme edge in cytochrome *c*. Moreover, the four fractions of the covalent complex seem to be structurally similar to one another and to the electrostatic complex.

When the acidic patch is blocked by chemical modification, plastocyanin fails to form the covalent complex with cytochrome *c* in the presence of EDC. All the fractions separated on the CM-52 column consisted of monomeric proteins (modified by the carbodiimide, as explained in the next subsection). Evidently it is the acidic patch that covers the heme edge in the covalent complex. The interaction domains in the cross-linked proteins are most likely the same as those determined for the electrostatically associated proteins, namely lysine residues 13, 25, 27, 86, and 87 in the horse cytochrome *c* and aspartate residues 43 and 45 and glutamate residues 44, 46, 60, 61, and 62 in the bean plastocyanin.

The intracomplex reaction in eq 1 is undetectably slow (less than 0.2 s^{-1}) in all four fractions of the covalent complex (7, 10). The lifetime of the triplet state is sensitive to protein docking, yet it is the same, $5.2 \pm 0.2 \text{ ms}$, in all eight fractions of the covalent complex $^3\text{Zncyt/pc(I)}$ (9). The rate constant k_t for the intracomplex reaction (eq 2) is also the same, $(2.2 \pm 0.5) \times 10^4 \text{ s}^{-1}$, in all eight fractions of the covalent complex $^3\text{Zncyt/pc(II)}$ (9). This uniform unreactivity, uniform photophysical properties, and uniform reactivity are additional evidence for structural uniformity of the fractions into which the covalent complex cyt/pc separates on the CM-52 resin.

Chromatographic Heterogeneity of the Covalent Complex cyt/pc. Since the diprotein complexes cyt(III)/

pc(II) and Zncyt/pc(II) are eluted from the cation exchanger CM-52 by dilute phosphate buffers, their overall charges must be relatively low. Indeed, the opposite charges of the individual proteins nearly neutralize each other upon association. Mobility of individual chromatographic fractions is characteristic of differences in total charge and in the distribution of charge (47). Besides efficiently and noninvasively cross-linking proteins, carbodiimide also modifies side chains (54, 55). Indeed, reaction of cytochrome *c* with EDC yields derivatives in which carboxylic groups, which are anions in neutral solution, have been converted into neutral *N*-acylurea groups according to eq 11 (56). We confirmed these



findings and also found similar conversions with plastocyanin. These derivatives of the individual proteins resembled the fractions of the covalent diprotein complex in their relative mobility on the CM-52 column. The attempt to cross-link cytochrome *c* to plastocyanin whose acidic patch had previously been modified by ethylenediamine yielded only the *N*-acylurea derivatives of the separate proteins.

Isoelectric points confirm that chromatographic fractions of the covalent complex differ from one another in charge. The values for the complex cyt/pc are 6.2, 6.8, 7.1, and 8.2; those for the complex Zncyt/pc are 6.2, 7.1, 8.0, 8.2, 8.5, 9.0, 9.6, and >9.6. Both of these series parallel the trends in mobility on the cation exchanger CM-52. These chromatographic fractions are derivatives with different numbers and locations of *N*-acylurea groups. This conclusion is supported by our detailed comparison of individual derivatives of the covalent complex Zncyt/pc(I) in their electron-transfer reactions according to eq 7 (12). Since peptide mapping is inapplicable to cross-linked complexes, these groups cannot be conclusively identified. Mass spectrometry with electrospray ionization (57, 58) may in the future become routinely applicable to protein complexes, but even this method would permit only quantitation, not location, of *N*-acylurea groups. Their identification in the derivatives of cytochrome *c* and of plastocyanin would be of little value because functional groups that are accessible in separate proteins may be inaccessible in the diprotein complex. Indeed, the change in the UV-vis spectrum that was attributed to modification of a propionate group in cytochrome *c* (56) is absent in the spectra of the cyt/pc derivatives. This propionate group, which is attached to heme and somewhat exposed to the protein exterior in native cytochrome *c*, becomes shielded when plastocyanin covers the heme edge. The rate constants for the reactions in eqs 1 and 2 are the same for all the derivatives. Since the lifetime of the triplet excited state and the intracomplex electron-transfer reactions do not depend on the number and location of *N*-acylurea groups on the surface, these groups were not examined further.

Electron-Transfer Reactions of Tethered Complexes cyt/pc. The rate constant at the ionic strength of 10 mM for the external reduction by riboflavin semiquinone is $5.4 \times 10^7 \text{ M}^{-1} \text{ s}^{-1}$ in the case of native ferricytochrome *c* (59) and $1.1 \times 10^7 \text{ M}^{-1} \text{ s}^{-1}$ in the case of the diprotein complex cyt(III)/pc(II) tethered by EGS (eq 12).

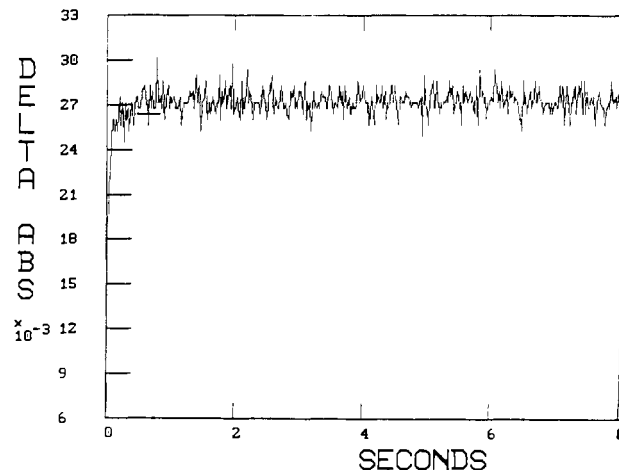
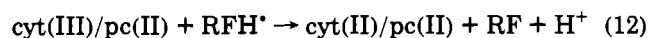


Figure 5. Reaction of riboflavin semiquinone with the covalent complex cyt(III)/pc(II) in which the protein molecules are tethered with EGS. Conditions: 10 μM cyt(III)/pc(II) in a phosphate buffer at pH 7.0, ionic strength 10 mM; absorbance at 550 nm.

Since riboflavin semiquinone reacts near the exposed heme edge (59), the inhibition of its attack at the diprotein complex indicates that the tether is attached to this area of cytochrome *c* surface, which is especially rich in lysine residues. Figure 5 shows the initial curvature, corresponding to the external reaction (eq 12) and a horizontal plot thereafter, corresponding to the lack of the internal (intracomplex) reaction (eq 1) at this low concentration of the diprotein complex. At higher concentrations the intercomplex reaction (eq 8) becomes evident. The complex cyt(III)/pc(II) tethered with DST gave similar absorbance traces.

The complexes cyt/pc with long tethers behave exactly like the complex cyt/pc with direct amide cross-links (7, 10). None of them undergoes the thermodynamically favorable internal reaction (eq 1). Although tethers allow some mobility of the protein molecules, the complexes apparently cannot adopt the reactive configuration (9, 42). Only the electrostatic complex cyt/pc, in which surface diffusion of the interacting protein molecules is unrestricted, can achieve the optimal configuration and undergo the internal reaction at a relatively fast rate (7, 10).

CONCLUSION

Direct cross-linking of proteins with carbodiimides produces multiple derivatives of the protein complexes, which need to be separated, purified, and examined. When the proteins form only one major electrostatic complex in solution or when multiple electrostatic complexes have similar configurations, the covalent complex is likely to be structurally homogeneous or heterogeneous beyond detection; this is the case with cytochrome *c* and plastocyanin. But when the proteins form different electrostatic complexes in appreciable amounts, structural heterogeneity of the covalent complex may be sufficient to allow separation of isomers; this may be expected of proteins that have on their surfaces multiple complementary patches of opposite charge. In either case, the covalent complex is likely to be heterogeneous in terms of net charge and of charge distribution on the surface. This heterogeneity may affect the interactions of the complex with other biomolecules and membranes.

ACKNOWLEDGMENT

This work was supported by NSF through a Presidential Young Investigator Award to N.M.K. (Grant CHE-8858387). We thank Dr. Venkatesh M. Shanbhag for dis-

cussions, Drs. Elizabeth D. Getzoff and Victoria A. Roberts for atomic coordinates of the cyt/pc complex, and Dr. Ling Qin and Longgen Zhu for electrophoretograms.

LITERATURE CITED

- (1) Sigel, H., and Sigel, A., Eds. (1991) Electron-Transfer Reactions in Metalloproteins. In *Metal Ions in Biological Systems*, Vol. 27, Marcel Dekker, Inc., New York.
- (2) Moore, G. R., Eley, C. G. S., and Williams, G. (1984) Electron Transfer Reactions of Class I Cytochromes *c*. *Adv. Inorg. Bioinorg. Mech.* 3, 1.
- (3) Cusanovich, M. A., Meyer, T. E., and Tollin, G. (1987) *c*-Type Cytochromes: Oxidation-Reduction Properties. *Adv. Inorg. Biochem.* 7, 37.
- (4) Sykes, A. G. (1991) Plastocyanin and the Blue Copper Proteins. *Struct. Bonding* 75, 175.
- (5) Christensen, E. M., Conrad, L. S., Mikkelsen, K. V., Nielsen, M. K., and Ulstrup, J. (1990) Direct and Superexchange Electron Tunneling at the Adjacent and Remote Sites of Higher Plant Plastocyanins. *Inorg. Chem.* 29, 2808.
- (6) Kostić, N. M. (1991) Diprotein Complexes and Their Electron Transfer Reactions. In *Metal Ions in Biological Systems* (H. Sigel, and A. Sigel, Eds.) Vol. 27, Chapter 4, Marcel Dekker, Inc., New York.
- (7) Peerey, L. M., and Kostić, N. M. (1989) Oxidoreduction Reactions Involving the Electrostatic and the Covalent Complex of Cytochrome *c* and Plastocyanin: Importance of the Protein Rearrangement for the Intracomplex Electron-Transfer Reaction. *Biochemistry* 28, 1861.
- (8) Zhou, J. S., and Kostić, N. M. (1991) Kinetics of Static and Diffusive Electron Transfer between Zinc-Substituted Cytochrome *c* and Plastocyanin. Indications of Nonelectrostatic Interactions between Highly Charged Metalloproteins. *J. Am. Chem. Soc.* 113, 6067.
- (9) Zhou, J. S., and Kostić, N. M. (1991) Reactions between Cytochrome *c* and Plastocyanin Indicate That Choice of Docking Sites on Protein Surfaces May Depend on Thermodynamic Driving Force for Electron Transfer. *J. Am. Chem. Soc.* 113, 7040.
- (10) Peerey, L. M., Brothers, H. M., II, Hazzard, J. T., Tollin, G., and Kostić, N. M. (1991) Unimolecular and Bimolecular Oxidoreduction Reactions Involving Diprotein Complexes of Cytochrome *c* and Plastocyanin. Dependence of Electron-Transfer Reactivity on Charge and Orientation of the Docked Metalloproteins. *Biochemistry* 30, 9297.
- (11) Zhou, J. S., and Kostić, N. M. (1992) Photoinduced Electron Transfer from Zinc Cytochrome *c* to Plastocyanin is Gated by Surface Diffusion within the Metalloprotein Complex. *J. Am. Chem. Soc.* 114, 3562.
- (12) Zhou, J. S., and Kostić, N. M. (1992) Photoinduced Electron-Transfer Reaction in a Ternary System Involving Zinc Cytochrome *c* and Plastocyanin. Interplay of Monopolar and Bipolar Electrostatic Interactions between Metalloproteins. *Biochemistry* 31, 7542.
- (13) Magner, E., and McLendon, G. (1989) Ground-State and Excited-State Electron-Transfer Reactions of Zinc Cytochrome *c*. *J. Phys. Chem.* 93, 7130.
- (14) Brautigan, D. L., Ferguson-Miller, S., and Margolias, E. (1978) Mitochondrial Cytochrome *c*: Preparation and Activity of Native and Chemically Modified Cytochromes *c*. *Methods Enzymol.* 53, 128.
- (15) Vanderkooi, J. M., and Erecinska, M. (1975) Cytochrome *c* Interaction with Membranes. Absorption and Emission Spectra and Binding Characteristics of Iron-Free Cytochrome *c*. *Eur. J. Biochem.* 60, 199.
- (16) Vanderkooi, J. M., Adar, F., and Erecinska, M. (1976) Metallocytochromes *c*: Characterization of Electronic Absorption and Emission Spectra of Sn^{4+} and Zn^{2+} Cytochromes *c*. *Eur. J. Biochem.* 64, 381.
- (17) Milne, P. R., and Wells, J. R. E. (1970) Structural and Molecular Weight Studies on the Small Copper Protein, Plastocyanin. *J. Biol. Chem.* 245, 1566.
- (18) Burkey, K. O., and Gross, E. L. (1982) Chemical Modification of Spinach Plastocyanin: Separation and Characterization of Four Different Forms. *Biochemistry* 21, 5886.
- (19) Anderson, G. P., Sanderson, D. G., Lee, C. H., Durell, S., Anderson, L. B., and Gross, E. L. (1987) The effect of ethylenediamine chemical modification of plastocyanin on the rate of cytochrome *f* oxidation and P-700⁺ reduction. *Biochim. Biophys. Acta* 894, 386.
- (20) Burkey, K. O., and Gross, E. L. (1981) Effect of Carboxyl Group Modification on Redox Properties and Electron Donation Capability of Spinach Plastocyanin. *Biochemistry* 20, 5495.
- (21) Geren, L. M., Stonehuerner, J., Davis, D. J., and Millett, F. (1983) The Use of a Water-soluble Carbodiimide to Cross-link Cytochrome *c* to Plastocyanin. *Biochim. Biophys. Acta* 724, 62.
- (22) Peerey, L. M., and Kostić, N. M. (1987) Transition-Metal Compounds as New Reagents for Selective Cross-Linking of Proteins. Synthesis and Characterization of Two Bis(cytochrome *c*) Complexes of Platinum. *Inorg. Chem.* 26, 2079.
- (23) Vickery, L. E. (1978) Spin States of Heme Proteins by Magnetic Circular Dichroism. *Methods Enzymol.* 54, 284.
- (24) Schlauder, G. G., and Kassner, R. J. (1979) Comparative Solvent Perturbation of Horse Heart Cytochrome *c* and *Rhodospirillum rubrum* Cytochrome c_2^* . *J. Biol. Chem.* 254, 4110.
- (25) Fiechtner, M. D., and Kassner, R. J. (1978) Axial Ligation and Heme Environment in Cytochrome *c*-555 from *Prosthecochloris aestuarii*. Investigation by Absorption and Solvent Perturbation Difference Spectroscopy. *Biochemistry* 17, 1028.
- (26) Lee, P. C., and Melsel, D. (1982) Adsorption and Surface-Enhanced Raman of Dyes on Silver and Gold Sols. *J. Phys. Chem.* 86, 3391.
- (27) Szymanski, T., Cape, T. W., Van Duyne, R. P., and Basolo, F. (1979) Determination of the Solution O—O Stretching Frequency of a Monomeric Dioxygen Cobalt Complex by Resonance Raman Spectroscopy. *J. Chem. Soc., Chem. Commun.* 5.
- (28) Ahmad, I., Cusanovich, M. A., and Tollin, G. (1982) Laser Flash Photolysis Studies of Electron Transfer between Semiquinone and Fully Reduced Free Flavins and the Cytochrome *c*-Cytochrome Oxidase. *Biochemistry* 21, 3122.
- (29) Simonsen, R. P., and Tollin, G. (1983) Transient Kinetics of Redox Reactions of Flavodoxin: Effects of Chemical Modification of the Flavin Mononucleotide Prosthetic Group on the Dynamics of Intermediate Complex Formation and Electron Transfer. *Biochemistry* 22, 3008.
- (30) Mauk, M. R., and Mauk, A. G. (1989) Crosslinking of Cytochrome *c* and Cytochrome b_5 with a Water-Soluble Carbodiimide. Reaction Conditions, Product Analysis and Critique of the Technique. *Eur. J. Biochem.* 186, 473.
- (31) Pierce Chemical Co. (1989) *Handbook & General Catalog*, p 289.
- (32) Erman, J. E., Kim, K. L., Vitello, L. B., Moench, S. J., and Satterlee, J. D. (1987) A Covalent Complex between Horse Heart Cytochrome *c* and Yeast Cytochrome *c* Peroxidase: Kinetic Properties. *Biochim. Biophys. Acta* 911, 1.
- (33) Moench, S. J., Satterlee, J. D., and Erman, J. E. (1987) Proton NMR and Electrophoretic Studies of the Covalent Complex Formed by Cross-linking Yeast Cytochrome *c* Peroxidase and Horse Cytochrome *c* with a Water-Soluble Carbodiimide. *Biochemistry* 26, 3821.
- (34) Augustin, M. A., Chapman, S. K., Davies, D. M., Sykes, A. G., Speck, S. H., and Margolias, E. (1983) Interaction of Cytochrome *c* with the Blue Copper Proteins, Plastocyanin and Azurin. *J. Biol. Chem.* 258, 6405.
- (35) Armstrong, G. D., Chapman, S. K., Sisley, M. J., Sykes, A. G., Aitken, A., Osheroff, N., and Margolias, E. (1986) Preferred Sites on Cytochrome *c* for Electron Transfer with Two Positively Charged Blue Copper Proteins, *Anabaena variabilis* Plastocyanin and Stellacyanin. *Biochemistry* 25, 6947.
- (36) Bagby, S., Barker, P. D., Guo, L.-H., and Hill, H. A. O. (1990) Direct Electrochemistry of Protein-Protein Complexes Involving Cytochrome *c*, Cytochrome b_5 , and Plastocyanin. *Biochemistry* 29, 3213.
- (37) Chapman, S. K., Knox, C. V., and Sykes, A. G. (1984) Kinetic Studies on 1:1 Electron-transfer Reactions involving Blue Copper Proteins. Part 10. The Assignment of Binding Sites in the Reactions of Plastocyanin (and Azurin) with Non-

- physiological Protein Redox Partners. *J. Chem. Soc., Dalton Trans.* 2775.
- (38) King, G. C., Binstead, R. A., and Wright, P. E. (1985) NMR and Kinetic Characterization of the Interaction Between French Bean Plastocyanin and Horse Cytochrome *c*. *Biochim. Biophys. Acta* 806, 262.
- (39) Bagby, S., Driscoll, P. C., Goodall, K. G., Redfield, C., and Hill, H. A. O. (1990) The Complex Formed Between Plastocyanin and Cytochrome *c*. Investigation by NMR Spectroscopy. *Eur. J. Biochem.* 188, 413.
- (40) Roberts, V. A., Freeman, H. C., Getzoff, E. D., Olson, A. J., and Tainer, J. A. (1991) Electrostatic Orientation of the Electron-Transfer complex Between Plastocyanin and Cytochrome *c**. *J. Biol. Chem.* 266, 13431.
- (41) Moore, G. R., Williams, R. J. P., Chien, J. C. W., and Dickinson, L. C. (1980) Nuclear Magnetic Resonance Studies of Metal Substituted Horse Cytochrome *c*. *J. Inorg. Biochem.* 13, 1.
- (42) Rush, J. D., Levine, F., and Koppenol, W. H. (1988) The Electron-Transfer Site of Spinach Plastocyanin. *Biochemistry* 27, 5876.
- (43) Takabe, T., and Ishikawa, H. (1989) Kinetic Studies on a Cross-Linked Complex between Plastocyanin and Cytochrome *f*. *J. Biochem.* 105, 98.
- (44) Morand, L. Z., Frame, M. K., Colvert, K. K., Johnson, D. A., Krogmann, D. W., and Davis, D. J. (1989) Plastocyanin Cytochrome *f* Interaction. *Biochemistry* 28, 8039. Correction: (1989) *Biochemistry* 28, 10093.
- (45) Wright, P. E., personal communication.
- (46) Chen, J., and Kostić, N. M. (1988) Binuclear Transition-Metal Complexes as New Reagents for Selective Cross-Linking of Proteins. Coordination of Cytochrome *c* to Dirhodium(II) μ -Tetraacetate. *Inorg. Chem.* 27, 2682.
- (47) Kostić, N. M. (1988) Selective Labeling, Cross-Linking, and Cleavage of Proteins with Transition-Metal Complexes. *Comments Inorg. Chem.* 8, 137.
- (48) Cotton, T. M., Schultz, S. G., and van Dyne, R. P. (1980) Surface-Enhanced Resonance Raman Scattering from Cytochrome *c* and Myoglobin Adsorbed on a Silver Electrode. *J. Am. Chem. Soc.* 102, 7960.
- (49) Hildebrandt, P., and Stockburger, M. (1989) Cytochrome *c* at Charged Interfaces. 1. Conformational and Redox Equilibria and the Electrode/Electrolyte Interface Probed by Surface-Enhanced Resonance Raman Spectroscopy. *Biochemistry* 28, 6710.
- (50) Cotton, T. M. (1988) The Application of Surface-Enhanced Raman Scattering to Biochemical Systems. In *Spectroscopy of Surfaces* (R. J. H. Clark, and R. E. Hester, Eds.) Chapter 3, John Wiley & Sons Ltd, New York.
- (51) Cotton, T. M., Kim, J.-H., and Chumanov, G. D. (1991) Application of Surface-Enhanced Raman Spectroscopy to Biological Systems. *Raman Spectrosc.* 22, 729.
- (52) Takabe, T., Ishikawa, H., Niwa, S., and Tanaka, Y. (1984) Electron Transfer Reactions of Chemically Modified Plastocyanin with P700 and Cytochrome *f*. Importance of Local Charges. *J. Biochem.* 96, 385.
- (53) Moore, G. R., and Pettigrew, G. W. (1990) Section 7.4.2. In *Cytochromes c. Evolutionary, Structural, and Physicochemical Aspects*. Springer-Verlag, Berlin.
- (54) Means, G. E., and Feeney, R. E. (1971) Sections 7-2 and A-4. In *Chemical Modification of Proteins*. Holden-Day, San Francisco, CA.
- (55) Carraway, K. L., and Koshland, D. E. (1972) Carbodiimide Modification of Proteins. *Methods Enzymol.* 25, 616.
- (56) Timkovich, R. (1977) Detection of the Stable Addition of Carbodiimide to Proteins. *Anal. Biochem.* 79, 135.
- (57) Prome, D., Blouquit, Y., Ponthus, C., Prome, J.-C., and Rosa, J. (1991) Structure of the Human Adult Hemoglobin Minor Fraction A_{1b} by Electrospray and Secondary Ion Mass Spectrometry. *J. Biol. Chem.* 266, 13050.
- (58) Katta, V., and Chait, B. T. (1991) Observation of the Heme-Globin Complex in Native Myoglobin by Electrospray-Ionization Mass Spectrometry. *J. Am. Chem. Soc.* 113, 8534.
- (59) Hazzard, J. T., Cusanovich, M. A., Tainer, J. A., Getzoff, E. D., and Tollin, G. (1986) Kinetic Studies of Reduction of a 1:1 Cytochrome *c*-Flavodoxin Complex by Free Flavin Semiquinones and Rubredoxin. *Biochemistry* 25, 3318.

Registry No. RFH*, 35919-91-6.

A Novel Method for the Incorporation of Glycoprotein-Derived Oligosaccharides into Neoglycopeptides

Stephen J. Wood and Ronald Wetzel*

Macromolecular Sciences Department, SmithKline Beecham Pharmaceuticals, 709 Swedeland Road, King of Prussia, Pennsylvania 19406. Received April 6, 1992

We describe a new method for the transfer of carbohydrate moieties to polypeptides in which complex carbohydrate, in the form of glycosyl amino acid, is removed from an available glycoprotein, derivatized, and reacted with a polypeptide via an iodoacetylated α -amino group. A family of oligomannose chains, N-linked to the side chain of Asn, was obtained from ovalbumin by pronase digestion and purified as previously described. A reactive sulfhydryl group was specifically placed on these molecules by reaction of 2-iminothiolane with the Asn α -amino group. Separately, the α -amino group of the peptide GGYR was specifically iodoacetylated by reaction with iodoacetic anhydride at pH 6. Reaction of the thiol-containing carbohydrate with iodoacetylated peptide at pH 8 gave in high yield the corresponding oligomannosyl-peptides, whose structures were confirmed by mass spectrometry. A peptide inhibitor of HIV protease was also oligomannosylated by this procedure. The principle advantage of this method is the efficiency of the reaction even when performed with stoichiometric amounts of the two molecules at low concentration. It should be feasible to extend this chemistry to larger polypeptides.

INTRODUCTION

There is increasing interest in the biological roles and potential therapeutic exploitation of the carbohydrate of glycoproteins, and many methods have been described for preparing conjugates of proteins and carbohydrate (1, 2). The available methods, however, are of limited value in carrying out a number of described transformations. In particular, there appear to be no methods available for efficiently attaching scarce, chemically complex carbohydrate to equally scarce polypeptide, with or without selectivity. Although biological methods are feasible in principle, our ignorance of the details of the cellular glycosylation process makes recombinant biosynthesis an unreliable approach to novel glycoproteins (3).

Of the many chemical methods which have been described, each suffers from one or more limitations. In many conjugation reactions, the amino groups of polypeptides are used as the attachment site, but it is often difficult to control the point of attachment and the extent of modification in a polypeptide containing a number of amino groups (4). Many of the available condensation reactions are relatively inefficient, requiring substantial excesses of carbohydrate (5, 6) or polypeptide (7) for significant conversion of a limiting, costly molecule. For example, for modification of scarce or costly polypeptides, reductive amination and similar methods are only feasible for simple, readily available saccharides. Bulk preparation of more complex carbohydrates by total chemical synthesis is not currently feasible. An alternative is to obtain complex carbohydrate of the desired structure from a plentiful glycoprotein. Classical methods which utilize available carbohydrate, however, suffer from relatively low yields of recovery of the required form of the carbohydrate from source glycoprotein, as well as low yields in the condensation reaction unless a large molar excess of carbohydrate or protein is used to achieve efficient utilization of the other molecule (7). Recently methods have been described for synthesis of neoglycoproteins which exploit the high reactivity and selectivity of the reaction between sulfhydryl groups and iodo- or bro-

moacetyl groups—the same reaction used in the method described here—for efficient cross-linking (8, 9). One of these methods uses as a starting material oligosaccharide derived from soy meal (8), while the other utilizes a monosaccharide derivative (9). It is not clear whether either of these methods will allow efficient use of carbohydrate derived from a natural glycoprotein.

We describe here a novel method for the synthesis of neoglycopeptides by the chemical conjugation of polypeptide to a carbohydrate moiety derived from a natural glycoprotein. In the method, a glycosylated amino acid is obtained by total digestion of a source glycoprotein with pronase followed by chromatographic purification, as previously described (10). The glycosyl-amino acid is then conjugated via its α -amino group in two high-yield steps. The chief advantages of the method are that both N- and O-linked carbohydrates can be utilized and the conjugation step involves highly efficient chemistry which can be conducted under mild conditions in small or large scale. In addition, the attachment point can be directed to the N-terminus of the polypeptide, especially in the case of peptides.

To illustrate the method we describe the conjugation of a family of related oligomannosyl-NAG₂-Asn¹ molecules to the N-terminal α -amino groups of the peptide glycylglycyltyrosylarginine (GGYR, 1) and the HIV-I protease inhibitor (4S,5S)-[4-hydroxy-5-[(alanylalanyl)amino]-6-phenylhexanoyl]valylvaline methyl ester (AAF Ψ GVV-OMe, 2, SKF# 107457) (11).

EXPERIMENTAL PROCEDURES

Materials and General Methods. The tetrapeptide GGYR (1) was synthesized by the standard Merrifield solid-phase method and supplied by Mike Burke of SmithKline Beecham Pharmaceuticals. The protease inhibitor SKF AAF Ψ GVV-OMe (2) (11) was supplied by Geoff Dreyer, SmithKline Beecham Pharmaceuticals.

¹ Abbreviations used: NAG = N-acetylglucosamine; 2-IT = 2-iminothiolane; TFA = trifluoroacetic acid; DTNB = 5,5'-dithiobis-2-nitrobenzoic acid; MES = 2-(N-morpholino)ethanesulfonic acid; EDTA = ethylenediaminetetraacetic acid; FAB = fast atom bombardment.

* Author to whom correspondence should be addressed.

Chicken egg ovalbumin (Grade V), dithiothreitol, DTNB and Protease type XV (Pronase E) were purchased from Sigma. Iodoacetic anhydride was from Aldrich Chemical Co. and 2-IT was from Pierce Chemical Co. HIV-I protease was provided by James Stickler of SmithKline Beecham. HIV-I protease inhibition was determined as previously described (12). HPLC was performed on a protein and peptide C18 column (Vydak) using linear gradients of buffer B (0.1% TFA in acetonitrile) in buffer A (0.1% TFA in water).

Isolation and Purification of Glycosyl-Asn. Asparagine-linked carbohydrate components of ovalbumin were isolated and purified according to the method of Huang et al. (10). Briefly, ovalbumin at pH 7.8 was heated to 80 °C for 15 min, cooled, and then digested with pronase at pH 7.4 for 24-h at room temperature. Oligomannosyl-NAG-NAG-Asn was separated from incompletely digested material by gel filtration on a Sephadex G-25 column (3.5 × 50 cm), and the incompletely digested ovalbumin fractions were pooled and digested further with pronase. This was repeated twice. Carbohydrate-containing fractions were identified with the phenol-sulfuric acid carbohydrate assay (13). Oligomannosyl-NAG-NAG-Asn containing fractions were pooled, desalted on a G-25 (3.5 × 50 cm), and fractionated on a Dowex AG-50W-X4 cation exchange column (1.6 × 90 cm).

Glycosyl-Asn/2-Iminothiolane Reaction. A pool of oligomannosyl-NAG-NAG-Asn fractions was prepared by mixing peaks A-E of the Dowex column, which behaved as described (10). A stock solution of 2-IT was freshly prepared by dissolving 2-IT in 50 mM potassium acetate buffer, pH 5, to a concentration of 100 mM, and an aliquot of this stock used to prepare the reaction mixture. A 1550- μ L reaction mixture consisting of 1 mM oligomannosyl-NAG-NAG-Asn (6) and 33 mM 2-IT in 1 mM EDTA, 33 mM potassium phosphate buffer, pH 7.0, was incubated at 37 °C. After 24 h, 500 μ L of 100 mM DTT was added and incubation at 37 °C continued. After 4 h the entire reaction mixture was chromatographed at room temperature on a G-10 gel filtration column (1.5 × 17 cm) equilibrated with 0.1% acetic acid. Fractions were assayed for carbohydrate using the phenol-sulfuric acid assay (13) and for the presence of free sulfhydryl using DTNB (14). Fractions testing positive for both carbohydrate and free sulfhydryl were freeze-dried and stored at -20 °C in 0.1% acetic acid (Figure 1).

Iodoacetic Anhydride Reactions. A stock solution of iodoacetic anhydride was prepared by dissolving iodoacetic anhydride in dry THF at a concentration of 250 mM (15). This solution was stored at -20 °C in microcentrifuge tubes which were stored inside 50-mL conical tubes with calcium carbonate dessicant and sealed with parafilm.

Derivatization of AAF Ψ GVV-OMe (2) with iodoacetic anhydride was accomplished at 0 °C as follows. To a 550- μ L reaction mixture containing 5 mM AAF Ψ GVV-OMe (2), 3.6 mM EDTA, and 100 mM MES, pH 6, were added three additions (30 μ L), with vortexing, of iodoacetic anhydride (0.25 M) at 3-min intervals. Following the final addition, 700 μ L of a 10% (v/v) methanol in chloroform solution was added and the mixture was vortexed for 1 min and then centrifuged for 5 min. The organic phase was removed into a fresh microcentrifuge tube, spun to dryness in a rotary evaporator, and stored at -20 °C.

Iodoacetylation of the tetrapeptide GGYR (1) was accomplished in the same manner with the exception that the organic extraction of the reaction product was not

performed. Instead, the iodoacetylated GGYR reaction product (4) was purified by reverse-phase HPLC (15).

Condensation Reactions. AAF Ψ GVV-OMe. To 500 μ L of a 4 mM solution of N α -iodoacetylated AAF Ψ GVV-OMe (5) in DMSO was added 1000 μ L of an approximately 2 mM solution of oligomannosyl-NAG₂-Asn-SH (8) in 20 mM acetic acid, 0.2 mM EDTA. The solution was brought to pH 8 by adding 500 μ L of 1 M potassium phosphate, pH 8.0, and the reaction incubated at 37 °C for 6 h.

GGYR. To 750 μ L of an approximately 50 μ M solution of oligomannosyl-NAG₂-Asn-SH (8) in 20 mM acetic acid, 1 mM EDTA was added 100 μ L of an aqueous solution 750 μ M in N α -iodoacetyl-GGYR (4). The solution was brought to pH 8 by addition of 500 μ L of 1 M potassium phosphate, pH 8.0, and the reaction incubated at 37 °C for 20 h.

Mass Spectrometry. Reaction products were analyzed by fast atom bombardment mass spectrometry on the first portion of a double focusing VG ZAB SE-4F tandem magnetic deflection mass spectrometer, which employs an accelerating voltage of 10 kV and a mass range of 12 500, or on a VG ZAB-HF magnetic deflection mass spectrometer, with an accelerating voltage of 8 kV and a mass range of 3000. The VG ZAB SE-4F was equipped with a flow FAB ion source and a Cs ion gun operated at 35 kV and a 2-4 μ A emission current. The VG ZAB-HF was also equipped with a standard flow FAB ion source, but employed an ION Tech FAB gun (operating voltage of 8 kV) which utilized a discharge current of 1 mA. All data was processed on a VG 11-250J data system. Most samples were analyzed by FAB-MS in a matrix of either thioglycerol or 1:1 thioglycerol-*m*-nitrobenzyl alcohol plus 1% trifluoroacetic acid.

RESULTS

The reactions described in this paper are summarized in Scheme 1. To simplify the scheme, the family of carbohydrates derived from ovalbumin, the major components of which are identified in the product as shown in Table I, is represented in a single structure, 6.

Digestion of ovalbumin with pronase generated a mixture of glycosylated asparagine derivatives giving a chromatogram on Dowex very similar to the published distribution (10). Fractions A-E (10), reported to contain glycosyl groups composed of 4-7 mannose units (plus the NAG-NAG bridge to the Asn side chain) (16), were pooled. This mixture was reacted with 2-iminothiolane (7) (17), which reacts with amino groups of proteins, peptides, and amino acids to generate a spacer terminating with a sulfhydryl group (15, 18-20). The reaction mixture was incubated with DTT to insure against loss of reactive thiolated carbohydrate by disulfide formation under reaction conditions. The desired product (8) was separated from 2-IT breakdown products and DTT by chromatography on Sephadex G-10. Figure 1 shows that the carbohydrate-containing fractions comigrate with the only macromolecular peak of DTNB-positive fractions. Further, there is good agreement between the estimated concentrations of Man_n-NAG-NAG-Asn-SH as assessed by both sulfhydryl and carbohydrate contents. This close agreement suggests that most of the Man_n-NAG-NAG-Asn α -amino groups have reacted. The DTNB estimate was taken as the correct concentration for setting up the condensation reactions. The results of these reactions, however, suggest that the DTNB-determined concentration may be an underestimate by approximately 50%.

Figure 2a shows the HPLC elution position of the peptide (4S,5S)-[4-hydroxy-5-[(alanylalanyl)amino]-6-phenylhexanoyl]valylvaline methyl ester (AAF Ψ GVV-

Scheme I

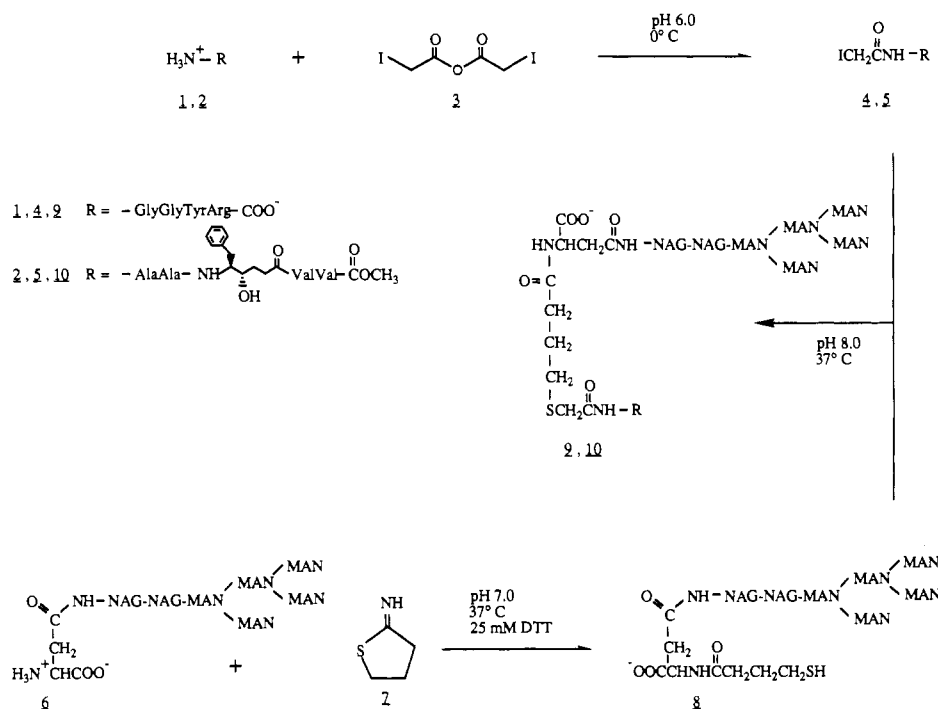


Table I. FAB-MS Parent Ions of the Major Components of Conjugates

oligomannosylated AAFΨGVV-OMe (10)		oligomannosylated GGYR (9)	
carbohydrate component ^a	M ⁺ , <i>m/z</i> (±2)	carbohydrate component	M ⁺ , <i>m/z</i> (±1.5)
Man ₅ NAG ₂	2070	Man ₅ NAG ₂	1943.3
Man ₆ NAG ₂	2232	Man ₆ NAG ₂	2105.5
Man ₇ NAG ₂	2394	Man ₆ NAG ₄	2349.7
Man ₈ NAG ₂	2556	Man ₅ NAG ₅	2553.2

^a Man = mannose, NAG = *N*-acetyl- β -D-glucosamine.

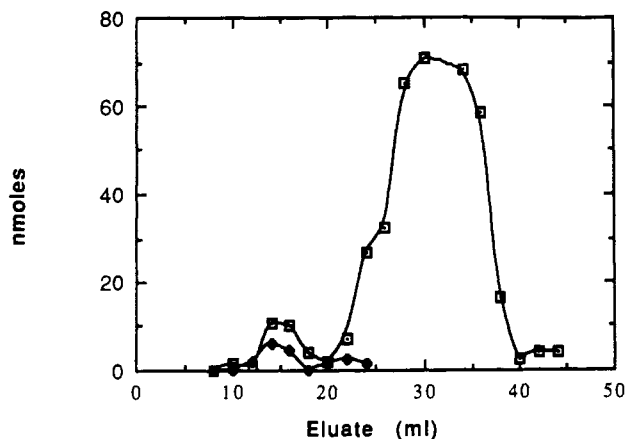


Figure 1. Estimate of 2-iminothiolane-derivatized carbohydrate eluting from a G-10 column based on the phenol-sulfuric acid carbohydrate assay (13) (♦) and the DTNB assay for free thiols (14) (□).

OMe) (2). Figure 2b shows the chromatogram of the reaction mixture of AAFVGVV-OMe with iodoacetic anhydride at pH 6, conditions previously described to be highly selective for iodoacetylation of the N^{α} -amino group of peptides (15, 21, 22). The major product peak elutes later than starting material, as expected for an iodoacetylated derivative (15). The yield of iodoacetylated peptide (5) is about 80%. Figure 2c shows the reaction mixture between the iodoacetylated peptide and the pool of Man-

NAG-NAG-Asn-SH (8) (which does not absorb at 215 nm) immediately after mixing at pH 2. Carbohydrate analysis (13) (not shown) indicates that Man_n-NAG-NAG-Asn-SH elutes in the injection peak. Figure 2d shows the chromatogram of the same mixture after the pH was adjusted to 8 and the mixture allowed to stand for 6 h at room temperature. The figure shows that the iodoacetylated peptide has disappeared and been replaced by an earlier-eluting peak of similar size. Earlier elution in an aqueous TFA, reversed-phase HPLC system is expected for the addition of carbohydrate to a peptide (4). Closer examination of the peak shows it to be asymmetric, consistent with its being a mixture of related structures. Figure 2d suggests that conversion of iodoacetylated peptide to the mannosylated peptide is essentially quantitative at relatively low reactant concentrations at a ratio of about 1:1.

Table I shows the MS analysis of this peak, which confirms that it is a mixture of glycosylated conjugates of AAFVGVV-OMe in the anticipated Man_n-NAG-NAG series. Three of the four carbohydrate structures found in the product are as expected from previous analysis of the heterogeneous oligosaccharide of ovalbumin (16). Analysis of inhibition of HIV-I protease by the conjugate mixture showed it to be only modestly reduced in inhibitory activity compared to the unmodified inhibitor ($K_i = 50$ and 10 nM, respectively, for oligomannosylated and unmodified inhibitor).

Figure 3a shows the chromatogram of the reaction mixture containing *N*- α -iodoacetyl-GGYR (4) and Man_{*n*}-NAG-NAG-Asn-SH (8) before adjusting the pH to 8. Figure 3b shows the same reaction mixture 20 h after adjusting the pH to 8 as described in the methods. The figure shows some residual, unreacted iodoacetylated peptide, which is expected given that the reaction mixture was adjusted to give a stoichiometry of about 1:2 carbohydrate to peptide. As mentioned above, the fact that the reaction appears to have progressed well beyond 50% suggests that the concentration of Man_{*n*}-NAG-NAG-Asn-SH was underestimated. The figure also clearly shows the heterogeneity in the product, which is expected on the basis of the known

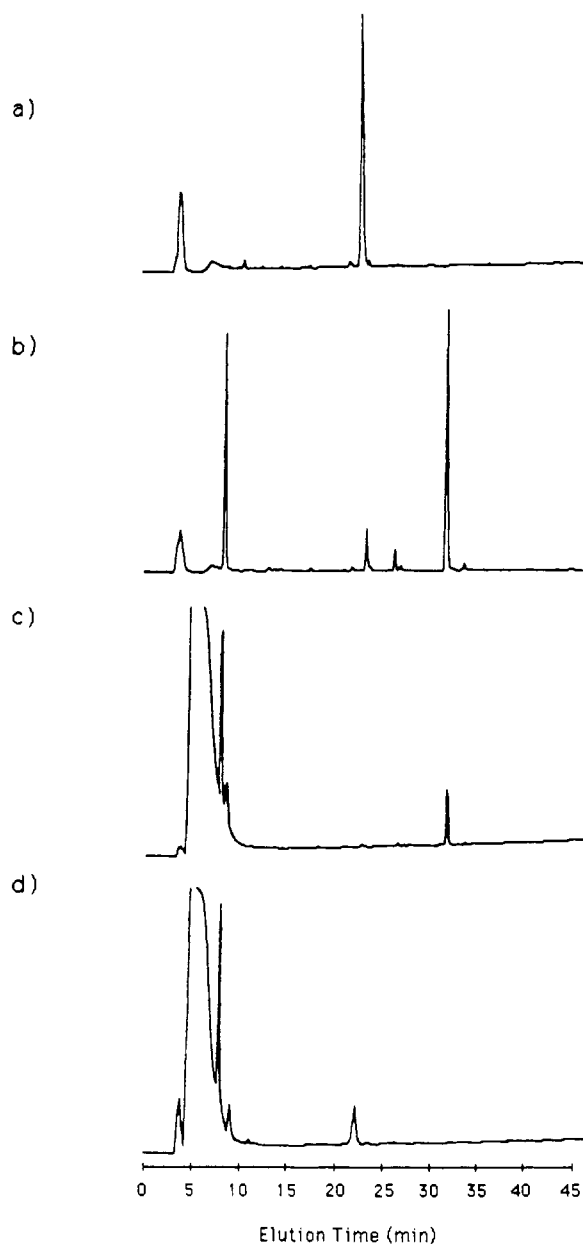


Figure 2. Reverse-phase HPLC chromatograms (A_{215}) of (a) pure HIV protease inhibitor, (b) reaction mixture from iodoacetylation of AAF Ψ GVV-OMe (2) with iodoacetic anhydride, (c) reaction mixture of iodoacetylated AAF Ψ GVV-OMe (5) and oligomannosyl-NAG₂-Asn-SH (8) at pH 2, and (d) reaction mixture of iodoacetylated AAF Ψ GVV-OMe (5) and oligomannosyl-NAG₂-Asn-SH (8) at pH 8 after 6 h at 37 °C.

heterogeneity of the carbohydrate. This broad peak was collected and submitted for MS analysis. Table I shows that the four major conjugate peaks are all expected from the previously characterized structures of ovalbumin's oligosaccharide component (16).

The MS parent ions listed in Table I are consistent with the molecular weights calculated for the suggested structures in Scheme I. The parent ions of 2-IT reaction products 8 suggest that the imino amide moiety expected in a 2-IT adduct hydrolyzes to the amide during the course of the reaction and workup. The scheme reflects this hydrolysis in the portrayed structures of 8–10. Hydrolysis of the imino amide to an amide is not surprising, based on the described chemistry of imino amides in general (23) and products of 2-IT reactions in particular (24).

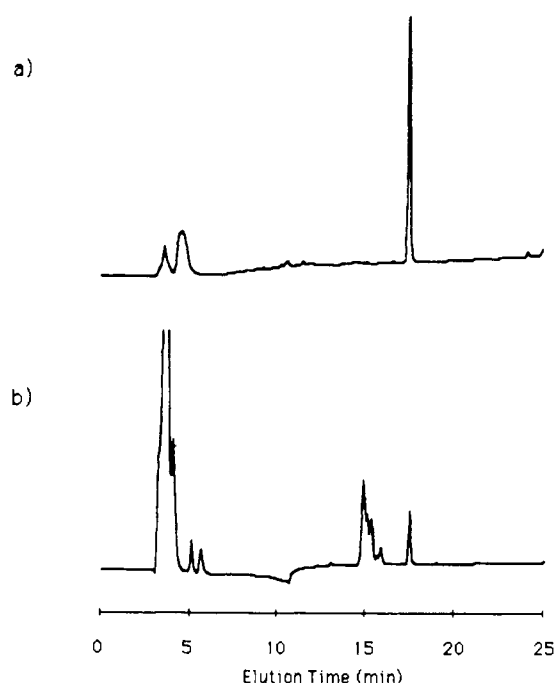


Figure 3. Reverse-phase HPLC chromatograms (A_{215}) of (a) reaction mixture of N^{α} -iodoacetyl-GGYR (4) with oligomannosyl-NAG₂-Asn-SH (8) at pH 2 and (b) reaction mixture of the N^{α} -iodoacetyl-GGYR (4) with oligomannosyl-NAG₂-Asn-SH (8) at pH 8 after 20 h at 37 °C.

DISCUSSION

The macrophage mannose receptor (25) requires multivalent mannose derivatives for endocytosis of the receptor–ligand complex (26). Multivalency can be achieved by modification of multiple lysines of a protein with simple mannose derivatives (5). However, such multivalent conjugates are not feasible for molecules containing only one potential attachment site. Furthermore, proteins hyperglycosylated at many lysine residues display carbohydrate in a significantly different way than do the multivalent, complex carbohydrates which are the presumed normal ligands of receptors like the macrophage mannose receptor. Other carbohydrate receptors might prove to have even higher requirements for native glycosyl chain structure than the mannose receptor. For these reasons, we set out to develop a general, efficient method which would allow one to borrow the glycosyl chains from a glycoprotein in hand and chemically transfer the intact carbohydrate to another protein or peptide with some control over the point of attachment.

Because of the difficulty in obtaining the carbohydrate moieties of glycoproteins in large amounts, we put a premium on conversion efficiency in choosing a condensation chemistry. We chose the reaction between the α -iodocarbonyl group and the thiol group, chemistry which can be controlled by pH and which can proceed with excellent yields under mild conditions without using large excesses or high concentrations of either reactant (14, 15).

The results described here support the merit of this choice of chemistry. The reaction of oligomannosyl-Asn with 2-IT appears to proceed in high yield, given the good agreement between measured SH and carbohydrate levels in the macromolecular fraction of the reaction mixture (Figure 1). Similarly, the condensation of the product Man_n-NAG-NAG-Asn-SH with iodoacetylated peptides also proceeds in high yields (Figures 2 and 3), even at low concentrations and 1:1 stoichiometries of reactants. These features should allow efficient use of available carbohy-

drate as well as polypeptide. Since the reaction with 2-IT simply requires any active amino group, the conjugation strategy should work equally well for O- and N-linked carbohydrate. Similarly, carbohydrate attached to Asn, Thr, or Ser which are incorporated into peptides (for example, as in the products of *incomplete* proteolytic digestion of a glycoprotein) should react equally well to give neoglycopolypeptides, albeit with longer, less well-defined spacer arms.

The chemistry also allows for varying degrees of homogeneity of the carbohydrate moiety. It should be possible to isolate and conjugate particular molecular species. In developing this chemistry we chose to use a mixture of glycosyl-Asn molecules obtained by pooling the chromatographic peaks from the separation of the products of pronase digestion of ovalbumin.

Carbohydrate hydroxyl groups can also react with 2-IT, especially at high pH values, at a rate estimated to be about 1% that of the reaction of 2-IT with amino groups (24). If a significant proportion of the product of 2-IT with oligomannosyl-NAG-NAG-Asn is modified at hydroxyl groups, it would thus be expected to produce a disubstituted molecule (with the amino group also modified), which would in turn produce a conjugate with two peptide groups per molecule of carbohydrate. We see no evidence for the formation of such conjugates in the MS data. However, the formation of a small amount of hydroxyl-modified conjugate cannot be discounted.

In contrast to one-step conjugation reactions such as reductive amination, the procedure described here also affords a degree of control over the attachment point, especially in the case of peptides. Reaction of peptides with iodoacetic anhydride at pH 6 has been shown previously to greatly favor the acylation of the N-terminal α -amino group, even in the presence of a number of unprotected lysine ϵ -amino groups (15). Furthermore, further control of the attachment site is possible since iodoacetylated peptides can be HPLC-purified, stored, and characterized before use in an alkylation reaction. (However, some care should be taken with iodoacetylated peptides containing Met, His, or Lys in the sequence, since, under appropriate conditions, such peptides can cyclize (22).)

Absolute specificity of attachment is more difficult to achieve with proteins containing many lysine groups, unless one of them is uniquely reactive. In cases where specificity is not possible, the iodoacetylation mediated attachment of carbohydrate described here still provides the advantage of finer control over the number of carbohydrate molecules bound per protein molecule. Where greater control over attachment point is desired, protein engineering methods might be utilized to construct mutants with uniquely reactive side chains which can be modified for specific reaction with a derivitized carbohydrate. Although logic dictates that additional steps in a synthetic route should generally decrease final yield, the strategy presented here, based on synthesis of reactive intermediates of both polymers, should lead to increased efficiency of use of these polymers, because of the high yields of all of the steps involved, including the final coupling step.

The cell-type specificity in the distribution of carbohydrate receptors makes drug targeting via added carbohydrate an attractive possibility (27, 28). Our results provide a new means to attachment of complex carbohydrates to potential drug molecules. In the example, attachment of a family of branched mannose oligosac-

charides to the N-terminus of an HIV-I protease inhibitor allowed good retention of biological activity.

ACKNOWLEDGMENT

We thank Geoff Dryer for the gift of SKF# 107457, Jim Strickler, and Tom Meek for help with the HIV-I protease inhibition assay, Steve Carr and Gerald Roberts for mass spectrometry, and Kalyan Anamula, Rich Kirsh, and Harma Ellens for helpful discussions.

LITERATURE CITED

- (1) Stowell, C. P., and Lee, Y. C. (1980) Neoglycoproteins: The preparation and application of synthetic glycoproteins. *Adv. Carbohydr. Chem. Biochem.* 37, 225-281.
- (2) Aplin, J. D., and Wriston, J. C., Jr. (1981) Preparation, properties and applications of carbohydrate conjugates of proteins and lipids. *CRC Crit. Rev. Biochem.* 10, 259-306.
- (3) Smith, P. L., Kaetzel, D., Nilson, J., and Baenziger, J. U. (1990) The sialylated oligosaccharides of recombinant bovine lutropin modulate hormone bioactivity. *J. Biol. Chem.* 265, 874-881.
- (4) Morehead, H., McKay, P., and Wetzel, R. (1982) High-performance liquid chromatography analysis in the synthesis, characterization, and reactions of neoglycopeptides. *Anal. Biochem.* 126, 29-36.
- (5) Lee, Y. C., Stowell, C. P., and Krantz, M. J. (1976) 2-imino-2-methoxyethyl 1-thioglycosides: New reagents for attaching sugars to proteins. *Biochemistry* 15, 3956-3963.
- (6) Marsh, J. W., Denis, J., and Wriston, J. C., Jr. (1977) Glycosylation of *Escherichia coli* L-asparaginase. *J. Biol. Chem.* 252, 7678-7684.
- (7) Mencke, A. J., and Wold, F. (1982) Neoglycoproteins: Preparation and *in vivo* clearance of serum albumin derivatives containing ovalbumin oligosaccharides. *J. Biol. Chem.* 257, 14799-14805.
- (8) Colon, M., Staveski, M. M., and Davis, J. T. (1991) Mild conditions for the preparation of high-mannose oligosaccharide oxazolines: Entry point for β -glycoside and neoglycoprotein synthesis. *Tetrahedron Lett.* 32, 4447-4450.
- (9) Davis, N. J., and Flitsch, S. L. (1991) A novel method for the specific glycosylation of proteins. *Tetrahedron Lett.* 32, 6793-6796.
- (10) Huang, C.-C., Mayer, H. E., Jr., and Montgomery, R. (1970) Microheterogeneity and Paucidisparity of Glycoproteins. *Carbohydr. Res.* 13, 127-137.
- (11) Dreyer, G. B., Lambert, D. M., Meek, T. D., Carr, T. J., Tomaszek, T. A., Jr., Fernandez, A. V., Bartus, H., Cacciavillani, E., Hassell, A. M., Minnich, M., Petteway, S. R., Jr., Metcalf, B. W., and Lewis, M. (1992) Hydroxyethylene isostere inhibitors of human immunodeficiency virus-1 protease: Structure-activity analysis using enzyme kinetics, X-ray crystallography, and infected T-cell assays. *Biochemistry* 31, 6646-6659.
- (12) Meek, T. D., Dayton, B. D., Metcalf, B. W., Dreyer, G. B., Strickler, J. E., Gorniak, J. G., Rosenberg, M., Moore, M. L., Magaard, V. W., and DeBouck, C. (1989) Human immunodeficiency virus 1 protease expressed in *Escherichia coli* behaves as a dimeric aspartic protease. *Proc. Natl. Acad. Sci. U.S.A.* 86, 1841-1845.
- (13) Dubois, M., Gilles, K. A., Hamilton, J. K., Rebers, P. A., and Smith, F. (1956) Colorimetric Method for Determination of Sugars and Related Substances. *Anal. Chem.* 28, 350-356.
- (14) Means, G. E., and Feeney, R. E. (1971) *Chemical Modification of Proteins*, p 220, Holden-Day, San Francisco.
- (15) Wetzel, R., Halualani, R., Stults, H. T., and Quan, C. (1990) A General Method for Highly Selective Cross-Linking of Unprotected Polypeptides via pH-Controlled Modification of N-Terminal α -Amino Groups. *Bioconjugate Chem.* 1, 114-122.
- (16) Kobata, A. (1984) The carbohydrates of glycoproteins. *Biology of Carbohydrates* (V. Ginsburg, and P. W. Robbins, Eds.), pp 87-161, John Wiley & Sons, New York.

- (17) Lambert, J. M., McIntyre, G., Gauthier, M. N., Zullo, D., Rao, V., Steeves, R. M., Goldmacher, V. S., and Blaettler, W. A. (1991) The galactose binding sites of the cytotoxic lectin ricin can be chemically blocked in high yield with reactive ligands prepared by chemical modification of glycopeptides containing triantennary N-linked oligosaccharides. *Biochemistry* 30, 3234–3247.
- (18) Traut, R. R., Bollen, A., Sun, T.-T., Hershey, J. W. B., Sundberg, J., and Pierce, L. R. (1973) Methyl 4-mercaptobutyrimidate as a cleavable cross-linking reagent and its application to the *Escherichia coli* 30S ribosome. *Biochemistry* 12, 3266–3273.
- (19) Jue, R., Lambert, J. M., Pierce, L. R., and Traut, R. R. (1978) Addition of sulfhydryl groups to *Escherichia coli* ribosomes by protein modification with 2-iminothiolane (methyl 4-mercaptobutyrimidate). *Biochemistry* 17, 5399–5406.
- (20) Goff, D. A., and Carroll, S. F. (1990) Substituted 2-iminothiolanes: reagents for the preparation of disulfide cross-linked conjugates with increased stability. *Bioconjugate Chem.* 1, 381–386.
- (21) Stults, J. T., Lai, J., McCune, S., and Wetzel, R. (1992) Simplification of high energy collision spectra of peptides by amino-terminal derivatization. Submitted for publication.
- (22) Wood, S. J., and Wetzel, R. (1992) A novel cyclization chemistry especially suited for biologically derived, unprotected peptides. *Int. J. Pept. Protein Res.* 39, 533–539.
- (23) De Wolfe, R. H. (1975) Kinetics and mechanisms of reactions of amidines. *The Chemistry of Amidines and Imidates* (S. Patai, Ed.) pp 349–387, Wiley, New York.
- (24) Alagon, A. C., and King, T. P. (1980) Activation of polysaccharides with 2-iminothiolane and its uses. *Biochemistry* 19, 4341–4345.
- (25) Taylor, M. E., Conary, J. T., Lennartz, M. R., Stahl, P. D., and Drickamer, K. (1990) Primary structure of the mannose receptor contains multiple motifs resembling carbohydrate-recognition domains. *J. Biol. Chem.* 265, 12156–12162.
- (26) Hoppe, C. A., and Lee, Y. C. (1983) The binding and processing of mannose-bovine serum albumin derivatives by rabbit alveolar macrophages. *J. Biol. Chem.* 258, 14193–14199.
- (27) Poznansky, M. J., and Juliano, R. L. (1984) Biological approaches to the controlled delivery of drugs: A critical review. *Pharm. Rev.* 36, 277–336.
- (28) Roche, A. C., Midoux, P., Pimpaneau, V., Negre, E., Mayer, R., and Monsigny, M. (1990) Endocytosis mediated by monocyte and macrophage membrane lectins—Application to antiviral drug targeting. *Res. Virol.* 141, 243–249.

Structural Features of the Antibody-A Chain Linkage that Influence the Activity and Stability of Ricin A Chain Immunotoxins

Alan J. Cumber,[†] John H. Westwood,[†] Raymond V. Henry,[†] Geoffrey D. Parnell,[†] Brian F. Coles,[†] and Edward J. Wawrzynczak^{*†}

Drug Targeting Group, Section of Immunology, Institute of Cancer Research, 15 Cotswold Road, Sutton, Surrey SM2 5NG, U.K., and CRC Molecular Toxicology Group, Department of Biochemistry, University College, Windeyer Building, London W16 6DB, U.K. Received April 13, 1992

The importance of the various structural elements constituting a ricin A chain immunotoxin to the stability of the disulfide bond between the antibody and A chain was examined using a panel of immunoconjugates prepared with the mouse monoclonal antibody Fib75. Analogues of the standard ricin A chain immunotoxin prepared with the *N*-succinimidyl 3-(2-pyridyldithio)propionate disulfide cross-linker included immunoconjugates made with *N*-succinimidyl 4-[(iodoacetyl)amino]benzoate the thioether cross-linker; with *N*-succinimidyl 3-(2-pyridyldithio)butyrate, the hindered disulfide cross-linker; with a peptide spacer between the antibody and cross-linker; or with the dodecapeptide corresponding to the C-terminus of ricin A chain. The cytotoxic activities of the immunoconjugates and their susceptibility to reduction by glutathione in vitro were compared. The thioether-linked immunotoxin could not be cleaved by glutathione in vitro and had low cytotoxic potency, consistent with the requirement of a reducible disulfide linkage for activity. The hindered disulfide-linked immunotoxin was 3-fold more stable to reduction than the immunotoxin containing a standard unhindered disulfide linkage, but the cytotoxic activities of the two constructs were indistinguishable. The introduction of a flexible peptide Ala-Ala-Pro-Ala-Ala-Ala-Pro-Ala-Pro-Ala between Fib75 and the disulfide linkage introduced by SPDP had no deleterious effect on cytotoxic activity and no effect on the susceptibility of the disulfide linkage to reduction. This finding suggests that the enforced proximity of the A chain to the antibody caused by the use of a short chemical cross-linker in a conventional immunotoxin has no influence on either of these properties in this system. In contrast, substitution of the ricin A chain by a dodecapeptide, 2,4-dinitrophenyl-Val-Tyr-Arg-Cys-Ala-Pro-Pro-Ser-Ser-Gln-Phe, greatly increased the extent to which the disulfide bond was cleaved by glutathione, demonstrating that the stability of the bond also depends upon the intact structure of the A chain.

INTRODUCTION

Immunotoxins are conjugates comprising a mAb¹ linked by chemical procedures to a protein toxin such as ricin, the toxin of *Ricinus communis* seeds, or its subunits (1, 2). The two-chain structure of ricin has been defined in studies of the primary structure by peptide sequencing (3) and nucleotide sequencing of the gene (4, 5), and the three-dimensional structure has been elucidated by X-ray crystallography (6). The A chain is a ribosome-inactivating protein which catalytically modifies the rRNA of the eukaryotic 60S ribosomal subunit by a site-specific *N*-glycanase activity (7). It consists of 267 amino acid residues and is linked by a disulfide bond from the Cys²⁵⁹ residue in the C-terminal region of the molecule to the B chain.

Ricin A chain ITs can exert highly potent and selective cytotoxic effects and have been used in several clinical trials (8, 9). The performance of such ITs in vivo is a function of both their activity and of their stability. To ensure maximal cytotoxic activity, it is necessary for the linkage between the mAb and the A chain to include a

disulfide bond (10). However, the disulfide linkage is sensitive to cleavage by reduction in the circulation with consequent dissociation into the constituent proteins (11, 12). Attempts to minimize this problem have concentrated on the use of a new generation of hindered cross-linking agents in which bulky side-chain groups proximal to the disulfide bond afford protection from nucleophilic attack (13, 14). Pharmacokinetic studies in several animal species have demonstrated that A chain ITs made with hindered disulfide cross-linkers have a longer half-life in vivo (13, 14) and an improved therapeutic index (15). We have further shown a correlation between breakdown in vivo and susceptibility to reduction by glutathione in vitro (16).

In this study, we have examined the importance of the various structural elements constituting a ricin A chain IT to the stability of the disulfide bond linking the mAb and A chain components. A series of immunoconjugates was prepared with the mouse mAb Fib75. Analogues of a standard ricin A chain IT prepared with SPDP as cross-linker included immunoconjugates made with SIAB, the thioether cross-linker; with SPDB the hindered disulfide cross-linker; with a peptide spacer between the mAb and the cross-linker; or with a dodecapeptide corresponding to the C-terminus of ricin A chain. The cytotoxic activities of the immunoconjugates and their susceptibility to reduction by glutathione in vitro were compared.

EXPERIMENTAL PROCEDURES

Materials. Ricin A chain and the mouse mAb Fib75 were prepared as described previously (11). *N*-Succinimidyl 3-(2-pyridyldithio)propionate, *N*-succinimidyl 3-(2-pyridyldithio)butyrate, and *N*-succinimidyl 4-[(io-

* To whom correspondence should be addressed.

[†] Institute of Cancer Research.

[†] University College.

¹ Abbreviations used: DNP, 2,4-dinitrophenyl; DTT, dithiothreitol; IT, immunotoxin; mAb, monoclonal antibody; NTB, nitrothiobenzoate; PAGE, polyacrylamide gel electrophoresis; PBS, phosphate-buffered saline; SDS, sodium dodecyl sulfate; SIAB, *N*-succinimidyl 4-[(iodoacetyl)amino]benzoate; SPDB, *N*-succinimidyl 3-(2-pyridyldithio)butyrate; SPDP, *N*-succinimidyl 3-(2-pyridyldithio)propionate.

doacetyl)amino]benzoate were prepared as described previously (13).

Peptide Synthesis, Sequencing, and Modification. The peptides used in this study, Ala-Ala-Pro-Ala-Ala-Ala-Pro-Ala-Pro-Ala (Ala₇Pro₃) and Val-Tyr-Arg-Cys-Ala-Pro-Pro-Ser-Ser-Gln-Phe (ricin A²⁵⁶⁻²⁶⁷), the C-terminus of native ricin A chain, were synthesized by conventional solid-phase Fmoc chemistry using a Milligen 9050 Pep-Synthesizer. Peptide purity and identity was confirmed by reversed-phase HPLC and sequencing by automated Edman degradation (23) using an Applied Biosystems 470A peptide sequencer and 120A HPLC system. The sequence of amino acid residues 256–267 present within the ricin A chain used for this study was determined directly by sequencing of the C-terminal fragment of the A chain generated by CNBr cleavage.

Ricin A²⁵⁶⁻²⁶⁷-DNP was synthesized by modifying the resin-bound side-chain-protected peptide intermediate selectively at the N-terminal amino group by reaction with 2,4-dinitrofluorobenzene in 1 M NaHCO₃/EtOH (1:2).

Ricin A chain and ricin A²⁵⁶⁻²⁶⁷ were substituted with the nitrothiobenzoate group by reaction with Ellman's reagent. The A chain at a concentration of 40 μ M was treated with a 24-fold molar excess of DTT for 1 h at 37 °C before addition of a 120-fold molar excess of 5,5'-dithiobis(2-nitrobenzoic acid) for 20 min at 37 °C. The A chain peptide at a concentration of 3 mM was treated with a 2-fold molar excess of Ellman's reagent for 1 h at room temperature. The derivatized ricin A-NTB and ricin A²⁵⁶⁻²⁶⁷-NTB were purified by gel filtration on Sephadex G25 and reversed-phase HPLC, respectively.

Immunoconjugate Preparation. Ricin A chain was attached to the Fib75 mAb using the SPDP, SPDB and SIAB cross-linkers as described previously (13).

The synthesis of the Fib75 immunoconjugate incorporating ricin A²⁵⁶⁻²⁶⁷-DNP via the SPDP linker was performed using the same basic methodology. The substitution ratio of this immunoconjugate was calculated from the introduced absorbance of the DNP group.

Fib75-Ala₇Pro₃-SPDP-ricin A was synthesized by the following procedure. (1) The Ala₇Pro₃ peptide was reacted with a 2-fold molar excess of SPDP in DMF/PBS (7:3) at room temperature to attach a PDP group to the single N-terminal amino group of the peptide. The product, Ala₇Pro₃-PDP, was purified by HPLC on a C₁₈ reversed-phase column using a 0.1% trifluoroacetic acid/acetonitrile gradient and freeze-dried by lyophilization. (2) Ala₇Pro₃-PDP was treated with a 5-fold molar excess of *N*-hydroxysuccinimide and *N,N'*-dicyclohexylcarbodiimide in DMF to activate the single C-terminal carboxyl group of the peptide. (3) A 10-fold molar excess of the activated Ala₇Pro₃ peptide was added to Fib75 and the Fib75-Ala₇Pro₃-PDP conjugate was purified by gel filtration on Sephadex G50. (4) Ricin A chain was coupled to Fib75-Ala₇Pro₃-PDP using the conditions previously described for the synthesis of conventional ricin A chain ITs (13).

Characterization of Immunoconjugate Preparations. The immunoconjugate preparations were analyzed by SDS-PAGE and gel permeation HPLC. Electrophoresis was performed on 4–12.5% gradient gels in the presence of 0.2% SDS solution. Samples were prepared for electrophoresis in the absence of reducing agent to preserve the disulfide bond between the mAb and the attached ricin A chain or A chain peptide. Protein bands were visualized by Coomassie Brilliant Blue staining. Gel permeation chromatography was performed on a TSK G3000SWXL column (60 cm \times 0.78 cm i.d.) as described previously (16).

Measurement of Cytotoxicity in Tissue Culture. Cytotoxicity experiments with the SW2 human small cell lung cancer cell line in tissue culture were conducted as described previously with slight modification (17). Briefly, 0.1-mL aliquots of a single-cell suspension of SW2 cells at a density of 2×10^5 cells/mL were distributed into the wells of a 96-well tissue culture plate. Samples of immunoconjugate prepared at different concentrations were added to the wells in 0.1-mL aliquots. Cultures were incubated for 48 h at 37 °C and then pulsed with 1 μ Ci of [³H]leucine for a further 24 h at 37 °C. Cells were harvested onto filters using an automated cell harvester, and the incorporation of [³H]leucine was determined by liquid scintillation counting.

Measurement of Immunoconjugate Breakdown. The release of ricin A chain from IT preparations following incubation with different concentrations (10, 1, 0.1 mM) of glutathione was measured directly by gel permeation HPLC as described previously (16). After incubation for 1 h at 37 °C under sterile conditions, iodoacetamide was added to a final concentration of 13 mM to block further reaction. Control samples were treated in an identical fashion except that glutathione was omitted.

Samples of the Fib75-SPDP-ricin A²⁵⁶⁻²⁶⁷-DNP conjugate were treated similarly to the Fib75 ITs. Following reaction, the immunoconjugate was gel filtered on Sephadex G25 and the fraction containing protein was collected and pooled before spectrophotometric analysis on a Beckman DU6 scanning spectrophotometer. The proportion of the peptide remaining in the immunoconjugate at each glutathione concentration was calculated from the ratio of the absorbances at 280 and 356 nm. Treatment with 100 mM DTT caused the complete release of the DNP-peptide.

Release of Nitrothiobenzoate from Ricin A-NTB and Ricin A²⁵⁶⁻²⁶⁷-NTB. Ricin A-NTB and ricin A²⁵⁶⁻²⁶⁷-NTB were treated with glutathione at a final concentration of 100 μ M in a sealed cell at 22.5 °C. The rate at which the nitrothiobenzoate anion was released was monitored continuously by spectrophotometric measurement at 412 nm in a Beckman DU6 spectrophotometer. In both cases, treatment of the derivatized peptides with 100 mM DTT gave an absorbance at 412 nm that corresponded to the calculated value for the complete release of the nitrothiobenzoate anion.

RESULTS

Immunoconjugate Characterization. The structures of the immunoconjugates examined in this study are shown in Figure 1. The panel is comprised of a conventional ricin A chain IT made with SPDP (A) and four analogues: an IT made with the linker SIAB introducing a nonreducible thioether bond (B), an IT made with the hindered disulfide linker SPDB (C), an IT in which the SPDP cross-linker is attached to the mAb via an Ala₇Pro₃ spacer (D), and an immunoconjugate in which the ricin A chain has been replaced by the C-terminal dodecapeptide labeled with a DNP reporter group (E).

The four ITs prepared with ricin A chain were of similar composition, consisting predominantly of one or two molecules of A chain coupled to a single molecule of mAb. Analysis by SDS-PAGE (Figure 2) identified the 1:1 conjugate as the major product in each case. The relative proportions of uncoupled antibody and more highly derivatized conjugate molecules were similar except in the case of the thioether-linked IT, where the higher level of 2:1 conjugate reflected the increased incorporation of cross-linker during the preparation of the conjugate. All four

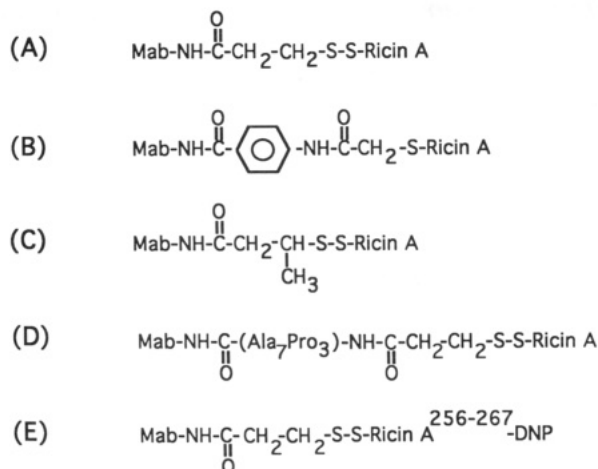


Figure 1. Chemical structures of the linkages in the series of Fib75 immunoconjugates. (A) Fib75-SPDP-ricin A, (B) Fib75-SIAB-ricin A, (C) Fib75-SPDB-ricin A, (D) Fib75-Ala₇Pro₃-SPDP-ricin A, (E) Fib75-SPDP-ricin A²⁵⁶⁻²⁶⁷-DNP.

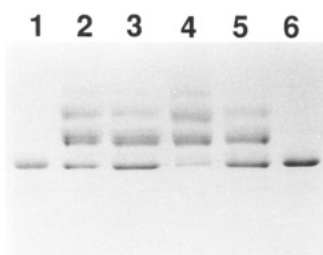


Figure 2. SDS-PAGE analysis of Fib75 mAb and immunoconjugates: lane 1, Fib75-SPDP-ricin A²⁵⁶⁻²⁶⁷-DNP; lane 2, Fib75-SPDP-ricin A; lane 3, Fib75-SPDB-ricin A; lane 4, Fib75-SIAB-ricin A; lane 5, Fib75-Ala₇Pro₃-SPDP-ricin A; lane 6, unconjugated Fib75.

IT preparations eluted from gel permeation HPLC columns with a characteristic pattern of peaks corresponding to the levels of A chain substitution (not shown). In no case was there any evidence of aggregated protein or breakdown products with a molecular weight lower than that of the mAb in these preparations.

The immunoconjugate prepared with ricin A²⁵⁶⁻²⁶⁷-DNP contained an average of two DNP-peptides per antibody molecule and its mobility was indistinguishable from that of unconjugated Fib75 by SDS-PAGE. When examined by gel permeation HPLC, the major peak eluted with the same retention time as the underivatized mAb but with a noticeably broader peak. A small proportion (<10%) of the product eluted with a shorter retention time than the main peak and probably consisted of immunoconjugate dimers.

Cytotoxic Activity in Tissue Culture. The ability of the immunoconjugates to inhibit protein synthesis in tissue culture was determined by measuring the incorporation of [³H]leucine by the SW2 cell line following a continuous 48-h incubation. A representative experiment is shown in Figure 3. The three ITs containing a disulfide bond, Fib75-SPDP-ricin A, Fib75-SPDB-ricin A, and Fib75-Ala₇Pro₃-SPDP-ricin A, had similar toxic effects upon the cells. [³H]Leucine incorporation was inhibited by 50% at a concentration of about 5×10^{-11} M, an effect at least 1000-fold more potent than that of unconjugated ricin A chain (not shown), and by 95% at an IT concentration of 1×10^{-9} M. The IT containing the thioether bond, Fib75-SIAB-ricin A, had no significant effect on [³H]leucine incorporation even at 1×10^{-8} M. As expected, the immunoconjugate lacking an intact A chain, Fib75-SPDP-ricin A²⁵⁶⁻²⁶⁷-DNP, also had no cytotoxic activity.

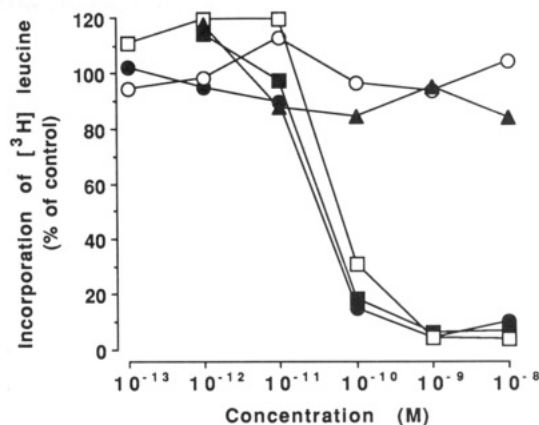


Figure 3. Cytotoxic effects of Fib75 immunoconjugates in tissue culture. SW2 small cell lung cancer cells were continuously exposed to Fib75 immunoconjugates at different concentrations for 48 h followed by a 24-h pulse with [³H]leucine: (●) Fib75-SPDP-ricin A, (○) Fib75-SIAB-ricin A, (■) Fib75-SPDB-ricin A, (□) Fib75-Ala₇Pro₃-SPDP-ricin A, (▲) Fib75-SPDP-ricin A²⁵⁶⁻²⁶⁷-DNP. Results shown are the mean values of quadruplicate determinations expressed as a percentage of the [³H]leucine incorporation of untreated control cultures. The standard deviations from the mean were less than 10% and have been omitted for clarity.

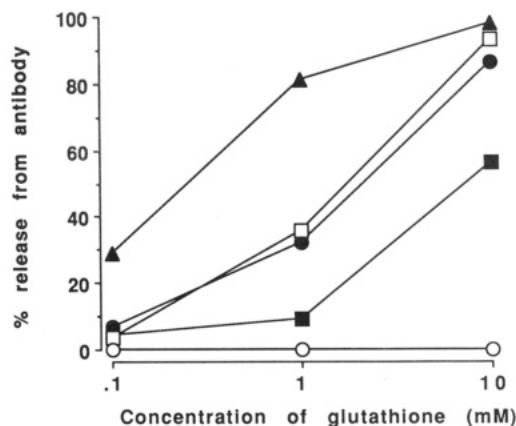


Figure 4. Release of ricin A chain or ricin A²⁵⁶⁻²⁶⁷-DNP from Fib75 immunoconjugates. The immunoconjugates were incubated with the stated concentrations of glutathione for 1 h at 37 °C. The amounts released were measured using gel permeation HPLC and have been expressed relative to the total content of A chain or peptide. (●) Fib75-SPDP-ricin A, (○) Fib75-SIAB-ricin A, (■) Fib75-SPDB-ricin A, (□) Fib75-Ala₇Pro₃-SPDP-ricin A, (▲) Fib75-SPDP-ricin A²⁵⁶⁻²⁶⁷-DNP.

Breakdown of Immunoconjugates. The release of ricin A chain or ricin A²⁵⁶⁻²⁶⁷-DNP from the corresponding Fib75 conjugates was measured following incubation with different concentrations of glutathione at 37 °C for 1 h. The IT containing the thioether bond, Fib75-SIAB-ricin A, showed no evidence of breakdown when treated with glutathione at any concentration, as expected (Figure 4). The three ricin A chain ITs containing a disulfide linkage broke down to release the A chain to an extent that depended upon the glutathione concentration. The extent of breakdown of the IT prepared with the SPDB linker was about 3-fold less than for that prepared with the SPDP reagent. At the intermediate concentration of glutathione used (1 mM), the relative percentages of A chain released were <10% and >30%, respectively. This difference reflects the greater steric hindrance afforded by the methyl group on the carbon atom adjacent to the disulfide bond in SPDB. In contrast, the introduction of the Ala₇Pro₃-PDP spacer into the linkage between the mAb and A chain had no effect upon the rate of breakdown

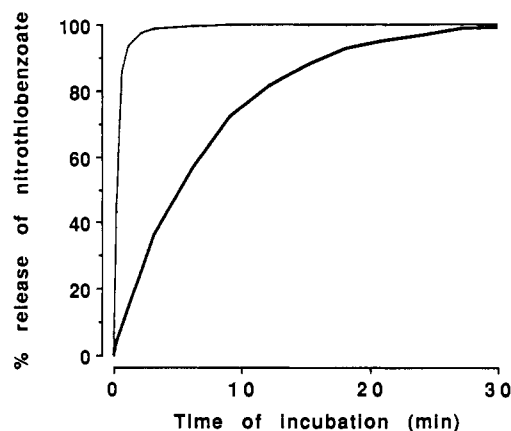


Figure 5. Release of nitrothiobenzoate anion from ricin A-NTB and ricin A²⁵⁶⁻²⁶⁷-NTB. Ricin A-NTB (—) and ricin A²⁵⁶⁻²⁶⁷-NTB (---) were treated with 100 μ M glutathione at 22.5 °C and the release of the nitrothiobenzoate anion monitored by the increase in absorbance at 412 nm. The results have been expressed relative to the maximal release of nitrothiobenzoate.

which was indistinguishable from that seen for the standard disulfide linked, IT, Fib75-SPDP-ricin A.

The release of the DNP-labeled peptide from Fib75-SPDP-ricin A²⁵⁶⁻²⁶⁷-DNP occurred at a considerably faster rate than that seen for Fib75-SPDP-ricin A, >80% of the peptide being released by the 1 mM glutathione treatment. Even at the lowest concentration of glutathione used (0.1 mM), 30% of the peptide was released whereas the release of ricin A chain from all the other disulfide-linked ITs was barely detectable under the same experimental conditions.

Release of Nitrothiobenzoate from Thiol-Substituted Ricin A Chain and Ricin A²⁵⁶⁻²⁶⁷. To investigate further the sensitivity of the disulfide linkage formed with Cys²⁵⁹ to reduction by glutathione, ricin A chain and ricin A²⁵⁶⁻²⁶⁷ were derivatized by reaction with Ellman's reagent under conditions leading to the introduction of a single activated disulfide bond into each molecule. The rates of reduction of the disulfide bonds were measured by following the release of the NTB anion. Upon treatment with 100 μ M glutathione, the times for 50% breakdown of ricin A-NTB and ricin A²⁵⁶⁻²⁶⁷-NTB were 6 min and 15 s, respectively (Figure 5), demonstrating a substantially greater stability in the case of the intact A chain.

DISCUSSION

The aim of the present study was to explore the contribution of the different components of ricin A chain ITs—the mAb, the cross-linker and the A chain—to the stability of the disulfide bond to reduction. To this end, we constructed a panel of immunoconjugates, each member of which was an analogue of a conventional IT, Fib75-SPDP-ricin A, and differed from it in a distinct defined way. The major findings of the study were firstly, that the introduction of a peptide spacer between the mAb and the cross-linker had no effect on disulfide bond stability and, secondly, that the intact structure of the A chain contributed to the stability of the disulfide linkage.

Four analogues of Fib75-SPDP-ricin A were compared. The first was an IT constructed with a nonreducible thioether linkage to act as a control for the reduction experiments with glutathione. The second was an IT made with the hindered disulfide cross-linker SPDB, which is known to be more resistant to reduction than SPDP (13). The third construct was an IT consisting of ricin A chain attached to Fib75 via an Ala₇Pro₃ peptide linker. The structure of the spacer was modeled upon the flexible pep-

tide sequences that allow the relative motion of folded polypeptide domains in the family of 2-oxo acid dehydrogenase multienzyme complexes (18). The aim was to prepare an IT in which the A chain was distanced from the mAb to prevent any enforced interaction between the two components. In the fourth immunoconjugate, ricin A chain was substituted with a dodecapeptide corresponding to the C-terminal region of the A chain, which had been labeled with the DNP reporter group, in order to determine the role of the A chain conformation around the Cys²⁵⁹ residue in the stability of the disulfide linkage.

The cytotoxic activities of the immunoconjugates were compared using a cell line expressing the target antigen recognized by the Fib75 mAb. The replacement of the standard disulfide linkage using SPDP by a hindered disulfide linkage with SPDB had no effect on the cytotoxic potency in the [³H]leucine incorporation assay. Similar results have been found for abrin A chain ITs made using the SPDP and SPDB linkers and a different mAb (19). These results are in accord with previous findings that the introduction of a hindered disulfide linkage has little or no effect on IT potency (14, 20), suggesting that intracellular reduction of the linkage occurs with high efficiency. The introduction of the Ala₇Pro₃ spacer between the mAb and the A chain had no significant effect on the cytotoxic activity of the Fib75 IT compared with that of the standard IT, suggesting that, in the experimental system examined, the release of the A chain within the cell was not influenced by the mode of attachment to the mAb.

The susceptibility to reduction of each of the conjugates was compared by measuring the release of ricin A chain or ricin A²⁵⁶⁻²⁶⁷ from mAb in the presence of glutathione. The SPDB-linked IT was considerably more stable than that made with the SPDP cross-linker. Studies with SPDB and other hindered disulfide cross-linkers have indicated that resistance to reduction is related to the degree of steric hindrance afforded by the chemical groupings adjacent to the disulfide bond (13, 14, 20, 21). In this study, we have actually demonstrated the enhanced chemical stability of the IT molecule itself when prepared with such a hindered disulfide bond.

The introduction of the Ala₇Pro₃ spacer between Fib75 and the disulfide linkage had no detectable effect upon the stability of the resulting IT compared with Fib75-SPDP-ricin A. This finding suggests that the spatial proximity of the mAb and the A chain components is not the principal factor influencing the stability of the disulfide bond in Fib75-ricin A chain ITs. In contrast, substitution of the ricin A chain component by a dodecapeptide corresponding to the C-terminus of the A chain and including the Cys²⁵⁹ residue had a profound effect upon the sensitivity of the immunoconjugate linkage to glutathione reduction. The peptide was released from the mAb at a much faster rate than the A chain itself. This finding implies that the stability of the disulfide bond depends critically upon the intact structure of the glycoprotein which cannot be mimicked by the A chain C-terminal peptide structure. This interpretation was supported by the finding that the rate of release of the nitrothiobenzoate anion from derivatives of ricin A chain and ricin A²⁵⁶⁻²⁶⁷ prepared by reaction with Ellman's reagent was considerably more rapid for the peptide than for the A chain.

The oligosaccharide side chains of the A chain play no role in protecting the disulfide bond against reduction because we have shown the stability of Fib75 ITs made with native ricin A chain, ricin A₁ chain, and aglycosyl recombinant ricin A chain to be identical (22). It is likely

therefore that the tertiary structure of the ricin A chain polypeptide surrounding the Cys²⁵⁹ residue inhibits the ability of glutathione to cleave the disulfide bond in the IT. Inhibition of disulfide reduction could occur either by means of steric hindrance to glutathione approach or as a consequence of electrostatic repulsion between the A chain and glutathione. We previously reported that a Fib75-SPDP-abrin A chain IT had greater stability in the presence of glutathione *in vitro* and a longer *in vivo* half-life than Fib75-SPDP-ricin A and speculated that the decreased susceptibility of the disulfide bond to cleavage might depend upon some intrinsic property of the abrin A chain (16). One possible explanation is that the linkage is strengthened by an interaction between the mAb and A chain components. A second explanation suggested by the findings reported herein is that abrin A chain itself may better protect the linking disulfide bond than ricin A chain.

In conclusion, we have demonstrated that the stability of the disulfide bond in a ricin A chain IT to reduction by glutathione depends on the structure of the cross-linker and the intact structure of the A chain but is apparently independent of the structure of the mAb component. These findings are potentially valuable for the design of novel ITs using genetically engineered proteins. Firstly, care will need to be taken in order to preserve the increased stability afforded by the structure of the native A chain molecule. Secondly, it may prove possible to attach A chains directly to engineered mAbs so that the structure of the mAb also provides stability to the disulfide linkage.

ACKNOWLEDGMENT

We thank the Cancer Research Campaign, London, U.K., for financial support. We are grateful to Professor W. C. J. Ross for his helpful comments on the manuscript.

LITERATURE CITED

- (1) Blakey, D. C., Wawrzynczak, E. J., Wallace, P. M., and Thorpe, P. E. (1988) Antibody toxin conjugates: A perspective. *Monoclonal Antibody Therapy. Progress in Allergy* 45 (H. Waldmann, Ed.) pp 50-90, S. Karger, Basel.
- (2) Vitetta, E. S., Fulton, R. J., May, R. D., Till, M., and Uhr, J. W. (1987) Redesigning nature's poisons to create anti-tumor reagents. *Science* 238, 1098-1104.
- (3) Funatsu, G., Yoshitake, S., and Funatsu, M. (1978) Primary structure of Ile chain of ricin D. *Agric. Biol. Chem.* 42, 501-503.
- (4) Lamb, F. I., Roberts, L. M., and Lord, M. J. (1985) Nucleotide sequence of cloned cDNA coding for preproricin. *Eur. J. Biochem.* 148, 265-270.
- (5) Halling, K. C., Halling, A. C., Murray, E. E., Ladin, B. F., Houston, L. L., and Weaver, R. F. (1985) Genomic cloning and characterization of a ricin gene from *Ricinus communis*. *Nucleic Acids Res.* 13, 8019-8033.
- (6) Montfort, W., Villafranca, J. E., Monzingo, A. F., Ernst, S. R., Katzin, B., Rutenber, E., Xuong, N. H., Hamlin, R., and Robertus, J. D. (1987) The three-dimensional structure of ricin at 2.8 Å. *J. Biol. Chem.* 262, 5398-5403.
- (7) Endo, Y., and Tsurugi, K. (1988) The RNA N-glycosidase activity of ricin A chain. *J. Biol. Chem.* 263, 8735-8739.
- (8) Wawrzynczak, E. J. (1991) Systemic immunotoxin therapy of cancer: advances and prospects. *Br. J. Cancer.* 64, 624-630.
- (9) Hertler, A. A., and Frankel, A. E. (1991) Immunotoxins in the therapy of leukemias and lymphomas. *Cancer Invest.* 9, 211-219.
- (10) Wawrzynczak, E. J., and Thorpe, P. E. (1988) Effect of chemical linkage upon the stability and cytotoxic activity of A chain immunotoxins. *Immunotoxins* (Frankel, A. E., Ed.) pp 239-251, Kluwer, Boston.
- (11) Worrell, N. R., Cumber, A. J., Parnell, G. D., Ross, W. C. J., and Forrester, J. A. (1986) Fate of an antibody-ricin A chain conjugate administered to normal rats. *Biochem. Pharmacol.* 35, 417-423.
- (12) Blakey, D. C., Watson, G. J., Knowles, P. P., and Thorpe, P. E. (1987) Effect of chemical deglycosylation of ricin A chain on the *in vivo* fate and cytotoxic activity of an immunotoxin composed of ricin A chain and anti-Thy1.1 antibody. *Cancer Res.* 47, 947-952.
- (13) Worrell, N. R., Cumber, A. J., Parnell, G. D., Mirza, A., Forrester, J. A., and Ross, W. C. J. (1986) Effect of linkage variation on pharmacokinetics of ricin A chain antibody conjugates in normal rats. *Anti-Cancer Drug Des.* 1, 179-188.
- (14) Thorpe, P. E., Wallace, P. M., Knowles, P. P., Relf, M. G., Brown, A. N., Watson, G. J., Knyba, R. E., Wawrzynczak, E. J., and Blakey, D. C. (1987) New coupling agents for the synthesis of immunotoxins containing a hindered disulphide bond with improved stability *in vivo*. *Cancer Res.* 47, 5924-5931.
- (15) Thorpe, P. E., Wallace, P. M., Knowles, P. P., Relf, M. G., Brown, A. N. F., Watson, G. J., Blakey, D. C., and Newell, D. R. (1988) Improved antitumor effects of immunotoxins prepared with deglycosylated ricin A chain and hindered disulfide linkages. *Cancer Res.* 48, 6396-6403.
- (16) Wawrzynczak, E. J., Cumber, A. J., Henry, R. V., May, J., Newell, D. R., Parnell, G. D., Worrell, N. R., and Forrester, J. A. (1990) Pharmacokinetics in the rat of a panel of immunotoxins made with abrin A chain, ricin A chain, gelonin, and momordin. *Cancer Res.* 50, 7519-7526.
- (17) Wawrzynczak, E. J., Derbyshire, E. J., Henry, R. V., Parnell, G. D., Smith, A., Waibel, R., and Stahel, R. A. (1991) Cytotoxic activity of ricin A chain immunotoxins recognising cluster 1, w4 and 5A antigens associated with human small cell lung cancer. *Br. J. Cancer* 63, Suppl. XIV, 71-73.
- (18) Perham, R. N. (1991) Domains, motifs and linkers in 2-oxo acid dehydrogenase multienzyme complexes: A paradigm in the design of a multifunctional protein. *Biochemistry* 30, 8501-8512.
- (19) Wawrzynczak, E. J., Zangemeister-Wittke, U., Waibel, R., Henry, R. V., Parnell, G. D., Cumber, A. J., Jones, M., and Stahel, R. A. (1992) Molecular and biological properties of an abrin A chain immunotoxin designed for therapy of human small cell lung cancer. *Br. J. Cancer*, in press.
- (20) Goff, D. A., and Carroll, S. F. (1990) Substituted 2-iminothiolanes: reagents for the preparation of disulfide cross-linked conjugates with increased stability. *Bioconjugate Chem.* 1, 381-386.
- (21) Greenfield, L., Bloch, W., and Moreland, M. (1990) Thiol-containing cross-linking agent with enhanced steric hindrance. *Bioconjugate Chem.* 1, 400-410.
- (22) Wawrzynczak, E. J., Cumber, A. J., Henry, R. V., and Parnell, G. D. (1991) Comparative biochemical, cytotoxic and pharmacokinetic properties of immunotoxins made with native ricin A chain, ricin A₁ chain and recombinant ricin A chain. *Int. J. Cancer* 47, 130-135.
- (23) Edman, P. (1950) Method for the determination of the amino acid sequence in peptides. *Acta Chem. Scand.* 4, 283-293.

Interferon Production of L929 and HeLa Cells Enhanced by Polyriboinosinic Acid-Polyribocytidylic Acid pH-Sensitive Liposomes

Pierre G. Milhaud,[†] Béatrice Compagnon,[‡] Alain Bienvenue,[‡] and Jean R. Philippot^{*‡}

Université Montpellier II, Sciences et Techniques du Languedoc, Département Biologie Santé, URA-CNRS 1191 Génétique Moléculaire, and URA-CNRS 530 Interactions Membranaires, 34095 Montpellier Cedex 5, France.
Received May 8, 1992

The double-stranded RNA polyinosinic acid-polycytidylic acid (PolyIC) is an inducer of interferons α and β (IFN) genes. With L929 and HeLa cells IFN pretreatment (priming) improves the IFN induction by PolyIC by several orders of magnitude. In the absence of the priming we demonstrate that PolyIC encapsulated into pH-sensitive liposomes (and not into pH-insensitive liposomes) enables L929 cells to secrete IFN efficiently and a low toxicity is observed; on primed cells pH-sensitive liposomes containing PolyIC trigger a high toxicity. With HeLa cells, the absence of the priming PolyIC encapsulated into pH-sensitive liposomes induces weak doses of IFN whereas free PolyIC was ineffective. Our experiments established that a pH drop (from 8 to 5.5) provoked a lipid mixing between pH-sensitive liposomes and cell membranes, likely by a fusion mechanism. Entrapment into pH-sensitive liposomes enhances the effect of PolyIC by several orders of magnitude, which might improve its therapeutic ability as an antitumor or anti-HIV agent.

INTRODUCTION

The double-stranded RNA polyriboinosinic acid-polyribocytidylic acid (PolyIC) is an inducer of interferon (IFN) α and β genes (Whatelet et al., 1987). Pretreating the cells with IFN (priming) (Stewart et al., 1971) enhances the response of L929 or HeLa cells to PolyIC powerfully (De Clercq, 1981).

On the other hand PolyIC induces a powerful toxicity against IFN-primed L929 cells (Stewart et al., 1972) the mechanism of which is not yet fully understood. However we have demonstrated that free PolyIC enters the cell through the acidic endocytic compartment before triggering that toxicity (Milhaud et al., 1987). Recently we demonstrated the induction of IFN by PolyIC loaded into liposomes which were targeted by antibodies to primed L929 cells (Milhaud et al., 1989). Surprisingly the IFN-PolyIC toxicity which goes with the endocytosis of PolyIC is highly increased by liposome-entrapped PolyIC. These results suggest that either a higher amount of intracellular PolyIC and/or a more appropriate intracellular delivery potentiate PolyIC efficacy.

Transfer of genetic material or synthetic nucleic acids interfering with gene expression (Leonetti et al., 1988) needs vectors to cross natural membranes, to escape degradative enzymes, and to reach their intracellular relevant targets. In several families of RNA viruses the delivery of the viral genome into the host cell cytoplasm is pH-dependent (Marsh & Helenius, 1989). At low pH, as encountered in the endocytic compartment, a viral protein triggers the fusion of the viral and endosomal membranes, thus allowing delivery of the viral genome into the cytoplasm. pH-sensitive liposomes have been devised which simulate viral behavior although the mechanisms are different (Connor et al., 1984; Ellens et al., 1984; Nayar & Schroit, 1985). Dioleoylphosphatidylethanolamine

(DOPE) and oleic acid (OA) liposomes are stable at neutral pH. The tendency to revert the HII phase occurs under conditions of acidic pH in which the OA component becomes protonated (Liu & Huang, 1989a). The lipid bilayer of such liposomes is destabilized at low pH and the loaded material enters the cytoplasm by a still unknown mechanism. Whatever the vector, virus, or liposome, the material to be delivered enters the cell by the endocytic pathway and escapes lysosomal degradation at least partially. The efficiency of pH-sensitive liposomes has been demonstrated in vitro with the help of encapsulated drugs such as antitumor drugs (Collins et al., 1988; Connor & Huang, 1986) or entrapped toxin (Collins & Huang, 1987; Chu et al., 1990) or fluorescent markers of aqueous compartment (Connor & Huang, 1985) or membrane lipids (Düzgünes et al., 1987). Efficient gene transfers have been performed in vivo (Wang & Huang, 1987b; Nayar & Schroit, 1989) and in vitro (Wang & Huang, 1987a; Wang & Huang, 1989).

These previous observations prompted us to test the efficiency of pH-sensitive liposomes for PolyIC delivery. In the present study we show that PolyIC entrapped into pH-sensitive liposomes induced the secretion of IFN from L929 cells in the absence of priming and only triggered a weak toxicity. However in the absence or in the presence of priming, PolyIC entrapped into pH-sensitive liposomes only induced a weak antiviral activity in HeLa cells.

EXPERIMENTAL PROCEDURES

Cell Lines and Viruses. Murine L929 cells (American Type Culture Collection, Rockville, MD; Ref. CCL 1) were grown in MEM medium (Gibco, Cergy Pontoise, France) supplemented with 5% (v/v) fetal bovine serum (FBS) and antibiotics. HeLa cells were obtained from G. Huez (Université libre de Bruxelles, Belgium); they were grown in RPMI 1640 medium enriched with glutamine and supplemented with 5% (v/v) FBS and antibiotics. The human lymphoblastic T CEM cells were cultured in RPMI 1640 supplemented with 10% FBS (v/v) and antibiotics.

Vesicular stomatitis virus (VSV) and encephalomyocarditis virus (EMCV) were grown and titrated on L929 cells.

Antibodies. Polyclonal rabbit antibodies to murine

* Corresponding author: Dr. J. R. Philippot, Université Montpellier II, Département Biologie Santé, URA-CNRS 530 Interactions Membranaires, Case 107, Place E. Bataillon, 34095 Montpellier Cedex 5, France. Phone: (33)67143741. Fax: (33)-67144286.

[†] URA-CNRS 1191 Génétique Moléculaire.

[‡] URA-CNRS 530 Interactions Membranaires.

IFN- α - β were obtained from Lee Biomolecular Research (San Diego, CA). The monoclonal murine antibodies (mAbs) to human IFN- α and to human IFN- β were obtained from Alpha Therapeutic Corp. (Los Angeles, CA). The murine mAbs UM21.1 (IgG_{2b}), a generous gift from Dr. Kraaijeveld and Dr. Snippe (State University of Utrecht, the Netherlands), are neutralizing antibodies to EMCV (Vlasploder et al., 1989). The goat peroxidase conjugated F(ab')₂ antibodies to whole mouse immunoglobulin G molecules were obtained from Immunotech (Marseille, France).

Interferon and Double-Stranded RNA. Murine IFN- α - β (specific activity 6×10^4 units/mg), a generous gift from Dr. G. Rossi (Istituto Superiore di Sanita, Roma), was diluted to 4×10^5 units/mL in phosphate-buffered saline (PBS: 137 mM NaCl, 2.7 mM KCl, 1.5 mM KH₂PO₄, 8.1 mM Na₂HPO₄, pH 7.4) containing 2 mg/mL bovine serum albumin and then aliquoted and frozen at -70 °C until use. Recombinant human interferon α 2a (HuIFN- α 2a) was similarly treated and stored.

A high molecular weight complex of PolyIC (Pharmacia, Uppsala, Sweden) (2 mg/mL) was sonicated (Branson, Danbury, CT, 20 W, 10 \times 30 s) until a mean length of 500–600 base pairs was obtained, as verified by 2% (w/v) agarose gel electrophoresis (buffer, 89 mM Tris-HCl, 89 mM borate, 1 mM EDTA (pH 7.5), 0.5 μ g/mL ethidium bromide).

PolyIC was labeled by [γ -³²P]ATP using polynucleotide kinase, according to standard protocols, to a final specific activity of 5×10^5 Bq/ μ mol.

Preparation of pH-Sensitive Liposomes. In routine experiments 20 μ mol of dioleoylphosphatidylethanolamine (DOPE), cholesterol (Chol), and oleic acid (OA) in the molar ratio 2:2:1 were dried from solvents to a thin film under a stream of nitrogen. Materials to be encapsulated (0.7–1.4 mg of PolyIC) were introduced in a high ionic strength [50 mM 4-(2-hydroxyethyl)-1-piperazineethanesulfonic acid (HEPES), 1 mM ethylenedis(oxyethylenetriyl)tetraacetic acid (EGTA) and 150 mM NaCl, pH 8.0] and lipids were hydrated for 30 min at 37 °C. A 100- μ mol portion of octyl glucoside in the corresponding buffer was added and the volume of the samples was adjusted to 0.5–0.65 mL with the buffer. After vigorous shaking the detergent was removed by dialysis against 50 mL of buffer containing 2 g of Amberlite XAD2 (Philippot et al., 1983). Liposome preparations were treated for 30 min at 37 °C with RNase A (EC 3.1.4.22) (25–100 μ g/mL) to digest unencapsulated polynucleotides. Liposomes were collected on a 5%–20% (w/v) dextran (average M_r = 162 000) gradient (Sigma) at 20 °C (45 min at 40 000 rpm). The yield of PolyIC encapsulated and the diameter of liposomes were measured for each sample. On a regular basis 2–4 μ g of PolyIC/ μ mol of lipid was encapsulated, and the diameters were around 450–650 nm.

The stability of the pH-sensitive liposomes was assessed as follows. pH-sensitive liposomes containing ³²P-labeled PolyIC were prepared and separated from nonincorporated PolyIC. The day following their preparation the liposomes were incubated in different media for 30 min and then loaded on a Biogel 5-m column (Bio-Rad) equilibrated with the buffer used for their preparation. The leakage was expressed as the ratio of the radioactivity trailing as a second peak to the total radioactivity eluted from the gel. The liposomes were incubated in the preparation buffer or in MEM without serum at 37 °C: the leakage was 23% and 44%, respectively (mean of two determinations, standard deviation = ± 0.6) in the first experiment; in the second independent experiment 38% and 63% were obtained. These experiments underscored the destabilizing effect of MEM on pH-sensitive liposomes.

As a rule we used the liposomes the day following their preparation.

Fluorescent pH-sensitive liposomes were prepared by replacing a few percent of DOPE by (4-nitrobenz-2-oxa-1,3-diazolyl)phosphatidylethanolamine (NBD-PE): DOPE/NBD-PE/Chol/OA, 1.75:0.25:2:1 (M/M).

Lipid Mixing Assays. Vesicle membrane fusion results in the communication between two aqueous compartments initially separated by the two fusing membranes: it involves intermixing of aqueous contents and intermixing of membrane components. The last event can be followed using a fluorescence method. The high concentration (5%) of NBD-PE (excitation, 460 nm; emission, 534 nm) present on the labeled pH-sensitive liposomes self-quenches its fluorescence. The fusion between these liposomes and cells dilutes the probe, resulting in an increase of NBD-PE fluorescence (Wilschut & Hoekstra, 1986). Kinetics were carried out at room temperature in the cell of a spectrofluorimeter.

Nonattached cells were used in this assay: 2.5×10^7 CEM cells in 1 mL (10 mM Tris, 150 mM NaCl) at pH 8 were mixed to 3 μ L of fluorescent liposomes and then the pH of the medium was shifted to pH 5.5 with 10% HCl (v/v) (zero time). At the plateau of the reaction, 10 μ L of Triton X100 (10%) was added and the fluorescence measured. Fluorescence changes were graphically estimated and expressed as percent of fluorescence variation between zero time and Triton X100 addition. In control experiments buffer was used instead of acidic solution.

Induction of IFN and of IFN-PolyIC Toxicity. IFN production was obtained by modification of published protocols (Milhaud et al., 1989). L929 cells were seeded at 10^5 cells/mL per well in 24-well tissue culture dishes and exposed to 800 U/mL IFN for 8 h. This step is defined as "priming" (Stewart et al., 1971). The cell monolayers (two wells per treatment) were washed and then various concentrations of free or liposome-encapsulated polynucleotides were added in serum-free medium and the dishes incubated for a further 2 h at 37 °C. Cell monolayers were washed with MEM supplemented with 5% (v/v) FBS and incubated at 37 °C for a further 18–20 h. The supernatant fluids were transferred to wells containing 10^5 L929 fresh cells, incubated for 20 h, and then challenged with 10^5 IU/mL VSV. The virus was titrated by end-point dilutions 24 h later.

Cell supernatants testing the antiviral activities induced by free or encapsulated PolyIC were incubated with antibodies to murine or human IFN- α - β (1000 neutralizing units) for 2 h; they were then incubated with L929 or HeLa cells and the antiviral activities were estimated by challenge with EMCV and the enzyme immunoassay as indicated below. The antiviral activities were completely neutralized, indicating that IFN- α and/or IFN- β were secreted by the cells treated with either free or liposome encapsulated PolyIC (data not shown).

Estimation of the PolyIC Toxicity. The toxicity was estimated on the primed and PolyIC-treated cells. As soon as a supernatant was transferred, 1 mL of diluted trypsin was added onto the cell monolayers, and the cells were counted with a Coulter counter (Coultronics). The results were expressed as the ratio of the number of the surviving cells after treatment with free or encapsulated PolyIC to the number of control cells (i.e. untreated or treated with empty liposomes, respectively).

Virus Titration by End-Point Dilution. Dishes containing L929 cells and virus were frozen and thawed twice, and the VSV titers measured by end-point dilutions on L929 cells seeded in 96-well tissue culture dishes. The number of infectious units (IU/mL) was estimated by the maximum likelihood method (Milhaud et al., 1983). The

99% confidence limits for the number M or IU/mL, obtained with a dilution factor 10 are $M \times 0.3 < M < M \times 3.38$.

Virus Titration by Enzyme Immunoassay. Relevant cells (L929 or HeLa) in 24-well Linbro dishes were pretreated by serial dilutions of the supernatants containing the secreted IFN. A dose effect of murine IFN- α - β (for L929 cells) or HuIFN- α 2a (for HeLa cells) was included in the assay. After a 20-h incubation the dishes were infected and reincubated for 5–7 h. The virus yield was estimated by a direct enzyme immunoassay of EMCV according to a modification of a previously published protocol (Vlasopolder et al., 1989). The immunoassay measured virus yields which in turn measured IFN concentrations. Briefly the cells were fixed by ethanol/acetone (1/1) and washed with PBS. mAbs UM 21.1 were added, incubated at 37 °C for 1 h, and then washed with PBS. Polyclonal antibody to whole mouse immunoglobulin, conjugated peroxidase, was added and incubated for 1 h at 37 °C and washed with PBS. The conjugated peroxidase was revealed with the help of 0.1 mM 2,2'-azino-bis(3-ethylbenzthiazoline-6-sulfonate) (Boehringer) or 4 mM 1,2-phenylenediamine (Fluka) as chromogen in the presence of 0.003% H_2O_2 as substrate. The colored reaction was read at 410 or 492 nm, respectively. Comparison between the results at 0.5 absorbance allowed an accurate titration of IFN.

RESULTS

Liposome Encapsulated PolyIC Resists RNase Treatment. Incubation of free PolyIC or that encapsulated into pH-sensitive liposomes with IFN-pretreated L929 cells induced a transferable antiviral activity to mouse cells.

To ascertain that the secreted antiviral activity could be only ascribed to the encapsulated PolyIC, a RNase treatment (50–100 μ g/mL) of the liposomes was carried out as indicated in the methods section. We checked for the efficacy of this step. PolyIC was encapsulated into pH-sensitive liposomes whereas pH-sensitive empty liposomes were incubated with labeled PolyIC; both liposome preparations were RNase treated as indicated in the methods. The induced antiviral capabilities of these liposomes were tested. PolyIC encapsulated into liposomes induced an antiviral activity while empty liposomes whose bound PolyIC had been chopped up by RNase were devoid of any activity.

Independent experiments ($n = 2$) showed that pH-sensitive liposomes, which had been pretreated with RNase as indicated above in the methods, were destroyed by a second harsh RNase treatment (50–100 μ g/mL). Table I shows that the activity of the encapsulated PolyIC was still shielded from a second weak RNase treatment (2 μ g/mL). These experiments emphasized that pH-sensitive liposomes provided PolyIC with protection.

PolyIC Encapsulated into pH-Sensitive Liposomes Induces IFN and a Weak Toxicity against Nonprimed L929 Cells. It has been reported that DEAE dextran is instrumental in enhancing the penetration of PolyIC into L929 cells (De Clercq, 1981) and triggers the induction of IFN in the absence of priming. Similarly pH-sensitive liposomes made it possible for the A chain of diphtheria toxin to penetrate and kill diphtheria-toxin-resistant L929 cells (Collins & Huang, 1987). We examined whether pH-sensitive liposomes could induce the production of IFN in the absence of priming.

As a preliminary experiment we titrated by ELISA the antiviral activity induced by free PolyIC from nonprimed and IFN-primed cells. As little as 0.02 μ g/mL of free

Table I. RNase Resistance of PolyIC-Encapsulated Preparations^a

liposome preparation ^b	untreated	RNase treated
free PolyIC	100	0
lip. pH-S-IC	99.4	98.5
lip. pH-S-0	0	0
lip. pHNS-IC	97.6	93.8
lip. pHNS-0	0	0

^a Free and encapsulated PolyIC (2 μ g/mL) were incubated in MEM in the absence or in the presence of RNase A (2 μ g/mL) at 37 °C. This was a second RNase treatment in addition to the initial one performed during liposome preparation. After 1-h incubation mixtures were checked for antiviral activity: virus growth was titrated by end-point dilution. The control viral growth was 1.3×10^7 IU/mL and in the presence of PolyIC was 1.3×10^4 IU/mL. The results are expressed as the percents of viral reductions ($1.3 \times 10^7 - Y/1.3 \times 10^7 - 1.3 \times 10^4$ IU/mL). The influence of RNase on virus growth was corrected accordingly. ^b lip. pH-S and lip. pHNS stand for pH-sensitive liposome and pH-insensitive liposome, respectively. -IC indicates that PolyIC was encapsulated, -0 indicates that the liposomes were empty.

Table II. Induction of IFN and Toxicity to L929 Cells of Free PolyIC and PolyIC Encapsulated into pH-Sensitive Liposomes^a

cell treatment	values at PolyIC concn, μ g/mL			
	free		encapsulated	
	0.2	2	0.2	2
untreated cells	<2 (0.98 \pm 0.04)	<2 (0.97 \pm 0.04)	12 (0.92 \pm 0.04)	512 (0.77 \pm 0.03)
primed cells	68 (0.40 \pm 0.02)	137 (0.02 \pm 0.01)	152 (0.77 \pm 0.03)	448 (0.18 \pm 0.03)

^a Results are expressed as units of IFN/mL. The toxicity is expressed as the fraction of surviving cells as detailed in Experimental Procedures and is in parentheses.

PolyIC produced a detectable antiviral activity on primed cells and the secreted antiviral activity reached the equivalent of 185 units of IFN at 1 μ g/mL. On the other hand 10 μ g/mL of PolyIC were required to obtain a detectable antiviral activity with unprimed cells and no more than the equivalent of 40 units of IFN/mL could be harvested after a treatment with 50–400 μ g/mL of free PolyIC. These results confirmed that IFN production by unprimed L929 cells required a 100-fold higher concentration of PolyIC than primed cells. Moreover the induction is weak and cannot be improved by a further increase of the dose of PolyIC (data not shown).

Comparable experiments ($n = 3$) were carried out with PolyIC encapsulated into pH-sensitive liposomes. The pH-sensitive liposomes induced an antiviral activity with primed and unprimed L929 cells (Table II). Further experiments ($n = 2$) showed that pH-insensitive liposomes failed to trigger any IFN production in nonprimed cells whereas they induced an antiviral activity in primed cells (data not shown).

Table II indicates in parentheses the relative toxicity of PolyIC loaded into pH-sensitive liposomes which was induced to nontreated or in IFN-pretreated L929 cells. At 2 μ g/mL PolyIC the toxicity to primed cells was 3–4-fold higher than on nonprimed cells. pH-insensitive liposomes did not induce any toxicity to nonpretreated L929 cells.

Comparison between pH-Sensitive and Insensitive Liposomes as Vectors for IFN-PolyIC Toxicity and IFN Induction on Primed L929 Cells. We compared the IFN-inducing activity of free PolyIC to that of PolyIC encapsulated into pH-sensitive or pH-insensitive liposomes. Figure 1 indicates that free PolyIC and PolyIC loaded into pH-sensitive or pH-insensitive liposomes essentially displayed the same IFN-inducing activities.

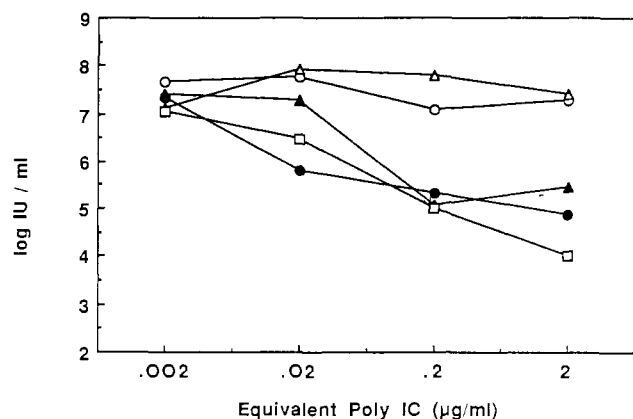


Figure 1. IFN activity induced by free and encapsulated PolyIC. Increasing doses of free PolyIC and PolyIC encapsulated into pH-sensitive and pH-insensitive liposomes were checked for antiviral activity. Results were plotted as log (IU/mL) (standard error = ± 0.205): free PolyIC (\square), pH-sensitive liposomes containing PolyIC (\bullet), pH-insensitive liposomes containing PolyIC (\blacktriangle), empty pH-sensitive liposomes (\circ), empty pH-insensitive liposomes (Δ).

Table III. IFN-PolyIC Toxicity Induced by Free and Encapsulated PolyIC^a

liposome preparation	toxicity at PolyIC concn, $\mu\text{g/mL}$		
	0.022	0.20	2.00
lip. pH-S-IC (Diameter 640 nm)	0.85 ± 0.03	0.59 ± 0.03	0.20 ± 0.01
lip. pHNS-IC (Diameter 492 nm)	0.98 ± 0.04	0.89 ± 0.04	0.59 ± 0.03
free PolyIC	0.99 ± 0.04	0.88 ± 0.04	0.50 ± 0.02

^a IFN pretreated L929 cells were incubated for 2 h with free or encapsulated PolyIC or empty liposomes. The cultures were washed with fresh medium, incubated for 18 h, and counted with a Coulter counter. Results are expressed as fractions of surviving cells as detailed in the Experimental Procedures. The error values were computed to allow for the errors on treated and untreated wells at 95% confidence limits. For abbreviations see legend of Table I.

The empty liposomes did not induce any transferable antiviral activity.

The IFN-PolyIC toxicity induced by free and encapsulated PolyIC is presented in Table III. Two independent experiments confirmed the higher toxicity of the PolyIC delivered by pH-sensitive liposomes as compared to pH-insensitive liposomes, and to free PolyIC. We had observed that small-sized liposomes loaded with PolyIC were more toxic in these experimental conditions independent of their lipid composition (data not shown). The higher toxicity of the pH-sensitive liposomes was not due to smaller size. Indeed the diameters of the pH-sensitive and the pH-insensitive liposomes were respectively 640 and 492 nm in that particular experiment. The empty liposomes did not display any toxicity. These results suggested a more efficient delivery of PolyIC from the pH-sensitive liposomes.

IFN Induction by Free and Encapsulated PolyIC into Nontreated and Primed HeLa Cells. HeLa cells are refractory to IFN induction by PolyIC unless a complex regimen is carried out including IFN priming and super-induction with PolyIC, cycloheximide, and actinomycin D (De Clercq, 1981). So we addressed the same questions for HeLa cells as we did for L929 cells previously. The HeLa strain we used was weakly induced (4 units IFN) by free PolyIC at 10 $\mu\text{g/mL}$ after priming with HuIFN- $\alpha 2a$. A better induction was obtained when the primed cells were treated with PolyIC and cycloheximide; a weak toxicity accompanied the IFN production (data not shown).

Table IV. IFN Production by Free and Encapsulated PolyIC in Nontreated and Primed HeLa Cells

cell treatment	IFN production at 2 $\mu\text{g/mL}$ PolyIC		
	free PolyIC	lip. pH-S-IC	lip. pHNS-IC
control	0	>0.5	0
priming	0	1.6	0

^a Antiviral activity were tested by ELISA; results are expressed as units of IFN/mL. For abbreviations see the legend of Table I.

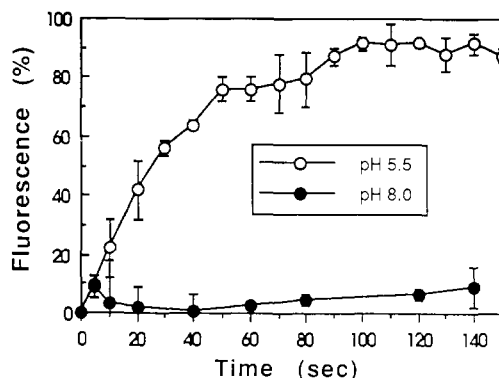


Figure 2. Mixing between liposome and cell membrane lipids. 2.5×10^7 CEM cells in 1 mL of buffer, pH 8, were set in the cell of a spectrofluorimeter under continuous magnetic stirring at room temperature. Then 3 μL of fluorescent liposomes were added and the suspension was allowed to equilibrate. At zero time the pH of the medium was shifted to pH 5.5 with 0.1 N HCl (0% fluorescence). The fluorescence emission of NBD-PE was monitored all along the kinetics for 200 s, then 10 μL of 10% Triton X100 was added to determine 100% fluorescence emission. In control experiments pH of the cell suspension stayed unchanged at pH 8.0.

Comparable experiments ($n = 2$) were performed with encapsulated PolyIC (2 $\mu\text{g/mL}$) on nonprimed and primed HeLa cells. A weak antiviral activity was only observed with pH-sensitive liposomes on nonprimed and primed cells: in both cases the antiviral activity was reproducibly weak but clear (around 1 unit IFN/mL) (Table IV). The immunoassay titrated less than 0.5 units of HuIFN/mL. In the same experiments no antiviral activity was detected for PolyIC loaded into pH-insensitive liposomes nor for empty liposomes.

Lipid Mixing between Liposomes and Cell Membranes. Liposomes do not spontaneously fuse with other liposomes or cells unless conditions are established to promote this event. It is a feature of pH-sensitive liposomes to undergo lipid mixing when they are exposed to an acidic environment (Collins et al., 1989). In order to evaluate the fusogenic ability of the pH-sensitive liposomes used throughout these studies we kinetically monitored the intensity of the fluorescence of NBD-PE embedded on the liposome membrane upon mixing of lipids between liposome and cell membranes. In this assay (Figure 2) fusion occurred at the plasma membrane level as the acidification was directly performed in the incubation medium. A shift to acidic medium induced an increase of fluorescence in suspensions containing fusogenic liposomes mixed with cells. Data from Figure 2 are the average of two assays. The phenomenon was completed in 2–3 min. Under control conditions fluorescent liposomes did not provoke any significant fluorescent change.

Electron microscopy and photon correlation spectroscopy indicated that the mean diameter of the liposomes was several-fold enlarged a few minutes after medium acidification (data not shown). These observations were consistent with a fusion process induced by the pH-sensitive liposomes.

DISCUSSION

Characteristics of the pH-Sensitive Liposomes.

Induction of IFN in the presence or in the absence of priming is a good model to demonstrate the efficiency of pH-sensitive liposomes in spite of their instability. The resistance of DOPE/OA liposomes has been improved by cholesterol so we adopted the composition DOPE/OA/CHOL, 4:2:4 (M/M), in accordance with published results (Liu & Huang, 1989b) without further investigation. However we have indicated in the methods section that pH-sensitive liposomes are leaky in the presence of MEM and cannot withstand a second harsh treatment with RNase A. The influence of the entrapped PolyIC on the stability of the liposomes cannot be excluded.

The liposome preparations were not extruded. Under standard conditions the mean diameter of the liposomes did not vary significantly unless the buffer composition was modified. L929 cells exhibit a high phagocytic ability so that large variations of liposome characteristics are required to obtain different biological responses.

Fusion of pH-Sensitive Liposomes. pH-sensitive liposomes are efficient vectors to introduce molecules into animal cells (Connor & Huang, 1985; Collins et al., 1988; Connor & Huang, 1986; Collins & Huang, 1987; Chu et al., 1990; Wang & Huang, 1987b; Nayar & Schroit, 1989; Wang & Huang, 1989). Among the possible mechanisms our results favor the fusion process; indeed the lipid experiments were performed with liposomes exhibiting larger diameters than CEM cell-coated pits (Carriere et al., 1989). First, the exposure of pH-sensitive liposomes to low pH at constant osmotic pressure led to a diameter increase. It was verified by electron microscopy that pH-sensitive liposomes did not aggregate upon medium acidification and remain paucilamellar. Moreover, mixing cellular membrane lipids and NBD-PE-associated liposomes induced fluorescence dequenching at low pH (Figure 2); such dequenching was observed with pH-sensitive liposomes only. Other indirect evidence using nonpermeant fluorescent dyes such as calcein have been published (Connor & Huang, 1985). We also observed a leakage of calcein from pH-sensitive liposomes by lowering the pH of the medium. These results reinforce but do not prove conclusively that fusion operates at the plasmic membrane level at low pH. However our results are not at variance with a fusion process at the endosome membrane following endocytosis, since L929 cells are able to internalize large diameter liposomes (Machy et al., 1987). Indeed, plasmatic or intracellular membrane-liposome fusion might occur through different mechanisms. Other mechanisms have been suggested to explain the delivery into the endosome and the escape from this compartment (Ellens et al., 1984).

Cytoplasmic Delivery. Induction of IFN along this work was carried out with encapsulated PolyIC. The liposomes were efficiently treated with RNase, which indicated that an important part of the liposome population shielded PolyIC; however, because of the leakage induced by MEM, a piggyback cell delivery cannot be ruled out. Indeed cell transfections with DNA bound at the external surface of pH-sensitive liposomes have already been reported (Wang & Huang, 1987b).

That at least part of the load of the pH-sensitive liposome is directly delivered into the cytoplasm has been demonstrated by means of fluorescent probes or drugs whose site of action are cytoplasmic as diphtheria toxin (Connor & Huang, 1985; Collins et al., 1988; Connor & Huang, 1986; Collins & Huang, 1987; Chu et al., 1990; Nayar & Schroit, 1989). The killing of diphtheria-toxin-resistant L cells by pH-sensitive liposomes loaded with diphtheria toxin A chain exemplifies such a cytoplasmic

delivery whereas comparable pH-insensitive liposomes failed to generate any toxicity (Collins & Huang, 1987).

Whether the improved biological activities of PolyIC encapsulated into pH-sensitive liposome stems from an appropriate or an increased cytoplasmic delivery cannot be formally demonstrated. Indeed neither IFN induction nor cytotoxicity triggered by PolyIC on IFN-treated cells is fully understood. Arguments which favor cytoplasmic targets for PolyIC have however been proposed. For example PolyIC inhibits translation by causing the inactivation of eIF-2 (eukaryotic initiation factor 2) and binds to this protein tightly. The PolyIC/eIF2 complex introduced into cells reduces the toxicity and increases IFN production, suggesting that eIF-2 is involved (Harary et al., 1990). The IFN-PolyIC toxicity would stem from the removal of eIF-2 from the translation machinery. This hypothesis does not explain the lytic event but implicates a cytoplasmic delivery.

Induction of IFN in the Absence of Priming. The present study shows that with L929 cells PolyIC loaded into pH-sensitive liposomes triggered a good induction of IFN (around 500 units of IFN/mL for 2 μ g/mL PolyIC) in the absence of priming (Table II) while large doses of free PolyIC (up to 200 μ g/mL) were unable to induce more than 40 units IFN/mL. As for HeLa cells we show that PolyIC loaded into pH-sensitive liposomes succeeded in inducing a reproducible but weak antiviral activity at doses where free PolyIC induced no IFN at all (Table IV). In both cases the efficiency of the PolyIC entrapped into pH-sensitive liposomes thus appeared several orders of magnitude better than that of free PolyIC or PolyIC loaded into pH-insensitive liposomes.

The induction obtained with L929 cells was far better than with HeLa cells; the difference might be explained both by the high endocytic capacity of L929 cells, which favors liposome internalization, and by cell-specific factors involved in the induction process (De Maeyer & De Maeyer, 1988). Using more appropriate pH-sensitive lipids, reducing liposome size for fitting with endocytic vesicles, and targeting with efficient antibodies should improve the overall results.

Whether the first role of priming is to induce the eIF-2 kinase which PolyIC will bind to (Harary et al., 1990) or fragilize the cells, rendering the access to cytoplasm easier (Milhaud et al., 1987), requires deeper investigations. Priming exerts important effects on IFN induction although its mechanism remains unclear, likely dependent on cell lines and IFN genes (Dron et al., 1990); however it is not compulsory to induce IFN. With L929 cells priming can be replaced by DEAE dextran which is reported to enhance PolyIC and polynucleotide intracellular penetration (De Clercq, 1981; Sompayrac & Danna, 1981). Likewise, microinjection of PolyIC with micropipets into HeLa cells has been reported to bring about IFN induction in the absence of any priming (Silhol et al., 1986).

We previously have shown that encapsulation of PolyIC into antibody-targeted liposomes protected the drug from nucleolytic attack and changed drastically its pharmacological characteristics. Here we show that encapsulation of PolyIC into pH-sensitive liposomes increases by several orders of magnitude its inducing capabilities. Such improvements might be beneficial if PolyIC or Ampligen, its analog, should be used as an antitumor (Chapekar & Glazer, 1985; Hubbell, 1986) or as an anti-HIV agent (Montefiori & Mitchell, 1987; Carter et al., 1987).

ACKNOWLEDGMENT

We thank B. Lebleu for advice and reading the manuscript. This work was supported by grants from Centre National de la Recherche Scientifique, Agence Nationale

de Recherches sur le SIDA, and Association pour le Developpement de la Recherche sur le Cancer to B. Lebleu (URA CNRS 1191) and independently to J. R. Philippot (URA CNRS 530).

LITERATURE CITED

- Carriere, D., Arcier, J. M., Derocq, J. M., Fontaine, C., and Richer, G. (1989) Antigenic modulation induced by four monoclonal antibodies adsorbed on gold particles (specificity anti-CD4, anti-CD5, anti-CD7, and anti-150-kDa antigen): relationship between modulation and cytotoxic activity of immunotoxins. *Exp. Cell Res.* 182, 114-128.
- Carter, W. A., Brodsky, I., Pellegrino, M. G., et al. (1987) Clinical, immunological, virological effects of Ampligen, a mismatched double-stranded RNA, in patients with AIDS or AIDS-related complex. *Lancet*, 1286-1292.
- Chapekar, M., and Glazer, R. I. (1985) Synergistic effect of human immune interferon and double-stranded RNA against human colon carcinoma cells *in vitro*. *Cancer Res.* 45, 2539-2544.
- Chu, C.-J., Dijkstra, J., Lai, M.-Z., Hong, K., and Szoka, F. C. (1990) Efficiency of cytoplasmic delivery by pH-sensitive liposomes to cells in culture. *Pharm. Res.* 7, 824-834.
- Collins, D., and Huang, L. (1987) Cytotoxicity of diphtheria toxin A fragment to toxin-resistant murine cells delivered by pH-sensitive immunoliposomes. *Cancer Res.* 47, 735-739.
- Collins, D., Norley, S., Rouse, B., and Huang, L. (1988) Liposomes as carriers for antitumor and antiviral drugs: pH-sensitive immunoliposomes and sustained release immunoliposomes. *Liposomes as Drug Carriers* (G. Gregoriadis, Ed.) pp 761-770, John Wiley, New York.
- Collins, D., Maxfield, F., and Huang, L. (1989) Immunoliposomes with different sensitivities as probes for the cellular endocytic pathway. *Biochim. Biophys. Acta* 987, 47-55.
- Connor, J., and Huang, L. (1985) Efficient cytoplasmic delivery of a fluorescent dye by pH-sensitive immunoliposomes. *J. Cell Biol.* 101, 582-589.
- Connor, J., and Huang, L. (1986) pH sensitive immunoliposomes as an efficient and target-specific carrier for antitumor drugs. *Cancer Res.* 46, 3431-3435.
- Connor, J., Yatvin, M. B., and Huang, L. (1984) pH-sensitive liposomes: Acid-induced liposome fusion. *Proc. Natl. Acad. Sci. U.S.A.* 81, 1715-1718.
- De Clercq, E. (1981) Interferon induction by polynucleotides, modified polynucleotides, and polycarboxylates. *Methods Enzymol.* 78, 227-236.
- De Maeyer, E., and De Maeyer, J. (1988) Induction of IFN- α and IFN- β . *Interferons and Other Regulatory Cytokines* (E. De Maeyer, and J. De Maeyer, Eds.) pp 39-66, John Wiley, New York.
- Dron, M., Lacasa, M., and Tovey, M. G. (1990) Priming affects the activity of a specific region of the promoter of the human beta interferon gene. *Mol. Cell. Biol.* 10, 854-858.
- Düzgünes, N., Allen, T. M., Fedor, J., and Papahadjopoulos, D. (1987) Lipid mixing during membrane aggregation and fusion: Why fusion assays disagree. *Biochemistry* 26, 8435-8442.
- Ellens, H., Bentz, J., and Szoka, F. C. (1984) pH-induced destabilization of phosphatidylethanolamine-containing liposomes: Role of bilayer contact. *Biochemistry* 23, 1538-1541.
- Harary, R., Gonsky, R., Itamar, D., and Kaempfer, R. (1990) Relief of cytotoxicity and enhancement of interferon inducer activity of double-stranded RNA by eukaryotic initiation factor 2. *Virology* 174, 494-503.
- Hubbell, H. R. (1986) Synergistic antiproliferative effect of human interferons in combination with mismatched double-stranded RNA on human tumor cells. *Int. J. Cancer* 37, 359-365.
- Leonetti, B., Rayner, B., Lemaître, M., Gagnor, C., Milhaud, P. G., Imbach, J. L., and Lebleu, B. (1988) Antiviral activity of conjugates between poly(L-lysine) and synthetic oligodeoxyribonucleotides. *Gene* 72, 323-332.
- Liu, D., and Huang, L. (1989a) Small, but not large, unilamellar liposomes composed of dioleylphosphatidylethanolamine and oleic acid can be stabilized by human plasma. *Biochemistry* 28, 7700-7707.
- Liu, D., and Huang, L. (1989b) Role of cholesterol in the stability of pH-sensitive, large unilamellar liposomes prepared by the detergent-dialysis method. *Biochim. Biophys. Acta* 981, 254-260.
- Machy, P., Truneh, A., Gennaro, D., and Hoffstein, S. (1987) Endocytosis and de novo expression of major histocompatibility complex encoded class I molecules: Kinetic and structural studies. *Eur. J. Cell Biol.* 45, 126-136.
- Marsh, M., and Helenius, A. (1989) Virus entry into animal cells. *Adv. Virus Res.* 36, 107-151.
- Milhaud, P. G., Silhol, M., Faure, T., and Milhaud, X. (1983) Numerical tables for the direct estimation of virus titres by the maximum likelihood method. *Ann. Virol. (Institut Pasteur)* 134E, 405-416.
- Milhaud, P. G., Silhol, M., Salehzada, T., and Lebleu, B. (1987) Requirement for endocytosis of poly(rI)-poly(rC) to generate toxicity on interferon-treated LM cells. *J. Gen. Virol.* 68, 1125-1134.
- Milhaud, P. G., Machy, P., Lebleu, B., and Leserman, L. (1989) Antibody targeted liposomes containing poly(rI)-poly(rC) exert a specific antiviral and toxic effect on cells primed with interferons α/β or γ . *Biochim. Biophys. Acta* 987, 15-20.
- Montefiori, D. C., and Mitchell, W. M. (1987) Antiviral activity of mismatched double-stranded RNA against human immunodeficiency virus *in vitro*. *Proc. Natl. Acad. Sci. U.S.A.* 84, 2985-2989.
- Nayar, R., and Schroit, A. J. (1985) Generation of pH-sensitive liposomes: Use of vesicles containing N-succinyldioleoylphosphatidylethanolamine. *Biochemistry* 24, 5967-5971.
- Nayar, R., and Schroit, A. J. (1989) pH-sensitive liposomes for the delivery of immunomodulators. *Liposomes in the Therapy of Infectious Diseases and Cancer* (G. Lopez-Berenstein, and I. J. Fidler, Eds.) pp 427-439, Alan R. Liss, New York.
- Philippot, J. R., Mutafschief, S., and Liautard, J. P. (1983) A very mild method allowing the encapsulation of very high amounts of macromolecules into very large (1000 nm) unilamellar liposomes. *Biochim. Biophys. Acta* 734, 137-143.
- Silhol, M., Huez, G., and Lebleu, B. (1986) An antiviral state induced in HeLa cells by microinjected Poly(rI)-Poly(rC). *J. Gen. Virol.* 67, 1867-1873.
- Sompayrac, L. M., and Danna, K. J. (1981) Efficient infection of monkey cells with DNA of simian virus 40. *Proc. Natl. Acad. Sci. U.S.A.* 78, 7575-7578.
- Stewart, W. E., Gosser, L. B., and Lockart, R. Z., Jr. (1971) Priming: A non viral function of interferon. *J. Virol.* 7, 792-801.
- Stewart, W. E., II, De Clercq, E., Billiau, A., Desmyter, J., and De Somer, P. (1972) Increased susceptibility of cells treated with interferon to the toxicity of polyribinosinic-polyribocytidylic acid. *Proc. Natl. Acad. Sci. U.S.A.* 69, 1851-1854.
- Vlasopolder, F., Donkers, E., Harmsen, T., Kraaijeveld, C. A., and Snippe, H. (1989) Rapid bioassay of human interferon by direct enzyme immunoassay of encephalomyocarditis virus in HEp-2 cell monolayers after a single cycle of infection. *J. Virol. Methods* 24, 153-158.
- Wang, C. Y., and Huang, L. (1987a) Plasmid DNA adsorbed to pH-sensitive liposomes efficiently transforms the target cells. *Biochem. Biophys. Res. Commun.* 147, 980-985.
- Wang, C. Y., and Huang, L. (1987b) pH-sensitive immunoliposomes mediate target cell-specific delivery and controlled expression of a foreign gene in mouse. *Proc. Natl. Acad. Sci. U.S.A.* 84, 7851-7855.
- Wang, C. Y., and Huang, L. (1989) Highly efficient DNA delivery mediated by pH-sensitive immunoliposomes. *Biochemistry* 28, 9508-9514.
- Whatelet, M. G., Clauss, I. M., Nols, C. B., Content, J., and Huez, G. (1987) New inducers revealed by the promoter sequence analysis of two interferon activated human genes. *Eur. J. Biochem.* 169, 313-321.
- Wilschut, J., and Hoekstra, D. (1986) Membrane fusion lipid vesicles as a model system. *Chem. Phys. Lipids* 40, 145-166.

A New Method to Specifically Label Thiophosphorylatable Proteins with Extrinsic Probes. Labeling of Serine-19 of the Regulatory Light Chain of Smooth Muscle Myosin

Kevin C. Facemyer and Christine R. Cremo*

Washington State University, Department of Biochemistry and Biophysics, Pullman, Washington 99164-4660.
Received May 28, 1992

We present a new method to specifically and stably label proteins by attaching extrinsic probes to amino acids that are thiophosphorylated by protein kinases and ATP γ S. The method was demonstrated for labeling of a thiophosphorylatable serine of the isolated regulatory light chain of smooth muscle myosin. We stoichiometrically blocked the single thiol (Cys-108) either by forming a reversible intermolecular disulfide bond or by reacting with iodoacetic acid. The protein was stoichiometrically thiophosphorylated at Ser-19 by myosin light chain kinase and ATP γ S. The nucleophilic sulfur of the protein phosphorothioate was coupled at pH 7.9 and 25 °C to the fluorescent haloacetate [3 H]-5-[[2-[(iodoacetyl)-amino]ethyl]amino]naphthalene-1-sulfonic acid ([3 H]IAEDANS) by displacement of the iodide. Typical labeling efficiencies were 70–100%. The labeling was specific for the thiophosphorylated Ser-19, as determined from the sequences of two labeled peptides isolated from a tryptic digest of the labeled protein. [3 H]IAEDANS attached to the thiophosphorylated Ser-19 was stable at pH 3–10 at 25 °C, and to boiling in high concentrations of reductant. The labeled light chains were efficiently exchanged for unlabeled regulatory light chains of the whole myosin molecule. The resulting labeled myosin had normal ATPase activities in the absence of actin, indicating that the modification of Ser-19 and the exchange of the labeled light chain into myosin did not significantly disrupt the protein. The labeled myosin partially retained the elevated actin-activated Mg $^{2+}$ -ATPase activity which is characteristic of thiophosphorylated myosin. This indicates that labeling of the thiophosphate group with [3 H]IAEDANS did not completely disrupt the functional properties of the thiophosphorylated protein in the presence of actin.

INTRODUCTION

The reversible phosphorylation of proteins is a common regulatory mechanism in biological processes. The mechanisms by which phosphorylation modulates protein function are largely unknown, although structural data for a few proteins have begun to answer this question (1, 2). Most phosphorylations are catalyzed by serine/threonine (3) and tyrosine protein kinases (4) and are reversed by the respective protein phosphatases. These enzymes finely regulate proteins in vivo by virtue of selective modification within consensus amino acid sequences for phosphorylation.

In general it appears that most protein kinases will accept the nonphysiological substrate ATP γ S¹ (5) in place of ATP (6). Kinases which are known to use ATP γ S as a substrate are phosphorylase kinase (7), cAMP dependent protein kinase (8–11), nuclear protein kinase II (12), cGMP dependent protein kinase (12), protein kinase C (13, 14), kinase F_A (15), heme-regulated protein kinase (16), myosin light chain kinase (17), calmodulin-dependent protein kinase II (18, 19), and EGF-receptor-associated protein kinase (20). A phosphorothioate instead of a phosphate is transferred to the acceptor protein with normal fidelity. In contrast, it appears that thiophosphorylated proteins tend to be poor substrates for phosphatases (6, 7, 17, 20, 21). Therefore, thiophosphorylated proteins mimic a stable phosphorylated state of a protein.

Although phosphorothioate and phosphate are structural analogs, they differ chemically in that phosphorothioate contains a nucleophilic sulfur (6). Nucleic acid chemists have made use of this nucleophile by attaching extrinsic probes to internucleotidic phosphorothioate diesters (22) or to single terminal phosphorothioate monoesters (23) of oligodeoxynucleotides. We have used this nucleophilic sulfur as a site to attach extrinsic probes to thiophosphorylated proteins. This approach to labeling of proteins promises to be generally useful because of the ubiquity of protein phosphorylation, the site specificity afforded by the kinases, and the expected stability of the linkage between the extrinsic probe and the protein.

Here we describe this new method and use it to modify Ser-19 on the RLC20 of smooth muscle myosin. RLC20 was chosen as a model to test the labeling method because it is a small protein (19 600 Da) of known sequence with one primary phosphorylation site and a single cysteine. This protein is of interest because phosphorylation of Ser-19 by myosin light chain kinase (3) is required for activation of smooth muscle contraction (24). We document the conditions and specificity of the labeling method and characterize myosin in which thiophosphate-labeled RLC20 has been exchanged for the native RLC20.

EXPERIMENTAL PROCEDURES

Reagents. ATP γ S (0.1 M solution) and MB-grade glycerol were from Boehringer Mannheim and ultrapure guanidine hydrochloride was from ICN Biochemicals. Sucrose was from Schwarz/Mann (density-gradient grade). [3 H]IAEDANS was synthesized and characterized by the method of Hudson and Weber (25) using [3 H]IAA (250 mCi/mmol) from NEN. IAEDANS was purchased from Sigma.

¹ Abbreviations used: IAA, iodoacetic acid; RLC20, 20-kDa regulatory light chain of chicken gizzard myosin; LC17, 17-kDa light chain of chicken gizzard myosin; DTE, dithioerythritol; [3 H]-IAEDANS, tritiated form of 5-[[2-[(iodoacetyl)amino]ethyl]amino]naphthalene-1-sulfonic acid; ATP γ S, adenosine, 5'-O-(3-thiotriphosphate).

Proteins. Gizzards from freshly killed chickens were cleaned, and the connective tissue was removed immediately prior to rapid freezing of the gizzards in liquid nitrogen and storage at -80°C for up to 6 months. Myosin was purified from the frozen gizzards by the method of Ikebe and Hartshorne (26) and stored on ice for up to 2 weeks. For longer storage, myosin solutions of up to 50% glycerol were made and stored at -20°C without loss of activity. A mixture of both types of myosin light chains (RLC20 and LC17) was isolated from the myosin by the method of Perrie and Perry (27). EtOH was then added to a final concentration of 82% to precipitate the RLC20 which was then resuspended in and dialyzed against 50 mM ammonium bicarbonate (pH 7.9). We routinely obtained an 80% yield of RLC20 which appeared to be free of LC17 and myosin heavy chains after analysis by both urea (see Figure 2 legend) and SDS gel electrophoresis. Sucrose (4 mg/mg of protein) was added prior to lyophilization and storage at -80°C . We determined the $\epsilon_{277}^{1\%}$ to be 3.35 by amino acid analysis, which is in agreement with the value determined by Hathaway and Haeberle (28) and by Sobieszek (29). The protein concentration of [^3H]IAEDANS-labeled RLC20 was determined by the bicinchoninic acid method (30). Myosin light chain kinase was purified by the method of Adelstein and Klee (31), except that the calmodulin-affinity chromatography step was omitted. Smooth muscle phosphatase SMP-I (32) was a generous gift of Dr. M. Pato. Actin was prepared by the method of Spudich and Watt (33).

Oxidation of Cys-108 to Cystine. RLC20 can be intermolecularly cross-linked by lyophilizing a 5 mg/mL protein solution in 50 mM ammonium bicarbonate, pH 7.9. The RLC20 dimers migrate above the monomers on urea gels (data not shown; DTE is omitted from the protein sample buffer).

Reduction and Alkylation of Cys-108. Lyophilized RLC20 was dissolved in 50 mM ammonium bicarbonate, pH 7.9, that had been purged with argon, and fresh DTE was added to 5 mM. After 2 h at 25°C under argon, IAA was added to 20 mM and reacted in the dark for 1 h at 25°C or on ice overnight.

Thiophosphorylation. When IAA was used to block Cys-108, RLC20 was dialyzed to remove excess IAA prior to thiophosphorylation. RLC20 was thiophosphorylated in 50 mM ammonium bicarbonate, pH 7.9, 0.2–1.0 mM ATP γ S, 1.5 mM CaCl₂, 5 mM MgCl₂, 4 $\mu\text{g}/\text{mL}$ myosin light chain kinase, 4 $\mu\text{g}/\text{mL}$ calmodulin (Sigma) for 1 h at 25°C or on ice overnight.

Labeling of Phosphorothioate with [^3H]IAEDANS. After thiophosphorylation, samples were dialyzed against 50 mM ammonium bicarbonate, 0.6 M KCl to remove excess ATP γ S. DTE (5 mM) was also included in this buffer if Cys-108 had been irreversibly blocked with IAA. The protein was then dialyzed into 50 mM ammonium bicarbonate (previously purged with argon) to remove excess salt and DTE (if added). [^3H]IAEDANS was added to a 5–10-fold excess over the protein concentration and allowed to react for 3 h at 25°C . Unreacted [^3H]IAEDANS was removed by Sephadex G-25 gel filtration in ammonium bicarbonate, or by precipitating twice from 2.5 M guanidine hydrochloride in 80% EtOH.

RESULTS AND DISCUSSION

Our strategy for specifically labeling thiophosphorylated proteins is shown in Figure 1. In most situations, cysteine sulphydryls are the only reactive protein side chains under conditions in which the thiophosphate group is labeled. We show two methods to block protein sulphydryls, either

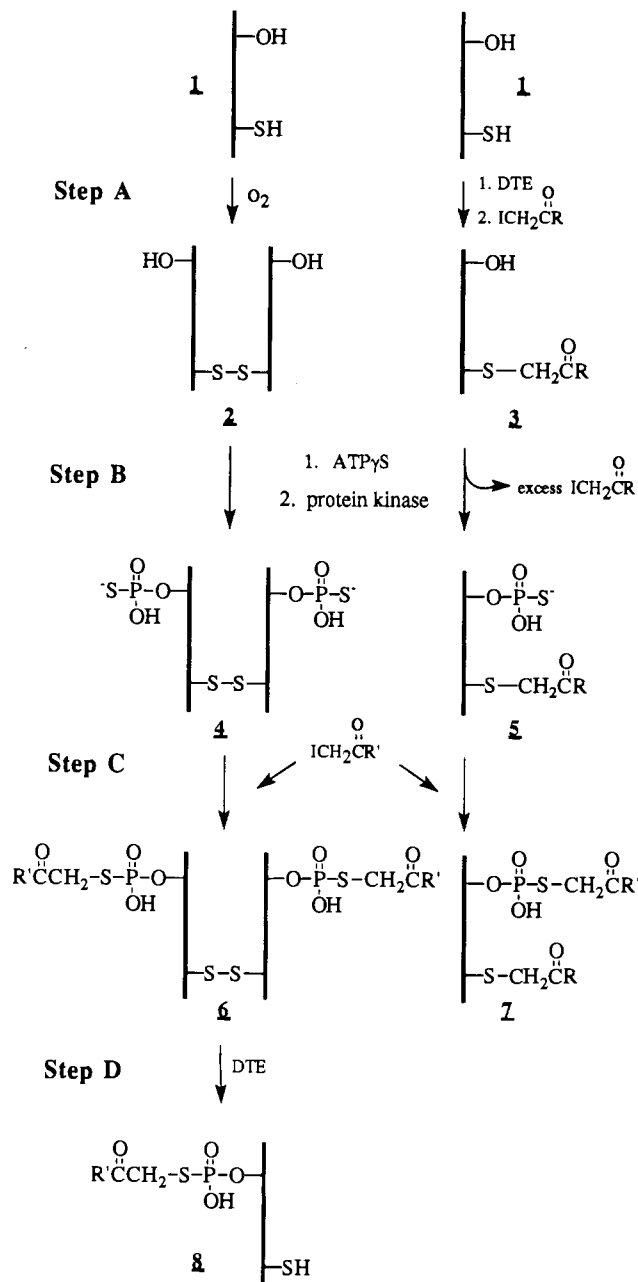


Figure 1. Outline of the method for specifically labeling thiophosphorylated proteins. Step A, blocking of thiol groups; step B, thiophosphorylation with kinase and ATP γ S; step C, reaction of phosphorothioate with haloacetate derivative; step D, reduction of reversibly blocked thiol groups. See the text for details.

reversibly (left side, Figure 1) or irreversibly (right side, Figure 1), in preparation for thiophosphate labeling of the RLC20 from smooth muscle myosin.

The native RLC20 (structure 1 in Figure 1) is shown schematically as a vertical line with the thiophosphorylatable Ser-19 at the top and the only cysteine, Cys-108, at the bottom. In step A, Cys-108 was blocked by one of two methods. For reversible thiol blocking, intermolecular disulfide bonds were formed by oxidation with molecular oxygen to produce structure 2. Other reversible methods of blocking are possible, such as methylthiolation with S-methylthio methanesulfonate and related reagents (34). Alternatively, the cysteine was irreversibly modified by reaction with a haloacetyl derivative ICH₂C(O)R (in our case, IAA) to produce structure 3. It is reasonable to assume that Cys-108 is the labeled amino acid because of the well-known specificity of haloacetates for sulphydryls

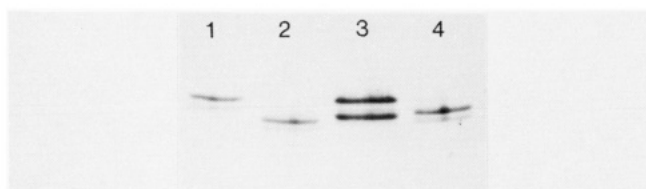


Figure 2. Urea gel assay for RLC20 modification. Protein samples were precipitated with 5 volumes of cold acetone and dissolved in 8 M urea, 10 mM DTE (freshly added), 0.2 mM EDTA, 33 mM Tris-glycine, pH 8.6, and applied to a 9% polyacrylamide, 8 M urea, 0.3 M Tris-HCl, pH 8.6, gel (10 cm \times 10 cm \times 0.75 cm) without a stacking gel. The running buffer was 60 mM Tris-glycine, pH 8.6. Gels were run at room temperature. Lane 1, unmodified RLC20 (1.5 μ g); lane 2, RLC20 (1.5 μ g) which is 100% IAA blocked at Cys-108 and 100% thiophosphorylated at Ser-19; Lane 3, smooth muscle myosin standard (30 μ g) showing RLC20 on top and LC 17 on bottom; Lane 4, RLC20 (1.5 μ g) which is 100% IAA blocked at Cys-108. The faint band below the RLC20 is due to a small amount of proteolytic cleavage which occurs during storage at 4 $^{\circ}$ C.

(35). The protein was thiophosphorylated in step B on Ser-19 by myosin light chain kinase, using ATP γ S as a substrate, to yield structures 4 and 5. The resonance structure of the phosphorothioate reflects the bond orders suggested by Frey and co-workers (36, 37). Following removal of excess ATP γ S, the haloacetate derivative ICH $_2$ C(O)R' (in our case [3 H]IAEDANS) is added in step C. The phosphorothioate group on the protein displaces halogen from the haloacetate to produce the stable structures 6 and 7. It is possible that maleimides may also be used in this step. However, we have not thoroughly explored this possibility as our initial studies indicated that maleimides react nonspecifically. The disulfide bond in structure 6 can be reversed by treatment with reductant such as DTE to yield structure 8.

The above reactions with RLC20 can be followed by urea gel electrophoresis (see Figure 2 for gel of samples which represent examples of structures 1, 3, and 5 from Figure 1). An increase of a single negative charge causes proteins to migrate faster in this gel system. Thus when IAA was used to block Cys-108 (structure 3) the protein migrated below native RLC20 (structure 1), reflecting the stoichiometric addition of a single negative charge. Addition of a negatively charged phosphorothioate to structure 3 to generate structure 5 caused an additional increase in the migration rate in the gel. In our case, 5 (Figure 2) and 7 (not shown) comigrate because a charge is both added and removed during the labeling of the phosphorothioate with [3 H]IAEDANS. These gel electrophoresis results indicate that both cysteine labeling and thiophosphorylation both proceed to essentially 100%. However, this assay was not useful to examine the reaction of the haloacetate with the thiophosphorylated serine (step C, Figure 1).

The time course of the reaction of thiophosphorylated Ser-19 with [3 H]IAEDANS was examined by precipitating the protein with acetone at various times after addition of [3 H]IAEDANS (Figure 3). The counts per minute in each thiophosphorylated protein pellet were corrected for background by subtracting the counts which were incorporated into an otherwise identical but phosphorylated protein sample. The raw data for one of the time courses is shown in the inset. The maximal labeling achieved under these conditions was 90%. These data show that the reaction is highly specific for the thiophosphate group and nearly stoichiometric labeling can be achieved under these conditions. We found that substoichiometric labeling would occur if the IAA-labeled RLC20 was not treated with DTE prior to labeling with [3 H]IAEDANS,

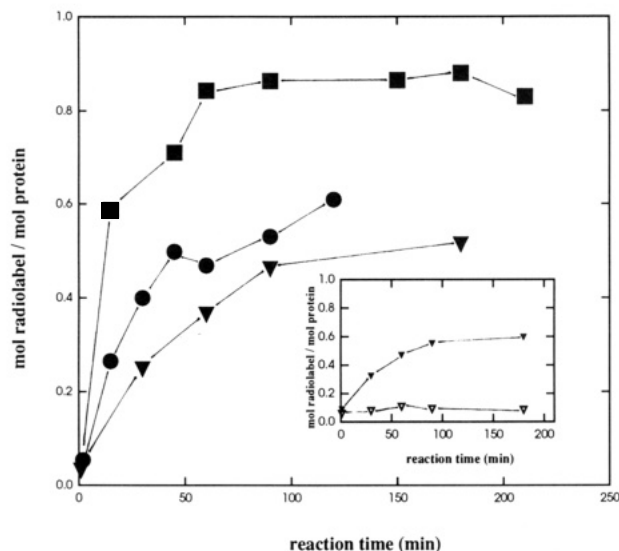


Figure 3. Time course of specific labeling of thiophosphorylated RLC20 at 25 $^{\circ}$ C. RLC20 (0.49 mg/mL; 25 μ M in ammonium bicarbonate, pH 7.9, 5 mM MgCl $_2$) was blocked at Cys-108 with IAA and then either phosphorylated or thiophosphorylated on serine-19 as described in the methods. At time = 0, [3 H]IAEDANS (4765 cpm/nmol) was added to the following final concentrations: ∇ , 250 μ M; \bullet , 500 μ M; \blacksquare , 750 μ M. At the indicated times, triplicate aliquots (0.03 mL) were removed and the protein was precipitated with 0.4 mL of ice-cold acetone to remove excess [3 H]IAEDANS. The mixture was vortexed and incubated at -20° C for 15 min prior to centrifuging at 4 $^{\circ}$ C in a microfuge (Beckman) for 2 min. The pellets were washed with cold acetone twice, dissolved in 4% sodium dodecyl sulfate, and transferred to scintillation counting vials. For each time point, the data are the averaged counts for the thiophosphorylated minus those for the phosphorylated RLC20. The inset shows the raw data for the time course at 250 μ M [3 H]IAEDANS (∇ , phosphorylated; \bullet , thiophosphorylated).

suggesting that some IAA remains bound to the protein during dialysis. Although the reactivity of the thiophosphate may differ from protein to protein, Baraniak and Frey (38) have used model compounds to predict that even shielded phosphorothioates that are ion paired with guanidinium or ammonium ions (as may be found in proteins) may have only modest perturbations in electronic distributions and thus may have similar chemical reactivity. Therefore it is likely that thiophosphorylated amino acids of other proteins will show a similar reactivity toward haloacetates as described here (Figure 3).

It should be noted that substoichiometric labeling could occur if the protein is partially phosphorylated during the thiophosphorylation reaction (step B, Figure 1) due to contaminating ATP in ATP γ S solutions. We tested for this possibility by treating thiophosphorylated RLC20 with light chain phosphatase [under the conditions described by Sellers et al. (39)], which is known to rapidly remove phosphate but not thiophosphate from RLC20. By urea gel electrophoresis (data not shown) we showed that all of the RLC20 was indeed thiophosphorylated, and was thus unresponsive to phosphatase treatment. This can be explained because our myosin light chain kinase is contaminated with phosphatase (31). Thus, during our thiophosphorylation reaction, the small percentage of RLC20 which was initially phosphorylated (by ATP) was eventually dephosphorylated and then thiophosphorylated. However, in general when it is important to achieve stoichiometric labeling, it may be useful to assay for complete thiophosphorylation prior to thiophosphate labeling.

We established directly the specificity of the phosphorothioate labeling by purifying and sequencing the labeled

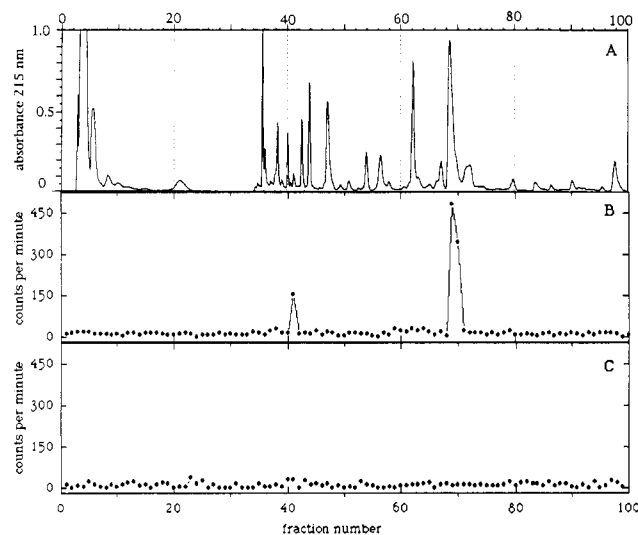


Figure 4. HPLC analysis of tryptic peptides. Labeled RLC20 (0.5 mg/mL) was digested at with three additions of 1/100 (w/w) trypsin (TPCK treated, Sigma) at 1-h intervals and then incubating overnight at 25 °C in 1 M urea, 1 mM CaCl_2 , 0.1 M HEPES, pH 7.0. After filtering, 17.5 nmol protein (0.34 mg) was applied to a Brownlee aquapore C8 RP 300 HPLC column (220 \times 4.6 mm) equilibrated in aqueous 5 mM potassium phosphate, pH 6.9. A linear gradient to 100% of 65% acetonitrile/35% H_2O was applied at a flow rate of 1 mL/min at room temperature and 1-mL fractions were collected. Panel A, HPLC chromatogram of tryptic digest of 7 (Figure 1), Cysteine-108 was modified with IAA to 100% and the Ser-19 phosphorothioate was labeled with [^3H]IAEDANS (using a 30-fold excess of [^3H]IAEDANS over protein) to 85%; panel B, radioactivity profile corresponding to panel A; panel C, radioactivity profile for a sample that was labeled to 100% on Cys-108 with IAA, phosphorylated, and then treated with [^3H]IAEDANS under conditions identical to those for the sample in panel A.

peptides from an enzymatic digest of structure 7 (Figure 1). Figure 4A shows the HPLC chromatogram of a trypsin digest of structure 7 (IAA on Cys-108, [^3H]IAEDANS on Ser-19). The profile of radioactivity shows that only two peptides were significantly labeled (Figure 4B). These two peptides contained 77% of the radioactivity which was applied to the column. An additional 11% of the radioactivity was estimated to elute throughout the chromatogram. As a control, Figure 4C shows that no labeled peptides resulted from treatment of phosphorothioate (rather than thiophosphorylated) structure 5 with [^3H]IAEDANS. This indicates that [^3H]IAEDANS is reacting only with the thiophosphate group.

The two radioactive peptides (fraction 69 and 41 from Figure 4B) were sequenced by Edman degradation. The results of seven cycles of sequencing of the predominant peptide (fraction 69 from Figure 4B) are shown in Figure 5. The sequence found (ATXNVFA) matches the known sequence of RLC20 from Ala-17 to Ala-23 (40), where X corresponds to Ser-19 in unmodified RLC20. Two pieces of evidence indicate that the thiophosphorylated Ser-19 is specifically labeled by [^3H]IAEDANS. First, the sequencing yield for all amino acids is low at cycle 3. The small amount of serine detected in this cycle indicates that some unlabeled serine may be generated under the sequencing conditions. Second, radioactivity begins to elute at cycle 3. The small number of counts eluted in cycle 3 (relative to the expected counts of about 1000) and the continued elution of radioactivity after cycle 3 are explained by a low extraction efficiency of the negatively charged modified serine residue from the filter. This poor extraction efficiency of negatively charged residues, such as phosphoamino acids, from the reaction filter has been

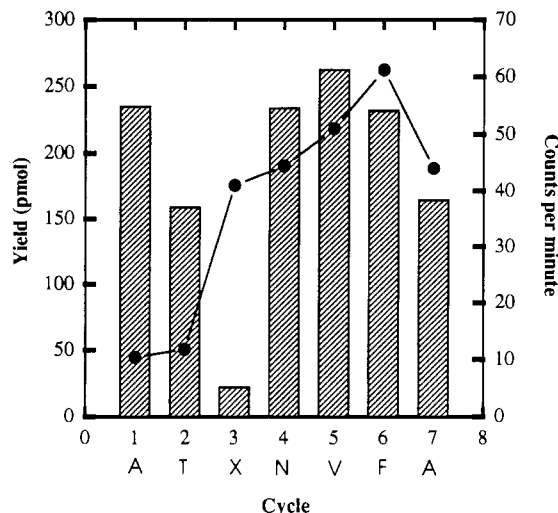


Figure 5. Amino acid sequence analysis of phosphorothioate-labeled peptide. Peptides were sequenced with an ABI Model 470-A gas-phase sequencer with Pulsed Liquid update (Applied Biosystems, Inc.) and ABI 120-APTH Analyzer. Data acquisition and analyses were performed with the standard program RUN 470-1 (ABI). One nanomole of peptide (4765 counts per cpm/nmol) from fraction 69 (see Figure 4) was applied to the filter. The initial yield is typically 50% for peptide standards on this instrument. The sample stream was split in half to simultaneously analyze the yield of each amino acid (bars) and the counts per minute corresponding to each cycle (filled circles). The sequence is indicated below the cycle numbers. X indicates that no known amino acid eluted in this cycle. The yield shown for cycle 3 is for serine.

noted by others (41). The sequence of the minor labeled peptide (fraction 41 from Figure 4B) and ATXNVFA, where X indicates that an unknown amino acid eluted at this position (data not shown). These data confirm that the labeling of structure 5 (Figure 1) by [^3H]IAEDANS was specific for the thiophosphorylated serine residue.

It was important to demonstrate that the linkage between the protein and the [^3H]IAEDANS in structure 6 was stable to reducing conditions (step D, Figure 1). We detected no loss of [^3H]IAEDANS from the protein after treatment with 1 mM β -mercaptoethanol for 120 h at 37 °C or after boiling for 30 min with 110 mM β -mercaptoethanol (data not shown). This is particularly important to those who may need to analyze labeled proteins by SDS gel electrophoresis, which often requires heating the protein with high concentrations of reductant. In addition we found that the [^3H]IAEDANS remained coupled to the protein after incubation at pH 3.0 to pH 10.5 for 23 h at 25 °C (data not shown). We did not test the stability of the linkage outside this pH range, but it is likely that strong base will cleave the C-S bond (5). This data indicates that the [^3H]IAEDANS-labeled protein is stable under most physiological conditions.

We provide evidence that the thiophosphate-labeled RLC20 remained in the native conformation by obtaining efficient exchange of thiophosphate-labeled RLC20 for unlabeled RLC20 of the whole smooth muscle myosin molecule. The resulting labeled myosin had normal K^+ , NH_4^+ -EDTA-, and Ca^{2+} -ATPase activities in the absence of actin (data not shown). This indicates that the modification of Ser-19 and the treatment required for exchange of the labeled light chain into myosin did not significantly disrupt the myosin. This also allowed us to specifically examine the effect of the thiophosphate labeling upon the actin-activated Mg^{2+} -ATPase activity of myosin which reflects its ability to generate force in the muscle (24).

Table I. Actin-Activated Mg^{2+} -ATPase Activities

myosin sample	RLC20 used during RLC20 exchange ^a	% of myosin sites exchanged ^b	actin-activated Mg^{2+} -ATPase activity ^c (nmol/min per mg)	
			-TP ^d	+TP ^d
control	none	—	0.74	25
exchanged	unmodified	—	0.78	23
control				
exchanged	thiophosphate labeled	50	2.9	14

^a We used the method of Dr. K. Trybus (unpublished results) to exchange light chains into whole myosin. Two mg/mL myosin and 1.6 mg/mL RLC20 (20-fold molar excess over myosin; either unlabeled or [³H]IAEDANS-thiophosphate-labeled with IAA on Cys-108) in 0.5 M NaCl, 5 mM EDTA, 10 mM DTE, 10 mM sodium phosphate, pH 7.5, 1 mM ATP, was incubated at 42 °C for 30 min. To stabilize the binding of the RLC20 to the myosin, $MgCl_2$ was added to 20 mM at 4 °C. The samples were dialyzed at 4 °C into 15 mM Tris, pH 7.5, 1 mM DTE, 10 mM $MgCl_2$, and the filamentous myosin was centrifuged. After the free light chains in the supernatant were removed, the pellet was resuspended and the centrifugation was repeated. This procedure was repeated once more and the pellet was resuspended in 15 mM Tris, pH 7.5 (at 25 °C), 5 mM $MgCl_2$, 0.1 mM EGTA prior to thiophosphorylation as described in the methods. The control was treated identically except that it was kept on ice and RLC20 was not added. ^b The extent of exchange of the RLC20 was calculated after determining the protein concentration by the bicinchoninic acid method (30) and counting the solution for [³H]IAEDANS. ^c A malachite green based spectroscopic method (49) was used to follow the generation of inorganic phosphate in the presence of 1 mg/mL myosin, 1 mg/mL actin in 15 mM Tris, pH 7.5 (at 25 °C), 5 mM $MgCl_2$, 0.1 mM EGTA, 30 mM KCl with 1 mM ATP at 25 °C. ^d +TP is thiophosphorylated and -TP is not thiophosphorylated.

Either phosphorylation or thiophosphorylation of Ser-19 increases the actin-activated Mg^{2+} -ATPase activity of smooth muscle myosin (24, 42). As shown in Table I, the activity of an untreated myosin sample increased 34-fold upon thiophosphorylation. Myosin that had been exposed to the exchange conditions in the presence of unlabeled light chains showed a similar level of activation upon thiophosphorylation (Table I), indicating that the exchange procedure does not alter this critical property of the protein. It has been shown previously that exchange with Cys-108-modified light chains does not alter the activity of smooth muscle myosin (43). After the exchange procedure in the presence of [³H]IAEDANS-thiophosphate-modified RLC20 (and IAA on Cys-108), 50% of the unmodified *in situ* light chains had been exchanged with modified ones (Table I). This preparation partially retained the elevated actin-activated Mg^{2+} -ATPase activity (2.9 nmol/min per mg) which is characteristic of thiophosphorylated myosin. This indicates that at least in this case, removal of the negative charge of the thiophosphate by modifying it with [³H]IAEDANS did not completely disrupt the actin-dependent functional properties of the protein. Further data is needed to establish the consequences and significance of modifications of this type.

Application of our strategy to other proteins may be limited. Specific labeling may not be achieved if a protein contains haloacetate reactive groups which may not be effectively blocked (44). In addition, this technique may not be useful to modify proteins which have many thiols that must be reversibly blocked. For example, we have had limited success applying the technique to thiophosphorylated smooth muscle myosin (45) which has many accessible thiols (46). In this case it was important to use a reversible method of thiol blocking, because thiol modification greatly altered the activity of the protein. We found that *S*-methylthiomethanesulfonate served as

an efficient thiol blocker, but we were able to return only limited activity to the protein after reduction with DTE. We had more success reversing the effects of 5,5'-dithiobis-(2-nitrobenzoic acid) (Ellman's reagent), which is a charged thiol blocker. These data suggest that activity-critical methylthio groups may become buried in the enzyme and are not accessible to DTE, as has been found for other proteins (47, 48). We are currently testing Bu_3P as an alternative reducing agent, which has the potential to access more hydrophobic sites on the protein (48). Despite these potential limitations, it is likely that our thiophosphate labeling approach will be useful for a variety of proteins.

In summary, we have demonstrated a new technique to specifically label thiophosphorylatable amino acids on proteins with extrinsic probes. Specifically, we have applied the technique to label a thiophosphorylatable serine residue of the RLC20 of smooth muscle myosin. We have focused on utilizing the thiophosphate labeling method to modify a serine; however, the method may also work for modifying threonines and tyrosines. The labeling reaction proceeds within hours at slightly alkaline pH and is highly specific for the thiophosphate moiety, and the product is stable to a wide pH range and to the presence of high concentrations of reductant. We feel that this approach to protein labeling is potentially useful for many proteins. By using various kinds of extrinsic probes, such as fluorophores, spin labels, electron-dense derivatives, and various antigens, this method may provide a new way to examine the structural aspects and functional implications of protein phosphorylation.

ACKNOWLEDGMENT

Dr. G. Munske performed the sequence analyses at the WSU Laboratory for Bioanalysis and Biotechnology. We thank M. Tibeau for technical assistance. We thank Dr. K. Nakamaye and Dr. L. McLaughlin, who gave advice and encouragement at the initiation of this project, Dr. K. Trybus for communicating her procedure for the exchange of RLC20 into smooth muscle myosin prior to publication, and Dr. M. Pato for providing valuable assistance concerning RLC20 phosphatases.

LITERATURE CITED

- Hurley, J. H., Dean, A. M., Sohl, J. L., Koshland, D. E. J., and Stroud, R. M. (1990) Regulation of an Enzyme by Phosphorylation at the Active Site. *Science* 249, 1012-1016.
- Sprang, S. R., Acharya, K. R., Goldsmith, E. J., Stuart, D. I., Varvill, K., Fletterick, R. J., Madsen, N. B., and Johnson, L. N. (1988) Structural changes in glycogen Phosphorylase induced by phosphorylation. *Nature* 336, 215-221.
- Edelman, A. M., Blumenthal, D. K., and Krebs, E. G. (1987) Protein Serine/Threonine Kinases. *Annu. Rev. Biochem.* 56, 567-613.
- Hunter, T., and Cooper, J. A. (1985) Protein-Tyrosine Kinases. *Annu. Rev. Biochem.* 54, 897-930.
- Goody, R. S., and Eckstein, F. (1971) Thiophosphate Analogs of Nucleoside Di and Triphosphates. *J. Am. Chem. Soc.* 93, 6252-6257.
- Eckstein, F. (1985) Nucleoside Phosphorothioates. *Annu. Rev. Biochem.* 54, 367-402.
- Gratecos, D., and Fischer, E. H. (1974) Adenosine 5'-0-(3-thiotriphosphate) in the Control of Phosphorylase Activity. *Biochem. Biophys. Res. Commun.* 58, 960-967.
- Moffett, R. B., and Webb, T. E. (1983) Characterization of a Messenger RNA Transport Protein. *Biochim. Biophys. Acta* 740, 231-242.

- (9) O'Brian, C. A., Rocznik, S. O., Bramson, H. N., Baraniak, J., Stec, W. J., and Kaiser, E. T. (1982) A Kinetic Study of Interaction of (R_p)- and (S_p)-Adenosine Cyclic 3',5'-Phosphorothioates with Type II Bovine Cardiac Muscle Adenosine Cyclic 3',5'-Phosphate Dependent Protein Kinase. *Biochemistry* 21, 4371-4376.
- (10) Watabe, S., Tsuchiya, T., and Hartshorne, D. J. (1989) Phosphorylation of Paramyosin. *Comp. Biochem. Physiol.* 94B, 813-821.
- (11) Sun, I. Y.-C., Johnson, M., and Allfrey, V. G. (1980) Affinity Purification of Newly Phosphorylated Protein Molecules. *J. Biol. Chem.* 255, 742-747.
- (12) Palvimo, J., Linnala-Kankkunen, A., and Maenpaa, P. H. (1985) Thiophosphorylation and Phosphorylation of Chromatin Proteins from Calf Thymus In Vitro. *Biochem. Biophys. Res. Commun.* 126, 103-108.
- (13) Sarafian, T., Pradel, L.-A., Henry, J.-P., Aunis, D., and Bader, M.-F. (1991) The Participation of Annexin II (Calpactin I) in Calcium-evoked Exocytosis Requires Protein Kinase C. *J. Cell. Biol.* 114, 1135-1147.
- (14) Giambalvo, C. (1988) Protein Kinase C and Dopamine Release. *Biochem. Pharm.* 37, 4001-4007.
- (15) Vandenheede, J. R., Yang, S.-D., Merlevede, W., Jurgensen, S., and Chock, B. (1985) Kinase F_A -mediated Regulation of Rabbit Skeletal Muscle Protein Phosphatase. *J. Biol. Chem.* 260, 10512-10516.
- (16) Ranu, R. S. (1986) Regulation of Protein Synthesis in Rabbit Reticulocyte Lysates. *FEBS Lett.* 208, 117-122.
- (17) Sherry, J. M. F., Gorecka, A. A., M. O., Dabrowska, R., and Hartshorne, D. J. (1978) Roles of Calcium and Phosphorylation in the Regulation of the Activity of Gizzard Myosin. *Biochemistry* 17, 4411-4418.
- (18) Ikeda, A., Okuno, S., and Fujisawa, H. (1991) Studies on the Generation of Ca^{2+} /Calmodulin-independent Activity of Calmodulin-dependent Protein Kinase II by Autophosphorylation. *J. Biol. Chem.* 266, 11582-11588.
- (19) Nichols, R. A., Sihra, T. S., Czernik, A. J., Nairn, A. C., and Greengard, P. (1990) Calcium/calmodulin-dependent Protein Kinase II Increases Glutamate and Noradrenaline Release from Synaptosomes. *Nature* 343, 647-651.
- (20) Cassel, D., and Glaser, L. (1982) Resistance to Phosphatase of Thiophosphorylation Epidermal Growth Factor Receptor in A431 Membranes. *Proc. Natl. Acad. Sci. U.S.A.* 79, 2231-2235.
- (21) Nichols, R. A., Sihra, T. S., Czernik, A. J., Nairn, A. C., and Greengard, P. (1990) Calcium/calmodulin-dependent protein kinase II increases glutamate and noradrenaline release from synaptosomes. *Nature* 343, 647-651.
- (22) Hodges, R. R., Conway, N. E., and McLaughlin, L. W. (1989) "Post-Assay" Covalent Labeling of Phosphorothioate-Containing Nucleic Acids with Multiple Fluorescent Markers. *Biochemistry* 28, 261-267.
- (23) Cosstick, R., McLaughlin, L. W., and Eckstein, F. (1984) Fluorescent labelling of tRNA and oligodeoxynucleotides using T4 RNA ligase. *Nucleic Acids Res.* 12, 1791-1810.
- (24) Hartshorne, D. J. (1987) Biochemistry of the Contractile Process in Smooth Muscle, 2nd ed. (L. R. Johnson, Ed.) pp 423-480, Raven Press, New York.
- (25) Hudson, E. N., and Weber, G. (1973) Synthesis and Characterization of Two Fluorescent Sulfhydryl Reagents. *Biochemistry* 12, 4154-4161.
- (26) Ikebe, M., and Hartshorne, D. J. (1985) Effects of Ca^{2+} on the Conformation and Enzymatic Activity of Smooth Muscle Myosin. *J. Biol. Chem.* 260, 13146-13153.
- (27) Perrie, W. T., and Perry, S. V. (1970) An Electrophoretic Study of the Low-Molecular-Weight Components of Myosin. *Biochem. J.* 119, 31-38.
- (28) Hathaway, D. R., and Haeblerle, J. R. (1983) Selective Purification of the 20,000-Da Light Chains of Smooth Muscle Myosin. *Anal. Biochem.* 135, 37-43.
- (29) Sobieszek, A. (1988) Bulk Isolation of the 20,000-Da Light Chain of Smooth Muscle Myosin: Separation of the Unphosphorylated and Phosphorylated Species. *Anal. Biochem.* 172, 43-50.
- (30) Smith, P. K., Krohn, R. I., Hermanson, G. T., Mallia, A. K., Gartner, F. H., Provenzano, M. D., Fugimoto, E. K., Goeke, N. M., Olson, B. J., and Klenk, D. C. (1985) Measurement of Protein Using Bicinchoninic Acid. *Anal. Biochem.* 150, 76-85.
- (31) Adelstein, R. S., and Klee, C. B. (1982) Purification of Smooth Muscle Myosin Light Chain Kinase. *Methods Enzymol.* 85, 298-308.
- (32) Pato, M., and Adelstein, R. S. (1982) Purification of Smooth Muscle Phosphatases. *Methods Enzymol.* 85, 308-315.
- (33) Spudich, J. A., and Watt, S. (1971) The Regulation of Rabbit Skeletal Muscle Contraction. *J. Biol. Chem.* 246, 4866-4871.
- (34) Smith, D. J., Maggio, E. T., and Kenyon, G. L. (1975) Simple Alkanethiol Groups for Temporary Blocking of Sulfhydryl Groups on Enzymes. *Biochemistry* 14, 766-771.
- (35) Means, G. E., and Feeney, R. E. (1971) *Chemical Modification of Proteins*, Holden-Day, Inc., San Francisco.
- (36) Frey, P. A., and Sammons, R. D. (1985) Bond Order and Charge Delocalization in Nucleoside Phosphorothioates. *Science* 228, 541-545.
- (37) Frey, P. A., Reimschuessel, W., and Paneth, P. (1986) Phosphorus-Sulfur Bond Order in Phosphorothioate Anions. *J. Am. Chem. Soc.* 108, 1720-1722.
- (38) Baraniak, J., and Frey, P. A. (1988) Effect of Ion Pairing on Bond Order and Charge Localization in Alkyl Phosphorothioates. *J. Am. Chem. Soc.* 110, 4059-4060.
- (39) Sellers, J. R., Pato, M. D., and Adelstein, R. S. (1981) Reversible Phosphorylation of Smooth Muscle Myosin, Heavy Meromyosin, and Platelet Myosin. *J. Biol. Chem.* 256, 13137-13142.
- (40) Matsuda, G. (1983) The Light Chains of Muscle Myosin: It's Structure, Function, and Evolution. *Adv. Biophys.* 16, 185-218.
- (41) Murakami, N., Healy-Louie, G., and Elzinga, M. (1990) Amino Acid Sequence around the Serine Phosphorylated by Casein Kinase II in Brain Myosin Heavy Chain. *J. Biol. Chem.* 265, 1041-1047.
- (42) Kenney, R. E., Hoar, P. E., and Kerrick, G. L. (1990) The Relationship between ATPase Activity, Isometric Force, and Myosin Light-chain Phosphorylation and Thiophosphorylation in Skinned Smooth Muscle Fiber Bundles from Chicken Gizzard. *J. Biol. Chem.* 8642-8649.
- (43) Morita, J.-I., Takashi, R., and Ikebe, M. (1991) Exchange of the Fluorescence-Labeled 20000-Dalton Light Chain of Smooth Muscle Myosin. *Biochemistry* 30, 9539-9545.
- (44) Gurd, F. R. N. (1967) *Methods Enzymol.* 11, 532-541.
- (45) Facemyer, K. C., and Cremo, C. R. (1991) Specific Labeling of Serine-19 of the Regulatory Light Chain of Chicken Gizzard Myosin. *Biophys. J.* 59, 436a.
- (46) Chandra, T. S., Nath, N., Suzuki, H., and Seidel, J. C. (1985) Modification of Thiols of Gizzard Myosin Alters ATPase Activity, Stability of Myosin Filaments, and the 6-10 S Conformational Transition. *J. Biol. Chem.* 260, 202-207.
- (47) Bednar, R. A., McCaffrey, C., and Shan, K. (1991) Introduction of Unnatural Amino Acids into Chalcone Isomerase. *Bioconjugate Chem.* 2, 211-216.
- (48) Nishimura, J. S., Kenyon, G. L., and Smith, D. J. (1975) Reversible Modification of the Sulfhydryl Groups of *Escherichia coli* Succinic Thiokinase with Methanethiolating Reagents, 5,5'-Dithio-bis-(2-Nitrobenzoic Acid), p-Hydroxymercuribenzoate, and Ethylmercurithiosalicylate. *Arch. Biochem. Biophys.* 170, 461-467.
- (49) Lanzetta, P. A., Alvarez, L. J., Reinach, P. S., and Candia, O. A. (1979) An Improved Assay for Nanomole Amounts of Inorganic Phosphate. *Anal. Biochem.* 100, 95-97.

Synthesis and High Stability of Complementary Complexes of *N*-(2-Hydroxyethyl)phenazinium Derivatives of Oligonucleotides

Sergei G. Lokhov, Mikhail A. Podyminogin, Dmitrii S. Sergeev, Vladimir N. Silnikov, Igor V. Kut'yavin, Gennadii V. Shishkin, and Valentina P. Zarytova*

Institute of Bioorganic Chemistry, Siberian Division of the Russian Academy of Sciences, Prospect Lavrent'eva, 8 Novosibirsk 630090, Russia. Received June 1, 1992

Two simple methods for the synthesis of oligonucleotides bearing a *N*-(2-hydroxyethyl)phenazinium (Phn) residue at the 5'- and/or 3'-terminal phosphate groups are proposed. By forming complexes between a dodecanucleotide d(pApApCpCpTpGpTpTpGpGpC), a heptanucleotide d(pCpCpApApApCpA), and Phn derivatives of the latter, it is shown that the introduction of a dye at the end of an oligonucleotide chain strongly stabilizes its complementary complexes. The T_{\max} and the thermodynamic parameters (ΔH , ΔS , ΔG) of complex formation were determined. According to these data, coupling of a dye with the 5'-terminal phosphate group is the most advantageous: $\Delta G(37^\circ\text{C})$ is increased by 3.59 ± 0.04 kcal/mol compared to 2.06 ± 0.04 kcal/mol for 3'-Phn derivatives. The elongation of the linker, which connects the dye to the oligonucleotide, from a dimethylene up to a heptamethylene usually leads to destabilization of the oligonucleotide complex. The complementary complex formed by the 3',5'-di-Phn derivative of the heptanucleotide was found to be the most stable among all duplexes investigated. Relative to the unmodified complex the increase in free energy was 4.96 ± 0.04 kcal/mol. The association constant of this modified complex at 37°C is $9.5 \cdot 10^6 \text{ M}^{-1}$, whereas the analogous value for the unmodified complex is only $3 \cdot 10^3 \text{ M}^{-1}$.

INTRODUCTION

Oligonucleotides bearing dye residues (1-4) are now under scrutiny by many nucleic acid chemists, as they are successfully used for directed effects on structure (5, 6) and functional activity (7-9) of nucleic acids. The oligonucleotide-dye conjugates have remarkable physicochemical and biochemical properties. Compared to unmodified oligomers, oligonucleotides covalently linked to intercalating dyes have a higher affinity for complementary targets (1-4) and are more resistant to cellular nucleases (10, 11). For example, oligodeoxyribonucleotides bearing an acridine derivative were found to be successful antisense agents for suppression of target nucleic acid expression not only in the *in vitro* experiments (7) but also in living cells (8, 9). According to some data (6, 12-14), the dye may play the role of a reactive agent under particular conditions.

In the present paper we describe the synthesis and hybridization properties of oligodeoxyribonucleotides bearing *N*-(2-hydroxyethyl)phenazinium residues (Phn¹) at the 3'- or 5'-end. Oligonucleotides which contain one or more phenazine quaternary salts form strong hybrids with complementary target strands due to stabilization by the phenazine residue. The phenazine residues were introduced by facile oxidative coupling of *N*-(2-hydroxyethyl)phenazinium chloride with readily prepared aminoalkyl-substituted oligonucleotides, a process which offers advantages of ease and quantitative yield. Based on the results obtained, we recommend Phn-oligonucleotide derivatives as promising starting materials for the design of nucleic acid targeted reagents and probes.

EXPERIMENTAL PROCEDURES

Chemicals. Chemicals used in the present work were from Fluka or Merck; T4-polynucleotide kinase was from Fermentas, [γ -³²P]ATP (specific radioactivity > 2000 Ci/mmol) was from Isotop. *p*-Chlorophenyl *N*-acyl-3'-*O*-levulinyl nucleoside 5'-phosphates, *p*-chlorophenyl β -cyanoethyl *N*-acyl nucleoside 5'-phosphates, 2,4,6-triisopropylbenzenesulfonyl chloride, and 4-chlorophenyl phosphorodichloridate were products of the Novosibirsk Institute of Organic Chemistry (Novosibirsk, Russia). Dimethyl sulfoxide was distilled under reduced pressure. Absolute pyridine was prepared by successive distillations under TPS, KOH, and P₂O₅. 2,2'-Dipyridyl disulfide, triphenylphosphine, 4-(dimethylamino)pyridine, polymethylenediamines, and polymethylenamine alcohols were commercially available and used without further purification.

Chromatography. Purification of unprotected oligonucleotides and their derivatives was by HPLC with a Beckman-332 system on Polisil SA (10 μm) anion-exchange and Lichrosorb RP 18 (5 μm) reverse-phase columns. The Polisil SA column was a gift of Dr. S. I. Yastrebov (Koltsovo, Russia).

Physical Measurements. UV-visible absorption spectra of dyes in water and oligonucleotide-dye conjugates in 0.16 M NaCl, 0.02 M Na₂HPO₄, and 0.1 mM EDTA (pH 7.4) were recorded in the 200-600-nm range on a UV-2100 spectrophotometer (Shimadzu). ¹H NMR spectra for dyes were run at 20 $^\circ\text{C}$, on a Bruker WP-200 spectrometer; chemical shifts are reported in ppm downfield from Me₄Si. Optical melting curves of oligonucleotide complexes were obtained on the UV detector of a Milichrom liquid chromatograph in a thermoregulated cell specially designed for this purpose. Speed of heating was 0.5-0.7 $^\circ\text{C}/\text{min}$. The melting curves were constructed by integrating over 500-600 data points obtained every 10 s from optical and thermal sensors. Optical noise did not exceed ± 0.001 A. The data were collected and processed on an Iskra-226 personal computer. Before the thermodynamic calculation, the melting curves were smoothed by a linear central

¹ Abbreviations used: Phn, *N*-(2-hydroxyethyl)phenazinium residue; TPS, 2,4,6-triisopropylbenzenesulfonyl chloride; MeIm, *N*-methylimidazole; (Ph)₃P, triphenylphosphine; (PyS)₂, 2,2'-dipyridyl disulfide; DMAP, 4-(dimethylamino)pyridine; d(pN...pN), unblocked oligonucleotide; d(pNpNpN...pN), blocked oligonucleotides; T_{\max} , melting temperature of a oligonucleotide duplex determined at the point of curve bending.

Table I. Physical Properties and Elemental Analysis Data of the Compounds of General Formula $\text{HO}(\text{CH}_2)_m\text{NHCOCF}_3$

<i>m</i>	<i>n</i> ₂₀ ^D	bp, °C (0.5 mmHg)	elemental analysis data					
			% found			% calcd		
			C	H	F	C	H	F
2 ^a		97–98	30.9	4.12	35.6	30.6	3.85	36.2
3	1.405	105–106	35.3	4.81	33.7	35.1	4.71	33.3
4	1.412	118–119	38.8	5.40	31.1	38.9	5.44	30.8
5	1.417	127–128	42.2	6.02	28.5	42.2	6.07	28.6

^a This compound is solid with mp 50–55 °C.

interpolation treatment of the data using a 2° window with consecutive averagings offset by 0.1°.

Thermodynamic Calculations. Thermodynamic parameters of complex formation were calculated according to a "two states" model by minimization of mean square errors between the calculated and experimental melting curves, where the ΔH and ΔS values were varied (15). Furthermore, these parameters were found to be similar to those obtained using the van't Hoff procedure for selected duplexes. The thermodynamic parameters were confirmed by the results of at least two experiments. The mean arithmetical errors of experiments are given in Table II. The melting temperatures of complexes (T_{max}) were determined at the points of curve bending.

Molar Extinction of Oligonucleotides. The concentration of the oligonucleotides and their derivatives was measured spectrophotometrically. The molar extinction of unmodified oligonucleotides was determined after complete hydrolysis by venom nuclease as described in ref 16. To determine the molar extinctions of dye-oligonucleotide conjugates, the starting unmodified oligonucleotides (~0.5 μmol) were labeled (~10–20 μCi) by reaction with T4-polynucleotide kinase, [γ -³²P]ATP, and ADP according to the technique described in ref 17. After purification of the labeled oligonucleotides by reverse-phase chromatography, they were used in the synthesis of the corresponding derivatives according to the methods described below. UV-visible absorption spectra of the starting oligonucleotides and then derivatives were recorded in the above buffer. Radioactivity of equal portions of these solutions was determined on an LKB scintillation counter by Cherenkov effect. Molar extinctions of oligonucleotide derivatives (ϵ_{260}^D) were calculated using the formula

$$\epsilon_{260}^D = \epsilon_{260}^S \frac{A^D R^S}{R^D A^S}$$

where A = optical density (260 nm) of the solution of starting oligonucleotide (A^S) and its derivative (A^D) and R = radioactivity of the aliquots of the corresponding solutions.

***N*-(2-Hydroxyethyl)phenazinium Chloride.** Ethylene oxide (50 mL) was added dropwise to a solution of phenazine (10 g) in 100 mL of glacial acetic acid at 10 °C. After 6 days of incubation in a closed flask at 20 °C, 10 mL of concentrated HCl was added and the reaction mixture was evaporated in vacuo. The dark-brown gum was twice treated with a mixture of toluene–heptane (1:1) and evaporated. Diethyl ether (150 mL) was added to form a suspension and to precipitate the product over 12 h. The precipitate was filtered and washed by acetone and diethyl ether. After the additional reprecipitation, 10.5 g of *N*-(2-hydroxyethyl)phenazinium chloride was obtained in a yield of 72%. Mp: 340–350 °C dec. UV-vis, λ_{max} , nm (log ϵ): 262 (4.89), 387 (4.39), 440 (3.47). ¹H NMR, δ , ppm (CD₃OD): 7.93–9.03 (arom H, 8 H, m), 5.45–5.95 (CH₂N⁺, 2 H, m), 4.20–4.44 (–CH₂O–, 2 H, m). Anal.

Calcd for C₁₄H₁₃ClN₂O: C, 64.5; H, 5.0; N, 10.7. Found: C, 64.5; H, 5.1; N, 10.5.

2-[(6-Aminohexyl)amino]-10-(2-hydroxyethyl)phenazinium Chloride. *N*-(2-Hydroxyethyl)phenazinium chloride (1 g) was dissolved in a solution of 2 g of 1,6-hexanediamine in 5 mL of dried methanol, and the reaction mixture was incubated at 20–23 °C for 1 day. The product was precipitated with diethyl ether (10 mL), reprecipitated from methanol, washed with diethyl ether, and dried. The yield of dye was 0.95 g (66%). To obtain a preparation of analytical grade, the dye was converted from the chloride to the perchlorate form by treatment of its concentrated aqueous solution with 10% aqueous LiClO₄ up to a 2-fold excess. The precipitated dye was filtered and crystallized from water. Mp: 123–125 °C. UV-vis, λ_{max} , nm (log ϵ): 237 (4.53), 295 (4.54), 380 (4.00), 394 (4.02), 530 (4.20). ¹H NMR, δ , ppm ((CD₃)₂SO): 7.94 (arom H, 6 H, m), 6.83 (arom H, 1 H, s), 5.10 (CH₂N, 2 H, t), 4.05 (CH₂O, 2 H, t), 3.58 (CH₂NH₂, 2 H, m), 2.81 (CH₂-HNAr, 2 H, m), 1.45 (–(CH₂)₄–, 8 H, m). Anal. Calcd for C₂₀H₂₆ClN₄O₅·1/2CO₃^{2–}: C, 53.7; H, 6.20; N, 11.9; Cl, 8.08. Found: C, 53.7; H, 6.15; N, 12.0; Cl, 7.94.

Synthesis of HO(CH₂)_{*m*}NHCOCF₃ (*m* = 2–5). The compounds of general formula HO(CH₂)_{*m*}NHCOCF₃ (*m* = 2–5) were prepared by treatment of the corresponding polymethylenamine alcohol (1 mol) with the ethyl ester of trifluoroacetic acid (1.3 mol) at 20 °C for 2 h. The desired product was isolated from the reaction mixture after two stages of distillation under low pressure (0.3–0.5 mmHg) with a yield of 50–70%. Some physical properties and elemental analysis data are summarized in Table I.

Blocked Oligonucleotides. The synthesis of blocked oligonucleotides was performed in chloroform by the triester method (18) starting with 5'-*p*-chlorophenyl *N*-acyl-3'-*O*-levulinyl nucleoside 5'-phosphates and *p*-chlorophenyl β-cyanoethyl *N*-acyl nucleoside 5'-phosphates. TPS and MeIm (1:2) were used as condensing reagents. The 3'-hydroxyl groups of the OH components were blocked by levulinate. The base residues were protected as in ref 18. At all stages the P and OH components were used at 0.2 M concentration and at a ratio close to equimolar. A 3-fold excess of the condensing reagents over the P components was used. The cyanoethyl groups were removed by a mixture of dry acetonitrile and triethylamine (1:1) (18). After the removal of the levulinate residue (19) the OH components were isolated by chromatography on silica gel in a gradient of methanol in chloroform.

Unblocked Oligonucleotides. The unblocked oligonucleotides were prepared from the corresponding products of the solid-phase phosphoramidite procedure using an automated Victoria 4M synthesizer (Novosibirsk, Russia) (20). Terminal phosphates were introduced by conversion of uridine 5'-phosphate residues by periodate oxidation and subsequent β-elimination as described (21). To prepare oligonucleotides containing these residues at the 3'- and 5'-termini, (iPr)₂N-P(OCH₃)OU(Bz)₂ was used

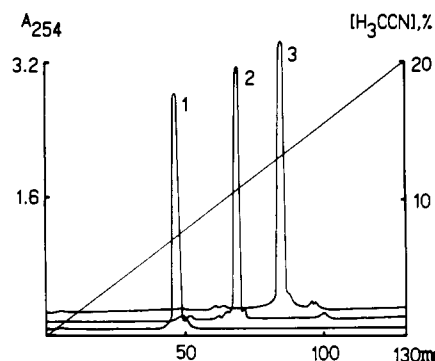


Figure 2. Results of isolation of Phn-NH(CH₂)₂NH-d(pCpCpApApCpA) (2) and Phn-NH(CH₂)₇NH-d(pCpCpApApCpA) (3) from the reaction mixture by a Lichrosorb RP 18 HPLC column (4 × 250 mm). Profile 1 is an analysis of the starting unmodified heptanucleotide d(pCpCpApApCpA). The flow rate was 3 mL/min with a linear gradient of acetonitrile from 0 to 20% in 0.05 M LiClO₄.

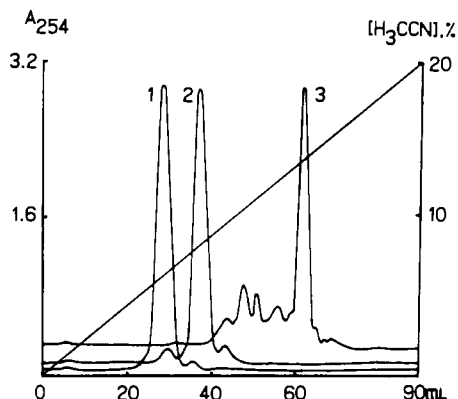


Figure 3. Results of isolation of d(pCpCpApApCpAp)-OCH₂-CH₂NH-Phn (2) and Phn-NH(CH₂)₂NH-d(pCpCpApApCpAp)-OCH₂CH₂NH-Phn (3) from the reaction mixture by a reverse-phase column. Profile 1 is analysis of the starting nucleotide d(pCpCpApApCpAp)-OCH₂CH₂NH₂. The flow rate was 2 mL/min; other conditions of isolation were the same as in Figure 2.

It is possible to prepare conjugates of an oligonucleotide with two Phn residues. The choice of a synthetic approach depends on whether protected or unprotected oligonucleotides are used as starting material. With unprotected oligonucleotides bearing two phosphate groups on the 3'- and 5'-end, we used approach A (Scheme I). Also for this purpose the 3'-Phn derivatives of oligonucleotides (final products of the approach B) were chosen. In contrast to the mono-Phn derivatives of oligonucleotides, the yields of the 3',5'-di-Phn derivatives (Figure 3) were considerably lower.

The structures of all oligonucleotide derivatives prepared were confirmed by different methods. Thus it was found that the dye is coupled only to the amino groups preliminarily introduced into the oligonucleotide structure. The unmodified oligonucleotides do not react with *N*-(2-hydroxyethyl)phenazinium chloride under these conditions. The UV-visible spectra of the Phn derivatives have absorption maxima corresponding to the oligonucleotide domain at 260 nm and to the 2-[(6-aminohexyl)amino]-10-(2-hydroxyethyl)phenazinium chloride moiety at 237, 290, 390, and 530 nm (Figure 4). Having compared spectral profiles of the oligonucleotide and dye with those of the Phn derivatives, we could confirm both the existence and the number of dye residues in the molecular structure. Phn derivatives are violet-pink in color, which makes them easily detectable. The chromatographic data was con-

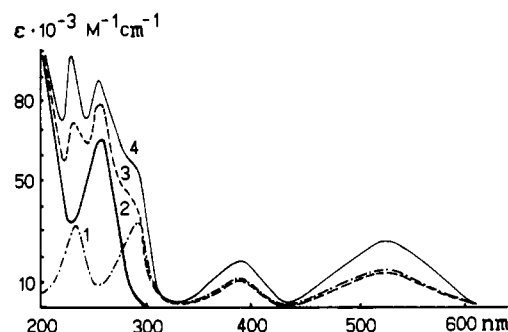
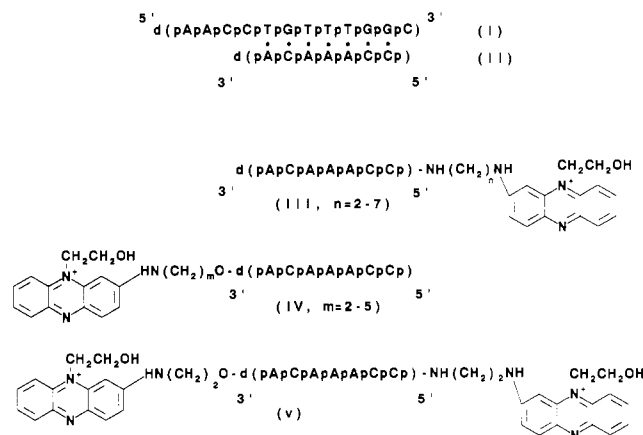


Figure 4. UV-visible spectra of 2-[(6-aminohexyl)amino]-10-(2-hydroxyethyl)phenazinium chloride (1), d(pCpCpApApCpA) (2), d(pCpCpApApCpAp)-OCH₂CH₂NH-Phn (3), and Phn-NH(CH₂)₂NH-d(pCpCpApApCpAp)-CH₂CH₂NH-Phn (4) in 0.16 M NaCl, 0.02 M Na₂HPO₄, and 0.1 mM EDTA (pH 7.4).

Scheme II



sistent with the suggested structures (Figures 2 and 3). Naturally, the mobility of the oligonucleotide derivatives during RPC falls with the introduction of the hydrophobic dye residues. As follows from the profile of Figure 2, the length of a polymethylene linker also affects the mobility of the Phn derivatives. A heptanucleotide derivative, Phn-NH(CH₂)₆NH-d(pCpCpApApCpCpA), was prepared using two methods: approach A (Scheme I) and a reaction between 2-[(6-aminohexyl)amino]-10-(2-hydroxyethyl)phenazinium chloride and a reactive 5'-phosphoryl 4-(dimethylamino)pyridine derivative of the heptanucleotide. The chromatographic and spectral characteristics of these heptanucleotide Phn derivatives prepared by the two methods were the same.

To elucidate the effect of the Phn residue on the stability of oligonucleotide complexes, we examined duplexes formed by dodecanucleotide (I), heptanucleotide (II), and modified heptanucleotide (III, *n* = 2–7; IV, *m* = 2–5; and V) derivatives (Scheme II). By analyzing temperature dependencies we determined that thermal stability of the duplexes increased passing from complex I + II to complexes I + III (*n* = 2–7) or I + IV (*m* = 2–5) and further to I + V apparently due to the introduction of the Phn residues (see Figure 5).

The melting points of all investigated complexes are listed in Table II. The thermodynamic parameters ΔH , ΔS , and ΔG were calculated on the basis of thermal denaturation curves of the complexes (Figure 5), including those derivatives in which the length of the polymethylene linker between the dye and the terminal phosphate group was varied. It is noteworthy that the introduction of Phn causes large changes in the thermodynamic properties of the complexes. For example, the enthalpy of the complexes formed by mono-Phn derivatives of heptanucleotide II is

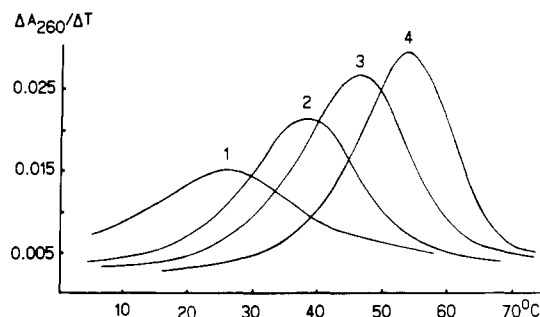


Figure 5. Differential melting curves for complexes of d(pApCpCpTpGpTpTpGpGpC) with d(pCpCpApApApCpA) (1), d(pCpCpApApApCpAp)-OCH₂CH₂NH-Phn (2), Phn-NH-(CH₂)₂NH-d(pCpCpApApApCpA) (3), and Phn-NH-(CH₂)₂NH-d(pCpCpApApApCpAp)-OCH₂CH₂NH-Phn (4) in the same buffer as in Figure 4.

Table II. Thermodynamic Parameters and Melting Points of Oligonucleotide Complexes Bearing an *N*-(2-Hydroxyethyl)phenazinium Residue^a

complex (<i>n</i> or <i>m</i>)	$\Delta H \pm 1$ kcal/mol	$\Delta S \pm 4$ cal/mol K	$\Delta G(37^\circ\text{C}) \pm$ 0.02 kcal/mol	$T_{\text{max}} \pm$ 0.1 °C
I + II	-37	-104	-4.93	27.2
I + III (2)	-53	-143	-8.30	47.4
I + III (3)	-54	-147	-7.99	45.0
I + III (4)	-60	-166	-8.52	47.1
I + III (5)	-54	-150	-7.92	44.5
I + III (6)	-53	-146	-7.76	43.7
I + III (7)	-49	-135	-7.41	41.9
I + IV (2)	-49	-134	-6.99	39.6
I + IV (3)	-46	-126	-6.74	37.7
I + IV (4)	-46	-127	-6.84	38.3
I + IV (5)	-44	-121	-6.75	37.8
I + V	-67	-183	-9.89	54.8

^a The conditions for thermal denaturation of the complementary complexes, from which all thermodynamic parameters and T_{max} 's were determined, are described in Figure 4.

increased by 7–23 kcal/mol compared to that of the unmodified counterpart. The corresponding change in free energy of complex formation at 37 °C is 1.81–3.59 kcal/mol, which is approximately equivalent to extending the duplex by one G-C or two A-T pairs (27). It should be pointed out that the contribution of the Phn residue to the enthalpy of the complementary complex I + III ($n = 4$) was more than twice as high as that of the acridine dye (10 kcal/mol) in a duplex formed by polydeoxyriboadenylic acid and a derivatized oligothymidylate (3).

As seen from Table II, the introduction of a dye into the 5'-terminal phosphate was the most advantageous. In the modified complex I + III ($n = 4$), ΔG increased by 3.59 kcal/mol (compared to 2.06 kcal/mol for the 3'-Phn derivative). The same effect was observed for DNA duplexes with an unpaired nucleoside residue at the 3'- and 5'-terminus (28). Elongation of the polymethylene chain connecting the dye to the oligonucleotide usually leads to destabilization of the hybrid complexes. Yet, in the case of the 5'-Phn derivatives of the heptanucleotide, the enthalpy and entropy of complex formation at first increases and then decreases with elongation of the linker chain from di- to heptamethylene. The complex I + III ($n = 4$) with a tetramethylene linker demonstrated the greatest stability. Its enthalpy mounted to 60 kcal/mol, whereas for complex I + III ($n = 2$) it was 7 kcal/mol lower. The difference between the ΔG values of these complexes is not as striking (~ 0.2 kcal/mol) because a pronounced enthalpy effect of the duplex I + III ($n = 4$) is compensated by a large entropy effect (23 cal/mol K). It is likely that a tetramethylene linker gives optimal conformational

freedom to the Phn residue, thus allowing maximal overlap between the heterocyclic system of the dye and the nearest base pair.

In contrast to the 5'-Phn derivatives III ($n = 2-7$), the 3'-Phn derivatives of the heptanucleotide do not have a smooth dependence of the energy of complex formation on the length of the polymethylene linker. It may only be stated that the complex I + IV ($m = 2$) is the most stable on the basis of the ΔG and T_{max} data. The analog with a trimethylene linker, on the contrary, is the least stable in the complexes I + IV ($m = 2-5$). Summarizing the thermodynamic data of complexes I + III ($n = 2-7$) and I + IV ($m = 2-5$), we discovered that complexes with an even number of methylene links are generally more stable than those with an odd number of methylene links. This fact and the expressed dependence of complex stability on the linker length were taken into account when synthesizing DNA-targeted oligonucleotide reagents (29, 30).

The complex I + V formed by the 3',5'-di-Phn derivative of heptanucleotide was the most stable among all the duplexes investigated (Figure 3, Table II). Its melting temperature was 54.8 °C. Relative to the unmodified complex I + II, the increase in free energy was 4.96 kcal/mol. It is likely that the Phn residues of oligonucleotide V affect the duplex I + V independently, as the value of the free energy change (4.96 kcal/mol) was very similar to the sum of the effects (5.43 kcal/mol) of complexes I + III ($n = 2$) and I + IV ($m = 2$). The association constant of complex I + V at 37 °C is $9.5 \cdot 10^6 \text{ M}^{-1}$, whereas the analogous value for the unmodified complex I + II is $3 \cdot 10^3 \text{ M}^{-1}$. Thus it may be possible to equalize affinities of the heptanucleotide II and its 3',5'-di-Phn derivative V during complex formation with dodecanucleotide I, if the di-Phn derivative is used at a concentration 3 orders of magnitude lower.

All the data discussed above show that introduction of a phenazine quaternary salt into oligonucleotides is an effective and promising approach for stabilization of nucleic acid complementary complexes and for directed influence on the functional activity of polynucleotide targets. So, it would not be groundless to consider Phn derivatives of oligonucleotides as promising antisense agents and for use as diagnostic probes.

LITERATURE CITED

- (1) Letsinger, R., and Schott, M. E. (1981) Selectivity in binding a phenanthridinium-dinucleotide derivative to homopolynucleotides. *J. Am. Chem. Soc.* 103, 7394–7396.
- (2) Asseline, V., Toulme, F., Thuong, N. T., Delarue, M., Montenay-Garestier, T., and Helene, C. (1984) Oligonucleotides covalently linked to intercalating dyes as base sequence-specific ligands. *EMBO J.* 3, 795–800.
- (3) Asseline, V., Delarue, M., Laucelot, G., Toulme, F., Thuong, N. T., Montenay-Garestier, T., and Helene, C. (1984) Nucleic acid-binding with high affinity and base sequence specificity: Intercalating agents covalently linked to oligodeoxynucleotides. *Proc. Natl. Acad. Sci. U.S.A.* 81, 3297–3301.
- (4) Gautier, C., Morvan, F., Rayner, B., Huynh-Dinh, T., Igolen, J., Imbach, J.-L., Paoletti, C., and Paoletti, J. (1987) α -DNA IV: α -Anomeric and β -anomeric tetrathymidylates covalently linked to intercalating oxazopyridocarbazole. Synthesis, physico-chemical properties and poly(rA) binding. *Nucleic Acids Res.* 15, 6625–6641.
- (5) Vlassov, V. V., Zarytova, V. F., Kutayin, I. V., Mamaev, S. V., and Podyminogin, M. A. (1986) Complementary addressed modification and cleavage of a single stranded DNA fragment with alkylating oligonucleotide derivatives. *Nucleic Acids Res.* 14, 4065–4076.
- (6) Le Doan, T., Perrouault, L., Praseuth, D., Habboub, N., Decout, J.-L., Thuong, N. T., Lhomme, J., and Helene, C. (1987) Sequence-specific recognition, photocrosslinking and cleavage

- of the DNA double helix by an oligo-[α]-thymidylate covalently linked to an azidoproflavine derivative. *Nucleic Acids Res.* 15, 7749-7760.
- (7) Toulme, J.-J., Krisch, H. M., Loreau, N., Thuong, N. T., and Helene, C. (1986) Specific inhibition of mRNA translation by complementary oligonucleotides covalently linked to intercalating agents. *Proc. Natl. Acad. Sci. U.S.A.* 83, 1227-1231.
 - (8) Cazenave, C., Loreau, N., Thuong, N. T., Toulme, J.-J., and Helene, C. (1987) Enzymatic amplification of translative inhibition of rabbit β -globin mRNA mediated by antimessenger oligodeoxynucleotides covalently linked to intercalating agents. *Nucleic Acids Res.* 15, 4717-4736.
 - (9) Zerial, A., Thuong, N. T., and Helene, C. (1987) Selective inhibition of the cytopathic effect of type A influenza viruses by oligonucleotides covalently linked to an intercalating agent. *Nucleic Acids Res.* 15, 9909-9919.
 - (10) Cazenave, C., Chevrier, M., Thuong, N. T., and Helene, C. (1987) Rate of degradation of [α]- and [β]-oligonucleotides in *Xenopus* oocytes. *Nucleic Acids Res.* 15, 10507-10521.
 - (11) Asseline, V., Thuong, N. T., and Helene, C. (1985) Oligonucleotides covalently linked to intercalating agents. Influence of positively substituents on binding to complementary sequences. *J. Biol. Chem.* 260, 8936-8941.
 - (12) Piles, U., and Englisch, U. (1985) Psoralen covalently linked to oligodeoxyribonucleotides: synthesis, sequence specific recognition of DNA and photo-cross-linking to pyrimidine residues of DNA. *Nucleic Acids Res.* 17, 285-291.
 - (13) Praseuth, D., Perrouault, L., Le Doan, T., Chassignol, M., Thuong, N. T., and Helene, C. (1988) Sequence-specific binding and photocrosslinking of [α] and [β]-oligodeoxynucleotides to the major groove of DNA via triple-helix formation. *Proc. Natl. Acad. Sci. U.S.A.* 85, 1349-1353.
 - (14) Perrouault, L., Asseline, U., Rivalle, C., Thuong, N. T., Bisagni, E., Giovannengeli, C., Le Doan, T., and Helene, C. (1990) Sequence-specific artificial photoinduced endonucleases based on triple helix-forming oligonucleotides. *Nature* 344, 358-360.
 - (15) Petershiem, M., and Turner, D. H. (1983) Base-stacking and base pairing contributions to helix stability: Thermodynamics of double-helix formation with CCGG, CCGGp, CCG-GAp, ACCGGp, CCGGUp and ACCGGUp. *Biochemistry* 22, 256-263.
 - (16) Shabarova, Z. A., Dolinnaya, N. G., Drutsa, V. L., Melnikova, N. P., and Pural, A. A. (1981) DNA-like duplexes with repetitions. III. Efficient template guided chemical polymerization of d(TGGGCCAAGCTp). *Nucleic Acids Res.* 9, 5747-5761.
 - (17) Berkner, K. L., and Folk, W. R. (1977) Polynucleotide kinase exchange reaction. Quantitative assay for restriction endonuclease-generated 5'-phosphoryl termini in DNAs. *J. Biol. Chem.* 252, 3176-3184.
 - (18) Zarytova, V. F., Ivanova, E. M., and Romanenko, V. P. (1983) Synthesis of oligonucleotides by phosphotriester approach in chloroform. *Bioorgan. Khimia (Russ.)* 9, 516-521.
 - (19) van Boom, J. H., and Burgers, P. M. J. (1976) Use of levulinic acid in the protection of oligonucleotides via the modified phosphotriester method: Synthesis of decaribonucleotide U-A-U-A-U-A-U-A-U-A. *Tetrahedron Lett.* 52, 4875-4880.
 - (20) Gryaznov, S. M., Gorn, V. V., Zarytova, V. F., Kumarev, V. P., Levina, A. S., Polishchuk, A. S., Potapov, V. K., Potemkin, G. A., Sredin, Yu. G., and Shabarova, Z. A. (1987) Automatic synthesis of oligodeoxyribonucleotides by phosphoramidite method at installation "Victoria-4M". *Izv. Sib. Otd. Akad. Nauk SSSR (Russ.)* 1, 119-123.
 - (21) Krynetskaya, N. F., Zayakina, G. V., Oretskaya, T. S., Volkov, E. M., and Shabarova, Z. A. (1986) Oligodeoxyribonucleotide-3'-phosphate synthesis by selective cleavage of 3'-terminal uridine. *Nucleosides Nucleotides* 5, 33-43.
 - (22) Bausk, E. V., Gorn, V. V., and Lebedev, A. V. (1985) General scheme of the solid-phase phosphotriester synthesis of 5'-phosphorylated-oligodeoxyribonucleotides on the basis of β -cyanoethyl *p*-chlorophenyl esters of *N*-acylnucleoside-5'-phosphates. *Bioorgan. Khimia (Russ.)* 11, 815-820.
 - (23) Dobrynin, V. N., Bystrov, N. S., Chernov, B. K., Severtsova, I. V., and Kolosov, M. N. (1979) Nucleophilic catalysis of phosphotriazolidine-effected phosphorylation in the triester synthesis of oligonucleotides. *Bioorgan. Khimia (Russ.)* 5, 1254-1256.
 - (24) Ambrose, B. J. B., and Pless, R. C. (1987) DNA sequencing: Chemical methods. *Methods Enzymol.* 152, 522-538.
 - (25) Knorre, D. G., Vlassov, V. V., Zarytova, V. F., and Karpova, G. G. (1986) Nucleotide and oligonucleotide derivatives as enzymes and nucleic acid targeted irreversible inhibitors. Chemical Aspects. *Advances in Enzyme Regulation* (G. Weber, Ed.) pp 277-300, Pergamon Press, Oxford.
 - (26) Swan, G. A. (1957) Phenazines. *The Chemistry of Heterocyclic Compounds*, 11 (A. Weissberger, Ed.) p 21, Interscience Publishers, New York.
 - (27) Breslauer, K. J., Frank, R., Blocker, H., and Marky, L. A. (1986) Predicting DNA duplex stability from the base sequence. *Proc. Natl. Acad. Sci. U.S.A.* 83, 3746-3750.
 - (28) Gaffney, B. L., Marky, L. A., and Jones, R. A. (1982) The influence of the purine 2-amino group on DNA conformation and stability. Synthesis and conformational analysis of d[T(2-aminoA)]₃. *Nucleic Acids Res.* 10, 4351-4361.
 - (29) Zarytova, V. F., Kutyavin, I. V., Silnikov, V. N., and Shishkin, G. V. (1986) Modification of nucleic acids in stabilized complementary complexes. I. Synthesis of alkylating derivatives of oligodeoxynucleotides having a 5'-terminal N-(2-hydroxyethyl)phenazinium residue. *Bioorgan. Khimia (Russ.)* 12, 911-920.
 - (30) Zarytova, V. F., Ivanova, E. M., Kutyavin, I. V., Sergeev, D. S., Silnikov, V. N., and Shishkin, G. V. (1989) Modification of nucleic acids in stabilized complementary complexes. III. Synthesis of oligonucleotide derivatives bearing N-(2-hydroxyethyl)phenazinium residue at their 3'-terminus. *Sib. Otd. Akad. Nauk SSSR (Russ.)* 6, 3-9.
- Registry No.** I-II, 143006-35-3; I-III *n*=2, 143036-82-2; I-III *n*=3, 143036-84-4; I-III *n*=4, 143006-37-5; I-III *n*=5, 143006-39-7; I-III *n*=6, 143006-41-1; I-III *n*=7, 143006-43-3; I-IV *m*=2, 143006-45-5; I-IV *m*=3, 143006-47-7; I-IV *m*=4, 143006-49-9; I-IV *m*=5, 143006-51-3; I-V, 143006-53-5; Phn⁺Cl⁻, 94496-01-2; (iPr)₂N-P(OCH₃)OU(Bz)₂, 118934-42-2; (DMTr)U(Ac), 142247-31-2; HO-(CH₂)₂NH₂, 141-43-5; HO(CH₂)₃NH₂, 156-87-6; HO(CH₂)₄NH₂, 13325-10-5; HO(CH₂)₅NH₂, 2508-29-4; HO(CH₂)₂NHCOCF₃, 6974-29-4; HO(CH₂)₃NHCOCF₃, 78008-15-8; HO(CH₂)₄NHCOCF₃, 128238-43-7; HO(CH₂)₅NHCOCF₃, 128238-44-8; NH₂(CH₂)₂NH₂, 107-15-3; NH₂(CH₂)₃NH₂, 109-76-2; NH₂(CH₂)₄NH₂, 110-60-1; NH₂(CH₂)₅NH₂, 462-94-2; NH₂(CH₂)₆NH₂, 124-09-4; NH₂(CH₂)₇NH₂, 646-19-5; phenazine, 92-82-0; ethylene oxide, 75-21-8; 2-[(6-aminohexyl)amino]-10-(2-hydroxyethyl)phenazinium chloride, 143036-80-0.

A Convenient and Flexible Approach for Introducing Linkers on Bifunctional Chelating Agents[†]

Martin Studer and Claude F. Meares*

Department of Chemistry, University of California, Davis, California 95616. Received July 15, 1992

The synthesis of a protected bifunctional analog of ethylenediaminetetraacetic acid (EDTA) is described. The molecule contains an aminobenzyl moiety that allows the easy attachment of the chelating agent to a wide variety of groups. Examples of reaction with the C-termini of two peptides are given. In the following paper, the two peptides are used to study the enzymatic cleavage of metal chelates from a monoclonal antibody.

INTRODUCTION

Due to their unmatched ability to form stable metal complexes with a great number of metal ions in different oxidation states, polyaminocarboxylate chelates are useful tools as probes of protein structure (1), contrast agents for magnetic resonance (2), and radiopharmaceuticals (3). In the development of bifunctional chelating agents that can be attached to biomolecules, there is still great interest in either optimizing syntheses for existing ligands (4) or developing compounds closely related to existing derivatives of ethylenediaminetetraacetic acid (EDTA) or diethylenetriaminepentaacetic acid (DTPA) (5, 6).

One problem generally encountered in such a synthesis is the high susceptibility of EDTA and DTPA derivatives to metal contamination after carboxymethylation of the amine precursors (7). Therefore, they have to be handled with extreme care to ensure that the ligand in the final product is still able to bind the desired metal ion. The poor solubility in solvents other than water is another drawback of polyaminocarboxylates. This limits considerably the chemistry that can be done with these compounds. The aminobenzyl group for example, often used as a precursor for linkages, is a poor nucleophile in aqueous solution. Highly reactive compounds like bromoacetyl bromide (8) or thiophosgene (9) must therefore be used to modify the amine.

To avoid such difficulties and to have a more versatile starting compound, we sought an alternative to the classical carboxymethylation. We decided to prepare an inert ester derivative of the well-known (*p*-aminobenzyl)-EDTA (3), following the suggestions of the literature (10-13). To show one of many possible applications of this new molecule, we linked it to an Ala-Leu-Ala-Leu moiety, which is known to be cleaved by liver peptidases *in vivo* and *in vitro* (14). By introducing such a peptide fragment we hoped to obtain a metal chelate that is easily separated from the antibody by enzymes in the liver (15), a strategy believed to improve the excretion of undesired radioactivity (16).

EXPERIMENTAL PROCEDURES

General. Proton NMR spectra were recorded on a General Electric QE 300 spectrometer at 300 MHz.

* Address correspondence to the author at the following address: Department of Chemistry, University of California, Davis, CA 95616. Phone: 916-752-0936. Fax: 916-752-8938.

[†] Abbreviations used: L-alanyl-L-leucine (Ala-Leu); *N*-(carbobenzoyloxy)-L-alanyl-L-leucine (CBZ-Ala-Leu); 1-hydroxybenzotriazole (HOBt); 1,3-dicyclohexylcarbodiimide (DCC).

Chemical shifts are relative to either HDO (4.70 ppm) or residual CHCl₃ (7.21 ppm). Mass spectra and exact mass measurements were obtained on a ZAB-HS-2F mass spectrometer (VG analytical instruments).

Chromatography. Thin-layer chromatography (TLC) was run on plastic-backed silica gel plates (Kieselgel 60 F₂₅₄, EM Science). For syntheses, various systems were used as described with individual experiments. For the metal-binding assays, a 10% (w/v) ammonium acetate/methanol (1:1 v/v) solution was used as the eluent (9).

Radiation Counting. γ -Counting was done in a Beckman Model 310 counter. TLC plates containing radiolabeled materials were visualized with an AMBIS radioanalytic imaging system. The HPLC effluent was counted by a flow-through Beckman 170 radioisotope detector.

Data Acquisition. Data acquisition (output of UV and radioactivity detectors) was done with a MacPacq unit (Biopac Systems) connected to a Macintosh computer.

Reagents. Pure water (18 M Ω cm⁻¹) was employed throughout. Carrier-free ⁵⁷CoCl₂ was obtained from ICN. (*S*)-1-(*p*-nitrobenzyl)ethylenediamine (1 (17)) was synthesized according to DeRiemer et al. (18). BrCH₂COOC(CH₃)₃, palladium on charcoal, and BrCH₂COBr were purchased from Aldrich Chemical Co.; 1-hydroxybenzotriazole (HOBt), 1,3-dicyclohexylcarbodiimide (DCC), L-alanyl-L-leucine (Ala-Leu), and *N*-(carbobenzoyloxy)-L-alanyl-L-leucine (CBZ-Ala-Leu) were from Sigma Chemical Co.; citric acid and CF₃COOH were from Fisher Scientific; silica gel (60-200 mesh) was from J. T. Baker.

Preparation of (*p*-Nitrobenzyl)-EDTA Tetra-*tert*-butyl Ester (2). To (*p*-nitrobenzyl)ethylenediamine dihydrochloride (1; 1.76 g, 6.56 mmol), suspended in 50 mL of dry CH₃CN, were added K₂CO₃ (4.66 g, 33.5 mmol) and KI (1.12 g, 6.75 mmol). While the reaction mixture was being stirred, BrCH₂COOC(CH₃)₃ (5.50 mL, 34.0 mmol) was added, and the reaction mixture was refluxed for 120 h in the dark. The mixture was evaporated to dryness, and, after treating it with 20 mL of CHCl₃, filtered through a glass frit (4.5 cm diameter, containing 2 cm of silica gel). The frit was washed with 500 mL of CHCl₃. The volume of the filtrate was reduced to 10 mL. The purification was carried out on an open silica gel column (35 \times 3.5 cm) eluted with CHCl₃. The fractions containing pure product (TLC *R*_f 0.3, CHCl₃/ethyl acetate 10:1) were collected and dried to give the yellow oil 2 (2.50 g, 3.84 mmol, 58%). ¹H NMR (CDCl₃): δ 1.20-1.50 (m, 36 H), 2.40 (m, 1 H), 2.80-3.50 (m 12 H), 7.40 (d, 2 H), 8.05 (d, 2 H). MS *m/e* for C₃₃H₅₃N₃O₁₀ (M + H⁺): 652.

Preparation of (*p*-Aminobenzyl)-EDTA Tetra-*tert*-butyl Ester (3). Compound 2 (110 mg, 0.169 mmol) was

dissolved in 3 mL of dry tetrahydrofuran (THF), and K_2CO_3 (30 mg, 0.217 mmol) and 10% palladium on charcoal (30 mg) were added. The reaction vessel was attached to an atmospheric-pressure hydrogenation apparatus. The mixture was purged with N_2 , and then filled with H_2 , and the reaction was stirred at 25 °C. The course of the reaction was monitored by the H_2 uptake. After 20 h, the solution was filtered through a glass frit (as for 2). The frit was washed with 100 mL of THF. The filtrate, positive to a test for primary amines using fluorescamine (19), was evaporated to dryness to give 3 (70 mg, 0.113 mmol, 67%). TLC R_f 0.3, $CHCl_3$ /ethyl acetate 3:1. 1H NMR ($CDCl_3$): δ 1.35–1.50 (m, 36 H), 2.40–2.60 (m, 2 H), 2.70–2.85 (m, 2 H), 3.05 (m, 1 H), 3.40–3.50 (m, 8 H), 6.55 (d, 2 H), 6.95 (d, 2 H). MS m/e for $C_{33}H_{55}N_3O_8$ ($M + H^+$): 622.

Preparation of CBZ-Ala-Leu-Ala-Leu (4). CBZ-Ala-Leu (0.50 g, 1.49 mmol) and HOBT· H_2O (228 mg, 1.49 mmol) were dissolved in 20 mL of dry N,N -dimethylformamide (DMF). After cooling to 0 °C, DCC (313 mg, 1.52 mmol) was added, and the mixture was held at 0 °C for 2.5 h and then at 25 °C for 4.5 h. Ala-Leu (340 mg, 1.68 mmol) was added, and the mixture was kept at room temperature for 10 h. After evaporation to dryness, the semisolid was taken up in 80 mL of ethyl acetate and 50 mL of aqueous citric acid (10% by weight) and transferred into a separatory funnel. The organic layer was extracted with citric acid (10% by weight, 3 × 30 mL) and saturated NaCl solution (10 mL). The ethyl acetate was dried over anhydrous Na_2SO_4 and evaporated to dryness to give 4 (0.60 g, 1.15 mmol, 77%). 4 was used without any further purification. MS m/e for $C_{26}H_{40}N_4O_7$ ($M + H^+$): 521.

Preparation of [*p*-(CBZ-Ala-Leu-Ala-Leu-amido)benzyl]-EDTA Tetra-*tert*-butyl Ester (5) and [*p*-(CBZ-Ala-Leu-amido)benzyl]-EDTA Tetra-*tert*-butyl Ester (9). Compound 4 (500 mg, 0.960 mmol) and HOBT· H_2O (160 mg, 1.04 mmol) were dissolved in 10 mL of dry DMF. After cooling to 0 °C, DCC (202 mg, 0.979 mmol) was added, and the mixture was held at 0 °C, for 2.5 h and then at 25 °C for 4.5 h. After the addition of 3 (715 mg, 1.15 mmol), dissolved in 10 mL of THF, the mixture was stirred for 16 h at 25 °C. The reaction was then evaporated to dryness; the semisolid was taken up in 80 mL of ethyl acetate and 50 mL of saturated K_2CO_3 and transferred into a separatory funnel. The organic layer was extracted with saturated K_2CO_3 (3 × 50 mL) and saturated NaCl solution (30 mL). The ethyl acetate was dried over anhydrous Na_2SO_4 and evaporated to dryness. The resulting yellow oil was dissolved in $CHCl_3$ and purification was carried out on an open silica gel column (50 × 2 cm) step eluted with 350 mL of $CHCl_3$, 350 mL of $CHCl_3$ /ethyl acetate (1:1), and 350 mL of ethyl acetate. The fractions containing pure product 5 (TLC R_f 0.2, ethyl acetate) were collected and dried (470 mg, 0.42 mmol, 44%). 1H NMR ($CDCl_3$): δ 0.90 (m, 12 H), 1.30–1.80 (m, 48 H), 2.55 (m, 2 H), 2.80 (m, 2 H), 3.10 (m, 1 H), 3.40–3.55 (m, 8 H), 4.20–4.70 (m, 4 H), 5.20 (s, 2 H), 7.10 (m, 2 H), 7.35 (m, 5 H), 7.70 (d, 2 H). MS m/e for $C_{59}H_{93}N_7O_{14}$ ($M + H^+$): 1125. The presence of a small amount of CBZ-Ala-Leu in the starting material 4 led to side product 9 (TLC R_f 0.55, ethyl acetate), which was collected and dried (100 mg, 0.106 mmol). 1H NMR ($CDCl_3$): δ 0.90 (m, 6 H), 1.20–1.90 (m, 42 H), 2.50–2.70 (m, 2 H), 2.75–3.00 (m, 2 H), 3.15 (m, 1 H), 3.35–3.55 (m, 8 H), 4.25 (m, 1 H), 4.55 (m, 1 H), 5.15 (s, 2 H), 5.35 (d, 1 H), 6.60 (d, 2 H), 7.15 (d, 2 H), 7.35 (m, 5 H), 7.50 (d, 2 H), 8.35 (s, 1 H). MS m/e for $C_{50}H_{77}N_5O_{12}$ ($M + H^+$): 941.

Preparation of [*p*-(Ala-Leu-Ala-Leu-amido)benzyl]-EDTA Tetra-*tert*-butyl Ester (6). Compound 5

(150 mg, 0.133 mmol) was dissolved in 5.5 mL of THF. After addition of 10% palladium on charcoal (30 mg) and K_2CO_3 (30 mg, 0.217 mmol), the reaction vessel was attached to an atmospheric-pressure hydrogenation apparatus. The mixture was purged with N_2 and then filled with H_2 . After 1 h, the solution was filtered through a glass frit (as for 2); the frit was washed with 500 mL of methanol. The filtrate, now positive to a test for primary amines using fluorescamine (19), was evaporated to dryness to give 6 (130 mg, 0.131 mmol, 99%). 1H NMR ($CDCl_3$): δ 0.80–1.00 (m, 12 H), 1.20–1.60 (m, 48 H), 2.20–3.50 (m, 13 H), 3.80–4.65 (m, 4 H), 6.95 (m, 2 H), 7.75 (d, 2 H). MS m/e for $C_{51}H_{87}N_7O_{12}$ ($M + Na^+$): 1012.

Preparation of [*p*-(Bromoacetyl)-Ala-Leu-Ala-Leu-amido]benzyl]-EDTA Tetra-*tert*-butyl Ester (7). Compound 6 (100 mg, 0.101 mmol) was dissolved in 10 mL of THF. While the reaction mixture stirred at room temperature, K_2CO_3 (374 mg, 2.71 mmol) and $BrCH_2COBr$ (0.175 mL, 2.02 mmol) were added in 3 portions over 3 h. Absolute ethanol (0.50 mL) was added, and after 1 h the mixture was filtered and evaporated to dryness under reduced pressure. Purification was carried out on an open silica gel column (40 × 2.5 cm), which was step eluted with 300 mL of ethyl acetate and 600 mL of ethyl acetate/methanol (1:1). UV-absorbing fractions that were also positive to a test for alkylating agents using 4-(*p*-nitrobenzyl)pyridine (20) were pooled and evaporated to dryness to give 7 (36 mg, 0.0324 mmol, 32%). 1H NMR ($CDCl_3$): New peak at δ 3.85 (s, 2 H) from $BrCH_2COR$. MS m/e for $C_{53}H_{88}BrN_7O_{13}$ ($M + Na^+$): 1134 (the typical two peaks for bromine compounds were observed).

Preparation of [*p*-(Bromoacetyl)-Ala-Leu-Ala-Leu-amido]benzyl]-EDTA (8). Compound 7 (15 mg, 0.014 mmol) was dissolved in 3 mL of neat CF_3COOH . After stirring for 3 h at room temperature, the mixture was evaporated to dryness. Addition of 0.5 mL of CH_3CN and 0.5 mL of H_2O gave a solution of 8 (still showing a positive test for alkylating agents (20)) that was frozen and stored at –80 °C. Yield of 8: 6.35 μ mol (47%), using the extinction coefficient of *p*-acetotoluidide (21) (λ_{max} = 244 nm, ϵ = 17724 $M^{-1} cm^{-1}$, concentration of 8: 6.35 mM). The metal binding capacity of the solution of 8 was determined to be 3.35 mM. 1H NMR (D_2O): The peak for the *tert*-butyl group disappeared, and the typical pattern for the Ala-Leu-Ala-Leu side chains was observed. The mass spectrum of this compound could not be obtained due to the low sensitivity of the instrument to alkyl bromides. Therefore, 8 was converted to the glycinamido derivative by stirring 50 μ L of 3.35 mM 8 with 50 μ L of 28–30% aqueous NH_4OH for 3 h at room temperature. The solution was lyophilized and redissolved in water. MS m/e for $C_{37}H_{58}N_8O_{13}$ ($M + Na^+$): 845.

Preparation of [*p*-(Ala-Leu-amido)benzyl]-EDTA Tetra-*tert*-butyl Ester (10). Compound 9 (5 mg, 9.53 μ mol) was dissolved in 5 mL of THF. After addition of 10% palladium on charcoal (10 mg) and K_2CO_3 (10 mg, 0.0724 mmol), the reaction vessel was attached to an atmospheric-pressure hydrogenation apparatus. The mixture was purged with N_2 and filled with H_2 . After 40 h at 25 °C, the solution was filtered. The filtrate, now positive to a test for primary amines using fluorescamine (19), was evaporated to dryness to give 10 (3 mg, 3.7 μ mol, 70%). 1H NMR ($CDCl_3$): 0.80–1.00 (m, 12 H), 1.20–1.60 (m, 48 H), 2.20–3.50 (m, 13 H), 3.80–4.65 (m, 2 H), 6.95 (m, 2 H), 7.75 (d, 2 H). MS m/e for $C_{42}H_{71}N_5O_{10}$ ($M + H^+$): 806.

Preparation of [*p*-(Ala-Leu-amido)benzyl]-EDTA (11). Compound 10 (3 mg, 3.7 μ mol) was dissolved in 2

ACKNOWLEDGMENT

We thank Habibe Diril, Michael McCall, and Tariq Rana for helpful discussions. Supported by Research Grant CA 16861 to C.F.M. and by Program Project CA 47829 (G.L. DeNardo, P.I.) from the National Cancer Institute, National Institutes of Health.

LITERATURE CITED

- (1) Rana, T. M., and Meares, C. F. (1990) Specific Cleavage of a Protein by an Attached Iron Chelate. *J. Am. Chem. Soc.* 112, 2457-2458.
- (2) Meares, C. F., and Wensel, T. G. (1984) Metal Chelates as Probes of Biological Systems. *Acc. Chem. Res.* 17, 202-209.
- (3) Lauffer, R. B. (1987) Paramagnetic Metal Complexes as Water Proton Relaxation Agents for NMR Imaging: Theory and Design. *Chem. Rev.* 87, 901-927.
- (4) Sundberg, M. W., Meares, C. F., Goodwin, D. A., and Diamanti, C. I. (1974) Selective Binding of Metal Ions to Macromolecules Using Bifunctional Analogs of EDTA. *J. Med. Chem.* 17, 1304-1307.
- (5) Gaudreault, R. C., and Noujaim, A. A. (1989) An improved synthesis of 1-(4-nitrobenzyl)-1,2-ethylenediamine, precursor of the corresponding ethylenediaminetetraacetic acid. *Org. Prep. Proc. Int.* 21 (5), 643-645.
- (6) Westerberg, D. A., Carney, P. L., Rogers, P. E., Kline, S. J., and Johnson, D. K. (1989) Synthesis of Novel Bifunctional Chelators and Their Use in Preparing Monoclonal Antibody Conjugates for Tumor Targeting. *J. Med. Chem.* 32, 236-243.
- (7) Keana, J. F. W., and Mann, J. S. (1990) Chelating Ligands Functionalized for Facile Attachment to Biomolecules. A Convenient Route to 4-Isothiocyanatobenzyl Derivatives of Diethylenetriaminepentaacetic Acid and Ethylenediaminetetraacetic Acid. *J. Org. Chem.* 55, 2868-2871.
- (8) Meares, C. F. (1986) Chelating Agents for the Binding of Metal Ions to Antibodies. *Nucl. Med. Biol., Int. J. Radiat. Appl. Instrum., Part B* 13, 311-318.
- (9) Mukkala, V. M., Mikola, H., and Hemmila, I. (1989) The Synthesis and Use of Activated *N*-Benzyl Derivatives of Diethylenetriaminepentaacetic Acids: Alternative Reagents for Labeling of Antibodies with Metal Ions. *Anal. Biochem.* 176, 319-325.
- (10) Meares, C. F., McCall, M. J., Reardan, D. T., Goodwin, D. A., Diamanti, C. I., and McTigue, M. (1984) Conjugation of Antibodies with Bifunctional Chelating Agents: Isothiocyanate and Bromoacetamide Reagents, Methods of Analysis, and Subsequent Addition of Metal Ions. *Anal. Biochem.* 142, 68-78.
- (11) Liberatore, F. A., Comeau, R. D., McKearin, J. M., Pearson, D. A., Belonga, B. Q., III, Brocchini, S. J., Kath, J., Phillips, T., Oswell, K., and Lawton, R. G. (1990) Site-Directed Chemical Modification and Cross-Linking of a Monoclonal Antibody Using Equilibrium Transfer Alkylating Cross-Link Reagents. *Bioconjugate Chem.* 1, 36-60.
- (12) Sergheraet, C., Mäes, P., and Tartar, A. (1986) Specific Covalent Fixation of Chelating Agents on Peptides. *J. Chem. Soc. Perkin Trans. 1*, 1061-1064.
- (13) Arya, R., and Gariépy, J. (1991) Rapid Synthesis and Introduction of a Protected EDTA-like Group during the Solid-Phase Assembly of Peptides. *Bioconjugate Chem.* 2, 323-326.
- (14) Cuenoud, B., and Schepartz, A. (1991) Synthesis of *N*- α -BOC-*N*- ϵ -tribenzyl EDTA-L-Lysine. An amino acid analogue suitable for solid phase peptide synthesis. *Tetrahedron* 47, 2535-2542.
- (15) Trouet, A., Masquelier, M., Baurain, R., and Deprez-De Campeneere, D. (1982) A covalent linkage between daunorubicin and proteins that is stable in serum and reversible by lysosomal hydrolases, as required for a lysosomotropic drug-carrier conjugate: *In vitro* and *in vivo* studies. *Proc. Natl. Acad. Sci. U.S.A.* 79, 626-629.
- (16) Studer, M., Meares, C. F., DeNardo, S. J., Kukis, D. L., and Kroger, L. A. (1992) Influence of a Peptide Linker on Biodistribution and Metabolism of Antibody Conjugated Benzyl-EDTAs. Comparison of Enzymatic Digestion in Vitro and in Vivo. *Bioconjugate Chem.*, following paper in this issue.
- (17) Deshpande, S. V., DeNardo, S. J., Meares, C. F., McCall, M. J., Adams, G. P., and DeNardo, G. L. (1989) Effect of Different Linkages Between Chelates and Monoclonal Antibodies on Levels of Radioactivity in the Liver. *Nucl. Med. Biol.* 6, 587-597.
- (18) For compounds 1-11, see also Scheme I.
- (19) DeRiemer, L. H., Meares, C. F., Goodwin, D. A., and Diamanti, C. I. (1981) BLEDTA II: Synthesis of a new tumor-visualizing derivative of cobalt(III)-bleomycin. *J. Labelled Compds. Radiopharm.* 18, 1517-1534.
- (20) Udenfriend, S., Stein, S., Bohlen, P., Wallace, D., Leimgruber, W., and Weigle, M. (1972) Fluorescamine: A reagent for assay of amino acids, peptides, proteins and primary amino acids in the picomolar range. *Science (Washington, DC)* 178, 871-872.
- (21) Kramer, S. P., Goodman, L. E., Dorfman, H., Solomon, R., Gutenberg, A. M., Pineda, E., Nason, L. L., Ulfohn, A., Gaby, S. D., Bakal, D., Williamson, C. E., Miller, J. I., Sass, S., Witten, B., and Seligman, A. M. (1963) Enzyme alterable alkylating agents VI. Synthesis, chemical properties, toxicities and clinical trial of haloacetates and haloacetamides containing enzyme susceptible bonds. *J. Natl. Cancer Inst.* 31, 297-326.
- (22) The Sadtler Standard Spectra, Published by Sadtler Research Laboratories, Subsidiary of Block Engineering, 3316 Spring Garden Street, Philadelphia, P.A., 19104, Spectrum UV 832, Recorded 1960.
- (23) Alner, D. J., Claret, P. A., and Osborne, A. G. (1972) Esterification of Ethylenediaminetetraacetic Acid. *J. Appl. Chem. Biotechnol.* 22, 1267-1276.
- (24) Mitchell, A. A., Verlander, M. S., and Goodman, M. (1980) Synthesis of 6-Aminoisoproterenol. *J. Org. Chem.* 45, 2750-2753.
- (25) *Methoden der Organischen Chemie (Houben Weyl)*, Band IV/1c (H. Kropf, Ed.) vierte Auflage (1980) Georg Thieme Verlag, Stuttgart.
- (26) Bodansky, M. (1988) *Peptide Chemistry, A Practical Textbook*, Springer Verlag, Berlin.
- (27) Bergmann, M., and Zervas L. (1932) A General Process for the Synthesis of Peptides. *Ber. Dtsch. Chem. Ges.* 65, 1192-1201.

Registry No. 1, 96813-21-7; 2, 143106-45-0; 3, 143106-46-1; 4, 143106-47-2; 5, 143106-48-3; 6, 143106-49-4; 7, 143106-50-7; 8, 143106-51-8; 9, 143106-52-9; 10, 143106-53-0; 11, 143106-54-1; BrCH₂COOC(CH₃)₃, 5292-43-3.

Influence of a Peptide Linker on Biodistribution and Metabolism of Antibody-Conjugated Benzyl-EDTA. Comparison of Enzymatic Digestion in Vitro and in Vivo

Martin Studer,[†] Linda A. Kroger,[‡] Sally J. DeNardo,[‡] David L. Kukis,[†] and Claude F. Meares^{*†}

Departments of Chemistry and Medicine, University of California, Davis, California 95616. Received July 15, 1992

Insight into the metabolism of radiolabeled antibodies is important for the design of better radioimaging and therapy agents. To test the effect of linkers that can be cleaved in vivo, we introduced Ala-Leu-Ala-Leu between the antibody Lym-1 and an ¹¹¹In-labeled benzyl-EDTA. For comparison, we studied a conjugate without the linker. Digestion of the two conjugates in vitro showed that the one with Ala-Leu-Ala-Leu was cleaved rapidly by the liver protease cathepsin B₁ ($T_{1/2} \approx 6$ h). After 100 h of digestion, reversed-phase HPLC product analysis of the Ala-Leu-Ala-Leu conjugate showed that 48% of the total radioactivity had the same retention time as (*p*-aminobenzyl)-EDTA(In), and 37% of the total radioactivity had the same retention time as [*p*-(Ala-Leu-amido)benzyl]-EDTA(In). After 97 h of digestion, the conjugate without the linker had 79% of the radioactivity activity still attached to the protein. We also tested the two conjugates in mice. Ala-Leu-Ala-Leu had only a moderate effect on the whole body and liver clearance in vivo. The excretion of the radioactivity was about 6% per day with the linker and about 3% per day without the linker. HPLC analysis of the urine of a single mouse showed products similar to the in vitro study; 54% of the excreted radioactivity had the same retention time as (*p*-aminobenzyl)-EDTA(In), while 10% had the retention time of [*p*-(Ala-Leu-amido)benzyl]-EDTA(In).

INTRODUCTION

Monoclonal antibodies are widely used for targeting cells, especially in the field of cancer diagnosis (1) and treatment (2). Due to their favorable physical properties, radioisotopes like ¹¹¹In, ^{99m}Tc, ⁶⁷Cu, and ⁹⁰Y are primary candidates for attachment to biomolecules. With the proper choice of chelating agents, these metal ions can be complexed in stable form in vivo, with only minimal loss from the antibody over days and even weeks (3). However, in contrast to radioiodinated antibodies, a significant fraction of the metallic radionuclides remains in the liver for an extended period (4-6). This decreases the target/nontarget ratio for imaging, and lowers the applicable dose for radiotherapy.

Several investigators have considered new approaches to lower the liver concentration of the radiopharmaceutical. Beatty et al. (7) showed that the liver accumulation can be reduced by pretreatment of the mice with unlabeled antibody. Paganelli et al. (8) biotinylated their antibodies, and let the unbound fraction clear before locating the bound part with a radiolabeled avidin. Rodwell (9) suggested reducing the size of the radioactive fragment to accelerate blood clearance.

Another promising route is the use of a cleavable linker between the protein and the chelating agent (10-12). Ester, peptide, thiourea, and disulfide linkers were investigated in the hope that they would be cleaved in the liver. The results showed that the liver clearance indeed depends on the linker. However, the observed effects were relatively small. Using ¹¹¹In complexes of benzyl-EDTA, Deshpande et al. (10) found with an Ala-Leu-Ala-Leu-Gly linker approximately 20% ID/g (injected dose/gram), and with a thiourea linker approximately 10% ID/g in the liver

during the whole 72-h period of their experiment. The desired fast liver clearance did not occur. Paik et al. (11) compared DTPA linked either by a diester or by the conventional amide bond formed by DTPA cyclic anhydride (13). Even though they found a somewhat improved tumor/blood ratio for the diester linker, the liver concentrations were still 6-9% ID/g. Since the absolute concentration of the radioactivity is lowered uniformly, the faster clearance is probably attributable to a decreased overall stability of the conjugate. Haseman et al. (12) also found with their ester-linked bifunctional chelate an increase in the tumor to blood ratio, but at the expense of an absolute decrease in tumor uptake and with only a small reduction in the liver concentration.

To gain better insight into what happens to chelate-tagged proteins in the liver, it is important to know what metabolic products are formed, and how the linkers are processed. Deshpande et al. (10, 14) could show that the radioactivity excreted in the urine was still essentially all bound by the chelator. More detailed information on the cleavage site of the chelate was not obtained. Jones et al. (15) injected ¹²⁵I (Iodogen method) and ¹¹¹In (cyclic DTPA method) labeled monoclonal antibodies into rats. They isolated the liver cells at different times to investigate the speed and the products of the metabolism. The rate of catabolism of the intact antibody was similar in both cases. However, the clearance from the liver was much more effective for the ¹²⁵I-labeled protein. The ¹¹¹In seemed to be trapped as low molecular weight In complexes (<1000 g/mol). The authors hypothesized that the main products were unaltered chelate complexes with one or more amino acids attached, but they were not identified.

In this study, we compared two antibody conjugates: one had a peptide Ala-Leu-Ala-Leu linker that is known to speed up drug metabolism in the liver (16) and another lacked this feature. We kept the conditions for the modification and the workup procedure as similar as practical. By attaching in both cases a bromoacetamido chelate to a 2-iminothiolane (2IT) modified protein, we

* Address correspondence to the author at the following address: Department of Chemistry, University of California, Davis, CA 95616. Phone: 916-752-0936. Fax: 916-752-8938.

[†] Department of Chemistry.

[‡] Department of Medicine.

aimed to obtain modified antibodies differing *only* in the linkages and not in other respects, such as number of chelates, amino acid side chain modified, and the location thereof. Since variations of this kind may have accounted for some of the measured effects in previously described work, we hoped to get a clearer determination of the influence of a cleavable linker by our approach.

Therefore, we examined the *in vitro* digestion of the labeled antibodies by proteases that are abundant in the liver (17). In parallel, we also investigated the metabolism of the same compounds in mice to get insight into the processing of the proteins and the linkers *in vivo*.

EXPERIMENTAL PROCEDURES

Chromatography. Thin-layer chromatography (TLC) was run on plastic-backed silica gel plates (Kieselgel 60 F₂₅₄, EM Science). For the analysis of the cathepsin digests and for the metal-binding assays, a 10% (w/v) ammonium acetate/methanol (1:1 v/v) mobile phase was used for the silica plates (18). Gel-filtration HPLC of the labeled immunoconjugates was performed on a TSK 3000SW (Bio-Rad) eluted with 0.1 M sodium phosphate buffer at pH 7.4 (1 mL/min). The fractions with a retention time from 9 to 11.5 min (molecular weight ca. 150 000 g/mol) were collected. Reversed-phase HPLC analysis of cathepsin digests and of mouse urine was run on a C₁₈ column (Dynamax A 300) with linear gradients. For the cathepsin digests, it was 20 min from 0.1 M ammonium acetate (pH 7.2) to 100% methanol with a flow of 1 mL/min. For the mouse urine it was 20 min from 0.1 M ammonium acetate (pH 7.2) to 66% methanol with a flow of 1.5 mL/min. An ISCO Model UA-5 detector (254 nm) was used for UV detection.

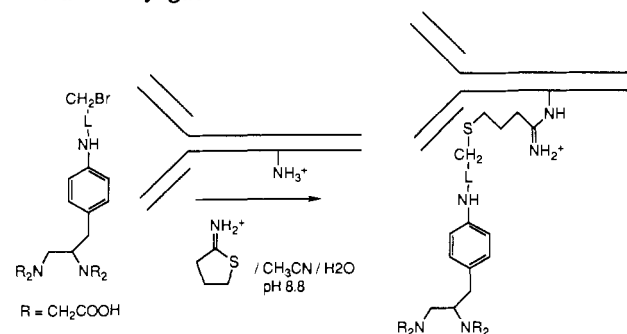
Radiation Counting. γ -Counting was done in a Beckman Model 310 counter. TLC plates containing radiolabeled materials were visualized with an AMBIS radioanalytic imaging system. The HPLC effluent was counted by a flow through Beckman 170 radioisotope detector.

Data Acquisition. Data acquisition (UV and radioactivity detectors) was done with a MacPac unit (Biopac Systems) connected to a Macintosh computer.

Reagents. Lym-1, an anti B cell lymphoma IgG_{2a} mAb (19), was obtained from Damon Biotech (Needham Heights, MA 02194; Encapcel murine Ab, lot #3-171-850718A). Pure water (18 M Ω cm⁻¹) was employed throughout. Carrier-free ¹¹¹InCl₃, ¹¹⁴InCl₃, and ⁶⁷CoCl₂ were purchased from Mallinckrodt, Du Pont, and ICN, respectively; cathepsin B₁ (EC 3.4.22.1), cathepsin D (EC 3.4.23.5), 2-iminothiolane (2IT), human serum albumin, and dithiothreitol (DTT) from Sigma Chemical Co.; citric acid, disodium ethylenediaminetetraacetic acid (disodium EDTA), and CF₃COOH from Fisher Scientific. (S)-1-[p-(Bromoacetamido)benzyl]-EDTA (BABE, see also Scheme I) was synthesized from (S)-1-(p-aminobenzyl)-EDTA (18) (ABE) according to Mukkala et al. (20) and McCall et al. (21). [p-(Alanyl-L-leucinamido)benzyl]-EDTA (AL-ABE) and [p-[(bromoacetyl)-L-alanyl-L-leucyl-L-alanyl-L-leucinamido]benzyl]-EDTA (BALAL-ABE) were prepared as described previously (22). All other reagents were at least reagent grade.

Labeling of ABE and AL-ABE (HPLC Standards) with ^{114m}In. ABE (5 mg, 3 μ mol) and AL-ABE (2 mg, 3.4 μ mol) were dissolved in 0.2 mL of 0.1 M sodium citrate buffer, pH 5.5, each. To both solutions was added 1 μ L of ^{114m}In (5 mCi/mL) in 0.5 M HCl. TLC analysis showed that after 30 min all the ^{114m}In was bound by the chelates. These preparations were used directly as HPLC standards.

Scheme I. Structure and Preparation of Antibody-Chelate Conjugates with Different Linkers.



^a L-NH stands for CO-NH (Lym-1-2IT-BABE) and for CO-Ala-Leu-Ala-Leu-NH (Lym-1-2IT-BALAL-ABE).

Lym-1-2IT-BABE Conjugations. The Lym-1 antibody solution (15–20 mg/mL) was prepared for conjugation with a centrifuged gel-filtration column (18, 23) (0.1 M sodium phosphate, pH 8.0, as column buffer). To the collected effluent was added, in order, BABE in aqueous solution, freshly prepared 2IT in 50 mM triethanolamine hydrochloride (pH 8.7), and acetonitrile (final approximate concentrations: 0.1 mM Lym-1, 2 mM BABE, 1 mM 2IT, 28% acetonitrile, v/v). Acetonitrile was included here so that the conditions for the conjugation would be comparable to the peptide-chelate conjugation. The pH of the solution was adjusted to 8.8 and the solution was incubated at 37 °C for 30 min. A Centricon apparatus (Amicon, Danvers, MA 01923) was used to remove the excess reagents and to change the buffer to 0.1 M ammonium citrate, pH 5.5. TLC analysis showed that the product was free from unbound chelate. A metal-binding assay (18) showed 1.4 chelates/antibody.

Lym-1-2IT-BALAL-ABE Conjugations. Conjugation using BALAL-ABE was done as above, except that the final pH was 8.7, the final acetonitrile concentration was 33% (v/v), and the final number of chelates/antibody was 1.6.

Labeling of the Immunoconjugates with ¹¹¹In. Two samples (4.6 mCi and 4.5 mCi) of ¹¹¹InCl₃ in 0.5 M HCl were dried at 80 °C under a gentle flow of N₂. Lym-1-2IT-BALAL-ABE (3.0 nmol dissolved in 230 μ L of 0.1 M ammonium citrate buffer, pH 5.5) and Lym-1-2IT-BABE (4.8 nmol in 99 μ L of the same buffer) were added to the dried ¹¹¹InCl₃ aliquots and incubated for 30 min at 25 °C. Na₂EDTA solution (10 mM final EDTA) was added to bind any previously unchelated ¹¹¹In, and after 5 min, 25% human serum albumin solution (1% final concentration) was added. The unbound ¹¹¹In and the other small molecules were removed with a centrifuged gel-filtration column (18, 23) (0.25% sterile saline as final medium). The conjugates were assayed to contain 7.7 mCi/mg (1.1 mCi/nmol) and 3.9 mCi/mg (0.60 mCi/nmol) ¹¹¹In; the final antibody concentrations were 1.5 mg/mL (9.7 μ M) and 4.9 mg/mL (32 μ M). The radiolabeling yields were 69% and 64%. It was shown by TLC that the products did not contain any ¹¹¹In that could be removed by 10 mM EDTA in 5 min at 25 °C. The labeled immunoconjugates were purified by HPLC as described above. The fractions containing the antibody monomer were diluted using 0.1 M sodium phosphate buffer at pH 7.4 to obtain final protein concentrations of 96 μ g/mL (235 μ Ci/mL) and 120 μ g/mL (and 150 μ Ci/mL), respectively.

In Vitro Digestion of Lym-1 Conjugates with Cathepsin B₁ and Cathepsin D. All experiments were run in triplicate. To 14 μ L of aqueous solutions of cathepsin B₁ (activity 1.08 units/mL (24)) or cathepsin D

Table I. Concentrations and Conditions for in Vitro Digestion^a

component	PB	PD	BB	BD	PBC	PDC	BBC	BDC
peptide conjugate (nM)	7.7	7.7	—	—	7.7	7.7	—	—
BABE conjugate (nM)	—	—	9.7	9.7	—	—	9.7	9.7
chelate (nM)	12	12	15	15	12	12	15	15
cathepsin B ₁ (unit/mL)	0.27	0.27	—	—	—	—	—	—
cathepsin D (unit/mL)	—	—	0.13	0.13	—	—	—	—

^a PB stands for Lym-1-2IT-BALAL-ABE exposed to cathepsin B₁, PD for Lym-1-2IT-BALAL-ABE exposed to cathepsin D, BB for Lym-1-2IT-BABE exposed to cathepsin B₁, BD for Lym-1-2IT-BABE exposed to cathepsin D. The same nomenclature applies to the controls (#C, same conditions, no enzymes added). The solutions were 7.5 mM in DTT and 75 mM in tetramethylammonium acetate, and the pH was 4.9–5.0 in all experiments.

(activity 0.50 unit/mL (25)) were added 14 μ L of 30 mM DTT and 14 μ L of 0.3 M tetramethylammonium acetate buffer, pH 4.8. After a 10-min incubation at 25 °C, 7 μ L of ¹¹¹In-labeled Lym-1-2IT-BALAL-ABE or Lym-1-2IT-BABE conjugates and 7 μ L of H₂O were added to give the approximate final concentrations listed in Table I.

At 0.17, 1, 12, 23, 47, and 97 h, 5- μ L aliquots were removed and spotted on a silica TLC plate. After drying of the plates, the TLC's were run immediately with 10% (w/v) ammonium acetate/methanol (1:1 v/v) as the eluent. Analysis was performed on an AMBIS radioanalytic imaging system (see Figure 1). Under the chosen TLC conditions, chelates cleaved from the protein had R_f 0.8, while the complexes still attached to the protein or a large fragment thereof remained at the origin.

Mouse Study. Healthy Balb/c mice (Simonson), fed Purina rodent chow ad libitum, were used for the study. Each mouse was given 17 μ Ci of one of the conjugates by tail vein injection. The initial injected dose and the whole-body retention of the radioactivity in each mouse were determined at different intervals by counting the mouse in a standardized dual sodium iodide crystal probe system. The results were decay-corrected to the time of injection. Mice were sacrificed at 5, 24, 48, and 72 h after injection; four animals were used for each data point. Means and standard deviations were calculated by standard methods. Mouse urine was collected at 5 and 24 h. Only the 5-h urine sample from one mouse injected with labeled Lym-1-2IT-BALAL-ABE contained enough radioactivity to be analyzed by HPLC.

RESULTS

Radiolabeling of the Conjugates with ¹¹¹In. By solid-phase assay (26), the immunoconjugates showed immunoreactivity of 74% (Lym-1-2IT-BALAL-ABE) and 53% (Lym-1-2IT-BABE). The radiolabeling yields were 69% and 64%, respectively.

In Vitro Digestion of the Conjugates with Cathepsin B₁ and Cathepsin D. In all experiments, enzyme was only added at time zero. The analysis was done on TLC plates; Figure 1 shows a AMBIS scan of one of the time points. The results of the whole study can be seen in Figure 2. Cathepsin B₁ cleaves more than 85% of the ¹¹¹In from Lym-1-2IT-BALAL-ABE with $T_{1/2} \approx 6$ h, producing low molecular weight complexes. The digestion leveled off at 13% chelate bound to the antibody or a large fragment thereof. The same immunoconjugate had 75% of the radioactivity associated with the protein after 97-h exposure to cathepsin D. In the other hand, the ¹¹¹In complex of Lym-1-2IT-BABE showed 79% (cathepsin B₁) and 86% (cathepsin D) uncleaved radiolabel after 97

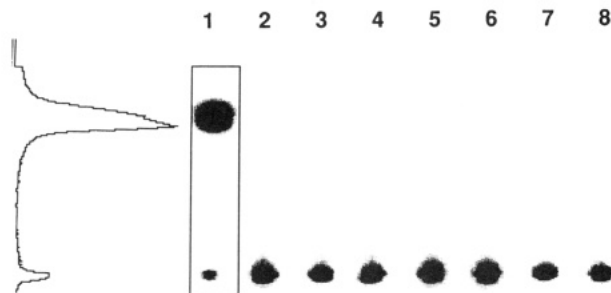


Figure 1. AMBIS scan of a TLC plate used to analyze the in vitro digestions (97-h incubation time; cleaved chelates, R_f 0.8; proteins, R_f 0–0.1): lane 1, Lym-1-2IT-BALAL-ABE exposed to cathepsin B₁, the quantitative profile of lane 1 shown at left; lane 2, Lym-1-2IT-BALAL-ABE exposed to cathepsin D; lane 3, Lym-1-2IT-BABE exposed to cathepsin B₁; lane 4, Lym-1-2IT-BABE exposed to cathepsin D. Lanes 5–8 represent the conjugates exposed to the same conditions with no enzymes added.

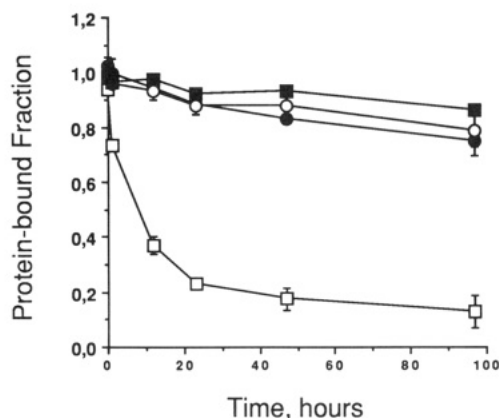


Figure 2. Digestion of Lym-1 conjugates exposed to cathepsins: \square , Lym-1-2IT-BALAL-ABE exposed to cathepsin B₁; \bullet , Lym-1-2IT-BALAL-ABE exposed to cathepsin D; \circ , Lym-1-2IT-BABE exposed to cathepsin B₁; \blacksquare , Lym-1-2IT-BABE exposed to cathepsin D.

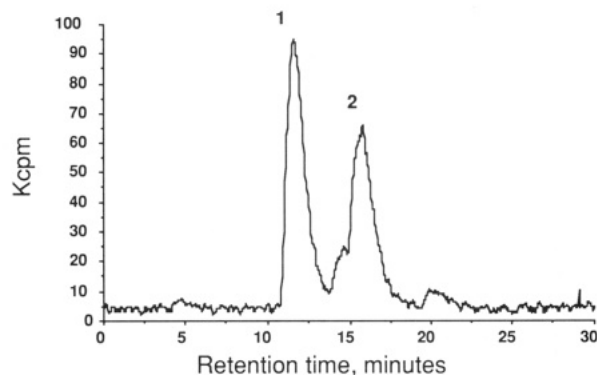


Figure 3. Radio-HPLC trace of Lym-1-2IT-BALAL-ABE exposed to cathepsin B₁ for 100 h: peak 1, 11.5-min retention time, 48% of total activity; peak 2, 15.9-min retention time, 37% of total activity, excluding the shoulder at 14–15 min.

h. The control experiment (same conditions, no enzymes added) showed that 92–95% of the radioactivity remained on the proteins.

HPLC Analysis of the Cathepsin B₁ and the Cathepsin D Digests. The samples, frozen after 100 h of incubation time, were analyzed by reversed-phase C₁₈ HPLC. Figure 3 shows the trace of the cathepsin B₁ digestion of Lym-1-2IT-BALAL-ABE recorded by the flow-through radioisotope detector. ^{114m}In-ABE and ^{114m}In-AL-ABE were independently prepared as standards as described above. Coinjection with the digestion product showed that peak 1 (11.5 min, 48% of total radioactivity)

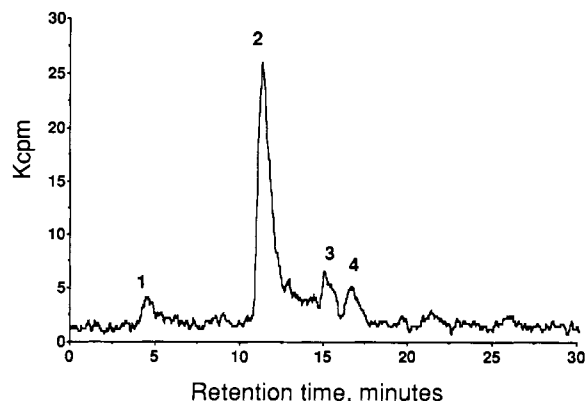


Figure 4. Radio-HPLC trace of the urine (5 h) of a mouse injected with labeled Lym-1-2IT-BALAL-ABE: peak 1, 4.4-min retention time, 6% of total activity; peak 2, 11.3-min retention time, 54% of total activity; peak 3, 15.2-min retention time, 10% of total activity; peak 4, 16.8-min retention time, 8% of total activity.

had the same retention time as ^{114m}In -ABE, and peak 2 (15.9 min, 37%) the same retention time as ^{114m}In -AL-ABE. The trace of the cathepsin B₁ digestion of Lym-1-2IT-BABE showed a major peak with a retention time of 14.0 min, which did not correspond to ^{114m}In -ABE or ^{114m}In -AL-ABE.

HPLC Analysis of the Mouse Urine. Figure 4 shows an HPLC trace of a urine sample of a mouse injected with labeled Lym-1-2IT-BALAL-ABE (5 h postinjection). The observed four radioactive peaks had retention times of 4.4 min (6% of total activity), 11.3 min (54%), 15.2 min (10%), and 16.8 min (5%). Coinjection of standards showed that the second peak had the same retention time as ^{114m}In -ABE and the third peak the same as ^{114m}In -AL-ABE. We were not able to identify the other, smaller peaks.

Mouse Study. The whole-body and the blood clearance can be seen in Figure 5. After 72 h, approximately 20% of the radioactivity had cleared the body for the ^{111}In -labeled Lym-1-2IT-BALAL-ABE, and 10% for the ^{111}In -labeled Lym-1-2IT-BABE. The blood clearance was similar in both cases. After 0.08 h, about 75% of the total radioactivity was located in the blood. This amount decreased to about 65% (1 h), 50% (5 h), 33% (24 h), and 16% (72 h).

The clearance of radioactivity from the organs and from the blood, expressed as % ID/g, can be seen in Figure 6. With both linkers, the radioactivity located in the liver decreased slightly over the time of the experiment (from 11% to 9% ID/g for Lym-1-2IT-BALAL-ABE, and from 14% to 10% ID/g for Lym-1-2IT-BABE). The kidneys showed a similar behavior; the decrease was from 10% to 7% ID/g for Lym-1-2IT-BALAL-ABE, and from 10% to 8% ID/g for Lym-1-2IT-BABE. In the spleen, a slight increase from 16% to 20% ID/g for Lym-1-2IT-BALAL-ABE and a fairly constant concentration of about 22% ID/g for Lym-1-2IT-BABE were observed.

DISCUSSION

There is great interest in the use of radioactive metal ions as imaging and therapeutic agents (1, 2). The early problems that resulted from the transchelation of the metal ions to serum proteins have largely been solved, and currently there are ligands and labeling procedures available that hold almost any metal ion stably bound in vivo for a long time (3). New procedures for the attachment of chelating agents to proteins have been improved to provide antibodies that show little or no loss of immunoreactivity after conjugation (21). Despite all these

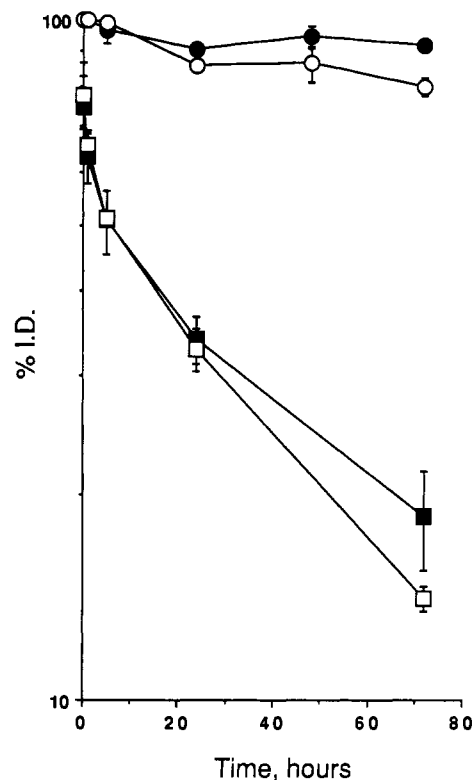


Figure 5. Decay-corrected whole-body and blood retention for ^{111}In -labeled Lym-1 conjugates in nontumored mice. For the whole-body data, ● stands for Lym-1-2IT-BABE and ○ for Lym-1-2IT-BALAL-ABE. For the blood data, ■ stands for Lym-1-2IT-BABE and □ for Lym-1-2IT-BALAL-ABE. The vertical scale is logarithmic. All of the data were decay-corrected to the time of injection. Error bars show standard deviations. Four animals were used for each data point.

improvements, the problem of the high liver uptake of radioactivity, especially in the case of ^{111}In , has not been solved. Twenty to fifty percent of the injected dose was found in this organ over a 7-day period if ^{111}In antibody (using the cyclic anhydride of DTPA for labeling) was employed (4–6, 27). This is in strong contrast to ^{131}I -labeled antibodies, which show only a small percentage of the injected dose in the liver (5, 6).

Of the several approaches to reduce this unwanted localization and to speed up the clearance (7–9), we decided to further investigate cleavable linkers (10–12). In order to be successful, they must be stable in serum but undergo cleavage in the liver. The pH change from serum to liver and/or the presence of different hydrolases or other enzymes could be used to achieve this. Even though it has been shown in vitro and in vivo that liver enzymes can effectively cleave a peptide bond between a drug and a carrier (16), the results of this approach for nuclear medicine have been disappointing so far.

One major drawback of the earlier studies was that the immunoconjugates evaluated may not be directly comparable. The number of chelates attached and possibly also their positions on the proteins varies greatly between the different immunoconjugates. In this study, we tried to keep everything except the linker the same. Both chelates were attached as a bromoacetamido compound to a 2-iminothiolane-modified antibody. The conditions for the conjugation and the labeling were kept as similar as practical. Both immunoconjugates were purified by HPLC and tested by TLC. They showed high radiochemical purity and good immunoreactivity.

In Vitro Digestion of the Conjugates. To model the processing of antibodies in the liver, we digested them

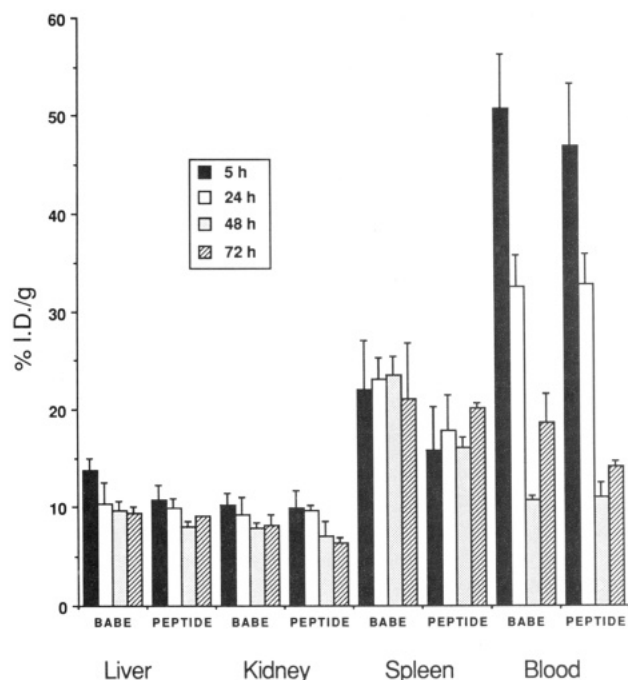


Figure 6. Clearance of radioactivity (liver, kidney, spleen, and blood) expressed as percent injected dose/gram for ^{111}In -labeled conjugates (BABE stands for Lym-1-2IT-BABE and PEPTIDE for Lym-1-2IT-BALAL-ABE) in nontumored mice. Time after injection is indicated. The data is decay-corrected to the time of injection. Error bars show standard deviations. Four animals were used for each data point.

with cathepsin B₁ and cathepsin D. These liver proteases are believed to be responsible for the biggest part of the protein turnover in this organ (17). Our *in vitro* conditions (pH 4.8–5.0, thiol groups present, activity of cathepsin B₁ 0.27 unit/mL, cathepsin D 0.13 unit/mL) were chosen to resemble those found in human liver *in vivo* (activity of cathepsin B₁ ca. 1.1–2.1 units/mL (17), cathepsin D ca. 0.17 unit/mL (25)).

Cathepsin B₁ (see Figure 2) was very efficient in cleaving the chelate from the protein, provided the complex was attached with an Ala-Leu-Ala-Leu linker. The $T_{1/2}$ of approximately 6 h for this cleavage showed the pronounced effect of the linker. This was in strong contrast to the compound without this feature, which, after 97 h of exposure to cathepsin B₁, had 79% of the radioactivity still attached to the protein. Even though cathepsin D was in a higher concentration than cathepsin B₁ relative to human liver, we observed a much lower activity toward Ala-Leu-Ala-Leu (86% uncleaved activity after 97 h). In the control experiments (same condition, no proteases), the conjugates lost 5–8% after the same time. This might be attributed to a slow hydrolysis of the linker, most probably at the amidine group.

The HPLC analysis of the same experiment after 100 h (Figure 3) showed two major peaks for cathepsin B₁ (48% and 37% of the total radioactivity). They coeluted with the independently prepared ^{114m}In complexes of ABE (peak 1) and Al-ABE (peak 2). This is a strong indication for the cleavage of the Ala-Leu-Ala-Leu by cathepsin B₁.

Lym-1-2IT-BABE with the same protease showed one major peak that did not coelute with the ^{114m}In complex of ABE. This may represent a 2IT-BABE chelate still attached to a lysyl side chain, a cleavage product similar to the ones suggested by Jones et al. (15).

Mouse Study. The whole-body clearance was slow for the two conjugates (Figure 5); after 72 h there was still 80% (Lym-1-2IT-BALAL-ABE) and 90% (Lym-1-2IT-

BABE) present in the body. This compares well to the results of Deshpande et al. (10), who found 70–85% of the injected dose of benzyl-EDTA- ^{111}In conjugates in the body after 72 h. On the other hand, it is slower than the clearance of the diester-linked DTPA reported by Paik et al. (11), who found only about 30% of the injected dose remaining in the body after 48 h. The accelerated excretion seems at least partially due to the reduced overall stability of the diester linkage.

For both our conjugates, the blood clearance results were similar to those of Deshpande et al. (10); after 72 h, there was roughly 20% of the initial dose left in the blood. For both conjugates, the liver clearance was slow. For Lym-1-2IT-BALAL-ABE, we observed approximately 10% ID/g in this organ throughout the experiment; for Lym-1-2IT-BABE it was 10–14%. The results for Lym-1-2IT-BABE again compare well to the results of Deshpande et al. (10), but our Ala-Leu-Ala-Leu linker showed only half the liver activity of the previously reported Ala-Leu-Ala-Leu-Gly. One explanation could be that the latter conjugate was prepared by direct alkylation of a lysyl residue, whereas our peptide was attached to a 2-iminothiolane-modified lysine (See Scheme I). Different numbers of chelates and different positions of attachment could also account for this effect.

Since Trouet et al. (16) have shown that an Ala-Leu-Ala-Leu linker is cleaved by liver enzymes quite effectively *in vitro* and that the effectiveness of a drug *in vivo* can be greatly enhanced by such a linker, the clearance of the radioactivity is disappointing. In agreement with the conclusion of Jones et al. (15), our data suggests that the chelates were cleaved in the liver and trapped there.

Analysis of the urine of a mouse injected with Lym-1-2IT-BALAL-ABE (Figure 4) supports this hypothesis. Of the four major peaks observed, peak 2 (54% of the total radioactivity) and peak 3 (10%) coeluted with the ^{114m}In complexes of ABE and AL-ABE, respectively, which is comparable to the *in vitro* results.

Our experiments suggest that our linker acts as expected in biological systems, being indeed cleaved by proteases. From the work of Jones et al. (15), we assume that the antibody conjugates studied here are taken into liver parenchymal cells. The disappointing biodistribution and clearance patterns observed so far are apparently due to cleaved chelates being trapped inside these cells. Accordingly, the emphasis of future research should be on a chelate that can be cleared from the liver cells, in combination with a cleavable linker. Changing the charge of the complex to 0 and/or making the ligand more lipophilic so it can penetrate membranes are approaches that could solve the first problem. The observations in this paper provide a solution to the second.

ACKNOWLEDGMENT

Supported by Research Grant CA 16861 to C.F.M. and by Program Project CA 47829 (G.L. DeNardo, P.I.) from the National Cancer Institute, National Institutes of Health, and by Research Grant DE-FG03-84ER60233 to S.J.D. from the Department of Energy.

LITERATURE CITED

- (1) Sands, H. (1990) Experimental Studies of Radioimmuno-detection of Cancer: An Overview. *Cancer Res.* 50 (Suppl.), 809s–813s.
- (2) Ford, C. H., Richardson, V. J., and Reddy, V. S. (1990) Antibody mediated targeting of radioisotopes, drugs and toxins in diagnosis and treatment. *Indian J. Pediatr.* 57 (1), 29–46.

- (3) Moi, M. K., and Meares, C. F. (1988) The Peptide Way to Macrocyclic Bifunctional Chelating Agents: Synthesis of 2-(p-Nitrobenzyl)-1,4,7,10-tetraazacyclododecane-*N,N',N'',N'''*-tetraacetic Acid and Study of Its Yttrium(III) Complex. *J. Am. Chem. Soc.* 110, 6266-6267. Meares, C. F., and Wensel, T. G. (1984) Metal Chelates as Probes of Biological Systems. *Acc. Chem. Res.* 17, 202-209.
- (4) DeNardo, S. J., DeNardo, G. L., Deshpande, S. V., Adams, G. P., Macey, D. J., Mills, S. L., Epstein, A. L., and Meares, C. F. (1987) The design of a radiolabeled monoclonal antibody for radioimmunodiagnosis and radioimmunotherapy. In *Radiolabeled Monoclonal Antibodies for Imaging and Therapy—Potential, Problems and Prospects* (S. Srivastava, Ed.) NATO Advanced Study Institute, Plenum, New York, in press.
- (5) Halpern, S. E., Hagan, P. L., Garver, P. R., Kozol, J. A., Chen, A. W. N., Frincke, J. M., Bartholomew, R. M., David, G. S., and Adams, T. H. (1983) Stability, characterization, and kinetics of ^{111}In labeled monoclonal antitumor antibodies in normal animals and nude-mouse human tumor models. *Cancer Res.* 43, 5347-5355.
- (6) Pimm, M. V., Perkins, A. C., and Baldwin, R. W. (1985) Differences in tumor and normal tissue concentrations of iodine- and indium-labelled monoclonal antibody. II. Biodistribution studies in mice with human tumor xenografts. *Eur. J. Nucl. Med.* 11, 300-304.
- (7) Beatty, B. G., Beatty, J. D., Williams, L. E., Paxton, R. J., Shively, J. E., and O'Connor-Tressel, M. (1989) Effect of Specific Antibody Pretreatment on Liver Uptake of ^{111}In -labeled Anticarcininoembryonic Antigen Monoclonal Antibody in Nude Mice Bearing Human Colon Cancer Xenografts. *Cancer Res.* 49, 1587-1594.
- (8) Paganelli, G., Riva, P., Deleide, G., Clivio, A., Chiolerio, F., Scassellati, G. A., Malcovati, M., and Siccaldi, A. G. (1988) In vivo labelling of biotinylated monoclonal antibodies by radioactive avidin: A strategy to increase tumor radiolocalisation. *Int. J. Cancer Suppl.* 2, 121-125.
- (9) Rodwell, J. D. (1989) Engineering monoclonal antibodies. *Nature* 342, 99-100.
- (10) Deshpande, S. V., DeNardo, S. J., Meares, C. F., McCall, M. J., Adams, G. P., and DeNardo, G. L. (1989) Effect of Different Linkages Between Chelates and Monoclonal Antibodies on Levels of Radioactivity in the Liver. *Nucl. Med. Biol.* 16, 587-597.
- (11) Paik, C. H., Yokoyama, K., Reynolds, J. C., Quadri, S. M., Min, C. Y., Shin, S. Y., Maloney, P. J., Larson, S. M., and Reba, R. C. (1989) Reduction of Background Activities by Introduction of a Diester Linkage Between Antibody and a Chelate in Radioimmunodetection of Tumor. *J. Nucl. Med.* 30, 1693-1701.
- (12) Haseman, M. K., Goodwin, D. A., Meares, C. F., Kaminski, M. S., Wensel, T. G., McCall, M. J., and Levy, R. (1986) Metabolizable ^{111}In -chelate conjugated anti-idiotypic monoclonal antibody for radioimmunodetection of lymphoma in mice. *Eur. J. Nucl. Med.* 12, 455-460.
- (13) Hnatowich, D. J., Layne, W. W., Childs, R. L., Lantaigne, D., Davis, M. A., Griffin, T. W., and Doherty, P. W. (1983) Radioactive labeling of antibody: a simple and efficient method. *Science (Washington, DC)* 220, 613-615.
- (14) Deshpande, S. V., Subramanian, R., McCall, M. J., DeNardo, S. J., DeNardo, G. L., and Meares, C. F. (1990) Metabolism of Indium Chelates Attached to Monoclonal Antibody: Minimal Transchelation of Indium from Benzyl-EDTA Chelate In Vivo. *J. Nucl. Med.* 31, 218-224.
- (15) Jones, P. L., Brown, B. A., and Sands, H. (1990) Uptake and Metabolism of ^{111}In -labeled Monoclonal Antibody B6.2 by the Rat Liver. *Cancer Res. Suppl.* 50, 852s-856s.
- (16) Trouet, A., Masquelier, M., Baurain, R., and Deprez-De Campeneere, D. (1982) A covalent linkage between daunorubicin and proteins that is stable in serum and reversible by lysosomal hydrolases, as required for a lysosomotropic drug-carrier conjugate: In vitro and in vivo studies. *Proc. Natl. Acad. Sci. U.S.A.* 79, 626-629.
- (17) Barrett, A. J., and Kirschke, H. (1981) Cathepsin B, Cathepsin H, Cathepsin L. *Methods Enzymol.* 80, 535-561.
- (18) Meares, C. F., McCall, M. J., Reardan, D. T., Goodwin, D. A., Diamanti, C. I., and McTigue, M. (1984) Conjugation of Antibodies with Bifunctional Chelating Agents: Isothiocyanate and Bromoacetamide Reagents, Methods of Analysis, and Subsequent Addition of Metal Ions. *Anal. Biochem.* 142, 68-78.
- (19) Epstein, A. L., Zimmer, A. M., and Spies, S. M. (1985) Radioimmunodetection of human B-cell lymphomas with a radiolabeled tumor-specific monoclonal antibody (Lym-1) In *Malignant Lymphomas and Hodgkin's Disease: Experimental and Therapeutic Advances* (F. Cavalli, G. Bonadonna, and M. Rozenzweig, Eds.) Chapter 14, 569-577, Martinus Nijhoff Publishing Co., Boston.
- (20) Mikkala, V. M., Mikola, H., and Hemmila, I. (1989) The Synthesis and Use of Activated *N*-Benzyl Derivatives of Diethylenetriaminetetraacetic Acids: Alternative Reagents for Labeling of Antibodies with Metal Ions. *Anal. Biochem.* 176, 319-325.
- (21) McCall, M. J., Diril, H., and Meares, C. F. (1990) Simplified Method for Conjugating Macrocyclic Bifunctional Chelating Agents to Antibodies via 2-Iminothiolane. *Bioconjugate Chem.* 1, 222-226.
- (22) Studer, M., and Meares, C. F. (1992) A Convenient and Flexible Approach for Introducing Linkers on Benzyl-EDTAs. *Bioconjugate Chem.*, previous paper in this issue.
- (23) Penefsky, H. S. (1979) A Centrifuged-Column Procedure for the Measurement of Ligand Binding by Beef Heart F_1 . *Methods Enzymol.* 56, Part G, 527-530.
- (24) Bajkowsky, A. S., and Frankfater, A. (1975) Specific Spectrophotometric Assays for Cathepsin B₁. *Anal. Biochem.* 68, 119-127.
- (25) Sigma Chemical Co. (1990) Personal communication. Barrett, A. J. (1970) Purification of Isoenzymes from Human and Chicken Liver. *Biochem. J.* 117, 601-607. Barrett, A. J. (1967) Lysosomal Acid Proteinase of Rabbit Liver. *Biochem. J.* 104, 601-608.
- (26) DeNardo, S. J., Peng, J.-S. B., DeNardo, G. L., Mills, S. L., and Epstein, A. L. (1986) Immunochemical Aspects of Monoclonal Antibodies Important for Radiopharmaceutical Development. *Nucl. Med. Biol.* 13, 303-310.
- (27) Murray, J. L., Rosenblum, M. G., Sobol, R. E., Bartholomew, R. M., Plager, C. E., Haynie, T. P., Jahns, M. F., Glenn, H. J., Lamki, L., Benjamin, R. S., Papadopoulos, N., Boddie, A. W., Frincke, J. M., David, G. S., Carlo, D. J., and Hersh, E. M. (1985) Radioimmunoinaging in Malignant Melanoma with ^{111}In -labeled Monoclonal Antibody 96.5. *Cancer Res.* 45, 2376-2381.

TECHNICAL NOTES

Preparation of 5- and 6-(Aminomethyl)fluorescein

Phillip G. Mattingly

Abbott Laboratories, Diagnostics Division, One Abbott Park Road, Abbott Park, Illinois 60064.

Received May 11, 1992

5(6)-Carboxyfluorescein is protected as the diacetate then reduced to 5(6)-(hydroxymethyl)fluorescein diacetate. The separated isomers are subjected to a Mitsunobu reaction with dibenzyl imidodicarbonate, yielding diprotected 5- and 6-(aminomethyl)fluorescein diacetate. Methanolysis of the acetates followed by deprotection with HBr/acetic acid gives 5- and 6-(aminomethyl)fluorescein hydrobromide.

INTRODUCTION

Many fluorescein derivatives have functional groups that are suitable for reaction with other molecules, and can therefore serve as labels in a variety of analytical applications ranging from probing cell functions (1) to monitoring the level of drugs in human fluids via immunoassays (2). The choice of the fluorescein derivative can be crucial to the optimal performance of the conjugate formed and cannot usually be made a priori. This is especially true when the conjugate is to be used in an immunoassay. In such cases a series of conjugates are prepared from a variety of fluorescein derivatives. Commonly used derivatives include 5- and 6-carboxyfluorescein, 5- and 6-aminofluorescein, 5- and 6-fluorescein isothiocyanate, and 4'-(aminomethyl)fluorescein (4'-AMF) (3). Of these, the 5- and 6-aminofluorescein compounds are the most difficult to work with since the amino group is not very nucleophilic. This is an expected consequence of the amino group being directly bound to the deactivating aromatic ring. 4'-(Aminomethyl)fluorescein was an earlier attempt to solve this problem by adding a methylene group between the amino group and the aromatic ring. While successful in restoring normal amino group reactivity, 4'-AMF derivatives do have some drawbacks, including a tedious purification in the preparation. In light of this, a fluorescein derivative substituted with a reactive amino group at the 5 or 6 position was desired. While 5-(aminomethyl)fluorescein has recently become commercially available, as of yet though there is not a reported preparation of the compound. The present work details the preparation of 5- and 6-(aminomethyl)fluorescein hydrobromide from the readily available mixture of 5(6)-carboxyfluorescein, thereby giving useful alternatives to currently used fluorescein labels.

EXPERIMENTAL PROCEDURES

General Comments. All reagents were purchased from Aldrich Chemical Company, Inc., Milwaukee, WI, and were used without further purification, except where noted. Solvents employed were of reagent or HPLC grade and were used as received. ^1H NMR spectra were recorded at 200 MHz on a Chemagnetics A-200 spectrometer in CDCl_3 with TMS as a standard. High-resolution mass spectra were recorded on a Kratos MS-50 double-focusing mass spectrometer.

5(6)-(Hydroxymethyl)fluorescein Diacetate (3a,b). 5(6)-Carboxyfluorescein diacetate was prepared from 5(6)-

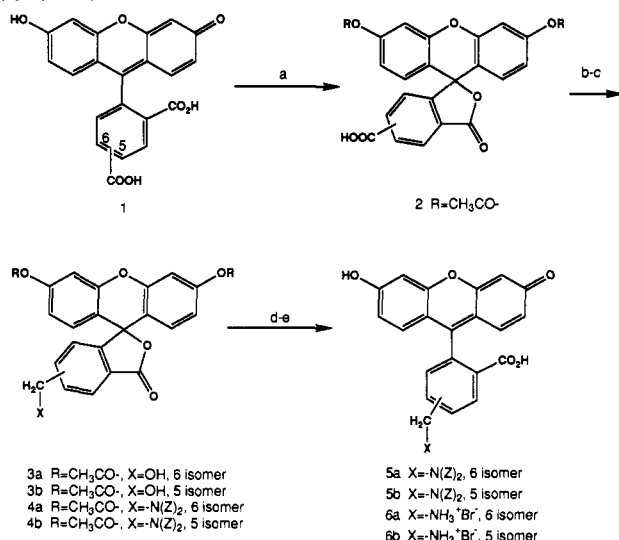
carboxyfluorescein (Eastman Chemicals) following the procedure for unsubstituted fluorescein (4). 5(6)-Carboxyfluorescein diacetate (2.5 g, 5.5 mmol) and triethylamine (845 μL , 6.0 mmol) are dissolved in THF (25 mL, distilled from benzophenone potassium ketyl) under a nitrogen atmosphere and cooled to 0 $^\circ\text{C}$. Ethyl chloroformate (845 μL , 6.0 mmol) was added at once and the mixture stirred for 1 h. Afterward, the mixture was filtered and added to sodium phosphate buffer (15 mL, 1 M, pH 6.0) which had been cooled to 0 $^\circ\text{C}$. NaBH_4 (500 mg, 13.2 mmol) in water (5 mL) was then added portionwise with efficient stirring over 5 min. The reaction was then immediately poured into cold water (100 mL) and extracted with ethyl acetate (3 \times 50 mL). The extract was washed with saturated sodium chloride (2 \times 25 mL), dried over anhydrous Na_2SO_4 , and evaporated to give the mixed 5(6)-(hydroxymethyl)fluorescein diacetate (1.73 g, 3.74 mmol, 68%). The mixture was separated by filtration through silica gel (5), eluting with methylene chloride/diethyl ether (9:1).

The first eluting compound was 3a. ^1H NMR (δ): 2.24 (6 H, s), 4.73 (2 H, d, $J = 4.9$ Hz), 6.86 (4 H, m), 7.1 (3 H, m), 7.55 (1 H, d, $J = 8.2$ Hz), 7.96 (1 H, d, $J = 8.2$ Hz). Calculated mass for $\text{C}_{25}\text{H}_{19}\text{O}_8$ 447.1080, found 447.1075.

The second eluting compound was 3b. ^1H NMR (δ): 2.29 (6 H, s), 4.82 (2 H, d, $J = 4.2$ Hz), 6.78 (4 H, m), 7.1 (3 H, m), 7.63 (1 H, d, $J = 8.2$ Hz), 8.0 (1 H, s). Calculated mass for $\text{C}_{25}\text{H}_{19}\text{O}_8$ 447.1080, found 447.1075.

5-[[N,N-Bis(carbobenzyloxy)amino]methyl]fluorescein Diacetate (4a). Compound 3a (1 g, 2.2 mmol), triphenylphosphine (690 mg, 2.6 mmol), and dibenzyl imidodicarbonate (640 mg, 2.2 mmol) are stirred in THF (50 mL, distilled from benzophenone potassium ketyl) under a nitrogen atmosphere. To this solution is added diethyl azodicarboxylate (415 μL , 2.6 mmol) in THF (25 mL) dropwise over 30 min. After stirring for an additional hour, the solution is evaporated and the residue purified by filtration through silica gel by eluting with methylene chloride/diethyl ether (9:1) to give 4a (923 mg, 1.3 mmol, 59%). ^1H NMR (δ): 2.32 (6 H, s), 4.9 (2 H, s), 5.14 (2 H, s), 5.16 (2 H, s), 6.73 (4 H, m), 6.94-7.35 (13 H, m), 7.47 (1 H, d, $J = 8.2$ Hz), 7.88 (1 H, d, $J = 8.2$ Hz). Calculated mass for $\text{C}_{41}\text{H}_{32}\text{NO}_{11}$ 714.1975, found 714.1977.

5-[[N,N-Bis(carbobenzyloxy)amino]methyl]fluorescein diacetate (4b) was prepared from 3b in the same manner as 4a. Compound 4b (1 g, 1.4 mmol, 61%). ^1H NMR (δ): 2.31 (6 H, s), 5.03 (2 H, s), 5.19 (2 H, s), 5.27 (2 H, s), 6.73 (4 H, m), 6.93-7.35 (13 H, m), 7.51 (1 H, d,

Scheme I^a

^a (a) acetic anhydride, sodium acetate; (b) (i) ethyl chloroformate, (ii) sodium borohydride, pH 6; (c) diethyl azodicarboxylate, triphenylphosphine, dibenzyl imidodicarbonate; (d) methanol, DMAP; (e) HBr/acetic acid.

$J = 8.2$ Hz), 7.92 (1 H, s, $J = 8.2$ Hz). Calculated mass for C₄₁H₃₂NO₁₁ 714.1975, found 714.1977.

6-(Aminomethyl)fluorescein Hydrobromide (6a). Compound 4a (675 mg, 0.95 mmol) was stirred at reflux in methanol (50 mL) containing 4-(dimethylamino)pyridine (10 mg) for 24 h. The solvent was evaporated to give 5a. ¹H NMR (δ): 4.92 (2 H, s), 5.13 (2 H, s), 5.20 (2 H, s), 6.61 (4 H, m), 6.94–7.35 (13 H, m), 7.49 (1 H, d, $J = 8.2$ Hz), 8.0 (1 H, d, $J = 8.2$ Hz). Calculated mass for C₃₇H₂₈NO₉ 630.1764, found 630.1763.

Without further purification 5a was dissolved in methylene chloride (50 mL, distilled from P₂O₅) and treated with HBr/HOAc (31%, 5 mL). After stirring for 4 h the reaction mixture was filtered and the precipitate dried in vacuo for 12 h to give 6a (410 mg, 0.93 mmol, 98%). ¹H NMR (δ , DMSO- d_6): 4.12 (2 H, m), 6.53 (4 H, m), 7.06 (1 H, s), 7.35 (2 H, d, $J = 8.2$ Hz), 7.76 (1 H, d), 8.2 (1 H, d, $J = 8.2$ Hz). Calculated mass for C₂₁H₁₆NO₅ 362.1028, found 362.1027. Compound 6a was 97% pure by HPLC [3.6 mm \times 25 cm μ Bondapak, C-18, 25:50:25 MeOH/H₂O/10% aqueous HOAc, 2 mL/min, $t_R = 4.97$ min] when monitored by UV (254 nm) or fluorescence (480_{ex}/520_{em}) detection.

5-(Aminomethyl)fluorescein hydrobromide (6b) was prepared from 4b (1 g, 1.4 mmol) by the procedure used for 6a. Compound 5b. ¹H NMR (δ): 5.03 (2 H, s), 5.20 (2 H, s), 5.27 (2 H, s), 6.78 (4 H, m), 6.94–7.35 (13 H, m), 7.54 (1 H, d, $J = 8.2$ Hz), 7.94 (1 H, s). Calculated mass for C₃₇H₂₈NO₉ 630.1764, found 630.1763. Compound 6b (600 mg, 1.36 mmol, 98%). ¹H NMR (δ , DMSO- d_6): 4.24 (2 H, br s), 6.53 (4 H, m), 6.7 (2 H, m), 7.35 (1 H, d, $J = 8.2$ Hz), 7.84 (1 H, d, $J = 8.2$ Hz), 8.1 (1 H, s). Calculated mass for C₂₁H₁₆NO₅ 362.1028, found 362.1027. Compound 6b was 94% pure by HPLC [3.6 mm \times 25 cm μ Bondapak, C-18, 25:50:25 MeOH/H₂O/10% aqueous HOAc, 2 mL/min, $t_R = 6.14$ min] when monitored by UV (254 nm) and 99% pure when monitored by fluorescence (480_{ex}/520_{em}) detection.

RESULTS AND DISCUSSION

5(6)-Carboxyfluorescein (1, roughly 40:60 mixture) was modified to increase its solubility in organic solvents and to differentiate the two carboxyl groups, by treatment with acetic anhydride (Scheme I). Once so treated the 5(6)-

carboxyfluorescein diacetate (2) (6) derivative was soluble in organic solvents commonly used for the reduction of carboxylic acid derivatives. The carboxylic acid was reduced to the alcohol by treatment with borane–tetrahydrofuran complex, or borane–dimethyl sulfide complex (7) over the course of 1–2 days. Loss of the acetyl groups was a concomitant side reaction which lessened the yield of the alcohol 3a,b. Alternatively, the carboxylic acid was converted into the mixed carbonic anhydride with ethyl chloroformate and reduced with NaBH₄ (8) in pH 6 buffered, aqueous THF (5 min, 0 °C) to the alcohol 3a,b. The mixture of alcohols thus formed were conveniently separated at this stage by chromatography on silica gel. The alcohol 3a or 3b was converted into the protected amine 4a, 4b under Mitsunobu conditions (9) using dibenzyl imidodicarbonate (10). Subsequent removal of the acetyl groups with methanol containing catalytic 4-(dimethylamino)pyridine, followed by treatment with HBr/acetic acid, gave (aminomethyl)fluorescein hydrobromide 6a or 6b.

ACKNOWLEDGMENT

Mass spectra were recorded by D418, PPD Structural Chemistry.

LITERATURE CITED

- (1) See, for example: (a) Dive, C., Cox, H., Watson, J. V., and Workman, P. (1988) Polar fluorescein derivatives as improved substrate probes for flow cytological assay of cellular esterases. *Mol. Cell. Probes* 2, 131. (b) Graber, M. L., DiLillo, D. C., Friedman, B. L., and Pastoriza-Munoz, E. (1986) Characteristics of fluoroprobes for measuring intracellular pH. *Anal. Biochem.* 156, 202.
- (2) See, for example: (a) Brynes, P. J., Martinus, J. A., Smith, C. M., Molina, C. M., and Vaughn, K. S. (1988) Fluorescence polarization immunoassay for amphetamine/metamphetamine. *Eur. Pat. Appl. EP279213 (Chem. Abstr. 110, 205680)*. (b) Wang, N. Y., Keegan, C. L., Hieman, D. F., Flentge, C. A., and Wang, P. P. (1988) New substituted 5-aryl-benzodiazepin-2-one compounds useful as immunogens and tracers for fluorescence polarization immunoassay of benzodiazepine derivatives. *Eur. Pat. Appl. EP264797 (Chem. Abstr. 110, 91693)*.
- (3) Fino, J. R., Shipchandler, M. T., Klein, L. D., and Kirkemo, C. L. (1987) 4'-[Aminomethyl]fluorescein and its N-alkyl derivatives: useful reagents in immunodiagnostic techniques. *Anal. Biochem.* 162, 89.
- (4) Orndorff, W. R., and Hemmer, A. J. (1927) Fluorescein and some of its derivatives. *J. Am. Chem. Soc.* 49, 1272.
- (5) Yau, E. K., and Coward, J. K. (1988) Filtering-column chromatography—a fast, convenient chromatographic method. *Aldrichimica Acta* 21, 106.
- (6) Bruning, J. W., Kardol, M. J., and Arnetzen, F. (1980) Carboxyfluorescein fluorochromasia assays. I. Non-radioactively labeled cell mediated lympholysis. *J. Immunol. Methods* 33, 33.
- (7) (a) Brown, H. C. (1972) *Boranes in Organic Chemistry*, Cornell University Press. (b) Lane, C. F. (1976) Reductions of organic compounds with diborane. *Chem. Rev.* 76, 773.
- (8) Ramasamy, K., Olsen, R. K., and Emery, T. (1982) Synthesis of N-t-Boc-L- α -amino adipic acid 1-t-butyl-6-ethyl ester from L-aspartic acid: a new route to L- α -amino adipic acid. *Synthesis* 42.
- (9) Mitsunobu, O. (1981) The use of diethyl azodicarboxylate and triphenylphosphine in synthesis and transformation of natural products. *Synthesis* 1.
- (10) Grehn, L., Lurdes, M., Almeida, S., and Ragnarsson, U. (1988) Convenient preparation of alkyl benzyl imidodicarbonates, useful reagents for the direct synthesis of protected amines. *Synthesis* 992.

Registry No. 1 (isomer A), 76823-03-5; 1 (isomer B), 3301-79-9; 2 (isomer A), 3348-03-6; 2 (isomer B), 79955-27-4; 3a, 143106-55-2; 3b, 143106-56-3; 4a, 143106-57-4; 4b, 143142-35-2; 5a, 143106-58-5; 5b, 143106-59-6; 6a, 143106-60-9; 6b, 143106-61-0.

Bioconjugate Chemistry

NOVEMBER/DECEMBER 1992

Volume 3, Number 6

© Copyright 1992 by the American Chemical Society

REVIEWS

Radiohalogenation of Proteins: An Overview of Radionuclides, Labeling Methods, and Reagents for Conjugate Labeling

D. Scott Wilbur

Department of Radiation Oncology, University of Washington, Seattle, Washington 98195. Received May 26, 1992

TABLE OF CONTENTS

I. Introduction	433	1. Maleimides	448
II. Radionuclides of Halogens	434	2. Acetyl Halides	450
A. Halogen Radionuclides for in Vitro Applications	435	C. Carbohydrate-Reactive Conjugates	450
B. Halogen Radionuclides for in Vivo Imaging	435	1. Amines	451
C. Halogen Radionuclides for Therapy	436	2. Hydrazines	452
D. Other Halogen Radionuclides	437	3. Hydroxylamines	452
III. Radiohalogen Labeling	437	D. Conjugates That React Nonspecifically	452
A. Halogen-Oxidizing Reagents	437	1. Diazonium Salts	453
B. Radiohalogenation Reaction Termination	438	2. Photogenerated Species	454
C. Radiohalogenation of Activated Aryl Compounds	438	E. Cross-Linking Reagents	454
1. Compounds Containing "Strongly Activating" Groups	438	1. Noncleavable	455
2. Compounds Containing "Mildly Activating" Groups	438	2. Cleavable	455
3. Direct Labeling of Proteins	439	V. Future Directions	457
D. Radiohalogenation of Nonactivated Compounds	439	A. Design of Conjugates	458
1. Diazonium Salts and Triazines	439	1. In Vivo Stability	458
2. Organometallic Intermediates	439	2. Cleavable Linkers	458
IV. Radiohalogenated Conjugates	440	3. Nonmetabolizable Linkers	460
A. Amine-Reactive Conjugates	440	B. Direct Labeling of Conjugates	460
1. Active Esters	440	VI. Radiation Safety Considerations	461
2. Imidate Esters	446	VII. Summary	461
3. Aldehydes	447	VIII. Acknowledgment	462
4. Isocyanates and Isothiocyanates	447	IX. Literature Cited	462
5. Activated Halides and Maleimides	448		
B. Sulfhydryl-Reactive Conjugates	448		

I. INTRODUCTION

Methods of radiolabeling proteins have been of interest for a variety of applications for several decades. Although many different radionuclides have been used to radiolabel proteins (1-7), the largest number of labeled-protein studies have used radionuclides of iodine, principally iodine-125 and iodine-131. These radionuclides of iodine have properties which are adequate for a number of different applications, and the radionuclides are relatively

easy to use and readily available at a nominal cost from commercial sources. Other radionuclides of the halogen group, while not studied extensively to date, could potentially be utilized in protein labeling. In fact, there are a number of radiohalogen nuclides, with a wide range of half-lives and radiochemical properties, which could be used for a variety of different purposes. As a group, radiohalogens may be particularly useful for radiolabeling of proteins because (a) their chemistry is well-understood (perhaps with the exception of astatine), (b) they form stable covalent bonds, (c) their steric and electronic nature can be expected to cause minimal alteration to the protein, (d) high specific activity radiolabeling can be accomplished, and (e) radionuclides with many different half-lives and photon or particle emissions are obtainable.

The first radiohalogen labeled protein studies may be that of radiobrominated human serum albumin (HSA) reported in 1943 by Fine and Seligman (8). Iodination of serum albumin was reported as early as 1945 (9); however, it appears that the first radioiodinated protein, iodine-131-labeled rabbit antiglobulin, was reported in 1948 by Pressman and Keighley (10). Radioiodination of proteins was quickly adopted in many studies and in 1957 Bale and Spar (11) wrote that "coupling of a radioactive halogen, almost always I^{131} , to an antibody or antigen has been the most widely used method of labeling with radioactivity for immunological purposes". They further stated that "coupling reactions are relatively easy to carry out in a routine fashion". In those early studies the radiohalogen label was used because prior studies involving labeling of the protein via incorporation of sulfur-35 ($t_{1/2} = 87$ d, β^-), tritium ($t_{1/2} = 12.35$ y, β^-) or carbon-14 ($t_{1/2} = 5730$ y, β^-) labeled amino acids resulted in very low efficiency of isotopic labeling. In a broader perspective, the advantages of using photon-emitting radionuclides rather than weak β -particle emitters such as tritium or carbon-14 for radiolabeling proteins went further than radiochemical yield. Importantly, counting biological samples labeled with photon (e.g. X-rays or γ -rays) emitting radionuclides can be done more easily than counting samples labeled with β -emitting radionuclides due to the need for tissue homogenization and mixing with scintillation cocktails for liquid scintillation counting. Perhaps more important though, many applications of radiolabeled proteins require that high specific activities be obtained for detection at very low levels of protein. As a comparison, the specific activity obtainable for iodine-125 (17 Ci/mg, 2125 Ci/mmol) or iodine-131 (10–50 Ci/mg, 1310–6550 Ci/mmol) labeled proteins allows for a much more sensitive assay of radioactivity, which has been estimated to be 75–150 times higher for radioiodine than for tritiated proteins and 35 000 times higher than for carbon-14-labeled proteins (12, 13). Indeed, it was the high specific activity obtainable with radioiodinated proteins which made the development of radioimmunoassay systems possible (14, 15).

The most common procedure employed in the radiohalogenation of proteins or peptides has been, and will likely continue to be, the reaction of an in situ prepared electrophilic radioiodine species with functional groups on a native protein, often referred to as "direct" labeling. The chemistry of direct labeling with radioiodine has been extensively studied and a number of reviews covering that chemistry have appeared in the literature (2, 3, 5, 16–18). Unfortunately, while direct labeling works very well for radioiodine, it is generally of little or no value for radiohalogenations with other elements in the halogen group. For example, direct labeling with bromine radionuclides requires harsh oxidizing conditions which can

cause denaturation of proteins, except when enzymes are used as the oxidants (19–21). However, routine use of enzymes for the radiobrominations is not practical at this time due to the cost and availability of the enzymes. Additionally, it might be expected that the harsh oxidizing conditions required to prepare electrophilic chlorine and fluorine would exclude use of radionuclides of these elements from direct radiohalogenations, and no reports of direct labeling radionuclides of these elements were found. Direct labeling of proteins with astatine nuclides can also be accomplished (22–25), but the astatine-protein bond produced has been found to be unstable (26, 27).

An alternative to direct radiohalogen labeling of proteins is conjugation of a small radiohalogenated molecule to the protein. Radiohalogenations using small molecule conjugates are more difficult to conduct because they involve more chemical steps, and often result in lower radiochemical yields, than direct labeling. However, conjugate labeling offers some benefits which cannot be obtained by direct labeling. Most important, perhaps, is the fact that conjugate labeling provides a method of introducing radiohalogens into proteins that cannot be directly labeled. Other benefits of conjugate labeling include providing (a) a method of stabilizing radiohalogens to in vivo dehalogenation by enzymes, (b) a method of labeling that does not expose the protein to harsh oxidants and reductants, (c) a method of labeling which permits dual-labeled-protein studies using the same molecule to attach two different halogen radionuclides, and (d) a method of labeling which can potentially provide some control of the secondary distribution of the radiohalogen.

This review focuses on protein labeling by conjugation of radiohalogenated small molecules. It is expected that peptides of less than 50 amino acids might be radiohalogenated in the same, or similar, manner as the larger proteins; however, they are not specifically addressed in the review. The chemistry of radiohalogenated conjugates in the review has been divided into three areas which are presented separately. The areas include (1) properties and chemistry of radiohalogens, (2) chemistry of radiohalogen labeling of small molecules, and (3) chemistry associated with conjugates for labeling proteins. A listing of radiohalogenated compounds that have been coupled (conjugated) to proteins is provided in Tables IV–IX. Structures for the compounds are provided in the tables and are referenced by compound number in the text. Some of the examples of conjugates cited are taken from preliminary communications (i.e. abstracts), because it was thought that this information should be included for completeness. In some literature citations, yields for the radiohalogenations or conjugations were not given directly, so where possible an estimation was made based on the information provided. When this was not possible, the notation of NR (not reported) was made.

Review of the literature has shown that there have been a large number of radiohalogenated protein conjugates prepared, with many new conjugates being reported within the past five years. Although an attempt was made to provide a complete list of halogenated conjugates studied to date, it is anticipated that some conjugates may have been overlooked as they have been reported in such diverse literature.

II. RADIONUCLIDES OF HALOGENS

A number of radionuclides, each with a different half-life and particle-emission properties, can be produced in the halogen group of elements. While iodine-125 and iodine-131 have been the radionuclides primarily used in

Table I. Selected Halogen Nuclides

nuclide	half-life	major route of decay ^a	ref
Iodine Nuclides			
¹¹⁹ I	19 min	β^+	29
¹²⁰ I	1.35 h	β^+ (81%)	32
¹²¹ I	2 h	β^+	29, 33
¹²² I	3.6 min	β^+ (76%)	30-32
¹²³ I	13.2 h	EC (100%)	28, 31, 32
¹²⁴ I	4.2 d	EC (70%), β^+ (30%)	29, 32, 45
¹²⁵ I	60.0 d	EC	29, 32
¹²⁶ I	13 d	EC (55%), β^- (44%), β^+ (1%)	29
¹²⁷ I	stable (100%)	none	29
¹²⁸ I	25 min	β^- (94%), EC (6%)	29, 32
¹²⁹ I	1.7×10^7 y	β^-	29
¹³⁰ I	12.5 h	β^-	29
¹³¹ I	8.04 d	β^-	29, 32
¹³² I	2.30 h	β^-	29, 32
¹³³ I	21 h	β^-	29, 32
¹³⁴ I	52.5 h	β^-	29
¹³⁵ I	6.7 h	β^-	29
Bromine Nuclides			
⁷⁴ Br	40 min	β^+ , EC	28, 29, 33
⁷⁵ Br	97 min	β^+ (75.5%), EC (24.5%)	28, 31, 32
⁷⁶ Br	16 h	β^+ (57%)	28, 32
⁷⁷ Br	57.1 h	EC (99.3%), β^+ (0.7%)	28
^{78m} Br	6.4 min	IT	29
⁷⁸ Br	<6 min	β^+	29
⁷⁹ Br	stable (50.5%)	none	29
^{80m} Br	4.5 h	IT	29, 31
⁸⁰ Br	18 min	β^- (92%), β^+ (3%), EC (5%)	29
⁸¹ Br	stable (49.5%)	none	29
⁸² Br	35.3 h	β^-	29, 32
⁸³ Br	2.4 h	β^-	29
⁸⁴ Br	32 min	β^-	29
Chlorine Nuclides			
^{34m} Cl	32.4 min	β^+ (53%), IT (47%)	29, 32
³⁵ Cl	stable (75.5%)	none	29
³⁶ Cl	3×10^5 y	β^- , β^+	29, 32
³⁷ Cl	stable (24.5%)	none	29
³⁸ Cl	37.2 min	β^-	29-32
³⁹ Cl	1 h	β^-	29
Fluorine Nuclides			
¹⁸ F	109.8 min	β^+ (97%), EC (3%)	28, 31, 32, 36
¹⁹ F	stable (100%)	none	
Astatine Nuclides			
²¹¹ At	7.21 h	α (42%), EC (58%)	28, 31, 32, 35

^a β^+ = positron emission, β^- = negatron (electron) emission, EC = electron capture, IT = isomeric transition.

protein labeling, there are a number of different halogen radionuclides that could be used for unique or specific applications. The choice of radionuclide to use for a particular application will be dependent on the nuclear emission properties, the physical half-life, the decay characteristics, the daughter nuclide characteristics, and the cost and availability. While many of the radiohalogen nuclides are not commercially available, most are obtainable through activation of the appropriate target materials using reactor (neutron) or cyclotron (proton, deuteron, or alpha) irradiations. However, it must be emphasized that even though a radionuclide can be produced, issues such as availability of target material, radioisotopic purity from the irradiation, quantity of radionuclide needed, and ultimately the cost may preclude its use in an application. Production of radionuclides of halogens is outside the scope of this review, but can be found in a number of articles from the literature (28-36).

The half-lives and primary emissions of halogen radionuclides which may have an application to protein labeling are given in Table I. Radionuclides with half-lives shorter than 3 min are not included, as these are unlikely to be of value for protein labeling. Since the ultimate use of the radiohalogen-labeled proteins will

define which of the radionuclides are of interest, the following discussion is structured according to application. The presentation is not a review of the area, but rather an overview with basic information to acquaint the reader with some of the important aspects of the area. There will be many potential applications not mentioned herein, and many more that have not yet been envisioned.

A. Halogen Radionuclides for in Vitro Applications. Iodine-125 has been the primary radionuclide for in vitro applications due to its 60-d half-life and low-energy photon emissions. The long half-life permits the preparation and storage of labeled protein for extended periods prior to usage. The lack of particulate emissions and low-energy photon emission makes it particularly attractive for storage, as minimal radiation damage to the labeled protein is expected. Specific activities that are very near the theoretical value (17.2 Ci/mg, 2175 Ci/mmol) are obtained with iodine-125. Its cost and availability are also very reasonable. In review other halogen radionuclides, it appears that there are no other radionuclides that can readily be used in the place of iodine-125 for in vitro studies.

B. Halogen Radionuclides for in Vitro Imaging. Any of the radionuclides of halogens which have X-ray or γ -ray (photon) emissions might be considered for in vivo imaging applications, but the extent of usefulness of the radionuclide to following the distribution and pharmacokinetics of a radiolabeled protein in vivo will be dependent on a number of factors. Most important are the energy and abundance of the photon emission(s) and the biological system studied. The application of radionuclides for measurement of receptor-ligand binding in vivo (37) has become less restricted through the advent of new imaging equipment and related computer image enhancement employed in single photon emission tomography (SPECT) and positron emission tomography (PET). Advancements are rapidly changing the detection limitations of specific radionuclides as outlined in the scientific highlights of the annual meeting of The Society of Nuclear Medicine presented by Dr. Wagner (38-40).

Evaluations of labeled proteins in vivo are very important applications of radiolabeled proteins. While analysis of materials in excrement (e.g. urine or fecal material) permits gaining information on the clearance rate of labeled protein and of some of the pathways in the metabolism of the labeled protein, it provides little knowledge of the in vivo distribution of protein. In vivo data can be obtained by sacrificing animals, excising tissue samples, and counting the radioactivity in an appropriate counter. Tritium- and carbon-14-labeled proteins can be used to obtain in vivo data, but due to the relative ease of counting tissue samples, the photo-emitting radionuclides iodine-125 and iodine-131 are routinely used. From experiments using iodine-125 and iodine-131, biodistribution data, pharmacokinetic data, and data on the metabolic fate of the radiolabel can readily be obtained. However, iodine-125 and iodine-131 are not optimal to assess the parameters in patients. Iodine-125, while it can be imaged by a thin-crystal γ -camera (marginally) when evaluating small animals such as mice, it is of little or no value in imaging patients due to the attenuation of the photons through tissues. Iodine-131 is often used for imaging with conventional γ -cameras, but its high-energy γ -emissions are not optimally counted, and its β -particle emission results in more radiation dose to the tissues than is desirable. An alternate radionuclide of iodine, iodine-123, has a reasonable half-life of 13 h and a nearly ideal γ -emission of 159 keV, in high abundance (100%) for imaging with the current γ -cameras. Unfortunately, production of this

radionuclide without radionuclidic impurities is expensive, which makes its general use impractical. Much controversy has accompanied this radionuclide as it has been felt that its use would be greatly expanded if it could be obtained inexpensively, while others have felt that it could be made inexpensively if its use was more in demand (41). Another γ -emitting radiohalogen that has been considered for in vivo diagnostics is bromine-77. While its emitted photons at 239 keV (24%) and 521 keV (23%) are high for efficient detection with current γ -cameras, bromine-77 has been used in imaging (42). Unfortunately, while it can be produced via a number of routes (28), routine production of curie quantities of bromine-77 by high-energy spallation reactions (34), which was carried out at Los Alamos National Laboratory, has stopped.

Perhaps the area that holds the greatest promise for new applications of radiohalogens is PET imaging in medicine (43). PET studies can provide quantitative data on the distribution and pharmacokinetics of radiohalogenated proteins in vivo (44). There are a number of positron-emitting radionuclides of halogens, with a variety of physical half-lives and emitted-positron energies. The positron energy (E_{\max}) is very important, as this defines the maximum distance that the positron will travel before its annihilation will occur, which in turn sets some limitations on the best resolution that can be obtained from the imaging device (i.e. tomograph). For positrons which have emission energies of 2 MeV or above, this distance may be in centimeters and can cause severe limitations in the resolution. However, radiohalogen nuclides with high-energy positrons may be useful in obtaining pharmacokinetic data.

The most widely used positron-emitting radiohalogen is fluorine-18. Fluorine-18 is likely to be the nuclide of choice in many protein-labeling applications as it (1) can be readily produced via a number of different methods (28, 36), (2) has a high positron abundance (97%), and (3) has a relatively low positron emission energy (0.635 MeV max), which limits its range to 2.3 mm in water (or tissue). However, fluorine-18's 110-min half-life may limit its use for some applications with proteins. Chlorine-34m is also a positron emitter, but it has a shorter half-life, lower positron-emission rate, and higher positron energy than fluorine-18 (28). Bromine-74m is another positron-emitting halogen radionuclide. It has a shorter half-life and a higher positron energy than fluorine-18 (28). Another bromine radionuclide, bromine-75 has a half-life of 97 min, which is similar to that of fluorine-18, but it has a positron emission of 1.74 MeV in 75% abundance. While bromine-75 may be produced at higher specific activities than fluorine-18, unless there are significant difficulties in labeling of proteins with fluorine-18, it is not likely to be used in its place. Yet another positron-emitting radionuclide or bromine, bromine-76, has a half-life of 16 h and appears to be an attractive candidate for labeling of proteins that have longer biological half-lives (e.g. 1–3 d). A positron-emitting radionuclide of iodine, iodine-122, will probably not be of general use for protein labeling due to its very short half-life (3.6 min). However, the fact that iodine-122 can be produced from a generator system makes it attractive when applicable (31). A longer lived positron-emitting radionuclide of iodine, iodine-124, has been investigated as a radiolabel. It has a 4.2 d half-life, but until recently it was not considered a reasonable candidate due to its complicated decay emission properties. However, it has been studied as a label for intact monoclonal antibodies since its half-life matches the biological half-life of antibody (45).

C. Halogen Radionuclides for Therapy. Radiohalogens with particulate emissions are being tested or considered for in vivo therapy of cancer, particularly in combination with monoclonal antibodies (46–49). Iodine-131 has been the most widely used therapeutic radionuclide for labeling antibodies. Due to its availability and cost, it is likely to continue to be used for this purpose, although iodine-131 does not have optimal characteristics for therapy (50) and its high energy (i.e. 364 keV) γ -emissions pose a radiation exposure risk to the people working with patients undergoing treatment. Thus, it is likely that other radionuclides may be used in the future (50–53). Of the β -particle-emitting radiohalogens, bromine-82 appears to be an alternative to iodine-131. A major difficulty with the use of bromine-82 is that it is generally produced from neutron irradiation of bromide salts (e.g. NH_4Br), which results in too low a specific activity for protein labeling. Further, the difficulties of working with patients treated with hundreds of millicuries of bromine-82 would be expected to be worse than that with iodine-131 as it has a number of high-energy γ -emissions (e.g. 554, 619, 776 keV). Other β -particle-emitting radiohalogens with shorter half-lives may be useful as well.

Potentially, the positron-emitting radiohalogens fluorine-18, bromine-75, bromine-76, and iodine-124 could be used for therapy, with the added benefit of being able to assess patient radiation dosimetry to tissues and monitor changes in tumor volume through PET scans. However, the difficulties mentioned regarding radiation risk to patient care providers would also apply since positron annihilation results in the emission of a 511 keV photon. Further, difficulties in producing some of the nuclides may limit their general use.

Another halogen radionuclide that may hold potential for some therapy applications is astatine-211 (54, 55). While its half-life of 7.2 h is relatively short, it decays by α -particle emission, which is extremely cytotoxic, such that it could be an effective therapeutic agent if it were specifically delivered to the cell or target material (53). Basic science studies are needed to understand the limitations of using proteins labeled with α -particle-emitting radionuclides for therapy. At present many investigators believe that astatinated antibodies may be limited to therapy of metastatic or blood-borne disease due to the short path length of the α -particle. Investigations on the therapeutic usefulness of astatine-211 have been very limited due to the difficulty in obtaining the radionuclide.

Auger electron emitters have been shown to be effective at cell killing if they can be incorporated into nuclear materials in cells (56). Iodine-125 decays with an emission of a number of Auger electrons; however, its 60-d half-life may be problematic if the turnover of labeled protein in the nucleus is considerably shorter than that. An antibody labeled with iodine-125 reactive against the α -epidermal growth factor receptor, which is internalized (57), in human glioma cells has been shown to be cytotoxic (58). Bromine-77 which decays by electron capture has also been tested for the cytotoxicity of the emitted Auger electrons, and found to be effective at cell killing when incorporated into nuclear material as [^{77}Br]bromodeoxyuridine (56). This radionuclide was thought to have the advantage that it had a shorter half-life than iodine-125 and that bromine was not taken up by the thyroid. Another iodine radionuclide, iodine-123, also has emission of Auger electrons. Due to its shorter half-life, and a γ -emission that is easily imaged, this radionuclide is an attractive candidate to study for therapeutic applications.

D. Other Halogen Radionuclides. Protein labeling with iodine-132 was reported in 1955 (59). Iodine-132 was obtained from tellurium-132, a fission product. It is interesting that this radionuclide, which has a much shorter half-life (2.3 h) than iodine-131, has not gained more prominence. However, the availability and cost of iodine-131 appears to have alleviated a need for it. More recently, the very long half-lived iodine-129 (1.57×10^7 y) has been used as an *in vivo* tracer for protein turnover (60). The plasma concentration of iodine-129 can be assessed accurately using by neutron-activation analysis. Unfortunately, while a patient may receive less of a radiation dose with this radionuclide, its use must be tempered by the need to dispose of such a long half-life radionuclide in the environment.

III. RADIOHALOGEN LABELING

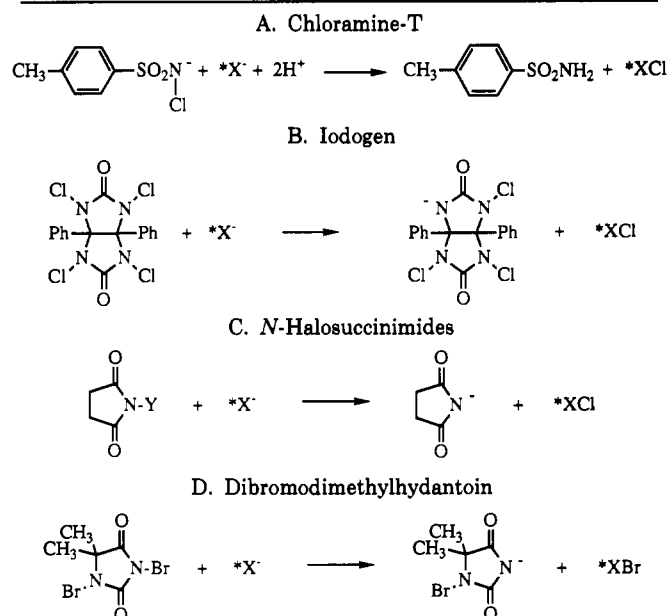
Methods for radiohalogenation of proteins, in general, should be rapid and give high radiochemical yields. The radiohalogenated protein that is obtained should be of high specific activity and should be labeled in a manner that results in a stable attachment of the radiohalogen. While the chemistry associated with radiolabeling using radiohalogens is the same as that of halogenation with stable nuclides, there are some distinct differences in reactions due to the fact that radiohalogenations are generally very dilute and contain many minor impurities from processing of the target material and in the chemicals used which are present in more mass than the radiohalogen itself. Thus, optimization of reaction parameters is almost always a requisite of radiohalogenations.

Stability of the radiohalogen-labeled protein is very important if one wants to be assured that the observation of radioactivity is a true indicator of what is happening with the protein. Most radiohalogenations, with the exception of fluorinations, are conducted as electrophilic substitution reactions (61). The rate of electrophilic substitution reactions is a distinct advantage with the dilute radiohalogens, allowing the reactions to occur rapidly under mild conditions. Electrophilic reactions require the production of an electrophilic radiohalogenation reagent through oxidation of halide ions. A section on oxidants used in electrophilic radiohalogenations is given below. Electrophilic radiohalogenation reactions are terminated prior to workup, and a section on this reaction step is also included below. Other parameters of radiohalogenations, such as solvent selection and purification method, are included in the discussion of these two topics and are not addressed separately.

Radiohalogenation reactions of proteins and small-molecule conjugates is presented below by the nature of the molecule being halogenated. A large amount of research has been conducted on high specific activity radiohalogenations of compounds for radiopharmaceutical development over the past 2 decades (62, 63). Many of the methods developed for high specific activity radiohalogenations can be, and in some examples have been, directly applied to radiohalogenation of proteins and small-molecule conjugates. Indeed, a number of the radiohalogenated small molecules used to prepare radiopharmaceuticals could potentially be used as protein conjugates.

A. Halogen-Oxidizing Reagents. Radiohalogens are generally obtained as their halide salts and must be oxidized to form an electrophilic halogenating species to label molecules. Oxidation of chloride, bromide, iodide, and astatide can readily be accomplished by inorganic reagents such as MnO_4^- , Ce^{4+} ion, $\text{Cr}_2\text{O}_7^{2-}$, and IO_3^- . However, the use of such strong oxidants is incompatible

Table II. *N*-Haloamine Oxidizing Reagents^a



^a Where X = F, Br, I, or At; Y = Cl (*N*-chlorosuccinimide), Br (*N*-bromosuccinimide), I (*N*-iodosuccinimide).

with most organic molecules and requires that the halogen be distilled from one vessel to another. Many of the early radiohalogenations of bromine used these oxidants (64–69), but the preferred approach for all of the radiohalogens today is to generate the electrophilic radiohalogenation reagent *in situ*. *In situ* oxidation can be accomplished by using dihalogens (X_2) of the same element, but in most examples this is not desired as the halogen being employed will react with the compound of interest and this will result in a decrease in the specific activity obtained. Further, oxidation to form a dihalogen species (${}^*\text{X}_2$) results in a maximum radiochemical yield of 50%. The maximum radiochemical yield can be increased to 100% when a mixed halogen species, such as halogen chloride (e.g. ICl), is generated.

There are very small quantities of radiohalide present when high specific activity solutions are employed, with the exception of radiohalogenations using therapeutic quantities of radiohalide. Even though microgram quantities of oxidant are used (often in the 10–100 $\mu\text{g}/\text{mCi}$ range), the stoichiometry of oxidizing reagent *in situ* is many times greater than that of the halide. This fact makes it necessary to have oxidants that do not adversely affect the molecules being labeled. For direct labeling of proteins (with radioiodine), the oxidant should be compatible with aqueous solutions of proteins, should not denature the protein, and should permit easy separation when done. Various oxidizing reagents have been used for *in situ* generation of mixed halogens. Iodine monochloride has been used as a method of iodination of proteins (70). The most common oxidizing reagents used are the *N*-haloamine compounds chloramine-T and iodogen shown in Table II (71, 72). These compounds are commercially available and the literature has many examples of their use. Chloramine-T, sodium *N*-chlorotoluenesulfonamide, has been used extensively for oxidation of halides and its chemistry is well-known. This reagent is water-soluble and has been utilized for *in situ* oxidation of iodide, bromide, and astatine. A similar reagent, iodogen, 1,3,4,6-tetrachloro-3 α ,6 α -diphenylglycoluril, has also been used extensively in radioiodinations. Iodogen (IODO-GEN) is very stable and is virtually insoluble in water. This latter

fact has made iodogen attractive because it is readily separated from the radiolabeled protein. Other related oxidizing reagents include IODO-BEADS, where chloramine-T is attached to a solid support (73).

Radiohalogenation of small molecules to be used as protein conjugates has different requirements of oxidizing reagents. Since the reactions are conducted in a separate vessel from the protein, stronger oxidizing reagents can be used without affecting the protein. Many examples of chloramine-T oxidations of halides for radiohalogenations of small molecules have been reported (74–76). The reactions have generally been conducted in aqueous solutions, but the salt is also soluble in some aprotic solvents such as trifluoroacetic anhydride (77). The use of various oxidizing reagents in high specific activity radiohalogenations has been reviewed by Coenen, Moerlein, and Stocklin (78). In preparing radiolabeled small molecules for protein conjugation, Zalutsky and co-workers have used *tert*-butyl hydroperoxide (TBHP) in chloroform/acetic acid solution to oxidize radioiodide and astatide (79, 80). In our protein conjugate studies, *N*-chlorosuccinimide (NCS) (see Table II) in methanol/acetic acid has been used for oxidation of radiobromide, radioiodide, and astatide (81–83). This reagent is readily available and presumably produces XCl when reacted with chloride, bromide, iodide, or astatide (84, 85). NCS has been attractive because it is a weaker oxidant than *tert*-butyl hypochlorite (86), *N*-chlorotetrafluorosuccinimide (87), or dichloramine-T (88). NCS does not halogenate phenolic compounds, and thus, does not dilute the specific activity of most radiohalogen-labeled compounds by producing chloro derivatives. A drawback to the use of NCS is the fact that only small quantities (<10%) of water can be present without adversely affecting the oxidation.

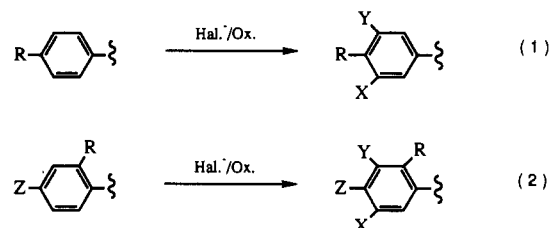
Another method of oxidizing radiohalogens in situ for labeling proteins or small molecules is to use oxidative enzymes. Radioiodinations and radiobrominations have been successfully conducted using enzymes (18). Lactoperoxidase, horseradish peroxidase, and myeloperoxidase, have been used for radioiodination of proteins. The enzymes chloroperoxidase (19), myeloperoxidase (20), and bromoperoxidase (21) have been successfully used in radiobrominations of monoclonal antibodies. While the use of enzymes in radiohalogenations offers a very mild method of oxidation, routine use of enzymes to radiohalogenate proteins is unlikely as (1) the enzymes can themselves be radiohalogenated, (2) the radioiodinated proteins have to be separated from the enzyme [although a solid support enzyme can be used (89)], and (3) the enzymes are more expensive and most are more difficult to obtain than the commonly used organic oxidants (i.e. chloramine-T, iodogen).

B. Radiohalogenation Reaction Termination. Electrophilic radiohalogenation reactions are routinely stopped (terminated) prior to workup due to concerns for volatile radiohalogens and subsequent undesired reactions. Depending upon the radionuclide, oxidant and solvent(s) used, and concentration of reagents (and perhaps the whim of the investigator), radiohalogenation reactions are allowed to proceed from 30 s to 30 min. Many radiohalogenation reactions are complete almost instantly. To terminate the reaction, an aqueous solution (or phosphate buffer solution) of the reductant sodium metabisulfite is generally added to reduce the electrophilic halogen species to the halide. A minimum amount of reducing agent should be added to quench (terminate) the reaction such that the possibility of side reactions is minimized. Investigators generally use quantities of sodium metabisulfite

ranging from 25 $\mu\text{g/mCi}$ (90) to 125 $\mu\text{g/mCi}$ (91) when terminating direct labeling reactions. In many direct radioiodination reactions of monoclonal antibodies, investigators have eliminated the reduction step and have simply put the radiolabeled protein over a size-exclusion column such as a Sephadex G-25 (PD-10) (92), Sephadex G-50 (93), Biogel P-60 (94), Pharmacia G-10 (95), or a Dowex column (96, 97). This process would be expected to leave the halogen on the column. One must be cautioned that this practice does require careful handling techniques and careful cleanup of reaction vial and column (see VI. Radiation Safety Considerations).

When a small molecule is radiolabeled prior to conjugation, it is necessary to quench unreacted halogen since any excess could react with the protein during the conjugation step. If one is concerned about deleterious effects of the metabisulfite on the protein, excess radiohalogen can be removed by an evaporation of the solvent under a gentle stream of N_2 or argon. The solvent evaporation must be done in an enclosed vessel which has an exit for the gas that passes through a charcoal bed. The volatilization of radiohalide should be avoided if at all possible, and other methods of terminating the reactions are preferred. Bolton has described the use of a cysteine solution for reaction termination (98). Another method of removal is to add a reactive species that can be readily separated from the labeled protein, such as phenol, to trap the electrophilic radiohalogen.

C. Radiohalogenation of Activated Aryl Compounds. 1. *Compounds Containing "Strongly Activating" Groups.* Aromatic ring compounds substituted with OH (phenols), NH_2 (anilines), or NHR or NR_2 (N-alkylanilines) are "strongly activated" toward electrophilic halogenation (99). These compounds react rapidly with electrophilic halogens, which is particularly attractive for reactions with the very dilute high specific activity radiohalogens. When the phenol hydroxyl ($\text{R} = \text{OH}$) or aniline amine ($\text{R} = \text{NH}_2$) is situated para to the aryl position containing the conjugation group, halogenation can lead to two products, as depicted in eq 1. These products are

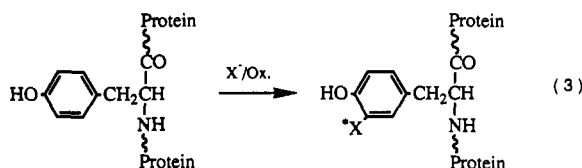


the monohalogenated product ($\text{X} = \text{halogen}$, $\text{Y} = \text{H}$) and the dihalogenated product ($\text{X} = \text{Y} = \text{halogen}$). When the activating substituent is in either the 2 or the 3 position of the aryl ring, three halogenated products can be obtained as depicted in eq 2. These products are either of the monosubstituted products ($\text{X} = \text{halogen}$, $\text{Y} = \text{H}$ or $\text{X} = \text{H}$, $\text{Y} = \text{halogen}$) or the disubstituted product ($\text{X} = \text{Y} = \text{halogen}$).

2. *Compounds Containing "Mildly Activating" Groups.* Aryl compounds containing OR (e.g. anisoles, where $\text{R} = \text{CH}_3$), NHCOR (e.g. acyl anilines), OCOR (e.g. phenolic esters), and SR (e.g. thiophenol ethers) can be considered "moderately activated" aromatic ring compounds in electrophilic aromatic substitution reactions (99). Depending on the nature of other substituents present, aromatic rings containing these functionalities can also be readily substituted with electrophilic halogen species. While mildly activated aryl compounds can be used for radiohalogenations, they are not as attractive as highly activated

aryl ring compounds as minor quantities of more reactive impurities could significantly lower radiochemical yields due to side reactions with the impurities. Additionally, the same type of mixtures of halogenated products can be obtained in the electrophilic aromatic substitution reactions as described for aryl compounds containing strongly activating groups.

3. Direct Labeling of Proteins. Several functional groups present in protein structures are reactive with electrophilic radioiodine. These include the highly activated phenolic ring of tyrosine residues, the imidazole ring of histidine residues, the benzene ring of phenylalanine residues, the indole ring of tryptophan residues, and the sulfhydryl groups of cysteine residues (100). The most readily iodinated residues are tyrosine, histidine, and cysteine. Under various reaction conditions (e.g. low pH) differing percentages of the tyrosyl, histidyl, and cysteinyl moieties have been observed to react with radioiodine (101). However, using commonly employed reaction conditions (i.e. pH 7.4, chloramine-T oxidant) a very large percentage of the radioiodine will be present on the phenolic tyrosine residues as depicted in eq 3 (102).



D. Radiohalogenation of Nonactivated Compounds.

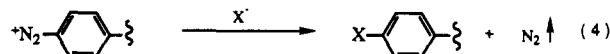
Radioiodination of activated aromatic ring conjugates has been very useful; however, not all halogens can be introduced by the use of activated aromatic compounds. For example, astatine labeling of phenolic compounds is not practical, as the phenolic ring is too activated to produce stable compounds with astatine nuclides (103–105). Furthermore, halogenated phenols and anilines are susceptible to dehalogenation by nucleophiles, and radioiodinated tyrosine derivatives (and to a lesser extent other radioiodinated phenols) are susceptible to *in vivo* enzymatic dehalogenation (106–108). Because of their higher stability, nonactivated aromatic ring compounds and halovinyl-substituted compounds are good alternatives to activated aromatic rings for halogens.

Fluorine labeling is somewhat different from the other radiohalogenations as fluorine is not readily displaced from aliphatic carbons and can be introduced into aromatic ring compounds via ipso displacement reactions. Electrophilic fluorination of activated aromatic compounds has been difficult due to the high oxidizing characteristics of fluorinating reagents (99). A number of reviews on the chemistry of fluorination (109–112) and radiofluorination (113–116) are in the literature.

Electrophilic chlorination and bromination of nonactivated aromatic ring compounds can be achieved directly (117, 118), but a catalyst is often used (99). Electrophilic iodination of nonactivated or deactivated aromatic ring compounds often requires that harsh reaction conditions or catalysts be employed (119–124). High specific activity radiohalogenation of nonactivated compounds can be particularly difficult in these reactions, as there are many impurities present that could react with the halogen before it reacted with the aromatic ring. These factors led investigators to find methods of regiospecifically introducing radiohalogens into nonactivated aromatic rings and vinyl moieties. Two methods of halogenation have been found to be suitable to fulfill these needs. These methods are incorporation of radiohalogens via decomposition of

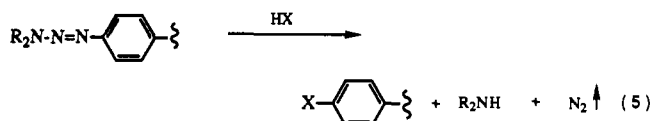
aryl diazonium salts and incorporation of radiohalogens in aromatic and vinyl positions in molecules using organometallic intermediates. Brief overviews of each of these methods of halogenation are given below.

1. Diazonium Salts and Triazines. One of the earliest methods developed for incorporation of halogens into nonactivated ring compounds was use of aryl diazonium salt decompositions [dediazoniations (125)] as depicted in eq 4. Reactions involving cuprous chloride and bromide



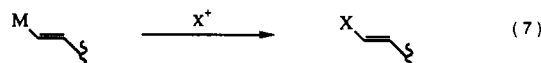
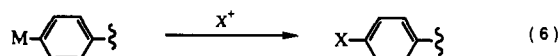
are commonly referred to as the Sandmeyer reaction (126, 127) and those involving HCl or HBr are referred to as the Gatterman reaction. There are a number of difficulties in using this method for radiohalogenations (78), with the most important being the low radiochemical yields that are generally obtained.

Introduction of astatine-211 via diazonium salt decomposition (128) gave higher radiochemical yields than those obtained for iodine-131 (129). Indeed, initial labeling reactions of organic compounds with astatine-211 were conducted with diazotized benzidine and *p*-aminobenzoic acid (130). Improvements in the stability of the aryl diazonium compounds and reaction conditions (e.g. no strong oxidants present) for halogenations and radiohalogenations were obtained by preparing triazines (131–134) as depicted in eq 5. This reaction is often referred to as the Wallach reaction.



Fluorination and radiofluorination have been accomplished by decomposition of the tetrafluoroborate salts of arene diazonium compounds, referred to as the Balz-Schiemann reaction (116) or Schiemann reaction (62). This reaction results in low specific activity labelings and is complicated by side products of the diazonium salt decomposition (135, 136).

2. Organometallic Intermediates. Radiohalogenation reactions using organometallic intermediates have been studied extensively. Halogen-reactive organometallic compounds have been studied as a means of efficiently, rapidly, and site-specifically incorporating radiohalogens into small molecules. Various research groups have investigated the use of organothallium compounds (137), organomercury compounds (138–141), organoboranes (142), organostannanes (143–147), organosilanes (148–154), organosilicates (155, 160), and organogermanes (157, 158). A generalized scheme for this reaction is given in eq 6. Small-molecule radiolabeling has been reviewed (78, 159) and will be only briefly discussed below.



There have been numerous studies by investigators involving radiohalogenations of aromatic compounds via organometallic intermediates. Based on the results obtained in studies of a particular organometallic intermediate, it is difficult to choose which one to use in designing

small molecules for protein conjugation. Some studies which have compared radiohalogenations of different organometallic intermediates have determined that for general applications organostannanes are probably the best candidates. For example, a comparative study of the application of arenes metalated with tin, mercury, germanium, boron, and silicon for introducing the very short half-life (3.6 min) iodine-122 into aromatic compounds has been reported by Moerlein, Mathis, and Yano (160). These investigators were interested in very fast (<5 min) and efficient reactions. They investigated a number of reaction parameters and concluded that high specific activity radioiodinations could be obtained in high yield (>90%) using aryltin or -mercury compounds, whether they were activated or deactivated toward electrophilic substitution. The investigators indicated that they felt that the arylstannane was the best candidate for labeling since the organomercury compounds were more difficult to obtain as a single regioisomer.

Our research group was also interested in comparing radioiodinations of organometallic compounds for incorporation of radioiodine into molecules that were being developed for protein labeling. Initial studies to assess which organometallic intermediate would be best for radiohalogenations were carried out in a comparison of low specific activity radioiodinations of 4-(methoxycarbonyl)mercuric halides, 4-(methoxycarbonyl)boronic acid, and 4-(tri-*n*-butylstannyl)benzoate (161). Later, no-carrier-added radioiodinations and astatine labeling of these compounds, along with 4-(tri-*n*-butylstannyl)toluene and potassium 4-tolypentafluorosilicate, were also carried out (162). On the basis of the results of those investigations, arylstannanes were chosen as the organometallic intermediate of choice for radiohalogen labeling. This choice was made, even though the phenylboronic acid gave very good radiohalogen labeling yields at the no-carrier-added level, because the boronic acid was more difficult to synthesize and purify. Additionally, purification of the radiohalogenated small molecule from aryltri-*n*-butylstannanes is not necessary in some labeled protein applications due to a partitioning of the highly lipophilic arylstannane from the aqueous medium.

Vinyl halides are also stabilized toward nucleophilic displacement and have therefore been used as labeling groups to introduce radiohalogens into small molecules. Introduction of halogens into vinyl positions is facilitated by the use of organometallic intermediates. Some of the organometallic intermediates give addition products when reacted with electrophilic halogens (163); however, vinyl boronic acids and vinyl stannanes are cleaved to yield the vinyl halide directly as depicted in eq 7. These reactions have been studied as a method of producing radiohalogenated compounds (164). Organoboronic acids and stannanes have been used extensively for preparing radiohalogenated steroids (165–168). In another reaction, halofluorination of alkenes via BrF or IF produced in situ by reaction of fluoride with *N*-haloamines (NBS, NIS or 1,3-dibromo-5,5-dimethylhydantoin; Table II) yields a mixture of isomers which could be dehydrohalogenated to give vinyl fluorides (169).

IV. RADIOHALOGENATED CONJUGATES

There are many reviews that describe the chemistry of protein modification through conjugation of small molecules (170–173). The principal functional groups on proteins which are used in conjugation reactions with other molecules are amines, sulfhydryls, and oxidized sugars; however, other reactive groups such as phenols, carbox-

Table III. Protein Modification Reagents^a

A. Sulfhydryl-Generating Reagents		
	HS-CH ₂ -CH ₂ -OH	HS-CH ₂ -CH(OH)-CH(OH)-CH ₂ -SH
2-Iminothiolane	β-ME	DTE or DTT
B. Protein Cross-Linking Reagents		
DSS	MBS	
DSP	SPDP	

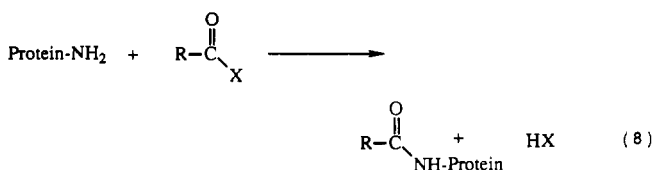
^a Where β-ME = 2-mercaptoethanol; DTT = dithiothreitol; DTE = dithioerythritol; DSS = disuccinimidyl suberate; MBS = *m*-maleimidobenzoyl *N*-hydroxysuccinimide ester; DSP = dithiobis(succinimidyl propionate); SPDP = *N*-succinimidyl 3-(2-pyridylthio)propionate

ylates, and imidazoles may also be used if desired. Additionally, a number of reagents have been developed which can be used to produce functional groups (e.g. sulfhydryls) or reactive entities (e.g. maleimides) on proteins for conjugation reactions with other molecules. Examples of these latter reagents are shown in Table III and examples of their use are described in the text.

One of the primary concerns in the design of new conjugates for radiohalogenation of proteins is which functional group will be utilized in the conjugation reactions. Thus, the following text is subdivided into sections on the basis of which protein functional group reactions are to be carried out with the small-molecule radiohalogenation reagents.

A. Amine-Reactive Conjugates. The most common functional group used for conjugation of radiolabeled molecules to proteins is the amine group, generally ε-amino groups of lysine residues. Many compounds reactive with lysines have been studied (176). Compounds that contain amine reactive functionalities such as active esters, imidates esters, aldehydes, and isothiocyanate groups have been used in protein conjugations. A large number of reaction conditions for conjugations with proteins have been studied. The primary considerations in the conjugation reactions are pH (usually >8.0) and concentrations of protein and reagents. A list of amine-reactive radiohalogenation reagents is given in Table IV. A brief description of the chemistry associated with radiohalogenated amine-reactive compounds is given in the following text.

1. Active Esters. Coupling of amines with "active" esters provides small-molecule conjugations which have amide linkages to the protein as shown in eq 8. There are



a large number of different active esters that may be synthesized. Fortunately, the choice of which active ester compound to prepare can be made more readily by reviewing the literature on the use of active esters in peptide synthesis (177, 178). For conjugates of radiohalogenated compounds the most commonly used active ester is the *N*-hydroxysuccinimide ester.

Perhaps the first activated carboxylic acid compound used for radiohalogenated-small-molecule conjugation of a protein was reported by Blau, Johnson, and Pressman (179). In their study, dual-labeled *p*-[¹³¹I]iodobenzoic [14C]acid, **2a**, was prepared by lithiation/carbonylation of diiodobenzene to incorporate a [14C]carboxylate into *p*-iodobenzoic acid, **1**, followed by ¹³¹I exchange at 250–260 °C for 10–12 h in a sealed ampule contained in a pressure bomb. In this early study the benzoic acid chloride, **2b**, was prepared for conjugation to the a rabbit γ -globulin. Although the labeling time was very long and the specific activity of the labeled product (estimated to be in the nCi/mg range based on Table I values for benzoate) was not as high as what would be desired (e.g. mCi/mg range), this very early dual-labeling experiment demonstrated that a radioiodinated protein conjugate could be prepared which was stable in vitro and in vivo.

The need to radiolabel proteins with high specific activity radioiodine led initially to protein conjugates which contained phenolic rings, as these were readily radioiodinated with high specific activity radioiodine. Some 16 y after the reported protein labeling of Blau et al., Bolton and Hunter reported a new method of labeling proteins which resulted in obtaining high specific activities of radioiodinated proteins (180). In the reported studies ¹²⁵I-labeled *N*-succinimidyl 3-(4-hydroxyphenyl)propionate, **4**, was prepared, producing a mixture of products (two radioactive spots by TLC analysis). The radiolabeled species were most likely the monoiodo derivative **4a** and the diiodo derivative **4b**. This mixture of labeled compounds was dried and reacted in a 3–4 mol ratio with a protein at pH 8.5. Three different protein hormones were radioiodinated, resulting in different (but high) specific activities for each protein. The authors found that the use of the new reagent (Bolton–Hunter reagent) was at least as good a method of radiolabeling as direct labeling, and in some examples was superior. They reported that the new labeling procedure generally gave specific radioactivities and biological activity of the labeled protein similar to those found with direct labeling with chloramine-T. However, it had a much broader application, as it could be used to label proteins which did not contain tyrosine residues, or which were sensitive to the oxidizing or reducing conditions of direct iodinations. Subsequent to the initial studies, the Bolton–Hunter reagent has been used for labeling many different proteins, and a description of large-scale radiolabeling procedure using the Bolton–Hunter reagent has been reported (181). Reviews of proteins labeled by the Bolton–Hunter reagent have appeared in the literature (182, 183). The Bolton–Hunter reagent has also been used to label cell surface (184) and platelet surface proteins (185). The Bolton–Hunter reagent is commercially available from several sources as a reagent for radioiodination, or in the monoradioiodinated (mixture or HPLC purified) and diradioiodinated (crude or HPLC purified) forms in specific activities of 2000–4000 Ci/mmol. A more water-soluble sulfohydroxysuccinimide ester is also commercially available. The sulfohydroxysuccinimide ester of the Bolton–Hunter reagent has been applied to labeling of cell surface proteins and is particularly attractive, as the charged sulfonate group

does not allow the radioiodinated reagent to cross the cell membrane (186).

The Bolton–Hunter reagent has also been used to obtain radiobrominated proteins. Attempts to obtain monobrominated ⁷⁷Br-labeled Bolton–Hunter reagent at Los Alamos National Laboratory resulted in mixtures of monobrominated (**4c**), dibrominated (**4d**), and nonbrominated (**3**) reagent using conventional oxidants (187). The fully dibrominated **4d** might have been achieved by adding carrier bromide, but it was felt that a lower specific activity material obtained would not be optimal for protein labeling. Knight et al. reported that the Bolton–Hunter reagent could be radiobrominated (⁷⁷Br) or radioiodinated (¹³¹I) by employing the enzyme chloroperoxidase and subsequently used to conjugate with fibrinogen and serum albumin (188). Low radiochemical yields were obtained using this method.

A reagent similar to the Bolton–Hunter reagent, *N*-succinimidyl (*tert*-butyloxycarbonyl)-L-[¹²⁵I]iodotyrosine (**5**), has been reported by Assoian et al. (189). This reagent was designed to be conjugated to a protein with subsequent removal of the *t*Boc protecting group to regenerate the positive charge lost in the conjugation step. Unfortunately, the deblocking step required that the iodinated protein be dried and 99% formic acid be added for 2–4 h at room temperature or overnight at 4 °C. These conditions were satisfactory for the peptides studied, but such conditions can be expected to cause deleterious effects to most proteins.

As mentioned previously, studies at Los Alamos which involved ⁷⁷Br-labeled monoclonal antibodies using the Bolton–Hunter reagent were unsuccessful (187). This led to the application of an arylsilane intermediate for regiospecific incorporation of bromine-77 into an amine-reactive compound. Thus, *N*-succinimidyl 3-[4-(trimethylsilyl)phenyl]propionate, **7a**, was synthesized and radiobrominated to form **8a** (190). Compound **7a**, an organometallic counterpart to the Bolton–Hunter reagent, was prepared and radiobrominated efficiently using NCS and Na^{77,82}Br in MeOH/HOAc at 50 °C for 5 min. However, radioiodination did not give the desired products under the conditions studied. There were no protein conjugations carried out with **8a**.

Radiohalogenated benzoic acids have been of interest for radiolabeling proteins and have been studied by a number of different research groups. The primary reason for the use of the more difficult to radiohalogenate, nonphenolic aryl ring benzoates was to stabilize the radiohalogen to in vivo dehalogenation. Additionally, the halogenated benzoyl conjugates were thought to be cleaved to benzoic acids which, for the *m*- and *p*-halobenzoic acid derivatives, would likely be rapidly converted in vivo to the corresponding hippuric acids and cleared through the renal system (191).

The earliest reported radiohalogen labeling of a benzoic acid was conducted by Hughes and Klinenberg, who demonstrated that 4-diazobenzoic acid, **9a**, could be used to prepare 4-astatobenzoic acid, **10a** (130). Subsequently, Friedman et al. demonstrated that 4-astatobenzoic acid, **10a**, could be used to stably radiolabel bovine serum albumin (BSA) by in situ formation of the isobutyl mixed anhydride **10b** (192). The experiments provided radiochemical yields of about 12% in the conjugation step. Vaughan was able to improve the radiochemical yield to 30–35% (10% overall labeling yield) when rabbit anti-mouse thymocyte IgG was labeled with the same reagent (193). Harrison and Royle also used the same approach to label a rabbit IgG with astatine-211 (194). These

Table IV. Amine-Reactive Radiohalogenation Reagents^a

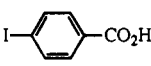
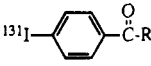
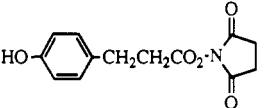
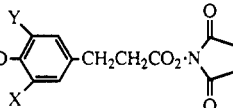
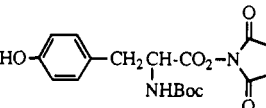
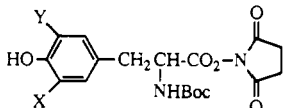
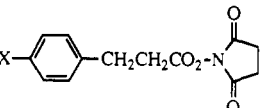
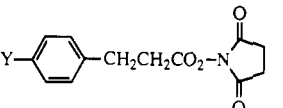
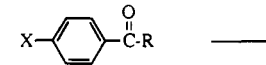
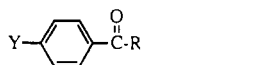
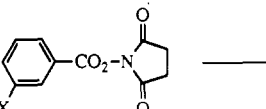
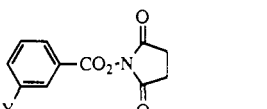
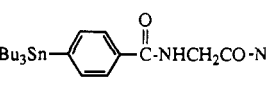
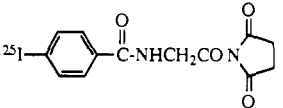
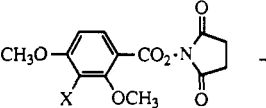
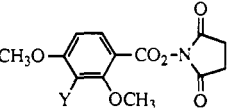
starting reagent	radiolabeled reagent (for protein conjugation)	% radiolab yield	% conjugn yield	ref
A. Activated Carboxylates				
 1	 2a: R = OH 2b: R = Cl	25-90	25-75	179
 3	 4a: X = ¹²⁵ I, ¹³¹ I, ¹²³ I; Y = H 4b: X = Y = ¹²⁵ I, ¹³¹ I, ¹²³ I 4c: X = ⁷⁷ Br; Y = H 4d: X = Y = ⁷⁷ Br	30-75 NR (to 85)	13-53 35-65	180 188
 5	 6a: X = ¹²⁵ I; Y = H 6b: X = Y = ¹²⁵ I	55-65	20-50	189
 7a: X = SiMe ₃ 7b: X = SnBu ₃	 8a: Y = ⁷⁷ Br, ⁸² Br 8b: Y = ¹²⁵ I	>80 51	NR NR	190 195
 9a: X = N ₂ ⁺ ; R = OH 9b: X = SnBu ₃ ; R = NHS 9c: X = SnBu ₃ ; R = CNP 9d: X = SnBu ₃ ; R = TFP 9e: X = SnBu ₃ ; R = PFP 9f: X = NO ₂ ; R = NHS 9g: X = NMe ₃ OTf; R = H	 10a: Y = ²¹¹ At; R = OH 10b: Y = ²¹¹ At; R = -OCO ₂ i-Bu 10c: Y = ¹²⁵ I, ¹³¹ I, ¹²³ I; R = NHS 10d: Y = ⁷⁷ Br; R = NHS 10e: Y = ²¹¹ At; R = NHS 10f: Y = ¹²⁵ I; R = CNP 10g: Y = ¹²⁵ I; R = TFP 10h: Y = ¹²⁵ I; R = PFP 10i: Y = ¹⁸ F; R = H 10j: Y = ¹⁸ F; R = OH 10k: Y = ¹⁸ F; R = NHS	NR 37-97 60-95 44-61 70-90 61-71 71-74 41-74 17-48	12-59 40-70 60-70 60-60 26 36 29	130 192-194 81 82 83 196 196 196
 11a: X = SnBu ₃ 11b: X = SnMe ₃ 11c: X = HgOAc	 12a: Y = ¹²⁵ I, ¹³¹ I 12b: Y = ²¹¹ At	85-90 67-95	33-65 39-65	79, 204, 205 80, 207
 13	 14	57	NR	195
 15a: X = Bu ₃ Sn 15b: X = Me ₃ Sn	 16: Y = ¹³¹ I	70-75	48-68	216

Table IV. (Continued)


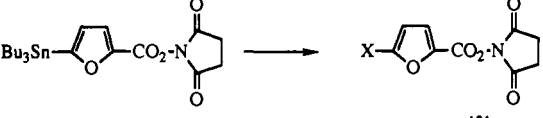
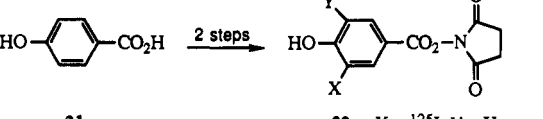
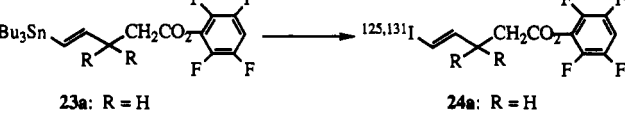

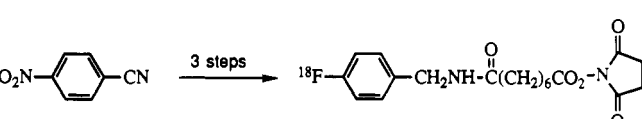
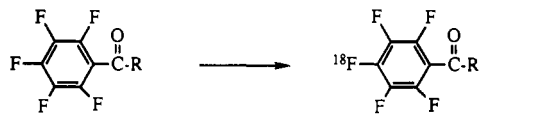


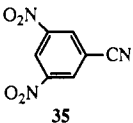
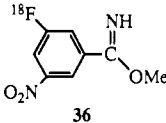
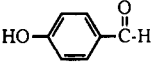
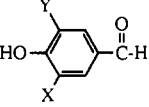
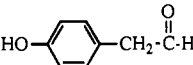
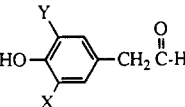
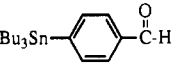
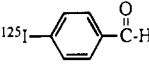
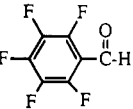

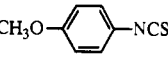
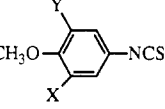
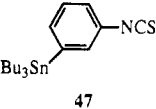
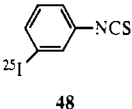
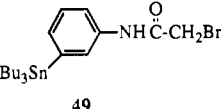
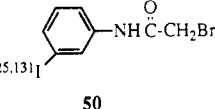
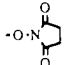
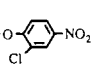
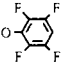
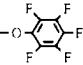
starting reagent	radiolabeled reagent (for protein conjugation)	% radiolab yield	% conjugn yield	ref
A. Activated Carboxylates (Continued)				
 <p>17a: X = Bu₃Sn 17b: X = Me₃Sn</p> <p>18: Y = ¹²⁵I, ¹³¹I</p>		80–88	56–65	217
 <p>19</p> <p>20a: X = ¹³¹I 20b: X = ²¹¹At</p>		70–80	38–58	218
 <p>21</p> <p>22a: X = ¹²⁵I; Y = H 22b: X = Y = ¹²⁵I</p>		50–90	10–15	219
 <p>23a: R = H 23b: R = CH₃</p> <p>24a: R = H 24b: R = CH₃</p>		70–95	25–50	222
 <p>25a: R = OH 25b: R = NHS 25c: R = NH-Protein 25d: R = OC(CH₃)₃</p> <p>26a: R = NH-Protein 26b: R = OH 26c: R = NHS</p>		90	NR	225
 <p>27</p> <p>28</p>		25–40	26–52	226
 <p>29a: R = phenol 29b: R = <i>p</i>-CN-phenol 29c: R = O-TFP</p> <p>30a: R = phenol 30b: R = <i>p</i>-CN-phenol 30c: R = O-TFP</p>		60 25 29	NR NR 52	227
B. Imidates				
 <p>31</p> <p>32a: X = ¹²⁵I; Y = H 32b: X = Y = ¹²⁵I</p>		60–80	20–30	230
 <p>33</p> <p>34</p>		55	NR	195

Table IV. (Continued)

starting reagent	radiolabeled reagent (for protein conjugation)	% radiolab yield	% conjugn yield	ref
B. Imidates (Continued)				
 35	 36	42-45	17-30	235
C. Aldehydes				
 37	 38a: X = ¹²⁵ I; Y = H 38b: X = Y = ¹²⁵ I	70-95	NR (est. 60%)	241
 39	 40a: X = ¹²⁵ I; Y = H 40b: X = Y = ¹²⁵ I	>90	8-58	242
 41	 42	NR	NR	240
 43	 44	60	NR	227
D. Isothiocyanates				
 45	 46a: X = ¹²⁵ I; Y = H 46b: X = Y = ¹²⁵ I	40-55	35-45	248
 47	 48	23-55	NR	249, 250
E. Acetyl Bromides				
 49	 50	80	48-60	251
^a Where NR = not reported; NHS =  ; CNP =  ; TFP =  ; PFP = 				

investigators were able to obtain a radiochemical yield of 50% (decay corrected). While the radiochemical yield of 50% was quite reasonable, the procedures used in astatine labeling were time-consuming, taking 3 h to complete (25% At-211 decay), and employed chemical extractions which could pose a safety risk when conducted.

Studies of radiohalogenation of proteins (antibodies) at NeoRx initially involved synthesis and radioiodination of *N*-succinimidyl 4-(tri-*n*-butylstannyl)benzoate, **9b**, *N*-

succinimidyl 3-[4-(tri-*n*-butylstannyl)phenyl]propionate, **7b**, *N*-succinimidyl 4-(tri-*n*-butylstannyl)hippuric acid, **13**, and methyl 4-(tri-*n*-butylstannyl)benzimidate, **33**. Synthesis of these compounds was readily accomplished using standard techniques (195). The radioiodinations were found to be facile in all examples studied, but the stability toward ester or imide hydrolysis (under the conditions studied) was markedly different, resulting in the large variations in radiochemical yields of desired product.

Because the benzoate ester **10c** was found to be the most stable radioiodinated compound toward hydrolysis, it was chosen for further study.

A large effort to optimize the chemistry of radioiodine labeling of **9b** and conjugation of the radioiodinated **10c** to monoclonal antibodies was conducted at NeoRx (196). The *N*-hydroxysuccinimide (NHS) ester had been found to be relatively stable to hydrolysis/methanolysis in the radiolabeling medium; however, it was of interest to determine whether other active esters might improve the conjugation yields. The stannylbenzoate esters of 2-chloro-4-nitrophenol (CNP), **9c**, 2,3,5,6-tetrafluorophenol (TFP), **9d**, and pentafluorophenol (PFP), **9e**, were prepared and studied. Radioiodination reactions were conducted in methanol, ethanol, and 2-propanol at room temperature and 55 and 75 °C. The results of those studies indicated that the radioiodination was similar for all of the different esters. Conjugation studies of the radioiodinated benzoate esters **10c,f-h** were carried out. All of the ester conjugations gave similar yields, but the NHS ester conjugation yields were slightly higher than the others. Further optimization of conjugation conditions was carried out on the NHS and TFP esters **10c** and **10g**. Again, the TFP ester **10g** gave similar conjugation yields to the NHS ester **10c** under optimized conditions, however, purification of the protein conjugated with the TFP ester was more difficult due to what appeared to be an "association" of the unreacted ester with the protein. Treatment of the radiolabeled protein with a 1 M lysine or glycine solution could be used to improve the radiochemical purity the protein conjugated with the TFP ester. This treatment was not necessary for purification of the NHS ester conjugated proteins, so the final choice of ester for use with the radiohalogenated benzoate was the NHS ester. Optimization studies of the benzoate NHS conjugations included the use of borate, phosphate, and carbonate buffers in conjugation reactions at various pHs. While borate buffer (pH 9.0) gave the highest conjugation yields (to 73%), bicarbonate/carbonate buffer (pH 8.5) was chosen due to concerns for borate buffer in an injectable preparation. Bicarbonate buffer gave good conjugation yields (to 60%). Indeed, under optimized conditions, where 1-mg quantities of protein at 3–5 mg/mL concentration were labeled, conjugation yields of 60–80% have been obtained using bicarbonate buffer.

The benzoate NHS has been used extensively for radioiodinated monoclonal antibodies in preclinical studies (81, 197–201). The studies have conclusively shown that free radioiodide is not released in vivo when the *p*-iodobenzoyl (PIB) labeling method is used, in contrast to antibodies that were radioiodinated by the direct labeling method. Radioiodinated monoclonal antibodies labeled with **10c** (iodine-123,125,131) have also been used in clinical studies (202, 203). Studies involving the use of the stannylbenzoate NHS ester **9b** with other radiohalogens have demonstrated that it can be used to radiolabel proteins with bromine-77 (82) and astatine-211 (83) as well.

Similar to our studies, Zalutsky and his co-workers have conducted a large number of studies on the use of *m*-halobenzoic acid conjugates of monoclonal antibodies (79, 80, 204–210). They have found iodine-125, iodine-131, or astatine-211 could be incorporated efficiently into the meta position of benzoic acid with either the tri-*n*-butylstannyl group, compound **11a** (*m*-BuATE), or the trimethylstannyl group, compound **11b** (*m*-MeATE). Higher yields were consistently observed using **11b** in the astatination reactions. The in vivo stability of the

radioiodinated **12a** was very good and the investigators have reported that they obtained enhanced tumor localization (206) and improved therapeutic efficacy (210) over the same antibodies directly labeled. Vaidyanathan and Zalutsky compared the stability of the radioiodine label on an antibody toward in vivo dehalogenation when it was labeled directly, labeled with **12a**, and labeled with the Bolton–Hunter reagent, **4a** (211). They found that the stability of the benzoyl label **12a** was highest, having about twice the stability of the Bolton–Hunter label. Both of the conjugates were considerably more stable than the direct label on the protein. Zalutsky and co-workers chose the meta isomer over the para isomer of benzoic acid, as they felt that it would be less susceptible to nucleophilic displacement of radioiodine. A comparison of the in vivo stability of coinjected, dual-labeled *p*-iodobenzoate **10c** and the *m*-iodobenzoate **12a** on an intact antibody provided data that suggested that the meta isomer was more stable (208). Comparative studies of coinjected, dual-labeled monoclonal antibody Fab fragment at NeoRx provided data suggesting that the radiolabels had essentially the same in vivo stability, but a large difference in the kidney retention of radioactivity was noted for radiolabeled antibody Fab fragments (197). Subsequent to those studies, Williams et al. compared the *m*- and *p*-iodobenzoyl conjugates with directly labeled antibody and found that the two conjugates were comparable, but an increased liver retention was noted for the meta isomer (212). Two other approaches to the preparation of **12a** have been described (213). A very complex approach involved radioiodination of aminobenzoic acid, removal of the amine through diazotization/decomposition, and preparation of NHS ester. As this procedure involves several steps with radiolabeled materials, it is quite undesirable. The second method of preparation of **12a** by the same investigators was the use of an organomercury intermediate, **11c**. The tetrafluorophenyl ester of *m*-iodobenzoic acid has also been prepared by Hanson et al. (214).

Vaidyanathan and Zalutsky have reported an investigation of the use of *N*-succinimidyl 4-¹⁸F fluorobenzoate, **10k**, for radiofluorination of monoclonal antibodies (215). An initial attempt to produce **10k** via nucleophilic displacement of an aromatic nitro group by [¹⁸F]fluoride on *N*-succinimidyl 4-nitrobenzoate, **9f**, was unsuccessful. However, fluorobenzaldehyde **10i** was obtained by [¹⁸F]-fluoride substitution on 4-formyl-*N,N,N*-trimethylanilinium triflate, **9g**, in 40–80% radiochemical yield. The radiofluorinated benzaldehyde **10i** was then oxidized to the corresponding benzoic acid **10j** in 55–80% radiochemical yield and esterified to produce the desired NHS ester **10k** in 31–89% yield (depending on time allowed). Total synthesis time was 100 min with about 25% (decay corrected) radiochemical yield (calculated 17–48%). Conjugation to a monoclonal antibody was achieved in good yield.

Zalutsky has also described several other new compounds for use as radiohalogenated conjugates of proteins (216–219). To incorporate a radioiodine into an aromatic ring which would have the halogen sterically blocked, the dimethoxy congener of *N*-succinimidyl *m*-iodobenzoic acid, **16**, was prepared and evaluated in vivo. *N*-Succinimidyl 2,4-dimethoxy-3-(tri-*n*-butylstannyl)benzoate, **15a** (220), and the corresponding trimethylstannyl compound, **15b** (216), were synthesized and radioiodinated. The in vivo data indicated that there was extensive in vivo deiodination. This result suggests that demethylation may be

occurring in vivo, resulting in an iodinated hydroxyphenol, which might be expected to undergo rapid deiodination.

Another radioiodinated conjugate that has been described by Zalutsky et al. is a pyridine derivative, *N*-succinimidyl 5- ^{131}I -3-pyridinecarboxylate, **18** (217, 218). The pyridine derivative was studied because its structure is dissimilar to the compounds, iodotyrosine and thyroxine, recognized by deiodinase enzymes. A similar protein conjugate, 5-iodopyridine-2-carboximide, has been described for preparing (nonradioactive) heavy-atom derivatives of protein (221). In the study of Zalutsky et al., *N*-succinimidyl 5-(tri-*n*-butylstannyl)-3-pyridinecarboxylate, **17a**, and *N*-succinimidyl 5-(trimethylstannyl)pyridinecarboxylate, **17b**, were synthesized and studied in radioiodination reactions. Radioiodinations required elevated temperatures (60–65 °C), but good radiochemical yields were obtained. *N*-Chlorosuccinimide (NCS) and *tert*-butyl hydroperoxide were studied as oxidants. The best yields were obtained with the trimethylstannyl intermediate **17b**, using NCS as the oxidant at 60–65 °C for 5 min. Conjugation reactions were conducted at pH 8.5 for 15 min and good yields were obtained. The iodinated pyridinecarboxylate (nicotinic acid) conjugates were found to be very stable toward in vivo deiodination.

A preliminary account of a furan ring conjugate, *N*-succinimidyl 5-(tri-*n*-butylstannyl)furan-2-carboxylate, **19**, has been reported by Zalutsky et al. (218). Studies have shown that this reagent can be radioiodinated to give **20a** in good yield. It has also been labeled with astatine-211 to prepare **20b**. The in vivo data from the radioiodinated furancarboxylate **20a** labeled antibody suggest that it is not as stable toward deiodination as the coinjected *m*-iodobenzoate **12a** labeled antibody.

In another investigation, Zalutsky et al. studied the use of *N*-succinimidyl 4-hydroxy-3- ^{131}I iodobenzoate, **22**, as a conjugate for monoclonal antibodies (219). This investigation was conducted to ascertain whether there was a difference in the in vivo stability between **22** and the Bolton-Hunter reagent, **3**, where there is a difference of two methylenes in the structures. Compound **22** was prepared from 4-hydroxybenzoic acid, **21**, followed by esterification. High yields for the radioiodination and esterification steps were obtained. No discussion of the possible mono- and diiodo products **22a** and **22b** was given. Conjugation yields were low compared with those of other benzoate reactions. There were no differences in thyroid activity (a measure of stability) at 24 h for coinjected antibodies labeled with hydroxybenzoyl- ^{131}I **22** and the similar nonphenolic ^{125}I **12a**. However, at later time points in the study differences in thyroid activity were observed which suggested that the hydroxy compound was less stable than the nonphenolic counterpart.

Two vinyl iodo compounds, 2,3,5,6-tetrafluorophenyl 5- $^{125,131}\text{I}$ iodo-4-pentenoate, **24a**, and 2,3,5,6-tetrafluorophenyl 3,3-dimethyl-5- $^{125,131}\text{I}$ iodo-4-pentenoate, **24b**, were prepared at NeoRx and studied as conjugates for monoclonal antibodies (222). The vinyl tri-*n*-butylstannyl derivatives **23a** and **23b** were synthesized from the corresponding acetylenic carboxylic acid methyl esters using hydrostannylation, followed by hydrolysis/reesterification with tetrafluorophenol. A more direct method of synthesizing **24a** involving stannylation of the tetrafluorophenyl ester of the alkyne has been described in a preliminary report by Hanson et al. (214). In our studies, esters **23a** and **23b** were radioiodinated using NCS as the oxidant, which resulted in good radiochemical yields of **24a** and **24b**. In vivo studies with a radiolabeled antibody Fab fragment indicated that the stability of the vinyl iodide in **24a** was not much higher than that obtained by direct

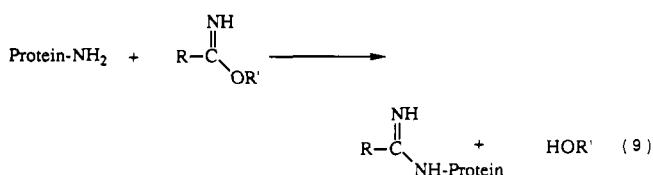
labeling with chloramine-T. However, the dimethyl vinyl iodo ester **24b** labeled Fab was found to have an intermediate stability toward dehalogenation compared with chloramine-T-labeled Fab. It had been anticipated that the dimethylpentenoic acid would be blocked from undergoing normal fatty acid catabolism (β -oxidation), as previously observed for dimethyl fatty acid derivatives (223, 224). With these limited studies it was concluded that vinyl iodides are not the conjugates of choice for protein labeling.

Reagents for radiofluorination of proteins which are conjugated by active esters have also been reported (225–227). For example, the NHS ester of α -bromo-*p*-toluic acid, **25b**, has been used to conjugate it to small peptides and amine-containing compounds. Once conjugated to the amine-containing peptide to give **25c**, the benzyl bromide was replaced with fluoride in refluxing acetonitrile in the presence of excess tetraalkylammonium fluoride, yielding radiofluorinated **26a**. This method would not be practical for fluorination of larger proteins. However, the investigators described another route for protein conjugation which uses the ^{19}F fluoro NHS ester **26c**. This route involves the fluorination of *tert*-butyl ester of α -bromo-*p*-toluic acid, **25d**, with tetrabutylammonium fluoride in acetonitrile, and has been accomplished in high yield (225). Subsequent cleavage of the *tert*-butyl group was accomplished in 10 min with exposure to neat trifluoroacetic acid and the NHS ester could be prepared in the usual manner. The authors did not report radiofluorinations using this reagent.

Zalutsky et al. have described the use of 4- ^{18}F -fluorobenzylamine, produced from the reaction of tetrabutylammonium ^{18}F fluoride with *p*-nitrobenzonitrile, **27**, and subsequent reduction with lithium aluminum hydride (226). The fluorobenzylamine was then reacted with disuccinimidyl suberate (DSS) to form the radiofluorinating reagent **28** in situ. It was found that the protein coupling yields could be improved by 15–40% when **28** was purified by HPLC. This difference in yield is believed to be brought about from excess DSS competing for amines on the protein. The synthesis times were long, 80–90 min, but good overall yields were obtained. Indeed, a preliminary study of the use of this reagent conjugated to an antibody and studied in a canine myocardial infarct model has been reported (228).

A preliminary investigation of the use of pentafluorobenzoate esters for radiofluorination of proteins has been reported (227). Pentafluorophenyl groups will undergo exchange (primarily in the position para to the non-fluorine group) with ^{18}F fluoride. The tetrafluorophenyl ester of pentafluorobenzoate, **29c**, was found to react rapidly (16 min) and was stable under the exchange conditions (tetrabutylammonium ^{18}F fluoride, heat, polar solvents). The product of the exchange reaction gave an overall labeling yield of 15% when reacted with human serum albumin. While reasonable yields were obtained, it should be noted that this labeling method suffers from the fact that low specific activity labeling would be expected, and this may cause problems with its general application.

2. Imidate Esters. Imidate esters react with protein amines to form amidine bonds as shown in eq 9. An



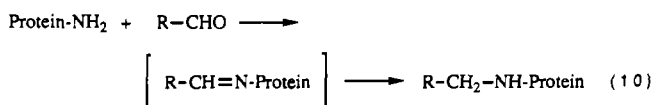
important characteristic of the amidine bond is that it is protonated at physiological pH, resulting in retention of the charge of the original amine. Thus, unlike the formation of amide bonds, the positive charge initially carried by the lysine amine is retained. The imide esters are more resistant to hydrolysis than many active esters, particularly *N*-hydroxysuccinimide esters, but the reaction rates for aminolysis of the methyl ester is also slower, resulting in longer overall reaction times. Conjugation reactions of imide esters are pH dependent, the extent of which has been shown to be a function of the amine and imido ester (229).

An imide ester of phenol which was used as a protein conjugate for radioiodination was described by Wood, Wu, and Gerhart (230). They synthesized methyl *p*-hydroxybenzimidate, 31, and prepared the mono- and di[¹²⁵I]-iodinated derivatives 32a and 32b in high specific activity. The overall labeling yields appear to be comparable to or slightly lower than those of the Bolton-Hunter reagent. This reagent (Wood's reagent) was reported to have the same advantages of mild protein labeling conditions as the Bolton-Hunter reagent, with the added advantage of retention of the positive charge on the amidine functionality. However, the authors point out the problem of ionization of the phenol when it is diiodinated. Thus, the net overall charge would be neutral, not retention of a positive charge. The Wood's reagent has been used to radiolabel proteins (231-233) and cell surface proteins (234).

An organometallic benzimidate, methyl *p*-(tri-*n*-butylstannyl)benzimidate, 33, was synthesized at NeoRx (195). This compound was radiolabeled efficiently (>90%) to give two radiolabeled products, but the desired iodo compound was obtained in only 55% yield. The other radioiodinated product was not identified but, due to its similar HPLC retention characteristics, was thought to be a radioiodinated phenyl compound. No further studies on the optimization of the radioiodination or on the conjugation with a protein have been done. However, the radioiodinated compound 34 remains of interest as it retains the positive charge without concern of an ionizable hydroxyl group being present.

A radiofluorinated benzimidate, 3-[¹⁸F]fluoro-5-nitrobenzimidate, 36, has been investigated for use in protein labeling by Kilbourn et al. (235). In conjugation reactions, effects of protein concentration, reaction time, and pH were studied. It was found that the conjugation yields did not increase appreciably above pH 7.5 but were increased dramatically with higher concentrations of protein. Conjugations were conducted at 47 °C, pH 8.0, for 1 h.

3. *Aldehydes*. Protein amines react with aldehydes to form imines (Schiff bases) which can subsequently be reduced with NaBH₄ (236-238) or NaBH₃CN (239) to form secondary amines as shown in eq 10. The reductions are



generally carried out at pH 9 when NaBH₄ is employed, but can be conducted as low as pH 5 for labeling of α -amino groups when the more stable NaBH₃CN is employed.

Conjugates containing phenolic rings for radiohalogenation and aldehyde functionalities for conjugation to proteins have been developed. Citing a need to preserve the nucleophilicity of conjugated amines of proteins for biological activity, particularly on small peptides, Su and

Jeng radioiodinated 4-hydroxybenzaldehyde, 37, and investigated conjugation of the radioiodinated product, 38, to glycine and lysine derivatives by reductive amination with sodium cyanoborohydride (240). Conjugation/reduction was conducted for 20 h at 37 °C. Two major products were observed, which the authors felt may have been mono- and di-*N*-alkylated products. Another explanation may be that the products obtained were the mono- and diiodinated conjugates of a monoalkylated product.

Panuska and Parker reported that protein labeling with 38 gave low yields, so they investigated the application of a similar reagent, (4-hydroxyphenyl)acetaldehyde, 39, for protein labeling (241). This reagent was used because the aldehyde group would be expected to be more reactive with protein amines due to its separation from the aromatic ring by the methylene group. In their studies, the enzyme β -galactosidase was reacted with radioiodinated 40 and NaBH₃CN at 4 °C for 24 h with no loss of enzymatic activity. The investigators found that conjugation could be accomplished over a range of pHs, allowing one to select an appropriate pH to minimize damage to the protein. They reported that "efficient incorporation" of radiolabel into the protein was obtained even at low concentrations of protein (e.g. 40 μ g/mL).

Nonphenolic radioiodinated aldehydes were prepared at NeoRx (242). An arylstannane, *p*-(tri-*n*-butylstannyl)benzaldehyde, 41, was prepared and radioiodinated. Synthesis of 41 was accomplished by stannylation of *p*-bromobenzyl alcohol using (Bu₃Sn)₂/Pd(PPh₃)₄ in toluene, followed by oxidation of the alcohol with pyridinium chlorochromate in CH₂Cl₂. (The phenacetaldehyde was also prepared in this manner, but a low yield was obtained and it was relatively unstable, so further studies were not pursued.) Radioiodination of 41 to prepare *p*-[¹²⁵I]-iodobenzaldehyde, 42, was facile giving radiochemical yields of >90%. Conjugations were conducted with 42 at pH 8.5-9.5 with various molar ratios of the reductant NaBH₃CN. Conjugation yields ranging from 8 to 58% were obtained after a 24-h reaction period.

A preliminary investigation of the use of pentafluorobenzaldehyde, 43, for radiofluorination to yield 44 and reductive alkylation to conjugate 44 with proteins has been reported by Herman et al. (227). The authors found that radiofluorination could be accomplished by exchange with tetrabutylammonium fluoride in DMSO to give 60% (decay corrected) yield within 30 min. Reductive alkylation of HSA using NaBH₄ in H₂O/DMSO for an additional hour gave an overall yield of 15% (decay corrected). Their brief report also indicated that when NaBH₃CN was used as the reductant, *in vivo* hydrolysis of the labeled aldehyde (imine) occurred.

4. *Isocyanates and Isothiocyanates*. Amines react with isocyanates (X = O) to form urea bonds (243) and isothiocyanates (X = S) to form thiourea bonds as depicted in eq 11. The isothiocyanate moiety is more stable toward

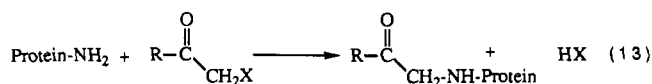
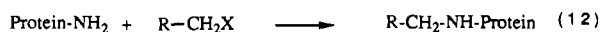


hydrolysis and is most often used for protein conjugation. Many conjugates of metal chelates have used isothiocyanates for conjugation (244-247), but few radiohalogen labeling reagents have been developed using this functionality.

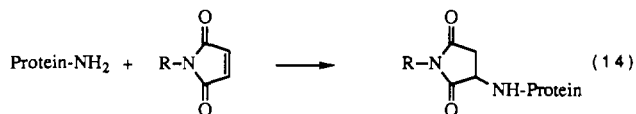
The use of *p*-methoxyphenyl isothiocyanate, 45, as a radioiodination reagent has been described in a preliminary report by Dewanjee et al. (248). Radioiodination of 45 yielded 46 with labeling efficiencies of 40-55%. Conju-

gation of 46 was achieved in radiochemical yields of 35–45%. In a recent publication, Ram and Buchsbaum have described preparation of 3-iodophenyl isothiocyanate, 48, for radioiodination of monoclonal antibodies (249). These investigators used a stannyl intermediate, 3-tri-*n*-butylstannylphenyl isothiocyanate, 47, to prepare the radioiodinated 48 in moderate to high yields. In a related preliminary report, these investigators reported a low yield for conjugation of 48 to a monoclonal antibody (250), but on the basis of other conjugations containing isothiocyanate functionalities, it is likely that the conjugation yields can be improved.

5. Activated Halides and Maleimides. Nucleophilic amines will react with compounds such as benzyl halides, acetyl halides, and maleimides to form alkylated amines as depicted in eqs 12–14. These types of compounds are



Where: X = I, Br, Cl, Tosylate, etc.



most often thought of as reagents for conjugations with thiol groups; however, depending on pH and availability of amines, conjugations with protein amines rather than thiol groups might be expected. Therefore, the conditions for conjugation of these groups must be carefully controlled.

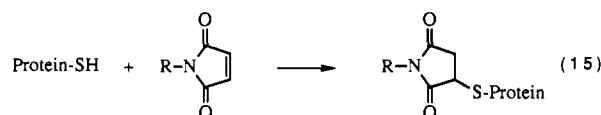
An example of conjugation with an acyl bromide, (3-[¹²⁵I,¹³¹I]iodophenyl)bromoacetamide, 50, to an antibody via amino groups has been reported by Khawli et al. (251). The radioiodination reagent 50 was prepared from [3-(tri-*n*-butylstannyl)phenyl]bromoacetamide, 49. The investigators conducted the reactions at pH 9.5 for 30 min and obtained good conjugation yields.

B. Sulfhydryl-Reactive Conjugates. The second most utilized functional group on a protein for formation of conjugates is the sulfhydryl (thiol) group present on cysteine residues. Thiols are nucleophiles like amines and will react with many of the functional groups described for conjugation of amines. Reaction with activated carboxylates yields thioesters which are themselves activated esters, and therefore are inherently unstable. However, reactions that form thioethers provide stable conjugates. Thiols can be reacted selectively in preference to the amines on a protein because they are better nucleophiles, particularly if the amines are protonated through adjustment of the pH (7 or less). Indeed, the most facile and highest yielding radiohalogenation reactions conducted in our laboratory have involved thiol conjugations.

There is a large amount of literature on the modification of thiols on proteins (252). Proteins which do not contain native thiols can be reacted with compounds such as 2-iminothiolane (which is commercially available as Traut's reagent) to generate them (253–255). Proteins lacking free sulfhydryl groups but containing disulfide bridges (e.g. antibodies) can be treated with thiol-containing reagents such as β-mercaptoethanol (256) or dithiothreitol (DTT, Cleland's Reagent) to produce free thiols (albeit transiently). These thiol-generating reagents are shown

in Table III. Thiol-reactive radiohalogenation reagents that have been studied are listed in Table V. A brief discussion of the chemistry involved in the thiol reactive conjugates is given in the following text.

1. Maleimides. Maleimide-containing compounds react with thiol groups to form thioethers as shown in eq 15.



Conjugation reactions are generally conducted at pH 7 or below and are complete within a few minutes.

A phenylmaleimide, *N*-(*p*-[¹²⁵I]iodophenyl)maleimide, 52, has been prepared and evaluated in protein conjugation reactions by Srivastava et al. (257). These investigators used the arylmercury intermediate *N*-[*p*-(acetylmercuric)-phenyl]maleimide, 51a, for radioiodination to prepare 52. Relatively low radioiodine labeling yields were obtained through a sequence of reaction/extraction/purification conducted over a 60-min period, with a maximum radiolabeling yield of 35%. Conjugation of the radioiodinated 52 also gave low radiochemical yields. Although a figure (Figure 2) in their report indicates that the reagent was conjugated by reaction of a free sulfhydryl group, it is unclear that sulfhydryls were present to react. Unless the antibody used had an available sulfhydryl for reaction with 52, it must be surmised that protein amines reacted in the conjugations.

Studies at NeoRx employed the arylstannane *N*-[*p*-(tri-*n*-butylstannyl)phenyl]maleimide, 51b, to prepare radioiodinated 52 (258). Much higher radiochemical yields were obtained using the arylstannane 51b than was reported for the arylmercury intermediate 51a. The maleimide ring of 51b was readily opened through alcoholysis with either methanol or ethanol to form the maleamic ester. This ring opening is a common side reaction of *N*-phenylmaleimides and is due to the conjugation of the nitrogen lone-pair electrons with the phenyl group (259). It was found that radioiodination reactions of 51b could be carried out without maleimide ring opening when 2-propanol/15% HOAc was used as the solvent. In this solvent mixture, the reactions were much slower than in the usual methanol/1% HOAc mixtures, but gave average radiochemical yields of 65%. The NeoRx studies used intact monoclonal antibodies and their Fab fragments which were pretreated with DTT to produce sulfhydryls for conjugation. Very careful handling of the DTT-treated antibodies provided conjugation reactions that were fast and gave high yields. The radioiodinated methyl maleimide derivative of 52 was (purposefully) produced in one experiment to ascertain if this compound would also conjugate to a DTT-treated antibody. It seemed reasonable that α,β-unsaturated amido compound might undergo a Michael type addition similar to maleimides. Indeed, this was the case with 80% conjugation yield being obtained at pH 6.0.

Khawli et al. have recently reported the preparation of *N*-(*m*-[¹²⁵I]iodophenyl)maleimide, 54 (260). The arylstannane *N*-[*m*-(tri-*n*-butylstannyl)phenyl]maleimide, 53 was prepared and radioiodinated in good yields to give 54. The investigators used a biphasic reaction mixture (H₂O/CH₂Cl₂) in the radioiodination step to effectively minimize the ring opening hydrolysis reaction. Conjugation of 54 with rabbit IgG and bovine serum albumin was accomplished by using the heterobifunctional coupling reagent *N*-succinimidyl 3-(2-pyridylthio)propionate (SPDP) for introduction of latent sulfhydryls. Reduction with dithio-

Table V. Thiol-Reactive Radiohalogenation Reagents^a

starting reagent	radiolabeled reagent (for protein conjugation)	% radiolab yield	% conjugn yield	ref
A. Maleimides				
<p>51a: X = HgOAc 51b: X = SnBu₃</p>	52	10–35 56–88	11–25 80–95	257 258
<p>53</p>	54	73	40–80	260
<p>55</p>	56	59–100	85	261
<p>57</p> <p>58a: X = ¹²⁵I, Y = H 58b: X = Y = ¹²⁵I</p>		NR	NR	262
<p>59</p>	60	15	NR	263
<p>61</p>	62	10	50	263
B. Acyl Halides				
<p>63a: Z = Cl 63b: Z = I</p> <p>64a: X = ¹²⁵I; Y = H; Z = Cl 64b: X = Y = ¹²⁵I; Z = Cl 64c: X = ¹²⁵I; Y = H; Z = I 64d: X = Y = ¹²⁵I; Z = I</p>		44–50 80–90	43–58 75–85	264 265
<p>65</p>	66	92–96	NR	266
<p>67a: Z = Br 67b: Z = I</p> <p>68a: Z = Br 68b: Z = I</p>		81–84	20–84	258
<p>61</p>	69	28–40	20–30	235

^a NR = not reported.

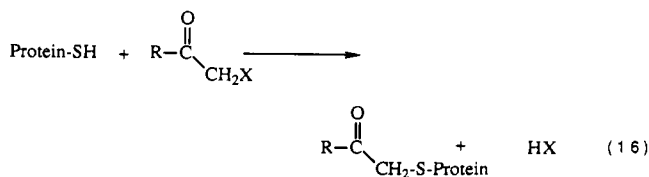
erythritol (DTE) resulted in conversion to the free sulfhydryl for conjugation with **54**. In the conjugation reaction, pH of 6.0–7.5 was found to be optimal. Sulfhydryls were also generated by treatment of intact antibody with DTE at pH 8. Interestingly, conjugation of **54** with the reduced disulfides prepared by the latter method were found to be pH sensitive, with the higher yields being obtained at pH 6.0 than obtained at pH 7.5.

As an alternative to *N*-phenylmaleimide **51b**, the phenethyl counterpart, *N*-[4-(tri-*n*-butylstannyl)phenethyl]maleimide, **55**, was synthesized and studied (261). Radioiodination of **55** could be conducted in the usual MeOH/1% HOAc solvent mixture to give very good radiochemical yields. The radiolabeling reaction was routinely conducted over 15 min, but it is likely that it was complete much sooner. Conjugation of the radioiodinated phenethylmaleimide **56** to DTT-treated antibody gave an average coupling yield of 85% in 20 min at room temperature.

A preliminary investigation of the synthesis and radioiodination of a tyramine maleimide derivative, *N*-[2-(3'-[¹²⁵I]iodo-4'-hydroxyphenyl)ethyl]maleimide, **58**, has been reported by Srivastava et al. (262). The investigators have reported radioiodinating **57** to produce the monoiodo maleimide **58a**. It is likely that they also produced some of the diiodo maleimide **58b** on the basis of other investigators' studies of radioiodinations of phenolic compounds. The investigators reported that a low thyroid uptake was obtained, indicating low *in vivo* deiodination, but it is unclear from the brief report what thyroid concentrations were obtained.

Preliminary studies of the use of two different maleimides for fluorine-18 labeling of antibodies have been reported by Shiue et al. (263). A phenylmaleimide, *N*-(*p*-[¹⁸F]fluorophenyl)maleimide, **60**, was prepared in four chemical steps from 1,4-dinitrobenzene. Preparation of **60** involved fluoride displacement of a nitro group on the aryl ring, followed by reduction of the remaining nitro group to an amine, condensation of the amine with maleic anhydride, and dehydration/ring closure. This process took 100 min from production of the fluorine-18 (from end-of-bombardment, EOB). The second fluorine-18-labeled maleimide, *m*-maleimido-*N*-(*p*-[¹⁸F]fluorobenzyl)-benzamide, **62**, was prepared in three steps from *p*-nitrobenzonitrile, **61**. In their preparation, the investigators displaced the nitro group with a fluoride and then reduced the nitrile to a fluorobenzylamine. The benzylamine was reacted with a cross-linking reagent, *m*-maleimidobenzoic acid *N*-hydroxysuccinimide ester (MBS), alleviating the need to prepare the maleimide. This synthesis took 70 min, but the reported yield was less than that for preparing **60**. The fluorine-18-labeled benzyl MBS derivative **62** was conjugated to rabbit IgG in 50% yield.

2. Acetyl Halides. Acetyl halides (α -halo ketones) are readily displaced by good nucleophiles such as thiol groups to form thioethers as shown in eq 16.



The preparation and radioiodination of *N*-(chloroacetyl)tyramine, **63a**, has been reported by Holowka (264). Initially, the investigators attempted to prepare the diiodo derivative **64b** by reaction with radioiodine containing 3 times the carrier sodium iodide, but they obtained a 1.7

mol of I/mol of *N*-(chloroacetyl)tyramine ratio of iodine in the product. This result and their observation of "the appearance of at least two distinct spots" by thin-layer chromatography suggests that they had a mixture that also contained the monoiodo compound **64a**. In later experiments they used no-carrier-added sodium [¹²⁵,¹³¹I]-iodide. DTT was used to produce sulfhydryl groups on the proteins studied. In the initial experiments, a large fraction of the labeled proteins were obtained as high molecular weight aggregates, which may have been formed from disulfide cross-linking. The investigators indicated that some of the radioiodinated tyramine derivative was nonspecifically bound to the protein.

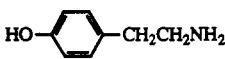
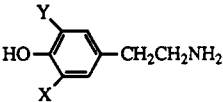
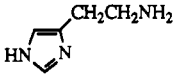
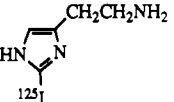
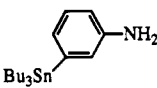
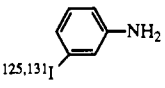
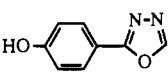
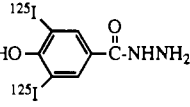
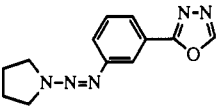
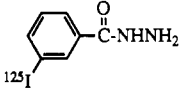
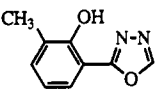
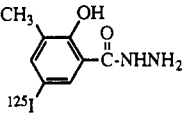
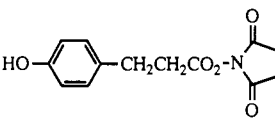
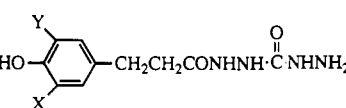
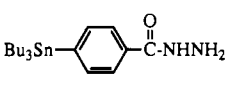
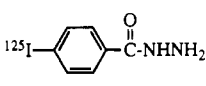
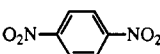
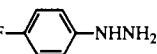
The rate of reaction of the chloroacetyl group with sulfhydryls is quite slow. Wyeth and Douglas reported obtaining higher conjugation yields with the iodoacetyl-derivatized tyramine **63b** (265). They also reported obtained much higher radioiodination yields. By reaction of the radioiodinated product **64c** (and **64d**?) with dithiothreitol (DTT) it was estimated that less than 5% of the radioiodine had exchanged with the iodoacetamido group.

In studies at NeoRx, the bromoacetyl derivatives of *p*-(tri-*n*-butylstannyl)aniline, **65**, and *p*-(tri-*n*-butylstannyl)phenethylamine, **67a**, were prepared (266). Initial studies were carried out with the bromo derivatives because it was felt that iodine exchange would occur with the iodoacetyl derivatives. While the bromo derivatives radiolabeled very well, their conjugation to DTT treated antibodies was quite slow. Conjugation with amines might have been conducted with these reagents as was done by Khawli et al. (251) with their similar reagent, **50**, but our goal was to develop a sulfhydryl conjugation reagent. Thus, to obtain higher conjugation yields, the iodoacetyl derivative of the phenethylamine **67b** was prepared and its radioiodination was studied (258). Very good radiochemical yields were obtained with no apparent exchange of the iodoacetyl iodide when the oxidant NCS was added to the radioiodide prior to adding the aryltin **67b**. Varying conjugation yields were obtained with radioiodination **68b** and were highest at pH 8, where the reaction of amines may effectively compete. The *in vitro* stability of the labeled proteins was found to be high, but because the reactions of thiols with the phenethylmaleimide **56** were much faster at lower pHs, no further studies with these agents were conducted.

Kilbourn et al. (235) have described the preparation of a radiofluorination reagent that contains an bromoacetyl group, 4-[¹⁸F]fluorophenacyl bromide, **69**. They were able to obtain good radiochemical (isolated) yields in a synthesis time of 75 min even though there are three chemical steps from the *p*-nitrobenzonitrile, **61**, starting material. In reactions conducted at 47 °C, pH 8.0, for 1 h, very good conjugation yields were obtained (>95%) when high concentrations of protein were used. When conducted at room temperature for 1 h, conjugation with fibrinogen was accomplished in 20–30% radiochemical yield.

C. Carbohydrate-Reactive Conjugates. Glycoproteins are important constituents of biological systems (267). Some proteins, such as monoclonal antibodies, have carbohydrate groups attached to specific regions of their structure, such as the "hinge region" (268) or the Fc region" (269). The fact that the carbohydrates are located at distinct areas of the antibody structures, away from the biologically active binding site, makes these functionalities attractive for "site-specific" conjugation of chemical species (270). A method of conjugation can be provided by oxidation of the oligosaccharide moieties to form reaction aldehyde functionalities on the glycoprotein molecules.

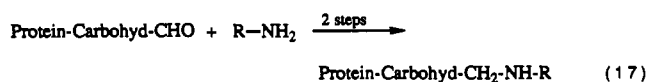
Table VI. Oxidized Carbohydrate-Reactive Radiohalogenation Reagents^a

starting reagent	radiolabeled reagent (for protein conjugation)	% radiolab yield	% conjugn yield	ref
A. Amines				
 70	 71a: X = ¹²⁵ I, Y = H 71b: X = Y = ¹²⁵ I	NR	NR	
 72	 73	70-90	NR	273
 74	 75	90	54-70	251
B. Acylhydrazines				
 76	 77	46	NR	274
 78	 79	12-30		275
 80	 81	80	25-40	276, 277
 3	 82a: X = ¹²⁵ I, Y = H 82b: X = Y = ¹²⁵ I	60-90	NR	278
 83	 84	20-40	NR	279
C. Phenylhydrazines				
 85	 86	NR	NR	280

^a NR = not reported.

Oxidation of carbohydrate moieties on antibodies is generally carried out with sodium periodate. The use of oxidized carbohydrates has permitted the addition of more moles of reagents per antibody without affecting the immunoreactivity than could be obtained by using lysines or aspartic and glutamic acid side chains in the preparation of immunoconjugates (271). A listing of radiohalogenated reagents which have been used (or conceived) for radiolabeling proteins via oxidized carbohydrates is given in Table VI. A discussion of the chemistry involved is given in the following text.

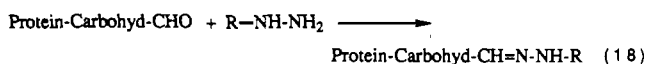
1. *Amines.* Standard condensation reactions of aldehydes with amines can produce imines. However, this reaction is reversible, so a second step involving reduction of the imine in situ must be conducted to form a stable attachment. The overall conjugation reaction of amines with oxidized glycoproteins is shown in eq 17.



A number of radiohalogenated amine-containing compounds have been prepared which could potentially be used to radiolabel proteins on oxidized carbohydrate moieties. Tyramine, 70, has been used in reductive aminations of cellobiose (272). Although carbohydrate adducts have generally been prepared prior to radioiodination, it should be possible to radioiodinate tyramine to prepare the mono- or diiodo derivatives 71a and 71b. On the basis of previous studies of radiohalogenations, the reactions will likely be better if the primary amine is protected as an amide or carbamate (e.g. tBoc group). Another amine that has potential in oxidized carbohydrate labeling is histamine, 72 (273). Radioiodinated histamine, 73, is commercially available (NEN Research Products/Du Pont) and has been used to radiolabel a number of compounds.

The preparation and conjugation of a radioiodinated iodoaniline with carbohydrate-oxidized monoclonal antibody has been described by Khawli et al. (251). These investigators prepared *m*-[¹²⁵I,¹³¹I]iodoaniline, 75, from the corresponding arylstannane, 74. An antibody was oxidized with NaIO₄ at pH 5.6 for 1 h at 4 °C and was reacted with 75 at a 1:1 molar ratio. The immunoreactivity of the radioiodinated antibody conjugate was decreased by 20% from a control, which they felt was due to damage from exposure to sodium periodate.

2. Hydrazines. Another amine reaction with aldehydes, that of hydrazines, produces a hydrazone derivative as shown in eq 18, which is stable to hydrolysis (274). In



reactions of oxidized carbohydrates (with excess hydrazine derivative) 2 equiv of the hydrazine derivative can react with the α -hydroxy aldehydes to form osazones.

A number of radiohalogenated benzoylhydrazine derivatives have been prepared. Heindel et al. have reported the use of a protective oxadiazole group as a synthon for the acylhydrazine group (275). They employed the synthon for acylhydrazine since iodination of *p*-hydroxybenzoic acid hydrazide failed to provide the desired iodinated (radioiodinated) compound. Iodination and radioiodination of 2-(4'-hydroxyphenyl)-1,3,4-oxadiazole, 76, was conducted with carrier-added iodide to prepare the diiodo derivative. The phenyloxadiazole was treated with refluxing concentrated HCl/THF for 3 h to generate the benzoylhydrazine 77, which was reacted in situ with *p*-(dimethylamino)benzaldehyde for 2 h at reflux to form the benzoylhydrazone for characterization. In a later publication (276), the authors used a triazine intermediate, 2-[3'-(3',3'-(1,4-butanediyl)triazeno]phenyl]-1,3,4-oxadiazole, 78, for preparing high specific activity radioiodinated *m*-[¹²⁵I]iodobenzoylhydrazine, 79. The high specific activity radiolabeling was conducted at 100 °C for 1 h, followed by addition of trifluoroacetic acid/H₂O and heating for an additional 1.5 h. A 12% radiochemical yield of 79 was isolated from an HPLC.

Rea et al. have investigated the use of 2-hydroxy-5-[¹²⁵I]iodo-3-methylbenzoylhydrazine, 81, for protein labeling (277). The radioiodinated 81 was prepared (carrier-added) from an acylhydrazine synthon, 1,3,4-oxadiazole derivative 80 (278), which was readily prepared from commercially available 3-methylsalicylic acid. This is an interesting phenolic compound as only one radiohalogenated isomer can be formed from a halogenation reaction due to the methyl substituent. Conjugation of the iodobenzoyl hydrazide 81 at pH 5 for 6–8 h with periodate-oxidized monoclonal antibody resulted in a conjugate

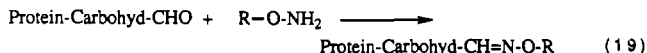
which was found to be unstable in vivo. Subsequently, reduction of the conjugated acylhydrazone with sodium cyanoborohydride provided a conjugate that was stable in vivo.

A radioiodinated acylhydrazone compound, 3-(3-[¹²⁵I]-iodo-4-hydroxyphenyl)propionyl carbohydrazide, 82a, has been prepared from the reaction of carbohydrazide with the Bolton–Hunter reagent, 3 (279). Good yields of the radioiodinated carbohydrazide were obtained. As with other phenolic reagents, two radioiodinated spots were observed by thin-layer chromatography, which the investigators attributed to the mono- and diiodo derivatives, 82a and 82b. The radioiodinated carbohydrazide was reacted with periodate-oxidized ribonucleosides (forming morpholine derivatives). Studies were also conducted with various other aldehydes and ketones to determine if this reagent could have a general application. The results suggest that it can; however, no studies of its application to oxidized glycoproteins were reported.

Studies were conducted at NeoRx to prepare *p*-[¹²⁵I]-iodobenzoylhydrazine, 84 (280). To prepare 84, the corresponding arylstannane, *p*-(tri-*n*-butylstannyl)benzoylhydrazine, 83, was synthesized from the reaction of hydrazine with methyl *p*-(tri-*n*-butylstannyl)benzoate. Radioiodination of 83 in CHCl₃ with carrier-added sodium [¹²⁵I]iodide resulted in a radiochemical yield of ca. 40% and a no-carrier-added yield of only 20%. Since the HPLC chromatograms indicated that only desired product and free iodide were present, higher amounts of the oxidant NCS were added. This resulted in production of unidentified polar products, with a decrease in overall radiochemical yields. An alternate path to the production of 84 was investigated. Very good radiochemical yields were obtained (>80%) when the *N*-hydroxysuccinimide ester 9b was reacted with a large excess of hydrazine. Separation of the excess hydrazine was accomplished on a reverse-phase C-18 Sep-Pak cartridge using MeOH as the solvent.

A preliminary investigation of the preparation of *p*-[¹⁸F]-fluorophenylhydrazine, 86, has been reported (281). The synthesis of 86 involved four steps: (1) preparation of *p*-[¹⁸F]fluoronitrobenzene by reaction of fluoride with dinitrobenzene, 85, (2) reduction of the nitro group to give *p*-[¹⁸F]fluoroaniline, (3) diazotization of the aniline, and (4) reduction of the diazonium salt with sodium cyanoborohydride. Phenylhydrazine 86 was generated in situ and reacted with keto compounds to form stable derivatives.

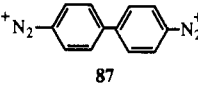
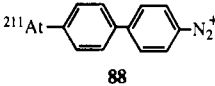
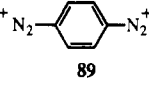
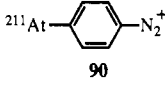
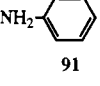
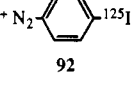
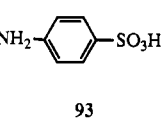
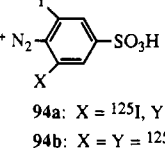
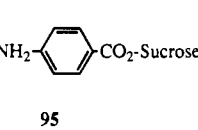
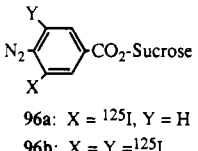
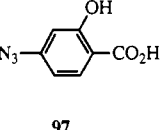
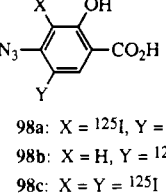
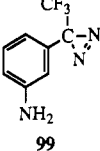
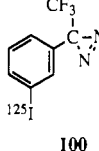
3. Hydroxylamines. A third aldehyde-reactive functionality is the hydroxylamine group. Reaction of hydroxylamines with aldehydes produce oximes as shown in eq 19, which are also stable functionalities (282).



No literature reports of radiohalogenation reagents which contain a hydroxylamine group were found. Preparation of such a reagent and its comparison in carbohydrate conjugations with amines, hydrazines, and acylhydrazines would be an important contribution to this area of study.

D. Conjugates That React Nonspecifically. Conjugation with specific chemical groups on proteins are most often sought; however, for some applications selectivity provided by reaction with a particular type of residue may not be important, or even desired. A listing of the reagents that I have classified as nonspecific conjugation reagents is given in Table VII. A description of some of the

Table VII. Radiohalogenation Reagents Which React in a Nonspecific Manner^a

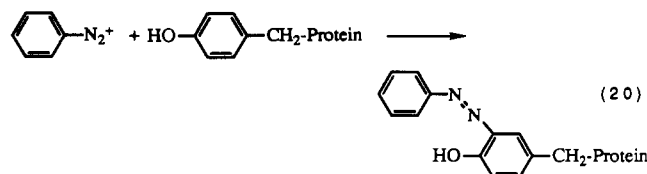
starting reagent	radiolabeled reagent (for protein conjugation)	% radiolab yield	% conjugn yield	ref
A. Diazonium Salts				
		NR	50 (overall)	130
		NR	23-57 (overall)	285
		NR	NR	286
		95	>85	287
		85-90	NR	288
B. Aryl Azides				
		NR	7-16 (not all covalent)	292
C. Diazirines				
		60-80	5%	293

^a NR = not reported.

chemistry related to the reagents classified in this manner is given in the following text.

1. *Diazonium Salts.* Diazonium salts can undergo a number of different reactions with functional groups (283). For example, under basic conditions aryl diazonium salts will react with aromatic ring compounds to form bis-aryl compounds. Diazonium salts will also react with amines under basic conditions to form triazines. Under neutral or basic conditions, diazonium salts will undergo electrophilic reactions with phenols (phenoxide ions) to form diazo linkages.

It is believed that a primary reaction of aryl diazonium salts with proteins is reaction of tyrosine residues as depicted in eq 20. Reaction with tyrosine can produce



either the mono- or disubstituted derivatives as is observed

in electrophilic halogenations. Similarly, histidine imidazole rings can undergo electrophilic substitution reactions. Amines on other amino acids also react with aryl diazonium salts, but their reactions are thought to take place at a slower rate than those of tyrosine or imidazole (284).

The use of diazonium salts to incorporate astatine-211 into aromatic compounds, as an alternative approach to direct labeling of proteins, was reported in 1955 (130). Indeed, in that very early report it was shown that diazotized benzidine, 87, could be halogenated with ²¹¹At to form the astatinated diazo compound 88, which was subsequently reacted with bovine serum albumin (BSA) to form a stable conjugate. Similarly, Wunderlich et al. reported that diaminobenzene could be diazotized to form *p*-diazobenzene, 89, labeled with astatine to form the astatinated diazobenzene 90, and conjugated with rabbit immunoglobulin (285). The conjugation reaction was conducted at pH 8 and room temperature for 1 h and was quenched by addition of an excess of phenol.

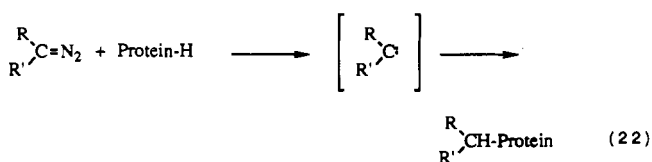
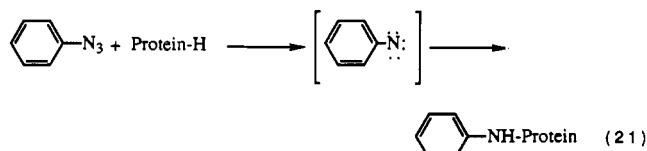
Hayes and Goldstein described the use of *p*-diazo[¹²⁵I]-iodobenzene, 92, for labeling proteins that contained

sulfhydryl groups which could not be modified without affecting the biological activity (e.g. enzymes) (286). Preparation of the radioiodinated diazonium salt **92** was accomplished through iodination of aniline, **91**, followed by diazotization. Conjugation with the protein was conducted at pH 9–10 for 1 h. The investigators indicated that a quantitative yield was obtained (Table 2 in that paper); however very few details on the results of labeling were given.

Labeling of proteins on red blood cell membranes with diazotized [¹³¹I]diiodosulfanilic acid, **94**, has been reported by Sears et al. (287). Radioiodinations of sulfanilic acid, **93**, gave the diiodosulfanilic acid, which was subsequently diazotized to form **94**. Conjugation of the radioiodinated diiodosulfanilic acid was carried out at 4 °C, pH 7.4. Raising the temperature in the conjugation to 24 or 37 °C gave lower conjugation yields, as did changing the pH to 7.0 or 7.8. The monoiodo derivative **94a** can be prepared from [¹²⁵I]iodosulfanilic acid, which is commercially available (NEN/Du Pont).

Another reagent that has been conjugated to proteins through reaction of a diazonium salt is *O*-(4-diazo-3,5-di-¹²⁵I)iodobenzoyl)sucrose, **96** (288). Preparation of **96** [structure not defined] was accomplished by radioiodination of (*p*-aminobenzoyl)sucrose, **95**, with (carrier) added NaI. The investigators reported that 1.7–1.8 equiv of iodine per molecule were obtained, indicating that a mixture of mono- and diiodo derivatives **96a** and **96b** may have been obtained. Conjugation was conducted at pH 8.1, 0 °C, for 2 h. It was postulated that the presence of sucrose on the radiolabeled compound would cause retention of the metabolized radioactivity in the organelles of the cells that metabolized it. Retention of activity was found to be largely in the mitochondrial and lysosomal fractions, and the investigators were able to determine the uptake of lactate dehydrogenase in the liver and spleen of rats using this reagent.

2. Photogenerated Species. Very fast, nonspecific reactions can be of value for coupling a radiohalogenated molecule with a protein. These types of reactions are used when attempting to detect interaction with "active sites" of proteins. They can also help provide information on such things as molecular structure of receptor proteins and transport proteins, membrane structure, protein-nucleic acid interactions, and antibody binding (289). The need to allow for an interaction prior to reaction makes the use of photolabile agents particularly attractive. There are two types of very reactive intermediates produced through photolysis of precursors that have been used extensively in protein labeling. These are aryl azides (290) and stabilized diazo compounds (i.e. acyl and phenyl substituted) (289). The photolysis of these reagents to produce aryl nitrenes and carbenes is shown in eq 21 and 22, respectively. Both of these reactive intermediates will



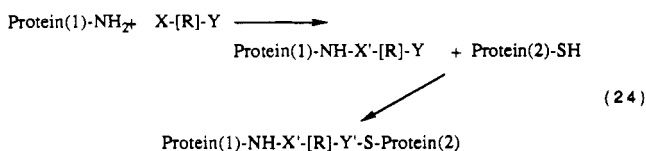
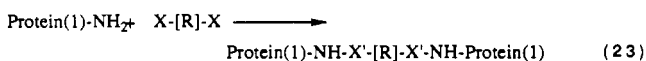
undergo nonspecific reactions (291) in the labeling of

proteins. For the purposes of this review, most of the applications of photolabeling reagents are included in the section on cross-linking of proteins.

An aryl azide radioiodinated photolabeling reagent (non-cross-linking) has recently been reported by Pandey et al. (292). The reagent, 4-azido-3-[¹²⁵I]iodo-2-hydroxybenzoic acid, **98**, was produced by radioiodination of 4-azidosalicylic acid, **97**. The investigators made no attempt to purify the radiolabeled **98** and did not determine whether it was the monoiodinated derivatives (**98a** and **98b**) or the diiodinated derivative (**98c**). They noted that two spots were observed by TLC which they believed could be the mono- and diiodo derivatives. As might have been expected for this type of reagent, low conjugation yields were obtained. Of the material associated with the protein after photolysis, a varying quantity (41–72%) was actually covalently attached to the protein.

A carbene-generating radioiodinated photolabeling reagent, 3-(trifluoromethyl)-3-(*m*-[¹²⁵I]iodophenyl)diazirine, **100**, has been reported for application to labeling in hydrophobic regions of membranes (293) and microsomal proteins (294). The structurally interesting diazirine group has been used for photolabeling (295, 296) and its chemistry has been reviewed (297). The diazirine **100** was produced from 3-(trifluoromethyl)-3-(*m*-aminophenyl)diazirine, **99**. Radioiodination of **99** was accomplished via two different synthetic routes. The initial studies incorporated the radioiodine in the first step of a multiple step synthesis and only 5% recovery of activity (as compound **100**) was obtained. A second route employed a diazonium salt decomposition for introducing the radioiodine in the final synthetic step. Very good radiochemical yields of the desired compound were obtained. Photolysis conducted at 0 °C under N₂ resulted in ca. 5% of the radioactivity being bound to protein.

E. Cross-Linking Reagents. Linking proteins to solid supports and other molecules (e.g. other proteins) has provided valuable tools to isolate, purify, stabilize, and elucidate biochemical interactions of the proteins. Discussion of the applications of cross-linking reagents is outside of the scope of this review, but can be found in a number of literature articles (170, 298–301). In essence there are two separate conjugation reactions occurring with the cross-linking reagents. Control of the two conjugation reactions when the reactive species are the same (homobifunctional) can be obtained by adjustments to the reaction conditions. More commonly the cross-linking compound will have two different reactive groups (heterobifunctional) for cross-linking of proteins. These two variations on cross-linking compounds are shown in eqs 23 and 24. Many of the cross-linking reagents contain a



photolysable aryl azide group. Radiohalogenation (generally with ¹²⁵I) of the protein can be carried out separate from the cross-linking process by direct labeling (302, 303) of the protein or through the use of conjugates such as the Bolton-Hunter reagent (304), but radiohalogen labeling of the cross-linking reagent allows for monitoring of the first conjugation reaction and, subsequently, the cross-linking reaction.

Cross-linking of proteins with other materials (e.g. proteins, solid supports) can be accomplished with reagents that form stable attachments, but for some applications cross-linking reagents that can be cleaved following cross-linking are desired. These two types of radiohalogen labeled cross-linking reagents are discussed separately in the following text. A list of cross-linking reagents that contain radiohalogens is given in Table VIII.

1. *Noncleavable*. Three cross-linking reagents, *N*-succinimidyl 4-azidosalicylate, 101, *N*-succinimidyl *N*-(4'-azidosalicyl)-6-aminocaproate, 103, and *N*-succinimidyl *N*-[*N*-(4-azidobenzoyl)glycyl]tyrosinate, 105, were prepared and radioiodinated by Ji et al. (305, 306). Initial radioiodinations were conducted in acetone and it was reported that "iodine-125 incorporates quickly and efficiently" into 101 and 103 (one major radioactive spot by TLC), but radioiodination of 105 "produced several radioactive spots". In a subsequent paper by these investigators, the radioiodination of salicylate 101 was increased from 3% in acetone to 63% when other solvents "such as aqueous acetonitrile, dimethylformamide, or dimethyl sulfoxide" were used. The radioiodinated salicylate 102 (a-c?) was conjugated and photolyzed to cross-link the α and β chains of human choriogonadotropin.

More recently fluorinated aryl azide containing compounds have been used for protein cross-linking. The fluorinated aryl azides have been used because singlet nitrenes are generated from them upon photolysis, and the singlet nitrenes have been found to be efficient at inserting into a variety of bond types (307). Also, the fluorinated aryl azides may be less selective in their reactivity than nonfluorinated aryl azides as they do not produce the ring-expanded azepine intermediates which are (selectively) reactive with nucleophiles such as lysine amines (308, 309).

Crocker et al. have described the synthesis and iodination of *N*-succinimidyl *N*-(4-azido-2,3,5,6-tetrafluorobenzoyl)tyrosinate, 107 (310). Iodination of 107 with an excess of iodide yielded the diiodo derivative 108b ($X = Y = ^{127}\text{I}$) in 81% isolated, purified yield. The radioiodination of 107 was not reported. Photolysis studies demonstrated that very good cross-linking yields could be obtained (to 40%). Similarly, Keana et al. have described fluorinated aryl azide cross-linking reagents that could be radioiodinated (311, 312). These investigators synthesized *N*-succinimidyl 2-amino-4-azido-3,5,6-trifluorobenzoate, 109, and *N*-succinimidyl 3-(4-azido-2,3,5,6-tetrafluorobenzamido)-5-aminobenzoate, 111. They iodinated these two compounds to prepare 110 and 112 by in situ generation of the respective diazonium salts. In the reaction of 109 incomplete iodination was obtained using an excess of NaI at 0 °C for 30 min. Iodination of 111 gave the desired compound by addition of a large excess of KI at 5 °C for 40 min. Photolysis of 110 and 112 gave results that indicated photodeiodination had occurred with both compounds. Photodeiodination had also been observed for nonfluorinated aryl azides (313).

Another cross-linking reagent that is activated by photolysis is 3-(trifluoromethyl)-3-(*m*-isothiocyanophenyl)diazirine, 113, which was reported by Dolder et al. (314). Radioiodination to form 114 was found to be difficult with low yields being obtained. A major iodinated byproduct was obtained which the authors felt did not contain the isothiocyanate functionality. Attempts to radioiodinate the amino precursor to the isothiocyanate also gave poor yields and a number of byproducts. The amino group was found to be very sensitive to oxidation and some attempts to halogenate the amino compound

caused the loss of the amino group. Low cross-linking yields were also reported. The radioiodinated diazirine 114 is commercially available (Amersham).

A homobifunctional radiohalogenated cross-linking reagent has been developed by Lawton et al. (315-317). The reagents, termed equilibrium transfer alkylation cross-link reagents (ETAC reagents), are believed to generate sequential α,β -unsaturated ketones which are reactive with nucleophilic functional groups on proteins. A radioiodinated cross-linking reagent, *N*-[4-[2,2-bis[(*p*-tolylsulfonyl)methyl]acetyl]benzoyl]-4-[^{125}I]iodoaniline, 116, was prepared by reaction of [^{125}I]iodoaniline with the carboxylic acid chloride 115. This reaction gave very low yields of the radioiodinated 116. However, cross-linking using 116 was accomplished in high yields. The cross-linking yields were quite dependent on pH and on the degree of antibody reduction with 2-mercaptoethanol.

In our recent studies at the University of Washington, a stannylphenethylamine derivative, *N*-[4-[2,2-bis[(*p*-tolylsulfonyl)methyl]acetyl]benzoyl]-4-(tri-*n*-butylstannyl)phenethylamine, 117, has been prepared and radioiodinated to give 118 in high yields (318). This method of radioiodination of the ETAC molecules was chosen as we wanted to obtain better radiolabeling yields and higher specific activity labeling of ETAC cross-linking molecules. Cross-linking of antibody Fab' fragments to prepare modified $\text{F}(\text{ab}')_2$ has been achieved in good yield with this reagent.

2. *Cleavable*. For some applications it is desirable to be able to separate the cross-linked proteins after isolation. To accomplish this, some radioiodinated cross-linking reagents that can be cleaved in vitro have been developed.

A radioiodinated cross-linking reagent, *N*'-sulfosuccinimidyl *N*-[4-[(*p*-azido-*m*-[^{125}I]iodophenyl)azo]benzoyl]-3-aminopropionate, 120, has been reported by Denny and Blobel (319). Preparation of 120 was accomplished by radioiodination of *N*-[4-[(*p*-aminophenyl)azo]benzoyl]-3-propionic acid, 119, followed by diazotization/azide incorporation and esterification. The overall incorporation of radioiodine was low due to the multiple steps involved and the chromatographic separation of the radioiodinated aniline from 119, although a high specific activity was obtained. A 44% incorporation of the radiolabeled 120 into protein A attached to a Sepharose support was obtained. The derivatized protein A-Sepharose was then photolyzed in the presence of human serum. The investigators indicated that using the 366-nm light for photolysis did not release any free iodide. Once irradiated, the proteins were treated with sodium dithionite which had been shown to reduce the azo bond in similar nonradio-labeled reagents (320). Murphy and Harris have reported that improved radioiodination yields (10-14%) for 120 were obtained when it was reacted with aminodextran prior to radioiodination (321). The radioiodinated reagent 120 (*N*-hydroxysuccinimide ester) is commercially available as the Denny-Jaffe reagent (NEN/Du Pont).

Another cleavable cross-linking reagent, *N*-sulfosuccinimidyl 2-(*p*-azidosalicylamido)-1,3'-dithiopropionate, 121, has been studied (322). Wollenweber and Morrison reported coupling 121 to a *Escherichia coli* lipopolysaccharide (LPS) and subsequently radioiodinating it. A moderate radiolabeling yield was obtained and no evaluation of the possible isomeric products (122a-c) was discussed. Cleavage of the disulfide in 122 with DTT indicated that the radioiodine had been incorporated into the phenolic ring as expected. Cross-linking of 122 with serum albumin proteins (for which an affinity with LPS had been previously noted) with UV irradiation at 254 nm

Table VIII. Radiohalogenation Reagents That Cross-Link^a

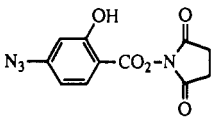
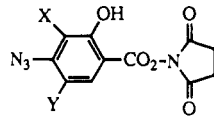
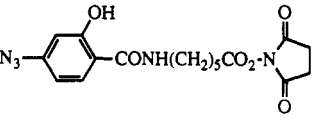
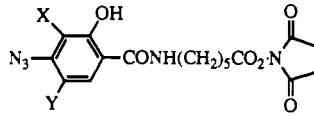
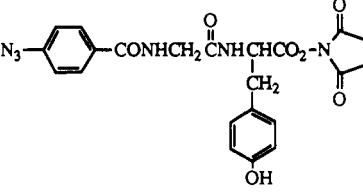
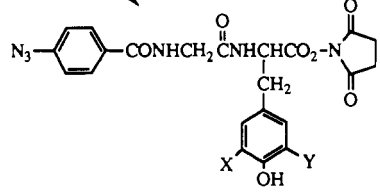
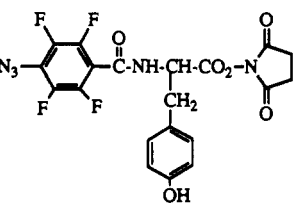
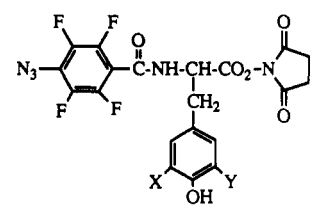
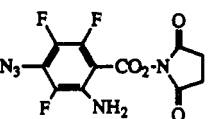
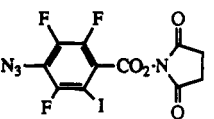
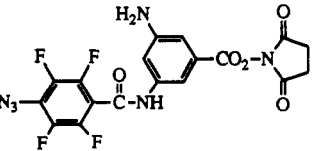
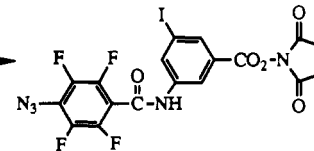
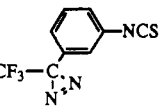
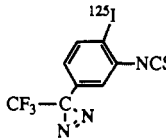
starting reagent	radiolabeled reagent (for protein cross-linking)	% radiolab yield	% cross-link yield	ref
A. Noncleavable Cross-Linking Reagents				
 101	 102a: X = ¹²⁵ I; Y = H 102b: X = H; Y = ¹²⁵ I 102c: X = Y = ¹²⁵ I	63	NR	306
 103	 104a: X = ¹²⁵ I; Y = H 104b: X = H; Y = ¹²⁵ I 104c: X = Y = ¹²⁵ I	NR	NR	305
 105	 106a: X = ¹²⁵ I; Y = H 106b: X = Y = ¹²⁵ I	NR	NR	305
 107	 108a: X = I; Y = H 108b: X = Y = I	NR	NR	310
 109	 110	NR	NR	311
 111	 112	NR	NR	311
 113	 114	<16	NR	314

Table VIII. (Continued)

starting reagent	radiolabeled reagent (for protein cross-linking)	% radiolab yield	% cross-link yield	ref
A. Noncleavable Cross-Linking Reagents (Continued)				
		1	30–85	315
		75–95	10–50	318
B. Cleavable Cross-Linking Reagents				
	 <p>120a: X = ¹²⁵I; Y = H 120b: X = Y = ¹²⁵I</p>	5	1	319
	 <p>122a: X = ¹²⁵I; Y = H 122b: X = H; Y = ¹²⁵I 124c: X = Y = ¹²⁵I</p>	30	NR	322

^a NR = not reported.

gave "significant incorporation of ¹²⁵I into the serum albumins". The radioiodinatable cross-linking reagent 121 is commercially available (Pierce).

V. FUTURE DIRECTIONS

Radiohalogenated proteins have been instrumental in gaining knowledge about many basic concepts of protein biochemistry and have been used in medical applications such as radioimmunoassay. However, it seems like that radiohalogenated protein conjugates will become increasingly important in future biochemical studies and will be used in many more medical applications. Although the

majority of studies and applications of radiohalogenated proteins in the future will likely continue to use direct labeling with radioiodine, some of the studies will be best conducted with radiohalogenated conjugates. While commercially available radioiodination reagents such as the Bolton-Hunter reagent will continue to be used, newer conjugation reagents containing organometallic intermediates should become commercially available in the near future because of the advantages that they can provide over phenolic conjugates. These considerations aside, further studies will be conducted involving radiohalogenated conjugates, either those described in this review or

newly designed conjugates. In a majority of protein conjugate studies, design and development of a new conjugate will not be necessary as it should be possible to adapt one of the compounds listed in the tables in this review. However, it should be noted that many of the compounds listed in Tables IV–IX have undergone limited investigation and will not be readily adaptable to all labelings without further investigation and optimization of the radiohalogenation chemistry or conjugation chemistry, or both. This review has been purposefully broad in its scope so decisions can be made on which chemistry might improve labeling or conjugation yields when new reagents are designed.

A. Design of Conjugates. Many of the future studies of radiohalogenated proteins will be conducted *in vivo*. One very important aspect of conjugate labeling of proteins is that desirable chemical properties can be designed into them. For instance, radiohalogenated protein conjugates can potentially offer some control of *in vivo* metabolism and secondary distribution, whereas direct labeling does not. Additionally, there is often a need to know with certainty that the radioactivity observed in *in vivo* evaluations of radiohalogenated proteins is indeed reflective of the distribution of that protein. This issue is one of *in vivo* stability, which can be addressed by designing conjugates that do not release the radiohalogen by the action of enzymes or nucleophiles found in the biological system. A brief discussion on what we have learned about *in vivo* stability is given in the next section.

Some control of the pharmacokinetics and *in vivo* distribution of labeled protein and its metabolites may also be possible through conjugate chemistry. While it is important to have control of *in vivo* stability, it may be desirable to have lower stability in certain tissues such as kidney and liver such that the radiation dose to these organs can be minimized. Design of conjugates which have chemical moieties that are selectively cleavable in tissues such as kidney and liver may provide a method of clearing those tissues faster than would otherwise be possible with stabilized conjugates. Another important function that may be designed into conjugates is a means of retention of the radiohalogen at a targeted tissue (e.g. tumor). A number of biochemical and/or chemical processes are available which could provide mechanisms (e.g. alkylation, metabolic trapping, etc.) by which retention or trapping of the radiohalogen at the target tissue could be obtained. Examples of radiohalogenated protein conjugates which were designed to be cleaved *in vivo* or be metabolically trapped are listed in Table IX. A discussion of the chemistry associated with the listed conjugates is given in the following text.

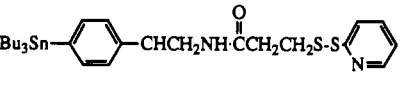
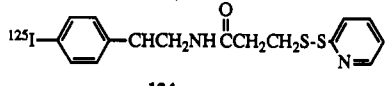
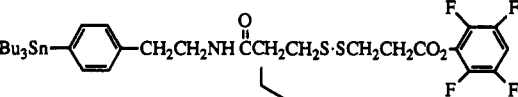
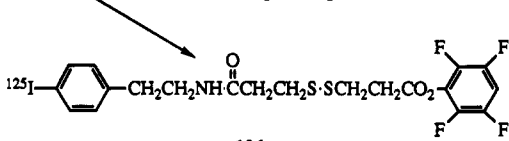
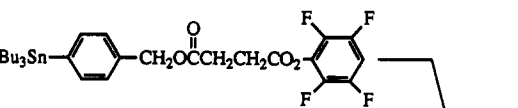
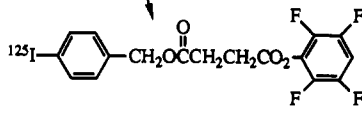
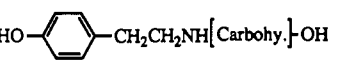
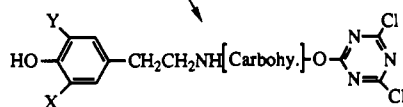
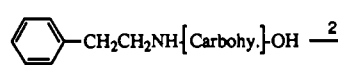
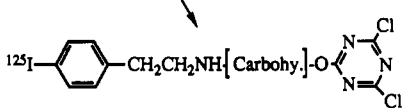
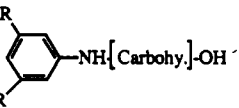



1. *In Vivo* Stability. A large amount of effort has been put into development of “stable” radiohalogenated conjugates because *in vivo* deiodination of directly labeled radioiodinated monoclonal antibodies, under investigation as imaging and therapeutic agents for cancer, has been considered a problem. Conjugates that contain phenolic rings have been shown to increase the *in vivo* stability relative to direct labeled counterparts, but some dehalogenation is still apparent. Importantly, it appears that the problem of *in vivo* dehalogenation has been solved by application of radiohalogenated nonactivated aromatic compounds such as the *p*-halobenzoate 10 and *m*-halobenzoate 12. However, it may be important to ask if the reason for the “stability” gained is really understood. Interpretation of what is occurring in the dehalogenation process is still not clear. That is, enzymatic dehalogenation (deiodination) has been perceived as a problem because

the presence of free radioiodide has been thought to be reflective of loss of radiolabel from the antibody, thus limiting the amount of activity that the antibody can deliver to the target tissue (e.g. cancer). However, the need to use “stable” conjugates may be dependent upon when the deiodination occurs. It may be that, as is widely held, deiodination occurs on the intact antibody (or fragment). On the other hand, deiodination may occur only after the protein has been metabolized to the individual amino acids and radioiodinated tyrosine is released. In this case, use of a stable radioiodination conjugation reagent may only provide a different excretion rate and secondary distribution of the radioiodine. The important point is that when a radiohalogenated protein or peptide is evaluated *in vivo*, metabolite studies must be conducted to help understand what is being observed when the tissues are counted. *In vitro* studies have shown that iodine can be lost from intact proteins (323), but questions of radiolysis of the label in those studies have been raised. Other investigators have interpreted observed differences in radioactivity of some tissues when radio-metal- and radioiodine-label antibodies are coinjected as being due to rapid deiodination of antibodies (324, 325), but it may simply be due to the fact that the radiometal is retained in tissue after catabolism while the radioiodide freely leaves the tissue (326). Studies of the metabolites of *p*-[¹²⁵I, ¹³¹I]iodobenzoyl-conjugated antibodies have demonstrated that the primary metabolites are lysine adducts of the benzoate (and the *N*-acetyl derivatives) (327, 328). Catabolism to single amino acids in organs (329) and metabolites of protein conjugates containing lysine adducts have been reported previously (329, 330). Contrary to this, Zalutsky and co-workers have reported that free *m*-[¹³¹I]iodobenzoic acid and *m*-[²¹²At]astatobenzoic acid have been observed as the major metabolites of radiolabeled antibodies when *m*-halobenzoate is used as a conjugate (211). Other investigators have also found examples where the free carboxylic acid has been released from protein lysine amine conjugates (331). The difference in metabolites for the two radiohalogenated benzoyl labels may help explain the tissue differences observed in comparative studies (197, 208, 212). These results indicate that small variations in the structure of radiohalogenated protein conjugates could dramatically alter the fate of the metabolites from labeled proteins *in vivo*.

2. *Cleavable Linkers.* Applications to therapy using radiolabeled antibodies have been hindered in some studies by accumulation of radioactivity in the liver or kidney. A major improvement in the agent might be obtained if a selective release of the radionuclide in excretory tissues (e.g. liver and kidney) without (or with minimal) effect on tumor-associated radioactivity. This concept has prompted the development of conjugates that have chemical moieties, or linkers, which are cleavable *in vivo*. Studies of protein drug and toxin conjugates (269) have provided examples of release of drug through esters (332), acid-cleavable linkers (333, 334), disulfide linkers (335), and proteolysis of peptides (336).

Studies involving synthesis, radioiodination, and conjugation of radioiodinated disulfide containing compounds were conducted at NeoRx (337). Reaction of *p*-(tri-*n*-butylstannyl)phenethylamine with *N*-succinimidyl 3-(2-pyridyldithio)propionate (SPDP, Pierce) provided disulfide-containing arylstannane 123. Radioiodination of 123 gave very high yields of the corresponding aryl iodide 124. Conjugation studies with radioiodinated 124 involving DTT-treated intact antibody gave highly variable yields. *In vitro* evaluation of an antibody conjugate of

Table IX. Radiohalogenation Reagents Containing Linker Functionalities

starting reagent	radiolabeled reagent (for protein conjugation)	% radiolab yield	% conjugn yield	ref
A. Metabolizable Linkers				
 123	 124	88-99	2-61	337
 125	 126	>90	25-50	337
 127	 128	>90	60	340
B. Nonmetabolizable Linkers				
 129a: Carbohy. = cellobiose	 130a: X = ¹²⁵ I, Y = H; Carbohy. = cellobiose 130b: X = Y = ¹²⁵ I; Carbohy. = cellobiose 130c: X = ¹²⁵ I, Y = H; Carbohy. = glucose 130d: X = Y = ¹²⁵ I; Carbohy. = glucose	80-95	46-70	344, 346 350, 351
129b: Carbohy. = glucose		83	55	350, 351
 131a: Carbohy. = cellobiose 131b: Carbohy. = glucose	 132a: Carbohy. = cellobiose 132b: Carbohy. = glucose	35 18	9-35 8-34	350, 351 350, 351
 133a: R = H; Carbohy. = cellobiose 133b: R = H; Carbohy. = glucose 133c: R = CH ₃ ; Carbohy. = cellobiose 133d: R = CH ₃ ; Carbohy. = glucose	 134a: R = H; Carbohy. = cellobiose 134b: R = H; Carbohy. = glucose 134c: R = CH ₃ ; Carbohy. = cellobiose 134d: R = CH ₃ ; Carbohy. = glucose	83 75 95 93	10-31 15-23 19-48 14-48	350, 351 350, 351 350, 351 350, 351
 135a: R = CH ₃ ; Carbohy. = cellobiose 135b: R = CH ₃ ; Carbohy. = glucose	 136a: R = CH ₃ ; Carbohy. = cellobiose 136b: R = CH ₃ ; Carbohy. = glucose	34 29	8-18 6-17	350, 351 350, 351

124 in PBS at 37 °C indicated that protein-bound radioactivity had only decreased to 82% by 6 days, and under the same conditions in serum it had decreased to 87%. In contrast to this, incubation of serum containing 2 and 4 mM cysteine decreased the protein bound activity to 18% and 9%, respectively, after 1.5 h at 37 °C. Problems with consistent conjugation yields led to a second approach to preparing disulfide conjugates.

A secondary approach to obtaining conjugates with disulfide bonds was to react *p*-(tri-*n*-butylstannyl)phenethylamine with another commercially available cross-linking compound, 3,3'-dithiobis(succinimidyl propionate) (DSP, Pierce). Initial attempts to produce the desired conjugate were fraught with difficulties as a mixture of desired compound, dimer containing two phenethylamines, and the compound where the *N*-hydroxysuccinimide ester was cleaved to the acid was obtained. Difficulties in purifying the desired compound from the mixture led to an alternate preparation. In the alternate preparation, an excess of DSP was used (to alleviate the dimer) and any *N*-hydroxysuccinimide ester remaining was hydrolyzed to the free acid prior to workup. Esterification of the free acid with DCC/tetrafluorophenol yielded the TFP ester of the DSP adduct of stannylphenethylamine, 125. Radioiodination of 125 was found to be facile with radiochemical yields consistently >90%. Conjugations with antibodies of radioiodinated 126 were conducted optimally at 37 °C for 30 min. The conjugate was purified by size-exclusion chromatography (Sephadex G-25; PD-10) to 94% with no high molecular weight aggregates being observed. In vitro evaluation of the radioiodinated DSP conjugate showed a minor drop in protein-associated activity at 37 °C in PBS for 2 h. Some aggregation or binding to serum proteins occurred in human serum over a 90-h period, but no loss of activity from proteins was noted. Treatment of an antibody conjugated to radioiodinated 126 with 10 mM DTT decreased the amount of protein-bound activity to 10% after 11 h, showing that the disulfide could be selectively cleaved. Unfortunately, the antibody conjugate of 126 was found to be quite unstable in vivo. Additional studies need to be conducted to determine if the in vivo stability could be increased by having hindered disulfides (338, 339).

Another cleavable linker that was studied at NeoRx was an ester-containing radioiodinated conjugate, tetrafluorophenyl *p*-[¹²⁵I]iodobenzyl succinate, 128 (340). Tetrafluorophenyl *p*-(tri-*n*-butylstannyl)benzylsuccinate, 127, was prepared by condensation of *p*-(tri-*n*-butylstannyl)benzyl alcohol with succinic anhydride, followed by esterification with DCC/tetrafluorophenol. Radioiodination of the ester was accomplished in high yield. Conjugations with an intact antibody and an antibody Fab fragment were accomplished in good yields at pH 8.5, 37 °C for 30 min. Evaluations of the radioiodinated ester, 128, conjugated Fab in saline indicated that minimal (<10%), if any, hydrolysis of the activity from the protein occurred over 30 h. In contrast to that, nearly 25% of the radioactivity was released from the protein in serum over that same period. In vivo evaluation of the Fab ester conjugate indicated that at 4 h, when a large differential would be of optimal value, its percent dose/gram (% D/g) in kidney was nearly identical to that of the same Fab radioiodinated with *p*-iodobenzoate, 10c. However, at 20 h the kidney activity (% D/g) was only 26% that of the *p*-iodobenzoyl-labeled Fab. These results might indicate that metabolism of the ester had occurred after metabolism of the protein. More rapid cleavage of the ester (i.e. from

the nonmetabolized Fab) might be attained if a diester was used as a linker (341–343).

3. Nonmetabolizable Linkers. In contrast to removal of activity from tissues, when delivering imaging or therapeutic radiohalogen nuclides to tumors it would be of great benefit to be able to trap (retain) the radionuclide at the tumor. Some studies in the literature have shown that it is possible to metabolically trap radioiodine (probably in lysosomes) by attaching a molecule containing the radioiodine (usually tyramine) to a carbohydrate moiety. Pittman et al. coupled tyramine to cellobiose by reductive alkylation with sodium cyanoborohydride to form the adduct 129a and radioiodinated the adduct (344). The radioiodinated tyramine–cellobiose was then coupled to cyanuric chloride (345) to form 130 (a,b?), which was immediately coupled to a protein by reaction at pH 7.0–7.5 for at least 1 h. Very good radiolabeling yields and protein conjugation yields were obtained using their procedures. High retention of activity (71%) was obtained after 24 h in the liver and bone marrow when asialotransferrin, a protein targeted for uptake in liver and bone marrow cells, was coupled with radioiodinated tyramine–cellobiose–cyanuric chloride and injected into rabbits.

Strobel et al. employed the same labeling method as Pittman et al. for radioiodination/conjugation of lactitol, cellobitol, dilactitol, and dicellobitol to a model carrier protein asialofetuin (ASF) (346). The results obtained indicated that radioiodinated glycoconjugates of ASF increased the liver retention, where ASF is metabolized, by a factor of 5 in 24 h. Disubstituted [¹²⁵I]tyramine glycoconjugates were retained more efficiently than the smaller monosubstituted conjugates. More recently, Maxwell et al. have described the use of much larger radioiodinated tyramine–inulin protein conjugates to slow the release of radiolabel (through catabolism) and improve the retention (347).

Ali et al. have used radioiodinated tyramine–cellobiose to radiolabel monoclonal antibodies in an attempt to increase the residence time of the radioactivity in a tumor model (348). These investigators found that good labeling and conjugation yields could be obtained while the immunoreactivity of the antibody was retained. They also found that tumor uptake and retention were greater with the radioiodinated tyramine–cellobiose conjugate than with directly labeled antibody, while other tissues were very similar. Welch et al. also investigated tyramine–cellobiose, 130, labeled antibodies (349). In contrast to the Ali et al. results, they found that the amount of antibody in the tumor was not increased but was retained longer. They also observed an increase in the liver activity over direct labeling. More recently, Ali et al. have reported the preparation, radioiodination, and conjugation of ten carbohydrate adducts (129a,b, 131a,b, 133a–d, 135a,b) (350, 351). In biodistribution studies, they found prolonged retention of the tyramine–cellobiose-labeled antibody in tumor over a direct-labeled control and again found normal tissues to be similar to the direct-labeled control.

B. Direct Labeling of Conjugates. It is very likely that new radiohalogenated conjugates will be developed which will have properties that are designed for specific applications; however, application of conjugate labeling methods may not be widely used even then, as the chemistry can be fairly difficult to conduct. Therefore, the challenge for the chemists will be to develop simple methods for radiolabeling proteins after the small molecule is conjugated. To do this, methods of producing rapid, high specific activity, high-yielding radiohalogenations of

proteins under mild conditions must be developed. This will be more challenging for some radionuclides than others, but all radionuclides will require developing compounds that are more reactive than any of the other reactive functional groups on the protein. Very reactive functional groups on proteins such as tyrosines (in electrophilic radiohalogenations) may have to be deactivated by reversible modification prior to the radiohalogenation reaction.

VI. RADIATION SAFETY CONSIDERATIONS

A detailed description of radiation safety procedures and shielding requirements when conducting experiments with radiohalogens is beyond the scope of this review. (This information can generally be obtained from radiation safety personnel at your institution.) However, the volatile nature of many radiohalogen species (e.g. dihalogens, acid halides) makes handling of these materials somewhat different than other radioactive materials. This is particularly true for handling radioiodine, as it is sequestered by the thyroid gland. Thus, a few statements about precautions that may be taken when conducting radiohalogenation reactions are given below.

The volatile nature of radiohalogen dictates that radiohalogenations always be conducted in a fume hood, vented glovebox, or (if large amounts of activity are used) in a "hot cell". For radioiodinations, a Plexiglas "iodination box" which has its own exhaust fan and charcoal filter is available commercially (Radiation Physics, Beltsville, MD). We have placed an iodination box within a fume hood and use it for all routine labelings. The charcoal filter in the unit is easily accessible and can be readily changed. Astatine-211 labelings are conducted in a glovebox which is vented through a charcoal filter into the iodination chamber, where its exhaust is passed through a second charcoal filter. Radiohalogenation reactions are routinely conducted in reaction vessels which are vented to the inside of the iodination box or glovebox through a (10-mL) syringe filled with charcoal. The effluent of the fume hood used for radioiodinations (other halogens?) should be monitored for release of radioactivity. While it may not be your task, an inexpensive method of monitoring for release of radiohalogens in the fume hood exhaust has been described by safety personnel at the University of Wisconsin which may be adapted to your facility (352).

As with handling any radioactive material, the appropriate laboratory attire must be worn. We routinely double glove (two gloves per hand) as a safety precaution against volatile halogens penetrating the first glove layer. We also use commercially available "sleeve protectors" to aid in decreasing the contamination of the lab coat sleeves when using the iodination box. Monitoring with appropriate equipment is conducted continually throughout an experiment. Between 24 and 72 h post radioiodinations, investigators should have a thyroid bioassay conducted. This is usually done by radiation safety personnel.

We have found that the radiation waste poses a significant health risk if it is not treated properly. This is particularly true of radioactivity that is left behind in glassware and on chromatography columns. Therefore, we routinely elute base (e.g. 0.1 N NaOH) over chromatography columns used in radiohalogenation reactions, rinse the reaction vessels and other glassware used in the labeling with base, and add base to any liquid waste from the radiohalogenations prior to storage or disposal. Once rinsed with base, the items are placed in a Zip-loc bag which contains charcoal to adsorb any volatile halogen.

Handling of astatine-211 is minimized, and all labeling glassware and equipment remain in the glove box for a minimum of 4 d (13 half-lives) before cleaning for the next experiment.

Radiohalogenations at high levels of activity can present a radiation risk. However, the risk is minimal if the protein labelings can be done remotely. In radioiodinations with **9b**, we conducted high-level radioiodination reactions involving up to 1 Ci of activity. In those experiments we found that all of the mixing and moving of radioactivity could be accomplished at a distance (remotely) from shielded sources. This was accomplished by using air pressure from syringes to move the activity from the reaction vessel into the protein solution and onto a purification column via sterile transfer tubes (cannulas). Indeed, several investigators have described similar remote labeling setups which could be adapted to almost any protein labeling experiment (353-355).

VII. SUMMARY

Direct labeling of proteins with radionuclides of iodine will continue to be the method of choice to answer questions addressed in many future studies. However, it seems likely that a increasing number of applications of radiohalogenated proteins will require, or benefit from, conjugate labeling. While many radiohalogen conjugates have been studied, a large proportion of them have only undergone preliminary studies to date, leaving a question of their overall utility. Phenolic conjugates give good radioiodination labeling yields, but mixtures of radiohalogenated products and problems with *in vivo* stability can be expected. This fact, along with the fact that phenolic compounds do not have a general application to radiohalogens, makes them less attractive than other alternatives.

Radiohalogen labeling through the use of organometallic intermediates has proven to be facile, resulting in high yields of high specific activity labeled small-molecule conjugates. Although the choice of which organometallic intermediate to use may depend somewhat on the radionuclide employed, arylstannanes appear to have the most general applicability. Fluorine-18 labeling of small-molecule conjugates has been best accomplished by ipso aromatic nucleophilic substitution (exchange) reactions. Radiohalogenated small molecules have been prepared which can be conjugated with specific functional groups (e.g. amines, sulfhydryl groups, and carbohydrates) or conjugated nonspecifically with groups in the proximity of the conjugate when it is photolyzed. On the basis of previous studies, good conjugation yields (i.e. 60-90%) can be expected for reactions with specific groups, whereas low yields (i.e. 1-5%) can be expected for conjugations with reactive nitrenes and carbenes. However, recent developments in the chemistry of conjugates that produce nitrenes and carbenes will likely improve the radiolabeling yields.

There have been too few comparative studies to readily assess which is the best approach to take when beginning a study involving radiohalogenation of a protein or peptide. However, it is clear that radiohalogenated conjugates of proteins can offer an advantage over direct labeling in that conjugates may be designed which provide some control over *in vivo* stability and secondary distribution of metabolites. Conjugates can be prepared which are designed to utilize *in vivo* biochemical processes to release a radiohalogenated small molecule from a tissue (i.e. kidney or liver) or retain the radioactivity at the target tissue (e.g. tumor). Aside from the designing of conjugates with

linking molecules for desired biological effects, the ultimate future goal for the radiolabeling chemist should be to prepare protein conjugates which can be radiohalogenated in a simple one-step procedure.

VIII. ACKNOWLEDGMENT

I would like to acknowledge all of the scientists that have contributed to the understanding of radiohalogenation reactions and development of radiohalogenated protein conjugates over the past 8 years. These include: Scott Rogers, Zita Svitra, Dr. Kent Anderson, and Wendy Stone for their assistance in organic synthesis and radiohalogen labeling at Los Alamos; Dr. Mark Hylarides, Dr. Stephen Hadley, Dr. David Jones, Joan Schroeder, Don Axworthy, Leah Grant, and Jerry Seubert for their assistance in organic synthesis and radiolabeling at NeoRx Corp.; Dr. Mary Ann Gray, Dr. Paul Beaumier, Karen Poole, Denise Dupont, and Joanne Stevens for their assistance in the animal studies conducted at NeoRx Corp.; Dr. Bob Vessella, James Stray, Dena Goffe, and Don Hamlin for their assistance in continuing studies at the University of Washington. I would also like to thank Dr. Robert Atcher, John Hines, and Ed Kemerite for their assistance in providing astatine-211 for our studies. I thank the following organizations for their support of radiohalogenated antibody research: DOE for support at Los Alamos National Laboratory and support in collaboration with Argonne National Laboratory; NIH for support under Grants N43-CM-57759, N43-CM-67759, and N43-CM-67939; NeoRx Corp. for their financial support; and University of Washington School of Medicine (BRSG 62-3126).

IX. LITERATURE CITED

- Magerstadt, M. (1991) *Antibody Conjugates and Malignant Disease*, pp 11-35, 79-93, CRC Press, Boca Raton, FL.
- Osterman, L. A. (1984) Labeling of Proteins. *Methods of Protein and Nucleic Acid Research*, pp 131-143, Springer-Verlag, New York.
- Kas, J., and Rauch, P. (1983) Labeled Proteins, Their Preparation and Applications. *Topics in Current Chemistry* (F. L. Boschke, Ed.) Vol. 112, pp 167-182, Springer-Verlag, NY.
- Srivastava, S. C., Ed. (1988) *Radiolabeled Monoclonal Antibodies for Imaging and Therapy*, Part III, pp 193-268, Plenum Press, New York.
- Regoezi, E., Ed. (1984) *Iodine-labeled Plasma Proteins*, Vols. I and II, CRC Press, Inc., New York.
- Eckelman, W. C., Paik, C. H., and Reba, R. C. (1980) Radiolabeling of Antibodies. *Cancer Res.* 40, 3036-3042.
- Fritzberg, A. R., Berninger, R. W., Hadley, S. W., and Wester, D. W. (1988) Approaches to Radiolabeling of Antibodies for Diagnosis and Therapy of Cancer. *Pharm. Res.* 5, 325-334.
- Fine, J., and Seligman, A. M. (1943) Traumatic Shock: IV. A Study of the Problem of the "Lost Plasma" in Hemorrhagic Shock by the Use of Radioactive Plasma Protein. *J. Clin. Invest.* 22, 285-303.
- Li, C. H. (1945) Iodination of Tyrosine Groups in Serum Albumin and Pepsin. *J. Am. Chem. Soc.* 67, 1065-1069.
- Pressman, D., and Keighley, G. (1948) The Zone of Activity of Antibodies as Determined by the Use of Radioactive Tracers; The Zone of Activity of Nephritox Antikidney Serum. *J. Immunol.* 59, 141-146.
- Bale, W. F., and Spar, I. L. (1957) Studies Directed Toward the Use of Antibodies as Carriers of Radioactivity for Therapy. *Adv. Biol. Med. Phys.* 5, 285-356.
- Bolton, A. E., and Hunter, W. M. (1986) Radioimmunoassay and related methods. *Handbook of Experimental Immunology. Volume 1: Immunochimistry*, 4th ed. (D. M. Weir, Ed.), pp 26.1-26.56, Blackwell Scientific Publications, London, England.
- Bolton, A. E. (1985) Selection of a Suitable Radioisotope. *Radioiodination Techniques*, 2nd ed., pp 14-15, Amersham Corp., Arlington Heights, IL.
- Berson, S. A., Yalow, R. S., Bauman, A., Rothschild, A., and Newerly, K. (1956) Insulin- I^{131} Metabolism in Human Subjects: Demonstration of Insulin Binding Globulin in the Circulation of Insulin Treated Subjects. *J. Clin. Invest.* 35, 170-190.
- Yalow, R. S., and Verson, S. A. (1960) Immunoassay of Endogenous Plasma Insulin in Man. *J. Clin. Invest.* 39, 1157-1175.
- Argentini, M. (1982) Labelling of Proteins and Peptides. *Labelling with Iodine. A Review of the Literature*, pp 255-285, Swiss Federal Institute for Reactor Research, Wuerenlingen, Switzerland (ISBN 3-85677-005-4).
- Eary, J. F., Krohn, K. A., Kishore, R., and Nelp, W. B. (1989) Radiochemistry of Halogenated Antibodies. *Antibodies in Radiodiagnosis and Therapy* (M. R. Zalutsky, Ed.) pp 83-102, CRC Press, Inc., Boca Raton, FL.
- Regoezi, E. (1984) Methods of Protein Iodination. *Iodine-labeled Plasma Proteins*, Vol. I, pp 35-102, CRC Press, Inc., New York.
- Knight, L. C., Krohn, K. A., Welch, M. J., Spomer, B. and Hager, L. P. (1975) ^{77}Br : A New Protein Label. *Radiopharmaceuticals* (G. Subramanian, B. A. Rhodes, J. F. Cooper, and V. J. Sodd, Eds.) pp 149-154, The Society of Nuclear Medicine, New York.
- McElvany, K. D., Barnes, J. W., and Welch, M. J. (1980) Characterization of Bromine-77-Labeled Proteins Using Myeloperoxidase. *Int. J. Appl. Radiat. Isot.* 31, 679-688.
- McElvany, K. D., and Welch, M. J. (1980) Characterization of Bromine-77-Labeled Proteins Prepared Using Bromoperoxidase. *J. Nucl. Med.* 21, 953-960.
- Hughes, W. L., and Gitlin, D. (1954) The Reaction of Astatine with Protein. *USAEC-D-BNL-314*, p 48.
- Hughes, W. L., and Gitlin, D. (1955) Astatinated (At^{211}) organic compounds for production of highly localized radiobiological effects. *Am. Soc. Biol. Chem.* 229 (abstract).
- Aaij, C., Tschroots, W. R. J. M., Lindner, L., and Feltkamp, T. E. W. (1978) The Preparation of Astatine Labeled Proteins. *Int. J. Appl. Radiat. Isot.* 26, 25-30.
- Vaughan, A. T. M., and Fremlin, J. H. (1978) The Preparation of Astatine Labeled Proteins Using an Electrophilic Reaction. *Int. J. Nucl. Med. Biol.* 5, 229-230.
- Visser, G. W. M., Diemer, E. L., Vos, C. M., and Kaspersen, F. M. (1981) The Biological Behavior of Some Organic Astatine Compounds in Rats. *Int. J. Appl. Radiat. Isot.* 32, 913-917.
- Visser, G. W. M., Diemer, E. L., and Kaspersen, F. M. (1981) The Nature of the Astatine-Protein Bond. *Int. J. Appl. Radiat. Isot.* 32, 905-912.
- Quaim, S. M., and Stocklin, G. (1983) Production of Some Medically Important Short-Lived Neutron-Deficient Radioisotopes of Halogens. *Radiochim. Acta* 34, 25-40.
- Kleinberg, J., and Cowan, G. A. (1960) *The Radiochemistry of Fluorine, Chlorine, Bromine, and Iodine*, National Academy of Sciences, National Research Council Nuclear Science Series, Office of Technical Services, Department of Commerce, Washington, DC.
- Yano, Y. (1975) Radionuclide Generators: Current and Future Applications in Nuclear Medicine. *Radiopharmaceuticals* (G. Subramanian, B. A. Rhodes, J. F. Cooper, and V. J. Sodd, Eds.) pp 236-245, The Society of Nuclear Medicine, New York.
- Lambrech, R. M. (1983) Radionuclide Generators. *Radiochim. Acta* 34, 9-24.
- Ruth, T. J., Pate, B. D., Robertson, R., and Porter, J. K. (1989) Radionuclide Production for the Biosciences. *Nucl. Med. Biol.* 16, 323-336.
- Waters, S. L., and Silvester, D. J. (1982) Inorganic Cyclotron Radionuclides. *Radiochim. Acta* 30, 163-173.
- Grant, P. M., Whipple, R. E., Barnes, J. W., Bentley, G. E., Wanek, P. M., and O'Brien, H. A. (1981) The Production and Recovery of ^{77}Br at Los Alamos for Nuclear Medicine Studies. *J. Inorg. Nucl. Chem.* 43, 2217-2222.
- Kirby, H. W. (1985) Production, Isolation, and Purification of Astatine Isotopes. *Gmelin Handbook of Inorganic Chem-*

- istry, Astatine, 8th ed. (H. K. Kugler, and C. Keller, Eds.) pp 95-106, Springer-Verlag, New York.
- (36) Kilbourn, M. R. (1990) Production of Fluorine-18. *Fluorine-18 Labeling of Radiopharmaceuticals*, pp 4-14, National Academy of Sciences, National Science Council Nuclear Science Series (NAS-NS-3203), National Academy Press, Washington, DC.
- (37) Schafer, D. E. (1983) Measurement of Receptor-Ligand Binding: Theory and Practice. *Lecture Notes in Biomathematics: Tracer Kinetics and Physiologic Modeling* (R. M. Lambrecht, and A. Rescigno, Eds.) pp 445-507, Springer-Verlag, New York.
- (38) Wagner, H. N. (1989) SNM Highlights-1989: Why Not? *J. Nucl. Med.* 30, 1283-1295.
- (39) Wagner, H. N. (1990) Scientific Highlights 1990: The Universe Within. *J. Nucl. Med.* 31, 17A-26A.
- (40) Wagner, H. N. (1991) Molecular Medicine: From Science to Service. *J. Nucl. Med.* 32, 11N-23N.
- (41) Consensus Panels (1985) *The Developing Role of Short-Lived Radionuclides in Nuclear Medicine Practice* (P. Paras, and J. W. Thiessen, Eds.) pp 497-544, Office of Scientific and Technical Information, United States Department of Energy, Conf-830523 (DE82008258).
- (42) McElvany, K. D., Katzenellenbogen, J. A., Shafer, K. E., Siegel, B. A., Senderoff, S. G., Welch, M. J., and the Los Alamos Medical Research Group (1982) $^{16}\alpha$ -[^{77}Br]Bromoestradiol: Dosimetry and Preliminary Clinical Studies. *J. Nucl. Med.* 23, 425-430.
- (43) Welch, M. J., and Kilbourn, M. R. (1986) Clinical Potential of Positron-Emitting Radiopharmaceuticals. *Radiopharmaceuticals, Progress and Clinical Perspectives*, Vol. II, pp 115-125, CRC Press, Inc., Boca Raton, FL.
- (44) Barrio, J. R., Hawkins, R. A., Mazziotta, J. C., and Phelps, M. E. (1986) Biochemical Strategies in Positron Emission Tomography. *Current Applications in Radiopharmacology. Proceedings of the Fourth International Symposium on Radiopharmacology*. (M. W. Billingham, Ed.) pp 2-16, Pergamon Press, New York.
- (45) Pentlow, K. S., Graham, M. C., Lambrecht, R. M., Cheung, N.-K. V., and Larson, S. M. (1991) Quantitative imaging of I-124 using positron emission tomography with applications to radioimmunodiagnosis and radioimmunotherapy. *Med. Phys.* 18, 357-366.
- (46) DeLand, F. H., and Goldenberg, D. M. (1986) Radiolabeled Antibodies: Radiochemistry and Clinical Applications. *Freeman and Johnson's Clinical Radionuclide Imaging*, 3rd ed., pp 1915-1992, Grune and Stratton, Inc., New York.
- (47) Lyster, D. M., and Alcorn, L. N. (1986) Antibody Imaging and Therapy in Human Cancer. In *Radiopharmaceuticals: Progress and Clinical Perspectives* (A. R. Fritzsche, Ed.) Vol. 1, pp 41-59, CRC Press, Inc., Boca Raton, FL.
- (48) Cobb, L. M., and Humm, J. L. (1986) Radioimmunotherapy of malignancy using antibody targeted radionuclides. *Br. J. Cancer* 54, 863-870.
- (49) Buchsbaum, D. J., and Lawrence, T. S. (1991) Tumor Therapy with Radiolabeled Monoclonal Antibodies. *Antibody, Immunoconjugate Radiopharm.* 4, 245-272.
- (50) Wessels, B. W., and Rogus, R. D. (1984) Radionuclide Selection and Model Absorbed Dose Calculations for Radiolabeled Tumor Associated Antibodies. *Med. Phys.* 11, 638-645.
- (51) Troutner, D. E. (1987) Chemical and Physical Properties of Radionuclides. *Nucl. Med. Biol.* 14, 171-176.
- (52) Wolf, W., and Shani, J. (1986) Criteria for Selection of the Most Desirable Radionuclide for Radiolabeling Monoclonal Antibodies. *Nucl. Med. Biol.* 13, 319-324.
- (53) Humm, J. L. (1986) Dosimetric Aspects of Radiolabeled Antibodies for Tumor Therapy. *J. Nucl. Med.* 27, 1490-1497.
- (54) Brown, I. (1986) Astatine Radiopharmaceuticals. Astatine-211: Its Possible Applications in Cancer Therapy. *Appl. Radiat. Isot.* 37, 789-798.
- (55) Wilbur, D. S. (1991) Potential Use of Alpha Emitting Radionuclides in the Treatment of Cancer. *Antibody, Immunoconjugate Radiopharm.* 4, 85-97.
- (56) Kassis, A. I., Adelstein, S. J., and Bloomer, W. D. (1987) Therapeutic Implications of Auger-Emitting Radionuclides. *Radionuclides in Therapy* (R. P. Spencer, R. H. Seevers, and A. M. Friedman, Eds.) pp 119-134, CRC Press, Inc., Boca Raton, FL.
- (57) Bender, H., Emrich, J., Glennon, P., Steplewski, Z., and Brady, L. W. (1992) Pharmacokinetic behavior and microdosimetry of ^{125}I -labeled α -epidermal growth factor receptor MAb 425 in human glioma cell in vitro. *Antibody, Immunoconjugate Radiopharm.* 5, 129 (abstract).
- (58) Bender, H., Morabito, M., Emrich, Rackover, M., Miyamoto, C., Woo, D. V., Steplewski, Z., and Brady, L. W. (1992) Pharmacokinetic behavior of ^{125}I -labeled α -epidermal growth factor receptor MAb 425 in high grade glioma patients. *Antibody, Immunoconjugate Radiopharm.* 5, 130 (abstract).
- (59) Veall, N., Pearson, J. D., and Hanley, T. (1955) The Preparation of ^{132}I and ^{131}I Labelled Human Serum Albumin for Clinical Tracer Studies. *Br. J. Radiol.* 28, 633-636.
- (60) De Kok, J., Van Den Hamer, C. J. A., and Goeij, J. J. M. (1990) Iodine-129 as a Protein Label for Studies of Plasma Protein Turnover and its Measurement with Neutron Activation Analysis. *Nucl. Med. Biol.* 17, 303-307.
- (61) de la Mare, P. B. D. (1976) *Electrophilic Halogenation*. Cambridge University Press, Cambridge, England.
- (62) Friedman, A. M., and Huang, C. C. (1983) Halogen Labeled Compounds. *Radiotracers for Medical Applications* (G. V. S. Rayudu, Ed.) Vol. I, pp 219-261, CRC Press, Inc., Boca Raton, FL.
- (63) Seevers, R. H., and Counsell, R. D. (1982) Radioiodination Techniques for Small Organic Molecules. *Chem. Rev.* 82, 575-590.
- (64) Murray, A., and Williams, D. L. (1958) Isotopic Halogen Compounds. *Organic Synthesis with Isotopes*, Part 2, pp 1147-1177, Interscience Publishers, Inc., New York.
- (65) Spicer, J. A., Preston, D. F., Robinson, R. G., Bradshaw, D. L., Stern, S. H., Dean, R. D., Martin, N. L., and Rhodes, B. A. (1977) A Case for ^{77}Br -Bromine Labelled Radiopharmaceuticals. *Int. J. Appl. Radiat. Isot.* 28, 163-168.
- (66) Eakins, M. N., and Waters, S. L. (1979) The Synthesis of ^{77}Br -labelled 5α -Dihydrotestosterone and a Comparison of Its Distribution in Rats with ^{77}Br -Bromide. *Int. J. Appl. Radiat. Isot.* 30, 701-703.
- (67) McElvany, K. D., Welch, M. J., Katzenellenbogen, J. A., Senderoff, S. G., Bentley, G. E., and Grant, P. M. (1981) Scope and Limitations of a Rapid Radiobromination Technique. *Int. J. Appl. Radiat. Isot.* 32, 411-416.
- (68) Malcolm-Lawes, D. J., and Massey, S. (1981) The Preparation of Radiobromine-Labelled Compounds. *J. Radioanal. Chem.* 64, 281-290.
- (69) Kulmala, H. K., Huang, C. C., Dinerstein, R. J., and Friedman, A. M. (1981) Specific In Vivo Binding of ^{77}Br -p-Bromospiroperidol in Rat Brain: A Potential Tool for Gamma Ray Imaging. *Life Sci.* 28, 1911-1916.
- (70) Doran, D. M., and Spar, I. L. (1980) Oxidative Iodine Monochloride Iodination Technique. *J. Immunol. Methods* 39, 155-163.
- (71) Greenwood, F. C., Hunter, M. W., and Glover, J. S. (1963) The Preparation of ^{131}I -Labelled Human Growth Hormone of High Specific Radioactivity. *Biochem. J.* 89, 114-123.
- (72) Salacinski, P. R. P., McLean, C., Sykes, J. E. C., Clement-Jones, V. V., and Lowry, P. J. (1981) Iodination of Proteins, Glycoproteins, and Peptides Using a Solid-Phase Oxidizing Agent, 1,3,4,6-Tetrachloro-3 α ,6 α -diphenyl Glycoluril (Iodogen). *Anal. Biochem.* 117, 136-146.
- (73) Markwell, M. A. K. (1982) A New Solid-State Reagent to Iodinate Proteins. I. Conditions for the Efficient Labeling of Antiserum. *Anal. Biochem.* 125, 427-432.
- (74) Hadi, U. A. M., Malcolm-Lawes, J., and Oldham, G. (1979) Rapid Radiohalogenations of Small Molecules-II. Radiobromination of Tyrosine, Uracil, and Cytosine. *Int. J. Appl. Radiat. Isot.* 30, 709-712.
- (75) Mazaitis, J. K., Francis, B. E., Eckelman, W. C., Gibson, R. E., Reba, R. C., Barnes, J. W., Bentley, G. E., Grant, P. M., and O'Brien, H. A. (1981) No-Carrier-Added Bromination of Estrogens with Chloramine-T and Na^{77}Br . *J. Labelled Compd. Radiopharm.* 18, 1033-1038.

- (76) Petzold, G., and Coenen, H. H. (1981) Chloramine-T for "No-Carrier-Added" Labelling of Aromatic Biomolecules with Bromine-75,77. *J. Labelled Compd. Radiopharm.* 18, 1319-1336.
- (77) Youfeng, H., Coenen, H. H., Petzold, G., and Stocklin, G. (1982) A Comparative Study of Radioiodination of Simple Aromatic Compounds via N-Halosuccinimides and Chloramine-T in TFAA. *J. Labelled Compd. Radiopharm.* 19, 807-819.
- (78) Coenen, H. H., Moerlein, S. M., and Stocklin, G. (1983) No-Carrier-Added Radiohalogenation Methods with Heavy Halogens. *Radiochim. Acta* 34, 47-68.
- (79) Zalutsky, M. R., and Narula, A. S. (1987) An Improved Method for the Radiohalogenation of Monoclonal Antibodies. *Immunological Approaches to the Diagnosis and Therapy of Breast Cancer* (R. L. Ceriani, Ed.) pp 187-203, Plenum Press, New York.
- (80) Zalutsky, M. R., and Narula, A. S. (1988) Astatination of Proteins using an N-Succinimidyl Tri-n-Butylstannyl Benzoate Intermediate. *Appl. Radiat. Isot.* 39, 227-232.
- (81) Wilbur, D. S., Hadley, S. W., Hylarides, M. D., Abrams, P. G., Beaumier, P. L., Morgan, A. C., Reno, J., and Fritzberg, A. R. (1989) Development of a Stable Radioiodinating Reagent to Label Monoclonal Antibodies For Radiotherapy of Cancer. *J. Nucl. Med.* 30, 216-226.
- (82) Wilbur, D. S., and Hylarides, M. D. (1991) Radiolabeling of A Monoclonal Antibody with N-Succinimidyl para-[⁷⁷Br]-Bromobenzoate. *Nucl. Med. Biol.* 18, 363-365.
- (83) Hadley, S. W., Wilbur, D. S., Gray, M. A., and Atcher, R. W. (1991) Astatine-211 Labeling of an Anti-Melanoma Antibody and its Fab Fragment using N-Succinimidyl p-[²¹¹At]Astatobenzoate: Comparisons in vivo with the p-[¹²⁵I]-Iodobenzoyl Conjugate. *Bioconjugate Chem.* 2, 171-179.
- (84) Wilbur, D. S., and Anderson, K. W. (1982) Bromine Chloride from N-Chlorosuccinimide Oxidation of Bromide Ion. Electrophilic Addition Reactions in Protic and Aprotic Solvents. *J. Org. Chem.* 47, 358-359.
- (85) Wilbur, D. S., and O'Brien, H. A. (1982) A-Ring Bromination of Estradiol and 17 α -Ethinylestradiol with N-Chlorosuccinimide and Bromide Ion. *J. Org. Chem.* 47, 359-362.
- (86) Wilbur, D. S., Anderson, K. W., Stone, W. E., and O'Brien, H. A. (1982) Radiohalogenation of Non-activated Aromatic Compounds Via Aryltrimethylsilyl Intermediates. *J. Labelled Compd. Radiopharm.* 19, 1171-1187.
- (87) Coenen, H. H., Machulla, H.-J., and Stocklin, G. (1979) Practically Carrier-Free Labeling of Aromatic Compounds with Bromine-77 via N-Chloro-Tetrafluorosuccinimide. *J. Labelled Compd. Radiopharm.* 16, 891-907.
- (88) Coenen, H. H., Petzold, G., and Stocklin, G. (1982) Recent Studies of Radiobromination and -Iodination (NCA) with Chloramine-T and Dichloramine-T in Aqueous and Organic Solvents. *J. Labelled Compd. Radiopharm.* 19, 1580-1581 (abstract).
- (89) Karonen, S.-L., Morsky, P., Siren, M., and Seuderling, U. (1975) An Enzymatic Solid-Phase Method for Trace Iodination of Proteins and Peptides with ¹²⁵Iodine. *Anal. Biochem.* 67, 1-10.
- (90) Goldenberg, D. M., Goldenberg, H., Sharkey, R. M., Higginbotham-Ford, E., Lee, R. E., Swayne, L. C., Burger, K. A., Tsai, D., Horowitz, J. A., Hall, T. C., Pinsky, C. M., and Hansen, H. J. (1990) Clinical Studies of Cancer Radioimmunodetection with Carcinoembryonic Antigen Monoclonal Antibody Fragments Labeled with ¹²³I or ^{99m}Tc. *Cancer Res.* 50, 909s-921s.
- (91) Pant, K. D., Zamora, P. O., Sass, K. S., Stewart, T. A., Valdez, E. F., O'Rourke, A. T., and Shah, V. O. (1987) A Comparison of Monoclonal Antibodies Against Distinct Colon Tumor-Associated Antigens in Immunohistochemistry and in Tumor Localization. *Nucl. Med. Biol.* 14, 81-89.
- (92) Bianco, J. A., Brown, P. A., Durack, L., Badger, C., Bernstein, I., Eary, J., Durham, J., Fisher, D., Sandmaier, B., Schuening, F., Storb, R., and Appelbaum, F. R. (1990) Effects of Propylthiouracil on Biodistribution of an Iodine-131-Labeled Anti-Myeloid Antibody in Normal Dogs: Dosimetry and Clinical Implications. *J. Nucl. Med.* 31, 1384-1389.
- (93) Sakahara, H., Endo, K., Nakashima, T., Koizumi, M., Kunimatsu, M., Kawamura, Y., Ohta, H., Nakamura, T., Tanaka, H., Kotoura, Y., Yamamuro, T., Hosoi, S., Toyama, S., and Torizuka, S. (1987) Localization of Human Osteogenic Sarcoma Xenografts in Nude Mice by a Monoclonal Antibody Labeled with Radioiodine and Indium-111. *J. Nucl. Med.* 28, 342-348.
- (94) Wahl, R. L., Geatti, O., Liebert, M., Wilson, B., Shreve, P., and Beers, B. A. (1987) Kinetics of Interstitially Administered Monoclonal Antibodies for Purposes of Lymphoscintigraphy. *J. Nucl. Med.* 28, 1736-1744.
- (95) Carrasquillo, J. A., Sugarbaker, P., Colcher, D., Reynolds, J. C., Estaban, J., Bryant, G., Keenan, A. M., Perentesis, P., Yokoyama, K., Simpson, D. E., Ferroni, P., Farkas, R., Schlom, J., and Larson, S. M. (1988) Radioimmunosintigraphy of Colon Cancer with Iodine-131-Labeled B72.3 Monoclonal Antibody. *J. Nucl. Med.* 29, 1022-1030.
- (96) Buraggi, G. L., Callegaro, L., Mariani, G., Turrin, A., Cascinelli, N., Attili, A., Bombardieri, E., Terno, G., Plassio, G., Dovis, M., Mazzuca, N., Natali, P. G., Scassellati, G. A., Rosa, U., and Ferrone, S. (1985) Imaging with ¹³¹I-Labeled Monoclonal Antibodies to a High-Molecular-Weight Melanoma-associated Antigen in Patients with Melanoma: Efficacy of Whole Immunoglobulin and its F(ab')₂ Fragments. *Cancer Res.* 45, 3378-3387.
- (97) Munz, D. L., Alavi, A., Koprowski, H., and Herlyn, D. (1986) Improved Radioimmunomaging of Human Tumor Xenografts by a Mixture of Monoclonal Antibody F(ab')₂ Fragments. *J. Nucl. Med.* 27, 1739-1745.
- (98) Bolton, A. E. (1985) Appendix I. Experimental Protocols for the Radioiodination of Proteins and Other Compounds. *Radioiodination Techniques*, 2nd ed., pp 58-59. Amersham Corp., Arlington Heights, IL.
- (99) March, J. (1985) Aromatic Electrophilic Substitution. *Advanced Organic Chemistry*, pp 447-511, John Wiley & Sons, New York.
- (100) Regoezi, E. (1984) Reactivities of Amino Acids and Proteins with Iodine. *Iodine-labeled Plasma Proteins*, Vol. I, pp 127-213, CRC Press, Inc., New York.
- (101) Knight, L. C., and Welch, M. J. (1978) Sites of Direct and Indirect Halogenation of Albumin. *Biochim. Biophys. Acta* 543, 185-195.
- (102) Hughes, W. L. (1957) The Chemistry of Iodination. *Ann. N.Y. Acad. Sci.* 20, 3-18.
- (103) Hughes, W. L., and Gitlin, D. (1955) Astatinated (At²¹¹) Organic Compounds for Production of Highly Localized Radiobiological Effects. *Am. Soc. Biol. Chem.* 14, 229.
- (104) Vaughan, A. T. M., and Fremlin, J. H. (1977) The Preparation of Astatotyrosine. *Int. J. Appl. Radiat. Isot.* 28, 595-598.
- (105) Visser, G. W. M., Diemer, E. L., and Kaspersen, F. M. (1979) The Preparation and Stability of Astatotyrosine and Astatiodotyrosine. *Int. J. Appl. Radiat. Isot.* 30, 749-752.
- (106) Regoezi, E. (1987) In Vivo Behavior of Catabolized Labels Derived from Iodoproteins. *Iodine-labeled Plasma Proteins*, Vol. II, Part B, pp 43-71, CRC Press, Inc., New York.
- (107) Engler, D., and Burger, A. G. (1984) The Deiodination of the Iodothyronines and of Their Derivatives in Man. *Endocr. Rev.* 5, 151-184.
- (108) Sinsheimer, J. E., Wang, T., Roder, S., and Shum, Y. Y. (1978) Mechanisms for the Biodehalogenation of Iodocompounds. *Biochem. Biophys. Res. Commun.* 83, 281-286.
- (109) Gerstenberger, M. R. C., and Haas, A. (1981) Methods of Fluorination in Organic Chemistry. *Angew. Chem., Int. Ed. Engl.* 20, 647-667.
- (110) Schlosser, M. (1978) Introduction of Fluorine into Organic Molecules: Why and How. *Tetrahedron* 34, 3-17.
- (111) Rozen, S., and Filler, R. (1985) α -Fluorocarbonyl Compounds and Related Chemistry. *Tetrahedron* 41, 1111-1153.
- (112) Hewitt, C. D., and Silvester, M. J. (1988) Fluoroaromatic Compounds: Synthesis, Reactions and Commercial Applications. *Aldrichimica Acta* 21, 3-10.
- (113) Palmer, A. J., Clark, J. C., and Goulding, R. W. (1977) The Preparation of Fluorine-18 Labelled Radiopharmaceuticals. *Int. J. Appl. Radiat. Isot.* 28, 53-65.
- (114) Tewson, T. J. (1982) Organic Synthesis Involving Fluorine-18. *Applications of Nuclear and Radiochemistry* (R. M. Lambrecht and N. Morcos, Eds.) pp 163-183, Pergamon Press, New York.

- (115) Fowler, J. S., and Wolf, A. P. (1982) *The Synthesis of Carbon-11, Fluorine-18, and Nitrogen-13 Labeled Radiotracers for Biomedical Applications*, National Academy of Sciences, National Research Council Nuclear Science Series—Nuclear Medicine, NAS-NS-3201 (DE82014870).
- (116) Kilbourn, M. R. (1990) *Methods of [¹⁸F]Fluorination. Fluorine-18 Labeling of Radiopharmaceuticals*, pp 15–69, National Academy of Sciences, National Science Council Nuclear Science Series (NAS-NS-3203), National Academy Press, Washington, DC.
- (117) Brown, H. C., and Stock, L. M. (1957) Relative Rates of Bromination of Benzene and Methylbenzenes. Partial Rate Factors for the Bromination Reaction. *J. Am. Chem. Soc.* 79, 1421–1425.
- (118) Brown, H. C., and Stock, L. M. (1957) Relative Rates of Chlorination of Benzene, Toluene, and the Xylenes. Partial Rate Factors for the Chlorination Reaction. *J. Am. Chem. Soc.* 79, 5175–5179.
- (119) Braendlin, H. P., and McBee, E. T. (1964) *Halogenation. Friedel-Crafts and Related Reactions* (G. A. Olah, Ed.) Vol. III, Part 2, pp 1517–1593, Interscience Publishers, New York.
- (120) Baird, W. C., and Surridge, J. H. (1970) Halogenation with Copper(II) Halides. The Synthesis of Aryl Iodides. *J. Org. Chem.* 35, 3436–3442.
- (121) Sugita, T., Idei, M., Ishibasha, I. Y., and Takegami, Y. (1982) Aromatic Iodination with Aluminum and Copper(II) Chlorides and Iodine. *Chem. Lett.* 1481–1482.
- (122) Radner, F. (1988) Lower Nitrogen Oxide Species as Catalysts in a Convenient Procedure for the Iodination of Aromatic Compounds. *J. Org. Chem.* 53, 3548–3553.
- (123) Pagni, R. M., Kabalka, G. W., Boothe, R., Gaetano, K., Stewart, L. J., Conaway, R., Dial, C., Gray, D., Larson, S., and Luidhardt, T. (1988) Reactions of Unsaturated Compounds with Iodine and Bromine on γ Alumina. *J. Org. Chem.* 53, 4477–4482.
- (124) Kahn, S. A., Munawar, M. A., and Siddiq, M. (1988) Monobromination of Deactivated Active Rings Using Bromine, Mercuric Oxide, and Strong Acid. *J. Org. Chem.* 53, 1799–1800.
- (125) Zollinger, H. (1978) Nitrogen as Leaving Group: Dediazoniations of Aromatic Diazonium Ions. *Angew. Chem., Int. Ed. Engl.* 17, 141–150.
- (126) Hodgson, H. H. (1947) The Sandmeyer Reaction. *Chem. Rev.* 40, 251–277.
- (127) Merkushev, E. B. (1988) Advances in the Synthesis of Iodoaromatic Compounds. *Synthesis* 923–937.
- (128) Visser, G. W. M., and Diemer, E. L. (1982) The Reaction of Astatine with Aromatic Diazonium Compounds. *Radiochem. Radioanal. Lett.* 51, 135–141.
- (129) Meyer, G.-J., Rossler, K., and Stocklin, G. (1979) Reaction of Aromatic Diazonium Salts with Carrier-Free Radioiodine and Astatine. Evidence for Complex Formation. *J. Am. Chem. Soc.* 101, 3121–3123.
- (130) Hughes, W. L., and Klinenberg, J. (1955) Astatine (At²¹¹) Incorporation into Aromatic Nuclei Via Diazonium Compounds. *USAEC-D-BNL-367*, pp 42–43.
- (131) Tewson, T. J., and Welch, M. J. (1979) Preparation of Fluorine-18 Aryl Fluorides: Piperidyl Triazines as a Source of Diazonium Salts. *J. Chem. Soc., Chem. Commun.* 1149–1150.
- (132) Foster, N. I., Heindel, N. D., Burns, H. D., and Muhr, W. (1980) Aryl Iodides from Anilines via Triazine Intermediates. *Synthesis* 572–573.
- (133) Foster, N. I., Dannals, R., Burns, H. D., and Heindel, N. D. (1981) A Condition Variation Study for Radioiodination via Triazine Intermediates. *J. Radioanal. Chem.* 65, 95–105.
- (134) Satyamurthy, N., Barrio, J. R., Schmidt, D. G., Kammerer, C., Bida, G. T., and Phelps, M. E. (1990) Acid-Catalyzed Thermal Decomposition of 1-Aryl-3,3-dialkyltriazines in the Presence of Nucleophiles. *J. Org. Chem.* 55, 4560–4564.
- (135) Bunnett, J. F., and Yijima, C. (1977) Thermolysis of Arenediazonium Ions in Acidic Methanol: Evidence for Competing, Independent Ionic and Radical Mechanisms. *J. Org. Chem.* 42, 639–643.
- (136) Broxton, T. J., Bunnett, J. F., and Paik, C. H. (1977) Thermolysis of Arenediazonium Salts in Acidic Methanol. Effects of Substituents, Atmospheres, and Added Substances on the Competition between Ionic and Radical Mechanisms. *J. Org. Chem.* 42, 643–649.
- (137) Gilliland, D. L., Basmajian, G. P., Marchand, A. P., Hinkle, G. H., Earlywine, A., and Ice, R. D. (1981) Iodine Labeled Pharmaceuticals from Arylthallium Bis(Trifluoroacetate) Intermediate. *J. Radioanal. Chem.* 65, 107–113.
- (138) Brown, I., and Mitchell, J. S. (1979) 6-[¹²⁵I]-Iodo-2-methyl-1,4-naphthoquinol Bis(diammonium phosphate): A New Potential Anti-tumour Drug. *J. Chem. Soc., Chem. Commun.* 659–660.
- (139) Flanagan, R. J., Charleson, P. P., and Synnes, E. I. (1985) Radiolabeling with Organomercury Compounds, Part 1. The Synthesis and Structure of 6-Halocholest-5-en-3 β -ols. *Can. J. Chem.* 63, 2853–2860.
- (140) Visser, G. W. M., Diemer, D. L., and Kaspersen, F. M. (1979) The Preparation of Aromatic Astatine Compounds Through Aromatic Mercury-Compounds. *J. Labelled Compd. Radiopharm.* 17, 657–665.
- (141) Visser, G. W. M., Bakker, C. N. M., v. Halteren, B. W., Herscheid, J. D. M., Brinkman, G. A., and Hoekstra, A. (1986) Fluorination and Fluorodemercuration of Aromatic Compounds with Acetyl Hypofluorite. *J. Org. Chem.* 51, 1886–1889.
- (142) Kabalka, G. W. (1984) Incorporation of Stable and Radioactive Isotopes via Organoborane Chemistry. *Acc. Chem. Res.* 17, 215–221.
- (143) Seitz, D. E., Tonnensen, G. L., Hellman, S., Hanson, R. N., and Adelstein, S. J. (1980) Iododestannylation. Position-specific Synthesis of Iodotamoxifen. *J. Organomet. Chem.* 186, C33–C36.
- (144) Coleman, R. S., Seevers, R. H., and Friedman, A. M. (1982) Aromatic Radiobromination without Added Carrier. *J. Chem. Soc., Chem. Commun.* 1276–1277.
- (145) Adam, J. J., Ruth, R. J., Homma, Y., and Pate, B. D. (1985) Radiobromination of Aromatic Compounds by Cleavage of Aryl-tin Bonds. *Int. J. Appl. Radiat. Isot.* 36, 935–937.
- (146) Milius, R. A., McLaughlin, W. H., Lambrecht, R. M., Wolf, A. P., Carrol, J. J., Adelstein, S. J., and Bloomer, W. D. (1986) Organoastatine Chemistry. Astatine via Electrophilic Destannylation. *Appl. Radiat. Isot.* 37, 799–802.
- (147) Hanson, R. N., Franke, L., Lee, S.-H., and Seitz, D. E. (1987) Radioiododestannylation: Preparation and Evaluation of Radioiodinated Thienyl Alcohols. *Appl. Radiat. Isot., Part A* 38, 641–645.
- (148) Wilbur, D. S., Anderson, K. W., Stone, W. E., and O'Brien, H. A. (1982) Radiohalogenation of Non Activated Aromatic Compounds via Aryltrimethylsilyl Intermediates. *J. Labelled Compd. Radiopharm.* 19, 1171–1188.
- (149) Speranza, M., Shuie, C. Y., Wolf, A. P., Wilbur, D. S., and Angelini, G. (1985) Electrophilic Radiofluorination of Aryltrimethylsilanes as a General Route to F-18 Labelled Arylfluorides. *J. Fluorine Chem.* 30, 97–107.
- (150) Wilbur, D. S., Stone, W. E., and Anderson, K. W. (1983) Regiospecific Incorporation of Bromine and Iodine into Phenols Using Trimethylsilylphenol Derivatives. *J. Org. Chem.* 48, 1542–1544.
- (151) Wilbur, D. S., and Svitra, Z. V. (1984) Electrophilic Radiobrominations of Hippuric Acid: An Example of the Utility of Aryltrimethylsilane Intermediates. *J. Labelled Compd. Radiopharm.* 21, 415–428.
- (152) Di Raddo, P., Diksic, M., and Jolly, D. (1984) The ¹⁸F Radiofluorination of Arylsilanes. *J. Chem. Soc., Chem. Commun.* 159–160.
- (153) Wilson, A. A., Dannals, R. F., Ravert, H. T., Burns, H. D., and Wagner, H. N. (1985) I-125 and I-123 Labeled Iodobenzyl Bromide, A Useful Alkylating Agent for Radiolabeling Biologically Important Molecules. *J. Labelled Compd. Radiopharm.* 23, 83–93.
- (154) Wilson, S. R., and Jacob, L. A. (1986) Iodination of Aryltrimethylsilanes: A Mild Approach to Iodophenylalanine. *J. Org. Chem.* 51, 4833–4836.
- (155) Wilbur, D. S., and Svitra, Z. V. (1983) Organopentafluorosilicates. Reagents for Rapid and Efficient Incorporation of No-Carrier-Added Radiobromine and Radioiodine. *J. Labelled Compd. Radiopharm.* 20, 619–626.
- (156) Speranza, M., Shuie, C. Y., Wolf, A. P., Wilbur, D. S., and Angelini, G. (1984) Regiospecific Radiofluorination of Aryl-

- pentafluorosilicates as a General Route to F-18-Labeled Arylfluorides. *J. Chem. Soc. Chem. Commun.* 1448-1449.
- (157) Moerlein, S. M. (1985) Regiospecific Incorporation of No-Carrier-Added Radiobromine and Radioiodine into Aromatic Rings via Halogendergemylation. *J. Chem. Soc., Perkin Trans. 1* 1687-1692.
- (158) Moerlein, S. M. (1987) Use of Aryltrimethylgermanium Substrates for Facile Aromatic Chlorination, Bromination, and Iodination. *J. Org. Chem.* 52, 664-667.
- (159) Kabalka, G. W., and Varma, R. S. (1989) The Synthesis of Radiolabeled Compounds via Organometallic Intermediates. *Tetrahedron* 45, 6601-6621.
- (160) Moerlein, S. M., Mathis, C. A., and Yano, Y. (1987) Comparative Evaluation of Electrophilic Aromatic Iodometallation Techniques for Labeling Radiopharmaceuticals with Iodine-122. *Appl. Radiat. Isot., Part A* 38, 85-90.
- (161) Hylarides, M. D., Wilbur, D. S., Hadley, S. W., and Fritzberg, A. R. (1989) Synthesis and Iodination of Methyl 4-Tri-*n*-Butylstannylbenzoate, 4-Carbomethoxyphenyl Mercuric Chloride and 4-Carbomethoxyphenyl Boronic Acid. *J. Organomet. Chem.* 367, 259-265.
- (162) Wilbur, D. S., Hylarides, M. D., and Fritzberg, A. R. (1989) Reactions of Organometallic Compounds with Astatine-211. Application to Protein Labeling. *Radiochim. Acta* 47, 137-142.
- (163) Grayson, E. J., and Whitham, G. H. (1988) Addition of Iodine-Based Electrophilic Reagent to Some Vinyl Silanes. *Tetrahedron* 44, 4087-4094.
- (164) Kabalka, G. W., Gooch, E. D., and Hsu, H. C. (1981) A Convenient Procedure for the Synthesis of Vinyl Iodides via the Reaction of Iodine Monochloride with Vinylboronic Acid. *Synth. Commun.* 11, 247-251.
- (165) Kabalka, G. W., Gooch, E. E., Hsu, H. C., Washburn, L. C., Sun, T. T., and Hayes, R. L. (1982) Rapid and Mild Synthesis of Radioiodinated Estrogen Derivatives via Organoborane Technology. *Applications of Nuclear and Radiochemistry* (R. M. Lambrecht, and M. Morcos, Eds.) pp 197-203, Pergamon Press, New York.
- (166) Hanson, R. N., Seitz, D. E., and Bottaro, J. C. (1984) Radiohalodestannylation: Synthesis of ^{125}I -Labeled 17α -E-Iodovinylestradiol. *Int. J. Appl. Radiat. Isot.* 35, 810-812.
- (167) Hanson, R. N., El-Wakil, H., Murphy, F., and Wilbur, D. S. (1989) Synthesis and Evaluation of ^{82}Br and ^{77}Br Labeled (17,20 E)-21-bromo-19-norpregna-1,3,5(10),20-tetraene-3,17-diol. *J. Labelled Compd. Radiopharm.* 27, 615-627.
- (168) DeSombre, E. R., Hughes, A., Mease, R., and Harper, P. V. (1990) Comparison of the Distribution of Bromine-77 Bromovinyl Steroidal and Triphenylethylene Estrogens in the Immature Rat. *J. Nucl. Med.* 31, 1534-1542.
- (169) Chi, D. Y., Kiesewetter, D. O., Katzenellenbogen, J. A., Kilbourn, M. R., and Welch, M. J. (1986) Halofluorination of Olefins: Elucidation of Reaction Characteristics and Applications in Labeling with the Positron-Emitting Radionuclide Fluorine-18. *J. Fluorine Chem.* 31, 99-113.
- (170) Means, G. E., and Feeney, R. E. (1990) Chemical Modification of Proteins: History and Applications. *Bioconjugate Chem.* 1, 2-12.
- (171) Feeney, R. E., Yamasaki, R. B., and Geoghegan, K. F. (1982) Chemical Modification of Proteins: An Overview. *Modification of Proteins. Food, Nutritional, and Pharmacological Aspects*, pp 3-55, Advances in Chemistry Series 198, American Chemical Society, Washington, DC.
- (172) Brinkley, M. (1992) A Brief Survey of Methods for Preparing Protein Conjugates with Dyes, Haptens, and Cross-Linking Reagents. *Bioconjugate Chem.* 3, 2-13.
- (173) Lundblad, R. L., and Noyes, C. M. (1984) *Chemical Reagents for Protein Modification*, Vol. I and II, CRC Press, Inc., Boca Raton, FL.
- (174) Atassi, M. Z. (1977) Chemical Modification and Cleavage of Proteins and Chemical Strategy in Immunochemical Studies of Proteins. *Immunochemistry of Proteins*, Vol. 1, pp 1-161, Plenum Press, New York.
- (175) Cohen, L. A. (1968) Group-Specific Reagents in Protein Chemistry. *Ann. Rev. Biochem.* 37, 683-726.
- (176) Lundblad, R. L., and Noyes, C. M. (1984) Modification of Lysine. *Chemical Reagents for Protein Modification*. Vol. 1, pp 127-170, CRC Press, Inc., Boca Raton, FL.
- (177) Bodanszky, M. (1979) Active Esters in Peptide Synthesis. *The Peptides. Analysis, Synthesis, Biology* (E. Gross and J. Meienhofer, Eds.) Vol. 1, pp 105-196, Academic Press, Inc., Orlando, FL.
- (178) Bodanszky, M. (1984) Activation and Coupling. *Principles of Peptide Synthesis*. pp 9-58, Springer-Verlag, New York.
- (179) Blau, M., Johnson, A. C., and Pressman, D. (1958) *p*-Iodobenzoyl Groups as a Paired Label for *in vivo* Protein Distribution Studies: Specific Localization of Anti-tissue Antibodies. *Int. J. Appl. Radiat. Isot.* 3, 217-225.
- (180) Bolton, A. E., and Hunter, W. M. (1973) The Labeling of Proteins to High Specific Radioactivities by Conjugation to a I-125 Containing Acylating Agent. *Biochem. J.* 133, 529-539.
- (181) Lucka, B., and Siuda, A. (1978) Preparation of Bolton and Hunter's Reagent for Labelling Proteins with Iodine-125. *J. Labelled Compd. Radiopharm.* 15, 495-497.
- (182) Langone, J. J. (1980) Radioiodination by Use of the Bolton-Hunter and Related Reagents. *Methods Enzymol.* 70, 221-243.
- (183) Langone, J. J. (1981) Radioiodination by Use of the Bolton-Hunter and Related Reagents. *Methods Enzymol.* 73, 113-127.
- (184) Katz, M. J., Lasek, R. J., Osdoby, P., Whittaker, J. R., and Caplan, A. I. (1982) Bolton-Hunter Reagent as a Vital Stain for Developing Systems. *Dev. Biol.* 90, 419-429.
- (185) Davies, G. E., and Palek, J. (1981) ^{125}I -Labeling of Platelet Proteins with Bolton-Hunter Reagent. *Anal. Biochem.* 115, 383-387.
- (186) Thompson, J. A., Lau, A. L., and Cunningham, D. D. (1987) Selective Radiolabeling of Cell Surface Proteins to a High Specific Activity. *Biochem.* 26, 743-750.
- (187) Roger, S. (deceased), Los Alamos National Laboratory, private communication, unpublished results.
- (188) Knight, L. C., Harwig, S. S. L., and Welch, M. J. (1977) *In Vitro* Stability and *In Vivo* Clearance of Fibrinogen or Serum Albumin Labeled with ^{77}Br , ^{131}I , or ^{125}I by Direct or Indirect Synthetic Methods. *J. Nucl. Med.* 18, 282-288.
- (189) Assoian, R. K., Blix, P. M., Rubenstein, A. H., and Tager, H. S. (1980) Iodotyrosylation of Peptides Using tertiary-Butyloxycarbonyl-L-[^{125}I]Iodotyrosine N-Hydroxysuccinimide Ester. *Anal. Biochem.* 103, 70-76.
- (190) Wilbur, D. S., Rogers, R. S., and Svitra, Z. V. (1984) Radiolabeled Phenylalkanoic Acids for Protein Labeling. Investigation of Arylsilanes as Intermediates for Radiolabeled Phenylpropionic Acids and Acid Derivatives. *Proceedings of 1984 International Chemical Congress of Pacific Basin Societies*, Honolulu, Hawaii, Dec 16-21 (abstract).
- (191) Quick, A. J. (1932) The Relationship between Chemical Structure and Physiological Response. I. The Conjugation of Substituted Benzoic Acids. *J. Biol. Chem.* 96, 83-101.
- (192) Friedman, A. M., Zalutsky, M. R., Wung, W., Buckingham, F., Harper, P. V., Scherr, G. H., Wainer, B., Hunter, R. L., Appelman, E. H., Rothberg, R. M., Fitch, F. W., Stuart, F. P., and Simonian, S. J. (1977) Preparation of a Biologically Stable and Immunogenically competent Astatinated Protein. *Int. J. Nucl. Med. Biol.* 4, 219-224.
- (193) Vaughan, A. T. M. (1979) The Labeling of Proteins with ^{211}At using an Acylation Reaction. *Int. J. Appl. Radiat. Isot.* 30, 576-577.
- (194) Harrison, A., and Royle, L. (1984) Preparation of a ^{211}At -IgG Conjugate Which Is Stable *in vivo*. *Int. J. Appl. Radiat. Isot.* 35, 1005-1008.
- (195) Wilbur, D. S., Jones, D. S., and Fritzberg, A. R. (1986) Synthesis and Radioiodinations of Some Aryltin Compounds for Radiolabeling of Monoclonal Antibodies. *J. Labelled Compd. Radiopharm.* 23, 1304-1306 (abstract).
- (196) Hadley, S. W., Grant, L. M., and Wilbur, D. S. (1987) Evaluation of Radioiodinations and Conjugations of 4-Iodobenzoates for Protein Labeling. *J. Nucl. Med.* 28, 725 (abstract).
- (197) Wilbur, D. S., Hadley, S. W., Grant, L. M., and Hylarides, M. D. (1991) Radioiodinated Iodobenzoyl Conjugates of a Monoclonal Antibody Fab Fragment. *In Vivo Comparisons with Chloramine-T Labeled Fab*. *Bioconjugate Chem.* 2, 111-116.
- (198) Badger, C. C., Wilbur, D. S., Hadley, S. W., Fritzberg, A. R., and Bernstein, I. D. (1990) Biodistribution of Para-

- Iodobenzoyl (PIP) Labeled Antibodies in a Murine Lymphoma Model. *Nucl. Med. Biol.* 17, 381-387.
- (199) Murray, J. L., Mujoo, K., Wilmanns, C., Mansfield, P., Wilbur, D. S., and Rosenblum, M. G. (1991) Variables Influencing Tumor Uptake of Antimelanoma Monoclonal Antibodies Radioiodinated Using the *para*-Iodophenyl (PIP) Technique. *J. Nucl. Med.* 32, 279-287.
- (200) Mujoo, K., Rosenblum, M. G., and Murray, J. L. (1991) Augmented Binding of Radiolabeled Monoclonal Antibodies to Melanoma Cells using Specific Antibody Combinations. *Cancer Res.* 51, 2768-2772.
- (201) Khawli, L. A., and Kassis, A. I. (1989) Synthesis of ^{125}I Labeled N-succinimidyl *p*-iodobenzoate for use in radiolabeling antibodies. *Nucl. Med. Biol.* 16, 727-733.
- (202) Wahl, R., Roberts, J., Hopkins, M., Dresschar, C., Fig, L., Mallette, S., Mudgett, E., Foisie, D., Schroff, D., Abrams, P., Fer, M., and Wilbur, S. (1990) Phase I Evaluation of I-131 PIP Labeled Antiovarian Carcinoma Antibody. *J. Nucl. Med.* 31, 777 (abstract).
- (203) Nelp, W., University of Washington, unpublished data.
- (204) Zalutsky, M. R., and Narula, A. S. (1987) A Method for the Radiohalogenation of Proteins Resulting In Decreased Thyroid Uptake of Radioiodine. *Int. J. Radiat. Appl. Inst. [A]*, 38, 1051-1055.
- (205) Zalutsky, M. R., and Narula, A. S. (1988) Radiohalogenation of a Monoclonal Antibody Using an N-Succinimidyl 3-(Tri-*n*-butylstannyl)benzoate Intermediate. *Cancer Res.* 8, 1446-1450.
- (206) Zalutsky, M. R., Noska, M. A., Colapinto, E. V., Garg, P. K., and Bigner, D. D. (1989) Enhanced Tumor Localization and in Vivo Stability of a Monoclonal Antibody Radioiodinated Using N-Succinimidyl 3-(Tri-*n*-butylstannyl)benzoate. *Cancer Res.* 49, 5543-5549.
- (207) Zalutsky, M. R., Garg, P. K., Friedman, H. S., and Bigner, D. D. (1989) Labeling monoclonal antibodies and $\text{F}(\text{ab})_2$ fragments with the alpha emitting radionuclide astatine-211: Preservation of immunoreactivity and in p250 localizing capacity. *Proc. Natl. Acad. Sci. U.S.A.* 86, 7149-7153.
- (208) Garg, P. K., Slade, S. K., Harrison, C. L., and Zalutsky, M. R. (1989) Labeling Proteins Using Aryl Iodide Acylating Agents: Influence of *Meta* vs *Para* Substitution on *In Vivo* Stability. *Nucl. Med. Biol.* 16, 669-673.
- (209) Garg, P. K., Harrison, C. L., and Zalutsky, M. R. (1990) Comparative Tissue Distribution in Mice of the α -Emitter ^{211}At and ^{131}I as Labels of a Monoclonal Antibody and $\text{F}(\text{ab})_2$. *Cancer Res.* 50, 3514-3520.
- (210) Schuster, J. M., Garg, P. K., Bigner, D. D., and Zalutsky, M. R. (1991) Improved Therapeutic Efficacy of a Monoclonal Antibody Radioiodinated Using N-Succinimidyl 3-(Tri-*n*-butylstannyl)benzoate. *Cancer Res.* 51, 4164-4169.
- (211) Vaidyanathan, G., and Zalutsky, M. R. (1990) Protein Radiohalogenation: Observations on the Design of N-Succinimidyl Ester Acylation Agents. *Bioconjugate Chem.* 1, 269-273.
- (212) Quadri, S. M., Zhang, Y.-Z., and Williams, J. R. (1991) Improvements in Radioiodination of Monoclonal Antibodies for Diagnosis and Treatment of Cancer. *Antibody, Immunoconjugate Radiopharm.* 4, 283-296.
- (213) Freud, A., Canfi, A., and Hirshfeld, N. (1991) N-Succinimidyl-3-Iodo- ^{125}I -Benzoate. A new compound for protein iodination. *J. Labelled Compd. Radiopharm.* 30, 203-204 (abstract).
- (214) Shen, X., Hanson, R. N., and Elmaleh, D. R. (1991) Synthesis and Evaluation of Radioiodinated Tetrafluorophenyl *m*-Iodobenzoate and Tetrafluorophenyl-5-Iodopentenoates as Conjugating Agents for Proteins and Antibodies. *J. Labelled Compd. Radiopharm.* 30, 222-223 (abstract).
- (215) Vaidyanathan, G., and Zalutsky, M. R. (1992) Labeling of Proteins with Fluorine-18 Using N-Succinimidyl 4- ^{18}F -Fluorobenzoate. *Nucl. Med. Biol.* 19, 275-281.
- (216) Vaidyanathan, G., and Zalutsky, M. R. (1990) Radioiodination of Antibodies via N-Succinimidyl 2,4-Dimethoxy-3-(trialkylstannyl)benzoates. *Bioconjugate Chem.* 1, 387-393.
- (217) Garg, S., Garg, P. K., and Zalutsky, M. R. (1991) N-Succinimidyl 5-(Trialkylstannyl)-3-pyridinecarboxylates: A New Class of Reagents for Protein Radioiodination. *Bioconjugate Chem.* 2, 50-56.
- (218) Garg, S., Garg, P. K., Bigner, D. D., and Zalutsky, M. R. (1991) Radioiodination and Astatination of Monoclonal Antibodies Using Heterocyclic Acylation Reagents. *J. Labelled Compd. Radiopharm.* 30, 207-208 (abstract).
- (219) Vaidyanathan, G., Affleck, D. J., and Zalutsky, M. R. (1992) Radioiodination of Proteins using N-Succinimidyl 4-Hydroxy-3-Iodobenzoate. *Proceedings of the 9th International Symposium on Radiopharmaceutical Chemistry*; pp 378-380, Paris, France, Apr 6-10 (abstract).
- (220) Narula, A. S., and Zalutsky, M. R. (1988) Synthesis of N-Succinimidyl-2,4-Dimethoxy-3-(Tri-*n*-butylstannyl)benzoate via Regio-specifically Generated Lithium 2,4-Dimethoxy-3-lithiobenzoate. *Tetrahedron Lett.* 29, 4385-4388.
- (221) Riley, M., and Perham, R. N. (1973) The Reaction of Protein Amino Groups with Methyl 5-Iodopyridine-2-carboximide. *Biochem. J.* 31, 625-635.
- (222) Hadley, S. W., and Wilbur, D. S. (1990) Evaluation of Iodovinyl Antibody Conjugates: Comparison with a *p*-Iodobenzoyl Conjugate and Direct Radioiodination. *Bioconjugate Chem.* 2, 154-161.
- (223) Otto, C. A., Brown, L. E., and Scott, A. M. (1985) Radioiodinated Branched-Chain Fatty Acids: Substrates for Beta Oxidation? Concise Communication. *J. Nucl. Med.* 25, 75-80.
- (224) Demaison, L., Dubois, F., Appar, M., Mathieu, J.-P., Vidal, M., Comet, M., and Cuchet, P. (1988) Myocardial Metabolism of Radioiodinated Methyl-Branched Fatty Acids. *J. Nucl. Med.* 29, 1230-1236.
- (225) Jacobson, K. A., Furlano, D. C., and Kirk, K. L. (1988) A Prosthetic Group for Rapid Introduction of Fluorine into Peptides and Functionalized Drugs. *J. Fluorine Chem.* 39, 339-347.
- (226) Garg, P. K., Garg, S., and Zalutsky, M. R. (1991) Fluorine-18 Labeling of Monoclonal Antibodies and Fragments with Preservation of Immunoreactivity. *Bioconjugate Chem.* 2, 44-49.
- (227) Herman, L. W., Elmaleh, D. R., Fischman, A. J., Hanson, R. J., and Strauss, H. W. (1991) The Use of Pentafluorophenyl Derivatives for the ^{18}F Labeling of Proteins. *J. Labelled Compd. Radiopharm.* 30, 205-206 (abstract).
- (228) Zalutsky, M. R., Garg, P. K., Johnson, S. H., Utsunomiya, H., and Coleman, R. E. (1992) Fluorine-18-Antimyosin Monoclonal Antibody Fragments: Preliminary Investigations in a Canine Myocardial Infarct Model. *J. Nucl. Med.* 33, 575-580.
- (229) Hunter, M. J., and Ludwig, M. L. (1962) The Reaction of Imidoesters with Proteins and Related Small Molecules. *J. Am. Chem. Soc.* 84, 3491-3504.
- (230) Wood, F. T., Wu, M. M., and Gerhart, J. C. (1975) The Radioactive Labeling of Proteins with an Iodinated Amidination Reagent. *Anal. Biochem.* 69, 339-349.
- (231) Tolan, D. R., Lambert, J. M., Boileau, G., Fanning, T. G., Kenny, J. W., Vassos, A., and Traut, R. R. (1980) Radioiodination of Microgram Quantities of Ribosomal Proteins from Polyacrylamide Gels. *Anal. Biochem.* 103, 101-109.
- (232) Praissman, M., Praissman, L., Kent, S. B., and Berkowitz, J. M. (1981) Preparation and Characterization of a Biologically Active Gastrin Derivative Modified with an ^{125}I -Labeled Imidoester. *Anal. Biochem.* 115, 287-297.
- (233) Bright, G. R., and Spooner, B. S. (1983) Preparation and Reactions of an Iodinated Imidoester Reagent with Actin and α -Actinin. *Anal. Biochem.* 131, 301-311.
- (234) Wall, K. A., and Fitch, F. W. (1985) Cell Surface Modification with an Iodinatable Imidoester to Enhance Radiolabeling. *J. Immunol. Meth.* 77, 1-8.
- (235) Kilbourn, M. R., Dence, C. S., Welch, M. J., and Mathias, C. J. (1987) Fluorine-18 Labeling of Proteins. *J. Nucl. Med.* 28, 462-470.
- (236) Means, G. E., and Feeney, R. E. (1968) Reductive Alkylation of Amino Groups in Proteins. *Biochemistry* 7, 2192-2201.
- (237) Rice, R. H., and Means, G. E. (1971) Radioactive Labeling of Proteins *In Vitro*. *J. Biol. Chem.* 246, 831-832.
- (238) Tack, B. F., and Wilder, R. L. (1981) Tritiation of Proteins to High Specific Activity: Application to Radioimmunoassay. *Methods Enzymol.* 73, 138-147.
- (239) Jentoft, N., and Dearborn, D. G. (1979) Labeling of Proteins by Reductive Methylation Using Sodium Cyanoborohydride. *J. Biol. Chem.* 254, 4359-4365.

- (240) Su, S.-N., and Jeng, I. (1983) Conversion of a Primary Amine to a Labeled Secondary Amine by the Action of Phenolic Group and Radioiodination. *Anal. Biochem.* 128, 405-411.
- (241) Panuska, J. R., and Parker, C. W. (1987) Radioiodination of Proteins by Reductive Alkylation. *Anal. Biochem.* 160, 192-201.
- (242) Hylarides, M., Hadley, S. W., and Seubert, J., unpublished data, NeoRx Corp.
- (243) Satchell, D. P. N., and Satchell, R. J. (1975) Acylation by Ketenes and Isocyanates. A Mechanistic Comparison. *Chem. Soc. Rev.* 4, 231-250.
- (244) Keana, J. F. W., and Mann, J. S. (1990) Chelating Ligands Functionalized for Facile Attachment to Biomolecules. A Convenient Route to 4-Isothiocyanatobenzyl Derivatives of Diethylenetriaminepentaacetic Acid and Ethylenediaminetetraacetic Acid. *J. Org. Chem.* 55, 2868-2871.
- (245) Rana, T. M., and Meares, C. F. (1990) N-Terminal Modification of Immunoglobulin Polypeptide Chains Tagged with Isothiocyanato Chelates. *Bioconjugate Chem.* 1, 357-362.
- (246) Gansow, O. A. (1991) Newer Approaches to the Radiolabeling of Monoclonal Antibodies by Use of Metal Chelates. *Nucl. Med. Biol.* 18, 369-381.
- (247) Yuanfang, L., and Chuanchu, W. (1991) Radiolabeling of Monoclonal Antibodies with Metal Chelates. *Pure Appl. Chem.* 63, 427-463.
- (248) Dewanjee, M. K., Ghafouripour, A. K., Ganz, W., Serafini, A. N., and Sfakianakis, G. N. (1991) Radioiodination of Proteins by a New Conjugation Technique with Activated Paramethoxyphenylisothiocyanate. *J. Labelled Compd. Radiopharm.* 30, 328-329 (abstract).
- (249) Ram, S., and Buchbaum, D. J. (1992) Development of 3-Iodophenylisothiocyanate for Radioiodination of Monoclonal Antibodies. *Appl. Radiat. Isotop.* in press.
- (250) Ram, S., Fleming, E., and Buchsbaum, D. J. (1992) Development of radioiodinated 3-iodophenylisothiocyanate for coupling to monoclonal antibodies. *J. Nucl. Med.* 33, 1029 (abstract).
- (251) Khawli, L. A., Chen, F.-M., Alauddin, M. M., and Epstein, A. L. (1991) Radioiodinated Monoclonal Antibody Conjugates: Synthesis and Comparative Evaluation. *Antibody, Immunoconjugate Radiopharm.* 4, 163-182.
- (252) Lundblad, R. L., and Noyes, C. M. (1984) The Modification of Cysteine. *Chemical Reagents for Protein Modification*. Vol. I, pp 55-93, CRC Press, Inc., Boca Raton, FL.
- (253) Lambert, J. M., Jue, R., and Traut, R. R. (1978) Disulfide Cross-Linking of *Escherichia coli* Ribosomal Proteins with 2-Iminoethiolane (Methyl 4-Mercaptobutyrimidate): Evidence That the Cross-Linked Protein Pore are Formed in the Intact Ribosomal Subunit. *Biochemistry* 17, 5406-5416.
- (254) Wower, I., Wower, J., Meinke, M., and Brimacombe, R. (1981) The Use of 2-iminoethiolane as an RNA-protein cross-linking agent in *Escherichia coli* ribosomes, and the localization on 23S RNA of sites cross-linked to proteins L4, L6, L21, L23, L27, and L29. *Nucleic Acids Res.* 9, 4285-4302.
- (255) Ghosh, S. S., Kao, P. M., McCue, A. W., and Chappelle, H. L. (1990) Use of Maleimide-Thiol Coupling Chemistry for Efficient Syntheses of Oligonucleotide-Enzyme Conjugate Hybridization Probes. *Bioconjugate Chem.* 1, 71-76.
- (256) Birnbaumer, M. E., Schrader, W. T., and O'Malley, B. W. (1979) Chemical Cross-Linking of Chick Oviduct Progesterone-Receptor Subunits by Using a Reversible Bifunctional Cross-Linking Agent. *Biochem. J.* 181, 201-213.
- (257) Srivastava, P. C., Buchsbaum, D. J., Allred, J. F., Brubaker, P. G., Hanna, D. E., and Spicker, J. K. (1990) A New Conjugating Agent for Radioiodination of Protein: Low *In Vivo* Deiodination of a Radiolabeled Antibody in a Tumor Model. *BioTechniques* 8, 536-545.
- (258) Wilbur, D. S., Hylarides, M. D., Hadley, S. W., Schroeder, J., and Fritzberg, A. R. (1989) A General Approach to Radiohalogenation of Proteins. Radiohalogenation of Organometallic Intermediates Containing Protein Reactive Substituents. *J. Labelled Compd. Radiopharm.* 26, 316-318 (abstract).
- (259) Hargreaves, M. K., Pritchard, J. G., and Dave, H. R. (1970) Cyclic Carboxylic Monoimides. *Chem. Rev.* 70, 439-469.
- (260) Khawli, L. A., van den Abbeele, A. D., and Kassis, A. I. (1992) N-(*m*-[¹²⁵I]iodophenyl)maleimide: An Agent for High Yield Radiolabeling of Antibodies. *Nucl. Med. Biol.* 19, 289-295.
- (261) Hylarides, M. D., Wilbur, D. S., Reed, M. W., Hadley, S. W., Schroeder, J. R., and Grant, L. M. (1991) Preparation and *in vivo* Evaluation of an N-(*p*-[¹²⁵I]iodophenethyl)maleimide-Antibody Conjugate. *Bioconjugate Chem.* 2, 435-440.
- (262) Srivastava, P. C., Allred, J. F., Lambert, C. R., and Kennel, S. J. (1990) No-Carrier-Added Preparation of a New Radioiodinated Maleimide as a Potentially Attractive Radioimmunoconjugator with Low *in vivo* Deiodination. *J. Nucl. Med.* 31, 906 (abstract).
- (263) Shuie, C.-Y., Wolf, A. P., and Hainfeld, J. F. (1989) Synthesis of ¹⁸F-Labelled N-(*p*-[¹⁸F]fluorophenyl)maleimide and its Derivatives for Labelling Monoclonal Antibody with ¹⁸F. *J. Labelled Compd. Radiopharm.* 26, 287-289 (abstract).
- (264) Holowka, D. (1981) N-Chloroacetyl-[¹²⁵I]iodotyramine: An Alkylating Agent with High Specific Activity. *Anal. Biochem.* 117, 390-397.
- (265) Wyeth, P., and Douglas, S. G. (1984) High Activity Antibody Radioiodination without Loss of Antigen Binding. *Proceedings of the Fifth International Symposium on Radiopharmaceutical Chemistry*, Tokyo, Japan, July 9-13, pp 100-101.
- (266) Hylarides, M. D., Wilbur, D. S., Schroeder, J. R., Grant, L. M., Seubert, J. R., Beaumier, P., and Fritzberg, A. R. (1988) Radioiodination of Monoclonal Antibodies. Labeling with Para-Iodophenyl (PIP) Derivatives using Protein Sulfhydryls. *Clin. Nucl. Med.* 13 (Suppl.) p 23 (abstract).
- (267) Smith, E. L., Hill, R. L., Lehman, I. R., Lefkowitz, R. J., Handler, P., and White, A. (1983) The Carbohydrates. *Principles of Biochemistry: General Aspects*. 7th ed., pp 96-105, McGraw-Hill Book Co., New York.
- (268) Day, E. D. (1990) The Secondary, Tertiary, and Quaternary Structures of Assembled Immunoglobulins. *Advanced Immunochimistry*. 2nd ed., pp 107-181, Wiley-Liss, New York.
- (269) Ohkura, T., Isobe, T., Yamashita, K., and Kobata, A. (1985) Structures of Carbohydrate Moieties of Two Monoclonal Human λ -Type Immunoglobulin Light Chains. *Biochemistry* 24, 503-508.
- (270) Upeslacijs, J., and Hinman, L. (1988) Chemical Modification of Antibodies for Cancer Chemotherapy. *Annu. Rep. Med. Chem.* 23, 151-160.
- (271) Rodwell, J. D., Alvarez, V. L., Lee, C., Lopes, A. D., Goers, J. W. F., King, H. D., Powsner, H. J., and McKearn, T. J. (1986) Site-Specific covalent modification of monoclonal antibodies: *in vitro* and *in vivo* evaluations. *Proc. Natl. Acad. Sci. U.S.A.* 83, 2632-2636.
- (272) Pittman, R. C., Carew, T. E., Glass, C. K., Green, S. R., Taylor, C. A., and Attie, A. D. (1983) A radioiodinated, intracellularly trapped ligand for determining the sites of plasma protein degradation *in vivo*. *Biochem. J.* 212, 791-800.
- (273) Slaunwhite, W. R. (1982) Ligand Compositions and Processes for Their Manufacture and Their Use in Radioimmunoassay. U.S. Patent 4,358,435.
- (274) Buckingham, J. (1969) The Chemistry of Arylhydrazones. *Q. Rev. Chem. Soc.* 23, 37-56.
- (275) Heindel, N. D., Van Dort, M., Cahn, M., Schneider, R., and Burns, H. D. (1985) The 1,3,4-Oxadiazole Moiety, A Protective Synthon for Indirect Radioiodination. *J. Heterocycl. Chem.* 22, 209-210.
- (276) Heindel, N. D., and Van Dort, M. (1985) Prosthetic Group Radioiodination at "No-Carrier-Added" Levels of Carbonyl-Containing Molecules. *J. Org. Chem.* 50, 1988-1990.
- (277) Rea, D. W., Ultee, M. E., Belinka, B. A., Coughlin, D. J., and Alvarez, V. L. (1990) Site-Specifically Radioiodinated Antibody for Targeting Tumors. *Cancer Res. (Suppl.)* 50, 857s-861s.
- (278) Belinka, B. A., Coughlin, D. J., and Alvarez, V. L. (1988) Radioiodinated site-specific monoclonal antibody conjugates for tumor therapy and imaging. *Biochemistry* 27, 3084 (abstract).
- (279) Randerath, K. (1981) 3-([¹²⁵I]iodo-4-hydroxyphenyl)-propionyl Carbohydrazide, a New Radioiodination Reagent for Ultrasensitive Detection and Determination of Periodate-

- Oxidized Nucleoside Derivatives and Other Carbonyl Compounds. *Anal. Biochem.* 115, 391-397.
- (280) Hylarides, M. D., Seubert, J., and Wilbur, D. S., NeoRx Corp., unpublished results.
- (281) Feliu, A. (1988) I. Preparation of [^{18}F]p-Fluorophenylhydrazine using Diazonium Chemistry. II. A Radiolabelled Glucocorticoid: [^{18}F]WIN 44577. *Proceedings of the Seventh International Symposium on Radiopharmaceutical Chemistry*, Groningen, The Netherlands, July 4-8, 1988.
- (282) Sandler, S. R., and Karo, W. (1972) Oximes. *Organic Functional Group Preparations*, Vol. 3, pp 365-405, Academic Press, New York.
- (283) Saunders, K. H., and Allen, R. L. M. (1985) *Aromatic Diazo Compounds*. 3rd ed., Edward Arnold (Publishers) Ltd., London, England.
- (284) Higgins, H. G., and Harrington, K. J. (1959) Reaction of Amino Acids and Proteins with Diazonium Compounds. II. Spectra of Protein Derivatives. *Arch. Biochem. Biophys.* 85, 409-425.
- (285) Wunderlich, G., Fischer, S., Dreyer, R., and Franke, W.-G. (1987) A Simple Method for Labelling Proteins with ^{211}At via Diazotized Aromatic Diamine. *J. Radioanal. Nucl. Chem., Lett.* 117, 197-203.
- (286) Hayes, C. E., and Goldstein, I. J. (1975) Radioiodination of Sulfhydryl-Sensitive Proteins. *Anal. Biochem.* 67, 580-584.
- (287) Sears, D. A., Reed, C. F., and Helmkamp, R. W. (1971) A Radioactive Label for the Erythrocyte Membrane. *Biochim. Biophys. Acta* 233, 716-719.
- (288) De Jong, A. S. H., Bouma, J. M. W., and Gruber, M. (1981) O-(4-Diazo-3,5-di[^{125}I]iodobenzoyl)sucrose, a novel radioactive label for determining organ sites of catabolism of plasma proteins. *Biochem. J.* 198, 45-51.
- (289) Chowdhry, V., and Westheimer, F. H. (1979) Photoaffinity Labeling of Biological Systems. *Annu. Rev. Biochem.* 48, 293-325.
- (290) Staros, J. V. (1980) Aryl azide photolabels in biochemistry. *Trends Biochem. Sci.* 320-322.
- (291) Isaacs, N. S. (1974) Carbenes (Methylenes). *Reactive Intermediates in Organic Chemistry*, pp 375-407, John Wiley & Sons, New York.
- (292) Pandey, R. N., Wilson, J. D., Zhao, X.-G., and Schlom, J. (1991) Photolabeling: A New Approach to Radioiodination. *Antibody, Immunoconjugate Radiopharm.* 4, 399-407.
- (293) Brunner, J., and Semenza, G. (1981) Selective Labeling of the Hydrophobic Core of Membranes with 3-(Trifluoromethyl)-3-(m -[^{125}I]iodophenyl)diazirine, a Carbene-Generating Reagent. *Biochemistry* 20, 7174-7182.
- (294) Frey, A. B., Kreibich, G., Washera, A., Clarke, L., and Waxman, D. J. (1986) 3-(Trifluoromethyl)-3-(m -[^{125}I]iodophenyl)diazirine Photolabels a Substrate-Binding Site of Rat Hepatic Cytochrome P-450 Form PB-4. *Biochemistry* 25, 4797-4803.
- (295) Brunner, J., Senn, H., and Richards, F. M. (1980) 3-Trifluoromethyl-3-phenyldiazirine. A New Carbene Generating Group for Photolabeling. *J. Biol. Chem.* 255, 3313-3318.
- (296) Baldini, G., Martoglio, B., Schachenmann, A., Zugliani, C., and Brunner, J. (1988) Mischarging *Escherichia coli* tRNA^{phe} with L-4'-[3-(Trifluoromethyl)-3H-diazirine-3-yl]-phenylalanine, a Photoactivatable Analogue of Phenylalanine. *Biochemistry* 27, 7951-7959.
- (297) Liu, M. T. H. (1987) Chemistry of Diazirines. Vols. I and II, CRC Press, Inc., Boca Raton, FL.
- (298) Lundblad, R. L., and Noyes, C. M. (1984) The Chemical Cross-Linking of Peptide Chains. *Chemical Reagents for Protein Modification*. Vol. II, pp 123-139, CRC Press, Inc., Boca Raton, FL.
- (299) Peters, K., and Richards, F. M. (1977) Chemical Cross-Linking: Reagents and Problems in Studies of Membrane Structure. *Annu. Rev. Biochem.* 46, 523-551.
- (300) Das, M., and Fox, C. F. (1979) Chemical Cross-Linking in Biology. *Annu. Rev. Biophys. Bioeng.* 8, 165-193.
- (301) Tae, H. J. (1979) The Application of Chemical Crosslinking for Studies on Cell Membranes and Identification of Surface Reporters. *Biochim. Biophys. Acta* 559, 39-69.
- (302) Ji, I., and Ji, T. H. (1981) Both α and β subunits of human chorionadotropin photoaffinity label the hormone receptor. *Proc. Natl. Acad. Sci. U.S.A.* 78, 5465-5469.
- (303) Schmitt, M., Painter, R. G., Jesaitis, A. J., Preissner, K., Sklar, L. A., and Cochrane, C. G. (1983) Photoaffinity Labeling of the N-Formyl Peptide Receptor Binding Site of Intact Human Polymorphonuclear Leukocytes. *J. Biol. Chem.* 258, 649-654.
- (304) Baenzinger, J. U., and Fiete, D. (1982) Photoactivatable Glycopeptide Reagents for Site-specific Labeling of Lectins. *J. Biol. Chem.* 257, 4421-4425.
- (305) Ji, T. H., and Ji, I. (1982) Macromolecular Photoaffinity Labeling with Radioactive Photoactivatable Heterobifunctional Reagents. *Anal. Biochem.* 121, 286-289.
- (306) Ji, I., Shin, J., and Ji, T. H. (1985) Radioiodination of a Photoactivatable Heterobifunctional Reagent. *Anal. Biochem.* 151, 348-349.
- (307) Soundararajan, N., and Platz, M. S. (1990) Descriptive Photochemistry of Polyfluorinated Azide Derivatives of Methyl Benzoate. *J. Org. Chem.* 55, 2034-2044.
- (308) Shields, C. J., Chrisope, D. R., Schuster, G. B., Dixon, A. J., Poliakoff, M., and Turner, J. J. (1987) Photochemistry of Aryl Azides: Detection and Characterization of a Dehydroazepine by Time-Resolved Infrared Spectroscopy and Flash Photolysis at Room Temperature. *J. Am. Chem. Soc.* 109, 4723-4726.
- (309) Schuster, G. B., and Liang, T. Y. (1987) Photochemistry of 3- and 4-Nitrophenyl Azides: Detection and Characterization of Reactive Intermediates. *J. Am. Chem. Soc.* 109, 7803-7810.
- (310) Crocker, P. J., Imai, N., Rajagopalan, K., Boggess, M. A., Kwiatkowski, S., Dwyer, L. D., Vanaman, T. C., and Watt, D. S. (1990) Heterobifunctional Cross-Linking Agents Incorporating Perfluorinated Aryl Azides. *Bioconjugate Chem.* 1, 419-424.
- (311) Keana, J. F. W., and Cai, S. X. (1990) New Reagents for Photoaffinity Labeling: Synthesis and Photolysis of Functionalized Perfluorophenyl Azides. *J. Org. Chem.* 55, 3640-3647.
- (312) Cai, S. X., Glenn, D. J., and Keana, J. F. W. (1992) Toward the Development of Radiolabeled Fluorophenyl Azide-Based Photolabeling Reagents: Synthesis and Iodinated 4-Azido-perfluorobenzoates and 4-Azido-3,5,6-trifluorobenzoates. *J. Org. Chem.* 57, 1299-1304.
- (313) Watt, D. S., Kawada, K., Leyva, E., and Platz, M. S. (1989) Exploratory photochemistry of iodinated aromatic azides. *Tetrahedron Lett.* 30, 899-902.
- (314) Dolder, M., Michel, H., and Segrist, H. (1990) 3-(Trifluoromethyl)-3-(m -Isothiocyanophenyl)diazirine: Synthesis and Chemical Characterization of a Heterobifunctional Carbene-Generating Cross-linking Reagent. *J. Protein Chem.* 9, 407-415.
- (315) Liberatore, F. A., Comeau, R. D., Mckearin, J. M., Pearson, D. A., Belonga, B. Q., Brocchini, S. J., Kath, J., Phillips, T., Oswell, K., and Lawton, R. G. (1990) Site-Directed Chemical Modification and Cross-Linking of a Monoclonal Antibody Using Equilibrium Transfer Alkylating Cross-Link Reagents. *Bioconjugate Chem.* 1, 36-50.
- (316) del Rosario, R. B., Wahl, R. L., Brocchini, S. J., Lawton, R. G., and Smith, R. H. (1990) Sulfhydryl Site-Specific Cross-Linking and Labeling of Monoclonal Antibodies by a Fluorescent Equilibrium Transfer Alkylation Cross-Link Reagent. *Bioconjugate Chem.* 1, 51-59.
- (317) Lawton, R. G., and Mitra, S. (1979) Reagents for the Cross-Linking of Proteins by Equilibrium Transfer Alkylation. *J. Am. Chem. Soc.* 101, 3097-3110.
- (318) Wilbur, D. S., Stray, J. E., Hamlin, D. K., Goffe, D. K., and Vessella, R. L. (1992) Synthesis and Radioiodination of an ETAC Reagent for Cross-Linking Antibody Fab' Fragments. *J. Nucl. Med.* 33, 943 (abstract).
- (319) Denny, J. B., and Blobel, G. (1984) ^{125}I -labeled crosslinking reagent that is hydrophilic, photoactivatable, and cleavable through an azo linkage. *Proc. Natl. Acad. Sci. U.S.A.* 81, 5286-5290.

- (320) Jaffe, C. L., Lis, H., and Sharon, N. (1980) New Cleavable Photoreactive Heterobifunctional Cross-Linking Reagents for Studying Membrane Organization. *Biochemistry* 19, 4423-4429.
- (321) Murphy, H. R., and Harris, H. W. (1987) Improved Synthesis and Iodination of a Cleavable Photoactivated Probe. *Anal. Biochem.* 165, 88-95.
- (322) Wollenweber, H.-W., and Morrison, D. C. (1985) Synthesis and Biochemical Characterization of a Photoactivatable, Iodinatable, Cleavable Bacterial Lipopolysaccharide Derivative. *J. Biol. Chem.* 260, 15068-15074.
- (323) Hidalgo, J. U., and Nadler, S. B. (1962) Stability Studies on I^{131} -labeled Albumin. *J. Nucl. Med.* 3, 268-272.
- (324) Stern, P., Hagan, P., Halpern, S., Chen, A., David, G., Adams, T., Desmond, W., Brautigam, K., and Royston, I. (1982) The Effect of Radiolabel on the Kinetics of Monoclonal Anti-CEA in a Nude Mouse-Human Colon Tumor Model. *Hybridomas in Cancer Diagnosis and Treatment* (M. S. Mitchell, and H. F. Oettgen, Eds.) pp 245-253, Raven Press, New York.
- (325) Sands, H., and Jones, P. L. (1987) Methods for the Study of the Metabolism of Radiolabeled Monoclonal Antibodies by Liver and Tumor. *J. Nucl. Med.* 28, 390-398.
- (326) De Nardo, G. L., De Nardo, S. J., Miyao, N. P., Mills, S. L., Peng, J. S., O'Grady, L. F., Epstein, A. L., and Young, W. C. (1988) Non-dehalogenation mechanisms for excretion of radioiodine after administration of labeled antibodies. *Int. J. Biol. Markers* 3, 1-9.
- (327) Axworthy, D. B., Wilbur, D. S., Schroff, R. W., Hadley, S. W., Hylarides, M. D., Collins, C., Nelp, W. B., and Fritzberg, A. R. (1988) Identification of the Major Urinary Metabolites of *para*-Iodobenzoate Conjugates of an Antibody Fragment in Humans: Comparison with Chloramine-T. *J. Nucl. Med.* 29, 1325 (abstract).
- (328) Axworthy, D. B., Vanderheyden, J. L., Wilbur, D. S., Hadley, S. W., Hylarides, M. D., Wahl, R. L., Hanelin, L., and Fritzberg, A. R. (1989) Urinary Metabolites of I-131 and Re-186 Radiolabeled Conjugates of Monoclonal Antibodies and Fragments in Patients. *J. Nucl. Med.* 30, 793 (abstract).
- (329) Maack, T., Park, C. H., and Camargo, M. J. F. (1985) Renal Filtration, Transport, and Metabolism of Proteins. *The Kidney, Physiology and Pathophysiology* (D. W. Seldin and G. Giebisch, Eds.) pp 1733-1803, Raven Press, New York.
- (330) Kitteringham, N. R., Maggs, J. L., Newby, S., and Park, B. K. (1985) Drug-Protein Conjugates-VIII. The Metabolic Fate of the Dinitrophenyl Hapten Conjugated to Albumin. *Biochem. Pharmacol.* 34, 1763-1771.
- (331) Christie, G., Kitteringham, N. R., and Park, B. K. (1987) Drug-Protein Conjugates-XIII. The Disposition of the Benzylpenicilloyl Hapten Conjugated to Albumin. *Biochem. Pharmacol.* 36, 3379-3385.
- (332) Zunino, F., Giuliani, F., Savi, G., Dasdia, T., and Gambetta, R. (1982) Anti-Tumor Activity of Daunorubicin Linked to Poly-L-Aspartic Acid. *Int. J. Cancer* 30, 465-470.
- (333) Mueller, B. M., Wrasidlo, W. A., and Reisfeld, R. A. (1990) Antibody Conjugates with Morpholinodoxorubicin and Acid-Cleavable Linkers. *Bioconjugate Chem.* 1, 325-330.
- (334) Srinivasachar, K. and Neville, D. M. (1989) New Protein Cross-Linking Reagents That Are Cleaved by Mild Acid. *Biochemistry* 28, 2501-2509.
- (335) Marinez, O. and Wofsy, L. (1986) Immunotoxins. *Handbook of Experimental Immunology, Vol. 1: Immunochimistry*, 4th ed. (D. M. Weir, Ed.) pp 37.1-37.11, Blackwell Scientific Publications, Oxford, England.
- (336) Trouet, A., Masquelier, M., Baurain, R., and Deprez-De Campeneere, D. (1982) A Covalent linkage between daunorubicin and proteins that is stable in serum and reversible by lysosomal hydrolases, as is required for a lysosomotropic drug-carrier conjugate: *in vitro* and *in vivo* studies. *Proc. Natl. Acad. Sci. U.S.A.* 79, 626-629.
- (337) Schroeder, J., Axworthy, D., Hadley, S. W., Hylarides, M. D., and Wilbur, D. S., unpublished results, NeoRx Corp.
- (338) Goff, D. A., and Carroll, S. F. (1990) Substituted 2-Iminothiolanes: Reagents for the Preparation of Disulfide Cross-Linked Conjugates with Increased Stability. *Bioconjugate Chem.* 1, 381-386.
- (339) Greenfield, L., Bloch, W., and Moreland, M. (1990) Thiol-Containing Cross-Linking Agent with Enhanced Steric Hindrance. *Bioconjugate Chem.* 1, 400-410.
- (340) Hadley, S. M., Grant, L. M., Hylarides, M. D., Fritzberg, A. R., and Wilbur, D. S. (1989), Synthesis, Radioiodination, and Evaluation of a *para*-Iodobenzyl Alcohol Ester Antibody Conjugate. *J. Nucl. Med.* 30, 924 (abstract).
- (341) Haseman, M. K., Goodwin, D. A., Meares, C. F., Kaminski, M. S., Wensel, T. G., McCall, M. J., and Levy, R. (1986) Metabolizable ^{111}In chelate conjugated anti-idiotypic monoclonal antibody for radioimmunodetection of lymphoma in mice. *Eur. J. Nucl. Med.* 12, 455-460.
- (342) Meares, C. F., McCall, M. J., Desphande, S. V., De Nardo, S. J., and Goodwin, D. A. (1988) Chelate Radiochemistry: Cleavable Linkers Lead to Altered Levels of Radioactivity in the Liver. *Int. J. Cancer (Suppl.)* 2, 99-102.
- (343) Paik, C. H., Yokoyama, K., Reynolds, J. C., Quadri, S. M., Min, C. Y., Shin, S. Y., Maloney, P. J., Larson, S. M., and Reba, R. C. (1989) Reduction of Background Activities by Introduction of a Diester Linkage Between Antibody and a Chelate in Radioimmunodetection of Tumor. *J. Nuc. Med.* 30, 1693-1701.
- (344) Pittman, R. C., Carew, T. E., Glass, C. K., Green, S. R., Taylor, C. A., and Attie, A. D. (1983) A radioiodinated, intracellularly trapped ligand for determining the sites of plasma protein degradation *in vivo*. *Biochem. J.* 212, 791-800.
- (345) Chaudhari, A. S., and Bishop, C. T. (1972) Coupling of Amino Acids and Amino Sugars with Cyanuric Chloride (2,4,6-Trichloro-s-triazine). *Can. J. Chem.* 50, 1987-1991.
- (346) Strobel, J. L., Baynes, J. W., and Thorpe, S. R. (1985) ^{125}I -Glycoconjugate Labels for Identifying Sites of Protein Catabolism *in vivo*: Effect of Structure and Chemistry of Coupling to Protein on Label Entrapment in Cells after Protein Degradation. *Arch. Biochem. Biophys.* 240, 635-645.
- (347) Maxwell, J. L., Baynes, J. W., and Thorpe, S. R. (1988) Inulin- ^{125}I -Tyramine, an Improved Residualizing Label for Studies on Sites of Catabolism of Circulating Proteins. *J. Biol. Chem.* 263, 14122-14127.
- (348) Ali, S. A., Eary, J. F., Warren, S. D., Badger, C. C., and Krohn, K. A. (1988) Synthesis and Radioiodination of Tyramine Cellobiose for Labeling Monoclonal Antibodies. *Nucl. Med. Biol.* 15, 557-561.
- (349) Welch, M. J., Mathias, C. J., Moerlein, S. M., Connett, J. M., and Philpott, G. W. (1989) Tyramine-Cellobiose (TC) Labeling of Antibodies: A Comparison with Other Labeling Techniques. *J. Labelled Compd. Radiopharm.* 26, 269-270 (abstract).
- (350) Ali, S. A., Warren, S. D., Badger, C. C., Eary, J. F., Press, O. W., Krohn, K. A., and Nelp, W. B. (1989) Synthesis and Radioiodination of Aryl-Carbohydrate Compounds for Attachment to Monoclonal Antibodies. *J. Labelled Compd. Radiopharm.* 26, 319-321.
- (351) Ali, S. A., Warren, S. D., Richter, K. Y., Badger, C. C., Eary, J. F., Press, O. W., Krohn, K. A., Bernstein, I. D., and Nelp, W. B. (1990) Improving the Tumor Retention of Radioiodinated Antibody: Aryl Carbohydrate Adducts. *Cancer Res. (Suppl.)* 50, 783s-788s.
- (352) Boeldt, E. J., Engelhardt, S., and Veleke, L. (1985) An Inexpensive Method for Monitoring Effluent Air from Iodination Hoods. *Health Phys.* 49, 1306-1307.
- (353) Ferens, J. M., Krohn, K. A., Beaumier, P. L., Brown, J. P., Hellstrom, I., Hellstrom, K. E., Carrasquillo, J. A., and Larson, S. M. (1984) High-Level Iodination of Monoclonal Antibody Fragments for Radiotherapy. *J. Nucl. Med.* 25, 367-370.
- (354) Weadock, K. S., Anderson, L. L., and Kassia, A. I. (1989) A Simple Remote System for the High-Level Radioiodination of Monoclonal Antibodies. *J. Nucl. Med. Allied Sci.* 33, 37-41.
- (355) Weadock, K. S., Sharkey, R. M., Varga, D. C., and Goldenberg, D. M. (1990) Evaluation of a Remote Radioiodination System for Radioimmunotherapy. *J. Nucl. Med.* 31, 508-511.

ARTICLES

Transition Metal Carbonyl Labeling of Proteins. A Novel Approach to a Solid-Phase Two-Site Immunoassay Using Fourier Transform Infrared Spectroscopy

Anne Varenne,[†] Michèle Salmain,[†] Chantal Brisson,[‡] and Gérard Jaouen^{*†}

Ecole Nationale Supérieure de Chimie de Paris, 11, rue Pierre et Marie Curie, 75231 Paris Cedex 05, France, and Clonatec, 60, rue de Wattignies, 75580 Paris Cedex 12, France. Received February 4, 1992

Labeling of bovine serum albumin (BSA) and anti-human thyroid stimulating hormone (hTSH) monoclonal antibodies (mAbs) was performed using (*N*-succinimidyl 4-pentynoate)hexacarbonyldicobalt (NSCo₂(CO)₆). Conditions of coupling were different depending on the protein to be labeled, denaturation of the mAbs occurring with high percentages of organic solvent in the reaction mixture. The influence of reaction time and initial concentration of NSCo₂(CO)₆ was examined. They were both shown to affect the final coupling rate of the metal carbonyl probe. Preservation of the immunoreactivity toward ¹²⁵I-hTSH was observed for five conjugates having different NSCo₂(CO)₆: mAb molar ratios when compared to unmodified and peroxidase-labeled mAbs. Finally, a preliminary study of the quantitative detection of the metal carbonyl mAbs on microtiter wells was achieved using Fourier transform infrared spectroscopy.

INTRODUCTION

The conjugation of metal-containing species to proteins and especially to antibodies has been described for a large variety of applications. Progress in fundamental biochemistry can be expected from protein topography, enzyme mechanism (Kostic, 1988), and 3-D structural analysis by X-ray crystallography (Petsko, 1985). In the case of medical diagnostics, radiometal labeling of monoclonal antibodies¹ offers a promising tool for in vitro (Goldenberg et al., 1980; Mirzadeh et al., 1990) and in vivo studies (Alvarez et al., 1988). In the case of quantitative assays, Miles and Hales (1965) had for the first time underlined the interest of using labeled antibodies in the assay of polypeptide antigens. Radiohalogens were the first probes used in immunometric assays. But rapidly, "cold" probes were suggested, giving birth for example to the popular ELISA tests where enzymes are conjugated to antibodies (Engvall, 1980).

Quantitative assays based on metallic probes are still little developed, since Cais et al. proposed the term "metalloimmunoassay" in 1977. However, many detection techniques can be associated to this type of labeling. When the probe is a coordination complex, atomic absorption spectroscopy (Cais, 1980; Chéret and Brossier, 1986; Mariet and Brossier, 1990), electrochemistry (Weber and Purdy, 1979; DiGleria et al., 1986), and fluorescence (Hemmilä et al., 1984; Diamandis and Morton, 1988) have been described as detection techniques for antigen assays.

A few years ago, we suggested the use of metal carbonyl moieties as markers for biological molecules (Jaouen et

al., 1985). The development of sensitive and easy-to-use Fourier transform infrared spectrometers should encourage this concept. Recently, we proposed the term "carbonyl metalloimmunoassay" (CMIA) to designate assays using labeled antigens (Salmain et al., 1991a, 1992). In the case of low molecular weight biomolecules like hormones and drugs, we synthesized metal carbonyl derivatives which still kept a very good recognition for the target protein (receptor or antibody) (Vessièrès et al., 1988; Gruselle et al., 1989). Additionally, a detection limit of 0.3 pmol of Co₂(CO)₆-labeled estradiol in solution has been obtained by optimizing the infrared measurements (Salmain et al., 1991b).

In order to enhance the sensitivity, an interesting solution is to increase the number of Co₂(CO)₆ fragments bound to the biomolecule. This idea, which is hardly applicable to haptens, could be easily applied to proteins (antibodies), which possess many potential reactive sites. CMIA tests for haptens and also for antigens could then be designed. Unfortunately, direct methods of complexation are not compatible with biological media where proteins are strictly soluble. We recently developed an indirect method of introduction of Co₂(CO)₆ fragments on biomolecules based on a Bolton-Hunter-like reagent, (*N*-succinimidyl 4-pentynoate)hexacarbonyldicobalt (NSCo₂(CO)₆).

In this paper, we describe the first example of labeling of proteins by Co₂(CO)₆ fragments, an immunoreactivity study of the metal carbonyl conjugates, and a preliminary study of FT-IR detection of the conjugates on microtiter plates.

EXPERIMENTAL PROCEDURES

Materials, Reagents, and Instrumentation. Inorganic salts were obtained from Merck (Darmstadt, Germany). Buffers were prepared from demineralized water as follows: phosphate-buffered saline (PBS), 0.01 M, 0.14

[†] Ecole Nationale Supérieure de Chimie de Paris.

[‡] Clonatec.

¹ Abbreviations used: BSA, bovine serum albumin; mAb, monoclonal antibody; hTSH, human thyroid stimulating hormone; NSCo₂(CO)₆, (*N*-succinimidyl 4-pentynoate)hexacarbonyldicobalt; FT-IR, Fourier transform infrared; PBS, phosphate-buffered saline; NS, number of scans; POX, (horse-radish) peroxidase.

M NaCl, pH = 7.2; carbonate buffer, 0.1 M, pH = 9.6. Acetonitrile and ethanol were obtained from Prolabo (Paris, France). Brilliant Blue G and bovine serum albumin (fraction V) were obtained from Sigma (St. Louis, MO). Anti-hTSH monoclonal antibodies JOSS 2-2 and microtiter wells (Maxisorb, Nunc, Denmark) were a gift from Dr. Brisson (CLONATEC, Paris, France). (*N*-Succinimidyl 4-pentynoate)hexacarbonyldicobalt $\text{NSCo}_2(\text{CO})_6$, was synthesized as described previously (Salmain et al., 1991a).

UV-visible data were measured on a Uvikon 860 spectrophotometer (Kontron, Switzerland). FT-IR measurements were obtained with a Michelson 100 spectrometer (Bomem, Quebec, Canada) equipped with a liquid nitrogen cooled InSb detector. Data were treated with a PC-AT computer (NEC) connected to the interferometer and the Bomem Spectracalc software package for peak absorbance measurements.

Labeling of BSA with $\text{NSCo}_2(\text{CO})_6$. BSA (21 nmol) in 1 mL of PBS was added to various quantities of $\text{NSCo}_2(\text{CO})_6$ in a fresh acetonitrile solution. The volume was brought to 2 mL with acetonitrile (final percentage 50%) and the pH was adjusted to 9.6 with carbonate buffer. The mixture was incubated at 4 °C for 18 h.

Purification and Analysis of the Conjugates. The conjugates were purified on a G-25 Sephadex PD10 gel filtration column (Pharmacia, Upsala) following the procedure recommended (elution with PBS). The first 10 fractions of 1 mL were collected and assayed for the presence of protein and $\text{Co}_2(\text{CO})_6$. The presence of protein in each tube was qualitatively and quantitatively determined by the Coomassie Blue method and the presence of $\text{Co}_2(\text{CO})_6$ fragments by FT-IR spectroscopy as follows: 20 μL of each sample tube was dropped on 15 mg of KBr powder (IR grade, Prolabo, France) and lyophilized. The powder was recovered and pressed into a 3-mm KBr disk. Tubes containing both species were pooled and analyzed. The protein concentration was remeasured using the Coomassie Blue method. The concentration of covalently bound $\text{Co}_2(\text{CO})_6$ fragments was determined either by UV spectroscopy at 348 nm, assuming an absorption coefficient of $3700 \text{ L mol}^{-1} \text{ cm}^{-1}$, or by FT-IR spectroscopy as described above ($\nu = 2052 \text{ cm}^{-1}$). For the labeling of BSA, the measures were confirmed by atomic absorption spectroscopy. The final $\text{Co}_2(\text{CO})_6$:protein molar ratio was compared to the initial $\text{Co}_2(\text{CO})_6$:protein molar ratio in order to calculate the coupling yield.

Labeling of JOSS 2-2 by $\text{NSCo}_2(\text{CO})_6$. JOSS 2-2 (6.6 nmol) in 1 mL of PBS was added to 165 nmol of $\text{NSCo}_2(\text{CO})_6$ in 165 μL of ethanol. The volume was brought to 2 mL with PBS and the pH was adjusted to 9.6 with carbonate buffer. The mixture was incubated for 15 h and the immunoconjugate was purified and analyzed as described above.

Effect of Reaction Time on the Labeling of JOSS 2-2 by $\text{NSCo}_2(\text{CO})_6$. A number of 2-mL mixtures containing 6.6 nmol of JOSS 2-2 and 231 nmol (35 equivalents) of $\text{NSCo}_2(\text{CO})_6$ with a final percentage of ethanol of 8% were incubated for variable periods at 4 °C. The immunoconjugates were purified and characterized as described above.

Effect of Concentration of $\text{NSCo}_2(\text{CO})_6$ on the Labeling of JOSS 2-2. A number of 2-mL mixtures containing 6.6 nmol of JOSS 2-2 and 10–45 equiv of $\text{NSCo}_2(\text{CO})_6$ (final ethanol percentage = 8%) were incubated for 3.5 or 15 h at 4 °C. The immunoconjugates were purified and characterized as described above.

Study of the Immunoreactivity of the Conjugates. Variable dilutions of JOSS 2-2, peroxidase-labeled JOSS

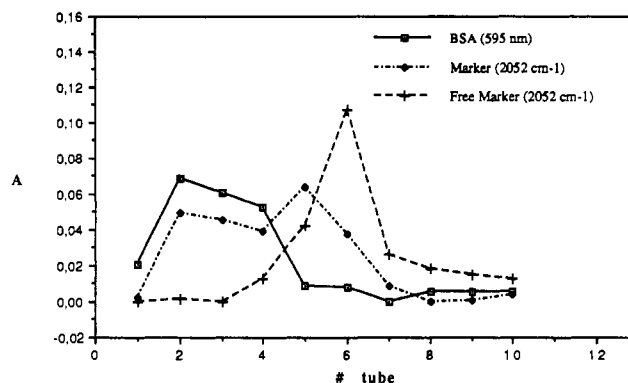


Figure 1. Protein elution profile (Coomassie Blue method), $\text{Co}_2(\text{CO})_6$ marker elution profile (infrared spectroscopic detection; 3-mm KBr pellets), and $\text{Co}_2(\text{CO})_6$ free marker elution profile (infrared spectroscopic detection; 3-mm KBr pellets).

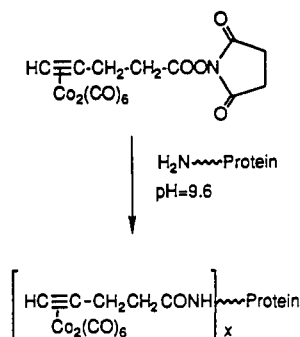
2-2, or $[\text{Co}_2(\text{CO})_6]_x$ -JOSS 2-2 ($x = 4, 11, 22, 25, 29, 31$) were assayed with ^{125}I -hTSH. After precipitation of the bound fractions by addition of anti-mouse IgG antibody, the binding of the tracer was plotted versus the dilution of the unconjugated or conjugated mAbs. The nonspecific binding of ^{125}I -prolactin to the mAbs (unconjugated or conjugated) was studied in the same manner.

Quantitative Detection of $[\text{Co}_2(\text{CO})_6]_{27}$ -JOSS 2-2 on Microtitration Wells by FT-IR Spectroscopy. A number of 26.8- μL samples of variable concentrations of $[\text{Co}_2(\text{CO})_6]_{27}$ -JOSS 2-2 in PBS were deposited on microtiter wells, quantities ranging from 4 to 33 pmol of protein. The solvent was evaporated off in a vacuum desiccator for 1 h and immediately analyzed by FT-IR spectroscopy ($\text{NS} = 10$). After baseline correction, the absorbance of the 2052-cm^{-1} νCO stretching band was plotted versus the quantity of protein deposited.

RESULTS AND DISCUSSION

Preliminary studies of protein labeling with the metal carbonyl probe $\text{NSCo}_2(\text{CO})_6$ were achieved with BSA as the model protein (Scheme I). $\text{NSCo}_2(\text{CO})_6$ is not readily soluble in water like other *N*-succinimidyl esters, so it had to be dissolved in a miscible organic solvent. Acetonitrile was chosen at first and added to the incubation mixture in a 1:1 proportion. Unreacted $\text{NSCo}_2(\text{CO})_6$ was removed by gel filtration chromatography on a Sephadex G-25 column (ready-to-use PD10), and the efficiency of this purification step was checked by a test chromatography of free $\text{NSCo}_2(\text{CO})_6$ alone and by extensive dialysis of the conjugate after gel filtration chromatography.

The purification of the reaction mixture was followed by infrared spectroscopy of the $\text{Co}_2(\text{CO})_6$ marker and by colorimetry of the BSA which reacted with Coomassie Blue. Both elution profiles are superposed as shown in Figure 1, together with the elution profile of the free marker alone. The $\text{Co}_2(\text{CO})_6$ marker gives two chromatographic peaks. By comparison of the elution profile of free $\text{NSCo}_2(\text{CO})_6$ alone, the marker eluted in tubes 5–9 is attributed to the free (unconjugated) form, so the two peaks correspond to the bound and free fractions, respectively. The BSA provides one peak, the form of which can be exactly superposed to the bound marker fraction peak (tubes 1–4). A coupling rate was calculated for each of the fractions (1–4), from standard straight lines for BSA and free marker obtained under the same conditions. It was found to be constant except for tube 4 which contains both forms of marker (free and conjugated), indicating that the labeling procedure provides conjugates with homogeneous coupling rates. Coupling rates measured by UV (348 nm) and IR

Scheme I. Preparation of the Metal Carbonyl-Protein Conjugates**Table I. Effect of Concentration of NSC₂(CO)₆ on the Labeling of BSA^a**

NSC ₂ (CO) ₆ :BSA ratio		% coupling yield ^b
initial	final	
10	8	80
30	26	87
40	37	92
60	40	67

^a [BSA] = 1.05×10^{-5} M; temperature = 4 °C; reaction time = 15 h; pH = 9.6; volume of reaction = 2 mL (acetonitrile = 50%).

^b Calculated from (final NSC₂(CO)₆:BSA ratio)/(initial NSC₂(CO)₆:BSA ratio) × 100.

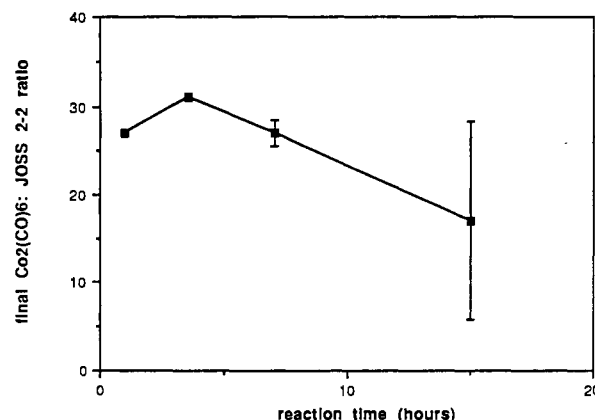
(2052 cm⁻¹) were identical, indicating that the 2052-cm⁻¹ peak absorbance is proportional to the number of Co₂(CO)₈ fragments bound to the protein. On the other hand, the coupling rate measured from the 2091-cm⁻¹ band is unexpectedly higher. In this case, the absorbance of the bound Co₂(CO)₈ fragments cannot be correlated to that of the free ones. We already observed such a difference of intensity in another series of Co₂(CO)₈-alkyne complexes (Salmann et al., 1991b), indicating a greater dependence of the intensity of this particular band with the substituent.

After pooling tubes 1–3, the average rate of Co₂(CO)₈ fragments bound to BSA was assayed by UV spectroscopy, assuming the same ϵ value as for the free NSC₂(CO)₆. This measure was confirmed by atomic absorption spectrophotometry (considered here as the reference method), justifying the above approximation. The coupling ratio remeasured after dialysis was identical. The other parameters, i.e. pH, reaction time, and protein concentration were not optimized.

We examined the influence of the initial NSC₂(CO)₆:BSA molar ratio on the final coupling yield (Table I). The yields reported are very high except for 60 equiv of NSC₂(CO)₆ where a final molar ratio of 40 to 1 is measured.

At pH = 9.6, NSC₂(CO)₆ is highly reactive toward free amino groups and is not subject to hydrolysis. Conjugates with a desired coupling rate can then be obtained by choosing the right initial equivalents of NSC₂(CO)₆. Among the 59 lysine residues contained in the primary structure of BSA, only 40 seem to be reactive under the conditions described. We suspect that the 40 residues are those located at the surface of protein which are readily accessible to solvent and reagents. The same value of 40 has been recently pointed out by Diamandis and Morton (1988) when they labeled BSA with an excess of BCPDA chelate. In addition, Bauminger and Wilchek (1970) noted earlier that only 30–35 out of the 59 lysine residues of BSA are usually accessible for coupling with haptens.

Coupling of NSC₂(CO)₆ to anti-hTSH mAbs JOSS 2-2 was tried first under the same conditions of reaction described for BSA. This experiment was unsuccessful and instead we observed a rapid denaturation (precipitation)

**Figure 2.** Effect of reaction period on the coupling rate of NSC₂(CO)₆ to JOSS 2-2. Experimental conditions: [JOSS 2-2] = 3.3×10^{-6} M; temperature = 4 °C; pH = 9.6, initial NSC₂(CO)₆: JOSS 2-2 molar ratio = 35; volume of reaction 2 mL (ethanol 8%).

of the protein. We checked that this phenomenon was essentially due to the presence of a high percentage (50%) of acetonitrile in the incubation mixture and not to the presence of the probe. Organic solvents are well-known to induce this kind of behavior, but we can still notice a great difference between BSA and JOSS 2-2. In a second experiment, we replaced acetonitrile by ethanol and reduced the final percentage of organic solvent to 8% in the reaction medium. The labeling of JOSS 2-2 was then successfully performed with 25 equiv of NSC₂(CO)₆ leading to a final coupling of 22 Co₂(CO)₈ fragments per protein molecule after a 15-h incubation time.

By reducing the percentage of organic solvent in the mixture, we were able to label, with a high yield, the monoclonal anti-hTSH antibody with the metal carbonyl probe, indicating that the protein contains at least 22 lysine residues accessible to the reagent. However, after several experiments, the results did not appear reproducible, so we went on studying the kinetics of the coupling reaction of NSC₂(CO)₆ to JOSS 2-2.

In a second set of experiments for the labeling of JOSS 2-2, we studied the influence of the reaction time on the coupling rate for an initial NSC₂(CO)₆:JOSS 2-2 molar ratio of 35:1. The results are presented in Figure 2. In 1 h, 27 out of the 35 equiv of NSC₂(CO)₆ added were coupled to the protein, indicating the reaction is complete in a very short period. The coupling rate remained approximately constant between 1 and 15 h of reaction. Protein recovery rates were about 50–60% of the initial molar quantity reacted even with the low percentage of ethanol used. A reaction time of 3.5 h seems a good compromise to obtain an efficient labeling of JOSS 2-2. We finally studied the effect of concentration of NSC₂(CO)₆ on the labeling of JOSS 2-2 for different reaction times.

In Figure 3, we present the plots of final NSC₂(CO)₆:JOSS 2-2 molar ratio versus initial NSC₂(CO)₆:JOSS 2-2 molar ratio for 3.5 and 15 h. The overall coupling yields are as high as for the other experiments except for the 15-h reaction time, for which they are low and unreproducible irrespective of the initial ratio. The coupling yield drops to 89% for 35 initial equivalents of NSC₂(CO)₆ and a 3.5 h reaction time. But when the initial NSC₂(CO)₆:JOSS 2-2 molar ratio reaches 45 the coupling rate is only 29, indicating a possible saturation value of the lysine sites accessible to the metal carbonyl reagent of approximately 30 residues.

As for BSA, immunoconjugates of various coupling rates can be easily obtained by selecting the proper value of

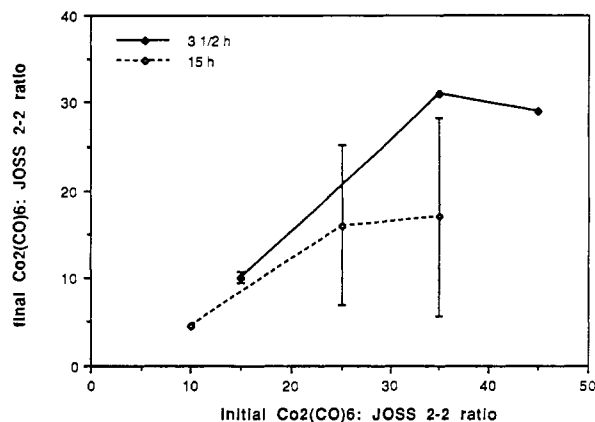


Figure 3. Effect of concentration of $\text{NSCo}_2(\text{CO})_6$ on the labeling of JOSS 2-2. Experimental conditions: $[\text{JOSS 2-2}] = 3.3 \times 10^{-6} \text{ M}$; temperature = 4°C ; pH = 9.6; volume of reaction = 2 mL (ethanol 8%).

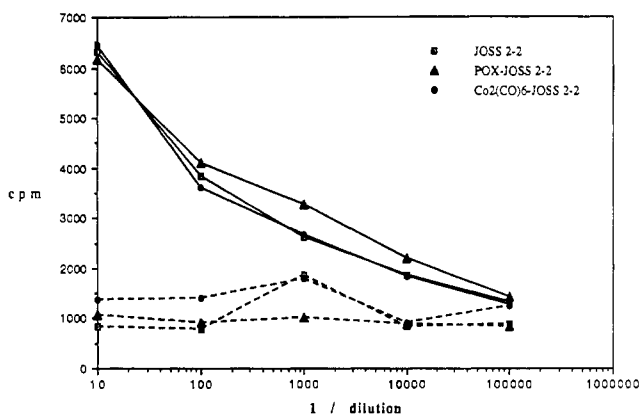


Figure 4. Immunoreactivity of JOSS 2-2, POX-JOSS 2-2, and $\text{Co}_2(\text{CO})_6$ -JOSS 2-2 (coupling ratio = 22). Dilution curves obtained in the presence of ^{125}I -hTSH (—) and ^{125}I -prolactin (- -).

initial equivalents of $\text{NSCo}_2(\text{CO})_6$. This is a very accurate point because the sensitivity of the FT-IR detection will be globally proportional to the number of $\text{Co}_2(\text{CO})_6$ fragments covalently bound to the protein. The introduction of such fragments on the monoclonal antibody is likely to interfere with the binding of the antigen, here hTSH. So the preliminary study concerning immunoconjugate requires an evaluation of their biological activity for different coupling rates.

The biological study of the metal carbonyl conjugates was assessed by performing a dilution assay of the mAbs in the presence of ^{125}I -hTSH as the tracer (specific binding) and in the presence of ^{125}I -prolactin (nonspecific binding). The dilution curves obtained from unconjugated JOSS 2-2, POX-JOSS 2-2, and $\text{Co}_2(\text{CO})_6$ -JOSS 2-2 (with a coupling ratio of 22) are reported Figure 4.

Moreover, the binding of ^{125}I -hTSH or ^{125}I -prolactin to equal dilutions of metal carbonyl conjugates with coupling ratios of 4, 11, 25, 29 and 31 was measured by comparison to unconjugated mAb (Table II). Using this assay, we cannot observe any significant difference of reactivity between unmodified and conjugated mAbs with variable coupling ratios.

The lysine residues involved in the conjugation of the $\text{Co}_2(\text{CO})_6$ fragments do not seem to interfere during the binding of hTSH to JOSS 2-2 and the labeling of the metal carbonyl probes does not alter the specificity of binding of the antibody. It is interesting to notice that a relatively high number of metal carbonyl fragments coupled are still compatible with a good immunoreactivity. This finding is remarkable since for radioisotopic labeling, a maximum

Table II. Effect of the $\text{NSCo}_2(\text{CO})_6$:BSA Ratio on the Immunoreactivity of the Protein

final $\text{NSCo}_2(\text{CO})_6$:BSA ratio	titration by ^{125}I -hTSH (cpm)	titration by ^{125}I -prolactin (cpm)
0	5457	1240
4	4770	948
11	4081	781
25	4261	813
29	4283	999
31	4368	942

of two ^{125}I atoms can be incorporated per protein without loss of immunoreactivity (Johnson et al., 1960). As for fluorescent dyes, conjugates with coupling ratios in the range of 4–6 are the best choice, essentially because of fluorescence quenching associated with higher substitution degrees (Brinkley, 1992). A coupling rate of 31:1 is a very positive point for the improvement of FT-IR detection sensitivity.

For heterogeneous assays, the use of antibody/antigen coated on solid phases can considerably simplify the procedures. Associated with two-site immunometric assays, polystyrene microtiter wells are widely used especially when the probe is an enzyme. We chose to study the feasibility of detection of metal carbonyl labeled antibodies on this solid phase because it seemed well-adapted for the design of an easy (ready-to-use) assay.

The first step was to examine the FT-IR transmission spectrum of a polystyrene well. In Figure 5 is presented its whole IR spectrum and an expansion of the $2200\text{--}1800\text{-cm}^{-1}$ region where νCO bands are expected. Two major observations can be drawn from these two spectra. First, polystyrene is an extremely absorbent material, but a spectral window (inset of Figure 5) can be observed between 2200 and 2000 cm^{-1} . Second, the alkyne- $\text{Co}_2(\text{CO})_6$ fragments are completely compatible with an IR detection on the polystyrene plate because they usually show their three νCO bands at wavenumbers above 2000 cm^{-1} .

The introduction of alkyne- $\text{Co}_2(\text{CO})_6$ fragments on the mAb JOSS 2-2 modifies its IR spectrum as illustrated on Figure 6 inset. When compared to the IR spectrum of unmodified JOSS 2-2, that of $[\text{Co}_2(\text{CO})_6]\text{-JOSS 2-2}$ presents three extra bands at 2093 , 2052 , and 2023 cm^{-1} , corresponding to stretching vibrations of the CO ligands bound to the metals and characteristic of the metallo-carbonyl fragments. Polystyrene being a highly absorbent material made it necessary to record the IR spectra on a very sensitive apparatus. For this purpose, we chose an InSb detector, previously shown as the most sensitive in the 2000-cm^{-1} region (Salmain et al., 1991b).

In order to detect the metal carbonyl conjugates on the microtiter wells, we deposited a constant volume of different concentrations of protein in PBS and evaporated the solutions in a vacuum dessicator. Wells were immediately analyzed. A blank well where a same volume of PBS had been evaporated was used for the reference spectrum.

A typical spectrum of the conjugate deposited on a microtiter well is shown in Figure 6. Again, each of the three bands can be clearly seen at 2093 , 2054 , and 2023 cm^{-1} . Actually, only the 2054-cm^{-1} band provides a good linearity because the 2093 cm^{-1} band is too low and the 2023 cm^{-1} band too close to the polystyrene cutoff. The plot of the 2052-cm^{-1} band absorbance versus the quantity of conjugate deposited is reported in Figure 7. It presents a fairly acceptable correlation coefficient over the range of study. Without precisely optimizing the IR measure-

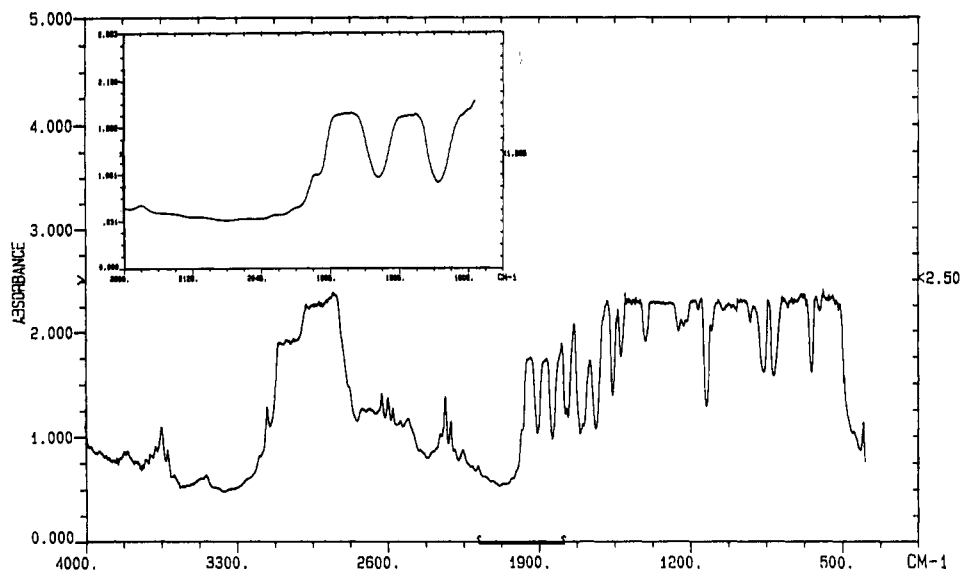


Figure 5. IR transmission spectrum of a polystyrene microtiter well (whole range = 400–4000 cm^{-1}). Inset: expansion of the 1800–2200- cm^{-1} region.

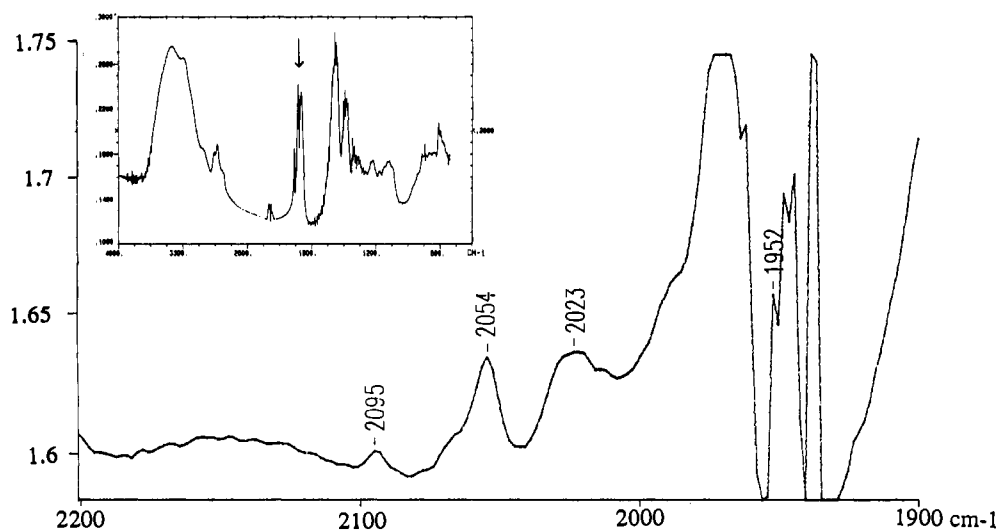


Figure 6. IR spectrum of $\text{Co}_2(\text{CO})_6$ -JOSS 2-2 on a microtiter well in the νCO region. Inset: IR spectrum of $\text{Co}_2(\text{CO})_6$ -JOSS 2-2 in KBr (whole range, 13-mm KBr pellet). The νCO bands are pointed with an arrow.

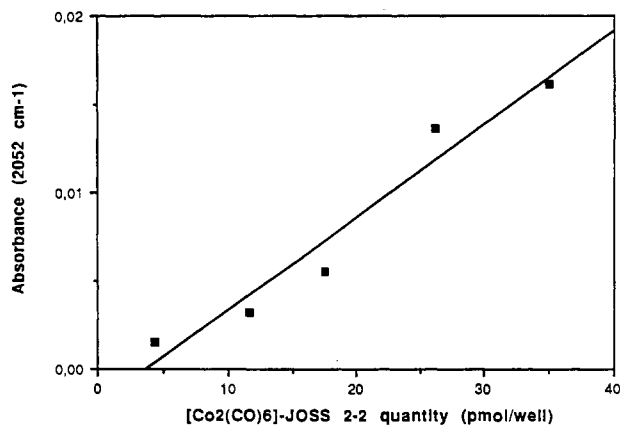


Figure 7. IR quantitative detection of $\text{Co}_2(\text{CO})_6$ -JOSS 2-2 on microtiter wells ($\nu = 2054 \text{ cm}^{-1}$; NS = 10; $y = -2.0124e^{-3} + 5.2847e^{-4}x$; $r^2 = 0.949$).

ments, we detected 4 pmol of $[\text{Co}_2(\text{CO})_6]_{27}$ -JOSS 2-2 on the microtiter wells. The position of the microtiter well must be carefully checked between the reference and the sample spectra in order to have a good compensation. Without a special mounting plate that could have kept the wells in the right position, it was extremely difficult

to obtain good spectra. We now need to build this instrument to improve the IR detection.

CONCLUSION

The coupling of biologically active proteins with an organometallic entity was performed in nondenaturing conditions with a specific labeling agent analogous to the Bolton-Hunter reagent. In the case of the monoclonal antibody, the percentage of organic solvent used to solubilize this reagent had to be carefully optimized in order to minimize the precipitation of the protein. We showed that the coupling ratio for both BSA and JOSS 2-2 reaches a plateau, indicating a saturation of the number of lysine residues involved in the coupling reaction with the metal carbonyl fragments. A good biological activity expressed as the immunoreactivity of the metal carbonyl conjugates toward ^{125}I -hTSH was retained even with high coupling rate conjugates, indicating that they may be included in an hTSH assay procedure. The IR detection of the modified mAb was performed on classical microtiter plates and this preliminary study showed that a fairly good linearity could be obtained between the quantity of conjugate deposited and the absorbance read at 2052 cm^{-1} .

Solid-phase immunoassays are now feasible once a special IR mounting plate for the microtiter plates is available.

ACKNOWLEDGMENT

This work was supported by Clonatec (Paris, France) who graciously supplied the monoclonal antibodies, the microtiter plates, and the gel filtration columns. We wish to thank F. Robillard from Clonatec for the immunological studies. This research was financially supported by an ANVAR grant. M.S. also wants to thank Dr. I.S. Butler for discussion and correction of the manuscript.

LITERATURE CITED

- Alvarez, V. L., Dwight Lopes, A., Rodwell, J. D., McKearn T. J., and Stuart, F. P. (1988) Radioimmunosintigraphy and radioimmunotherapy in nude mouse models. *Antibody-mediated delivery systems* (J.D. Rodwell, Ed.) pp 99-118, Marcel Dekker, New York.
- Bauminger, S. J., and Wilchek, M. (1980) The use of carbodiimides in the preparation of immunizing conjugates. *Methods Enzymol.* 70, 151-159.
- Brinkley, M. (1992) A brief survey of methods for preparing protein conjugates with dyes, haptens and cross-linking reagents. *Bioconjugate Chem.* 3, 2-13.
- Cais, M. (1980) Specific binding assay method and reagent means. U.S. Patent No. 4,205,952.
- Cais, M., Dani, S., Eden, Y., Gandolfi, O., Horn, M., Isaacs, E. E., Josephi, Y., Saar, Y., Slovin, E., and Snarsky, L. (1977) Metalloimmunoassay. *Nature* 270, 534-535.
- Chéret, P., and Brossier, P. (1986) Metalloimmunoassay of antidepressant drugs: Production and characterization of antiserum. *Res. Commun. Pathol. Pharmacol.* 54, 237-253.
- Diamandis, E. P., and Morton, R. C. (1988) Time-resolved fluorescence using an europium chelate of 4,7-bis-(chlorosulfonyl)-1,10-phenanthroline-2,9-dicarboxylic acid (BCPDA). *J. Immunol. methods* 112, 43-52.
- Di Gleria, K., Allen, H., Hill, O., McNeil, J., and Green, M. J. (1986) Homogeneous ferrocene-mediated amperometric immunoassay. *Anal. Chem.* 58, 1203-1205.
- Engvall, E. (1980) Enzyme immunoassay ELISA and EMIT. *Methods Enzymol.* 70, 419-439.
- Goldenberg, D. M., Edmundkim, E., Deland, F. H., Bennett, S., and James Prims, F. (1980) Radioimmunodetection of cancer with radioactive antibodies to carcinoembryonic antigen. *Cancer Res.* 40, 2984-2992.
- Gruselle M., Deprez, P., Vessièrès, A., Greenfield, S., Jaouen, G., Larue, J. C., and Thouvenot, D. (1989) Cobalt and molybdenum carbonyl clusters in immunology. Synthesis and binding properties of mycotoxin derivatives of zearalenone. *J. Organomet. Chem.* 359, C53-C56.
- Hemmilä, I., Dabuku, S., Mukkala, V. M., Siitari, H., and Lovgren, T. (1984) Europium as a label in time-resolved immunofluorometric assays. *Anal. Biochem.* 137, 353-343.
- Jaouen, G., Vessièrès, A., Top, S., Ismail, A. A., and Butler, I. S. (1985) Metal-carbonyl fragments as a new class of markers in molecular biology. *J. Am. Chem. Soc.* 107, 4778-4780.
- Johnson, A., Day, E. D., and Pressman, D. (1960) The effect of iodination on antibody activity. *J. Immunol.* 84, 213-220.
- Kostic, N. M. (1988) Selective labeling, cross-linking and cleavage of proteins with transition-metal complexes. *Comm. Inorg. Chem.* 8, 137-162.
- Mariet, F., and Brossier, P. (1990) A new power association for immunoassay: organometallic label conjugated to solvent separation method. *Res. Commun. Chem. Pathol. Pharmacol.* 68, 251-262.
- Miles, L. E., and Hales, C. N. (1968) Labelled antibodies and immunological assay systems. *Nature* 219, 186-189.
- Mirzadeh, S., Brechbiel, M. W., Atcher, R. W., and Gansow, D. A. (1990) Radiometal labeling of immunoproteins: Covalent linkage of 2-(4-isothiocyanatobenzyl)diethylenetriaminepentaacetic acid ligands to immunoglobulin. *Bioconjugate Chem.* 1, 59-65.
- Petsko, G. H. (1985) Preparation of heavy-metal derivatives. *Methods Enzymol.* 114, 147-156.
- Salmain, M., Vessièrès, A., Butler, I. S., and Jaouen, G. (1991a) (N-Succinimidyl 4-pentynoate)hexacarbonyl: a transition-metal carbonyl complex having similar uses to the Bolton-Hunter reagent. *Bioconjugate Chem.* 2, 13-15.
- Salmain, M., Vessièrès, A., Jaouen, G., and Butler, I. S. (1991b) Fourier Transform infrared spectroscopic method for the quantitative trace analysis of transition metal carbonyl-labeled bioligands. *Anal. Chem.* 63, 2323-2329.
- Salmain, M., Vessièrès, A., Brossier, P., Butler, I. S., and Jaouen, G. (1992) Carbonylmetal immunoassay (CMIA) a new type of non-radioisotopic immunoassay. Principles and application to phenobarbital assay. *J. Immunol. Methods* 148, 65-75.
- Vessièrès, A., Jaouen, G., Gruselle, M., Rossignol, J. L., Savignac, M., Top, S., and Greenfield, S. (1988) Synthesis and receptor binding of polynuclear organometallic estradiol derivatives. *J. Steroid Biochem.* 30, 301-305.
- Weber, S. G., and Purdy, W. C. (1979) Homogeneous voltammetric immunoassay: A preliminary study. *Anal. Lett.* 12, 1-9.

Registry No. NSCo₂(CO)₆, 132178-38-2; TSH, 9002-71-5.

Site-Specific Conjugation of Chain-Terminal Chelating Polymers to Fab' Fragments of Anti-CEA mAb: Effect of Linkage Type and Polymer Size on Conjugate Biodistribution in Nude Mice Bearing Human Colorectal Carcinoma

M. A. Slinkin,*† C. Curtet,† C. Sai-Maurel,† J. F. Gustin,† V. P. Torchilin,‡ and J. F. Chatal†

Laboratoire Biophysique-Cancerologie, INSERM U.211, Plateau Technique CHR, Quai Moncousu, 44035 Nantes Cedex 01, France, and Center for Imaging and Pharmaceutical Research, Massachusetts General Hospital, Charlestown, Massachusetts 02129. Received February 6, 1992

Polylysine-based chelating polymers were used for site-specific modification of anti-CEA mAb Fab' fragments via their SH group distal to the antigen-binding site of the antibody molecule. Conjugation was performed using chain-terminal (pyridyldithio)propionate or 4-(*p*-maleimidophenyl)butyrate moieties to form reducible (S-S) or stable (S-C) bonds between a polymer and Fab' molecule, respectively. One S-S conjugate (S-S₉) and two different S-C conjugates (S-C₃ and S-C₉) were prepared using 3- and 9-kDa molecular weight polymers. No significant loss of immunoreactivity was observed in solid-phase immunoassay, 90-95% of ¹¹¹In-labeled conjugates being bound to CEA-coated Sepharose beads. After labeling with ¹¹¹In, the conjugates had a specific radioactivity of 90-120 µCi/µg. Injected in nude mice bearing LS 174T carcinoma, the conjugates produced different biodistribution patterns. S-S₉ was practically unable to accumulate in tumor and produced very rapid blood clearance of radioactivity and high uptake of radioactivity in liver, spleen, and especially kidneys (225% ID/g 24 h postinjection). S-C₃ and S-C₉ produced practically the same blood clearances (much slower than that of S-S₉) and significant tumor uptake (9-10% ID/g at 24 h). S-C₃ gave significantly lower radioactivity in spleen, skin, and bones, and cleared more rapidly from liver and kidneys. Renal uptake for S-C₃ and S-C₉ was rather high (45% ID/g at 24 h), but much lower than for S-S₉.

INTRODUCTION

The use of chelating polymers for mAb modification was initially proposed as a means of increasing the number of heavy-metal ions which could be bound to mAb molecule without loss of its immunoreactivity (1-3). The main purpose was to use immunoreactive mAb molecules highly loaded with Gd atoms as an immunospecific contrast agent in magnetic resonance imaging. Subsequently, biodistribution studies using different animal models also showed some unexpected and very favorable effects of mAb coupling with chelating polymers in target visualization in immunoscintigraphy (4,5), thus enhancing the potential role of such polymers as mAb modifiers.

We recently proposed the use of chain-terminal polylysine-based chelating polymers to reduce the risk of antibody inactivation during its modification with chelating polymer (6). Our approach allows every polymer chain to be coupled to an antibody molecule strictly via a single amino acid residue, thereby providing a high yield during the conjugation reaction. However, the choice of an "anchor" residue for polymer attachment to antibody remains to be determined. If it were adjacent to the antigen-binding site, this would result in some loss of antibody immunoreactivity upon its modification. Therefore, it would be advisable to ensure polymer binding to antibody molecule via the amino acid residue, which is undoubtedly located distal to the antibody hypervariable region (i.e., near the hinge region), in order to ensure site-specific binding of polymer to antibody. The conjugate could thus be prepared with exact knowledge of the molecular structure.

This approach was applied in the present work to modification of SH groups of anti-CEA Fab' fragments by polymer chain-terminal groups. Reducible disulfide (S-S) or stable thioether (S-C) bonds were used to test whether the type of Fab'-polymer molecule binding has an effect on conjugate biodistribution. The S-C bond was formed using a maleimide-terminal polymer not previously described. As we were also interested in the possible effect of polymer size, conjugates were prepared using two different maleimide-terminal polymers with 3- and 9-kDa molecular weights (MW).

EXPERIMENTAL PROCEDURES

Anti-CEA mAb F6, and IgG₁ specific for human gastrointestinal tract adenocarcinomas, was kindly provided by the CIS Biointernational Co. (Saclay, France) (7). F(ab')₂ fragments were obtained by pepsin digestion.

As starting polymers, ϵ -N-(carbobenzoxy)poly(D,L-lysine) with 3 and 9-kDa MW were used (PL-Z). PL-Z, N-succinimidyl 3-(pyridyldithio)propionate (SPDP), 2-(methylsulfonyl)ethyl N-succinimidyl carbonate (MSOC-NHS), N-succinimidyl 4-(*p*-maleimidophenyl)butyric acid (SMPB), diethylenetriamine-N,N,N',N'',N'''-pentaacetic acid cyclic anhydride (caDTPA), trinitrobenzenesulfonic acid (TNBS), dithitritol (DTT), and 5,5'-dithiobis(2-nitrobenzoic acid) (DTNB) were obtained from Sigma Chemical Co. (La Verrillière, France). Buffer solution components and organic solvents were obtained from Aldrich (St. Quentin Fallavier, France) and carriers for gel chromatography from Pharmacia-LKB (St. Quentin en Yvelines, France).

F(ab')₂ Reduction and Activation with Ellman's Reagent. Fab' fragments were prepared from F(ab')₂ as described in ref 8. Briefly, a portion of F(ab')₂ was reduced by addition of 2-mercaptoethylamine to a concentration

* Laboratoire Biophysique-Cancerologie.

† Center for Imaging and Pharmaceutical Research.

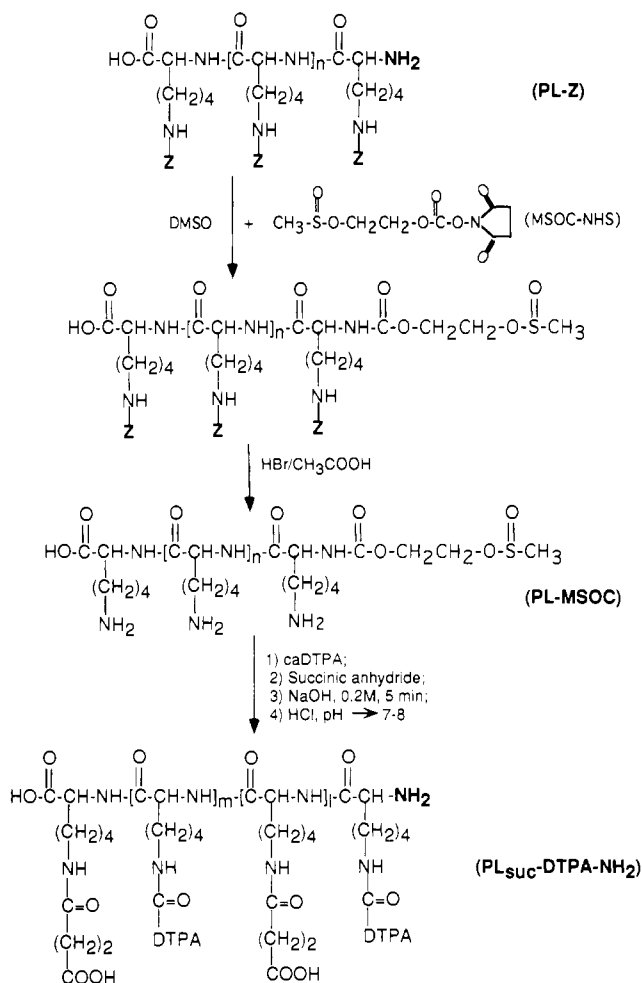


Figure 1. Preparation of amino chain-terminal chelating polymer based on polylysine. Z is a benzoyloxycarbonyl residue.

of 1 mM, EDTA to 1 mM, and NaAsO₂ to 10 mM. After incubation of the solution at room temperature for 18 h, solid Ellman's reagent (DTNB) was added to 20 mM. After a further 3 h, excess reagents were removed by centrifugal gel filtration (9) on Sephadex G-25, pre-equilibrated with 0.1 M sodium phosphate and 1 mM EDTA, pH 6.8. Recovery of Fab'-thionitrobenzoate (Fab'-TNB) derivatives was 80–85%. A small sample of each Fab'-TNB was analyzed by HPLC at 0.7 mL/min on a TSK 3000-SW gel filtration column fitted with a guard column packed with TSK 2000-SW. The column (7.5 mm × 30 cm) was equilibrated to 0.1 M sodium phosphate, pH 6.8. Absorbance was monitored at 254 and 330 nm. F(ab')₂ emerged at 13 min and Fab'-TNB at 15 min in this system.

Polymer Synthesis. PL_{suc}-DTPA-PDP. Chelating polymer PL-DTPA-PDP was prepared based on caDTPA and PL-Z with an average MW of 9 kDa as described in ref 6. This polymer was further modified to prepare succinylated polymer (PL_{suc}-DTPA-PDP) by addition of 10–20-fold molar excess of succinic anhydride (with respect to the polymer unit) in 0.1 M carbonate, pH 8 (concentrated NaOH solution being used to maintain the pH at 8–9 during the reaction). The absence of free NH₂ groups in PL_{suc}-DTPA-PDP was confirmed immediately after reaction by colorimetric assay with 2,4,6-trinitrobenzenesulfonic acid (10).

PL_{suc}-DTPA-NH₂. Amino chain-terminal polymer PL_{suc}-DTPA-NH₂ prepared according to Figure 1 was used as a precursor to introduce the MPB functional moiety at the polymer terminus. Twenty milligrams of PL-Z with 3- or 9-kDa MW was dissolved in 0.5 mL of DMSO, and

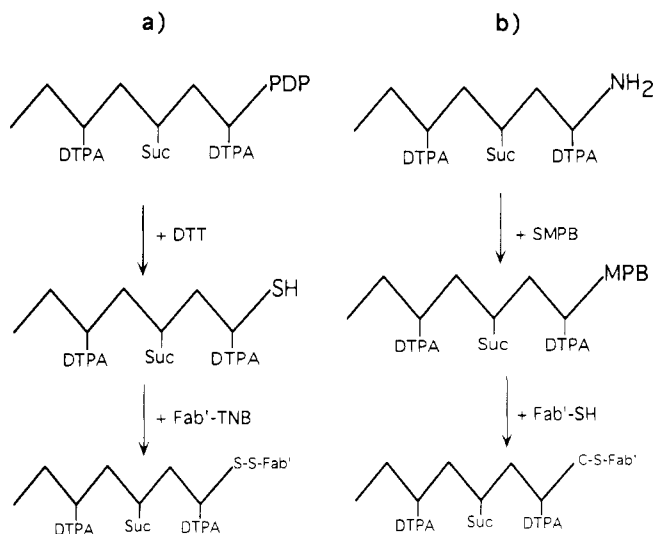


Figure 2. Synthetic schemes for the preparation of bioconjugates with disulfide (a) or thioether (b) bonds.

a 2-fold molar excess of triethylamine was added with respect to the polymer molecule. An 8-fold molar excess of MSOC-NHS was then added and the mixture was incubated at room temperature overnight. The terminal-modified polymer was then separated, Z residues deprotected, and DTPA groups introduced as previously described (6), to obtain PL-DTPA-MSOC. The remaining free ε-amino groups of lysine monomers were subsequently modified with succinic anhydride in the same way as indicated above for PL_{suc}-DTPA-PDP, producing PL_{suc}-DTPA-MSOC, which gave no color reaction with TNBS reagent. To deprotect the MSOC group, solid NaOH was added to the solution of the latter polymer up to a concentration of 0.2 M. After 5 min of incubation, pH 7–8 was restored with concentrated HCl.

The appearance of chain-terminal amino groups after the deprotection step was tested by TNBS reaction using aliquots from the solutions of both polymers at a concentration of 2 mg/mL (with respect to initial PL-MSOC). Briefly, 75 μL of polymer solution were added to 125 μL of water + 200 μL of 0.1 M borate, pH 9.2. To this mixture was added 100 μL of 5.7 mM TNBS solution. After 1 h of incubation, 100 μL of the solution of 2 M NaH₂PO₄ + 20 mM Na₂SO₃ were added, and optical densities at 420 nm were measured.

After the deprotection step, Sephadex G-25 column centrifugation was performed to separate all low molecular weight compounds and to change the buffer to 0.1 M phosphate, pH 7.0.

Conjugate Preparation. Fab'-S-S-PL_{suc}-DTPA (S-S₉) (Figure 2a). Immediately before the conjugation reaction, the SH group was generated on the terminus of the polymer chain. PL_{suc}-DTPA-PDP was reduced with dithiothreitol (DTT) added to the polymer solution (0.2 mg, 2 mg/mL) to a final concentration of 25 mM. The mixture obtained was then incubated for 20 min. Reduced polymer was separated from low molecular weight impurities (including DTPA) by centrifugal gel filtration on Sephadex G-25 columns equilibrated with 0.1 M sodium phosphate, pH 6.5. Immediately after separation, SH polymer solution was added to 0.5 mg of anti-CEA Fab'-TNB (3 mg/mL), and the mixture was then incubated for 18 h at 4 °C. This reaction formed the disulfide bond between the polymer and Fab' molecules. A small aliquot from the solution was then analyzed by HPLC as described above, with the resulting single broad peak at 13 min indicating the absence of free Fab' in the mixture. To

purify the conjugate from a free polymer, gel chromatography of the mixture was performed on a Sephadex G-100 column.

Fab'-S-C-PL_{suc}-DTPA (S-C₃ and S-C₉) (Figure 2b). A 0.4-mg sample of both of the PL_{suc}-DTPA-NH₂ prepared as described above were modified with a 3-fold molar excess (with respect to polymer molecule) of SMPB reagent. The reaction was performed for 2 h in 0.1 M phosphate, pH 7.0, under a polymer concentration of 2 mg/mL. The low molecular weight substances were then separated by Sephadex G-25 column centrifugation, and PL_{suc}-DTPA-MPB polymers were obtained in 0.1 M phosphate/1 mM EDTA, pH 6.8.

Simultaneously, 1 mg of Fab'-TNB in 0.1 M phosphate/1 mM EDTA (3 mg/mL) was reduced with 1 mM of 2-mercaptoethylamine for 1 h, and the Fab'-SH produced was purified by Sephadex G-25 column centrifugation. Immediately after the polymer and Fab'-SH purification step, reactions were allowed to proceed between 0.3–0.4 mg of every PL_{suc}-DTPA-MPB and 0.5 mg of Fab'-SH in 0.1 M phosphate/1 mM EDTA, pH 6.8, for 1 h. They were then stopped by addition of 1 mg of DTNB. The conjugates were subsequently separated from nonreacted Fab' fragments and polymers by DEAE-Sephadex A-25 anion-exchange chromatography as described in ref 4. Briefly, nonreacted protein was washed from the column with the starting buffer (0.05 M acetate, pH 6.0), conjugates were washed with a 0.45 M NaCl step gradient, and highly negatively charged polymers were washed only with a 0.95 M NaCl step gradient.

Sodium dodecyl sulfate–polyacrylamide gel electrophoresis [4–16% (w/v) gel gradient] was done to control the purity, molecular weight, and stability of the conjugates prepared (see Figure 5 for details).

¹¹¹In Conjugate Labeling. To label polymeric conjugates with ¹¹¹In, 10 μg of every conjugate was incubated for 2 h in 0.02 M citrate + 0.1 M acetate, pH 5, with 1.4 mCi ¹¹¹indium chloride. Free ¹¹¹In was then separated in an Amicon C-30 ultrafiltration cell, and bound and total radioactivities were counted in a Medi 202 γ counter (Medisystem, France).

Immunoreactivity Assay. Two parameters of conjugate immunoreactivity were studied: apparent affinity and the immunoreactive fraction.

To estimate the apparent affinity of anti-CEA F(ab')₂ or Fab' preparations, tubes coated with anti-CEA (CIS Biointernational Co., Saclay, France) were used. First, the antigen solution in 0.05 M citrate, pH 5.0, was added to the tubes and incubated at 45 °C for 3 h. Each tube was then washed twice with 3 mL of 0.05% Tween-20 solution, and serial dilutions of the preparation were done in the presence of a constant amount of ¹²⁵I-anti-CEA. The tubes were subsequently incubated overnight at room temperature, washed twice with 0.05% Tween, and counted in a Compugamma LKB γ counter. The apparent affinity of conjugates was estimated by the half-binding point derived from the titration curves obtained.

The immunoreactive fraction of ¹¹¹In-labeled conjugates was determined by a binding assay using CEA-coated Sepharose beads (11). Briefly, a 200-μL aliquot of ¹¹¹In-labeled conjugate, previously diluted with PBS to a protein concentration of 50 ng/mL, was added to 0.2 mL of a 50% (v/v) CEA-coated bead suspension, previously incubated with BSA for 1 h, in an Eppendorf test tube. The test tube was counted in a γ counter, and the contents were mixed under vortexing at room temperature for 1 h. The tube was then centrifuged and the pellet of beads collected and washed twice by resuspension in 0.5 mL of

PBS and recentrifugation. The final bead pellet was counted in a γ counter, and the percentage of radiolabeled conjugate bound to the CEA-coated beads was determined by comparing the net cpm of test tube contents before and after washing.

Biodistribution Studies. Nude mice (8-weeks-old) were injected subcutaneously in the right flank with 10⁷ LS 174T cells. Twelve to fifteen days later, the mice were injected in the tail vein with 100 μL of ¹¹¹In-labeled conjugate in 0.9% NaCl (1 μg of protein). The radioactivity injected was 3.44–5.18 MBq for polymeric conjugates.

After anesthesia, mice were killed by cervical dislocation 4, 24 and 96 h after injection. All organs were removed from each animal, washed, dried, and weighed. Tumor weight at the time of removal ranged from 0.2 to 0.5 g. Radioactivity was measured on a γ counter, and results were expressed as the percentage (mean ± SEM) of injected dose per gram of tissue (% ID/g) and in tumor-to-normal tissue ratios for an average of four or five mice injected at each time interval.

RESULTS

Synthesis of PL_{suc}-DTPA-MPB Polymers. To introduce the MPB moiety at the terminus of the polylysine chain, a synthetic route (see Figure 1) somewhat longer than that used for the synthesis of PL_{suc}-DTPA-PDP was chosen. Introduced in the first step (as in the case of the PDP group), the maleimide function would obviously react with deprotected ε-amino groups of lysine monomers under the conditions of polymer modification with cadTPA and succinic anhydride. As there is no simple way to conserve a maleimide group in the protected state (as in the case of the SH group), we decided to use the MSOC group well known in peptide chemistry (12, 13) to protect the NH₂-terminal group of PL-Z at the first step. This protecting group could easily be eliminated after introduction in the polymer chain of DTPA and succinic acid residues, with release of the terminal NH₂ group available for reaction with SMPB reagent.

TNBS reagent analysis of the terminal amino groups in both PL_{suc}-DTPA-NH₂ polymers prepared (based on PL-Z of 3- and 9-kDa MW) showed a 3-fold difference in their content which correlated well with the molecular weight differences of the corresponding PL-Z polymers. When the same TNBS reaction of NH₂-terminal polymers was used after the column centrifugation step, recovery of polymers with initial MW of 3 and 9 kDa after separation was found to be 70% and 85%, respectively.

Conjugate Preparation and Analysis. S-S₉. Figure 3a,b shows the HPLC chromatograms of Fab'-TNB and the aliquot from the reaction mixture after Fab'-TNB conjugation with PL_{suc}-DTPA-SH, demonstrating the complete incorporation of Fab'-TNB in conjugate and the absence of any aggregate formation during the modification procedure. The shifting and broadening of the conjugate peak, easily apparent compared to that of Fab'-TNB alone, can be attributed to an increase in protein molecular weight after conjugation to a polymer with a rather broad molecular weight distribution. The absence of free Fab'-TNB in the mixture after conjugation was independently proven by DEAE-Sephadex ion-exchange chromatography under the conditions described above for S-C conjugates (see Experimental Procedures), which gave no protein peak washed with the starting buffer (0.05 M acetate, pH 5.5). This high reaction yield allowed purification of the conjugate to be carried out by Sephadex G-100 gel chromatography alone, which easily allowed separation of much smaller molecules of free polymer (see Figure 4).

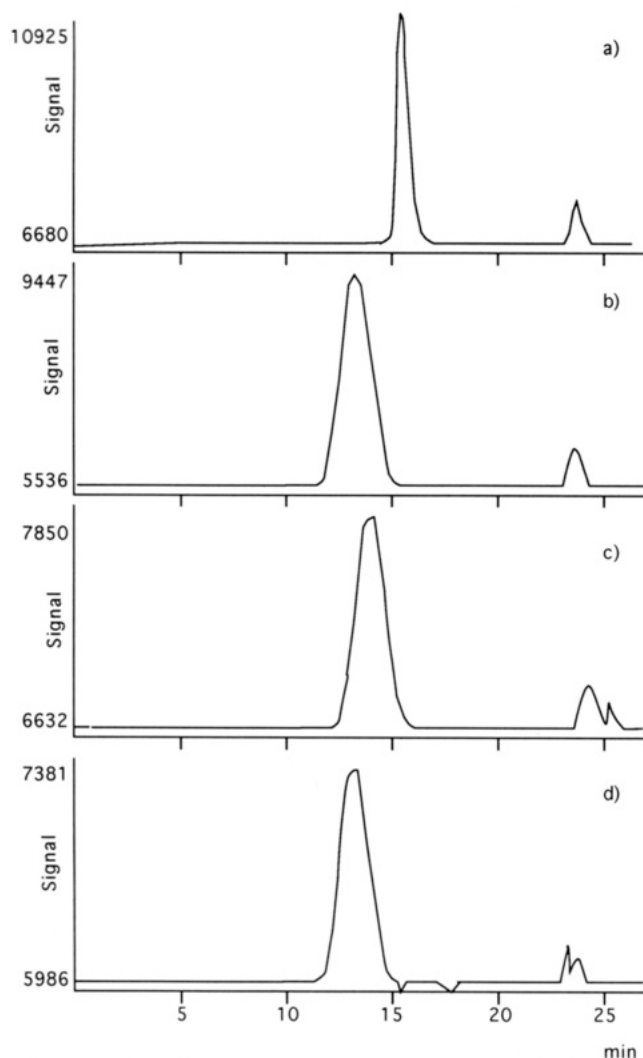


Figure 3. HPLC elution profiles of Fab'-TNB (a), S-S₉ in the mixture after conjugation reaction (b), and purified S-C₃ (c) and S-C₉ (d), as detected by UV adsorption at 280 nm. Size-exclusion column chromatography (TSK G3000SW, 7.5 × 300 mm) was followed by elution with 0.1 M acetate + 0.1 M NaCl (pH 5.0) at a flow rate of 0.7 mL/min.

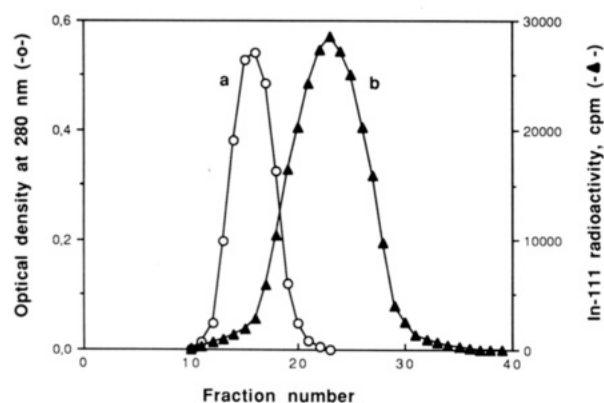


Figure 4. Gel chromatography of the reaction mixture after conjugation of Fab'-TNB with PL_{suc}-DTPA-SH (a) and of ¹¹¹In-PL_{suc}-DTPA-PDP (b) on a Sephadex G-100 column (1.0 × 20 cm) equilibrated with 0.01 M acetate + 0.02 M citrate + 0.08 M NaCl, pH 5.0. Fractions (0.6 mL) were collected, and optical density and γ radioactivity were measured.

Molecular weight increase and the absence of aggregates were also demonstrated by using SDS-polyacrylamide gel electrophoresis (see Figure 5). Under nonreducing conditions, Fab'-TNB migrated as a narrow band of apparent MW 50 000, whereas S-S₉ migrated as a broad band of

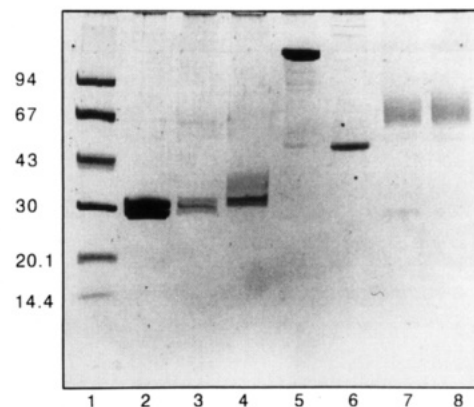


Figure 5. Analysis of the conjugates by SDS-PAGE (4.5–16%) was done under reducing (lanes 2–4) and nonreducing (lanes 5–8) conditions: lanes 2 and 6, anti-CEA Fab'-TNB; lanes 3 and 7, S-S₉; lanes 4 and 8, S-C₉; lane 5, anti-CEA F(ab')₂. The gel was calibrated with the marker proteins (lane 1).

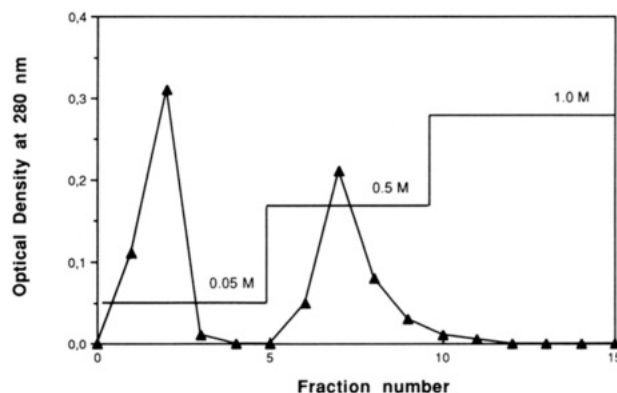


Figure 6. Ion-exchange chromatography on DEAE-Sephadex A-25 (1 × 2 cm) of the reaction mixture after conjugation of Fab'-SH with PL_{suc}-DTPA-MPB. Total salt concentrations are indicated above the gradient steps. Fraction volume is 1 mL.

apparent MW 55–70 000. Under reducing conditions, the complete splitting of S-S₉ conjugate showed two bands of apparent MW 28 000 and 30 000 corresponding to fragments of light and heavy chains with no evidence of polymer coupled to these fragments.

S-C₃ and S-C₉. HPLC chromatography on a TSK 3000 column showed that the coupling efficiency of PL_{suc}-DTPA-MPB polymers with Fab'-SH was not as high as that of PL_{suc}-DTPA-SH with Fab'-TNB. For both polymers only 30–35% of protein was incorporated into the conjugate. Therefore, these conjugates had to be purified using DEAE-Sephadex ion-exchange chromatography, which allowed the separation of unbound Fab' fragments and polymers from the conjugate via application of different salt concentrations. Figure 6 illustrates such separation in the case of S-C₉. The protein peak washed in 0.05 M acetate + 0.45 M NaCl, pH 5.5, was used for ¹¹¹In labeling, and ¹¹¹In-labeled S-C₉ gave a single peak on Sephadex G-100 column chromatography, showing the absence of free polymer (data not shown). HPLC chromatography of purified S-C₃ and S-C₉ (Figure 3c,d) showed some molecular weight difference and the absence of aggregates in both preparations.

Purified S-C₉ was also analyzed by SDS-polyacrylamide gel electrophoresis (Figure 5). While under nonreducing conditions it gave practically the same band as S-S₉, reducing conditions revealed the difference between these two preparations. S-C₉ then showed one narrow band of apparent MW 30 000 corresponding to chain fragments and one broad band of MW 35–40 000 obviously corre-

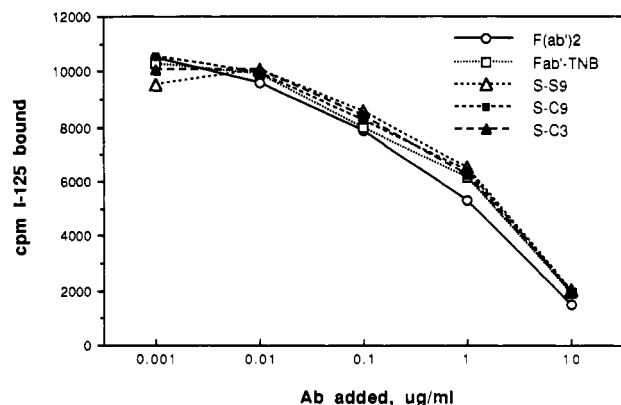


Figure 7. Comparison of the apparent affinity of different anti-CEA $F(ab')_2$ - and Fab' -based preparations by solid-phase competitive radioimmunoassay.

sponding to polymer-modified chain fragments. Such splitting proves that there was indeed a single coupling point between the polymer and Fab' molecules. When modified with a polymer carrying randomly distributed protein-reactive groups, Fab' fragments do not split at all in reducing conditions due to their intramolecular cross-linking with the polymer molecule (14).

Specific Conjugate Radioactivity and Immunoreactivity. The maximal specific radioactivity attained for ^{111}In -labeled conjugates was 90–120 $\mu Ci/\mu g$ of protein, which is much higher than that of Fab or $F(ab')_2$ fragments labeled via low molecular weight chelating agents (15, 16), indicating that a large number of DTPA residues were incorporated into the conjugate.

Figure 7 compares the apparent affinity of the conjugates prepared with those of anti-CEA $F(ab')_2$ and Fab' -TNB. There was some decrease in the immunoreactivity of Fab' as compared to $F(ab')_2$ (a well-known phenomenon in immunochemistry), but there was practically no further immunoreactivity loss for polymer-modified Fab' fragments. The absence of adverse affection of Fab' immunoreactivity was also confirmed by measurement of the immunoreactive fraction: the percentage of binding of ^{111}In -labeled conjugates with CEA-coated microbeads in conditions of approximately infinite antigen excess was 90–95%, indicating excellent retention of initial Fab' fragment immunoreactivity during conjugate preparation.

Biodistribution Studies. The results of biodistribution in human colorectal carcinoma tumor-bearing athymic mice for ^{111}In -labeled $S-C_3$, $S-C_9$, and $S-S_9$ are summarized in Table I. At 4 h postinjection, blood radioactivity for $S-S_9$ was already much lower than for both of the thioether conjugates, obviously due to the breakdown of the disulfide bond in vivo. Such rapid blood clearance of radioactivity appears to be the main reason for the very low accumulation of $S-S_9$ radioactivity in tumor, which was 3.5 and 9 times as low as for the other two conjugates at 4 and 24 h postinjection, respectively. At the same time, compared with $S-C$ conjugates, $S-S_9$ produced significantly higher radioactivities in liver, spleen, and especially kidneys, apparently reflecting the biodistribution of ^{111}In -labeled PL_{suc} -DTPA-SH released from $S-S_9$.

When the biodistribution of $S-C_3$ and $S-C_9$ is compared, a difference can be noted in the kinetics of radioactivity clearance from liver, kidneys, spleen, skin, and bone. Whereas the concentrations of conjugates in these organs 4 h postinjection did not differ statistically, $S-C_3$ radioactivity was significantly lower at 24 and especially 96 h compared to that of $S-C_9$. Conversely, tumor concentrations revealed the same kinetics for both conjugates,

with some slight increase in tumor radioactivity between 4 and 24 h postinjection and a significant decrease between 24 and 96 h. Such biodistribution patterns resulted in significantly higher tumor:blood, tumor:liver, and tumor: kidney ratios for $S-C_3$ as compared to $S-C_9$ at 24 and 96 h postinjection (Table II).

DISCUSSION

The present work describes a simple approach for site-specific conjugation of chain-terminal chelating polymers with Fab' fragments of IgG antibody. This approach ensures a single binding site between the chelating polymer chain and Fab' distal to the hypervariable region of the antibody molecule. It combines the advantages of chain-terminal chelating polymer and site-specific antibody modification; i.e., it completely excludes the possibility of inter- and intramolecular cross-linking of the modified antibody and dramatically reduces the risk of its inactivation due to modification of amino acid residues essential to maintain the spatial organization of the antigen-binding site. A priori, it seems unlikely that antibody immunoreactivity would be changed by such modification unless there were some sort of unfavorable polymer-protein interaction not connected with the polymer-binding site.

The method used for Fab' -TNB preparation allowed the generation of two or three protected SH groups depending on the subclass of IgG (17), thus enabling two or three polymer chains to be coupled to an antibody molecule.

Two different methods of Fab' modification were performed in order to prepare conjugates with two different linkages between Fab' and polymer molecules. The simpler way of preparing the conjugate consisted of the formation of a disulfide bond using Fab' -TNB and PL_{suc} -DTPA-SH. Under the conditions described, Fab' fragments were completely incorporated into the conjugate without aggregate formation. Preparation of the conjugate with a thioether bond was more complicated, requiring in particular the synthesis of PL_{suc} -DTPA-MPB through the PL_{suc} -DTPA-MSOC and PL_{suc} -DTPA- NH_2 polymers. Furthermore, the previous reduction of Fab' -TNB and separation of the Fab' -SH obtained were indispensable to the conjugation reaction. The efficiency of this reaction was not as high as for disulfide bond formation since only 35–40% of Fab' -SH was incorporated into the conjugate.

The synthetic scheme elaborated for the preparation of PL_{suc} -DTPA- NH_2 seems somewhat more flexible than that for PL_{suc} -DTPA-PDP since it allows the introduction at the polymer chain terminus of any functional moiety able to react with amino groups. The only prerequisite is to block all deprotected lysine monomer ϵ -amino groups. This can easily be performed with a suitable acylating agent selected according to the net electron polymer charge required. The choice of acetic instead of succinic anhydride allows the preparation of a polymer not carrying such a high negative charge (unpublished results).

In keeping with the main idea behind the approach used in this study, the immunoreactivity of Fab' fragments was completely preserved after their conjugation with polymers. Interestingly, the apparent affinity of Fab' was tested using nonlabeled conjugates, whereas immunoconjugates highly labeled with ^{111}In were used to determine the immunoreactive fraction. The results suggest that DTPA residue saturation with a heavy metal had no influence on the immunoreactivity of the conjugates.

The different stability of $S-S$ and $S-C$ linkages between Fab' and polymer molecules was clearly demonstrated by SDS gel electrophoresis since the former was completely

Table I. Biodistribution of S-C₃, S-C₉, and S-S₉ in Athymic Mice Bearing Human Colorectal Carcinoma Tumor^a

organ	S-C ₃			S-C ₉			S-S ₉		
	4 h	24 h	96 h	4 h	24 h	96 h	4 h	24 h	96 h
tumor	8.2 ± 2.1	9.7 ± 1.9	4.2 ± 0.6	8.9 ± 1.6	9.3 ± 0.2	5.1 ± 1.0	2.6 ± 0.5	1.0 ± 0.1	0.6 ± 0.2
blood	15.8 ± 2.8	1.3 ± 0.3	0.16 ± 0.01	16.0 ± 1.7	1.8 ± 0.1	0.21 ± 0.06	1.9 ± 0.4	1.2 ± 0.4	0.04 ± 0.01
liver	8.0 ± 1.2	6.2 ± 0.9	4.2 ± 1.0	8.4 ± 2.1	10.1 ± 1.6	9.1 ± 0.9	25.4 ± 4.2	18.7 ± 3.1	11.8 ± 1.4
kidney	48.4 ± 12.5	43.5 ± 5.7	13.2 ± 3.1	32.5 ± 8.9	45.5 ± 2.3	24.0 ± 5.7	121.2 ± 9.8	223.4 ± 9.4	62.6 ± 4.3
spleen	4.6 ± 0.6	2.2 ± 0.2	2.0 ± 0.6	4.7 ± 1.0	4.3 ± 0.8	5.9 ± 1.0	9.8 ± 1.7	17.3 ± 2.4	6.5 ± 1.0
bone	2.7 ± 1.2	1.2 ± 0.1	1.0 ± 0.2	4.5 ± 1.4	3.4 ± 0.7	4.1 ± 0.8	1.5 ± 0.2	3.9 ± 1.5	3.0 ± 0.4
skin	2.9 ± 0.8	2.7 ± 0.1	1.6 ± 0.2	2.9 ± 1.1	4.9 ± 1.1	4.1 ± 0.8	1.4 ± 0.6	4.3 ± 2.2	2.6 ± 0.8

^a Organ levels of radioactivity are expressed as percentage of injected dose/gram of tissue (mean ± SD, *n* = 4–5) after iv injection of 1 µg of the corresponding conjugate.

Table II. Tumor-to-Organ Ratios of S-C₃ and S-C₉ at 4, 24, and 96 h Postinjection

tumor/organ ratio	S-C ₃			S-C ₉		
	4 h	24 h	96 h	4 h	24 h	96 h
tumor/blood	0.50	7.46	26.25	0.55	5.17	24.28
tumor/liver	1.03	1.56	1.00	1.06	0.92	0.56
tumor/kidney	0.17	0.22	0.31	0.27	0.20	0.21
tumor/spleen	1.78	4.40	2.10	1.89	2.16	0.86
tumor/bone	3.03	8.08	4.20	1.98	2.73	1.24

broken down under reducing conditions. The disulfide bond is also known to be labile and unstable in circulation (18, 19), apparently because of the presence of low concentrations of reduced glutathione which is continually being manufactured by the liver and is maintained in plasma at a level of about 24 µM (20). Our biodistribution data, in particular the very fast blood clearance of radioactivity for S-S₉, as compared to S-C conjugates, also strongly suggest a breakdown of S-S₉ in vivo. High accumulation of radioactivity in kidneys can obviously be related to the biodistribution of released ¹¹¹In-PL_{suc}-DTPA-SH. Such accumulation seems strange in the light of the results reported for the highly negatively charged compound ¹¹¹In-antimyosin-Fab-succinimidyl-PL_{suc}-DTPA (4) which demonstrated low kidney concentration in a canine model of myocardial infarction. The unexpected accumulation of this rather low molecular weight negatively charged polymer could be due to the role of the polymer terminal SH group available for some modifications in vivo. This could have changed the biodistribution pattern of the polymer, which could also account for the relatively high accumulation of S-S₉ radioactivity in liver.

Even S-C₃ and S-C₉ conjugates with stable thioether linkages demonstrated relatively high kidney accumulation of radioactivity, with rather unfavorable tumor:kidney ratios for tumor imaging. However, renal uptake for both these conjugates in a nude mouse model was much lower than that of Fab' or Fab fragments labeled with ¹¹¹In using caDTPA. Thus, the renal uptake of ¹¹¹In after injection of ¹¹¹In-labeled anti-CEA C198 Fab was approximately 60% of the whole body activity at 72 h postinjection (21), and ¹¹¹In-labeled MoAb OV-TL 3 Fab' produced 150% ID/g in kidneys 24 h postinjection (22). It is not absolutely clear from this study whether decreased renal uptake of polymeric as compared to DTPA-modified conjugates is due to negative polymer charge or simply to the somewhat higher molecular weight of the former. It is possible that both effects are involved. In any event, liver uptake of radioactivity for S-C₃ and S-C₉ was 2–3 times as great as that of ¹¹¹In-labeled Fab (or Fab') fragments in the studies just mentioned. This suggests that for Fab'-polymer conjugates as opposed to Fab(Fab')-DTPA the organ catabolizing the immunoconjugate shifts to some extent from kidneys to liver. It is also noteworthy that comparison of the biodistribution of S-C polymeric conjugates with that of ¹¹¹In-OV-TL 3 Fab'-DTPA shows a significant

decrease in blood clearance for the former. Instead of 3% ID/g of radioactivity remaining in blood 4 h after injection of ¹¹¹In-Fab', there was about 16% ID/g of ¹¹¹In-labeled S-C₃ and S-C₉ still circulating. Such a decrease is obviously related to the increased molecular weight of the polymeric conjugates.

The differences in S-C₃ and S-C₉ biodistribution could also be related to differences either in the conjugate electron charges or molecular weight. The fact that S-C₃ clears from kidneys and liver significantly faster than S-C₉ suggests that negatively charged ¹¹¹In-labeled digestion products from S-C₃ leave these organs more easily than do those from S-C₉ because of their lower molecular weight. However, the real mechanism accounting for these differences is still not clear. From a practical point of view, it would be of interest to decrease renal and liver uptake of polymeric conjugates further by using chelating agents which provide more stable metal complexes capable of metabolism in liver and kidney (23).

It may be concluded that the simple chemical approach described in this paper could allow the preparation of a number of immunoreactive conjugates highly charged with metal ions. Easily available S-S conjugate characterized by a poor biodistribution pattern could be used for some in vitro applications, e.g., the enhancement of the sensitivity of time-resolved fluorescence immunoassay (after labeling with Eu³⁺ or Tb³⁺) (24). However, for in vivo applications only conjugates with a relatively stable linkage between a polymer and Fab' fragments would seem suitable. Labeled with Gd³⁺, such conjugates could be used as immunospecific contrasts agents for magnetic resonance imaging (25), or when labeled with a cytotoxic radioactive isotope up to high specific radioactivity, they could also be used in radioimmunotherapy to reduce the amount of administered xenoprotein and hence the risk of anti-murine antibody response (26).

LITERATURE CITED

- (1) Shreve, P., Aisen, A. E. (1986) Monoclonal antibodies labeled with polymeric paramagnetic ion chelates. *Magn. Res. Med.* 3, 336–340.
- (2) Manabe, Y., Longley, C., and Furmanski, P. (1986) High-level conjugation of chelating agents onto immunoglobulins: use of intermediary poly(L-lysine)-diethylenetriaminepentaacetic acid carrier. *Biophys. Biochem. Acta* 883, 460–467.
- (3) Torchilin, V. P., Klibanov, A. L., Nossiff, N. D., Slinkin, M. A., Strauss, W., Haber, E., Smirnov, V. N., and Khaw, B. A. (1987) Monoclonal antibody modification with chelate-linked

- high-molecular-weight polymers: major increases in polyvalent cation binding without loss of antigen binding. *Hybridoma* 6, 229-240.
- (4) Khaw, B. A., Klivanov, A., O'Donnell, S. M., Saito, T., Nossiff, N., Slinkin, M. A., Newell, J. B., Strauss, H. W., and Torchilin, V. P. (1991) Gamma imaging with negatively charge-modified monoclonal antibody: Modification with synthetic polymers. *J. Nucl. Med.* 32, 1742-1751.
- (5) Wang, T. S. T., Fawwaz, R. A., and Alderson, P. O. (1992) Reduced hepatic accumulation of radiolabeled monoclonal antibodies with indium-111-thioether-poly-L-lysine-DTPA-monoclonal antibody-TP41.2F(ab')₂. *J. Nucl. Med.* 33, 570-574.
- (6) Slinkin, M. A., Klivanov, A. L., and Torchilin, V. P. (1991) Terminal-modified polylysine-based chelating polymers: Highly efficient coupling to antibody with minimal loss in immunoreactivity. *Bioconjugate Chem.* 2, 342-348.
- (7) Accolla, R. S., Carrel, S., and Mach, J. P. (1980) Monoclonal antibodies specific for carcinoembryonic antigen and produced by two hybrid cell lines. *Proc. Natl. Acad. Sci. U.S.A.* 77, 563-566.
- (8) Brennan, M. (1986) A chemical technique for the preparation of bispecific antibodies from Fab fragments of mouse monoclonal IgG1. *BioTechniques* 4, 424-427.
- (9) Parkinson, A. J., Scott, E. N., and Muchmore, H. G. (1981) Purification of labeled antibody by minicolumn gel centrifugation. *Anal. Biochem.* 118, 401-404.
- (10) Fields, R. (1972) The rapid determination of amino groups with TNBS. In *Methods of Enzymology* (Hirs C. H. W., and Timasheff, S. N., Eds.) Vol. XXV, Part B, pp 464-468, Academic Press, New York.
- (11) Sumerdon, G. A., Rogers, P. E., Lombardo, C. M., Scnobrich, K. E., Melvin, S. L., Hobart, E. D., Tribby, I. I. E., Stroupe, S. D., and Johnson, D. K. (1990) An optimized antibody-chelator conjugate for imaging of carcinoembryonic antigen with indium-111. *Nucl. Med. Biol.* 17, 247-254.
- (12) Wolters, E. T. M., Tesser, G., and Nivard, R. (1974) Synthesis of the A 14-21 sequence of ovine insulin by the solid-phase technique. *J. Org. Chem.* 39, 3388-3392.
- (13) Tesser, G. I., and Balvert-Geers, I. C. (1975) The methyl-sulfonyl-ethoxycarbonyl group, a new and versatile amino protective function. *Int. J. Pept. Protein Res.* 7, 295-305.
- (14) Slinkin, M. A., Klivanov, A. L., Khaw, B. A., and Torchilin, V. P. (1990) Succinylated polylysine as a possible link between the antibody molecule and deferoxamine. *Bioconjugate Chem.* 1, 291-295.
- (15) Khaw, B. A., Yasuda, T., Gold, H. K., Leinbach, R. C., Johns, J. A., Kanke, M., Barlai-Kovach, M., Strauss, H. W., and Haber, E. (1987) Acute myocardial infarct imaging with indium-111 labeled monoclonal antimyosin Fab. *J. Nucl. Med.* 28, 76-82.
- (16) Yemul, S., Leon, J. A., Seldin, D. M., Link, M. J., Kramer, P., Mesa-Tejada, R., and Estabrook, A. (1991) Tumor localization in nude mice bearing human breast carcinoma xenografts using ¹¹¹In-DTPA conjugates of monoclonal antibodies. *Nucl. Med. Biol.* 18, 295-304.
- (17) Svasti, J., and Milstein, C. (1972) The disulfide bridges of a mouse immunoglobulin G₁ protein. *Biochem. J.* 126, 837-850.
- (18) Paik, C. H., Quadri, S. M., and Reba, R. C. (1989) Interposition of different chemical linkages between antibody and ¹¹¹In-DTPA to accelerate clearance from non-target organs and blood. *Nucl. Med. Biol.* 16, 475-481.
- (19) Blakey, D. C., Watson, G. L., Knowles, P. P., and Thorpe, P. E. (1987) Effect of chemical deglycosylation of ricin-A chain on the in vivo fate and cytotoxic activity of an immunotoxin compound of ricin-A chain and anti-Thy 1.1 antibody. *Cancer Res.* 47, 947-952.
- (20) Thorpe, P. E., Wallace, P. M., Knowles, P. P., Relf, M. G., Brown, A. N. F., Watson, G. J., Knyba, R. E., Wawrzynczak, E. J., and Blakey, D. C. (1987) New coupling agents for the synthesis of immunotoxins containing a hindered disulfide bond with improved stability in vivo. *Cancer Res.* 47, 5924-5931.
- (21) Andrew, S. M., Pimm, M. V., Perkins, A. C., and Baldwin, R. W. (1986) Comparative imaging and biodistribution studies with an anti-CEA monoclonal antibody and its F(ab')₂ and Fab fragments in mice with colon carcinoma xenografts. *Eur. J. Nucl. Med.* 12, 168-175.
- (22) Massuger, L. F. A. G., Claessens, R. A. M. J., Pak, K. Y., Boerman, O. C., Daddona, P. E., Koenders, E. B., Kenemans, P., and Corstens, F. H. M. (1991) Tissue distribution of ^{99m}Tc, ¹¹¹In and ¹²³I-OV-TL3 Fab' in ovarian carcinoma bearing nude mice. *Nucl. Med. Biol.* 18, 77-83.
- (23) Paik, C. H., Yokoyama, K., Reynolds, J. C., Quadri, S. M., Min, C. Y., Shin, S. Y., Maloney, P. J., Larson, S. M., and Reba, R. C. (1989) Reduction of background activities by introduction of a diester linkage between antibody and a chelate in radioimmunodetection of tumor. *J. Nucl. Med.* 30, 1693-1701.
- (24) Hemmila, I. (1985) Fluoroimmunoassays and immunofluorometric assays. *Clin. Chem.* 318, 359-370.
- (25) Anderson-Berg, W. T., Strand, M., Lempert, T. E., Rasenbaum, A. E., and Joseph, P. M. (1986) Nuclear magnetic resonance and gamma camera tumor imaging using Gd-labeled monoclonal antibodies. *J. Nucl. Med.* 27, 829-833.
- (26) Pimm, M. V., Perkins, A. C., Armitage, N. C., and Baldwin, R. W. (1985) The characteristics of blood-born radiolabels and the effect of anti-mouse IgG antibodies on localization of radiolabeled monoclonal antibody in cancer patients. *J. Nucl. Med.* 26, 1011-1023.

Identification and Characterization of a Nucleotide Binding Site on Recombinant Murine Granulocyte/Macrophage-Colony Stimulating Factor

Michael A. Doukas,*† Ashok J. Chavan,‡ Cecelia Gass,† Thomas Boone,§ and Boyd E. Haley†

Colleges of Medicine and Pharmacy, Lucille P. Markey Cancer Center, University of Kentucky and Veterans Affairs Medical Center, Lexington, Kentucky 40536-0093, and Amgen, Inc., Amgen Center, Thousand Oaks, California 91320. Received March 26, 1992

Granulocyte/macrophage-colony stimulating factor (GM-CSF) is a regulatory cytokine important in the proliferative and functional activation of hematopoietic cells. It belongs to a family of 20 kDa or less acidic glycoprotein molecules found in a broad range of cellular sources. On the basis of the previously reported nucleotide-binding properties of interleukin-2 (IL-2), atrial natriuretic factor (ANF), and glucagon, the interaction of GM-CSF with nucleotides was investigated. Using radiolabeled 8-azidoadenosine-containing photoprobes of ATP ($[\gamma\text{-}^{32}\text{P}]\text{-}8\text{N}_3\text{ATP}$) and Ap_4A , the putative biological alarmone ($[\beta'\text{-}^{32}\text{P}]\text{-}8\text{N}_3\text{Ap}_4\text{A}$), we have identified a nucleotide binding site on recombinant murine GM-CSF (rmGM-CSF). Specificity of binding was demonstrated by saturation and competition experiments. Saturation of photoinsertion by $[\gamma\text{-}^{32}\text{P}]\text{-}8\text{N}_3\text{ATP}$ and $[\beta'\text{-}^{32}\text{P}]\text{-}8\text{N}_3\text{Ap}_4\text{A}$ occurs with apparent K_d 's of 10 and 0.7 μM , respectively. Using an immobilized Fe^{3+} affinity chromatography technique, developed specifically for the isolation of photolabeled peptides, a single radiolabeled peptide was isolated. It was identified as amino acids 5-14 near the N-terminus of GM-CSF. This peptide region has been shown in previous studies to be critical for biological activity. Also consistent with this observation is our finding that the photolabeled GM-CSF has lost most, if not all, of its biological activity, as determined by a cellular proliferation assay.

INTRODUCTION

Granulocyte/macrophage-colony stimulating factor (GM-CSF)¹ has a broad range of proliferative, differentiating, and activating effects upon inflammatory cells and their precursors (1, 2). While original work focused primarily on neutrophils, monocytes, and their precursors, the activities of GM-CSF are now known to include effects upon the eosinophil and basophil lineages. GM-CSF *in vitro* has additive effects (to IL-5) on eosinophil colony formation (3) and in clinical trials provokes a profound eosinophilia and neutrophilia (4). This cytokine also activates the mature eosinophils and neutrophils with regard to cellular activities (2). GM-CSF also promotes basophil production in liquid culture (5). This broad range of activities for GM-CSF supports the view that this cytokine is central, or certainly contributory, to most inflammatory processes.

Receptor binding of GM-CSF appears to be mediated by at least two membrane glycoproteins (α and β) which together bind GM-CSF with high affinity and transduce a biological signal (6). On some cell lines, however, there

are only low affinity (α) GM-CSF receptors, which apparently do not transduce a signal and whose function is unclear at this time (7). Indirect evidence as to the activities of the receptors in subsequent signal-transduction events confirms the importance of protein kinase activation (8) and specifically tyrosine phosphorylation (9). While experimentation has revealed parts of the puzzle regarding receptor physiology and subsequent signal transduction, no clear view has yet emerged as to the signaling events triggered by cytokines which lead to cellular proliferation and specific gene transcription. The mature murine GM-CSF consists of a polypeptide chain of 124 amino acids with a great deal of hydrophobicity and conformational stability (10). The three-dimensional structure of GM-CSF has been predicted by molecular modeling techniques (11). The initial report on the crystal structure of the human GM-CSF indicates that it crystallizes with two molecules in the asymmetric unit (12, 13).

As an energy source for certain cellular signaling mechanisms, nucleotides are critical in the regulation of biological systems. Much of our knowledge concerning regulation of these systems comes from research utilizing analogs of the various nucleotides. Nucleotide photoaffinity probes have been very effectively used for this purpose (14, 15). A possible role for nucleotides in the mechanism of action of small peptide hormones and cytokines has been suggested by demonstration of specific nucleotide binding sites on IL-2, ANF, and glucagon. IL-2 has high affinity for ATP and NAD^+ (16), whereas ANF and glucagon has high affinity for GTP (17, 18). In the present study, utilizing the nucleotide photoaffinity probes $[\gamma\text{-}^{32}\text{P}]\text{-}8\text{N}_3\text{ATP}$ and $[\beta'\text{-}^{32}\text{P}]\text{-}8\text{N}_3\text{Ap}_4\text{A}$, we have detected, characterized, and identified a nucleotide binding site on GM-CSF. We describe the detection and specificity of binding and the identification of the peptide region of the

* Author to whom correspondence should be addressed: Hematology/Oncology Section (111-E/CDD), Veterans Affairs Medical Center, 2250 Leestown Road, Lexington, KY 40511-1093. Phone No. (606) 281-4956; Fax No. (606) 257-1020.

† College of Medicine, University of Kentucky and Veterans Affairs Medical Center.

‡ College of Pharmacy, University of Kentucky Medical Center.

§ Amgen, Inc.

¹ Abbreviations used: GM-CSF, granulocyte/macrophage colony stimulating factor; IL, interleukin; ANF, atrial natriuretic factor; $8\text{-N}_3\text{ATP}$, 8-azidoadenosine triphosphate; $8\text{-N}_3\text{GTP}$, 8-azidoguanosine triphosphate; $8\text{-N}_3\text{Ap}_4\text{A}$, 8-azidoadenosine 5',5'''- P_1P_4 -tetrakisphosphate adenosine; SDS-PAGE, sodium dodecyl sulfate polyacrylamide gel electrophoresis; CBB, Coomassie Brilliant Blue; TNF, tumor necrosis factor.

GM-CSF molecule which is involved in nucleotide binding. The specificity and very low concentrations at which nucleotide binding occurs, and the loss of biological activity of GM-CSF with covalently attached nucleotide, indicate a possible physiological role for these novel interactions.

EXPERIMENTAL PROCEDURES

Materials. rmGM-CSF (*Escherichia coli* derived) was kindly provided by Amgen, Inc., and was >95% pure by SDS-PAGE and reverse-phase HPLC analysis. Protein molecular weight standards were obtained from Bio-Rad. All other reagents were analytical grade and obtained from Sigma or Aldrich. $\text{H}_3^{32}\text{PO}_4$ was from ICN.

Synthesis of Nucleotide Photoaffinity Probes. $[\gamma\text{-}^{32}\text{P}]\text{-}8\text{N}_3\text{ATP}$ and $[\gamma\text{-}^{32}\text{P}]\text{-}8\text{N}_3\text{GTP}$ (5–30 mCi/ μmol) were synthesized using the previously published procedures (14, 19). $[\beta'\text{-}^{32}\text{P}]\text{-}8\text{N}_3\text{Ap}_4\text{A}$ (5–15 mCi/ μmol) was synthesized as described elsewhere (20).

Photolabeling of rmGM-CSF. Samples containing 0.2 μg of rmGM-CSF in 40–60 μL of photolysis buffer (20 mM NaH_2PO_4 , pH 4.5) were incubated at 4 °C in Eppendorf tubes with photoprobe for 15 s, followed by a 45-s irradiation at 4 °C with a hand-held 254-nm UV lamp (intensity = 7200 $\mu\text{W}/\text{cm}^2$). The reaction was quenched by addition of a protein-solubilizing mixture consisting of 10% SDS, 3.6 M urea, 162 mM dithiothreitol, pyronin Y (tracking dye), and 20 mM Tris (pH 8.0). For protection studies, rmGM-CSF was first incubated for 60 s at 4 °C with the competitor, followed by incubation with photoprobe for 15 s at 4 °C and photolysis for 45 s at 4 °C. For the multiple photolysis experiments, 0.2 μg of rmGM-CSF was incubated sequentially with either 16.7, 12.5, and 10 μM $[\beta'\text{-}^{32}\text{P}]\text{-}8\text{N}_3\text{Ap}_4\text{A}$ or 167, 125, and 100 μM $[\gamma\text{-}^{32}\text{P}]\text{-}8\text{N}_3\text{ATP}$ for 15 s each at 4 °C and photolyzed for 45 s between each sequential addition of the probe at 4 °C. The samples photolyzed once, twice, and three times were analyzed separately by SDS-PAGE to determine the percent photoincorporation after each step. The percent modification of cytokine was calculated by converting the cpm in gel pieces to mCi. Then, by making use of specific activity of the probe used, picomole of probe present with cytokine in the gel piece was calculated. Knowing the picomole of cytokine used for the experiment and assuming a single binding site on each cytokine molecule, the ratio of picomole of probe to picomole of cytokine afforded the percent modification.

SDS-Polyacrylamide Gel Electrophoresis. Solubilized protein samples were subjected to electrophoresis in a 10% polyacrylamide separating gel with a 4% stacking gel according to the method of Laemmli (21). Gels were either stained with Coomassie Brilliant Blue R, destained overnight, and dried on a slab gel dryer or fixed and dried without staining. Gels were subjected to autoradiography and ^{32}P incorporation was quantified by excision of the labeled protein bands and liquid scintillation counting utilizing a Packard Minaxi or Tri-Carb scintillation counter (counting efficiency, 99% for ^{32}P).

Isolation of the Photolabeled Tryptic Peptides of rmGM-CSF Photolabeled with $[\beta'\text{-}^{32}\text{P}]\text{-}8\text{N}_3\text{Ap}_4\text{A}$. (a) *Photolabeling and Trypsin Digestion.* Two hundred micrograms of rmGM-CSF was incubated with photoprobe (cytokine to probe ratio of 1:5, sp act. = 3.9 mCi/ μmol) for 45 s at 4 °C and photolyzed for 90 s at 4 °C. This was followed by a second incubation with nonradioactive photoprobe (cytokine to probe ratio of 1:5) for 45 s at 4 °C and photolysis for 90 s at 4 °C. The cytokine was precipitated by adding an equal volume of ice-cold 7%

perchloric acid. Trypsin digestion was done according to a procedure described elsewhere (22). The photolabeled cytokine was carboxamidomethylated on cysteine residues with iodoacetamide and then digested with modified trypsin (5% w/w and 5% w/w after 3 h) for 18 h at 37 °C.

(b) *Immobilized Fe^{3+} Affinity Chromatography.* In a plastic column 300 μL of resin, iminodiacetic acid-epoxy activated Sepharose 6B fast flow (Sigma), was washed successively with 10 mL of water, 10 mL of 50 mM ferric chloride, 20 mL of water, 15 mL of buffer A (100 mM ammonium acetate, pH 8.0), 10 mL of buffer A containing 0.5 M NaCl, 10 mL of buffer A, 10 mL of buffer A containing 4 M urea, and 10 mL of buffer A. The tryptic digest from part (a) above was diluted with buffer A and passed through the resin very slowly. More than 90% of the radioactivity was retained on the resin. The resin was then successively washed with 15 mL of buffer A, 10 mL of buffer A containing 0.5 M NaCl, 10 mL of buffer A, 10 mL of buffer A containing 4 M urea, and 10 mL of buffer A. Finally the photolabeled peptides were eluted with 10 mL of buffer A containing 5 mM K_2HPO_4 . During washings 1.5-mL fractions were collected and assayed for radioactivity. Greater than 90% of the radioactivity was eluted with the phosphate wash. About 5% eluted with the other washes.

(c) *Reverse-Phase High-Performance Liquid Chromatography of Photolabeled Peptides.* The fractions containing radioactivity from the metal affinity chromatography were pooled, concentrated, and analyzed by reverse-phase HPLC using an Aquapore RP-300 C8 column (220 \times 4.6 mm, Brownlee Labs). Absorbance was monitored using a diode-array spectral detector. The gradient used was 0.1% TFA at 0 min, 0.1% TFA at 5 min, 0.1% TFA in 70% acetonitrile at 65 min at 0.5 mL/min, and 0.5-mL fractions were collected. The fractions were assayed for radioactivity. The fractions containing radioactivity and indicating UV absorbance at 214 nm were subjected to amino acid sequence analysis using Applied Biosystems 477A pulse liquid protein sequencer with on-line PTH identification at the University of Kentucky Macromolecular Sequencing Facility.

Isolation of the Photolabeled Tryptic Peptide of rmGM-CSF Photolabeled with $[\gamma\text{-}^{32}\text{P}]\text{-}8\text{N}_3\text{ATP}$. The procedure described above for the isolation of photolabeled peptide was followed for 150 μg of rmGM-CSF which was photolabeled twice with $[\gamma\text{-}^{32}\text{P}]\text{-}8\text{N}_3\text{ATP}$ as described earlier (cytokine to probe ratio of 1:5, sp act. = 8.0 mCi/ μmol).

Bioassay. The $8\text{-N}_3\text{Ap}_4\text{A}$ photolabeled rmGM-CSF samples were prepared by incubating 5 μg of cytokine with 16.5 μM probe for 45 s at 4 °C and then photolyzing for 90 s at 4 °C. This was followed by two more additions of 12.5 and 10 μM probe and photolysis. The control sample was photolyzed for 4.5 min before the probe was added in three additions of 16.5, 12.5, and 10 μM , respectively.

FDCEP-1D cells were seeded (1×10^4 /well) into 96 well microtiter plates which contained rmGM-CSF standards or photolabeled samples in 1:2 serial dilutions starting at 200 ng/mL. The assay mixture in a final volume of 200 μL /well was then incubated for 48 h at 37 °C in a 5% CO_2 humidified incubator and pulsed with $[\text{H}^3]\text{thymidine}$ (1 μCi /well) for the final 4 h. The contents of the wells were harvested onto glass-fiber filters and $[\text{H}^3]\text{thymidine}$ incorporated into DNA was determined.

Digestion of the Photolabeled and Nonphotolabeled rmGM-CSF with Trypsin and Chymotrypsin. Two micrograms of the cytokine were photolabeled with 1 μM $[\beta'\text{-}^{32}\text{P}]\text{-}8\text{N}_3\text{Ap}_4\text{A}$. To this was added 5% w/w trypsin or chymotrypsin followed by incubation at room temperature

Table I. Effect of pH on the Photoincorporation of the Photoprobe into rmGM-CSF

pH	% ³² P incorp ^a		pH	% ³² P incorp ^a	
	[β'- ³² P]-8N ₃ Ap ₄ A	[γ- ³² P]-8N ₃ ATP		[β'- ³² P]-8N ₃ Ap ₄ A	[γ- ³² P]-8N ₃ ATP
4.0	94 ± 6	87 ± 8	6.5	39 ± 7	60 ± 5
4.5	100	100	7.0	30 ± 1	67 ± 8
5.0	91 ± 7	92 ± 6	7.5	20 ± 9	60 ± 9
5.5	65 ± 2	92 ± 4	8.0	11 ± 3	51 ± 12
6.0	49 ± 1	52 ± 1	8.5	8 ± 3	51 ± 9

^a Mean ± SEM of two experiments.

for 1 h. Two micrograms of the nonphotolabeled cytokine was also treated with trypsin or chymotrypsin in an identical fashion. The proteolyzed samples were separated by 12% SDS-PAGE. The gel was dried on a transparent cellophane sheet. Autoradiography exposure was for 12 h. The CBB-stained protein bands from the gel and the autoradiogram were quantified by LKB 2202 Ultrosan laser densitometer.

Boronate Affinity Chromatography. rmGM-CSF (50 μg) was photolabeled sequentially three times with [β'-³²P]-8N₃Ap₄A as described earlier. The unbound nucleotide was removed by gel filtration on G-25. The photolabeled cytokine was applied to 3 mL of Affi-Gel 601 (Bio-Rad) equilibrated with 250 mM ammonium acetate, pH 8.8, and purified as described elsewhere (23). The equivalent amounts of cytokine present in unbound fractions (fractions 2–5 pooled) and bound fractions (fractions 41–49 pooled) in Figure 8A were determined by reverse-phase HPLC analysis and assayed for biological activity using [³H]thymidine uptake assay as described elsewhere in this paper.

RESULTS

Characterization of Nucleotide Binding and Specificity. In order to investigate the nucleotide binding properties of rmGM-CSF, it was photolabeled with the nucleotide photoaffinity probes [γ-³²P]-8N₃ATP, [γ-³²P]-8N₃GTP, and [β'-³²P]-8N₃Ap₄A. The latter is an analog of Ap₄A, the putative biological alarmone. The photolabeling was optimized for pH, buffer, temperature, preincubation time, and time of photolysis. Although significant labeling was observed over a wide pH range, the optimum photolabeling in 20 mM NaH₂PO₄ buffer was at pH 4.5 (Table I). At pH values above 4.5 the photoincorporation of [β'-³²P]-8N₃Ap₄A was greatly reduced whereas that with [γ-³²P]-8N₃ATP was not greatly affected and seemed to have leveled off at pH 7.0. The photolabeling was optimized for preincubation time and time of photolysis. rmGM-CSF exhibited rapid binding in that a short preincubation time of 15 s and photolysis for 45 s at 4 °C seemed to give maximum photolabeling (data not shown).

The UV light did not have any major effect on rmGM-CSF. Pre-exposure to UV light for up to 2.5 min and subsequent photolabeling yielded photoincorporation similar to the control labeling (data not shown). Also, prephotolysis did not affect biological activity (data not shown). Photoincorporation was dependent upon UV light since in the absence of light less than 0.2% ³²P incorporation was observed as compared to control (data not shown). This also proves the absence of phosphorylation under these conditions. A 45-s photolysis of the probe prior to the immediate addition of rmGM-CSF resulted in less than 1% of labeling compared to control (data not shown). This indicated the absence of pseudoaffinity labeling that may result due to any long-lived chemically

Table II. Effect of Various Divalent Metal Ions and Metal Ion Chelators on [β'-³²P]-8N₃Ap₄A Photoincorporation into rmGM-CSF

metal ion/ chelator at 2 mM	% ³² P incorp ^a	metal ion/ chelator at 2 mM	% ³² P incorp ^a
control	100	CoCl ₂	58 ± 13
MgCl ₂	112 ± 20	CuCl ₂	37 ± 14
MnCl ₂	72 ± 9	EDTA	119 ± 23
CaCl ₂	107 ± 19	EGTA	65 ± 21
ZnCl ₂	71 ± 4		

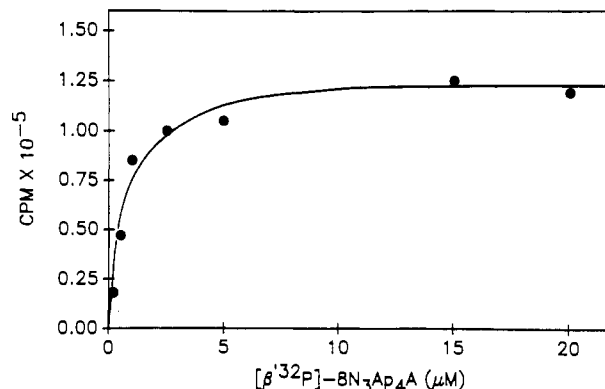
^a Mean ± SEM of four experiments.

Figure 1. Saturation of [β'-³²P]-8N₃Ap₄A photoincorporation into rmGM-CSF: rmGM-CSF (0.2 μg) in 40 μL of photolysis buffer was incubated with increasing concentrations of the photoprobe (sp act. = 10.9 mCi/μmol) for 15 s at 4 °C, photolyzed for 45 s at 4 °C, and subjected to 10% SDS-PAGE analysis and autoradiography. ³²P incorporation was quantified by cutting out appropriate protein bands and determining radioactivity by liquid scintillation counting. The result shown is representative of two trials.

reactive intermediate generated by photolysis and rearrangement of the nitrene.

The effect of various metal ions and chelators on [β'-³²P]-8N₃Ap₄A photolabeling is summarized in Table II. Mg²⁺ and Ca²⁺ increased the photoincorporation to a small extent whereas Mn²⁺, Zn²⁺, Co²⁺, and Cu²⁺ decreased it to varying degrees. EDTA increased the photoincorporation whereas EGTA decreased it. The concentration of metal ions present in the rmGM-CSF supplied was not determined.

To show the specificity of nucleotide interaction, the photolabeling should be saturable and protected by the parent compound at physiologically relevant concentrations. In the case of [β'-³²P]-8N₃Ap₄A the saturation of labeling was achieved at approximately 10 μM concentration with an apparent K_d of approximately 0.7 μM (Figure 1). At a saturating concentration of 8-N₃Ap₄A (15 μM), a minimum of 39 ± 5% of the cytokine was modified.

Protection studies with a wide variety of nucleotides at 100 μM concentration showed that the best competitor for 8-N₃Ap₄A binding and photoincorporation was Ap₄A (Table III). When rmGM-CSF was photolabeled with 0.7 μM [β'-³²P]-8N₃Ap₄A in the presence of increasing concentrations of Ap₄A, close to 90% protection of photolabeling was achieved at 200 μM Ap₄A with half-maximal protection at 30 μM concentration (Figure 2).

Weak protection against [β'-³²P]-8N₃Ap₄A photoincorporation by triphosphosphate and pyrophosphate was also noted with half-maximal protection occurring at approximately 100 μM (data not shown), indicating a role for a polyphosphate moiety in the binding site. This was confirmed by the sequential reduction of the inhibitory effect of adenosine nucleotides with fewer phosphate

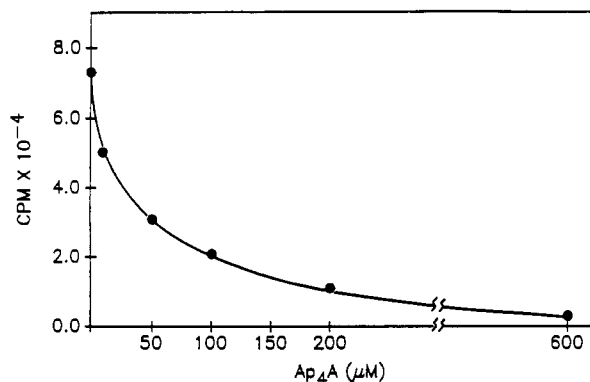


Figure 2. Protection of $[\beta'\text{-}^{32}\text{P}]\text{-}8\text{N}_3\text{Ap}_4\text{A}$ photoincorporation into rmGM-CSF by Ap_4A : rmGM-CSF ($0.2\text{ }\mu\text{g}$) was incubated in photolysis buffer with indicated concentrations of Ap_4A for 60 s at 4°C then with $0.7\text{ }\mu\text{M}$ of the photoprobe (sp act. = $11.0\text{ mCi}/\mu\text{mol}$) for 15 s and photolyzed. SDS-PAGE analysis and determination of ^{32}P incorporation was done as in Figure 1. The result shown is representative of three trials.

Table III. Protection of $0.7\text{ }\mu\text{M}$ $[\beta'\text{-}^{32}\text{P}]\text{-}8\text{N}_3\text{Ap}_4\text{A}$ Photoincorporation into rmGM-CSF by Various Competitors

competitor at $100\text{ }\mu\text{M}$	% ^{32}P incorp ^a	competitor at $100\text{ }\mu\text{M}$	% ^{32}P incorp ^a
no competitor	100	GTP	73 ± 16
Ap_4A	40 ± 9	NAD ⁺	78 ± 17
ATP	65 ± 4	CTP	93 ± 10
ADP	86 ± 10	UTP	87 ± 8
AMP	100 ± 14	TTP	85 ± 10
adenosine	94 ± 6		

^a Mean \pm SEM of three experiments.

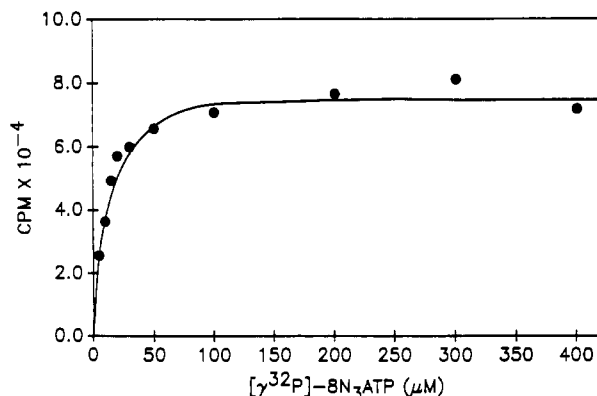


Figure 3. Saturation of $[\gamma\text{-}^{32}\text{P}]\text{-}8\text{N}_3\text{ATP}$ photoincorporation into rmGM-CSF: rmGM-CSF ($0.2\text{ }\mu\text{g}$) in $40\text{ }\mu\text{L}$ of photolysis buffer was incubated with increasing concentrations of photoprobe (sp act. = $5.3\text{ mCi}/\mu\text{mol}$) for 15 s at 4°C and photolyzed for 45 s at 4°C . SDS-PAGE analysis and determination of ^{32}P incorporation was done as in Figure 1. The result shown is representative of two trials.

groups (Table III). Additionally, a comparison of the protective effect on $[\beta'\text{-}^{32}\text{P}]\text{-}8\text{N}_3\text{Ap}_4\text{A}$ photoinsertion by Ap_3A , Ap_4A , and Ap_5A at $100\text{ }\mu\text{M}$ levels indicated that the polytetraphosphate gave a maximum protective effect. Ap_3A decreased $[\beta'\text{-}^{32}\text{P}]\text{-}8\text{N}_3\text{Ap}_4\text{A}$ photoinsertion by 50% while Ap_4A and Ap_5A both gave a 75% decrease (data not shown).

With $[\gamma\text{-}^{32}\text{P}]\text{-}8\text{N}_3\text{ATP}$, saturation of labeling was achieved at approximately $100\text{ }\mu\text{M}$ concentration with an apparent K_d of $10\text{ }\mu\text{M}$ (Figure 3). At the saturation concentration of $100\text{ }\mu\text{M}$, $43 \pm 5\%$ of the cytokine was modified.

When rmGM-CSF was photolabeled with $20\text{ }\mu\text{M}$ $[\gamma\text{-}^{32}\text{P}]\text{-}8\text{N}_3\text{ATP}$ in the presence of increasing concentrations of ATP, 70% of the photoincorporation was protected by

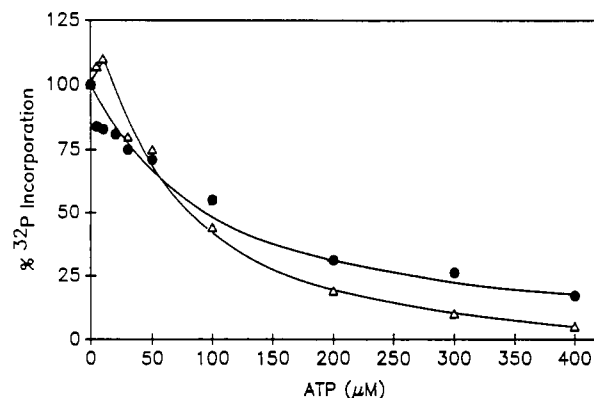


Figure 4. Protection of $[\gamma\text{-}^{32}\text{P}]\text{-}8\text{N}_3\text{ATP}$ photoincorporation into rmGM-CSF by ATP: rmGM-CSF ($0.2\text{ }\mu\text{g}$) in $40\text{ }\mu\text{L}$ of photolysis buffer was incubated with indicated concentrations of ATP for 60 s at 4°C and then with either $2.0\text{ }\mu\text{M}$ photoprobe (Δ) or $20\text{ }\mu\text{M}$ photoprobe (\bullet) (sp act. = $17.6\text{ mCi}/\mu\text{mol}$) for 15 s at 4°C and photolyzed for 45 s at 4°C . SDS-PAGE analysis and determination of ^{32}P incorporation was done as in Figure 1. The result shown is representative of four trials.

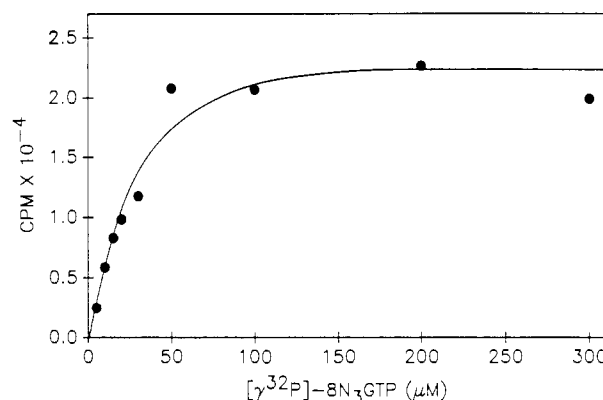


Figure 5. Saturation of $[\gamma\text{-}^{32}\text{P}]\text{-}8\text{N}_3\text{GTP}$ photoincorporation into rmGM-CSF: rmGM-CSF ($0.2\text{ }\mu\text{g}$) in $40\text{ }\mu\text{L}$ of photolysis buffer was incubated with increasing concentrations of photoprobe (sp act. = $12.8\text{ mCi}/\mu\text{mol}$) for 15 s at 4°C , photolyzed for 45 s at 4°C , and subjected to SDS-PAGE analysis and autoradiography. ^{32}P incorporation was quantified as in Figure 1. The result shown is representative of two trials.

$200\text{ }\mu\text{M}$ ATP with half-maximal protection being achieved at approximately $100\text{ }\mu\text{M}$ ATP (Figure 4). When this protection experiment was repeated with $2\text{ }\mu\text{M}$ $[\gamma\text{-}^{32}\text{P}]\text{-}8\text{N}_3\text{ATP}$, which is well below the saturation concentration, a reproducible increase of $16 \pm 7\%$ in photoincorporation was observed at $10\text{--}15\text{ }\mu\text{M}$ ATP in each of four experiments (Figure 4). This indicates a possible cooperative allosteric effect involving higher order ligand-protein interactions.

To increase the level of photoinsertion, rmGM-CSF was photolabeled in three sequential steps as described in the experimental procedures. With $[\gamma\text{-}^{32}\text{P}]\text{-}8\text{N}_3\text{ATP}$, sequential photolyses with 167 , 125 , and $100\text{ }\mu\text{M}$ probe resulted in 38% , 58% , and 60% total modification of the cytokine after one, two, and three photolysis events, respectively. With $[\beta'\text{-}^{32}\text{P}]\text{-}8\text{N}_3\text{Ap}_4\text{A}$, sequential photolyses with 16.7 , 12.5 , and $10\text{ }\mu\text{M}$ probe resulted in 38% , 41% , and 44% total modification of the cytokine, respectively (data not shown).

rmGM-CSF was also photolabeled with $[\gamma\text{-}^{32}\text{P}]\text{-}8\text{N}_3\text{GTP}$. The labeling was determined to be similar to that with $8\text{-N}_3\text{ATP}$. The photolabeling was saturable at approximately $100\text{--}125\text{ }\mu\text{M}$ with an apparent K_d of $25\text{--}30\text{ }\mu\text{M}$ (Figure 5). GTP and ATP protected $8\text{-N}_3\text{GTP}$ photoinsertion to the same extent (data not shown).

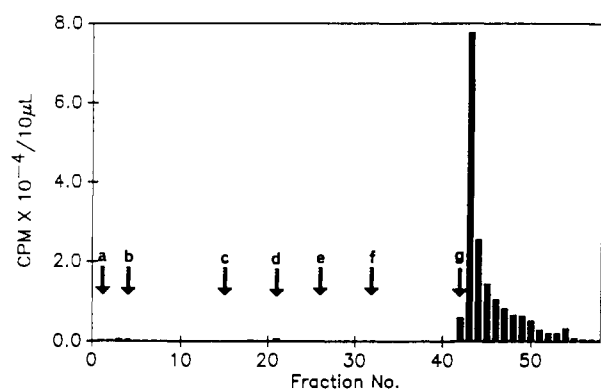


Figure 6. Radioactivity elution profile for Fe^{3+} affinity chromatography of tryptic digest of rmGM-CSF photolabeled with [β - ^{32}P]-8N $_3$ Ap $_4$ A: 200 μg of rmGM-CSF was photolabeled with the photoprobe, digested with trypsin, and loaded onto a 300- μL Fe^{3+} affinity column as described in Experimental Procedures. (a) Tryptic digest loaded, washed with (b) buffer A, (c) buffer A containing 0.5 M NaCl, (d) buffer A, (e) buffer A containing 4 M urea, (f) buffer A, and (g) buffer A containing 5 mM K_2HPO_4 . The fractions collected (1.5 mL) were assayed for radioactivity by liquid scintillation counting.

Table IV. Resistance of Photolabeled rmGM-CSF to Trypsin and Chymotrypsin Digestion

		% remaining			
		trypsin		chymotrypsin	
		0 h	1 h	0 h	1 h
nonphotolyzed	protein	100	22	100	6
photolyzed	protein	100	19	100	3
	cpm	100	60	100	23

Proteolysis of Photolabeled rmGM-CSF. The photolabeled rmGM-CSF was more resistant to proteolysis with trypsin and chymotrypsin than the unmodified material (Table IV). With trypsin, while only 19% of CBB-stained protein band remained, 60% of the radioactivity was still undigested after 1 h. With chymotrypsin, 3% of the CBB-stained protein band remained whereas 23% of radioactivity remained. All of our studies, including those done under denaturing conditions, indicated that proteolysis of photolabeled rmGM-CSF took longer than expected when compared to the nonphotolabeled material. We were able to digest the photolabeled protein with protease K. However, this resulted in a complex mixture of peptides which could not be easily resolved and was not used to identify the photolabeled peptide. We observed that carboxamidomethylation of rmGM-CSF cysteine residues, followed by prolonged digestion with a more active modified trypsin (Promega), proved to be the most successful procedure for generating small peptides.

Immobilized Metal Affinity Chromatography. The use of immobilized Fe^{3+} affinity chromatography was recently developed in our laboratory to isolate photolabeled peptides (20). When the tryptic digest of the photolabeled rmGM-CSF was passed through the Fe^{3+} affinity column, the bulk of the tryptic peptides were in the flow through (Figure 7A). However, greater than 90% of the radioactivity was retained on the column (Figure 6). To elute any peptides bound to the resin other than through phosphate- Fe^{3+} interaction, the column was washed with 100 mM ammonium acetate containing salt (0.5 M NaCl) and 4 M urea. These washes resulted in elution of less than 5% of the eluted radioactivity. However, when these washes were analyzed by reverse-phase HPLC, the presence of nonlabeled peptides was observed (data not shown). The photolabeled peptides were eluted with a 5 mM potassium phosphate wash as indicated by the elution of

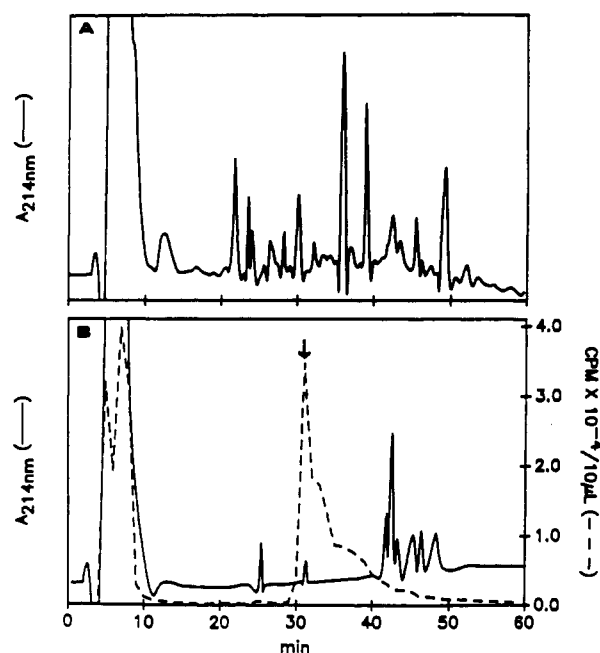


Figure 7. Reverse-phase HPLC analysis of fractions collected from Fe^{3+} affinity chromatography: (A) UV elution profile of reverse-phase HPLC analysis of flow-through fractions 1–10 from Figure 6, and (B) UV and radioactivity elution profile of reverse-phase HPLC analysis of fractions 42–46 from Figure 6 as described in experimental procedures. The peak indicated by the arrow was subjected to amino acid sequence analysis.

Table V. Amino Acid Sequence Analysis of the Photolabeled Tryptic Peptides of rmGM-CSF

cycle no.	amino acid no.	amino acid (pmol)	
		8-N $_3$ Ap $_4$ A	8-N $_3$ ATP
1	5	S (21)	S (16)
2	6	P (24)	P (14)
3	7	I (29)	I (20)
4	8	T (17)	T (12)
5	9	V (17)	V (16)
6	10	T (15)	T (12)
7	11	R (8)	R (7)
8	12	P (4)	P (4)
9	13	W (ND) ^a	W (ND) ^a
10	14	K (5)	K (5)

^a ND, picomole not determined.

radioactivity (Figure 6). The radioactivity obtained in the phosphate wash represented approximately 90% of the eluted radioactivity and 30–50% of the loaded radioactivity.

When the phosphate wash from the Fe^{3+} affinity column was analyzed by reverse-phase HPLC, as described in the Experimental Procedures, two radioactive peaks containing approximately 50% each of the total radioactivity were obtained (Figure 7B). The first peak, which was in the flow through volumes, did not contain any peptide. The second peak which eluted at 31 min, was subjected to amino acid sequence analysis and gave data consistent for a peptide corresponding to residues 5–14 (SPITVTRPWK) located near the N-terminus of rmGM-CSF (Table V). Approximately 5–15% of the loaded radioactivity eluted with the peptide. The site of modification could not be determined with certainty. Based on the picomole recovery, the site of modification may be on the residue number 12, proline. The picomole recovery of tryptophan residue could not be determined since diphenylurea coeluted with it during sequencing. Picomole recovery of peptide upon sequence analysis was in excess of 70% of

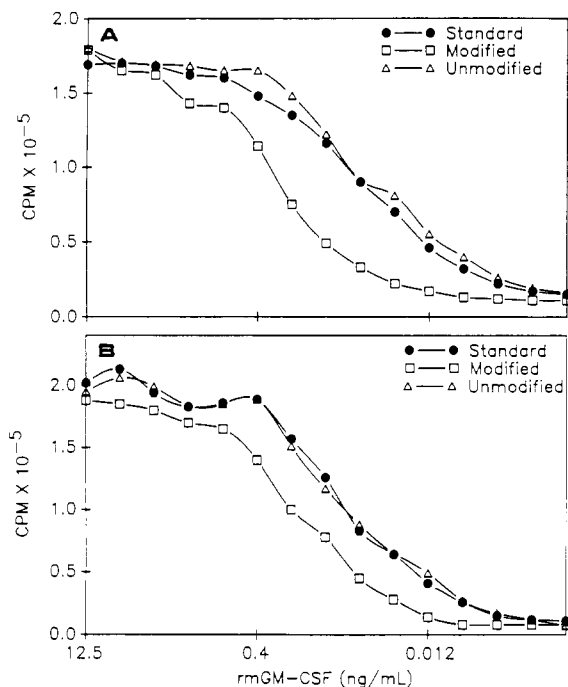


Figure 8. Bioassay of the rmGM-CSF photolabeled with (A) 8- N_3 ATP and (B) 8- N_3 Ap $_4$ A: 5 μ g of rmGM-CSF was photolabeled with the photoprobe and assayed for biological activity using [3 H]thymidine uptake assay as described in Experimental Procedures; (●) standard rmGM-CSF, (□) rmGM-CSF photolabeled with the photoprobe, (Δ) rmGM-CSF photolyzed in the absence of photoprobe and then photoprobe added to it. Each point is mean of three observations.

that used for sequencing based on the specific activity of the photoprobe used.

In one experiment two radioactive peaks with corresponding peptides were obtained during HPLC. Besides the peak at 31 min, indicated in Figure 7B, the second was obtained at 36 min. Amino acid sequence analysis revealed it to be a longer version of the peptide obtained at 31 min (i.e. residues 5–20, SPITVTRPWKHVEAIK). The other UV-absorbing peaks eluting after 40 min in Figure 7B were either due to some peptides being nonspecifically adsorbed or some non-peptide UV-absorbing material being eluted from the resin in the phosphate wash. This was confirmed since these peaks were also present in a control experiment where rmGM-CSF was photolyzed in the absence of probe. Additionally the peak at 31 min in Figure 7B which was due to the photolabeled peptide was absent in the control experiment. This provided additional evidence for the peptide sequenced being the photolabeled peptide.

When this peptide isolation procedure was repeated using [γ - 32 P]-8- N_3 ATP, the same peptide consisting of residues 5–14 was isolated (Table V), indicating that both the probes were binding to the same domain.

Bioassay of Photolabeled rmGM-CSF. The initial cell proliferation bioassays were conducted on the rmGM-CSF photolabeled sequentially three times with 8- N_3 Ap $_4$ A and 8- N_3 ATP as described in the Experimental Procedures, without removing the unbound nucleotide, since we could photomodify it over 40%. The assays indicated that the photolabeled rmGM-CSF was much less active than the control. In the case of 8- N_3 ATP, the half-maximal cell proliferation, or unit activity, for the photolabeled sample was obtained at approximately 0.3 ng/mL compared to 0.04 ng/mL for the control reflecting a difference of approximately 3.5 dilutions, which would be equivalent to approximately 85% modification of the cytokine (Figure

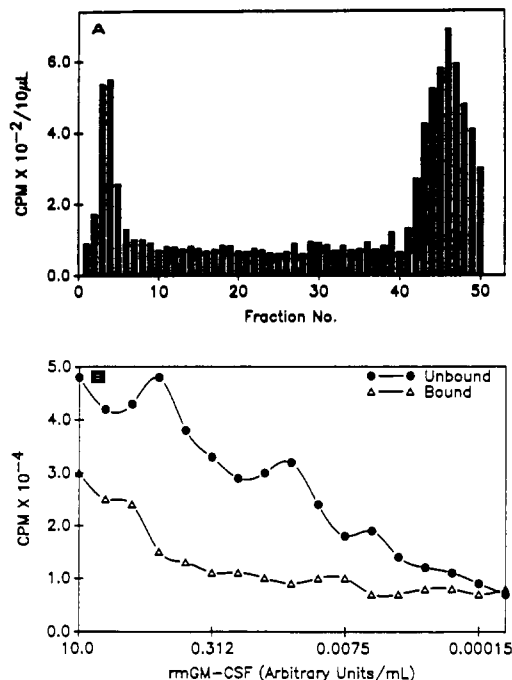


Figure 9. (A) Separation of photolabeled rmGM-CSF from nonphotolabeled rmGM-CSF using boronate affinity chromatography: rmGM-CSF (50 μ g) was photolabeled sequentially three times with [β' - 32 P]-8- N_3 Ap $_4$ A and purified on Affi-Gel 601 as described in Experimental Procedures. (B) Bioassay of rmGM-CSF purified by boronate affinity chromatography: Biological activity of rmGM-CSF present in unbound fractions (fractions 2–5 pooled) and bound fractions (fractions 41–49 pooled) from boronate affinity chromatography was determined by [3 H]thymidine uptake assay as described in the Experimental Procedures. Each point is mean of three observations.

8A). The covalent linkage of the photoprobe was essential for this inactivation since rmGM-CSF containing non-photolyzed probe did not show this effect. When the bioassay was conducted with rmGM-CSF photolabeled sequentially three times with 8- N_3 Ap $_4$ A, the unit activity indicated a difference of approximately 1.5 dilutions, which would be equivalent to approximately 65% modification of the cytokine (Figure 8B).

To confirm that photolabeling inactivated rmGM-CSF, 50 μ g of the cytokine was photolabeled sequentially three times with [β' - 32 P]-8- N_3 Ap $_4$ A and the unbound nucleotide was removed by gel filtration on G-25. Taking advantage of the two ribose rings present on Ap $_4$ A, the photolabeled rmGM-CSF was separated from the nonphotolabeled rmGM-CSF by boronate affinity chromatography on Affi-Gel 601 as described in the Experimental Procedures. Since the recovery of rmGM-CSF from the boronate affinity resin was low, the equivalent amount of cytokine present in unbound and bound fractions (Figure 9A) was determined by reverse-phase HPLC analysis (data not shown). The nonphotolabeled rmGM-CSF was in the flow through (unbound, fractions 2–5 pooled) whereas the photolabeled cytokine stayed attached until released by a pH change (bound, fractions 41–49 pooled). The unbound fractions contained most of the nonphotolabeled rmGM-CSF, whereas the bound fractions, which contained most of the radioactivity and hence most of the photolabeled cytokine showed a difference in unit biological activity of approximately six dilutions as shown in Figure 9B.

DISCUSSION

Many cytokines and growth factors such as GM-CSF are of appreciable molecular weight, greater than that

which might be expected to be necessary for receptor interaction alone. On the basis of the observation that IL-2 (16), ANF (17), and glucagon (18) possessed specific nucleotide binding sites, we decided to study the possible nucleotide binding properties of the growth factor GM-CSF.

To show the specificity of a nucleotide binding site using photoaffinity probes the photolabeling should be saturable and be protected by the natural compound at physiologically relevant concentrations. rmGM-CSF was initially photolabeled with $[\gamma\text{-}^{32}\text{P}]\text{-}8\text{-N}_3\text{ATP}$ and $[\gamma\text{-}^{32}\text{P}]\text{-}8\text{-N}_3\text{GTP}$. Photolabeling with $[\gamma\text{-}^{32}\text{P}]\text{-}8\text{-N}_3\text{ATP}$ was saturable at approximately 100 μM with an apparent K_d of 10 μM . In the presence of increasing concentrations of ATP, 70% of the photolabeling with 20 μM $[\gamma\text{-}^{32}\text{P}]\text{-}8\text{-N}_3\text{ATP}$ was protected by 200 μM ATP with half-maximal protection being achieved at approximately 100 μM ATP.

Photolabeling with $[\gamma\text{-}^{32}\text{P}]\text{-}8\text{-N}_3\text{GTP}$ was saturable at approximately 100–125 μM with an apparent K_d of 25–30 μM . GTP at a concentration of 500 μM afforded approximately 90% protection of 10 μM $[\gamma\text{-}^{32}\text{P}]\text{-}8\text{-N}_3\text{GTP}$ photolabeling. Overall, GTP exhibited similar affinity. NAD^+ was a poor protector of either 8- N_3ATP or 8- N_3GTP photolabeling, indicating a different kind of nucleotide binding site compared to IL-2 (affinity for both ATP and NAD^+) and ANF and glucagon (affinity specific for GTP).

The photoincorporation with these probes was light dependent, indicating the absence of phosphorylation. Photolysis of the probe prior to incubation with protein resulted in less than 2% of photoincorporation compared to control, indicating the absence of pseudoaffinity labeling resulting from any long-lived chemically reactive intermediate.

To obtain binding site peptide purification and to develop a procedure for purifying the photolabeled GM-CSF from the nonphotolabeled GM-CSF we photolabeled rmGM-CSF with $[\beta\text{-}^{32}\text{P}]\text{-}8\text{-N}_3\text{Ap}_4\text{A}$. It is a photoaffinity probe of a biological stress-related nucleotide Ap_4A (24). This dinucleotide binds boronate affinity resin by virtue of two ribose rings possessing *cis*-hydroxyl groups as in the case of NAD^+ (23 and references therein). The lower apparent K_d value of 0.7 μM and saturation at 10 μM obtained for this analog compared to $[\gamma\text{-}^{32}\text{P}]\text{-}8\text{-N}_3\text{ATP}$ prompted us to study the binding properties with 8- $\text{N}_3\text{-Ap}_4\text{A}$ in detail. Protection experiments indicated that 90% of the photolabeling was protected by approximately 200 μM Ap_4A with half-maximal protection at approximately 30 μM Ap_4A . Protection of 8- $\text{N}_3\text{Ap}_4\text{A}$ photolabeling with other nucleotides indicated decreased protection in the order of ATP, ADP, AMP, and adenosine. In addition, tripolyphosphate and pyrophosphate also afforded 50% protection at 100 μM concentration, indicating that the phosphate binding region is also contributing to the specificity of this nucleotide binding domain.

The divalent metal ions did not show any significant effect on photolabeling. Mn^{2+} , Zn^{2+} , Co^{2+} , and Cu^{2+} showed an inhibitory effect on photoinsertion. Photoincorporation increased 7% in the presence of Ca^{2+} and decreased 35% in the presence of EGTA.

When rmGM-CSF was photolabeled with 2 μM $[\gamma\text{-}^{32}\text{P}]\text{-}8\text{-N}_3\text{ATP}$, which is below the saturation concentration, an increase in photoincorporation was observed at low (10–15 μM) concentrations of competing ATP. This could be interpreted as cooperative binding as observed with multisubunit enzymes (25). GM-CSF is a monomeric protein (1), and no data on higher order (quaternary) structures in solution are known to us. However, in preliminary crystal structure work on hGM-CSF, crys-

tallization occurs with two molecules in the asymmetric unit (12, 13). The possibility of higher order structures of GM-CSF molecules in solution could explain what appears to be a cooperative effect of 8- N_3ATP binding with the addition of low concentrations of ATP. GM-CSF may be like IL-6 and TNF where dimers and trimers are apparently the dominant forms in solution (26, 27).

When the photolabeled rmGM-CSF was subjected to proteolysis for the purpose of generating small peptides, it exhibited considerable resistance compared to nonphotolabeled samples. This has also been observed in our study of nucleotide binding properties of other cytokines (unpublished results). Standard trypsin and chymotrypsin were unsuccessful in digesting the photolabeled rmGM-CSF to an appreciable extent. The covalently attached nucleotide appears to interfere with the digestion procedure. This result may be indicative of a possible protective role for nucleotide interaction *in vivo*. Use of a more active, modified trypsin (Promega) achieved success in generating small peptides.

The problems encountered in isolating photolabeled peptides, especially with reverse-phase HPLC are well-described (28). The problems stem either from lability of the photoinserted bond and/or the lability of N-glycosidic bond to HPLC. Also, the phosphates which carry the radioactive tag may be lost during the purification procedure.

To overcome these problems, recent efforts in this laboratory have concentrated on using a mild purification procedure prior to reverse-phase HPLC for the isolation of photolabeled peptides. Boronate affinity chromatography and to some extent anion exclusion chromatography have been useful for this purpose (23, 29). However, we still lacked an effective procedure for isolating peptides photolabeled with nucleoside triphosphates. Photolabeling with 8- $\text{N}_3\text{Ap}_4\text{A}$ was tested assuming that it would be able to interact with the ATP binding site and could be used to provide us with a procedure for isolating photolabeled peptide using boronate affinity chromatography. The observed low apparent K_d for 8- $\text{N}_3\text{Ap}_4\text{A}$ was not expected. Boronate affinity chromatography did afford a satisfactory resolution of the intact photolabeled rmGM-CSF from the nonphotolabeled rmGM-CSF. However, it was not very effective in terms of material recovered. Also, the separation of smaller photolabeled peptides from nonphotolabeled peptides was not as good as obtained using the following procedure.

Immobilized Fe^{3+} affinity chromatography has been previously used for the isolation of phosphoproteins and phosphopeptides (30). Recently, using a modification of these procedures we have developed metal affinity chromatography for the isolation of photolabeled peptides (20). This procedure is based on the principle that the photolabeled peptides carrying photoinserted phosphates will form a complex with transition-state metals immobilized on a Sepharose support. The complex is relatively stable to salt washes, as well as to urea washes, which can be used to dissociate peptides retained nonspecifically due to ionic, electrostatic, or hydrophobic interactions. Using this method, in combination with reverse-phase HPLC, we selectively isolated a heavily radiolabeled (3.4×10^4 cpm/10 μL of 0.5 mL fraction), single peptide consisting of residues 5–14 near the N-terminus of GM-CSF and suggest that this domain is involved in nucleotide binding. During this study and several other in this laboratory we have determined that the radiolabel retained with the photolabeled peptide during reverse-phase HPLC is dependent

rmGM-CSF (5-13)	S P I T V T R P W
T2 (161-169)	T P V D V T C P W
T4 (160-168)	T P V D V T C P W
T6 (161-169)	T P V D V T C P W

Figure 10. Amino acid sequence comparison of the photolabeled peptide of rmGM-CSF with other nucleotide-binding proteins. The method used for sequence comparison was that of Needleman and Wunsch (31) as implemented by Dayhoff (32) and Doolittle (33). The scan was done using a Dayhoff MDM-78 matrix with a bias of 60 and a gap penalty of 60.

upon the flow rate. Approximately 80% more of the radiolabel was lost at 1 mL/min compared to 0.5 mL/min flow rate.

Also, photolysis with [γ - 32 P]-8-N₃ATP resulted in the isolation of the same peptide indicating that both the probes were interacting with the same region on GM-CSF. We isolated only one peptide in the case of 8-N₃Ap₄A which can potentially interact with two binding regions due to the presence of two adenine rings. This indicates that this binding domain has higher affinity for the 8-azido-adenine ring than for the adenine ring. The site of modification could not be determined with certainty. Strictly on the basis of the picomole recovery of residues, proline may be the site of photoinsertion.

When this peptide sequence was analyzed for sequence homology with other proteins by scanning Swiss prot 16 database using the PC-Genes program, it showed sequence homology with several nucleotide binding proteins (Figure 10). Of interest was the approximately 84% sequence homology with single-stranded DNA binding protein from bacteriophage T2, T4, and T6.

This sequence comparison was also carried out in the case of our IL-2 work where the ATP/NAD⁺ binding domain has been identified.² The peptide regions in the nucleotide binding domain on IL-2 showed greater than 90% sequence homology with sequences on several nucleotide binding proteins, the most interesting one being the sequence on subunit 1 from *Bordetella pertussis*, which has been implicated in the NAD⁺ binding and ADP ribosylating activity. A similar sequence was also observed in cholera toxin.

The three-dimensional structure of GM-CSF has been predicted by molecular modeling techniques (11). The preliminary crystallographic examination confirms the presence of four α helices (12, 13). The areas of the GM-CSF molecule critical to bioactivity have been described by a variety of techniques. Small N-terminal and C-terminal deletions do not adversely affect activity, nor does glycosylation (34, 35). Regions critical to bioactivity are arrayed throughout the molecule. On the basis of scanning-deletion analysis, residues 18-22 near the N-terminus of mGM-CSF were determined to be important for biological activity (36). On the basis of mutagenesis studies, residues 11-15 near the N-terminus have also been implicated in biological activity (37). The nucleotide binding domain identified by photoaffinity labeling lies within or in close proximity to this critical region near the N-terminus. Most neutralizing antibody epitopes reported are in the C-terminus half of the human GM-CSF molecule, leaving certain biologically critical regions in the N-terminus portion with no receptor binding function described (38, 39). We suggest, due to the specificity and avidity of

the binding site described, that this nucleotide interaction is critical for GM-CSF signal transduction in a novel fashion. Possible candidate roles include modulation of receptor affinity after internalization, protection of GM-CSF against proteolytic digestion, endosomal trafficking of internalized GM-CSF (the optimum pH of 4.5 of nucleotide binding is interesting in this regard), or possible catalytic activity.

We tested the bioactivity of rmGM-CSF photolabeled with either 8-N₃Ap₄A or 8-N₃ATP in a cell-proliferation assay using [3 H]thymidine uptake. The photolabeled samples, without removal of any unbound nucleotide, indicated decreased bioactivity compared to a control sample as well as to a sample which was prephotolyzed, photoprobe being subsequently added to it. In the case of 8-N₃Ap₄A the difference in bioactivity was equivalent to approximately 1.5 dilutions, which would be equivalent to approximately 65% modification of the cytokine. The percent modification determined by quantifying 32 P incorporation after SDS-PAGE separation was 44%. This is a minimal percent due to inherent loss of peptide and instability of the photolabel to SDS-PAGE and gel staining and drying procedures. In the case of 8-N₃ATP the difference in bioactivity was equivalent to approximately 3.5 dilutions, which would be equivalent to approximately 85% modification of the cytokine. The percent modification observed based on SDS-PAGE analysis in this case was 60%. The percent modification in the case of 8-N₃Ap₄A was lower compared to that in the case of 8-N₃ATP. This is probably due to the non-azido adenine ring staying intact after photolysis of 8-N₃Ap₄A and being able to act as a competitor for the second and third addition and photolysis of 8-N₃Ap₄A.

The inactivation of the photolabeled rmGM-CSF was further confirmed by partial purification of the photolabeled cytokine from the non-photolabeled cytokine using boronate affinity chromatography. The bound material and the unbound material indicated a difference of approximately 6 dilutions in bioactivity, indicating that more than 90% of rmGM-CSF in the bound fractions was modified. The bioactivity result would be consistent with the hypothesis that the critical region near the N-terminus, for which no clear function is yet ascribed, is being interfered with by the covalent attachment of nucleotide analog. However, the possibility of inability of covalently modified GM-CSF molecule to bind to the receptor does exist. Such a possibility of modulation of receptor binding via nucleotide binding site occupancy is being investigated. The observation of this nucleotide binding site opens new avenues for exploring the physiology of cytokine signal transduction which is currently not fully understood.

ACKNOWLEDGMENT

We thank the National Institutes of Health (Grant GM 35766), the Lexington Clinic Foundation (B.E.H.), and the Association for Medical Research (M.A.D.) for their generous financial support.

LITERATURE CITED

- (1) Metcalfe, D. (1986) The Molecular Biology and Functions of the Granulocyte-Macrophage Colony-Stimulating Factor. *Blood* 67, 257-267.
- (2) Metcalfe, D., Begley, C. G., and Johnson, G. R. (1986) Biologic Properties *In Vitro* of a Recombinant Granulocyte-Macrophage Colony-Stimulating Factor. *Blood* 67, 37-45.
- (3) Clutterbuck, E. J., Hirst, E. M. A., and Sanderson, C. J. (1989) Human Interleukin-5 (IL-5) Regulates the Production of

² (a) Campbell, S. R., and Haley, B. E., manuscript under preparation. (b) Campbell, S. R. (1991) Ph.D. Thesis, Department of Biochemistry, University of Kentucky.

- Eosinophils in Human Bone Marrow Cultures: Comparison and Interaction With IL-1, IL-3 and GM-CSF. *Blood* 73, 1504-1512.
- (4) Phillips, N., Jacobs, S., Stoller, R., Earle, M., Przepiorka, D., and Shadduck, R. (1989) Effect of Recombinant Human Granulocyte-Macrophage Colony Stimulating Factor on Myelopoiesis in Patients with Refractory Metastatic Carcinoma. *Blood* 74, 26-34.
- (5) Favre, C., Saeland, S., Caux, C., Duvert, V., and DeVries, J. E. (1990) Interleukin-4 has Basophilic and Eosinophilic Cell Growth-Promoting Activity on Cord Blood Cells. *Blood* 75, 67-73.
- (6) Nicola, N. A., and Meltcalf, D. (1991) Subunit Promiscuity Among Hemopoietic Growth Factor Receptors. *Cell* 67, 1-4.
- (7) Baldwin, G. C., Golde, D. W., Widhopf, G. F., Economou, J., and Gasson, J. C. (1991) Identification and Characterization of a Low-Affinity Granulocyte-Macrophage Colony-Stimulating Factor on Primary and Cultured Human Melanoma Cells. *Blood* 78, 609-615.
- (8) Khwaja, A., Roberts, P. J., Jones, H. M., Yeng, K., Jaswon, M. S., and Linch, D. C. (1990) Isoquinolinesulfonamide Protein Kinase Inhibitors H7 and H8 Enhance the Effects of Granulocyte-Macrophage Colony-Stimulating Factor on Neutrophil Function and Inhibit GM-CSF Receptor Internalization. *Blood* 76, 996-1003.
- (9) Kanakura, Y., Druker, B., Cannistra, S. A., Farukawa, Y., Torimoto, Y., and Griffin, J. D. (1990) Signal Transduction of the Human GM-CSF and IL-3 Receptors Involves Tyrosine Phosphorylation of a Common Set of Cytoplasmic Proteins. *Blood* 76, 706-715.
- (10) Wingfield, P., Graber, P., Moonen, P., Craig, S., and Pain, R. H. (1988) The Conformation and Stability of Recombinant-Derived Granulocyte-Macrophage Colony Stimulating Factors. *Eur. J. Biochem.* 173, 65-72.
- (11) Kaushansky, K., Brown, C. B., and O'Hara, P. J. (1990) Molecular Modeling of Human Granulocyte-Macrophage Colony Stimulating Factor. *Int. J. Cell Cloning* 8, 26-34.
- (12) Diederichs, K., Jacques, S., Boone, T., and Karplus, P. A. (1991) Low Resolution Structure of Recombinant Human Granulocyte-Macrophage Colony Stimulating Factor. *J. Mol. Biol.* 221, 55-60.
- (13) Diederichs, K., Boone, T., and Karplus, P. A. (1991) Novel Fold and Putative Receptor Binding Site of Granulocyte-Macrophage Colony-Stimulating Factor. *Science* 254, 1779-1782.
- (14) Czarnecki, J., Geahlen, R. T., and Haley, B. E. (1979) Synthesis and Use of Azido Photoaffinity Analogs of Adenine and Guanine Nucleotides. *Methods Enzymol.* 56, 642-653.
- (15) Potter, R. L., and Haley, B. E. (1982) Photoaffinity Labeling of Nucleotide Binding Sites with 8-azidopurine Analogs. *Methods Enzymol.* 91, 613-633.
- (16) Campbell, S., Kim, H., Doukas, M. A., and Haley, B. E. (1990) Photoaffinity Labeling of ATP and NAD⁺ Binding Sites on Recombinant Human Interleukin-2. *Proc. Natl. Acad. Sci. U.S.A.* 87, 1243-1246.
- (17) Mann, D. M., Haley, B. E., and Greenberg, R. N. (1991) Photoaffinity Labeling of Atrial Natriuretic Factor Analog Atriopeptin III with [γ -³²P]8N₃GTP. *Pept. Res.* 4, 79-83.
- (18) Shoemaker, M., Lin, P. C., and Haley, B. E. (1992) Identification of the Guanine Binding Domain Peptide of the GTP Binding Site of Glucagon. *Protein Sci.* 1, 884-891.
- (19) Geahlen, R. L., and Haley, B. E. (1977) Interactions of a Photoaffinity Analog of GTP with the Proteins of Microtubules. *Proc. Natl. Acad. Sci. U.S.A.* 74, 4375-4377.
- (20) Salvucci, M. E., Chavan, A. J., and Haley, B. E. (1992) Identification of Peptides From the Adenine Binding Domains of ATP and AMP in Adenylate Kinase: Isolation of Photoaffinity Labeled Peptides by Metal-Chelate Chromatography. *Biochemistry* 31, 4479-4487.
- (21) Laemmli, U. K. (1970) Cleavage of Structural Proteins During the Assembly of the Head of Bacteriophage 4. *Nature* 227, 680.
- (22) Stone, K. L., LoPresti, M. B., Myron Crawford, J., DeAngelis, R., and Williams, K. R. (1989) Enzymatic Digestion of Proteins and HPLC Peptide Isolation. *A Practical Guide to Protein and Peptide Purification for Microsequencing* (P. T. Matsudaira, Ed.) pp 37-42, Academic, San Diego.
- (23) Kim, H., and Haley, B. E. (1991) Identification of Peptides in the Adenine Ring Binding Domain of Glutamate and Lactate Dehydrogenase Using 2-Azido-NAD⁺. *Bioconjugate Chem.* 2, 142-147.
- (24) Andersson, M. (1989) Diadenosine Tetraphosphate (Ap₄A): Its Presence and Functions in Biological Systems. *Int. J. Biochem.* 21, 707-714.
- (25) Levitzki, A., and Koshland, D. E., Jr. (1972) Ligand-Induced Dimer-TO-Tetramer Transformation in Cytosine Triphosphate Synthetase. *Biochemistry* 11, 247-252.
- (26) May, L. T., Santhanam, U., and Sehgal, P. B. (1991) On the Multimeric Nature of Natural Human Interleukin-6. *J. Biol. Chem.* 266, 9950-9955.
- (27) Jones, E. Y., Stuart, D. I., and Walker, N. P. C. (1989) Structure of Tumor Necrosis Factor. *Nature* 338, 225-228.
- (28) Haley, B. E. (1991) Nucleotide Photoaffinity Labeling of Protein Kinase Subunits. *Methods Enzymol.* 200, 477-487.
- (29) Chavan, A. J., Kim, H., Haley, B. E., and Watt, D. S. (1990) A Photoactive Phosphonamide Derivative of GTP for the Identification of the GTP-Binding Domain in β -Tubulin. *Bioconjugate Chem.* 1, 337-344.
- (30) Andersson, L., and Porath, J. (1986) Isolation of Phosphoproteins by Immobilized Metal (Fe³⁺) Affinity Chromatography. *Anal. Biochem.* 154, 250-254.
- (31) Needleman, S. B., Wunsch, C. D. (1970) A General method applicable to the search for similarities in the amino acid sequence of two proteins. *J. Mol. Biol.* 48, 443-453.
- (32) Dayhoff, M. O. (1978) A model of evolutionary change in proteins. Matrices for detecting distant relationships. In *Atlas of Protein Sequence and Structure* (M. O. Dayhoff, Ed.) Vol. 5, suppl. 3, pp 1-8, National Biomedical Research Foundation, Washington, D.C.
- (33) Feng, D. F., Johnson, M. S., Doolittle, R. F. (1985) Aligning Amino Acid Sequences: Comparison of commonly used methods. *J. Mol. Evol.* 21, 112-125.
- (34) LaBranche, C. C., Clark, S. C., Johnson, G. D., Ornstein, D., Sabath, D. E., Tushinski, R., Paetkau, V., and Prystowsky, M. B. (1990) Deletion of Carboxy-terminal of Murine Granulocyte-Macrophage Colony Stimulating Factor Results in a Loss of Biologic Activity and Altered Glycosylation. *Arch. Biochem. Biophys.* 276, 153-159.
- (35) Clark-Lewis, I., Lopez, A. F., To, L. B., Vadas, M. A., Schrader, J. W., Hood, L. E., and Kent, S. B. H. (1988) Structure-Function Studies of Human Granulocyte-Macrophage Colony Stimulating Factor. *J. Immunol.* 141, 881-889.
- (36) Shanafelt, A. B., and Kastelein, R. A. (1989) Identification of Critical Regions in Mouse Granulocyte-Macrophage Colony Stimulating Factor by Scanning Deletion Analysis. *Proc. Natl. Acad. Sci. U.S.A.* 86, 4872-4876.
- (37) Gough, N., Grail, D., Gearing, D. P., and Metcalf, D. (1987) Mutagenesis of murine Granulocyte/Macrophage Colony Stimulating Factor Reveals Critical Residues near the N-Terminus. *Eur. J. Biochem.* 169, 353-358.
- (38) Brown, C. B., Hart, C. E., Curtis, D. M., Bailey, M. C., and Kaushansky, K. (1990) Two Neutralizing Monoclonal Antibodies Against Human Granulocyte-Macrophage Colony Stimulating Factor Recognize the Receptor Binding Domain of the Molecule. *J. Immunol.* 144, 2184-2189.
- (39) Nice, E., Dempsey, P., Layton, J., Morstyn, G., Cui, D. F., Simpson, R., Fabri, L., and Burgess, A. (1990) Human Granulocyte-Macrophage Colony Stimulating Factor (hGM-CSF): Identification of a Binding Site for a Neutralizing Antibody. *Growth Factors* 3, 159-169.

Registry No. GM-CSF, 83869-56-1.

Imidazoles as Well as Thiolates in Proteins Bind Technetium-99m

Paul O. Zamora* and Buck A. Rhodes

RhoMed Inc., 4261 Balloon Park Road NE, Albuquerque, New Mexico 87109. Received April 13, 1992

^{99m}Tc is widely thought to directly bind proteins through thiolate groups of cysteine residues, resulting in Tc-cysteiny-protein bonds. Chemical reduction of disulfide bonds in proteins is widely used to generate thiolates with the goal of increasing ^{99m}Tc binding. This strategy is used because most proteins contain no thiolates, but many do contain disulfide bonds. In this study, we have evaluated the hypothesis that imidazole groups of histidine are also involved in direct ^{99m}Tc binding to proteins. Human γ -globulin was used as the model protein in these studies. The immunoglobulin was used (a) without reduction or was (b) treated with stannous ions to reduce disulfide bonds thereby increasing thiolate concentration. These proteins were used to evaluate the hypothesis that imidazole as well as thiolate groups bind Tc. The proteins were evaluated by (a) using free amino acids to compete with proteins for ^{99m}Tc and (b) by chemical modification of amino acid side chains. In addition, peptides known to contain either cysteine or histidine, but not both, were also successfully directly labeled with ^{99m}Tc . These results indicate that in proteins (and peptides) imidazole-containing groups as well as thiolate-containing groups bind Tc.

INTRODUCTION

Technetium-99m is the most widely used radionuclide in nuclear medicine and considerable effort has been focused on directly binding it to proteins for diagnostic imaging of human diseases (Eckelman & Steigman, 1991; Rhodes, 1991). Clinical-grade Tc is normally produced from a $^{99}\text{Mo}/^{99m}\text{Tc}$ generator as sodium pertechnetate (NaTcO_4); in that form it does not bind to proteins. Tc can bind to proteins when the pertechnetate [Tc(VII)] ion is chemically reduced to a lower oxidation state (Steigman & Eckelman, 1992).

In most proteins, endogenous Tc-binding capacity is easily saturated, and consequently the Tc-binding efficiency is low. To increase the Tc-binding efficiency, a number of investigators have chemically treated one class of proteins, immunoglobulins, with reducing agents (stannous ions, dithiothreitol, 2-mercaptoethanol, and the like) with the goal of generating reactive thiolates for subsequent Tc binding (see Rhodes, 1991 for specific references). This strategy is based on the well-known ability of reduced Tc to bind to thiolate-containing molecules (cysteine, penicillamine, mercaptoacetyl triglycine) (Dewanjee, 1990).

Stannous ions reduce the disulfide bonds in proteins and generate cysteine thiolates. Excess tin ions presumptively bind thiolates, forming Sn-cysteiny-protein bonds, and thereby minimizing disulfide bond reformation. On addition of pertechnetate, stannous effects reduction of the pertechnetate, and the Tc then undergoes a replacement reaction with the bound tin, forming strongly bound Tc-cysteiny-protein (Hawkins et al., 1990). As applied to immunoglobulins, this approach results in immunoreactive antibody preparations which are radiolabeled with high efficiency in a single step, using a methodology suited to diagnostic imaging.

In spite of the attention focused on direct binding of Tc to thiolates in proteins, little is known about the environment of thiolate binding site(s) and the extent to which other binding sites contribute to overall Tc binding. That

proteins contain multiple types of Tc-binding sites has been inferred by a number of investigators (Steigman et al., 1975; Lantagne & Hnatowich, 1984; Paik, et al., 1985; 1986).

Since Tc is a transition metal (group VIIb), it might be expected to share some of the protein-binding characteristics of other transition metals such as iron, cobalt, copper, zinc, molybdenum, and ruthenium. We have pointed out the similarity of Cu and Tc binding in immunoglobulins (Zamora et al., 1992). In general, proteins form stable coordination complexes with transition metals (including Cu) by interactions not only with thiolates in cysteine but also with imidazoles of histidine (Arnold & Haymore, 1991). For example, ruthenium(III), which is adjacent to Tc on the periodic chart, forms stable coordination complexes with peptides containing histidine (Ghardiri & Fernholz, 1990).

This report describes results which validate the hypothesis that Tc can directly bind to proteins via at least two different types of binding sites. Human IgG was used in these studies as a model protein and was selected, in part, due to the wide interest in direct labeling of antibodies for clinical diagnostic imaging. The results show that one type of binding site involves thiolates of cysteine, resulting in Tc-cysteiny-protein bonds. Another type of binding site, however, involves imidazoles of histidine, resulting in Tc-histidiny-protein bonds. This report appears to be the first description of Tc binding to imidazoles of histidine in proteins.

EXPERIMENTAL PROCEDURES

Preparation of Immunoglobulin Kits for ^{99m}Tc Labeling. Human γ -globulin (Gamimune N, Cutter Biological, Elkhart, IN) was used as a source of immunoglobulin and was used without additional purification. Two types of immunoglobulin labeling kits were used. One type of kit was prepared using unmodified immunoglobulin, and is referred to as an IgG kit. The other type of kit was prepared using stannous ion-reduced immunoglobulin and is referred to as an IgG-r kit. The IgG and the IgG-r kit contents were the same except that the immunoglobulin in the latter was pretreated with stannous ions to increase the thiolate concentration. All immunoglobulin prepa-

* Address correspondence to Dr. Paul O. Zamora, RhoMed Inc., 4261 Balloon Park Road NE, Albuquerque, NM 87109. Telephone: (505) 344-7200. Telefax: (505) 344-9460.

rations were prepared aseptically using nitrogen-purged solutions, and whenever feasible under an atmosphere of nitrogen.

To prepare IgG labeling kits, the immunoglobulin was diluted to a final concentration of 1.4 mg/mL in chilled, nitrogen-purged 10 mM tartrate/40 mM phthalate buffer, pH 5.6 (P/T buffer). The antibody solution was mixed (7:3) with P/T buffer containing 1.25 mM stannous tartrate and excipients. Aliquots (typically 0.5 mL containing 500 μ g of antibody) were then dispensed into individual vials and lyophilized.

To prepare IgG-r labeling kits, immunoglobulin was treated with stannous ion to increase the amount of thiolates (Rhodes et al., 1986; Hawkins et al., 1990). To do this, the immunoglobulin was diluted to 8.3 mg/mL in P/T buffer and the resulting solution mixed (3:2) in an amber vial with P/T buffer containing 5 mM stannous tartrate. The head-space gas was purged with nitrogen, the vial sealed, and the reaction allowed to proceed for 21 h at room temperature. At the end of the incubation period, the solution was filtered through a 0.22- μ m filter and chromatographed over Sephadex G-25 pre-equilibrated in P/T buffer, thereby removing uncomplexed tin ions. Protein concentration was determined by use of a commercially available dye binding assay (Commassie Blue G-250) using unmodified human γ -globulin as the standard. After determining the protein concentration, the IgG-r was mixed (7:3) with P/T buffer containing 1.25 mM stannous tartrate and excipients. Aliquots of 0.5 mL were then dispensed into individual vials and lyophilized.

^{99m}Tc Labeling. To radiolabel, the lyophilized kits were reconstituted with 0.5 mL of water (or 0.9% saline); each rehydrated kit contained 0.5 mg of IgG, 40 mM phthalate, 10 mM tartrate, and 22 μ g of stannous tartrate. The labeling reaction was accomplished by the addition of 0.5–2.0 mCi of ^{99m}Tc (sodium pertechnetate in saline). Radiochemical analysis began 30 min after the introduction of the pertechnetate.

Radiochemical Analysis by High-Performance Liquid Chromatography. To determine the relative amount of ^{99m}Tc bound to a given antibody preparation, aliquots of the ^{99m}Tc -labeled preparations were analyzed by HPLC at a flow rate of 1 mL/min phosphate-buffered saline (0.01 M phosphate, pH 7.0, containing 0.15 M NaCl) using a 7.5 \times 300 mm TSK G3000SW column with a TSK-SW 7.5 \times 7.5 mm guard column (TosoHaas, Philadelphia, PA) and a UV and radioisotope detector in series. Additional information on analysis of radiolabeled antibodies by this method can be found elsewhere (Hawkins et al., 1990).

The following points are noted with regard to this analytical system: (a) free pertechnetate was quantitatively recovered, (b) reduced Tc bound to carrier molecules (chelators, proteins) was recovered in high yield, and (c) uncomplexed reduced Tc was quantitatively adsorbed onto the column and could not be subsequently eluted. According to information supplied by the manufacturer, the HPLC separation and guard columns are packed with a porous, hydrophilic silica support housed in stainless steel columns. It is not known what component of the chromatography system binds uncomplexed, reduced Tc.

Thin-Layer Chromatography (TLC). TLC was used to measure the amount of protein-bound (and unbound) ^{99m}Tc . ITLC-SG (Gelman Sciences, #61886) chromatography paper was cut into 1.5 \times 10 cm strips and activated by heating for 30 min at 110 $^{\circ}\text{C}$, as per the manufacturer's instructions. After heating, the strips were stored at room temperature until use.

Protein-bound ^{99m}Tc in the radiolabeled antibody preparations was measured using TLC in an organic solvent (85% aqueous methanol). The organic solvent separated the soluble, unbound ^{99m}Tc (which migrated with the solvent front) from ^{99m}Tc bound to the protein (which remained at the origin). The method of use and subsequent processing of data were similar to that described elsewhere (Rhodes et al., 1986). Both cysteine and histidine, as used in the competition studies, are soluble in alcohols, and their ^{99m}Tc complexes were found in control studies to migrate with the solvent front.

The percentage of protein-bound ^{99m}Tc was the ratio of the cpm in the origin half of the strip minus the background divided by the total cpm. The total cpm was the cpm in the origin half of the strip minus the background plus the cpm in the solvent front half of the strip minus the background cpm.

Competition for ^{99m}Tc by Free Amino Acids. Individual lyophilized kits of IgG or reduced IgG were hydrated with 40 mM phthalate/10 mM tartrate buffer, pH 5.6, containing various concentrations of free amino acids. Histidine was used at concentrations of 50, 5, 0.5, 0.05, 0.005, 0.0005, and 0.0 mM (control). Cysteine was used at concentrations of 5, 0.5, 0.05, 0.005, 0.0005, and 0.0 mM (control). The labeling reaction was initiated by adding 0.5–2.0 mCi of ^{99m}Tc (sodium pertechnetate in saline) to the vial. Radiochemical analysis was begun 30 min after the introduction of the pertechnetate.

Modification of Imidazole Groups. Commercially available DEPC (diethyl pyrocarbonate, Aldrich Chemical Co., Milwaukee, WI) was used to modify the imidazole groups on histidine, and presumptively block potential binding. DEPC, a liquid (6.9 M), was diluted with anhydrous acetonitrile. DEPC has a half-life of 24 min at room temperature pH 6.0 (Miles, 1979), and was prepared immediately prior to use.

The final concentration of DEPC used in this study was 7 mM. The working dilution was prepared from a 0.69 M working stock solution. An aliquot of 3 mL of immunoglobulin solution (50 mg/mL) was placed in an amber vial and 60 μ L of stock solution of DEPC was added with mixing. The mixture was incubated either at room temperature for 1 h or at 4 $^{\circ}\text{C}$ overnight, and the volume was then adjusted to 10 mL with 0.9% NaCl. The mixture was chromatographed through Sephadex G-25 to remove unreacted components. The void volume, containing the immunoglobulin, was collected and filtered through a 0.22- μ m filter. This preparation was analyzed by HPLC and found to be chromatographically uniform, with a single peak which eluted at a time corresponding to the molecular weight of standard IgG. The sample was then divided into two aliquots and further processed into IgG and IgG-r labeling kits as described above, except that the kits were frozen at -70°C until use, rather than lyophilized.

Modification of Thiolate Groups. *N*-Ethylmaleimide (NEM) was used as a thiolate blocking agent. It was prepared fresh in an amber vial as a 100 mM stock solution in 95% ethanol. Actual modification mixtures contained either 60 mg of IgG or IgG-r in 0.9% NaCl prepared by buffer exchange over Sephadex G-25. The pH was adjusted to 8.1 by the addition of 1:10 volume of 0.1 M phosphate buffer, pH 8.1. The reaction was started by adding NEM stock solution to a final concentration of 1 mM NEM. The reaction was allowed to proceed for 30 min at room temperature and was terminated by precipitation of the antibody in approximately 20% polyethylene glycol (MW 8000, 52% PEG stock solution). The precipitated antibody was collected by centrifugation (1000g

for 15 min) and the supernatant discarded. The precipitate containing the antibody was dissolved in 0.9% NaCl and chromatographed over Sephadex G-25 in degassed 0.9% NaCl. The eluate was collected and filtered through a 0.22- μm filter. The IgG and IgG-r preparations were then prepared for labeling as described above, except that the final kits were stored frozen rather than lyophilized.

Modification of Both Thiolate and Imidazole Groups. Immunoglobulin (300 mg) was reacted with 7 mM DEPC for 1 h at room temperature. After incubation, the solution was chromatographed over Sephadex G-25 (0.9% NaCl equilibration and elution buffer) and the void volume containing the antibody was collected. The DEPC-treated immunoglobulin was then split into two aliquots. One aliquot was treated with NEM and used to prepare IgG labeling kits. The other aliquot was reduced with stannous ions, treated with NEM, and used to prepare IgG-r labeling kits.

For treatment with NEM, one aliquot of DEPC-treated IgG was incubated in 10 mM NEM in 0.01 M phosphate buffer, pH 8.0, for 30 min. Unreacted NEM was separated from the antibody by chromatography over Sephadex G-25 (0.9% NaCl equilibration and elution). The antibody was then subjected to buffer exchange by chromatography over Sephadex G-25 (equilibrated and eluted with 40 mM phthalate/10 mM tartrate, pH 5.6). The immunoglobulin was made into IgG labeling kits as described above, and frozen until used.

The other aliquot of DEPC-treated immunoglobulin was first reduced with stannous ions and then treated with NEM. The DEPC-treated immunoglobulin was reduced in phthalate/tartrate buffer, pH 5.6, containing 2 mM stannous tartrate for 21 h. The stannous ions were removed by chromatography over Sephadex G-25 (0.9% NaCl equilibration and elution). The IgG-r was then incubated in 10 mM NEM in 0.01 M phosphate buffer, pH 8.0, for 30 min. The unreacted NEM was separated from the antibody by chromatography over Sephadex G-25 (0.9% NaCl equilibration and elution). The IgG-r was subjected to buffer exchange by chromatography over Sephadex G-25 (equilibrated and eluted with 40 mM phthalate/10 mM tartrate, pH 5.6). The immunoglobulin was made into IgG-r labeling kits as described above, and frozen until used.

Sham DEPC- and NEM-modified kits were also made, in which immunoglobulin was subjected to the pH shifts, buffer exchanges, and column chromatography steps, without addition of either DEPC or NEM. These IgG and IgG-r kits were used as controls in DEPC- and NEM-modified kit experiments, to insure that the reaction conditions did not affect ^{99m}Tc binding.

Preparation of Peptides for Labeling. Synthesized peptides were obtained commercially as lyophilized preparations. Each peptide was dissolved directly in P/T buffer, resulting in a peptide concentration of 1.4 mg/mL. This solution was mixed (7:3) with P/T buffer containing 1.25 mM stannous tartrate. Aliquots of 0.5 mL were dispensed into individual vials and stored frozen until used. Each kit contained 0.5 mg of peptide, 40 mM phthalate, 10 mM tartrate, and 22 μg of stannous tartrate. All preparations were labeled with ^{99m}Tc using methods similar to those described above.

RESULTS

The IgG labeling kits were found to have 0.6 thiolates/molecule as determined by use of Ellman's reagent (Jocelyn, 1987). The IgG-r labeling kits, treated with stannous ions to reduce disulfide bonds and increase

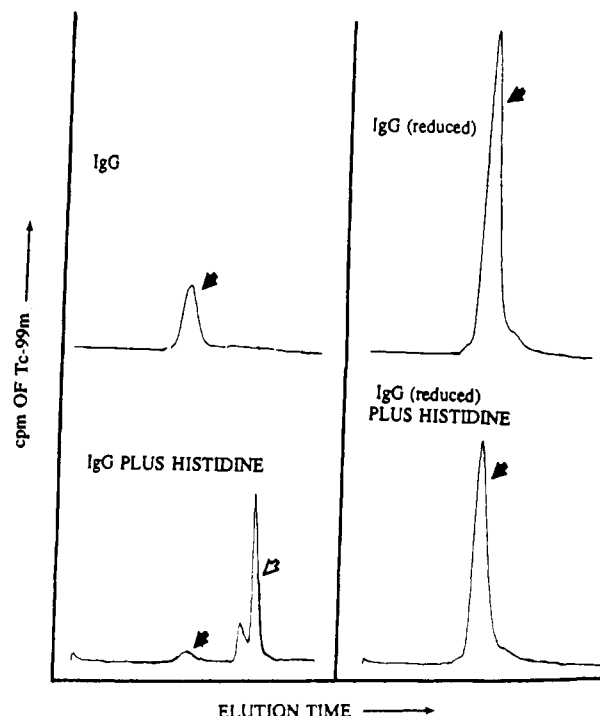


Figure 1. Radiochemical analysis by high-pressure liquid chromatography of IgG and IgG-r after labeling with ^{99m}Tc in the absence (controls) or presence of 0.5 mM histidine. Similar amounts of protein and ^{99m}Tc were used, and the incubation and analytical conditions were also similar. The dark arrows indicate protein-bound ^{99m}Tc (elution time = 9.3 min). The outlined arrow indicates ^{99m}Tc presumably bound to histidine (elution time = 14.2 min).

thiolate concentration, were found to have 6–8 thiolates/molecule. The IgG kits consistently bound some, but not all, of the ^{99m}Tc ($34.0 \pm 6.0\%$ total ^{99m}Tc , $n = 10$) as determined by quantitative radio-HPLC. The IgG-r kits consistently bound nearly all the ^{99m}Tc ($96.5 \pm 2.0\%$ total ^{99m}Tc , $n = 40$).

Competition for ^{99m}Tc with Free Histidine and Cysteine. To evaluate the hypothesis that both imidazoles in histidine and thiolates in cysteine bind ^{99m}Tc , competition studies were performed in which either histidine or cysteine was added during hydration of IgG and IgG-r labeling kits.

Histidine, in concentrations ranging from 0.005 to 50 mM, was able to compete for ^{99m}Tc with the immunoglobulin in IgG labeling kits, as is illustrated in Figures 1 and 2. At a concentration of 0.05 mM histidine, approximately 50% of the ^{99m}Tc was removed from the protein. However, the immunoglobulin in IgG-r labeling kits was able to bind approximately 90% of the ^{99m}Tc , even in the presence of 50 mM histidine. IgG labeling kits were very sensitive to histidine, while IgG-r kits were relatively insensitive. In those cases where histidine was able to compete with the antibody protein for ^{99m}Tc , HPLC profiles revealed a second, low molecular weight radioactive peak which was consistent with the known elution time of histidine. As an aside, in control experiments where free histidine, but no protein, was used, a discrete peak of radioactivity was associated with the histidine.

Cysteine, in concentrations ranging from 0.005 to 5 mM, was able to compete successfully for ^{99m}Tc in both IgG and IgG-r labeling kits (Figure 2). The competition curves demonstrate that IgG kits were more sensitive to competition with free cysteine than were IgG-r kits.

In studies where glycine was used as a competitor, no effect on the binding of ^{99m}Tc with either IgG or IgG-r kits

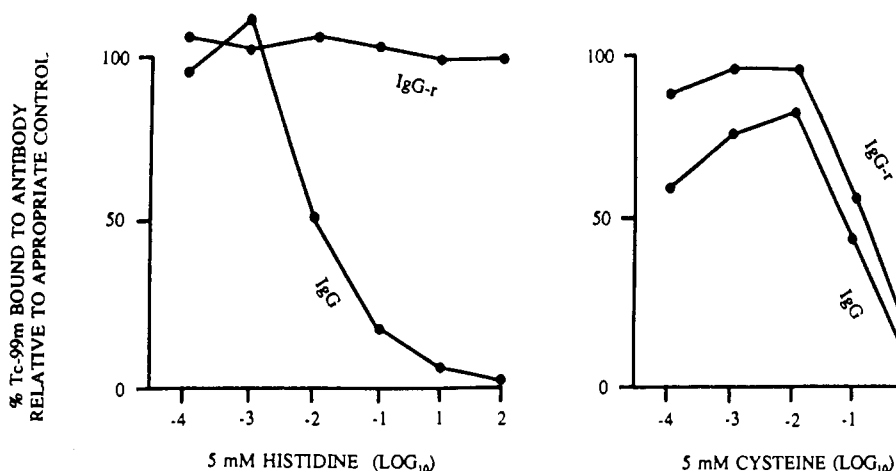


Figure 2. Comparative effect of adding histidine or cysteine to IgG and IgG-r prior to radiolabeling with ^{99m}Tc . All experimental values are expressed as a percentage of the appropriate control value, e.g. the percentage of ^{99m}Tc bound to either IgG or IgG-r containing 0 mM free amino acid. Note the dissimilarity in the shape of the curves obtained with histidine and the overall similarity of the curves obtained with cysteine.

Table I. Comparison of the Relative Percentage of ^{99m}Tc Bound in IgG and IgG-r Kits, Both with and without Chemical Modification of Amino Acid Side Chains^a

group modified	% of total ^{99m}Tc protein-bound	
	IgG	IgG-r
none	30.2	100.0
histidine only	5.7	85.0
thiolate only	38.8	60.1
histidine and thiolate	0.5	11.5

^a Histidine was modified by the use of diethyl pyrocarbonate. Thiolates were modified by use of *N*-ethylmaleimide. All values are compared relative to IgG-r labeling. See methods section for details on modification conditions. All evaluations were performed using an equivalent amount of protein and radionuclide, and similar labeling conditions.

was detected at any concentration of glycine tested (up to 20 mM). Similarly, essentially no effect was noted when 5 mM of either lysine or arginine was used as competitors.

Amino Acid Side Chain Modification. In both IgG and IgG-r labeling kits, the relative percentages of immunoglobulin-bound ^{99m}Tc , as determined by quantitative HPLC, changed depending on whether (a) histidines were modified with diethyl pyrocarbonate (DEPC), (b) thiolates were modified with *N*-ethylmaleimide (NEM), or (c) both histidines and thiolates were modified. A summary of the results of these experiments is shown in Table I.

When histidine groups of IgG were modified with DEPC, the subsequent labeling of the IgG kits with ^{99m}Tc labeling was greatly inhibited. This is illustrated by the HPLC profiles shown in Figure 3. However, when DEPC-modified IgG-r kits were labeled with ^{99m}Tc , the amount of ^{99m}Tc bound to immunoglobulin was only slightly reduced compared to that in unmodified, control kits (IgG-r). Some dimerization or aggregation was noted with the DEPC-modified IgG-r kits, but an evaluation of the absorbance profile at 280 nm suggested that little or no immunoglobulin was lost during the evaluation.

With NEM-modified IgG kits, in which thiolate groups were presumptively blocked, ^{99m}Tc labeling was slightly higher than in control IgG kits (Table I). This higher value is believed to be within experimental error. However, NEM-modified IgG-r kits showed a sharp decrease in labeling efficiency.

When both imidazole and thiolate groups in the immunoglobulin were modified, ^{99m}Tc labeling universally decreased. With DEPC- and NEM-modified IgG kits,

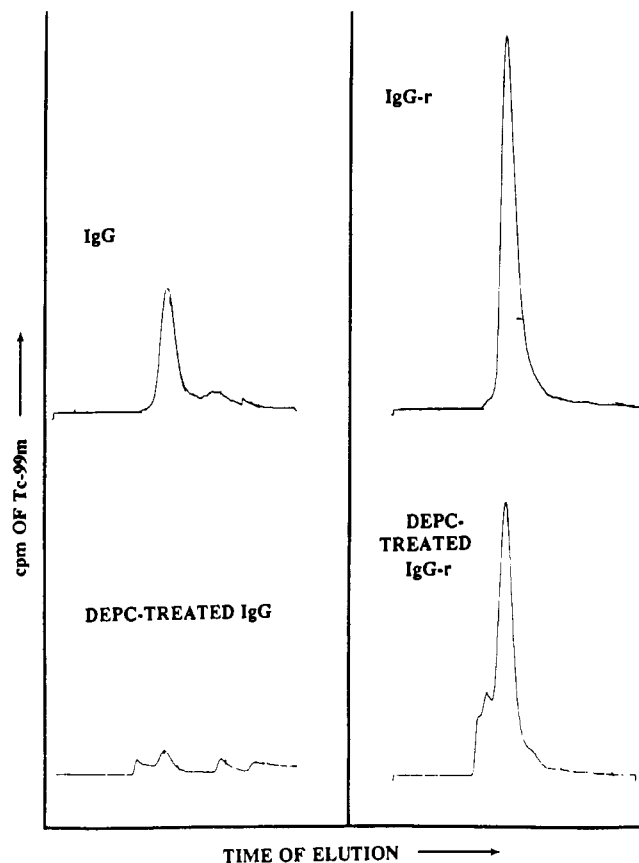


Figure 3. The effect of diethyl pyrocarbonate (DEPC), a chemical modifier of histidine, on the subsequent ^{99m}Tc labeling of IgG as determined by radio-HPLC. The profiles in the top panels are paired controls for the DEPC-treated preparations in the bottom panels. In the left panels are results obtained with IgG. In the right panels are results obtained with IgG-r.

^{99m}Tc labeling was negligible, approximately 0.5%. With DEPC- and NEM-modified IgG-r kits, labeling efficiency was substantially reduced, but was not eliminated.

In studies with preparations receiving sham treatments, in which the steps for NEM and DEPC modification were followed, but without addition of either NEM or DEPC, IgG kits were determined to bind approximately 30% total ^{99m}Tc , and IgG-r kits essentially 100% total ^{99m}Tc (Table I). Results with sham treatments were thus similar to results with regular IgG and IgG-r kits.

It should be noted that selection of NEM as a thiolate modifying agent was based on a series of preliminary studies evaluating a number of thiolate blocking agents (iodoacetamide, dibromobimane, monobromobimane, *N*-(iodoethyl)trifluoroacetimide) (Dailey, 1984). NEM was found to decrease the number of thiolates in IgG-r from 6–8 thiolates/molecule to approximately 1 thiolate/molecule, and was the most effective thiolate-modifying agent evaluated. These preliminary studies showed a direct relationship between the number of thiolates/molecule and ^{99m}Tc labeling efficiency in IgG-r kits. IgG-r kits with 6 or more thiolates/molecule labeled with essentially 100% efficiency, with the labeling efficiency decreasing approximately 20% for every decrease of 2 thiolates/molecule.

Labeling Synthesized Peptides Containing Histidine or Cysteine. To further evaluate the potential binding of ^{99m}Tc to histidine as well as cysteine, we evaluated ^{99m}Tc binding in three peptides with known amino acid sequences. These peptides were specifically selected to be unrelated to IgG. One peptide, with the amino acid sequence $\text{H}_2\text{N-Cys-Asp-Pro-Gly-Tyr-Ile-Gly-Ser-Arg}$, contained a single cysteine residue and no histidines. Another peptide, with the sequence $\text{Ac-Asp-Arg-Val-Ile-His-Pro-Phe-His-Leu-Val-Ile-His-Asp}$, contained histidine residues but no cysteines or cystine. The control, polytyrosine, contained neither histidine nor cysteine.

The histidine-containing peptide bound some but not all of the added ^{99m}Tc (Figure 4). The cysteine-containing peptide bound essentially all of the added ^{99m}Tc (Figure 4). Polytyrosine, the negative control material, did not label. These results were confirmed by conventional thin-layer chromatography. To further confirm that ^{99m}Tc could bind to histidine-containing peptides, a number of other peptides were examined and found to bind ^{99m}Tc . These peptides include the following: *N*-acetylrenin substrate tetradecapeptide ($\text{Ac-Asp-Arg-Val-Ile-His-Pro-Phe-His-Leu-Val-Ile-His-Asp}$), renin inhibitor ($\text{Pro-His-His-Pro-Phe-His-Phe-Phe-Leu-Val-His}$), angiotensin ($\text{Asp-Arg-Val-Tyr-Ile-His-Pro-Phe-His-Leu}$), hypercalcemia of malignancy factor (PTH-like) 1–16 ($\text{Ala-Val-Glu-His-Gln-Leu-Leu-His-Asp-Lys-Gly-Lys-Gly-Ser-Ile-Gln}$), and polyhistidine. Polyhistidine was found to have very limited solubility under the conditions of the experiment, but nonetheless, evidenced ^{99m}Tc binding. ^{99m}Tc binding was also observed in poly(His,Glu)-poly-Ala-poly-Lys, and to a much larger extent than poly(Tyr,Glu)-poly-Ala-poly-Lys.

DISCUSSION

Rhodes et al. (1980) were the first to develop an "instant" labeling kit for immunoglobulins in which stannous ions were used to reduce proteins, thereby generating reactive thiolates, for subsequent direct labeling with ^{99m}Tc . This strategy, applied primarily to monoclonal antibodies, has been widely emulated using a number of reducing agents (for reviews see Eckelman & Steigman, 1991; Rhodes, 1991; also Schwarz & Steinstrasser, 1987, and Mather & Ellison, 1990). Thakur et al. (1991) has directly related the type of reducing agent to the number of thiolate groups produced in antibodies and the resulting radiochemical incorporation. Thakur also suggested treating reduced antibody with iodoacetate to validate the hypothesis that thiolate groups provide the binding sites for ^{99m}Tc .

Thiolate groups in cysteine have long been implicated in the direct labeling of proteins with Tc (Steigman et al., 1975). In spite of the implication that ^{99m}Tc is bound to reduced immunoglobulin via the thiolates of cysteine

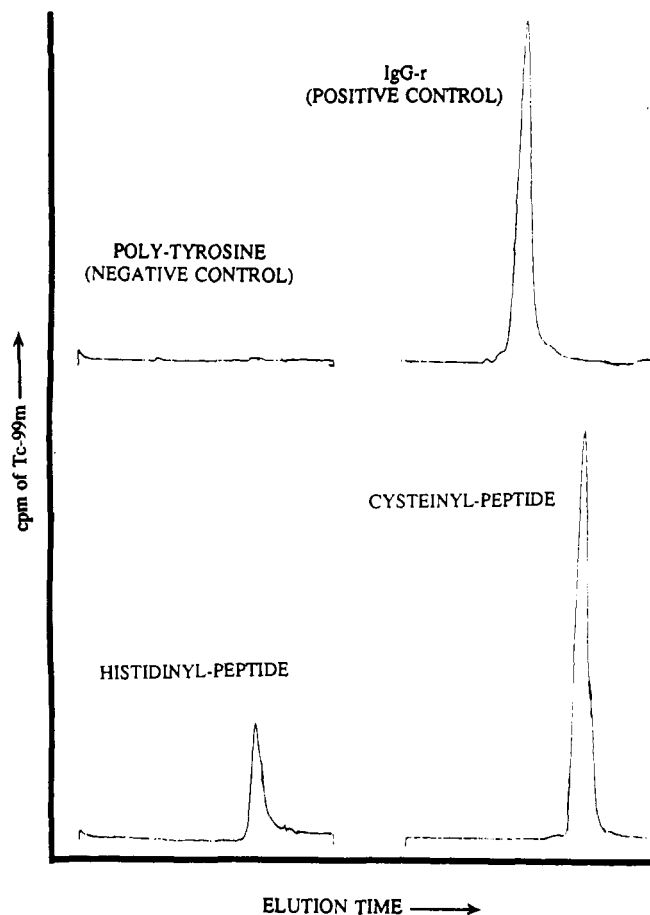


Figure 4. The binding of ^{99m}Tc to synthesized peptides as determined by radio-HPLC. Polytyrosine (negative control) was used as an example of a peptide containing neither histidine nor cysteine. IgG-r was used as a positive control material. One peptide, $\text{Ac-Asp-Arg-Val-Ile-His-Pro-Phe-His-Leu-Val-Ile-His-Asp}$ (elution time = 13.8 min), contained histidine but no cysteine or cystine. Another peptide, $\text{H}_2\text{N-Cys-Asp-Pro-Gly-Tyr-Ile-Gly-Ser-Arg}$ (elution time = 13.9 min), contained a single cysteine but not histidine.

residues (Rhodes, 1991), a number of other amino acids may be involved in the direct binding of ^{99m}Tc to proteins, analogous to the binding that takes place with other transition metals (Henkin, 1975). Histidine, for example, is well-known for its ability to coordinate metals, and as a free amino acid binds ^{99m}Tc (Seifert et al., 1983).

The results of Steigman et al. (1975) and Lantaigne and Hnatowich (1984) clearly indicate that proteins contain thiolate binding sites as well as other Tc-binding sites. Lantaigne and Hnatowich (1984), for example, were able to Tc label myoglobin, a molecule which contains neither cystine nor cysteine. Immunoglobulins (the constituent component of IgG kits of this study) contain histidines in both the light and heavy chains (Edelman et al., 1969), and while they do not normally contain reactive thiolates, they do contain significant numbers of disulfide bridges. Reduced immunoglobulin (the constituent component in the IgG-r kits used in this study) contains 6–8 reactive thiolates per molecule.

In the study reported here, when histidine was added immediately prior to radiolabeling, it was able to successfully compete for ^{99m}Tc with immunoglobulin, but not reduced immunoglobulin. This suggests that the primary binding site in unreduced immunoglobulin is related to histidine groups. This observation explains reports of direct labeling of unmodified immunoglobulins, albeit with low radiochemical incorporations (Pettit et al., 1980). The

inability of histidine to compete with reduced immunoglobulin for ^{99m}Tc does not necessarily preclude Tc-histidinyl-protein bond formation. The results do suggest that a different site, presumably involving thiolates, is predominant in reduced immunoglobulin.

When cysteine was added immediately prior to radio-labeling, it successfully competed for ^{99m}Tc with both immunoglobulin and reduced immunoglobulin. Since immunoglobulin contains virtually no reactive thiolates, these observations suggest that cysteine may be involved in binding to reduced immunoglobulin. However, since cysteine is a reducing agent known to bind ^{99m}Tc , an alternative explanation is that the cysteine reduced Tc-protein bonds and subsequently competed for the released Tc.

To further explore the relative involvement of imidazoles and thiolates in ^{99m}Tc binding, we monitored the labeling of IgG and IgG-r labeling kits with amino acid side chain modification (Means and Feeney, 1990). The results indicate that the primary ^{99m}Tc binding site in unreduced immunoglobulin is related to imidazole groups, and not to thiolates. In IgG-r kits, containing reduced immunoglobulin, both imidazole and histidine groups are involved in ^{99m}Tc binding. It is clear that reduction of IgG to generate thiolates is required to obtain radiochemical incorporations of ^{99m}Tc which approach 100%.

In the immunoglobulin preparations tested, residual stannous ions used to reduce pertechnetate could potentially reduce disulfide bonds, and complicate the interpretation of the results. We thus evaluated the binding of ^{99m}Tc to peptides with defined amino acid sequences. One peptide contained a terminal cysteine residue, but no histidines, while the other peptide contained histidine residues, but no cysteine or cystine. Both peptides were found to label with ^{99m}Tc , while in control studies, a peptide free of cysteine and histidine did not label. The utility of histidine group binding in peptides and proteins lacking cysteine remains to be fully developed, but suggests that such a labeling strategy deserves further study.

In conclusion, both histidine and cysteine groups of proteins can bind ^{99m}Tc . When cysteine is not available in IgG, ^{99m}Tc binds to histidine groups, and the binding efficiency is only moderate. When cysteine is available, as in reduced IgG, ^{99m}Tc binds to the protein almost quantitatively, and the binding is essentially to cysteinyl groups.

ACKNOWLEDGMENT

This study was funded by Small Business Innovative Research Grant 2 R44 CA50877-02 from the National Cancer Institute, Department of Health and Human Services. The editorial assistance of T. Coons and S. Slusher is gratefully acknowledged, as is the technical assistance of P. Budd, C. Lambert, and K. Sass. The professional expertise of M. Marek in preparation of some of the immunoglobulin kits is also gratefully acknowledged.

LITERATURE CITED

- Arnold, F. H., and Haymore, B. L. (1991) Engineered metal-binding proteins: Purification to protein folding. *Science* 252, 1796-1797.
- Dailey, H. A. (1984) Effect of sulfhydryl group modification on the activity of bovine ferrochelatase. *J. Biol. Chem.* 259, 2711-2715.
- Dewanjee, M. K. (1990) The chemistry of ^{99m}Tc -labeled radiopharmaceuticals. *Semin. Nucl. Med.* 20, 5-27.
- Eckelman, W. C., and Steigman, J. (1991) Direct labeling with ^{99m}Tc . *Nucl. Med. Biol.* 18, 3-7.
- Edelman, G. M., Cussingham, B. A., Gall, W. E., Fottlieb, P. D., Rutinhasuer, U., and Waxdal, M. L. (1969) The covalent structure of an entire gamma-G immunoglobulin molecule. *Proc. Nat. Acad. Sci. U.S.A.* 63, 78-85.
- Ghardiri, M. R., and Fernholz, A. K. (1990) Peptide architecture. Design of stable α -helical metalloproteins via a novel exchange-inert Ru^{III} complex. *J. Am. Chem. Soc.* 112, 9633-9635.
- Hawkins, E. B., Pant, K. D., and Rhodes, B. A. (1990) Resistance of direct Tc-99m-protein bond to transchelation. *Antibody Immunoconjugate Radiopharm.* 3, 17-25.
- Jocelyn, P. C. (1987) Spectrophotometric assay of thiols. *Methods Enzymol.* 143, 44-67.
- Lanteigne, D., and Hnatowich, D. J. (1984) The labeling of DTPA-coupled proteins with ^{99m}Tc . *Int. J. Appl. Radiat. Isot.* 35, 617-621.
- Mather, S. J., and Ellison, D. (1990) Reduction-mediated technetium-99m labeling of monoclonal antibodies. *J. Nucl. Med.* 31, 692-697.
- Means, G. E., and Feeney, R. E. (1990) Chemical modifications of proteins: History and applications. *Bioconjugate Chem.* 1, 2-12.
- Miles, E. W. (1979) Modification of histidinyl residues in proteins by diethylpyrocarbonate. *Methods Enzymol.* 49, 431-442.
- Paik, C. H., Phan, L., Hong, J. J., Sahami, M. W., Heald, S. C., Reba, R. C., Steigman, J., and Eckelman, W. C. (1985) The labeling of high affinity sites of antibodies with ^{99m}Tc . *Int. J. Nucl. Med. Biol.* 12, 3-8.
- Paik, C. H., Eckelman, W. C., and Reba, R. C. (1986) Transchelation of ^{99m}Tc from low affinity sites to high affinity sites of antibody. *Nucl. Med. Biol.* 139, 359-362.
- Pettit, W. A., DeLand, F. H., Bennett, S. J., and Goldenberg, D. M. (1980) Radiolabeling of affinity-purified goat anti-carcinoma embryonic antigen immunoglobulin G with Technetium-99m. *Cancer Res.* 40, 3043-3045.
- Rhodes, B. A. (1991) Direct labeling of proteins with ^{99m}Tc . *Nucl. Med. Biol.* 18, 667-676.
- Rhodes, B. A., Torvestaad, D. A., Burchiel, S. W., and Austin, R. K. (1980) A kit for direct labeling of antibody and antibody fragments with Tc-99m. *J. Nucl. Med.* 21, 80 (abstract).
- Rhodes, B. A., Zamora, P. O., Newell, K. D., and Valdez, E. F. (1986) Technetium-99m labeling of murine monoclonal antibody fragments. *J. Nucl. Med.* 27, 685-693, 1986.
- Schwarz, A., and Steinstrasser, A. (1987) A novel approach to Tc-99m-labelled monoclonal antibodies. *J. Nucl. Med.* 28, 721 (abstract).
- Seifert, S., Munze, R., and Johannsen, B. (1983) Technetium-99 and 99m chelates with N-donor ligands: A new class of potential cationic radiopharmaceuticals. In *Technetium in Chemistry and Nuclear Medicine* (E. Deutsch, M. Nicolini, and H. N. Wagner, Jr., Eds.) pp 19-23, Cortina International, Verona.
- Steigman, J., and Eckelman, W. C. (1992) *The Chemistry of Technetium in Medicine*, National Academy Press, Washington, DC.
- Steigman, J., Williams, H. P., and Solomon, N. A. (1975) The importance of the protein sulfhydryl group in HSA labeling with Technetium-99m. *J. Nucl. Med.* 16, 573 (abstract).
- Thakur, M. L., DeFulvio, J., Richard, M. D., and Park, C. H. (1991) Technetium-99m labeled monoclonal antibodies: Evaluation of reducing agents. *Nucl. Med. Biol.* 18, 227-233.
- Zamora, P. O., Mercer-Smith, J. A., Marek, M. J., Schulte, L. D., and Rhodes, B. A. (1992) Similarity of copper and technetium binding sites in human IgG. *Nucl. Med. Biol.* 19, 797-802.

Registry No. ^{99m}Tc , 14133-76-7; Cys, 52-90-4; His, 71-00-1; Ac-Asp-Arg-Val-Ile-His-Pro-Phe-His-Leu-Val-Ile-His-Asp, 143790-84-5; $\text{H}_2\text{N-Cys-Asp-Pro-Gly-Tyr-Ile-Gly-Ser-Arg}$, 110590-60-8; imidazole, 288-32-4.

1-(*m*-[²¹¹At]Astatobenzyl)guanidine: Synthesis via Astatodemetallation and Preliminary in Vitro and in Vivo Evaluation

Ganesan Vaidyanathan* and Michael R. Zalutsky

Department of Radiology, Duke University Medical Center, Durham, North Carolina 27710. Received June 1, 1992

No-carrier-added 1-(*m*-[²¹¹At]astatobenzyl)guanidine ([²¹¹At]MABG) was synthesized by astatodemetallation using two different routes. The overall yield for the two-step approach from 3-(tri-*n*-butylstannyl)benzylamine was 13%. *N*-Chlorosuccinimide-mediated astatodesilylation of 1-[3-(trimethylsilyl)benzyl]guanidine in acetic acid gave poor yields. In trifluoroacetic acid, the reaction worked well. The radiochemical yield was independent of reaction time and the amount of precursor used; however, the temperature of the reaction had a marked effect. Yields of 85% were obtained in 5 min at 70 °C using 0.5 μmol of the precursor. The percentage specific binding in vitro of [²¹¹At]MABG was nearly constant over a 2-log activity range and was comparable to that of no-carrier-added [¹³¹I]MIBG. The accumulation of [²¹¹At]MABG in the heart and adrenals of normal mice was similar to that observed for no-carrier-added [¹³¹I]MIBG.

INTRODUCTION

Radioiodinated 1-(*m*-iodobenzyl)guanidine (MIBG)¹ was synthesized by Wieland (1) for use as a radiopharmaceutical for the imaging of adrenomedullary diseases. Since that time, [¹³¹I]MIBG has been applied in the therapy of neuroendocrine tumors such as neuroblastoma (2, 3) and pheochromocytoma (4). In some patients with neuroblastoma, [¹³¹I]MIBG administration has reduced tumor volume, but remissions have been rare and generally of only several month's duration. Higher doses could be more effective in controlling tumor but pose the risk of toxic reactions, especially to the hematologic system (5). The problem has been attributed to the physical characteristics of ¹³¹I, for which the absorbed dose declines as the tumor size decreases and many neuroblastomas are small, with diameters below 1 mm (6, 7). Because the lower energy emissions of iodine-125 are fully absorbed by smaller volume tumors, MIBG labeled with this isotope alone or in combination with [¹³¹I]MIBG has been suggested for the treatment of neuroblastoma (6).

Because of the short range of its α particles (55–80 μm), astatine-211 might be an ideal nuclide for use in the treatment of neuroblastoma. α particles are attractive for radiotherapeutic applications because they are radiation of high linear energy transfer (8), making them more cytotoxic than β-emitting nuclides such as ¹³¹I. Since astatine is a halogen, the substitution of ²¹¹At for iodine in MIBG might offer an improved agent for the treatment of neuroendocrine tumors. Indeed, Mairs et al. (9) have suggested that 1-(*m*-[²¹¹At]astatobenzyl)guanidine ([²¹¹At]MABG) could be more effective in the treatment of neuroblastoma, provided that its specificity of uptake is the same as that of MIBG. Kemshead et al. (10) and Shapiro and Gross (11) also have commented on the prospective use of [²¹¹At]MABG in the treatment of neuroblastoma. McEwan et al. (12) have predicted that

[²¹¹At]MABG also could be advantageous in the treatment of pheochromocytoma.

Previously we found that [¹³¹I]MIBG could be prepared in no-carrier-added levels using the iodo demetallation approach (13). In this paper, we have modified these methods in order to prepare [²¹¹At]MABG. In vitro cell-binding studies and tissue-distribution measurements in normal mice suggest that the biological properties of [²¹¹At]MABG are quite similar to those of [¹³¹I]MIBG.

EXPERIMENTAL PROCEDURES

General. Astatine-211 was produced on the Duke University Medical Center cyclotron by 27–28 MeV α-particle-beam bombardment of a natural bismuth target. The activity was distilled and trapped into chloroform (or in some cases 0.1 N NaOH) as previously described (14). 1-(*m*-Iodobenzyl)guanidine sulfate was prepared following a literature procedure (15). [¹³¹I]MIBG prepared by isotopic exchange was obtained in 5 mM acetate buffer (pH 4.5) from the Duke University radiopharmacy. The specific activity was in the range of 2–10 mCi/mg, and the radioactivity concentration was about 2.5 μCi/μL.

The neuroblastoma cells SK-N-SH and SK-N-MC (16) were purchased from American Type Culture Collection (Rockville, MD). The incubation medium for the in vitro studies was made by mixing 440 mL of RPMI 1640, 50 mL of 10% Serum Plus, 5 mL of penicillin-G/streptomycin (5000 unit of penicillin and 5000 μg of streptomycin in 1 mL) and 5 mL of L-glutamine (200 mM in saline). All of these ingredients were obtained from JRH Biosciences (Lenexa, KS).

High-pressure liquid chromatography was conducted with two LKB Model 2150 pumps, an LKB Model 2152 control system, an LKB Model 2138 fixed-wavelength UV detector, and a Beckman Model 170 radioisotope detector. Peak analysis was performed using a Nelson Analytical software package on an IBM computer. Silica gel HPLC was performed using an Alltech silica gel column (Patrisil silica 10 μ, 250 × 4.6 mm). The solvent used for this was ethyl acetate/methanol/28% NH₄OH (90:8:2, v:v:v) and the flow rate was 1 mL/min. For reverse-phase chromatography, a Waters μ Bondapak C18 column (10 μm, 3.9 × 300 mm) was used. Two solvent systems were used: (A) 0.2 M NH₄H₂PO₄/tetrahydrofuran (80:20, v:v), at a flow rate of 0.8 mL/min (17), and (B) H₂O/tetrahydrofuran:

* Address correspondence to Ganesan Vaidyanathan, Ph.D., Duke University Medical Center, Box 3808, Room 161A, Bryan Research Building, Durham, North Carolina 27710; (919) 660-2711 ext 4411; FAX (919) 684-4211.

¹ Abbreviations used: MIBG, 1-(*m*-iodobenzyl)guanidine; MABG, 1-(*m*-astatobenzyl)guanidine; NCS, *N*-chlorosuccinimide.

triethylamine/ H_3PO_4 (96.5:2.0:1.0:0.5, v:v:v:v), at a flow rate of 2 mL/min (18).

Preparation *m*-(Tri-*n*-butylstannyl)benzylamine. *m*-(Tri-*n*-butylstannyl)benzylamine was prepared as reported (13). Briefly, a solution of 3-bromobenzylamine in 10 mL of dry tetrahydrofuran (distilled over LiAlH_4) at -100°C was treated with 3 equiv of *n*-butyllithium. After stirring for 30 min, 3 equiv of tri-*n*-butylstannyl chloride was added. The reaction mixture, after stirring at room temperature overnight, was partitioned between ether and water. The compound was isolated from the ether layer by evaporation of ether and silica gel chromatography.

Preparation of 1-[3-(Trimethylsilyl)benzyl]guanidine. This compound was prepared from 3-bromotoluene as previously described (13). 3-(Trimethylsilyl)benzylamine was prepared using a slight modification of a literature procedure (19). The hydrochloride salt of this benzylamine (500 mg, 2.3 mmol) and cyanamide (291 mg, 6.9 mmol) were heated at 100°C for 4 h. The guanidine, thus formed, was converted to its bicarbonate salt by adding a solution of 230 mg of KHCO_3 in 1 mL of water to the solution of residual reaction mixture in 1.2 mL of water. The precipitated bicarbonate salt was isolated by filtration, dried, and converted to the sulfate salt by recrystallization from 11 mL of 0.28 N H_2SO_4 (15). 1-[3-(Trimethylsilyl)benzyl]guanidine was obtained in a yield of 58%. The spectral and analytical data were in excellent agreement with the structure of the compound.

Preparation of ^{211}At]MABG. Two methods were used to synthesize 1-(*m*- ^{211}At]astatobenzyl)guanidine: a two-step method from 3-(tri-*n*-butylstannyl)benzylamine and a one-step procedure from 1-[3-(trimethylsilyl)benzyl]guanidine. For the first approach, the ^{211}At activity was trapped in 0.1 N NaOH (when the ^{211}At activity was trapped in chloroform, a lower yield resulted). In a Reacti vial (Pierce), 50 μL of the ^{211}At solution was combined with 20 μL of peracetic acid (prepared by mixing 130 μL of 30% hydrogen peroxide and 50 μL of glacial acetic acid and leaving the mixture at room temperature for 2 h) and 5 μL (0.5 μmol) of 3-(tri-*n*-butylstannyl)benzylamine in chloroform. The reaction mixture was stirred at room temperature for 30 min and injected into a silica gel HPLC column. A hot peak having a retention time similar to that of *m*-iodobenzylamine (8.0 min) was collected. This peak contained about 50% of the activity injected onto the HPLC column.

Only one experiment was performed for the conversion of *m*- ^{211}At]astatobenzylamine to ^{211}At]MABG. The solvent from the HPLC fraction was removed by a stream of argon. To the test tube containing the *m*- ^{211}At]astatobenzylamine was added 100 μL of methanol and 5 μL (1 mg) of cyanamide solution in water. After heating for 30 min at 128°C , a hot peak coeluting with an authentic sample of MIBG was collected that contained 25% of the injected activity. The overall radiochemical yield for this two-step synthesis was 13%.

For the one-step experiment using 1-[3-(trimethylsilyl)benzyl]guanidine, fresh solutions of *N*-chlorosuccinimide (NCS) and precursor were prepared. To 1 μL of 0.1 N NaOH in a 1 mL of Reacti vial was added 100 μL of the chloroform solution containing the ^{211}At activity. After the solution was vortexed, the chloroform was evaporated with a gentle stream of argon, and little or no activity was lost. The process was repeated, if necessary, in order to obtain the required amount of activity in 0.1 N NaOH. For kinetic runs, about 100 μCi of ^{211}At activity was used. For in vitro studies and biodistribution measurements, 300–700 μCi were used. To the ^{211}At activity was added

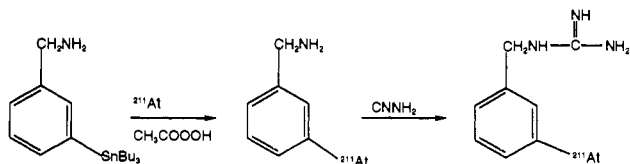
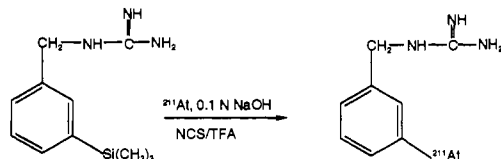
10 μL of a solution of NCS in trifluoroacetic acid (TFA) (0.4 mg in 10 μL), followed by 5 μL of precursor solution (0.5–2 μmol). After the mixture was vortexed, the capped vial was left at 20 – 70°C for 5–30 min (Heating was achieved by an oil bath with an immersion heater, and the temperature was maintained within $\pm 1^\circ\text{C}$). At the end of the reaction, the entire reaction mixture was injected into a reverse-phase HPLC. For kinetic runs, HPLC solvent system A was used, and for biological experiments, solvent system B was used. The yield of ^{211}At]MABG was calculated as the percentage of injected activity that eluted with the retention time of an MIBG standard.

In Vitro Binding to Neuroblastoma Cells. Human neuroblastoma cell lines SK-N-SH (target) and SK-N-MC (control) were used to determine the specific binding of ^{211}At]MABG. The HPLC fraction containing the ^{211}At]MABG activity was stripped of tetrahydrofuran using a stream of argon for 5–10 min. The remaining solution was passed through an activated C18 Sep-Pak, and the Sep-Pak was washed further with 2×5 mL of water and 2×500 μL of 5 mM sodium acetate buffer (pH 4.5). The Sep-Pak was eluted with 250- μL portions of methanol, and 75–80% of ^{211}At]MABG was isolated in fractions 2–4. The methanol was removed with an argon stream, and the activity was reconstituted in 5 mM sodium acetate buffer (pH 4.5). Doses of 10 000–2 000 000 counts per minute of ^{211}At]MABG in 500 μL of the incubation medium were prepared. Both SK-N-SH and SK-N-MC cells, 4×10^5 per well, were incubated in quadruplicate in 24 well plates with ^{211}At]MABG for 3 h at 37°C . This protocol also was used, in parallel, to determine the specific binding of ^{131}I]MIBG prepared by the isotopic exchange method. After incubation, the cells were washed twice with phosphate-buffered saline and lysed with 500 μL of 0.5 N NaOH for 30 min at room temperature. The solubilized cells were harvested by aspiration and wiped with cotton swabs. These were counted, along with input standards, using an automated γ counter (LKB 1282). The percentage of specific binding was calculated as the difference between the percentage bound to the target cells and that bound to the controls.

Biodistribution in Normal Mice. The HPLC fraction containing ^{211}At]MABG was desalted by passing it through a C18 Sep-Pak as described above and reconstituted in phosphate-buffered saline. BALB/c mice were injected in the tail vein with 4–5 μCi of ^{211}At]MABG in 100 μL of phosphate-buffered saline. Groups of five mice were given a halothane overdose at 1–24 h. Tissues of interest were isolated after dissecting, washed with saline, and counted for ^{211}At activity in an automated γ counter. The results were expressed as the percentage of injected dose per gram of tissue (% ID/g). Standards of appropriate count rates were used to calculate the above values. Data for the tissue distribution of no-carrier-added ^{131}I]MIBG were used for comparison (13).

RESULTS AND DISCUSSION

The goal of this investigation was to develop a method for the synthesis of ^{211}At]MABG and to compare its in vitro binding and in vivo tissue distribution with that of no-carrier-added ^{131}I]MIBG. Astatate demetalation was explored because of the successful application of this approach to the synthesis of other ^{211}At -labeled compounds. The radioastatination of a wide variety of organic compounds using organomercury precursors has been described by Visser and co-workers (20–22). Initial studies using trialkylstannyl precursors required the use of iodide carrier to obtain reasonable ^{211}At labeling yields (23). More

Scheme I. Synthesis of [²¹¹At]MABG: Two-Step MethodScheme II. Synthesis of [²¹¹At]MABG: One-Step Method

recently, astatination via electrophilic destannylation without the use of iodide carrier has been reported (14, 24, 25), and a number of other astatine demetalation precursors also have been investigated (25). Previous attempts to prepare a tin precursor from which [²¹¹At]MABG could have been obtained in a single step were not successful (13). Like [¹³¹I]MIBG, however, the feasibility of [²¹¹At]MABG preparation in two steps from 3-(tri-*n*-butylstannyl)benzylamine could be demonstrated (Scheme I). In the few experiments performed using this route, the overall yield was 13%. This low yield might be due to the considerable amount of water present in the activity (see below), and better yields might be obtainable with smaller volumes of 0.1 N NaOH. Since this approach involved an extra step after the introduction of ²¹¹At, we focused our attention on the preparation of [²¹¹At]MABG in a single step, from 1-[3-(trimethylsilyl)benzyl]guanidine (Scheme II).

Substantial amounts of water decreased the yield of radiohalo desilylation of 1-[3-(trimethylsilyl)benzyl]guanidine. This generally was not a problem with ¹³¹I, since it is commercially available in high radioactivity concentrations (0.5–1.0 mCi/μL). With our current astatine target distillation system, a minimum volume of 100–200 μL trapping medium is necessary. As a result, if the astatine activity were trapped directly in sodium hydroxide solution, the resulting radioactivity concentration would be very low. Fortunately, it was possible to extract the astatine activity into as small a volume as 1 μL of 0.1 N NaOH from chloroform solutions without sacrificing the reactive quality or quantity of the activity. Using trifluoroacetic acid as the oxidant, astatine desilylation of 1-[3-(trimethylsilyl)benzyl]guanidine could be accomplished in the presence or absence of chloroform. Although yields of 50% sometimes were obtained, reproducibility with this oxidant was less than ideal.

Unlike iodination, astatine desilylation of 1-[3-(trimethylsilyl)benzyl]guanidine using NCS as the oxidant and acetic acid as the medium gave poor yields, even at 70 °C. This observation is similar to that reported by Hadley et al. (26) with regard to the halo demetalation of *N*-succinimidyl *p*-(tri-*n*-butylstannyl)benzoate. They found that using this tin precursor, larger quantities of reagents were necessary for NCS-mediated astatine destannylation to obtain yields comparable to those obtained with iodo destannylation. A plausible explanation for this behavior could be the increased steric hindrance caused by the bulky astatine atom.

With trifluoroacetic acid as the medium, better yields were obtained. The effect of temperature, time, and precursor amount on the yield of astatine desilylation using NCS as the oxidant in trifluoroacetic acid was studied, and the results are shown in Figure 1. The yield did not

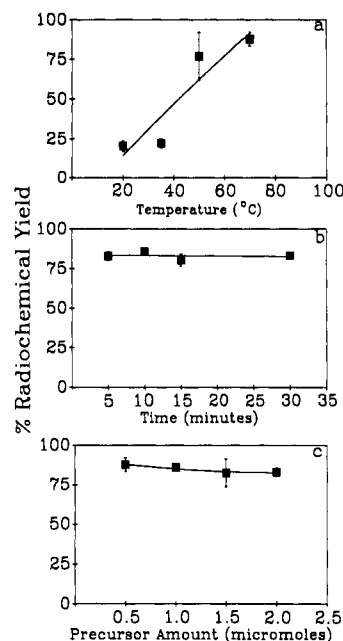


Figure 1. NCS-mediated astatine desilylation of 1-[3-(trimethylsilyl)benzyl]guanidine in trifluoroacetic acid showing effect of temperature, reaction time, and precursor on yield. *N*-Chlorosuccinimide (0.4 mg) dissolved in 10 μL of trifluoroacetic acid was added to the astatine activity in 1 μL 0.1 N NaOH followed by the desired amount of precursor in 5 μL of trifluoroacetic acid: (a) Reaction time = 5 min, 0.5 μmol of precursor, *n* = 3–5; (b) reaction temperature = 70 °C, 2 μmol of precursor, *n* = 3; (c) reaction time = 5 min, reaction temperature = 70 °C, *n* = 3.

depend on the reaction time (83.0 ± 2.6% in 5 min vs 83.2 ± 1.7% in 30 min) or precursor amount (87.7 ± 4.3% with 0.5 μmol vs 83.0 ± 2.6% with 2.0 μmol). Temperature, however, had a remarkable influence on the yield. At temperatures of 20 and 30 °C, yields of only 20–25% were obtained, while at 50 and 70 °C, the yields were 77.0 ± 15.1% and 87.7 ± 4.3%, respectively. Like [¹³¹I]MIBG, [²¹¹At]MABG could be separated, by HPLC solvent system B, from possible byproducts such as 1-benzylguanidine and 1-(*m*-chlorobenzyl)guanidine. Within the limits of detection, no coeluting, UV-absorbing mass peak was observed.

Before [²¹¹At]MABG can be considered as a potential therapeutic agent, it is critical to demonstrate that substitution of astatine for iodine in MIBG would not alter its specificity. In order to evaluate the uptake of [²¹¹At]MABG, we performed in vitro experiments using neuroblastoma cells SK-N-SH as the target and SK-N-MC as the control. Specific binding was defined as the difference in binding to the two cell lines. Binding to the SK-N-MC control line was 2–3% for both [²¹¹At]MABG and [¹³¹I]MIBG at all dose levels. As shown in Figure 2, the percentage of specific binding of [²¹¹At]MABG remained fairly constant over a 2-log activity range and was comparable to that reported previously for no-carrier-added [¹³¹I]MIBG (13). In comparison, the specific binding of [¹³¹I]MIBG prepared by isotopic exchange decreased with increasing dose presumably due to the saturation of cellular uptake due to the presence of carrier MIBG in this preparation. Thus, astatine for iodine substitution did not compromise the specificity of uptake of this 1-(halobenzyl)guanidine analog, at least, in the case of SK-N-SH cells.

To determine whether the biodistribution of [²¹¹At]-MABG was similar to that of [¹³¹I]MIBG, we used normal mice to compare the percentage of the injected dose localized per gram of tissue (% ID/g) for [²¹¹At]MABG

Table I. Tissue Distribution of [^{211}At]MABG and No-Carrier-Added [^{131}I]MIBG in Normal Mice

tissue	% injected dose per gram ^a					
	1 h		4 h		24 h	
	[^{211}At]MABG	[^{131}I]MIBG ^b	[^{211}At]MABG	[^{131}I]MIBG ^b	[^{211}At]MABG	[^{131}I]MIBG ^b
liver	9.17 \pm 0.80 ^c	7.45 \pm 1.06	4.81 \pm 0.59	4.08 \pm 0.70	1.54 \pm 0.11 ^c	0.95 \pm 0.13
spleen	3.87 \pm 0.69	4.55 \pm 0.84	3.40 \pm 0.42	3.22 \pm 0.22	2.65 \pm 0.88	1.82 \pm 0.14
lungs	7.42 \pm 1.84	7.62 \pm 1.41	3.84 \pm 0.77	3.69 \pm 0.87	1.26 \pm 0.32	1.10 \pm 0.34
heart	20.61 \pm 2.71	24.88 \pm 3.75	12.97 \pm 1.58 ^c	16.14 \pm 2.60	4.42 \pm 0.51	3.75 \pm 0.54
kidney	2.83 \pm 0.29	2.52 \pm 0.18	2.24 \pm 0.21 ^c	1.62 \pm 0.19	1.01 \pm 0.05 ^c	0.72 \pm 0.19
thyroid	2.83 \pm 0.61	2.85 \pm 0.99	2.24 \pm 0.32	2.38 \pm 0.50	2.47 \pm 0.52	2.60 \pm 0.34
blood	0.87 \pm 0.05	0.99 \pm 0.13	0.52 \pm 0.11	0.52 \pm 0.08	0.21 \pm 0.06 ^c	0.10 \pm 0.02
adrenals	20.33 \pm 5.06	16.85 \pm 2.98	16.67 \pm 1.91	16.15 \pm 4.54	20.79 \pm 5.53	26.73 \pm 6.10

^a Mean \pm SD ($n = 5$). ^b No-carrier-added preparation. ^c Uptake of the two agents determined to be statistically significant by a two-sided t test; differences found to be significant are indicated ($p < 0.05$).

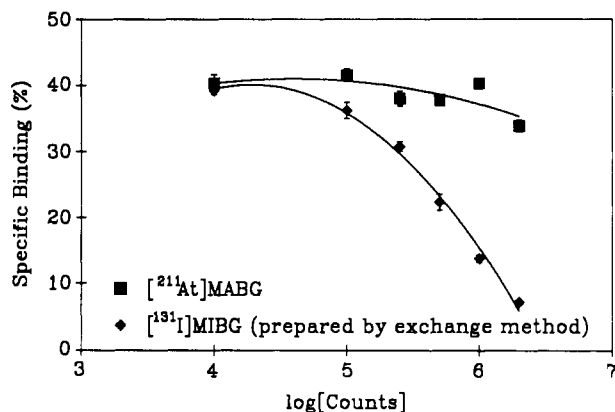


Figure 2. Binding of [^{211}At]MABG and [^{131}I]MIBG, prepared by an exchange method, to SK-N-SH neuroblastoma cells: percentage of specific binding (percent bound to SK-N-SH minus percent bound to SK-N-MC) as function of input dose.

with the results obtained earlier (13) for no-carrier-added [^{131}I]MIBG (Table I). As is evident from these data, the tissue distribution of [^{211}At]MABG was quite similar to that observed for [^{131}I]MIBG. With most tissues, the differences in the uptake of [^{211}At]MABG and [^{131}I]MIBG were not statistically significant ($p > 0.05$ using a two-sided t test). Because of the known specific localization of MIBG in adrenals and heart (1), the relative uptake of the two labeled 1-(halobenzyl)guanidines in these tissues was of particular interest. Differences in the adrenal uptake of the two compounds were not statistically significant for all the time points studied. The heart uptake of [^{211}At]MABG was 80–83% of that seen for no-carrier-added [^{131}I]MIBG at 1 and 4 h; however, the difference was statistically significant only at 4 h ($13.0 \pm 1.6\%$ vs $16.1 \pm 2.6\%$; $p < 0.05$). At 24 h, the value for [^{211}At]MABG was about 1.2-fold that of [^{131}I]MIBG, but the difference was not significant. These data suggest that the specificity of uptake is not changed significantly when astatine is substituted for iodine in MIBG.

A potential concern with using [^{211}At]MABG as a radiotherapeutic agent is the in vivo stability of the carbon-astatine bond, which would be expected to be lower than the corresponding carbon-iodine bond in MIBG. Nevertheless, uptake of [^{211}At]MABG in the thyroid was comparable to that of [^{131}I]MIBG, suggesting a low degree of dehalogenation for both compounds. It is important to note that the uptake of astatide in mouse thyroid is only 10–50% that of iodide over the time course of these experiments (27). In addition, spleen and lungs are two organs with relative selectivity for astatide about 10 times that seen for iodide (27). In the current study, the uptake of [^{211}At]MABG and [^{131}I]MIBG in these tissues was nearly identical, suggesting that [^{211}At]MABG may be reasonably stable in vivo.

In conclusion, we have developed a one-step method for the preparation of 1-(m -[^{211}At]astatobenzyl)guanidine. Results from in vitro experiments using SK-N-SH neuroblastoma cells and tissue-distribution studies in normal mice suggest that [^{211}At]MABG has biological properties similar to MIBG. Whether [^{211}At]MABG will be a useful agent for the radiotherapy of neuroendocrine tumors remains to be ascertained, particularly in light of the significant accumulation of activity in normal adrenals and heart. This issue will be addressed in the future in an athymic mouse neuroblastoma model.

ACKNOWLEDGMENT

The excellent technical assistance of Donna Affleck, Susan Slade, and Phil Welsh is greatly appreciated. The authors are grateful to Sandra Gatling and Ann Tamariz for help in preparing the manuscript. This research was supported in part by Grants CA 42324 and CA 14236 from the National Cancer Institute.

LITERATURE CITED

- Wieland, D. M. (1986) Radiopharmaceutical Design: The Adrenal Medulla and Its Diseases. In *Radiopharmaceuticals: Progress and Clinical Perspectives* (A. R. Fritzberg, Ed.) Vol. 1 pp 117–153, CRC Press, Inc., Boca Raton, FL.
- Voûte, P. A., Hoefnagel, C. A., de Kraker, J., Valdes Olmos, R., Bakker, D. J., and van de Kleij, A. J. (1991) Results of Treatment with ^{131}I -metaiodobenzylguanidine (^{131}I -MIBG) in Patients with Neuroblastoma. Future Prospects of Zeto-therapy. In *Advances in Neuroblastoma Research 3* (A. E. Evans, G. J. D'angio, A. G. Knudson, Jr., and R. C. Seeger, Eds.) pp 439–445, Wiley-Liss, Inc., New York (Progress in Clinical and Biological Research, Vol. 366).
- Caraventa, A., Guerra, P., Arrighini, A., Bertolazzi, L., Bestagno, M., De Bernardi, B., Lanino, E., Villavecchia, G. P., and Claudiani, F. (1991) Treatment of advanced neuroblastoma with ^{131}I -meta-iodobenzylguanidine. *Cancer* 67, 922–928.
- Sisson, J. C., Shapiro, B., Beierwaltes, W. H., Glowniak, J. V., Nakajo, M., Mangner, T. J., Carey, J. E., Swanson, D. P., Copp, J. E., Satterlee, W. G., and Wieland, D. M. (1984) Radiopharmaceutical treatment of malignant pheochromocytoma. *J. Nucl. Med.* 24, 197–206.
- Sisson, J. C., Hutchinson, R. J., Carey, J. E., Shapiro, B., Johnson, J. W., Mallette, S. A., and Wieland, D. M. (1988) Toxicity from treatment of neuroblastoma with ^{131}I -meta-iodobenzylguanidine. *Eur. J. Nucl. Med.* 14, 337–340.
- Sisson, J. C., Hutchinson, R. J., Shapiro, B., Zasadny, K. R., Normolle, D., Wieland, D. M., Wahl, R. L., Singer, D. A., Mallette, S. A., and Mudgett, E. E. (1990) Iodine-125-MIBG to treat neuroblastoma: Preliminary report. *J. Nucl. Med.* 31, 1479–1485.
- O'Donoghue, A., Wheldon, T. E., Babich, J. W., Moyes, J. S. E., Barrett, A., and Meller, T. (1991) Implications of the uptake

- of ¹³¹I-radiolabelled meta-iodobenzylguanidine (MIBG) for the targeted radiotherapy of neuroblastoma. *Br. J. Radiol.* 64, 428-434.
- (8) Hall, E. J. (1988) LET and RBE. *Radiobiology for the Radiologist*, pp 161-177, Lippincott, Philadelphia.
- (9) Mairs, R. J., Angerson, W. J., Babich, J. W., and Murray, T. (1991) Differential Penetration of Targeting Agents into Multicellular Spheroids Derived from Human Neuroblastoma. In *Advances in Neuroblastoma Research 3* (A. E. Evans, G. J. D'Angio, A. G. Knudson, Jr., and R. C. Seeger, Eds.) pp 495-501, Wiley-Liss, Inc., New York (Progress in Clinical and Biological Research, Vol. 366).
- (10) Kemshead, J. T., Pizer, P. L., and Patel, K. (1990) Neuroblastoma: Perspectives for future research. In *Neuroblastoma: Tumor Biology and Therapy* (C. Pochedly, Ed.) pp 381-395, CRC Press, Boca Raton, FL.
- (11) Shapiro, B., and Gross, M. D. (1987) Radiochemistry, biochemistry, and kinetics of ¹³¹I-metaiodobenzylguanidine (MIBG) and ¹²³I-MIBG: Clinical implications of the use of ¹²³I-MIBG. *Med. Pediatr. Oncol.* 15, 170-177.
- (12) McEwan, A. J., Wyeth, P., and Ackery, D. (1986) Radioiodinated iodobenzylguanidines for diagnosis and therapy. *Appl. Radiat. Isot.* 37, 765-775.
- (13) Vaidyanathan, G., and Zalutsky, M. R. (1992) No-carrier-added synthesis of meta-[¹³¹I]iodobenzylguanidine. *Appl. Radiat. Isot.* In press.
- (14) Zalutsky, M. R., Garg, P. K., Friedman, H. S., and Bigner, D. D. (1989) Labeling monoclonal antibodies and F(ab')₂ fragments with the α -particle-emitting nuclide astatine-211: Preservation of immunoactivity and in vivo localizing capacity. *Proc. Natl. Acad. Sci. U.S.A.* 86, 7149-7153.
- (15) Wieland, D. M., Wu, J.-I., Brown, L. E., Mangner, T. J., Swanson, D. P., and Beierwaltes, W. H. (1980) Radiolabeled adrenergic neuron-blocking agents: Adrenomedullary imaging with [¹³¹I]iodobenzylguanidine. *J. Nucl. Med.* 21, 349-353.
- (16) Biedler, J. N., Helson, L., and Spengler, B. A. (1973) Morphology and growth, tumorigenicity, and cytogenetics of human neuroblastoma cells in continuous culture. *Cancer Res.* 33, 2643-2652.
- (17) Wieland, D. M., Mangner, T. J., Inbasekaran, M. N., Brown, L. E., and Wu, J.-I. (1984) Adrenal medulla imaging agents: A structure-distribution relationship study of radiolabeled aralkylguanidines. *J. Med. Chem.* 27, 149-155.
- (18) Iwata, R., and Ido, T. (1983) Production of [¹¹C]cyanamide as a new precursor for [¹¹C]benzylguanidine synthesis. *Int. J. Appl. Radiat. Isot.* 34, 973-976.
- (19) Gertner, D., Rosen, H., and Zilkha, A. (1965/66) Synthesis of some silicon-containing β -amino acids. *Israel J. Chem.* 3, 235-238.
- (20) Visser, G. W. M., Diemer, E. L., and Kaspersen, F. M. (1980) The preparation of aromatic astatine compounds through aromatic mercury compounds. *J. Labelled Compd. Radiopharm.* 17, 657-665.
- (21) Visser, G. W. M., Diemer, E. L., and Kaspersen, F. M. (1981) The preparation of aromatic astatine compounds through aromatic mercury compounds. Part II: Astatination of pyrimidines and steroids. *J. Labelled Compd. Radiopharm.* 18, 799-807.
- (22) Visser, G. W. M., Diemer, E. L., and Kaspersen, F. M. (1980) The preparation and stability of ²¹¹At-astato-imidazoles. *Int. J. Appl. Radiat. Isot.* 31, 275-278.
- (23) Milius, R. A., McLaughlin, W. H., Lambrecht, R. M., Wolf, A. P., Carroll, J. J., Adelstein, S. J., and Bloomer, W. D. (1986) Organoastatine chemistry. Astatination via electrophilic destannylation. *Appl. Radiat. Isot.* 37, 799-802.
- (24) Zalutsky, M. R., and Narula, A. S. (1988) Astatination of proteins using an *N*-succinimidyl tri-*n*-butylstannylbenzoate intermediate. *Appl. Radiat. Isot.* 39, 227-232.
- (25) Wilbur, D. S., Hyalarides, M. D., and Fritzberg, A. R. (1989) Reactions of organometallic compounds with astatine-211. Application to protein labeling. *Radiochem. Acta* 47, 137-142.
- (26) Hadley, S. W., Wilbur, D. S., Gray, M. A., and Atcher, R. W. (1991) Astatine-211 labeling of an antimelanoma antibody and its Fab fragment using *N*-succinimidyl *p*-astatobenzoate: Comparisons in vivo with the *p*-[¹²⁵I]iodobenzoyl conjugate. *Bioconjugate Chem.* 2, 171-179.
- (27) Garg, P. K., Harrison, C. L., and Zalutsky, M. R. (1990) Comparative tissue distribution in mice of the α -emitter ²¹¹At and ¹³¹I as labels of a monoclonal antibody and F(ab')₂ fragment. *Cancer Res.* 50, 3514-3520.
- Registry No.** [²¹¹At]MABG, 127367-45-7; *m*-(tri-*n*-butylstannyl)benzylamine, 143773-91-5; 3-[(trimethylsilyl)benzyl]guanidine, 143773-92-6; *m*-[²¹¹At]astatobenzylamine, 143773-93-7.

Use of Microsphere-Antibody Conjugates in Microparticle-Enhanced Nephelometric Immunoassay

Paul Montagne,* Rachida El Omari, Florence Cliquet, Marie Louise Cuillière, and Jean Duheille

Immunology Laboratory, Faculty of Medicine, BP 184, F-54505 Vandoeuvre les Nancy Cedex, France. Received June 1, 1992

A new microparticle-enhanced nephelometric immunoassay has been recently described as a sensitive, accurate, and easy-to-perform competitive immunoassay for various analytes. As initially described, this test is based on the nephelometric quantification of the inhibition, by the antigen to be assayed, of immunoagglutination of microparticle-antigen conjugates. Its applicability as a competitive immunoassay is thus limited by the necessary availability of pure antigens to prepare microparticle-antigen conjugates. In this paper, we report an adaptation of this initial test, where microparticles are coated by monoclonal antibodies, eliminating the need for purified antigens. The new configurations of particle agglutination-based immunoassays described include use of these microparticle-antibody conjugates with microparticle-antigen conjugates, free antigen, and anti-mouse immunoglobulins antiserum. The feasibility of such configurations is studied with human chorionic gonadotropin hormone, human thyroid stimulating hormone, and human myoglobin as antigens. Capture of the analyte by microparticle-antibody conjugates is evidenced by inhibition of their agglutination with microparticle-antigen conjugates and by agglutination in a sandwich assay with a complementary monoclonal antibody or polyclonal antiserum. The use of a second xenogenic antibody enhances the agglutination process and increases the assay sensitivity. Microparticle-antibody conjugates may extend the applications of microparticle-enhanced nephelometric immunoassays to unavailable analytes.

INTRODUCTION

A microparticle-enhanced nephelometric immunoassay has been recently described as a new method for quantitation of various analytes in human serum (Cuillière et al., 1991; Gartner et al., 1991; Montagne et al., 1991b, 1992a-c) and bovine milk (Collard-Bovy et al., 1991; El Bari et al., 1991; Marchal et al., 1991; Montagne et al., 1991a). It was a competitive immunoassay based on the inhibition, by free antigen, of the microparticle-antigen conjugate agglutination occurring in the presence of monoclonal antibody or specific antiserum. Measurement of the light scattered by conjugate clusters during this inhibition with an adapted nephelometer allowed the quantitation of free antigen. Thus developed, microparticle-enhanced nephelometric immunoassay was a sensitive (about 10^{-14} mol/mL of analyte significantly detected), accurate (variation coefficients lower than 10% in within- and between-assay reproducibility), and easy-to-perform (one-step assay without washing or phase separation) method. However, it required the availability of pure antigens to prepare microparticle-antigen conjugates. This necessity restricted its application to the assay of readily available antigens. The use of microparticle-antibody conjugates to trap the antigen to be assayed followed by a conjugate agglutination disclosing this capture and permitting its nephelometric quantification may allow further developments of the method.

We report here the immunonephelometric study of hydrophilic microspheres (MS)¹ specifically designed for microparticle-enhanced nephelometric immunoassay and covalently coated with monoclonal antibody (mAb). The reactivity of these MS-mAb conjugates with MS-antigen

conjugate, free antigen, and anti-mouse immunoglobulins (Ig) antiserum (As) is described. The use of MS-mAb conjugates is evaluated in various configurations of particle agglutination-based immunoassays. Different procedures, schematized in Table I, are thus studied to show the capture of the antigen to be assayed by MS-mAb conjugate: competitive inhibition of coagglutination between MS-mAb and MS-antigen conjugates (Table I, configuration I) or direct agglutination of MS-mAb/antigen complexes by a complementary mAb (Table I, configuration II) or polyclonal As (Table I, configuration IV). The use of a second xenogenic antibody to produce or amplify the agglutination reaction is also described (Table I, configurations III and V) and discussed. Possible applications to human chorionic gonadotropin hormone (hCG), human thyroid stimulating hormone (hTSH), and human myoglobin (hMb) are depicted. They allowed evaluation of the characteristics and showed the feasibility of these new configurations of particle agglutination-based immunoassay.

EXPERIMENTAL PROCEDURES

Reagents. 2-Hydroxyethyl methacrylate, acrolein, and methacrylic acid were purchased from Merck (Darmstadt, Germany). *N,N'*-Methylenebisacrylamide was a product of Eastman Kodak Co. (Rochester, NY). Other chemical reagents were analytical-reagent-grade from Prolabo-Rhône Poulenc (Paris, France). Immunonephelometric assays were performed with the phosphate buffer for nephelometry, pH 7.2, supplied by Diagnostics Pasteur (Marnes, France).

hCG (3326 IU/mg) from human pregnancy urine and hTSH (7 IU/mg) from human pituitary, standardized according to the international preparations, were purchased from Sigma (St. Louis, MO). hMb was obtained from Dakopatts (Glostrup, Denmark).

Murine mAbs, produced by standard hybridoma technology and purified from ascites fluid (Paolucci et al., 1986),

* Author to whom correspondence should be addressed.

¹ Abbreviations used: MS, microsphere; mAb, monoclonal antibody; Ig, immunoglobulins; As, antiserum; hCG, human chorionic gonadotropin hormone; hTSH, human thyroid stimulating hormone; hMb, human myoglobin.

Table I. Configurations of Microparticle-Enhanced Nephelometric Immunoassay Using MS-mAb Conjugates

test	reagents	analyte	reaction and nephelometric observation
I	MS-mAb MS-hCG	hCG	formation of MS-mAb/hCG complexes with inhibition of MS-mAb/MS-hCG agglutination
II	MS-mAb mAb* ^a	hCG	formation of MS-mAb/hCG complexes and agglutination MS-mAb/hCG/mAb*
III	MS-mAb mAb* ^b anti-mouse Ig As	hCG (hTSH)	formation of unagglutinating MS-mAb/hCG (hTSH)/mAb* complexes and agglutination by anti-mouse Ig As
IV	MS-mAb rabbit anti-hMb As	hMb	formation of MS-mAb/hMb complexes and agglutination by rabbit anti-hMb As
V	MS-mAb rabbit anti-hMb As anti-rabbit Ig As	hMb	formation of unagglutinating MS-mAb/hMb/anti-hMb complexes and agglutination by anti-rabbit Ig As

^a mAb* is complementary to the mAb bound to MS in MS-mAb conjugate. ^b mAb* is present in the reaction mixture at a concentration inhibiting the MS-mAb agglutination by anti-mouse Ig As.

were supplied by Sanofi Research (Montpellier, France). Six of the mAbs used (A1, B1, D2, F3, G4, and H5) reacted with five complementary regions of the hCG molecule. Four of them (A1, B1, D2, and F3) were specific for its β chain. Two mAbs (Ib and IIa) were directed against two complementary epitopes, located on the β and α chain, respectively, of the hTSH molecule. One anti-hMb mAb was also used. The affinity constant of these mAbs was determined by the Scatchard's method (Scatchard, 1949) and ranged from 10^8 to 10^{10} M⁻¹. Rabbit anti-hMb and rabbit anti-mouse Ig As were purchased from Dakopatts. Goat anti-rabbit Ig As was produced by Diagnostics Pasteur.

Preparation of MS and MS-Protein Conjugates. Polyfunctional (hydroxyl, aldehyde, and carboxyl functions) hydrophilic MS [diameter = 200 nm, (SD = 6 nm) and diameter = 295 nm (SD = 4 nm)] were synthesized and characterized as previously reported (Montagne et al., 1992c). Mixtures (100 and 120 g/L) of acrylic monomers: 2-hydroxyethyl methacrylate, acrolein, methacrylic acid, and *N,N'*-methylenebisacrylamide (49.7%, 47%, 2%, and 1.3% (v/v) of total monomers, respectively) were copolymerized in the presence of 0.6 and 0.9 g/L sodium dodecyl sulfate under γ -irradiation (75 krad/cm²) from a ⁶⁰Co source (CENG, Grenoble, France).

Protein-coated MS were prepared as previously described (Marchand et al., 1992) by formation of covalent imine bonds between aldehyde groups on MS and primary amino groups of proteins. Briefly, MS-hCG conjugate was obtained by mixing 1.6 mg of hCG with 10 mg of MS (200 nm in diameter) in 1 mL of 0.005 M phosphate buffer, pH 7.2. After gentle stirring for 18 h at 4 °C and blocking of the unreacted aldehyde groups on MS by 2-aminoethanol (0.12 M, pH 8, 4 h, room temperature), MS-hCG were collected by centrifugation (10000g, 1 h, 4 °C) on a discontinuous sucrose gradient (200/800 mg/mL) and stored in 0.1 M phosphate buffer, pH 7.2, containing 2 mg/mL sodium azide. MS-mAb conjugates were similarly produced by covalent coating of hydrophilic MS (295 nm in diameter, 4 mg) with 0.4 mg of various mAbs (anti-hCG mAb B1, D2, F3 and G4; anti-hTSH mAb Ib; anti-hMb mAb) in 1 mL of 0.1 M borate buffer, pH 9. MS-mAb were stored in this same borate buffer containing sodium

azide after elimination of uncoupled mAbs by centrifugation (8000g) on a sucrose gradient.

The amounts of hCG in MS-hCG conjugate (1000 hCG molecules per MS) and of immunoreactive mAb in MS-mAb conjugates (120–190 antibody sites per MS, according to the mAb bound) was assessed by radioimmunological assays (Montagne et al., 1992c) using ¹²⁵I-antigen probes prepared by the chloramine-T method (Greenwood & Hunter, 1963) and free hCG or free mAbs as calibrators. The stability and immunoreactivity of MS-protein conjugates was preserved for several months when stored at 4 °C (Marchand et al., 1992).

Immunonephelometric Study of MS-mAb Conjugates. The immunonephelometric reactivity of MS-mAb conjugates with MS-antigen conjugate, free antigen, and anti-mouse Ig As was studied by measurement of the light scattered during conjugates agglutination using the Diagnostics Pasteur nephelometer Nephelia N 600 (Montagne et al., 1992c). Controls consisting of reaction mixture containing the conjugate alone or total reaction mixture without analyte were systematically performed in each test to measure the intensity of the light scattered by dispersed conjugate, at 0% agglutination or at 100% agglutination in inhibition procedures. This allowed calculation of the light-scattering amplification, defined as the ratio of the light scattered by conjugate clusters to the light scattered by dispersed conjugate alone. They also permitted the determination of analyte concentrations significantly detectable at those yielding a light-scattering amplification different from the noise [intensity of light scattered 3 SD ($n = 30$) higher than the mean of the intensity of the light scattered by control without analyte]. All dilutions and dispensations were performed in the buffer for nephelometry with an automated dilutor (Hamilton, Bonaduz, Switzerland) in disposable microcuvettes (Nephelia microcuvette, 1-cm light path, 0.3-mL reaction volume).

Reaction of anti-hCG MS-mAb Conjugates with MS-hCG Conjugate. The reaction between each anti-hCG MS-mAb conjugate and MS-hCG was performed by mixing serial concentrations of MS-B1, MS-D2, MS-F3, and MS-G4 (between 5 and 520 μ g/mL) with MS-hCG (20 μ g/mL). The light scattered by each mixture was measured after 2 h. Inhibition of conjugate coagglutination by free hCG (Table I, configuration I) was assayed by adding serial concentrations of hCG (0.016–8.2 IU/mL) to MS-mAb conjugate (30 μ g/mL). After incubation for 30 min at room temperature, MS-hCG conjugate (20 μ g/mL) was added to the mixtures and the scattered light was measured after 2 h.

Reaction of Anti-hCG MS-D2 Conjugate with Free hCG. Capture of hCG by MS-mAb D2 conjugate was performed by incubation for 30 min at room temperature of the conjugate (30 μ g/mL) with serial concentrations of hCG (0.02–5 IU/mL). Anti-hCG mAbs A1, B1, F3, G4, and H5, specific to an hCG epitope different from that recognized by mAb D2, were then separately added at serial concentrations (0.36–11.40 μ g/mL), and the light scattered by conjugate clusters was measured after 2 h of reaction (Table I, configuration II).

Reaction of Anti-hCG MS-D2 Conjugate with Anti-Mouse Ig As. Agglutination of MS-mAb D2 conjugate by anti-mouse Ig As was carried out by adding serial dilutions (1/1000 to 1/256 000) of As to 30 μ g/mL of conjugate. Inhibition of this agglutination by free anti-hCG mAbs was assayed by mixing together MS-D2 conjugate (30 μ g/mL), 32 000-fold-diluted anti-mouse Ig As, and serial concentrations (0.11–7.20 μ g/mL) of each of

the other anti-hCG mAbs. The agglutination of MS-mAb conjugate by anti-mouse Ig As, inhibited by free complementary mAb, was used to the quantitation of hCG in the following procedure (Table I, configuration III): 0.02–5 IU/mL hCG was mixed with MS-D2 conjugate (30 μ g/mL) and incubated for 1 h at room temperature. The complementary mAb A1 was added at a concentration able to inhibit the conjugate agglutination by xenogenic antibodies (0.9 μ g/mL), and after a further 1 h of incubation, 32 000-fold-diluted anti-mouse Ig As was then added. The intensity of light scattering was measured with the nephelometer after 30 min.

Use of MS-mAb Conjugate for the Quantitation of hTSH. Use of MS-mAb conjugate for the quantitation of hTSH was performed in the same way as the procedure just described for hCG (Table I, configuration III). Serial concentrations of hTSH (3.9–500 μ IU/mL), anti-hTSH conjugate MS-mAb Ib (30 μ g/mL), and free complementary mAb IIa (0.25 μ g/mL) were mixed together. Anti-mouse Ig As (1/64 000) was added after an incubation period of 4 h at room temperature, and measurement of the light scattered was performed after 30 min.

Use of MS-mAb Conjugate for the Quantitation of hMb. Two configurations were assayed for the rapid quantitation of hMb by trapping the molecule between an anti-hMb conjugate and polyclonal rabbit anti-hMb As. In the first (Table I, configuration IV), MS-mAb conjugate (80 μ g/mL), hMb (3–192 ng/mL), and 600-fold-diluted anti-hMb As were mixed together. In the second (Table I, configuration V), 500-fold-diluted goat anti-rabbit Ig As was added to the mixtures of MS-mAb conjugate (80 μ g/mL), hMb (1.125–72 ng/mL), and rabbit anti-hMb As (1/800). Measurement of the scattered light was performed after 30 min at room temperature in both cases.

Evaluation of this last configuration was performed in human serum. A calibration curve was obtained by mixing reagents with 50-fold-diluted negative serum and serial concentrations of hMb (56–3600 ng/mL). For within-run precision, three samples with low, middle, and high hMb levels were assayed 20 times during the same run. Between-run precision for the middle hMb concentration was determined in five successive assays. For the recovery study, 60 assays were performed with negative serum samples overloaded with known concentrations of pure hMb (92, 370, and 900 ng/mL).

RESULTS

Reaction of Anti-hCG MS-mAb Conjugates with MS-hCG Conjugate. Reaction between MS-hCG and MS-B1, MS-D2, or MS-G4 conjugates produced an agglutination with formation of conjugates clusters scattering the light (Figure 1A), but no agglutination was observed when the MS-F3 conjugate was used. The MS-mAb conjugate concentrations necessary to obtain the same agglutination were different according to the mAb bound to MS: with 20 μ g/mL MS-hCG conjugate in the reaction mixture, a nephelometric signal of 200 mV was obtained with 12, 50, and 450 μ g/mL of MS-D2, MS-B1, and MS-G4 conjugate, respectively.

Coagglutinations between MS-hCG and anti-hCG MS-mAb conjugates were inhibited by free hCG (Table I, configuration I). Figure 1B shows the changes in light-scattering amplification during inhibition of the agglutination obtained with MS-D2 conjugate. The inhibition curve covered hCG concentrations ranging from 0.016 to 8.2 IU/mL, and the level of hCG yielding 50% inhibition was 0.5 IU/mL.

Reaction of Anti-hCG MS-D2 Conjugate with Free hCG. Agglutination of MS-D2 conjugate with hCG was

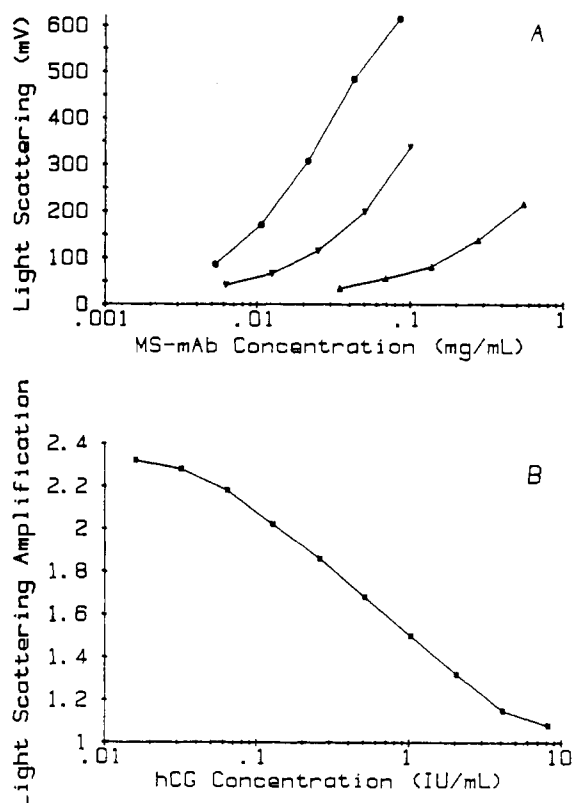


Figure 1. Reaction between anti-hCG MS-mAb and MS-hCG conjugates. (A) Agglutination as a function of MS-mAb concentration: MS-B1, ∇ ; MS-D2, \bullet ; MS-G4, \blacktriangle ; MS-hCG concentration, 20 μ g/mL; reaction time, 2 h. (B) Inhibition (Table I, configuration I) by free hCG of agglutination between anti-hCG MS-D2 (30 μ g/mL) and MS-hCG (20 μ g/mL) conjugates; total reaction time, 2.5 h.

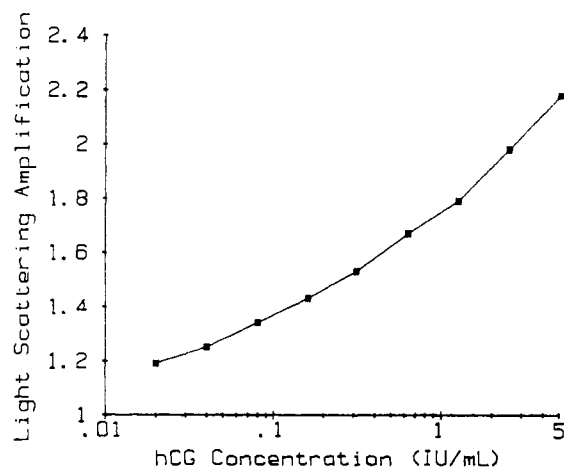


Figure 2. Agglutination (Table I, configuration II) by trapping hCG between anti-hCG MS-D2 conjugate (30 μ g/mL) and free anti-hCG mAb B1 (5.7 μ g/mL); total reaction time, 2.5 h.

observed when one of the free anti-hCG mAbs used (A1, B1, G4, or H5) complementary to mAb D2 was present in the reaction mixture (Table I, configuration II), but no agglutination was observed when mAb F3 was used. The agglutination curve obtained with mAb B1 (5.7 μ g/mL) is shown in Figure 2. A concentration of 0.02 IU/mL hCG produced a detectable agglutination (light-scattering amplification = 1.2, significantly different from background as defined above) and 1 IU/mL of hCG in the reaction mixture yielded a light-scattering amplification of 1.75.

Reaction of Anti-hCG MS-D2 Conjugate with Anti-mouse Ig As. As shown in Figure 3A, MS-D2 conjugate was agglutinated by very diluted anti-mouse Ig As (last

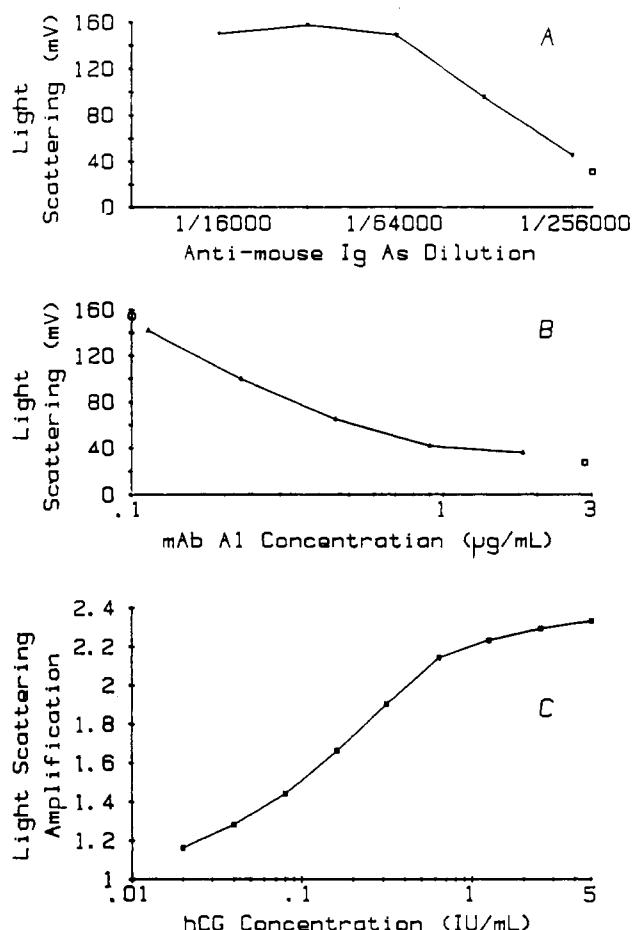


Figure 3. (A) Agglutination of anti-hCG MS-D2 conjugate (30 µg/mL) by anti-mouse Ig As as a function of As dilution: light scattered by MS-D2 conjugate alone, □; reaction time, 2 h. (B) Inhibition by free anti-hCG mAb A1 of the MS-D2 conjugate (30 µg/mL) agglutination obtained with 32 000-fold-diluted anti-mouse Ig As: light scattered by MS-D2 conjugate alone, □; light scattered by clusters of MS-D2 produced by 32 000-fold-diluted As, ○; reaction time, 2 h. (C) Agglutination (Table I, configuration III) by trapping hCG between anti-hCG MS-D2 conjugate (30 µg/mL) and anti-hCG mAb A1 (0.9 µg/mL) in the presence of anti-mouse Ig As (1/32 000); total reaction time, 2.5 h.

agglutinating dilution, 1/256 000). Such an agglutination by xenogenic antibodies could be totally inhibited by any of the other anti-hCG mouse mAb complementary to mAb D2. Figure 3B shows the inhibition of MS-D2 agglutination observed with free mAb A1 as a function of its concentration in the reaction mixture. Conjugate agglutination by anti-mouse Ig As was restored (Table I, configuration III) when serial concentrations of hCG were mixed with MS-D2 conjugate and a concentration of mAb A1 (0.9 µg/mL) able to inhibit conjugate agglutination by xenogenic antibodies. The agglutination curve observed (Figure 3C) was a function of the hCG concentration in the reaction mixture. As in the previous configuration (Figure 2), 0.02 IU/mL of hCG was significantly detected, but in these conditions, 1 IU/mL of hCG produced a higher light-scattering amplification (2.2).

Use of MS-mAb Conjugate for the Quantitation of hTSH. Application of the procedure just described for hCG (Table I, configuration III) to the quantitation of hTSH provided the agglutination curve shown Figure 4. The concentration of measurable hTSH ranged from 4 µIU/mL (concentration significantly detected) to 500 µIU/mL with a large variation of scattered light (230 mV, 30 min only after the addition of anti-mouse Ig As).

Use of MS-mAb Conjugate for the Quantitation of

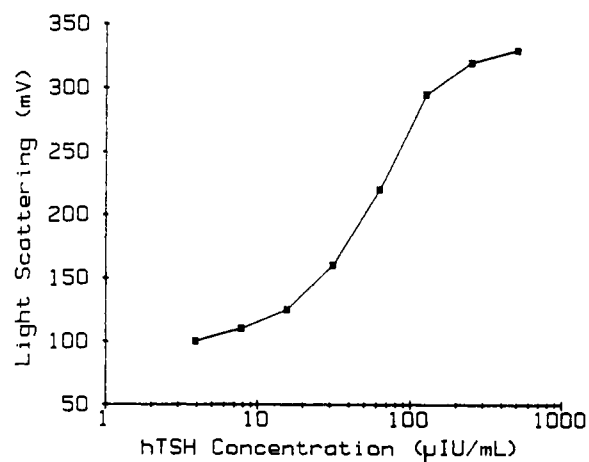


Figure 4. Application to microparticle-enhanced nephelometric immunoassay of hTSH. Agglutination (Table I, configuration III) by trapping hTSH between anti-TSH MS-mAb Ib conjugate (30 µg/mL) and anti-TSH mAb IIa (0.25 µg/mL) in the presence of anti-mouse Ig As (1/64 000); total reaction time, 4.5 h.

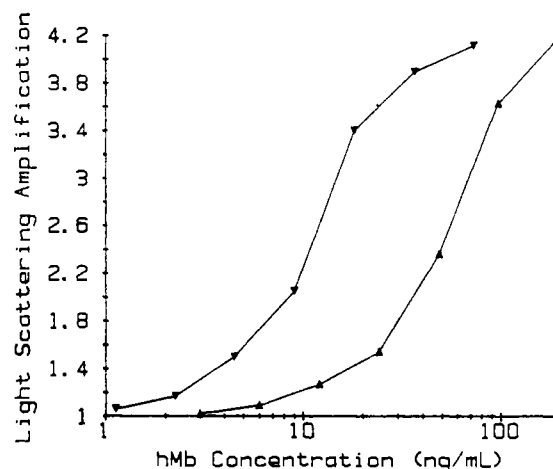


Figure 5. Application to microparticle-enhanced nephelometric immunoassay of hMb (reaction time, 30 min): agglutination (Table I, configuration IV) by trapping hMb between anti-hMb MS-mAb conjugate (80 µg/mL) and antibodies of rabbit anti-hMb As (1/600), ▲; agglutination (Table I, configuration V) by trapping hMb between anti-hMb MS-mAb conjugate (80 µg/mL) and antibodies of rabbit anti-hMb As (1/800) amplified by goat anti-rabbit Ig As (1/500), ▼.

hMb. Capture of hMb by MS-mAb conjugate could be disclosed by agglutination using anti-hMb polyclonal rabbit As (Table I, configuration IV). Figure 5 shows the curve obtained after a total reaction time of 30 min: 10 ng of hMb was detected as producing a significant light-scattering amplification (1.2) for concentrations ranging up to 200 ng/mL. When goat anti-rabbit Ig As was added (Table I, configuration V), the same hMb concentration of 10 ng/mL induced a higher amplification of the light scattered (2.3) and a lower concentration was significantly detected.

The calibration range for the determination of hMb in human serum, using this last configuration, extended from 56 to 3600 ng/mL. Precision was assessed by within-run CVs (mean = 94.3 ng/mL, SD = 5.4 ng/mL, CV = 5.7%; mean = 282.4 ng/mL, SD = 22.7 ng/mL, CV = 8.0; mean = 869.9 ng/mL, SD = 76.5, SD = 8.8%) and between-run CV (mean = 351 ng/mL, SD = 20.5 ng/mL, CV = 5.8%). A linear profile ($n = 60$, $r = 0.994$) was observed for recovery of hMb (mean percentage = 92%, SD = 13%) in overloaded sera.

DISCUSSION

Preliminary unreported results had shown free hCG to be unable to induce MS-mAb conjugate agglutination, owing to the nonrepetition of epitopes on the hCG molecule. The immunonephelometric reactivity of anti-hCG MS-mAb conjugates was thus first studied in a reaction involving MS-hCG conjugate. Mixing of MS-hCG with MS-B1, MS-D2, or MS-G4 conjugates, but not with MS-F3, produced conjugate agglutination. The agglutination capacity differed according to the mAb bound on MS in spite of comparable numbers of immunoreactive paratopes on each MS-mAb conjugate (120–190 immunoreactive paratopes per MS). MS-D2 appeared as the most reactive anti-hCG conjugate (12 $\mu\text{g/mL}$ of conjugate able to produce large agglutination with 20 $\mu\text{g/mL}$ of MS-hCG conjugate) and was thus retained for all other nephelometric studies.

Inhibition by free hCG of the agglutination occurring between MS-B1, MS-D2, or MS-G4 and MS-hCG conjugates demonstrated the immunological specificity of the agglutination and allowed consideration of a possible competitive assay of hCG (Table I, configuration I; Figure 1B). Such a competitive assay using coagglutination between MS-mAb and MS-antigen conjugates presented the interest that the antigen to be assayed did not itself produce the nephelometric signal. It provided a possibility to assay haptens and eliminated the risk of underevaluation in antigen excess conditions (hook effect). However, it presented the same limitation as the microparticle-enhanced nephelometric immunoassays previously described because it required the preparation of MS-antigen conjugate (Montagne et al., 1992c) and thus the availability of purified antigen.

Anti-hCG MS-mAb conjugates were agglutinated by hCG in the presence of a complementary mAb. No conjugate agglutination was induced by the capture of hCG by MS-mAb conjugate, but this reaction could be evidenced by the agglutination of resulting MS-mAb/hCG complexes, after addition of free complementary anti-hCG mAbs. The trapping of hCG between MS-mAb conjugate and free complementary mAb thus allowed sandwich nephelometric quantitation of hCG (Table I, configuration II; Figure 2).

Another interesting configuration was also optimized to detect the antigen capture. A new nephelometric immunoassay configuration (Table I, configuration III), using agglutination of MS-mAb conjugate by anti-mouse Ig antiserum, was developed for the detection of hCG (Figure 3C) and hTSH (Figure 4). In a first reaction step, hCG (or hTSH) was trapped between the mAb bound on MS (anti-hCG MS-mAb or anti-hTSH MS-mAb conjugate) and another mAb, complementary to the first and present in the mixture at a concentration sufficient to inhibit conjugate agglutination by anti-mouse Ig antiserum. The formation of sandwich complexes of MS-mAb/hCG (or hTSH)/complementary mAb used up the free complementary mAb which inhibited the xenogenic reaction. In the second step, the addition of anti-mouse Ig antiserum induced the agglutination of such complexes as a function of the trapped amount of hCG or hTSH. In the hCG assay, the concentration of free complementary mAb used was lower (0.9 instead of 5.70 $\mu\text{g/mL}$) than in the previous sandwich configuration (Table I, configuration II) and was too low to induce direct agglutination. The sensitivity of the quantitation was improved by the larger light-scattering amplification obtained although the detection threshold (0.02 IU/mL of hCG) was unchanged. This reaction configuration was also used for the quan-

titation of hTSH with an assay range reaching 2×10^{-14} mol/mL of hTSH (according to the conversion factor, 7 IU/mg, given for the hTSH preparation used as calibrator).

The capture of hMb by anti-hMb MS-mAb conjugate could be shown by the agglutination of MS-mAb/hMb complexes induced by rabbit anti-hMb. As in the case of hCG measurement, such a sandwich configuration assay was usable in hMb quantitation (Table I, configuration IV; Figure 5). However, when xenogenic antibodies such as goat anti-rabbit Ig As were added (Table I, configuration V; Figure 5), they allowed a greater dilution of the hMb-specific As and thus improved the assay sensitivity (2.5 instead of 10 ng/mL hMb). The use of anti-rabbit Ig As was different from the use of anti-mouse Ig As in the configuration III assay (Table I) perfected for hCG and hTSH. The xenogenic reaction involved MS-mAb/hMb/antibodies complexes as a function of the concentration of hMb in the reaction mixture, but could not react directly with the MS-mAb conjugate. In addition to their better sensitivity, these systems using xenogenic antibodies were interesting because they did not require the antigen to be assayed to supply the major part of the nephelometric signal. The immunocapture of antigen alone was not sufficient to induce conjugate agglutination. The agglutination reaction, depending on a secondary xenogenic reaction, was dissociated from the antigen/antibody reaction specific of the analyte. This may be considered a general procedure suitable for a large variety of analytes.

Hydrophilic MS specifically designed for competitive immunonephelometry using MS-antigen conjugate (Montagne et al., 1992c) thus also appear to be usable in sandwich immunoassays, when they are covalently coated with mAb. The various configurations described in this report for microparticle-enhanced nephelometric immunoassay using such mAb-coated microparticles may allow new developments of this analytical method to analytes not easily available for the preparation of antigen-coated particles.

ACKNOWLEDGMENT

Dr. F. Paolucci from Sanofi Research (Montpellier, France) and Dr. D. Riochet from Diagnostics Pasteur (Marnes, France) are gratefully acknowledged for providing us with monoclonal antibodies and microparticles. P.M. is research engineer, Institut National de la Santé et de la Recherche Médicale. M.L.C. is study engineer, Centre National de la Recherche Scientifique.

LITERATURE CITED

- Collard-Bovy, C., Marchal, E., Humbert, G., Linden, G., Montagne, P., El Bari, N.; Duheille, J., and Varcin P. (1991) Microparticle-enhanced nephelometric immunoassay: I. Measurement of α - and κ -casein. *J. Dairy Sci.* 74, 3695–3701.
- Cuillière, M. L., Montagne, P., Bessou, Th., El Omari, R., Riochet, D., Varcin, P., Laroche, P., Prud'homme, Ph., Marchand, J., Flecheux, O., Pau, B., and Duheille J. (1991) Microparticle-Enhanced Nephelometric Immunoassay (Nephelia) for Immunoglobulins G, A, and M. *Clin. Chem.* 37, 20–25.
- El Bari N., Montagne, P., Humbert, G., Cuillière, M. L.; Varcin, P., Linden, G., and Duheille, J. (1991) Development of a microparticle-enhanced nephelometric immunoassay for the quantification of beta-casein in milk. *Food Agric. Immunol.* 3, 63–71.
- Gartner, A., Carles, C., Montagne, P., Cuillière, M. L., and Duheille, J. (1991) A microparticle-enhanced nephelometric immunoassay (Nephelia) applied to thymulin measurement. *J. Immunoassay* 12, 521–542.

- Greenwood, F. C., and Hunter, W. M. (1963). The preparation of ^{131}I -labeled growth hormone of high specific activity. *Biochem. J.* 89, 114-121.
- Marchal, E., Collard-Bovy, C., Humbert, G., Linden, G., Montagne, P., Duheille, J., and Varcin P. (1991) Microparticle-enhanced nephelometric immunoassay: II. Measurement of alpha-lactalbumin and beta-lactoglobulin. *J. Dairy Sci.* 74, 3702-3708.
- Marchand, J., Varcin, P., Riochet, D., Montagne, P., Cuillière, M. L., Duheille, J., and Pau, B. (1992) Synthesis of new hydrophilic microspheres: Optimized carriers for microparticle-enhanced nephelometric immunoassays. *Biopolymers* 32, 971-980.
- Montagne, P., Gavriloff, C., Humbert, G., Cuillière, M. L., Duheille, J., and Linden, G. (1991a) Microparticle-enhanced nephelometric immunoassay for immunoglobulins G in cow's milk. *Lait*. 71, 493-499.
- Montagne, P., Laroche, P., Cuillière, M. L., Riochet, D., Flecheux, O., Varcin, P., Marchand, J., Pau, B., and Duheille, J. (1991b) Polyacrylic microspheres as a solid phase for microparticle-enhanced nephelometric immunoassay (Nephelia) of transferrin. *J. Immunoassay* 12, 165-183.
- Montagne, P., Laroche, P., Cuillière, M. L., Varcin, P., Pau, B., and Duheille, J. (1992a) Microparticle-enhanced nephelometric immunoassay for human C-reactive protein. *J. Clin. Lab. Anal.* 6, 24-29.
- Montagne, P., Laroche, P., Bessou, T., Cuillière, M. L., Varcin, P., and Duheille, J. (1992b) Measurement of eleven serum proteins by microparticle-enhanced nephelometric immunoassay. *Eur. J. Clin. Chem. Clin. Biochem.* 30, 217-222.
- Montagne, P., Varcin, P., Cuillière, M. L., and Duheille, J. (1992c) Microparticle-enhanced nephelometric immunoassay with microsphere-antigen conjugates. *Bioconjugate Chem.* 3, 187-193.
- Paolucci, F., Basuyaux, B., Clavies, C., Piechaczyk, M., and Pau, B. (1986) Lymphocyte hybridization: basic principles and selection of monoclonal antibodies directed against hormones. *Serono Symposia Vol. 30* (G. Forti, M. B. Lipsett, and M. Serio, Eds.) pp 3-13, Raven Press, New York.
- Scatchard, G. (1949) The attractions of proteins for small molecules and ions. *Ann. N. Y. Acad. Sci.* 51, 660-672.
- Registry No.** TSH, 9002-71-5; CG, 9002-61-3.

Evaluation of Peptide Libraries: An Iterative Strategy To Analyze the Reactivity of Peptide Mixtures with Antibodies

James Blake* and Leonora Litzi-Davis

Bristol-Myers Squibb Pharmaceutical Research Institute, 3005 First Avenue, Seattle, Washington 98121. Received June 10, 1992

Peptide libraries corresponding to a presumed mixture of 50 625 tetrapeptides or 16 777 216 hexapeptides were each prepared in a single assembly by standard solid-phase peptide synthesis. By enzyme-linked immunosorbent assay, the tetrapeptide library was shown to inhibit the binding of an antiserum to FMRF amide with an FLRF capture antigen; the hexapeptide library was shown to inhibit the binding of a monoclonal antibody to a 28 amino acid peptide with the corresponding peptide capture antigen. An iterative strategy of variation was used to determine for each position in the tetra- or hexapeptides which amino acid contributed the most to activity. As a result we were able to logically select out of the tetrapeptide library the sequence FLRF and to select out of the hexapeptide library a sequence that differed from the apparent probable epitope but was twice as active. A single amino acid substitution in the logically derived sequence gave a peptide that was 35 times as active as the hexapeptide sequence in the original 28 amino acid peptide.

INTRODUCTION

Recent advances in peptide chemistry have resulted in the development of methods for the preparation and evaluation of peptide libraries. Large numbers of randomly or specifically directed peptides have been synthesized (1-9) and assayed for activity, usually binding to an antibody to determine the epitope. The strategies employed may be divided into two categories. In the first, a mixture of peptides is exposed to a receptor and the resultant binding is used to separate the active peptides from the inactive peptides. The identity of the active peptides is then determined by the techniques of molecular biology (1-3) or peptide chemistry (4). In the second strategy, the synthesis of the peptide analogs is compartmentalized and this knowledge is used to determine the identity of the active peptides (5-9). We now report a strategy wherein a mixture of peptides is synthesized and evaluated, and subsequent iterative variations in the mixture allow deduction about the structure of the active peptide.

EXPERIMENTAL PROCEDURES

Peptide Synthesis. Peptides and peptide mixtures were synthesized by the solid-phase method (10) on an Applied Biosystems peptide synthesizer, Model 430A, using Boc amino acids. *p*-Methylbenzhydrylamine resin was the starting resin for all syntheses. All mixtures of Boc amino acids were coupled by reaction with DCC/HOBT; individual amino acids were coupled as recommended by Applied Biosystems—DCC/HOBT or preformed symmetric anhydride. Boc amino acids used for the preparation of mixtures were purchased from Bachem. Side chain protecting groups were as follows: Ser, Bzl; Thr, Bzl; Glu, Bzl; Asp, Bzl; Tyr, BrZ; Lys, 2-ClZ; Arg, Tos; His, Bom. In the synthesis of peptides 2 and 3 the side chain of cysteine was protected by an ethylcarbamoyl group (11, 12).

* Author to whom correspondence should be addressed.

¹ Abbreviations used: Boc, *tert*-butoxycarbonyl; HRP, horse radish peroxidase; DCC, *N,N'*-dicyclohexylcarbodiimide; HOBT, 1-hydroxybenzotriazole; ELISA, enzyme-linked immunosorbent assay; BSA, bovine serum albumin.

The Boc amino acids were divided into three groups which were α (L, A, V, T, F, Y, in molar ratios 1, 1, 2, 2, 1, 1.4), β (G, S, P, D, E in molar ratios of 1, 1, 1, 1, 1), and γ (K, R, H, N, Q in molar ratios of 1, 2, 1, 1, 1). X designates a mixture of all of the amino acids in the indicated proportions. In the experiments with the antiserum to FMRF amide, the Boc amino acid mixtures were dissolved in DMF and aliquots were added to the amino acid cartridges. In the later experiments with the mAb to peptide 3 it was found to be easier to prepare stock mixtures of the solid derivatives which were ground together with a mortar and pestle to give a fine powder and then weighed into the amino acid cartridges. In the $\beta_2\gamma$ coupling mixtures indicated in the tables, the molar ratios of the β group amino acids were twice those of the γ group, and the amino acids of the α group were absent. As an example for other mixtures shown in the tables, KRH₃ indicates that the molar ratio of H to K or R was three times greater than it was in the primary X or γ mixtures, and Q and N were absent.

The peptides were cleaved from the resin and deprotected on their side chains by reaction with 90% HF/10% anisole for 1 h at 0 °C. After evaporation of HF, the mixture was washed with ethyl acetate, and the peptides were dissolved in 50% acetic acid. The peptide solution was diluted with water and lyophilized. In the case of peptide mixtures the residue from lyophilization was used in immunoassay without further purification. In the case of individual peptides, purification was achieved by preparative HPLC on a Rainin Dynamax 300-Å, C-8 column, 22 × 250 mm, by a gradient of acetonitrile in 0.1% trifluoroacetic acid. The purified peptides were characterized by analytical HPLC, amino acid analysis, and mass spectrometry. Peptide 2 was treated with aqueous sodium hydroxide to remove the ethylcarbamoyl group as previously described (12), and the peptide was coupled through its side chain thiol group to BSA that had been previously reacted with the heterobifunctional reagent sulfosuccinimidyl 4-(*N*-maleimidomethyl)cyclohexane-1-carboxylate (Pierce). Amino acid analysis of the resulting conjugate indicated that it contained 15% by weight of peptide 2.

ELISA Procedure. ELISA was performed on Dynatech Immulon 96-well plates. All operations were performed at room temperature. Rabbit antiserum to FMRF amide was obtained as a dry powder from Peninsula Laboratories (Cat. No. RAS8755) and mouse mAb to peptide 3 was obtained by standard procedures.

The plates were coated overnight with bicarbonate solutions (pH 9.6) of peptide 2-BSA or peptide 3 at concentrations of 10 or 0.2 $\mu\text{g/mL}$, respectively. The plates were washed with saline/Tween and then incubated with a skimmed milk blocking agent for 1–2 h and then washed again. The next step varied slightly in the two experiments. In the case of the antiserum to FMRF amide, 25- μL aliquots of the peptide mixtures at serially diluted concentrations were added to each of the wells, followed by the addition of 75 μL of antiserum powder dissolved (2.6 mg/mL) in 0.1% Triton X-100 (Sigma). For the mAb to peptide 3, 75- μL aliquots of the peptide mixtures were preincubated with 25 μL of mAb in PBS, 0.08 $\mu\text{g/mL}$, for 15 min, and then added to the wells. After 1-h incubation in the wells, the plate was washed and incubated with goat anti-rabbit γ -globulin-HRP conjugate or goat anti-mouse γ -globulin-HRP conjugate for 1 h. Subsequent treatment with tetramethylbenzidine gave a signal (absorbance at 450 nm) that was measured on a microplate reader. The concentration of peptide or peptide mixture that gave a 50% reduction in $A_{450\text{nm}}$ is shown in the tables.

RESULTS AND DISCUSSION

As an initial model problem we chose to examine a commercially available antiserum to FMRF amide. The peptides FLRF amide (1) and GCGGGGFLRF amide (2) were synthesized and peptide 2 was conjugated to BSA through its cysteine residue. We substituted leucine for methionine because we had decided to exclude methionine from our peptide library and thus avoid the chemical problems it presents, and because of indications that leucine substitution would not markedly affect the cross reactivity of the peptide with anti-FMRF amide. The peptide 2-BSA conjugate was used as a capture antigen in ELISA and was shown to bind anti-FMRF amide. Peptide 1 was able to compete with the capture antigen for binding to anti-FMRF amide and a concentration of 0.5 μg of peptide 1/mL gave a 50% reduction in signal obtained for anti-FMRF amide.

A tetrapeptide mix XXXX was then synthesized where each X represented a mixture of 15 amino acids. The amino acids were A, L, V, F, Y (subgroup α), G, S, P, D, E (subgroup β), K, R, H, N, and Q (subgroup γ). Methionine, as indicated above, plus cysteine and tryptophan were excluded to avoid the chemical problems that they present. We also believed that valine is a suitable general substitute for isoleucine, and threonine was excluded to simplify the problem. The fifteen amino acids were used in equimolar mixtures with the exception that the proportions of V, Y, and R were increased because of their lower relative coupling efficiency (see Experimental Procedures). The presumed mixture of 15⁴ (50 625) peptides was shown to competitively inhibit the binding of anti-FMRF amide to the capture antigen by the decreased signal obtained in ELISA (Table I).

The problem was then to logically deduce the structure of a single highly active peptide in the mixture of 50 625 peptides. To do this we employed a bogus coin strategy—a strategy wherein one tries to learn which one of a group of coins has a different weight than the others using a minimum number of weighings or trials. This strategy involved dividing the objects (coins or amino acids) into

Table I. Ability of Synthetic Peptide Mixtures To Inhibit Binding of FMRF Amide Antiserum with FLRF-BSA in ELISA

peptide sequence ^a				$C_{1/2}$ ^b	deduced key residues ^c
AA ₁	AA ₂	AA ₃	AA ₄		
X	X	X	X	1400	
$\beta_2\gamma$	X	X	X	>2500	α
χ	$\beta_2\gamma$	X	X	>2500	α
X	X	$\beta_2\gamma$	X	1450	γ
X	X	X	$\beta_2\gamma$	>2500	α
α	α	γ	α	35	
LAV ₃	α	γ	α	>500	F or Y
α	LAV ₃	γ	α	44	A or L
α	α	KRH ₃	α	41	K or R
α	α	γ	LAV ₃	>500	F or Y
FY	AL	KR	FY	2.8	
F	AL	KR	FY	1.9	F
FY	A	KR	FY	20	L
FY	AL	K	FY	>70	R
FY	AL	KR	F	1.4	F
F	L	R	F	0.5	

^a All peptides have carboxyl terminus amide. ^b Concentration ($\mu\text{g/mL}$) of peptide or peptide mixture with antiserum that gave 50% of the signal obtained with antiserum alone. ^c The amino acids or amino acid mixtures that were deduced to make the greatest contribution to binding activity.

three groups. The proportion of the first group (α) was decreased, the proportion of the second group (β) was increased, and the proportion of the third group (γ) was unchanged. The effect on the activity—decreased, increased, or unchanged—indicated which of the groups was contributing the most to the activity.

Four peptide mixtures were synthesized in which three positions contained 15 amino acids and one position contained none of the amino acids of subgroup α , approximately twice the proportion of the amino acids of the subgroup β , and approximately the same proportion of the amino acids of subgroup γ . The effect of this change is shown in Table I. As an example, the peptide mixture that contained the $\beta_2\gamma$ mix in position 1 required a higher concentration for 50% inhibition than the XXXX peptide; hence this altered mixture was much less active than the XXXX peptide. Therefore, at position 1 of the peptide the amino acids of the α subgroup contributed the most to the activity of the peptide mixture. The results indicate that for positions 1, 2, 3, and 4 in the peptide mixture the greatest contribution to activity was by the subgroups α , α , γ , and α , respectively. Synthesis of a new tetrapeptide mixture containing only five amino acids at each position, $\alpha\alpha\gamma\alpha$, resulted in a 40-fold increase in activity.

The process was repeated and each subgroup was divided into three sections. As an example for the α group: F and Y were decreased (i.e., omitted from the coupling mixture), V was increased; and A and L were unchanged. Four syntheses and subsequent immunoassay reduced to two the number of key amino acids in each position. Synthesis of a new mixture with two amino acids in each position gave a 12-fold increase in activity. Single amino acid substitutions led to the final deduction that the amino acids which contributed most to the activity of the original peptide mixture XXXX were F at position 1, L and position 2, R at position 3, and F at position 4. This corresponds to the sequence of the capture antigen and can be safely presumed to be one of the most active peptides in the original mixture of 50 625 peptides.

As a second model problem we chose a mAb raised against a 28 amino acid peptide, acetyl-RTPALG-PQAGIDTNEIAPLEPDAPPDAC amide (3). Since the epitope had not been previously characterized, this constituted a problem with an unknown answer. Pre-

Table II. Ability of Synthetic Peptide Mixtures To Inhibit Binding of the mAb to Peptide 3 with Peptide 3 in ELISA

peptide sequence						A ₄₅₀ ^a	deduced ^b key residues
AA ₁	AA ₂	AA ₃	AA ₄	AA ₅	AA ₆		
X	X	X	X	X	X	0.356	
$\beta_2\gamma$	X	X	X	X	X	0.336	γ
X	$\beta_2\gamma$	X	X	X	X	0.352	γ
X	X	$\beta_2\gamma$	X	X	X	0.427	α
X	X	X	$\beta_2\gamma$	X	X	0.232	β
X	X	X	X	$\beta_2\gamma$	X	0.368	γ
X	X	X	X	X	$\beta_2\gamma$	0.234	β
						0.740 ^c	

^a Signal obtained at a peptide concentration of 7500 $\mu\text{g/mL}$. Determinations were in quadruplicate and the standard deviation for all measurements was 0.01–0.02 absorbance units. ^b See Table I.

^c Signal obtained in the absence of peptide.

liminary results (data not shown) indicated that a hexapeptide mixture was able to block the binding of the mAb to peptide 3 as a capture antigen. Lesser though measurable blocking was obtained with a pentapeptide mixture and no blocking could be detected in a pentapeptide mixture containing only D-amino acids.

The hexapeptide mixture contained 16 amino acids (including threonine) at each position and presumably corresponded to 16^6 or 16 777 216 peptides. Inhibition of ELISA signal by XXXXXX and the corresponding $\beta_2\gamma$ substitution mixtures showed (Table II) that substitution of positions 1, 2, and 5 did not affect activity (deduced γ group), substitution at positions 4 and 6 increased activity (deduced β group), and substitution at position 3 decreased activity (deduced α group). A new mixture, $\gamma\gamma\alpha\beta\gamma\beta$ amide, gave increased activity compared to the activity of XXXXXX (Table III).

The iterative process was continued, and the results (Table III) obtained for the KRH₃ substitutions are illustrative. At position 1, KRH₃ substitution gave essentially the same activity, and therefore K or R were

deduced to be the key residues; at position 2, KRH₃ substitution gave reduced activity and therefore the missing residues, Q or N, were deduced to be the key residues; at position 5, KRH₃ substitution gave increased activity and therefore H was deduced to be the key residue.

The final deduced peptide was RQVGHD amide (4). A comparison to the sequence of peptide 3 points up the segment PQAGID (5), which is identical to peptide 4 at positions 2, 4, and 6 and has nonconservative differences at positions 1, 3, and 5. The activity of peptides 4, 5, and several analogs is shown in Table IV. The results indicated that (a) the full length of peptide 4 is necessary for high activity; (b) peptide 4 is ca. twice as active as the "natural" sequence, peptide 5; (c) the nonconservative replacements at positions 3 or 5 increase activity compared to the "natural" sequence; and (d) the nonconservative replacement at position 1 decreases activity compared to the "natural" sequence. It is of interest that the substitutions at positions 3 and 5 gave a peptide, PQVGHD amide, that is 35 times more active than the "natural" sequence peptide 5.

In conclusion, we believe that the method presented here can prove useful in logically searching through a mixture of thousands or even millions of peptides to pick out the peptides that have binding activity or any activity that correlates directly with binding. The principal advantage is that these results can be obtained by conventional solid-phase peptide synthesis on commercially available synthesizers that are designed for the syntheses of single peptides. It remains to be determined whether this strategy can be extended to peptide mixtures longer than six residues. The geometric decrease in the concentration of individual peptides for each extra residue and the limits of detection in most biological assays suggest that six residues may be at or near the maximum useful length.

Table III. Ability of Synthetic Peptide Mixtures To Inhibit Binding of the mAb to Peptide 3 with Peptide 3 in ELISA

peptide sequence						C _{1/2} ^a	deduced key residues
AA ₁	AA ₂	AA ₃	AA ₄	AA ₅	AA ₆		
X	X	X	X	X	X	6500	
γ	γ	α	β	γ	β	860	
KRH ₃	γ	α	β	γ	β	975	K or R
γ	KRH ₃	α	β	γ	β	>4500	N or Q
γ	γ	L ₂ A ₂ VT	β	γ	β	810	V or T
γ	γ	α	GSP ₃	γ	β	950	G or S
γ	γ	α	β	KRH ₃	β	580	H
γ	γ	α	β	γ	GSP ₃	>4500	D or E
KR	NQ	VT	GS	H	DE	14	
K	NQ	VT	GS	H	DE	28	R
KR	N	VT	GS	H	DE	>75	Q
KR	NQ	V	GS	H	DE	11	V
KR	NQ	VT	G	H	DE	7	G
KR	NQ	VT	GS	H	E	>75	D

^a See Table I.

Table IV. Ability of Synthetic Peptides To Inhibit Binding of the mAb to Peptide 3 with Peptide 3 in ELISA

peptide sequence						C _{1/2} ^a
AA ₁	AA ₂	AA ₃	AA ₄	AA ₅	AA ₆	
R	Q	V	G	H	D	1.2
	Q	V	G	H	D	>750
R	Q	V	G	H		128
E	Q	V	G	H	D	14
P	Q	V	G	H	D	0.08
R	Q	A	G	H	D	4.0
R	Q	V	G	I	D	17
P	Q	A	G	I	D	2.8

^a See Table I.

ACKNOWLEDGMENT

The authors thank Becky Woodworth and Virginia Smith for their skilled technical assistance, Dale Yelton and Ursula Garrigues for the monoclonal antibody, and Ana Wieman for preparation of the manuscript.

LITERATURE CITED

- (1) Cwirla, S. E., Peters, E. A., Barrett, R. W., and Dower, W. J. (1990) Peptides on phage: A vast library of peptides for identifying ligands. *Proc. Natl. Acad. Sci. USA* 87, 6378-6382.
 - (2) Devlin, J. J., Panganiban, L. C., and Devlin, P. E. (1990) Random peptide libraries: A source of specific protein binding molecules. *Science* 249, 404-406.
 - (3) Scott, J. K., and Smith, G. P. (1990) Searching for peptide ligands with an epitope library. *Science* 249, 386-390.
 - (4) Lam, K. S., Salmon, S. E., Hersh, E. M., Hruby, V. J., Kazmierski, W. M., and Knapp, R. J. (1991) A new type of synthetic peptide library for identifying ligand-binding activity. *Nature* 354, 82-84.
 - (5) Geysen, H. M., Meloen, R. H., and Barteling, S. J. (1984) Use of peptide synthesis to probe viral antigens for epitopes to a resolution of a single amino acid. *Proc. Natl. Acad. Sci. U.S.A.* 81, 3998-4002.
 - (6) Geysen, H. M., Rodda, S. J., and Mason, T. J. (1986) The delineation of peptides able to mimic assembled epitopes. *Synthetic Peptides as Antigens. Ciba Foundations Symposium 119* (R. Porter and J. Wheelan, Eds.) pp 131-149, Wiley, New York.
 - (7) Houghten, R. A. (1985) General method for the rapid solid-phase synthesis of large numbers of peptides: Specificity of antigen-antibody interaction at the level of individual amino acids. *Proc. Natl. Acad. Sci. U.S.A.* 82, 5131-5135.
 - (8) Houghten, R. A., Pinilla, C., Blondelle, S. E., Appel, J. R., Dooley, C. T., and Cuervo, J. H. (1991) Generation and use of synthetic peptide combinatorial libraries for basic research and drug discovery. *Nature* 354, 84-86.
 - (9) Fodor, S. P. A., Read, J. L., Pirrung, M. C., Stryer, L., Lu, A. T., and Solas, D. (1991) Light-directed, spatially addressable parallel chemical synthesis. *Science* 251, 767-773.
 - (10) Merrifield, R. B. (1963) Solid phase synthesis. I. The synthesis of a tetrapeptide. *J. Am. Chem. Soc.* 85, 2149-2154.
 - (11) Guttman, St. (1966) Synthesis of glutathione and oxytocin using a new protecting group for the thiol function. *Helv. Chim. Acta* 49, 83-96.
 - (12) Blake, J., Woodworth, B. A., Litzi-Davis, L., and Cosand, W. L. (1992) Ethylcarbamoyl protection for cysteine in the preparation of peptide-conjugate immunogens. *Int. J. Pept. Protein Res.* in press.
- Registry No.** 1, 80690-77-3; 2, 143924-37-2; 3, 143924-38-3; 4, 143924-39-4; 5, 143924-40-7; FMRF amide, 64190-70-1; PQVGHD amide, 143924-41-8.

Acidic Derivatives of Homocysteine Thiolactone: Utility as Anionic Linkers

W. J. Leanza, L. S. Chupak, R. L. Tolman, and S. Marburg*

Department of Medicinal Chemistry, Merck Research Laboratories, Box 2000, Rahway, New Jersey 07065.
Received June 15, 1992

Homocysteine thiolactone (2) derivatives in which the nitrogen is acylated with groups containing acidic functionalities have been synthesized. These include the succinyl (3), the carboxymethylglutaryl (4), the 3-phosphonopropionyl (7), and the 3-sulfopropionyl (8) derivatives. These thiolactones can be used to introduce a thiol functionality into proteins such as the outer membrane protein complex of *Neisseria meningitidis* (OMPC) allowing conjugation with electrophilic ligands. This chemistry is the same as with *N*-acetylhomocysteine thiolactone (1), but their pK_a values are such that at pH 7 concomitant negative charge is introduced into the conjugate. Such negative charge should neutralize some excess positive charge introduced when arginine- and lysine-rich peptides are bonded as ligands. In the case of OMPC, introduction of such positive charge appears to effect irreversible precipitation. The system has been studied using the maleimidopropionyl and bromoacetyltriarginine (9 and 10) derivatives as models. In select instances anionic spacers reduce the degree of precipitation relative to *N*-acetylhomocysteine thiolactone derivatives.

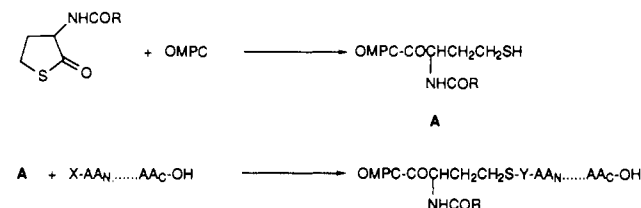
INTRODUCTION

The outer membrane protein complex of *Neisseria meningitidis*^{1,2} (OMPC) is a very effective immunogenic carrier of polysaccharide antigens (1, 2) and has been approved by regulatory agencies worldwide as a vaccine component (PedvaxHIB). It follows that OMPC is a potential immunogenic carrier for peptide antigens, especially those derived from the V3 domain of gp120, an envelope protein of the human immunodeficiency virus. The principal neutralization determinant of this V3 domain has been extensively mapped (4) and has been shown to reside in the V3 disulfide loop. Indeed, substantial antipeptide responses are observed for such OMPC-peptide conjugates (unpublished data).

These peptide conjugates were prepared by reacting an electrophilic derivative of the peptide with a thiol derivative of OMPC which was obtained by reacting the protein with *N*-acetylhomocysteine thiolactone, 1 (R = methyl), as outlined in Scheme I. This thiolactone has been used to introduce a thiol functionality into small molecules and macromolecules for a variety of purposes outlined in Table I and has been particularly useful because it unambiguously defines covalency by a "bigeneric spacer" concept (1).

Frequently, however, the OMPC-peptide preparations were characterized by the very poor protein recoveries (<15%) due to irreversible precipitation of the conjugate. This prevented use as a vaccine material and it became obvious that practical considerations required a solution to this

Scheme I. ^a Thiolation and Peptide Conjugation of OMPC



^a AA_N = N-terminal amino acid residue and AA_C = C-terminal amino acid residue. X = electrophilic group such as bromoacetyl or 3-(maleimidopropionyl). Y = methylenecarbonyl or 3-*N*-succinimidylpropionyl.

Table I. Application of 1 as a Thiolating Agent

molecule type thiolated	utility	ref
aminoglycoside	protein conjugation	5
muramyl dipeptide	polysaccharide conjugation	6
HSA	drug conjugation	7
enzymes	polystyrene conjugation	8
albumin microspheres	peptide-protein conjugation	9
cell surface carbohydrate	cell surface labeling	10
lactoglobulin	increased heat stability	11
oligonucleotide	fluorescence labeling	12
amino lipid	liposome preparation	13

problem. Examination of the peptide sequences that were conjugated to OMPC revealed that all were positively charged in that they contained one or more of the basic amino acids arginine, histidine, and lysine and none of the acidic ones such as glutamic and aspartic acids. This is in contrast to the polysaccharide conjugates which are almost always acidic polymers (that form anions at neutral pHs) and that do not suffer the precipitation problems observed with the peptide conjugates. It was therefore inferred that the precipitation was linked to the increased positive charge in the conjugate. It seemed that introduction of negative charge concomitant with conjugation of the peptide might attenuate this problem. *N*-Acylated derivatives of homocysteine thiolactone (2) which incorporate one or two acidic functionalities are linking molecules which will impart one to two negative charges per ligand in the conjugate at neutral pHs.

* Author to whom correspondence should be addressed.

¹ Abbreviations used: AAA, amino acid analysis; DIEA, diisopropylethylamine; DMF, dimethylformamide; DTT, dithiothreitol; EDTA, ethylenediaminetetracetic acid disodium salt; HSA, human serum albumin; MS FAB, mass spectrum (fast atom bombardment); OMPC, outer membrane protein complex of *N. meningitidis*; OMPC-SH, thiolated OMPC; SCMHC, *S*-(carboxymethyl)homocysteine; TFA, trifluoroacetic acid.

² OMPC is an aggregate consisting of approximately 50% of a 42 000-Da protein, 45% of four other proteins, and 5% of lipopolysaccharide. The molecular weight of the complex has been estimated between 30 and 50 million and the material exists in water as a stable colloidal suspension (3).

Since the HIV peptides in question were available in limited quantities and expressed a variety of other characteristics (e.g. hydrophobic groups) which could effect the solubility of the product, a standard peptide seemed necessary for adequate comparison of the different spacers. Triarginine, which as the maleimidopropionyl derivative **9** or bromoacetyl derivative **10** introduces a net increase of one positive charge after conjugation to thiolated OMPC, seemed an appropriate model to test our hypothesis. Preliminary conjugation experiments, in which OMPC that had been thiolated with **1** was reacted with **10** (resulting in almost complete precipitation) or bromoacetyltriglycine (no precipitation), supported this view.

In this paper we report the syntheses of various acidic derivatives of **2** and demonstrate that they undergo the same chemistry as **1**. Their effect on the precipitation of conjugates is evaluated using the triarginine model.

EXPERIMENTAL PROCEDURES

General. All manipulations of thiolated OMPC were carried out in a nitrogen-purged dry-box. The nitrogen was sterilized by passage through a 0.2- μ M (Gelman Acro 50) filter. An effort was made to keep reagents and equipment sterile. Buffers were prepared from dibasic sodium phosphate and the pH adjusted with concentrated phosphoric acid. All centrifugations unless otherwise noted were performed in a Beckman L-80 Optima centrifuge using a 80 Ti rotor and 10-mL polycarbonate tubes. All centrifugations were effected at 43 000 rpm, for 2 h at 4 °C unless otherwise noted. Amino acid analyses were done on a Beckman 6300 amino acid analyzer by Mr. G. Kolodin of these laboratories. NMR spectra were obtained on Varian 300- and 400-MHz instruments (all *J* values are in hertz). The protein titers were determined by the method of Lowry (14) using a Zymate II robotic system by Mr. W. Clark of these laboratories; thiol titers were determined by the method of Ellman (15); *pK_a* values were determined by titration by Dr. J. McCauley of these laboratories.

D,L-N-Succinylhomocysteine Thiolactone (3). D,L-Homocysteine thiolactone hydrochloride, **2** (1.84 g, 12 mmol), was suspended in 20 mL of DMF, and to it were added 1.04 g (10 mmol) of succinic anhydride and 1.79 mL of *N,N*-diisopropylethylamine (DIEA) (10 mmol). The mixture was stirred at room temperature for 1 h after which an additional 0.9 mL of DIEA (0.5 mmol) was added. Stirring was continued for another 45 min, after which a third charge of DIEA (0.9 mL, 5 mmol) was added. After stirring for an additional 2 h at room temperature the mixture was stored at 4 °C overnight. It was then quenched onto 22 g of ice (pH = 7.1) and the solution applied to a 30 mL column of Dowex 1 (acetate form). This was washed free of thiolactone and then eluted with 2 M formic acid. The UV-positive fractions were concentrated to 2.13 g of *N*-succinylhomocysteine thiolactone, mp 128–135 °C. FAB MS showed the major peak at *m/e* 218 (MH⁺). A small amount (47 mg) of this material was recrystallized by dissolving in acetonitrile, filtering, and precipitating crystals with equal volumes of chloroform and cyclohexane, affording pure product: mp 140–142 °C; ¹H NMR (CDCl₃) δ 4.67 (dd, 1 H, *J* = 7.0, 12.7), 3.44 (dt, 1 H, *J* = 5.4, 11.5), 3.33 (ddd, 1 H, *J* = 1.2, 7.1, 11.5), 2.55–2.7 (m, 5 H), 2.20 (dq, 1 H, *J* = 7.1, 12.2). Anal. Calcd for C₉H₁₁NO₄S: C, 44.24; H, 5.07; N, 6.45; S, 14.75. Found: C, 44.17; H, 5.04; N, 6.43; S, 14.48.

N-[3-(Carboxymethyl)glutaryl]homocysteine Thiolactone (4). A mixture of 3-(carboxymethyl)glutaric anhydride (**16**) (1.72 g, 10 mmol) and homocysteine

thiolactone hydrochloride (1.85 g, 12 mmol) in dry DMF (10 mL) was stirred in a flask capped with a septum and cooled in an ice bath, and DIEA (4.3 mL, 25 mmol) was added via syringe through the septum over a period of 15 min. After aging the mixture for 2 h, a stream of nitrogen was passed through the solution for 15 min to remove excess amine and then 15 g of ice was added. The pH at this point was 7. The solution was applied to a column of Dowex 1 (acetate form, 80 mL), which was eluted with water (250 mL) followed by 2 N formic acid (350 mL). The acidic fraction was concentrated to 20 mL and applied to a column of neutral polystyrene resin (80 mL of HP-20, Pharmacia Fine Chemicals) and washed with 150 mL of water. The product was recovered by elution with 250 mL of 12% acetonitrile–water and lyophilized. This afforded 2.2 g of a material which was crystallized from acetonitrile–water, affording 1.9 g of **4**: mp 149–150 °C; FAB MS *m/e* 290 [MH⁺]; ¹H NMR (D₂O) δ 4.68 (dd, 1 H, *J* = 7.0, 12.8), 3.45 (dt, 1 H, *J* = 5.5, 11.4), 3.35 (ddd, 1 H, *J* = 1.3, 7.0, 11.4), 2.71 (m, 1 H, *J* = 7.0), 2.62 (m, 1 H), 2.52 (d, AB q, 2 H), 2.50 (d, 2 H, *J* = 7.0), 2.43 (d AB q, 2 H), 2.22 (dq, 1 H, *J* = 7.0, 12.8). Anal. Calcd for C₁₁H₁₅NO₆: C, 45.67; H, 5.23; N, 4.84; S, 11.08. Found: C, 45.64; H, 5.34; N, 5.05; S, 11.28.

D,L-N-(3-Bromopropionyl)homocysteine Thiolactone (5). D,L-Homocysteine thiolactone hydrochloride, **2** (52.0 g, 0.34 mol), was dissolved in 135 mL of water and covered with 300 mL of ethyl acetate. While being stirred at 0 °C, 39 mL of 3-bromopropionyl chloride (0.78 mol) was added in 2-mL aliquots. After each aliquot of bromopropionyl chloride, 20 mL of 2.5 N sodium hydroxide was added to maintain the pH at 7.35. After aging at room temperature for 1 h without stirring, a yellow precipitate (76 g) was filtered. This precipitate was dissolved in 600 mL of refluxing ethyl acetate and filtered, hot, through Celite. After 72 h at 4 °C compound **5** (40.5 g, 0.16 mol) was obtained. The supernatant fluid was reduced to 200 mL and seeded. After 18 h at 4 °C an additional 9.6 g was obtained. A total of 50.1 g of compound **5** was isolated (58% yield): mp 142.5–149.1 °C; ¹H NMR (CDCl₃) δ 6.06 (s, 1 H), 4.51 (pentet, 1 H, *J* = 8.4), 3.6 (m, 2 H), 3.36 (dt, 1 H, *J* = 6.8, 15), 3.26 (dd, 1 H, *J* = 8.8, 15), 2.98 (m, 1 H), 2.81 (m, 2 H), 1.94 (dq, 1 H, *J* = 9.2, 16.6). Anal. Calcd for C₇H₁₀NO₂SBr: C, 33.34; H, 4.01; N, 5.56; S, 12.72; Br, 31.69. Found: C, 33.60; H, 3.88; N, 5.51; S, 12.86; Br, 31.78.

D,L-N-[3-(Dimethylphosphono)propionyl]homocysteine Thiolactone (6). D,L-N-(3-Bromopropionyl)-homocysteine thiolactone, **5** (5 g, 19.8 mmol), was covered with 60 mL of trimethyl phosphite. This solution, with nitrogen bubbling through it, was refluxed at 119 °C for 7 h. The excess trimethyl phosphite was removed by distillation at 48 °C under vacuum (110 mmHg), leaving a clear yellow oil. Ethyl ether was slowly added to the oil with vigorous stirring to produce a white precipitate (5.7 g). The precipitate was recrystallized by dissolving it in 200 mL of boiling toluene and adding hexane to the cloud point. White crystals, compound **6** (3.4 g, 61%), were filtered after aging for 72 h at 4 °C: mp 109.5–111.5 °C; ¹H NMR (CDCl₃) δ 6.5 (s, 1 H), 4.50 (pentet, 1 H, *J* = 6.5), 3.72 (d, 6 H), 3.33 (dt, 1 H, *J* = 5.1, 11.5), 3.24 (ddd, 1 H, *J* = 1.3, 7.0, 11.5), 1.86 (m, 1 H), 2.53 (m, 2 H), 2.1 (dt, 2 H, *J* = 7.75, 17.86), 1.95 (dq, 1 H, *J* = 7.1, 12.4). Anal. Calcd for C₉H₁₆NPO₅S: C, 38.43; H, 5.74; N, 4.98; P, 11.01; S, 11.40. Found: C, 38.31; H, 5.59; N, 4.90; P, 11.24; S, 11.30.

D,L-N-(3-Phosphonopropionyl)homocysteine Thiolactone (7). D,L-N-[3-(Dimethylphosphono)propionyl]-

homocysteine thiolactone, **6** (1.0 g, 3.6 mmol), was dissolved in 18 mL of dichloromethane, bromotrimethylsilane (7.5 mL, 56.8 mmol) added, and the reaction aged at 25 °C for 16 h. The solvent and volatiles were removed with a stream of N₂, 100 mL of methanol was added, and the solution was aged at 25 °C for 2 h. The methanol was then removed in vacuo. The remaining orange oil was dissolved in 8 mL of water and charged to 7 mL of Dowex 1X8 (200–400 mesh, acetate form) and the column then washed with 250 mL of water. Compound **7** was eluted with 200 mL of 2 N formic acid. Complete removal of formic acid under reduced pressure gave a clear oil (0.78 g, 3.1 mmol, 87% yield) which crystallized after 24 h at 25 °C: ¹H NMR (D₂O) δ 4.71 (dd, 1 H, *J* = 7.1, 12.6), 3.47 (dt, 1 H, *J* = 5.4, 11.5), 3.36 (dd, 1 H, *J* = 7.1, 11.5), 2.54–2.68 (m, 3 H), 2.23 (dq, 1 H, *J* = 7.1, 12.6), 2.06 (dt, 2 H, *J* = 8.7, 17.4); FAB MS *m/e* 252 (MH⁺). Anal. Calcd for C₇H₁₂NPO₅S·0.25H₂O: C, 32.62; H, 4.89; N, 5.44; P, 12.02; S, 12.44. Found: C, 32.59; H, 4.81; N, 5.43; P, 12.03; S, 12.33.

***N*-(3-Sulfopropionyl)homocysteine Thiolactone Sodium Salt (8).** A solution of *N*-(3-bromopropionyl)-homocysteine thiolactone, **5** (1.0 g, 3.9 mmol), in DMF (6 mL) was added dropwise to a solution of sodium bisulfite (1.25 g, 12 mmol) in 16 mL of a 3:1 H₂O–DMF mixture. The pH was adjusted to 8.8 by the addition of DIEA (1.5 mL) and the milky suspension stirred at room temperature for 18 h. The mixture was filtered to remove undissolved sodium sulfite and the filtrate evaporated in vacuo to a solid. This solid was redissolved in 10 mL of water, charged to a 60-mL column of Dowex 50X4 (H⁺ form), and eluted with 125 mL of water. The eluate was evaporated to 5 mL, adjusted to pH 7.2 with 5 N NaOH, and applied to a column of brominated polystyrene resin (90 mL, SP-207, Mitsubishi Chemical Co.). The column was eluted with water and after a forerun of 90 mL (AgNO₃ positive), 200 mL (UV positive) was collected and evaporated to dryness. The solid was dissolved in 15 mL of water and the product precipitated by the slow addition of 15 mL of absolute ethanol, yielding 0.6 g (54%) of an amorphous white solid: ¹H NMR (D₂O) δ 4.70 (dd, 1 H, *J* = 7, 12.5), 3.46 (dt, 2 H, *J* = 5.5, 11.7), 3.36 (ddd, 1 H, *J* = 1.4, 7.0, 11.1), 3.19 (m, 2 H), 2.74 (m, 2 H), 2.64 (dddd, 1 H, *J* = 1.4, 5.5, 7.0, 12.5), 2.22 (dq, 1 H, *J* = 7, 12.5). Anal. (Dried 80 °C/4 h.) Calcd for C₇H₁₀NO₅S₂Na: C, 30.54; H, 3.66; N, 5.09; S, 23.29. Found: C, 30.28; H, 3.54; N, 4.98; S, 23.54.

(β-Maleimidopropionyl)-L-arginyl-L-arginyl-L-arginine (9). To a solution of L-arginyl-L-arginyl-L-arginine (triarginine) triacetate (18 mg, 0.027 mmol) in 1 mL of 60% acetonitrile–water was added 0.324 mL of 0.5 M sodium bicarbonate (6 equiv) followed by β-maleimidopropionic acid *N*-hydroxysuccinimide ester (9 mg, 0.034 mmol). The solution was stirred at 0 °C and the progress of the reaction was monitored by HPLC [C₁₈ reverse phase 4.6 mm × 25 cm 8% acetonitrile–water–0.1% TFA; flow rate, 2 mL/min; retention time (min), starting material, 2.9; product, 4.8; β-maleimidopropionic acid, 3.9]. After 2 h the reaction was quenched by the addition of TFA (13 μL), filtered through a 0.2-μm syringe filter and purified by HPLC (2.12 × 25 cm, C₁₈, 10 mL/min of 8% MeCN–0.1% TFA). The peak at 9–13 min was concentrated in vacuo and lyophilized, affording 18 mg (68%) of the tris-TFA salt of (β-maleimidopropionyl)triarginine: FAB MS *m/e* 637 (MH⁺); ¹H NMR (D₂O) δ 6.85 (s, 1 H), 4.38 (dd, 1 H, *J* = 5.0, 9.0), 4.32 (dd, 1 H, *J* = 6.1, 8.1), 4.22 (dd, 1 H, *J* = 6.1, 8.1), 3.79 (t, 2 H, *J* = 6.4), 3.2 (m, 6 H), 1.5–2.0 (m, 12 H). The amino acid analysis exhibited an arginine to β-alanine ratio of 3:1.

***N*-(α-Bromoacetyl)-L-arginyl-L-arginyl-L-arginine (10).** Resin-bound triarginine which was tris-guanidino protected by (4-methoxy-2,3,6-trimethylphenyl)sulfonyl (Mtr) groups was synthesized on a 0.18-mmol scale on a Milligen Model 9050 peptide synthesizer. Preloaded Fmoc-Arg(Mtr)-OPKA resin (Milligen Co.) was coupled with Fmoc-Arg(Mtr) pentafluorophenyl esters using single 60-min reactions and a piperidine deprotection. The final resin was rinsed with methylene chloride and ether and dried in vacuo. A Kaiser test was positive for amine. This resin with the bound tripeptide derivative was swollen in 7 mL of *N*-methylpyrrolidine (NMP), and then 31 μL of DIEA and 85 mg of *p*-nitrophenyl bromoacetate were added. The resin was agitated at room temperature until a negative Kaiser test was observed. The bromoacetylated peptidyl resin was then washed with DMF (50 mL), methylene chloride (50 mL), and ether (50 mL). Cleavage from the resin was effected by TFA (20 mL) containing 3% thioanisole for 7 h at room temperature. The resin was removed by filtration and washed with TFA (3 × 20 mL), and the combined filtrates were concentrated in vacuo. The residue was triturated with ether, affording crude product (82 mg) which was purified by HPLC (Waters RCM 25 × 10 Delta Pack C₁₈, 10 mL/min, using a gradient [8% to 15% acetonitrile (0.1% TFA) in 20 min] to give 14.6 mg of *N*-(α-bromoacetyl)-L-arginyl-L-arginyl-L-arginine: FAB MS *m/e* 607 (MH⁺).

Thiolation of OMPC with *N*-Acetylhomocysteine Thiolactone and the Anionic Homocysteine Thiolactones. Evaluation of Irreversible Precipitation. The degree of irreversible precipitation was evaluated by examining the protein remaining in the supernatants after reaction with alkylating reagents **9** and **10**. It was quantified by an amino acid analysis (AAA) and calculating the amount of protein using the factor 420 nmol of lysine/mg of OMPC. This factor was obtained from AAA (triplicate) of unmodified OMPC and several of its derivatives (unpublished data). Since it had been observed that solubility of OMPC conjugates varied with ionic strength, the initially formed precipitate was subjected to further solubilization by dilution of the residual supernatant buffer with water. Thus solubility values in Table II are given at 0.1 and 0.02 M sodium phosphate. The total solubility is the sum of the residual protein in the supernatants in both molarities of phosphate.

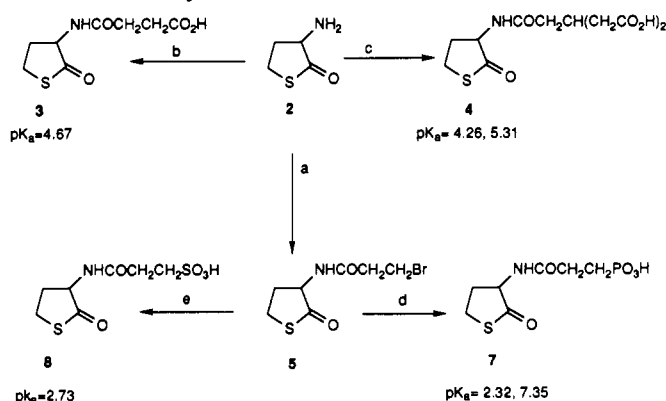
The thiolation procedure for *N*-acetylhomocysteine thiolactone is as follows: OMPC (5 mL, 3.8 mg/mL) was ultracentrifuged and the pellet resuspended, using a Dounce tissue homogenizer, in 6 mL of a thiolating solution (86 mg of EDTA, 17 mg of DTT, and 46 mg of *N*-acetylhomocysteine thiolactone in 10 mL of 0.1 M, pH 11 borate buffer). After 1 h, 1 M KH₂PO₄ (2.5 mL) was added and the mixture transferred to a centrifuge tube with a rinse of 1.5 mL of pH 7 phosphate buffer. (In another run the reaction time was extended to 1.5 h.) The mixture was pelleted by ultracentrifugation and the pellet resuspended in 10 mL of 0.1 M, pH 7 phosphate buffer and recentrifuged. After a final resuspension of the pellet in 5 mL of 0.1 M pH 8 phosphate buffer, the solution of thiolated OMPC was sampled for an Ellman assay and amino acid analysis.

Aliquots (1.0 mL) of the thiolated OMPC were pipetted into each of three 1.5-mL polypropylene tubes containing 1.5 mg each of (tube 1) iodoacetamide, (tube 2) bromoacetyltriarginine, and (tube 3) (β-maleimidopropionyl)-triarginine. The tubes were capped, shaken to dissolve the reagent, and aged at room temperature for 2 h and then in a refrigerator overnight. Tubes 2 and 3 were

Table II. Comparative Solubilities of OMPC-Triarginine Conjugates

characterization of reactant OMPC-SH solution				% conjugate in product supernatant using 9 and 10 ^d			
thiolactone	$\mu\text{mol SH}^a/\mu\text{mol Lys}^a$	SCMHC/Lys ^b	mg OMPC/mL ^c	0.1 M PO ₄		0.02 M PO ₄	
				10	9	10	9
1 ^e	0.23	0.21	3.2	<5	<5	<5	<5
1 ^f	0.29	0.26	3.2	<5	<5	<5	<5
3	0.29	0.26	3.3	<5	9	8	6
4	0.22	0.20	3.2	87	12	<5	81
7	0.25	0.23	3.2	31	10	<5	25
8	0.28	0.24	3.2	<5	<5	6	<5

^a Calculated from Ellman assay and Lys (AAA). ^b From AAA. ^c From Lys (AAA)/420. ^d From Lys (AAA)/420 divided by values in column 4. ^e 1-h reaction. ^f 1.5-h reaction.

Scheme II. ^a Synthesis of Anionic Thiolactones

^a Reagents: (a) bromopropionyl chloride; (b) succinic anhydride; (c) (carboxymethyl)glutaric anhydride; (d) trimethyl phosphite then trimethylsilyl bromide; (e) sodium bisulfite.

centrifuged for 2 min at 3000 rpm in a clinical centrifuge, and 0.8 mL of supernatant was removed. Water (0.8 mL) was added to the precipitate and the suspension tumbled on an Adams nutator for 2 h and again centrifuged for 2 min. All supernatants were sampled for amino acid analysis. The contents of tube 1 was dialysed vs 4 L of 0.01 M, pH 8 phosphate buffer overnight and the dialysate sampled for amino acid analysis.

For thiolation of OMPC with anionic thiolactones and reaction with the triarginine reagents 9 and 10, OMPC (5 mL, 3.8 mg/mL) was ultracentrifuged as above and the pellet thiolated with a similar borate buffer containing 80–90 mg of the selected anionic thiolactone reagents. The reaction was aged at room temperature overnight then transferred to a centrifuge tube with a rinse of 0.1 M pH 8 phosphate buffer. The remaining workup and reactions were carried out exactly as above.

RESULTS AND DISCUSSION

Synthesis. The syntheses of the various anionic thiolactones, shown in Scheme II, were effected either by direct acylation of homocysteine thiolactone, 2, or by conversion to the bromopropionyl derivative 5, followed by displacement of the bromine with the appropriate nucleophiles. The preparation of the phosphonic acid 7 proceeded via the phosphono dimethyl ester 6, which was demethylated with trimethylsilyl bromide (17).

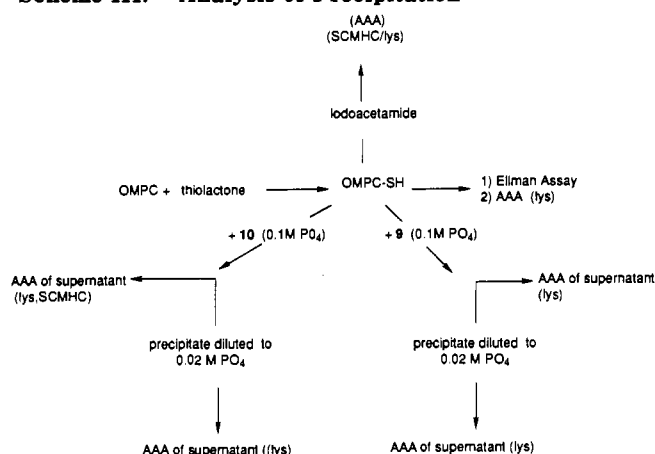
Conjugation. The role of a homocysteine thiolactone in the conjugation chemistry of OMPC involves acylation of the amino groups of OMPC to append a thiol group to the protein. This thiol group is then alkylated by an electrophile, such as a bromoacetyl group, which is incorporated into the molecule (i.e. peptide) to be conjugated. This is outlined in Scheme I. The stable thioether formed in the process not only affords the covalent bond between OMPC and the ligand (peptide) but also in

appropriate cases allows the degree of ligand binding to be evaluated. In the case of a bromoacetylated ligand and *N*-acetylhomocysteine thiolactone, the readily assayed *S*-(carboxymethyl)homocysteine (SCMHC) is formed and its titer can be used to evaluate the degree of conjugation. The anionic thiolactones experience the same chemistry with no problems. This can be inferred from the data in Table II, as follows: (a) the Ellman assay of the thiolated protein (column 2 in Table II) normalized to the amount of lysine in the sample indicates that about 25% of the lysines are derivatized; (b) after alkylation of the thiol with iodoacetamide, hydrolysis, and amino acid analysis, the ratio SCMHC/lysine (column 3) is congruent to the thiol/Lys ratio. Since alkylation of thiols by iodoacetamide is a facile process, this result implies that the hydrolysis of the homocysteine amide bonds is not disturbed by the presence of the acidic groups. The slightly lower ratio in column 3 could possibly be due to loss of SCMHC by oxidation during the analysis. Unfortunately, the maleimido electrophiles are not as useful in this regard as they afford the two diastereomeric forms of the *S*-(2-succinyl)-homocysteine, neither of which appears in a "window" in the amino acid analysis spectrum (unpublished data).

Comparison Strategy. For comparisons of the various types of thiolactones to be valid, the level of thiolation on each OMPC particle would have to be the same. This would result in equal levels of triarginine conjugation and hence equal levels of charge on each OMPC molecule. The effect of charge could then be more precisely evaluated. The maximum thiolation levels using anionic thiolactones are only about 60% of that achieved by 1 and seem to be related to the amount of negative charge that an OMPC particle can accommodate. In an experiment where the thiolation product of OMPC with 4 was rethiolated with the uncharged 1, a doubling of the thiol titer was observed (unpublished results). Since 1 is the key thiolactone for comparison purposes, we reduced its OMPC thiolation level by reducing its reaction time with OMPC so that the resulting degree of thiolation was roughly equal to that of the anionic thiolactones. Thiol levels were quantitated by normalizing the Ellman assays to the lysine levels (AAA) in OMPC-SH (column 2, Table II). This AAA method, for defining the protein titer, was employed since the commonly used Lowry method is standard dependent and each different thiolated OMPC might have a different response to the Lowry reagent.

The evaluation strategy is outlined in Scheme III and the results are summarized in Table II.

Table II shows that the SH/Lys ratio (column 2) varied by about 30% from the lowest (0.22) to the highest value (0.29) and it is possible that this variation may account for the larger amount of the irreversible precipitation observed with thiolactones 3 and 8 compared to 4 and 7. That is the higher level of thiolation of 3 and 8 result in more positive charge per OMPC molecule. However

Scheme III. ^a Analysis of Precipitation

^a Amino acid analysis (AAA) affords protein concentration from the formula 420 nmol Lys/mg OMPC; SCMHC/Lys affords degree of reaction with haloacetyl reagents.

comparison of 4 and 7 (both dianions at pH 7) with 1 indicates that diminishing the positive charge has some merit in preventing precipitation. In the case of 4 only about 10% of the OMPC is irreversibly lost. That the soluble protein in the case of 4 and 7 was a peptide conjugate was confirmed by appropriate SCMHC/Lys ratios in the experiments of 4 and 7 involving the bromoacetyl reagent 10.

With more complex peptide ligands (unpublished) the effect of the anionic spacers was not predictable, making it clear that the solubility of derivatized proteins is dependent on many factors. However the availability of these anionic thiolactones for use as linking molecules offers the possibility of changing the physical properties of the thiolated forms of the various types of macromolecules listed in Table I, thus affording fruitful conjugations and usable materials.

ACKNOWLEDGMENT

We would like to thank Dr. V. R. Lombardo and Ms. S. Halko for help preparing additional quantities of reagents.

LITERATURE CITED

- (1) Marburg, S., Jorn, D., Tolman, R. L., Arison, B.; McCauley, J., Kniskern, P. J., Hagopian, A., and Vella, P. P. (1986) Bimolecular chemistry of macromolecules: Bacterial polysaccharide conjugates of *Neisseria meningitidis* membrane protein. *J. Am. Chem. Soc.* 108, 5282-5287.
- (2) Marburg, S., Tolman, R. L., and Kniskern, P. J. (1987) Covalently modified polyanionic bacterial polysaccharides, stable covalent conjugates of such polysaccharides and im-

munogenic proteins with bigeneric spacers and methods of preparing such polysaccharides and conjugates and confirming covalency. U.S. patent 4,695,624.

- (3) Ip, C. C. Y., and Miller, W. J. (1992) Monosaccharide compositional analysis of *Haemophilus influenzae* type b conjugate vaccine-A method for in-process analysis. In *Chromatography in Biotechnology* (C. Horvath and L. S. Ettre, Eds.) American Chemical Society, Washington, DC, in press.
- (4) Emini, E. A., and Conley, A. J. (1992) The Development of an AIDS Vaccine: Progress and Perspectives. In *Challenges of the 1990's. New Diseases and New Therapies: Acquired Immunodeficiency Syndrome (AIDS)* (R. P. Luthy and R. G. Douglas, Eds.) Hanley and Belfus, Philadelphia, pp 85-91, (references cited therein).
- (5) Singh, P., Pirio, M., Leung, D. K., and Tsay, Y. G. (1984) Controlled coupling of aminoglycoside antibiotics to proteins for use in homogeneous enzyme immunoassays. *Can. J. Chem.* 62, 2471-2477.
- (6) Ponpipom, M. M., and Rupprecht, K. M. (1983) Methyl β -glycosides of N-acetyl-6-O-(omega-aminoacyl)muramyl-L-alanyl-D-isoglutamines, and their conjugates with meningococcal group C polysaccharide. *Carbohydr. Res.* 113, 45-56.
- (7) Christie, G., Breckenridge, A. M., and Park, B. K. (1989) Detection of antibodies towards the antimalarial amodiaquine and its quinone imine metabolite in man and the rat. *Biochem. Pharmacol.* 38, 1451-1458.
- (8) Manecke, G., and Middeke, H. J. (1980) Enzyme immobilization by reactive carriers containing maleimide groups. *Angew. Makromol. Chem.* 91, 179-201.
- (9) Martodam, R. R., Twumasi, D. Y., Liener, I. E., Powers, J. C., Nishino, N., and Krejcarek, G. (1979) Albumin microspheres as carrier of an inhibitor of leukocyte elastase: Potential therapeutic agent for emphysema. *Proc. Natl. Acad. Sci. U.S.A.* 76, 2128-2132.
- (10) Taylor, K. E., and Wu, Y. C. (1980) A thiolation reagent for cell surface carbohydrate. *Biochem. Int.* 1, 353-358.
- (11) Kim, S. C., Olson, N. F., and Richardson, T. (1990) Thiolation of β -lactoglobulin with N-acetylhomocysteine thiolactone (N-AHTL) and S-acetylmercaptosuccinic anhydride. *Milch-wissenschaft* 45, 580-583.
- (12) Kumar, A., Advani, S., Dawar, H., and Talwar, G. P. (1991) A simple method for introducing a thiol at the 5' end of synthetic oligonucleotides. *Nucleic Acids Res.* 19, 4561.
- (13) Ishimori, Y. (1990) Thiol group-containing lipids for preparing liposomes for lysis immunoassay. *Jpn Kokai Tokkyo Koho JP* 02,150,991.
- (14) Lowry, O. H., Rosebrough, N. J., Farr, A. L., and Randall, R. J. (1951) Protein measurement with the Folin phenol reagent. *J. Biol. Chem.* 193, 265-275.
- (15) Ellman, G. L. (1959) Tissue sulfhydryl groups. *Arch. Biochem. Biophys.* 82, 70-77.
- (16) Casas, J., Valls, J., and Serratos, F. (1977) *Anal. Quim.* 73, 260-264.
- (17) Chakravarty, P. K., Combs, P., Roth, A., and Greenlee, W. J. (1987) An efficient synthesis of gamma-amino- β -ketoalkylphosphonates from alpha-amino acids. *Tetrahedron Lett.* 28, 611-612.

Complete Protection of Antisense Oligonucleotides against Serum Nuclease Degradation by an Avidin-Biotin System

Ruben J. Boado* and William M. Pardridge

Department of Medicine, Division of Endocrinology, and Brain Research Institute, UCLA School of Medicine, Los Angeles, California 90024. Received June 18, 1992

It has been recently demonstrated that a complex of avidin, a cationic protein, and a monobiotinylated antisense oligonucleotide for the GLUT1 glucose transporter mRNA is taken up by cells in vitro and by organs in vivo via absorptive-mediated endocytosis. In the present study, a GLUT1 biotinylated oligonucleotide-avidin construct showing complete protection against serum 3'-exonuclease-mediated degradation is described. 21-mer antisense oligonucleotides complementary to nucleotides 162-182 and 161-181 of the bovine GLUT1 glucose transporter mRNA were synthesized with a 6-aminodeoxyuridine at positions 3 and 20, respectively, biotinylated with NHS- or NHS-XX-biotin to yield near 5'- or near 3'-biotinylated oligonucleotide (bio-DNA), and 5'- and 3'-end radiolabeled. Serum induced a rapid degradation of unprotected (no avidin) [5'-³²P]-5'-bio-DNA (>95% at 30 min). Avidin partially protected this construct (~31% of intact 21-mer oligo remained at 1 h). Similar results were obtained with the [3'-³²P]-5'-bio-DNA; however, no degradation products of varying size were observed, confirming that the degradation is mediated primarily by a 3'-exonuclease. Incubation of the [5'-³²P]-3'-bio-DNA with serum showed a rapid conversion to the 20- and 19-mer forms ($t_{1/2} \sim 13$ min). Conversely, avidin totally protected this construct against the serum 3'-exonuclease. In conclusion, avidin fully protects antisense oligonucleotides biotinylated at the near 3'-terminus against serum 3'-exonuclease degradation, and this property may be useful for avidin-mediated drug delivery of oligonucleotides to tissues in vivo or to cultured cells in vitro.

INTRODUCTION

The glucose transporter type I (GLUT1), a member of the Na⁺-independent glucose transporter supergene family (1-9), is overexpressed in malignancy and by cellular transformation and oncogenes (1, 10-12). Therefore, inhibition of the GLUT1 gene in cancer cells may result in glucose deprivation to the malignancy and potential inhibition of cell division. Antisense oligonucleotides are potential specific chemotherapeutic agents for the treatment of cancer, viral infections, and other disorders (13-15). However, major problems limiting the therapeutic efficacy of these agents in vivo are the minimal transcapillary transport or cellular uptake of the highly charged oligonucleotide and the rapid degradation by serum nucleases (16, 17), which have recently been shown to be predominantly 3'-exonucleases (17). Owing to these two problems, antisense oligonucleotides must be added to cells in tissue culture in high concentrations ranging from 10-100 μ M to achieve biological effects (18-22). Even higher concentrations will be required in vivo, where capillary barriers retard the delivery of oligonucleotides to cells. In particular, the delivery of these therapeutics to brain is impaired by the poor transport of these molecules through the brain capillary wall, which makes up the blood-brain barrier (BBB) in vivo (23). Although recent advances have shown that the use of methylphosphonate or phosphorothioate linkages protect antisense oligonucleotides against serum nuclease degradation, this protection was shown to be partial (18, 19, 24).

Given these considerations with regard to poor transport and rapid serum metabolism of antisense oligonucleotides, it would be advantageous to conjugate the antisense

oligonucleotide to a transport vector via high-affinity binding that is stable in the circulation but is labile in cells. A single solution to these multiple problems is potentially offered by the avidin-biotin system. Avidin binds biotin with very high affinity (i.e., $K_D = 10^{-15}$ M and dissociation $t_{1/2} = 89$ days) (25), and the avidin-biotin reaction is stable in the circulation but is labile in cells (26). Finally, avidin may act as a transport vector for mediating the uptake of biotinylated antisense oligonucleotide or biotinylated peptide by tissues in vivo. Avidin is a polycationic protein and recent studies have shown that avidin, like other polycationic proteins such as cationized albumin (27), is taken up by cells in vitro via absorptive-mediated endocytosis through a reaction that is inhibited by other polycationic proteins such as protamine (28). In addition, avidin enhances the organ delivery of biotinylated antisense oligonucleotides or peptides in vivo (29).

In addition to catalyzing the endocytosis of biotinylated antisense oligonucleotides, it is possible that the avidin-biotin system may protect the oligonucleotide from serum 3'-exonuclease activity by selectively biotinylating the oligonucleotide at the 3'-terminus. Data reported here demonstrate that avidin fully protects antisense oligonucleotides biotinylated at the near 3'-terminus against serum nuclease-mediated degradation.

EXPERIMENTAL PROCEDURES

Materials. [γ -³²P]Adenosine 5'-triphosphate (ATP) (3000 Ci/mmol), [α -³²P]deoxyadenosine 5'-triphosphate (dATP) (3000 Ci/mmol), and Cronex lighting plus intensifying screens were purchased from Du Pont-NEN (Boston, MA). T₄ polynucleotide kinase was obtained from Promega Corp. (Madison, WI), and terminal deoxynucleotidyl transferase was purchased from BRL (Gaithersburg, MD). Acrylamide, N,N'-methylenebisacrylamide, urea, and ammonium persulfate were purchased from

* Author to whom correspondence should be addressed: Ruben J. Boado, Ph.D., Department of Medicine, UCLA School of Medicine, Los Angeles, CA 90024. Phone: (310) 825-8858. FAX: (310) 206-5163.

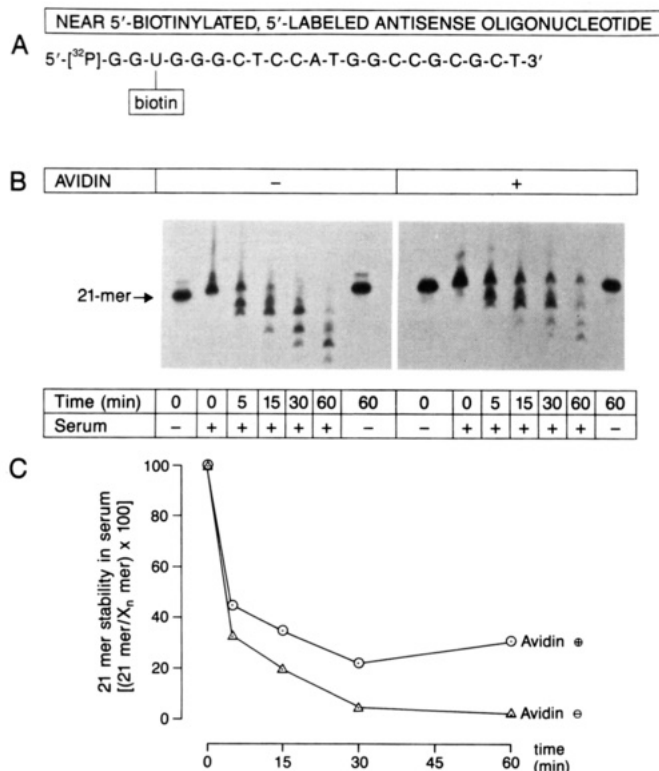


Figure 1. Avidin protection of near 5'-biotinylated [5'-³²P]-ant sense oligonucleotide in serum. (A) A 21-mer antisense oligonucleotide complementary to nucleotides 162-182 of the bovine GLUT1 glucose transporter mRNA was synthesized with an extended primary amine group by replacement of the deoxythymidine that corresponds to position 180 with 6-amino-deoxyuridine and biotinylated with NHS-biotin. (B) Effect of avidin on the stability of the near 5'-biotinylated oligonucleotide in serum. Six femtomole (26 400 dpm; specific activity = 2.0 μ Ci/pmol) of [5'-³²P]-5'-bio-oligonucleotide or [5'-³²P]-5'-bio-oligonucleotide/avidin complex was incubated with buffer or rat serum at 37 °C for the time indicated in the figure. Samples were resolved in a 15% polyacrylamide/7 M urea sequencing gel. The autoradiogram of the gel is shown in part B of the figure. (C) Quantitation of the autoradiogram by laser scanning densitometry. Results expressed as percent 21-mer [³²P]oligonucleotide/ X_n [³²P]oligonucleotides (degradation products). There is a consistent slightly lower migration of labeled product through the gel in the lanes containing serum.

Schwartz/Mann Biotech (Cleveland, OH). *N*-Hydroxy-succinimide ester of biotin (NHS-biotin) was obtained from Pierce Chemical Co. (Rockford, IL). Avidin and all other reagents were obtained from Sigma Chemical Co. (St. Louis, MO). Customized oligonucleotides were obtained from Genosys Biotechnologies, Inc. (The Woodlands, TX).

Synthesis of Biotinylated Oligonucleotides. Two 21-mer antisense oligonucleotides complementary to nucleotides 162-182 (Figure 1A) and 161-181 (Figure 3A) of the bovine GLUT1 glucose transporter mRNA (30) were synthesized with an extended primary amino group by replacement of the deoxythymidine at position 3 and 20, respectively, with 6-aminodeoxyuridine (aU) (Genosys Biotechnologies). This yielded the following oligonucleotides: 5'-GGaUGGGCTCCATGGCCGCGCT-3' (3-amino oligonucleotide) and 5'-GTGGGCTCCATGGCCGCGCaUG-3' (20-amino oligonucleotide). The size of these oligonucleotides was determined by the manufacturer by comparing migration distances with that of a parallel oligonucleotide standard using a 20% polyacrylamide/7 M urea gel electrophoresis.

The gel-purified 3-amino oligonucleotide was biotinylated to yield the 5'-biotinyl oligonucleotide (5'-bio-

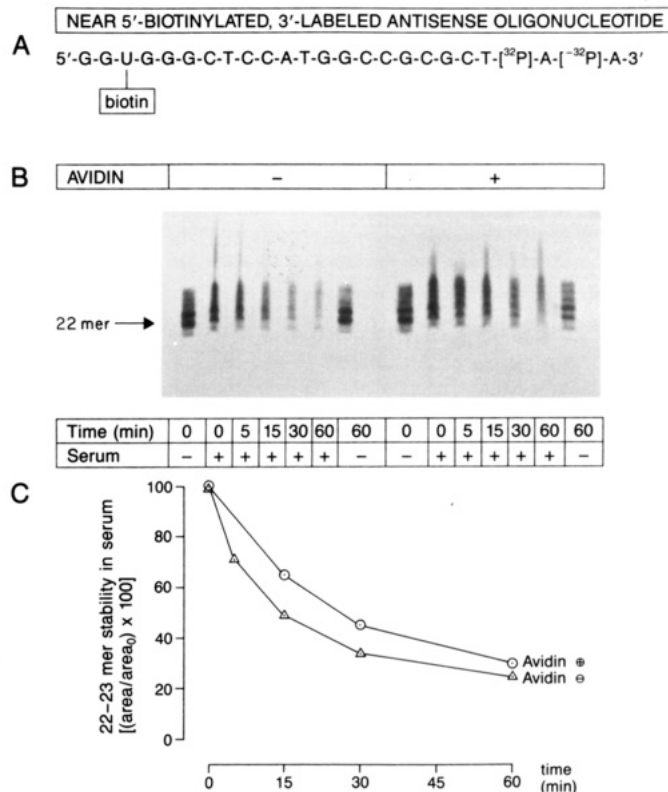


Figure 2. Avidin protection of the near 5'-biotinylated [3'-³²P]-labeled oligonucleotide in serum. (A) The 21-mer oligonucleotide described in Figure 1 was labeled at the 3'-terminus with [α -³²P]-dATP and terminal deoxynucleotidyl transferase and purified by gel electrophoresis. (B and C) The experiment was performed under identical conditions as those described in Figure 1 using 6 fmol of [3'-³²P]-5'-bio-oligonucleotide (29 000 dpm; specific activity = 2.2 μ Ci/pmol). Since no degradation products of varying size were seen in the [3'-³²P]-labeled experiment (B) due to action of 3'-exonucleases, results were expressed as integrated area/area₀, where area₀ = area at time zero. The initial labeled oligonucleotide mainly contains 1 and 2 molecules of [³²P]dATP and trace amounts containing up to 5 dATP molecules/molecule of oligonucleotide. A consistent slightly slower migration of labeled product through the gel was observed in the lanes containing serum.

oligonucleotide) by incubation with a 10.6 M excess ratio of NHS-biotin (31) to oligonucleotide in 0.125 M NaHCO₃ at pH = 9 for 16 h at 22 °C. Following biotinylation, the excess of NHS-biotin was removed from the 5'-bio-oligonucleotide by Sephadex G-25 spin-column chromatography (32) (Boehringer Mannheim, Indianapolis, IN).

The 20-amino oligonucleotide was similarly biotinylated with NHS-XX-biotin (X = 6-aminohexanoyl; Glen Research, Herndon, VA) to yield the 3'-bio-oligonucleotide. The 3'-bio-oligonucleotide was purified by high-pressure liquid chromatography using a 5- μ m C18 reverse-phase column (10 \times 250 mm) with a 300-Å pore size. The liquid phases were A, 0.1 M triethylammonium acetate in water, pH = 7, and B, 100% acetonitrile. The gradient was 30-38% B over 40 min. Under these conditions, biotinylation produced a 5-min shift in the retention of the oligonucleotide. Tubes corresponding to the biotinylated oligonucleotide were pooled and concentrated. The extinction coefficient (ϵ) was calculated as described previously (32), and it was found to be 207 mM⁻¹. The concentration of oligonucleotides [equal to optical density (OD)₂₆₀/ ϵ] was determined in all samples after measuring OD₂₆₀ in a Beckmann 34 UV spectrophotometer (Irvine, CA).

Preparation of [³²P]-Labeled Oligonucleotides. Aliquots of 15 pmol of 5'- and 3'-bio-oligonucleotide were

Near 3'-Biotinylated, 5'-Labeled Antisense Oligonucleotide

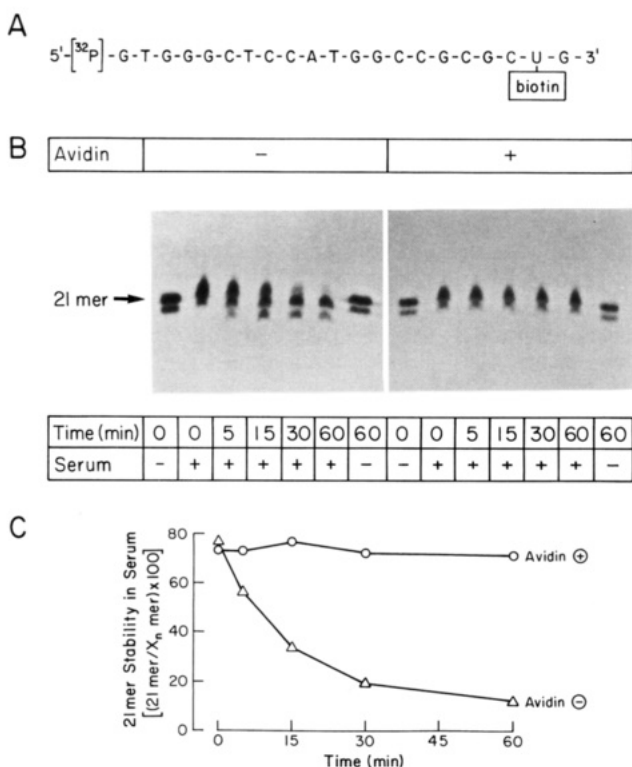


Figure 3. Avidin protection of near 3'-biotinylated [5'-³²P]-antisense oligonucleotide in serum. (A) A 21-mer antisense oligonucleotide complementary to nucleotides 161-181 of the bovine GLUT1 glucose transporter mRNA was synthesized with an extended primary amine group at position 20 and biotinylated with NHS-XX-biotin. (B and C) The experiment was performed under identical conditions as those described in Figure 1 using 6 fmol of [5'-³²P]-3'-bio-oligonucleotide (26 400 dpm, specific activity = 2.0 μ Ci/pmol). The initial labeled oligonucleotide is 80% 21-mer and 20% 20-mer [³²P]oligonucleotide, respectively, as determined by scanning laser densitometry (methods). There is a consistent slightly slower migration of labeled product through the gel in the lanes containing serum.

labeled at the 5'-end with 50 μ Ci of [γ -³²P]ATP and 8 units of T₄ polynucleotide kinase in a 20- μ L reaction containing 50 mM TRIS at pH = 7.6, 10 mM MgCl₂, 5 mM DDT, 0.1 mM spermidine-HCl, and 0.1 mM EDTA for 45 min at 37 °C. The labeled product was purified through a Sephadex G-25 spin column (32). The 5'-bio-oligonucleotide (15 pmol) was also labeled at the 3'-end with 100 μ Ci of [α -³²P]dATP and 15 units of terminal deoxynucleotidyl transferase (33) in a 10- μ L reaction containing 0.1 M potassium cacodylate (pH = 7.2), 2 mM CaCl₂, and 0.2 mM DTT for 2 h at 37 °C. The [3'-³²P]-labeled 5'-bio-oligonucleotide was purified by electrophoresis on a 15% denaturing polyacrylamide/7 M urea gel (32). The labeled oligonucleotide, mainly containing 1 and 2 molecules of [³²P]dATP/molecule of oligonucleotide, was identified by autoradiography and eluted from gel slices in 0.5 M NH₄ acetate/1 mM EDTA for 16 h at 22 °C, concentrated in a vacuum centrifuge evaporator (Savant), and suspended in H₂O.

The efficiency of the labeling procedure using either T₄ polynucleotide kinase or terminal deoxynucleotidyl transferase was determined by adsorption to DE-81 filters (Whatman International, Ltd., Maidstone, England) as described previously (32). Briefly, aliquots of the labeled reaction were applied to the positively charged DE-81 filters and dried at room temperature. In order to remove

all the free [³²P]dATP and -ATP, filters were individually washed three times in 50 mL of 0.5 M phosphate buffer, pH = 7, and one time in 70% ethanol. Filters were then dried, and the radioactivity was determined in a Packard scintillation counter Tri-carb 4530 (Downers Grove, IL) using SCINT-A XF scintillation cocktail (Packard). The percentage of incorporation was determined as (dpm in washed filters/dpm in unwashed filters) \times 100. The specific activity of the [³²P]-labeled oligonucleotides, calculated as percentage of incorporation \times amount of radioactivity used (μ Ci)/mass of oligonucleotide (15 pmol) \times 100, was 2.0 and 2.2 μ Ci/pmol for the 5'- and 3'-labeling reaction, respectively. The purity of the [³²P]-labeled oligonucleotides was determined after the purification steps (G-25 spin column for the T₄ kinase reaction and polyacrylamide gel electrophoresis for the terminal transferase reaction) by adsorption to the DE-81 filters as described above and was more than 99% pure.

For the serum protection studies, aliquots of 12.8 pmol of [³²P]-5'- or -3'-bio-DNA were incubated with 140 μ g of avidin in 100 μ L of PBST (PBST = 10 mM phosphate buffer, pH = 7.5; 0.15 M NaCl; 0.1% bovine serum albumin; 500 μ g tRNA/mL) at room temperature for 15 min. The avidin/[³²P]bio-oligonucleotide complex was purified from unbound [³²P]-labeled oligonucleotide, if any, by Sephadex G-75 spin-column chromatography prior to the experiment.

Serum Protection Studies. The effect of avidin on the stability of biotinylated oligonucleotide in serum was studied in 4 μ L of PBST containing 6 fmol (26 400 and 29 000 dpm for 5'- and 3'-labeled oligonucleotide, respectively, calculated using the specific activity and μ Ci = 2.2×10^6 dpm) of [³²P]bio-DNA or [³²P]bio-DNA/avidin complex, which were incubated with PBST or rat serum pool (16 μ L) at 37 °C for 0, 5, 15, 30, or 60 min. The final concentration of avidin in the reaction tube was 3.5 μ g/mL. The reaction was stopped by transferring tubes onto an ice bath and adding 2 volumes of 8 M urea/10% glycerol. Samples were heated for 5 min at 95 °C and incubated for 5 min on ice immediately before resolving them in a 0.4 mm 15% polyacrylamide/7 M urea sequencing gel (32). The gel was fixed for 10 min in 5% methanol/10% acetic acid, washed for 10 min in H₂O, and dried on Whatman 3 MM using a gel drier (Bio-Rad 583, Richmond, CA). Autoradiography was performed at -70 °C with intensifying screens for 1-3 days. Results were quantified by laser scanning densitometry (LKB Model 2202 ultrascan laser densitometer, Bromma, Sweden) of the autoradiogram, which yielded the area of each radioactive peak. In Figures 1 and 3, the area of the individual bands corresponding to labeled oligonucleotides of varying size was determined and expressed as percent 21-mer [³²P]oligonucleotide/ X_n , where X_n = the sum of all [³²P]oligonucleotides (degradation products). Since no degradation products of varying size were seen in the [3'-³²P]-labeled experiment (Figure 2) due to action of 3'-exonucleases, the results were expressed as integrated area for each peak/area₀, where area₀ is the area at zero time.

The rat serum pool was obtained from anesthetized animals killed by decapitation. Blood was collected by draining the trunk and serum obtained by centrifugation. The serum pool was kept at -20 °C, and aliquots were thawed once.

RESULTS

The protective effect of avidin from serum nuclease degradation of biotinylated oligonucleotides is shown in Figures 1-3. Incubation of the unprotected (i.e., no avidin) [5'-³²P]-5'-bio-antisense oligonucleotide (Figure 1) with

serum showed a rapid conversion to degradation products (20–16-mer) (Figure 1, B and C). In the absence of avidin, more than 95% of the labeled oligomer was degraded during the first 30 min of incubation. Incubation with avidin partially protected the near 5'-biotinylated [5'-³²P]-oligomer against degradation by the serum-mediated nucleases, as 31% of intact 21-mer labeled oligonucleotide was left at the end of the 1-h incubation period (Figure 1, B and C).

The degradation of the [5'-³²P]-5'-bio-oligonucleotide in serum was sequential (Figure 1); this observation, in conjunction with the absence of small degradation products, suggests the participation of a serum exonuclease. To test this hypothesis, the serum protection experiment was repeated with the near 5'-biotinylated oligonucleotide labeled with [α -³²P]dATP at the 3'-end with terminal transferase (Figure 2). The labeled product mainly contains 1 and 2 molecules of [³²P]dATP and traces containing up to 5 dATPs/molecule of oligonucleotide (Figure 2B). Avidin also protected the [3'-³²P]-5'-bio-oligomer partially and in a similar manner as it protected the [5'-³²P]-5'-bio-oligonucleotide (shown in Figure 1). In these studies, no degradation products of varying molecular size were observed in the presence of absence of avidin, confirming that the degradation of oligonucleotides in the present study was mainly mediated by a serum 3'-exonuclease.

Since avidin partially protects the 5'-bio-DNA against the serum 3'-exonuclease degradation, its effect was tested on the second oligomer which is biotinylated near the 3'-end (Figure 3). The labeled oligonucleotide was 80% 21-mer and 20% 20-mer [³²P]oligonucleotide. Incubation of the [5'-³²P]-3'-bio-oligonucleotide with serum without avidin showed a rapid conversion to degradation products (20- and 19-mer) with a half-life ($t_{1/2}$) of approximately 13 min. Conversely, incubation with avidin totally protected the [5'-³²P]-3'-bio-oligonucleotide against degradation by the 3'-exonuclease in serum during the incubation period (Figure 3).

DISCUSSION

The present study demonstrates that biotinylation of the oligonucleotide near the 3'-end (at nucleotide 20 of the 21-mer, Figure 3A) and avidin binding fully protects the oligomer against serum 3'-exonuclease degradation (Figure 3). On the other hand, when the oligonucleotide was biotinylated near the 5'-terminus (Figure 1) and incubated in serum, avidin partially protected the oligomer and degradation products of varying size (from 20- to 16-mer) were observed. Interestingly, the avidin/3'-biotinylated oligomer conjugate was totally resistant to the serum nuclease action, whereas when incubated in the absence of avidin, a rapid conversion of the 3'-biotinylated 21-mer/20-mer mixture to a 20-mer/19-mer mixture was observed, indicating that biotinylation, per se, at the 3'-terminus but not the 5'-terminus (Figure 1), protects against 3'-exonuclease-mediated degradation. This represents an important characteristic of 3'-biotinylated oligonucleotides, and suggests that after the biotin-avidin bond is cleaved in the cell, the 3'-bio-antisense oligonucleotide may still be stable to cellular 3'-exonuclease.

The model antisense oligonucleotide therapeutic employed in these studies was designed to contain only a single primary amino group available for biotinylation. The presence of multiple biotin groups on the therapeutic compound would cause the formation of high molecular weight aggregates owing to the multivalency of avidin binding of biotin (25). Although the GLUT1 antisense

oligonucleotide was selected as a model therapeutic, since the GLUT1 glucose transporter gene is overexpressed in malignancy (1, 10), this system is applicable to other antisense oligonucleotides. Whether biotinylated antisense oligonucleotides still bound to avidin retain their ability to hybridize to specific targets is at present unknown. However, the release of the biotinylated oligonucleotide from the avidin carrier may be facilitated by employing sulfosuccinimidyl 2-[2-(biotinamido)ethyl]-1,3'-dithiopropionate (NHS-SS-biotin), a disulfide-based biotinylation analogue that has been used previously to biotinylate oligonucleotides (34) or peptides (28, 29).

Overall, the present study shows that biotinylation of antisense oligonucleotides at the 3'-terminus and avidin binding provides complete protection against serum nuclease degradation. This property, in conjunction with previous studies showing endocytosis of avidin-drug conjugates (28, 29), may be useful for drug delivery of antisense oligonucleotides to tissues in vivo or to cultured cells in vitro using the avidin-biotin system.

ACKNOWLEDGMENT

The authors are indebted to Sherri J. Chien and Sara Morimoto for skillful preparation of the manuscript. This work was supported by NIH Grant RO1-AI28760.

LITERATURE CITED

- (1) Mueckler, M., Caruso, C., Baldwin, S. A., Panico, M., Blench, I., Morris, H. R., Allard, W. J., Lienhard, G. E., and Lodish, H. F. (1985) Sequence and Structure of a Human Glucose Transporter. *Science* 229, 941–945.
- (2) Birnbaum, M. J., Haspel, H. C., and Rosen, O. M. (1986) Cloning and Characterization of a cDNA Encoding the Rat Brain Glucose-Transporter Protein. *Proc. Natl. Acad. Sci. U.S.A.* 83, 5784–5788.
- (3) Thorens, B., Sarkar, H. K., Kaback, H. R., and Lodish, H. F. (1988) Cloning and Functional Expression in Bacteria of a Novel Glucose Transporter Present in Liver, Intestine, Kidney, and β -Pancreatic Islet Cells. *Cell* 55, 281–290.
- (4) Fukumoto, H., Seino, S., Imura, H., Seino, Y., Eddy, R. L., Fukushima, Y., Byers, M. G., Shows, T. B., and Bell, G. I. (1988) Sequence, Tissue Distribution, and Chromosomal Localization of mRNA Encoding a Human Glucose Transporter-Like Protein. *Proc. Natl. Acad. Sci. U.S.A.* 85, 5434–5438.
- (5) Kayano, T., Fukumoto, H., Eddy, R. L., Fan, Y.-S., Byers, M. G., Shows, T. B., and Bell, G. I. (1988) Evidence for a Family of Human Glucose Transporter-Like Proteins. Sequence and Gene Localization of a Protein Expressed in Fetal Skeletal Muscle and Other Tissues. *J. Biol. Chem.* 263, 15245–15248.
- (6) James, D. E., Strube, M., and Mueckler, M. J. (1989) Molecular Cloning and Characterization of an Insulin-Regulatable Glucose Transporter. *Nature* 338, 83–87.
- (7) Birnbaum, M. J. (1989) Identification of a Novel Gene Encoding an Insulin-Responsive Glucose Transporter Protein. *Cell* 57, 305–315.
- (8) Charron, M. J., Brosius, F. C., III, Alper, S. L., and Lodish, H. F. (1989) A Glucose Transport Protein Expressed Predominantly in Insulin-Responsive Tissues. *Proc. Natl. Acad. Sci. U.S.A.* 86, 2535–2539.
- (9) Kayano, T., Burant, C. F., Fukumoto, H., Gould, G. W., Fan, Y.-S., Eddy, R. L., Byers, M. G., Shows, T. B., Seino, S., and Bell, G. I. (1990) Human Facilitative Glucose Transporters. Isolation, Functional Characterization, and Gene Localization of cDNAs Encoding an Isoform (GLUT5) Expressed in Small Intestine, Kidney, Muscle, and Adipose Tissue and an Unusual Glucose Transporter Pseudogene-Like Sequence (GLUT6). *J. Biol. Chem.* 265, 13276–13282.
- (10) Yamamoto, T., Seino, Y., Fukumoto, H., Koh, G., Yano, H., Ingaki, N., Yamada, Y., Inoue, K., Manabe, T., and Imura, H. (1990) Over-Expression of Facilitative Glucose Transporter

- Genes in Human Cancer. *Biochem. Biophys. Res. Commun.* 170, 223-230.
- (11) Birnbaum, M. J., Haspel, H. C., and Rosen, O. M. (1987) Transformation of Rat Fibroblasts by FSV Rapidly Increases Glucose Transporter Gene Transcription. *Science* 235, 1495-1498.
- (12) Flier, J. S., Mueckler, M. M., Usher, P., and Lodish, H. F. (1987) Elevated Levels of Glucose Transport and Transporter Messenger RNA are Induced by *ras* and *src* Oncogenes. *Science* 235, 1492-1495.
- (13) Weintraub, H., Izant, J. G., and Harland, R. M. (1985) Antisense RNA as a Molecular Tool for Genetic Analysis. *Trends Gene.* 1, 22-25.
- (14) Dolnick, B. J. (1991) Antisense Agents in Cancer Research and Therapeutics. *Cancer Invest.* 9, 185-194.
- (15) Cohen, J. S. (1991) Antisense Oligodeoxynucleotides as Antiviral Agents. *Antiviral Res.* 16, 121-133.
- (16) Wickstrom, E. (1986) Oligodeoxynucleotide Stability in Subcellular Extracts and Culture Media. *J. Biochem. Biophys. Methods* 13, 97-102.
- (17) Tidd, D. M., and Varenus, H. M. (1989) Partial Protection of Oncogene, Anti-Sense Oligodeoxynucleotides Against Serum Nuclease Degradation Using Terminal Methylphosphonate Groups. *Br. J. Cancer* 60, 343-350.
- (18) Smith, C. C., Aurelian, L., Reddy, M. P., Miller, P. S., and Ts'o, P. O. P. (1986) Antiviral Effect of an Oligo(nucleoside methylphosphonate) Complementary to the Splice Junction of Herpes Simplex Virus Type 1 Immediate Early Pre-mRNAs 4 and 5. *Proc. Natl. Acad. Sci. U.S.A.* 83, 2787-2791.
- (19) Marcus-Sekura, C. J., Woerner, A. M., Shinozuka, K., Zon, G., and Quinnan, G. V. Jr., (1987) Comparative Inhibition of Chloramphenicol Acetyltransferase Gene Expression by Antisense Oligonucleotide Analogues Having Alkyl Phosphotriester, Methylphosphonate and Phosphorothioate Linkages. *Nucleic Acids Res.* 15, 5749-5763.
- (20) Letsinger, R. L., Zhang, G. R., Sun, D. K., Ikeuchi, T., and Sarin, P. S. (1989) Cholesteryl-Conjugated Oligonucleotides: Synthesis, Properties, and Activity as Inhibitors of Replication of Human Immunodeficiency Virus in Cell Culture. *Proc. Natl. Acad. Sci. U.S.A.* 86, 6553-6556.
- (21) Leonetti, J. P., Machy, P., Degols, G., Delbeu, B., and Leserman, L. (1990) Antibody-Targeted Liposomes Containing Oligodeoxyribonucleotides Complementary to Viral RNA Selectively Inhibit Viral Replication. *Proc. Natl. Acad. Sci. U.S.A.* 87, 2448-2451.
- (22) Morrison, R. S. (1991) Suppression of Basic Fibroblast Growth Factor Expression by Antisense Oligodeoxynucleotides Inhibits the Growth of Transformed Human Astrocytes. *J. Biol. Chem.* 266, 728-734.
- (23) Pardridge, W. M. (1991) *Peptide Drug Delivery to the Brain*, Raven Press, New York, NY, pp 1-356.
- (24) Matsukura, M., Shinozuka, K., Zon, G., Mitsuya, H., Reitz, M., Cohen, J. S., and Broder, S. (1987) Phosphorothioate Analogs of Oligodeoxynucleotides: Inhibitors of Replication and Cytopathic Effects of Human Immunodeficiency Virus. *Proc. Natl. Acad. Sci. U.S.A.* 84, 7706-7710.
- (25) Green, N. M. (1975) Avidin. *Adv. Protein Chem.* 29, 85-133.
- (26) Wei, R. D., Koou, D. H., and Hoo, S. L. (1970) Dissociation of Avidin-Biotin Complex in vivo. *Experientia* 27, 366-368.
- (27) Kumagai, A. K., Eisenberg, J., and Pardridge, W. M. (1987) Absorptive-Mediated Endocytosis of Cationized Albumin and a β -Endorphin-Cationized Albumin Chimeric Peptide by Isolated Brain Capillaries. Model System of Blood-Brain Barrier Transport. *J. Biol. Chem.* 262, 15214-15219.
- (28) Pardridge, W. M., and Boado, R. J. (1991) Enhanced Cellular Uptake of Biotinylated Antisense Oligonucleotide or Peptide Mediated by Avidin, a Cationic Protein. *FEBS Lett.* 288, 30-32.
- (29) Pardridge, W. M., Boado, R. J., and Buciak, J. L. (1992) Drug Delivery of Antisense Oligonucleotides or Peptides to Tissues in Vivo Using an Avidin-Biotin System. *Drug Targeting Delivery*. In press.
- (30) Boado, R. J., and Pardridge, W. M. (1990) Molecular Cloning of the Bovine Blood-Brain Barrier Glucose Transporter cDNA and Demonstration of Phylogenetic Conservation of the 5'-Untranslated Region. *Mol. Cell. Neurosci.* 1, 224-232.
- (31) Langer, P. R., Waldrop, A. A., and Ward, D. C. (1981) Enzymatic Synthesis of Biotin-Labeled Polynucleotides: Novel Nucleic Acid Affinity Probes. *Proc. Natl. Acad. Sci. U.S.A.* 78, 6633-6637.
- (32) Sambrook, J., Fritsch, E. F., and Maniatis, T. (1989) *Molecular Cloning: A Laboratory Manual*, Cold Spring Harbor Laboratory Press, Cold Spring Harbor.
- (33) Collins, M. L., and Hunsaker, W. R. (1985) Improved Hybridization Assays Employing Tailed Oligonucleotide Probes: A Direct Comparison with 5'-end labeled Oligonucleotide Probes and Nick-Translated Plasmid Probes. *Anal. Biochem.* 151, 211-224.
- (34) Shimkus, M., Levy, J., and Herman, T. (1985) A Chemically Cleavable Biotinylated Nucleotide: Usefulness in the Recovery of Protein-DNA Complexes From Avidin Affinity Columns. *Proc. Natl. Acad. Sci. U.S.A.* 82, 2593-2597.

Sulfomethylation of Di-, Tri-, and Polyazamacrocycles: A New Route to Entry of Mixed-Side-Chain Macrocyclic Chelates

Jeroen van Westrenen and A. Dean Sherry*

Department of Chemistry, The University of Texas at Dallas, P.O. Box 830688, Richardson, Texas 75083-0688. Received June 29, 1992

The sulfomethylation of piperazine and the polyazamacrocycles, [9]aneN3, [12]aneN3, [12]aneN4, and [18]aneN6 with formaldehyde bisulfite in aqueous medium at various pH values is described. The number of methanesulfonate groups introduced into these structures was found to be largely determined by pH. At neutral pH, disubstituted products of [9]aneN3, [12]aneN3, [12]aneN4 are formed and, in the latter case, the *trans*-1,7-bis(methanesulfonate) isomer was predominant. Similarly, a single, symmetrical trisubstituted product was formed with [18]aneN6 at neutral pH. Monomethanesulfonated products of these same polyaza compounds were formed at more acidic pH's. These sulfomethylated products were used as an entry into a series of mono- and diacetate, phosphonate, and phosphinate derivatives of [9]aneN3, [12]aneN3, and [12]aneN4. The sulfonate groups may be converted to acetates without isolation of intermediates by using cyanide to displace the sulfonate(s) followed by acidic hydrolysis. The aminomethanesulfonates may also be oxidatively hydrolyzed by using aqueous triiodide as a prelude to the preparation of aminomethanephosphonates or aminomethanephosphinates.

INTRODUCTION

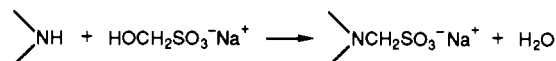
The high thermodynamic stability and kinetic inertness of chelates formed between lanthanide(III) cations and polyazamacrocyclic ligands having either carboxylate or phosphonate pendant donor groups have led to considerable interest in their application as NMR shift reagents in biological systems or as magnetic resonance imaging (MRI) contrast agents (1). The protonation schemes that have emerged from prior potentiometric and NMR pH titrations show that these ligands have unique protonation patterns resulting from the close proximity of the ring nitrogens (2-7).

The triazamacrocycles with ring sizes varying from 9 to 12 typically have one acidic nitrogen, one quite basic nitrogen, and a third nitrogen with a pK_a near neutrality (Table II). For polyazamacrocycles with an even number of nitrogens, such as tetraazacyclododecane and hexaazacyclooctadecane, a sharp division in pK_a 's is shown upon half-protonation. To our knowledge, no advantage has been taken of these pK_a differences in a synthetic sense. We considered that sulfomethylation may be especially well-suited for taking advantage of such pK_a differences because the reaction is a Mannich-type reaction that works both in neutral and basic pH ranges (8) and indeed found that the sulfomethylation products of these polyazamacrocycles seem to be largely pH determined. We report here the synthesis of mono- and disulfomethylated triazamacrocycles, the preparation of a symmetrical disulfomethylated tetraazamacrocyclic and a trisulfomethylated hexaazamacrocyclic, and the conversion of several sulfomethylated products into carboxylate(s), phosphonate(s), or phosphinate(s). We show that sulfomethylation provides a convenient synthetic entry into selective geometrical isomers of macrocyclic chelates having more than one type of side-chain chelating group.

RESULTS AND DISCUSSION

Sulfomethylation Using $\text{HOCH}_2\text{SO}_3\text{Na}$. The sulfomethylation of amines by a Mannich-type reaction with

formaldehyde and sodium bisulfite has been described previously. (9-13) The reaction may be carried out in aqueous solution using the commercially available sodium salt of formaldehyde bisulfite. The degree of sulfome-



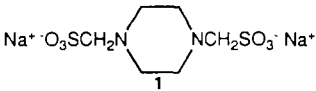
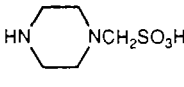
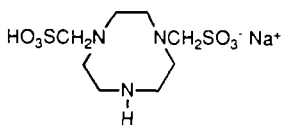
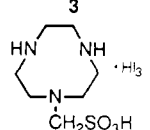
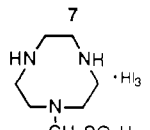
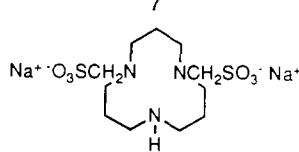
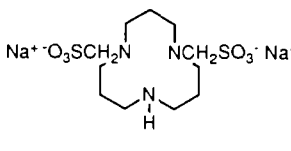
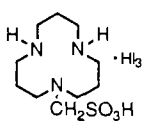
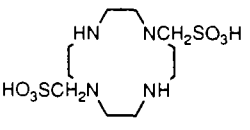
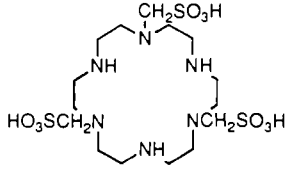
thylation of macrocyclic amines was found to be quite pH dependent. For example, piperazine forms a disulfomethylated product at pH 9-10 and a monosulfomethylated product at pH 6 (see Table I). A similar pH selectivity was observed for sulfomethylation of the triazamacrocycles. Disulfomethylated [9]aneN3 and [12]aneN3 were obtained in high yields by using stoichiometric amounts of formaldehyde bisulfite at pH values between 7 and 9 (Table I), while monosulfomethylated products were formed exclusively at pH 4, even with formaldehyde bisulfite in a 3-fold excess over the amine. Trisulfomethylated products were only formed under conditions where all three macrocyclic nitrogens are known to be largely deprotonated (above pH 11-12). These observations suggest that protonation of a secondary amine dramatically decreases its reactivity with formaldehyde bisulfite and that the distinct pK_a differences of the nitrogens within a given polyazamacrocyclic give rise to this rather unusual chemical selectivity.

The tetraazamacrocyclic, [12]aneN4, has two high and two low pK_a values (Table II), so at neutral pH, [12]aneN4 $\cdot 2\text{H}^+$ is virtually the only ionic form present. As predicted, sulfomethylation of [12]aneN4 with formaldehyde bisulfite at pH 7 yields the disulfomethylated product exclusively. Furthermore, of the two possible regioisomers, the 1,7-*trans* isomer is the predominant product (>90%). This observation is consistent with the microprotonation sequence of [12]aneN4 as determined by NMR (2), which indicates that the first two protonations occur at nitrogens *trans* to one another. Thus, at pH 7, two *trans* nitrogens are largely protonated while two remain nonprotonated and thus available to react with formaldehyde bisulfite.

Regioisomers should also be formed in the reaction of

* Author to whom correspondence should be addressed.

Table I. Sulfomethylation Products and Yields of Di-, Tri-, and Polyazamacrocycles

starting amine (A)	reactant (R) (mole ratio, R/A)	conditions	product	% isolated yield
piperazine	HOCH ₂ SO ₃ ⁻ Na ⁺ (2.0)	pH 9–10, 70 °C, 2 h	 1	51
piperazine	HOCH ₂ SO ₃ ⁻ Na ⁺ (1.05)	pH 6, 40 °C, 2 h	 2	51
[9]aneN3	HOCH ₂ SO ₃ ⁻ Na ⁺ (2.1)	pH 9.5, 40 °C, 16 h	 3	>95
[9]aneN3	(CH ₃) ₂ NH ⁺ CH ₂ SO ₃ ⁻ (1.5)	(a) pH 3.9, 25 °C, 16 h (b) NaI/I ₂	 7	93
[9]aneN3	H ₂ NCH ₂ SO ₃ ⁻ Na ⁺ (1.3)	(a) pH 4, 75 °C, 16 h (b) NaI/I ₂	 7	50
[12]aneN3	HOCH ₂ SO ₃ ⁻ Na ⁺ (2.1)	pH 9.6, 40 °C, 16 h	 4	>95
[12]aneN3	HOCH ₂ SO ₃ ⁻ Na ⁺ (9)	pH 4, 40 °C, 16 h	 4	>95 ^a
[12]aneN3	(CH ₃) ₂ NH ⁺ CH ₂ SO ₃ ⁻ (1.5)	(a) pH 4.3, 25 °C, 16 h (b) NaI/I ₂	 8	65
[12]aneN4	HOCH ₂ SO ₃ ⁻ Na ⁺ (2.1)	pH 7, 40 °C, 16 h	 5	95
[18]aneN6	HOCH ₂ SO ₃ ⁻ Na ⁺ (7.5)	pH 7, 25 °C, 3 days	 6	53

^a Estimated from ¹³C NMR.

formaldehyde bisulfite with [18]aneN6, yet the symmetrical 1,7,13-trisubstituted derivative was the main product observed when the reaction was carried out at pH 7. Again, this likely occurs because three nitrogens are largely protonated at this pH (Table II) and one might expect that the three protonations would occur at nitrogen

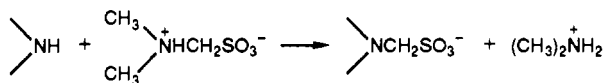
positions which give the least electrostatic repulsions. Interestingly, when this reaction was carried out in a Na₂HPO₄ and KH₂PO₄ buffer, trisulfomethylated [18]aneN6 crystallized from the reaction mixture as a HPO₄²⁻ adduct. **Sulfomethylation by Amine Exchange with (CH₃)₂NCH₂SO₃H.** As indicated above, monosubstituted de-

Table II. Protonation Constants of Amines (25 °C)

amine	log K_1	log K_2	log K_3	log K_4
(CH ₃) ₂ NH	10.77			
piperazine	9.83	5.56		
[9]aneN3 ^a	10.42	6.82	low	
[12]aneN3 ^a	12.60	7.57	2.41	
[12]aneN4 ^b	10.6	9.6	low	low
[18]aneN6 ^c	10.07	9.11	8.61	3.97

^a 0.1 M KNO₃, ref 6. ^b 0.1 M NaClO₄, ref 26. ^c 0.1 M NaClO₄, refs 5 and 26.

derivatives of [9]aneN3 and [12]aneN3 may be synthesized at pH 4 in the presence of excess formaldehyde bisulfite. When 1.5 mol of formaldehyde bisulfite per [12]aneN3 was used, only 30% of the amine was converted to a monosubstituted product during a 16 h period at 50 °C. Longer reaction times at this temperature leads to extensive decomposition of the desired product, as indicated by ¹³C NMR. Alternatively, (dimethylamino)-methanesulfonic acid may be used as a sulfomethylating agent via an amine exchange reaction.



The reaction of [9]aneN3 with 1.5 equiv of (dimethylamino)methanesulfonic acid at pH 3.8 shows complete conversion to the monosulfomethylated product plus dimethylammonium ion after 16 h at 25 °C, as indicated by NMR. This reaction likely proceeds via a reverse Mannich-type reaction, with the iminium ion or its hydrated form reacting with a nonprotonated triazamacrocyclic amine to liberate the dimethylammonium ion. The resulting macrocyclic iminium ion could then react with hydrogen sulfite to form the macrocyclic aminomethanesulfonate. The large p*K* differences between dimethylamine and the p*K*₃'s of [9]aneN3 or [12]aneN3 (Table II) result in an equilibrium which lies heavily in favor of the monosulfomethylated macrocycle at pH 4. The commercially available aminomethanesulfonic acid also undergoes an amine exchange reaction, but the rate of exchange is slower. After stirring of [9]aneN3 with 1.3 equiv of aminomethanesulfonic acid at 25 °C, pH 4, for 16 h, about 50% of the starting amine was converted to a monosubstituted product. The rate of this exchange might be affected by the low solubility of aminomethanesulfonic acid, however, since this compound has limited solubility in water.

Conversion of Aminomethanesulfonates to Aminomethanecarboxylates. The conversion of aminomethanesulfonates to amino acids via nucleophilic substitution of cyanide for sulfonate has been known for some time. (13–15) Cyanide substitution can be performed at 25 °C without isolation of the sulfomethylated product by adding NaCN directly to the reaction mixture. (13) After stirring of 1.5 equiv of NaCN with monosulfomethylated [9]aneN3 (prepared in situ) for 16 h at room temperature, a ¹³C NMR spectrum of the reaction mixture indicates that *N*-(cyanomethyl)-1,4,7-triazacyclononane was the main product formed, with about 15–20% of unsubstituted [9]aneN3 remaining. Both dimethylamine and a small amount of (CH₃)₂NCH₂CN [formed by CN[−] substitution with (dimethylamino)methanesulfonic acid] were present in the reaction mixture as well. The desired product was purified by cation-exchange chromatography in an isolated yield of 32%.

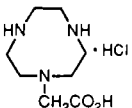
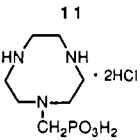
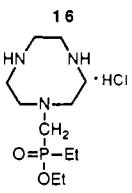
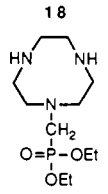
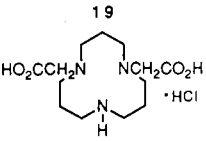
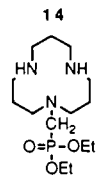
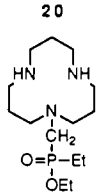
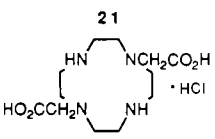
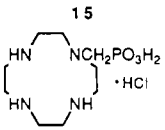
Subsequent hydrolysis of the nitrile in HCl was followed by ¹H NMR. Refluxing the nitrile for 30 min in 20% HCl

regenerates about 25% of the original amine, [9]aneN3. Reducing either the temperature or the acid concentration reduced the amount of decarboxylation but led to extended reaction times for the hydrolysis. Since reformation of at least some [9]aneN3 appeared inevitable during acidic hydrolysis, a one-pot synthesis of 1,4,7-triazacyclononane-*N*-acetic acid was developed with the optimum hydrolysis conditions being about 10% HCl, 75 °C, for 4 days. These conditions gave the monoacetic acid derivative in an isolated yield of 32%, after purification by cation-exchange chromatography (see Table III).

As noted above, formaldehyde bisulfite was used for disulfomethylation of the triaza and tetraaza macrocycles. Unlike (*N,N*-dimethylamino)methanesulfonic acid, which forms unreactive (CH₃)₂NCH₂CN during nucleophilic displacement by CN[−], the formaldehyde adduct forms HOCH₂CN under similar conditions (confirmed by ¹³C NMR in a separate experiment) and this is known to react with free amines to give aminomethanenitriles. (16,17) The reactivity of HOCH₂CN was particularly evident during the conversion of disulfomethylated [12]aneN3 to the dinitrile. When [12]aneN3 was sulfomethylated by using 4 mol of formaldehyde bisulfite per mole of [12]aneN3 in a concentrated buffer medium at pH 7, ¹³C NMR indicated that the major product was disulfomethylated [12]aneN3. However, upon addition of 4 mol of NaCN to this same reaction mixture, the tricyanomethylated derivative of [12]aneN3 crystallized from the reaction mixture in 52% yield. The same phenomena was observed when [12]aneN4 was reacted with 5.5 mol of formaldehyde bisulfite at pH 7 followed by the addition of 5.5 mol of NaCN in a second step. In this case, the tetracyanomethylated derivative of [12]aneN4 crystallized from the reaction mixture in 61% yield. Therefore, if the desired product is a dicyanomethylated triaza- or tetraazamacrocyclic, the cyanide substitution reaction must be carried out after formaldehyde bisulfite is completely consumed. Fortunately, disulfomethylated derivatives of [9]aneN3, [12]aneN3, and [12]aneN4 can be prepared quantitatively using stoichiometric amounts of formaldehyde bisulfite. Thus, the pure 1,7-diacetic acid derivative of [12]aneN4 may be isolated in 80% yield (after purification by cation-exchange chromatography) by reacting [12]aneN4 with 2 equiv of formaldehyde bisulfite at pH 7, adding NaCN without a reaction workup, followed by hydrolysis in refluxing 20% HCl for 48 h (Table III). The 1,4-disubstituted regioisomer that is formed in small quantities during sulfomethylation is not detected by ¹H or ¹³C NMR after column purification. Acidic hydrolysis of the dicyanomethylated [12]aneN4 product does not appear to require the same mild acidic conditions to prevent decarboxylation, for reasons that are not fully understood. This same reaction sequence has been used to prepare the diacetic acid derivative of [12]aneN3 in 19% yield with 95% purity (Table III). In this case, a small amount of the monoacetic acid derivative is present after purification by cation-exchange chromatography.

The Reaction of Macrocyclic Aminomethanesulfonates with Triiodide. Disubstituted aminomethanesulfonic acids can undergo oxidative hydrolysis to aminomethanol derivatives by reaction with triiodide, the rate-limiting step being the formation of the sulfite ion via the reverse Mannich reaction prior to its oxidation to sulfate. (18) ¹H NMR studies by Burg (19) have shown that the reaction of triiodide with Me₂NCH₂SO₃[−] proceeds almost quantitatively to Me₂NCH₂OH in a few minutes as judged by NMR. Similarly, the reaction of bis-(sulfomethyl)piperazine with 2 mol of triiodide in aqueous

Table III. Summary of Reactions Used To Convert Sulfomethylated Polyazamacrocycles into Carboxylates, Phosphonates, or Phosphinates

sulfomethylated amine	reactant(s) and conditions	product	% isolated yield
7	(a) NaCN, pH 3.5 (b) 37% HCl, 75 °C, 4 days		32
7·HI ₃	molten H ₃ PO ₃ , 80 °C		21
7·HI ₃	HP(O)(OEt)Et, 25 °C		43
7·HI ₃	HP(O)(OEt) ₂ , 25 °C		24
4	(a) NaCN, 25 °C, 24 h (b) 20% HCl, reflux, 3 days		19
8·HI ₃	HP(O)(OEt) ₂ , 25 °C		31
8·HI ₃	HP(O)(OEt)Et, 25 °C		73
5	(a) NaCN, 22 h, 25 °C (b) 37% HCl, reflux, 65 h		80
5	(a) 10% HCl, NaI ₃ , ppt, 25 °C (b) molten H ₃ PO ₃ , 80 °C, 3 h		24
		22	

solution at 25 °C resulted in a color change from brown to colorless after about 2 min. This event was followed by the formation of a white precipitate, which was isolated in 34% yield. An IR spectrum of the isolated solid showed a broad absorption from 2534 to 2342 cm⁻¹, indicative of a protonated quaternary nitrogen. Elemental analysis was

consistent with formation of the dihydrated form of the diiminium ion. The addition of sodium triiodide to either monosulfomethylated [9]aneN3 or [12]aneN3 resulted in formation of brown precipitates, which were isolated in high yields. These proved to be simple triiodide salts of the monosulfomethylated triaza compounds, which have

limited water solubility at room temperature. The triiodide salt of monosulfomethylated [9]aneN3 does dissolve in water at 40 °C and this solution gradually becomes colorless over a 3-h period, indicating that triiodide had completely reacted with the monosulfomethylated amine. The expected hydrolysis product was confirmed by ^1H NMR, which showed broad peaks for the [9]aneN3 protons (3.61 ppm) and the NCH_2OH methylene protons (4.58 ppm). Resonances at 4.81 and 3.69 ppm indicated that some further hydrolysis to HOCH_2OH and unsubstituted [9]aneN3 had occurred. Dissolution and subsequent reaction of monosulfomethylated [12]aneN3 goes even slower; complete oxidative hydrolysis was not observed after 16 h at 40 °C. It also proved possible to reduce the triiodide salt of monosulfomethylated [9]aneN3 to iodide without altering the methanesulfonate group on the macrocycle by suspending the salt in ethanol and adding excess diethyl phosphite.

Conversion of Aminomethanesulfonates to Aminomethanephosphonates and Aminomethanephosphinates. Although the mechanisms of sulfonate displacement by cyanide has not been described, other strong nucleophiles such as the malonate anion apparently react similarly. (13) However, the nucleophilicity of $\text{HP}(=\text{O})(\text{OH})_2$ or its conjugate base is too low to displace the sulfonate group as no phosphorylation seems to occur even with a large excess of $\text{HP}(=\text{O})(\text{OH})_2$. As indicated above, some aminomethanesulfonates may be converted to the corresponding aminomethanol derivatives, and these in turn are reactive intermediates in the Mannich reaction. As one example, the addition of a 10-fold excess of phosphorus acid to $(\text{CH}_3)_2\text{NCH}_2\text{OH}$ (formed in situ by reaction of $\text{Me}_2\text{NCH}_2\text{SO}_3^-$ with triiodide) gave quantitative yields of (dimethylamino)methanephosphonate after 4 h at reflux. Partial hydrolysis to dimethylammonium and formaldehyde was observed when a 5-fold excess of phosphorus acid was used.

Oxidative hydrolysis of the disulfomethylated derivative of piperazine with triiodide gave a bis(hydroxymethyl)-piperazine salt that precipitated from solution. Addition of 1 mmol of this salt to a 10 M phosphorous acid solution resulted in the formation of di- (17%) and monomethylenephosphonate (50%) derivatives of piperazine plus free piperazine after 4 h at reflux. However, this undesired reaction was prevented by carrying out the reaction in molten phosphorous acid at 80 °C. These conditions gave *N,N'*-bis(methylenephosphonate) piperazine as the only product (Table III).

The partially substituted methanesulfonate derivatives of the tri- and tetraaza macrocycles have an additional problem in that intermolecular reactions result in polymers. To suppress this side reaction, the phosphorylation was carried out in 20% HCl to insure that all amino groups were fully protonated. When the oxidized product of 1,7-disulfomethylated [12]aneN4 was refluxed with a 10-fold excess of phosphorous acid per hydroxymethylene group, extensive hydrolysis of the hydroxymethylene group still occurred, giving a mixture of monomethylphosphonylated [12]aneN4 and "free" [12]aneN4 with no trace of the expected disubstituted methanephosphonate.

Phosphonylation of the tri- and tetraazamacrocycles cannot be carried out under anhydrous conditions such as those described for the piperazine derivative because the aminomethanol derivatives are not isolated in pure form as a solid. However, the HI_3 salts of the monomethanesulfonic acids of [9]aneN3 and [12]aneN3 may be used directly. When these triiodide salts were added to molten phosphorous acid at 80 °C or to neat $\text{HP}(=\text{O})\text{Et}(\text{OEt})$ or

$\text{HP}(=\text{O})(\text{OEt})_2$ at 25 °C, exothermic reactions occurred, yielding the monomethanephosphonate, the monomethane-*P*-ethylphosphinate ethyl ester, and the monomethanephosphonate diethyl ester, respectively, of [9]aneN3 and [12]aneN3 nearly quantitatively within a few seconds (Table III). The yields reported in Table III are isolated yields of the pure compounds. Isolation of the pure product is somewhat more elaborate due to the presence of a large excess of H-P compound and small amounts of the unsubstituted product. Both the monomethanephosphonate diethyl ester and the monomethane-*P*-ethylphosphinate ethyl ester of [9]aneN3 crystallized in pure form in ethanol. The corresponding [12]aneN3 derivatives are more soluble in ethanol whereas unsubstituted [12]aneN3 precipitated in ethanol. *N*-Methylation products that are commonly observed as side products in a Mannich reaction involving H-P compounds were not detected by ^1H NMR in these reactions. This makes this a very attractive method for preparing monomethylphosphonylated and monomethylphosphinated triazamacrocycles. The yields could undoubtedly be improved upon by altering the workup procedure.

CONCLUSIONS

Sulfomethylation of di-, tri-, and tetra-, and hexaazamacrocyclic amines may be carried out successfully over a wide pH range, from 3 to 11. The selectivity of this reaction appears to arise from the substantial pK_a differences of the nitrogens in these polyazamacrocycles. Monosubstituted products may be obtained in high yields at pH 4 while regioselective partially substituted products may be obtained at pH 7. At neutral pH, a sharp division of pK_a 's for [12]aneN4 and [18]aneN6 results in selective formation of disubstituted [12]aneN4 and trisubstituted [18]aneN6. In each case, the nitrogens were sulfomethylated in alternating positions as evident by NMR. This is consistent with the premise that microscopic protonation of the macrocyclic nitrogens determines the degree of sulfomethylation.

(Dimethylamino)methanesulfonate was also found to donate sulfomethyl groups selectively to nonprotonated amines in [9]aneN3 or [12]aneN3, thus providing a simple synthetic route to the monosulfomethylated analogs. It was also possible to oxidatively hydrolyze the sulfomethylated piperazines, monosulfomethylated [9]aneN3, and, to a lesser extent, monosulfomethylated [12]aneN3 using triiodide. Surprisingly, monosulfomethylated [9]aneN3 and [12]aneN3 react so slowly with triiodide that these compounds may be isolated as stable triiodide salts.

Although there may be no obvious advantage of using this method over direct alkylation methods to prepare mono- or diacetate derivatives of a triaza macrocycle (20), it does offer the versatility of preparing a variety of mono- and disubstituted phosphonate, phosphonate monoester, and alkyl phosphinate derivatives of the triaza macrocycles which may be difficult to prepare using more direct methods.

One major advantage of the sulfomethylation route became evident by the observation that alternately substituted tetraaza and hexaaza macrocycles were prepared easily in excellent yields, without the use of amine protective groups. There has been considerable interest in preparing the triacetate derivative of [12]aneN4 (DO3A) (21) in bulk quantities as a starting material for MRI contrast agents. Dischino, et al. (22) obtained DO3A in 26% yield by the direct alkylation route (which produces a mixture of products that must be separated by ion-exchange chromatography) versus in approximately 69%

yield via a monoformyl tetraaza macrocyclic intermediate. The preparation of particular disubstituted geometric isomers of [12]aneN4 is even more problematical. For example, Aime et al. (23) have recently reported isolating both the *cis* and *trans* isomers of a particular dialkylated [12]aneN4 in 25% and 8% yield, respectively. Another very recent report (24) describes the preparation of several *trans*-1,7-diprotected [12]aneN4 derivatives in yields ranging from 49% to 77%. The method presented here allows preparation of the *trans*-1,7-bis(methanesulfonate) [12]aneN4 product in about 90% yield which, in turn, may be converted to a variety of products (acetates, phosphonates, phosphinates, etc.) with differing chelating tendencies.

EXPERIMENTAL PROCEDURES

The macrocycles 1,4,7-triazacyclononane ([9]aneN3), 1,5,9-triazacyclododecane ([12]aneN3), [12]aneN3-3HBr, 1,4,7,10,13,16-hexaazacyclooctadecane ([18]aneN6), and [18]aneN6-3H₂SO₄, the formaldehyde sodium bisulfite addition compound, aminomethanesulfonic acid, dichloroethylphosphine, and diethyl phosphite were obtained from Aldrich Chemical Co. (Milwaukee, WI). 1,4,7,10-Tetraazacyclododecane tetrahydrochloride ([12]aneN4-4HCl) was obtained from Parish Chemical Co. (Orem, UT). (Dimethylamino)methanesulfonic acid was prepared in 40% yield with a 92% purity (iodometric assay) according to a modified Backer and Mulder procedure (9). All NMR spectra were recorded on a JEOL JNM-FX200; the methyl group of *tert*-butyl alcohol was used as internal reference at 1.2 ppm (¹H NMR) or at 31.2 ppm (¹³C NMR). Elemental analysis were performed by ONEIDA Research Service, Inc.

Disodium Piperazine-*N,N'*-bis(methanesulfonate) (1). An aqueous solution (5 mL) containing piperazine (10 mmol, 0.86 g) and HOCH₂SO₃Na (20 mmol, 2.68 g) was heated for 2 h at 70 °C. The precipitate which formed was filtered off and washed with ethanol (10 mL) and ether (10 mL). The product was obtained in 51% yield (1.79 g). ¹H NMR (D₂O): 3.81 (s, 4 H), 2.91 ppm (s, 8 H). ¹³C NMR (D₂O): 73.0, 51.5 ppm. Anal. Calcd for C₆H₁₂N₂S₂O₆Na₂·2H₂O: C, 20.34; H, 4.55; N, 7.91; S, 18.10. Found: C, 20.34; H, 4.54; N, 7.82; S, 18.22.

Piperazinomethanesulfonic Acid (2). An aqueous solution (3 mL) containing piperazine (2 mmol, 0.172 g) neutralized with hydrochloric acid (2 mmol) and HOCH₂SO₃Na (2.1 mmol, 0.282 g) was heated for 2 h at 40 °C. Ethanol (10 mL) was added to the solution and after a few hours a white product crystallized. The crystals were suitable for X-ray diffraction. (25) Yield: 51% (1.02 mmol, 0.188 g). ¹H NMR (D₂O): 3.82 (s, 2 H), 3.24 (m, 4 H), 3.12 ppm (m, 4 H). ¹³C NMR (H₂O/D₂O): 72.95, 49.14, 44.27 ppm. Anal. Calcd for C₅H₁₂N₂SO₃·0.25H₂O: C, 32.51; H, 6.77; N, 15.16; S, 17.36. Found: C, 32.63; H, 6.59; N, 15.25; S, 19.03.

Hydrogen Sodium 1,4,7-Triazacyclononane-*N,N'*-bis(methanesulfonate) (3). [9]aneN3-3HCl (1 mmol, 0.239 g) was dissolved in water (3 mL), neutralized with NaOH (1.342 mL, 1.49 M), and mixed with HOCH₂SO₃Na (2.1 mmol, 0.282 g). The final solution pH was 6.9. After heating for 16 h at 40 °C the reaction was complete. Ethanol (10 mL) was added and the product slowly crystallized. The crystals were filtered and washed with ethanol and ether to yield 97% (0.373 g). Recrystallization in 50/50 water/ethanol gave crystals that were suitable for X-ray diffraction. (25) ¹H NMR (D₂O): 3.98 (s, 4 H), 3.17 (s, 8 H), 3.01 ppm (s, 4 H). ¹³C NMR (D₂O/H₂O): 73.58, 51.76, 49.36, 46.07 ppm. Anal. Calcd for

C₈H₁₈N₃S₂O₆Na·2.5H₂O: C, 25.00; H, 6.03; N, 10.93; S, 16.68. Found: C, 24.81; H, 5.78; N, 10.85; S, 17.45.

Disodium 1,5,9-Triazacyclododecane-*N,N'*-bis(methanesulfonate) Hydrochloride (4). [12]aneN3 (1.206 mmol, 0.206 g) was dissolved in water (3 mL), neutralized with HCl (1.047 mL, 1.152 M), and mixed with HOCH₂SO₃Na (2.533 mmol, 0.340 g). The final solution pH was 9.6. The reaction was complete after 16 h at 40 °C. Ethanol was added and the solution was evaporated in vacuo at 40 °C. The resulting precipitate was treated with acetone (50 mL), filtered, and washed with ether. Yield: 98% (0.540 g). ¹H NMR (D₂O): 3.74 (s, 4 H), 3.13, 3.03, 2.78 (bs, 4 H), 1.88 ppm (bs, 6 H). ¹³C NMR (D₂O/H₂O): 69.0, 55.48, 48.40, 47.58, 23.20, 22.40 ppm. Anal. Calcd for C₁₁H₂₃N₃S₂O₆Na₂·HCl·H₂O: C, 28.85; H, 5.72; N, 9.18; S, 14.00. Found: C, 28.83; H, 5.49; N, 8.25; S, 13.89.

1,4,7,10-Tetraazacyclododecane-*N,N'*-bis(methanesulfonic Acid) (5). [12]aneN4-4HCl (1 mmol, 0.318 g) was dissolved in water (3 mL), neutralized with NaOH (1.342 mL, 1.49 M), and mixed with HOCH₂SO₃Na (2.1 mmol, 0.282 g). The final pH of the mixture was 7. After heating for 16 h at 40 °C the reaction was complete. Ethanol (10 mL) was added and the reaction mixture was evaporated. Addition of fresh ethanol gave an oil that slowly crystallized. The crystals were filtered and washed with ethanol and ether to yield 0.565 g (95%). Sodium chloride was present in the solid as well. The ratio of 1,7-disubstituted:1,4-disubstituted was about 9:1. The product was further purified by fractional recrystallization in ethanol/water. NaCl crystallized first, whereafter adding extra ethanol to the reaction mixture produced large needle-shaped crystals of pure 1,7-disubstituted product which were suitable for X-ray diffraction. (25) ¹H NMR (D₂O): 3.83 (s, 4 H), 3.12 (s, 16 H) ppm. ¹³C NMR (D₂O/H₂O): 71.61, 51.56, 45.67 ppm. Anal. Calcd for C₁₀H₂₄N₄S₂O₆·2H₂O: C, 30.29; H, 7.12; N, 14.13. Found: C, 30.25; H, 7.05; N, 13.98.

1,4,7,10,13,16-Hexaazacyclooctadecane-*N,N',N'''*-tris(methanesulfonate) (6). [18]aneN₆-3H₂SO₄ (1 mmol, 0.556 g) was dissolved in water (10 mL) and neutralized with NaOH (2.105 mL, 1.424 M). HOCH₂SO₃Na (7.53 mmol, 1.01 g) and Na₂HPO₄/KH₂PO₄ (pH 7 buffer: pHydryon dry, 4.85 g) were added. The mixture was stirred at room temperature for 3 days, during which time a product crystallized from solution. The product was filtered off and washed with ethanol (50 mL) and ether (50 mL). Yield: 52.5% (0.284 g). ¹H NMR (D₂O): 3.93 (s, 6 H), 3.30 (bs, 12 H), 3.18 ppm (bs, 12 H). ¹³C NMR (D₂O): 69.83, 53.20, 47.64 ppm. Anal. Calcd for C₁₅H₃₆N₆S₃O₁₃K₃·H₃PO₄·1.5H₂O: C, 23.10; H, 5.06; N, 10.81; S, 12.37. Found: C, 23.24; H, 5.28; N, 10.66; S, 12.30. ³¹P NMR (H₂O, pH 7, ref 85% H₃PO₄/H₂O): 1.66 ppm.

1,4,7-Triazacyclononane-*N*-methanesulfonate Hydrotriiodide (7). [9]aneN3 (8.79 mmol, 1.136 g) was dissolved in water (10 mL) and 17.6 mL of 1.0 M HCl added followed by 1.84 g of (CH₃)₂NCH₂SO₃H. The pH of the resulting mixture was 3.8. After 16 h at 25 °C the reaction was complete. ¹³C NMR (D₂O/H₂O): 72.93, 50.93, 45.81, 44.10, 36.43 ppm ((CH₃)₂NH₂⁺). ¹H NMR (D₂O): 4.026 (s, 2 H), 3.689 (s, 2 H), 3.347 (bs, 8 H), 2.692 ppm (s, 6 H, (CH₃)₂NH₂⁺). An aqueous solution (7 mL) containing iodine (13.21 mmol, 3.353 g) and sodium iodide (26.42 mmol, 3.96 g) was added to the reaction mixture. Almost immediately, a brown precipitate was formed. The precipitate was filtered off and washed with ethanol (50 mL) and ether (50 mL), yielding brown crystals in 93%

yield (4.492 g). Anal. Calcd for $C_7H_{18}N_3SO_3I_3 \cdot 0.5H_2O$: C, 13.69; H, 3.12; N, 6.84; S, 5.22. Found: C, 13.69; H, 3.01; N, 6.70; S, 5.53.

1,4,7-Triazacyclononane-*N*-methanesulfonate hydrotriiodide can be reduced to the hydroiodide salt by diethyl phosphite. The I_3 salt (0.11 mmol, 66.7 mg) was suspended in ethanol (0.5 mL) and $HP(O)(OEt)_2$ (21.3 μ L) was added. The brown solid completely decolorized upon reaction. The precipitate was filtered off and washed with ether (10 mL). Yield: 35.79 mg. This salt was now readily soluble in D_2O . 1H NMR (D_2O): 3.98 (s, 2 H), 3.67 (s, 4 H), 3.33, 3.29 ppm (2 bs, 8 H).

1,5,9-Triazacyclododecane-*N*-methanesulfonate Hydrotriiodide (8). [12]ane-3HBr (2.42 mmol, 1 g) was dissolved in water (4 mL) and neutralized with NaOH (1.696 mL, 1.424 M). After adding 0.504 g of $(CH_3)_2NCH_2SO_3H$, the pH of the reaction mixture was 4.3. After 16 h at room temperature the reaction was complete. ^{13}C NMR (D_2O/H_2O): 70.78, 54.84, 46.23, 43.64, 23.27, 21.63 ppm. A $(CH_3)_2NH_2^+$ resonance was present at 36.43 ppm. An aqueous solution (2 mL) containing iodine (2.42 mmol, 0.61 g) and sodium iodide (4.83 mmol, 0.724 g) was added and the HI_3 salt was isolated as described for 7. Yield: 65% (1.0722 g). Anal. Calcd for $C_{10}H_{24}N_3SO_3I_3 \cdot H_2O$: C, 18.06; H, 3.94; N, 6.32; S, 4.82. Found: C, 18.01; H, 3.62; N, 6.33; S, 4.46.

Piperazine-*N,N'*-bis(hydroxymethane) Sodium Hydrogen Sulfate (9). Iodine (2.09 mmol, 0.530 g) and sodium iodide (2.00 mmol, 0.30 g) were dissolved in 4 mL of water. The iodine that did not dissolve was filtered off prior to the addition of disodium piperazine-*N,N'*-bis(methanesulfonate) (1; 1.01 mmol, 0.322 g). Two minutes after the addition, the solution turned clear and a white precipitate formed. The crystals were filtered and washed with ethanol and ether. Yield: 34% (0.111 g). IR (cm^{-1}): 3459, 3421 (O-H), 3026, 2970 (C-H), 2534–2342 (N^+-H), 1629, 1463 (C-N). Anal. Calcd for $C_6H_{14}N_2O_2 \cdot NaHSO_4 \cdot 0.25NaI \cdot H_2O$: C, 22.40; H, 5.32; N, 8.71; I, 9.86. Found: C, 22.50; H, 5.22; N, 9.10; I, 9.67. 1H NMR (D_2O): 4.02 (s, 4 H), 3.39 ppm (s, 8 H).

***N*-(Cyanomethyl)-1,4,7-triazacyclononane Hydrochloride (10).** Triazacyclononane (2.32 mmol, 0.300 g) was dissolved in 3 mL water and neutralized with HCl (4.64 mL, 1.0 M). $(CH_3)_2NCH_2SO_3H$ (3.20 mmol, 0.485 g) was added to the solution to give a final pH of 3.1. The reaction mixture was stirred for 24 h at 25 °C. Sodium cyanide (3.483 mmol, 0.171 g) was added and the reaction mixture was stirred for another 16 h at 25 °C. The reaction product was purified on Dowex 50X8 (bed volume, 25 mL). A 25-mL portion of ethanol was added to the oily residue obtained from the column to yield the pure product as a white powder. Yield: 33% (0.187 g). 1H NMR (D_2O): 4.013 (s, 1 H), 3.79 (s, 2 H), 3.54 (t, 2 H, $^3J = 6.1$ Hz), 3.23 ppm (t, 2 H, $^3J = 6.1$ Hz). ^{13}C NMR (D_2O/H_2O): 118.0, 49.61, 45.18, 44.04 ppm. Anal. Calcd for $C_8H_{14}N_4 \cdot 1.5HCl \cdot 1.5H_2O$: C, 38.75; H, 7.52; N, 22.60. Found: C, 38.99; H, 7.56; N, 22.71.

1,4,7-Triazacyclononane-*N*-acetic Acid Hydrochloride (11). Compound 10 was prepared as described above starting from [9]aneN3 (3.075 mmol, 0.397 g) and $(CH_3)_2NCH_2SO_3H$ (4.61 mmol, 0.642 g) at pH 3.5. Sodium cyanide (4.24 mmol, 0.227 g) was added. After the substitution was complete, the reaction mixture (10 mL) was directly acidified with 4 mL of concentrated HCl (37%) and heated at 75 °C for 4 days. The solution was evaporated under vacuum. After addition of 10 mL of concentrated HCl (37%), NaCl crystals were filtered off, and the brownish solution was concentrated to 3 mL.

Addition of 3 mL of ethanol to the filtrate gave a white precipitate (0.418 g), which was further purified using Dowex 50X8 (bed volume, 9 mL). Absolute ethanol (10 mL) was added to the fraction containing the product, whereupon a white solid was formed. The solid was filtered off and washed with ethanol and ether. Yield: 32% (0.259 g). 1H NMR (D_2O): 3.66 (s, 2 H), 3.62 (s, 1 H), 3.30 (t, 2 H, $^3J = 6.1$ Hz), 3.09 ppm (t, 2 H, $^3J = 6.1$ Hz). ^{13}C NMR (D_2O): 178.40, 57.23, 50.92, 46.36, 45.05 ppm. Anal. Calcd for $C_8H_{17}N_3O_2 \cdot 2HCl$: C, 36.93; H, 7.36; N, 16.15. Found: C, 36.66; H, 7.25; N, 15.89.

***N,N,N'*-Tris(cyanomethyl)-1,5,9-triazacyclododecane (12).** [12]aneN3 (1.52 mmol, 0.26 g) was dissolved in 6.2 mL water and neutralized with a HCl solution (1.32 mL, 1.15 M) followed by addition of pH 7 buffer (Metrepack pHHydron tablet, 0.75 g) and $HOCH_2SO_3Na$ (6.08 mmol, 0.815 g). The solution was stirred for 16 h at 25 °C followed by addition of sodium cyanide (6.08 mmol, 0.298 g). The reaction mixture was then heated to 50 °C for 6 h. The product precipitated from the reaction mixture in pure form. The white precipitate (0.173 g) was filtered off and washed with water (5 mL, 0 °C). The pH of the remaining filtrate was adjusted to 10 by adding a few drops of 1 M NaOH and the solution extracted with dichloromethane (3×50 mL). After evaporation of dichloromethane, the residue was dissolved in water (5 mL). Small white needle-shaped crystals (0.0702 g) were formed over several hours. The overall yield was 55% (0.243 g, 0.84 mmol). 1H NMR ($CDCl_3$): 3.54 (s, 1 H), 2.63 (t, 2 H), 1.65 (m, 1 H), 1.65 ppm (s, 0.3 H, 1 H_2O). ^{13}C NMR ($CDCl_3$): 115.4, 49.2, 42.7, 22.7 ppm.

***N,N,N',N''*-Tetrakis(cyanomethyl)-1,4,7,10-tetraazacyclododecane (13).** [12]aneN4 (1.00 mmol, 0.318 g) was dissolved in 2 mL of water and neutralized with NaOH (1.34 mL of 1.49 M). $HOCH_2SO_3Na$ (5.50 mmol, 0.738 g) was added and the reaction mixture was stirred for 2 h at 25 °C. Sodium cyanide (5.5 mmol, 0.27 g) was added and the reaction mixture was stirred an additional 3 days at 25 °C. The white precipitate that formed was filtered off and washed with water (5 mL, 0 °C) and dried under vacuum over H_2SO_4 . Yield: 61% (0.61 mmol, 0.21 g). 1H NMR ($CDCl_3$): 3.59 (s, 1 H), 2.76 ppm (s, 2 H). ^{13}C NMR ($CDCl_3$): 114.8, 51.4, 43.54 ppm.

1,5,9-Triazacyclododecane-*N,N'*-diacetic Acid Hydrochloride (14). 1,5,9-Triazacyclododecane trihydrobromide (0.414 g, 1 mmol) was dissolved in 3 mL of water and neutralized with NaOH (1.342 mL, 1.49 M). $HOCH_2SO_3Na$ (0.268 g, 2 mmol) was added and the reaction mixture was heated for 16 h at 40 °C. Sodium cyanide (0.103 g, 2.1 mmol) was added and the mixture was stirred for 24 h at 25 °C. ^{13}C NMR (D_2O/H_2O): 117.5, 56.6, 51.1, 50.2, 48.3, 23.2, 22.9 ppm. The reaction was worked up by adding NaOH (1.4 mL, 1.49 M) and the product was extracted into dichloromethane (3×100 mL). The dichloromethane was removed by evaporation under vacuum and the residue was dissolved in 20 mL of HCl (20%) and refluxed for 3 days. The solution was evaporated under vacuum and the excess HCl was removed by coevaporation with 10 mL of water. The product was purified on Dowex 50X8 (bed volume 5 mL). The solid obtained after lyophilization was dissolved in 3 mL of ethanol and precipitated upon addition of 20 mL of ether. The white solid was filtered off and washed with ether. Yield: 19% (0.084 g). 1H NMR (D_2O): 3.73 (s, 4 H), 3.12 (m, 12 H), 2.00 (m, 4 H), 1.97 ppm (m, 2 H). ^{13}C NMR (D_2O): 172.2, 56.67, 53.92, 52.08, 45.86, 21.84, 21.30 ppm. The product was 95% pure as judged by ^{13}C NMR (a small amount of the monoacetate derivative was present). Anal.

Calcd for $C_{13}H_{25}N_3O_4 \cdot 2.5HCl \cdot 3H_2O$: C, 36.10; H, 7.81; N, 9.71. Found: C, 35.87; H, 7.86; N, 9.62.

1,4,7,10-Tetraazacyclododecane-*N,N'*-diacetic Acid Hydrochloride (15). [12]aneN4-4HCl (1 mmol, 0.318 g) was dissolved in 3 mL of water and neutralized with NaOH (1.34 mL, 1.49 M). $HOCH_2SO_3Na$ (2.1 mmol, 0.28 g) was added and the solution heated at 40 °C for 16 h. ^{13}C NMR indicated that approximately 90% the 1,7-bis(methanesulfonate) derivative and 10% of the corresponding 1,4-isomer was present. Sodium cyanide (2 mmol, 0.098 g) was added. After 6 h at 25 °C an additional amount of sodium cyanide (0.5 mmol, 0.0243 g) was added and the reaction mixture was stirred for another 16 h. At the end of this period, ^{13}C NMR showed that the 1,7-bis(cyanomethyl) derivative had formed. ^{13}C NMR (D_2O/H_2O): 119.2, 51.52, 45.51, 45.15 ppm. The reaction mixture was acidified by adding HCl (37%, 20 mL) and the cyano groups were hydrolyzed by refluxing the solution for 65 h. The solution was evaporated to dryness under vacuum and coevaporated with 2 \times 20 mL of water. The product was purified on Dowex 50X8-200 (bed volume 20 mL). The product fraction was evaporated under vacuum and lyophilized. Ethanol (2 mL) was added to the solid and the white solid filtered and washed with 5 mL of ether. Yield: 80% (0.314 g). ^{13}C NMR (D_2O/H_2O): 176.3, 55.2, 50.75, 44.23 ppm. 1H NMR (D_2O): 3.53 (s, 1 H), 3.18 (bs, 2 H), 3.06 (bs, 1 H), 2.90 ppm (bs, 1 H). Anal. Calcd for $C_{12}H_{24}N_4O_4 \cdot 2.5HCl$: C, 37.98; H, 7.04; N, 14.76. Found: C, 37.87; H, 6.91; N, 14.61.

1,4,7-Triazacyclononane-*N*-methanephosphonic Acid Dihydrochloride (16). Phosphorous acid (4.77 g, 58.2 mmol) was melted at 75 °C and 7 (1.418 g, 2.34 mmol) was added in small portions while the temperature was maintained near 80 °C. After each addition, the brown solid dissolved and rapidly decolorized. Vapors evolved that were likely SO_2 , H_2S , and I_2 . Five minutes after the final addition, 15 mL of ether was added. The product that precipitated was filtered, washed with 5 mL of ether, redissolved into 6 mL water, and purified on a Dowex 50X8 ion-exchange column (bed volume, 14 mL). The fractions containing product were lyophilized to give a white hygroscopic solid. The yield of 16 as a dihydrochloride salt was 21% (0.145 g, 0.48 mmol). 1H NMR (D_2O): 3.63 (s, 2 H), 3.32 (t, 2 H, $^3J = 6.1$ Hz), 3.11 (t, 2 H, $^3J = 6.1$ Hz), 3.01 ppm (d, 1 H, $^2J_{HP} = 8.6$ Hz).

Ethyl Ethylphosphonite (17). Dichloroethylphosphine (Caution: *Reacts explosively with water at 25 °C*) (19.3 g, 0.15 mmol) was added dropwise to 40 mL of absolute ethanol and 11.9 mL of pyridine at 0 °C within 30 min. The reaction mixture was stirred for an additional 30 min at 25 °C. The pyridine hydrochloride salt that is formed is filtered off prior to distillation of the product under reduced pressure (75–78 °C, 15 mmHg). The product was obtained in 80% yield (14.8 g, 0.12 mol). 1H NMR ($CDCl_3$): 7.06 (d, 1 H, $^1J_{HP} = 527$ Hz), 4.11 (m, 2 H), 1.78 (m, 2 H), 1.37 (t, 3 H), 1.16 ppm (dt, 3 H, $^3J_{HP} = 20$ Hz).

***P*-Ethyl 1,4,7-Triazacyclononane-*N*-methanephosphinate Ethyl Ester Hydrochloride (18).** Compound 7 (0.607 g, 1.00 mmol) was added to 1 mL of 17 at 0 °C. The resulting orange solution was warmed to room temperature and the reaction mixture turned yellow and gases evolved in about 1 min. Ethanol (12 mL) was added and the solution was kept at 0 °C for several hours. The white crystals that formed were filtered and washed with ethanol (0 °C) and ether (crystals turned light yellow probably as a result of iodide oxidation by ether peroxides). Yield: 43% (0.227 g). 1H NMR (D_2O): 4.15 (dt, 2 H), 3.65

(s, 4 H), 3.36 (bs, 6 H), 3.20 (bt, 4 H), 1.98 (m, 2 H), 1.35 (t, 3 H), 1.14 ppm (dt, 3 H, $^3J_{HP} = 18.3$ Hz). Anal. Calcd for $C_{11}H_{26}N_3PO_2 \cdot 2HI \cdot 0.33H_2O$: C, 25.16; H, 5.50; N, 8.00. Found: C, 25.12; H, 5.35; N, 7.99. Ether (10 mL) was added to the filtrate, which gave another precipitate that was filtered off and was washed with ether. Yield: 0.167 g. This product contained about 10% [9]aneN3 and 10% of another phosphorylated product, as evidenced by 1H NMR.

1,4,7-Triazacyclononane-*N*-methanephosphonate Diethyl Ester (19). This compound was prepared using procedures described for 18, starting with 7 (0.341 g, 0.564 mmol) and 0.630 mL of diethyl phosphite. After 5 min, ethanol (1 mL) was added to the reaction mixture and the product was precipitated from this solution by adding 3 mL of ether while stirring vigorously. The ethanol/water was decanted and the precipitate was washed with 5 mL of ether. The precipitate was dissolved in 1 mL of ethanol and crystallized after 10 min. The crystals were filtered off and washed with ether. The precipitate was dissolved in water (5 mL). The pH of the water layer was adjusted to 13 by addition of NaOH. The product was extracted from the water layer with $CHCl_3$ (50 mL). The latter $CHCl_3$ layer was dried with Na_2SO_4 for several hours before evaporation in vacuum gave a colorless oil. Yield: 24% (0.034 g). 1H NMR ($CDCl_3$): 4.08 (dt, 4 H), 2.97 (d, $^1J_{HP} = 8.5$ Hz, 2 H), 2.73 (s, 4 H), 2.70 (s, 8 H), 2.35 (bs, 2 H, NH), 1.28 ppm (t, $^3J_{HP} = 7.3$ Hz). ^{13}C NMR ($CDCl_3$): 61.71, 54.65, 52.28 ($^1J_{CP} = 158$ Hz), 46.99, 46.38, 16.52 ppm.

1,5,9-Triazacyclododecane-*N*-methanephosphonate Diethyl Ester (20). This compound was prepared as described for 19, starting with 8 (0.280 g, 0.441 mmol) and 0.625 mL of diethyl phosphite. The reaction was worked up by addition of 4 mL of ether giving a precipitate. The precipitate was washed with 2 \times 4 mL of ether and then dissolved in 4 mL of ethanol. 1,5,9-Triazacyclododecane itself did not dissolve. The precipitate was removed by centrifugation. Ether (4 mL) was added to the clear ethanol solution and the product precipitated. The product was filtered off under nitrogen and was washed with ether (4 mL). The solid was extracted into $CHCl_3$. Yield: 31% (0.044 g). 1H NMR ($CDCl_3$): 4.03 (dt, 4 H), 2.69 (m, 16 H), 1.57 (m, 6 H), 1.24 ppm (t, 6 H, $^3J_{HP} = 7.3$ Hz). ^{13}C NMR ($CDCl_3$): 61.25, 53.36, 49.33, 47.19 ($^1J_{CP} = 150.9$), 25.78, 25.66, 16.37 ppm.

***P*-Ethyl 1,5,9-Triazacyclododecane-*N*-methanephosphinate Ethyl Ester (21).** This compound was prepared as described for 20, starting with 8 (0.314 g, 0.495 mmol) and 0.625 mL of 17. Yield: 73% (0.111 g). 1H NMR ($CDCl_3$): 3.96 (dt, 2 H), 2.80 (bs, 2 H, NH), 2.63 (m, 14 H), 1.69 (m, 2 H), 1.55 (m, 6 H), 1.20 (t, 3 H), 1.04 ppm (dt, 3 H, $^3J_{HP} = 17.7$ Hz). ^{13}C NMR ($CDCl_3$): 59.90, 52.74, 50.49 ($^1J_{CP} = 104$ Hz), 48.63, 46.15, 25.72, 20.82 ($^1J_{CP} = 87.9$ Hz), 16.55, 5.65 ppm.

1,4,7,10-Tetraazacyclododecane-*N*-methanephosphonic Acid Hydrochloride (22). Compound 5 was prepared as described previously (1 mmol). After lyophilization, the resulting solid was added to 4 mL of 20% HCl containing iodine (0.51 g, 2 mmol) and NaI (0.30 g, 2 mmol). NaCl precipitated together with a brown gum. After 10 min, the solution was filtered over a cotton plug and phosphorous acid (0.82 g, 10 mmol) was added. This solution was boiled for 3 h. The solution was evaporated to dryness and coevaporated with 20 mL of water. The solid was dissolved in 5 mL of water and purified on Dowex 50X8 (bed volume, 40 mL). The product fraction was evaporated under vacuum and lyophilized. The oily

material was treated with ether (10 mL) giving a white powder. Yield: 24% (0.103 g). ^1H NMR (D_2O): 3.32 (bs, 4 H), 3.28 (bs, 8 H), 3.08 (bs, 4 H), 2.97 ppm (d, 2 H, $^2J_{\text{HP}} = 9.8$ Hz). ^{13}C NMR ($\text{D}_2\text{O}/\text{H}_2\text{O}$): 52.46, 50.54, 44.42, 43.98 ppm. ^{31}P NMR ($\text{D}_2\text{O}/\text{H}_2\text{O}$): 22.92 ppm. Anal. Calcd for $\text{C}_9\text{H}_{23}\text{N}_4\text{O}_3\text{P}\cdot 4\text{HCl}\cdot 0.5\text{H}_2\text{O}$: C, 25.67; H, 6.70; N, 13.30. Found: C, 25.57; H, 6.74; N, 13.77.

ACKNOWLEDGMENT

This research was supported by grants from the Robert A. Welch Foundation (AT-584) and the Meadows Foundation.

LITERATURE CITED

- Bunzli, J.-C. G. and Choppin, G. R., Eds. (1989) *Lanthanide Probes in Life, Chemical, and Earth Sciences: Theory and Practice*, Chapters 4 and 5, Elsevier, New York.
- Desreux, J. F., Merciny, E., and Loncin, M. F. (1981) Nuclear magnetic resonance and potentiometric studies of the protonation scheme of two triazatetraacetic macrocycles. *Inorg. Chem.* 20, 987-991.
- Geraldes, C. F. G. C., Sherry, A. D., Marques, M. P. M., Alpoim, M. L., and Cortes, S. J. (1991) Protonation scheme for some triaza macrocycles studied by potentiometry and NMR spectroscopy. *Chem. Soc. Perkin Trans. 2* 137-146.
- Geraldes, C. F. G. C., Sherry, A. D., and Cacheris, W. P. (1989) Synthesis, protonation sequence, and NMR studies of polyazamacrocyclic methylenephosphonates. *Inorg. Chem.* 28, 3336-3341.
- Kimura, E., Sakonaka, A., Yatsunami, T., and Kodama, M. (1981) Macromonocyclic polyamines as specific receptors for tricarboxylate-cycle anions. *J. Am. Chem. Soc.* 103, 3041-3045.
- Zompa, L. J. (1978) Metal complexes of cyclic triamines 2: Stability and electronic spectra of nickel(II), copper(II) and zinc(II) complexes containing nine- through twelve-membered cyclic triamine ligands. *Inorg. Chem.* 17, 2531-2536.
- Yang, R., and Zompa, L. J. (1976) Metal complexes of cyclic triamines 1: Complexes of 1,4,7-triazacyclononane ([9]aneN3) with nickel(II), copper(II) and zinc(II). *Inorg. Chem.* 15, 1499-1502.
- Gilbert, E. E. (1965) *Sulfonation and Related Reactions*, Chapter 5, Interscience, New York.
- Backer, H. J., and Mulder, H. (1933) Acyl derivatives of aminomethanesulfonic acid. *Recl. Trav. Chim. Pays-Bas* 52, 454-468.
- Reinking, K., Dehnelt, E., and Labhardt, H. (1905) *Chem. Ber.* 38, 1069.
- Bucherer, H., and Schwalbe, A. (1906) *Chem. Ber.* 39, 2796.
- Backer, H. J., and Mulder, H. (1934) Acetylation of some 1,1 aminosulfonic acids and 1,1 hydrazinesulfonic acids. *Recl. Trav. Chim. Pays-Bas* 53, 1120-1127.
- Neelakantan, L., and Hartung, W. H. (1959) α -aminoalkane sulfonic acids. *J. Org. Chem.* 24, 1943-1948.
- Knoevenagel, E. (1904) *Chem. Ber.* 37, 4073.
- Miller, W. v., and Plöchl, J. (1892) *Chem. Ber.* 25, 2020.
- Ulrich, H., and Ploetz, E. Amino carboxylic acid nitriles. US patent 2,205,995; *Chem. Abstr.* 34, 7298.
- Smith, R., Bullock, J. L., Bresworth, F. C., and Martell, A. E. (1950) Carboxymethylation of amines. I. Preparation of ethylenediamine tetraacetic acid. *J. Org. Chem.* 14, 355-361.
- Steward, T. D., and Brabley, W. E. (1932) Rate of reaction of disubstituted aminomethanesulfonic acids with iodine. *J. Am. Chem. Soc.* 54, 4183-4188.
- Burg, A. B. (1989) Restudy of the action of sulfur dioxide on dry trimethylamine oxide: Iodine oxidation and Lewis acid chemistry of the most reactive product, $(\text{CH}_3)_2\text{H}(\text{NCH}_2\text{SO}_3)$. *Inorg. Chem.* 28, 1295-1300.
- Neves, A., Walz, W., Wieghardt, K., Nuber, B., and Weiss, J. (1988) Kinetics and the mechanism of outer-sphere electron-transfer-induced formation of cis-dioxovanadium(V) species from vanadyl(IV) complexes. Crystal structure of $[\text{VO}(\text{TCDAA})\cdot\text{H}_2\text{O}]$ and $[\text{VO}_2(\text{TCDAAH})\cdot 2\text{H}_2\text{O}]$ (TCDAA = 1,4,7-triazacyclononane-N,N'-diacetate). *Inorg. Chem.* 27, 2484-2489.
- Tweedle, M. F., Gaughan, G. T., and Hagan, J. J. (1987) Preparation of 1-substituted-1,4,7-tris(carboxymethyl)-1,4,7-tetraazacyclododecane and analogs as medical imaging agents. *Eur. Pat. Appl.* EP 232,751.
- Dischino, D. D., Delaney, E. J., Emswiler, J. E., Gaughan, G. T., Prasad, J. S., Srivastava, S. K., and Tweedle, M. F. (1991) Synthesis of nonionic gadolinium chelates useful as contrast agents for magnetic resonance imaging: 1,4,7-tris(carboxymethyl)-10-substituted 1,4,7,10-tetraazacyclododecanes and their corresponding gadolinium chelates. *Inorg. Chem.* 30, 1265-1269.
- Aime, S., Botta, M., Ermondi, G., Fedell, F., and Uggeri, F. (1992) Synthesis and NMRD studies of Gd^{3+} complexes of macrocyclic polyamino polycarboxylic ligands bearing beta-benzoyloxy-alpha-proponic residues. *Inorg. Chem.* 31, 1100-1103.
- Anelli, P. F., Murru, M., Uggeri, F., and Virtuani, M. (1991) Highly regioselective synthesis of 1,7-diprotected 1,4,7,10-tetraazacyclododecane derivatives. *J. Chem. Soc., Chem. Commun.* 1317-1318.
- The crystal structure will be reported elsewhere.
- Smith, R. M., and Martell, A. E., Eds. (1980) *Critical Stability Constants*, Vol. 6, Plenum Press, New York and London.

Registry No. 1, 144003-13-4; 2, 144003-14-5; 3, 144003-15-6; 4, 144003-16-7; 5, 144003-17-8; 6, 144003-18-9; 7-HI, 144003-20-3; 7-HI, 144003-21-4; 7 free base, 144003-19-0; 8, 144003-23-6; 8 free base, 144003-22-5; 9, 144003-24-7; 10, 144017-94-7; 11, 144017-95-8; 12, 144003-25-8; 13, 144003-26-9; 14, 144003-27-0; 15, 144003-28-1; 16, 144003-29-2; 17, 998-80-1; 18, 144017-96-9; 19, 144003-30-5; 20, 144003-31-6; 21, 144017-97-0; 22, 144003-32-7; [9]aneN3, 4730-54-5; [9]aneN3-3HCl, 58966-93-1; [12]aneN3, 294-80-4; [12]aneN3-3HBr, 35980-62-2; [12]aneN4-4HCl, 10045-25-7; [18]aneN6-3H₂SO₄, 56187-09-8; HOCH₂SO₃Na, 870-72-4; (CH₃)₂, 68507-34-6; piperazine, 110-85-0; dichloroethylphosphine, 1498-40-4; 1,4,7,10-tetraazacyclododecane-1,4-bis(methanesulfonic acid), 144003-33-8; 1,7-bis(cyanomethyl)-1,4,7,10-tetraazacyclododecane, 144003-34-9.

Gene Transfer into Hepatocytes Using Asialoglycoprotein Receptor Mediated Endocytosis of DNA Complexed with an Artificial Tetra-Antennary Galactose Ligand

Christian Plank, Kurt Zatloukal, Matt Cotten, Karl Mechtler, and Ernst Wagner*

Research Institute of Molecular Pathology, Dr. Bohr-Gasse 7, A-1030 Vienna, Austria. Received July 14, 1992

We have constructed an artificial ligand for the hepatocyte-specific asialoglycoprotein receptor for the purpose of generating a synthetic delivery system for DNA. This ligand has a tetra-antennary structure, containing four terminal galactose residues on a branched carrier peptide. The carbohydrate residues of this glycopeptide were introduced by reductive coupling of lactose to the α - and ϵ -amino groups of the two N-terminal lysines on the carrier peptide. The C-terminus of the peptide, containing a cysteine separated from the branched N-terminus by a 10 amino acid spacer sequence, was used for conjugation to 3-(2-pyridyldithio)propionate-modified polylysine via disulfide bond formation. Complexes containing plasmid DNA bound to these galactose-polylysine conjugates have been used for asialoglycoprotein receptor-mediated transfer of a luciferase gene into human (HepG2) and murine (BNL CL.2) hepatocyte cell lines. Gene transfer was strongly promoted when amphipathic peptides with pH-controlled membrane-disruption activity, derived from the N-terminal sequence of influenza virus hemagglutinin HA-2, were also present in these DNA complexes. Thus, we have essentially borrowed the small functional domains of two large proteins, asialoglycoprotein and hemagglutinin, and assembled them into a supramolecular complex to generate an efficient gene-transfer system.

INTRODUCTION

During the last few years gene-transfer methods have been developed that adopt natural receptor-mediated endocytosis pathways for the delivery of DNA into eukaryotic cells. Ligands for cellular receptors, such as transferrin (1, 2), viral proteins (3), insulin bound to albumin (4), or asialoorosomucoid (5, 6) have been successfully used for the import of DNA molecules. For this purpose these ligands have been conjugated to DNA-binding compounds, such as a polycation or an intercalating agent. Incubating DNA with these protein conjugates generates ligand-coated DNA which can bind receptors on the cell surface and is subsequently internalized. Small synthetic, rationally designed compounds that bind specifically to a cellular receptor may be useful, well-defined alternatives for large protein ligands.

In this paper we describe the synthesis of polylysine conjugates containing an artificial ligand for the asialoglycoprotein receptor (7). This hepatocyte-specific receptor recognizes exposed galactose on serum glycoproteins that have lost the terminal sialic acids and rapidly removes these glycoproteins from the circulation to the liver. The artificial ligand we designed displays four galactoside residues on a branched carrier peptide possessing a C-terminal cysteine as a ligation site for coupling to the DNA-binding polycation polylysine. Using this protein-free, synthetic polylysine conjugate, luciferase gene transfer into cultured hepatocytes is possible with an efficiency similar to that achieved with a natural ligand, asialofetuin, conjugated to polylysine. One limit to receptor-mediated gene delivery may be the accumulation of the delivered DNA complexes in intracellular vesicles (2, 3, 8). To overcome this barrier, we have developed strategies that utilize the endosome disruption activity of either defective adenovirus particles (9, 10) or synthetic, amphipathic peptides (11), derived from the N-terminus of the influenza virus hemagglutinin HA-2 protein (12). Further goals of this work have been to prepare DNA complexes containing both the synthetic galactose-ligand and the amphipathic

peptides, and to subsequently investigate whether these protein-free DNA complexes have improved gene transfer efficiencies.

EXPERIMENTAL PROCEDURES

Materials and Conjugates. The DNA plasmid pCMVL, containing the *Photinus pyralis* luciferase gene under control of the cytomegalovirus enhancer/promoter, was prepared by removing the *Bam*HI insert of the plasmid pSTCX556 (13), treating the plasmid with Klenow fragment, and ligating with the *Hind*III/*Ssp*I and Klenow-treated fragment from the plasmid pRSVL (14), which contains the sequence coding for luciferase. Human transferrin-poly(L-lysine) conjugates with an average chain length of 190 lysines (TfpL190¹) or 290 lysines (TfpL290) were prepared as described (15). Mouse transferrin-poly(L-lysine) conjugates (mTfpL290) were synthesized using the method described in ref 1. Conjugate InflupL, containing the peptide derived from influenza virus hemagglutinin (Gly-Leu-Phe-Glu-Ala-Ile-Ala-Gly-Phe-Ile-Glu-Asn-Gly-Trp-Glu-Gly-Met-Ile-Asp-Gly-Gly-Gly-Cys) coupled to polylysine pLys₃₀₀, was synthesized as described in ref 11. Synthesis of N^ε-lactosylated polylysine (pLys-lactose) was performed as follows: to a solution of 16.5 mg (0.44 μ mol) of pLys₂₀₀, acetate salt, in 0.46 mL of 100 mM sodium acetate (pH 5.0) was added 90 mg (0.26 mmol) of lactose (Sigma), which dissolved upon agitating within 30 min at 37 °C. The solution was kept at this temperature while four 3-mg portions of sodium cyanoborohydride were added in about 10-h intervals. The reaction mixture was left for an additional 21 h at 37 °C; then 15 μ L of acetic acid was added, and the reaction

¹ Abbreviations used: TfpL, transferrin-poly(L-lysine) conjugate; AFP_L, asialofetuin-poly(L-lysine) conjugate; pLys₂₀₀ and pLys₂₉₀, poly(L-lysine) with an average chain length of 200 or 290 lysine monomers; HEPES, 4-(2-hydroxyethyl)-1-piperazineethanesulfonic acid; HBS, HEPES-buffered saline (150 mM NaCl, 20 mM HEPES, pH 7.3).

mixture was subjected to gel filtration (Sephadex G25-PD10) in 100 mM sodium acetate (pH 5.0). The product-containing fraction (identified by ninhydrin assay and staining with anisaldehyde after spotting 1- μ L samples on TLC plates) was dialyzed against 20 mM sodium acetate overnight and then against 0.05% acetic acid. Lyophilization gave 26.5 mg of pLys₂₀₀, acetate salt, with about 75–80% of the N^ε-lysine amino groups lactosylated, as determined by ninhydrin analysis and NMR analysis [¹H NMR (D₂O, 250 MHz, solvent suppression): δ (ppm) = 4.51 (d, J = 7.2 Hz, galactose-1H), 4.22–4.34 (lysine α -H), 4.1–4.22 (sugar H), 2.9–4.0 (lysine ϵ -H and sugar H), 1.91 (acetate, CH₃), 1.1–2.0 (aliphatic CH₂ of lysine)].

Assays. The amount of dithiopyridine linkers in modified asialofetuin or polylysine was determined after reduction of an aliquot with dithiothreitol followed by absorption measurement of released pyridine-2-thione at 340 nm. The polylysine content of fractions was estimated spectrophotometrically by ninhydrin assay. The amount of free mercapto groups in modified polylysine or peptides was determined using 5,5'-dithiobis(2-nitrobenzoic acid) (16) and measurement at 412 nm. The asialofetuin content of fractions was determined by UV measurement at 280 nm and correction of the value (where necessary) by subtraction of the corresponding UV absorption of dithiopyridine or buffer at 280 nm. Lactosylation was monitored by staining with anisaldehyde reagent (*p*-anisaldehyde/sulfuric acid/ethanol, 1/1/18) on TLC plates (silica gel), by ¹H-NMR analysis, and/or spectrophotometrically by the anthron assay (17) using lactosylated polylysine as standard.

Asialofetuin-Polylysine Conjugate Synthesis. Asialofetuin-polylysine conjugate (AFpL) was synthesized by coupling asialofetuin to polylysine via disulfide bonds after modification of asialofetuin with the bifunctional reagent succinimidyl 3-(2-pyridyldithio)propionate (SPDP, Pharmacia) in a similar fashion as described (1). To a solution of 100 mg (2.2 μ mol) of asialofetuin (Sigma) in 4 mL of 100 mM HEPES buffer, pH 7.9, was added 330 μ L of a 15 mM ethanolic solution of SPDP (5.0 μ mol) with vigorous mixing. After 1 h at room temperature, purification was performed by gel filtration (Sephadex G25; 100 mM HEPES buffer, pH 7.9) to give 5 mL of a solution of 1.4 μ mol of asialofetuin modified with 2.25 μ mol of dithiopyridine linker. This solution was mixed under an argon atmosphere with a solution of 0.33 μ mol of poly(L-lysine) with an average chain length of 190 lysine monomers (pLys₁₉₀), modified with 1.07 μ mol of 3-mercaptopropionate groups as described in ref 1, in 6.5 mL of 200 mM HEPES buffer, pH 7.6. The reaction mixture was kept for 24 h at room temperature. Conjugates were isolated from the reaction mixture by cation-exchange chromatography (Mono S column HR 10/10, Pharmacia; gradient elution with buffer A, 50 mM HEPES, pH 7.9, and buffer B, buffer A plus 3 M NaCl). Sodium chloride was added to the reaction mixture (final concentration 0.6 M) before loading the column, and the gradient was started at this salt concentration. The product was eluted at a NaCl concentration of ca. 1.5 M. After dialysis against HBS, conjugates containing 0.24 μ mol of pLys₁₉₀ modified with 0.52 μ mol asialofetuin were obtained.

Synthesis of Tetragalactose-Peptide-Polylysine Conjugate (gal)4pL. (A) *Lactosylated Peptide 1b.* Freeze-dried, branched peptide 1a (3.5 mg, 1.92 μ mol) with the sequence α, ϵ -(Lys)₂-Lys-Gly-(Ser-Gly-Gly)₃-[S-(2-pyridyldithio)]Cys, synthesized by the Fmoc procedure (18, 19) using an Applied Biosystems 431A peptide synthesizer and α, ϵ -bis(Fmoc)-protected lysine (Bachem), was treated

with a solution of 7.85 mg (23 μ mol) of lactose in 40 μ L of 10 mM aqueous sodium acetate, pH 5 at 37 °C. To the solution were added four 0.6 mg (10 μ mol) portions of sodium cyanoborohydride at 10-h intervals. After a total of 64 h at 37 °C, 0.5 mL of HEPES, pH 7.3, and 15 mg of dithiothreitol were added. After 30 min, fractionation by gel filtration (Sephadex G10, 12 \times 130 mm, eluent 20 mM NaCl) under argon yielded a 3.6-mL solution of lactosylated peptide 1b in the free mercapto form (1.73 μ mol, according to an assay with Ellman's reagent, an 84% yield). Samples of the modified peptide showed a color reaction with anisaldehyde, but no color reaction with ninhydrin; this is consistent with the assumption that all four N-terminal amino groups have been lactosylated. ¹H-NMR analysis (D₂O, 250 MHz, solvent suppression) demonstrated that the group of five α -H signals, δ (ppm) = 4.58 (1 H, Cys), 4.52 (3 H, 3 Ser), 4.35 (1 H, Lys), found in the spectrum of the precursor peptide is overlaid by the signal of four galactose-1H protons at 4.51 ppm (4 H). Time-of-flight mass spectrum performed with a Bio Ion ²⁵²Cf PD-MS instrument (Uppsala, Sweden) showed a major mass peak of 2473 (MH⁺ of product 1b) and a minor peak of 2146 (presumably traces of tris-lactosylated peptide).

(B) *3-Dithiopyridinepropionate-Modified Polylysine 2.* To a gel-filtered solution of 0.60 μ mol of pLys₂₉₀ (hydrobromide, Sigma) in 1.2 mL of 100 mM HEPES buffer, pH 7.9, was added 400 μ L of a 15 mM ethanolic solution of SPDP (6.0 μ mol) with vigorous mixing. One hour later 500 μ L of 1 M sodium acetate, pH 5, was added; gel filtration (Sephadex G25, 100 mM sodium acetate, pH 5) yielded a 2.4 mL solution of 2, containing 0.56 μ mol of pLys₂₉₀ modified with 5.77 μ mol of dithiopyridine linker.

(C) *Conjugation of Peptide with Polylysine.* Conjugates were prepared by mixing 1.5 μ mol of lactosylated peptide 1b in 3 mL of 20 mM NaCl with 0.146 μ mol of modified polylysine 2 in 620 μ L of 100 mM sodium acetate buffer, pH 5, under an argon atmosphere. After the addition of 100 μ L of 2 M HEPES, pH 7.9, the reaction mixture was kept for 18 h at room temperature. The salt concentration was brought to 0.66 M by addition of NaCl, and conjugates were isolated by cation-exchange chromatography (Pharmacia Mono S column HR 5/5; gradient elution with buffer A, 50 mM HEPES, pH 7.3, and buffer B, buffer A plus 3 M NaCl). The product fractions were eluted at salt concentrations around 1.2–1.8 M and pooled. After dialysis against 25 mM HEPES, pH 7.3, conjugate 3, "(gal)4pL", was obtained, containing 49 nmol of pLys₂₉₀ modified with ca. 380 nmol of ligand moieties (i.e. 1.5 μ mol of lactosamine groups).

Cells and Transfections. HepG2 cells (ref 20, a kind gift of Prof. M. Spiess, Basle) were grown in DMEM plus 10% FCS, 100 units/mL penicillin, 100 μ g/mL streptomycin, and 2 mM glutamine in 25 cm² flasks. The mouse embryonic liver cell line BNL CL2 (ATCC TIB 73; ref 21) was grown in 6-cm plates in high glucose DMEM (0.4% glucose) supplemented with 10% heat-deactivated FCS, with 100 units/mL penicillin, 100 μ g/mL streptomycin, and 2 mM glutamine at 37 °C in a 5% CO₂ atmosphere. Transfections were performed at a density of 300 000–400 000 cells per flask (or plate). Before transfection, cells were supplied with fresh serum-supplemented medium. The cells were harvested for the luciferase assay (3) 24 h after transfection. Values shown in the figures represent the total luciferase activity in the transfected cells. The filled bars represent mean values, the bracket above each bar indicates one standard deviation.

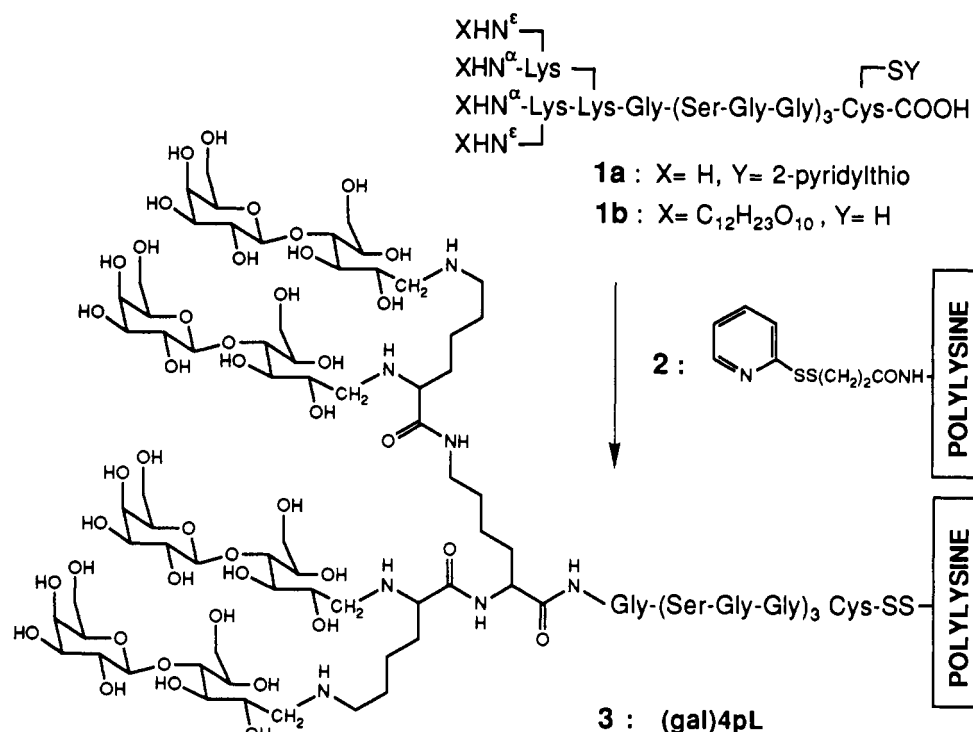


Figure 1. Artificial galactoside ligand-polylysine conjugate.

RESULTS

Synthesis. We wanted to construct a tetra-antennary ligand containing four galactoside residues that should serve for binding to the asialoglycoprotein receptor. For this purpose, the branched peptide **1a** (see Figure 1) was prepared by automated solid-phase synthesis using the Fmoc procedure (18). Branching at the N-terminus was the result of coupling two lysines to the α - and ϵ -amino groups of a further lysine, utilizing a concept similar to that described for the preparation of MAPs (multiple antigenic peptides, ref 22). The four amino groups of **1a** were modified with lactose (0.6 M lactose, i.e. 12 equiv/peptide; 37 °C) by aldimine formation followed by reduction with sodium cyanoborohydride to the secondary amines. The resulting glycopeptide **1b**, containing the clustered carbohydrate groups separated from a C-terminal cysteine by a 10 amino acid long Gly/Ser spacer sequence, was isolated in the reduced, sulfhydryl-containing form. Modification of all four amino groups was indicated by a ninhydrin assay and confirmed by proton NMR analysis and time-of-flight mass spectroscopy. The C-terminal cysteine served for coupling to pyridyldithiopropionate-modified polylysine **2** (average chain length of ca. 290 L-lysine monomers per molecule) via disulfide bond formation in the next step. Conjugate **3**, "(gal)4pL", was isolated by ion-exchange chromatography and characterized by determination of lysine and carbohydrate content. The conjugate contains, on average, 8 glycopeptide ligands per polylysine chain, which corresponds to 1 ligand per 36 lysine residues.

As reference compounds, asialofetuin-polylysine conjugates, AFpL, and N⁶-lactosylated polylysine, pLys-lactose, were synthesized (see Experimental Procedures). The synthesis of AFpL conjugates involved the modification of one to two amino groups on the asialofetuin molecule with succinimidyl 3-(2-pyridyldithio)propionate, followed by ligation to similarly modified polylysine **2** through the formation of disulfide bonds. N⁶-Lactosylated polylysine was prepared by reductive coupling of lactose to the polylysine amino groups. The chosen conditions

(0.6 M lactose, corresponding to 3 equiv of lactose/amino group, 37 °C, 60 h) resulted in modification of ca. 75–80% of the N⁶-lysine amino groups.

Gene Transfer to Hepatocyte Cultures. We tested whether DNA complexed with (gal)4pL would be bound by and internalized into cells expressing the hepatocyte-specific asialoglycoprotein receptor. Different DNA transport complexes were prepared by mixing plasmid DNA pRSVL [encoding *P. pyralis* luciferase as a reporter gene, under the control of the Rous sarcoma virus long terminal repeat enhancer/promoter (14)], with either (gal)4pL or various other ligand-polylysine conjugates. Under these conditions the polylysine moiety of the conjugates neutralizes a large proportion (ca. 50–100%) of the DNA charge (see the legend of Figure 2). These complexes were applied onto HepG2 cells (which express high levels of the asialoglycoprotein receptor); the cells were harvested 24 h later and assayed for luciferase activity. Expression of luciferase (Figure 2), as an indication of successful gene transfer into HepG2 cells, was found using transferrin, asialofetuin, or the artificial galactose-containing peptide as ligands (Figure 2, lanes 1–3), but only if the cells were also incubated in the presence of the lysosomotropic agent chloroquine, which prevents acidification and activation of lysosomal degradative enzymes, but may also act by osmotic destabilization of intracellular acidic vesicles upon internal accumulation of the agent (2–3, 8, 23). The highest luciferase activities have been obtained with the asialofetuin conjugates (Figure 2, lane 2) and the synthetic (gal)-4pL conjugates (Figure 2, lane 3). Proper structural arrangement of the galactosides on the ligand seems to be essential for gene transfer. DNA complexed with lactosylated polylysine (pLys-lactose, see Experimental Procedures) was not expressed at significant levels (Figure 2, lane 4). DNA complexes containing neutralizing or slightly higher amounts of unmodified polylysine (Figure 2, lane 5) show low, but significant, receptor-independent uptake into HepG2 cells. This unspecific effect of polylysine has been observed in certain adherent cell lines in experiments at low (2% or less) serum levels.

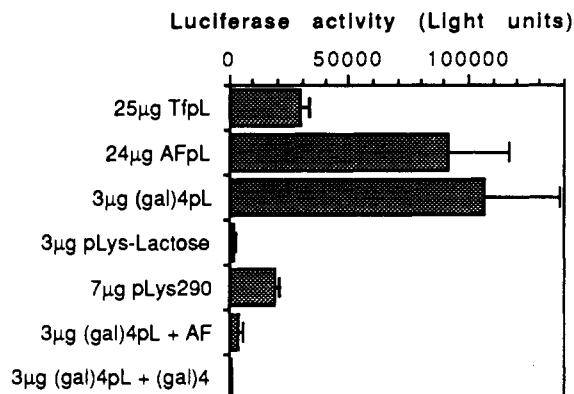


Figure 2. Luciferase gene delivery to HepG2 cells using different ligand-polylysine conjugates. pRSVL DNA (10 µg) in 330 µL of HBS was mixed with the indicated amounts of TfPL190B conjugate, asialofetuin-polylysine AFpL, polylysine (pLys₂₉₀), or (gal)4pL, in 170 µL HBS. Optimum ratios of DNA/conjugate have been determined in preliminary titrations by assaying the resulting gene-transfer efficiency (data not shown). The amounts (µg) of conjugate or polycation refer, in the case of pLys₂₉₀ or (gal)4pL, to the content of polylysine calculated as hydrobromide salt and, in the case of TfPL (or AFpL), to the transferrin (asialofetuin) content. In the competition experiments 240 µg (13 equiv) of asialofetuin (AF) or 30 µg (25 equiv) of lactosylated peptide (gal)4 was added after 30 min. The DNA complex mixture was then added to HepG2 cells (400 000 cells per flask) in 4 mL of medium containing 10% FCS; just prior to transfection, chloroquine (Sigma) was added to a final concentration of 100 µM in the transfection medium. The cells were incubated at 37 °C for 4 h, and then the transfection medium was replaced by 4 mL of fresh DMEM plus 10% FCS. Harvesting of cells and luciferase assays were performed 24 h after transfection as previously described (1). Light unit values as shown represent the total luciferase activity of the transfected cells. The filled bars represent mean values; the bracket above each bar indicates one standard deviation.

We next asked if the delivery of DNA/(gal)4pL complexes truly involved interactions with the asialoglycoprotein receptor. If this is the case, including excess levels of free ligand [either (gal)4 peptide or asialofetuin] should compete with DNA complexes for receptor binding and lower the subsequent luciferase gene expression. We found that inclusion of either excess free asialofetuin or free (gal)4 peptide blocks luciferase gene delivery to these cells (Figure 2, lanes 6 and 7) indicating that gene delivery occurs by binding to the asialoglycoprotein receptor. In this experiment, where only half of the DNA charge was neutralized by (gal)4pL conjugates, the unspecific effect of polylysine (compare Figure 2, lane 5) has been largely eliminated.

Augmentation of Gene Delivery by Replication-Defective Adenovirus Particles. Gene transfer into the murine embryonic hepatocyte line BNL CL.2 is shown in Figure 3. Again, complexes containing the hepatocyte-specific ligands, AF or (gal)4, showed the highest gene transfer activities in the presence of chloroquine (Figure 3B). In the absence of chloroquine only modest expression levels (Figure 3A) near the background of 150–200 light units were obtained. Although the plasmid DNA pCMVL, containing the *P. pyralis* luciferase gene under control of the more efficient cytomegalovirus immediate-early promoter/enhancer, was used, the transfection efficiencies have been moderate even in the presence of chloroquine. An alternate measure to prevent accumulation of the delivered DNA in intracellular vesicles is the use of replication-defective adenoviruses, which, as a result of their endosome-disrupting activity, have been found to strongly enhance transferrin-polylysine-mediated gene transfer into HeLa cells (9). Addition of adenovirus dl312

particles to the transfection medium resulted in a strong augmentation of gene expression both in BNL CL.2 cells (Figure 3C) and HepG2 cells (data not shown). The augmentation (30–500-fold over the level of chloroquine-augmented transfections, ca. 10⁶-fold over the level of control transfections) was most pronounced in the case of polylysine-rich DNA complexes (Figure 3C, "(gal)4pL"), which tend to bind adenovirus particles by ionic interaction between polylysine and the acidic viral capsid proteins (our unpublished observations). DNA/transferrin-polylysine complexes which are physically linked to the virus (10) have been found to be a most efficient means for gene transfer, as colocalization of the DNA complex and virus particle in the same endosome is guaranteed.

Enhanced Gene Transfer Using DNA Complexes Containing Galactose-Ligand and Influenza Peptides. Polylysine-conjugated peptides containing sequences derived from the N-terminus of the influenza virus hemagglutinin HA-2 subunit have been found to substantially augment transferrin-polylysine-mediated gene transfer (11). We have prepared similar complexes (Figure 4A) containing the plasmid pCMVL, the tetra-antennary galactose ligand linked to polylysine, and the polylysine-modified influenza peptide InflupL (see Experimental Procedures and ref 11). Conditions were chosen so that the ligand-polylysine conjugate neutralized half of the DNA charge and the remainder of the charge was used to load the complexes with influenza peptide-polylysine conjugate. Delivery of these complexes into BNL CL.2 hepatocytes resulted in luciferase gene expression (Figure 4B) that was significantly higher than the expression obtained with transferrin as ligand. The expression was more than 500-fold higher than in control experiments using DNA complexes lacking the influenza peptides, but containing the same amount of transferrin or (gal)4pL conjugates and polylysine (Figure 4B). The activity obtained in the presence of the modified influenza peptide was ca. 10-fold higher than that obtained with DNA/(gal)4pL complexes incubated with cells in the presence of chloroquine (see Figure 3B), and ca. 10⁴-fold higher than in the control experiment (Figure 3A).

DISCUSSION

Our aim is to develop a synthetic gene transfer system based on receptor-mediated endocytosis, a natural mechanism that is utilized for uptake of macromolecules such as proteins or viruses into cells. For this purpose, a number of groups (4, 6, 24), including our own, have synthesized DNA-binding conjugates of proteins that are ligands for cellular receptors. When DNA complexes prepared with the iron transporter transferrin, conjugated to polycations or other DNA-binding components (1, 15), are incubated with cells, the complexes bind to transferrin receptors, and subsequent uptake into the cells results in expression of the gene contained on the DNA (2, 25). In many cases the protein conjugation chemistry is difficult to control in terms of positions and numbers of polycation ligation sites, as a consequence of multiple potential reactive groups on the large protein ligands. In the case of transferrin conjugates, a specific ligation procedure involving modification of the transferrin carbohydrate moiety has been described (15) which allows defined, site-specific polycation attachment.

Another approach to obtain structurally well-defined DNA-binding ligand conjugates is the replacement of large protein ligands by smaller, synthetic compounds that mimic ligand-binding to a receptor. For this purpose we have synthesized an artificial ligand for the asialoglyco-

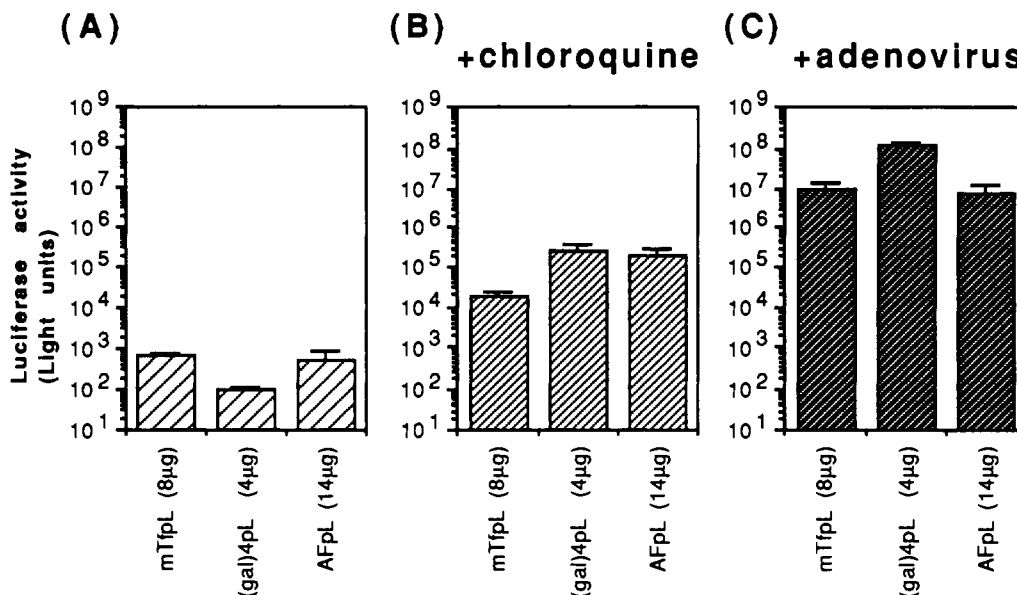


Figure 3. Transfection of BNL CL.2 hepatocytes and its augmentation by the endosome-disruption activity of defective adenovirus particles. Solutions of 6 µg of pCMVL DNA in 330 µL of HBS were mixed with the indicated amounts of mouse TfPL290 conjugate, asialofetuin-polylysine (AFpL), or (gal)4pL, in 170 µL HBS, and left for 30 min at room temperature. The DNA complexes were added to BNL CL.2 cells (300 000 cells per plate) cultured with 1 mL of fresh medium containing 2% FCS without (A) or with (B) chloroquine (final concentration 100 µM). Cells were incubated at 37 °C for 2 h, and then 1.5 mL of medium containing 10% FCS without (A) or with (B) 100 µM chloroquine was added. Two hours later the transfection medium was replaced by 4 mL of fresh high-glucose DMEM plus 10% FCS. (C) Instead of including chloroquine in the cell culture medium, to each DNA/conjugate complex was added 1 mL of DMEM containing 2% FCS and 50 µL of adenovirus dl312 stock solution (ca. 10⁹ viral particles). Incubation of the cells with the complexes and further manipulations were performed as described above, but in the absence of chloroquine. Assays were performed as described in Figure 2.

protein receptor. This hepatocyte-specific receptor has already proven to be suitable for gene delivery using asialoorosomucoid-polylysine conjugates (5). The interaction of this receptor with its ligand is well-studied and occurs via recognition of (preferentially) three terminal galactose residues on the asialoglycoprotein ligand by the trimeric subunits of the receptor (7). Triantennary or tetra-antennary oligosaccharides (that are present, for example, on asialofetuin or asialo-orosomucoid) with three or four terminal galactose residues are rapidly endocytosed by hepatocytes, whereas there is no evidence of efficient endocytosis of biantennary oligosaccharides (26) or asialoglycoproteins containing biantennary oligosaccharides (27). The clustering effect has also been described for the binding of neoglycoproteins containing covalently attached synthetic galactosides at various sugar densities (28). Synthetic cluster glycosides containing three galactosyl or lactosyl residues are bound to the asialoglycoprotein receptor and endocytosed by hepatocytes (29, 30).

We have synthesized a tetra-antennary ligand, (gal)4, containing galactoside residues bound to a branched peptide backbone which should provide appropriate structural arrangement of the carbohydrate groups (Figure 1). This synthetic ligand, if conjugated to polylysine, binds to DNA and delivers the gene contained on the DNA into cultured hepatocytes. The uptake most likely proceeds through binding to the asialoglycoprotein receptor followed by endocytosis, because the gene expression can be inhibited by addition of compounds that compete for binding to the asialoglycoprotein receptor (Figure 2).

After endocytosis, in the natural context, asialoglycoproteins are targeted to lysosomes and degraded by hydrolytic enzymes. The accumulation in lysosomal compartments may present a major limit to receptor-mediated gene delivery. A related hurdle seems to be present in the case of gene transfer by calcium phosphate precipitation, where over 50% of the DNA was found degraded in lysosomes (31). Nevertheless, successful

receptor-mediated gene transfer has been found using asialoorosomucoid-polylysine conjugates (5, 6). In our hands, the expression levels in hepatocyte gene transfer experiments with asialofetuin or the (gal)4 conjugates were very low unless further supporting measures (see below) were taken. Some rationalizations for the difference to the published data (5, 6) are as follows: (i) we are working with a slightly different system (ligand, conjugate, reporter gene, complex formation, amount of reagents, cell culture conditions); (ii) we believe that the gene transfer in the published system (5, 6) may be considerably augmented by the use of supporting agents such as chloroquine or adenovirus. In our experiments, efficient gene transfer was found when we included either chloroquine, which may protect to some extent internalized material from lysosomal degradation and/or may destabilize intracellular vesicles, or agents that promote the release of internalized DNA complexes from endosomes. A particularly effective measure consists of the use of defective adenovirus particles with endosome-disruption activity (9, 32), which (in comparison to chloroquine) results in a 500-fold enhancement of gene expression mediated by the (gal)4-containing DNA complexes (Figure 3).

Instead of using whole viral particles, it would be desirable to generate completely synthetic gene transfer complexes that utilize cellular mechanisms for entry. We intended to separate the endosome-release function of viruses from the whole virus particles. In this context, we have recently demonstrated that small synthetic peptides derived from influenza virus hemagglutinin that are able to disrupt membranes specifically under acidic conditions, if included in DNA complexes, promote transferrin-mediated gene transfer (11). We have shown here that DNA complexes containing both the synthetic ligand for endocytosis, (gal)4, and the synthetic membrane-active influenza peptide can deliver genes to hepatocytes with an efficiency approximately 500-fold higher than complexes lacking the influenza peptide (Figure 4), but still

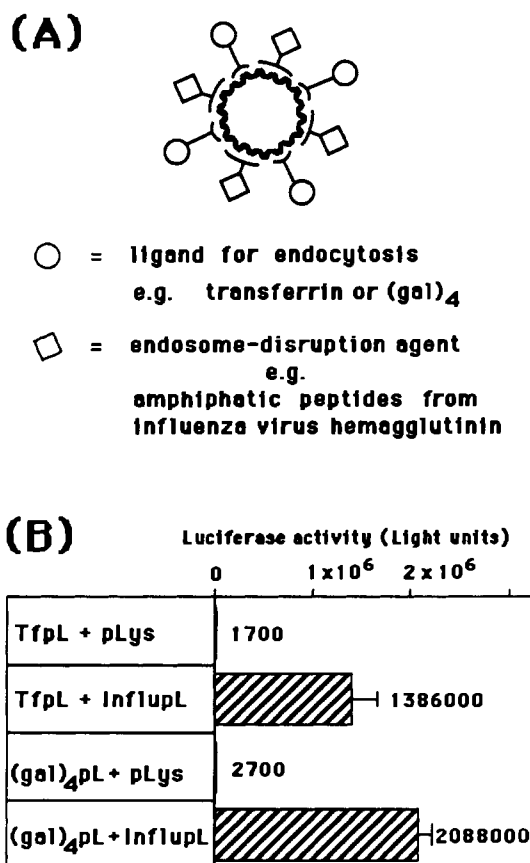


Figure 4. Gene transfer using combination complexes containing receptor ligands and membrane-active peptides. (A) Schematic drawing of DNA complexes containing both a ligand for endocytosis and a membrane-active component for endosome disruption. (B) Luciferase gene transfer into BNL CL.2 hepatocytes. DNA combination complexes were prepared by mixing first 6 μ g of pCMVL-DNA in 160 μ L of HBS with 4 μ g of TfpL₂₉₀ or 2 μ g of (gal)₄pL in 160 μ L of HBS and, after 15–30 min at room temperature, subsequent mixing with 20 μ g of the influenza HA-2 N-terminal peptide-poly(L-lysine) conjugate (InflupL) or with 20 μ g of unmodified poly(L-lysine) (pLys), in 160 μ L of HBS. Addition of the DNA complexes to the cells (in the absence of chloroquine) and further treatment of the cultures was performed as described in Figure 3A. Cell culture samples were harvested and assayed for luciferase activity as described in Figure 2.

approximately 50-fold lower than with adenovirus particles (Figure 3C). Our synthetic ligand for the asialoglycoprotein receptor functions comparably to a natural ligand and, with respect to hepatocytes, even better than transferrin as ligand in gene-transfer experiments. We hope that gene-transfer systems containing synthetic, well-defined ligands such as the (gal)₄ described here, combined in a modular manner with other functional components such as synthetic membrane-disrupting peptides, will prove useful for targeted gene-transfer applications.

ACKNOWLEDGMENT

We thank Prof. Dr. Martin Spiess (Basle) for providing HepG2 cells. We also thank Helen Kirlappos for technical assistance. We thank Prof. Dr. Max L. Birnstiel for support and helpful discussions. We further appreciate the critical reading of this paper by Drs. Lisa Ballou and Berndt Oberhauser. We are grateful to Dr. Horst Ahorn for the help in preparing time-of-flight mass spectra.

LITERATURE CITED

- (1) Wagner, E., Zenke, M., Cotten, M., Beug, H., and Birnstiel, M. L. (1990) Transferrin-polycation conjugates as carriers for DNA uptake into cells. *Proc. Natl. Acad. Sci. U.S.A.* 87, 3410–3414.
- (2) Cotten, M., Langle-Rouault, F., Kirlappos, H., Wagner, E., Mechtler, K., Zenke, M., Beug, H., and Birnstiel, M. L. (1990) Transferrin-polycation-mediated introduction of DNA into human leukemic cells: stimulation by agents that affect the survival of transfected DNA or modulate transferrin receptor levels. *Proc. Natl. Acad. Sci. U.S.A.* 87, 4033–4037.
- (3) Cotten, M., Wagner, E., and Birnstiel, M. L. (1992) Receptor mediated transport of DNA into eukariotic cells. *Methods Enzymol.*, in press.
- (4) Hockett, B., Ariatti, M., and Hawtrey, A. O. (1990) Evidence for targeted gene transfer by receptor-mediated endocytosis. *Biochem. Pharmacol.* 40, 253–263.
- (5) Wu, G. Y., and Wu, C. H. (1987) Receptor-mediated in vitro gene transformation by a soluble DNA carrier system. *J. Biol. Chem.* 262, 4429–4432.
- (6) Wu, C., Wilson, J., and Wu, G. (1989) Targeting genes: Delivery and persistent expression of a foreign gene driven by mammalian regulatory elements in vivo. *J. Biol. Chem.* 264, 16985–16987.
- (7) Spiess, M. (1990) The asialoglycoprotein receptor: A model for endocytic transport receptors. *Biochemistry* 29, 10009–10018.
- (8) Zatloukal, K., Wagner, E., Cotten, M., Phillips, S., Plank, C., Steinlein, P., Curiel, D., and Birnstiel, M. L. (1992) Transfection: A highly efficient way to express gene constructs in eukariotic cells. *Ann. N.Y. Acad. Sci.* 660, 136–153.
- (9) Curiel, D. T., Agarwal, S., Wagner, E., and Cotten, M. (1991) Adenovirus enhancement of transferrin-polylysine-mediated gene delivery. *Proc. Natl. Acad. Sci. U.S.A.* 88, 8850–8854.
- (10) Wagner, E., Zatloukal, K., Cotten, M., Kirlappos, H., Mechtler, K., Curiel, D. T., and Birnstiel, M. L. (1992) Coupling of adenovirus to transferrin-polylysine/DNA complexes greatly enhances receptor-mediated gene delivery and expression of transfected genes. *Proc. Natl. Acad. Sci. U.S.A.* 89, 6099–6103.
- (11) Wagner, E., Plank, C., Zatloukal, K., Cotten, M., and Birnstiel, M. (1992) Influenza virus hemagglutinin HA-2 N-terminal fusogenic peptides augment gene transfer by transferrin-polylysine/DNA complexes: Towards a synthetic virus-like gene transfer vehicle. *Proc. Natl. Acad. Sci. U.S.A.* 89, 7934–7938.
- (12) Wharton, S. A., Martin, S. R., Ruigrok, R. W. H., Skehel, J. J., Wiley, D. C. (1988) Membrane fusion by peptide analogues of influenza virus haemagglutinin. *J. Gen. Virol.* 69, 1847–1857.
- (13) Severne, Y., Wieland, S., Schaffner, W., and Rusconi, S. (1988) Metal binding 'finger' structures in the glucocorticoid receptor defined by site-directed mutagenesis. *EMBO J.* 7, 2503–2508.
- (14) DeWet, J., Wood, K., DeLuca, M., Helinski, D., and Subramani, S. (1987) Firefly luciferase gene: Structure and expression in mammalian cells. *Mol. Cell. Biol.* 7, 725–737.
- (15) Wagner, E., Cotten, M., Mechtler, K., Kirlappos, H., and Birnstiel, M. L. (1991) DNA-binding transferrin conjugates as functional gene-delivery agents: Synthesis by linkage of polylysine or ethidium homodimer to the transferrin carbohydrate moiety. *Bioconjugate Chem.* 2, 226–231.
- (16) Ellman, G. L. (1959) *Arch. Biochem. Biophys.* 82, 70.
- (17) Seifter, S., Dayton, S., Novic, B., and Muntwyler, E. (1950) *Arch. Biochem.* 25, 191.
- (18) Atherton, E., Gait, M. J., Sheppard, R. C., and Williams, B. J. (1979) The polyamide method of solid phase peptide synthesis and oligonucleotide synthesis. *Bioorg. Chem.* 8, 351.
- (19) Atherton, E., and Sheppard, R. C. (1989) *Solid Phase Peptide Synthesis, The Practical Approach Series*. IRL Press, Oxford, England.

- (20) Knowles, B. B., Howe, C. C., and Aden, D. P. (1980) Human hepatocellular carcinoma cell lines secrete the major plasma proteins and hepatitis B surface antigen. *Science* 209, 497-499.
- (21) Patek, P. Q., Collins, J. L., and Cohn, M. (1978) Transformed cell lines susceptible or resistant to in vivo surveillance against tumorigenesis. *Nature* 276, 510-511.
- (22) Tam, J. P. (1988) Synthetic peptide vaccine design: Synthesis and properties of a high-density multiple antigenic peptide system. *Proc. Natl. Acad. Sci. U.S.A.* 85, 5409-5413.
- (23) Corley Cain, C., Sipe, D. M., and Murphy, R. F. (1989) Regulation of endocytic pH by the Na, K-ATPase in living cells. *Proc. Natl. Acad. Sci. U.S.A.* 86, 544-548.
- (24) Rosenkranz, A. A., Yachmenev, S. V., Jans, D. A., Serebryakova, N. V., Murav'ev, V. I., Peters, R., and Sobolev, A. S. (1992) Receptor-mediated endocytosis and nuclear transport of a transfecting DNA construct. *Exp. Cell Res.* 199, 323-329.
- (25) Zenke, M., Steinlein, P., Wagner, E., Cotten, M., Beug, H., and Birnstiel, M. L. (1990) Receptor-mediated endocytosis of transferrin polycation conjugates: An efficient way to introduce DNA into hematopoietic cells. *Proc. Natl. Acad. Sci. U.S.A.* 87, 3655-3659.
- (26) Baenziger, J. U., and Fiete, D. (1980) Galactose and N-acetylgalactosamine-specific endocytosis of glycopeptides by isolated rat hepatocytes. *Cell* 22, 611-620.
- (27) Ashwell, G., and Morell, A. G. (1974) The role of surface carbohydrates in the hepatic recognition and transport of circulating glycoproteins. *Adv. Enzymol.* 41, 99-128.
- (28) Lee, Y. C. (1989) Binding modes of mammalian hepatic Gal/GalNAc receptors. *Carbohydrate Recognition in Cellular Function*. (Ciba Foundation Symposium 145) pp 80-95, Wiley, Chichester.
- (29) Connolly, D. T., Townsend, R. R., Kawaguchi, K., Bell, W. R., and Lee, Y. C. (1982) Binding and endocytosis of cluster glycosides by rabbit hepatocytes. *J. Biol. Chem.* 257, 939-945.
- (30) Kempen, H. J. M., Hoes, C., van Boom, J. H., Spanjer, H. H., de Lange, J., Langendoen, A., and van Berkel, T. J. C. (1984) A water-soluble cholesteryl-containing trisgalactoside: Synthesis, properties, and use in directing lipid-containing particles to the liver. *J. Med. Chem.* 27, 1306-1312.
- (31) Orrantia, E., and Chang, P. L. (1990) Intracellular distribution of DNA internalized through calcium phosphate precipitation. *Exp. Cell Res.* 190, 170-174.
- (32) Cotten, M., Wagner, E., Zatloukal, K., Phillips, S., Curiel, D. T., and Birnstiel, M. L. (1992) High-efficiency receptor-mediated delivery of small and large (48kb) gene constructs using the endosome disruption activity of defective or chemically inactivated adenovirus particles. *Proc. Natl. Acad. Sci. U.S.A.* 89, 6094-6098.

Preparation and Characterization of Biologically Active 6'-O-(6-Aminocaproyl)-4'-O-monophosphoryl Lipid A and Its Conjugated Derivative

Kent R. Myers,^{*,†} J. Terry Ulrich,[†] Nilofer Qureshi,^{‡,§} Kuni Takayama,^{‡,§} Rong Wang,^{||} Ling Chen,^{||} W. Bart Emary,^{||} and Robert J. Cotter^{||}

Ribi ImmunoChem Research, Inc., 553 Old Corvallis Road, Hamilton, Montana 59840, Mycobacteriology Research Laboratory, William S. Middleton Memorial Veterans Hospital, Madison, Wisconsin 53705, Department of Bacteriology, College of Agriculture and Life Sciences, University of Wisconsin, Madison, Wisconsin 53706, and Department of Pharmacology and Molecular Sciences, The Johns Hopkins University School of Medicine, Baltimore, Maryland 21205. Received August 7, 1992

N-tert-butyloxycarbonyl (*t*-Boc) protected 6-aminocaproic (Cap) anhydride was reacted with unprotected hexaacyl-4'-O-monophosphoryl lipid A (MLA) obtained from the lipopolysaccharide of *Escherichia coli* J5 to yield *t*-Boc-Cap-MLA. After a column purification step, the *t*-Boc group was removed by incubating the sample at low temperature in the presence of acid to yield Cap-MLA. This product was analyzed by californium plasma desorption mass spectrometry (PDMS). Purified *t*-Boc-Cap-MLA was further fractionated by reverse-phase high-performance liquid chromatography as its methyl ester and characterized by laser desorption mass spectrometry, PDMS, and proton nuclear magnetic resonance spectroscopy. These analyses revealed that the Cap group was selectively introduced into the 6'-position of MLA. To demonstrate that Cap-MLA can be conjugated to other compounds, it was reacted with biotin-Cap *N*-hydroxysuccinimide ester to yield biotin-(Cap)₂-MLA. Analysis of this product by PDMS confirmed its expected molecular weight of 2171 and showed the presence of fragments containing the biotin and Cap groups. Monoclonal antibodies and streptavidin were used to show the presence of both lipid A and biotin in this conjugated product. These two novel lipid A derivatives were then tested for their bioactivities. Although both Cap-MLA and biotin-(Cap)₂-MLA showed mitogenic activity using murine splenocytes, they were about 4-8 times less active than MLA at 20 µg/mL or less and only one-half as active at 100 µg/mL. In the induction of tumor necrosis factor release by RAW 264.7 murine macrophage cell line, the biotin-(Cap)₂-MLA showed 7-9-fold lower activity than MLA at the concentration range of 0.1-1.0 µg/mL. These results showed that Cap-MLA is a biologically active lipid A derivative that can be conjugated to other compounds through its free amino group to form new and active derivatives. It should thus be a useful reagent to study the biological properties of lipid A.

INTRODUCTION

The lipopolysaccharide (LPS)¹ of Gram-negative bacteria plays a key role in the pathophysiology of Gram-negative sepsis and septic shock (1). This potent molecule is able to stimulate a wide range of responses in humans at levels as low as 1 ng/kg (2). It is now well-established that essentially all of the biological activity of LPS resides in the lipid A portion of the molecule, although other structures present in LPS can potentiate these activities (3, 4). The medical importance of Gram-negative sepsis

and septic shock makes the mode of action of LPS and lipid A a topic of significant research interest.

The exquisite sensitivity of certain cell types to LPS suggests that recognition occurs via one or more high-affinity receptors. Considerable effort has been directed at identifying the receptor structures that mediate LPS recognition by responsive cells (5). An important strategy for identifying potential LPS receptors involves the use of probes prepared by conjugation of the LPS molecule to appropriate reporter functionalities. One particularly useful derivative is ¹²⁵I-ASD-LPS, which can be used to covalently label LPS binding structures with ¹²⁵I (6). This derivative has made it possible to identify and initiate characterization of several candidate receptors (7, 8).

Preparation of derivatives such as ¹²⁵I-ASD-LPS requires the presence of free amino groups in LPS that can react with appropriately activated groups such as *N*-hydroxysuccinimide esters. Amino-containing substituents, such as phosphorylethanolamine and 4-deoxy-4-aminoarabinose, do occur in the core and/or the lipid A regions of LPS from many species of bacteria (9, 10). However, these substituents are generally present in nonstoichiometric amounts and also may occur at more than one position in the LPS molecule (9, 10). In addition, it is not known if the fatty acid distribution in the lipid A portion of LPS varies depending on the presence and location of amino-containing substituents; this possibility is suggested

* Author to whom correspondence should be addressed. Telephone: (406) 363-6214. Fax: (406) 363-6129.

[†] Ribi ImmunoChem Research, Inc.

[‡] University of Wisconsin.

[§] William S. Middleton Memorial Veterans Hospital.

^{||} Johns Hopkins University.

¹ Abbreviations used: LPS, lipopolysaccharide; ¹²⁵I-ASD-LPS, ¹²⁵I-iodinated form of 2-[2-(*p*-azidosalicylamido)ethyl]-3-dithiopropionate-coupled LPS; SASD, sulfosuccinimidyl 2-[2-(*p*-azidosalicylamido)ethyl]-3-dithiopropionate; MLA, monophosphoryl lipid A (hexaacyl); *t*-Boc, *tert*-butoxycarbonyl; Cap, 6-aminocaproyl; TLC, thin-layer chromatography; HPLC, high-performance liquid chromatography; LDMS, laser desorption mass spectrometry; PDMS, plasma desorption mass spectrometry; FAB-MS, fast atom bombardment mass spectrometry; TNF, tumor necrosis factor; ELISA, enzyme-linked immunosorbent assay.

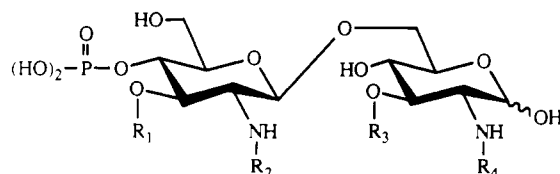


Figure 1. Structure of MLA from *E. coli*. R_1 and R_2 are 3-(acyloxy)myristoyl groups; R_3 and R_4 are 3-hydroxymyristoyl groups. See Table I for further definition of R_1 and R_2 .

by the observation that the polysaccharide and fatty acid contents of LPS are inversely correlated (11). These ambiguities complicate the interpretation of experiments performed with derivatives such as ^{125}I -ASD-LPS.

We now report on the selective introduction of a 6-aminocaproyl group to the 6'-O-position of 4'-O-monophosphoryl lipid A (MLA) obtained from the LPS of *Escherichia coli* (Figure 1). The product, 6'-O-(6-aminocaproyl)-MLA (Cap-MLA), contains a free amino group to which substituents such as SASD can be attached. As an example of the utility of this derivative, the conjugate of biotin and Cap-MLA was prepared. The resulting material, biotin-(Cap) $_2$ -MLA, retained the biological activity of unconjugated MLA with respect to activation of murine B-cells and macrophages, and exhibited high affinity for streptavidin.

An additional result of this study was the observation of heterogeneity in the lipid A structure due to variability in the (acyloxy)acyl residues at both the 2'-O- and 3'-O-positions. This heterogeneity is evidently of biosynthetic origin.

EXPERIMENTAL PROCEDURES

Reagents and Supplies. 6-Aminocaproic acid, 2-[[[(*tert*-butoxycarbonyl)oxy]imino]-2-phenylacetoneitrile, dicyclohexylcarbodiimide, trifluoroacetic acid, and HCl(g) were obtained from Aldrich Chemical Co. Biotin-Cap *N*-hydroxysuccinimide ester and polymyxin B were purchased from Sigma Chemical Co. All reagents were of the highest grades available, and were used without further purification. HPLC grade solvents were purchased from J. T. Baker, Inc. Chloroform and pyridine used in reactions were dried by storage over molecular sieves (4A). Chloroform treated in this way was free of residual alcohols or moisture as judged by IR spectroscopy. Chromatographic media used in this study were Kieselgel 60 TLC plates, 250 μm (EM Science); Empore soft TLC plates, silica (Analytichem International, Inc.); Biosil HA silicic acid (Bio-Rad Laboratories—Chemical Division); Nova-Pak radial compression cartridge, C_{18} -bonded and capped 4 μm silica, 8 mm \times 10 cm (Waters Associates, Inc.); and Accell Plus QMA ion-exchange packing (Waters Associates, Inc.). ELISA binding assays were performed on Immulon 2 microtiter plates (Dynatech Laboratories, Inc.). Culture reagents were RPMI-1640, antibiotics (Sigma Chemical Co.); fetal calf serum (Hyclone Laboratories, Inc.); [^3H]thymidine (NEN Research Products); and anti-lipid A monoclonal antibodies DS77 and DS35 (Ribi ImmunoChem Research, Inc.). Female C3H/HeJ and C3H/HeSnJ mice 6–8 weeks of age were obtained from Jackson Laboratories. ICR mice were obtained from the mouse colony at Ribi ImmunoChem.

Analytical Techniques. All TLC analyses were carried out using a solvent system consisting of chloroform/methanol/water/ammonium hydroxide (50:31:6:2, v/v). Bands on the developed plates were visualized by spraying with 10% (w/v) phosphomolybdic acid in ethanol followed by charring or 0.2% (w/v) ninhydrin in *n*-butanol/water/

acetic acid (95:4.5:0.5, v/v) followed by brief heating at 100 $^\circ\text{C}$. TLC plates (visualized with phosphomolybdic acid) were analyzed by scanning densitometry with a Shimadzu CS9000U dual-wavelength flying spot scanner (Shimadzu Corp.), using a scanning wavelength of 520 nm. Phosphorus was determined by the method of Bartlett (12), and free amino groups were assayed by the procedure of Ghuysen and Strominger (13), using the modification of Jiao et al. (11). Amino sugar and amino acid analyses were carried out using Pico-Tag chemistry (Waters Associates, Inc.).

Growth of Bacteria. *E. coli* J5 cells were grown in sparged culture at 37 $^\circ\text{C}$ in M9 media containing 16 g/L glucose. Cells were harvested at stationary phase with an Amicon hollow fiber system (Amicon Corp.), recovered as a pellet, and lyophilized.

Isolation of LPS and Preparation of MLA. The rough chemotype LPS (Rc chemotype LPS) was extracted from the lyophilized cells of *E. coli* J5 by the method of Galanos et al. (14), as modified by Qureshi et al. (15). This crude RcLPS preparation (614 mg) was hydrolyzed in 0.1 N HCl (3 mg/mL) at reflux for 20 min. The reaction mixture was cooled in an ice bath and then extracted with 2.5 volumes of chloroform/methanol (2:1, v/v) to yield crude MLA (290 mg). This material was applied to an anion-exchange column (Accell Plus QMA) and MLA was eluted using chloroform/methanol/60 mM ammonium acetate (2:3:1, v/v). The recovery of the purified MLA was 154.5 mg. A portion of this material (152 mg) was applied to a 3 cm \times 30 cm Biosil HA silicic acid column and eluted with a linear gradient of 0–24% methanol/water (95:5, v/v) in chloroform over 3.6 L at a flow rate of 2 mL/min. Fractions (12 mL) were collected and analyzed for MLA content by TLC. Fractions 132–187 were pooled, evaporated to dryness, and weighed, yielding 78 mg of the desired pure MLA (hexaacyl).

Preparation of *t*-Boc-Cap-MLA. *t*-Boc-Cap-MLA was prepared by reaction of MLA with 6-(*t*-Boc-amino)caproic anhydride. 6-Aminocaproic acid was first *N*-protected by reaction with 2-[[[(*tert*-butoxycarbonyl)oxy]imino]-2-phenylacetoneitrile, using the procedure of Paleveda et al. (16). The anhydride was formed using dicyclohexylcarbodiimide in chloroform, and was recrystallized from diethyl ether/hexane (approximately 65:5, v/v). MLA (69.1 mg, 40 μmol) and 6-(*t*-Boc-amino)caproic anhydride (53.9 mg, 121 μmol) were then combined in 3.4 mL of chloroform/pyridine (1:1, v/v) and stirred at 23 $^\circ\text{C}$ for 24 h. The reaction was quenched by addition of 3.4 mL of 0.1 M Na_2CO_3 (pH 10) followed by vigorous stirring for 30 min. The resulting mixture was extracted with 8.5 mL of chloroform/methanol (2:1, v/v). The phases were separated by centrifugation and the lower (organic) phase was washed with four 5-mL portions of 1.0 N HCl and once with 5 mL of water. The organic phase was then evaporated to dryness, yielding 90.7 mg of crude product mixture. A portion (84.5 mg) of this material was purified on Biosil HA silicic acid using the procedure described above, except that the linear gradient in this case was 0–18% methanol/water (95:5, v/v) in chloroform over 2.7 L at a flow rate of 2 mL/min. Fractions (10 mL) were collected and were pooled on the basis of their appearance on TLC. Three pools were obtained: I, fractions 70–72, 2.4 mg; II, fractions 73–76, 12.8 mg; and III, fractions 77–170, 51.1 mg. Pool III represented the desired product, *t*-Boc-Cap-MLA.

Deprotection of *t*-Boc-Cap-MLA. In general, *t*-Boc-Cap-MLA was deprotected either by dissolving in trifluoroacetic acid at -20 $^\circ\text{C}$ and stirring for 20 min or by

bubbling HCl(g) through a solution of the Boc-protected material in chloroform at -5°C . The following is a representative example of the latter method: a solution of 14.0 mg of *t*-Boc-Cap-MLA (pool III, 7.2 μmol) in 1.0 mL of anhydrous chloroform was stirred at -5°C while being sparged with HCl(g). The reaction was followed by analytical TLC and was complete within 40 min. Two milliliters of 5% NaHCO₃ and 5 mL of chloroform/methanol (2:1, v/v) were then added to the reaction solution, and the resulting mixture was vortexed and centrifuged. The organic phase was recovered, washed once with 2 mL of water, and evaporated to dryness. The yield was 12.5 mg of Cap-MLA (6.8 μmol , 94% yield), which appeared as a single ninhydrin-positive spot by analytical TLC.

Preparation of Biotin-(Cap)₂-MLA. Cap-MLA (9.5 mg, 5.2 μmol) and biotin-Cap *N*-hydroxysuccinimide ester (4.1 mg, 9.0 μmol) were stirred in 0.8 mL of chloroform/pyridine (1:1, v/v) for 41 h at 23°C . The reaction was then worked up by adding 5 mL of chloroform/methanol (2:1, v/v) and washing twice with 2 mL of 1.0 N HCl and once with water. The organic phase was evaporated, yielding 9.9 mg of crude product. The major product was purified by preparative TLC using the solvent system described earlier, resulting in 6.2 mg of purified biotin-(Cap)₂-MLA.

HPLC Fractionation of MLA Derivatives. HPLC was performed with two Waters 6000A solvent-delivery systems (Waters), a Waters 660 solvent programmer, a Waters U6K Universal liquid chromatograph injector, a variable-wavelength detector (Model LC-85B, Perkin-Elmer Corp.), and a radial compression module (Model RCM-100, Waters Associates, Inc.).

Cap-MLA or *t*-Boc-Cap-MLA were first converted to the free acid form by passage through sulfonic acid resin (H⁺ form) followed immediately by methylation of the phosphate group with diazomethane. Samples were then analyzed by reverse-phase HPLC using a Nova-Pak cartridge (8 mm \times 10 cm). A linear gradient of 20–80% 2-propanol in acetonitrile over 60 min at a flow rate of 2 mL/min was used. The wavelength of the detector was set at 210 nm. Typically, 2–3 mg of sample were injected per run, and an AUFS setting of 0.15 was used.

LDMS. Laser desorption mass spectra were obtained on a CVC-2000 (Rochester, NY) time-of-flight mass spectrometer equipped with a Tachisto (Needham, MA) Model 215G pulsed carbon dioxide laser as previously described (17, 18).

PDMS. Californium plasma desorption mass spectra were obtained on a BIO ION Nordic (Uppsala, Sweden) BIN-10K time-of-flight mass spectrometer, with a ²⁵²Cf fission-fragment ionization source. Samples were dissolved in chloroform/methanol (1:1, v/v) saturated with the tripeptide glutathione (19) to a concentration of approximately 0.5 μg of sample/mL, and 10 μL of this sample was electrosprayed on the aluminum foil sample holder. Mass spectra were obtained by accumulating the ion signal to a preset value of 5×10^6 primary ion events.

FAB-MS. Fast atom bombardment mass spectra were obtained on a AEI/Kratos (Manchester, England) mass spectrometer using 8 KeV xenon atoms (15, 20). The matrix consisted of dithiothreitol/dithioerythritol (3:1, v/v). Mass calibration was achieved by measurement of cesium iodide ions over the mass range from 800 to 2300.

Proton NMR Spectroscopy. Spectra were recorded on a Bruker AM 500 spectrometer operating at 500 MHz. The spectrometer was equipped with an Aspect 3000 computer and digital pulse shifter. HPLC-purified dimethyl-*t*-Boc-Cap-MLA, peak III-C (8.0 mg; see below),

was dissolved in 0.5 mL of CDCl₃/CD₃OD (8:1, v/v). A two-dimensional proton correlation (COSY) spectrum was obtained under conditions described previously (21, 22).

ELISA Binding Assay. Immulon 2 microtiter plates were washed with 15% 1-propanol and then coated for 2 h at 37°C with 100 μL /well of either MLA or biotin-(Cap)₂-MLA at 10 μg /mL in 0.05 M sodium bicarbonate/carbonate (pH 9.5) buffer. The plates were then washed three times with water, and 100 μL of antibody in ELISA buffer (0.01 M Tris, pH 7.2, 25% v/v FCS, 2 mg/mL EDTA, and 0.1% v/v Tween 20) or ELISA buffer alone was added to each well. The plates were incubated for 1 h and washed as above. Horse radish peroxidase-goat anti-mouse IgG (100 μL /well in ELISA buffer) was added to wells containing antibody. Horse radish peroxidase-streptavidin (100 μL /well in ELISA buffer) was added to wells to be analyzed for streptavidin binding. Horse radish peroxidase-streptavidin concentrations were tested in quadruplicate. Plates were incubated at 37°C for 1 h and then washed. *o*-Phenylenediamine reagent (0.4 mg/mL in 0.1 M citrate phosphate buffer, pH 5.0, containing 0.01% v/v H₂O₂; see ref 23) was added to each well, and plates were incubated for an additional 15 min. The reaction was stopped by addition of 50 μL of 1 N H₂SO₄, and the optical density was read at 490 nm.

Stimulation of Lymphocyte Blastogenesis. Mitogenic activities of test materials were assessed according to standard procedures (24). Splenocytes were obtained from either C3H/HeJ, C3H/HeSnJ, or ICR mice, and were cultured in 96-well plates at a density of $2\text{--}3 \times 10^5$ cells/well in RPMI-1640 media containing 10% fetal calf serum, 2 μg /mL Fungizone, 50 μg /mL gentamycin, 2 mM L-glutamine, and varying concentrations of test materials. Test materials were assayed in triplicate at each concentration. One group of three wells, to be used for estimation of background activity, received all media components but did not receive any added mitogens. After 36–48 h, 200 μL (1 μCi) of [³H]thymidine was added to each well, and the cells were incubated for an additional 6–8 h. Cells were then harvested onto fiberglass filter pads and their [³H]thymidine uptake was determined by liquid scintillation counting. Stimulation indices were calculated as the ratio of ³H counts in cells exposed to mitogen versus media alone. For assays involving polymixin B inhibition, test materials were combined with appropriate concentrations of polymixin B in ELISA buffer and incubated at 37°C for 30 min prior to addition to microtiter wells.

Induction of TNF- α . The abilities of various materials to induce release of TNF- α were assessed in the RAW 264.7 cell line. Cells were cultured according to the procedures of Virca et al. (25), in 24-well plates at a cell density of 5×10^6 cells/well. Experiments involved exposing cells to varying amounts of test materials in serum- and antibiotic-free RPMI-1640 media containing 2 mM L-glutamine for 8 or 20 h. Cells exposed to media alone, without added test substances, were used to estimate background TNF-inducing activity. Conditioned supernatant fractions were analyzed in duplicate for the presence of TNF- α using an ELISA assay (obtained from Genzyme, Inc.). The TNF- α induced by each test substance was calculated as the difference between TNF- α elicited in the presence of the test material and TNF- α elicited by media alone.

RESULTS

Preparation of CAP-MLA and Derivatives. The reaction of MLA (69.1 mg) with the *t*-Boc-protected anhydride of 6-aminocaproic acid proceeded readily at

room temperature in the presence of pyridine to yield *t*-Boc-Cap-MLA. TLC of the product mixture followed by charring and scanning densitometry revealed one major product spot ($R_f = 0.59$, 80%), a smeared region containing one distinct spot ($R_f = 0.65$, 14% for the smear), and a minor spot ($R_f = 0.69$, 4%). A small amount of material migrating with the same R_f as the starting material ($R_f = 0.33$, 2%) was also evident. In other experiments, addition of further anhydride and incubation for longer times did not reduce the intensity of the lower spot, suggesting that it did not correspond to MLA starting material.

Fractionation of the crude *t*-Boc-Cap-MLA on a silicic acid column yielded three major fractions: pool III, the largest fraction with $R_f = 0.59$; pool I, a minor component with $R_f = 0.65$; and pool II, a mixture of pools I and III. Pools I and III were further analyzed.

The *t*-Boc-Cap-MLA (pool III) was deprotected by treatment with HCl(g) in chloroform at -5°C . The yield of Cap-MLA was greater than 90%. On TLC, this product appeared as a single, ninhydrin-positive spot with an R_f slightly less than that of the starting MLA. It was determined to have a molar ratio of phosphorus to free amino groups of 1.00:1.13, whereas the starting MLA had a ratio of 1.00:0.01. Amino acid analysis of acid-hydrolyzed sample confirmed the presence of glucosamine and 6-aminocaproic acid in the Cap-MLA product (data not shown).

The reaction of Cap-MLA with 1.7 equiv of biotin-Cap *N*-hydroxysuccinimide ester yielded a product with an R_f intermediate between that of the two starting materials. This product was identified to be biotin-(Cap)₂-MLA. The reaction reached completion in 18 h at 23°C .

STRUCTURAL CHARACTERIZATION OF CAP-MLA AND DERIVATIVES

HPLC Purification of Dimethyl-*t*-Boc-Cap-MLA. Pools I and III from the silicic acid column fractionation were methylated with diazomethane and analyzed by reverse-phase HPLC. Methylated pool I gave a single major peak (I-A) which was recovered and analyzed by FAB-MS (to be discussed later). The chromatographic profile of pool III is shown in Figure 2. It contained two prominent and two minor peaks (III-A through III-D). The relative abundances of these four components, based on integrated absorbance at 210 nm, are given in Table I.

Mass Spectrometry of HPLC-Purified Pools I and III. LDMS of the major HPLC peak III-C (Figure 2) gave a molecular ion $M + K^+$ at 1999 and $M + Na^+$ at 1983 (Figure 3). The molecular weight of this product is 1960. A major fragmentation resulted from cleavage of the hydroxymyristoyl group (R_3) at the 3'-O-position of the glucosamine disaccharide with proton transfer from the sugar (243 amu + H) to yield peaks at 1754 and 1738 (containing K^+ and Na^+ , respectively). The loss of both R_3 and *t*-Boc-Cap (243 + 230 amu) from 1999 gave a peak at 1524.

The second major fragmentation pathway was cleavage of the O-C₁ and C₄-C₅ bonds of the reducing-end sugar to give the "distal ions" at 1426 (17, 18). The mass of this ion suggests that the *t*-Boc-Cap group is attached to the distal glucosamine. If the group were attached to the reducing-end glucosamine, then the distal ion would have a mass of 1213, which is not observed. The proposed structure of *t*-Boc-Cap-MLA is shown in Figure 4.

The origin of the peak at 1451 is not clear. However, we suggest that it is a two-bond ring cleavage carrying an additional ethylene group. The three peaks at 1426, 1451, and 1524 all represent ions in which the only ester-linked fatty acid on the reducing end (R_3) has already been lost.

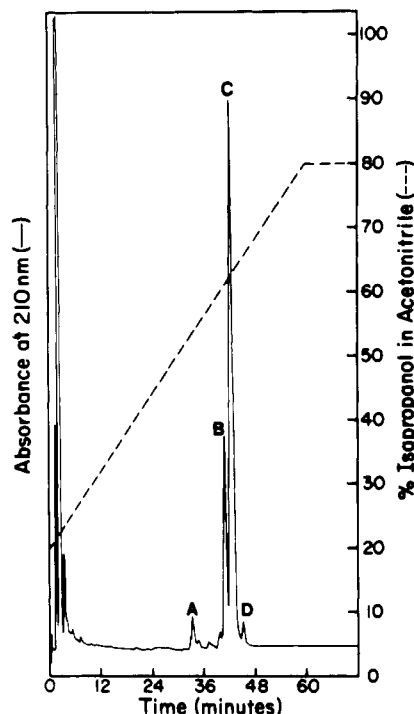


Figure 2. HPLC chromatogram of dimethyl-*t*-Boc-Cap-MLA, pool III. A C₁₈-bonded silica cartridge was used. The mobile phase was a linear gradient of 20–80% 2-propanol in acetonitrile at a flow rate of 2 mL/min over a period of 60 min. The absorbance units at full scale was set at 0.064 for 2.0 mg of dimethyl-*t*-Boc-Cap-MLA. Baseline correction was made by the Perkin-Elmer LC-85B detector.

The only possible additional fragment ions would involve losses of the myristic and lauric acids attached to R_1 and R_2 , respectively. These are lost as the neutral acids (228 and 200 amu). All of the remaining peaks in the mass spectrum can be explained as losses of either lauric acid, myristic acid, or both. If one observes the loss of R_3 from the peak at 1999, then one should also observe an additional loss of R_1 (i.e., from the peak at 1754). This minor peak appeared at 1315.

LDMS of the HPLC peak III-B gave a molecular ion $M + K^+$ at 1971 and $M + Na^+$ at 1955 (Figure 5). The molecular weight of this product is 1932. A major fragmentation resulted from cleavage of R_3 to yield peaks at 1726 and 1710 (containing K^+ and Na^+ , respectively). The loss of both R_3 and *t*-Boc-Cap gave a peak at 1494.

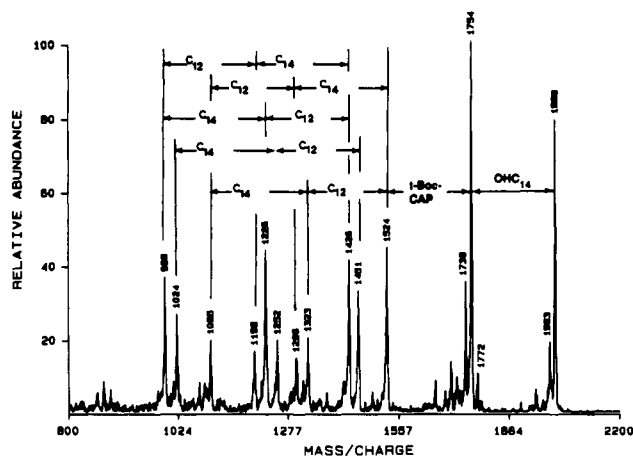
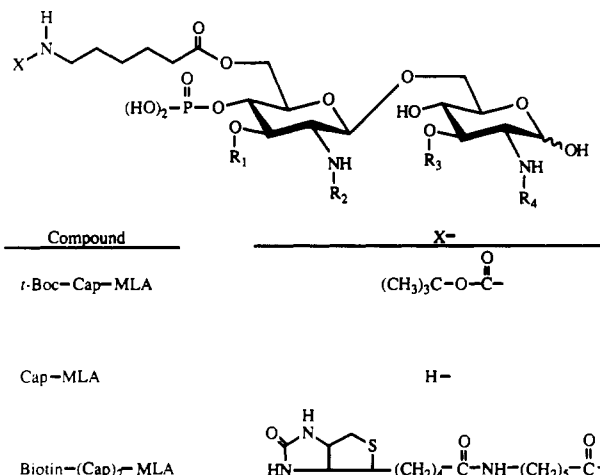
The peak at 1398 is the distal portion plus $OCH_2CH=O$ plus K^+ . The mass again suggests that the *t*-Boc-Cap is attached to the distal sugar and that the 28 amu difference between peaks III-B and III-C is located on the distal portion. The peak at 1382 is the distal portion plus $OCH_2CH=O$ plus Na^+ . The 1398 ion further fragments to form the ions at 1196 and 996, representing the successive losses of two laurate groups. Similarly, the ion at 1494 showed the same two losses of lauric acid to yield fragments at 1296 and 1095; the ion at 1420 lost successive lauric acid units to form the ions at 1224 and 1022. These fragment ions would suggest that both R_1 and R_2 are 3-(lauroyloxy)-laurate, so that the 28 amu difference between this product and III-C resulted from the substitution of lauric acid for myristic acid in R_1 .

It could be argued that R_1 is 3-(myristoyloxy)myristate and R_2 is 3-(caproyloxy)myristate. The ion at 1224 would then represent the loss of caproic acid from 1398, followed by the loss of myristic acid to give the peak at 996. However, if that were the case, one should also observe the loss of myristic acid from 1398 first at 1170, which is

Table I. Structure of Dimethyl-*t*-Boc-Cap-MLA Species Isolated from Pool III by HPLC, As Determined by Mass Spectrometry and Nuclear Magnetic Resonance^a

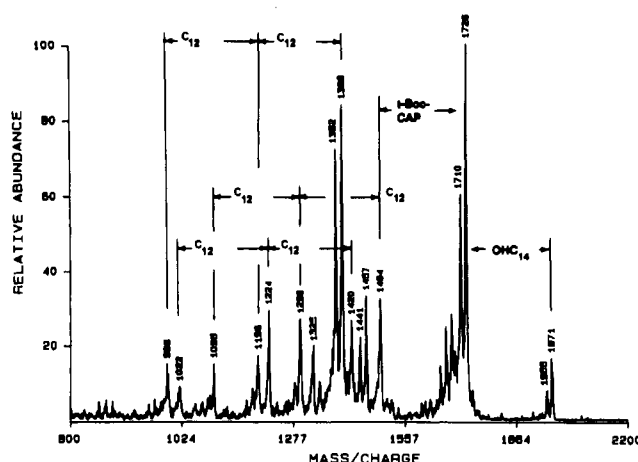
HPLC peak	Mr	position of <i>t</i> -Boc-Cap group	relat abund	fatty acid distribution ^b			
				R ₁	R ₂	R ₃	R ₄
III-A	1960	unk	6	C ₁₄ OC ₁₄	C ₁₂ OC ₁₄	OHC ₁₄	OHC ₁₄
III-B	1932	6'	38	C ₁₂ OC ₁₄	C ₁₂ OC ₁₄	OHC ₁₄	OHC ₁₄
III-C	1960	6'	100	C ₁₄ OC ₁₄	C ₁₂ OC ₁₄	OHC ₁₄	OHC ₁₄
III-D	1988	6'	4	C ₁₄ OC ₁₄	C ₁₄ OC ₁₄	OHC ₁₄	OHC ₁₄

^a HPLC chromatogram of pool III is shown in Figure 2. R₁, R₂, R₃, and R₄ correspond to fatty acyl groups shown in Figure 4. ^b Abbreviations used: OHC₁₄, 3-hydroxymyristate; C₁₂OC₁₄, 3-(lauroyloxy)myristate; C₁₄OC₁₄, 3-(myristoyloxy)myristate; unk, unknown.

**Figure 3.** Laser desorption mass spectrum of HPLC peak III-B.**Figure 4.** Structures of *t*-Boc-Cap-MLA, Cap-MLA, and biotin-(Cap)₂-MLA. The structure for *t*-Boc-Cap-MLA corresponds to peaks III-B, -C, and -D (see text and Table I for further explanation). R₁ and R₂ are 3-(acyloxy)myristoyl groups; R₃ and R₄ are 3-hydroxymyristoyl groups. See Table I for further definition of R₁ and R₂.

not observed. Thus, the major contribution to HPLC peak III-B must be a dimethyl-*t*-Boc-Cap-MLA, in which a lauric acid has been substituted for a myristic acid in R₁.

PDMS were obtained for the HPLC peak fractions III-A, -B, -C, and -D, and the resulting molecular weight data are summarized in Table I. The M + Na⁺ molecular ion for III-C confirmed its molecular weight and the PDMS spectra of III-B and -D confirmed that they were 28 amu below and above III-C, respectively. For all three of these fractions, the loss of R₃ was the predominant fragment ion and confirmed that R₃ was in all cases ω-hydroxymyristate. The distal ions were also observed and, in the case of III-D, this ion was shifted 28 amu higher than in III-C, suggesting that in III-D both R₁ and R₂ were 3-(myristoyloxy)myristate. The PDMS of HPLC peak III-A indicated that it had a molecular weight equivalent

**Figure 5.** Laser desorption mass spectrum of HPLC peak III-C.

to that of III-C. However, the major fragment ion was the loss of *t*-Boc-Cap rather than R₃, suggesting attachment of the *t*-Boc-Cap moiety directly to the sugar ring or to the 3-hydroxymyristate at R₃ or R₄. The available positions on the reducing-end glucosamine would be the 1- and 4-positions. The results of the mass spectral analysis of the products are summarized in Table I.

FAB-MS of HPLC peak I-A (from silicic acid column fraction pool I) gave a pseudomolecular ion at 2074. Assuming that this corresponds to M + H⁺, the molecular weight for this compound is 2073. This represents a difference of 113 amu relative to the mass of peak III-C, the main species present in pool III. The additional mass in I-A may reflect the presence of a moiety with an elemental composition of C₆H₁₁NO, corresponding to -NH(CH₂)₅CO-. Such a product could arise if unblocked 6-aminocaproic acid was present during preparation of the *t*-Boc-Cap anhydride. Unblocked material would readily undergo amide bond formation in the presence of dicyclohexylcarbodiimide to yield 6-(6'-aminocaproyl-amido)caproic acid, which would in turn undergo anhydride formation.

Proton NMR of Dimethyl-*t*-Boc-Cap-MLA. Proton NMR was used to determine the linkage between *t*-Boc-Cap and MLA. A two-dimensional COSY experiment was performed to assign the relevant protons in the spectrum of HPLC-purified *t*-Boc-Cap-MLA (peak III-C). Figure 6A gives the correlations that led to the identification of these protons, and the proton assignments are shown in Figure 6B. It showed H-1, H-3, H-3', Hβa, and Hβb resonances within the region from 5.1 to 5.4 ppm. The signal for H-1 was downfield from that of H-1'. These are normal for lipid A (21, 22, 26). However, the H-6'a resonance appeared at 4.25 ppm, which is consistent with substitution of the 6'-O-position of MLA with a *t*-Boc-Cap group.

PDMS of Monomethyl-Cap-MLA. Preparative-TLC-purified Cap-MLA was methylated with diazomethane to

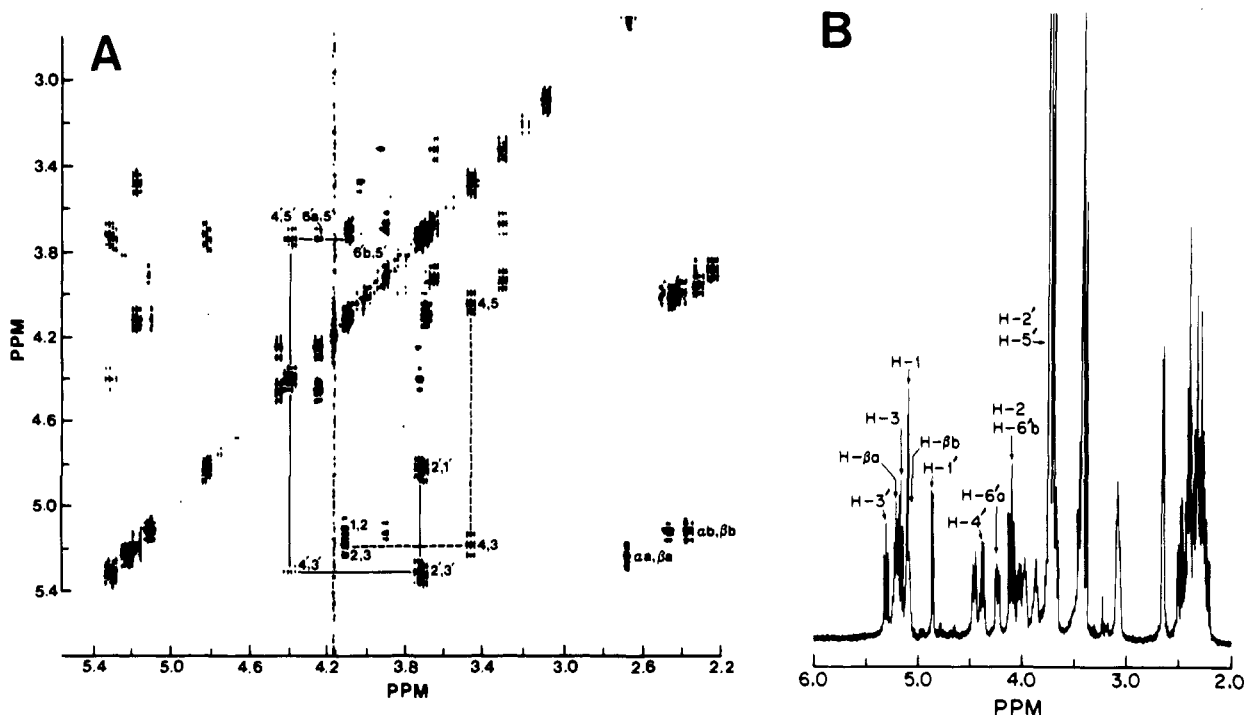


Figure 6. Two-dimensional proton correlation (COSY) spectrum (A) and partial proton NMR spectrum (B) at 500 MHz of the dimethyl-*t*-Boc-Cap-MLA (III-C) dissolved in $\text{CD}_3\text{Cl}/\text{CD}_3\text{OD}$ (8:1, v/v). Scalar coupling connectivities for the sugar ring systems are shown in panel A, with dashed lines for the reducing-end sugar and solid lines for the distal sugar. Cross peaks are also shown for the (acyloxy)acyl methylene groups ($\alpha\alpha$, $\beta\alpha$ and $\alpha\beta$, $\beta\beta$).

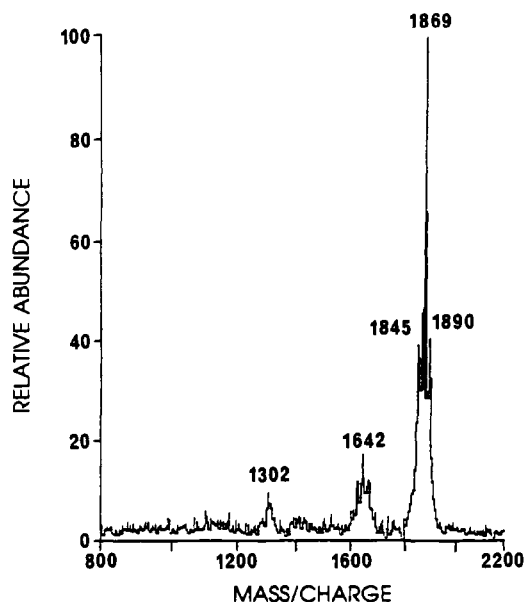


Figure 7. Partial plasma desorption mass spectrum of monomethyl-Cap-MLA.

form monomethyl-Cap-MLA,² purified by reverse-phase HPLC and analyzed by positive ion PDMS. The resulting spectrum in the high mass region showed peaks at 1845, 1869, and 1890 representing $M + H^+$, $M + Na^+$, and $M + 2Na^+ - H$, respectively (Figure 7). The calculated value for $M + Na^+$ is 1868.1 amu. The loss of the O-linked hydroxymyristoyl group at the 3-O-position of the MLA

² We were neither able to completely methylate the phosphate group in Cap-MLA with diazomethane nor achieve good separation of the structural components of the methyl ester by reverse-phase HPLC. This might be due to the neighboring free amino group. We have found that the phosphate group of the amino-protected *t*-Boc-Cap-MLA can be completely methylated and that this product is suitable for HPLC fractionation.

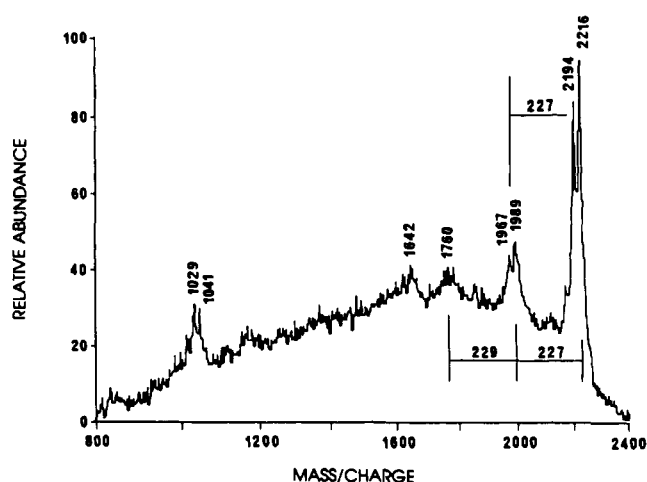


Figure 8. Plasma desorption mass spectrum of biotin conjugate of MLA.

moiety accompanied by H-transfer, leaving an OH group at that position, gave an ion at 1642. The ion at 1302 represented the result of a two-bond cleavage.³ These results, taken together with the structure of the precursor *t*-Boc-Cap-MLA, support the structure for Cap-MLA shown in Figure 4.

Mass Spectrometry of Biotin-(Cap)₂-MLA. PDMS (positive ion) of preparative TLC-purified biotin-(Cap)₂-MLA in the high-mass region gave pseudomolecular ions corresponding to $M + Na^+$ at 2194 and $[M + 2Na - H]^+$ at 2216 (Figure 8). These values yield a molecular weight estimated for the product of 2171, in agreement with the calculated average molecular weight for biotin-(Cap)₂-MLA. The major fragment ions (1967 and 1989) corresponded to loss of myristic acid (227 amu) from each of

³ Two-bond cleavages of the disaccharide backbone of lipid A are observed in LDMS (18) and in positive-ion PDMS (R. Wang and R. J. Cotter, unpublished results).

Table II. Recognition of Biotin-(Cap)₂-MLA Conjugate by Both Anti-Lipid A Antibodies and Streptavidin

probe	reciprocal ELISA titers ^a	
	MLA	biotin-(Cap) ₂ -MLA
streptavidin	<1 000 ^b	4 000 ^c
DS77	>1 024 000	512 000
DS35	1 024 000	256 000

^a Reciprocal of highest dilution which gave OD₄₉₀ > 0.1. ^b OD₄₉₀ = 0.010 at 1/1000 (lowest dilution tested). ^c OD₄₉₀ = 0.383 at 1/4000.

Table III. Mitogenic Activity of Lipid A Derivatives in Murine Splenocytes

test material	strain	stimulation index ^a			
		0.80 ^b	4.0	20	100
<i>E. coli</i> J5 LPS	C3H/HeSnJ	59	73	81	94
	C3H/HeJ	1.1	1.7	2.4	2.5
MLA	C3H/HeSnJ	14	28	45	42
	C3H/HeJ	1.3	1.7	2.5	2.8
Cap-MLA	C3H/HeSnJ	1.9	4.4	12	20
	C3H/HeJ	1.2	1.1	1.6	1.5
biotin-(Cap) ₂ -MLA	C3H/HeSnJ	3.5	3.7	9.5	27
	C3H/HeJ	1.5	1.5	1.8	2.8
biotin ^c	C3H/HeSnJ	1.6	2.2	2.6	1.9
	C3H/HeJ	1.3	1.3	1.2	1.0

^a Ratios of ³H counts in treated versus untreated splenocytes. Untreated splenocytes from C3H/HeSnJ mice had 1125 cpm, while those from C3H/HeJ mice had 517 cpm. ^b Treatment concentrations in μg/mL. ^c Biotin tested at 0.16, 0.8, 4, and 20 μg/mL, reflecting the approximate molar contents of biotin in the respective 0.8, 4, 20, and 100 μg/mL treatment groups for biotin-(Cap)₂-MLA.

the pseudomolecular ions. Loss of this fragment was also observed during PDMS of dimethyl-*t*-Boc-Cap-MLA. The spectrum was also examined in the low-mass region (110–600 amu) and it revealed the presence of ions for a biotin fragment at 143, biotin at 228, and biotin-(Cap)₂ + Na⁺ at 494 (data not shown). The presence of these fragmentation ions allowed us to verify the sequence order of biotin-Cap-Cap-MLA. These results are consistent with the structure for biotin-(Cap)₂-MLA shown in Figure 4.

FUNCTIONAL CHARACTERIZATION OF CAP-MLA AND DERIVATIVES

Binding of Streptavidin and Anti-Lipid A Antibodies to Biotin-(Cap)₂-MLA. Biotin-(Cap)₂-MLA should contain binding loci characteristic of both MLA and biotin. The data in Table II demonstrate that the conjugate was in fact recognized by monoclonal antibodies directed against lipid A (DS77 and DS35), and by streptavidin. On the other hand, unconjugated MLA bound the anti-lipid A antibodies but was not recognized by streptavidin. Monoclonal antibodies directed against non-lipid A epitopes did not react with either MLA or biotin-Cap₂-MLA (data not shown).

Mitogenic Activity of Cap-MLA and Biotin-(Cap)₂-MLA. MLA retains the ability of LPS to stimulate polyclonal proliferation of splenocytes from murine LPS-responder strains (27). The data in Table III demonstrate that attachment of a Cap moiety to the 6'-O-position of MLA attenuates but does not eliminate this activity. For example, MLA showed significant mitogenic activity at a concentration of 0.8 μg/mL (stimulation index 14), but it required 20 μg/mL of Cap-MLA to reach this level of activity (stimulation index = 12). Coupling a biotin-Cap group to Cap-MLA did not appear to further attenuate this mitogenic activity, as can be seen from the comparable stimulation indices attained with Cap-MLA and biotin-(Cap)₂-MLA at all concentrations tested. The activity observed with biotin-(Cap)₂-MLA was not attributable

Table IV. Effect of Polymixin B on Mitogenic Activity of LPS, MLA, Cap-MLA, and Biotin-(Cap)₂-MLA in Murine Splenocytes

treatment	treatment dose (μg/mL)	stimulation index ^a			
		0 ^b	80	400	2000
LPS	100	77	48	11.4	0.3
	20	72	18	6.3	0.3
	0.8	61	6.5	4.9	0.2
MLA	100	30	8.4	1.4	0.1
	20	31	13	1.8	0.2
	0.8	22	6.2	1.2	0.1
Cap-MLA	100	19	4.5	0.6	0.2
	20	13	2.9	0.7	0.3
	0.8	3.7	1.3	0.3	0.2
biotin-(Cap) ₂ -MLA	100	25	5.1	0.6	0.1
	20	10	3.2	0.4	0.1
	0.8	2.5	1.6	0.2	0.1

^a Ratios of ³H counts in treated versus untreated splenocytes. Untreated splenocytes from mice in the groups receiving LPS and MLA had 1650 cpm, while those in the groups receiving Cap-MLA and biotin-(Cap)₂-MLA had 1134 cpm. ^b Polymixin B concentrations, in μg/mL.

to the presence of biotin, since biotin itself did not exhibit significant activity at comparable molar concentrations (Table III).

Two lines of evidence suggest that the mitogenic activity observed with the Cap-MLA and biotin-(Cap)₂-MLA preparations was lipid A-related and not due to contaminating protein mitogens. First, as shown in Table III, these preparations were only slightly active in splenocytes obtained from C3H/HeJ (LPS-nonresponder) mice. For example, biotin-(Cap)₂-MLA at 100 μg/mL gave a stimulation index of 2.8 when tested in nonresponder cells, compared to a value of 27 in responder cells. All of the endotoxin-derived materials showed similar levels of activity in the nonresponder splenocytes. Second, data in Table IV show that the mitogenic activity of Cap-MLA and biotin-(Cap)₂-MLA was eliminated in a dose-responsive manner by addition of polymixin B. Both preparations were inactive even at 100 μg/mL in the presence of 400 μg/mL polymixin B. In comparison, both LPS and MLA retained some mitogenic activity in the presence of 400 μg/mL polymixin B, but were devoid of activity at 2000 μg/mL polymixin B. It should be noted that all of the materials exhibited stimulation indices well below 1.0 at the higher concentrations of polymixin B. This may reflect either residual endotoxin contamination of the fetal calf serum used during cell culture or toxicity of polymixin B toward these cells at higher concentrations.

Stimulation of TNF-α Release by Biotin-(Cap)₂-MLA. The ability of Biotin-(Cap)₂-MLA to induce release of TNF-α was evaluated in the RAW 264.7 cell line. Cells were cultured in the presence of varying concentrations of biotin-(Cap)₂-MLA for 8 and 20 h, and the supernatant fractions were evaluated for TNF-α content by ELISA. MLA and LPS were also tested for comparison. The data, summarized in Table V, show that biotin-(Cap)₂-MLA exhibited appreciable TNF-inducing activity in this cell line at concentrations as low as 1 μg/mL. MLA at 100 pg/mL was comparable to biotin-(Cap)₂-MLA at 1 μg/mL in terms of TNF-α-inducing activity. LPS was fully active even at 10 pg/mL, the lowest concentration tested. In this experiment, biotin-(Cap)₂-MLA at 10 μg/mL appeared to induce higher amounts of TNF-α than did either MLA or LPS at that concentration. A second experiment confirmed the induction of TNF by biotin-(Cap)₂-MLA at 1 and 10 μg/mL, although the levels were below those elicited by MLA and LPS (data not shown). All of the TNF-α-inducing activity of biotin-(Cap)₂-MLA at 10 μg/

Table V. Induction of TNF- α Release from RAW 264.7 Cells by LPS, MLA, and Biotin-(Cap)₂-MLA

sample	time ^a	TNF- α concentration ^c (ng/mL)			
		0.01 ^b	0.1	1.0	10.0
LPS	8	31	23	30	44
	20	26	26	22	26
MLA	8	1.5	12	34	45
	20	1.9	12	25	27
biotin-(Cap) ₂ -MLA	8	1.4	1.3	5.0	>48 ^d
	20	1.4	1.3	15	>31 ^d

^a Time (h) of exposure to stimulus. ^b Concentration (μ g/mL) of test substances in culture media. ^c Determined by ELISA assay. Values are corrected for TNF- α elicited in the absence of test materials. ^d These samples had $A_{490} > 2.8$, which was the maximum readable absorbance. Concentrations correspond to $A_{490} = 2.8$, after correction for the background levels of TNF- α present at 8 and 20 h, respectively.

mL was blocked in the presence of 200 or 1000 μ g/mL polymyxin B (data not shown).

DISCUSSION

Unprotected MLA was reacted with 6-(*t*-Boc-amino)caproic anhydride and the resulting product mixture was analyzed in some detail. It was found that greater than 90% of the material in the main product fraction (peaks III-B, -C, -D in Figure 2) was *t*-Boc-Cap-MLA substituted at the 6'-O-position (Table I). The remainder of pool III (peak III-A) was monosubstituted at a different position with the *t*-Boc-Cap moiety. No disubstituted species were observed in any of the analyzed materials. Pool III, obtained by reaction of unprotected MLA followed by a simple chromatographic procedure, therefore represented an overall yield of monoacylated product of about 70%.

The ease and selectivity with which the 6'-O-position of MLA reacted with 6-(*t*-Boc-amino)caproic anhydride was unexpected. The 4'-O-phosphate may play a role in predisposing the hydroxyl at the 6'-O-position to undergo reaction. Consistent with this possibility is the observation that blocking of the 4'-O-phosphate by methylation with diazomethane reduced greatly the rate of reaction of MLA with 6-(*t*-Boc-amino)caproic anhydride.⁴ A plausible mechanism for this participation involves initial reaction of 6-(*t*-Boc-amino)caproic anhydride with the 4'-O-phosphate, giving rise to a mixed anhydride which can then undergo nucleophilic substitution by the 6'-hydroxyl.

HPLC fractionation of the dimethyl-*t*-Boc-Cap-MLA resolved the mixture into three interesting fractions (Table I). The major fraction (III-C) contained 3-(myristoyloxy)myristate as R₁ and 3-(lauroyloxy)myristate as R₂, a minor fraction (III-B) contained 3-(lauroyloxy)myristate as both R₁ and R₂, and a trace fraction (III-D) contained 3-(myristoyloxy)myristate as both R₁ and R₂ in the structure of lipid A. These results showed that structural heterogeneity of the lipid A moiety of *E. coli* J5 LPS exists due to variation in the chain length of the normal fatty acids (within lauric and myristate only). This is consistent with recent data suggesting that the lauroyl transferase involved in lipid A biosynthesis can also catalyze myristoyl transfer (28). Structural determinations of lipid A that have assumed complete enzyme specificity may have to be reconsidered in light of these findings (29).

The usefulness of conjugates prepared from Cap-MLA depends on their ability to interact with biological systems in ways that are characteristic of unmodified MLA. In this study, MLA was compared with a prototypical conjugate, biotin-(Cap)₂-MLA, in several assays of bio-

logical recognition or activity. It was found that the activity of MLA in these assays was retained following conjugation via the 6'-O-position. For example, biotin-(Cap)₂-MLA was recognized by monoclonal antibodies specific for the nonreducing end of lipid A (Table I). This conjugate was also bound by streptavidin, indicating that the biotinyl domain was accessible. Both anti-lipid A antibodies showed a higher binding affinity for MLA than for biotin-Cap₂-MLA. In this regard, it has been observed that both DS77 and DS35 react equally well with diphospholipid A and MLA and less well with ReLPS.⁵ This suggests that substitution at the 6'-O-position of lipid A may partially obscure the epitope(s) recognized by these monoclonal antibodies, consistent with our results.

MLA, like LPS and diphosphoryl lipid A, is a potent mitogen for splenocytes from LPS-responder mice (27). Both Cap-MLA and biotin-Cap₂-MLA are active in this model, although less so than underivatized MLA. Cap-MLA was found also to be active in stimulating the 70Z/3 pre-B cell line, although again it was less active than MLA.⁶

Another biological activity characteristic of LPS and lipid A is the stimulation of TNF- α release from macrophages and macrophage-like cell lines (30). MLA has also been shown to induce the release of TNF- α in mice primed with *Listeria monocytogenes* or *Mycobacterium bovis* BCG (31, 32) and in the RAW 264.7 cell line.⁷ In the present study, biotin-Cap₂-MLA at 1.0 μ g/mL was able to induce release of TNF- α in the RAW 264.7 cell line. Unlike MLA, the conjugate did not show appreciable activity below 1.0 μ g/mL. The response elicited by biotin-Cap₂-MLA was blocked in the presence of polymyxin B. These data indicate that biotin-Cap₂-MLA retains at least some of the ability of MLA to interact with a macrophage cell line and to stimulate release of TNF- α .

The presence of between 1 and 5% unmodified MLA in Cap-MLA and biotin-Cap₂-MLA could account for the observed mitogenic and TNF- α -inducing activities of these materials. This does not seem likely, since (1) no unmodified MLA was detected by HPLC and MS in the peak III fraction of *t*-Boc-Cap-MLA that was used to prepare both Cap-MLA and biotin-Cap₂-MLA and (2) biotin-Cap₂-MLA was purified by preparative TLC prior to use, and no unmodified MLA was detected by TLC after this purification step (detection limit of 0.1–0.5%). Furthermore, in a separate series of experiments, binding of biotin-Cap₂-MLA to murine peritoneal exudate cells was observed directly using flow cytometry.⁸ This demonstrated that intact biotin-Cap₂-MLA is capable of interacting with murine macrophages.

The free amino group in Cap-MLA makes it possible to attach a wide range of amino-reactive materials to MLA via the 6'-O-position. Biotin-Cap₂-MLA is an example of a conjugate prepared via reaction of Cap-MLA with an *N*-hydroxysuccinimide ester. Such well-characterized lipid A derivatives, uniformly modified at a defined location, should have considerable utility in studies directed at identification, isolation, and characterization of lipid A binding structures.

ACKNOWLEDGMENT

PDMS and LDMS mass spectral determinations were carried out at the Middle Atlantic Mass Spectrometry Laboratory, a National Science Foundation Shared In-

⁴ K. R. Myers, unpublished results.

⁵ J. T. Ulrich, unpublished results.

⁶ T. N. Kirkland and K. Takayama, unpublished results.

⁷ J. T. Ulrich, unpublished results.

⁸ J. L. Cantrell, unpublished results.

strument Facility, The Johns Hopkins University School of Medicine. FAB-MS determinations were carried out by Dr. Joe Sears, director of the Mass Spectrometry Facility housed in the Department of Chemistry at Montana State University. Nuclear magnetic resonance services were provided by the staff of the National Magnetic Resonance Facility, Department of Biochemistry, University of Wisconsin—Madison, which is supported in part by NIH Grant RR02301 from the Biomedical Research Technology Program, Division of Research Resources. Equipment in the facility was purchased with funds from the University of Wisconsin, the NSF Biological Instrumentation Program (Grant PCM-8415048), the NIH Biomedical Research Technology Program (Grant RR-02031), the NIH Shared Instrumentation Program (Grant RR02781), and the U.S. Department of Agriculture. We thank Dr. Frank Robey for performing the amino acid and amino sugar analyses, and Mr. Mark Livesay for preparation of the structure figures. This work was supported by Ribi ImmunoChem Research, Inc., Veterans Administration Medical Research Service, National Science Foundation Grants CHE 84-10506 and BBS 85-15390, and National Institutes of Health Grant GM-36054.

LITERATURE CITED

- Morrison, D. C., and Ryan, J. L. (1987) Endotoxins and disease mechanisms. *Ann. Rev. Med.* 38, 417-432.
- Engelhardt, R., Mackensen, A., Galanos, C., and Andreesen, R. (1990) Biological response to intravenously administered endotoxin in patients with advanced cancer. *J. Biol. Resp. Mod.* 9, 480-491.
- Galanos, C., Lüderitz, O., Rietschel, E. Th., Westphal, O., Brade, H., Brade, L., Freudenberg, M., Schade, U., Imoto, M., Yoshimura, H., Kusumoto, S., and Shiba, T. (1985) Synthetic and natural *Escherichia coli* free lipid A express identical endotoxic activities. *Eur. J. Biochem.* 148, 1-5.
- Haeflner-Cavaillon, N., Caroff, M., and Cavaillon, J.-M. (1989) Interleukin-1 induction by lipopolysaccharides: Structural requirements of the 3-deoxy-D-manno-2-octulosonic acid (KDO). *Mol. Immunol.* 26, 485-494.
- Morrison, D. C. (1989) The case for specific lipopolysaccharide receptors expressed on mammalian cells. *Microb. Pathog.* 7, 389-398.
- Wollenweber, H.-W., and Morrison, D. C. (1985) Synthesis and biochemical characterization of a photoactivatable, iodinated, cleavable bacterial lipopolysaccharide derivative. *J. Biol. Chem.* 260, 5068-5074.
- Lei, M.-G., and Morrison, D. C. (1988) Specific endotoxic lipopolysaccharide-binding proteins on murine splenocytes. I. Detection of lipopolysaccharide-binding sites on splenocytes and splenocyte subpopulations. *J. Immunol.* 141, 996-1005.
- Kirkland, T. N., Virca, G. D., Kuus-Reichel, T., Multer, F. K., Kim, S. Y., Ulevitch, R. J., and Tobias, P. S. (1990) Identification of lipopolysaccharide-binding proteins in 70Z/3 cells by photoaffinity cross-linking. *J. Biol. Chem.* 265, 9520-9525.
- Rietschel, E. Th., Wollenweber, H.-W., Russa, R., Brade, H., and Zähringer, U. (1984) Concepts of the chemical structure of lipid A. *Rev. Infect. Dis.* 6, 432-438.
- Rietschel, E. Th., Brade, L., Holst, O., Kulshin, V. A., Lindner, B., Moran, A. P., Schade, U. F., Zähringer, U., and Brade, H. (1990) Molecular structure of bacterial endotoxin in relation to bioactivity. *Endotoxin Research Series* (Nowotny, A., Spitzer, J. J., and Ziegler, E. J., Eds.) Vol. 1, pp 15-32, Elsevier Science Publishers B.V., The Netherlands.
- Jiao, B., Freudenberg, M., and Galanos, C. (1989) Characterization of the lipid A component of genuine smooth-form lipopolysaccharide. *Eur. J. Biochem.* 180, 515-518.
- Bartlett, G. R. (1959) Phosphorus assay in column chromatography. *J. Biol. Chem.* 234, 466-468.
- Ghuysen, J.-M., and Strominger, J. L. (1963) Structure of the Cell Wall of *Staphylococcus aureus*, strain Copenhagen. I. Preparation of Fragments by Enzymatic Hydrolysis. *Biochemistry* 2, 1110-1119.
- Galanos, C., Lüderitz, O., and Westphal, O. (1969) A new method for the extraction of R lipopolysaccharides. *Eur. J. Biochem.* 9, 245-249.
- Qureshi, N., Takayama, K., Heller, D., and Fenselau, C. (1983) Position of ester groups in the lipid A backbone of lipopolysaccharides obtained from *Salmonella typhimurium*. *J. Biol. Chem.* 258, 12947-12951.
- Paleveda, W. J., Holly, F. W., and Veber, D. F. (1984) Tert-butoxycarbonyl-L-phenylalanine (L-phenylalanine, N[(1,1-dimethylethoxy)carbonyl]-). *Org. Synth.* 63, 171-174.
- Takayama, K., Qureshi, N., Hyver, K., Honovich, J., Cotter, R. J., Mascagni, P., and Schneider, H. (1986) Characterization of a structural series of lipid A obtained from the lipopolysaccharides of *Neisseria gonorrhoeae*. *J. Biol. Chem.* 261, 10624-10631.
- Cotter, R. J., Honovich, J., Qureshi, N., and Takayama, K. (1987) Structural determination of lipid A from Gram negative bacteria using laser desorption mass spectrometry. *Biomed. Environ. Mass Spectrom.* 14, 591-598.
- Alai, M., Demirev, P., Fenselau, C., and Cotter, R. J. (1986) Glutathione as a matrix for plasma desorption mass spectrometry of large peptides. *Anal. Chem.* 58, 1303-1307.
- Qureshi, N., Cotter, R. J., and Takayama, K. (1986) Application of fast atom bombardment mass spectrometry and nuclear magnetic resonance on the structural analysis of purified lipid A. *J. Microbiol. Methods* 5, 65-77.
- Takayama, K., Qureshi, N., and Mascagni, P. (1983) Complete structure of lipid A obtained from the lipopolysaccharides of the heptoseless mutant of *Salmonella typhimurium*. *J. Biol. Chem.* 258, 12801-12803.
- Qureshi, N., Mascagni, P., Ribi, E., and Takayama, K. (1985) Monophosphoryl lipid A obtained from lipopolysaccharides of *Salmonella minnesota* R595. *J. Biol. Chem.* 260, 5271-5278.
- Smith, R. A., and Ulrich, J. T. (1983) Enzyme-linked immunosorbent assay for quantitative detection of *Bacillus thuringiensis* crystal protein. *Appl. Environ. Microbiol.* 45, 586-590.
- Oppenheim, J. J., and Rosenstreich, D. L. (1976) Lymphocyte transformation: Utilization of automatic harvesters. In *Vitro Methods in Cell Mediated and Tumor Immunity* (Bloom, B. R., and David, J. R., Eds.) pp 573-585, Academic Press, New York.
- Virca, G. D., Kim, S. Y., Glaser, K. B., and Ulevitch, R. J. (1989) Lipopolysaccharide induces hyporesponsiveness to its own action in RAW 264.7 cells. *J. Biol. Chem.* 264, 21951-21956.
- Strain, S. M., Armitage, I. M., Anderson, L., Takayama, K., Qureshi, N., and Raetz, C. R. H. (1985) Location of polar substituents and fatty acyl chains on lipid A precursors from a 3-deoxy-D-manno-octulosonic acid-deficient mutant of *Salmonella typhimurium*. *J. Biol. Chem.* 260, 16089-16098.
- Ribi, E., Cantrell, J. L., Takayama, K., Qureshi, N., Peterson, J., and Ribi, H. O. (1984) Lipid A and immunotherapy. *Rev. Infect. Dis.* 6, 567-572.
- Brozek, K. A., and Raetz, C. R. H. (1990) Biosynthesis of lipid A in *Escherichia coli*. *J. Biol. Chem.* 265, 15410-15417.
- Johnson, R. S., Her, G.-R., Grabarek, J., Hawiger, J., and Reinhold, V. N. (1990) Structural characterization of monophosphoryl lipid A homologs obtained from *Salmonella minnesota* Re595 lipopolysaccharide. *J. Biol. Chem.* 265, 8108-8116.
- Beutler, B., Greenwald, D., Hulmes, J. D., Chang, M., Pan, Y.-C. E., Mathison, J., Ulevitch, R., and Cerami, A. (1985) Identity of tumour necrosis factor and the macrophage-secreted factor cachectin. *Nature* 316, 552-554.
- Kiener, P. A., Marek, F., Rodgers, G., Lin, P.-F., Warr, G., and Desiderio, J. (1988) Induction of tumor necrosis factor, IFN- γ , and acute lethality in mice by toxic and non-toxic forms of lipid A. *J. Immunol.* 141, 870-874.
- Bennett, J. A., Peters, J. H., Chudacoff, R., and McKneally, M. F. (1988) Endogenous production of cytotoxic factors in serum of BCG-primed mice by monophosphoryl lipid A, a detoxified form of endotoxin. *J. Biol. Response Modif.* 7, 65-76.

Determination of Immunoreactivity of Doxorubicin Antibody Immunoconjugates by a Le^y Competitive RIA

Huiru Zhao,* David Willner, Jeffrey S. Cleaveland, Gary R. Braslawsky, and Joseph P. Brown

Bristol-Myers Squibb Company, Pharmaceutical Research Institute, Wallingford, Connecticut 06492. Received August 11, 1992

Many monoclonal antibody-drug immunoconjugates have been evaluated for their ability to deliver cytotoxic drugs to tumors. It is essential to establish that the ability of the conjugates to bind antigen, i.e. their immunoreactivity, is not adversely affected by the drug conjugation procedure. We have described herein a measurement of the immunoreactivity of BR96-DOX, a conjugate comprised of BR96, a chimeric monoclonal antibody specific for the Le^y tetrasaccharide commonly expressed on human carcinomas, and doxorubicin, an anticancer agent in widespread clinical use. We have employed a competitive RIA, in which microtiter wells were coated with synthetic Le^y conjugated to human serum albumin and then incubated with ¹²⁵I-labeled antibody BR96 in the presence of test conjugate or intact BR96 mAb. The test conjugates were found to compete as effectively as unconjugated BR96. This assay is highly applicable to QC processes with the intra-assay CV = 2.0% and the interassay CV = 4.3%.

Doxorubicin (DOX¹)-monoclonal antibody conjugates have been developed to increase a drug's specificity and selectivity to tumor cells and to decrease its toxicity, particularly its dose-limiting cardiac toxicity and myelosuppression (1-5). In these targeted delivery systems, DOX was coupled to monoclonal antibodies (mAbs) with an acid-labile hydrazone linker. In general, effective cancer chemotherapy utilizing antibody-drug conjugates requires that the mAbs transport DOX in an antigen-specific manner. Once bound to tumor cells the conjugate is internalized and free DOX is released from lysosomes to function as a DNA alkylator (6, 7). In our study, chimeric BR96 mAb was selected as a drug carrier for the following features: high tumor reactivity, rapid internalization, and direct cytotoxicity on antigen-positive tumor cells as well as mediation of ADCC and CDC (8). Preliminary studies have indicated that at least a portion of the epitope recognized by BR96 is a Le^y carbohydrate chain (8). Animal studies have established that BR64-DOX immunoconjugates, in which BR64 binds the same antigen as BR96, kill tumor cells in an antigen-specific manner *in vitro* and *in vivo* against human breast, colon, lung tumor xenograft (9). All those results imply that BR96-DOX immunoconjugates have the potential to be clinically effective antineoplastic drugs in tumor chemotherapy.

Antibodies may undergo structural changes after conjugation and this may affect their binding characteristics and their efficacy as selective carrier vehicles (10). In most circumstances, the more drug molecules that were directly coupled to a mAb via amide or ester bonds, the lower the immunoreactivity (binding avidity) of the conjugate (11). Therefore, our major concern is to determine the immunoreactivity of the drug-modified BR96 mAb as compared to that of intact BR96 mAb.

Furthermore, there is substantial need for a precise assay to probe structural variations and binding avidities in the conjugates.

In this study, a 96-well microtiter plate was coated with synthetic Le^y conjugated to human serum albumin. This plate was then incubated with ¹²⁵I-labeled antibody BR96 in the presence of test conjugates or standard BR96 to evaluate BR96-DOX immunoconjugates. Moreover, a comparative study has also been carried out with fluorescence-activated cell sorter on MCF₇ cells. There is a 10% difference in the binding avidity between these two assays. However, the ease, speed, and reproducibility of microtiter-based assay overcome some of the drawbacks which occur in cell-based immunoassays such as their manipulative inconvenience and widely variant results.

EXPERIMENTAL PROCEDURES

Materials. HSA-Le^y antigen was purchased from ChemBiomed, Alberta, Canada. The 96-well microtiter plates (Immulon-2) were purchased from Dynatech Laboratory Inc., Chantilly, VA; BSA, EDTA, Tris, and sucrose were from Sigma Chemical Co., St. Louis, MO; Dulbecco's phosphate-buffered saline (D-PBS, 1X) was from GIBCO Laboratories, Grand Island, NY; sodium carbonate was from EM Science, Gibbstown, NJ; Tween-20 was from Bio-Rad, Richmond, CA; and chimeric BR96 mAb (IgG1) was obtained from Bristol-Myers Squibb Biotechnology Purification Pilot Plant, Syracuse, NY. FITC-labeled goat anti-human Ig κ chains F(ab)₂ was purchased from Boehringer Mannheim Corp., Indianapolis, IN. All other reagents were purchased from Fisher Scientific, Springfield, NJ.

Equipment. A Waters (Milford, MA) HPLC system, equipped with a 600 E system controller, 490E programmable multiwavelength detector, 700 Satellite WISP autosampler, and Maxima 820 computer-controlled data processor was employed for analytical study. A Supelco 7.8 × 300 mm size-exclusion HPLC column (Rohm and Haas Co.), a Progel-TSK G3000 SWXL column, and a guard column of the same type of packing (6.0 × 40.0 mm) were used for determining the quality of the immunoconjugates.

* Author to whom correspondence should be addressed.

¹ Abbreviations used: DOX, doxorubicin; BR96 mAb, chimeric BR96 monoclonal antibody; ADCC, antigen-dependent cellular cytotoxicity; CDC, complement-dependent cytotoxicity; BR96-DOX, doxorubicin-BR96 antibody immunoconjugates; RIA, radioimmunoassay; D-PBS, Dulbecco's phosphate-buffered saline; HSA, human serum albumin; Le^y, Lewis^y hapten; FBS, fetal bovine serum; FITC, fluorescein isothiocyanate.

Immobilization of Le^y Antigen Plates. The 96-well microtiter plates were coated by treatment with 100 μ L of Le^y antigen at a concentration of 15–20 μ g/mL in 0.1 M sodium bicarbonate/carbonate buffer (pH 9.0) for 16–20 h at 4 °C. The antigen-coated plates were then blocked with 200 μ L of 2% BSA/1 mM EDTA/5% sucrose in Tris buffer (pH 7.2) and were incubated at ambient temperature for 2 h. The blocked plates were dried on absorbent paper and stored desiccated at 4 °C for subsequent use.

Selection of Optimal Conditions for Competitive RIA. Microtiter plates were coated with 100 μ L of a serial dilution of Le^y antigen solution in 0.1 M bicarbonate/carbonate buffer, pH 9.0, at concentrations of 3.12, 6.25, 12.5, 25.00, 50.00, and 100.00 μ g/mL. 2% BSA and D-PBS buffer were used as controls. The plates were immobilized and dried as described above. Each point was measured in quadruplicate.

To wells containing the same concentration of Le^y antigen, four series of ¹²⁵I-labeled chimeric BR96 mAb at 1.3, 2.6, 6.6, and 13.0 μ g/mL in 2% BSA phosphate buffer were added. ¹²⁵I-labeled BR96 mAb was prepared by the chloramine-T method (12) with a specific activity of 6.3 mCi/mg. The plates were sealed and incubated at 37 °C for 2 h. Plates were then washed four times with 0.05% Tween-20/PBS and dried on absorbent paper at ambient temperature. To each well was added 1 M sodium hydroxide. The solution in each well was then transferred into individual scintillation tubes. ¹²⁵I counts bound per well (cpm) were recorded on a LKB gamma counter and a correction was made for nonspecific binding.

From the above experiment, optimum concentration for ¹²⁵I-labeled BR96 mAb was selected as 5 μ g/mL. Several different parameters were selected to search for the optimum conditions for the binding study. Among these, two densities of Le^y antigen at concentrations of 10 and 2.5 μ g/mL were chosen, and two competition reaction periods of 2 and 3 h at 37 °C were adopted. The standard unmodified chimeric BR96 mAb was diluted 2-fold serially with 1% BSA/PBS to concentrations of 200, 100, 50, 25, 12.5, and 3.12 μ g/mL. The above standard mAb solution was mixed with an equal volume of ¹²⁵I-labeled BR96 mAb and was added to the immobilized Le^y antigen plates. The plates were sealed and incubated at 37 °C for 2 or 3 h. The repetitive sequences were carried out as described above.

Competitive RIA for the Evaluation of BR96–DOX Immunoconjugates. Based on the competitive RIA studies described above, optimum concentrations for Le^y antigen and ¹²⁵I-BR96 mAb were selected as 10 and 5 μ g/mL, respectively. The competitive reaction period was selected as 2 hours. Antibody conjugates with a drug load of between 6 and 8 mol of DOX and standard unmodified chimeric BR96 mAb were diluted 2-fold serially with 1% BSA/PBS to concentrations of 200, 100, 50, 25, 12.5, and 6.25 μ g/mL. The immunoreactivities were determined as described above.

All assays were performed in duplicate or triplicate. Additional controls were used to determine the maximal cpm bound as well as the specificity of binding by using 1% BSA in PBS, and polyclonal human IgG–DOX and free DOX in 1% BSA phosphate buffer, respectively. The percent avidity was determined as the concentration of BR96 mAb at 50% bound (IC_{50}) divided by the concentration of the conjugate at 50% bound.

The purity of the BR96–DOX immunoconjugates was analyzed on a Progel-TSK G3000 SWXL HPLC column (7.8 \times 300 mm) with a guard column (6.0 \times 40.0 mm) of the same type of packing. The eluant for the HPLC system was 50 mM phosphate buffer. A series of molecular weight

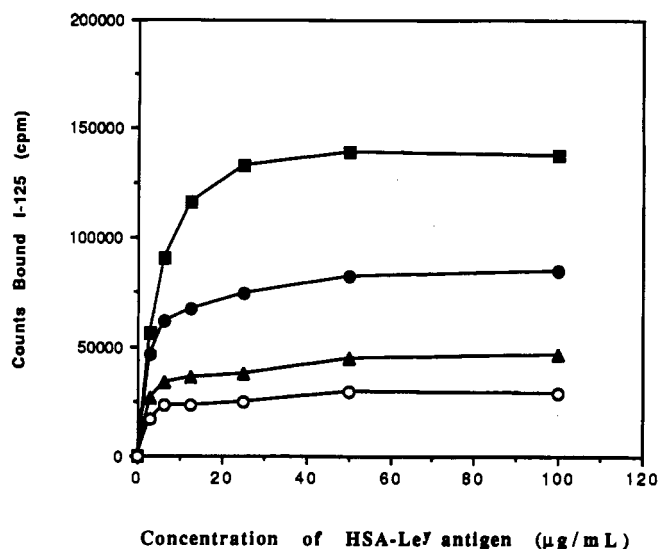


Figure 1. Direct binding RIA with a serial dilution of HSA–Le^y antigen on Immulon-2 microtiter plates. At each concentration of antigen, ¹²⁵I-BR96 mAb was selected at concentrations (μ g/mL) of 1.3 (○), 2.6 (▲), 6.6 (●), and 13.0 (■).

standards were used to calibrate the HPLC column. The peaks were monitored at two wavelengths, 220 and 495 nm, at which only DOX has absorbance. The peak heights or areas of the aggregates and the monomeric conjugates were measured which had absorbance at both 220 and 495 nm. There was less than 5% aggregates in the synthesized conjugates.

The concentration of BR96 mAb in BR96–DOX conjugates was calculated spectrophotometrically at two wavelengths, 280 and 495 nm (5). The amount of conjugated DOX in antibody was determined by absorbance at 495 nm ($\epsilon_{495} = 8030$). To correct for the overlap of DOX absorbance at 280 nm, the following equation was used:

$$\text{mAb (mg/mL)} = [A_{280} - (0.72 \times A_{495})]/1.4$$

Determination of Immunoreactivities of BR96–DOX on MCF₇ Cells by FACS. Assays were performed by fluorescence as previously described (20). Briefly, target cells were harvested in the logarithmic phase using EDTA in calcium- and magnesium-free PBS. The cells were washed twice in PBS containing 1% bovine serum albumin and resuspended to 1×10^7 /mL in PBS containing 1% BSA. Cells (0.05 mL) were mixed with standard BR96 mAb, BR96–DOX with a drug load of 6.9, and nonbinding human IgG at concentrations of 66, 33, 6.66, 3.33, 0.66, 0.33, and 0.066 nM. The cells were then incubated for 45 min at 4 °C. The cells were washed two times in 1% FBS/PBS buffer and resuspended in 0.1 mL of an appropriate concentration of FITC-labeled goat anti-human IgG κ chains F(ab)₂. Cells were incubated for 45 min, washed two times, and kept on ice until analyzed on a Coulter EPICS 753 fluorescence-activated cell sorter. Data are expressed as the mean channel number of specific versus control antibody.

RESULTS

Selection of the Optimum Conditions in the Competitive RIA. The standard curve of direct binding ¹²⁵I-BR96 mAb to HSA–Le^y antigen on microtiter plates is shown in Figure 1. There was no significant increase of counts bound at antigen excess with antibody concentrations above 6.6 μ g/mL. As compared by assays at different antigen densities in immobilization, a Le^y antigen

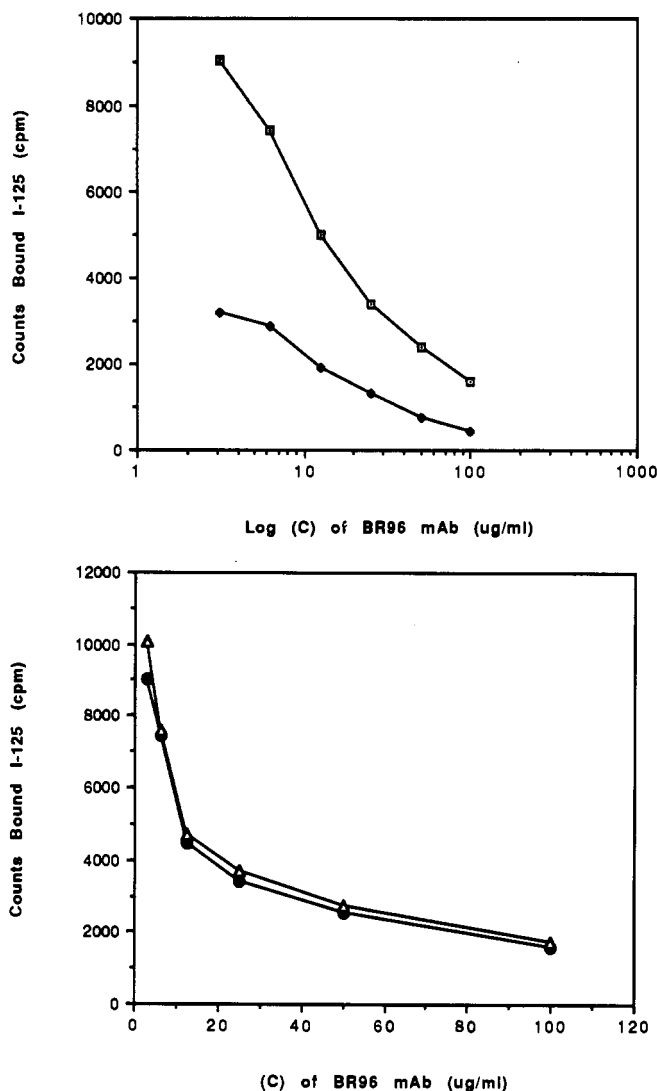


Figure 2. (a) Competitive RIA for standard BR96 mAb with HSA-Le^y antigen in plate at concentrations of 10 µg/mL (□) and 2.5 µg/mL (◇). The ¹²⁵I-BR96 concentration was 5 µg/mL. (b) Competitive RIA for standard BR96 mAb at HSA-Le^y antigen in plate (10 µg/mL) with an immunoreaction period of 2 h (●) and 3 h (▲). The rest parameters were same as above. The X-axis represents the concentration of competing BR96 mAb while the Y-axis represents percent the counts bound of ¹²⁵I-BR96 mAb.

concentration of 10 µg/mL would provide more information content (Figure 2a). Thus, the Le^y antigen concentration for immobilization was selected as 10 µg/mL, and the labeled antibody concentration as 5 µg/mL. From Figure 2b, we see that equilibrium for the competition reaction has been reached at 2 h. There is no significant difference in results between 2 and 3 h. Therefore, 2-h incubation at 37 °C was selected for the following RIA.

Assay Sensitivity and Reproducibility. As observed in the competitive assay for BR96 mAb (Figure 2a), the standard dilutions ranged from 6.25 to 100 µg/mL. The curve was linear between 10 and 30 µg/mL on the log plot and this portion of the plot can be utilized for more quantitative determination of immunoconjugates. The sensitivity of this assay is as low as 3 µg/mL. The intra-assay coefficient of variation (cpm) was 2.0%, and the interassay coefficient of variation was 4.3%. The titer of the assay is 10⁴ at an antigen concentration of 10 µg/mL. The titer of the assay will increase as the concentration of antigen goes up in the plate.

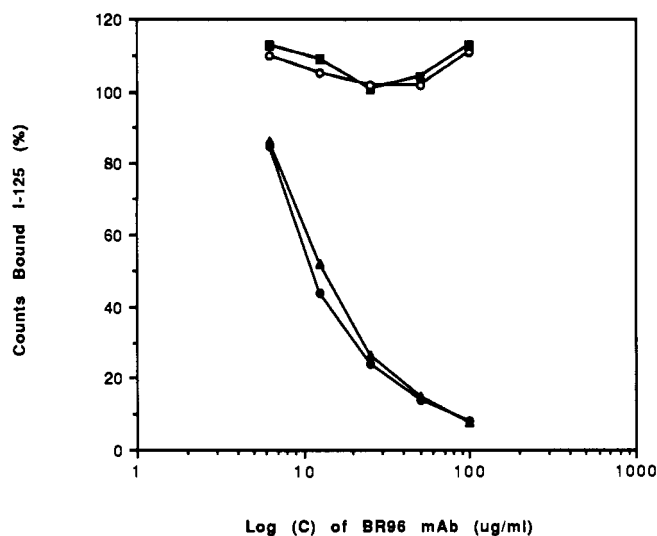


Figure 3. Competitive RIA for standard BR96 mAb (●), human IgG-DOX (drug load = 8.2) (■), BR96-DOX (drug load = 7.8) (▲), and free DOX (○) under the same conditions as in Figure 2b with a 2-h reaction period.

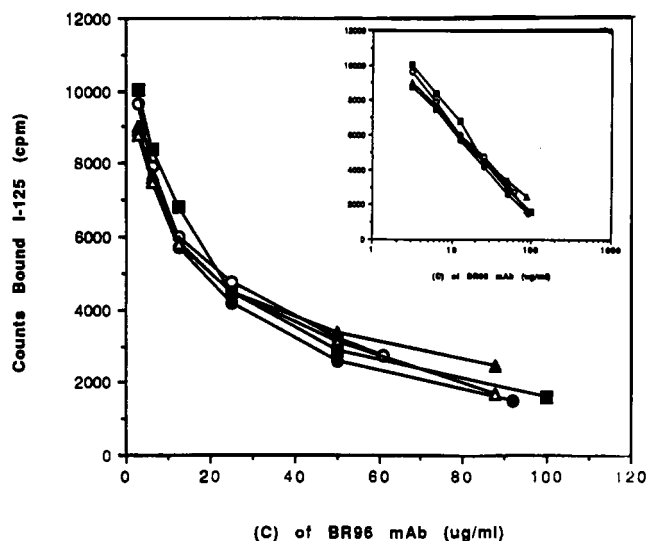


Figure 4. Determination of immunoreactivities of BR96-DOX immunoconjugates by competitive RIA under the same conditions as described previously. ● represents BR96 mAb. Drug loads in BR96-DOX are 6.9 (▲), 7.0 (○), 7.7 (■), and 8.0 (△). The log-scale plot is inset.

Antibody Specificity. The competitive RIA for intact and modified BR96 mAb is displayed in Figure 3. The human polyclonal antibody IgG-DOX was selected as a negative control as also was free DOX. Le^y antigen, which is the tumor-cell-associated antigen (13), competes with BR96 mAb and modified BR96 conjugate (drug load = 8.0). The binding affinity constant of BR96 mAb to Le^y antigen is in the range of 10⁻⁶–10⁻⁷ M, which corresponds to the same level as that of BR96 mAb to H3396 breast adenocarcinoma line (8).

Competitive RIA Evaluation of BR96-DOX Immunoconjugates. The binding curve for modified BR96 mAb conjugates with a doxorubicin load of 6–8 mol/mol of antibody is shown in Figure 4. The percent avidities were determined as the concentration of control (BR96) at 50% bound divided by the concentration of the conjugate at 50% bound. These results are shown in Table I. The IC₅₀ values for both unmodified BR96 and BR96-DOX were obtained from the log scale regression of experimental data by using the Cricket graph program.

Table I. Binding Avidities of BR96-DOX Immunoconjugates with Drug Loads of 6–8 mol/mol of mAb^a

BR96-DOX drug load	IC ₅₀ values (μg/mL)	binding avidity (%)	BR96-DOX drug load	IC ₅₀ values (μg/mL)	binding avidity (%)
6.9	16.2	80	7.7	13.1	98
7.0	14.0	92	8.0	14.3	90

^a These data were calculated from a regression of the experimental data (in log scale) of Figure 4 by using the Cricket graph program.

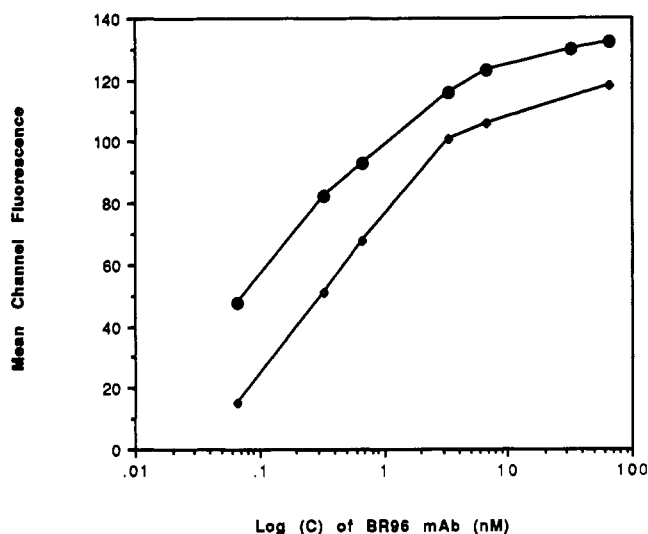


Figure 5. FACS profile for BR96 mAb (●) and BR96-DOX with a drug load of 6.9 (◊) on MCF₇ cells. The X-axis represents the concentration of mAb on a log scale (nM) while the Y-axis represents the mean channel fluorescence.

Table II. Determination of Immunoreactivity of BR96-DOX with a Drug Load of 6.9 with Comparison of Competitive RIA and FACS

	IC ₅₀ (μg/mL)	binding avidity (%)
RIA	16.2	80
FACS	0.38	71

Comparative Study of Two Assays in Determination of the Immunoreactivity of BR96-DOX. The binding profile of BR96-DOX on MCF₇ cells by FACS is shown in Figure 5. In this assay the binding avidity was expressed as the concentration of the conjugate at 50% bound divided by the concentration of BR96 mAb at 50% bound. The binding avidities of BR96-DOX were determined and found to be 71% in the FACS assay. Whereas in competitive RIA the binding avidity for BR96-DOX (drug load = 6.9) was 80%. There was about 10% difference between these two assays. The comparative data are listed in Table II.

DISCUSSION

BR96 monoclonal antibody is specific for Le^y antigen, which is highly expressed in tumor-associated cells. BR96 and its immunoconjugates might be expected to be more potent and more effective cancer chemotherapeutics. The assay established here is based on the interaction of BR96 mAb with Le^y antigen. As observed in Figure 1, HSA-Le^y antigen has high binding affinity to BR96 mAb at 10⁻⁷ M. This antigen is also readily immobilized onto Immulon-2 microtiter plates through hydrophobic interaction. Data derived from sucrose-coated aged plates (2 weeks old) stored desiccated at 4 °C was consistent with that obtained with freshly prepared plates. The antigen plates can stay desiccated for 1 month without losing potency. The

reported procedure for binding antigen and blocking nonspecific binding was a minor modification of a previous immobilization protocol employed in our laboratory; i.e., the antigen plates were blocked with 2% BSA, washed with 0.05% Tween-20, and dried on absorbent paper for immediate use. Our present blocking technique is described in the Experimental Procedures section. Results from both protocols are in agreement, allowing for preparation of large numbers of antigen-coated 96-well plates.

The data in Figure 3 indicate that Le^y antigen specifically competes with BR96 mAb and its modified conjugates. Le^y antigen was expressed at higher levels in tumor-associated cells (such as MCF₇ cells and RCA cells) even though it is also present to a lesser degree in many other tissues in the form of glycolipid and glycoproteins derivatives (16, 17). The binding affinity between Le^y antigen and human IgG-DOX is very low as evidenced by the noncompetitive nature of IgG-DOX conjugates in this assay. Also, free DOX, which might be generated during storage, did not interfere with this assay. Therefore, this assay provides a generic protocol for the determination of the immunoreactivity of BR96 mAb conjugates including drug-antibody conjugates, immunotoxin conjugates, and radionuclides conjugates.

Other considerations in assay development include both time and economic efficiency. The traditional cell-based immunoassay (11) requires at least one entire day for the analysis of one or two conjugates and large numbers of cells are required for five or six samples. The microtiter-based RIA reported here is efficient and allows for higher throughput. It requires about 4–5 h to evaluate approximately six samples with potential for the evaluation of many more. Thus this assay allows for the efficient evaluation of many more samples in less time than previous methodologies.

Most of the synthetic immunoconjugates have preserved reasonable binding avidity as displayed in Table I. Higher loads of drug up to 8.0 mol/antibody do not structurally alter the antibody binding avidity. This implies that doxorubicin would not be conjugated to the antigenic binding sites (V_H region) of the antibody.

It is very interesting to notice that there is some difference in the binding avidity between competitive RIA and FACS in assessment of BR96-DOX immunoconjugates. FACS assay is based on direct binding mAb on the target MCF₇ cells, in which the Le^y antigen was expressed at higher density. The binding ability to the cells was detected by the second antibody, F(ab)₂-FITC. Whereas in competitive RIA, the labeled antibody and test conjugates competed for the excess amount of purified Le^y antigen. The data from these assays were all acceptable as evidenced by antigen-specific cell killing in vitro for this batch of the immunoconjugate (unpublished results). Thus, BR96-DOX with a drug load of 6.9 has relatively preservable immunoreactivity. With respect to speed, simplicity, and replicability, the competitive RIA is more suitable as a quality control process.

ACKNOWLEDGMENT

The authors wish to express appreciation to Dr. Ned Heindel, Lehigh University, for revising the manuscript.

LITERATURE CITED

- (1) Kaneko, T., Willner, D., Monkovic, I., Knipe, J. O., Braslawsky, G. R., Greenfield, R. S., and Vyas, D. M. (1991) New hydrazone derivatives of adriamycin and their immunocon-

- jugates—A correlation between acid stability and cytotoxicity. *Bioconjugate Chem.* 2, 133–144.
- (2) Yang, H. M., and Reisfeld, R. A. (1988) Doxorubicin conjugated with a monoclonal antibody directed to a human melanoma-associated proteoglycan suppresses the growth of established tumor xenografts in nude mice. *Proc. Natl. Acad. Sci. U.S.A.* 85, 1189–1193.
- (3) Dillman, R. O., Jojnsen, D. E., Shawler, D. L., and Koziol, J. A. (1988) Superiority of an acid-labile daunorubicin-monoconjugate compared to free drug. *Cancer Res.* 48, 6097–6102.
- (4) Braslawsky, G. R., Edson, M. A., Pearce, W., Kaneko, T., and Greenfield, R. (1990) Antitumor activity of adriamycin (hydrazone-linked) immunoconjugates compared with free adriamycin and specificity of tumor cell killing. *Cancer Res.* 50, 6608–6614.
- (5) Greenfield, R., Kaneko, T., Daves, A., Edson, M. A., Frtzgerald, K. A., Olech, L. J., Grattan, J. A., Spitalny, G. L., and Braslawsky, G. R. (1990) Evaluation in vitro of adriamycin immunoconjugates synthesized using an acid-sensitive hydrazone linker. *Cancer Res.* 50, 6600–6607.
- (6) deDuve, C. (1983) Lysosome revisited. *Eur. J. Biochem.* 137, 391–397.
- (7) Pastan, I. H., and Willingham, M. C. (1985) Pathway of Endocytosis. In *Endocytosis* (I. H. Pastan, and M. C. Willingham, Eds.) pp 1–44, Plenum Publishing Corp., New York.
- (8) Hellstrom, I., Garrigues, H. J., Garrigues, U., and Hellstrom, K. E. (1990) Highly tumor-reactive, internalizing, mouse monoclonal antibodies to Le^v-related cell surface antigens. *Cancer Res.* 50, 2183–2190.
- (9) Trail, P. A., Willner, D., Lasch, S. J., Henderson, A. J., Greenfield, R. S., King, D., Zoeckler, M. E., and Braslawsky, G. R. (1992) Antigen-specific activity of carcinoma reactive BR64-Adriamycin conjugates evaluated in vitro and in human tumor xenograft models. *Cancer Res.* In press.
- (10) Tyle, P., and Ram, B. P. (1990) *Targeted Therapeutic System* (P. Tyle and B. P. Ram, Eds.) pp 9–10, Marcel Dekker, Inc., New York.
- (11) Pierce, D. L., Heindel, N. D., Schray, K. J., Jetter, M. M., Emrich, J. G., and Woo, D. V. (1990) Misonidazole conjugates of the colorectal tumor associated monoclonal 17-1A. *Bioconjugate Chem.* 1, 314–318.
- (12) Hunter, R. M., and Greenwood, F. C. (1962) Preparation of iodine-131 labeled human growth hormone of high specific activity. *Nature* 194, 495–496.
- (13) Shestowsky, W., Fallavollita, L., and Brodt, P. (1990) A monoclonal antibody to lewis lung carcinoma variant H-59 identifies a plasma membrane protein with apparent relevance to lymph node adhesion and metastasis. *Cancer Res.* 50, 1948–1953.
- (14) Hunger, H. D., Flachmeier, C., Schmidt, G., Behrendt, G., and Coutelle, Ch. (1990) Ultrasensitive enzymatic radioimmunoassay using a fusion protein of protein A and neomycin phosphotransferase II in two-chamber-well microtiter plates. *Anal Biochem.* 187, 89–93.
- (15) Cleaveland, J. S., Kiener, P. A., Hammond, D. J., and Schacter, B. Z. (1990) A microtiter-based assay for the detection of protein tyrosine kinase activity. *Anal Biochem.* 190, 249–253.
- (16) Waldock, A., Ellis, I. O., Armitage, N., Turner, D. R., Hardcastle, J. D., and Embleton, J. (1989) Differential expression of the lewis Y antigen defined by monoclonal antibody C14/1/46/10 in colonic polyps. *Cancer Res.* 49, 414–421.
- (17) Bara, J., Mollicone, R., Herrero-Zabaleta, E., Gautier, R., Daher, N., and Oriol, R. (1988) Ectopic expression of the Y (Le^v) antigen defined by monoclonal antibody 12-4LE in distal colonic adenocarcinomas. *Int. J. Cancer* 41, 683–689.
- (18) Heindel, N. D., Zhao, H., Egolf, R. A., Chang, C. H., Schray, K. J., Emrich, J. G., McLaughlin, J. P., and Woo, D. V. (1991) A novel heterobifunctional linker for formyl to thiol coupling. *Bioconjugate Chem.* 2, 427–430.
- (19) de Rosario, R. B., Wahl, R. L., Brocchini, S. J., Lawton, R. G., and Smith, R. H. (1990) Sulfhydryl site-specific cross-linking and labeling of monoclonal antibodies by a fluorescent equilibrium transfer alkylation cross-link reagent. *Bioconjugate Chem.* 1, 51–59.
- (20) Hellstrom, I., Hom, D., Linsley, P., Brown, J. P., Brankovan, V., and Hellstrom, K. E. (1986) Monoclonal mouse antibodies raised against human lung carcinoma. *Cancer Res.* 46, 3917–3923.

Synthesis and Properties of an Oligodeoxynucleotide Modified with a Pyrene Derivative at the 5'-Phosphate

Jeffrey S. Mann, Yoko Shibata, and Thomas Meehan*

Division of Toxicology and Department of Pharmacy, University of California, San Francisco, California 94143.
Received March 23, 1992

The synthesis of an oligonucleotide (ODN) modified with pyrene (pyr) on the 5'-phosphate is described. The ODN and pyrene are joined through a linker composed of four methylene groups. Modification of the oligonucleotide was effected via condensation of the 2-cyanoethyl *N,N*-diisopropylphosphoramidite of 4-(1-pyrenyl)butanol (pyr-m₄OPAm, 2) with the 5'-OH of an ODN. This derivative is suitable for incorporation into automated solid-phase DNA synthesis and was attached to the 5' terminus of the DNA chain through a phosphodiester linkage. The properties of the 5'-(pyr-m₄)d(T)₁₅ (3) and the duplex it formed with d(A)₁₅ were investigated by fluorescence and absorbance spectroscopy. The pyrene fluorescence in the modified duplex was quenched 96.3% relative to an identical concentration of free 4-(1-pyrenyl)butanol. The ultraviolet spectrum of the 5'-(pyr-m₄)-d(T)₁₅ and 5'-(pyr-m₄)-d(T)₁₅-d(A)₁₅ modified duplex, in the 320-360-nm region, was red-shifted 6 nm relative to the free 4-(1-pyrenyl)-butanol. The *T_m* values of the unmodified and modified duplexes at 0.1 M NaCl were 34.9 and 41.9 °C, respectively. The pyrene-induced stabilization corresponds to a free energy change ($\Delta\Delta G^\circ$) of -2.6 kcal/mol.

INTRODUCTION

Antisense oligodeoxynucleotides (ODN) are widely used for sequence-specific, down-regulation of gene expression (1). The replication of vesicular stomatitis virus (2), herpes simplex virus (3), influenza virus (4), and HIV (5, 6) has been arrested by synthetic oligonucleotides complementary to sequences within the viral genome. Antisense oligonucleotides have also been used to inhibit leukemia cell proliferation (7) and the production of gene products from a number of oncogenes such as *ras* (8), *c-myc* (9), *c-myc* (10), and *N-ras* (11).

The development of clinically useful antisense drugs is limited in part by the expense of synthesizing ODNs. This problem is magnified by the low cellular uptake of ODNs and their susceptibility to degradation by nucleases. Our goal is to introduce chemical modifications into ODNs that will increase cellular uptake, nuclease resistance, and the binding affinity of the modified ODNs to their target sequences.

Derivatization of ODNs with a neutral polycyclic aromatic hydrocarbon such as pyrene is clearly a promising approach. Pyrene is nonmutagenic and has a high LD₅₀ (250 mg/kg, mice), which makes it an attractive candidate for in vivo applications (12). Analogous to ODNs derivatized with cholesterol (13) or phospholipids (14), an ODN derivatized with the lipophilic pyrene moiety is expected to show enhanced cell association, which may lead to increased transport of the ODNs across cell membranes. Recent work has indicated that placement of a polymethylene tail on an acridine-modified ODN led to a substantial increase in antisense activity, that may be due in part to increased ODN transport (15). Further, pyrene intercalates between the base pairs of both single-stranded and double-stranded nucleic acids (16) and, therefore, should stabilize the duplex between the modified ODN and its target sequence. Charged intercalator-derivatized oligonucleotides are known to exhibit enhanced binding affinity for complementary sequences. For example, the melting temperature (*T_m*) of the duplex formed between an octathymidylate derivatized with the intercalator acridine and its complementary sequence was found to be twice

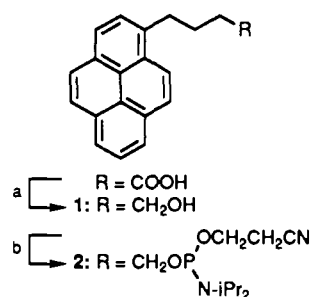
that of the unmodified duplex (17). Charged intercalating groups attached at the 3' and/or 5' ends of the ODN also impart nuclease resistance to the modified ODN. Asseline, et al. (18) reported that an octa- β -D-thymidylate derivatized at both the 3' and 5' ends with acridine was resistant to degradation by exonucleases. Compared to ODN derivatization with positively charged intercalators, such as acridine, little attention has been paid to the rational conjugation of pyrene to synthetic oligonucleotides (19-21). As yet pyrene-modified ODNs have not been evaluated for antisense activity. Since neutral intercalators would be expected to enhance the transport of ODNs and they undergo significantly different interactions with nucleic acids compared to charged intercalators (16), we have embarked upon a program to evaluate the utility of neutral intercalator-modified ODN. In this paper we describe the synthesis of a pyrene derivative (2) tethered to a phosphoramidite via a linker arm composed of four methylene groups. The pyrene phosphoramidite was incorporated into the solid-phase synthetic cycle and attached to the 5' end of d(T)₁₅. Spectroscopic and thermodynamic data indicate that the pyrene interacts strongly with both single strand and duplex DNA, most likely in an intercalative or stacking manner.

RESULTS

Synthesis of Pyr-m₄OPAm (2). The 2-cyanoethyl *N,N*-diisopropylphosphoramidite of 4-(1-pyrenyl)butanol, 2, was synthesized as shown in Scheme 1. The commercially available pyrenebutyric acid was reduced to the corresponding alcohol 1 in 87% yield with LiAlH₄ in THF at 25 °C. Alcohol 1 was treated with diisopropylethylamine and 2-cyanoethyl *N,N*-diisopropylphosphoramidochloridite in THF. The desired product 2 was isolated by silica gel chromatography in 78% yield. The structure of phosphoramidite 2 was confirmed by ¹H and ³¹P NMR spectroscopy and chemical ionization (CI) mass spectrometry.

Synthesis of Oligonucleotide-Pyrene Conjugate 5'-(pyr-m₄)d(T)₁₅ (3). Oligonucleotides were synthesized using automated solid-phase phosphoramidite method-

Scheme 1 *



* (a) LiAlH_4 , THF; (b) $\text{CIPN}-(i\text{Pr})_2(\text{OCH}_2\text{CH}_2\text{CN})$, $\text{EtN}(i\text{Pr})_2$.

ology starting with 5'-DMT-dT attached to a CPG support. Phosphoramidite 2 was introduced in the 15th cycle using a procedure which incorporated lengthened reaction times and increased addition of activator and phosphoramidite relative to the standard coupling. The overall yield of coupling reactions 1–14 was estimated to be 86–89% from the height of the peak at $\lambda = 504$ nm in the absorbance spectrum of the DMT cation produced in the deblocking step. The extent of 5' derivatization with pyrene was estimated at approximately 85% from HPLC analysis of the crude oligonucleotide mixture. The oligonucleotides were purified by reverse-phase HPLC using 0.1 M triethylammonium acetate (pH 7) and a 40-min linear acetonitrile gradient (0–80% CH_3CN) at a flow rate of 1.0 mL/min. The major peak ($t_R = 28.4$ min) was collected and lyophilized, affording 28 A_{260} units of purified oligomer 3. The purified oligonucleotide was digested using snake venom phosphodiesterase and analyzed by reverse-phase HPLC using 0.1 M triethylammonium acetate (pH 7) and a 50-min linear acetonitrile gradient (0–100% CH_3CN) at a flow rate of 1.0 mL/min. The column effluent was monitored by UV (260 nm) and fluorescence (245-nm excitation and >320-nm emission). The resulting chromatogram showed a UV peak which coeluted with deoxythymidine 5'-monophosphate ($t_R = 9.2$ min) and a peak which exhibited both fluorescence and UV absorbance with the same retention time as an authentic sample of 4-(1-pyrenyl)butanol ($t_R = 41.2$ min). The identity of the fluorescent peak was confirmed by CI mass spectrometry ($m/z = 274.4$).

Physical Properties of 5'-(pyr- m_4)d(T)₁₅ (3). The properties of the 5'-pyrene derivatized ODN, 5'-(pyr- m_4)d(T)₁₅ and the duplex it formed with d(A)₁₅ were investigated by fluorescence and UV spectroscopies. Relative to the free 4-(1-pyrenyl)butanol, the fluorescence yield of pyrene in the single- and double-stranded ODN was approximately 9.0% and 3.7%, respectively (Figure 1). The maxima in the UV spectra of the modified single- and double-stranded oligomers were red-shifted by 6 nm (346 nm vs 340 nm) relative to those of an aqueous solution of 4-(1-pyrenyl)butanol (Figure 2).

The thermal stability of the modified duplex relative to the native duplex was measured over a range of NaCl concentrations (0.02–0.52 M). Both the modified and native duplexes displayed cooperative transitions over the range of salt concentrations employed. The modified duplex exhibited a sharper melting transition than the unmodified duplex indicating an enhanced cooperativity (Figure 3). A plot of T_m versus $\log [\text{Na}^+]$ was linear and displayed a steady increase in transition temperature (T_m) for both the native and modified duplexes (Figure 4). Cooperativity was confirmed by the linearity exhibited in the $1/T_m$ vs $\ln C_t$ plot, which was constructed from data obtained at single-strand concentrations (C_t) between 1.2 and 4.8 μM (Figure 5).

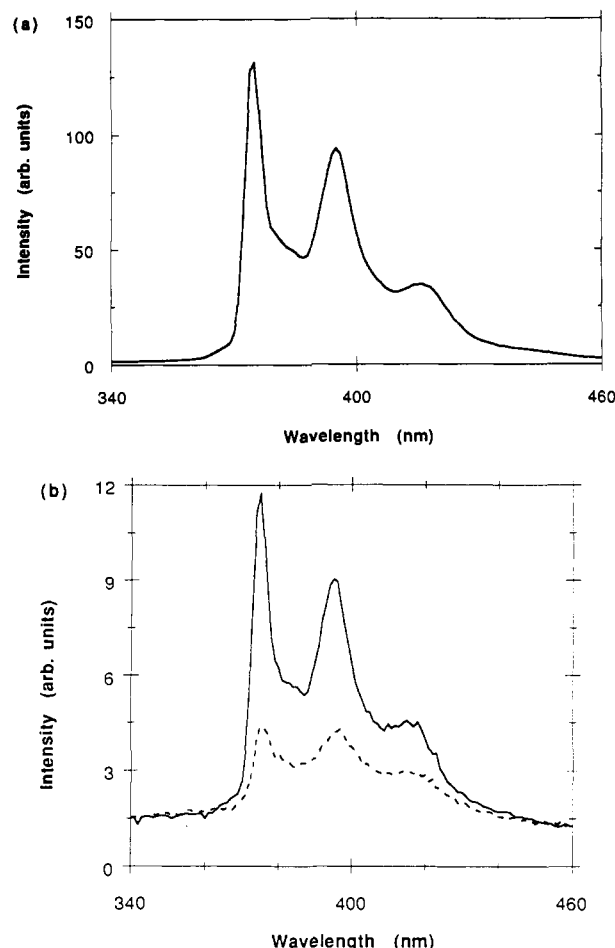


Figure 1. (a) Fluorescence emission spectrum of a 0.12 μM solution of 4-(1-pyrenyl)butanol. (b) Fluorescence emission spectra of the pyrene-modified dT₁₅ single-strand (—) and the pyrene-modified duplex dT₁₅-dA₁₅ (---). Both spectra were measured on solutions which were 0.12 μM in pyrene-modified dT₁₅. All samples were dissolved in 0.1 M NaCl, 0.01 M sodium phosphate (pH 7) and recorded with the excitation monochromator at 276 nm. Although fluorescence intensity is in arbitrary units, the relative intensities of the spectra in a and b are as shown.

DISCUSSION

Synthesis of Pyrene-Oligonucleotide Conjugate 5'-(pyr- m_4)d(T)₁₅ (3). The synthesis of derivatives which can be incorporated into the solid-phase synthetic cycle is central to our strategy for preparing pyrene-labeled oligonucleotides. This approach avoids the difficulties of solution-phase oligonucleotide synthesis and the structural ambiguity encountered in the course of postsynthetic modification of oligonucleotides. Additionally, the synthesis of pyrene phosphoramidites, such as 2, provides a versatile and convenient avenue in order to vary linker-arm length and composition without prior attachment to a nucleotide monomer. This strategy places no restrictions on oligonucleotide length or base sequence. It will also allow a systematic investigation into the linker-length parameter and its effect on antisense activity and the physical properties of pyrene-modified ODNs.

Duplex Stability. Model (CPK) building studies indicate that pyrene attached to an oligonucleotide via a linker arm composed of four methylene groups is fairly constrained yet has three possible modes of interaction with the duplex: intercalation, end stacking, and, less likely, groove binding. Stacking and intercalation are shown in Figure 6. The quenching of the pyrene fluo-

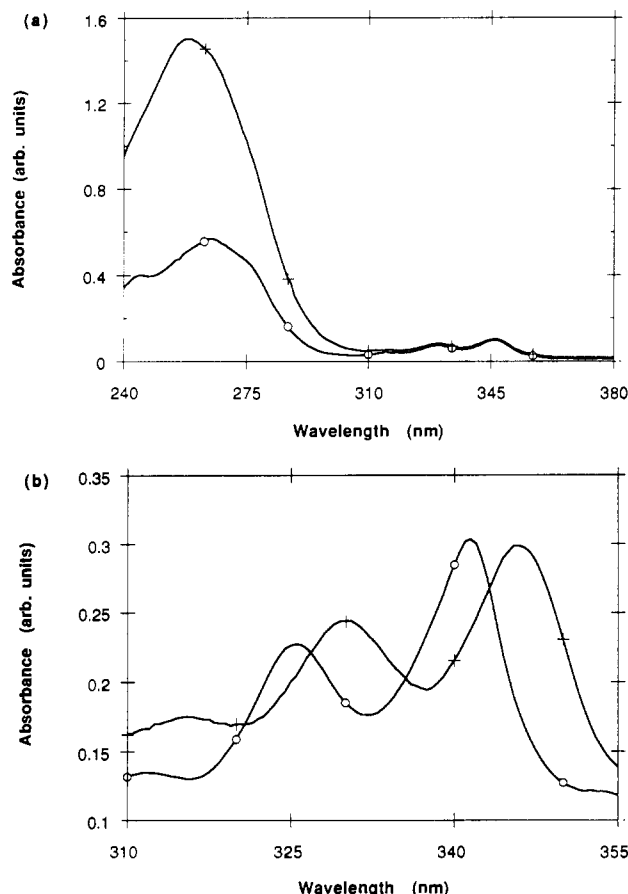


Figure 2. (a) Comparison of the UV absorbance spectra of the pyrene-modified dT₁₅ single-strand (O) and pyrene-modified dT₁₅-dA₁₅ duplex (+). (b) Comparison of the UV absorbance spectra of 4-(1-pyrenyl)butanol (O) and the red-shifted (6 nm) pyrene-modified duplex dT₁₅-dA₁₅ (+), in the 300–360-nm region. All samples were dissolved in 0.1 M NaCl, 0.01 M sodium phosphate (pH 7).

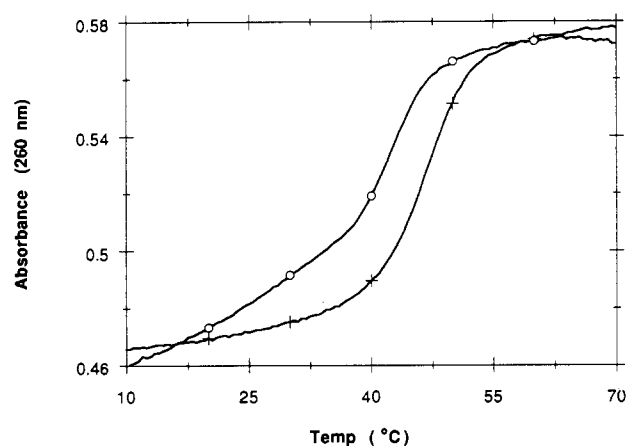


Figure 3. Melting curves for unmodified (O) and pyrene modified (+) d(T)₁₅-d(A)₁₅ in 0.3 M NaCl, 0.01 M sodium phosphate (pH 7).

rescence, increase in duplex stability, and the magnitude of the red-shift in the UV spectrum of the duplex indicate that the pyrene interacts strongly with one or more nucleobases; possibly stacking on the exterior of the ultimate base pair or intercalating between the ultimate and penultimate base pairs. Both models might be used to explain the enhanced stability of the modified duplex relative to its unmodified counterpart. Groove binding would be expected to lead to less significant duplex stabilization and quenching of the pyrene fluorescence

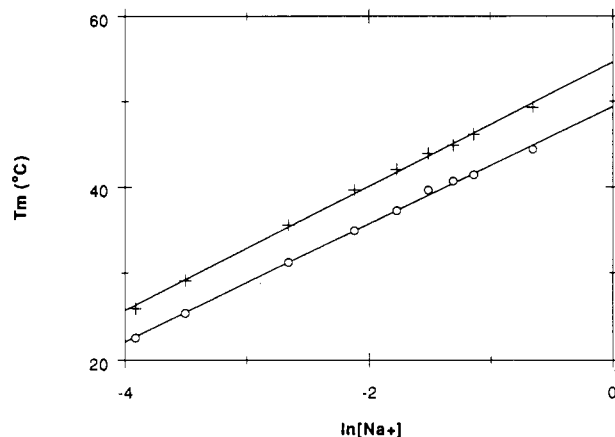


Figure 4. Dependence of the duplex melting temperature (T_m) on sodium ion concentration $[Na^+]$ for pyrene-modified dT₁₅-dA₁₅ (+) and unmodified dT₁₅-dA₁₅ (O) duplexes at a total strand concentration of 4.5 μ M in 0.01 M sodium phosphate (pH 7).

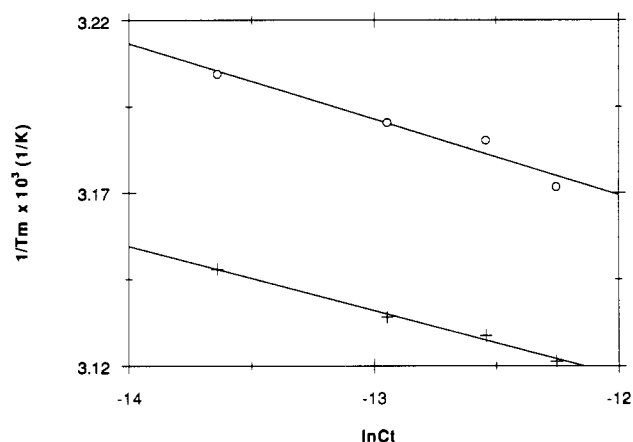


Figure 5. Dependence of duplex melting temperature (T_m) on single-strand concentration (C_t) for the pyrene-modified (+) and unmodified (O) duplexes in 0.10 M NaCl, 0.1 M sodium phosphate (pH 7).

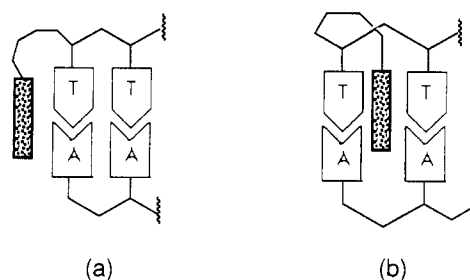


Figure 6. Two possible modes of pyrene-duplex interaction: (a) stacking on the ultimate base pair and (b) intercalation between duplex base pairs.

(17). Pyrene fluorescence is also quenched in the single strand, but to a lesser degree than in the double-stranded oligomer. Pyrene fluorescence in the double-stranded sample is reduced by a factor of 96.3% relative to the free pyrenebutanol and 60% compared to the pyrene-modified single-stranded sample. Previous work in this laboratory has shown that benzo[a]pyrene derivatives and pyrene interact strongly with single-stranded DNA at high salt concentrations (16). This binding probably results from intercalation into loosely ordered intrastrand duplexes which can be more easily unwound to accommodate the hydrocarbon than the native duplex. Inspection of the thermodynamic parameters calculated from plots of $1/T_m$ vs $\ln C_t$ for both the modified and unmodified duplexes reveals a free energy difference ($\Delta\Delta G^\circ$) of -2.6 kcal/mol

at 25 °C. The stabilization of the pyrene-modified duplex results from a reduction of the transition enthalpy ($\Delta\Delta H^\circ = -16.5$ kcal/mol) and in the transition entropy ($\Delta\Delta S^\circ = -46.8$ cal/mol K) of the modified duplex relative to the unmodified duplex.

EXPERIMENTAL SECTION

Materials and Methods. Pyrenebutyric acid, lithium aluminum hydride (1.0 M in THF), and 2-cyanoethyl *N,N*-diisopropylphosphoramidochloridite were purchased from Aldrich. Diisopropylethylamine (Aldrich) was distilled from NaOH under N_2 and stored over molecular sieves (4 Å). THF (Fisher) was distilled from sodium metal under N_2 immediately prior to use. Column chromatography and TLC were performed on 230–400 mesh, 60-Å silica gel (Aldrich), and Rediplates, 250 μ m (Fisher), respectively. Reverse-phase HPLC was performed on a C_{18} Zorbax ODS column (4.6 mm \times 25 cm) on an HPLC composed of an Altex Model 110A pump and a Kratos Spectroflow 430 gradient programmer. The column effluent was monitored at 260 nm with a Hitachi 100-40 UV detector linked in tandem with a Schoeffel FS 970 LC fluorometer. 1H NMR spectra were recorded on a G.E. QE 300 spectrometer. The samples were dissolved in $CDCl_3$, and the absorbance of the residual solvent protons was used as a reference. ^{31}P NMR spectra were measured on a Bruker 300 MHz instrument and were referenced to an external standard of 85% H_3PO_4 .

Synthesis of 4-(1-Pyrenyl)butanol (1). Pyrenebutyric acid (888.1 mg, 3.08 mmol) was dissolved in anhydrous THF (20 mL) with stirring under argon. To this solution was carefully added $LiAlH_4$ (1.0 M in THF, 4.0 mL). The resulting solution was stirred for 4 h, then EtOAc (15 mL) was added dropwise and the solution was poured into ice-cold 10% H_2SO_4 giving a bright yellow mixture. The mixture was transferred to a separatory funnel and the organic layer was removed. The aqueous layer was extracted with EtOAc (3 \times 20 mL). The organic layers were pooled, washed with 10% K_2CO_3 (1 \times 20 mL) and H_2O (1 \times 20 mL), dried (Na_2SO_4), and evaporated to dryness, giving 739 mg (87%) of the alcohol as a pale yellow solid. TLC (CH_2Cl_2): R_f 0.26. NMR ($CDCl_3$): δ 1.62–1.88 (m, 4 H), 3.34 (t, $J = 7.8$ Hz, 2 H), 3.64 (t, $J = 6.5$ Hz, 2 H), 7.84–8.28 (m, 9 H).

4-(1-Pyrenyl)butanol, 2-Cyanoethyl *N,N*-Diisopropylphosphoramidite (2). 4-(1-Pyrenyl)butanol (1; 161.5 mg, 0.60 mmol) was dissolved in anhydrous THF (500 μ L) under Ar with stirring. Diisopropylethylamine (152 mg, 1.2 mmol) was added via syringe followed by 2-cyanoethyl *N,N*-diisopropylphosphoramidochloridite (142 mg, 0.60 mmol). Within one min a voluminous white precipitate had formed. The reaction mixture was stirred for 40 min then the precipitate was removed by filtration. The filtrate was diluted to 25 mL with EtOAc and washed with 0.1 M NaH_2PO_4 , pH 7.0 (1 \times 10 mL). The organic layer was removed, dried (Na_2SO_4) and rotary evaporated to dryness affording 304 mg of a pale yellow oil. The crude product was chromatographed on silica (1 cm \times 10 cm) eluted with EtOAc/hexanes (1:3). A fast-moving fraction was isolated and evaporated to dryness, affording 213 mg (75%) of the desired product as a fluorescent pale yellow oil. 1H NMR ($CDCl_3$): δ 1.15 (t, $J = 6.9$ Hz, 12 H), 1.82 (m, 2 H), 1.96 (m, 2 H), 2.56 (t, $J = 6.3$ Hz, 2 H), 3.38 (t, $J = 7.5$ Hz, 2 H), 3.68 (m, 6 H), 8.08 (m, 9 H). ^{31}P NMR ($CDCl_3$): δ 147.85. Mass spectrum (ammonia CI): calcd for $C_{29}H_{35}N_2O_2P$ 474.6, found 475.0.

DNA Synthesis and Purification. The unmodified and modified oligonucleotides were synthesized on a 1.0-

μ mol scale with a Biosearch 8600 DNA synthesizer using phosphoramidite chemistry (23). The standard coupling program (6.5 min) was used for the synthesis of d(A)₁₅ and d(T)₁₅. The coupling program was modified to include a 60-min coupling cycle and two extra additions of pyrene phosphoramidite 2 and tetrazole at the final step of the synthesis. The oligonucleotides were deprotected by treatment with concentrated NH_4OH for 5 h at 55 °C. The deprotected oligonucleotides were evaporated to dryness and taken up in 400 μ L of 100 mM triethylammonium acetate, pH 7.0, and purified by reverse-phase HPLC eluting with 100 mM triethylammonium acetate with a gradient of acetonitrile. The gradient was developed linearly from 0%–80% acetonitrile over 40 min at a flow rate of 1 mL/min.

T_m Determination. T_m values were determined using a Gilford 2600 spectrophotometer. The temperature was controlled by a Gilford 2527 thermal programmer. Data points were collected every 0.5 min. Single-strand concentration was determined from the calculated UV extinction coefficients of the individual strands. The spectral overlap contributions from the pyrene in the modified strand were determined and found to be negligible. Thermodynamic parameters were calculated from plots of $1/T_m$ vs $\ln C_t$, where C_t is the total single-strand concentration, using a previously published procedure (24).

Nuclease Digestion of Modified and Unmodified Oligonucleotides. The oligonucleotide (2 OD units) was diluted to 3.0 mL with a buffer solution composed of 0.11 M Tris-HCl, 0.11 M NaCl, and 0.15 mM $MgCl_2$ (pH 8.9). Snake venom phosphodiesterase (0.1 Kunitz unit) was added, the mixture was vortexed and left overnight at 23 °C. In order to precipitate the protein prior to HPLC analysis, the digest mixture was reduced in volume to 250 μ L followed by the addition of 750 μ L of acetonitrile. The mixture was vortexed and then centrifuged and the aqueous acetonitrile supernatant containing the mononucleotide and 4-(1-pyrenyl)butanol was drawn off. The protein was redissolved and the precipitation carried out two more times. The three aqueous acetonitrile supernatants were combined, evaporated to dryness, and reconstituted in 200–400 μ L of 0.1 M triethylammonium acetate before HPLC analysis.

ACKNOWLEDGMENT

This work was supported in part by NIH Grant 40598 and the Elsa U. Pardee Foundation. We thank Alan R. Wolfe for helpful discussions and his generous assistance in the preparation of the manuscript. CIMS was carried out at the Bioorganic and Biomedical Mass Spectrometry Facility of the University of California, San Francisco.

LITERATURE CITED

- (1) For a review, see: Helene, C., and Toulme, J.-J. (1990) Specific regulation of gene expression by antisense, sense and antigene nucleic acids. *Biochim. Biophys. Acta* 1049, 99–125.
- (2) Leonetti, J. P., Rayner, B., LeMaitre, M., Gagnor, C., Milhaud, P. G., Imbach, J. L., and LeBleu, B. (1988) Antiviral activity of conjugates between poly-(L-lysine) and synthetic oligodeoxynucleotides. *Gene* 72, 323–31.
- (3) Miller, P. S., and Ts'O, P. O. P. (1987) A new approach to chemotherapy based on molecular biology and nucleic acid chemistry: Matagen (Masking tape for gene expression). *Anticancer Drug Des.* 2, 117–27.
- (4) Zerial, A., Thuong, N. T., and Helene, C. (1987) Selective inhibition of the cytopathic effect of type A influenza viruses by oligodeoxynucleotides covalently linked to an intercalating agent. *Nucleic Acids Res.* 15, 9909–19.

- (5) Vickers, T., Baker, B. F., Cook, P. D., and Zomes, M. (1991) Inhibition of HIV-LTR gene expression by oligonucleotides targeted to the TAR element. *Nucleic Acids Res.* 19, 3359-68.
- (6) Laurence, J., Sikder, S. K., Kulkosky, Miller, P., and Ts'O, P. O. P. (1991) Induction of chronic human immunodeficiency virus infection is blocked in vitro by a methylphosphonate oligodeoxynucleoside targeted to a U3 enhancer element. *J. Virol.* 65, 213-9.
- (7) Szczylic, C., Skorski, T., Nicolaides, N. C., Manzella, L., Malaguarnera, L., Venturelli, D., Gewirtz, A. M., and Calabretta, B. (1991) Selective inhibition of leukemia cell proliferation by BCR-ABL antisense oligonucleotides. *Science* 253, 562-5.
- (8) Chang, E. H., Miller, P. S., Cushman, C., Devadas, K., Pirollo, K. F., Ts'O, P. O. P., and Yu, Z. P. (1991) Antisense inhibition of ras-p21 expression that is sensitive to a point mutation. *Biochemistry* 30, 8283-6.
- (9) Degols, G., Leonetti, J.-P., Meehti, N., and LeBleu, B. (1991) Antiproliferative effects of antisense oligonucleotides directed to the RNA of the c-myc oncogene. *Nucleic Acids Res.* 19, 945-8.
- (10) Gewirtz, A. M., and Calabretta, B. (1988) A c-myc antisense oligodeoxynucleotide inhibits normal human hematopoiesis. *Science* 242, 1303-6.
- (11) Tidd, D. M., Hawley, P., Warenius, H. M., and Gibson, I. (1988) Evaluation of N-ras oncogene antisense, sense and nonsense sequence methylphosphonate oligonucleotide analogues. *Anticancer Drug Des.* 3, 117-27.
- (12) Karcher, W., Fordham, R. J., Dubois, J. J., Glaude, P. G. J. M., and Ligthart, J. A. M. (1985) *Spectral Atlas of Polycyclic Aromatic Compounds*, p 91, D. Reidel Publishing Co., Dordrecht.
- (13) Letsinger, R. L., Zhang, G., Sun, D. K., Ikeuchi, T., and Sarin, P. S. (1989) Cholesteryl-conjugated oligonucleotides: Synthesis properties and activity as inhibitors of replication of human immunodeficiency virus in cell culture. *Proc. Natl. Acad. Sci. U.S.A.* 86, 6553-6.
- (14) Shea, R. G., Marsters, J. C., and Bischofberger, N. (1990) Synthesis, hybridization properties and antiviral activity of lipid-oligodeoxynucleotide conjugates. *Nucleic Acids Res.* 18, 3777-83.
- (15) Saison-Behmoaras, T., Tocqué, B., Rey, I., Chassignol, M., Thuong, N. T., and Helene, C. (1991) Short modified antisense oligonucleotides directed against Ha-ras point mutation induce selective cleavage of the mRNA and inhibit T25 cells proliferation. *EMBO J.* 10, 1111-8.
- (16) Wolfe, A., Shimer, G. H., Jr., and Meehan, T. (1987) Polycyclic aromatic hydrocarbons physically intercalate into duplex regions of denatured DNA. *Biochemistry* 26, 6392-6.
- (17) Thuong, N. T., Asseline, U., and Montenay-Garestier, T. (1989) Oligodeoxynucleotides covalently linked to intercalating and reactive substances: synthesis, characterization and physicochemical studies. In *Oligodeoxynucleotides: Antisense inhibitors of gene expression* (Cohen, J. S., Ed.) pp 25-47, CRC Press Boca Raton, FL.
- (18) Asseline, U., and Thuong, N. T. (1988) Oligothymidylates substitués par un dérivé de l'acridine en position 5' à la fois en position 5' et 3' on sur un phosphate internucleotidique. *Nucleosides Nucleotides* 7, 431-55.
- (19) Casale, R., and McLaughlin, L. W. (1990) Synthesis and Properties of an oligodeoxynucleotide containing a polycyclic aromatic hydrocarbon site specifically bound to the N² amino group of a 2'-deoxyguanosine residue. *J. Am. Chem. Soc.* 111, 5264-71.
- (20) Yamana, K., and Letsinger, R. L. (1985) Synthesis and properties of oligonucleotides bearing a pendant pyrene. *Nucleic Acids Res.* 16, 169-72.
- (21) Yamana, K., Ohashi, Y., Nunota, K., Kitamura, M., Nakano, H., Sangen, O., and Shimidzu, T. (1991) Synthesis of oligonucleotide derivatives with pyrene group at sugar fragment. *Tetrahedron Lett.* 32, 6347-50.
- (22) Lee, H., Hinz, M., Stezowski, J. J., and Harvey, R. G. (1990) Synthesis of polycyclic aromatic hydrocarbon-nucleoside and nucleotide adducts specifically alkylated on the amino functions of deoxyguanosine and deoxyadenosine. *Tetrahedron Lett.* 31, 6773-6.
- (23) McBride, L. J., and Carruthers, M. H. (1983) An investigation of several deoxynucleoside phosphoramidites useful for synthesizing deoxyoligonucleotides. *Tetrahedron Lett.* 24, 245-8.
- (24) (a) Marky, L. A., and Breslauer, K. J. (1987) Calculating thermodynamic data for transitions of any molecularity from equilibrium melting curves. *Biopolymers* 26, 1601-20. Alberg, D. D., Marky, L. A., Breslauer, K. J., and Turner, D. H. (1981) Thermodynamics of (dC-dG)₃ double-helix formation in water and deuterium oxide. *Biochemistry* 20, 1409-13.

TECHNICAL NOTES

Reagent for Introducing Pyrene Residues in Oligonucleotides

Vladimir A. Korshun, Nikolai B. Pestov, Klara R. Birikh, and Yuri A. Berlin*

M. M. Shemyakin Institute of Bioorganic Chemistry, Russian Academy of Sciences, Miklukho-Maklaya 16/10, Moscow 117871, Russia. Received April 20, 1992

A novel pyrenyl-containing phosphoramidite reagent, *N*-[4-(1-pyrenyl)butyryl]-*O*¹-(4,4'-dimethoxytrityl)-*O*²-[(diisopropylamino)(2-cyanoethoxy)phosphino]-3-amino-1,2-propanediol (**5**), has been synthesized from 4-(1-pyrenyl)butanoic acid in four steps with the 52% overall yield and used to incorporate pyrene residue(s) into oligonucleotides. Oligonucleotides **6** and **7**, bearing one or two pyrenes at the 5'-terminus, have been prepared by means of that reagent, characterized with fluorescence spectra, and successfully used as primers in a polymerase chain reaction.

Nonradioactive labeling of low molecular compounds and biopolymers is widely used in studying their interactions and transformations. For fluorescent labeling of oligonucleotides or studies on carcinogenesis, pyrene (a well-known fluorophore) was attached, through linker arms of various lengths, to internucleotide phosphates (**1**), the N⁴-atom of deoxycytidine (**2**, **3**), the N²-atom of deoxyguanosine, the N⁶-atom of deoxyadenosine (**4**), and the O²-atom of uridine (**5**). Recently, the difference in fluorescence spectra of the pyrene monomer and its excimer was used to detect duplex DNA (**6**). A similar energy transfer was observed and applied for study of the interaction, on a complementary template, of two oligonucleotides, one of which is 3'-labeled with pyrene and the other is 5'-labeled with P(V) porphyrin (**7**). Pyrene-labeled oligonucleotides are able to intercalate into DNA duplexes (**1**, **3**, **4**), thus increasing the duplexes stability.

Among compounds which could serve as a linker between an oligonucleotide and its labeling group, 3-amino-1,2-propanediol is of undoubted interest. In fact, its primary and secondary hydroxyl groups, imitating 5'- and 3'-hydroxyl groups of deoxynucleosides, can be used to elongate the nucleotide chain, whereas the amino group is a reactive site to be easily coupled with various modifiers. These features and the availability of the starting compound allowed one to synthesize reagents for incorporating aliphatic amino groups into synthetic oligonucleotides (**8**, **9**). In the present paper we describe the use of 3-amino-1,2-propanediol for the synthesis of a convenient reagent for introduction of pyrenyl residues into biopolymers and some properties of pyrene-containing oligonucleotides.

EXPERIMENTAL PROCEDURES

General Procedures. *N,N'*-Dicyclohexylcarbodiimide (DCC) and solvents were purchased from Merck (Darmstadt, FRG), 4,4'-dimethoxytrityl chloride (DMTCI) was from Aldrich Chemical Co. (Milwaukee, WI), and 3-amino-1,2-propanediol and pentafluorophenol were from Fluka (Buchs, Switzerland). Pyridine and acetonitrile were distilled over CaH₂, THF was distilled over LiAlH₄, and diethyl ether was passed through a column of alumina I activity (Merck). 4-(1-Pyrenyl)butanoic acid was prepared from pyrene by the Friedel-Crafts acylation with succinic anhydride/AlCl₃ (**10**) followed by the Wolf-Kishner reduction (**11**), and diisopropylammonium tet-

razolide and bis(diisopropylamino)(2-cyanoethoxy)phosphine were prepared as described (**12**). NMR spectra were obtained on a Bruker AC-500 spectrometer. IR spectra were performed with a UR-20 spectrophotometer. Mass spectral data were obtained on a Varian MAT-44S (electron impact) or a Kratos MS 50TC (fast atom bombardment); mass spectrum of phosphoramidite **5** was obtained on a plasma desorption spectrometer using ionization with products of ²⁵²Cf fission (Electron, Sumy, Ukraine). Melting points were determined on a Boetius instrument and are uncorrected. TLC was run on Kieselgel 60 F₂₅₄ plates (Merck). Column chromatography was carried out with silica gel 60 (40-63 μm; Merck). Oligonucleotides were synthesized on an Applied Biosystems 380B instrument. Fluorescence spectra were measured with a Hitachi MPF-4 spectrofluorimeter.

4-(1-Pyrenyl)butanoic Acid Pentafluorophenyl Ester (2). To a magnetically stirred and cooled (0 °C) solution of 4-(1-pyrenyl)butanoic acid (**10**, **11**) (1.44 g, 5.0 mmol) and pentafluorophenol (0.96 g, 5.2 mmol) in THF (15 mL) was added a solution of DCC (1.07 g, 5.2 mmol) dropwise, the mixture was stirred overnight, the *N,N'*-dicyclohexylurea formed was filtered off and washed with CH₂Cl₂, and the combined organic solutions were evaporated under reduced pressure. The crude product was purified by flash chromatography (CH₂Cl₂) to give ester **2** (2.18 g, 96%) as light yellow crystals: mp 135-136 °C (CHCl₃-hexane); TLC (CHCl₃) *R*_f 0.66; MS (*m/z*) 454 (M⁺); IR (KBr) 1779 cm⁻¹ (C=O); ¹H NMR (CDCl₃, δ, ppm) 8.3-7.9 (m, 9 H, ArH), 3.50 (t, 2 H, *J* = 6 Hz, ArCH₂), 2.81 (t, 2 H, *J* = 6 Hz, CH₂CO), 2.35 (quintet, 2 H, *J* = 6 Hz, CH₂CH₂CH₂).

***N*-[4-(1-Pyrenyl)butyryl]-3-amino-1,2-propanediol (3).** To a magnetically stirred solution of ester **2** (2.04 g, 4.5 mmol) in THF (40 mL) was added 3-amino-1,2-propanediol (0.70 mL, 9.0 mmol). After the reaction was completed (TLC), the solvent was removed under reduced pressure and the residue was chromatographed on silica gel in a methanol gradient (0 → 10%) in chloroform. The major fraction was coevaporated with dry pyridine and toluene and triturated with diethyl ether to give the light yellow crystalline amide **3**: yield 1.80 g (90%); mp 110-111 °C (CHCl₃); TLC (CHCl₃-MeOH 9:1) *R*_f 0.21; MS (*m/z*) 361 (M⁺); IR (KBr) 1550 (amide), 1643 (C=O), 3325, 3420 (OH...O) cm⁻¹; ¹H NMR (DMSO-*d*₆, δ, ppm) 8.4-7.9

(m, 9 H, ArH), 7.84 (br t, 1 H, NH), 4.73 (d, 1 H, $J = 4.5$ Hz, CHOH), 4.53 (t, 1 H, $J = 5.5$ Hz, CH₂OH), 3.51 (m, 1 H, CHO), 3.34–3.29 (m, 4 H, ArCH₂, CH₂O), 3.28–3.32, 3.07–3.01 (m, 2 H, NCH₂), 2.28 (t, 2 H, $J = 7$ Hz, CH₂CO), 2.02 (quintet, 2 H, $J = 7$ Hz, CH₂CH₂CO).

N-[4-(1-Pyrenyl)butyryl]-O¹-(4,4'-dimethoxytrityl)-3-amino-1,2-propanediol (4). Compound 3 (1.45 g, 4.0 mmol) was coevaporated twice with pyridine, dissolved in dry pyridine (20 mL), and cooled down to 0 °C, and after addition of DMTCl (1.49 g, 4.4 mmol), the stirred mixture was allowed to warm up to 20 °C. After disappearance of the starting material (about 2 h) the reaction was quenched with methanol (0.5 mL), evaporated to one-third its original volume, diluted with CHCl₃ (150 mL), washed with 5% NaHCO₃ and water, and dried (Na₂SO₄). The solvents were evaporated under reduced pressure; the crude product was coevaporated with toluene, purified by column chromatography (50 → 0% hexane in CHCl₃ containing 0.5% Et₃N), and dried in vacuo (0.04 Torr, 12 h) to give 4 (2.42 g, 91%) as a yellowish foam: TLC (CHCl₃-MeOH 9:1) R_f 0.68; FAB MS (m/z) 664 (M⁺); ¹H NMR (DMSO-*d*₆, δ , ppm) 8.4–7.9 [m, 9 H, ArH (pyrene)], 7.76 (br t, 1 H, NH), 7.4–6.7 [m, 13 H, ArH (DMT)], 5.03 (d, 1 H, $J = 6$ Hz, OH), 3.73 (m, 1 H, CHO), 3.64 (s, 6 H, OCH₃), 3.32–3.26, 3.10–3.03 (m, 2 H, NCH₂), 3.24 (t, 2 H, $J = 7$ Hz, ArCH₂), 2.91 (m, 2 H, CH₂O), 2.21 (t, 2 H, $J = 7$ Hz, CH₂CO), 1.95 (quintet, 2 H, $J = 7$ Hz, CH₂CH₂CO).

N-[4-(1-Pyrenyl)butyryl]-O¹-(4,4'-dimethoxytrityl)-O²-(diisopropylamino)(2-cyanoethoxy)phosphino]-3-amino-1,2-propanediol (5). Compound 4 (0.75 g, 1.13 mmol) was coevaporated with MeCN, dissolved in dry MeCN, and then diisopropylammonium tetrazolide (0.34 g, 2.0 mmol) and bis(diisopropylamino)(2-cyanoethoxy)phosphine (0.43 mL, 1.35 mmol) were added. The reaction mixture was stirred magnetically under argon; after reaction completion (about 1 h, TLC), the solvent was removed under reduced pressure and the residue was purified by column chromatography (hexane-CHCl₃ 1:1 with 0.5% Et₃N) and dried in vacuo (0.04 Torr, 12 h) to give 5 (0.75 g, 78%) as a yellowish foam. It was dissolved in toluene (3 mL), precipitated in pentane (300 mL), filtered off, dissolved in dry MeCN, evaporated to dryness, and dried in vacuo (0.04 Torr, 24 h) to give 5 in a form suitable for direct use in a synthesizer: yield 0.66 g (67%); TLC (CHCl₃-hexane-Et₃N 5:5:1) R_f 0.43, 0.54 (diastereomers); MS (m/z) 863, 5 (M⁺); ¹H NMR (CDCl₃, δ , ppm) 8.3–7.8 [m, 9 H, ArH (pyrene)], 7.5–6.7 [m, 13 H, ArH (DMT)], 6.07 (br t, 0.5 H, NH), 5.68 (br t, 0.5 H, NH), 4.05 (m, 1 H, CHO), 3.82–3.48 (m, 12 H, OCH₃, ArCH₂, NCH₂, NCH), 3.37 (m, 2 H, POCH₂), 3.29–3.09 (m, 2 H, CH₂-ODMT), 2.45–2.12 (m, 6 H, CH₂CH₂CO, CH₂CN), 1.11 (m, 12 H, CH(CH₃)₂).

Modified Oligodeoxynucleotides 6 and 7. The 20-meric nucleotide part of the conjugates 6 and 7 was synthesized by the solid-phase phosphoramidite method (12) from 0.2 μ mol thymidine immobilized through its 3'-hydroxyl and a succinate grouping on aminoalkylated CPG-500; the oligonucleotide chain was elongated with deoxynucleoside β -cyanoethyl (diisopropylamino)-phosphites. After the oligonucleotide chain was completed and detritylated, it was phosphorylated with 0.2 M reagent 5 in the presence of 0.5 M tetrazole in acetonitrile solution (45 s) and oxidized with iodine under standard conditions. Then the support containing the oligonucleotide was divided in two equal parts, one was used for the isolation of the monopyrenyl derivative 6 whereas from the other, after repeating the previous step, was obtained dipyrenyl

Chart I. Synthesis of the Phosphoramidite Reagent with a Pyrene Residue

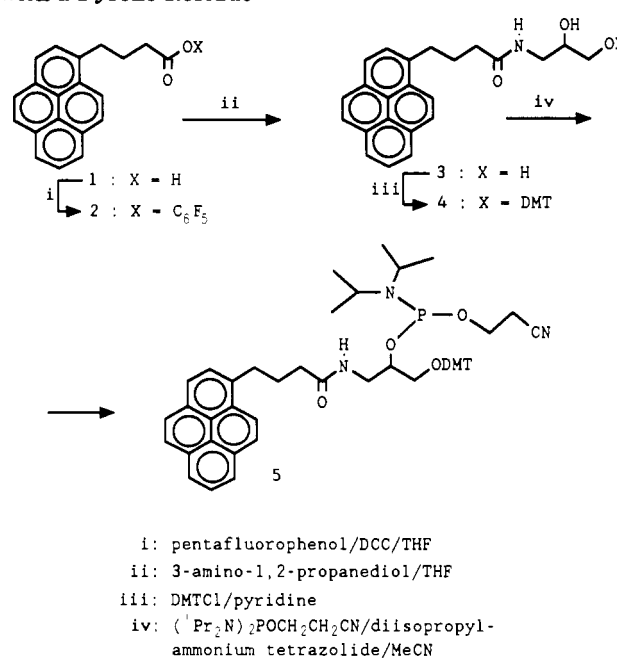
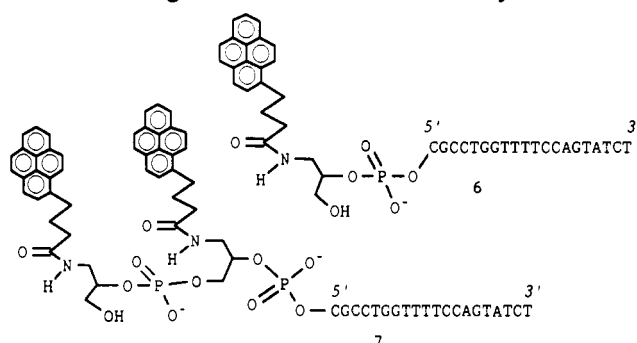


Chart II. Oligonucleotides Labeled with Pyrene



derivative 7. The oligonucleotides were finally deprotected by treatment with ethanolamine-ethanol 1:1, 65 °C, 30 min (13) and purified by 15% PAGE.

Amplification in Vitro (PCR). Amplification of the proximal part of exon 7 of the IL-1 α gene was carried out according to the modified method (14) in a 100- μ L incubation mixture containing 20 ng of a recombinant plasmid bearing the synthetic IL-1 α gene insert and 30 pmol each of upstream and downstream primers as described (15).

RESULTS AND DISCUSSION

Initial 4-(1-pyrenyl)butanoic acid (1) (Chart I) was transformed into pentafluorophenyl ester 2, which acylated (\pm)-3-amino-1,2-propanediol to give amido diol 3. The latter was dimethoxytritylated and phosphitylated, yielding the final phosphoramidite 5 as a mixture of diastereomers. The reagent 5 is soluble in acetonitrile and therefore could be easily employed in the automated oligonucleotide synthesis to yield mono- and dipyrenyl oligonucleotide derivatives 6 and 7 (Chart II). Earlier described nucleoside phosphoramidites containing pyrene residues (2, 4, 5) were much more complicated to obtain due to the multistep schemes used for their syntheses. Moreover, they may affect—just because of the extra base—hybridization properties of the corresponding labeled probe. On the other hand, when the modifying reagent contains only a functionalized pyrene and the acyl-

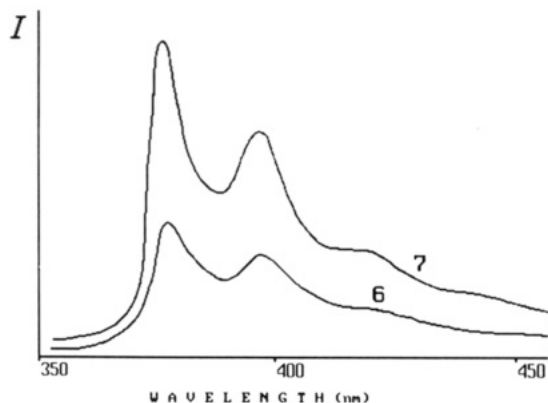


Figure 1. Fluorescence spectra of pyrene-labeled oligonucleotides 6 and 7 in aqueous solution: excitation at 330 nm, $A_{350} = 0.12$.

ation proceeds at an exogenous amino group of oligonucleotide (3), experimental problems arise due to dramatically different solubilities of the reagent and oligonucleotide. The reagent 5, with a relatively simple synthetic pathway to yield it and a solubility similar to that of protected oligonucleotides, apparently obviates all these complications. Its chirality, though being a source of diastereomers after conjugation with an oligonucleotide, does not hinder the conjugates' purification nor affect in any significant degree other properties of these compounds (e.g., hybridization or elongation). It should be noted, by the way, that almost any polyfunctional linker is chiral or at least prochiral [e.g., glycerol used in the synthesis of conjugates with biotin by Misiura et al. (16)], what amounts to the same, once the conjugate has formed.

In synthesizing oligonucleotides with several pyrene residues we anticipated their use in the direct detection of complex formation of pyrene-containing probes with DNA. It might be expected that two hydrophobic pyrenyl residues in an oligonucleotide conjugate in aqueous solution would interact to reveal an excimeric effect. In that case formation of a duplex with the complementary single-stranded DNA would lead to intercalation of one of the pyrene residues in the double helix formed and therefore uncoupling of its interpyrenyl interaction. This, in turn, should be accompanied by the disappearance of the excimer, easily monitored by the change in the fluorescence spectrum (cf. ref 6). However, the fluorescence spectra of oligonucleotides 6 and 7 in aqueous solution proved to be similar, substance 7 showing no excimer fluorescence (Figure 1). This fact can be explained by a significant distance between the pyrene residues divided by an 18-atom chain (low concentration—about 10^{-6} M—prevents intermolecular effects), shorter arms being a prospective object of study. At the same time, the lack of the excimer would naturally lead to the additivity of the fluorescence and therefore increase the sensitivity upon detection of oligonucleotide probes labeled with several pyrenyl residues.

We used the reagent 5 to synthesize a 20-meric oligodeoxynucleotide [the downstream primer for amplification in vitro of the seventh exon of the human interleukine 1 α gene (15)] containing one (6) or two pyrene residues (7) at the 5'-terminus. The condensation yield with the reagent 5 determined on the basis of the ion DMT⁺ absorption (17) was 93%.

It has been shown that the modified oligonucleotides 6 and 7 can be used as primers in PCR. As a result, a 195 base pair double-stranded proximal segment of exon 7 of the gene for human interleukin 1 α 5'-labeled with one or

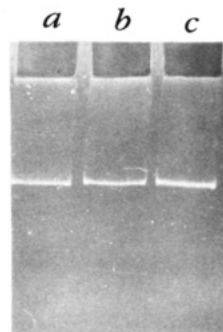


Figure 2. Electrophoresis in 10% PAG of the amplification products of exon 7 of the IL-1 α gene (in all PCRs a nonlabeled upstream primer ATGCCTGAGATACCCAAAAC was used): a, nonlabeled downstream primer (control); b, downstream primer 6; c, downstream primer 7. Detection was by staining with ethidium bromide.

two pyrene residues, respectively, has been obtained (Figure 2). Though these polynucleotides could not be visually detected in gel, at least on a 30-pmol scale (we therefore used staining with ethidium bromide), other experiments carried out by us showed that with multiple pyrene labels (eight and more) visual detection becomes possible (to be published).

As can be seen from Figure 2, the intensity of the PAGE band corresponding to the PCR product upon ethidium bromide staining of the electrophoregram is essentially the same no matter what kind of oligonucleotide (non-labeled, monolabeled or double-labeled) is used as a downstream primer (upstream primer was nonlabeled in all three cases shown in Figure 2). It indicates that pyrene residue(s) at the 5'-terminus do not hinder the hybridization and extension of oligonucleotide primers. It still remains to be seen if pyrenyl residues could even stimulate primer's hybridization, for instance, due to an interaction between the pyrene moiety and the template.

Capacity of nonisotopically 5'-labeled oligonucleotides to serve as primers in PCR is promising in many aspects, for example, in a broad use of the reverse dot-blot technique (18) for identification of genomic mutations.

ACKNOWLEDGMENT

We are grateful to I. A. Kudelina for fluorescence spectra, to T. A. Balashova and K. V. Pervushin for NMR spectra, to Yu. P. Kozmin for plasma desorption mass spectra, and to O. V. Plutalov for helpful advice.

LITERATURE CITED

- (1) Yamana, K., and Letsinger, R. L. (1985) Synthesis and properties of oligonucleotides bearing a pendant pyrene group. *Nucleic Acids Symp. Ser. No. 16*, 169–172.
- (2) Roget, A., Bazin, H., and Teoule, R. (1989) Synthesis and use of labelled nucleoside phosphoramidite building blocks bearing a reporter group: biotinyl, dinitrophenyl, pyrenyl and dansyl. *Nucleic Acids Res.* 17, 7643–7651.
- (3) Tesler, J., Cruickshank, K. A., Morrison, L. E., and Netzel, T. L. (1989) Synthesis and characterization of DNA oligomers and duplexes containing covalently attached molecular labels: comparison of biotin, fluorescein, and pyrene labels by thermodynamic and optical spectroscopic measurements. *J. Am. Chem. Soc.* 111, 6966–6976.
- (4) Lee, H., Hinz, M., Stezowski, J. J., and Harvey, R. G. (1990) Syntheses of polycyclic aromatic hydrocarbon-nucleoside and oligonucleotide adducts specifically alkylated on the amino functions of deoxyguanosine and deoxyadenosine. *Tetrahedron Lett.* 31, 6773–6776.
- (5) Yamana, K., Gokota, T., Ohashi, Y., Ozaki, H., Kitamura, M., Nakano, H., Sangen, O., and Shimidzu, T. (1990) Oligo-

- nucleotides with pyrene fluorophore at the sugar fragment: synthesis and properties in binding to complementary polynucleotide. *Nucleic Acids Symp. Ser. No. 22*, 103-104.
- (6) Kitamura, M., Nimura, A., Yamana, K., and Shimidzu, T. (1991) Oligonucleotides with *bis*-pyrene adduct in the backbone: syntheses and properties of intramolecular excimer forming probe. *Nucleic Acids Symp. Ser. No. 25*, 67-68.
- (7) Kitamura, M., Nimura, A., Kunimoto, K., Segawa, H., and Shimidzu, T. (1991) Synthesis and properties of oligonucleotide derivative with P(V) porphyrin. *Nucleic Acids Symp. Ser. No. 25*, 13-14.
- (8) Arnold, L. J., Reynolds, M. A., and Bhatt, R. S. (1987) Non-nucleotide linking reagents for nucleotide probes. Pat. PCT WO 89/02439.
- (9) Nelson, P. S., Sherman-Gold, R., and Leon, R. (1989) A new and versatile reagent for incorporating multiple primary aliphatic amines into synthetic oligonucleotides. *Nucleic Acids Res.* 17, 7179-7186.
- (10) (a) Cook, J. W., and Hewett, C. L. (1933) The isolation of a cancer-producing hydrocarbon from coal tar. Part III. Synthesis of 1,2 and 4,5-benzpyrenes. *J. Chem. Soc.* 398-405. (b) Winterstein, A., Vetter, H., und Schön, K. (1935) Zur Synthese der krebs-erregenden 3,4-Benzpyrenes (Synthesis of carcinogenic 3,4-benzopyrene). *Chem. Ber.* 68, 1079-1085.
- (11) Bachmann, W. E., Carmack, M., and Safir, S. R. (1941) Some modifications of the synthesis of 3,4-benzpyrene from pyrene. *J. Am. Chem. Soc.* 63, 1682-1685.
- (12) Caruthers, M. H., Barone, A. D., Beaucage, S. L., Dodds, D. R., Fisher, E. F., McBride, L. J., Matteucci, M., Stabinsky, Z., and Tang, J.-Y. (1987) Chemical synthesis of deoxy-oligonucleotides by the phosphoramidite method. *Methods Enzymol.* 154, 287-313.
- (13) Polushin, N. N., Pashkova, I. N., and Efimov, V. A. (1991) Rapid deprotection procedures for synthetic oligonucleotides. *Nucleic Acids Symp. Ser. No. 24*, 49-50.
- (14) Saiki, R. K., Gelfand, D. H., Stoffel, S., Scharf, S. J., Higuchi, R., Horn, G. T., Mullis, K. B., and Ehrlich, H. A. (1988) Primer-directed enzymatic amplification of DNA with a thermostable DNA polymerase. *Science* 239, 487-491.
- (15) Lebedenko, E. N., Birikh, K. R., Plutalov, O. V., and Berlin, Yu. A. (1991) Method of artificial DNA splicing by directed ligation (SDL). *Nucleic Acids Res.* 19, 6757-6761.
- (16) Misiura, K., Durrant, I., Evans, M. R., Gait, M. J. (1990) Biotinyl and phosphotyrosinyl phosphoramidite derivatives useful in the incorporation of multiple reporter groups on synthetic oligonucleotides. *Nucleic Acids Res.* 18, 4345-4354.
- (17) Sproat, B. S., and Gait, M. J. (1984) Solid-phase synthesis of oligodeoxyribonucleotides by the phosphotriester method. In *Oligonucleotide Synthesis: A Practical Approach* (M. J. Gait, Ed.) pp 83-115, IRL Press, Oxford.
- (18) Saiki, R. K., Walsh, P. S., Levenson, C. H., Ehrlich, H. A. (1989) Genetic analysis of amplified DNA with immobilized sequence-specific oligonucleotide probes. *Proc. Natl. Acad. Sci. U.S.A.* 86, 6230-6234.

Registry No. 1, 3443-45-6; 2, 143039-32-1; 3, 143039-33-2; 4, 143039-34-3; 5 (isomer 1), 143039-35-4; 5 (isomer 2), 143039-36-5; 6, 143170-79-0; 7, 143170-78-9; (Pr₂N)₂POCH₂CH₂CN, 102691-36-1; pentafluorophenol, 771-61-9.

Large-Scale Synthesis of the Bifunctional Chelating Agent 2-(*p*-Nitrobenzyl)-1,4,7,10-tetraazacyclododecane-*N,N',N'',N'''*-tetraacetic Acid, and the Determination of Its Enantiomeric Purity by Chiral Chromatography

Oliver Renn and Claude F. Meares*

Department of Chemistry, University of California, Davis, California 95616. Received May 15, 1992

The attachment of radiometals to monoclonal antibodies for medical applications requires extreme stability under physiological conditions, with no significant release of metal. Chelators that can hold radiometals like ^{111}In , ^{67}Ga , and ^{90}Y with high stability under these conditions are essential for radiotherapy or immunoscintigraphy. 2-(*p*-Nitrobenzyl)-1,4,7,10-tetraazacyclododecane-*N,N',N'',N'''*-tetraacetic acid (nitrobenzyl-DOTA) is one of the most promising bifunctional chelating agents. A large-scale synthesis of nitrobenzyl-DOTA is described. The overall yield for the nine-step synthesis sequence starting from nitrophenylalanine is 5.6%. Synthesis of nitrobenzyl-DOTA according to the new procedure yields up to ~10 g without special apparatus. Both enantiomers of the chiral chelate nitrobenzyl-DOTA have been prepared, and their enantiomeric purity has been checked by chiral chromatography.

INTRODUCTION

Radiolabeled monoclonal antibodies (mAbs)¹ have shown considerable promise in the detection and therapy of cancer (1-5). Radionuclides of interest for radioimmunotherapy and radioimmunoimaging are metals such as ^{111}In , ^{90}Y , ^{67}Cu , ^{55}Co , and ^{68}Ga (6-9). Chelators that can hold these radiometals with high stability under physiological conditions are essential to avoid excessive radiation damage to nontarget cells (10). Bifunctional chelating agents (11, 12) are compounds with a strong metal-chelating group at one end and a reactive functional group at the other. When conjugated to mAbs, these agents act as carriers of radiometals for tumor targeting and radiotherapy. Methods to attach these chelates to mAbs have gained growing attention in the last several years (13, 14) and are now well-developed (15).

Among the metallic radionuclides for therapy, yttrium-90 is of particular interest due to its superior properties, including pure β -emission and the high dose yield per nanomole (16).

We have recently developed a new macrocyclic bifunctional chelating agent, 2-(*p*-nitrobenzyl)-1,4,7,10-tetraazacyclododecane-*N,N',N'',N'''*-tetraacetic acid (10, nitrobenzyl-DOTA, Figure 1), that holds yttrium with extraordinary stability under physiological conditions in human serum (17).

Radiopharmaceuticals prepared from this DOTA analog have gained growing attention. Nitrobenzyl-DOTA binds an interesting variety of metals better than any other chelator we have studied so far. It binds both yttrium and indium with superior stability, so it should be possible to use DOTA chelates of the γ -emitting ^{111}In as a tracer for DOTA chelates of the β -emitting ^{90}Y to gain accurate measurements of radiation dosimetry.

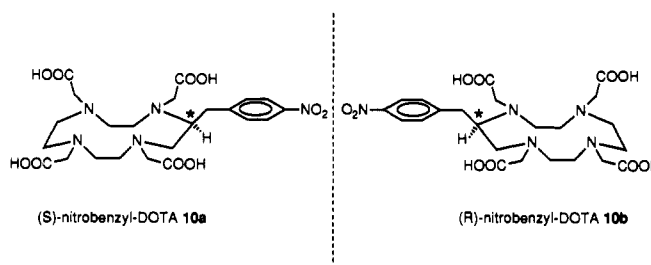


Figure 1. Schematic structures of (*R*)- and (*S*)-nitrobenzyl-DOTA.

In addition, the stability of nitrobenzyl-DOTA chelates with other metals such as copper (Cu-nitrobenzyl-DOTA has shown a better serum stability than any other copper chelate studied so far) suggest that it will be useful in a variety of applications to biological systems. Nitrobenzyl-DOTA has also been used as a precursor for the synthesis of a new chelate conjugate for pretargeted diagnosis and therapy (18), which is now in clinical trials.

The growing demand for large amounts of 10 encouraged us to develop a large-scale synthesis. This compound is prepared in a nine-step synthesis from nitrophenylalanine. The synthesis, described by Moi and Meares (17), was originally devised for lab-scale, giving final yields of less than 100 mg. In this report we describe a large-scale synthesis procedure that produces amounts up to ~10 g.

Like many of the drugs in current use, 10 incorporates a chiral center. The majority of such compounds are marketed as racemates. Generally differences in activity may occur between enantiomers. Thus it is important to control enantiomeric purity. Of particular importance in the case of 10, which is prepared either from L- or D-nitrophenylalanine, different immunogenicity could result when the protein-conjugated chelate is administered as a radiopharmaceutical (19). We have prepared (*S*)-nitrobenzyl-DOTA (10a) as well as (*R*)-nitrobenzyl-DOTA (10b) and have explored several chromatographic methods for chiral discrimination. Chromatography with a chiral stationary phase (Cyclobond column) gave good resolution of 10a and 10b, showing no detectable contamination by one enantiomer in preparations of the other.

* Address correspondence to Claude F. Meares, Department of Chemistry, University of California, Davis, CA 95616. Telephone: 916-752-0936. FAX: 916-752-8938.

¹Abbreviations used: BOC, *tert*-butoxycarbonyl; BOC-ON, 2-[[*tert*-butoxycarbonyloxy]imino]-2-phenylacetone nitrile; DMF, *N,N*-dimethylformamide; DOTA, 1,4,7,10-tetraazacyclododecane-*N,N',N'',N'''*-tetraacetic acid; mAb, monoclonal antibody; THF, tetrahydrofuran; TFA, trifluoroacetic acid; TsCl, *p*-toluenesulfonyl chloride.

EXPERIMENTAL PROCEDURES

All reagents and solvents were the purest commercially available and were used without further purification, if not stated otherwise. Borane-THF (1 M) in Sure/Seal bottles was purchased from Aldrich. Pure water (18 M Ω cm⁻¹) was employed throughout. Metal-free conditions were maintained during synthetic chemistry. All glass labware was washed with a mixed acid solution and thoroughly rinsed with deionized, distilled water (20). All plastic labware was washed with 3 M HCl and thoroughly rinsed. Reagent-grade THF was distilled from benzophenone sodium ketyl immediately before use.

Thin-Layer Chromatography. TLC was run on plastic backed silica gel plates (0.2 mm thick silica gel 60 F₂₅₄, E. Merck, Germany) using a 10% (w/v) aqueous ammonium acetate/CH₃OH (1:1 v/v) solution as the eluent. In this system, unchelated cobalt and conjugates remain at the origin while free chelates migrate to *R_f* 0.5–0.7.

High-Performance Liquid Chromatography. HPLC was carried out on a Rainin Rabbit HPX System (Rainin Instrument, Woburn, MA) equipped with titanium piston washing pump heads. Solvents were mixed using a Dynamax dual-chamber dynamic mixer (Titanium). UV absorbance was measured using an absorbance/fluorescence monitor (ISCO Model UA-5) at 254 or 345 nm. A Gilson Model 201 Fraction collector (Gilson Medical Electronics, Middleton, WI) was used. The HPLC system was controlled by Dynamax software on a Macintosh Plus computer.

Normal-phase HPLC was performed at room temperature with a Dynamax 21.4 \times 250 mm silica column using a gradient of CH₂Cl₂ and CH₃CN. For detailed descriptions of the gradients, see below.

Reversed-phase HPLC was performed at room temperature with a Dynamax 21.4 \times 250 mm C₁₈ column, generally using gradients of CH₃OH or CH₃CN and 0.1 M ammonium acetate (pH 6) with a flow rate of 12.5 mL/min.

All solvents for HPLC and reaction mixtures were filtered through a nylon 66 Millipore filter (0.45 μ m) prior to use.

Chiral Chromatography. This was done using the system described above. The following procedures were tried: (i) Chromatography was performed on a Pirkle covalent D-phenylglycine column (250 \times 4.6 mm), obtained from Regis Chemical Co. (Morton Grove, IL). Mobile phases of mixtures of dimethyl sulfoxide, CH₂Cl₂, CH₃CN, and 2-propanol at 1 mL/min were used. (ii) Chromatography was performed on ASTEC Cyclobond I columns (250 \times 4.6 mm) with Cyclobond guard columns, purchased from Rainin Instruments (Woburn, MA). Mobile phases of aqueous ammonium acetate, ammonium phosphate, triethylammonium acetate, and ammonium citrate buffers (0.1 to 0.01 M or 1% to 0.1%) with varying amounts of CH₃OH and CH₃CN at different pH values were used. Flow rates were between 0.7 and 1.4 mL/min. (iii) For chiral derivatization, Marfey's reagent [(1-fluoro-2,4-dinitrophenyl-5)-L-alanine amide] from Peptides International, Louisville, KY, was used. The derivatization was carried out as recommended by Peptides International; however the reaction temperature and time had to be increased to 65 $^{\circ}$ C and to 2 h. Chromatography was performed on a C₁₈ reversed-phase column, with mobile phases of 0.1 M ammonium acetate and varying amounts of CH₃CN or CH₃OH at a flow rate of 12.5 mL/min. (iv) Chromatography was performed on a C₁₈ reversed-phase

column, with a mobile phase of aqueous L-lysine (1 \times 10⁻² to 5 \times 10⁻³ M) as a chiral additive, at a flow rate of 12.5 mL/min.

Ultraviolet Spectrophotometry. Optical density measurements at 280 nm were made on a Gilford Model 250 spectrophotometer using a 1-cm pathlength microcell. Optical densities were measured at dilutions which gave absorbance readings of 0.1–1.0.

Radiation Counting. γ -counting was done in a Beckman Model 310 counter with the appropriate energy windows set for ⁵⁷Co. TLC plates containing radiolabeled materials were visualized with an AMBIS radioanalytical imaging system.

NMR Spectroscopy. Proton NMR spectra were obtained on a GE QE 300 Spectrometer at 300 MHz or a Bruker AC 200 at 200 MHz. Chemical shifts were relative to either HDO (4.70 ppm) or residual CHCl₃ (7.24 ppm). For D₂O solutions, 0.4 unit was added to the pH meter reading.

Mass Spectroscopy. Mass spectra and exact mass measurements were obtained on a ZAB-HS-2F mass spectrometer (VG Analytical, Wythenshawe, UK). During mass spectroscopic measurements, either 3-nitrobenzyl alcohol or dithiothreitol/dithioerythritol (3:1 w/w) was used as a matrix along with small amounts of *p*-toluenesulfonic acid. High-resolution FAB spectra contained polyethylene glycol or polyethylene glycol methyl ether as reference compound.

Preparation of 2-(*p*-Nitrobenzyl)-1,4,7,10-tetraazacyclododecane-*N,N,N',N''*-tetraacetic Acid (10). Total yields for each step are given in Table I.

(*S*)-*p*-Nitrophenylalanine. (*S*)-Phenylalanine (80 g, 0.48 mol) was dissolved in 215 mL of concentrated sulfuric acid over the course of 5 h at 0 $^{\circ}$ C. Concentrated nitric acid (27 mL) was added dropwise over the course of 2 h at 4–8 $^{\circ}$ C. The reaction mixture was poured over 300 mL of ice and carefully neutralized with small additions of (NH₄)₂CO₃. On neutralization, (*S*)-*p*-nitrophenylalanine precipitated. The precipitate was collected and recrystallized from water. Yield: 61.63 g (61%). ¹H NMR (300 MHz, D₂O, pH 6): δ 3.18 (q, 1 H), 3.23 (q, 1 H), 3.90 (t, 1 H), 7.40 (d, 2 H), 8.10 (d, 2 H).

***N*-(*tert*-Butoxycarbonyl)-(*S*)-*p*-nitrophenylalanine (1).** (*S*)-*p*-Nitrophenylalanine (61.63 g, 293.2 mmol) in 176 mL of H₂O was reacted with BOC-ON (79.5 g, 323 mmol) in 171 mL of dioxane and 62 mL of triethylamine (4 h, room temperature, N₂ atmosphere). The reaction mixture was poured into 500 mL of water and extracted with ether (5 \times 400 mL) and the pH of the aqueous layer adjusted to 1 with 6 M HCl. This solution was extracted with ethyl acetate (5 \times 400 mL), and the extracts were taken to dryness. The yellow material was dissolved in 300 mL ether, the solvent was removed under reduced pressure, and the residue was lyophilized to give the product, *N*-(*tert*-butoxycarbonyl)-(*S*)-*p*-nitrophenylalanine (1) as a white powder. Yield: 77.97 g (86%). ¹H NMR (300 MHz, CDCl₃): δ 1.30 (d, 9 H), 3.10 (m, 2 H), 4.50 (q, 1 H), 7.40 (d, 2 H), 9.80 (s, 1 H).

***N*-(*tert*-Butoxycarbonyl)-(*S*)-*p*-nitrophenylalanine *N*-Hydroxysuccinimide Ester (2).** *N*-Hydroxysuccinimide (29 g, 252 mmol) was added to a solution of 1 (77.97 g, 252 mmol) and dicyclohexylcarbodiimide (57 g, 275 mmol) in 1250 mL of dioxane (room temperature, 17 h, N₂ atmosphere). The resulting precipitate was filtered off and the filtrate taken to dryness. The residue was dissolved in 1000 mL of 2-propanol and the undissolved material was filtered off. The filtrate was taken to dryness, giving *N*-(*tert*-butoxycarbonyl)-(*S*)-*p*-nitrophenylalanine

N-hydroxysuccinimide ester (2). Yield: 87.03 g (82%). ¹H NMR (300 MHz, CDCl₃): δ 1.40 (s, 9 H), 2.90 (s, 4 H), 3.40 (m, 2 H), 5.00 (s, 1 H), 7.50 (d, 2 H), 8.20 (d, 2 H).

***N*-(*tert*-Butoxycarbonyl)-(*S*)-*p*-nitrophenylalanyl-glycylglycylglycine (3).** Compound 2 (93.00 g, 219 mmol) in 415 mL of DMF was added to a solution of 58.25 g (307 mmol) of triglycine and 34.42 g of sodium bicarbonate in 820 mL of water and the solution stirred for 5 h at room temperature (nitrogen atmosphere). The reaction mixture was filtered and 1770 mL of water was added. The product, *N*-(*tert*-butoxycarbonyl)-(*S*)-nitrophenylalanyl-glycylglycylglycine (3), was precipitated from solution by the addition of concentrated HCl (final pH 1). The mixture was held at 4 °C for 12 h, and the precipitate was filtered off, washed with ether, and dried in a desiccator under reduced pressure. Yield: 104.09 g (99%). ¹H NMR (300 MHz, D₂O, pH 11): δ 1.10 (s, 3 H), 1.25 (s, 6 H), 3.15 (m, 2 H), 3.65 (s, 3 H), 3.85 (s, 3 H), 4.40 (m, 1 H), 7.25 (d, 2 H), 8.05 (d, 2 H). FAB-MS: *m/e* calcd (M + Na⁺) 504, found 504.

(*S*)-*p*-Nitrophenylalanyl-glycylglycylglycine (4). Compound 3 was dissolved in trifluoroacetic acid at 0 °C and stirred for 1 h. The solvent was removed under reduced pressure to give (*S*)-*p*-nitrophenylalanyl-glycylglycylglycine (4) as the trifluoroacetate salt in quantitative yield. This material is very hygroscopic; the preparation of 4 was always done immediately before the reduction, or the sample was stored under high vacuum. FAB-MS: *m/e* calcd (M + H⁺) 382, found 382.

(*S*)-11-(*p*-Nitrobenzyl)-3,6,9,12-tetraazadodecanol (5, 6). **Caution:** *BH₃·THF* can cause explosions and/or fire if not used properly. Protect from sparks, water, etc. Handle only in a hood behind sufficient shielding. Use a fiberglass tray under the reaction apparatus. In our hands, reductions with up to 1.6 L *BH₃·THF* (1 M) can be done safely using the following equipment and precautions.

Glassware was carefully checked and oven-dried at 200 °C prior to use. A 5-L three-neck round-bottom flask was equipped with a water-cooled condenser (5 × 60 cm) and an addition funnel (500 mL). The addition funnel was sealed with a rubber septum. A low nitrogen flow was applied through this septum into the reaction flask. A large gas bubbler (1.0-cm diameter) filled with mineral oil was connected to the condenser with Tygon tubing. Due to the possible high pressures during the addition of borane and the reduction, the system has to be carefully checked for a safe release of high pressure. All glassware was fixed with metal clamps. Tubing must be secured too, because the tubing material may weaken and become kinked during the reaction, resulting in a closed system. Also, the tubing softens during the HCl workup. Borane from Sure/Seal bottles was added using the double-needle technique (see Aldrich information: Handling Air Sensitive Reagents) through the septum into the addition funnel. A 500-mL addition funnel was chosen to keep the volume of *BH₃·THF* near the reaction flask low; addition of *BH₃·THF* solution in 500-mL aliquots was repeated as necessary.

For efficient stirring of the large volume (up to 2.3 L), it was necessary to use an egg-shaped stir bar and a magnetic stirrer with electronic speed control (Model RET, IKA, Germany). A heating mantle was used for heating the reaction mixture. The 5-L round-bottom flask was doubly clamped on a rigid support high enough to change the ice bath and heating mantle easily, without moving the heavy reaction vessel.

Compound 4 (44.52 g, 90 mmol) was dissolved in 420 mL of freshly distilled THF, and after cooling to 0 °C,

1600 mL of 1 M *BH₃·THF* complex (1600 mmol) was added slowly. The mixture was refluxed for 17 h, cooled to 0 °C, quenched with 200 mL of CH₃OH, saturated with HCl gas, and refluxed again for 17 h. The solvent was removed by evaporation under reduced pressure. The remaining viscous, colorless solution was decanted. The white, gummy precipitate was washed with CHCl₃, dissolved in 1000 mL of water, and washed again with 3 × 200 mL CHCl₃. The solvent was evaporated under reduced pressure and lyophilized to give 5 as a white powder. Yield: 42.5 g (93%). The resulting hydrochloride salt 5 was dissolved in a minimum amount of water by adjusting the pH to 10 with 10 M NaOH. The basic solution was continuously extracted with CHCl₃ for 8 h. The organic layer was taken to dryness under reduced pressure to give (*S*)-11-(*p*-nitrobenzyl)-3,6,9,12-tetraazadodecanol (6). Yield: 95%. ¹H NMR (300 MHz, D₂O, pH 11): δ 2.25 (br s, 6 H), 2.50–3.00 (m, 14 H), 3.10 (m, 1 H), 3.60 (t, 2 H), 7.35 (d, 2 H), 8.15 (d, 2 H). FAB-MS: *m/e* calcd (M + H⁺) 326, found 326.

(*S*)-11-(*p*-Nitrobenzyl)-*N,N,N',N''*-O-pentakis(tolylsulfonyl)-3,6,9,12-tetraazadodecanol (7): Freshly prepared 6 (30.9 g, 94 mmol) was dissolved in 480 mL of CH₃CN, 240 mL of triethylamine, and 240 mL of CH₂Cl₂. *p*-Toluenesulfonyl chloride (90.0 g, 471 mmol) was added and the mixture was stirred for 5 h under N₂. The solvent was removed under reduced pressure. The residue was taken up in CHCl₃, washed with aqueous HCl, and prepurified by open silica gel chromatography (4 × 8 cm, 60–200 mesh); the eluent was CHCl₃, followed by CH₃CN. Final purification was done by normal-phase HPLC to give the product (*S*)-11-(*p*-nitrobenzyl)-*N,N,N',N''*-O-pentakis(tolylsulfonyl)-3,6,9,12-tetraazadodecanol (7). Yield: 26.80 g (26% after HPLC purification). Normal-phase HPLC: solvent A, CH₂Cl₂; solvent B, CH₃CN; 2–5% B, 0–21 min; 5–100% B, 21–23 min; 100–2% B, 25–29 min; UV detection at 345 nm; product peak, 26 min; 245 runs (172 h) to purify 41.5 mmol of 7. ¹H NMR (300 MHz, CDCl₃): δ 2.30 (s, 3 H), 2.50 (m, 12 H), 2.60–3.50 (m, 14 H), 3.75 (m, 1 H), 4.20 (t, 2 H), 5.30 (d, 1 H), 7.00–7.90 (m, 24 H). High-resolution FAB-MS: *m/e* calcd (M + H⁺) 1096.263; found 1096.265.

(*S*)-2-(*p*-Nitrobenzyl)-*N,N,N',N''*-tetrakis(tolylsulfonyl)-1,4,7,10-tetraazacyclododecane (8). Compound 7 (45.43 g, 41.5 mmol) was dissolved in 4200 mL of DMF, CsCO₃ (13.4 g, 42 mmol) was added, and the mixture was stirred at 60 °C for 5 h under N₂. The solvent was removed under reduced pressure, and the residue was taken up in CHCl₃ and washed with 0.1 M HCl (3 × 250 mL). The solvent was again removed under reduced pressure to give the crude compound 8. The residue was dissolved in 200 mL of CHCl₃ and purified by open silica gel chromatography (4 × 8 cm, 60–200 mesh, eluent CHCl₃). The volume was reduced to ≈100 mL, and CH₃OH and ethyl acetate (≈200 mL each) were slowly added in equal portions until the first precipitate appeared. (*S*)-2-(*p*-Nitrobenzyl)-*N,N,N',N''*-tetrakis(tolylsulfonyl)-1,4,7,10-tetraazacyclododecane (8) was collected after cooling to 4 °C. Yield: 22.05 g (58%). Analytical normal-phase HPLC: solvent A, CH₂Cl₂; solvent B, CH₃CN; 2–3.7% B, 0–12 min; 3.7–4.1% B, 12–14 min; 4.1–100% B, 14–16 min; 100% B, 16–17 min; 100–2% B, 17–18 min; 2% B, 18–21 min; product peak, 18 min. ¹H NMR (300 MHz, CDCl₃): δ 2.40–2.60 (m, 12 H), 3.00–4.20 (m, 16 H), 4.50 (m, 1 H), 7.00–7.50 (m, 12 H), 7.60–7.90 (m, 6 H), 8.15 (d, 2 H). FAB-MS: *m/e* calcd (M + H⁺) 924.24; found 924.25.

(*S*)-2-(*p*-Nitrobenzyl)-1,4,7,10-tetraazacyclododecane (9). Compound 8 (13.03 g, 14.1 mmol) was dissolved

in 600 mL of concentrated H_2SO_4 , and 22.5 g of phenol was added. The mixture was heated to 100°C and stirred for 56 h under N_2 . The mixture was poured on to 2 L of ice and neutralized with ≈ 3.3 kg of barium hydroxide. During neutralization, more water must be added to make the mixture easy to stir, yielding a final volume of 16 L. The neutral suspension was held at 4°C for 12 h. The large amount of barium sulfate could be removed easily by filtration through funnels with fritted discs (9-cm diameter) of decreasing porosity (coarse, medium, fine). The remaining solution (9.5 L) was evaporated to a small volume (about 300 mL) under reduced pressure and purified by reversed-phase HPLC to give the product (S)-2-(p-nitrobenzyl)-1,4,7,10-tetraazacyclododecane (9). Yield after HPLC purification: 6.28 g of 9-2.5 CF_3COOH (84%). Reversed-phase HPLC: solvent A, 0.1% trifluoroacetic acid in water; solvent B, CH_3CN ; 15–20% B, 0–20 min; 20–60% B, 20–21 min; 60–15% B, 21–23 min; 15% B, 23–31 min; product peak, 18 min; 121 runs (64 h) to purify 16.6 mmol of 9. ^1H NMR (300 MHz, D_2O , pH 2): δ 2.80–3.50 (m, 17 H), 7.50 (d, 2 H), 8.20 (d, 2 H). FAB-MS: m/e calcd ($\text{M} + \text{H}^+$) 308.210, found 308.209.

(S)-2-(p-Nitrobenzyl)-1,4,7,10-tetraazacyclododecane-*N,N',N'',N'''*-tetraacetic Acid (10). Bromoacetic acid (10.14 g, 73.0 mmol) was added to a solution of 9 (8.83 g of 9-2.5 CF_3COOH , 16.6 mmol 9) in 45 mL of water at pH 11. The mixture was stirred at 70°C , while the pH was maintained at 10 using a pH-stat with 3 M NaOH. After 5 h the solution was neutralized with 6 M HCl and purified by reversed-phase HPLC to give the product (S)-2-p-nitrobenzyl-1,4,7,10-tetraazacyclododecane-*N,N',N'',N'''*-tetraacetic acid (10). Yield: 6.50 g (73%), based on $^{57}\text{Co}^{2+}$ metal-binding assay (14). Reversed-phase HPLC: solvent A, 0.1 M ammonium acetate, pH 6; solvent B, CH_3OH ; 15–30% B, 0–20 min; 30–100% B, 20–25 min; 100–15% B, 25–30 min; product peak, 10 min; 123 runs (70 h) to purify 12.05 mmol of 10. ^1H NMR (200 MHz, D_2O , pH 5.8): δ 2.80–3.96 (complex multiplet, 25 H), 7.54 (d, 2 H, $J = 8.39$ Hz), 8.25 (d, 2 H, $J = 8.57$ Hz). FAB-MS: m/e calcd ($\text{M} + \text{H}^+$) 540, found, 540.

RESULTS AND DISCUSSION

Large-Scale Synthesis of Nitrobenzyl-DOTA (Figure 2). Originally, 2-(p-nitrobenzyl)-DOTA (Figure 1) was synthesized by a nine-step procedure (17). The last four steps required preparative HPLC to purify the products. We tried to avoid these time-consuming, costly HPLC purification procedures and develop a synthesis procedure that gives a final yield of several grams of 10 without special apparatus.

Since nitrobenzyl-DOTA has one chiral carbon atom, starting from L-phenylalanine or D-phenylalanine results in either the *S*- or *R*-enantiomer of 2-(p-nitrobenzyl)-DOTA. We have prepared both enantiomers and developed an analytical method to check their enantiomeric purity by chiral chromatography.

(S)-p-nitrophenylalanine is commercially available or can be prepared using common procedures from phenylalanine. After protection of the α -amino group with BOC-ON, the carboxyl terminus of 1 was activated using dicyclohexylcarbodiimide and *N*-hydroxysuccinimide coupling to give 2. The tetrapeptide 3 was prepared in 99% yield by reaction with triglycine. The *t*-BOC group was removed using neat CF_3COOH to give 4 in quantitative yield.

The first critical step of the synthesis is the borane reduction of 4 to the polyamino alcohol 5. On the original scale, the reduction step required 68 mL of 1 M $\text{BH}_3\cdot\text{THF}$.

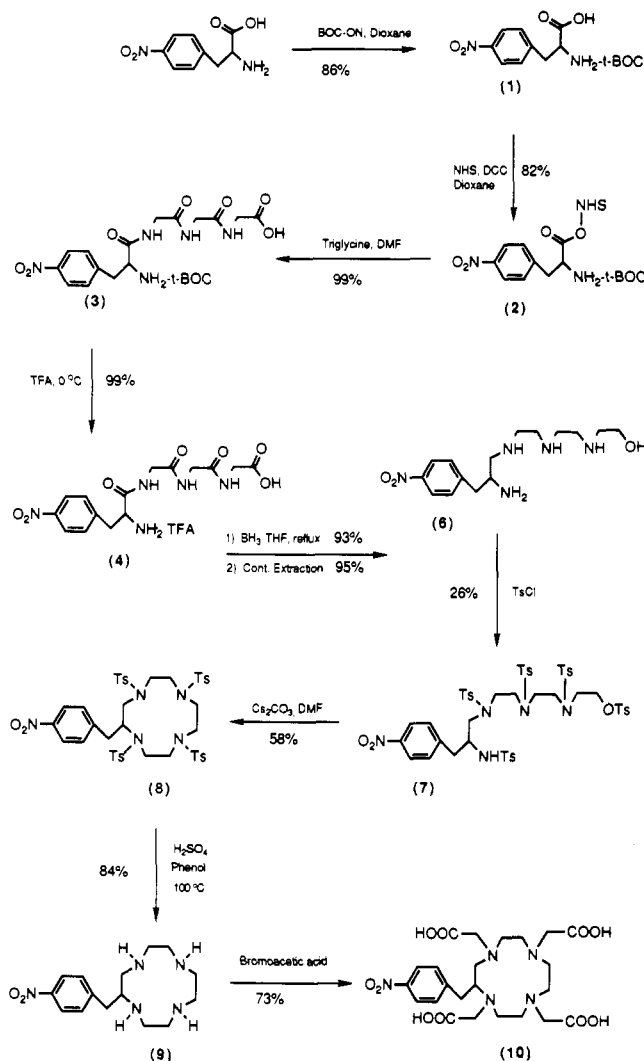


Figure 2. Reaction scheme for the large-scale synthesis of nitrobenzyl-DOTA (10) from nitrophenylalanine.

Starting the synthesis with 0.29 mol of phenylalanine gives about 140 g (0.22 mol) of deprotected tetrapeptide. Since four $\text{C}=\text{O}$ groups must be reduced, a total of 4.8 L of 1 M $\text{BH}_3\cdot\text{THF}$ is necessary for 0.22 mol of 4.

To reduce 0.22 mol, it proved most convenient to carry out three 0.7-mol reductions of 4. From readily available components, we designed a reduction apparatus where reductions with up to 1.6 L $\text{BH}_3\cdot\text{THF}$ can be done safely. Particular caution was taken regarding possible high H_2 pressures in the apparatus, which might occur when handling these large amounts of material. High pressure has to be released safely; it is therefore very important that the reaction mixture, which may be viscous at the beginning, is always stirred efficiently. General precautions and procedures are described in the experimental part.

The workup was improved to give 5 in yields up to 93% as the hydrochloride, a white powder. Several attempts were made to convert the hydrochloride 5 directly to the tosylated polyamino alcohol 7. However, none of the attempts to generate the free base 6 by ion exchange or by the use of Ag_2O gave satisfactory results, partly due to the instability of the polyamine. Finally, 6 was prepared using continuous liquid-liquid extraction into an organic phase.

The tosylation of polyamino alcohol 6 is a multistep reaction, which involves the alkylation of four amines and a primary alcohol. This reaction is a difficult step in the

Table I. Stepwise Yields for Nitrobenzyl-DOTA Synthesis

product	yield (%)
<i>N</i> -(<i>tert</i> -butoxycarbonyl)- <i>p</i> -nitrophenylalanine (1)	86
<i>N</i> -(<i>tert</i> -butoxycarbonyl)- <i>p</i> -nitrophenylalanine <i>N</i> -hydroxysuccinimide ester (2)	82
<i>N</i> -(<i>tert</i> -butoxycarbonyl)- <i>p</i> -nitrophenylalanyl-glycylglycylglycine (3)	99
<i>p</i> -nitrophenylalanyl-glycylglycylglycine (4)	99
11-(<i>p</i> -nitrobenzyl)-3,6,9,12-tetraazadodecanol hydrochloride (5)	93
11-(<i>p</i> -nitrobenzyl)-3,6,9,12-tetraazadodecanol (6)	95
11-(<i>p</i> -nitrobenzyl)- <i>N,N',N'',N'''</i> , <i>O</i> -pentakis(tolylsulfonyl)-3,6,9,12-tetraazadodecanol (7)	26
2-(<i>p</i> -nitrobenzyl)- <i>N,N',N'',N'''</i> -tetrakis(tolylsulfonyl)-1,4,7,10-tetraazacyclododecane (8)	58
2-(<i>p</i> -nitrobenzyl)-1,4,7,10-tetraazacyclododecane (9)	84
2-(<i>p</i> -nitrobenzyl)-1,4,7,10-tetraazacyclododecane- <i>N,N',N'',N'''</i> -tetraacetic acid (10)	73
overall yield	5.6

synthesis, since the yield is low due to side reactions (inter- and intramolecular condensation reactions involving partially tosylated intermediates are possible). We explored different solvents, bases, reaction temperatures, and procedures [e.g., different concentrations of 6 or addition of a catalyst (21)]. On this scale, tosylation of 6 using *p*-toluenesulfonyl chloride in a mixture of triethylamine/ $\text{CH}_3\text{CN}/\text{CH}_2\text{Cl}_2$ (1:2:1) at room temperature gave the best yields (26%). The large number of side products (up to eight according to HPLC) requires purification by HPLC. Reasonable HPLC runtime was made possible by using a prepurification step (open silica column) to remove the oily byproducts.

The cyclization step was carried out in DMF (0.01 M 7 at 60 °C). In the original synthesis procedure preparative HPLC was necessary for purification of the cyclic tetra-tosylamide; on this scale, attempts to precipitate 8 were successful and 8 could be obtained as a clean, white powder.

Removal of the tosylamide to generate the free cyclic tetraamine in neat H_2SO_4 with phenol gives the detosylated product. Neutralization of the sulfuric acid solution with barium hydroxide results in large amounts of precipitated barium sulfate. However, we found that barium sulfate could be removed easily after aging the precipitate, by using a series of three glass frits with decreasing porosity. Most of the barium sulfate was retained by the coarse filter, allowing a short filtration time. Preparative HPLC was used to separate the product 9 from the phenol in the mixture. The concentrated solution contained the product 9 in good purity, so that relatively large amounts of the crude product could be injected.

Finally, the cyclic amine was alkylated with bromoacetic acid under basic conditions to give the product, nitrobenzyl-DOTA. From the reaction mixture, the tetraalkylated compound was obtained in high yield. For medical applications, 10 was purified by HPLC.

Table I gives the yields of all the steps involved in the reaction sequence. The overall yield is 5.6%; starting with 300 mmol of *p*-nitrophenylalanine gives a yield of 9.15 g (17 mmol) nitrobenzyl-DOTA. The reaction sequence involves three preparative HPLC purification steps: the first step was improved in terms of separation, with a 30% reduction of run time so that the relative amounts of solvents were considerably less than previously reported (17). The second HPLC purification was done under aqueous conditions; CH_3CN was decreased by 60%, resulting from a change in the solvent gradient and a 30% reduction of run time.

While this paper was in preparation, a synthesis of bifunctional tetraazamacrocycles was published (22). That report describes the synthesis of 10 by two different routes; both start from nitrophenylalanine, but in each case the macrocycle is formed by bimolecular cyclization. Yields of the cyclization steps are lower (40% and 44%) than for the intramolecular cyclization described here (58%). The bimolecular cyclization step is also a limiting factor for

scaling up those syntheses because these reactions are done under high dilution and by using a special apparatus. Thus final yields of 1 or 2 g, depending on the route, result (22).

The cyclized products in ref 22 are reduced to yield the substituted macrocyclic tetraamine. We experienced generally higher yields when the linear molecule 5 was reduced; reduction of a macrocyclic amide with borane may be hindered sterically, resulting in lower yields. Thus a reduction followed by a cyclization step seems to be a better reaction sequence, giving yields of 93% (reduction of 5) and 58% (cyclization of 7) compared to 40% (44%) and 55% (37%) when the reduction is done after the cyclization. However, the low yield of the tosylation step in our synthesis scheme lowers the overall yield.

For the final alkylation to prepare nitrobenzyl-DOTA, the yields differ considerably. In ref 22 the reported conditions (pH 8.5, excess of $\text{BrCH}_2\text{CO}_2\text{H}$) give a 48% yield, compared with 73% for the alkylation of 9 at pH 11.

Determination of the Enantiomeric Purity of 10 by Chiral Chromatography. The introduction of a side chain into DOTA, giving a C-functionalized macrocycle, results in a chiral molecule since the C(2) atom is chiral (Figure 1). Nitrobenzyl-DOTA, when reduced and conjugated to a tumor-targeting antibody, could thus form diastereomeric radiopharmaceuticals. These might have different biological properties, including immunogenicity (19).

The determination of enantiomeric purity is of particular interest, since it is known that the enantiomeric forms of a drug may have different biological activities (24). Methods available to analyze enantiomers include chromatography on chiral stationary phases, the use of chiral additives in the mobile phase, derivatization to yield diastereomers, chiral detectors, NMR, and enantiomer specific immunoassays. Until chiral stationary phases were developed, chiral derivatization was the most common method. As diastereomers differ in their physical properties, they may be separated on achiral stationary phases. However, for derivatization the reagent must be obtainable in chemically and optically pure form, and the derivative must be formed in high yield. For simplicity, the direct use of chiral liquid chromatography (25–27) is the most common first approach to enantiomeric analysis.

We tried four different chiral HPLC systems to determine the enantiomeric purity of 10. Chiral stationary phases tested included a Pirkle column and a Cyclobond column. For the resolution of enantiomers on an achiral stationary phase, chiral derivatization using Marfey's reagent (28) was investigated. In addition, we briefly examined chiral ion-pair chromatography.

Chiral Stationary Phases for Enantiomeric Resolution of 10. When choosing a chiral stationary phase for enantiomeric resolution, the different characteristics of the phase have to be considered in order to match the structural features of the solute and the mobile phase. We

first tried a π -electron acceptor column. The first commercially available chiral stationary phase for HPLC was a 3,5-dinitrobenzoyl-D-phenylglycine "Pirkle" column (29), bound covalently to a silica support. However, our attempts to develop a method for the analysis of the enantiomeric purity of 10 using a Pirkle column were unsuccessful. Strongly anionic or cationic complexes with 10 are not easily resolved on this stationary phase, which may make derivatization necessary. Since 10 is only soluble in polar solvents such as water, dimethyl sulfoxide or DMF, it proved impossible to add enough nonpolar organic modifier into the mobile phase.

We next tried a cyclodextrin-based column, used in the reversed-phase mode. Cyclodextrins form chiral cavities that are bound to a silica support through a spacer. The cyclodextrin structure can be viewed as a cone open at both ends; the interior of the cone is relatively hydrophobic. If a chiral molecule fits into the cavity and has functional groups that interact with the secondary hydroxyl groups at the wider opening of the cone, then chiral separation may occur. Cyclodextrin columns are available in three different sizes, which allow separation of enantiomers of different sizes. The nitrobenzyl group of 10 fits well into the cavity of a β -cyclodextrin, so a Cyclobond I column was chosen.

Besides the nitrobenzyl group, nitrobenzyl-DOTA has two other types of functional groups: four carboxylic moieties and four tertiary amine moieties. In reported stereochemical resolutions of chiral molecules containing a carboxylic moiety, this function has to be attached to the C*, which appears to be the major structural requirement. In 10, the amine group is closer to the chiral C*. However, the flexibility of the carboxymethyl group might make its involvement in the process of chiral recognition possible. Steric hindrance at the C* may increase the stereochemical resolution. It is recommended (30) that the aromatic moiety is at the C*, as with nitrobenzyl-DOTA.

Mobile phase additives such as buffer salts can help improve column efficiency and resolution. We therefore investigated a number of different buffers: ammonium acetate, ammonium nitrate, ammonium phosphate, ammonium citrate, and triethylammonium acetate. When determining the optimum pH, the nearest hydrogen bonding group to the stereogenic center has to be considered. As an amine group is closest to C*, buffers of low pH were investigated first. Using gradients down to pH 4.0, the time difference between the elution of the two isomers was increased, but the α -value increased only slightly (from 1.08 to 1.09). However, this also resulted in long retention times (71 and 78 min for 95:5 (v/v) 0.1 M ammonium acetate pH 4.75/CH₃CN), and the peaks became extremely broad and flat. CH₃CN as the organic modifier gave generally better results than CH₃OH.

We also studied the influence of buffers with higher pH, as recommended for the resolution of carboxylic acids. A pH 7.5 ammonium acetate buffer containing 10% CH₃CN gave α 1.23 and sufficiently sharp peaks (Figure 3). The *S*-isomer 10a elutes first at 11.6 min; the *R*-isomer 10b elutes at 13.6 min. As can be seen from Figure 3, no cross-contamination could be detected, demonstrating that this synthesis does not involve significant racemization.

Among all buffers investigated, ammonium acetate seemed to work best. Triethylammonium acetate buffers caused strong retention of 10 on the column. An ammonium phosphate buffer might also work well, but closer investigation was impossible due to the relatively short lifetime of the Cyclobond columns. To achieve these

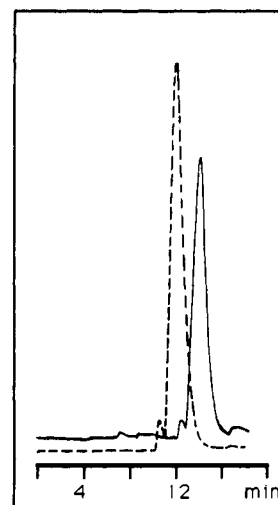


Figure 3. Determination of the enantiomeric purity of (*S*)-nitrobenzyl-DOTA (10a) (dashed line), and (*R*)-nitrobenzyl-DOTA (10b) (solid line) using a Cyclobond column: mobile phase, isocratic 90% 0.1 M ammonium acetate, pH 7.5, 10% CH₃CN; flow rate, 1.0 mL/min. The small peaks in front of 10a and 10b are unidentified impurities that are also evident on achiral C₁₈ HPLC. They may be metal chelates formed from trace metal impurities in the system.

results, two Cyclobond columns were consumed. This clearly demonstrates the major disadvantage of Cyclobond columns: the short lifetime, especially when gradients with high aqueous content are used.

Chiral Derivatization for Enantiomeric Resolution. Because of the short lifetime of Cyclobond columns, we also investigated other methods. Marfey's reagent (28), which provides a quantitative method of separating L- and D-amino acids, has been used to analyze the optical purity of peptides. In one study, 22 derivatives of 11 amino acids were studied on a C₁₈ column in a single reversed-phase chromatographic run (31). Even though the complete separation of all 22 derivatives studied was not achieved, the derivative of each enantiomer was well resolved from that of its enantiomeric counterpart. This prompted us to test Marfey's reagent for chiral derivatization. As an amine function is necessary to form the covalent bond to the reagent, we used 2-(*p*-aminobenzyl)-DOTA, which was prepared from 10a and 10b according to ref 23. However, no resolution could be obtained even with extremely shallow solvent gradients.

Chiral Ion-Pair Chromatography. We also investigated chiral ion-pair chromatography (32, 33). The separation of enantiomers on chiral stationary phases involves the reversible formation of diastereomeric complexes. In favorable cases, it is possible to achieve separation by adding a chiral reagent to the mobile phase and using nonchiral stationary phases. Organic acids and bases are able to interact with ion-pairing reagents in the mobile phase by forming less polar ion pairs. In some cases it is assumed that in situ coating of the column to form a temporary stationary phase is responsible for separation. Chiral mobile phases work with less expensive column packing, since the normal achiral materials can be used. However, due to the large amounts of the chiral additive needed, chiral ion-pair chromatography can be costly.

A study of the mechanism of anionic chelate retention in ion-pair reversed-phase chromatography was recently published (34). We tried the conditions recommended there and used L-lysine as a chiral counterion, but we were unable to resolve 10 using this system. Ion-pair chromatography in reversed-phase systems may be not sufficient

for some enantiomeric separations, since the undesired dissociation and solvation effects of water present in the eluent affect the intimate contact between the hydrophobic surfaces of the solute and the reagent molecule (35).

ACKNOWLEDGMENT

We thank Min Li and Douglas P. Greiner for helpful discussions. This work was supported by NIH-NCI Grants CA 16861 and CA 47829.

LITERATURE CITED

- (1) Yuanfang, L., and Chuanchu, W. (1991) Radiolabeling of monoclonal antibodies with metal chelates. *Pure Appl. Chem.* 3, 427-463.
- (2) Meares, C. F., Moi, M. K., Diril, H., Kukis, D. L., McCall, M. J., Deshpande, S. V., DeNardo, S. J., Snook, D., and Epenetos, A. A. (1990) Macrocyclic chelates of radiometals for diagnosis and therapy. *Br. J. Cancer* 62, Suppl. X, 21-26.
- (3) Bloomer, W. D., Lipsztein, R., and Dalton, J. F. (1985) Antibody mediated radiotherapy. *Cancer* 55, 2229-2233.
- (4) DeNardo, S. J., DeNardo, G. L., Peng, J.-S., and Colcher, D. (1983) Monoclonal Antibody Radiopharmaceuticals for Cancer Radioimmunotherapy. *Radioimmunology and Radioimmunotherapy* S. Burchiel, and B. Rhodes, Eds. pp 409-417, Elsevier, New York.
- (5) DeNardo, G. L., DeNardo, S. J., O'Grady, L. F., Levy, N. B., Adams, G. P., and Mills, S. L. (1990) Fractionated radioimmunotherapy of B-cell malignancies with ^{131}I -Lym-1. *Cancer Res.* 50 (3 Suppl), 1014s-1016s.
- (6) Halpern, S. E., Hagan, P. L., Garver, P. R., Kozial, J. A., Chen, A. W. N., Frincke, J. M., Bartholomew, R. M., David, G. S., and Adams, T. H. (1983) Stability characterization and kinetics of indium-111-labeled monoclonal antitumor antibodies in normal animals and nude mouse-human tumor models. *Cancer Res.* 43, 5347-5355.
- (7) Hnatowich, D. J., Layne, R. L., Lantaigne, D., and Davis, M. A. (1982) Radioactive labeling of antibody: a simple and efficient method. *Science* 220, 613-615.
- (8) Deshpande, S. V., DeNardo, S. J., Kukis, D. L., Moi, M. K., McCall, M. J., DeNardo, G. L., and Meares, C. F. (1990) Yttrium-90-labeled monoclonal antibody for therapy: Labeling by a new macrocyclic bifunctional chelating agent. *J. Nucl. Med.* 31, 473-479.
- (9) Kozak, R. W., Raubitschek, A., Mirzadeh, S., Brechbiel, M. W., Junghaus, R., Gansow, O. A., and Waldmann, T. A. (1989) Nature of the bifunctional chelating agent used for radioimmunotherapy with yttrium-90 monoclonal antibodies: Critical factors in determining in vivo survival and organ toxicity. *Cancer Res.* 49, 2639-2644.
- (10) Klein, J. L., Nguyen, T. H., Laroque, P., Kopfer, K. A., Williams, J. R., Wessels, B. W., Dillehay, L. E., Frincke, J., Order, S. E., and Lechner, P. K. (1989) Yttrium-90 and iodine-131 radioimmunoglobulin therapy of an experimental human hepatoma. *Cancer Res.* 49, 6383-6389.
- (11) Sundberg, M. W., Meares, C. F., Goodwin, D. A., and Diamanti, C. T. (1974) Chelating agents for the binding of metal ions to macromolecules. *Nature* 250, 587-588.
- (12) Meares, C. F., and Wensel, T. G. (1984) Metal chelates as probes of biological systems. *Acc. Chem. Res.* 17, 202-209.
- (13) Yeh, S. M., Sherman, D. G., and Meares, C. F. (1979) A new route to "bifunctional" chelating agents: Conversion of amino acids to analogs of ethylenedinitrilotetraacetic acid. *Anal. Biochem.* 100, 152-159.
- (14) Meares, C. F., McCall, M. J., Reardan, D. T., Goodwin, D. A., Diamanti, C. I., and McTigue, M. (1984) Conjugation of antibodies with bifunctional chelating agents: Isothiocyanate and bromoacetamide reagents, methods of analysis, and subsequent addition of metal ions. *Anal. Biochem.* 142, 68-78.
- (15) Brinkley, M. (1992) A brief survey of methods for preparing protein conjugates with dyes, haptens and cross-linking agents. *Bioconjugate Chem.* 3, 2-13.
- (16) Wessels, B. W., and Rogus, R. D. (1984) Radionuclide selection and model absorbed dose calculations for radiolabeled tumor associated antibodies. *Med Phys.* 11, 638-645.
- (17) Moi, M. K., Meares, C. F., and DeNardo, S. J. (1988) The peptide way to macrocyclic bifunctional chelating agents: Synthesis of 2-(p-nitrobenzyl)-1,4,7,10-tetraazacyclododecane-N,N',N'',N'''-tetraacetic acid and its study of its yttrium (III) complex. *J. Am. Chem. Soc.* 110, 6266-67.
- (18) Renn, O.; Goodwin, D. A., Paganelli, G., Studer, M., and Meares, C. F. Manuscript in preparation.
- (19) Kosmas, C., Snook, D., Gooden, C. S., Courtenay-Luck, N. S., McCall, M. J., Meares, C. F., and Epenetos, A. A. (1992) Development of Humoral Immune responses against a Macrocyclic Chelating Agent (DOTA) in Cancer Patients Receiving Radioimmunoconjugates for Imaging and therapy. *Cancer Res.* 52, 904-911.
- (20) Thiers, R. C. (1957) Contamination in trace element analysis and its control. *Methods Biochem. Anal.* 5, 273-335.
- (21) Börjesson, L., and Welch, C. J. (1991) An alternative synthesis of cyclic aza compounds. *Acta Chem. Scand.* 45, 621-626.
- (22) McMurphy, T. J., Brechbiel, M., Kumar, K., and Gansow, O. A. (1992) Convenient Synthesis of Bifunctional Tetraaza Macrocycles. *Bioconjugate Chem.* 3, 108-117.
- (23) McCall, M. J., Diril, D., and Meares, C. F. (1990) Simplified method for conjugating macrocyclic bifunctional chelating agents to antibodies via 2-Iminothiolane. *Bioconjugate Chem.* 1, 222-226.
- (24) Stevenson, D., and Williams, G. A. (1988) The biological importance of chirality and methods available to determine enantiomers. *Chiral Separations*. D. Stevenson, and I. D. Wilson, Eds. pp 1-9, Chromatographic Society Symposiums; Plenum Press, New York.
- (25) Lough, W. J. (Ed.) (1989) *Chiral liquid Chromatography*. Chapman and Hall, New York.
- (26) Stevenson, D., and Wilson, I. D. (Eds.) (1990) *Recent advances in chiral separations*. Chromatographic Society Symposium, Plenum Press, New York.
- (27) Zief, M., and Crane, L. J. (Eds.) (1988) *Chromatographic Chiral Separations*. *Chromatographic Science*, Vol. 40, Marcel Dekker, New York.
- (28) Marfey, P. (1984) Determination of D-Amino Acids. II. Use of a bifunctional Reagent, 1,5-Difluoro-2,4-dinitrobenzene. *Carlsberg Res. Commun.* 49, 591-594.
- (29) Pirkle, W. H., and House, D. W. (1979) Chiral high-pressure liquid chromatographic stationary phases. 1. Separation of the enantiomers of sulfoxides, amines, amino acid alcohols, hydroxy acids, lactones and mercaptans. *J. Org. Chem.* 44, 1957-1960.
- (30) Wainer, I. W., Stiffin, R. M., and Chu, Y.-Q. (1988) Drug Analysis using High-Performance Liquid Chromatographic chiral stationary phases: Where to begin and which to use. *Chiral Separations*, (D. Stevenson, and I. D. Wilson, Eds.) p 11-21, Chromatographic Society Symposiums, Plenum Press, New York.
- (31) Collicott, R. J. (1990) A note on some examples of chiral high performance liquid chromatographic resolution in the pharmaceutical industry. *Recent advances in chiral separations* (D. Stevenson, and I. D. Wilson Eds.), pp 25-30. Chromatographic Society Symposium, Plenum Press, New York.
- (32) Pettersson, C., and Schill, G. (1981) Separations of enantiomeric amines by ion-pair chromatography. *J. Chromatogr.* 204, 179-183.
- (33) Knox, J. H., and Jurand, J. (1982) Separation of optical isomers by zwitter ion-pair chromatography. *J. Chromatogr.* 234, 222-224.
- (34) Timerbaev, A. R., and Petrukhin, O. M. (1991) Liquid chromatography of chelates. Mechanism of anionic chelate retention in ion-pair reversed-phase chromatography (Review). *J. Anal. Chem. USSR* 46, 153-162.
- (35) Szepesi, G. (1989) Ion-pairing. *Chiral liquid Chromatography* (W. J. Lough, Ed.) pp 199-202. Chapman and Hall, New York.